Indexes

ENGINEERING LIBRARY

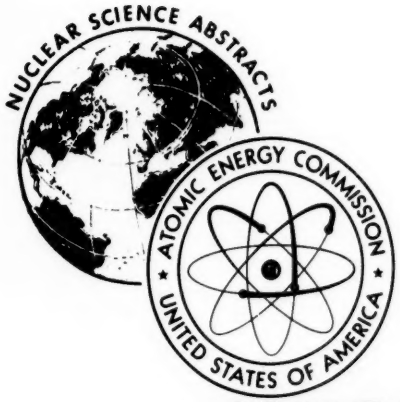

THE UNIVERSITY OF MICHIGAN
DEC 29 1966
ENGINEERING LIBRARY

NUCLEAR SCIENCE ABSTRACTS

Volume 20 Number 22

Abstracts 40493 – 42695

November 30, 1966

UNITED STATES ATOMIC ENERGY COMMISSION
Division of Technical Information

DEPOSITED BY THE UNITED STATES OF AMERICA

USAEC DEPOSITORY LIBRARIES

Collections of USAEC reports are maintained in the libraries of the organizations listed below for reference use by the general public. Facilities for making photocopies are available. The USAEC also makes available through these libraries atomic energy reports of countries other than the U. S. that are abstracted in *Nuclear Science Abstracts*.

ALABAMA
Auburn, Auburn University
ALASKA
College, University of Alaska
ARIZONA
Tucson, University of Arizona
ARKANSAS
Fayetteville, University of Arkansas
CALIFORNIA
Berkeley, University of California
Davis, University of California
Los Angeles, University of California
San Diego, Public Library
Stanford, Stanford University
COLORADO
Boulder, University of Colorado
Denver, Public Library
CONNECTICUT
New Haven, Yale University
DELAWARE
Newark, University of Delaware
DISTRICT OF COLUMBIA
Washington, Library of Congress
FLORIDA
Coral Gables, University of Miami
Gainesville, University of Florida
Tallahassee, The Florida State University
GEORGIA
Atlanta, Georgia Institute of Technology
HAWAII
Honolulu, University of Hawaii
ILLINOIS
Chicago, John Crerar Library
Chicago, University of Chicago
Evanston, Northwestern University
Urbana, University of Illinois
INDIANA
Bloomington, Indiana University
Lafayette, Purdue University
IOWA
Ames, Iowa State University
KANSAS
Manhattan, Kansas State University
KENTUCKY
Lexington, University of Kentucky
Louisville, University of Louisville
LOUISIANA
Baton Rouge, Louisiana State University
New Orleans, Tulane University
MARYLAND
Baltimore, Johns Hopkins University
College Park, University of Maryland
MASSACHUSETTS
Cambridge, Harvard University
Cambridge, Massachusetts Institute of Technology
MICHIGAN
Ann Arbor, University of Michigan
Detroit, Public Library
East Lansing, Michigan State University
MINNESOTA
Minneapolis, University of Minnesota
MISSISSIPPI
State College, Mississippi State University
MISSOURI
Kansas City, Linda Hall Library
Rolla, University of Missouri School of Mines and Metallurgy
St. Louis, Washington University
MONTANA
Bozeman, Montana State College
NEVADA
Las Vegas, Nevada Southern University
Reno, University of Nevada
NEW JERSEY
Princeton, Princeton University
Teaneck, Fairleigh Dickinson University
NEW MEXICO
Albuquerque, University of New Mexico
NEW YORK
Albany, The University of the State of New York
Buffalo, State University of New York at Buffalo
Ithaca, Cornell University
New York, Atomic Industrial Forum, Inc.
New York, Columbia University
New York, New York University
Rochester, University of Rochester
Schenectady, Union College
Syracuse, Syracuse University
Troy, Rensselaer Polytechnic Institute
NORTH CAROLINA
Charlotte, Public Library of Charlotte and Mecklenburg County
Durham, Duke University
Raleigh, North Carolina State College
NORTH DAKOTA
Grand Forks, University of North Dakota
OHIO
Cincinnati, University of Cincinnati
Cleveland, Public Library
OHIO (CONT.)
Columbus, Ohio State University
Toledo, University of Toledo
Youngstown, Youngstown University
OKLAHOMA
Norman, University of Oklahoma
Stillwater, Oklahoma State University
OREGON
Corvallis, Oregon State University
Portland, Reed College
PENNSYLVANIA
Philadelphia, University of Pennsylvania
Pittsburgh, Carnegie Library
University Park, Pennsylvania State University
PUERTO RICO
Rio Piedras, University of Puerto Rico
RHODE ISLAND
Providence, Brown University
SOUTH CAROLINA
Columbia, University of South Carolina
TENNESSEE
Knoxville, University of Tennessee
Memphis, Public Library
Nashville, Joint University Libraries
Oak Ridge, Oak Ridge Associated Universities
TEXAS
Austin, University of Texas
College Station, Texas A & M University
Dallas, Southern Methodist University
Houston, Rice University
Lubbock, Texas Technological College
San Antonio, Public Library
UTAH
Salt Lake City, University of Utah
VIRGINIA
Blacksburg, Virginia Polytechnic Institute
Charlottesville, University of Virginia
Norfolk, Old Dominion College
WASHINGTON
Pullman, Washington State University
Seattle, University of Washington
WEST VIRGINIA
Morgantown, West Virginia University
WISCONSIN
Madison, University of Wisconsin
Milwaukee, Public Library
WYOMING
Laramie, University of Wyoming

DEPOSITED BY THE
UNITED STATES OF AMERICA

Volume 20, Number 22, November 30, 1966

NUCLEAR SCIENCE ABSTRACTS

A semimonthly publication of the USAEC Division of Technical Information, Edward J. Brunenkant, Director. Published by the USAEC Division of Technical Information Extension, Robert L. Shannon, Extension Manager.

Nuclear Science Abstracts covers the international literature on nuclear science and technology and provides the only comprehensive abstracting and indexing of this body of information. Published twice each month since 1947, *NSA* covers technical reports of the U. S. Atomic Energy Commission and its contractors, technical reports of U. S. Government agencies and other governments, universities, industrial and research organizations, as well as patents, books, and journal literature on a world-wide basis. Nearly 350,000 abstracts have appeared in *NSA* through Volume 19. The subject matter covered in *NSA* is described in issue Number 1 and in TID-4552, *Subject Scope of Nuclear Science Abstracts*, available free from the U. S. Atomic Energy Commission, Division of Technical Information Extension, P. O. Box 62, Oak Ridge, Tennessee 37830.

Abstracts are arranged according to a number of subject categories and subcategories. Definitions of categories appear in issues Number 1 and 13. If the language of the original item is not English, the language will be indicated. Translations are not abstracted where an abstract of the original item has appeared in *NSA*.

INDEXES TO NSA

Corporate author, personal author, subject, and report number indexes appear in each issue and are cumulated quarterly, semiannually, and annually. Multi-volume cumulations have been issued as indicated on the following page. Report number indexes for all volumes (1–18) were issued at the end of Vol. 18. At the end of Vol. 19, the indexes for Vols. 1–15 were reissued to include additional public availability information. This cumulation will be a permanent shelf item and will not be reissued. Report number indexes for Vol. 19 are included as a cumulation beginning with Vol. 16.

AVAILABILITY OF PUBLICATIONS ABSTRACTED

The public availability of all U. S. Atomic Energy Commission reports is indicated in the report number indexes. The availability of other reports, when known, is also indicated. The availability of some unnumbered reports is given in the abstract.

Dissertations abstracted in *Dissertation Abstracts* and included in *NSA* are available from University Microfilms, Inc., 315 N. First Street, Ann Arbor, Michigan 48103.

Most of the published literature abstracted in *NSA* is on deposit at the Library, Oak Ridge Associated Universities, Oak Ridge, Tennessee, (a USAEC depository library) and is available through interlibrary loan. When requesting papers from this source, it is important that *NSA* volume and abstract number be cited.

HOW TO OBTAIN NUCLEAR SCIENCE ABSTRACTS

NSA is available on an exchange basis to universities, research institutions, industrial firms, and publishers of scientific information. Inquiries should be directed to the U. S. Atomic Energy Commission, Division of Technical Information Extension, P. O. Box 62, Oak Ridge, Tennessee 37830.

Government agencies may obtain *NSA* free of charge.

NSA is available to the general public on a subscription basis from the Superintendent of Documents, U. S. Government Printing Office, Washington, D. C. 20402, as follows:

For the 24 regular issues, $30.00 domestic, $37.00 foreign. A single issue costs $1.75, plus 25 per cent for foreign mailing. Domestic rates apply to the United States, Canada, Mexico, and Central and South American countries except Argentina, Brazil, Guyana and French Guiana, Surinam, and British Honduras. Foreign rates apply to the countries excepted above and to all other countries throughout the world.

For the quarterly, semiannual, and annual indexes, $22.00 domestic, $25.00 foreign.

Multivolume subject and author indexes are available as follows:

Vols. 1–4 (1948–1950) Johnson Reprint Corporation, 111 Fifth Avenue, New York, N. Y. 10003, $30.00.

Vols. 5–10 (1951–1956) Superintendent of Documents, U. S. Government Printing Office, Washington, D. C. 20402, $5.25.

Vols. 11–15, Subjects, Superintendent of Documents, U. S. Government Printing Office, Washington, D. C. 20402, $19.00.

Vols. 11–15, Personal Authors, Superintendent of Documents, U. S. Government Printing Office, Washington, D. C. 20402, $14.25.

Vols. 11–15, Corporate Authors, Superintendent of Documents, U. S. Government Printing Office, Washington, D. C. 20402, $2.50.

Cumulative Report Number Index, Vols. 1–15, Revised, is available from the Superintendent of Documents, U. S. Government Printing Office, Washington, D. C. 20402, $4.00.

Cumulative Report Number Index, Vols. 16–19, is available from the Superintendent of Documents, U. S. Government Printing Office, Washington, D. C. 20402, $2.50.

Annual Indexes are available separately from the U. S. Government Printing Office as follows:

Vol. 16, Subject and Authors, $9.75.
Vol. 17, Subject and Authors, $12.25.
Vol. 18, Subject and Authors, $12.50.
Vol. 19, Subject and Authors, $12.50.

ACKNOWLEDGMENTS

Agreements between the United States Atomic Energy Commission and the following organizations with regard to providing continuing services and specific literature coverage for *Nuclear Science Abstracts* are gratefully acknowledged:

American Institute of Physics; Atomic Energy of Canada Limited; Atomic Energy Research Establishment, United Kingdom; European Atomic Energy Community (EURATOM); Gmelin Institute; International Atomic Energy Agency; Japan Atomic Energy Bureau — Japan Atomic Energy Research Institute; Netherlands Patent Office; Reactor Centrum Nederland.

TABLE OF CONTENTS

Volume 20, Number 22, November 30, 1966

Category	Page
BIOLOGY AND MEDICINE	4925
General	4925
Ecology	4928
Metabolism, Tissue Distribution, and Toxicology	4931
Radiation Effects on Biochemicals	4938
Radiation Effects on Tissues	4941
Radiation Effects Therapy and Countermeasures	4959
Radiation Hazards and Protection	4960
Radiotherapy and Radiodiagnosis	4962
CHEMISTRY	4971
General	4971
Analytical Procedures	4971
Inorganic and Physical Chemistry	4978
Organic Chemistry	4987
Radiation Chemistry	4988
Radiochemistry	4997
Separation Processes and Procedures	5000
ENGINEERING	5004
General	5004
Applications of Nuclear Explosions	5004
Facilities and Equipment	5005
Heat Transfer and Fluid Flow	5008
Materials Testing	5009
Protective Structures	5010
Space Propulsion	5011
Vacuum Engineering	5012
GEOLOGY, METEOROLOGY, AND MINERALOGY	5013
General	5013
Meteorology	5013
Natural Radioactivity and Fallout	5013
Site Survey and Selection	5016
Techniques and Equipment	5016
Thorium and Uranium Minerals	5019
HEALTH AND SAFETY	5021
INSTRUMENTATION	5028
General	5028
Radiation Detection	5032
Radiation Effects	5044
ISOTOPE TECHNOLOGY	5045
General	5045
Industrial Applications	5045
Power Application	5047
Separation and Production	5048
MATHEMATICS AND COMPUTERS	5050
METALS, CERAMICS, AND OTHER MATERIALS	5051
General	5051
Corrosion	5051
Fabrication	5053
Properties and Structure	5054
Radiation Effects	5061
PHYSICS	5065
General	5065
Accelerators	5067
Astrophysics and Cosmology	5073
Atomic Physics	5076
Cosmic Radiation	5082
Direct Energy Conversion	5083
Elementary Particles and Radiations	5108
Field Theory, Scattering Theory, and Symmetries	5121
Fluid Physics and Thermodynamics	5131
Geophysics	5132
Gravitation, Quantum Mechanics, and Relativity Theory	5136
Low Temperature Physics	5139
Neutron Physics	5143
Nuclear Properties and Reactions	5144
Plasma Physics and Thermonuclear Processes	5169
Shielding	5185
Solid State Physics	5186
REACTOR TECHNOLOGY	5193
General	5193
Auxiliaries and Components	5193
Criticality Studies	5195
Design and Feasibility	5196
Fuels	5196
Power and Power-Breeder Reactors	5197
Process Heat Reactors	5202
Production Reactors	5202
Propulsion and Space	5202
Research and Test Reactors	5203
WASTE DISPOSAL AND PROCESSING	5206
GENERAL AND MISCELLANEOUS	5207
CORPORATE AUTHOR INDEX	INDEX-1
PERSONAL AUTHOR INDEX	INDEX-10
SUBJECT INDEX	INDEX-58
REPORT NUMBER INDEX	INDEX-159

STAFF OF NUCLEAR SCIENCE ABSTRACTS

MANAGING EDITOR

John W. Norris

ASSISTANT MANAGING EDITOR

Donald D. Davis

ASSOCIATE EDITORS

Lawrence T. Whitehead
David E. Bost
Robert C. Kelly
Lee M. Thompson

SUBJECT INDEX EDITOR

Everett J. Hoffman

EVALUATORS

William D. Matheny
John H. Mitchell
Mary H. Newman

ABSTRACTORS

F. S. Armstrong (AECL)
Jane G. Buchanan
D. Lamar Cason
Bennie G. Di Bona
Helen G. Donald
James R. Dulaney
Wells L. Green
Mary Catherine Grissom
Fernando J. Hamilton
Phyllis C. Hansen
Carolyn D. Houston
Rose V. Jermain
Betty L. McDowell
Jean F. Peckham
Mona H. Raridon
Julia S. Redford
Francis L. Sachs
Lila B. Smith
Charles E. Stuber
Martha J. Thomas
Anne G. Ward
David C. West
Milton O. Whitson
Gabriel O. Ycaza

SUBJECT HEADING SPECIALIST

Robert E. Upchurch

CORPORATE AUTHOR SPECIALIST

Clara L. Fox

DESCRIPTIVE CATALOGING SPECIALIST

J. Paul Meredith

SCHEDULING AND PUBLISHING COORDINATOR

Brainard L. Patton

Communication concerning the editorial policy and content of *NSA* should be addressed to the Managing Editor, *Nuclear Science Abstracts*, AEC Division of Technical Information Extension, P. O. Box 62, Oak Ridge, Tennessee 37830.

Use of funds for printing this publication approved by the Director of the Bureau of the Budget, June 28, 1966.

Volume 20, Number 22 November 30, 1966

NUCLEAR SCIENCE ABSTRACTS

BIOLOGY AND MEDICINE

General

Refer also to abstract 40626.

40493 (ANL-7300) LABORATORY ANIMAL SCIENCE: A REVIEW OF THE LITERATURE FOR JANUARY, FEBRUARY, AND MARCH 1966. Abstracts 1–123. Flynn, Robert J. (Argonne National Lab., Ill.). June 1966. Contract W-31-109-eng-38. 55p. Dep. mn. CFSTI $3.00 cy, $0.50 mn.

This annotated bibliography contains 123 references to journal articles on laboratory animal management, technology and medicine. A species index is included. (H.L.W.)

40494 (COO-1329-3) POPULATION DYNAMICS, MOVEMENT, AND HOME RANGE OF BLACK-TAILED JACKRABBITS (LEPUS CALIFORNICUS) IN CURLEW VALLEY, NORTHERN UTAH. Technical Progress Report, July 15, 1965–July 14, 1966. Wagner, Frederic H. (Utah State Univ., Logan. Dept. of Wildlife Resources). Contract AT(11-1)-1329. 32p. Dep. mn. CFSTI $2.00 cy, $0.50 mn.

Progress is reported on studies of population dynamics, movement and home range, and effects of x irradiation on ecological parameters in black-tailed jackrabbits. Population density continued the decline initiated in 1960. Reproductive performance was characterized by constant reproductive rates per female and length of breeding season in the period 1963-65 and by gradual advancement in breeding season phenology during the period of study. Thus, the progressive decrease in population density was attributed to mortality rates, the one year mortality averaging 5%. Progress in movement and home range studied during the report period was confined to development and refinement of telemetry facilities. Animal exposure facilities for head irradiation were designed and used to determine the $LD_{50(30)}$. Results indicated that the $LD_{50(30)}$ lay somewhere between 6000 and 6900 R. (H.G.D.)

40495 (NYO-901-54) PROGRESS REPORT NO. 28 [ON BIOLOGICAL PROBLEMS IN CANCER AND RADIATION], MAY 1, 1965–APRIL 30, 1966. (New England Deaconess Hospital, Boston, Mass. Cancer Research Inst.). Contract AT(30-1)-901. 62p. Dep. mn. CFSTI $3.00 cy, $0.75 mn.

Separate abstracts were prepared for the six sections of this report. (C.H.)

For abstracts of individual sections see: 40533, 40615, 40616, 40734, 40745, and 40810.

40496 (NYO-1753-3) PROGRESS REPORT [ON PRESERVATION OF HUMAN PLATELETS], 1966. (Children's Cancer Research Foundation, Boston, Mass.). June 1966. Contract AT(30-1)-1753. 87p. Dep. mn. CFSTI $3.00 cy, $0.75 mn.

Progress is reported on investigations of methods for the preservation of human blood platelets and granulocytes. Clinical studies on preserved platelets were continued. The ability of frozen human platelets to remain in the circulation when infused into thrombocytopenic recipients was further substantiated. A previously unknown cryoprotective agent, Dimethylacetamide (DMAC) was tested. It is superior to DMSO (dimethylsulfoxide) for the preservation of animal (rat) platelets. The simultaneous presence of dextrose increased the cryoprotective effect of both agents. Many other agents, including glycerol, were considerably less effective whether used alone or in combination with sugars. Removal of DMAC prior to the infusion of the platelets may be possible. Persistence in the circulation of preserved frozen human leukocytes in rats made leukopenic with Cytoxan was demonstrated. The increments in the WBC counts were 30 to 60% of those observed with infusions of fresh human leukocytes. This observation is consistent with previous data on phagocytosis by frozen human granulocytes. Methods for the better separation and harvesting of granulocytes as a by-product of platelet procurement are being developed. Adjustment of the hematocrit in the separated buffy coat to less than 40% increases the yield of granulocytes. A synthetic polypeptide, JFB-17, was found to be superior to dextran or phytohemagglutinin for the separation of granulocytes from red cells by sedimentation. Platelet components responsible for the formation of heterologous antibodies which affect vascular permeability and reduced platelet counts were demonstrated in a platelet extract previously shown to reduce vascular fragility. The fractionation and separation of these components is in progress. (18 references.) (auth)

40497 (NYO-3400-1) HUMAN CHROMOSOME ANALYSIS BY A SEMI-AUTOMATIC SYSTEM. Final Report for Four-Month Extension Period. Neurath, Peter W. (Research and Advanced Development Div., Avco Corp., Wilmington, Mass.); Falek, Arthur (New York State Psychiatric Inst., New York). Nov. 2, 1965. Contracts AT (30-1)-3400; AT(30-1)-3381. 47p. Dep. mn. CFSTI $2.00 cy, $0.50 mn.

During the extension period of the contract for the development of Human Chromosome Analysis by a Semi-Automatic System, several objectives were reached. First of all, the resolution of our system was considerably improved. This had to be done without having a better camera available and was accomplished by dividing the chromosome spread into four quadrants, then taping each quadrant separately and finally recombining all four quadrants during the computer analysis of the spread. Secondly, the computer program was rearranged systematically and fully documented so as to enable additions and changes to be made more easily and by programming personnel not familiar with the work from the beginning. The considerable portions of the effort devoted to documentation were not anticipated earlier, but were forced upon us at the beginning of this period by unexpected personnel changes involving the two programmers who originally worked on this problem as well as

by further anticipated moves. During this process, improvements in the program itself were also made. Finally, a fairly large number of chromosome spreads were prepared for taping by this latest procedure and several of these were carried through the whole process. The results reflect the improvements in resolution and in program and look very encouraging. They do, at the same time, show up some of the remaining problems more clearly, particularly in connection with arm ratio determinations. Progress was also made in improving slide preparations and staining. At least one promising variation for better spreading was turned up. (auth)

40498 (ORNL–3922) BIOLOGY DIVISION SEMIANNUAL PROGRESS REPORT FOR PERIOD ENDING JANUARY 31, 1966. (Oak Ridge National Lab., Tenn.). May 1966. Contract W-7405-eng-26. 207p. Dep. mn. CFSTI $6.00 cy, $1.25 mn.

Separate abstracts were prepared for the 25 sections of the report. (H.S.D.)

For abstracts of individual sections see: 40499–40508, 40535, 40581, 40582, 40623–40632, 40718, and 40719.

40499 (ORNL–3922, pp 69-79) CELL GROWTH AND DIFFERENTIATION. (Oak Ridge National Lab., Tenn.).

Research is reported on: a general method for the isolation and purification of phosvitin from vertebrate eggs; effects of alchol treatment on the lens-inducing ability of the optic cup in an in vitro system of Xenopus laevis; the appearance and accumulation of a fine, fibrous component in the nucleus during cellular differentiation in the lens regenerate and its possible relation to gamma crystallins; changes in the pattern of ribosomes during cellular differentiation of the lens regenerate; enhancement of nucleic acid synthesis in the iris epithelium caused by lens removal in Amblystoma opacum; continued growth of the regenerating lens in vitro; depigmentation and fiber differentiation of the Wolffian lens during regeneration in a chemically defined medium; and the membranous component of amphibian oocyte nucleoli. (H.G.D.)

40500 (ORNL–3922, pp 109-12) CELL PHYSIOLOGY. (Oak Ridge National Lab., Tenn.).

Calorimetric determinations were made of bound water in biological systems and the density of bacteriophages T4B and $T4BO_1$ were determined as a function of dilution treatment. (H.G.D.)

40501 (ORNL–3922, pp 113-14) NUCLEIC ACID CHEMISTRY. (Oak Ridge National Lab., Tenn.).

Various fractions and one highly purified product ($tRNA^{Phe}$) obtained by the chromatographic separation of crude tRNA from E. coli were analyzed for their base ratios and end groups. No correlation was found between base ratios and chromatographic position of the various tRNA species. (H.G.D.)

40502 (ORNL–3922, pp 115-27) PATHOLOGY AND PHYSIOLOGY. (Oak Ridge National Lab., Tenn.).

Research is reported on late hematologic effects of 14 Mev neutrons in mice; the effect of vinblastine on megakaryocytes and platelets; induction of resistance to a transplantable homologous lymphoid leukemia; the effect of microbial flora on aging in ICR mice; growth in semisolid agar of cells infected with the Rauscher leukemia virus; transplantability and leukemogenic activity of myxofibrosarcomas induced by the Rauscher virus; viral transmission of radioinduced myeloid leukemia; an optical-density analyzer; discontinuous, vertical flat-bed electrophoresis as a preparative system; separation and purification of erythropoietin; and an autoradiographic study of vaginal epithelia of mice by serial biopsy. (H.G.D.)

40503 (ORNL–3922, pp 137-45) ENZYMOLOGY. (Oak Ridge National Lab., Tenn.).

Research is reported on: the role of membranous particle fractions in protein synthesis; studies of the ribosomes of Clostridium pasteurianum; biosynthesis of cytochrome; configuration studies on E. coli polysomes; physical studies on E. coli phenylalanine transfer RNA; clearance of sheep and rat erythrocytes in mice using ^{75}Se as a tracer; antibody biosynthesis; phenylalanyl-RNA synthetase; the effect of methylation on phenylalanine transfer RNA from E. coli; ribosome-RNA synthetase separation by molecular sieving; purification and properties of alcohol dehydrogenase from Drosophila; use of lactate dehydrogenase as a marker in rat-mouse chimeras; lactate dehydrogenases from rodents; and inhibition of valyl-tRNA synthetase by oligonucleotides. (H.G.D.)

40504 (ORNL–3922, pp 146-60) BIOPHYSICS. (Oak Ridge National Lab., Tenn.).

Research is reported on: thymine dimer formation in uv-irradiated DNA at 77°K vs. room temperature; endothermic decay of long-lived free radicals induced in amino acids by x rays; repair of uv damage in differentiating bacterial spores; uv-induced breaks in the bromouracil-substituted DNA of phage T3; dosimetry of chronic neutron sources; the relative response of NaI(Tl) and anthracene to ^{32}P beta rays under conditions of partial absorption; the attachment of f1 bacteriophage to male strains of E. coli; the transducing bacteriophage P1kc; DNA transfer in bacterial conjugation; purification of nucleic acid polymerases; DNA polymerase activity in puromycin-treated synchronized mammalian cells; dimer formation and monomerization in the presence of proflavine; in vitro excision of pyrimidine dimers; repair of uv damage in T3 phage by E. coli B/r; transfer of thymine dimers from parent to progeny phage $T4_v$; and biological parameters involved in repair of x-ray damage. (H.G.D.)

40505 (ORNL–3922, pp 167) MICROBIOLOGY. (Oak Ridge National Lab., Tenn.).

The properties of malic-lactic transhydrogenase were used to study the complex formation between substrate and enzyme-bound pyridine nucleotide. Transhydrogenase was prepared in homogeneous form from two different species of Micrococcus lactilyticus. (H.G.D.)

40506 (ORNL–3922, pp 168-73) BIOCHEMICAL REGULATION. (Oak Ridge National Lab., Tenn.).

Research is reported on; participation of protein hormones in control of the synthesis of a steroid inducible enzyme in liver; hormonal control of enzyme levels in the Reuber hepatoma in vitro; RNA synthesis in fetal rat liver; charging of transfer RNA's with amino acids in adult and fetal rat liver; the mechanism of the in vitro inactivation of tyrosine α-ketoglutarate transaminase from rat liver; and studies of the mechanism of pyridoxine induction of tyrosine α-ketoglutarate transaminase in rat liver. (H.G.D.)

40507 (ORNL–3922, pp 191-6) AEC–NIH ZONAL ULTRACENTRIFUGE DEVELOPMENT. (Oak Ridge National Lab., Tenn.).

Progress is reported on: new gradient separation methods; separation of rat liver cell components by the B-XV zonal centrifuge rotor; respiratory syncytial virus studies in the B-IX zonal rotor: and evaluation of the k-1 zonal rotor. (H.G.D.)

40508 (ORNL–3922, pp 196-9) AEC–NASA SPACE BIOLOGY. (Oak Ridge National Lab., Tenn.).

Research is reported on: biocompatibility tests of the prototype packages for the Neurospora biosatellite experiment under simulated flight conditions, and a simulated space flight test for Habrobracon. The Gemini-3 s-4 space flight interaction experiment is discussed. (H.G.D.)

40509 (TID–22965) REVERSION FREQUENCY OF WAXY POLLEN TYPE IN NORMAL AND HYPOPLOID MAIZE PLANTS. Bianchi, A.; Tomassini, C. (Milan Univ. (Italy). Istituto di Genetica. Universita Cattolica del Sacro Cuore di Milano, Piacenza (Italy). Istituto di Genetica Vegetale). [1965]. Contract AT(30-1)2613. 22p. ORAU.

Maize pollen grains of constitution Yg I Sh Bz Wx were used to fertilize a stock possessing the corresponding recessive genetic markers yg C sh bz wx of the short arm of chromosome 9. Appropriate screening of the ensuing seedlings, together with the results of proper test-crossing and scoring of the pollen, made it possible to isolate hypoploid plants in which the chromosome 9 carrying the dominant

markers had lost at least the Wx gene, known to affect the chemical nature of the starch both in endosperm and in pollen grains. The pollen produced by such plants was, then, only influenced by the wx gene of the undamaged chromosome. The reversion rate of this gene, on the basis of the appearance of pollen grains giving the Wx chemical reaction (with iodine solution), was measured and compared with the reversion rate of normally diploid wx wx plants. On the basis of results with yeast, the expectation was that the normal chromosome condition should have produced a higher reversion rate than the genotype in which the hypoploid condition associated with the deficiency of the genetically marked region provided no opportunity for pairing and crossing-over, which was supposed to be responsible for that high reversion rate. In maize the experimental data failed to confirm a similar behavior. This finding suggests that the wx alleles investigated are likely to be due to base substitution. In such a case unequal crossing-over, causing base losses and insertions in DNA and, therefore, restoration of a sequence compatible with normal functioning, appears unlikely. Mutagenesis in these cases appears to rely only on mutational events s.s. and is associated with a suppressor system. In maize such a requirement seems to be met with the controlling elements. (auth)

40510 (TID-23137) COMPARATIVE MUTAGENESIS IN NEUROSPORA. Comprehensive Report, June 15, 1963-September 14, 1966. Brockman, Herman (Illinois State Univ., Normal. Dept. of Biological Sciences). June 1966. Contract AT(11-1)-1314. 14p. Dep. mn. CFSTI $1.00 cy, $0.50 mn.

Progress is reported on studies of mutagenesis in Neurospara crassa. Results are reported from studies on the effects of certain chemical mutagens, with emphasis on the action of acridines at the ad-3 region of N. crassa. (32 references.) (C.H.)

40511 (UCRL-16776) EFFECTS OF THYROID HORMONES ON CULTURED MAMMALIAN CELLS. Siegel, Edward (Lawrence Radiation Lab., Univ. of California, Berkeley). Mar. 1966. Contract W-7405-eng-48. 151p. Dep. mn. CFSTI $5.00 cy, $1.00 mn.

Thesis.

Monolayer tissue culture techniques and autoradiography were used to study the effects of thyroid hormones on the growth of mammalian cells. The influence of L-thyroxine and L-triiodothyronine on human kidney epithelial cells closely paralled the in vivo response to these hormones and limited corroborative studies were carried out on human heart and hamster bone marrow cell lines. Cellular proliferation and surface area, as well as plating efficiency, were affected by physiological and pathological concentrations of the hormones and biphasic response or negative feedback patterns were related to dose. The findings are discussed in relation to possible mechanisms of hormonal action, with the nucleus as the primary site of action. It is postulated that the hormones interact either directly with the genome or with the nuclear membrane to cause stimulation of m-RNA and protein synthesis. (145 references.) (C.H.)

40512 GENETIC CONTROL OF THE GERM CELL FORMATION. Gottschalk, W. (Univ., Bonn). Atompraxis, 12: 353-6(July 1966). (In German).

A large number of radioinduced mutant types of the pea (Pisum sativum), showing specific defects in the course of meiosis, were studied. Four different groups of genes were found to influence the germ cell formation in various ways. Certain of them become effective before meiosis starts and prevent the differentiation of the sporogenic tissue. Other genes influence the pairing of the homologous chromosomes or the chiasmatic formation, causing a strong reduction of the portion of functionable germ cells. A large group of recessive genes induces the complete breakdown of meiosis in certain meiotic stages, and in these cases germ cell formation does not take place. (auth)

40513 CHIMERICAL STRUCTURE OF M_1 PLANTS AND ITS BEARING ON THE DETERMINATION OF MUTATION FREQUENCIES IN ARABIDOPSIS. Mueller, A. J. (Research Inst. of Cultivated Plants, Gatersleben, Ger.). pp 46-52 of Induction of Mutations and the Mutation Process. Veleminsky, Jiri; Gichner, Tomas (eds.). Prague, Publishing House of the Czechoslovak Academy of Sciences, 1965.

A technique is described for scoring mutation frequencies in M_1 plants of Arabidopsis thaliana. Lethal embryos and chlorophyll deficiencies in the cotyledons in this plant were detected in seed pods under a binocular microscope. The seed pods of plants grown from mutagen treated seeds were examined shortly before the ripening of the seeds. (C.H.)

40514 MEASUREMENT OF CORONARY CIRCULATION TIME WITH A CATHETER-TYPE MICRO G-M COUNTER. Ueda, Hideo; Koide, Tadashi; Ito, Masahiro; Nakanishi, Atsuo; Ito, Iwao (Tokyo Univ.). Jap. Heart J., 527-33 (Nov. 1965).

A newly developed instrument and technique were used in experiments on dogs to evaluate coronary hemodynamics. Fifty to 600 μC of ^{32}P, as sodium orthophosphate, was injected quickly into the left ventricle via a No. 6 Cournand catheter, which was inserted through a femoral artery. Radioactivity was detected continuously by a catheter-type micro G-M counter inserted into right side of the heart through the internal jugular or femoral vein. The external diameter of the G-M counting tube was 2, 3, 4, or 5 mm and the effective length was 8, 10, 12, or 20 mm, respectively. The tubes were shielded with 25% chromium steel, with a thickness of 0.1 mm, or 100 mg/cm^2. As the ^{32}P solution was injected into the left ventricle, its arrival into the right side of the heart was monitored in situ with the G-M counter. A biphasic curve was recorded in the right ventricle, of which the earlier peak was related to coronary circulation, and the later one to systemic circulation. The early peak was inscribed also in the right atrium and coronary sinus, but in neither the superior nor the inferior vena cava. The average coronary circulation time from the left ventricle to the right ventricle was 2.2 ± 1.0 (S.D.) sec, ranging from 0.9 to 3.8 sec, in 9 dogs, when measured as the transit time of peak radioactivity. The value thus obtained was appreciably shorter than that reported previously. Since a probable reason for this discrepancy is the inadequate accuracy of conventional methods, the superiority of this technique is emphasized. (BBB)

40515 SOME UNUSUAL TOPICS IN RADIATION BIOLOGY. Zimmer, K. G. (Kernforschungszentrum, Karlsruhe, Ger.). Radiat. Res., 28: 830-43(Aug. 1966).

Three topics are discussed in this lecture which was presented at the fourteenth annual meeting of the Radiation Research Society, Coronado, California: (1) Single-Hit Effects in Radiobiology. Experiments with Drosophila on sex-linked lethal mutations indicate a single-hit effect. The influence of the stage of germ cells on x-ray-induced mutations is shown by dose effect curves for various stages of germ cells. Radiation studies on water snails demonstrate that single-hit curves can arise through superposition of multihit curves. Gamma radiation experiments with RNase in air and in nitrogen result in single-hit inactivation curves. (2) Energy transfer by elastic nuclear collisions as related to radiobiology. The cross section for inactivation of dry RNase was measured for protons of various energies. The results demonstrate the importance of elastic nuclear collisions for causing damage. (3) Protective Substances. Experiments on inactivation of T1 phage by gamma radiation show that inactivation is slower in the presence of SH compounds. (H.L.W.)

40516 APPLICATION OF THYROID SCANNING TO THE STUDY OF TRANSPLANTATION. Mizock, Bernard J.; Ferguson, Donald J.; Harper, Paul V. Jr. (Argonne Cancer Research Hospital, Ill.). Surg. Forum, 16: 226-7(1965).

A method was developed for demonstrating the role of thyroid deficiency in the host on the survival of autografted and homografted thyroid tissue. It clearly demonstrates that 8- to 9-day-old homografts exhibit a functional dependence on thyroid status which does not characterize the function of autografts. One millimeter slices of thyroid

tissue were implanted into the ear lobe of dogs. Simultaneous photo and dot scans of the ears were made 0.5 to 1.5 hr after intravenous administration of 1 mC of pertechnetate-99m. This isotope was used because of its 6 hr half-life, permitting repeated observations, its trivial radiation dosage to thyroid tissue, and its ready accessibility. It is concentrated by the ion-trapping mechanism of thyroid tissue to about the same degree as iodide. In 6 hemithyroidectomized dogs, each dog having a homograft in 1 ear and an autograft in the other, all 6 autografts scanned positive, whereas all 6 homografts scanned negative at 8 to 9 days. In 10 dogs rendered athyroid at the time of grafting, all 10 homografts scanned positive at 8 to 9 days; 5 dogs had control autografts in the opposite ear which also scanned positive. Microscopic study of the grafts revealed intact follicles with colloid in the 9-day homografts and autografts, irrespective of thyroid status. Data from totally thyroidectomized dogs indicate it is possible to undertake a series of scans on each experimental animal at 2- to 3-day intervals. By this means, it is possible to determine a mean functional survival time of the in situ homograft indicated by conversion of a previously positive scan to negative. (BBB)

Ecology

Refer also to abstract 40573.

40517 (BNL–9457) EFFECTS OF CHRONIC GAMMA IRRADIATION ON LICHEN COMMUNITIES OF A FOREST. Woodwell, G. M.; Gannutz, T. P. (Brookhaven National Lab., Upton, N. Y.). [1965]. Contract AT(30-2)-Gen-16. 19p. Dep. mn. CFSTI $1.00 cy, $0.50 mn.

Chronic gamma irradiation on an oak-pine forest on Long Island reduced populations of corticolous and terrestrial lichens in approximate proportion to the rate of irradiation. The decline in species diversity was approximately linearly related to logarithmic increases in daily radiation exposure. While a daily exposure of 800 R/day was estimated to have reduced diversity by 50% in the first year, a linear extrapolation of diversity, coefficient of community and similarity curves to zero suggested that certain lichen populations would survive 3 years' exposure at daily rates up to 15,000–20,000 R. There was an apparent threshold at 100–200 R/day for radiation effects on the composition of lichen communities. The crustose forms were more resistant than foliose or fruticose forms, an observation which parallels previous observations that the most radioresistant higher plants tend to be of short stature. (auth)

40518 (CEX–63.10) DESIGN OF A SHIELDED SOURCE FOR THE IRRADIATION OF NATURAL ANIMAL POPULATIONS. Lucas, A. C.; Burson, Z. G.; Lagerquist, R. E. (Edgerton, Germeshausen and Grier, Inc., Santa Barbara, Calif.). Feb. 1966. Contract AT(29-1)-1183. 44p. (EGG–1183-2054). Dep. mn. CFSTI $1.00 cy, $0.50 mn.

This report discusses the design of a radiation source and shield that provides dose rates in the range 0.38 to 0.75 R/hr over a 20-acre circular plot. Calculations of the primary and secondary radiations contributing to the dose distribution at the soil surface were utilized in predicting the amount of shielding necessary to provide a uniform dose rate. The source is placed on a 50-foot tower in the center of the irradiation site. A manually operated winch is used to raise and lower the source. (auth)

40519 (NP–16259) POVEDENIE ZHIVYKH ORGANIZMOV V POLYAKH IZLUCHENII. (The Behavior of Live Organisms in Radiation Fields). Darenskaya, N. G.; Pravdina, G. M.; Khrushchev, V. G. (Institut Atomnoi Energii, Gosudarstvennyi Komitet po Ispol'zovaniyu Atomnoi Energii SSSR, Moscow). 1965. 19p. Dep. mn.

The paper describes in considerable detail a method for estimating the reaction of animals to small constant doses of γ-rays based on changes in water and food consumption from feeding places inside and outside the radiation field. Results show that 1) animals react to very small doses of irradiation which are of the order of 1-2 R when exposing sections of the head or abdomen, or to 0.001-0.05 R during whole body exposure; 2) mice, rats, guinea pigs, and monkeys were able to determine the position of the radiation source and avoid the water container located within the radiation field; and 3) the radiation reaction threshold for guinea pigs is 0.0017 R/sec, for mice 0.0023 R/sec, and for rats 0.0127 R/sec. The ionizing radiation seems to belong to the class of general nonspecific irritants. (JPRS)

40520 (NP–16261) O PODVIZHNOSTI I FORMAKH NAKHOZHDENIYA ^{90}Sr, STABIL'NOGO STRONTSIYA I KAL'TSIYA V DERNOVO-PODZOLISTOI I CHERNOZEMNOI POCHVAKH. (The Mobilities and Forms of ^{90}Sr, Stable Strontium, and Calcium in Turf-Podzolic and Black Earth Soil). Pavlotskaya, F. I.; Zatsepina, L. N.; Tyuryukanova, E. B.; Baranov, V. I. (Institut Atomnoi Energii, Gosudarstvennyi Komitet po Ispol'zovaniyu Atomnoi Energii SSSR, Moscow). 1965. 21p. Dep. mn.

While numerous experimental investigations established the ion exchange effects during ^{90}Sr migration in soil, the migration of this isotope under natural conditions in different types of soil is not sufficiently understood. Consequently, in August of 1961 and 1963 the authors carried out comprehensive studies of strontium 90, stable strontium, and calcium mobilities. In arable turf-podzolic soil, the mobilities of these three isotopes are almost identical and are of the order of 90%; in typical black earth soil the radioactive and stable strontium mobilities are about 65%, while that of calcium is 85%. The mobility is defined here as the ratio of the total content in the water soluble and exchangeable states, to the content of acid-soluble states, expressed in percent. Differences found in the mobilities of the two types of soils and between the mobilities in cultivated and virgin land are determined basically by the amounts of these isotopes found in water-soluble form. Under otherwise equal conditions, more ^{90}Sr is water-soluble than the other two isotopes. In addition to the physical and chemical properties of the soil, the forms in which ^{90}Sr, stable strontium, and calcium appear and their distributions and mobilities are affected significantly by the form in which they appear, the peculiarities of the composition of virgin soil, and the agricultural techniques employed. (JPRS)

40521 (NP–16270) ENVIRONMENTAL RADIOACTIVITY IN NEW ZEALAND. Quarterly Report, January–March 1966. (National Radiation Lab., Christchurch (New Zealand)). 24p. (NRL-F–20). Dep. mn.

In September 1957 the Department of Health was charged under a cabinet directive, with the responsibility for the monitoring of environmental radioactive contamination in New Zealand and the Pacific areas with which it is associated. Subsequently the network of collecting stations has been established to provide the necessary samples of air, water, soil and milk. The collections and measurements are being made on a routine basis and the results are published in the present series of Quarterly Reports, i.e., "Fallout in New Zealand," DXRL-F1 to F9 and NRL-F10 onwards. The selection of rainwater collecting stations was based on the requirement that an adequate geographical coverage of the country must be made, taking account of natural features, such as mountain ranges which, particularly in the South Island, account for the extremes in rainfall. Furthermore, proximity of rainwater collecting sites to milk producing areas is desirable, so that comparisons between levels of contamination in rain and milk can be made. The selection of milk producing areas was based not only on geographical coverage and routine availability of samples but also on population distribution, so that the average result of all stations would be representative of the contamination in the average New Zealand diet. (auth)

40522 (NYO–3273-7) RADIOCHEMICAL AND RADIOECOLOGICAL STUDIES ON BRAZILIAN AREAS OF HIGH NATURAL RADIATION. Annual Report. Penna Franca, E.

(Brazil Univ., Rio de Janeiro. Instituto de Biofisica). July 30, 1966. Contract AT(30-1)-3273. 115p. Dep. mn. CFSTI $4.00 cy, $0.75 mn.

This report covers programs under-way in three different Brazilian areas of high natural radioactivity: Guarapary-Meaipe, in the monazite sand region, Araxá and Morro do Ferro, both located in areas of volcanic intrusives. The following main objectives are pursued: Selection of individuals receiving known doses of external radiation within the range of 0.5–2.0 rad/year in the monazite sand area. Estimation of their body-burden of heavy radionuclides. Selection of individuals with higher than normal radium and thorium body-burdens in the Araxá area. In both groups, studies of the frequency of somatic chromosome aberrations are under way. Cataloguing of flora and fauna at Morro do Ferro and nearby control areas, and characterization of the radiation environment, as basic work for radioecological studies. Radioecological studies with selected organisms at Morro do Ferro. (auth)

40523 (RLO–1750-8(Vol.1)) ECOLOGICAL STUDIES OF RADIOACTIVITY IN THE COLUMBIA RIVER AND ADJACENT PACIFIC OCEAN. Progress Report, July 1, 1965–June 30, 1966. McCauley, James E. (comp. and ed.) (Oregon State Univ., Corvallis. Dept. of Oceanography). July 1966. Contract AT(45-1)-1750. 296p. Dep. mn. CFSTI $6.00 cy, $1.50 mn.

The Hanford reactors are a source of several radionuclides (^{65}Zn, ^{51}Cr, ^{54}Mn, ^{60}Co, ^{124}Sb, and ^{46}Sc) that appear in the Columbia River estuary and provide an opportunity to carry out radioecological studies under natural conditions. Both ^{65}Zn and ^{51}Cr are generally found in sediments, water, and biota, while the other radioisotopes favor one or another phase. Water samples collected monthly at 4 sampling stations are analyzed salinity and dissolved oxygen and temperature measurements are made and water samples from 3 depths at each station are analyzed for nutrients. Samples of silts and biota are collected from trawls or dredges with the aid of a 300-ft monofilament gill net of 0.25 to 4-in. mesh. Additional 25 hr samplings are made at various seasons. Results are reported from studies of distribution, abundance, species composition, and ecology of benthic and pelagic fauna in the Columbi River estuary and Northeast Pacific Ocean off the Oregon coast, with emphasis on fishes and plankton found at various depths during the various seasons. Data are also included from studies on the effects of sediment composition on the fauna, factors affecting vertical migration and distribution, the content of ^{65}Zn in Columbia River sediments and the content of ^{65}Zn and ^{54}Mn in marine organisms, the total radioactivity in sediments and soluble and particulate radionuclides in the water, and the abundance of Hanford-induced radionuclides in the various portions of the ecosystem. Instruments developed for use in the studies included a sediment probe, a large volume precipitation separator, and instruments for the in situ measurements of turbidity, salinity, temperature, and suspended and soluble radioactivity. Analytical techniques for the determination of CO_2 in sea water and for measurements of the electrolytic properties of sea water were evaluated. (C.H.)

40524 (TID–23271) THE UPTAKE OF STRONTIUM BY VARIOUS TYPE CROPS AND FACTORS AFFECTING UPTAKE AND TRANSLOCATION OF STRONTIUM AND CALCIUM NATIVE TO SOIL. Technical Progress Report. (Arizona Agricultural Experiment Station, Tucson). [1966]. Contract AT(11-1)-947. 36p. Dep. mn. CFSTI $2.00 cy, $0.50 mn.

This study has shown that certain species of algae absorb calcium preferentially over strontium. However, it has also been demonstrated that certain species of algae are capable of absorbing large amounts of strontium even in the presence of quantities of calcium sufficient to fill the needs of the organism. In all but one of the species studied strontium did not appear to compete in the absorption of calcium by algal cells, but was absorbed in addition to the needed calcium. Not only has it been shown that algae attempt to use strontium in the absence of needed calcium, but that strontium actually competes with calcium in absorption and metabolism by certain algae (in particular Chlorococcales scenedesmus). Increased microbial activity reduces radiostrontium movement and, in the presence of large amounts of organic matter, decreases the amount of sodium acetate extractable strontium-89 in calcareous soils. Movement of radiostrontium from algal tissues is low, as is the case with movement of radiostrontium from other plant tissues. This study shows that the major portion of contamination radiostrontium is found in the surface layer of the soil. Preliminary experiments have shown that certain fungi can absorb radiostrontium from a liquid culture medium. However, the fungi tested discriminate highly in favor of calcium, and apparently strontium does not compete with calcium in the absorption by certain fungi. (H.L.W.)

40525 CLINICAL AVIATION AND AEROSPACE MEDICINE. A CRITIQUE OF THE BIOLOGICAL SIGNIFICANCE OF THE SUPERSONIC TRANSPORT RADIATION ENVIRONMENT. Nold, Max M.; Adams, Duane A.; Supko, Peter R. (Air Force Weapons Lab., Kirtland AFB, N. Mex.). Aerospace Med., 37: 829-34(Aug. 1966).

There are several poorly defined aspects of the ambient space radiations, which relate to their biological significance. Although the magnitudes of doses expressed in physical units are low, even for transient solar flare encounters, some concern has been expressed by others regarding the high cell damaging potential of the heavily ionizing component of galactic primary radiations, secondary galactic radiations, and of the alpha particle component of solar particle eruptions. This paper compares the approaches taken by several authors to delineate the radiation problem at 70,000 feet and comments on the assumptions used for lack of measured parameters. The problems of physiological aging and increased genetic burden are considered, and the status of the fractional cell lethality concept is discussed. Finally, an experimental program is discussed in which the Federal Aviation Agency, Air Force Weapons Laboratory, and National Aeronautics and Space Administration will cooperate to better define the environment at 70,000 feet. The FAA-AFWL experiment will use tissue-equivalent sensors to measure absorbed dose and LET spectra while NASA will measure neutron and charged particle fluxes and spectra. Measurements will be made in high flying aircraft stationed throughout the world. (auth)

40526 STUDIES ON ECOLOGICAL EFFECTS OF SHORT TERM EXPOSURES OF IONIZING RADIATION. Cotter, David J. (Alabama Coll., Montevallo). J. Ala. Acad. Sci., 36: 143-56(Oct. 1965).

This review surveys the effects of radiation on biological systems. Only effects of short-term radiation from point sources are dealt with. High-level radiation acts as a stress on individuals, populations, communities, and ecosytems, different portions of which have varying abilities to compensate for the effects of radiation. Thus survival is dependent upon the reaction of the individual parts. For example, if the root systems are more radiation resistant or receive a sublethal exposure, recovery from radiation may be initiated by the growth of underground sprouts, even though the aerial portions were killed. Survival is a common index of radiation damage, but involves two different concepts: sensitivity and resiliency. Following release from sublethal radiation stress, recovery ensues, and here major differences in the responses of different systems may be seen. The degree of resiliency of a system is affected by the amount of radiation-induced damage, but it is also influenced by other factors. Radiation is merely the accelerator that releases these recovery responses to a greater or lesser degree. The factors which affect recovery vary with respect to the system being analyzed. On the organismal level it may be the available food supply for growth, auxin metabolism, or some other factor only partially affected by sublethal exposure; on the population level it could be the genetic diversity, or the ability to respond to a changed micro-environment; on the community level it may be changes in the biotic relations

and on the ecosystem level it may be the complexity of the system. Additional changes may occur in these systems as they recover from the effects of radiation and set in motion a whole spectrum of secondary responses. (85 references) (BBB)

40527 BIOLOGICAL CONSEQUENCES OF RADIOACTIVE CONTAMINATION OF WATER BODIES. Polikarpov, G. G.; Kardashev, A. V.; Barinov, G. V.; Ivanov, V. N.; Shekhanova, I. A.; Parchevskii, V. P.; Pomanova, E. S.; Fleishman, D. G. (Kovalevskii Inst. of Tropical Marine Biology, Sevastopol. All-Union Research Inst. for Sea Fisheries and Oceanography, Moscow). Vienna, International Atomic Energy Agency, 1966, Preprint SM-72/56, 34p. (In Russian). (CONF-660507-32). ORAU.

From Symposium for the Disposal of Radioactive Wastes into Sea, Oceans, and Surface Waters, Vienna.

From data based on the statistical theory of complex isotopic exchange, formulae and methods for calculating the build-up factor for numerous radionuclides in the hydrosphere and the rates of hydrobiont deactivation are presented. The relationships derived between the build-up factors for various radionuclides and other accumulation parameters may serve as basis for the conduct of rapid and more complete assessments of radioecological situations, i.e., the degree of contamination of hydrobionts used for human consumption and the doses received by them. It is recommended that maximum permissible doses be established for hydrobionts. The harmful effects of very low concentrations of various radionuclides, particularly strontium and the rare-earth elements on fish spawning were investigated. Studies were made of radiation effects on the morphology, cytology, physiology and biochemistry of fish embryos and prelarvae. The effects of radioactivity on the rate of cell division in microphytes were determined. The conclusions convincingly demonstrate that further radioactive contamination of the hydrosphere should not be permitted and that it is essential to prohibit the disposal of radioactive wastes into the hydrosphere. (TCO)

40528 UPTAKE OF RADIONUCLIDES BY MARINE INVERTEBRATES FROM THE WEST COAST OF INDIA. Patel, B.; Bhatt, Y. M.; Naidu, J. R.; Krishnamurthy, T. M.; Doshi, G. R.; Bhattathiri, P. M. A.; Unni, C. K.; Viswanathan, R. (Atomic Energy Establishment, Trombay, India). Vienna, International Atomic Energy Agency, 1966, Preprint SM-72/36, 32p. (CONF-660507-24). ORAU.

From Symposium for the Disposal of Radioactive Wastes into Sea, Oceans, and Surface Waters, Vienna.

Studies have been made on the uptake, loss and retention of radionuclides by selected species of marine invertebrates from the Bombay region of the West Coast of India. The species investigated included two lamellibranches, Anadara granosa (Linn.) and Katelysia marmorata Lam. and a crab, Scylla serrata (Forskal). In laboratory experiments with Anadara granosa, the rate of uptake of manganese-54 was higher in the smaller-sized animals. In the edible portion, the maximum concentration factor of 10-12 (after 6 to 7 days' exposure) was observed in the mantle folds along with adductor muscle and labial palps. The exposed and equilibrated animals lost about 50% of their radioactivity in 15 days' immersion in inactive sea water. Analogous to manganese, zinc (as zinc-65) was also concentrated to a greater extent in the edible portion than in the shell. The pattern of uptake of cobalt, reported in Anadara, was repeated in Katelysia marmorata with the concentration factors being generally higher with lower amounts of carrier-cobalt in the medium (water). Tissue-wise, distribution studies on Anadara specimens exposed to solutions containing uranium indicated that the shell accumulated more uranium than the edible portion. About 50% of the uranium was lost within 3 days of transfer to non-active medium. Uptake of cesium-137 by Katelysia marmorata reached a steady state after 65 hours of exposure when the clam had concentrated the fission product tenfold in the edible portion. In the crab, Scylla serrata, concentration factors for cesium-137 in the soft portions, as also the rates of uptake, varied with the sex of the animal. In addition, field observations were made on Anadara granosa specimens exposed continuously to secondary coolant effluent from the Canada India Reactor. The exposed animals were found to have accumulated zirconium-95, cesium-137 and cerium-144. Data on the uptake of radionuclides by marine invertebrates have been discussed with reference to the determination of maximum permissible concentrations of radioisotopes in the sea and allied aspects of radioactive waste disposal. (auth)

40529 BACTERIAL TRANSPORT OF RADIOPHOSPHORUS IN A STREAM ECOSYSTEM. Hooper, Frank F. (Inst. for Fisheries Research, Ann Arbor, Mich.); Ball, Robert C. Vienna, International Atomic Energy Agency, 1966, Preprint SM-72/32, 16p. (CONF-660507-21). ORAU.

From Symposium for the Disposal of Radioactive Wastes into Sea, Oceans, and Surface Waters, Vienna.

Escherichia coli cells were cultured in a phosphorus-poor medium containing 25 mC of ^{32}P. The procedures used allowed virtually complete uptake of the radioactive phosphorus by the cells. Cells were filtered from the medium, mixed with stream water, and released into a small cold-water stream during a 33-minute period. In moving downstream approximately 90% of the radioactivity remained inside the bacterial cells while 10% diffused from the cells and appeared in the water in filterable form. There was a grateful loss of radioactivity from the water. In a distance of 4 km, only 48% of the activity was lost compared to more than 95% in previous experiments in which ^{32}P was put into the stream in soluble form. Loss of radioactivity from the water appeared to be chiefly due to the fallout of labeled cells but there was also uptake by filter feeding invertebrates. A small fraction of the ^{32}P released in soluble form by the bacterial cells was taken up by periphyton and aquatic macrophytes. Among the consumer organisms in the ecosystem only four species accumulated ^{32}P that had entered the food chain by way of bacteria. These were the caddisflies (Hydropsyche and Brachycentrus), the snail (Physa), and ammocoetes of the brook lamprey (Lampetra). Other species, including fish, accumulated only small amounts of activity; the quantity was in all cases about that expected if the source had been only the soluble phosphorus released by the bacterial cells. Failure to find important concentrations of radioactivity in any part of the chain or in the environment suggests that E. coli cells effectively disperse radioactive phosphorus and minimize the transfer activity through segments of the food web leading to man. The ecological implications of the low efficiency of the endogenous system for removal of E. coli cells are discussed. (auth)

40530 CYTOGENETIC STUDY OF A NATURAL POPULATION OF CHIRONOMIDAE INHABITING AN AREA CONTAMINATED BY RADIOACTIVE WASTE. Blaylock, B. G. (Oak Ridge National Lab., Tenn.). Vienna, International Atomic Energy Agency, 1966, Preprint SM-72/55, 16p. (CONF-660507-31). ORAU.

From Symposium for the Disposal of Radioactive Wastes into Sea, Oceans, and Surface Waters, Vienna.

The aquatic larvae of Chironomus tentans, one of the midges, inhabit the radioactive bottom sediments of White Oak Lake and White Oak Creek in large numbers. This aquatic habitat has received varying quantities of radioactive waste released from the Oak Ridge National Laboratory since 1943. Dosimetric measurements and calculations based on radionuclide content of the bottom sediments indicate that these larvae were receiving 230 rad/year. It is estimated that 130 generations have been exposed to this or greater dose rates for the past 22 years. During the past five years the incidence of chromosomal aberrations in the salivary gland chromosomes of larvae collected seasonally from the radioactive and control habitats was measured. Chromosomal polymorphism is prevalent in C. tentans in this locality and six endemic inversion heterozygotes were found in all populations. Three of these inversions occurred at relativity high frequencies (.09 to .22), but these frequencies did not fluctuate seasonally nor change significantly in the irradiated populations

for five years. Also, the frequencies of endemic inversions in the irradiated populations were not significantly different from a control populations. In addition to the six endemic inversions found in all populations, ten inversions and one deletion were observed only one time in 755 larvae from the radioactive habitat, while no additional aberrations were observed in 714 larvae from the control habitats. It is concluded that the ionizing radiation from the radioactive waste was increasing the frequency of new chromosomal aberrations in the White Oak Lake and White Oak Creek populations, but these new aberrations were eliminated by selection. Also, this level of chronic radiation, which was capable of producing a detectable increase of new chromosomal aberrations, has not affected the fitness of the population by producing a change in the frequencies of the endemic inversions. (auth)

Metabolism, Tissue Distribution, and Toxicology

Refer also to abstracts 40524, 40590, 40790, and 40830.

40531 (A/AC.82/G/L-1045(Rev.1)) REPORT ON NATURALLY OCCURRING RADIONUCLIDES IN HUMAN TISSUES. Ichikawa, R. (International Atomic Energy Agency, Vienna (Austria)). Mar. 1966. 24p.

Results are summarized from measurements of naturally occurring radionuclides in human tissues sampled throughout the world. Data are presented on the content of ^{226}Ra in bones and teeth; the content of ^{228}Ra or ^{228}Th in bone; the content of ^{210}Pb or ^{210}Po in bone and teeth; the content of ^{226}Ra in soft tissues; and the content of ^{210}Po in soft tissues and placenta. Emphasis was placed on data from areas of high natural radioactivity such as Kerala, India and the Araxá and Tapira regions of Brazil, and the arctic region of Canada. Lung tissues of cigarette smokers were also examined and were found to have a higher ^{210}Po content than that of non-smokers. (28 references.) (C.H.)

40532 (COO-1097-17) GENETIC CONTROL OF PHYSIOLOGICAL PROCESSES IN HIGHER PLANTS. Technical Progress Report, 1965-66. Rasmusson, D. C.; Smith, L. H.; Kleese, R. A.; Rust, R. H. (Minnesota Univ., Minneapolis). [1966]. Contract AT(11-1)-1097. 32p. Dep. mn. CFSTI $2.00 cy, $0.50 mn.

Six kinds of plant populations were grown in the field to provide information on extent of genetic variation in accumulation of stable elements. Two crosses of barley were used in a study of heritability of strontium-89 and calcium-45 accumulation in seedling plants. The evidence indicates that the differences in strontium/calcium ratio among F3 lines did not have a genetic basis. Evidence from a selection experiment involving one barley and one wheat population indicates that strontium accumulation is highly amenable to selection. Significant differences were observed among varieties of barley in accumulation of calcium, potassium and phosphorus. These differences were observed in grain and in shoots of seedling plants grown in soil and in nutrient culture. Physiological studies included the role of the stem and root in determining genotypic differences in strontium-89 and calcium-45 accumulation in soybeans, photophosphorylation in barley, kinetic studies of strontium accumulation by barley genotypes, and influence of translocation on strontium accumulation in grain of barley genotypes. Studies were conducted on variability of ion content of soils. The analysis of variance indicates a significant difference between crop areas (wheat and barley) on Waukegan soil for magnesium, potassium and pH and between crop areas of Webster soil for zinc, iron, and manganese and pH. (H.L.W.)

40533 (NYO-901-54, pp 16-19) BIOLOGICAL CHEMISTRY. (New England Deaconess Hospital, Boston, Mass. Cancer Research Inst.).

Progress is reported in the development of standardized methods for the activation of tryptophan pyrrolase and tyrosine transaminase. Levels of these enzymes provide indices of adrenal glucocorticoid secretion, which is altered by irradiation and in animals bearing transplanted radioinduced tumors. Mechanisms involved in activation of these enzymes and the properties of these enzymes were investigated. The sequential enzymes of tryptophan metabolism were investigated in Pseudomonas and the tyrosine transaminase and tryptophan pyrrolase levels and their elevation by hydrocortisone were documented in developing postnatal rats. A method for the determination of tryptophan was developed. Data were compiled on enzyme reactions in neoplastic cells. (C.H.)

40534 (NYO-3621-1) NUCLEAR METABOLISM OF DNA AND RNA AND THE SITES OF RADIATION SENSITIVITY. Progress Report, October 1965-July 1966. Abrams, Richard (Pittsburgh Univ., Pa. Dept. of Biochemistry and Nutrition). July 15, 1966. Contract AT (30-1)-3621. 10p. Dep. mn. CFSTI $1.00 cy, $0.50 mn.

Investigations were carried out in several parallel areas related to macro-molecular metabolism in mammalian nuclei. Methods were developed for fractionation of histones with a view toward finding polylysine as a protein product coded for by the polyadenylate that had previously been found in thymus nuclei. A technique for analytical electrophoresis on polyacrylamide gels was developed using 8M urea to prevent artifacts due to aggregation. Histones from thymus and from Ehrlich ascites carcinoma were shown to consist of 6 major bands, one of which was a very-lysine-rich component. This component was easily prepared in a homogeneous state by extraction and precipitation techniques. The analytical gel analysis indicated that none of the conventional chromatographic or other methods of histone fractionation led to homogeneous proteins for the other histone components. No evidence was found for a component consisting solely of lysine. By using specific inhibitors of protein and DNA synthesis (particularly cycloheximide and hydroxyurea) it was shown in Ehrlich ascites cells that there was no mandatory coupling between DNA synthesis and any of the detectable histone fractions. The nature and turnover of rapidly labeled RNA in ascites cell nuclei was investigated. Pulse labeled RNA was found to be heterogeneous (4s to 55s) with the major component in the 45s region. In the presence of actinomycin D much of this RNA was degraded to an acid soluble state and evidence was obtained that a Mg^{++} dependent nuclease was responsible for this hydrolysis. The heavy RNA (centering around 45s) was most susceptible, and evidence was obtained indicating that the most susceptible fraction was the newly made, chromatin-bound RNA. The properties of a soluble, nuclear, Mg^{++}-activated nuclease were investigated. The enzyme was shown to be an exonuclease, generally similar to snake-venous phosphodiesterase in that the hydrolysis product was exclusively 5'-nucleoside monophosphate. However, it acted only on polyribonucleotides (not on DNA or a DNase digest of DNA), preferentially attacked phosphodiester bonds on purine nucleosides, and required a single stranded substrate without a hydrogen-bonded secondary structure. The rise in enzyme levels associated with DNA synthesis that occurs at entry into S phase was shown not to be a sequential series of derepressions dependent upon accumulation of substrate (deoxyribonucleoside triphosphates). DNA polymerase appears and cells enter S (become x-ray resistant) whether or not dNTP synthesis occurs normally or is blocked. (auth)

40535 (ORNL-3922, pp 128-35) NUCLEIC ACID ENZYMOLOGY. (Oak Ridge National Lab., Tenn.).

Research is reported on: attempts at isolation of bacteriophage messenger RNA; oligodeoxyribonucleotide transferase system of T2-infected E. coli; inhibitory action of colicins E2 on bacteriophage R17-infected cells; partition studies of transfer RNA; multiple aminoacyl-RNA synthetase systems; fractionation, coding properties, and interspecies reactions of sRNA in Neurospora; an autoradiographic and biochemical study of amphibian lethal hybrid development; a uracil-containing compound in amphibian eggs; and priming ability of brine shrimp DNA isolated from developing embryos. (H.G.D.)

40536 (ORO–3461-1) THE TOXICOLOGY OF NICKEL CARBONYL. Progress Report. Sunderman, F. William Jr. (Florida Univ., Gainesville. Dept. of Pathology). July 1, 1966. Contract AT(40-1)-3461. 11p. Dep. mn. CFSTI $1.00 cy, $0.50 mn.

The toxic effects of nickel carbonyl in rats were studied after intravenous, intraperitoneal, or subcutaneous administration. The LD_{50} values ranged from 1.3 mg Ni/100 gm of tissue to 2.2 mg Ni/100 gm of tissue, depending on administration route. Acute clinical and pathological reactions, which appeared primarily in lungs and to a lesser extent in liver, are described. Preliminary results are reported from studies of carcinogenic effects, biochemical changes associated with nickel carbonyl toxicity, and the metabolism of $^{63}Ni(CO)_4$ and $^{63}NiCl_2$. The therapeutic use of sodium diethyldithiocarbamate in acute nickel carbonyl poisoning and acute thallium sulfate poisoning in man is reported. (C.H.)

40537 (TID–23052) DIFFERENTIAL ABSORPTION OF STRONTIUM BY PLANTS. Final Report. Mayberry, B. D. (Tuskegee Inst., Ala.). Mar. 23, 1966. Contract AT(40-1)-2749. 19p. Dep. mn. CFSTI $1.00 cy, $0.50 mn.

The factors which influence the accumulation of strontium in edible plant parts were studied. Lima beans, squash, potatoes, and tomatoes were grown in the greenhouse and in the growth chamber. The growing medium was Norfolk loamy sand of low (5.7) initial pH. Plant nutrients, other than calcium, were added in calculated optimum amounts. Calcium was added to the potted soil at the calcium carbonate equivalent of 0, 405, 810, and 1350 pounds/acre. The plants were grown under these conditions to the stage of harvest for commercial purposes. Analysis and evaluation of results involved the use of isotopic techniques, with ^{89}Sr used as the indicator. The practice of succession cropping did not significantly decrease strontium absorption, since the amount of strontium uptake by each crop was a very small fraction of the total dose and had no effect on the uptake by successive crops. The uptake of strontium by plants, irrespective of species, was decreased with increase in calcium content of the acid soil up to the point of 100% of base saturation. The total uptake of strontium by plants differed with the species. (19 references.) (C.H.)

40538 (TID–23238) REPLICATION AND GENETIC EXCHANGE IN THE GENOME OF ESCHERICHIA COLI K-12. PART I. INVERTED AND NONINVERTED TRANSPOSITIONS. PART II. REPLICATION. Berg, Claire Marjorie (Oak Ridge National Lab., Tenn.). 1966. Contract W-7405-eng-26. 71p. Dep. mn. CFSTI $3.00 cy, $0.75 mn.

Thesis. Submitted to Columbia Univ., [New York].

The current models for replication of the bacterial genome have been tested by analyses of relative transductant frequencies in Escherichia coli K-12. The method developed proved to be reproducible and capable of detecting differences in gene frequency. Phage Plkc was grown on a series of isogenic F^-, F^1, Hfr and transposition strains, which on any unique-origin model for replication were expected to differ systematically in the position of certain genes relative to the origin. In a chromosome population growing exponentially at a constant rate from a single origin, marker frequency is a function of the distance of the gene from the origin of replication; hence these strains were expected to differ in the frequency with which regions of the bacterial genome were recovered in transducing phage. No such difference was observed. Thus, the results favor either of two modes of chromosome replication: (1) there is not a unique site from which replication is always initiated, but rather alternative origins, or (2) there is a unique origin, but the direction of replication is not fixed. (auth)

40539 (UCD–472-113) ANNUAL REPORT: FISCAL YEAR 1966. (California Univ., Davis. School of Veterinary Medicine). June 1966. Contract AT(04-3)-472. 69p. Dep. mn. CFSTI $3.00 cy, $0.75 mn.

Separate abstracts were prepared on two sections of this report. (C.H.)

For abstracts of individual sections see: 40540 and 40638.

40540 (UCD–472-113, pp 17-56) RADIONUCLIDE TOXICITY. (California Univ., Davis. School of Veterinary Medicine).

Results are summarized from long-term (1961 to 1966) studies on the toxic effects of various doses of ^{90}Sr and ^{226}Ra in dogs. Annual examinations of experimental dogs included complete skeletal radiographic surveys. No radiation effects were observed in dogs examined during the first 3 or 4 years of life. Hematological studies showed a decrease in leukocytes following the administration of ^{90}Sr or ^{226}Ra by mouth or intravenously. No changes were seen in blood serum chemistry values. Pathological findings are reported on dogs that died since the experiment started. Data are included from studies on the translocation of ^{90}Sr from maternal skeleton to progeny during gestation and lactation, Sr/Ca discrimination in puppies, and the content of Sr and Zn in newborn and aged beagles. (C.H.)

40541 (UCD–34P104-3) ^{90}Sr AND ^{137}Cs FOOD CHAIN RELATIONSHIPS TO DEER AND SHEEP. III. FACTORS INFLUENCING BODY ACCUMULATION OF RADIONUCLIDES. Progress Report, September 1, 1965–June 15, 1966. Longhurst, William M.; Kepner, Richard E. (California Univ., Davis). Contract AT(11-1)-34. 56p. Dep. mn. CFSTI $3.00 cy, $0.50 mn.

Progress is reported on studies of factors influencing the body accumulation of fallout radionuclides, with emphasis on ^{137}Cs and ^{90}Sr, in ruminants, particularly deer and sheep ingesting forage plants. Gas chromatography was used to identify volatile compounds in forage plants that affect their palatability for deer and sheep. Data are presented on volatile components identified in young green tips of Douglas and white fir trees. The relationship between palatability, substrate level, essential oil content, and rumen microbial digestibility of certain browse plant species was investigated in deer and sheep. Preliminary results are included from studies on the transfer of ^{45}Ca, ^{137}Cs, ^{35}S, and ^{85}Sr from blood to rumin of deer and sheep; the determination of blood urea nitrogen levels in deer and sheep; measurements of total body water and body water turnover in deer and sheep, in which T_2O was used as a tracer; a study of the anatomy of the digestive tract of deer and sheep as compared with other ruminants; and measurements of the ^{90}Sr content in mandibles and femurs of yearling deer sampled during Aug. and Sept. 1965. (C.H.)

40542 INDEX OF ^{85}Sr UPTAKE IN LEG FRACTURES. Mangiaracina, A.; Gennari, C. (Univ., Siena, Italy). Atti Accad. Fisiocritici Siena, Sez. Med.-Fis., 12: 1567-75(1963). (In Italian).

Strontium-85 incorporation in bone fractures of 22 patients was studied up to 24 months after fracture. Reasons for using ^{85}Sr in clinical studies rather than various calcium radioisotopes are explained. Strontium-85, a γ-emitter with a half life of ~65 days, is superior for such studies to ^{47}Ca. Strontium-85 was administered as the carrier-free chloride salt intravenously in a dose of 20 to 30 μC. A scintillation meter was used to register counts over the fracture and a control site on the contralateral, normal leg. In subjects tested at various intervals after fracture, a progressive increase in ^{85}Sr uptake was seen from the first to eight month. It then began to decline, fairly sharply for the next 8 months, and less sharply from the 16th to the 24th month. At the peak ^{85}Sr uptake at the eighth month, the ratio of pathologic/normal bone reached 20 and by the 24th month had fallen to 2. The uptake of ^{85}Sr corresponded to the osteogenic activity of the healing bone and callus. Radiographs of the fractured bone are shown to illustrate the degree of calcification of the pathologic zone in relation to radioactivity measurements. (BBB)

40543 PHOTOREACTIVATING ENZYME IN THE SEA URCHIN EGG. Cook, John S.; Setlow, Jane K. (Oak Ridge National Lab., Tenn.). Biochem. Biophys. Res. Commun., 24: 285-9(Aug. 12, 1966). (ORNL-P-2246).

The heat lability and trypsin sensitivity of the Arbacia extract indicate that its photoreactivating capacity is due to an enzyme. Photoreactivation of Hemophilus influenzae transforming DNA by yeast enzyme repairs around 90% of the damage from 2537 A radiation (Setlow, 1963). Since the Arbacia extract photoreactivates this DNA to approximately the same extent as the yeast enzyme, there must be a large, if not complete, overlap in the types of lesions repaired by the yeast and Arbacia extracts. Photoreactivation of transforming ability in UV-irradiated H. influenzae DNA by yeast extract is the result of monomerization of pyrimidine dimers (Setlow, 1966), and it may be inferred that the Arbacia extract probably acts by the same mechanism. It is therefore likely that most or all of the photoreactivable lesions which cause cleavage delay in Arbacia punctulata are pyrimidine dimers. (auth)

40544 A COMPARATIVE STUDY OF THE FIXATION OF ^{75}Se AND ^{35}S ONTO PROTEIN-POLYSACCHARIDES OF BOVINE COSTAL CARTILAGE. Campo, Robert D.; Wengert, Paul A. Jr.; Tourtellotte, Charles D.; Kirsch, Michael A. (Temple Univ., Philadelphia). Biochim. Biophys. Acta, 124: 101-8(July 27, 1966).

^{75}Se- and ^{35}S-labeled protein-polysaccharides were isolated from slices of bovine costal cartilage which had been incubated in media containing $^{75}SeO_4^{2-}$ or $^{35}SO_4^{2-}$. Analysis of the protein-polysaccharides revealed that the ^{75}Se was attached to the protein moiety. The chondroitin sulfate was labeled with ^{35}S but not with ^{75}Se. Only very small amounts of ^{75}Se were fixed to the protein-polysaccharides of preboiled slices of cartilage or onto protein-polysaccharide itself if these were incubated in the media containing $^{75}SeO_4^{2-}$. These results suggest that the binding to protein of ^{75}Se derived from $^{75}SeO_4^{2-}$ is dependent upon cellular activity. (auth)

40545 THE METABOLISM OF ^{47}Sc PRODUCED BY THE DECAY OF ^{47}Ca IN VIVO. Taylor, D. M. (Inst. of Cancer Research, Belmont, Sutton, Eng.). Brit. J. Radiol., 39: 620-2(Aug. 1966).

The metabolic behavior of ^{47}Ca and ^{47}Sc have been compared in rats after intravenous injection of a ^{47}Ca + ^{47}Sc mixture. The results suggest that the ^{47}Sc initially present in the mixture follows the normal pathways of scandium metabolism, but that 90 per cent or more of the ^{47}Sc by the decay of ^{47}Ca in bone is retained in the skeleton. (auth)

40546 BIOLOGICAL CONCENTRATION FACTORS IN MARINE MEDIA. APPLICATION TO THE PROBLEMS OF RADIOACTIVE POLLUTIONS. Michon, G. (CEA, Fontenay-aux-Roses, France). Cah. CERBOM (Cent. Etud, Rech. Biol. Oceanogr. Med.), 17: 125-47(1965). (In French).

The mechanisms for the fixation of fallout radioisotopes by marine organisms are outlined. The methods by which it is possible to determine the equilibrium levels that can be established between pollution of a given type and that of the media are discussed. The principal isotopes accumulated by marine organisms are listed in order of their biological importance. It is pointed out that phytoplankton represents the greatest surface area for radioisotope uptake of all marine organisms and its importance in the absorption and transport of radioisotopes and in their uptake by mollusks, crustacea, and fish is discussed. The use of fallout radioisotopes as tracers to determine the content and distribution of stable elements in marine organisms and in studies of marine pollution are discussed. (C.H.)

40547 USE OF ^{99m}Tc IN STUDYING THYROID PHYSIOLOGY IN THE MOUSE: DOUBLE LABEL EXPERIMENT WITH ^{99m}Tc AND ^{125}I. Schindler, W. J.; McHorse, T. S.; Krause, D. M. (Baylor Univ., Houston, Tex.). Endocrinology, 79: 281-8(Aug. 1966).

Mice were maintained for 72 hr prior to the experiment at 30, 24 or 5 C to induce hypoactive, normal, or hyperactive thyroids, respectively. Pertechnetate is concentrated by the thyroid, probably by a transport mechanism similar to that for iodide, but is not bound or metabolized there. Carrier-free ^{99m}Tc in the form of pertechnetate was used to determine thyroid/serum (T/S)[3] ratios in the mouse thyroid gland not blocked by goitrogens. These T/S[TcO_4^-] ratios were similar to T/S[I^-] or T/S[TcO_4^-] ratios determined in goitrogen-blocked mouse thyroids. The T/S ratios of all groups of mice were inversely related to environmental temperature. One group of mice at each temperature receiving no goitrogen was injected with both $^{99m}TcO_4^-$ and $^{125}I^-$ 1 hr prior to killing. Radioactivity of each of these radioisotopes was determined in plasma and thyroid glands by γ-ray spectrometry in a well-type scintillation counter. In this double label experiment, 3 thyroidal responses were determined in each animal: 1) an estimate of the "thyroidal iodide pump" (T/S[TcO_4^-]) comparable to the T/S ratio of a blocked gland; 2) an estimate of the "thyroidal iodide pump" (T/S[I^-]) in the unblocked gland; 3) an estimate of thyroid radioiodide uptake and binding. By combining all 3 thyroidal responses for each animal into one composite response metameter, more accurate discrimination of overall thyroid status was made between groups of mice at each temperature. (auth)

40548 EFFECT OF RADIATION ON THE COMPOSITION OF DEOXYRIBONUCLEIC ACID IN PLANTS. Klechkovskii, V. M.; Evdokimova, T. P.; Zyulikova, A. G. Dokl., Moskov. Sel'skokhoz. Akad., No. 79, 235-42(1962). (In Russian).

From the test data it was concluded that incorporation of radiophosphorous at doses inhibiting the normal development of the plants is not accompanied by a statistically proved change of the nucleotide composition of the desoxyribonucleic acid. (tr-auth)

40549 COMPARISON OF THE EFFECTS OF RADIATION AND INHIBITORS OF OXIDATIVE PHOSPHORYLATION ON THE NUCLEAR STRUCTURE OF RAT THYMOCYTES. Whitfield, J. F.; Youdale, T. (National Research Council, Ottawa). Exp. Cell Res., 43: 153-66 (Aug. 1966).

The most striking visible consequence of irradiation of the thymocyte is the complete disappearance of nuclear structure. Since the primary metabolic effect of irradiation seems to be the inhibition of oxidative phosphorylation, we have determined and compared the nuclear changes caused by radiation with those caused by 2,4-dinitrophenol, parathyroid extract and oligomycin, all of which inhibit oxidative phosphorylation but have different effects on respiration and the uptake of inorganic phosphate. Those compounds (parathyroid extract and low concentration of oligomycin) which inhibit oxidative phosphorylation, but do not affect phosphate uptake caused the disappearance of nuclear structure. On the other hand, 2,4-dinitrophenol, known to inhibit both oxidative phosphorylation and phosphate uptake, strongly inhibited the loss of nuclear structure in irradiated and unirradiated cell suspensions as well as in the irradiated rat. The metabolic prerequisites for nuclear structural homogenization therefore seem to be a loss of the ability to carry out oxidative phosphorylation combined with a continuing ability to accumulate phosphate. It is suggested that the loss of nuclear structure is the result of a dissociation of histone from DNA in the chromatin granules of the nucleus and this dissociation is itself caused by accumulated inorganic phosphate. (auth)

40550 SIGNIFICANCE OF CHROMOSOMAL ABERRATIONS IN CANCEROSTATIC EFFECTIVITY OF SOME CHEMOTHERAPEUTIC AGENTS. Schoeneich, J. (Research Inst. of Cultivated Plants, Gatersleben, Ger.). pp 109-14 of Induction of Mutations and the Mutation Process. Veleminsky, Jiri; Gichner, Tomas (eds.). Prague, Publishing House of the Czechoslovak Academy of Sciences, 1965.

The significance of chromosomal aberrations in determining the cancerostatic effectiveness of certain radiomimetic chemotherapeutic agents was investigated in mouse Ehrlich ascites carcinoma and S-2-sarcoma cells. The chromosome breaking effectiveness of nitrogen mustard, and triethyleneamine, with and without added nicotinic amide, was scored on ideograms. Results indicated that induced chromosomal aberrations were without significance for tumor regression induced by the cancerostatic agents

used in this study. It was concluded that the significant reactions initiated by these agents and leading to lethal effects take place within the cytoplasm and not within the nucleus. (C.H.)

40551 INTRACELLULAR DISTRIBUTION OF CALCIUM IN THE MUCOSA OF THE AVIAN SHELL GLAND. Hohman, Wayne; Schraer, Harald (Pennsylvania State Univ., University Park). J. Cell Biol., 30: 317-31(Aug. 1966).

The intracellular distribution of calcium has been studied in the mucosa of the avian shell gland, a tissue which transports large quantities of calcium during discrete time intervals. ^{45}Ca was administered to hens either in a single dose followed by sacrifice 5 min later or in repeated doses over an extended period followed by sacrifice 2 hr or 24 hr after the last injection. Subcellular fractions were isolated by differential centrifugation and analyzed for ^{45}Ca. The ^{45}Ca was located principally in the particulate fractions; the concentration (CPM ^{45}Ca/Mg N) was highest in the mitochondrial fraction. Comparisons of (1) the ^{45}Ca distribution in shell gland cells with that of liver cells, (2) the alterations which occur due to the phase of the egg laying cycle, (3) the effects due to the time elapsed since the last injection of ^{45}Ca, and (4) the ^{45}Ca distribution of the short term experiments with that of the long term experiments revealed that the mitochondrial fraction of the shell gland appeared to be active in the movement of calcium. The microsomal fraction showed increased values in CPM ^{45}Ca/mg N when calcification was occurring, which may indicate that the subcellular components of this fraction have a role in calcium transport. The nuclear and supernatant fractions did not seem to be involved in the transport process. The implications of these results concerning the manner by which calcium may be controlled on a cellular level in this system are discussed. (auth)

40552 COMPARISON BETWEEN THE RESULTS OF RADIOCALCIUM STUDIES AND HISTOLOGICAL FINDINGS IN A CASE OF PRIMARY HYPERPARATHYROIDISM (OSTEITIS FIBROSA CYSTICA GENERALISATA OF VON RECKLINGHAUSEN) BEFORE AND AFTER REMOVAL OF PARATHYROID ADENOMA. Caniggia, Angelo; Gennari, Carlo; Guideri, Renzo; Cesari, Leone (Univ. of Siena, Italy). J. Clin. Endrocrinol. Metab., 26: 867-74 (Aug. 1966).

^{45}Ca dynamics and intestinal absorption of ^{45}Ca (or ^{47}Ca) have been performed on a case of primary hyperparathyroidism with osteitis fibrosa cystica generalisata of von Recklinghausen, and compared to the histological findings of iliac crest biopsy before the extirpation of a parathyroid adenoma and after 2 and 45 weeks. The elevated values of Ca miscible pool, Ca turnover rate, accretion and resorption rates decreased 45 weeks after the operation (when the osteoid tissue had completely disappeared). The intestinal hyperabsorption of radiocalcium was already lowered 2 weeks after the operation. (auth)

40553 PROCEDURE FOR THE DETERMINATION OF TOTAL IODINE IN RADIOACTIVE IODIDE PREPARATIONS OF HIGH SPECIFIC ACTIVITY. Helmkamp, R. W.; Contreras, Ma. de los Angeles; Bale, W. F. (Univ. of Rochester, N. Y.). J. Nucl. Med., 7: 491-500(July 1966).

A method, based on radioactivity measurements, is described for determining total iodine in highly radioactive iodide samples. In ^{131}I-labeling of protein or other substances, by procedures in which ^{131}I as iodide is oxidized to positive iodine, this analysis permits calculation of the amount of iodine incorporated in the labeled product. When the iodinating agent is iodine monochloride, into which ^{131}I is introduced by isotopic exchange, this analysis makes it possible to predict the fraction of the ^{131}I used that will be in the iodinated substance. (auth)

40554 STUDY OF THE METABOLISM OF ^{18}F IN DOGS AND ITS SUITABILITY FOR BONE SCANNING. Dworkin, H. J.; Moon, N. F.; Lessard, R. J.; LaFleur, P. (Univ. of Michigan, Ann Arbor). J. Nucl. Med., 7: 510-20(July 1966).

Twenty-five dog experiments were performed using orally and intravenously administered ^{18}F as carrier free NaF. Bone scans and external point counting indicated that the uptake of ^{18}F by bone reached a maximum within one hour and that scans of good quality could be achieved after that time. A rapid fall in blood radioactivity was found as well as rapid urinary excretion of ^{18}F; 50% of the administered dose was found in the urine within six hours. Bone radioactivity usually was more than five fold that found in soft tissues (except kidney) as determined by well counting. Autoradiographs revealed nonhomogeneity of ^{18}F distribution in bone; 0.12 rad/mC is the estimated radiation dose to bone using the usual methods of calculations. (auth)

40555 STUDY OF THYROID PHYSIOLOGY UTILIZING INTRAVENOUS SODIUM PERTECHNETATE. Sodee, D. Bruce (Doctors Hospital and Renner Clinic Foundation, Cleveland Heights, Ohio). J. Nucl. Med., 7: 564-7(July 1966).

In this preliminary report we have presented 34 patients studied with ^{131}I and ^{99m}Tc to determine whether Tc has a place in the study of thyroid physiology. In this study the euthyroid range of Tc concentration at one hour is 1.5-to-4 per cent. In the three hyperthyroid patients, Tc concentration at one hour post dose was between 10-to-20 per cent. The Tc uptake is also decreased in hypothyroidism whether it be primary or secondary. The Tc scans may be performed in conjunction with the uptake and are comparable to the 24 hour ^{131}I scans. Because of the low radiation dose delivered to the thyroid and to the whole body (1), these studies indicate the possiblity of extending the thyroid physiology studies into children and the pregnant women. This study would suggest that sodium pertechnetate warrants further investigation as an indicator of thyroid physiology. (auth)

40556 INFLUENCE OF DIETARY CALCIUM, ZINC, AND OIL UPON THE IN VITRO UPTAKE OF ^{65}Zn BY PORCINE BLOOD CELLS. Berry, R. K.; Bell, M. C.; Wright, P. L. (Univ. of Tennessee, Oak Ridge). J. Nutr., 88: 248-90(Mar. 1966).

This study was conducted to ascertain whether the in vitro uptake of ^{65}Zn by porcine blood cells could be altered by dietary calcium, zinc, or corn oil and to compare uptake of various other radioisotopes. Weanling barrows were fed variable levels of either calcium, zinc, or fat for 16 weeks to determine effects on ^{65}Zn retention by blood cells. Five ml of freshly drawn whole blood obtained at 2-week intervals was treated with 200 mμC ^{65}Zn. After incubation under O_2 atmosphere at 38° for a 2-hr period, the cells were separated from the plasma and their radiozinc content was determined. Average percentages cellular ^{65}Zn uptake per treatment (after packed-cell volumes were adjusted to 40) were: basal, 34; basal +71 ppM Zn, 26; basal +0.6% Ca, 55; basal +71 ppM Zn + 0.6% Ca, 28; basal +5% oil, 34; basal +0.6% Ca + 5% oil, 51. Dietary calcium increased, whereas dietary zinc decreased, in vitro uptake ^{65}Zn throughout the experiment. Added oil exerted no significant effect on ^{65}Zn uptake in vitro. Dietary treatment had no detectable effect on the stable zinc content of these cells. Also tested was the the in vitro uptake by red cells of other isotopes (^{131}I, ^{75}Se, ^{137}Cs, ^{60}Co, ^{59}Fe, ^{54}Mn, ^{115}Cd, and ^{64}Cu). Calcium feeding increased ^{137}Cs retention. The ^{59}Fe in vitro uptake was variable. Calcium and zinc increased ^{59}Fe uptake when added to the ration separately; however, when both were added simultaneously, they decreased ^{59}Fe activity. Dietary zinc in the presence of added calcium decreased in vitro ^{64}Cu activity of blood cells, but ^{131}I, ^{75}Se, ^{60}Co, ^{54}Mn, and ^{115}Cd retention was not significantly affected by dietary treatment. (BBB)

40557 DISTRIBUTION OF ^{47}Ca IN THE RAT. Anderson, J.; Tomlinson, R. W. S. (King's Coll. Hospital, London). J. Physiol. (London), 182: 664-70(Feb. 1966).

Plasma sp activities were measured at various times after the intravenous injection of calcium-47 in four different age groups of rats. The data could be represented as two power functions. The change in power function occurs at a set time which is significantly different in three of the age groups. Various bones, muscle, and skin all

show different uptakes of the calcium-47 and the change in the power function of the plasma data probably represents an equilibrium of the soft tissue calcium. From the data presented on muscle, skin and bone it would appear that there are no fixed compartments of any size which exchange at a fixed rate. Skin exchanges rapidly at first but does not reach the plasma sp act. during the duration of this study. Muscle and bone likewise have different uptake patterns. The uptakes of calcium-47 into the skull and the epiphyses and metaphyses of the femur were all different. Thus each bone in the skeleton and even different parts of the same bone takes up calcium at an independent rate. The usefulness of the study of plasma sp act. data is limited because of the difficulty of interpretation. The proof that it measures bone accretion has never been established. The present study suggests that it represents the end result of a complex equilibrium and that if bone formation is to be measured other techniques will have to be developed, such as the tetracycline labelling of Haversian systems. (BBB)

40558 DYNAMICS OF THE MINERALIZATION OF THE FETAL SKELETON OF CHICKENS BY THE USE OF ^{32}P AND ^{45}Ca. **Draganovic, B. Mededel. Landbouwhogeschool Opzoekingssta. Staat. Gent, 30: 797-805(1965). (In French).**

During the osteogenesis and ossification of the chicken fetus skeleton, the formation of the bone matrix and its mineralization can be distinguished. The dynamics of these processes were studied by using ^{32}P and ^{45}Ca. Incubated eggs from the white leghorn were used as research materials. The radioisotopes were administered on the sixth day of incubation and the mineralization elements were evaluated on the tibia of the chicken fetus. From the analysis of the results obtained by measuring the tracing doses of ^{32}P and ^{45}Ca by radiometric methods, the volume and intensity of the ossification produced in the skeleton and the dynamics of the mineralization of cartilege can be deduced. These studies have shown that the calcium to phosphorus ratio remains constant during these phenomena. Although the calcium and phosphorus are primarily osteotropic, the distribution of the phosphorus has a more pronounced intensity, since it is also present in other tissues. Thus it is possible to follow phosphorus metabolism not only in the bone but in the epiphysis cartilege. The radial calcium is primarily a tracer of the skeleton in the ossification phase. Therefore calcium can be used to follow the changes in the dynamics of the ossification, in the evolution, and in the growth of the bone. Autohistoradiograms of the tibia have shown that the process of mineralization is most intense in the period from the 12th to the 18th day of incubation, that it is propagated from the center of the diaphysis to the epiphysis, and that it is accelerated on the proximal epiphysis. During the fetal evolution of the chicken, the phosphorus and the calcium show that the bone of the skeleton are modeled and ossified up to the metaphysis itself, which in the postfetal evolution are the carriers of the growth potential with respect to length. (tr-auth)

40559 CONTAMINABILITY OF EGGS BY RADIONUCLIDES IN CONDITIONS OF EXTERNAL RADIOCONTAMINATION. **Petrovic, B. (L'institut pour l'application de l'energie nucleaire, Belgrade). Mededel. Landbouwhogeschool Opzoekingssta. Staat Gent, 30: 1223-6(1965). (In French).**

The problem of the external radiocontamination of eggs suitable as food was examined. The radioactive contamination of eggs by the isotopes ^{90}Sr, ^{137}Cs, ^{144}Ce, and ^{131}I was examined. Basic information on the degree of external radiocontamination by these radiosiotopes was obtained from the biological viewpoint. Data were also presented on the speed of the penetration of the shell and on the radioisotopic distribution in the internal layers of the eggs as a function of time. The data obtained can be used for the hygiene-radiological determination of this food. (tr-auth)

40560 THE MECHANISM OF CERIUM UPTAKE BY SACCHAROMYCES CEREVISIAE. **Johnson, G. T.; Kyker, G. C. (Oak Ridge Associated Universities, Tenn. Univ. of Arkansas, Fayetteville). Mycologia, 58: 91-9(Jan.-Feb. 1966). (TID-21223).**

A large fraction of the total uptake of cerium-144 by washed resting yeast cells occurs quite rapidly (less than 15 min). Optimum uptakes occur in acidic environments (pH 2.5–4.0). The cells show a relatively constant cerium binding capacity (about 3×10^{-4} mg/mg dry wt), measured by radioactive tracer techniques after 2 hr contact time. The uptake is independent of temperature over the range from 4 to 38 C, is as high under anaerobic as under aerobic conditions, and is not affected by the common inhibitors of respiratory and glycolytic pathways. The cerium of labeled cells is rapidly removed by the hydrogen ion, complexing agents, and an excess of cerium cations. The data presented suggest cerium uptake by yeast involves primarily an adsorption of the element by some solid phase in or on the cell rather than an active transport process in which metabolic energy is required. (auth)

40561 ^{59}Fe INCORPORATION INTO RAT ERYTHROCYTES AFTER A SINGLE DOSE OF L-METHIONINE SULPHOXIMINE AND AFTER 600 r X-RAY IRRADIATION. **Kolousek, J.; Gyoergyi, S. (Charles Univ., Prague. Budapest Univ. of Medicine). Neoplasma, 13: 289-93(1966).**

We have examined the rate of incorporation of radioactive iron (^{59}Fe) into the erythrocytes of rats after irradiation with 600 R x-ray dose on the whole body as well as after a single dose of L-methionine sulphoximine. Similarly we have examined the ^{59}Fe-content and the water-content of the plasma and urine. Within 6 hours after the irradiation and the application of L-methionine sulphoximine respectively we did not find any essential difference between the specific activities of the plasma or urine of the treated and control groups respectively. As a consequence of both treatments the rate of incorporation of ^{59}Fe into the erythrocytes decreased significantly; this difference remained even after the material had remained at room temperature for 18 hours. There was no significant change in the water-content of urine or plasma within 6 hours. The results obtained are indicative of the fact that ionizing irradiation as well as methionine sulphoximine after permeability of erythrocytes and that their rate of incorporation of ^{59}Fe is influenced presumably by irritation or destruction of the neurosecretory centers of the hypothalamus. (auth)

40562 IMITATION OF POST-RADIATION DAMAGE TO THE DNA UNDER INFLUENCE OF EXTRACTS FROM IRRADIATED POTATO BULBS. **Kuzin, A. M.; Tokarskaja, B. I.; Kopylow, B. A.; Mielnikowa, S. K. (Inst. of Biophysics, Moscow). Nowotwory, 17: 127-30(Apr.-June 1966). (In Polish).**

The effects of toxic extracts from irradiated tissue on DNA synthesis were studied in potato tubers. A decrease in DNA synthesis averaging 50% resulted from the action of the radiotoxins, and the adenine to thymine ratio was affected in test material. (H.G.D.)

40563 THE METABOLISM OF ^{65}Zn BY RATS UNDER THE INFLUENCE OF PREDNISOLONE OR DEXAMETHASONE. **Glaubitt, D.; Nordmeyer, P.; Asam, U. (Univ., Hamburg). Nucl.-Med., 5: 250-5(19660. (In German).**

Dexamethasone-21-o-phosphate and, less markedly, Prednisolone-21-hemisuccinate-sodium reduced the biological half-life of whole-body radioactivity in 60 male Wistar rats after intraperitoneal administration of ^{65}Zn. Radioactivity in the pancreas and, less so, in the kidneys decreased more rapidly in the dexamethasone animals than in the controls. (auth)

40564 MINIMUM DOSE OF POTASSIUM IODIDE WHICH INHIBITS THE THYROIDAL RADIOIODINE UPTAKE. **Koutras, D. A.; Livadas, D. (Univ. of Athens). Nucl.-Med., 5: 256-61(1966).**

The thyroidal uptake of ^{131}I was measured 2 and 24 hrs after an oral tracer dose in 60 persons receiving KI in doses ranging from 5 to 80 mg. The results show that 40 mg of KI is the minimal dose required for a complete inhibition of thyroidal uptake. In cases when it becomes desirable to block entirely the uptake of radioactive isotopes of iodine by the human thyroid, KI should be given in an initial dose of 40 mg, with a minimal maintenance dose of 3.3 mg/day. (auth)

40565 TEST OF THE THEORY OF ALKALINE EARTH METABOLISM BY THE BEHAVIOUR OF ^{133}Ba IN RATS. Domanski, T. M.; Depczyk, D.; Liniecki, J. (Inst. of Occupational Medicine, Lodz, Poland). Phys. Med. Biol., 11: 461-70(1966).

Fractional biological retention of intravenously injected ^{133}Ba of high specific activity was followed in adult rats for about 460 days. The specific activity of serum and of whole body was determined in serially killed groups of rats. The data were used to test Marshall's theory of the metabolism of alkaline-earth elements. Observed values of retention were expressed as a power function of time, and monoexponential termination of retention was observed directly at a time exceeding by far the value predicted by the theory from observation of serum and body-specific activity. The integral of real retention between time = 0 and infinity was greater by a factor of ten than the value postulated by the theory. In the light of these observations some of the basic assumptions of the theory are questioned. (auth)

40566 RAPID DETECTION OF TUMOR HORMONE DEPENDENCY BY RADIOISOTOPES. White, Richard L.; Herter, Frederic P. (Columbia Univ., N. Y.). Surg. Forum, 16: 69-71(1965).

Animal and clinical experiments were performed in the development of a new radioisotope method to detect the response of tumors to hormones. Small Geiger tubes were embedded in 3-methylcholanthrene-induced, hormone-dependent breast carcinomas in female Sprague-Dawley rats. Continuous uptake records were obtained for 45 to 146 hr after a single 0.05 $\mu C/g$ ^{32}P injection. All tumors which continued to grow after the ^{32}P uptake test demonstrated a peak of ^{32}P accumulation at 39 to 53 hr. Half the tumors showed a steady gradual accumulation of ^{32}P after injection, but the other half first reached a vascular peak at 2 hr. These latter tumors then lost 26% of this ^{32}P in 9 hr before reaccumulating ^{32}P to reach the 41 hr peak (23% above initial vascular peak). All showed a fourth phase wherein accumulated ^{32}P was conserved with a count-rate decrease only 33.9% faster than the count loss due to ^{32}P physical decay. This uptake pattern, associated with uninterrupted tumor growth, was seen in 7 of 13 untreated control tumors; 1 of 12 tumors treated with dihydrotestosterone; and 2 tumors which, after initial regression with daily androgen, recurred and were then retested. To assess the usefulness of this method in rapidly evaluating nonoperative forms of cancer treatment in humans, Geiger tubes were embedded in the superficial tumors of 14 patients with inoperable carcinoma. All patients received a single intravenous injection of 308 to 500 μC of $Na_2H^{32}PO_4$. Five patients, 3 with breast carcinomas, 1 with an undifferentiated clavicular metastasis, and 1 with a sacral chordoma showed no growth response to hormone or chemotherapy in a 4 to 7 month follow-up. All showed a characteristic pattern of ^{32}P incorporation in tumor consisting of a rapidly attained vascular peak at 2 hr, a subsequent 32% loss of ^{32}P over 20 hr, and a third phase of prolonged conservation of ^{32}P for 130 hr. This third phase count-rate decrease paralleled the loss of count resulting from the physical decay of ^{32}P in 3 cases and in 2 others equaled 53.0% and 89.6%. In contrast the 3 tumors which, with hormonal or chemotherapy, lost 22 to 96% of their mass over a 2.5 to 9 month follow-up respectively, demonstrated striking differences in the ^{32}P uptake pattern. These observations suggest that prolonged hormone dependency or responsiveness to chemotherapy can be predicted rapidly by monitoring ^{32}P uptake in tumors. (BBB)

40567 THE USE OF RADIOAUTOGRAPHY IN INVESTIGATING PROTEIN SYNTHESIS. CONFERENCE, MONTREAL, 1965. Leblond, C. P. (McGill Univ., Montreal); Warren, Katherine Brehme (eds.). Symp. Int. Soc. Cell Biol., 4: 1-348(1965).

Papers are presented on autoradiographic techniques and methods applicable to studies of protein synthesis. Studies on protein synthesis in the cell nucleus, in various types of cells, and in secretory processes are included. (H.G.D.)

40568 INFLUENCE OF CALCIUM AND STRONTIUM IN THE DIET ON THE ELIMINATION OF ^{85}Sr AND ^{89}Sr BY GOATS. Prinz, W. (Tieraerztliche Hochschule, Hannover). Zentralbl. Veterinaermed., 12: 580-6(Dec. 1965). (In German).

Studies on strontium excretion were carried out on male animals, on female pregnant and lactating goats, and on kids. The animals received over several months either a diet deficient in calcium (calcium content 0.2%) or adequate in calcium (0.77% Ca). Radiostrontium was given in capsules over a ten-day period. Male animals of the group deficient in calcium excreted during a three-week balance period only 50-60% of the radiostrontium given by mouth, whereas the animals on a diet with optimal calcium content excreted 70–90% in the urine and feces. Feeding stable strontium had no effect if the diet contained an adequate amount of calcium but on calcium-deficient diets the excretion of strontium in the urine after doses of the stable element was reduced. Lactating animals of all ages on a diet abundant in calcium excreted 1 to 3% of radiostrontium in the milk. Young animals on a calcium-deficient diet eliminated up to 20% of strontium in the milk, whereas eight-yr-old goats on this diet eliminated only 2 to 3% in the milk, i.e., no more than on calcium-rich diets. With diets deficient in calcium, larger amounts of strontium were deposited in the skeleton, up to 10% of the dose given. (BBB)

40569 DEPOSITION AND DISTRIBUTION OF STRONTIUM IN HEN EGGS. Schmid, A.; Zipf, K. (Univ., Munich). Zentralbl. Veterinaermed., 12: 613-16(Dec. 1965). (In German).

Hens were given a mash containing Sr for 180 days, followed by a mash in which Ca was substituted for Sr for 218 days, and for 209 days a mash that contained neither element. Estimation of the Ca in the egg whites gave a value of 1.47 ± 0.57%. Two days after the start of the Sr supplementation the Sr concentration of the whites was 0.07%, which was 5 or 10 times greater than normal. This value ranged, after this, from 0.05 to 0.30%. On the 77th day the extreme value was 0.30%. When the Sr was no longer given, the concentration in the whites fell to 0.05%. This value was found after 40 days on the Sr-free diet. The rate of deposition of Sr occurred in the order, shell, albumin, yolk. Concentration of Sr was in the same order. Distribution of Ca in the three egg components was similar to that of Sr. (BBB)

40570 UMWELTRADIOAKTIVITAET UND STRAHLENBELASTUNG. Bericht IV/65. (Environmental Radioactivity and Radiation Burden. Fourth Quarterly Report, 65). Bad Godesberg, Ger., Bundesminister fuer Wissenschaftliche Forschung, 1966. 208p. DM 10.--.

The content of the radioactive materials in air, water, soil, and food materials and the radiation burden of the population in the German Federal Republic measured during the fourth quarter of 1965 are reported in graphic and tabular form. (J.S.R.)

40571 OXIDATIVE PHOSPHORYLATION IN FRACTIONATED BACTERIAL SYSTEMS. XXII. THE EFFECT OF NEAR-ULTRAVIOLET IRRADIATION ON THE SUCCINATE OXIDASE PATHWAY OF MYCOBACTERIUM PHLEI. Ramakrishna, C. K.; Brodie, Arnold F. (Univ. of Southern California, Los Angeles). 32p. (CONF-660539-3). ORAU. Gmelin, AED-CONF-66-114-3.

From American Society for Microbiology, 66th Annual Meeting, Los Angeles.

The succinate oxidase activity of Mycobacterium phlei was sensitive to irradiation with light at 360 mμ. The loss of activity was due to a lesion occurring in the electron transport chain between the flavoprotein and cytochrome b regions. The activity lost was not restored by addition of vitamin K_1 or other cofactors, but could be restored by the addition of the supernatant fraction. The factor responsible for the restoration of the succinate chain has been purified. It was sensitive to heat and irradiation and appeared to be protein in nature. It activated both oxidation and phosphorylation in irradiated particulate systems. The proteins which restored the two activities could not be separated. (auth)

40572 MINOR-ELEMENT AND TRACE-ELEMENT CONTENT OF THE MARINE ENVIRONMENT ON THE WEST COAST OF INDIA. Sreekumaran, C.; Bhatt, Y. M.; Naidu, J. R.; (and others) (Atomic Energy Establishment, Trombay, India). Vienna, International Atomic Energy Agency, 1966, Preprint SM-72/36A, 24p. (CONF-660507-25). ORAU.

From Symposium for the Disposal of Radioactive Wastes into Sea, Oceans, and Surface Waters, Vienna.

In view of the affinity of marine organisms and sediments for minor and trace elements and their radioisotopes, analyses were carried out on marine-environmental samples at five stations on the West Coast of India (Bombay, Veraval, Ratnagiri, Mangalore and Cochin) during the period 1962 to 1965. The following ranges of concentrations were observed in sea water: potassium, 362 to 722 ppm; calcium 398 to 448 ppm; strontium, 2.8 to 13.6 ppm; phosphorus, 60 to 214 μg/l; iron, 1 to 13 μg/l; copper, 0.5 to 22 μg/l; manganese, 2 to 17 μg/l; uranium, 1.3 to 4.2 μg/l. Analyses were also carried out on sea water samples collected from the Indian Ocean during the International Indian Ocean Expedition. The samples from the coastal waters differed from the open ocean samples mainly in their contents of phosphorus and manganese, the concentration ranges for the two elements in the open ocean being respectively 17 to 128 μg/l and 2 to 20 μg/l. From the observations on the elemental concentrations in marine organisms, it appeared that the following would serve well as indicators for zinc and manganese respectively: Crassostrea gryphoides (190 to 400 ppm) and Sunetta donacina (50 to 84 ppm). Data on fallout activities (^{137}Cs, ^{90}Sr, and ^{106}Ru) were included to indicate calculation of specific activities of the elements available for organisms. (auth)

40573 FLUX OF ^{32}P AND ^{65}Zn THROUGH A SALT-MARSH ECOSYSTEM. Pomeroy, L. R.; Odum, E. P.; Johannes, R. E.; Roffman, B. (Univ. of Georgia, Sapelo Island. Univ. of Georgia, Athens). Vienna, International Atomic Energy Agency, 1966, Preprint SM-72/10, 16p. (CONF-660507-9). ORAU.

From Symposium for the Disposal of Radioactive Wastes into Sea, Oceans, and Surface Waters, Vienna.

Flux of ^{32}P and ^{65}Zn was studied by introducing 100 mc of each simultaneously into the water of a tidal creek with a drainage area of 7 hectares. Components of the system were sampled over a period of months. The clay minerals of the sediments (kaolinite and montmorillonite) provided sites for adsorption. Since the amount of stable isotopes already adsorbed was large compared to the amount present in the water, uptake of corresponding radionuclides was rapid and subsequent loss was slow. Bacteria in the sediments competed for the radionuclides and reduced the amount taken up by the sediments. Higher plants of the marsh did not take up the radionuclides used. Populations of diatoms and other algae in the sediments did not become as radioactive as the sediments in which they live. A dinoflagellate bloom did take up measurable amounts of the radionuclides. Those animal populations that consumed sediments, either as their food or incidentally in their feeding, removed the radionuclides from the sediments. Probably the digestion of bacteria from the sediments by sediment-feeding animals was an important step in the flux from sediments to biota. It is concluded that when the radionuclides are introduced into marsh water or to the surface of marsh sediments, they will be adsorbed rapidly by the sediments and bacteria. From there they move slowly into the biota over a period of days or months. The radionuclides that we used do not enter the salt-marsh biota at the level of primary producers (except via dinoflagellate blooms) but rather at the level of bacteria, filter-feeding organisms, and sediment-feeding organisms. Losses of the radionuclides from the marsh will be through desorption from sediments to the water and subsequent flushing out of the water by tidal action, and also by the removal of radioactive organisms from the system. Most removal of organisms will occur at the level of secondary and tertiary consumers. Loss through this route is, therefore, slow. (auth)

40574 EFFECT OF IRRIGATION ON ABSORPTION AND LOCALIZATION OF CESIUM AND STRONTIUM IN ORYZA SATIVA L. Myttenaere, C.; Masset, M. (EURATOM, Ispra, Italy). Vienna, International Atomic Energy Agency, 1966, Preprint SM-72/30, 40p. (In French). (CONF-660507-20). ORAU.

From Symposium for the Disposal of Radioactive Wastes into Sea, Oceans, and Surface Waters, Vienna.

Factors affecting absorption of Cs and Sr by a particular variety of lowland rice grown on irrigated, non-irrigated, desiccated and submerged soils were investigated. The radioisotopes (^{137}Cs and ^{85}Sr) were applied to the surface at the same time as the mineral fertilizer. Distribution of the chemical forms differed greatly between the two ions concerned. Irrigation affected the distribution of exchangeable K in the soil but not that of ^{137}Cs, a feature less marked in the case of Ca and ^{85}Sr ions. The distribution of ^{137}Cs (in % of the total activity of the plant) was affected by the methods of cultivation. The roots contained 50% of the total activity of the plant in an irrigated medium, as against 35% by normal cultivation. This result was due partly to the development of the root system. Distribution differed widely with the isotope. Under submerged cultivation, lowland rice accumulates more Cs and Sr than by normal cultivation (^{137}Cs 62% against 0.13%; ^{85}Sr 16% against 2%) and, in addition, the normal preferred sequence of uptake was reversed. The activity of the various parts of the panicle was slightly lower in irrigated soil. This would seem to indicate that factors other than irrigation (and its consequences) underlie the results observed in the field. Among the stable isotopes determined (Mn, Sr, Ca, K and Cs), Mn appears best to respond to irrigation conditions (higher Mn content on irrigated soil). (auth)

40575 UPTAKE AND ACCUMULATION OF ^{51}Cr BY THE CLAM, TAPES DECUSSATUS, IN RELATION TO PHYSICAL AND CHEMICAL FORM. Chipman, Walter A. (IAEA, Monaco). Vienna, International Atomic Energy Agency, 1966, Preprint SM-72/35, 20p. (CONF-660507-23). ORAU.

From Symposium for the Disposal of Radioactive Wastes into Sea, Oceans, and Surface Waters, Vienna.

Experiments were made using the clam, Tapes decussatus, to examine the uptake and accumulation of ^{51}Cr when added to the sea water in different chemical and physical forms. The addition of ^{51}Cr as trivalent chromic chloride resulted in precipitation with the greater part of the radionuclide present as filterable particles. There was also considerable loss from adsorption to surfaces. Clams exposed to this sea water rapidly became radioactive from their filtering activity and from adsorption. The radioactive particles were quickly eliminated by the clams, but the adsorbed radioactivity was lost almost exclusively by decay of the radionuclide. When the trivalent ^{51}Cr was added as an EDTA chelate, the radioactivity was not filterable. Clams maintained in this sea-water solution failed to take up and accumulate the radionuclide. The addition of ^{51}Cr in the form of hexavalent sodium chromate to sea water resulted in a solution containing radioactive ions. The radionuclide in this form was rapidly taken up by the clams through the absorptive surfaces of the body. Following the more rapid initial uptake, there was a slow continued uptake without an apparent lessening in rate over an observation time of 20 days. Accumulation in this length of time was not great. The amount of chromium and ^{51}Cr entering the clams was related to concentration in the sea water, accumulation apparently being a passive process. The greater part of the radioactivity was accumulated within the soft body tissues and much in the body liquids. The radionuclide was tightly bound in tissues and biological retention time of the radioactivity was long when the animals were returned to normal sea water. (auth)

40576 NUTRITIONAL VALUE OF IRRADIATED POTATOES. Lang, K.; Baessler, K. H. (Univ. of Mainz). Vienna, International Atomic Energy Agency, 1966, Preprint SM-73/39, 4p. (CONF-660609-16). ORAU.

From International Symposium on Food Irradiation, Karlsruhe, Ger.

Rats received dried potatoes, irradiated with 10 krad, in an amount of 72% of the diet. Control groups received the same amount of non-irradiated potatoes. Up to date there is no difference between the groups fed with irradiated potatoes and the controls as far as weight gain and protein efficiency are concerned. Another experiment has been running for 12 weeks under the same conditions except that the radiation dose was 100 krad. Here, too, no difference to the control groups can be observed. (auth)

40577 NUCLEIC ACID METABOLISM IN THE THYMUS AND RELATED ORGANS OF MICE AFTER ESTRADIOL AND IRRADIATION. Thompson, J. S. 5p. (CONF-660428-1). ORAU. Gmelin, AED-CONF-66-075-2.

From Federation of American Societies for Experimental Biology, 50th Meeting, Atlantic City.

The effect of estradiol on the lymphatic tissues and immune system was studied in normal adult mice, newborn mice, and lethally irradiated adult mice transplanted with syngeneic marrow. Estradiol did not alter the nucleic acid metabolism in the mesenteric lymph node, and both DNA and RNA syntheses were stimulated in the spleen within 24 hrs of administration. Like irradiation, estradiol administration caused thymic involution characterized by cellular loss and destruction, decreased DNA and RNA content, and depressed DNA synthesis. Results support the premise that estradiol action in newborn and irradiated mice is mediated by the thymus. (H.G.D.)

40578 ACCUMULATION OF RADIONUCLIDES BY AQUATIC ORGANISMS OF ECONOMIC IMPORTANCE IN THE UNITED KINGDOM. Bryan, G. W. (Marine Biological Association of the United Kingdom, Plymouth, Eng.); Preston, A.; Templeton, W. L. Vienna, International Atomic Energy Agency, 1966, Preprint SM-72/39, 18p. (CONF-660507-26). ORAU.

From Symposium for the Disposal of Radioactive Wastes into Sea, Oceans, and Surface Waters, Vienna.

A survey was made of some of the more recent work done in the United Kingdom on the extent to which radionuclides can be accumulated by edible plants, molluscks, crustaceans and fish in the sea and fresh water. Results from laboratory experiments on rates of uptake and factors affecting them have been combined with results from field work at Windscale, from fallout studies, and from stable isotope analyses. (auth)

40579 ACCUMULATION OF BETA ACTIVITY FROM FALLOUT ON LEAVES. Gallant, Esther M. 19p. (CONF-660430-3). ORAU. Gmelin, AED-CONF-66-105-2.

From Ohio Academy of Science, 75th Annual Meeting, Columbus, Ohio.

This study is concerned with mechanisms by which fission products accumulate in leaves. The objective was to determine the pattern of accumulation of radioactive particles by leaves of selected trees during an entire growing season. Leaves were collected from four species of trees, silver maple, horsechestnut, boxelder, and Scotch pine. The leaves were dried, ground and ashed. Samples were affixed to stainless steel planchets with a film of hydroxyethyl cellulose. The samples were counted with a Baird-Atomic model 132 gas flow counter in a model 750 automatic sample changer. A variety of plants, such as mullein, goldenrod, burdock, lichens and Scotch pine, were collected and sampled for gross beta activity. Annual or first year plants had lower activity than perennials. When different parts of the same plant were sampled, the leaves and bark always counted significantly higher than xylem and roots. Grass from a flooded stream bank has less activity than grass from a high flat field. Levels of activity on leaves were not lowered by rinsing with detergent or acetone. When leaves from which surface hairs had been removed were rinsed with EDTA and detergent, the beta activity was reduced. With regard to beta activity during the growing season, the highest peaks of activity were reached early in the growing season; by the middle of June the count rates were declining; the general trend was gradual reduction during the season. Reduction of activity could be explained by decay of initially absorbed radionuclides, leaching by rain, and dilution by leaf growth. The main part of the beta activity results from radioactive particles deposited on and absorbed by the young leaves which are more capable of foliar absorption than are mature leaves. Data are presented in the form of tables and graphs. (H.L.W.)

Radiation Effects on Biochemicals

See also CHEMISTRY — Radiation Chemistry

40580 (NYO-2804-8) THE EFFECTS OF IRRADIATED MEDIUM ON SOME CELLULAR FUNCTIONS OF E. COLI. Frey, Harold E. Jr. (Pennsylvania State Univ., University Park. Dept. of Biophysics). June 1966. Contract AT(30-1)-2804. 64p. Dep. mn. CFSTI $3.00 cy, $0.75 mn.

Thesis.

The effects of irradiated medium on a bacterial cell were studied with primary emphasis on where in the cell the damage was occurring. It was shown that the agent causing the damage was a peroxide, quite possibly hydrogen peroxide. The study also shows that the structural integrity of a cellular system is important for cells to remove peroxide. Finally, it is concluded that irradiated medium affects the respiratory pathway in the bacterial cell, possibly by interfacing with electron transport along the cytochrome system. (auth)

40581 (ORNL-3922, pp 50-1) BIOPHYSICAL AND BIOCHEMICAL CYTOLOGY. (Oak Ridge National Lab., Tenn.).

Progress is reported on: the effects of ultraviolet radiation on human leukocytes; the effects of thymidine on incorporation of deoxycytidine into DNA; and diminution of x-radioinduced chromosome aberrations by treatment with actinomycin D. Stirred samples of human leukocytes were irradiated with uv from a large monochromator at 2500, 2650, 2800, 2900, 3000, and 3100 A. At all wavelengths except 3100 A, cells would not undergo mitosis. Experiments in which the cells were exposed to tritiated thymidine showed that after uv irradiation, fewer lymphocytes became transformed, there was an inhibition of incorporation of label into DNA, and some cells became necrotic. Cells of Vicia faba grown in various concentrations of thymidine for 60 min showed an inhibition of ^{3}H-deoxycytidine incorporation into the DNA of root treated with high concentration. However thymidine had no apparent physiological effects on root cells. Therefore, it was suggested that the presence of a high concentration of exogenous thymidine affects the pathways of pyrimidine synthesis and causes an increase in the size of the deoxycytidine pool within the cell. Soaked seeds of Vicia faba were: x-irradiated (600 R, 200 R/min) followed by 3 hr immersion in actinomycin D; pretreated with actinomycin D for 3 hrs prior to x-irradiation; or exposed to x rays during a 3 hr treatment with actinomycin D. Metaphase cells in the resulting root-tip smears were analyzed for chromosome aberrations and it was found that the number of such aberrations seen in actinomycin D-treated roots was consistently reduced from the control value by 75%. (H.G.D.)

40582 (ORNL-3922, pp 65-8) CYTOCHEMISTRY AND CELL REPRODUCTION. (Oak Ridge National Lab., Tenn.).

Super-suppressors as addition-deletion mutations were studied in Saccharomyces. It was concluded that neither the suppressible nor the super-suppressors show a meiotic effect. A fragment of tryptophan synthetase in a super-suppressible mutant of yeast was assayed by ^{14}C tracer techniques, and it was found that super-suppressible mutants of yeast make prematurely terminated proteins. Further a region in the tryptophan synthetase of yeast contained a region that was very similar to the A protein of the E. coli enzyme. Estimates of the ratios of diapause larvae to adults was made for vials of Mormoniella. Distribution of the vials as to none, few, several, many, or all according to age of the mother is tabulated. (H.G.D.)

40583 EFFECTS OF WHOLE-BODY IRRADIATION BY ^{60}Co ON THE LEVEL OF REDUCED NICOTINAMIDE NUCLEOTIDES IN RAT LIVER HOMOGENATES. Sonka, J.; Hilgertova, J.; Pospisil, J.; Dienstbier, Z. (Charles Univ., Prague). Atompraxis, 12: 350-2(July 1966).

Rats were subjected to whole-body irradiation by ^{60}Co (dose 800 R). The level of the total of reduced pyridine nucleotides (NADH + NADPH) was measured in their livers using glutathione-reductase, the decrease of extinction being 340 mμ. Radiation caused a loss of reduced pyridine nucleotides reaching at 0 time 39%, at 3 hours 43%, at 6 hours 26%, and at 12 hours following treatment 24%, relative to non-irradiated controls (100%). This drop in the level of reduced pyridine nucleotides is discussed in view of previous findings showing a decrease of reductive processes, especially of reductive syntheses. (auth)

40584 RADIOCHEMICAL METHOD FOR THE ESTIMATION OF CHOLINE ACETYLTRANSFERASE. Fonnum, F. (Agricultural Research Council, Cambridge, Eng.). Biochem. J., 100: 479-84(Aug. 1966).

A radiochemical method for the estimation of choline acetyltransferase (choline acetylase) has been devised which involves the formation of labeled acetylcholine from labeled acetate. [1-^{14}C]Acetate and coenzyme A are preincubated in the presence of non-rate-limiting concentrations of acetylcoenzyme. A synthetase to give [1-^{14}C]acetyl-coenzyme A, which then reacts with choline in the presence of the acetyltransferase to give [^{14}C]acetylcholine. Any [^{14}C]-acetylcoenzyme A remaining at the end of the reaction is destroyed by the addition of excess of hydroxylamine, and [^{14}C]acetylcholine is freed from other labeled compounds by precipitation with sodium tetraphenylborate (Kalignost). The washed precipitate is dissolved in acetonitrile–benzyl alcohol and estimated by scintillation counting. Advantages over other methods are discussed. (auth)

40585 IRRADIATION OF DEOXYRIBONUCLEOHISTONE SOLUTIONS. I. AMINO ACID DESTRUCTION. Robinson, M. G.; Weiss, J. J.; Wheeler, C. M. (Univ. of Newcastle upon Tyne, Eng.). Biochim. Biophys. Acta, 124: 176-80(July 27, 1966).

^{60}Co-γ-irradiation of deoxynucleohistone and of histone solutions has been carried out in order to determine the nature and the extent of amino acid destruction. The results show that amino acids are attacked, in both cases, to an extent depending upon their reactivity towards hydroxyl radicals and upon their relative concentration in the histone. Comparison of the total attack on deoxynucleohistone and on histone shows these to be approximately equal, thus confirming previous suggestions that the DNA in deoxynucleohistone is protected to a large extent from attack by the radiation-produced active species. (auth)

40586 IRRADIATION OF DEOXYRIBONUCLEOHISTONE SOLUTIONS. II. LABILIZATION OF THE DNA-HISTONE LINKAGE. Robinson, M. G.; Weiss, J. J.; Wheeler, C. M. (Univ. of Newcastle upon Tyne, Eng.). Biochim. Biophys. Acta, 124: 181-6(July 27, 1966).

Experiments have been carried out in order to determine the effect of ^{60}Co γ-irradiation on the binding of histone to DNA in deoxyribonucleohistone. Only small amounts of histone (~4% at 160 krad) are released by irradiation alone. However, if NaCl is added to the solution after irradiation this has a very marked effect as it labilizes the binding of the histone to the DNA as compared with the unirradiated deoxynucleohistone. This difference is particularly marked in the range of 0.4–0.8 M NaCl. Amino acid analyses which have been carried out on the histone released or labilized by γ-irradiation show that this has a relative composition differing from that of the total histone. (auth)

40587 PREMATURE INCORPORATION OF TRITIATED THYMIDINE AFTER POST-MITOTIC IRRADIATION OF FIBROBLAST AND MYOBLAST OF CHICKEN EMBRYOS. Liebecq-Hutter, S.; Donoel, C.; Beaumariage, M. L. (Univ., Liege). Compt. Rend. Soc. Biol., 159: 2268-71 (1965). (In French).

An immediate and premature incorporation of tritiated thymidine was detected in synchronous cultures of embryonic chick fibroblast and myoblast given a total x-ray dose of 400 R at the beginning of interphase. The incorporation is probably independent of DNA synthesis during mitosis, being attributed to synthesis that normally occurs toward the 20th hr of incubation. (H.G.D.)

40588 STUDIES ON ALLOGENIC INHIBITION. II. INHIBITION OF MOUSE TUMOR CELL GROWTH BY IN VITRO CONTACT WITH CELLS CONTAINING FOREIGN H-2 ANTIGENS. Bergheden, C.; Hellstroem, K. E. (Karolinska Institutet Medical School, Stockholm). Int. J. Cancer, 1: 361-9(July 15, 1966).

Mouse lymphoma cells were inoculated into preirradiated syngenetic hosts after incubation with lymph-node, spleen, liver, or lymphoma cells from different sources in the presence of phytohemagglutinin. Neutralization of tumor growth was detected after incubation of lymphoma target cells with added untreated or x-irradiated normal lymphoid or liver cells, or with x-irradiated intact or ultrasonically disintegrated lymphoma cells in all cases where the added cells contained H-2 isoantigens that were foreign to the targets. (auth)

40589 STUDIES OF HYDROGEN-BONDED SYSTEMS. IV. RADIATION-INDUCED TUNNELING AND TAUTOMERIC EQUILIBRIA IN THE GUANINE–CYTOSINE BASE PAIR. Rein, Robert; Harris, Frank E. (Uppsala Univ.). J. Chem. Phys., 45: 1797-9(Sept. 1, 1966).

Electronic energies were calculated for the ground states of the cation and anion of the guanine–cytosine base pair, using an approximate self-consistent-field method. The calculations were made for a series of positions of the hydrogen-bonded protons, all three of which are explicitly included in the formulation. The results are used to discuss equilibria and proton tunneling between tautomeric forms, and an indication is given of the possible connection between these phenomena and radioinduced mutation. (auth)

40590 HISTOCHEMICAL ASSAYS ON THE PRESENCE OF CERTAIN ENZYMES IN THE CEREBRAL TISSUE IN VARIOUS PHASES OF THE ACUTE IRRADIATION SYNDROME. Jonek, Jan; Kosmider, Stanislaw; Jonek, Teresa. Pol. Przegl. Radiol. Med. Nuklearnej, 30: 307-15(May-June 1966). (In Polish).

The publication presents histochemical assays on the presence of certain enzymes as DPNH-diaphorase alkalic and acid phosphatase, ATP-ase in the cerebral tissues of guinea pigs in various phases of acute irradiation disease. It was stated, that in the course of development of the irradiation syndrome the DPNH-diaphorase activity decreases in the cerebral cells—which may be due to a fall of the oxygenation processes. In the initial period of the disease the alkalic phosphatase increases and in further phase its decrease may be detected. The ATP-ase increases throughout the evolution of the irradiation syndrome. The mentioned enzymes activities alterations after the irradiation influence the active transportation of substrates from the plasma to the cell cytoplasm. The observed increase of the acid phosphatase activity in some groups of the ganglionar cells may be an effect of postirradiation catabolic processes. The presented changes of certain enzymes activities in the cerebral tissue, observed after irradiation, may be responsible for certain functional disturbances observed in the course of acute irradiation disease. (auth)

40591 DEPOLYMERIZATION OF HYALURONIC ACID BY AUTOXIDANTS AND RADIATIONS. Matsumura, Go; Herp, Anthony; Pigman, Ward (New York Medical Coll., New York). Radiat. Res., 28: 735-52(Aug. 1966).

The effects of x rays, β rays (^{32}P internally), and autoxidants were compared for the depolymerization of hyaluronic acid in the presence of air. A 0.02 mM solution of ascorbic acid reduced the viscosity of hyaluronic acid solutions at about the same rate as 2400 rads of x rays or β rays. The yields (G values) were low, about 0.015. Visible light also caused the degradation of hyaluronic acid in the presence of riboflavin as a sensitizer. A survey of compounds with possible autoxidant properties showed that the following

structures were associated with such activity: enediols (reduced or oxidized), quinones and hydroquinones, many thiols (not disulfides), m-nitrophenol, and a few metallic ions, especially Cu^{+}, Fe^{2+}, and Sn^{2+}. Antioxidant activity was tested extensively for the system hyaluronic acid–ascorbic acid, and some were studied in the radiation systems. The effects in both systems were similar, but were less extensive in the radiation system. (auth)

40592 ELECTRON SPIN RESONANCE AND THE EFFECTS OF RADIATION ON BIOLOGICAL SYSTEMS. Proceedings of a Conference Held at Gatlinburg, Tenn. May 10–12, 1965. Snipes, Wallace (ed.). Nuclear Science Series Report Number 43. Washington, D. C., National Academy of Sciences–National Research Council, 1966. 204p. $4.00. (CONF-650561).

Proceedings are presented on the correlation of radiation-produced electron spin resonance signals and biological effects. Separate abstracts of seven of the eight papers have been prepared. The eighth paper has appeared previously in NSA 20: 8588. (W.E.B.)

For abstracts of individual papers see: 40593–40598 and 42433.

40593 RADIATION-PRODUCED ELECTRON SPIN RESONANCE SIGNALS IN NUCLEIC ACIDS. Mueller, Adolph (Kernforschungszentrum, Karlsruhe, Ger.). pp 29-45 of Electron Spin Resonance and the Effects of Radiation on Biological Systems. Snipes, Wallace (ed.). Washington, D. C., National Academy of Sciences–National Research Council, 1966.

This paper presents results of qualitative and quantitative studies of ESR spectrometry of dried nucleic acids and their components and of radicals in biologically active nucleic acid from bacteriophage. Radical yield as a function of radiation dose was studied, and an expression for the relation is given. It was found that increases in radical yield proportional to radiation dose was found only at doses below about 1 Mrad. (W.E.B.)

40594 ELECTRON SPIN RESONANCE OF IRRADIATED DEOXYRIBONUCLEIC ACID. Shulman, R. G. (Bell Telephone Labs., Inc., Murray Hill, N. J.); Rahn, R. O.; Pershan, P. S.; Longworth, J. W.; Eisinger, J. pp 46-80 of Electron Spin Resonance and the Effects of Radiation on Biological Systems. Snipes, Wallace (ed.). Washington, D. C., National Academy of Sciences–National Research Council, 1966.

Three areas of radiation damage to DNA are mentioned—electronic excitation, stable chemical damage, and biological damage. This paper deals only with the first area by ESR studies of events before the stable chemical change stage. A discussion is given on the ESR spectra of free radicals formed by gamma irradiation and uv irradiation of DNA and on the excited triplet state induced in DNA by uv irradiation. (W.E.B.)

40595 ELECTRON SPIN RESONANCE SIGNALS IN IRRADIATED PROTEINS. Henriksen, Thormod (Univ. of California, Berkeley). pp 81-100 of Electron Spin Resonance and the Effects of Radiation on Biological Systems. Snipes, Wallace (ed.). Washington, D. C., National Academy of Sciences–National Research Council, 1966.

The paper covers ESR signals observed in proteins which were irradiated by 6.5 Mev electrons and measured at room temperature, proposed mechanisms for formation of protein radicals, and correlation between radiation-induced free radicals and biological effects, i.e., the dose of enzymatic activity. (W.E.B.)

40596 RADIATION CHEMISTRY OF PROTEINS IN THE DRY STATE. Tolbert, Bert M. (Univ. of Colorado, Boulder). pp 101-36 of Electron Spin Resonance and the Effects of Radiation on Biological Systems. Snipes, Wallace (ed.). Washington, D. C., National Academy of Sciences–National Research Council, 1966.

This paper presents information on enzyme inactivation. First-order inactivation is discussed in terms of the one-hit model. Effects of irradiation on enzyme activity, on conformational structure on disulfide linkages, on primary structure, and on the interrelationships of these properties are given. (W.E.B.)

40597 CONTRIBUTIONS OF ELECTRON PARAMAGNETIC RESONANCE TECHNIQUES TO THE UNDERSTANDING OF RADIATION BIOLOGY. Powers, E. L. (Argonne National Lab., Ill.). Contract AT-(40-1)-3408. pp 137-59 of Electron Spin Resonance and the Effects of Radiation on Biological Systems. Snipes, Wallace (ed.). Washington, D. C., National Academy of Sciences–National Research Council, 1966.

This paper treats the idea that radioinduced biological damage results from free radicals. The existing evidence for effects of free radicals, the needed evidence, and the use of ESR in developing the evidence are discussed. Data are given from effects of temperature, NO, oxygen, and water on irradiated organisms. (W.E.B.)

40598 SIGNIFICANCE OF ELECTRON SPIN RESONANCE MEASUREMENTS ON IRRADIATED BIOLOGICAL MACROMOLECULES. Alexander, Peter (Chester Beatty Research Inst., London). pp 162-76 of Electron Spin Resonance and the Effects of Radiation on Biological Systems. Snipes, Wallace (ed.). Washington, D. C., National Academy of Sciences–National Research Council, 1966.

The author feels that ESR is not very useful in determining the nature of the primary lesions responsible for cell death, but that the technique is useful for determining the mechanism of radioprotective or radiosensitizing procedures for dose modification. Studies are reported on effects of 2-amino ethanethiol (MEA) on trypsin inactivation and on other free radical reactions, the effects of oxygen and iodoacetic acid on free radical reactions, and the formation of ions in proteins containing sulfur. (W.E.B.)

40599 EFFECTS OF GAMMA RADIATION ON THE CONSTITUENTS OF WHEAT FLOUR. Deschreider, A. R. (Central Lab. of the Ministry of Economic Affairs, Brussels). Vienna, International Atomic Energy Agency, 1966, Preprint SM-73/4, 16p. (In French). (CONF-660609-27). ORAU.

From International Symposium on Food Irradiation, Karlsruhe, Ger.

Physical, chemical, and biochemical changes occurring in the constituents of wheat exposed to gamma radiation are discussed. The extent of these changes depends on the origin of the wheat and on the radiation dose. The carotenoids of the oily fraction of the wheat are reduced by the effects of the radiation, disappearing when the dose reaches 4 mrad. However, the chemical composition of the lipids, which are the seat of reactions similar to those giving rise to hydroperoxides, remains virtually unchanged even at very high doses. The substantial degradation of the starch indicates that the polysaccharides of the wheat are the fractions most severely affected by radiation. This leads to an increase in the reducing substances already present and in the maltose index as the dose rises. However, the increase in autolytic production of reducing sugars in the irradiated wheat is due to the greater susceptibility of the starch to hydrolysis by the diastases. The denaturation of the polysaccharide reduces the viscosity of the starch pastes thanks to an increase in the solubility of the amylopectin. Gamma irradiation generally reduces the proteolytic activity of flour, and, in the case of high doses, causes not only a partial denaturation of the proteins but also their polymerization and/or condensation. This polymerization may be explained by the reaction of free radicals with the gluten proteins having –SH groups and by the interaction of primary radicals in the protein macromolecules (these phenomena occurring during irradiation). The modifications in the proteins cause variations in the solubility of the albumin, gliadin and glutenin, and also in the percentage distribution of the groups of which they consist. It was found that low gamma radiation doses (20,000 to 150,000 rad) produce a maximum in the curves of starch viscosity, sub-

stances capable of precipitation by electrodialysis, gliadin solubility, and the Hagberg index. This anomaly explains the improvement in baking properties that certain authors have noted in the case of wheat receiving small gamma radiation doses. (auth)

40600 RADIATION RESISTANCE OF ENZYMES IN FOODS IRRADIATED AGAINST MICROBIAL DAMAGE. Vas, K. (FAO/IAEA, Vienna). Vienna, International Atomic Energy Agency, 1966, Preprint SM-73/12, 15p. (CONF-660609-24). ORAU.

From International Symposium on Food Irradiation, Karlsruhe, Ger.

Enzyme behavior in food tissues subjected to radiation doses adequate for microbiol control is reviewed. Generally speaking, enzyme radioresistance in situ is about an order of magnitude higher than that of the microorganisms causing spoilage or public health hazards. Thus, radiation doses adequate to microbiological stabilization, and at present considered just feasible economically, are insufficient to prevent enzymatic deterioration. To date, work in radiation enzymology has, to a large extent, been carried out in systems of medical interest. Hence, the mechanism of inactivation, as well as the roles of enzyme concentration, water activity of the medium, oxygen concentration, pH, and temperature have been studied intensively. Since radiomodifying substances are known to exert a decisive influence on the radiation inactivation of enzymes, it is felt that much more work is still needed on radioprotectors and radiation sensitizers in combination with highly-purified enzymes. The usual great radiosensitivity of high-purity enzymes and the contrasting extreme resistance of enzymes in the tissues and in their unpurified extracts certainly indicate the need for finding the reasons for this difference in order to facilitate possibly a rational approach of controlling enzyme activity in food irradiation. Effects on enzyme action of combining irradiation with heating, refrigeration, or physiological methods are discussed. (H.G.D.)

40601 THEORETICAL AND APPLIED ASPECTS OF RADIATION D-VALUES FOR SPORES OF CLOSTRIDIUM BOTULINUM. Grecz, N. (Illinois Inst. of Tech., Chicago). Vienna, International Atomic Energy Agency, 1966, Preprint SM-73/67, 16p. (CONF-660609-5). ORAU.

From International Symposium on Food Irradiation, Karlsruhe, Ger.

The index of radioresistance is the D_{10}-value defined as the dose necessary to inactivate one log cycle (90%) of a given spore population and $12 \times D$ has been arbitrarily defined as the safe radiation preservation dose for food products. Extensive data from our laboratory revealed that the D_{10}-value of a particular Clostridium botulinum strain depended on temperature, medium, and size of spore inoculum. Methods of calculation also affected to D_{10} values significantly. Irradiation temperature was shown to influence formation, chemical reactivity, extent of annealment, and diffusion of free radicals indirectly, especially during liquid-solid transition of the medium around 0°C. A combination of these temperature dependent effects explains why spores are most sensitive when irradiated at 0°C as compared with higher or lower temperatures. In addition to the indirect effect on radicals, temperature also affects the vibrational state and extent of hydration of the DNA molecules. The apparent hydration of DNA is related to the range of action of indirect effects, which can be calculated for C. botulinum 33A to add an additional 30 A to the radius of DNA (10.5A), hence almost tripling the effect of radiation. This change in radiosensitive volume is reflected by a corresponding change in D_{37} value from 1.6×10^5 rad for the dry spore to 6.6×10^4 rad for the wet spore. (H.G.D.)

Radiation Effects on Tissues

Refer also to abstracts 40494, 40502, 40791, 41187, 41207, and 41388.

40602 (AD-624934) EFFECT OF IONIZING RADIATION ON ANIMALS AND PLANTS. Compilation of Abstracts. Smith, Janice L. (Aerospace Technology Div., Library of Congress, Washington, D. C.). Dec. 8, 1965. 22p. (N-66-14667; ATD-65-110). CFSTI $1.00 cy, $0.50 mn.

Abstracts are presented on 10 experimental and theoretical studies on ionizing radiation effects on living organisms. Comparative studies of the radiosensitivity of different animal strains and species, determination of the RBE of different types of ionizing radiation, and investigation of the relationship between the age of animals and their radiosensitivity are considered. Newer research areas include protein metabolism in animals under the influence of radiation, changes in the proteolytic activity of blood during irradiation, and the neurohumoral mechanism of remote radiation effect. (C.H.)

40603 (AD-635086) ERYTHROCYTE STEM CELL KINETICS IN THE POSTRADIATION RAT. Baum, S. J. (Armed Forces Radiobiology Research Inst., Bethesda, Md.). May 1966. 28p. (AFRRI-SR-66-4). CFSTI $2.00 cy, $0.50 mn.

In rats exposed to 300 R of 250 kvp x rays erythropoiesis, as measured by ^{59}Fe uptake, diminished greatly for 48 hours followed by a rapid recovery approaching near normal values approximately 6 days after radiation. It has been postulated that the rate of recovery was primarily due to accelerated release of noninjured stem cells. The present experiment was designed to test this hypothesis. The polycythemic rat preparation was used since it permits the experimenter to control the release of erythrocyte stem cells. In polycythemic rats observed for 17 days postradiation, stem cell release diminished to 8 percent of the control values during the first 24 hours. This was followed by a rapid recovery from the 2nd to the 5th day. A second decrease was noted from the 6th to the 9th day and a third depression from the 9th to the 12th day. Thereafter, the oscillations diminished indicating a possible return toward the preradiation normal state. An attempt was made to correlate these findings with a kinetic model of erythropoiesis. It was suggested that the initial depression in stem cell release might be due to cellular destruction and inhibitions of cellular release mechanisms. The oscillations of the recovery curve were ascribed to possible rate differences in cellular movements from one precursor compartment to the subsequent one, and to competitive stimulations for progenitor cells from related cellular systems of the hematopoietic system. (auth)

40604 (AD-635251) TREADMILL EXERCISE PERFORMANCE BY THE AGEING IRRADIATED RAT. Jones, D. C.; Osborn, G. K.; Kimeldorf, D. J. (Naval Radiological Defense Lab., San Francisco, Calif.). May 5, 1966. 22p. (USNRDL-TR-1017). CFSTI $1.00 cy, $0.50 mn.

The ability of male Sprague-Dawley rats irradiated as young adults to perform on an inclined treadmill was evaluated at 3, 10, 16, 22, and 28 months of age. Irradiated groups received whole-body sublethal (30-day) or lethal-range doses of x rays (430 or 680 rads) or fast neutrons (230 or 320 rads) after the first treadmill tests. In spite of reductions in treadmill speed, the proportion of the control group which completed the task declined gradually through the first two years, then decreased markedly at 28 months. The gradual progressive decrement in the proportion of the group which completed the task was also apparent in the irradiated animals but the rapid deterioration in performance ability occurred at 22 months of age. The terminal deterioration appeared associated with approaching death, and its earlier appearance in irradiated groups was associated with radiation-induced lifespan shortening. For those control animals able to complete the task, there was an abrupt rise in heart rate with the onset of exercise, little or no change during the remainder of the one-hour exercise period, and a return to preexercise levels within a half-hour after cessation. The pattern of heart rate with exercise was not markedly affected by age and only occasional differences between irradiated and control groups were noted. Although colonic temperature

increased with the initiation of exercise at all ages, the pattern during the remainder of exercise varied with age at the time of test. At younger (3 months) or older (21, 28 months) ages, temperature either decreased or remained stable until the end of exercise. At 10 and at 16 months of age, temperature continued to increase beyond the initial moments of exercise in controls so that heat was accumulated rather than dissipated. With rest, temperatures returned to pre-exercise levels within about 15 minutes at all ages. In irradiated groups, the accumulation of heat at 10 and 16 months was not observed. Differences between colonic temperatures of irradiated and control groups appear related to the loss of body weight, induced by radiation, and its effect on the work load involved in the test. (auth)

40605 (AD-635735) RECOVERY FROM RADIATION INJURY IN SWINE AS EVALUATED BY THE SPLIT-DOSE TECHNIQUE. Nachtwey, D. S.; Ainsworth, E. J.; Leong, G. F. (Naval Radiological Defense Lab., San Francisco, Calif.). May 18, 1966. 23p. (USNRDL-TR-1025). CFSTI $1.00 cy, $0.50 mn.

With 1 Mvp x rays, the acute $LD_{50/30}$ (midline air dose) of 8 to 9 month old Duroc gilts was determined to be 399 R (95% confidence interval: 371 to 424 R). The pattern of recovery from the effects of 240 or 265 R of x rays was studied by means of the split-dose technique, which consists of conditioning the animals with a sublethal exposure and redetermining the LD_{50} at various times thereafter. By this criterion, the swine had recovered from 51% of the initial injury by three days. By seven days, they appeared to have recovered from about 65% of the initial injury, but the data suggest that part of the population had recovered completely while part was still about as sensitive as at three days. By twenty days, the entire population appeared to be radioresistant: the redetermined LD_{50} was 164% of the LD_{50} of unconditioned animals. Radioresistance was also evident at 61 and 107 days: at 61 days, 734 R killed eight out of 15 animals conditioned with 265 R whereas, the same exposure killed 15 of 15 unconditioned animals; at 107 days, none of nine conditioned animals died after 399 R. The pattern of systemic recovery and the period of radioresistance are not clearly reflected in the pattern of hematological changes that follow a conditioning exposure. (auth)

40606 (BMWF-FBK-66-02) ENTWICKLUNG EINER MODELLVORSTELLUNG ZUR ERREGUNG EINER NERVENFASER AUF GRUND VON EXPERIMENTELLEN UNTERSUCHUNGEN UEBER DEN EINFLUSS WEICHER ROENTGENSTRAHLEN AUF DIE REIZSCHWELLE DER PERIPHEREN NERVENFASER. (Development of a Pattern with Regard to the Stimulation of a Nerve Fiber Based upon Experimental Studies on the Influence Exerted by Soft X Rays on the Stimulus Threshold of the Peripheral Nerve Fiber). Vanselow, K. (Kiel Univ. (West Germany). Institut fuer Angewandte Physik). Mar. 1966. 25p. Dep. mn.

By the charging of the axon membrane there originates an electrostatic pressure of approximately 50 cm water column at 70 mv. When assuming a pore membrane, which will be deformed insignificantly by the influence of pressure, there can be explained a series of membrane properties and some phenomena in the development of the action potential. Ionizing radiation modifies the elastic consistence of the membrane. The changed equilibrium explains a series of radiobiological phenomena. (auth)

40607 (BNL-10518) NECTURUS MACULOSUS AS AN EXPERIMENTAL ANIMAL TO STUDY CELLULAR INJURIES OF THE IRRADIATED GUT IN VIVO. Prasad, Kedar N. (Brookhaven National Lab., Upton, N. Y.). Aug. 10, 1966. Contract AT(30-2)-Gen-16. 18p. (CONF-660917-1). Dep. mn. CFSTI $1.00 cy, $0.50 mn.

From Gastrointestinal Radiation Injury Symposium, Richland, Washington.

The small intestines of adult male rats were exteriorized and x-irradiated. Small regenerating foci lined by hyperchromic cells with frequent mitosis appeared in the deeper mucosa after 4 days. From the 8th to the 20th day there was a gradual epithelial change in the crypts and villi. There was considerable decrease in mucosal uptake of iron-59 in irradiated animals. Necturi (Amphibia) were anesthetized and exposed to x-irradiation; the animals were arranged so that the abdomen was irradiated while the rest of the body was shielded with lead. Radioautographic studies of the small intestine showed that there was no labeling of epithelial cells with tritiated thymidine either 3 hours or 3 days after injection. Cells lining the villi were decreased in number and exhibited swelling and nuclear fragmentation. The cells in the crypts were more basophilic than those of the rat intestines, and differed from the rat intestine in that there were no mitotic figures. In comparison with rats, the Necturi were very resistant to abdominal radiation and the progression of mucosal injuries was slow. Hence, Necturus is a more desirable animal for studies on intestinal cell populations. (H.L.W.)

40608 (CEA-R-3001) ETUDE CLINIQUE ET SYMPTOMATOLOGIQUE CHEZ LE PORC SOUMIS A UNE IRRADIATION GAMMA TOTALE A DOSE LETALE. (Clinical and Symptomatological Study of Pigs Subjected to a Lethal Dose of Integral Gamma Irradiation). Vaiman, Marcel; Guenet, Jean-Louis; Maas, Jean; Nizza, Pierre (Commissariat a l'Energie Atomique, Fontenay-aux-Roses (France). Centre d'Etudes Nucleaires). May 1966. 21p. Dep. mn.

Results are reported from a clinical and hematological study on a Corsican species of pigs wholly exposed to an approximately lethal dose of γ radiation. The aim of this work was to examine the changes in the irradiation syndrome of irradiation for pigs to make it thus possible to devise further experiments, in particular in the therapeutic field. The dose received was 285 rads (measured as the absorption in the vertical antero-posterior mesial plane). Data are presented on cyto-haematological changes in the blood circulating immediately after irradiation, and followed up to death, and changes in the medullary cytology after irradiation. The clinical picture of lethal radiation injury in swine is described. (C.H.)

40609 (CONF-660418-1) REPAIR OF CHROMOSOMAL DAMAGE. Wolff, Sheldon (California Univ., San Francisco. Medical Center). [1965]. Contract AT(11-1)-Gen-10. 13p. Dep. mn. CFSTI $1.00 cy, $0.50 mn.

From IAEA Meeting on the Genetical Aspects of Radiosensitivity: Mechanisms of Repair, Vienna.

Data are reviewed from a number of studies of the repair of chromosomal damage after exposure of plant or animal cells to uv, x radiation, neutrons, or radiation from incorporated radioisotopes. Results are reviewed from studies on Tradescantia, Vicia faba seeds, bacteriophages, cultured hamster cells, and other cells. Classes of radioinduced aberrations and various aspects of repair mechanisms are discussed. (23 references.) (C.H.)

40610 (COO-895-9) THE EFFECTS OF IONIZING RADIATION ON THE FUNCTIONAL AND STRUCTURAL STATUS OF THE BULL TESTICLE. Technical Progress Report, 1965-66. Carlson, W. D. (Colorado State Univ., Fort Collins. Coll. of Veterinary Medicine). Contract AT(11-1)-895. 35p. Dep. mn. CFSTI $2.00 cy, $0.50 mn.

The effects of single whole-body doses of 400 R x radiation or fractionated radiation doses delivered at the rate of 80 R/day for 5 days to a total dose of 400 R on the function and structure of the testicle were studied in 2-yr-old bulls. Semen samples were collected weekly for one year after irradiation and smears were examined microscopically by counting 100 sperm and classifying them as normal, or having primary or secondary abnormalities. Semen samples were also evaluated for sperm concentration, percentage of live sperm, and sperm mobility. Biochemical studies of seminal fructose content were made to evaluate the effects of radiation on the functional behavior of the interstitial cells of the testis and oxygen consumption of sperm was measured as an indication of metabolic activity. Histological examinations of testicular tissues and accessory organs taken from bulls at various times after irradiation were also used to evaluate the effects of single or fractionated radiation exposure. (C.H.)

40611 (COO–1421-2) GAMMA IRRADIATION EFFECTS ON TOXIC RESPONSES OF FISH. Progress Report, June 1, 1965 to May 31, 1966. Neuhold, John M. (Utah State Univ., Logan). Contract AT(11-1)-1421. 26p. Dep. mn. CFSTI $2.00 cy, $0.50 mn.

The effects of doses of 200 to 20,000 R γ radiation on mortality and signs of radiation injury of rainbow trout were studied. Fish weighing 55g responded to irradiation doses earlier than both larger and smaller fish and there appeared to be a definite relationship between the response and dose distribution. A peak in response occurred at approximately 200 R, an intermediate response occurred at 2,000 R, and a high response occurred again at 20,000 R dose level. The effects of water hardness on absorbed dose, the effects of biological stress due to high population density in aquaria, and the effects of oxygen consumption on radiation response were also studied. (C.H.)

40612 (EUR–2711.f) INFLUENCE DE CERTAINS FACTEURS SUR LE NOMBRE DE LEUCOCYTES DANS LE SANG. (Influence of Certain Factors on the Number of Leukocytes in the Blood). Tanguy, H. (European Atomic Energy Community, Ispra (Italy). Joint Nuclear Research Center). 1966. 8p. Dep. mn.

The influence of a certain number of factors on the number of leucocytes in the blood of 706 individuals was studied. The average number of leucocytes per cubic millimeter was found to be 8,218, with slight variations according to the year; there was a relatively important diminution in 1964. The individual variations are worth noting (4.4% of the cases have an average lower than 6000; 8.5% an average higher than 10,000); but sex has no influence on the number. This average number of leucocytes varied also according to the season for no apparent reason, with a strong rise in September, October, and December. Emotions have only a slight influence, and if so, cause a rise in the number of leucocytes. Race and origin had a more important role; the Italians have a notably higher average in relation to the Germans, Belgians, French, and Dutch. Individuals who received low doses of ionizing radiations were compared with those who had not been exposed to radiations, and no difference in the number of leucocytes was found. (auth)

40613 (N–66-18147) DISCUSSION ON THE POSSIBILITIES OF PRODUCING MUTANTS RESISTANT TO PERONOSPORA TABACINA (BLUE MOLD DISEASE) OF TOBACCO PLANTS BY SEED TREATMENT WITH IONIZING RADIATION. Polar, Emine (Cekmece Nuclear Research Center, Atomic Energy Commission, Istanbul (Turkey)). Nov. 1964. 22p. (CNAEM–18). CFSTI $1.00 cy, $0.50 mn.

A literature survey concerned with the possibility of obtaining disease resistant tobacco plants by producing mutants treated with ionizing radiation is presented. The survey shows that a decision about the minimum dose that should be given tobacco seeds can be facilitated by an estimation of the radiosensitivity of the seeds, from the knowledge of their biological trait and chemical composition. The literature has some controversy as to whether there is a differential efficiency when using neutrons, x rays, and γ rays. In determining radiation dosage, great importance should be given to work on seeds of similar states as their ontogenetic development, dormancy, moisture, and oxygen content. Environmental variables like time between irradiation and germination, storage conditions, and temperature before and after irradiation, chemical composition of the soil, and planting technique should be carefully recorded. (STAR)

40614 (NYO–901-39) LUNG CARCINOMAS IN IRRADIATED PARABIOTIC RATS. Goldenberg, Victor E.; Chute, Rosanna N.; Warren, Shields (Francis Delafield Hospital, New York. Dept. of Pathology. Columbia Univ., New York. Coll. of Physicians and Surgeons. New England Deaconess Hospital, Boston, Mass. Cancer Research Inst.). Sept. 22, 1965. Contract AT(30-1)-901. 17p. Dep. mn. CFSTI $1.00 cy, $0.50 mn.

Eight primary pulmonary carcinomas were found in 600 parabiotic pairs of rats after one partner had received 1000 R of total-body irradiation. Five tumors occurred in irradiated and three in nonirradiated partners. Irradiation carcinogenesis is implicated in the former, while the cause of the latter remains obscure. No hormonal or viral effects were demonstrated. (auth)

40615 (NYO–901-54, pp 26-8) BIOSTATISTICS AND ADMINISTRATION. (New England Deaconess Hospital, Boston, Mass. Cancer Research Inst.).

Preliminary results are summarized from a survey of the radiation exposure, health, and fertility of Massachusetts dentists. A statistical analysis of the life span of radiologist and causes of death was almost completed. Preliminary data indicate that since 1935 the evidence of life shortening in radiologists has decreased and no evidence of life shortening was apparent among them by 1960. The excessive incidence of leukemia in radiologists decreased in recent years. The data indicate that current occupational maximal permissible dose levels provide adequate protection. (C.H.)

40616 (NYO–901-54, pp 48-50) RADIOBIOLOGY. (New England Deaconess Hospital, Boston, Mass. Cancer Research Inst.).

Data are presented from a study on the effect of radiation from various doses of ^{131}I on the incorporation of ^{3}H-thymidine by thyroid cell nuclei as measured 56 days after ^{131}I injection. (C.H.)

40617 (NYO–2740-3) ANNUAL REPORT ON RESEARCH PROJECT. (Columbia Univ., New York. Radiological Research Lab.). Jan. 1, 1966. Contract AT(30-1)-2740. 261p. Dep. mn. CFSTI $6.00 cy, $1.25 mn.

Separate abstracts were prepared on three sections of this report. (C.H.)

For abstracts of individual sections see: 40618, 40619, and 41268.

40618 (NYO–2740-3, pp 166-215) BIOPHYSICS. (Columbia Univ., New York. Radiological Research Lab.).

Progress is reported on studies of the relative biological effects (RBE) of 0.43 and 1.8 Mev neutrons relative to x radiation on lens opacification and cataract induction in mice and rabbits; the cytogenetic effects of 14 Mev neutrons on maize; the RBE of 0.43 Mev neutrons and x radiation on embryo lethality following exposure of pregnant mice; the effects of low doses (below 25 rad) of x radiation on the survival of cultured mammalian cells (HeLa and Chinese hamster V79) grown in standard medium with and without the addition on ^{14}C-colchicine or unlabeled colchicine; the ultraviolet radiosensitivity of developing Escherichia coliphage complexes; the effects of post-irradiation dark treatments on the ultraviolet sensitivity of E. coli; and a comparison of the mutagenic and lethal effects of ultraviolet radiation, x radiation, and thymine deprivation on Escherichia coli grown in high concentrations of glucose or treated with acriflavine. (C.H.)

40619 (NYO–2740-3, pp 216-57) RADIOBIOLOGY. Rugh, R. (Columbia Univ., New York. Radiological Research Lab.).

Progress is reported on studies on the effects of AET on x irradiated Arbacia eggs; the effects of exposure of mice embryos of various gestation ages to 100 R x radiation on cataract development; the effects of 100 R x radiation delivered at various gestation ages from fertilization 18 days to mouse embryos on fertility and anomaly induction in offspring of both sexes; the effects of localized doses of 200 to 400 R x radiation to the gravid uterus of pregnant monkeys on the weight skeletal measurements, brain development, retinal damage, and other biological and physiological parameters in offspring. (C.H.)

40620 (NYO–2804-9) A STUDY ON DNA DEGRADATION IN ESCHERICHIA COLI PRODUCED BY IONIZING RADIATION. Achey, Phillip Mueller (Pennsylvania State Univ., University Park. Dept. of Biophysics). Mar. 1966. Contract AT(30-1)-2804. 65p. Dep. mn. CFSTI $3.00 cy, $0.75 mn.

Thesis.

Escherichia coli 15 T⁻L⁻ was used to investigate the action of gamma radiation on DNA metabolism, with the emphasis on DNA degradation. E. coli 15 T⁻L⁻ readily incorporates thymine and, thus, allows the fate of the DNA to be easily followed by introducing radioactive thymine into its DNA. An oxygen potentiating effect is found for the action of radiation on DNA synthesis, DNA degradation, and colony-forming ability. Degradation can only be initiated by direct radiation action on the cell, and not by an indirect radiation effect such as irradiated medium. Completion of chromosome replication, incorporation of 5-BU, and the use of succinate as a carbon source instead of glucose all change the amount of degradation. In addition to these treatments prior to irradiation, post-irradiation changes in medium, temperature, and the type of gas bubbled through the culture alter the amount of degradation. It is concluded that there are two aspects of degradation: the initiation of degradation, requiring radiation action within the cell and the expression of degradation following the irradiation, dependent on post-irradiation environmental conditions. An autoradiographic study indicates that degradation occurs to nearly the same extent from cell to cell. A chromatographic study of the label lost by the cells into the medium identifies it as thymine, and not a phosphorylated derivative of the base as would normally be expected from the action of a nuclease. (36 references.) (auth)

40621 (NYO-3086-5) A STUDY OF THE DISTRIBUTION OF ^{226}Ra, ^{228}Ra, ^{210}Pb, AND ^{228}Th IN BONE AND SOFT TISSUE OF RADIUM DIAL PAINTERS. Petrow, Henry G. (New York Univ., N. Y. School of Engineering and Science). Apr. 1966. Contract AT(30-1)-3086. 157p. Dep. mn. CFSTI $5.00 cy, $1.00 mn.

Thesis.

A comprehensive investigation was made of Ra-226, Ra-228, Th-228 and Pb-210 concentrations in bone and Ra-226 and Pb-210 concentrations in soft tissue obtained from two deceased radium dial painters. Both painters had carried their radium burdens for nearly 50 years. Approximately 0.05% of the terminal Ra-226 burden and 0.65% of the terminal Pb-210 burden was found in soft tissue, with aorta and thyroid having the highest concentration of both radionuclides. It is felt that the aorta and thyroid concentrations reflect blood concentrations of Ra-226 and Pb-210 during the last few years of life, and that during exposure, when the blood concentrations of Ra-226 were high, the dose received by both the aorta and the thyroid may have been high. The ratio of Pb-210 to Ra-226 in the skeleton indicates that both radionuclides are cleared from the skeleton at the same rate, a result confirmed by excreta analysis. Variations in the value of this ratio from site to site in the skeleton are considerable. For long bones, low ratios are found in the ends of the bone, and high ratios in shafts. Low ratios are found in vertebra and high ratios in rib. For a given bone, the higher the ratio, the lower the Ra-226 concentration. The cause of the variability in ratio is believed to be either variable in the radon retention factor from site to site in the skeleton because of structural variations in bone mineral, or the result of a selective translocation process. Analysis of the bone of one of the dial painters for Th-228 and Ra-228 indicated that the biological half-life for radium was of the order of 10 years, and that there was a significant amount of thorium translocation. Dose calculations were made and these indicate that both painters received about one-half their alpha dose from the Ra-226 chain and one-half from the Ra-228 chain. Approximately 5% of the alpha dose from the Ra-226 chain came from Po-210. (auth)

40622 (NYO-3096-8) PROGRESS REPORT [ON GENETIC STUDIES], JUNE 1, 1965–JUNE 1, 1966. Dobzhansky, Theodosius (Rockefeller Univ., New York). Contract AT(30-1)-3096. 13p. Dep. mn. CFSTI $1.00 cy, $0.50 mn.

Progress is reported on studies of the genetic consequences of the exposure of experimental populations of Drosophila melanogaster maintained under conditions of relaxed natural selection to an accumulated dose of 120,000 R x radiation administered at rates of 2000, 4000, and 6000 R per generation for 60, 30, and 20 generations, respectively. Data are included from studies of genetic loads in natural Drosophila populations, chromosomal polymorphism in natural and experimental populations, and genetic diversity and selection in Drosophila populations. The hypothesis that some of the chromosomes in irradiated populations are lethal, semilethal, or subvital when homozygous but are heterotic when heterozygous was tested and findings are compared with published data from similar studies. (25 references.) (C.H.)

40623 (ORNL-3922, pp 32-49) CYTOLOGY AND GENETICS. (Oak Ridge National Lab., Tenn.).

Progress is reported in studies of mitosis and mutation induction in Paramecium following exposure to x radiation; studies on the growth of Paramecium aurelia; the effects of 5 kR x radiation on cell division of the ciliate Spathidium spathula; the effect of inorganic phosphate on the growth of Tetrahymena pyriformis; the uv inactivation of transforming DNA in Hemophilus influenzae; the genetic effects of uv radiation in bacteriophage; the effects of uv radiation on the cell cycle of Chinese hamster tissue culture cells; DNase and DNA polymerose activity during Drosophila development; the effects of x radiation on the survival of cultured human cells; the use of gonal centrifugation to isolate particles from mice spleen that contain transplantation antigens; and the cytology and metabolism of the protozoan Rhynchosciara angelae. (C.H.)

40624 (ORNL-3922, pp 52-8) FUNGAL GENETICS. (Oak Ridge National Lab., Tenn.).

Studies in fungal genetics were made with Neurospora. Progress is reported on: modification of impaired complementation between nonallelic mutations; qualitative and quantitative aspects of photoreactivating forward mutations, and carbon dioxide stimulation of the ad-3 mutants. (H.G.D.)

40625 (ORNL-3922, pp 59-64) DROSOPHILA CYTOLOGY AND GENETICS. (Oak Ridge National Lab., Tenn.).

Research progress in Drosophila cytology and genetics is reported on: a tandem duplication that lowers recombination throughout a chromosome arm; translocations as crossover suppressors; the frequency of x-radioinduced crossover-suppressing aberrations recovered from oocytes; scintillation counting of tritiated thymidine transferred to females by labeled males; a mutation induced by ethyl methanesulfonate that alters electrophoretic mobility of alcohol dehydrogenase isoenzymes; the meiotic origin of temperature-induced crossing over; and the effects of exchange and structural zygosity on radioinduced non-disjunction and loss. (H.G.D.)

40626 (ORNL-3922, pp 80-3) RADIATION IMMUNOLOGY. (Oak Ridge National Lab., Tenn.).

Research is reported on: the relationship of senescence to the secondary antibody-forming potential of mice; homeostatic regulation and the depletion of immunologically competent cells by exposure to excess antigen; the possibility of determining the absolute number of hemagglutinating antibody molecules in antisera; functional ribosomes in antibody-forming cells; and the effect of prior stimulation of donors on the in vitro engulfing capacity of peritoneal phagocytes. (H.G.D.)

40627 (ORNL-3922, pp 84-8) MAMMALIAN GENETICS. (Oak Ridge National Lab., Tenn.).

Research is reported on: mutation frequency in mouse spermatogonia at high dose rates; radioinduced sex chromosome abnormalities in various stages of germ cells in female mice; the radiation response of human spermatogonia; genetic control of radiosterilization in female mice; and tests for possible mutagenic effects of DNA in mice. (H.G.D.)

40628 (ORNL-3922, pp 89-93) HUMAN CYTOGENETICS. (Oak Ridge National Lab., Tenn.).

Research is reported on: induction of chromatid aberrations by tritiated thymidine and the origin of sister chromatid exchanges. (H.G.D.)

40629 (ORNL–3922, pp 94-8) RADIATION MICROBIOLOGY. (Oak Ridge National Lab., Tenn.).

Research is reported on: radioresistance and macromolecular synthesis; the role of donor pili in specific pair formation and chromosome transfer in E. coli K-12; mechanisms of chromosome transfer by F^+ donors of E. coli; the role of the F^- parent during bacterial conjugation in E. coli; the pro-lac region of the E. coli K-12 genome; genetically marked E. coli strains for studies of intestinal flora in mice; inverted and noninverted transpositions in the genome of E. coli K-12; the mechanism of photoreactivation in Neurospora crassa; and radioresistant mutants of E. coli K-12. (H.G.D.)

40630 (ORNL–3922, pp 106-8) SUBCELLULAR AND VIRAL PHYSIOLOGY. (Oak Ridge National Lab., Tenn.).

Progress is reported on: attempts to isolate substances that promote division in filament-forming strains of E. coli and studies on the genesis of ribosomes in Tetrahymena pyriformis. (H.G.D.)

40631 (ORNL–3922, pp 161-6) PLANT PHYSIOLOGY AND PHOTOSYNTHESIS. (Oak Ridge National Lab., Tenn.).

Progress is reported on: electron spin resonances induced by seed hydration and physical characteristics; developmental studies of auxin effects on wheat parenchyma growing without cell division; base composition of nucleic acid fractions in root cells of Vicia faba; microspectrophotometry of wheat nuclei; studies on the endogenous electron spin resonance signal in lettuce seeds; and photosynthesis. (H.G.D.)

40632 (ORNL–3922, pp 175-91) AEC–NIH CHEMICAL CARCINOGENESIS. (Oak Ridge National Lab., Tenn.).

Research is reported on: the mechanism of action of the Shope papilloma virus; a soluble amino-acid-incorporating system from trout liver; protein synthesis in normal and cancerous trout liver; hepatomatous trout; development of tissue culture lines for studies on chemical carconogenesis; aminoacyl-sRNA synthetases from normal and neoplastic human cells; mitosis and mutation induction by TEM (triethylene melamine); a method for solving protein structures; phase determination for protein crystals by a combination of isomorphous replacement and anomalous scattering data; single-crystal equatorial-plane diffractometry with a plane monochromator; genetic alterations in EMS-induced as-3B mutants of Neurospora; the mutagenicity of dimethylnitrosamine and diethylnitrosamine in Neurospora crassa; inhalation carcinogenesis; morphologic changes in spleen lymphatic tissue during antibody production; the physiology of virus-host interaction; aminoacyl-sRNA synthetase systems of viral-infected cell systems; the diffusion chamber technique for cytokinetic studies of antibody response; the binding power and photodynamic effect of benzopyrene on bacterial DNA; thymineless bacteria; and metabolism of 1-(4-dimethylaminobenzyl-idene)-indene. (H.G.D.)

40633 (ORNL–P–2287) INFLUENCE OF AGE AT IRRADIATION ON SUSCEPTIBILITY TO RADIATION-INDUCED LIFE-SHORTENING IN RF MICE. Upton, A. C.; Conklin, J. W.; Popp, R. A. (Oak Ridge National Lab., Tenn.). [1966]. Contract W-7405-eng-26. 18p. (CONF-660635–2). Dep. mn. CFSTI $1.00 cy, $0.50 mn.

From International Colloquium on Radiations and Aging, Semmering, Austria.

Non-inbred male and female RF mice were exposed to 50 to 400 R whole-body x rays at ages ranging from $9\frac{1}{2}$ days after conception to 1 year after birth. In mice of both sexes, irradiation after birth shortened the life span, the effect per unit dose being largest at the higher dose levels (300 to 400 R) and in the groups exposed at 40 to 70 days of age. In mice exposed before birth, life-shortening was consistently less marked than in those exposed after birth, except in the males irradiated early in development at the highest dose level administered prenatally (i.e., 300 R at $14\frac{1}{2}$ days after conception). These males died with runting and microcephaly after a mean survival time of only 6 to 7 months from causes yet to be determined. They failed to show the typical spectrum of neoplastic and non-neoplastic lesions associated with life-shortening and aging in the other groups. The relatively low susceptibility of all other prenatally irradiated mice to radiation-induced life-shortening and carcinogenesis is paradoxical and remains to be explained. (auth)

40634 (ORNL-P–2312) AN IN VITRO BONE MARROW SYSTEM FOR STUDYING RECOVERY FROM RADIATION INJURY. Smith, L. H. (Oak Ridge National Lab., Tenn.). [nd]. Contract W-7405-eng-26. 5p. (CONF-660634–1). Dep. mn. CFSTI $1.00 cy, $0.50 mn.

From Conference on the Recovery of Irradiated Cells by Nucleic Acids, Herceg Novi, Yugoslavia.

Using the spleen ^{59}Fe method, a survival curve was constructed for in vitro radiosensitivity of the erythropoietic compartment of mouse bone marrow. The exponential survival curve indicated at D_{37} of about 75 R and an extrapolation to zero x-ray dose at about 1.6. Environmental effects on recovery of marrow cells in vitro were investigated, and temperature was found to be the major variable. Data indicated that recovery cannot be enhanced by manipulating temperature, but that the expressions of x-ray injury may be a temperature-dependent event. The efficacy of tissue extracts was tested, but no substance was found that, when present in the postradiation environment for up to 24 hrs, would effect recovery from x-ray injury. Studies comparing single vs divided exposure showed that mouse marrow cells may recover from the first increment of a divided dose. (H.G.D.)

40635 (ORNL-TM–1550) SYNERGISTIC EFFECT OF ZERO-G AND RADIATION ON WHITE BLOOD CELLS. AN EXPERIMENT FOR THE GEMINI III MANNED SPACE FLIGHT. Annual Report, Period Ending June 30, 1965. Bender, M. A. (Oak Ridge National Lab., Tenn.). Aug. 1966. Contract W-7405-eng-26. 43p. Dep. mn. CFSTI $2.00 cy, $0.50 mn.

The design and execution of an experiment on the synergistic effect of zero-G and radiation on white blood cells, which was successfully carried out during the Gemini III manned space flight of March 23, 1965, are described. The experiment consisted of the irradiation of samples of human leukocytes with ^{32}P beta particles during the orbital phase of the mission, and the subsequent cytogenetic analysis of the material to determine chromosomal aberration rates. Preparation of the experiment included the design, fabrication, and testing of the necessary hardware and equipment. The experimental data showed that although there was no significant difference between the yields of multiple-break chromosome aberrations induced on the ground and induced during orbital flight, the frequency of single-break aberrations was significantly higher in the flight samples. Several lines of evidence rule out the possibility that this difference arose from differences in absorbed dose, temperature, oxygen tension, or other parameters known to influence chromosome aberration yields. That the space flight itself induced aberrations is ruled out by the experiment control samples and also by preflight and postflight blood samples obtained from the Gemini III flight crew. A synergism between radiation and some space-flight parameter thus appears to exist for human chromosome aberration production. (C.H.)

40636 (ORO–1747-12) RADIATION GENETICS AND RADIATION RESISTANCE IN PEANUTS. Annual Report, July 1, 1965–June 30, 1966. Emery, Donald A. (North Carolina State Coll., Raleigh). Aug. 1, 1966. Contract AT(40-1)-1747. 15p. Dep. mn. CFSTI $1.00 cy, $0.50 mn.

A study was made of genetic components of variance in a cultivated variety (NC2) of peanuts (Arachis hypogaea) following radiation with 20 Kr of gamma rays. A hierarchial analysis of variance of pedigreed progenies in the M_4 and C_4 generation showed residual variance to be significant and confirmed the presence of radiation effects. The genetic

model was constructed on the premise that the alleles at a polygenic locus have functionally two states, one which has a positive effect on the expression of a character and one which has a negative effect. The number of chimeral sectors in an M_1 plant proved to be a problem of vital importance in the development of the genetic model. Three alternative models were proposed based on the number of chimeral sectors sampled in the M_1 plant. In Model One it was assumed that two M_2 seed from the same M_1 plant always came from the same sector, which could be ++, +−, or −−. In Model Two the M_1 plant was assumed to have the sectors which could be of the same or different genotypes. The two M_2's would be drawn at random from the possible combinations of genotypes. For Model Three the two M_2 seed were assumed to be randomly drawn from M_1 plants which always had a large number of chimeral sectors. Each model resulted in a different joint frequency distribution of M_n relatives derived from a common M_1 plant. The distribution of genotypes in the M_2 and M_2 generations was not affected by the number of chimeral sectors in the M_1 plant. The correlation of additive scales of two M_n relatives from a common ancestor, i.e., an M_1, and M_2 or an M_3 plant, was derived for each of the three models. The effect of residual variance occurred in the correlation of additive scales. The correlations were shown to be a function of the gene frequency in the original population and the mutation rate. Three populations representing radioresistant, radiosensitive and radioresistant-radiosensitive hybrids were developed and the X_1 generation evaluated in 1956, the X_3X_1 generation in 1959, and the $X_5X_3X_1$ generation in 1961. Results have been submitted on these generation-treatments in earlier Progress Reports. In 1965 four mixtures of Golden and Recurved marked genotypes were planted in an isolated field near Snow Hill, North Carolina. The Golden macromutant in these mixtures included 10 Kr, 15 Kr, 20 Kr, 25 Kr and Control treatments. The total number of plants harvested in 1965 was 564 for the controls, 45 for the 10 Kr irradiated, and 17 for the 15 Kr irradiated. The total number of progeny for the control group was 7613, for the 10 Kr irradiated, 161, and for the 15 Kr irradiated, 36. (H.L.W.)

40637 (ORO-2754-7) THE EFFECTS OF GAMMA RADIATION ON SOIL MICROORGANISMS AND THEIR METABOLIC PROCESSES. Final Report. Eno, Charles F. (Florida Univ., Gainesville. Dept. of Soils). [1966]. Contract AT(40-1)-2754. 36p. Dep. mn. CFSTI $2.00 cy, $0.50 mn.

In general, the effects of gamma irradiation on soil organisms and their metabolic processes were negative. Soil fungi were slightly more sensitive to gamma radiation than were bacteria, which were considerably more radiosensitive than algae. Combined observations from chemical and biological studies clearly established the fact that the P and N status of the soil is altered by gamma radiation and that these changes can affect growth in higher plants. Available N and P increased in irradiated soils, and the amounts released were closely related to soil type (organic content). When gamma radiation was compared with steam and methyl bromide as a soil sterilizing agent, it was found that: cation exchange capacity was not significantly altered by any of the treatments; amounts of N, P, and S were increased and moisture content decreased by steam, gamma ray and methyl bromide sterilization generally increased N, P, and S; and the magnitude of all parameters was closely related to organic matter content. Radiation recovery of soil microorganisms was satisfactory at 50 and 200 kR doses, but recovery from 500 kR doses was never more than 6% of the control. In pure culture studies with algae, Chlorella appeared to grow after somewhat higher doses than Chlorococcum. Red wigglers were much more resistant to environmental stresses than the African giants. However the African giants survived much longer than the red wigglers following irradiation at doses of 16, 32, and 64 kR. Rotifers were affected rather severely by low dose rates, although more than 600 kR were required for an immediate effect. At 50 kR no effects were observed at moisture contents below 12%. (H.G.D.)

40638 (UCD-472-113, pp 1-16) X-IRRADIATION EFFECTS. (California Univ., Davis. School of Veterinary Medicine).

Data are summarized from a long-term (1951 to 1966) study on the effects of 100 or 300 R whole-body x irradiation on the life span, clinical conditions, incidence of neoplasms, and reproductive performance of beagles. (C.H.)

40639 SOLAR-FLARE INDUCED INCREASES IN SEA-LEVEL COSMIC-RAY INTENSITIES AND OTHER GEOPHYSICAL PHENOMENA IN RELATION TO MULTIPLE SCLEROSIS. Barlow, John S. (Massachusetts General Hospital, Boston). Acta Neurol. Scand., 42: Suppl. 19, 118-36(1966).

Analysis of the results of recent epidemiological surveys on multiple sclerosis confirms that the geographical distribution of this disease is more closely correlated with geomagnetic latitude than with geographic latitude. This geomagnetic latitude effect for the disease resembles that for the increases in the nucleonic component of cosmic rays at the earth's surface which occurs for several hours following major solar flares, of which there have been 10 in the last 20 years. The pathogenesis of multiple sclerosis might be related to cosmic-ray phenomena through a chain of events entailing cosmic-ray induced radioactivity, mutations in immunologically important cells, and a consequently altered immune response on the part of susceptible individuals. In persons so affected, specific demyelinative episodes might be precipitated by entirely unrelated factors, and the clinical course of the disease might be largely independent of geographical movements of the patients, except that such precipitating factors might be modified. In many areas, the amount of ionizing radiation from terrestrial sources exceeds that from cosmic rays. However, reasons why ionizing radiation from terrestrial sources of radioactivity (even if ingested) are not implicated are suggested. Multiple sclerosis is not especially prevalent in areas of relatively high terrestrial background radiation nor does it appear that x-ray personnel have a predilection for the disease. In Czechoslovakia, multiple sclerosis is not unusually prevalent where ores containing several radioactive elements are mined, nor is the prevalence ratio for the country as a whole unusually high. The geographic distribution of multiple sclerosis appears to resemble the nucleonic, (e.g., protons and neutrons) rather than the ionizing component of cosmic radiation at the earth's surface. (TCO)

40640 POLYGENIC VARIABILITY IN IRRADIATED CULTIVATED RICE N.P. 130. Venkatanadhachari, G. (Sugar Cane Research Station, Anakapalle, India). Andhra Agr. J., 10: 37-47(1963).

Polygenic variability was studied in the M_2 generation of irradiated, cultivated rice, variety N. P. 130, treated with x rays, thermal neutrons, and β rays (^{35}S). Large numbers of abnormalities, i.e., variation in width, length, thickness of grain, width of leaf, length of awn, and flowering duration were observed. Three lines, L. 4-7-1 (x ray: 11 kR), L. 13-11-1 (x ray: 33 kR), and L. 34-12-2 (neutrons: $4.32 \times 10^{12}/cm^2$), exhibited a wide variability in the size of the leaf. Statistical analysis revealed that the leaf breadth of L. 4-7-1 and L. 34-12-1 was significantly different from the controls. The variety N. P. 130 is tip awned, and the awn length ranges from 0.0 to 1.9 cm, mean 0.49 cm. The mean awn lengths in 3 lines were 1.288, 1.256 and 1.554 cm, respectively, and differed significantly from the parent. The grain size in rice is one of the most stable characters by which a variety can be characterized. The variety N. P. 130 has a mean length of 9.412 mm, a width of 2.536 mm, and a thickness of 1.905 mm. In 20 cultures originating from the treatments of x rays, thermal neutrons, and ^{35}S, wide differences in grain size were noted. Plants with reduced grain width in comparison to control were also observed. None of the 20 plants that were selected gave greater grain thickness than the control. In addition to the variation in grain size, some of the plants were fully awnless. (TCO)

40641 CYTOLOGICAL ABNORMALITIES IN IRRADIATED RICE. Venkatanadhachari, G. (Sugar Cane Re-

search Station, Anakapalle, India). Andhra Agr. J., 10: 93-100(1963).

Dry, dormant seeds of rice, variety N.P. 130, were irradiated with x rays, thermal neutrons, and β particles (^{35}S). For β irradiation, dehusked seeds of rice were soaked in diluted solution of $H_2{}^{35}SO_4$. Analysis of chromosomes in pollen mother cells was done at pachytene, diakinesis, and metaphase-1 stages of meiosis, and confined to the lines which exhibited chlorophyll mutations. The major class of cytological abnormalities observed at pachytene in plants heterozygous for chlorophyll-developing gene in M_2 generation was differential segments. Similar segments have occurred in some interspecific hybrids and intervarietal hybrids and are indications of structural hybridity. While the metaphase stage revealed regular bivalents in these lines, the detection of these abnormalities at pachytene indicates that only a small portion of the chromosome breaks are observable at metaphase I. Typical deficiency configurations were not observed at pachytene. The gene mutation may cover a small region not analyzable at pachytene or the region where deletion occurred, although large, may be nonhomologously paired by adjustment of the adjacent regions and hence is not analyzable. The independent assortment of the chromosomes leading to the deficiencies in some gametes may be responsible for the observed chlorophyll mutations or the observed abnormalities may have no relation to the origin of chlorophyll mutations. The occurrence of chlorophyll-deficient types in the progenies of intervarietal rice hybrids and their occurrence along with the structural changes revealed by differential segments suggest that some of the chlorophyll mutants caused by radiation may be of this type. (TCO)

40642 ANTIOXIDANT AND PROOXIDANT ACTIVITY IN ASCITES TUMORS. Lash, Edward D. (Univ. of Illinois, Urbana). Contract AT(11-1)-878. Arch. Biochem. Biophys., 115: 332-6(Aug. 1966). (COO-878-12).

In contrast to liver, brain, and other tissues, homogenates of Ehrlich and Krebs-2 ascites tumor cells formed no lipid peroxides upon aerobic incubation. These tumor cells contained two antioxidant components (measured by their inhibition of lipid peroxidation in liver homogenates): a heat-stable supernatant fraction, and a heat-labile pellet fraction. Also present was a dialyzable, heat-labile supernatant prooxidant. Ultraviolet irradiation of tissue homogenates caused considerable peroxidation in liver but had little effect on the tumors. However, extracted tumor lipids were shown to be capable of forming peroxides. Tumor antioxidant activity was reduced by ultraviolet light, but x-irradiation of tumor cells in vitro and of tumor-bearing animals had little effect on antioxidant activity. (auth)

40643 IS THE BRAIN AN IMMUNOLOGICALLY PRIVILEGED SITE? II. STUDIES IN INDUCED HOST RESISTANCE TO TRANSPLANTABLE MOUSE GLIOMA FOLLOWING IRRADIATION OF PRIOR IMPLANTS. Scheinberg, Labe C.; Levy, Arnoldo; Edelman, Fredkic (Albert Einstein Coll. of Medicine, Bronx, N. Y.). Arch. Neurol., 13: 283-6(Sept. 1965).

In view of previous reports that the brain is immunologically unresponsive, experiments were performed to ascertain whether it would respond to isologous tumors, later eradicated by irradiation, by rejecting subsequent implants of the tumor. When gliomas were transplanted to the brains of isologous mice and cured by irradiation, subsequent tumor isotransplants to the skin or brain were rejected in significant numbers when compared to unexposed hosts. Gliomas transplanted to subcutaneous tissues of isologous mice and cured by irradiation resulted in still greater rejection of subsequent intracerebral or subcutaneous transplants. Prior irradiation of normal brain did not affect growth of subsequent tumor implants. The x rays were administered in five doses of 500 R to give a total of 2500 R. Following irradiation cure of an intracerebral tumor, 37% of second intracerebral implants and 43% of subcutaneous implants were rejected. This difference was not significant. Following irradiation cure of a subcutaneous tumor, 64% of the subcutaneous implants and 83% of second subcutaneous implants were rejected. This difference was also not significant and indicated that prior growth of a tumor in the brain or skin imparts some immunity to subsequent tumor growth in these areas. Prior growth in the skin imparts greater immunity to subsequent growth in the brain. Also, prior growth in the skin imparts greater immunity to subsequent growth in the skin than does prior growth in the brain. These results have significance in the pathogenesis of certain diseases of the central nervous system (CNS) which are possibly autoimmune (post-infectious encephalomyelitis, and multiple sclerosis). The CNS antigens may gain access to the reticuloendothelial system generally and stimulate the formation of cellular or humoral autoantibodies are then believed to enter the CNS where they attack myelin or glial cells and as a result produce demyelinating lesions. This investigation raises the possibility that the alleged autoantibodies are formed in situ and directly attack the neural antigens of the CNS. (BBB)

40644 HISTOLOGIC AND KARYOMETRIC CHANGES IN THE MINOR AND MAJOR SALIVARY GLANDS IN MAN FOLLOWING EXPOSURE TO IONIZING RADIATION (^{60}Co). Gruenberg, H. (Univ.-HNO-Klinik, Wuerzburg, Ger.). Arch. Ohren, Masen, Kehlkopfheilk., 184: 235-48(Dec. 4, 1964). (In German).

Salivary gland sections were obtained from patients irradiated preoperatively with 3000- to 6000-R doses of ^{60}Co, given at 150 R/dose, from 8 days to 5 months after termination of the irradiation series. There were no basic morphological differences between glands that received 3000 and 6000 R. In the serous portions the average dia of the nuclei was increased above normal. Dyschylia was observed, the saliva being qualitatively as well as quantitatively different from normal. The parts of the glands that appeared to be atrophic were more extensive after irradiation. The radio-induced enlargement of the cell nuclei was detectable for months after the irradiation had ended. The average nuclear size at 2 to 4 weeks as compared to 6 to 12 weeks after irradiation did not differ greatly. A similar average nuclear size was observed in these patients as compared to patients whose irradiation had been terminated less than ½ yr before larygeal extirpation. Thus the nuclear enlargement induced by irradiation appears to be irreversible for long periods, and seems to be related to disturbance of function. Although there is no evidence to indicate the minimum dose that may produce this type in injury, the results indicate that the radiosensitivity of the salivary glands is high since they appear to have little ability to regenerate. These results are similar to morphological changes and functional disturbances observed in salivary and mucosal glands in the respiratory tract, nasopharynx, oropharynx, and tracheal tree. (BBB)

40645 LESIONS OF THE GASTROINTESTINAL TRACT IN CHRONIC RADIATION SICKNESS CAUSED BY MULTIPLE X IRRADIATION. Lebedeva, G. A. Ark. Patol., 24: 21-6(Oct. 1962). (In Russian).

Studies were made in 12 dogs which had been subjected to x rays 1 to 5 times per week in doses of 5, 10, or 30 R per day at intervals from 1 to 2 months for a duration of 4 months to 7 yr. Total doses of 1540 to 6950 R were administered. Chronic radiation sickness developed in the animals. Post-mortem investigation showed hemorrhages in the wall of the gastrointestinal tract, moderate atropy of the mucous membrane of the stomach and intestine, sclerotic changes, disturbances of the vascular, lymphatic, and nervous tissue, and a change in the cellular composition of the stroma. In one dog, which died 7 years after irradiation (total dose of 6950 R) malignant changes were discovered. The extent of injury to various segments of the gastrointestinal tract differed; the most pronounced changes occurred in the stomach. There appeared to be no strict relation between the severity of pathologic changes and the radiation dose. (BBB)

40646 MORPHOLOGICAL CHANGES AND SOME HISTOCHEMICAL ALTERATIONS IN THE EYES OF MONKEYS AFFECTED WITH RADIATION SICKNESS. Abdullaev, V. M. (Inst. of X-Radiation, Ministerium of Health

Preservation, Azerbaijan SSR). Ark. Patol., 27: 45-52 (1965). (In Russian).

A study was made of the eyes of 30 monkeys 1.5 to 2.5 years old, affected with radiation sickness, while 5 monkeys served as controls. The monkeys were subjected to 620 R γ irradiation from a ^{60}Co source. Changes in various characteristics appeared in all membranes and cell layers of the eyes of the irradiated monkeys. After the monkeys died (10 to 36 days after irradiation), the eyes were sectioned for histologic study. The earliest development of a radiation reaction in the eye was seen in the concentrations of glycogen and ascorbic acid as well as degenerative changes of the interstitial substances, usually preceded by alterations in cell structure. In most cases, marked vascular changes were noted, which were accompanied by hemorrhages in the vitreous and retina. The rod and cone layer, and also cells of the pigment epithelium, underwent degenerative changes. In interpreting the pathogenesis of radiation manifestations in the eye it is necessary to consider the complexity of morphological and histochemical changes of all its membranes and cell layers; some were also present in healthy monkey eye tissue. (BBB)

40647 MORPHOLOGICAL CHANGES IN THE THYROID GLAND FOLLOWING RADIOIODINE ADMINISTRATION. Kalinin, A. P.; Odinokova, V. A.; Talantov, V. V. Arkh. Patol., 28: No. 5, 3-10(1966). (In Russian).

Due to the application of the methods of histological analysis many important data were obtained concerning morphological changes of the thyroid parenchyma in ^{131}I action. A study of the structure and properties of the thyroid tissue in conditions of experimental ^{131}I administration offered a possibility of approaching the assessment of the ^{131}I therapeutic effect with greater precision. Taking into consideration the species ^{131}I sensitivity of the thyroid gland experimental and clinical analysis data should not be considered as identical. Data on morphological changes developing in the thyroid gland as a result of ^{131}I therapy require a further study. Mostly these changes are dystrophic and necrobiotic lesions with subsequent fibrosis; regenerative processes occur more seldom. These theoretical data are of practical significance for the solution of the problem concerning radioiodine therapy of goiter and thyroid gland tumors. (auth)

40648 ACUTE EFFECTS OF X-RADIATION UPON THE MOUSE ELECTROCARDIOGRAM. Mason, H. C.; Moos, W. S. (Arkansas State Hospital, Little Rock, Univ. of Illinois, Chicago). Atompraxis, 12: 347-50(July 1966).

Irradiation of mouse hearts with x rays (10 min with 2×10^5 R/min) caused heart blockage initiated by injuries to the ventricles and pacemaker that eventually resulted in a simulated Adam-Stokes attack. Atrial flutter-fibrillation appeared somewhat later, after the abnormal and bizarre ventricular complexes began to fail. Reversal of the QRST complex is not a common finding in mice exposed to high dose heart irradiation. The results reported herein occurred rather consistently in mice exposed to the cardiac irradiation through the chest wall. Mice can and do temporarily survive the injury, and the heart apparently recovers from exposure to this dose of radiation, (the smaller the animal's heart, the better the chance for restoration of normal rhythm) although oxygen uptake is decreased about one-third in heart irradiated mice. The severe damage to the heart does not appear to be quantitatively reduced to the degree of EKG abnormality; also the ability of x-irradiated cardiac musculature to withstand subsequent superimposed stresses is not presently known. (auth)

40649 SEQUELAE OF THE LD/50 X-RAY EXPOSURE OF THE PRE-IMPLANTATION MOUSE EMBRYO: DAYS 0.0 TO 5.0. Rugh, R.; Duhamel, L.; Somogyi, C.; Chandler, A.; Cooper, W. R.; Smith, R.; Stanford, G. (Columbia Univ., New York). Contract AT(30-1)-2740. Biol. Bull., 131: 145-54(Aug. 1966).

Either x rayed or control male mice had average weights in excess of the females at a comparable age. Pre-implantation mouse embryos, subjected to x rays and surviving for 24 months, showed no gross adverse weight effects of the exposure. In some instances those with a radiation history were heavier, probably because they came from depleted litters which had more growing space within the uteri. Whole blood counts indicated that mice x irradiated in the pre-implantation stage tended to have slightly higher white cell counts and slightly lower red cell counts than their parallel controls. Otherwise any possible hematological damage appears to have been rectified. There were no permanent skeletal effects on mice x irradiated in utero during the pre-implantation stages of 0.0 to 5.0 days, as determined by radiographs of five selected bones and two skull measurements at 2 months of age. Mice x rayed at fertilization or at 5 days gestation showed almost as good survival as did the controls, but those x rayed on days 1, 2, 3, and 4 showed slightly reduced survivals. Corneal opacities occur frequently in these mice. Their eyes appear to be anesthetized to the particulate material in the bedding. There appeared to be no direct relationship between corneal opacities and the development of cataracts. Many mice with corneal opacities at two months recovered normal corneas at a later date. Mouse cataracts appear to arise as nuclear or cortical sclerosis of the lens, but those arising in the nuclear region appear to be in the majority. The ultimate cataract, regardless of its origin, appeared to be similar in its involvement. At any test period the percentage incidence of cataracts among the survivors was always higher among those x rayed in utero than among the parallel controls. Variations in cataractogenesis existed between males and females similarly x rayed, as had also been shown in the previous study with the uniform exposure of 100 R x rays. There appeared to be a sex differential in cataractogenesis of x-ray origin. The fact that cataracts appeared earlier and to a greater extent among the x-irradiated mice than among the controls suggests that x-rays may hasten the onset of the usual senile cataracts. There appears to be a greater incidence of bilateral as opposed to unilateral cataracts, and this seems to be particularly true for the females. The incidence of cataracts in one eye leading to bilateral cataracts occurred more frequently in mice x-rayed at fertilization and in females x-rayed at 1.0 and 5.0 days gestation. Thus, there was no clear-cut evidence of uni- leading to bilateral cataract development except possibly among some potential females. The precursors of the two eyes of any mouse at these early stages presumably received the same degree of radiation insult. Since this study is based entirely upon x-irradiation of the early mouse embryo from fertilization to 5 days gestation, and since it has been demonstrated that x-rays during this period do in fact increase the incidence of cataracts, it must be presumed that the damage is done to the precursors of the lens since lens development is not initiated until about 11 days gestation. It is suggested that the etiology of these radiation-induced cataracts may be through an interference with the developmental process, originating with damage to chromosomes insufficient to be lethal. (auth)

40650 LEUKOCYTE RESPONSE FOLLOWING SIMULTANEOUS IONIZING AND MICROWAVE (RADAR) IRRADIATION. Thomson, R. A. E.; Michaelson, S. M.; Howland, J. W. (Univ. of Rochester, N. Y.). Blood, 28: 157-62(Aug. 1966).

Simultaneous microwave and x-irradiation at a sublethal x-ray dose level modify the hematologic response to x-irradiation. Earlier neutrophil recovery and delayed lymphocyte and hematocrit recovery resulted following simultaneous microwave and x-ray exposure. (auth)

40651 IMMUNOLOGICAL TOLERANCE IN PARENTAL STRAIN MICE INDUCED BY F_1 HYDRID SPLEEN CELLS. Silobrcic, V. (Inst. Rudjer Boskovic, Zagreb). Brit. J. Exp. Pathol., 46: 583-91(Dec. 1965).

A high degree of specific immunological tolerance was induced in strain A and CBA newborn recipients of $(A \times CBA)F_1$ spleen cells. Spleen cells from $(C_{57} \times CBA)F_1$ hybrids produced a high degree of tolerance in 88% of CBA newborn recipients, while no highly tolerant animals were found among C_{57} hosts. Post-mortem findings in highly

tolerant mice were mostly within normal limits. Tolerant animals were cellular chimeras containing only a small percentage of donor cells in their spleens. Experiments were also conducted with x rays to test the possible immunological reactivity of $ABAF_1$ and $BBAF_1$ mice against their parents. Groups of 10 hybrids received skin grafts from one or the other parent. After all grafts were fully tolerated for 100 to 120 days, second-set grafts were transplanted from the same source, to boost the putative sensitivity. Eighteen to 20 days after transplantation of the second graft, all hybrid recipients were x irradiated with 1000 R and injected with 7×10^6 nucleated bone marrow cells from the skin donor strain. No significant difference in postirradiation mortality was seen between sensitized (2 parental skin grafts) and nonsensitized hybrids. Both parental grafts in all F_1 hybrid hosts were fully tolerated through the period of observation. (BBB)

40652 EFFECT OF SINGLE DOSES OF X RADIATION ON MANDIBULAR GROWTH. Adkins, K. F. (Univ. of Queensland, Brisbane). Brit. J. Radiol., 39: 602-6 (Aug. 1966).

The short-term effects of localised X radiation applied in single doses of 110, 550 and 1,100 R on mandibular growth in the rat were examined. Intravital staining with the fluorochrome alizarin red S had labelled the bone mineralised immediately before irradiation and permitted recognition of that level in subsequent examinations. Microscopic measurements were taken from the labelled line to the periphery of the bone at the lingual alveolar plate, the inferior border and the condyle. Gross measurements taken were from the gnathion to condyle and gnathion to gonion. Analysis of results revealed a marked reduction in growth in every area examined in animals receiving 1,100 R of X radiation. The greatest reductions, were in the lingual alveolus (63 per cent) and the condyle (36 per cent). The lowest dose to produce any significant retardation of bone growth was 550 R where reductions of 12 per cent in the inferior border and 9 per cent in the condyle were recorded for male animals. At the 110 R level there was no measurable reduction of bone growth. (auth)

40653 USE OF X RAYS TO PRODUCE TRANSMISSION PICTURES OF VIRUS MODELS. Fletcher, E. W. L.; Almeida, June D. (St. Thomas's Hospital, London). Brit. J. Radiol., 39: 623-6(Aug. 1966).

The use of x rays to record the transmission images of models to simulate virus particles is described. By this means it is possible to view the models under conditions similar to that by which virus particles are recorded in the electron microscope. The radiographic patterns so obtained enabled several controversial virus structures to be elucidated. (auth)

40654 CONDITIONED REFLEXES IN RATS SUBJECTED TO PRENATAL IONIZING IRRADIATION IN A DOSE OF 1 r. Semagin, V. N. (Inst. of Higher Nervous Activity and Neurophysiology, Moscow). Byull. Eksp. Biol. Med., 60: No. 9, 43-6(Sept. 1965). (In Russian).

Higher nervous activity was studied in 26 rats fetally irradiated on the 18th day of gestation with a 1 R dose and in 25 control rats beginning with the 45th day after birth. In the irradiated rats the conditioned reflexes to sound and light signals stabilized more slowly than in the control group. Almost all indices of the conditioned, unconditioned and inter-signal reflexes in irradiated rats were significantly worse than the corresponding indices in control rats. In the irradiated rats the excitation and inhibition processes were weakened, and the stabilizing function of the brain was disturbed. (auth)

40655 REACTION OF THE HYPOPHYSEAL-ADRENAL SYSTEM OF IRRADIATED RATS TO REPEATED STRESS. Bagramyan, E. R. (Inst. of Experimental Endocrinology, Moscow). Byull. Eksp. Biol. Med., 60: No. 11, 15-19(Nov. 1965). (In Russian).

The response of the hypophyseal-adrenal system of irradiated rats to a repeated action of unfavorable factors was studied. Excision of the left adrenal led to an ascorbic acid in the right adrenal both in intact and irradiated rats. Repeated irradiation of rats at the height of radiation sickness caused the same reduction of the ascorbic acid depletion in the adrenals as primary irradiation. Irradiated rats, just as the normal ones, developed compensatory hypertrophy of the remaining gland in response to excision of its counterpart. (auth)

40656 BEHAVIOR OF FISH IN THE ZONE OF RADIATION SOURCES. Pravdina, G. M. Byull. Eksp. Biol. Med., 60: No. 11, 88-91(Nov. 1965). (In Russian).

Methods were used for a free selection of food by fish (carp) in a radiation zone and outside thereof. Fish were found to be capable of determining the location of gamma-radiation sources in an aquarium and of avoiding the radiation zone. The dose intensity of radiation sources measured at a distance of 15 mm was 2.48 rad/min. The possibility of the action of radiation as an external inhibitor is discussed. (auth)

40657 MODIFICATION OF RADIOSENSITIVITY BY PORPHYRINS. II. TRANSPLANTED RHABDOMYOSARCOMA IN MICE. Cohen, Leon; Schwartz, Samuel (Hebrew Univ., Jerusalem. Univ. of Minnesota, Minneapolis). Cancer Res., 26: 1769-73(Aug. 1966).

Eight days after intramuscular injection of rhabdomyosarcoma into the thighs of mice, the tumors were irradiated with 2750 R. Three hr before X-irradiation the mice were given injections intraperitoneal of 0.5 ml of 0.75% sodium bicarbonate alone or of 0.01, 0.05, 0.25, or 1.25 mg of crude "hematoporphyrin," a copper "hematoporphyrin" nitrate. The tumor response varied significantly with the dose of porphyrin given: tumors of all 27 mice (100%) who received 0.05 mg of "hematoporphyrin" or its copper complex showed grossly complete regression and did not recur during the following 84–86-day study period, while such regression was seen in only 5 of 126 mice (4%) treated by injection with the other dose levels of porphyrin or with vehicle alone prior to X-irradiation. Normal mice receiving total body X-irradiation showed no similar porphyrin effect, suggesting an increase in the therapeutic ratio (cancer effect/whole body effect) by the 0.05 mg of porphyrin administered. Little, if any, modification of radiosensitivity was produced by the copper "hematoporphyrin" nitrate. Other findings related to the observed porphyrin dose-dependent response curve are discussed. (auth)

40658 PREVENTION OF X-RAY-INDUCED LEUKEMIA IN MICE. I. ACTION OF A RADIATION LEUKEMIA PROTECTION FACTOR IN SEVERAL MOUSE STRAINS FOLLOWING LEUKEMOGENIC OR SUBLETHAL DOSES OF X-RAY. Hodes, M. E.; Clewell, Don B.; Hubbard, J. Donald; Yu, Pao-lo (Indiana Univ., Indianapolis). Contract AT(11-1)-1391. Cancer Res., 26: 1780-6(Aug. 1966). (COO–1391-5).

Leukemia was induced in 6- to 8-week-old male and female mice by exposure to fractional doses of x-irradiation. Half the animals were given injections immediately after exposure of 40% extracts of sheep spleen according to the procedure of Berenblum et al. (2) or with 10% extracts. The extracts caused a highly significant difference in leukemia incidence in C57BL/6 and BALB/C mice, and no effect on a small group of RF mice. There was no significant difference in leukemia incidence between the sexes. X irradiated C3H/eb mice died within hours of the 4th or 5th injection, apparently in anaphylactic shock. Similar highly significant decreases in leukemia incidence in C57BL/6 mice were produced by 40% bovine spleen extracts. Bovine serum albumin was devoid of effect, whereas bovine serum γ-globulin exerted a significantly protective action. Three strains of mice were used in an attempt to demonstrate an antilethal effect of the sheep spleen extracts. In 2 experiments in which Swiss mice and 1 in which C57BL/6 mice were exposed to single doses of 550 R, significant decreases in mortality, measured at 30 days, were noted. In the remaining 15 experiments, the differences either were not significant, or the extracts seemed to exert a deleterious

action. An experiment with BALB/C mice infected with Rauscher virus failed to demonstrate an antiviral effect of sheep spleen extract. (auth)

40659 IATROGENICS. Cade, Stanford (Westminister Hospital, London). Clin. Radiol., 17: 193-202(July 1966).

Some of the radioinduced disabilities following radiotherapy are considered. The damaging effects on subcutaneous tissue, bone, the kidney, the lungs, the central nervous system, and the abdominal and pelvic viscera are reviewed, and the functional disabilities resulting from radiation induced damage are considered. Attention is drawn to the prevention of such Iatrogenic effects by changes in technique. Reference is made to metabolic disturbances following the use of radioactive iodine. The carcinogenic effects of radiation are briefly mentioned. (auth)

40660 HYPOPITUITARY DWARFISM FOLLOWING RADIOTHERAPY FOR NASOPHARYNGEAL CARCINOMA. Tan, B. C.; Kunaratnam, N. (General Hospital, Singapore). Clin. Radiol., 17: 302-4(July 1966).

Radiation is a rare cause of hypopituitary dwarfism. The authors present what is probably the first patient with pituitary dwarfism following deep x-ray therapy for carcinoma of the nasopharynx, and discuss the effects of pituitary irradiation during radiotherapy for nasopharyngeal carcinoma. Pituitary dysfunction is practically unknown in such patients, presumably because the pituitary gland is relatively radioresistant to external irradiation, as shown by animal experiments and human studies. In this patient, there is incomplete pituitary inhibition. (auth)

40661 NEW STUDIES MADE IN RATS CARRYING A LYMPHOBLASTIC LYMPHOSARCOMA EXPOSED TO THE EFFECT OF ELECTROMAGNETIC WAVES ASSOCIATED WITH MAGNETIC FIELDS. Riviere, Marcel-Rene; Guerin, Maurice (Institut de Recherches Scientifiques sur le Cancer, Villejuif, France). Compt. Rend., Ser. D, 262: 2669-72(June 20, 1966). (In French).

In experiments with a new modulated electromagnetic wave and magnetic field generator comparable results were obtained. In effect, the rats having lymphoblastic lymphosarcoma, exposed to this device, present a regression process of their tumor in a considerable percentage of cases when the treatment is conducted satisfactorily. When the treatment is insufficient, the samples die after an appreciable survival time, significantly valid in comparison with the controls. The rats clinically cured showed specific immunization phenomena several months later that were biologically indicated by the resorption of a second isologous graft of the same tumor. The rats succumb to the implantation of a homologous tumor of different histologic type. (tr-auth)

40662 INFLUENCE OF IONIZING RADIATIONS ON HUMAN HEREDITY. Vallebona, A. (Univ., Genoa). pp 9-18 of Convego della Salute, Ferrara, May 20-1, 1961. Modena, Italy, Stabilimento Poligrafico Artioli. (In Italian).

An assessment is made of the possible genetic influence of ionizing radiations from natural and artificial sources. Natural sources (cosmic radiation, terrestrial radiation, and internal sources, such as ^{14}C and ^{40}K) account for an average gonadal dose of 2 to 5 R over a 30-yr period. Populations living at high altitudes or under elevated terrestrial radiation levels receive higher doses. Artificial sources, which are enumerated, result in an ~equivalent dose, that is, 2 to 3 R over a 30-yr period. With the introduction of nuclear energy exploitation, the ambient radioactivity to which man is exposed has increased. The nature of radioinduced mutations and their development from internal and external radiation sources are discussed. Data derived from animal experimentation are reviewed and their applicability to human heredity is examined. It is concluded that the radiosensitivity of the genetic apparatus in man is reasonably similar to that of higher mammals, and that the doubling dose of 50 R found in mice is probably applicable to man. Linearity and threshold of the genetically effective dose is also considered. (BBB)

40663 STUDIES ON LYMPHOPOIESIS. IV. A COMPARISON OF TWO APPROACHES FOR THE DETERMINATION OF THE GENERATION TIME IN THORACIC DUCT CELLS WITHOUT DETECTABLE CYTOPLASMIC DIFFERENTIATION. Janett, A. (Univ. of Bern); Wagner, H. P.; Jansen, C. R.; Cottier, H.; Cronkite, E. P. Europe. J. Cancer, 2: 231-6(Aug. 1966).

In vivo cytokinetic studies on calf thoracic duct lymphoid cells using tritiated thymidine as a cell marker served as a model for the discussion of the relative validity of two methods of investigation of cell lines without detectable cytoplasmic differentiation. The combined analysis of the change of the mitotic labelling index and of the mean grain count per labelled mitotic figure as a function of time after a single injection of thymidine-^{3}H gave more reliable data on the generation cycle than the analysis of the decrease of the mean grain count per labelled cell in interphase and the determination of the mean grain count halving time. For in vivo studies of the proliferative pattern of human malignant cell lines, clinical situations should be sought, in which evaluation of the mitotic labelling index as a function of time after a single administration of thymidine-^{3}H is feasible without disturbing the steady state. (auth)

40664 EFFECT OF RADIOPROTECTORS ON DAMAGE INDUCED BY ALKYLATING AGENTS ON TUMOURAL AND NORMAL TISSUES. Garattini, S.; Palma, V.; Reyers-Degli Innocenti, I.; Guaitani, A. (Istituto di Ricerche Farmacologiche Mario Negri, Milan). Europe. J. Cancer, 2: 237-44(Aug. 1966).

A quantitative investigation was carried out to establish the usefulness of radioprotector drugs in combination with alkylating agents for the chemotherapy of Ehrlich carcinoma and Sarcoma 180 in mice. Tumoural growth, spleen weight and number of blood white cells were measured. The results show that a protection against the damage induced by alkylating agents on spleen and white cells was always achieved at doses of radioprotectors able to prevent also the antitumoural activity of the same alkylating agent. Despite the large range of doses and schedule of treatment tried it was impossible to produce evidence that the combination radioprotectors + alkylating agents was useful. (auth)

40665 COMPARISON OF THE EFFECTS OBTAINED ON HUMAN BLOOD CELL CHROMOSOMES IRRADIATED IN VITRO BY MEANS OF X-RAYS, GAMMA RAYS FROM ^{60}Co AND ELECTRONS OF HIGH ENERGY. Feremans, W. (Univ., Brussels). Europe. J. Cancer, 2: 279-84(Aug. 1966). (In French).

Human blood cells were cultured according to the method of Moorhead and Hungerford and irradiated with three types of radiations: x rays of 200 kV, gamma rays of ^{60}Co, electrons of 20 Mev. The doses varied between 50 and 600 R. The chromosomal aberrations observed 24 hr after irradiation were: achromatic gaps, chromatid breaks, chromatid exchanges, ring chromosomes, polyploidies, and endoreduplications. The rates of abnormal mitoses were compared in the cultures irradiated with x-rays, with gamma-rays and with electrons. No statistical difference was observed. Nevertheless, it is possible that a difference exists in the number and in the chromosomal aberration types observed per cell. The demonstration of this point constitutes a second step—not yet finished—in the study of the Relative Biological Efficiency of the three types of radiations. (auth)

40666 ^{125}I-DU (5-IODO-2'-DEOXYURIDINE) IN AUTORADIOGRAPHIC STUDIES OF CELL PROLIFERATION. Feinendegen, L. E.; Bond, V. P.; Hughes, W. L. (Institut du Radium, Paris. Brookhaven National Lab., Upton, N. Y. Tufts Univ., Boston). Exp. Cell Res., 43: 107-19 (Aug. 1966). (BNL-9974).

5-^{125}I-2'-deoxyuridine (^{125}I-DU) was used as thymidine analogue for autoradiography of bone marrow cells of the rat. It was shown that ^{125}I (gamma, 35 kev) gives an autoradiographic resolution sufficient for determining the relative labeling intensities of single cells. ^{125}I-DU is incorporated, following a single injection, into the same type of bone marrow cells and yield labeling indices nearly

identical to those observed with ^{3}H-thymidine. A comparison of the relative labeling intensity of myelocytes and segmented neutrophiles at 1 hr, 1 day, and 3 days after injection of ^{125}I-DU indicates that IDU is not lost from the DNA in these cells during division and subsequent maturation. The data obtained with ^{3}H-thymidine is comparable to that obtained with ^{125}I-DU. Since IDU is reutilized inefficiently or not at all on DNA catabolism in contrast to thymidine, single cell autoradiography can be used to study the effect of thymidine reutilization on measurements of cell proliferation and DNA renewal made with labeled thymidine. An investigation of the distribution of labeled cells of the megacaryocytic series at 1 hr and 3 days after a single injection of ^{125}I-DU or of ^{3}H-thymidine shows the effect of thymidine reutilization likely responsible for a near 100 per cent labeling of all megacaryocytic forms at day 3 after injection of ^{3}H-thymidine. The data also indicate that a "quiescent stem cell" with regard to DNA synthesis cannot be assumed to be the only immediate precursor for megacaryoblasts. These precursor cells must synthesize DNA at least once within 3 days prior to differentiating into recognizable megacaryocytic elements. The overall mitotic index in the bone marrow did not change over a period of 3 days attesting the lack of recognizable radiation effects from ^{125}I and of metabolic toxicity of IDU at the dose level used in the experiments. The autoradiographic efficiency of ^{125}I in comparison with ^{3}H under the conditions of the experiment is discussed. (auth)

40667 EFFECTS OF X-RAY DOSAGES ON DEVELOPMENT OF HETERAKIS GALLINARUM. Ostlind, D. A.; Hansen, M. F. (Kansas State Univ., Manhattan). Exp. Parasitol., 18: 41-8(Feb. 1966).

The importance of H. gallinarum in relation to blackhead disease in turkeys and chickens prompted this study to: (1) determine effects of x irradiation on rate of embryogenesis, (2) determine the reproducibility of x irradiation results, and (3) record by photomicrographs abnormalities in cleavage patterns. In two experiments egg cultures were irradiated with 4000, 16,000, and 64,000 R. In another experiment eggs were exposed (250 R/min, 90 kv) to 30,000, 60,000, and 120,000 R. Doses up to 64,000 R retarded embryogenesis and 120,000 R appeared lethal. At 64,000 R, most eggs required 15 days longer incubation to develop to infective larvae than did the controls. Lethal effects of 64,000 R were manifested early (fertile to 5-cell stage) in embryogeny. The effective dose (ED_{50}) which would result in 50% of the eggs failing to reach infective stage after 14 days incubation was 39,120 R (uncorrected) or 49,550 R (corrected). Reproducibility of results was better for replications within an experiment than repeating experiments at different times. Morphological effects of x rays on eggs were seen as abnormal cleavage and differentiation as well as vacuolation. Vacuolation is a general biological effect of x irradiation indicating abnormal permeability of the enclosing membranes or abnormal functioning of the permeability regulatory mechanism. (BBB)

40668 RADIOSENSITIZING ACTION OF SOME NATURALLY OCCURRING PYRIMIDINES. Pol'kina, R. I. (Inst. of Oncology, Academy of Medical Sciences, USSR). Federation Proc., Transl. Suppl., 25: T283-4(Mar.-Apr. 1966).

Translated from Vop. Onkol., 11: 57(1965).

The radiosensitizing actions of cytosine, thymine, and uracil were studied in mice with Ehrlich's tumor implants under the skin of the flank. Five to 7 days after implantation, when the tumors had reached a mean diameter of up to 0.5 cm, the animals were given one of the test preparations and 1.5 hrs later the tumors were exposed to 3382 R x radiation. The animals were sacrificed 25 to 30 days later and the mean weight and mean tumor weights were calculated. Only uracil, at a dose of 10 mg/kg, increased the sensitivity of the tumor tissue to the action of x radiation. (C.H.)

40669 "BLACK" EYE COLORS OF MORMONIELLA. Whiting, P. W. (Oak Ridge National Lab., Tenn.). Genetics, 54: 639-55(Aug. 1966). (ORNL-P-82).

Eye-color mutations in Mormoniella may be grouped as "bright" and "black," the former occurring much more frequently. Of 13 separate black mutations, eight were "eb (ebony) black" and five were "bk (black) black." Combinations were made with R-locus dahlia, da, scarlet, st, and orange, or. da eb is black phenotypically, da bk lavender; st eb is scarlet, st bk white; or eb and or bk are both white. Because some of the ebonies and blacks are difficult or impossible to distinguish from wild type by inspection, the white combinations were used in determining homology, white offspring from crosses indicating homology, colored indicating nonhomology. The eight ebonies proved homologous. The five bk blacks included two pairs of alleles and a third gene linked with R giving 20.1% crossovers. F_2 males from crosses of blacks and R-locus genes and between nonhomologous blacks gave data indicating linked viability depressors, linkage between a black and R, and linkage of black loci (repulsion phase) resulting in excess of whites. Several of these linkages are probably spurious owing to chromosomal irregularities. Deficiency of whites from some crosses may be due to reduced viability of the double recessives. One of the ebony genes depresses viability to 50% of normal, and a bk-black gene depresses viability to less than 90%. Differences in intensity of black between different stocks may be caused by the state of the black genes themselves, some being weak enough to give a wild phenotype, or there may be suppressors at other loci. Gene formulae for the black genes may be expressed in terms of factor states as in the R alleles. (auth)

40670 FURTHER EVIDENCE DEMONSTRATING GERMINAL SELECTION IN EARLY PREMEIOTIC GERM CELLS OF DROSOPHILA MALES. Abrahamson, S.; Meyer, Helen Unger; Himoe, E.; Daniel, G. (Univ. of Wisconsin, Madison). Genetics, 54: 687-96(Aug. 1966).

Drosophila males were irradiated with cesium-137 gamma rays, and germ cells which were early spermatogonia at the time of irradiation were scored for X-chromosome and second chromosome lethals. Only the primary, or pre-definitive gonial cells were tested and the experimental procedures avoided the inclusion of clusters of identical mutations in the data. The ratio of induced x to autosome lethals recovered was 1:5.5 providing further evidence that germinal selection has occurred in these cells. (auth)

40671 CHANGES IN QUANTITATIVE TRAITS OF TRIBOLIUM UNDER IRRADIATION AND SELECTION. Bartlett, Alan C.; Bell, A. E.; Anderson, V. L. (Purdue Univ., Lafayette, Ind.). Contract AT(11-1)-965. Genetics, 54: 699-713(Aug. 1966).

The consequences of various combinations of selection (high and random) and levels of X-irradiation (0, 100, and 1000 R per generation) on pupal weights were investigated in two strains of Tribolium castaneum for 11 generations. Reproductive fitness was measured each generation in terms of sterility, adult mortality, and number of offspring. The Foundation Strain was an unselected panmictic population with an initial weight of 2.10 mg. The second strain, Large, had originated earlier from Foundation and had been selected for large pupal weight for 44 generations. At the beginning of the present study its average pupal weight was 5.66 mg. High selection contributed to significant responses in pupal weight, but the degree of response was negatively correlated with the level of irradiation. Even though an increase in heritability and phenotypic variance was observed in some irradiated lines, a decline in reproductive fitness contributed to smaller selection differentials and in turn less selection response. Several strain by treatment interactions possibly were related to the previous selection history of the genetic material. For example, reproductive fitness increased with high selection in Foundation and responded inversely in the Large Strain. Yet the latter was more resistant to the deleterious effects of irradiation than was the Foundation Strain. (auth)

40672 SOME OBSERVATIONS ON THE FINE STRUCTURE OF THE LUTEIN CELLS OF X-IRRADIATED RAT

OVARY. Flaks, Bojan; Bresloff, Paul (Univ. of Leeds, Eng.). J. Cell Biol., 30: 227-36(Aug. 1966).

The ovaries of 10- to 13-week-old rats were exteriorized and irradiated with sterilizing doses of X-rays. Following treatment, the animals entered a phase of constant vaginal cornification. Animals were killed 8 to 12 wk after the onset of this phase, and their ovaries were prepared for electron microscopy. Tissue was fixed in glutaraldehyde, postfixed in osmium tetroxide (Millonig's, phosphate-buffered), and embedded in Epon. Lutein cells from these ovaries were compared with those from sham-irradiated controls. The cytoplasm of lutein cells from experimental animals was characterized by an increase in the amount of agranular endoplasmic reticulum and by an increase in the number of mitochondria. These mitochondria are more variable in external form and often possess increased numbers of villiform cristae. Other features noted were a decrease in the amount of cytoplasmic lipid granules and an increase in cell size and surface irregularity. The significance of the morphological findings is discussed in relation to ovarian hormone production in animals sterilized by x irradiation. (auth)

40673 MATING COMPETITION OF GAMMA-IRRADIATED AND NONIRRADIATED MALE TROGODERMA GLABRUM HERBST. Tilton, Elvin W.; Burkholder, Wendell E.; Cogburn, Robert R. (Dept. of Agriculture, Hyattsville, Md.). J. Econ. Entomol., 59: 168-9(Feb. 1966).

Attempts were made to develop a sterile-male irradiation technique for field tests for eradication of this insect. Male T. glabrum are capable of copulation after treatment with a dose of γ irradiation as high as 100,000 rad, but complete sterility occurs at 25,000 rad. Longevity of the treated males is not significantly shortened by 25,000 rad. The results of a preliminary study to determine the mating competition by male T. glabrum irradiated at 25,000 rad are reported. When an irradiated male and a nonirradiated male were placed with a virgin female, 57% of the females produced viable eggs, as compared with 97% for the females with a nonirradiated male only. These results indicate that males of T. glabrum sterilized at 25,000 rad do compete favorably with nonirradiated males. If small numbers of males of this species should escape sterilization during irradiation of a commodity, the presence of large numbers of sterilized males should provide a significant factor in population depletion. Since multiple matings are common in this species, of interest is the high incidence of females that produced no progeny, indicating the high priority for fertilization of one of the matings or the dominance of one of the males. (BBB)

40674 GAMMA RADIATION-INDUCED DOMINANT LETHALITY TO THE SPERM OF THE OLIVE FRUIT FLY. Tzanakakis, M. E.; Tsitsipis, J. A.; Papageorgiou, M.; Fytizas, E. (Democritus Nuclear Research Center, Athens). J. Econ. Entomol., 59: 214-16(Feb. 1966).

In efforts to develop a sterile male irradication technique, pupae of the olive fruit fly, Dacus oleae, were exposed to 8, 10, and 12 krad of γ rays. Permanent dominant lethality was caused in sperm to a degree considered satisfactory for practical purposes. It was shown also that 6 krad was a satisfactory male-sterilizing dose. At these doses not more than 2.6% of the progeny of irradiated males mated with normal females reached the first larval instar, and not more than 0.3% reached the pupal stage, as compared with 82.3% and 41.4% of the controls, respectively. When females 24 to 30 days old, exposed as pupae to 6, 8, and 12 krad of γ rays, were dissected, no mature eggs were found in their ovaries in contrast to normal females. The size of their ovaries was the same or smaller than that of nonirradiated 1-day-old females. Thus, doses of γ rays which cause dominant lethality to the male will permanently sterilize the female, the reproductive system of which seems to be more sensitive to radiation than that of the male. No increased adult mortality in the irradiated males as compared with the nonirradiated males was seen, and the radiation doses used did not seem to affect the time or the percent of adult emergency. (BBB)

40675 AN IMPROVED METHOD FOR RADIOAUTOGRAPHY OF ERYTHROPOIETIC CELLS LABELED WITH ^{55}Fe OR ^{59}Fe. Fowler, J. H.; McCulloch, E. A.; Till, J. E.; Siminovitch, Louis (Univ. of Toronto). J. Lab. Clin. Med., 68: 523-30(Sept. 1966).

A radioautographic method is described which permits the quantitative estimation of the number of labeled cells present in a suspension of mouse hematopoietic cells labeled with ^{55}Fe or ^{59}Fe, in vitro or in vivo. The method makes use of Millipore filters to minimize cell loss and cell damage during the preparation of the cells for radioautography. Other advantages of the method include a random distribution of the cells over the filter surface, ease in adjustment of concentration of cells per unit area, firm binding of emulsion to the filter, and excellent retention of isotope in the cell, permitted by use of the fixer glutaraldehyde. The usefulness of ^{55}Fe for radioautography has been investigated and compared with that of ^{59}Fe. ^{59}Fe appears to be the isotope of choice where grain counting is desired, whereas ^{55}Fe is to be preferred for determinations of the percentage of labeled cells, especially since the availability of carrier-free ^{55}Fe makes it possible to obtain satisfactory radioautographs within 12 hours after the labeled cells are coated with emulsion. (auth)

40676 COMPARISON OF ULTRAVIOLET SENSITIVITY OF BACILLUS SUBTILIS BACTERIOPHAGE SP02 AND ITS INFECTIOUS DNA. Okubo, S. (Okaka Univ.). J. Mol. Biol., 14: 130-42(Nov. 1965).

In the infection of competent bacteria with phage DNA, two modes of DNA infectivity can be distinguished: group I DNA, which yields titers of infectious centers strictly proportional to the DNA concentration, and group II DNA, which yields titers of infectious centers proportional to a higher power of the DNA concentration. The effect of uv irradiation on phage SP02 DNA, which belongs to group I, is reported, and a hypothesis is presented suggesting that host cell reactivation occurs in SP02 phage-infected cells, but occurs to only a limited extent in SP02 DNA-infected cells. DNA extracted from a clear plaque mutant of the temperate phage, SP02, was infectious when incubated with competent cultures of Bacillus subtilis 168 M. The relation between numbers of infectious centers and DNA concentration was linear. The sensitivity of the infectious DNA to uv light was much greater than that of the free phage when B. subtilis 168 M wa used as host. Acriflavin, which inhibits host cell reactivation, increased the rate of uv inactivation of the free phage so that it approached the inactivation rate of the phage DNA. Acriflavin had little effect on the survival curves of the infectious DNA. Nonhost-reactivating mutants (hcr$^-$) of B. subtilis 168 M were isolated. The survival curves of SP02 phage were much steeper when the hcr$^-$ mutant was used as a host than those obtained when the hcr$^+$ parental strain was used as a host. The uv sensitivity of the phage DNA was still greater than that of the free phage even when B. subtilis hcr$^-$ was used as host, but the difference in sensitivity was much less than the difference obtained with B. subtilis hcr$^+$ as a host. (BBB)

40677 PATHOGENESIS OF RADIATION-INDUCED THYMIC LYMPHOMA IN MICE. Siegler, Richard; Harrell, Wilhelmina; Rich, Marvin A. (Albert Einstein Medical Center, Philadelphia). J. Nat. Cancer Inst., 37: 105-21(Aug. 1966).

Previous observations on the pathogenesis of thymic lymphoma in mice indicate that the two thymic masses on either side of the trachea behave independently during leukemogenesis and should be considered as separate organs—the right and left thymuses. After each of 4 weekly doses of radiation, both thymuses showed lymphocyte depletion, followed by lymphocyte regeneration. The rate and degree of the depletion and subsequent regeneration, quantitated by individual thymus weights, were identical. This synchronous thymic response to the direct effect of the radiation was in contrast to the later, nonsynchronous, independent thymic lymphoma response, which in this study was always unilateral. Changes in Hassall's corpuscles were noted in the period preceding the development of the thymic lym-

phoma. The pathogenesis of radiation-induced lymphoma was similar to that of virus-induced lymphoma. (auth)

40678 AVERAGE DIAMETER OF ERYTHROCYTES UNDER THE EFFECT OF SMALL DOSES OF IONIZING RADIATION IN THE HUMAN. Goldberg, E. D. (Tomsk Medical Inst., USSR). Lab. Delo, 9: 9-11(Feb. 1966). (In Russian).

Hematologic patterns in x-ray and radiological workers were studied. Of the 252 persons observed working under conditions exposing them to ionizing radiation (x-ray apparatuses, betatrons operating at 25 and 31 Mev, radium, radioactive cobalt, iodine, phosphorus, sulfur, mercury, and others), 173 were women and 79 men. Generally, the daily dose of irradiation was not higher than 0.02 to 0.04 R, with a few persons in the betatron lab receiving doses up to 0.06 once or twice a month. Even in persons with more than 15 yr service using x rays and radium, the average diameter of erythrocytes (ADE) did not show large deviations from normal (ADE = 7.65 μ). The observed increase of ADE (7.76−8.2 μ) in radiologists was accompanied by an increase in the average volume of erythrocytes (AVE), while the AVE in x-ray workers were within the limits of the normal. Macrocytosis was also discovered in some persons exposed in the betatron and radioisotope laboratories. In these groups the increase of ADE was accompanied by a small increase of AVE. A tendency toward the development of macrocytosis in the observed persons was not associated with disturbances in erythropoiesis aside from the increase in size of the blast cells. Apparently, the increase in red blood cell size is a result of low-dose irradiation (0.02 to 0.04 R/day) in these occupationally exposed workers. (BBB)

40679 CLINICAL STUDY ON GENERALIZED AND MULTIPLE ERUPTIONS DURING ^{60}Co RADIOTHERAPY OF FEMALE GENITAL CANCER. Matsuoka, Yoshito (Kumamoto Medical Univ., Japan). Nippon Sanfrejinka Zasshi, 17: 1029-38(Sept. 1965). (In Japanese).

The generalized cutaneous reaction during the radiotherapy of a gynecological cancer is a complication, not well understood yet. Therefore, no systematic studies of the clinical symptoms, causes and treatment have been reported so far. Clinical studies were made in 22 cases with these complications during the ^{60}Co radiotherapy of gynecological cancers. The results obtained are as follows: (1) The symptoms appeared in 9.4% of cases. (2) The complication appeared only in cervical and vaginal cancers, and no symptoms appeared in other genital cancers. (3) Nineteen of the 22 cases were associated with radiotherapy alone and the remaining three with the postoperative radiotherapy. (4) The period from the initation of radiotherapy to the appearance of eruption was 43 days on the average. (5) Previous allergic histories were noted in 5 of the 22 cases. (6) Eczematous, toxicodermatous and erythematous eruptions were observed in almost all of the cases. (7) Many of the cases complained of skin itching and radiation sickness. (8) Significant eosinophilia and moderate liver damage were observed in many of the cases and in whose vaginal discharge, staphylococcus, streptococcus and coliform bacteria were detected. (9) The allergic reaction due to denatured tissue products following the radiotherapy was considered as the possible etiology, but bacterial flora in the genital and intestinal tracts probably played an important role also as its causative agents. (auth)

40680 ANALYTICAL CONSIDERATION OF FETAL GONAD BURDEN IN ISOTOPE PLACENTOGRAPHY. Tautz, M. (Staedtishe Klinikum, Berlin). Nucl.-Med., 5: 272-84(1966). (In German).

Using a spherical cap as a geometrical approximation of the placenta, the exposures to the fetal gonads are calculated for human serum albumin labeled with ^{131}I, ^{132}I, ^{51}Cr, or ^{99m}Tc. The effects of tissue absorption on the results of these calculations are discussed. Additional doses resulting from possible diaplacental passage are reported. The overall results indicate that ^{131}I-labeled albumin causes the highest gonadal dose and should, therefore, no longer be used for radioisotope placentography. (auth)

40681 USE OF GAMMA RADIATION IN JUTE BREEDING. Mia, M. M.; Ali, S. M.; Shaikh, A. Q. Nucl. Sci. Appl., 2: 13-17(Apr. 1966).

Dry seeds of Corchorus capsularis var. D-154 and Corchorus olitorius var. C. G. were irradiated with doses of cobalt-60 gamma rays ranging from 70 kR to 100 kR. Tests from germination percentage, seedling height and survival percentage revealed that C. olitorius was more sensitive towards radiation than C. capsularis. It seems that a dose between 90 and 100 kR is the critical dose for mutation research in jute. In the M_1 generation different morphological changes in the leaves and stems, variation in the chlorophyll contents in the leaves and the time of flowering were also noted. In some cases it was found that the flower petals were transformed into full-fledged leaves. Most of the abnormal looking plants were completely sterile. Some were fertile but their offspring did not inherit the parental characters. In the M_2 generation dwarf, early and late flowering types were isolated. They were completely fertile. A hybrid of the cross female C. G. (0 kR) X male 154 (80 kR) was obtained. These hybrids inherited the bilobed and krinkled leaf characters of the parental male plants. In meiotic studies on the plants raised from the gamma treated seeds different kinds of chromosomal aberrations were observed. (auth)

40682 POPULATION OF GERM CELLS IN IMMATURE MALE RATS FOLLOWING IRRADIATION AT BIRTH. Mandl, Anita M. (Univ. of Birmingham, Eng.). Proc. Roy. Soc. (London), Ser. B, 165: 103-35(July 19, 1966).

Male rats were irradiated with 19 R on the day of birth, and killed at intervals ranging from 5 to 18 days. Estimates were made of the absolute and relative numbers of germ cells at different stages of spermatogenesis in 64 irradiated and 61 untreated specimens. In the normal rat, the calculated population of germ cells increased from about 160,000 at 5 days to 30 million at 18 days. Only negligible numbers of primordial germ cells (gonocytes and transitional cells) persisted beyond the age of 10 days. Small numbers of spermatogonia type A appeared at 5 days (15,000) and their population rose to about 1 million at 12 days, and 2 million at 18 days (7% of all germ cells). Intermediate spermatogonia first occurred in appreciable numbers (23,000 to 55,000) at 8 or 9 days, when the population of type-A spermatogonia was 360,000. The subsequent rise in the population of intermediate spermatogonia was more rapid than that of type A (4 million at 18 days). Spermatogonia type B and primary spermatocytes appeared at 9 to 10 days, and their numbers rose more steeply still (6.5 and 16 million at 18 days, respectively). Irradiation at birth exerted no rapid effect on the cytological appearance of primordial germ cells. Transformation from gonocytes to transitional cells appeared to proceed normally and the estimated total population of germ cells at 5 days was no smaller than in the controls. Subsequently, however, many of the transitional cells failed to divide: they enlarged to form giant cells, acquired bizarre nuclear outlines, and persisted for unusually long periods. Some degenerated at mitotic prophase or metaphase, while a few seemed to die at interphase, without entering division. The calculated total population of germ cells in irradiated rats rose from 160,000 at 5 days to 9.4 million at 18 days. Small numbers of spermatogonia type A, presumably derived from such primordial germ cells as were able to complete mitosis, appeared some 2 to 3 days later than in controls. The number of type-A spermatogonia in 7-day-old irradiated rats was 44,000, cf. 215,000 in controls; the difference became less pronounced with time, and by the age of 18 days, the population of 1.9 million was comparable to that estimated for the controls. Small numbers of intermediate spermatogonia appeared on the 9th (8000) and 10th day (35,000), when the population of type-A spermatogonia was about 110,000 and 260,000 respectively. By the 18th day, intermediate spermatogonia numbered 2 million. The populations of type-B spermatogonia and primary spermatocytes rose from 11,000 to 13,000 at 10 days to 1.6 and 3.4 million, respectively, at 18 days. The difference in the absolute and rela-

tive numbers of germ cells between normal and irradiated testes widened progressively with advance in the developmental stage of the germ cells. Analysis of the results indicates that in the reduced population of spermatogonia type A after irradiation, the pattern of spermatogonial mitoses is modified so as to favor the formation of more type-A, in preference to intermediate, spermatogonia. (auth)

40683 ULTRASTRUCTURE OF MALE GERM CELLS IN RATS X IRRADIATED AT BIRTH. Franchi, L. L.; Mandl, Anita M. (Univ. of Birmingham, Eng.). Proc. Roy. Soc. (London), Ser. B, 165: 136-54(July 19, 1966).

A histological and ultrastructural study was made of the testes of rats, aged 1 to 15 days that had received partial-body x-irradiation (ca. 100 R) on the day of birth. Nineteen serially sectioned testes were subjected to a quantitative analysis including counts of germ cells and measurements of nuclear volume. The type, position, and general form of germ cells, together with the incidence of various organelles, were assessed semi-quantitatively from 533 electron micrographs of irradiated (370) and normal (163) tissues. Exposure to 100 R at birth has no marked effect on the total population of germ cells during the first 5 days. The transformation of gonocytes into transitional cells is not affected. Subsequently, the treated testes differ from those of coeval controls by the almost complete absence of germinal mitoses and, consequently, of spermatogonia type A. Many of the transitional cells grow into irregularly shaped giant cells, usually with a highly lobed nucleus and enlarged nucleoli. Although some cells show condensation of chromatin which may indicate the onset of mitotic prophase, the majority appear to degenerate at interphase. By 10 days, the testes contain only a fraction of the original population of germ cells. No significant changes are detectable in the ultrastructure of germ cells up to 4 days after irradiation. The treatment only induces the sporadic appearance of two minor features (pinocytotic vesicles containing electron-dense material; peripheral granular bodies with some internal organization), which are normally absent from corresponding cells in the controls. Electron micrographs of giant transitional cells confirmed the cytological observations of irregularity of nuclear outline and nucleolar enlargement. The nucleoli are frequently irregular in shape and contain material of two distinct electron densities. In general, the organelles of giant transitional cells are normal and healthy in appearance. With advancing age, an increasing proportion of germ cells show degenerative changes leading to pyknosis. Dead cells appear to be engulfed by neighboring somatic cells. In both normal and irradiated testes, the simple form of Golgi apparatus in the gonocyte changes to a more complex type in the transitional cells. The persistence of giant cells is associated with a tendency for the Golgi apparatus to revert to the simple type, or to disperse into a number of small simple units. The most striking feature is the relatively high incidence of centrioles, suggesting that radiation-induced mitotic inhibition and gigantism may be accompanied by endomitosis. Irradiation does not markedly affect the appearance and incidence of A- and B-bodies. These organelles tend, however, to persist over a longer period in irradiated than in untreated young rats. (auth)

40684 ACCRETION AND EXCHANGE OF ^{85}Sr IN TRABECULAR AND CORTICAL BONES. Gong, J. K.; Burgess, E.; Bacalao, P. (State Univ. of New York, Buffalo). Contract AT(30-1)-3234. Radiat. Res., 28: 753-65(Aug. 1966).

Accretion and exchange of ^{85}Sr in trabecular and cortical bones were determined in dogs. The respective A's and E's found were, for cortical bone, 0.45 mg Ca/day/gm ash and 4.6 mg Ca/gm ash; and for trabecular bone, 2.59 mg Ca/day/gm ash and 39.0 mg Ca/gm ash. When the overall A and E values calculated from the above ash values and based on the total estimated trabecular and cortical ash amounts in the average dog were compared with the A and E values obtained from whole-body in vivo countings, they were found to be similar: A = 0.80 mg Ca/day/gm ash, and E = 10.3 mg Ca/gm ash. The influence of the adjacent fraction on normal A's and E's, as well as the effect of dead and callus bones in the overall accretion and exchange of the various sections of the femur and tibia, was also described and discussed. (auth)

40685 RESPONSE OF ISOLATED LEUKOCYTE LYSOSOMES TO GAMMA IRRADIATION. Harris, John W. (Australian Atomic Energy Commission Research Establishment, Sutherland, N. S. W.). Radiat. Res., 28: 766-78 (Aug. 1966).

Lysosomes isolated from rabbit polymorphonuclear leukocytes were irradiated in vitro at 0° to 4°C with 1 to 50 krads of γ radiation and subsequently incubated for 1 hour at 0° to 4°C, 28°C, or 37°C. Irradiation of lysosome suspensions resulted in a rapid drop in their optical density (520 mμ). The rate at which this fall occurred during the first 15 minutes postirradiation was dose-dependent. The magnitude of the decrease in turbidity resulting from irradiation was less during incubation at 0° to 4°C than at higher temperatures; at all temperatures the effect showed a tendency to level off during the latter portion of the incubation period. Irradiated lysosome suspensions had increased amounts of protein in the granule-free suspending medium. At high doses this effect was greater, relative to controls, at 0° to 4°C than at higher incubation temperatures. It was concluded that radiation may have produced some form of damage in or near the membrane of the isolated lysosome and that subsequent stress (in the form of heating) resulted in an exaggerated response (fall in optical density). The leakage of protein, on the other hand, occurred in the absence of such extreme stress and may represent a more sensitive indicator of lysosomal damage. The possible relationship of these data to the role of the lysosome in the initiation or exacerbation of cellular radiation damage was discussed. (auth)

40686 THE KINETICS OF CHROMATID ABERRATIONS INDUCED IN CHINESE HAMSTER CELLS BY TRITIUM-LABELED THYMIDINE. Brewen, J. G.; Olivieri, G. (Oak Ridge National Lab., Tenn.). Radiat. Res., 28: 779-92 (Aug. 1966). (ORNL-P-1563).

Dose curves were obtained for the induction of the various types of chromatid aberrations by tritiated thymidine. When the yields of aberrations were plotted against the number of grains in the autoradiograms, terminal deletions and chromatid exchanges exhibited one-hit and two-hit components in their dose curves, and isochromatid deletions exhibited linear kinetics. Since the numbers of silver grains obtained for a given film exposure time were measures of relative dose rates, it was assumed that they were also an accurate estimation of the total relative doses. The great majority of the data available on the induction of aberrations by chronic ionizing radiations indicate that when both a one-hit and a two-hit component are present in an acute radiation dose curve, the two-hit component is severely reduced when chronic radiation is employed and the dose curve approaches linearity. The present data are not in agreement with these findings. If stage sensitivity and mitotic delay are taken into consideration, however, an equation can be constructed which satisfactorily explains the shapes of the dose curves obtained and shows that linear kinetics hold for all classes of aberrations. The nonlinear portions of the dose curves apparently arise from variation, with dose, in the time spent in cell stages of different sensitivity. (auth)

40687 RESPONSE OF THE DBA/2J MOUSE STRAIN TO ACUTE IONIZING RADIATION: THE BIPHASIC DEATH PATTERN. Yuhas, John M.; Jacobus, David P.; Crenshaw, John W. (Walter Reed Army Inst. of Research, Washington, D. C. Univ. of Maryland, College Park). Radiat. Res., 28: 804-10(Aug. 1966).

The DBA/2J strain of mice responds to lethal irradiation by way of a fourth-week syndrome in addition to the normal medullary syndrome. This fourth-week syndrome, which is not seen in the outbred WR-BS strain, is induced at a lower dose than is the medullary syndrome. Increases in the medullary deaths, mediated by joint housing with the

WR-BS after irradiation, do not eliminate the fourth-week syndrome from the lethal response of the DBA/2J. Intrastrain crowding has been shown to increase the lethal efficiency of the fourth-week syndrome. (auth)

40688 LOCOMOTOR BEHAVIOR AND NEUROMORPHOLOGIC ANOMALIES IN PRENATALLY AND POSTNATALLY IRRADIATED RATS. Lipton, James M. (Univ. of Michigan, Ann Arbor). Contract AT(11-1)-1201. Radiat. Res., 28: 822-9(Aug. 1966).

Locomotor performance of rats X-irradiated with 200 R at 1 or 3 days postnatally was compared with that of animals irradiated 17 days postconception and with that of controls. The locomotor tasks required the rats to traverse narrow bridges or parallel rods to obtain food. Rats irradiated 17 days postconception showed the greatest locomotor deficits. The 3-day postnatally irradiated animals showed less deficit than the 17-day group, though their performance was still significantly below that of controls. There was no difference in locomotor performance between the group irradiated 1 day after birth and controls. Neuromorphologic patterns resulting from irradiation at these stages of development and their relations with locomotor performance are discussed. (auth)

40689 COMPLICATIONS AND LATE CHANGES FOLLOWING RADIATION THERAPY FOR CARCINOMA OF THE EYELID AND CANTHI. Levitt, S. H.; Bogardus, C. R. Jr.; Brandt, E. N. Jr. (Medical Coll. of Virginia, Richmond). Radiology, 87: 340-7(Aug. 1966).

Sixty-three patients treated for carcinoma of the eyelid and canthi with radium and x ray between 1946 and 1962 were statistically analyzed as to the effects of various factors in the development of complications. Those treated with radium showed a statistically significant increase in ocular complications. In all cases radium to tumor doses of over 5,000 R resulted in ocular complications, most of a severe nature. The cure rate was similar for patients treated with x ray and radium. It is concluded that radium implantation without special precautions should not be routine in the treatment of eyelid and canthal lesions. (auth)

40690 METHOD OF RADIATION CATARACT ANALYSIS AND ITS USES IN EXPERIMENTAL FRACTIONATION STUDIES. Focht, Elizabeth F. (Cornell Medical Center, New York); Merriam, George R. Jr.; Schwartz, Melvin; Velasquez, Joseph; McNeill, Daniel. Radiology, 87: 465-74(Sept. 1966).

A method of inducing and of evaluating radiation cataracts has been devised. An "isoeffect" method of comparing the doses of two different radiation conditions containing different parameters has been described. In the present study an appreciable difference with fractionation was statistically determined. This difference is in time of onset, but otherwise biologically equivalent for the criteria used here. The effect of fractionation as defined was not found to be different for doses from 2,000 to 500 rads. There were insufficient data to determine whether or not the result was a function of the stage. These methods of irradiation, of scoring, and of data analysis, are applicable to radiation cataract studies in general. Some of the aspects of irradiation dosimetry and procedure and of isoeffect and data analysis are applicable to radiobiological studies in general. (auth)

40691 PHYSIOLOGICAL IMPLICATIONS OF LASER BEAMS. THE VERY HIGH RADIATION FLUX DENSITIES OF OPTICAL MASERS POINT TO IMPORTANT BIOMEDICAL APPLICATIONS. Solon, Leonard R.; Aronson, Raphael; Gould, Gordon (TRG, Inc., Syosset, N. Y.). Science, 134: 1506-8(Nov. 10, 1961).

Calculations are presented which are of physiological interest in terms of the hazard associated with laser beams and their potential employment as biological and clinical tools. From the point of view of physiological interest, two important properties of laser beams are the extremely collimated character of the light and its high degree of monochromaticity. The collimation property implies the possibility of obtaining large energy densities in narrow beams. The optimum divergence angle of a laser beam is limited only by the wavelength of the light emitted and the dia of the laser source in accord with the Frauhofer diffraction relation. The spectral line of laser light is potentially much narrower than the spectral lines achievable by ordinary excitation processes in gas discharge tubes or arcs, which are limited by the Doppler widths of spontaneous radiative transitions of individual atoms. Laser light, comprised as it is of coherent superposed wave trains emitted during induced transitions, is not so limited. Spectral lines narrow as the power of the laser source increases; lines as narrow as 10^{-6} of a Doppler width have been observed. Retinal energy density from laser beams is discussed, and formulas are given for retinal spot size and light intensity under various conditions. The existence of an intensity or energy density rate-dependence is shown. It is probable that there is a short integration time within which retinal damage is proportional to the integrated intensity, irrespective of the rate. If this time is very much shorter than 10 sec, the integrated intensity obtained with the 0.5-msec duration of the Vireo I laser pulse may be considerably more than 6 times that required to produce a retinal lesion. It is concluded that the laser, being an emitter of high-intensity light, is a new energy source to be explored with regard to its effects on ocular and other tissues with a view toward biomedical application. Persons working with laser light sources should be alerted to the potential occupational hazard. (BBB)

40692 OCULAR LESIONS PRODUCED BY AN OPTICAL MASER (LASER). Zaret, Milton M. (New York Univ., N. Y.); Breinin, Goodwin M.; Schmidt, Herbert; Ripps, Harris; Siegel, Irwin M.; Solon, Leonard R. Science, 134: 1525-6(Nov. 10, 1961).

Ocular lesions were experimentally produced in rabbit by a laser. The high-energy density delivered in a single 0.5-msec pulse was sufficient to cause instantaneous thermal injury to the pigmented retina and iris of the brown rabbit. Ophthalmoscopically, the retinal lesions resembled flash burns from an atomic fireball. The lesion consists of blanched, coagulated retina elevated in crater fashion and containing a small, centrally placed hemorrhage. Five days later, the appearance was that of a flat white scar with pigment clumping in and around the exposed area. A lesion produced by a single laser pulse was observed in the iris immediately after exposure and was characteristically a dark brown, irregularly shaped burn. When the eye was examined several days later, the pupil constricted in a grossly eccentric manner suggestive of internal damage to the iris. The ocular effects described were produced by a coherent source of intense field strength. As amplified light systems are developed and adapted to fulfill military, industrial, and medical objectives, it is essential that attending personnel be fully cognizant of this potential hazard. (BBB)

40693 THE LETHAL EFFECTS OF ^{60}Co ON MATURE WHITE LEGHORN CHICKENS (AN LD 50/30 STUDY). Banks, W. C.; Hensley II, J. C.; Krueger, W. F.; Runnels, Sandra (Texas A and M Univ., College Station). Southwestern Vet., 17: 15-18(Fall 1963).

A flock of selected pedigreed male and female White Leghorn chickens in early sexual maturity was exposed to ^{60}Co-γ radiation at the rate of 50 R/h for total dose levels ranging from 200 to 1600 R. Observation of death rate for 30 days post irradiation resulted in an LD_{50} of 742 R. Probit analysis revealed a difference of 210 R in the female radioresistance (LD_{50}) as compared to males. Post irradiation symptomatology and post mortem findings are listed. This group of birds closely parallels commercial and farm flocks common today. (auth)

40694 COMPARISON OF RADIATION SICKNESS CHARACTERISTICS IN VARIOUS SPECIES OF MAMMALS, INCLUDING PRIMATES. Semenov, L. F.; Yakovleva, L. A. (Inst. of Experimental Pathology and Therapy, Academy of Sciences, USSR). Vestn. Akad. Med. Nauk SSSR, No. 9, 11-13(1965). (In Russian).

The literature is reviewed, and experimental data are presented on acute radiation sickness in mice, rats,

guinea pigs, rabbits, dogs, and monkeys. Irradiations were carried out with the RUM-3 x-ray machine and a ^{50}Co source (70 to 110 rad/min). Data on the effects of total and localized irradiation (abdomen and head) in monkeys (1650 to 25000 rad) and the survival time (in hrs) are given. The disruption of the leukopoiesis mechanism accompanying acute radiation sickness is described. Information on infectious diseases (gingivitis, pneumonia, enteritis and colitus) with which the various animals were affected (in addition to acute radiation sickness) is presented in tabular form. It is concluded that radiation sickness in humans most closely resembles that in monkeys. (ATD)

40695 EFFECT OF WHOLE-BODY X-RAY IRRADIATION ON ACTIVITY OF ATP-ASE IN RAT LIVER MITOCHONDRIA. Khanson, K. P. (Central State Research Inst. for Radiology and Roentgenology, Leningrad). Vop. Med. Khim., 12: 256-8(May-June 1966). (In Russian).

No changes in activity of ATP-ases (stimulated by DNP and magnesium ions) could be observed in mitochondria within liver 24 hours after whole-body irradiation (800 R) of rats. Alterations, characteristic for aging mitochondrial preparations, were observed earlier on incubation in isotonic sucrose solutions of mitochondria from livers of irradiated animals as compared with the mitochondria from non-irradiated controls. (auth)

40696 INJURIES OF THE SKIN CAUSED BY LIGHT. Niebauer, G. Wien. Med. Wochensch., 114: 879-82 (Dec. 5, 1964). (In German).

The author summarizes and reviews the normal and pathological reactions of skin to various wavelengths of solar radiation. Over the range from 760 mμ to 5 μ irradiation produces a warming effect, resulting in hyperemia. Visible light, extending from 400 to 760 mμ has no known pathological effects. The normal effect of exposure to μv light from 315 to 400 mμ (uv A) is direct pigmentation within a few minutes without subsequent erythema. It is probable that during this time colorless precursors of melanin pigment that are present in the skin are oxidized. Phototoxic reactions and dermatitis may result from overexposure. Exposure to uv light from 280 to 315 mμ (uv B) produces erythema, edema, indirect pigmentation, thickening of the horny layer, and formation of vitamin D. Sunburn and actinic elastosis result from excessive exposure. Several other complications of uv light include light urticaria, porphyria, and xeroderma pigmentosum. In sunburn the uv B penetrates only the outer epidermis, but it causes secondary effects such as vasodilatation, fluid diapedesis, and leukodiapedesis. A classic example of a dermatosis induced by light is pellagra, which results from a deficit of B vitamin. A clinically similar picture is also caused by inborn defects of tryptophan metabolism. Xeroderma pigmentosum may also be caused by disturbance of amino acid metabolism. In this rare disease the first visible changes usually appear in early childhood after the first exposure to sunlight. The histologic skin changes resemble those seen in actinic elastosis and may develop into carcinoma. (BBB)

40697 CHANGES IN TOTAL LEUKOCYTE COUNTS AFTER EXPOSURE TO VARIOUS WHOLE-BODY DOSES OF IONIZING RADIATION. Schmid, A.; Zipf, K.; Gutschow, K. (Univ., Munich). Zentralbl. Veterinaermed., 12: 563-6(Dec. 1965). (In German).

Hourly counts of leukocytes were made in adult male rats exposed to 1-, 10-, or 100-rad doses of 55-kv x rays at 4.9 rad/min. Total leukocyte counts were depressed 1 hr after all three doses, to 50% of normal after 100 rad. Counts began to rise and reached a slightly higher level after all three doses in the 2nd hour. In the 1- and 10-rad groups the counts continued to rise, reaching normal by the 6th hr in the 1-rad group and remaining 20% below normal in the 10-rad group. However, in the rats exposed to 100 rad, the counts continued to fall after the 2nd hr, reaching a minimum level 40% of normal by the 6th hr. The postirradiation rise of peripheral leukocytes (at 2 hr) is interpreted as reflecting a discharge of leukocytes into the circulation from tissue stores, while the progressive decline of counts after high doses is taken as a sign of exhaustion of depot leukocytes. (BBB)

40698 X-RAY INDUCED HYPOTHYROIDISM IN THE DOG. Quinlan, W. J.; Michaelson, Sol. 3p. (CONF-660212-11). ORAU. Gmelin, AED-CONF-66-016-11.

From Radiation Research Society, 14th Annual Meeting, Coronado, Calif.

Brief exposure of the upper part of the body of the dog to 1200 to 1820 R of 1000 KVP x-rays results in hypothyroidism between 2 and 4 years after irradiation, as evidenced by physical signs, depressed uptake of ^{131}I by the thyroid gland, lowered serum PBI levels, and increased cholesterol levels. The uptake of ^{131}I and the serum PBI levels are both refractory to the administration of exogenous TSH, which suggests primary involvement of the thyroid rather than the pituitary in the observed hypothyroidism. (auth)

40699 RADIATION RESISTANCE OF SPORES OF CLOSTRIDIUM BOTULINUM TYPE E. Segner, W. P.; Schmidt, C. F. (Continental Can Co., Inc., Chicago). Vienna, International Atomic Energy Agency, 1966, Preprint SM-73/28, 14p. (CONF-660609-19). ORAU.

From International Symposium on Food Irradiation, Karlsruhe, Ger.

The resistance of spores of Clostridium botulinum Type E to ^{60}Co was determined in 1:2 haddock homogenate and in neutral phosphate buffer. Inoculated samples were irradiated at 0.1 mrad internal doses at 35°F (1.7°C). The number of survivors at each dose was determined in a medium consisting of 5% peptone, 16% gelatin, and 0.1% sodium thioglycollate, using a replicate deep-tube recovery method and incubation at 68°F (20°C) and 46°F (7.8°C). Survivor curves were constructed by plotting log percent survivors against dose. The viable counts of unirradiated spores at 68°F and 46°F were used to calculate the respective percent survivors. Survivor curves for spores of the Beluga, 8E, Alaska, and Minneapolis strains in both substrates and at both temperatures were characterized by a pronounced shoulder or lag during the first log cycle of reduction followed by exponential destruction. Lag values, defined as the dose in mrad for a survivor curve to traverse the first log cycle of reduction, were larger with haddock than with buffer and larger with incubation at 68°F than at 46°F. Lag values of spores in haddock at 68°F ranged from 0.29 to 0.43 mrad. At 46°F, the lag values equalled approximately 0.25 mrad. In buffer at 68°F, the lag values ranged from 0.21 to 0.30 mrad versus 0.13 to 0.20 mrad at 46°F. D-values, defined as the dose for 90% reduction from the exponential portion of a survivor curve, equalled 0.22 mrad in haddock and 0.08 to 0.11 mrad in buffer at 68°F. D-values of 0.08 to 0.11 mrad were obtained in both haddock and buffer at 46°F. From partial spoilage data at 85°F (29.4°C), spores of the 8E and Minneapolis strains showed D-values equal to 0.25 mrad. More than a twofold reduction in resistance was observed with incubation at 46°F. D-values for 10^6 inactivation from extrapolation of the survivor curves compared closely to those calculated from partial spoilage results. The survivor curve for spores of the Beluga strain irradiated in trypticase-peptone-glucose medium with recovery in peptone-agar at 85°F was indistinguishable from the survivor curve of spores of the same strain irradiated in haddock with recovery at 68°F. (auth)

40700 EFFECTS OF X-IRRADIATION ON VARIOUS STAGES OF THE LIFE CYCLE OF PHYSA ACUTA, DRAP., A FRESHWATER GASTROPOD. Ravera, O. (EURATOM, Ispra, Italy). Vienna, International Atomic Energy Agency, 1966, Preprint SM-72/52, 19p. (CONF-660507-30). ORAU.

From Symposium for the Disposal of Radioactive Wastes into Sea, Oceans, and Surface Waters, Vienna.

The effects of x rays on the mortality, fecundity, fertility, egg viability, and embryonal development of Physa acuta, Drap were studied. The embryos were irradiated with a single dose of 200 R to 3200 R of unfiltered 300 kV x rays, delivered at 200 $R \cdot min^{-1}$. The mortality of the embryos increased with dose and their radiosensitivity decreased

with increasing age. Thus, up to 3200 R the mortality of the oldest irradiated embryos (veliger and hippostage) was very similar to that of the controls, whereas the LD_{50} was 2400 R for trocophora and 1100 R for blastula. There was no evident delay in the development of the hippostage between 200 and 3200 R, whereas in the other stages, delay increased with dose and was more marked in the youngest ones. Adults were irradiated with a single dose ranging from 2 kR to 220 kR at dose rates of 1 kR and 2 kR $\cdot$ min^{-1}. The mortality of the animals exposed to 10 kR was not different from that of the controls. Significant effects on the mortality of the animals irradiated with 28 kR became evident only 20 days after irradiation. Fecundity, fertility and egg viability were decreased. A dose of 100 kR completely abolished the reproductive capacity of the adult. Temporary sterility (50 days) was produced at 10 kR. Thereafter there was a progressive recovery in fertility to levels almost similar to those of controls. (auth)

40701 STUDIES OF THE EFFECT OF SINGLE AND FRACTIONATED X IRRADIATION ON HOMOZYGOTE PARENT VARIETIES AND THEIR CROSSED POPULATIONS OF BARLEY (HORDEUM VULGARE L.). Siegert, W. Jena, Ger., Univ., Jena, 1965. 58p. $2.00 Gmelin, AED-Diss. 65-328.

Thesis.

Radiation sensitivity in heterozygote crossed populations of barley is lower than that of the corresponding parent varieties. Fractionated irradiations increase the mutation rate significantly. It is recommended to use heterozygote genotypes as starting material for mutation breeding. (Gmelin Inst.)

40702 RADIATION REACTIONS OF THE LOCALLY X-IRRADIATED RAT SPLEEN ISOLATED BY OPERATION. Kemmuna, A. Mainz, Univ., Mainz, 1965. 21p. $2.00 Gmelin, AED-Diss. 65-273.

Thesis.

After irradiation of isolated rat spleens with 600 R a marked injury of the white spleen pulpa occurs. Maximum injury occurs after 6 hrs. Regeneration takes place after 1 day. Results indicate that the regeneration of spleen tissue occurs more rapidly after local irradiation than after whole-body irradiation with the same dose. (Gmelin Inst.)

40703 DELAYED REACTIONS OF THE URINARY SYSTEM AND THE INTESTINE AFTER IRRADIATION OF UTERINE CARCINOMA. Sina, H. Muenster, Ger., Univ., Muenster, 1965. 60p. $2.00 Gmelin, AED-Diss. 65-307.

Thesis.

Delayed effects in 741 female patients with uterine carcinomas treated by irradiation were investigated by cytoscopic and pyelographic methods. In 365 patients delayed effects on the urinary system were observed. Therapy of delayed injuries is discussed. (Gmelin Inst.)

40704 EXPERIMENTAL STUDIES ON THE SINGLE AND COMBINED ACTION OF ^{60}Co γ RAYS AND TRENIMON (TRIETHYLENEIMINO BENZOQUINONE) ON THE NUCLEUS AND NUCLEOLUS OF CANCER CELLS (TYPE HeLa) IN THE INTERPHASE IN VITRO. Stein, G. Tuebingen, Ger., Univ., Tuebingen, 1964. 86p. $2.00 Gmelin, AED-Diss. 64-1080.

Thesis

Hela cell cultures were irradiated with 250 to 1000 R ^{60}Co γ rays and treated with trenimon in a concentration of 1:20 millions. Areas of nuclei and nucleoli were determined by planimetric methods. A significant dose dependent increase of nucleus area was observed. Radiation effects are enhanced by trenimon. (auth)

40705 INDUCTION OF MUTATIONS AND THE MUTATION PROCESS. Proceedings of a Symposium Held in Prague, September 26–28, 1963. Veleminsky, Jiri; Gichner, Tomas (eds.). Prague, Publishing House of the Czechoslovak Academy of Sciences, 1965. 143p. (CONF-630916).

Separate abstracts were prepared on fourteen papers. One paper was abstracted previously and appeared in NSA Vol. 19: 19527. (C.H.)

For abstracts of individual papers see: 40513, 40550, and 40706–40717.

40706 BIOLOGICAL ORGANIZATION IN RELATION TO DIFFERENTIAL GENE RESPONSE TO MUTAGENS. Fahmy, O. G.; Fahmy, Myrtle J. (Royal Cancer Hospital, London). pp 14-25 of Induction of Mutations and the Mutation Process. Veleminsky, Jiri; Gichner, Tomas (eds.). Prague, Publishing House of the Czechoslovak Academy of Sciences, 1965.

Theories on chromosome structure and mutagenesis are reviewed. Results are reported from studies in Drosophila on the effects of x radiation or the chemical mutagens, triethylenemelamine or a mustard derivative of phenylalanine, that demonstrated the relevance of each unit of biological structure to the process of mutagenesis, starting from the cell level through the chromosome and the gene to the subgenic elements that approach macromolecular dimensions. The degree of differential mutagenicity induced by x radiation and the chemicals was assessed by determining the absolute mutation rate at 11 specific loci. The relative response of each locus to the different mutagens was compared and a complementation map was prepared of the rudimentary locus and the distribution of cistons damaged by the various mutagens. Studies on the mutagenic specificity of DNA showed that both homologous and heterologous DNA are effective in the induction of small chromosome deletions resulting in the autosomal dominants known as minutes, and to a lesser extent in the induction of point mutation visibles. It was also shown that a great many polymers of natural and synthetic origin possess the DNA type of mutagenicity. The specificity of action of DNA was studied on the IVth chromosome by comparing the distribution of minutes with that induced by x radiation and recovered under the same conditions. The implications of the specific action of one mutagen on one locus and the possible genetic effects of synthetic macromolecules specific to particular loci are discussed. (C.H.)

40707 INFLUENCE OF INTERACTION BETWEEN EDTA AND X-RAYS ON MUTATION AND CROSSOVER FREQUENCIES IN DROSOPHILA MELANOGASTER. Ondrej, M. (Inst. of Experimental Botany, Prague). pp 26-9 of Induction of Mutations and the Mutation Process. Veleminsky, Jiri; Gichner, Tomas (eds.). Prague, Publishing House of the Czechoslovak Academy of Sciences, 1965.

Results are reported from studies on the effects of ethylenediaminetetraacetic acid (EDTA) and x radiation on mutation and cross-over frequencies in Drosophila melanogaster. The medium in which the whole generation was reared had 2×10^{-3} M concentration of EDTA added and the sensitivity of the different stages of spermatogenesis to the effects of EDTA and x radiation was studied. Results showed the effect of EDTA was on the border line of significance and the effect of x radiation was not increased by the action of EDTA. The influence of both agents and their interactions on crossing over was studied in females homozygous for certain traits and mated to recessive males after injection of EDTA. The flies were transferred to fresh media every second day and after the third transfer a significant increase in the recombination frequency was noted. However, the frequency did not significantly exceed the sum of activities induced by EDTA or x radiation alone. It was concluded that the time interval between pretreatment and x irradiation did not allow interaction to occur and that the sensitization of chromosomes by EDTA does not occur in all systems. (C.H.)

40708 SOME ASPECTS OF MUTAGENESIS IN MAIZE. Bianchi, A. (Univ., Milan. Univ. Cattolica, Piacenza, Italy). pp 30-7 of Induction of Mutations and the Mutation Process. Veleminsky, Jiri; Gichner, Tomas (eds.). Prague, Publishing House of the Czechoslovak Academy of Sciences, 1965.

Analysis of the genetic variability detectable in open-

pollinated populations of maize revealed that mutations occurring in nature are almost exclusively point events, while the majority of artificially induced mutations are of the chromosome type. Results are summarized from studies on the analysis of genetic material in mutations induced by doses of 560 to 1680 R x radiation or by chemical mutagens such as diepoxybutane and ethyl methanesulfonate administered to the pollen mother cell, pollen grain, or seed. Factors such as x ray dose and dose fractionation, temperature, moisture content, and storage time were varied with the consequence of sometimes changing the total effect significantly, but it was exceedingly difficult to alter the type of response. Results indicate the induction of artificially obtained back mutations in maize. (auth)

40709 EFFECTS OF TWO ENDOGENOUS FACTORS ON ARTIFICIAL MUTAGENESIS IN ARABIDOPSIS THALIANA. Roebbelen, G. (Univ., Goettingen, Ger.). pp 42-5 of Induction of Mutations and the Mutation Process. Veleminsky, Jiri; Gichner, Tomas (eds.). Prague, Publishing House of the Czechoslovak Academy of Sciences, 1965.

Results of studies on the effects of endogenous factors on artificial mutagenesis in Arabidopsis thaliana, in which biological components were kept constant. The effects of ontogenetic development on mutations induced by the treatment of seeds or germ cells with a chemical mutagen, phenyl ethylurethan, or x radiation were studied. Results indicated that different physiological conditions or developmental stages had a marked effect on mutagenic reactions in the same plant. (C.H.)

40710 INDUCTION OF CHLOROPHYLL CHIMERAS BY X RAYS AND ETHYL METHANESULFONATE (EMS) IN DIFFERENT HETEROZYGOUS STRAINS OF ARABIDOPSIS THALIANA. Gichner, T.; Veleminsky, J. (Inst. of Experimental Botany, Prague). pp 54-6 of Induction of Mutations and the Mutation Process. Veleminsky, Jiri; Gichner, Tomas (eds.). Prague, Publishing House of the Czechoslovak Academy of Sciences, 1965.

Seeds of different heterozygous strains of Arabidopsis thaliana were treated with ethyl methanesulfonate (EMS) and 50 kr x radiation. The dose of x radiation used did not induce any chimeras in homozygous plants. Seeds from heterozygous plants, carrying genes for lethal chlorophyll mutants, were treated with EMS and x radiation. After sowing these seeds, the chlorophyll mutants died in an early stage of development and the rest of the viable plants were heterozygotes and homozygotes in the proportion 2 to 1, as distinguished by analysis of pods. Analysis of the types of heterozygotes showed that three mutants were induced by x radiation and three by EMS, all segregated 3 normal to 1 mutant and the relationship of heterozygous and homozygous plants in heterozygous strains was clearly 2 to 1. The results indicated that after EMS treatment the frequency of chimeras was higher in heterozygous strains, but the frequency differed in different strains. After x radiation treatment the frequency of chimeras was very low and the differences between individual strains were not significant. Possible explanations for the origin of chimeras in heterozygous plants are discussed. (C.H.)

40711 SELECTION IN M_1 GENERATION AFTER MUTAGENIC TREATMENT OF BARLEY SEEDS. Gaul, H. (Max-Planck Inst. of Plant Breeding, Cologne). pp 62-72 of Induction of Mutations and the Mutation Process. Veleminsky, Jiri; Gichner, Tomas (eds.). Prague, Publishing House of the Czechoslovak Academy of Sciences, 1965.

Results are summarized from studies on diplontic selection and the effect of selecting certain M_1 seedlings as well as that of selecting M_1 spikes of different degrees of sterility after the x irradiation of barley seeds. Results showed that selection of M_1 seedlings with reduced vigor may result in higher M_2-mutation rates as compared with the selection of vigorous M_1 seedlings. Different mutation rates of different M_1 seedling height classes were only found after exposure to low doses of x radiation. Selection of fertile M_1 spikes did not result in reduced M_2 chlorophyll mutation frequency. (C.H.)

40712 EXPERIMENTS ON USE OF INDUCED MUTANTS TO HYBRIDIZATION BREEDING IN BARLEY. Scholz, F. (Research Inst. of Cultivated Plants, Gatersleben, Ger.). pp 73-9 of Induction of Mutations and the Mutation Process. Veleminsky, Jiri; Gichner, Tomas (eds.). Prague, Publishing House of the Czechoslovak Academy of Sciences, 1965.

Experiments over a 15-year period with barley seeds treated by x radiation or ethyl methanesulfonate have resulted in a mutant collection of nearly 1,000 lines. The mutant lines have been used for studies of morphological changes, the protein content in grain, plant breeding, genetic factors, taxonomy, evolution, and the inheritance of agronomically important characters. Application of induced mutants in the hybridization breeding of barley for the development of agronomically desired characters is discussed in detail. (C.H.)

40713 ALLELE-INDUCED INSTABILITY (SOMATIC CONVERSION) IN THE TOMATO. Hagemann, R. (Research Inst. of Cultivated Plants, Gatersleben, Ger.). pp 80-4 of Induction of Mutations and the Mutation Process. Veleminsky, Jiri; Gichner, Tomas (eds.). Prague, Publishing House of the Czechoslovak Academy of Sciences, 1965.

The genetic analysis of mutations induced by x irradiation of seeds of the Lukullus variety of tomatoes (Lycopersicon esculentum) revealed gene instability due to somatic gene conversion. The existence of plants with green, variegated, or pure yellow branches made it possible to study the nature of the variegation of heterozygous plants. Results of these studies are reported. (C.H.)

40714 EXPERIMENTAL INDUCTION OF CHROMOSOMAL ABERRATIONS IN PLANTS. Rieger, R. (Research Inst. of Cultivated Plants, Gatersleben, Ger.). pp 85-100 of Induction of Mutations and the Mutation Process. Veleminsky, Jiri; Gichner, Tomas (eds.). Prague, Publishing House of the Czechoslovak Academy of Sciences, 1965.

Data are reviewed from a number of studies on the induction of chromosomal aberrations in plants by physical and chemical agents. Topics discussed include the types of aberrations and the sensitivity pattern of the cell cycle to the various mutagens; the kinetics of aberration production by ionizing radiations and chemicals; and the distribution of aberrations between cells and between, as well as within, the chromosomes. Data are tabulated on the distribution of chemically induced chromosome aberrations of Vicia faba, the classification of chromosome- breaking agents on the basis of the influence of oxygen and respiration inhibitors, and the interaction of chromatid breaks induced by various agents in Vicia. Emphasis is placed on the induction of aberrations by x or γ radiations, or neutrons, ethyl methanesulfonate, myeleran, nitrogen mustards, di(2,3-epoxypropyl) ether, beta propiolactone, azoserine, ethyl alcohol, butyl hydroperoxide, potassium cyanide, oxygen under pressure, N-nitroso-N-methylurethane, 8-ethoxycaffeine, maleic hydrozide, mitomycin C, diepoxybutane, 2,2 bipyridine, 5-fluorodeoxyuridine, alone or in various combinations. It is concluded that higher plants and animals are very complex test systems for chromosome aberrations, that the agents start numerous reactions on the cellular level that may or may not be of major importance in aberration production, that aberration production is a complicated process that may start at the chromosome or elsewhere in the cell, that chromosomes are highly organized structures, and that the relationship between chromosome structure during mitotic and meiotic divisions and the interphase state of chromosomes is more or less obscure. (C.H.)

40715 CHELATE FORMATION AS A SENSITIZING FACTOR IN PRODUCTION OF CHROMATID ABERRATIONS BY RADIOMIMETIC AGENTS. Michaelis, A.; Rieger, R. (Research Inst. of Cultivated Plants, Gatersleben, Ger.). pp 101-6 of Induction of Mutations and the Mutation Process. Veleminsky, Jiri; Gichner, Tomas

(eds.). Prague, Publishing House of the Czechoslovak Academy of Sciences, 1965.

Results are reported from a study of the influence of two chelating compounds, ethylenediaminetetraacetic acid and 2,2'-bipyridine, on the frequency of chromosomal aberrations induced by various radiomimetic agents in primary roots of Vicia faba. Possible modes of action of the two chelators are discussed. (C.H.)

40716 EFFECTS OF CHRONIC IRRADIATION ON FREQUENCY OF CHROMOSOME ABERRATIONS IN ROOT TIP MERISTEM OF BARLEY. Honcariv, R.; Misutova, O.; Honcarivova, K. (Safarik Univ., Kosice, Czechoslovakia). pp 107-8 of Induction of Mutations and the Mutation Process. Veleminsky, Jiri; Gichner, Tomas (eds.). Prague, Publishing House of the Czechoslovak Academy of Sciences, 1965.

Germinating seeds of barley were irradiated continuously for 92 hr at a dose rate of 10mR/hr to 3.22 R/hr using a ^{60}Co γ source. Control specimens were kept under identical conditions but without irradiation. The roots were fixed immediately after completion of irradiation and the frequency of chromosome bridges and acentric fragments in anaphases were determined in chromosome preparations. Data are tabulated on the number of cells counted, dose rate, and frequency of aberrations. Results showed that with increasing dose rate the percentage of chromosome bridges also increased up to a dose rate of 1.170 R/hr. A small increase in the frequency of acentric fragments was also observed at the dose rate of 1.170 R/hr. An equation is included for the mathematical analysis of the frequency of chromosome bridge steps. (C.H.)

40717 FACTORS AFFECTING THE BIOLOGICAL ACTION OF MUTAGENS. Konzak, C. F.; Nilan, R. A.; Froese-Gertzen, Edith E.; Foster, R. J. (Washington State Univ., Pullman). pp 123-32 of Induction of Mutations and the Mutation Process. Veleminsky, Jiri; Gichner, Tomas (eds.). Prague, Publishing House of the Czechoslovak Academy of Sciences, 1965.

Results are reported from studies of factors that affect the biological action of chemical mutagens on barley seeds. The physical and chemical properties of diethyl sulfate (DS) and ethyl methanesulfonate (EMS) and factors influencing their activity were examined in in vitro and in vivo experiments. Emphasis was placed on differences in reaction rates of the agents as estimated from hydrolysis data, the over-all toxicity, the diffusion rate, and the effects of temperature. Results are included from preliminary mutation studies on barley that indicate that n-butyl methanesulfonate is an effective mutagen. Data are included on the mutagenic effects of alkylating sulfonates on barley as compared with the effects of x radiation. (C.H.)

Radiation Effects Therapy and Countermeasures

40718 (ORNL-3922, pp 99-105) MAMMALIAN RECOVERY. (Oak Ridge National Lab., Tenn.).

Research is reported on: modification of secondary disease mortality; secondary mortality and body weight loss in lethally irradiated mice given small doses of isologous bone marrow cells; effects of immunization with living parental cells; and polycythemic mice produced by hypoxia in silicone rubber membrane enclosures. (H.G.D.)

40719 (ORNL-3922, pp 136) CHEMICAL PROTECTION AND ENZYME CATALYSIS. (Oak Ridge National Lab., Tenn.).

The effects of chemicals (glutathione and AET) and combined preirradiation treatment with chemicals and postirradiation treatment with isologous bone marrow on the $LD_{50/30}$ in BC3F1 mice were determined in x-irradiated animals. The $LD_{50/30}$ values for the combined treatments were close to the values one would expect by adding the increments for each agent alone. (H.G.D.)

40720 THYMIC AND SPLENIC IRRADIATION IN TREATMENT OF ACUTE LYMPHATIC LEUKEMIA. Fish, V. J.; Winchell, H. S.; Lawrence, J. H. (Palo Alto Medical Clinic, Calif. Univ. of California, Berkeley). Amer. J. Roentgenol., Radium Therapy Nucl. Med., 97: 989-90 (Aug. 1966).

Each of four patients received an estimated tissue dose of 3,000 rads to the thymus and 1,000 rads to the spleen, delivered within a 2 week period, using a telecobalt 60 unit. Data are given in a table which shows time elapsed between completion of radiation therapy to the thymus and spleen, the time of reinstitution of drugs and the patient's time of death. It is deduced that only one patient had definite therapeutic benefit from radiation therapy to thymus and spleen. (H.L.W.)

40721 INCREASED RADIOSENSITIVITY OF SKIN AND NORMAL TISSUES IN HIGH PRESSURE OXYGEN. van den Brenk, H. A. S. (Cancer Inst. Board, Melbourne). Amer. J. Roentgenol., Radium Therapy Nucl. Med., 97: 1007-18(Aug. 1966).

Experimental and clinical studies are reviewed which provide evidence in respect to enhancement of radiosensitivity of normal tissues in vivo by exposure to hyperbolic oxygen. The results of further studies of radiation reactions and damage in rat skin are presented which confirm previous observations that skin irradiated in air tolerates doses 20–30 percent higher than doses administered in hyperbaric oxygen. The application of these results to clinical studies and trials, designed to evaluate the use of hyperbaric oxygen in radio therapy of cancer, is considered. It is suggested that doses prescribed in air in such trials should be suitably corrected for this oxygen enhancing effect of hyperbaric oxygen exposures. (auth)

40722 EFFECT OF POSTIRRADIATION BLEEDING ON PROLIFERATION OF BONE MARROW CELLS IN MICE IRRADIATED WITH 350 r. AUTORADIOGRAPHIC EXAMINATION USING THYMIDINE-^3H. Karanovic, Dobrila; Karanovic, Jovo; Hajdukovic, Srdjan. Bull. Boris Kidrich Inst. Nucl. Sci., 17: 49-55(Jan. 1966).

In normal animals bleeding leads to increase of labeling activity of erythroid, myeloid and reticular cells; the increase is much lower in reticular cells. Postirradiation bleeding causes an earlier onset and peak of proliferation of erythroid cells in comparison with the behavior of proliferation of erythroid cells in mice only irradiated. The application of the method of labeling cells (with thymidine-^3H) in evaluating the proliferation of myeloid elements after irradiation must be accepted with suspicion, at least if doses near semilethal are concerned, because the stopping of mitotic activity causes the appearance of atypical cells labeled with marked intensity. Labeling of these cells is the result of the disturbance of mitosis more than the sign of immediate mitoses. Different behavior of erythroid and myeloid cells seems to be connected with their different radiosensitivity. Effect of postirradiation bleeding on the proliferative activity of reticular cells is stimulative, but spontaneous postirradiation regeneration indicates that it does not favor it. (auth)

40723 INFLUENCE OF DNA ISOLATED FROM DIFFERENT ORGANS ON THE REPARATION OF GERMINAL EPITHELIUM AND MORPHOLOGICAL CHANGES OF SPERMATOZOA OF TOTAL-BODY X-IRRADIATED RATS. Savkovic, N.; Kacaki, J.; Hajdukovic, S. Bull. Boris Kidrich Inst. Nucl. Sci., 17: 57-66(Jan. 1966).

A study was made of the effects of homologous liver, thymus, spleen, testes, brain and kidney DNA's on the reparation of germinal epithelium and morphological changes of spermatozoa of rats irradiated with a dose of 600 R. The results show that animals irradiated and treated with DNA from different organs show marked signs of reparation of spermatogenesis. They also show that DNA from different organs markedly decrease the number of morphologically abnormal spermatozoa. (auth)

40724 PROTECTIVE ACTION OF PHOSPHORORGANIC PREPARATION OF NIBUFIN ON ALBINO MICE IRRADI-

ATED WITH LETHAL DOSES OF X RAYS. Goldshtein, M. I.; Berezovskii, B. S. (Kazan Medical Inst.). Byull. Eksp. Biol. Med., 60: No. 10, 68-9(Oct. 1965). (In Russian).

Prophylactic administration of anticholinesterase phosphororganic preparation (nibufin) to albino mice produced a certain protective effect against lethal doses of x rays. Survival time was increased though mortality rate was not reduced, and radiation sickness was undiminished. (TCO)

40725 REVERSIBLE AND IRREVERSIBLE EFFECTS OF DENSELY IONIZING RADIATIONS UPON THE REPRODUCTIVE CAPACITY OF CULTURED HUMAN CELLS. Todd, Paul (Univ. of California, Berkeley). Med. Coll. Va. Quart., 1: No. 4, 2-14(Winter 1966).

Work with human kidney T1 cells is summarized to demonstrate that environmental factors that alter the sensitivity of the reproductive capacity of cultured mammalian cells to the effects of x and gamma radiation fail to alter the effects of densely-ionizing particulate radiations, or alter them less effectively. Modifying conditions considered are: oxygen, dose fractionation, chemical protection with cysteamine, and the thymidine analogs IUdR and BUdR. It was found that chronic exposure must be considered equivalent to acute exposure whenever evaluating the hazards of heavily ionizing radiations. (H.G.D.)

40726 STUDIES ON THE BONE MARROW TRANSPLANTATION FOR THE HEMATOPOIETIC DISTURBANCE PART I. PRELIMINARY REPORT. Iwamori, Shigeru; Shigemitsu, Takao; Tanimoto, Junichi; Hamada, Katsuhiro; Matsumura, Hideaki; Imada, Yukuo; Nagata, Nobuo; Ohshiro, Koji; Nakamae, Tsunenori. Proc. Res. Inst. Nucl. Med. Biol., No. 7, 99-107(1966). (In Japanese).

Five cases of hematopoietic anomalies resulting from cancer chemo- or radiotherapy and treated with autologous or homologous bone marrow are reported. Homologous transplantation showed a remarkable effect on severe hematopoietic disturbance induced by alternating massive doses of mitomycin and telecobalt and on agranulocytosis induced by mercazol therapy for hyperthyroidism. (TCO)

40727 INTERRELATIONSHIPS OF MYELOID AND LYMPHOID CELLS: STUDIES WITH CHROMOSOME-MARKED CELLS TRANSFUSED INTO LETHALLY IRRADIATED MICE. Micklem, H. S.; Ford, C. E.; Evans, E. P.; Gray, Joyce (Medical Research Council, Harwell, Eng.). Proc. Roy. Soc. (London), Ser. B, 165: 78-102 (July 19, 1966).

Lethally irradiated CBA mice were injected with a mixture of two cell suspensions, syngeneic with each other and with the host, but distinguished by the presence of either one or two T6 marker chromosomes. One of the cell suspensions was derived from adult bone marrow (10^5 cells), the other from adult thymus or pooled lymph nodes or thoracic duct lymph (10^7 cells). The recipients were killed between one day and one year after irradiation, having been injected 1½ hr previously with Colcemid. Their bone marrow, spleen, thymus, and lymph nodes were studied cytologically, and counts were made of the numbers of mitotic cells derived from the two donor cell suspensions and from the irradiated host. Bone marrow, spleen and thymus were all recolonized predominantly or exclusively by descendants of injected bone marrow cells. Descendants of injected lymphoid cells were seen in substantial numbers only in the lymph nodes, where they formed the majority of the total dividing cells between 1 and 3 weeks after irradiation. After that the proportion of such cells in the lymph nodes decreased gradually, in favor of bone marrow-derived cells, but they did not disappear completely. Lymphoid cells were equally unsuccessful at recolonizing the myeloid and thymic tissues of mice given a high sublethal dose of irradiation (800 rad) without bone marrow therapy. The normality of the repopulated lymph nodes and thymus was verified histologically and by two functional tests involving the capacity of cells rapidly to recolonize the lymph nodes or form macroscopic hematopoietic nodules in the spleen of further lethally irradiated mice. A small and decreasing amount of hematopoiesis was found in the lymph nodes during the first 2 months after irradiation, but not in the thymus. (auth)

40728 INFLUENCE OF X-IRRADIATION ON EXPERIMENTAL ALLERGIC ENCEPHALOMYELITIS IN RATS. Vitale, Branko; Allegretti, Niksa; Matosic, Miloje (Institut Rudjer Boskovic, Zagreb. Univ. of Zagreb). Radiat. Res., 28: 727-34(Aug. 1966).

Irradiation with x rays reduced the incidence of experimental allergic encephalomyelitis (EAE) in rats sensitized in a relatively short time interval after irradiation and, concomitantly, postponed the onset of disease. By increasing the time interval between irradiation and sensitization (10 to 14 days), the normal incidence of disease was reached. At the same time, none of the sick animals was overcome by disease. Rats irradiated following sensitization developed EAE after a slight delay but with increased lethality. Lethal outcome was greater when the time interval between these two events was shorter. Sensitized nonirradiated and paralyzed rats succumbed to EAE only if paralysis occurred within the first 13 days. In rats sensitized prior to irradiation the lethal outcome of disease was observed even in animals developing EAE symptoms within a 20-day period following sensitization. (auth)

40729 PROTECTIVE ACTION OF CYSTEINE ON GONAD DEVELOPMENT OF IN UTERO IRRADIATED RATS. Heidemann, B. Hamburg, Univ., Hamburg, 1964. 35p. $2.00 Gmelin, AED-Diss. 64-1081.

Thesis.

Sixty-eight gravid rats were x-irradiated with 300 R on the 16th day after mating. Thirty-nine rats were given 1 ccm of a 5% cysteine solution by intravenous injection 5 min before irradiation. Survival times, weight curves, and gonad weights of the offspring of the animals given cysteine are significantly higher than for untreated animals. (auth)

40730 DATA FROM RADIATION PROTECTION PROGRAMS. VOLUME 3, NUMBER 5. Ottawa, Department of National Health and Welfare, Radiation Protection Division, 1965. 34p.

Separate abstracts were prepared for each of the three chapters in the publication. (H.G.D.)

For abstracts of individual sections see: 41136, 41208, and 41209.

40731 PROBLEMY POSTRADIATSIONNOGO VOSSTANOVLENIYA. (Problems of Post-Radiative Cell Restoration). Korogodin, V. I. Moscow, Atomizdat, 1966. 391p.

A brief survey is given of the methods for determining radiobiological characteristics of cells and the possibilities of their post-radiative modification and restoration. An analysis is made of various facts indicating the existence of restorative effects. The concept of potential cell injuries, realization and indications of cell injuries, metabolic aspects of the restoration, statistical modes and wide range of general biological aspects of post-radiative restoration of multicellular organisms are discussed. 737 references are included. (R.V.J.)

Radiation Hazards and Protection

See also HEALTH AND SAFETY

Refer also to abstracts 41215, 41216, and 41561.

40732 (AD-636209) RADIATION-PROTECTION AND RECOVERY FROM RADIATION INJURY IN ENDOTOXIN-TREATED MICE: HEMATOPOIETIC RECOVERY AND SENSITIVITY TO A SECOND RADIATION EXPOSURE. Ainsworth, E. J.; Kendall, K.; Mitchell, F. A.; Phillips, T. L. (Naval Radiological Defense Lab., San Francisco, Calif.). May 23, 1966. 43p. (USNRDL-TR-1023). CFSTI $2.00 cy, $0.50 mn.

The present data confirm and extend earlier protection

studies in mice and show that the protective effect of endotoxin was additive with the protection afforded by hypoxia. The mechanism of endotoxin-protection is thought to involve stimulation of hematopoietic recovery, and the primary objective of the present study was to examine the process of hematopoietic recovery in endotoxin-protected mice. Hematologic studies showed that endotoxin-treated mice had more circulating granulocytes than did controls during the second and third weeks after exposure to 428 R. Although the endotoxin-treated animals showed evidence of accelerated hematopoietic recovery, as estimated by numbers of circulating and mobilizable granulocytes, no overall increase was observed in the rate at which they returned toward a normal radiosensitivity. The possibility is discussed that in endotoxin-treated mice, the extent of granulocytic recovery is not necessarily indicative of a sustained increase in the rate of hematopoietic stem cell repopulation. The split dose recovery data are discussed in terms of the general question of rate(s) of recovery from radiation injury in the mouse. (TCO)

40733 (ISS–66/16) LA PROTEZIONE DALLE RADIAZIONI NEGLI IMPIANTI A RAGGI X PER USO MEDICO. (Protection Against X Rays From Apparatus for Medical Use). Missoni, G. (Istituto Superiore di Sanita, Rome (Italy). Laboratori di Fisica). Apr. 20, 1966. 37p. Dep. mn.

The hazards of the use of x rays in diagnosis and therapy are reviewed. The organization of protection from a technical and a legal point of view is illustrated and useful recommendations for carrying out the controls are given. (auth)

40734 (NYO–901–54, pp 24–5) BIOPHYSICS AND RADIATION PROTECTION. (New England Deaconess Hospital, Boston, Mass. Cancer Research Inst.).

Progress is reported in the development of equipment for use with radioisotopes used for diagnostic or therapeutic purposes. A number of spectrometers were evaluated for performance; silver activated metaphosphate glass rods were tested as dosimeters in mice with small pellets of ^{60}Co implanted; and an apparatus to detect minute amounts of ^{14}C in the atmosphere was tested. (C.H.)

40735 (NYO–2744–37) ACCUMULATION OF Ca, Sr, Mg, P AND Zn BY GENOTYPES OF CORN (ZEA MAYS L.) UNDER DIFFERENT SOIL FERTILITY LEVELS. Baker, Dale E.; Bradford, R. R.; Thomas, W. I. (Pennsylvania State Univ., University Park. Dept. of Agronomy). [1964]. Contract AT(30-1)-2744. 16p. (CONF-660912-1). Dep. mn. CFSTI $1.00 cy, $0.50 mn.

From FAO/IAEA Symposium on the Use of Isotopes in Plant Nutrition and Physiology Studies, Vienna, Austria.

Single-cross hybrids of Zea mays were selected for investigation on the basis of the chemical element accumulation characteristics of the parental inbred lines in other single-cross hybrids. Among the single-cross hybrids selected, high and low accumulations of Ca, Sr, Mg, K, and P were predicted for ear leaf samples removed about 30 days post-silk. Accumulations of Ca, Sr, Mg and other elements by four corn hybrids were studied under greenhouse conditions at four rates of calcitic and dolomitic limestone each in the presence and absence of K. The same hybrids were grown in the field on the same soil type under similar soil fertility conditions. Four single-cross hybrids, predicted to accumulate different amounts of P, were grown on 44 different soils under greenhouse conditions. The same four hybrids, another single-cross and one double-cross hybrid were grown in the field on virgin Huntington silt loam at four rates of P. Chemical element accumulation characteristics of the corn hybrids grown in the greenhouse were determined by chemical analyses of whole plants when they were four to six weeks of age. In addition to whole plants, ear leaves from plants grown in the field were removed for analysis about 30 days post-silk. With respect to concentrations of the different chemical elements in ear leaves of plants grown in the field, the corn hybrids generally ranked in the order predicted from the performance of the parental inbred lines. Accumulations of Ca and Sr were highly associated in hybrids grown on soil treated uniformly. The significant differences in Ca : Sr ratios among field grown hybrids indicated different capacities to selectively absorb Ca in preference to Sr or vice versa. The same hybrids were not different when grown in the greenhouse where the plant roots were restricted to a homogeneous substrate. These data suggest that significant differences in Ca : Sr ratios among corn hybrids in the field resulted from inherent differences in depth of rooting among the hybrids. The corn hybrids differed greatly with respect to accumulation of P in ear leaves. The concentrations of P in young plants were not related to the concentrations of P in the ear leaves of the hybrids. The concentration of P in ear leaves of some hybrids was not a satisfactory measure of the availability of P in the soil, but the concentration of P in young plants provided an accurate measure of the availability of P in the soil. Additional evidence was obtained which indicated that concentrations of Ca, Sr, Mg, P, Zn and other elements, as well as ionic ratios, including P : Zn. Mg : Sr and Ca : Mg, were under partial genetic control. Possible applications in the development of agronomic practices which would reduce the amounts of ^{137}Cs, ^{90}Sr, and other radioactive elements from fallout entering the food chain are discussed. (21 references.) (C.H.)

40736 RADIOPROTECTIVE AND ANTI-TUMOR EFFECT OF MIXED BACTERIAL TOXINS AND ANTHRAMYCIN. Cole, Donald R.; Dreyer, Brenda B.; Rousselot, Louis M.; Tendler, Moses D. (St. Vincent's Hospital and Medical Center, New York. New York Univ., New York). Amer. J. Roentgenol., Radium Therapy Nucl. Med., 97: 997-1002(Aug. 1966).

Our studies indicate that increased host resistance to irradiation is produced when mixed bacterial toxins (M.B.T.) or anthramycin is injected prior to exposure. The mechanism of protection with a therapeutic dose of M.B.T. or anthramycin is thought to be through stimulation of the hematopoietic and reticuloendothelial systems—usually sites of severe irradiation injury. Lysosome studies have been conducted on microscopic sections of liver and spleen of mice treated with M.B.T. and anthramycin 24 hours prior to lethal irradiation of 700 R and, in contrast, of control mice treated with saline and like irradiation. Immediately following irradiation and on day 7, 14, and 21 post total body exposure, the organs were removed and the animals sacrificed. The tissues were fixed and stained according to the method of Barka and Anderson. Microscopic examination was made of the prepared slides to determine evidence of stimulation of the hematopoietic or reticuloendothelial systems through this medium. To date, insufficient evidence is available to clearly define the mode of action of these drugs. Additional clinical and experimental studies are needed to establish the active principle(s) the anthramycin and M.B.T. furnish for protection of a host against lethal irradiation and to evaluate the specific mode of action producing this effect. (auth)

40737 A NEW RADIOPROTECTOR IN ESCHERICHIA COLI. Pittillo, Robert F.; Lucas, Mary B.; Blackwell, Robert T.; Davis, Carl W. (Southern Research Inst., Birmingham, Ala.). Contract PH43-62-485. Radiat. Res., 28: 811-21(Aug. 1966).

3,3'-[(p-Sulfamoylphenyl)arsylenedithio]dialanine (SPATA) has been found to protect several strains of Escherichia coli against the lethal action of ionizing irradiation. SPATA must be present during the irradiation to exert a protecting effect. Several other bacteria tested were not protected by SPATA against radiation damage. In E. coli, SPATA was found to diminish the radiation-sensitizing effects of aminopterin, 2-fluoradenosine, and sparsomycin. (auth)

40738 DISCUSSION OF PROJECT HARBOR SUMMARY REPORT AND OF CNI CRITICISM OF HARBOR. Sci. Citizen, 7: No. 9, 1-28(Aug. 1965).

Biological and sociological effects of nuclear weapons are discussed in view of defense against such effects. It is concluded that: any civil defense program can be rendered useless by an enemy step-up in offensive power; sociologi-

cal and economic recovery pose more difficulties than indicated in the Project Harbor Summary; biological damage from a nuclear war may be much more severe than estimated by the Harbor Study; and civil defense cannot provide enough defense in large-scale nuclear war to make such a war a rational measure of national policy. (H.G.D.)

40739 GUIDELINES FOR RADIATION PROTECTION IN HOSPITALS AND CLINICS. Verslag. Mededel. Betreffende Volksgezondheid, No. 9, 1405-1559(Sept. 1965). (In Dutch).

The guidelines formulated by the Commission of Health for the utilization of radiation in hospitals and clinics are given. (J.S.R.)

Radiotherapy and Radiodiagnosis

Refer also to abstracts 40566, 40644, 40679, 40691, 41299, 41312, 41321, 41323, 41555, and 41564.

40740 (ACRH-25) SEMIANNUAL REPORT TO THE ATOMIC ENERGY COMMISSION. Jacobson, Leon O.; Doyle, Margot (eds.) (Argonne Cancer Research Hospital, Chicago, Ill.). Mar. 1966. Contract AT(11-1)-69. 143p. Dep. mn. CFSTI $4.00 cy, $1.00 mn.

Separate abstracts were prepared on two sections of this report. Abstracts on two conference papers included were prepared previously and appeared in NSA Vol. 20 as numbers 26732 and 28929. (C.H.)

For abstracts of individual papers see: 40741 and 40742.

40741 (ACRH-25, pp 15-23) DETERMINATION OF ABSORBED DOSE FOR ELECTRON BEAM THERAPY. Lanzl, L. H.; Skaggs, L. S.; Rozenfeld, M. L. (Argonne Cancer Research Hospital, Chicago, Ill.). (CONF-650969-1).

From International Meeting on Physical and Clinical Dosimetry of Fast Electrons, Rome.

The apparatus and procedures used for measurements of the absorbed dose during therapy using a highly monoenergetic electron beam are described. The electron source is a traveling-wave linear accelerator whose energy can be controlled to give a sharp spectrum with a peak of from 5 to 50 Mev. The deflecting and scanning unit includes a triple magnet system, counterweight, rotating shield, and treatment cot. The electron beam striking the patient is contained within a vacuum chamber with a transmission ionization chamber at the beam exit. The ionization chamber is used to determine the beam current that strikes the absorbing medium, and current calibration is carried out with a Faraday cup composed of graphite and backed by lead to minimize bremsstrahlung production. Compton electrons escaping from the cup assembly are measured using an insulated graphite block behind the lead. Detailed checks must be made to provide an absolute measurement of the electron current of the high-energy beam and a few of these are discussed. (C.H.)

40742 (ACRH-25, pp 24-9) THIN FOIL CALORIMETER FOR ELECTRON BEAM DOSIMETRY. Skaggs, L. S. (Argonne Cancer Research Hospital, Chicago, Ill.). (CONF-650965-2).

From 1st International Conference on Medical Physics, Harrogate, Eng.

A calorimetric method of measuring electron beam dose rate during therapy is described. The beam passes through a very thin metallic foil, normally within the vacuum system of the accelerator, releasing a small amount of energy as heat in the foil due to electron collision losses. Heat is conducted from the foil through its supporting heat leaks to the reference system so that the foil quickly comes to an equilibrium temperature that is proportional to the electron beam current. A thermocouple is used to measure the temperature difference between the foil and the reference system and the dose rate is calculated from the data. (C.H.)

40743 (BNL-9374) TRITIATED THYMIDINE AS A CYTOCIDAL AGENT IN HUMAN LEUKEMIA. Greenberg, Michael L.; Chanana, Arjun D.; Cronkite, Eugene P.; Schiffer, Lewis M.; Stryckmans, Pierre A. (Brookhaven National Lab., Upton, N. Y. Mount Sinai Hospital, New York, Dept. of Hematology). July 15, 1965. Contract AT(30-2)-Gen-16. 18p. Dep. mn. CFSTI $1.00 cy, $0.50 mn.

Two patients had partial remissions of acute leukemias after ten intravenous injections of H^3Tdr (Sp.Ac. 1.9 or 13.0 c/mM), each 0.25 μc/gm body weight, given over five days. Some aspects of the cytotoxic effects of H^3Tdr are reviewed. The radiation dose to the nucleus of bone marrow cells was estimated in autoradiograms. Evidence for the observed remissions being due to H^3Tdr is presented (21 references.) (C.H.)

40744 (BNL-10403) EXTRACORPOREAL IRRADIATION OF THE BLOOD AND LYMPH: EXPERIMENTAL STUDIES ON HOMOTRANSPLANTATION AND HUMAN LEUKEMIA. Cronkite, E. P. (Brookhaven National Lab., Upton, N. Y.). [1966]. Contract AT(30-2)-Gen-16. 4p. (CONF-660548-1). ORAU.

From Freiburg Medical Society Meeting, Freiburg, Germany.

Extracorporeal irradiation of blood is a technique by which a fraction of the cardiac output is diverted through an irradiation field and results in the destruction of radiosensitive lymphocytes. Within a few hours of treatment, the blood lymphocyte level falls from roughly 6000/mm^3 to as low as 100/mm^3 and 48 hrs of continuous irradiation of the blood results in a marked depletion of lymphocytes in the cuff surrounding the germinal centers of the spleen, a diminution in the thickness of the cortical densely packed small lymphocytes of lymph nodes, and a diminution in the thickness of the cortex of the thymus. The thoracic duct can be canulated to divert the lymph either through a continuous flow centrifuge or an irradiator to deplete the animal of lymphocytes. Depletion of lymphocytes causes prolonged skin homograft acceptance time. The procedure of extracorporeal irradiation of blood was used to treat acute myelocytic, chronic granulocytic, and chronic lymphocytic leukemia in man. Each case of acute leukemia showed a drop in the peripheral blood count and some patients survived for over a year with no other treatment. Some individuals became susceptible to chemotherapy once again after treatment with extracorporeal irradiation of the blood. One patient was carried through pregnancy by this treatment. The partial remission obtained in cases of chronic granulocytic leukemia was short-lived. (C.H.)

40745 (NYO-901-54, pp 29-47) EXPERIMENTAL PATHOLOGY. (New England Deaconess Hospital, Boston, Mass. Cancer Research Inst.).

Preliminary results are summarized from a study of the incidence of leukemia and other hematopoietic disorders in patients with cancer of the cervix uteri treated with radiation. The incidence of leukemia was comparable to that of a control population. Chromosome studies in persons exposed to radiation and aged individuals were continued. Results are summarized for 51 inhabitants of the Marshallese Islands, 43 of whom were exposed to approximately 175 R fallout radiation in 1954. The data indicate a small but significant amount of residual chromosome damage in the exposed population 10 years after exposure. Preliminary data are presented from histopathological studies of bone pathology and bone tumors in mice injected with ^{239}Pu, some of which were treated with diethylenetriaminepentaacetic acid (DTPA). Bone tumor incidence was significantly reduced by DTPA treatment when Pu was administered in the polymeric form but not when it was administered in the monomeric form. Generalized disorganization of bone architecture was noted in some animals without malignant bone tumors. Studies of tumor-host relationships, and the effects of radiation, surgery, and other types of therapy on the control of the growth of tumor cells at metastatic sites, were continued with emphasis on material from patients with cancer of the cervix, breast cancer, and cancer of the bladder, tumor-bearing hamsters, and rats bearing transplanted tumors. Preliminary results indicate that blood vessel invasion, lymph node involvement, the frequency of mitoses in endocervical glandular cells, and the uptake of ^3H-thymidine by cervical tissues are of prognostic value in

patients with carcinoma of the uterine cervix; blood vessel invasion is of prognostic significance in breast cancer cases in which regional lymph nodes are negative; and the frequency of mitoses and data on tryptophan metabolism in tumor sections were of prognostic significance in cancer of the urinary bladder. (C.H.)

40746 (NYO–3510-2) BIOLOGICAL AND CLINICAL DOSIMETRY. Annual Progress Report, July 1, 1965–June 30, 1966. Laughlin, John S. (Sloan-Kettering Inst. for Cancer Research, New York). July 7, 1966. Contract AT(30-1)-3510. 32p. Dep. mn. CFSTI $2.00 cy, $0.50 mn.

The microcalorimeter was employed to verify and define the extent of the energy dependence of lithium fluoride dosimeters for high energy radiation. Further comparison of calorimetric and ionometric determinations of absorbed dose were undertaken using an extrapolation chamber, and some inherent problems in this comparison were investigated. Extensive measurements of the radiation field around various isotope sources used in implant therapy were performed, and the differences between theoretical and actual dose distributions in an implant were investigated by use of a computer. This work conducted in conjunction with the Medical Physics Department of Memorial Hospital was reported at the annual meeting of the RSNA and is being prepared for publication. A total intensity calorimeter providing absolute dose measurements for the field emission electron generator was constructed and preliminary data obtained. In the area of research intended to clarify problems of standarization of dose measurement for high energy radiation, an intercomparison of the Sloan-Kettering Institute and Argonne National Laboratory calorimeters has been initiated. Measurements in the short circuit mode of p-i-n junctions indicate that only diodes with shallow lithium drifts or undrifted p-n junctions are suitable for calibrations as x-ray dosimeters due to the appearance of a large negative temperature coefficient (~1%/°C) in units drifted beyond ~.3 mm. RMS noise measurements and spectral (FWHM) measurements using Bi-207 and Cs-137 were made on diodes fabricated at Sloan-Kettering yielding noise levels of 40 to 90 kev. A device based upon the combination of a plastic scintillator and a pair of silicon diodes is being developed, which is expected to measure absorbed dose from high energy electrons with a sensitivity two orders of magnitude greater than an ionization chamber of equal volume. (auth)

40747 (UCRL–14866) GAMMA MAPPING OF THE LIVER WITH THE DIGITAL COMPUTER. Werner, Richard W.; Govan, Ian O. (Lawrence Radiation Lab., Univ. of California, Livermore). June 1, 1966. Contract W-7405-eng-48. 34p. Dep. mn. CFSTI $2.00 cy, $0.50 mn.

High-speed digital computers can be used for analytical support of existing scintillation cameras for detecting and analyzing space-occupying abnormalities such as tumors in the human liver, kidney, brain, and other organs of the body in vivo. Detection of the abnormalities is based on the selective absorption or non-absorption of a gamma-emitting isotope compound which has been deliberately introduced into the body. This report contains test data obtained on the human liver and liver models and the detection of flaws or anomalies in these organs. The techniques illustrated are extendable to other organs. The three-element analytical system consists of a pulse-height analyzer for data-gathering and interim storage, and magnetic tape unit for dynamic storage and data resurrection, and the CDC 3600 computer for detailed analysis of system output. The system is based on a 64 × 64 data location matrix and produces output in the following forms: (1) numerical form showing gamma count level as a function of location; (2) traverses or vertical slices through the data field; (3) contours or horizontal slices through the data field at selected isoactivity levels; and (4) summation of contours (i.e., a gamma topographic map). An adjunct to the basic program provides for computer-corrected errors generated in the image detector. (auth)

40748 RADIOISOTOPE SCANNING WITH A SYSTEM FOR TOTAL INFORMATION STORAGE AND CONTROLLED RETRIEVAL. Rejali, Abbas M. (Western Reserve Univ., Cleveland); Friedell, Hymer L.; Gregg, Earle C. Contract W-31-109-eng-78. Amer. J. Roentgenol., Radium Therapy Nucl. Med., 97: 837-49(Aug. 1966).

This presentation emphasizes the improved clinical results obtained from our present radioisotope scanner and data presentation system. The essence of the system is that all available information received by the detector is stored without prior modification in a permanent memory. A special vidicon television replay system under carefully controlled circumstances permits immediate and innumerable degrees of erase and contrast enhancement to be applied to the stored data in a few seconds. A profile representing the count rate through any slice in the scanned area may be performed to determine relative distribution. At present, the method appears to be particularly valuable in identifying small differences and presenting them in a clearly demonstrable fashion. (auth)

40749 VISUALIZATION OF THE LUNG BY METHODS OF SCINTIPHOTOGRAPHY. Loken, Merle K.; Bugby, Robert D. (Univ. of Minnesota, Minneapolis). Amer. J. Roentgenol., Radium Therapy Nucl. Med., 97: 850-9(Aug. 1966).

Scintiphotograms of the lung using macroaggregates of albumin tagged with iodine 131 and technetium 99m were obtained on 115 patients. Seventy-eight of these have had sufficient follow-up to be included here. The dose administered intravenously was 300 μC in patients receiving the iodine 131 macroaggregates of albumin and up to 5 mc in patients receiving technetium 99m macroaggregates of albumin. The macroaggregates ranged in size from 10 to 100 μ. These studies have indicated the sites and magnitude of pulmonary arterial obstruction whether they were recognizable roentgenographically or not. Areas of decreased activity on the scintiphotograms relate to areas of ischemia, which are frequently due to pulmonary embolization but also can be secondary to pneumonia, atelectasis, emphysematous blebs, abscesses and cysts. We have used either a rectilinear scanner or scintillation camera for these studies. The two major disadvantages of rectilinear scanning relate to the time required to perform the scan and, secondly, to the prone positioning of the patient, which is desirable for best results but is different to obtain, particularly if the patient is severely ill. The scintillation camera obviates these problems but has the disadvantage of a restricted field size, making it necessary to obtain several studies in large patients. Scintiphotography of the lungs using macroaggregates of albumin is considered to be an excellent screening test prior to subjecting a patient to pulmonary angiography. Serial scintiphotograms can be very helpful in following closely disease processes within the pulmonary parenchyma. We are presently exploring the use of xenon 133 for studies of pulmonary function and perfusion. Preliminary results indicate that xenon 133 offers significant advantages over the use of macroaggregates, providing a device such as the scintillation camera is available for obtaining the scintiphotograms. (auth)

40750 RADIOISOTOPE SCINTIPHOTOGRAPHY WITH ^{99m}Tc AND THE GAMMA SCINTILLATION CAMERA. Gottschalk, Alexander (Univ. of Chicago. Argonne Cancer Research Hospital, Cnicago). Amer. J. Roentgenol., Radium Therapy Nucl. Med., 97: 860-8(Aug. 1966).

The physical properties of ^{99m}Tc allow millicurie quantities to be administered to a patient without radiation hazard. Its clean 140 kev γ ray makes it an ideal agent for use with the scintillation camera. Count rates as high as 700,000 per minute are achieved and consequently, multiple views can easily be obtained, thus enhancing diagnostic accuracy. It is now possible to use exposures so short that they can be made while the patient holds his breath. This eliminates the resolution loss caused by respiration in scanning moving organs such as liver and spleen. Several chemical forms of technetium are now available for radioisotope imaging.

These include pertechnetate for thyroid and brain; sulfur for liver, spleen and marrow; iron complex for kidney; albumin for blood pool; and aggregated albumin for lung. Examples of the clinical use of these agents with the gamma scintillation camera are described. (auth)

40751 THYROID SCANNING USING THE GAMMA CAMERA. Wang, Yen (Presbyterian-University Hospital, Pittsburgh. St. Francis General Hospital, Pittsburgh). Amer. J. Roentgenol., Radium Therapy Nucl. Med., 97: 869-73(Aug. 1966).

Scanning time for a thyroid gland using a 3 by 2 inch crystal scanner usually takes about 12 to 16 minutes, provided there is an adequate count in the thyroid. Ordinarily, the oral tracer dose for thyroid scanning is in the range of 50 to 100 μC of ^{131}I. With the same amount of radioactivity and by using the scintillation camera, the scanning time is about 4 to 6 minutes. The real difference between these two systems of thyroid scanning is the time required and the location of an anatomic landmark. Although with the scintillation camera, the scanning time is less than half of that using a mechanical scanner, the mechanical scan gives a life sized picture with a clear anatomic landmark. As far as the actual resolution is concerned, there is probably very little difference between these two systems. We have been able to demonstrate a nodule as small as 1.5 to 2.0 cm in diameter by either scanning system. (auth)

40752 RADIONUCLIDE VENOGRAPHY USING ^{99m}Tc PERTECHNETATE AND THE GAMMA-RAY SCINTILLATION CAMERA. Rosenthall, Leonard (Montreal General Hospital). Amer. J. Roetgenol., Radium Therapy Nucl. Med., 97: 874-9(Aug. 1966).

The ^{99m}Tc venogram obtained with the γ-ray scintillation camera is adequate to provide information on patency and gross displacement on the major vessels. It serves as a valuable, simple and quick screening procedure. The resolution of the radionuclide venogram does not compare favorably with the contrast venogram, but it can select patients for the more detailed roentgenographic procedure when necessary. Illustrations of ^{99m}Tc venograms of the trunk and lower extremities are presented. (auth)

40753 SIMPLIFIED PREPARATION OF ^{99m}Tc SULFIDE COLLOID FOR LIVER SCANNING. Patton, Dennis D.; Garcia, Eugene N.; Webber, Milo M. (Univ. of California, Los Angeles) Amer. J. Roentgenol., Radium Therapy Nucl. Med., 97: 880-5(Aug. 1966).

Technetium 99m sulfide colloid can be prepared rapidly and conveniently by precipitation from pertechnetate eluted from a ^{99m}Tc generator, using rhenium as a carrier, through the action of sodium thiosulfate. The use of presterilized reagents yields a sterile product, which is ready for use without further processing. Gelatin is added as a protective colloid. No toxic materials or odoriferous gases are used. The product contains virtually no soluble technetium and no macroaggregates. Preparation time is less than 10 minutes, and can be done in a small area of any radioisotope clinic. Liver scans of high resolution and excellent counting statistics can be obtained with minimal patient radiation dose. (auth)

40754 TANDEM ELUTION OF ^{99m}Tc GENERATORS. Bogardus, Carl R. Jr. (Univ. of Oklahoma, Oklahoma City); Levitt, Seymour H.; Ficken, Vernon J. Amer. J. Roentgenol., Radium Therapy Nucl. Med., 97: 886-7(Aug. 1966).

A simple method was devised whereby the elution efficiency could be increased by utilizing a fresh technetium generator coupled in tandem to the previous week's generator. A special barn was constructed so that the generators may be housed with a minimum amount of handling and be milked in tandem with ease. (auth)

40755 PRACTICAL MODIFICATION OF THE RECTILINEAR SCANNER. Atkins, H. L. (Brookhaven National Lab., Upton, N. Y.). Amer. J. Roentgenol., Radium Therapy Nucl. Med., 97: 888-95(Aug. 1966). (BNL–9956).

It is possible, with minimum expense, to adapt a standard rectilinear scanner for the data-blending technique developed by others. A method of using this technique is described. Scans produced with this method appear to be of superior quality and are more confidently interpreted. Full advantage may be taken of the high statistical reliability and improved resolution possible with ^{99m}Tc, but the method is also valuable with other isotopes. (auth)

40756 ADVANTAGE OF THREE COMBINED DIAGNOSTIC PROCEDURES WITH ^{131}I FOR THE EVALUATION OF THYROID DISORDERS. Maglione, Anthony A.; Collica, Carl J.; Rubenfeld, Sidney (Bellevue Hospital Center, New York). Amer. J. Roentgenol., Radium Therapy Nucl. Med., 97: 896-900(Aug. 1966).

The results of 24 hour ^{131}I uptake, 24 hour PB^{131}I conversion ratio, and salivary ^{131}I/plasma PB^{131}I ratio in 1,086 patients are analyzed. A very high percentage of correlation (above 90 percent) between the real clinical status and these tests can be obtained if comprehensive interpretation of their values is carried out. The salivary ^{131}I/plasma PB^{131}I ratio is established as a useful indirect index of thyroid activity. (auth)

40757 RADIOISOTOPIC SCANNING AS AN AID IN PLANNING RADIATION THERAPY. Tefft, M. (Children's Hospital Medical Center, Boston). Amer. J. Roentgenol., Radium Therapy Nucl. Med., 97: 920-2(Aug. 1966).

In the past, we had attempted to use intravenous pyelography for demonstrating the position of the kidney in this situation. This was not too satisfactory, both because it was difficult to differentiate liver from renal shadows and because of the effect of magnification on the 40 inch intravenous pyelogram compared to portal roentgenograms. It appears that the relatively simple use of radioisotopes to outline these organs in relation to the volume under radiation therapy, without the complication of magnification and with the sharp demarcation possible, would make this a worthwhile procedure. (auth)

40758 RADIATION THERAPY IN THE CONTROL OF PERSISTENT THYROID CANCER. Sheline, Glenn E.; Galante, Maurice; Lindsay, Stuart (Univ. of California, San Francisco). Amer. J. Roentgenol., Radium Therapy Nucl. Med., 97: 923-30(Aug. 1966).

Between 1935 and 1964, 58 patients received external radiation therapy for local control of thyroid cancer. In each instance the residual cancer tissue was not resected because thyroid cartilage, trachea, or hypopharynx was invaded. In 33 patients the extrathyroidal extension was grossly evident. In the other 25, there was presumed microscopic involvement of 1 or more of these structures. Patients in whom the extrathyroidal disease was limited to resectable structures are not included in the study. Of the 9 patients given radiation therapy at least 5 years ago for grossly evident papillary carcinoma, 5 have survived 5, 6, 10, 14, and 25 years without recurrence, 1 is living with recurrence at 5 years, and the other 3 have died of recurrence at periods between 5 and 18 years after treatment. All 12 patients with probable microscopic persistent papillary cancer have been observed at least 5 years and 6 have been observed for more than 10 years; none has shown evidence of local recurrence to date. In patients with follicular carcinoma, the long periods of control of several tumors suggest that some do respond to local radiation therapy even though control is less reliable than in the papillary carcinomas. Of the 8 patients with follicular carcinoma treated at least 5 years ago, 6 are without local recurrence. Three of 7 observed 10 years or more are without recurrence at 10, 16, and 18 years after treatment. For patients with locally persistent follicular carcinoma and no evidence of distant spread, local radiation therapy should be attempted before resorting to systemic therapy with radioiodine. Three of the 7 patients with anaplastic carcinoma obtained some benefit from radiation treatment. One was without local recurrence for 6 years, then died of distant metastases. A second patient has been free of disease for 2 years and in a third recurrence developed only after 3 years. All 5 patients with giant cell carcinoma were dead within 2 months. Of 6 patients with lymphosar-

coma initially limited to the thyroid, 3 were observed without evidence of the lymphoma locally or elsewhere for periods of 3, 17, and 20 years. (auth)

40759 RADIATION THERAPY OF CARCINOMA OF THE VOCAL CORD WITHOUT MUCOSAL REACTION. Vaeth, Jerome M.; Buschke, Franz (San Francisco Medical Center). Amer. J. Roentgenol., Radium Therapy Nucl. Med., 97: 931-2(Aug. 1966).

Twenty-one patients with carcinoma of the vocal cord were treated at the University of California Hospital, San Francisco, with 1 Mev irradiation and a protraction of the over-all treatment time of 7 weeks for 5,500 R midline dose or 8 weeks for 6,000 R, an average of 53 days for 6,000 R instead of the previous average protraction of 40 days for 6,000 R (30 percent). With this greater protraction, morbidity was markedly reduced; formation of a false membrane and the previously common late edema were not observed. Seven of 9 carcinomas, Stage I, and 7 of 12, Stage II, were controlled. Cordectomy in 2 patients with Stage I uncontrolled or recurrent disease was done in lieu of total laryngectomy, without any surgical complications or recurrent disease to date. In 4 instances of uncontrolled disease in Stage II, laryngectomies were done without ensuing complications. (auth)

40760 EXPERIMENTAL DETERMINATION OF THE PULMONARY TISSUE FACTOR IN ^{60}Co TELETHERAPY. Voutilainen, Antero; Vaehaetalo, Soini (Univ. Central Hospital, Helsinki). Amer. J. Roentgenol., Radium Therapy Nucl. Med., 97: 939-43(Aug. 1966).

To determine the pulmonary tissue factor in cobalt-60 teletherapy, the dose of radiation was measured in vivo within the field of radiation by introducing Sievert chambers into the patient's esophagus. At the same time, the dose received as determined from a water phantom at the same depth was also measured. By comparing these results, the tissue factor was calculated. The result obtained agreed with those employing other types of measurements. It was also found that the doses delivered craniad over the thorax are larger than those delivered caudad, due to the fact that the thoracic thickness decreases craniad. The pulmonary tissue factor also depends on the consistency of the tumor in the lung. (auth)

40761 PREGNANCY FOLLOWING OVARIAN IRRADIATION. Vuksanovic, Mario M. (Univ. of Miami, Fla.). Amer. J. Roentgenol., Radium Therapy Nucl. Med., 97: 951-6(Aug. 1966).

Two patients in late stages of pregnancy, who were affected by invasive carcinoma of the cervix and were treated in the immediate postpartum period by intracavitary cobalt 60 sources to a dose which resulted in permanent control of the tumors and who subsequently became pregnant are reported. One of the patients delivered an infant who has remained apparently normal up to the age of 4½ years when he was last seen. A brief review of 11 similar cases from the literature is presented. It is concluded that the position of the ovaries immediately postpartum often results in a relatively low dose of radiation to the ovaries, and the ovarian function is resumed after variable intervals of dysfunction. All but 1 of these cases were treated by some form of intracavitary application. A follow-up study in 7 of 13 infants born to these mothers, ranging from 2 to 7 years showed no gross abnormalities in health and development. (auth)

40762 THE EFFECT OF COMBINED RADIATION AND ACTINOMYCIN D THERAPY ON INCOMPLETELY REMOVED MOUSE TUMORS. Tefft, Melvin; Brown, Barbara L.; Maddock, Charlotte L.; D'Angio, Giulio J. (Children's Hospital Medical Center, Boston. Harvard Medical School, Boston). Amer. J. Roentgenol., Radium Therapy Nucl. Med., 97: 991-6(Aug. 1966).

In an experimental situation, viz., excised ROS in the AKD_2F_1 mouse, simulating incomplete surgical removal of tumor, it was shown that roentgen therapy at 1,500 R and actinomycin D at 150 μg/kg, both applied once, very significantly improved the outcome, as compared to surgery alone. Results were measured by two parameters, i.e., survival time and tumor growth rate. When survival times were compared, surgery followed by combined therapy always produced results superior to those obtained by surgery followed by either modality; however, when tumor growth rates were assessed, only in the first experiment were better results obtained, when combined therapy was used after surgery. (auth)

40763 MODIFICATION OF RADIATION RESPONSE OF TISSUE BY COLCHICINE. A CLINICAL EVALUATION. Griem, Melvin L.; Malkinson, Frederick D. (Univ. of Chicago. Argonne Cancer Research Hospital, Chicago). Amer. J. Roentgenol., Radium Therapy Nucl. Med., 97: 1003-6(Aug. 1966).

A clinical evaluation of the combined use of colchicine and irradiation is presented. Adenocarcinoma of the gastrointestinal tract as well as mycosis fungoides showed favorable response. A number of other tumors was surveyed. (auth)

40764 RELATION OF DOSE-FRACTIONATION OF X RAYS AND ITS SPACING IN TIME TO SKIN DAMAGE. EXPERIMENTAL STUDIES. van den Brenk, H. A. S. (Cancer Inst. Board, Melbourne). Amer. J. Roentgenol., Radium Therapy Nucl. Med., 97: 1023-31(Aug. 1966).

Prolongation of fractionation times greatly modifies the intensity of the reactions, irrespective of the number and size of fractions delivered. This is due to a perturbation of cell population dynamics and the time factors involved in the onset of reactive hyperplasia. The results indicate that iso-effect dose formulae for fractionated treatments in radiotherapy, based on experimental animal and cell survival data, are of doubtful validity if dose-time factors which modify repopulation dynamics are ignored. This particularly applies to treatments in which a limited number of large fractions are used. For large dose increments in the range 1,200–1,800 rads, spacings in excess of 14 days between successive fractions do not improve tissue tolerance but tissue tolerance decreases progressively as the interval is reduced to approximately 6 days, below which a further decrease has little effect in modifying damage. Doses of 600 rads produced similar effects but prolongation of such treatments with spacings between fractions in excess of 3 days did not improve tissue tolerance further. In the various tissues of different species, the results of fractionation in respect to time differ according to cell turnover rates, the capacity of tissues to regenerate and undergo hyperplasia in reaction to damage. These factors invalidate an oversimplification of tissue tolerance and effects in terms of any single "iso-effect-dose" formula designed to provide the radiotherapist with a "ready-reckoner" for calculation of doses. (auth)

40765 COMPUTER DOSIMETRY SYSTEM FOR RADIUM IMPLANTS. Rose, Joseph A.; Bloedorn, Fernando G.; Robinson, J. Eugene (Univ. of Maryland Hospital, Baltimore). Amer. J. Roentgenol., Radium Therapy Nucl. Med., 97: 1032-40(Aug. 1966).

A system has been developed to calculate and plot the radiation fields produced by radium needle implants. An IBM 7094 computer system is used to perform the necessary calculations and a Calcomp Digital Incremental Plotter is used to place the data in graphic form. A program was written which uses the four Sievert Integrals to calculate and permanently store on magnetic tape the data describing the radiation fields around the various single needles in our stock. A second program utilizes these precalculated tables to compute and plot the radiation fields around radium implants. The system is versatile enough to allow for the computation and plotting of the radiation fields on any planes in any position in the vicinity of a radium implant. (auth)

40766 THERMOLUMINESCENT DOSIMETRY OF BETA DEPTH DOSE. Hendee, William R. (Univ. of Colorado Medical Center, Denver). Amer. J. Roentgenol., Radium Therapy Nucl. Med., 97: 1045-8(Aug. 1966).

Radiothermoluminescent measurements have been made of ^{90}Y β depth dose from a commercially available ^{90}Sr–^{90}Y beta applicator. Good agreement of the resulting beta depth

dose curve with those obtained by film and extrapolation chamber techniques of measurement suggests the usefulness of radiothermoluminescent dosimetry as a rapid and convenient approach to the measurement of relative absorbed dose. (auth)

40767 CHANGES IN THE RELATIVE BIOLOGICAL EFFECTIVENESS OF A 35 Mev ELECTRON BEAM AS A FUNCTION OF TISSUE DEPTH. Schwarz, George; Berg, Roger; Botstein, Charles (Montefiore Hospital and Medical Center, New York). Amer. J. Roentgenol., Radium Therapy Nucl. Med., 97: 1049-52(Aug. 1966).

Survival curves obtained by in vivo total body irradiation of young CF_1 mice indicate a change in the RBE (relative biological effectiveness) of 35 Mev electrons as they penetrate through tissue. The results suggest a long plateau region of low LET (linear energy transfer) followed by a terminal rise. They indicate a minimal three-fold increase in the terminal portion LET as compared to the plateau region if the log-linear relation between LET and RBE holds. The relatively large cross-section of the test object may have concealed an even higher RBE peak. Studies using a smaller test object are now in progress. (auth)

40768 RESULTS OF SUPERVOLTAGE THERAPY IN GYNECOLOGY. Schubert, G.; Uhlmann-Hamburg, G. (Univ.-Frauenklinik, Hamburg). Arch. Gynaekol., 202: 263-73(1964). (In German).

Results obtained in the treatment of vulva carcinoma with a 15-Mev betatron and of uterine carcinoma with ultrahard radiation and telecobalt beams are reported. It is concluded that supervolt therapy represents simple technique and gives an exceptionally good dose distribution in the small pelvic. In combination with radium therapy the optimum dose output can be obtained at the focus. It produces few urological and intestinal complications. (J.S.R.)

40769 EXPERIENCES OF THE RADIUM CLINIC IN STOCKHOLM WITH HIGH-VOLTAGE THERAPY OF UTERINE CARCINOMA. Kottmeier, H.-L. Arch. Gynaekol., 202: 305-9(1964). (In German).

The therapy used in various stages of uterine carcinoma with combined cobalt and intracavity radium treatment is reported with examples given of cobalt treatment plans. The dose distribution with conventional x ray treatment and with the cobalt therapy is illustrated. (J.S.R.)

40770 EFFECT OF X-RAY QUALITY AND OVARIAN LOCATION ON GENETIC EXPOSURE IN GYNAECOLOGICAL EXAMINATIONS. Nikl, I. (Frederic Joliot-Curie National Research Inst. for Radiobiology and Radiohygiene, Budapest). Brit. J. Radiol., 39: 607-11(Aug. 1966).

Dosimetric measurements are carried out on an inhomogeneous anatomical phantom of definite size to assess both incident skin and ovary doses resulting from certain routine pelvic radiographs and fluoroscopic examinations, as a function of X-ray quality and ovarian position. (auth)

40771 RADIATION CATARACT: NEW EVIDENCE ON RADIATION DOSAGE TO THE LENS. Britten, M. J. A.; Halnan, Keith E.; Meredith, W. J. (Christie Hospital and Holt Radium Inst., Manchester, Eng. Manchester Royal Eye Hospital, Eng.). Brit. J. Radiol., 39: 612-17(Aug. 1966).

The eyes of 104 patients treated for 106 tumors of the eyelids in 1952–53 and 1957–58, have been examined in 1964. Fourteen cases of radiation cataract (only six seriously affecting visual acuity) were found in 38 patients treated by radon gold seed implant. The five major cataracts began to affect vision at 3, 7, 10, 10 and 11 years after treatment. These cataracts are probably progressive between six and 11 years after treatment, since the incidence after radon seed implant was three out of 16 1957–58 cases and 11 out of 22 1952–53 cases, all five major cataracts being in the latter group. Many of these radiation cataracts have not had significant effect on visual acuity, even though they were clearly distinguishable when the lens was examined by slit-lamp ten or more years after radiotherapy. Radiation doses to the lens have been calculated. After a radon gold seed implant, 4,000 R to the centre of the lens appear to lead to cataract in all cases, less than 2,000 R to no cataracts. Only one case of radiation cataract was found in 57 patients treated by superficial X-ray therapy, and this was in the contralateral eye. The radiation dose to the whole of this lens was approximately 950 rads given as a single treatment and the lens dose on the treated side was about 16 rads. (auth)

40772 CERVICAL CANCER. STUDY OF A SERIES OF PATIENTS TREATED BY RADIATIONS. De Paepe, J.-C. Bull. Soc. Roy. Belge Gynecol. Obstet., 34: 37-50(1964). (In French).

A series of 220 cases of cervical carcinoma has been studied; follow-up observations have been made for five years on 112 of these. The patients were treated with radium (the method being a modification of the Manchester procedure) and x rays. For patients in the first two stages of the disease, the rate of cure was 68%. Various factors influencing the fate of patients are discussed. (tr-auth)

40773 INCIDENCE OF RADIATION FIBROSIS AFTER USE OF A STANDARDIZED TECHNIQUE OF RADIOTHERAPY FOR BREAST CANCER. Greenberg, Harry B.; Jacobs, Sydney (Tulane Univ., New Orleans). Cancer, 19: 1289-92(Sept. 1966).

To determine whether the use of a standardized technique of radiotherapy for breast cancer was followed by roentgenographic evidence of pulmonary fibrosis, a survey was made of the serial chest roentgenograms of 42 patients with breast cancer who had received such radiotherapy 2½ years previously. Also reviewed, to aid in identification of roentgenographic changes caused by other disease, were their clinical notes, hospital records and, in 5 instances, autopsy protocols. Evidence of slight pulmonary fibrosis appeared on the chest roentgenograms of 6 patients as one or more fibrotic strands, 2 or 3 cm long, in the lung underlying x-irradiated regions of the thoracic wall. The affected lungs were not retracted or distorted. Evidence of radiation fibrosis did not appear on the serial chest roentgenograms of the other 36 patients. Among these 42 disparate patients with breast cancer observed for at least 2½ years this standardized technique of radiotherapy did not cause roentgenographic evidence of significant pulmonary fibrosis. (auth)

40774 PREDICTION OF THE DOSE OF RADIOACTIVE PHOSPHORUS IN THE TREATMENT OF POLYCYTHEMIA VERA. Hume, R.; Cowell, Mary A. C.; Goldberg, A. (Western Infirmary, Glasgow). Clin. Radiol., 17: 295-8 (July 1966).

Red cell volume (RCV) measurements were carried out before and 3 to 4 months after a single therapeutic dose of ^{32}P in 18 patients with polycythemia vera. It was found that the absolute fall in RCV correlated with the dose of ^{32}P. ($P < 0.01$). Because the RCV is directly related to lean body mass (LBM) the statistical significance of LBM to ^{32}P dose requirement was also assessed but was found not to be significant. From the correlation of isotope dose and absolute fall in RCV a scale was constructed for the prediction of ^{32}P dosage in other patients on the basis of an absolute increased level in RCV. This scale proved to be useful, and it was found to be more accurate than the total weight method when predicting the dose of isotope. The technique reduced the total dose of ^{32}P administered over 6 and 18 month periods as compared to the figures published by Lawrence (1955), using a titration method of ^{32}P administration, which is important because of the association of terminal acute leukemia and previous radiation therapy. (auth)

40775 RADIOISOTOPE RENOGRAPHY IN DIAGNOSIS OF A "SILENT" KIDNEY. Aksel'dorf, A. L.; Gleizer, Yu. Ya. (Moscow Medical Inst.). Federation Proc., Transl. Suppl., 25: T683-T5(July-Aug. 1966).

Translated from Sovet. Med., 28: No. 8, 52(1965).

The contrast material, which is injected intravenously, is Hippuran with one iodine molecule replaced by the isotope iodine-131. The passage of the isotope through all parts of the kidney is detected by scintillators containing a sodium

crystal. The curves obtained are used to judge the characteristics of kidney function. In a renographic investigation of 58 patients with a "silent" kidney, it was found that the renal function in 33 cases was still preserved, although modified. Parallel with renography, in 22 patients renal angiography was performed; in 20 cases the results of renography and aortography were in agreement. Experience with the use of isotope renography confirms the high diagnostic value of this method in patients with a "silent" kidney. (H.L.W.)

40776 APPLICATIONS OF THE LASER BEAM IN CANCER BIOLOGY. Goldman, Leon (Children's Hospital Research Foundation, Cincinnati). Int. J. Cancer, 1: 309-18(July 15, 1966).

The use of lasers in cancer research and therapy is reviewed. Laser microprobes have the advantage of permitting spectroscopy of living cancer tissues without significant destruction of the specimen. The most successful application of lasers in cancer therapy has been with melanomas. A variety of skin lesions, adenocarcinomas, and brain tumors has been treated with lasers. It is pointed out that a thorough knowledge of laser technology is necessary for the planning of adequate personnel protection. (H.G.D.)

40777 COLLOIDAL ALBUMIN ^{131}I AS AN AGENT FOR SCANNING LIVER AND SPLEEN. AN EXPERIMENTAL STUDY IN ANIMALS AND MAN. Loken, Merle K.; Staab, Edward V.; Shea, Andrew W. (Univ. of Minnesota, Minneapolis). Invest. Radiol., 1: 295-300(July-Aug. 1966).

Following intravenous injection, 131 iodine colloidal albumin is rapidly taken up by cells of the reticuloendothelial system and as such may serve as an agent for visualization of the liver and spleen. However, measurements made of the clearance of colloidal albumin from these organs in C-3H mice and in our patients have shown that colloidal albumin is usually cleared too rapidly from these organs to permit a uniform scan to be obtained. The simultaneous administration of 4 mg/kg of stable colloidal albumin will increase the clearance time sufficiently so that essentially uniform scans may be obtained. Liver scans performed with ^{131}I colloidal albumin under carefully controlled conditions (control of time of scan and the addition of stable colloidal albumin) are satisfactory for clinical evaluation and in some situations are preferred to scans obtained with ^{131}I Rose Bengal and colloidal 198-gold. Advantages of colloidal albumin relate to lower radiation dosage to the patient as well as to its more rapid clearance so that repeat studies or other radioisotope studies may be performed the following day without interference from the ^{131}I colloidal albumin. Although success has been achieved in visualization of the spleen with colloidal abumin, the authors believe that a relatively new agent, ^{197}Hg mercurihydroxypropane, is much better for spleen scanning and also permits information to be derived on splenic function. (auth)

40778 RADIOTHERAPY, CHEMOTHERAPY, AND SURGERY IN THE CURATIVE TREATMENT OF INOPERABLE CERVICAL CANCER. REPORT OF ONE CASE WITH FIVE-YEAR SURVIVAL. Kemp, William N. J. Amer. Med. Ass., 196: 292-3(Apr. 18, 1966).

Ineffectiveness of radiotherapy alone in advanced cervical cancer is discussed, and a case is presented wherein Ra and external ^{60}Co therapy combined with drugs and surgery was effective in curing an apparently inoperable tumor. In the case described, triweekly administration of 100 mg of testosterone propionate preceded radiotherapy. One radium implantation was carried out, but the principal radiation was given by 20 external exposures to a high level dose of cobalt-60 radiotherapy. Immediately following the final cobalt-60 dose, the patient received 100 mg of testosterone propionate intramuscularly once daily, 40 mg of fluoxymesterone daily in four divided doses by mouth, and 200 mg of cyclophosphamide intravenously twice daily. Possibly due to the anabolic effect of testosterone propionate, the patient was free of radiation sickness while receiving radiotherapy. When a modified Wertheim hysterectomy was performed, no macroscopic evidence of carcinoma was found and only after a prolonged search were the remnants of a carcinoma in the myometrium found. Five years later the patient was found to be in good health and completely free of any recurrence of cervical cancer. (TCO)

40779 SCINTILLATION SCANNING WITH AN EIGHT-INCH DIAMETER SODIUM IODIDE (Tl) CRYSTAL. McAfee, J. G.; Mozley, J. M.; Natarajan, T. K.; Fueger, G. F.; Wagner, H. N. Jr. (Johns Hopkins Medical Institutions, Baltimore). J. Nucl. Med., 7: 521-47(July 1966).

The use of an eight-inch diameter sodium iodide crystal with focusing collimator for rectilinear scanning has been shown to improve the quality of scanning images and to shorten significantly the procedure times compared with a three-inch diameter crystal detector. The large crystal scanner has been superior for all types of organ scanning with the exception of the liver. Because of the greater number of patient studies which can be completed per day compared with a three-inch scanner, the increase in cost of the eight-inch scanner can be justified economically. The large crystal scanner is electronically less complex and less expensive than any type of scintillation camera. So far, the collimators designed for this instrument have had the same optical resolution as those in common use for three-inch scanners (R = 0.25 to 0.5 inches). In the future, however, an improvement in the radius of resolution by a factor of two is theoretically feasible, particularly for radionuclides with weak gamma energies of 150 kev or less. The present limitation in the use of this instrument is imposed by engineering difficulties in the precise fabrication of focusing collimators for low gamma energies with extremely thin septa and a large number of channels. The maximum linear scanning speed of the unit described herein is 96 inches per minute; however, this should be increased to 400 inches per minute in the immediate future. Using such high scanning speeds, analog methods of photorecording are completely unsatisfactory. The need for high contrast photorecording, used extensively with three-inch scanners is considerably less with the larger crystal, because of the marked improvement in counting statistics. For certain organs, such as the brain, liver and lungs, the optimal crystal geometry may consist of two opposing five-inch crystal detectors, rather than a single eight-inch crystal. Although the "double five-inch scanner" has an overall efficiency equivalent to a single eight-inch scanner, its cost is considerably greater because of the duplication in electronic components and image recording systems. (auth)

40780 LONG-TERM INCIDENCE OF MYXEDEMA APPEARING AFTER RADIOTHERAPY FOR CANCER OF THE LARYNX. Felix, H.; Dupre, N.; Drape, M.; Court, L. (Hopital Militaire d'Instruction Desgenettes, Lyon). Lyon Med., 206: 1043-50(Nov. 12, 1961). (In French).

The occurrence of myxedema after x-ray or radioiodine treatment of hyperthyroidism is examined, and a case history of this x-ray-induced late complication is presented to exemplify some of the problems involved. The normal thyroid gland is relatively radioresistent, and postirradiation myxedema is a rarity in patients submitted to radiotherapy of the head and neck region. In the case described, that of a 38-yr-old woman with a family history of goiter, x-ray therapy was given because of an epithelioma of the vocal cords which was first noted when the patient was 31 years of age. Over a three-month period irradiation was given over three fields (4500 R to two lateral fields and 2400 R to the anterior field of the larynx) for a total of 11,400 R. No untoward effects were noted, and the tumor was apparently eradicated, until nine years later, when myxedema was diagnosed. Tests with ^{131}I showed a 6-hr uptake value of only 1.6% and a 24-hr value of 2.7% (of the dose administered). This indicated almost total absence of functioning thyroid tissue. Substitutive therapy with a thyroid preparation was effective in alleviating symptoms of thyroid insufficiency. Whereas a dose of 30,000 R is required to inactivate healthy thyroid tissue, it is evident that a dose much less than 11,400 R destroyed a large portion of the goitrous gland in the present case. (BBB)

40781 X-RAY TELEVISION USING THE PLUMBICON. Feddema, J.; Marquerinck, J. E. (Philips Labs., Eindhoven, Netherlands). Med. Biol. Illus., 16: 33-6(Jan. 1966).

Instrumentation is described and illustrated which allows a marked reduction in radiation dose to patient and operator in fluoroscopy. The advantages of television monitoring applied to x-ray fluoroscopy (in conjunction with an image intensifier) are that x-ray dose reduction is derived from image intensification and gain in image brightness obviates the need to carry out fluoroscopic examination in a darkened room. There is freedom of choice of the positions in which one or more monitors may be placed and the position of the observer is not restricted. Other recording devices (e.g., for blood pressure and pulse rate) may be grouped around the television monitor and checked simultaneously, more than one person can conveniently see the results of the examination, and the television image may be filmed or video taped, thus providing a permanent record. The principal disadvantages of the technique are the cost of the equipment and the reduced image detail arising from the introduction of another step in the transmission line. A schematic representation of the television system is presented. (BBB)

40782 COMBINED TREATMENT OF TUMOURS OF THE OTO-RHINO-LARYNGEAL REGION BY METHOTREXATE AND IRRADIATION. Mechl, Z.; Kadlecova, D.; Konecny, M. (Oncological Inst., Brno). Neoplasma, 13: 327-33(1966).

The effect of a combination of systematically applied Methotrexate with actinotherapy in the treatment of some tumors of the oto-rhino-laryngeal region was studied. They obtained relatively good results, which were, however, limited in their duration. When comparing these results with those gained by regional administration of Methotrexate, they point out the advantages of its systemic application. (auth)

40783 COMPLICATIONS OF EXTRAPERITONEAL SURGICAL RADIATION (HIROSAKI). PARESIS-LIKE SYMPTOMS AND PAINS OF THE LEGS. Onodera, Norihiko (Hirosaki Univ., Japan). Nippon Sanfrejinka Zasshi, 17: 1115-21(Oct. 1965). (In Japanese).

In the clinical uses of the "extraperitoneal surgical radiation-Hirosaki" the paresis-like symptoms or pains of the legs have frequently been observed, in the region of the lymphocysts of the extra-peritoneal space. The complications were found in 23 of the 65 patients (35%). Although both the etiology and treatment of these complications remain unsolved, the following deserve mentioning here. (1) The complications of this kind can be divided into two, i.e., paresis-like symptoms, and pains of the legs. The former are usually combined with some functional disturbances in the lower extremities: that is, difficulties in sitting down and standing up promptly, in using geta or zori (footwear), or in going up stairs. Pains of the legs are usually found not diffusely but localized in some areas innervated by such nerves as N. fibularis, N. tibialis, N. cutaneous femoris lateralis, N. glutaeus, etc. (2) These are found on the average on the 24th day of postoperative course. More exactly, the disturbance or pains were noticed in 14 of the 23 cases (60%) within 10 days, 16 cases (70%) within 30 days, and the remaining cases (30%) later than 30 days, respectively. (3) The incidence of these disturbances on the left side was somewhat higher than on the right side. (4) These disturbances remained in 14 cases (60%) for 3 months; but, there were 6 cases (26%) the complaints lasted more than 6 months. (5) No definite correlations was found between the dosage of gamma rays delivered by the interstitial radiation and the incidence of these complications. In some cases, when the interstitial radiation was carried out only on one side, the disturbances were found exceptionally on the opposite side. (auth)

40784 TEN-YEAR SURVIVAL OF PATIENTS WITH LYMPHOGRANULOMATOSIS, FOLLOWING RADIATION THERAPY. Glinska, Halina (Inst. of Oncology, Krakow). Nowotwory, 16: 163-6(Apr.-June 1966). (In Polish).

Experience with forty-one patients given radiotherapy for lymphogranulomatosis (Hodgkin's Disease) is reported. Diagnosis of the disease was confirmed microscopically in all cases. Seventeen percent of those receiving radiotherapy survived over 10 yrs. Results indicated that the stage of advancement of the disease is a basic prognostic factor. (H.G.D.)

40785 SURGERY COMPARED WITH RADIOIODINE THERAPY IN THE TREATMENT OF HYPERTHYROIDISM. Costa, A.; Cottino, F.; Zoppetti, G. (Mauriziano Hospital, Turin). Panminerva Med., 7: 238-42(June 1965).

Advantages and disadvantages of radioiodine treatment of hyperthyroidism are discussed with reference to 700 patients treated with ^{131}I. In hyperthyroid patients under 21 years of age who do not respond or who exhibit intolerance of drug treatment, surgery is preferable to radiation therapy. However, the authors do not believe that radioisotopes are contraindicated in patients under 40 years of age. Radioisotope therapy is absolutely contraindicated in pregnancy. Surgery is preferred for hyperthyroidism due to toxic goiter and a hot nodule. There are many advantages of radioisotope therapy. Radioisotope therapy is associated with an almost zero mortality rate; nevertheless, a few deaths can be ascribed to thyroid storm or the failure of an arrhythmic, decompensated heart caused by radioisotope therapy. No scars remain after radioisotope therapy, and there is no damage inflicted on the vocal cords or parathyroids. There is no danger of aggravating a pre-existing exophthalmos or thyrotoxic myopathy. Radioisotope therapy can be performed tentatively; in particularly severe cases, small repeated doses of the radioisotope can be given and it can be repeated in cases of relapse with little risk of psychological or physical trauma (unlike surgery). Hospital admission is not usually required, and the cost of radioisotope therapy is negligible. Some disadvantages of radioisotope therapy are that there is little or no effect on pre-existing goiters and it does not reveal the nature of the goiter or nodule. Transitory and sometimes long-lasting hypothyroid states may be caused more frequently than with surgical removal owing to the difficulty of calculating dosage; determining the exact dose required is an even more speculative procedure than establishing how much of the gland tissue should be removed. The period of treatment is a long one and follow-up must be made for a year or longer. There are unknown factors such as the risk of a carcinogenic or genetic changes. It is concluded from a survey of clinical results that the two methods are not mutually exclusive but complementary. (TCO)

40786 MANAGEMENT OF CANCER OF THE LUNG. Sellors, Thomas Holmes (Middlesex Hospital, London). Practitioner, 196: 17-22(Jan. 1966).

Use of radiation in the treatment of pulmonary carcinoma, as well as other methods, is reviewed, with data on survival, complications, and future prospects. In general, results of radiotherapy in lung cancer are poor. Treatment produces considerable alleviation of symptoms and even radiological regression of some tumors, but complete resolution is rare. Modern apparatus and methods give better results, but radiation should only be accepted if surgery is not practicable. Radiation is not recommended for patients with tuberculous lesions or with lung sepsis, but it may give relief in patients with venous obstruction, persistent hemoptysis and bone pain. For patients regarded as suitable for radiotherapy the full course aims at delivering a tumor dose of 4500 to 6000 R through several ports of entry. Modern techniques avoid producing fibrosis of the lung, a serious complication. Careful observation of the blood count is necessary during the whole course of treatment which lasts for four to six weeks. Loss of appetite, sickness, and malaise are suffered by some patients and towards the end of treatment painful swallowing due to esophagitis may occur. Preoperative radiation is not successful owing to interference with healing, particularly of the bronchus stump. It is concluded that surgery alone offers much hope of cure, and that successful excision is followed by a reasonable proportion of five-year survivals. Radiotherapy, though essentially palliative at present, may

produce better results as the techniques improve, and a break-through with the discovery of new cytotoxic drugs could revolutionize the picture. (BBB)

40787 CONSIDERATIONS OF RADIATION QUANTITIES AND UNITS IN THE SENSE OF THEORY OF ENERGY TRANSFER. Papageorciou, Th. (Univ.-Geschwulstklinik der Charite, Berlin). Radiobiol. Radiotherap., 7: 215-24(1966). (In German).

Each radiation must be considered by the Poynting vector. The divergence of this vector characterizes the emission state of a substance as well as its absorption state. Considering the productiveness of an emission source from the point of view of the theory of energy transfer it is characterized by the positive divergence of the field around the source. The specific activity with the positive divergence is identical with the positive divergence, j, of the field. The negative divergence, j, of an acting field is a measure of the energy absorbed by a substance. It is necessary in order to be able to determine the absorption power of the substance. Consequently, negative divergence may be used as a base of dosimetry. The transfer of energy from a ^{60}Co γ source is used as an example. (C.H.)

40788 EXTENSION OF THE MEMORIAL SYSTEM FOR IMPLANT DOSIMETRY. Balter, Stephen; Freed, Barry R.; Ragazzoni, Gian D.; Siler, William; Laughlin, John S. (Memorial Hospital for Cancer and Allied Diseases, New York). Radiology, 87: 475-82(Sept. 1966).

The Memorial system for implant dosimetry has been extended to provide further information on the actual dose distributions in interstitial radioactive seed implants. The system is capable of providing complete isodose distributions for real implants of radioactive seeds. The computer programs and ancillary technics employed are discussed. Several concepts, such as implanted volume, average dose to an implant, dose-frequency histogram, etc., are introduced. The computer programs and sample output are available from the authors on request. (auth)

40789 CRESCENT PATTERN OF INCREASED RADIOACTIVITY IN BRAIN SCANNING. Heiser, William J.; Quinn III, James L.; Mollihan, William V. (Northwestern Univ., Chicago. Chicago Wesley Memorial Hospital). Radiology, 87: 483-8(Sept. 1966).

The pattern of a crescent-shaped area of increased uptake in the brain scan as seen on the anterior and/or posterior views is nonspecific. It may be observed in patients with subdural hematoma, granulomatous pachymeningitis, scalp trauma, craniotomy scalp abrasions, craniotomy defect, cerebral ischemia, metastatic carcinoma, unilateral Paget's disease in the skull, and occlusion of the common carotid artery. Total patient evaluation is required for the scan interpreter to approach the differential diagnosis of this pattern more intelligently, but in the majority of instances cerebral arteriography and/or craniotomy are necessary for definitive diagnosis. (auth)

40790 RESULTS OF THE RADIOIODINE TREATMENT IN DIABETES MELLITUS ASSOCIATED WITH HYPERTHYROIDISM. Gligore, V.; Motocu, M.; Fekete, T.; Gherman, Gr.; Holan, T.; Dumitrescu, Gr. (Institutul de Medicina Nucleara, Cluj). Stud. Cercet. Endocrinol., 17: 43-8(1966). (In Rumanian).

Thirteen patients were treated with ^{131}I. Basal metabolism and pulse was decreased in all cases, and glucose levels in blood and urine were decreased in nine cases. (W.E.B.)

40791 THE OPTICAL MASER AS A RETINAL COAGULATOR: AN EVALUATION. Campbell, Charles J. (Coll. of Physicians and Surgeons of Columbia Univ., New York); Rittler, M. Catherine; Koester, Charles J. Trans. Amer. Acad. Ophthalmol. Otolaryngol., 67: 58-67 (Jan.-Feb. 1963).

This report describes the design and construction of an experimental instrument for retinal coagulation which utilizes an optical maser as the source. The results obtained with the new instrument are illustrated with microscopic sections and fundus photographs. The equipment consisted of a ruby maser excited by a xenon lamp. The output of the maser was a collimated beam of light, deep red in color, measuring 6943 Å. The pulses were of extremely short duration measuring 1 msec or less. Experiments were performed on adult pigmented rabbits utilizing both the maser and the xenon arc photocoagulator. Therapeutic retinal burns have been produced satisfactorily in a small series of human subjects. The extremely short duration of the maser emission is important clinically in reducing the effects of eye movements by the patient. From the point of view of patient management, the maser coagulator has significant advantages. No patient reported pain or even discomfort from the maser treatments. These experiments demonstrated the feasibility and suggested the desirability of producing coagulations of the retina with a maser. (BBB)

40792 INVESTIGATION OF THE SPECTRUM OF SCATTERED GAMMA RADIATION OF ^{137}Cs IN A PARAFFIN PHANTOM. Jagielak, J.; Kotonski, Z. (Warsaw Polytechnic). Zeszyty Nauk. Politech. Warszaw., No. 118, 63-76(1965). (In Polish).

A method was used which makes possible measurements by using low activity sources of the order of mC. From the measurement, the spectral distribution was calculated at different depths. The ratio of $(D_r/D_r + D_p)$, where D_r and D_p are the doses of scattered and primary radiation correspondingly, was ascertained as a function of the distance from the phantom surface. Comparison of spectral distribution, as obtained by this method, with the results of investigations using different equipment and high activity sources up to hundreds of Curie is also presented. (ATD)

40793 DOES PROPHYLACTIC RADIOTHERAPY GIVEN FOR CANCER OF THE BREAST PREDISPOSE TO METASTASIS? Chu, Florence C. H.; Lucas, John C. Jr.; Farrow, Joseph H.; Nickson, James J. (Memorial Hospital, New York. James Ewing Hospital, New York). 25p. (CONF-660433-2). ORAU. Gmelin, AED-CONF-66-064-3.

From American Radium Society, 48th Annual Meeting, Phoenix, Ariz.

The results of 674 clinic patients with primary cancer of the breast, who had radical or extended radical mastectomies, with or without postoperative radiotherapy were analyzed. Patients who received postoperative irradiation had more advanced disease as indicated by more frequent and more extensive axillary nodal metastases. Survival rates of the patients with the same stage of disease were similar except that there was a statistically significant higher survival rate at the five year level for the irradiated patients who had metastases in the apical axillary lymph nodes. The incidence of lung, pleura, and skin metastases was the same in the irradiated and non-irradiated patients who were compared according to their axillary lymph nodal status. There was a lower incidence of and a delay in the appearance of metastatic lymph nodes in the prophylactically irradiated supraclavicular fossa. Serious irradiation complications consisting of chronic ulceration and/or radiation osteitis occurred in 5% of the patients who received the orthovoltage postoperative irradiation. (auth)

40794 VALUE OF ^{85}Sr BONE SCANNING IN RADIATION THERAPY. Sklaroff, David M.; Charkes, N. David (Albert Einstein Medical Center, Philadelphia). 9p. (CONF-660433-3). ORAU. Gmelin, AED-CONF-66-064-4.

From American Radium Society, 48th Annual Meeting, Phoenix, Ariz.

Experiences with ^{85}Sr for bone scanning are reviewed, and eight case histories are presented to illustrate specific applications of the technique. Scanning with ^{85}Sr was used: to determine the presence or absence of metastases; to determine whether metastases are local or generalized; to locate areas requiring therapy; to check the accuracy of portals; and to locate suitable sites for bone biopsy in cancer suspects. In about 2% of the series, the scan was negative despite the radiographic presence of bone lesions. These lesions were usually radiolucent. Bone biopsies in these patients revealed no evidence of reactive bone forma-

tion to the invading tumor, but extensive destruction was present. The mean radiation dose to bone in the scans was approximately 1.6 to 4.6 rads per 100 uc administered. (H.G.D.)

40795 STUDIES OF THE PANORAMIX RADIOGRAPHIC TECHNIQUE AND OF RADIATION DOSE DURING PANORAMIX AND MOUTH FILM EXPOSURE. Heger, H. Tuebingen, Ger., Univ., Tuebingen, 1964. 58p. $2.00 Gmelin, AED-Diss. 64-1079.

Thesis.

The Panoramix radiographic system with a rod-like anode that can be inserted in the patient's mouth is described. Optimal exposure data are discussed. Gonad doses during jaw radiography are given. (Gmelin Inst.)

CHEMISTRY

General

Refer also to abstract 41442.

40796 (IS–1500(Sect. C)) ANNUAL SUMMARY RESEARCH REPORT IN CHEMISTRY. (Ames Lab., Iowa State Univ. of Science and Tech.). 111p.

Research progress on physical and inorganic chemistry, analytical chemistry, spectrochemistry, radiochemistry, structural chemistry, and theoretical chemistry is reported. (M.C.G.)

Analytical Procedures

See also Separation Processes and Procedures

Refer also to abstracts 41037, 41068, 41112, 41168, 41415, 41416, and 41526.

40797 (AECL–2524) THE MICRODETERMINATION OF CARBON AND HYDROGEN IN HYDROGENATED POLYPHENYLS, FOULING FILMS, AND TERPHENYL MIXTURES. Grant, M. A.; Stewart, R. B. (Atomic Energy of Canada Ltd., Pinawa (Manitoba). Whiteshell Nuclear Research Establishment). Jan. 1966. 13p. Dep. mn. AECL $0.50.

A procedure for the determination of carbon and hydrogen in hydrogenated polyphenyls, fouling films, and terphenyl mixtures based on the classical method by Pregl is described. For hydrogenated polyphenyls standard deviations of 0.08% for the hydrogen percentage and of 0.35% for the carbon percentage were found. For a mixture of terphenyl isomers standard deviations of 0.10% for the hydrogen percentage and of 0.23% for the carbon percentage were found. (auth)

40798 (ANL–7209) AVERAGES OF INTERFEROMETRIC MEASUREMENTS OF THORIUM LINES. Giacchetti, Athos (Argonne National Lab., Ill.). May 1966. Contract W-31-109-eng-38. 26p. Dep. mn. CFSTI $2.00 cy, $0.50 mn.

Interferometric measurements of thorium lines are compiled. Data on 701 lines are collected in Table I, including vacuum and air wavelengths, intensity and ion classification, average deviations, number of measurements, and deviations for each independent measurements. In Table II are 40 lines not included in Table I nor in the computation of averages. (M.C.G.)

40799 (CEA-R–2887) INSTALLATION DE CHIMIE ANALYTIQUE SOUS RAYONNEMENT. (Installation for Analytic Chemistry Under Irradiation). Fradin, Jean; Azoeuf, Pierre; Guillon, Andre (Commissariat a l'Energie Atomique, Saclay (France). Centre d'Etudes Nucleaires). May 1966. 119p. Dep. mn.

An installation was set up for carrying out manipulations and chemical analyses on radioactive products. It is completely remote-controlled and is of linear shape, 15-m long; it is made up of three zones: an active zone containing the apparatus, a rear zone giving access to the active zone, and a forward zone independent of the two others and completely protected. It is from this zone that the remote-control of the apparatus is effected. The whole assembly was designed so that each apparatus corresponding to an analytical technique is set up in a sealed enclosure. The sealed enclosures are interconnected by a conveyor. After three years operation, a critical review is made of the installation. (auth)

40800 (CNAEM–35) NEUTRON ACTIVATION ANALYSIS OF ROMAN COPPER COINS FROM 250–500 A. D. PART II. Zuber, Kurt (Cekmece Nuclear Research Center, Atomic Energy Commission, Istanbul (Turkey)). May 1966. 38p. Dep. mn.

Tin can be detected in a copper coin by observing the 9.7-min ^{125}Sn activity if epicadmium neutrons are used for the activation. Activation with epicadmium neutrons is also useful for the determination of indium. For cobalt the 5.1-yr activity has to be observed if only traces are present. The problem of shielding is important for the activation by epicadmium neutrons. The observed experimental values of the calibration constants are compared with the values calculated by using the atomic and nuclear constants. The mass-ratios of Ag, Au, Sn, Sb, Co, and In to copper are given for the coins. The elder of these coins shows, in general, stronger alloying with silver and tin, whereas antimony is present up to nearly 1% in the younger coins. Gold is detected as an impurity of the silver used for the alloying. Cobalt is found in the coins minted under Constantine I and later. Indium was also detected as an impurity. The measured values of the resonance integrals of three tin isotopes are given in an appendix. The effective resonance integral of ^{64}Cu was determined for 0.36 to 1.1 g/cm^2 copper. (auth)

40801 (EUR–2957.d,f,e) PRACTICAL ASPECTS OF ACTIVATION ANALYSES WITH CHARGED PARTICLES. Proceedings of the Meeting held at Grenoble, France, June 23, 1965. (European Atomic Energy Community). 1966. 185p. (CONF-650667). Dep. mn.

In Dutch, French, and English.

Discussions on the chief practical problems encountered by specialists in charged-particle activation analysis are presented. (P.C.H.)

40802 (HW–65402(Rev.1)) URANIUM TRIOXIDE PRODUCT SPECIFICATION ANALYSES. Downey, C. L.; Zimmer, W. H. (General Electric Co., Richland, Wash. Hanford Atomic Products Operation). May 5, 1964. Contract AT(45-1)-1350. 8p. Dep. mn. CFSTI $1.00 cy, $0.50 mn.

The methods used in meeting product specifications for both enriched and depleted UO_3 are described. The uranium content of UO_3 is determined gravimetrically by the indirect conversion of UO_3 to U_3O_8. All of the impurity elements are determined by emission spectrography. Alternate methods are available for Fe, Cr, Ni, Na, and Ca. Particle size determinations are performed by placing weighed samples of UO_3 powder on the top screen of an assembly of standard sieve screens. The percentage of UO_3 powder that passes through each specified screen is calculated directly from the weight fractions collected. Fission product content of the UO_3 powder is defined in the product specifications in terms of the percentage beta and percentage gamma count in excess of that found in aged natural uranium. Plutonium content is determined by extraction and alpha counting of plutonium. ^{235}U content is determined by mass spectrometry. (M.C.G.)

40803 (KFK–387) ABTRENNUNG UND RADIOCHEMISCHE BESTIMMUNG VON SPALTELEMENTAKTIVITAETEN. (Separation and Radiochemical Determination of Fission Element Activities). Baeckmann, A. v.; Schroeder, H.; Stamm, H. H.; Wertenbach, H. (Kernforschungsanlage, Juelich (West Germany). Institut fuer Radiochemie). Dec. 1965. 118p. Dep. mn.

Laboratory methods for the separation of fission elements and determination of their relative activity are described. The separation of Sr, Zr, Mo, Lu, Te, I, Cs, Ba, and Ce from fission product solutions are considered, and the reproducibility of the methods used is discussed. (J.S.R.)

40804 (KR–108) THE REFRACTOMETRIC DETERMINATION OF U(VI) IN AQUEOUS AND IN TBP SOLUTIONS. Joon, K.; Deurloo, P. A. (Institutt for Atomenergi, Kjeller (Norway)). June 1966. 16p. Dep. mn.

From measurements on the system $UO_2(NO_3)_2-H_2O-HNO_3$ in the concentration range up to 300 gU/l and up to

9 M in HNO_3, a linear relation between the refractive index (n) and the U concentration of the solution was obtained. The increase of the refractive index per gram of U is inversely proportional to the nitric acid concentration. If this system is extracted with a tri-n-butyl phosphate–dodecane mixture, the refractive index of the organic solution also increases linearly with the U concentration. In this case the slope of the n-[U] curve is directly proportional to the logarithm of the HNO_3 concentration in the aqueous phase from which the U was extracted. Provided that the HNO_3 concentration of a sample is known, the measurement of the refractive index can be applied for a quantitative U determination. If an Abbé-type refractometer is used, the error can be less than 1 g U/l for the aqueous, and less than 1.1 g U/l for the organic solutions. (auth)

40805 (MLM–1325, pp 63-70) ANALYTICAL AND INSTRUMENTATION. (Mound Lab., Miamisburg, Ohio).

The development and use of various instruments for analytical purposes are reported. Methods for determining the presence of nitrogen dioxide, impurities in plutonium, and trace amounts of Te in Bi metal were developed using gas chromatography, optical emission spectroscopy, and atomic absorption spectrophotometry, respectively. Quadrupolar coupling between nitrogen and hydrogen atoms in formamide was demonstrated by NMR. A general program that is applicable to all seven crystal systems for the determination of precision lattice parameters using the least-squares analytical method was written in Fortran II for the IBM-1620 computer. Potassium bromide windows for infrared analysis of heavy metal systems were coated with 2 μ thick polyethylene to prevent interactions between the heavy metal and bromine. (P.C.H.)

40806 (NAS-NS-3110) ACTIVATION ANALYSIS WITH CHARGED PARTICLES. Tilbury, R. S. (Union Carbide Corp., Tuxedo, N. Y. [Mining and Metals Div.]). [1966]. Contract AT(30-1)-2975. 47p. Dep. mn. CFSTI $1.00 cy, $0.50 mn.

Nuclear Science Series of the National Academy of Science–National Research Council, Washington, D. C. Committee on Nuclear Science.

A review of charged-particle activation analysis is presented. Charged particles are compared and contrasted with uncharged particles for activation analysis and a brief discussion is given of the machines available for particle acceleration. Thick and thin targets are compared followed by the specific use in activation analysis of protons, deuterons, helium-3 ions, alpha particles, tritons, and recoil particles in a nuclear reactor. (auth)

40807 (NLCO–976) THE EFFECTS OF VARIOUS GRADES OF GRAPHITE ELECTRODES ON THE CARRIER DISTILLATION OF IMPURITIES IN U_3O_8. Supplemental Report: MB-100 and Ex-11 Graphites. Pepper, C. E.; Duff, C. E.; Pardi, A. J. (National Lead Co. of Ohio, Cincinnati). Sept. 1966. Contract AT(30-1)-1156. 7p. Dep. mn. CFSTI $1.00 cy, $0.50 mn.

Two new grades of spectroscopic graphite were evaluated for use as electrodes in the determination of impurities in U_3O_8 samples. A 10% AgCl–LiF carrier-distillation technique was employed. Random samples of the test electrodes were checked for purity and conformity with specifications for electrode geometry. The sensitivities and precisions of seven elements (Al, B, Cr, Cu, Fe, Ni, and Si) were determined and compared with those obtained for reference graphite electrodes. (auth)

40808 (NP–16212) DEVELOPMENT OF A METHOD OF NON DESTRUCTIVE ANALYSIS OF IRRADIATED FUEL ELEMENTS FOR ^{235}U AND PLUTONIUM CONTENT BY MONITORING AND SPECTROMETRY. Final Report. (Societa Nazionale Metanodotti, Milan (Italy). Laboratori Reuniti Studi e Ricerche). Nov. 30, 1963. 80p. Dep. mn.

Development of a method of nondestructive analysis of irradiated fuel elements for ^{235}U and Pu by monitoring and spectrometry is described. The problem consisted in finding a suitable detector to be attached to the surface of a fuel element so the concentrations of ^{235}U and Pu could be determined at the end of the irradiation, only by examining the monitor itself, without any interference from the fuel element. The irradiation of thin U films contained in suitable boxes attached on the surface of the fuel elements and the subsequent counting of the spectrum of the alpha emitters when the elements are discharged are proposed. The ratios of the areas of the ^{235}U and Pu lines to the area of the ^{238}U line should determine (taking into account the disintegration constants also) the concentration of ^{235}U and Pu. These values can afterwards be correlated with the amounts of these isotopes in the fuel element itself by means of theoretical calculations. Preliminary studies indicated that a resolution of 2% in alpha spectra, such as provided by most commercial ionization chambers, is adequate for Pu analysis. Determination of ^{235}U was considered likely to be more difficult because the alpha spectrum of ^{235}U is composed of three lines over an interval of 0.18 Mev and because of the small quantity of ^{235}U in natural U, it is necessary to use U enriched in ^{235}U. The enrichment is generally obtained via gaseous diffusion, with a consequent enrichment also in ^{234}U, the alpha line of which is adjacent to the lines of ^{235}U and many times higher. During irradiation, a fraction of the ^{235}U is converted to ^{236}U, the alpha line of which falls between the ^{235}U and ^{234}U lines. These facts cause a number of lines to be placed in a small energy range and, to resolve from them the line of ^{235}U a resolution of the order of 0.5 to 1% is required. Semiconductor detectors for alpha particles were tested, and, with the addition of a particular circuit to reduce the noise, resolution values in the range from 0.8 to 0.4% were attained. After irradiation of 20% enriched U, it was found that the alpha spectrum measurements are influenced by the high beta background due to activation of the uranium film. This background caused such an enlargement of the alpha lines that there was no possibility of distinguishing the peaks due to the various isotopes. To eliminate this background, methods of reprocessing the uranium film were developed. The application of these methods to fuel elements rests on the possibility of obtaining a correlation between the quantities of those isotopes in the specimens attached externally on the fuel elements and the quantities of the same isotopes in the fuel elements. (auth)

40809 (NP–16235) RADIONUCLIDE ANALYSIS OF ENVIRONMENTAL SAMPLES: A LABORATORY MANUAL OF METHODOLOGY. Krieger, Herman L.; Velten, Richard J.; Burmann, Franz J. (eds.) (Public Health Service, Washington, D. C.). Dec. 1959. Revised Feb. 1966. 74p. (R–59-6).

Actual laboratory procedures for separating a particular nuclide from the remainder of the radionuclides in an environmental sample are presented. For each procedure, the method capabilities represent the statistical evaluation of the analysis, and the actual procedure time does not include such processes as long evaporation, digestion, and equipment preparation. Decontamination factors were determined for those fission products most likely to be present and are based on their separation from ~100,000 dpm of the interfering nuclides. Instrumentation, methodology, and reagent preparation are discussed for determinations of tritium, ^{89}Sr, ^{90}Sr, ^{131}I, ^{137}Cs, ^{226}Ra, Rn, Ca, and stable Sr. (M.C.G.)

40810 (NYO–901-54, pp 20-3) BIOPHYSICS: ACTIVATION ANALYSIS IN FORENSIC MEDICINE. (New England Deaconess Hospital, Boston, Mass. Cancer Research Inst.).

Progress is reported in preliminary work on the application of activation analysis to legal medical evidence with emphasis on the usefulness of activation analysis as a means of identifying human tissue by its micro-constituents. A computer program was written for the subdivision of complex spectra into their component parts using a reference library containing spectra of the appropriate elements. An investigation was started in conjunction with

members of the Harvard Law School to set forth the legal and scientific principles and criteria necessary for a satisfactory presentation of evidence in court. (C.H.)

40811 (ORO–2670–13) THE DETERMINATION OF BROMINE IN TERRESTRIAL AND EXTRATERRESTRIAL MATERIALS BY NEUTRON ACTIVATION ANALYSIS. Lieberman, Kenneth W. (Kentucky Univ., Lexington. Dept. of Chemistry). July 1, 1966. Contract AT(40-1)-2670. 179p. Dep. mn. CFSTI $5.00 cy, $1.00 mn.

The geochemical behavior of Br in terrestrial and extraterrestrial materials was investigated. A method was developed to accurately determine Br in a silicate matrix for abundance levels of 1 ppM or less, using neutron activation. Irradiated samples were dissolved in a Na_2O_2–NaOH fusion mixture and Br was separated by treatment with a series of selective oxidizing and reducing agents in conjunction with a solvent extraction procedure. Analytical determinations for Br were conducted on specimens from the major chondrite and achondrite classifications, australites and other tektites, igneous rocks from the Palisades Sill and the Oslo plutonic sequence, specimens from other intrusive and extrusive igneous formations, eight standard rocks, some possible upper mantle materials, and on two deep-sea sediment cores. Br was found to be fractionated among the three major chondrite groups; carbonaceous, enstatite, and ordinary. It becomes progressively depleted in going from carbonaceous to the ordinary chondrites. Br was depleted during fractionation of a magma in the formation of the Oslo plutonic sequence, and was enriched during the fractionation of the Palisades magma. The geochemical behavior of Br during differentiation of the Palisades Sill is comparable to the behavior of F in the Great Lake Sheet. The abundance of Br in igneous rocks was relatively uniform and for the majority of analyses ranged from 0.15–1.5 ppM. The Br abundance data for the australites suggest a geographical trend with generally higher concentrations in the east and a progressive depletion toward the west. Br was enriched in the deep-sea sediments investigated with respect to oceanic water. (161 references). (P.C.H.)

40812 (ORO–2980–14) ELEMENTAL TRACE ANALYSIS BY CHARGED PARTICLE AND NEUTRON ACTIVATION. Blake, K. R.; Parker, C. V.; England, L. D.; Morgan, I. L. (Texas Nuclear Corp., Austin). Aug. 17, 1966. Contract AT(40-1)-2980. 44p. Dep. mn. CFSTI $2.00 cy, $0.50 mn.

Elemental trace analysis was conducted by measurement of charged particle induced delayed gamma activity and of charged particle induced prompt gamma activity, and by neutron activation analysis. Beryllium metal surfaces were analyzed for carbon, oxygen, and nitrogen by 2.7 Mev deuteron activation analysis. Delayed gamma activities provided a measure of each of the three elemental concentrations. Standard sized samples were bombarded in a vacuum chamber. Results of C, O, and N analysis are presented and oxygen surface determinations were compared with measurements of total oxygen content independently determined by fast neutron activation analysis. Trace analyses of impurities in metal surfaces were accomplished by deuteron bombardment and analysis of prompt emitted gamma radiation. Studies of a complex nickel base alloy resulted in carbon and aluminum analysis down to 200 ppM. Other trace elements that were determined included boron and magnesium. The limits of sensitivity were dependent upon concentrations of competing elements. Fast neutron activation analysis was used in a pilot plant facility to measure the aluminum and silicon content of bauxite. A brief description of the facility is presented. Results of studies with bauxite containing 27% aluminum, 3% silicon, and 8% iron are presented. (P.C.H.)

40813 (RFP–271) AN OPTICAL EMISSION SPECTROGRAPHIC METHOD FOR THE DETERMINATION OF ^{240}Pu IN PLUTONIUM MATERIALS. Vejvoda, E. (Rocky Flats Div., Dow Chemical Co., Denver, Colo.). Sept. 12, 1962. Contract AT(29-1)-1106. 19p. Dep. mn. CFSTI $1.00 cy, $0.50 mn.

An optical emission isotopic spectrographic method was developed for the determination of ^{240}Pu in plutonium dioxide. The analysis is based on the resolution of the isotope spectral shift for ^{240}Pu using a plate-grating spectrograph in the 6th order with a 15,000 LPI grating. The method is applicable to materials that can be converted to plutonium dioxide. (M.C.G.)

40814 (RFP–664) A MODIFIED PYROELECTRIC SODIUM FLUORIDE CARRIER DISTILLATION METHOD FOR THE SPECTROGRAPHIC ANALYSIS OF IMPURITIES IN PLUTONIUM. Schreiber, G. A.; Barrick, C. W. (Rocky Flats Div., Dow Chemical Co., Golden, Colo.). Aug. 1966. Contract AT(29-1)-1106. 31p. (CONF-660810–2). Dep. mn. CFSTI $2.00 cy, $0.50 mn.

From 8th Annual Rocky Mountain Spectroscopy Conference, Denver, Colo.

A modification of the pyroelectric sodium fluoride carrier distillation method for analysis of impurities in plutonium metal is described. The metal is dissolved. Plutonium is precipitated and treated with nitric acid. The slurry obtained is dried and ignited. The resultant low-density oxide is mixed with sodium fluoride and pressed into a pellet for arcing. Cobalt is used as the internal standard for densitometric determinations of six elements. Additional elements are determined using visual comparisons against prepared standards. The procedural modifications improve reproducibility and sensitivity of most of the elements involved. (auth)

40815 (RFP–698) THE DETERMINATION OF IRON AND NICKEL IN URANIUM BY ATOMIC ABSORPTION SPECTROPHOTOMETRY. Shepherd, G. A.; Johnson, A. J. (Rocky Flats Div., Dow Chemical Co., Golden, Colo.). Aug. 1966. Contract AT(29-1)-1106. 23p. (CONF-660810–3). Dep. mn. CFSTI $1.00 cy, $0.50 mn.

From 8th Annual Rocky Mountain Spectroscopy Conference, Denver, Colo.

Uranium was analyzed for iron and nickel by atomic absorption spectrophotometry. Iron and nickel were determined in the samples under three different experimental conditions: in solutions containing uranium, in solutions extracted from uranium, and by the method of additions. The results obtained were compared. A comparison was also made of results reported by atomic absorption, emission spectrography, and colorimetric methods. The relative standard deviation for iron at 165 ppm was, 6.3, 4.3, and 7.9%, respectively. Relative standard deviation for nickel at 20 ppm was, 7.9, 2.8, and 36.0%, respectively. The ppm values are in terms of original uranium sample weight. (auth)

40816 (RFP–699) ANALYSIS OF RADIOACTIVE METALS BY SPARK SOURCE MASS SPECTROGRAPHY. Johnson, A. J.; Kozy, A.; Morris, R. N. (Rocky Flats Div., Dow Chemical Co., Golden, Colo.). Aug. 1966. Contract AT(29-1)-1106. 30p. (CONF-660810–1). Dep. mn. CFSTI $2.00 cy, $0.50 mn.

From 8th Annual Rocky Mountain Spectroscopy Conference, Denver, Colo.

A spark-source mass spectrograph was adapted for the analysis of plutonium and americium metals. Over 70 elements can be determined in these metals on the same analysis. Elements such as Cl, F, S, Ta, W, and rare earths, which require involved procedures for determination by emission spectrographic or chemical methods, can be readily determined by mass spectrography. A comparison was made between results obtained by mass spectroscopy and by conventional methods for impurity elements. The operations involved in handling radioactive materials in the mass spectrograph are also discussed. (auth)

40817 (UCRL–14959) CATHODIC ETCHING TO PREPARE RADIOACTIVE SAMPLES FOR OXYGEN DETERMINATION. Hill, John H.; Morris, C. J.; Frazer, Jack W. (Lawrence Radiation Lab., Univ. of California, Livermore). Apr. 18, 1966. Contract W-7405-eng-48. 6p. Dep. mn. CFSTI $1.00 cy, $0.50 mn.

A cathodic etching method was developed to clean the

surfaces of radioactive metal samples prior to oxygen determinations. The sample becomes the cathode in a low pressure argon-ion discharge. The argon ions bombard the surface of the sample and remove the oxide film by an etching process. The oxygen content of ^{238}U samples cleaned by cathodic etching is consistently lower than the oxygen content of samples cleaned by either acid etching or filing. In addition, the hazards of radioactive contamination are minimized because the sputtered metal deposits on surfaces inside the etcher assembly. (auth)

40818 (UJV–1368) STANOVENI WOLFRAMU V ZELEZE AKTIVACNI ANALYZOU. (Determination of Tungsten in Iron by Activation Analysis). Slunecko, J.; Kukula, F.; Simkova, M. (Ustav Jaderneho Vyzkumu, Ceskoslovenska Akademie Ved, Rez). June 1966. 16p. Dep. mn.

A sensitive method for the nondestructive analysis of W in zone-purified iron by means of the ^{187}W isotope is described. For calculation of the W content, 0.48-Mev photons and x-ray peaks at 0.06 kev on the γ spectrum were used. By irradiation of the sample in cadmium foils in the thermal channel of the reactor, the activities of ^{59}Fe and ^{54}Mn were reduced in comparison with the activity of ^{187}W. The sensitivity of the determination is 0.03 ppM, five times higher than in irradiations without cadmium foils. (tr-auth)

40819 (CEA-tr–A-1883) METHODE SIMPLE POUR DOSER LA RADIOACTIVITE NATURELLE ET ARTIFICIELLE DANS L'EAU EN S'APPUYANT SUR DES EFFETS DE COPRECIPITATION ET D'ADSORPTION. (Simple Method for Determination of Natural and Artificial Radioactivity in Water; Its Dependence on the Effects of Coprecipitation and Adsorption). Dannecker, A. ([Technische Hochschule, Karlsruhe (West Germany)]). Translated into French from a Thesis. 63p. Dep. mn. JCL $6.60 fs, $2.09 mf.

A concentration method for measurement of radioactivity in water was developed. It is based on coprecipitation and adsorption phenomena. The efficiency of the methods was determined for fallout, fission products formed by irradiation of natural uranium by slow neutrons, and for the radioisotopes ^{137}Cs, $^{90}Sr + ^{90}Y$, ^{141}Ce, ^{204}Tl, ^{124}Sb, ^{99}Tc, ^{60}Co, ^{106}Ru, ^{106}Rh, ^{192}Ir, ^{131}I, and ^{32}P. The activities of the precipitates were measured by internal counters. It is necessary to apply to the measured counting rate corrections due to adsorption in the preparation and back-scattering from the subjacent layer. These two depend on the mass covering of the preparation and the β energy. Since a theoretical estimation was impossible, it was necessary to establish correction curves (counting rate as a function of the layer thickness for a given decay rate) for the different emitters. The efficiency of the internal counter was determined with K. The measurements made showed that the method of adsorption and coprecipitation can be used with success. The efficiency of the method is, on an average, 95% for cations, whereas that for the common evaporation methods is at most 50 to 60%. Moreover, there is the advantage that a tenfold quantity of water can be analyzed in $\frac{1}{5}$ the time. The total experimental precision is increased and short-lived isotopes can be measured. (tr-auth)

40820 (IS-Trans–37) THE BEHAVIOR OF DEFINITE NITRIDES IN TITANIUM AND ZIRCONIUM BY THE DETERMINATION OF NITROGEN. Fischer, W.; Steinruecken, D. Translated by Wayne E. Dallmann (Ames Lab., Iowa), from pp 81-9 of Nitrogen in Metals, Academy Publishing House, Berlin, 1965. 21p. Dep. mn. JCL $2.60 fs, $0.83 mf.

Studies were made on the difference between results obtained by the hot extraction and Kjeldahl procedures used for determining the nitrogen content in Ti and Zr materials in order to determine which of the two methods provides the correct results. As a preliminary step, it was determined that sample form did not influence the results. The Kjeldahl method, in all examined cases, provided uniformly good and demonstrable correct results. From the hot extraction experiments, essentially no difference in behavior between normal metal samples and definite nitride samples was observed. Consequently, nitrogen bound as nitrides of Ti or Zr can be recovered by hot extractions under application of the metal bath. (P.C.H.)

40821 STUDY OF MASS DISCRIMINATION DURING MEASURING OF ISOTOPIC COMPOSITION OF STRONTIUM AND RUBIDIUM MADE IN MASS SPECTROMETER MI-1305 BY SURFACE IONIZATION METHOD. Gorokhov, I. M. pp 182-92 of Absolyutnyi Vozrast Dokembriiskikh Porod SSSR, Akademiya Nauk SSSR, Laboratoriya Geologii Dokembriya. (In Russian).

Data from mass spectrometric measurements of Sr and Rb samples (in a mixture of natural Sr or Rb with synthesized stable indicators enriched by ^{84}Sr or ^{87}Rb) were evaluated by statistical processing to determine whether it is necessary to introduce into a measured $^{87}Sr : ^{86}Sr$ ratio the semiempirical correction made on the basis of measuring the $^{86}Sr : ^{88}Sr$ ratio. Isotopic compositions of the elements were measured in a mass spectrometer with a homogeneous magnetic field, 60° angular deviation, and accelerating voltage of 4 kv. The ions were produced on the hot surface of a W filament in the ion source at $\leqq 2 \times 10^{-6}$ mm Hg. The results of the statistical analysis showed that the deviations in measuring the isotopic ratios were accidental. The effect of isotopic fractionation was insignificant. Results on isotopic composition of Sr in ocean water, obtained by surface ionization made on single, double, and triple-filament ion sources, were in good agreement. (P.C.H.)

40822 ADSORPTION OF A NUMBER OF ELEMENTS FROM SULFURIC ACID SOLUTIONS BY ANION EXCHANGE. Danielsson, L. (Swedish Inst. of Metal Research, Stockholm). Acta Chem. Scand., 19: 670-8 (1965).

The adsorption on Dowex 1-X8 (SO_4^{2-} form) of 26 metal ions from 0.1N to 10N – H_2SO_4 solution was investigated as a basis for the study of adsorption from some mixed-acid systems used in analysis of metals and alloys. Elements were determined colorimetrically, by complexometric titration, or by x-ray fluorescence analysis. Beryllium, Mg, La, Ce(III) V(IV), Mn(II), Fe(II), Co, Ni, Cu, Ag, Zn, Cd, Al, As(III), Sb(V), Sn(IV), and Sb(III) were not adsorbed. From solutions < N in H_2SO_4, Ti(IV), V(V), Cr(III), Fe(III), As(V), and Bi were adsorbed; and adsorption decreased with increasing H_2SO_4 concentration. Only Zr(IV) and Mo(VI) were strongly adsorbed, but again, adsorption decreased with increasing H_2SO_4 concentration. The effect of H_2O_2 on adsorption from H_2SO_4 solution was also studied. (Anal. Abstr., Vol. 13, No. 8, Aug. 1966).

40823 RADIOMETRIC METHOD FOR DETERMINING NEOMYCIN ON COTTON. Seaman, W.; Stewart, D. Jr. (American Cyanamid Co., Bound Brook, N. J.). Amer. Dyestuff Rep., 54: 104-5(1965).

Neomycin is determined by causing its amino-groups to react with CS_2, treating the dithiocarbamate so formed with $^{110}AgNO_3$, and measuring the radioactivity of the resulting $^{110}Ag_2S$. For up to 25 μg of neomycin in the sample (≃25 mg of cloth), the graph of activity vs neomycin content is rectilinear. Sources of error are discussed, and it is suggested that the method should also be useful for determining aliphatic primary and secondary amines. (Anal. Abstr. Vol. 13, No. 8, Aug. 1966).

40824 RELEASE OF NITROGEN FROM AMINO ACIDS WITH NINHYDRIN FOR ^{15}N ANALYSIS. Kennedy, I. R. (Univ. of Western Australia, Perth). Anal. Biochem., 11: 105-10(Apr. 1965).

A quantitative method for the specific release of α-amino nitrogen of amino acids as ammonia is described. The amino nitrogen of γ-amino-n-butyric acid is also released. The method was applied to the determination of ^{15}N enrichment in amino acids of legume root nodules exposed to $^{15}N_2$. (auth)

40825 QUANTITATIVE DETERMINATION OF COPPER IN POTATO TISSUE USING NEUTRON ACTIVATION ANALYSIS AND ELECTRODEPOSITION OF COPPER. Brown, Roger C.; Weaver, Merle L.; Steen, Heather (Washington State Univ., Pullman). Anal. Biochem., 16: 119-31(July 1966).

The quantitative determination of copper in biological tissue samples in amounts of 0.01 to 10 μg is described. Tissue samples were activated in a 100-kw nuclear reactor for 30 to 180 min, after which the samples were digested in HNO_3 (conc.) and H_2SO_4 (conc.). The free copper was then electroplated on to a brass or copper screen, and the screen was counted for the 0.511-Mev positron annihilation radiation associated with the decay of ^{64}Cu. There is a linear relation between the observed count rate and the quantity of copper present in the tissue. The electrodeposition removes the copper from the presence of the interfering radioactive isotopes of ^{24}Na, ^{42}K, and ^{56}Mn normally found in activated potato tissue. This separation is so nearly complete that there is essentially no contribution to the count rate from these other radioactive elements. It was demonstrated that it is possible to determine accurately the quantity of copper in 50-mg samples of potato tissue. (auth)

40826 CONCENTRATION OF WATER SAMPLES FOR THE DETERMINATION OF TRITIUM. Zel'venskii, Ya. D.; Nikolaev, D. A.; Tatarinskii, V. S.; Shalygin, V. A. At. Energ. (USSR), 18: 367-72(1965). (In Russian).

Conditions were studied for the concentration of ^3H in water by rectification in vacuo under stationary and nonstationary conditions. The degree of enrichment was determined by monitoring the change in concentration of ^{18}O or ^2H in the rectified water; the concentration of ^3H is then determined from the known ratio of ^{18}O or ^2H to ^3H in the enriched water. Optimum enrichment was achieved at 100 to 120 torr. (Anal. Abstr., Vol. 13, No. 8, Aug. 1966).

40827 RECENT ADVANCES IN ION-EXCHANGE-RESIN SPOT TESTS: 1960 TO 1964. [PART] I. Fujimoto, Masatoshi (Tokyo Univ.). Chem. Analyst, 54: No. 2, 58-62(1965).

A summary is given of the various techniques used, and some ion exchangers that serve as reaction media are described. Known spot tests for inorganic ions are summarized in a table, and details are given of tests for Au(III), Cd(II), Cu(II), Fe(III), heavy metals, Hg(II), Mo(VI), U(VI), Ti(IV) and Tl(I). (50 references). (Anal. Abstr., Vol. 13, No. 8, Aug. 1966).

40828 ANALYSIS OF GASES BY ABSORPTION OF SOFT γ RADIATION. Dresia, H.; Tetzlaff, K. H.; Voelker, W. (Staatliche Ingenieur-Schule fuer Maschinenwesen, Essen). Chem.-Ing.-Tech., 38: 871-6(Aug. 1966). (In German).

The quantum absorption of soft γ rays is made use of in determination of the various components of a gaseous mixture. The physical basis, sources of error, and accuracy of the method, are discussed. The construction of a measuring instrument is also described. The efficiency of the method was tested by determining the SO_2 content of waste gases with ^{55}Fe used as the radiation emitter. (auth)

40829 NONDESTRUCTIVE ACTIVATION ANALYSIS OF ANTIQUE GOLD COINS. Das, H. A.; Zonderhuis, J. (Reactor Centrum, Petten, Netherlands). Chem. Weekbl., 61: 215-18(1965). (In Dutch).

Coins were irradiated in a neutron flux of $\simeq 2.9 \times 10^{10}$ neutrons per cm^2 per sec, and ^{198}Au, ^{110m}Ag, and ^{64}Cu were then determined by γ spectrometry. Results are discussed. (Anal. Abstr., Vol. 13, No. 8, Aug. 1966).

40830 DETERMINATION OF INCORPORATION OF ^{59}Fe IN HEMIN OF PERIPHERAL RED BLOOD CELLS AND OF RED CELLS IN BONE-MARROW CULTURES. Thunell, S. (Univ. of Lund, Sweden). Clin. Chim. Acta, 11: 321-33(1965).

The plasma from 0.02 to 0.4 ml of blood is added to an equal volume of H_2O, and the mixture is stirred to accelerate hemolysis. Ethyl acetate-anhydrous acetic acid (3:1) (3 ml) is added, and the precipitated proteins are ground with a glass rod against the side of the tube; N-HCl (3 ml) is added, and the phases are mixed by stirring; the mixture is then centrifuged at 3000 g for 3 min. The acetate–acetic acid phase (1.0 ml) is removed, and the radioactivity is determinined by counting for 3 min. Further acetate–acetic acid mixture (4.0 ml) is added, with mixing, and the extinction is read at 540 mμ in a 1-cm cell. The specific activity of hemin is then equal to—counts per 3 min per ml/$(1000 \times E^{540}_{1cm})$. (Anal. Abstr., Vol. 13, No. 8, Aug. 1966).

40831 ERRORS OF THE METHOD OF DIRECT AND INVERSE ISOTOPE DILUTION ANALYSIS CAUSED BY INEXACTNESS OF THE RADIOACTIVITY MEASUREMENTS OF THE SAMPLES AND BACKGROUND. Klas, J. (Slovak Inst. of Tech., Bratislava). Collect. Czech. Chem. Commun., 31: 3119-26(Aug. 1966).

The analytical errors of the direct and inverse isotope dilution method were studied theoretically. The errors are caused by insufficient precision of measurement of the radioactivity of the samples and background. Conditions were investigated under which the analytical error is minimal or close to minimum. (auth)

40832 DETERMINATION OF LANTHANIDES IN URANIUM BY ACTIVATION ANALYSIS. Vobecky, M.; Mastalka, A.; Marecek, J. (Inst. of Nuclear Research, Czechoslovak Academy of Sciences, Rez. Research Inst. of Inorganic Chemistry, Usti nad Labem, Czechoslovakia). Collect. Czech. Chem. Commun., 31: 3309-14(Aug. 1966).

A method for the determination of lanthanides in uranium by means of neutron activation analysis is described. Determination by activation was made possible by quantitative separation of uranium on an anion exchanger before activation of the sample. Final isolation of the individual lanthanides after irradiation of the sample was carried out chromatographically on a cation exchanger by elution with a concave gradient of the ammonium α-hydroxyisobutyrate concentration (pH 4.8). This procedure made possible full utilization of the extreme sensitivity of the activation analytical method. (auth)

40833 DETERMINATION OF SMALL SPECIFIC ACTIVITIES BY MEASUREMENTS OF HIGH-ENERGY β-RADIATION. Dementev, V. A.; Furman, A. O. Dokl., Ross. Sel'skokhoz. Akad., No. 99, 537-46(1964). (In Russian).

Beta radiation of ^{40}K in KCl was measured by anticoincidence techniques using two series of Geiger-Mueller counters. The lead shielding (5cm) and the anticoincidence shielding resulted in efficient β particle measurements. The results are given as a function of the number of counters in the series and the weight of the measured sample. (D.H.M.)

40834 INVESTIGATION OF THE GEOGRAPHICAL AND VERTICAL DISTRIBUTION OF SEVERAL TRACE ELEMENTS IN SEA-WATER BY NEUTRON-ACTIVATION ANALYSIS. Schulz, D. F.; Turekian, K. K. (Yale Univ., New Haven). Geochim. Cosmochim. Acta, 29: 259-313 (1965).

Methods for the determination of Hg, Se, Sb, Cr, Rb, Cs, Ag, Au, Zr, Hf, Ta, Zn, Co, Fe, Sc, Ba, and Sr in sea water are described, with details of sampling procedure, radiochemical separations, and counting procedures. Strontium is used as an internal flux-monitor. Results are shown to be independent of the major analytical variables, and coefficients are ± 23%. (Anal. Abstr. Vol. 13, No. 8, Aug. 1966).

40835 DETERMINATION OF GOLD, IRIDIUM, AND PLATINUM IN METEORITES AND NATURAL MATERIALS BY THERMAL-NEUTRON ACTIVATION ANALYSIS. Boedecker, P. A.; Ehmann, W. D. (Univ. of Kentucky, Lexington). Geochim. Cosmochim. Acta, 29: 329-42(1965).

The experimental techniques used for Ir are those of Rushbrook and Ehmann (Analyt. Abstr., 1962, 9, 5210). For Au and Pt, the flux monitors used are squares of high-purity aluminium foil, on to which are evaporated aliquots of a standard flux-monitor solution. This solution is prepared by dissolving metal (10 μg of platinum and 1 μg of gold) of 99.9% purity in aqua regia and diluting to the desired concentration. The flux-monitor foil and its cover are sandwiched between two blank aluminum foils, which

are counted separately after irradiation to allow for impurities in the aluminum foil. The flux-monitor package is wrapped around the quartz vial containing the sample for irradiation. Full details are given for the radiochemical separations. Gold is determined by counting the 0.411-Mev photopeak of 2.7-day ^{198}Au produced by (n,γ) reactions on the 100% naturally abundant ^{197}Au. Platinum is determined from the 0.158-Mev photopeak of 3.14-day ^{199}Au in the extracted gold sample, produced by the β-decay of the 31-min ^{199}Pt, which in turn is produced by (n,γ) reactions on 7.2% naturally abundant ^{198}Pt. The absolute error for Au and Ir is estimated to be ±10%, and that for Pt ±20%. (Anal. Abstr., Vol. 13, No. 8, Aug. 1966).

40836 ISOTOPIC FRACTIONATION IN THE WATER OF CRYSTALLIZATION OF CALCIUM SULFATE. Fontes, J. C. (Faculte des Sciences, Sorbonne, Paris). Geol. Rundsch., 55: 172-8(1966). (In French).

The fractionation of ^{18}O between the mother liquor and the water of crystallization of gypsum was experimentally determined. A special apparatus was used for extraction of the water of crystallization and its analysis. A 20-g sample of gypsum was placed in a Pyrex tube which was evacuated to remove traces of adsorbed water. The sample was then heated to 400°C, and the released water collected by condensation in liquid N_2. Almost 100% of the water of crystallization was released after 40 min of heating. The water of crystallization was then equilibrated at 25.2°C with CO_2, and the isotopic composition of the carbon dioxide determined by mass spectrometry. The mean value of ^{18}O was −0.45% for synthetic crystalline calcium sulfate hydrate and the value for natural gypsum varied from −0.36 to −0.42%, with a mean value of −0.39%. The mean error was estimated to be ±0.03%. The isotopic fractionation factor in the crystallization of gypsum ($^{18}O/^{16}O$ for water of crystallization: mother liquor) was found to vary from 1.0029 to 1.0041. The geologic significance of these results are discussed and they are applied to paleoclimatic and paleogeographic interpretations. (BBB)

40837 DETERMINATION OF ^{85}Sr, ^{106}Ru, ^{137}Cs, AND ^{144}Ce BY γ-SPECTROSCOPY OF THEIR MIXTURES USING SIMULTANEOUS EQUATIONS. Knezevic, Zvonko (Institut za Kemiju, Prirodno-Matematicki Fakultet, Sarajevo, Ys.); Pujic, Zdravko; Maric, Stjepan. Glas. Hemicara Technol. Bosne Hercegovine, 12: 81-8(1963). (In Croatian).

The nuclides Sr-85, Ru-106, Cs-137, and Ce-144 were determined by automatic single-channel gamma spectroscopy. Simultaneous equations describing mutual interferences of the nuclides were used. Precision and accuracy for determination of microcurie level was about ±15%. (auth)

40838 THE DETECTION OF SILVER IN RAINWATER: ANALYSIS OF PRECIPITATION COLLECTED FROM CLOUD-SEEDING EXPERIMENTS. Warburton, J. A.; Maher, C. T. (CSIRO, Sydney). J. Appl. Meteorol., 4: 560-4(Oct. 1965).

Measurements were made of the concentration of silver in precipitation samples collected in areas of Australia where cloud seeding with silver iodide had occurred. Silver was detected in 41 of 63 "seeded" samples and in three of 23 "unseeded" ones. Values of concentration of the silver were between 3×10^{-12} gm ml^{-1} and 4.8×10^{-11} gm ml^{-1}. There is some evidence that silver is detected more frequently when the precipitation falls from seeded clouds which have top temperatures < −15°C. (auth)

40839 THE DETECTION OF SILVER IN RAINWATER: FURTHER DEVELOPMENTS OF TECHNIQUE. Warburton, J. A. (CSIRO, Sydney). J. Appl. Meteorol., 4: 565-8(Oct. 1965).

Details are presented of the experimental processes involved in the concentration of silver ions from water. Monitoring procedures, which lead to improvements in reliability in the techniques, are described. The performance of the detection system using better quality ion-exchange resins, was measured using the radioisotopes ^{110}Ag and ^{131}Ba in dilute aqueous solutions. The lower limit of detection was extended to ion-exchange column loadings of 4×10^{-8} g of silver. (auth)

40840 DETERMINATION OF FLUORIDE IN FLUORINATED URANIUM COMPOUNDS WITHOUT PREVIOUS SEPARATION. Lievens, F.; Lecocq, A. (CEN, Mol, Belg.). J. Inorg. Nucl. Chem., 28: 1871-5(Sept. 1966).

An electrolytic cell composed of an aluminium−platinum couple in a molar acetic acid medium does not yield an appreciable current unless fluoride ions are present. This cell can be used to determine traces of fluoride in the presence of uranium. Fluoride contents are then measured down to the microgram scale. The accuracy on the determination of 10 μg of fluoride in the presence of 10 mg of uranium is of the order of 1 per cent. (auth)

40841 REVIEW ON THE ANALYTICAL METHODS FOR THE STABLE AND RADIOACTIVE CESIUM. Yamagata, Noboru (Inst. of Public Health, Tokyo). Contract 140/R2/RB. Koshu Eiseiin Kenkyu Hokoku, 14: 59-86(1965).

Radiochemical separation methods as well as analytical methods for stable cesium in trace amounts are reviewed. (251 references). (P.C.H.)

40842 DETERMINATION OF COLLOIDAL GOLD BY THERMAL NEUTRON RADIOACTIVATION. Pijck, J. (Univ., Ghent). J. Pharm. Belg., 20: 300-10(July-Aug. 1965). (In French).

Detailed information is presented for a method whereby traces of colloidal gold may be determined by nondestructive neutron activation analysis with γ spectrometric measuring techniques. The reproducibility of analyses on pure diluted gold colloid solutions was good. It was, however, impossible to obtain reproducible results when analyzing a complex mixture containing an excess of Cu and Ag. In all analyses of pharmaceutical preparations containing traces of colloidal gold, important losses of gold were noted, due to adsorption on the glass containers. Reproducibility of the method described varied from 1.5% for a gold solution of 1 mg/ml to 4.8% for a 2 μg/ml solution. Gold can be assayed to sample contents as low as 30 ppB. The neutron activation reaction for stable gold is as follows: $^{197}Au(n,\gamma)^{198}Au(n,\gamma)^{199}Au$. The 0.411-Mev γ emission of ^{198}Au was measured. The γ spectrum of Au and other radioisotopes is illustrated and some theoretical aspects of neutron-activation assay are discussed. (BBB)

40843 VARIATION OF THE ISOTOPIC CONCENTRATION IN SEPARATED RARE EARTHS. THEIR ACTIVATION IN RADIOACTIVATION ANALYSIS OF THESE ELEMENTS. Sautin, A.; Tousset, J. (Institut de Physique Nucleaire, Lyon). pp 1-10 of Journee de Radiochimie Analytique. Villeurbanne, France, Institut de Physique Nucleaire de Lyon, 1965. (In French).

In the determination of Gd by neutron activation in a mixture of rare earths, errors can result according to the isotope, ^{159}Gd or ^{153}Gd, used. Studies showed that there is an isotopic variation of ^{152}Gd in standards that introduces an error of approximately 50% in determinations made on this isotope. It is suggested that the separation of the standards, during which they are submitted to a number of separations and often to ion exchange purification, can be responsible for this variation of the ^{152}Gd. (J.S.R.)

40844 APPLICATION OF RADIOISOTOPIC DILUTION WITH INCOMPLETE EXTRACTION TO THE DETERMINATION OF THE OLIGOELEMENTS IN BIOLOGY. Bizollon, Ch. A.; Moret, R. (Pharmacie Centrale des Hopitaux, Lyon). pp 11-20 of Journee de Radiochimie Analytique. Villeurbanne, France, Institut de Physique Nucleaire de Lyon, 1965. (In French).

The use of radioisotopic dilution for determination of trace elements in biology is reviewed. The addition of incomplete extraction to improve the determination of trace elements is reviewed. Studies made on determination of Cu, Zn, and ceruloplasmin in the blood using the isotopic dilution method combined with incomplete extraction are outlined. The method is outlined in detail and the results are tabulated. They show that the method is simple, rapid, exact, and usable in series determinations. (J.S.R.)

40845 DETERMINATION OF FLUORINE IN GELS OF SILICA–ALUMINA CONTAINING LEAD FLUORIDE BY FAST NEUTRON RADIOACTIVATION. Bussiere, Paul (CNRS, Villeurbanne, France). pp 31-8 of Journee de Radiochimie Analytique. Villeurbanne, France, Institut de Physique Nucleaire de Lyon, 1965. (In French).

The radioactivation method used for determination of fluorine in gels of silica–alumina containing lead fluoride is outlined. An internal standard of alumina was used because of the reaction $^{27}Al(n,\alpha)^{24}Na$. The preliminary results obtained with the method are given. (J.S.R.)

40846 PRECISION AND CALIBRATION IN THE DETERMINATION OF OXYGEN BY NEUTRONS AT 14 Mev. Lepetit, H.; Tousset, J. (Institut de Physique Nucleaire, Lyon). pp 39-76 of Journee de Radiochimie Analytique. Villeurbanne, France, Institut de Physique Nucleaire de Lyon, 1965. (In French).

Experimental studies on the neutron activation determination of oxygen in boron are reported. Two methods of measurement were used, one with a secondary standard and the other with an internal standard. The principal causes of error are reviewed and a critique of the two methods is given. Results showed that the internal standard method offers the most advantages. With the internal standard, flux variations can be neglected and samples of any geometric form can be used. The limit of detection approaches 10 ppM of oxygen, but depends on the mass of the sample. (J.S.R.)

40847 SEPARATION OF SILVER FROM MIXTURES BY CATION-EXCHANGE CHROMATOGRAPHY. Rangnekar, Asha V.; Khopkar, S. M. (Indian Inst. of Tech., Bombay). Mikrochim. Ichnoanal. Acta, No. 4, 642-6 (1965).

The elution of Ag from a column (1.4 cm × 19 cm) of Dowex 50W-X8 (H^+ form) by solution of ammonium acetate, NH_4NO_3, $NaNO_3$, HNO_3, H_2SO_4, and citric, tartaric, and acetic acids was studied. Elution of 26 mg of Ag is complete with 200 ml of HNO_3 (3 to 6M), H_2SO_4 (M to 4M), ammonium acetate (3 to 4M), NH_4NO_3 (2 to 5M), or $NaNO_3$ (4 to 5M). Techniques were developed for the separation of Ag from Ce, Zr, Th, Bi, Fe, Cu, U, Al, Zn, Ba, Sr, Sb, and As. Attempts to separate Ag from Cd and Hg were not successful. (Anal. Abstr., Vol. 13, No. 8, Aug. 1966).

40848 ACTIVATION ANALYSIS IN THE METALS INDUSTRY. Wood, Donald E. (Kaman Nuclear Div., Kaman Aircraft Corp., Colorado Springs). Nucl. News, 9: No. 9, 12-17(Sept. 1966).

A description of the activation analysis systems used at Kaman Nuclear Laboratory; Dow Chemical Company (analysis of oxygen in beryllium); Plessey Nucleonic (analysis of oxygen in steel); General Motors (analysis of silicon in iron); United States Geological Survey (silver ore location); U. S. Steel Corporation (oxygen in steel); and Texas Nuclear Corporation (conveyor belt for several applications) is given. The potential and future prospects of activation analysis are discussed. (D.H.M.)

40849 BIS-2-PYRIDYL GLYCOL AS A REAGENT FOR GRAVIMETRIC DETERMINATION OF URANIUM, ALUMINIUM, AND BERYLLIUM. Bhat, A. N.; Gupta, R. D.; Jain, B. D. (Univ. of Delhi). Proc. Indian Acad. Sci., Sect. A, 63: 356-60(June 1966).

Bis-2-pyridyl glycol was used for the gravimetric determination of uranium, aluminum, and beryllium. The reagent quantitatively precipitates uranium from uranyl nitrate solution at pH 5.0 to 8.0, aluminum from potash alum solution at pH 5.2 to 8.5, and beryllium from beryllium sulfate solution at pH 7.5 to 9.5. The precipitate in each case was ignited to the corresponding oxide and weighed. (auth)

40850 SEPARATION AND ENRICHMENT OF TRACE COMPONENTS IN ANALYTICAL CHEMISTRY. Minczewski, J. (Warsaw Technical Univ. Inst. for Nuclear Research, Warsaw). Pure Appl. Chem., 10: 567-78(1965).

Trace analysis of inorganic compounds is discussed. Two types of trace analysis considered are: those in which the analysis aims at the determination of traces of the desired element present in the sample; and those in which, on the basis of analytical results, the purity of the examined substance must be evaluated and all, or at least a significant number, of impurities present in the samples must be determined. The technological processes are discussed according to the basic ability of elements to undergo the fundamental chemical reactions: acid-base, redox, precipitation, and complexing reactions. (D.H.M.)

40851 CHROMATOGRAPHIC SEPARATION OF SOME XENON AND IODINE OXYGEN COMPOUNDS. Mosevich, A. N.; Kuznetsov, N. P.; Gusev, Yu. K. Radiokhimiya, 7: 678-87(1965). (In Russian).

By means of radioactive tracers, the behavior of XeO_3 and the anions 10_3^- and 10_4^- on the ionites aluminum oxide, zirconium hydroxide, zirconium phosphate, and Amberlite IRA-400 was investigated and the conditions for separating XeO_3 from solutions containing iodate and periodate were determined. It was found that when gaseous xenon is present in the solutions, it is eluted from the XeO_3 on cleared columns of aluminum oxide, zirconium hydroxide, and Amberlite IRA-400. The chromatographic separation of the mixture $XeO_3 - 10_3^- - 10_4^-$ on zirconium hydroxide, zirconium phosphate, and Amberlite IRA-400 was carried out. Chemically bound xenon-131m, formed as a result of the β decay of ^{131}I in the compound HIO_3, was separated in pure form by the addition of XeO_3 as carrier. (tr-auth)

40852 DETERMINATION OF ^{131}I. Degtyarev, Yu. N.; Belosiyudova, G. A. Radiokhimiya, 7: 729-32(1965). (In Russian).

The substitution of aqueous solutions saturated with gaseous sulfur for sodium bisulfate during the determination of radioactive isotopes of iodine in milk and vegetable rinses simplified the analytical process. The method for the determination of iodine-131 in fresh mixtures of radioactive isotopes is presented. (tr-auth)

40853 COMBINED DETERMINATION OF ^{90}Sr AND ^{137}Cs. Degtyarev, Yu. N. Radiokhimiya, 7: 733-6 (1965). (In Russian).

A method for the combined separation and determination of ^{90}Sr and ^{137}Cs in samples of the surface atmosphere, food products, and the biosubstratum was developed. The yield of the carrier strontium varied from 40 to 80%. The yield of carrier Cs was of the order of 80%. (tr-auth)

40854 ^{90}Sr CONTENT IN MILK IN MEXICO. Nulman, Rebeca M.; Baez, A. P. (Comision Nacional de Energia Nuclear, Mexico City). Rev. Mex. Fis., 15: 177-99(1966).

A simple and economic method for determining ^{90}Cr content in milk was developed. This method permits running several samples simultaneously with little supervision. The recovery of the activity due to ^{90}Sr is of the order of 90%. The sampling method and detailed radiochemical separation procedure are described and the results for 1963, 1964, and the first eight months of 1965 are given. The ^{90}Sr content in Mexican milk is low compared to those reported for milk in the United States of America. (auth)

40855 ANION-EXCHANGE SEPARATION TECHNIQUES WITH METHANOL–WATER SOLUTIONS OF HYDROCHLORIC AND NITRIC ACIDS. Morrow, Richard J. (Univ. of California, Livermore). Talanta, 13: 1265-74(Sept. 1966). (UCRL–14312).

Mixed methanol-water systems were shown to be of use in analysis of samples containing 500-mg amounts of metallic impurities for rare earths and actinides. Detailed study of the hydrochloric acid-methanol system led to improved separation of einsteinium and californium from americium and curium as well as to lanthanide-actinide separations. Comparisons of elution orders are also drawn between these systems and the corresponding lithium salt systems, with emphasis on ion-hydration theories. (auth)

40856 SEPARATION OF TECHNETIUM FROM RHENIUM BY LIQUID-LIQUID EXTRACTION WITH POTASSIUM XANTHATE. Kiba, T.; Terada, K.; Okawa, N.;

Osaki, S. (Kanazawa Univ., Japan). Talanta, 13: 1385-8(Sept. 1966).

A method is described for separating technetium from rhenium in hydrochloric acid medium by liquid-liquid extraction using potassium xanthate and carbon tetrachloride. The effects of the concentration of various acids, concentration of xanthate, different solvents, and diverse ions were investigated. (auth)

40857 DETERMINATION OF ISOTOPIC COMPOSITION OF URANIUM IN SAMPLES BY ABSORPTION OF α-RADIATION. Lenin, S. S. Vop. Rudn. Geofiz., Min. Geol. Okhrany Nedr. SSSR, No. 5, 20-4(1965). (In Russian).

The ratio $^{234}U:^{238}U$ was determined by measuring the α radiation filtered through thin films with the accuracy provided by alpha spectrometers of high resolving power. Al foil, thin condenser paper, polyethylene, and polyfluoroethylene films can be used as absorbers. A plate with a luminous compound is set directly on the cathode, the absorber is then set on the plate, and the source is attached closely to the absorber without an air clearance. The thickness of the absorber was selected so that during the registering of α particles the count rate with the absorber is 0.07 of that without the absorber. Two-layer absorbers made from condenser foil and metallized polyethylene film satisfied the requirements best. The measurements showed good agreement with data obtained using a pulse ionization chamber. Systematic errors of ~10 and 30% resulted when the densities of uranium layers were 160 and 300 γ/cm^2. (P.C.H.)

40858 CONTRIBUTION TO THE SEPARATION OF ^{90}Sr, ^{89}Sr, AND ^{140}Ba FROM THE ASHES OF BEEF BONES, MILK, AND FISH. Niepel, J. (Bereitstellung der Forschungsmittel, Berlin). Z. Lebensm.-Untersuch. Forsch., 128: 144-53(1965). (In German).

The common separation of strontium and barium from the ashes of beef bones, milk, and fish was obtained by two nitrate precipitations at HNO_3 concentrations of 67 and 68% and a calcium content of the final precipitation 1.5% with yields of 90 to 93%. The nitrate percipitate can be filtered from concentrated HNO_3 in a polyvinyl chloride filtration device with a removable upper part on normal filter paper of hard gradation. The calcium constituent of the nitrate precipitate was determined by a modified method. (tr-auth)

40859 DETERMINATION OF LANTHANUM IN CERIUM OXIDE USING PAPER CHROMATOGRAPHY. Babko, A. K.; Vdovenko, M. E. (Inst. of General and Inorganic Chemistry, Academy of Sciences, Ukrainian SSR). Zavodsk. Lab., 32: 783-4(1966). (In Russian).

A method was developed for determining 5 to 40% La in cerium oxides within ±5%. The preliminary separation is achieved by paper chromatography. A direct photometric analysis of the chromatographic spots in reflected light is used to determine the content of lanthanum. (R.V.J.)

40860 PHOTOMETRIC DETERMINATION OF LANTHANUM BY XYLENOL ORANGE IN THE PRESENCE OF COMPLEXONE III. Vdovenko, M. E. (Inst. of General and Inorganic Chemistry, Academy of Sciences, Ukrainian SSR). Zavodsk. Lab., 32: 785-6(1966). (In Russian).

Lanthanum determination in Complexone III solutions was carried out using Xylenol Orangé with calcium nitrate acting as a buffer. The equilibrium in the solutions shifted to the side of lanthanum Xylenol Orange complex formation. (R.V.J.)

40861 ISOTOPIC SPECTRAL ANALYSIS OF HELIUM WITH THE USE OF AN ISOTOPIC FILTER. Lvov, B. V.; Mosichev, V. I. Zh. Prikl. Spektrosk., Akad. Nauk BSSR, 4: 491-6(June 1966). (In Russian).

A simple photoelectric method of isotopic analysis of helium ($^3He-^4He$) was worked out at the 10830 Å He ($2\,^3P_{0,1,2}-2\,^3S_1$). It is based on the absorption of ^4He components in an absorption tube filled with natural helium. The calibration curve is in good agreement with the calculated one. The single measurement error does not exceed 0.2-0.3 at. % ^3He. The range of concentrations determined is 1-99% of one of the isotopes. (auth)

40862 SELECTIVE ACTIVATION IN NEUTRON ACTIVATION ANALYSIS. Mozeck, P. Dresden, Technische Univ., 1965. 159p. $2.00 Gmelin, AED-Diss. 65-293. Thesis.

Selective activation using special neutron filters for the suppression of self-shielding in neutron activation samples with high cross section was studied. Determination of thermal and epithermal neutron flux is described. Maximum quantities of isotopes for 5 and 10% error from self-shielding are tabulated. (Gmelin Inst.)

40863 CHARACTERISTICS OF THE CONCENTRIC TUBE AND PARALLEL PLATE ELECTRON CAPTURE DETECTORS. Hartmann, C. Harold; Oaks, Dudley M.; Dimick, Keene P. (Varian Aerograph, Walnut Creek, Calif.). 12p. (CONF-660201-3). ORAU. Gmelin, AED-CONF-66-117-2.

From Conference on Analytical Chemistry and Applied Spectroscopy, Pittsburgh.

The effect of nonelectron adsorbing materials, such as hydrocarbons, on the response of the electron capture detector is described. Linearity, sensitivity, and baseline stability were studied using both the concentric tube and parallel plate detectors. Also studied were the merits of pulsed versus d-c voltage, and nitrogen versus argon-methane as carrier gas for both detectors. (J.F.P.)

Inorganic and Physical Chemistry

Refer also to abstracts 41064, 41411, 41412, 41438, and 41455.

40864 (BMwF-FBK-66-10) ELEKTROLYTISCHE ABSCHEIDUNG VON BERYLLIUM AUS METALLORGANISCHEN KOMPLEXSALZEN. (Electrolytic Deposition of Beryllium From Metallorganic Complex-Salts). Strohmeier, W. (Wuerzberg Univ. (West Germany). Institut fuer Physikalische Chemie). May 1966. 14p. Dep. mn. DM 1,60.

The electrodeposition of beryllium as a coherent film is possible from beryllium organic complex-salts of the type $MX \cdot n \cdot Be(C_2H_5)_2$ in the temperature range from 60 to 100°C on copper or silver electrodes. The exact analysis of the deposited beryllium showed, however, that, simultaneously at the cathode, Be_2C is formed, which becomes immersed in the beryllium deposit. The amount of Be_2C in Be is about 20 to 30%. (auth)

40865 (CNLM-4461) HEAT CAPACITY AND ENTHALPY OF URANIUM MONONITRIDE FROM 0 TO 1200C (32 TO 2200F). Harrington, L. C. (Pratt and Whitney Aircraft, Middletown, Conn. Connecticut Advanced Nuclear Engineering Lab.). Mar. 8, 1963. Contract AT(30-1)-2789. 2p. Dep. mn. CFSTI $1.00 cy, $0.50 mn.

40866 (EUR-2954.e) ISOTHERMAL TRANSPORT PROCESSES IN MOLTEN SALTS BINARY SYSTEMS. Berlin, A.; Forcheri, S.; Langevin, B.; Wagner, V. (European Atomic Energy Community, Ispra (Italy). Joint Nuclear Research Center). 1966. 12p. (CONF-650975-1). Dep. mn.

From 16th Meeting of the International Committee of Thermodynamics and Electrochemical Kinetics, Budapest, Hungary.

Transport number determinations in the molten systems $(Cs-Ag)NO_3$ at T = 240°C, $(Na-Tl)NO_3$ at T = 320°C and in the $CsNO_3$-rich region of the $(Na-Cs)NO_3$ system at T = 440°C, were carried out by means of an ionophoretic technique. The inert support was provided by a thin layer of fritted porous ceramic oxides (Al_2O_3, MgO, or ZrO_2) fixed on strips of sintered ceramic oxides (Al_2O_3 or ZrO_2) with zero open porosity. In both $(Cs-Ag)NO_3$ and $(Na-Tl)NO_3$ the measured transport numbers varied in a non-linear way with composition, indicating that ionic mobilities are not constant. From the transport parameters liquid junction potentials were calculated. These values never exceed 8 mv $(Cs-Ag)NO_3$, and 3 mv $(Na-Tl)NO_3$. (auth)

40867 (KFK-385) UEBER DOPPELFLUORIDE DER VIERWERTIGEN ACTINIDENELEMENTE THORIUM, URAN,

NEPTUNIUM UND PLUTONIUM VOM TYP $Me^{II}Me^{IV}F_6$ MIT LaF_3-STRUKTUR. (Double Fluorides of Tetravalent Actinide Elements Thorium, Uranium, Neptunium, and Plutonium of the Type $Me^{II}Me^{IV}F_6$ With LaF_3 Structure). Salzer, Manfred (Kernforschungsanlage, Juelich (West Germany). Institut fuer Radiochemie). Feb. 1966. 68p. Dep. mn.

The preparation and properties of the double fluorides of some actinide elements with the general formula $Me^{II}Me^{IV}F_6$ (where Me^{II} = Ca, Sr, Ba, Pb, Cd, Eu and Me^{IV} = Th, U, Np, and Pu) were investigated. The compounds $CaThF_6$, $CaUF_6$, $CaNpF_6$, $CaPuF_6$, $SrThF_6$, $SrUF_6$, $SrNpF_6$, $SrPuF_6$, $BaThF_6$, $BaUF_6$, $BaNpF_6$, $PbThF_6$, $PbUF_6$, $PbNpF_6$, $CdThF_6$, and $EuThF_6$ were prepared by solid state reactions in the temperature interval from 800 to 1,100°C. The compounds $CaThF_6$, $SrThF_6$, $SrUF_6$, $SrNpF_6$, $SrPuF_6$, $SrCeF_6$, $BaThF_6$, $BaUF_6$, $PbThF_6$, $PbUF_6$, $PbCeF_6$ were prepared by precipitation reactions from aqueous solutions. All the compounds prepared from aqueous solutions crystallized in the hexagonal LaF_3 lattice. The lattice constants of all compounds prepared were determined. In the framework of solubility studies on the systems MeF_2-MeXF_6 (Me = Ca, Sr, Ba, and Pb and X = Th, U, Np, and Pu) and MeF_2-XF_3 (Me = Ca, Sr, and Ba and X = Ce, Pu, and Am) it was found that between 25 and 27 mole % of MeF_2 dissolves in $Me^{II}Me^{IV}F_6$. A solubility of $Me^{II}Me^{IV}F_6$ in MeF_2 could be detected only in the system $BaThF_6-BaF_2$. A solubility of MeF_2 in MeF_3 could be found only in the system SrF_2-CeF_3. By density measurement it was determined that in the solubility of MeF_2 in $Me^{II}Me^{IV}F_6$ an ion vacancy is formed. The results of x-ray studies of the double fluorides are tabulated. (tr-auth)

40868 (LA–3523) THE SOLUBILITIES OF SELECTED ELEMENTS IN LIQUID PLUTONIUM. VIII. MOLYBDENUM. Bowersox, D. F.; Leary, J. A. (Los Alamos Scientific Lab., Univ. of California, N. Mex.). May 24, 1966. Contract W-7405-eng-36. 11p. Dep. mn. CFSTI $1.00 cy, $0.50 mn.

The solubility of Mo in liquid Pu was measured over the temperature range 700 to 1000°C. The solubility increased from 0.63% Mo (by weight) at 700°C to 2.07% Mo at 1000°C. The data fit the equation $\log N_{Mo} = 0.329 - 2.06 \times 10^{-3}\ T^{-1}$, where N_{Mo} is the solubility expressed as the mole fraction and T is the temperature in degrees Kelvin. (auth)

40869 (MCW–1473) CALIBRATION OF A WESTPHAL BALANCE AND PLUMMET. Christopherson, H. L. (Mallinckrodt Chemical Works, Weldon Spring, Mo. Uranium Div.). Aug. 12, 1966. Contract W-14-108-eng-8. 6p. Dep. mn. CFSTI $1.00 cy, $0.50 mn.

Equations were derived for the relationships that must exist among the volume of the plummet; the masses of the plummet, weights, and reference; and the densities of air and the reference fluid to obtain direct readings of either density or specific gravity. Suggestions are made for obtaining the relationships. A procedure is given for calibrating the Westphal beam notches. (auth)

40870 (NAA-SR-Memo-7310) A POSSIBLE MECHANISM FOR THE ACTIVATION OF URANIUM MONOCARBIDE. Colby, L. J. Jr. (Atomics International, Canoga Park, Calif.). Apr. 11, 1962. Contract AT(11-1)-Gen-8. 9p. Dep. mn. CFSTI $1.00 cy, $0.50 mn.

A mechanism is proposed to explain the activation of UC. The chemical reactivity of UC is a sensitive function of its hydrogen content. It is suggested that UH_3 acts as a catalyst in the reaction of UC with O_2, N_2, CO_2, and H_2O. (auth)

40871 (NIRL-R-95) TABLES OF VAPOUR PRESSURE AND MOLAR VOLUME FOR LIQUID HYDROGEN AND DEUTERIUM. Tapper, R. J. (comp.) (Rutherford High Energy Lab., Science Research Council, Chilton (England)). Mar. 1965. 16p. Dep. mn. BIS $0.60. HMSO 3s.

Tables of published empirical equations for vapor pressures and molar volumes of liquid hydrogen and deuterium are presented. The tables were prepared for use in accurate total cross section measurements using liquid hydrogen and deuterium as target materials. (M.C.G.)

40872 (NP–16254) ZUR CHEMIE DES PROMETHIUMS. (Chemistry of Promethium). Scherer, Volker (Munich Univ. (West Germany)). 1966. 97p. Dep. mn. Thesis.

The fluoride, chloride, bromide, oxyhalides, iodate, oxides hydroxide, phosphate, arsenate, chromate, vanadate, scandate, borate, indate, tungstate, molybdate, and chromate of Pm were prepared. Pm salts of some acids were also prepared. These included the dihydrate of Pm carbonate, the decahydrate of Pm oxalate, Pm formate, and Pm trichloroacetate. X-ray diffraction patterns were obtained for all compounds prepared. The ion radius of the Pm(III) ion was determined and found to lie between that of Nd and Sm. (79 references). (J.S.R.)

40873 (NYO–3462-2) STABLE ISOTOPE STUDIES. Annual Progress Report, July 15, 1965–August 15, 1966. Spindel, William (Belfer Graduate School of Science, Yeshiva Univ., New York). Aug. 15, 1966. Contract AT(30-1)-3462. 67p. Dep. mn. CFSTI $3.00 cy, $0.75 mn.

Experimental results are reported on the fractionation factor for nitrogen-15 between nitric oxide and nitric acid solutions at various temperatures below room temperature. Additional reactivity of nitric oxide with the acid solutions at lower temperature appears to limit the magnitude of the fractionation factor. Partition function ratios for nitrogen and oxygen exchange were calculated over a wide range of temperatures for about 14 different inorganic oxy-nitrogen molecules from the best available spectroscopic data. Partition function ratios calculated by approximation methods were compared to results obtained by an "exact" equation. Equilibrium constants for both N and O exchange among all the molecules were calculated and a large number of instances of "inversion" of isotope fractionation was found, including several cases of multiple inversions. Further studies are in progress on the "inversions" of isotope effect and the relationship between isotope effects and individual interatomic motions in the molecules. (auth)

40874 (ORNL-RMIC–5) LISTS OF AVAILABLE AND DESIRED MATERIALS AND AVAILABLE CRYSTAL-GROWTH REFERENCES (ULTRAPURE INORGANIC RESEARCH MATERIALS). Connolly, T. F. (Oak Ridge National Lab., Tenn.). Aug. 1966. Contract W-7405-eng-26. 52p. Dep. mn. CFSTI $3.00 cy, $0.50 mn.

40875 (ORNL-TM–1599) A COMPUTER PROGRAM TO CALCULATE HIGH-TEMPERATURE THERMODYNAMIC FUNCTIONS. Godfrey, T. G.; Leitnaker, J. M. (Oak Ridge National Lab., Tenn.). Sept. 1966. Contract W-7405-eng-26. 37p. Dep. mn. CFSTI $2.00 cy, $0.50 mn.

A computer program, PLOTHEAT, was written which uses the method of least squares to fit high-temperature enthalpy data to one or several selected functions. From the generated equation the heat capacity, C_T^0, the enthalpy, $H_T^0 - H_{298}^0$, the entropy, S_T^0, and the free energy function, $(F_T^0 - H_{298}^0)/T$, are calculated and tabulated at 100° increments. (The last two quantities assume a knowledge of the entropy at 298.15°K, S_{298}^0.) A subroutine package can be used with the program to plot the computed equation together with the input data using different symbols for each set of data. (auth)

40876 (ORO–1797-2) THE EFFECT OF CHANGES IN THE IONIC MEDIUM ON THE STABILITY CONSTANT OF $Eu(NO_3)^{+2}$. Choppin, G. R.; Kelly, D. A.; Ward, E. H. (Florida State Univ., Tallahassee. Dept. of Chemistry). July 1, 1966. Contract AT(40-1)-1797. 21p. (CONF-660805–2). Dep. mn. CFSTI $1.00 cy, $0.50 mn.

From International Conference on Solvent Extraction, Goteberg, Sweden.

The stability constant of $(EuNO_3)^{2+}$ was measured in vari-

ous ionic media. Correlation of the values with the viscosity B coefficient indicated that the differences are related to the effect of ionic media on the structure of the solvent water. Correction of the measured stability constants by appropriate activity coefficients brought the values in the different media within experimental error of each other. The use of a constant ionic medium in determination of stability constants of inorganic complexes is a common practice. Relatively few experiments have been reported that study specifically the effect of changes in the constitution of the ionic medium. In studies of the weak ion-pairing of lanthanide ions by halide and nitrate anions, it was necessary to change significantly the constitution of the ionic medium; therefore, an investigation of possible medium effects in these systems seemed desirable. Formation of $(EuNO_3)^{2+}$ seemed to be a promising reaction as this weak, outer sphere complex should be relatively sensitive to medium effects. In this study both cation and anion species were varied separately. (auth)

40877 (RL-SEP-823) THERMAL STABILITY OF NITRATE FORM ANION RESINS IN A VENTED SYSTEM. Fullam, H. T. (General Electric Co., Richland, Wash. Hanford Atomic Products Operation). Dec. 1965. Contract AT(34-1)-1350. 37p. Dep. mn. CFSTI $2.00 cy, $0.50 mn.

Studies were made on factors affecting the self-ignition temperature for nitrate-form anion resins. The results indicated that the thermal stability of vented nitrate-form anion resin is lower than that previously anticipated, especially when the effect of Pu loading is considered. The lowest ignition temperature measured was 135°C, which was obtained with Pu-loaded resin; however, this was with a small volume of resin. With larger volumes of Pu-loaded resin, the ignition temperature would be much lower. For production-scale vented ion exchange columns (4-in. dia), the critical ignition temperature for loaded resin would be well below 100°C. Recommendations for reducing hazards involved in using nitrate-form anion resins are listed. (P.C.H.)

40878 TRI(CYCLOPENTADIENYL)AMERICIUM(III). Baumgaertner, F.; Fischer, E. O.; Kanellakopulos, B.; Laubereau, P. (Kernforschungszentrum, Karlsruhe, Ger.). Angew. Chem. Int. Ed. Engl., 5: 134-5(1966).

The first organometallic derivative of americium was prepared by treatment of $AmCl_3$ with molten $Be(C_5H_5)_2$ at 65°C: $2AmCl_3 + 3Be(C_5H_5)_2 \rightarrow 2Am(C_5H_5)_3 + 3BeCl_2$. In 4 batches, 0.6 g of $^{241}AmO_2$ was converted into rose-colored $AmCl_3$ by passage of a Cl_2/CCl_4/argon stream over it at 650°C for several hours. The yield of $Am(C_5H_5)_3$ from freshly prepared, powdered $AmCl_3$ was 50% (calculated on $AmCl_3$) after 12 hr; it was less if fused $AmCl_3$ cake or older $AmCl_3$ powder was used. $Am(C_5H_5)_3$ can be separated in an analytically pure state by fractional sublimation at 10^{-5} mm and 160–205°C as a flesh-colored compound which glows in the dark with a pale light. It does not melt below 330°C when heated in argon. At higher temperatures it darkens. It decomposes only slowly in air. The compound is not pyrophoric, unlike $Pu(C_5H_5)_3$, but discolors quickly during C–H analysis in pure oxygen, with formation of a black decomposition product. The compound is decomposed by water or dilute acids, with gas evolution and deposition of white flocks, to give a rose-colored Am(III) solution. Infrared spectra, taken for polycrystalline samples in Nujol or poly(tetrafluoroethylene), show the presence of symmetrical five-membered rings. The high specific radioactivity of the preparation requires measurement of the spectra by a special compensation technique. $Am(C_5H_5)_3$ and $Pu(C_5H_5)_3$ have analogous structures. The higher sublimation temperature, the greater thermal stability, the behavior in solution, and the absorption at 768/788 cm^{-1}, i.e., at lower wave numbers than for $Pu(C_5H_5)_3$, indicate that $Am(C_5H_5)_3$ resembles the cyclopentadienyl complexes of lanthanides more closely than does $Pu(C_5H_5)_3$. (BBB)

40879 SYNTHESIS AND STUDIES OF GALLIUM YTTRIUM SULFIDES ($YGaS_3$) AND INDIUM YTTRIUM SULFIDES ($YInS_3$). Karaev, Z. Sh.; Keiserukhskaya, L. G.; Alieva, Sh. A.; Gadymov, A. M. (Inst. of Inorganic and Physical Chemistry, Academy of Sciences, Azerbaidzhan SSR). Azerbaidzh. Khim. Zh., No. 1, 112-15(1966). (In Russian).

It is shown that the synthesized ternary compound $YGaS_3$ crystallizes into the hexagonal system and $YInS_3$ into the rhombic. The specific resistance of $YGaS_3$ is $\sim 10^8$ ohm·cm and that of $YIns_3$ is $\sim 10^7$ ohm·cm. Both compounds are stable in water and air and do not disintegrate in alkali and organic solvents. Reactions with hydrochloric and sulfuric acids release hydrogen sulfide. (R.V.J.)

40880 NOTE ON THE URANIUM AND COBALT COMPLEXES OF HETEROCYCLICALLY SUBSTITUTED FORMAZANS. Seyhan, Muvaffak; Sargin, Necla (Univ. of Istanbul). Chem. Ber., 99: 2072-4(1966). (In German).

For U complexing studies, the following formazans were prepared: N-phenyl-N′-(2-carboxyphenyl)-C-[isoquinolyl-(3)]-formazan, N-phenyl-N′-(2-carboxyphenyl)-C-[6-ethoxyquinolyl-(2)]-formazan, and N-phenyl-N′-(2-carboxyphenyl)-C-[antipyryl-(4)]-formazan. These were prepared by the reaction of diazotized anthranilic acid with the phenylhydrazones of 3-formylisoquinoline, 2-formyl-6-ethoxyquinoline, and 4-formylantipyrine, respectively. The first two form complexes with U on warming with ethanolic UO_2Ac_2 for a short period of time. These have a UO_2/formazan ratio of 1:1. The coordination number of U is five in these complexes, the sixth position being occupied by the electron pair of N. The third formazan yields a complex with Co on warming with ethanolic $CoCl_3 \cdot 6H_2O$. (BBB)

40881 STRUCTURE OF THE URANYL TRIPEROXIDE ION. Alcock, N. W. (Cambridge Univ., Eng.). Chem. Commun., No. 15, 536-7(Aug. 10, 1966).

An x-ray investigation was made on the crystal structure of the uranyl triperoxide ion, $(UO_8)^{4-}$. Structural data are given for crystals of the sodium salt of this ion, which were prepared by the reaction of uranium tetroxide with an excess of hydrogen peroxide in 10 M sodium hydroxide. The structure of the UO_8^{4-} ion is illustrated. There is a linear UO_2 group, with mean U—O distance 1.88 A, surrounded equatorially by three peroxide groups, mean U—O distance 2.27 A, mean O—O in the peroxide groups 1.51 A. (P.C.H.)

40882 THE PREPARATION, CRYSTAL STRUCTURE, AND MAGNETIC PROPERTIES OF PENTAFLUOROXENONYL HEXAFLUOROPLATINATE(V), $[XeF_5]^+[PtF_6]^-$. Bartlett, Neil; Einstein, Fred; Stewart, D. F.; Trotter, James (Univ. of British Columbia, Vancouver). Chem. Commun., No. 15, 550-2(Aug. 10, 1966).

Studies were made on the crystal structure and magnetic properties of $F_{11}PtXe$ formed during reactions between xenon, fluorine, and platinum pentafluoride. A single-crystal x-ray structure determination of $F_{11}PtXe$ disclosed a molecular geometry consistent with an ionic formulation $(XeF_5)^+(PtF_6)^-$. The magnetic susceptibility of the compound obeys the Curie-Weiss Law in the range 77 to 298°K with $\theta = 35°$. The crystals are orthorhombic with unit-cell dimensions: a = 8.16, b = 16.81, c = 5.73 A, V = 785.4 A^3. The geometric arrangement of the atoms is illustrated. Binding energies for the compound are discussed. (P.C.H.)

40883 HYDRIDO-DEUTERIO-COMPLEXES OF IRIDIUM. Vaska, L. (Mellon Inst., Pittsburgh. Clarkson Coll. of Tech., Potsdam, N. Y.). Chem. Commun., No. 17, 614-6(Sept. 7, 1966).

Two synthetic routes to hydrido-deuterio complexes, compounds in which the two hydrogen isotopes are simultaneously bonded to the same metal atom and occupy specific stereo-chemical positions, were investigated, and the structures of the resulting products examined by infrared spectroscopy. The reaction of $[IrCl(CO)(Ph_3P)_3]$ with hydrogen, using hydrogen deuteride as addendum, was studied. Crystals of the five-co-ordinated hydride complex $[IrH(CO)(Ph_3P)_3]$ reacted almost immediately with gaseous hydrogen halides. The structure and the

infrared data of the cation $[IrH_2(CO)(Ph_3P)_3]^+$ and its isotopic analogues are given. (D.H.M.)

40884 PARTICLE TRAJECTORIES IN RADIATION AND CHEMICAL PROCESSES IN A PSEUDO-LIQUEFIED LAYER. Kheifets, L. I.; Mukosei, V. I.; Dzhagatspanyan, R. V. Dokl. Akad. Nauk SSSR, 166: 1405-8(Feb. 21, 1966). (In Russian).

An attempt was made to take into account the effect of the suspended-particle trajectories in studies relating to the radiochemical chlorination and sulfochlorination processes of polymers in pseudo-liquefied layers; the diffusion model was used. It was assumed that diffusion inside the particles (all particles are isotropic spheres) is the limiting factor of the stationary radiochemical chlorination process of polyethylene, and that the gas volume does not change during the experiment,-i.e., for each mole of reacted chlorine, a mole of hydrogen chloride is formed. The trajectory distribution probability in the pseudo-liquefied layer was calculated for a given hydrodynamic model of the apparatus. It was suggested that the equations derived might be used as a basis for the calculations of fluidized-bed reactors. (C.E.S.)

40885 INFLUENCE OF ACID LIGANDS ON COMPLEXING OF URANYL WITH TRI-n-BUTYL PHOSPHINE OXIDE. Sinitsyna, S. M.; Sinitsyn, N. M. Dokl. Akad. Nauk SSSR, 168: 110-12(May 1, 1966). (In Russian).

The reaction of complex uranyl salts with tri-n-butylphosphine oxide (TBPO) was studied, and the properties of the complexes formed were investigated. Tris-tri-n-butylphosphine oxidosulfatouranyl, decakis-tri-n-butylphosphine oxidotetrasulfatotetrauranyl, tri-n-butylphosphine oxidooxalatouranyl, tris-tri-n-butylphosphine oxidotetraacetodiuranyl, bis-tri-n-butylphosphine oxidodiperchloratouranyl and tris-tri-n-butylphosphine oxidodithiocyanatouranyl were produced by adding a 20% solution of TBPO in heptane to a sample of the uranyl salt in the strictly stoichiometric amount. The compositions of the uranyl compounds obtained indicated that with decreasing displacing ability of the singly charged acido-ligands $CH_3COO^- > NO_3^- > ClO_4^- > CNS^-$, there is a tendency for an increase in the number of TBPO molecules in the inner sphere of the complexes. An analogous dependence can be noted for doubly charged acido-ligands: displacing ability $CO_3^{-2} \geq C_2O_4^{-2} > SO_4^{-2}$, number of TBPO molecules in the stable complex from zero for CO_3^{-2} to three SO_4^{-2}. The coordination number of the UO_2^{+2} group in complex compounds with TBPO in the inner sphere was found to depend on the nature of the acido-ligands, while the complex formation of RBPO even with monotypic uranyl salts cannot be described by one general equation. The nature of the acido-ligands substantially influences the composition, structure, and properties of coordination compounds of uranyl formed in extraction processes. (JPRS)

40886 INFRARED ABSORPTION SPECTRA OF LANTHANUM, GADOLINIUM, AND YTTRIUM NITRATES. Kharitonov, Yu. Ya.; Babievskaya, I. Z. (Kurnakov Inst. of General and Inorganic Chemistry, Academy of Sciences, USSR). Dokl. Akad. Nauk SSSR, 168: 615-17(May 21, 1966). (In Russian).

Rare earth bonding with the nitrate group in prepared compounds of $La(NO_3)_3 \cdot 6H_2O$, $Gd(NO_3)_3 \cdot 4H_2O$, $Y(NO_3)_3 \cdot 4H_2O$, and $Y(NO_3)_3 \cdot 2NH_4NO_3$ was studied using a spectrophotometer. The infrared absorption spectra and wave numbers of the maximum absorption bands are tabulated. A tendency toward strengthening of the coordination bonds between the central atom and nitrate groups was observed in the nitrates of Ce, La, Sm, Gd, and Y. The strongest coordination bonds were observed in the complex nitrate, $(NH_4)_2Y(NO_3)_5$. (R.V.J.)

40887 EFFECT OF DEUTERATION ON FLUORESCENCE LIFETIMES OF SOME URANYL SALTS. Pant, D. D.; Pande, D. N.; Pant, H. C. (DSB Government Coll., Nainital, India). Indian J. Pure Appl. Phys., 4: 289(1966).

The effect of substituting hydrogen by deuterium on the lifetimes of uranyl sulphate and potassium uranyl sulfate was studied. While uranyl sulfate shows an increase in the lifetime on deuteration, no such effect is observed in potassium uranyl sulfate. This is attributed to the fact that the quantum yield of the latter compound is unity. No changes in the nonradiative temperature dependent constants are indicated. (auth)

40888 LATTICE CONSTANTS OF 1:1 LITHIUM TETRAVALENT ACTINIDE PENTAFLUORIDES. Keenan, Thomas K. (Los Alamos Scientific Lab., N. Mex.). Inorg. Nucl. Chem. Lett., 2: 153-6(June 1966). (LA-DC-7886).

The compounds $LiNpF_5$, $LiPuF_5$, $LiAmF_5$, and $LiCmF_5$ were prepared and their lattice constants determined. The compounds are isostructural and tetragonal. A steady decrease in atomic volume was noted throughout the series. (D.H.M.)

40889 THERMAL STABILITY OF SAMPLES OF URANIUM FISSION PRODUCTS IN MONOCRYSTALLINE MUSCOVITE UNDER EXPERIMENTAL CONDITIONS FOR CHEMICAL ETCHING. Geguzin, Ya. E.; Berzina, I. G.; Vorob'eva, I. V. (Univ., Kharkov). Izv. Akad. Nauk SSSR, Ser. Geol., No. 6, 21-6(June 1966). (In Russian).

The real structure of a defect zone may be obscured by the closure of a defect, if another is formed with a lower chemical potential than the original. Mirror surfaces were obtained for sections across the surface of the sample. One of these was then heated in air to 500 or 600°C for one hour, and then the appearance of the etching surface was compared for the two faces. All surfaces were lightly etched. The number of deep and lightly etched features found compared to the total originally observed at 20°C was studied as a function of the temperature to which the sample was heated prior to etching. The number of both types remains similar to the low temperature values until about 425°C when the percentage of deep features begins to decrease and that of light features begins to increase; at 650°C only light features remain, but the quantity of even these begins to decrease slightly above this point. At 750°C it is half its maximum value. (BBB)

40890 INVESTIGATION OF THE SORPTION OF RUTHENIUM BY NATURAL SORBENTS. Sinitsyn, N. M. (Kurnakov Inst. of General and Inorganic Chemistry, Moscow). Izv. Sibirsk. Otd. Akad. Nauk SSSR, Ser. Khim. Nauk, No. 3, 87-93(1965). (In Russian).

The effect of the chemical state of radioruthenium in solution on its sorption by various natural sorbents was studied. The procedure and equipment used in the experiments are described. The percentage of sorption of radioruthenium depends primarily on the properties of the sorbent. Irrespective of the chemical form of radioruthenium in solution, the lowest sorption coefficient is shown by sand and clay, and the highest by peat and silt containing a maximum amount of humus and exchange calcium. The chemical state of ruthenium in solution has a considerable effect on the percentage of sorption. Irrespective of the nature of the sorbent, the highest sorption coefficient is shown by radioruthenium in solution in the form of nitroso nitrate complexes, and the lowest by the nitroso-nitro-, nitrosochloro-, and chloro complexes of ruthenium. The effect of hydrolysis of compounds in solution on the percentage of sorption is noted. The percentage of sorption also depends, to a considerable degree, on the time of contact of the sorbent with the ruthenium solution. An increase in the pH of the solution from 2 to 9 for clay as well as for soil causes an increase in the percentage of sorption. It was concluded that the behavior of radioruthenium during sorption by natural sorbents is extremely complicated, unique, and is fundamentally different from that of other long-lived fission products. The characteristic of the coordination chemistry of ruthenium and the chemical forms of finding it in solutions substantially affect the sorption of radioruthenium by natural sorbents. (ATD)

40891 OPTICAL SPECTRA OF TRIPOSITIVE ^{244}Cm IN LANTHANUM TRICHLORIDE. Gruber, John B. (Univ. of California, Los Angeles); Cochran, William R.; Conway, John G.; Nicol, Ann T. Contract AT(11-1)-34. J. Chem. Phys., 45: 1423-7(Sept. 1, 1966).

Absorption and emission optical spectra are reported for Cm^{3+} in $LaCl_3$ between 3000 and 8000 Å. These data are explained in terms of the Racah, spin-orbit, and configuration-interaction parameters: $E^0 = 4939.29$, $E^1 = 4621.47$, $E^2 = 17.70$, $E^3 = 399.42$, $\zeta = 2841.66$, $\alpha = 57.08$, $\beta = -4761.60$ cm^{-1}, respectively. Crystal-field splitting of the ground state $^8S_{7/2}$ was observed. (auth)

40892 NUCLEAR MAGNETIC RESONANCE AND RELAXATION OF HEXAFLUORIDE MOLECULES IN THE SOLID. Blinc, R.; Pirkmajer, E.; Slivnik, J.; Zupancic, I. (Nuclear Inst. Josef Stefan, Ljubljana, Yugoslavia). J. Chem. Phys., 45: 1488-95(Sept. 1, 1966).

The ^{19}F magnetic resonance absorption spectra and spin-lattice relaxation times of polycrystalline UF_6, PuF_6, WF_6, OsF_6, PtF_6, MoF_6, and XeF_6 were studied as a function of temperature and magnetic field. In all investigated metal hexafluorides the chemical shifts were quite large, exceeding the dipole–dipole broadening in the solid, and allowing an unambiguous determination of the tetragonal distortion of the hexafluoride octahedra in the low-temperature orthorhombic phase. The fluorines can occupy either axial or equatorial sites. The chemical shifts of the axial and equatorial fluorines (σ_0, axial = –5350 ppM, σ_0, equatorial = –2800 ppM) with respect to HF, and the anisotropies of the ^{19}F screening tensors in PtF_6, $|\sigma_{||} - \sigma_\perp|_a = 1300 \pm 100$ ppM and $|\sigma_{||} - \sigma_\perp|_e = 1380 \pm 100$ ppM seem to be the largest of all known fluorine compounds. A slow, thermally activated motion where each fluorine atom is alternatively axial and equatorial, and which consists of a hindered rotation and subsequent distortion of the octahedron in the crystalline field of its neighbors, produced at higher temperatures a coalescence of the spectrum into a single, narrow line. The same fluorine motion was found to influence the spin-lattice relaxation both by a direct modulation of the resonance fields due to anisotropic chemical shifts tensors and by a modulation of the dipole–dipole coupling. The solid-solid transitions to the cubic phase in PtF_6, WF_6, and MoF_6, were accompanied by a very sharp increase in T_1 and a lowering of the activation energy for molecular motion. (auth)

40893 CALCULATED ION-TO-MOLECULE-ION RATIOS FOR ELECTRON-BOMBARDMENT STUDIES OF MOLECULAR HYDROGEN AND ITS ISOTOPES. Cashion, J. K. (Harvard Univ., Cambridge, Mass.). J. Chem. Phys., 45: 1663-6(Sept. 1, 1966).

Recent calculations of the H_2^+ and H_2 potentials were used in computing the ratios X^+/X_2^+ (where X is H, D, or T) that arise from the electron bombardment of hydrogen and its isotopes. Values are given for a range of electron energies for the ground vibrational states. Values for 30-v electrons are given for those vibrationally excited states that would contribute to the ratio in shock-tube studies. All these values should be limited in accuracy only by the assumption of the Franck-Condon principle, which underlies the calculation. Comparison with experiments showed discrepancies of +6%, –16%, and –11% for hydrogen, deuterium, and tritium, respectively. (auth)

40894 DEUTERON QUADRUPOLE COUPLING CONSTANT IN CH_3D. Caves, T.; Karplus, M. (Columbia Univ., New York). J. Chem. Phys., 45: 1670-3(Sept. 1, 1966).

The deuteron electric-field gradient q_D and quadrupole coupling constant $(eqQ/h)_D$ for CH_3D were calculated from extended basis-set LCAO-MO-SCF wave functions determined by Woznick for this system. Comparison of the results for different wave functions and different distances suggest that a reasonable theoretical estimate is $(eqQ/h)_D = 210 \pm 30$ kc/sec. Since this disagrees significantly with the present experimental estimate [$(eqQ/h)_D = 100 \pm 50$ kc/sec], a more refined measurement would be desirable. Simplified schemes are examined for calculating $(eqQ/h)_D$ with neglect of three-center integrals or introduction of a two-center model; errors of 5 to 20% result. (auth)

40895 INFRARED SPECTRA OF HCl AND DCl IN SOLID RARE GASES. II. POLYMERS. Keyser, L. F.; Robinson, G. W. (California Inst. of Tech., Pasadena). J. Chem. Phys., 45: 1694-1702(Sept. 1, 1966).

Dimers and trimers of HCl, of DCl, and of mixed isotopic composition were identified from their infrared absorption spectra in rare-gas host matrices. One dimer and at least two different trimers were found. The vibrational frequencies of these aggregates can be quantitatively explained on the basis of a model where: the molecules are situated at substitutional sites in the close-packed rare-gas crystal; nearest-neighbor intermolecular resonance interactions, identical in magnitude with those in the pure HCl or DCl crystal, act to split the states of the aggregate into components about a "center of gravity"; and the position of the "center of gravity" depends upon the size but not the shape of the aggregate, decreasing in frequency toward the pure crystal limit as the aggregate grows. From an explanation of a portion of the trimer spectra, the sign of the intermolecular coupling constant was found to be positive. The relative intensities of the various spectral components are used to estimate the intermolecular orientations within the aggregate. While these estimates, which are based on an "oriented gas model," should be viewed with caution, the data suggest that the relative nearest-neighbor orientation approaches that of the crystal as the polymer size increases. The orientation in the dimer was very different from that in the crystal while the orientation in the trimer was intermediate between these two extremes. There is no obvious relationship between the HCl dimer observed in the rare-gas matrix and that observed by Rank, Sitaram, Glickman, and Wiggins in the gas phase. (auth)

40896 ATOM-ATOM IONIZATION CROSS SECTIONS OF THE NOBLE GASES: ARGON, KRYPTON, AND XENON. Kelly, Arnold J. (California Inst. of Tech., Pasadena). Contract AF 49(638)-1285. J. Chem. Phys., 45: 1723-32 (Sept. 1, 1966).

An experimental investigation of the initial phase of shock produced ionization in argon, krypton, and xenon was conducted in order to elucidate the atom-atom ionization reaction and to determine the atom-atom ionization cross sections. A high-purity shock tube was employed to heat these gases to temperatures in the range from 5000 to 9000°K at neutral particle densities of 4.4×10^{17}, 7.0×10^{17}, and 13.3×10^{17} cm^{-3}, and impurity levels of approximately 10^{-6}. A K-band (24-GHz) microwave system situated so that the microwave-beam propagation direction was normal to the shock tube, monitored the ionization relaxation process occurring immediately after the passage of the shock front. Electron density was calculated from the microwave data using a plane-wave–plane-plasma slab interaction theory corrected for near field effects associated with the coupling of the microwave energy to the plasma. These data, adjusted to compensate for the effects of shock attenuation, verified that the dominant electron-generation process involves a two-step, atom-atom ionization reaction and that the first step (excitation to the first excited states) is rate determining. The quadratic dependence on neutral density associated with this reaction was experimentally demonstrated (with an uncertainty of ±15%). The cross section, characterized as having a constant slope from threshold (first excited energy level), represented as the cross-sectional slope constant C, was equal to $1.2 \times 10^{-19} \pm 15\%$, $1.4 \times 10^{-19} \pm 15\%$, and $1.8 \times 10^{-20} \pm 15\%$ cm^2/ev for argon, krypton, and xenon, respectively. The electron-atom elastic momentum-exchange cross sections derived from the microwave data correlated quite well with Maxwell-averaged beam data, the agreement for the case of argon being ±20%; krypton, ±30%; and xenon, within a factor of 2. (auth)

40897 SOLUBILITY AND THERMODYNAMICS OF SOLUTION OF ARGON IN MIXTURES OF H_2O AND D_2O. Ben-Naim, A. (Hebrew Univ., Jerusalem). J. Chem. Phys., 45: 1848-9(Sept. 1, 1966).

Measurements of the solubility of argon in three mixtures of D_2O and H_2O are reported. The measurements were made to determine the effect of the amount of D_2O

added to water on the "degree of crystallinity" of the solvent. The thermodynamic functions, $\Delta\mu_t^0$, $\Delta\bar{S}t^0$, and $\Delta\bar{H}_t^0$, which were calculated for the transfer of argon from pure water into mixtures of D_2O and H_2O, showed a monotonic (nearly linear) change when changing the solvent from pure water to pure D_2O. This indicated that the O–D bonds not only fit into the framework of the clusters of O–H bonds, but also increase gradually in average size in passing from H_2O to D_2O. (D.H.M.)

40898 SPECTROPHOTOMETRIC AND CONDUCTOMETRIC STUDIES OF THE COMPLEXES BETWEEN UO_2^{2+} AND 2-HYDROXY-3-NAPHTHOIC ACID IN AQUEOUS MEDIUM. Gupta, S. L.; Soni, R. N. (Birla Inst. of Tech. and Science, Pilani, India). J. Indian Chem. Soc., 43: 311-15(May 1966).

The orange-colored, water-soluble complex, formed by the interaction of uranyl ion and 2-hydroxy-3-naphthoic acid, was studied spectrophotometrically in aqueous solutions of different ionic strengths and at different temperatures. It has an absorption maximum at 450 mμ and a flat region thereafter. The optimum pH range is 4.5 to 4.8 and it is stable towards time. The formula of the complex, established spectrophotometrically and conductometrically, is UO_2R (R = reagent). The molecular extinction coefficient is 4.16×10^2. The dissociation constant of the complex was determined for different ionic strengths and temperatures. The values of ΔH and ΔS were found to be –5.104 kcal and 37.2 ± 0.2 eu, respectively. The probable structure of the complex is also suggested. (auth)

40899 KINETICS OF THERMAL DECOMPOSITION OF UO_3. PART I. α-UO_3. Dharwadkar, S. R.; Karkhanavala, M. D. (Atomic Energy Establishment, Trombay, India). J. Indian Chem. Soc., 43: 363-7(May 1966).

Kinetics of thermal decomposition of α-UO_3 was studied thermogravimetrically. The decomposition was found to proceed according to the scheme: α-$UO_3 \rightarrow UO_{2.9} \rightarrow UO_{2.67}$. The rate-dependent parameters, viz., the order of reaction n, activation energy ΔE, and entropy of activation ΔS for the two steps: (i) α-$UO_3 \rightarrow UO_{2.9}$ and (ii) $UO_{2.9} \rightarrow UO_{2.67}$, were determined. (auth)

40900 DIFFERENTIAL THERMAL ANALYSIS OF OXALATE HYDRATES OF RARE EARTH METALS. Moebius, R.; Dietzold, W.; Matthes, F. (Technische Hochschule fuer Chemie, Merseburg, Ger.). J. Inorg. Nucl. Chem., 28: 1847-53(Sept. 1966). (In German).

Congruence of curves, obtained by differential thermal analysis of thermal decomposition of oxalate hydrates of the rare earths was found in several studies. Opinions are divergent regarding the decomposition of the anhydrous oxalates, following the dehydration. Factors that influence the results are discussed in detail. (auth)

40901 THE MAGNESIUM, STRONTIUM, AND BARIUM POLYURANATES. Klima, J.; Jakes, D.; Moravec, J. (Inst. of Nuclear Research, Prague). J. Inorg. Nucl. Chem., 28: 1861-9(Sept. 1966).

Magnesium mono- and triuranates were prepared by ignition of $MgCl_2$ with U_3O_8. A nonstoichiometric phase, as yet uncharacterized was formed when $SrCl_2$ was annealed with U_3O_8(Sr : U = 1 : 1). Barium mono- and diuranates were prepared by sintering barium carbonate and U_3O_8. Phases not fully identical with those reported by others were obtained by ignition of strontium and barium uranyl acetates. New reflection planes on $MgUO_4$, MgU_3O_{10}, and $BaUO_4$ were found and indexed in known lattice parameters. Infrared spectra were obtained for all uranates. It was found that infrared spectroscopy could be used as a rapid and sensitive analytical method for the qualitative determination of uranates. (auth)

40902 STABILITY OF SOME LANTHANIDE COMPLEXES WITH MANDELATE AND ATROLACTATE. Thun, H.; Verbeek, F.; Vanderleen, W. (Ghent Univ.). J. Inorg. Nucl. Chem., 28: 1949-54(Sept. 1966).

The successive formation constants were determined for mandelate and atrolactate complexes of several lanthanide elements by potentiometric titration. The formation constants increase as a function of the atomic numbers for both ligands. For atrolactate the usual irregularities in the trend in the Eu–Gd region are observed. For a given lanthanide the order of complex stability is atrolactate > mandelate ≅ α-hydroxyisobutyric acid > lactate > glycolate. The average ligand number per metal ion exceeding a value of three, indicates the formation of ML_4^- complexes. The acid dissociation constant for each of the ligands was also calculated. (auth)

40903 STUDY OF THE NATURE AND STABILITY OF THE SYSTEM URANYL-BENZOHYDROXAMIC ACID IN ACID MEDIUM. Maggio, F.; Romano, V.; Cefalu, R. (Univ., Palermo, Italy). J. Inorg. Nucl. Chem., 28: 1979-84(Sept. 1966).

Spectrophotometric and conductometric measurements made in aqueous acid solutions containing UO_2^{2+} and benzohydroxamic acid (HB), showed the formation of the complex ion UO_2B^+. The stability constant of this ion is 5.2×10^7 at 20°C and at ionic strength 1.0. The value of the stability constant shows that the complex ion is very stable at pH values between 2.3 and 2.8. The results confirm that under such experimental conditions protonic displacement from benzohydroxamic acid by the uranyl ion occurs $HB + UO_2^{2+} \rightleftharpoons UO_2B^+ + H^+$. (auth)

40904 EQUILIBRIUM STUDY OF THE CHLORIDE AND NITRATE SYSTEMS OF PRASEODYMIUM AND NEODYMIUM WITH TRIBUTYL PHOSPHATE AND ACID. Gray, J. A.; Smutz, M. (Ames Lab., Ames, Iowa). Contract W-7405-eng-42. J. Inorg. Nucl. Chem., 28: 2015-24(Sept. 1966). (IS-1235).

An equilibrium study was made of the solvent extraction systems, $Nd(NO_3)_3$–$Pr(NO_3)_3$–HNO_3–H_2O–TBP and $NdCl_3$–$PrCl_3$–HCl–H_2O–TBP. Comparison of a rigorous expression for the separation factor with available data, indicates that for the nitrate system the increase in the separation factor with increasing concentration is caused by variation of the activity coefficient term. It is shown that a good correlation is obtained when the separation factor, $\beta_{Nd/Pr}$, is expressed as a function of the equivalents of nitrate per 1000 g of solvent in the organic phase. The separation factor for the nitrate system was found to be a function of the ratio of the two rare earths only at very high acid concentrations and at very high mole ratios of neodymium to praseodymium. The separation factors, $\beta_{Nd/Pr}$, for the chloride system were less than unity, and not ratio dependent, for all concentrations and acidities used. The fact that for the previously studied system $SmCl_3$–$NdCl_3$–HCl–H_2O–TBP, the separation factor, $\beta_{Sm/Nd}$, was greater than unity was postulated to be the result of samarium having a lower hydration number than neodymium and praseodymium. (auth)

40905 HYDROLYSIS OF URANIUM, THORIUM, AND ALUMINUM CARBIDES IN D_2O. Sears, M. Bradley; Ferris, L. M. (Oak Ridge National Lab., Tenn.). Contract W-7405-eng-26. J. Inorg. Nucl. Chem., 28: 2055-9(Sept. 1966). (ORNL-P-1794).

The reactions of thorium and uranium carbides with D_2O at 80°C were identical to previously reported reactions with H_2O except that deuterium was substituted for hydrogen in the products. Within the limits of experimental error the rates of gas evolution, volumes of gas evolved, and amounts of wax formed were the same with D_2O as with H_2O. Isotopic analysis by mass spectroscopy indicated that the gaseous products were greater than 96% deuterated compared with 99% in the original D_2O. Production of methane by hydrolysis of aluminum carbide at 80°C was four times as rapid in H_2O as in D_2O. The rate-determining step in the hydrolysis of thorium and uranium carbides probably does not involve cleavage of the H–O bond in the water since the reaction shows no isotope effect. This is in contrast to the hydrolysis of aluminum carbide where the cleavage of H–O is the rate-determining step. (J.G.B.)

40906 RAMAN SPECTRUM AND HYDROLYSIS STUDIES ON HYDROGEN FLUORIDE SOLUTIONS OF XENON OXIDE TETRAFLUORIDE. Selig, H. H.; Quarter-

man, L. A.; Hyman, H. H. (Argonne National Lab., Ill.). J. Inorg. Nucl. Chem., 28: 2063-5(Sept. 1966).

Previous studies indicated the possible existence of the compound xenon dioxide difluoride in an incompletely hydrolyzed sample of xenon hexafluoride. An attempt was made to characterize this compound through its Raman spectrum. It was found that the Raman spectrum of xenon oxide tetrafluoride as a solute in hydrogen fluoride is similar to that of pure liquid oxide tetrafluoride. When a small amount of water was added to the solution, no new hydrogen fluoride soluble species was observed. An unstable white precipitate was formed, probably xenon trioxide. No evidence was found for the existence of xenon dioxide difluoride. (J.G.B.)

40907 ON THE UNIT CELL OF γ-UO_3. Hoekstra, H.; Siegel, S.; Gebert, E. (Argonne National Lab., Ill.). J. Inorg. Nucl. Chem., 28: 2056-6(Sept. 1966).

Single crystals of γ-UO_3 were grown from a $ZnCl_2$ melt. A mixture of γ-UO_3 and anhydrous $ZnCl_2$ was heated for several weeks in sealed silica tubes at ~625°C. Some reaction (to form ZnU_3O_{10}) occurred, but most of the UO_3 was recovered as crystals measuring up to 1.0 mm in diameter. Although these crystals exhibited a pronounced polysynthetic twinning, they can be indexed on the basis of orthorhombic symmetry. A comparison of the single crystal measurements with previously reported data is given. It was concluded that only one form of γ-UO_3 exists. (J.G.B.)

40908 PMR SPECTRA OF SOME NEOPENTYL DERIVATIVES OF MERCURY. LONG-RANGE ^{199}Hg-^{1}H COUPLING. Singh, Gurdial (E. I. du Pont de Nemours and Co., Inc., Wilmington, Del.). J. Organometal. Chem. (Amsterdam), 5: 577-9(June 1966).

In continuation of studies on the long-range interaction of protons with hetero nuclei, it was found that ^{199}Hg (spin $\frac{1}{2}$, 16.86% natural abundance) couples strongly with protons over four single bonds. Neopentyl derivatives, prepared by the usual methods, were used as model compounds because of the simplicity of their proton magnetic resonance (PMR) spectra. The ^{199}Hg-H_γ coupling could be measured easily as the two peaks of the split γ protons were located symmetrically about the resonance of the corresponding unsplit protons. It was found that $J(^{199}Hg\text{-}H_\gamma)$ experiences the same substituent effect as $J(^{199}Hg\text{-}H_\alpha)$ [$J(^{199}Hg\text{-}H_\alpha)/J(^{199}Hg\text{-}H_\gamma)$] = ~15.5 ± 1.5), suggesting that both α and γ protons couple with mercury via the same mechanism. The dominant contribution to $J(^{199}Hg\text{-}H_\alpha)$ arises from the contact term. However, the coupling mechanism of mercury with γ protons is complex, and the possibility of any contribution through space cannot be excluded. The substituents alter significantly the shielding of α protons, but have only little effect on the electronic environment of the γ protons. The effect of solvent on the chemical shifts of α and γ protons and their coupling constants with mercury was examined. As expected, in neopentylmercurie halides, the coupling constants increased with the polarity of the solvent. The greater shielding of protons in more polar solvents is explainable by the facile solvation of mercury compounds in polar solvents. The mercury atom in $RHg^{\delta+}$ can easily accept one or more pairs of electrons into its empty 6p orbitals from the solvents such as dimethyl sulfoxide-d_6 and thus cancel, at least partly, the partial charge on it. Consequently, depending upon the nature of the solvating media, the α and γ protons should be more shielded. In the case of dineopentylmercury, there is only little solvent effect on δ(H) and $J(^{199}Hg\text{-}H)$, in accord with the above explanation. The proton chemical shifts and their coupling constants with mercury remained virtually unchanged when the molarity of the solution was reduced from 2 to 1. (BBB)

40909 CHEMISTRY OF THE RARE EARTH METALS. XI. YTTRIUM TARTRATE COMPLEXES IN THE ACID REGION. Pastorek, Richard; Brezina, Frantisek; Rosicky, Jaroslav (Univ., Olomouc, Czech.). Monatsh. Chem., 97: 452-9(1966). (In German).

A systematic investigation of the system $Y^{3+} - H_4T$ in the acidic range was undertaken. The equilibrium constants for dissociation of the complexes $(YH_3T)^{2+}$, $(YH_2T)^{+}$, $(Y_2H_2T)^{4+}$, $(Y(H_2T)_2)^{-}$ and HYT were determined from pH measurements to be $(1.51 \pm 0.12) \times 10^{-3}$, $(8.45 \pm 0.15) \times 10^{-5}$, $(1.08 \pm 0.04) \times 10^{-6}$, $(1.30 \pm 0.08) \times 10^{-7}$, and $(1.36 \pm 0.11) \times 10^{-13}$, respectively. The compounds $Y_2(H_2T)_3 \cdot 8H_2O$, $Y_2(H_2T)_3 \cdot 5H_2O$, and $H(Y(H_2T)_2) \cdot 3H_2O$ were isolated. Thermal decomposition curves are provided; decomposition is found as follows for each compound respectively: beginning of decomposition, 50°, 50°, 60°; plateau, -, -, -; first acceleration of decomposition, 207°, 207°, 153°C; second acceleration, 340°, 355°, 347°C; end of decomposition, 740°, 740°, 730°C. The ir spectra of $Y_2(H_2T)_3 \cdot 8H_2O$ and $H(Y(H_2T)_2) \cdot 3H_2O$ are tabulated, as are the debyeograms for $Y_2(H_2T)_3 \cdot 5H_2O$ and $H(Y(H_2T)_2) \cdot 3H_2O$. The results are compared with similar data for the tartrate complexes of the lanthanides. (BBB)

40910 LIQUID IMMISCIBILITY IN THE RARE EARTH OXIDE–BORIC OXIDE SYSTEMS. Levin, E. M. (National Bureau of Standards, Washington, D. C.). Phys. Chem. Glasses, 7: 90-3(June 1966).

Three experimental methods were used to determine the composition of the modifier-rich liquids in the following binary systems with B_2O_3: La_2O_3, Nd_2O_3, Sm_2O_3, Eu_2O_3, Gd_2O_3, Dy_2O_3, Y_2O_3, Ho_2O_3, Er_2O_3, Tm_2O_3, Yb_2O_3, Lu_2O_3, and and Sc_2O_3. The first method consisted of gravity separation of the light and heavy liquids. The second method consisted of constructing a plot of the index of refraction of the quenched glass against composition, in the region just beyond the immiscibility zone. Construction of the liquidus curve from quench data for all the compositions studied in the vicinity of the immiscibility region was the third method for estimating the limiting composition. With decreasing ionic radius (increasing atomic number), the extent of immiscibility increased from 21.5 mole % for the La_2O_3 system to 34.0 mole % for the Sc_2O_3 system. With the exception of the La_2O_3 and Nd_2O_3 systems, temperatures of the monotectics increased monotonically from 1136°C for Sm_2O_3 to 1526°C for Sc_2O_3. Index of refraction of the quenched modifier-rich liquid was a maximum (1.732) for Eu_2O_3. Competing ionic field strengths between the glass-forming and modifier cations with oxygen govern the existence of immiscibility. Structural considerations governing the number of oxygens associated per modifier cation determine the extent of immiscibility. (TCO)

40911 EFFECT OF COMPLEXING AGENTS ON THE DISPROPORTIONATION OF URANIUM(V). Mehta, M. M.; Saraiya, S. C.; Sundaram, A. K. (Atomic Energy Establishment, Trombay, India). Proc. Indian Acad. Sci., Sect. A, 63: 371-5(June 1966).

The effect of lactate, thiocyanate, sulfate, oxalic acid, and fluoride on the disproportionation of uranium(V) formed at the dropping mercury electrode was studied. The rate constants for the disproportionation reaction are calculated and the results are discussed on the basis of the stability of the complexes. (auth)

40912 ELECTROMIGRATION METHOD FOR STUDYING COMPLEX FORMATION OF TRIVALENT PLUTONIUM IN ETHYLENEDIAMINETETRAACETIC ACID SOLUTIONS. Stepanov, A. V.; Makarova, T. P. Radiokhimiya, 7: 664-9 (1965). (In Russian).

The complexing of Pu^{3+} with EDTA was investigated by the electric migration method with μ = 0.1, t° = 25°, and pH = 1.1 to 3.5. It was established that under these conditions two forms of the complex ions $[Pu(ENTA)]^0$ and $[PuH(ENTA)]^-$ (EDTA = H_4ENTA) are produced. The latter predominated in solutions with pH > 3. The instability constants of the trivalent plutonium complexes were determined as -15.0 ± 0.3 and -4.6 ± 0.3, respectively. (tr-auth)

40913 ELECTROMIGRATION METHOD FOR STUDYING COMPLEX Am(III) OXALATES. Stepanov, A. V.; Makarova, T. P. Radiokhimiya, 7: 670-3(1965). (In Russian).

By means of the electromigration method, the formation of the complex of Am(III) in oxalic acid solution was investigated. It was established that in moderately acid solu-

tions at pH 1.5 to 3.7 the complexes $(AmOx)^+$ and $(AmOx_2)^-$ are formed. It was shown that under the experimental conditions hydrogen-containing complexes of americium oxalate are not formed. The stability constants of the ions $(AmOx)^+$ and $(AmOx_2)^-$ were calculated at $\mu = 0.1$ and $t° = 25°C$ as equal to $\beta_1 = (1.4 \pm 0.5) \times 10^6$ and $\beta_2 = (3.5 \pm 1.5) \times 10^{10}$. (tr-auth)

40914 BEHAVIOR OF MICROQUANTITIES OF YTTRIUM AND CERIUM IN THE SOIL. Molchanova, I. V.; Titlyanova, A. A. Radiokhimiya, 7: 687-92(1965). (In Russian).

The sorption of microquantities of yttrium by soil was found to be almost complete over a wide range of solution acidity and yttrium concentration. When hydrolyzing elements, such as Al and Fe are in the solution, the sorption of yttrium decreases in the weakly acid and neutral pH range which probably is explained by the formation of negatively charged absorbed yttrium colloids. The sorption of microquantities of yttrium by the soil depends on cerium concentration, solution pH, and presence of hydrolyzing elements. In the alkaline range, the cerium sorption decreases with increase of its concentration and also with the presence of Fe and Al in the solution which is probably connected with the formation of negatively charged cerium colloids. (tr-auth)

40915 ADSORPTION OF MICRO-AMOUNTS OF CESIUM ON FLUOROPLAST-4, POLYETHYLENE, AND GLASS FROM AQUEOUS SOLUTIONS OF SODIUM TETRAPHENYLBORATE. Skulskii, I. A.; Glazunov, V. V. Radiokhimiya, 7: 703-9(1965). (In Russian).

Adsorption of cesium from aqueous solutions onto polyethylene and Fluoroplast-4 [Soviet Teflon] dropped sharply when sodium tetraphenylborate was added. Cesium adsorbed on the surface of polyethylene and Fluoroplast-4 was readily desorbed by acetone and nitrobenzene. Liquids with low dielectric constant (benzene and ether) were poor desorbents. On the basis of adsorption and desorption, it is proposed that on the nonionogenic hydrophobic surfaces of polyethylene and Fluoroplast-4, cesium is present as a complex with a tetraphenylborate anion. In complex solutions containing specific organic anions, adsorption of alkaline cations on nonionogenic hydrophobic surfaces is possible. This process can be of special significance in biological systems. If organic anions exist in biological systems which specifically interact with alkaline ions, then apparently surface phenomena can play as large a role in cell selectivity as processes of ion exchange in polyelectrolytic gels or the passage of lyophylic complexes through nonaqueous membranes. (CFSTI)

40916 ABSORPTION SPECTRA OF URANIUM OXIDES. I. INFRARED SPECTRA OF U_2O_5 ABSORPTION. Ilinskaya, T. A.; Kuzin, V. I.; Tolmachev, Yu. M. Radiokhimiya, 7: 722-5(1965). (In Russian).

The absorption spectra of pentavalent uranium was determined in the range of 4800 to 400 cm^{-1}. The spectrum of U_2O_5 prepared from solutions of U_3O_8 in sulfuric acid, as distinguished from the spectra of U_3O_8 and U_2O_5 prepared by reduction with hydrogen, is characterized by the presence of absorption bands with maxima at 916 and 670 cm^{-1}. In the lattice of pentavalent uranium, chains of the atoms U–O–U–O– are present just as in U_3O_8 and α-UO_3. The range of stability of the compound U_2O_5, prepared from solutions of U_3O_8 in sulfuric acid, is below 400°C. (tr-auth)

40917 DISSOLUTION OF $UO_2C_2O_4$ BY ION EXCHANGE RESINS. Bogatyrev, V. L.; Sokolova, S. I. Radiokhimiya, 7: 725-7(1965). (In Russian).

The dissolution of the slightly soluble salt $UO_2C_2O_4$ was investigated using mixtures of the cationite KU-2 and the ionite AB-17. The effects of the quantity of ion exchange resins, weighed portion of the salt, temperature, and total impurities on the speed of dissolution of the precipitant are discussed. (tr-auth)

40918 PAPER CHROMATOGRAPHIC STUDY OF THE SOLUTION CHEMISTRY OF TECHNETIUM IN HYDROBROMIC ACID AT VARIOUS TEMPERATURES. Shukla, Shyama Kant (Univ., Rome. CNR, Rome). Ric. Sci. Riv., 36: 447-52(June 1966).

Studies were made on the reactions between concentrated hydrobromic acid and pertechnetate ion at 24, 8, and 0°C, and the chromatographic behavior of Tc(IV), Tc(V), and Tc(VII) in hydrobromic acid in the concentration range 0.125 to 8.7 N. Variations in R_f values for the three valence states are presented graphically. The conditions under which technetium(V) can be stabilized were also determined. (P.C.H.)

40919 GROWING OF RARE EARTH SILICATE SINGLE CRYSTALS OF OXYORTHO- AND DIORTHO-TYPE FROM A SOLUTION MELT. Bondar, I. A.; Koroleva, L. N.; Toropov, N. A. (Inst. of Crystallography, Academy of Sciences, USSR). Rost Kristallov., Akad. Nauk SSSR, Inst. Kristallogr., 6: 111-15(1965). (In Russian).

Attempts were made to prepare oxyortho- ($Ln_2O[SiO_4]$) and diorthosilicates ($Ln_2Si_2O_7$) of lanthanum, samarium, ytterbium, yttrium, and scandium in single crystal form by growing from a solution-melt. Potassium fluoride was chosen as the solvent and mineralizer. Coprecipitation with NH_4OH was used to achieve an intimate mixture of silica and rare earth oxide. The mixture was then heated in a crucible to 1300–1320°C for 8 hr, kept at this temperature for 4–6 hr, then slowly cooled from 1320 to 850°C. The experiment lasted 300 hr. La, Sm, Yb, Y, Sc oxyorthosilicate and Yb diorthosilicate crystals measuring 4 × 3 × 2 mm and less were obtained. Their quality was checked by x-ray phase analysis, microscopic analysis, and infrared spectroscopy, and the corresponding data are tabulated. (ATD)

40920 GROWING OF RARE EARTH ALUMINATE SINGLE CRYSTALS WITH A PEROVSKITE STRUCTURE. Zonn, Z. N.; Ioffe, V. A. (Inst. of Crystallography, Academy of Sciences, USSR). Rost Kristallov., Akad. Nauk SSSR, Inst. Kristallogr., 6: 122-6(1965). (In Russian).

Single crystals of $LaAlO_3$, $PrAlO_3$, $SmAlO_3$, and $NdAlO_3$ measuring up to 15 × 10 × 10 mm were obtained from an equimolar mixture of PbO and PbF_2 (ratio of crystallized substance to solvent, 1:8). The Pr, Nd, and Sm crystals were prepared from a mixture obtained by coprecipitation with NH_3. Observations with a high-temperature polarization microscope showed the presence of two phase transitions in $PrAlO_3$ (1000 and 1500–1600°C) and $NdAlO_3$ (950 and 1400°C). $LaAlO_3$ single crystals were prepared by heating to 1300°C, then cooling at the rate of 4.5° per hour, and also by heating to 1200°C, holding for 24 hr, and lowering the temperature at the rate of 1.5–2° per hour. These crystals contained up to 18% of the palladium group ions and up to 2% lead ions as impurities. X-ray-powder data for all four types of crystals are tabulated. (ATD)

40921 THERMODYNAMIC PROPERTIES OF URANIUM COMPOUNDS. PART 2. LOW-TEMPERATURE HEAT CAPACITY AND ENTROPY OF THREE URANIUM NITRIDES. Counsell, J. F. (National Physical Lab., Teddington, Eng.); Dell, R. M.; Martin, J. F. Trans. Faraday Soc., 62: 1736-47(July 1966).

The heat capacities of UN, $UN_{1.59}$, and $UN_{1.73}$ were measured from 11 to 320°K. The C_p curves for the three compounds show anomalies at 52, 94, and 33°K, respectively, corresponding to magnetic ordering phenomena. The values of the standard thermodynamic functions are tabulated, together with heats and entropies of the magnetic transitions. UN undergoes type 1 antiferromagnetic ordering at 52°K; the entropy increment associated with this ordering (0.15 cal deg^{-1} $mole^{-1}$) is substantially less than the expected magnetic entropy. Comparison is made with magnetic transitions in other uranium compounds, notably UO_2 and US whose magnetic entropies may be calculated with reasonable accuracy. It seems that the entropy of spin ordering represents only a part of the total magnetic entropy. Possible reasons for this are discussed. (auth)

40922 ACTIVITY OF UCl_3 IN THE EUTECTIC MELT LiCl–KCl. Knacke, O.; Krahe, J.; Mueller, F. (Technische Hochschule, Aachen. Kernforschungsanlage, Jue-

lich, Ger.). Z. Phys. Chem. (Frankfurt), 50: 91-104(July 1966). (In German).

The activity of the UCl_3 was determined by EMF measurements on Ag/U/LiCl–KCl–UCl_3//LiCl–KCl–AgCl/Ag cells. At U concentrations of the melt up to 0.5 mol % UCl_3 and at temperatures from 450 to 650°C, the activity of the UCl_3 is approximately equal to its mol fraction in pure liquid UCl_3 as reference state. The thermochemical data on UCl_3 and AgCl given in the literature were compiled and evaluated. For the chemical ground potentials of UCl_3 and AgCl as pure solid materials, pure melts, and in infinite dilutions at concentrations through the mol fraction, the following relations in cal/mol are given: $\mu°UCl_3$, sol. = −199.350 −64.60 T (700 to 950°K); $\mu°UCl_3$, liq. = −188,250 −74.60 T (700 to 950°K); $\mu°UCl_3$, gel. = −188,500 −74.81 T (700 to 870°K); $\mu°AgCl$, sol. = −23,900 −35.90 T (550 to 728°K); $\mu°$ AgCl, liq. = −20,800 −40.16 T (728 to 1000°K); $\mu°AgCl$, gel. = −20,400 −39.60 T (700 × 850°K). (tr-auth)

40923 ANODIC POLARIZATION OF UC IN THE MELT LiCl–KCl. Knacke, O.; Krahe, J.; Mueller, F. (Technische Hochschule, Aachen. Kernforschungsanlage, Juelich, Ger.). Z. Phys. Chem. (Frankfurt), 50: 105-12(July 1966). (In German).

The anodic polarization of a UC electrode was investigated by plotting the stationary voltage-current curve by the commutator method at 500°C. Liquid tin or liquid lead was used as the cathode and the electrolyte was the eutectic melt LiCl–KCl with uranium contents between 3 and 8 wt. % UCl_3. The Ag/AgCl electrode was the reference electrode. Three characteristic potentials were established. According to thermodynamic calculations, these potentials are limited by saturation of the electrode/electrolyte phase-boundary on UCl_3 or UCl_4 or the elimination of gaseous chlorine. In the region of the saturation on UCl_4, a limiting current of about 2.5 amp/cm² was observed. The phase USn_3 or UPb_3 was separated on the cathode after a brief electrolysis time. The polarization of the two-phase cathode Sn–USn_3 was insignificant up to current densities of −50 mamp/cm². (tr-auth)

40924 THERMODYNAMIC REGULARITIES IN ISOTOPIC EXCHANGE. I. THE METHOD FOR COMPUTING THE SUM OF STATES. Knyazev, D. A.; Bantysh, A. N.; Ivlev, A. A. Zh. Fiz. Khim., 40: 32-7(Jan. 1966). (In Russian).

In order to formulate the principles of the oriented selection of the chemical exchange system for separation of isotopes and to resolve the questions on the possibility of the use of chemical methods for isotope separation of heavy elements the knowledge of the general regularities of the thermodynamics of isotopic exchange reactions is necessary. For clarification of these regularities, sufficiently abundant numerical material is necessary for evaluation of the sum of states of isotopic molecules (β factors), including compounds with a variety of chemical nature. Precise evaluation of the β factors for a large number of molecules can be obtained by calculations using as original data the fundamental frequencies of the compounds. With accurate selection of the potential function of the molecules the comparative errors in the calculation of β-1 can be reduced to a completely satisfactory size (±4%). (tr-auth)

40925 VISCOSITY OF MOLTEN LANTHANUM TRICHLORIDE AND ITS MIXTURES WITH LANTHANUM DICHLORIDE. Smirnov, M. V.; Khokhlov, V. A.; Stepanov, V. P. Zh. Fiz. Khim., 40: 1248-51(June 1966). (In Russian).

The dependence of viscosity on the temperature of pure molten lanthanum trichloride and solutions of metallic lanthanum saturated with lanthanum trichloride, corresponding to the composition formula $LaCl_{2.14}$, was measured by the torsion balance method. Expressions for the temperature dependence of the viscosity coefficients of the solution studied were found to be $\lg\eta$ (in centipoises) = 1.686 + 2852/T ± 0.004 for $LaCl_3$ and $\lg\eta$ (in centipoises) = −2.135 + 3019/T ± 0.002 for $LaCl_{2.14}$. The viscosity of the melts $LaCl_3$ and $LaCl_{2.14}$ satisfactorily agrees with data on the viscosity of molten chlorides representing ionic liquids. (tr-auth)

40926 MIXED SULFOSALICYLATE COMPLEXES OF RARE EARTH ELEMENTS. Poluektov, N. S.; Mishchenko, V. T. Zh. Neorg. Khim., 10: 2275-81(Oct. 1965). (In Russian).

The formation of mixed polynuclear complexes (rare earth complexes) with sulfosalicylic acid in neutral and weakly alkaline media was studied by spectrophotometric and fluorometric methods. The absorption spectra of sulfosalicylate solutions of neodymium and erbium changed in the presence of such complexes of other rare earths (yttrium and lanthanum). The greatest change was observed in absorption bands having peaks at λ = 575.5 mm (Nd) and 523.0 nm (Er) in chloride solutions. The data obtained for the properties of complexes studied spectrophotometrically pertain to the pH range of 5.5 to 9.5. In a mixed sulfosalicylate complex, the element with the smaller ionic radius (Y, Nd) stands in the ratio of 1 : 2 to the element with the larger radius (Nd, La), i.e., the mixed complexes formed are trinuclear. A fluorometric study of the formation of mixed complexes by terbium and europium in sulfosalicylic acid solutions showed that the formation is due to a transfer of energy from Tb^{3+} to Eu^{3+}, as indicated by the phenomenon of sensitized fluorescence of europium in the presence of terbium. (ATD)

40927 ABSORPTION PROPERTIES AND STABILITY OF SOME URANYL COMPOUNDS AT INCREASED TEMPERATURES. Umreiko, D. S. Zh. Prikl. Spektrosk., Akad. Nauk BSSR, 4: 523-8(June 1966). (In Russian).

The temperature dependence of absorption spectra and the acidity of some aqueous, acidic, and organic solutions of uranyl salts and complexes were investigated at increased temperatures. The results obtained indicate considerable stability in a certain temperature range of uranyl compounds present in these solutions. For a number of substances (uranyl-sulfate in sulfuric acid at t = 135°C, uranyl nitrate in cyclohexanone at t = 70°C) irreversible chemical reactions were observed leading to the formation of some new compounds. Analysis of their absorption spectra on the basis of the available reference data allowed the conclusion that in the first case (uranyl sulfate in H_2SO_4) a new compound is formed at t = 135°C which seems to contain tetravalent uranyl and in the second case (uranyl nitrate in cyclohexanone) the temperature increase up to 70°C leads to the formation of uranium protoxide-oxide, U_3O_8. (auth)

40928 INFLUENCE OF A SOLVENT ON THE PARAMAGNETIC RELAXATION CONSTANT IN LIQUID SOLUTIONS OF GADOLINIUM NITRATE. Vishnevskaya, G. P.; Kozyrev, B. M. Zh. Strukt. Khim., 7: 24-9(Jan.-Feb. 1966). (In Russian).

The paramagnetic absorption was measured by the parallel field method and the paramagnetic relaxation constants ρ_L, ρ_s, and b/c were calculated for liquid solutions of gadolinium nitrate. The change of the solvate cloud around the Gd^{3+} ion is reached by using a wide range of solvents, such as alcohols, dioxane, and acetone. A study of the effect of concentration and temperature on the paramagnetic relaxation constant in different solvents showed that the change of the approximate vicinity around the Gd ion significantly affects ρ_L, ρ_s, and b/c. (tr-auth)

40929 SOLUTIONS FOR THOMAS-FERMI-DIRAC EQUATION TAKING INTO ACCOUNT CORRELATIONS FOR DIVALENT RADIUM IONS. Vdovenko, V. M.; Dubasov, Yu. V. Zh. Strukt. Khim., 7: 60-5(Jan.-Feb. 1966). (In Russian).

Solution of the Thomas-Fermi-Dirac equation is described. One of the solutions, characteristic with the ion Z_i = 1.910, was used for calculating the electron polarizability, α, and the diamagnetic susceptibility, χ_d, of the Ra^{2+} ion. The theoretically calculated α and χ_d are in satisfactory agreement with experimental values. (tr-auth)

40930 THE INFLUENCE OF SOLUTION STRUCTURE ON THE MOBILITY OF ISOTOPIC IONS $^6Li^+$ AND $^7Li^+$.

Bakulin, E. A.; Aleksandrov, B. P. Zh. Strukt. Khim., 7: 179-83(Mar.-Apr. 1966). (In Russian).

The dependence of the comparative difference of mobilities, ϵ, of the isotopic ions $^6Li^+$ and $^7Li^+$ on the concentration (in the range from 3.45 to 22.6 g-equiv./1000 g H_2O) and temperature from 20 to 70° of $LiNO_3$ solution was investigated by the ion mobility method. For concentrations from 9 to 10 g-equiv./1000 g H_2O an abrupt change in the pattern of the dependence of $\epsilon(^6Li^+, ^7Li^+)$ on the concentration of the $LiNO_3$ solution was detected, which can perhaps be explained by the attainment of "the boundary of complete solvation." (tr-auth)

40931 NUCLEAR MAGNETIC RESONANCE AND ELECTRON STRUCTURE OF URANIUM, THORIUM, AND ZIRCONIUM. Gabuda, S. P.; Gagarinskii, Yu. V.; Lundin, A. G. Zh. Strukt. Khim., 7: 192-9(Mar.-Apr. 1966). (In Russian).

The chemical displacements of the nuclear magnetic resonance of ^{19}F in UF_4, ThF_4, ZrF_4 and the anisotropy of the constantly shielded fluorine nucleus in ThF_4 and ZrF_4 were investigated. On the basis of the data obtained, a series of parameters was determined that characterize the electron state and nature of the chemical bonds in these compounds. It was found that the state of the electron shell of the fluorine ions depends noticeably on the spacing density of these ions in the structure. (tr-auth)

40932 CRYSTAL STRUCTURE OF $Cs_3[UO_2(NCS)_5]$. Arutyunyan, E. G.; Porai-Koshits, M. A. Zh. Strukt. Khim., 7: 393-8(May-June 1966). (In Russian).

The structure of $Cs_3[UO_2(NCS)_5]$ was determined by 3-dimensional distribution of the electron density and made more precise by the least squares method. The structure is isolated. The coordination polyhedron of uranium is a distorted pentagonal bipyramid with the spacing: U–O = 1.60 and 1.73 Å and U–N = 2.88 and 2.48 Å. (tr-auth)

40933 A THEORETICAL AND EXPERIMENTAL STUDY OF GERMANIUM ISOTOPE FRACTIONATION. Brown, H. M. Edmonton, Alta., Univ. of Alberta, 1962. 94p.

Thesis.

A theoretical study is given on the isotopic compounds of germanium. Isotopic vibrational frequencies were calculated for various ^{70}Ge- and ^{76}Ge-containing compounds. From these, the ratios of the corresponding isotopic vibrational partition functions were computed. These ratios were then used to calculate the equilibrium constants for various $^{70}Ge-^{76}Ge$ exchange reactions at different temperatures. In such equilibria, variations in the $^{70}Ge/^{76}Ge$ ratio of up to 3.5% were predicted provided that such exchanges could be effected experimentally. Calculations of the minimum and maximum kinetic isotope effects to be expected in the breaking of various diatomic bonds also predicted isotope effects of the same order. An experimental study of the reductions: $^{70}GeO_2 \xrightarrow{k_1} {}^{70}GeO$ and $^{76}GeO_2 \xrightarrow{k_2} {}^{76}GeO$ showed the ratio of the rate constants k_1/k_2 to be 1.012 at 100°C. This result was in agreement with a simplified theoretical model of the reaction. (auth)

40934 URANIUM AND LANTHANIDE ACTIVATED ALKALINE EARTH MOLYBDATE AND TUNGSTATE PHOSPHORS. Vogel, Marcel J. (to International Business Machines Corp.). U. S. Patent 3,265,628. Aug. 9, 1966. Filed Mar. 23, 1962.

The use of lanthanide and uranium ions as activators and sensitizers in alkaline earth metal phosphors is described. The combination of lanthanide and uranium can be used to increase perceptibly the emission of the rare earth ion while substantially extinguishing the uranium emission. The addition of the tungstate enhances the emission of the alkaline earth oxides. These phosphors are prepared by fusing a uniform mixture of a calcium compound such as calcium oxide or calcium carbonate with a lanthanide and uranium salt, and then fusing the calcium compound with a tungstate or molybdate oxide or acid to form the phosphor. (J.F.P.)

40935 IMPROVEMENTS IN OR RELATING TO THE PREPARATION OF URANIUM TETRAFLUORIDE. Taylor, Herbert Arthur; Lloyd, James Elgie (to United Kingdom Atomic Energy Authority). British Patent 1,037,291. July 27, 1966. Filed June 20, 1962.

In a fluidized-bed process for the preparation of UF_4 from UO_2, a fluidizing medium and anhydrous HF vapor are fed to the UO_2 in a fluidized bed reactor. The HF offgases diluted by the reaction are condensed, and the dilute aqueous HF condensate is collected. At an intermediate stage in the process, the liquid HF solution is substituted as feed to the UO_2 before the reaction is complete. As a final stage before the reaction is complete, the anhydrous HF vapor is resubstituted for the aqueous solution of HF. Use of the aqueous solution of HF from the condensed offgases introduces a simple economy into the process. (B.L.M.)

40936 URANIUM MONOSULFIDE–URANIUM MONOPHOSPHIDE SOLID SOLUTIONS. Baskin, Yehuda; Shalek, Peter D. (to U. S. Atomic Energy Commission). U. S. Patent 3,264,223. Aug. 2, 1966.

A new composition, consisting of a solid solution of uranium monosulfide and uranium monophosphide, is reported. (AEC)

40937 METHOD OF ROUNDING ACTINIDE OXIDE GEL PARTICLES. Hamner, R. L.; Smith, W. H. Jr. (to U. S. Atomic Energy Commission). U. S. Patent 3,264,379. Aug. 2, 1966.

A method of preparing spherical actinide oxide gel particles is reported. By this method irregularly shaped, slightly water-soluble oxide gel particles are contacted with a solution comprising 25 to 75 vol % water and the balance a water-miscible inert organic liquid thereby wetting the surface of the particles and thereafter tumbled to remove the irregular projections on the particles. (AEC)

40938 INTERACTION OF TRITIUM IONS IN SELECTED ENERGY RANGES WITH GASEOUS BUTANE. Paulus, J. (Centre de Recherches Nucleaires, Strasbourg). 17p. (CONF-660431–4). ORAU. Gmelin, AED-CONF-66-120-4.

From Symposium on Hot Atom Chemistry, Lafayette, Ind.

A mass spectrometer was designed for a study of the interaction of tritium ions with gaseous compounds in an energy range between 3 and 6000 ev. Butane was chosen as the target gas. The experiments were performed at gas pressures between 10^{-2} and 10^{-1} mm Hg. The experimental arrangement is described and some typical results are given. (W.D.M.)

Organic Chemistry

Refer also to abstract 40504.

40939 CALCULATIONS OF KINETIC ISOTOPE EFFECTS FOR THE IODIDE EXCHANGE AND FOR THE SOLVOLYSIS OF METHYL IODIDE. Willi, Alfred V. (Brookhaven National Lab., Upton, N. Y.). Can. J. Chem., 44: 1889-97(Aug. 15, 1966). (BNL–9690).

Kinetic deuterium and ^{13}C isotope effects were calculated for the S_N2 exchange reaction of CH_3I with $*I^-(131)$ and for CH_3I solvolysis in water. The normal vibrational frequencies of CH_3I and of the transition state $I \ldots CH_3 \ldots X$(X = I or OH_2) were evaluated from force constants by solving the secular equation with an IBM 7094 computer. Values for force constants of the planar CH_3 moiety (with an sp^2 C atom) in the transition state were obtained by comparison with suitable stable molecules. For the iodide exchange reaction, there was not much dependence of the calculated D isotope effect on the particular choice of f_{CI} and f_{I2} (interaction between CI stretches) if these force constants were within reasonable limits. The bending force constant $f_{HCI}(\ddagger)$ may then be adjusted to reproduce the experimental D isotope effect. Based on the simple transition state model $CH_3^{\delta+} \ldots I^{\delta-}$, it was not possible to obtain agreement with

the experimental D effect in the solvolysis reaction without assuming an extremely high value of f_{HCl}. It was concluded that a water molecule is probably involved in the transition state. On the basis of the model I ... CH_3 ... OH_2, the experimental D effect may be reproduced with a suitable choice of f_{HCl} and f_{HCO}. It is shown that, under favorable circumstances, experimental temperature dependence data may be applied for a distinction between different sets of f_{CH}, f_{HCH}, and f_{HCl} (or f_{HCO}), which reproduce the experimental isotope effect at one temperature. (auth)

40940 SYNTHESIS AND SEVERAL PROPERTIES OF DEUTERATED ORGANIC COMPOUNDS. Weening, W. E. (Rijksuniversiteit, Groningen, Netherlands). Chem. Weekbl., 62: 153-7(1966). (In Dutch).

General methods of deuteriation by exchange, addition, and substitution reactions are reviewed. Specific methods are outlined for the preparation of substituted alkanes, alkenes, alkynes, alcohols, halogen compounds, amines, ethers, aldehydes, ketones, acids, aromatic hydrocarbons, and heterocyclic compounds, with some emphasis on the preparation of substituted thiophenes and bromothiophenes. A short summary of the more important physical characteristics of organic C compounds is given, with the foundation of physical-organic chemical variations. Infrared spectral, NMR, and mass spectrometric applications are discussed. The use of D compounds in structural investigations and in biochemistry are touched upon. (75 references). (BBB)

40941 THE SYNTHESIS OF ^{14}C-LABELLED BIPYRIDYLIUM SALTS. Dunn, M. J.; Martin, R. J.; Roberts, N. L.; Slade, P.; Standen, H.; Walker, P. (Imperial Chemical Industries Ltd., Runcorn, Eng.). J. Chem. Soc., No. 16, 1468-72(1966).

[2,3-$^{14}C_2$] Pyridine was prepared from [1,2-$^{14}C_2$] acetylene and converted into the corresponding [$^{14}C_4$]2,2′- and [$^{14}C_4$]4,4′-bipyridyls. NN′-Ethylene-[$^{14}C_4$]2,2′-bipyridylium dibromide and NN′-dimethyl-[$^{14}C_4$]4,4′-bipyridylium dichloride and di(methyl sulfate), which possess herbicidal activity, were prepared for biological tracer studies. (auth)

40942 HYDROGEN EXCHANGE BETWEEN HYDROGEN, ETHYLENE, OR ETHANE DURING THE PROGRESS OF THE CATALYZED HYDROGENATION OF ETHYLENE IN THE PRESENCE OF NICKEL. Matsuzaki, Isao; Nakajima, Tsuyoshi (Hokkaido Univ., Sapporo). J. Res. Inst. Catalysis, Hokkaido Univ., 13: 44-54(July 1965).

Hydrogen-deuterium exchange from ethane to hydrogen or ethylene during nickel catalyzed hydrogenation of ethylene was studied in the temperature range from 50 to 150°C and interpreted on the basis of the associative mechanism put forward previously, indicating that the extent of the exchange was beyond mass spectrometric detection. The catalyzed interaction between H_2, C_2H_4, and C_2D_6 (~30% D content), each at 10 mm Hg partial pressure, was observed at 50, 100, and 150°C in the presence of nickel wire to check this conclusion. Mass spectrometry showed that no exchange of deuterium from ethane to hydrogen or to ethylene was observed, which verified the above conclusions. (TCO)

40943 INVESTIGATION ON PROMOTING ACTION OF RARE EARTH OXIDES ON DEHYDROGENATING CHARACTERISTICS OF ALUMINUM OXIDE–CHROMIUM OXIDE CATALYSTS. Minachev, Kh. M.; Khodakov, Yu. S.; Sterligov, O. D. (Inst. of Organic Chemistry, Academy of Sciences, USSR). Neftekhimiya, 6: 361-6(May-June 1966). (In Russian).

The effects of an addition of the oxides of neodymium and praseodymium (from 0.5 to 2.2 wt %) on the properties of aluminum oxide–chromium oxide catalysts were investigated in the dehydrogenation of butane. It was established that catalysts activated by rare earth oxides in the active layer are significantly more active and selective than the aluminum oxide–chromium oxide–potassium oxide catalysts. Under the experimental conditions the highest yield of butene and divinyl, calculated on the basis of the butane, amounted to 13 to 25 and 30 to 33 wt % at selectivities of 47 to 64 and 66 to 77% in comparison with the aluminum oxide–chromium oxide–potassium oxide catalysts and the aluminum–chromium catalysts containing neodymium or praseodymium oxides. (tr-auth)

40944 THE PREPARATION OF ^{99m}Tc-LABELED HUMAN SERUM ALBUMIN. Kazem, I.; Maier-Borst, W. (Krebsforschungszentrum, Heidelberg). Nucl.-Med., 5: 285-9(1966). (In German).

A method for the preparation of ^{99m}Tc-labeled serum albumin is described. Certain modifications of the original technique developed by Stern et al., that improve the yield are presented. (auth)

40945 NMR STUDIES OF A HYDROGEN–DEUTERIUM EXCHANGE IN CARBONIUM ION SYSTEMS. Kingsbury, Charles A. (Iowa State Univ., Ames). Tetrahedron Lett., No. 23, 2539-44(June 1966).

Deuterium exchange was examined in a series of cations derived from several 1,1-diarylethylenes. The effect of substituents on the rate of exchange suggests that exchange directly involves the cation, rather than the 1,1-diarylethylene itself. The intermediate in the former case would be a dication. NMR studies of H-D exchange in other carbonium ion systems have shown that exchange occurs very slowly, probably due to the deactivating influence of the positive charge. The dication intermediate would be markedly destabilized by charge repulsion. Other studies have shown that organic dications are extremely unstable species. However, older work showed that tetraanisyl pinacol yielded a dication in concentrated acid solution. In this case each charge possesses its own separate resonance pathway, and coulombic repulsions may be significantly reduced. The olefinic substrate is almost 100% converted to the diaryl cation in 96% H_2SO_4. Nevertheless, H-D exchange may take place in the small amount of olefin present in the equilibrium studied. The anisyl ring proton spectra may be approximated as an AB pattern. As deuteration progresses the resonance absorption of proton B diminishes while that of proton A is converted from a doublet to a broad singlet. The same type of behavior occurs for the other aromatic protons except at a much slower rate (depending upon the electron donating character of the substituent). Representative spectra illustrating this effect are given. The data fit a first-order rate equation. (BBB)

Radiation Chemistry

See also BIOLOGY AND MEDICINE — Radiation Effects on Biochemicals Radiation Effects on Tissues

Refer also to abstracts 41067 and 41691.

40946 (AECL–2589) THE RADIOLYSIS OF ORTHO- AND META-TERPHENYL. II. WITH GAMMA RAYS AT DOSE RATES OF 0.15–0.2 Wg^{-1}. Boyd, A. W.; Connor, H. W. J.; Miller, O. A. (Atomic Energy of Canada Ltd., Chalk River (Ontario)). June 1966. 11p. Dep. mn. AECL $0.50.

Ortho- and meta-terphenyl were irradiated at dose rates of 0.15 to 0.2 Wg^{-1} inside cadmium annuli at temperatures from 180 to 458°C. Over 99% of the energy deposition was due to gamma absorption. Disappearance, high boiler, biphenyl, total gas, and hydrogen G values were determined. G values for the disappearance of ortho increased from 0.23 at 235°C to ~4.5 at 450°C and of meta from 0.15 at 180°C to ~2 at 458°C. Comparisons with fast neutron-γ-irradiations and electron irradiations showed there are both LET and dose rate effects. A reaction scheme to explain these effects is proposed. (auth)

40947 (BMwF-FBK–66-14) STRAHLENCHEMISCHE REAKTIONEN IN GEMISCHEN DES PHOSPHORTRICHLORIDS MIT OLEFINEN. (Radiation Chemical Reactions in Mixtures of Phosphorus Trichloride With Olefines). Wunder, K. (Technische Universitaet, Berlin (West Germany)). June 1966. 10p. Dep. mn.

1-Chlorocyclohexyl-phosphorus dichloride is formed in a Kharasch type chain reaction when γ rays act on mixtures of phosphorus trichloride and cyclohexene. The G-value is proportional to the reciprocal square root of the dose rate and reaches a maximum at 100°C. The activation energy of the rate determining step $PCl_2C_6H_{10} + PCl_3 \rightarrow PCl_2C_6H_{10}Cl + PCl_2$ was found to amount to 6.7 kcal/mole. At higher temperatures, the yield strongly decreases since another chain reaction predominates which produces cyclohexyl-phosphorus dichloride. The two chains have a common propagation step. (auth)

40948 (COO-578-3-32) RADIATION SYNTHESIS INVOLVING HALOGEN COMPOUNDS. Final Report, May 1, 1960–October 31, 1965. Feng, Paul Y. (IIT Research Inst., Chicago, Ill.). May 5, 1966. Contract AT(11-1)-578. 76p. Dep. mn. CFSTI $3.00 cy, $0.75 mn.

Developments in studies on the radiation chemistry of selected fluorocarbons and the mechanism and reaction kinetics of the radioinduced fluorination process are reported. Studies on the radiation chemistry of fluorocarbons were carried out either by using only a selected fluorocarbon as the irradiated material or by using the fluorocarbon mixed with other compounds that could react with the intermediate product by radiation. The radiation chemistry of CF_3Cl, CF_3Br, and CF_4 has been studied. The results show that despite the well-established thermal and chemical stability of the C–F bond, the radiation stability of the fluorocarbons is comparable with, though somewhat higher than, that of the hydrocarbons. Both ionic and radical intermediates are produced, and the primary G values are of the order of 2 to 3 or less. In addition, the C–F bond was found to be subject to attack by ionic intermediates, such as CF_3^+, leading to the formation of the fluorine abstraction product, CF_4. Irradiation of mixtures of the simple fluorocarbons with aromatic hydrocarbons led to the formation of aromatic fluorine compounds with G ~ 2 to 3. Both radical and ionic processes contribute to the observed reaction process. The temperature effects for these processes, however, differ and thus afford a means of controlling the course of the radioinduced fluorination reaction. (P.C.H.)

40949 (NYO-3003-29) SOME STUDIES OF CRYSTAL ORIENTATION IN IRRADIATED POLYETHYLENE. Final Report, May 1, 1962–April 30, 1966. Stein, Richard S. (Massachusetts Univ., Amherst. Polymer Research Inst.). Contract AT(30-1)-3003. 11p. Dep. mn. CFSTI $1.00 cy, $0.50 mn.

Methods and procedures were developed for the study of the morphology, texture, crystallinity, and kinetics of crystallization of polymers and also radiation cross-linked films. Microscopic observations and light scattering studies demonstrated that the crystals in a polycrystalline polymer are not independent entities but exist in superstructures in which their orientation and location are correlated. Deformation of this structure resulted in orientation of the crystals and a change in the birefringence. The orientation distribution obtained from an x-ray-diffraction-determined pole figure was compared with that predicted theoretically. Unoriented polymers and scattering were also studied. Specific results are given for polyethylene and polypropylene. (P.C.H.)

40950 (PRNC-88) MATRIX ISOLATION STUDIES OF PRODUCTS OF GAMMA-RADIOLYSIS OF HETEROCYCLIC MOLECULES. Progress Report No. 1, Fiscal Year 1966. Grimison, Alec (Puerto Rico Nuclear Center, Mayaguez). Contract AT(40-1)-1833. 20p. Dep. mn. CFSTI $1.00 cy, $0.50 mn.

Two designs of optical dewars were tested for the examination of optical spectra at liquid nitrogen temperatures. Preliminary qualitative results were obtained by gamma irradiation of a wide variety of heterocyclic molecules in methyltetrahydrofuran and 3-methylpentane glassy solutions at 77°K. Color formation was examined visually. Theoretical studies were made using the valence-bond technique and the molecular-orbital technique. (M.C.G.)

40951 (RPI-321-6) DECONTAMINATION OF PRODUCTS FROM CHEMONUCLEAR REACTIONS. Zipprich, F.; Dondes, S.; Harteck, P. (Rensselaer Polytechnic Inst., Troy, N. Y.). July 1966. Contract AT(30-3)-321. 138p. Dep. mn. CFSTI $4.00 cy, $1.00 mn.

Investigations were carried out to determine the extent of contamination and methods of decontamination of products from chemonuclear reactions. Previous work by others in this laboratory showed that radiolysis of CO and mixtures of N_2 and O_2 with fission fragments produces solid carbon suboxide polymer and nitrogen dioxide, respectively. Enriched uranium incorporated in the structure of thin fibers provided the source of fission fragments and the means for their escape into the irradiated phase. The percentage of the fission fragments that escape the glass fibers was determined and several specific isotopes were investigated to elucidate their behavior relative to the bulk activity. The glass fibers were surrounded by gas at about 10 atm during the irradiation and had a diameter of 5 μ. The results indicated that 60% of the gross activity escaped and remained outside the fibers and fission products such as Ru, Cs, Ce, Sr, and Sb followed a similar pattern. The percent escaping was somewhat less than expected since it was calculated that 90% should escape. Several methods for decontamination of carbon suboxide polymer were examined. Alternate precipitation-dissolution cycles and ion exchange techniques were attempted. These procedures proved to be ineffective, i.e., gave a decontamination factor of less than 100 for mixtures of fission products and for elements such as Cs, Sr, Y, and Ru. The results are explained by formation of compounds between the various cations investigated and the polymer. Additional experiments with I_2 and carbon suboxide showed that compounds can be expected to form between the polymer and the halogens. Since the polymer was not fully identified, it was concluded that additional work is needed on this aspect and on determination of its properties before other decontamination techniques are attempted. Decontamination of nitrogen dioxide by evaporation was studied. The magnitude of the decontamination factor, the optimum boil-up-rate, and the presence of volatile activity that would limit the effectiveness of the evaporation technique were determined. Evaporation of NO_2 from nonvolatile ^{137}Cs gave decontamination factors of 10^7 to 10^8 at boil-up-rates of 300 to 400 lbs/hr-ft^2. Additional experiments with mixtures of fission products indicated I, Xe, and possibly Tc were volatile under the conditions used. Decay measurements on condensate samples showed at least two nuclides in addition to I and Xe were present while aluminum absorption and gamma spectrometric analysis showed the presence of a weak beta emitter that gave off only a small amount of gamma rays at 0.070, 0.095, and 0.335 Mev. Identification was not possible because of the small amount of activity present. (auth)

40952 (SC-DC-66-1823) PHOTOCONDUCTIVITY PROCESSES IN LOW MOBILITY ORGANIC MATERIALS. Coppage, F. N.; Kepler, R. G. (Sandia Corp., Albuquerque, N. Mex.). July 1966. Contract AT(29-1)-789. 6p. (CONF-660705-3). Dep. mn. CFSTI $1.00 cy, $0.50 mn.

From IEEE Annual Conference, Palo Alto, Calif.

Recent studies on photoconductivity processes in anthracene crystals made it possible to calculate the number of carriers created in polymers when they are subjected to high-energy radiation. The results are described and applied to some recently reported measurements on polystyrene. Reasonable values were found for such quantities as carrier mobility and trap densities. (auth)

40953 RADIATION-INDUCED GRAFTING OF MIXED MONOMERS ON COTTON FABRIC. Gupta, Sharda Das (Atomic Energy of Canada Ltd., Ottawa). Amer. Dyestuff Rep., 55: 59-66(Mar. 14, 1966).

Experiments are reported on attempts to graft mixtures of monomers on cotton fabric using low doses of γ radiation. The material used was broadcloth and the monomer mixtures were styrene–methyl methacrylate, acrylic acid–styrene and acrylonitrile–methyl methacrylate. The simultaneous irradiation method was employed for grafting.

The amount of grafting was found to increase linearly with radiation dose up to 2×10^5 rad. Further increase did not have any significant value. With styrene–methylmethacrylate when the total irradiation dose of 5×10^5 rad and the styrene and water concentrations were kept constant at 10%, the percentage weight increase due to the total grafting increased linearly with the concentration of methyl methacrylate. Both in the case of styrene–methyl methacrylate and acrylonitrile–methyl methacrylate mixtures, the percentage weight increases due to total grafting increased with the concentration of water added. The grafted products with weight increase of 15% or more were insoluble in cupriethylenediamine, a solvent that dissolves cellulose. The physical properties of the grafted products were greatly superior to those of the starting materials especially as regards tensile strength, crease recovery, retention of crease after treatment with chlorinated solvents, resistance to water and fungus growth (rot), and dye acceptability. The optimum range of conditions that yielded styrene–methyl methacrylate grafted cotton fabrics having these improved properties is given. For 10 parts of styrene, methylmethacrylate can be varied from 3 to 8 parts. The solvents that can be used for the monomers are methanol, methyl–hydrate, or ethanol. Addition of up to 10% water increased grafting 5 to 10 fold. The total volume of monomers should be between 12–18% of the total grafting media, and total irradiation dose required is 3 to 5×10^5 rad. Dose rates can be varied from 1×10^5 to 7×10^5 rad/hr. (BBB)

40954 SPECTRAL SHIFT PHENOMENON OF CHLOROQUINE. Sams, W. Mitchell Jr.; Carroll, Nicholas V. (Letterman General Hospital, San Francisco). Arch. Dermatol., 93: 123-8(Jan. 1966).

Ultraviolet irradiation of chloroquine diphosphate in 0.1M phosphate buffer pH 7.4 results in a marked depression of the characteristic spectral peaks at 3280 and 3420 Å, and a significant increase of absorption in the 2670-3000 Å range. This spectral shift phenomenon is probably due to radiation between 2900 and 3100 Å. Under the conditions of the experiments it did not occur when uv irradiation was carried out on chloroquine-containing serum, sweat, or homogenized epidermal cells. Nor did it occur when chloroquine was extracted from the skin of rats that were uv irradiated after a single intraperitoneal injection of the drug. In addition, it did not occur at pH below 5.0. Paper chromatography of the uv-irradiated chloroquine afforded isolation of one of the compounds responsible for the spectral shift. The separation of two compounds from uv-irradiated chloroquine indicates that the original molecule has been broken at one point at least. That it may have been split at more than one point cannot be dismissed at this time. The site of the break is at present unknown. The spectral shift phenomenon described for chloroquine is probably not the mechanism whereby the drug exerts its beneficial effect in polymorphic light eruption. It may represent no more than an interesting laboratory observation. The important observation with chloroquine is that the absorption increases greatly in the erythema zone before it is destroyed. (TCO)

40955 ELECTRON SPIN RESONANCE SPECTRA OF ^{15}N-CENTERED RADICALS AT LOW TEMPERATURES. II. THE RADIOLYSIS OF POTASSIUM SULFAMATE. Morton, J. R.; Smith, D. R. (Atomic Energy of Canada Ltd., Chalk River, Ont.). Can. J. Chem., 44: 1951-5 (Aug. 15, 1966). (AECL–2465).

Single crystals of potassium sulfamate, KNH_2SO_3, enriched in the isotope ^{15}N, were γ-irradiated, and examined at 77°K by electron spin resonance. Two intermediates, neither of which are present on examination at 300°K, were identified as NH_2 and NH_2SO_3. A possible radiolysis mechanism is discussed. (auth)

40956 ELECTRON SPIN RESONANCE SPECTRA OF $N_2H_4^+$ AND PF_2. Wan, J. K. S.; Morton, J. R.; Bernstein, H. J. (National Research Council, Ottawa). Can. J. Chem., 44: 1957-9(Aug. 15, 1966). (NRC–9057).

The radicals $N_2H_4^+$ and PF_2 were detected by electron spin resonance in γ-irradiated NH_4PF_6. The radical $N_2H_4^+$ was formed from NH_3^+ radicals detectable after low-temperature irradiation. (auth)

40957 RADIATION CHEMISTRY OF SOLUTIONS OF CHLOROMETHANES IN CYCLOHEXANE. Sherman, Warren V. (Soreq Nuclear Research Centre, Yavne, Israel). Chem. Commun., No. 15, 489-90(Aug. 10, 1966).

The γ radiolysis of cyclohexane solutions containing methyl chloride, methylene chloride, chloroform, and carbon tetrachloride was studied to determine the exact nature of the transfer mechanism, i.e., whether via thermal electrons or excitation energy. The sole radiolytic product gaseous at liquid-air temperature in solutions of CH_2Cl_2, $CHCl_3$, and CCl_4 was hydrogen; while in the CH_3Cl-cyclohexane system methane was identified in addition to hydrogen. $G(H_2)$ decreased with increasing solute concentration in the solutions of all four solutes. It was concluded that while it is possible to explain at least part of the reduction in hydrogen yields brought about by the presence of the chloromethanes by an electron-capture process, the latter cannot be of major importance in the formation of HCl. (P.C.H.)

40958 TO THE THEORY OF RADIATION CHEMISTRY. I. APPLICATION OF PRINCIPLES OF THE SIMPLIFIED QUASI-EQUILIBRIUM THEORY OF MASS SPECTRA TO THE DETERMINATION OF RADIATION CHEMICAL YIELDS OF A GAS PHASE RADIOLYSIS. Prasil, Z. (Inst. of Nuclear Research, Czechoslovak Academy of Sciences, Rez). Collect. Czech. Chem. Commun., 31: 3252-62(Aug. 1966).

A spontaneous decomposition of molecules and ions, electronically excited by ionizing radiation, taking place in the time interval between their formation and the first collision, is treated according to the principles of the simplified quasi-equilibrium theory of mass spectra. The optical approximation was used to determine the energetical distribution of excited particles. The limits of applicability of the calculation procedure are discussed. (auth)

40959 TO THE THEORY OF RADIATION CHEMISTRY. II. CALCULATION OF RELATIVE RADIATION CHEMICAL YIELDS OF THE GAS PHASE RADIOLYSIS OF METHANOL. Prasil, Z. (Inst. of Nuclear Research, Czechoslovak Academy of Sciences, Rez). Collect. Czech. Chem. Commun., 31: 3263-79(Aug. 1966).

Primary and total radiation chemical yields of products of the gas-phase radiolysis of methanol were calculated using the quasi-equilibrium theory of mass spectra in the semiclassical approximation. A modified mechanism of the decomposition of an excited molecular ion CH_3OH^{+*} was suggested, which is more suitable for the calculation of the mass spectrum. Special attention was paid to the influence of some of the parameters on the final yields, especially to the influence of the distribution function of excited states, estimated with the aid of the optical approximation. The role of superexcited states in these processes is discussed. Calculated results are in relatively good agreement with experimental data. (auth)

40960 KINETICS OF THE DECOMPOSITION OF RADICALS IN FROZEN AQUEOUS SOLUTIONS OF $NaClO_4$ AND $HClO_4$. Belevskii, V. N.; Bugaenko, L. T.; Golubev, V. B. (Moscow State Univ.). Dokl. Akad. Nauk SSSR, 168: 122-5(May 1, 1966). (In Russian).

Kinetics of the disappearance of the hydrogen atoms (I) and hydroxyl (II) and chlorine trioxide (III) radicals in a frozen aqueous solution of $NaClO_4$ and $HClO_4$ irradiated with ^{60}Co γ rays were investigated by means of ESR to clarify the mechanism by which the molecular products of radiolysis are formed. Solutions were frozen in glass ampules 2 to 2.5 mm thick and irradiated with γ rays in doses of 3×10^{16} ev/ml/sec at –196°C. For short reaction times the process was strictly of second order for I and III, but of mixed order for II. For an extended reaction time the process was of the first order for all investigated radicals. Activation energies for the disappearance of I and III were determined, and it was found that the activation energy of

the disappearance of H in $HClO_4$ is twice that in $NaClO_4$. (ATD)

40961 DETERMINATION OF THE RADIATION YIELD OF THE FORMATION OF TRIPLET MOLECULES IN THE RADIOLYSIS OF BENZENE. Samokhvalova, L. I.; Krongauz, V. A. (Karpov Inst. of Physics and Chemistry, Academy of Sciences, USSR). Dokl. Akad. Nauk SSSR, 168: 154-7(May 1, 1966). (In Russian).

The benzene-sensitized trans-cis isomerization of stilbene was used to determine the radiation yield of triplet molecules under the action of gamma rays on benzene. The radiation yields of the isomerization of stilbene increased with increasing concentration of the solutions approximately up to 10^{-3}M; with further increases in concentration, the yields reached limiting values, and remained constant within the range of concentrations investigated (up to 0.1M). The limiting radiation yield of the isomerization of trans-stilbene in cyclohexane was greater than that in benzene. Isomerization of trans-stilbene occurs not only in benzene, but also in cyclohexane, which has no stable excitation levels, indicating that it is due substantially to interaction of stilbene with radicals formed in the radiolysis of the solvents. At stilbene concentrations less than 10^{-3}M, the reaction of primary free radicals with stilbene competes with their mutual recombination, whereas at higher stilbene concentrations, all the primary free radicals formed from the solvent cause isomerization of stilbene. Isomerization of stilbene induced by free radicals was inhibited by conducting the radiolysis of stilbene solutions in benzene and cyclohexane in the presence of additions of vinyl monomers: styrene and methylmethacrylate, which are effective radical acceptors. A comparison with the sensitized photolysis of benzene solutions of trans-stilbene in the presence of styrene and methylmethacrylate indicates that under the action of gamma rays, a substantial fraction of the triplet benzene molecules that induce isomerization of styrene are formed from higher excited states or in the neutralization of ions. (JPRS)

40962 DETERMINATION OF THE YIELD OF STABILIZED CHARGES IN LOW-TEMPERATURE RADIOLYSIS OF ORGANIC SYSTEMS. Tochin, V. A.; Nikolskii, V. G.; Buben, N. Ya. (Inst. of Chemical Physics, Academy of Sciences, USSR). Dokl. Akad. Nauk SSSR, 168: 360-3 (May 11, 1966). (In Russian).

The electron paramagnetic resonance method was used to obtain quantitative data on the yields and limiting concentrations of ion radicals stabilized in the low-temperature radiolysis of organic substances. The accumulation of paramagnetic particles during irradiation within the dose interval 0.2 to 30 Mrad and the change in the EPR spectra under the action of visible light were investigated on a broad range of organic substances, including saturated hydrocarbons (hexane, n-decane, 2,7-dimethyloctane, cyclohexane, dicyclohexyl-4-decane, polyethylene), aromatic hydrocarbons (benzene, toluene, ethylbenzene, styrene, cumene, diphenylmethane, polystyrene), alcohols (ethyl, isopropyl, polyvinyl), ketones (acetone, methyl ethyl ketone, acetophenone), heterocyclic compounds (tetrahydrofuran, 2-methyltetrahydrofuran, dioxane), and certain ethers and organosilicon compounds. The influence of visible light and the addition of electron acceptor additives (CCl_4, CS_2, naphthalene, and diphenyl) on the EPR signal were studied. (JPRS)

40963 ULTRAVIOLET SPECTROSCOPY OF IRRADIATED POLYETHYLENE. Bodily, David M.; Dole, Malcolm (Northwestern Univ., Evanston, Ill.). J. Chem. Phys., 45: 1428-32(Sept. 1, 1966). (COO-1088-18).

When polyethylene was irradiated with high-energy radiations, ultraviolet absorption bands with peaks at 229, 236, 245, 258, 264, 275, 285, 288, 307, 323, 340, 359, and 396 mμ were observed. The bands were most clearly distinct at liquid-nitrogen temperature, but some could only be observed after decay of free radicals on admission of oxygen at room temperature. The assignment of these bands to conjugated polyene and polyenyl free-radical groups is given and discussed. (auth)

40964 RADIATION CHEMISTRY OF POLYETHYLENE. VIII. KINETICS OF GROWTH AND DECAY OF POLYENE AND POLYENYL FREE RADICAL GROUPS. Bodily, David M.; Dole, Malcolm (Northwestern Univ., Evanston, Ill.). J. Chem. Phys., 45: 1433-9(Sept. 1, 1966). (COO-1088-19).

Free radicals produced as intermediates during the radiolysis of polyethylene were studied using ultraviolet absorption spectroscopy because the uv absorption bands of the allyl, dienyl, and trienyl conjugated free radicals are well separated on the wavelength scale and do not overlap as do the ESR signals from these intermediates. Stable polyenes were also produced by the radiolysis and were studied quantitatively by ultraviolet spectroscopy. In contrast to the diene groups whose concentration grew linearly with the dose, the allyl and dienyl free radicals as well as conjugated trienes grew with increasing rates as the irradiation proceeded. A statistical calculation of the triene growth reaction rate constant in terms of the diene concentration and a probability factor based on the vinylene growth rate was successful. From this result and others it was concluded that trienes and allyl, dienyl, and trienyl free radicals were not primary products of the irradiation. The effect of ultraviolet light on the allyl and dienyl free radicals was studied. Uv light decreased the allyl free radical concentration; however, the dienyl and trienyl concentrations increased. On standing after the uv irradiation the allyl groups recovered practically their initial abundance, but the dienyl and trienyl free radical concentrations continued to grow. Various mechanisms are discussed. (auth)

40965 PHOTO- AND RADIATION-INDUCED cis-TRANS ISOMERIZATION OF SEVERAL 2-OLEFINS. Golub, M. A.; Stephens, C. L.; Brash, J. L. (Stanford Research Inst., Menlo Park, Calif.). J. Chem. Phys., 45: 1503-5(Sept. 1, 1966).

Benzene photo- and radiation-sensitized cis-trans isomerization of 2-pentene, 2-hexene, 2-heptene, and 2-octene all yielded the same photo- and radiostationary trans/cis ratio, viz., 1.0. The G value for benzene triplet formation is estimated at 5.0. G values for the radioinduced unsensitized isomerization of the above olefins are 2.50, 2.13, 1.85, and 1.67, respectively. (auth)

40966 ELECTRON SPIN RESONANCE IDENTIFICATION OF AN N_2^- DEFECT IN X-IRRADIATED SODIUM AZIDE. Gelerinter, Edward; Silsbee, Robert H. (Cornell Univ., Ithaca, N. Y.). J. Chem. Phys., 45: 1703-9(Sept. 1, 1966). (NYO-2150-12).

A defect was produced in sodium azide (NaN_3) by exposing it to x rays and was studied using the ESR (electron spin resonance) technique in the frequency range from 10 to 70 kMc/sec. The observed spectrum agreed with the theoretical predictions made using a model of an N_2^- ion in the azide position with the surroundings frozen in a Jahn-Teller distortion. Since the azide ion was in a position of trigonal symmetry, there were three such distortions, and there was experimental evidence that these three distortions are equally populated. The absence of experimental evidence for tunneling does not necessarily imply correspondingly low tunneling matrix elements, but instead may be the result of stabilization of the static states by the strain which is known, from x ray data, to be present. These strains were also responsible for some of the observed line broadenings. The available crystals were heavily twinned, so that it is necessary to correlate x ray and ESR data in order to remove the ambiguities associated with this twinning. (auth)

40967 ESR OF FREE RADICALS TRAPPED IN INERT MATRICES AT LOW TEMPERATURE: P, PH_2, AND As. Morehouse, Roger L.; Christiansen, Joern J.; Gordy, Walter (Duke Univ., Durham, N. C.). J. Chem. Phys., 45: 1747-51(Sept. 1, 1966).

Free radicals produced by γ irradiation of PH_3 and of AsH_3 in dilute solution in a krypton matrix at 4.2°K were studied by electron spin resonance. For the PH_3 solution, PH_2 radicals as well as H and P atoms were observed.

For the AsH_3 solutions, only H and As atoms were observed. For the PH_2 radicals, the observed ESR constants are: $A_f(^{31}P)$ = 80 G, $A_f(H)$ = 18 G, and g = 2.0087. For the P atoms, $A_f(^{31}P)$ = 30.5 G and g = 2.0027. For the As atoms, $A_f(^{75}As)$ = 11.2 G and g = 1.9975. From the P and H couplings it was concluded that the P bonding orbitals of PH_2 are sp_2 hybrids with 27% s character. From the line shapes it was concluded that the PH_2 radical rotates in the krypton matrix. (auth)

40968 ESR OF FREE RADICALS TRAPPED IN INERT MATRICES AT LOW TEMPERATURE: CH_3, SiH_3, GeH_3, AND SnH_3. Morehouse, Roger L.; Christiansen, Joern J.; Gordy, Walter (Duke Univ., Durham, N. C.). J. Chem. Phys., 45: 1751-8(Sept. 1, 1966).

The free radicals CH_3, SiH_3, GeH_3, and SnH_3 were produced in a krypton matrix at 4.2°K by γ irradiation of the matrix containing dilute concentrations of CH_4, SiH_4, GeH_4, and SnH_4. The electron spin resonances indicated free or restricted rotation for all the radicals in the matrix. Observed anisotropies in g showed that SiH_3, GeH_3, and SnH_3 execute restricted rotation about an axis perpendicular to the symmetry axis. From the observed values for the rotating radicals, the axially symmetric principal g values for the static radicals were derived as follows: for SiH_3, $g_{||}$ = 2.003, $g_\perp$ = 2.007; for GeH_3, $g_{||}$ = 2.003, $g_\perp$ = 2.017; for SnH_3, $g_{||}$ = 2.003, $g_\perp$ = 2.025. Hyperfine structure caused by ^{29}Si was observed for SiH_3 with isotropic coupling constant A_f = 266 G and anisotropic coupling $A_{||}$ = 24 G. These couplings revealed 22% s character in the orbital of the unpaired electron, which indicated that the radical was nonplanar with bond angles of 110.6°. Probably GeH_3 and SnH_3 are also nonplanar. The magnitudes of the isotropic proton couplings are: 23, 8.1, 15, and 26 G, respectively, for CH_3, SiH_3, GeH_3, and SnH_3. The coupling of SiH_3 is probably negative like that for CH_3, but that of GeH_3 and of SnH_3 may be positive. (auth)

40969 ELECTRON SPIN RESONANCE SPECTRUM OF ClO_4 TRAPPED IN IRRADIATED $KClO_4$. Morton, J. R. (National Research Council, Ottawa). J. Chem. Phys., 45: 1800-2(Sept. 1, 1966).

Two paramagnetic centers were detected in $KClO_4$ crystals γ irradiated at 77°K. After consideration of the various possibilities it was concluded that the centers may be described as ClO_4 radicals trapped in magnetically distinct sites. (auth)

40970 CHARGE RECOMBINATION IN GAMMA-IRRADIATED ALKANE GLASSES. Funabashi, Koichi; Magee, John L. (Univ. of Notre Dame, Ind.). J. Chem. Phys., 45: 1851-2(Sept. 1, 1966).

The nature of the charge carrier in recombination processes in gamma-irradiated alkane glasses was studied and found to depend on the purity (or chemical composition) of the sample and the method of bleaching. In the case of pure alkane glasses and thermal bleaching, the positive charge was the principal moving entity; in the case of doped alkane and thermal bleaching, the electron became the moving entity. In the case of optical bleaching, the electron was essentially the only charge carrier. (D.H.M.)

40971 RADIATION-INITIATED CODIMERIZATION OF METHALLYL CHLORIDE WITH UNSATURATES. Gale, L. H. (Shell Development Co., Emeryville, Calif.). J. Org. Chem., 31: 2475-80(Aug. 1966).

Ionizing radiation initiates the codimerization of methallyl chloride with a variety of unsaturated compounds including 1-pentene, maleic anhydride, allyl acetate, and vinyl acetate. The general product from this free-radical reaction with $CH_2{=}CHR$ is a codimer, $Cl(CH_2CHR)CH_2C(CH_3){=}CH_2$. With favorable raction conditions (150°C, 0.1 Mrad/hr), G values for codimer formation range from 50 to 250. Higher molecular weight trimers of the general structure $Cl(CH_2CHR)_2CH_2C(CH_3){=}CH_2$ and $CH_3C(CH_2CL)_2(CH_2CHR)CH_2C(CH_3){=}CH_2$ may also be formed. A major side reaction is the formation of methylallyl chloride dimer. A free-radical chain reaction is proposed for the codimerization, and ratios of rate constants for a number of the intermediate reaction steps were determined from the product distributions resulting from variation of the methallyl chloride-unsaturated mole ratios. (auth)

40972 ELECTRON SPIN RESONANCE OF IRRADIATED $NaH_3(SeO_3)_2$ AND $NaD_3(SeO_3)_2$. Blinc, R.; Pobera], S.; Schara, M.; Stepisnik, J. (Stefan Nuclear Inst., Ljubljana, Yugoslavia. Univ. of Ljubljana, Yugoslavia). J. Phys. Chem. Solids, 27: 1391-1400(Sept. 1966).

ESR spectra of γ-irradiated $NaH_3(SeO_3)_2$ and $NaD_3(SeO_3)_2$ single crystals were investigated, and the principal stable damage centers were identified as SeO_3^-. The spectra consist of a central part, due to those SeO_2^- groups, which are composed of spinless isotopes of Se, and of a number of satellites due to hyperfine interaction with ^{77}Se. At room temperature four physically non-equivalent free radicals were found in the unit cell of nonpolar $NaH_3(SeO_3)_2$ and $NaD_3(SeO_3)_2$; two of them were also chemically non-equivalent and the complete g and hyperfine coupling tensors were determined. A tentative model of the electronic structure of the damage center is proposed. Significant changes were found in the spectra on cooling the samples below the corresponding ferroelectric $NaH_3(SeO_3)_2$ or antiferroelectric $NaD_3(SeO_3)_2$ transition points, which were explained by reversible reorientations of the SeO_2^- radicals. (auth)

40973 RADIATION-INDUCED COPOLYMERIZATION OF FORMALDEHYDE AND STYRENE. Castille, Y. P.; Stannett, V. (Research Triangle Inst., Durham, N. C.). J. Polym. Sci., Pt. A-1, 4: 2063-79(Sept. 1966).

The radioinduced copolymerization of styrene with liquid formaldehyde in bulk and in solution was studied at low temperatures. In bulk and in methylene chloride solution copolymerization took place, whereas in diethyl ether solution only homopolymerization of the formaldehyde was found. At –78°C, in bulk and in methylene chloride solution, no evidence of polystyrene blocks could be found, at –30°C in bulk, about 30% of the styrene content of the copolymer was in the form of high molecular weight blocks. The rate of copolymerization in methylene chloride solution was found to be first-order with respect to dose rate and third-order with respect to formaldehyde concentration similar to results reported for formaldehyde in toluene solution. The thermal stabilities of the copolymers were found to be intermediate between those of pure polyoxymethylene and commercially stabilized polymers. Since the latter were of higher molecular weight and contained added stabilizers, the increased thermal stabilities of the copolymers were considered to be particularly significant. (auth)

40974 IRRADIATION OF SOME POLYSILOXANES IN VARIOUS GASES. Jenkins, Robert K. (Northrop Space Labs., Hawthorne, Calif.). J. Polym. Sci., Pt. A-1, 4: 2161-70(Sept. 1966).

The changes produced by γ irradiation on two polysiloxanes in several gaseous atmospheres were studied by both sequential and parallel exposures with an in situ vibrating reed technique. Irradiation in atmospheres of N_2O, He, air, and a mixture of 20% NO_2 and 80% N_2, caused reduction in the crosslinking rates of the polymers as compared to vacuum. Marked discolorations of the samples occurred when irradiations were conducted in air, N_2O, and 20% NO_2–80% N_2. Similarities in crosslinking rates and color changes were obtained when the polymers were irradiated in either or the gas mixture. (auth)

40975 INFLUENCE OF ADDITION OF ETHYLENE ON THE γ-RAY-INDUCED ALTERNATING COPOLYMERIZATION OF ETHYLENIMINE AND CARBON MONOXIDE. Kagiya, Tsutomu (Kyoto Univ.); Narisawa, Shizuo; Ichida, Taizo; Fukui, Kenichi; Yokota, Hisao. J. Polym. Sci., Pt. A-1, 4: 2171-8(Sept. 1966).

The influence of the addition of ethylene on the γ-induced alternating copolymerization of ethylenimine and carbon monoxide was investigated. A mixture of ethylenimine, carbon monoxide, and ethylene was irradiated to produce a polymer containing these monomeric units. The infrared

spectrum of the copolymer showed the characteristic absorption peaks of the secondary amide and ketone bond and was different from that of the reaction product of polyketone with ethylenimine and that of the γ irradiation product of ethylene and poly-β-alanine. The x-ray diffraction diagram of the copolymer was different from those of poly-β-alanine and polyketone and exhibited an amorphous structure. Paper chromatographic analysis showed that the hydrolysis product of the copolymer contained β-alanine and δ-aminovaleric acid. These results indicated that terpolymerization of ethylenimine, carbon monoxide, and ethylene took place under γ irradiation and gave an amorphous polymer containing the units $(-CH_2CH_2NHCO-)$, $(-CH_2CH_2CO-)$, and $(-CH_2CH_2CH_2CH_2NHCO-)$. (auth)

40976 RADIATION-INDUCED POLYMERIZATION OF HEXAFLUOROPROPYLENE AT HIGH TEMPERATURE AND PRESSURE. Lowry, R. E.; Brown, D. W.; Wall, L. A. (National Bureau of Standards, Washington, D. C.). J. Polym. Sci., Pt. A-1, 4: 2229-40(Sept. 1966).

The radioinduced polymerization of hexafluoropropylene was studied at pressures from 4,500 to 15,000 atm and temperatures from 100 to 230°C, respectively. Retardation was a serious problem; data thought to apply to the unretarded polymerization are summarized. At 1,500 rad/hr the polymerization rate was 15%/hr at 230°C and 15,000 atm. The activation enthalpy and volume were 9.5 kcal/mole and −10 cc/mole, respectively. The rate varied as the square root of the radiation intensity. The highest intrinsic viscosity of the polymer was 2.0 dl/g; values increased with temperature and pressure. At 130°C and 10,000 atm the intrinsic viscosity was the same at two radiation intensities. (auth)

40977 RADIATION-INDUCED SOLID-STATE POLYMERIZATION IN BINARY SYSTEMS. II. RELATIONSHIP BETWEEN POLYMERIZATION RATE AND PHYSICAL STRUCTURE OF BINARY SYSTEMS. Kaetsu, Isao (Sekisui Chemical Co., Osaka); Sagane, Norio; Hayashi, Koichiro; Okamura, Seizo. J. Polym. Sci., Pt. A-1, 4: 2241-51(Sept. 1966).

The radioinduced solid-state polymerization of binary systems consisting of acrylic monomer (acrylamide, acrylic acid) and organic compounds was investigated. The mechanism of rate increase was investigated by examination of phase diagrams, viscosities, and surface tension of the binary systems. Viscosity and surface tension are the measure of the molecular interaction of the two-component systems. The effect of linear crystal growth rate and the half maximum width of the x-ray-diffraction diagram of the crystallization process were determined. The larger the molecular interaction between the two components, the slower the linear crystal growth rate of monomer. The size of the monomer crystal decreased and the dislocation density of the monomer crystals increased in systems with large molecular interaction. It was concluded that the physical structure of a binary solid system is the most important parameter determining the rate increase of solid-state polymerization. Dislocation on the grain boundary is more important than defects inside of the crystal lattice. The acceleration of polymerization rate was found to be large in binary systems with larger molecular interaction. In some systems such as organic acid−amide systems with strong hydrogen bonds, glassy phases may be formed in which monomer may readily polymerize at very low temperature. (auth)

40978 γ-RADIATION-INDUCED IONIC POLYMERIZATION OF PURE LIQUID STYRENE. [PART] II. Potter, R. C.; Bretton, R. H.; Metz, D. J. (Brookhaven National Lab., Upton, N. Y.). J. Polym. Sci., Pt. A-1, 4: 2295-2306 (Sept. 1966).

Additional evidence is presented that the γ-induced polymerization of very pure, ultradry styrene exhibits kinetics that can best be explained as due to one or more ionic processes, depending on the dryness of the sample. The effect of the various steps in the drying procedure on the observed kinetics was studied and a preparative procedure, which yields good reproducibility among independently prepared samples is described. Under these conditions, the rate of polymerization was proportional to the 0.70 power of the dose rate at 0°C; there appeared to be no wall effect; and the temperature coefficient for the process appeared to be a complicated function, most probably a small negative value at 0 to 50°C and the dose rates ($\sim 10^3$ to 10^5 rad/hr) covered in this study. The maximum G value for disappearance of monomer was of the order of 6×10^5 molecules of monomer/100 ev at 0°C and a dose rate of 2×10^3 rad/hr. (auth)

40979 CHARGE-TRANSFER THEORY FOR THE INTERPRETATION OF RADIATION-INDUCED GRAFTING OF MONOMERS TO CELLULOSE. Dilli, S.; Garnett, J. L. (Univ. of New South Wales, Kensington). J. Polym. Sci., Pt. A-1, 4: 2323-4(Sept. 1966).

A charge-transfer hypothesis is presented to help interpret radioinduced grafting reactions. Using styrene-cellulose as a model system, it was shown how adsorption phenomena and "inaccessible" radical sites may both contribute to the nature of bonding if the concept of a charge-transfer interaction is invoked. (D.H.M.)

40980 SOLID-STATE POLYMERIZATION OF DIACETONE ACRYLAMIDE. Marans, N. S.; Ehrig, R. J. (Grace (W. R.) and Co., Clarksville, Md.). J. Polym. Sci., Pt. A-1, 4: 2330-5(Sept. 1966).

The polymerization of diacetone acrylamide (N-(1,1-dimethyl-3-oxobutylacrylamide), irradiated by an electron beam from a Van de Graaff accelerator, in both the solid and liquid state, was studied. With decreasing monomer purity, the percentage conversion to polymer increased in the solid state. The final solid-state-prepared polymer did not replicate the crystalline structure of the initial monomer in either the pure or impure monomer. In the liquid state polymer conversion was higher than that in the solid state. Results showed that conversion increased with increasing dose, with a holding of the sample at an elevated temperature after irradiation, and with increasing temperature of irradiation. The polymer conversion was reduced when the monomer sample was melted and resolidified into a continuous film and when air was present during the irradiation. (D.H.M.)

40981 ESR STUDY ON THE RADIATION-INDUCED POLYMERIZATION OF NITROETHYLENE. Tsuji, Kozo (Kyoto Univ.); Yamaoka, Hitoshi; Hayashi, Koichiro; Kamiyama, Hideo; Yoshida, Hiroshida. J. Polym. Sci., Pt. B, 4: 629-31(Sept. 1966).

During gamma-induced polymerization of nitroethylene, results were obtained, mainly by ESR methods, which suggested that polymerization in a mixture of nitroethylene and 2-methyltetrahydrofuran was initiated by anion radicals of nitroethylene formed by the capture of an electron from 2-methyltetrahydrofuran. (D.H.M.)

40982 GRAFTING OF VINYL CHLORIDE ONTO POLYETHYLENE BY THE PRE-IRRADIATION METHOD. Ueda, Kazuo (Electrical Communications Lab., Tokyo). Kobunski Kagaku, 23: 222-8(Apr. 1966). (In Japanese).

Vinyl chloride was grafted to high- and low-density polyethylenes by decomposing the peroxides and hydroperoxides, which were previously formed in the polymers by irradiating with γ rays in the air. The influence of several parameters such as grafting temperature (55 to 100°C) and preirradiation dose (1.27 to 5.23 mR) on the rate of graft polymerization, degree of covalent grafting, and grafting efficiency was studied. The experimental results are discussed and explained on the basis of the chain transfer to monomer and diffusion of monomer to polyethylene. The degree of covalent grafting lies between 40 to 100%, depending on the grafting condition and kind of polyethylene samples. The Arrhenius plots of the rate of covalent graft copolymerization exhibit a break point at 80°C, and the overall activation energy is 11 Kcal/mole above and 18 Kcal/mole below the point; the overall activation energy of homopolymerization is 22 Kcal/mole. Graft efficiency lies between 5 to 30%, and the efficiency decreases as the temperature increases. The molecular weight of homopolymers formed in polyethylene has a

similar value to that in liquid phase, and depends mainly on the grafting temperature. Uniform distribution of graft concentration across the section is observed. (auth)

40983 RADIATION CHEMICAL OXIDATION OF BUTANOL IN AQUEOUS SOLUTION AT INCREASED TEMPERATURE. Komarov, P. N.; Barelko, E. V.; Proskurnin, M. A. (Scientific Research Physicochemical Inst., USSR). Neftekhimiya, 5: 715-20(1965). (In Russian).

The development of the reaction of branched chain oxidation in butanol dissolved in water was studied. This system represents an acceptor, the reaction of which consists of transfer of alpha hydrogen of the alcohol molecule to a hydrogen atom or to a free hydroxyl, with the formation of the alcohol radical and H_2 or H_2O, respectively. The dependence of the formation of products in the oxidation of n-butanol in aqueous solution on the temperature and dose rate of ^{60}Co gamma radiation were studied. At temperatures above 100°, a chain reaction develops, the rate of which is approximately an order of magnitude below that in the oxidation of the pure alcohol. At 20°, the effective activation energy is 1 kcal/mole. In the region of 104–150°, it increases to 5 kcal/mole. During the initial period the reaction rate is proportional to the radiation dose rate. The temperature dependence is compared with that in the reaction of aqueous solutions of benzene. In both cases the data may be treated as the result of an activated removal of radicals from the cell. In contrast to benzene, for which such a temperature dependence in the initial period is maintained almost up to 200°, in an aqueous alcohol solution, the process of chain propagation proceeds more readily than in the case of benzene, and at comparatively low temperatures chain acceleration of the reaction and the related more complex temperature dependence become appreciable. (CFSTI)

40984 INFLUENCE OF THE DOSE RATE OF THE GAMMA RADIATION OF ^{60}Co ON THE KINETICS OF THE INITIAL STEP IN THE RADIATION-CHEMICAL OXIDATION OF BUTANOL IN AQUEOUS SOLUTION. Komarov, P. N. (Scientific Research Physicochemical Inst., USSR). Neftekhimiya, 5: 721-4(1965). (In Russian).

The dependence of the formation of products in the oxidation of n-butanol in aqueous solution on the dose rate of ^{60}Co gamma radiation was investigated. The linear dependence of the reaction rate on the dose rate is due to the fact that the reaction is a chain process with short chains (two to three links). The chain length is approximately quadrupled in the case of oxidation of the pure alcohol. When the rate of initiation is large and the chains are short, a substantial portion of the reaction products are recombination products of peroxide radicals; when the dose rate is lowered, the proportion of recombination products drops, and, correspondingly, the proportion of products formed in the development of the basic reaction chain increases. The oxidation products in the radiochemical oxidation of n-butanol in a 0.98 M aqueous solution are peroxides, aldehydes, and acids; the dose rate dependence of the accumulation of peroxides and the data of polarographic and iodometric analyses of the peroxides indicate that the latter are formed only as a result of development of the basic chain. The aldehydes and acids, at least in the initial period of the oxidation, are produced chiefly by chain termination, and the rate of accumulation of each of the products increases in direct proportion to the gamma dose rate. (CFSTI)

40985 INTERMEDIATES OF α-METHYLSTYRENE POLYMERIZATION STUDIED BY MEANS OF PULSE RADIOLYSIS. Katayama, Meiseki (Hokkaido Univ., Sapporo); Hatada, Motoyoshi. Nippon Kagaku Zasshi, 87: 37-9(Jan. 1966). (In Japanese).

The decay of optical absorption at 3663 Å was observed in very dry α-methylstyrene by means of pulse radiolysis using a photoelectric method of recording. Two kinds of decay rates were observed, both of which obeyed the first order reaction kinetics with a half life of about 25 μsec and 5 msec, respectively. Since it can be estimated from previous reports that ionic polymerization is some hundred times faster than radical polymerization, the fast decay is regarded as the reaction of ionic species, or more specific, anion radicals, and the slow decay, probably as that of free radicals. (auth)

40986 MECHANISM OF RADIATION-THERMAL LIQUID PHASE CONVERSIONS OF n-ALKANES. Brodskii, A. M.; Lavrovskii, K. P.; Titov, V. B.; Eglit, A. Kh. (Topchiev Inst. of Petrochemical Synthesis, Academy of Sciences, USSR). Petrol. Chem. (USSR) (Eng. Transl.), 5: No. 2, 120-33(1966).

A detailed study was made of the temperature dependence of radiation-thermal, liquid-phase breakdown of hydrocarbons by following the degradation of $C_{34}H_{70}$ normal paraffin (tetratriacontane) in the mixed radiation field of a nuclear reactor at 150 to 400°. All experiments on the irradiation of tetratriacontane and its solutions in p-terphenyl were carried out with an integral dose of 6×10^{21} ev/g. Up to this dose, a linear dependence of the radiation-chemical yields of the bulk of the radiolytic products on the dose was observed. It was found that the decomposition of secondary hydrocarbon radicals (isoradicals) is important mainly in the formation of low-molecular weight radiation-thermal breakdown products of tetratriacontane; consequently processes of formation of low-molecular weight saturated and unsaturated hydrocarbons have the same activation energies. Processes taking place in a liquid envelope, particularly during the formation of high-boiling radiolytic products (polymers) are important in the mechanism of radiation-thermal liquid phase conversions. The concentrations of various types of radicals were evaluated in the envelope and outside the envelope, and it was found that, during the primary event of radiation, rupture of C–C bonds takes place mainly with the formation of primary hydrocarbon radicals (normal) in the envelope, while outside the envelope hydrocarbon radicals mainly consist of secondary radicals formed by reactions of substitution from normal radicals. Pre-exponential factors of the rate constant were evaluated for the breakdown of secondary hydrocarbon radicals. The results of radiolysis after addition of inhibitors showed that p-terphenyl addition does not affect the yields of light gaseous products and polymers. An inhibiting effect of p-terphenyl was noted only in the formation of dienes. (BBB)

40987 IMPORTANT EARLY STAGES IN THE RADIOLYSIS OF SOLID AND LIQUID SYSTEMS. Dainton, F. S. (Univ. of Leeds, Eng.). Pure Appl. Chem., 10: 395-411 (1965).

A review of the early stages of the radiolysis of solid and liquid systems is given, starting with the change of emphasis from exclusively ionic to free-radical mechanisms. Topics discussed are: initial excitation and ionization, deceleration of electrons, fate of electrons in non-polar media, fate of electrons in polar media, properties and uses of solvated and trapped electrons, fate of positive ions, the role of excited states, and energy transfer in solids. It was concluded that positive ions, electrons, free radicals, and excited states may all contribute to the extent and nature of the final product in degrees that depend on the polarity and state of aggregation of the solvent and the nature of the solute. (D.H.M.)

40988 PROGRESS IN CHEMONUCLEAR AND RADIATION CHEMICAL PROCESS DEVELOPMENT. Steinberg, M. (Brookhaven National Lab., Upton, N. Y.). Pure Appl. Chem., 10: 425-40(1965).

Principal factors involved in the development of chemonuclear and radiation chemical processes are discussed with respect to economics of the system, including both the cost of producing the product and its quality or marketability. A number of endothermic chemical reactions considered or proposed for chemonuclear synthesis are listed. A summary of work on the fixation of nitrogen for chemonuclear process development and the polymerization of ethylene in the field of radiation chemical processing is given. (D.H.M.)

40989 HETEROGENEOUS PROCESSES IN RADIATION CATALYSIS. Polak, L. S.; Pshezhetskii, S. Ya. (Mos-

cow State Univ. Karpov Physics-Chemical Research Inst., Moscow). Pure Appl. Chem., 10: 441-57(1965).

The evidence available in the field of radioinduced catalysis is discussed with respect to excitation, ionization, and recombination of free charge carriers formed by irradiation of solid catalysts, dielectrics, or semiconductors. The topics considered are: general characteristics of the effect of ionizing radiation in solids; radiation chemisorption of hydrogen; processes in radiation catalysis; adsorption of radicals and possible "centers" of radiation catalysis; selectivity of "radiation-catalytic" processes; chain processes in radiation catalysis; and radioactive catalysts. (D.H.M.)

40990 ALPHA-PARTICLE RADIOLYSIS OF THE CYCLOHEXANE–SULFUR SYSTEM. Blackburn, R.; Charlesby, A.; Read, J. F. (Royal Military Coll. of Science, Shrivenham, Swindon, Eng.). Radiat. Res., 28: 793-803(Aug. 1966).

The presence of sulfur in cyclohexane reduced the α-particle and γ-photon radiolysis yields of dimer. This is ascribed to scavenging of cyclohexyl radicals by sulfur or its immediate radiation products, thus reducing the reaction of these species with each other. The scavenging process is less effective in the case of high-LET radiation, and this is ascribed to dimerization reactions within the track. The agreement of the experimental results with the Fricke one-radical model is consistent with a set of radical reactions rather than with reaction of very short-lived excited species. The existence of a track effect suggests that the part played by large excited domains, if they exist, is small. (auth)

40991 THERMAL AND RADIOCHEMICAL STABILITY OF CERTAIN AROMATIC AND HETEROCYCLIC HYDROCARBONS. Girier, J. P. (Institut Francais du Petrole, Grenoble, France). Rev. Inst. Franc. Petrole Ann. Combust. Liquides, 21: 103-8(Jan. 1966). (In French).

Naphthalene, quinoline, isoquinoline, and several of their methyl substitution products were subjected to thermal and radiochemical degradation, and the results compared with the ionization potentials of the compounds and the appearance potentials of the (M – 1) and (M – 15) ions. A good correlation was found for the threshold temperature for thermal degradation and the appearance potential of the (M – 1) peak. The radiochemical yields found for naphthalene, 2-methylnaphthalene, 1-methylnaphthalene, quinoline, isoquinoline, and 3-methylisoquinoline are 0.379, 0.388, 0.437, 0.616, 0.701, 0.726 (G values), respectively. This sequence does not correlate with the appearance potentials of the (M – 1) ions; but initiation stage of a radiochemical reaction depends on ionization probability of the molecule, and therefore its ionization potential. A correlation was found between the sequence of G values and the ionization potentials, which are 8.12, 7.95, 8.00, 7.75, 7.65, and 7.00 ev, respectively. The reversal of the two methylnaphthalenes was determined by the weakness of the C–H bond in each compound. (BBB)

40992 RADIATION-INDUCED GRAFT COPOLYMERIZATION OF STYRENE TO POLYVINYL CHLORIDE. I. COMPARISON OF THE RATES OF GRAFTING IN LIQUID PHASE AND IN VAPOR PHASE OF STYRENE MONOMER. Takamatsu, Toshiaki (Inst. of Physical and Chemical Research, Tokyo). Rika Gaku Kenkyusho Hokoku, 40: 203-8(1964). (In Japanese).

Graft copolymerization of poly(vinyl chloride) films was carried out in liquid styrene or in its vapor by γ irradiation from ^{60}Co or by electrons accelerated with a Van de Graaff generator. The relation between the degree of grafting and total dose of radiation and between the rate of grafting and the dose rate was studied. When the polymer is irradiated in monomer liquid in the dose rate range from 4.2×10^2 to 1.7×10^5 R/hr, the rate of grafting is proportional to the square root of dose rate. On the other hand, when the polymer is irradiated in monomer vapor, the rate of grafting is proportional to the square root of dose rate only in the range below 4.8×10^3 R/hr. At higher dose rates the rate of grafting tends to be independent of dose rate and reaches a constant value at 2×10^4 R/hr. The rate of grafting in monomer vapor is much larger than that in monomer liquid. The efficiency of grafting initiated by exposure to high-energy electrons is much smaller than by γ irradiation. When the polymer is immersed in monomer liquid, the concentration of monomer absorbed in the polymer film quickly attains its equilibrium value, but with the polymer in monomer vapor, the concentration of monomer in the polymer film slowly increases with time and does not reach an equilibrium value. The difference between the rate of grafting in monomer liquid and that in monomer vapor is due to the difference of monomer concentration during irradiation. (BBB)

40993 RADIATION-INDUCED GRAFT COPOLYMERIZATION OF STYRENE TO POLYVINYL CHLORIDE. II. RELATION BETWEEN THE RATE OF GRAFTING AND THE CONCENTRATION OF STYRENE ABSORBED IN POLYVINYL CHLORIDE. Takamatsu, Toshiaki (Inst. of Physical and Chemical Research, Tokyo). Rika Gaku Kenkyusho Hokoku, 40: 209-14(1964). (In Japanese).

The rate of grafting of styrene to poly(vinyl chloride) by exposure to γ rays was studied as a function of monomer concentration absorbed in the polymer. The rate of grafting initially increases with the increase of monomer concentration, and reaches a maximum value at the concentration of 3.5 mole/l, then decreases to a minimum value at the concentration of 5.2 mole/l which is the value at absorption equilibrium. The kinetics of this grafting reaction were considered by the analogy of homogeneous homopolymerization, and the value of k_p^2/k_t for vapor and liquid-phase graft polymerization have been derived, where k_p is the rate constant of propagation and k_t is the rate constant of termination. The value of k_t is calculated by assuming that the value of k_p is the same as that for the homopolymerization reaction. The value of k_t increases greatly when the monomer concentration becomes more than 3.5 mole/l. This increase in k_t may be explained as follows: When styrene is absorbed into poly(vinyl chloride), it acts as a plasticizer and increases the molecular motion of the polymer. As the concentration of styrene becomes more than 3.5 mole/l, the transition temperature of the swollen polymer decreases to a value lower than room temperature. Consequently, the recombination of growing radicals is greatly promoted, resulting in a large value of k_t. (BBB)

40994 ESR INVESTIGATION OF RADICAL REACTIONS IN γ-IRRADIATED FROZEN AQUEOUS SOLUTIONS OF FORMIC ACID AND FORMATE. Getoff, N.; Guetlbauer, F.; Schenck, G. O.; Wolgast, R. (Max-Planck-Institut fuer Kohlenforschung, Muelheim-Ruhr, Ger.). Tetrahedron Lett., No. 24, 2725-31(June 1966).

Electron spin resonance (ESR) experiments on the formation of the intermediate ($COO^-.OCH.O^-$) radical ion in the radiolysis of deaerated aqueous solutions of carbon dioxide, bicarbonate, carbonate, formic acid, and formate are reported. ESR signals of the radicals formed in aerated water by ^{60}Co γ irradiation at 77°K were interpreted as being due to OH and HO_2 radicals. On warming the samples, the signals of the OH radical disappear between 90 and 110°K and those of the HO_2 radical at 145°K. ESR spectra were recorded as a function of temperature up to 250°K. For solutions of formic acid at 77°K the ESR signal (I) of the irradiated solutions proved to be identical with that of pure water. In formic acid, as well as in the other solutions the signal (I) decayed rapidly between 85–95°K and simultaneously a new signal (II) was formed at higher field strengths. In irradiated formate solutions essentially the same signal (II) was formed when the temperature was raised to 120°K. The signal was stable up to 170°K and, with rising temperature, its intensity decreased slowly until it disappeared above 240°K. The intensity at 120°K was greater by a factor of 3 as compared to formic acid solution. In interpreting the ESR spectra it was concluded that the signals do not arise from HO_2 radicals. The radicals of the solutes are not formed directly as a consequence of the irradiation but are products of a secondary reaction between the water radicals and the solute. From a consideration of the reaction mechanism of radioinduced carboxyl-

ation of formic acid and formates, the ESR results in frozen aqueous solutions point to the radical intermediate $COO^-.OCH.O^-$. (TCO)

40995 POST-IRRADIATION GRAFTED VINYL CELLULOSE COPOLYMERS. Blouin, Florine A.; Morris, Nelle J.; Arthur, Jett C. Jr. (Dept. of Agriculture, New Orleans). Textile Res. J., 36: 309-16(Apr. 1966).

Studies were made to evaluate further a previously described post-irradiation grafting technique which utilizes as the reaction medium a strong swelling agent for the cellulose, to evaluate the properties of the grafted vinyl-cellulose copolymers produced by this technique, and to evaluate the effect of monomers used and other experimental variables on the properties of the resultant copolymers. Purified cotton cellulose fibers, yarns, and fabrics were grafted with vinyl acetate, acrylonitrile, and methyl methacrylate, using a post-irradiation grafting technique. The cottons were irradiated dry and in nitrogen with γ rays from a cobalt-60 source to a dose of 1 MR and treated at about 23°C with a 15% monomer solution in 70, 75, or 80% aqueous zinc chloride. The rates of graft polymerization of these were 6400 to 75,000 molecular actions per 100 ev. The rate of reaction and maximum yield were also dependent on the physical state of the cotton. Yarns and fabrics containing 50 and 25% grafted polymer, respectively, were prepared for property evaluations. Grafted yarns showed a marked increase in elongation-at-break and a decrease in average stiffness. Polyacrylonitrile-cotton yarns exhibited significant rot resistance. The vinyl grafted yarns were thermoplastic. Two different distributions of the vinyl polymers were observed on examination of cross sections of grafted fibers. The molecular weights of the vinyl polymers were very high (1 to 3×10^6). Both the polyvinyl acetate- and the polyacrylonitrile-cotton fabrics exhibited marked improvements in abrasion resistance. (BBB)

40996 MECHANISM OF RADIOLYSIS OF CARBON DIOXIDE. Anbar, M.; Perlstein, P. (Weizmann Inst. of Science, Rehovoth, Israel. Soreq Nuclear Research Center, Yavne, Israel). Trans. Faraday Soc., 62: 1803-11(July 1966).

The radiolytic behavior of CO_2 was investigated following the $C^{16}O_2-{}^{18}O_2-C^{16}O$, $C^{18}O_2-{}^{18}O_2-C^{16}O$, $C^{18}O_2-C^{16}O$, $C^{16}O_2-{}^{18}O_2$, ${}^{13}CO-C^{16}O_2-{}^{18}O_2$ as well as the $C^{18}O_2-C^{16}O_2$ and ${}^{18}O_2-{}^{16}O_2 + CO_2$ isotopic exchange reactions. CO is formed as primary product with a G value of approximately 11. O_2 was a secondary product presumably formed by the decomposition of CO_3 molecules. The latter species was suggested for the oxidation of CO to CO_2, for the perpetuation of the CO_2-CO_2 isotopic exchange as well as for the inhibition of the O_2-O_2 exchange. (auth)

40997 RADIATION CHEMISTRY OF LIQUID HYDROGEN SULFIDE. McNaughton, G. S. (DSIR, Lower Hutt, N. Z.). Trans. Faraday Soc., 62: 1812-21(July 1966).

$G(H_2)$ for cobalt-60 γ-irradiated liquid hydrogen sulfide at −78°C is 8.1 ± 0.3 and is unaffected by the addition of I_2 or 2,2-diphenyl-1-picrylhydrazyl (DPPH). G(S) is 6.6 ± 0.7 for the pure liquid, and when DPPH is present increases through a flat maximum about 8 at DPPH concentrations of 10^{-4} to 10^{-3} M, thereafter decreasing to 3 in 10^{-2} M DPPH. The yields suggest that H atoms abstract hydrogen atoms from the solvent, and SH radicals combine to form H_2S and S atoms which later polymerize. Although H_2S_2 was not detected, the lack of stoichiometry suggests it is formed in the pure liquid and the following yields were calculated assuming G_{H_2} is zero. $G_H = G_{-H_2S} = 8.1 \pm 0.3$; $G_{SH} = 5.1 \pm 1.7$; $G(H_2S_2) = 1.5 \pm 1.0$. The value for G_{-H_2S} is greater than the maximum value calculated from mass spectrometric and ionization efficiency data for the reactions of the primary ions alone and suggests that some decomposition may result from excitation also. The ineffectiveness of I_2 and DPPH in changing $G(H_2)$ is probably due to an inability to add sufficient of these solutes to compete with solvent for H atoms. In iodine solutions, sulfur is formed in a chain reaction. (auth)

40998 RADIATION EFFECTS ON ION AND ELECTRON PROCESSES OCCURRING IN CONDENSED-PHASE HYDROCARBONS. Frankevich, E. L. (Inst. of Chemical Physics, Moscow). Usp. Khim., 35: 1161-85(1966). (In Russian).

In evaluating the role of charged particles formed during exposure to radiation, the ionic aspects of radiolysis were examined. Processes occurring in the condensed phase were chosen because gas-phase processes were studied exhaustively. The condensed-phase processes usually cannot be examined in the ionization chamber of a mass spectrometer. Action of penetrating radiations, such as γ quanta, x rays, and electrons on matter is primarily due to the interaction between fast primary quanta and electrons with the electrons of the electron shell of atoms and molecules; interaction with nuclei may neglected in radiation chemical studies. The radiation-generated conductivity in the condensed phase is due to the formation of ions and electrons; it may also reflect charges other than the "free" electrons formed during ionization. In addition to electric methods, others based on determination of the magnetic moment, absorption spectra, and light emission during recombination of ions and electrons are also widely used. The various charged-particle reactions in the condensed phase are described. As the lifetimes of the ions greatly exceed the period between collisions (10^{-13} sec), the ionization products also participate in recombination reactions. (116 references). (TTT)

40999 STUDY OF KINETICS OF POLYMERIZATION OF UNSATURATED OLIGOMERS WITH ^{60}Co γ-RAYS BY MEANS OF ELECTROCONDUCTIVITY METHOD. Kurilenko, A. I.; Nikulina, I. G.; Faizi, N. H. Vysokomol. Soedin., 8: 1180-4(July 1966). (In Russian).

The changes of electric resistance (ρ_v) of the polyester resin PN-1 (67% solution of diethyleneglycol maleate naphthalate in styrene) during ^{60}Co γ-ray-induced polymerization were compared with changes of C=C bond concentration measured by infrared spectroscopy and with gel-fraction content obtained by extraction. The possibility of studying polymerization kinetics induced by ionizing radiation by means of ρ_v measurements was confirmed. (J.G.B.)

41000 RADIATION EFFECTS ON THE RATE OF SILVER NITRITE THERMAL DISINTEGRATION. Boldyrev, V. V.; Eroshkin, V. I. Zh. Fiz. Khim., 40: 3-4(Jan. 1966). (In Russian).

Experiments showed that the change in the rate of thermal dissociation of silver nitrite at 80°C as a function of the dose of absorbed x radiation is complex in character: as the dose increases, the rate decreases at first, then increases, but always remains less than the value obtained for nonirradiated samples. The deceleration of the thermal dissociation of silver caused by x rays may be due to one of two causes: The atomic centers of silver formed by the x irradiation of $AgNO_2$ display donor properties during heating, causing the conduction band to be enriched with electrons and thus decreasing the rate of thermal decomposition. The conditions of contact at the $AgNO_2-Ag$ interface are such that the metal particles do not capture electrons, as would be the case during the action of light on silver halides and silver azide; on the contrary, electrons are transferred from the metal particle, so that the electron concentration of the conduction band increases, and the rate of thermal dissociation drops. (ATD)

41001 INVESTIGATION BY THE EPR METHOD OF THE ULTRAVIOLET AND γ-RADIATION INDUCED FREE RADICALS IN H_2O_2 IN NH_3 SOLUTIONS. Roginskii, V. A.; Komov, A. G. Zh. Fiz. Khim., 40: 175-7(Jan. 1966). (In Russian).

The differences in behavior in the NH_2 radical produced as a result of ultraviolet and γ irradiation on frozen solutions of H_2O_2 in NH_3 was investigated by the EPR method. The lower thermal stability of the NH_2 radicals formed by ultraviolet radiation was connected with the pair stabilization. The latter is the result of the reaction of 2 hydroxyl radicals, produced by photodissociation of H_2O_2 molecules, with 2 molecules of NH_3. The low-temperature reaction of

the NH_2 radicals with molecules of H_2O_2 yielding peroxide radicals was detected. (tr-auth)

41002 OXIDATION OF p-XYLENE INDUCED BY γ RADIATION. Komarov, P. N. Zh. Fiz. Khim., 40: 243-7 (Jan. 1966). (In Russian).

The effects of temperature and γ irradiation dose on the kinetics of the initial stages in the oxidation of p-xylene in the liquid phase were investigated. It was found that in the temperature interval from 80 to 125°C the oxidation reaction of p-xylene represents a chain degeneration-branching process with long chains of 11 to 35 members. At doses of 3.5 to 5 Mrad the oxidation products are p-xylene hydroxide, p-toluyl alcohol, and p-toluyl aldehyde. The activation energy for the prolongation of the chain reaction was determined as E_2 = 7.2 kcal/mole. The experimental data obtained indicate the participation of irradiation in the branching reaction. Possible mechanisms of such a process are considered. (tr-auth)

41003 RADIOLYSIS OF MIXED Co(III) NITROAMMONIATES AND Co(III) HEXANITRITES. Shagisultanova, G. A.; Neokladnova, L. N.; Koval'chuk, M. A. (Belorussian State Univ., USSR). Zh. Fiz. Khim., 40: 446-50 (Feb. 1966). (In Russian).

The behavior of aqueous solutions of the complex salts $[Co(HN_3)_4(NO_2)_2]NO_3$, $[Co(NH_3)_3(NO_2)_3]$, and $Na_3[Co(NO_2)_6]\cdot \frac{1}{2}H_2O$ under the action of gamma and ultraviolet radiation was studied. Data in support of an oxidation-reduction mechanism for radiation chemical transformations are presented. The yields of the radiation chemical reactions are calculated. According to the measure of conversion from $[Co(NO_2)_6]^{3-}$ to $[Co(NH_3)_3(NO_2)_3]$ and $[Co(NH_3)_4(NO_2)_2]^{1+}$, i.e., according to the increase of ammonium groups in the internal sphere of the complex ion and the decrease in the number of coordinated acid groups, (NO_2^-), the yield of the radiation chemical reaction drops off (based on Co(II)). The greatest initial acidification of the solution and the highest yield of the reduced ions of cobalt occurs in the case of $[Co(NO_2)_6]^{3-}$. The high pH values, as a rule, inhibit the transition Co(III) → Co(II). (CFSTI)

41004 COMPOSITION OF PRODUCTS OF RADIATIVE METHANOL OXIDATION. Ladygin, B. Ya.; Saraeva, V. V. Zh. Fiz. Khim., 40: 497-9(Feb. 1966). (In Russian).

In the radiation oxidation of methanol, peroxide compounds and formaldehyde are formed. The composition of the peroxide compounds depends on the condition of irradiation and can be represented by hydrogen peroxide, performic acid, and its methyl esters. (tr-auth)

41005 RADIATION-INDUCED ELECTRIC AND PHOTOCONDUCTIVITY IN FROZEN HEPTANE. Yakovlev, B. S.; Frankevich, E. L. Zh. Fiz. Khim., 40: 1327-32 (June 1966). (In Russian).

Recombination of the current, generated by irradiation in frozen heptane, originates by first order reactions in the holes. During radiolysis new holes appear which are free radicals. In the irradiated samples, the photoelectric effect was detected, dependent on the release of the current from the hole. The dependence of photocurrent on irradiation dose made it possible to trace the kinetics of the accumulation of electrons in the hole present in the heptane before irradiation. Under conditions of high concentrations of deep holes in the solid phase, electrons, not emerging from the area in which the potential of Coulomb attraction to its own ions is larger than kT, may participate in the electric conductivity. (tr-auth)

41006 RADIOLYSIS OF ISOPROPANOL AND SOLUTIONS OF BENZOPHENONE AND NAPHTHALENE IN ISOPROPANOL IN THE LIQUID STATE AT 30 DEG C AND IN THE VITREOUS STATE AT -196 DEG C. Kish, F.; Bagdasar'yan, Kh. S. Zh. Fiz. Khim., 40: 1339-46 (June 1966). (In Russian).

During radiolysis of vitreous isopropanol at 77°K the formation of solvated electrons and hydroxyisopropyl radicals was observed. In the presence of benzophenone, ketyl radicals and anionic radicals of benzophenone were also formed; in the presence of naphthalene, anionic radicals of naphthalene were formed. During irradiation with light at λ > 340 mμ the solvated electrons very quickly disappeared, but the anionic radicals of benzophenone were stable. Desolvation of electrons with light did not increase the concentration of the hydroxyisopropyl radicals and did not change the yields of hydrogen, methane, and acetone. During radiolysis of liquid isopropanol, the yield of acetone depends on the concentration of added benzophenone and passes through a maximum which is explained by the superposition of the reaction $2(CH_3)_2\dot{C}OH \rightarrow (CH_3)_2C=O + (CH_3)_2CHOH$ and reactions of acceptance of H atoms by benzophenone molecules. The addition of naphthalene decreased the yield of all radiolysis products. (tr-auth)

41007 MECHANISM OF RADIOLUMINESCENCE IN CRYSTAL PHOSPHORS OF ALKALI METAL HALIDES. Sooyik, T. Zh. Prikl. Spektrosk., Akad. Nauk BSSR, 3: 279-82(1965). (In Russian).

Comparison of recent data on the luminescence yield, I_0/I_∞ ratio, the effectiveness of Tl-activated potassium halides, and of Tl-activated potassium and rubidium iodides is given to explain the reason iodide is the only Tl-activated alkali metal halide that is practical as a scintillator. The high scintillating properties of KI(Tl) phosphors may be explained by the exciton mechanism of the luminescence excitation in this phosphor. (D.H.M.)

41008 METHOD OF PRODUCING HYDRAZINE. Steinberg, M.; Pruzansky, J.; Kramer, H. (to U. S. Atomic Energy Commission). U. S. Patent 3,265,602. Aug. 9, 1966.

A method for radiolytically converting ammonia to hydrazine is given. The ammonia was absorbed on a substrate of finely divided alumino-silicate during the irradiation step. (AEC)

Radiochemistry

See also Separation Processes and Procedures

Refer also to abstracts 40825, 41199, and 41334.

41009 (AERE-R-3268) IRRADIATION EXPERIMENTS WITH PLUTONIUM DIOXIDE SUSPENSIONS. Harder, B. R.; Sowden, R. G. (Atomic Energy Research Establishment, Harwell (England)). Mar. 1960. 22p. Dep. mn.

The effects of exposing dilute aqueous plutonia suspensions to pile irradiation were investigated. Solids of high specific surface area (~30 $m^2\ gm^{-1}$) undergo rapid fragmentation; colloidal suspensions are formed, which are stable indefinitely at room temperature but flocculate slowly at 200°C. The degree of fragmentation per unit of dose decreased with the specific surface area of the suspended plutonia, but the effect was still measurable with high-fired material (< 0.3 $m^2\ gm^{-1}$). Fragmentation may occur exclusively along crystallite boundaries, or extend to comminution of the crystallites themselves. Measurements were made of the distribution of selected fission products between the plutonia surface and the aqueous phase following short irradiations at pile temperature. Barium was retained exclusively in the aqueous phase under all conditions, while molybdenum, zirconium, and iodine were predominantly adsorbed by the solid surface. The distribution of cerium and tellurium was sensitive to the pH of the suspension. Cerium was entirely adsorbed on the surface after irradiation at pH 6, but after irradiation at pH < 2 it was found exclusively in the aqueous phase. The implications of these findings on the feasibility of continuous fission product removal in a suspension reactor are discussed. (auth)

41010 (DP-1048) QUANTITATIVE ELECTRODEPOSITION OF ACTINIDES FROM ISOPROPYL ALCOHOL. Donnan, M. Yates; Dukes, E. Kenneth (Du Pont de Nemours (E. I.) and Co., Aiken, S. C. Savannah River Lab.). Aug. 1966. Contract AT(07-2)-1. 10p. Dep. mn. CFSTI $1.00 cy, $0.50 mn.

An electrodeposition method was developed for the preparation of thin, uniform alpha sources for precise counting and accurate pulse height analysis. The method employs an isopropanol electroplating medium and is applicable to deposition of actinides for both organic and aqueous media. Moderate amounts of aluminum and iron do not decrease deposition yields. (auth)

41011 (SGAE-CH-34/1966) MOLECULAR PLATING. [PART] V. THE INFLUENCE OF SOME EXPERIMENTAL FACTORS ON THE DEPOSITION YIELD. Getoff, N.; Bildstein, H.; Proksch, E.; Saukel, H. (Oesterreichische Studiengesellschaft fuer Atomenergie G.m.b.H., Seibersdorf. Institut fuer Chemie). May 1966. 15p. Dep.

The effects of cathode diameter, electrode distance, initial current and temperature on the deposition yield using the molecular plating method were studied. $^{90}Sr/^{90}Y$ was used as a model nuclide. The best conditions for obtaining a uniform layer with 100% yield are reported. (auth)

41012 A COMBINED SLIT-COLLIMATOR FOR MEASURING THE DISTRIBUTION OF ISOTOPES WITH γ ACTIVITY. Inzelt-Gerber, E.; Molnar, S. (Lorand Eoetvoes Univ., Budapest. Quality Control Co., Budapest). Acta Chim. Acad. Sci. Hung., 49: 29-56(1966).

A combined slit-collimator for measuring linear γ-activity distribution, e.g., in a capillary tube, is described. The efficiency of the slit-collimator, using an ^{131}I point source, is 48% and the stripe width, B_{50}, is 1.5 mm, so that measurements of considerable accuracy can be performed with the instrument. The high efficiency reduces the expenses for health protection, since the measurements may be carried out at lower activities. (auth)

41013 SYNTHESIS OF ROTENONE-6-^{14}C ON A SEMI-MICRO SCALE. Nishizawa, Yoshihiko; Casida, John E. (Univ. of California, Berkeley). Agr. Food Chem., 13: 522-4(Nov.-Dec. 1965).

Preparation of carbon-14-labeled rotenone was accomplished by reaction of 2 mmoles of methyl bromoacetate-1-^{14}C with 3 mmoles of derritol to produce 6a,12a-dehydrorotenone-6a-^{14}C in 50% yield. Sodium boron hydride reduction gave the 12-hydroxy-6a-^{14}C intermediate and subsequent Oppenauer oxidation produced rotenone-6a-^{14}C. Yields for conversion of nonradioactive 6a,12a-dehydrorotenone to rotenone were 17 to 25% but, with radioactive material of 2.36 mC per mmole, the yield was only 7.5%. Other oxidation procedures for the reduction product of 6a,12a-dehydrorotenone are considered, as are possible explanations for the lower yield with the radioactive material. A possibility for the lower rotenone-6a-^{14}C yield and formation of the by-product, deoxy-12,12a-dehydrorotenone-6a-^{14}C, might be a radioinduced autoxidation during the sodium boron hydride reduction of 6a,12a-dehydrorotenone-6a-^{14}C, but no information is available on the specific intermediates formed. (TCO)

41014 SYNTHESIS OF METHYLENE-^{14}C-DIOXYPHENYL COMPOUNDS: RADIOACTIVE SAFROLE, DIHYDROSAFROLE, MYRISTICIN, PIPERONYL BUTOXIDE, AND DIASTEREOISOMERS OF SULFOXIDE. Kuwatsuka, Shozo; Casida, John E. (Univ. of California, Berkeley). Agr. Food Chem., 13: 528-33(Nov.-Dec. 1965).

Five radiolabeled methylenedioxyphenyl compounds, all active as insecticide synergists, were prepared. Methylene-^{14}C iodide, prepared by reduction of iodoform-^{14}C was made to react with the appropriate catechol to yield the following methylene-^{14}C-dioxyphenyl compounds with a specific activity of 1.0 mC/mmole: safrole, dihydrosafrole, myristicin, sulfoxide synergist {1,2-methylenedioxy-4-[2-(octylsulfinyl)propyl]benzene}, and piperonyl butoxide {α-[2-(2-butoxyethoxy)ethoxy]-4,5-(methylenedioxy)-2-propyltoluene}. Yields from iodoform-^{14}C were 31 to 55% on a 0.5 to 0.8-mmole scale except with piperonyl butoxide, where the yield appeared to be related to the specific activity of the methylene-^{14}C iodide used. The octylthio, octylsulfinyl, and octylsulfonyl analogs of sulfoxide synergist, substituted on the 1-, 2-, or 3-position of the propyl group, were prepared in nonradioactive form for comparative purposes. Sulfoxide synergist and the 1-octylsulfinyl analog were resolved by chromatography into the enantiomorphs of the diastereoisomers about the sulfoxide grouping and the asymmetric carbon of the propyl grouping. The potency as synergists for the insecticidal activity of carbaryl (1-naphthyl methylcarbamate) and pyrethrum with houseflies (Musca domestica) was compared for all the nonradioactive methylenedioxyphenyl compounds prepared. Carbaryl was highly synergized in its toxicity to houseflies by safrole, dihydrosafrole, and piperonyl butoxide, but less effectively by analogs of sulfoxide synergist. The three (octylthio)propyl analogs were more effective than their sulfoxides and sulfones for carbaryl synergism and, in each series, the potency decreased in the order of 1 > 2 > 3 for the position of sulfur attachment to the propyl group. (BBB)

41015 SYNTHESIS OF d-TRANS-CHRYSANTHEMUMIC ACID-1-^{14}C AND ITS ANTIPODE ON A SEMIMICRO SCALE. Nishizawa, Yoshihiko; Casida, John E. (Univ. of California, Berkeley). Agr. Food Chem., 13: 525-7(Dec. 1965).

A semimicro scale (4 mmole) procedure is reported for: preparation of dl-cis,trans-chrysanthemumic acid-1-^{14}C; chromatographic separation of the cis and trans isomers; cis-trans isomerization; and resolution of the l-trans isomer as a quinine salt and the d-trans isomer as a l-α-methylbenzylamine salt. Pure d-trans- and l-trans-chrysanthemumic acids-1-^{14}C (1.3 to 2.7 mC/mmole) were obtained. dl-trans-chrysanthemumic acid-1-^{14}C was prepared in 45% yield from 4 mmole of ethyl glycinate-1-^{14}C. Yield of the trans-acid was increased by isomerization of methyl cis-chrysanthemumate-1-^{14}C with sodium tert-amylate. Geometrical isomers of the acid were separated by column chromatography, and optical isomers of the trans-acid were resolved as a quinine salt for the l-isomer and an l-α-methylbenzylamine salt for the d-isomer. Overall yields of trans-chrysanthemumic acids-1-^{14}C, based on radioactivity from ethyl glycinate-1-^{14}C (2.7 mC/mmole), were: 22.8% of impure d-isomer, 10.4% of pure l-isomer, and 7.0% of pure d-isomer. (BBB)

41016 PREPARATION OF RADIOACTIVELY LABELED PYRIDOXAL-5'-PHOSPHATE. Stock, Arthur; Ortanderl, Franz; Pfleiderer, Gerhard (Univ., Frankfurt am Main). Biochem. Z., 344: 353-60(1966). (In German).

Detailed instructions are given for the preparation of ^{32}P- and ^{3}H-labeled vitamin B_6 derivatives. For the synthesis of ^{32}P-labeled pyridoxal-5'-phosphate, isopropylidene-pyridoxine was allowed to react in chloroform with ^{32}P-$POCl_3$ and the product of the reaction was partially hydrolyzed in potassium bicarbonate solution. After the isopropylidene residue had been removed with 1 N perchloric acid, the ^{32}P-pyridoxine-5'-phosphate was oxidized to ^{32}P-pyridoxal-5'-phosphate with freshly prepared manganese dioxide in 4 N perchloric acid at low temperature. The crude product was purified by chromatography on Dowex 1X8 in acetic acid. Pyridoxal-5'-phosphate was also labeled with tritium by reduction with ^{3}H-$NaBH_4$ to ^{3}H-pyridoxine-5'-phosphate which was oxidized to ^{3}H-pyridoxal-5'-phosphate, and purified as described above. The specific activities of the ^{32}P- and ^{3}H-labeled products were 0.56 and 28 mC/mmole, respectively. (BBB)

41017 NOTE ON HYDROGEN EXCHANGE IN γ-LACTONES. Theilacker, Walter; Bremer, Karl-Heinz (Technische Hochschule, Hanover). Chem. Ber., 99: 2066-9 (1966). (In German).

Experiments on the catalyzed exchange reaction incorporating ^{3}H into the α-position of γ-butyrolactone are described. The product was analyzed by oxidation to succinic acid and counting with a liquid scintillation counter. Without a catalyst, a 1:1 mixture of labeled water and lactone showed only 0.001% exchange after 100 hours at 100°C. In the presence of triethylamine (mole ratio of lactone : amine = 4:1 to 5:1) up to 56% exchange was observed, as measured by the activity in percent of activity of the water used. The best conditions found involved a mole ratio of water : lactone : amine of 0.136 : 0.234 : 0.052, with heating at 100°C for 133 hours. If the labeled water is in excess,

the incorporation is greatly slowed because equilibrium between the lactone and the hydroxy acid is shifted unfavorably. Only slow exchange was observed at room temperature. An enolate ion as intermediate is suggested since no exchange was found for α,α-dimethyl-γ-butyrolactone under analogous conditions. (BBB)

41018 EFFECT OF RADIOACTIVE DECAY IN SOLIDS ON THEIR RELAXABILITY. Pavlyuchenko, M. M.; Prodan, E. A.; Slyshkina, S. A. (Inst. of General and Inorganic Chemistry, Academy of Sciences, Belorussian SSR). Dokl. Akad. Nauk BSSR, 9: 736-9(1965). (In Russian).

The influence of radioactive decay on the reactivity of solids was studied with two identically prepared cadmium carbonate samples, one of which contained ^{14}C. The ^{14}C-labeled cadmium carbonate with a specific activity of 0.5 $\mu C/g$ had a relatively higher reactivity, lower thermal stability, lower values of pre-exponential Arrhenius multiple ($10^{9.4}$ against $10^{13.9}$ min^{-1}), and lower disintegration activation energy (14.1 kcal/mole), (than the nonactivated sample). The high reactivity of labeled cadmium carbonate is related to the radioactive decay, which induced various defects in the initial crystals. (R.V.J.)

41019 RADIOCHROMATOGRAPHY IN THE GAS PHASE: CONSTRUCTION OF AN APPARATUS AND STUDY OF THE IODIDE ISOTOPIC EXCHANGE REACTION. Machiroux, R. (Univ., Liege). Ind. Chim. Belge, 31: 10-18(Jan. 1966). (In French).

A detailed description is given for building an apparatus for gas radiochromatography. The thermostatic chamber, heating and injection systems, columns, and detectors are diagrammed. The apparatus is provided with two detectors: one Lovelock ionization detector and one scintillation crystal detector and ratemeter. The electrometer associated with the ionization detector is of the inverted triode type. The temperature obtained is near 250°C with a stability of ±0.5°C up to 150°C and of ±1°C above this value. This apparatus can easily detect 0.05 μg of CCl_4 (1.6×10^{-9} mg/ml) with a reproductibility of ±0.7%. With this apparatus, it was also possible to study the ionic character of the exchange reaction of radioiodine between CH_3I and C_2H_5I and to reveal the existence of a secondary reaction between basic hydroxy compounds and alkyl iodides: $RI + R'OH \rightarrow R-O-R' + HI$. (BBB)

41020 PREPARATION OF SOME ^{18}F LABELLED FLUORIDES. Azeem, M.; Gillespie, R. J. (McMaster Univ., Hamilton, Ont.). J. Inorg. Nucl. Chem., 28: 1791-3(Sept. 1966).

The fluorides BF_3, POF_3, PF_5, AsF_5, SF_4, SOF_2, and SeF_4 were labeled with ^{18}F by passing them over heated $Li^{18}F$. A mechanism for the exchange reactions is suggested. Labeled lithium fluoride was prepared from lithium carbonate by irradiation with thermal neutrons. (auth)

41021 SOLVENT EXTRACTION OF ^{18}F AS TETRAPHENYLSTIBONIUM FLUORIDE. Bowen, L. H.; Rood, R. T. (North Carolina State Univ., Raleigh). J. Inorg. Nucl. Chem., 28: 1985-90(Sept. 1966).

A rapid separation procedure was developed for producing carrier-free ^{18}F. After neutron irradiation of Li_2CO_3, the sample is dissolved in H_2SO_4, and ^{18}F extracted into CCl_4 as tetraphenylstibonium fluoride, which is back extracted into dilute base. This procedure gives >80% recovery of ^{18}F from a 20 g Li_2CO_3 target in 30 min. The variation of distribution ratio with pH, tetraphenylstibonium, fluoride, and salt concentration has been studied. A pronounced maximum at about pH 3 is observed. (auth)

41022 TRITIUM LABELLING OF COMPOUNDS: AN ASSESSMENT. Jones, J. R. (Battersea Coll. of Technology, London). Lab. Pract., 14: 433-40(Apr. 1965).

A comprehensive assessment of the chemical and physical methods available in tritium labeling and their current position in the light of recent advances is discussed. (auth)

41023 PREPARATION OF CARRIER FREE ^{111}Ag. FORMATION OF ^{111}Ag AND ^{110m}Ag BY IRRADIATION OF PALLADIUM WITH NEUTRONS. Levin, V. I.; Kozlova, M. D.; Malinin, A. B. Radiokhimiya, 7: 673-7(1965). (In Russian).

A method is described for the preparation of carrier-free ^{111}Ag from neutron-irradiated palladium. The method is based on the utilization of extraction chromatographs on columns of inert carrier (Fluoroplast-4) covered with tributyl phosphate film. The ^{111}Ag obtained by this method contains only 0.015 to 0.025% ^{110m}Ag at the time of termination of the irradiation. Other radioactive admixtures were not detected. It was found that the admixture of long-lived silver isotopes is explained by the chain reaction $^{108}Pd(n,\gamma)^{109}Pd \xrightarrow{\beta^-} {}^{109}Ag(n,\gamma)^{110m}Ag$. (tr-auth)

41024 SYNTHESIS OF RADIOACTIVELY LABELED COMPOUNDS. XV. SYNTHESIS OF γ-AMINO-(^{15}N)-α-HYDROXYBUTYRIC ACID AND (^{15}N)-METHYLANTHRANILIC ACID. Johne, S.; Groeger, D. (Institut fuer Biochemie der Pflanzen, Berlin). Z. Chem., 6: 149-50 (Apr. 1966). (In German).

The synthesis of γ-amino-(^{15}N)-α-hydroxybutyric acid was achieved by the following route: K phthalimide-(^{15}N) was reacted with γ-butyrolactone in refluxing dimethylformamide. The resulting γ-phthalimidobutyric acid-(^{15}N) (73%) was brominated with P and Br_2 under cooling, yielding γ-phthalimido-α-bromobutyric acid-(^{15}N) (88%). This was converted to the Ba salt hexahydrate of the hydroxy acid by treatment with freshly precipitated $BaCO_3$ in boiling water (83%). Hydrolysis of the phthalimido residue was achieved by 12-hour treatment with 25% HCl on the waterbath, and the final product was purified by chromatography of the filtrate over Dowex 50 × 4 (H form, 200-400 mesh), eluting with 1 N NH_4OH. The compound (79%) was compared paper chromatographically with an authentic sample of the acid. The preparation of methylanthranilic acid-(^{15}N) was carried out by refluxing anthranilic acid-(^{15}N) with dimethyl sulfate 70 min, concentrating in vacuum, precipitation with ether, salting out with $NaC_2H_3O_2$ solution, and purification either by recrystallization from ethanol (68%) or by thin layer chromatography. (BBB)

41025 MEASUREMENT OF THE DOSE RATE OF UNKNOWN γ-RADIOACTIVE SUBSTANCES. Jatczak, Jerzy; Lipinski, Andrezej; Orlik, Leszek (Univ., Lodz, Poland). Zesz. Nauk, Uniw. Lodz., Ser. II, 19: 55-60(1965). (In Polish).

A method for the measurement of the dose rate of unknown γ radioactive substances is described. The γ active isotope was identified by measurement of the γ energy spectrum and by analysis of the spectrum. (tr-auth)

41026 METHOD FOR SEPARATING CARRIER-FREE RADIOACTIVE IODINE (^{131}I) FROM NEUTRON-IRRADIATED TELLURIUM OXIDE. Spanish Patent 311,107. July 1, 1965. Filed Mar. 27, 1965.

Reactor-irradiated TeO_2 was dissolved in 20% NaOH, and silver nitrate was added to produce silver hydroxide, which precipitated, carrying the ^{131}I present. The iodine was dissolved in alkaline peroxide, and after destruction of the peroxide in phosphoric acid solution, was distilled off with a current of nitrogen, and collected in an alkaline hyroxide solution (pH greater than 6.5). (IIC-MG)

41027 RADIOAKTIVNYE IZOTOPY V KHIMICHESKIKH ISSLEDOVANIYAKH. (Radioactive Isotopes in Chemical Research). Nefedov, V. D.; Toropova, M. A.; Krivokhatskaya, I. V.; Sinotova, E. N. Moscow, Izdatel'stvo Khimiya, 1965. 301p.

Theoretical data are presented on preparation and separation of isotopes of various elements and methods for preparing labeled compounds. Applications of radioactive isotopes in analytical, inorganic, physical, and organic chemistry are discussed in detail. (523 references). (R.V.J.)

41028 JOURNEE DE RADIOCHIMIE ANALYTIQUE, LYON, 13 MAI 1965. (Conference on Analytical Radiochemistry, Lyon, May 13, 1965). Villeurbanne, France, Institut de Physique Nucleaire de Lyon, 1965. 79p. (CONF-650573).

Four of the papers presented at the conference were ab-

stracted individually. The remaining paper concerns a method for determining acrylic sizing residues on polyamide fibers. (D.H.M.)

For abstracts of individual papers see: 40843–40846.

Separation Processes and Procedures

See also Analytical Procedures
ISOTOPE TECHNOLOGY — Separation and Production

Refer also to abstract 41067.

41029 (BNWL–279) CHLORINE RECOVERY AND RADIOIODINE BEHAVIOR IN THE SALT CYCLE PROCESS. Mudge, L. K.; Lundquist, J. R. (Battelle-Northwest, Richland, Wash. Pacific Northwest Lab.). July 1966. Contract AT(45-1)-1830. 22p. Dep. mn. CFSTI $1.00 cy, $0.50 mn.

Engineering-scale tests of Cl recovery by liquefaction at –100°C showed it to be nearly 100% of that theoretically obtainable (as calculated from vapor pressure measurements). Caustic usage in the down-stream caustic scrubber was reduced by a factor of ten by operation of the Cl liquefier, and can be further decreased by reduction of the air in-leakage to the system. In operation of the pilot plant apparatus, it was observed that the volatility of an I compound was limiting the removal of ^{131}I from the gas stream by the action of the liquid Cl scrubber. A laboratory investigation of the vapor pressure of I over liquid Cl showed that the observed volatilization of I in the pilot plant apparatus was due to part of the I not reacting with the liquid Cl. Reaction of I with liquid Cl forms a precipitate of ICl_3, which subsequently volatilizes with decomposition to form ICl vapor. Estimation of the equilibrium constants for vaporization at 0°C and –45.2°C indicated that much greater I decontamination of the off-gas could have been obtained if good contact of the off-gas with the liquid Cl had been made. (auth)

41030 (CEA-R–2994) FIXATION D'ACETATES METALLIQUES DANS UNE RESINE ECHANGEUSE D'ANIONS. (Fixation of Metallic Acetates on an Anion-Exchange Resin). Brigaudeau-Vaissiere, Michele (Commissariat a l'Energie Atomique, Fontenay-aux-Roses (France). Centre d'Etude Nucleaires). June 1966. 64p. Dep. mn.

Theoretical principles governing the fixation of anionic complexes of metallic elements on an anion exchange resin are reviewed, and the particular case of uranyl acetate considered. By plotting the partition curves, the exchange constants in the resin could be calculated. By studying the changes in the logarithm of the limiting partition coefficient as a function of the logarithm of the free acetate ion concentration, it was possible to calculate the dissociation constants for the complexes in solution. The fixation of a large number of metallic acetates was studied. All the tests were negative except in the case of mercury. The possibility of separating uranium from a certain number of elements was considered. Some of these separations are possible even in the presence of interfering anions such as chlorides, which have a greater affinity for the resin than have the acetate ions. In the case of water–ethanol and water–isopropanol mixtures, the conditions under which copper acetate and mercury acetate may be fixed were improved. The dissociation constant was calculated for the $CuAc_3^-$ complex in the mixtures water + 40% (by weight) isopropanol and water + 50% (by weight) isopropanol. (auth)

41031 (DP–717) DISSOLUTION OF ION EXCHANGE RESINS IN ALKALINE PERMANGANATE. Snyder, Mark D. (Du Pont de Nemours (E. I.) and Co., Aiken, S. C. Savannah River Lab.). July 1962. Contract AT(07-2)-1. 10p. Dep. mn. CFSTI $1.00 cy, $0.50 mn.

A process was developed for the dissolution of radioactive ion exchange resins by heating in mildly alkaline potassium permanganate solutions. The resins were oxidized to carbon dioxide and aqueous-soluble organic compounds, and the permanganate was reduced to granular manganese dioxide. At 70°C all of the carbon dioxide remained in solution as bicarbonate and at 100°C about one-third was evolved as gas. "Dowex" 1 anion resin required 0.6 kg of $KMnO_4$ per liter of resin for dissolution and "Permutit" SK anion resin required 3.2 kg of $KMnO_4$. The alkaline oxidizing medium suppressed the volatilization of ruthenium and retained 99.95 to 99.99% of the total radioactivity adsorbed on the resin. (auth)

41032 (DP–1010) CURIUM PROCESS DEVELOPMENT, III-1. ANALYTICAL TECHNIQUES FOR CHARACTERIZING SOLVENT. Narvaez, Richard (Du Pont de Nemours (E. I.) and Co., Aiken, S. C. Savannah River Lab.). July 1966. Contract AT(07-2)-1. 22p. Dep. mn. CFSTI $2.00 cy, $0.50 mn.

Gas and thin-layer chromatographic techniques were developed to use with infrared spectrometry for analyzing virgin or degraded solvent for the curium purification process. A separation scheme was developed to facilitate analysis of highly degraded solvent. (auth)

41033 (INR–678/IV/C) BADANIE MOZLIWOSCI WYDOBYCIA TORU Z KRAJOWYCH SUROWCOW TOROWYCH. (The Studies on the Possibilities of Thorium Recovering from Polish Thorium Ores). Szymanska, Danuta (Institute of Nuclear Research, Warsaw (Poland)). Dec. 1965. 10p. Dep.

The possibility of recovering thorium from native thorium ores by chemical methods was studied on a laboratory scale. It was found that 90% of Th may be extracted from "Sz" ores by leaching with concentrated H_2SO_4 at 100°C. In the case of "Op" ores 95% extraction may be attained by leaching with 5 and 10% H_2SO_4 at 100°C. (auth)

41034 (JEN–160-DQ/I-54) ESTUDIO DE LOS PRODUCTOS DE FISION DE PERIODO CORTO. SEPARACION DE LOS RADIONUCLIDOS DE FISION DEL YODO Y DEL XENON. (Study of the Short-Lived Fission Products. Separation of Iodine and Xenon Fission Radionuclides). Barrachina, M.; Villar, M. A. (Junta de Energia Nuclear, Madrid (Spain). Division de Quimica). 1965. 24p. Dep. mn.

A method for the separation of the iodine isotopes (8-day iodine-131, 2,3-hr iodine-132, 21-hr iodine-133, 53-min iodine-134, and 6.7-hr iodine-135) present in a U sample after different irradiation and cooling times by distillation in sulfuric acid- or phosphoric acid-hydrogen peroxide medium is described. The use of active charcoal columns for the retention of Xe isotopes (5.27-day xenon-133 and 9.2-hr xenon-135) either released during dissolution of irradiated uranium samples or generated along the fission isobaric chains in solutions of distillated iodine is also reported. In both cases the radiochemical purity of the separated products was established by gamma spectrometry. The separation methods described allow radioisotopes with a high specific activity to be obtained. (auth)

41035 (LA–2758) LARGE-SCALE ELECTROREFINING OF PLUTONIUM FROM GALLIUM ALLOYS. Mullins, L. J.; Leary, J. A.; Morgan, A. N. (Los Alamos Scientific Lab., Univ. of California, N. Mex.). Aug. 1962. Contract W-7405-eng-36. 32p. Dep. mn. CFSTI $2.00 cy, $0.50 mn.

Electrorefining processes were developed for the recovery of plutonium from plutonium–gallium alloys on the 3.5-kg. scale. The process can be controlled to produce Pu metal containing <100 ppM of metallic impurities with recovery yields of ~85%. The theory of Pu alloy electrorefining is discussed, and a method based on back emf measurements for controlling the process automatically is presented. (auth)

41036 (MCW–1494) ELECTROLYTIC RECOVERY OF SCRAP URANIUM METAL. Fleming, W. S.; Piper, R. D.; Kennelley, J. A. (Mallinckrodt Chemical Works, Weldon Spring, Mo. Uranium Div.). Aug. 19, 1966. Con-

tract W-14-108-eng-8. 15p. Dep. mn. CFSTI $1.00 cy, $0.50 mn.

An electrolytic process for recovery of scrap uranium metal was developed on a laboratory scale. In this process, uranium oxides on the scrap react with a consumable graphite anode to form uranium metal and carbon monoxide. Operation at 1150°C in a fused $BaF_2-LiF-UF_4$ electrolyte produces molten metal at the cathode by a combination of electrolytic reduction of the oxides, electrolytic transfer of the metal, and thermal melting of the metal. Scrap type, cell design, electrolyte composition, and cathode current density were found to be major factors affecting current efficiency and metal quality. (auth)

41037 (MLM–1325) MOUND LABORATORY QUARTERLY PROGRESS REPORT, JANUARY–MARCH 1966. Eichelberger, J. F.; Grove, G. R.; Jones, L. V. (Mound Lab., Miamisburg, Ohio). Mar. 31, 1966. Contract AT(33-1)-Gen-53. 67p. Dep. mn. CFSTI $3.00 cy, $0.75 mn.

Two sections are included on radioelements and analytical instrumentation. Separate abstracts were prepared for each. (P.C.H.)

For abstracts of individual sections see: 40805 and 41038.

41038 (MLM–1325, pp 9-62) RADIOELEMENTS. (Mound Lab., Miamisburg, Ohio).

Developments are reported for studies on: gamma spectra of ^{227}Th, ^{223}Fr, ^{223}Ra, ^{211}Pb, ^{228}Ac, and ^{212}Pb; and ^{233}U; half life determination of ^{210}Po by decaying pairs; separation and half life determination of ^{223}Fr; nuclear levels in ^{223}Ra populated by the decay of ^{227}Th and ^{223}Fr; weak alpha and electron-capture decay in ^{208}Po and ^{209}Po; radiolysis of uranyl nitrate; structure of plutonyl nitrate; valence wandering of ^{238}Pu; residue adsorption of Th-228/229 from U-232/233; ^{234}U recovery from aged ^{238}Pu; and ^{229}Th recovery from ^{233}U. (P.C.H.)

41039 (ORNL–3880) TRANSURANIUM QUARTERLY PROGRESS REPORT FOR PERIOD ENDING FEBRUARY 28, 1965. Burch, W. D. (comp.) (Oak Ridge National Lab., Tenn.). Jan. 1966. Contract W-7405-eng-26. 60p. Dep. mn. CFSTI $3.00 cy, $0.75 mn.

Recovery of gram amounts of heavy actinide elements for research work is accomplished in the Transuranium Processing Plant (TRU). Process development, work in the Curium Recovery Facility, experimental engineering studies, design and development of target fabrication processes and equipment, design of equipment and construction of the Transuranium Processing Plant, corrosion studies, and development of analytical methods B are reviewed. (M.C.G.)

41040 (ORNL-TM-1342) SEPARATION OF STRONTIUM AND BARIUM BY CATION EXCHANGE USING POLYAMINEPOLYCARBOXYLIC ACIDS AS ELUANTS. Wamanacharya, G. S. (Oak Ridge National Lab., Tenn.). Sept. 1966. Contract W-7405-eng-26. 11p. Dep. mn. CFSTI $1.00 cy, $0.50 mn.

Strontium and barium were separated on a cation-exchange column using 2-hydroxyethylethylenediaminetriacetic acid (HEDTA) and diethylenetriaminepentaacetic acid (DTPA) as eluants. Separations were equally good but not as fast as with citric acid, the eluant now used; however, the polyaminepolycarboxylic acids were more easily removed from the product. (auth)

41041 (PG-Report-698) METHOD FOR THE PREPARATION OF PURIFIED U_3O_8 FROM IRRADIATED URANIUM (FOR MASS SPECTROMETRY). (Production Group, United Kingdom Atomic Energy Authority, Sellafield (England)). 1966. 10p. Dep. BIS $0.30. HMSO 1s. 9d.

Uranium is purified by extraction into diethyl ether, followed by a basic ferric acetate scavenge. These processes are repeated if necessary until the plutonium and β and γ activities in the uranium are below the required specification level. Finally, ammonium diuranate is precipitated and ignited to U_3O_8. This purification is an intermediate process in the preparation of uranium hexafluoride for determination of uranium isotopic abundance by mass spectrometry. The method described is applicable to solutions of uranium from which most of the plutonium and β and γ activities were previously removed so that all manipulations may be carried out in a fume hood. (auth)

41042 (PG-Report–722) METHOD FOR THE DISSOLUTION AND PRELIMINARY PURIFICATION OF IRRADIATED URANIUM FUEL SPECIMENS (PREPARATION FOR MASS SPECTROMETRY). (Production Group, United Kingdom Atomic Energy Authority, Sellafield (England)). 1966. 5p. Dep. BIS $0.30. HMSO 1s. 3d.

The preliminary treatment needed to obtain samples suitable for mass spectrometry from irradiated U metal containing up to 3% Mo is described. A portion of the solution produced is diluted to a suitable concentration for the determination of Pu/U ratio and isotopic abundance. Separation from fission products and Pu is necessary before the U hexafluoride mass spectrometer can be used for determining U isotopic abundances. (P.C.H.)

41043 PURIFICATION OF PROTACTINIUM FROM NATURAL SOURCES. Kirby, H. W.; Figgins, P. E. (Monsanto Research Corp., Miamisburg, Ohio). Colloq. Int. Centre Nat. Rech. Sci. (Paris), No. 154, 275-81(1966).

Protactinium was separated from ten times as much niobium by selective precipitation from oxalic-hydrochloric acid mixtures. Data are presented, which show that the stability of the niobium oxalate complex is 100 times as great as that of protactinium oxalate. The addition of hydrochloric acid, by repressing the ionization of oxalic acid, greatly reduced the solubility of protactinium while having relatively little effect on that of niobium. The final product, obtained by dissolution and recrystallization of protactinium from concentrated sulfuric acid, contained 0.5 microgram of niobium per milligram of protactinium. A solution containing 90 mg/ml of protactinium in approximately 5N sulfuric acid showed no hydrolysis or gel formation after more than four years. (auth)

41044 HYDROLYTIC SEPARATIONS OF PROTACTINIUM. Kirby, H. W. (Monsanto Research Corp., Miamisburg, Ohio). Colloq. Int. Centre Nat. Rech. Sci. (Paris), No. 154, 283-91(1966).

Milligram amounts of ^{231}Pa were separated from its decay products, ^{227}Ac, ^{227}Th, and ^{223}Ra by hydrolysis from 1 and 6N hydrochloric acid. Separation from thorium was accomplished by hydrolysis in 1N nitric acid and from niobium by hydrolysis in a mixture of oxalic and hydrochloric acids. Iron was separated by selective dissolution of its hydroxide in dilute hydrochloric acid. Micrograms of protactinium were separated from its decay products by adsorption on glass wool from a dilute sulfuric acid solution, by the method of residue adsorption, and selective desorption from a gold surface. The application of the adsorption technique to the problem of "inextractable polymers" is discussed briefly. (auth)

41045 SEPARATION OF RARE-EARTH METALS BY REVERSED-PHASE PAPER CHROMATOGRAPHY. THE TRIBUTYL PHOSPHATE–NITRIC ACID–AMMONIUM THIOCYANATE SYSTEM. Chang, Chu-Chun; Yang, Hsiu-Hsia (Northwestern Univ., China). Hua Hsueh Hsueh Pao, 31: 182-5(1965). (In Chinese).

The rare earth metals, U, and Th are separated by reversed-phase paper chromatography, with tributyl phosphate as the stationary phase and acidified 0.2M-NH_4SCN as the developing solvent. The spots are located by saturated ethanolic alizarin. The R_F values for these metals decrease with increase in concentration of NH_4SCN (up to 2%), but increase with HNO_3 concentration (0.1 to 0.5N). Satisfactory separations are quoted for mixtures of rare earth metals, U, and Th with a developing solvent containing 0.2M-NH_4SCN and 0.1N-HNO_3. (Anal. Abstr., Vol. 13, No. 8, Aug. 1966).

41046 SEPARATION OF LANTHANIDES BY THIN-LAYER HIGH-VOLTAGE ELECTROPHORESIS. Baechmann, K.; Goerisch, H. (Technische Hochschule, Darm-

stadt, Ger.). J. Chromatog., 23: 336-8(July 1966). (In German).

The thin-layer high-voltage electrophoretic separation of lanthanides was tested on mixtures of Ce, Pm, and Eu. The results showed that the optimum conditions for thin-layer electrophoresis are 1.1M α-HlBA (α-Hydroxyisobutyric acid) at a pH of 2.4. The separation effect is somewhat better in thin-layer electrophoresis than in paper electrophoresis. The separation times for thin-layer and paper electrophoresis are approximately equal. Larger amounts of material can be separated with thin-layer electrophoresis than with paper electrophoresis. Of the thin-layer substances tested cellulose gave the best results. (J.S.R.)

41047 LIQUID-LIQUID EXTRACTION OF NONFERROUS METALS. REVIEW OF THE ART. Smithson, G. R. Jr.; Shea, J. F.; Tewksbury, T. L. (Battelle Memorial Inst., Columbus, Ohio). J. Metals, 18: 1037-46(Sept. 1966).

Developments in processes and equipment for liquid-liquid extraction of nonferrous metals are reviewed. The extracts most commonly used and the metals commonly recovered by hydrometallurgical techniques are grouped into various categories. (P.C.H.)

41048 FRACTIONAL CONDENSATION OF THE CHLORIDE VAPOR FROM CHLORINATED URANIUM ORE. Ino, Shiro; Tomizawa, Satoshi (Government Chemical Industrial Research Inst., Tokyo). Kogyo Kagaku Zasshi, 68: 2360-6(Dec. 1965). (In Japanese).

The condensates obtained from Ningyotoge uranium ore, by chlorination at 900 to 950°C, contain the various chlorides derived from the components of the ore besides the uranium chloride, and the concentration of the uranium chloride in the total condensate is less than 4%. The fractional condensation of chloride vapors was, therefore, investigated for the purpose of concentrating the uranium. When fractional condensation was carried out using the condenser previously added along with a small quantity of NaCl, 98% of the vaporized uranium chloride was condensed in the temperature zone higher than 650°C according to the chlorination condition, and concentration of the uranium chloride up to about 30% was attained. The interaction of chloride components greatly affected the condensation and led to results which differed from those inferred from the vapor pressures of the individual chlorides. (auth)

41049 SEPARATION OF ^{32}P FROM A ^{32}P–^{35}S MIXTURE BY CO-PRECIPITATION WITH FERRIC HYDROXIDE, USING SEVERAL ORGANIC BASES AS PRECIPITANTS. Koda, Yoshio; Ito, Masayuki. Nagoya Kogyo Gijutsu Shikensho Hokoku, 15: No. 3, 96-102(1966). (In Japanese).

The separation of carrier-free ^{32}P from a $H_3{}^{32}PO_4$–$H_2{}^{35}SO_4$ mixture by coprecipitation with ferric hydroxide is described. To maintain a pH value of a test solution in a narrow range without buffer solution, organic bases such as pyridine, α-picoline, benzylamine, and ethylamine were used as precipitants, in addition to ordinary precipitants, ammonia, and sodium hydroxide. Carrier-free ^{32}P was co-precipitated with yields above 80% within the range of pH 4 to 10, however yields decreased above pH 10. Carrier-free ^{35}S was coprecipitated below pH 6, and yields rapidly decreased above this pH value. Addition of a sulfate ion to a test solution as carrier brought about a further decrease in coprecipitation of ^{35}S. The suitable condition of separation of carrier-free ^{32}P from a ^{32}P–^{35}S mixture by coprecipitation was in the range of pH 8 to 10, and in this range ^{35}S contents could be decreased under 1/1,000 by a single operation. (auth)

41050 MECHANISM OF THORIUM AND URANIUM EXTRACTION BY MONO- AND DIISOPENTYL ESTERS OF METHYLPHOSPHONIC ACID. Ukraintsev, E. V. Radiokhimiya, 7: 641-8(1965). (In Russian).

The extraction of thorium by diisopentyl esters of methylphosphonic acid was investigated. It was found that the extraction of thorium by this reagent is accompanied in the organic phase by the formation of di- and tri-solvates. The effective constants of the formation reaction are equal to 5.75×10^3 and 3.1×10^4 at constant ionic strength of approximately 2. A mechanism for the extraction of uranium and thorium by the monoisopentyl ester of methylphosphonic acid (MPMPA) in the form of the complexes $UO_2(MPMPA)_2$ and $Th(MPMPA)_4$ is suggested. The constants of the formation reaction were calculated at $3.2 \times 10^3 \pm 250$ and $4.75 \times 10^5 \pm 350$. The extraction of uranium and thorium by MPMPA was used for dilute solutions (10^{-4} to 10^{-5} M), during which the coefficients for the separation of thorium from uranium were determined by the equation $\beta = 0148 \pm 1.4 \times MPMPA/[H^+]$. (tr-auth)

41051 ZIRCONIUM EXTRACTION BY DI- AND MONOISOPENTYL ESTERS OF METHYLPHOSPHONIC ACID. Ukraintsev, E. V. Radiokhimiya, 7: 648-57 (1965). (In Russian).

The extraction of zirconium from nitric acid solutions by diisopentyl esters of methylphosphonic acid (DPMPA) was studied as a function of the composition of the aqueous and organic phase. It was shown that the zirconium is extracted in DPMPA in the form of mono- and disolvates of acid zirconyl nitrate with the composition $H_2ZrO(NO_3)_4 \cdot MPMPA$ and $H_2ZrO(NO_3)_4 \cdot DPMPA$. The effective constants for the formation reaction were $(62.0 \pm 2) \times 10$ and $(32.0 \pm 1) \times 10^2$. The composition of the lower solvate was confirmed by chemical analysis. The product of the interaction of gram quantities of zirconium nitrate and the monoisopentyl esters of methylphosphonic acid (MPMPA) appeared to have the composition $ZrO(MPMPA)_2$. The composition of products was determined by the methods of extraction and chemical analysis. The effective interaction constants of microquantities of zirconium with MPMPA was calculated to be $(15 \pm 1) \times 10^3$. The presence of MPMPA in quantities of several percent in DPMPA sharply increases the coefficient of distribution of microquantities of zirconium in weakly acid solutions. (tr-auth)

41052 EXTRACTION METHOD FOR COMPLEX FORMATION OF POLONIUM WITH CHLORINE AND PERCHLORATE IONS. Starik, I. E.; Ampelogova, N. I. Radiokhimiya, 7: 658-63(1965). (In Russian).

The solvent extraction of polonium from chloride and perchlorate solutions with TBP solutions in benzene was investigated as a function of the concentration of TBP in the organic phase and H^+ and Cl^- ions in the aqueous phase at pH 1, 3, and 6. The effective formation constants for complexes of polonium with chloride and perchlorate ions were calculated. (tr-auth)

41053 URANIUM EXTRACTION BY TRIOCTYLAMINE-DIISOPENTYL PHOSPHORIC ACID MIXTURE. Smelov, V. S.; Strakhova, A. V. Radiokhimiya, 7: 718-19(1965). (In Russian).

The conditions under which the maximum value of the synergistic effect was obtained are described. Special attention was given to the comparative mechanism of the extraction mixture trioctylamine–diisopentyl phosphate. (tr-auth)

41054 SEPARATION OF XeO_3 AND HIO_3 IN ZIRCONIUM PHOSPHATE. Kirin, I. S.; Gusev, Yu. K.; Mosevich, A. N.; Kuzhetsov, N. P.; Guselnikov, V. S. Radiokhimiya, 7: 736-8(1965). (In Russian).

It was found that zirconium phosphate can be used successfully for the separation of XeO_3 from HIO_3. The xenon trioxide, labeled with ^{131m}Xe, was formed from products of β decay of ^{131}I in iodates. (tr-auth)

41055 PREPARATION OF GRANULATED ZIRCONYL PHOSPHATE BY FREEZING AND ITS ION EXCHANGE PROPERTIES. Sharygin, L. M.; Pospelov, A. A.; Chukhlantsev, V. G. Radiokhimiya, 7: 744-7(1965). (In Russian).

A method for the preparation of granulated vitreous inorganic ionites by means of freezing out the original gelatinous products was developed. The ion exchange properties of the granulated zirconyl phosphate were investigated, and it was found suitable for separation of cation pairs. (tr-auth)

41056 IMPROVEMENTS IN OR RELATING TO ELECTROLYTIC DISSOLUTION OF SPENT URANIUM FUEL

ELEMENTS. Raviv, Szmuel; Levin, Iddo. British Patent 1,037,524. July 27, 1966. Priority date May 6, 1963, Israel.

In a process for the dissolution of a spent reactor fuel element having an outer envelope of Al or Al alloy and a core of U metal or U alloy, an electrolytic circuit is established in which the fuel element is the positive electrode and the electrolyte is an aqueous sodium or potassium hydroxide solution whose concentration does not exceed 15% by weight. The electrolytic dissolution is initiated by establishing a potential difference that does not exceed 30 v between the anode and the cathode. The dissolution is allowed to proceed at this voltage as long as current continues to flow through the system. Then the alkaline solution is exchanged for an aqueous nitric acid solution whose concentration (3 to 5 m/l) does not dissolve the core to any appreciable extent, and electrolytic dissolution is started to dissolve the core in the acid solution. (B.L.M.)

41057 METHOD FOR EXTRACTION OF ^{137}Cs SALTS FROM IRRADIATED NUCLEAR FUEL. Baehr, Werner; Vogg, Hubert (to Gesellschaft fuer Kernforschung mbH). German Patent 1,217,351. May 26, 1966. Filed July 6, 1963.

The method comprises the steps of decomposing the fuel in an oxidizing, alkaline melt, of leaching out the solidified melted material with water or sodium hydroxide, and of separating the mother liquor in which the ^{137}Cs is dissolved from the precipitation. (Gmelin Inst.)

41058 SEPARATION OF RADIOACTIVE IONS FROM THEIR SOLUTIONS. Riesenhuber, Heinz. German Patent 1,218,964. June 8, 1966. Filed Mar. 20, 1963.

A radioactive salt of low solubility is obtained by filtering the solution through a layer of a substance of low solubility with an ionic bond, which is deposited on a filter. The substance comprises an inactive isotope of the radionuclide to be separated, the atoms of which are arranged on regular lattice points. (Gmelin Inst.)

41059 PROCESS FOR EXTRACTION OF THORIA AND CERIA FROM RARE EARTH ORES. Kraitzer, Ian C. (to Associated Minerals Consolidated Ltd.). U. S. Patent 3,252,754. May 24, 1966. Priority date Oct. 12, 1959, Australia.

A process for the recovery of thoria and ceria from rare earth ores, such as monazites, includes digesting the ground ore with caustic soda to yield the mixed hydroxides, slurrying the hydroxide with a sodium bicarbonate solution, rapidly heating to about 80°C, and adding solid sodium bicarbonate to a pH value of 9.5 to 10. At this point the thoria is solubilized as the double carbonate, and the insoluble lanthanon double carbonate is separated by decantation or filtration. The pregnant leach liquor containing the thorium double carbonate is digested with caustic soda to yield thoria which may be dried to yield a 55-60% product or calcined to yield a 90-95% product. The insoluble lanthanon double carbonate is metathesized with caustic soda at boiling temperatures, and the resulting lanthanon compounds are dried until the Ce has been oxidized to the quadrivalent state. The ceric compound is then leached out in the same manner as used for the thorium compound to yield the soluble ceric double carbonate; subsequently, the ceria is removed from solution by the addition of caustic soda in the same manner as for thoria to yield a product that calcines to yield a 95% ceria. (B.L.M.)

41060 REMOVAL OF STAINLESS-STEEL CLADDINGS FROM NUCLEAR FUEL ELEMENTS. Ramaswami, Devabhaktuni; Levitz, Norman M.; Jonke, Albert A. (to U. S. Atomic Energy Commission). U. S. Patent 3,268,303. Aug. 23, 1966.

A process of dissolving stainless-steel cladding from ceramic nuclear reactor fuel elements by contacting the fuel elements with liquid atomized aqueous hydrochloric acid while in an oxygen-containing-gas fluidized bed at from 25 to 100°C is reported. (AEC)

41061 DECONTAMINATION OF RADIOACTIVE SOLUTIONS. Crawley, Ralph Hugh Alfred; Hudson, Michael John Bedenham (to English Electric Co. Ltd.). British Patent 1,034,817. July 6, 1966. Filed June 29, 1962.

A method is described for decontaminating cooling-pond water from a nuclear reactor installation. The pH of the water is adjusted to a value in the range of 5 to 7 by saturation with CO_2, and the water is then pumped through solid sodium aluminosilicate having the general formula $Na_2O \cdot Al_2O_3 \cdot nSiO_2$, where "n" is 4, 5, or 6, to remove the radioactive cations by ion exchange. Alternatively, the water may be pumped directly through a strong-base cationic ion exchanger without the pH adjustment to transfer substantially all the radioactive ions to a regeneration liquor which is then neutralized and passed through the sodium aluminosilicate. (B.L.M.)

41062 REMOVAL OF ACTINIDE HALIDES FROM ALUMINA. Ramaswami, D.; Levitz, N. M.; Jonke, A. A. (to U. S. Atomic Energy Commission). U. S. Patent 3,264,070. Aug. 2, 1966.

A process for removing adsorbed actinide halide from refractory material by reacting the material first with a gas containing a low proportion of fluorine and a high proportion of nitrogen at a low temperature, and then with a gas containing a high proportion of fluorine and a low proportion of nitrogen at a higher temperature to volatilize the actinide halide as the hexafluoride is presented. (AEC)

ENGINEERING

General

41063 (BNL–997) CALCULATIONS OF HARD SPHERE PACKINGS IN LARGE CYLINDERS. Clancy, B. E. (Brookhaven National Lab., Upton, N. Y.). June 1966. Contract AT(30-2)-Gen-16. 23p. Dep. mn. CFSTI $2.00 cy, $0.50 mn.

A procedure is described for generating numerical models of various arrangement of hard spheres packed in a cylindrical vessel. Calculations of a variety of configurations have been carried out on a digital computer for two packing models. The results are compared with measurements of the packing density in experimental configurations and with other measured properties of the packings. (auth)

41064 (IS–1500(Sect. E)) ANNUAL SUMMARY RESEARCH REPORT IN ENGINEERING. (Ames Lab., Iowa State Univ. of Science and Tech.). 34p.

Research progress on chemical engineering, ceramic engineering, and mechanical engineering is reported. (R.C.K.)

41065 (TID–4100(Suppl.34)) SUPPLEMENTAL INSERT SHEETS FOR ENGINEERING MATERIALS LIST. (Division of Technical Information Extension (AEC), Oak Ridge, Tenn.). Aug. 1966. 36p. Dep. DTI Extension Free.

Supplementary insert sheets are presented for 35 packages of engineering drawings. These sheets should be inserted in the proper numerically CAPE-numbered sequence in TID-4100. The drawings describe computers, glove boxes, samplers, reactor equipment, spectrometers, radiation detection instruments, and other instruments. (F.S.)

41066 RADIOACTIVE METHOD OF DETECTION OF HIDDEN EXPLOSIVES. Johnston, William H. (to William H. Johnston Labs., Inc.). U. S. Patent 3,255,352. June 7, 1966. Filed Sept. 6, 1962.

A method of detecting hidden explosives in or on carriers such as airline baggage and airline passengers depends upon detecting radiation of both a time and direction coincidence on the carriers as they or the baggage pass rapidly through an air terminal. A radioactive material would have to be associated with at least one of the constituents at the time of manufacture of the explosive. This radioactive material would be operative to cause the simultaneous emission of several gamma rays during decay and yet not be present in the explosive in a quantity that might be harmful to people using the explosive. Preferably, the constituent would be a positron emitter associated with the detonator in the amount of 0.1 to 1 μC in each detonator. The positron emitter would function to emit a first gamma ray and a positron in time coincidence and a pair of oppositely-directed gamma rays by positron annihilation in substantially time coincidence with the first gamma rays. The detection would be performed at three positions adjacent to the carriers, and an indication would be furnished only when detections occur simultaneously at all positions. (B.L.M.)

Applications of Nuclear Explosions

41067 (ORNL-TM–1582) CHEMICAL APPLICATIONS OF NUCLEAR EXPLOSIONS (CANE). Progress Report, April 1–June 30, 1966. Blake, C. A. Jr.; Brown, K. B.; Crouse, D. J. (comps.) (Oak Ridge National Lab., Tenn.). July 29, 1966. Contract W-7405-eng-26. 14p. Dep. mn. CFSTI $1.00 cy, $0.50 mn.

Studies were continued on the possible behavior of radionuclides that would be present in the usual copper recovery process as a result of using nuclear explosives for breaking the ore. More than 20 exchangers tested were found to be inefficient in removing ruthenium from a synthetic leach liquor. Preliminary tests of the recently proposed solvent extraction process for treating copper ore showed that copper was efficiently extracted from a synthetic liquor with LIX-64. Tritium and hydrogen exchange between tritiated water and methane is linear with time and occurs at the rate of 0.6×10^{-4} mC/liter-day in a 1-liter flask containing methane at approximately 1 atmosphere and ~50 mC tritium in tritiated water. A 2-g gold target supported in a 3½-in.-diam copper cone was fired in the jet sampler test setup at Frankford Arsenal. There was good recovery of the copper at the receiver, but the tests indicate that lack of uniformity in thickness and irregularity of shape in the gold plating prevented proper focusing of the jet. Additional cone-target assemblies are being made with high precision. (auth)

41068 (PNE–5006) TRACE ELEMENTS IN COMMON ROCK TYPES AND THEIR RELATIVE IMPORTANCE IN NEUTRON-INDUCED RADIOACTIVITY CALCULATIONS. Paul, Roger A.; Day, Walter C. (Army Engineer Nuclear Cratering Group, Livermore, Calif.). June 1966. Contract W-7405-eng-48. 31p. Dep. mn. CFSTI $1.50 cy, $0.50 mn.

The chemical composition of the rock surrounding an underground nuclear detonation must be known or assumed when calculations of the resulting neutron-induced radioactivity are attempted. A typical chemical analysis of rock samples does not include certain trace elements which have high neutron-capture cross sections. A literature search was undertaken to determine the average and range of content of these trace elements in common rock types to permit an evaluation of their relative importance in neutron-induced radioactivity calculations. The elements considered in the study were Dy, Gd, Eu, Sm, Nd, Cd, Ag, Co, Cr, V, Sc, Cl, S, B, and Li. Data are reported giving contents of these elements in ten igneous rock types and three sedimentary rock types. The five elements Gd, Eu, Sm, B, and Cl were found to occur in most rock types in quantities which would significantly affect neutron-induced radioactivity calculations. Calculations of induced radioactivity were performed for granite using maximum, average, and minimum trace element values obtained from the literature search. Calculations were also performed using average trace element values for four other igneous rocks and two sedimentary rocks. It is concluded that, in general, use of the average values for trace elements presented in this report is adequate for assessing the production quantities of radionuclides induced external to the device for use in feasibility studies for large scale excavation projects and other underground nuclear detonations when detailed chemical analyses of emplacement media are not available. (auth)

41069 (SC-RR–66-324) CRATERS FROM SHORT-ROW CHARGES AND THEIR INTERACTION WITH PRE-EXISTING CRATERS. Vortman, L. J. (Sandia Corp., Albuquerque, N. Mex.). July 1966. Contract AT(29-1)-789. 82p. Dep. mn. CFSTI $2.00 cy, $0.75 mn.

All charges were buried at a depth which would maximize single-charge crater dimensions, and adjacent charges were separated by a uniform distance between 1 and 1.1 times the maximum single-charge crater radius. Short rows of simultaneously detonated charges produced craters which differed only slightly from single-charge craters in volume per charge and in width and depth. Ejecta perpendicular to the row was appreciably greater than the average ejecta for a single charge, but each additional charge beyond the second charge made a smaller contribution to the lateral ejecta than did its predecessor. As expected, ejecta off the end ordinarily did not exceed that for a single charge. One, two, or five charges were detonated simultaneously adjacent to the preexisting craters formed by one, two, three, or five charges. Crater dimensions were not appreciably different because of the pre-existing craters, but the detonation of

two or five charges against craters from three or five charges, respectively, caused a barrier to be formed in the near end of the pre-existing craters. Preferential venting in the direction of the pre-existing crater caused a preponderance of ejecta to be distributed in that direction. The barrier was larger for the larger number of charges. (auth)

41070 (VUF–3021) TIMING AND FIRING. Final Report. Project DRIBBLE, Salmon Event. Colman, J. M.; Planchet, R. P. (Edgerton, Germeshausen and Grier, Inc., Bedford, Mass.). Jan. 1965. 43p. Dep. mn. CFSTI $1.50 cy, $0.50 mn.

Timing and firing services for the Salmon event of the Dribble Program are described. In addition to the Salmon event timing and firing services for two high-explosive confirmation experiments conducted under the technical direction of the Lawrence Radiation Laboratory are also described. All monitors at the control point indicated that the performance of the timing system was completely satisfactory on both the Salmon event and the two confirmation experiments. Both hardwire and radio signals were transmitted to the experimenters as requested. Instrumentation for the Salmon event included (1) the special mobile control point built for the Dribble Program, (2) a zero site station housed in a wooden structure located in the area adjacent to surface zero, (3) radiotone barrels for use of experimenters located at positions remote from the control point, and (4) communications nets essential to the transmission of long-range, local, and worldwide countdown. (R.C.K.)

41071 AN APPLICATION OF NUCLEAR EXCAVATION TO RAILROAD USE. Beeder, R. H. (Atchison, Topeka and Santa Fe Railway, Los Angeles, Calif.). Amer. Railway Eng. Ass. Bull., 67: 742-7(June-July 1966).

Project Carryall, a study to investigate the economic feasibility of using nuclear excavation to cut a channel 2 miles long through the Bristol Mountains in California to relocate a 78-mile segment of double-track railroad is described. The study, conducted by railway, highway, and government engineers, concluded that Project Carryall was technically and economically feasible. It was estimated that the use of nuclear explosions to excauate the channel would save about $8,000,000 over the cost of a route location by conventional construction methods. (R.C.K.)

41072 NUCLEAR EXPLOSIVES IN CIVIL ENGINEERING. Comit. Naz. Energ. Nucl. Notiz., 12: No. 6, 54-60 (June 1966). (In Italian).

An extensive discussion of the past, current, and planned activities in the United States concerning the peaceful uses of nuclear explosives, particularly for industrial purposes, is given. (auth)

41073 ATOMIC TOOLS IN DEVELOPING WATER. Piper, Arthur M. (Geological Survey, Menlo Park, Calif.). 9p. (CONF-650973–1). ORAU.

From National Water Well Association Conference, Houston, Tex.

Potential advantages and limitations of using nuclear explosives at suitable depths as a tool in the development and management of water are discussed. The results of a 1 kt detonation in silicate and carbonate rocks are described. Liability and legal obstacles are reviewed. (F.S.)

Facilities and Equipment

Refer also to abstracts 41125 and 42685.

41074 (AECL–2551) PERFORMANCE TESTING OF CONICAL-FACE HIGH PRESSURE ROTARY SHAFT SEALS. Watson, R. D. (Atomic Energy of Canada Ltd., Chalk River (Ontario)). Nov. 1965. 36p. Dep. mn. AECL $1.00.

The performance characteristics of a special type rotary shaft seal have been determined at pressures up to 1000 lbf/in.^{2}, gage and speeds to 1900 rev/min. The seal is made up of two rings, with one flat face ring in contact with the very slightly cone-shaped face of the other ring. The channel, which is formed by the two faces in contact, converges in the direction of the leakage flow. The taper on the cone-shaped ring was varied from 0.00032 in./in. to 0.0024 in./in. and the seal characteristics were determined for each different taper. The leak rate of the conical-face seal was found to vary with rotary speed. The larger the ratio of tangential seal velocity to radial leakage velocity the greater the percentage change in leak rate with speed. Concave twisting of a seal produced by pressure induced unbalanced moments on the seal rings has been shown to cause the leak rate of a seal to decrease as the pressure is increased, when normally the reverse is true. For a given set of conditions the leak rate of the conical-face seal was found to decrease with increasing viscosity. At zero speed the leak rate is approximately proportional to the reciprocal of viscosity. When the seals are running this is no longer true because the effect of rotational velocity on leak rate varies with viscosity. (auth)

41075 (AERE–R–5217) THE DEVELOPMENT OF A HIGH TEMPERATURE GRAPHITE RIG FOR SCATTERING LAW EXPERIMENTS. Bedford, L. A. W. (Atomic Energy Research Establishment, Harwell (England)). July 1966. 17p. Dep. BIS $0.60. HMSO 3s.

A rig for maintaining a thin specimen of reactor grade graphite at temperature up to 2000°C for long periods in scattering-law experiments is described. The specimen is placed in a beam of neutrons and the scattered particles recorded in counters set up at angles around it. The development was carried out in two stages. A Mark I rig was built and run at a maximum temperature of 1500°C using an argon atmosphere. This rig has been used successfully on the Phased Rotor Neutron Spectrometer at Chalk River. Experience gained with Mark I enabled a Mark II rig to be built and this has been tested at a maximum temperature of 2000°C for long periods. It was possible to run this rig into a vacuum and enabled a reduction in power input to be made compared with the same specimen temperature in Mark I. The two rigs both used the specimen as its own resistance heater. Radiation shields of minimum number and thickness are used together with a local thin section in the containment vessel, to reduce scattering from materials other than the specimen. A demountable, circumferential thin metal window was developed for Mark II and has proved very reliable. (auth)

41076 (EUR–2750.e) PROCEEDINGS OF THE CONFERENCE ON MEGAGAUSS MAGNETIC FIELD GENERATION BY EXPLOSIVES AND RELATED EXPERIMENTS, SEPTEMBER 21–23, 1965. Knoepfel, H.; Herlach, F. (eds.) (Laboratorio Gas Ionizzati, Comitato Nazionale per l'Energia Nucleare, Frascati (Italy)). July 1966. 538p. (CONF-650937). Belgian American Bank and Trust Co., New York $12.00.

Separate abstracts were prepared for 22 of the included 26 papers. For abstracts of the remaining 4 papers see CONF-650937 in the report number index. In addition, an abstract was prepared for abstracts of 8 Russian papers which were to have been presented at the conference. (M.O.W.)

For abstracts of individual papers see: 41081–41096, 41515, 41684–41687, 42434, and 42526.

41077 (INR-696/I/PL) UKLAD AUTOMATYCZNEGO STEROWANIA TRANSPORTEM PROBEK (SAMOCZYNNA "POCZTA"). (The Automatic Control-System for Samples Transport). Lenartowicz, J.; Turos, A. (Institute of Nuclear Research, Warsaw (Poland)). Feb. 1966. 22p. Dep.

A device for automatic transport of small samples between two terminal positions is described. At one of those positions samples can be activated and the activities are counted at the other position according to the prescribed routine. The system allows for programming of irradiation and counting time at each of the two extreme positions, and disposing of them when automatic taking samples from the stack, the measurement cycle is over. The main rea-

son for construction of the system was to use it in connection with a 100 channel analyzer for the investigation of nuclear reaction products with decay periods of 0.5–10 sec. There are other possibilities for the applications of this device. Practical sample transport time obtained so far amounts to about 1 sec in a distance of 4 m. (auth)

41078 (ORNL–3875, pp 91-100) PROCESS INSTRUMENTATION AND CONTROL SYSTEMS ENGINEERING. (Oak Ridge National Lab., Tenn.).

A report is presented on process instrumentation and control systems engineering at ORNL. Topics include system design group activities, thorium utilization program, instrumentation for a ^{233}U liquid storage facility, transuranium processing plant valves, nuclear safety pilot plant, startup of the high-radiation-level analytical laboratory, containment research installation, project salt vault, and a thermocouple scanner. (B.G.D.)

41079 (RFP–666) MIMIC TOOL SETTER. Larson, R. A. (Rocky Flats Div., Dow Chemical Co., Golden, Colo.). Aug. 17, 1966. Contract AT(29-1)-1106. 6p. Dep. mn. CFSTI $1.00 cy, $0.50 mn.

The mimic tool setter was designed to "set" single point tool bits on two-axis numerical control turning machines. The prime design considerations were economy, accuracy, and operational speed. The tool setter retains manual operation, but eliminates operator "feel." By retaining manual operation, the cost of the setter is kept low, and reliability is kept high. By eliminating operator "feel," accuracy is increased, and operational time is reduced. (F.S.)

41080 (UCRL–14831) VERY HIGH MAGNETIC FIELDS PRODUCED BY CAPACITOR-BANK DISCHARGE. Shearer, James W. (Lawrence Radiation Lab., Univ. of California, Livermore). Apr. 13, 1966. Contract W-7405-eng-48. 16p. (CONF-660921–1). Dep. mn. CFSTI $1.00 cy, $0.50 mn.

From International Colloquium on Intense Magnetic Fields, their Production and their Application, Grenoble, France.

It is calculated that transient magnetic fields in the range of 2 to 8 MG can be produced in an initial volume of ≃0.1 cc by discharging large capacitor banks into properly designed loads. The value of the peak magnetic field in a given geometry is shown to depend primarily on the voltage of the capacitor bank and the compressibility of the walls. A magnetic field of 2.1 MG was measured in an experiment for which 2.6 MG was calculated by numerical computation methods. Heating of the wires of the induction probe used to measure this field is negligible when thin enough wire is used. Pulsed x ray radiography is used to study the geometry of the compression distribution in the metal wall surrounding the high-field volume This compression distribution is then compared to the numerical computations. At these high fields the metal load explodes as violently as TNT, and the experiments must be performed in a blast-proof room. However, this blast energy is small in comparison with that of typical high-explosive magnetic-field implosion experiments. Thus the high-voltage capacitor bank should be an economically useful means of producing multi-megagauss fields. (auth)

41081 MAGNETIC FIELD COMPRESSION. Brin, A.; Besancon, J. E.; Champetier, J. L.; Plantevin, J. P.; Vedel, J. (Commissariat a l'Energie Atomique, Paris). pp 21-36 of EUR–2750.e.

The basic principles of a magnetic field compression are given with an analysis of the factors intervening in the experience: field diffusion, explosive pressure, appearance of jets due to the slot of the liner and of the solenoid coil, probe destruction occurring before the turnaround. The first experiences were tried with a 50 mm i.d. implosive charge and a 110 koersted initial field. The mean final field was of 3.5 moersted. The last experiences utilize a 100 mm i.d. implosive charge, a 52 koersted initial field and the final field obtained with a stainless steel liner attained 10 moersted. Applications are foreseen for the study of magnetism in the pulsed high fields. (auth)

41082 MAXIMUM MAGNETIC FIELDS OBTAINABLE BY FLUX COMPRESSION: LIMITATION DUE TO THE DIFFUSION OF MAGNETIC FIELD. Lehner, G. (Laboratorio Gas Ionizzati, Frascati, Italy). pp 55-66 of EUR–2750.e.

The maximum magnetic fields obtainable by the compression of magnetic flux are limited by the finite conductivity of the liner. They depend decisively on the behavior of the conductivity as a function of the temperature. If one assumes that the conductivity varies as 1/T, the maximum fields are not extremely large. However, such an assumption is too pessimistic. A discussion shows that the conductivity decreases as 1/T only in the early stages of the compression (i.e., at relatively low temperatures) while it should tend towards an almost constant value later (i.e., at very high temperatures). In such a case the limitation due to field diffusion is not serious and the maximum magnetic field obtainable in compression experiments is governed by other effects. (auth)

41083 MAGNETIC FIELDS OBTAINED BY FLUX COMPRESSION. LIMITATION DUE TO THE DYNAMICS OF THE CYLINDRICAL LINER. Somon, J. P. (Laboratorio Gas Ionizzati, Frascati, Italy). pp 67-99 of EUR–2750.e.

The dynamics of a cylindrical metallic liner compressing an axial magnetic field is studied for the range of typical experimental situations. The liner should behave like a perfect fluid of infinite electrical conductivity. The maximum magnetic field and its characteristic time decay is evaluated as a function of two reduced parameters. Some details of the dynamics are investigated. (auth)

41084 DEVELOPMENT OF MAGNETIC FIELD COMPRESSION TECHNIQUES FOR METALLIC PARTICLE ACCELERATION. Chapman, R. L. (Aerojet-General Nucleonics, San Ramon, Calif.). pp 107-45 of EUR–2750.e.

The development of techniques for achieving magnetic field gradients in the megagauss/millimeter range are described. These gradients are used to provide a strong force for accelerating milligram mass metal spheres to hypervelocities. A unique feature of this device is the flux concentrator which significantly increases the obtainable magnetic field strengths and establishes the field gradient. Electric currents are induced on the surface of the sphere by the explosively compressed magnetic field. This creates a dipole field which interacts with the axial field gradient to accelerate the projectile. Maximum theoretical velocity of a projectile of density ρ is $v \approx (3/\rho)^{1/2} H_{max}/5$ kilometers/second where H is in megagauss. Design and fabrication details of the initial magnetic field system, the high explosive system, flux compression and concentration components, and instrumentation are also discussed. Starting with 40 kilogauss, peak magnetic field strengths in excess of 7 megagauss were achieved. Recent projectile acceleration test results are discussed. (auth)

41085 RESULTS AND LIMITATIONS OF CYLINDRICAL FLUX COMPRESSION EXPERIMENTS. Herlach, F.; Knoepfel, H. (Laboratorio Gas Ionizzati, Frascati, Italy). pp 147-66 of EUR–2750.e.

Results of work on cylindrical flux compression devices are given. The experiments have shown up very large technical difficulties for the generation of magnetic fields above 4 MG, indicating that a great technical effort is needed to produce reliable fields in this region. These and connected problems are discussed in detail. (auth)

41086 ENERGY CONVERSON EFFICIENCY IN FLUX COMPRESSION. Cowan, M. Jr. (Sandia Lab., Albuquerque, N. Mex.). pp 167-81 of EUR–2750.e.

The conversion of chemical energy of explosives to electromagnetic energy by flux compression is discussed. An example of the chemical-to-mechanical phase is shown where as much as 35% of the explosive energy is converted to the original kinetic energy of the liner. For plane and cylindrical flux compression with constant liner resistivity and implosion speed, equations are developed for magnetic field and energy amplifications and for Joule heat in the

liners. Using these equations, the mechanical-to-electrical energy conversion efficiencies are also expressed for conditions which lead to liner turnaround by magnetic field pressure. Mechanical-to-electrical efficiencies greater than 90% result if the magnetic Reynolds number $R_m = l\sigma\mu_0\nu_0$ just prior to turnaround is greater than about 200 for plane compression or for cylindrical compression if $R_m = 2r\sigma\mu_0\nu_0$ is greater than 10^3. (auth)

41087 THE EFFECT OF JOULE HEATING ON THE DIFFUSION OF MEGAGAUSS FIELDS INTO METALS. Bryant, A. R. (Atomic Weapons Research Establishment, Aldermaston, Eng.). pp 183-201 of EUR-2750.e.

The diffusion of megagauss magnetic fields into a plane metal slab is discussed theoretically. The electromagnetic diffusion equations, together with the equations of compressible hydrodynamic flow, are briefly derived, and specialized to the case of an intense hydromagnetic disturbance propagating at constant velocity, for which an exact solution is derived. It is found that a solution arises for magnetic intensities sufficient to lead to vaporization of the metal which bears a close resemblance to a chemically driven detonation wave in explosives. The Joule heating region drives ahead of it an inert shock wave similar to the von Neumann "spike." The nonconducting metal vapor behind the Joule heating region expands adiabatically to form a rarefaction which keeps in step with the motion of the Joule heating region providing a Chapman-Jouget-like condition to determine the whole motion. Unlike chemical detonations, a wide range of intensities and propagation velocities are possible corresponding to the range of values of the external electrical power source. Numerical values are determined for a number of magnetic detonation waves in copper using the thermodynamic equation of state of Morris. The partition of energy into mechanical, thermal, and electrical is discussed. (auth)

41088 NUMERICAL COMPUTATION METHODS FOR IMPLOSION PROCESSES. Albertoni, S.; Cercignani, C.; Taroni, A.; Guerri, L. pp 203-33 of EUR-2750.e.

The methods used in actual calculations of an implosion experiment are described. After a review of the basic equations, the calculation methods employed for the detonation phase are described in detail and the accuracy of the obtained results pointed out. The general properties of the numerical scheme employed for the second phase (propagation of the shock wave into the liner and liner's motion) are discussed. The results obtained in simple test problems are also described. Finally the results obtained for the whole problem of the implosion experiment are given. (auth)

41089 MAGNETIC FIELDS OBTAINED BY FLUX COMPRESSION. LIMITATION DUE TO THE DIFFUSION OF THE FIELD IN THE CYLINDRICAL LINER. Somon, J. P. (Laboratorio Gas Ionizzati, Frascati, Italy). pp 235-62 of EUR-2750.e.

The diffusion of an axial magnetic field compressed by a cylindrical incompressible metallic liner is studied. The maximum magnetic field is evaluated and the main results given for the range of typical experimental situations. Numerical calculations were made for the case of a constant surface velocity and for a constant or 1/T electrical conductivity. Extensions to other velocity or conductivity laws are considered. (auth)

41090 THEORY OF MAGNETIC FIELD COMPRESSION DIFFUSION, SURFACE INSTABILITIES. Besancon, J. E.; Champetier, J. L.; Leclanche, Y.; Plantevin, J. P. (Commissariat a l'Energie Atomique, Paris). pp 263-86 of EUR-2750.e.

Calculations were made to point out the influence of various parameters in an experiment of implosed magnetic field. If the magnetic field is trapped in an infinite cylinder, with an infinite conductivity, infinite thinness, a cylinder on which the explosive makes a known pressure during the whole implosion, the problem is a simple one and a few interesting laws are discussed. The following imperfections are discussed: (1) the liner being but an imperfect conductor, there is a diffusion of the magnetic field, (2) the presence of a slit causes metal to be thrown out, and (3) as the cylinder is not infinite, there are end-effects. It is shown that the most serious imperfection is the second one. The various conclusions can be proved experimentally. (auth)

41091 MAGNETIC FIELD AND CURRENT AMPLIFICATION WITH NON-CYLINDRICAL EXPLOSIVE SYSTEMS. Herlach, F.; Knoeppel, H.; Luppi, R. (Laboratorio Gas Ionizzati, Frascati, Italy). pp 287-304 of EUR-2750.e.

Magnetic flux compression experiments are described in which the initial magnetic flux is trapped by a plane plate conductor system and finally pushed into a one-turn solenoid. These compression devices are characterized by the separation of the compression region from the volume where the megagauss fields are finally used. Starting from initial fields of about 60 kG, final fields in excess of 2 MG were produced in volumes of the order of 10 cm^3. Experiments, with compression factors ranging from 6 to 30, are analyzed and discussed. (auth)

41092 USE OF A PULSE TRANSFORMER TO GENERATE MULTI-MEGAMPERE CURRENTS FOR HIGH-FIELD RESEARCH. Furth, H. P.; Waniek, R. W. (Advanced Kinetics, Inc., Costa Mesa, Calif.). pp 305-14 of EUR-2750.e.

Experiments with megagauss fields generally call for input currents in the multi-megampere range, because the high-current low-voltage input regime maximizes the physical strength of conductors and minimizes the electrical stress on insulators. Standard capacitor banks of moderate size, however, typically do not store sufficient charge to supply such current pulses for times longer than 10 μsec. An analysis is presented of optimum pulse transformer design and it is shown that arbitrarily high efficiency can be achieved in principle. A small (.2 m^3) air-core pulse transformer suitable for conversion of a 10 kv, 440 kA input pulse into a 2.2kv, 2000 kA output pulse, with 70 μsec half-cycle time was constructed. The initial energy of 50 kJ can be transferred with 80% efficiency. Fields of 600 kG will be obtainable in a single-turn load of 2.5 cm ID and height; and fields above 1 MG for 1 cm ID and height. The advantages of the transformer-powered single-turn coil over the single-layer multi-turn coil and the flux concentrator are discussed. (auth)

41093 MAGNETIC-FLUX COMPRESSION IN AN EXPLOSION GEOMETRY. Lukasik, S. J. (Stevens Inst. of Tech., Hoboken, N. J.); Zepko, G. W.; Jameson, R. L. pp 397-419 of EUR-2750.e.

A series of experiments was performed to explore the utility of an explosion geometry for the compression of magnetic flux. Typically about 9,000 J of capacitively stored energy is discharged into a single turn load coil having an inductance of about 40 nhy. The magnetic field so generated has a value at maximum discharge current of about 100 kg and a quarter-period of about 5 μsec. At this time the current supply is crowbarred, either by the 176-gm explosive compressor system located within the load coil or by means of an auxiliary explosive system. Thereafter, the radial expansion of the explosively driven liner compresses the magnetic flux within the load coil. Field-compression ratios in the range from 4 to 26 were observed. The process terminates due to mechanical failure of the liner resulting from the magnetic pressure of the compressed field. The maximum field achieved in the experiments reported here was 1.33 megagauss; the field exceeded 1 MG for 1.7 μsec. The hydrodynamic behavior of the expanding liner and the liner-load coil interaction were studied by means of high-speed photography. A series of animated framing-camera records in color was assembled to illustrate the process. (auth)

41094 SIMPLE FLUX COMPRESSION DEVICES WITH A SMALL EXPLOSIVE CHARGE. Di Gregorio, C.; Herlach, F.; Knoepfel, H. (Laboratorio Gas Ionizzati, Frascati, Italy). pp 421-35 of EUR-2750.e.

A simple flux compression device with a quasi-cylindrical implosion geometry and with small explosive loadings was developed. Its reproducible performance and the good

implosion symmetry enables one to make an extensive and comparative study of the flux compression process up to final fields of about 3 MG. In particular, a "turnaround" behavior was observed, i.e., the situation when the moving liner is stopped and pushed back by the magnetic pressure. (auth)

41095 ELECTRICAL PULSES FROM HELICAL AND COAXIAL EXPLOSIVE GENERATORS. Cummings, D. B.; Morley, M. J. (Aerojet-General Nucleonics, San Ramon, Calif.). pp 451-70 of EUR-2750.e.

Two designs of explosive generators are described and discussed. These generators, which produce electrical energy from chemical energy, use the principle of compresing and doing work upon a magnetic field by an explosively driven conductor. The basic theory together with the description and operation of coaxial and helical generators are given. Generator performance, limitations and loss mechanisms are discussed. A technique for coupling generators into large inductive loads is also discussed. (auth)

41096 ABSTRACTS SUBMITTED BY RUSSIAN AUTHORS. pp 515-17 of EUR-2750.e.

Abstracts are presented of 8 articles submitted by Russian authors who did not participate in the conference. All deal with magnetic field compression. (M.O.W.)

41097 HIGH-STRENGTH CONDUCTORS FOR SUPERMAGNETS. Montgomery, D. Bruce (Massachusetts Inst. of Tech., Cambridge). IEEE (Inst. Elec. Electron. Eng.), Spectrum, 3: 111-14(Aug. 1966).

With the introduction of powerful magnets such as the National Magnet Laboratory's 225-kG device that recently went into continuous operation, it has become necessary to consider the structural problems that arise because of the high stresses and high temperatures involved. Primarily, a magnet material must be provided that possesses strength as well as porosity. Various combinations of ETP copper, steel, beryllium–copper, and zirconium–copper have proved effective. It is pointed out that stresses can be reduced by proper arrangement of the coils, and that there is an advantage to using high-strength materials in stress-limited magnets despite their increased resistivity. (auth)

41098 HOT LABORATORIES. Nucl. Eng., 11: 603-5(Aug. 1966).

Consolidation of techniques and better understanding of hazards is the current pattern of development in high activity laboratory work. The UKAEA is producing good results by adapting available components. By establishing standard routines and techniques with equipment having many standard parts, it has been possible to pass responsibility, for as much as 90% of the work, from highly qualified scientists to skilled or semiskilled operators. Some of the adopted procedures on remote handlers and transfer systems are explained. (F.S.)

41099 NUCLEAR TELEVISION. Oudin, J. (Compagnie Francaise Thomson Houston, Paris). Nucl. Eng., 11: 609-10(Aug. 1966).

Television designed to function in a nuclear atmosphere must have a camera fabricated from metals free of contaminants, such as cobalt, which have long half lives. Glass used for optical parts of the camera must be resistant to nuclear radiations. Electronic vacuum tubes, such as the Nuvistor, must replace semiconductors. The new cameras are used to supervise charging circuits, channel exploration, observe gas release at the surface of the pressure tubes in pool reactors, and survey the condition of welds. (F.S.)

41100 COUPLINGS FOR TUBULAR MEMBERS. Robinson, John Albert (to Nuclear Power Plant Co. Ltd. AEI-John Thompson Nuclear Energy Co. Ltd.). British Patent 1,032,585. June 15, 1966. Filed Mar. 16, 1964.

A coupling for tubular members includes end fittings for fixing one to each of the members to be coupled and a tubular coupling member adapted to slide over the end fittings. The end fittings have radially extending lugs that extend axially for a portion of the length of the end fitting on its outer periphery. The lugs are spaced around the periphery. The tubular coupling member has lugs on its inner periphery that are adapted to pass between adjacent lugs on the end fitting and which, on rotation of the coupling member, enter a recess between each lug on an end fitting to limit axial movement of the end fittings relative to one another. Means are provided on adjacent faces of the end fittings and coupling member to prevent relative rotation of one with another when the end fittings and coupling member are in the correct engaged position. (B.L.M.)

Heat Transfer and Fluid Flow

See also PHYSICS — Fluid Physics and Thermodynamics

Refer also to abstracts 41440, 42036, and 42602.

41101 (NAA-SR-Memo-10848) EFFECTS OF THE MOLECULAR DIFFUSION OF HEAT ON FLUID VELOCITY MEASUREMENTS ACCOMPLISHED BY THERMOCOUPLE CROSS-CORRELATION. Bailey, R. E. (Atomics International, Canoga Park, Calif.). Mar. 28, 1965. Contract AT(11-1)-Gen-8. 26p. Dep. mn. CFSTI $2.00 cy, $0.50 mn.

An attempt was made to find a minimum velocity for fluids, with low Prandtl number, above which cross correlation techniques between thermocouples, one downstream from the other, could be used to measure the transit time of an eddy of fluid between the two thermocouples. A point source of heat in an infinite medium was used to represent an eddy of fluid. The criteria used to find the minimum velocity was that the eddy of fluid must pass between the thermocouples much more quickly than the maximum of a thermal wave generated by a point source located at the upstream thermocouple. Two methods of analysis are presented along with a more refine mathematical formulation of the problem. A family of curves is also presented which relates the minimum allowable velocity of the eddy to the distance between thermocouples for fluids of different thermal diffusivities. The analysis presented indicates the feasibility of the cross correlation technique. It was recommended that the technique be calibrated by an instrument which can be used as a primary standard before further mathematical studies are initiated. (auth)

41102 (NYO-2930-6) SOLID DENSITY DISTRIBUTION IN GAS-SOLID PIPE FLOW. Technical Report No. 108-ME-F. Baw, P. S.; Peskin, R. L. (Rutgers–The State Univ. of New Jersey, New Brunswick. Dept. of Mechanical Engineering). Apr. 1966. Contract AT(30-1)-2930. 48p. Dep. mn. CFSTI $2.00 cy, $0.50 mn.

The solid phase density distribution in gas-solid turbulent flow was measured by optical techniques. Density profile computations were attempted using a Reynolds averaging technique and it was found that the mean density profile depends on the correlation of axial and transverse particle velocity. (auth)

41103 (RT-ING-(65)7) MISURA DELLA FRAZIONE VOLUMETRICA DI VAPORE IN UN CANALE BOLLENTE CON METODO AD IMPEDENZA. (Void Fraction Measurement in a Boiling Channel Using the Impedance Method). Cimorelli, L.; Di Bartolomeo, M.; Premoli, A. (Comitato Nazionale per l'Energia Nucleare, Rome (Italy)). Oct. 1965. 53p. Dep. mn.

A capacitance method is described for measuring void fractions in a boiling channel. Results obtained at atmospheric pressure under subcooled boiling conditions are presented. (F.S.)

41104 (UCRL-14841) THE "LONG JOHN" THERMOGASDYNAMIC RESEARCH FACILITY. Pitts, J. H.; Van Sant, J. H.; Corallo, R. A. (Lawrence Radiation Lab., Univ. of California, Livermore). Apr. 20, 1966. Contract W-7405-eng-48. 31p. Dep. mn. CFSTI $2.00 cy, $0.50 mn.

A research facility has been developed for experimental studies of heat and momentum transfer to gases flowing inside long channels. Design specifications and operating capacities and capabilities are described for the major components of the flow system and the instrumentation equipment. The facility has been designed so that investigations with flow channels of various lengths and shapes can be conducted over a large range of pressures, temperatures, and flow rates. Acquisition of final results is expedited by automatic recording of test data and by using digital computers for calculating and plotting the required data. (auth)

41105 HEAT TRANSFER TO MHD FLOW IN THE THERMAL ENTRANCE REGION OF A FLAT DUCT. Hwang, Ching-lai; Knieper, P. J.; Fan, Liang-tseng (Kansas State Univ., Manhattan). Int. J. Heat Mass Transfer, 9: 773-89(Aug. 1966).

Heat transfer to an MHD fluid in the thermal entrance region of a flat duct has been investigated. The flow is laminar and fully developed Hartmann flow, and heat flux at the wall is considered to be constant. The development temperature profiles as well as the local Nusselt number are presented graphically for the heat generation parameter of −1.0, −0.5, 0, 0.5 and 1.0; for the Hartmann number of 0, 4 and 10; and for the electric field factor of 0.5, 0.8 and 1.0. The results presented are applicable for the cases with any Prandtl number. Comparisons are presented for certain cases with the previous work. (auth)

41106 NONUNIFORM COOLING OF A HEAT-GENERATING CYLINDER OR SPHERE. Fagan, Walter (Peat, Marwick, Caywood, Schiller, and Co., Chicago); Leipziger, Stuart. J. Heat Transfer, 88: 257-64(Aug. 1966).

A heat-generating solid cylinder or sphere is cooled in steady state with a heat transfer coefficient which varies arbitrarily on the surface. A solution is obtained which permits exact calculation of the temperature distribution. Simple approximate solutions are also obtained for the two cases where (a) the heat transfer coefficient does not differ greatly from its average value, and (b) the coefficient differs greatly from its average value. Numerical studies are made, and the errors resulting from the approximate solutions are calculated. (auth)

41107 MAXIMUM TWO-PHASE VESSEL BLOWDOWN FROM PIPES. Moody, F. J. (General Electric Co., San Jose, Calif.). J. Heat Transfer, 88: 285-95(Aug. 1966).

Existing flow models are applied to predict maximum two-phase flow from a constant area, adiabatic pipe with friction. Graphs are given for maximum steam/water flow rate in terms of pipe f(L/D) and entrance stagnation properties. Theoretical blow-downs are graphed for 1000 and 2000 psia saturated-water systems with f(L/D) ranging from 0.0 to 100. Estimated pipe flow rates and blowdown transients are compared with steam/water data. Reasonable agreement is shown. (auth)

41108 RADIATIVE HEAT TRANSFER THROUGH AN ABSORBING BOUNDARY LAYER. Fritsch, C. A. (Bell Telephone Labs., Inc., Whippany, N. J.); Grosh, R. J.; Wildin, M. W. J. Heat Transfer, 88: 296-304(Aug. 1966).

An analytical investigation is made of a method of shielding a surface from parallel beams of thermal radiation by distributed injection of a fluid containing absorbing particles into the boundary-layer flow over the surface near the stagnation point. Superposition of various solutions is used to obtain results for a wide range of parameter values from a relatively small number of functions. Three optical conditions of the surface are considered: Specular reflection, diffuse reflection, and black. It is found that injection of absorbing particles helps to shield the surface if the injection rate is relatively high. (auth)

41109 FUEL ELEMENT HEAT TRANSFER NEAR DIMPLE BRACES. Wilkie, D.; White, L. (United Kingdom Atomic Energy Authority, Windscale, Eng.). Nucl. Eng., 11: 596-9(Aug. 1966).

Heat and mass transfer experiments were performed on AGR type fuel rods to illustrate the usefulness and possibilities of the analogy between mass and heat transfer for determining heat transfer properties. If greater accuracy can be achieved, heat transfer experiments would possibly be unnecessary. Many heat transfer experiments are complicated by the damping effects of thermal conduction, and in these cases the mass transfer approach should be considered. (F.S.)

41110 LAMINAR ELECTROHYDRODYNAMIC FLOW IN A PLANE EXIT CONE WITH BARODIFFUSION OF SPACE CHARGE TAKEN INTO ACCOUNT. Mkhitaryan, A. M.; Kas'yanov, V. A. (Inst. of Civil Aviation, Kiev). Zh. Tekh. Fiz., 36: 860-7(May 1966). (In Russian).

Two-dimensional electrohydrodynamic flow in a plane exit cone was calculated. It is believed that the results may be of assistance in evaluating the possibilities of the electrohydrodynamic technique for influencing the flow of liquid and gaseous dielectrics. Among the simplifying assumptions employed in the calculations are the following: the vertex angle of the exit cone is small; the electrical Reynolds number is small; the azimuthal component of the electric current vanishes; the component of the radical electric current due to the space charge field is small compared with that due to the external radial electric field; and the plane dielectric walls of the exit cone are neither charged nor polarized. The flowing medium is assumed to carry a space charge. The electrohydrodynamic equations of motion are derived under these assumptions with barodiffusion taken into account. These equations are linearized by the technique of Targ and approximate solutions of them are obtained. Formulas for the total pressure drop and the position at which the flow breaks from the wall of the exit cone are given in terms of the total flux and other parameters of the problem. Velocity profiles are presented graphically for two specific cases. (ATD)

41111 USE OF ATTENUATION TECHNIQUES FOR THE DETERMINATION OF VOID FRACTIONS IN TWO-PHASE POTASSIUM FLOW. Balzhiser, R. E.; Farvar, M. A.; Gahman, R. L. (Univ. of Michigan, Ann Arbor). 32p. (CONF-660506-5). ORAU. Gmelin, AED-CONF-66-133-6.

From American Inst. of Chemical Engineers, Nuclear Engineering Div. Symposium, Columbus, Ohio.

Collimated gamma beam from a ^{170}Tm source is partially attenuated in passing through a pipe containing all vapor flows of potassium. The intensity of the attenuated beam is measured by a scintillation detector. Void fractions were measured for qualities up to 4%. Above 7% quality no difference in attenuation was detectable for potassium flows at pressure level of 6−10 psia. The scatter of the void fraction result was reduced considerably by controlling the temperature of the scintillation crystal, by improving alignment and collimation of the apparatus and by eliminating the low energy portion of the energy spectrum through the use of a pulse height selector. Coincidence counting techniques are discussed as a possible method for enlarging the range of qualities and pressures over which void fractions might be obtained for metallic fluids. (auth)

Materials Testing

Refer also to abstract 41197.

41112 (IITRI-578P11-54) EVALUATION OF THERMAL NEUTRON CAPTURE GAMMA RAY TECHNIQUES FOR NONDESTRUCTIVE ANALYSIS OF REACTOR BURNABLE POISONS. Greenwood, R. C.; Spalek, Jan (IIT Research Inst., Chicago, Ill.). Oct. 27, 1965. Contract AT (11-1)-578. 48p. (IITRI-1193-54). Dep. mn. CFSTI $2.00 cy, $0.50 mn.

The feasibility of using the measurement of thermal neutron capture gamma rays as a nondestructive technique for determination of concentrations and distributions of burn-

able poisons in reactor fuel materials is described. Data were obtained using samples simulating fully enriched U fuel elements containing B, Cd, Sm, Eu, Gd, Dy, and Hf each used as burnable poison material, and using fuel pellets from a core loading of the EBWR reactor. The EBWR fuel pellets were 6% enriched and contained Eu and Sm as a mixed burnable poison. For these analyses, the fuel-poison samples were irradiated with a thermal neutron beam from the IITRI Research Reactor and the prompt gamma rays were detected in a 3 in. × 3 in. NaI(Tl) scintillation detector. The data show that variations in burnable poison content can be detected which are smaller than 2% of the total macroscopic absorption cross section of the fuel element, and significant improvements in this sensitivity can be anticipated with improved systems design. (auth)

41113 IMPACT TESTING OF RADIOACTIVE SAMPLES. Stagg, M. S. (Berkeley Nuclear Labs., Bristol, Eng.). Nucl. Eng., 11: 606-8(Aug. 1966).

Equipment and procedures used in impact testing of steels for embrittlement caused by neutron irradiation are described. The equipment has proved to be so efficient that an operator can produce complete transition curves in 30 min. (F.S.)

41114 RADIOACTIVE KRYPTON SIMPLIFIES TEMPERATURE MAPPING OF TURBINE BLADES. Wisnieff, Stanley F.; Bardach, Herbert (Lycoming Div., Avco Corp., Stratford, Conn.). SAE (Soc. Automotive Eng.) J., 74: 56-9(Aug. 1966).

A new technique was developed employing ^{85}Kr. Krypton-85 may be introduced into the metal by ion bombardment (2–5 kev) or by forcible diffusion of a 5% ^{85}Kr–95% ^{84}Kr mixture into the metal in a pressure vessel at 600°C for 48 hr. The krypton atoms are captive in the lattice structure of the material. Using heat as a means of liberation, three specific techniques were developed: residual counting method, gas evolution method, and ratio test method of approximation. The residual counting method is based on the fact that if the kryptonated material is reheated in an inert atmosphere at temperatures lower than its previous maximum temperature of heating, there will be no significant activity losses. Reheating to temperatures higher than the previous maximum temperature will, however, produce significant activity losses. In the gas evolution method, devised to overcome the shortcomings of the residual counting method, the krypton gas evolved during heating was counted rather than the kryptonated material after heating. The ratio test method, used to approximate the maximum temperature, involves taking the ratio of the residual activity after heating to the residual activity before heating and comparing it to a standard ratio test curve derived for an equivalent period of heating. (BBB)

41115 RADIOACTIVITY APPARATUS FOR INDICATING PROPERTIES OF MATERIALS. Carver, Robert L.; Shevick, Philip (to Nuclear-Chicago Corp.). U. S. Patent 3,256,434. June 14, 1966. Filed Nov. 20, 1963.

A portable radioactivity device is provided for measuring certain characteristics of materials, such as moisture content of soil. The device comprises a lead shield, a number of slow neutron detectors in a plane defining a detecting area, a fast neutron reflector between and immediately adjacent to the central portion of the detecting area and the lead shield, a gamma-emitting fast neutron source, and a lead shielding sleeve containing the source in the central portion of the detecting area. Means are provided for moving the source from the shield through an aperture in the reflector into the shielding sleeve for making the measurement on a surface upon which the housing is placed. The sensitivity of the neutron detectors spaced side-by-side is inversely proportional to neutron velocity to form a detecting area of dimensions of from 6 to 8 in. in each direction in the plane of the detectors. The detectors are BF_3 counters, and the source is alpha-activated Be. The response of the detector array is a linear function of moisture content over the range of 2 to 40% in soils when the device is used for moisture detection. (B.L.M.)

41116 IMPROVEMENTS IN OR RELATING TO RADIOGRAPHIC EXAMINATION TECHNIQUES. Cotterell, Kenneth (to United Kingdom Atomic Energy Authority). British Patent 1,038,711. Aug. 10, 1966. Filed May 24, 1962.

A method of examining the internal structure of a specimen, such as a reactor fuel element, in which the specimen is scanned using x or gamma radiation and a scintillation detector is described. The signal from the detector is supplied to a facsimile recorder, driven in synchronism with the scanning of the specimen. A pictorial representation of the internal structure of the specimen, dependent upon variations in the levels of radiation detected by the scintillation detector, is produced. (F.S.)

Protective Structures

41117 SITE TESTING FOR EMP (ELECTROMAGNETIC PULSE) HARDNESS. Molmud Paul; Arnush, Donald (TRW Systems, Inc., Redondo Beach, Calif.). IEEE (Inst. Elec. Electron. Eng.) Trans. Aerospace Electron. Systems, AES-2: 455-60(July 1966).

Buried command posts and missile launch complexes are hardened against the overpressure produced by the explosions of nuclear weapons. They must also be hardened against the EMP effects of the weapons. EMP refers to electromagnetic pulse or the large amplitude electric and magnetic fields which are produced by the detonation. These fields are strong enough to destroy unprotected circuitry and impair the performance of unshielded, delicate equipment. EMP is caused mainly by the radial flow of γ photons from the weapon, causing radial flow of Compton electrons when the photons interact with the electrons in the atmosphere. This radial current flow is asymmetric because of the presence of the earth, asymmetries in the nuclear detonation, and the earth's magnetic field, and thus can radiate electromagnetic energy. In view of the EMP effects, circuits and equipment must be protected and shielded. Even after some equipment is shielded and some obvious circuits are protected, there still remain some unanswered questions: (1) Is the shielding adequate? (2) Are there any circuits which have been overlooked? (3) Are there any accidental or deliberate penetrations of the site which make it more susceptible to EMP? (4) Does the extended nature of the source provide some unexpected integrated effects? A test procedure was developed to answer these questions. The procedure is to determine the Green's or transfer function of the site using infinitesimal electric and magnetic dipole oscillators. The Green's function is comprised of the set of measured electric and magnetic fields when the oscillators are operated at each point, with each orientation and frequency. It is shown how the fields within the site are predicted, given knowledge of the currents in air producing the EMP, or the tangential components of the fields on the earth's surface. (BBB)

41118 DEVICES FOR PROTECTION AGAINST RADIOACTIVE FALLOUT. Stark, Virgil. U. S. Patent 3,256,440. June 14, 1966. Filed Dec. 20, 1961.

A structure for shielding against gamma radiation resulting from a nuclear explosion consists of one or more layers of flowable material between several walls or panels to serve as a variable thickness with relation to the attenuation factor for the radiation. The panels may be collapsible, fixed, or movable; may be located parallel or at an angle to each other; and in combination may constitute a container or series of containers inside each other forming separate compartments. The flowable material may be solid particles such as sand, iron oxide, etc., or slurries of solid materials in liquid carriers, or liquids such as water, oil, mercury, etc. The containers may take the form of a suit for encasing the human body, a rigid enclosed movable device for one or several people, variable barrier shielding for windows, doors, or automobiles. (B.L.M.)

41119 BOMB AND FALL-OUT SHELTERS. Trice, Siebert W. U. S. Patent 3,251,159. May 17, 1966. Filed Oct. 27, 1961.

A precast concrete fallout shelter for installation in a predug hole and designed to be covered with earth is patented. The shelter is suitable for individual family units or small groups of individuals and is inexpensive to construct. All sections of the shelter, including walls, floor, and roof, are formed with a rabbet along four edges for interlocking with each other and with the hatchway and blast wall. The parts are assembled and grouted at the joints to form a tight seal unit with no straight through passages for radiation entry. An exit hatch opening is provided in the roof section, and a precast hatchway is interlocked into projections provided in the roof section to join the hatchway in a tight seal to the roof section. A blast wall, engaging with the roof, with the floor and with one side wall, but terminating short of the other side wall, forms an entry way beneath the hatch opening and separates the main room from the hatch and entry way. (B.L.M.)

Space Propulsion

See also ISOTOPE TECHNOLOGY — Power Application
REACTOR TECHNOLOGY — Propulsion and Space

41120 STUDIES ON IONIZATION PHENOMENA ASSOCIATED WITH SOLID-PROPELLANT ROCKETS. Capener, E. L.; Chown, J. B.; Dickinson, L. A.; Nanevicz, J. E. (Stanford Research Inst., Menlo Park, Calif.). Contract NAS7-179. AIAA (Amer. Inst. Aeronaut. Astronaut.) J., 4: 1349-54(Aug. 1966).

A series of studies was made with a view to determining the magnitude of the microwave attenuation problem associated with the exhaust plasma of typical state-of-the-art solid propellants. Propellants studied have included nonaluminized and aluminized composite propellants using both polyurethane and polybutadiene based binders. Two-frequency microwave diagnostic probing was used for the study of the rocket motor exhaust plasma. Within the combustion chamber, electron density was measured using ionization probes. Experiments showed, for a combustion chamber pressure of 300 psi, that equilibrium ionization conditions held down to an expansion ratio of about 40; below this point frozen flow occurred. It also was found that, initially, ionization was below the equilibrium value expected from the theoretical calculations (these included attachment to Cl) and that it increased progressively with time. Electron leakage to ground from an insulated motor was measured, and this also was found to be progressive with time. (auth)

41121 NEUTRAL MASS DENSITY MEASUREMENTS IN A REPETITIVELY PULSED COAXIAL PLASMA ACCELERATOR. Karras, T.; Gorowitz, B.; Gloersen, P. (General Electric Co., King of Prussia, Pa.). Contract NASw-1044. AIAA (Amer. Inst. Aeronaut. Astronaut.) J., 4: 1366-70(Aug. 1966).

A detailed study of the time-dependent gas density profile within various modifications of a repetitively pulsed coaxial plasma accelerator was initiated. A fast pressure probe was used which sampled a volume of only 0.5 cm^3 at one time so that adequate resolution was available to observe fine structure. Initial measurements showed that no more than 15% of the injected propellant was present within the accelerator barrel at any one time. Guided by these measurements, propellant injector port modifications were made which raised this figure to over 90%. Controlled triggering of the discharge simultaneous with this maximum propellant fraction in turn led to a marked increase in engine efficiency. In addition, detailed examination in both axial and radial positions indicated a nonoptimum gas density distribution for coupling with the field. More judicious propellant placement, as well as further increase in the propellant fraction acted on, is discussed, and detailed plots of the gas density distribution as a function of time and axial and radial position are presented. The advantages of directed axial propellant injection at a downstream point near the inner electrode are emphasized. (auth)

41122 DEVELOPMENT OF A REGENERATIVE COLLECTOR TARGET FOR LONG-TERM TESTING OF ELECTRICAL PROPULSION SYSTEMS. Trolinger, James D.; Shipp, John I. (ARO, Inc., Arnold Air Force Station, Tenn.). New York, American Inst. of Aeronautics and Astronautics, 1966, Preprint No. 66-500, 17p., $1.50. (CONF-660632-6). ORAU.

From American Inst. of Aeronautics and Astronautics, 4th Aerospace Sciences Meeting, Los Angeles, Calif.

The design and experimental results of a newly developed collector target complex is reported. The problems of target lifetime and contamination of test equipment by sputtered target material are eliminated with the new concept. The target comprises a metal which can be easily liquified. Sputtered material is trapped on cold surfaces surrounding the target which are specially designed so that the condensed material may be melted and returned to the target housing when required. The target can be regenerated either in this manner or from an external source without breaking vacuum. Metals under consideration have vapor pressures low enough to meet vacuum requirements and simultaneously high enough to prevent contamination by plating of test equipment with target material. An experimental evaluation of the operating characteristics of the complex, using a ten cm electron bombardment engine and a Hg target, indicates this technique is practical and economical—particularly for long-term testing. The results of additional experiments to ascertain emission properties of a Hg target under Hg^+ bombardment, as a function of target temperature and beam energy, are also reported. (auth)

41123 PLASMA CHARACTERISTICS OF THE ELECTRON BOMBARDMENT ION ENGINE. Masek, Tommy D. (California Inst. of Tech., Pasadena). 69p. (CONF-660414-7). ORAU. Gmelin, AED-CONF-66-119-8.

From 2nd International Conference on Electron and Ion Beam Science and Technology, New York.

Nonlinear partial differential equations requiring numerical solutions are used to describe plasma as it relates to the electron bombardment ion engine. General characteristics of plasma are presented in terms of collision times, collision and ionization cross sections, ion production coefficients, and general equations of plasma. The equation for axial ion flux, in terms of ion density gradient, is compared to measured beam current densities. (F.S.)

41124 SOLAR-ELECTRIC PROPULSION SYSTEM PERFORMANCE FOR THE 0.1-AU SOLAR PROBE MISSION. Strack, William C. (National Aeronautics and Space Administration, Cleveland, Ohio). New York, American Inst. of Aeronautics and Astronautics, 1966, Preprint No. 66-496, 26p., $1.50. (CONF-660632-5). ORAU.

From American Inst. of Aeronautics and Astronautics, 4th Aerospace Sciences Meeting, Los Angeles, Calif.

Saturn IB/Centaur and Atlas/Centaur launched electric propulsion vehicles employing present or near-future state-of-the-art solar cell power supplies (50 to 100 lb/kw(e)) are shown to be attractive systems for performing the 0.1-AU solar probe mission. This result compares favorably with the alternative systems composed of the same boosters but with chemical or nuclear final stages—which are inadequate for this mission. The performance calculations for the electric propulsion systems include the optimization of the launch vehicle burnout velocity, the electric stage specific impulse and power level, and the thrust orientation for constant specific impulse thrustors. Two sets of results are presented. The first set is associated with constant power operation of the thrustors as would be the case for nonsolar dependent power supplies such as nuclear-electric systems. The second set of data represents solar-cell-powered electric systems. In this case the thrustor power is a function of the sun-vehicle distance. The power is varied by adjustment of the propellant flow rate. Of special interest is the fact that absolute optimal trajectories for the solar cell systems belong to

an entirely different class than those optimals associated with constant power systems. (auth)

Vacuum Engineering

41125 (SGAE-PH-41/1966) VORRICHTUNG ZUR BEWEGUNGSUBERTRAGUNG IN EIN VAKUUMSYSTEM. (Apparatus for Motion Transfer in a Vacuum System). Edl, F. W. (Oesterreichische Studiengesellschaft fuer Atomenergie G.m.b.H., Seibersdorf. Physik-Institut). 1966. 6p. Dep. mn.

A device is described which makes it possible to transfer, by a combination of simple constructional elements, 6 different motions in a vacuum system. (tr-auth)

GEOLOGY, METEOROLOGY, AND MINERALOGY

General

Refer also to abstracts 40811 and 40836.

41126 MULTIPLE SUBSURFACE SPALLING BY UNDERGROUND NUCLEAR EXPLOSIONS. Eisler, J. D. (Stanford Research Inst., Menlo Park, Calif.); Chilton, F.; Sauer, F. M. Contract W-7405-eng-48. J. Geophys. Res., 71: 3923-7(Aug. 15, 1966). (UCRL-13195(Rev.1)).

Multiple spalling of subsurface layers in the earth accompanies the detonation of contained underground nuclear shots. Interpretation of available data for shots detonated in tuff, halite, and alluvium points to the existence of ascending and descending waves which produce spall gaps in the subsurface. The records of particle acceleration at depth indicates an upward-traveling sequence of closures of these gaps. The pattern of spallation is similar for the tuff and halite shots. For an alluvium shot, spallation appears to be largely the consequence of slumping of the cavity rather than of tensile stress waves reflected from the free surface. (auth)

41127 RADIOCARBON CONTENT OF DEEP AND SURFACE WATERS OF THE NORTH INDIAN OCEAN (SEA OF OMAN). Thommeret, Jean; Thommeret, Yolande; Galliot, Jean (Centre Scientifique, Monaco). Radioact. Sea, No. 18, 1-8(1965). (In French).

Ten carbon-14 concentration measurements of surface and deep sea water samples of the north Indian ocean (Arabian sea), collected in August and September 1963, during the International Indian Ocean Expedition (Atlantis II), have confirmed previous results obtained in 1960 in the same ocean (south-east part). The mixing of surface water, above the thermocline, takes several years and affects only a thin surface layer of the sea. A marked increase in the carbon-14 content of surface waters has been observed in 1963. There is no significant difference of age between deep waters from water masses of the Pacific for which a northward speed component of 0.05 cm/sec was calculated. An age difference of 400 years was measured by radiocarbon, between 40°S and 40°N of the Pacific. (auth)

41128 STUDY OF BOTTOM LAYERS IN THE DEEP PARTS OF THE MEDITERRANEAN SEA. Romanovsky, V. (Centre de Recherches et d'Etudes Oceanographiques, Paris). Vienna, International Atomic Energy Agency, 1966, Preprint SM-72/26, 11p. (In French). (CONF-660507-17). ORAU.

From Symposium for the Disposal of Radioactive Wastes into Sea, Oceans, and Surface Waters, Vienna.

Devices were developed for dispensing Rhodamine B solutions that were either lighter or heavier than sea water, and whose dispersion was photographed at regular intervals by under-water cameras. For sampling the water in contact with the bottom, where the immobility of the water prevents use of conventional apparatus, an instrument was developed which pumps the sample and guarantees its origin. Measurements carried out at between 500 and 2700 meters depth indicated that there was a substantial current gradient within a few tens of meters of the bottom, but that there was, in contact with the sediment, an absolutely immobile layer where no turbulence was evident. The thickness of this layer varies with the depth of the water and disappears as soon as the bottom rises above 2000 meters; it is therefore found only in the great abyssal plain. On the average it is a few decimeters thick. Water samples showed that there was a strong dissolved oxygen gradient above the bottom, thus confirming the measurements made by a number of others. However, very large gradients which have not so far been ported were described. The measurements show that the study of the bottom layers at great depths presents a very promising line of investigation and throws fresh light on problems of exchange between the sea and the bottom. (auth)

Meteorology

See also Site Survey and Selection

Refer also to abstract 40838.

41129 FORECASTING STRONG SOUTHWEST WINDS AT THE NATIONAL REACTOR TESTING STATION (NRTS). Richter, Alden P. (Air Resources Field Research Office, Idaho Falls, Idaho). 14p. (CONF-660330-1). ORAU. Gmelin, AED-CONF-66-072-1.

From Conference on Modern Methods of Weather Forecasting and Analysis, Chicago.

Strong southwest wind patterns at the NRTS are generally divided into two classes. Class 1 is characterized by strong southwest winds over only the southern portion of the NRTS. Class 2 is characterized by strong southwest winds over the entire NRTS. Tests at the northern area of the NRTS under meteorological control generally require class 2 winds for safety reasons. Synoptic differences between class 1 and 2 winds are investigated by construction of seasonal maps of sea level pressure and of 500 mb data for the western United States. Maps of long period normals and composite maps of class 1 and 2 wind days from a three year dependent data sample and sea level pressure and 500 mb height gradients computed from the above maps are discussed. It is concluded that the topography of the northern area of the NRTS requires a unique synoptic pattern for the occurrence of class 2 winds. Three features of this pattern revealed by this study are a northerly directed sea level pressure gradient of sufficient magnitude, a northwesterly directed 500 mb height gradient of sufficient magnitude and advection of 500 mb height falls near 100 meters into the Great Basin area. Verification of trial predictors on a year of independent data show little skill. A computer program of the screening procedure and multiple linear regression will be run on the dependent data sample. Hopefully, it will yield a useful objective technique from which the hours of class 2 and class 1 winds can be predicted. (auth)

Natural Radioactivity and Fallout

See also HEALTH AND SAFETY

Refer also to abstracts 40531, 40546, 40574, 40639, 40730, 41198, and 41277.

41130 (COO-1407-10) RAIN SCAVENGING STUDIES: DATA ANALYSIS, SYNTHESIS, AND INTERPRETATION. Progress Report No. 2. Dingle, A. Nelson; Gatz, Donald F. (Michigan Univ., Ann Arbor. Dept. of Meteorology and Oceanography). May 1966. Contract AT(11-1)-1407. 37p. Dep. mn. CFSTI $2.00 cy, $0.50 mn.

Progress is reported in research on several problems associated with the deposition of atmospheric particulate matter by convective storms. Low altitude (below 650 mb) inflow to the convective storm of May 10, 1964, provided sufficient fallout radioactivity to account for observed deposition. A physical mechanism is proposed to explain observed concentration-rainfall rate relationships. The process involves the deposition of large amounts of contaminant in the first rain to fall at a point from a moving shower and the subsequent depletion of contaminants in the heavy rain. It is postulated that the raindrop evaporation process contributes to concentration fluctuations and especially to the high concentrations found in the light rain at the start of a shower. Concentration variations in severe storm cells appeared to be significantly different from those in less severe convective systems. The Chinese nuclear test of May 14, 1965, provided a source of high-altitude tracers. Rain water samples collected at various locations in the U. S. and Canada were analyzed for fresh

fission products. Data on content and age determinations of ^{144}Ce, ^{144}Pr, ^{125}Sb, ^{137}Cs, ^{95}Zr, and ^{95}Nb are presented. Results indicated that rain scavenging of the fresh debris was delayed at least one day, and in some cases up to 6 days, from the date the high level debris plume was believed to have passed the collecting station. (C.H.)

41131 (HASL–172) HEALTH AND SAFETY LABORATORY FALLOUT PROGRAM. Quarterly Summary Report, March 1, 1966–June 1, 1966. Hardy, Edward P. Jr.; Rivera, Joseph (Health and Safety Lab., New York Operations Office (AEC), N. Y.). July 1, 1966. 523p. Dep. mn. CFSTI $8.00 cy, $2.25 mn.

Current data are presented from the HASL Fallout Program, Environmental Science Services Administration, National Radiation Laboratory in New Zealand, Argonne National Laboratory, and the EURATOM Joint Nuclear Research Centre. Radionuclide levels in fallout, milk, tap water, diet, surface, and high-altitude air, are given in tabular form. The initial section includes interpretive reports and data summaries covering the following topics: strontium-90 concentrations in the waters of Lake Michigan and a comparison with the cumulative land deposit; a summary of the air filter samples collected during 1965 at balloon-borne altitudes; the results of an experiment to determine how much fallout debris is collected on the balloon-borne filtering devices during ascent and descent; stratospheric strontium-90 concentrations from January 1963 and predictions to August 1968; plutonium-238 in the stratosphere from SNAP-9A; vertical profiles of particulate radioactivity in the atmosphere during February 1965; gross gamma measurements in surface air from July 1965 to February 1966; global deposit of strontium-90 through 1965 and prediction for 1966; monthly averages of strontium-90 fallout and precipitation by 10° bands of latitude; and strontium-90 in human vertebrae sampled in 1965. A bibliography of recent publications related to radionuclide studies is included. (auth)

41132 (NYO–3364–20) ^{137}Cs IN MILK IN NORWAY 1962–1966. Madshus, Kjell (Norsk Hydro's Inst. for Cancer Research, Oslo); Stroemme, Aksel (Norsk Radiumhospital, Oslo); Koren, Kristian (Statens Radiologisk-Fysiske Laboratorium, Oslo (Norway)). Contract AT(30-1)-3364. 42p. Dep. mn. CFSTI $2.00 cy, $0.50 mn.

A survey of ^{137}Cs-contamination in cows' milk in Norway during the period March 1962 to May 1966 is presented. Curves showing the seasonal variations of ^{137}Cs in milk based upon monthly observations and over 3000 single observations in milk samples from late winter and spring are included. Cesium-137 was determined by gamma-spectrometric methods, using a ϕ 2½'' by 3'' NaI(Tl) crystal and multichannel kicksorters (R.C.L. 256 channels, Intertechnique SA 40, 400 channels). The time for analysis was usually 50 minutes, and the standard error was generally considered to be better than ±5%. Measured and calculated data are approximated to the nearest 5 pCi or percent. (TCO)

41133 (SC-CR-66-2030) PARTICLE FALLOUT AND DISPERSION IN THE ATMOSPHERE. Quarterly Report No. 3. Hage, K. D.; Brown, P. S.; Arnason, G.; Bowne, N. E. (Travelers Research Center, Inc., Hartford, Conn.). Apr. 1966. Contract AT(29-1)-789, Subcontract No. 48-2417. 70p. Dep. mn. CFSTI $3.00 cy, $0.75 mn.

For Sandia Corp., Albuquerque, N. Mex.

Progress is described on the development of a three-dimensional model (Model B) for estimating the transport and dispersion of falling particles released from an instantaneous point or line source located at altitudes of 10 to 90 km. The Runge-Kutta-Gill fourth-order numerical method was found to be fast, accurate, and stable for the integration of particle trajectories, and was selected for use in the model. The minimum time-step length needed for specified absolute accuracy of particle position depends on the amplitude and wavelength of disturbances in the wind field. These relationships were investigated for floating particles in a large-scale, stationary wind field. Vertical profiles and maps of total stream function illustrate the mathematical functions that are used to simulate the mean wind flow and the planetary or long-wave velocity components. The equations that are used for the simulation of short-wave wind velocity components are described. Draft specifications and flow diagrams for the Model B computer program are given in an appendix. (27 references.) (auth)

41134 (SFL–A3) RADIOSTRONTIUM IN MILK, GRASS AND SOME OTHER BIOLOGICAL SAMPLES IN FINLAND. Paakkola, O. (Institute of Radiation Physics, Helsinki (Finland)). Apr. 1966. 34p. Dep. mn.

Results are presented from country-wide survey of ^{90}Sr content in dried milk and $^{90}Sr/g$ Ca in milk samples collected in Finland from 1960 through 1965. The results of the daily dried milk samples for ^{90}Sr show that the rise of the summer maxima began in 1963 and 1964 in the end of June and reached its highest value in one month. The daily and geographical variations in $^{90}Sr/Ca$ ratios in Finland were not large. Strontium-89 from north Finland was measured in milk. In August 1963, ^{89}Sr reached its maximum, a value of about 200 pCi/g Ca. The observed ratios found in summer 1963 for two farms were on the average 0.05. During February 1964, daily diets in one hospital in Helsinki had a mean $^{90}Sr/Ca$ ratio of 30.4 pCi/g, i.e., about 25% higher than $^{90}Sr/Ca$ ratio in milk during the same period. During the spring of 1965 the $^{90}Sr/Ca$ ratio was about 1.0 pCi/g for Baltic herring caught in the coastal waters of Finland. (auth)

41135 SULFUR ISOTOPE ABUNDANCES IN EVAPORITES AND IN THE ANCIENT OCEANS. Thode, H. G.; Monster, J. (McMaster Univ., Hamilton, Ont.). pp 589-600 of Chemistry of the Earth's Crust, Memorial to V. J. Vernadsky. Vol. 2. Moscow, 1964. (In Russian).

A detailed study was made of the distribution of sulfur isotopes in the evaporites of ten sedimentary basins of several continents in an attempt to establish the sulfur isotope ratio for the various ancient oceans and to establish the pattern of change. Results showed that there are gypsum evaporites forming today in marine lagoons with sulfur isotope ratios almost identical with that of the ocean sulfate from which they are derived. Also, some of the samples show ^{34}S enrichment with respect to the present day ocean sulfate, indicating bacterial action and isotope fractionation. These results confirm that marine evaporites will either have the same isotope ratio as that of the contemporaneous oceans or be enriched in ^{34}S. In a narrow horizon of gypsum or anhydrite evaporite covering a large area of a sedimentary basin, the sulfur isotope ratios are remarkably uniform. Within a unit or formation within a sedimentary basin, there are fluctuations in the sulfur isotope content of the evaporites from bed to bed at different depths. These fluctuations within a fairly narrow time interval probably reflect the isotope ratio of the sedimentary basin, rather than that of the contemporaneous oceans. The fact that the minimum ^{34}S δ values of contemporaneous evaporite beds from widely separated sedimentary basins coincide, whereas the maximum values vary considerably, indicates that the isotopic content of the basins has fluctuated more rapidly than the large reservoir of sulfate in the contemporaneous oceans. The results confirm conclusively that the ^{34}S content of the oceans has changed with time, the total variation being at least 20 ppm from Precambrian time to the present. The changes in the ^{34}S content of the oceans have been somewhat cyclic in nature. A maximum enrichment seems to occur in Cambrian time, and a minimum enrichment in Permian time. (TCO)

41136 REACTOR ENVIRONMENT MONITORING FOR APRIL, 1965. Samuels, E. R.; Mohindra, V. K. pp 27-32 of Data from Radiation Protection Programs. Vol. 3, No. 5. Ottawa, Department of National Health and Welfare, Radiation Protection Division, 1965.

Data from monitoring studies conducted during April 1965, near the sites of the Chalk River reactors, the Nuclear Power Demonstration Reactor (NPD), and the Doug-

las point (Candu) reactor are presented. Total alpha activity and total beta activity determinations, as well as ^{89}Sr, ^{90}Sr, and ^{137}Cs analyses were made on water samples from selected areas above and below the reactors. Air filter samples were collected daily in the vicinity of the McMaster University reactor. All data were in general agreement with observations made in the fallout program, and no anomalies attributable to release of contaminants from the reactors were shown. (H.G.D.)

41137 POSSIBILITY OF IMPROVING THE ROUTINE MEASUREMENTS OF ARTIFICIAL BETA ACTIVITY IN THE AIR. **Mattsson, R. (Finnish Meteorological Office, Helsinki). Geophysica (Helsinki), 7: 245-9(1963).**

Routine measurement of gross β activity is discussed, and it is shown that if the aerosol β activity is measured with two different absorbers, considerably more information is achieved, e.g., the age of fission products can be estimated from relatively small samples. A method is described which provides a simple way to get comparable results from the air filter measurements and in addition some extra information that is usually connected with more laborious measurements. The hard component of the β activity is first measured with a counter that has a window thickness of 30 to 50 mg/cm^2. This system is calibrated against ^{40}K and ^{36}Cl by measuring filters prepared with standard solutions of these radioisotopes. The unknown filters as well as the standard ^{40}K and ^{36}Cl filters are then measured directly from the surface with a thin window counter. This counter does not necessarily cover the whole filter area. On the contrary, more information can be achieved by measuring several spots on the same filter. The error due to absorption in the filter is corrected by measuring the filter with the exposed side to the counter (A_1), with the unexposed side to the counter (A_2), and with a clean filter between the exposed side and the counter (A_3). A corrected value, A_0, is then obtained: $A_0 = A_1\sqrt{A_2/A_3}$. Each filter is then characterized by a β-energy index i.e., the ratio between the count rate from a thick-window counter to that from a thin-window one. This ratio is high if hard β rays dominate and γ activity is subtracted. This energy index together with the usually convenient measurement with thick window counters, gives a good value for the total activity on the filter, and, in addition, some extra information. Some data collected from aerosol samples collected in Finland in 1962 are charted and correlated with nuclear weapon test detonations. The advantages of measuring with two different absorber values, as described, over measurements made with only one absorber value are enumerated. (BBB)

41138 HIGHLY ACTIVE SINGLE PARTICLES IN RADIOACTIVE FALLOUT. Murayama, N. Kishocho Kenkyu Jiho, 17: 308-16(1965). (In Japanese).

Radioactive particles in the fallout from the nuclear explosions in fall of 1962 and October of 1964 were found in airborne dusts near the ground using a continuously driven dust sampler. Characteristics of the particles were examined by their radioactivity decays. These particles (about 10 μ in dia.) were transported from 4,000 to 5,000 km in 3 to 5 days by the westerly wind in the troposphere. (auth)

41139 RADIOAKTIVNOST' POCHV I METODY EE OPREDELENIYA. (Radioactivity of Soils and Methods of Measurement). Antipov-Karataev, I. N. (ed.). Moscow, Izdatel'stvo Nauka, 1966. 258p.

A series of twelve articles on the radioactivity of soils and methods of measurement are compiled. The topics discussed are the accumulation and distribution of ^{90}Sr in the soils from radioactive precipitations, behavior of radioisotopes in soils, uptake of radioisotopes by plants, natural radioactive sources in soil, and methods for the determination of small quantities of radioisotopes. (J.S.R.)

41140 ABSORPTION OF ARTIFICIAL RADIONUCLIDES BY MARINE DETRITUS UNDER NATURAL OCEAN CONDITIONS. Patin, S. A.; Popov, N. I. (Inst. of Oceanography, Moscow). Vienna, International Atomic Energy Agency, 1966, Preprint SM-72/28, 8p. (In Russian). (CONF-660507-18). ORAU.

From Symposium for the Disposal of Radioactive Wastes into Sea, Oceans, and Surface Waters, Vienna.

The distribution of various radionuclides as between suspended material and sea water solution was evaluated. A radiochemical and γ-spectrometric analysis was carried out on samples of detritus separated from large volumes of water in the Indian Ocean. The concentrations of fission products in samples of water were determined at the same time. In spite of the relatively large amounts of suspension analyzed, the activity of ^{90}Sr and ^{137}Cs in the samples investigated proved to be below the sensitivity of the methods of measurement used. The maximum possible content of these isotopes does not exceed 0.1 to 0.3 pCi/g dry weight, representing the build-up factor (the ratio between the concentrations of the isotope in the suspension and in the water) of less than 1000. The relative content of these nuclides in the solid phase amounts under these conditions to less than 0.01% of the total content per unit volume of water. The measured content of ^{144}Ce and ^{106}Ru in the suspension is about 2 pCi/g dry weight. This represents build-up factors of from 10,000 to 50,000. The relative content of the latter isotopes in the solid phase does not exceed 1%. (auth)

41141 NUMERICAL MODEL FOR THE HYDROLOGIC TRANSPORT OF RADIOACTIVE AEROSOLS FROM PRECIPITATION TO WATER SUPPLIES. Huff, Dale D.; Kruger, Paul (Stanford Univ., Calif.). 30p. (CONF-651108-6). ORAU. Gmelin, AED-CONF-65-347-11.

From Symposium on Isotope Techniques, Urbana, Ill.

Preparation of a numerical model of the transport of nuclear debris from the atmosphere by precipitation through the surface-water portion of the hydrologic cycle is described. The model collates the significant parameters involved, such as the physical and chemical properties of biologically-important radionuclides (e.g., ^{90}Sr) in aerosols, their deposition by precipitation under Pacific Coast cyclonic conditions, and their movement through the catchment basin during precipitation and runoff. The model is based upon the quantitative estimation of these parameters under conditions given by an existing computer model which traces the movement of water through the basin to predict the runoff hydrograph. The numerical model should serve as an index of predictability for radionuclide concentration in water supplies originating from atmospheric sources, and as a means to locate areas where additional numerical knowledge of hydrologic processes is needed. (auth)

41142 AN EVALUATION FROM THE HEALTH POINT OF VIEW OF FACTORS DETERMINING THE MOVEMENT OF ^{90}Sr FROM FRESH WATER BODIES INTO THE HUMAN ORGANISM. Marei, A. N.; Saurov, M. M. (Ministry of Health Inst. of Biophysics, Moscow). Vienna, International Atomic Energy Agency, 1966, Preprint SM-72/33, 12p. (In Russian). (CONF-660507-22). ORAU.

From Symposium for the Disposal of Radioactive Wastes into Sea, Oceans, and Surface Waters, Vienna.

Strontium-90 migrates from water bodies into the human organism as a result of the use of water for drinking and through the food chain. This phenomenon acquires greatest importance in rural communities, where locally-produced commodities predominate in the diet of the population. The intake of ^{90}Sr with food products depends on the natural features of the locality, on economic conditions, and on dietary structure. Intake of ^{90}Sr with the various food products is determined principally by the levels of accumulation of the isotope in the food product concerned, by the amount of the product consumed, and by the method of culinary preparation. The degrees of accumulation of ^{90}Sr in individual food products are expressed by the value of the accumulation multiplicity factor (AMF): AMF = [(Ci/kg of food product)/(Ci/l of water from water-body)]. They depend on the degree of mineralization of the water (Ca), the nature of the food product in question, the soil and climatic conditions of the locality, and other factors. As applied to the conditions

obtaining in the central zone of the USSR the value of the AMF for individual food products lies in the range 0.01 to 1.3 for fish products and 0.01 to 0.3 for milk, fruit, meat and other commodities. For the adult population the overall coefficient of intake (OCI) values vary between 0.3 and 2.0. The number of persons in whose diet the OCI values were at maximum represents 10 to 20% of the total population in the riparian zone. It is clear from the research data that the intake of ^{90}Sr with the diet due to its movement into the food chain from fresh water is quite large and that under certain conditions may exceed the intake from drinking water. The logical conclusion is that differential standards for ^{90}Sr content in ordinary water-bodies and in drinking water must be established. (TCO)

41143 2me REUNION INTERNATIONALE D'OCEANOGRAPHIE MEDICALE. COLLOQUE INTERNATIONAL SUR "LA POLLUTION DU MILIEU MARIN." PART II. LA RADIOACTIVITE DU MILIEU MARIN. (Second International Assembly of Medical Oceanography. International Symposium on Pollution of Marine Media, Nice, France, September 15–17, 1964. Part II. The Radioactivity of Marine Media.). Cah. CERBOM (Cent. Etud. Rech. Biol. Oceanogr. Med.), 17: 1-153(1965). (CONF-640931).

Separate abstracts were prepared on six papers presented at this conference. (C.H.)

For abstracts of individual papers see: 40546, 41144–41147, and 42687.

41144 RADIOACTIVITY OF THE SEA DUE TO NATURAL PRODUCTS AND ARTIFICIAL RADIOACTIVITY PRODUCED BY FALLOUT. Lambert, G. (Centre d'Etudes Nucleaires, Saclay, France. Centre des Faibles Radioactivites, Gif-sur-Yvette, France). Cah. CERBOM (Cent. Etud. Rech. Biol. Oceanogr. Med.), 17: 15-34(1965). (In French).

Almost all of the total artificial radioactivity in the sea is introduced by nuclear explosions. The fission products produced in such explosions and the dissemination of these fission products are discussed. The horizontal and vertical distributions of the artificial radioisotopes in the ocean are described and their accumulation in the ocean is considered. (J.S.R.)

41145 METHODS AND RESULTS OF THE MEASUREMENT OF THE RADIOACTIVITY IN THE SEA. Chesselet, R.; Lalou, C.; Nordemann, D. (Centre d'Etudes Nucleaires, Saclay, France. Centre des Faibles Radioactivites, Gif-sur-Yvette, France). Cah. CERBOM (Cent. Etud. Rech. Biol. Oceanogr. Med.), 17: 35-65(1965). (In French).

Gamma spectrometric analysis of sea water makes possible the direct determination of concentration gradients for ^{95}Zr, ^{95}Nb, ^{103}Ru, and ^{106}Ru. The depth of fission product diffusion is connected with the depth of the thermocline. These gradients were used for a quantitative study of fallout in the eastern Mediterranean and the Bay Biscay in 1963. The ratios between the specific activities of the fallout in the sea and the specific activities of fallout in terrestrial collectors are always higher than 1. The discussion of these results leads to the re-evaluation of the collecting efficiency of marine species with respect to that of the continents for radioactive fallout. (tr-auth)

41146 RECENT STUDIES ON THE RADIOACTIVITY OF PLANKTON AND OF ORGANIC REFUSE. Chesselet, R. (CNRS, Gif-sur-Yvette, France); Lalou, Cl; Aubert, M.; Gambarotta, J.-P. Cah. CERBOM (Cent. Etud. Rech. Biol. Oceanogr. Med.), 17: 67-97(1965). (In French).

A systematic study of the Nice coastal zone of the Mediterranean Sea from January 1963 to December 1963 showed the very important role of plankton and organic debris as the concentrating agent of certain artificial radioisotopes present in fallout. These include ^{95}Zr, ^{95}Nb, ^{103}Ru, ^{106}Ru, ^{141}Ce, and ^{144}Ce. A comparative study made on the effects of fallout rate on the activity of sea water and on the activity of the plankton lead to the conclusion that for the radioisotopes studied the contamination of the zoo plankton by atmospheric fallout is related principally to the injection conditions of the particles rather than to the specific activity of the sea water in which the plankton live. (tr-auth)

41147 FUTURE OF THE "IN SITU" DIRECT DETECTION METHOD OF THE γ ACTIVITY OF SEAWATER. Thommeret J.; Galliot, J. (Centre Scientifique, Monaco). Cah. CERBOM (Cent. Etud. Rech. Biol. Oceanogr. Med.), 17: 103-7(1965). (In French).

The development of an immersible scintillation probe for use in the direct measurement of γ activity in sea water at depths up to 4000 meters is described. The influence of environmental factors, such as temperature, salinity, transparency, oxygen tension, and radioactivity of the water, on counting results are discussed. Good results are reported when the equipment was used for measurements of radioactivity in the Atlantic Ocean. Indian Ocean, and Mediterranean Sea. (C.H.)

Site Survey and Selection

41148 (AAEC-TM-316) THE STABILITY OF THE LUCAS HEIGHTS AREA AGAINST POSSIBLE SEISMIC EVENTS. Mumme, I. A. (Australian Atomic Energy Commission Research Establishment, Lucas Heights). Apr. 1966. 16p. Dep. mn.

Available geophysical and geological data are reviewed in considering the stability of the Lucas Heights site against possible seismic events. The region is seismically inactive and no tremors of magnitude greater than 6 have been recorded in the last 55 years. If we assume the worst probable case based on previous records, the maximum probable earthquake, occurring at Lucas Heights, would have a magnitude 6, and an intensity of VII–VIII on the modified Mercalli scale. The dominant rock formation outcropping in the region is Hawkesbury sandstone which is about 750 feet thick with an average compression strength of about 3000 psi. The steady state stresses in the rock formations are due to gravitational effects. It is necessary to consider whether allowance should be made for resistance of structures to earthquake forces. As an example, the problem of the design of a fuel storage facility consisting of a pattern of drill-holes is considered. The geometry of the holes is such that displacements under horizontal accelerations of the order of 130 cm/sec^2 (corresponding to a magnitude 6 earthquake) would not induce collapse as the rock would behave elastically. It was recommended that steel linings be grouted into the facility to prevent collapse of weathered rock into the holes or the influx of ground water. (auth)

Techniques and Equipment

Refer also to abstracts 41115 and 42062.

41149 (AD-632956) BUFF. Long-Range Seismic Measurements [of] VELA UNIFORM. Seismic Data Laboratory Report No. 143. (Teledyne Industries, Inc., Alexandria, Va. Earth Sciences Div.). Dec. 16, 1965. Contract AF 33(657)-15919. 41p. CFSTI $2.00 cy, $0.50 mn.

An analysis was made of seismological data from an underground nuclear explosion as part of a continuing study to aid in distinguishing between earthquakes and explosions. A table of travel-times and amplitudes of P, Pg, Lg, and surface waves are included along with other unidentified phases. (auth)

41150 (AECL-2576) THE USE OF RADIOACTIVE TRACER GASES TO STUDY THE RATE OF EXCHANGE OF WATER VAPOR BETWEEN AIR AND NATURAL SURFACES. Barry, P. J. (Atomic Energy of Canada Ltd., Chalk River (Ontario). Chalk River Nuclear Labs.). June 1966. 9p. (CONF-651108-7). Dep. mn. AECL $0.50.

From Symposium on Isotope Techniques, Urbana, Ill.

Radioactive tracers have been used to measure the flux of matter at the surface of snow. By the use of two tracers having markedly different molecular diffusivities it is pos-

sible to study turbulent and molecular transports separately. The results are compared with existing evaporation equations for surface-to-air concentration gradients and none of those equations studied was found to predict rates of evaporation satisfactorily. (auth)

41151 BACTERIOGENIC SULFUR ISOTOPIC RATIOS IN GEOLOGY. **Jensen, M. L. (Yale Univ., New Haven). Beitr. Mineral. Petrogr., 11: 405-14(1965).**

Stable sulfur isotopes may aid in distinguishing sulfides of a magmatic hydrothermal origin from sulfides containing biogenic sulfur. For those sulfide ore deposits that are intimately associated with the intrusive body from which it is inferred their ore solutions were derived, the variation in $\delta^{34}S$ values is generally less than ±5 per mill. Biogenic sulfides, on the other hand, exhibit a broad spread in $\delta^{34}S$ values that is rately less than a few per mill. The reason for this is that the sulfur produced, as hydrogen sulfide by anaerobic bacteria, is isotopically fractionated by variable amounts resulting in a relatively broad spread in $\delta^{34}S$ values. Raw culture experiments have illustrated the isotopic effects resulting from reduction of sulfate to hydrogen sulfate by sulfate reducing bacteria. The characteristics of enrichment of ^{32}S to a highly variable extent in hydrogen sulfide is verified by these experiments. In addition, a series of closed system raw culture experiments resulted in fractionation factors between 1.043 to 1.062 which are similar to variations in $\delta^{34}S$ between juxtaposed sulfides in nature produced by bacteriogenic processes. (auth)

41152 SEISMOLOGY AND FUNDAMENTAL GEOLOGY. **Thirlaway, Henry I. S. (Atomic Weapons Research Establishment, Aldermaston, Eng.). Discovery, 27: No. 5, 43-8(May 1966).**

A world-wide network of seismic installations has been developed to detect large underground nuclear explosions. These stations provide help in studies of the earth's structure and the dynamic processes involved in its evolution. (F.S.)

41153 ISOTOPIC EVIDENCE FOR UPPER-CAMBRIAN OR LOWER-ORDOVICIAN GRANITE EMPLACEMENT IN THE VIGO AREA, NORTHWESTERN SPAIN. **Priem, H. N. A.; Boelrijk, N. A. I. M.; Verschure, R. H.; Hebeda, E. H.; Floor, P. (Laboratorium voor Isotopen-Geologie, Amsterdam). Geol. Mijnbouw, 45: 36-40(Feb. 1966).**

Determinations were made of $^{87}Sr/^{86}Sr$ ratio, and total Sr and Rb contents on whole-rock samples and separated minerals from riebeckite granite-gneiss and biotite granite-gneiss. The specimens were collected along the coast 0.5 km south of La Guia, Vigo, and 0.5 km west of Rebullon, east of Vigo, respectively. The isotopic age determinations on the riebeckite granite-gneiss from the Vigo area indicated an emplacement age of 486 ± 24 Myr at least and 544 ± 16 Myr at the highest (Upper-Cambrian/Lower-Ordovician and Upper-Cambrian, respectively). Field evidence indicated that the emplacement of the riebeckite granite was younger than that of the biotite granite of the same area, for which an emplacement age of 500 ± 25 Myr is probable. The age of the latest metamorphic recrystallization was established to be 278 ± 10 Myr for the riebeckite granite-gneiss and 292 ± 15 Myr for the biotite granite-gneiss. The weighted mean for the time of latest Hercynian metamorphic recrystallization in this area was 282 ± 8 Myr (Upper-Carboniferous). This age accords well with the isotopic ages of late-Hercynian, post-tectonic granite emplacement and associated thermal metamorphism established elsewhere in north-western Spain and in Portugal. (BBB)

41154 DETERMINATION OF THE DENSITY OF ROCK BY THE γ-ABSORPTION METHOD USING A NARROW BEAM OF RAYS WITH THE SCINTILLATION COUNTER. **Volker, A. R. (Karl-Marx-Univ., Leipzig). Geophys. Geol., Folge 7: 84-95(1965). (In German).**

The physical principles of the γ-absorption technique are reviewed, and the possibilities for application of the γ collimation method in practice are outlined. The construction of apparatus and choice of operating conditions for individual γ-absorption investigations are outlined, and the apparatus used for determination of density of rock is illustrated schematically. Time resolution is 12.6 μsec, geometry factor is 1.02×10^{-4}, total null effect is 300 imp/min through 57 mm Pb. Distance from sample to detector was 350 mm; 2 mm bore in the sample and 4 mm in the detector crystal serve to collimate the photon beam. Determination of density of rock in the air-dried state is outlined. Data by this method are compared with results from the hydrostatic method, and a set of calibration curves is prepared. Comments on the water content determination of lignite by this technique and on the determination of moist raw density and water content using neutron and γ rays are given. One hundred four references are cited. (BBB)

41155 EARTHQUAKE OR EXPLOSION? THE SCIENCE OF NUCLEAR TEST DETECTION. **Lindgren, Nilo. IEEE (Inst. Elec. Electron. Eng.), Spectrum, 3: 66-75 (Aug. 1966).**

Problems of underground detection and identification are outlined. Criteria whereby underground events are discriminated are given and the present state of the art is assessed. The Large Aperture Seismic Array is described, and its use in the detection of earthquakes and underground explosions is described. (F.S.)

41156 TWO-PROBE NUCLEAR DEVICE FOR DETERMINING THE DENSITY OF SEDIMENTS. **McHenry, J. Roger (Dept. of Agriculture, Oxford, Miss.). pp 189-202 of International Association of Scientific Hydrology. Land Erosion, Precipitation, Hydrometry, Soil Moisture. Ghent-Brugge, Belgium. 1964.**

The development, calibration, testing, and application of a dual probe employing radioactivity for the measurement of sediment density and concentration in situ are described. The dual-probe system used consisted of a γ source, a scintillation detector, a fixed dual access-tube assembly for spacing the probe and source, and a suitable power supply and electronic read-out device. The γ radiation was produced by a 7-mC ^{137}Cs source placed in the smaller access tube. The detector was a sodium iodide (thallium-activated) scintillation crystal and the electronic read-out system employed a modified integral discriminator so that only the γ rays exceeding 0.65 Mev were recorded by the scaler-ratemeter. Excellent precision and accuracy were obtained with the dual probe in lab experiments. The maximum thickness of the measured volume of sediment was less than 1-in., permitting the use of this technique for measurement of densities of thin sediment layers and at phase interfaces. The performance of the dual probe was compared in a field survey with the single probe which utilizes the reflection technique of measuring γ attenuation. The dual probe performed satisfactorily in the field and in addition offered the advantage of determining densities of narrow sediment bands and at interfaces. Sediment densities were determined at 1-in. intervals through sediments up to 3 ft deep beneath as much as 15 ft of water. In its present state of development the dual probe is not as rugged as the γ probe and is not recommended for use in routine field surveys. However, the dual probe provides the means of measuring accurately the variation of density within a sediment and near interfaces and as such extends the utility of the γ attenuation method of measuring sediment density. (BBB)

41157 APPLICATION OF DELAYED NEUTRONS FOR CORELESS DETERMINATION OF URANIUM CONTENT IN BOREHOLES. **Igumnov, S. A. (Vakhrushev Mining Inst., Sverdlovsk, USSR). Izv. Vyssh. Ucheb. Zaved., Gorn. Zh., 9: No. 2, 3-6(1966). (In Russian).**

A polonium-beryllium neutron source (10^7 n/sec) was inserted into a model borehole containing water for determination of U content. The neutron source was removed after 15 sec and replaced with a scintillation counter (B + ZnS) to determine the delayed neutrons due to the fission of ^{235}U. It was concluded that, for the ores containing ~0.5% U, an accuracy of 15% in the determination of U could be achieved in 20–30 min with the neutron source emitting 2×10^7 n/sec. (R.C.K.)

41158 AMPLITUDE VARIABILITY OF EXPLOSION WAVES AT LONG RANGES. Reed, Jack W. (Sandia Lab., Albuquerque, N. Mex.). J. Acoust. Soc. Amer., 39: 980-1(May 1966). (SC-R-66-886).

Three airburst high-explosive calibration shots were fired at H − 2, H + 4, and H + 7 min to determine the air-blast wave amplitude transmitted from an underground nuclear test. Microbarograms, made at long range from the three 10^9-g high explosives, were compared to show atmospheric propagation variability. Records made at 40–250-km ranges gave amplitude repeatability with a logarithmic-normal standard deviation of 0.49. (F.S.)

41159 RADIOMETRIC AGES OF SOME PRECAMBRIAN ROCKS FROM THE NORTHWEST DIVISION OF WESTERN AUSTRALIA. Leggo, P. J. (Bureau of Mineral Resources, Canberra); Compston, W.; Trendall, A. F. J. Geol. Soc. Austral., 12: 53-66(1965).

The $^{87}Rb/^{86}Sr$ and $^{87}Sr/^{86}Sr$ ratios are reported in the course of age measurements for acid volcanic rocks, a tuffaceous siltstone, and two granites, all of Precambrian age, from the northwest division of Western Australia. On field evidence these samples are of the same age, so that the Rb–Sr data were interpreted as giving ~2100 Myr for this age, assuming a variation in initial $^{87}Sr/^{86}Sr$ ratio of 0.700 to 0.720. The tuffaceous siltstone, from the overlying Wyloo Group, has a maximum indicated age of 1850 Myr. This value is subject to uncertainty since only one sample was analyzed, but nevertheless it is significantly younger than the Woongarra Volcanics, in accordance with its stratigraphic position, and it is likewise consistent with concordant total-rock and mineral ages of 1720 Myr measured in the Boolaloo Granite, which is intrusive into the Syloo Group. Owing to suspected later metamorphism only broad limits of 2300 to 3000 Myr can be set for the age of an Archaean granite which is older than the oldest Proterozoic sediments. Two previously unpublished U–Pb and Rb–Sr ages from the same area are also reported. (BBB)

41160 USE OF TRITIUM TO MEASURE THE MOVEMENT OF GROUNDWATER TOWARD IRRIGATION WELLS IN WESTERN FRESNO COUNTY, CALIFORNIA. Haskell, E. E. Jr. (Dept. of Agriculture, Fresno, Calif.); Leventhal, J. S.; Bianchi, W. C. J. Geophys. Res., 71: 3849-59(Aug. 15, 1966).

The tritium content of water from irrigation wells along two east-west traverse lines was used in estimating groundwater velocities in the San Joaquin Valley. Tritium peaks due to nuclear weapons tests were identified within the groundwater body. The estimated velocities were comparable with velocities expected in the coarse parts of the aquifers. The ratio of tritium in the well water to that in the rain was inconsistent with predicted recharge, indicating that recharge was localized and that water flowed to the sampled wells through the coarse aquifers. (auth)

41161 ORIGIN OF SALINE FORMATION WATERS. 1. ISOTOPIC COMPOSITION. Clayton, R. N. (Univ. of Chicago); Friedman, I.; Graf, D. L.; Mayeda, T. K.; Meents, W. F.; Shimp, N. F. J. Geophys. Res., 71: 3869-82 (Aug. 15, 1966).

The content of total dissolved solids and δD and $\delta^{18}O$ values are given for 95 oil-field brines from the Illinois, Michigan, and Alberta basins and the Gulf Coast. The variation in deuterium content among basins is found to be much greater than that within each basin. Oxygen isotopic composition, on the other hand, shows a large range in each basin, strongly correlated with salinity. The relationships between isotopic and chemical compositions of the brines lead to the following conclusions: (a) the water is predominantly of local meteoric origin; (b) the deuterium content has not been greatly altered by exchange or fractionation processes; (c) extensive oxygen exchange has taken place between water and reservoir rocks. Several samples contain water which appears to have originated as precipitation during Pleistocene glacial periods. (auth)

41162 RARE-GAS CHRONOLOGY OF CALCIUM-RICH ACHONDRITES. Megrue, G. H. (Brookhaven National Lab., Upton, N. Y.). Contract AT(30-2)-Gen-16. J. Geophys. Res., 71: 4021-7(Aug. 15, 1966). (BNL-9963).

The isotopes of He, Ne, and Ar from pyroxene and feldspar concentrates of the Estherville mesosiderite and Haraiya, Juvinas, Shergotty, and Stannern achondrites were analyzed. Concordant K-Ar ages of 3.6×10^9 years (Haraiya) and 4.0×10^9 years (Estherville, Juvinas, Shergotty, Stannern) indicate that diffusion of radiogenic Ar after crystallization has been negligible. One separate of the severely shocked Shergotty meteorite gave an age of 2.2×10^9 years, which may represent the time at which the meteorites broke up. Cosmic-ray exposure ages have been calculated from the ^3He and ^{21}Ne content of the pyroxene separates and production rates derived from the pyroxene data of the Estherville mesosiderite. The radiation ages vary between 10 My (Juvinas) and 60 My (Shergotty). Haraiya and Stannern have similar radiation ages of 32 My. The age values of Juvinas and Stannern was greater than were found in previous determinations made on the entire meteorite. This is primarily the result of recent ^3He and Ne diffusion from feldspar. U and ^4He concentrations from pyroxene and feldspar concentrates of the Estherville mesosiderite can be altered by simple leaching. This suggests that U is associated with a highly soluble mineral such as whitlockite. Interpretation of the thermal history of the parent body from (U, Th)-He ages may be incorrect because the loss of radiogenic ^4He accompanying the recent diffusion of cosmogenic ^3He and Ne is unknown. (auth)

41163 ISOTOPIC AGES FROM SOUTHWESTERN MONTANA. Giletti, Bruno J. (Brown Univ., Providence). J. Geophys. Res., 71: 4029-36(Aug. 15, 1966).

Potassium–argon and rubidium–strontium age measurements for the southwest Montana basement show that a regional metamorphism occurred 1.6 ± 0.1 gigayears (Gy) ago and was accompanied by igneous intrusion (Dillon granite gneiss). The southeastern margin of this metamorphism is found in the Gravelly Range and the Gallatin River canyon. Rocks to the southeast of the margin yield ages from 2.1 to 3.2 Gy. Some of the gneisses in the 1.6-Gy terrane may be 3.1 Gy old. The Laramide Boulder and Tobacco Root batholiths sharply reduced the isotopic ages of the Precambrian rocks they intruded in a narrow belt around their contacts. Deposition of the Belt series postdates the 1.6-Gy age. (auth)

41164 DISTRIBUTION IN FRACTURE PERMEABILITY OF A GRANITIC ROCK MASS FOLLOWING A CONTAINED NUCLEAR EXPLOSION. Boardman, C. R.; Skrove, J. (Univ. of California, Livermore). J. Petrol. Technol., 619-23(May 1966). (UCRL-14292(Rev.2)).

In situ permeability of the rock outside the Hardhat chimney was determined by pressurization of long holes with air. Experimental data indicated a remarkable difference between fracture permeability of the rock near the chimney and that at a considerable distance. Although permeable fault zones were known to exist in the granite stock, the measurements of background permeability were quite low, on the order of tenths to several millidarcies. The observed difference is about two or three orders of magnitude above this background in the region 125 to 215 ft radially from the shot point, or 80 to 165 ft radially from the vertical axis of the chimney. The presence of a collapsed drift immediately beyond this region precluded measurements which could have defined the maximum extent of the zone of high permeability. (auth)

41165 ELECTRODE CALIBRATION FOR NUCLEAR DIAGRAPHY. Comanescu, V.; Oncescu, M.; Sandru, P.; Topa, A. Teh. Nucl., 8: 289-94(June 1965). (In Rumanian).

A new method for electrode calibration was tested to compare the diagraphs obtained from oilwells prospected by gamma spectrometry with those of electrodes. Basically the method consists in drawing the calibration line for gamma rays of various energies and following the stability

of that line. ^{203}Hg, ^{131}I, ^{198}Au, ^{137}Cs, ^{22}Na, ^{65}Zn, and ^{60}Co were used as gamma sources. After calibration, the spectrometric gamma electrode may be used for prospecting and for operations involving the simultaneous injection of gamma-active tracers in oil well holes. (R.C.K.)

41166 APPLICATION OF NEUTRON-CAPTURE γ SPECTROSCOPY FOR ANALYTICAL PURPOSES ESPECIALLY FOR BORE-HOLE EXPLORATION OF IRON ORE. Loetzsch, W. Freiberg i. B., Bergakademie, 1965. 108p. $2.00 Gmelin, AED-Diss. 65-344.

Thesis.

The design and construction of a neutron capture spectrometer for use in bore holes are described. PoBe is used as neutron source. High energy count rate (>7 Mev) is proportional to iron content. Results are compared with data from samples irradiated in a reactor beam, and iron contents of samples from several iron mines are reported. (Gmelin Inst.)

41167 TRITIUM MEASUREMENTS OF SUBTERRANEAN WATERS IN SOME SOUTH AFRICAN SITES. Verhagen, B. Th.; Sellschop, J. P. F. (Univ. of the Witwatersrand, Johannesburg). 3p. (CONF-650652-20). ORAU. Gmelin, AED-CONF-66-176-2.

From 6th International Conference on Radiocarbon and Tritium Dating, Pullman, Wash.

A counting system used in tritium measurement of subterranean water supplies in South Africa is described. The system consists of a gas proportional counter shielded by an anticoincidence ring of G-M counters. The system is not able to go below 5 TU. (F.S.)

41168 PROBLEMS IN THE ENRICHMENT OF TRITIUM BY THE THERMAL DIFFUSION TECHNIQUE. Verhagen, B. Th.; Sellschop, J. P. F. (Univ. of the Witwatersrand, Johannesburg). 21p. (CONF-650652-21). ORAU. Gmelin, AED-CONF-66-176-1.

From 6th International Conference on Radiocarbon and Tritium Dating, Pullman, Wash.

Thermal diffusion equipment for low-level assay of natural waters is described. The TD column consists of two vertical concentric tubes, the inner heated and the outer cooled. The mixture of gas is introduced between the tubes. Superposition of horizontal mass separation and vertical convection set up a vertical concentration gradient, the heavier molecules collect near the bottom. The enrichment is independent of the concentration tested. (F.S.)

41169 AMPLITUDES AND ENERGIES OF PRIMARY SEISMIC WAVES NEAR THE HARDHAT, HAYMAKER, AND SHOAL NUCLEAR EXPLOSIONS. Trembly, Lynn D.; Berg, Joseph W. Jr. (Oregon State Univ., Corvallis). 22p. (CONF-650448-1). ORAU. Gmelin, AED-CONF-65-227-1.

From Seismological Society of America, Annual Meeting, St. Louis.

Records of near-source (0.3 to 20 km) primary seismic waves generated by the Hardhat, Haymaker, and Shoal underground nuclear explosions were analyzed in terms of displacement amplitude and energy variations with distance. The observed data were compared to similar data from a theoretical source model to determine the adequacy of the theoretical model. There was evidence that a long-period displacement field existed near the explosions as predicted by the theoretical source. Scatter in the observed amplitude data made it difficult to distinguish between the long-period and the radiation fields. The variation of total energy of the observed primary seismic waves with distance showed the presence of the long-period field. The comparison of observed and theoretical data indicates that a theoretical elastic source model approximated the observed sources. (auth)

41170 SYSTEM FOR DETERMINING FLUID FLOW RATE IN BOREHOLES. Cobb, Lewis A.; Marshall, Wilton R.; Sumner, Cyril R.; Walker, Terry (to Halliburton Co.). U. S. Patent 3,255,347. June 7, 1966. Filed Nov. 20, 1962.

In a well logging system for measuring flow rates of fluids within a borehole, an elongated logging tool is adapted for suspension within the borehole by means of a wireline from the earth's surface and tracer ejector means and radioactive detector means are mounted on the tool. At the upper end the tool is provided with a bore having its axis inclined with respect to the axis of the tool. Detector means are provided on the tool and below the bore. A decentralizer means on the tool is arranged to urge the tool against the wall of the borehole and to angularly orient the tool so that the radial plane extends substantially diametrically through the borehole. In response to signal communication from the earth, a seal is destroyed and the material is expelled from the bore into the fluids at high velocity as compared to the fluid velocity in the borehole in a generally downward direction towards the detector means. The detectors serve to note the rate of fall of the tracer as it passes the detectors. (B.L.M.)

41171 APPARATUS FOR NUCLEAR WELL LOGGING WHILE DRILLING. Scherbatskoy, Serge A. U. S. Patent 3,255,353. June 7, 1966. Filed Dec. 21, 1962.

An anticipatory type well logging apparatus is adapted to provide the driller not only with information about the formation traversed by the borehole but also with information concerning the unpenetrated formation below the bottom of the borehole toward which the drilling is proceeding. The apparatus comprises a drill string, a drill bit, a gamma source within the drill string for irradiating the formations below the end of the borehole, a directionally sensitive radiation detector within the drill string positioned to respond preferentially to gamma rays emitted from below the drill bit and directed upwardly. The information derived from the output of the detector is transmitted to a point outside the borehole. (B.L.M.)

Thorium and Uranium Minerals

41172 NOTES ON THE MINERALOGY OF SWEDEN. 4. NEW DISCOVERIES OF SECONDARY URANIUM MINERALS. Welin, Eric. Ark. Mineral. Geol., 4: 267-75 (1966).

The occurrence of secondary U minerals in Sweden is very sparse. Some uranyl carbonates (andersonite, liebigite and schroeckingerite) are very recent depositions on the walls of the drifts in Stripa iron ore mine. The present investigation has shown the presence of six other secondary minerals (uranophane, beta-uranophane, zippeite, vandendriesscheite, phosphuranylite and kasolite). These minerals occur as coatings along cracks in the matrix adjacent to the radioactive minerals or as coatings along joint planes or on the surface of outcropping igneous rocks, which have a slight content of uraniferous minerals, usually uraninite. Secondary U minerals on the surface of rock outcrops are of postglacial age, but this may not be the case for those on joint planes and cracks. (auth)

41173 ACCESSORY THOROURANINITE IN TUVA NEPHELINE SYENITES. Kapustin, Yu. L. At. Energ. (USSR), 20: 501-6(June 1966). (In Russian).

Data on the detection of uraninites in nepheline syenites in Tuva are reported. The uraninites displayed two generations and were characterized by anomolous composition; hexavalent uranium and lead were absent. The uraninite investigated contained only 27% ThO_2, which is unusual. The minerals have the cerium composition of rare earths. With respect to physical properties, the minerals are close to the theoretical compound $(U, Th)O_2$. (tr-auth)

41174 RADIOACTIVITY OF PHOSPHORITES. Bliskovskii, V. Z.; Smirnov, A. I. Geokhimiya, No. 6, 744-7 (June 1966). (In Russian).

The increased radioactivity of phosphorites to the crust is due to the presence of uranium and its decay products. This problem was further investigated on Siberian and Kazakhstan phosphorites, determining the composition of the ore and the gangue in the weathering products. It was found that activity at great depths is usually lower than on

the surface. The increased uranium concentration was assumed to have originated in marine sedimentation and weathering zones. The easily sorbed U^{4+} may enter the crystal lattice by being replaced by the Ca^{2+} ion. Weathering results in the leaching out of carbonates and oxidation of pyrites, resulting in an increase of the radioactivity in areas near cracks. During the second stage, the fluorocarbonate apatite is recrystallized into fluoro apatite. During later stages of weathering, the apatite lattice is decomposed and calcium–aluminum phosphates with increased uranium and rare-element content are formed. This increased content renders this mineral a potential source for uranium. Geophysical and radiometric prospecting methods are useful for weathered locations. (TTT)

41175 URANIUM AND ARSENIC IN HYDROTHERMAL PROCESS. Boytsov, V. E.; Kaykova, T. M. Int. Geol. Rev., 8: 912-17 (Aug. 1966).

An account is given of the peculiarities of the geologic structure of hydrothermal uranium deposits and of the mineral composition of their ores. The deposits belong to the sulfide-uranium category. Mineralization occurred in stages. The peculiarity of the ore composition lies in the extensive development of native arsenic, forming a paragenetic association with pitchblende. Analysis of the mineral composition of the ores and of the patterns of paragenesis formation suggests the presence of a high arsenic concentration in the hydrothermal solutions from which the pitchblende was deposited. The most important characteristic of the deposits described is the extensive development of a quartz-pitchblende-native arsenic association in the veinlets of the ore stage. This association is possibly accompanied also by coffinite, particularly in the ores from deposits situated at the exocontact. The solutions from which the pitchblende was deposited were at first distinguished by a high sulfur concentration and, slightly later and before the end of the period of pitchblende deposition, by a high concentration of successively oxidized arsenic. This is shown by the fact that in the successively formed arsenical minerals As^{1-} (in arsenopyrite) alternated with As (in native arsenic), while As^{3+} appeared (in realgar) after the separation of pitchblende. Such arsenical minerals as native arsenic and realgar provide indirect evidence that the deposits formed at a small depth. Evidently these minerals and pitchblende were deposited from the hydrothermal solutions at low temperatures. (BBB)

41176 EVALUATION OF THE DECAY CONSTANT OF ^{235}U FROM LEAD ISOTOPE RATIOS. Banks, Philip O. (Western Reserve Univ., Cleveland); Silver, Leon T. J. Geophys. Res., 71: 4037-46 (Aug. 15, 1966).

The decay constant of ^{235}U has been evaluated from the radiogenic $^{207}Pb/^{206}Pb$ ratios of several cogenetic fractions of zircon and uranothorite, analyzed by conventional mass spectrometric methods. Variation of the $^{206}Pb/^{238}U$ apparent ages among the mineral fractions demonstrates that some form of isotopic disturbance has occurred during their geologic history. Arguments are presented to show that the method of calculating λ_{235} is relatively insensitive to such disturbances because of the young geologic age of the samples and the probability that zircon and uranothorite experience isotopic disturbance by partial loss of Pb. Inaccuracy in the calculated value is further reduced by deducing, from geologic and isotopic considerations, the most likely limits to the apparent ages to which the $^{207}Pb/^{206}Pb$ ratios should correspond. Although the uncertainties in the method do not permit a unique derivation of the decay constant, the results suggest that the currently accepted value is probably accurate to within 1%, relative to the accepted values for the decay constant of ^{238}U and the isotopic composition of natural U. (auth)

HEALTH AND SAFETY

See also BIOLOGY AND MEDICINE — Radiation Hazards and Protection
GEOLOGY, METEOROLOGY, AND MINERALOGY — Natural Radioactivity and Fallout

Refer also to abstracts 40691, 40738, 41220, 41234, 41540, and 42677.

41177 (AD–632211) OPERATIONAL AND MANAGEMENT ASPECTS OF PERIPHERAL RADIOLOGICAL COUNTERMEASURES. Final Report. Van Horn, William H. (URS Corp., Burlingame, Calif.). Mar. 1966. 153p. (USNRDL-TRC–5; URS–646–4). CFSTI $5.00 cy, $1.00 mn.

The four peripheral countermeasures studied, postattack evacuation, applied shielding, dose equalization (including group shielding), and exposure scheduling, can be used by the local civil defense organization to provide a significant degree of control over radiation exposure during the early postattack period, resulting in the reduction of dose to personnel and/or the time of emergence from shelter. Operational constraints on the implementation of peripheral countermeasures can be lessened by a limited preattack planning effort on the part of the local civil defense organization. Such planning includes recognition of postattack demands for peripheral countermeasures and the probable response capability. Postattack implementation of peripheral countermeasures, although optimized by preattack planning, can be accomplished using planning aids and procedures, developed in the report, which permit the rapid evaluation of available inputs. These aids emphasize predicting dose (both accumulated dose and equivalent residual dose) for complex radiological environments. Response time, which is a major management constraint, can best be minimized by delegating authority for local action to the lowest echelon, normally the shelter itself. It is concluded that the planning necessary for the use of peripheral countermeasures can be integrated into the present civil defense organization with relatively minor difficulty, resulting in an appreciable payoff in postattack capabilities. (auth)

41178 (AD–635547) FALLOUT SIMULANT DEVELOPMENT: THE SORPTION REACTIONS OF CERIUM, CESIUM, RUTHENIUM, STRONTIUM, AND ZIRCONIUM–NIOBIUM. Lane, William B. (Stanford Research Inst., Menlo Park, Calif.). Nov. 1965. Contract N228-(62479)65414. 30p. CFSTI $2.00 cy, $0.50 mn.

This report describes the preparation of synthetic fallout. Methods are discussed for simulating selected properties of radioactive fallout so that experiments can be conducted to evaluate radiological hazards. The experiments measured solubility of radionuclides which would be available to cycle in the food chains. Heating the fallout particles to high temperatures reduced the solubility of all nuclides studied. The methods described can be used by other researchers to prepare synthetic fallout with selected solubility and availability properties. (auth)

41179 (AD–635821) RADIOLOGICAL RECOVERY REQUIREMENTS, STRUCTURES, AND OPERATIONS RESEARCH. VOLUME I. GENERAL CONSIDERATIONS. Final Report. Ryan, J. T.; Johnson, T.; Walker, S. M. (Research Triangle Inst., Durham, N. C.). June 6, 1966. Contract N228(62479)-68153. 94p. (USNRDL-TRC–16 (Vol.1)). CFSTI $3.00 cy, $0.75 mn.

The application of decontamination strategies to extensive urban areas is discussed. Urban areas of various sizes (from a few acres to an interconnected system involving hundreds of acres) are examined with regard to decontaminating vital sections and their connecting links. The task of creating decontaminated islands of marshaling areas is determined to be feasible. The nature and scope of command and control system elements required for conducting effective decontamination in practical situations is determined together with the preattack and postattack data required by such a system. Several models were developed and are discussed. (auth)

41180 (AD–635822) RADIOLOGICAL RECOVERY REQUIREMENTS, STRUCTURES, AND OPERATIONS RESEARCH. VOLUME II. DEVELOPMENT OF ANALYTICAL, COMPUTER, AND SYSTEMS MODELS IN SUPPORT OF DECONTAMINATION ANALYSES. Final Report. Ryan, J. T.; Johnson, T. (Research Triangle Inst., Durham, N. C.). June 6, 1966. Contract N228(62479)-68153. 243p. (USNRDL-TRC–16(Vol.2)). CFSTI $6.00 cy, $1.25 mn.

The cost and effectiveness of the radiological decontamination of urban areas in the event of radiological warfare were analyzed. Analytical, computer, and systems models used in the analysis are presented. These include models for approximating gamma ray intensity at a single detector location, a feasibility study of the application of analog computers to the analysis of decontamination, a FORTRAN program for decontamination analysis, and a study of the nature and scope of command and control systems required for conducting effective decontamination in municipalities. (C.H.)

41181 (AD–635823) RADIOLOGICAL RECOVERY REQUIREMENTS, STRUCTURES, AND OPERATIONS RESEARCH. VOLUME III. DECONTAMINATION ANALYSIS OF SELECTED SITES AND FACILITIES IN SAN JOSE, CALIFORNIA. Final Report. Walker, S. M. (Research Triangle Inst., Durham, N. C.). June 6, 1966. Contract N228(62479)-68153. 240p. (USNRDL-TRC–16(Vol.3)). CFSTI $6.00 cy, $1.25 mn.

The cost and effectiveness of the radiological decontamination of urban areas in the event of radiological warfare were analyzed. Sixteen sites and facilities located in San Jose, California, were selected for study. Facilities decontaminated include a telephone company, a pharmaceutical laboratory, a bus depot, a newspaper office, and the like. Supporting data related to the decontamination analysis are presented. (C.H.)

41182 (AD–635824) RADIOLOGICAL RECOVERY REQUIREMENTS, STRUCTURES, AND OPERATIONS RESEARCH. VOLUME IV. DECONTAMINATION ANALYSIS OF SELECTED SITES AND FACILITIES IN DETROIT, MICHIGAN. Final Report. Ryan, J. T. (Research Triangle Inst., Durham, N. C.). June 6, 1966. Contract N228(62479)-68153. 285p. (USNRDL-TRC–16(Vol.4)). CFSTI $6.00 cy, $1.50 mn.

The cost and effectiveness of the radiological decontamination of urban areas in the event of radiological warfare were analyzed. Twelve sites and facilities located in Detroit, Michigan, were selected for study. Facilities decontaminated include a hospital, department store, water pumping station, a power plant, an airport, a public building, and the like. Supporting data related to the decontamination analysis are presented. (C.H.)

41183 (AD–635931) AREA-WIDE SHELTER SYSTEMS. Condit, Richard I. (Stanford Research Inst., Menlo Park, Calif.). Dec. 1965. 370p. CFSTI $6.00 cy.

Many reports of previous research describe particular aspects of civil defense, such as identifying fallout protection in existing buildings, designing new blast shelters, providing warning, ensuring emergency communications, etc. — detailed considerations of restricted subject areas. This report is broader in nature, combines such partic-

ularized results, and shows how the people of a region may make integrated arrangements for community protection—how they may develop area-wide shelter systems. It describes the general principles of community-wide protection, while applying them specifically to the City of San Jose, California. Based on the knowledge of what it takes to provide various degrees of protection from the effects of nearby and distant nuclear explosions, the planning of area-wide shelter systems starts with an inventory of the existing community resources of possible value for protection. In San Jose, this includes the results of the National Fallout Shelter Survey, improving those spaces with additional ventilation, and upgrading them against blast and fire; home basements; special facilities; covered storm drains; and the protection potential of creeks and standing water. To these are added the possibilities for new construction, stretching from emergency trenches and fox holes to carefully prepared blast and fallout shelters. Eight area-wide shelter systems are worked out and presented for San Jose—four for protection against direct effects and fallout, and four for protection against radioactive fallout only. Both sets of four attempt to span the range of possibilities from doing the best you can with what you have, to building a new system to fit the needs. Accompanying procedures for increasing emergency-readiness in case of a warning rise in international tensions are also indicated. (TCO)

41184 (AD–637806) SHELTER HABITABILITY IN EXISTING BUILDINGS UNDER FIRE EXPOSURE. Summary of Research Report. Waterman, Thomas E. (IIT Research Inst., Chicago, Ill.). June 1966. Contract N228(62479) 68355. 148p. (NRDL-TRC–16). CFSTI $4.00 cy, $1.00 mn.

Experiments were performed in full scale buildings to obtain information regarding the habitability of fallout shelters in existing buildings under fire exposure. One two-story and two three-story buildings of masonry and wood joist construction were used. The fire load of the room of fire origin consisted of a large crib (2 × 4 inch lumber) with the remainder of the structures loaded with furniture typical of residential construction. In two of the buildings, the spread of heat, smoke and toxic gases was monitored throughout the buildings for fires contained within one room. In the other building, conditions (temperature, pressure, and CO concentration) were monitored in and around a fire-resistive basement shelter during complete burnout of the structure. Radiant heat fluxes emitted at window openings were measured in all of the experiments. Results indicate that oxygen depletion in an active fire zone will be reproduced throughout interconnecting spaces. Carbon monoxide concentrations of 75 percent of those in the active fire zone were found at places removed from the fire but on the same or higher levels. For these buildings, wind-induced pressure differences were greater than fire-induced pressure differences and thus would have had greater effect on the infiltration of fire gases through shelter barriers. The long lasting effects of debris fires in contact with the shelter were found to produce dangerous heating of the shelter. In addition to other pertinent observations, the experiments have also demonstrated that local fire and engineering services, if given proper guidance, can collect meaningful data from building burns. (auth)

41185 (AECL–2594) TRITIUM HAZARDS. Bush, W. R. (Atomic Energy of Canada Ltd., Chalk River, (Ontario). Chalk River Nuclear Labs.). June 1966. 16p. Dep. mn. AECL $0.50.

This publication is based on various talks on the radiation hazards of tritium oxide which have been given by the author to process operators and supervisors, to laboratory technicians, and to mechanical tradesmen. The absorption of tritium oxide into the body through the skin and lungs, its excretion in urine, and the administrative controls ("removal, caution, minor and negligible") are described. The concentration of tritium in air, expressed as $(MPC)_a$, and the radiation dose resulting from a number of $(MPC)_a$-hours of exposure are explained. Finally, the methods for protecting against tritium (ventilation, air-supplied masks, and plastic clothing) are discussed. (auth)

41186 (ARCRL–15) RADIOACTIVITY IN MILK, 1965. Interim Report. Bruce, R. S. (ed.) (Agricultural Research Council, Wantage (England). Radiobiological Lab.). Feb. 1966. 10p. Dep. mn. BIS $0.50. HMSO 2s. 6d.

Measurements of strontium-90 and cesium-137 in milk show that the downward trend in the levels of contamination continued between July and December 1965. The average ratio of strontium-90 to calcium in milk from throughout the United Kingdom during 1965 was 19 pCi ^{90}Sr/g.Ca; the mean concentration of cesium-137 was 98 pCi/litre. Both figures are about two-thirds of the values in 1964. (auth)

41187 (BNL–9468) INTERPRETATION OF MICROBEAM EXPERIMENTS FOR MANNED SPACE FLIGHT. Curtis, Howard J. (Brookhaven National Lab., Upton, N. Y.). [1965]. Contract AT(30-2)-Gen-16. 15p. (CONF-650924–1). Dep. mn. CFSTI $1.00 cy, $0.50 mn.

From Workshop Conference on Space Radiation Biology, Berkeley, Calif.

Previously reported work with a deuteron microbeam, which simulates the biological action of heavy particles, has shown 1) that the brain is very insensitive to this type of radiation, 2) that the epithelial cells of the lens of the eye are quite sensitive, but it takes more than a very few abnormal cells to form a cataract and 3) the hair follicles are quite sensitive, and a relatively small dose will cause the hair from an irradiated follicle to turn gray. These results are quite in accord with modern concepts in radiobiology which have been deduced from many different kinds of experiments. From these considerations one can estimate the effect of these particles on other organs of the body. It is then possible to predict with considerable confidence from the known fluxes that the heavy cosmic ray particles will not constitute an appreciable hazard for space flights of some months duration. (auth)

41188 (BNWL–235-1) PACIFIC NORTHWEST LABORATORY ANNUAL REPORT FOR 1965 IN THE PHYSICAL SCIENCES. VOLUME 1. ATMOSPHERIC SCIENCES. Pearce, D. W.; Green, J. K. (eds.) (Battelle-Northwest, Richland, Wash. Pacific Northwest Lab.). May 1966. Contract AT(45-1)-1830. 38p. Dep. mn. CFSTI $2.00 cy, $0.50 mn.

Washout coefficients for inorganic iodides present in process stock gases were measured in three snowfalls and one rainfall. Results indicated a linear relation of scavenging and snowfall rate. Organic iodides were scavenged in rainfall with only about 1% of the inorganic iodides. A pair of equations are presented for use in the prediction of exposures from an elevated particulate source in which plume width and height parameters are related to travel time. Modifications of the grid consisting of data gathering stations on and peripheral to the Hanford reservation are reported. Data on wind, temperature, and radiation are integrated on a real-time basis and radio-telemetered to an accumulation and print-out facility where the hourly data of all stations are automatically programmed for incorporation into climatological data for use in hazards evaluations, diffusion experiments, and related studies. Data on the spectral distribution of atmospheric turbulence during the past two years are presented. A Beechcraft A-Queen-Air-80 aircraft was fitted with a zinc sulfide detection system to permit the use of the aircraft in atmospheric diffusion studies involving zinc sulfide tracer. Installation and calibration of the detection equipment are described. A MIDAS (Modified Integral Digital Analog Simulator) computer program was prepared for use in evaluation of evaporative losses of falling rain drops. A MIDAS computer program was also prepared for use in calculations of stream functions for long-range trajectory construction on constant-entropy surfaces. (C.H.)

41189 (CEA-R–3020) LES RETOMBEES RADIOACTIVES EN FRANCE APRES LA SECONDE EXPLOSION NUCLEAIRE CHINOISE: PROCESSUS DE TRANSFERTS

ATMOSPHERIQUES. (Radioactive Fallout in France After the Second Chinese Nuclear Explosion: Atmospheric Transfer Processes). Doury, Andre; Bourgeon, Pierre (Commissariat a l'Energie Atomique, Fontenay-aux-Roses (France). Centre d'Etudes Nucleaires). May 1966. 32p. Dep. mn.

The products liberated into the atmosphere by the second Chinese nuclear explosion were detected and measured in France during the months of May, June and July 1965. The main results are presented here and discussed. They are considered in particular in the light of the meteorological conditions as a function of the most recent hypotheses concerning transfer processes. (auth)

41190 (CONF-660621-4) PORTABLE INSTRUMENTATION FOR DETECTION OF MAXIMUM PERMISSIBLE BURDEN OF INSOLUBLE ^{60}Co LUNG CONTAMINATION. Zendle, R.; Feinberg, R. J. (Knolls Atomic Power Lab., Schenectady, N. Y.). June 28, 1966. Contract W-31-109-eng-52. 18p. Dep. mn. CFSTI $1.00 cy, $0.50 mn.

From Health Physics Society, 11th Annual Meeting, Houston, Tex.

A procedure for in vivo detection of small quantities of insoluble ^{60}Co contamination in human lungs was tested for sensitivity. A masonite phantom was constructed to simulate the geometry and density of the chest and lungs. A variety of sources were prepared of known ^{60}Co activity which were placed in the phantom to simulate various distributions and quantities of insoluble lung contamination. A portable scintillation probe survey meter with a 2 × 2-inch NaI(Tl) detector was used to measure the ^{60}Co γ response at the surface of the phantom versus the quantities placed in the phantom. It was concluded that, in the prevalent natural background of .02 mR/hr, the procedure and instrument used reliably indicated the presence of 0.1 microcuries of ^{60}Co in the phantom regardless of its distribution, with the unshielded detector at the surface of the masonite. The investigation included calculations that showed that the maximum permissible lung burden may be estimated as about 1.2 μC of insoluble ^{60}Co and that at least 10 percent of this activity deposited originally would probably remain in the lungs for six months. (auth)

41191 (HUX-3170-1) ANALYSIS OF BONE SAMPLES FROM PATIENTS WITH PROVEN OSTEOGENIC SARCOMA FOR NATURALLY-OCCURRING RADIOISOTOPES. ANALYSIS OF SOFT TISSUES FOR ALPHA-EMITTING RADIOELEMENTS, WITH PARTICULAR REFERENCE TO POLONIUM INHALED IN CIGARETTE SMOKE AS A SOURCE OF RADIATION EXPOSURE. Final Report, March 1, 1963–June 30, 1966. Whittenberger, James L. (Harvard School of Public Health, Boston, Mass.). Contract AT(30-1)-3170. 60p. Dep. mn. CFSTI $3.00 cy, $0.75 mn.

The studies described in this report, with one exception, have been concerned with low levels of naturally-occurring radioelements, levels normally found in our environment. The concentrations of ^{210}Pb, ^{226}Ra, and ^{228}Th observed in the bones of individuals with osteogenic sarcoma were found to be no higher than those found in the bones of a group of controls. Although osteogenic sarcoma is a known result of higher concentrations of these isotopes in the skeleton, it is obvious that the present study does not directly implicate them as agents in the spontaneous production of osteogenic sarcoma in populations without occupational or iatrogenic exposure to internal emitting bone-seeking radioelements. Radiochemical analyses of bone samples of populations exposed to higher radiation dose, together with large scale epidemiologic surveys, such as Argonne National Laboratory has under study, may throw more light on the relationship between radiation dose and osteogenic sarcoma. The observation that ^{210}Po is attached to tobacco smoke particles has raised the possibility that the low dose which ^{210}Po atoms could deliver to bronchial epithelium may be a factor in carcinogenesis. Our calculation of the radiation dose to the bronchial epithelium has been questioned by Skrable, et al. (1964), Hill (1965), and Rajewsky and Stahlhofen (1966). However, the uncertainty of the radiation dose should possibly be considered as secondary to the question of whether any radiation dose, however low, can contribute to cancer production. The synergistic action of ionizing radiation and cigarette smoke condensate has been shown in experimental carcinogenesis (Bock and Moore, 1959). But, the quantitative aspects of the action of co-carcinogens are virtually unknown. This is particularly the case of the role of ionizing radiation as an initiator. Further studies should be directed towards identifying as far as possible the physiological and biochemical factors which affect the delivery of a dose of radiation from ^{210}Po atoms to the bronchial epithelium in the lungs of smokers. The role of ionizing radiation in the process of carcinogenesis has been long recognized in the case of high radiation doses. Low radiation doses can only be regarded as a strong suspect in epidemiologic studies of leukemia and cancer of the thyroid. The possibility is presented that the bovine eye could be a useful organ for the study of some of the questions raised by our research into low levels of ionizing radiation. Naturally-occurring alpha-emitting radioelements are concentrated in the choroid and iris and the overlying cells at the corneo-sclereal junction are particularly susceptible to squamous cell carcinoma. The radiation dose to the choroid and iris has been estimated to be 5.3 Mev per year. It would be of considerable interest to observe the effects of such a dose with time on the cells at risk. (TCO)

41192 (IDO-12053) CONTROLLED ENVIRONMENTAL RADIOIODINE TESTS. Progress Report No. 2. Bunch, D. F. (ed.) (Idaho Operations Office (AEC), Idaho Falls. Health and Safety Div.). Aug. 1966. 39p. Dep. mn. CFSTI $2.00 cy, $0.50 mn.

The Controlled Environmental Radioiodine Test (CERT) program consists of a series of field releases of various types of radioiodine over different vegetation and under various meteorological conditions to obtain data on the hazard of iodine and on the quantitative movement of iodine through the air-vegetation-cow-milk-human chain. Results of the sixth and seventh tests in the series and laboratory experiments to support the field studies are reported. The laboratory experiments consisted of measuring the deposition and retention of the various forms of radioiodine on vegetation in an environmental chamber and the development of sampling techniques. Results of field studies using ^{131}I as tracer indicated that the deposition of methyl iodide (CH_3I) on grass is at least a factor of 100 less than I_2 (iodine vapor) under similar conditions and that the dose potential (defined as the ratio of standard-man ingestion dose to inhalation dose) is at least a factor of 400 less. The metabolic behavior of CH_3I in humans appeared to be very similar to other chemical forms of iodine. Information was obtained on the movement of radioiodine under typical late-fall or early-winter conditions. An analytical model was derived which makes possible rapid and reasonably accurate assessment of levels of ^{131}I activity in milk as well as the expected thyroid dose. The dose potential was evaluated as a function of season and age groups, and it is estimated that the probable ingestion dose to children under typical adverse weather conditions is about 400 times that for the standard-man inhalation dose. Results indicated that iodine concentrations in milk may be relatively greater in fall than in spring or summer months, probably due to an increased rate of secretion of iodine in milk. (34 references.) (C.H.)

41193 (IDO-12054) DOSE TO VARIOUS BODY ORGANS FROM INHALATION OR INGESTION OF SOLUBLE RADIONUCLIDES. Bunch, D. F. (Idaho Operations Office (AEC), Idaho Falls. Health and Safety Div.). Aug. 1966. 28p. Dep. mn. CFSTI $2.00 cy, $0.50 mn.

The International Commission on Radiological Protection has published two reports that provide biological data on the retention of various radionuclides in the body. These data were used to compile a list of dose conversion factors so that rapid approximations of dose from inhalation or ingestion of soluble radioactive materials may be made. Included are tables of rem per curie inhaled, rem per curie-sec/m^3 (time integrated concentration), rem per curie in the organ of interest, and rem per curie ingested. In addition, the parameters and

values used to derive these factors are presented and discussed. (auth)

41194 (LA–3516) BETA-GAMMA RADIOACTIVITY IN ENVIRONMENTAL AIR AT LOS ALAMOS, NEW MEXICO, FOR 1965. Kennedy, W. R.; Aeby, Jack W. (Los Alamos Scientific Lab., Univ. of California, N. Mex.). Jan. 1966. Contract W-7405-eng-36. 22p. Dep. mn. CFSTI $2.00 cy, $0.50 mn.

The radioactivity in samples of atmosphere particulates and precipitation was measured in samples collected daily during 1965. Levels of radioactivity declined throughout the year. No fallout which could be attributed to atmospheric testing was detected. (C.H.)

41195 (LA–3519) KIWI TRANSIENT NUCLEAR TEST DOSE RATE SURVEY. Lee, P. K.; Fultyn, R. V. (Los Alamos Scientific Lab., Univ. of California, N. Mex.). Mar. 1966. Contract W-7405-eng-36. 51p. Dep. mn. CFSTI $3.00 cy, $0.50 mn.

Following the KIWI TNT event, intensive, accurate dose rate surveys were taken of the contaminated areas surrounding the test point. The data collected during these surveys, and decay relations derived therefrom, are presented. (auth)

41196 (LA-DC–7996) SOME (SECOND) THOUGHTS ON TRITIUM CONTAMINATION. Coffin, Don O. (Los Alamos Scientific Lab., Univ. of California, N. Mex.). [nd]. Contract W-7405-eng-36. 12p. (CONF-660621–6). Dep. mn. CFSTI $1.00 cy, $0.50 mn.

From Health Physics Society, 11th Annual Meeting, Houston, Tex.

The procedure of sealing contaminated objects in plastic bags to retard the spread of air-borne contamination was investigated. It was concluded that plastic bags should not be used when dealing with tritium leakage or contamination. In a few hours a plastic bag can raise the personnel exposure rate from a contaminated object by as much as a thousandfold. Data on the diffusion of tritium through plastic are presented. The use of double-walled tritium containers during intra-laboratory operations was also examined and it was found that these vessels tend to increase the potential radiation hazards to those handling them. Where this type of container is still required, as for shipment between installations, some design changes should be made to decrease the inherent danger from HTO build-up. (C.H.)

41197 (NP–16172) THE DEVELOPMENT OF A STANDARD METHOD FOR TESTING PACKAGING OF RADIOACTIVE MATERIALS FOR RADIATION LEAKAGE. Report No. 3 (Final), February 1, 1964–October 1, 1965. Domanus, Jozef (Instytut Elektrotechniki, Warsaw (Poland). Zaklad Radiologii Przemyslowej). IAEA Contract 251/RB. 219p. Dep. mn.

The IAEA and ISO directives for the safe transport of radioactive materials prescribe that radiation leakage tests on containers be performed by either autoradiography or radiometry but the field of application of these methods is not defined. Detailed tests of both methods were performed. For the autographic method, high speed x-ray films with Pb intensifying screens gave best results. Characteristic curves are presented that were computed for different thicknesses of Pb that correspond to the thickness of shielding of transport containers and using ^{192}Ir, ^{137}Cs, and ^{60}Co as sources. Measurements were also made on containers with holes drilled to simulate activity released by container rupture. Radiometric investigations were performed using a scintillation counter with one- and 2-in. crystals and different Pb collimators, a portable scintillation counter with three crystals, and a portable ionization chamber dosimeter. Higher detection sensitivity was obtained with the autoradiographic method. Recommendations are presented for standardized tests for leaks in containers used for shipping radioactive materials. (C.H.)

41198 (NP–16192) DATA FROM RADIATION PROTECTION PROGRAMS. Volume 4, Number 5. (Department of National Health and Welfare, Ottawa (Ontario). Radiation Protection Div.). May 1966. 31p. Dep. mn.

Results are reported from fallout and reactor environs monitoring in Canada, April 1966. Data are included on total β activity in atmosphere and precipitation samples collected throughout the country, ^{137}Cs and ^{90}Sr content in liquid milk, the ^{90}Sr and Ca content of wheat samples, and radioactivity of the environs of Canadian reactors. (C.H.)

41199 (ORNL-TM–626) OPERATING GUIDE FOR RADIOCHEMICAL LABORATORIES AT VARIOUS ACTIVITY LEVELS. Guthrie, C. E.; Beauchamp, E. E.; Corbin, L. T.; Burnett, T. J.; Arehart, T. A. (Oak Ridge National Lab., Tenn.). July 22, 1963. Contract W-7405-eng-26. 7p. Dep. mn. CFSTI $1.00 cy, $0.50 mn.

A guide for radiochemical laboratory safety is presented. Various types of laboratory facilities are classified as to the quantity and radiotoxicity of isotopes that may be handled safely. It is pointed out that both radiation and contamination hazards must be considered in the radiochemical laboratory. Approximately 150 radioisotopes are classified as to relative toxicity, based on inhalation or immersion hazard, when compared to one gram of ^{239}Pu. (C.H.)

41200 (ORNL-TM–1551) URETHANE SPRAY FOAMING. Pierce, G. E. (Oak Ridge National Lab., Tenn.). Aug. 1966. Contract W-7405-eng-26. 10p. Dep. mn. CFSTI $1.00 cy, $0.50 mn.

The penthouse negative pressure was increased from 0.15 to 0.30 in. H_2O by urethane foam spraying on the interior walls and ceiling. The penthouse at Building 3019 serves as a secondary containment area above seven shielded cells located below. It has a volume of 101,000 ft^3 and receives ten air changes per hour. The total area sprayed in the penthouse was 13,730 ft^2 at an average cost of $0.57/$ft^2$. The insulation value of the room was improved by the addition of the $\frac{3}{4}$-in.-thick foam blanket. (auth)

41201 (RRA–T55 and Summary) AN ANALYSIS OF THE PERFORMANCE OF ENCLOSURE SHIELDS IN A REAL FALLOUT FIELD. Final Report. French, R. L.; Price, J. H.; Tompkins, K. W. (Radiation Research Associates, Inc., Fort Worth, Tex.). Dec. 31, 1965. Contract DA-23-072-AMC-332(X). 130p.

State-of-the-art shield calculational techniques were applied in the analysis of an experiment in which spherical and cubical multilayer iron and water enclosure shields were exposed in a real fallout field. The calculations were divided into three steps; 1) specification of the time-dependent energy spectrum of the gamma rays emitted by the fallout, 2) determination of the energy and angular distribution of the resultant gamma rays incident upon the shields, and 3) calculation of the penetration of the gamma rays into the shields. Monte Carlo air- and ground-scattering data along with a limited amount of measured data were employed in establishing the radiation distribution incident upon the shields. Monte Carlo procedures were used to compute the penetration into the shields. The results were expressed as dose transmission factors (inside dose divided by outside dose) and compared with corresponding factors from the experiment. Both sets of results indicated that the shields were least effective during the first few hours and that the dose transmission factors decreased by as much as 50 percent by the end of the first day. However, the calculated results were found to be consistently higher than the measured results by as much as a factor of two depending upon the particular source term. After investigating several possible causes, it was concluded that the discrepancy was probably the cumulative effect of a deficiency of low energy photons in the calculated source terms, of support structure inside the enclosure shields, and of neglecting the effects of ground roughness in the calculations. (auth)

41202 (UCRL–14990) MECHANISMS THAT AFFECT THE ADSORPTION OF METHYL IODIDE ON CHARCOAL UNDER HUMID CONDITIONS. Ackerman, Frank J.; Grens,

John Z. (Lawrence Radiation Lab., Univ. of California, Livermore). [1966]. Contract W-7405-eng-48. 20p. (CONF-660904-6). Dep. mn. CFSTI $1.00 cy, $0.50 mn.

From 9th Air Cleaning Conference, Boston.

Breakthrough curves of the adsorption of methyl iodide from air on charcoal were experimentally measured over the range of 20–100% humidity. The observed breakthrough curves can be explained by assuming two rate controlling mechanisms for mass transfer; bulk diffusion was found to control the adsorption rate during the early period, while pore diffusion was found to control later in the adsorption process. Water vapor greatly limits the external surface adsorption capacity of the charcoal for methyl iodide. Water vapor also hinders the rate of mass transfer by pore diffusion. (auth)

41203 (UCRL–16259) EXPLOSION TESTS IN A GLOVED BOX WITH ETHER-AIR MIXTURES. Young, Jensen; Phillips, Will D. (Lawrence Radiation Lab., Univ. of California, Berkeley). July 12, 1965. Contract W-7405-eng-48. 12p. Dep. mn. CFSTI $1.00 cy, $0.50 mn.

A number of tests were carried out in a gloved box with ether–nitrogen and ether–air mixtures to evaluate their explosion potential. Spark plugs were used in the box as the source of ignition while the air flow, ether volume, and hot-plate temperature were all varied. It was found that nitrogen–ether concentrations were safe under the test condition, rapid vaporization of ether in air produced local explosive concentrations that were unpredictable, explosions occur if hot-plate temperatures approach 180°C, slow evaporation of ether at low air flow was safe, the lower explosive limit of ether–air mixtures in a gloved box of 12 ft^3 was about 3% by volume, the gloved box withstood many vigorous explosions; the explosive force was vented through the gloved ports and out the gasket seal around the window. (auth)

41204 (Y–1544-A) CHARACTERIZATION OF Y-12 URANIUM PROCESS MATERIALS CORRELATED WITH IN VIVO EXPERIENCE. Steckel, L. M.; West, C. M. (Union Carbide Corp., Oak Ridge, Tenn. Y-12 Plant). July 28, 1966. Contract W-7405-eng-26. 44p. Dep. mn. CFSTI $3.00 cy, $0.50 mn.

Twenty-two process materials from the Y-12 enriched uranium area were selected as suspect exposure materials to five employees showing internal chest burdens with long biological half lives. As a means of establishing which of these were the most likely exposure materials, measures were made of their solubility in a simulated lung fluid; each was characterized as to particle size, uranium composition, and other contaminants. Similar analyses were made on oxides prepared at known temperatures to further study the insolubility parameters. The studies indicated that three process combustion ashes, containing uranium octoxide (U_3O_8), were the most likely exposure materials. These materials apparently differed from those used in previous animal studies in thermal history, particle size, and level of contamination. In view of these differences and the paucity of such animal data, it was recommended that animal experiments be conducted using these three ashes. (auth)

41205 (JPRS–36341) LABOR HYGIENE AND OCCUPATIONAL DISEASES. Translation of Gig. Truda Prof. Zabolev., 10: No. 4, 3-64(1966). 102p. (TT–66-32773). CFSTI $4.00 cy, $0.75 mn.

A separate abstract was prepared on one section of this translation of the Russian language journal Gigiyena Truda i Professional'nyye Zabolevaniya, Vol. X, No. 4, April 1966. Twenty-two additional articles discuss various aspects of industrial hygiene. (C.H.)

For an abstract of the individual section see: 41206.

41206 (JPRS–36341, pp 10-17) CLINICAL AND DOSIMETRIC DATA ON PERSONNEL OPERATING A 10 Gev SYNCHROPHASOTRON. Lebedev, V. N.; Gus'kova, A. K.; Ponizovskaya, A. I.; Denisova, E. A.; Gribova, I. A.; Salatskaya, M. I.; L'vovskaya, E. N. Translated from Gig. Truda Prof. Zabolev., 10: No. 4, 9-14(1966).

Dosimetry data obtained over an 8-yr period on personnel operating a 10-Bev accelerator were compared with results of clinical studies on personnel made during the same time period. Observations on 254 persons indicated that the working conditions of those serving in a high-energy laboratory were satisfactory. The amount of radiation received by the individuals during 8 years of observation were within permissible limits. No significant differences were found in the blood picture, crystalline lens, or other clinical criteria of operations and research personnel and a control group. All those examined were essentially healthy. The most consistent changes noted in the highly sensitive organs and systems in the course of careful clinical observation were mostly within the limits of physiological fluctuations. (C.H.)

41207 CARCINOGENIC AND LEUKEMIC ACTIVITY OF IONIZING RADIATIONS. Vallebona, A. (Univ., Genoa). pp 179-96 of Convego della Salute, Ferrara, May 25-6, 1963. Modena, Italy, Stabilimento Poligrafico Artioli. (In Italian).

This review considers radiocarcinogenesis and leukemogenesis from the point of view of exposure to ionizing radiations occupationally, medically, and experimentally, also the influence of dose, its spatial distribution, and latent period before the appearance of malignancy. Occupational carcinogenesis has largely involved radiologists and other workers with x-ray apparatus, resulting in skin tumors, and ingestion of Ra, resulting in bone tumors. Degenerative changes in skin or bone have preceded the development of tumors by many years. Present-day precautions taken by workers in nuclear fields have largely eliminated this type of radiocarcinogenesis. Data on the origin of tumors from medical sources of radiation have been largely accumulated from late effects of radiotherapy, particularly in the thyroid gland and hematopoietic system. Results of animal experimentation in this field are also reviewed. This survey indicates that certain doses of radiation predispose some tissues to neoplastic changes, which makes it essential to reduce human exposure to ionizing radiation to a minimum. However, protective measures allow the essential use of radiation for diagnostic and other medical purposes. (BBB)

41208 SAFETY OF RADIOISOTOPES IN INDUSTRY. Booth, A. H. pp 3-13 of Data from Radiation Protection Programs. Vol. 3, No. 5. Ottawa, Department of National Health and Welfare, Radiation Protection Division, 1965.

Although potentially, the application of radioisotopes in industry involves a risk of accidents, just as with any other toxic substance, in practice it has been found that such accidents are extremely rare. The reasons for this are: the high degree of public interest in radiation and awareness of the hazard; the safety features incorporated by manufacturers in the design of radioisotope devices; the comprehensive and effective regulatory controls established by government agencies; and the back-up services provided by health departments. It is suggested that the safety record of radioisotope uses in industry can be held up as a showpiece in the general field of industrial safety. It indicates what can be done to minimize accidents when the four factors mentioned above combine effectively. (auth)

41209 CANADIAN FALLOUT DATA FOR APRIL, 1965. Samuels, E. R.; Mohindra, V. K. pp 14-26 of Data from Radiation Protection Programs. Vol. 3, No. 5. Ottawa, Department of National Health and Welfare, Radiation Protection Division, 1965.

Data on fallout analyses carried out on samples of air, precipitation and milk collected in April, 1965 are presented. Daily air data in terms of gross beta activity in the air samples did not vary significantly from that observed during previous months. The average Cs and Sr concentrations in precipitation for the month of April were twice the values obtained during the month of March, probably due to higher levels of precipitation during April. Strontium-90 levels in liquid milk samples were the same as in March. However ^{137}Cs concentrations showed a de-

crease of 16pCi/l from essentially a constant level of about 162pCi/l observed during previous months. (H.G.D.)

41210 COMPARISON OF MEASURED AND CALCULATED DOSES IN RADIATION TREATMENT OF NEOPLASMAS OF THE HEAD AND NECK. Skolyszewski, Jan; Kujawska, Janina; Szymczyk, Wislawa (Inst. of Oncology, Krakow). Nowotwory, 16: 195-7(Apr.-June 1966). (In Polish).

The doses of x rays, measured in the anatomical phantoms of head and neck, are compared with doses calculated from tables. The differences between measured and calculated doses appear: when tumor is screened by thick layer of bone (nasopharynx); and when bolus material is applied for filling the space between the patients body and the surface of the applicator. Technical difficulties in homogeneous filling of this space result in increase of proposed doses. (auth)

41211 SCATTERED RADIATION FROM A CUBOID PHANTOM. McEwan, A. C. (National Radiation Lab., Christchurch, N. Z.). Phys. Med. Biol., 11: 395-403 (1966).

The angular variation of the intensity and HVT of scattered radiation from a cuboid shaped tissue-equivalent phantom, using square fields and for primary beams in the range 50 to 250 kv (1.63 mm Al to 3.13 mm Cu HVT) was experimentally determined. The effect of varying the thickness of the phantom, the area of the field and the distance from the edge of the field to the edge of the phantom was studied. It was found that in the range 50 to 100 kv the HVT of the scattered radiation was generally greater than that of the primary beam. (auth)

41212 RADIATION PROTECTION IN INDUSTRIAL RADIOGRAPHY. Domanus, Jozef; Wolski, Maciej. Polska Akad. Nauk, Zeszyty Probl. Nauki Polskiej., No. 26, 65-70(1965). (In Polish).

In industrial radiography both x-ray machines and gamma radiography sources are used. These sources of radiation constitute a potential danger to the health of persons in charge of those machines as well as for persons working in the vicinity of radiographic laboratories. Therefore it is necessary to have all those persons under a constant radiation protection control. This control consists of a permanent, systematic and periodic individual dose measurements for all the personel of radiographic laboratories as well as periodic measurements of dose rates around the radiation sources. The test-film method was adapted for the evaluation of individual doses of x- and gamma-radiation. As x- and gamma-ray energies used in industrial radiography range from about 50 to 1250 kev it was impossible to use only one brand of x-ray films for the dose measurements. Therefore two brands of films were used (made in Poland). One was used without screens (for x-rays) and the other with lead intensifying screens (for gamma-rays). In 1960 measurements were made in 43 industrial laboratories for 405 persons. Altogether 3908 films were evaluated. In the same period test-film measurements were also made for the medical personel and the total of films evaluated in 1960 was 22,555. The test-film measurements have shown that there was less than 1 per cent of persons who received radiation doses in excess to the permissible level. (W.E.B.)

41213 OBSERVATIONS DERIVED FROM FILM PACKS USED IN A NATION-WIDE X-RAY EXPOSURE STUDY. Chadwick, Donald R.; Spector, Mozart I.; Kincaid, Caleb B. (Department of Health, Education and Welfare, Washington, D. C.). Radiology, 87: 321-7(Aug. 1966).

A Public Health Service nation-wide x-ray exposure study is described, and selected information derived from more than 4,000 film packs employed to corroborate and supplement the technical x-ray examination factors reported by practitioners identified in the study is summarized. The analysis is based on 2,330 radiographic, 258 fluoroscopic, and 1,491 dental film packs for which relatively complete data were obtainable. (auth)

41214 COMPOSITIONS AND PROCESS FOR REMOVAL OF RADIOACTIVE CONTAMINANTS. Pariseau, Paul R. (to Purex Corp., Ltd.). U. S. Patent 3,255,119. June 7, 1966. Filed Oct. 30, 1962.

A process is described for the decontamination and removal of scale from Al, Zr, or their alloys without corroding the surfaces. The surface is subjected to treatment with an aqueous solution consisting of about 0.2 to 15 wt % sulfamic acid and about 0.2 to 15 wt % of a member chosen from a group consisting of sulfuric acid and the alkali metal and ammonium bisulfates, having a pH not greater than 3 and being substantially free of halides. The metal is treated with the solution at temperatures 20 to 100°C. Alternatively, the metal surface may be treated at room temperatures with the composition with no water added. (B.L.M.)

41215 RADIOLOGICAL HEALTH PROBLEMS ASSOCIATED WITH THE OPERATION OF NEUTRON GENERATORS. Boggs, Richard F.; Jacobs, Robert; Leupold, Rodger L. (Dept. of Health, Education and Welfare, Rockville, Md.). 13p. (CONF-660621-13). ORAU. Gmelin, AED-CONF-66-193-5.

From 11th Annual Meeting Health Physics Society, Houston, Tex.

The number of and uses for neutron generators has increased at a rapid rate during the past 15 years. More than 300 neutron generators have been sold, and about 200 of these units are located in the United States. A majority of the machines is controlled by neither Federal nor State agencies; however, licensing for the use of tritium targets is the responsibility of the Atomic Energy Commission or the "agreement" States. Most of the machines now in use are of the Cockcroft-Walton type in which deuterons are accelerated onto a tritium target with the subsequent release of 14 Mev neutrons. Many of these relatively inexpensive machines are operated in areas where little or no health physics capability is available and, until recently, minimal information concerning the associated health hazards has been available. This paper attempts to present additional and current information related to the production of tritium x rays, neutrons, and the resultant need for adequate shielding. (auth)

41216 HEALTH PHYSICS PROBLEMS IN OIL AND GAS WELL LOGGING. Fontaine, Jack H.; Flora, David H. (Texas State Dept. of Health, Austin). 17p. (CONF-660621-10). ORAU. Gmelin, AED-CONF-66-193-2.

From 11th Annual Meeting Health Physics Society, Houston, Tex.

The use of radioactive material in oil and gas well logging began in the 1930's when radium was used as the radioactive source. Radium is still being widely used but is being replaced by reactor-produced radioactive material. Sealed sources are used for a number of logging applications ranging from "neutron logging" to tagging casing collars. Today, large quantities of radioisotopes are being used as down-hole tracers for multiple aplications. The widespread uses of unsealed radioactive material and sealed sources constitute a unique health physics problem, not only regarding personnel exposure but in environmental contamination. Being developed today is a down-hole accelerator which will produce higher energy neutrons than can be produced from an isotopic source. Its use in logging will be included in this paper. (auth)

41217 HAZARDS RESULTING FROM DISCHARGE OF RADIOACTIVE WASTES INTO MUNICIPAL SEWER SYSTEMS. Aurand, K.; Wolter, R. (Bundesgesundheitsamt, Institut fuer Wasser-, Boden-und Lufthygiene, Berlin). Vienna, International Atomic Energy Agency, 1966, Preprint SM-72/44, 16p. (CONF-660507-27). ORAU.

From Symposium for the Disposal of Radioactive Wastes into Sea, Oceans, and Surface Waters, Vienna.

Hazards to persons working in sewers and to the population from discharge of radioactive materials into sewer systems are considered. It is concluded that incorporation of radioisotope-contaminated sewage can be excluded as a possible hazard to sewer workers. However, contamination

of drinking water and agricultural products must be considered along with incorporation of contaminated sewage when evaluating the hazard to the population. Therefore, it is recommended that limits be set for the concentration and total sum of radionuclides permissible in sewage, particularly where radionuclides are discharged in considerable amounts and have long half-lives. (H.G.D.)

41218 STUDY OF THE BIOLOGICAL CLEANABILITY OF SURFACES USING RADIOISOTOPE TRACER TECHNIQUES. **Gelezunas, V. L.; Bryce, A. J. (General Electric Co., King of Prussia, Pa.). 17p. (CONF-660432–1). ORAU. Gmelin, AED-CONF-66-077-1.**

From Aerospace Medical Assn., 37th Annual Scientific Meeting, Las Vegas, Nev.

Radioisotope tracer techniques were used as a basis for evaluating biological cleanability. Various surfaces were used and special emphasis was placed on low contamination levels. Either labeled bacteria or compounds of biological interest were deposited on surfaces, and exposed for varying ultrasonic cleaning times. The residual contaminant remaining on the surface after cleaning was inferred by measuring the activity in a low-level counting system. It was shown that relative cleanability can be a function of wash time and that removal of thin chemical films and bacteria follow similar kinetics. Ultrasonic cleanability data were found to fit the following equation: $F = Be^{-at} + (1-B)e^{-bt}$ where F is the residual fraction of initial contaminant remaining after washing time t, while B, and a and b are cleanability parameters. Calculations indicate that ^{32}P labeled bacteria can be detected (counting precision ±5%) to at least 1 bacterium/cm^2 in reasonable times. (auth)

41219 CURRENT AND PROPOSED MANNED SPACECRAFT CENTER RADIATION SAFETY PROGRAM. **Martin, Shell E. (Manned Spacecraft Center, Houston, Tex.). 21p. (CONF-650540–7). ORAU.**

From American Industrial Hygiene Association Meeting, Houston, Tex.

The NASA-Manned Spacecraft Center (MSC) has unique missions and functions which require a complex pattern of organizational integration. Missions fall into two general areas, spacecraft development and space-flight operations, and include: research and development, preliminary design studies, contractor management, tests, and evaluations, special equipment development, mission design, ground and flight crew training, spacecraft preparation, mission control and recovery. The following activities are programmed: Flight mission exposure to space radiation; Damage and malfunction studied on electronic systems; Space radiation shielding studies on space systems; Space radiation instrument calibration and dosage; Radiation techniques for heat shield ablation sensors; Ion sources for gas analysis; Radioactivated luminous phosphors for spacecraft control devices, and others. (H.L.W.)

INSTRUMENTATION

General

Refer also to abstract 41648.

41220 (BNWL–214) PHYSIOLOGICAL DATA TELEMETRY SYSTEM. Hoitink, N. C.; Porter, N. S. (Battelle-Northwest, Richland, Wash. Pacific Northwest Lab.). July 1966. Contract AT(45-1)-1830. 12p. Dep. mn. CFSTI $1.00 cy, $0.50 mn.

A physiological data telemetry system, comprising both commercial and developed solid state circuits, was developed and is being used to monitor, on a continuous basis, body temperatures and heart function (ECG data) of two maintenance technicians working under high temperature conditions. The completed system includes two miniature transmitters, ECG electrodes, thermistor temperature probes, two FM receivers, a developed demodulator unit, and a dual channel recorder. Satisfactory performance is being achieved over 200 ft ranges in general field operation. (auth)

41221 (COO–1471-1) HELICOPTER CLOSE ORDER FORMATION KEEPING SYSTEM. Progress Report, May–July 1965. (Industrial Nucleonics Corp., Columbus, Ohio). July 23, 1965. Contract AT(11-1)-1471. 41p. Dep. mn. CFSTI $2.00 cy, $0.50 mn.

Progress is reported on an isotopic γ-ray signaling system which will permit close-order formation flying in helicopters. Each helicopter will be provided a source and a detector. Studies and experiments in the following areas are reported: dynamic range and response function, angular dependence of the collimated detector aperture, improvement in measurement capabilities of the system, feasibility of stationary array directional detectors, choice of sources and detectors (including health hazard considerations), and angular dependence of detector efficiency. (F.S.)

41222 (DP–900) CONTROL SYSTEM FOR X-RAY DIFFRACTOMETER SCANNING. Cook, L. H. Jr. (Du Pont de Nemours (E. I.) and Co., Aiken, S. C. Savannah River Lab.). Aug. 1966. Contract AT(07-2)-1. 11p. Dep. mn. CFSTI $1.00 cy, $0.50 mn.

A time-based program controller using a prepunched tape was developed for automatic goniometer scanning of an x-ray diffractometer in which the locations of the diffraction lines are known. The program controller consists of a dual-speed drive unit which moves the goniometer rapidly over portions of the diffraction pattern not under observation and slowly over the diffraction lines to be observed, and an electronic control system which will scan the selected diffraction lines, print the accumulated data for each line, reset the goniometer, rewind the control tape, and then either stop or repeat the cycle. The control accuracy is within 0.01° Bragg 2θ angle. (auth)

41223 (EGG–1183-1244) PHOTO-OPTICAL INSTRUMENTATION AT THE NUCLEAR ROCKET DEVELOPMENT STATION. Lockwood, Harold E. (Edgerton, Germeshausen and Grier, Inc., Las Vegas, Nev.). [nd]. Contract AT(29-1)-1183. 18p. (CONF-660804–1). ORAU.

From Society of Photo-optical Instrumentation Engineers, 11th Annual Symposium, St. Louis, Mo.

Prolonged and frequently interrupted tests, low frequency vibrations, and extreme environments impose severe requirements on photographic techniques and equipment design. Photographic objectives fall into two categories; Studies of fuel lines for leaks, and studies of the plane for symmetry and the existence of foreign material. Infrared and color film are the two principal photosensensitive materials used in these studies. Equipment and station design criteria must provide for extended time coverage and remote operation of the cameras, protection of the film from extreme environments, particularly radiation, and the elimination of vibration. (R.C.K.)

41224 (EGG–1183-2078) MOTION SENSING AND ITS APPLICATION TO PROJECT WISP. Report No. S-319-R. Hudson, C.; Lagerquist, R.; Rutland, D. (Edgerton, Germeshausen and Grier, Inc., Santa Barbara, Calif.). Feb. 1966. Contract AT(29-1)-1183. 89p. (UCRL–13206). Dep. mn. CFSTI $3.00 cy, $0.75 mn.

The field of motion sensing for possible solutions to motion sensing problems associated with Project WISP are examined. Motion sensing principles are outlined, devices and systems are evaluated, and promising avenues for further research are recommended. (auth)

41225 (NYO–3622-4) APPLICATIONS OF ULTRASONIC ENERGY: ULTRASONIC INSTRUMENTATION FOR NUCLEAR APPLICATIONS. Bimonthly Progress Report No. 29, June 1, 1966–July 31, 1966. (Aeroprojects, Inc., West Chester, Pa.). Aug. 1966. Contract AT(30-1)-3622. 12p. Dep. mn. CFSTI $1.00 cy, $0.50 mn.

Initial tests with an acoustic flowmeter showed promise for the technique, and satisfactory performance should be achieved after minor transmission problems are solved. Study of ultrasonic techniques for measuring pressure in high-temperature systems was initiated. Promising techniques involving measurement of acoustic impedance and resonant frequency are being analyzed. (auth)

41226 (ORNL–3875) INSTRUMENTATION AND CONTROLS DIVISION ANNUAL PROGRESS REPORT FOR PERIOD ENDING SEPTEMBER 1, 1965. (Oak Ridge National Lab., Tenn.). Aug. 1966. Contract W-7405-eng-26. 187p. Dep. mn. CFSTI $5.00 cy, $1.00 mn.

Separate abstracts were prepared for the 15 sections included in the progress report. (B.G.D.)

For abstracts of individual sections see: 41078, 41227–41233, 41269–41272, 41541, 42581, and 42585.

41227 (ORNL–3875, pp 1-3) NANOSECOND CIRCUITRY AND TECHNIQUES. (Oak Ridge National Lab., Tenn.).

The noise and amplification characteristics of several h-f transistors were evaluated. Low-noise, h-f, wide-bandwidth amplifiers utilizing these transistors were developed. A pulse generator was designed that produces 2 kv pulses. The pulse rise and fall times are less than 1 nsec, the pulse widths are between 2 and 20 nsec, and the repetition rates are between 2 and 70 pulses/sec. (B.G.D.)

41228 (ORNL–3875, pp 15-20) MISCELLANEOUS ELECTRONICS DEVELOPMENT. (Oak Ridge National Lab., Tenn.).

Various aspects on electronics development are presented. Topics included are a magnetometer for superconducting materials, tests on 20-pin Amperex photomultiplier tube socket, transfer-function simulation of a pulse amplifier for aerosol particle-size analysis, remotely operated range wheel, high-voltage power supply for electron heating, and noise-signal pickup in instrumentation circuits. (B.G.D.)

41229 (ORNL–3875, pp 21-3) FABRICATION AND MAINTENANCE OF ELECTRONIC INSTRUMENTS. (Oak Ridge National Lab., Tenn.).

Product design, fabrication, and quality control for electronic instruments are discussed along with servicing and maintenance. (B.G.D.)

41230 (ORNL–3875, pp 24-34) INSTRUMENTATION FOR AUTOMATIC CONTROL. (Oak Ridge National Lab., Tenn.).

Instrumentation for automatic control is discussed. Topics included are furnace power controller, adjustable ramp generator for power controller, eliminating the thermal conductivity response of catalytic combustion detectors in gas chromatography, automatic welding, elec-

tronic etch controller for electron microscope specimens, computer-controlled x-ray diffractometer, automatic sample changer, and automatic control for a microfiche printer. (B.G.D.)

41231 (ORNL–3875, pp 35-43) INSTRUMENTATION FOR BIOMEDICAL RESEARCH. (Oak Ridge National Lab., Tenn.).

Instrumentation developments in biomedicine research are discussed. Topics included are delayed-light measurements using a Kerr-cell shutter, electromechanical aids to chromosome length measurement, and application of a digital memory oscilloscope to delayed-light measurements. (B.G.D.)

41232 (ORNL–3875, pp 75-90) DATA COLLECTION AND ANALYSIS. (Oak Ridge National Lab., Tenn.).

A report is presented on data collection and analysis at ORNL. Topics discussed are activities of the data processing and analysis group, data collection and analysis system for the MSRE, MSRE computer programming, data acquisition system for reactor division experiments, time-of-flight system using an on-line computer, data center for connecting experiment stations to the CDC 160A computer, high-speed punch-control and readout scanner for an ND-160 analyzer, thermocouple calibration computer program, smoothed thermocouple tables of extended significance, and a computer program for flow calculations. (B.G.D.)

41233 (ORNL–3875, pp 101-24) PROCESS INSTRUMENTATION DEVELOPMENT. (Oak Ridge National Lab., Tenn.).

A report is presented on process instrumentation development at ORNL in three parts: temperature, level of molten metal and molten salt differential pressure, and turbopump speed. Topics discussed are testing of temperature-measurement sensors, linearizers for platinum thermocouples, thermal emf of three types of thermocouple lead-wire connectors, thermocouple-scanner reference voltage supply, differential thermal analysis system, temperature measurements by infrared methods, nozzle flow stability in pneumatic temperature measurements, experiment simulator for high temperature fuel studies, high temperature thermometry, summary of experience with high-temperature thermocouples used in the ORNL–GCR program fuel irradiation experiments, molten metal and salt indicators, high temperature NaK differential pressure transmitter, and turbopump speed detector. (B.G.D.)

41234 (ORNL-P-2436) CHARACTERIZATION OF RADIOACTIVE PARTICULATE AEROSOLS BY THE FIBROUS FILTER ANALYZER. Silverman, M. D.; Truitt, J.; Browning, W. E. Jr.; Franzen, L. F.; Adams, R. E. (Oak Ridge National Lab., Tenn.). [1965]. Contract W-7405-eng-26. 20p. (CONF-660904–10). Dep. mn. CFSTI $1.00 cy, $0.50 mn.

From 9th Air Cleaning Conference, Boston, Mass.

The fibrous filter analyzer (FFA) was developed for measuring the characteristics of radioactive aerosols in terms of their response to filtration processes by determining their distribution vs depth in a filter under carefully controlled conditions. Moisture was shown to have no significant effect on the performance of the FFA, although the test aerosol itself was affected by moisture. The filtration efficiency data obtained agreed well with the theoretical treatment of filtration developed by Torgeson. The analyzer was calibrated against particles having diameters from 150 to 1500 Angstroms, measured by electron microscopy. (auth)

41235 DESIGN OF RADIOACTIVE ISOTOPE INSTRUMENTS IN CONSIDERATION OF APPARATUS ERRORS AND STATISTICAL CHARACTERISTICS OF THE INPUT SIGNAL. Klempner, K. S.; Cherednichenko, I. M.; Shumilovskii, N. N. Avtometriya, No. 2, 84-91(1965). (In Russian).

Problems of accuracy in measurements with the aid of radioactive isotope instruments are discussed, in consideration of the statistical characteristics of the input signal and apparatus errors of all types. An accounting is made of apparatus errors, dependent and independent of the intensity of the current being measured. A general expression is developed which connects the error in measurement Δx, sensitivity of method of measurement γ and signal to noise ratio z. Conditions of measurement are found at which the maximal signal to noise ratio is to be obtained. It is shown that identical measurement accuracy may be attained by instruments with different apparatus errors by changing the sensitivity of the method of measurement. (ATO)

41236 RECENT STATE AND DEVELOPMENT OF MANUFACTURING ISOTOPIC AND NUCLEONIC DEVICES IN POLAND. Kernenergie, 9: 169-76(May 1966). (In German).

A brief review is given of the production of Polish isotopic and nucleonic devices. The characteristics of newly developed instruments are briefly reported. (J.S.R.)

41237 CONTRIBUTION TO AN EXPERIMENTAL AND THEORETICAL STUDY OF FLUCTUATIONS OF AN INTEGRAL LOGARITHMIC PERIOD METER IN THE RANDOM REGION. Van der Beken, H.; Bonnet, G.; Delcroix, V. (CEA-CEN, Grenoble, France). Nucl. Instrum. Methods, 43: 298-311(Aug. 1966). (In French).

First are stated again the main characteristics of the functioning of a diode pump in the recurrent state. Then it is shown that, in a fairly wide field this system can be represented by a linear filter. In the randomly occurring state, the study of the spectral density of a series of impulses, deriving from a Poisson distribution through erasure of period 2, provides the elements necessary to the calculation of the mean values and variances of the level of the output "power" and "period" of the complete channel of the type "log. period". The experimental verifications were affected by a technique of sampling, which leads to a successful match between theory and measurements. The formulas reached in this way must, in spite of their complexity, allow an a priori determination of the basic elements of such a channel. (auth)

41238 MOESSBAUER EFFECT VELOCITY DRIVE LINEARIZED BY SHAPE CORRECTION. Zane, R. (Univ. of California, Berkeley). Nucl. Instrum. Methods, 43: 333-7(Aug. 1966). (UCRL–16401).

An electromechanical feedback system for the measurement of Mössbauer effect spectra in multiscaler mode of operation of a pulse-height analyzer is described. The equations of motion of the system were examined analytically (through use of an IBM 7094 and Cal-Comp plotter). The velocity drive was linearized by introduction of a correction term in the Fourier expansion of acceleration. (auth)

41239 ENERGY DISTRIBUTION OF He^+ IONS PRODUCED BY A SOURCE WITH HIGH-FREQUENCY ELECTRIC EXCITATION. Benoit-Cattin, P.; Blanc, D.; Bordenave-Montesquieu, A.; Dagnac, R.; Vacquie, S. (Faculte des Sciences, Toulouse). Nucl. Instrum. Methods, 43: 349-54(Aug. 1966). (In French).

A study of the energy spectra of helium ions emitted from a h-f ion source was performed with a sector shaped electrostatic analyzer. The ion energy distribution curve shows a fundamental maximum, the half-width of which does not exceed 50 ev and secondary maxima extending toward lower energies. These maximum amplitudes are 50 to 100 fold less than the fundamental maximum amplitude. Peak-amplitude variations and fundamental maximum half-widths are given vs source working parameters. These data provide optimal working conditions for minimum energy dispersion. (auth)

41240 A MODULAR 100-Mc DIGITAL TIMER. Eckhause, M.; Siegel, R. T.; Welsh, R. E. (College of William and Mary, Williamsburg, Va.). Nucl. Instrum. Methods, 43: 365-7(Aug. 1966).

A digital time analyzer employing flexible plug-in logic and time base frequencies up to 100 Mc is described. Tests

and performance in muon and pion lifetime experiments indicate linearity to better than 0.1%. The analyzer is comprised entirely of commercially available modular circuit elements. (auth)

41241 PHASE-SETTING CIRCUIT AT A FREQUENCY OF 100 MHz BY TRANSISTORS IN THE AVALANCHE REGION. Goursky, V.; Guillon, H. (Centre d'Etudes Nucleaires, Saclay, Gif-sur-Yvette, France). Nucl. Instrum. Methods, 43: 376-8(Aug. 1966). (In French).

A phase setting circuit for pulse analyzers and time-of-flight measurements is described. The circuit diagram is shown in which a binary scale is used to improve the time resolution. Various wave forms and pulses are shown. (J.F.P.)

41242 NOMOGRAM FOR DESIGNING TUNNEL DIODE MONOSTABLE CIRCUITS. Abbattista, N.; Coli, M.; Plantamura, V. L. (Istituto di Fisica, Bari, Italy. CNEN, Frascati, Italy). Nucl. Instrum. Methods, 43: 383-4(Aug. 1966).

A nomogram for a straight design of a tunnel diode monostable circuit with linear and nonlinear biasing is described. The parameters of this nomogram for solving the design problems of a tunnel diode are given, and an application for the nomogram is discussed. (J.F.P.)

41243 CHARGED PARTICLE IDENTIFICATION SYSTEM USING A FAST MULTIPLIER. Mark, S. K.; Moore, R. B. (McGill Univ., Montreal). Nucl. Instrum. Methods, 44: 93-7(Sept. 1966).

A charged particle identification system based on the principle $(E + E_0 + kdE/dx)dE/dx$ is described. It is found that charged particles with energy in the range from 20 to 100 Mev can be separated by using plastic scintillator Naton 136 for the measurement of E and dE/dx of the particles. A relatively fast transistor multiplication circuit is presented together with its performance. The performance of the system in separating deuterons from protons is given. (auth)

41244 CIRCUIT FOR PREVENTING ACCUMULATION OF EXPERIMENTAL DATA WHEN THE NUCLEAR REACTION RATE EXCEEDS A PRESET VALUE. Gupta, S. K. (Tata Inst. of Fundamental Research, Bombay); Iyengar, K. V. K.; Bhalerao, P. J. Nucl. Instrum. Methods, 44: 123-4(Sept. 1966).

A circuit was devised to restrict accumulation of (n,γ) angular correlation data in $A(x,n\gamma)B$ type reactions only to periods when the counting rate in the γ detector is below the fatigue level of the photomultiplier and its gain insensitive to changes in the counting rate. (auth)

41245 APPROXIMATIONS TO IMMERSION TYPE ELECTROSTATIC LENSES. Paris, Gy. (Central Research Inst. of Physics, Budapest). Nucl. Instrum. Methods, 44: 137-40(Sept. 1966).

The rigorous solution of the paraxial ray equation for the potential distribution $V = \gamma + th\omega z$ with $\gamma = 1$ is given. Immersion-type lenses similar to the unipotential lens described by Glaser are analyzed by means of Lamé- and Hill-type differential equations. The paraxial ray equation can be always transformed in the case of lenses with focal planes to a Hill-type equation. It is found that in terms of voltage multiplications any lens may be either focusing or defocusing. (auth)

41246 SUGGESTIONS FOR IMPROVEMENTS OF TIMING CIRCUITS WITH TUNNEL DIODES. Abbattista, N.; Coli, M.; Plantamura, V. L. (Univ., Bari, Italy. CNEN, Frascati, Italy). Nucl. Instrum. Methods, 44: 153-4(Sept. 1966).

The minimum slewing time of a zero crosser circuit using a tunnel diode is calculated. The analysis is devoted to the synchronizing circuit of P. Orman (Nucl. Instr. and Meth., 21: 121 (1963)). (J.F.P.)

41247 TRANSISTORIZED NUCLEAR MAGNETOMETER. Wolski, W. (Wroclaw Polytechnic Inst.). Przegl. Elektron., No. 3, 138-42(1966). (In Polish).

The principles of measurement of magnetic field intensity using the nuclear resonance phenomenon are described. The advantages of using an autodyne generator for detecting nuclear absorption are briefly discussed. The measuring system and the transistorized autodyne generator developed are shown and described. Glycerine (of about 70 cu. mm in volume) was used as the absorption substance. The system can measure field intensity from 2300 to 5500 oersted. The measurement range was chosen so that the system can be used in conjunction with an electron-resonance spectrometer. The measurement accuracy is not less than 0.01%. The amplifier of the absorption signal is described. It has a voltage gain of 5×10^3, sensitivity better than 5 microvolts, its bandwidth is from 80 to 1000 cps, and it can transmit absorption signals with the modulation frequency of the measured field within the limits of from 50 to 200 cps. The factors influencing the signal-to-noise ratio of the system are briefly discussed. The signal-to-noise ratio of the system was in excess of 25 db. The procedure to be followed in using the instrument is described (it is stipulated that the measured field must be uniform; its gradient cannot exceed 2 Oe/cm). (ATD)

41248 DESIGN OF A HIGH-IMPEDANCE VACUUM TUBE VOLTMETER FOR USE IN THE RADIOISOTOPE LABORATORY. Bogardus, Carl R. Jr.; Levitt, Seymour H. Radiology, 87: 357-8(Aug. 1966).

A reliable, yet simple, high-impedance vacuum tube voltmeter for use in a radioisotope laboratory is described. The instrument has a d-c input resistance of 110 M ohms, so that negligible drain is placed on the system to be measured. Two voltage ranges are provided, and the meter may be used with either positive or negative power supplies. Multiple coaxial connector inputs are employed. Final calibration showed that the meter was linear with the calibrating power supply within ±10v. This gives an overall error of ±0.7% full scale. (R.C.K.)

41249 AUTODYNE INSTALLATION FOR EXPERIMENTS ON DYNAMIC POLARIZATION OF NUCLEI. Draghicescu, M.; Ianculovici, B. (Inst. of Atomic Physics, Bucharest). Rev. Roum. Phys., 11: 213-24(1966). (In French).

An installation for the detection of the nuclear magnetic resonance signal under the specific conditions of a dynamic polarization experiment was described. The conditions of oscillation and sensitivity for the autodyne working along a cable were analyzed. The auxiliary installation of the autodyne, the frequency sweep and variation circuits, and the stabilization circuit of the oscillation level are transistorized. A compact device was constructed with the following characteristics: region of operation from 5 to 36.5 MHz, frequency sweep up to 2 MHz, level of the radiofrequency voltage controllable from several mv to 100 mv and constant at ±1%/MHz during the frequency sweep, and the sample reel at several meters from the oscillator. (tr-auth)

41250 CONSIDERATIONS AFFECTING DESIGN OF ATOMIC AND MOLECULAR BEAM RESONANCE APPARATUS EMPLOYING TWO-POLE STATE SELECTORS. McColm, Douglas (Univ. of California, Berkeley). Rev. Sci. Instrum., 37: 1115-23(Sept. 1966). (UCRL-11670-(Rev.)).

Optimum design criteria for atomic and molecular beam apparatus are discussed, and signal strengths under a number of conditions are calculated. Signal strength and signal-to-noise ratios are shown graphically as functions of the design parameters. (auth)

41251 EXTRACTION OF POSITIVE IONS FROM ELECTRODELESS DISCHARGE. Williams, J. F. (Australian National Univ., Canberra, Aust.). Rev. Sci. Instrum., 37: 1205-10(Sept. 1966).

The positive ion current extracted from an electrodeless discharge is studied as a function of the discharge parameters of oscillator input power and frequency, gas pressure, magnetic field, extraction voltage, and extraction electrode geometry. A greatly enhanced ion current is obtained by

operating the discharge at a pressure of several microns of mercury and applying a static magnetic field either parallel or perpendicular to the magnetic component of the high frequency electromagnetic field. Mean beam energies up to 200 ev above the extraction voltage and beam energy spreads of 50 ev are observed and studied as functions of the discharge parameters. (auth)

41252 MICRON REGION PRESSURE STANDARD FOR URANIUM HEXAFLUORIDE. Pappas, W. S. (Oak Ridge Gaseous Diffusion Plant, Tenn.). Rev. Sci. Instrum., 37: 1217-19(Sept. 1966). (K-L-6096).

A standard was developed for calibrating uranium hexafluoride pressure gages in the micron region. The device employs the equilibrium dissociation pressure of uranium hexafluoride furnished by the sodium fluoride complex salt at easily controlled temperatures above ambient. The pressure signal obtained is in good agreement with reported dissociation pressure measured by the transpiration method. The principles are applicable to noncorrosive gas-solid systems; for example, some oxides, carbonates, and hydrates dissociate reversibly to give a definite oxygen, carbon dioxide, or water vapor pressure at a given temperature. (auth)

41253 WIDE RANGE THERMOSTAT FOR MOESSBAUER SPECTROSCOPY. Sharon, B.; Treves, D. (Weizmann Inst. of Science, Rehovoth, Israel). Rev. Sci. Instrum., 37: 1252-4(Sept. 1966).

A vacuum thermostat for Mössbauer effect studies permitting temperature control from 85 to 870°K is described. Any temperature in this range can be maintained for long periods, utilizing an appropriate electronic temperature stabilizer. Temperature inhomogeneity over the sample is estimated to be less than 1°K. This thermostat can transmit radiation with a conical angle of 12°. Operation is simple and samples can be quickly interchanged. (auth)

41254 METHOD FOR DETERMINING SPLITTING IN NUCLEAR-RESONANCE SPECTRA. Chizhik, V. I.; Ryl'kov, V. V. (Leningrad State Univ.). Zavodsk. Lab., 32: 683-6(1966). (In Russian).

A method for the determination of the frequency shift between two linear nuclear magnetic resonance spectra was described. The method is based on the separation of pulsed frequencies from 3-echo signals. Experimental verification showed that the precision of the method given exceeds the precision of measurements made with a high resolution spectrometer. (tr-auth)

41255 HIGH RESOLUTION NUCLEAR MAGNETIC RESONANCE SPECTROSCOPY. VOLUME I. Emsley, J. W.; Feeney, J.; Sutcliffe, L. H. Oxford, Pergamon Press, 1965. 709p.

A detailed account of the basic theory for high-resolution nuclear magnetic resonance spectroscopy and a survey of the major applications to problems in physics and chemistry are presented. The topics covered are the general theory of nuclear magnetic resonance, the origin of chemical shifts and spin-spin coupling, calculation of shielding constants of nuclei in molecules, theoretical calculations of spin-spin coupling constants of simple molecules, NMR spectrometers and their accessories, and experimental procedures. Also included are the analysis of high-resolution spectra, and the effects of chemical equilibria and molecular conformational motion on NMR spectra. (J.F.P.)

41256 INSTRUMENTATION NUCLEAIRE. (Nuclear Instrumentation). Paris, Commissariat a l'Energie Atomique, 1966. 210p.

A parallel column French and English catalog of electronic instruments and equipment currently used in the nuclear establishments of C.E.A. is presented. (G.O.Y.)

41257 MEASUREMENT OF ATMOSPHERIC DENSITY USING GAMMA BACKSCATTER TECHNIQUES. Hakewessell, David B. (Giannini Controls Corp., Duarte, Calif.). 26p. (CONF-660207-25). ORAU. Gmelin, AED-CONF-66-011-38.

From Radioisotope Applications in Aerospace Symposium, Dayton, Ohio.

The use of gamma scattering for the measurement of atmospheric density is presented. Theoretical and experimental data are given showing the relation between scattered gamma radiation measurements and atmospheric density. Test results of measurements made in large altitude chambers, from balloon payloads and from sounding rocket payloads, are included. The rocket flight results demonstrate the high altitude capability of the technique; the balloon flights demonstrate the accuracy capability of the technique. The radioisotopes used in this experimentation are ^{144}Ce, ^{75}Se, and ^{241}Am. The ^{144}Ce and ^{75}Se radioisotopes are used as sources of low energy gamma radiation for scattering and the ^{241}Am is used as a source of alpha radiation for reference. (auth)

41258 IMPROVEMENTS IN OR RELATING TO ELECTRIC CONTROL OR MONITORING EQUIPMENT OR APPARATUS. Thompson, Willie Ellison; Allen, Philip (to Ekco Works). British Patent 1,036,720. July 20, 1966. Filed Aug. 21, 1962.

In a monitoring system for a control circuit, a module includes a transistor connected between supply lines having a substantially constant applied voltage and means for applying to the module one or more signals to control the operation of the transistor. The continuity of each signal path is controlled by a device, e.g., a relay, operable by the circuit. The module also has means for receiving a checking pulse, and a pulse corresponding with the checking pulse is developed at an output of the transistor only when at least a predetermined number of one or more signals is or are fed to the module. An amplifier is provided to respond to the presence in the output of a pulse corresponding with the checking pulse. In a monitoring means for control and/or interlock circuit, a number of these modules are connected in cascade, and the first of the modules has a first a-c signal impressed on it. In normal operation, this signal will be available at the output of the last module of the cascade. The modules each comprise a trip circuit which determines the transfer of the signal through that module in dependence on a separate a-c signal(s) impressed upon it from circuit connections each controlled by at least one of the elements. Such devices are required to monitor the instruments which in turn monitor the operation of equipment in a nuclear reactor. (B.L.M.)

41259 IMPROVEMENTS IN AND RELATING TO SEPARABLE ELECTRIC CONNECTORS. Buckland, Ernest Clifford (to M. B. Metals Ltd.). British Patent 1,037,783. Aug. 3, 1966. Filed Apr. 10, 1962.

A separable electric connector is described that is suitable for use at high temperatures, particularly for thermocouples of nuclear reactor fuel elements. The connector is made up of two separable connector members with a number of discrete electrical contacts making surfaces on each member to provide a number of discrete electrical connections. Further engaging surfaces, at least one of which is C, are provided on the members. (B.L.M.)

41260 PROTECTIVE CIRCUIT FOR NUCLEAR PHYSICS MEASURING APPARATUS. Gaertner, Rudolf (to VEB Vakutronik Dresden). German Patent 1,216,996. May 18, 1966. Filed Dec. 2, 1963.

A circuit is given for the protection of the input stage of a linear amplifier from the voltage peaks generated by turning on or switching off the high voltage of the detector. The amplifier the input of which is connected to the high voltage source by means of a coupling capacitor, is provided with a glow lamp intermediate between the grid of the input valve and a point of fixed voltage which is grounded via a capacitor. (Gmelin Inst.)

41261 MASS SPECTROMETER. Geerk, Jens; Jenckel, Ludolf (to Atlas-Werke Aktiengesellschaft). German Patent 1,219,254. June 16, 1966. Filed Feb. 5, 1960.

A mas spectrometer is described which comprises a magnetic analyzer in the form of a homogeneous sectorial magnetic field, an electron bombardment ion source with a drawing out plate parallel to the flat ionization zone, and collimating electrodes with slits focusing the ion beam upon the entrance slit of the magnetic field. The direction

of the flat ionizing electron beam in the ion source, the flat ionization zone, and the drawing out slit are arranged perpendicular to the lines of force and to the entrance slit of the magnetic analyzer. The focusing electrode system is composed of circularly curved electrodes the center of curvature of which is situated at the entrance slit. (Gmelin Inst.)

Radiation Detection

Refer also to abstracts 40741, 40742, 41147, 41190, 41543, and 42311.

41262 (BNWL-SA-619) A NEW NEUTRON AND HIGH ENERGY PARTICLE DOSIMETER FOR MEDICAL DOSIMETRY APPLICATIONS. Baumgartner, W. V.; Brackenbush, L. W.; Unruh, C. M. (Battelle-Northwest, Richland, Wash. Pacific Northwest Lab.). July 20, 1966. Contract AT(45-1)-1830. 15p. (CONF-661005-1). Dep. mn. CFSTI $1.00 cy, $0.50 mn.

From Symposium on Solid-State and Chemical Radiation Dosimetry, Vienna, Austria.

Principles, design, and performance of solid state track dosimeters are discussed. For neutron detection, a strip of plastic is used with a fissionable foil attached to it. Neutrons induce fission in the foil, and the fission tracks in the plastic can be detected by using etchants which preferentially attack the damaged areas. For proton detection, proton-fissionable foils can be used. Alpha particles and higher nuclei leave their own tracks directly in appropriate plastic detectors. However, large fluxes and doses of particles on photons, which do not provide a minimum critical rate of energy loss in traversing a material, do not leave tracks. Cobalt-60 gamma radiation doses to 10^5 R have not produced observable damage. Flat, cylindrical, and spherical detector designs are described. Methods of determining dose from exposed devices are given. (W.E.B.)

41263 (CERN-66-23) A TRACK CENTERING SYSTEM FOR IEPs USING A VIBRATING REED TRACK DETECTOR (VIBRATRON). Moore, M. F. C.; Anders, H. (European Organization for Nuclear Research, Geneva (Switzerland)). June 28, 1966. 51p. Dep. mn.

A track centering and following system is described. The system was designed for use with an instrument for the evaluation of photographs (IEP). The vibrating reed which forms the basic element of the system (Vibratron) is described along with the complete system. Operating instructions for the use of the device are presented. The system logic is also described. (B.G.D.)

41264 (DP-552) FISSION COUNTER FOR THE ROUTINE ISOTOPIC ANALYSIS OF PLUTONIUM. Goosey, Malcolm H. (Du Pont de Nemours (E. I.) and Co., Aiken, S. C. Savannah River Lab.). Mar. 1961. Contract AT(07-2)-1. 11p. Dep. mn. CFSTI $1.00 cy, $0.50 mn.

A fission counter for routine analyses of the ^{240}Pu content in Pu samples is described. The instrument is designed for operation by non-technical personnel and features a minimum of external controls. Experimental comparison with a mass spectrograph demonstrated agreement within ±2%. (auth)

41265 (INR-704/III/PL) DETERMINATION OF STATISTICAL PARAMETERS OF THE TRIPLE COINCIDENCE CIRCUIT ON THE BASIS OF A SINGLE EMPIRICAL DELAYED COINCIDENCE CURVE. Kalisz, J. (Institute of Nuclear Research, Warsaw (Poland)). Apr. 1966. 24p. Dep.

Two mathematical methods for determination of the main coincidence-circuit parameters resolving time, jitter breadth, and efficiency on the basis of a single empirical delayed-coincidence curve are described. The general approach based on the assumption of Gaussian jitter distributions is presented and some particular cases are considered. (auth)

41266 (LAL-1028) THE SECONDARY EMISSION MONITOR. Aggson, Th. L. (Laboratoire de l'Accelerateur Lineaire, Univ. de Paris, Orsay (France)). Feb. 14, 1962. Contract DA-91-591-EUC-2011. 34p.

A short experimental study of the secondary emission properties of the secondary emission monitor is presented. A theoretical search for the origins of the energy dependence of the secondary emission monitor which has been observed with relativistic electron beams is outlined. (auth)

41267 (MPI-PAE-P1-30/66) PHOTOELEKTRISCHES SPEKTROGRAPHEN-REGISTRIERPHOTOMETER HOHER EMPFINDLICHKEIT UND PRAEZISION. (Photoelectric Recording Device of High Sensitivity and Accuracy for Spectrographs). Vidal, C.-R. (Max-Planck-Institut fuer Physik und Astrophysik, Munich (West Germany)). May 1966. 11p. Dep. mn.

For the wavelength region 1,800–10,000 Å a photoelectric device was developed for recording spectral line intensities with high sensitivity and accuracy. This was achieved by guiding the exit slit of the spectrograph in the plane of the plate by means of a spring parallelogram free from play and by reducing the dark current of the multipliers by several orders of magnitude. The uv multiplier was cooled by immersion into liquid nitrogen and the infrared multiplier by using Peltier batteries. Furthermore the dark current of the multiplier was reduced by a little permanent ring magnet, which restricts the sensitive region of the photocathode to the actually illuminated area of about 3 mm diameter. (auth)

41268 (NYO-2740-3, pp 5-165) RADIOLOGICAL PHYSICS. (Columbia Univ., New York. Radiological Research Lab.).

The design of a capacitor type ionization chamber for the dosimetry of monoenergetic neutrons in hydrogenous materials (plant or animal tissues) is described. The chamber wall and collector are a thermosetting epoxy plastic mixture that gives an exact duplicate of the hydrogen nitrogen composition of the tissue and a mixture of methane, nitrogen, and CO_2 is used as the filling gas for the sensitive chamber volume. A small capacitor type ionization chamber that employs tissue equivalent (muscle) plastic walls and atmospheric air in the sensitive volume was fabricated for use in neutron dosimetry. Preliminary calibration studies are reported. Experiments were conducted to test the stability of sealed gas multiplication tissue equivalent ionization chambers as a function of applied potential and pressure with time. Equipment designed for the dosimetry of a 2.2 Bev proton beam, consisting of an ionization chamber, positioning equipment, reading and timing circuitry, was tested using one beam shape and two different phantom configurations. Computer programs were written to obtain sums of all the chamber readings during a given run, ratios of monitor chamber to flux readings, and of depth-dose to monitor readings as well as mean values and deviations as required. Depth dose studies in mouse phantoms exposed to fission neutrons and γ radiation from the ORNL Health Physics Research Reactor are described in detail. Emphasis was placed on the shielding and scattering effects produced when several unrestrained mice share the same cage during irradiation. Measurements of the microscopic distribution of radiation energy are reported. The depth dose measurements for 14.7 Mev neutrons were extended to 10 to 20 mps at five energies ranging from 0.43 Mev to 1.8 Mev using the (p,T) reaction. All measurements were made with a 1-in. diameter proportional counter and the dose and event size distributions and other parameters pertaining to distribution were calculated with the aid of an IBM 7090 computer. Data are presented on the gas multiplication and resolution characteristics of 1-in. and 2-in. diameter tissue equivalent spherical proportional counters and design modifications of a wall-less tissue equivalent proportional counter used in measurements of the microscopic distribution of radiation energy. A summary of quantities and functions employed in microdosimetry is included. Event size distributions due to ^{60}Co γ rays were measured with a 1-in. diameter tissue equivalent proportional counter employing a low-noise preamplifier. Measurements were made for a

range of sizes from 0.5μ to 20μ. The relative responses of cylindrical and spherical proportional counters were evaluated and the distribution of path length in a prolate spheroid was measured as part of an evaluation of wall less counters. Measurements were also made of α path length distribution in a sphere and the frequency of multiple tracks in tissue equivalent cavities of varying density. The design of a device for plating active deposits is described and a schematic sketch is included. Breakdown protection of a proportional counter was obtained by the use of circuit incorporating a locked grid thyratron in parallel with the counter. A sketch of the circuit is included. (C.H.)

41269 (ORNL–3875, pp 4–12) PULSE COUNTING AND ANALYSIS. (Oak Ridge National Lab., Tenn.).

A progress report is presented on pulse counting and analysis. Topics discussed are gating of a large-area-photocathode PM tube, wide-band low-noise charge-sensitive preamplifier, undesirable undershoot in the operation of nuclear pulse amplifiers, minimum noise pulse shaping with new double delay-line filters in nuclear pulse amplifiers, versatile scaler with d-c to 100 Mc capabilities, electronic gain control, stabilization system for a nuclear spectrometer, E·dE/dX system for identifying and analyzing charged particles, and optimization of semiconductor preamplifiers for use with semiconductor detectors. (B.G.D.)

41270 (ORNL–3875, pp 13–14) ELECTROMETERS AND ACCESSORIES. (Oak Ridge National Lab., Tenn.).

Significant characteristics of metal-oxide-semiconductor field-effect transistors (MOSFET) are studied. A differential electrometer with two MOSFET's in the input stage is constructed. A passive Fourier comb filter is developed. (B.G.D.)

41271 (ORNL–3875, pp 44–52) DETECTORS OF IONIZING PARTICLES AND RADIATION. (Oak Ridge National Lab., Tenn.).

A report is presented on detectors of ionizing particles and radiation. Topics discussed are production and encapsulation of lithium-drifted germanium detectors, basic instrumentation in radioisotope applications, alpha scintillation detector response in gamma ray and neutron backgrounds, ion-chamber current fluctuations produced by neutron and gamma sources, PCP III ionization chamber, spherical BF_3 proportional counters, and radiation damage in cadmium sulfide and cadmium telluride. (B.G.D.)

41272 (ORNL–3875, pp 53–74) RADIATION MONITORING. (Oak Ridge National Lab., Tenn.).

A report is presented on radiation monitoring in two parts: operation and maintenance of systems and development of instruments and components. Topics discussed are modernization and expansion of ORNL radiation warning and communication systems, waste effluent monitoring, environmental monitoring, nonproject engineering activities of the monitoring systems development group, performance of the radiation warning and communication system at ORR, ORNL radio communication system, radio telemetry perimeter air monitoring system, maintenance activities of the monitoring systems development group, accelerator radiation protection, HFIR cladding-failure detector, investigation of CD-V-742 dosimeter failures, shoe contamination monitor, stack effluent monitor for alpha radiation, gamma process monitor, thermal neutron survey meter, alpha survey meter, alpha monitor for heavy-element chemistry, compacted ^{10}B absorbers, remotely operated low-energy neutron spectrometer, and detector for radioactive-gas monitor. (B.G.D.)

41273 (ORNL–TM–1295) TEMPERATURE DEPENDENCE OF THE RESPONSE OF LITHIUM-DRIFTED GERMANIUM DETECTORS TO GAMMA RAYS. El-Shishini, M. M.; Zobel, W. (Oak Ridge National Lab., Tenn.). Sept. 1966. Contract W-7405-eng-26. 78p. Dep. mn. CFSTI $3.00 cy, $0.75 mn.

Thesis. Submitted by M. M. El-Shishini to Univ. of Tennessee, Knoxville.

While it has generally been stated that lithium-drifted germanium detectors must be operated at liquid-nitrogen temperature for optimum performance, no systematic investigation to prove or disprove this statement has been reported. The closest experiment is that of Tavendale who, however, only investigated the resolution as a function of temperature for one low-energy gamma ray. The resolution and efficiency of two lithium-drifted germanium detectors, approximately 20-mm diameter and 3-mm thickness, were studied in the temperature range from 85 to 160°K, using gamma-ray sources whose energies varied from 279 to 1332 kev. It was found that, contrary to the results of Tavendale, the resolution of the detectors had a pronounced peak at about 105°K. The origin of this peak is not known, but is not due to changes in diode capacitance or leakage current. The efficiency of the diodes is approximately constant for each energy over the temperature range. (auth)

41274 (ORNL–TM–1581) ESTIMATION OF BETA RADIATION DOSE TO THE SKIN BY MEANS OF FIELD INSTRUMENT MEASUREMENTS. Gupton, E. D. (Oak Ridge National Lab., Tenn.). July 29, 1966. Contract W-7405-eng-26. 9p. Dep. mn. CFSTI $1.00 cy, $0.50 mn.

There are two basic problems in beta dosimetry monitoring for dose rates to the skin from small-area sources: one is that of determining the dose rate when the source is in contact with the skin; the other is when the beta-emitter is a contaminant on or in the skin. In neither case do the readings which may be obtained with field-type survey instruments represent directly the dose rate to the skin. In fact, the skin dose rate may be as much as 1000 times the observed instrument reading, even though the instrument is very near the source when the reading is obtained. The response of field-type radiation survey instruments to beta radiation from small-area sources was determined. Observational readings were made with a β scintillator referenced to an extrapolation chamber and photographic films at various distances from beta sources (^{32}P, ^{89}Sr, ^{111}Ag, ^{36}Cl, ^{185}W, ^{147}Pm, and ^{60}Co) which were prepared for the purpose. The dose rates to the skin from such sources, at various source-to-skin distances, were derived from measurements and calculations. From the data obtained in these experiments and from calculations it appears that, by proper interpretation of the measurements, field-type instruments may be used to obtain an adequate estimate of skin dose rates from small-area beta sources. Proposed methods are outlined for estimating the dose rate from a source in contact with the skin and the dose rate from contamination on the skin. (C.H.)

41275 (RFP–777) A COMPACT, LOW-COST ALPHA COUNTER. Tyree, W. H. (Rocky Flats Div., Dow Chemical Co., Golden, Colo.). Aug. 17, 1966. Contract AT(29-1)-1106. 7p. Dep. mn. CFSTI $1.00 cy, $0.50 mn.

An alpha counter with meter readout is described. The cost of the counter including an air proportional detector and rechargeable batteries is less than $65.00. (auth)

41276 (UCRL–16769) SOME RECENT DEVELOPMENTS IN TECHNIQUE FOR MONITORING HIGH-ENERGY ACCELERATOR RADIATION. McCaslin, Joseph B.; Patterson, H. Wade; Smith, Alan R.; Stephens, Lloyd D. (Lawrence Radiation Lab., Univ. of California, Berkeley). Aug. 1966. Contract W-7405-eng-48. 21p. (CONF-660920–5). Dep. mn. CFSTI $1.00 cy, $0.50 mn.

From 1st International Congress of the International Radiation Protection Assn., Rome, Italy.

In order to accurately evaluate the exposures received by individuals working near high-energy accelerators it is necessary to measure the separate components in the radiation field and to determine their energy spectrum. Since no single instrument or detector will do this, a variety of different detectors and instruments must be used. Three recent developments in technique for monitoring particulate radiation above 20 Mev use nuclear emulsion, elemental mercury, and ^{7}Be production in light elements; below 20

Mev, the use of moderated foils of In, Au, and Co has been extended to include Ta. When emulsion is used, the number of stars formed by high-energy inelastic collisions is counted, together with the number of gray prongs. The ratio of gray prongs per star was previously found to be linearly related to the energy of the neutron which formed the star, over the energy range 20 to 300 Mev. This technique is used to measure average neutron energy and to estimate spectrum shape for neutron energies above 20 Mev. A second technique makes use of the spallation of Hg to ^{149}Tb, an alpha emitter of 4.12-hour half-life. The threshold for this reaction is near 500 Mev, and it therefore extends the use of threshold detectors for the estimation of spectrum shape to a new energy domain and gives some additional confidence in previous estimates of spectrum shape made with Bi fission, $^{12}C(n,2n)^{11}C$, and $^{27}Al(n,\alpha)^{24}Na$. Thirdly, production of ^{7}Be from ^{12}C, ^{14}N, and ^{16}O was studied; it offers a method of high-energy neutron threshold detection with practical thresholds extending from 30 to 40 Mev for carbon to 45 to 55 Mev for oxygen. The practical sensitivity can be arbitrarily high without making the extraction process either too lengthy or unwieldy. Another recent development involves the inclusion of Ta in the class of detectors which use a thermal-neutron-sensitive activation element inclosed in a Cd-clad hydrogenous moderator to allow an integration period of a few months and a sensitivity considerably greater than with Co. Finally, recent improvements in the performance of our large parallel-plate Bi fission chamber are discussed. (auth)

41277 (UCRL-16952) A SIMPLE AND INEXPENSIVE SYSTEM FOR MEASURING CONCENTRATIONS OF ATMOSPHERIC ^{222}Rn. Jones, Gary E.; Kleppe, Lowell M. (Lawrence Radiation Lab., Univ. of California, Berkeley). June 27, 1966. Contract W-7405-eng-48. 21p. Dep. mn. CFSTI $2.00 cy, $0.50 mn.

A radon-222 sampling system was designed and built which uses a charcoal absorption technique for collecting and analyzing that gas in a simple, inexpensive, reliable way. Results of measurements made with the system, although only preliminary, are in agreement with data obtained by other investigators. (auth)

41278 (UCRL-70000) A STUDY OF FISSION γ RAYS USING A Ge(Li) DETECTOR IN CONJUNCTION WITH A BENT-CRYSTAL SPECTROMETER IN CAUCHOIS GEOMETRY. White, D. H.; John, W.; Saunders, B. G.; Groves, D. J. (Lawrence Radiation Lab., Univ. of California, Livermore). July 20, 1966. Contract W-7405-eng-48. 7p. (CONF-660906-24). Dep. mn. CFSTI $1.00 cy, $0.50 mn.

From International Conference on Nuclear Physics, Gatlinburg, Tenn.

The high-resolution capability of the bent-quartz-crystal spectrometer in Cauchois geometry was extended above 400 kev by replacing the photographic emulsion with a Ge(Li) detector and using multichannel pulse height analysis. By proper collimation at the focal circle, extended spectral bands of fission γ rays are recorded which are free of Compton edges and other secondary processes. (auth)

41279 (AEC-tr-6698) APPLIED SPECTROMETRY OF IONIZING RADIATION. Stolyarova, E. L. Translation of Prikladnaya Spektrometriya Ioniziruyushchikh Izluchenii, Atomizdat, Moscow, 1964. 505p. Dep. mn. CFSTI $8.25 cy, $2.25 mn.

41280 (NP-tr-1410) MULTISPHERE TECHNIQUE. I. GENERAL CHARACTERISTICS AND APPLICATIONS. Zaborowski, H. (Commissariat a l'Energie Atomique, Cadarache (France). Centre d'Etudes Nucleaires). Translated by R. R. Inston (Atomic Energy Research Establishment, Harwell, Eng.), from report PAS-63/72. 52p. Dep. mn. JCL $5.60 fs, $1.76 mf.

A study is made of the general characteristics and applications of the multisphere technique for flux measurement, dosimetry and spectrometry of neutron sources from thermal energies to 7 Mev. Equations are given relating to three fluxmeters (equivalent long counters) for flux measurements. Other equations have also been derived for: multiple collision dosimetry (in rads and rems) and first collision dosimetry (in rads); and the spectrometry and dosimetry of neutrons in five energy bands in accordance with a method similar to that employed by threshold detectors. (auth)

41281 THE MEASUREMENT OF THE RADIOACTIVITY OF ^{14}C USING A COUNTER WITHOUT A WINDOW. Genunche, Ana; Frangopol, Maria (Institutul de Fisica Atomica, Bucharest). Acad. Repub. Pop. Romine, Stud. Cercet. Chim., 13: 1271-81(Dec. 1965). (In Rumanian).

Methods of measurement of ^{14}C are reviewed; the applicability of each depends to some extent on whether the sample is a solid, liquid, or gas. Use of a Geiger counter with a window is particularly adapted for solids, with the usual error 5%. Proportional counters, ionization chamber devices, scintillation counters and autoradiography are also compared with respect to accuracy and sensitivity. With windowless counters, measurements may be made in heterogeneous or homogeneous media; the former is measured in a continuous flow of gas. Solids are studied by placing them below the anode of the detector and a constant stream of He or Ar saturated with a mixture of 96% anhydrous ethanol and 4% ether is passed over the sample. Detectability is to 10^{-10} C, error 5%, voltage 1400-1700 v as a function of gas flow and temperature of saturation. Techniques used are discussed, and the statistical treatment of results is outlined. (BBB)

41282 STUDIES OF IRON-FREE ASYMMETRIC TWO-LENS β SPECTROMETER WITH CORRECTING COILS. Bonchev, Tsv.; Ormandzhiev, Sl.; Zlatareva, A.; Mitrikov, M.; Todorov, P.; Manushev, B. Ann. Univ. Sofia, Fac. Sci. Phys., 59: No. 5, 119-37(1964-65). (In Russian).

Descriptions are given of a two-lens β spectrometer with a correction coil between the main focusing coils which improved the light power and tapered the spherical image. The spectrometer was equipped with varying entrance and exit diaphragms with 4π changing from 0 to 6% and resolving power $\eta = (\Delta\rho/\rho)$ varying from 0.8 to 2%. (R.V.J.)

41283 RECOMBINATION LOSSES AND THEIR INFLUENCE ON THE ENERGY RESOLVING POWER OF p-i-n DETECTORS. SOME METHODS OF MEASURING τ, μ, AND HOMOGENEITY. Kuhn, A. (Inst. of Crystal Research, Turnov, Czech.). Czech. J. Phys., 16: 697-722 (1966). (In German).

The general solution for the recombination losses was derived and some simpler equations for the different cases of irradiation were found. The theoretical spectrum of pulses for irradiation perpendicular to the field as a result of the general solution was proved experimentally. Some new methods of measuring the lifetime and mobility in p-i-n-type counters by means of the voltage dependence of the recombination losses and the transit time and new methods of measuring the detector homogeneity were developed. Different influences on the fluctuations of recombination losses and energy resolution, surface recombination, and the voltage and temperature dependence of the pulse spectra are treated in turn. (auth)

41284 A NEW INSTRUMENT FOR DETERMINING THE INTENSITY OF GAMMA RADIATION: GAUSS QUANTUM METER. Komar, A. P.; Kruglov, S. P.; Lopatin, I. V. (Ioffe Inst. of Physics and Tech., Leningrad). Dokl. Akad. Nauk SSSR, 167: 785-8(Apr. 1, 1966). (In Russian).

An instrument is described in which the intensity of γ radiation, as measured by its absorption in a substance, is determined integrating the area under the transition curves. The integration is by means of a quadrature formula under the main area of the curve and by means of a six-point Gaussian approximation. The thicknesses of the absorbing copper plates and the widths of the gaps between them are calculated to obtain the best quadrature integration. (ATD)

41285 TESTING COUNTERS OF NUCLEAR RADIATIONS OF THE T-25-BFL TYPE BY THE AID OF AN

AUTOMATIC APPARATUS. Furman, A. O.; Kobazev, E. I. Dokl., Moskov. Sel'skokhoz. Akad., No. 79, 259-68 (1962). (In Russian).

An automatic device for testing the counting characteristics of the T-25-BFL counter was developed, constructed, and put into production. The automatic device made it possible to increase the work output during control countings by 4 to 5 times by comparison with the common test counters. The form of the counting characteristics of the T-25-BFL was investigated in dependence on the type of radiation. The dependence of the pulse amplitude produced by α and β particles and the recovery time on the feed voltage was determined. (tr-auth)

41286 CHARACTERISTICS OF SELF-EXTINGUISHING GEIGER-MULLER COUNTING TUBES. Vodros, Daniel (Research Group for Medical Radiology, Hungarian Academy of Sciences). Meres Automat., 13: 314-17(1965). (In Hungarian).

For the assembling of a multiple radiation detector it was necessary to determine the characteristics of 21 Geiger-Mueller counting tubes. The results were presented and discussed to indicate the ranges of characteristics (such as, starting voltage, plateau angle and length, sensitivity, dead-time, directional sensitivity effects, etc.) encountered in such tubes of similar nominal values. The methods employed in the measurements were described and it was noted that some characteristics can be described by limit values only. Generally, the sensitivity of cylindrical tubes is highest in the perpendicular direction to the axis and lowest in the anode extension direction. These differences are especially large in end-window tubes. The delay-time was approximately inversely proportional to the voltage differential between the electrodes. (CFSTI)

41287 SHORT REVIEW ON THE DEVELOPMENT AND USE OF SEMICONDUCTOR DETECTORS. Kuhn, L. Mitteilungsbl. Strahlungsmessgeraete, 7: No. 15, 13-15 (Apr. 1966). (In German).

The development and use of semiconductor detectors are briefly reviewed. The results obtainable with semiconductor detectors are compared with results obtainable by other detection devices. Data on the special electronics for the operation of semiconductor detectors are tabulated. (J.S.R.)

41288 THE ACCURATE MEASUREMENT OF THE RELATIVE EFFICIENCY OF Ge(Li) GAMMA-RAY DETECTORS IN THE ENERGY RANGE 500 to 1500 kev. Freeman, J. M.; Jenkin, J. G. (Atomic Energy Research Establishment, Harwell, Eng.). Nucl. Instrum. Methods, 43: 269-77(Aug. 1966). (AERE-R-5142).

A method is discussed for obtaining empirically the relative total-energy-peak efficiency, ϵ, over the gamma-ray energy range 500 to 1500 kev, for any given Ge(Li) detector in a specific geometry. Use is made of sources for which the relative emission rates of pairs of gamma rays are precisely known. An accuracy of about 1% in the relative efficiency curve is obtainable by use of the semi-empirical formula $\epsilon \propto \tau + \sigma A \exp(-BE)$, where τ and σ are photoelectric and Compton absorption coefficients respectively, E is the gamma-ray energy and A and B are constants determined from the gamma-ray measurements. (auth)

41289 WEDGE-SHAPED SCINTILLATION DETECTOR FOR A MAGNETIC SPECTROMETER. Calderbank, M.; Burge, E. J.; Edwards, V. R. W. (London Univ.). Nucl. Instrum. Methods, 43: 317-24(Aug. 1966).

The performance of a wedge-shaped scintillation detector, for use in the focal plane of a double focusing magnetic spectrometer, was investigated both theoretically and experimentally. Computations for 50 and 30 Mev protons for a variety of geometrical arrangements and the optimum orientation of the detector, are discussed. In experimental tests, overall resolutions of about 100 kev were obtained, corresponding to a detector with about 30 channels of resolved position indication. (auth)

41290 DIAMOND AS A NEUTRON SCINTILLATION COUNTER. Miller, T. G. (Redstone Arsenal, Ala.). Nucl. Instrum. Methods, 43: 338-42(Aug. 1966).

The scintillation properties of diamond w. e investigated when neutrons and gamma rays are incident on the diamond. The neutrons are produced by the D(d,n) reaction and the response to neutrons and background gamma rays is separated by time-of-flight techniques. The full width at half maximum of the neutron time-of-flight spectrum when diamond pulses are used as start for the time converter is essentially equal to the neutron burst width indicating fast rise time for the pulses, but the energy resolution is poor, possibly due to after pulsing. (auth)

41291 RANDOM EVENTS, PILE-UP, AND SUMMATION IN A FAST-SLOW COINCIDENCE. Lange, D.; Eckert, H. G.; Haupt, W. (Univ., Goettingen, Ger.). Nucl. Instrum. Methods, 43: 343-8(Aug. 1966). (In German).

Examples are given for coincidence-spectra which are distorted by chance-coincidences in the slow part of a conventional fast-slow-coincidence and also by pile-up and summation-effects. By measuring at two different geometries a simple procedure was developed to subtract these unwanted effects. (auth)

41292 METHOD FOR ANALYSIS OF PULSE-HEIGHT SPECTRA. Graber, H. D. (Cornell Coll., Mt. Vernon, Iowa); Watson, D. D. Nucl. Instrum. Methods, 43: 355-60 (Aug. 1966).

An analytic method for computer analysis of gamma-ray pulse-height spectra is discussed and some results of the computer program are presented. The method allows the determination by the computer of the number and energies of the constituent gamma rays as well as their relative intensities. (auth)

41293 COMPACT LOW-INDUCTANCE SPARK CHAMBER PULSER. Parker, S. I.; Rey, C. A. (Univ. of California, Berkeley). Nucl. Instrum. Methods, 43: 361-4 (Aug. 1966). (UCRL-16654).

A small low-inductance spark chamber pulser of simple construction is described. It has a capacity of 16000 pF, a series inductance of 8 nH exclusive of the spark inductance and will drive a 5500-pF load with a rise time of 14 nsec. The complete pulser measures $1.8 \times 6 \times 18$ cm. An avalanche transistor Marx circuit that can be used to drive the pulser is also described. It triggers on 2-v pulses and drives the spark gap trigger electrode with a 1.2-kv pulse having a delay time of 4 nsec and a rise time of 2 nsec. (auth)

41294 PRESSURIZED DISCHARGE CHAMBER. Kajikawa, R.; Kobayakawa, H.; Masaike, A.; Ohashi, Y.; Okada, A. (Univ. of Nagoya, Japan). Nucl. Instrum. Methods, 43: 373-5(Aug. 1966).

Preliminary results of an experiment operating a three-dimensionally localized discharge chamber at pressures up to 33 kg/cm^2 at room temperature is described. The design of the chamber is given, and the threshold voltage curve of the spark for helium gas is shown. Photographs of cosmic ray particles passing through the chamber in various directions to the electric field are presented. The preliminary results indicate that the streamers in the high energy and pressure gas are sufficiently localized under certain conditions of operation giving space resolution better than that of conventional spark chambers operated at atmospheric pressure. (J.F.P.)

41295 A Ge(Li)–NaI(Tl) COINCIDENCE SYSTEM WITH MULTICHANNEL ANALYSIS. Ramayya, A. V.; Van Nooijen, B.; Carter, H. K.; Hamilton, J. H. (Vanderbilt Univ., Nashville). Nucl. Instrum. Methods, 43: 379-80 (Aug. 1966).

A Ge(Li)-NaI(Tl) coincidence arrangement, which works satisfactorily and can be easily assembled from instruments which are commercially available, is described. A block diagram of the coincidence system and spectra from ^{154}Eu decay for single and coincident gamma spectra are shown. (J.F.P.)

41296 MODIFIED HYPODERMIC SYRINGE FOR LIQUID DEPOSITION OF BETA SPECTROMETER SAMPLES. Pinajian, J. J. (Oak Ridge National Lab., Tenn.).

Nucl. Instrum. Methods, 43: 385(Aug. 1966). (ORNL-P-2122).

The modification of the hypodermic syringe described involves drawing out the tip of the barrel so that a fine capillary is obtained. The required technique for this design modification and the advantages of such a modified syringe are discussed. (J.F.P.)

41297 DESIGN AND PERFORMANCE OF AN ON-LINE WIRE SPARK CHAMBER SPECTROMETER FOR 5 TO 30 Gev/c PARTICLES. Bleser, E. (Brookhaven National Lab., Upton, N. Y.); Collins, G. B.; Fischer, J.; Fujii, T.; Heller, S.; Higinbotham, W.; Menes, J.; Pate, H.; Turkot, F.; Hien, N. C. Nucl. Instrum. Methods, 44: 1-17(Sept. 1966). (BNL-9897).

The design and performance of a wire spark chamber spectrometer system connected on-line to a PDP-6 computer are described. The system analyzes particles of 5 to 30 Bev/c momentum scattered at angles from 0 to 15° with a momentum resolution of 0.5% and an angular resolution of 0.5 mrad. The chambers can be sparked every 1.25 msec and the computer can analyze up to 150 events in the 2 sec between AGS beam spills. (auth)

41298 STUDY OF THE RESOLUTION OF A CHARGE PREAMPLIFIER. Libs, G.; De Rosny, G. (Departement d'Electronique Generale, Saclay, France). Nucl. Instrum. Methods, 44: 39-44(Sept. 1966). (In French).

Two spectrometric experiments for accurately measuring the noise performance of a hybrid preamplifier are described. Moreover the noise of valve, two-pole and field-effect transistor preamplifier is studied with respect to detector leakage current. (auth)

41299 IMAGERY OF X AND γ RAYS BY MEANS OF GAS-FILLED IMAGE INTENSIFIER OPERATING IN EITHER THE SPARK OR THE AVALANCHE REGION. Lansiart, A.; Morucci, J. P.; Roux, G.; Leloup, J. (CEN de Saclay, Gif-sur-Yvette, France). Nucl. Instrum. Methods, 44: 45-54(Sept. 1966). (In French).

A new gas filled avalanche or spark producing image intensifier detector for x and γ rays was developed. This instrument was used for visualization of radioisotopes fixed in human organs. Essentially, the detector is composed of three plane parallel electrodes; incident photons are detected between cathode and grid, electronic avalanches take place between grid and anode. Depending on the applied grid-anode voltage, sparks are directly recorded on camera, or small luminous avalanches are focused on an image intensifier. When the electric field permits sparking, an electronic circuit triggered by initiation of the spark was used to discharge the grid anode capacitance. Approximately, every photon absorbed by gas between cathode and grid produces a spark. High yield is obtained with xenon. (auth)

41300 REVERSE CURRENT OF HIGH-RESISTIVITY SILICON SURFACE-BARRIER COUNTERS. Langmann, H. J.; Meyer, O. (Karlsruhe Nuclear Research Center, Ger.). Nucl. Instrum. Methods, 44: 55-60(Sept. 1966).

The reverse current of surface barrier counters made of high-resistivity n-silicon was analyzed. It was compared with theoretical calculations using measured values for the specific resistivity and the effective lifetime. It is shown that the reverse current of carefully fabricated metal-semiconductor diodes at voltages above about 5 v has mainly two components: the diffusion and the generation current. The condition of the surface is of extreme importance even in the case when surface currents are negligible. The influence of the surface current is discussed. The diffusion current is dependent on the thickness of the undepleted material of the base of the diode and to some extent on the condition of the back contact. (auth)

41301 NUMERICAL ANALYSIS OF THE TIME SPECTRUM OF DELAYED COINCIDENCES. [PART] I. Bostroem, L. (Uppsala Univ.); Olsen, B.; Schneider, W.; Matthias, E. Nucl. Instrum. Methods, 44: 61-4(Sept. 1966).

An improved computer method was developed for the analysis of time spectra obtained from multichannel analyzers. It allows control of drifts between the measurement of the prompt and the delayed curve. No previous fitting procedure is applied to the experimental prompt curve. (auth)

41302 NUMERICAL ANALYSIS OF THE TIME SPECTRUM OF DELAYED COINCIDENCES. [PART] II. Olsen, B.; Bostroem, L. (Uppsala Univ.). Nucl. Instrum. Methods, 44: 65-72(Sept. 1966).

A convolution method to evaluate the decay constant λ of excited nuclear levels in multichannel coincidence measurements is investigated. The experimental prompt curve is used in the convolution. The results are compared with those obtained from the slope method (when applicable) and the first three moment methods. The different methods are tested with simulated theoretical decay curves with true statistical errors. The investigations concern, e.g., the dependence on drifts in the equipment and the inaccuracy in determination of accidentals. The convolution method is shown to be the most stable one against a combination of these errors. The procedure is demonstrated in the cases of the 81 kev level in ^{133}Cs, the 66 kev level in ^{73}As, the 114 kev level in ^{149}Pm and the 113 kev level in ^{177}Hf. (auth)

41303 CONTINUOUS MONITOR FOR RADIOACTIVE FALLOUT IN THE AIR. Thukral, S. P.; Vohra, K. G. (Atomic Energy Establishment, Trombay, India). Nucl. Instrum. Methods, 44: 73-6(Sept. 1966).

An instrument for continuously recording the level of long-lived beta activity in the air is described. This instrument can be used as a continuous monitor for radioactive fallout in the air. The beta activity of fallout produced radionuclides is distinguished from that of natural radon and thoron daughters by providing a delay between collection and recording of activity. The activity is collected on a rotating annular ring of filter paper and a shielded G-M counter is used as a detector. In its initial performance test the instrument recorded the variations in airborne radioactivity at a high altitude station in India after the second Chinese test. The instrument can also be adopted for continuously monitoring the airborne radioactivity in laboratories handling radioisotopes. A special feature of the instrument is its utility in providing periodic records of the increase in air activity. (auth)

41304 FACTORS INFLUENCING THE DEVELOPING OF THE DISCHARGE ALONG THE TRAJECTORY OF A PARTICLE IN A SPARK CHAMBER. Bolotov, V. N.; Devishev, M. I.; Klimanova, L. F. (Lebedev Inst. of Physics, Moscow). Nucl. Instrum. Methods, 44: 77-80 (Sept. 1966).

The influence of gas filling and pressure, and the amplitude of the supplying pulse, on the maximum angle of the spark following along the particle trajectory in a spark chamber was investigated. (auth)

41305 IMPROVEMENT OF SIGNAL-TO-NOISE RATIO BY DOUBLE INTEGRATION APPLICATION TO NUCLEAR MAGNETIC RESONANCE. Gagnaire, D. (CEN, Grenoble, France); Spivak, V.; Sicard, F.; Magneron, P. Nucl. Instrum. Methods, 44: 81-9(Sept. 1966). (In French).

A method improving the signal to noise ratio in the case of repetitive signals is reported. By a double integration, matched to the parameters of the noise in which the signal is buried, the number of channels is artificially increased to obtain the best sampling conditions. The method is applied to nuclear magnetic resonance in the case of the use of a multichannel analyzer Intertechnique SA 40 with a spectrometer Varian A-60. (auth)

41306 BROAD-RANGE MAGNETIC SPECTROGRAPH SYSTEM FOR ROUTINE ANGULAR DISTRIBUTION DETERMINATIONS. Feldl, E.; Fetrow, C.; Moore, C. F. (Florida State Univ., Tallahassee). Nucl. Instrum. Methods, 44: 98-102(Sept. 1966).

A broad-range magnetic spectrograph system for charged particle reaction analysis, utilizing nuclear track emulsion plates, was built. The magnetic spectrograph is a broad-range, high-resolution instrument with an analysis range

similar to that of a Browne-Buechner spectrograph. The system features speed and ease of operation without loss of precise relative alignment of slits, target, magnet and emulsion plates. Change of nuclear emulsion plates in the focal plane, angle change of the spectrograph and target interchange or rotation are accomplished in less than 5 min without breaking vacuum. (auth)

41307 PEAK-TO-TOTAL RATIOS AND EFFICIENCIES FOR A 5 in. DIA. BY 5 in. NaI CRYSTAL. Young, F. C.; Heaton, H. T.; Phillips, G. W.; Forsyth, P. D.; Marion, J. B. (Univ. of Maryland, College Park). Nucl. Instrum. Methods, 44: 109-13(Sept. 1966).

The peak-to-total ratio and absolute efficiency of a 5'' dia × 5'' NaI crystal for γ-ray energies from 0.4 to 9.2 Mev were measured by using a magnetic spectrometer to isolate nuclear states which decay by only one γ transition. Particle-γ-ray coincidence measurements provide the pulse-height spectrum for a single γ-ray energy. The detector efficiency is determined by detecting only those particles leading to the nuclear state which provides the desired γ ray. The efficiency is given by the ratio of the coincidence counts in the γ spectrum to the particle counts in the spectrometer. The peak-to-total ratio data were supplemented by singles measurements from some γ sources and (p,γ) and $(p,\alpha\gamma)$ reactions. (auth)

41308 DIODE FUNCTION GENERATOR FOR IDENTIFICATION OF CHARGED PARTICLES. Turos, A. (Inst. for Nuclear Research, Warsaw); Zieminski, A. Nucl. Instrum. Methods, 44: 119-22(Sept. 1966).

A simple, low-cost diode function generator for identifying charged particles with different mass and/or charge, is described. The circuit is capable of handling input pulses as narrow as 0.5 μsec. The accuracy of a function approximation of 0.5% with good stability and reliability can be obtained. The possibilities of the application of this circuit for different methods of particle identification are discussed. (auth)

41309 A b = 1.0 TOROIDAL BETA RAY SPECTROMETER. Bartis, F. J. (Univ. of Washington, Seattle. Indiana Univ., Bloomington). Nucl. Instrum. Methods, 44: 125-32(Sept. 1966).

A 38 gap toroidal spectrometer was designed for the study of short-period beta emitters. The spectrometer is portable, yet capable of focusing 10-Mev electrons. It has 1.4% transmission and 2.2% resolution for a 4-mm diameter source. Unlike other toroidal spectrometers with $b > 0.6$, its transmission is nearly equal to its gathering power. Its performance can be explained by the azimuthal focusing effect of the coil geometry. The same effect may also account for the high luminosity of b = 0.6 toroidal spectrometers. (auth)

41310 DETERMINATION OF RELATIVE EFFICIENCIES FOR A MULTIDETECTOR SYSTEM. Crannell, H. L.; Suelzle, L. R. (Stanford Univ., Calif.). Nucl. Instrum. Methods, 44: 133-6(Sept. 1966).

The greater accuracy of multidetector systems used in conjunction with magnetic spectrometers in high-resolution electron scattering experiments has raised the problem of determining accurately the relative efficiencies of the individual detectors. A calibration technique utilizing an unknown spectrum of high-energy scattered electrons is presented. Application to present equipment at Stanford University is discussed. (auth)

41311 REDRIFT TREATMENT OF Li-DRIFTED SILICON DETECTORS. Jaskola, M.; Nyboe, K. (Univ. of Copenhagen). Nucl. Instrum. Methods, 44: 141-2(Sept. 1966).

The performance of some redrift-treated detectors which were used for the detection of protons and deuterons in a (d,p) experiment with 12-Mev deuterons is reported. The detectors were cooled to –50°C during the experiment. After an exposure of about $2(10)^8$ the energy resolution changed from 18.5 to 35 kev fwhm for 12-Mev deuterons. The leakage current at room temperature remained unchanged. The resolution obtained for one of the detectors before and after the redrift treatment and the performance of some detectors are shown. Detectors which had some energy resolution before the redrift treatment usually recovered after 48 hr of redrift, while those which were insensitive to radiation before redrift needed a much longer redrift time. (J.F.P.)

41312 VALLEY-TO-PEAK RATIOS FOR ZERO-THICKNESS SOURCES. Mohindra, V. K.; Green, R. M.; McNeil, K. G. (Univ. of Toronto). Nucl. Instrum. Methods, 44: 143-4(Sept. 1966).

Changes in shapes of scintillation spectra obtained with thallium-doped sodium iodide crystals are studied for the purpose of determining the location and shape of radioactive deposits in the body. Results for the valley-to-peak ratio for zero-thickness sources are shown as a function of source energy. It is seen that the ratio passes through a minimum with γ energy. (J.F.P.)

41313 GALLIUM ARSENIDE SURFACE BARRIER DIODE AS CHARGED PARTICLE SPECTROMETER. Kobayashi, T.; Takayanagi, S. (Tokyo Shibaura Electric Co., Ltd.). Nucl. Instrum. Methods, 44: 145-6(Sept. 1966).

The performance of gallium arsenide surface barrier diodes as a charged particle spectrometer is described. An outline is given of the detector fabrication. The spectral response to α particles from ^{239}Pu of the GaAs surface barrier detector SG-11 at 30 v bias and room temperature is shown. Also shown is the charge collection efficiency versus the reverse bias voltage of this detector. (J.F.P.)

41314 DISPLAY LAMP FOR COUNTER LOGIC. Bowen, T.; Jones, J. J. (Univ. of Arizona, Tucson). Nucl. Instrum. Methods, 44: 151-2(Sept. 1966).

A test lamp circuit for particle counting high-speed logic is described. This lamp is an easily observed indicator of the overall scintillation counter and logic system operation and of accelerator beam spill characteristics. The circuit diagram is shown. (J.F.P.)

41315 RELIABILITY OF FRACTIONAL REGISTRY OF NUCLEAR SPECTRA. Bilaniuk, O. M.; Elmore, W. C. (Swarthmore Coll., Pa.). Nucl. Instrum. Methods, 44: 157-9(Sept. 1966).

Statistical aspects of scanning are examined, and criteria for expedient scanning are obtained. The validity of fractional scanning (scanning in swaths separated by unscanned gaps) is considered, and the limits for reliability of such scanning are established. It is shown that absolute peak intensity can be obtained by fractional scanning without significant loss of accuracy, provided the widths of scans and of unscanned gaps are appropriately chosen. The question of gaps between individual detectors in nuclear spectrographic multi-unit arrays is discussed. (J.F.P.)

41316 MONTE CARLO CALCULATION OF SOURCE-TO-DETECTOR GEOMETRY. Williams, I. R. (Oak Ridge National Lab., Tenn.). Nucl. Instrum. Methods, 44: 160-2(Sept. 1966). (ORNL-P-2306).

A computer program which performs a Monte Carlo calculation for obtaining the source-to-detector geometry to any desired degree of accuracy is presented. It requires less than 3 minutes to obtain a result with a 1% standard deviation when the source is smaller than the detector. A computer is made to perform a "ljedanken" experiment to simulate the isotropic emission of particles uniformly situated on a hypothetical disc. The program used random numbers to give the point of origin of the disintegration and the direction cosines, then ascertains whether a line with the randomly selected direction originating at the randomly chosen point on the disc intersects a circular disc representing the detector. This program permits a choice of the number of interactions (disintegrations) thus controlling the time and accuracy of the calculation. The method of calculation, written in FORTRAN, is outlined. (J.F.P.)

41317 DETECTION OF DIVERGENT ALPHA-RAYS AND NEUTRONS WITH MULTIPLE-WIRE SPARK COUNTERS OF THREE TYPES. Kawata, S. (Konan Univ., Japan). Nucl. Instrum. Methods, 44: 163-6(Sept. 1966).

The characteristics of three multiple-wire spark counters are compared by irradiation of ^{241}Am alpha particles. The variation of cpm is shown when the source was moved vertically above about the middle point of the array of the wires, also the variation of cpm with the horizontal displacement of the source, and with applied voltage. The voltage characteristic for narrow beams is also shown. Experiments for the detection of neutrons were also carried out and the performance of the three detectors given. (J.F.P.)

41318 SIMPLE PULSE INTERVAL ANALYZER FOR SCINTILLATION SCANNING. Erban, J.; Husak, V.; Wiedermann, M. (Univ. Hospital, Olomouc, Czech.). Nucl.-Med., 5: 290-7(1966).

A simple pulse interval analyzer that efficiently suppresses the background of scintiscans was developed. The analyzer was used both for mechanical and optical records, the latter exploiting a television cathode-ray tube. Electronic details of the apparatus and examples of its use are given. (auth)

41319 DIGITAL COMPUTERS IN NUCLEAR RADIATION COUNTING. Nodine, John H. (Hahnemann Medical Coll. and Hospital, Philadelphia). Nucleus (Chicago), No. 19, 1-11(Mar. 1965).

The capabilities of computers are reviewed. The ability of the digital computer to rapidly and accurately carry out an appropriate sequence of calculations spares the radioisotope investigator and staff from much of the tedium of radiation counting. Calculations which ordinarily must be done by one person and checked by another can be carried out far more rapidly and accurately with an appropriate computer program. Even a slow computer may carry out as many as 200,000 additions and subtractions per second with an accuracy far exceeding that which can be obtained manually in much longer periods of time. An appropriately programmed digital computer can extend manyfold the useful research time of an investigator and his staff. A stable and increasingly fruitful relation between isotope technology and computer methodology seems apparent both now and in the forseeable future. (auth)

41320 PRECISION DETECTOR FOR HIGH-ENERGY NEUTRAL PIONS. Bellettini, G. (Univ., Pisa, Italy. Istituto Nazionale di Fisica Nucleare, Pisa, Italy); Bemporad, C.; Braccini, P. L.; Benvenuti, P.; Foa, L. Nuovo Cimento (10), 44A: 946-64(Aug. 21, 1966).

A system of eight lead-glass Cherenkov counters, each coupled to a veto scintillation counter, was used at Frascati in a measurement of the Primakoff effect in the π^0 photoproduction on complex nuclei. The system as a whole is a precision π^0 detector: pion angle and energy are measured with a precision near to the limit attainable with present-day techniques. In the first part of the work the problem of measuring with high resolution the four-momentum of neutral pion of ≈ 1 Bev energy is discussed. In the second part, the Monte Carlo calculation of the detector efficiency is described. (auth)

41321 THE PINHOLE CAMERA IN THE STUDY OF THE SECONDARY EMISSION IN BODIES EXPOSED TO TELECOBALT IRRADIATION. Bergonzi, L.; De Maria, D. (Univ., Modena, Italy). Radiobiol. Radioterap. Fis. Med., 21: 99-111(Mar.-Apr. 1966). (In Italian).

The characteristics of the pinhole γ camera are reviewed and uses in clinical medicine are discussed. Applications in the study of secondary emission from bodies with compositions similar to human tissue, induced by ^{60}Co teletherapy, are described. The method proposed, based on the use of special γ cameras, must be integrated with electronic devices for thorough investigations. (tr-auth)

41322 SPECTRAL MEASUREMENTS OF 200- TO 300-kv X RAYS. Goodwin, Paul N. (Johns Hopkins Hospital, Baltimore). Radiology, 87: 205-13(Aug. 1966).

Measured spectral distributions are given for 21 different therapy beams in the 200 to 300 kvp region. It was shown that a knowledge of the half-value layer is sufficient to obtain reasonably accurate values for the rads per R conversion factors. The spectra occurring at depths of 2, 6, and 15 cm in water were calculated, and the rads per R factors determined. The results are presented in the form of graphs, from which it is possible to determine the energy absorption in bone placed at various depths in water or soft tissue, when the treatment field size and the half-value layer of the primary beam are known. An example is given of the application of these results in a clinical situation. (auth)

41323 AUTOMATIC ELECTRON DOSIMETRY SYSTEM FOR A MICROWAVE LINEAR ACCELERATOR. Cook, Kenneth J.; Mantel, Joseph. Radiology, 87: 353 (Aug. 1966).

A review of the literature was made to find a solution to the problem of dosage control in the use of a linear accelerator as an electron source in tumor therapy. To overcome this problem, an automatic dosimetry system for electron beam therapy, which terminates treatment at an exactly predetermined dose, is described. The system is presently being tested on a 6-Mev linear accelerator. Preliminary results indicate that it is an improvement over other methods of dosage control for high-intensity electron beams. (R.C.K.)

41324 RESPONSE OF SILICON FISSION DETECTORS TO CHANNELED ^{127}I AND ^{40}Ar IONS. Moak, C. D.; Dabbs, J. W. T.; Walker, W. W. (Oak Ridge National Lab., Tenn.). Contract W-7405-eng-26. Rev. Sci. Instrum., 37: 1131-4(Sept. 1966). (ORNL-P-2198).

When very heavy ions were directed along the crystalline channels of Si fission detectors, a three-fold improvement in energy resolution was obtained for particles remaining in the channels. For such channeled particles the usual pulse height defect was reduced by more than a factor of 10. The results seem to fit certain theoretical explanations of detector nonlinearities found in which the nonlinearities are ascribed to the predominance of atomic collision processes near the end of the range. (auth)

41325 NANOSECOND TIME RESOLUTION IN FISSION FRAGMENT X-RAY LIFETIME EXPERIMENTS USING THIN PLASTIC AND NaI(Tl) SCINTILLATION DETECTORS. Bridwell, L.; Wyman, M. E. (Univ. of Illinois, Urbana). Rev. Sci. Instrum., 37: 1145-50(Sept. 1966).

Apparatus for the half-life measurements of x rays from fission fragments is described. The fission fragment detector was an ultrathin plastic scintillator and the x-ray detector was a 1 mm NaI(Tl) crystal. Both detectors were mounted on fast (56 AVP) photomultipliers. The details of the design of the plastic scintillator are given and curves showing the double humped fission fragment kinetic energy spectrum are illustrated. A systematic study of the x-ray energy detection characteristics of the NaI(Tl) on a 56 AVP is given. The pulse heights were determined to be linear with x-ray energy and the spectra were shown to follow Poisson's statistics. The number of photoelectrons produced at the photocathode was determined to be 3.2 per kiloelectron volt. The time measuring device was a conventional time to amplitude converter using pulse overlap methods. The prompt response of this converter could be predicted from the results gained in the energy detector study. Both the width and the apparent half-life were consistent with the assumption that the time to amplitude converter was triggered on a single photoelectron. (auth)

41326 LITHIUM COMPENSATED SILICON FOCAL PLANE DETECTORS FOR ELECTRON SCATTERING SPECTROMETERS. Dodge, W. R.; Coleman, J. A.; Domen, S. R.; Whittaker, J. K. (National Bureau of Standards, Washington, D. C.). Rev. Sci. Instrum., 37: 1151-9(Sept. 1966).

In order to utilize the inherent resolving power of a double focusing, 169.8°, 76.2 cm radius of curvature magnetic spectrometer being constructed at the National Bureau of Standards for elastic and inelastic electron nuclear

scattering studies, focal plane counters were needed whose dimension along the direction of momentum dispersion was 1 mm. The fabrication techniques and performance of lithium compensated silicon 1 × 1 × 60 mm radiation detectors which seem well suited for use as focal plane detectors for the above spectrometer are described. Differential and integral pulse height distributions for 10–40 Mev electrons incident on the counters are presented as a function of the temperature and bias voltage. Effects due to the finite width of the counters are discussed. A tunnel diode discriminator which provides the desired binary information to the NBS data processing system is described. (auth)

41327 CONTINUOUS AVERAGING TECHNIQUE FOR AVOIDING DRIFT EFFECTS IN X-RAY SCATTERING MEASUREMENTS. **Peters, C. R.; Milberg, M. E. (Ford Motor Co., Dearborn, Mich.). Rev. Sci. Instrum., 37: 1186-9(Sept. 1966).**

A continuous averaging technique for avoiding the effects of long period drift in x-ray scattering measurements was developed. Only minor changes in conventional diffractometer equipment are required. A high speed drive motor is substituted for the conventional one in the diffractometer, and the scattered intensities are stored on paper tape. Thus, the sum of many rapid scans is substituted for one slow scan and the effective drift time is reduced to a negligible value. The actual summation of scattering patterns in proper register is done with an electronic computer. The scattering patterns obtained in this manner are expected to provide better structural information than was previously available concerning amorphous substances. Comparison of conventional and continuous averaging scattering patterns with and without an artificially imposed drift demonstrates that the method is effective. (auth)

41328 TO ENCAPSULATE EFFECTIVELY SCINTILLATION CRYSTALS FOR X-RAY DIFFRACTION WORK. **Samson, Sten (California Inst. of Tech., Pasadena). Rev. Sci. Instrum., 37: 1255(Sept. 1966).**

A technique for sealing a scintillation crystal inside a capsule in order to prevent the crystal from deteriorating is described. A thin layer of resin is used for the sealing process. Several crystals prepared by this process have been used for more than a year and show no sign of deterioration. (J.F.P.)

41329 LOW TEMPERATURE SPARK CHAMBER. **Leontic, B. A. (Brookhaven National Lab., Upton, N. Y.). Rev. Sci. Instrum., 37: 1255-6(Sept. 1966).**

A description is given of a spark chamber operated with helium and neon gas at liquid nitrogen temperatures. A schematic diagram of the apparatus and a typical track in neon are shown. A major departure from the spark chamber behavior at normal temperature was observed in that both gases showed considerable postdischarge phosphorescence, greenish in appearance. The recovery time appeared independent of the clearing field as long as the latter was maintained below 500 v/cm. When the value of the clearing field was increased above 1000 v/cm in either direction, the afterglow and the recovery time became noticeably longer. (J.F.P.)

41330 SIMPLE MARX HIGH VOLTAGE PULSE GENERATOR FOR WIDE GAP SPARK CHAMBERS. **Keller, L. P. (Argonne National Lab., Ill. Oklahoma State Univ., Stillwater); Walschon, E. G. Rev. Sci. Instrum., 37: 1258-9(Sept. 1966).**

A low-inductance high-capacitance Marx pulse generator built for use with a high precision wide gap spark chamber system which requires a rapidly rising 100 kv pulse is described. The circuit diagram and a pictorial drawing of the unit are shown. The observed pulses from the wide gap spark chamber and from a 200Ω resistive load are given. (J.F.P.)

41331 PULSE AMPLITUDE SHIFTS IN GAS PROPORTIONAL X-RAY DETECTORS. **Burkhalter, P. G.; Brown, J. D.; Myklebust, R. L. (College Park Metallurgy Research Center, Md.). Rev. Sci. Instrum., 37: 1267-8 (Sept. 1966).**

X-ray detectors were tested and compared for peak shifts under a variety of experimental conditions including gas flow, detector anode potential, amplifier gain, x-ray energy, and anode wire contamination. The pulse amplitude shifts with x-ray intensity and pulse amplitude shifts versus the detector anode potential are shown. (J.F.P.)

41332 ELIMINATION OF INTENSITY DEPENDENT SHIFTS IN PROPORTIONAL COUNTER PULSE HEIGHT DISTRIBUTIONS. **Spielberg, N. (Philips Labs., Briarcliff Manor, N. Y.). Rev. Sci. Instrum., 37: 1268-9 (Sept. 1966).**

It is postulated that the density of the positive ion space charge and hence its ability to screen the anode wire should depend upon the diameter of the anode wire in gas-filled proportional counters. It is shown that the use of sufficiently larger anode wires almost completely eliminates the shift of the pulse height distribution from the intensity effect. (J.F.P.)

41333 FAST NEUTRON MEASUREMENTS BY MEANS OF THRESHOLD DETECTORS IN THE PRESENCE OF 32 Mev X-RAYS. **Brenner, Marten W. (Univ. Central Hospital, Helsinki). Soc. Sci. Fenn., Comment. Phys.-Math., 31: No. 3, 13p(1965).**

The value of P, Al, Si, Fe as (n,p) detector and Al as (n,α) detector for neutrons in the presence of strong x-radiation of 32 Mev maximum energy, was studied. Only the activities due to (n,p) reactions in P and Al could be used to obtain information on the neutron flux, while the other detectors had to be discarded because of strongly competing photoreactions. The counting efficiency was determined experimentally using known activities produced in a reactor. The neutron flux of a betatron at the clinic for radiation therapy in Helsinki was determined. (auth)

41334 SENSITIVITY THRESHOLDS OF RADIOMETRIC ANALYSIS. **Baranov, V. I. pp 16-19 of Sovremennye Metody Analiza, Metody Issledovaniya Khimicheskogo Sostava i Stroeniya Veshchestv, Akademiya Nauk SSSR, Institut Geokhimii i Analiticheskoi Khimii im. V. I. Vernadskogo. Moscow, Izdatel'stvo Nauka, 1965. (In Russian).**

By variations in the disintegration of nuclear samples as well as variations in background activity the sensitivity of radiometric analysis was determined. The stability of the system and external conditions are important aspects of this sensitivity. It is shown that it is impossible to measure the activity of a sample with a high degree of accuracy (10%) when the background activity is greater than 10 times the activity of the sample. (B.G.D.)

41335 DETECTOR OF FAST NEUTRONS WITH A MODERATOR. **Braun, R.; Lipinskii, A.; Malecki, H.; Przytula, M. (Lodz Univ., USSR). Zesz. Nauk. Univ. Lodz., Ser. II, No. 17, 79-82(1964). (In Russian).**

A scintillation detector, consisting of a scintillator from silver-activated zinc sulfide and boron sinter, a plexiglas moderator, and two photomultiplier tubes, is described. Five layers of sinter 1 mm in thickness are inserted between the six plates of plexiglas, and neutrons falling perpendicularly to the plates are slowed down in the plexiglas. The slowing down takes place also in an additional moderator 16 mm in thickness placed in front of the detector. A 16 mm plexiglas layer placed behind the detector serves as a neutron reflector. Light flashes in the zinc sulfide produced by alpha particles from the reaction of the slowed-down neutrons are recorded by two photomultiplier tubes. This setup is advantageous in that a small number of photomultiplier tubes can record light flashes from a large surface. The pulses from the photomultiplier tubes are transferred first to simple cathode followers and then to a 20-meter concentric cable connected to an amplifier, discriminator, and computer. At 100 cm^2 of active detector surface the efficiency for neutrons from a Po-Be source amounts to about 5%. Detector sensitivity to gamma and x radiation is negligible under these conditions. (JPRS)

41336 GAMMA-RAY SCINTILLATION SPECTROMETER WITH NaI(Tl) SINGLE CRYSTAL. **Braun, Ryszard;**

Lipinski, Andrzej; Malecki, Henryk; Przytula, Marian. Zeszyty Nauk. Uniw. Lodz., Ser. II, 17: 83-8(1964). (In Polish).

This spectrometer is designed for the study of spectra of gamma rays emitted during the inelastic scattering of neutrons. The NaI(Tl) crystal is 38 mm in diameter and 38 mm in height. Pulses from the photomultiplier tube cathode are transferred to a WI-1 amplifier via cathode follower and a 20-meter concentric cable. Amplified pulses are analyzed by means of an AAI-02 analyzer. Spectra of gamma rays from ^{137}Cs, ^{65}Zn, and Po–Be sources and from the ^{11}B(p,γ)^{12}C reaction are produced. The resolving power of the spectrometer at E = 661 kev is 9.6%. Work is proceeding on two other single-crystal spectrometers and efforts are being made to improve their resolving power. (ATD)

41337 TWO-IMPULSE NEUTRON DETECTOR WITH PLASTIC SCINTILLATOR. Czepelska-Sulkowska, Barbara; Lipinski, Andrzej; Przytula, Marian (Univ., Lodz, Poland). Zesz. Nauk. Uniw. Lodz., Ser. II, 19: 31-3 (1965). (In Polish).

A scintillation detector with a plastic scintillator (3.2 cm × 3.2 cm) was constructed. The scintillator was covered with an external powder of zinc sulfide containing boron. Fast neutrons striking the detector can produce two pulses: the first is protons from the output of the plastic scintillator and the second is from α particles from ^{10}B(n,α)^{7}Li reaction in the zinc sulfide. By the method of delayed coincidences the time distribution of the secondary pulses is found with respect to the first in the presence of a Po–Be neutron source. The delayed coincidence curve with ^{60}Co γ sources was also shown. The results of the measurement of the neutron spectra were not reported as the counting statistics were not very reliable. (tr-auth)

41338 EFFICIENCY OF A HODOSCOPE FOR THE REGISTRATION OF CHARGED PARTICLES. Bonczak, Bazyli; Firkowski, Ryszard; Jarecki, Tadeusz; Jatczak, Jerzy (Univ., Lodz, Poland). Zesz. Nauk. Uniw. Lodz., Ser. II, 19: 35-45(1965). (In Polish).

A hodoscope was constructed from 30,000 Conversi detectors. The efficiency of the Conversi detector plates for the recording of charged particles in large air showers of cosmic radiation was investigated. Two methods were used for the measurement of the efficiency: comparison of the mean density of recorded particles from G-M counters and from the hodoscope and determination of the ratios of the number of ignited detectors and the number of detectors which a particle penetrates. It was shown that the efficiency of the Conversi detectors is 49% ± 1.3%. (tr-auth)

41339 MEASUREMENT OF EFFICIENCY OF LIQUID SCINTILLATION COUNTERS OF LARGE AREA. Bonczak, Bazyli; Jatczak, Jerzy; Lipinski, Andrzej; Stepinski, Marian (Univ., Lodz, Poland). Zesz. Nauk. Uniw. Lodz., Ser. II, 19: 47-53(1965). (In Polish).

The method of measuring the efficiency of large-area liquid scintillation counters is described, and results are given. The relative efficiency dependence on the distance of the γ incidence from the counter axis is determined from ^{60}Co γ rays. The pulse-forming systems from such a counter are discussed. (tr-auth)

41340 PYROGALLOL–AMIDOL DEVELOPER FOR NUCLEAR PHOTOEMULSIONS. Zakharov, V. I.; Novikova, N. R.; Perfilov, N. A.; Fadina, E. V. Zh. Nauch. Prikl. Fotogr. Kinematogr., 9: 422-5(Nov.-Dec. 1964). (In Russian).

The effect of a "leveling" developer with phenidone and some fast developers on nuclear photographic PR-2 exposed to relativistic electrons was examined. It was established that the best photographic properties were obtained by the use of pyrogallol–amidol developer. The grain density in the track after development in this developer increased approximately 25% with respect to the density obtained in the ID-19 developer and amidol. Moreover, pyrogallol–amidol developer guaranteed high homogeneity at greater depths than other developers studied. (tr-auth)

41341 MECHANISM FOR INCREASING LOW-TEMPERATURE SENSITIVITY OF NUCLEAR PHOTOGRAPHIC EMULSIONS. Kartuzhanskii, A. L.; Matvienko, V. I. Zh. Nauch. Prikl. Fotogr. Kinematogr., 11: 217-19(May-June 1966). (In Russian).

It was reported earlier that the temperature sensitivity toward the α radiation of ^{235}U of various nuclear emulsions sensitized with triethylamine (TEA) in the +20 to –196°C range increases more rapidly than the sensitivity of the unsensitized emulsions. The low-temperature sensitization by TEA was therefore more closely examined. It was found that TEA quenches the low-temperature fluorescence of the emulsion, without changing the spectral composition, or the quantum yield. The phenomenon is true quenching, rather than reabsorption. It was assumed that the phenomenon is similar to that occurring when iodide is eliminated from the system. However, it was demonstrated that TEA acts by means of a surface effect and the iodide through a volume effect. Whenever the presence of AgI stimulates the photographically ineffectual fluorescence, the quenching mechanism of TEA plays an important role by making use of the halide's luminescence energy. This recovery of energy is effective only if the silver halide crystals are able to absorb effectively the relatively long-wavelength radiation of the fluorescence. (TTT)

41342 TEMPERATURE LUMINESCENCE DECAY OF ZnS:Ag MONOCRYSTALS AT THE EXCITATION OF IONIZING RADIATION. Besel, V. S.; Gavrilov, F. F.; Bronnikov, V. K. Zh. Prikl. Spektrosk., Akad. Nauk BSSR, 3: 176-8(Aug. 1965). (In Russian).

The effect of the specific excitation density of the ionizing-particle track on the scintillation-pulse amplitude and temperature decay processes is considered. It is shown that the regularities observed can be explained if the possibility is assumed of a limitation of the excitation channel due to the action of electrostatic forces. (auth)

41343 MECHANISM OF RADIOLUMINESCENCE OF ALKALI METAL HALIDE CRYSTAL PHOSPHORS. Soovik, T. A. Zh. Prikl. Spektrosk., Akad. Nauk BSSR, 3: 279-82(Sept. 1965). (In Russian).

The causes of the great difference in the scintillation efficiency of members of the homologous series KI(Tl), KBr(Tl), and KCl(Tl) are discussed. For these phosphors experimental data are presented on the yield of stationary luminescence optically excited in the zone-to-zone transition region and in the long-wave exiton absorption band and on the relative scintillating efficiency. For KI(Tl) the dependence of these quantities on the concentration of the activator and the nature of the kinetics of photo- and cathode-luminescence are found. The facts presented are considered as strong evidence in favor of the important role of exiton processes in the phenomenon of scintillation in activated potassium halides. (auth)

41344 EFFECT OF PLASTIC DEFORMATION ON LIGHT STORAGE IN CRYSTALS OF NaI(Tl). Baturicheva, Z. B.; Gurevich, N. Yu.; Tsirlin, Yu. A. Zh. Prikl. Spektrosk., Akad. Nauk BSSR, 3: 282-4(Sept. 1965). (In Russian).

It is shown that the light stored in crystals of NaI(Tl), x irradiated at room temperature, is in the main due to thallium capture centers. The nature of capture centers in NaI(Tl) crystals, and also crystals of LiI(Tl), KI(Tl), and CsI(Tl) is discussed. (auth)

41345 DURATION OF SCINTILLATION OF MONOCRYSTALS OF CsI(Te) AS A FUNCTION OF THE CONCENTRATION OF THE ACTIVATOR. Vasileva, N. N. Zh. Prikl. Spektrosk., Akad. Nauk BSSR, 3: 470-2(Nov. 1965). (In Russian).

The dependence of warmup time of a protracted activator component of scintillation on the concentration of the activator is established. (auth)

41346 PLASTIC SCINTILLATOR WITH LIGHT YIELD PROPORTIONAL TO THE ENERGY OF OUTER ELECTRONS. Tsirlin, Yu. A.; Sokolovskaya, T. I.; Nikulina,

R. A.; Nagornaya, L. L.; Malkes, L. Ya.; Shubina, L. V. Zh. Prikl. Spektrosk., Akad. Nauk BSSR, 3: 571-3(Dec. 1965). (In Russian).

A plastic scintillator (polystyrenol +1% PBE) with light yield proportional to the energy of the outer electrons was developed. This scintillator has a higher light yield than other plastic scintillators at low energies (0 to 20 kev) which makes it convenient for detecting low energy electrons. (auth)

41347 THE EFFECT OF ANION ADMIXTURES ARISING IN THE PROCESS OF GROWTH ON LUMINESCENCE AND SCINTILLATION PROPERTIES OF MONOCRYSTALS NaI(Tl). Kostenko, N. S.; Mokhir, E. P.; Mustafina, R. Kh. Zh. Prikl. Spektrosk., Akad. Nauk BSSR, 3: 573-5(Dec. 1965). (In Russian).

The formation of impurities of carbonate and iodate in growing crystals of NaI in air, their effect on the inertia properties, and scintillation characteristics of crystals (light yield, energy, and time resolving power) is studied. (auth)

41348 A SVARTHOLM-SIEGBAHN TYPE BETA SPECTROMETER WITH ADJUSTABLE ANGULAR SEPARATION BETWEEN SOURCE AND DETECTOR. Bobykin, B. V.; Babenkov, M. I. Zh. Tekh. Fiz., 36: 931-6(May 1966). (In Russian).

The performance is described of a double focusing magnetic beta spectrometer with iron pole pieces in which the approximately $\pi\sqrt{2}$ angular separation between the source and the detector was made adjustable to compensate for the deviation of the magnetic field from the ideal distribution and the variation of field distribution with field strength due to the nonlinear magnetic properties of the pole pieces. The radius of the electron-optical axis was 24.3 cm, and the position on this axis of the detector, consisting of two Geiger-Müller counters in coincidence, could be varied through an angle of about 10° by means of a micrometer screw working through a Wilson vacuum joint. The instrument was operated with the detector at the position of best radial focus, the consequent deterioration of vertical focusing being compensated by lengthening the entrance slit to the detector. The optimum position of the detector for each magnetic field strength (electron energy) was determined by repeatedly measuring the width of a conversion line in the corresponding energy region with the detector in different positions. The optimum angle decreased by about 4° as the $H\rho$ value was increased from 700 to 1100 Oe cm and remained nearly constant with further increase of $H\rho$ to 3500 Oe cm. The optimum angle also depended appreciably on the magnetic history of the pole pieces, but the relation between optimum angle and electron energy was adequately reproducible when the pole pieces were suitably prepared between measurements. The measured full width at half-maximum of the 74.9-kev conversion line from 1 × 20 mm ^{152,154}Eu source was 0.15% when the 1.2 × 20 mm entrance slit to the detector was at the optimum position. Shifting the detector position by 3° to either side of the optimum position increased the measured half-width to 0.17%. Relative intensities of conversion lines were correctly measured even when the position of the detector was as much as 8-10° from the optimum position. (ATD)

41349 GAMMA DIRECTIONAL SENSOR (Engineering Materials). (Goodyear Atomic Corp., Portsmouth, Ohio). (CAPE-1472).

10 drawings.

A portable sensor used in finding the source of a nuclear excursion is designed. The device, based on the use of a Geiger-Mueller gamma survey meter, can locate an excursion within ±5° by triangulation, without endangering the surveyor. Elevation and azimuth angles can be measured. The device can be used in large one-floor or multi-storied storage areas or processing facilities. (F.S.)

41350 ULTRAHIGH VACUUM GRATING SPECTROGRAPH WITH GLACING INCIDENCE FOR STUDIES OF VERY SOFT X RAYS. MEASUREMENTS WITH Si, Al, Be, Cb, AND Mo. Wiech, G. Munster, Ger., Univ., Munster, 1965. 100p. $2.00 Gmelin, AED-Diss. 65-301.

Thesis.

Design and construction of a grating spectrograph for soft x rays is described. L and K emission bands of various substances are studied. Dependence of line energy and shape on chemical composition is investigated for elements and oxides. (Gmelin Inst.)

41351 DETECTION OF SLOW ELECTRONS PRODUCED IN A HIGH VACUUM BY MEANS OF A FLOW COUNTER WITH PRESSURE STAGE. Zimmer, F. Dresden, Technische Hochschule, 1965. 110p. $2.00 Gmelin, AED-Diss. 65-295.

Thesis.

A proportional counter for low energy electrons is described. 8-kev electrons which are produced in a high vacuum are passed through a pressure difference stage into the counter. Thermal- and photo-emission of electrons is discussed. (Gmelin Inst.)

41352 SEMICONDUCTOR COUNTERS FOR NUCLEAR RADIATIONS. Second Edition. Dearnaley, G.; Northrop, D. C. New York, John Wiley and Sons, Inc., 1966. 477p. $12.75.

The discussion of semiconductor counters for nuclear radiations includes the properties of nuclear radiations and their absorption in solids. The principles of operation of other types of detectors are summarized, and comparisons are drawn. The behavior and requirements of semiconductors such as low noise, large volume, and good absorption are considered, and semiconductor diodes, preparation and testing of detectors, and their applications are discussed. Also considered are the effects of radiation damage. (J.F.P.)

41353 PRACTICAL GAMMA SPECTROMETRY. Duivenstijn, A. J.; Venverloo, L. A. J. Philips Technical Library Series. Springfield, Ill., Charles C Thomas, 1963. 152p.

Translated from the Dutch by G. du Cloux.

An introduction to practical gamma spectrometry is presented. Stable and radioactive atoms, radiation and matter, radiation detectors, the gamma spectrometer, qualitative and quantitative interpretations of gamma spectra measurements and special spectrometer techniques are discussed. (J.F.P.)

41354 CONSTRUCTION OF A CURRENT GENERATOR FOR A PRECISION β SPECTROMETER AND MEASUREMENTS OF CONVERSION LINES. Kuntze, M. Heidelberg, Univ., Heidelberg, 1965. 52p. $2.00 Gmelin, AED-Diss. 65-310.

Thesis.

An iron free precision β spectrometer with a new focusing principle is described. The exit slit is curved. A highly inhomogeneous magnetic field is produced by 5 coil pairs. Focusing of electrons up to 4.4 Mev is possible. A magnet current generator with a stability of 2×10^{-5} is described. Resolution is 1.3×10^{-4}. Preliminary data of ^{192}Ir conversion spectra are reported. Natural line width of the F line of ThB is 80 ± 10 ev. (Gmelin Inst.)

41355 CONSTRUCTION OF A β SPECTROMETER WITH A FOCUSING ANGLE $(\pi/2)\cdot\sqrt{13}$. Jahn, P. Heidelberg, Univ., 1964. 56p. $2.00 Gmelin, AED-Diss. 64-2003.

Thesis.

Design and construction of a flat magnetic β spectrometer with a new focusing principle is described. Focusing angle is 324.5° and the radius of the stationary orbit 30 cm. The spectrometer was tested with conversion lines. Best resolution is 1.3×10^{-4}. Effective solid angle is larger than that of comparable double focusing spectrometers. (Gmelin Inst.)

41356 CONSTRUCTION OF A HIGH PRESSURE DIFFUSION CLOUD CHAMBER AND STUDIES OF ITS OPERATION PROPERTIES. Greiner, E. Jena, Ger., Univ., 1964. 111p. $2.00 Gmelin, AED-Diss. 64-1085.

Thesis.

A theory of the diffusion cloud chamber using Volmer's theory of drop formation is given. Construction of a cloud chamber for pressures up to 65 atm is described. The chamber was tested with 14-Mev neutrons. Methods for stereographic analysis are discussed. (Gmelin Inst.)

41357 A NEW METHOD FOR THE DETERMINATION OF ELECTRON LIFETIME IN BF_3 PROPORTIONAL COUNTERS. Froehlich, H. Jena, Ger., Univ., 1965. 63p. $2.00 Gmelin, AED-Diss. 65-356.

Thesis

Electron lifetime and electron loss factors in BF_3 counters are calculated from differential pulse height spectra. Lifetime depends on field strength and has a maximum value at the anode. An empirical equation relating electron lifetime to the amplitude of pulses starting near anode and cathode is given. (Gmelin Inst.)

41358 DEVICE FOR THE MEASUREMENT OF NEUTRON RADIATION. Pychlau, Herbert (to Physikalisch-Technische Werkstaetten). German Patent 1,215,263. Apr. 28, 1966. Filed Jan. 29, 1964.

A single, short-time neutron pulse generated by a reactor accident or the explosion of a nuclear bomb is detected by the neutron activation of a substance, e.g. gold. A foil metal of the substance to be activated is placed in front of a counter tube, and an electrostatic relay, which is actuated by means of an ionization chamber exposed to the neutron radiation, switches on the counter tube after the decay of the neutron pulse. (Gmelin Inst.)

41359 CLOSING DEVICE FOR LARGE-SURFACE FORMED METHANE FLOW COUNTER. Kimmel, Hermann. German Patent 1,216,444. May 12, 1966. Filed July 1, 1961.

The body of the counter is made of sheet metal formed by noncutting shaping, and comprises an upper piece containing the sensitive counter volume and constructed in the shape of an inverted pot, and a lower base plate on which the sample to be measured is located. The base plate is pressed against the edges of the upper piece of the counter body by means of an eccentric press, the sealing being provided by compression across the edges which are covered with U-shaped profile washers of rubber. (Gmelin Inst.)

41360 METHOD FOR THE GAMMA COMPENSATION OF AN IONIZATION CHAMBER FOR THE DETECTION OF A NEUTRON FLUX IN NUCLEAR REACTORS. Schmid, Paul; Comunetti, Angeolo; Huerlimann, Theodor (to Technische Hochschule, Zurich). German Patent 1,218,626. June 8, 1966. Priority date Mar. 1, 1963, Switzerland.

The ionization chamber comprises a measuring electrode in the middle of the chamber forming, with the bias electrode on one side of the chamber, a neutron reaction space, and with the compensation electrode on the other side of the chamber, a gamma reaction space. The bias voltage is positive for the time intervals dT and negative for time intervals T−dT; dT/T is adjustable between 0.1 and 0.4. The chamber is overcompensated. The resulting current in the chamber has a mean value proportional to the mean neutron flux. The interval dT is chosen for allowing the restoration of the ions to equilibrium. (Gmelin Inst.)

41361 SEMICONDUCTOR AMPLIFYING RADIATION DETECTOR. Bergstrom, James W.; Bockemuehl, Robert R. (to General Motors Corp.). U. S. Patent 3,265,899. Aug. 9, 1966. Filed July 25, 1962.

A radiation detector means which is capable of controlling sizable currents and has a short time of response even at high frequencies is described. The design of this semiconductor amplifying radiation detector is shown and discussed. (J.F.P.)

41362 NEUTRON DOSIMETER. Fendler, Heinz-Gerhard (to Licentia Patent-Verwaltungs-GmbH). German Patent 1,216,997. May 18, 1966. Filed Oct. 30, 1964.

A neutron dose-rate meter for measuring the dose rates of fast, intermediate and thermal neutrons comprises a neutron sensitive scintillation crystal surrounded by a liquid moderator which is contained in a chamber with flexible walls. The volume of the chamber is varied by changing the pressure and the quantity of the liquid moderator within the chamber. (Gmelin Inst.)

41363 METHOD FOR THE PRODUCTION OF SURFACE-BARRIER DETECTORS FOR NUCLEAR RADIATION. Kaufmann, Klaus (to Deutsche Akademie der Wissenschaften). German Patent 1,218,073. June 2, 1966. Filed Nov. 18, 1963.

The method comprises the steps of treating p-type silicon discs with an amine containing substance, e.g., epoxies with amine containing hardeners, of storing the discs on air, and of depositing gold by evaporation. (Gmelin Inst.)

41364 DEVICE FOR DETECTING AND MEASURING HIGH ENERGY PARTICLES OF A PREDETERMINED ENERGY LEVEL. Baker, Edward J. (to U. S. Army). U. S. Patent 3,265,895. Aug. 9, 1966. Filed June 8, 1965.

A detection device is designed in which a resonator structure is disposed within a cylindrical chamber and is provided with several angularly disposed cavity resonators. At least one of the cavity resonators is provided with an output loop for coupling energy developed by the resonator structure to a spectrum analyzer or other type of indicator. A window is provided in the peripheral wall of the casing. The casing is evacuated and is supported between the poles of a powerful magnet. The device is capable of detecting the presence of particles of a preselected level in a radiation environment. (L.B.S.)

41365 RADIATION GAUGING SYSTEM WITH COMPENSATION FOR HIGH BACKGROUND RADIATION INTENSITIES. Brunton, Donald C.; McMullen, James M. (to Industrial Nucleonics Corp.). U. S. Patent 3,255,346. June 7, 1966. Filed Oct. 30, 1961.

A radiation gaging system is provided for use in situations having a high background radiation, e.g. in measurement of liquid level in the heat exchanger of a nuclear reactor. The apparatus includes a radiation source, a pair of radiation detectors, and shielding means for the source and the detectors. One detector receives the combined radiations of both the material and the field to produce a signal that is a function of the intensity of the combined radiations. A second detector is shielded from the material radiation and provides a signal responsive to the background radiation. These signals are combined to obtain an output signal that is a function of the material properties being measured irrespective of variations in the intensity of the background radiation. (B.L.M.)

41366 SCINTILLATION ALPHA COUNTER. Moon, Jack L. (to Eberline Instrument Corp.). U. S. Patent 3,256,436. June 14, 1966. Filed May 22, 1963.

A counter for alpha particles is provided in which the material to be counted may be placed either within a drawer in the instrument or opposed to a hand probe and the integrated magnitude of the radiation is continuously indicated on indicators reading in decades. The device is constructed on three chassis which are mounted within a housing or cabinet. The first chassis includes control and power supply components; the second, detector components; and the third, indicator components. The power supply includes a high voltage supply, a first conductor connected between the high voltage supply and the detector head, and a-c impedance tapping the conductor, and a second conductor from the impedance to the counter to transmit pulses on the first conductor to the counter. A trigger is interposed between the second conductor and the counter, and a control relay is interposed between the trigger and the counter. The counter is provided with a safety device to prevent injury to the detector due to too much light striking the detector upon opening the drawer. The detector material is zinc sulfide mounted on an adhesive substance. This combination is placed over the open end of a torus having the other open end abutting a photomultiplier tube. (B.L.M.)

41367 IMPROVEMENTS RELATING TO SOLID-STATE RADIATION DETECTORS. Freck, David Vernon; Wakefield, James (to Associated Electrical Industries Ltd.). British Patent 1,038,041. Aug. 3, 1966. Filed Oct. 4, 1961.

A method is described for manufacturing a solid state p-i-n junction radiation detection apparatus consists in heating a member formed of a p-type semiconductor element having an atomic number of at least 30, preferably Ge, in a stream of Li in an inert gas formed by passing the gas over a Li-source heated to about 700°C while the Ge is heated to about 200°C to diffuse the Li into the semiconductor to form a p-n junction. A reverse electrical bias is then applied across the junction while the semiconductor is heated to about 70°C to increase the thickness of the depletion zone and form a p-i-n junction device. The device is then connected in circuit with a voltage pulse height analyzer. (B.L.M.)

41368 IMPROVEMENTS RELATING TO RADIATION DETECTOR APPARATUS. Freck, David Vernon (to Associated Electrical Industries Ltd.). British Patent 1,038,042. Aug. 3, 1966. Filed Apr. 19, 1962.

A radiation detection apparatus includes a solid state detector feeding a pulse height analyzer apparatus providing both a required channel output and unwanted channel outputs adjacent to the required channel. The unwanted channel outputs are provided at both higher and lower energies than the required channel output, and means are provided for averaging the adjacent channel outputs and subtracting the mean value from the required channel output. (B.L.M.)

41369 PARTICLE DETECTOR OF THE SEMI-CONDUCTOR TYPE. Walsh, Charles J.; Sandborg, Alan O. (to Nuclear Diodes, Inc.). U. S. Patent 3,255,351. June 7, 1966. Filed Apr. 19, 1963.

In a system for particle identification an energy detecting device is provided in which the mass-charge-energy detector and the energy detector are both interchangeable and can be substituted conveniently without endangering the semiconductor barriers. The first detector includes a first apertured conductive housing in which is supported an insulator plate that is apertured concentrically with the housing. A first semi-conductor barrier is mounted to the insulator plate at its aperture and is of a thickness so as to dissipate in the barrier without totally absorbing the energy of any one of the intercepted radiation particles. A conductive coating is provided between the one surface of the first semiconductor barrier and the conductive housing, and a first electrode extends from the other surface of the semiconductor barrier. A second apertured conductive housing of the second detector is coaxially aligned with the aperture of the first housing and is detachably engaged to the first housing. The second detector is formed essentially like the first except the second conductive barrier is of a thickness so as to absorb substantially all the remaining energy of one intercepted particle. A conductive base connector is formed to detachably engage the second conductive housing for applying a reference voltage to the first and second housings and to the surfaces of the first and second barriers electrically connected to the housings. At the first electrode a potential can be established across the first barrier, and changes in the potential responsive to dissipation in the barrier of the energy of one radiation particle can be detected; while at the second electrode a potential can be established across the second barrier, and changes in potential responsive to absorption in the barrier of energy of the radiation particle can be detected. (B.L.M.)

41370 THERMOLUMINESCENT DOSIMETRY METHOD. Fix, Richard C. (to Controls for Radiation, Inc.). U. S. Patent 3,255,350. June 7, 1966. Filed Dec. 10, 1962.

A thermoluminescent dosimeter is provided that provides an accurate indication of neutral particle doses and that simulates tissue response to both charged and uncharged radiation. A thermoluminescent material in powdered form is disposed in intimate contact with a hydrogenous material capable of being completely removed from the thermoluminescent material. The preferred combination is ^{7}LiF in alcohol in which the alcohol can be removed by evaporation. The dosimeter is not restricted to the use of this combination, and other hydrogenous materials that may be used are powdered acrylic resins of a different sieve size than the thermoluminescent material which may be removed by mechanical separation or materials capable of complete separation from the thermoluminescent material by a flotation process. The mixture of materials is placed in a dosimeter capsule or container of non-hydrogenous material whose constituents all have a low atomic number, preferably below 10. The dosimeter is coupled with duplicate dosimeter that does not incorporate the hydrogenous material. Both dosimeters are irradiated; and after the hydrogenous material is removed from the one, the pure luminescent material from both is heated to provide an indication of the total radiation in the case of the dosimeter containing the hydrogeneous material and of the charged particle radiation in the case of the other dosimeter. The difference of the output of the two dosimeters provides an indication of the neutral particle radiation. (B.L.M.)

41371 GAMMA-GAMMA DIRECTIONAL CORRELATION. Clark, Gary Edwin (Kansas State Univ., Manhattan). 9p. (CONF-660550-1). ORAU. Gmelin, AED-CONF-66-139-1.

From Kansas Academy of Science, 98th Annual Meeting, Topeka, Kan.

The coefficients A_0, A_2, and A_4 are found for the directional correlation function, $W(e) = A_0P_0 + A_2P_2(\cos e) + A_4P_4(\cos e)$, which expresses the dependence of the coincident cascade gamma rays on the angle between the detectors. It is assumed that the A's must be normalized, and thus W(e) is the actual coincidence counting rate. (J.F.P.)

41372 RADON EFFECT WITH A COPPER COUNTING TUBE. Freundlich, J. 3p. (CONF-650652-19). ORAU. Gmelin, AED-CONF-65-158-28.

From 6th International Conference on Radiocarbon and Tritium Dating, Pullman, Wash.

A low but quantitatively measurable alpha count rate is observed with a proportional counter made of high purity copper tubing, the observed time dependence of which corresponds to ^{222}Rn (namely, a half life of approx. 4 days). A series of checks was made in order to test the relevance of alternative assumptions for explaining the effect. Their results are, however, in accord with the ^{222}Rn assumption. The time dependent increase of count rate in the alpha channel is accompanied by an equivalent increase of count rate in the anticoincidence line, which shows to be three times that of the alpha count rate. (auth)

41373 DEVELOPMENT OF THERMOLUMINESCENT DOSIMETERS AT TROMBAY. Nambi, K. S. V.; Gurg, R. P.; Sunta, C. M. (Atomic Energy Establishment, Trombay, India). 15p. (CONF-660621-15). ORAU. Gmelin, AED-CONF-66-193-8.

From Health Physics Society, 11th Annual Meeting, Houston, Tex.

A preliminary report on work being done on thermoluminescent dosimetry at Trombay is presented. Some thermoluminescent materials were prepared and their sensitivities are compared with natural calcium fluoride and Harshaw's lithium fluoride. A dosimeter using natural calcium fluoride was developed and calibrated for use for specific purposes. It consists of a Kanthal strip on which is firmly deposited a thin layer of the thermoluminescent material. The reader system consists of an assembly in which the dosimeter strip is heated by passing a heavy electric current to release the glow which is measured by a photomultiplier tube. Doses above 10 mr can be read. In the study of composition and preparation of thermoluminescent materials of possible use in dosimetry, calcium fluoride samples doped with uranium, thorium, manganese, samarium, cerium, etc., were prepared and tested. Promising results were obtained with some of them. Lithium

fluoride samples were also prepared and tested. The various observations in detail are given. (auth)

41374 HIGH TEMPERATURE RUGGEDIZED MULTIPLIER PHOTOTUBES. Rome, Martin (Electro-Mechanical Research, Inc., Princeton, N. J.). 21p. (CONF-660207-24). ORAU. Gmelin, AED-CONF-66-011-33.

From Radioisotope Applications in Aerospace Symposium, Dayton, Ohio.

The design and performance of a highly ruggedized multiplier phototube for use in scintillation counting at high temperatures are described. The tube, with a 1" diameter photocathode of approximately 20% quantum efficiency, is capable of withstanding shock in excess of 1000 g. The dark current rate at room temperature is 100 counts/second, doubling with approximately every 9°C increase in temperature. A comparison of pulse height resolution of the tube alone (using a CRT light source) and the resolution of a scintillation crystal-tube combination shows the crystal to be the principal cause of line width spread. At 150°C the increase in pulse height resolution with temperature of the crystal is twice that of the tube. The room temperature pulse height spectrum of ^{55}Fe (6 kev x-ray) obtained with a beryllium window NaI(Tl) crystal and an ASCOP 541N tube shows a clear separation between the photopeak and the dark current pulses. At 100°C a dark current count rate of approximately 10 cps is estimated from the tube data presented. (auth)

41375 LASER INDUCED PREBREAKDOWN AND BREAKDOWN PHENOMENA OBSERVED IN CLOUD CHAMBERS. Naiman, C. S.; Schwartz, J.; DeWolf, M. Y.; Goldblatt, I. (MITHRAS, Inc., Cambridge, Mass.). 22p. (CONF-660438-2). ORAU. Gmelin, AED-CONF-66-078-5.

From International Quantum Electronics Conference, Phoenix, Ariz.

Direct observation of initiating electrons is reported and ascribed to photoionization. Sensitive cloud chamber techniques were applied to the search for soft x-ray luminescence and upper limits were determined. (auth)

41376 VACUUM ENCAPSULATED LITHIUM-DRIFT DETECTOR TELESCOPE. Hayashi, I.; Kern, H. E.; Rodgers, J. W.; Wheatley, G. H. (Bell Telephone Labs., Inc., Murray Hill, N. J.). 26p. (CONF-660304-22). ORAU. Gmelin, AED-CONF-66-020-44.

From Institute of Electrical and Electronics Engineers, Scintillation and Semiconductor Counter Symposium, Washington, D. C.

Fabrication techniques for producing lithium-drifted telescopes for space experiments were developed. High resistance grooves were obtained in lithium-drifted silicon detectors which can separate the detector into independent regions having small cross-talk as well as sharp spatial definition. This indicates the possibility of making integrated arrays of lithium-drifted detectors in a single substrate. The origin of leakage current and noise is not yet clear. The surface condition of the n-i junctions can be a contributing factor. In addition, there are indications that the surface barrier plays a prominent role in this problem. Results of environmental life tests show that the methods of detector fabrication and vacuum encapsulation are capable of providing detectors with the stability required for space experiments. (auth)

41377 DIRECT READING INTRACAVITARY DOSIMETER FOR USE IN RADIUM THERAPY. Baily, Norman A.; Norman, Amos; Hilbert, Jerald W. (Univ. of California, Los Angeles). 16p. (CONF-660433-1). ORAU. Gmelin, AED-CONF-66-064-2.

From American Radium Society, 48th Annual Meeting, Phoenix, Ariz.

Direct dosimeter systems used in treating cancer of the vagina, cervix, or body of the uterus with intracavitary radium or external radiation are discussed. Instrumentation parameters and clinical experience are presented for silicon particle detectors operated in a mode where the carrier generation due to gamma rays interacting with the bulk silicon is measured by means of the open circuit voltage induced by these carriers. The dosimeter described is characterized by high sensitivity, rapid response, simple readout, and flexibility. (H.G.D.)

41378 A 73 WATT, 3 DEG K HELIUM REFRIGERATOR USING GAS BEARING TURBINES. Firth, M.; Ward, D. E.; Gardner, J. B. (British Oxygen Cryoproducts, London). 14p. (CONF-660628-4). ORAU. Gmelin, AED-CONF-66-173-9.

From International Institute of Refrigeration Commission Meeting, Boulder, Colo.

A refrigerator built to operate with an 80-cm helium bubble chamber at a temperature as low as 3°K is described. The control systems and turbines are discussed, and the general arrangement of the fixed plant is shown. A general view of the mobile part of the plant is included, and performance of the plant is discussed. (J.H.M.)

Radiation Effects

Refer also to abstract 42536.

41379 PHOTOCONDUCTIVITY OF p-TYPE SILICON IRRADIATED BY FAST ELECTRONS. Sevchenko, A. N.; Tkachev, V. D. (Lenin Belorussian State Univ., USSR). Dokl. Akad. Nauk BSSR, 10: 80-2(Feb. 1966). (In Russian).

The kinetics of formation and the stability of radiation damage in p-type silicon exposed to 1-Mev electrons at integral doses of 10^{13} to 10^{18} electrons/cm^2 were investigated. The radiation damage is due to impurities in the starting material; therefore, care was taken that the concentration of residual chemical impurities with energy levels in the forbidden zone should not exceed 4 to 6×10^{11} cm^{-3}. It was found that the radiation caused the formation of centers which introduced the following local energy levels: $E_v + 0.30$ ev, $E_v + 0.38$ ev and $E_v + 0.45$ ev. As the total flux is increased, the shape of the photoconductivity spectrum is changed, indicating changes in the appearance of radiation damage. The $E_v + 0.30$ centers were found to be the most effective ones; further increase of the electron flux resulted in the disappearance of the structure at the long-wave-length portion of the spectrum, indicating that effectiveness of formation of the radiation damage is indeed dependent on the impurities within the starting material. The results were ascribed in part to a redistribution of the point damage between several impurity atoms. (TTT)

ISOTOPE TECHNOLOGY

General

Refer also to abstract 41264.

41380 (IFA-IS-36) STABLE ISOTOPES APPLICATIONS. I. APPLICATIONS IN PHYSICS, CHEMISTRY, AND GEOLOGY. Vasaru, Gheorghe (Institutul de Fizica Atomica, Academia R. P. R., Bucharest (Romania)). Translated from Stud. Cercet. Fiz., 16: 701-28(1964). 47p. Dep. mn. JCL $4.60 fs, $1.61 mf.

Stable isotopes may be used either as tracers or as pure monoisotopic materials. As a tracer, the stable isotope will follow the chemical which it represents. When using it as a pure material, it influences the process in which it takes part. Applications of stable isotopes in geology, chemistry, and physics are described. One hundred thirty-two references are included. (F.S.)

41381 MEASUREMENT OF GAS VELOCITIES BY THE RADIATION-MODULATION TECHNIQUE. Loeffler, Helmut; Richter, Karl (Institut fuer Anwendung Radioaktiver Isotope, Aussenstelle Pirna-Copitz, Pirna-Copitz, Ger.). Wiss. Z. Tech. Univ. Dresden, 14: 1131-3(1965). (In German).

Periodic labeling of a gas stream with ions permits determination of the gas velocity by determining the transit time of the ions. An apparatus for using this radiation modulation technique is described; it is designed for measurements in the velocity range from 2 to 20 m/sec. The source of radiation is a ^{85}Kr preparation; a mechanical modulator produces ions periodically. Two ion detectors operating on the influence principle are used for finding the transit time. The impulse from each detector is amplified and univibrated, giving a bistable inclined gradation. The duration of the inclined impulse is identical to the time separation of the detector emission impulse. After integration the signal can be recorded. Preliminary results are shown. Continuous measurement is provided. There is no cross section contraction, as is found with other measuring devices. (BBB)

41382 RADIOACTIVE MATERIALS. Catalog and Price List. Pittsburgh, Nuclear Science and Engineering Corporation, 1965. 72p.

Availability, specifications, and prices are presented for ~95 radioisotopes. The principal specifications for radioisotopes are specific activity, radiochemical purity, and concentration. (R.C.K.)

Industrial Applications

Refer also to abstracts 40699, 41319, and 42687.

41383 (CONF-650552) RADIATION PRESERVATION OF FOODS. A Symposium held May 19, 1965 in Conjunction with 25th Annual Meeting, Institute of Food Technologists, Kansas City, Missouri. (Division of Isotopes Development (AEC), Washington, D. C.). Aug. 1966. 106p. Dep. mn. CFSTI $1.25 cy, $0.75 mn.

Major developments in the research programs on the radiation preservation of foods in the United States in the past twenty-five years are outlined. As further research information has become available, greater awareness of the potential for selected applications of radiation both at "sterilization" and at "pasteurization" doses has become evident. Intensive studies on quality factors (flavor, color, texture, nutritive value and wholesomeness) in foods as influenced by radiation and alternate processing systems show that radiation is technically feasible in several instances. The transition from "scientific feasibility" to "commercial feasibility" is now being approached. (auth)

41384 (TID-22833) STUDY OF IRRADIATED-PASTEURIZED FISHERY PRODUCTS. Period Covering October 1, 1964–September 30, 1965. Slavin, Joseph W.; Ronsivalli, Louis J.; Kaylor, John D.; Carver, Joseph H. (Bureau of Commercial Fisheries, Gloucester, Mass. Technological Lab.). Contract AT(49-11)-1889. 190p. Dep. mn. CFSTI $5.00 cy, $1.00 mn.

Cooked, air-packed lobster meat was successfully radiopasteurized at levels ranging from 150,000 to 450,000 rads γ radiation. All samples were considered good throughout a 4 week storage period at 33 to 35°F. Cod fillets radiopasteurized at 15,000 rads and held for 4 weeks at 33°F were judged organoleptically acceptable by taste panels. Fillets cut from one to two day old fish stored for one day at 42°F had a post-irradiation shelf life of 8 to 13 days at 33°F. Many available flexible plastic materials having low gas permeability were found acceptable for packaging radiopasteurized fish. Bacterial permeability of plastic films presented no problem. Carbonyl and sulfide compounds that affect the flavor and odor of cod fillets and clam meat were identified by the use of classical methods, gas chromatography, and mass spectrometry in raw and cooked, fresh and stored, and irradiated and non-irradiated samples. Generally, the number of volatile compounds and the concentration of some compounds increased with increasing doses of ionizing radiation but apparently no abnormal compounds formed. Studies to determine the reliability of microbiological sampling techniques showed that a 50 gram sample was satisfactory for estimating the average total aerobic bacterial count of a fillet. Haddock fillets irradiated at 150,000 rem had a maximum shelf life of about 24 days, but this was found to be shorter than the time required for the development of Clostridium botulinum Type E toxin in heavily inoculated fillets. Tests showed that botulism toxin was destroyed by ordinary cooking methods. A tracer technique was developed that showed that certain Na salts, which inhibit the growth of Clostridium when used in dips, penetrate throughout the fillet to effective concentrations. Preliminary studies indicated the Marine Products Development Irradiator is basically suitable for the irradiation of commercial shipments of fish. (C.H.)

41385 (TID-23136) GAMMA RADIATION OF FRUITS TO EXTEND MARKET LIFE. Marketing Research Report No. 717. Bramlage, William J.; Couey, H. Melvin (Department of Agriculture, Washington, D. C.). Nov. 1965. Contract AT(49-11)-2342. 27p. Dep. mn. GPO $0.15.

Eleven kinds of fresh fruits were irradiated to determine possible extension of the market life. Gamma irradiation of strawberries and two varieties of fig extended the market life by several days through reduction of decay, without apparent impairment of fruit quality. Brown rot, but not Rhizopus rot, of peaches and nectarines was controlled; the peaches softened during irradiation and subsequently developed more red color but less flavor than the controls. Radiation inhibited blue coloring of plums and increased softening of the fruits. Low doses inhibited ripening of pears by several days, but the resultant ripening was abnormal. Decay of grapes was controlled less effectively by radiation than by the customary sulfur dioxide fumigation. Radiation increased rind pitting of oranges without reducing decay during semicommercial tests. Irradiated apples were softer, more shriveled, and had less flavor than the controls following storage for 3 to 6 months. Avocados and olives were severely discolored both internally and externally by radiation. Individual varieties of peaches and figs responded quite differently to radiation. Water on the surface of peaches during irradiation caused spotting of the skin. The stage of development of fungal infections determined the effectiveness of radiation as a decay-control agent for oranges. Fruit maturity within the limits of these experiments did not affect the responses to radiation. (auth)

41386 (JPRS-36895) ACTIVITIES OF THE ISOTOPE INSTITUTE OF THE NATIONAL ATOMIC ENERGY COMMITTEE. Tetenyi, Pal. Translated from Magyar Tud. Akad. Kem. Tud. Osztalyanak Kozlem., 25: 419-29(1966). 15p. (TT-66-33325). CFSTI $1.00 cy, $0.50 mn.

The production of isotope preparations, development of isotope applications, and utilization of the Isotope Institute of the National Atomic Energy Committee of Hungary are reviewed. (F.S.)

41387 MICROBIOLOGICAL STUDIES ON THE INFLUENCE OF COMBINED PROCESSES OF HEAT AND IRRADIATION ON THE SURVIVAL OF SACCHAROMYCES CEREVISIAE VAR. ELLIPSOIDEUS. Stehlik, G.; Kaindl, K. (Reactor Center, Seibersdorf, Austria). Vienna, International Atomic Energy Agency, 1966, Preprint SM-73/43, 7p. (CONF-660609-14). ORAU.

From International Symposium on Food Irradiation, Karlsruhe, Ger.

The effect of heat and irradiation treatments on the survival of yeast cells (colony formation) is described. A highly radioresistant strain, Saccharomyces cerevisiae var. ellipsoideus, grown in a semi-synthetic medium, was given a combined treatment of heating and gamma-irradiation (^{60}Co source) at the beginning of its log-phase. The heat treatment was applied either immediately before, during, or immediately after the irradiation process. The temperature was varied between 20°C and 52.5°C. The irradiation treatment was carried out with a dose range up to 0.3×10^6 rads in a well-aired glass tube. The inhibiting effect of this combined treatment depends upon the sequence of heating and irradiation and shows the following results: the most effective combination is the simultaneous treatment of heating and irradiation; less effective is the combination wherein irradiation at room temperature follows the heating procedure; and most ineffective is heating after irradiation at room temperature. The combined heat/irradiation treatment results in survival curves (survival fractions) that are straight lines in relation to the irradiation dose at a semi-logarithmic scale in the temperature range between room temperature and 45°C. Above 45°C the curves show at doses lower than 30 krad an increase of the survivals compared with the unirradiated sample. By comparing the slopes of the survival curves obtained at different temperatures, it is shown that in the case of irradiation at temperatures higher than 40°C, there is a high synergistic effect for the simultaneous treatment, e.g., about 2 orders of magnitude at 150 krad. (auth)

41388 GENERAL PRINCIPLES IN THE MICROBIOLOGY OF IRRADIATED FOODS. Ingram, M.; Roberts, T. A. (Agricultural Research Council, Cambridge, Eng.). Vienna, International Atomic Energy Agency, 1966, Preprint SM-73/14, 17p. (CONF-660609-25). ORAU.

From International Symposium on Food Irradiation, Karlsruhe, Ger.

The important microbiological objectives of irradiation treatments are reviewed, with special reference to the definitions of the proposed new terms radappertisation, radicidation and radurisation. Emphasis is placed on the nature of the food in determining the microbiological requirements of the irradiation treatment. It is suggested that, just as with heat-processed foods, classifications into the major groups of acid or cured foods will remain valid with the irradiation process, and that different microbiological criteria will apply to these different classes of foods. The differences depend in part on the influence which the nature of the food has on the effectiveness of the irradiation treatment itself, but more especially on the way in which the nature of the food affects the activities of those microorganisms which might survive irradiation. The principles used to calculate the appropriate doses of radiation are discussed, with comments on the reliability of the fundamental assumptions or the need for further experimentation. The microbiological characteristics of irradiated foods are compared with those of corresponding heat-processed foods, to emphasize points of difference, with special reference to the appropriateness of suggested classifications for heat-processed foods. Finally, some general difficulties are considered, such as uncertainty about the significance and behavior of food-borne viruses, and about the significance of the mutations which might conceivably be induced in microorganisms surviving an irradiation process. (auth)

41389 NEED FOR MICROBIOLOGICAL CONTROLS IN LEGISLATION ON IRRADIATED FOOD. Goresline, H. E. (FAO/IAEA, Vienna). Vienna, International Atomic Energy Agency, 1966, Preprint SM-73/20, 9p. (CONF-660609-20). ORAU.

From International Symposium on Food Irradiation, Karlsruhe, Ger.

The objectives of food preservation by radiation treatment can be divided into three categories: destruction of spoilage and pathogenic microorganisms in the food (radappertization), so that microbial spoilage will not take place regardless of the storage conditions; treatment of food to destroy viable non-spore-forming pathogenic microorganisms (radicidation); and reduction of numbers of spoilage microorganisms sufficient to enhance the keeping quality of the food (radurization). In any legislation on the radiation treatment of food there is need for microbiological control to ensure that the objectives of the treatment are met or that a public health hazard is not likely. If claims are made that a process accomplishes any of these objectives, there must exist microbiological methods and techniques with which to establish proof of attainment of that objective. This points to the need for standardized microbiological procedures to be incorporated into control legislation. Discussion on the various problems is presented. (auth)

41390 PERSPECTIVES FOR THE USE OF IONIZING RADIATION IN THE DECONTAMINATION ("SALMONELLA RADICIDATION") OF SOME FROZEN PROTEINACEOUS STAPLE FOODS AND DRY MIXED FEED COMPONENTS. Mossel, D. A. A. (Central Inst. for Nutrition and Food Research, Zeist, Netherlands. San Marcos Univ., Lima). Vienna, International Atomic Energy Agency, 1966, Preprint SM-73/19, 16p. (CONF-660609-21). ORAU.

From International Symposium on Food Irradiation, Karlsruhe, Ger.

Radiopreservation of proteinaceous food is reviewed with emphasis on Salmonella radicidation. Topics discussed include: epidemiological background; microbiological indications for radiation decontamination; the feasibility of radicidation treatments applied to frozen meats, frozen poultry and game, and dry animal feeds; wholesomeness; and requirements in development, laboratory control, and training. It is concluded that tentative commercial-scale decontamination experiments in the region of production can now be undertaken, and it is suggested that Latin American countries might be the most promising areas for the first tests of this sort. (H.G.D.)

41391 BIOLOGICAL EFFECTS OF IRRADIATED FATS. Lang, K.; Baessler, K. H. (Univ. of Mainz). Vienna, International Atomic Energy Agency, 1966, Preprint SM-73/38, 18p. (CONF-660609-17). ORAU.

From International Symposium on Food Irradiation, Karlsruhe, Ger.

Rats were fed with a diet containing 20% of irradiated oils. If the oils were irradiated with 2.5 mrad, there was no indication of detrimental effects during the course of 80 weeks. Oils irradiated with 10 mrad, however, caused an increase in lethality after a lag period of 9 to 12 months. Irradiation with 50 mrad caused weight losses after 24 weeks, disturbed liver function, and hypoproteinemia with a relative increase in gamma-globulins. No animal of this group exceeded a life span of 75 weeks. Irradiation with 100 mrad caused immediate toxic symptoms and a high lethality. There is no indication for peroxides to be responsible for the toxicity of the irradiated oils. Because of the high content of dimeric products in the irradiated oils it is assumed that dimerization of fatty acids is the cause of damage. (auth)

41392 RADIATION INACTIVATION OF FOOT AND MOUTH DISEASE VIRUS IN THE BLOOD, LYMPHATIC GLANDS AND BONE MARROW OF THE CARCASSES OF INFECTED ANIMALS. Massa, D. (Istituto Zooprofilattico Sperimentale dell'Umbria e delle Marche, Perugia, Italy). Vienna, International Atomic Energy Agency, 1966, Preprint SM-73/18, 40p. (CONF-660609-22). ORAU.

From International Symposium on Food Irradiation, Karlsruhe, Ger.

The effects of gamma radiation on foot and mouth disease (FMD) virus cultures in vitro were studied. According to the results, a dose of 3 mrad when the virus is in the liquid state, and of 4 mrad when it is in the dry state, is necessary to reduce the number of virus particles from 10^7 to 1. The D_{10} value for the liquid FMD virus is equivalent to 481 krad; the D_{10} value for the dried virus is equivalent to 626 krad. The effects of gamma radiation on FMD virus in situ were studied. According to these results, to inactivate the FMD virus in the experimentally-infected pigs' tissues where the viral contents are the highest (blood, bone marrow, lymphatic glands), doses of 2 mrad for the blood and bone marrow and of 1.5 mrad for the lymphatic glands are necessary. The results show that it is possible to sterilize by means of gamma radiation the carcasses of foot and mouth disease virus-infected animals provided that high doses of gamma radiation (2 mrad) are employed, which gives rise to a series of biochemical problems in connection with edibility of the irradiated meats. (auth)

41393 RADIOISOTOPES FOR LIGHTING. (American Atomics Corp., Tucson, Ariz.). 22p. (CONF-660207-23). ORAU. Gmelin, AED-CONF-66-011-34.

From Radioisotope Applications in Aerospace Symposium, Dayton, Ohio.

Applications of radioisotopes for the production of visible light are considered. Emphasis is placed on self-luminous sources having brightness levels greater than 2 foot-lamberts. The applications described include area locators, information markers, runway markers, interior illumination and reference sources. Theory and future developments are also covered. (J.F.P.)

41394 NUTRITION EXPERIMENTS IN PIGS FATTENED WITH HEAT-DECONTAMINATED, GAMMA-IRRADIATED AND UNTREATED FEEDS. Dammers, J.; Kampelmacher, E. H.; Edel, W.; Van Schothorst, M. (Research Inst. for Animal Nutrition, Hoorn, Netherlands. National Inst. of Public Health, Utrecht). Vienna, International Atomic Energy Agency, 1966, Preprint SM-73/32, 8p. (CONF-660609-18). ORAU.

From International Symposium on Food Irradiation, Karlsruhe, Ger.

Three groups of 8 pigs each were raised: on meal that had been irradiated with 1 mrad of ^{60}Co γ-rays; on heat-decontaminated; or on untreated meal. Allowance was made for geographical factors. Heat-decontamination was carried out at 80 to 85°C during 30 minutes. Counts of Enterobacteriaceae of the untreated meal amounted to 1.0×10^5/g. After both treatments of decontamination 30 samples of 50 grams were taken at random from the decontaminated consignments and examined for Enterobacteriaceae by enrichment. Among the heat-treated meal samples, five, and, from the irradiated meal samples, two were not found entirely free from these bacteria; these can yet be considered adequately decontaminated as far as Salmonella is concerned. In one experiment the pigs were fattened for approximately 100 days, reaching a weight of approximately 100 kg. The average growth in grams per animal per day, was 767 for the group fed untreated meal, 770 for the group receiving heat-treated meal, and 800 g for the irradiated-meal group. The feed intake in kg/kg growth for the above-mentioned groups amounted to 2.85, 2.81, and 2.74, respectively. Other pigs were fattened during approximately 155 days reaching a weight of almost 116 kg. The average growth in grams per animal per day, was, for the groups fed untreated, heat-treated, and irradiated meal 627, 643, and 625, respectively. The feed figures, in kg intake per kg growth were for these groups 3.30, 3.23, and 3.24, respectively. From these results the conclusion can be drawn that neither irradiation nor heat-decontamination had any adverse effect on the nutritional value of meals in these tests. In all instances the required vitamins were added to the meals subsequent to the decontamination treatment. As a further study on the effect of the bacteriological quality of a feed on Salmonella, feces samples were examined for the presence of Salmonella twice a week from each animal. In the untreated meal group Salmonellae were isolated in 13 cases. Feces of pigs fed irradiated or heat-treated meal were free from Salmonellae throughout the whole test period. This demonstrates at the same time the efficiency of the decontamination treatments used and the efficacy of such processing methods in the prevention of the occurrence of healthy Salmonella-carriers among pigs. (H.W.)

41395 NUCLEAR STATIC ELIMINATORS DESIGN AND DEVELOPMENT. Walz, Richard N. (Minnesota Mining and Manufacturing Co., St. Paul). 7p. (CONF-660549-1). ORAU. Gmelin, AED-CONF-66-141-1.

From 6th Annual Packaging Industry Technical Conference, Hartford, Conn.

The nuclear static eliminater was developed using ^{210}Po. The radioisotope is contained in a small, spherical, ceramic bead carrier too heavy to become airborne. The ceramic bead is chemically, physically, and biologically stable. To fabricate the static eliminator the beads are held on an aluminum foil by a radiation resistant binder. The radioactive surface is protected by an aluminum housing. The static eliminator is useful in handling or processing plastic films and papers and minimizing static electricity in the production of transistors and capacitors. (F.S.)

Power Application

See also ENGINEERING — Space Propulsion

41396 (STL-517-0042) RADIOISOTOPE PROPULSION TECHNOLOGY PROGRAM (POODLE). Quarterly Progress Report, January 1–March 31, 1966. (TRW Systems, Redondo Beach, Calif.). Apr. 1966. Contract AT(04-3)-517. 185p. Dep. mn. CFSTI $5.00 cy, $1.00 mn.

Creep of heat source capsules under the action of internal He pressure was studied for operating durations of 30 days at temperatures in the vicinity of 2000°C. Three capsules were made of W-25Re. Oxidation protection must be provided for the refractory alloy capsule structure. Oxidation kinetics and cladding/substrate compatibility were investigated for several Rh–Ir alloys, since these appear to be most promising. Because flow at the POODLE nozzle throat is in the laminar regime, a rapid growth of the boundary takes place in the diverging section. Experimental and analytical tasks are underway to clarify the behavior of low-thrust nozzles and to enable the selection of an optimum design. Further research on heat source simulation is described. (M.O.W.)

41397 ISOTOPIC POWER SOURCES. O'Brien, J. F. 13p. (CONF-660419-3). ORAU. Gmelin, AED-CONF-66-057-3.

From IEEE Region 6 Annual Conference, Tucson, Ariz.

The accomplishments achieved in the development of isotopic power sources are outlined. The present status of these energy sources including the manufacture, separation, and packaging of radioactive elements are examined. Future prospects for the power sources are explored. Characteristics of SNAP-3, 7, 9, 15, 19, 21, 23, and 29 are reviewed. (F.S.)

41398 ISOTOPIC POWER SYSTEMS FOR MANNED MISSIONS. Gingrich, James E. (North American Aviation, Inc., Canoga Park, Calif.). 25p. (CONF-650412-2). ORAU.

From IEEE Convention, Las Vegas, Nev.

The first phase of an engineering study of radioisotope dynamic electrical power systems for Manned Mars/Venus

Missions is summarized. Power levels for the systems ranged from 4 to 8 kw(e), with mission lengths of from 359 to 682 days. The objective was to develop necessary power conversion cycle information and system parametric data from which the working fluid could be selected and detailed designs could be completed. The Brayton and Rankine power conversion cycles were both evaluated with a number of working fluids and the optimum fluid for each cycle was selected on the basis of mission constraints, cycle characteristics, and cost. The Brayton cycle was studied with helium, neon, argon, krypton, xenon, and various mixtures. The Rankine cycle working fluids considered were water, mercury, Dowtherm-A, ortho xylene, sodium, potassium, and rubidium. The objective was not to compare the Brayton and Rankine cycle systems, but to arrive at an optimum design of each with respect to manned interplanetary spacecraft and mission requirements. (auth)

Separation and Production

See also CHEMISTRY — Separation Processes and Procedures

41399 (IEA–110) PREPARACADO DO ^{131}I A PARTIR DO TELLURIO ELEMENTAR IRRADIADO. (Preparation of Carrier-Free ^{131}I from Irradiated Elemental Tellurium). da Silva, Constancia Pagano; Ramaniah, V. M. (Instituto de Energia Atomica, Sao Paulo (Brazil)). Dec. 1965. 10p. (CONF-650974–1). Dep. mn.

From 15th Brazilian Congress, Rio de Janeiro, Brazil.

A method is described for obtaining ^{131}I by irradiation of tellurium, followed by a sodium hydroxide–hydrogen peroxide dissolution of tellurium. This chemical treatment is made in such a way to obtain a suspension of sodium tellurate to which sulfuric acid is added. The resulting solution is heated and the iodine distilled and received into a reducing solution containing thiosulfate in a carbonate-bicarbonate buffer. The elemental tellurium can be irradiated in a high neutron flux for several hours without dehydration and agglomeration of the irradiated mass. The yield of the proposed method is of about 95%. This method differs from the classical one using elemental tellurium, by the fact that the dissolution is not violent as it is when a sulfochromic mixture is used. The method also makes it possible to obtain a pure product after only one distillation. (M.C.G.)

41400 (ORNL–3301(Suppl.1)) PREPARATION OF CHARGE MATERIALS FOR ORNL ELECTROMAGNETIC ISOTOPE SEPARATORS. Sheridan, C. W.; Gwinn, H. R.; Love, L. O. (Oak Ridge National Lab., Tenn.). Sept. 1966. Contract W-7405-eng-26. 15p. Dep. mn. CFSTI $1.00 cy, $0.50 mn.

The preparation of those charge materials that result in either greater ion output, better isotopic purity, higher ion retention, or smoother operation in the separator is discussed (P.C.H.)

41401 (ORNL–4006) REVIEW OF ORNL ELECTROMAGNETIC SEPARATIONS PROGRAM, 1965. Love, L. O.; Bell, W. A. (Oak Ridge National Lab., Tenn.). Aug. 1966. Contract W-7405-eng-26. 37p. Dep. mn. CFSTI $2.00 cy, $0.50 mn.

The effort in the electromagnetic separations program was divided between separating materials for requirements and developing techniques and equipment needed for the separations program to keep pace with stated or anticipated requirements in quantity and isotopic purity of product samples. In >50% of the separations completed this year, operations improved in one or more of the parameters used in judging separation performance. The first major electromagnetic separation of beta-gamma material was completed in the heavy-element section of the program. Ion sources, isotope receivers, ion implantation, contamination studies, vacuum improvement, developments incorporated into scheduled separations, 180° sector separator development, heavy-element separations, and stable isotope separations are discussed. (M.C.G.)

41402 SEPARATION OF LITHIUM ISOTOPES BY COUNTERCURRENT-EXCHANGE-ELECTROLYSIS. Arkenbout, G. J.; Boerboom, A. J. H.; Smit, W. M. (TNO, Utrecht). Ber. Bunsenges. Physik. Chem., 70: 658-64 (Aug. 1966).

The separation of lithium isotopes by countercurrent-exchange-electrolysis was investigated. In this process the separation is based on an exchange between a lithium amalgam and a solution of a lithium salt, transported in countercurrent through a column. It appeared possible to obtain a satisfactory countercurrent transport in a packed column. Sand with a particle size between 0.35 and 0.5 mm was found to be a suitable packing material. The reflux at the bottom of a column, where the lithium is transported from the amalgam to the electrolyte solution (anodic reflux) was realized by a continous method based on exchange-electrolysis. The cathodic reflux was obtained by evaporating the solvent dimethyl formamide, transferring the lithium chloride into water, and electrolyzing the lithium chloride solution in water. Experiments carried out for 20 to 40 hrs in an exchange-column with a length of 1 to 2 m resulted in an increase of ^{6}Li content from 7.5 to 13% at the bottom of the column and a decrease of ^{6}Li content from 7.5 to 5.3% at the top of the column. (auth)

41403 FEATURES OF A PLASMA ION SOURCE WITH A HOT CATHODE GAS DISCHARGE. Ciampi, M.; Talini, N. (CAMEN, Pisa, Italy). Nucl. Instrum. Methods, 43: 325-32(Aug. 1966).

The main features and the results of a plasma ion source for electromagnetic separators of isotopes are described. Hydrogen, argon and nitrogen are employed in the source and ion currents of about 6 mamp are obtained with a yield higher than 80%. Particular attention is devoted to the various arc conditions in the discharge chamber and to the dependence of ion currents on the extraction potentials in different operating conditions. (auth)

41404 GASEOUS CENTRIFUGE AND SEPARATION OF ARGON ISOTOPES. Oyama, Yoshitoshi; Yamaguchi, Kenji; Tonooka, Yasuhiko; Nangu, Makoto; Sakata, Harumi; Takashima, Yoichi (Inst. of Physical and Chemical Research, Tokyo). Rika Gaku Kenkyusho Hokoku, 40: 215-32(1964). (In Japanese).

Two gaseous centrifuges with an upper-driven long rotor, UBT-1 and UBT-2, were constructed. Their dimensions and specifications are given. The damping bearings of the UBT-2 are different from those of the UBT-1. The power consumption of the UBT-1 is about 1.5 kw at 20,000 rpm. That of the UBT-2 is 2.0 kw at 14,000 rpm and 2.6 kw at 16,000 rpm. The rotor of the latter could not be operated beyond 16,000 rpm due to vibration. Difficulties in the drawing of the rotor material and its lath processing, fitting of the endplates, and sealing are discussed. After long-run endurance tests of the mechanical elements of each centrifuge were conducted, experiments on the separation of argon isotope ^{36}Ar from ^{40}Ar were performed by concurrent and countercurrent flow methods. The separation factor for UBT-1 for countercurrent flow varied from 1.01 to 1.07 in the range of gas flow rate 0.5 to 6 l/min at 20,000 rpm, and it was 1.015 (max) for concurrent flow. The factor for UBT-2 at 16,000 rpm ranged from 1.01 to 1.03. (BBB)

41405 IMPROVEMENT OF THE PROFILE OF LINEAR SHIMS DESIGNED FOR THE SEPARATION OF HEAVY ISOTOPES. $\Delta M/M = 1/235$. Gendreau, G.; Hamelin, J.; Trahin, M. (CEN de Saclay, Gif-sur-Yvette, France). 11p. (In French). (CONF-578-17). ORAU.

From Conference on the Physics of Electromagnetic Separation Methods, Orsay, France, July 1962.

The use of linear shims to increase the separation of beams with large angular aperture and significant axial dimensions was analyzed for beams of isotopes differing by only one main unit. The polar profile corresponding to the shims was represented mathematically with the aid of

a distribution of currents localized at the surface of plane polar pieces. The image of a focused beam after a deflection of 180° and the equipotential of the corresponding shim was determined using an IBM computer. The configuration of the optimum field gives a residual aberration corresponding to 0.75 mass units for an angular aperture of approximately ±0.15 radians and an axial dimension of 12 cm. (tr-auth)

MATHEMATICS AND COMPUTERS

41406 (IS–1500(Sect. M and C)) ANNUAL SUMMARY RESEARCH REPORT IN MATHEMATICS AND COMPUTER RESEARCH. (Ames Lab., Iowa State Univ. of Science and Tech.). 8p.

A report is presented on mathematics and computer programming research. Topics discussed are a two parameter homogeneous mean value, a property of the hypergeometric mean value, computation of elliptical integrals, hypergeometric functions, real time control system, selective dissemination of information, and language development. (B.G.D.)

41407 (ORNL–4004) DATA ON A SET OF TRINOMIAL DISTRIBUTIONS. Uppuluri, V. R. Rao; Bowman, Kimiko O. (Oak Ridge National Lab., Tenn.). Sept. 1966. Contract W-7405-eng-26. 86p. Dep. mn. CFSTI $3.00 cy, $0.75 mn.

A Fortran IV program is briefly described which can be used to study any trinomial distribution exactly, for sample sizes ranging from 5 to 75. In the case of a set of eleven trinomial probability vectors which have arisen naturally in connection with a multi-judge reliability problem (which seem to be a representative set), tables are given for n = 10, 15 and 20 which contain information on the exact trinomial probabilities associated with each partition of n, and the distribution of the likelihood ratio test criterion and the distribution of Pearson's X^2 statistic. (M.O.W.)

41408 APPLICATIONS OF THE LEAST SQUARES METHOD. I. (REVIEW). Balogh, Tibor. ATOMKI (Atommag Kut. Intez.) Kozlem., Mellek., 8: 55-62(1966). (In Hungarian).

One of the most frequent questions posed by persons who make use of applied mathematics, involves the correlation between the variables x and y: $y = a_0 + a_1 x + a_2 x^2 \ldots +$ $a_s x^s = P_s(x)$ ($s \geq 0$ an integer), in which the parameters a_0, $a_1 \ldots a_s$ are not known; it is desired to determine these parameters by means of the least squares method, finding out the effect of an error in these values on the total error of $P_s(x)$ for given values of x. The cases differ, depending on whether the scatter of the measured data change markedly or are identical. The solution derived is presented, pointing out that if the parameters continue to increase, the explicit expressions of the approximation functions and of the squares of their scatter become increasingly complicated. There is, however, a simplified method, rendering the equations more manageable; it will be presented in a follow-up paper. (Review article). (TTT)

41409 VARIATIONAL DESCRIPTION OF DISSIPATIVE PROCESSES. Pomraning, G. C. (General Atomic Div., General Dynamics Corp., San Diego, Calif.). J. Nucl. Energy: Pt. A and B, 20: 617-34(Aug. 1966).

The Roussopoulos variational formalism is applied to equations with a first-order time derivative. The resulting functional is a very general variational characterization of dissipative processes in that it admits trial functions which do not satisfy the equation of interest, do not satisfy the boundary conditions, and are not continuous. It is shown that the previous functionals presented in the literature for this type of problem are special cases of this more general functional. The use of this variational principle to estimate a rather general class of characteristics of interest is discussed. It is also pointed out that this general functional is not unique and arguments are given to deal with this non-uniqueness. The variational description of the Sturm–Liouville equation is considered in this same generality. This leads to a generalization (to a more complete class of admissible trial functions) of the classical Rayleigh quotient for estimating eigenvalues. (auth)

METALS, CERAMICS, AND OTHER MATERIALS

General

Refer also to abstract 41064.

41410 (EURAEC–1612) INVESTIGATION WITH REGARD TO THE BREAKING STRENGTH OF WELDMENTS ON HEAVY GAGE TENSILE STEELS, ON THE BASIS OF FRACTURE CRITERIA WHICH ARE IN TURN BASED ON THE EFFECT OF THE DEFORMATION VELOCITY. Quarterly Report No. 1, September 1–December 31, 1965. Schnadt, H. (Oerlikon Elektrodenfabrik Eisenberg G.m.b.H. (West Germany)). Contract 049-65/9-TEED. 10p. (EUR–2825). Dep. mn. CFSTI $1.00 cy, $0.50 mn.

Work Performed under United States–Euratom Joint Research and Development Program.

41411 (IS–1379) URANIUM METAL BY CARBON REDUCTION OF URANIUM OXIDE IN VACUUM. Wilhelm, H. A.; Strain, R. V.; Neubauer, E. P. (Ames Lab., Iowa State Univ. of Science and Tech.). June 14, 1966. Contract W-7405-eng-42. 37p. (CONF-660630–1). Dep. mn. CFSTI $2.00 cy, $0.50 mn.

From Vacuum Metallurgy Conference, New York.

In the reduction of uranium oxides by C under vacuum conditions below 1000°C, it appears that any higher uranium oxide is reduced to the dioxide. The reduction of UO_2 to form carbide takes place at 1300 to 1550°C. Lower oxides are formed at temperatures up to around 1800°C. The final stage of the reaction is between UC and residual oxide and requires temperatures between 1900 and about 2100°C. A container for the charge and primary metal product at the highest temperatures is of major concern Slip-cast Y_2O_3 crucibles have been used in this capacity for studying the reduction and preparing primary metal for subsequent treatments. UO_2 can be reduced by C in a vacuum to give at least 90% yield of primary metal containing about 0.25% C. Most of this C precipitates in the form of UC dendrites as the liquid metal cools to its solidification temperature. Granulation or fragmentation of the dendrites followed by segregation of the UC by liquation permits recovery of a major part of the primary metal with relatively low C content. (auth)

41412 (IS–1500(Sect. M)) ANNUAL SUMMARY RESEARCH REPORT IN METALLURGY. (Ames Lab., Iowa State Univ. of Science and Tech.). 97p.

Results of research are reported on metals preparation and purification, phase studies, thermodynamic properties studies, reactor materials properties and fabrication, separation research, and structure of materials. (J.R.D.)

41413 CHOICE OF MATERIALS IN NUCLEAR TECHNOLOGY. De Meester, P. (Studiecentrum voor Kernenergie, Mol, Belg.). Ing. Bl. (Antwerp), No. 10, 1-8 (1965). (In Dutch). (BLG–351).

A survey is given of the demands that should be satisfied by the materials used in nuclear technology. The main technological factors that may influence the choice of the materials are investigated. Radiation effects in different materials and means to reduce these effects are briefly discussed. (tr-auth)

41414 ELECTRICAL AND THERMAL CONDUCTIVITIES OF METALS OVER THEIR ENTIRE LIQUID RANGE, i. e., FROM MELTING POINT TO CRITICAL POINT, AND THE CONTAINMENT OF METALLIC SUBSTANCES UP TO 5000 DEG K FOR SUBSTANTIAL PERIODS OF TIME. PART III. THE CONTAINMENT OF LIQUID METALLIC SUBSTANCES UP TO 5000 DEG K. Grosse, Aristid V. (Temple Univ., Philadelphia). Rev. Hautes Temp. Refract., 3: 139-46(Apr.-June 1966).

The containment of liquid TaC heated to 5,000°K by a high intensity electric arc, for substantial periods of time, in a rotating graphite crucible, is described. Experimental temperature and graphite sublimation rates measurements mutually support each other. Possible practical applications for nuclear rockets (specific impulses up to 2,000 sec) and magnetohydrodynamic power generators are discussed. (J.R.D.)

41415 DETERMINATION OF RARE EARTH INCLUSIONS IN STEEL. Raybeck, R. M.; Pasztor, L. C. (Jones and Laughlin Steel Corp., Pittsburgh). 24p. (CONF-650311–6). ORAU.

From Conference on Analytical Chemistry and Applied Spectroscopy, Pittsburgh.

An electrolytic procedure developed for isolation of total precipitated rare earths from steel employed an electrolyte with a composition of 5% Na citrate, 2% KBr, and 1% KCNS and a natural pH of 8. For the selective isolation of rare earth oxides, sulfides, and carbides from the resultant residue, the carbides were first dissolved in a $Cu(NH_4)_2Cl_4$ solution. The sulfides were then removed by direct chlorination, leaving the oxides. Finally, the residues were analyzed spectrographically for Ce, La, and Nd. Reproducibility of the procedure was good. (A.G.W.)

41416 CONFERENCE INTERNATIONALE SUR LA METALLURGIE DU BERYLLIUM, GRENOBLE, 17–20 MAI 1965. (International Conference on Beryllium Metallurgy, Grenoble, May 17–20, 1965). Paris, Presses Universitaires de France, 1966. 702p. (CONF-650508).

Information is presented on Be purification, analysis, and its reactions with other metals. Results of physical studies on Be lattices and the structure of Be point defects are summarized. Information is also included on mechanical properties of single- and bi-crystal Be, properties of polycrystalline Be, and manufacture and properties of wrought Be products. The information was presented at the conference as two main lectures and 60 papers. The two lectures are in English along with about half of the papers and most of the discussions. Other information is in French. (J.R.D.)

41417 TERMODINAMICHESKIE SVOISTVA NEORGANICHESKIKH VESHCHESTV (SPRAVOCHIK). (Thermodynamic Properties of Inorganic Substances (Handbook)). Veryatin, U. D.; Mashirev, V. P.; Ryabtsev, N. G.; Tarasov, V. I.; Rogozkin, B. D.; Korobov, I. V. Moscow, Atomizdat, 1965. 460p.

The handbook includes the data on the heat of formation, entropy, heat capacity thermodynamic potentials of formation of oxides, hydrides, halides, sulfates, and high melting point compounds. Thermal phase transformation, vapor pressure and crystalline structure of inorganic substances are discussed. Methods for computing thermodynamic and thermochemical values of the compounds are given. 70 references are included. (R.V.J.)

Corrosion

Refer also to abstract 41449.

41418 (GEAP–5150) STAINLESS STEEL FAILURE INVESTIGATION PROGRAM. Fourth Quarterly Progress Report, January–March 1966. Duncan, R. N. (comp.) (General Electric Co., San Jose, Calif. Vallecitos Atomic Lab.). Apr. 1966. Contract AT(04-3)-189. 42p. (EURAEC–1633). Dep. mn. CFSTI $2.00 cy, $0.50 mn.

Work Performed under United States–Euratom Joint Research and Development Program.

Corrosion testing of high-purity austenitic alloys with controlled impurity additions in $HNO_3 + Cr^{+6}$ indicated that Si is of major importance in determining the intergranular corrosion resistance of austenitic alloys. C additions also affect the intergranular corrosion resistance but is highly

dependent on heat treatment prior to testing. Mn was shown to have very little effect. Measurements of the anodic polarization characteristics of austenitic tricrystals indicate that the rate of dissolution of the grain boundary is nearly two orders of magnitude higher than the rate of dissolution of the grain centers. Corrosion tests permformed on irradiated type-304 stainless steel cladding samples in aqueous $FeCl_2$ at 650°F (0.1 g/l) indicates that irradiation increases the susceptibility of the stainless steel to intergranular attack. Fuel cladding from fuel rods fabricated by co-extrusion showed less susceptibility, in either irradiated or non-irradiated condition, than any other cladding when tested in aqueous $FeCl_2$ at 650°F. A neutron activation analysis technique for chloride in a sample of corrosion product from a reactor was developed. Electrochemical corrosion studies of stainless steel were extended to 300°C. Potentiostatic curves were obtained on various type-304 stainless steel samples. Intergranular attack of stressed type-304 stainless steel samples ocurred at 650°F in HCl and NaCl solutions in addition to the $FeCl_2$ solution. Room temperature H_2 embrittlement tests were completed. The tests were inconclusive as to the role H_2 may play in the intergranular failure of type-304 stainless steel fuel rod cladding. (auth)

41419 (GMAD-3643-5) INVESTIGATION OF BIMETALLIC LIQUID METAL SYSTEMS. Progress Report, February 1–May 31, 1966. (Allison Div., General Motors Corp., Indianapolis, Ind.). June 20, 1966. Contract AT(30-1)-3643. 66p. (EDR-4719). Dep. mn. CFSTI $3.00 cy, $0.75 mn.

Examination and analysis of material from bimetallic (AISI 316 SS and Nb-1% Zr) liquid K systems are being conducted. These systems operate between 1200 and 1500°F for times up to 8000 hr. Results to date indicate that phase changes in the AISI 316 SS involve formation of complex carbides ($Cr_{23}C_6$) and chi phases. Stress rupture testing of loop-exposed specimens shows a decrease in this property. Low cycle fatigue testing is proceeding. N_2 gradients in the stainless steel containment were obtained and are providing the basis for kinetics analyses of N_2 transport. No area of outward diffusion of N_2 through the stainless steel was found. Detailed chemical and metallurgical analyses of a loop which operated for 8000 hr is also being used for kinetics analysis of N_2, C, and O_2 transport. Preliminary results of kinetics correlations show diffusion coefficients for C in stainless steel to be at least an order of magnitude greater than those in the refractory alloy. Qualitative examination of air-side surfaces indicated no catastrophic oxidation of stainless steel surfaces when surface temperatures did not exceed 1500°F. Ni fins became embrittled (probably due to O_2 diffusion) after 8000 hr of operation at 1400 to 1500°F. (auth)

41420 (MSAR-66-149) EFFECT OF HIGH TEMPERATURE SODIUM ON AUSTENITIC AND FERRITIC STEELS. MECHANICAL PROPERTIES OF MATERIALS. Quarterly Progress Report, April–June 1966. (MSA Research Corp., Evans City, Pa.). July 1966. Contract AT(11-1)-765. 66p. Dep. mn. CFSTI $3.00 cy, $0.75 mn.

The mechanical strengths of candidate structural materials in various environments were studied. A test of 304 ss in 1200°F high-O_2 (300 ppm) Na was conducted. Unstressed specimens were also exposed to the high-O_2 Na environment and a He environment for subsequent mechanical testing. The testing of these exposed materials is in progress. A test of 304 ss in 1200°F high-C Na also was conducted. The fatigue tests are continuing, and the testing of exposed specimens was initiated. The base-line air data (creep, creep-rupture and tensile) tests for this heat of 304 ss are in progress. Fatigue tests are in progress in a He environment. The preliminary results of completed tests to date are presented. Metallographic studies were used to trace anomalies in fatigue data of high-O_2 Na environment to differences in C absorption. All other metallographic monitoring of specimens and tabs in either environment reveals no deviations of trends noted in testing. The testing of the initial out-of-house Linear Variable Differential Transformer (LVDT) units resulted in satisfactory performance of the units and associated auxiliary equipment up to ~800°F. However, at a temperature of 1200°F, the performance is erratic. Modification and testing are continuing. Analytical studies are in progress on cold traps operated in environments of high-C and high-O_2 (300 ppm) Na. The cold traps were sampled by coring. Preliminary data are included on the concentrations found regarding O_2, H_2, C (both in the Na and in the mesh), N_2, and metal elements. (J.R.D.)

41421 EFFECT OF YTTRIUM ON HIGH TEMPERATURE OXIDATION OF MOLYBDENUM. Cheng, I-p'ng; Yin, Yao-te; Li, Hsun. Chin Shu Hsueh Pao, 9: 107-9 (Jan. 1966). (In Chinese).

Molybdenum alloys containing 0, 0.3, 1.0, 3, and 8% by weight of yttrium were prepared; their hardness and appearance of a dark structure were found to increase with increasing yttrium content. All oxidations were carried out under pressure of 76 millimeters of mercury. The volumetric method was used for oxidation at 600°C, and differences in oxidation pattern and the rate of oxidation of molybdenum alloys and those of pure molybdenum were negligible. A quartz spring balance was used to determine the weight loss of samples during oxidation at 900°C, and rates of oxidation of molybdenum alloys were all lower than that of pure molybdenum. After one hour of oxidation, a layer of brownish black molybdenum dioxide was found on the surface of pure molybdenum whereas alloys had an outer layer of loose white oxide of $Y_2O_3 \cdot 3MoO_3$ and an inner brownish black layer containing MoO_2 and a minute amount of yttrium. X-ray analysis showed that the oxidation product of alloys at 600°C was molybdenum trioxide, which was basically the same as that of pure molybdenum. (CFSTI)

41422 ZIRCONIUM AND ITS ALLOYS AS SPECIAL MATERIALS FOR WATER-COOLED NUCLEAR REACTORS. Rosler, U. Siemens Rev., 33: 211-16(1966).

A review of Zr alloy development is presented. Properties of Zr–Nb alloys and Zircaloy-2 are compared for use in water-cooled reactors, and it is noted that the Zr–Nb alloys have superior corrosion resistance and better high-temperature embrittlement characteristics than Zircaloy-2. (J.R.D.)

41423 AQUEOUS CORROSION OF ZIRCONIUM SINGLE CRYSTALS. Bibb, A. E.; Fascia, J. R. (General Electric Co., Schenectady, N. Y.). Trans. Met. Soc. AIME, 230: 415-19(Apr. 1964). (KAPL-P-2280).

Single-crystal wafers of Zr were exposed to 680°F neutral water. The single crystals were of known orientation, and weight-gain data as a function of crystal orientation were obtained. The data show that corrosion of all crystal faces studied obeyed a cubic rate law out to the time of transition whereupon the crystals corroded at an approximately linear rate. The time to transition varied from 114 days for $(10\bar{1}4)$ crystals to about 325 days for the $(21\bar{3}0)$ faces. The epitaxial relationship between metal and monoclinic oxide was found to be $(0001) \parallel (1\bar{1}1)$ and $[11\bar{2}0] \parallel [10\bar{1}]$. A black tight adherent oxide layer was formed on the crystals in the pretransition range. This black oxide was found to be monocrystalline. The white corrosion product produced after transition was found to be polycrystalline but highly oriented. X-ray line-broadening studies found that the black oxide was a highly strained structure whereas the white oxide was relatively strain-free. These results indicate a strain-induced recrystallization or fragmentation accompanies the change from protective black oxide to nonprotective white oxide. (auth)

41424 OXIDATION STUDIES OF COMPLEX SILICIDES FOR PROTECTIVE COATINGS. Regan, R. E.; Baginski, W. A.; Krier, C. A. (Boeing Co., Seattle). 35p. (CONF-660505-11). ORAU. Gmelin, AED-CONF-66-103-14.

From American Ceramic Society Meeting, Washington, D. C.

Oxidation tests of bulk phase complex silicides, performed under flowing air conditions at both atmospheric and 0.5 torr total pressure and 2800 to 2900°F, demon-

strated the effectiveness of alloying to improve the oxidation resistance of the simple refractory metal disilicides. Substantial improvements to the oxidation performance at reduced pressure were afforded the $NbSi_2$, $MoSi_2$, $TaSi_2$, and WSi_2 systems by additions of Cr, Ti, V, Al, and B. From a group of more than 375 compositions tested less than 10 outstanding ones were found. A discussion of development philosophy, specimen preparation, and testing methods is presented. Both steady-state and simulated service profile oxidation tests were employed to compare systems. Weight change data and visual appearance records are included. (auth)

Fabrication

Refer also to abstract 42586.

41425 (IITRI-578-P29-2) RESEARCH ON ZIRCALOY BRAZE ALLOY DEVELOPMENT. [Progress Report], April 1–June 30, 1966. Saperstein, Z. P. (IIT Research Inst., Chicago, Ill.). July 18, 1966. Contract AT(11-1)-578. 14p. (EURAEC-1679; IITRI-B6064-2). Dep. mn. CFSTI $1.00 cy, $0.50 mn.

Work Performed under United States–Euratom Joint Research and Development Program.

A program was initiated to develop a braze filler alloy and brazing procedure suitable for the fabrication of pressurized-water reactor fuel-element assemblies. The initial work which was undertaken during the first quarterly period is described. The first experimental effort will involve the preparation and evaluation of a large number of Zr-base binary systems. More complex second-generation alloys will be developed in later stages of the program. (auth)

41426 (LA-3493) STUDIES ON THE FORMATION OF Pu_2O_3 IN THE SINTERING OF PuO_2. Pritchard, W. C.; Nance, R. L. (Los Alamos Scientific Lab., Univ. of California, N. Mex.). Dec. 1965. Contract W-7405-eng-36. 34p. Dep. mn. CFSTI $2.00 cy, $0.50 mn.

The effects of sintering atmospheres and temperatures on the composition of pellets of PuO_2 powder prepared from oxalate and peroxide methods were investigated. The effects of ball milling, binder additions, and cold compacting pressures were also studied. Metallographic examination as well as lattice constant results were correlated with conditions conducive to the formation of bcc Pu_2O_3. The consequences of Si as a sintering furnace contaminant were also noted. (auth)

41427 (NASA-TM-X-53453(Vol.1)) FABRICATION OF BERYLLIUM. VOLUME I. A SURVEY OF CURRENT TECHNOLOGY. Williams, R. F. (Lockheed Missiles and Space Co., Palo Alto, Calif.); Gerds, A. F.; Boulger, F. W. (Battelle Memorial Inst., Columbus, Ohio). July 1966. Contracts NAS 8-11798; DA-01-021-AMC-203(Z). 139p.

Fabrication of Be and its alloys into space vehicle structures is discussed. Currently used methods for fabricating the metal into sheets, rods, and other forms are summarized. Some of the difficulties that have been encountered in various aspects of fabrication, especially regarding the inherent brittleness of the metal, are enumerated along with the means that have been used to circumvent these problems. The survey includes 102 references to articles and papers in the unclassified literature, most of them having been published since 1960. The data on Be prior to 1960 were covered in two reports issued by the Defense Metals Information Center, DMIC Reports 106 and 168. (auth)

41428 (SCL-DC-66-57) PRESSING HOLLOW SHAPES FROM HIGH-STRENGTH BERYLLIUM. Johnson, D. M. (Sandia Corp., Livermore, Calif.). [1966]. Contract AT(29-1)-789. 20p. Dep. mn. CFSTI $1.00 cy, $0.50 mn.

Efforts to fabricate and test hollow or shaped pressings from Be powder are discussed. The pressing process was unsuccessful when applied to large frustums, but the possibility of producing Be pressings having a yield strength of 55,000 psi was demonstrated. The feasibility of hollow pressings was demonstrated, and the addition of Si to the Be powder was found to promote sintering at reduced pressure. (J.R.D.)

41429 (USBM-RC-1249) QUARTERLY METALLURGY PROGRESS REPORT NUMBER 31, APRIL 1–JUNE 30, 1966. (Bureau of Mines, Albany, Oreg. Albany Metallurgy Research Center). Contract AT(11-1)-599. 51p. Dep. mn. CFSTI $3.00 cy, $0.50 mn.

Development of production methods for high-temperature metal-C specimens for property studies is reported. Trial runs using a newly constructed carbide-casting furnace are discussed. Castings of ZrC, TiC, and NbC were evaluated for quality during the quarter. Data were also obtained on hot hardness of HfC, TaC, and NbC specimens. Air oxidation data are included on HfC, TaC, and NbC samples. Research on Th–ThO_2 systems is reported. One series of studies is concerned with submicron ThO_2 additions aimed at production of high-strength cermets. Another series of studies is concerned with micron-sized ThO_2 additions aimed at production of simulated reactor fuels composed of 15 to 20% ThO_2. Results of mechanical property and electrical measurements on these cermets are discussed. Development work on furnaces for induction melting of reactive metals is reported. Preparation and evaluation of N-containing oxycarbides are reported. Data are included on U–C–O–N systems at 1700°C, and on production of UCO specimens. In W–Re–Mo alloy development, analyses of tubular W–Re and W–Re–Mo samples were completed. Arc-melted W–25Re extruded tube specimens were examined, and pressing of W–25Re sleeves was completed. Methods of W–Re alloy scrap recovery were investigated. (J.R.D.)

41430 FABRICATION OF THIN PLATES FROM REFRACTORY CARBIDES. Ignat'ev, B. G.; Nezhevenko, L. B.; Kovalev, A. V.; Poltoratskii, N. I.; Fomin, G. S.; Yakutovich, M. V. At. Energ. (USSR), 20: 489-94(June 1966). (In Russian).

The technology of the fabrication of thin plates of ZrC was explained for 2 methods: compression with high temperature activated soldering, and rolling of carbide powders in strips with subsequent sintering. The preferred method was sintering, which made it possible to produce thin plates with densities of approximately 97% of the theoretical density. (tr-auth)

41431 STABILIZATION OF URANIUM MONOCARBIDE AND PRODUCTION OF THE SINGLE-PHASE CARBIDE. Huet, J. J.; Vangeel, J. (Centre d'Etude de l'Energie Nucleaire, Mol, Belg.). Metallurgie (Mons, Belg.), 2: 31-42(1964). (In French). (BLG-348).

To obtain single-phase uranium carbide, uranium carbide with 3.5 to 8 wt. % of carbon was subjected to arc melting in a mixed argon–nitrogen atmosphere and a mixed argon–air atmosphere. The carbon and nitrogen contents of the final product were checked and found to depend on the partial pressure of nitrogen and oxygen. As a result of melting in an argon–nitrogen atmosphere some nitrogen goes into the carbide. The carbon content also increases as a result of contamination by the graphite electrode. By this process, a substoichiometric carbide could be made stoichiometric. The melting in a mixed argon–nitrogen–oxygen atmosphere produces a decrease in the carbon content as a result of a reaction between the carbides and the oxygen. The nitrogen content also increases. The nitrogen reacts with the free uranium to form uranium mononitride, which passes in solution into the uranium monocarbide. Thus, the melting of uranium carbides in the presence of oxygen and nitrogen yields a single-phase uranium carbon nitride. (tr-auth)

41432 HOT DRAWING OF THIN WALLED ZIRCALOY-2 TUBES. Timmermans, W. (SCK-CEN, Mol, Belg.). Metallurgie (Mons, Belg.), 2: 43-8(1964). (In Dutch). (BLG-347).

Zircaloy-2 and zirconium tubes were drawn down to

0.22 mm wall thickness. Some factors affecting the finished product were studied: lubrication, shape of the dies, and thermal treatment after each pass. The lubrication mechanism during the drawing demonstrated the necessity of a well-bonded underlayer to fix the lubricant. As underlayers oxide, phosphate, and bonderisation layers were studied; the latter is to be preferred. Good results were obtained with tungsten carbide dies having an entry angle of 30° and a cylindrical part of 3 mm length. The optimum temperature for thermal treatment is between 400 and 500°C; the grain size and the hardness remain constant in this range. On a tube with a 0.22-mm wall thickness variations of −0.025 to +0.010 mm were measured with an ultrasonic apparatus. The accuracy obtained is quite satisfactory. (tr-auth)

41433 DUCTILITY OF CROSS-ROLLED BERYLLIUM SHEET: BARRIER OR CHALLENGE. Ingels, S. E. (Lockheed Missiles and Space Co., Palo Alto, Calif.). 23p. (CONF-660437–1). ORAU.

From Society of Automotive Engineers, National Aeronautic Meeting, New York.

Production techniques required for the severe forming of commercially available cross-rolled beryllium sheet are described. Configurations prepared with these techniques include straight bends, curved channels, hemispherical segments, and semicylinders with spherical ends. A minimum acceptable bend radius of 5 t, an optimum forming temperature of 1350°F, and shrink and stretch values of 9.0 and 13.0%, respectively, are established by statistical, metallographic, and dimensional analysis. The feasibility of the extreme forming of cross-rolled sheet material, as required for many aerospace applications, is clearly demonstrated. (auth)

41434 INNOVATIONS IN ELECTRON-BEAM ZONE REFINING OF MOLYBDENUM. Prekel, H. L.; Lawley, A. (Franklin Inst. Research Labs., Philadelphia). 22p. (CONF-660414–4). ORAU. Gmelin, AED-CONF-66-119-4.

From 2nd International Conference on Electron and Ion Beam Science and Technology, New York.

Modifications to a conventional electron beam floating zone unit are described. The filament is hidden from the specimen, and this results in increased stability of operation, longer filament life, and excellent uniformity of crystal diameter (0.130'' ± 0.001''). Molybdenum single crystals grown from vacuum arc-cast and hot swaged stock contain inclusions, and the crystals exhibit a high grown-in dislocation density $\sim 6 \times 10^7$ cm^{-2}; 90% of these dislocations are associated with and are attributable to the inclusions. Variations in zoning speed, number of zone passes, and annealing treatments at 1700°C in vacuum or in argon have no appreciable effect on the number of inclusions. The inclusions are effectively removed from zoned crystals by annealing in hydrogen at ~2000°C; this is accompanied by a decrease in dislocation density to $\sim 10^6$ cm^{-2}. Hydrogen annealing of the as-received material followed by zone melting gives inclusion-free crystals, and a dislocation density $\sim 4.5 \times 10^6$ cm^{-2}; a further hydrogen anneal after zone melting reduces the density to $\sim 2 \times 10^5$ cm^{-2}. The observation that crystals grown from hydrogen annealed stock are inclusion-free provides proof that there is no significant re-contamination of the molybdenum during zone melting. The effectiveness of the dual approach of hydrogen annealing and zone melting is considered in the light of the associated surface and underlying structures. (auth)

41435 IMPROVEMENTS IN OR RELATING TO STRUCTURAL MATERIALS. Strong, Robert Edmund; Berry, Arnold (to United Kingdom Atomic Energy Authority). British Patent 1,036,646. July 20, 1966. Filed June 5, 1964.

A method is described for producing structural members such as bricks, blocks, walls, pillars, roofs, etc., of a mixture of granular and/or powdered U depleted of ^{235}U using cement or its substitute. The powdered and/or granular U and the cement are mixed with a curing agent. The mixture is formed into a suitable shape, and the formed member is allowed to set either with or without the incorporation of reinforcement. (B.L.M.)

41436 IMPROVEMENTS IN OR RELATING TO GAUGING INSTRUMENTS. Statham, Eric; James, Clifford (to United Kingdom Atomic Energy Authority). British Patent 1,032,121. June 8, 1966. Filed July 30, 1962.

A gaging instrument for indicating ovality of a bore comprises a tubular member with a rod slidable in the tubular member and interconnected to the tubular member by two diametrically opposed pairs of toggle linkages. During a gaging operation the two knuckles of the toggle linkages bear against the surface of the bore and upon relative rotation between the instrument and the bore, ovality of the bore effects pivoting of the linkages and is indicated by corresponding longitudinal movement of the rod. The instrument may include an indicator for indicating the extent of longitudinal movement of the rod and therefore the amount of ovality of the bore, and the instrument may be calibrated to show when a predetermined degree of ovality is exceeded. The instrument is particularly applicable to checking the ovality and parallelism of a bore that is restricted at one end, as for example, the bore of a hollow rod of fissile material for a nuclear reactor fuel element. (B.L.M.)

Properties and Structure

See also CHEMISTRY — Inorganic and Physical Chemistry
PHYSICS — Solid State Physics

Refer also to abstracts 40874, 41429, 41729, 41738, 41762, 42535, and 42618.

41437 (AERE-R–5210) TWO CRYSTALLOGRAPHIC COMPUTER PROGRAMMES FOR LATTICE PARAMETER REFINEMENT AND FOR CALCULATING EXPECTED LINE POSITIONS. Marples, J. A. C.; Shaw, J. L. (Atomic Energy Research Establishment, Harwell (England)). May 1966. 62p. Dep. BIS $1.60, HMSO 8s.

The Cohen Program can be used to calculate the lattice parameters which give the best fit to a set of indexed ''d'' or ''2θ'' values for the hexagonal, tetragonal, orthorhombic, monoclinic or triclinic systems. The Genstruck Program can be used to calculate the $1/d^2$,d,2θ and $\sin^2\theta$ values expected for all the above systems (and for rhombohedral) given the lattice parameters. If observed ''d'' or 2θ values are also read in, these can be indexed by the program and cards punched suitable for the input of Cohen. Both programmes are written in S2 Fortran. (auth)

41438 (AGN–8187) ALKALI METALS EVALUATION PROGRAM. Quarterly Progress Report, January 1–March 31, 1966. Achener, P. Y.; Parr, E. D. (Aerojet-General Nucleonics, San Ramon, Calif.). Contract AT(04-3)-368. 28p. Dep. mn. CFSTI $2.00 cy, $0.50 mn.

Efforts directed toward determination of Rb and Cs thermodynamic and transport properties for space power systems are reported. Four experimental runs to determine pressure-volume-temperature relations were conducted for Cs and three similar runs were conducted for Rb. Resulting data are included. Data are also presented from Cs viscosity experiments at 55 to 1063°C. Equipment and procedures are being developed to measure specific heats, vapor, viscosities and vapor thermal conductivities of Cs and Rb. Preparations for investigations of alkali metals for heat pipe applications are discussed. (J.R.D.)

41439 (AGN–8198) ALKALI METALS EVALUATION PROGRAM. Quarterly Progress Report, April 1–June 30, 1966. Achener, P. Y. (Aerojet-General Nucleonics, San Ramon, Calif.). Aug. 1966. Contract AT(04-3)-368. 15p. Dep. mn. CFSTI $1.00 cy, $0.50 mn.

Work toward obtaining pressure-volume-temperature relations in Cs is briefly described. Apparatus for measure-

ment of the thermal conductivity of Cs and Rb vapors at 1000 to 2000°F is described along with apparatus for Cs vapor viscosity and specific heat at 2000°F. Research on latent heat of vaporization of Na, vapor pressure of Li, surface properties of liquid Na and Li, viscosities of liquid Li and Na, and specific heats of liquid Li and Na is briefly summarized. Topical reports are being prepared on most of these tasks. No data are included. (J.R.D.)

41440 (ALO–3632-4) RESEARCH AND DEVELOPMENT IN A THERMAL INSULATION STUDY. Quarterly Progress Report, April–June 1966. DeWitt, W. D. (Union Carbide Corp., Tonawanda, N. Y. Linde Div.). July 26, 1966. Contract AT(30-1)-3632. 94p. Dep. mn. CFSTI $3.00 cy, $0.75 mn.

The insulation materials study to evaluate the use of Al, Cu, and Ni foils as thermal radiation shields was completed, and a parametric study showing foil life as a function of operating temperature with foil thickness as a parameter is presented. This study showed that for a mission life of 1 to 5 yr the use of Ni foil at 1700 to 1800°F is questionable. Ta foil was recommended as a substitute for Ni at these temperatures, and the feasibility, of producing Ta flake opacified spacer as a substitute for Ni flake opacified spacer is being investigated. Experiments evaluating potential foil cleaning techniques for Al, Cu, and Ni foils were completed, and a Linde foil cleaning process was selected. A data survey of the properties of the candidate spacer materials was completed, and a laboratory analysis for residual C content of these materials — in the as-received condition — with the exception of the metal flake opacified spacers was completed. A theoretical study based on reaction rate and mass transfer phenomena was carried out to investigate the processing of candidate spacers. Experiments based on this work were conducted; and a correlation relating processing time, processing temperature, oxidizer gas concentration, spacer C content, and exhaust gas stream CO_2 concentration was developed. Physical stability testing was begun, and experiments were performed on quartz fiber cloth and quartz fiber paper candidates. An offgassing test apparatus was assembled and testing was initiated. Fabrication of the thermal conductivity test apparatus, and fixtures for the insulation preliminary vibrational tests has begun. The vacuum enclosure materials study disclosed three potential problem areas: the permeation of super alloys by air components at elevated temperature, the vaporization of high vapor pressure constituents of the super alloys during long-term exposure to elevated temperature, and intergranular oxide penetration. (auth)

41441 (BNWL–224) MELTING POINTS OF HYPOSTOICHIOMETRIC URANIUM DIOXIDE. Bates, J. Lambert (Battelle-Northwest, Richland, Wash. Pacific Northwest Lab.). June 1966. Contract AT(45-1)-1830. 5p. Dep. mn. CFSTI $1.00 cy, $0.50 mn.

Melting points were measured for hypostoichiometric $UO_{2.00}$ to $U_{1.67}$. The melting points decrease with decreasing O:U ratio below 2.00, and the data suggests a possible maximum in the melting point curve between $UO_{2.00}$ and $UO_{1.93}$. (D.L.C.)

41442 (CNLM–2393) DATA BOOK ON PHYSICAL PROPERTIES OF MATERIALS. (Pratt and Whitney Aircraft, Middletown, Conn. Connecticut Advanced Nuclear Engineering Lab.). Mar. 15, 1960, Revised June 15, 1960. Contract AT(30-1)-2789. 79p. Dep. mn. CFSTI $3.00 cy, $0.75 mn.

The data are grouped under metals, alloys, ceramics and cermets, and liquid metals. (J.R.D.)

41443 (COO–588-12) TRANSFORMATION CHARACTERISTICS OF ZIRCONIUM–NIOBIUM ALLOYS. Interim Technical Report No. 9. Yaffe, P. E.; Perkins, A. J.; Hehemann, R. F. (Case Inst. of Tech., Cleveland, Ohio. Dept. of Metallurgy). July 31, 1966. Contract AT(11-1)-588. 27p. Dep. mn. CFSTI $2.00 cy, $0.50 mn.

Transmission electron microscopy was used to investigate the formation of athermal and isothermal omega in a series of Zr-Nb alloys. Athermal omega is a quenched 12% Nb alloy exists as discrete platelets parallel to {112} beta planes and approximately 150Å in dia and 20 to 40Å thick. These platelets are arranged in a periodic fashion in ⟨112⟩ and ⟨110⟩ beta directions. A modulated structure rather than discrete particles characterizes athermal omega in a 17% Nb alloy and corresponds to what has been termed in the literature diffuse omega. This structure is replaced by periodically arranged discrete particles during aging. A preliminary study of low temperature aging of a 50% Nb alloy, which does not form omega on quenching, provides evidence for segregation within the beta phase and concurrent formation of diffuse omega in regions of low Nb content. (auth)

41444 (COO–1477-5) FRACTURE TOUGHNESS OF REACTOR PRESSURE VESSEL STEELS. Development of Test Procedures, June 1–July 31, 1966. Ripling, E. J.; Crosley, Phillip (Materials Research Lab., Inc., Richton Park, Ill.). Aug. 15, 1966. Contract AT(11-1)-1477. 8p. Dep. mn. CFSTI $1.00 cy, $0.50 mn.

Fracture toughness testing procedures are being developed to evaluate the toughness of medium-strength steels such as A 302 B at room temperature. Impulsive loading (a triangular displacement pulse of approximately 100 milliseconds) is being used. Using this procedure, room-temperature initiation toughness is found to be slightly higher in two-in.-thick than in one-in.-thick specimens. The arrest toughnesses for the two are essentially identical however. These data indicate that valid toughness can be measured at room temperature in reasonable sized specimens. The use of smaller specimens and higher loading rates will be investigated. (J.R.D.)

41445 (EURAEC–1622) RESEARCH TO DETERMINE THE LONG-TERM MECHANICAL PROPERTIES OF METALS SUBJECTED TO MECHANICAL STRESS AT ELEVATED TEMPERATURES AND NEUTRON IRRADIATION. Quarterly Report No. 13, January 1–March 31, 1966. Siegfried, W.; Zimering, S. (Battelle Memorial Inst., Geneva (Switzerland)). May 1966. Contracts 100-62-12-RDS; 057-64-7-TEES(RD). 16p. (EUR–2835). Dep. mn. CFSTI $1.00 cy, $0.50 mn.

Work Performed under United States–Euratom Joint Research and Development Program.

Work devoted to separating the mechanisms of structural changes from those of deformation and formation of rupture, on the basis of the energies of activation is reported. Development work on procedures and apparatus for time-to-rupture tests on pure Fe is summarized. Methods for extrapolation of time-to-rupture tests by means of the exponential function of real order were investigated. Rupture mechanisms were investigated via time-to-rupture tests on CrMoV-steel, Alloy S 590, Alloy S 816, and steel type 304. (J.R.D.)

41446 (EURAEC–1624) A STUDY OF PLASTIC FATIGUE EMBRITTLEMENT OF REACTOR VESSEL STEELS. Quarterly Report No. 9. (Centre National de la Recherche Scientifique, Paris (France)). May 1966. Contract 005-63-12TEEB. 32p. (EUR–2837). Dep. mn. CFSTI $2.00 cy, $0.50 mn.

Work Performed under United States–Euratom Joint Research and Development Program.

Research concerning the effects of small-amplitude deformations on fatigue of pressure-vessel steels is summarized. Results are included on plastic fatigue to breaking point, and brittleness after fatigue at 20 and 300°C. It is concluded that first embrittlement occurs at low fatigue damage. Discussions of embrittlement mechanisms are included. (J.R.D.)

41447 (EURAEC–1669) STUDY OF THE BASE METAL INTENDED FOR RESEARCH ON THE BRITTLE FRACTURE OF LARGE WELDMENTS. Technical Report No. 2, May 1, 1965–April 30, 1966. (Institut de Recherches de la Siderurgie, St. Germaine-Enlaye (France)). Apr. 30, 1966. Contract 031-64-TEEF(RD). 31p. Dep. mn. CFSTI $2.00 cy, $0.50 mn.

Work Performed under United States–Euratom Joint Research and Development Program.

Results of studies concerning super Elso Ni–Cr–Mo steel revealed that the optimal stress-relief treatment corresponds to a residence time of 2 hr at 600°C. It was also found that the use of fast heat cycles decreases the critical quench rate and has a small effect on transformation. Studies of Mn–Mo–V Ammo steels are reported on composition, dilatometry, quenching, and tensile properties. Tests to determine brittle fracture strength are reported along with results of structural transformation studies. (J.R.D.)

41448 (EURAEC–1670) INVESTIGATION WITH REGARD TO THE BREAKING STRENGTH OF WELDMENTS ON HEAVY-GAGE HIGH-TENSILE STEELS, ON THE BASIS OF FRACTURE CRITERIA WHICH ARE IN TURN BASED ON THE EFFECT OF THE DEFORMATION VELOCITY. Quarterly Report No. 2, January 1–March 31, 1966. (Oerlikon Elektrodenfabrik Eisenberg G.m.b.H. (West Germany)). Contract 049-65/9-TEED. 8p. (EUR–2862). Dep. mn. CFSTI $1.00 cy, $0.50 mn.

Work Performed under United States–Euratom Joint Research and Development Program.

41449 (EURAEC–1676) THE RELATIONSHIP OF NITROGEN CONTENT OF AUSTENITIC STAINLESS STEELS TO STRESS CORROSION. Quarterly Report No. 438-8, [March 1–May 31, 1966]. Ferry, B. N.; Eckel, J. F. (Virginia Polytechnic Inst., Blacksburg. Dept. of Metals and Ceramic Engineering). June 1966. Contract AT(40-1)-3208. 26p. Dep. mn. CFSTI $2.00 cy, $0.50 mn.

Work Performed under United States–Euratom Joint Research and Development Program.

Results of studies associated with dilatometry of AiSi type 304 steel wire are reported. A linear regression analysis was performed on the dilatometer calibration curve to obtain values for sigma and the confidence interval at the mean temperature of each line segment. Resulting data are included. Specimens of nitrided type 304 stainless steel were tested in the dilatometer at 50 to 170°C. An analysis of dilatometer test results is included with plates showing wire microstructure changes. (J.R.D.)

41450 (EURAEC–1684) APPLICATION OF THE SUBMERGED ARC WELDING PROCESS TO THICK PLATES. Quarterly Report No. 5, April 1–June 30, 1966. Leymonie, C. (Chantiers de l'Atlantique Pehoet-Loire, Paris (France)). July 7, 1966. Contract 054-61-12-RDF. 6p. (EUR–2871). Dep. mn. CFSTI $1.00 cy, $0.50 mn.

Work Performed under United States–Euratom Joint Research and Development Program.

Results of investigations are discussed concerning austenization, dilatometry, and stress relief in steels designated as 15 MDV, 1.2 MD 07, Wel-Monix, WB 35, and PM 24. (J.R.D.)

41451 (GA–7101) A RESEARCH PROGRAM ON THE EFFECT OF SUBSTRUCTURE ON THE IRRADIATION STABILITY OF ASTM A302 GRADE B STEEL. Quarterly Progress Report No. 4. Trozera, T. A.; Flynn, P. W. (General Dynamics Corp., San Diego, Calif. General Atomic Div.). Apr. 12, 1966. Contract AT(04-3)-167. 15p. (EURAEC–1634). Dep. mn. CFSTI $1.00 cy, $0.50 mn.

Work Performed under United States–Euratom Joint Research and Development Program.

Results of further cold work and heat treatments were the basis of a selection of 0.03 and 0.06 prestrains and 450°C heat treatment for steel irradiations. Capsule and specimen fabrication is continuing. A servovalve and controller were added to the pressurization unit. A modified extensometer was made and is being evaluated. The Charpy instrumentation was tested and is discussed. Warm work of A302-B steel was done at several temperatures and reductions with significant increase in the tensile strength were achieved. (J.R.D.)

41452 (MLM–1172) DIFFERENTIAL THERMAL ANALYSIS STUDY OF IMPURITIES IN PLUTONIUM. Etter, D. E.; Wittenberg, L. J. (Mound Lab., Miamisburg, Ohio). Oct. 31, 1963. Contract AT(33-1)-Gen-53. 17p. Dep. mn. CFSTI $1.00 cy, $0.50 mn.

Differential thermal analysis (DTA) was used to detect phase transformations caused by small quantities of certain alloy elements in high purity Pu and in delta-stabilized Pu with one weight per cent Ga. Each alloy composition was sealed in a Ta capsule, heated to 1200°C, shaken, then cooled rapidly to produce a fine-grained, homogeneous alloy. DTA traces from the alloys were compared to a trace of high purity Pu. Fe, Co, or Ni at 0.1 atom per cent (0.0240 wt %) caused additional phase transformations between 405 and 412°C. Fe or Co at 0.1 atom per cent in delta-stabilized Pu caused additional phase transformations at 405°C. The combined presence of Fe and Ni, each at 0.05 atom per cent, depressed the Pu–Fe phase transformation 10 to 15 degrees, to 390–395°C, for both Pu and the delta-stabilized alloy. DTA traces for samples of production-grade Pu and delta-stabilized alloy quantitatively indicated the presence of Fe and Ni. A sample of delta-stabilized Pu was melted, cooled at a rate of three degrees per minute to room temperature, and analyzed; the DTA trace indicated the presence of approximately six per cent alpha phase. (auth)

41453 (NUMEC–3428-21) GROWTH OF SINGLE CRYSTALS OF PLUTONIUM. Quarterly Progress Report, January 1, 1966–March 30, 1966. (Nuclear Materials and Equipment Corp., Apollo, Pa.). Apr. 29, 1966. Contract AT(30-1)-3428. 17p. Dep. mn. CFSTI $1.00 cy, $0.50 mn.

Efforts directed toward setting up zone melting equipment to determine the feasibility of zone refining C-contaminated Pu–Ga alloy rods and to evaluate the potential of zone refining as a means of producing single-crystal delta Pu are described. Results of chemical analyses of zone refined material show that zone melting did not result in transport of impurities along the rod. Strain anneal and secondary recrystallization were selected as the methods for use in delta stabilized Pu single-crystal studies. (J.R.D.)

41454 (NYO–2394-22) CONTINUUM THEORY OF PLASTICITY ON THE MACROSCALE AND THE MICROSCALE. Technical Report No. 22. Drucker, D. C. (Brown Univ., Providence, R. I. Div. of Engineering). June 1966. Contract AT(30-1)-2394. 67p. (CONF-660627–3). Dep. mn. CFSTI $3.00 cy, $0.75 mn.

From American Society for Testing and Materials, 69th Annual Meeting, Atlantic City.

Concepts of the mathematical theory of plasticity and of their relations with the analysis and design of structures, machines, or continua, and for an understanding of metalworking processes are reviewed. Direct application of the theory on a microscale is shown to provide a reasonable explanation and prediction of flow and fracture features such as transition temperature, the fracture strength of sintered carbides, the effects of grain size, and the qualitative differences between the stress-strain curves for pearlitic and spherodized steels. Limitations imposed by atomic scale, however, lie outside of conventional plasticity theory. Familiar theorems, including the limit theorems, do not hold. Dispersion and precipitation hardening are discussed in these terms along with other effects of size on the microscale. (auth)

41455 (NYO–2731-7) PHASE EQUILIBRIA AND SPECIFIC VOLUMES OF LIQUID METALS AND ALLOYS. Report No. V. Progress Report, August 1, 1965–July 31, 1966. Kanda, Frank A. (Syracuse Univ. Research Inst., N. Y. Dept. of Chemistry). May 1966. Contract AT(30-1)-2731. 83p. Dep. mn. CFSTI $3.00 cy, $0.75 mn.

Investigations were conducted to extend results already obtained and to obtain values on systems not previously studied. Results are presented from studies of Na–Li immiscibility regions. Data on densities of liquid Na–Li alloys as a function of composition and temperature are included. Data and information are also included on densities and intermetallic compounds formed in liquid Cd–Sb alloys. Other data are included on densities of liquid Bi–Te and Tl–Te systems including possible telluride structures. Re-

sults of developmental work on viscometers for use in liquid metal investigations are summarized. Design and operation of distillation apparatus for preparation of high-purity Ca is described. Investigation of the properties and structure of Mg–Sr intermetallic compounds are reported. (J.R.D.)

41456 (ORNL–3992) CREEP-RUPTURE PROPERTIES OF TUNGSTEN AND TUNGSTEN-BASE ALLOYS. McCoy, H. E. (Oak Ridge National Lab., Tenn.). Aug. 1966. Contract W-7405-eng-26. 51p. Dep. mn. CFSTI $3.00 cy, $0.50 mn.

The creep-rupture properties of two types of unalloyed W and two W-base alloys were determined at 1650 and 2200°C for times of at least 500 hr. The materials studied were wrought powder-metallurgy W, several lots of thermochemically deposited (TCD) W, W–2% ThO_2, and Sylvania A (W–0.5% Hf–0.02% C). At 1650°C, the order of strengths from the greatest to least was W–2% ThO_2, Sylvania A, and TCD and powder-metallurgy W. At 2200°C the order of strengths from greatest to least was W–2% ThO_2, TCD and powder-metallurgy W, and Sylvania A. The ductility of the TCD W was low at 1650°C, but was good at 2200°C. The W–2% ThO_2 showed moderate ductility at both temperatures. The ductility of the Sylvania A improved from moderate at 1650°C to good at 2200°C. The powder-metallurgy W had good ductility at both test temperatures. All of the materials studied exhibited better high-temperature grain-size stability than the powder-metallurgy material. Voids formed in the TCD W at 2200°C and grew to quite large sizes under an imposed stress. These voids were thought to be associated with impurities. (auth)

41457 (ORO–3291-3) APPLICATION OF ADIABATIC CALORIMETRY TO METAL SYSTEMS. Progress Report, September 1, 1965–August 31, 1966. Stansbury, E. E.; Brooks, C. R. (Tennessee Univ., Knoxville. Dept. of Chemical and Metallurgical Engineering). June 1966. Contract AT(40-1)-3291. 36p. Dep. mn. CFSTI $2.00 cy, $0.50 mn.

Development of equipment and methods for calorimetry are are summarized. Data on the specific heat of Cu obtained using a Ni-component calorimeter are included along with data from the literature on Cu specific heat. Data and discussion are presented concerning specific heat, electric properties, and phases of Mo–Ni alloys and Ni_4Mo. Data on the specific heat of Cu_3Au are included. Phase studies of Ti–Zr alloys were conducted and data concerning phases are presented as shown by electric conductivity. (J.R.D.)

41458 (TID–23268) CONTRIBUTION TO THE UNDERSTANDING OF THE HIGH TEMPERATURE OXIDATION OF METALS. Final Report, February 1, 1962–May 31, 1966. Wagner, J. Bruce Jr. (Northwestern Univ., Evanston, Ill. Technological Inst.). June 17, 1966. Contract AT(11-1)-1126. 81p. Dep. mn. CFSTI $3.00 cy, $0.75 mn.

Investigations of doping semiconducting oxides are summarized. Li-doped NiO and CoO are discussed as examples of the doping process. Investigations are also reported on equilibrium vacancy concentrations in the Wüstite phase field around a reported P-to-n transformation at 950 to 1250°C. Transformation mechanisms are discussed. Results of studies concerning oxidation of iron alloys containing 0.59 to 1.06 at. % Ti at 900 to 1100°C in CO_2–CO mixtures are presented. An investigation to determine the mechanisms of oxidation of Cu and Cu–Au alloys in CO_2 at 1000°C is summarized. Results of thermogravimetric and Seebeck effect measurements on Li-doped CoO crystals are included. (J.R.D.)

41459 (TID–23288) AN INVESTIGATION OF THE MECHANICAL BEHAVIOR OF GRADES RVD AND AGOT GRAPHITES. Final Report. Woodard, John D. (Southern Research Inst., Birmingham, Ala.). Apr. 20, 1966. Contract AT(40-1)-2073. 166p. Dep. mn. CFSTI $5.00 cy, $1.00 mn.

For Union Carbide Corp., Y-12 Plant, Oak Ridge, Tenn.

The evaluation of RVD graphite covered the range in temperature from 1000 to 5500°F and consisted of short-time uniaxial response at constant strain rate in tension and compression, short-time uniaxial response with a change of strain rate in tension and compression, uniaxial creep response in tension and compression, uniaxial response under cyclic loads in tension, uniaxial response with a period of stress relaxation in tension, short-time torsional response with a constant axial tensile load, and the dynamic modulus of the material. For the AGOT graphite, short-time uniaxial evaluations were performed from 70 to 4500°F, and shear evaluations were performed at 70°F. Bulk density was determined for all specimens. (auth)

41460 (TIM–793) VISCOSITY OF LIQUID POTASSIUM TO 900 DEG C. Rigney, D. V.; Kapelner, S. M.; Cleary, R. E. (Pratt and Whitney Aircraft, Middletown, Conn. Connecticut Advanced Nuclear Engineering Lab.). June 22, 1964. Contract AT(30-1)-2789. 17p. Dep. mn. CFSTI $1.00 cy, $0.50 mn.

An oscillating pendulum viscometer was designed and constructed to determine the viscosity of liquid metals and was used to measure the viscosity of liquid K to 908°C. The temperature dependency of the viscosity was found to fit an Arrhenius equation and the Andrade equation to 500°C with a change in slope to a similar function from 500°C to 908°C. At 85 to 501°C $\log_{10}\eta = 3.1530 + 308.26/T$, $\sigma_{\log_{10}\eta} = \pm 0.011$ and from 500 to 908°C, the data best followed a second function $\log_{10}\eta = 3.3584 + 466.77/T$, $\sigma_{\log_{10}\eta} = \pm 0.010$, where T is in degrees Kelvin. The change in slope may indicate some change in the mechanisms of momentum transfer. (auth)

41461 (UCRL–7361(Pt.3)) SOME EXPERIENCES WITH NOBLE-METAL, METAL-SHEATHED THERMOCOUPLES THIRD AND FINAL REPORT. Bostwick, William E. (Lawrence Radiation Lab., Univ. of California, Livermore). Sept. 15, 1965. Contract W-7405-eng-48. 14p. Dep. mn. CFSTI $1.00 cy, $0.50 mn.

Tests were conducted on MgO, Y_2O_3, Al_2O_3 (both α and γ types), and BN, to determine their insulating capability for Pt 10%-Rh/Pt metal-sheathed thermocouple application at temperatures above 2400°F. Presintered (α) Al_2O_3 appeared to be the best although it resintered during testing. MgO and Y_2O_3 likewise sintered. BN did not. Sheathed thermocouple material should be checked carefully if flexibility is desired or required. Metal-sheathed thermocouple material from seven manufacturers were inspected for possible damage during the manufacturing process. It was concluded that if damage to the wires, and/or sheath nonuniformity and hardness cannot be tolerated, sampling and inspection of the material during both production and preproduction runs are required. (auth)

41462 (USBM-RC–1245) SELECT PROPERTIES OF THORIUM WITH LOW THORIA ADDITIONS. Topical Report, July 1, 1965–June 30, 1966. O'Hare, S. A.; Armantrout, C. E. (Bureau of Mines, Albany, Oreg. Albany Metallurgy Research Center). July 1966. Contract AT(11-1)-599. 18p. Dep. mn. CFSTI $1.00 cy, $0.50 mn.

Results of investigations are presented concerning submicron ThO_2 particles and their effect on hardness properties, tensile properties, and electrical resistivity of Th. Temperatures considered were ambient to 800°C for the hot hardness, 400 to 800°C for the tensile study, and 20°C for the electrical resistivity. Composition variation did not have any significant effect on the hardness or tensile properties but did affect the electrical resistivity. Increasing the ThO_2 content increased the electrical resistivity. (auth)

41463 THERMAL DESORPTION OF INERT GASES FROM TUNGSTEN MONOCRYSTALS. Kornelsen, E. V.; Sinha, M. K. (National Research Council, Ottawa). Appl. Phys. Lett., 9: 112-14(Aug. 1, 1966).

Clean W surfaces were bombarded with inert gas ions at energies of 50 to 5000 ev. The targets were then heated at a known rate, and the resulting rate of change of pressure in an isolated volume was recorded to form desorption spectra. Desorption spectra obtained following bombardment with 1500-ev Ne^+ ions show that the desorption

depends strongly on the crystal face bombarded. Evidence is also presented that some of the sites from which the desorption takes place are located within a few atomic layers of the crystal surface. (A.G.W.)

41464 THE ISOTHERMAL SECTIONS AT 1200 C OF THE EQUILIBRIUM DIAGRAMS OF THE SYSTEMS Mo–Ti–Zr AND Mo–Nb–Zr. Chuang, Yu-chih; T'ang, Ch'uang-hung; Chuang, Hsiang-lin. Chin Shu Hsueh Pao, 9: 63-71 (Jan. 1966). (In Chinese).

The isothermal sections at 1200°C of the systems Mo–Ti–Zr and Mo–Nb–Zr were determined by metallographic and x-ray-diffraction methods supplemented by hardness measurements. The constitutions of these two systems are strikingly similar; besides a bcc ternary terminal solid solution and a ternary Laves phase isomorphous with $MgCu_2$ structure, no new intermediate phase was found. In the Mo–Ti–Zr system the lattice parameter of the ternary solid solution increases with the increase of Ti or Zr in solid solution, and the ternary Laves phase is (Ti,Zr) Mo_2. In the Mo–Nb–Zr system, the lattice parameter of the ternary solid solution also increases with the increase in the Nb- or Zr content, and the ternary phase in this case is $Zr(Mo,Nb)_2$. The isohardness contours of the Mo–Ti–Zr system tend to expand towards the titanium corner as the Ti content is increased, whereas those of the Mo–Nb–Zr system expand towards the niobium corner with the increase in Nb content in a like manner. (CFSTI)

41465 STUDY OF MOLYBDENUM–GADOLINIUM PHASE DIAGRAMS. Chuang, Yu-chih; Li, Chao-wu; Chuang, Hsiang-lin; Kao, Lien-mei. Chin Shu Hsueh Pao, 9: 110-12(Jan. 1966). (In Chinese).

The Pirani method was used to determine the fusion temperature and the peritectic temperature of molybdenum–gadolinium alloys, and Cu K radiation was used for powder x-ray analysis. Solid solubility of gadolinium in molybdenum was 1.1% at 2400°C, 0.4% at 2200°C, 0.3% at 2000°C, 0.2% at 1800°C and 0.15% at 1600°C after molybdenum alloy containing 0.09 to 5% of gadolinium was kept at 1600 to 2400°C and then hardened. Fusion temperatures of Mo–Gd (0.09–24.5%) alloys were determined and the peritectic temperature of Mo–Gd alloy was found to be 2457°C. The average fusion temperature of gadolinium-rich alloys was 1305°C. The transformation temperature of α Gd $\rightleftharpoons$ β Gd of the gadolinium-rich phase was determined by thermal analysis to be 1270°C, and that of β Gd $\rightleftharpoons$ L_{II} was 1314°C. The transformation temperature of pure gadolinium's α Gd $\rightarrow$ β Gd was 1288°C and that for β Gd $\rightarrow$ liquid was 1328°C. The fact that the hardness of alloys decreases with increasing gadolinium content shows the absence of an intermediate phase in Mo–Gd binary alloy. (CFSTI)

41466 INVESTIGATION OF THE AGING KINETICS OF MOLYBDENUM-BASE ALLOYS. Goltsev, V. P. (Nuclear Power Inst., Academy of Sciences, USSR). Dokl. Akad. Nauk BSSR, 10: 385-7(1966). (In Russian).

Sheet specimens 1 mm thick of molybdenum–zirconium, molybdenum–titanium, and molybdenum–hafnium alloys containing 0.003 to 0.005% carbon, 0.01 to 0.20% oxygen, and up to 0.06% nitrogen were aged at 1300°, 1400°, and 1500°K in vacuum for 1.8 to 108 ksec. In all three alloys, the aging-induced changes in microhardness and lattice parameter "a" were found to follow roughly the same pattern. In molybdenum–hafnium alloy the final drop in microhardness brought about by prolonged aging or by aging at higher temperature is a result of the redissolution of the strengthening phase precipitated in the first stages of aging. However, a similar drop in microhardness in molybdenum–zirconium and molybdenum–titanium alloys was found to be the result of the coagulation of the strengthening phase. In all three alloys, age hardening was caused by the precipitation of finely dispersed oxides of alloying elements. (ATD)

41467 ELECTRON MICROSCOPIC AND MICRODIFFRACTION ANALYSIS OF NONMETALLIC INCLUSIONS IN MOLYBDENUM AND ITS ALLOYS. Ageev, N. V.; Ignatov, D. V.; Kantor, M. M. (Baykov Inst. of Metallurgy, USSR). Dokl. Akad. Nauk SSSR, 167: 635-6 (Mar. 21, 1966). (In Russian).

The electron microscope was used for studying nonmetallic inclusions in molybdenum and its alloys melted by various methods. The phase composition and distribution of the inclusions were determined in specimens of molybdenum produced by electron-beam melting and in molybdenum alloys containing carbon (0.003 to 0.021%), titanium (0.02 to 0.3%), and zirconium (0.01 to 0.15%), produced by arc melting and fusion melting. The specimens were studied in the cast, deformed, and annealed states. The method used for producing the replicas is briefly described. Photomicrographs and diffraction patterns show that the inclusions consist basically of Mo_2C. This is probably due to the melting conditions and heat treatment of the specimens. The electron-beam melting and annealing were done in a vacuum of 10^{-4} to 10^{-5} Hg mm. Oil vapor diffusion pumps were used for producing the vacuum. Apparently the main residual gas consists of the oil vapors, which decompose to form carbon. This carbon diffuses into the metal and forms carbides. (ATD)

41468 MORPHOLOGY AND TEXTURE OF MOLYBDENUM AND TUNGSTEN CARBONYL DEPOSITS. Matyushenko, N. I.; Rozen, A. A.; Sagalovich, V. V. Fiz. Metal. Metalloved., 21: 403-8(Mar. 1966). (In Russian).

The morphology and textures of deposits obtained in thermal decomposition of molybdenum and tungsten carbonyls were studied over the temperature range from 150 to 1050°C. X-ray-diffraction patterns and particle size of the deposits, obtained at different temperatures of the deposition surface, were determined. It was found that there exist two morphological transition temperatures, at 250 and 750°C and 350 and 800°C for Mo and W respectively. The first transition temperature is related to the rupture of carbonyl molecule and the second to the condensation from supercooled liquid or, at higher temperature (i.e., $T > \theta_2$), to the formation of crystal nuclei. (ATD)

41469 THE STRUCTURES OF POLONIUM AND ITS COMPOUNDS. I. α AND β POLONIUM METAL. DeSando, R. J.; Lange, R. C. (Mound Lab., Miamisburg, Ohio). Contract AT(33-1)-Gen-53. J. Inorg. Nucl. Chem., 28: 1837-46(Sept. 1966). (MLM-1313J).

The crystal structures of alpha and beta Po metal were redetermined from x-ray-diffraction powder photographs using monochromatic radiation and a He atmosphere by employing an isotopic mixture of ^{208}Po and ^{209}Po. Electron distribution curves as a function of interatomic distance were also computed. Previous x-ray data obtained from ^{210}Po (half life of 138.4 days), were influenced by the growth of Pb at the rate of 0.5 per cent per day and self-heating effects. The half lives of ^{208}Po and ^{209}Po are 2.8 and 103 yr, respectively. The growth rate of Pb and the thermal effects from self-heating are reduced to four per cent of those in ^{210}Po. Alpha Po is simple cubic and in space group Pm3m with a = 3.359 ± 0.001 Å and ρx ray = 9.142 g/cm^3. Beta Po is rhombohedral and a space group R3m (A10 type) with α = 3.368 ± 0.001 Å, α = 98° 14.4′ and ρx ray = 9.392 g/cm^3. The structure of Po and its relationship to elements in Group VIB are discussed. (auth)

41470 STRUCTURAL CHANGES IN URANIUM DUE TO THERMAL CYCLES. Slancar, F.; Shlantsar, F. (Inst. for Nuclear Research, Czechoslovak Academy of Sciences, Rez). Kovove Mater., No. 1, 20-33(1965). (In Czech).

Experimental tests are described on 99.82% pure U specimens—4-mm-diameter extruded wire, 4.15-mm-diameter forged wire, and shapes 30 mm in diameter. The first two types were heat treated at 720°C, quenched in water, and then annealed at 500°C for two hours. They were then examined for internal slip and twinning, boundary slip, grain polygonization, and micro cracks. Methods of preparing metallographic samples of each type of test material are described, including electrolytic polishing,

ion bombardment, and buffing with diamond paste. Structural changes were studied with a heat microscope over a range from 80 to 550°C, maintained for 13 minutes and followed by quenching in oil for two minutes. The heat cycles were arranged in a special apparatus in which the temperature rose from 50 to 550°C in 12 minutes, with the maximum maintained for 10 minutes. The results are given in a series of metallographic photomicrographs and show that coarse-grained U is highly deformed in each time cycle, but fine-grained metal shows no discernible deformation. Boundary slip was very noticeable in fine-grained U. Grain polygonization occurred equally in both 90-μ and 70-μ average grain sizes, which are most widely used in reactors, and increased through 800 times cycles, but the grain size did not change from that point up to 2000 cycles. Micro cracks originated in occlusions of U(OCN), spread to the grain boundary, then progressed between grains. These cracks lengthened as the time cycles increased, and formed dense networks after 1600 or 2000 cycles. (JPRS)

41471 INVESTIGATION OF ALLOYS OF THE Zr–C SYSTEM. Godin, Yu. G.; Evstyukhin, A. I.; Emelyanov, V. S.; Rusakov, A. A.; Suchkov, I. I. Met. Metalloved. Chistykh Metal., Sb. Nauchn. Rabot, No. 5, 25-32(1966). (In Russian).

A series of zirconium–carbon alloys containing 0.1 to 68 at. % C were made by compacting powdered 99.5%-pure zirconium and carbon by sintering green ingots in vacuum at 2000°C with subsequent arc melting in an inert atmosphere, or by direct arc melting of solid 99.8%-pure zirconium with carbon. The alloys were water-quenched from 750 to 862°C or oil quenched from 1100 to 2400°C. A phase diagram of the Zr–C system, based on physicochemical analyses, is shown. Two-phase alloys containing 0.05 to 5.4 wt. % C consist of grains of zirconium carbide and the α phase, which is a supersaturated solid solution of carbon in zirconium formed with the $\beta \rightarrow \alpha'$ transformation during quenching. Alloys with a carbon content ranging from 6.0 wt. % to that of zirconium carbide (11.63 wt. % C) consist of a solid solution of zirconium in carbide. With a further increase in the carbon content, free carbon is precipitated both as eutectic and as primary carbide grains. Quenching of alloys from 2400, 1700, or 1100°C had no substantial effect on the alloy structure; the solubility of carbon in the β zirconium at 1100°C was less than 0.1 wt. %. The microstructure of the alloys containing 7.1 to 10.5 wt. % C quenched at lower temperatures (to 750°C) consists of a solid solution of zirconium in carbon; the solubility of carbon in α zirconium at 820°C is about 0.3 wt. %. X-ray diffraction confirmed the existence of a single carbide phase in the Zr–C system. Two-phase alloys quenched from 2400°C have a lattice constant of 4.695 Å, compared to 4.693 Å for the same alloys quenched from 1700°C. The microhardness of cast and quenched zirconium alloys increases with increasing carbon content, reaches a maximum of 2150 kg/mm^2 at a composition corresponding to zirconium carbide, and then decreases with further increase in the carbon content because of the appearance of free carbon in the form of both a eutectic and of primary grains. The microhardness of α' zirconium (180 kg/mm^2) remains constant with increasing carbon content and is higher than the hardness of α zirconium. This probably is caused by the solubility of carbon in zirconium and by the $\beta \rightarrow \alpha$ martensitic transformation. (ATD)

41472 PROCEEDINGS OF THE BRITISH CERAMIC SOCIETY. No. 6. MECHANICAL PROPERTIES OF NON-METALLIC CRYSTALS AND POLYCRYSTALS. Proc. Brit. Ceram. Soc., No. 6, 1-334(June 1966).

A total of 27 papers were presented at meeting. Separate abstracts were prepared for three of the papers. Papers for which no abstracts were prepared are concerned with strength of non-metallic crystals, interpretation of data on complex ceramics, plastic flow of polycrystalline material, and dislocation phenomena. (J.R.D.)

For abstracts of individual papers see: 41473–41475.

41473 OBSERVATIONS ON THE STRENGTH AND YOUNG'S MODULUS OF BeO AS A FUNCTION OF DENSITY AND GRAIN SIZE. O'Neill, J. S.; Hill, N. A.; Livey, D. T. (Atomic Energy Research Establishment, Harwell, Eng.). Proc. Brit. Ceram. Soc., No. 6, 95-101(June 1966).

The variations in modulus of rupture and Young's modulus as a function of grain size and density are presented for BeO of 94 to 99% theoretical density. The modulus of rupture by three-point bending reached a maximum of ~40,000 p.s.i. at ~97% theoretical density and a grain size of 3 to 5 mμ. The Young's modulus increased with density to 56 × 10^6 psi at 99% theoretical density. (auth)

41474 CREEP OF ThO_2 AND ThO_2–CaO SOLID SOLUTIONS. Morgan, C. S.; Hall, L. L. (Oak Ridge National Lab., Tenn.). Proc. Brit. Ceram. Soc., No. 6, 233-8(June 1966).

Compressive creep tests at elevated temperatures were carried out on polycrystalline ThO_2 and ThO_2–CaO specimens. At 1465°C a stress of 8000 psi caused appreciable long-term creep in ThO_2 bushings. At the same temperature, specimens that contained small quantities of CaO deformed initially at an order of magnitude lower stress. The creep rate of the material containing CaO decreased steadily with time, and after several hundred hours was about the same as that for pure ThO_2 specimens. Metallographic examination of the specimens after creep test revealed evidence of polygonization in ThO_2 specimens, and grain growth in ThO_2–CaO specimens. (auth)

41475 EFFECT OF STOICHEIOMETRY ON THE YIELD STRESS OF TiC AND TiO_2. Hollox, G. E.; Smallman, R. E. (Univ. of Birmingham, Eng.). Proc. Brit. Ceram. Soc., No. 6, 317-24(June 1966).

Non-stoichiometric defects tend to raise the yield stress of TiO_2, but have the opposite effect in TiC, the former behavior being typical of the interaction of vacancies with dislocations. The latter can be explained by considering that the deformation mechanisms of TiC are governed by a fcc Ti lattice with a frictional drag resulting from a covalent interaction with C interstitial atoms, the magnitude of which decreases with increasing non-stoichiometry. (auth)

41476 ELECTRICAL AND THERMAL CONDUCTIVITIES OF METALS OVER THEIR ENTIRE LIQUID RANGE, i. e., FROM MELTING POINT TO CRITICAL POINT, AND THE CONTAINMENT OF METALLIC SUBSTANCES UP TO 5000 DEG K FOR SUBSTANTIAL PERIODS OF TIME. PART I. ELECTRICAL CONDUCTIVITIES. Grosse, Aristid V. (Temple Univ., Philadelphia). Rev. Hautes Temp. Refract., 3: 115-27(Apr.-June 1966).

The electrical conductivity of Hg was previously measured over the entire liquid range. It was found recently that a hyperbolic relation of the form $(\kappa_{red.} + b)(\theta + b) = a$ exists between the reduced conductivity, $\kappa_{red.} = \kappa_T/\kappa_{m.p.}$ and the reduced temperature, $\theta = (T - T_{m.p.})/(T_{c.p.} - T_{m.p.})$, a and b in the above equation are constants of the hyperbola, both dependent on the distance, Δ, of the vertex of the hyperbola from either the $\kappa_{red.}$ axis or θ axis. Experimental data on the electrical conductivity of liquid Na, K, Rb, and Cs are now available over a substantial liquid temperature range. These alkali metals also show, within experimental error, the same hyperbolic relationship as Hg. Cu, Ag, Au, Al, and Sn also conform, as far as the experimental data now available go, with the empirical hyperbolic relationship. Experimental data on Li and Zn (and to a lesser extent on Cd) indicate an exception to the hyperbolic relation. Data on these metals are included. (J.R.D.)

41477 ELECTRICAL AND THERMAL CONDUCTIVITIES OF METALS OVER THEIR ENTIRE LIQUID RANGE, i. e., FROM MELTING POINT TO CRITICAL POINT, AND THE CONTAINMENT OF METALLIC SUBSTANCES UP TO 5000 DEG K FOR SUBSTANTIAL PERIODS OF TIME. PART II. THERMAL CONDUCTIVITIES. Grosse, Aristid V. (Temple Univ., Philadelphia). Rev. Hautes Temp. Refract., 3: 127-39(Apr.-June 1966).

The thermal conductivity of liquid Hg, Na, K, Rb, and Ce

can be estimated using the Wiedemann-Franz-Lorentz law $\lambda_{therm.} = L\mathcal{K}.T$, where L is the Lorentz constant = $2.443 \cdot 10^{-8}$ watts/ohm/(°K)^2. Independently from any assumption involving the free electron theory of metals, the thermal conductivity at the critical point can be estimated for these metals by approaching the critical point from the saturated vapor side, where $\lambda_{therm.}$ is $\simeq 0$. The thermal conductivity of the saturated vapor of Hg and the above alkali metals was measured and agrees well with the calculations based on the kinetic theory. Using a hyperbolic relation and the Wiedemann-Franz-Lorentz law, it is possible to estimate the thermal conductivity of liquid Hg and the four alkali metals mentioned, over their entire liquid temperature range. In addition, the thermal conductivities of many other metals can be estimated, since the $\mathcal{K}_{m.p.}$ values of most metals are known and $\mathcal{K}_{c.p.} \simeq 0$, even if these estimates are of a preliminary nature. From the known electrical conductivities of the monetary metals—Cu, Ag, and Au—the $\lambda_{therm.}$ vs T functions can be estimated. (J.R.D.)

41478 THE DEPENDENCE ON MICROSTRUCTURE OF THE HIGH TEMPERATURE PROPERTIES OF URANIUM OXIDE. MOLYBDENUM AND URANIUM OXIDE. TUNGSTEN CERMETS. Amato, I.; Colombo, R. L.; Polin, F. (FIAT, Sezione Energia Nucleare, Turin). Rev. Hautes Temp. Refract., 3: 189-96(Apr.-June 1966).

Specimens of UO_2–Mo and UO_2–W were prepared and their electric conductivities were measured as a function of microstructure. One series of specimens were prepared by sintering pressed UO_2 powders with W or Mo powders. Another series was prepared by mixing green spheroidal agglomerates of UO_2 powder in slurries of Mo or W dispersed in acrylic cement, drying, and sintering. A third series of specimens were prepared by sintering green agglomerate UO_2 spheroids, coating them with Mo or W and hot pressing. Results are presented graphically. (J.R.D.)

41479 THERMAL DIFFUSIVITY AND CONDUCTIVITY MEASUREMENTS ON METALS AND OXIDES AT HIGH TEMPERATURES. Iacobelli, R.; Moretti, S. (CNEN, Centro Studi Nucleari Della Casaccia, Rome). Rev. Hautes Temp. Refract., 3: 215-28(Apr.-June 1966).

A discussion is presented concerning experimental facility used and the results obtained by applying a transient method and implementing generalized equations for measuring thermal diffusivity at high temperatures. The method consists in exposing a thin slab of the material under test to a very short pulse of radient energy and in following the thermal history at the face of the slab opposite to the one at which the energy is deposited. The thermal diffusivity is derived by measuring the time ($t_{½}$) at which the temperature of the opposite face reaches one half of its maximum value. The experiments were performed under vacuum, so that the radiation heat losses from the surfaces of the specimen were easily defined. The method was first tested for stainless steel and then applied to UO_2. (auth)

41480 PREPARATION OF SINGLE CRYSTALS OF REFRACTORY COMPOUNDS FROM BINARY OR MULTICOMPONENT SYSTEMS AND EFFECT OF TEMPERATURE CONDITIONS OF GROWTH ON THEIR FORM AND FACETING. Izvekov, V. N.; Sysoev, L. A.; Obukhovskii, Ya. A.; Birman, B. I. (Inst. of Crystallography, Academy of Sciences, USSR). Rost Kristallov., Akad. Nauk SSSR, Inst. Kristallogr., 6: 116-21(1965). (In Russian).

The growth of cadmium sulfide single crystals from melts of cadmium chloride and iodide and their mixtures, and the growth of single crystals of α-corundum (ruby), rutile, strontium titanate, and calcium tungstate from fluorides were studied. CdS single crystals with a wurtzite lattice were obtained in the 600 to 380°C range from the $CdS–CdCl_2–CdI_2$ system. The oxide crystals were grown in platinum crucibles in the 1200 to 700°C range with slow cooling. An important feature revealed by these experiments is the dependence of the crystal habit of the crystals obtained on the temperature range of the crystallization. This phenomenon is explained by differences in the growth rates of faces having different crystallographical indices, particularly surface roughness. The concept of the influence of surface roughness on the growth forms of crystals is extended to binary and multicomponent systems. (ATD)

41481 GROWING AND PLASTIC DEFORMATION OF THE SINGLE CRYSTALS OF REFRACTORY METALS AND ALLOYS. Savitskii, E. M.; Burkhanov, G. S.; Kopetskii, Ch. V.; Chuprikov, G. E. Rost Kristallov., Akad. Nauk SSSR, Inst. Kristallogr., 6: 308-18(1965). (In Russian).

The physical and mechanical properties of single crystals of tungsten, molybdenum, rhenium, tantalum, niobium, vanadium, and their alloys grown from melts of vacuum-arc melted or sintered metals were investigated. Crystals up to 12 to 14 mm in diameter and 150 to 250 mm long were grown in an electron-beam furnace developed for vacuum zone melting of refractory metals. The crystal purity was found to be two orders higher than that of the initial metals and alloys. For instance, the oxygen content dropped from 0.05 and 0.012% in the sintered and in vacuum-arc melted rhenium, respectively, to 0.001% in single crystals. The removal of interstitial impurities decreased the tensile strength and appreciably increased the ductility of all investigated metals. For example, the tensile strength of sintered and arc-melted rhenium, 115 and 65.8 kg/mm^2, respectively, decreased to 42.5 kg/mm^2 for rhenium single crystals. At the same time, elongation increased from 12.1 and 16.1% to 41%. Molybdenum single crystals sustained a bend angle of 180° at room temperature and a 60° bend angle at −196°C. At room temperature, tungsten and niobium single crystals sustained a bend angle of 90 and 180°, respectively, and rhenium sustained a bend angle of 90° at −196°C. Molybdenum single crystals 13 mm in diameter and 250 mm long were drawn into wire 50 μm in diameter or rolled into 50 μm-thick foil without process annealing. Single crystals of some alloys in the region of solid solutions of the Mo–Nb, Mo–W, Mo–Ti, and W–Nb systems were also grown from electron beam-melted single crystals of the respective metals. The single crystals obtained had essentially the same substructures as the initial components; they also had good ductility and a tensile strength higher than that of the initial metals. (ATD)

41482 EFFECT OF THE ANNEALING TEMPERATURE AND MEDIUM ON THE PROPERTIES OF MOLYBDENUM. Khoroshailov, V. G.; Bogoyavlenskii, K. N.; Rossomakho, Ya. V. (Leningrad Polytechnic Inst.). Tr. Leningr. Politekhn. Inst., No. 251, 28-30(1965). (In Russian).

Cold-rolled strips of 99.9%-pure sintered molybdenum, 150 to 180 × 0.2 × 400 to 800 mm, were annealed in a vacuum of 1.5 to 1.4×10^{-2} mm Hg or in dry hydrogen at 800 to 1400°C for 45 min to determine the optimum conditions for heat treatment. In the as-delivered condition, molybdenum had a hardness HV of 275 to 300, a tensile strength of 100 to 130 kg/mm^2, and an elongation of 0.5 to 2%; the microstructure was typical for a cold-worked metal. Annealing lowered the hardness and strength and increased the ductility. The decrease in tensile strength and hardness by annealing at 800 to 950°C is associated with the relieving of stresses caused by cold working. The texture disappeared completely after annealing at 1100°C; grain growth began at 1200°C. Annealing at 1200°C for more than 45 min had no additional effect on the strength and ductility. The temperature of recrystallization for vacuum-annealed metal was 100 to 150°C higher than that for metal annealed in hydrogen; this was attributed to some leak of air through the walls of the quartz ampules at high temperatures. (ATD)

41483 REDKOZEMEL'NYE FERROMAGNETIKI I ANTIFERROMAGNETIKI. (Rare Earth Ferromagnetics and Antiferromagnetics). Belov, K. P.; Belyanchikova, M. A.; Levitin, R. Z.; Nikitin, S. A. Moscow, Izdatel'stvo Nauka, 1965. 319p.

On the basis of work published by Soviet and foreign scientists and engineers, a review of the recent theoretical and experimental investigations of the ferromagnetism and antiferromagnetism of the rare earth metals, alloys, and compounds is given. The results of original investi-

gations by authors of various monographs are included. A section on the ferromagnetism of rare earth ferrites is also included. (G.O.Y.)

41484 NEW METHODS FOR THE MEASUREMENT OF DIFFUSION OF α-EMITTING ATOMS IN SOLIDS. DIFFUSION OF ACTINIDE ELEMENTS IN UO_2. Schmitz, F. K. Brunswick, Technische Hochschule, 1965. 70p. $2.00 Gmelin, AED-Diss 65-272.

The diffusion of Pu in UO_2 was determined by 3 methods, the sectioning method, surface decrease method, and by α energy degradation. Activation energies obtained by these methods are in satisfactory agreement. Diffusion mechanisms of actinide elements in UO_2 are discussed. (Gmelin Inst.)

41485 SOME OBSERVATIONS ON THE PRESSURE-TEMPERATURE PHASE DIAGRAM OF BERYLLIUM. Contre, M.; Francois, D. 20p. (CONF-660205-6). ORAU. Gmelin, AED-CONF-66-021-8.

From Metallurgical Society of the American Institute of Mining, Metallurgical, and Petroleum Engineers, New York.

At atmospheric pressure, the α-β transformation of beryllium occurs at 1264°C and involves an increase in resistivity amounting to about 50%. The range of stability of the β phase increases with pressure. A slight change in slope and a marked arrest in the resistance curve below the α-β transition temperature are attributed to recrystallization under pressure of the sample, which is severely cold worked as pressure is increased. From first experimental results a provisional pressure-temperature phase diagram of pure beryllium is drawn. According to this diagram enthalpy change at α-β transition would be about 1.8 kcal/mole at atmospheric pressure; the change in volume on melting would be an increase of about 10%. (auth)

41486 DIFFUSE REFLECTANCE CHARACTERISTICS OF MONOCLINIC ZrO_2 AS A FUNCTION OF PURITY. Sarver, J. F. (General Electric Co., Cleveland). 21p. (CONF-660505-6). ORAU. Gmelin, AED-CONF-66-103-6

From American Ceramic Society Meeting, Washington, D. C.

Diffuse reflectance spectra of monoclinic ZrO_2 from several commercial sources are compared with the spectrum of high-purity ZrO_2 prepared from $ZrOCl_2 \cdot 8H_2O$ purified by recrystallization from an HCl solution. The purified oxide exhibits greater than 98% reflectance relative to CaF_2 above 3250 Å. Below 3000 Å, the lattice absorption of ZrO_2 increases and the reflectance decreases to a minimum of about 10% at 2300 Å. Ti^{4+} in solid solution introduces a very strong absorption band in the ultraviolet, and all commercial sources of ZrO_2 as well as other sources of high-purity oxides exhibited an absorption band attributable in part to titanium. The presence of iron causes a further lowering of the reflectance in the visible range. (auth)

41487 ELECTRODEPOSITION OF COPPER-MOLYBDENUM ALLOYS. Bohn, Carole W. 19p. (CONF-660430-5). ORAU. Gmelin, AED-CONF-66-105-3.

From Ohio Academy of Science, 75th Annual Meeting, Columbus, Ohio.

The effects of each of the following variables on electrodeposition of Cu–Mo alloys were studied: current density, plating time, temperature, and pH and composition of the plating bath. Under optimal conditions plates containing about 8% Mo, 87% Cu, and 5% nonmetallic material were obtained. The plates were shiny and light pink when fresh but tarnished badly on standing. The composition was reproducible to ±0.5%. (A.G.W.)

Radiation Effects

See also CHEMISTRY — Radiation Chemistry

Refer also to abstracts 41113, 41418, 41445, 41451, 42527, 42530, 42533, 42543, 42547–42549, 42551, 42553–42557, 42562, 42564, 42566, and 42567.

41488 (EGG-1183-2013) TRANSIENT RADIATION EFFECTS, OPTICAL. Quarterly Progress Report. Smith, W. A. Jr.; Walsh, G. E. (Edgerton, Germeshausen and Grier, Inc., Santa Barbara, Calif.). Jan. 1965. Contract AT(29-1)-1183. 8p. Dep. mn. CFSTI $1.00 cy, $0.50 mn.

Equipment for use in measurements of transient optical effects produced in materials by electron or gamma pulses is described. Construction and modification of sample container, vacuum system, and optical system are discussed. (J.R.D.)

41489 (EGG-1183-2014) TRANSIENT RADIATION EFFECTS, ELECTRICAL. Quarterly Progress Report. Smith, W. A. Jr.; Walsh, G. E. (Edgerton, Germeshausen and Grier, Inc., Santa Barbara, Calif.). Jan. 1965. Contract AT(29-1)-1183. 3p. Dep. mn. CFSTI $1.00 cy, $0.50 mn.

Research on radioinduced electric conductivity changes in organic polymers is briefly summarized. Most of the effort during the quarter was devoted to equipment design, fabrication and testing. Modifications of the sample support structure and vacuum system were completed. Plans are discussed to correlate temperature-dependent electric conductivity changes with optical emission changes to gain information on polymer radiation damage. Only administrative data are included. (J.R.D.)

41490 (EGG-1183-2029) TRANSIENT RADIATION EFFECTS, ELECTRICAL. Quarterly Progress Report. Smith, W. A. Jr. (Edgerton, Germeshausen and Grier, Inc., Santa Barbara, Calif.). May 1965. Contract AT (29-1)-1183. 3p. Dep. mn. CFSTI $1.00 cy, $0.50 mn.

This is an administrative-type report containing no data. (J.M.J.)

41491 (EGG-1183-2030) TRANSIENT RADIATION EFFECTS, OPTICAL. Quarterly Progress Report. Smith, W. A. Jr.; George, W. D.; Walsh, G. E. (Edgerton, Germeshausen and Grier, Inc., Santa Barbara, Calif.). May 1965. Contract AT(29-1)-1183. 13p. Dep. mn. CFSTI $1.00 cy, $0.50 mn.

Development of components for optical systems to be used in measurements on samples irradiated by pulsed electrons or gamma radiation is described. Work is reported on sample holders, solenoid-activated shutters, filter holders, light source monitors, and vacuum pumps. (J.R.D.)

41492 (EGG-1183-2039) TRANSIENT RADIATION EFFECTS, OPTICAL. Quarterly Progress Report. McGuire, R.; Walsh, G.; George, W. (Edgerton, Germeshausen and Grier, Inc., Santa Barbara, Calif.). Aug. 1965. Contract AT(29-1)-1183. 11p. Dep. mn. CFSTI $1.00 cy, $0.50 mn.

Development and testing of components for optical systems to be used in measurements on samples irradiated by pulsed electrons or gamma radiation are described. Results of optical emission measurements on electron bombardment KCl crystals are included. (J.R.D.)

41493 (EGG-1183-2052) TRANSIENT RADIATION EFFECTS IN ELECTRONIC MATERIALS. Quarterly Progress Report. McGuire, R. L.; Walsh, G. (Edgerton, Germeshausen and Grier, Inc., Santa Barbara, Calif.). Oct. 1965. Contract AT(29-1)-1183. 8p. Dep. mn. CFSTI $1.00 cy, $0.50 mn.

Research on radioinduced optical effects in transparent materials is summarized. F-center production in KCl in response to pulsed electron beams at 11 Mev was observed. Measurements and observations from the F-center experiments were used as a basis for equipment design for transmission measurements. Studies were initiated on optical emission of various materials associated with weapons testing. (J.R.D.)

41494 (EURAEC-1617) A NEW DETERMINATION OF THE EMBRITTLEMENT IN STEEL USING SMALL SPECIMENS (~0.2 cc) IN PARTICULAR WITH RESPECT TO IRRADIATION. Progress Report, January 1, 1966–March 31, 1966. van Elst, H. C. (Nijverheidsorgan-

depends strongly on the crystal face bombarded. Evidence is also presented that some of the sites from which the desorption takes place are located within a few atomic layers of the crystal surface. (A.G.W.)

41464 THE ISOTHERMAL SECTIONS AT 1200 C OF THE EQUILIBRIUM DIAGRAMS OF THE SYSTEMS Mo–Ti–Zr AND Mo–Nb–Zr. Chuang, Yu-chih; T'ang, Ch'uang-hung; Chuang, Hsiang-lin. Chin Shu Hsueh Pao, 9: 63-71 (Jan. 1966). (In Chinese).

The isothermal sections at 1200°C of the systems Mo–Ti–Zr and Mo–Nb–Zr were determined by metallographic and x-ray-diffraction methods supplemented by hardness measurements. The constitutions of these two systems are strikingly similar; besides a bcc ternary terminal solid solution and a ternary Laves phase isomorphous with $MgCu_2$ structure, no new intermediate phase was found. In the Mo–Ti–Zr system the lattice parameter of the ternary solid solution increases with the increase of Ti or Zr in solid solution, and the ternary Laves phase is (Ti,Zr) Mo_2. In the Mo–Nb–Zr system, the lattice parameter of the ternary solid solution also increases with the increase in the Nb- or Zr content, and the ternary phase in this case is $Zr(Mo,Nb)_2$. The isohardness contours of the Mo–Ti–Zr system tend to expand towards the titanium corner as the Ti content is increased, whereas those of the Mo–Nb–Zr system expand towards the niobium corner with the increase in Nb content in a like manner. (CFSTI)

41465 STUDY OF MOLYBDENUM–GADOLINIUM PHASE DIAGRAMS. Chuang, Yu-chih; Li, Chao-wu; Chuang, Hsiang-lin; Kao, Lien-mei. Chin Shu Hsueh Pao, 9: 110-12(Jan. 1966). (In Chinese).

The Pirani method was used to determine the fusion temperature and the peritectic temperature of molybdenum–gadolinium alloys, and Cu K radiation was used for powder x-ray analysis. Solid solubility of gadolinium in molybdenum was 1.1% at 2400°C, 0.4% at 2200°C, 0.3% at 2000°C, 0.2% at 1800°C and 0.15% at 1600°C after molybdenum alloy containing 0.09 to 5% of gadolinium was kept at 1600 to 2400°C and then hardened. Fusion temperatures of Mo–Gd (0.09–24.5%) alloys were determined and the peritectic temperature of Mo–Gd alloy was found to be 2457°C. The average fusion temperature of gadolinium-rich alloys was 1305°C. The transformation temperature of α Gd $\rightleftharpoons$ β Gd of the gadolinium-rich phase was determined by thermal analysis to be 1270°C, and that of β Gd $\rightleftharpoons$ L_{II} was 1314°C. The transformation temperature of pure gadolinium's α Gd $\rightarrow$ β Gd was 1288°C and that for β Gd $\rightarrow$ liquid was 1328°C. The fact that the hardness of alloys decreases with increasing gadolinium content shows the absence of an intermediate phase in Mo–Gd binary alloy. (CFSTI)

41466 INVESTIGATION OF THE AGING KINETICS OF MOLYBDENUM-BASE ALLOYS. Goltsev, V. P. (Nuclear Power Inst., Academy of Sciences, USSR). Dokl. Akad. Nauk BSSR, 10: 385-7(1966). (In Russian).

Sheet specimens 1 mm thick of molybdenum–zirconium, molybdenum–titanium, and molybdenum–hafnium alloys containing 0.003 to 0.005% carbon, 0.01 to 0.20% oxygen, and up to 0.06% nitrogen were aged at 1300°, 1400°, and 1500°K in vacuum for 1.8 to 108 ksec. In all three alloys, the aging-induced changes in microhardness and lattice parameter "a" were found to follow roughly the same pattern. In molybdenum–hafnium alloy the final drop in microhardness brought about by prolonged aging or by aging at higher temperature is a result of the redissolution of the strengthening phase precipitated in the first stages of aging. However, a similar drop in microhardness in molybdenum–zirconium and molybdenum–titanium alloys was found to be the result of the coagulation of the strengthening phase. In all three alloys, age hardening was caused by the precipitation of finely dispersed oxides of alloying elements. (ATD)

41467 ELECTRON MICROSCOPIC AND MICRODIFFRACTION ANALYSIS OF NONMETALLIC INCLUSIONS IN MOLYBDENUM AND ITS ALLOYS. Ageev, N. V.; Ignatov, D. V.; Kantor, M. M. (Baykov Inst. of Metallurgy, USSR). Dokl. Akad. Nauk SSSR, 167: 635-6 (Mar. 21, 1966). (In Russian).

The electron microscope was used for studying nonmetallic inclusions in molybdenum and its alloys melted by various methods. The phase composition and distribution of the inclusions were determined in specimens of molybdenum produced by electron-beam melting and in molybdenum alloys containing carbon (0.003 to 0.021%), titanium (0.02 to 0.3%), and zirconium (0.01 to 0.15%), produced by arc melting and fusion melting. The specimens were studied in the cast, deformed, and annealed states. The method used for producing the replicas is briefly described. Photomicrographs and diffraction patterns show that the inclusions consist basically of Mo_2C. This is probably due to the melting conditions and heat treatment of the specimens. The electron-beam melting and annealing were done in a vacuum of 10^{-4} to 10^{-5} Hg mm. Oil vapor diffusion pumps were used for producing the vacuum. Apparently the main residual gas consists of the oil vapors, which decompose to form carbon. This carbon diffuses into the metal and forms carbides. (ATD)

41468 MORPHOLOGY AND TEXTURE OF MOLYBDENUM AND TUNGSTEN CARBONYL DEPOSITS. Matyushenko, N. I.; Rozen, A. A.; Sagalovich, V. V. Fiz. Metal. Metalloved., 21: 403-8(Mar. 1966). (In Russian).

The morphology and textures of deposits obtained in thermal decomposition of molybdenum and tungsten carbonyls were studied over the temperature range from 150 to 1050°C. X-ray-diffraction patterns and particle size of the deposits, obtained at different temperatures of the deposition surface, were determined. It was found that there exist two morphological transition temperatures, at 250 and 750°C and 350 and 800°C for Mo and W respectively. The first transition temperature is related to the rupture of carbonyl molecule and the second to the condensation from supercooled liquid or, at higher temperature (i.e., $T > \theta_2$), to the formation of crystal nuclei. (ATD)

41469 THE STRUCTURES OF POLONIUM AND ITS COMPOUNDS. I. α AND β POLONIUM METAL. DeSando, R. J.; Lange, R. C. (Mound Lab., Miamisburg, Ohio). Contract AT(33-1)-Gen-53. J. Inorg. Nucl. Chem., 28: 1837-46(Sept. 1966). (MLM-1313J).

The crystal structures of alpha and beta Po metal were redetermined from x-ray-diffraction powder photographs using monochromatic radiation and a He atmosphere by employing an isotopic mixture of ^{208}Po and ^{209}Po. Electron distribution curves as a function of interatomic distance were also computed. Previous x-ray data obtained from ^{210}Po (half life of 138.4 days), were influenced by the growth of Pb at the rate of 0.5 per cent per day and self-heating effects. The half lives of ^{208}Po and ^{209}Po are 2.8 and 103 yr, respectively. The growth rate of Pb and the thermal effects from self-heating are reduced to four per cent of those in ^{210}Po. Alpha Po is simple cubic and in space group Pm3m with a = 3.359 ± 0.001 Å and ρx ray = 9.142 g/cm^3. Beta Po is rhombohedral and a space group R3m (A10 type) with α = 3.368 ± 0.001 Å, α = 98° 14.4′ and ρx ray = 9.392 g/cm^3. The structure of Po and its relationship to elements in Group VIB are discussed. (auth)

41470 STRUCTURAL CHANGES IN URANIUM DUE TO THERMAL CYCLES. Slancar, F.; Shlantsar, F. (Inst. for Nuclear Research, Czechoslovak Academy of Sciences, Rez). Kovove Mater., No. 1, 20-33(1965). (In Czech).

Experimental tests are described on 99.82% pure U specimens — 4-mm-diameter extruded wire, 4.15-mm-diameter forged wire, and shapes 30 mm in diameter. The first two types were heat treated at 720°C, quenched in water, and then annealed at 500°C for two hours. They were then examined for internal slip and twinning, boundary slip, grain polygonization, and micro cracks. Methods of preparing metallographic samples of each type of test material are described, including electrolytic polishing,

ion bombardment, and buffing with diamond paste. Structural changes were studied with a heat microscope over a range from 80 to 550°C, maintained for 13 minutes and followed by quenching in oil for two minutes. The heat cycles were arranged in a special apparatus in which the temperature rose from 50 to 550°C in 12 minutes, with the maximum maintained for 10 minutes. The results are given in a series of metallographic photomicrographs and show that coarse-grained U is highly deformed in each time cycle, but fine-grained metal shows no discernible deformation. Boundary slip was very noticeable in fine-grained U. Grain polygonization occurred equally in both 90-μ and 70-μ average grain sizes, which are most widely used in reactors, and increased through 800 times cycles, but the grain size did not change from that point up to 2000 cycles. Micro cracks originated in occlusions of U(OCN), spread to the grain boundary, then progressed between grains. These cracks lengthened as the time cycles increased, and formed dense networks after 1600 or 2000 cycles. (JPRS)

41471 INVESTIGATION OF ALLOYS OF THE Zr–C SYSTEM. Godin, Yu. G.; Evstyukhin, A. I.; Emelyanov, V. S.; Rusakov, A. A.; Suchkov, I. I. Met. Metalloved. Chistykh Metal., Sb. Nauchn. Rabot, No. 5, 25-32(1966). (In Russian).

A series of zirconium–carbon alloys containing 0.1 to 68 at. % C were made by compacting powdered 99.5%-pure zirconium and carbon by sintering green ingots in vacuum at 2000°C with subsequent arc melting in an inert atmosphere, or by direct arc melting of solid 99.8%-pure zirconium with carbon. The alloys were water-quenched from 750 to 862°C or oil quenched from 1100 to 2400°C. A phase diagram of the Zr–C system, based on physicochemical analyses, is shown. Two-phase alloys containing 0.05 to 5.4 wt. % C consist of grains of zirconium carbide and the α phase, which is a supersaturated solid solution of carbon in zirconium formed with the $\beta \rightarrow \alpha'$ transformation during quenching. Alloys with a carbon content ranging from 6.0 wt. % to that of zirconium carbide (11.63 wt. % C) consist of a solid solution of zirconium in carbide. With a further increase in the carbon content, free carbon is precipitated both as eutectic and as primary carbide grains. Quenching of alloys from 2400, 1700, or 1100°C had no substantial effect on the alloy structure; the solubility of carbon in the β zirconium at 1100°C was less than 0.1 wt. %. The microstructure of the alloys containing 7.1 to 10.5 wt. % C quenched at lower temperatures (to 750°C) consists of a solid solution of zirconium in carbon; the solubility of carbon in α zirconium at 820°C is about 0.3 wt. %. X-ray diffraction confirmed the existence of a single carbide phase in the Zr–C system. Two-phase alloys quenched from 2400°C have a lattice constant of 4.695 Å, compared to 4.693 Å for the same alloys quenched from 1700°C. The microhardness of cast and quenched zirconium alloys increases with increasing carbon content, reaches a maximum of 2150 kg/mm^2 at a composition corresponding to zirconium carbide, and then decreases with further increase in the carbon content because of the appearance of free carbon in the form of both a eutectic and of primary grains. The microhardness of α' zirconium (180 kg/mm^2) remains constant with increasing carbon content and is higher than the hardness of α zirconium. This probably is caused by the solubility of carbon in zirconium and by the $\beta \rightarrow \alpha$ martensitic transformation. (ATD)

41472 PROCEEDINGS OF THE BRITISH CERAMIC SOCIETY. No. 6. MECHANICAL PROPERTIES OF NON-METALLIC CRYSTALS AND POLYCRYSTALS. Proc. Brit. Ceram. Soc., No. 6, 1-334(June 1966).

A total of 27 papers were presented at meeting. Separate abstracts were prepared for three of the papers. Papers for which no abstracts were prepared are concerned with strength of non-metallic crystals, interpretation of data on complex ceramics, plastic flow of polycrystalline material, and dislocation phenomena. (J.R.D.)

For abstracts of individual papers see: 41473–41475.

41473 OBSERVATIONS ON THE STRENGTH AND YOUNG'S MODULUS OF BeO AS A FUNCTION OF DENSITY AND GRAIN SIZE. O'Neill, J. S.; Hill, N. A.; Livey, D. T. (Atomic Energy Research Establishment, Harwell, Eng.). Proc. Brit. Ceram. Soc., No. 6, 95-101(June 1966).

The variations in modulus of rupture and Young's modulus as a function of grain size and density are presented for BeO of 94 to 99% theoretical density. The modulus of rupture by three-point bending reached a maximum of ~40,000 p.s.i. at ~97% theoretical density and a grain size of 3 to 5 mμ. The Young's modulus increased with density to 56 × 10^6 psi at 99% theoretical density. (auth)

41474 CREEP OF ThO_2 AND ThO_2–CaO SOLID SOLUTIONS. Morgan, C. S.; Hall, L. L. (Oak Ridge National Lab., Tenn.). Proc. Brit. Ceram. Soc., No. 6, 233-8(June 1966).

Compressive creep tests at elevated temperatures were carried out on polycrystalline ThO_2 and ThO_2–CaO specimens. At 1465°C a stress of 8000 psi caused appreciable long-term creep in ThO_2 bushings. At the same temperature, specimens that contained small quantities of CaO deformed initially at an order of magnitude lower stress. The creep rate of the material containing CaO decreased steadily with time, and after several hundred hours was about the same as that for pure ThO_2 specimens. Metallographic examination of the specimens after creep test revealed evidence of polygonization in ThO_2 specimens, and grain growth in ThO_2–CaO specimens. (auth)

41475 EFFECT OF STOICHEIOMETRY ON THE YIELD STRESS OF TiC AND TiO_2. Hollox, G. E.; Smallman, R. E. (Univ. of Birmingham, Eng.). Proc. Brit. Ceram. Soc., No. 6, 317-24(June 1966).

Non-stoichiometric defects tend to raise the yield stress of TiO_2, but have the opposite effect in TiC, the former behavior being typical of the interaction of vacancies with dislocations. The latter can be explained by considering that the deformation mechanisms of TiC are governed by a fcc Ti lattice with a frictional drag resulting from a covalent interaction with C interstitial atoms, the magnitude of which decreases with increasing non-stoichiometry. (auth)

41476 ELECTRICAL AND THERMAL CONDUCTIVITIES OF METALS OVER THEIR ENTIRE LIQUID RANGE, i. e., FROM MELTING POINT TO CRITICAL POINT, AND THE CONTAINMENT OF METALLIC SUBSTANCES UP TO 5000 DEG K FOR SUBSTANTIAL PERIODS OF TIME. PART I. ELECTRICAL CONDUCTIVITIES. Grosse, Aristid V. (Temple Univ., Philadelphia). Rev. Hautes Temp. Refract., 3: 115-27(Apr.-June 1966).

The electrical conductivity of Hg was previously measured over the entire liquid range. It was found recently that a hyperbolic relation of the form $(\kappa_{red.} + b)(\theta + b) = a$ exists between the reduced conductivity, $\kappa_{red.} = \kappa_T/\kappa_{m.p.}$ and the reduced temperature, $\theta = (T - T_{m.p.})/(T_{c.p.} - T_{m.p.})$, a and b in the above equation are constants of the hyperbola, both dependent on the distance, Δ, of the vertex of the hyperbola from either the $\kappa_{red.}$ axis or θ axis. Experimental data on the electrical conductivity of liquid Na, K, Rb, and Cs are now available over a substantial liquid temperature range. These alkali metals also show, within experimental error, the same hyperbolic relationship as Hg. Cu, Ag, Au, Al, and Sn also conform, as far as the experimental data now available go, with the empirical hyperbolic relationship. Experimental data on Li and Zn (and to a lesser extent on Cd) indicate an exception to the hyperbolic relation. Data on these metals are included. (J.R.D.)

41477 ELECTRICAL AND THERMAL CONDUCTIVITIES OF METALS OVER THEIR ENTIRE LIQUID RANGE, i. e., FROM MELTING POINT TO CRITICAL POINT, AND THE CONTAINMENT OF METALLIC SUBSTANCES UP TO 5000 DEG K FOR SUBSTANTIAL PERIODS OF TIME. PART II. THERMAL CONDUCTIVITIES. Grosse, Aristid V. (Temple Univ., Philadelphia). Rev. Hautes Temp. Refract., 3: 127-39(Apr.-June 1966).

The thermal conductivity of liquid Hg, Na, K, Rb, and Ce

can be estimated using the Wiedemann-Franz-Lorentz law $\lambda_{therm.} = L\varkappa T$, where L is the Lorentz constant = $2.443 \cdot 10^{-8}$ watts/ohm/(°K)^2. Independently from any assumption involving the free electron theory of metals, the thermal conductivity at the critical point can be estimated for these metals by approaching the critical point from the saturated vapor side, where $\lambda_{therm.}$ is $\simeq 0$. The thermal conductivity of the saturated vapor of Hg and the above alkali metals was measured and agrees well with the calculations based on the kinetic theory. Using a hyperbolic relation and the Wiedemann-Franz-Lorentz law, it is possible to estimate the thermal conductivity of liquid Hg and the four alkali metals mentioned, over their entire liquid temperature range. In addition, the thermal conductivities of many other metals can be estimated, since the $\varkappa_{m.p.}$ values of most metals are known and $\varkappa_{c.p.} \simeq 0$, even if these estimates are of a preliminary nature. From the known electrical conductivities of the monetary metals—Cu, Ag, and Au—the $\lambda_{therm.}$ vs T functions can be estimated. (J.R.D.)

41478 THE DEPENDENCE ON MICROSTRUCTURE OF THE HIGH TEMPERATURE PROPERTIES OF URANIUM OXIDE. MOLYBDENUM AND URANIUM OXIDE. TUNGSTEN CERMETS. Amato, I.; Colombo, R. L.; Polin, F. (FIAT, Sezione Energia Nucleare, Turin). Rev. Hautes Temp. Refract., 3: 189-96(Apr.-June 1966).

Specimens of UO_2–Mo and UO_2–W were prepared and their electric conductivities were measured as a function of microstructure. One series of specimens were prepared by sintering pressed UO_2 powders with W or Mo powders. Another series was prepared by mixing green spheroidal agglomerates of UO_2 powder in slurries of Mo or W dispersed in acrylic cement, drying, and sintering. A third series of specimens were prepared by sintering green agglomerate UO_2 spheroids, coating them with Mo or W and hot pressing. Results are presented graphically. (J.R.D.)

41479 THERMAL DIFFUSIVITY AND CONDUCTIVITY MEASUREMENTS ON METALS AND OXIDES AT HIGH TEMPERATURES. Iacobelli, R.; Moretti, S. (CNEN, Centro Studi Nucleari Della Casaccia, Rome). Rev. Hautes Temp. Refract., 3: 215-28(Apr.-June 1966).

A discussion is presented concerning experimental facility used and the results obtained by applying a transient method and implementing generalized equations for measuring thermal diffusivity at high temperatures. The method consists in exposing a thin slab of the material under test to a very short pulse of radient energy and in following the thermal history at the face of the slab opposite to the one at which the energy is deposited. The thermal diffusivity is derived by measuring the time ($t_{\frac{1}{2}}$) at which the temperature of the opposite face reaches one half of its maximum value. The experiments were performed under vacuum, so that the radiation heat losses from the surfaces of the specimen were easily defined. The method was first tested for stainless steel and then applied to UO_2. (auth)

41480 PREPARATION OF SINGLE CRYSTALS OF REFRACTORY COMPOUNDS FROM BINARY OR MULTICOMPONENT SYSTEMS AND EFFECT OF TEMPERATURE CONDITIONS OF GROWTH ON THEIR FORM AND FACETING. Izvekov, V. N.; Sysoev, L. A.; Obukhovskii, Ya. A.; Birman, B. I. (Inst. of Crystallography, Academy of Sciences, USSR). Rost Kristallov., Akad. Nauk SSSR, Inst. Kristallogr., 6: 116-21(1965). (In Russian).

The growth of cadmium sulfide single crystals from melts of cadmium chloride and iodide and their mixtures, and the growth of single crystals of α-corundum (ruby), rutile, strontium titanate, and calcium tungstate from fluorides were studied. CdS single crystals with a wurtzite lattice were obtained in the 600 to 380°C range from the $CdS-CdCl_2-CdI_2$ system. The oxide crystals were grown in platinum crucibles in the 1200 to 700°C range with slow cooling. An important feature revealed by these experiments is the dependence of the crystal habit of the crystals obtained on the temperature range of the crystallization. This phenomenon is explained by differences in the growth rates of faces having different crystallographical indices, particularly surface roughness. The concept of the influence of surface roughness on the growth forms of crystals is extended to binary and multicomponent systems. (ATD)

41481 GROWING AND PLASTIC DEFORMATION OF THE SINGLE CRYSTALS OF REFRACTORY METALS AND ALLOYS. Savitskii, E. M.; Burkhanov, G. S.; Kopetskii, Ch. V.; Chuprikov, G. E. Rost Kristallov., Akad. Nauk SSSR, Inst. Kristallogr., 6: 308-18(1965). (In Russian).

The physical and mechanical properties of single crystals of tungsten, molybdenum, rhenium, tantalum, niobium, vanadium, and their alloys grown from melts of vacuum-arc melted or sintered metals were investigated. Crystals up to 12 to 14 mm in diameter and 150 to 250 mm long were grown in an electron-beam furnace developed for vacuum zone melting of refractory metals. The crystal purity was found to be two orders higher than that of the initial metals and alloys. For instance, the oxygen content dropped from 0.05 and 0.012% in the sintered and in vacuum-arc melted rhenium, respectively, to 0.001% in single crystals. The removal of interstitial impurities decreased the tensile strength and appreciably increased the ductility of all investigated metals. For example, the tensile strength of sintered and arc-melted rhenium, 115 and 65.8 kg/mm^2, respectively, decreased to 42.5 kg/mm^2 for rhenium single crystals. At the same time, elongation increased from 12.1 and 16.1% to 41%. Molybdenum single crystals sustained a bend angle of 180° at room temperature and a 60° bend angle at −196°C. At room temperature, tungsten and niobium single crystals sustained a bend angle of 90 and 180°, respectively, and rhenium sustained a bend angle of 90° at −196°C. Molybdenum single crystals 13 mm in diameter and 250 mm long were drawn into wire 50 μm in diameter or rolled into 50 μm-thick foil without process annealing. Single crystals of some alloys in the region of solid solutions of the Mo–Nb, Mo–W, Mo–Ti, and W–Nb systems were also grown from electron beam-melted single crystals of the respective metals. The single crystals obtained had essentially the same substructures as the initial components; they also had good ductility and a tensile strength higher than that of the initial metals. (ATD)

41482 EFFECT OF THE ANNEALING TEMPERATURE AND MEDIUM ON THE PROPERTIES OF MOLYBDENUM. Khoroshailov, V. G.; Bogoyavlenskii, K. N.; Rossomakho, Ya. V. (Leningrad Polytechnic Inst.). Tr. Leningr. Politekhn. Inst., No. 251, 28-30(1965). (In Russian).

Cold-rolled strips of 99.9%-pure sintered molybdenum, 150 to 180 × 0.2 × 400 to 800 mm, were annealed in a vacuum of 1.5 to 1.4×10^{-2} mm Hg or in dry hydrogen at 800 to 1400°C for 45 min to determine the optimum conditions for heat treatment. In the as-delivered condition, molybdenum had a hardness HV of 275 to 300, a tensile strength of 100 to 130 kg/mm^2, and an elongation of 0.5 to 2%; the microstructure was typical for a cold-worked metal. Annealing lowered the hardness and strength and increased the ductility. The decrease in tensile strength and hardness by annealing at 800 to 950°C is associated with the relieving of stresses caused by cold working. The texture disappeared completely after annealing at 1100°C; grain growth began at 1200°C. Annealing at 1200°C for more than 45 min had no additional effect on the strength and ductility. The temperature of recrystallization for vacuum-annealed metal was 100 to 150°C higher than that for metal annealed in hydrogen; this was attributed to some leak of air through the walls of the quartz ampules at high temperatures. (ATD)

41483 REDKOZEMEL'NYE FERROMAGNETIKI I ANTIFERROMAGNETIKI. (Rare Earth Ferromagnetics and Antiferromagnetics). Belov, K. P.; Belyanchikova, M. A.; Levitin, R. Z.; Nikitin, S. A. Moscow, Izdatel'stvo Nauka, 1965. 319p.

On the basis of work published by Soviet and foreign scientists and engineers, a review of the recent theoretical and experimental investigations of the ferromagnetism and antiferromagnetism of the rare earth metals, alloys, and compounds is given. The results of original investi-

gations by authors of various monographs are included. A section on the ferromagnetism of rare earth ferrites is also included. (G.O.Y.)

41484 NEW METHODS FOR THE MEASUREMENT OF DIFFUSION OF α-EMITTING ATOMS IN SOLIDS. DIFFUSION OF ACTINIDE ELEMENTS IN UO_2. Schmitz, F. K. Brunswick, Technische Hochschule, 1965. 70p. $2.00 Gmelin, AED-Diss 65-272.

The diffusion of Pu in UO_2 was determined by 3 methods, the sectioning method, surface decrease method, and by α energy degradation. Activation energies obtained by these methods are in satisfactory agreement. Diffusion mechanisms of actinide elements in UO_2 are discussed. (Gmelin Inst.)

41485 SOME OBSERVATIONS ON THE PRESSURE-TEMPERATURE PHASE DIAGRAM OF BERYLLIUM. Contre, M.; Francois, D. 20p. (CONF-660205-6). ORAU. Gmelin, AED-CONF-66-021-8.

From Metallurgical Society of the American Institute of Mining, Metallurgical, and Petroleum Engineers, New York.

At atmospheric pressure, the α-β transformation of beryllium occurs at 1264°C and involves an increase in resistivity amounting to about 50%. The range of stability of the β phase increases with pressure. A slight change in slope and a marked arrest in the resistance curve below the α-β transition temperature are attributed to recrystallization under pressure of the sample, which is severely cold worked as pressure is increased. From first experimental results a provisional pressure-temperature phase diagram of pure beryllium is drawn. According to this diagram enthalpy change at α-β transition would be about 1.8 kcal/mole at atmospheric pressure; the change in volume on melting would be an increase of about 10%. (auth)

41486 DIFFUSE REFLECTANCE CHARACTERISTICS OF MONOCLINIC ZrO_2 AS A FUNCTION OF PURITY. Sarver, J. F. (General Electric Co., Cleveland). 21p. (CONF-660505-6). ORAU. Gmelin, AED-CONF-66-103-6.

From American Ceramic Society Meeting, Washington, D. C.

Diffuse reflectance spectra of monoclinic ZrO_2 from several commercial sources are compared with the spectrum of high-purity ZrO_2 prepared from $ZrOCl_2 \cdot 8H_2O$ purified by recrystallization from an HCl solution. The purified oxide exhibits greater than 98% reflectance relative to CaF_2 above 3250 Å. Below 3000 Å, the lattice absorption of ZrO_2 increases and the reflectance decreases to a minimum of about 10% at 2300 Å. Ti^{4+} in solid solution introduces a very strong absorption band in the ultraviolet, and all commercial sources of ZrO_2 as well as other sources of high-purity oxides exhibited an absorption band attributable in part to titanium. The presence of iron causes a further lowering of the reflectance in the visible range. (auth)

41487 ELECTRODEPOSITION OF COPPER-MOLYBDENUM ALLOYS. Bohn, Carole W. 19p. (CONF-660430-5). ORAU. Gmelin, AED-CONF-66-105-3.

From Ohio Academy of Science, 75th Annual Meeting, Columbus, Ohio.

The effects of each of the following variables on electrodeposition of Cu–Mo alloys were studied: current density, plating time, temperature, and pH and composition of the plating bath. Under optimal conditions plates containing about 8% Mo, 87% Cu, and 5% nonmetallic material were obtained. The plates were shiny and light pink when fresh but tarnished badly on standing. The composition was reproducible to ±0.5%. (A.G.W.)

Radiation Effects

See also CHEMISTRY — Radiation Chemistry

Refer also to abstracts 41113, 41418, 41445, 41451, 42527, 42530, 42533, 42543, 42547–42549, 42551, 42553–42557, 42562, 42564, 42566, and 42567.

41488 (EGG-1183-2013) TRANSIENT RADIATION EFFECTS, OPTICAL. Quarterly Progress Report. Smith, W. A. Jr.; Walsh, G. E. (Edgerton, Germeshausen and Grier, Inc., Santa Barbara, Calif.). Jan. 1965. Contract AT(29-1)-1183. 8p. Dep. mn. CFSTI $1.00 cy, $0.50 mn.

Equipment for use in measurements of transient optical effects produced in materials by electron or gamma pulses is described. Construction and modification of sample container, vacuum system, and optical system are discussed. (J.R.D.)

41489 (EGG-1183-2014) TRANSIENT RADIATION EFFECTS, ELECTRICAL. Quarterly Progress Report. Smith, W. A. Jr.; Walsh, G. E. (Edgerton, Germeshausen and Grier, Inc., Santa Barbara, Calif.). Jan. 1965. Contract AT(29-1)-1183. 3p. Dep. mn. CFSTI $1.00 cy, $0.50 mn.

Research on radioinduced electric conductivity changes in organic polymers is briefly summarized. Most of the effort during the quarter was devoted to equipment design, fabrication and testing. Modifications of the sample support structure and vacuum system were completed. Plans are discussed to correlate temperature-dependent electric conductivity changes with optical emission changes to gain information on polymer radiation damage. Only administrative data are included. (J.R.D.)

41490 (EGG-1183-2029) TRANSIENT RADIATION EFFECTS, ELECTRICAL. Quarterly Progress Report. Smith, W. A. Jr. (Edgerton, Germeshausen and Grier, Inc., Santa Barbara, Calif.). May 1965. Contract AT (29-1)-1183. 3p. Dep. mn. CFSTI $1.00 cy, $0.50 mn.

This is an administrative-type report containing no data. (J.M.J.)

41491 (EGG-1183-2030) TRANSIENT RADIATION EFFECTS, OPTICAL. Quarterly Progress Report. Smith, W. A. Jr.; George, W. D.; Walsh, G. E. (Edgerton, Germeshausen and Grier, Inc., Santa Barbara, Calif.). May 1965. Contract AT(29-1)-1183. 13p. Dep. mn. CFSTI $1.00 cy, $0.50 mn.

Development of components for optical systems to be used in measurements on samples irradiated by pulsed electrons or gamma radiation is described. Work is reported on sample holders, solenoid-activated shutters, filter holders, light source monitors, and vacuum pumps. (J.R.D.)

41492 (EGG-1183-2039) TRANSIENT RADIATION EFFECTS, OPTICAL. Quarterly Progress Report. McGuire, R.; Walsh, G.; George, W. (Edgerton, Germeshausen and Grier, Inc., Santa Barbara, Calif.). Aug. 1965. Contract AT(29-1)-1183. 11p. Dep. mn. CFSTI $1.00 cy, $0.50 mn.

Development and testing of components for optical systems to be used in measurements on samples irradiated by pulsed electrons or gamma radiation are described. Results of optical emission measurements on electron bombardment KCl crystals are included. (J.R.D.)

41493 (EGG-1183-2052) TRANSIENT RADIATION EFFECTS IN ELECTRONIC MATERIALS. Quarterly Progress Report. McGuire, R. L.; Walsh, G. (Edgerton, Germeshausen and Grier, Inc., Santa Barbara, Calif.). Oct. 1965. Contract AT(29-1)-1183. 8p. Dep. mn. CFSTI $1.00 cy, $0.50 mn.

Research on radioinduced optical effects in transparent materials is summarized. F-center production in KCl in response to pulsed electron beams at 11 Mev was observed. Measurements and observations from the F-center experiments were used as a basis for equipment design for transmission measurements. Studies were initiated on optical emission of various materials associated with weapons testing. (J.R.D.)

41494 (EURAEC-1617) A NEW DETERMINATION OF THE EMBRITTLEMENT IN STEEL USING SMALL SPECIMENS (~0.2 cc) IN PARTICULAR WITH RESPECT TO IRRADIATION. Progress Report, January 1, 1966–March 31, 1966. van Elst, H. C. (Nijverheidsorgan-

isatie (TNO), The Hague (Netherlands)). Apr. 14, 1966. Contract 060-64-11-TEEN. 25p. (EUR–2830). Dep. mn. CFSTI $1.00 cy, $0.50 mn.

Work Performed under United States–Euratom Joint Research and Development Program.

The determination of the embrittlement of pressure vessel steels, such as T_1(U.S.S.), Soudotenax (Cockerill-Ougrée), HSB 55 C (Phoenix Rheinrohr) and 1.2 MD 07 (Creusot) after increasing neutron radiation doses at 80°C was continued. Series of small samples of these steels irradiated with fluxes of 1×10^{18} to 13×10^{18} n/cm^2 were tested by stress wave attenuation. In the ductile region a decrease of energy absorption after irradiation occurred. The shift in the brittle-ductile region was nuclear owing to a remaining finite slope of the energy-absorption-versus-temperature curve outside transition region and to the decrease of this slope within the transition region, which causes a blurring of the transition phenomenon of the steel. After a neutron dose of 12.571×10^{18} n/cm^2, the energy absorption for T_1-steel was about constant at increased temperature and smaller than in the unirradiated brittle state. Such behavior is also sometimes found at notch impact testing of steel after severe shockloading. After the smaller neutron doses, an increase of energy absorption in the brittle region was observed with the HSB 55-steel. (auth)

41495 (EURAEC–1621) RESEARCH TO DETERMINE THE LONG-TERM MECHANICAL PROPERTIES OF METALS SUBJECTED TO MECHANICAL STRESS AT ELEVATED TEMPERATURES AND NEUTRON IRRADIATION. Annual Report, 1965. Siegfried, W.; Zimering, S. (Battelle Memorial Inst., Geneva (Switzerland)). Apr. 1966. Contract 100-62-12RDS. 24p. (EUR–2834). Dep. mn. CFSTI $1.00 cy, $0.50 mn.

Work Performed under United States–Euratom Joint Research and Development Program.

An investigation was initiated to determine the extent to which temperature-extrapolation methods already known can be applied to rupture time tests under neutron irradiation. Programs were established to develop suitable working hypotheses on the basis of scientific results of solid-state physics, and to develop a new basis for the evaluation of technological rupture time tests. For evaluation of technological rupture-time tests, a new mathematical function was introduced which determines the shape of rupture-time curves by means of a few parameters much better than all functions hitherto known. This is the exponential function of real order, which was developed recently. By means of this function, the problem of scattering and the evaluation of practical rupture-time tests can be put on a new basis. (J.R.D.)

41496 RADIATION CROSS LINKING OF CABLE POLYETHYLENE INSULATION ON LARGE SCALE. Berlyant, S. M.; Drozdov, V. E.; Finkel, E. E.; Orlenko, P. A.; Suroegin, L. M.; Breger, A. Kh.; Karpov, V. L.; Zorin, V. A. At. Energ. (USSR), 21: 64-6(July 1966). (In Russian).

Crosslinking of cable polyethylene by irradiation with 100-Mrad doses in the air improved thermal resistance and extended cable working life at 150°C to ~5000 or 6000 hr and at 200°C to ~100 or 150 hr. In oxygen-free media, the life of polyethylene specimens increased to many thousands of hours. (R.V.J.)

41497 ANISOTROPY OF DISPLACEMENTS OF THE ATOMS IN THE CRYSTAL LATTICE OF THE ALPHA PHASE OF NEUTRON-BOMBARDED CARBON STEEL. Kritskaya, V. K.; Ilina, V. A.; Kuznetsova, A. P.; Sharov, B. V. (Bardin Central Scientific Inst. of Ferrous Metals and Inst. of Theoretical and Experimental Physics, USSR). Dokl. Akad. Nauk SSSR, 167: 789-91(Apr. 1, 1966). (In Russian).

Earlier work in which anomalies were observed in the attenuation of certain x-ray reflections from neutron-bombarded steels was continued, using the α phase of U-9 steel. The preparation of the samples, the heat treatment, the neutron-bombardment conditions, and the x-ray photography procedure were the same as before, except that a mechanical pulse counter was added to the apparatus to improve the reliability and the accuracy. To determine the variation of the intensity of the x-ray reflections from different crystallographic planes, the integral intensities of the x-ray interferences of a large number of reflections with different multiple values of h, k, and l were measured. The results show that neutron bombardment decreases the intensity of the scattered x rays more for some planes than for others. This is taken as convincing proof that the crystallographic orientation plays an important role in the formation of point defects by neutron bombardment. The distribution of these defects is anisotropic. The mean displacement of the atoms was 0.04 Å for the (h00) and (hhh) planes, as against 0.025 Å for most other planes. Certain planes (for example (631)) experienced no change in scattering ability at all after bombardment. (ATD)

41498 CHANGES IN THE ANTIFRICTION AND STRENGTH CHARACTERISTICS OF STRUCTURAL MATERIALS SUBJECTED TO NEUTRON IRRADIATION. Markovskii, E. A.; Krasnoshchekov, M. M.; Kochegura, N. M. (Inst. of Foundry Problems, Kiev). Fiz.-Khim. Mekh. Mater., 1: 552-6(1965). (In Russian).

Changes in the antifriction parameters of some structural metals and alloys subjected to various degrees of neutron irradiation in an operational neutron reactor were studied. Simultaneously, the changes in some of the strength characteristics of the materials are also determined. The materials studied were steel No. 45, various types of cast iron, copper, and SB-30 lead bronze. The results obtained give evidence that the accelerated process of stress relaxation under the effect of irradiation may take place not only for stressed materials but also for metastable hardened structures. An attempt is made to explain the time-dependent decrease in the strength of steel subjected to irradiation, but it is not sufficiently grounded. The work performed showed that the materials tested, after undergoing a stage of relative decrease in strength, obtain under prolonged neutron irradiation satisfactory antifriction and strength characteristics and may be successfully used in friction joints. It is suggested that work in this field should be directed toward the study of the wear resistance and setting of materials under neutron irradiation, in vacuum, at high temperatures, and in special media. (ATD)

41499 EXPERIMENTAL RESULTS OBTAINED IN LOW TEMPERATURE ELECTRON IRRADIATION OF Pd, Mo, Zn, AND α-U. Lucasson, A.; Lucasson, P. (Univ., Paris, Orsay, France). J. Phys. Chem. Solids, 27: 1423-9(Sept. 1966).

Electron irradiations of metals were performed at temperatures ranging from 11 to 7°K. Low-temperature isochronal recovery (stage I) studies of the electrical resistivities of the bombarded specimens were made. The results obtained in non-cubic metals (Zn and α-U) were tentatively related to the atomic elastic properties of the metals, and particularly, to their thermal expansion behaviors in the stage I temperature domains. (auth)

41500 DYNAMIC MECHANICAL PROPERTIES OF POLYOXYMETHYLENE. [PART] I. Miki, Kyosuke; Yokokawa, Yukimoto; Hikichi, Kunio; Furuichi, Jiro (Hokkaido Univ., Sapporo). Jap. J. Appl. Phys., 5: 818-23 (Sept. 1966).

Dynamic mechanical properties of melt grown polyoxymethylene were studied for specimens with different lamella thicknesses and for irradiated specimens over a range of temperature from −30 to 150°C. The apparent relaxation strength of the mechanical α dispersion is proportional to the lamella thickness. This result qualitatively satisfies the requirements of Okano's theory of crystalline dispersion. The apparent relaxation strength of the α dispersion for irradiated specimens increases with increasing irradiation dose. This behavior is not due to the growth of lamella thickness with irradiation, but due to other effects, such as the occurrence of lattice defects in crystallites by irradiation. Thus it is impossible to explain this behavior in terms of Okano's theory.

The apparent activation energy of the α dispersion does not change with γ irradiation, which indicates that the irradiation does not essentially influence the molecular mechanism of the dispersion. (auth)

41501 EFFECT OF GAMMA RADIATION ON THE MECHANICAL CHARACTERISTICS OF POLYETHYLENE TEREPHTHALATE FILM. Kallinnikov, A. E. (Moscow Higher Technical School). Mekhan. Polimerov, Akad. Nauk Latv. SSR, No. 3, 461-2(1966). (In Russian).

The mechanical characteristics of polyethylene terephthalate (PETP) films were determined after irradiation in air by gamma rays from a Co-60 source to evaluate the radiation effect on this polymer material as a function of the absorbed energy of ionizing radiation. Experimental stress-strain diagrams and the plots of ultimate strength and critical elongation vs gamma-radiation dosage indicated an improvement in the mechanical characteristics of the films at radiation doses up to about 10^6 rad. A radiation dose of 10^8 rad caused a decrease in ultimate strength and critical elongation. Complete loss of original characteristics of the film concurrently with self-destruction (conversion to a powder) occurred at a dose of 6×10^8 rad. (ATD)

41502 RADIATION OPTICAL STABILITY OF QUARTZ GLASS. Brekhovskikh, S. M.; Landa, L. M. Zh. Prikl. Spektrosk., Akad. Nauk BSSR, 2: 374-6(1965). (In Russian).

The effect of investigated of γ radiation and protons on the optical transmission of two brands of quartz glass (KI and KV). The KV contains far fewer impurities than KI. Both glasses were exposed to γ rays from ^{60}Co with exposure doses of 10^4, 10^5, 10^6, and 10^7 r and with $\sim 1.75 \times 10^{13}$, 2×10^{14}, and 10^{15} protons of energy 4.8×10^6 ev in the cyclotron of the Tomsk Polytechnic Institute. The light transmission of the samples was measured with the SF-10 instrument in the visible part of the spectrum, SF-4 in the ultraviolet, and IF-16 for the integral light transmission at wavelength 0.55 μ. The KV glass did not change its transmission even at a 10^7 r dose, whereas the KI became completely opaque at that dose. A similar situation arises following proton bombardment. The endurance of the glass varies with the wavelength of the light. The results are interpreted from the point of view of discoloring and coloring action of the radiation at different wavelengths, and the difference in the color centers produced by the various impurities in the glass. (ATD)

41503 GAMMA RADIATION EFFECTS ON MAGNET WIRE. McClenahan, Donald L. (Schenectady Chemicals, Inc., N. Y.). 4p. (CONF-650962-3). ORAU. Gmelin, AED-CONF-65-240-2.

From 6th Electrical Insulation Conference, New York.

Samples of magnet wire covered with different types of film insulation were exposed to doses of 1×10^7 to 1×10^{10} R of gamma radiation from a ^{60}Co source and from spent fuel elements. After irradiation samples were tested for the following: film build, flexibility and adhesion, scrape abrasion, thermoplastic flow, solvent resistance, breakdown voltage, and infrared absorption. Results are presented in tabular and graph form. For each type of magnet wire a failure point was determined, and a relative order of resistance to radiation for the materials tested is given. Infrared absorption curves indicated that radiation changed or broke certain chemical bonds within the polymers. These changes are related to the observed chemical, electrical, and mechanical failures of the samples. (A.G.W.)

41504 TWO-CAPSULE PROGRAM FOR COMPARING A302B STEEL FROM TWO MANUFACTURERS UNDER SPECIFIC IRRADIATION CONDITIONS. Stern, G. (United Nuclear Corp., White Plains, N. Y.); Shimokawa, K.; Knopf, N. R.; Cihi, J. 64p. (CONF-660627-5). ORAU. Gmelin, AED-CONF-66-198-3.

From American Society for Testing and Materials, 69th Annual Meeting, Atlantic City.

A two-capsule program compared the effects of irradiation on A302 Grade B steel from two different sources. The comparison was made with 36 impact and 12 tensile specimens representing two 4-in. thick plates as well as weld metal deposited in a joint made from one of the plates. The properties compared were tensile, hardness, impact, and microstructure, and meaningful results were obtained. The irradiation conditions were nominal integrated fast fluxes of 10^{19} and 10^{20} nvt (>1 Mev) and a temperature of 200 to 300°F. Details of the capsule design are given. An appendix, outlining theories of irradiation effects on steel, is included. The results obtained confirm the effects of irradiation on A302 Grade B steel. These include increase in hardness, increase in yield and tensile strength, decrease in ductility, and decrease in fracture toughness. Microstructure was not changed by irradiation. A quantitative comparison between the two steels tested was possible. (auth)

41505 EFFECTS OF SPACE RADIATIONS ON REFRACTIVE PROPERTIES OF OPTICAL GLASSES. Malitson, Irving H.; Dodge, Marilyn J.; Gonshery, Marvin E. (National Bureau of Standards, Washington, D. C. Frankford Arsenal, Philadelphia). 4p. (CONF-660542-1). ORAU.

From Society of Photographic Scientists and Engineers Meeting, San Francisco.

Initial results are reported from a laboratory study of the effects of ^{60}Co γ radiation and electrons on the refractive index of regular and Ce-protected borosilicate (BSC 517) and dense flint (DF 649) glasses and high-purity fused silica. Radiation doses used were 10^6 rad of γ and 10^{15} e/cm^2 at 2.0 Mev. The refractive index was measured at various intervals of time after exposure at 9 visible wavelengths from 0.4 to 0.7 μ. The results demonstrated that radiation may cause a change in refractive index even though there is no color change in glasses. No significant changes in transmittance and refractive index were observed in high-purity silica after irradiation. (A.G.W.)

41506 IRRADIATION EFFECTS ON THE MECHANICAL PROPERTIES OF VANADIUM-BASE ALLOYS. Boehm, H.; Dienst, W.; Hauck, H.; Laue, H. J. (Kernforschungszentrum, Karlsruhe, Ger.). 14p. (CONF-660627-4). ORAU. Gmelin, AED-CONF-66-198-2.

From American Society for Testing and Materials, 69th Annual Meeting, Atlantic City.

Experiments were carried out to establish the influence of neutron irradiation (1.4×10^{21} n/cm^2, E > 100 kev) on the mechanical properties between room temperature and 750°C of different V-base alloys. The radioinduced increase in the absolute values of the yield strength in the binary V–Ti alloys is independent of Ti content, but in the V–Ti–Nb alloys with a constant Nb content of 20% the degree of increase in the yield strength falls with increasing Ti content. At 650°C it was observed that in the binary V–Ti alloys and in ternary V alloys containing Ti, there was a complete recovery of irradiation damage at Ti contents of 10% or more, while at lower Ti content there was still a clear indication of unrecovered radiation damage. The strong influence of Ti on the annealing of radiation damage was determined experimentally by means of irradiated specimens whose mechanical properties were determined at room temperature after a 5-hr anneal at 600°C. At 650 and 750°C the V alloys showed no indication of high-temperature embrittlement. (auth)

41507 THE THEORY OF SECONDARY EMISSION AND OF ELECTRON INDUCED CONDUCTIVITY IN INSULATORS. Harth, W. Munich, Technical Univ., 1965. 144p. $2.00 Gmelin, AED-Diss. 65-355.

Thesis.

The transport of internal secondary electrons in insulators can be described by a Boltzmann equation. Solutions of this equation are in agreement with experimental data. Temperature dependence of energy distribution and yield is calculated. Conductivity induced by electron bombardment can be described by Ohm's law and a Poisson distribution. Induced current density is proportional to primary current density and independent on temperature. (Gmelin Inst.)

41508 ELECTRON RADIATION DAMAGE IN SEMICONDUCTORS AND METALS. Corbett, James W. Solid State Physics. Advances in Research and Applications. New York, Academic Press, 1966. 419p. $16.50.

A review of radiation damage in semiconductors and metals is presented. Radioinduced lattice defects affecting physical properties are given special attention along with the technology of radiation damage mechanisms and the theory of electron radiation damage. The information is grouped in sections on background material, elemental semiconductors, compound semiconductors, pure metals, and alloys. (J.R.D.)

PHYSICS

General

41509 (AD–638830) CLASSICAL STATISTICAL MECHANICS OF THE HARD-CORE POTENTIAL. Cooper, Martin J. (Brandeis Univ., Waltham, Mass.). June 1966. Contract NONR-1677-04. 75p. CFSTI $3.00 cy, $0.75 mn. Thesis.

An investigation was made to discuss the difficulties associated with representing the strong short ranged forces between the particles of a many-body system and to describe a method by which a more exact treatment of the N-body system becomes available without restricted domains or excluded volume regions provided that certain physical properties of the two-body scattering are retained. The method employed, that of an extended canonical point-transformation, is based on providing an equivalent non-singular Hamiltonian which is both Hermitian and Fourier analyzable. The price of such a transformation is the introduction of non-local velocity dependent interactions between the particles. But such forms are well known in classical mechanics and can be treated in a statistical mechanical context without difficulty. This approach allows for an immediate means of analysis of the role of the hard-core interactions in a many-body system which may be treated by any of the conventional methods of statistical physics. Direct contact is made with the more usual expressions for a hard-sphere many-body system and it is explicitly demonstrated that the real advantage of this canonical reformulation of the strong interactions in terms of an equivalent momentum potential lies in allowing the repulsion to be treated in the same manner as any weak long ranged interaction. The role of the excluded volume regions in the condensation of a real fluid of weakly attractive particles is investigated. A description of the approach to equilibrium of a hard-sphere gas is obtained by means of VHP Master Equation formalism. (auth)

41510 (MIT–2098-251) PHYSICS PROGRESS REPORT, NOVEMBER 1, 1964–DECEMBER 31, 1965. (Massachusetts Inst. of Tech., Cambridge. Lab. for Nuclear Science). Contract AT(30-1)-2098. 110p. Dep. mn. CFSTI $4.00 cy, $0.75 mn.

Separate abstracts are prepared for 7 of the 8 sections presented. One paper was in summary form only and was not abstracted for NSA. (B.G.D.)

For abstracts of individual sections see: 41667, 41795, 41796, and 42165–42168.

41511 (RLO–1388-501) PROGRAM B: THEORETICAL NUCLEAR PHYSICS PROGRAM. Progress Report, September 16, 1965–September 15, 1966. (Washington Univ., Seattle. Dept. of Physics). Contract AT(45-1)-1388. 30p. Dep. mn. CFSTI $2.00 cy, $0.50 mn.

Summaries of the present research programs at the University of Washington are presented. These are divided into the topics: nuclear reactions and structure, quantum statistical mechanics and the many body problem, field theory and elementary particles, astrophysics and general relativity, and atomic and molecular physics. (B.G.D.)

41512 (UCRL–14744) PHYSICS DEPARTMENT PROGRESS REPORT, OCTOBER 1965–JANUARY 1966. (Lawrence Radiation Lab., Univ. of California, Livermore). Contract W-7405-eng-48. 52p. Dep. mn. CFSTI $3.00 cy, $0.50 mn.

Separate abstracts were prepared for the 3 included sections. (M.O.W.)

For abstracts of individual sections see: 41513, 42169, and 42418.

41513 (UCRL–14744, pp 19-36) THERMODYNAMIC PROPERTIES OF MATTER. (Lawrence Radiation Lab., Univ. of California, Livermore).

Brief summaries of research progress are presented for the following: profile of shock waves in solids, asymptotic expansion of operator sums over a large number of quantum states, phase change for a hard-square lattice gas, equation of state of I, Hugoniot equation of state of Mg alloy AZ31B, shock induced demagnetism, shock-induced solid-solid phase transformation in Bi, and Brillouin scattering behind shock fronts. (M.O.W.)

41514 (AI-Trans–209) POWER SUPPLY INSTALLATIONS FOR FUTURE SPACECRAFT. Grob, Franz; Langpape, Reinhart; Stahl, Kurt Translated for Atomics International, Canoga Park, Calif., from BBC-Nachr., 48: 156-72(1966). 20p. Dep. mn. JCL $1.60 fs, $0.80 mf.

A detailed comparison of the different methods of energy production in space is presented. The advantages and disadvantages of each are outlined. (M.H.R.)

41515 FARADAY ROTATION IN MEGAGAUSS FIELDS. Herlach, F.; Knoepfel, H.; Luppi, R.; Van Montfoort, J. E. (Laboratorio Gas Ionizzati, Frascati, Italy). pp 471-82 of EUR–2750.e.

The Faraday effect for quartz and crown glass in megagauss fields was measured. Experiments were done both with plane and cylindrical compression devices. They demonstrate both the flexibility and the limitation of these devices from the point of view of application of the megagauss fields. Experimental arrangements are described and particular experimental difficulties are discussed, also in view of related experiments. (auth)

41516 EFFECT OF THE DOSE OUTPUT ON THE ELECTRET EFFECT IN PARAFFIN WAX. Bernadzikowski, R.; Gomulkiewicz, J. (Landwirtschaftliche Hochschule, Wroclaw). Exp. Tech. Phys., 14: 57-62(1966). (In German).

The effect of the dose output of β emitters on the electret effect in paraffin wax was investigated. The dependence of the electret charge on the irradiation time was experimentally determined for several values of the dose output and the dependence of the electret charge on the dose output was determined for a fixed irradiation time. A comparison of the results with theory shows that the centers producing the polarization underlie the recombination and that this recombination has an essentially bimolecular character. (tr-auth)

41517 DYNAMICS OF CERTAIN SPHERICAL CHARGE DISTRIBUTIONS. Liboff, Richard L. (Cornell Univ., Ithaca, N. Y.). J. Math. Phys. (N. Y.), 7: 991-7(June 1966).

Two initial-value problems are solved in the Lagrange representation. The initial configuration of the first is an isolated, negative, finite spherical gas. In the second a fixed, infinitely thin, positive, permeable, spherical shell is placed concentric and exterior to the negative gas of the first configuration. The charge of the total system is zero. The first system is totally soluble. Application to the special case of uniform initial density gives that the charge density at a point far removed from the initial sphere decays as the inverse cube of time, and is independent of radius. In the second configuration if a is the radius of the positive shell and b the initial radius of the negative gas, then for uniform initial distribution, all charge in the shell $b(b/a)^{\frac{1}{2}} \leq r \leq b$ escapes. The remaining charge oscillates and is randomized by phase mixing. (auth)

41518 DETERMINATION OF NON-LINEAR PARAMETERS AND THEIR STANDARD DEVIATIONS FROM LEAST-SQUARES RESIDUALS. Archer, N. P.; Prestwich, W. V.; Keech, G. L. (McMaster Univ., Hamilton, Ont.). Nucl. Instrum. Methods, 44: 114-18(Sept. 1966).

The mathematical relation existing between the sum of the squares of weighted residuals, χ^2 and the parameters determined by least-squares fitting procedures is investigated. This relation is shown to contain explicitly the

variance of the calculated parameters. Examples are given in which this formulation is used in the least-squares estimation of nonlinear parameters and their standard deviations. (auth)

41519 INTERACTION OF ELECTRON BEAMS WITH A MODULATED REACTANCE SURFACE. Neureuther, A. R.; Mittra, R. (Univ. of Illinois, Urbana). Proc. IEEE (Inst. Elec. Electron. Eng.), 54: 1100-1(Aug. 1966).

A theoretical investigation of the sinusoidally modulated reactance surface is presented which gives an indication of the influence of the synchronism condition on the interaction resistance. It illustrates how the complex dispersion characteristics can be used to determine both the synchronism condition and its relative influence for the various modes on a structure. (M.H.R.)

41520 ON THE GRADIENT INVARIANCE OF THE LAGRANGIAN OF A PARTICLE WITH NONLOCAL POTENTIAL. Korolev, A. M. (Inst. of Physics, Kiev). Ukr. Fiz. Zh., 11: 711-20(1966). (In Ukrainian).

The lagrangian of a particle with nonlocal potential, invariant during gradient transformations, is constructed. It is shown that from the requirements of gradient invariance of the lagrangian there follows an additional interaction of the charged particle with the electromagnetic field. This interaction, which is associated with the dependence of the nonlocal potential on the momentum, is a consequence of the existence of additional electric currents in the system. A complete expression for current density is obtained on considering an infinitesimal variation of the field during gradient transformation. It is shown that nonlocal currents do not affect the value of the probabilities of electric multipole transitions, but substantially affect the value of magnetic transitions. (auth)

41521 SOME RELATIONS GOVERNING THE P-T PHASE DIAGRAMS AND POLYMORPHIC TRANSFORMATIONS OF ELEMENTS UNDER HIGH PRESSURES. Evdokimova, V. V. Usp. Fiz. Nauk, 88: 93-123(Jan. 1966). (In Russian).

Data published up to May, 1965, dealing with the use of P-T phase diagrams to predict the transitions that alter the crystal structures of various substances in their high-pressure phases, are discussed. Using the available sequences of the polymorphic modifications within each group of the periodic table, the presently known data on the types of crystal structure and their changes, which occur in each of the elements for which P-T diagrams are presently known, are reviewed. The results to date indicate that the periodicity of the elements applies also to their phase diagrams, so that the P-T diagrams of elements in one group are very similar, but they gradually contract toward lower pressures and temperatures as the atomic number increases. The variety of elements is reflected in the variety of the forms of the phase boundaries. The general effect of pressure is to make the looser crystal structures more closely packed and acquire larger coordination numbers although some exceptions to this rule are also observed. In some cases the P-T diagram of an element has much in common with the diagrams of elements in the neighboring group. Some predictions are made regarding high-pressure modifications of elements which have not yet been investigated by x-ray analysis. (auth)

41522 NATURAL SYSTEM OF UNITS IN CLASSICAL ELECTRODYNAMICS AND ELECTRONICS. Kapitsa, S. P. (Inst. for Physical Problems, Academy of Sciences, USSR). Usp. Fiz. Nauk, 88: 191-4(Jan. 1966). (In Russian).

A system of units is proposed which may be called natural for classical electrodynamics. The point of such a system is to introduce scales for numerical evaluations of various electronic phenomena and to simplify the writing of formulas. The proposed system uses the classical electron radius r_0 as the unit of length, electron rest energy mc^2 as the unit of energy, and electron mass as the unit of mass. Planck's constant is found to equal 137 in the proposed system. The new system is considered convenient for the solution of problems in classical electrodynamics and electronics and gives units for voltage, current, and power to demonstrate this. The value obtained for power is characteristic of relativistic electronic devices and occurs in the theory of electron accelerators. No new physical findings will result from the use of the proposed system, but it should be handy for calculating phenomena and for explaining and teaching electrodynamics. (CFSTI)

41523 DIFFRACTION RADIATION. Bolotovskii, B. M.; Voskresenskii, G. V. (Lebedev Inst. of Physics, Moscow). Usp. Fiz. Nauk, 88: 209-51(Feb. 1966). (In Russian).

A class of radiation effects connected with scattering of the wave components of the field associated with charges moving past optical inhomogeneities in a medium is reviewed. The optical inhomogeneities considered are ideally conducting surfaces of various forms (plane screens, waveguides, and periodic structures). This type of radiation and the features distinguishing it from other effects is described such as Cherenkov or transition radiation or radiation from a source in nonuniform motion, mathematical techniques necessary to get exact solution of diffraction-radiation problems are presented, and various specific cases of diffraction radiation from uniformly charged wires or line currents are treated. It is pointed out that in all cases there are several common characteristic properties: (1) the radiation energy is independent of the mass of the particle, but is determined by its velocity and charge; (2) the character of the diffraction radiation depends on the form of the scattering obstacle; (3) the angular and frequency distributions of the radiation are determined by the velocity of the source and the shape of the scattering obstacle; (4) the intensity of the radiation falls off exponentially at high frequencies; and (5) the energy loss in diffraction radiation from line sources is proportional to the first power of the velocity when the velocity is low, and becomes dependent on the form of the line source and the shape of the obstacle at relativistic velocities. (ATD)

41524 THEORY OF REGULAR ELECTROSTATIC CHARGED PARTICLE BEAMS. Syrovoi, V. A. Zh. Prikl. Mekh. Tekh. Fiz., No. 1, 3-7(Jan.-Feb. 1966). (In Russian).

Investigations of regular electrostatic flows make extensive use of a procedure which consists of shifting to a system of coordinates related to the trajectory. In such a system, the velocity vector has only one component, so that the flow takes place in the x^1 direction (x^1 flow). This flow is termed one-dimensional. The procedure may prove to be effective in the search for a broad class of flows. The system of coordinates, which postulate flows in the x^1 direction, is a problem more particular than the general problem of the separation of variables. The concept of x^1 flow is discussed from the viewpoint of its usefulness in obtaining solutions to equations of a regular electrostatic beam. It is shown that the shift to the system of coordinates related to the trajectory is justifiable for only four orthogonal systems: the Cartesian, cylindrical, spiral cylindrical, and spherical systems. For the case of the two-dimensional system on a plate with a conformal metric it is shown that the necessary condition of the probability of x^1 flow and the Euclidean condition of space may be effectively used for the establishment of the fact of existence in the prescribed class of the system of coordinates of the x^1 flow which does not initiate from a real emitter. (ATD)

41525 THE INTEGRAL RADIANT EMISSIVITY OF TUNGSTEN IN THE TEMPERATURE INTERVAL FROM 1200 TO 2800 DEG K. Dmitriev, V. D.; Kholopov, G. K. Zh. Prikl. Spektrosk., Akad. Nauk BSSR, 3: 72-5(July 1965). (In Russian).

The integral radiant emissivity of tungsten in the temperature interval from 1200 to 2800°K is calculated according to data on spectral radiant emissivity. (auth)

41526 USE OF THE HOLLOW CATHODE FOR THE DETERMINATION OF GASES IN SOLIDS BY THE ISOTOPIC EQUILIBRIUM METHOD. Shvangiradze, R. R.; Oganezov,

K. A.; Chikhladze, B. Ya. Zh. Prikl. Spektrosk., Akad. Nauk BSSR, 3: 300-5(Oct. 1965). (In Russian).

The use of a hot hollow cathode makes it possible to obtain isotopic equilibrium at a temperature to 2000°C, for the purpose of the spectral isotopic determination of gases in solids. A temperature value somewhat exceeding the melting point of the materials analyzed is optimal for isotopic equilibrium. It is unnecessary to make corrections on the control experiment because of the possibility of complete preliminary degassing of the pipe. The method makes it possible to determine gases in solids to thousandths of one percent. (auth)

41527 MATERIAL RADIATION ENVIRONMENT. Muehlhause, C. O. 8p. (CONF-660505-5). ORAU. Gmelin, AED-CONF-66-103-4.

From American Ceramic Society Meeting, Washington, D. C.

The general arrangement of components in a basic reactor system, the radiation environment prevailing in the system, and the primary radiation processes involved are reviewed. (A.G.W.)

41528 APPARATUS FOR ALTERNATE ELECTRON AND ION TREATMENT OF SURFACES WITH A MICRON SIZE SPOT. Heil, H.; Scott, B. W. (Hughes Research Labs., Malibu, Calif.). 16p. (CONF-660414-2). ORAU. Gmelin, AED-CONF-66-119-3.

From 2nd International Conference on Electron and Ion Beam Science and Technology, New York.

An apparatus which will alternately produce an electron or an ion beam of micron size is described. Only electrostatic focusing and deflecting fields are used. Therefore, the type of beam, either electron or ion, is readily changed by reversing the sign of all potentials. A tungsten hairpin is used as the electron source as well as the source of cesium ions. The latter are formed by surface ionization at the hairpin. A very small amount of atomic cesium is produced from a mixture of cesium chloride and calcium, mounted next to the hairpin and heated separately. The device can be repeatedly exposed to the atmosphere without affecting the cesium source. In this apparatus the beam is stationary and the target is moved. Thus, simple post acceleration focusing from a small aperture over a small distance is possible, and very small spots are obtainable. The ability to switch from ion beam to electron beam without breaking the vacuum and without moving the target makes it very easy to inspect the working area with the electron beam. (auth)

41529 STUDIES OF MULTIPLE EMISSION IN ELECTRON EMISSION PROCESSES. Herrmann, M. Mainz, Univ., Mainz, 1965. 63p. $2.00 Gmelin, AED-Diss. 65-308.

Thesis.

Multiple emission in various electron emission processes is studied using post-acceleration and proportional-counter spectroscopy. Multiple processes are very rare in all cases Distributions can be described approximately by Poisson curves. (Gmelin Inst.)

Accelerators

Refer also to abstracts 41266, 41276, 41314, and 41323.

41530 (ANL-7196) MEASUREMENT OF BEAM PROFILES WITH THERMOLUMINESCENT DOSIMETERS. Lucks, Herbert; Marcowitz, Stewart M.; Wheeler, Robert V. (Argonne National Lab., Ill.). Apr. 1966. Contract W-31-109-eng-38. 9p. Dep. mn. CFSTI $1.00 cy, $0.50 mn.

Thermoluminescent dosimeters have been used to determine the profile of the 12.5-Bev external beam of the Zero Gradient Synchrotron at Argonne National Laboratory. The total number of particles in the beam, the distribution of particles, and the shape of the beam were determined. The results are in excellent agreement with results obtained by other techniques used for determination of beam profiles. Using only one accelerator pulse, a beam of comparable size with intensity up to 10^{12} particles per pulse and as low as 10^6 particles per pulse could be analyzed. (auth)

41531 (BNL-10528) GROWTH OF PHASE SPACE IN HIGH INTENSITY PROTON BEAMS DUE TO NONUNIFORM RADIAL CHARGE DISTRIBUTION. Turner, C. M.; Bennett, G. W. (Brookhaven National Lab., Upton, N. Y.). July 28, 1966. Contract AT(30-2)-Gen-16. 22p. Dep. mn. CFSTI $1.00 cy, $0.50 mn.

Experimental results are presented of work aimed at establishing quantitative information on the rate of growth of apparent emittance area in the drifting high-intensity proton beams with nonuniform radial charge distributions considered by Blewett. (B.G.D.)

41532 (BNL-10559) 600 MHz RF SYSTEM FOR 200 Bev ACCELERATOR. Halama, H. J. (Brookhaven National Lab., Upton, N. Y.). Aug. 5, 1966. Contract AT(30-2)-Gen-16. 18p. Dep. mn. CFSTI $1.00 cy, $0.50 mn.

A discussion is presented on an r-f system which combines the advantages of both linear and circular accelerators. This is achieved by employing five iris-loaded structures which are grouped together in one long straight section (34m) forming a traveling wave linac. The whole accelerating system is confined to one location only, thus eliminating long cable runs, and the r-f control station is located directly above the iris-loaded structures. (B.G.D.)

41533 (CERN-66-27) STUDIES ON CAPTURE EFFICIENCIES OF SYNCHRO-CYCLOTRONS. Kullander, S. (European Organization for Nuclear Research, Geneva (Switzerland)). Aug. 31, 1966. 32p. Dep. mn.

The starting phase of the particles in relation to the radio frequency affects the capture time considerably. This is found from numerical computations in which both the equilibrium phase and the starting phase have been varied. The total capture time per acceleration cycle was derived from an integration over the starting phase interval 0-60°. The phase oscillations are damped with increasing energy; this fact was used to minimize the acceleration time. The frequency range will be reduced considerably if radially increasing magnetic fields are employed. The capture efficiency, however, does not differ compared to that which can be obtained for actual linearly sloping fields. Intensities are estimated by means of the presented results and from available space-charge theories. A synchrocyclotron of 600 Mev energy can be improved to deliver at least 60 μA of protons. (auth)

41534 (DESY-66/18) ABSCHIRMUNG HOCHENERGETISCHER ELEKTRONEN: DIE NEUTRONEN- UND MYONENKOMPOENTE. (Shielding High-Energy Electrons: The Neutron and Muon Components). Bathow, G.; Freytag, E.; Tesch, K. (Deutsches Elektronen-Synchrotron, Hamburg (West Germany)). July 1966. 18p. Dep. mn.

Heavy concrete shielding measurements were extended to thicknesses from 200 to 400 cm using 4- and 6-Bev electron beams. High-energy neutrons and secondary low-energy neutrons as well as muons were measured. Flux densities, attenuation coefficients, and lateral distributions are given. The experimental results agree with the estimates. (auth)

41535 (DNPL-1) NINA: THE 4 Gev ELECTRON SYNCHROTRON OF THE NATIONAL INSTITUTE FOR RESEARCH IN NUCLEAR SCIENCE. (Daresbury Nuclear Physics Lab. (England)). [nd]. 22p. Dep. mn.

A progress report is presented on the 4 Bev electron synchrotron NINA. Topics discussed are laboratory buildings, magnet, magnet power supply, r-f accelerating system, vacuum system, and injection system. (B.G.D.)

41536 (DNPL-2) 4 Gev ELECTRON SYNCHROTRON. Progress Report to 31st October, 1965. (Daresbury Nuclear Physics Lab. (England)). 31p. Dep. mn.

A progress report is presented on the 4 Bev electron synchrotron, NINA. Topics discussed are magnets, magnet power supplies, vacuum system, r-f accelerating system, injection equipment, control and instrumenta-

tion, accelerator development, physics apparatus, and services group. (B.G.D.)

41537 (LA–3587) QUARTERLY STATUS REPORT ON THE MEDIUM-ENERGY PHYSICS PROGRAM FOR PERIOD ENDING JULY 30, 1966. (Los Alamos Scientific Lab., Univ. of California, N. Mex.). Aug. 1966. Contract W-7405-eng-36. 94p. Dep. mn. CFSTI $3.00 cy, $0.75 mn.

A progress report is presented on the medium energy physics program at Los Alamos Scientific Laboratory. Topics discussed are: accelerator structures such as waveguides, Alvarez drift tubes, and injectors; R-F power sources such as an 805-MHz power amplifier and control systems, a 201.25 MHz amplifier, power supply studies; accelerator control and instrumentation, accelerator physics, and building and site planning. (B.G.D.)

41538 (LNF–66/29) COMPUTATION OF THE EFFECTS OF ERRORS OF A MAGNETIC CHANNEL ON THE FINAL BEAM PARAMETERS. Note No. 323. Bassetti, M.; Buonanni, R. M. (Laboratori Nazionali di Frascati, Comitato Nazionale per l'Energia Nucleare (Italy)). May 30, 1966. 30p. Dep. mn.

Computation of the correlation between the beam parameter at the output of a magnetic channel and the errors due to the channel assembly and to the variations of current supply is reported. (B.G.D.)

41539 (MIT–2098–259) EXPERIMENTS AND TARGET-GAS STORAGE AT THE CEA AT THE TIME OF THE JULY 5, 1965 ACCIDENT AND FIRE. Biron, R. D. (Massachusetts Inst. of Tech., Cambridge. Lab. for Nuclear Science). May 18, 1966. Contract AT(30-1)-2098. 14p. (CONF-660605–9). Dep. mn. CFSTI $1.00 cy, $0.50 mn.

From Cryogenic Engineering Conference, Boulder, Colo.

The experimental systems and materials which contributed to the explosion and fire of July 1, 1965 at the Cambridge Electron Accelerator are discussed. The experimental setups, arrangements for flammable gases, and the probable sequence of events in the accident are considered. (J.F.P.)

41540 (NYO–3364-7(Rev.)) INDUCED RADIOACTIVITY IN THE COLLIMATOR SYSTEM OF A 31 Mev BROWN BOVERI BETATRON. Stroemme, Aksel (Norsk Radiumhospital, Oslo). [nd]. Contract AT(30-1)-3364. 9p. Dep. mn. CFSTI $1.00 cy, $0.50 mn.

An investigation of the induced radioactivity in the collimator system of the BBC 12 Mev betatron is presented. Handling of the collimator system by personnel and radiation hazards due to induced radioactivity are discussed. (B.G.D.)

41541 (ORNL–3875, pp 159–63) SUPPORT FOR THE HIGH-VOLTAGE ACCELERATOR PROGRAM. (Oak Ridge National Lab., Tenn.).

A progress report is presented on the high-voltage accelerator program at ORNL. Topics discussed are vacuum techniques, control console for the 5 Mw Van de Graaff, scattering chamber for gaseous targets, duoplasmatron arc-current regulator, energy calibration system for the Tandem Van de Graaff, pulsing equipment for the Tandem accelerator, Tandem operations for 1964-65, and developments in gridded ion lenses. (B.G.D.)

41542 (RHEL/R–125) THE NIMROD ELECTROSTATIC INFLECTOR. Srivastava, K. D. (National Inst. for Research in Nuclear Science, Chilton (England). Rutherford High Energy Lab.). July 1966. 16p. Dep. mn. BIS $0.50. HMSO 2s. 6d.

The development of the electrostatic inflection system used on NIMROD, the 7-Bev proton synchrotron, is described. The work was aimed at improving its operational reliability. (auth)

41543 (RPP–R–2) NEUTRON DOSIMETRY METHODS AND EXPERIENCE ON THE 7 Gev PROTON SYNCHROTRON, NIMROD. Perry, D. R. (National Inst. for Research in Nuclear Science, Chilton (England). Rutherford High Energy Lab.). 1966. 22p. (CONF-660807–2). Dep. mn.

From Symposium on Neutron Monitoring for Radiological Protection, Vienna, Austria.

The stray radiation field around a high energy accelerator contains many types of radiation, each with a wide energy spectrum. The pulsed nature of this radiation adds to the problems of measurement. Neutrons are always a major component of this field, and around Nimrod comprise more than 50% of the dose equivalent in occupied areas. The methods which have been used, and the results obtained, in measurements of neutron flux, dose equivalent, dose rate, and energy spectrum are described. These methods include threshold activation detectors, moderated foils, photographic films, nuclear track emulsion, thermoluminescent detectors, proton recoil counters, BF_3 counters, and LiI scintillators in various moderating assemblies, and ionization chambers. The suitability of different detectors for fixed point measurements, routine surveys, personal dosimetry and special investigations was assessed by trials and intercomparisons in typical Nimrod fields and with standard sources. Comparisons between detectors with differing thresholds or characteristics show that the energy spectrum varies from place to place but always falls off rapidly with increasing energy Most of the neutron flux and dose equivalent is due to neutrons with energies between 0.1 and 10 Mev: the dose contributions from thermal and very high energy neutrons are both very small. Examples of surveys carried out for routine purposes and for shielding design studies are given. A summary of radiation levels and personal doses with internal and external (extracted beam) targets, and a discussion of the practical problems of dosimetry arising both from present operations and from proposed accelerator developments are presented. (auth)

41544 (SLAC–63) DESIGN OF BEAM POSITION AND CHARGE MONITORING CIRCUITS FOR THE STANFORD TWO-MILE ACCELERATOR. Larsen, R. S. (Stanford Linear Accelerator Center, Stanford Univ., Calif.). May 1966. Contract AT(04-3)-400. 93p. Dep. mn. CFSTI $3.00 cy, $0.75 mn.

The beam position and charge monitoring circuits for the Stanford two-mile accelerator are described. Circuit design and performance are outlined. (B.G.D.)

41545 (AD–631586) LABORATORY AND DEMONSTRATION HEAVY-PARTICLE ACCELERATORS. Kuz'menko, G. I. Translated from Izv. Vyssh. Ucheb. Zaved., Fiz., No. 4, 174-5(1965). 6p. (FTD-HT–66-191). CFSTI $1.00 cy, $0.50 mn.

Experimental results on the simplified manufacture and operation of accelerator-dischargers for laboratory and demonstration applications are presented. The proton and deuterium accelerator-dischargers are discussed. (B.G.D.)

41546 RESOURCE LETTER PA-1 ON PARTICLE ACCELERATORS. Blewett, John P. (Brookhaven National Lab., Upton, N. Y.). Amer. J. Phys., 34: 742-52 (Sept. 1966). (BNL–10021).

A brief history of the development of charged particle accelerators is given. A list of the published proceedings of conferences on accelerators is also given. (J.F.P.)

41547 COUPLING BETWEEN THE HF CAVITIES AND THE POSITION OF PROTONS IN A SYNCHROTRON. THE NON-LINEAR TECHNIQUE. Loeb, Julien. Automatisme, 9: 513-18(Dec. 1964). (In French).

The inadequacy of the linear approximation for the description of coupling in a synchrotron is shown. The cavity-phase transfer function of protons is examined by using the nonlinear technique. The properties of the simple pendulum are derived, and transitory regimes are considered. (J.S.R.)

41548 LINEAR ACCELERATOR SIMULATOR. Green, Miles F. (Inst. of Radiotherapy, Shenton Park, Australia). Brit. J. Radiol., 39: 635-7(Aug. 1966).

The simulator here described is in many respects similar to that described by Greene et al., (1964); its ability to

produce verification films is greater than that machine, in that all set-ups possible on a linear accelerator are also possible on the simulator and therefore there is never any need for the treatment room to be delayed while marking up is in progress. Having the pedestal mimic that of the linear accelerator also makes the machine a useful training tool for the indoctrination of cadet radiographers in the principles of radiotherapy positioning, when using a linear accelerator. (auth)

41549 SUPERCONDUCTING CAVITIES FOR MICROTRONS. Combe, Rene; Caillaud, Alain (Univ., Paris, Clermont-Ferrand, France). Compt. Rend., Ser. B, 263: 131-4(July 11, 1966). (In French).

Calculation methods and fabrication procedures for superconducting resonant cavities for microtrons are briefly discussed. The techniques used to measure the characteristic parameters are also treated. The experimental results obtained for three temperatures (295, 77, and 4.2°K) are given. (tr-auth)

41550 AUTOMATIC BEAM CURRENT CONTROL ON THE ELECTRON ACCELERATOR. Pluemer, F. (Institut fuer Physik und Physikalische Chemie der Hochpolymeren, Deutsche Akademie der Wissenschaften, Leipzig). Exp. Tech. Phys., 14: 20-4(1966). (In German).

A control device was described that makes it possible to maintain the beam current of the linear electron accelerator constant under given conditions in order to have available an invariable dose output at given irradiations. The value was selected so that this dose output could be preset within given limits. For the control engagement no supplementary devices, that can themselves affect the electron beam, are necessary on the accelerator. (tr-auth)

41551 FOCUSING OF AN ELECTRON BEAM FROM A LOW-NOISE GUN WITH DIFFERENT MAGNET SYSTEMS. PART II. TRAJECTORIES OF THE OUTER-EDGE ELECTRON IN AN INITIALLY PERTURBED BEAM FOCUSED BY A UNIFORM MAGNETIC FIELD. Chen, Tsung-Shan (Radio Corp. of America, Harrison, N. J.). Int. J. Electron., 20: 193-215(1966).

Computer solutions are considered for the profiles of an electron beam which is launched into a constant magnetic field with either positive or negative boundary slope and with initial radius greater or less than the cathode radius. It was found that the outermost electron traces sine waves and executes limited excursions when the initial boundary slope corresponds to angles up to ±1% no matter whether the initial radius is 0.90 or 1.10 times the radius of the cathode. For initial inclination angles close to ±2°, the beam boundary does not preserve a sinusoidal shape; this holds true for focusing magnetic flux densities varying from 200×10^{-4} to 700×10^{-4} weber/m^2. The variations of the beam radius and rippling wavelength along the axis of the electron flow as obtained by the computer are compared with the results calculated from formulas derived on the basis of linearization of the paraxial-ray differential equation. With an initially perturbed electron beam, the linearization process is applicable only to cases where the initial boundary slope is small, corresponding to angles within the limits ±1°, and the focusing magnetic field exceeds 300×10^{-4} weber/m^2. (BBB)

41552 FOCUSING OF AN ELECTRON BEAM FROM A LOW-NOISE GUN WITH DIFFERENT MAGNET SYSTEMS. PART III. TRAJECTORIES OF THE EDGE-ELECTRON IN A BEAM FOCUSED BY MEANS OF A LONG-PERIOD REVERSED-FIELD MAGNET. Chen, Tsung-Shan (Radio Corp. of America, Harrison, N. J.). Int. J. Electron., 20: 241-72(1966).

The focusing of an electron beam which is produced by a magnetically immersed gun and confined by a long-period reversed-field magnet is considered. The trajectories of the edge electron in the beam were determined by solving the paraxial-ray differential equation of the outermost electron on a computer. The flux distribution of the magnet required to minimize the beam scalloping caused by the flux reversal was determined for three types of long-period magnets: peak-field compensation, dip-peak-field compensation, and dip-field compensation. The correct length of the unit structure, which contains two regions of flux reversals, was found for each of the three types of magnets. The long-period magnet producing the dip-field compensation results in a beam contour with min rippling and represents the optimum focusing system. When the electron beam is focused by a long-period, reversed-field magnet the beam rippling results in the different uniform-field regions assume regular, sinusoidal and shallow waves in lieu of the short and jerky up-and-down motions occurring in a beam focused by a short-period periodic permanent magnet. This is believed to be one reason why a lower noise figure can be obtained with a long-period magnet tube than that prevailing in a tube focused by a short-period magnet. (BBB)

41553 DEVICE FOR MEASURING MEDIAN PLANES OF MAGNETIC FIELDS IN ACCELERATORS. Kuzmin, V. N.; Petrov, Yu. K. Izv. Tomsk. Politekh. Inst., 122: 89-93(1962). (In Russian).

Permalloy transducers for measuring the median surface of the magnetic field in accelerators present the advantage of small size and high sensitivity. Such a device was developed on the basis of the determination of the location of points in the gap, at which the radial component of the magnetic field is zero. A driving mechanism allowed movement of the device within the air gap of the electromagnet. The transducer consisted of a strip of $0.02 \times 0.1 \times 25$ mm Permalloy, to which a 400-ohm coil was attached. Errors in the measurements are due to the faulty determination of the zero point of the magnetic field, the actual location of the device and its deviation from a strictly horizontal position. The tests yielded satisfactory results as the errors amounted to only ±0.14 mm, but the device was not suitable for dynamic measurements. It is planned to improve the system by using an iron probe for determining the zero point of the field which promises to reach an accuracy of 1×10^{-4} oersted. (TTT)

41554 MAGNETIC ACCELERATION OF A SUPERCONDUCTING SOLENOID TO HYPERVELOCITIES. Winterberg, F. (Univ. of Nevada, Reno). J. Nucl. Energy: Pt. C, 8: 541-53(Sept.-Oct. 1966).

A new method is described which promises to accelerate large macroscopic particles up to meteoric velocities and beyond. In this method a superconducting solenoid is trapped and accelerated in front of a magnetic travelling wave. The magnetic travelling wave is generated by a lumped parameter transmission line. It is demonstrated that with relatively modest accelerator dimensions velocities in the meteoric range of 10^6 cm/sec up to 10^7 cm/sec may be attainable. To reach a velocity of 10^8 cm/sec the length of the accelerator will be at least of the order of a few kilometers. At velocities of 10^8 cm/sec the controlled release of thermonuclear power should become feasible. The high pressure generated at impact should make it possible to study matter under conditions similar to those that exist in the interior of planets and stars. For velocities of 10^8 cm/sec and beyond it should be possible to observe the Lorentz contraction. (auth)

41555 35-Mev BETATRON. Tanaka, Osamu; Takakura, Koichi (Mitsubishi Electric Mfg. Co., Ltd., Japan). Mitsubishi Denki Giho, 40: 1025-9(June 1966). (In Japanese).

A 35-Mev betatron was constructed for use in medical treatment and industry. Unlike the 30 Mev-field bias-type betatron built formerly, it has an electromagnet of simple construction and also a simple electric circuit so as to reduce troubles in operation. This qualifies the machine as excellent in practical service. It is in successful operation and well adapted to radiography and x-ray and electron irradiation experiments. The maximum energy obtained is 34 Mev, and x-ray output available is 50 r/min-met with the energy of 30 Mev. The design, construction, field characteristics, radiation and electron orbit of the magnet of the betatron are described. (auth)

41556 FAST NEUTRON SPECTROSCOPY USING THE YALE ELECTRON LINAC AND A NEW NANOSECOND

TIME-OF-FLIGHT SYSTEM. Firk, F. W. K. (Yale Univ., New Haven). Nucl. Instrum. Methods, 43: 312-16 (Aug. 1966).

The Yale electron linac was modified to provide pulses ≲10 ns wide and ≲1.5 A peak current. The useful range of electron energy is from 10 to 70 Mev. A time-to-time converter and synchronized oscillator provide a flexible timing system with channel widths between 2 and 10 ns. An overall resolution of 0.2 ns/m is achieved. The favorable ratio of signal-to-background observed for the system permits investigations of a wide range of fast neutron experiments previously the prerogative of Van de Graaff accelerators. The differential elastic scattering of neutrons from the $^{12}C(n,n)^{12}C$ reaction was measured with high resolution at several angles for energies between 1 and 10 Mev. As a further example, polarization effects in the yield of photo-neutrons from the giant dipole resonance region of the $^{16}O(\gamma,n)^{15}O$ reaction were studied by left-right scattering from a ^{12}C analyzer. (auth)

41557 VARIABLE ENERGY BEAM EXTRACTION FROM THE MANITOBA CYCLOTRON. Burgerjon, J. J. (Univ. of Manitoba, Winnipeg, Can.). Nucl. Instrum. Methods, 43: 381-2(Aug. 1966).

The design of the Manitoba cyclotron with a variable-energy external beam is given. The performance of this system, which has been in operation for two months is described. It allows energy changes to be made in a few minutes. (J.F.P.)

41558 MOTION OF A CHARGED PARTICLE IN AN AXIALLY SYMMETRIC NONSTATIONARY MAGNETIC FIELD. Stanic, B. V. (Univ. of Belgrade). Nucl. Instrum. Methods, 44: 147-8(Sept. 1966).

An approximate method is given for analyzing the motion of charged particles in time-varying magnetic fields with axial symmetry. A high-speed computer is not necessary for numerical calculations using this method. (J.F.P.)

41559 RECENT PROGRESS IN THE TECHNIQUE OF PARTICLE ACCELERATORS: STORAGE AND COLLISION RINGS. Blanc-Lapierre, A. (Faculte des Sciences, Orsay, France). Onde Elec., 46: 726-39(June 1966). (In French).

The advantages of head-on collisions between two particles arranged in such a manner that the mass center does not move is first of all described: the system in which this mass-center exists is at rest relative to that of the laboratory and all the energy available in the latter is also available in the former. Storage and collision rings create these conditions of operation. Their general characteristics and the main problems encountered in their realization and operation are analyzed. In particular, certain fundamental phenomena such as synchrotron radiation, space-charge effects, phenomena determining particle lifetimes, and instability due to the resistivity of the vacuum chamber walls are reviewed. A description of the Orsay collision ring A.C.O. together with a report on the test schedule and on the performance results so far obtained are also presented. (auth)

41560 ELECTRON INJECTION INTO BETATRON. Hattori, Hiroyuki (Shimadzu Seisakusho Ltd., Japan). Oyo Butsuri, 35: 410-6(June 1966). (In Japanese).

For electron injection into a betatron acceleration tube, there are an optimum angle of incidence and an optimum position of the electron gun for rendering the amplitude of electron oscillation to a minimum. In general, the oscillation amplitude of tangentially incident electrons becomes smaller as the field bumps are smaller, their phase angle is nearer $\pi/2$ and the voltage of incident electrons is higher. Hence, with a Kerst type magnet, the maximum x-ray output is easily obtained by placing the electron gun right under the magnet yoke, whereby the optimum angle of electron incidence becomes independent of the voltage of incident electrons and excitation current of the magnet. On the assumption that the x-ray output is proportional to the reciprocal of electron oscillation amplitude, the relation between the angle of electron incidence and the x-ray output can be explained. (auth)

41561 BETATRON AND THE PROBLEM OF PROTECTION IN ITS USE. Hrabovcova, Alojzia (Research Inst. for Work Hygiene and Occupational Diseases, Bratislava). Prac. Lek., 18: No. 1, 21-9(Jan. 1966). (In Czech).

Protection from the radiation emitted by a betatron must be based on its high-energy content electromagnetic radiation and its electron emission, while respecting the interactions between the radiation and the materials which are irradiated by it. The intensity of the primary and secondary radiation must be measured. Protection against hard x radiation is the most important feature. It is usually difficult to determine the amount of radiation affecting a given location, and an overall protective scheme must be devised. (JPRS)

41562 SCANNING ELECTRON BEAM PROFILE MONITOR. Reagan, Daryl (Stanford Linear Accelerator Center, Stanford, Calif.). Contract AT(04-3)-400. Rev. Sci. Instrum., 37: 1190-1(Sept. 1966). (SLAC-PUB-186).

A scanning beam profile monitor is described that was developed for use along the Stanford 3 km linear accelerator. The maximum beam loss due to scattering caused by this monitor can be made to be a small fraction of that which would be caused by the Čerenkov radiator or scintillating screen. (auth)

41563 HEAVY ION ACCELERATOR OF THE ORSAY NUCLEAR PHYSICS LABORATORY. Lot, Fernand. Sci. Progr.-Nature, No. 3375, 247-51(July 1966). (In French).

The characteristics and construction of the Orsay cyclotron are described. (J.S.R.)

41564 SHIMADZU 26-Mev MEDICAL BETATRON. Toriyama, Hideaki; Hattori, Hiroyuki (Shimadzu Seisakusho Ltd., Japan). Shimazu-Hyoron, 23: 5-14(Mar. 1966). (In Japanese).

In 1965, two 24 Mev medical betatrons were installed in Osaka and Matsuyama, and one improved type has just been installed in Tokyo. The rated energy of this machine is 26 Mev. These machines can produce ultra-hard x-rays and high energy electron beams. To date, machines capable of producing energy around 24 Mev weigh 3 tons or more. But the magnet of this betatron weighs less than 2 tons and the total weight is about 2.5 tons. The betatron head is supported by only one axis as if it were cantilevered from the wall. This arrangement, while being convenient for doctors and nurses, necessitates the betatron head being of very rigid construction. But, this problem was solved by a unit construction of the magnet yoke, which also assured its very accurate construction and lowered the noise level in operation. The operation of this betatron is very simple. The radiation energy is selected by a dial, which is graduated from 4 to 26 Mev in 2 Mev steps. The only meters on the panel are the radiation monitor and the dose integrator. The only regulator is the radiation intensity regulator. The radiation output is about 40 r/min at 1m for x-rays and about 1,000 r/min for electron beams. (auth)

41565 INVESTIGATION OF THE INFLUENCE OF INJECTION PULSE DURATION ON THE CAPTURE OF ELECTRONS IN A BETATRON. Tulinova, N. I. Zh. Tekh. Fiz., 36: 937-41(May 1966). (In Russian).

A continuation is presented of earlier work of the author and collaborators on the influence of injection pulse duration on the intensity of the x rays from a betatron. The intensity of x rays from the betatron was measured as a function of the duration of the injection pulse, the injection current, and the injection potential. The injection pulse duration was varied from about 10 to 150 nanosec (corresponding to 4 revolutions of an electron in the betatron orbit); the injection current was varied from 3.5 to 175 mA; and the injection potential was varied from 0.5 to 1.2 kv. For fixed injection current and potential the x-ray intensity was maximum for a certain optimum pulse duration and decreased toward zero with further increase of the pulse duration. For fixed injection potential the pulse duration for maximum x-ray intensity was inversely pro-

portional to the injection current, and thus corresponded to injection of a certain optimum charge into the machine. The optimum injected charge increased with increasing injection potential. The radial position of the electron beam in the betatron was explored with a probe, and it was found that the beam was shifted toward the center of the chamber with increasing injection pulse duration. The observed results cannot be explained by interaction between successive turns of the beam in the betatron, for the maximum x-ray intensity frequently occurred for a pulse duration much shorter than the time required for even a single revolution of the electrons in the betatron orbit. It is hypothesized that the variation of x-ray intensity with injection pulse duration is due to enhancement of betatron oscillation by the space charge of secondary electrons knocked from the walls of the chamber by a fraction of the electrons of the injected beam. This hypothesis is discussed in a quantitative way, and it is concluded that it can account for the observed behavior. (ATD)

41566 RADIATION SHIELDING AT THE NRL LINAC FACILITY. Zimmer, Glenn W.; Murray, Kenneth M. (Naval Research Lab., Washington, D. C.). 20p. (CONF-651101-85). ORAU. Gmelin, AED-CONF-65-332-139.

From 13th Conference on Remote Systems Technology, Washington, D. C.

High-intensity radiation conditions were established and radiation surveys were conducted under several conditions of operation to verify the shielding calculations which were made previously, and to determine the effectiveness of the shielding. Problems associated with monitoring x rays and neutrons from pulsed radiation sources are discussed, along with the calibration and surveying. The results of the studies showed that the effectiveness of the shielding for x rays could be calculated, but such calculations for neutrons predicted the shielding to be more effective than actually observed. Suggestions for additional work are made, which should help improve the correlation between the calculated and the measured neutron fluxes. (auth)

41567 PHASE SPACE REPRESENTATIONS OF CHARGED PARTICLE BEAMS. Crawford, C. K.; Brody, M. D. (Massachusetts Inst. of Tech., Cambridge). 19p. (CONF-660414-6). ORAU. Gmelin, AED-CONF-66-119-5.

From 2nd International Conference on Electron and Ion Beam Science and Technology, New York.

Charged-particle motion study by plotting the particle trajectories in phase space is considered. The Γ and μ spaces and their applications to charged-particle optics and mass spectrometer design are discussed. (J.F.P.)

41568 THE 10 Gev ELECTRON SYNCHROTRON AT CORNELL. Wilson, R. R. (Cornell Univ., Ithaca, N. Y.). 46p. (CONF-660104-2). ORAU. Gmelin, AED-CONF-66-174-1.

From Symposium on Magnet Flat Topping for Rapid Cycling Particle Accelerators, Princeton, N. J.

The design and technical details of the 10-Bev electron synchrotron at Cornell are described. The discussion includes the buildings, magnet construction and excitation, the r-f system, injection, the lattice, the vacuum system, ultimate energy and intensity, and monitoring of the beam position. Also given are adjustments and corrections, magnetic measurements, controls, construction schedule and costs, and a listing of the synchrotron parameters. (J.F.P.)

41569 DIVERSE SCHEMES FOR FLAT TOPPING THE PPA. Isaila, M.; Morris, C. (Princeton Univ., N. J.). 16p. (CONF-660104-3). ORAU. Gmelin, AED-CONF-66-174-2.

From Symposium on Magnet Flat Topping for Rapid Cycling Particle Accelerators, Princeton, N. J.

Flat topping of the Princeton-Pennsylvania Accelerator by the introduction of one or two properly phased harmonically related tank circuits in series with each magnet is considered. A feedback loop and a power amplifier are included for higher order corrections. Another scheme achieves the same degree of flat topping by storing most of the flat topping energy in capacitors and exchanging this energy between the capacitor bank and an inductor. In the last scheme considered one additional storage filter reduces the size of the power amplifier and the power waste but somewhat limits the flexibility of the flat top fine structure. (J.F.P.)

41570 A MEASURING METHOD FOR THE INTERNAL BEAM OF A SECTOR FOCUSSED CYCLOTRON WITHOUT DISTURBING THE BEAM. Feldmann, H.-H. Berlin, Technische Univ., 1964. 142p. $2.00 Gmelin, AED-Diss. 64-2009.

Thesis.

An apparatus for the measurement of the phase behavior of circulating ion bursts as a criterion for the magnetic field precision is described. Influence electrodes reacting on the corresponding electromagnetic field are used. Results of measurements at the Karlsruhe cyclotron are given. (Gmelin Inst.)

41571 DUOPLASMATRON AS NEGATIVE ION SOURCE. Rau, G. Heidelberg, Univ., Heidelberg, 1965. 37p. $2.00 Gmelin, AED-Diss. 65-312.

Thesis.

Production of a negative Li ion beam by direct extraction from a duoplasmatron source is studied. The dependence of ion current on geometrical and electric source parameters is investigated. Results indicate that electron capture with triple collision is the most probable process for negative ion production. Maximal Li^- ion current was 55 mamp. (Gmelin Inst.)

41572 ACCELERATOR. Iwashita, Fumio (to Tokyo Shibaura Electric Co., Ltd.). Japanese Patent 1965-20838. Sept. 15, 1965. Filed July 31, 1964.

In the proposed type of accelerators like a betatron with a ring-shaped accelerating tube, the acceleration can be done at the constant electron current, from the high to low-energy condition, or vice versa. The electrons are accelerated in the accelerating tube at the optimum accelerating conditions corresponding to the particle energy conditions. The accelerator consists of an accelerating tube, an electron gun to inject the electrons into this tube, the main electromagnetic device for accelerating the injected electrons in a given orbit in the accelerating tube, the auxiliary electromagnetic device attached to the main device for adjusting the orbit of the accelerated electrons, and a device installed on the accelerating tube for drawing out the accelerated electrons whose orbit is adjusted by the auxiliary electromagnetic device. The electrons injected into the accelerating tube are accelerated, orbit-adjusted and drawn out of the maximum magnetic field of the main electromagnetic device corresponding to the acceleration condition. (auth)

41573 BETATRON AND SIMILAR ACCELERATORS. Iwashita, Fumio (to Tokyo Shibaura Electric Co., Ltd.). Japanese Patent 1965-20837. Sept. 15, 1965. Filed July 27, 1964.

A betatron and similar accelerators are proposed in which the electrons accelerated are ejected from the accelerating orbit very favorably by means of a device installed on the outer surface of the accelerating tube for taking out the accelerated electrons without disturbing the main magnetic fluxes from their orbit. The proposed accelerator consists of the following: a (ring-shaped) accelerating tube; an electron gun attached to the accelerating tube for injecting the electrons into this tube; a main electromagnetic device installed so as to accelerate the injected electrons in a circular orbit; the auxiliary electromagnetic device installed near the main device for adjusting the electron-accelerating orbit; a device installed on the accelerating tube which takes out the accelerated electrons tangentially from their accelerating circular orbit by decreasing stepwise the magnetic field of the (said) main electromagnetic device; and an exit on the accelerating tube for the accelerated electrons thus led out by the device. (auth)

41574 DEVICE FOR ACCELERATING AN ELECTRON BEAM. Iwashita, Fumio (to Tokyo Shibaura Electric Co., Ltd.). Japanese Patent 1965-20836. Sept. 15, 1965. Filed June 11, 1964.

The proposed electron-beam accelerating device has an unusual irradiation window with two windows for obtaining the vacuum of an accelerating tube and protecting from the air pressure, respectively. The irradiation window of the electron beam accelerator consists of the following: a window with a metal membrane for producing the vacuum attached in an air-tight manner to the end of the accelerating tube; a window with a metal membrane for protecting from the air pressure attached opposedly to the other (said) window; and a kind of blower, which cools forcedly the two membranes by blowing cooled air into the space formed by the two windows. The two metal membranes are fixed onto the respective window frames by the use of a heat-hardening resin. Such irradiation windows are most suitable for large electron currents. (auth)

41575 METHOD FOR DEFLECTING ACCELERATED CHARGED PARTICLE. Iwashita, Fumio (to Tokyo Shibaura Electric Co., Ltd.). Japanese Patent 1965-20835. Sept. 15, 1965. Filed Sept. 30, 1964.

A method is proposed, which is very suitable for deflecting charged particles accelerated to a very high speed and energy. Employing the method proposed, an irradiation apparatus, which is capable of irradiating a target material or film uniformly (this increases the life of a target material) can be had at low cost, with its function being stable and maintenance expense low. The device employing the method uses an electromagnet, energized by means of an induction regulator, which produces a revolving magnetic flux; and a charged-particle beam duct, piercing through the (said) revolving magnetic flux. By rotating at a suitable period the rotator of the regulator, the magnitude of the revolving magnetic flux is changed periodically, thereby deflecting the accelerated charged particles so as to describe a spiral scanning line. (auth)

41576 DEVICE FOR PRODUCING A PULSED CHARGED-PARTICLE BEAM. Komai, Kenichiro (to Hitachi, Ltd.). Japanese Patent 1965-20834. Sept. 15, 1965. Filed Sept. 12, 1964.

In the device proposed for producing a pulsed charged-particle beam, pulses of very short time-interval are obtained in order to improve the energy resolution of the charged-particle beam accelerated and to make the overall dimensions compact. The device consists of the following: a place where the charged-particle beam is produced; an electrode impressed by the basic voltage to pulse the charged-particle beam; a deflecting electrode, impressed by the voltage to deflect the basic particle-pulse once at least; a collecting electrode, impressed by the voltage to collect time-wise the charged-particle beam, synchronized with the basic pulses; and the space where the beam is accelerated. Necessary voltages are applied to the (said) respective electrodes and the (said) space through the pulse transformer made by winding a coaxial cable to obtain the secondary windings. (auth)

41577 PARTICLE ACCELERATING TUBE. Iwashita, Fumio (to Tokyo Shibaura Electric Co., Ltd.). Japanese Patent 1965-20959. Sept. 17, 1965. Filed Dec. 30, 1964.

A particle accelerating tube on which the high-voltage-producing circuits are installed, making the whole one body, is proposed. The high-frequency power source, including condensers and other circuits, is made compact, which is all supported by the hoops of the accelerating tube, and this power source is embodied with the latter. As a result, the accelerating tube as a whole is made small in size, thus increasing the usefulness of the accelerating tube obtained. It consists of the following: the accelerating-tube body; hoops arranged at equal intervals on the outside of the tubular body; and the high-voltage-producing circuits, employing an h-f power source as their charge source, which are installed close to the outside of the accelerating-tube body, supported by the hoops. (NSA of Japan)

41578 PARTICLE ACCELERATOR. Iwashita, Fumio (to Tokyo Shibaura Electric Co., Ltd.). Japanese Patent 1965-20960. Sept. 17, 1965. Filed Dec. 25, 1964.

In the particle accelerator proposed, the ion source is supported by means of transparent supporting rods; and instruments are installed near the end of the supporting rods in the particle-source compartment. Thus, by watching the instruments through the transparent supports, accidents such as the destruction of an ion source can be prevented. It consists of the following: the accelerating tube; an ion source attached at the end of the accelerating tube; and the transparent insulating support rods for supporting the ion source, which penetrate through the base plate to the ion source. Instruments are installed, in the ion-source compartment, very close to the end of the support rods, and these are watched from the other end of the supporting rods. (NSA of Japan)

41579 PORCELAIN TUBES. Manaka, Kazuo; Maruyama, Masuo (to Tokyo Shibaura Electric Co., Ltd.). Japanese Patent 1965-22291. Oct. 4, 1965. Filed Nov. 5, 1963.

Porcelain tubes for use in an accelerating tube are proposed; the charged particles are accelerated in this tube maintained under high vacuum, by applying a high voltage. In such accelerators, the accelerating tube is constructed by arranging alternately and attaching together a plurality of porcelain tubes and of metal electrode discs. In this case, when attaching together the two kinds of members, it is required that the sticking together of the porcelain tube and the metal disc is strong; there is no air leakage at these joints; the sticking is not destroyed or the porcelain tubes themselves are not damaged, due to the difference in the thermal expansion coefficients of the porcelain tubes and metal discs, and so on. To meet these requirements, in the method proposed, a nylon film on which epoxide resin was pasted is applied between the respective porcelain tubes. The stable sticking power is obtained (the flexibility of the nylon remaining absorbs the (said) difference in the thermal expansion coefficients) by inducing a hardening reaction by heating. A nylon film pasted with epoxide resin is applied between the porcelain tubes, and by heating the accelerating-tube members cohere. (NSA of Japan)

41580 PARTICLE ACCELERATOR. Iwashita, Fumio (to Tokyo Shibaura Electric Co., Ltd.). Japanese Patent 1965-26720. Sept. 10, 1965. Filed June 11, 1964.

A particle accelerator with a forced cooling device is proposed. By this method, the temperature of the transformers, connected in cascade in the tank, can be cooled below the tolerance level. The particle accelerator proposed consists of the following: a high-voltage-producing device consisting of a plurality of transformers connected in cascade; the accelerating tube in which the charged particles are accelerated by means of the high voltage produced; a tank, filled with an insulating gas and containing part of the accelerating tube, the (said) high voltage producing device and other electrical equipment; at least one pair of piping, which enters the tank at the top and leaves it at the bottom; and a device for circulating forcedly an insulating gas through the tank, and a heat exchanger for cooling the heated gas, which are connected in series outside the tank between the upper and lower parts of the (said) piping. (NSA of Japan)

41581 APPARATUS FOR THE ACCELERATION OF CHARGED PARTICLES. van de Graaff, Robert Jemison (to High Voltage Engineering Corp.). German Patent 1,219,140. June 16, 1966. Filed June 15, 1961.

An apparatus for the acceleration of charged particles by means of high voltages, charge transfer processes and multiple stripping of electrons (tandem acceleration) is discussed. The apparatus comprises a tank filled with an insulating gas under pressure, a long column supported within this tank and provided with three high voltage terminals, the central high voltage terminal being raised to a high positive voltage and the other two terminals being raised to a high negative voltage, and a single insulating belt within the tank, each end of which is supported on two pulleys in order that the two runs of the belt may be as close together as possible. (Gmelin Inst.)

41582 ELECTRON LINEAR ACCELERATOR PHASING METHOD INVOLVING ALTERNATELY TURNING ON AND TURNING OFF THE ELECTROMAGNETIC DRIVER OF THE SECTION BEING PHASED. Goerz, David J. Jr.; Neal, Richard B.; Mallory, Kenneth B. (to U. S. Atomic Energy Commission). U. S. Patent 3,264,568. Aug. 2, 1966.

A method of phasing individual klystron tubes which supply driving energy to respective sections of a multisection linear accelerator is given. With klystron energy removed from a section to be tuned, the phase difference between an arbitrary reference voltage and a voltage induced solely by an electron beam at the output of the section is determined. Then with klystron energy applied to the section being tuned, the phase of the klystron voltage is adjusted until the resultant wave at the output of the section is 180° out of phase with respect to the phase of the voltage induced by the beam alone. (Gmelin Inst.)

41583 COLLINEAR TERMINATION FOR HIGH ENERGY PARTICLE LINEAR ACCELERATORS. Haimson, Jacob (to Varian Associates). U. S. Patent 3,264,515. Aug. 2, 1966. Filed June 29, 1961.

A description is given of a method and apparatus for attenuating radio-frequency waves at the end of particle accelerating structures such as linear accelerators. (L.B.S.)

Astrophysics and Cosmology

Refer also to abstract 41162.

41584 (UCRL-Trans-10040) REMARKS ON STELLAR EVOLUTION. PART III. INTERPRETATION OF AXIAL ROTATIONS. Schatzman, E. Translated for Univ. of California Lawrence Radiation Lab., Livermore, from Ann. Astrophys., 17: 300-11(1954). 19p. Dep. mn. JCL $1.60 fs, $0.80 mf.

Assuming that the stars in the first part of the main sequence are formed by the contraction of large rotating masses, it is shown that it is possible to explain quantitatively the observed distribution of rotational velocities for stars of different spectral types in the first part of the main sequence. The pre-stellar medium is turbulent. (auth)

41585 (UCRL-Trans-10041) REMARKS ON STELLAR EVOLUTION. PART V. ON THE FORMATION OF STELLAR SYSTEMS. Schatzman, E. Translated for Univ. of California Lawrence Radiation Lab., Livermore, from Ann. Astrophys., 17: 382-97(1954). 27p. Dep. mn. JCL $2.60 fs, $1.01 mf.

If one considers the internal and turbulent energy of gas masses capable of separation into stars by gravitational consideration, it seems that the energy of stellar systems thus formed is necessarily negative. A nonstationary aggregation leads to a stellar escape about fifteen times greater than in the case of a stationary grouping; the residue is a system with large negative energy. The formation of stationary aggregations, or aggregations with positive energy, is not compatible with the proposed model. (auth)

41586 DYNAMICAL STABILITY AND BOUNDARY PERTURBATIONS OF THE SOLAR WIND. Carovillano, R. L.; King, J. H. (Boston Coll., Chestnut Hill, Mass.). Astrophys. J., 145: 426-44(Aug. 1966).

The stationary-state theory of solar and stellar winds of E. N. Parker is examined for its dynamical stability properties and for the response of its critical transonic flow curve to arbitrary first-order perturbations. The ideal gas law and the hydrodynamical equations of motion and continuity are employed, while the temperature is phenomenologically related to the density by a polytrope law. A set of linearized coupled differential equations is obtained for the independent spatial and temporal modes. By choosing boundary conditions such that disturbances vanish at the source of the flow, it is shown that there are no non-trivial solutions of the perturbation equations. This yields the important conclusion that Parker's steady-state theory is dynamically stable. Stationary-state disturbances are examined with spherical symmetry as asymmetry. With symmetry, a complete specification of first-order variables in terms of zero-order variables is obtained. For asymmetric disturbances, it is shown that special conditions must be satisfied by the variables at the base of the flow; exact solutions are given in the limit of asymptotically large radial distance. The transonic point of the zero-order flow is a singular point of the perturbation equations. This leads to the interpretation that the zero-order flow is unstable under all time-dependent boundary perturbations which do not meet the (specified) regularity condition at its transonic point. (auth)

41587 RED GIANTS OF POPULATION II. IV. Haerm, R.; Schwarzschild, M. (Princeton Univ., N. J.). Astrophys. J., 145: 496-504(Aug. 1966).

The evolutionary phases of a Population II star through the helium flash were recomputed with improved representations for several of the relevant physical processes. The new computations show that the helium flash is less extreme than indicated by the earlier, less accurate computations; the nuclear-energy release reaches only 10^{11} $L_\odot$ at the peak, and the rate of evolutionary changes now appears to be too slow for major hydrodynamic effects. On the other hand, the new computations confirm the earlier results indicating that the convective core at its greatest extent (after the flash) misses the hydrogen-rich region by about two density scale heights. Accordingly, in view of the very small overshooting from convective cores found in a recent separate investigation, it now appears highly likely that the helium flash does not lead to mixing in the star. (auth)

41588 CATALOG OF METHODS FOR STUDYING THE NORMAL MODES OF RADIAL PULSATION OF GENERAL-RELATIVISTIC STELLAR MODELS. Bardeen, James M. (California Inst. of Tech., Pasadena); Thorne, Kip S.; Meltzer, David W. Astrophys. J., 145: 505-13(Aug. 1966).

A catalogue is presented of various methods now available for studying the normal modes of radial pulsation of stars in general relativity theory. The methods are classified according to the normal-mode properties which they investigate; and the relative merits of the methods are discussed. (auth)

41589 NORMAL MODES OF RADIAL PULSATION OF STARS AT THE END POINT OF THERMONUCLEAR EVOLUTION. Meltzer, David W.; Thorne, Kip S. (Princeton Univ., N. J.). Astrophys. J., 145: 514-43(Aug. 1966).

The lowest three normal modes of radial pulsation are studied for stellar configurations at the end point of thermonuclear evolution. Two alternative equations of state are assumed—the Harrison-Wheeler equation of state and the Skyrme-Cameron-Saakyan equation of state. The adiabatic index is discussed for each equation of state, taking into account the extent to which periodic changes in nuclear composition are produced by stellar pulsation. The periods and e-folding times of the lowest three normal modes of a wide range of configurations are calculated to an accuracy of ±1%. The eigenfunctions of some of the normal modes and the pulsation energy which they can store are also calculated; and a discussion is presented of the damping of neutron-star pulsations and of the consequent heating of the star. (M.O.W.)

41590 PERTURBATIONS OF AN EXPANDING UNIVERSE. Hawking, S. W. (Cambridge Univ., Eng.). Astrophys. J., 145: 544-54(Aug. 1966).

Perturbations of a spatially homogeneous isotropic universe are investigated in terms of small variations of the curvature. It is found that rotational perturbations die away. Density perturbations grow relatively to the background, but galaxies cannot be formed by the growth of perturbations that were initially small. In the steady-state universe small rotational and density perturbations die away. The behavior of gravitational radiation in expanding

universes is also investigated. Its "energy density" decreases at the same rate as that of electromagnetic radiation, although its active gravitational effect is only half as great. If a small amount of viscosity is present, gravitational radiation will be completely absorbed in the steady-state universe but not in an evolutionary universe. (auth)

41591 CLOSED MODEL UNIVERSES WITH A COSMOLOGICAL CONSTANT. Omer, Guy C. Jr. (Univ. of Florida, Gainesville); Vanyo, James P. Astrophys. J., 145: 555-9(Aug. 1966).

Families of closed cosmological models were calculated for two values of the Hubble expansion parameter, 7.5×10^{-11} yr^{-1} and 10×10^{-11} yr^{-1}. These parameters correspond to 73 km/sec/Mpc and 100 km/sec/Mpc. The results are given as two diagrams in which the calculated age of the model, the deceleration parameter, and the cosmological constant are plotted against the average density of matter and the radius of curvature. Thus the entire cosmological siutation is displayed as a single schematic. It was hoped that more realistic model ages could be obtained from this study. (auth)

41592 ENERGY SPECTRUM OF RADIATION IN THE EXPANDING UNIVERSE. Weymann, Ray (Univ. of Arizona, Tucson). Astrophys. J., 145: 560-71(Aug. 1966).

A combination of theoretical arguments and observational evidence suggests the existence of a moderately hot, fully ionized intergalactic gas. In the process of heating this gas distortions of the residual black-body radiation could arise. (This black-body radiation has been detected by several workers and seems to have a temperature of about 3°K.) This possibility is investigated by integrating the differential equations describing the evolution of the radiation field subject to interaction with a hot gas by Compton-scattering, bound-free, and free-free processes. It is suggested that, in addition to the x-ray emission produced by a hot gas, it would be useful to attempt to find distortions of the black-body-curve around 300 μ and 30 cm. Failure to find such distortions would exclude the possibility that the gas was heated at very early epochs in the expansion. (auth)

41593 SIMPLE METHOD FOR STUDYING FRAGMENTATION IN ASTROPHYSICAL SYSTEMS. Arny, Thomas T. (Univ. of Arizona, Tucson). Astrophys. J., 145: 572-82 (Aug. 1966).

The growth of a density perturbation in a spherically symmetric collapsing gas cloud is studied by following the motion of points on the periphery of the perturbation. This technique makes possible solutions including the effects of nonlinearity, nonuniformity, and radiation. Magnetic and rotational effects are ignored. A comparison with the linearized theories of Hunter and Savedoff and Vila shows excellent agreement in the linear regime. It is found that the nonlinearity enhances the growth rate relative to the linearized solutions. In the zero-pressure case the nonuniformity retards growth. The inclusion of radiation gives a roughly isothermal collapse for the conditions anticipated in an H I cloud and the intergalactic medium. (auth)

41594 RADIO ELECTRONS AND MAGNETIC FIELDS IN THE GALACTIC HALO. Felten, James E. (Univ. of California, San Diego, La Jolla). Contract AF49(638)-1527. Astrophys. J., 145: 589-94(Aug. 1966).

The density of radiating electrons in the galactic halo is re-examined in the light of recent cosmic-ray data. A flux $\phi_h(E) \approx 0.8 \times 10^{-2}\ E^{-2.4}$ (cm^2 sec ster Bev)$^{-1}$ in 0.6–3.5 Bev is proposed; this is 1–2 per cent of the quiescent primary proton flux and is higher than estimates used previously in deriving the halo magnetic field from radio brightness measurements and models of the halo. The halo field implied by such a flux is $\approx (2-3.5) \times 10^{-6}$ gauss; the lower figure corresponds to the uniform radio emissivity originally given for the halo by Baldwin, the higher to Mills' value for the central regions. Higher field estimates obtained analogously by other authors are discussed. (auth)

41595 INTERSTELLAR CLOUDS AND PETSCHEK'S MECHANISM FOR DISSIPATING MAGNETIC FIELDS. Wentzel, Donat G. (Univ. of Michigan, Ann Arbor). Astrophys. J., 145: 595-615(Aug. 1966).

Petschek's mechanism ("P.M.") for reconnecting and dissipating magnetic fields is summarized, critically evaluated, and subsequently applied to interstellar clouds. It leads to the following observational and theoretical consequences: (1) If P.M. occurs in H I regions, they involve streams of gas with densities $\simeq 100$ atoms cm^{-3} and speeds $\simeq \pm 3$ km/sec. Such streams should be recognizable in 21-cm emission, even more in 21-cm absorption. They actually dominate the absorption lines of Ca^+ and Na, requiring a recomputation of the abundances of interstellar Ca and Na. The inhomogeneous density distribution also allows significant variations in temperature. (2) The clouds may be disconnected from the general galactic magnetic field. It follows that spiral arms must be gravitational in orgin and the galactic field must be nearly force-free. The alignment of interstellar polarization implies slightly elongated clouds. (3) The evolution of clouds can be meaningfully discussed. A lifetime of the order of 10^8 years may start at the time of a supernova, involves gradual dissipation of internal magnetic fields and a consequent increase in density, and may end by star formation. (auth)

41596 TRAJECTORIES OF MASSLESS PARTICLES IN SUPERDENSE STARS. Kuchowicz, B. (Univ., Warsaw). Bull. Acad. Pol. Sci., Ser. Sci. Math. Astron. Phys., 14: 255-7(1966).

The motion of a massless neutrino in the interior of a superdense star is described in terms of classical theory partially developed by Landau and Lifshitz. (M.O.W.)

41597 RADIATION OF A COLLAPSING AND ANTI-COLLAPSING BODY. Pachner, J. (Astronomical Inst., Prague). Bull. Astron. Inst. Czech., 17: 183-7(1966).

Investigated is a monochromatic electromagnetic radiation of a body with zero internal pressure collapsing or anticollapsing with parabolic velocity. Analytical expressions for four functions are deduced: for the dependence of the radius of the body, measured by rigid rods, on the proper time, for the dependence of the radius of the body emitting from its surface an electromagnetic radiation on the proper time of the reception of this radiation by a very distant observer at rest, for the dependence of the proper time of the reception of the electromagnetic radiation by a very distant observer at rest on the proper time in which this radiation was emitted from the surface of the body, and for the dependence of the ratio of the received frequency to the emitted one on the proper time of the reception by a very distant observer at rest. These four functions are for a certain special case graphically represented in four diagrams. The transformation of the Schwarzschild metric to the metric with co-moving coordinates is carried out. The free fall of a test body in the Schwarzschild field is described. (auth)

41598 OBSERVATIONS OF INTENSITY FLUCTUATIONS IN RADIO EMISSION FROM THE QUASI-STELLAR SOURCE 3C-48 CAUSED BY HETEROGENEITIES OF THE INTERPLANETARY PLASMA. Vitkevich, V. V.; Antonova, T. D.; Vlasov, V. I. (Lebedev Inst. of Physics, Moscow). Dokl. Akad. Nauk SSSR, 168: 55-8(May 1, 1966). (In Russian).

Heterogeneities in the solar supercorona with velocities reaching several thousand km per second were observed at distances of up to 100 solar radii. Using the east-west line of the Radioastronomical Station of the Institute of Physics of the Academy of Sciences SSSR, systematic investigations of the quasi-stellar 3C-48 source were made on the 3.5-m wavelength. In February, the source approached the sun. In March, fluctuations in the brightness of the source began. Fluctuations increased with the decrease in angular distance between the source and the sun, attaining the maximum in April and May when the minimum angular distance occurred. The mean period of fluctuations was 3 and 4 seconds. A weak second period of 6 and 7 seconds may be identified. This is related to the 3.5-m wavelength. An attempt to continue the investigation on the 7.9-m wavelength was unsuccessful. The area of scattered light at a distance of one astronomical unit with a diameter of 500 to 1000 km is seen at an angle of 0.7 to 1.4''. The

effective angular diameter of the source was accepted as equal to 0.1". (ATD)

41599 STATIONARY DUST-FILLED COSMOLOGICAL SOLUTION WITH $\Lambda = 0$ AND WITHOUT CLOSED TIME-LIKE LINES. Maitra, S. C. (Univ. of Maryland, College Park). J. Math. Phys. (N. Y.), 7: 1025-30(June 1966).

An analytic and complete solution of Einstein's field equations without the Λ term is presented for a dust-filled universe ($p = 0$). The solution is stationary and inhomogeneous and does not contain any closed time-like lines. Also some of the properties of the solution are studied. (auth)

41600 SOME PROBLEMS OF NUCLEAR ASTROPHYSICS. Reeves, H. (Univ., Montreal. Laboratoire Joliot-Curie de Physique Nucleaire, Orsay, France). J. Phys. (Paris), Colloq., No. 1, 28-32(1966). (In French).

The development of astrophysics requires knowledge of the cross sections of certain nuclear reactions. A few of the cases in which cross-section values are most urgently needed are presented, briefly situated in their context. (auth)

41601 ROLE OF THERMAL INSTABILITIES IN STAR FORMATION. Hunter, J. H. Jr. (Yale Univ., New Haven). Mon. Notic. Roy. Astron. Soc., 133: 239-45(1966).

The stability of a uniform medium is discussed including thermal and magnetic effects. The new stability criteria are shown to be fundamentally different from those of Jeans (1928) and Chandrasekhar & Fermi (1953), and they reduce to Field's (1965) thermal instability criteria when self gravitation is neglected. It is shown that Field's (1962) model for the intercloud component of the interstellar medium can lead to the formation of condensations having masses on the order of 100 $M_\odot$ in a time scale of between 10^9 and 10^{10} years by the two step process of thermal instability at pressure equilibrium followed by gravitational collapse. (auth)

41602 THE MAGNETIC FIELD OF A CONTRACTING GAS CLOUD. I. STRICT FLUX-FREEZING. Mestel, L. Mon. Notic. Roy. Astron. Soc., 133: 265-84(1966).

A gravitationally-bound, isothermal, spherical magnetic cloud is imagined formed by non-homologous, spherically-symmetric compression of a uniform medium permeated by a uniform magnetic field. The field structure is derived assuming strict flux-freezing, and the consequent magnetic forces computed. Within the cloud the results do not differ much from the predictions of the virial theorem. Outside the cloud, magnetic pinching generates a strongly compressed equatorial zone, with the radial magnetic force locally much greater than the mean value as given by the virial theorem. However, spontaneous straightening of the external field-lines and flow of gas down the field into the zone rapidly bring the magnetic and gravitational forces into local balance. Relaxation of the field into a dipole-type structure which does not exert excessive pinching forces, and with the cloud field effectively detached from the background field, is impossible as long as the constraint of strict flux-freezing is imposed. (auth)

41603 PRODUCTION OF MESONS IN THE NUCLEI OF GALAXIES. Falla, D. F. (University Coll. of Wales, Aberystwyth). Nature, 211: 165-8(July 9, 1966).

A model is proposed in which a process whereby new material is accreted from intergalactic space by a galactic nucleus consisting of hydrogen already at an advanced stage of condensation. The situation for which this material before its entry into the galactic nucleus has acquired an energy exceeding the threshold for the production of π mesons and antinucleons is investigated. It is suggested that such a process centered on a galactic nucleus of radius somewhat greater than its Schwarzchild limit could lead to the production of π mesons and antinucleons: decay of the π mesons would give rise to fast electrons while the antinucleons would give the same ultimate decay products but by way of π-meson production from the annihilation process. (J.F.P.)

41604 APPARENT CORRELATION BETWEEN THE LUNAR ECLIPSE BRIGHTNESS AND THE SOLAR WIND. Matsushima, Satoshi (Univ. of Iowa, Iowa City). Nature, 211: 1027-8(Sept. 3, 1966).

An investigation was made on the relation of the brightness of the moon during a lunar eclipse and the interplanetary plasma. Brightness and plasma flux diagrams are described, and it is concluded that the relationship is due to luminescence on the moon. (M.O.W.)

41605 NEUTRINO ENERGY LOSSES FROM VIBRATING NEUTRON STARS. Hansen, C. J. (Yale Univ., New Haven. Goddard Inst. for Space Studies, New York). Nature, 211: 1069-70(Sept. 3, 1966).

An investigation was made to determine whether significant amounts of vibrational energy can be stored for long times in vibrating neutron stars. The temperature effect is excluded by considering only zero temperature neutron stars. (M.O.W.)

41606 FREQUENCY SPLITTING OF SOLAR RADIO BURSTS. Ellis, G. R. A.; McCulloch, P. M. (Univ. of Tasmania, Australia). Nature, 211: 1070-1(Sept. 3, 1966).

A brief discussion is presented on radio wave measurements in which frequency splitting shows up in their spectra. A possible explanation of these split pairs is given as the excitation of electromagnetic waves near the ordinary and extraordinary mode critical frequencies. (M.O.W.)

41607 ANTI-MATTER CONTENT OF THE TUNGUSKA METEOR. Gentry, Robert V. (Columbia Union Coll., Takoma Park, Md.). Nature, 211: 1071-2(Sept. 3, 1966).

An extension of earlier work of Cowan et al., is presented on the anti-matter content of the Tunguska meteor. The $p\bar{p}$ annihilation reactions and charged pion production are discussed. (M.O.W.)

41608 QUASI-STELLAR RADIO SOURCES. Hahn, H. (Brookhaven National Lab., Upton, N. Y. Faculte des Sciences, Orsay, France). Onde Elec., 46: 715-25(June 1966). (In French).

After a summary review of astronomical data and methods of identification of optical and radio sources in the universe, the observed characteristics of quasi-stellar radio sources or quasars are described: optical luminosity, radio structure, spectrum and variations as a function of time. The mechanism of a hypothetical gravitational collapse is analyzed which could explain the enormous amount of energy radiated during the life-time of a quasar. Various models are developed from first principles as examples consistent with observed characteristics. (auth)

41609 ELECTROMAGNETIC FIELDS AND ROTATING MASSES. Cohen, Jeffrey M. (Yale Univ., New Haven, Conn.). Phys. Rev., 148: 1264-8(Aug. 26, 1966).

In addition to their "Machian" effects on inertial frames, rotating bodies also have "Machian" effects on electromagnetic fields. It is well known that a rotating charged shell in flat space exhibits an electromagnetic field within it. However, if this rotating charged shell is surrounded by a (concentric) slowly rotating mass shell which rotates with the same angular velocity, the electromagnetic field within the charged shell decreases as the mass of the outer shell increases. Finally, as the gravitational radius approaches the radius of the mass shell, the electromagnetic field within the rotating charged shell vanishes. If in this limit the two shells rotate with different angular velocities, one cannot distinguish (even with electromagnetic fields reaching beyond the mass shell) whether the charged shell is rotating or the mass shell is rotating in the opposite direction. Therefore, in a certain cosmological model of our universe, the electromagnetic field within a rotating charged shell vanishes when the latter rotates with the same angular velocity as the bulk of the matter in the universe. (auth)

41610 SEPARATION OF THE RELATIVISTIC PERIHELION PRECESSION FROM THE PRECESSION DUE TO THE GRAVITATIONAL QUADRUPOLE MOMENT. Goldberg, I. (Clarkson Coll. of Technology, Potsdam, N. Y.). Phys. Rev., 149: 1010-12(Sept. 30, 1966).

The gravitational quadrupole moment is considered insofar as its effect on the perihelion precession of Mercury and pericenter precession of satellites is concerned. It is found possible to separate the quadrupole precession from

the precession due to the general theory of relativity. As a corollary, it is found that an exchange of angular momentum between planet and sun takes place due to the quadrupole moment. This exchange may help to explain the phenomenon of sunspots and solar flares. (auth)

41611 ARROW OF TIME IN HOMOGENEOUS COSMOLOGICAL MODELS. Banerji, S. (Univ. of Burdwan, India). Proc. Phys. Soc. (London), 89: 393-9(1966).

Hogarth, Sciama and Hoyle and Narlikar applied the Wheeler–Feynman absorber theory of radiation to the Einstein–de Sitter universe and to the steady-state universe and have shown that, while the advanced solution is consistent in the former, the retarded solution is consistent in the latter. Both these models have the spatial curvature k = 0. It is shown that the retarded solutions remain inconsistent even if we introduce spatial curvature in homogeneous cosmological models in relativistic cosmology (with the cosmological constant $\Lambda = 0$). They are, however, the only consistent solutions for homogeneous models with spatial curvature in Hoyle's cosmology. (auth)

41612 APPLICABILITY OF A DUST-LIKE MODEL TO A COLLAPSING OR ANTI-COLLAPSING STAR AT HIGH TEMPERATURE. Nariai, Hidekazu; Tomita, Kenji (Hiroshima Univ.). Progr. Theoret. Phys. (Kyoto), 35: 777-85(May 1966).

The applicability of the concept of a model-star with uniform density and negligible pressure to the problem of gravitational collapse or anti-collapse is critically examined by comparing the radiation density with the matter density taking into account the energy loss due to the process $e^+ + e^- \rightarrow \nu + \bar{\nu}$. The neutrino surface intensity and the neutrino energy to be lost during some characteristic time interval are also calculated on the assumption that the neutrino production is going on uniformly throughout the stellar interior. It is shown that the model is applicable to a star with $M \lesssim 10^6 M_\odot$ before or after some characteristic stage according as the star is collapsing or anti-collapsing. (auth)

41613 BEHAVIOR OF THE CENTRAL REGION OF A COLLAPSING STAR WITH SPHERICAL SYMMETRY AND PRESSURE GRADIENT. Nariai, Hidekazu (Hiroshima Univ.). Progr. Theoret. Phys. (Kyoto), 35: 786-97(May 1966).

The behavior of the central region of a collapsing star with spherical symmetry and a finite pressure gradient is studied from the standpoint of boundary conditions at the center r = 0. In the case of adiabatic collapse, Einstein's equations supplemented by an equation of state are reduced to four independent equations for five unknown functions of the time variable t only. This arbitrariness is analogous to that in the selection of initial Cauchy data at t = 0 in the Misner-Sharp approach and it permits the construction of a variety of models for the central region regular at all times. The case of nonadiabatic collapse is also mentioned by introducing a suitable parameter whose reciprocal stands for the time-scale of the energy flow near r = 0. (auth)

41614 GAMMA-SPECTROMETRIC DETERMINATION OF SPECIAL REACTION PRODUCTS OF COSMIC RADIATION IN METEORITES. Woelfle, R.; Herpers, U. (Univ., Cologne. Kernforschungsanlage, Juelich, Ger.). Raumfahrtforschung, 10: 110-13(July-Sept. 1966). (In German).

Numerous stable and unstable nuclides extremely small in quantity (about 10^{-10} g/g) are formed in meteorites by cosmic-ray bombardment while traversing space. With regard to the exact analytical determination of these "spallation" products both neutron activation and γ-spectrometry which also allows nondestructive analyses recently became increasingly important. On the basis of their γ,γ-coincidences the ^{26}Al-contents of a number of stone and iron meteorites were measured. Furthermore the spallation nucleus ^{53}Mn was determined by neutron capture as ^{54}Mn. Disturbing reactions were allowed. From ^{36}Cl/^{36}Ar proportions information about "radiation ages" of the analyzed iron meteorites may be gained. (auth)

41615 WAVE-PARTICLE INTERACTIONS IN THE SOLAR WIND. Scarf, Frederick L. (TRW Systems, Redondo Beach, Calif.). Raumfahrtforschung, 10: 114-22 (July-Sept. 1966).

Recent fluid dynamic calculations which include thermal conduction, viscosity and the rotating magnetic field of the sun appear to explain the transition from a nearly static corona to the supersonic solar wind; however the conventional fluid equations are not valid when the mean free paths become large. In interplanetary space the solar wind represents a collisionless magnetized plasma, and various plasma instabilities become significant as wave-particle interactions replace particle-particle scattering. The extent to which the interplanetary plasma can be considered a fluid is assessed using recent experimental data, the possible forms of local acceleration processes are discussed, and some classes of experiments which might help to understand these phenomena are described. (auth)

41616 MAGNETIC FIELDS OF THE SUN AND STARS. Severnyi, A. B. Usp. Fiz. Nauk, 88: 3-50(Jan. 1966). (In Russian).

Although much research has been devoted to the problem of the existence of magnetic fields on the sun and stars, the nature of solar and stellar magnetic fields has not been thoroughly investigated. Many hypotheses have been developed, but none of them can explain these phenomena in detail. The stellar magnetic field must be stable because of high temperatures and good plasma conductivity. Observations prove a variable stellar field with a sudden change in stellar plasma. Stellar magnetic fields of the intensity of 34 kgs have been found. Methods of measurements and observations of the solar field are discussed in detail. (ATD)

41617 STELLAR WINDS AND THE DISTRIBUTION OF ELECTROSTATIC POTENTIALS ABOUT STARS. Lam, S. H. (Princeton Univ., N. J.); Sandri, G. 8p. (CONF-660411–36). ORAU. Gmelin, AED-CONF-66-060-75.

From American Physical Society Meeting, Washington, D. C.

A number of important features arise when the individual components of the solar wind are treated in their own right. In the absence of an electrostatic field, electrons from the ionized stellar atmosphere will escape with a much higher rate than the more massive ions. In the quasi-steady-state situation, the star must acquire a positive electrostatic potential so that the net escape rates of the positive and negative charges are the same. A calculation is presented of the electrostatic potential distribution about the star by a detailed analysis of the dynamics of the stellar wind. (W.D.M.)

41618 SOME PROBLEMS OF RADIATIVE TRANSFER IN AN ATMOSPHERE HAVING A STELLAR WIND. Delache, Philippe (Observatoire de Paris, Meudon, France). 8p. (CONF-660217–3). ORAU. Gmelin, AED-CONF-66-013-7.

From Symposium on Interdisciplinary Aspects of Radiative Energy Transfer, Philadelphia.

Some physical phenomena are described which take place in the transition region between the chromosphere and the corona in the presence of a stellar wind. The effects of these phenomena on interpreting coronal emissions is considered. Velocities in the temperature gradient region and departure of the stationary state from chemical equilibrium are discussed. (W.D.M.)

Atomic Physics

Refer also to abstracts 41250, 41809, and 42445.

41619 (CEA-R–3042) TABLES OF RANGE AND STOPPING POWER OF CHEMICAL ELEMENTS FOR CHARGED PARTICLES OF ENERGY 0,5 TO 500 Mev. Williamson, Claude Francis; Boujot, Jean-Paul; Picard, Jean (Commissariat a l'Energie Atomique, Saclay (France). Centre d'Etudes Nucleaires). 1966. 370p. Dep. mn.

The range, energy loss, and differential of rate of energy loss were tabulated for 37 target materials for all hydrogen and helium ions. The incident energy range covered is from 0.1 to 500 Mev. (auth)

41620 (NIJS-R-471) MASSENSPEKTROMETRISCHE UNTERSUCHUNGEN UEBER DEN ISOTOPIEEFFEKT BEI DER SEKUNDAERELEKTRONENAUSLOESUNG AN METAL LOBERFLAECHEN DURCH POSITIVE IONEN. (Mass Spectrometric Study on the Isotope Effect in Secondary Electron Emission from Metal Surfaces by Positive Ions). Debevec, L.; Heldt, E.; Krebs, K. H.; Marsel, J. (Nuklearni Institut Jozef Stefan, Ljubljana (Yugoslavia)). Dec. 1965. 6p. (CONF-650836-3). Dep. mn.

From 7th International Conference on Phenomena in Ionized Gases, Beograd, Yugoslavia.

From earliest studies it is well known that the secondary electron factor $\overline{\gamma}$($\overline{\gamma}$ = the mean number of secondary electrons per ion) has a dependence on the isotope mass of the ion emitted by the metal surface. In contrast to earlier measurements which treated only the secondary electron emission by two isotope ions of an element, measurements were made with elements which have more than two stable isotopes. The isotope ions of the elements Sr, Sm, Ba, W, Cr, Ne, Kr, Xe, and Hg with an energy of 5 kev were reflected on a CuBe surface in vacuum at 10^{-6} torr and the isotope ions of Ne, Ar, Kr, Xe, and Hg with energies from 12 to 25 kev were reflected on a Ni surface in vacuum of 10^{-7} torr. The $\overline{\gamma}$ values were measured. The results of all measurements were clear and show a nonlinear dependence on the isotope mass. The results were discussed and the possibilities of error in connection with the ion detection with a photomultiplier tube were considered. (tr-auth)

41621 (ORNL-TM-1565) LOW ENERGY ELECTRON STUDIES IN INDIUM AND MAGNESIUM. Pray, H. L.; Birkhoff, R. D.; Nakai, M. Y.; Ritchie, R. H. (Oak Ridge National Lab., Tenn.). Sept. 1966. Contract W-7405-eng-26. 67p. Dep. mn. CFSTI $3.00 cy, $0.75 mn.

Thesis. Submitted to Univ. of Tennessee, Knoxville.

Low energy electron transmission of thin films of magnesium and indium was investigated. For magnesium, as the electron energy was increased, direct observations were made for interactions of the electron beam with the surface plasma, volume plasma, conduction electrons, and the L_I and L_{II} electron shells. The L_I and L_{II} ionization potentials were measured as 49.5 ev and 76.7 ev, respectively. The stopping power for magnesium was measured as 2.49 ev/Å at 1460 ev, 2.54 ev/Å at 1775 ev, 2.5 ev/Å at 1870 ev, and 2.38 ev/Å at 1930 ev. For indium, direct observations were made for interactions with the surface plasma, volume plasma, conduction electrons with N_I electron shell. The ionization potential for the N_I shell was measured as 130 ev. (M.O.W.)

41622 (SC-DC-66-1564) RANGE AND TOTAL IONIZATION OF LOW-ENERGY RECOIL IONS FROM α DISINTEGRATIONS IN PURE AND BINARY GASES. Cano, G. L. (Sandia Corp., Albuquerque, N. Mex.). July 1966. Contract AT(29-1)-789. 10p. (CONF-660811-1). Dep. mn. CFSTI $1.00 cy, $0.50 mn.

From American Physical Society Meeting, Mexico City, N. Mex.

Energy and range loss measurements were made for the $^{210}Po(\alpha)^{206}Pb$ reaction in argon gas. The 5.3-Mev α particles were used primarily for calibration purposes. The ^{206}Pb recoil particle nascent velocity was $V = 0.142\ V_0$. The kinetic energy in the center-of-mass system between the ^{206}Pb particle and Ar gas atoms initially was 16.8 kev. The range and average energy loss per ion pair produced by the slow, heavy Pb recoil particle was determined as a function of the gas. Results are presented for Ar, Ar + C_2H_4, C_2H_4, N_2, and N_2 + C_2H_4. (M.O.W.)

41623 (UCRL-14904) FINITE TEMPERATURE THERMODYNAMICS FOR THE MODIFIED HARTREE-FOCK ELECTRON GAS. Stuart, Richard N.; Schwartz, Judah L. (Lawrence Radiation Lab., Univ. of California, Livermore). Sept. 1, 1966. Contract W-7405-eng-48. 87p. CFSTI $3.00 cy.

The density, screening length, and energy of the modified Hartree-Fock electron gas were calculated self-consistently for a wide range of temperatures and chemical potentials. Selected results are presented. (auth)

41624 (UCRL-17034) APPROXIMATIONS IN THE THEORY OF REARRANGEMENT COLLISIONS AND APPLICATIONS TO A TRACTABLE MODEL OF CHARGE EXCHANGE SCATTERING. Quong, James (Lawrence Radiation Lab., Univ. of California, Berkeley). Aug. 19, 1966. Contract W-7405-eng-48. 79p. Dep. mn. CFSTI $3.00 cy, $0.75 mn.

Thesis.

The approximation ideas and methods and the historic difficulties involved with the calculation of ion-atom rearrangement scattering are examined and redeveloped. Five approximation schemes are selected to be tested. The transition probability for symmetric resonant charge exchange is calculated by these methods for a model one-dimensional scattering system whose exact solution, serving as the basis for comparison, is also attainable by numerical techniques. The impact parameter ideas concerning the uncoupling of the internal and external dynamics are built into the model. None of the high energy theories are found to be adequate beyond the upper intermediate range; this suggests at least that the convergence of perturbation expansion is slow. The two improved first-order schemes, for which the effects of nonorthogonality have been eliminated, are adequate only at upper intermediate energies. The Born approximation always gives results too high. An exchange mechanism is found to be operative for all energies up through the intermediate range. The two two-component coupled-channel schemes, one employing atomic form factors, the other molecular form factors, together covers accurately this span of the spectrum. Asymmetric resonant and nonresonant exchange are examined briefly at low and intermediate energies, to confirm predictions drawn from the previous work. The new results are that asymmetric resonant systems are qualitatively indistinguishable from symmetric resonant systems, and that the exchange mechanism is present also for nonresonant systems and may even be the controlling mechanism over the upper portion of the range of energy mentioned. At decreasing energies, however, the mechanism of the adiabatic approximation, tending to suppress exchange in nonresonant systems, becomes progressively more important and eventually becomes decisive. The formal statement is that the coupled-channel schemes provide an adequate theory for calculating the exchange probability, within the limitation imposed by off-manifold processes, over the low and intermediate ranges of energy for all three types of scattering systems. (auth)

41625 MEASUREMENT OF THE CROSS SECTION OF COHERENT AND INCOHERENT SCATTERING OF 662-kev γ RAYS ON BOUND ELECTRONS. Di Lazzaro, Maria A.; Missioni, Guido (Instituto Superiore di Sanita, Rome). Ann. Ist. Super. Sanit., 1: 1-60(1965). (In Italian).

The differential cross sections for the incoherent scattering of 662-kev gamma rays on the K electrons of U and Zn and on the L electrons of Au and U were measured. Data on the spectral distribution of photons scattered at 75° by K electrons of Au and U and at 26° by K electrons of Au atoms were also obtained. In addition, the cross section for the coherent scattering of 662-kev gamma rays on Au was measured. The experimental results were compared with theoretical predictions. (D.C.W.)

41626 FREE-FREE TRANSITIONS OF ELECTRONS IN GASES. Dalgarno, A.; Lane, N. F. (Queen's Univ., Belfast). Astrophys. J., 145: 623-33(Aug. 1966).

A simple formula is derived for estimating the absorption coefficient for free-free transitions at long wavelengths in gases with temperatures of a few thousand degrees, and tables of the auxiliary functions that enter are presented. The procedure makes use of experimental or theoretical data on elastic scattering cross-sections. Explicit results are given for the gases H, He, N, O, Ne, H_2, N_2 and O_2. (auth)

41627 THE USE OF ALPHA-PARTICLE IRRADIATION IN IONIZATION COEFFICIENT MEASUREMENTS IN GASES. Blair, D. T. A. (Univ. of Strathclyde, Glasgow). Brit. J. Appl. Phys., 17: 1051-60(Aug. 1966).

The determination of ionization coefficients from the measured spatial growth of ionization in a uniform-field discharge gap irradiated by an α-particle source is considered; this provides a more stable initial ionization than does the more usual ultraviolet source. Theoretical expressions are calculated for the gas-amplified current i as a function of gap length d for the case of an electron-attaching gas, with a secondary mechanism producing electron emission at the cathode. Experiments in nitrogen have yielded values of Townsend's first coefficient, at a pressure of about 300 torr, over the range of E/p (where E is electric field strength and p is gas pressure) from 39.7 to 45.7 v cm^{-1} $torr^{-1}$, and the results are in good agreement with those obtained by other authors using ultraviolet irradiation. The experimental (log i, d) plots in nitrogen differ in detail from those predicted by theory. It is suggested that this discrepancy is due to an additional photocurrent initiated at the cathode surface by radiation from molecules excited by α-particle collision, and experiments have given some support to this suggestion. The occurrence of this additional photocurrent would make the method used here unsatisfactory in electron-attaching gases but it is shown that a modification of this method, involving the use of α particles of reduced range, would not have this disadvantage. (auth)

41628 CALCULATED MAGNETIC ELECTRON DRIFT VELOCITIES IN H_2, N_2, O_2, AIR AND C_3H_8 FOR $10 \leq E/p \leq 10^4$ V m^{-1} $torr^{-1}$. Heylen, A. E. D.; Dargan, C. L. (Univ. of Leeds, Eng.). Brit. J. Appl. Phys., 17: 1075-82(Aug. 1966).

The influence of the ratio of magnetic field to gas pressure on the perpendicular and transverse drift velocity of an electron swarm is examined quantitatively for H_2, N_2, O_2, air and C_2H_6 for mean energies from 0.1 to 10 ev. Whereas the perpendicular drift velocity reaches a peak value when the electron collision frequency is approximately equal to the cyclotron frequency, the transverse velocity starts to decline when this equality is reached. In contrast, the ratio of the perpendicular to transverse velocity, which is shown to be an important quantity governing gaseous discharge movement, continues to increase with B/p; the increase is almost linear throughout except for gases exhibiting the Townsend-Ramsauer effect. Expressions are derived for the low and high magnetic field case and values in the intermediate region, which lies in the range $10^{-3} \lesssim B/p \lesssim 10^{-1}$ Wb m^{-2} $torr^{-1}$, are obtained numerically. The mobility values for the different gases at a fixed value of mean energy and B/p differ by up to a factor of 10, and this should allow discharge propagation velocities to be identified with particular movement mechanisms unless obscured by feedback processes. At low magnetic fields the perpendicular drift velocity is derived as a function only of B/p and E/p. If the equivalent pressure concept were used in the derivation of Ampère's law, the magnitude of the force on a conductor in a crossed magnetic field would be higher than hitherto accepted. The relevance and application of the calculated magnetic transport data to practical discharges are mentioned briefly. (auth)

41629 BOUND STATE OF THE POSITRON IN CERTAIN FINELY DIVIDED OXIDES. Paulin, Robert; Ambrosino, Georges (Commissariat a l'Energie Atomique, Gif-sur-Yvette, France). Compt. Rend., Ser. B, 263: 207-9(July 11, 1966). (In French).

Results of some experiments that elucidate the origin and the long lifetime of the positron in certain powders are presented. It is concluded that the long-lived bound state (6 to 7×10^{-8} sec) formed by the positron in some powdered oxides, seems to have a direct relation to the large specific surfaces and to the adsorption properties exhibited by these substances in their multicrystalline powder state. (tr-auth)

41630 ELECTRON CORRELATION IN ATOMS AND MOLECULES. Kapuy, Ede (Theoretical Physics Research Group, Academy of Sciences, Hungary). Fiz. Szemle, 16: 209-11(June 1966). (In Hungarian).

One of the chief functions of atomic and molecular quantum theory is the determination of the energy eigenvalues of stationary states and the derivation of eigenfunctions. The Hartree-Fock model is considered very suitable for computer applications but does not take the electron correlation and the relativistic effects into account. The correlation energy is roughly proportional with the number of electrons but it varies within a given period. The following methods may be used for calculating the correlation energy: the perturbation calculation, in which the Hartree-Fock state is considered as not perturbed and the difference between the potential energies of the particle and the actual interaction as perturbed, allowing to calculate the correlation energy of the high-density homogeneous electron gas; the configuration interaction method, by means of which wave functions are developed, using a linear combination of determinants of one-particle functions. Several other approximation methods are also evaluated. (TTT)

41631 HARTREE-FOCK PARAMETERS FOR THE ATOMS HELIUM TO RADON. Froese, Charlotte (Univ. of British Columbia, Vancouver). J. Chem. Phys., 45: 1417-20(Sept. 1, 1966).

Numerical Hartree-Fock calculations for ground-state or near-ground-state configurations were performed for the neutral atoms helium to radon. Some typical results in the form of tables of atomic parameters are reported for La, Ce, Pr, and Nd. (auth)

41632 ATOM-ATOM IONIZATION MECHANISMS IN ARGON–XENON MIXTURES. Kelly, Arnold J. (California Inst. of Tech., Pasadena). Contract AF 49(638)-1285. J. Chem. Phys., 45: 1733-6(Sept. 1, 1966).

The atom–atom ionization process occurring in high-purity argon–xenon mixtures was investigated by means of a conventional shock tube employing a microwave probe to monitor the electron-generation rate. All tests were conducted at approximately atmospheric pressure and at temperatures in the range from 5000 to 9000°K, corresponding to a neutral-particle density of 7.0×10^{17} cm^{-3}. The cross-sectional slope constant for xenon ionized by collision with an argon atom is 1.8×10^{-20} cm^2 ev± 20%, that is, equal to that for xenon ionized by collision with another xenon atom. The data for the reaction of argon ionizing xenon are consistent with an activation energy of 8.315 ev, that is, of the xenon–xenon, atom–atom ionization process. No data were obtained for xenon ionizing argon. Good correlation was obtained between the cross sections for electron elastic momentum exchange derived from the microwave experiment and those obtained from beam experiments. The argon–xenon ionization cross section implied that, for atom–atom processes in the noble gases at pressures ~1 atm and temperatures ~⅔ ev, the ionization cross section is independent of the electronic structure of the projectile atom. (auth)

41633 GENERALIZED DISCRETE-CONTINUUM RADIAL INTEGRALS WITH COULOMB FUNCTIONS. Bebb, H. Barry (Univ. of Rochester, N. Y.). J. Math. Phys. (N. Y.), 7: 955-9(June 1966).

Simple closed-form computational formulas involving only elementary functions are obtained for the hydrogenic, discrete-continuum matrix elements $\langle k, l' | r^m | n, l \rangle$. The results allow for different effective charge parameters Z and Z′ for the discrete and continuum functions. The central radial integral computed is sufficiently general to allow the evaluation of matrix elements of $r^m \exp(-r/\epsilon)$ between the Coulomb continuum functions and any discrete function formed from $r^k \exp(-r/A)$. Results are also given for the free-particle limit as $Z' \to 0$. (auth)

41634 FORMATION OF EXCITED HYDROGEN ATOMS BY CHARGE EXCHANGE IN GROUND STATE ATOMS. Hiskes, J. R. (Univ. of California, Livermore). Contract

W-7405-eng-48. J. Nucl. Energy: Pt. C, 8: 577-8(Sept.-Oct. 1966). (UCRL-14678).

Calculations were performed to determine the population distributions of excited hydrogen atoms produced by charge exchange in several ground-state atoms. The population ratios are presented for the $2s^22p^r$ sequence: B, C, O, Ne; and for the ns^2 sequence: He, Be, Mg, Ca, Sr, and Ba. The calculational model used employs the Brinkman-Kramer post interaction and assumes that all electrons in the target, or neutralizer, contribute independently; the total cross section for capture into a particular level is taken as the sum of capture cross sections due to the individual target electrons. (W.D.M.)

41635 THERMODYNAMIC PROPERTIES OF BLOCH ELECTRONS IN A MAGNETIC FIELD. Glasser, M. Lawrence (Battelle Memorial Inst., Columbus, Ohio). J. Phys. Chem. Solids, 27: 1459-67(Sept. 1966).

The free energy and zero field magnetic susceptibility for electrons in a potential, periodic along the uniform magnetic field, were obtained. The de Haas–van Alphen effect is discussed for a simple band structure and is shown to be consistent with the semiclassical theory. The magnetic susceptibility is proportional to the density of states as the free electrons. The relevance of the model to experiment is discussed briefly. (auth)

41636 EXTENSION OF THE PERIODIC TABLE. Smith, S. Nature, 211: 1085-6(Sept. 3, 1966).

In earlier investigations on the behavior of orbital objects around a nucleus, in which the properties of various simple theoretical models were studied to determine under what conditions the exchange of radiation and/or particles obeying the inverse square law could account for other interaction laws, the following series was found: $n_1/1^2 + n_2/2^2 + n_3/3^2 + \ldots = 2k$ (k = 1, 2, 3, etc.). This equation is used to predict electronic structures of the elements $Z \leq 118$. (M.O.W.)

41637 MOESSBAUER RECOILLESS FRACTION IN TIN COMPOUNDS. Stoeckler, H. A.; Sano, H. (Rutgers State Univ., New Brunswick, N. J.). Nucl. Instrum. Methods, 44: 103-8(Sept. 1966).

The error analysis for the determination of the recoilless fractions, *f*, in tin made by Hohenemser was extended to include the effect of vibrations due to the bubbling of low temperature coolants. These vibrations cause a decrease in the effect magnitude and broadening of the linewidth. It is shown that this error is minimized when the area under the resonance curve is considered. The minimum thickness of palladium necessary to attenuate the Sn x-rays was revaluated and is found to be 4.0 mil for a $Mg_2{}^{119m}Sn$ source and 3.0 mil for a $Pd^{119m}Sn$ source. Internal attenuation of Sn x-rays was found to occur in the $Pd^{119m}Sn$ source. The only Mössbauer sources found acceptable for *f* measurements of tin compounds are $Mg_2{}^{119m}Sn$ and $Pd^{119m}Sn$. Disadvantages of other sources are discussed. (auth)

41638 SIMPLE FORMULA FOR THE TRANSMISSION AND ABSORPTION OF MONOENERGETIC ELECTRONS. Subba Rao, B. N. (Tata Inst. of Fundamental Research, Bombay). Nucl. Instrum. Methods, 44: 155-6(Sept. 1966).

A simple formula is described, which is of the Fermi-function type and which gives good-fit to many of the available transmission and absorption curves for monoenergetic electrons. (M.O.W.)

41639 HYPERFINE AND ISOTOPE STRUCTURE IN THE PLUTONIUM SPECTRUM AND ITS CLASSIFICATION. Korostyleva, L. A.; Striganov, A. R. Opt. Spectros. (USSR) (Engl. Transl.), 20: 309-12(Apr. 1966).

Translated from Opt. Spektros., 20: 545-53(Apr. 1966).

A supplementary analysis of hyperfine and isotope structure in the plutonium spectrum was carried out. As a result, new data on the classification of the plutonium spectrum were obtained. (auth)

41640 RAMAN ANALOG OF ELECTRONIC AND NUCLEAR SPIN INDUCTION AND ECHO. Shubina, R. V. Opt. Spectros. (USSR) (Engl. Transl.), 20: 369-72(Apr. 1966).

Translated from Opt. Spektros., 20: 661-8(Apr. 1966).

The Schroedinger equation was solved for a system of particles with a discrete energy spectrum exposed to the simultaneous action of two pulse generators. It is seen from the solutions obtained that a pulse excitation of a system of particles through many-quantum transitions allows one to examine a large variety of nonequilibrium states of a system with a discrete spectrum which were not investigated until the present. It is shown that the system can radiate electromagnetic and sound signals, acting as the Raman analogs of spin and sound echo and of free induction. (auth)

41641 RESONANCE PHENOMENA IN THE ELASTIC SCATTERING OF ELECTRONS BY HELIUM ATOMS. II. Zhikhareva, T. V. Opt. Spectros. (USSR) (Engl. Transl.), 20: 402-4(Apr. 1966).

Translated from Opt. Spektros., 20: 724-7(Apr. 1966).

The behavior of the cross section of the elastic scattering of electrons by helium atoms near the threshold is discussed assuming coupling of the $1^1S-2^3S-2^1S$ states of the helium atom. This makes it possible to explain the second resonance observed previously below the threshold of excitation of the 2^3S level of He which is due to the formation of the metastable $1s2s2p^2P$ state of He^-. (M.H.R.)

41642 CONVERGENCE BEHAVIOR OF THE BORN SERIES FOR REARRANGEMENT COLLISIONS. Dettmann, K.; Leibfried, G. (Technische Hochschule, Aachen. Kernforschungsanlage Juelich, Ger.). Phys. Rev., 148: 1271-3(Aug. 26, 1966).

It is shown that the commonly used arguments to prove the divergence of the Born series for rearrangement collisions at all energies do not hold. As counterexample, a one-dimensional three-body collision with δ-function interactions is treated in detail. (auth)

41643 GENERATORS OF O(4,1) FOR THE QUANTUM-MECHANICAL HYDROGEN ATOM. Musto, R. (Syracuse Univ., New York). Phys. Rev., 148: 1274-5(Aug. 26, 1966). (NYO-3399-50).

It is well known that the noncompact group O(4,1) is an imbedding group for the symmetry group O(4) of the hydrogen atom. The expressions for the generators of O(4,1) in terms of the dynamical variables r and p have been calculated by Bacry in the classical case. These generators in the quantum-mechanical case also were calculated. The classical expressions of Bacry are obtained in the limit $\hbar \to 0$.

41644 GENERATORS OF THE DE SITTER GROUP FOR THE HYDROGEN ATOM. Pratt, R. H.; Jordan, R. F. (Univ. of Pittsburgh). Phys. Rev., 148: 1276-9 (Aug. 26, 1966).

Explicit Hermitian operator functions of q and p are constructed for the generators of the de Sitter group O(4,1) on the bound-state wave functions for the hydrogen atom. This is done for each of the one-parameter family of irreducible representations of O(4,1) in which the irreducible representations of the four-dimensional rotation group O(4) correspond to the degeneracy subspaces of the bound-state energy levels. The commutation relations and the values of the invariants which label the representation of O(4,1) are verified by direct operator calculations. (auth)

41645 EXCITATION OF HYDROGEN MOLECULES BY ELECTRON IMPACT. Khare, S. P. (Goddard Space Flight Center, Greenbelt, Md.). Phys. Rev., 149: 33-7(Sept. 9, 1966).

Using one-center wave functions of Huzinaga for the hydrogen molecule together with the Born and Ochkur approximations, the excitation of the molecule from the ground state to the B and C electronic states by electron impact was investigated. The shape of the curves for the differential cross section and for the oscillator strength is in accord with the experimental results of Geiger. The effect of exchange is to reduce the scattering cross sections. (auth)

41646 CHARGE EXCHANGE AND DISSOCIATION CROSS SECTIONS FOR H_1^+, H_2^+, AND H_3^+ IONS OF 2- TO 50-kev ENERGY INCIDENT UPON HYDROGEN AND THE INERT GASES. Williams, J. F.; Dunbar, D. N. F. (Australian National Univ., Canberra). Phys. Rev., 149: 62-9(Sept. 9, 1966).

Within the energy range 2 to 50 kev, the cross sections for the single-electron capture by protons, for dissociation of H_2^+ ions into H_1^+ and H_1^- ions, and for dissociation of H_3^+ ions into H_2^+, H_1^+, and H_1^- ions, have been measured in hydrogen, nitrogen, and inert-gas targets. The dissociation cross sections were found to decrease by as much as 30% for changes in the operating conditions of the electrodeless discharge-type ion source. The dissociation cross sections were independent of changes in the oscillator frequency, the rf input power, and the d-c ion extraction voltage. Changes in both the source gas pressure and transverse magnetic field cause variations in the mean energy and the energy spread of the positive ions extracted from the source; these variations have been related to the population of the vibrationally excited states of the primary molecular ions. The measured cross-section values are accurate relative to one another within 5%. It is shown that the measurements are not invalidated by effects such as competing capture and loss processes outside the collision cell, beam size, and dissociation-product scattering. (auth)

41647 SOME HEAVY-ION STOPPING POWERS. Moak, C. D.; Brown, M. D. (Oak Ridge National Lab., Tenn.). Contract W-7405-eng-26. Phys. Rev., 149: 244-5(Sept. 9, 1966). (ORNL-P-2121).

Multicomponent Br and I beams from the Oak Ridge Tandem Accelerator have been used to measure the stopping powers of Be, C, Al, Ni, Ag, and Au over the energy range 10 to 100 Mev. (auth)

41648 NUCLEAR QUADRUPOLE RESONANCE BY NUCLEAR INDUCTION: THEORY AND EXPERIMENT; WITH AN EXTENSION OF THE THEORY TO ABSORPTION METHODS. Smith, George W. (General Motors Corp., Warren, Michigan). Phys. Rev., 149: 346-67 (Sept. 9, 1966).

A theory is presented for nuclear quadrupole resonance (NQR) by means of nuclear induction and is extended to absorption methods. Based on the Bloch-type equations of Bloom, Robinson, and Volkoff, the theory is derived for the case $I = 1$, $\eta = 0$. For the induction method to work, a small magnetic field must remove the degeneracy of the $m_= \pm 1$ levels; in practice this is done by an audio-frequency modulation field. Phase-sensitive detection methods are then used to minimize noise. The theory predicts the effect of modulation field, static magnetic field, and r-f field on the slow-passage induction signal. Theory and experiment agree that magnetic fields (modulating or static) broaden the line, but for low enough fields, the true NQR derivative line is observed. Sufficiently large static fields introduce complex structure into the line shape. The effect of r-f is given by a modified form of the Bloembergen-Purcell-Pound saturation curves. Experiments on polycrystal hexamethylenetetramine yield good agreement with all aspects of the theory. The extension of the theory to single-coil (absorption) NQR methods predicts that sinusoidal magnetic modulation and phase-sensitive detection will produce zero signal in a single-coil experiment. In addition it yields the proper line shapes for Zeeman modulation and and frequency modulation methods and predicts the effects of modulation amplitude and magnetic fields in both cases. A brief qualitative discussion of cases other than $I = 1$, $\eta = 0$ indicates that the induction method can be used for half-integral spins with any η, but that it is applicable to integral spins only when η is small. In other words the induction method can be used for any case to which the Zeeman-modulated absorption method is applicable. (auth)

41649 DOUBLE POLES AND NONEXPONENTIAL DECAYS IN ATOMIC PHYSICS. Lassila, K. E. (Stanford Univ., Calif. Iowa State Univ., Ames); Ruuskanen, Vesa. Phys. Rev. Lett., 17: 490-2(Aug. 29, 1966).

Atomic resonance fluorescence is examined as a scattering problem, and Goldberger-Watson double poles are found to occur in situations producible in the laboratory. Systematic study of this effect and associated nonexponential decay thus appears possible. (auth)

41650 SPIN EXCHANGE BETWEEN THE SINGLY IONIZED Xe^+ GROUND STATE AND THE METASTABLE STATE OF NEUTRAL XENON. Hadeishi, Tetsuo; Liu, Chung-Heng (Univ. of California, Berkeley). Phys. Rev. Lett., 17: 513-15(Sept. 5, 1966).

Spin-exchange collisions were observed between the singly ionized $^2P_{\frac{1}{2}}$ ground state of Xe and the $^3P_2$ metastable state of neutral Xe, both formed and aligned by electronic-impact excitation under space-charge neutralization. Extension to the r-f spectroscopy of the ionized ground state of other noble-gas atoms seems promising. (auth)

41651 LOCALIZED VIBRATIONS OF TRAPPED MOLECULES. Downes, J. S. (Oxford Univ.); White, J. W.; Egelstaff, P. A.; Rainey, V. Phys. Rev. Lett., 17: 533-6(Sept. 5, 1966).

The spectrum of motions of molecules trapped in molecular cages has been previously studied in detail by neutron inelastic- and elastic-scattering methods. Experiments on methane, methyl cyanide, and methanol trapped in fully deuterated β-quinol clathrates, and on methyl cyanide, methanol, water, and ammonia in molecular sieves are described. The apparatus used has been previously described. A selection of results is presented. (W.D.M.)

41652 ELECTRON COLLISIONS IN NITROGEN. Daly, N. R.; Powell, R. E. (Atomic Weapons Research Establishment, Aldermaston, Eng.). Proc. Phys. Soc. (London), 89: 273-80(1966).

A mass spectrometer has been used to study electron collisions in nitrogen. The cross section for the ionization of N_2 to form N_2^{2+} by electron impact has been measured up to 240 ev. By a comparison with the results of Peterson the dissociative ionization cross section of N_2 has also been measured. N^{3+} formed from N_2 has been observed and its appearance potential determined. The method developed by Baker and Hasted to study electron–ion collisions has been used to look at the following processes: $N^+ + e \rightarrow N^{2+} + 2e$; $N_2^+ + e \rightarrow N_2^{2+} + 2e$; $N_2^{2+} + e \rightarrow N^{2+} + N + e$. Reaction (3) appears to have a very large cross section. (auth)

41653 ELECTRON IONIZATION OF He^+ AND THE DESTRUCTION OF He^{2+} BY CHARGE TRANSFER PROCESSES IN A SPACE-CHARGE TRAP. Daly, N. R.; Powell, R. E. (Atomic Weapons Research Establishment, Aldermaston, Eng.). Proc. Phys. Soc. (London), 89: 281-7(1966).

The method developed by Baker and Hasted to study electron–ion collision was applied to the electron-helium ion collision. Helium ions were trapped in the space charge of a magnetically confined electron beam and the reactions taking place were studied using a mass spectrometer. The ionization of He^+ was clearly demonstrated. The destruction of He^{2+} ions in the trap, probably by radiative charge transfer, $He^{2+} + He \rightarrow He^+ + He^+ + h\nu$ was also shown to take place. (auth)

41654 IMPACT PARAMETER TREATMENT OF THE EXCITATION OF ATOMS BY CHARGED PARTICLES. Stauffer, A. D. (London Univ.); McDowell, M. R. C. Proc. Phys. Soc. (London), 89: 289-98(1966).

The work of Seaton and Stauffer and McDowell is generalized to any non-exchange atomic transition (excluding s–s transitions), the contributions from all multipoles in the expansion of the interaction potential being included. Numerical results are presented for a few selected transitions. (auth)

41655 ELECTRON-IMPACT-INDUCED $n \rightarrow n'$ TRANSITIONS IN H ATOMS. Pluta, K. M.; McDowell, M. R. C. (Univ. of Durham, Eng.). Proc. Phys. Soc. (London), 89: 299-304(1966).

A semiclassical impact parameter treatment with a cutoff is used to estimate the cross sections for electron-impact-induced transitions between sets of levels of principal quantum numbers n and n' ($n' > n$) in atomic hydrogen.

The results are in closer accord at moderate and low energies with classical calculations based on Stabler's model than with those of Kingston, and agree closely with the Born approximation values at high energies, provided $n' - n \leq 2$. (auth)

41656 ELECTRON RESONANCES OF THE H_2^- ION. Bardsley, J. N.; Herzenberg, A.; Mandl, F. (Univ. of Manchester, Eng.). Proc. Phys. Soc. (London), 89: 305-19(1966).

The calculation of resonances according to the definitions of Siegert and of Kapur and Peierls is illustrated for s waves of a single particle in a potential well. A variational principle incorporating outgoing-wave boundary conditions is used. It picks out a resonance from the continuum of unbound states and yields simultaneously both the resonance energy and the decay width. The variational principle is applied to calculate the two simplest $^2\Sigma^+$ electron resonances of the H_2^- ion, both of which go over into H + H^- for large separations of the nuclei. For small separations they have the electronic configurations $(1s\sigma_g)^2(2p\sigma_u)\ ^2\Sigma_u^+$ and $(1s\sigma_g)(2p\sigma_u)^2\ ^2\Sigma_g^+$. (auth)

41657 VIBRATIONAL EXCITATION AND DISSOCIATIVE ATTACHMENT IN THE SCATTERING OF ELECTRONS BY HYDROGEN MOLECULES. Bardsley, J. N.; Herzenberg, A.; Mandl, F. (Univ. of Manchester, Eng.). Proc. Phys. Soc. (London), 89: 321-40(1966).

The processes of vibrational excitation and dissociative attachment in the bombardment of hydrogen molecules by electrons of energies up to about 12 ev are discussed. The assumption is made that only the two simplest electron resonances in H_2^- need be taken into account. The lower of these resonances, $(1s\sigma_g)^2(2p\sigma_u)\ ^2\Sigma_u^+$, gives rise to a broad peak, extending from 2 to 6 ev, in the cross section for the excitation of the two lowest excited vibrational states in H_2. The upper resonance, $(1s\sigma_g)(2p\sigma_u)^2\ ^2\Sigma_g^+$, leads mainly to dissociative attachment, with a prominent peak in the cross section extending from about 8 to about 12 ev. The calculated cross sections are in good qualitative and semi-quantitative agreement with experiment. In particular, the shapes and ratios of the peaks in the vibrational cross sections and the shape and isotope effect in the dissociative attachment cross sections around 10 ev are accounted for. (auth)

41658 LOWER BOUND TO THE RECIPROCAL OF THE SCATTERING LENGTH. [PART] II. Houston, S. K.; Moiseiwitsch, B. L. (Queen's Univ., Belfast). Proc. Phys. Soc. (London), 89: 341-51(1966).

It is shown that, for the scattering of zero-energy particles by a compound system, Kohn's variational method used in conjunction with inappropriately normalized trial functions provides an absolute lower bound to the reciprocal of the scattering length in the following cases: (i) there exists no composite bound state and the Born approximation to the scattering length $a_B < 0$; (ii) there exists one composite bound state, $a_B < 0$ and the exact scattering length $a \geq 0$; (iii) there exists no composite bound state and $a \geq 0$. The theorems are illustrated by the calculations of the scattering lengths for collisions of electrons and positrons and hydrogen atoms and helium atoms (auth)

41659 EFFECT OF VIBRATIONAL-ROTATIONAL MOTION ON THE ELECTRIC AND MAGNETIC PROPERTIES OF DIATOMIC MOLECULES. Jain, D. C.; Sahni, R. C. (New York Univ., New York). Proc. Phys. Soc. (London), 89: 409-13(1966).

The vibrational wave functions appropriate to the Rydberg–Klein–Rees (RKR) potential energy curves and corrected for rotational motion were employed for calculating the magnetic susceptibility and the rotational magnetic moment of H_2, HD and D_2. The results were compared with the experimental data as well as with those reported by others. (auth)

41660 FORBIDDEN TRANSITION $L_{II}N_{II}$ IN THE SPECTRUM OF PLATINUM. Gokhale, B. G.; Nigam, A. N. (Univ. of Locknow, India). Proc. Phys. Soc. (London), 89: 475-6(1966).

The presence of the line corresponding to the forbidden transition $L_{II}N_{II}$ in the spectrum of platinum was established using a 40 cm curved mica crystal spectrograph of the transmission type. The reported value of the wavelength of this line (λ = 977.2 x.u.) agrees more closely with the value calculated from the energy levels than does the one (980.5 x.u.) reported by Cauchois. A possible reason for the discrepancy is given. (auth)

41661 RECENT EXPERIMENTS ON MUONIUM. Hughes, V. W.; Amato, J.; Mobley, R.; Rothberg, J.; Thompson, P. (Yale Univ., New Haven). pp 377-409 of Proceedings of the Williamsburg Conference on Intermediate Energy Physics. Vol. I. Williamsburg, Va., College of William and Mary, 1966.

The hyperfine structure of muonium, which was determined by observing an induced transition in weak magnetic fields, is discussed. Also considered is the interaction of muonium with atoms and molecules. (J.F.P.)

41662 MEASUREMENT OF THE ASYMMETRY OF BREMSSTRAHLUNG FROM TRANSVERSALLY POLARIZED ELECTRONS. Guenthner, K. Erlangen-Nuernberg, Ger., Univ., 1964. 27p. $2.00 Gmelin, AED-Diss. 64-1096. Thesis.

The asymmetry function of external bremsstrahlung from 300-kev electrons was determined. Results are not in agreement with calculations using Born's approximation but have the opposite sign. (Gmelin Inst.)

41663 VIBRATIONAL DISSOCIATION AND DISSOCIATION IN CASCADE OF H_2^+ IONS BY COLLISIONS WITH MOLECULES OF A GAS. Valckx, F. P. G.; Verveer, P. (EURATOM-CEA, Fontenay-aux-Roses, France). 19p. (In French). (CONF-650833–1). ORAU. Gmelin, AED-CONF-65-315-46.

From Fourth International Conference on the Physics of Electronic and Atomic Collisions, Quebec.

Protons produced by collisional dissociation of H_2^+ ions have an energy spectrum with a narrow central peak. The protons in this peak are produced by vibrational dissociation and by a cascade of two collisions. For H_2^+ ions of 50 to 150 kev the cross section for vibrational dissociation is about 4.1×10^{-19} cm^2/mol. in hydrogen and 1.1×10^{-18} cm^2/mol. in argon. (auth)

41664 EFFECTIVE MASS OF POSITIVE AND NEGATIVE IONS IN LIQUID HELIUM. Dahm, A. J. 7p. (CONF-651015-26). ORAU. Gmelin, AED-CONF-65-312-61.

From American Physical Society Meeting, Chicago.

Measurements were made on ions taken from alpha tracks with a ^{210}Po source submerged in liquid helium. A measurement of the mobility yields the ratio of the current relaxation time to the effective mass. The current relaxation time was measured and the effective mass determined. (W.D.M.)

41665 ANALYSIS OF π^--MESONIC ATOMS. Seki, Ryoichi; Cromer, Alan H. (Northeastern Univ., Boston). 18p. (CONF-660411-41). ORAU. Gmelin, AED-CONF-66-060-112.

From American Physical Society Meeting , Washington, D. C.

A phenomenological analysis of the π^--mesonic atom in light nuclei was made by use of a new approximation technique on the exterior wave function outside of the region of strong interaction. This approximation is a functional expansion of the Whittaker function in terms of the energy level shift ratio $\Delta E_{1S}/E_{1S}$. Using the Stearns' data it is found that the S-state potential has no obvious isotopic spin dependence. The exact scattering lengths calculated from these potentials come out to be independent of the atomic number of the nuclei, which is in serious disagreement with the common π^--mesonic atom analyses based on the hypothesis of the additivity of the scattering length. It is found that the volume integral of the potential is shape independent. The probability that the π^--meson is inside the nucleus is reduced by half the value given by Born approximation. (auth)

41666 CONTRIBUTION TO A STUDY OF INELASTIC INTERACTIONS BETWEEN TWO ION BEAMS. Guidini, J.; Manus, C.; Sinda, T.; Watel, G. (CEN de Saclay, Gif-sur-Yvette, France). 7p. (In French). (CONF-650833-2). ORAU. Gmelin, AED-CONF-65-315-18.

From Fourth International Conference on the Physics of Electronic and Atomic Collisions, Quebec.

The cross section for the production of neutral and charged particles during the passage of molecular hydrogen ions H_2^+ across a medium constituted of charged N_2^+ particles was measured. The two reactions expected are $H_2^+ \rightarrow H^0 \ldots \sigma_0$ and $H_2^+ \rightarrow H_1^+ \ldots \sigma_+$, where σ_0 and σ_+ are the corresponding cross sections. The apparatus used is described and causes the right angle intersection of two ion beams. The H_2^+ beam has an intensity of the order 5×10^{-7} amp and energy between 20 and 250 kev. The N_2^+ beam constitutes the ionized target medium and its energy is 2.5 kev. It has a density of 2×10^7 cm^{-3} and a cross section of 4×0.4 cm. The reaction products are detected on scintillation counters. (tr-auth)

Cosmic Radiation

See also Elementary Particles and Radiations
Nuclear Properties and Reactions

Refer also to abstract 41603.

41667 (MIT–2098-251, pp 1-13) COSMIC RAY GROUP. (Massachusetts Inst. of Tech., Cambridge. Lab. for Nuclear Science).

A progress report is presented on the research activities of the cosmic ray group of M.I.T. Topics discussed are x-ray astronomy, high energy gamma-ray astronomy, interplanetary plasma, deuterium detector, Bolivian air shower joint experiment, composition of primary cosmic rays, theoretical studies of cosmic rays as a relativistic gas, infrared astronomy, solar neutrons and gamma rays, time variations of cosmic rays, supernova x rays, and supernova visible light at times close to outburst. (B.G.D.)

41668 STUDY OF ASYMMETRY IN THE LATERAL DISTRIBUTION OF SHOWER PARTICLES NEAR SEA LEVEL. Rao, A. Bhaskara; Gill, P. S. (Indian Inst. of Tech., New Delhi. Central Scientific Instruments Organization, Chandigarh, India). Indian J. Pure Appl. Phys., 4: 287-8(1966).

Experimental observations made at Aligarh (altitude, 205 m.), using two Geiger-Müller counter telescopes, on the azimuthal asymmetry in the distribution of shower particles around the shower axis, indicate an asymmetry of about 6 per cent due to both the electronic and μ-meson components of showers. (auth)

41669 ORIGIN OF COSMIC PARTICLES. Lequeux, J. (Faculte des Sciences, Paris). Onde Elec., 46: 702-6 (June 1966). (In French).

After a brief description of secondary and primary cosmic radiation, a close relationship is shown between sources of cosmic particles and sources of electromagnetic wave in the radio part of the spectrum. Various sources are reviewed, together with the known propagation characteristics obtained from terrestrial sources. From this analysis, the most probable sources of observed primary particles in view of their relatively low energies must be in supernovas and in our own galaxial center. (auth)

41670 COSMIC-RAY MODULATIONS IN THE SOLAR SYSTEM AND IN INTERSTELLAR SPACE. Silberberg, Rein (Naval Research Lab., Washington, D. C.). Phys. Rev., 148: 1247-59(Aug. 26, 1966).

The intensity of cosmic-ray protons between 1959 and 1963 (i.e., near solar maximum and near solar minimum) was modulated twice as much as the intensity of helium at the same velocity, for energies from 0.2 to 0.7 Bev/nucleon. Similar results were obtained by other authors for the modulation between 1963 and 1964 when the intensities of protons and helium nuclei were measured by many investigators. It has been shown by other authors that the ratio of helium nuclei to protons of the same velocity decreases with increasing cosmic-ray energy from about 0.3 to about 0.05 in the energy interval 0.2 to 10 Bev/nucleon. These observations are shown to be in agreement with Dorman's modification of Parker's solar-modulation theory for intermediate values of rigidity, i.e., with a modulation function of the form exp $[-K(t)/R\beta]$, where R and β are the rigidity and velocity of the cosmic-ray particle, respectively, t is time, and K(t) depends on various solar-wind parameters. Additional investigations show that while Dorman's expression fits the data well between rigidities of 1.5 and 15 Bv, it no longer does so at lower rigidities at certain times of the solar cycle. A transition to Parker's modulation function exp $[-K(t)/\beta]$ seems to occur. Also a purely rigidity-dependent modulation function of the form exp $[-K(t)/R]$ fits nearly all of the experimental data. The local interstellar spectra of cosmic-ray protons and helium are investigated, assuming that these spectra are similar in shape between energy values of 1 and 10 Bev/nucleon. Using these results, such parameters of the interplanetary medium as the number of scattering centers along the cosmic-ray path and the radial extent of the cosmic-ray convection and diffusion region are evaluated, and are found to agree with those proposed by Parker. The scale factors of the scattering centers are found to be distributed between 6×10^{10} cm and 10^{12} cm, or more, provided that the magnetic field strength of the scattering centers do not vary beyond the earth's orbit with the radial distance from the sun. (auth)

41671 ELECTRON-INDUCED CASCADE SHOWERS IN COPPER AND LEAD AT 1 Gev. Nelson, Walter R.; Jenkins, Theodore M.; McCall, Richard C.; Cobb, Joseph K. (Stanford Linear Accelerator Center, Calif.). Contract AT(04-3)-400. Phys. Rev., 149: 201-8(Sept. 9, 1966). (SLAC-PUB–163).

The radial and longitudinal development of electron-photon showers has been measured in copper and lead at 1 Bev. A new technique using the thermoluminescent property of LiF was employed to measure energy deposition. The resultant radial distributions and transition curves show good agreement with Monte Carlo calculations. (auth)

41672 OBSERVATION ON THE ELEMENTAL ABUNDANCES OF LOW-ENERGY COSMIC RAYS IN JULY 1964. Reames, D. V.; Fichtel, C. E. (Goddard Space Flight Center, Greenbelt, Md.). Phys. Rev., 149: 991-5(Sept. 30, 1966).

In a sounding rocket experiment flown at Fort Churchill, Manitoba in July 1964, nuclear emulsion detectors were used to study the composition and fluxes of primary cosmic-ray nuclei with charge $Z \geq 3$ above the atmosphere in the region of kinetic energy from 40 to 200 Mev/nucleon. The results show a flux ratio for light ($3 \leq Z \leq 5$) to medium ($6 \leq Z \leq 9$) nuclei of 0.16 ± 0.07 in the 40- to 100-Mev/nucleon region and a ratio for heavy ($Z \geq 10$) to medium nuclei of 0.42 ± 0.11 in the 70- to 160-Mev/nucleon interval. The elemental structure of the medium nuclei is found to contain $(40 \pm 7)\%$ carbon, $(10^{+4}_{-6})\%$ nitrogen, and $(48 \pm 7)\%$ oxygen. Extrapolating the fluxes back through approximately 2.5 g/cm^3 of interstellar hydrogen to the source, one finds a flux of nitrogen consistent with zero. (auth)

41673 SOURCE SPECTRA AND COMPOSITION OF COSMIC RAYS IMPLIED BY AN ANALYSIS OF INTERSTELLAR AND INTERPLANETARY TRAVEL. Fichtel, C. E.; Reames, D. V. (Goddard Space Flight Center, Greenbelt, Md.). Phys. Rev., 149: 995-1007(Sept. 30, 1966).

The implications of a simple set of assumptions related to galactic cosmic rays are examined and compared with the existing data. These assumptions are that (a) the multiply charged cosmic-ray nuclei all have the same spectral shape at the source, (b) the relative abundances of ^{3}He and light nuclei ($3 \leq Z \leq 5$) are negligible at the source, and (c) the average amount of interstellar material traversed is independent of particle energy. The results show that within

the present uncertainties of the experimental data and of the interaction cross sections, the data agree with the predictions without additional assumptions if the differential source spectra are relatively flat at low energies and the average interstellar path is 2.8 ± 0.4 g/cm^2. In particular, the nearly constant relative abundances of the helium, medium ($6 \leq Z \leq 9$), and ($Z \geq 10$) nuclei for different values of energy/nucleon can be explained, and the observed variation of the flux ratio of light to medium nuclei with energy/nucleon can be brought into fair agreement with predictions. The calculations also imply that, if the analysis does represent the true situation, then there is little or no solar modulation of the cosmic rays near solar minimum, and protons and helium nuclei have different source spectra. (auth)

41674 COSMIC-RAY ELECTRON FLUX ABOVE 4.7 Bv. Smith, Lawrence H.; Frye, Glenn M. Jr. (Case Inst. of Tech., Cleveland). Contract AT(11-1)-818. Phys. Rev., 149: 1013-17(Sept. 30, 1966). (COO-818-79).

The cosmic-ray electron flux was measured at 2.16 g/cm^2 and 4.35 g/cm^2 residual atmosphere, using a lead-plate spark chamber to detect the soft showers. Both flights were made from Palestine, Texas, where the vertical geomagnetic cutoff is 4.7 Bv. A twelve-gap spark chamber containing seven lead plates of 6.28 g/cm^2 each and five magnesium plates of 1.1 g/cm^2 was used to detect the electrons. Six hundred and eighty five "electron-type" events were detected at 4.35 g/cm^2, and 197 at 2.16 g/cm^2. The number of electron showers was deduced from the data by utilizing the difference between the cascade length and the nuclear interaction length. In the first three lead plates, 97% of the electrons initiate substantial showers. The nuclear particles interact almost equally in the seven lead plates, and the number of nuclear interactions in the first three plates is deduced from the observed rate in 4 through 7. The excess interactions observed in the first three lead plates are caused by electrons. The electron flux was determined at 4.35 g/cm^2 residual atmosphere to be 16.3 ± 5.3 electrons/sr m^2 sec and at 2.16 g/cm^2 residual atmosphere to be 4.8 ± 5.4 electrons/sr m^2 sec. The upper limit to the primary flux is 5.5 electrons/sr m^2 sec when both statistical and instrumental uncertainties are included. The penetrating particle flux was monitored throughout the flight at 4.35 g/cm^2 as 684 ± 40 penetrating particles/sr m^2 sec and at 2.16 g/cm^2 as 750 ± 41 penetrating particles/sr m^2 sec. (auth)

41675 MATTER TRAVERSED BY LOW-ENERGY COSMIC-RAY NUCLEI IN SPACE. Biswas, S.; Ramadurai, S.; Sreenivasan, N. (Tata Inst. of Fundamental Research, Bombay). Phys. Rev., 149: 1037-40(Sept. 30, 1966).

The amount of matter traversed in space by the primary cosmic-ray nuclei of energy 50–150, 200–500, 500–1000, and >1500 Mev/nucleon are obtained as 5.5 ± 1.4, 9.1 ± 0.9 5.3 ± 0.4 g cm^{-2} of hydrogen, respectively, using recent measurements of spallation cross sections with proton beams from accelerators and Li/M ratios of cosmic-ray nuclei (where M denotes nuclei with $6 \leq Z \leq 9$). These results and other evidence seem to suggest the hypothesis of two distinct sources (or propagation paths) of cosmic-ray nuclei, one responsible for nuclei of energy roughly 50–150 Mev/nucleon and the other energies greater than this. (auth)

41676 SEARCH FOR HEAVY MAGNETIC MONOPOLES. Carithers, W. C.; Stefanski, R.; Adair, R. K. (Yale Univ., New Haven. Brookhaven National Lab., Upton, N. Y.). Phys. Rev., 149: 1070-7(Sept. 30, 1966).

The discovery of an apparent breakdown in time-reversal invariance in K_2^0 decays demands further investigation into the symmetry properties of the fundamental interactions. Since a simple model of electric charge and magnetic poles leads to an electrodynamics which is not time-reversal invariant, it appeared essential to extend previous investigations concerning the possible existence of magnetic monopoles to regions of higher monopole mass and lower production cross section. An experiment was designed to detect monopoles produced in the earth's atmosphere by the primary cosmic radiation following a method introduced by Malkus. A solenoid with a magnetic moment of 3×10^5 A m^2 was used to collect monopoles moving along the earth's lines of magnetic flux and to accelerate them through scintillation counters, a spark chamber, and into emulsions. The negative results of the search show that the monopole flux at the surface of the earth is less than 10^{-6}/cm^2 year. Using for the sake of comparison, a simple model of monopole production such that the cross section is constant above threshold, this result shows that the cross section for the production of monopoles by nucleon-nucleon interactions is less than $10^{-6}(\hbar/Mc)^2$ for a monopole mass M of 15 Bev/c^2. The limit on the production of monopoles by photonucleon interactions is about 10^3 times higher. In both cases the cross-section limit varies with monopole mass approximately as $M^{3.4}$. (auth)

41677 MEASUREMENTS OF THE CHARGE RATIO OF COSMIC-RAY MUONS. Aurela, A. M.; MacKeown, P. K.; Wolfendale, A. W. (Univ. of Durham, Eng.). Proc. Phys. Soc. (London), 89: 401-8(1966).

Results are presented of two independent determinations of the charge ratio of cosmic-ray muons, at energies up to several hundred Bev. In one case the data are based on 19,235 particles collected in a smaller angular range about the vertical, and in the other case measurements refer to the range of zenith angles 77.5° to 90° and comprise 10,832 particles. The various factors relevant to a transformation of the observed charge ratio to that at production are considered, after which a comparison is made both between the two series and with the result of other authors. The charge ratios observed in the two directions are very similar. No supporting evidence is found for a pronounced minimum in the charge ratio in the region of 50 to 100 Bev. (auth)

Direct Energy Conversion

Refer also to abstract 41514.

41678 (IPP-3/40) ANLAGE ZUM BETRIEB EINES MHD-GENERATORS MIT EINEM GASKREISLAUF UND DER EINRICHTUNG FUER STROMDICHTEMESSUNGEN. (Device for Operating a Closed-Loop MHD Generator With Current Density Measuring Facilities). Brederlow, G.; Salvat, M. (Institut fuer Plasmaphysik, G.m.b.H., Garching (West Germany)). June 1966. 16p. Dep. mn.

A description of an experimental segmented electrode generator operating with potassium-seeded argon at 100 gr/sec mass flow and permitting the measurement of the current distribution at different electrode geometries is given. The purpose of this design is to gain practical experience in the construction of closed-cycle generators and to obtain additional information regarding the effect of the surface to volume ratio upon the experimental results. The major components of the system are as follows: The plasma jet, the potassium injection system with the corresponding mixing chamber, the MHD generator with measuring facilities, the potassium separator, and the compressor. The individual components of the system are described in detail. Particular attention is given to the potassium injector which assures a constant seeding ratio at any selected value of the seed mass flow within a range of 0.04 to 2.9%, and to the potassium separator yielding a continuous separation at a sufficiently low pressure drop. Technical and technological details related to the design of such components as the plasma arc heater, the mixing chamber, the generator, and the monitoring facilities are also given. (auth)

41679 (NASA-CR-543) THERMAL INTEGRATION OF ELECTRIC POWER AND LIFE SUPPORT SYSTEMS FOR MANNED SPACE STATIONS. Woods, R. W.; Erlanson, E. P. (General Electric Co., Philadelphia, Pa. Missile and Space Div.). Sept. 1966. Contract NAS 3-6478. 321p. CFSTI $4.25 cy, $1.50 mn.

Rankine and Brayton Cycle electric power systems using Isotopic and Solar Sources are analyzed and thermally integrated with attitude control, refrigeration, life support and cabin environmental control systems. The resulting system design with the most potential for use with a six-man orbiting station is a combined life support-solar Bray-

ton system weighing 3593 pounds. The electrical power requirements were reduced from eight kilowatts for a non-integrated system to five kilowatts for an integrated system with the use of power system waste thermal energy. The two-man lunar shelter considered had an integrated electrical power reduction of 1.2 kilowatts. (auth)

41680 (NYO-3642-2) THE DEVELOPMENT OF AN ADSORPTION CESIUM RESERVOIR. Second Quarterly Technical Report. (Radio Corp. of America, Lancaster, Pa. Direct Energy Conversion Dept.). June 1966. Contract AT(30-1)-3642. 39p. Dep. mn. CFSTI $2.00 cy, $0.50 mn.

Research is described leading to the development of a thermionic converter with a self-contained, self-regulating, high-temperature, adsorption reservoir for the automatic control of cesium pressure. A study of reservoir materials and geometries is described. Liquid reservoirs are compared with adsorption reservoirs. (M.O.W.)

41681 (UCRL-11857) SURFACE IONIZATION OF CESIUM AND THERMIONIC EMISSION FROM PLANAR SINGLE CRYSTALS OF TUNGSTEN. Koenig, Daniel Rene (Lawrence Radiation Lab., Univ. of California, Berkeley). June 1966. Contract W-7405-eng-48. 305p. Dep. mn. CFSTI $7.00 cy, $1.50 mn.

Thesis.

The thermal emission of electrons, and cesium atoms and ions from two large (≈1.5 cm^2), flat, monocrystalline, tungsten surfaces oriented in the [100] and [110] crystallographic directions was investigated. All experimental results were obtained by measuring the current-voltage-time characteristics of two diodes, each having one of the tungsten single crystals for the cathode (emitter). A guard ring in the plane of the collector ensured accuracy of the current measurements. The work function ϕ_0 of each crystal surface was determined from measurements of the field-free thermionic emission in vacuum in the temperature range 1400 to 2200°K. The desorption energies ϕ_{io} and ϕ^*_{ao} of cesium ions and atoms, respectively, evaporating from the (essentially) bare crystal surfaces were determined from measurements of the evaporation rates of these particles in the temperature range 1000 to 1500°K. The change in the work function of each crystal surface due to adsorption of cesium was evaluated from measurements of both the field-free electron and cesium-ion emissions in the surface-temperature range 850 to 1450°K and the cesium-reservoir temperature range 0 to 100°C. Excellent agreement was found between these two independent determinations. Much of the data obtained from the (110) crystal exposed to cesium could not be confidently related to the vacuum data because the crystal surface was believed to have become contaminated. The flux of cesium vapor in equilibrium with its condensed phase was measured in the temperature range 0 to 120°C. (auth)

41682 (LA-tr-66-32) GENERATION OF THERMIONIC ELECTRICITY FROM THE THERMAL ENERGY FROM NUCLEAR COMBUSTION. Sankavich, Melvin F.; Schutt, Paul F. Translated for Los Alamos Scientific Lab., N. Mex., from French Patent 1,336,354. 16p. Dep. mn. JCL $1.60 fs, $0.80 mf.

This invention includes a cell adapted to the thermionic generation of electricity from thermal energy from a nuclear fuel irradiated by neutrons. The cell contains a pair of thermionic conversion elements involving cathodes on the respective faces of a mass of nuclear fuel and a thermal exchange relationship with the latter. There are associated anodes adapted for liquid cooling with arrangements for receiving the electrons emitted thermionically by the corresponding cathodes. (M.H.R.)

41683 MODULATED CONDUCTIVITY INDUCTION SYNCHRONOUS MAGNETOGASDYNAMIC GENERATOR. Nilewski, J.; Szewalski, R. (Inst. of Fluid Flow Machines, Danzig). Bull. Acad. Pol Sci., Ser. Sci. Tech., 13: 277-83(1965). (In Polish).

The results are described of an earlier study concerning the operation of a synchronous generator fed with a jet of a working medium with different conductivity. The layout and working characteristics of an asynchronous generator with a traveling-wave magnetic field are, to a certain extent, similar to those of the synchronous generator under consideration. There are two essential differences: (a) in a synchronous generator, the modulated-conductivity working-medium flow is indispensable, whereas with an asynchronous generator, constant conductivity may be used, and (b) an asynchronous generator needs a much higher value of the working medium conductivity than the synchronous generator. The main difference between the asynchronous and the synchronous generator is that the asynchronous generator meets and the synchronous generator does not meet the applicability requirement of magnetic Reynolds numbers for the medium flow in the generator duct. (ATD)

41684 FERROELECTRIC TRANSDUCERS. Besancon, J. E.; David, J.; Vedel, J. (Commissariat a l'Energie Atomique, Paris). pp 315-29 of EUR-2750.e.

Polarized ferroelectric materials, shock loaded by high explosive, generate electrical charges on the electrode area. All of the successful experiments were made using different types of barium titanate and lead zirconate ceramics. There is not a transducer effect. Theoretical models are given for the cases where the shock front moves in a direction normal or perpendicular to the polarization. The released-to-bound-charges ratio as function of the output impedance is ranging from 15 to 60%. The models are compared with the experimental results given by several curves. (auth)

41685 EXPLOSIVE DRIVEN LINEAR MHD GENERATORS. Jones, M. S. Jr. (MHD Research, Inc., Newport Beach, Calif.); McKinnon, C. N. Jr. pp 349-66 of EUR-2750.e.

A series of experiments was conducted in explosive driven linear MHD generator channels of three different sizes to determine the scaling parameters. The results of these sealing experiments are predicted by an intermediate magnetic Reynolds number theory which suggests that the magnetic Reynolds number in the explosive driven MHD channel approaches unity and therefore self-induced magnetic fields must be included in the theoretical description. Data are presented giving voltage and current characteristics for a variety of conditions. These data include information regarding the slowing of the plasma mass as kinetic energy is converted to electrical energy. The use of explosive driven plasmas for magnetic field compression experiments is also suggested. (auth)

41686 SOME EXPERIMENTS RELATED TO EXPLOSIVE DRIVEN MHD CONVERTERS. Burnham, M. W. (Falcon Research and Development Co., Denver, Colo.); Marshall, S. J. pp 367-86 of EUR-2750.e.

High speed color photographs of the explosively produced plasmas at 2×10^6 frames/sec are shown and these, along with Lin coil measurements, are discussed in the light of models in the literature. Application of the results to a breadboard type generator with a curved duct is discussed. Considerable increase in output was observed for the curved duct geometry. Experiments reported consist of (a) plasma geometry experiments, (b) plasma conductivity measurements, (c) plasma density estimates, (d) studies of the cohesive properties discussed by Cook and Keyes, and the results of the breadboard application using curved ducts in which currents in the Kiloampere range were converted. (M.O.W.)

41687 PULSED ELECTRICAL POWER GENERATION FROM MAGNETICALLY LOADED EXPLOSIVES. McKinnon, C. N. Jr. (Univ. of Missouri, Columbia); Jones, M. S. Jr. pp 437-50 of EUR-2750.e.

Recent work with detonation driven linear MHD channels has indicated that it is possible to generate high power electrical pulses using the expanded products of high explosives. One disadvantage of this method is the need for an externally applied d-c magnetic field, which at the present state of the art can only be supplied by a conventional electromagnet. Since the reaction zone in a solid explosive can be made almost as conducting as the expanded seeded products, it appears feasible to supply the

magnetic field directly to the undetonated explosive in the form of uniformly distributed permanent magnet particles dispersed in the explosive. This may be termed a magnetically located explosive. Upon detonation, the highly ionized reaction zone interacts with the magnetic field to produce the U × B voltage. Electrodes in contact with the explosive allow current to flow through a connected load. Electrodeless coupling is also possible. The electrical power output is found to be strongly dependent on the electrical conductivity of the detonation products and the magnetic permeability of the undetonated composite. (auth)

41688 INVESTIGATION OF D-C ELECTROMAGNETS WITH IRON CORES IN MHD GENERATOR APPLICATIONS. Shakhtarin, V. N. Magnit. Gidrodinamik., Acad. Nauk Latv. SSR, No. 2, 151-8(1965). (In Russian).

Methods and results to determine leakage coefficients in iron-core electromagnets are presented. Two forms of iron cores, C and E types, are considered in detail. Graphical magnetization results are given for both types of magnets with rectangular cross section of the pole faces. Also, using the analogy between two-dimensional electric potential on a resistive sheet and the two dimensional magnetic vector potential, a method for determining leakage coefficients is described. The resistive-paper method results are then compared with test measurements for the two types of magnets and show good agreement. The method is recommended, together with some detailed instructions, for design of electromagnets for MHD generators. (CFSTI)

41689 ELECTRODE PROTECTION FOR MAGNETOHYDRODYNAMIC GENERATORS. Way, Stewart; Young, William E.; Hundstad, Richard L. (to Westinghouse Electric Corp.). U. S. Patent 3,259,767. July 5, 1966. Filed July 13, 1962.

A method is outlined for protecting the carbon electrodes in MHD cells from oxidation. The method involves providing continuously a layer of protection material to the electrodes. (M.O.W.)

41690 MAGNETO HYDRODYNAMIC GENERATOR. (to Brown, Boveri and Co. Ltd.). British Patent 1,035,522. July 13, 1966. Priority date Jan. 17, 1962, Switzerland.

A MHD generator is described in which the pressure gradient along the duct is made at least substantially independent of changes in the load. A number of pairs of electrodes are spaced along the duct in the direction in which the gas flows and perpendicular to the direction of gas flow and to the magnetic field. The electrodes are connected in series and are connected to a load resistance. The ratio of the longitudinal distance between two adjacent serially connected pairs of electrodes to the transverse distance between the electrodes is at least equal to the ratio of the Hall voltage to the resistive voltage in the duct. (B.L.M.)

41691 MEANS FOR CONVERTING HIGH ENERGY RADIATION TO ELECTRICAL ENERGY. Ghormley, John A. (to Union Carbide Corp.). U. S. Patent 3,255,046. June 7, 1966. Filed Feb. 16, 1961.

A system is provided for the conversion of high-energy radiation, electromagnetic radiation having a wavelength shorter than the visible spectrum, to electrical energy by irradiation of a working solution, such as an aqueous solution of ferrous sulfate, with an external radiation source to alter the working solution in such a manner as to provide species capable of being discharged by a recombination cell with the accompanying release of electrochemical energy directly as electricity. The highly efficient process is cyclic and may be run continuously by reirradiating the working solution after it is discharged through the recombination cell. (B.L.M.)

41692 EXPERIMENTAL INVESTIGATION OF FLUCTUATIONS IN A NONEQUILIBRIUM MHD PLASMA. Dethlefsen, Rolf; Kerrebrock, Jack L. (Massachusetts Inst. of Tech., Cambridge). 29p. (CONF-660326-2). ORAU. Gmelin, AED-CONF-66-047-1.

From 7th Symposium on Engineering Aspects of Magnetohydrodynamics, Princeton, N. J.

Measurements of the electrical fluctuations in an argon-potassium nonequilibrium plasma are presented and correlated with the theories of electrothermal and magneto-acoustic waves. A very high fluctuation intensity at Hall parameters above 2 and electron densities above 2×10^{13} cm^{-3} correlates well with the former. A sizeable reduction of effective conductivity is associated with the noise in this regime. The low noise level observed for Hall parameters below 2, and electron densities above 2×10^{13} cm^{-3} is in accord with the predictions of both theories. (auth)

41693 MAGNETOHYDRODYNAMIC POWER GENERATION. Tsu, T. C. (Westinghouse Electric Corp., Pittsburgh). New York, Inst. of Electrical and Electronics Engineers, 1966, Paper No. 31PP66-453, 15p., $1.00. (CONF-660708-3). ORAU.

From IEEE Summer Power Meeting, New Orleans.

An outline is given of the broad field of magnetohydrodynamic power generation, starting with the principle of MHD power generation and taking up the coal-burning MHD-steam power plant, the noble-gas MHD generator with a nuclear heat source, and the liquid-metal MHD generator. Emphasis is placed on central station power generation. It is concluded that the coal-burning MHD-steam power plant is closest to technical reality. (W.D.M.)

41694 THEORY AND ANALYSIS OF THE CYLINDRICAL INDUCTION TYPE MAGNETOHYDRODYNAMIC a-c POWER GENERATORS. Rashad, A. R. M. (Memphis State Univ., Tenn.). 21p. (CONF-660419-2). ORAU. Gmelin, AED-CONF-66-057-2.

From IEEE Region 6 Annual Conference, Tucson, Ariz.

The theory and performance of this type of MHD generators is investigated in detail. The generator's output power, conversion efficiency, and equivalent circuit are derived. It is found that the performance of this type of generator can be represented in a similar way to that of a conventional induction generator. (auth)

41695 INFLUENCE OF NEGATIVE IONS ON CESIATED EMITTERS. Rasor, N. S. (Brown, Boveri and Co., Heidelberg). 9p. (CONF-660324-5). ORAU. Gmelin, AED-CONF-66-036-5.

From 26th Annual Conference on Physical Electronics, Cambridge, Mass.

A previous formalism for alkali metal adsorption is extended to include two-electron or "negative ion" states of the adsorbed particle. It is estimated that a work function increase can occur with initial cesium adsorption on surfaces having vacuum work functions below 3 ev. In addition, in an independent computation, it is estimated that in a Cs + CsF vapor system, electron emission can become limited by the space charge of emitted negative fluorine ions. This should occur for conditions typical in a thermionic converter when the CsF reservoir temperature exceeds the emitter temperature divided by 2.5. (auth)

41696 TWO-DIMENSIONAL ELECTRO-FLUID DYNAMIC CHANNEL FLOW. Chiu, H. H. (New York Univ., New York); Kahn, B.; Brandmaier, H. E. 16p. (CONF-660326-1). ORAU. Gmelin, AED-CONF-66-047-4.

From 7th Symposium on Engineering Aspects of Magnetohydrodynamics, Princeton, N. J.

Results are presented from a detailed two-dimensional analysis of flow in an axisymmetric electro-fluid generator, showing the effects of radial fields and viscous forces on performance characteristics. Of particular importance is the effect on the electrical breakdown of the gas. Comparisons are made with measured radial potential distributions and with a typical load characteristic. The electro-fluid dynamic generator is described. (auth)

41697 CARROUSEL MAGNETOAERODYNAMIC GENERATOR. de Simone, Jean Claude; Klein, Georges; Dubois, Pierre (Centre de Recherches de la Compagnie Generale d'Electricite, Marcoussis, France). Vienna, International Atomic Energy Agency, 1966, Preprint No. SM-74/147, 28p. (In French). (CONF-660704-92). ORAU.

From Magnetohydrodynamic Electrical Power Generation, 2nd International Symposium, Salzburg.

In the magnetoaerodynamic generators normally considered, the flow of ionized gas passing through the conversion duct is equal to the mass flow of gas produced by the heat source. In a "carrousel" generator, on the contrary, the mass flow of gas in the conversion duct is a high multiple of the gas flow produced by the heat source. A substantial part of the gas flow leaving the conversion duct is returned to the entrance of the latter while the remainder is discharged to the outside. This partial recycling of the gas leaving the duct is obtained by supersonic injection upstream from the conversion duct of the gas flow produced by the heat source. The equations governing the development of the thermodynamic and electrical characteristics of the plasma in the generator are defined, and experiments carried out in the cold state are described, the results of which agree with these equations. Reference is made to the principal advantages of the system, which include reduction of wall losses, a shorted conversion duct, and the possibility of designing generators of moderate electric capacity. (auth)

41698 PLASMA FLOW IN THE DUCT OF A SERIES-FLOW MHD GENERATOR. Kovbasuk, V. I.; Medin, S. A. (Moscow State Univ.). Vienna, International Atomic Energy Agency, 1966, Preprint No. SM-74/225, 8p. (In Russian). (CONF-660704-93). ORAU.

From Magnetohydrodynamic Electrical Power Generation, 2nd International Symposium, Salzburg.

For Hall numbers comparable to unity, a series-flow MHD generator has an advantage over Faraday, segmented, or Hall-type MHD generators, since it admits of a high degree of electrode segmenting for a limited number of different loads and gives a high conversion efficiency. The plasma flow in the generator duct has a number of special characteristics, determined by changes in the physical properties of the working fluid along the duct and by changes in the local load factor for a given electrode configuration. A study of plasma movement in the duct of a series-flow MHD generator is considered. A general statement of the problem is formulated and conditions are determined for the validity of a quasi-unidimensional flow model. Flow conditions close to the optimum are calculated and analyzed. Using a graphical analysis method a simple interpretation is given for the results obtained. (auth)

41699 INVESTIGATION OF A DISINTEGRATING ARGON–CESIUM PLASMA BY THE MICROWAVE METHOD. Kuleshov, V. P. (Kurchatov Inst. of Atomic Energy, Moscow). Vienna, International Atomic Energy Agency, 1966, Preprint No. SM-74/91, 8p. (In Russian). (CONF-660704-94). ORAU.

From Magnetohydrodynamic Electrical Power Generation, 2nd International Symposium, Salzburg.

Measurements were made of the effective recombination coefficient, $\alpha_{3\phi}$, of a disintegrating argon–cesium plasma with hot electrons at various argon pressures. The measurements were made at a frequency of 75 Gc/s using a microwave interferometer, in the electron concentration range $7 \times 10^{12}-4 \times 10^{13}$. The plasma was generated by a pulsed discharge in glass tubes 56 mm in diameter. In the experimental conditions the argon temperature was considerably lower than the electron temperature. The measured values of $\alpha_{3\phi}$, of the order of 10^{-10} cm^2/s^{-1}, were explained by the quasi-steady-state change in the parameters of the plasma, the Saha ionization equilibrium being maintained. In this case the rate of de-ionization was determined by the change in electron temperature T_e, according to the equation: $[(I + 3/2kT_e)(\delta n_e/\delta t)] = W$ where I is the ionization temperature and W is the power loss by the electrons in inelastic collisions with the atoms of the gas. An increase in $\alpha_{3\phi}$ occurred with increase in argon pressure. (auth)

41700 INTERNAL RESISTANCE AND POTENTIAL DROP IN MHD GENERATORS. Lengyel, L.; Salvat, M. (Institut fuer Plasmaphysik, Garching, Ger.). Vienna, International Atomic Energy Agency, 1966, Preprint No. SM-74/16, 20p. (CONF-660704-95). ORAU.

From Magnetohydrodynamic Electrical Power Generation, 2nd International Symposium, Salzburg.

The electromotive force produced by the Hall effect in Faraday-type MHD generators is compensated by an electrostatic field in the main part of the plasma flow. No such compensation is possible, however, in the vicinity of the electrodes. As a result of this, the electromagnetic force acting on the charge carriers changes periodically along the electrode walls; the longitudinal component of the induced Hall-emf remains uncompensated along the electrodes and vanishes completely along the insulator sections. Such a discontinuous force distribution makes the current distribution in the neighborhood of the electrodes strongly nonuniform. Thus the internal resistance, which is expressible in terms of the total current and the associated internal potential drop between the electrodes, becomes a function of the current distribution itself. At constant electrical conductivity, the perturbation of the current distribution depends upon the geometry and the relative position of the electrodes; and upon the Hall parameter $\beta = \omega\tau$. The numerical calculations performed by Z. N. Celinski and F. W. Fischer for Faraday-type generators with segmented electrodes led to an empirical formula yielding the ratio of the ideal (corresponding to $\beta = 0$ and infinitely segmented electrodes, i.e., to a uniform current distribution) and the actual internal resistance as a function of the geometric parameters of the generator duct and the magnitude of β. It is shown that the same expression can be obtained on the basis of purely physical considerations. The nonuniformity of the current distribution in Faraday-type generators with segmented electrodes can be reduced by shifting the electrodes relative to each other (staggered electrode geometry). Such a displacement of the electrodes has two immediate consequences: it affects the current distribution and at the same time it changes the absolute distance between the electrodes (thus affecting the magnitude of the "unperturbed" internal resistance). A numerical method was developed for the calculation of the current and potential distributions corresponding to staggered electrode geometry. The internal resistance as a function of the electrode displacement is considered in detail. (auth)

41701 APPLICABILITY OF THE ELECTRODYNAMIC APPROXIMATION IN THE THEORY OF LIQUID-METAL, INDUCTION MHD CONVERTERS. Lielpeter, Ya. Ya. (Inst. of Physics, Academy of Sciences, Latvian SSR). Vienna, International Atomic Energy Agency, 1966, Preprint No. SM-74/240, 12p. (In Russian). (CONF-660704-96). ORAU.

From Magnetohydrodynamic Electrical Power Generation, 2nd International Symposium, Salzburg.

Questions relating to the theory of induction MHD converters are considered. Theoretical expressions characterizing the ideal induction MHD machine and defining the influence of the surface effect in the secondary circuit of the machine, the transverse edge effect, the longitudinal edge effect, and the higher spatial harmonics of the magnetic field are presented. Expressions are given for the basic energy characteristics, the power factor for a generator converting the energy of liquid-metal pressure, and the power factor for a pump. Those questions that have not been studied sufficiently are mentioned, such as the longitudinal edge effect, and the results of new solutions for generators converting the kinetic energy of liquid metal are presented. The limits of applicability of the electrodynamic approximation are discussed. The results of new experiments carried out on a device that permits measurement of the external characteristics of an induction MHD machine and also measurement of the electromagnetic strength of the reaction acting on the stator of the apparatus are described. Data were obtained concerning the electromagnetic pressure, the distribution of pressure in the duct, and the magnetohydrodynamic losses. The results were compared with the electrodynamic approximation theory and with experimental data

obtained using a model with a revolving disc. Experimental data concerning the optimum duct shape are presented for the case where the Stewart number is considerably less than unity. The basic characteristics (power, efficiency, and power factor) of the induction MHD device when operating as a generator and as a pump are compared. (auth)

41702 VELOCITY AND DENSITY PROBE FOR STEADY NONEQUILIBRIUM, SUPERSONIC FLOW. Loth, J. L. (Univ. of Illinois, Urbana). Vienna, International Atomic Energy Agency, 1966, Preprint No. SM-74/7, 16p. (CONF-660704-97). ORAU.

From Magnetohydrodynamic Electrical Power Generation, 2nd International Symposium, Salzburg.

To avoid the difficulties, inherent in using the various probes, a new type has been developed and tested at the University of Illinois. Its main advantage is that there is no need to know anything about the chemical or physical nature of the flow. This probe measures directly the mass and momentum influx of a captured streamtube of a cross-sectional area equal to the inlet area of the probe. The captured flow is stagnated and cooled down to an equilibrium temperature, and the mass flow rate is metered, either through a sonic nozzle or a timed inflow into an evacuated vessel of known volume. The minimum free stream Mach number is 1.5 so as to prevent spillage and force the normal shock to occur inside the probe. Because of the special construction of the probe, the measured thrust equals the influx of momentum and does not include the other possible thrust contributions. The pressure thrust can be ignored for high Mach number flows, because for $M_\infty > 5$ its value is always less than 3%. However, for low Mach number flows the ambient pressure of the probe should be adjusted to equal the free stream pressure, so that the pressure thrust will cancel out. To avoid external drag on the probe it is necessary to surround it entirely with a stationary shroud. The captured mass leaves the probe through radial outlets and consequently the exit momentum does not contribute to the axial thrust. The free stream velocity is computed by dividing the measured axial thrust by the captured mass flow rate. The free stream density equals the square of the mass flow rate divided by the product of the axial thrust and the probe inlet area. For thermal equilibrium flow the experimental results were compared with a pitot tube reading, and a deviation of less than 4.5% was observed. As the free stream Mach number increases, both the dimensionless thrust, $F/P_0 \cdot A_{in}$, and the dimensionless mass flow rate, $\dot{m}\sqrt{R.T_0}/P_0 \cdot A_{in}$, which are functions of M_∞, decrease rapidly. For $M_\infty = 10$, both values are about 0.005 and about one percent of their values at $M_\infty = 1.5$. This limits the practical application of the probe to a range of free stream Mach numbers: $1.5 < M_\infty < 10$. It is expected that this simple and rugged probe will find a wide range of applications in supersonic, nonequilibrium flow analysis. (auth)

41703 STUDIES ON AN ALKALI SHOCK TUBE AND ON AN MHD GENERATOR WIND TUNNEL. Louis, Jean F. (Avco-Everett Research Lab., Everett, Mass.). Vienna, International Atomic Energy Agency, 1966, Preprint No. SM-74/172, 20p. (CONF-660704-98). ORAU.

From Magnetohydrodynamic Electrical Power Generation, 2nd International Symposium, Salzburg.

An alkali shock tube has been successfully developed for two applications: to study the kinetics of the alkalies at high temperature; and to simulate the flow and MHD phenomena in large MHD generators. The 15-cm shock tube makes use of a suspension of alkali aerosols of 0.2-μ size in flowing argon. For such particles, the settling velocity is negligible compared to the gas velocity. The production of the suspension, size distribution, and measurements to verify the uniformity of the gas sample are described. Measurements of electron density and conductivity behind the incident shock are given. Results on the ionization kinetics of cesium in argon obtained behind the reflected shock are given and analyzed. It was found that the transfer of resonance radiation plays a role in the kinetics of cesium ionization in argon. The shock tube delivers the high-temperature seeded gas obtained behind the reflected shock to an MHD generator duct. The use of the reflected shock allows the expansion to start with a gas at known thermodynamic stagnation conditions. In its present design, the 15-cm shock tube can deliver high mass flows (10 kg/s) and heat input up to 20 Mw to the MHD device. The shock tube has the further advantages of high reservoir temperature flexibility and short flow times of the order 1 ms which eliminate the materials problems. Further, a disk geometry was chosen for the MHD duct to eliminate the axially located electrodes of linear channels. The pulsed magnet delivers magnetic fields up to 2.6 Tesla which allows a good interaction and the addition of a wide range of $\omega\tau$. By having eliminated the problems related to heat transfer and electrodes and by working at high values of the Reynolds number and good interaction, the purpose of the experiment was to ascertain the controlled conditions of Mach numbers, temperature, and Hall coefficients for which large inert gas MHD generators are stable and efficient. (auth)

41704 AVERAGING MAGNETOHYDRODYNAMIC FLOWS AND THE APPLICABILITY OF THE HYDRAULIC APPROXIMATION FOR CALCULATING MAGNETOHYDRODYNAMIC FLOW IN DUCTS. Lyubimov, G. A. (Moscow State Univ.). Vienna, International Atomic Energy Agency, 1966, Preprint No. SM-74/207, 12p. (In Russian). (CONF-660704-99). ORAU.

From Magnetohydrodynamic Electrical Power Generation, 2nd International Symposium, Salzburg.

The problem of the various approaches to the hydraulic description of nonhomogeneous MHD flow in ducts is discussed. It is shown that the hydraulic calculation of MHD flow using the mean temperature value to calculate the mean conductivity may in a number of cases give results which are far from accurate, even for flows with a relatively slight degree of nonhomogeneity in the distribution of parameters over the cross section of the duct. It is also demonstrated that in a number of cases of practical interest the hydraulic approach using a canonical flow homogeneous with respect to all parameters may be fundamentally inapplicable for calculating MHD flow in ducts. Ways of introducing basic improvement into methods for these calculations are indicated. (auth)

41705 ELECTROSTATIC PROBES FOR DIAGNOSTICS IN A COLLISION-DOMINATED WEAKLY IONIZED PLASMA. McKee, H. B.; Mitchner, M. (Stanford Univ., Calif.). Vienna, International Atomic Energy Agency, 1966, Preprint No. SM-74/174, 12p. (CONF-660704-100). ORAU.

From Magnetohydrodynamic Electrical Power Generation, 2nd International Symposium, Salzburg.

Previous studies of Langmuir-type probes as possible diagnostic devices for use in collision-dominated partially ionized gases have not considered the effects of volume ionization and recombination. Because the probe acts as a sink for charged particles, the electron number density near the probe will be depressed compared to its equilibrium value, even when the temperature is uniform. Since the ionization rate will exceed the recombination rate near the probe, there will be a tendency for the degree of ionization to be augmented. The effect of this mechanism is to decrease the spatial extent of the perturbation of the density and potential profiles by the probe and to increase the current collected at a given biasing voltage. Results were obtained in terms of four parameters, an ionization-recombination parameter, a pair of parameters reflecting the ratio of probe size to mean-free-path for ions and electrons, and the ratio of ion to electron mobility. Supporting calculations indicated that the ionization is important in a typical system near atmospheric pressure involving potassium seed in argon for temperatures above about 1700°K. Comparison of the calculated current-voltage characteristics with experimentally obtained data permitted determination of the plasma electron number density and an indication of the electron temperature. The governing equations for the problem were the electron and ion conservation equations with fluxes caused by density and electric potential gradients. A free-fall electrical sheath at the probe and uniform number density and potential at infinity were assumed for the boundary conditions.

Charge neutrality permitted solution for the ambipolar number density and the electric potential without recourse to Poisson's equation. The potential was eliminated from the ambipolar-flux differential equations, and the number density was obtained by solving the remaining nonlinear ordinary differential equation. Substitution of the density profile thus obtained into either of the original flux equations for a combination thereof permitted the determination of the potential profile. Currents were then determined simply from the density profiles and the sheath-drop voltage and matched with the potential profiles to obtain current-voltage characteristics. (auth)

41706 BRAYTON CYCLE MAGNETOHYDRODYNAMIC POWER GENERATION. McNary, Charles A.; Jackson, William D. (Massachusetts Inst. of Tech., Cambridge). Vienna, International Atomic Energy Agency, 1966, Preprint No. SM-74/162, 14p. (CONF-660704-101). ORAU.

From Magnetohydrodynamic Electrical Power Generation, 2nd International Symposium, Salzburg.

A detailed study of the single-loop MHD Brayton cycle is reported, with emphasis on data for comparison of this system with other competitive power generation techniques. The current state of the art in reactor design, high-temperature materials technology, and magnetics was taken into account to fix upper limits on the operation of the cycle and its components. Conductivity calculations based on the Kerrebrock nonequilibrium conductivity theory are included for helium, argon, and neon. The subsequent cycle analysis was performed for neon, the preferred working fluid, with a maximum reactor fuel rod temperature of 2300°C and a reactor configuration similar to the Peach Bottom gas-cooled reactor. The principal results of the analysis are given. (W.D.M.)

41707 EXPERIMENTAL INVESTIGATION OF MHD CHANNEL FLOWS AT HIGH HARTMANN AND REYNOLDS NUMBERS. Maciulaitis, A.; Loeffler, A. L. Jr., Calcanes, P. J. (Grumman Aircraft Engineering Corp., Bethpage, N. Y.). Vienna, International Atomic Energy Agency, 1966, Preprint No. SM-74/195, 16p. (CONF-660704-102). ORAU.

From Magnetohydrodynamic Electrical Power Generation, 2nd International Symposium, Salzburg.

The experiments described essentially complete the first phase of a fundamental investigation of MHD turbulence using liquid mercury flowing through channels of various cross sections. During this phase of work, friction factors were determined for fully developed flow through a dielectric circular pipe and preliminary measurements were taken for flow through an insulated rectangular channel of 5 to 1 aspect ratio, both in the presence of a uniform transverse magnetic field. The experimental apparatus was designed and sized with the objective in mind of taking detailed velocity profile measurements; this large size led to high values of Reynolds number and Hartmann number. Friction factors were obtained for circular pipe at Reynolds numbers ranging up to 3×10^6 and Hartmann numbers up to 3×10^3. For the rectangular channel, the corresponding range will be up to 10^6 and 4×10^3, respectively. The reported results were new and represent a significant extension of available data. Comparisons were made with existing data and theory. For the laminar flow in the circular pipe, friction factors fell on a straight line when plotted against the Hartmann/Reynolds number ratio (M/Re), but were about 10% higher than predicted by the approximate theory. Transition from laminar to turbulent flow was shown to occur over a narrow range of M/Re values. Good agreement with accepted turbulent data for zero magnetic field was demonstrated. An error analysis was carried out to estimate the uncertainty intervals of the presented results. (auth)

41708 EXPERIMENTAL INVESTIGATION OF PLASMA USING MODEL MHD GENERATORS. Maslennikov, N. M.; Germanyuk, V. N. (Lenin All-Union Electrotechnical Inst., Moscow). Vienna, International Atomic Energy Agency, 1966, Preprint No. SM-74/236, 12p. (In Russian). (CONF-660704-103). ORAU.

From Magnetohydrodynamic Electrical Power Generation, 2nd International Symposium, Salzburg.

In an applied electric field a voltage distribution is obtained in the interelectrode space normal to an argon–potassium plasma flow (at atmospheric pressure, a gas temperature of 1700 to 2400°K, and a cathode temperature of 1300 to 2400°K). Most of the applied voltage is concentrated in the cathode layer. As the cathode temperature rises, emission from the cathode increases and there is a drop in voltage at the cathode. This causes an increase in the voltage applied directly to the plasma, which in its turn leads to heating of the electrons and increased electric conductivity. The voltage drop at the anode is only weakly dependent on its temperature. When the gas temperature is 1600°K and the temperature of the tungsten cathode more than 2600°K, the electric conductivity of the interelectrode space is 650 times greater than that of the same space when occupied by an equilibrium plasma. In the induced field, tests were carried out at a pressure of 0.08 atm for the purpose of ascertaining the feasibility of operating at high values of $\omega_e \tau_e$ (of the order of 100 to 140). The rate of gas flow was 4.5 g/sec, the temperature 1300 to 2400°K, induction 10^4 G, velocity 660 to 900 m/sec, and voltage under open-circuit conditions 14 to 16 V. Under short-circuit conditions without cathode heating there is a general voltage drop in the cathode layer. As the cathode temperature increases the voltage drop decreases and the current between the electrodes rises. This current causes a voltage drop in the anode layer, the drop being considerably greater than the voltage drop caused by corresponding currents in the applied field. The increased voltage drop is due to the concentration of current at the anode edge, which is equivalent to a decrease in its surface. At a gas temperature of 1300°K the electric conductivity is 7×10^{-2} mho/cm, and exceeds the equilibrium value by a factor of 500. If the length of the electrodes is reduced relative to the optimum, the discharge does not develop and the excess of electric conductivity is insignificant. If the length of the electrodes is increased, the excess of electric conductivity decreases, since the Hall field is short-circuited. Figures are presented showing oscillograms and tables are given of experimental results. (auth)

41709 SELF-EXCITED MHD GENERATORS. Mattsson, Arne C. J.; Brogan, Thomas R. (Avco-Everett Research Lab., Everett, Mass.). Vienna, International Atomic Energy Agency, 1966, Preprint No. SM-74/168, 16p. (CONF-660704-104). ORAU.

From Magnetohydrodynamic Electrical Power Generation, 2nd International Symposium, Salzburg.

Design considerations and results obtained for a self-excited Faraday-type MHD generator having multi- or single-circuit net power outputs are presented. A large combustion driven self-excited MHD generator (the Mark V) designed for multicircuit net output of 20,000 kw was designed and built. The design of this generator is discussed and includes consideration of working fluid and its electrical properties, mass flow, channel configuration, and the strength of the magnetic field, along with a description of the analysis of the MHD generator flow and the manner in which that analysis is coupled with the magnet design so as to provide self-excitation. The design of the major generator components is also reviewed. The generator was tested over a wide range of operating conditions, and provided a maximum net power output of 23,600 kw with a gross power output of 32,000 kw. The initial testing of the generator was aimed at the achievement of self-excitation. Significant results from tests in the self-excitation study are presented along with data for net power output performance of the generator. Various problems encountered during the testing program are discussed. Since the effective use of a generator having multiple output circuits is limited, the generator was modified to give single circuit output of 20,000 kw at an output voltage of 1000 volts. Single circuit output implies shorted Hall potential throughout the entire generator; therefore, the single circuit design consists of finding a suitable efficient Hall field shorted configuration which provides a good impedance match with

the magnet and rapid excitation. These and other important design considerations for single circuit operation are presented. (auth)

41710 ELECTRODELESS CONDUCTIVITY MEASUREMENTS WITHIN THE REACTION ZONE OF A COMBUSTION CHAMBER. Milde, Helmut; Gallant, Hermann (Brown Boveri and Cie., Baden, Switzerland). Vienna, International Atomic Energy Agency, 1966, Preprint No. SM-74/21, 12p. (CONF-660704-105). ORAU.

From Magnetohydrodynamic Electrical Power Generation, 2nd International Symposium, Salzburg.

The degree of ionization within the reaction zone of a Bunsen-type flame is many times greater than would be expected by purely thermal ionization. The purpose of this experiment was to determine if such nonequilibrium ionization also occurs in a combustion process typical of an MHD generator and whether such ionization could be utilized. The combustion chamber consisted of one centrally located and eight circularly arranged fuel atomizers surrounded by a water-cooled chamber. Pre-heated air (from 500 to 850°K) was introduced from the bottom of the combustion chamber. Another atomizer was positioned within the pre-heated air duct for the addition of water or water-dissolved seeding material. Commercial fuel oil with a C/H ratio of 0.53 was used. A Laval-type nozzle was attached to the top of the combustion chamber. Adjoining this nozzle was the actual test section where the gas temperature was measured by the sodium line reversal method and the electrical conductivity determined by the HF coil method. The distance between the fuel atomizers and the test section could be varied from 0.25 m to 1 m thus permitting the investigation of the gas properties at different stages of combustion. The conductivity measuring coil was embedded in a streamlined cyclinder in such a way that the magnetic field lines were perpendicular to the gas velocity vector. The coil was introduced into the gas stream by pneumatic means for about half a second and then removed. During that period the change of the coil impedance was registered by a recording instrument. To avoid gas disturbances while measuring, the coil piece was joined to a water-cooled stainless steel cylinder of the same cross-sectional dimensions. This cyclinder was kept within the gas stream during periods of non-measurement. To obtain optimum measuring sensitivity of the coil and minimum temperature influence, a large coil diameter of 3 cm and a high-energizing frequency of 15.9 Mc/s were chosen. The experimental results obtained showed a relatively high non-equilibrium conductivity over the entire region investigated. The magnitude of the conductivity was of the order of 1 mho/m and varied with the air pre-heat temperature, stoichiometric ratio, and the distance between fuel atomizers and test area. It was also observed that the nonequilibrium conductivity was strongly affected by the introduction of seeding material. By adding small amounts of seeding material the conductivity, for example, dropped to a value roughly corresponding to thermal ionization. By further increasing the seeding concentration, the conductivity would go up initially and then decrease on account of the strong temperature drop due to the introduction of the water-dissolved seeding. While measuring the temperature drop due to the addition of water a very marked influence of the water on the nonequilibrium ionization was discovered. (auth)

41711 STRIATED FLOW IN THE INDUCTION SYNCHRONOUS MAGNETOGASDYNAMIC GENERATOR. Milewski, J. (Inst. of Fluid-Flow Machines, Danzig). Vienna, International Atomic Energy Agency, 1966, Preprint No. SM-74/58, 16p. (CONF-660704-106). ORAU.

From Magnetohydrodynamic Electrical Power Generation, 2nd International Symposium, Salzburg.

Striated-layer flow of the working medium is considered in the duct of an induction synchronous magnetogasdynamic generator. The electric characteristics and approximate gasdynamic characteristics of the generator have been presented previously. A more accurate solution of the equations of flow in generator duct is given, and attention is drawn to the problems of stability. A gaseous working medium is assumed. The experimental apparatus and mode of operation are discussed. The analysis is based on the equations of nonstationary, quasi-one-dimensional flow of a partly conducting gaseous medium. The solution is obtained by successive approximations on the linearized set of equations. As first approximation, the solutions for the mean values of parameters are obtained in which the three particular cases are considered: constant velocity flow, flow in duct of constant area, and flow at constant Mach number. Expressions for the magnitudes of parameters pulsation with basic frequency are found in the second approximation. Only in the third approximation is the examination possible of flow stability by a classical small perturbation method, but here the analysis is confined to the case of inviscid flow. (W.D.M.)

41712 SOME PROPERTIES OF A PLASMA IN HELIUM AND ARGON WITH ADDED CESIUM AND POTASSIUM VAPORS. Morgulis, N. D.; Polushkin, I. N. (Kiev State Univ.). Vienna, International Atomic Energy Agency, 1966, Preprint No. SM-74/234, 16p. (In Russian). (CONF-660704-107). ORAU.

From Magnetohydrodynamic Electrical Power Generation, 2nd International Symposium, Salzburg.

The investigation is described of some physical properties of a binary pulsed-discharge plasma in an inert gas (helium and argon) at a constant pressure, P, of approximately 100 torr, to which is added cesium and potassium vapor at a controlled lower ($p \ll P$) pressure in the range 10^{-3} to 0.5 torr, the discharge current density, j, being varied between 1 and 50 A/cm^2. This and similar (e.g., He–Cs) systems are physical models of a gas-plasma extrinsic semiconductor whose properties and parameters can be varied simply and in a controlled manner by varying the relative concentration of the added vapor. The electric conductivity of the plasma, the strength of the electric field in the plasma, some of its spectral properties, the electron temperature, etc., were determined for the given ranges of values of p and j; for these values the conditions for obtaining a homogeneous plasma column were selected. As the density of the discharge current increased, it was found that: (1) at first only the added vapor was ionized, while the behavior of the inert gas remained neutral (extrinsic semiconductor); (2) as the added vapor became almost totally ionized the gradually increasing ionization of the inert gas was superimposed ("mixed" semiconductor), etc. Investigations were also carried out on some phenomena of the nonsteady state during the formation and decay of such a plasma: variations in the ionic fractions and the electron temperature, charge recombination, etc. The experimental data obtained are discussed. (auth)

41713 CONDUCTIVITY OF A GAS WITH SUSPENSION. Mori, F.; Fushimi, K.; Honma, T. (Ministry of International Trade and Industry, Tokyo). Vienna, International Atomic Energy Agency, 1966, Preprint No. SM-74/128, 16p. (CONF-660704-108). ORAU.

From Magnetohydrodynamic Electrical Power Generation, 2nd International Symposium, Salzburg.

A discussion is presented on the possibility of giving a required conductivity to the working fluid in an MHD generator using thermionic emission from a suspended powder of LaB_6. The results of analytical calculations showed that an electron density of 10^{14} per cubic centimeter was attained with a powder density of 10^{13}/cc for the case of the LaB_6 solid particles of 10^{-5} cm radius at 2300°K. The fundamental properties of gas with suspension are thought to be different from those of a usual ionized plasma at various points, such as transport and relaxation phenomena, the magnetohydrodynamical properties, and the mobility of solid particles in the fluid. The conductivity of a mixture of nitrogen gas and powder of LaB_6 was calculated from the collision frequencies of an electron with solid particles and neutral molecules. The mechanism of the collision between electrons and solid particles is more complicated with that of electrons and ions. The effect of collisions was analyzed and the results were divided into the following three types: (1) The grazing collisions due to the attractive force between electrons and charged solid particles, (2) distant encounters between them, (3) the

collisions between electrons and neutral molecules. For nitrogen gas the Maxwell-averaged cross-section is reportedly 7.45×10^{-16} cm^2, thus the maximum conductivity is expected to be about 10 mho/m for a powder density of 10^{13}/cc (r = 10^{-5} cm) at 2300°K. Other transport coefficients, such as viscosity and thermal conduction were also calculated; however these values were not appreciably affected by the powder suspension. The relaxation times between electron temperature and solid temperature of particles, and between gas temperature and solid temperature are discussed by considering inelastic collisions. The electron density produced by the thermal emissivity from the powder was determined by the solid temperature of suspension. The evaluation of the solid temperature was not so easily raised by the elevated electron temperature. The magnetohydrodynamic equations of the powder suspension gas were deduced from the microscopic properties. The current equation shows the considerably reduced effect of ion slip. (auth)

41714 MHD POWER GENERATOR; E.T.L. MARK II. Mori, F. (Ministry of International Trade and Industry, Tokyo); Fushimi, K.; Yamamoto, M. Vienna, International Atomic Energy Agency, 1966, Preprint No. SM-74/133, 10p. (CONF-660704-109). ORAU.

From Magnetohydrodynamic Electrical Power Generation, 2nd International Symposium, Salzburg.

Major components parts of the E.T.L. Mark II generator are described. The combustion chamber was designed for a thermal output of 24 Mw by burning 0.6 kg/sec of kerosene with 1.8 kg/sec of oxygen. Separated 30 pairs of graphite electrodes are used with the insulation of magnesia slabs. The flow channel is of the conventional rectangular type with a cross-section of 10 × 10 cm at inlet, and a length of 120 cm. The ratio of the cross-sectional area at the outlet to the inlet is about 2.5. The magnetic field is provided by an iron-core electromagnet. The weights of the iron and the copper coil are approximately 70 t and 10 t respectively. The end face of the pole piece is 26 × 120 cm and the nominal air gap is 16 cm. The magnet, designed and tested by small models, can be run at 3.5 t with an exciting power of 1200 kw for five minutes. (W.D.M.)

41715 SHOCK TUBE STUDIES OF MAGNETICALLY INDUCED NON-EQUILIBRIUM IONIZATION IN POTASSIUM SEEDED ARGON PLASMA. Mori, Y. (Tokyo Inst. of Tech.); Kawada, H.; Yamamoto, M.; Imani, K. Vienna, International Atomic Energy Agency, 1966, Preprint No. SM-74/134, 24p. (CONF-660704-110). ORAU.

From Magnetohydrodynamic Electrical Power Generation, 2nd International Symposium, Salzburg.

The interaction of a moderately supersonic potassium-seeded argon plasma with a transverse magnetic field was investigated with various geometries of Faraday, straight-segmented Hall, ring and continuous electrodes in a conventional shock tube made of seven centimeter inner-diameter stainless tube. The flow velocity of test plasma varied from 1070 to 1150 m/sec and the corresponding gas temperature, pressure, and K number density were 1460 to 1950°K, 0.92 to 0.43 atm and 1.4×10^{15} to 1.6×10^{15}/cc, respectively. With five pairs of Faraday-type electrodes made of Mo or stainless steel at room temperature, it was possible to extract 10 amperes (0.4 A/cm^2) from the plasma at 1460°K, 0.92 atm, 1070 m/sec, and 1.4×10^{15}/cc K number density that is the lowest limit of gas temperature for MHD power generation. If the tube was evacuated to 100 ppM impurity level in order to avoid K oxidation and inelastic electron energy loss, a power as high as 21 watts (0.2 watt/cc) could be generated from the same plasma with an average magnetic field strength of 7050 gauss. Although the electrode drop especially at cathode was dominant, these values were found to be about two orders of magnitude greater than the theoretical equilibrium values with a reasonable agreement to the nonequilibrium theory including radiation loss. By the average method for bulk plasma diagnostics, the quasi-equilibrium electrical conductivity, electron density, and temperature were 0.1 mhos/m, 9×10^{10}/cc, and 1530°K respectively, when a normal and Hall-current short-circuit was imposed to the same test plasma. Under the same conditions, Hall parameter was found to be 2.8. Therefore, the momentum transfer cross section for 1530°K electron to argon was 1.6×10^{-16} cm^2 that was larger than the value from d-c discharge. When the opposed electrodes were short-circuited (one ohm) and Hall-opened, the nonequilibrium electrical conductivity, electron density, electron temperature, Hall parameter, and the cross section were 13 mhos/m, 2.7×10^{13}/cc, 2460°K, 2.2 radians, and 9.8×10^{-17} cm^2. The analysis of the electron energy balance showed that the elastic heat transfer to Ar overwhelmed the radiation loss above 10^{13}/cc electron density. The nonuniformity created by the Hall field over electrode walls could not seriously hamper the performance of the MHD generator, perhaps because of the low Hall parameter, cold surface temperature, and coarse geometry of electrodes. (auth)

41716 END LOSSES IN MHD CHANNELS OF VARIABLE CROSS SECTION AND THEIR REDUCTION. Moszynski, Jerzy R. (Argonne National Lab., Ill.). Vienna, International Atomic Energy Agency, 1966, Preprint No. SM-74/194, 12p. (CONF-660704-111). ORAU.

From Magnetohydrodynamic Electrical Power Generation, 2nd International Symposium, Salzburg.

Recently described schemes of MHD power generation, employing liquid metals, offer relatively high power densities with attendant low aspect ratios. Some of these schemes employ variable, rather than constant, area generator channels. The success of these schemes depends in a large measure on the reduction of end shunt losses. These have been shown to be capable of preventing power generation in the MHD channel for sufficiently low aspect ratios. Methods of calculation of these losses, available in the literature, are restricted to channels of constant cross section. In the present paper the method of Sutton, Hurvitz, and Poritsky is extended to channels of linearly variable area under the assumption of large Reynolds number and small magnetic Reynolds number. Under those conditions, and with the use of an "equivalent channel geometry" a conformal mapping technique permits the exact calculation of the net electrode current. Methods of reduction of the end losses, both in constant and in variable area channels, by employing insulating vanes parallel to the flow, were investigated. The effectiveness of such vanes is best expressed in terms of the gain in the maximum possible efficiency of the generator, as compared with the unvaned case. Simple vane configurations, amenable to analytical treatment, were found to be relatively ineffective and to require generally very long vanes with attendant large viscous losses. Thus, for example, a channel with an aspect ratio of 2 : 1 is capable of a maximum efficiency of 40.4%, if no attempt is made to reduce and losses. Very long vanes on the centerline of such a duct both upstream and downstream change the effective aspect ratio to 4 : 1 with an attendant maximum possible efficiency of 52.1%. More complex vane configurations, involving short vanes, were studied by an analog method and a most promising configuration was found to offer a maximum possible efficiency of 66% with the same aspect ratio of 2 : 1. Applied to the 4 : 1 aspect ratio channel, this vane configuration would promise a maximum possible efficiency of 74%. A number of channel and vane configurations and attempts to obtain an optimum considering both electrical and viscous losses are described. (auth)

41717 PLASMA DIAGNOSTICS BY MICROWAVE INTERFEROMETRY IN MHD CHANNELS WITH THE AID OF AN OPEN WAVEGUIDE. Muenkel, J. (Technische Hochschule, Aachen). Vienna, International Atomic Energy Agency, 1966, Preprint No. SM-74/155, 10p. (CONF-660704-112). ORAU.

From Magnetohydrodynamic Electrical Power Generation, 2nd International Symposium, Salzburg.

A new method of plasma diagnostics by microwave interferometry is described. Use is made of an open nonconventional waveguide in the test path of the microwave bridge. This waveguide, the so-called groove guide, consists of two parallel metal plates or bands with a shallow axially

directed groove in each. The plasma stream to be tested flows between these plates in a direction perpendicular to the direction of propagation of the microwaves. The groove guide has similar properties as the ideal parallel-plate guide with infinite sidewise extension, but the energy flow is caused to be concentrated in the middle region by the grooves. An approximate analysis, the transverse-resonance analysis, was used to calculate the field distribution and propagation characteristics of the guide. Because of the cross-sectional dimensions of the MHD channe in question (height 16 mm) and the wavelength chosen (4 mm) the groove guide had to be built for use in oversized quasi-optic technique. The transition from rectangular guide to the open guide was done in two steps. A commercial transition element from E-band to X-band waveguide was used, while a special launcher for transforming the TE_{10}-mode of the rectangular guide to the dominant mode of the groove guide was to be designed and constructed. With a good knowledge of the groove guide data and an appropriate theory of propagation of electromagnetic waves in ionized media, measuring phase shift and additional damping of the microwaves by introduction of the ionized gas allowed an evaluation of electron density and collision frequency, two of the most important plasma parameters. This new method of microwave plasma diagnostics is felt to be the best and most apt for obtaining reliable information in small MHD channels. (auth)

41718 PREPARATION AND TEST OF MHD DUCT WALL AND ELECTRODE MATERIALS. Nagahiro, A. (Asahi Glass Co., Yokohama, Japan); Shiota, M.; Fukui, T.; Amemiya, Y.; Hosoda, T.; Matoba, T.; Iida, S.; Takahashi, S. Vienna, International Atomic Energy Agency, 1966, Preprint No. SM-74/130, 24p. (CONF-660704–113). ORAU.

From Magnetohydrodynamic Electrical Power Generation, 2nd International Symposium, Salzburg.

Several insulating duct-wall and electrode materials were produced and their physical properties at high temperature were determined. Corrosion tests were also carried out and the changes in microstructure of test specimens were precisely observed and compared with each other. High-purity magnesia and stabilized or semi-stabilized zirconia refractories were selected as the wall materials. The starting materials were electrofused or hard-sintered high-purity grains of various mesh sizes, and some high-pressure forming techniques with special attention to the size distribution in the batch mix were adopted. The electrode materials were zirconium diboride and its alloys. They were prepared by a hot pressing method and the effect of their composition, press pressure, and press temperature on their quality was studied. The heat conductivity and the electric conductivity in the temperature range around 2000°C as well as the electron emissivity of the electrode were determined utilizing newly designed measuring apparatus. Long-time corrosion tests were performed at a hot-wall surface temperature above 2300°C, The seeding material was in the form of an alcoholic solution of potassium acetate and was spurted continuously with oxygen into the combustion chamber from the rear of the burner. The results of tests were inspected with petrographic microscope, x-ray diffraction analysis, and electron-probe microanalyzer. After 10 hr at 2400°C, the magnesia refractory showed hardly any trace of melting but a maximum loss of 5 mm in thickness due to evaporation and ablation was found. At the hot surface the growth of periclase crystals was marked and the striking tendency to form large single crystals was observed. The chemical reaction with the seed was not apparent. Based on several experiments with various product specimens and combustion conditions, the availability of these materials for hot-wall and semi-hot-wall open cycle MHD ducts was discussed. (auth)

41719 CRITERIA FOR USE OF RANKINE-MHD SYSTEMS IN SPACE. Nichols, Lester D. (Lewis Research Center, Cleveland). Vienna, International Atomic Energy Agency, 1966, Preprint No. SM-74/190, 16p. (CONF-660704–114). ORAU.

From Magnetohydrodynamic Electrical Power Generation, 2nd International Symposium, Salzburg.

Rankine cycles using an MHD generator can be considered for use in space. These systems must be evaluated on the basis of minimum weight, which generally means minimum radiator area to reject the cycle waste heat. On the basis of material limitations, maximum available magnetic field strength limitations, and limitations imposed by the MHD generation process itself, a restricted range of working fluid temperature and density is delineated. The maximum temperature, which is set by materials limitations, and the minimum radiator criterion can be used to specify the operating temperature extremes. The electrical conductivity of the working fluid must be about 1.0 mho/meter in order to achieve a reasonable power density. Since the conductivity decreases with increasing density this imposes a restriction on the working fluid in the generator. Since the generator can be shown to be less efficient at high Mach numbers and to generate a lower power density at a low Mach number, a compromise Mach number of 1.0 is selected. For this Mach number and the maximum allowable working fluid density in the generator, the density at the high-cycle temperature is specified. With this temperature fixed, the pressure is determined. Because a condensable vapor is used in the Rankine cycle, this combination of temperature and pressure requirements dictate the working fluid to be used. As a result, the condensor pressure is also specified because the radiator temperature is fixed. Within the framework of these restrictions certain freedom in the design of the generator system is possible. Nonequilibrium ionization can be used to enhance the conductivity of the working fluid at the prescribed conditions. In the case of magnetically induced ionization this effect is limited, however, by the maximum magnetic field strength that can be attained. Also, the generator cross-sectional area can be determined so as to minimize the generator volume consistent with the condition that the inlet and exit pressure is specified. Calculations based upon all of these criteria indicate that lithium is a good choice for a working fluid. If lithium is boiled at 1365°K, superheated to 1645°K and condensed at 1100°K the radiator weight is minimized for a generator efficiency of 0.80. For these conditions in a Faraday segmented generator operating with the entrance Mach number of 1.0 and a load parameter of $\frac{3}{4}$ with a magnetic field strength of 15 Tesla, the magnetically induced nonequilibrium ionization can produce an electrical conductivity of about $\frac{1}{2}$ mho/meter, corresponding to a power density of about 10^7 watts/cubic meter. The MHD system radiator area is about the same as for a turbo-electric system with the same temperature limits. The weights of these systems are comparable if a superconducting magnet is used in the MHD system and if the nuclear reactors for the two systems are of comparable weight. However, if larger magnetic field strengths and/or higher maximum cycle temperatures are attainable then it may be possible to reduce the weight of the MHD system. (auth)

41720 ANALYSIS OF A MAGNETOHYDRODYNAMIC AMPLIDYNE. Nowacki, Pawel Jan (Inst. of Nuclear Research, Warsaw. Technical Univ., Warsaw). Vienna, International Atomic Energy Agency, 1966, Preprint No. SM-74/52, 12p. (CONF-660704–115). ORAU.

From Magnetohydrodynamic Electrical Power Generation, 2nd International Symposium, Salzburg.

A new type of d-c generator, called the MHD amplidyne, is described. This type consists of n pairs of segmented electrodes, which are series-connected, the output electrode of the nth pair being connected through a load-resistance R_L with the input electrode of the first pair of electrodes. The electromotive force E_1 across the first pair of electrodes is created by an external magnetic field, e.g., a permanent magnet, whereas each following electrode pair is excited by a set of coils shunt-connected to the preceding electrode pair. The analysis is carried out for a case in which the Hall coefficient β can be neglected, the velocity of the gas being constant. By means of the chosen type of electrodes and coils connections, consider-

able output voltages can be obtained. The equations for the load current and electric output power are derived and optimal working conditions are discussed. Despite the inconvenience that the proposed generator type must be equipped with as many magnetic circuits as it has electrode pairs, it represents certain useful properties, especially it is a high-voltage source with moderate current and only one load-resistance. (auth)

41721 NON-EQUILIBRIUM MHD GENERATOR USING A NON-SEEDED INERT GAS AS WORKING FLUID. Ohlendorf, W. (Institut fuer Plasmaphysik, Garching, Ger.). Vienna, International Atomic Energy Agency, 1966, Preprint No. SM-74/31, 20p. (CONF-660704-116). ORAU.

From Magnetohydrodynamic Electrical Power Generation, 2nd International Symposium, Salzburg.

For the most successful operation of an MHD generator, two conditions must be fulfiled: (1) The electrodes must have a low enough work function so that they may emit the necessary current thermionically. The working fluid must have a certain degree of pre-ionization before it enters the MHD channel. The low electrode work function is necessary to avoid a cathode fall and to ensure that the current is uniformly distributed along the electrode perpendicular to the gas flow direction. This would not be the case for, for example, an arc-type discharge. Pre-ionization is necessary so that the discharge is not blown out downstream. In a MHD generator using inert gases such as argon as the working fluid, these two conditions are usually obtained by using an alkali-metal vapor as a seed material. The alkali-metal covers the electrodes and lowers the work function of the surface. At a gas temperature of 1500 to 2000°K, the thermal ionization of the seed material provides enough electrons so that the discharge is not carried downstream. These two conditions can however, be achieved with no seed material by: Using special electrodes with a low work function. For example, one can use commercially produced sinter electrodes which are coated or impregnated with barium- or strontium oxide. Pre-ionization to satisfy the second condition may be produced in various ways. One may use a small auxiliary discharge with d-c, a-c, or r-f supply, photoionization by uv light or x rays, electron beams, and so on. Theory and experiment show that the decay time for the electron density is of the order of hundreds of microseconds. The gas can be pre-ionized nonthermally before it reaches the channel entrance, and enough electrons remain at the channel entrance to fulfill the second condition. A simple theory shows that the nonequilibrium generator without seeding is comparable with a generator using seed. In addition, the non-seeded generator has many technical advantages over a seeded generator. Experiments have been set up to check these ideas. (auth)

41722 PERFORMANCE OF SPATIALLY CONSTANT B/ρ-TYPE MHD GENERATOR WITH ENERGY DISSIPATION. Ozawa, Yasutomo; Kayukawa, Naoyuki (Hokkaido Univ., Sapporo). Vienna, International Atomic Energy Agency, 1966, Preprint No. SM-74/139, 16p. (CONF-660704-117). ORAU.

From Magnetohydrodynamic Electrical Power Generation, 2nd International Symposium, Salzburg.

Numerical calculations were carried out on the electrical potential drop due to electrical boundary effects near the electrodes, the momentum drop due to viscous boundary layers, and the dissipation of thermal energy due to wall cooling. The effects of shock locations in the generator duct upon the generator performance of the generator proposed were calculated by taking into account the experimental results of the large-scale MHD generator, it was shown that the spatially constant B/ρ-type MHD generator had much higher conversion efficiencies than that of the conventional constant-velocity-type converter for moderate interaction parameters. (auth)

41723 QUASI-ONE-DIMENSIONAL ANALYSIS OF MAGNETOGASDYNAMICS. Pai, S. I. (Univ. of Maryland, College Park). Vienna, International Atomic Energy Agency, 1966, Preprint No. SM-74/1, 14p. (CONF-660704-118). ORAU.

From Magnetohydrodynamic Electrical Power Generation, 2nd International Symposium, Salzburg.

The basic equations of quasi-one-dimensional MGD flow are rigorously derived and the accurate expression of the electrical current density is obtained. The flow of an electrically conducting gas in a channel of slowly varying cross-section area A(x) with transverse externally applied electromagnetic fields is considered. For simplicity, it is assumed that the axis of the channel is straight and is denoted as the x axis. In quasi-one-dimensional analysis, the average values of MGD variables are used over each section x of the channel such that $\bar{Q}(x,t) = [1/A(x)] \int\int Q(x,y,z,t)\, dy\, dz$ where $Q(x,y,z,t)$ may be any one of the MGD variables and $\bar{Q}(x,t)$ is the corresponding average value used in quasi-one-dimensional analysis. The average process to the three-dimensional MGD equations with scalar electrical conductivity is applied and a system of exact quasi-one-dimensional MGD equations is obtained. The importance of many covariance coefficients of MGD has been pointed out. For instance, the exact equation of continuity for a steady flow should be $\bar{\rho}\,\bar{u}\,A = A\,\bar{\rho}\,\bar{u} + A\,\mathrm{cov}(\rho,u) = \text{constant} = k_\rho \bar{\rho}\,\bar{u}$ (say) where bar refers to the average value of a quantity and cov(ρ,u) is the covariance of ρ and u and k_ρ is a covariance coefficient introduced by the author. The value of k_ρ depends on the shape of the channel and its operating conditions. Actually k_ρ is a function of the Mach number of the channel flow. Further study of these covariance coefficients is recommended. The exact quasi-one-dimensional MGD equations are discussed and their relations with the conventional analyses are given. The exact Maxwell equation in quasi-one-dimensional analysis is $(1/A)(\delta A\bar{H}y/\delta x) = k_0\bar{\sigma}(\bar{E}_z + k_J\bar{u}\,\bar{B}y)$ where k_0 and k_J are two covariance coefficients. For approximate one-dimensional MGD flow, $k_0 = 0$ while for strictly one-dimensional analysis, $k_0 = 1$. But actually the value of k_0 lies between 0 and 1. Some simple solutions of exact quasi-one-dimensional MGD equations are given, which include both the steady and the unsteady flows of a viscous, heat-conducting and electrically conducting gas. (auth)

41724 APPLICATION OF FLUID SWITCHING TO MHD ENERGY CONVERSION. Pavlin, C.; Pascual, L. (Ste Bertin et Cie, Plaisir, France). Vienna, International Atomic Energy Agency, 1966, Preprint No. SM-74/66, 10p. (In French). (CONF-660704-119). ORAU.

From Magnetohydrodynamic Electrical Power Generation, 2nd International Symposium, Salzburg.

By using two fluid multivibrators operating in phase opposition—one fed with seeded hot gas and the other with cooler gas— it is possible to obtain striated flows without the use of any moving component. The fronts separating the sections are very clearly demarcated. A preliminary laboratory-scale experiment has been set up by the Ste Bertin et Cie. The switching frequency is high on a small scale (several hundred Hz). A large-scale project has yet to be carried out by experience with rocket-jet deflection by gas injection, which is based on the same principle, has shown that the response time for the establishment of the aerodynamic profile is extremely short. It is difficult to see how alternating current can be extracted directly from conventional MHD conversion units. To the extent that sufficiently fine and clearly demarcated fluid sections can be obtained—and this seems feasible with fluid switching—it will be possible to group electrodes so as to ensure alternating-current operation. By interposing nonconducting sections between conducting sections it will be possible to achieve direct elimination of the Hall currents, which would permit the use of quasi-continuous electrodes. A number of flow arrangements are outlined. (auth)

41725 BEHAVIOR OF ELECTRODES WITH ELECTRICALLY-CONDUCTING CERAMIC FRONTAL FACES ON THE RENARDIERES 8Mw-TEST RIG (ELECTRICITE DE FRANCE). Pericart, M. J. (Electricite de France, Paris); Yerouchalmi, M. D. Vienna, International Atomic Energy Agency, 1966, Preprint No. SM-74/63, 16p. (In French). (CONF-660704-120). ORAU.

From Magnetohydrodynamic Electrical Power Generation, 2nd International Symposium, Salzburg.

Ceramics were first considered from the point of view of electric conductivity, which had to be mainly electronic in view of the direct current generated with MHD. Stabilized cubic zirconias were gradually replaced by rare-earth chromites and mixed rare-earth zirconias and chromites. The materials considered were used in the form of cast cements or sintered pieces. In addition, the thermal fluxes were considered and evaluated with a view to making controlled-temperature ceramic-faced composite cooled electrodes placed against a metal case with water circulation. Various geometric solutions were used for fixing the ceramics on the cases, for ensuring electric relay of the current generated, and for satisfactory evacuation of the thermal flux. (auth)

41726 DESIGN AND TESTING OF INSULATING WALLS AND ELECTRODES FOR MHD CONVERTERS. Pericart, J. (Electricite de France, Paris); Dubois, A. Vienna, International Atomic Energy Agency, 1966, Preprint No. SM-74/65, 10p. (In French). (CONF-660704-121). ORAU.

From Magnetohydrodynamic Electrical Power Generation, 2nd International Symposium, Salzburg.

The insulating walls consist of cooled metallic elements mounted on large plates made of insulating material. The metal elements are separated by refractory ceramic joints. The electrodes consist of metallized ceramic elements brazed onto a cooled metallic support. An account is given of the results obtained from preliminary trials on test rigs of limited thermal power. This led to development of designs selected so as to ensure — from the viewpoints of mechanical strength, removal of high thermal fluxes, electrical insulation of the insulating wall elements, and electrode emissivity — satisfactory behavior of the components coming into contact with potassium-seeded combustion gases moving at high speed. The results of tests with insulating walls and electrodes designed and constructed in the light of the data obtained from the preliminary trials are described. (auth)

41727 SOME ASPECTS ON THE USE OF CRYOGENICALLY-COOLED PRIMARY-WINDINGS-SYSTEM FOR AN A-C MHD GENERATOR. Peschka, W.; Carpetis, C.; Gann, A.; Tries, B. (Deutsche Versuchsanstalt fuer Luft- und Raumfahrt eV, Stuttgart). Vienna, International Atomic Energy Agency, 1966, Preprint No. SM-74/115, 32p. (CONF-660704-122). ORAU.

From Magnetohydrodynamic Electrical Power Generation, 2nd International Symposium, Salzburg.

Two configurations of cryogenically cooled windings systems for a-c-MHD converters are proposed, one for a liquid nitrogen cooling system and the second for a liquid hydrogen cooling system. Real machine data are considered and the characteristics of the converter are given, mainly by considering the circle diagram of the machine (current vector as a function of slip s). An a-c-MHD converter, based on the first windings configuration and cryogenically cooled with liquid nitrogen and working with mercury is now running in order to study the predicted performance, and the technological problems. The data and construction characteristics of this machine are reported. Measurements of flow velocity, pressure drop along the MHD channel, temperature of mercury, losses in mercury, power flow between working fluid and cryogenically cooled windings, and the power factor $\cos\varphi$ are reported and compared to the theoretical values. The power of the heat pump needed for the cooling is considered. This power must be only a fraction of the MHD power, i.e., in order to have a sufficient efficiency of the system, very low cooling temperatures are needed. By use of nitrogen cooling the ohmic losses are high, and the power needed from the heat pump is generally higher than that of the MHD generator. But for a cooling temperature in the range of 20°K the heat pump power will be about 10 to 15% of the MHD power and the specific mass of the heat pump about 10 kg/kw of the MHD power. (auth)

41728 MHD GENERATORS OPERATING WITH TWO-PHASE LIQUID METAL FLOWS. Petrick, Michael (Argonne National Lab., Ill.). Vienna, International Atomic Energy Agency, 1966, Preprint No. SM-74/196, 20p. (CONF-660704-123). ORAU.

From Magnetohydrodynamic Electrical Power Generation, 2nd International Symposium, Salzburg.

A simplified one-component liquid metal MHD cycle which utilizes two-phase mixtures passing directly through the generator has been proposed and is being studied. Analysis indicates that a nuclear dual-cycle power system utilizing the proposed liquid metal conversion scheme as a topping cycle has overall efficiencies that are comparable to a plasma dual-cycle system at much lower temperatures. The key to the potential of this cycle is the performance of the MHD generator operating with two-phase mixtures. A large NaK–N_2 loop capable of accommodating both d-c conduction or a-c induction generators operating with either single-phase or two-phase flows has been built and recently put into operation. Recirculating NaK flow rates up to 200 gal/min and gas flows of 750 cu-ft/min can be obtained. The efficiency of a generator operating with two-phase flow will depend upon the nature of the flow and the degree to which the total entering liquid flow interacts with the magnetic field. Because the flow pattern of a two-phase mixture changes from a dispersion of gas in liquid to a dispersion of liquid in gas as the mixture quality is increased, two different types of generators are proposed and are being studied. In the first generator, referred to as a film generator, the two-phase mixture enters at a slight angle to the lower surface of the generator. The liquid is separated by impingement. The high-velocity free surface liquid film that is formed interacts with a transverse magnetic film. The efficiency of this type of generator is a function of the separation ratio, skin friction and momentum losses. A 2-kw version of the generator has been built and is currently being run. Initial tests up to 250 watts have been made which have shown that the generator concept is feasible and that the flow is stable. Thus far, this generator has run with inlet qualities to 0.05 and magnetic fields up to 12,000 gauss. Measured voltages and amperages have ranged to 0.60 volts and 60 amps. It is planned to continue with a sequence of tests wherein the generator performance will be studied at mixture qualities up to 50%. The trends of the data accumulated to date have been verified by analysis. A second generator wherein the two-phase mixture is passed directly through the generator with no deliberate attempt to form a film is also being studied. Experimental studies of air–water mixtures have shown that the conductivity of two-phase mixtures does not deteriorate excessively until mixture qualities of 30% are reached. A continuous functional relationship between the quality and conductivity exists even though the flow pattern traverses the gambit of two-phase flow regimes — from bubble to dispersed annular. From these tests, it appears that the electrical conduction is also through an annular film which exists in the various flow regimes. Such a generator has been operated successfully at very low qualities and flow rates, <5%; currently its performance characteristics in the higher quality regimes are being investigated. (auth)

41729 EXPERIMENTAL DETERMINATION OF THE ELECTRIC RESISTANCE AND THE TOTAL HEMISPHERIC AND MONOCHROMATIC RADIATION CAPACITY ($\lambda = 0.06$ μm) OF NIOBIUM AND ZIRCONIUM CARBIDES AT TEMPERATURES BETWEEN 1200° and 3500°K. Petrov, V. A.; Chekhovskoi, V. Ya., Sheindlin, A. E. (Moscow State Univ.). Vienna, International Atomic Energy Agency, 1966 Preprint No. SM-74/230, 12p. (In Russian). (CONF-660704-124). ORAU

From Magnetohydrodynamic Electrical Power Generation, 2nd International Symposium, Salzburg.

High-temperature carbides of zirconium and niobium can be used in MHD generators and other devices operating at high temperatures. Some of the thermophysical properties of these carbides at extremely high temperatures were investigated. The experimental determination of the total hemispheric radiation capacity of the carbides was performed calorimetrically. A sample in the form of a rod was heated by means of an alternating current. On the basis of measurements of the strength of the current passing through the sample, the voltage drop across the iso-

thermal working portion and the true temperature of the radiating surface of the sample, calculations were made of the total radiation capacity. At the same time the monochromatic radiation capacity for a wavelength of 0.66μm and the specific electric resistance were determined. The total radiation capacity, the monochromatic radiation capacity, and the specific electric resistance of niobium and zirconium carbides were measured at temperatures between 1200 and 3500°K. (auth)

41730 PROSPECTS FOR THE UTILIZATION OF CHEMICAL IONIZATION PHENOMENA IN MHD. Poncelet, J.; Harris, G.; Lozano, L. (Institut Francais du Petrole, Rueil-Malmaison, France). Vienna, International Atomic Energy Agency, 1966, Preprint No. SM-74/122, 19p. (In French). (CONF-660704-125). ORAU.

From Magnetohydrodynamic Electrical Power Generation, 2nd International Symposium, Salzburg.

A method has been developed for measuring the mean electrical conductivity of the reaction zone of pre-mixed hydrocarbon and air flames varying in composition and oxygen enrichment. The action of certain additives selected on the basis of currently accepted chemical ion formation mechanisms and capable of increasing the rate of ion formation was studied. The conditions necessary for possible application to MHD energy conversion and the problems involved in this connection are discussed. (auth)

41731 EXPERIMENTAL INVESTIGATION OF THE IONIZATION AND CONDUCTIVITY OF HYDROCARBON FUEL COMBUSTION PRODUCTS IN THE PRESENCE OF SOLID PARTICLES WITH A SMALL ELECTRON WORK FUNCTION. Popov, V. A.; Zimin, E. P. (Krzhizhanovskii Inst. of Power Engineering, Moscow). Vienna, International Atomic Energy Agency, 1966, Preprint No. SM-74/243, 10p. (In Russian). (CONF-660704-126). ORAU.

From Magnetohydrodynamic Electrical Power Generation, 2nd International Symposium, Salzburg.

A study is presented of the electrophysical parameters of the combustion products of methane in the presence of solid particles of matter possessing a small electron work function. The investigations were carried out in the combustion product zone of a methane–oxygen flame into which barium oxide and calcium oxide particles were introduced. The experimental conditions were as follows: total pressure 1 atm, temperature 2200 to 2530°K, activity radius of the particles $\sim 10^{-5}$ cm, and particle concentration up to $\sim 10^{9}$ cm^{-3}. The measurements were carried out by means of microwave probes. By using radio waves of two frequencies (35.4 and 70 kMHz) it was possible to measure simultaneously the free electron concentration and the effective frequency of the collisions between electrons and other particles. The particle size distribution was measured directly in the combustion zone and the activity radius of the particles thereby determined. The conductivity of the combustion products of methane and coal was also measured. (auth)

41732 APPLICATION IN NUCLEAR MHD CYCLES OF NON-EQUILIBRIUM IONIZATION FROM METASTABLE MOLECULAR STATES EXCITED BY FISSION FRAGMENTS. Powell, J.; Zucker, M. (Brookhaven National Lab., Upton, N. Y.). Vienna, International Atomic Energy Agency, 1966, Preprint No. SM-74/192, 16p. (CONF-660704-127). ORAU.

From Magnetohydrodynamic Electrical Power Generation, 2nd International Symposium, Salzburg.

Nonequilibrium ionization by the Kerrbrock effect (ohmic heating) has the disadvantage that energy input and conductivity are dependent on current density. This may lead to serious inhomogeneities and short circuits in the plasma. An alternative method of nonequilibrium ionization is proposed, whereby fission fragments emitted from thin uranium-bearing foils in the nuclear reactor excite long-lived states in the plasma. If a mixture of nitrogen, inert gas, and cesium vapor is used, the excitation and ionization will persist till the gas leaves the MHD generator. Three modes of excitation are examined in detail: monatomic nitrogen, metastable electronic, and metastable vibrational states of nitrogen. In the conditions of interest all have lifetimes of a few milliseconds or greater. The main reactions are: $N + N + Cs \rightarrow N_2^*$ electronic $+ Cs^+ + e^-$; N_2^* electronic $+ Cs \rightarrow N_2^*$ vibrational $+ Cs^+ + e^-$; N_2^* vibrational $+ Cs \rightleftharpoons N_2$ ground $+ Cs^+ + e^-$; N_2^* vibration $+ x \rightarrow N_2$ ground $+ x +$ K.E.; and $e^- + x \rightarrow e^- + x$ (K.E.). The system of equations is solved for a concentration and conductivity in a variety of conditions, using experimental rate and equilibrium constants. Typically, if 5% of the reactor power is deposited in the gas by fission fragments, excited species concentrations are 10^{16} cm^{-3}. Conductivities are on the order of 10 mho/meter and persist for 5 to 10 milliseconds in a gas at 2 atm and 1500°K. The nonequilibrium heating rate is several watts/cc, comparable to the ohmic heating method. Analyses of MHD generators with simultaneous ohmic and metastable nonequilibrium heating are presented. Because of variations in gas density operating conditions should be chosen to maximize the energy in vibrational metastables, otherwise conductivity variations become excessive along the generator. Some experiments relating to lifetime of the metastable electronic species in nitrogen are described. Afterglow plasmas of several hundred milliseconds duration at 1 to 2 atm have been obtained. (auth)

41733 ANALYTICAL AND EXPERIMENTAL RESULTS OF THE FLUID METAL MHD POWER CONVERSION PROGRAM. Prem, Lawrence L. (Atomics International, Canoga Park, Calif.). Vienna, International Atomic Energy Agency, 1966, Preprint No. SM-74/184, 16p. (CONF-660704-128). ORAU.

From Magnetohydrodynamic Electrical Power Generation, 2nd International Symposium, Salzburg.

The fluid metal MHD power conversion cycle developed by Atomics International was described at the 1964 Paris Conference. The analytical and experimental results accomplished during the past two years are summarized. One of the most significant achievements has been the design and construction of a 350 cps, 10-pole pair, flat channel, constant fluid velocity induction generator which was tested in a NaK blowdown facility. Net power of 1840 watts at 215 volts was generated, with an electrical efficiency of 36%. Evaluation of these tests shows that a sinusoidal magnetic field and induced current and voltage can be produced and that the predicted efficiency for a large generator will be 70% or better. Additional generator studies presently under way are: construction of a variable fluid velocity and variable magnetic field velocity generator, stator performance tests for a variable field velocity, and continuing analytical studies of the induction generator concept. Problems associated with the thermodynamics of the cycle are currently being investigated in a 1600°F potassium test loop which is now in operation. Frictional pressure drop tests of two-phase potassium have been completed. One of the results indicates that the frictional losses in the generator power. Another experiment concerning the mass heat transfer between an accelerated vapor and a subcooled liquid is presently being performed to determine: condensation of vapor as a function of mass flow rate and degree of subcooling, optimum method of injecting subcooling liquid, geometric configuration of the drift tube, and preferred pressure and temperature profiles from nozzle to generator inlet. These tests are expected to be concluded by the end of 1966. A liquid metal facility for operation at ambient temperatures has also been constructed for use in testing generators and other system components, such as diffusers and nozzles. This is a 1500-lb capacity NaK blowdown facility which can supply NaK at velocities of 250 ft/sec for a test period of 60 sec. Analytical studies of the overall cycle are also continuing using computer techniques, and the following parameters were investigated further; use of various alkali metals as working fluid, multipoint injection and expansion, and use of mixtures of two alkali metals as working fluid. These studies have shown that efficiencies of systems utilizing a working fluid composed of a mixture of lithium and cesium, or lithium and potassium are greater than those for single-fluid systems. (auth)

41734 ENERGY CONVERSION WITH LIQUID METAL WORKING FLUIDS IN MHD STAUSTRAHLROHR. Radebold, R. (AEG-Forschungsinstitut, Berlin); Lang, H.; Schulz, T.; Weh, H.; Klein, E.; Wagner, K. H. Vienna, International Atomic Energy Agency, 1966, Preprint No. SM-74/30, 20p. (CONF-660704-129). ORAU.

From Magnetohydrodynamic Electrical Power Generation, 2nd International Symposium, Salzburg.

The theoretical background of this project was described in a paper presented at the MHD Symposium in 1964 in Paris. It was pointed out that the thermodynamic acceleration of the liquid metal was the most serious problem of this energy conversion process. To reduce impact losses due to the injection of a sub-cooled liquid for condensation of the expanded vapor stepwise expansion and injection was proposed. The basic idea of this thermodynamic transformation was to convert the available energy of the gaseous phase into kinetic energy of the liquid phase, the latter being increased stepwise in mass flow rate. Condensation of the gaseous phase takes place in the last step of transformation by injecting sub-cooled liquid, the mass flow rate of which being comparable to that of the two-phase flow leaving the nozzle of this stage. A transformation of this kind assumes the liquid phase to be distributed as minute droplets into the gaseous phase, otherwise the slip in velocity between the two phases may not be neglected. The questions to be answered are how to convert a liquid into a fog-like two-phase flow in the heat source, how to disperse the liquid injected in the different steps of transformation and how to condense the fog flow? The problems involved in these questions are nucleation in liquids, growth of embryos, and explosion of bubbles. These processes were studied and the parameters influencing the spectra of droplets in the fog both in theory and experiment were analyzed. It should be noted that the strong coupling of both the gaseous and liquid phase gives a maximum of simplicity and reliance in respect to the conversion process, due to lack of superheating the gaseous phase and separation of the entrained liquid, as known from the Clausius-Rankine process. The theory of inductive extraction of electric energy from the liquid metal working fluids in the MHD converter was improved. A new concept of calculating end effects was developed and tested on a rotating machine. The effect of non-rectangular velocity profile in the liquid was analyzed and the losses due to current failing to reach bus bars estimated. A 50-cycle, three-phase, 380 volts inductive MHD converter ran several hours to prove the basic assumptions of the theory. The converter ran with NaK as a working fluid fed by a rotating pump. Deliberations for the realization of this energy conversion process led to the conclusion that a 20 kw(e) unit is a suitable one for space power applications, the heat source of which is a nuclear reactor, and the radiator to sub-cool the liquid for condensation is the surface of the last stage of the rocket. Passing the working fluid through the reactor does not seem to be opportune because of activation; a separate reactor circuit including pumps and heat exchanger to create the fog flow for thermodynamic transformation, however, destroys the concept of a simple and reliable power plant. At first sight, transfer of fission heat by heat pipes, in which the condensed phase of the metal enclosed is recirculated due to capillary forces, seems to be very promising; the problems involved in this concept proposed by Neu and co-workers (in respect to thermoionic conversion) are, however, not yet fully recognized. (auth)

41735 MAGNETIC HYDRODYNAMICS OF FLOW IN MHD DUCTS. Rakhimov, A. T.; Ulinich, F. R. (Kurchatov Inst. of Atomic Energy, Moscow). Vienna, International Atomic Energy Agency, 1966, Preprint No. SM-74/98, 10p. (In Russian). (CONF-660704-130). ORAU.

From Magnetohydrodynamic Electrical Power Generation, 2nd International Symposium, Salzburg.

Problems of the magnetohydrodynamics of flow with hot electrons in MHD ducts at low magnetic Reynolds numbers are discussed. The work deals principally with boundary-layer and impact-wave theory. In connection with boundary-layer theory, the conditions of the occurrence of detachment and the jump in condensation associated with it are discussed for a supersonic flow. The methods of preventing detachment are discussed; in particular the required degree of exhaustion of the plasma from the boundary layer is calculated. The wave resistance to supersonic flow which arises from the uneven distribution of the current on the electrode wall of the duct is considered. In connection with the theory of impact waves in a plasma with hot electrons, the structure of these waves in relation to the rate of ionization is considered, together with their stability. The problems related to the appearance of parasitic closed currents, with a strong reduction in conductivity of the plasma beyond the front of the impact wave and a change in the regime to accelerating, are also dealt with. (auth)

41736 MHD POWER GENERATION EXPERIMENTS USING SEEDED INERT GASES. Ralph, J. C.; Bainton, K. F. (Atomic Energy Research Establishment, Harwell, Eng.). Vienna, International Atomic Energy Agency, 1966, Preprint No. SM-74/12, 16p. (CONF-660704-131; AERE-R-4901). ORAU.

From Magnetohydrodynamic Electrical Power Generation, 2nd International Symposium, Salzburg.

The design and operation of a low-temperature MHD test rig is described, in which attempts are being made to study the feasibility of operating in the nonthermal ionization mode and still produce reasonable power levels. The basic facility which is described in some detail consists of an alumina pebble bed heated by graphite resistance elements. The heat capacity and heat transfer in this bed are such that at least 300 kw of heat energy can be transferred to the inert gas under test (usually argon) for several minutes with gas outlet temperatures stable and within 90°C of the initial center bed temperature. The design at present permits gas temperatures up to 1500°K to be obtained, this being a conservative estimate of what could be achieved by a high-temperature gas-cooled reactor within the next decade. A rig of this type naturally required some development in the early stages of commissioning and the various problems which have arisen on this apparatus are discussed. There are a number of novel features on the rig, such as a dew point method of measuring seed fraction, a porous Inconel seed evaporator, and the method of seed injection used; these are also described. The experimental program on this apparatus has just started and the observations on the first generation ducts are given. Initial indications are that the very low thermal ionization levels for potassium seeded argon at 1400°K require extremely high levels of duct insulator resistance in order to observe any output voltage or current when only thermal ionization takes place, which has so far been the case. (auth)

41737 TECHNIQUE FOR MEASURING THE SCALAR AND TENSOR PLASMA CONDUCTIVITY USING AN INDUCTION TYPE MHD DEVICE. Rashad, A. R. M. (Memphis State Univ.). Vienna, International Atomic Energy Agency, 1966, Preprint No. SM-74/3, 12p. (CONF-660704-132). ORAU.

From Magnetohydrodynamic Electrical Power Generation, 2nd International Symposium, Salzburg.

A new technique is described for accurately measuring the scalar and tensor a-c electrical conductivity of plasmas used in a-c MHD generators and accelerators. The device consists of a cylindrical plasma column (region 1) moving with a regulated axial velocity V_{opz}. An external magnetic field structure is located outside the plasma, and separated from it by a thin annular homogeneous medium (region 2). The magnetic field system is properly designed to produce in the plasma a constant axial magnetic field B_{opz} and a traveling-wave magnetic field B_t. The coils of the latter magnetic field system are excited in a certain way so as to produce radial, azimuthal, axial magnetic field components alone or any combination of them as required. This field design permits measuring the scalar and tensor components of the plasma conductivity directly. The theory of the apparatus is presented analytically in detail. The design features of the device are properly chosen so as to simu-

late the actual operating conditions of traveling magnetic wave a-c plasma accelerators and generators. It permits also accurate measurements of the plasma conductivity in these specific applications. Further, the results of this study are compared to those of the actual conductivity measurements obtained from the actual generator and accelerator experiments. Good agreement between the results was observed. It is concluded that the technique permits accurate measurements of the plasma conductivity under similar operating conditions to those of MHD generators and accelerators. (auth)

41738 PROCESSES OF INTERACTION BETWEEN HIGH-TEMPERATURE MATERIALS AND GAS FLOWS IN THE DUCT OF AN MHD GENERATOR. Rekov, A. I.; Romanov, A. I.; Ivanov, A. B. (Moscow State Univ.). Vienna, International Atomic Energy Agency, 1966, Preprint No. SM-74/228, 8p. (In Russian). (CONF-660704-133). ORAU.

From Magnetohydrodynamic Electrical Power Generation, 2nd International Symposium, Salzburg.

The behavior of a wide range of materials was studied in conditions simulating the operating conditions of open- and closed-cycle MHD generators. A number of possible electrode and insulating materials are discussed, in particular the oxides ZrO_2, MgO, BeO, and Al_2O_3; the carbides SiC, TiC, ZrC, and NbC; the borides ZrB_2, TiB_2, and LaB_6; and various composition materials. The possibility of using high-temperature concretes for electrical insulation is considered. (auth)

41739 MHD GENERATOR PERFORMANCE PREDICTION INCLUDING TWO-DIMENSIONAL EFFECTS AND WALL LEAKAGE. Reseck, Karl G.; Eustis, Robert H.; Kruger, Charles H. (Stanford Univ., Calif.). Vienna, International Atomic Energy Agency, 1966, Preprint No. SM-74/175, 12p. (CONF-660704-134). ORAU.

From Magnetohydrodynamic Electrical Power Generation, 2nd International Symposium, Salzburg.

The Stanford MHD generator operates on the combustion products of ethyl alcohol, oxygen, nitrogen, and KOH seed. The active part of the generator test section is 19 inches in length with a constant cross section of $1\frac{1}{4} \times 4$ inches. Thirteen pairs of electrodes can be connected for segmented, continuous, Hall, or other modes of operation. At normal conditions about 0.16 lbm per second of alcohol is burned with stoichiometric oxygen and an equal mass of nitrogen, resulting in a total throughput of about 0.80 lbm per second and a thermal input of about 2 Mw. The Mach number at the entrance to the test section is about 0.6 and the flow is choked at the exit. The exhaust pressure is atmospheric. Performance calculations based on simple one-dimensional analysis do not agree well with the observed data. Electric field probes in the side walls clearly show large voltage losses associated with the electrodes and the thermal boundary layers. The load voltage is less than predicted by simple theory, and the discrepancy increases with both magnetic field intensity and axial position down the channel. At B = 2.6 Tesla, the average open-current load voltage is approximately 20% low. An analytical model has been postulated which considers the gas as a one-dimensional core enclosed by four viscous and thermal boundary layers. Since the magnetic interaction in the Stanford generator is small, the fluid mechanics and electromagnetic effects are assumed to be uncoupled. Flat-plate boundary layer theory with one-seventh power velocity and static enthalpy profiles are used. Properties are evaluated at a reference temperature in the boundary layer and the flow is assumed in local thermal equilibrium with dissociation effects accounted for. Load currents and leakage currents (boundary layer and conducting wall) are considered in both the axial and transverse directions. The final equations express the axial and transverse electric fields in the gas core as functions of observed load currents and two leakage resistances—one axial and one transverse. Quantitative performance of the generator is established by selecting one set of values for the two resistances which are then used to predict power generation performance for segmented, continuous, and Hall electrode configurations. (auth)

41740 OPTIMIZATION OF GENERATOR PARAMETERS AND OF OVERALL THERMAL EFFICIENCIES FOR AN MHD REACTOR SYSTEM. Rice, G.; Parsons, M. J. (Atomic Energy Research Establishment, Harwell, Eng.). Vienna, International Atomic Energy Agency, 1966, Preprint No. SM-74/251, 14p. (CONF-660704-135). ORAU.

From Magnetohydrodynamic Electrical Power Generation, 2nd International Symposium, Salzburg.

The basic parameters for a direct-cycle gas-cooled reactor MHD generating plant are considered. The reactor coolant temperature is limited to within the range 1600 to 2000°K. Increased gas pressure normally implies reduced reactor plant size. In an MHD plant, however, increased pressure will normally result in reduced specific power, for which a lower limit of 5 to 10 Mw/m^3 is assumed. Extra thermal ionization due to enhanced electron temperature is assumed. The gases helium and argon with potassium and cesium seeding are considered. Computed values of power density for the generator are presented for various gas temperatures between 1010 and 2000°K, magnetic field strengths up to 8 T and a generator coefficient of 0.8. The effect of varying Mach number, for mainly subsonic flow, is illustrated in plots of power density versus seed pressure. Optimum seed fraction values result in increase in conductivity of a few orders of magnitude when compared to results computed at seed fractions appropriate to optimized thermal conditions. For argon–potassium the optimum seed for nonequilibrium conditions is in general an order of magnitude less than that for thermal conditions. Plots of computed values of electric field for varying degrees of ionization, at fixed current density, illustrate the effect of reduced conductivity on optimum seed fraction. Comparison is made with similar results obtained by static gas discharge experiments. It is shown that helium is worse than argon by a factor 10 on pressure, for the same MHD power density. For helium at a temperature of 1000°K, "ion-slip" starts to become dominant and subatmospheric operation is necessary for attaining power densities as low even as 2 Mw/m^3. The ionic mobility of helium–potassium is, in fact, much higher than for argon–potassium and for the former combination especially, and in particular for a segmented geometry generator, the effect on Hall field is of considerable importance. Using the values of pressure and temperature suggested by this study the thermal efficiency of a combined reactor-MHD-steam plant is established for the various values of reactor outlet temperature, MHD duct inlet and outlet temperatures, and steam generator inlet and outlet temperatures. The gas side was taken to operate on a Brayton cycle with heat exchange and the steam plant on a Rankine cycle with superheat, reheat as necessary both with and without regenerative heating. An expression for the thermodynamic efficiency of the combined gas-steam cycle is derived taking account of the heat lost in the cooler. The procedure for establishing temperatures at inlet and outlet to the steam generator to ensure maximum overall efficiency is described and the variation of efficiency with recuperator ratio is illustrated. These results show that a recuperator ratio of 1 gives almost the same overall efficiency as a ratio of 0 and intermediate values result in a lower efficiency. The size of reactor, MHD duct, and steam generator are compared for the conditions implied by the duct and cycle analysis. (auth)

41741 EXPERIMENTAL INVESTIGATIONS OF CLOSED-LOOP MPD POWER GENERATION. Rosebrock, T. L.; Tipton, D. L.; Clingman, D. L.; Koch, R. L.; Whitaker, R. O. (General Motors Corp., Indianapolis). Vienna, International Atomic Energy Agency, 1966, Preprint No. SM-74/181, 14p. (CONF-660704-136). ORAU.

From Magnetohydrodynamic Electrical Power Generation, 2nd International Symposium, Salzburg.

Modifications and previously unreported results of recent closed-loop MPD generator testing are reported. Theoretical calculations of loop performance are presented and correlated with experimental data for the various electrode configurations. Tests were conducted on a generator designed to incorporate an electrode structure for elimination of electrode shorting and increased length to provide more

time for relaxation of nonequilibrium effects. The magnetic field was 2 Teslas with an effective generator length of 45 cm. Electrode shorting due to cesium coverage was apparently eliminated. Cesium was metered as a liquid by positive displacement, evaporated, and injected as a vapor through a multi-orifice manifold. Injection rate was electronically controllable over a seed ratio from 0.1 to 1.0 per cent. Hall current leakage was minimized by use of boron nitride flow guides at the generator inlet and exit. The channel Mach number was approximately 0.5. The static pressure was limited to approximately 0.5 atm at a static temperature of 1700°K by maximum heater power. Consideration was given to the measurement of plasma properties under conditions of nonthermodynamic equilibrium between electron temperatures and electron density. Theoretical calculations are presented for equilibrium and nonequilibrium generator performance. Equilibrium plasma properties were computed by use of a computer program for a four-component, two-temperature plasma. Electrical conductivities were computed using energy-dependent electron cross sections. Assuming resonance lines to be broadened by Doppler and Lorentz effects, the radiation loss from the plasma was computed by adding elastic energy losses to the radiation losses. Inlet relaxation lengths of electron temperature and electron density elevation were computed for a dense helium–cesium plasma. The ionization rate coefficient was based on ionization from excited states. The effect of recombination and plasma properties on inlet relaxation are considered. Experimental performance data are presented for continuous, Hall, and segmented generator configurations. Electrical conductivity data at generator inlet and exit allowed determination of magnetoactive ionization and nonequilibrium relaxation. (auth)

41742 EFFICIENCY OF CLOSED-LOOP MHD GENERATORS UTILIZING THERMAL NON-EQUILIBRIUM IONIZATION. Rosner, M. (Brown, Boveri and Co. Ltd., Baden, Switzerland). Vienna, International Atomic Energy Agency, 1966, Preprint No. SM-74/29, 12p. (CONF-660704–137). ORAU.

From Magnetohydrodynamic Electrical Power Generation, 2nd International Symposium, Salzburg.

In an earlier paper for the case of the open-loop MHD cycle, the advantage of presenting the thermal efficiency as a function of the net MHD-output density (including compressor power) has been shown, all other operating parameters being held constant. This method is used for presenting the efficiencies of the closed-loop MHD cycle. Taking the example of the simple combined MHD-steam power station, working with He/Cs, the effect of gas velocity in the MHD channel, the wall friction, the channel heat losses, the segmentation of the electrodes, and the seeding concentration on the optimum overall efficiency is discussed in detail. The calculations were made with the intention of stimulating further investigations to answer the ultimate question of whether future high-temperature gas-cooled reactors in combination with MHD generators will eventually be more economical than the proposed conventional energy converters, perhaps even at the same thermal efficiency. (auth)

41743 OIL FIRED MHD POWER PLANT. Rosner, M. (Brown, Boveri and Co. Ltd., Baden, Switzerland). Vienna, International Atomic Energy Agency, 1966, Preprint No. SM-74/28, 20p. (CONF-660704–138). ORAU.

From Magnetohydrodynamic Electrical Power Generation, 2nd International Symposium, Salzburg.

As a possible pilot plant, a heavy fuel oil-fired MHD-steam power station is described. A pilot plant with natural gas as fuel cannot be considered as representative. On the other hand, residual fuel oil has been steadily increasing in significance in European power station practice over the past few decades. The MHD pilot plant must be as simple as possible in concept, so that the question of its reliability can be answered. The two essential unknowns are the design of the MHD duct and the large superconducting magnets. Both pre-heating of the air above about 800°C and oxygen enrichment should be dispensed with for the time being. The combustion chamber should be constructed according to well-proved principles. It is proposed as well that the seeding problem should be solved with simple methods. In the example which is discussed, it does not seem impossible that the specific plant costs of the whole power station will be kept to the level prevailing for steam power stations of the same output, while the thermal efficiency, after taking into account all the losses which can at the moment be assessed, is still 15% higher than that of the power station in comparison. If only the proposed pilot plant is considered, then the enormous development costs for the high temperature pre-heater and other costly items can be postponed until a later date, when the further development of the open-cycle MHD-power station can be fully justified. (auth)

41744 EFFECTIVENESS OF THE OXYGEN ENRICHMENT OF AIR IN MHD GENERATOR ASSEMBLIES. Rossievskii, G. I.; Monastyrskaya, A. R.; Koryagina, G. M.; Goncharova, V. S.; Iglova, L. V.; Vinokurov, E. K. (Ordzhonikidze Inst. of Engineering Economy, Moscow). Vienna, International Atomic Energy Agency, 1966, Preprint No. SM-74/201, 16p. (In Russian). (CONF-660704–139). ORAU.

From Magnetohydrodynamic Electrical Power Generation, 2nd International Symposium, Salzburg.

Oxygen enrichment of air in MHD generator assemblies is considered as a means of lowering the temperature of the oxidizer and raising the initial temperature of the cycle. The initial parameters of the cycle are shown to depend on the composition of the oxidizer and its pre-heat temperature when the final parameters are fixed; the maximum temperatures attainable in the cycle are also given. The effective degree of oxidizer pre-heating as a function of its composition is discussed. The limitations, associated with the increase in the initial pressures, that prevent the use of a high degree of oxygen enrichment are analyzed. The results are presented of heat flow calculations for large power stations incorporating MHD generators and for the MHD generators themselves, using oxygen enrichment. A comparison is also made between the power-generating characteristics of MHD installations operating with oxygen-enriched air and those of MHD generators in which normal air is pre-heated to high temperatures. It is concluded that, for oxygen to be used effectively in MHD power generation, it must be produced more economically. (auth)

41745 CONSTRUCTION AND TESTING OF AUXILIARY-ARC ELECTRODES. Rostas, Francois; Destree, Rene (Centre de Recherches de la Compagnie Generale d'Electricite, Marcoussis, France). Vienna, International Atomic Energy Agency, 1966, Preprint No. SM-74/146, 12p. (In French). (CONF-660704–140). ORAU.

From Magnetohydrodynamic Electrical Power Generation, 2nd International Symposium, Salzburg.

Auxiliary-arc electrodes which have been constructed and tested seem to provide a solution both of the cold boundary layer problem and of the cathode emissivity problem. For this purpose an arc is established between a refractory metal cathode placed behind and clear of the generator wall and an anode forming part of the wall. The arc column can be activated by a rotational movement under the effect of a magnetic field, which may be that of the machine itself. The mechanical arrangement of the electrodes is such that, with a weak flow of gas (argon for example), it is possible to maintain a protective atmosphere around the arc cathode, while the arc anode is strongly cooled by the wall. The gas flow also has the effect of forcing the arc column towards the stream, thus increasing the conductivity of the boundary layer. Furthermore, the arc column behaves as a virtual cathode, from which a sizeable electron current can be extracted. Electrodes constructed on this principle were tested on gas streams composed of fuel-oil combustion products. By using them as cathodes it was possible to extract a current of 5 A without the voltage drop between the electrode and the gas exceeding 10 v. Comparative tests were carried out with cooled metal electrodes, in which case the voltage drop was of the order of 120 v. The arc electrodes operated for several hours without any apparent

damage. In spite of the energy which had to be dissipated in the arc, the energy balance was extremely favorable and from this point of view the situation was as if the drop at the electrodes had been reduced from 120 to 20–30 v. Independently of the overall energy balance, the total elimination of voltage drop at the electrodes could make it possible to carry out conversion tests on streams generating low power. In addition, the fact that the metal components of these electrodes are swept by a gas such as nitrogen or argon should ensure, with electrodes of this type, the long lifetimes required for magnetoaerodynamic generators. (auth)

41746 METHOD OF OPTIMALIZING THE ELECTROMAGNET OF A DIRECT-CURRENT MHD GENERATOR. Schenk, J. (Higher Technical School, Brno). Vienna, International Atomic Energy Agency, 1966, Preprint No. SM-74/83, 20p. (In Russian). (CONF-660704–141). ORAU.

From Magnetohydrodynamic Electrical Power Generation, 2nd International Symposium, Salzburg.

A calculation method is given for evolving a combined technical and economic project of a ferromagnetic electromagnet to be used in a direct-current MHD generator. The method is based on the factors determining the estimated costs of the electromagnet. These estimates, including capital and operating components, are determined using data on dimensions and costs. A further factor is the "magnetic condition" linking the dimensional data with the electromagnetic values. Using the method of optimalization which has been worked out, and with known magnetic induction and known dimensions of the air gap, it is possible to determine from the above two factors the size of electromagnet at which the estimated costs will be lowest. This method was used to calculate for an industrial MHD generator, the specific estimated costs and the specific power required of the electromagnet as a function of the magnetic induction in the air gap; these parameters also serve as a basis for the general design of an MHD generator or an MHD power station. It is interesting to note that, over the relatively wide range of change in magnetic induction in the air gap from 2.0 to 3.5 Teslas, the minimum costs are obtained at the same relatively low current loads of the exciting coils $I = 3.2 \times 10^6$ to 4.0×10^6 A/m^2. The same current load on copper is encountered in normal machines. The preliminary calculation for a given electromagnet is reproduced as a descriptive example; it shows the possibility of the economic use of electromagnets with ferromagnetic materials in the industrial application of direct energy conversion. The fraction of the total capital outlay spent on the electromagnet and the portion required by the power station are within economically acceptable limits. The derivation of an approximate relation for calculating the magnetomotive force of the magnetic circuit required to solve the "magnetic condition" is given. Calculated relations are also given for determining changes in magnetic induction in the air gap of the electromagnet. The accuracy and applicability of these relations have been checked on an experimental electromagnet. (auth)

41747 EXPERIMENTAL INVESTIGATION OF CLOSED-LOOP MPD POWER GENERATION. Schneider, R. T.; Wilhelm, H. E. (Univ. of Florida, Gainesville). Vienna, International Atomic Energy Agency, 1966, Preprint No. SM-74/160, 18p. (CONF-660704–142). ORAU.

From Magnetohydrodynamic Electrical Power Generation, 2nd International Symposium, Salzburg.

Results of a closed loop MPD power generation experiment are reported. Objective of the experiment was to investigate whether nonequilibrium ionization exists and whether this effect is of sufficient magnitude to make closed loop MPD power generation feasible to low operation temperatures. It was observed that the generator can be operated in two different modes—the nonsaturated mode and the saturated mode. In the latter, the U-B curves show not only a saturation at medium magnetic fields but also a decrease of the output voltage at higher magnetic fields. An explanation of this "saturation effect" is proposed. Experiment and theory are compared. (auth)

41748 EXPERIMENTAL DETERMINATION OF THE INTERNAL RESISTANCE MATRIX OF MHD GENERATOR WITH TENSOR CONDUCTIVITY USING A SEMICONDUCTING MODEL OF HIGH ELECTRON MOBILITY. Schultz-Grunow, F.; Denzel, D. L. (Technische Hochschule, Aachen). Vienna, International Atomic Energy Agency, 1966, Preprint No. SM-74/72, 18p. (CONF-660704–143). ORAU.

From Magnetohydrodynamic Electrical Power Generation, 2nd International Symposium, Salzburg.

The electrical characteristics of an MHD generator with an arbitrary electrode configuration, finite electrode number, and full consideration of end effects were investigated. The influence of Hall effect, ion slip effect, and an arbitrary velocity profile were considered. The potential of the laboratory co-ordinate system is transformed by an integral relation to the moving frame potential Φ, which satisfies Laplace's equation. With the form of the expression for the conformal transformation of the generator duct onto a plane with homogeneous current density, it is shown that the (n-1) potential differences $(\Phi_i - \Phi_1)$ of the n electrodes can be expressed as a linear function of each of the (n-1) electrode currents I_i. The interrelation of (n-1) potential differences and (n-1) electrode currents form an array of elements which is called the internal resistance matrix. Each element of this internal resistance matrix can be clearly defined by the generator geometry, the conductivity and by the angle of the conductivity tensor. In contrast to the scalar conductivity case, it is shown that Maxwell's reciprocity theorem is not valid. For tensor conductivity, the internal resistance matrix is not symmetric, so the derivation of an equivalent circuit for the generator under general loading condition is not possible. For real channel geometry, the calculation of elements of the internal resistance matrix is not possible by any analytical method. All the elements of the internal resistance matrix can be determined by simple terminal measurements at semiconducting models of high-load carrier mobility in a magnetic field. Such a channel replication is provided with electrodes in conformity with the MHD channel geometry. At given plasma parameters the corresponding model parameters are formulated. (auth)

41749 MHD ROTATING MACHINE: NEW TYPE OF A-C MAGNETOHYDRODYNAMIC POWER GENERATOR AND TURBINE. Sekiguchi, T.; Katsurai, M.; Yokoyama, K. (Tokyo Univ.). Vienna, International Atomic Energy Agency, 1966, Preprint No. SM-74/137, 8p. (CONF-660704–144). ORAU.

From Magnetohydrodynamic Electrical Power Generation, 2nd International Symposium, Salzburg.

In order to remedy unfavorable present situation for a-c MHD generators based upon the induction principle, a new type of MHD machine is proposed. The conceptual structure of the machine is very similar to that of the conventional three-phase rotating synchronous machine which consists of the rotor for the excitation of the mechanically rotating d-c magnetic field and the stator with conventional three-phase a-c windings. The only difference in concept is the existence of the MHD working fluid flowing in the duct space between the rotor and the stator in the direction of rotation of the rotor. Results of the preliminary theoretical analysis of the machine are presented. It is shown that the machine may be operated as an a-c MHD electrical power generator or as an electrically controlled MHD turbine or as the combination of these. As an a-c generator, the machine may be regarded as the combination of the synchronous and asynchronous (or induction) generator, and can be operated under such a condition that the rotor is in the self-rotating condition at the synchronous speed, or in other words, the external driving of the rotor is not required so that all the energy of the MHD working fluid, except the Joule loss in the fluid itself, is converted into a-c electrical power. On the other hand, as an MHD turbine, the d-c magnetic field of the rotor plays the role of the turbine blades, and in this case a small a-c current in the stator windings can control the mechanical power output transferred from the working fluid to the turbine rotor.

The very interesting results as an a-c electrical power generator from the practical viewpoint are that (1) under the self-rotating condition the lag power-factor operation ($0.8 \sim 1.0$) is possible in contrast with the case of the MHD induction generator, and (2) the machine is practically feasible not only by utilizing the combination of the liquid-metal working fluid and a relatively low d-c exciting magnetic field, but also by the use of the gaseous-plasma working fluid and a very high d-c magnetic field excitation. (auth)

41750 ANALYSIS OF SHOCK WAVE PROPAGATION IN CESIUM VAPOR, WITH ALLOWANCE FOR RADIATION. Seryakov, K. I. (Moscow State Univ.). Vienna, International Atomic Energy Agency, 1966, Preprint No. SM-74/219, 12p. (In Russian). (CONF-660704-145). ORAU.

From Magnetohydrodynamic Electrical-Power Generation, 2nd International Symposium, Salzburg.

The propagation of a shock wave in cesium vapor is characterized by a number of features. The thermodynamic properties of a cesium plasma depend to a considerable extent on the interaction of free charged particles (electrons and ions) with each other and with neutral atoms in highly excited states. The influence of these effects on the thermodynamic and gas dynamic parameters of a shock wave was investigated. Even at relatively low temperatures, the energy losses due to radiation become comparable with the rate of transformation of the kinetic energy of the flow into the thermal energy in the shock wave, especially upon propagation in a tube of finite diameter. The significance of this process is considered with regard to the possible formation of cesium plasma in a shock tube. (auth)

41751 EXAMINATION OF THE VALIDITY OF THE SAHA EQUATION IN A GAS DISCHARGE. Shaw, J. F.; Kruger, C. H.; Mitchner, M.; Viegas, J. R. (Stanford Univ., Calif.). Vienna, International Atomic Energy Agency, 1966, Preprint No. SM-74/176, 10p. (CONF-660704-146). ORAU.

From Magnetohydrodynamic Electrical Power Generation, 2nd International Symposium, Salzburg.

The electron number density, n_e, and the number densities of the various states, $n_k (k = 1, 2, \ldots N)$, in a steady-state partially ionized gas are determined by a set of rate equations which describe the collisional and radiative rates at which the various states are populated and depopulated. Symbolically, these algebraic equations in n_e and n_k have the form $F_e[n_e, n_k; f(\vec{v})] = 0$, $F_k[n_e, n_k; f(\vec{v})]$, $(k = 1, 2, \ldots N)$ where $f(\vec{v})$ is the free electron velocity distribution function. On the other hand, $f(\vec{v})$ is determined by electron Boltzmann equation. In the case of an applied electric field $\vec{E}$, this is an integro-differential equation which may be written symbolically $G[f(\vec{v}); n_e, n_k; T, \vec{E}] = 0$, where T denotes the temperature of the heavy particles. It is apparent that a rigorous solution for the degree of ionization (and consequently the electrical conductivity) requires simultaneous solution of these coupled equations. Using numerical procedures, solutions of these coupled equations were obtained which describe an alkali-metal-seeded noble gas at atmospheric pressure. Results are presented showing the effect of non-equilibrium phenomena on the degree of ionization and the electrical conductivity of the plasma. The effects, both of photon escape and of a non-Maxwellian distribution function with depleted tail, are considered. Under some conditions, either mechanism may produce a degree of ionization considerably different from that predicted by the Saha equation at the electron temperature. (auth)

41752 SPECIAL THERMODYNAMIC FEATURES OF HIGH-TEMPERATURE OPEN CYCLES. Shchegolev, G. M. (Ukrainian Academy of Sciences, Kiev). Vienna, International Atomic Energy Agency, 1966, Preprint No. SM-74/235, 10p. (In Russian). (CONF-660704-147). ORAU.

From Magnetohydrodynamic Electrical Power Generation, 2nd International Symposium, Salzburg.

At high temperatures the extraction of work from the working cycle of any motor, particularly an MHD generator, involves, in addition to the dissipative losses characteristic of all motors, inevitable losses through cooling and, when there is a fast gas flow in the working zone, losses due to imbalance of the expansion process. The most convenient way of performing the calculations for this work extraction process is to take a final point in the cycle at which the temperature is determined by the minimum acceptable gas conductivity; it is then possible and sufficient for purposes of the calculations to determine the increase in the entropy due to each class of losses indicated above. The method of calculation is simple if an IS diagram allowing for heat of dissociation is constructed for the working fluid under consideration. In order to allow for losses due to imbalance of the work extraction process, a special IS diagram can be constructed and dS/dI values superposed for adiabatic processes with a gas composition that is completely fixed. Although the necessary data for making corrections to the diagram when the gas composition is only partly fixed are not yet available, they can be obtained in the form of a relationship between the degree to which the gas composition is fixed and the actual composition of the gas and its rate of cooling. High-temperature cycles possess special features connected mainly with dissociation processes. A high-temperature cycle can be defined in such a way as to distinguish it from ordinary cycles (the maximum calorific value of the fuel is less than the thermal charge of the cycle). Of particular importance in MHD-generator cycles is the temperature beyond the duct, which is determined by the conductivity. A reduction in this temperature has a very positive effect on the cycle; when the temperature is high the pressure in the combustion chamber is at one or the other extreme. As a consequence the different types of loss have different and unusual effects on the thermodynamic characteristics of the cycle. In addition to the normal cycle with adiabatic expansion, it is useful to consider cycles in which heat is imparted while work is being extracted and which, in an idealized form, convey the idea of a cycle with an isothermal work extraction process. Such a cycle has somewhat poorer thermodynamic characteristics, but can lead to a reduction in the size of the chamber. If, on the other hand, as a result of an increase in conductivity during combustion, it becomes possible to reduce the temperature beyond the duct, this leads to an improvement—rather than a deterioration—in the thermodynamic characteristics of the cycle. Open-cycle MHD generators with oxygen enrichment of the air are the only types that are feasible in stationary power generation without involving other, i.e., non-MHD, scientific and technological problems. Analysis of such a cycle on the basis of various initial data has confirmed the fundamental ideas concerning the increase in the efficiency of a cycle as oxygen is added (assuming that the oxidizer is always preheated to the same temperature). It follows from the same analysis that cooling of the duct walls, which is essential for ensuring reliable operation of the MHD generator over a long period, can have a considerable effect on the thermodynamic characteristics of the cycle. This effect can be counterbalanced by adding more oxygen. The feasibility of increasing the amount of added oxygen and hence the efficiency of the cycle is limited by the increase in pressure in the combustion chamber. It is concluded that it is possible to construct a power station of considerable capacity and with an efficiency of the order of 50% using MHD generation with oxygen enrichment and a steam-turbine cycle. No new materials would have to be developed and no very expensive existing materials would need to be used; moreover, hardly any research work would be required. (auth)

41753 EXPERIMENTAL PROGRAM TO EVALUATE THE FEASIBILITY OF JET COMPRESSORS FOR CLOSED-BRAYTON-CYCLE MHD SYSTEMS. Shih, C.; Bienert, W. B. (Martin Co., Baltimore). Vienna, International Atomic Energy Agency, 1966, Preprint No. SM-74/186, 20p. (CONF-660704-148). ORAU.

From Magnetohydrodynamic Electrical Power Generation, 2nd International Symposium, Salzburg.

The application of jet compressors to closed Brayton cycle MPD systems has been suggested previously. The

feasibility of jet compression for MPD systems was investigated and some preliminary test results from a single-stage jet compressor loop are given. The purpose of the experimental program was to simulate the operation of a jet compressor under conditions comparable to those of an actual MPD plant, and to study the physics of momentum transfer of two high-velocity gas (or vapor) streams of highly different molecular weights. A jet compressor in which both gases mix at equal forward velocity has the same theoretical compression ratio as a reversible engine. The upper limit for the compression ratio achievable for a given set of input parameters (stagnation properties of both gases) can be calculated from purely thermodynamic principles. The expressions for the performance of an ideal jet compressor were applied to two typical high-temperature MPD cycles. The overall cycle efficiency is somewhat lower than obtainable with rotating machinery, but acceptable for special applications. In the experimental program a single-stage test facility was designed and operated. The driving gas was cesium vapor, the driven gas, helium. In the design of the system the objective was to simulate the temperatures, pressures, and working media of an MPD plant on a small scale. The facility is capable to handle up to 12 g/sec of the primary stream (cesium) and up to 2.5 g of the secondary stream (helium). The cesium is fed by a diaphragm pump into a refractory metal boiler at a pressure of up to 8.0 atmospheres and then superheated to approximately 1700°K. The superheated vapor expands in a supersonic nozzle and transfers part of its momentum to the low-temperature helium stream. The helium is circulated in a closed loop which is equipped with a throttle valve to simulate the pressure drop which would occur in an MPD generator. During some preliminary experiments the test loop was successfully operated at a cesium vapor temperature of 1590°K, and a helium pressure rise of 36% at a flow rate of 1.12 g/sec was achieved. The experimental results were reasonably close to the expected values. Experimental results with the single-stage compressor are presented. (auth)

41754 INFLUENCE OF WALL RADIATION ON THE NON-EQUILIBRIUM ELECTRICAL CONDUCTIVITY AND ON THE IONIZATION REACTION TIME OF A He–Cs PLASMA. Staehle, M.; Burkhardt, H. (Technische Hochschule, Stuttgart). Vienna, International Atomic Energy Agency, 1966, Preprint No. SM-74/47, 18p. (CONF-660704–149). ORAU.

From Magnetohydrodynamic Electrical Power Generation, 2nd International Symposium, Salzburg.

Electrical conductivity and ionization time constants of a He–Cs plasma were calculated as a function of pressure, temperature, and effective electrical field intensity. The flux of ionizing radiation within the MGD channel is defined by the wall temperature rather than by the electron temperature. Up to an electron density of 10^{15} cm^{-3} remarkable differences to the results of the usual calculation with the aid of Saha equation using electron temperature were observed. Measurements of the nonequilibrium electrical conductivity show an almost constant conductivity in a certain range of low current densities. Previous calculations of the nonequilibrium conductivity do not explain this experimentally observed effect at low current densities. By using Saha's equation with electron temperature, these calculations imply the assumption, that the radiation flux within the plasma is at equilibrium with the electron temperature. The electron density and electrical conductivity were calculated in a certain range of effective electrical field intensity, pressure, and gas temperature using dynamic equilibrium of ionization and recombination reactions. The results show a constant and even a decreasing electrical conductivity with current density at low values of current density, as has been experimentally observed. Due to the influence of external radiation there results not only an explanation of the character of the curves, but, depending on gas pressure, also an essential difference in the value of the nonequilibrium electrical conductivity at higher values of current densities, as compared to the calculations with the Saha equation. This implies the use of high-temperature, uncooled walls for MGD channels with nonequilibrium seeded noble gas flow. Another point of view for understanding of the experiments in MGD-channel flows is the retarded achievement of the stationary nonequilibrium value of the electron density after the entrance of the plasma into the magnetic field region. The equations were linearized and approximate solutions were achieved which are described by the sum of two ionization-reaction time constants. A survey is given of the solutions including the effect of radiation by calculating the time constants as functions of parameters p, T, and E*. It is interesting to observe that in the nonequilibrium case, the ionization-reaction time increases with increasing plasma density. It is not certain that the stationary nonequilibrium value of the electron density is achieved within the time of transition of the plasma through a convertor channel of technically feasible length. (auth)

41755 EXPERIMENTS WITH AN MHD GENERATOR MODEL. Strashinin, E. P. (Inst. of Electrodynamics, Kiev); Karp, I. N.; Mazur, N. I.; Kristofovich, B. G. Vienna, International Atomic Energy Agency, 1966, Preprint No. SM-74/206, 16p. (In Russian). (CONF-660704–150). ORAU.

From Magnetohydrodynamic Electrical Power Generation, 2nd International Symposium, Salzburg.

The relationships between the true and brightness temperatures of combustion products, on the one hand, and the oxygen/fuel ratio, the relative amount and the concentration in solution of the seeding material, and the total rate of the fuel mixture on the other, were investigated experimentally with short runs under open-flame conditions. The electrical conductivity of the plasma was also determined for the same mode of operation. The characteristics of an MHD generator under conditions of load, of open circuit and of short circuit, and the Hall potential distribution along the duct, were investigated with the help of a model. The volt-ampere characteristics at the cold and hot electrodes were investigated with the experimental device operating as a motor and with control of the flow temperature and the potential distribution between the electrodes. (auth)

41756 INVESTIGATION OF PHENOMENA AT THE CATHODE OF AN OPEN-CYCLE MHD GENERATOR. Strashinin, E. P.; Mazur, N. I.; Shtefan, V. V. (Inst. of Electrodynamics, Kiev). Vienna, International Atomic Energy Agency, 1966, Preprint No. SM-74/209, 12p. (In Russian). (CONF-660704–151). ORAU.

From Magnetohydrodynamic Electrical Power Generation, 2nd International Symposium, Salzburg.

Using an experimental device, phenomena at the cathode of an open-cycle MHD generator were investigated. Hot and cold cathodes were investigated. In the case of the cold cathodes there was observed a stable threshold voltage below which there was virtually no current through the plasma region. In the case of hot graphite electrodes, the current rose smoothly until a certain voltage was reached, after which there was a cascade-like rise to a limit imposed by the conductivity of the plasma. In addition to the volt-ampere characteristics, the plasma temperature was measured by spectral line inversion and also by means of a special semiconducting optical pyrometer. The addition of potassium and the coefficient of completeness of combustion varied within wide limits. Theoretical investigations were carried out of the volt-ampere characteristics of a plasma diode, considered as the model of an MHD channel, employing probe theory and allowing for the effect of the electric field on emission. The ionization coefficients were calculated and the special features of ionization near the cathodes investigated. (auth)

41757 ROLE OF EXCITED ATOMS ON NONEQUILIBRIUM OF PARTIALLY IONIZED PLASMA (USE OF KLEIN EFFECT). Suita, T. (Osaka Univ.); Fujiie, Y. Vienna, International Atomic Energy Agency, 1966, Preprint No. SM-74/129, 16p. (CONF-660704-152). ORAU.

From Magnetohydrodynamic Electrical Power Generation, 2nd International Symposium, Salzburg.

Realization of effective nonequilibrium ionization in low-temperature and partially ionized plasma is one of the most important problems in direct energy conversion systems. The Klein effect, a new method of direct energy conversion to electricity, shows that the second kind of collisions of electrons with excited atoms and molecules present in plasma are indispensable to keep the electron temperature much higher than those of neutral particles and ions in working gas or vapors. Therefore, the use of excited atoms or molecules for obtaining nonequilibrium ionization can be an excellent method in such a case as the direct energy conversion with a fission reactor as heat source, where excited atoms or molecules are produced by various radiations and fission products. Mercury vapors and inert gases are selected as working fluids because both can work as the reactor coolant and have the monoatomic properties which are advantageous in some respects. The mercury closed-cycle system consists of a boiler and superheater section, a duct section which includes nozzle and electrodes placed under magnetic field, and a condenser which is connected to a vacuum system and return path to boiler. Mercury vapors are electrically ionized and excited by r-f or d-c discharge and electron bombardment instead of nuclear radiation. In this device, not only the superposition of the Klein effect and MHD generation, but also the basic properties of flow channel and mercury vapor were measured, for example, V-I characteristics, gas temperature, gas flow velocity, and so on. The experimental results of these measurements were compared with theoretical values and discussed with respect to some problems. In order to investigate the behaviors of excited atoms, monoenergetic electron beams are injected into mercury vapors to measure the relaxation of the radiation intensity from excited mercury atoms along the vapor flow direction under the various conditions; the energy dependence of incident electrons on the intensity relaxation was also examined. From these results, the excitation cross section of a mercury atom and the relaxation time of excited atoms were estimated. In the case of inert gas, the experiment was performed using the argon plasma jet in the stainless duct. To show the significance of the excited atoms in the plasma of inert gases, the temperatures of the gases and electrons were measured. (auth)

41758 EXPERIMENTAL STUDY OF PHYSICAL PROPERTIES OF COMBUSTION GAS. Sumida, A. (Mitsubishi Heavy Industries, Ltd., Kobe, Japan); Ito, T.; Morikawa, T.; Murai, Y.; Matsubara, S. Vienna, International Atomic Energy Agency, 1966, Preprint No. SM-74/136, 16p. (CONF-660704-153). ORAU.

From Magnetohydrodynamic Electrical Power Generation, 2nd International Symposium, Salzburg.

An experimental study on physical properties of combustion gases as the MHD working fluid is reported. The combustion gas was generated by an acetylene–oxygen burner with mass flow rate of 20 to 60 g/sec. The combustion chamber was constructed with a water-cooled metal wall. In the chamber, potassium as the seed material and nitrogen were mixed with the high-temperature flame generated by the burner. The seeded gas thus obtained was forced to flow through the duct for measurement, in which the high-velocity fluid with the velocity of 300 m/s ~ 400 m/s was generated and various measurements were carried out for the fluid. The temperature was measured with the Na–D line reversal method by means of a device which was specially constructed to minimize various errors in the measurement. The conductivity of gas was measured with the following two methods. With the first method, the conductivity of gas as well as the electrode voltage drop was estimated from the voltage-current characteristics which were obtained by impressing a d-c voltage from batteries to the electrodes. With the second method, the conductivity was calculated from Q values of high frequency coil, inside which the conductive gas flows. The conductivity of the gas was obtained as a function of gas temperature, seeding ratio, and mixing ratio of nitrogen. In addition, the phenomena over electrode surfaces were observed optically through the observation windows which were set to take both the side view and the front view of the electrodes. The functional relations between the conductivities and the temperature as well as the mixing ratio of nitrogen showed a fairly good agreement with the theoretical values which were calculated with the method proposed by Frost. The current could flow even in the case of cold copper electrodes with the electrode drop of only 40 to 50 volts. Rates of heat transfer were measured at the wall of the combustion chamber and at the surface of the electrodes with calorimeters and heat flux meters. It was found that the heat transfer rate at the combustion chamber showed fairly good agreement with that calculated by taking into account radiation loss. The heat transfer at the electrode surface was higher than that predicted from the theory of the convective heat transfer in turbulent flow. (auth)

41759 CURRENT DISTRIBUTION IN A FARADAY-TYPE SEGMENTED-ELECTRODE GENERATOR. Lo Surdo, C. (CNEN, Frascati, Italy). Vienna, International Atomic Energy Agency, 1966, Preprint No. SM-74/22, 18p. (CONF-660704-154). ORAU.

From Magnetohydrodynamic Electrical Power Generation, 2nd International Symposium, Salzburg.

The current and potential distribution in the low magnetic Re number steady-state regime of a segmented-electrode conversion duct has been studied previously using conformal mapping technique. The plasma is considered to be in thermal equilibrium, flowing with uniform velocity across a uniform magnetic field and the existence of an asymptotic region (remote from the walls), where all the spatial gradients vanish, is assumed. The last limitation can be easily removed when the problem is solved by expanding a suitable unknown by Fourier series. An interesting extension of this problem consists in taking into account nonequilibrium ionization effects described by a reasonably simple microscopic model. For instance, conductivity σ and Hall parameter β can be readily expressed in terms of current density if the plasma is treated as a two-temperature fluid. (auth)

41760 TRANSITION PROCESSES IN SUPERCONDUCTING MAGNETIC SYSTEMS. Sychev, V. V.; Zenkevich, V. B.; Andrianov, V. V. (Moscow State Univ.). Vienna, International Atomic Energy Agency, 1966, Preprint No. SM-74/229, 16p. (In Russian). (CONF-660704-155). ORAU.

From Magnetohydrodynamic Electrical Power Generation, 2nd International Symposium, Salzburg.

The prospects for using MHD energy conversion depend in many ways on the feasibility of superconducting magnetic systems. The construction of large, efficient superconducting magnets requires in its turn detailed information about the phenomena occurring in the superconducting windings. The properties of superconducting windings are determined largely by the characteristic features of magnetic field penetration into the volume of the superconductor and by the processes associated with the transition of a part of the windings to the normal state. Accordingly, the program for the development of a superconducting magnetic system for MHD generation includes investigations of these processes, in which the properties of superconducting windings are brought out most clearly. The experiments were carried out with a small solenoid. The results show that the transition of the superconducting windings to the normal state follows certain patterns. Processes associated with current variations in a superconducting solenoid were investigated; for example, the relation between the interlinkage of electric and magnetic circuits in the solenoid and the current, the residual interlinkage, the relation between inductance and current, and the losses when the magnetic polarity of the solenoid is reversed, etc. (auth)

41761 HALL CONFIGURATION MHD GENERATOR STUDIES. Teno, J.; Brogan, T. R.; DiNanno, L. R. (Avco-Everett Research Lab., Everett, Mass.). Vienna, International Atomic Energy Agency, 1966, Preprint No. SM-74/50, 16p. (CONF-660704-156). ORAU.

From Magnetohydrodynamic Electrical Power Generation, 2nd International Symposium, Salzburg.

Studies performed with a large combustion driven transverse (Faraday) segmented electrode MHD generator have

been previously reported. A maximum output power of 1480 kilowatts to 50 loads was achieved. Experimental results and predicted performance were in good agreement. The object of the work reported here is to obtain a detailed understanding of the fluid mechanics of the Hall MHD generator under conditions where the magnetohydrodynamic effects dominate the flow. For high efficiency, a Hall generator should operate at a high value of the Hall parameter which leads to operation at low static pressure with supersonic flow. Further, the condition that the axial current is a constant leads naturally to operation of the Hall generator at high inlet velocity with power extraction from the kinetic energy of the flow at nearly constant gas state. With such conditions, the stability of the electrode boundary layer under the influence of the magnetic forces is a prime consideration. The basic conditions of operation for the Hall generator are reviewed. The experimental program was carried out using two different channels in a basic MHD generator fluid dynamic facility which is described. Tests were performed to study the effects of varying a selected number of parameters on generator performance. In particular voltage-current and power-current characteristics were observed for different mass flows and seeding rates. The maximum output of the modified rectangular channel operating in the Hall mode was one megawatt at 5510 volts. The maximum output is two-thirds of that obtained for the same channel in the Faraday configuration while the conductivity is 10 to 30% of the Faraday generator values. The high relative output of the Hall mode is due to the increased flow speed. The maximum output obtained using the circular channel, whose volume is three-fourths of the volume of the rectangular channel, was 930 kilowatts at 2860 volts. The maximum Hall coefficient employed for the experiments was four. The observed performance can be explained with a simple theory which considers a one-dimensional inviscid core flow in the MHD channel and a boundary layer flow on the channel walls. (auth)

41762 EXPERIMENTAL INVESTIGATION OF THE TOTAL HEMISPHERICAL DEGREE OF BLACKNESS (EMISSIVITY), ELECTRIC CONDUCTIVITY AND THERMAL CONDUCTIVITY COEFFICIENT FOR A NUMBER OF HIGH-MELTING METALS IN THE TEMPERATURE RANGE 1300 TO 3000 DEG K. Timrot, D. L.; Peletskii, V. E.; Voskresenskii, V. Yu. (Moscow State Univ.). Vienna, International Atomic Energy Agency, 1966, Preprint No. SM-74/224, 10p. (In Russian). (CONF-660704-157). ORAU.

From Magnetohydrodynamic Electrical Power Generation, 2nd International Symposium, Salzburg.

The high-melting metals molybdenum, tantalum, niobium, and others serve as a basis for modern vapor-tight structural materials in new technical fields, and in particular for MHD generators. They are becoming increasingly widely used both in the pure form and in the form of alloys and chemical compounds. The investigation of their thermophysical properties, in particular the thermal conductivity coefficient, the specific electric resistance and the total degree of blackness (emissivity), is a very pressing problem, important both from the strictly applied and from the theoretical point of view. Experimental methods of studying these characteristics are based on electron heating. This has made it possible to experiment with samples of simple geometry (short cylinders 10 to 12 mm in diameter), and in practice to remove restrictions on the temperature levels attainable. All the properties concerned are studied together on two experimental rigs of original design, and measurements may be made on one and the same sample. The error of the measurements does not exceed ±1 to 1.5% for electric conductivity, ±6 to 8% for the total hemispherical degree of blackness, and ±10 to 12% for the thermal conductivity coefficient. Molybdenum (poly- and monocrystalline), tantalum, niobium, and hafnium iodide were investigated. The data obtained made it possible to gain a more precise idea of the accuracy of the Wiedemann-Franz-Lorentz relationship for this group of metals in the high temperature region. Data were obtained for the first time for a number of temperature ranges of niobium, tantalum, and hafnium. (auth)

41763 SPATIAL EFFECTS IN AN MHD DUCT WITH SEGMENTED ELECTRODES. Tolmach, I. M. (Electro Research Inst., Kharkov). Vienna, International Atomic Energy Agency, 1966, Preprint No. SM-74/248, 16p. (In Russian). (CONF-660704-158). ORAU.

From Magnetohydrodynamic Electrical Power Generation, 2nd International Symposium, Salzburg.

A general analytical description is found for the current density distribution in an MHD duct with sectioned electrodes of finite size that are interconnected arbitrarily, the flow velocity, duct cross section, induction, and Hall parameters being constant. In the non-periodic version of the problem, with an arbitrary but limited number of electrodes and insulating gaps (Hilbert boundary problem for a strip electrode), an equation for the current density distribution is given. In the second version, when the number of similar sections with electrodes is extremely large and the problem can be assumed to be periodic, a solution is obtained by way of double-periodic functions (Hilbert boundary problem for double-periodic functions). Expressions are derived for voltage, useful power and efficiency, and numerical calculations are carried out for a wide combination of parameters; these calculations are compared with the extreme case, considered by de Montardi, in which the dimensions of the electrode and insulating sections are infinitely small and the current density is uniform. Appropriate graphs and figures illustrating the current density distribution are presented. When the insulating gaps are narrow (for example, ten times smaller than the electrodes) the current flows back along the insulator. This does not occur when the insulators are wider. When the ratio of flow width to electrode repeat distance is smaller (2-3), there is a considerable deterioration in efficiency (several times over) relative to the extreme (de Montardi) case. As the ratio increases the position improves, and when the electrode and insulating sections are equal, efficiency and power values close to the extremes are obtained even at ratios of 8 to 10; when the insulators are narrow, such values are obtained at ratios greater than 40, with a dependence on the Hall parameter also becoming evident. Such a ratio can be achieved in large systems. The analytical solution is in satisfactory agreement with the experimental results obtained by Korkosak and Hoffman with a two-electrode duct. (auth)

41764 THEORY OF THE STABILITY OF SOUND IN A NON-HOMOGENEOUS PLASMA. Triger, S. A. (Moscow State Univ.). Vienna, International Atomic Energy Agency, 1966, Preprint No. SM-74/223, 6p. (In Russian). (CONF-660704-159). ORAU.

From Magnetohydrodynamic Electrical Power Generation, 2nd International Symposium, Salzburg.

Problems of the stability of a weakly ionized plasma have recently become of great interest in connection with magnetohydrodynamics. Using the three-liquid MHD model in the linear approximation, the potential oscillation spectrum of a weakly ionized plasma with a current flowing perpendicular to the magnetic field is considered. A differential equation is obtained for oscillations propagated in such a system across the external magnetic field; this is then analyzed in the geometrical optics approximation. It is shown that in a dissipative medium a considerable effect on the stability of sound oscillations results from systematically taking into account the nonhomogeneity of the ground state of the system. Increments of the sound oscillations are found, and stability criteria are obtained which differ from those previously known. The low-frequency and high-frequency (in relation to sound) limits of the equation obtained are discussed. (auth)

41765 OPTIMIZATION STUDIES OF MHD-STEAM PLANTS. Tsu, T. C. (Westinghouse Electric Corp., Pittsburgh); Young, W. E.; Way, S. Vienna, International Atomic Energy Agency, 1966, Preprint No. SM-74/179, 18p. (CONF-660704-160). ORAU.

From Magnetohydrodynamic Electrical Power Generation, 2nd International Symposium, Salzburg.

Previous optimization studies of MHD power generation have usually considered the generator passage alone, with

attempts made to maximize power, and minimize length. In the present investigation, interrelation of all the components of the MHD-steam plant are included. One is chiefly interested in discovering the design for the most efficient plant and the lowest possible cost. Since cost of the final plant is strongly influenced by the cost of the air pre-heater and the superconducting magnet, the important parameters are air pre-heat temperature and factors affecting magnet cost, such as maximum field strength and generator size. Other parameters which are varied include gas type (working fluid), pressure ratio, generator coefficient, variation of gas velocity and magnetic field along generator duct, etc. Several hundred cycles were calculated on a computer and the "best" cycle was selected according to a set of criteria which in essence specify the upper limits of maximum gas temperature, air pre-heat temperature, and generator length. It is also required that the generator geometric configuration be reasonable, and the weight of superconducting magnet wire be minimum. A best cycle was selected with coal as fuel and another with char as fuel. Plant efficiency exceeds 50% in each case. Char appears to have some advantage over coal in that it requires a shorter generator duct, less superconducting wire, lower air pre-heat temperature, and results in lower Hall voltage. Alternatively, with char, the generator length could be kept at the same value as for coal, with realization of higher overall efficiency. Among the gas types selected for study were combustion products with various seeding conditions. It was found that optimum seeding level was much lower than the value which gives maximum electrical conductivity. (auth)

41766 RELAXATION PROCESSES IN NON-EQUILIBRIUM PLASMA. Ulyanov, K. N. (Lenin All-Union Electrotechnical Inst., Moscow). Vienna, International Atomic Energy Agency, 1966, Preprint No. SM-74/237, 8p. (In Russian). (CONF-660704-161). ORAU.

From Magnetohydrodynamic Electrical Power Generation, 2nd International Symposium, Salzburg.

The Boltzmann kinetic equation method is used to describe processes of the nonsteady state in nonequilibrium plasma. A plasma with local collisions is considered, in which the concentration of particles at a point is determined by the collision processes at that point and by the radiation field. Variations in the plasma parameters with time can be calculated by means of equations of particle and energy balance if the symmetrical part of the electron velocity distribution function is known. A method is proposed for solving the system of equations of particle and energy balance. In the case of nonsteady-state processes, quasi-stationary values can often be used for the photon frequency distribution and electron velocity distribution functions. Moreover, it can be assumed that the distribution of excited atoms with respect to states is also quasi-stationary in character. In a plasma consisting of a mixture of an inert gas and alkali metal vapor and capable of being used in MHD generators the situation becomes even simpler. For virtually all regimes of interest from the point of view of MHD conversion, processes of the nonsteady state are quasi-stationary in character, i.e., the concentrations of electrons and atoms in all states of the discrete energy spectrum become adjusted to the changing temperature. This is due to the fairly uniform arrangement of levels in the term diagram of the alkali metal atoms and to the high intensity of bound-bound transitions. If the electron concentration is greater than 10^{13} and the geometric dimensions greater than 1 cm, the distribution of excited atoms with respect to states and the degree of ionization are in equilibrium with the electron temperature when more than 1% of the additive is ionized. Simple formulas are derived for calculating the concentrations and temperatures of the plasma components as functions of time. When it is possible to neglect variations in the temperature of the heavy particles, the equations are solved by quadrature. Simple criteria are obtained for the quasi-stationary state, for thermodynamic equilibrium, and for the presence of local collisions; these criteria take into account nonuniformity of the irradiation field and deviations from the equilibrium electron velocity distribution function. If any of these criteria are not fulfilled it is necessary to use the general theory of nonsteady-state processes in a nonequilibrium plasma. (auth)

41767 MHD DUCT DESIGN. Urusov, I. D. (All-Union Electromechanics Research Inst., Moscow). Vienna, International Atomic Energy Agency, 1966, Preprint No. SM-74/242, 20p. (In Russian). (CONF-660704-162). ORAU.

From Magnetohydrodynamic Electrical Power Generation, 2nd International Symposium, Salzburg.

MHD generators for use in large-scale power generating systems have become the object of many design and technical-economic studies and comparisons. Accordingly it has become necessary to determine correctly the basic dimensions and the active volume of MHD ducts as functions of the parameters adopted for the working fluid and its physical properties. Formulas are given for the length and active volume of an MHD duct with allowance for the influence of variable electric conductivity and the escape of heat to the surrounding space. The two most typical types of duct are analyzed: U ducts and T ducts. The solutions are derived by quadrature using the probability integral and the results are presented in the form of tabulated dimensionless coefficients. From an analysis of the MHD process in T-S space a formula is derived for the thermal efficiency of the duct with allowance for the factors indicated above. (auth)

41768 EFFECTIVE CONDUCTIVITY OF NON-HOMOGENEOUS PLASMA IN A MAGNETIC FIELD. Vedenov, A. A.; Dykhne, A. M. (Kurchatov Inst. of Atomic Energy, Moscow). Vienna, International Atomic Energy Agency, 1966, Preprint No. SM-74/94, 10p. (In Russian). (CONF-660704-163). ORAU.

From Magnetohydrodynamic Electrical Power Generation, 2nd International Symposium, Salzburg.

The problem of finding the effective conductivity tensor (which links the mean values of the electric field and the current density) of a nonhomogeneous plasma situated in a homogeneous external magnetic field is discussed theoretically. The spatial fluctuations of the conductivity tensor, caused by fluctuations in degree of ionization, density and temperature of the plasma, are regarded as fixed. For the case of high Hall parameters evaluations are obtained for the components of the effective conductivity tensor which determine the mean conductivity current and the mean Hall current with a set mean electric field. (auth)

41769 EFFECT OF THE CAPACITY OF ELECTRIC POWER STATIONS WITH MHD GENERATORS ON THEIR THERMAL EFFICIENCY. Vinokurov, E. K.; Rossievskii, G. I.; Shumyatskii, B. Ya. (Ordzhonokidze Inst. of Engineering Economy, Moscow). Vienna, International Atomic Energy Agency, 1966, Preprint No. SM-74/204, 16p. (In Russian). (CONF-660704-164). ORAU.

From Magnetohydrodynamic Electrical Power Generation, 2nd International Symposium, Salzburg.

Experiments to determine the effect of the capacity of electric power stations with open-cycle MHD generators both on the performance of the actual MHD generators and on the steam-turbine sections of the power stations were performed. The method of analysis and the structure of the formulas for determining the thermal efficiency of such power stations are presented. The results are given of MHD generator calculations based on different working fluid flow rates, electrical efficiencies, and initial parameters. The effect of the various types of loss on the power generation characteristics of MHD generators is analyzed as a function of working fluid flow rate. It is found that the power generation characteristics of relatively large MHD generators are stable over a wide range of working fluid flow rates and that the total capacity of a power station has a considerable effect on the performance of the steam-turbine section. (auth)

41770 INVESTIGATION OF AN ELECTRICAL DISCHARGE IN A MAGNETIC FIELD IN THE PRESENCE OF A FLOW OF GAS. Vitshas, A. F.; Golubev, V. S.; Malikov, M. M. (Kurchatov Inst. of Atomic Energy, Moscow). Vienna, International Atomic Energy Agency, 1966, Preprint No. SM-74/85, 28p. (In Russian). (CONF-660704-165). ORAU.

From Magnetohydrodynamic Electrical Power Generation, 2nd International Symposium, Salzburg.

Direct current electrical discharges were investigated in a flow of gas (argon and argon with cesium) in a magnetic field perpendicular to the direction of flow. The direction of the electric current of the arc differed in the various tests: perpendicular to the direction of flow and to the magnetic field; perpendicular to the direction of flow but parallel to the magnetic field; and parallel to the direction of flow and perpendicular to the magnetic field. Arcs with combinations of all the above three cases were also investigated. The experiments were carried out under two typical sets of conditions: (1) Argon density ~1 atm, rate of flow up to 10^5 cm/s (Mach No. M = 1.5–2), magnetic field strength up to 2.5×10^4 Oe, arc current 10^2–10^3 A, cesium concentration up to 10^{16} cm^{-3}; (2) Argon density up to 200 mm/Hg, rate of flow up to 10^3 cm/s, magnetic field strength up to 10^4 Oe, arc current 1–10 A. The aims of the experiments were: (1) To determine the relaxation length of conductivity as a function of the electric power supplied to the arc (by joule heating of electrons) and of the direction of the current in the arc. (2) To determine the extent to which the arc was driven from the entrance to the duct into the duct itself as a function of the strength of the magnetic field, the rate of flow, and the arc current. (3) To investigate the stability and degree of homogeneity of the plasma in the arc with various current directions. The following results were obtained from the experiments: (1) The relaxation length of conductivity is determined principally by energy losses on heating the atoms of the gas and also on producing ions. Losses on radiation do not play an important part. (2) Expulsion of the arc can be prevented by selecting the strength of the current and of the magnetic field so that the amperage maintains the arc at the entrance (when the direction of the arc current is perpendicular to the direction of flow and to the magnetic field). Expulsion is also considerably reduced when the arc current is directed along the flow of gas. (3) The most stable arc is that in which the current is directed along the flow of gas with the anode located upstream. The most homogeneous plasma in an arc situated at the entrance to the duct is formed when cesium is introduced in such an amount that it is almost completely ionized. (auth)

41771 DETERMINATION OF CONCENTRATION OF CESIUM ATOMS IN A FLOW OF ARGON AND CESIUM BY THE RADIATION ABSORPTION METHOD. Vitshas, A. F.; Golubev, V. S.; Zhibritskii, V. K. (Kurchatov Inst. of Atomic Energy, Moscow). Vienna, International Atomic Energy Agency, 1966, Preprint No. SM-74/87, 12p. (In Russian). (CONF-660704-166). ORAU.

From Magnetohydrodynamic Electrical Power Generation, 2nd International Symposium, Salzburg.

The cesium atom concentration n_{Cs} in the range 10^{14} to 10^{17} cm^{-3} was determined in an argon–cesium mixture with an argon density of 0.25 to 5 atm. The determination was carried out by measuring the absorption of radiation from an incandescent lamp in the region of the Cs 4555 Å resonance line, the width of the entry slit in the monochromator being 1 to 4 Å. The measurement of n_{Cs} in a mixture with argon or another inert gas can be carried out using a simple spectroscopic device of moderate resolving power ($\Delta\lambda$ = 1 Å); this is explained by the considerable widening of the radiation and absorption lines by impacts of the atoms of the inert gas. The signal was recorded using a photomultiplier and an electron oscillograph. The method was calibrated in conditions where the cesium atom concentration corresponded to even pressure of a saturated vapor at known saturation temperature. Since the argon temperature in the experimental device and on the calibrating rig was 400 to 800°C, the material used for the walls of the tubes through which the mixture of argon and cesium passed was stainless steel, while the windows for radioscopy were of sapphire. The method has advantages over other methods in that the concentration of the cesium vapor only is determined and the concentration can be measured under pulsed conditions. (auth)

41772 ELECTRICAL CONDUCTIVITY AND ELECTRON ENERGY BALANCE IN NON-EQUILIBRIUM PLASMA. Volkov, Yu. M. (Kurchatov Inst. of Atomic Energy, Moscow). Vienna, International Atomic Energy Agency, 1966, Preprint No. SM-74/86, 20p. (In Russian). (CONF-660704-167). ORAU.

From Magnetohydrodynamic Electrical Power Generation, 2nd International Symposium, Salzburg.

Pulsed discharge in mixtures of argon or helium (at a pressure of 100 mm/Hg at room temperature) with cesium in long sealed tubes was studied. The current, the longitudinal electric field, the radius of conductivity, the distribution of electron concentration over the radius, and the mean electron temperature and concentration were measured as a function of time. It was possible to determine from these measured quantities the local values of electron temperature and concentration, current density and conductivity. (W.D.M.)

41773 RESULTS OF THEORETICAL INVESTIGATIONS OF MHD FLOWS. Vulis, L. A.; Dzhaugashtin, K. E. Vienna, International Atomic Energy Agency, 1966, Preprint No. SM-74/244, 18p. (In Russian). (CONF-660704-168). ORAU.

From Magnetohydrodynamic Electrical Power Generation, 2nd International Symposium, Salzburg.

Results are given of theoretical investigations of plane laminar flows of a conducting fluid and a gas in an external magnetic field. Two types of MHD flow are considered: (1) A free, semi-bounded stream and a fluid stream in a duct; (2) Very simple flows that show strong temperature dependence. Both types of flow are considered in the induction-free approximation. In the first case the well-known solutions are reviewed and compared, and a number of new results presented. The solutions of the equations for the MHD boundary layer are derived both by the asymptotic layer method and the finite-thickness layer method. Numerical integration methods are used in solving the Navier-Stokes equations. Some of the solutions take into account the effect of the non-isothermal nature of the flow with an approximate value for the temperature-dependence of the conductivity. A more detailed investigation of the effect of the non-linear temperature-dependence of conductivity on the MHD flows is made with reference to work on the second type of MHD flow. On the basis of an approximate method of calculation, a qualitative explanation is given for the hysteretic effects peculiar to low-temperature plasma flows. The quantitative results obtained for Couette flows and for the boundary layer are compared with precise calculations. Similar approximate estimates are made for one-dimensional flows of a conducting gas in an MHD converter duct. The significance of the fact that the characteristic dependences are many-valued and the probability associated with this fact, of the occurrence of unstable flows, and the influence of temperature pulsations on the effective conductivity of a low-temperature plasma are discussed. (auth)

41774 OBSERVATIONS OF MERCURY FLOWING ALONG A TROUGH IN A TRANSVERSE MAGNETIC FIELD. Vulis, L. A.; Yaglenko, V. T. (Electro Research Inst., Kharkov). Vienna, International Atomic Energy Agency, 1966, Preprint No. SM-74/249, 20p. (In Russian). (CONF-660704-169). ORAU.

From Magnetohydrodynamic Electrical Power Generation, 2nd International Symposium, Salzburg.

The results obtained from observations of a steady-state mercury flow along a horizontal trough in a transverse magnetic field are reported. The results of experiments carried out with subcritical and supercritical

mercury flows are given for Froude numbers between 0.1 and 3.0, for extremely low Reynolds magnetic numbers, and high Hartman numbers (above 100). The basic parameters of the device were as follows: channel dimensions 40 × 200 mm, velocity of mercury flow to 1.2 m/sec, and magnetic induction to 1.2 Tesla. Experimental data relating to changes in the local and total level of the fluid are compared with calculations carried out in the one-dimensional approximation for continuous flows in ducts of constant and variable cross-section. Detailed characteristics were obtained for the hydraulic jump in the transverse field, its structure and modification, total height losses, etc. The movement of mercury in a duct having insulated walls and electrodes with external resistance was studied. The basic method of observation used was photographic; in addition, the electric and hydraulic characteristics were measured. The investigation showed that a one-dimensional design diagram satisfactorily describes a continuous flow in a duct. A number of particular features inherent in the phenomena considered and caused by the action of the magnetic and electric fields were detected. In particular, a virtually smooth transition through the critical velocity was obtained in a diverging duct when certain relationships held. Limitations associated with the superposition of a magnetic field were established, in addition to the usual hydrogas analogy. (auth)

41775 PART LOAD OPERATION OF MHD POWER PLANTS. Way, Stewart (Univ. of California, Santa Barbara). Vienna, International Atomic Energy Agency, 1966, Preprint No. SM-74/180, 12p. (CONF-660704–170). ORAU.

From Magnetohydrodynamic Electrical Power Generation, 2nd International Symposium, Salzburg.

Part-load operation of an open cycle MHD-steam power plant presents certain problems because of interactions of various components in the system, desirability of minimizing voltage variation, and necessity for operating the MHD generator duct at an off-design condition. It is highly desirable that the part-load operation be realized with a corresponding reduction in fuel flow to maintain good efficiency. The desired reduced fuel flow must be matched to a certain degree by a reduced air flow in order to maintain adequate electrical conductivity. Reduction of power output could be accomplished by reduction of fuel flow alone, but the fuel reduction from this means would by no means correspond to the power reduction. It thus appears desirable to reduce load by reducing both air and fuel flow in such a way that the product of generator total enthalpy drop and gas flow rate (with correction for duct wall heat loss) is equal to the desired power level. It is important that the generator outlet total temperature does not increase during the load change as this would endanger the air preheater; it is also important that it does not decrease appreciably as this adversely affects conductivity. Conversion efficiency in the MHD duct will not change greatly during the load shift, and the generated voltage will also remain fairly constant, especially if diagonal electrode inter-connections are used. These questions are discussed and the method of analyzing the MHD duct at off-design conditions is described. An example is given for a large MHD-steam central station plant of the type currently envisaged, and the state of affairs at part-load conditions is evaluated. The necessity for reduced air flow, with lower end-to-end pressure drop in the MHD duct, calls for operation of the compressors at reduced speed under part-load. A separate turbine drive for the compressors, rather than drive from the main turbine shaft at constant speed, is thus very desirable. The steam side of the power plant will also put out less power, about in proportion to the reduced gas flow. (auth)

41776 END LOSSES IN MHD GENERATORS. Welly, J. D. (Siemens-Schuckertwerke AG, Erlangen, Ger.). Vienna, International Atomic Energy Agency, 1966, Preprint No. SM-74/110, 12p. (CONF-660704–171). ORAU.

From Magnetohydrodynamic Electrical Power Generation, 2nd International Symposium, Salzburg.

MHD generators may be operated economically only when the magnetic flux densities are sufficiently high (30 to 100 kG). Since the capital costs of the magnet represent a considerable proportion of the total costs of an MHD plant, it is essential to use as much as possible of the available magnetic flux for energy conversion. This is done by suitable arrangement of electrodes and by optimum loading. Such optimization presents no difficulties, provided that the current and field distribution is homogeneous. This is not so, however, at the beginning and end of the magnetic field. In these zones, the electrical output generated is normally less by an amount ΔP than that produced in a zone of equal size in the middle of the field with homogeneous field distribution. This amount ΔP is called the end loss. The end loss is calculated for a given magnetic field, depending on the electrode arrangement and the load. A number of formulas are established for calculating ΔP. These formulas are generally derived by conformal mapping, expansion into series, or Fourier transformation. Prerequisite conditions are that the problem may be dealt with two-dimensionally, and that the conductivity, the flow velocity, and the duct width remain constant. The magnetic field strength may vary in any way with x, where x is the co-ordinate parallel to the duct axis. The electrodes are generally assumed to be continuous or infinitely segmented. The influence of the Hall effect is taken into account where possible. As a result of nonhomogeneous field distribution and eddy currents at the ends of the magnetic field, the gas discharge and the pressure drop will also differ by ΔPg and Δp respectively. If F is the cross-sectional area of the duct, $\Delta p = \Delta Pg/vF$. Formulae are also given to calculate the additional gas discharge ΔPg, which may be positive or negative. (auth)

41777 WALL LOSSES BY RADIATION IN OIL-FIRED MHD GENERATOR. Wittel, H. (Siemens-Schuckertwerke AG, Erlangen, Ger.). Vienna, International Atomic Energy Agency, 1966, Preprint No. SM-74/109, 16p. (CONF-660704–173). ORAU.

From Magnetohydrodynamic Electrical Power Generation, 2nd International Symposium, Salzburg.

The properties of a radiating gas layer are governed by two parameters. One of these is the emission coefficient (ϵ) which indicates the radiation power of 1 cm^3 of the gas per steradian. The other is the absorption coefficient (k) having the dimension cm^{-1} and indicates the degree by which the radiation is weakened by absorption when passing through a gas layer 1 cm thick. Both coefficients vary with the frequency. The radiation power can assume large values with low absorption when the radiating gas layer is sufficiently thick, i.e., if the product of the absorption coefficient k and the thickness d, the optical density, is sufficiently big. The value of k is not known for the combustion plasma of an MHD generator, while d can reach values up to 1 metre in an actual plant. Conclusions are drawn as to the expected thermal loading of the duct walls by determining the integrated emission coefficient $\bar{\epsilon}$ for all frequencies and a mean absorption coefficient $\bar{k}$. The mutual radiation of the hot duct walls is neglected in this connection. The measuring apparatus consists of a system of two plane mirrors and a number of diaphragms limiting a parallel bundle of rays and allowing its passage for measurement. The radiation receiver is a thermocouple which is directly exposed to the radiation without intermediate optical lenses in order to cover the whole spectral range. Since the lack of such intermediate lenses results in low intensities, special measures are necessary to maintain the cold junction of the receiver at a constant temperature. The absorption is measured by displacement of the mirrors, thereby varying the thickness of the radiating gas layer in steps. Reflection losses at the mirrors are determined in a special apparatus in the light given off by the plasma itself. For plasma at 3000°K and 1 atm with an addition of 10% K_2CO_3 an emission coefficient $\bar{\epsilon} = 0.75$ W/cm^3 sterad is obtained. Without K_2CO_3, $\bar{\epsilon} = 0.26$ W/cm^3 sterad. The absorption measurement shows that the intensity rises up to a value of d approximately 30 cm. Greater

thicknesses are too inaccurate for interpretation, owing to increasing angle and reflection losses. Taking into consideration all geometrical factors these figures give heat loading of the wall of approximate 18 W/cm^2 from a hemisphere of 30 cm radius. In consequence, no significant radiation loading of the wall need be expected for an MHD duct having a width of approximately 50 cm. (auth)

41778 THERMODYNAMICS OF A TWO-COMPONENT LIQUID-METAL POWER MHD ASSEMBLY WITH INJECTOR. Yakimovich, K. A.; Shpilrain, E. E.; Syaskin, Yu. M. (Moscow State Univ.). Vienna, International Atomic Energy Agency, 1966, Preprint No. SM-74/218, 12p. (In Russian). (CONF-660704-174). ORAU.

From Magnetohydrodynamic Electrical Power Generation, 2nd International Symposium, Salzburg.

A thermodynamic analysis was carried out of the efficiency of a two-component vapor-liquid injector, making allowances for the impact loss upon the mixing of the streams. The thermal efficiency of the cycle of a power generating MHD plant with a two-component working fluid was considered, and relationships for calculating the efficiency of a vapor-liquid injector and the cycle as a whole with a two-component working fluid were derived. It is shown that for a given combination of liquid metals at a maximum cycle temperature of 1200°K, the internal efficiency of a vapor-liquid injector may amount to about 80%, and the thermal efficiency of the cycle to about 30%. (auth)

41779 CALCULATION OF THE BOUNDARY LAYER AT THE ELECTRODE OF A PLANE MHD GENERATOR. Yakubenko, A. E. (Moscow State Univ.). Vienna, International Atomic Energy Agency, 1966, Preprint No. SM-74/245, 10p. (In Russian). (CONF-660704-175). ORAU.

From Magnetohydrodynamic Electrical Power Generation, 2nd International Symposium, Salzburg.

The problem of the flow of an electrically conducting gas through crossed electric and magnetic fields in a plane MHD generator with ideally conducting walls is solved. The conditions for solving independently problems relating to the boundary layer at the electrodes and to the heart of the flow are set forth. The conditions at the heart of the flow are calculated numerically by means of one-dimensional theory for subsonic and supersonic velocities. The dependences of the flow characteristics on the load parameter are found. The non-automodel boundary-layer equations are solved numerically for small Reynolds magnetic numbers at one of the MHD generator electrodes. The dependence of the resistive force and the Nusselt number on the load parameter and the co-ordinate along the electrode is found. It is shown that the resistive force and the heat flow described by the Nusselt number increase considerably relative to the case of a nonconducting gas. This is because the gas conductivity falls sharply and the release of joule heat increases near the cooled wall. The point is found where the boundary layer detaches itself from the electrode in cases of supersonic motion at the heart of the flow. (auth)

41780 EXPERIMENTAL STUDIES OF OIL-FIRED MHD POWER GENERATION. Yamamoto, M.; Tamaoki, T.; Saito, Y. (Tokyo Shibaura Electric Co., Ltd.). Vienna, International Atomic Energy Agency, 1966, Preprint No. SM-74/135, 16p. (CONF-660704-176). ORAU.

From Magnetohydrodynamic Electrical Power Generation, 2nd International Symposium, Salzburg.

To understand the characteristics of MHD power generation and the technical difficulties of its practical development, a 7-Mw thermal input oil-fired MHD generator was constructed and experiments were conducted under various conditions. On this scale of experiment, the heat loss should be minimized to preserve the high temperature of gas, so the combustor was lined with MgO bricks of 50 mm thickness and the generating channel was composed of MgO insulating walls and 19 pairs of graphite electrodes. A divergent channel was used, which had cross sections of 50 × 120 mm^2 at inlet, 50 × 240 mm^2 at outlet and an active length of 1000 mm, and was supplied with a 20 kG magnetic field. Since the 19 pairs of segmented electrodes were connected to separate variable resistors, the relation between terminal voltage and current along the channel could be established. Seeding was supplied in form of potassium soap which was blended into the fuel. Light oil was used as fuel. Following the heating, the fuel was burned with gaseous oxygen. The experiments were carried out under subsonic and supersonic flow, the electrical data and hydraulic data along the generating channel were measured. For example, the maximum value of voltage, current and electrical power was about 400 V, 1200 A, and 100 kw, respectively, and the location of the shock wave could be determined from the pressure distribution along the channel. The analysis of the generator was done assuming one-dimensional flow and compared with experiments. This analysis could represent the reality in subsonic condition with fairly high fidelity, if properties of high temperature gas are known as a function of temperature and pressure. Even for supersonic flow, one-dimensional flow analysis is appropriate with no shock wave in the generating channel, but at a low gas flow rate shock occurred due to the discontinuity of induced voltage at the point of the shock wave, simple one-dimensional flow analysis could not be applied. In these experiments, to minimize heat loss, MgO insulating walls were used in combustor and channel, but in the practical stage, water-cooled metal walls should be developed. (auth)

41781 MHD POWER GENERATION EXPERIMENTS WITH POTASSIUM-SEEDED ARGON PLASMAS. Yano, S.; Hiramoto, T.; Matsunaga, S.; Shirakata, H.; Fujino, H.; Sasaki, Y. (Japan Atomic Energy Research Inst., Tokyo). Vienna, International Atomic Energy Agency, 1966, Preprint No. SM-74/131, 18p. (CONF-660704-177). ORAU.

From Magnetohydrodynamic Electrical Power Generation, 2nd International Symposium, Salzburg.

The JAERI MHD experimental facility was almost completed by 1965. An outline of the JAERI MHD experimental facility and the results of recent power generation experiments are given. Subsonic argon flows up to 4000°K can be obtained at almost atmospheric pressure in the MHD channels. A magnetic field of about 2 Wb/m^2 is produced over a volume of 200 × 100 × 800 mm^3 in the air gap of the magnet. Seeding potassium, with flow rates of 0.1 to 0.5 g/s, is carried by an auxiliary argon gas into a mixing chamber as a mist of 20 μ of the average diameter. The potassium reservoir in the seeding apparatus contains about 2 kg of melted potassium. The output characteristics of generators are recorded on two X-Y recorders, while the loads for Faraday or Hall generators are automatically varied. Both electron temperatures and gas temperatures in the MHD channels can also be measured by two spectroscopes. More than 10 generator channels were tested using K_2CO_3-seeded argon gas for the study of generator configurations with continuous electrodes and segmented electrodes. In the experiment on generators with segmented electrodes, the open circuit voltages, short circuit currents, and voltage-current characteristics were measured in the Faraday and Hall connections. Internal voltages in the generators were also measured by probes in the generators. The generator with segmented graphite electrodes in the Faraday connection generated a power of about 10 watts between each pair of opposed electrodes having the surface area of 1.5 cm^2. The open circuit voltage in the Faraday direction was about 40 volts, and the short circuit current was 1 to 2 A for the pair. Open Hall voltages of 40 to 50 volts were observed between the upstream and downstream electrodes separated by about 13 cm. The short circuit Hall current was 0.5 to 1 A. Generators with continuous graphite electrodes were tested under nearly the same plasma conditions for the segmented electrode generators. From dependence of the short circuit current upon the magnetic field, the Hall parameters of the plasma were estimated to be in the range of 1 to 10 at a magnetic field of 2 Wb/m^2, as the seeding ratio varied from 10^{-2} to 10^{-4}. In the generators with graphite-segmented electrodes, the Hall field varied almost proportionally to the magnetic field, and the increase in the short

circuit current with the magnetic field was smaller than that which is directly proportional with the field. These results were considered to be due to the nonuniformity of plasma in the MHD channels. The results of various generator characteristics are discussed and the problem of MHD power generation with K-seeded Ar plasma is also discussed for nonequilibrium ionization. (auth)

41782 CHARACTERISTICS OF PLASMA PROBES IN AN MHD WORKING FLUID. Whitman, Alan M.; Yeh, Hsuan (Univ. of Pennsylvania, Philadelphia). Vienna, International Atomic Energy Agency, 1966, Preprint No. SM-74/250, 22p. (CONF-660704–178). ORAU.

From Magnetohydrodynamic Electrical Power Generation, 2nd International Symposium, Salzburg.

Plasma probes have been in use for a long time in determining experimentally the electron temperature, ion temperature, and charged-particle number density. The use of these devices, however, has been limited to lower pressure ranges due to the lack of a suitable theory for high-pressure plasmas. The purpose of this study was to extend the theory of plasma probes to nonequilibrium plasmas at pressures of the order of one atmosphere such as existing in an MHD power generator. It is shown that in such cases, the recombination of electrons and ions is an important consideration. The analysis is based on the assumption that the three-body recombination and ionization is the dominant process. In a typical MHD working fluid, say an argon gas seeded with 1% cesium at 2000°K and one atmosphere of pressure, the penetration length l of ions and electrons, i.e., the distance that an ion or electron diffuses before recombination, is of the order of 10^{-3}. (It is to be noted that ambipolar diffusion prevents the electrons from traveling much faster than the ions.) Thus a situation where $(l/L) \ll 1$, $\leftarrow (\lambda/l) \ll 1$, $\leftarrow$ and $(\lambda/R_D) \gg 1$ where L is the characteristic dimension of the probe, λ is the mean free path and R_D the Debye length. Because of the last condition, i.e., $R_D \ll \lambda$, the space charge region is contained wholly in a "free-falling' zone in the immediate neighborhood of the probe. Since, also, $(R_D/l) \ll 1$, the region outside of the "free-falling" zone is in a state of "quasi-neutrality," i.e., the number densities of electrons and ions are approximately equal. In this latter region, the mechanisms of diffusion and recombination are both important. The two regions must of course be matched at their connecting boundaries. The complete equations were solved on a computer without the assumption of quasi-neutrality in the outer region. With such an assumption, analytic solutions were obtained in closed form. It was found that the predictions of the theory agreed, in all the cases considered, with existing experimental findings. A notable success of the theory was the prediction of the correct value of ion-saturation current obtained experimentally by Rohatgi and Emmons for a typical MHD working fluid. However, results showed that the use of such a probe to measure ion temperature very accurately would require a better knowledge of recombination coefficients than is presently available. (auth)

41783 MAGNETOHYDRODYNAMIC POWER GENERATION AS AFFECTED BY VISCOSITY AND NON-EQUILIBRIUM IONIZATION. Yen, James T. (Catholic Univ. of America, Washington, D. C.). Vienna, International Atomic Energy Agency, 1966, Preprint No. SM-74/187, 8p. (CONF-660704–179). ORAU.

From Magnetohydrodynamic Electrical Power Generation, 2nd International Symposium, Salzburg.

The phenomenon of non-equilibrium ionization has been studied by Kerrbrock, Robbens and others. Due to this phenomenon, local electron temperature is enhanced, with a resulting increase in the electrical conductivity and an improvement in the performance of MHD generators. Also due to this phenomenon, local electrical conductivity becomes dependent on the local electrical current density. This dependence may be expressed as a hyperbolic relation, such as that studied by Robbens. Based on this hyperbolic relation, channel flow and power generation of a Faraday type MHD generator were studied. The basic model was the same as that of Yen where effects of viscosity and Hall currents are included. Attention is focused on the influence of nonequilibrium ionization. The channel is taken as of a constant cross section, with a large aspect ratio and finely segmented electrodes. Viscous effects of these electrodes are neglected while that of the insulating walls are included. A sufficient Hall electric field is applied along the channel to make the net Hall currents vanish. The magnitude of this electric field as dependent on the external loading parameter, the Hartmann number, and the Hall parameter (i.e., the Cowling number) is determined. In the constant conductivity cases of Yen, complex variables are found to be useful in simplifying the analysis. In the present case, no analytic solution is obtainable. The problem is solved by iteration on an IBM 7094 computer, starting with the constant conductivity solution. A good convergence is obtainable in general after several iterations. The efficiency of the Faraday generator is found to increase with both the Hartmann number M and the Cowling number W, in a rate faster than the constant conductivity case. For the same M and W, it achieves a maximum efficiency at a critical value of the external loading parameter. The location of this critical loading depends again on M and W, and is generally of a larger value, with some exceptions, than that of the constant conductivity case. Numerical results are presented in detail. (auth)

41784 TESTING OF MATERIALS AND STRUCTURES INTENDED FOR MHD CONVERSION IN A 200-kw EXPERIMENTAL DUCT. Yerouchalmi, D. (CEN, Saclay, Gif-sur-Yvette, France). Vienna, International Atomic Energy Agency, 1966, Preprint No. SM-74/144. 16p. (In French). (CONF-660704–180). ORAU.

From Magnetohydrodynamic Electrical Power Generation, 2nd International Symposium, Salzburg.

The choice of materials and the design of the structures were dictated by the necessity of operating with frontal faces of insulating and conducting walls (electrodes) whose temperature is fixed between 1900 and 2000°K, depending on the thermal flux traversing the walls of the duct. This temperature limitation of the insulating and conducting walls is due to the interplay of two factors. The insulating walls no longer insulate at temperatures of over 1900 to 2000°K, and the composite electrodes used would only function properly below these reference limits. It was also necessary to take account of transversal and longitudinal thermal expansion and to provide assemblies which would prevent the continuity of the wall surfaces of the duct from being interrupted at any time or from being subjected to destructive stresses. Studies were also made of an appropriate type of segmentation for the ceramic materials with a view to taking into account the precautions specified above and to guarding against the possibility of damage by thermal shocks. Systematic investigations were made with a view to choosing high-temperature materials as a function of their intrinsic properties of insulation, conductivity, and pyroscopic and corrosion resistance. The duct is preceded by a converging part which provides a rectangular section for the hot seeded gases coming from the combustion chamber. This converging part, which has partially cooled refractory walls, forms the flow of gas which passes at a boundary layer temperature of about 2000°K. Along the length of the duct there are ten electric modulation elements and ten MHD conversion elements, placed between the poles of the electromagnet. Each element has, facing one another, two insulating walls and two electrodes mounted in units on a structure which forms the framework of the element. These structures are interconnected by metal diaphragms which function as springs and ensure wall-surface continuity whatever the direction of the thermal stress at startup or shutdown. In addition there are springs to accommodate the mechanical stresses produced by thermal expansion in the transverse section plane of the duct. The technological study of the overall and detailed design has been pursued with a view to achieving MHD conversion in an inhomogeneous-flow closed-cycle system for a period of a few hours. (auth)

41785 COMPOSITION AND THERMODYNAMIC PROPERTIES OF THE COMBUSTION PRODUCTS OF NATURAL FUELS WITH IONIZING ADDITIVES. Yungman, V. S.; Gurvich, L. V.; Rtishcheva, N. P. (Moscow State Univ.). Vienna, International Atomic Energy Agency, 1966, Preprint No. SM-74/217, 12p. (In Russian). (CONF-660704-181). ORAU.

From Magnetohydrodynamic Electrical Power Generation, 2nd International Symposium, Salzburg.

The engineering calculations for natural-fuel MHD-generator processes require the use of data on the thermodynamic properties and equilibrium compositions of the combustion products of the fuels in question, employed in conjunction with ionizing additives to improve the electrical characteristics of the system. The basic principles involved in calculating the thermodynamic properties and equilibrium compositions of chemically reacting mixtures were examined, taking ionization into account, and calculations were performed for cases where methane and fuel-oil are burned in air with the addition of potassium over a wide range of variations in initial composition, temperature, and pressure. The results of the calculations and the role played by molecular potassium compounds in the system are discussed. (auth)

41786 EXPERIMENTAL STUDY OF THE RELAXATION PROCESS AND THE MAGNITUDE OF NON-THERMAL IONIZATION IN AN MHD GENERATOR. Zauderer, Bert (General Electric Co., King of Prussia, Pa.). Vienna, International Atomic Energy Agency, 1966, Preprint No. SM-74/182, 16p. (CONF-660704-182). ORAU.

From Magnetohydrodynamic Electrical Power Generation, 2nd International Symposium, Salzburg.

It has been previously reported that in a study of magnetically induced ionization it was observed that a number of mechanisms contributed to the ionization process. The aim of the present work was to obtain experimental data of magnetically induced ionization which would allow separation of the effect of electron heating from the other ionization mechanisms. In addition, a study was made of the ionization relaxation process in the generator. The pertinent experimental conditions were as follows: the MHD channel was 5 × 5 cm square × 30 cm long; the electrodes were at room temperature; the magnetic field was 0.7 to 2.25 T; the test gas was shock-heated xenon with a 100 m/s velocity and 200 mhos/m equilibrium conductivity; and the current per electrode pair ranged from 5 to 100 amperes. The major result obtained was that the electron density and conductivity computed from the nonequilibrium electron energy balance equation, using the Saha equation at the electron temperature, was in excellent agreement with the experimental data. It should be noted that radiation losses were negligible for the present experimental conditions. The effect of ohmic gas heating and compressional heating on the ionization increase was readily calculable, and it was found to be small compared to the electron-induced nonthermal ionization. The ionization relaxation process performed in the generator proceeds in two consecutive stages. Since the electrodes are nonemitting, it is first necessary to strike a cold cathode arc discharge at the electrodes. Once the electrodes are in the arc mode of operation, the current level and the electron density increase extremely fast to the final equilibrium value. The total ionization relaxation time for both of the above stages was about 100 microseconds for the present experiments. This corresponds to the time a gas particle traverses one-third of the generator length. This relaxation time is consistent with the theoretical value obtained by solving the ionization kinetics equation. (auth)

41787 ELECTRICAL LOSS MECHANISMS IN LINEAR MHD GENERATORS OPERATING AT LARGE HALL PARAMETERS. Zauderer, Bert (General Electric Co., King of Prussia, Pa.). Vienna, International Atomic Energy Agency, 1966, Preprint No. SM-74/183, 16p. (CONF-660704-183). ORAU.

From Magnetohydrodynamic Electrical Power Generation, 2nd International Symposium, Salzburg.

The purpose of this experimental study was to determine the causes of the appreciable power output and Hall potential reduction in linear, high $\omega\tau$ MHD generators. The origin of this reduction does not appear to be due primarily to nonthermal ionization, since it has been observed in equilibrium and nonequilibrium mode of generator operation. Accordingly, measurements were made of the electrical load characteristics of a linear Hall and a linear Faraday generator operating in both ionization modes. In addition, time-resolved photographs were taken of the discharge pattern in the MHD generator. The plasma conductivity ranged from an equilibrium value of 100 mhos/m to a nonequilibrium value of 800 mhos/m, and the $\omega\tau$ value ranged from 3 to 11. With the generator operating at current levels below 30 amperes/electrode and in the equilibrium mode, the major loss mechanism was the high resistance of the aerodynamic boundary layer in front of the electrodes. The inclusion of this loss in the data analyses gave voltage-current characteristics which were in agreement with the uniform Faraday generator theory and the Hall generator theory. At transverse current levels greater than 30 amperes per electrode, additional power and Hall potential losses are caused by the formation of a high-conductivity layer along the anode wall. The experiments show that this layer originates primarily from the following effects; namely, gas dynamic flow disturbances, Lorentz forces, and the large value of the Hall parameter. In addition the experiments indicate that magnetically induced ionization is a secondary loss mechanism which merely aggravates the power losses in the channel. It is concluded that by appropriate changes in the MHD channel design, the external load connections, and the current level per electrode, it should be possible to greatly reduce all of the above-mentioned loss mechanisms. (auth)

Elementary Particles and Radiations

See also Field Theory, Scattering Theory, and Symmetries

Refer also to abstracts 41371, 41671, 42005, 42104, 42184, 42185, 42304, 42312–42321, 42386, and 42523.

41788 (BMwF-FBK-66-12) PERIPHERES MODELL MIT ABSORPTION FUER DEN ERZEUGUNGSPROZESS $\bar{p} + p \rightarrow \bar{N}^* + N^*$. (Peripheral Model with Absorption for the Production Process $\bar{p} + p \rightarrow \bar{N}^* + N^*$). Ebel, G. (Technische Hochschule, Karlsruhe (West Germany). Institut fuer Theoretische Kernphysik). May 1966. 19p. Dep. mn. DM 3,00.

The differential cross section for the production process $\bar{p} + p \rightarrow \bar{N}^{*--} + N^{*++}$ is calculated in the one-pion exchange model. The isobar is treated as an elementary particle of spin $^3/_2$. The absorption in the initial and final state is included according to the distorted wave Born approximation, the absorption parameters being determined by the elastic scattering. (auth)

41789 (DESY-66/16) STRAHLUNGSKORREKTUREN ZU BREMSSTRAHLUNG UND PAARERZEUGUNG BEI HOHEN ENERGIEN. (Radiative Corrections to Bremsstrahlung and Pair Production at High Energies). Schulz, Hans Dietrich (Deutsches Elektronen-Synchrotron, Hamburg (West Germany)). June 1966. 105p. Dep. mn.

Radiative corrections to bremsstrahlung should show up in a precision measurement of the bremsstrahlung spectrum as deviations from first-order cross sections. If this measurement is done with a pair spectrometer, radiative corrections to pair production will contribute as well. The results of such a measurement are presented. Theoretical cross sections for bremsstrahlung and pair production at high energies are discussed, including Coulomb correction, effects of the atomic electrons, and second-order effects (radiative corrections). It is shown that at high energies and with high-Z target nuclei the various

approximations made in deducing the first order cross sections plus Coulomb correction contribute an error of less than 0.5% to the cross section integrated over all angles, whereas neglect of radiative corrections causes errors of up to 4%. A description of the experimental setup and procedure is given. Experimental conditions were chosen in such a way that pure thin-target spectra integrated over the emission angles of photons were measured. Experimental results are compared to theoretical predictions, and possible systematic errors are discussed. Deviations from first-order cross sections plus Coulomb correction are observed which are distinctly outside the error limit of 1% and which cannot be traced to systematic errors inherent in the apparatus. Magnitude and sign of the deviations correspond to the radiative corrections to bremsstrahlung and pair production as recalculated by the method of Mork and Olsen, taking into account the special experimental conditions. Radiative corrections amount to +2.5% for relative photon energies below $k/E_0 = 0.9$ and drop to −3% at $k/E_0 = 0.99$. Roughly one fifth of the correction stems from the bremsstrahlung process and four fifths from pair production. (auth)

41790 (DESY-66/17) DIE ANWENDUNG DER MAXIMUM LIKELIHOOD METHODE IN DER HOCHENERGIEPHYSIK. (Applications of the Maximum Likelihood Method in High Energy Physics). Swanson, W. P. (Deutsches Elektronen-Synchrotron, Hamburg (West Germany)). June 1966. 32p. Dep. mn.

A lecture on applications of the Maximum Likelihood Method in high energy physics is presented. Both the ordinary and extended MLM are introduced. Four practical examples are given: the analysis of proton polarization by scattering on carbon; the determination of spin density matrix elements; the determination of amounts, masses, and widths of resonances plotted on a triangle plot; and the determination of branching ratios in a two-step decay process. Minimization processes are described in detail. Likelihood ratios for hypothesis discrimination are defined and the meaning of these ratios is discussed. References to other examples in the literature are given. (auth)

41791 (DESY-66/20) SMALL ANGLE ELECTRON PROTON ELASTIC SCATTERING CROSS SECTIONS FOR MOMENTUM TRANSFERS BETWEEN 10 AND 105 F^{-2}. Bartel, W.; Dudelzak, B.; Krehbiel, H.; McElroy, J. M.; Meyer-Berkhout, U.; Morrison, R. J.; Nguyen-Ngoc, H.; Schmidt, W.; Weber, G. (Deutsches Elektronen-Synchrotron, Hamburg (West Germany). Hamburg Univ. (West Germany). II. Institut fuer Experimentalphysik). July 1966. 14p. Dep. mn.

A report is presented on the results of an electron-proton scattering experiment in which the elastic scattering cross section for momentum transfers between 10 and 105 F^{-2} was measured with a precision of about 5%. (B.G.D.)

41792 (INR-708/VI/PL) BADANIA NAD ODDZIALYWANIEM ANTYPROTON-PROTON BEZ EMISJI LUB Z EMISJA DWOCH CZASTEK NALADOWANYCH W PRZEDZIALE PEDU PIERWOTNEGO 3-4 Gev/c. (Study of Zero and Two Prong Antiproton-Proton Interactions at 3-4 Gev/c Primary Momentum). Czyzewski, Oleg (Institute of Nuclear Research, Warsaw (Poland)). May 1966. 61p. Dep.

About 4000 two and zero prong $\bar{p}$-p interactions at 3, 3.6, and 4 Bev/c primary momentum were measured. Results concerning single pion production were compared with predictions of the Ferrari and Selleri OPE model. Satisfactory agreement at 4 Bev/c was obtained after the modification of the form factors. In the process $\bar{p} + p \rightarrow \bar{n} + n + \pi^+ + \pi^-$ strong production of N* (1688) was observed. N* (1688) decays in cascade. Four-momentum transfer distribution for the charge-exchange process is found to be more flat, than in the case of reaction $p + n \rightarrow n + p$. This distribution, as well as the energy dependence of the charge-exchange cross-section are satisfactorily described by the OPE model with absorption. (auth)

41793 (JINR-E-2822) DISPERSION SUM RULES FOR STRONG AND ELECTROMAGNETIC INTERACTIONS. Matveev, V. A.; Pisarenko, V. G.; Struminskii, B. V. (Joint Inst. for Nuclear Research, Dubna (USSR). Lab. of Theoretical Physics). 1966. 8p. Dep. mn.

Dispersion sum rules for strong and electromagnetic interactions of nucleons are considered. In the resonance approximation the relations between coupling constants and magnetic moments of nucleons are obtained. The results are in good agreement with the experiment. (auth)

41794 (JINR-E-2860) RECOIL PROTON POLARIZATION IN ELASTIC π^--p SCATTERING AT 300 Mev AND THE PHASE SHIFT ANALYSIS OF PION-NUCLEON SCATTERING. Vasilevskii, I. M.; Vishnyakov, V. V.; Ivanchenko, I. M.; Lapidus, L. I.; Silin, I. N.; Tyapkin, A. A.; Shchegel'skii; V. A. (Joint Inst. for Nuclear Research, Dubna (USSR). Lab. of Nuclear Problems). 1966. 8p. Dep. mn.

New measurements of recoil proton polarization in 300 Mev Π^--p-scattering have been carried out. The phase shift analysis of all available data on Π-N interactions at 310 Mev was performed. A Geiger counter hodoscope with controlled pulse supply was used for measurements. The asymmetry of recoil proton scattering on carbon was detected with a spark chamber. The SPDF analysis was made. The experimental data are described which is similar to that of Vik and Rugge. (auth)

41795 (MIT-2098-251, pp 21-36) HIGH ENERGY ACCELERATOR PHYSICS GROUP. (Massachusetts Inst. of Tech., Cambridge. Lab. for Nuclear Science).

A progress report is presented on the research activities of the high energy accelerator physics group at M.I.T. Topics discussed are photoproduction, spark chamber activities, and electron and photon interaction work. (B.G.D.)

41796 (MIT-2098-251, pp 74-103) THEORETICAL GROUP. (Massachusetts Inst. of Tech., Cambridge. Lab. for Nuclear Science).

A progress report is presented on the research activities of the Theoretical Group at M.I.T. Topics discussed are particle theory, SU(6) symmetry and its $\tilde{U}(12)$ generalization, relativistic three-body and N-body problems, field theory (particularly quantum electrodynamics), strong interactions, nuclear theory, nuclear reactions, and optical model studies. (B.G.D.)

41797 (MIT-2098-264) SEARCH FOR FRACTIONALLY CHARGED, WEAKLY INTERACTING PARTICLES. Foss, J.; Garelick, D.; Homma, S.; Lobar, W.; Osborne, L. S.; Uglum, J. (Massachusetts Inst. of Tech., Cambridge). Sept. 1, 1966. Contract AT(30-1)-2098. 2p. (CONF-660808-10). Dep. mn. CFSTI $1,00 cy, $0.50 mn.

From 13th International Conference on High Energy Physics, Berkeley, Calif.

Characteristics of an experiment for photon-produced weakly-interacting fractionally-charged particles are discussed. (B.G.D.)

41798 (MIT-2098-265) π^0 PHOTOPRODUCTION AT 3.0, 4.0, AND 5.0 Gev FOR BARYON FOUR MOMENTUM TRANSFERS BETWEEN 0.5 AND 4.0 $(Gev/c)^2$. Bolon, G. C.; Garelick, D.; Homma, S.; Luckey, D.; Lewis, R.; Osborne, L. S.; Uglum, J. (Massachusetts Inst. of Tech., Cambridge). Sept. 1, 1966. Contract AT(30-1)-2098. 13p. (CONF-660808-9). Dep. mn. CFSTI $1.00 cy, $0.50 mn.

From 13th International Conference on High Energy Physics, Berkeley, Calif.

Preliminary results of measurements of the cross sections for the reaction $\gamma + p \rightarrow \pi^0 + p$ are reported. From the energy variations of the cross sections and the dip at momentum transfer of −0.8 it is suggested that the ρ is important in meson (π^0) photoproduction. (J.F.P.)

41799 (ORO-2504-96) INVESTIGATIONS ON THE PROPERTIES OF K MESONS AND HYPERONS AND RELATED TOPICS IN HIGH ENERGY PHYSICS. Technical Report No. 614. Snow, G. A. (Maryland Univ., College Park. Dept. of Physics and Astronomy). Aug. 1966. Contract AT(40-1)-2504. 24p. Dep. mn. CFSTI $1.00 cy, $0.50 mn.

A progress report is presented on bubble and spark chamber experiments with mesons (K) at the University of Maryland. Also included are summaries of theoretical work in progress such as baryon-baryon reactions and SU(3) symmetry, determination of NAK coupling constant from KN dispersion, $\pi\pi$ effective mass anomaly in low energy $\pi^-p \rightarrow \pi^+\pi^-n$ and the Olsson-Yodh model, reaction predictions of higher symmetries, assignment of Y_1^* (1765) and Y_0^* (1520) into the 1134 representation of SU(6), and nonlinear density effect in the transmission of K_2^0-mesons through matter. (B.G.D.)

41800 (UCRL-14716) ELASTIC AND INELASTIC PROTON-PROTON SCATTERING: A BIBLIOGRAPHY. Schauer, Carlotta V. (Lawrence Radiation Lab., Univ. of California, Livermore). Mar. 28, 1966. Contract W-7405-eng-48. 24p. Dep. mn. CFSTI $1.00 cy, $0.50 mn.

A selective bibliography is presented on elastic and inelastic proton-proton scattering covering the period 1960 to January 1966. References were compiled from Chemical Abstracts, Nuclear Science Abstracts, and Physics Abstracts. (B.G.D.)

41801 (UCRL-16003) A MEASUREMENT OF THE RELATIVE BRANCHING RATIO $K^+ \rightarrow \mu^+ + \nu/K^+ \rightarrow \pi^+ + \pi^0$. Beck, Robert Lamar (Lawrence Radiation Lab., Univ. of California, Berkeley). July 28, 1966. Contract W-7405-eng-48. 62p. Dep. mn. CFSTI $3.00 cy, $0.75 mn.

Thesis.

K^+ mesons in a momentum-analyzed beam were identified by a velocity selecting Cherenkov counter and brought to rest in a beryllium target which served as a source for a broad-range magnetic spectrometer. Muons and pions from the decay modes $K^+_{\mu 2} \rightarrow \mu^+ + \nu$ (P_μ = 236 Mev/c) and $K^+_{\pi 2} \rightarrow \pi^+ + \pi^0$ (P_π = 205 Mev/c) were identified by momentum and range, and a value 2.31 ± 0.24 for the relative branching ratio $K\mu 2/K\pi 2$ was obtained. The value is compared with results of other experiments. (auth)

41802 (UCRL-16832) PRODUCTION OF $K\bar{K}$ PAIRS IN π^-p INTERACTIONS. Hess, Richard Irwin (Lawrence Radiation Lab., Univ. of California, Berkeley). June 24, 1966. Contract W-7405-eng-48. 86p. Dep. mn. CFSTI $3.00 cy, $0.75 mn.

Thesis.

The 72-inch hydrogen bubble chamber was exposed to a beam of π^- mesons having laboratory momenta of 2.0, 3.1, and 4.0 Bev/c. The final states containing a $K\bar{K}$ pair included many cases of resonance production. In particular evidence for production of the ϕ, A_2, D, and E mesons was found. The cross sections at 3.1 Bev/c are $\sigma(\pi^-p \rightarrow pA_2^-, A_2^- \rightarrow K\bar{K}) = 18 \pm 4$ μb, $\sigma(\pi^-p \rightarrow nA_2^0, A_2^0 \rightarrow K\bar{K}) = 36 \pm 10$ μb, $\sigma(\pi^-p \rightarrow nD, D \rightarrow K^0K^\pm\pi^\mp) = 7 \pm 2$ μb, and $\sigma(\pi^-p \rightarrow nE, E \rightarrow K^0K^\pm\pi^\mp) = 17 \pm 5$ μb. The reaction $\pi^-p \rightarrow n\phi$ proceeds with a cross section of 30 ± 8 μb at 2.0 Bev/c. The quantum numbers $I^GJ^P = 1^-$ even$^+$ (J = 0 excluded) were established for the A_2 meson; though our determination is not conclusive, $I^GJ^P = 0^+1^+$ for both the D and E mesons are favored. (auth)

41803 (UCRL-16863) PHYSICS DIVISION SEMI-ANNUAL REPORT, NOVEMBER 1965–APRIL 1966. (Lawrence Radiation Lab., Univ. of California, Berkeley). May 15, 1966. Contract W-7405-eng-48. 71p. Dep. mn. CFSTI $3.00 cy, $0.75 mn.

A progress report is presented for the Physics Division of Lawrence Radiation Laboratory. Topics discussed are elementary particle research, development and operation of bubble chambers, use and programming of computers, nuclear emulsions in space research, S-matrix theory, mesic atoms, field theory, nuclear physics, gravitational studies, and development and operation of accelerators. (B.G.D.)

41804 (UCRL-17003) K^+p INELASTIC INTERACTIONS AT 2.7 Bev/c. Newman, Riley David (Lawrence Radiation Lab., Univ. of California, Berkeley). July 1966. Contract W-7405-eng-48. 73p. Dep. mn. CFSTI $3.00 cy, $0.75 mn.

Thesis.

An analysis is presented of an exposure of the hydrogen bubble chamber to a 2.65 Bev/c separated K^+ beam. Channel cross sections are presented for K^+p interactions, except those corresponding to a two prong topology. A detailed study is made of the final states $K^0p\,\pi^+$ and $K^+p\,\pi^+\pi^-$, which are dominated by the production of K*(891) and N*(1236). The reaction $K^+p \rightarrow K^*p$ is analyzed in terms of a one-meson-exchange model modified by form factors, and results are compared with data at other energies. The model is found to give a very unsatisfactory account of the energy dependence of K* production. The reaction $K^+p \rightarrow K^{*0}N^{*++}$ is analyzed in terms of a pion exchange model modified to include the effects of absorption in initial and final states. No evidence is found for production of resonant states other than K*(891), N*(1236), and ω. Relations between three body final states of K^+p reactions implied by SU_3 symmetry are derived and tested. (auth)

41805 (SLAC-Trans-46) ELECTROPRODUCTION OF VERY HIGH-ENERGY MUONS. Clement, G.; Kessler, P. Translated by Benjamin Thayne for Stanford Linear Accelerator Center, Stanford Univ., Calif., from Nuovo Cimento (10), 37: 876-7(1965). 19p. Dep. mn. JCL $1.60 fs, $0.80 mf.

The muon beam intensities which might be obtained from existing and projected high-energy electron accelerators are evaluated. First the cross-section for the photoproduction of a μ (+ or −) in a forward cone of small angle is presented taking into account a nuclear form factor. The number of muons of given energy produced by an electron is then obtained by integration over the thick target gamma spectrum. For this calculation several approximations are made which are subsequently discussed; this leads to the suggestion that a few radiation lengths of a heavy element (e.g., 1 or 2 inches of lead) will give the best results. Finally an estimate is given for the pion contamination; the ratio of pions to muons is roughly of the order of unity, provided that the angle of the production cone is taken sufficiently small (a few degrees). The results of the calculations are displayed in curves, which show the muon intensities which might be obtained from 6, 12, and 25 Bev electron accelerators; other curves show the pion contamination. (auth)

41806 ARE ZERO REST MASS PARTICLES NECESSARILY STABLE? Havas, Peter (Temple Univ., Philadelphia). Amer. J. Phys., 34: 753-7(Sept. 1966).

It was stated recently that particles of zero rest mass are necessarily stable as a consequence of known conservation laws or of requirements of relativistic invariance. It is shown that such a conclusion is not warranted. A proper relativistic characterization of unstable particles of zero rest mass is given, and examples of decay schemes of the photon and the neutrino not forbidden by general considerations are indicated. The questions of experimental evidence and detection of photon decay are briefly discussed. The problem whether photon decay is allowed by quantum electrodynamics is outlined; no definite conclusions can be drawn from available calculations. (auth)

41807 THEORY OF CLASSICAL PARTICLES WITH DIPOLE MOMENTS. Zastavenko, L. G. (Joint Inst. for Nuclear Research, Dubna, USSR). Ann. Univ. Sofia, Fac. Sci. Phys., 59: No. 5, 17-24(1964-65). (In Russian).

A simplified Price method was used to obtain a regularized energy-momentum tensor for an electromagnetic field in the presence of a particle with a dipole moment. The use of generalized functions permitted a direct generalization of the method for particles of arbitrary spin or for any multipole order in the particle field. (G.O.Y.)

41808 THEORY OF DIRAC'S CLASSICAL ELECTRON. Zastavenko, L. G. (Joint Inst. for Nuclear Research, Dubna, USSR). Ann. Univ. Sofia, Fac. Sci. Phys., 59: No. 5, 25-34(1964-65). (In Russian).

Dirac's classical electron theory is discussed in terms of point motion and a simplified Price energy-momentum tensor is derived. A set of standard equations, along with the asymptotic conditions for the four-momentum and the

angular momentum, are derived also. The equations of permissible motion are considered. (G.O.Y.)

41809 RADIATIVE ABSORPTION OF STOPPED PIONS BY DEUTERONS. Reitan, Arne (Norges Tekniske Hoegskole, Trondheim, Norway). Ark. Fys. Seminar Trondheim, No. 1, 1-20(1966).

The ratio between the absorption rates for non-radiative and radiative absorption of stopped pions by deuterons is calculated for atomic s-orbits. Agreement with experiments is obtained for a reasonable value of the $\pi N\gamma$ coupling constants. (auth)

41810 [THE MUON] "WHO EVER ORDERED THAT?" CERN Cour., 6: 152-54(Aug. 1966).

An experiment designed to measure the anomalous magnetic moment of the muon to a very high order of accuracy has completed a preliminary trial run at the CERN proton synchrotron. The run has already confirmed the results of an experiment, known as the "g minus 2" experiment, carried out at CERN five years ago and more detailed measurements are now under way. The experiment and its relevance to the understanding of the muon is described. (auth)

41811 ON THE REAL PART OF THE AMPLITUDE OF ELASTIC SCATTERING OF PROTONS ON DEUTERONS AT AN ENERGY OF 8 Gev. Korbel, Z. (Czech Technical Univ., Prague). Czech. J. Phys., 16: 643-53(1966).

The elastic scattering of a proton on a deuteron at an energy of 8 Bev is studied by the method of multiple transitions of protons through a target 1.5 μ thick, made from $(CD_2)_n$. Altogether 27,385 reflected deuterons were recorded and measured by means of nuclear emulsions. From an analysis of the course of the differential cross section as a function of the scattering angle in the limits of 1.4 to 8.9° ($|t| = 0.0042 - 0.1750$ (Bev/c)^2) the ratio of the real and imaginary parts of the scattering amplitude $\alpha = \mathrm{Re}\,A(0)/\mathrm{Im}\,A(0) = -0.36 \pm 0.08$ was determined. The total cross section for elastic scattering (p-d) in the given interval of scattering angles was σ_{el}(p-d) = (9.5 ± 0.7) mb. The effective radius of interaction between the proton and deuteron at elastic scattering was r = (2.26 ± 0.04) Fermi. (auth)

41812 PHOTOFORMATION OF MESONS ON NUCLEONS AND SU(6) SYMMETRY. Akhiezer, A. I.; Rekalo, M. P. (Inst. of Physics and Tech., Academy of Sciences, Ukrainian SSR). Dokl. Akad. Nauk SSSR, 166: 60-2(Jan. 1, 1966). (In Russian).

The relation between the amplitudes of formation of p-state mesons in the case of interaction of magnetic dipole-type γ quanta with nucleons was investigated within the framework of the SU(6) symmetry. In this case, the photoformation process involves two partial amplitudes, one of which corresponds to the total angular momentum $I = \frac{1}{2}(M_{11})$, and the other to the total momentum $I = \frac{3}{2}(M_{13})$. The spin structure of the photoformation amplitude of pseudoscalar mesons in the center of inertia system is described on the basis of the polarization vector of the γ quantum. The magnetic dipole type γ quanta are identified in the SU(6) symmetry by a second-order tensor. A series of correlations were established between the various amplitudes of photoformation; some of them are derived from known transformation properties of the Hamiltonian of electromagnetic interactions; another group is satisfied by the criteria of the SU(3) symmetry while the third group applies only for the SU(6) symmetry. (TTT)

41813 RELATIONSHIP BETWEEN STRUCTURE AND POLARIZATION OF PARTICLES IN $1 + \tilde{1} \rightleftharpoons p + \tilde{p}$ REACTIONS. Sokolov, A. A.; Kerimov, B. K.; Dzhafarov, I. G.; Yakh'yaev, R. Sh. (Moscow State Univ.). Dokl. Akad. Nauk SSSR, 166: 337-40(Jan. 11, 1966). (In Russian).

Depending on the experimental conditions, colliding beams of particles and antiparticles may result in scattering or annihilation processes. Determination of the formfactors of elementary particles requires experiments with extended polarized particles. The annihilation process $e^-(\mu^-) + e^+(\mu^+) \rightleftharpoons p + \tilde{p}$ was investigated with extended polarized particles. The electron (μ meson) was considered as a point particle without an anomalous magnetic moment. It was found that a study of the longitudinal polarization alone is not sufficient to determine the time formfactors of the particles; experiments with transversally polarized particles are also required. The formfactors in the one-photon approximation include radiative and meson corrections; the two-photon approximation does not affect the total cross section and the angular distribution of the reaction products. Formulas were derived for calculating the differential cross section of formation of arbitrarily polarized, extended protons and antiprotons, taking into account the longitudinal polarization and formfactors of the annihilating electrons and positrons. In view of the difficulties encountered in the study of the polarization of the ultimate particles, the following annihilation process of arbitrarily polarized protons and antiprotons in the lepton-antilepton pair $p + \tilde{p} \rightarrow e^- + e^+$, $p + \tilde{p} \rightarrow \mu^- + \mu^+$ is best suited for the study of proton formfactors. (TTT)

41814 IONIZATION OF RELATIVISTIC ELECTRONS. Padmavathi, S. V.; Kamal, A. A. (Osmania Univ., Hyderabad, India). Indian J. Pure Appl. Phys., 4: 291-2(1966).

Ionization and multiple scattering measurements on electron pair tracks scanned in a stack of G_5 emulsions exposed to a beam of 17-Bev/c negative pions, indicate that the observations are inconsistent with the existence of Tsytovich effect. (auth)

41815 A MODIFIED ONE-NUCLEON EXCHANGE MODEL IN π-N SCATTERING. Caprasse, H. (Univ., Liege). Nucl. Phys., 87: 100-6(1966).

A modified version of the one-nucleon exchange model for π-N scattering which may satisfy the unitary sum rule associated with the partial wave dispersion relation is studied. It is shown that the model is compatible with the Froissart bound in the u-channel for $l = 0$ and $l = 1$. Using the N/D technique the model was tested numerically for the $l = 0$, $T = \frac{3}{2}$ and $l = 1$, $J = \frac{3}{2}$, $T = \frac{3}{2}$ waves. For the former a quantitative evaluation of the inability of the nucleon exchange approximation to give a correct prediction is given. For the latter it is shown that "exact" numerical solutions already given in the past do not satisfy the unitary sum rule. A new solution not suffering from this drawback is given and predicts qualitatively the (3, 3) resonance. Further improvements of it are suggested and the relevance of the unitary sum rule to study short-range forces is pointed out. (auth)

41816 PHOTOPRODUCTION OF POSITIVE PIONS FROM HELIUM AND HYDROGEN. Lawson, E. M.; Little, R. (Glasgow Univ.). Nucl. Phys., 87: 121-30(1966).

Absolute yields of π^+ mesons photoproduced from helium and hydrogen were measured at 65, 90, 110, and 135° to the 320-Mev bremsstrahlung beam of the Glasgow electron synchrotron. Pions in the energy ranges 11–37 and 63–69 Mev were detected in a scintillation counter telescope using a delayed coincidence technique. The photoproduction of π^+ mesons from a bound proton in the helium nucleus is compared to that from a free proton. (auth)

41817 PHOTOPRODUCTION OF CHARGED PIONS FROM HELIUM AND HYDROGEN. Thomas, D. L.; Hogg, W. R.; Mann, B. (Glasgow Univ.). Nucl. Phys., 87: 131-7(1966).

Relative yields were measured of π^- and π^+ mesons photoproduced from helium and π^+ mesons photoproduced from hydrogen at 67, 88, and 112° to a bremsstrahlung beam of maximum energy 330 Mev. A magnetic spectrometer was used to detect the pions in energy bands centered on 19, 36, and 66 Mev (67°) and on 16, 34, and 65 Mev (88 and 112°). (auth)

41818 THE SCHROEDINGER THEORY OF THE STATIC πN INTERACTION. Petras, M. (Komenskeho Univ., Bratislava). Nucl. Phys., 87: 141-52(1966).

The p-wave Klein-Gordon equation is used for a description of the static πN interaction. An inversion problem for the determination of the corresponding potentials from unphysical singularities of the scattering amplitude is formulated and solved approximately. (auth)

41819 PERIPHERAL MODEL FOR K^--p COLLISIONS. Gupta, Y. M.; Agarwal, B. K. (Univ. of Allahabad, India). Nucl. Phys., 87: 170-6(1966).

The one-particle exchange model was extended to study the interference between the two charge states of Y_1^*. (auth)

41820 DISTORTED-WAVE ONE-PION-EXCHANGE MODEL FOR INELASTIC PROTON-PROTON SCATTERING. Yock, P. C. M. (Massachusetts Inst. of Tech., Cambridge). Contract AT(30-1)-2098. Nuovo Cimento (10), 44A: 777-83(Aug. 1, 1966). (MIT-2098-246).

The one-pion-exchange model, modified to allow for initial- and final-state interactions, is applied to those inelastic two-body proton-proton scattering processes involving the excitation of the two lightest nucleon isobars. The model apparently overestimates the N^{*+} (1238) production cross-section, but gives a satisfactory account of N^{*+} (1430) production. (auth)

41821 (γ,ρ^0) AS TWO-PION EXCHANGE. Peaslee, D. C. (Australian National Univ., Canberra). Nuovo Cimento (10), 44A: 784-93(Aug. 1, 1966).

The reaction $N(\gamma,\rho^0)N$ is remarked as unique in having practically no allowed one-boson exchange processes, so that it serves as a sort of "laboratory" for studying two-boson (pion) exchange. The two-pion term can be evaluated absolutely and is estimated crudely for large s and small t; it is found to account well for a couple of measured forward cross sections. The forms are different from those of the diffraction treatment: No one-pion exchange need be invoked, and the ρ^0 is polarized transverse to the incident beam only for $\theta = 0^\circ$; at finite angles the ρ^0 has a component parallel to the incident direction. For small angles and high energies this component represents transverse polarization of the ρ^0 relative to its own direction of motion. (auth)

41822 CROSS-SECTION FOR ANNIHILATION OF A PAIR IN TWO PHOTONS WITH GAUGE-INVARIANT MODIFICATION OF THE ELECTRON PROPAGATOR. Calucci, G. (Univ., Trieste, Italy. Istituto Nazionale di Fisica Nucleare, Trieste, Italy). Nuovo Cimento (10), 44A: 809-17(Aug. 1, 1966).

The cross section for annihilation in two photons of an electron-positron pair with a single modification of the electronic propagator is calculated. In order to conserve the gauge invariance, besides the modification of the vertex prescribed by the Ward-Takahashi identity and proposed by McClure and Drell, also the intervention of a two-photon vertex is considered. First the problem of the general construction of such a vertex is dealt with; afterwards, this result is applied in the simplest form, to compute differential and total cross sections. The calculation is done in view of the experiments of pair annihilation planned in order to test in this way the validity of quantum electrodynamics. (auth)

41823 P-WAVE $\pi\pi$-$K\bar{K}$ CROSS-SECTION IN THE T = 1 STATE. Nath, R. (Moscow State Univ.). Nuovo Cimento (10), 44A: 826-8(Aug. 1, 1966).

A calculation of the P-wave $\pi\pi$-$K\bar{K}$ cross section in the T = 1 state was made by taking into account the absorption effects, due to the presence of the other opening channels. This was done by employing the multichannel approach developed by Lichtenberg and Williams, in which starting from the Born amplitudes for the elastic and inelastic scattering one can calculate the absorption effects arising from the unitarity of the S matrix. (J.F.P.)

41824 FIELD-THEORETICAL SUM RULES AND MASS-DIFFERENCE CALCULATIONS. Bassetto, A.; Paccanoni, F. (Univ., Padua. Istituto Nazionale di Fisica Nucleare, Padua). Nuovo Cimento (10), 44A: 839-42(Aug. 1, 1966).

An approach, based on the axioms of field theory, to the general problem of the mass differences is presented using the examples of a proton-neutron case and the case of a meson (ρ). The starting point is the sum rule obtained in terms of the spectral functions of the inverse of the renormalized propagator for the probability, Z of finding the bare particle into the physical one. Also according to the current philosophy of considering the hadrons as composite particles, the condition Z = 0 is imposed. (J.F.P.)

41825 PHASE-SHIFT ANALYSIS OF K^+-PROTON ELASTIC SCATTERING AT 910 Mev/c. Warty, M. D. (Univ. of Delhi). Nuovo Cimento (10), 44A: 878-86(Aug. 21, 1966).

Equations for the coefficients of the angular distribution for K^+-proton elastic scattering and polarization are presented in terms of the phase shifts with the help of which the phase-shift analysis is done at 910 Mev/c for this reaction. It is a characteristic feature of the angular distribution that it depends critically on the angular momentum of the resonating state but not on the parity, however the coefficients of cos θ into which the angular distribution is expanded can be affected by the parity. This is particularly used in the study of K^+-proton reaction at 910 Mev/c by taking into account the production of Λ^* at this momentum. The conclusion drawn is that the S-wave which is dominant and repulsive at lower momenta continues to remain so even at 910 Mev/c. (auth)

41826 RATE OF ENERGY LOSS FOR POSITIVE AND NEGATIVE PIONS. Ekspong, A. G.; Yamdagni, N. K. (Univ. of Stockholm). Nuovo Cimento (10), 44A: 887-94 (Aug. 21, 1966).

With the use of a high-resolution magnetic spectrometer, the ranges of pions in nuclear emulsions were measured at two momenta: 78 Mev/c and 90 Mev/c. The pions were produced in the CERN synchrocyclotron. It was found that the ranges of positive and negative pions are equal within ±0.5%. Any possible difference in the rate of energy loss must have saturated at a much lower momentum. (auth)

41827 MULTIPLE EMISSION OF FRAGMENTS WITH CHARGE ≥3 AFTER DISINTEGRATION OF HEAVY NUCLEI IN IONOGRAPHIC EMULSIONS. Stein, R. (Centre de Recherches Nucleaires, Strasbourg). Nuovo Cimento (10), 44A: 895-902(Aug. 21, 1966). (In French).

A study was made of the fragment emission in nuclear emulsions for incident-proton energy of 25 Bev and also of double and multiple fragment emission for charges ≥3. To discriminate the simple fragments, a photometrical method was applied and at least 250 stars were observed which emit two or more fragments of charges ≥3. An analysis of the results indicates a good agreement with the Russian results and it seems that, for fragments of energy lower than 4.5 Mev per nucleon, the emissions of the two fragments would be interdependent. (auth)

41828 THE MASS SPECTRA OF RECOIL NUCLEON STATES FROM INELASTIC ρ^0 PRODUCTION BY PIONS OF 12 AND 18 Gev/c. Jones, L. W.; Bleuler, E.; Caldwell, D. O.; Elsner, B.; Harting, D.; Middelkoop, W. C.; Symons, C. R.; Zacharov, B. (CERN, Geneva). Nuovo Cimento (10), 44A: 915-26(Aug. 21, 1966).

The mass spectra of recoil nucleon states from the inelastic production of ρ^0 mesons by incident pions of 12 and 18 Bev/c were studied in a spark chamber experiment. From over 2000 events, qualitative agreement with a one-pion-exchange calculation is found, both in the magnitudes of the cross sections and in the missing mass spectra of the nucleon states. The dominance of this channel over elastic ρ^0 production and the consequences of extending the model to very high energies are discussed. (auth)

41829 ANGULAR DISTRIBUTION OF MESONS FROM SLIGHTLY PERTURBED PROTON-NUCLEON COLLISIONS AT 20 Gev/c. Manz, A. (Max-Planck-Institut fuer Physik und Astrophysik, Munich). Nuovo Cimento (10), 44A: 966-73(Aug. 21, 1966). (In German).

Multiple production of mesons by collisions of protons from the CERN synchrotron at 20 Bev/c on nucleons in nuclear emulsions was investigated. The angular distribution for 90 minimum stars, indicated by the number of mesons produced, were compared with unified models of the theory of hard cosmic-shower jets. The best agreement for stars with more than four mesons produced was found with a model of isotropic production in the cm sys-

tem and a meson energy spectrum that decreases as $1/\gamma_{ss}^2$. For stars with two mesons a deviation from anisotropy was found. (tr-auth)

41830 MEASUREMENT OF THE π^+p TOTAL EFFECTIVE CROSS SECTION AT T_π = 300 TO 700 Mev. Bizard, G. (Univ., Caen, France); Duchon, J.; Seguinot, J.; Yonnet, J.; Bareyre, P.; Bricman, C.; Valladas, G.; Villet, G. Nuovo Cimento (10), 44A: 999-1014(Aug. 21, 1966). (In French).

π^+p total cross sections were measured in the 300 to 700 Mev incident-pion kinetic-energy range. A particular emphasis was given to the leptonic contamination of the pion beam. The results are compared with previous measurements. (auth)

41831 SEMI-PHENOMENOLOGICAL ANALYSIS OF NONLEPTONIC HYPERON DECAYS IN $\tilde{U}(12)$. Hussain, F.; Rotelli, P. (Imperial Coll. of Science and Tech., London). Nuovo Cimento (10), 44A: 1047-54(Aug. 21, 1966).

A semi-phenomenological theory of nonleptonic hyperon decay based on the current-current hypothesis is presented. Explicit U_{12} forms are used for the currents and the effects of strong interactions are considered in the simplest possible way. (auth)

41832 S-WAVE PION-PION SCATTERING. Kamal, A. N. (Univ. of Alberta, Edmonton). Nuovo Cimento (10), 44A: 1055-67(Aug. 21, 1966).

An S-matrix calculation is made using the N/D method for the low-energy S-wave π-π scattering. The approximation involves replacing the left-hand cut by two poles whose positions are fixed a priori. Their residues are then determined using the approximate crossing relations at the symmetry point. The calculations suggest that satisfactory solutions are obtained with $A_0^0(\nu_0)$ ($\approx -5\lambda$) = –0.6. The S-wave phase shifts are repulsive in both isobaric spin states with scattering lengths a_I (sign convention: $\delta = -ak$, $k \to 0$): $a_0 \approx +1.1$, $a_2 \approx +0.5$. (auth)

41833 ELECTROMAGNETIC FORM FACTOR OF THE PION. Antoine, J.-P. (Univ., Louvain, Belg.). Nuovo Cimento (10), 44A: 1068-80(Aug. 21, 1966).

The formalism recently proposed by Schiff for evaluating the electromagnetic form factor of the pion is analyzed. For reasons of consistency, the long-range cut-off R was introduced from the beginning and the cross section is required to be independent of R, i.e., remain finite when $R \to \infty$. This requirement leads to a set of identities between partial amplitudes which must be satisfied in each order of the perturbation expansion in powers of the Coulomb interaction. Finally it is shown that the identity corresponding to the most diverging term—the only one that can be evaluated without specifying a model for the potentials—is in fact verified in each order. This result gives strong support to the first-order treatment of the Coulomb interaction, and to Schiff's method of which this is the key. (auth)

41834 NOVEL APPROACH TO NONLEPTONIC WEAK HYPERON DECAYS. Roman, P.; Yun, S. K. (Boston Univ.). Nuovo Cimento (10), 44A: 1091-1109(Aug. 21, 1966).

A phenomenological theory of nonleptonic hyperon decays is proposed which does not rely on octet dominance and on R or RP invariance. Postulating SU_3 symmetry and a certain space-time behavior, a minimal H_W is uniquely obtained. All S- and P-wave amplitudes are computed and expressed in terms of five parameters. Experimentally correct relations are deduced. (auth)

41835 TWO-PION DECAYS OF KAONS IN A NOVEL APPROACH TO NONLEPTONIC WEAK PROCESSES. Roman, P.; Yun, S. K. (Boston Univ.). Nuovo Cimento (10), 44A: 1110-19(Aug. 21, 1966).

The $K \to \pi\pi$ decays are studied in the framework of a recently proposed phenomenological theory of nonleptonic weak processes (P. Roman and S. K. Yun, Nuovo Cimento, 44A: 1091(1966)). The same hamiltonian is used as the one which applies for nonleptonic hyperon decays. Without further assumptions, all decay amplitudes are calculated and expressed in terms of five parameters. Three relations between the amplitudes are obtained. Comparison is made with experiment and with related work by other authors. (auth)

41836 OBSERVATIONS CONCERNING PRODUCTION AMPLITUDES AND MODELS FOR $J^P = \frac{3}{2}^+$ BARYONS. Grisaru, M. T. (Brandeis Univ., Waltham, Mass.); Kane, G. L. Nuovo Cimento (10), 44A: 1120-38(Aug. 21, 1966).

The effect of inelastic processes (pion production) on single-channel bootstrap calculations for $J^P = \frac{3}{2}^+$ baryons is considered, with particular reference to the Ω^- and to some of the difficulties of working with production amplitudes in such a context. (auth)

41837 VECTOR MESON BOOTSTRAP FROM SINGULAR N/D EQUATIONS. Bassetto, A.; Paccanoni, F. (Univ., Padua. Istituto Nazionale di Fisica Nucleare, Padua). Nuovo Cimento (10), 44A: 1139-47(Aug. 21, 1966)

The P-wave scattering amplitude of two pseudoscalar mesons is studied with the forces coming only from one-vector-meson exchange. The exact solution of the singular N/D equations leads to bootstrap conditions without any free parameter. The ρ-meson mass and width are predicted in agreement with experiment. (auth)

41838 THREE-NUCLEON POTENTIAL. Quang, Ho-kim (Massachusetts Inst. of Tech., Cambridge). Nuovo Cimento (10), 44A: 1148-62(Aug. 21, 1966).

The interaction between three nucleons is studied on the basis of the covariant Green's function. A three-nucleon potential is derived from the scattering matrix and is characterized by an expansion in number of mesons exchanged. The complete definition of the potential now depends on the knowledge of the basic meson-nucleon interaction amplitudes to which each term of the expansion is connected. With the neglect of pion-pion interactions, the lowest-order potential, which involves the exchange of two quanta, is given in terms of the renormalized coupling constant and the total cross section for meson-nucleon scattering. It is argued that in low energies and at large distances, the higher terms in the expansion give no appreciable contribution and so the lowest order suffices for most purposes. (auth)

41839 SHADOW MODEL FOR THE HIGH-ENERGY PION-PROTON ELASTIC BACKWARD PEAK. Bertocchi, L.; Capella, A. (CERN, Geneva). Nuovo Cimento (10), 44A: 1194-1209(Aug. 21, 1966).

A model is proposed in which the elastic backward peak for high-energy pion-nucleon scattering is explained as the shadow of the production processes. The small height of the backward peak as compared to that of the forward one is due to the forward-backward asymmetries in the angular distributions of the secondaries in πp collisions. The application of the model to π^+p scattering at 8 Bev/c gives the right order of magnitude for the height of the backward peak and a width approximately equal to that of the forward one. (auth)

41840 EFFECTIVE $\Delta I = \frac{1}{2}$ RULE IN THE THREE-PION DECAYS OF KAONS. Roman, P.; Yun, S. K. (Boston Univ.). Nuovo Cimento (10), 44A: 1210-18(Aug. 21, 1966).

The universal nonleptonic weak hamiltonian previously proposed (Nuovo Cimento, 44A: 1091-1110(1966)) is used to compute, without further dynamical assumptions, the decay amplitudes for all $K \to \pi\pi\pi$ processes. The results can be expressed in terms of two parameters. An effective $\Delta I = \frac{1}{2}$ rule is obtained, and some interesting structural features are noted. (auth)

41841 EXTENSION OF THE AXIOMATIC ANALYTICITY DOMAIN OF SCATTERING AMPLITUDES BY UNITARITY. [PART] II. Martin, A. (CERN, Geneva). Nuovo Cimento (10), 44A: 1219-44(Aug. 21, 1966).

The second of a series on the subject is entirely devoted to the pion-pion scattering amplitude. The main results are: (1) The scattering amplitude can be continued till the

border-line of the double-spectral function, except for $8\,\mu^2 < s < 32\,\mu^2$. Hence the nearest singularities are really induced by two-particle unitarity. Another consequence is that the only possible static potential describing low-energy pion-pion scattering is a Yukawa superposition. The domain of validity of fixed-transfer dispersion relations is slightly enlarged, as compared to I. (2) A partial analytic completion is carried out by various methods. As a result a very large domain of analyticity is found for the fixed-angle amplitude and the partial-wave amplitudes; this domain extends from $s = -28\,\mu^2$ to $s = +\infty$. However, only in the interval $-28\,\mu^2 < Res < 78\,\mu^2$ the extension in Ims is appreciable ($|Ims|max = 70\,\mu^2$). (3) The result of Bros, Epstein, and Glaser on the validity of fixed, negative-t quasi-dispersion relations is extended to any t inside the parabola with focus $t = 0$ and summit $t = \mu^2$. (auth)

41842 REGGE POLE ANALYSIS OF $\pi^+p \rightarrow \pi^0\Delta^{*++}$. Caprasse, H. (Department de Physique Mathematique, Liege); Stremnitzer, H. Nuovo Cimento (10), 44A: 1245-9 (Aug. 21, 1966).

An attempt is made to show that the behavior in t and in s of the differential cross section for the reaction $\pi^+p \rightarrow \pi^0\Delta^{*++}$ can be explained by a simple Regge pole model. Curves of the differential cross section vs the momentum transfer squared obtained from the model are compared with experimental data at 4 and 8 Bev/c. The good fit obtained both at 4 and 8 Bev/c for small t shows that the s dependence of the differential cross section is substantially improved compared to that obtained by the absorption model in which an elementary ρ is exchanged. It is remarked that the slopes of the differential cross section for the reactions $\pi^+p \rightarrow pA_2$ and $\pi^+p \rightarrow pA_1$ are approximately the same as for the reaction $\pi^+p \rightarrow \pi^0\Delta^{*++}$, which indicate that they are also dominated by the ρ Regge trajectory. (L.B.S.)

41843 BARYON RESONANCE DECAYS IN BROKEN $U_3 \times U_3$. Mahanta, P. (Imperial Coll. of Science and Tech., London). Nuovo Cimento (10), 44A: 1250-1(Aug. 21, 1966).

A new sum rule for baryon resonance decays is presented, which assumes an interaction that breaks SU_3 to first order within the context of the symmetry scheme of $U_3 \times U_3$. (L.B.S.)

41844 ABSORPTION CORRECTION IN HIGH-ENERGY PHOTOPRODUCTION OF PIONS. Ar-Rashid, Harun; Kawaguchi, M. (International Atomic Energy Agency, Trieste, Italy. International Center for Theoretical Physics, Trieste, Italy). Nuovo Cimento (10), 44A: 1252-5 (Aug. 21, 1966).

The pion pole diagram is evaluated in order to investigate the effect of absorption in the final state on the one-pion-exchange model of pion photoproduction. It is found that the effect reduces the Born approximation considerably but not sufficiently to bring about agreement with experiment. (L.B.S.)

41845 TRANSVERSE-MOMENTUM DISTRIBUTION OF SECONDARY PARTICLES FROM HIGH-ENERGY COLLISIONS. Jones, F. C. (Goddard Space Flight Center, Greenbelt, Md.). Nuovo Cimento (10), 44A: 1256(Aug. 21, 1966).

It is argued that the proof of Aly, Kaplon, and Shen (Nuovo Cimento, 31: 905(1964)) that only a Boltzmann-type distribution in transverse momentum of particles emitted in a high-energy collision is compatible with axial symmetry about the collision axis is in error, and that in fact the Boltzmann-type distribution does not follow from axial symmetry alone. (L.B.S.)

41846 CURRENT ALGEBRAS AND MESON-NUCLEON SCATTERING LENGTHS. Balanchandran, A. P.; Gundzik, M. G.; Nicodemi, F. (Syracuse Univ., N. Y.). Nuovo Cimento (10), 44A: 1257-61(Aug. 21, 1966). (NYO-3399-63).

π-N and K-N scattering lengths are computed in terms of the PCAC constant using current algebra techniques. The derivation employs a formulation that avoids completely the use of unsubtracted dispersion relations in energy. (L.B.S.)

41847 $p\bar{p}$ ANNIHILATIONS AT REST WITH REPRESENTATION MIXING IN SU_{6w}. Hussain, F.; Rotelli, P. (Imperial Coll. of Science and Tech., London). Nuovo Cimento (10), 44A: 1262-4(Aug. 21, 1966).

Representation mixing in broken inhomogeneous $U_{6,6}$ or equivalently in SU_{6w} is used for the collinear process of $p\bar{p}$ annihilation at rest into two mesons. Calculations are made of the ratios of the rates for the pseudoscalar-pseudoscalar and pseudoscalar-vector modes. (L.B.S.)

41848 STATIC BARYON-MESON BOOTSTRAPS AND SU_6 SYMMETRY. Kanazawa, A.; Saito, M.; Sakuma, T.; Seto, K.; Tokuda, N. (Tokyo Univ. Hokkaido Univ., Sapporo). Nuovo Cimento (10), 44A: 1265-7(Aug. 21, 1966).

It is shown that the self-consistent bootstrap equations for the coupling constants of the meson-baryon interaction yields the SU(6) symmetry in the static limit. (L.B.S.)

41849 CP VIOLATION AND THE NEUTRAL KAON COMPLEX. Mathur, V. S. (Univ. of Rochester, N. Y.). Nuovo Cimento (10), 44A: 1268-71(Aug. 21, 1966). (UR-875-129).

It is pointed out that the assumption of CP violation in the $K_L^0 \rightarrow \pi^+ + \pi^-$ decay leads to the complication that the neutral kaon complex contains arbitrary parameters. It is shown that considerations of K_s^0 and K_l^0 as their own anti-particles introduce a simplification in the description of the neutral kaon complex, which has some experimentally interesting consequences. (L.B.S.)

41850 MEASUREMENT OF THE BRANCHING RATIO $\omega \rightarrow$ NEUTRALS/$\omega \rightarrow \pi^+ + \pi^- + \pi^0$. Di Giugno, G. (Univ., Naples. Istituo Nazionale di Fisica Nucleare, Naples); Peruzzi, I.; Troise, G.; Vanoli, F.; Giorgi, M.; Schiavon, P.; Silvestrini, V. Nuovo Cimento (10), 44A: 1272-5(Aug. 21, 1966).

The branching ratio $(\omega \rightarrow \text{neutrals})/(\omega \rightarrow \pi^+ + \pi^- + \pi^0)$ was measured to be $(13.4 \pm 2.6)\%$ in an experiment performed at CERN using a counter technique. Some details of the experimental technique and method are given. (L.B.S.)

41851 USE OF MULTIPOLES IN THE FIXED-t DISPERSION RELATIONS FOR PHOTOPION PRODUCTION. Shaw, G. (London Univ.). Nuovo Cimento (10), 44A: 1276-8(Aug. 21, 1966).

The approximation of the absorptive parts of the fixed-t dispersion relations for photopion production by the first few terms of their multipole expansions is discussed. It is argued that the method should work well up to energies of about 900 Mev. An arbitrary assumption in the use of Omnès method to solve the equations for the resonant multipoles is pointed out. (L.B.S.)

41852 CONNECTION BETWEEN THE COMPLEX LORENTZ GROUP WITH A REAL METRIC AND THE $U_{3,1}$ GROUP. Santilli, R. M. (Univ., Turin). Nuovo Cimento (10), 44A: 1784-9(Aug. 21, 1966).

In order to show that the 16-parameter complex Lorentz group with a real metric is isomorphic to the $U_{3,1}$ group the transition between the commutation relations of the two groups is investigated by introducing a suitable realization of their generators. It is also shown that the 15-parameter semisimple Λ_+ subgroup of the Λ group is isomorphic to the $SU_{3,1}$ group. (L.B.S.)

41853 EFFECTIVE MASS OF THE POSITRON IN SODIUM. Majumdar, Chanchal K. (Carnegie Inst. of Tech., Pittsburgh). Phys. Rev., 149: 406-8(Sept. 9, 1966).

The band effective mass of the positron in sodium is computed by the standard method of Wigner, Seitz, and Bardeen. The result is $m^* = 1.06m$, where m is the free-particle mass. Combining it with the results of the many-body calculations of the effective mass of a positron interacting with a Fermi sea of electrons, one can conclude that the theoretical value is much smaller than the experimentally observed effective mass. (auth)

41854 SEARCH FOR C VIOLATION IN $\eta \rightarrow \pi^+\pi^-\pi^0$. Contract W-7405-eng-48. Phys. Rev., 149: 1044-51 (Sept. 30, 1966). (UCRL-16693).

A search was made for charge asymmetry in the decay distribution of or combined sample of 1300 η decays. The Dalitz plot is divided into six azimuthal sectors, where sectors 1, 2, and 3 are the charge conjugates of sectors 6, 5, and 4, respectively. It is found that $R = (N_1 + N_2 + N_3 - N_4 - N_5 - N_6)/N_{total} = +0.058 \pm 0.034$, and $R' = (N_1 - N_2 + N_3 - N_4 + N_5 - N_6)/N_{total} = +0.068 \pm 0.033$. A more detailed parametrization is also given; it yields results consistent with those for R and R'. The largest theoretical estimates give about 5% for R. Thus the observed asymmetry admits the possibility of a C violation as large as the theoretical maximum. Since the asymmetry differs from zero by only two standard deviations, no definite conclusion is reached. (auth)

41855 K_L^0 THREE-BODY DECAYS AND THE $|\Delta I| = \frac{1}{2}$ RULES. Auerbach, L.; Bowen, D.; Dobbs, J. M.; Lande, K.; Mann, A. K.; Sciulli, F. J.; Uto, H.; White, D. H.; Young, K. K. (Univ. of Pennsylvania, Philadelphia). Phys. Rev., 149: 1052-62(Sept. 30, 1966).

The absolute decay rate of K_L^0 into three-body charged modes, Γ_L (ch), was measured in a spark-chamber-counter experiment. The result is Γ_L (ch) = $(15.1 \pm 1.9) \times 10^6$ sec^{-1}. The partial rates in K_L^0 decay are obtained from this value and previously measured branching ratios. The results are in agreement with values obtained by requiring internal consistency among all measured K_L^0 decay rates, absolute and relative. Comparison with conjugate K^+ partial decay rates is in agreement with the predictions of the $|\Delta I| = \frac{1}{2}$ rules for both leptonic and nonleptonic decays. As by-products of this investigation (a) the lifetime of K_S^0 was measured, (b) a search was made for coherent interference between K_L^0 and K_S^0 through their decays into two charged pions, and (c) the vector nature of the coupling in the leptonic decays of K_L^0 was verified. (auth)

41856 QUESTION OF A K^+K^+ RESONANCE. Erwin, A. R.; Walker, W. D.; Weinberg, A. (Univ. of Wisconsin, Madison). Contract AT(11-1)-881. Phys. Rev., 149: 1062-9(Sept. 30, 1966).

Using a separated 3.535-Bev/c K^+ beam, the reactions $K^+p \rightarrow K^+K^+\Lambda^0$ and $K^+p \rightarrow K^+K^+\Sigma^0$ were examined for indications of a K^+K^+ resonance. No statistically significant evidence was found for such a resonance either in the K^+K^+ effective-mass distributions or in the spectrum of invariant momentum transfer to the hyperon. Calculation of a K^+K^+ scattering cross section from the data using a peripheral absorption model suggests $\sigma_{KK} \approx \pi\lambda_\rho^2$, which is too small for a resonance at the previously reported mass of 1280 Mev/c^2. In addition, considerable evidence that K^+K^+ scattering does not dominate the production mechanism and that instead the two K's may originate from different vertices in a vector exchange model was found. (auth)

41857 DIFFERENTIAL CROSS SECTIONS FOR $\pi^\pm$p ELASTIC SCATTERING IN THE MOMENTUM RANGE 875-1579 Mev/c. Duke, P. J.; Jones, D. P.; Kemp, M. A. R.; Murphy, P. G.; Prentice, J. D.; Thresher, J. J. (National Inst. for Research in Nuclear Science, Chilton, Eng.). Phys. Rev., 149: 1077-89(Sept. 30, 1966).

Measurements were made of the differential cross sections for π^+p and π^-p elastic scattering at incident beam momenta in the range 875 to 1579 Mev/c. Two arrays of scintillation counters were used to detect pions scattered from a liquid-hydrogen target in coincidence with recoiling protons. In each of the 25 angular distributions, data were obtained at 18 center-of-mass angles varying from $\cos\theta^* = -0.97$ to $\cos\theta^* = 0.75$. The differential cross sections were expressed as series of the form $d\sigma^\pm/d\Omega = \Sigma_n C_n^\pm P_n \times (\cos\theta^*)$. The energy dependence of the coefficients $C_n^\pm$ suggests that N*(1688) has J = 5/2, I = 1/2, that N*(1928) has J = 7/2, I = 3/2, and that these two resonances have the same parity. The "shoulder" in the π^+p total cross section at about 950 Mev/c probably occurs in a J = 1/2 wave. (auth)

41858 PION-PION INTERACTIONS IN π^-p REACTIONS AT 2.1 Bev/c. West, E.; Boyd, J. H.; Erwin, A. R.; Walker, W. D. (Univ. of Wisconsin, Madison). Contract AT(11-1)-881. Phys. Rev., 149: 1089-1113(Sept. 30, 1966). (COO-881-59).

An analysis is given of the interactions of two pions as they result from the reactions of negative pions incident upon protons with a momentum of 2.1 Bev/c. A historical background of the motivation for the experiment is given and experimental techniques for dealing with the data are described, from the points of view of both event-by-event analysis and the physical theories which aid in the understanding of the results. Cross sections are given for the various reactions and are inferred by Chew-Low methods for pion-pion scattering. Evidence is presented which indicates that two resonant states in addition to the ρ meson and N*(1238) are present in these reactions: (1) the N* (1920), whose existence in other reactions is well established, and (2) the T = 0, s-wave pion-pion interaction, which is still in doubt, known as the ϵ^0, the evidence for which stems from an analysis of the decay distribution of the ρ^0. Finally, corrections to the one-pion-exchange model which involve pion-nucleon scattering vertices are made in an attempt to determine more accurately the low-energy, T = 0, s-wave pion-pion scattering cross sections, the results suggesting a range of about 10–15 mb in the region below the ρ. (auth)

41859 W-MESON PRODUCTION IN $\pi^- + p \rightarrow W^- + p$ INTERACTIONS. Sullivan, J. D. (Stanford Linear Accelerator Center, Stanford, Calif.). Contract AT(04-3)-400. Phys. Rev., 149: 1114-21(Sept. 30, 1966). (SLAC-PUB-144).

The cross section for production of W bosons in the reaction $\pi^- + p \rightarrow W^- + p$ is calculated on the basis of single-particle exchange for W masses in the region 2–5 Bev. Corrections for absorption in the initial channel are included. Pion exchange is found to dominate rho exchange and gives $(4-12)|F_\pi(m_W{}^2)|^2 \times 10^{-34}$ cm^2 as an estimate of the total production cross section. Here $F_\pi(m_W{}^2)$ is the pion electromagnetic form factor evaluated at the W-meson mass. (auth)

41860 EVALUATION OF MESON-BARYON COUPLING CONSTANTS FROM CURRENT DIVERGENCES. Raman, K. (Syracuse Univ., N. Y.). Contract AT(30-1)-3399. Phys. Rev., 149: 1122-5(Sept. 30, 1966). (NYO-3399-52).

It is examined how in broken SU_3 symmetry the strong coupling constants may be obtained in terms of the d/f ratio of the weak axial-vector current and the physical baryon masses by making suitable assumptions, particularly the hypothesis of partially conserved axial-vector current and Cabibbo's assumptions about leptonic decays. The derivation suggests that the correct starting point for calculations in broken SU_3 assigns the pseudovector couplings (rather than the pseudoscalar couplings) the values of the corresponding structure constants of the exact symmetry. (auth)

41861 UNSUBTRACTED DISPERSION RELATIONS AND CONSISTENCY CONDITIONS ON THE STRONG INTERACTIONS. Fuchs, Norman H. (Univ. of Pennsylvania, Philadelphia). Phys. Rev., 149: 1145-9(Sept. 30, 1966).

Consistency conditions involving strong interactions alone are derived from the assumption that the divergence of the $\Delta S = 0$, $\Delta I = 1$ axial-vector current is a highly convergent operator obeying unsubtracted dispersion relations which are dominated by nearby pole terms. The results are compared with those previously obtained by Adler under the assumption that the axial-vector current divergence is proportional to the pion field operator. The case of pion-pion scattering is treated in some detail, and it is found that the σ-meson (T = 0 = J, 400 Mev) model for low-energy pion-pion scattering fits in well, while the scattering-length approximation is incompatible with the conditions derived on pion-pion scattering. (auth)

41862 LIE GROUP OF THE STRONG-COUPLING THEORY. II. EQUIVALENCE WITH STATIC BOOTSTRAP THEORY AND APPLICATION TO PION-HYPERON SCATTERING. Singh, Virendra; Udgaonkar, Bhalchan-

dra M. (Tata Inst. of Fundamental Research, Bombay). Phys. Rev., 149: 1164-71(Sept. 30, 1966).

The mathematical equivalence of the Lie-group approach of Cook, Goebel, and Sakita to strong-coupling theory and certain conventional static bootstrap models is established. This equivalence is exploited to explicitly exhibit a new irreducible representation of the strong-coupling group $[SU(2) \otimes SU(2)] \times T_9$. This new representation is suitable for accommodating the Y = 0 hyperon isobars and has the spin-isospin content $J = I \pm \frac{1}{2} = \frac{1}{2}, \frac{3}{2}, \frac{5}{2}, \ldots$. It is found that $\Gamma(Y_1^* \to \Sigma\pi)/\Gamma(Y_1^* \to \Lambda\pi) = 12\%$ [SU(3) prediction 16%; observed ratio 11%]. The ratio of $(Y_1^* \to \Lambda\pi)$ to $(\Sigma \to \Lambda\pi)$ coupling and the isovector magnetic moments are in agreement with SU(6), while the ratio of $\Sigma\Sigma\pi$ to $\Sigma\Lambda\pi$ coupling has the SU(3) sign and approximately the SU(3) magnitude corresponding to $D/F = \frac{3}{2}$. (auth)

41863 PHOTON DISSOCIATION MODEL FOR VECTOR-MESON PHOTOPRODUCTION. Ross, Marc (Univ. of Michigan, Ann Arbor); Stodolsky, Leo. Contract AT(30-2)-Gen-16. Phys. Rev., 149: 1172-81(Sept. 30, 1966). (BNL-10146).

It is shown how the diffraction-dissociation approach can be formulated and used to yield detailed results for photoproduction of photon-like states such as ρ, ω, and φ. The model is shown to yield a coherent description of both the qualitative and quantitative aspects of the relevant experiments, including the size and behavior of the cross sections, the mass shifting of the ρ peak, and the nuclear A dependence. Scattering cross sections for the vector mesons and their effective photon couplings can be extracted from experiment, which are in accord with other data, insofar as they are available. A number of interesting experiments are suggested that can be used to test the model and the φ-ω mixing theory for the SU_3 structure of the photon. (auth)

41864 MODIFIED EFFECTIVE-RANGE APPROXIMATION BASED ON REGGE POLES. APPLICATION TO LOW-ENERGY π-N PHASE SHIFTS. Trivedi, U. (Tata Inst. of Fundamental Research, Bombay). Phys. Rev., 149: 1181-7(Sept. 30, 1966).

An improved form of the Khuri-Udgaonkar ansatz is presented. Its justification was sought in the domain of scattering by Yukawa potentials. The ansatz is then applied to P_{11} and P_{33} amplitudes of the π-N scattering for low energies, assuming that the principal contributions arise from nucleon, N*, and ρ exchanges. It is found that the ρ-exchange contribution is responsible for a turning of the P_{11} phase shift. (auth)

41865 S-MATRIX METHOD FOR CALCULATION OF RADIATIVE CORRECTION FOR $\pi^+ \to \pi^0 e^+ \nu$. Watanabe, Keiji (Dublin Inst. for Advanced Studies). Phys. Rev., 149: 1188-90(Sept. 30, 1966).

Dashen and Frautschi's method of calculating the p-n mass difference is extended to the electromagnetic correction of πe_3 decay. The $\gamma \to 3\pi$ contribution is evaluated. (auth)

41866 η-NUCLEON INTERACTION AND η PRODUCTION IN π-NUCLEON SCATTERING. Ball, James S. (Univ. of California, Los Angeles). Phys. Rev., 149: 1191-5(Sept. 30, 1966).

A dynamical model of the η-nucleon interaction is constructed which satisfies the requirements of analyticity and unitarity as well as including the most important single-particle exchange terms as an interaction. The resulting model depends on two parameters: the η-nucleon coupling constant g_η and a cutoff. It is found that a reasonably good fit to the η-production data and the π-nucleon phase-shift analysis can be obtained. Finally it is shown that the strong rise in η production just above the threshold implies the existence of a $J = \frac{1}{2}$ odd-parity nonstrange baryon of mass 1420-1460 Mev. (auth)

41867 SIMPLE $\pi\pi\rho$ BOOTSTRAP MODEL. Leon, M. (Carnegie Inst. of Tech., Pittsburgh). Phys. Rev., 149: 1195-9(Sept. 30, 1966).

A bootstrap model of the $\pi\pi\rho$ system is studied using a simple and somewhat unusual approach. An attempt is made to bootstrap both the ρ and the π; it is found that self-consistency can be achieved in the ρ channel, but not in the π channel. Two adjustable (cutoff) parameters can then be used to fit both the observed ρ mass and width. (auth)

41868 PARITY-CONSERVING HYPERON DECAY AND THE POLE MODEL. Pakvasa, S. (Syracuse Univ., N. Y.); Graham, R. H.; Rosen, S. P. Phys. Rev., 149: 1200-2(Sept. 30, 1966).

B. W. Lee has shown that, in the limit $\delta = 0$, where $\delta = (m_\Sigma - m_\Lambda)/(m_\Xi - m_N)$, a λ_6-type pole model for parity-conserving (p.c.) hyperon decay gives rise to an effective interaction which behaves like λ_7. Here this result is generalized to include a 27-plet baryon pole, and it is shown that, under certain plausible conditions, the generalization holds to first order in δ. As a result of this generalization, the p.c. decay amplitudes satisfy two sum rules which have previously been derived for parity-violating amplitudes from the SU(3) properties of the Cabibbo current × current interaction. (auth)

41869 VECTOR DOMINANCE AND MESON PHOTOPRODUCTION. Beder, Douglas S. (Univ. of California, Berkeley). Contract W-7405-eng-48. Phys. Rev., 149: 1203-7(Sept. 30, 1966). (UCRL-16781).

It is assumed that matrix elements of currents are dominated by vector-meson intermediate states. This assumption is then used to relate pseudoscalar-meson photoproduction to the (strong-interaction) production of vector mesons. Numerical comparison is hindered by the lack of "overlapping" data for the above two reactions, but predictions appear to be in rough agreement with extrapolated data for photoproduction of K's and π's. If valid, this vector dominance assumption could be a useful tool for high-energy photoproduction prediction. (auth)

41870 COUPLED-EQUATIONS METHOD FOR THE SCATTERING OF IDENTICAL PARTICLES. [PART] II. Levin, F. S. (Atomic Energy Research Establishment, Harwell, Eng.). Phys. Rev., 149: 1212-16(Sept. 30, 1966).

The set of coupled, inhomogeneous equations describing the scattering of a fermion by a system of identical fermions, previously derived from the integral equation for scattering, is shown to follow directly from the Schroedinger equation and the symmetry properties of the exact scattering wave function. (auth)

41871 ANALYSIS OF THE REACTION $\pi^- + p \to \eta + n$ NEAR THRESHOLD. Uchiyama-Campbell, F.; Logan, R. K. (Univ. of Illinois, Urbana). Phys. Rev., 149: 1220-4(Sept. 30, 1966).

A successful fit of both the total and the differential cross sections for the reaction $\pi^- + p \to \eta + n$ in the region of T_π^- from the threshold (558 Mev) to 900 Mev was made with both multichannel Breit-Wigner and effective-range formulas. It is found that an S-wave resonance accounts for the enhancement of the reaction near threshold. A comparison is made of the various πp S_{11} phase-shift analyses with the phase shifts predicted by our multichannel fits. A search was made for the S-matrix poles of our Breit-Wigner and effective-range solutions on the various sheets of the energy plane. (auth)

41872 CP VIOLATION WITH $|\Delta T| > \frac{1}{2}$: A RE-EXAMINATION OF TRUONG'S MODEL FOR $K_L^0 \to 2\pi$. Barshay, Saul (Rutgers-The State Univ. of New Jersey, New Brunswick). Phys. Rev., 149: 1229-33(Sept. 30, 1966).

The possibility of the failure of CP invariance in an electromagnetic interaction provokes interest in the possibility that CP-violating amplitudes with $|\Delta T| > \frac{1}{2}$ play a significant role in the decays $K_L^0 \to \pi^+\pi^-$ and $K_L^0 \to 2\pi^0$. Such a model has been invented by Truong. A reformation of this model is given, which is characterized by an exceedingly simple derivation. The assumptions or approximations made at any point can be clearly stated and simply understood. Using a representative value of the pion-pion S-wave coupling parameter, and the measured branching ratio $|\eta^{+-}|^2$ for $K_L^0 \to \pi^+\pi^-$ to $K_S^0 \to \pi^+\pi^-$, estimates were made on the basis of this model of (I) the branching ratio for $K_L^0 \to 2\pi^0$ to $K_L^0 \to \pi^+\pi^-$ to be about 1.8; (II) the branch-

ing ratio for $K_L^0(K_S^0) \rightarrow l^- + \pi^+ + \bar{\nu}_l$ to $K_L^0(K_S^0) \rightarrow l^+ + \pi^- + \nu_l$ to be about 1 ± 0.0001 (with $\Delta S = \Delta Q$); (III) the magnitude of the mass difference between K_S^0 and K_L^0 to be $|\Delta m| = |m_S - m_L| \cong 0.42$, in units of the K_S^0 decay rate; (IV) the phase of η^{+-} to be η (or $\pi + \eta$) $\cong 1.2$ radians for $\Delta m > 0$, or $\cong 1.9$ radians for $\Delta m < 0$. The first two numbers are significantly different from those given earlier by Truong. The predictions (I) and (II) differ decidedly from the corresponding predictions of the theory with "superweak," CP-violating, $|\Delta S| = 2$ interactions. If the amplitude for $K_S^0 \rightarrow 2\pi$ is depressed by SU(3) symmetry by a factor $\cong 3$, it is found that the real and imaginary parts of the $|\Delta T| > \frac{1}{2}$ amplitude in $K^0(\bar{K}^0) \rightarrow 2\pi$ are comparable in magnitude, as might be expected if they arise from a CP-violating electromagnetic correction to a $|\Delta T| = \frac{1}{2}$ interaction, or, more generally, if CP violation is intrinsic to whatever causes $|\Delta T| > \frac{1}{2}$. (auth)

41873 TWO-PION-EXCHANGE EFFECTS IN NN SCATTERING AND CONSISTENCY WITH πN SCATTERING. Durso, John W. (Michigan State Univ., East Lansing). Contract AT-(11-1)-1051. Phys. Rev., 149: 1234-42 (Sept. 30, 1966). (TID-22834).

The two-pion-exchange contribution to nucleon-nucleon scattering was recalculated using the method of Amati, Leader, and Vitale: previous errors were eliminated. The new results show that low-energy pion-nucleon scattering phenomena and two-pion exchange effects in nucleon-nucleon scattering can be explained in a consistent way. The results also show that the two-pion parts of the NN phase shifts are dominated by the cross-channel s-wave contribution, in contrast to the results of Amati et al. The cutoff sensitivity of both the total and high-wave cross-channel contributions is examined, and arguments are presented to explain the strong sensitivity of the high-wave part. (auth)

41874 ARE THE POSITIVE-PARITY MESONS IN THE 405 MULTIPLET? Resnikoff, M. (Univ. of Maryland, College Park); Silbar, R. R. Contract AFOSR 500-66. Phys. Rev., 149: 1245-7(Sept. 30, 1966).

The 405 multiplet mass formulas, derived previously, are used to predict the masses of the positive-parity mesons. Using three 2^+ mesons (f_0,A_2,K**) as input, the f' is predicted in agreement with experiment, and the states of the 2^+ 27-plet are found to lie higher, but in the accessible experimental region. The existence of the 27-plet states is a clear test of whether the 405 multiplet exists. When the 1^+ mesons D(1286) and E(1420) are taken together with the three 2^+ mesons as input, the remaining $J = 0^+$, 1^+ mesons are predicted. Mass-difference equalities are presented and comparison is made with experiment. (auth)

41875 THICK-TARGET BREMSSTRAHLUNG AND TARGET CONSIDERATIONS FOR SECONDARY-PARTICLE PRODUCTION BY ELECTRONS. Tsai, Y. S.; Whitis, Van (Stanford Linear Accelerator Center, Calif.). Contract AT(04-3)-400. Phys. Rev., 149: 1248-57(Sept. 30, 1966). (SLAC-PUB-184).

Bremsstrahlung spectra as a function of target thickness up to several radiation lengths, to be used for particle production in high-energy electron machines, are investigated. The shower equations are cast in integral forms, which are then solved by iteration. The iterations are performed up to the second-generation photons; and the numerical results show that for most experiments the first-generation photons alone will give sufficiently accurate results. For example, for a target thickness of two radiation lengths and for $k/E_0 = 0.5$, where k is the photon energy and E_0 is the incident electron energy, the ratio of the second- to the first-generation photon intensity is 8%. This ratio decreases rapidly as one increases k/E_0 and decreases the target thickness. A very simple formula which approximates the first-generation photon spectra as a function of target thickness is derived. This approximate formula is shown to be accurate enough for estimating the secondary-beam production by electrons. As by-products of our investigation the first- and the second-generation electron and positron spectra were obtained as functions of target thickness. These spectra are useful in estimating the electron and positron background. Some aspects of target considerations for the secondary-beam production are given as an illustration of the use of our formulas. (auth)

41876 CONNECTION BETWEEN BBP AND VPP VERTICES IN THE QUARK MODEL. Becchi, C.; Morpurgo, G. (Univ., Genoa. Istituto Nazionale di Fisica Nucleare, Genoa). Phys. Rev., 149: 1284-7(Sept. 30, 1966).

It is shown that in the quark model it is possible to express the $N_{33}^* N\pi$ vertex and the $\rho\pi\pi$ vertex in terms of the axial-vector quark-pion coupling constant. By expressing then this constant in terms of the NNπ coupling constant f, results in fair agreement with the experimental data are obtained for the above vertices. A detailed comparison of this calculation with that of Gürsey, Pais, and Radicati is made, illustrating the different points of view and the different assumptions of the two procedures. (auth)

41877 LARGE-ANGLE NEUTRON-PROTON C_{NN} PARAMETER AT 23.1 Mev. Malanify, J. J.; Bendt, P. J.; Roberts, T. R.; Simmons, J. E. (Los Alamos Scientific Lab., N. Mex.). Phys. Rev. Lett., 17: 481-4(Aug. 29, 1966). (LA-DC-7537)

The neutron-proton spin-correlation parameter, C_{NN}, was measured at $\theta_n = 140$ and 174° c.m., by scattering polarized neutrons from a polarized proton target. Comparison to recent phase-shift analyses is made, and a sensitivity of the S-D coupling parameter to the data is noted. (auth)

41878 SIGN OF THE K_1^0–K_2^0 MASS DIFFERENCE. Meisner, Gerald W.; Crawford, Bevalyn B.; Crawford, Frank S. Jr. (Univ. of California, Berkeley). Phys. Rev. Lett., 17: 492-5(Aug. 29, 1966). (UCRL-16938).

Evidence is presented that the long-lived neutral K is heavier than the short-lived. (auth)

41879 NEW Σ DECAY PARAMETERS AND TEST OF $\Delta I = \frac{1}{2}$ RULE. Bangerter, Roger O.; Barbaro-Galtieri, Angela; Berge, J. Peter; Murray, Joseph J.; Solmitz, Frank T.; Stevenson, M. Lynn; Tripp, Robert D. (Univ. of California, Berkeley). Phys. Rev. Lett., 17: 495-8 (Aug. 29, 1966). (UCRL-16939)

New values for the three decay asymmetry parameters in the nonleptonic decays of Σ hyperons are presented. The selection rule $\Delta I = \frac{1}{2}$ is found to be well satisfied. (auth)

41880 EXCHANGE OF EVEN- AND ODD-PARITY BARYON-MESON RESONANCES AND BACKWARD ELASTIC SCATTERING. Desai, Bipin R. (Univ. of California, Riverside). Phys. Rev. Lett., 17: 498-501(Aug. 29, 1966).

If there are two meson-baryon resonances or bound states with opposite parities but with the same remaining internal quantum numbers including signature, one at c.m. energy W_1 with $l = J - \frac{1}{2}$ and the other at W_2 with $l = J + \frac{1}{2}$, then the residue of the Regge trajectory on which they lie must change sign between W_1 and $-W_2$. Consequences of the exchange of such a trajectory to backward elastic scattering are discussed. (auth)

41881 NEW DETERMINATION OF THE φ SPIN AND G PARITY. Gray, L. (Syracuse Univ., N. Y.); Kalogeropoulos, T.; Nicodemi, G.; (and others). Phys. Rev. Lett, 17: 501-4(Aug. 29, 1966).

Determination of the ϕ spin which is independent of any assumption on the structure of the ϕ is reported; at the same time confirmation that $G_\phi = -1$ is obtained. (B.G.D.)

41882 ENERGY DEPENDENCE OF PROTON-PROTON BREMSSTRAHLUNG. Slaus, Ivo; Verba, J. W.; Richardson, J. Reginald; Carlson, R. F.; van Oers, W. T. H.; August, L. S. (Univ. of California, Los Angeles). Phys. Rev. Lett., 17: 536-8(Sept. 5, 1966).

An accurate measurement of the proton-proton bremsstrahlung cross section which can be compared with the independent measurement at 48 Mev by Warner (Phys. Letters 18: 289(1965)) is presented, in order to investigate the energy dependence of the cross section, and to investigate the angular distribution of gamma rays for a fixed pair of proton angles. (B.G.D.)

41883 ROLE OF MESON CURRENT IN THE DETERMINATION OF NEUTRON FORM FACTORS FROM ELASTIC ELECTRON-DEUTERON SCATTERING. Dietz, Klaus; Month, Melvin (Univ. of Illinois, Urbana). Phys. Rev. Lett., 17: 546-8(Sept. 5, 1966).

Elastic electron-deuteron scattering data are used to determine the electromagnetic form factors of neutrons. A comparison is made with previous results (DeVries, et al., Phys. Rev. 134: B848(1964)) using only inelastic electron-deuteron scattering data. (B.G.D.)

41884 PRECISE MEASUREMENTS OF THE K^+/K^- AND π^+/π^- LIFETIME RATIOS. Lobkowicz, F. (Univ. of Rochester, N. Y.); Melissinos, A. C.; Nagashima, Y.: Tewksbury, S.; von Briesen, H. Jr.; Fox, J. D. Phys. Rev. Lett., 17: 548-52(Sept. 5, 1966). (UR-875-152).

An experiment to measure the ratio $\tau(K^+)/\tau(K^-)$ is described. As a check on the experimental proceedure the lifetime ratio of the π mesons was also measured. (B.G.D.)

41885 RELATION BETWEEN THE PION-NUCLEON AND THE ρ-MESON COUPLING CONSTANTS FROM PION SCATTERING LENGTHS. Sakurai, J. J. (Univ. of Chicago). Phys. Rev. Lett., 17: 552-3(Sept. 5, 1966).

The scattering length of a pion on an isospin-bearing target can be computed either by applying the U(2) ⊗ U(2) current algebra or by assuming ρ dominance in the t channel. Comparing the two approaches, the relation $(f_\rho^2/4\pi) = (G_{\pi NN}^2/4\pi)(g_V/g_A)^2(m_\rho^2/2m_N^2)$, is established which was previously obtained on the basis of current algebra applied to $\rho \to 2\pi$. (auth)

41886 Y_1^* RESONANT AMPLITUDES BETWEEN 1600 AND 1900 Mev. Smart, Wesley M.; Kernan, Anne; Kalmus, George E.; Ely, Robert P. Jr. (Univ. of California Berkeley). Phys. Rev. Lett., 17: 556-61(Sept. 5, 1966). (UCRL-16961).

A partial-wave analysis of the reaction $K^- + n \to \Lambda + \pi^-$ has confirmed the spin-parity assignments for Y_1^* (1765) and Y_1^* (2030) and measured the mass, width, and $\Lambda\pi$ branching ratio of Y_1^* (1765) as 1776 ± 6 Mev, 129 ± 16 Mev and 0.14 ± 0.02, respectively. A tentative spin-parity assignment for Y_1^* (1660) and Y_1^* (1915) is also made. The resonant amplitudes Y_1^* (1765) and Y_1^* (1915) are in phase at the resonant energy and are 180° out of phase with Y_1^* (1660) and Y_1^* (2030). (auth)

41887 CHARGE INDEPENDENCE IN HIGH-ENERGY SCATTERING FROM DEUTERONS. Wilin, Colin (Brookhaven National Lab., Upton, N. Y.). Phys. Rev. Lett., 17: 561-3(Sept. 5, 1966).

It is shown that the usual shadow correction for high-energy scattering of particles by deuterons violates charge independence in the case of pions. Alternative formulas are derived which are applicable to this case. (auth)

41888 REGENERATION EFFECTS IN ω-φ PRODUCTION. Ross, Marc (Massachusetts Inst. of Tech., Cambridge); Stodolsky, Leo. Phys. Rev. Lett., 17: 563-8(Sept. 5, 1966). (BNL-10386).

It is shown that effects closely analogous to the K^0 mixing phenomena (particle mixing) should exist for high-energy ω-ϕ production. (B.G.D.)

41889 PHOTOPRODUCTION OF ETA MESONS FROM 950 TO 1100 Mev. Heusch, C. A.; Prescott, C. Y.; Bloom, E. D.; Rochester, L. S. (California Inst. of Tech., Pasadena). Phys. Rev. Lett., 17: 573-6(Sept. 5, 1966).

Experimental results are presented on the photoproduction of η mesons. The purpose of the experiment was to extend cross section data to higher energies, and specifically, to investigate a possible contribution of an isobar diagram to the photoproduction mechanism. (B.G.D.)

41890 POLARIZATION IN PION-PROTON SCATTERING. Grannis, P. D. (Univ. of California, Berkeley). pp 175-86 of Proceedings of the Williamsburg Conference on Intermediate Energy Physics. Vol. I. Williamsburg, Va., College of William and Mary, 1966.

Experiments for measuring the polarization parameter in π-p scattering are considered. The left-right asymmetry in scattering from a 100% polarized proton target is measured. These results are presented and show rapid changes in the polarization in the region of the resonances in the π-N nucleon. (J.F.P.)

41891 COMPARISON OF THE LIFETIMES OF POSITIVE AND NEGATIVE PIONS. Ayres, David S. (Univ. of California, Berkeley); Eandi, Richard D.; Greenberg, Arthur S.; Kenney, Robert W.; Kurz, Richard J.; Macdonald, Burns; Caldwell, David O.; Stearns, Brenton F. pp 419-25 of Proceedings of the Williamsburg Conference on Intermediate Energy Physics. Vol. I. Williamsburg, Va., College of William and Mary, 1966.

An experiment for measuring the total lifetime of positive and negative mesons (π) and the ratio of these lifetimes is described. The lifetime measurement for the negative mesons (π) in flight is performed, and the positive (π) lifetimes are determined by measuring the attenuation due to decay as a function of distance of nearly identical beams of mesons (π^+) and (π^-). The results are 26.26 ± 0.08 nsec for mesons (π^+) and 25.80 ± 0.21 for mesons (π^-) lifetimes. (J.F.P.)

41892 INTERMEDIATE BOSON PRODUCTION BY NUCLEON-PAIR ANNIHILATION. Yamaguchi, Yoshio (CERN, Geneva). Progr. Theoret. Phys. (Kyoto), 35: 914-33(May 1966).

The intermediate boson production in antinucleon-nucleon annihilation $\bar{N} + N \to W \to l \pm \nu$ is discussed. A comparison with the electromagnetic process $\bar{N} + N \to \bar{l} + l$ was also made. The total decay rate of W, which is important for our production rate, is estimated from several models. (auth)

41893 VERTEX FUNCTION AND RENORMALIZATION CONSTANT Z_1. Kubo, Reijiro (Tokyo Inst. of Tech.). Progr. Theoret. Phys. (Kyoto), 35: 962-4(May 1966).

The S-state scattering of two scalar mesons with equal mass is treated, and the general form of the proper vertex function in the limit $Z_1 = 0$, where Z_1 is the renormalization constant is studied. (J.F.P.)

41894 EVIDENCE FOR EXISTENCE OF A REPULSIVE CORE IN THE Λ-N INTERACTION. Kanada, Hiroyuki; Otsuki, Shoichiro; Sakai, Kenji; Yasuno, Masaru (Univ. of Nagoya, Japan). Progr. Theoret. Phys. (Kyoto), 35: 971-3 (May 1966).

Evidence for the existence of a repulsive core in the Λ-N interaction in the S state is reported. It is concluded that a repulsive core in the Λ-N system certainly exists in the $^1S_0$ state and probably in the $^3S_1$ state, and if the repulsive core is approximated by a hard core, the values of its radius in both states seem equal to or larger than that in the N-N $^1S_0$ state. (J.F.P.)

41895 LARGE ANGLE PROTON-PROTON SCATTERING AND REAL PART OF THE SCATTERING AMPLITUDE. Yamamoto, Yoshitaka (Tokyo Univ.). Progr. Theoret. Phys. (Kyoto), 35: 809-20(May 1966).

The large angle P-P scattering in the accelerator energy region is discussed. This large angle scattering is assumed to be due to the real part of the scattering amplitude. The real amplitude for an arbitrary angle is derived, by using only the experimental information on the imaginary amplitude for small momentum transfer, and the ratio of the real to the imaginary forward amplitude. A model for the central collision is introduced. The differential cross section for large momentum transfer and the total elastic cross section can be obtained from this real amplitude. They fit the experimental curves well, and support the assumption. It is also inferred from the real amplitude that the region of the central collision is of the order of a nucleon Compton wave length. (auth)

41896 LARGE-ANGLE ELASTIC PROTON-PROTON SCATTERING AT HIGH ENERGY. Bando, Masako; Takada, Yoshio (Kyoto Univ.). Progr. Theoret. Phys. (Kyoto), 35: 834-9(May 1966).

A possible explanation of the characteristic features of large angle elastic proton-proton scattering at high energies is suggested. The effect of the diffraction scattering

of a cloud pion of the target proton from the incident proton is calculated; this gives the main contribution in the region II where the scattering angle ranges from 20 to 70°. (auth)

41897 LARGE t LIMIT OF COMPTON SCATTERING OF A VECTOR PHOTON BY A SCALAR NUCLEON IN THE SIXTH-ORDER DIAGRAM. Otokozawa, Jun (Nihon Univ., Tokyo). Progr. Theoret. Phys. (Kyoto), 35: 881-8(May 1966).

The sixth order diagrams for the Compton scattering of a massless vector photon by a scalar nucleon are evaluated in the large t limit. The leading term in t for the largest invariant amplitude is found to be ln^4t compared to ln^2t for the case of scattering of a finite mass photon. The same situation also holds for other smaller invariant amplitudes, that is, the magnitude in the large t limit increases by a factor lnt or ln^2t if the photon mass is zero. The Regge behavior in this case is discussed in detail. (auth)

41898 EXPLICIT CALCULATION OF THE CROSS SECTION OF THE REACTION K + N → K* + N. Berzi, Vittorio (Univ., Milan); Recami, Erasmo. Rendic. Ist. Lombardo Sci. Lett., A, 99: 911-20(1965). (In Italian).

The contribution of the exchange of a single pion to the cross section amplitude of a reaction of the type P + B = V + B′ is evaluated. P and B indicate, respectively, a pseudoscalar particle with spin 0 and a particle with vectoral character and spin 1 and negative parity; B and B′ indicate particles with spin ½ having the same parity relative to space. (tr-auth)

41899 ONE-BOSON EXCHANGE POTENTIALS IN NUCLEON-NUCLEON SCATTERING. Cronstroem, C.; Laurikainen, K. V. (Univ. of Helsinki). Soc. Sci. Fenn., Comment. Phys. Math., 31: No. 4, 1-16(1965).

The N-N scattering was investigated assuming one-boson exchange process only. In addition to the OPEP, potentials corresponding to η-, ρ- and ω-meson exchange and a hard core are included in the N-N interaction. The results are not sufficiently compatible with all experimental phase shifts, and it is observed that the agreement could be improved by introducing a potential term corresponding to a hypothetical isotriplet scalar boson. (auth)

41900 THEORY OF REACTIONS WITH FORMATION OF THREE PARTICLES NEAR THRESHOLD. Anisovich, V. V.; Ansel'm, A. A. Usp. Fiz. Nauk, 88: 287-326 (Feb. 1966). (In Russian).

A theoretical interpretation of reactions with multiple production of particles is presented with emphasis on the determination of the scattering amplitudes of unstable particles at zero energy. The approach used is based on an investigation of processes connected with formation of several particles near the threshold, when the total released kinetic energy is lower than the mass of any particle, and makes it possible to develop a consistent theory that describes reactions with creation of low-energy particles in terms of a certain number of independent parameters and in terms of the scattering amplitudes of the pairs of produced particles. The analysis is limited to three-particle production. Kinematic relations are derived for the transformation of two particles into three, and rules for selecting the proper Feynman diagrams are formulated. It is shown that in the case of low-energy nucleon-nucleon scattering the selection rules lead directly to the Bethe-Peierls effective-radius theory. Topics discussed are kinematics, fundamental principles of diagram selection, scattering of particles near threshold, expansion of the amplitude in terms of states with different total angular momenta, unitarity condition and calculation of discontinuities, linear and quadratic terms in the expansion of the amplitude with L = 0 in terms of the threshold momenta, cubic terms in the expansion in terms of the threshold momenta and the general structure of the expansion of the amplitude with L = 0, production of three particles in a state with unity total angular momentum, resonant interaction of produced particles, the reactions $\pi + N \to N + \pi + \pi$, $\gamma + N \to N + \pi + \pi$, and $K \to 3\pi$ decay. (ATD)

41901 POLARIZATION EFFECTS IN THE PHOTOPRODUCTION OF W-MESON PAIRS ON A NUCLEUS. Bolsun, A. I. Vestsi Akad. Navuk Belarusk. SSR, Ser. Fiz.-Mat. Navuk, No. 1, 134-6(1966). (In Russian).

The observation of lepton pairs which are emitted in a direction opposite to that of the photon beam, during photoproduction on lead-208 at high energies is used as an indication of the intermediate formation of a vector meson (W). The cross section for the formation of a pair of circularly polarized mesons (W) decaying to form lepton pairs for a photon energy of 50 Bev and a maximum momentum transfer of 0.126 Bev is given as $0.12\ (10)^{-30}$. (J.F.P.)

41902 SPONTANEOUS POLARIZATION OF NEUTRONS IN MAGNETIC AND ELECTRIC FIELDS. Lyuboshits, V. L. Yadern. Fiz., 4: 269-71(Aug. 1966). (In Russian).

An elementary derivation is given of the formula for the spontaneous polarization probability of relativistic neutrons in external magnetic fields. The spontaneous radiation neutrons in a homogeneous electric field is considered. The obtained expressions describe the dependence of the mean spontaneous polarization time for charged particles with spin ½ on the energy, field intensity, and magnetic moment, correctly up to a factor. (auth)

41903 SEARCH FOR NEW DECAY MODES OF THE K_2^0-MESONS. Anikina, M.; Vardenga, G.; Zhuravleva, M.; Kotlyarevskii, D.; Novikov, V.; Okonov, E.; Takhtamyshev, G.; Wu, Tsung-fan; Chkhaidze, L. Yadern. Fiz., 4: 360-4(Aug. 1966). (In Russian).

The kinematical analysis of 1116 well measurable K_2^0 decays recorded in a Wilson chamber yields no decays of the type $K_2^0 \to e^+e^-$, $K_2^0 \to \mu^+e^-$ and $K_2^0 \to \mu^+\mu^-$. This gives $W \lesssim 1.2 \cdot 10^4\ sec^{-1}$ for the upper limit of the probability of these processes. Events of the mode $K_2^0 \to \pi^+\pi^-\gamma$ in which the γ-quantum produces an electron-positron pair in a lead plate have also not been observed, so that $W(K_2^0 \to \pi^+\pi^-\gamma) \lesssim 2 \cdot 10^5\ sec^{-1}$. Among the decays analyzed no events were found with anomalously large decay energy. (auth)

41904 CROSS SECTION FOR DOUBLE BREMSSTRAHLUNG IN ee-COLLISIONS IN THE SMALL ANGLES APPROXIMATION. Synakh, V. S. (Computer Center, Siberian Division, Academy of Sciences, USSR). Yadern. Fiz., 4: 365-6(Aug. 1966). (In Russian).

The cross section for double bremsstrahlung in e-e interactions is integrated over angular variables in cms. (auth)

41905 ON THE POSSIBLE EFFECTS OF THE VIOLATION OF CP-INVARIANCE IN THE RADIATIVE DECAYS OF NEUTRAL K-MESONS. Dolgov, A. D.; Ponomarev, L. A. (Inst. of Theoretical and Experimental Physics, State Atomic Energy Commission, USSR). Yadern. Fiz., 4: 367-70(Aug. 1966). (In Russian).

The possible manifestation of CP-nonconservation in the decays $K^0 \to 2\pi\gamma$, $2\pi e^+e^-$ is discussed. It is shown that the $\pi^+\pi^-$ asymmetry can attain several percents in K_2^0-decays. Some polarization effects are considered. (auth)

41906 ISOSPIN AMPLITUDE FOR S-STATE PION PHOTOPRODUCTION ON NUCLEONS. Govorkov, B. B.; Denisov, S. P.; Minarik, E. V. (Lebedev Inst. of Physics, Moscow). Yadern. Fiz., 4: 371-8(Aug. 1966). (In Russian).

The energy dependence of the $\gamma + p \to p + \pi^0$ differential cross section for the pion emission angle 90° was measured for photons with energies in the region 158 to 200 Mev. The S-state π^0-meson photoproduction amplitude was determined as $(-0.26 \pm 0.04) \times 10^{-15}$ cm by extrapolating the empirical energy dependence to the threshold. The isovector E_{0+}^+ part of the S-amplitude was determined, as well as the amplitudes of certain isospin states. These quantities were compared with dispersion theory predictions. (auth)

41907 RELATIVISTIC SCATTERING OF ELECTRONS ON NUCLEI WITH ARBITRARY SPINS. Marinov, M. S. (Inst. of Theoretical and Experimental Physics, State Atomic Energy Commission, USSR). Yadern. Fiz., 4: 379-86(Aug. 1966). (In Russian).

The method of helicity amplitudes is used to consider the

electromagnetic interaction of relativistic polarized particles (in the first Born approximation). Polarization effects in the scattering of electrons on deuterons are found, in particular the polarization correlations which could be due to the existence of an electric dipole moment of the deuteron. (auth)

41908 RADIATIVE DECAYS OF VECTOR MESONS IN THE SU(6) SYMMETRY. Rekalo, M. P. Yadern. Fiz., 4: 387-90(Aug. 1966). (In Russian).

Relations between the amplitudes for the decays of vector mesons into a pair of pseudoscalar mesons and a γ quantum are investigated on the basis of the SU(6) symmetry. The influence of a possible resonance interaction of the final state mesons is studied in detail. (auth)

41909 PARTICLE DECAY DESCRIBED BY THE LEE MODEL WITH COULOMB INTERACTION. Hannover, H. Muenster, Ger., Univ., 1965. 105p. $2.00 Gmelin, AED-Diss. 65-353.

Thesis.

The influence of the electromagnetic field on the decay of a V particle into charged N and Θ particles as described by the Lee decay interaction is studied. Approximate solutions are obtained by perturbation theory. (Gmelin Inst.)

41910 DETECTION AND PROPERTIES OF π^0 MESONS IN MULTIPLE PROCESSES. Klugow, J. Berlin, Humboldt Univ., 1965. 38p. $2.00 Gmelin, AED-Diss. 65-350.

Thesis.

The mesons (π^0) from high-energy (8 Bev/c) multiple production processes are detected by decay electron pairs. Kinematic properties of mesons (π^0) are calculated. Energy spectra of γ quanta are compared to momentum spectra of π^0 particles and used for studies of radiation decays of resonance particles. No η resonance was found, the cross section for π^--nucleon interactions is therefore smaller than 0.5 mb. (Gmelin Inst.)

41911 PRODUCTION OF HYPERFRAGMENTS BY 1.5-Bev/c K^- MESONS AND STUDIES OF THEIR DECAY PROPERTIES. Harmsen, D.-M. Hamburg, Univ., Hamburg, 1965. 92p. $2.00 Gmelin, AED-Diss. 65-303.

Thesis.

Production of hyperfragments in a nuclear emulsion stack exposed in the CERN K^- beam is studied. 1270 hyperfragments were observed in 40–100 beam particle interactions. 87 hyperfragments decayed with π^- meson emission, one with π^+ emission. 40 of these meson decaying fragments were identified. Nonmesonic decay takes place by neutron stimulation. (Gmelin Inst.)

41912 PROCEEDINGS OF THE WILLIAMSBURG CONFERENCE ON INTERMEDIATE ENERGY PHYSICS, FEBRUARY 10–12, 1966. VOLUME II. Williamsburg, Va., College of William and Mary, 1966. 338p. (CONF-660209(Vol.2)).

The conference included 17 papers, 8 of which were abstracted previously in NSA. For abstracts of these papers see CONF 660209 in the Report Number Index. Separate abstracts were prepared for 9 papers. (J.F.P.)

For abstracts of individual sections see: 41913–41916, 41992, and 42276–42279.

41913 PION-NUCLEON PHASE SHIFT ANALYSES. Roper, L. David. pp 495-515 of Proceedings of the Williamsburg Conference on Intermediate Energy Physics. Vol. II. Williamsburg, Va., College of William and Mary, 1966.

Phase shift calculations and analyses that attempted to determine the phase shifts over wide energy ranges are reviewed. The discussion includes theoretical calculations, resonances in phase shift analyses, and nonresonant phases. (J.F.P.)

41914 n-n S-WAVE SCATTERING LENGTH FROM THE NEUTRON SPECTRA OF THE REACTION $\pi^- + d \rightarrow 2n + \gamma$. Salter, R. M. Jr. (Univ. of California, Los Angeles); Zeller, M.; Haddock, R. P.; Czirr, J. B.; Nygren, D. R. pp 569-94 of Proceedings of the Williamsburg Conference on Intermediate Energy Physics. Vol. II. Williamsburg, Va., College of William and Mary, 1966.

A determination of the neutron-neutron S-wave scattering length giving $a_{nn} = -16.47F \pm 1.27F$.is reported. The neutron time-of-flight and angle spectra from the reaction $\pi^- + d \rightarrow 2n + \gamma$ were recorded and are shown. (J.F.P.)

41915 MEASUREMENTS OF THE DIFFERENTIAL CROSS-SECTION AND POLARIZATION IN PROTON-PROTON SCATTERING AT ABOUT 143 Mev. Jarvis, O. N.; Cox, G. F.; Eaton, G. H.; Rose, B.; Van Zyl, C. P. (Atomic Energy Research Establishment, Harwell, Eng.). pp 595-601 of Proceedings of the Williamsburg Conference on Intermediate Energy Physics. Vol. II. Williamsburg, Va., College of William and Mary, 1966.

Measurements of the differential cross section and polarization in proton-proton interactions at 143 Mev were repeated with improved accuracy. The cross section data were obtained to a relative precision of better than ±0.5% and the absolute scale was determined to ±0.8%. The polarization data were determined to a relative precision of about 1% of the maximum value and the absolute scale to 0.85%. These data are shown. (J.F.P.)

41916 EXPERIMENTAL ASPECTS OF NUCLEON-NUCLEON SCATTERING AND POLARIZATION BELOW 1 Bev. Rose, B. (Atomic Energy Research Establishment, Harwell, Eng.). pp 603-47 of Proceedings of the Williamsburg Conference on Intermediate Energy Physics. Vol. II. Williamsburg, Va., College of William and Mary, 1966.

The present state of nucleon-nucleon data is reviewed. There has been a resurgence of interest in the problem at 300–700 Mev, partly stimulated by the availability of polarized targets. Some of the new data is clearing away old discrepancies and some revealing new ones. The precision of existing data is rarely as high as claimed, and much greater precision will be needed if unique energy independent analyses are to be carried out at the higher energies. Twice as many experimental papers are published on the p-p as on the n-p system. It is proposed that more attention be devoted to the neutron proton system with neutron beams, in preference to quasi-free experiments using the deuteron as a neutron target. The problems of doing so are discussed. Recent results on nuclear bremsstrahlung are briefly mentioned. (auth)

41917 APPLICATION OF π-N SCATTERING RESULTS TO Λ-K^0 PRODUCTION. Rush, J. E. (Univ. of the South Sewanee, Tenn. Vanderbilt Univ., Nashville, Tenn.); Holladay, W. G. 42p. (CONF-660411-27). ORAU. Gmelin, AED-CONF-66-060-62.

From American Physical Society Meeting, Washington, D.C.

The appearance of numerous phase-shift analyses of pion-nucleon scattering and the tentative identification of resonances in that process lead naturally to an application of these results to processes involving other decay channels. The three isospin-$\frac{1}{2}$ resonances of the π-N system on which there seems to be the widest agreement are chosen and their effect on the process $\pi^- + p + \Lambda + K^0$ near 900 Mev is considered. The background term used is a K^* pole modified by an arbitrary constant factor of modulus unity. A comparison with available data is given for various resonance pairs and for the three resonances together. (auth)

41918 DIFFRACTION MODEL FOR BOSON PRODUCTION AT SEVERAL Bev. Smrz, Pavel; von Baeyer, Hans C. (McGill Univ., Montreal). 16p. (CONF-660411-30). ORAU. Gmelin, AED-CONF-66-060-57.

From American Physical Society Meeting, Washington, D. C.

The two-meson (π) exchange contribution to high-energy interactions is calculated. A model for any two-meson (π) exchange graph is proposed and applied to the photoproduction of the meson (ρ^0) on protons and to three processes of meson (π^+)-proton interactions which cannot proceed via one pion exchange. (J.F.P.)

41919 STUDY OF SIX-PRONGED INTERACTIONS IN π^+p COLLISIONS AT 7 Bev/c. Slattery, Paul F.; Kraybill, Henry L. 9p. (CONF-660107-55). ORAU. Gmelin, AED-CONF-66-003-122.

From American Physical Society Meeting, New York.

A preliminary investigation of 3200 six-pronged events occurring in an exposure of a hydrogen bubble chamber to a 6.9-Bev/c beam of positive mesons (π) is reported. Some of the more interesting effective mass spectra are presented. The evidence for various resonances in these spectra is discussed. (J.F.P.)

41920 NEUTRAL PION PRODUCTION IN P-P INTERACTIONS AT 2.8 Bev/c. Schmidt, D. L.; Ijaz, M. A. (Virginia Polytechnic Inst., Blacksburg). 18p. (CONF-660547-4). ORAU. Gmelin, AED-CONF-66-121-1.

From Virginia Academy of Science, 44th Annual Meeting, Harrisonburg.

Two-prong events of the type $p + p \rightarrow p + p + \pi^0$ are analyzed from measurements taken from the Brookhaven 20 in. liquid hydrogen bubble chamber which was now exposed to a 2.8-Bev/c proton beam. Momentum and Q-value distributions for the $p\pi^0$ systems are presented together with predictions of the isobar model. Peaks corresponding to the $N^*_{\frac{3}{3}}$ (1236) and $N^*_{\frac{1}{1}}$ (1518) resonances were observed. Some indication of $N^*_{\frac{3}{3}}$ (1312) was also found. (L.B.S.)

41921 P-P BREMSSTRAHLUNG CALCULATIONS. Signell, P. (Michigan State Univ., East Lansing); Marker, D. 12p. (CONF-660209-14; TID-22859). ORAU. Gmelin, AED-CONF-66-023-14.

From Williamsburg Conference on Intermediate Energy Physics, Va.

The predictions for p,pγ interactions are calculated from potentials of four types using the two-potential formalism of Gell-Mann and Goldberger: hard-core, long-range finite core, weak momentum dependent, and nonlocal separable potential. The results for the 50 Mev calculations are discussed, and discrepancies between theory and data are analyzed. (L.B.S.)

41922 MEASUREMENT OF THE $K^0_S - K^0_L$ MASS DIFFERENCE BY THE TIME DEPENDENCE OF STRANGENESS. Camerini, U.; Cline, D.; English, J. B.; Fischbein, W.; Fry, W. F.; Gaidos, J. A.; Hantman, R. L.; March, R. H.; Stark, R. (Univ. of Wisconsin, Madison). 27p. (CONF-660411-44; COO-881-68). ORAU. Gmelin, AED-CONF-66-060-106.

From American Physical Society Meeting, Washington, D. C.

The magnitude of the $K^0_S - K^0_L$ mass difference was measured by monitoring the time dependence of the strangeness of neutral K's produced in hydrogen and deuterium in the LRL 25" hydrogen bubble chamber. The particles originate as $\overline{K}^0$ in K^- charge-exchange scatters at .85 to 1.15 Bev/c; the signature for an S = −1 reaction is the production of a hyperon. Seventy-seven events were found, obtaining $\Delta\omega = 0.50 \pm 0.15$, measured in units of inverse K^0_S lifetime. This and two other recent measurements using the same method are consistent with one another and with measurements of $\Delta\omega$ by other means. A combined "world average" of nine reasonably consistent measurements gives $\Delta\omega = 0.60 \pm 0.06$ (auth)

Field Theory, Scattering Theory, and Symmetries

See also Elementary Particles and Radiations

41923 (BNL-956) SYMMETRY PRINCIPLES IN PHYSICS. Brookhaven Lecture Series Number 50. Yang, C. N. (Brookhaven National Lab., Upton, N. Y.). Oct. 13, 1965. Contract AT(30-2)-Gen-16. 10p. Dep. mn. CFSTI $1.00 cy, $0.50 mn.

A discussion is presented on symmetry principles in physics. Topics discussed are historical origins of symmetry principles; effectiveness of symmetry considerations in quantum mechanics; C, P, and T invariances; and symmetries in elementary particle physics. (B.G.D.)

41924 (DESY-66/19) CURRENT COMMUTATION RELATIONS IN THE FRAMEWORK OF GENERAL QUANTUM FIELD THEORY. Revised Version. Schroer, B. (Hamburg Univ. (West Germany). II. Institut fuer Experimentalphysik); Stichel, P. (Physikalisches Staatsinstitut, Hamburg (West Germany). Deutsches Elektronen-Synchrotron, Hamburg (West Germany)). July 1966. 38p. Dep. mn.

A rigorous formulation of Gell-Mann's equal time commutation relations in the framework of general quantum field theory is presented. It is shown that this can be achieved despite the nonexistence of charge operators for nonconserved currents. Starting from the properly formulated equal time commutation relations of generalized charges, the application of the Gauss-Theorem is justified and the limits for large times of time dependent generalized charges are discussed. The Jost-Lehmann-Dyson representation is used in order to show that the equal time commutation relations always lead to exactly one frame independent sum rule. The connection between properties of the Jost-Lehmann-Dyson spectral function and the convergence of Adler-Weisberger type sum rules is also discussed. (auth)

41925 (JINR-P-2756) INTERPRETATSIYA PARAPOLYA KAK OBYCHNOGO POLYA S VNUTRENNEI STEPEN'YU SVOBODY. (Interpretation of Parafield as an Usual Field With an Inner Degree of Freedom). Govorkov, A. B. (Joint Inst. for Nuclear Research, Dubna (USSR). Lab. of Theoretical Physics). 1966. 12p. Dep. mn.

Paraquantization is another form of writing the fact that usual fermion and boson fields have an inner degree of freedom. (auth)

41926 (JINR-P-2777) MATRICHNYE ELEMENTY PREOBRAZOVANIYA LORENTSA DLYA UNITARNOGO PREDSTAVLENIYA. (Matrix Elements of Lorentz Transformation for Unitary Concept). Tao Wong Tek; Nguyen Van Hieu (Joint Inst. for Nuclear Research, Dubna (USSR). Lab. of Theoretical Physics). 1966. 7p. Dep. mn.

An expression was derived for the matrix elements of Lorentz transformation in the case of unitary (infinite) concept. The expression was based on the canonical concept executed in the Hilbert space L_2 (z). (tr-auth)

41927 (JINR-P-2797) VOSSTANOVLENIE ENERGETICHESKOGO SPEKTRA NESTABIL'NYKH CHASTITS PO IKH RASPADAM. (Reduction of the Energy Spectra of Non-Stable Particles According to Their Decay). Kopylov, G. I. (Joint Inst. for Nuclear Research, Dubna (USSR). Lab. of High Energy). 1966. 20p. Dep. mn.

If the direction and magnitude of the momentum of only part of the decay products of unstable particles are measured, then this is sufficient for the determination of the energy of the particle if the direction is known. However the energy spectrum of unstable particles can be reduced from the integral equation relating the characteristics of the primary and secondary particles. It was shown that the equations appear especially simple if the particle motion characterizes either their longitudinal speed or the sum (difference) of their energies and longitudinal momentum. The kernel of the equation for the most important cases was described, and their solutions were reduced. (tr-auth)

41928 (NP-16191) LECTURES ON HIGHER SYMMETRIES OF HADRONS. Lectures Delivered at the Summer School of Theoretical Physics, Dalhousie (Panjab), India, May 25–June 15, 1965. Sakita, B. (Delhi Univ. (India). Dept. of Physics and Astrophysics). July 27, 1965. 106p. Dep. mn.

Notes Compiled by S. Rai Choudhury.

A series of lectures are presented on higher symmetries of elementary particles. Topics discussed are historical survey, SU_6 symmetry scheme, problems of relativization of SU_6, phenomenological approach to relativistic SU_6, and Lie group of strong coupling theory. (B.G.D.)

41929 YANG-MILLS GROUPS AND FIELDS. Dotson, Allen C. (Western Michigan Univ., Kalamazoo). Amer. J. Phys., 34: 670-6(Aug. 1966).

A review is given of the procedure by which the electrodynamic gauge group was used as a guide in the construc-

tion of a more complicated gauge group, known as a Yang-Mills group. The field which plays, in this new case, a role analogous to that of the electromagnetic field is discussed. Reference is also made to several recent attempts to relate the quanta of such fields to some of the vector mesons of elementary particle physics. (auth)

41930 ORIGIN OF SU_3 SYMMETRY IN ELEMENTARY PARTICLES. Sen, P. (National Physical Lab., New Delhi). Amer. J. Phys., 34: 690-1(Aug. 1966).

The similarity between the energy density tensors of an isotropic harmonic oscillator and an isolated tube of fluid indicates that they are equivalent models for the description of elementary particles. In the latter model the wave equation for quantization of masses of elementary particles is already known and is explicitly stated. (auth)

41931 FIELD-THEORETICAL METHOD IN THE MANY-BODY PROBLEM. I. THE FIELD-THEORETICAL METHOD. Kisdi, David. ATOMKI (Atommag Kut. Intez.) Kozlem., Mellek., 8: 27-53(1966). (In Hungarian).

The field-theory method bypasses the wave functions, eliminating the necessity to carry out long calculations. The following data were considered as being of special interest for the multibody problem: energy of the ground state, excitation spectrum of the quasiparticles, density and pulse distribution, and pair-correlation functions. Approximation methods, such as those developed by Bethe and Goldstone, Brueckner, and Hugenholtz are presented. These modern methods are better suited to the analysis of actual problems than the elementary quantum-mechanical approximation methods but they are rapidly becoming obsolescent; this fact emphasizes the efficiency of the field-theory method. (TTT)

41932 GENERALIZATIONS OF ISOPARITY. Biedenharn, L. C.; Nuyts, J.; Ruegg, H. (CERN, Geneva). Commun. Math. Phys., 2: 231-50(1966).

The generalization of the isoparity (G-parity) for an arbitrary internal symmetry group is the problem of adjoining appropriately the charge conjugation operation, thereby extending the group. A complete solution to this problem is given, and explicitly detailed for the four families of compact, simple and simply connected Lie groups (SU_n, R_{2k+1}, R_{2k} and Sp_n). The extended isoparity is shown to depend upon the structure of the groups in question, and the required structure is developed and summarized. The properties of the extended isoparity are discussed and two special cases—'strong G-parity' and 'weak G-parity'—are treated in more detail. (auth)

41933 ANALYTIC CONTINUATION OF GROUP REPRESENTATIONS. Hermann, R. (Argonne National Lab., Ill.). Commun. Math. Phys., 2: 251-70(1966).

Some general methods for analytically continuing group representations are presented. In favorable cases, this enables the generalization of the principal, discrete and supplementary series to be recognized. (auth)

41934 SCHROEDINGER EQUATION FOR QUANTUM FIELDS WITH NONLINEAR NONLOCAL SCATTERING. Glimm, James (Massachusetts Inst. of Tech., Cambridge. Aarhus Univ., Denmark). Commun. Math. Phys., 2: 271-300(1966).

Perturbations $H = H_0 + \epsilon V$ of the hamiltonian operator H_0 of a free scalar boson field are considered. V is polynomial in the annihilation creation operators. Terms of any order are allowed in V, but point interactions, such as $\int :0(x)^4 : dx$, are not considered. Unnormalized solutions for the Schrödinger equation are found. For $\epsilon \to 0$, these solutions have a partial asymptotic expansion in powers of ϵ. The set of all possible perturbation terms V forms a Lie algebra. General properties of this Lie algebra are investigated. (auth)

41935 PROOF OF THE BOGOLIUBOV-PARASIUK THEOREM ON RENORMALIZATION. Hepp, Klaus (Inst. for Advanced Study, Princeton, N. J.). Commun. Math. Phys., 2: 301-26(1966).

A new proof is given that the subtraction rules of Bogoliubov and Parasiuk lead to well-defined renormalized Green's distributions. A collection of the counter-terms in "trees" removes the difficulties with overlapping divergences and allows fairly simple estimates and closed expressions for renormalized Feynman integrals. The renormalization procedure, which also applies to conventionally nonrenormalizable theories, is illustrated in the ϕ^4 theory. (auth)

41936 ANALYTIC PROPERTIES OF SCATTERING AMPLITUDES IN TWO VARIABLES IN GENERAL QUANTUM FIELD THEORY. Lehmann, H. (Institut des Hautes Etudes Scientifiques, Bures-sur-Yvette, France). Commun. Math. Phys., 2: 375-83(1966).

It is shown that scattering amplitudes have analytic properties as functions of momentum transfer not only for physical, but also for complex energies. This follows from local relativistic field theory for all reactions for which an ordinary dispersion relation can be proved. It is further shown that such amplitudes are boundary values of analytic functions of the two variables energy and momentum transfer. A domain of holomorphy is given explicitly. It follows then that partial waves can be analytically continued to complex energies. (auth)

41937 ON THE PHYSICAL REPRESENTATIONS OF AN INFINITE-DIMENSIONAL LIE ALGEBRA. Havlicek, M. (Czech Technical Univ., Prague); Votruba, J. Czech. J. Phys., 16: 631-42(1966).

Irreducible Hermitian representations of the infinite-dimensional Lie algebra, presented and suitable for the classification of elementary particles, are characterized by assumptions given. All representations of this kind are found explicitly. (auth)

41938 THEORY OF A NEUTRAL MASSIVE TENSOR FIELD WITH SPIN 2. Ogievetskii, V. I.; Polubarinov, I. V. (Joint Inst. for Nuclear Research, Dubna, USSR). Dokl. Akad. Nauk SSSR, 166: 839-42(Feb. 1, 1966). (In Russian).

An interacting symmetrical tensor field $h^{\gamma\mu}$ ($h^{\gamma\mu} = h^{\mu\gamma}$) may define spins 2 and 1 and two spins 0. A theory of such interacting mass tensor field was developed, deriving a supplementary Hilbert-Lorentz type generalized condition from the equation of motion. In this theory, the $h^{\mu\gamma}$ field may define only spins 2 and 0, excluding the other 0 spin and the spin 1 because the sign of the spin 1 energy is opposite of that of spins 2 and 0. The interaction of the tensor field with itself and with the scalar field was examined; a two-parameter family of nonequivalent theories was obtained for the mass tensor field. The equation obtained differed from Einstein's equation by possessing a cosmological term which disturbs the general covariance and the theory of equivalence. (TTT)

41939 ON THE STRUCTURE OF VECTOR AND AXIAL CURRENTS IN BROKEN $\tilde{U}(12)$ SYMMETRY. Winternitz, P.; Makarov, A. A.; Nguyen van Hieu; Tkachev, L. G.; Uhlir, M. (Joint Inst. for Nuclear Research, Dubna, USSR). Dokl. Akad. Nauk SSSR, 166: 1323-5(Feb. 21, 1966). (In Russian).

The SL(6) or $\tilde{U}(12)$ symmetry represents the generalization of the SU(6) symmetry. If the usual four-momentum of particles are considered as tensor components, transformed into the corresponding tensor spinors of the SL(6) group, the wave equations are invariant with respect to the SL(6) group. This makes it possible to study the SL(6) symmetry, taking into account the internal disturbance due to the wave functions. The problem was further examined by studying the general structure of the matrix elements of the vector and axial currents for baryons in the $\tilde{U}(12)$ symmetry. The matrix element of the current is derived from a generalization of the Bargman Wigner equation for a given baryon multiplet. As a result, the matrix elements in the $\tilde{U}(12)$ symmetry of the octet vector and axial currents for particles in the 56-plet of the SU(6) group are expressed through three independent functions. The correlations were verified experimentally by studying weak lepton interactions, such as lepton decay of baryons and Ω hyperons, generation of baryons and baryon resonances in neutrino experiments. (TTT)

41940 UNIFIED UNITARY REPRESENTATION OF THE POINCARE GROUP FOR PARTICLES OF ZERO AND POSITIVE REST MASS. Chakrabarti, A. (Ecole Polytechnique, Paris). J. Math. Phys. (N. Y.), 7: 949-55(June 1966).

As is well known, Wigner's construction of the unitary representations in terms of little groups gives quite dissimilar forms for the cases m = 0 and m > 0, while the spinor representation which does give a unified description of the above two cases is not unitary. It is pointed out that it is quite possible to give a unified unitary representation for both cases. This is achieved simply by noting that, while the factorization of $U(\Lambda)$ corresponding the choice of the little group of (1,0) is not valid for m = 0, the explicit final expression for the Wigner rotation R_w and the corresponding infinitesimal generators remain perfectly well defined for m = 0, and continue to furnish a unitary (discrete spin) representation for this case, which is compatible with the restriction of helicity to a particular fixed value. Moreover, the representation thus obtained has a very simple and direct geometrical significance. The relation of the formulation with that of Wigner is studied and the comparison with the spinor representations is given. The representation is rederived, starting from a particular simple condition which holds for both cases (m = 0, m > 0). The application of the unified formulation to the reduction of direct products, involving particles of positive and zero rest mass, is then considered, comparing the result with that of helicity coupling. Certain remarks concerning the Hermiticity of the generators and the possibility of defining a position operator for m = 0 are made. Comparison with Foldy's representation is given, explaining why his representation cannot be considered to be strictly unitary, though the relation with the unitary case is quite a simple one. (auth)

41941 q-EQUIVALENT PARTICLE HAMILTONIANS. I. THE CLASSICAL ONE-DIMENSIONAL CASE. Currie, Douglas G.; Saletan, Eugene J. (Northeastern Univ., Boston). J. Math. Phys. (N. Y.), 7: 967-74(June 1966).

The classes of equivalent Lagrangians in one-dimensional particle dynamics are found. These classes contain not only Lagrangians yielding the same equations of motion (Lagrangians differing by a total time derivative), but also those implying each other's equations of motion. The corresponding classes of hamiltonians, all of which give the same orbits in configuration space, but in general different orbits in phase space, are also found. Some specific examples are presented. (auth)

41942 FINITE-DIMENSIONAL REPRESENTATIONS OF SOME NON-SEMISIMPLE LIE ALGEBRAS. George, Claude (Institut Elie Cartan, Nancy); Levy-Nahas, Monique. J. Math. Phys. (N. Y.), 7: 980-8(June 1966).

The finite-dimensional representations of nonsemisimple Lie algebras are studied. Some general properties are given and applied to the case of the motion group and of the inhomogeneous Lorentz group. (auth)

41943 HIGHER-ORDER POLES IN THE S-MATRIX. Hagen, C. R. (Univ. of Rochester, N. Y.). J. Math. Phys. (N. Y.), 7: 989-90(June 1966). (UR-875-107).

The question of the possible existence of multiple poles in the S-matrix is discussed. It is shown by means of a simple model that such poles are not generally incompatible with Lagrangian field theory and can only be excluded in axiomatic formulations by the assumption of a unique correspondence between stable particles and the poles of the S-matrix on the physical sheet. (auth)

41944 THE MOST GENERAL CLEBSCH-GORDAN COEFFICIENTS OF THE UNIVERSAL COVERING GROUP OF THE INHOMOGENEOUS LORENTZ GROUP. Kummer, Martin (Univ. of Michigan, Ann Arbor). J. Math. Phys. (N. Y.), 7: 997-1015(June 1966).

The most general Clebsch-Gordan coefficients to reduce the physically most important n-fold product representations of the groups $\tilde{P}_+\uparrow$ and $\tilde{P}$ (Universal covering groups of the restricted and full inhomogeneous Lorentz groups) are derived. They are used to answer the question: What can be said about the S-matrix if only Lorentz invariance is postulated? (auth)

41945 THEOREM ON THE CLEBSCH-GORDAN SERIES IN SU(n). Nussinov, S. (Univ. of Washington, Seattle). Contract AT(45-1)-1388. J. Math. Phys. (N. Y.), 7: 1046-8(June 1966).

A theorem on the Clebsch-Gordan series conjectured by B. Vitale is proved using simple Young diagram techniques. (auth)

41946 ALTERNATE COMMUTATION RELATIONS. Parks, W. F. (Kansas State Univ., Manhattan). J. Math. Phys. (N. Y.), 7: 1049-53(June 1966).

An alternate quantization procedure for Bose fields is proposed. This procedure leads to a field algebra which is related to that of angular momentum rather than momentum. With this algebra is associated a maximum (n_0) to the number of particles allowed in a given momentum state. It is indicated by the investigation of models that physical observables converge for large n_0 to those obtained using the canonical commutation relations. (auth)

41947 POLYNOMINAL BASES AND ISOSCALAR FACTORS FOR SU(3). Sharp, R. T.; von Baeyer, Hans (McGill Univ., Montreal). J. Math. Phys. (N. Y.), 7: 1105-22(June 1966).

The generators of SU(3) are represented by differential operators which act on states represented by functions of six independent variables. Orthonormal bases for irreducible representations are presented in the form of polynomials. These are used to construct bases for product representations, to derive the Clebsch-Gordan series, and to find explicit expressions for certain special isoscalar factors. The general isoscalar factors are then expressed as sums over products of these special ones. Also, two types of recursion relation are derived for the general isoscalar factors; the method of deriving these is illustrated by deriving recursion relations for SU(2) which were obtained recently by other means. (auth)

41948 S-MATRIX FORMALISM, CHARGE RENORMALIZATION, AND DEFINITION OF THE HAMILTONIAN IN A SIMPLE FIELD-THEORETICAL MODEL. Yndurain, F. J. (Univ., Saragossa, Spain). J. Math. Phys. (N. Y.), 7: 1133-6(June 1966).

A field-theoretical model (the relativistic version of the Lee model) is exhibited for which one can rigorously prove that the essential features of the S-matrix formalism (in particular analyticity) hold, even for point coupling, and that all charge renormalizations are finite. It is also shown that, although the interaction-picture description fails, the total hamiltonian may still be defined as a symmetric operator and it governs the dynamics of the interaction. Finally, it is pointed out that the usual pathologies which appear in the current (static) version of the model are not an intrinsic feature of the theory, but rather the result of too crude oversimplifications. (auth)

41949 SOME CONSEQUENCES OF THE ALGEBRA OF WEAK AND ELECTROMAGNETIC CURRENTS. Polyakov, A. M. JETP Lett. (USSR) (Engl. Transl.), 4: 50-3(July 15, 1966).

Translated from Zh. Eksp. Teor. Fiz., Pis'ma Redaktsiyu, 4: 74-7(July 15, 1966).

Several valid relations in the limit as $m_\pi \to 0$ are obtained on the basis of Nambu's hypothesis and under the assumption of weak and electromagnetic currents from an SU(3) × SU(3) algebra. (J.F.P.)

41950 CONSTRAINTS ON THE STATISTICAL TENSOR FOR LOW-SPIN PARTICLES PRODUCED IN STRONG INTERACTION PROCESSES. Dalitz, R. H. (Oxford Univ.). Nucl. Phys., 87: 89-99(1966).

The requirement that all the eigenvalues of the spin density matrix ρ are positive imposes a set of constraints on the values possible for the statistical tensors t_L^M which characterize ρ. Here, these constraints on t_L^M are given explicitly for spin values $J \leqq 2$ for the case of particles produced in strong interaction processes. The constraints

on ρ itself are given as a set of inequalities, valid for arbitrary J. (auth)

41951 CUTKOSKY-LEON NORMALIZATION CONDITIONS. Agrawala, V. K.; Belinfante, J. G.; Renninger, G. H. (Carnegie Inst. of Tech., Pittsburgh). Nuovo Cimento (10), 44A: 740-4(Aug. 1, 1966).

The Cutkosky-Leon normalization conditions for Bethe-Salpeter amplitudes play an important role in relativistic bootstrap models. These normalization conditions are here derived in several elementary ways for ordinary quantum mechanics with an energy-dependent potential, thereby exploiting the well-known and useful similarity between the techniques used for the relativistic Bethe-Salpeter theory of composite particles and the familiar methods of ordinary nonrelativistic quantum mechanics. (auth)

41952 PARTIAL CONSERVATION OF TENSOR CURRENT AND ELECTROMAGNETIC FORM FACTORS. Krolikowski, W. (IAEA, Trieste, Italy). Nuovo Cimento (10), 44A: 745-54(Aug. 1, 1966).

A conjecture of "the partial conservation of a tensor current" is applied to the electromagnetic structure of strongly interacting particles. Some relations corresponding to the Goldberger-Treiman relation are obtained. The electromagnetic form factors of the nucleon are discussed. (auth)

41953 PHASE-SPACE INTEGRALS AND INVARIANT-MASS DISTRIBUTIONS WITH MONTE CARLO TECHNIQUES. McCall, J. R.; Parks, J. G. (Univ. of California, Livermore). Contract W-7405-eng-48. Nuovo Cimento (10), 44A: 768-76(Aug. 1, 1966). (UCRL-14667).

A method is presented in which a Monte Carlo approach is used for evaluating multi-particle phase-space integrals and individual-particle energy distributions in systems of nonzero total momentum. A technique is also developed for the computation of invariant-mass distributions. (auth)

41954 CERTAIN PHYSICAL-REGION SINGULARITIES IN S-MATRIX THEORY. Bloxham, M. J. W. (Cambridge Univ., Eng.). Nuovo Cimento (10), 44A: 794-808(Aug. 1, 1966).

Discontinuities of the four-to-four particle amplitude across the cuts in the physical region associated with two quadrilateral singularities are evaluated by S-matrix methods. The Cutkosky formula and positive-α criterion for these singularities are deduced. (auth)

41955 INFORMATION ON THE AXIAL-VECTOR COUPLING CONSTANT THROUGH DIFFERENT CURRENT ALGEBRAS. Beckers, J. (Univ., Liege). Nuovo Cimento (10), 44A: 822-5(Aug. 1, 1966).

It is shown that by considering the collinear SU(2) $\otimes$ SU(2) and SU(3) $\otimes$ SU(3) algebras and by taking matrix elements between one-particle states with zero momentum, information is obtained on the sign of the strangeness-conserving axial vector coupling constant in correlation with Adler-Weisberger and Amati-Bouchiat-Nuyts results. (J.F.P.)

41956 COMMUTATION RULES BETWEEN AXIAL CHARGES AND AXIAL DIVERGENCES. Soliani, G. (Univ., Turin). Nuovo Cimento (10), 44A: 829-33(Aug. 1, 1966).

It is shown that commutators between axial charges and divergences can be used to yield new sum rules from which one can obtain much information. The advantages of these relations are demonstrated by using the commutator within the framework of SU(3) $\otimes$ SU(3). (J.F.P.)

41957 PERTURBATIONS OF INELASTIC UNITARITY ON DYNAMICAL CALCULATIONS. Nath, P. (Univ. of Pittsburgh. Univ. of California, Riverside); Srivastava, Y. N. Nuovo Cimento (10), 44A: 834-7(Aug. 1, 1966).

Perturbative effects of inelasticity on dynamical calculations performed with elastic unitarity for 2-particle channels are studied. The on-the-mass-shell S-matrix method is used to compute first-order changes in amplitudes and, in particular, changes in the masses and coupling constants of composite states following Dashen and Frautschi. (J.F.P.)

41958 NOTE ON THE DERIVATION OF SUM RULES FROM THE EQUAL-TIME COMMUTATION RELATIONS FOR THE SPACE COMPONENTS OF CURRENT DENSITIES. Bouchiat, C.; Meyer, Ph. (Faculte des Sciences, Orsay, France). Nuovo Cimento (10), 44A: 843-5(Aug. 1, 1966).

It is shown that if the assumptions made to obtain the sum rules are valid, the equal-time commutation relations of the space components of the current can only be evaluated in the Breit frame. (J.F.P.)

41959 REDUCED-AMPLITUDE EQUATIONS FOR TWO- AND THREE-PARTICLE SYSTEMS. [PART] II. Taha, M. O. (Cambridge Univ., Eng.). Nuovo Cimento (10), 44A: 849-70(Aug. 21, 1966).

Reduced amplitudes are simultaneously defined for two particle $\rightarrow$ three particle and three particle $\rightarrow$ three particle processes. They are shown to lack the physical-region singularities: the subenergy cuts, the total discontinuity, the separate energy cuts and, in 3 $\rightarrow$ 3, the cross-energy poles. A reduced amplitude for two particle $\rightarrow$ two particle scattering lacking the three-particle, as well as the two-particle, cut is also defined. This simultaneously involves the three particle $\rightarrow$ two particle interaction for which a reduced amplitude is thus obtained. This analysis is relativistic and nonpotential-theoretic. (auth)

41960 COVARIANT DENSITY MATRICES FOR ARBITRARY SPINS. Zaman, Arif Uz; Liu, Y. S. (Middle East Technical Univ., Ankara). Nuovo Cimento (10), 44A: 903-14(Aug. 21, 1966).

Covariant density matrices for free particles are written in terms of $D^{(j,0)} \oplus D^{(0,j)}$ spinors and it is shown that they can be expanded in terms of the covariant matrices of the corresponding representation. The tensor indices of these matrices are contracted with the tensor indices of the four tetrad vectors and the coefficients (which are linear combinations of the probabilities W.) were determined for spin $\frac{1}{2}$, 1, and $\frac{3}{2}$. (auth)

41961 ANALYTIC AND ASYMPTOTIC PROPERTIES OF SOLUBLE N/D MODELS. Contogouris, A. P. (CERN, Geneva). Nuovo Cimento (10), 44A: 927-44(Aug. 21, 1966).

A class of relativistic models, defined in terms of the N/D equations for asymptotically varying left-hand discontinuities and constant inelasticity, is considered. This is shown to present an alternative, analogous in certain respects to, but simpler than, the class of models based on the ladder approximation of the Bethe-Salpeter equation. In terms of an N/D amplitude with an asymptotically vanishing left-hand discontinuity an approximate strong-coupling calculation of the Pomeranchuk trajectory in agreement with the Regge pole analysis of the diffraction scattering experimental data is given; the corresponding residue function is also determined. An N/D amplitude with an asymptotically constant left-hand discontinuity is shown to be associated with a nonshrinking diffraction peak. Certain analogies to the solutions for nonrelativistic scattering by regular or singular energy-independent potentials are also discussed. (auth)

41962 CONDITIONS OF MACROSCOPIC CAUSALITY FOR THE SCATTERING MATRIX. Blokhintsev, D. I.; Kolerov, G. I. (Joint Inst. for Nuclear Research, Dubna, USSR). Nuovo Cimento (10), 44A: 974-83(Aug. 21, 1966).

The condition of macroscopic causality for the scattering matrix is formulated. An example of the unitary but nonlocal scattering matrix which satisfies the requirements of macroscopic causality is given. (auth)

41963 THEOREM ON HIGH-ENERGY SCATTERING AMPLITUDES. Sommer, G. (Freie Univ., Berlin). Nuovo Cimento (10), 44A: 984-98(Aug. 21, 1966).

A theorem is presented which allows, starting from amplitudes with well-defined high-energy behavior, to construct a new amplitude, which turns out to be asymptotically larger than the original ones. Application to amplitudes represented by certain classes of any kind of graphs (e.g. A^3 theory or multiperipheral graphs) leads to a statement on the actual high-energy scattering amplitude T. If it has a high-energy behavior of the form $f \cdot s^{\alpha}(\log s)^{\beta}(\log_2 s)^{\gamma_2} \ldots (\log_n s)^{\gamma_n}$ the class of graphs corresponding to T must include generalized ladder diagrams which contain every 2-particle irreducible graph

with 4 external lines an infinite number of times as generalized rungs. (auth)

41964 INCONSISTENCY OF CANONICAL COMMUTATION RELATIONS AMONG CURRENT DENSITIES. Okubo, S. (International Atomic Energy Agency, Trieste, Italy). Nuovo Cimento (10), 44A: 1015-30(Aug. 21, 1966).

Ordinary commutation relations among current densities are shown to lead to inconsistency without assuming the conservation law of currents. Also it is demonstrated that the ordinary PS-PV meson theory and also the σ-model will give rise to similar inconsistencies in general. (auth)

41965 DEPARTURES FROM $\tilde{U}_{12}$ IN A RELATIVISTIC QUARK MODEL. Daboul, J.; Delbourgo, R. (Weizmann Inst. of Science, Rehovoth, Israel). Nuovo Cimento (10), 44A: 1031-46(Aug. 21, 1966).

Adopting a $\tilde{U}_{12}$-invariant four-quark interaction as the potential input to the Bethe-Salpeter equation for the quark-antiquark system nonets of bound 0^- and 1^- meson states can be obtained. Owing to the presence of a spin-splitting term in the kernel, the masses and coupling constants of the composites deviate from the common values used in a phenomenological $\tilde{U}_{12}$ field theory of quarks and mesons; the magnitudes of these changes are calculated in detail. (auth)

41966 CROSS-DISCONTINUITY CONDITION IN S-MATRIX THEORY. Branson, D. (Univ. of California, Berkeley). Nuovo Cimento (10), 44A: 1081-90(Aug. 21, 1966). (UCRL-16702).

In recent work on S-matrix discontinuity equations it has been conjectured that the terms in a unitarity equation associated with a normal threshold discontinuity in one channel have no normal threshold singularities in overlapping crossed channels. An S-matrix theory proof of this conjecture is given for simple cases, but it is shown that when intermediate states of four or more particles are involved, the conjecture is true only if the particles in the intermediate state are sufficiently near threshold. The impact of this result on previous work is discussed. (auth)

41967 SYSTEMATICS OF HADRONS UNDER NON-COMPACT GROUPS. Kantorovich, A.; Nguyen-Duc, T. (Tel-Aviv Univ., Israel). Nuovo Cimento (10), 44A: 1184-93(Aug. 21, 1966).

The baryon and meson states are classified in irreducible representations of the noncompact groups $U_{6,6}$, $U_6 \times U_6 \times O_{3,1}$ and $U_6 \times U_6 \times SI_{3,R}$. The possible use of the double noncompact groups, $U_{6,6} \times O_{3,1}$ and $U_{6,6} \times SI_{3,R}$, is introduced. (auth)

41968 SATURATION OF THE SU_6 ALGEBRA AND A POSSIBLE CLASSIFICATION GROUP FOR HADRONS. Gatto, R. (Univ., Florence. Istituto Nazionale di Fisica Nucleare, Florence); Maiani, L.; Preparata, G. Nuovo Cimento (10), 44A: 1279-83(Aug. 21, 1966).

The problem of saturation of the SU_6 algebra is considered in light of a possible classification group for hadrons. Predictions of various mixing schemes for baryons are tabulated. A scheme is proposed for a compact group structure, which gives both SU_6- and L-excitation. Irreducible representations of the compact SU_{18} group are analyzed in terms of $SU_6 \otimes O_3$ multiplets for mesons and for baryons. Some consequences of the scheme are discussed, in particular, its relevance in supplying a set of states within which the commutation relations of charges are to be saturated. (L.B.S.)

41969 CONSTRUCTION OF NONTRIVIAL SYMMETRY-BREAKING SOLUTIONS IN FIELD THEORY. Guralnik, G. S.; Hagen, C. R. (Univ. of Rochester, N. Y.). Contract AT(30-1)-875. Phys. Rev., 149: 1017-26(Sept. 30, 1966). (UR-875-125).

Although the hope has often been expressed that the Green's functions of a given theory may possess a lower symmetry than that of the corresponding Lagrangian, there has thus far been no adequate demonstration of the possibility of such symmetry-breaking solutions in the domain of particle physics. The validity of this conjecture is further suggested by showing that in the Lee model such solutions can exist in the case that the θ meson has vanishing mass. It is further demonstrated that the corresponding broken-symmetry states may alternatively be viewed as the eigenstates of a new hamiltonian of reduced symmetry. Because the nonrelativistic property of the model is relevant only to the extent that it renders the theory soluble, it is argued that in general the presence of a massless particle in a theory implies the existence of an infinite set of symmetry-breaking solutions to the field equations. (auth)

41970 ONE-GRAVITON EXCHANGE INTERACTION OF ELEMENTARY PARTICLES. Barker, Bruce M.; Gupta, Suraj N.; Haracz, Richard D. (Wayne State Univ., Detroit). Phys. Rev., 149: 1027-32(Sept. 30, 1966).

The interaction of elementary particles of several different spins due to the exchange of a graviton is investigated. The exact one-graviton exchange potentials are obtained, and then simplified by making various approximations. The gravitational interaction is found to be independent of the spins of the particles, provided that the distance between them is large compared with their Compton wavelengths. It is pointed out that the spin-dependent interaction terms, whose range is of the order of the Compton wavelength, may be of interest in the theory of gravitational collapse. It is shown that the gravitational particle-antiparticle interaction differs from the corresponding particle-particle interaction only by contact interaction terms. (auth)

41971 PHOTON STATISTICS AND CLASSICAL FIELDS. Mandel, L.; Wolf, E. (Univ. of Rochester, N. Y.). Phys. Rev., 149: 1033-7(Sept. 30, 1966).

In view of the misunderstanding which surrounds the use of semiclassical methods in the treatment of optical coherence problems, a simple analysis is given which illustrates the generality of these methods. In particular, it is pointed out that, under commonly occurring circumstances, these methods apply at arbitrarily low light levels and give correct results for the photoelectric counting of photons. The conclusions are illustrated by treating the interference between laser light and thermal light to demonstrate that this nontrivial case, recently treated by quantum field theory, is correctly described by semiclassical methods (auth)

41972 COMBINED SPIN AND G_2 SYMMETRY. Garibotti, C. R. (Princeton Univ., N. J.). Phys. Rev., 149: 1125-7(Sept. 30, 1966).

The algebra of the group D_5 is the most direct generalization of that of the direct product of G_2 with the ordinary spin group SU_2. Furthermore it also contains that of R_7 times SU_2. The particle classification provided by D_5 is analyzed; it is found that a 16-dimensional representation appears to contain the baryons and gives results for the magnetic moment and mass formula equivalent to those obtained with the nonbroken $G_2 \otimes SU_2$ group, but now the Λ particle is directly included. The 45-dimensional regular representation of D_5 provides an appropriate basis for the proposed $G_2 \otimes SU_2$ representations of the mesons and boson resonances. (auth)

41973 M(12) POTENTIAL MODEL FOR NUCLEON-NUCLEON SCATTERING INCLUDING KINETIC ENERGY AND SU(3) BREAKING EFFECTS. O'Donovan, Patrick J. (Univ. of Chicago). Contract AT(11-1)-264. Phys. Rev., 149: 1128-31(Sept. 30, 1966). (COO-264-321; EFINS-66-40).

The predictions of exact M(12) symmetry for NN scattering are shown to be severely affected by mass splittings among the 0^- and 1^- mesons which contribute to the NN potential. A potential for the NN problem is derived from the meson-baryon vertices given by M(12) symmetry. It is shown that ρNN couplings, which are experimentally reasonable, result in the $L \cdot S$ part of the potential that is too small. It is suggested that, unless the ρNN couplings are to be arbitrarily increased as is done in certain N/D calculations, the solution to the discrepancy lies in treating the NN system as one channel in a multichannel problem which includes the $N^*_{33}N^*_{33}$ and $N^*_{33}N$ channels as well. (auth)

41974 SATURATION OF QUARK FORCES IN ZERO-TRIALITY STATES. Peres, Asher (Israel Inst. of Tech., Haifa). Phys. Rev., 149: 1131-3(Sept. 30, 1966).

The Han-Nambu quark model is considered, in which the internal symmetry group of hadrons is SU(3) ⊗ SU(3)′, and an attempt is made to find a mechanism such that the masses of SU(3)′ singlets are much lower than those of other SU(3)′ multiplets. One possibility is to assume the existence of a massive vector "supermeson" strongly coupled to the (1,8′) part of the quark current. The lowest energy state of the supermeson field would favor SU(3)′ singlets, just as the lowest energy state of the electromagnetic field is reached when all matter is neutral. These supermesons, if sufficiently massive, would be rather difficult to observe. Another possibility (which effectively corresponds to the limit of supermesons with infinite mass) is to assume a four-quark interaction of the current-current type. With a suitable form of this interaction, SU(3)′ singlets again have masses much lower than those of other SU(3)′ multiplets. (auth)

41975 DYNAMICAL CALCULATION OF EXTINCT BOUND STATES. Atkinson, D.; Halpern, M. B. (Univ. of California, Berkeley). Phys. Rev., 149: 1133-7 (Sept. 30, 1966).

Aspects of the possible dynamical extinction of a bound state (coincident zero in N and D) are discussed within the single and multichannel ND^{-1} framework. A surprising result is that, within any one-channel calculation, the "mass" of the extinct bound state cannot be calculated. This may be reflected in the multichannel formulation by a particular sensitivity of the "mass" to the input. (auth)

41976 BARYON MASS DIFFERENCES IN A MODEL OF BROKEN UNITARY SYMMETRY. Cohen, S. L.; Hagen, C. R. (Univ. of Rochester, N. Y.). Contract AT(30-1)-875. Phys. Rev., 149: 1138-44(Sept. 30, 1966). (UR-875-138).

Proceeding from the assumption that the breaking of unitary symmetry within the baryon octet can be described as a low-energy effect generated by the pseudoscalar-meson mass differences, a model is proposed which relates the departure from full SU_3 symmetry within these two octets. Although it is assumed that the corrections to the low-energy behavior of the baryon two-point functions are dominated by the least massive two-particle intermediate states, no condition is required on the strength of the baryon-meson coupling. Using the experimentally observed mass differences, one can calculate within the framework of this model the SU_3-invariant baryon-meson coupling constants, the results being in reasonable agreement with currently accepted values. (auth)

41977 BARYON-ANTIBARYON SCATTERING AND THE COLLINEAR U(3) X U(3) SYMMETRY. Tripathy, Kishore Chandra (Univ. of Delhi). Phys. Rev., 149: 1149-51(Sept. 30, 1966).

Baryon-antibaryon scattering processes are considered in collinear U(3) × U(3) symmetry. Simple relations between the differential cross sections are found and have been compared with the available experimental data. (auth)

41978 DYNAMICS OF STRONGLY BOUND SYSTEMS. Domokos, G.; Palmer, W. (Johns Hopkins Univ., Baltimore). Phys. Rev., 149: 1152-7(Sept. 30, 1966).

A dispersion-theoretic approach is developed for systems with large binding energies. Strong binding can be obtained if the one-particle exchange force is singular at short distances. Many-meson exchange forces play an important role and are described by a suitable asymptotic expression. The method is used to construct a relativistic degenerate quark model of mesons. The model is unsatisfactory in the sense that, while yielding a sufficiently strong binding, the symmetry required for SU_6-invariant vertices in the static limit is destroyed by the relativistic motion of the quarks. It is conjectured that a realistic quark model of mesons necessarily requires the existence of long-range, "superstrong" interactions. (auth)

41979 DIFFRACTION SCATTERING AND FORM FACTORS. Beder, Douglas S. (Univ. of California, Berkeley). Contract W-7405-eng-48. Phys. Rev., 149: 1208-12(Sept. 30, 1966). (UCRL-16728).

The asymptotic feature of diffraction scattering of hadrons is tentatively assumed to mean asymptotically pure-imaginary partial waves. An essential requirement is then inferred to be the existence of an infinity of reaction channels and asymptotically infinite inelasticity (assuming asymptotic vanishing of partial-wave amplitudes). This view is supported by construction of a physically sensible inelastic model which has all the above features. Finally, these assumptions are shown to imply asymptotic vanishing of form factors; this resolves a puzzling feature of conventional dispersion-theory solutions for form factors. (auth)

41980 CONNECTION BETWEEN THE ELECTROMAGNETIC FORM FACTOR AND THE PROPAGATOR NORMALIZATIONS. Cawley, Robert G. (Clarkson Coll. of Technology, Potsdam, N. Y.). Phys. Rev., 149: 1224-8 (Sept. 30, 1966).

The Ward identity is used to display the connection between the electromagnetic form factor and propagator normalizations. (auth)

41981 WEAK AXIAL-VECTOR CURRENTS AND THE BARYON FIELD. Gleeson, Austin M. (Syracuse Univ., N. Y.). Phys. Rev., 149: 1242-4(Sept. 30, 1966).

A postulated commutation relation between the chiral charge and the nucleon field is studied. This relationship is used to generate a sum rule between $g_{\rho\pi\pi}$, $g_{\pi NN*}$, and g_r. It is found that the ρ meson and N* baryon are insufficient to saturate the sum rule. The addition of strong S-wave dipion scattering is found to be adequate to explain the discrepancies of the above sum rule. (auth)

41982 NONCOMPACT GROUPS IN CLASSIFYING HADRONS. Freund, P. G. O. (Univ. of Chicago). Contract AT(11-1)-264. Phys. Rev., 149: 1257-9(Sept. 30, 1966). (COO-264-316; EFINS-66-32).

It is shown that the noncompact groups U(6,6), GL(6,C), and U(6) × U(6) × O(3,1) proposed by many authors to underlie a classification of hadrons can be excluded on the basis of existing information on the hadron spectrum. A scheme which at least avoids the obvious difficulties of the above noncompact groups is mentioned. (auth)

41983 LORENTZ- AND SPIN-INVARIANT ELASTIC SCATTERING OF TWO SPIN-1/2 PARTICLES. Bebie, H. (Syracuse Univ., N. Y.). Contract AT(30-1)-3399. Phys. Rev., 149: 1260-3(Sept. 30, 1966). (NYO-3399-49).

The elastic scattering of two spin-½ particles is considered. For each particle (n = 1,2) a spin-like vector $\Sigma^{(n)}$ is constructed in terms of the variables of the nth particle alone in such a way that the conservation of $\Sigma = \Sigma^{(1)} + \Sigma^{(2)}$ is compatible with Lorentz invariance. However, the unitarity of the scattering operator restricts the possible processes to forward and backward scattering. (auth)

41984 PERMUTATION SYMMETRY IN STRONG INTERACTIONS. Tanaka, K. (Ohio State Univ., Columbus). Contract AT(11-1)-1545. Phys. Rev., 149: 1264-8 (Sept. 30, 1966). (COO-1545-4).

It is assumed that there exist three basic fields Φ_1, Φ_2, and Φ_3 and the Sakata triplet p, n, and Λ which is related to the basic fields by a unitary transformation. Then, a meson-baryon interaction hamiltonian that is invariant under SU(3) is derived under the requirement that it should be invariant under permutations of Φ_1, Φ_2, and Φ_3 and conserve charge and baryon number. A singlet fermion field is introduced in addition to the Sakata triplet in order to define the baryons in the octet case. Invariance under one permutation and conservation of isotopic spin, charge, and baryon number yield a hamiltonian that is SU(3)-invariant. An explanation is given of how permutation symmetry S_3, the aforementioned unitary transformation, and two conservation laws lead to SU(3) symmetry. (auth)

41985 NECESSITY OF ADDITIONAL UNITARY-ANTISYMMETRIC q-NUMBER TERMS IN THE COMMUTATORS OF SPATIAL CURRENT COMPONENTS. Buccella, F. (Univ., Florence); Veneziano, G.; Gatto, R.; Okubo, S. Phys. Rev., 149: 1268-72(Sept. 30, 1966).

It is proved that to maintain consistency of the commutation relations among spatial current components with the Jacobi identity, a Schwinger term antisymmetric with respect to interchange of isotopic (or unitary) indices is needed. The proof is based on the use of the Jacobi identity for triple commutators and of the Lehman-Källen expression for the vacuum expectation value of a current commutator. Additional conditions to be satisfied by the new Schwinger term are derived from an analysis of the origin of a discrepancy between the Lee-Dashen-Gell-Mann and the Cabibbo-Radicati sum rules for magnetic moments, and a solution of the discrepancy is proposed. (auth)

41986 LEHMANN-SYMANZIK-ZIMMERMANN FORMALISM IN THE LEE MODEL (V-θ SECTOR). Maxon, M. Stephen (Univ. of California, Livermore). Phys. Rev., 149: 1273-83(Sept. 30, 1966).

The Lehmann-Symanzik-Zimmermann formalism is used to solve the V-θ sector of the Lee model. The solution to one singular integral equation solves the entire sector, giving the two elastic-scattering amplitudes and the production amplitude. The behavior of the various amplitudes and phase shifts is discussed as a function of energy and coupling constant. Also, the bound-state problem is discussed. This approach is compared with the eigenvalue and dispersion treatments of this sector found in the literature. (auth)

41987 LEPTONIC DECAYS OF HADRONS. Brene, N. (Univ. of Copenhagen); Veje, L.; Roos, M.; Cronstroem, C. Phys. Rev., 149: 1288-93(Sept. 30, 1966).

The experimental data on leptonic decays of baryons were re-examined in the light of a two-angle Cabibbo theory, where the two angles, θ_V and θ_A, are characteristic of the vector and axial-vector baryon currents, respectively. With certain assumptions about the energy dependence of the form factors in the vector (K_{e3}) and axial-vector ($K_{\mu 2}, \pi_{\mu 2}$) decays of mesons, it can be shown that the angles θ_V and θ_A derived from baryon decays are compatible with the corresponding angles derived from meson decays, thus justifying our use of a two-angle theory. There is no discrepancy between the information from hyperon and meson decays and the information from the superallowed nuclear beta decays (^{14}O, ^{34}Cl, etc.). Using the assumptions about the meson form factors, a fit of all data on leptonic decays of hadrons gives the values $\theta_V = 0.212 \pm 0.004$, $\theta_A = 0.268 \pm 0.001$, $\alpha = 0.665 \pm 0.018$, where the parameter α defines the relative content of D coupling in the baryonic axial-vector current. (auth)

41988 DIVERGENCE CONDITIONS AND SUM RULES. Veltman, M. (Brookhaven National Lab., Upton, N. Y.). Phys. Rev. Lett., 17: 553-6(Sept. 5, 1966).

The first-order electromagnetic and weak interaction effects on the divergence condition $\partial_\mu J_\mu^V = 0$ by Feynman and Gell-Mann for the vector current of hadrons that is coupled to leptons and photons are discussed. Axial and vector current sum rules are derived from this divergence condition. (B.G.D.)

41989 REGGE POLES IN UNEQUAL-MASS SCATTERING PROCESSES. Freedman, Daniel Z.; Wang, Jiunnming (Univ. of California, Berkeley). Phys. Rev. Lett., 17: 569-72(Sept. 5, 1966).

The kinematical ambiguity as to whether the Regge asymptotic form $s^{\alpha(u)}$ holds in the backward region of high-energy πN backscattering is discussed. Interesting features of the unequal-mass scattering problem and of the Regge-pole theory in general are also discussed. (B.G.D.)

41990 COULOMB SCATTERING FOR ARBITRARY SPIN. Dowker, J. S. (Univ. of Manchester, Eng.). Proc. Phys. Soc. (London), 89: 353-64(1966).

Explicit cross sections are derived to lowest order in e^2 for the Coulomb scattering of a charged particle of arbitrary spin. The interaction employed is one derived from a consistent theory of interacting particles of any spin which was developed earlier. This theory is further discussed in the nonrelativistic and classical limits and it is shown that it predicts a magnetic moment of $e/2\kappa$. (auth)

41991 VARIATIONAL PRINCIPLE FOR THE SCATTERING PHASE MATRIX. Seaton, M. J. (London Univ.). Proc. Phys. Soc. (London), 89: 469-70(1966).

A variational principle for scattering phases was discussed by Demkov in 1958 and Percival in 1960. A generalized theory is presented for the many-channel scattering phase matrix. (auth)

41992 NON-DYNAMICAL STRUCTURE OF PARTICLE REACTIONS. Moravcsik, Michael J. (Univ. of California, Livermore). pp 517-43 of Proceedings of the Williamsburg Conference on Intermediate Energy Physics. Vol. II. Williamsburg, Va., College of William and Mary, 1966.

The method of invariant amplitudes or form factors which is applicable to all spins and energies is discussed. Within this framework the properties of the form factors and the relation between physical observables which are determined by the form factors are considered. The discussion is carried out in terms of the M-matrix of a reaction. (J.F.P.)

41993 FREDHOLM THEORY OF SCATTERING. Kanki, Takeshi; Kawaguchi, Masaaki (Osaka Univ.). Progr. Theoret. Phys. (Kyoto), 35: 821-33(May 1966).

The Fredholm theory of integral equations is applied to the nonrelativistic theory of scattering. Divergence difficulties are overcome by using the Poincaré-Hilbert formula. It is shown that the Fredholm determinant has a zero of order $2l + 1$ corresponding to a bound state or a resonance with orbital angular momentum l. In order to see the speed of convergence of the Fredholm determinant as a power series in the coupling constant, scattering by the Yukawa potential and the exponential potential is studied. Application of the method to the Bethe-Salpeter equation is also discussed. (auth)

41994 BROKEN SYMMETRY AND STABILITY OF PARTICLE-LIKE STATES. Okabayashi, Takao; Naito, Seiichi (Tokyo Univ.). Progr. Theoret. Phys. (Kyoto), 35: 840-57(May 1966).

The relation between broken symmetry and the stability of particle-like states (bound states and resonance states) is discussed through a simple soluble model. It is shown that the formalism on the physical sheet succeeds in realizing all the properties of the multichannel problem with broken symmetry which are expected from physical insight: First, the components of a composite system with some multiplicity in the symmetrical world correspond to the ones in the physical world. Secondly, there exists a critical value of the strength of the symmetry violating interaction such that some members of a multiplet, which is a bound state (a resonance state) in the symmetrical world, become resonance states (bound states). Further, the ratios between the mass differences relative to a standard component depend on the strength of the symmetry violating interaction. The behavior of the complex poles in the formalism on the Riemann sheets is also analyzed, and the peculiar results given by the formalism are disclosed. (auth)

41995 SUM RULES FOR FORM FACTORS OF PSEUDOSCALAR HADRON DENSITIES. Matsuda, Satoshi (Tokyo Univ.). Progr. Theoret. Phys. (Kyoto), 35: 858-65 (May 1966).

Sum rules for the form factors of the pseudoscalar hadron densities in the high-energy limit are derived on the basis of their current commutation relations. It is shown that, according to these sum rules, the form factors of the pseudoscalar hadron densities at high energy become of pure f-type in the limit of SU(3) symmetry, while it is also shown that a d-type contribution results from the effects of various symmetry breaking interactions at low energy. (auth)

41996 SELF-CONSISTENT METHOD FOR ANOMALOUS MAGNETIC MOMENTS OF BARYONS. Yamada,

Masao (Tokyo Univ.). Progr. Theoret. Phys. (Kyoto), 35: 866-80(May 1966).

Meson photoproduction amplitudes with $J^P = \frac{1}{2}^+$ are analyzed in detail, and some self-consistency conditions are derived in a general form for the anomalous magnetic moments of the baryons. The equations are applied to the SU(2) and the SU(3) symmetry schemes of strong interactions. It is shown that the results are in good agreement with the experimental values of the moments of the nucleons. The results are discussed in connection with the bootstrap mechanism of the baryons. (auth)

41997 REMARK ON THE CONDITION, $Z_3 = 0$. CASE OF MANY PARTICLES WITH IDENTICAL QUANTUM NUMBERS. Yabuki, Haruichi (Tokyo Univ.). Progr. Theoret. Phys. (Kyoto), 35: 889-96(May 1966).

The Z_3 factors for particles with the same quantum numbers are investigated. In the presence of many particles in the same channel there are two kinds of renormalization constants corresponding to the Z_3 factor of the one-particle case. One of these (denoted by C_{ij}) is the generalization of the wave function renormalization constant and the other (denoted by Z_{ij}) is that of the propagator renormalization constant. The relation between Z_{ij} and C_{ij} is given. Properties of Z_{ij} and C_{ij} are discussed with particular attention to the limit, $Z_{ij} = 0$. It is shown that $\Sigma_i |C_{ij}|^2$, which represents the probability of bare states in the j-th physical one, is always different from zero. A certain peculiar situation not known in the one-particle case arises. (auth)

41998 3*-PLET MODEL OF ELEMENTARY PARTICLES. Hayashi, Takemi (Univ. of Nagoya, Japan); Nakagawa, Masami; Toyoda, Akira; Umemura, Isao. Progr. Theoret. Phys. (Kyoto), 35: 897-907(May 1966).

With the aim of establishing a simple composite model in which the fundamental particles have integral charges and baryon numbers, a model which is the complex conjugate of the Sakata model is examined. The $\frac{1}{2}^+$ baryons belong to a 15 dimensional representation in this model. However, the extra baryons A(Y = –2, I = 1) and C(Y = –1, I = $\frac{3}{2}$) are shown to have masses higher than those of the eight known baryons. Properties of baryons in the 15 dimensional representation—electromagnetic form factors and weak currents—are also discussed and presented in detail in comparison with those of the eightfold way and shown to be not inconsistent with the experimental data. A new sum rule for the S-wave amplitudes of the non-leptonic weak decay of hyperons is obtained and shown to be consistent with the experimental data. (auth)

41999 DYNAMICAL APPROACH TO THE LEPTONIC DECAYS OF BARYONS. Kanazawa, Akira; Sakuma, Tetsuro (Hokkaido Univ., Sapporo). Progr. Theoret. Phys. (Kyoto), 35: 908-13(May 1966).

The leptonic decays of hyperons are analyzed using the dynamical self-consistency requirement and the assumption that the leptonic decay processes originate in a driving weak interaction of the current-current type. The hadron currents are assumed to transform like an octet component of SU(3). It is shown that the axial vector amplitude can have a resonance with almost the same values of the parameters as were fixed previously to explain the non-leptonic decays of hyperons in the same spirit as mentioned above. The enhancement mechanism can predict the D/F ratio of the axial vector amplitude; this is found to be 2.5, which is not inconsistent with experiment. (auth)

42000 NON-TRIVIAL EXAMPLE OF A RELATIVISTIC QUANTUM THEORY OF PARTICLES WITHOUT DIVERGENCE DIFFICULTIES. Kita, Hideji (Kyoto Univ.). Progr. Theoret. Phys. (Kyoto), 35: 934-59(May 1966).

A simple but nontrivial set of generators P_μ and $M_{\mu\nu}$ of the Poincaré group is obtained in terms of creation- and annihilation operators of particles. P_4 contains a cutoff form factor, which is a function of the square of the invariant momentum transfer at the interaction vertex. The relativistic quantum theory of particles thus obtained has no divergence difficulties. It is shown that the theory differs from the ordinary quantized field theory in the point that the former is not "manifestly" invariant although it still satisfies the symmetry requirements of special relativity. The method used is of rather general character, and the essential points, which have to be taken into consideration for the application to more realistic systems of particles, are discussed. (auth)

42001 MASSES OF HADRONS AND PAIR STATES OF QUARKS. Iwasaki, Yoichi (Tokyo Univ.). Progr. Theoret. Phys. (Kyoto), 35: 960-2(May 1966).

The masses of all the hadrons were calculated by introducing only two parameters. The two assumptions on which the calculation is based are: $H = H_0 + aS_0 + bS_8$ where H_0 is invariant under the chiral $U(3) \times U(3)$ ($S_i = \int q^* \beta \lambda_i q(x)/2d^3x$) and the nonchiral $U(3) \times U(3)$, which is generated by $F_i^{\pm} = \frac{1}{2}(S_i \pm V_i)$ where $V_i = \int (q^* \lambda_i q)/2d^3x$. is a good dynamical symmetry. (J.F.P.)

42002 HIDDEN CHANNELS AND ELEMENTARITY. Kinoshita, Kisei (Tokyo Univ.). Progr. Theoret. Phys. (Kyoto), 35: 964-5(May 1966).

The S-wave two-channel scattering of two spinless particles, $A\bar{A}$ in the first channel and $B\bar{B}$ in the second channel, is studied. It is assumed that the matrix amplitude has no left-cut and no zero and satisfies elastic unitarity. (J.F.P.)

42003 STRUCTURE OF BARYONS. Matumoto, Ken-iti (Kanazawa Univ., Japan). Progr. Theoret. Phys. (Kyoto), 35: 966-7(May 1966).

The structure of the hadron is investigated concretely using a mass formula. The model of the baryons is taken as $ttt\bar{R}^*$ (the urbaric charge of R is –3), and $t\bar{t}$ is the model of the mesons. A Rutherford-type model is found with central forces three times larger than the inter-urbaryon force, and these central forces play a dominant role in the binding. (J.F.P.)

42004 SUB-HADRONIC AND HADRONIC DYNAMICS. Matumoto, Ken-iti (Kanazawa Univ., Japan). Progr. Theoret. Phys. (Kyoto), 35: 967-9(May 1966).

From previous work on the structure of hadrons it is tentatively concluded that the suppression of the urbaryon-pair effect is a universal feature in subhadronic dynamics, although the true reason is unknown. Various deductions from this conclusion are considered. (J.F.P.)

42005 X-η MIXING AND B_8 MASS SPLITTINGS. Hirayama, Minoru (Kyoto Univ.). Progr. Theoret. Phys. (Kyoto), 35: 969-71(May 1966).

The X-η mixing in addition to ϕ-ω mixing is considered for obtaining the Gell-Mann-Okubo mass relations for various SU(3) multiplets. It is concluded that there is no definite reason to believe that one of the ϕ-ω and X-η is more fundamental than any other. (J.F.P.)

42006 PICTURE OF STRONG INTERACTIONS. Tati, Takao (Kanazawa Univ., Japan). Progr. Theoret. Phys. (Kyoto), 35: 973-4(May 1966).

It is noted that the main features of hadrons are described by a basic field the Lagrangian of which is given. The energy dependence of the hadron dynamics expected from this viewpoint is emphasized. It is concluded that for relatively low-energy phenomena strong interactions are described effectively by phenomenological boson-fermion Yukawa interactions although all the strongly interacting hadrons including the superstrongly interacting boson are described by a basic operator. (J.F.P.)

42007 COMPOSITION OF HADRONS AND MASS SPLITTINGS. Tanaka, Sho (Kyoto Univ.). Progr. Theoret. Phys. (Kyoto), 35: 975-6(May 1966).

It is shown that detailed studies of the mass splitting of hadron multiplets may provide a powerful clue to the inner structure and dynamics of the hadron. The P_8 meson composition and the mass splittings of the P_8 and V_8 meson octets are discussed in the light of the results obtained. (J.F.P.)

42008 S_3 INVARIANCE AND BROKEN U_3 SYMMETRY. Katayama, Yasuhisa (Kyoto Univ.). Progr. Theoret. Phys. (Kyoto), 35: 977-8(May 1966).

The use of the permutation group among three kinds of

ur-particles with the same mass, showing that the permutation invariant system allows the existence of a doublet with the same mass and a singlet with a different mass as in the case of molecular spectra, is generalized to the case of broken U(3) symmetry. It is shown that the permutation invariant system allows the validity of the mass formula derived from the broken U(3) symmetry. It is noted that the deviation from complete U(3) symmetry corresponds to the off-diagonal permutation invariant terms which are interpreted from an analogy to the deformation of an elastic body. (J.F.P.)

42009 WEAK INTERACTIONS OF LEPTONS WITH $\tilde{U}(12)$ SYMMETRY. Seto, Kenji (Hokkaido Univ., Sapporo). Progr. Theoret. Phys. (Kyoto), 35: 980-2(May 1966). (In French).

Generalizations for the weak magnetism, which is important in the theory of beta decay, are established for baryons using the method of $\tilde{U}(12)$ symmetry. A spurion formalism for weak interactions similar to the electromagnetic formalism for weak interactions in the $\tilde{U}(12)$ symmetry scheme is adopted, and it is assumed that the lepton current has the property of transforming the 143-dimensional representation, which is the same as that for the meson field. (J.F.P.)

42010 SOME MATRIX ELEMENTS AND NORMALIZATION COEFFICIENTS IN SU_n. Brody, T. A.; Moshinsky, M.; Renero, I. (Univ. Nacional de Mexico). Rev. Mex. Fis., 15: 145-65(1966).

The derivation of recursion relations for the Wigner coefficients of SU_n, based on the concept of auxiliary Wigner coefficient, for which the multiplicity problem does not arise, was described previously. The coefficients in the recursion relations are explicitly obtained here, and the polynomials in the creation operators which constitute the basis for the irreducible representation of SU_n are normalized, after a preliminary result concerning the expansion of determinants in the creation operators is obtained. (auth)

42011 SYMMETRY PROPERTIES OF THE STRONG INTERACTIONS. Engelbrecht, C. A. Tydskr. Natuurwetenskappe, 5: 67-88(June 1965). (In Afrikaans).

The introduction of isospin is clarified by means of an analogy with electrons in a magnetic field. Following a review of particles and resonances discovered up to the end of 1963, the same techniques are used to introduce the concepts of unitary symmetry. By means of simple group theoretical arguments further parallels between isospin invariance and unitary symmetry are drawn. This is followed by a demonstration of the way in which the known particles and resonances can be accommodated in the octet model. (auth)

42012 FRYE-WARNOCK EQUATION AND THE FROISSART N/D METHOD. Chermalykh, G. N. (Kiev Inst. of Physics). Ukr. Fiz. Zh., 11: 590-3(1966). (In Ukrainian).

The Frye-Warnock equation and the corresponding equation of the Froissart N/D-method are considered with $\eta(\nu) \propto \ln^{-\beta}\nu$, $\nu^{-\beta}$, $\exp(-c\nu^{\beta})$, where $\eta(\nu)$ is the inelasticity coefficient. It is pointed out that in the case of $\eta(\nu) \propto \nu^{-\beta}$ the first equation can be the Fredholm one for $1 > \beta$, while the second equation can be such for every $\beta \geq 0$. (auth)

42013 RELATIONS BETWEEN INTERACTION CONSTANTS OF VECTOR MESONS WITH BARYONS. Rekalo, M. P. (Inst. of Physics and Technology, Kharkov). Ukr. Fiz. Zh., 11: 697-703(1966). (In Ukrainian).

Eight relations between 14 independent interaction constants of vector mesons with baryons g(B*, BV) are found within the framework of unitary symmetry with moderately strong interaction (B* is the baryon from the unitary decuplet, B is the baryon from the unitary octet, V is the vector meson). (auth)

42014 PRINCIPLE OF MICROCAUSALITY AND "LACK OF REMOTE ACTION" IN ELEMENTARY PARTICLE THEORY. Lomsadze, Yu. M.; Krivskii, I. Yu. (Uzhgorod State Univ., USSR). Ukr. Fiz. Zh., 11: 721-9 (1966). (In Ukrainian).

An attempt is made to formulate in its most general aspect one of the fundamental problems of the axiomatic approach of Bogolyubov—Medvedev—Polivanov in elementary particle theory—the problem of ascertaining the properties of amplitudes or on the basis of postulates of the theory. This formulation of the problem requires investigation of an arbitrary regular generalization of the concept of the sum of the series implicit in the symbol Σ_v in the most general symbolic form of the generalized function $T(\tau)$, actually realized in the definition of this generalized function. In this general formulation the problem is practically boundless. The problem is then discussed with limited generality, assuming Σ_v to have the sense of a symbol of ordinary summation. Two possible strict formulations are presented both of the microcausality principle and the principle of "lack of remote action", based on recent researches. It is shown that limitation of the amplitude T(k) of an arbitrary linear exponent when $k \to \infty$ in the upper k-half-plane, which follows both from the first and second formulations of the principle of "lack of remote action," cannot be obtained solely from the principle of microcausality in any formulation whatever, even if the problem is set with the above-mentioned limitation of generality. In this connection the possibility of obtaining physical consequences from the principle of microcausality alone involves more refined characteristics of the generalized functions than the integral characteristic ρ. (auth)

42015 ASYMPTOTIC RELATIONS BETWEEN THE SCATTERING AMPLITUDES IN LOCAL FIELD THEORY. Logunov, A. A.; Nguyen Van Hieu; Todorov, I. T. (Joint Inst. of Nuclear Research, Dubna, USSR). Usp. Fiz. Nauk, 88: 51-91(Jan. 1966). (In Russian).

The derivation of rigorous asymptotic relations between the scattering amplitudes in high-energy interactions and the resultant relations between such characteristics as cross sections, polarizations, and others, from the point of view of their agreement with the most recent experimental data are discussed. Special attention is paid to the hypotheses on whose basis the asymptotic relations are derived. The asymptotic relations derived by many earlier investigators are reviewed as well as related papers dealing with the derivation of asymptotic relations in the presence of higher symmetries of strong interactions and in processes involving particle production. (ATD)

42016 REMARKS ON THE $SU(6)_w$ SYMMETRY. Bokov, O. G. Yadern. Fiz., 4: 391-4(Aug. 1966). (In Russian).

The symmetry scheme $SU(6)_w$ is discussed. The meson-baryon vertex is considered and relations between form factors are obtained. It is shown that some of these relations are not relativistically invariant. The origin of this noncovariance is investigated, as well as the possibility of introducing covariant techniques for the $SU(6)_w$ symmetry. (auth)

42017 QUARK STRUCTURE AND MASSES OF STRONGLY INTERACTING PARTICLES. Zeldovich, Ya. B.; Sakharov, A. D. Yadern. Fiz., 4: 395-406(Aug. 1966). (In Russian).

A baryon resonance with the charge 3e, recently reported in the papers of Goldhabers and collaborators and by Alexander and collaborators can be explained by assuming its quark structure to be 4 quarks and 1 antiquark $(4q,\bar{q})$. It is suggested that such a structure is a leading one (i.e., it is contained in the superposition of structures with the maximal weight) for all baryons, including the 56-plet for which the minimal quark structure is 3q. A unified mass formula (linear in the masses) for mesons and baryons is proposed, based on the assumption that the spin and annihilation interactions involving strange quarks are suppressed (in the same degree for mesons and baryons). (auth)

42018 NON-LINEAR HEISENBERG OPERATORS IN QUANTUM FIELD THEORY. Sukhanov, A. D. (Moscow Inst. of Radioelectronics and Mining Electromechanics). Yadern. Fiz., 4: 407-17(Aug. 1966). (In Russian).

The problem is considered of determining nonlinear Heisenberg operators in quantum field theory as local

functions of Heisenberg fields. It is shown that the quasi-normal product of Heisenberg fields with equal arguments plays a specific role in the theory. This is used to develop the Lagrange and Hamilton methods in the Heisenberg representation, in particular to obtain the equations of motion. The expression for the Heisenberg current, figuring in the equations, is equal, in renormalizable theories, to the expression for the same operator obtained in the axiomatic method. (auth)

42019 ANALYTICAL PROPERTIES OF THE NON-RELATIVISTIC AMPLITUDE IN A SOLUBLE THREE-PARTICLE MODEL. Vashakidze, I. Sh.; Chilashvili, G. A. (Tbilisi State Univ., Georgian SSR). Yadern. Fiz., 4: 418-24(Aug. 1966). (In Russian).

The analytical properties of the three-particle inelastic scattering amplitude are investigaged for a factorizable potential for which the problem is solved exactly. It is shown that in the complex angular momentum plane the amplitude has an infinite number of cuts. (auth)

42020 LAGRANGIAN AND HAMILTONIAN FOR VECTOR ELECTRODYNAMICS IN HEISENBERG REPRESENTATION. Slavnov, A. A.; Sukhanov, A. D. (Steklov Inst. of Mathematics, Academy of Sciences, USSR). Yadern. Fiz., 4: 425-31(Aug. 1966). (In Russian).

Mathematical techniques developed previously were used to investigate problems of the lagrangian and hamiltonian in vector electrodynamics. A closed expression for the interaction hamiltonian is obtained in the interaction representation. The problem of the unitarity of the S-matrix and the connection between various operators in the Heisenberg and interaction representations are discussed. (auth)

42021 ANALYTICAL PROPERTIES OF EUCLIDEAN AMPLITUDES. Efimov, G. V. Yadern. Fiz., 4: 432-42 (Aug. 1966). (In Russian).

The Cutkossky rule for normal thresholds is proved for arbitrary Feynman diagrams in the euclidean formulation of quantum field theory. (auth)

42022 PAULI PRINCIPLE AND UNSTABLE ELEMENTARY PARTICLES. Khalfin, L. A. (Steklov Inst. of Mathematics, Leningrad). Yadern. Fiz., 4: 443-5(Aug. 1966). (In Russian).

An analog of the Ehrenfest–Oppenheimer theorem and specifically the symmetrization principle for unstable particles is investigated. Several experimental tests about the symmetrization principle are described. With the help of these tests one can solve the problem of the dependence of some properties of unstable elementary particles on the method of production. (auth)

42023 NONLEPTONIC BARYON DECAYS IN THE STATIC MODEL WITH SU(6) SYMMETRY. Rekalo, M. P. Yadern. Fiz., 4: 446-8(Aug. 1966). (In Russian).

Investigations were made of hadron decays with SU(6) symmetry based on the static model. In such a model the infinitely heavy nucleon interacts with a pseudo scalar meson at p-distance. Under such conditions the meson has an effective moment equal to one and positive parity. Such a situation is achieved in baryon hadron decays with conservation of parity. Equations were developed for the amplitude of baryon hadron decays. The relativistic generalization of SU(6) proved to be in better agreement with experimental data than the nonrelativistic SU(6) symmetry. (R.V.J.)

42024 RELATIVISTIC THEORY OF REACTIONS. Model Independent Methods. Werle, J. New York, John Wiley and Sons, Inc., 1966. 475p. $17.50.

The problems of the relativistic theory of reactions which can be solved by model independent methods are considered. Only the general principles of relativistic quantum mechanics and the symmetry properties of the S-matrix elements are used. A unified treatment of all the problems considered is achieved by extensive use of group theoretical methods. A compact and comprehensive review of the theory of groups and their representations is included. The topics covered are vector space and linear operations, groups and group representations, general principles of the relativistic theory of reactions, description of free-particle states, transition amplitudes, cross sections and their p-wave expansions, selection rules, and relations between different reactions. (J.F.P.)

42025 REGGE SYMMETRIES OF CLEBSCH-GORDAN COEFFICIENTS AS A PROPERTY OF SYMMETRIC FUNCTIONS. Giovannini, Alberto (Duke Univ., Durham, N. C.). 16p. (CONF-660411-40). ORAU. Gmelin, AED-CONF-66-060-109.

From American Physical Society Meeting, Washington, D. C.

Regge has given a relation between 3 × 3 determinants and the (3j) coefficients. It is shown that this relation may be rewritten in terms of symmetric functions, and one may accordingly establish a distinction between the classical symmetries and the Regge symmetries of the (3j) symbols. It is remarked that the Regge symmetries are consequences of the symmetry of each function with respect to its variables. This remark permits a geometrical picture to be given for all (3j) coefficient symmetries in the space of the variables of the above symmetric functions. (auth)

42026 REPRESENTATIONS OF STRONG COUPLING GROUPS. Goebel, C. (Univ. of Wisconsin, Madison). 16p. (CONF-660540-3). ORAU. Gmelin, AED-CONF-66-113-2.

From Conference on Non-Compact Groups in Particle Physics, Milwaukee.

For the discussion of strong coupling group representations the dynamics of static models (meson field interacting with an infinite mass scatterer) in the strong coupling limit is described completely by two sets of given equations. These equations were derived from field theory and from Chew-Low theory. Restriction is made to rigid rotator models. (J.F.P.)

42027 INFINITY OF POTENTIAL STRENGTH. Tani, S. (Marquette Univ., Milwaukee, Wis.). 47p. (CONF-660411-39). ORAU. Gmelin, AED-CONF-66-060-90.

From American Physical Society Meeting, Washington, D. C.

The infinity of the potential strength is studied as a preliminary to singular potential scattering. The strong coupling theory of a potential of finite rank, which is a potential composed of a sum of a finite number of separable potentials, is considered, and a discussion is given for the K-matrix at infinity of potential strength for a potential of finite rank. The K-matrix for a hard core is derived by applying the results obtained to a repulsive hard core potential. Strong coupling theory is introduced, and the difference between attraction and repulsion is discussed. Also the limiting process in which the depth of an attractive square well tends to infinity is considered. (J.F.P.)

42028 FORWARD SCATTERING AMPLITUDE AT HIGH ENERGY. Kinoshita, Toichiro (Cornell Univ., Ithaca, N. Y.). 14p. (CONF-660411–45). ORAU. Gmelin, AED-CONF-66-060-104.

From American Physical Society Meeting, Washington, D. C.

Recently Martin has enlarged the domain of analyticity of the scattering amplitudes substantially within the framework of axiomatic field theory. Although it is still much smaller than that assumed in the Mandelstam representation, it already imposes rather strong restrictions on the properties of the scattering amplitude. A review is given of some recent results concerning the high energy behavior of forward scattering amplitudes which are derived from unitarity and rigorously proved analyticity. (auth)

42029 DYNAMICAL STUDY OF THE QUARK-MESON SYSTEM. Nieto, Michael Martin (Cornell Univ., Ithaca, N. Y.). 64p. (CONF-660411–47). ORAU. Gmelin, AED-CONF-66-060-102.

From American Physical Society Meeting, Washington, D. C.

In order to investigate a possible Quark-Meson bootstrap, triplet scattering off of an octet of degenerate

pseudoscalar mesons (0.49 Bev) was studied. The exchange forces in the u channel were the triplets and any other p-wave multiplets that bootstrapped, and in the t channel were an assumed octet of vector mesons (0.89 Bev) with experimental values for G^V and G^T. A first order N/D iteration technique was used, and a successful NN* bootstrap was obtained to check the calculational method. From an initial triplet, the masses and coupling constants obtained from one iteration were used as starting points for the next. Although a $\underline{3}\ P_{\frac{1}{2}}$, $\underline{6}^*\ P_{\frac{1}{2}}$, $\underline{15}\ P_{\frac{1}{2}}$ bootstrap appeared possible, the solutions iterated into "ghosts" for large values of the coupling constants or cut-offs, and the triplet solution collapsed for smaller values. The interpretation is that one should not expect to find low mass (≈1 Bev) quarks. (auth)

42030 BEYOND SU(6). Fronsdal, Christian (Univ. of California, Los Angeles). 11p. (CONF-651213-5). ORAU. Gmelin, AED-CONF-65-400-3.

From American Physical Society, Winter Meeting in the West, Los Angeles.

The phenomenological mass formulas for the 56-dimensional baryon multiplet and the 35-dimensional meson multiplet are discussed. Also symmetries beyond SU(6) and supermultiplets larger than those of SU(6) are considered. (J.F.P.)

42031 SEVEN TYPES OF U(6). Coleman, Sidney (Univ. of California, Berkeley). 25p. (CONF-660545-1). ORAU. Gmelin, AED-CONF-66-140-1.

From Midwest Conference on Theoretical Physics, Bloomington, Ind.

The construction of a relativistic U(6) theory is considered. The structure of theories rather than their predictions is discussed. (J.F.P.)

42032 THE UNIVERSALITY OF LORENTZ INVARIANCE IN PARTICLE PHYSICS. Dresden, M. (State Univ. of New York, Stony Brook). 11p. (CONF-660540-6). ORAU. Gmelin, AED-CONF-66-113-3.

From Conference on Non-Compact Groups in Particle Physics, Milwaukee.

The status of groups and symmetries for investigating the theoretical structure of elementary particles is reviewed. Comments are made on the quark picture and the fundamental theoretical picture. Possible modifications of the Poincare group for incorporating some symmetry structure in a dynamic scheme are discussed, with particular reference to Lorentz transformations. (L.B.S.)

42033 PROBLEMS OF PHYSICAL INTERPRETATION CONNECTED WITH NONCOMPACT GROUPS IN PARTICLE PHYSICS. Roman, P. (Boston Univ.). 11p. (CONF-660540-1). ORAU. Gmelin, AED-CONF-66-113-1.

From Conference on Non-Compact Groups in Particle Physics, Milwaukee.

A construction of representations for arbitrary groups in a Hilbert space such that all physical requirements of interpretation are met is suggested. An application of non-compact groups for obtaining, without symmetry breaking, a mass spectrum in theories which possess a symmetry group containing both internal and external (space-time) symmetry operations is discussed. (J.F.P.)

42034 $SU(6)_W$ AND COMPOSITE MODELS OF HADRONS. Capps, Richard H. (Northwestern Univ., Evanston, Ill.). 18p. (CONF-660411-38). ORAU. Gmelin, AED-CONF-66-060-89.

From American Physical Society Meeting, Washington, D. C.

The composite model of hadrons discussed is basically an extension of the Chew-Low model in which relativistic interactions are considered. It is assumed that the most important constituent states in composite models of the lighter hadrons are two-particle states made up of the lightest multiplets, that the dominant force mechanisms are one-particle exchange mechanisms involving the lightest multiplets, and that the particles are degenerate in a given multiplet. The meson bootstrap model and some predictions concerning meson and baryon resonances are considered. (J.F.P.)

Fluid Physics and Thermodynamics

See also Plasma Physics and Thermonuclear Processes

Refer also to abstracts 41774 and 41778.

42035 (IPP-2/41) MONTE-CARLO-SIMULATION DER STROEMUNG EINES KNUDSEN-GASES UNTER BERUECKSICHTIGUNG DER VERWEILZEIT. (Monte Carlo Simulation of the Flow of a Knudsen Gas With Due Allowance for the Sojourn Time). Gorenflo, R.; Pacco, M. G.; Scherzer, B. M. U. (Institut fuer Plasma-physik, G.m.b.H., Garching (West Germany)). Nov. 1965. 38p. (IPP-6/46). Dep. mn.

The initial flow of a Knudsen gas through a long, thin tube is discussed. The intention is to determine from the measured intensity of the outflow at the end of the tube the distribution density of the sojourn of the gas molecules on the tube wall. For this purpose an integral equation is formed. Because of the complications involved, a numerical solution was not contemplated, an attempt being made instead to approximate the known intensity of the outflow by trial substitution of various sojourn distributions. This was abandoned owing to the enormous computing time required. Further simulation was made to investigate the degree of approximation with which the flow may be regarded as a diffusion process, i.e., the approximation with which the flow may be treated with the aid of the diffusion equation and appropriate initial and boundary conditions. It was found that the flow was not a diffusion process. The deviation is caused by 5 to 9% of the particles (those travelling too far). (auth)

42036 (SC-RR-66-356) A GENERALIZED MAGNETOHYDRODYNAMIC ENTRANCE FLOW MODEL. I. MOMENTUM INTEGRAL METHOD. Saric, W. S.; Touryan, K. J. (Sandia Corp., Albuquerque, N. Mex.). Aug. 1966. Contract AT(29-1)-789. 51p. Dep. mn. CFSTI $3.00 cy, $0.50 mn.

The hydromagnetic flow of a conducting, incompressible fluid is analyzed by using a two-conductivity model and a momentum integral method. The model implies a highly conducting viscous layer with Hall effects and a cool inviscid core. (auth)

42037 (UTIAS-115) MAGNETOHYDRODYNAMIC FLOW IN THE SHOCK TUBE BOUNDARY LAYER WITH TRANSVERSE MAGNETIC FIELD. Dukowicz, J. K. (Toronto Univ. (Ontario). Inst. for Aerospace Studies). May 1966. 103p.

Some cases of boundary layer flow in a shock tube with insulated walls and a transverse magnetic field are investigated experimentally and theoretically. The configuration is similar to the insulator boundary layer in an MHD generator channel with a loading parameter equal to unity. With argon as the test gas, the experimental results show some cases where the heat flux to the wall is uninfluenced by the magnetic field, and others where a strong effect is observed. A Couette flow calculation, incorporating all relevant physical phenomena and representing the conditions encountered in the experiment, was carried out. The results indicate that the Hall effect has an important influence in such a way that when Hall currents are unrestricted there is little change in the heat flux. The strong interaction observed may be explained by the absence of Hall currents, or possibly by the occurrence of an electron thermal instability predicted by Kerrebrock at high Hall parameters (auth)

42038 (NASA-TT-F-360) NUMERICAL METHODS IN GAS DYNAMICS. Roslyakov, G. S.; Chudov, L. A. (eds.). Translation of Chislennye Metody v Gazovoi Dinamike from Sb. Rabot, Vychisl. Tsentr Moskov. Univ., Vol. II. 170p. (TT-65-50138; IPST-Cat.-1456). CFSTI $5.00 cy, $1.00 mn.

A collection of 17 papers dealing with various aspects of steady gas flow, boundary layer, viscous flow, and seepage problems is presented. (M.O.W.)

42039 MAGNETOHYDRODYNAMIC BOUNDARY LAYER BETWEEN PARALLEL STREAMS OF DIFFERENT MAGNETIC FIELDS AND TEMPERATURES. Pao, H. P.; Chang, C. C. (Catholic Univ. of America, Washington, D. C.). Contract NsG-586. AIAA (Amer. Inst. Aeronaut. Astronaut.) J., 4: 1313-20(Aug. 1966).

An analysis and calculations of the free laminar boundary-layer flow between parallel streams of different magnetic fields and temperatures were made for an incompressible, viscous, thermally, and electrically conducting fluid. The parallel magnetic field is directed in the fluid stream direction. Small perturbation and approximate solutions were given. The approximate solution, when magnetic Prandtl number is unity, gives quite a satisfactory flowfield that only involves a discrepancy of 1% from the exact numerical solution in most cases. The integration of the exact boundary-layer equations was carried out, and some sample calculations were shown in the graphs. No steady-state solution exists when the Alfvén speed is greater than the fluid speed. The magnetic field thickens the flow boundary layer and thus indicates a stabilizing effect on the flowfield. The possibility of an extension to parallel streams of two different fluids also is investigated. (auth)

42040 INSTABILITY OF NONUNIFORM CURRENT AND FIELD DISTRIBUTION. Gurevich, L. E.; Ioffe, V. I. Dokl. Akad. Nauk SSSR, 168: 65-7(May 1, 1966). (In Russian).

It is shown that magnetohydrodynamic instability may be produced not only by a gradient in the concentration of current carriers, but also by a mobility gradient or instability in the external electric and magnetic fields. Gradient instability in semiconductors is considered. This type of instability (in an electric field at a frequency much lower than the collision frequency) requires conditions opposite to those necessary for "drift" instability: a temperature gradient or pronounced nonisothermicity in the plasma, a strong external magnetic field with no electric field and a low collision index. It is assumed that the nonhomogeneities are of such a nature that the Wentzel-Kramers-Brillouin approximation may be used. Expressions are given for longitudinal and transverse instability with respect to current. Calculations show that instability of this type is possible only in materials with a low carrier concentration. Specific cases of gradient instability are considered with respect to critical electric fields and electron temperatures. (ATD)

42041 CRITICAL WAVELENGTH IN THE SYSTEM OF A COLLISIONLESS GAS AND SOLID MEDIUM IN A HOMOGENEOUS MAGNETIC FIELD. Maksumov, M. N.; Dobrovolskii, O. V. (Inst. of Physics and Tech., Academy of Sciences, Tadzhik SSR). Dokl. Akad. Nauk Tadzh. SSR, 9: No. 3, 17-20(1966). (In Russian).

The critical wavelength λ_{cr} within a gravitating system determines the limit of the stability of small-amplitude flat waves within that system. The critical wavelength is studied in an infinite homogeneous system consisting of a collisionless gas and self-gravitating particles. The gas has infinite conductivity in a homogeneous magnetic field. The dynamics of such a system is expressed by equations of magnetohydrodynamics, by Boltzmann's integral for the function of particle distribution in a collisionless gas, and by Poisson's equation of the gravitational potential of a self-coordinated field. Equations are developed for determining small deviations from equilibrium values in the magnetic field, in hydrodynamic velocity, in density, in the gravitational potential, and in the distribution function of the collisionless gas. The solution of the equation system yielded a system of algebraic equations characterizing perturbed values of parameters. Individual algebraic equations characterize a subsystem of magnetohydrodynamic waves, which are independent of gravity and compressibility. The equation dealing with interstellar gas contains the relative phase velocity of the wave, which determines the position of the wave in the gas. (ATD)

42042 MAGNETOHYDRODYNAMICS OF CONDENSED MEDIA. Kirko, I. Latvijas PSR Zinat. Akad. Vestis, No. 7, 22-6(1965). (In Russian).

After briefly sketching the history, scope, and applications of magnetohydrodynamics, the contributions are listed of Soviet and particularly Latvian scientists in this field. The Laboratoriya Magnitnoy Gidravliki Instituta Fiziki AN Latviyskoy SSR (Magnetic Hydraulics Laboratory, Institute of Physics, AN Latvian SSR), headed by O. A. Liyelausis, has studied flow phenomena of liquid metals in magnetic fields, and the effect of the latter on flow around bodies. The laboratory headed by Ya. Liyelpeter is studying phenomena in a traveling magnetic field as a medium for exerting a noncontact influence on liquid metals. The SKB Instituta Fiziki (SKB of the Institute of Physics) and TsKTBMiA Latviyskogo Sovnarkhoza (TsKTBMiA of the Latvian Council of National Economy) have constructed a series of modern electromagnetic pumps. Several inventions were made in the field of induction pumps by researchers at the "VEF" plant. Yu. Birzvalk is directing major research in the field conduction MHD machines for liquid metals. Inventions pertaining to noncontact methods of measuring the velocity of a liquid metal are mentioned together with the inventors names. Work on applications in ferrous and nonferrous metallurgy, casting, chemical, and semiconductor industry is being carried out at the TsKTBMiA Latviyskogo Sovnarkhoza in Riga. Studies in the field of simulation of MHD phenomena are being conducted at the Riga Polytechnic Institute. An important role in the development of MHD is played by the Vychislitel'nyy Tsentr Latviyskogo Gosudarstvennogo Universiteta (Computer Center of the Latvian State University). (ATD)

42043 TSCHEBYSCHEFF APPROXIMATION IN PARTIAL FUNCTIONS. Schlender, B.; Traving, G. Z. Astrophys., 61: 92-4(1965). (In German).

The introduction of Tschebyscheff approximation in partial functions is investigated. The results were used in numerical calculations, and values obtained for hydrogen are given as an example of the validity of the Tschebyscheff approximation introduction. (J.S.R.)

42044 SELF-SIMILAR SOLUTION OF NONSTEADY-STATE EQUATIONS OF A PLANE, LAMINAR, MAGNETOHYDRODYNAMIC BOUNDARY LAYER. Boev, A. G. Zh. Prikl. Mekh. Tekh. Fiz., No. 1, 15-20(Jan.-Feb. 1966). (In Russian).

Self-similar solutions of nonsteady-state equations of a magnetohydrodynamic plane boundary layer are found. Use is made of the shift to curvilinear coordinates of a special type. The selection of the type depends on the requirements necessary to reduce the boundary layer equations to a system of ordinary differential equations. The Weyl iteration method is employed to solve equations which describe flow on an impulsively driven plate. (ATD)

42045 PERFECT THERMODYNAMIC VAPOR. Hammitt, A. G.; Cecil, R. A. (TRW Systems, Redondo Beach, Calif.). 8p. (CONF-660326-3). ORAU. Gmelin, AED-CONF-66-047-3.

From 7th Symposium on Engineering Aspects of Magnetohydrodynamics, Princeton, N. J.

A "perfect thermodynamic vapor" is postulated which may be considered to be the vapor analogy of a perfect gas. The thermodynamic properties of the vapor are derived and shown to compare favorably with a real vapor. The usefulness of the concept is demonstrated by deriving an analytic relation for the efficiency of two Rankine cycles of interest. (auth)

Geophysics

Refer also to abstract 42453.

42046 (RM-4988) THE DEVELOPMENT OF A RADIO SIGNAL FROM A NUCLEAR EXPLOSION IN THE ATMOSPHERE. Gilinsky, Victor (RAND Corp., Santa Monica, Calif.). Aug. 1966. 19p.

The dipole radio signal from a low altitude atmospheric nuclear explosion of low yield is computed by numerically integrating Maxwell's equations. The source is described by a simple model. The function describing the time history

of the rate of gamma output is taken to be an isosceles triangle with a base equal to a fraction of a microsecond. The asymmetry necessary for radiation comes entirely from the variation of air density with altitude. The dipole fields are shown as functions of position for various times after the explosion. These curves form, in effect, a motion picture of the development of the signal. (auth)

42047 RELATIONS BETWEEN CERTAIN FORMS OF IONOSPHERIC ABSORPTION AND SOLAR AND GEOPHYSICAL PHENOMENA. **Pick, M. (Observatoire, Meudon, France). Ann. Geophys., 22: 310-19(1966). (In French).**

Some optical and radioelectric properties of solar flares associated with three types of events are discussed, namely, sudden ionospheric disturbances, polar cap absorption, and sudden onset of solar storms. The sun emits x rays over a large spectral range, but in a solar flare it is the 1- to 10-Å radiation which is responsible for ionization in the D layer of the ionosphere. This is manifested by sudden ionospheric disturbances affecting radio wave propagation. These sudden disturbances can be closely correlated with the time of eruption of sun spots. It has been shown that the optical importance of an eruption is of less significance than the radioelectric effect. There are two characteristic flares associated with radioelectric effects, type II and type IV. Type II flares correspond to a solar corona velocity of ~1000 km/sec, and this type flare is associated with an immediate geomagnetic storm. (BBB)

42048 THE CONTRIBUTION OF THE IONOSPHERIC F REGION TO COSMIC NOISE ABSORPTION. **Taubenheim, J.; Hense, U.; Lippert, W. (Heinrich-Hertz-Institut, Berlin). Ann. Geophys., 22: 320-2(1966).**

Two approaches were made to determine the F region contribution to cosmic noise absorption. First, an experimental study was made of the solar eclipse effect on A1 and A2 absorption, and a theoretical estimate of collisional absorption in the F region was obtained. The experimental evidence from solar eclipse measurements and theoretical model calculations are discussed. The results show the existence of a considerable F region absorption which, however, cannot be quantitatively explained by collisional losses alone, but by the additional presence of noncollisional loss processes, which seem to be more intense at lower than at higher solar activity. (M.O.W.)

42049 OBSERVATIONS OF THE DETERMINATION OF THE ELECTRON CONTENT OF THE IONOSPHERE FROM THE FARADAY EFFECT OF THE IONOSPHERE. **Schoedel, Juergen-Peter (Max-Planck-Institut fuer Aeronomie, Lindau, Ger.). Arch. Elek. Uebertr., 20: 353-6(June 1966). (In German).**

Some limitations for the calculation of the total electron content of the ionosphere deduced from the Faraday effect of the ionosphere are discussed. These include the influence of different propagation paths of the ordinary and extraordinary rays of a radio wave, consideration of the geometry of the measuring system satellite-fixed receiving dipole, the irregular structures of the ionosphere, and consideration of the terrestrial magnetic field. A method for determination of the electron content is established and some results for the content over Lindau for 15 passes of the BE-B satellite, calculated from the Faraday effect for two close frequencies. Results compare closely with values obtained by the difference Doppler effect method. (BBB)

42050 CONTINUOUS RECORDING OF SMALL AIR IONS IN CLOSED ROOMS. **Siksna, Reinhards; Eichmeier, Joseph (Univ. of Uppsala). Ark. Geofys., 4: No. 29, 563-76(1965).**

High concentrations of naturally produced air ions were measured in different closed rooms at the Institute of High-Tension Research in Uppsala. The diversity of the ionic conditions in the air in different rooms appeared to be great and therefore the variations in the concentration of small air ions were investigated by continuous recording over long periods of time. (M.O.W.)

42051 THE IONOSPHERIC ABSORPTION OF SHORT WAVES DURING THE SOLAR ECLIPSE ON 15 FEBRUARY, 1961. I. MEASUREMENTS WITH THE PULSE REFLECTION METHOD (A1). **Bischoff, K.; Boehm, S.; Kretschmer, R.-G.; Taubenheim, J. (Heinrich-Hertz-Institut fuer Schwingungsforschung, Berlin). Beitr. Geophys., 73: 13-20 (1964). (In German).**

The nonselective ionospheric absorption of short waves is essentially determined by the electron concentration and its spatial distribution in the lower ionosphere (D and E layers). Measurement of ionospheric absorption during a solar eclipse can provide information on physical processes dependent on the electron concentration. To provide such data, measurements of ionospheric absorption by the pulse reflection method (A1) during the solar eclipse of the 15th of February, 1961 were made at two stations in Germany and two stations of the solar-eclipse expedition into the zone of totality in Bulgaria. The solar-eclipse effect showed a min of absorption at the time of totality, about 7 db below the values of the control days. The time variation of the effect was nonsymmetrical. The undisturbed values of the absorption were reached a few min after the fourth contact. (BBB)

42052 THE IONOSPHERIC ABSORPTION OF SHORT WAVES DURING THE SOLAR ECLIPSE OF 15 FEBRUARY 1961. II. INTERPRETATION OF THE SOLAR-ECLIPSE EFFECT BY A1 MEASUREMENTS. **Bischoff, K.; Taubenheim, J. (Heinrich-Hertz-Institut fuer Schwingungsforschung, Berlin). Beitr. Geophys., 73: 93-101(1964). (In German).**

The measurements described were made at two stations in Germany and at two stations in Bulgaria in the zone of totality. The time-variation of ionospheric absorption at 3.86 and 3.18 Mcps in the region of total solar eclipse (pulse reflection method, A1) was compared to model calculations based upon the usual ionospheric continuity equation. The best fit to the solar eclipse effect was given by a two-layer model, in which about one half of the total absorption is attributed to the E region, whereas the remaining absorption is contributed by a part of the D region, probably situated at a height between 60 and 80 km. (BBB)

42053 THE IONOSPHERIC ABSORPTION OF SHORT WAVES DURING THE SOLAR ECLIPSE ON 15, FEBRUARY 1961. III. MEASUREMENT WITH THE COSMIC NOISE METHOD. **Lippert, W. (Heinrich-Hert-Institut fue Schwingungsforschung, Berlin). Beitr. Geophys., 73: 199-208(1964). (In German).**

During a solar eclipse, changes occur in the ionizing irradiation from the sun and such variations cause changes in the electron density of the ionosphere which can be detected by its effect on the absorption of short-wave radio transmission. The ionospheric absorption of short radio waves was recorded during a total solar eclipse both by the pulse reflection method (A1) and by the cosmic noise method (A2). This report deals with cosmic noise observations at 25 Mcps, made in Bulgaria during the total eclipse of 15 February, 1961. With increasing occultation of the sun's disc by the moon, the ionospheric absorption showed the expected decrease, reaching its max 40 sec after totality. Thereafter, the absorption increased more slowly than it had decreased earlier. The intensity of cosmic noise was higher on the days around the 15th of February than on other days of the month. (BBB)

42054 CORRELATIONS BETWEEN ELECTROMAGNETIC PULSATIONS AND THE F2 LAYER. **Hollo, L.; Veroe, J. (MTA Geofizikai Kutato Laboratoriuma, Sopron, Hung.). Beitr. Geophys., 74: 353-6(1965). (In German).**

A correlation between electron concentration in the F2 region and amplitudes of earth-current pulsations with periods of 2-6 min is established. The correlation of the logarithmic decrement with f_0F2 is described, with a correlation of −0.25; the increase of electron concentration with pt pulsation occasions the decrease of the damping. Three groups of pt cases were defined with limiting frequencies 4.0 – 5.5 Mcps, 5.6 – 7.0 Mcps, >7.0 Mcps, and the damping curves were prepared. For lower concentrations, the first amplitude is large, but the later ones fall off more rapidly than for greater concentrations. For

all three classes the damping curves are concave left from below. The low correlation between damping and electron concentration indicates that propagation of pulsations at lower latitudes probably occurs through magnetoacoustic waves which propagate perpendicular to the field lines. If the propagation proceeded through ionospheric currents, the correlation would be better. (BBB)

42055 SOLAR MINIMUM MEASUREMENTS OF FAST NEUTRONS AT HIGH ALTITUDE. Baird, G. A.; Wilson, B. G. (Univ. of Calgary, Alta.). Can. J. Phys., 44: 2131-6(Sept. 1966).

Several rocket and balloon measurements of neutron intensity above Fort Churchill, Canada, were made during 1964 and 1965. The detector in each case was an anthracene–plastic "phoswich" using pulse-shape discrimination to distinguish between neutrons, gamma rays, and charged particles. Neutrons were recorded in the energy range 2 to 11 Mev. Measurements indicate that the albedo neutron flux is somewhat lower than theoretical predictions but is in agreement with reasonable extrapolations to zero atmospheric depth of measurements within the atmosphere made by other workers. The exponent of the differential energy spectrum appears to change from −1.4 at large atmospheric depths to −0.8 outside the atmosphere. (auth)

42056 ORIGIN OF ELECTRON PRECIPITATIONS IN THE AURORAL ZONES. Coppi, Bruno; Laval, Guy; Pellat, Rene (EURATOM-Commissariat a l'Energie Atomique, Fontenay-aux-Roses, France). Compt. Rend., Ser. B, 263: 128-30(July 11, 1966). (In French).

It is shown that an instability developing in the outer magnetosphere could explain certain auroral phenomena. The theoretical analysis takes account of the movement of auroral arcs, of their localization and geometrical structure. The characteristic times of evolution and the particle energy responsible for the auroral luminescence are also in good agreement with the theoretical results. (G.O.Y.)

42057 MOVEMENTS OF RADIO AURORA. Oksman, J. (Geophysical Observatory, Sodankylae, Finland). Geophysica (Helsinki), 9: 235-50(1966).

Measurements were made, from March to August 1963, of the field strength of 88.9 Mcps transmission to investigate backscattering of radio waves from auroral ionization, called radio aurora. Bistatic measurements of radio aurora between the transmitter at Mikkeli and the receiver at Sodankylae were analyzed and the results compared with calculated reflection conditions. Bending of radio waves in the E region of the ionosphere and change in the inclination of the geomagnetic field due to the auroral electrojet were estimated. Meridional and longitudinal motions of auroral ionization were deduced from the measurements. The relatively frequent occurrence of auroral echoes between the station pair Mikkeli-Sodankylae, in spite of the poor predictions based on the calculated geometry, is explained by the finite scattering beam width of auroral irregularities, bending of radio waves in the ionospheric E (or E_s) layer and change of the inclination due to the auroral electrojet. North-south movements of auroral ionization were estimated by comparing the statistics of auroral echoes with the statistics of geomagnetic disturbances. The right direction was obtained but the magnitude of the velocity was too low. East-west motions were studied by comparing the strength of echoes received by the two antennae used in the measurement. (BBB)

42058 A LIMITED SURVEY OF THE F1 REGION IN SUMMER AT SOLAR MINIMUM. King, G. A. M.; Lawden, M. D. (DSIR, N. Z.). J. Atmos. Terrest. Phys., 28: 871-7(Sept. 1966).

Ionograms obtained at Campbell Island during December 1963 and January 1964 were analyzed by the "method of overlays" to provide measures of the rates of electron production and loss, and of the scale height, in the lower F region. The results indicate that the ratio between the concentrations of atomic oxygen and of molecules, which determines the rate of loss, changed suddenly during the period investigated; it also changed with (even weak) storm activity in such a way as to increase the rate of loss. (auth)

42059 ENHANCED ACTIVITY IN THE IONOSPHERE E REGION AT CAPE HALLETT AND CAMPBELL ISLAND. Bullen, J. M. (DSIR, Christchurch, N. Z.). J. Atmos. Terrest. Phys., 28: 879-89(Sept. 1966).

Analysis of ionospheric recordings of enhanced E at Cape Hallett (−74.7° Geomag. Lat.) and Campbell Island (−57.3° Geomag. Lat.) during 1958 and 1963 supplies information on the diurnal variation and sunspot cycle changes of overhead auroral activity. Enhancements of the E-region at Campbell occur mainly at night during magnetic disturbance. They are most frequent at equinox, show small seasonal change and decrease in number and intensity from sunspot maximum to minimum. At Hallett, on the opposite side of the maximum auroral zone, enhanced E is more frequent but is mainly minor and unrelated to magnetic disturbance. Minor enhancements occur most often in the morning hours, are more easily observed in winter than summer, and increase in number towards the solar cycle minimum. In summer there is a contrasting decrease from sunspot maximum to minimum of intense enhancement associated with major magnetic disturbance. Estimates of electron fluxes required to produce enhanced E of different intensities agree with those obtained from in situ observations of the aurora. Enhanced E is an indicator of electron conductivity and aurorae and is potentially useful in investigations of the solar plasma stream and its terrestrial effects. (auth)

42060 A PROPOSED POLAR AURORAL RADAR SYSTEM. Bates, Howard F. (Univ. of Alaska, College). J. Atmos. Terrest. Phys., 28: 903-7(Sept. 1966).

The position of the auroral belt can be reliably determined through the use of an h-f multifrequency backscatter sounder. Auroral echoes recorded at Thule show that aspect-sensitive auroral backscatter can be obtained from the south in the northern hemisphere. In comparing simultaneous Thule and College records, the auroral belt latitude data were found to be independent of the latitude of the auroral radar. It is proposed that one multifrequency h-f backscatter sounder installed at the north geomagnetic pole could provide real-time information on the position of the entire auroral belt around the northern hemisphere. (auth)

42061 ISOTOPIC COMPOSITION OF LITHIUM IN CHONDRULES. Dews, Jon R. (Univ. of California, Berkeley). J. Geophys. Res., 71: 4011-20(Aug. 15, 1966).

Trace quantities of Li in chondrules from the Bruderheim and Bjurböle meteorites were isolated by chemical procedures that yielded more than 90% of the Li in the sample. The isotopic composition of Li in two samples of Bruderheim chondrules and one sample of Bjurböle chondrules was measured on a 9-inch-radius-of-curvature, single-focusing mass spectrometer. The problem of mass fractionation which occurs during the mass analysis was solved by an integration procedure. The isotopic composition of Li from two samples of "whole-rock" Bruderheim and one sample of the granite G-1 was also measured for comparison. The $^7Li/^6Li$ ratios for the chondrules, whole-rock Bruderheim, and G-1 were found to be identical within 3.3% (at the 95% confidence level). The Li content of all the samples was determined by isotope dilution analyses of aliquots of each sample. The contents found were 0.404 ppm for whole-rock Bruderheim, 0.267 ppm for Bruderheim chondrules, 0.089 ppm for a large lath chondrule from Bruderheim, 0.134 ppm for Bjurböle chondrules, and 20.8 ppm for G-1. Blanks were less than 0.3% of the sample sizes in our experiments. A previous report of a 15% excess of ^6Li in the Bruderheim meteorite was confirmed. (auth)

42062 CONCENTRATION AND ISOTOPIC COMPOSITION OF LEAD IN TOLUCA IRON METEORITE. Ostic, Ronald G. (Univ. of California, San Diego, La Jolla). J. Geophys. Res., 71: 4060-3(Aug. 15, 1966).

Lead extracted from several Fe meteorites was found to be more radiogenic than can be accounted for by the amount of U and Th present. The Pb from one such meteorite, Toluca, was studied in several laboratories. An analysis of the data indicated that the isotopic composition

of the Pb was similar to that for Pb in Canyon Diablo, Burgavli, and Aroos troilites. (R.C.K.)

42063 INTERPRETATION OF PLASMA RESONANCES ON TOPSIDE IONOGRAMS. Wallis, G. (Heinrich-Hertz-Institut fuer Schwingungsforschung, Berlin). Monatsber. Deut. Akad. Wiss. Berlin, 6: 914-17(1964). (In German).

The singularity regions for the square of the refractive index were examined by the magnetoionic theory. These regions were then examined on a plot of the transmission frequency vs plasma frequency, both normalized by the gyrofrequency. The magnetoionic theory cannot explain the existence of characteristic spikes on the topside ionograms. Several discrepancies exist between intensities and width of the resonance lines which might be eliminated by detailed models for the boundary layers found by the Alouette satellite at 1000 km and their interaction with spiraling electrons. Alternately, the anharmonic parts of the electrons are produced by thermal motion, which is ignored in the magnetoionic theory; but the refractive index possesses singularities at harmonics of the gyrofrequency, when calculated by the kinetic theory using the linearized Boltzmann equation, if the propagation vector lies normal to the magnetic field. It appears difficult to distinguish between the two approaches experimentally. (BBB)

42064 COMPOSITION OF METEORITES. Vinogradov, A. P. (Vernadskii Inst. of Geochemistry and Analytical Chemistry, Moscow). Pure Appl. Chem., 10: 459-93 (1965).

A study of meteorites is presented. The topics discussed are: the composition and classification of meteorites; fractionation of the chemical composition of meteorites; products of cosmic irradiation of meteorites; meteorite composition with respect to meteorite belt material; origin of meteorites; and problems of cosmic chemistry in the immediate future. Tables are given of the chemical composition of chondrites, achondrites, feldspathic achondrites, stony-iron, and iron meteorites. The contents of alkali metals, alkaline earth metals, uranium, thorium, halides, sulfur, selenium, tellurium, heavy metals, platinoids, gold, and silver in various meteorites are given. (D.H.M.)

42065 ADVANCES IN IONOSPHERIC PHYSICS IN THE ROCKET AND SATELLITE ERA. Schmerling, E. R. (National Aeronautics and Space Administration, Washington, D. C.). Rev. Geophys., 4: 329-62(Aug. 1966).

With the systematic use of rockets and satellites, a great deal of progress has been made in increasing our knowledge and understanding of the ionosphere and the interaction of radio waves with a magnetoplasma. The major results obtained during the last six years are summarized. During this period, helium was found to be an important atmospheric constituent; topside sounders produced the first survey of the electron distribution above the peak of the F region; several types of plasma resonance were discovered; electron temperatures were observed to be systematically in excess of neutral temperatures, even at night; and new types of whistlers were observed. Steady progress was made in establishing the sources of ionization, from the cosmic rays effective below 70 km to the particular regions in the solar x-ray and uv emissions responsible for ionization at greater altitudes. Less progress has been made in understanding the mechanisms of electron loss, since uncertainties still exist about reaction rates, the role of minor constituents, and the contributions of electrodynamic transport. As a result of the observations made during the past six years, a new picture of the ionosphere is emerging which is very different from the old one of layers produced in an isothermal atmosphere by monochromatic radiation. Although the new picture is much more complicated, it is firmly based on observation, and it holds out a real hope that the solution of some outstanding problems is now within reach. (auth)

42066 WORLD WIDE SURVEY OF VERTICAL COSMIC-RAY CUTOFF RIGIDITIES DETERMINED BY THE TRAJECTORY-TRACING METHOD. Shea, M. A. (Cambridge Research Labs., Bedford, Mass.). 13p. (CONF-660411-28). ORAU. Gmelin, AED-CONF-66-060-61.

From American Physical Society Meeting, Washington, D. C.

Since the advent of high-speed digital computers, the trajectory-tracing process has been employed by several researchers to calculate the cutoff rigidity for specific locations of geophysical interest. Previously, because of the tremendous amount of computer time necessary, only a limited number of these trajectory-derived cutoff rigidities have been obtained and these were primarily used to correct presently published rigidity tables. This trajectory-tracing method, using the Finch and Leaton 6th-degree simulation of the quiescent geomagnetic field, was utilized to complete a uniform 15-degree world grid of vertical cutoff rigidities with a finer 5×15-degree grid in process. When cosmic-ray threshold rigidities interpolated from this grid are used to order cosmic-ray intensity data, good coherence of the data is obtained, even in magnetically anomalous areas. However, slight variations are indicative of the fact that a limitation of the usefulness of vertical cutoff rigidities was reached. (auth)

42067 THE WIND SHEAR THEORY OF THE FORMATION OF TEMPERATE ZONE SPORADIC E LAYERS. Axford, W. I. (Cornell Univ., Ithaca, N. Y.). 17p. (CONF-660439-2). ORAU. Gmelin, AED-CONF-66-063-2.

From Conference on Ground-Based Aeronomic Studies of the Lower Ionosphere, Ottawa, Ontario, Canada.

The wind shear theory provides the most attractive mechanism so far proposed for the formation of temperate zone blanketing sporadic E layers. The basis of the theory is outlined and a review is presented of some recent developments. (J.H.M.)

42068 STRUCTURE OF THE MAGNETOPAUSE CURRENT LAYER. Sonnerup, B. (Dartmouth Coll., Hanover, N. H.); Cahill, L. J. Jr. 17p. (CONF-660401-11). ORAU. Gmelin, AED-CONF-66-061-18.

From American Meteorological Society, American Geophysical Union, Annual Joint Meeting, Washington, D. C.

Explorer 12 magnetometer data are used to determine the magnetic field component perpendicular to the magnetospheric boundary, to study its magnetic structure and to calculate its attitude. A summary of the results show: (1) that the normal field component is, with a few notable exceptions, very small, (2) that two fundamentally different current layer structures exist, (3) that systematic deviations of the boundary shape occurs when the solar wind is not perpendicular to the dipole axis, and (4) that waves or bumps in the magnetospheric surface occur. (J.H.M.)

42069 PENETRATION OF SOLAR WIND PARTICLES INTO EARTH'S MAGNETOSPHERE. Yen, James T. (Catholic Univ. of America, Washington, D. C.). New York, American Inst. of Aeronautics and Astronautics, 1966, Preprint No. 66-510, 12p., $1.50. (CONF-660632-8). ORAU.

From American Inst. of Aeronautics and Astronautics, 4th Aerospace Sciences Meeting, Los Angeles, Calif.

An equation of Parker of the current density transverse to magnetic fields in a collisionless plasma is applied to the magnetopause. The basic mechanism is a "pressure drift," explained first by Spitzer for confined plasmas. By considering the magnetopause as a finite transition permeable to tangential pressure gradients, as supported by the IMP-1 data of Serbu, it is found that solar wind particles may enter the magnetosphere near the equatorial plane and near the neutral points, as well as at any point where this mechanism is effective. Such entrances are also substantiated by the IMP-1 data. [Space Res., 5: 564-74 (1965)]. (auth)

42070 STUDY OF BLANKETING SPORADIC E. Matsushita, S. 9p. (CONF-660401-8). ORAU. Gmelin, AED-CONF-66-061-15.

From American Meteorological Society, American Geophysical Union, Annual Joint Meeting, Washington, D. C.

The daytime behavior of mid-latitude sporadic E on magnetically quiet days is described as revealed by an

investigation of the fbEs values of 1958. The IGY data obtained at 80 stations are grouped and analyzed in terms of three longitudinal zones. The distribution of stations in the three zones is shown. The fbEs values on 15 magnetically quiet days in each season were averaged for each station at each hour. These average values are plotted as a function of dip latitude. Typical variations of fbEs with local time at different dip latitudes are presented and contours of equal fbEs values are shown in the local time vs. dip latitude domain. The frequency of occurrence of fbEs ≥ 2.0 mc/s was studied and data are presented. (J.H.M.)

Gravitation, Quantum Mechanics, and Relativity Theory

Refer also to abstracts 41643 and 41970.

42071 (JINR-P-2785) KLASSIFIKATSIYA SISTEM OBOBSHCHENNYKH VOLNOVYKH FUNKTSII, REALIZUYUSHCHIKH PREDSTAVLENIYA L(m,n) I P(m,n) GRUPP. (Classification of Systems of Generalized Wave Functions, Realizing the Representations of L(m,n) and P(m,n) Groups). Sheftel, M. B. (Joint Inst. for Nuclear Research, Dubna (USSR). Lab. of Theoretical Physics). 1966. 20p. Dep. mn.

The class of unitary irreducible representations of the groups L(m,n) and P(m,n) is considered which is dependent on one parameter only and realized in the eigenfunction space of the multidimensional Laplacian for the space R. The rules for constructing coordinate systems in R are formulated which are necessary for the classification of the basis functions corresponding to any given chain of subgroups and also the rules are formulated for constructing the system of the basis functions itself in these coordinates. The problem is discussed of the normalization of the basis by methods of the integral geometry. (auth)

42072 LORENTZ PRINCIPLE AND THE GENERAL THEORY OF RELATIVITY. PART I. HOMOGENEOUS PROPAGATION OF LIGHT. Janossy, L. (Central Research Inst. for Physics, Budapest). Acta Phys. Acad. Sci. Hung., 21: 1-15(1966).

The formulation of the general theory of relativity in terms of the Lorentz principle is attempted. The Lorentz transformation is generalized so as to be applicable to parts of space where light is propagated homogeneously but possibly unisotropically. It is shown that the Lorentz principle in its ordinary form remains valid for such regions. (auth)

42073 LORENTZ PRINCIPLE AND THE GENERAL THEORY OF RELATIVITY. PART II. INHOMOGENEOUS PROPAGATION OF LIGHT. Janossy, L. (Central Research Inst. for Physics, Budapest). Acta Phys. Acad. Sci. Hung., 21: 17-32(1966).

The generalization of the Lorentz transformation to regions where light is propagated inhomogeneously is given, and it is shown that the Lorentz principle can be maintained in its ordinary form provided the Lorentz transformation is taken in its more general form formulated for such regions. The well-known equations for the geodetic lines in a gravitational field are obtained from the Lorentz principle thus generalized. (auth)

42074 VARIATIONAL PRINCIPLE IN DESCRIBING A MANY-PARTICLE SYSTEM. Pompe, W.; Elk, K.; Macke, W. (Institut fuer Theoretische Physik, Dresden). Acta Phys. Acad. Sci. Hung., 21: 55-105(1966). (In German).

A general survey is given on applications of variational principles to the solutions of many body problems. Following a discussion of general conditions for the existence of variational principles their use in the classical equilibrium and nonequilibrium statistics is investigated. Methods for calculation of stationary and nonstationary quantum mechanical systems are summarized. Irreversible phenomena is described with the principle of the extremal entropy production. In particular, methods for solution of the Boltzmann equation are treated. (tr-auth)

42075 SPACE RELATIVITY: SPACE RESEARCH AND THEORY OF RELATIVITY. Ginzburg, V. L. (Lebedev Inst. of Physics, Moscow). Astronaut. Acta, 12: 136-52(Mar.-Apr. 1966).

Problems which are connected with the theory of relativity, and at the same time, with the use of rockets, satellites and space probes are discussed. The following questions are considered: experimental verification of the general theory of relativity, that is, of relativistic theory of the gravitational field; cosmological problem, which is closely related to the general theory of relativity; high-energy physics in the limits connected with the analysis of the existing concepts of the special theory of relativity, when they are applied to very small space-time regions or to particles with very large energy and momentum. In the field of verification of the general theory of relativity the most valuable satellite and probe experiments are observations of the relativistic precession of the axis of a gyroscope and, perhaps also, measurements of the relativistic effect of the turn of the perihelion of an artificial planet and extra eclipse observations of the deflection of light-rays in the sun's field. Cosmological interest is focused on mainly satellite measurements of the intensity of extra-galactic electromagnetic radiation in the microwave, infrared and visible portions of the spectrum, and also the far ultraviolet, x-ray and γ-ray portions. The use of heavy satellites is most promising (at least to the next decade) for the investigation of interactions between nucleons in the region of energies higher than $10^{11}-10^{12}$ ev and up to 10^{15} ev. (auth)

42076 THEOREM ON CANONICAL COMMUTATION AND ANTICOMMUTATION RELATIONS. Dell'Antonio, G.-F. (Institut des Hautes Etudes Scientifiques, Bures-sur-Yvette, France); Doplicher, S.; Ruelle, D. Commun. Math. Phys., 2: 223-30(1966).

The aim of this note is to characterize representations of the canonical commutation or anticommutation relations which, on a subspace of the "space of test functions," reduce to a sum of copies of the Fock representation. (auth)

42077 REPRESENTATION OF AN ELECTRON BY A CHARGED AND COHERENT FLUID, BOHR'S RELATION $\Delta E = h\nu$, AND THE DURATION OF THE QUANTUM TRANSITIONS. Fer, Francis (Institut de Physique Nucleaire, Orsay, France. Ecole des Mines, Paris). Compt. Rend., Ser. B, 263: 103-6(July 11, 1966). (In French).

A theoretical representation of the electron as a charged and coherent fluid is presented. Using this equation and the relation $\Delta E = h\nu$, an explanation of the dynamic quantum transitions is formulated. (G.O.Y.)

42078 EINSTEIN'S EQUATIONS AS DESCRIBING A MASSLESS TENSOR FIELD WITH SPIN 2. Ogievetskii, V. I.; Polubarinov, I. V. (Joint Inst. for Nuclear Research, Dubna, USSR). Dokl. Akad. Nauk SSSR, 166: 584-7 (Jan. 21, 1966). (In Russian).

The concept of the spin of an interacting field and the principle of limitation of the spin results in the reduction of classes of interacting spin 1 vector fields. In this connection, the theory of the interacting $h^{\mu\nu}$ spin 2 tensor field was examined. It was found that the equation of motion of this theory coincides with Einstein's gravitational field equations. In examining the minimal interaction theory of the tensor field, it was shown that in the case of a massless tensor field, the equation of motion coincides with Einstein's equations only in the case of one theory. The approach used for this study differed from that employed by Yang and Mills. (TTT)

42079 SPINOR CALCULUS IN RIEMANNIAN MANIFOLDS. Cap, F.; Majerotto, W.; Raab, W.; Unteregger, P. (Univ. of Innsbruck). Fortschr. Phys., 14: 205-33 (1966).

A general introduction of the spinor concept into the Riemannian space of general relativity is presented. Topics discussed are spinor calculus in Lorentz space, spinors in Riemannian space, transformation behavior

of spinors, applications, spin and angular momentum, and general remarks on conservation laws in general relativity. A survey of publications is also presented. (B.C.D.)

42080 DEVELOPMENT OF THE COVARIANT FORMULATION OF THE CONSERVATION LAWS OF GENERAL RELATIVITY. Davis, W. R.; Moss, M. K. (North Carolina State Univ., Raleigh). J. Math. Phys. (N. Y.), 7: 975-6(June 1966).

A method of obtaining Komar's covariant formulation of the conservation laws of general relativity directly from the variation of the scalar curvature density is presented. The procedure of obtaining this expression is free of the addition of arbitrary elements and only tensorial terms and operations are employed in the development. (auth)

42081 QUANTUM-MECHANICAL EXTENSION OF THE LEBOWITZ-PENROSE THEOREM ON THE VAN DER WAALS THEORY. Lieb, Elliott (Yeshiva Univ., New York). J. Math. Phys. (N. Y.), 7: 1016-24(June 1966).

Recently Lebowitz and Penrose gave a rigorous derivation of the van der Waals–Maxwell theory of the liquid-vapor transition, and showed how the Maxwell equal area-rule could be obtained from a proper statistical mechanical calculation. Their results are quite general—being valid in any number of dimensions and for a broad class of pair potentials—but they were proved only for classical mechanics. The proof is extended to quantum systems with any statistics—Boltzmann, Bose, or Fermi. One corollary of this extended theorem is a model of a Bose gas with a first-order phase transition. (auth)

42082 DERIVATION OF THE GENERALIZED BOLTZMANN EQUATION IN QUANTUM STATISTICAL MECHANICS. Morita, Tohru (Catholic Univ. of America, Washington, D. C.). J. Math. Phys. (N. Y.), 7: 1039-45 (June 1966).

The hierarchy of the equations of motion for the reduced density matrices in quantum statistical mechanics is solved and the (cumulant) reduced density matrices at a time t are expressed in terms of those at an earlier time t_0. Diagrams are introduced to express the results. With the aid of the technique of partial summations, the general term in the kinetic equation for the one-particle reduced density matrix or the generalized Boltzmann equation in quantum statistical mechanics is obtained. The equation is non-Markovian. A method of reducing the equation to Markovian is sketched. (auth)

42083 AN AXIOMATIC APPROACH TO THE FORMALISM OF QUANTUM MECHANICS. I. Prugovecki, Eduard (Princeton Univ., N. J.). J. Math. Phys. (N. Y.), 7: 1054-69(June 1966).

An axiomatic formulation of a quantum mechanical formalism is given. The formulation is not in terms of objects associated with the Hilbert space, but in terms of a different kind of objects for which the name "complex probability measures" has been chosen. It is shown that the conventional Hilbert-space formalism obeys the given axioms. A few consequences of the axioms are investigated. (auth)

42084 AN AXIOMATIC APPROACH TO THE FORMALISM OF QUANTUM MECHANICS. II. Prugovecki, Eduard (Princeton Univ., N. J.). J. Math. Phys. (N. Y.), 7: 1070-96(June 1966).

Another axiom has to be introduced to make the formalism given in Part I physically equivalent to the conventional Hilbert-space formalism. Then it is shown that, given a certain fundamental set of observables, a B*-algebra U can be built into which the set O_b of all bounded observables can be mapped injectively. The closure of the algebra generated by the image of O_b into U is U itself. A Hilbert space H exists into which the set S_0 of all pure physical states can be mapped injectively. The closure of the subset of H which is the image of this mapping is H itself. The algebra U can be mapped in such a fashion into the C*-algebra B(H) of all bounded observables that these mappings provide, essentially, just a translation of the original formalsim in a Hilbert-space formalism. (auth)

42085 DIRAC BRA AND KET FORMALISM. Roberts, J. E. (Emmanuel Coll., Cambridge, Eng.). J. Math. Phys. (N. Y.), 7: 1097-1104(June 1966).

The place of the Dirac formalism in quantum theory is investigated using rigged Hilbert spaces. Emphasis is laid on the representation of observables by continuous linear operators and on the existence of sufficient eigenkets. Using the concept of labeled observables, a canonical procedure is given for constructing a rigged Hilbert space and the bra and ket spaces are constructed for nonrelativistic quantum systems of n interacting particles. Spectral theory is investigated in this framework and the results are compared with the Dirac formalism. (auth)

42086 TOPOLOGY OF SOME SPHEROIDAL METRICS. Zipoy, David M. (Univ. of Maryland, College Park). J. Math. Phys. (N. Y.), 7: 1137-43(June 1966).

The solutions of Einstein's vacuum field equations, $R\mu\nu = 0$, are found when quasi-oblate and prolate spheroidal coordinates are used. The solutions for the "Newtonian" potential can be written as a linear combination of Legendre polynomides of integral order l. For oblate coordinates the solutions for each l have a ring singularity and have a double sheeted topology; one can get from one sheet to the other by going through the ring. When the $l = 0$ and $l = 1$ solutions are combined an infinite-sheeted topology results from the nonlinear character of the field equations. In general the geometry is asymptotically flat on only one sheet; on the others it is highly distorted. In some cases the region near the "ring singularity" opens out into a multisheeted infinite space. For the prolate coordinates the solutions contain a line singularity of finite length. In general, the prolate coordinate solutions are much less rich in varied topologies than are the oblate solutions. (auth)

42087 SOLUTION OF THE ELECTROMAGNETIC EQUATIONS FOR ROTATING SYSTEMS. Wolk, I.; da Costa, R. C. T. (Centro Brasileiro de Pesquisas Fisicas, Rio de Janeiro). Notas Fis., Cent. Brasil. Pesqui. Fis., 12: 1-11(1965).

The electromagnetic equations relative to a rotating system are introduced with the help of the space-time metric discussed by Kursonoglu, and its solution in the case of an electric current flowing parallel to the rotation axis is investigated. It was found that in the stationary case the rotation effects manifest themselves through a change in the argument of the Bessel function giving the radial solution, this change being absent for problems with cylindrical symmetry about the axis of rotation. However, in the time-dependent case even the symmetric solutions are modified, the Bessel functions being substituted by hypergeometric functions. The dependence in θ and z (the angular and axial coordinates) of the separated solutions is unaffected in all cases. (auth)

42088 INTERACTION OF THE GRAVITATIONAL AND SPINOR FIELDS. Oliveira, Colber G.; Vidal, Alberto (Centro Brasileiro de Pesquisas Fisicas, Rio de Janeiro). Notas Fis., Cent. Brasil. Pesqui. Fis., 12: 15-27(1965).

The interacting system of the gravitational and spinor fields is studied from the point of view of the three-dimensional geometry and under the condition that the gravitational field is a linear field (weak field approximation), the transformation law for the spinor field is then interpreted as a gaug ransformation in the three-dimensional hypersurface of constant time where the state of the system is given. An expression for a gauge invariant quantity involving the spinor field is derived; this expression is a linear functional of the spinor field. (B.G.D.)

42089 SYMMETRIZATION POSTULATE AND CLUSTER PROPERTY. Steinmann, O. (Institut des Hautes Etudes Scientifiques, Bures-sur-Yvette, France). Nuovo Cimento (10), 44A: 755-67(Aug. 1, 1966).

A quantum-mechanical system of identical particles is considered. It is shown that only totally symmetric or to

totally antisymmetric wave functions are compatible with the cluster property. As a consequence it follows that no particles with a statistical behavior different from that of ordinary bosons or fermions can exist. Para-fields can under certain conditions be used for the description of particles with an internal degree of freedom. Their use is then, however, optional. From a purely field-theoretical point of view there are no objections against the use of para-fields. (auth)

42090 IS THE HEISENBERG PICTURE BETTER THAN THE SCHROEDINGER PICTURE? Katz, A. (Weizmann Inst. of Science, Rehovoth, Israel). Nuovo Cimento (10), 44A: 871-6(Aug. 21, 1966).

In an infinite system of spins, it is shown that rotations may be represented equivalently in Schrödinger or Heisenberg picture. The operator of finite rotations which connects the two pictures acts over a nonseparable Hilbert space and is unitary. It is not however differentiable with respect to the angle of rotation. Consequently, infinitesimal rotations can only be described in the Heisenberg picture. It is argued that a similar case may arise concerning time development of a system of an infinite number of degrees of freedom. If it does, we have within a nonseparable Hilbert space unitarily equivalent Schrödinger and Heisenberg pictures. But differential equations of motion may be stated in the Heisenberg picture only, except in the subspace of "physical states." (auth)

42091 EQUILIBRIUM OF A LARGE ASSEMBLY OF PARTICLES IN GENERAL RELATIVITY. Bonazzola, S. (Univ., Rome); Pacini, F. Phys. Rev., 148: 1269-70 (Aug. 26, 1966).

A new approach to the problem of the equilibrium of a relativistic configuration is proposed, taking into account quantum-gravitational effects. This approach is based upon the quantization of the motion of the particles in the gravitational field. The case of an assembly of spinless particles is investigated by using the formalism of second quantization and starting from a Klein-Gordon equation which includes in the operator $\nabla_i\nabla^i$ the gravitational field. The mean values $\langle T_{ik} \rangle$ of the operator T_{ik} are computed. It is then possible to derive from the Einstein equations a system of differential equations which represents the equilibrium state for an assembly of a large number of particles. The corresponding problem for Fermi particles can be investigated in a similar way. (auth)

42092 SUM RULES FOR A GENERALIZED FREQUENCY DISTRIBUTION FUNCTION. Singwi, K. S.; Tosi, M. P. (Argonne National Lab., Ill.). Phys. Rev., 149: 70-2(Sept. 9, 1966).

The first few positive even moments of the Fourier transform of the velocity autocorrelation function of a particle in a condensed system are shown to be expressible in terms of thermal expectation values of the derivatives of the potential energy. (auth)

42093 THEORETICAL BASIS OF THE SYMMETRIZATION POSTULATE. Bros, J.; Messiah, A. M. L.; Williams, D. N. (Centre d'Etudes Nucleaires, Saclay, France). Phys. Rev., 149: 1008-9(Sept. 30, 1966).

The postulate of symmetrization for identical particles in quantum mechanics does not necessarily follow from the condition of the indistinguishability. Greenberg and Messiah have shown that, under suitable conditions, the selection rule implied by the postulate of symmetrization actually follows from the indistinguishability complemented by some broad assumptions about the quantum system. It is shown that the most restrictive of these extra assumptions, namely, PCT or time-reversal invariance, is unnecessary. (auth)

42094 GEOMETRY AND NEWTONIAN PHYSICS. Cohn, Jack (Univ. of Oklahoma, Norman). Phys. Rev., 149: 1040-3(Sept. 30, 1966).

The question is raised whether there is any physical content in the requirement that freely moving particles move along geodesics in 4-space. The question is partially answered in the affirmative by demonstrating that some motions cannot be expressed as geodesics in any 4-space under certain conditions. In particular, it is shown that the trajectories of the Newtonian equations of motion for any type of nonvanishing conservative force field cannot be expressed as geodesics in any static 4-space when it is required that the metric have the diagonal form (1, 1, 1, constant) at infinity. (auth)

42095 RADIATIVE CORRECTIONS TO HIGH-ENERGY INELASTIC ELECTRON SCATTERING. Henry, G. Reading (Harvard Univ., Cambridge). Contract AT(30-1)-2752. Phys. Rev., 149: 1217-19(Sept. 30, 1966).

Radiative corrections to inelastic electron scattering are estimated in terms of the inelastic form factors. The application of these corrections to experiments measuring these form factors is discussed briefly. (auth)

42096 RELATIVISTIC QUANTUM CONCEPT OF GRAVITATION. Sofonea, Liviu (Polytechnic Inst., Brasov, Romania). Studii Cercet. Mat., 17: 1089-1107(1965). (In Rumanian).

The various interpretations of gravitation according to the classic Newtonian theory and the general theory of relativity are examined from a historical perspective. The quantum theory of the gravitational radiation and problems connected with the quantizing of the gravitational field are considered, with special attention concerning the development of the unified field theory. The analogy with the quantized electromagnetic field concept during the first period of the development of the theory is pointed out. The phenomenological concept of the gravitational charge is discussed, setting it equal or closely related with the mass. This charge of elementary microparticles is much smaller than the electric or meson charges but it is physically present. On the other hand, gravity plays an important role for macroscopic bodies, as in the case of celestial mechanics. The probability of gravitational transformations increases rapidly with energy; for $E = 10^{21}\ mc^2$ it is of the order of magnitude of electromagnetic forces. The emerging electric–gravitational–mesodynamic–atomistic theory suggests a generalized structure of matter based on quantized fields and interchangeable microparticles. (TTT)

42097 ACCURATE AND STABLE NUMERICAL SOLUTIONS TO THE SCHROEDINGER EQUATION. Rouse, Carl A. (Naval Research Lab., Washington, D. C. Univ. of California, Berkeley). 52p. (CONF-660411-26). ORAU. Gmelin, AED-CONF-66-060-67.

From American Physical Society Meeting, Washington, D. C.

A new method is presented for accurate and stable numerical solutions of ordinary differential equations. Applied to the Schrödinger equation, the basic numerical equations are two simultaneous Taylor expansions between space steps of both the wavefunction ($R(\rho)$), and the slope of the wavefunction ($m(\rho)$). The present results represent the accurate and stable numerical solutions of the radial hydrogenic Schrödinger equation. With the ability to calculate eigenvalues to nine or more significant figures and eigenfunctions to nine or more decimal places, the method becomes an alternative to perturbation and variational methods. (auth)

42098 REVISED MECHANICS. Selzer, Adolph. 60p. (CONF-660440-1). ORAU. Gmelin, AED-CONF-66-106-3.

From American Physical Society, New England Section, Spring Meeting, Providence, R. I.

It is shown that the Einstein theory led to the clock paradox, due to the fact that the four-dimensional space, which is only a convenient geometrical model in practical cases, cannot be taken literally. A correct theory can only be established through a rigorous postulation of the absolute character of energy. It is shown that the equivalence of mass and energy follows from the conservation laws a priori. The important mass formula and the velocity-addition theorem are derived by pure mechanical considerations. The mass formula leads to a second kind of mass which has a speed higher than the speed of light. Together with a corresponding momentum equation it represents the

basic concept for the establishment of quantum mechanics in terms of determinism. A rigorous examination of the Schroedinger wave is made which shows that this wave can be given a realistic meaning. (W.D.M.)

Low Temperature Physics

Refer also to abstracts 41378, 41727, 41760, 42523, 42531, and 42534.

42099 (AD-636625) EFFECTS OF DESOLVATION OF A Pb-Sb ALLOY ON THE CRITICAL CHARACTERISTICS OF SUPERCONDUCTORS. Chang, Che-ray; Tsao, Shao-wen; Guan, Wein-yen. Translated from Wu Li Hsueh Pao, 20: 568-70(1964). 9p. (FTD-TT-65-887). CFSTI $1.00 cy, $0.50 mn.

The effects of desolvation of a Pb–Sb alloy on the $j_c(H)$ curve were considered. It was shown experimentally that the high critical fields of superconductors in strong magnetic fields and their high current densities have entirely different origins. (M.O.W.)

42100 EXPERIMENTS ON THE PROPAGATION OF NORMAL REGION IN A SUPERCONDUCTING MAGNET. Shimamoto, Susumu; Todoriki, Itaru; Ushio, Kazuhiro; Ohtsuki, Soji. Denki Shikensho Iho, 30: 417-26(May 1966). (In Japanese).

The propagation of a normal region at the quenching of a superconducting magnet was investigated in a Nb–25% Zr solenoid. For the purpose of measuring the initiation and propagation of a normal region, taps were attached to the solenoid and the voltages between them were measured during the s-n transition. The quantitative analysis revealed that the normal region appeared in the innermost layer in most cases and that the propagation was three-dimensional. (auth)

42101 SUPERCONDUCTIVITY OF LaAg. Chao, C. C. (California Inst. of Tech., Pasadena); Luo, H. L.; Smith, T. F. J. Phys. Chem. Solids, 27: 1555-7(Sept. 1966).

The intermetallic compound LaAg was found to become superconducting at 0.9°K. The pressure dependence of the superconducting transition was correlated with the La–La nearest-neighbor separation. (P.C.S.)

42102 SPIN-LATTICE RELAXATION IN DIRTY SUPERCONDUCTING ALLOYS IN HIGH FIELDS. Cyrot, Michel (Faculte des Sciences, Orsay, France). J. Phys. (Paris), 27: 283-6(May-June 1966). (In French).

Spin lattice relaxation time of a dirty type II superconductor in the mixed state for fields close to the upper critical field H_{c2} is discussed. This relaxation time is space varying and to order $|\Delta|^2$ depends only on the local value of the order parameter $\Delta(r)$. $T_1(r)$ as a function of the local magnetic field is derived and the space average $\langle T_1(r)\rangle$ is shown to be smaller than the normal relaxation time for $0.6\ T_c < T < T_c$. (auth)

42103 DISTRIBUTION OF NORMAL REGION AFTER S-N TRANSITION IN A SUPERCONDUCTING MAGNET. Shimamoto, Susumu; Ushio, Kazuhiro (Electrotechnical Lab., Tokyo). Jap. J. Appl. Phys., 5: 836-7(Sept. 1966).

The distribution of the normal region in a superconducting solenoid after quenching was measured by varying the quenching current. A heater on the inside layer of the solenoid was used for quenching. It was found that after quenching the normal region disappeared in the inside part and remained in the middle part of the solenoid. The solenoid had 4953 turns of Nb–25% Zr wire (0.254 mm) coated with 0.03 mm copper and insulated with epoxy enamel. (W.D.M.)

42104 SUPERCONDUCTING FOCUSING SYSTEMS IN HIGH-ENERGY PHYSICS. Smith, P. F.; Haskell, G. P. (National Inst. for Research in Nuclear Science, Chilton, Eng.). Nucl. Instrum. Methods, 43: 285-97(Aug. 1966).

Optimized focusing systems using superconducting and conventional quadrupoles are compared, with particular reference to particle beams in the momentum range 1 to 1000 Bev/c. It is shown that, provided certain limitations in superconductor technology can be overcome, high field superconducting lenses could make possible order-of-magnitude reductions in the cost of focusing high energy beams and at the same time allow substantially shorter object-to-image distances than those which are practicable with conventional quadrupoles. A detailed analysis of focusing systems using superconducting solenoids, suggests that in general the latter should become competitive with quadrupoles for beam divergences of 0.1 rad or greater. Beam transport systems are considered separately and it is shown that in a freely designed system conventional quadrupoles should maintain their superiority at all energies; however, any restrictions on length, periodicity or maximum aperture, will increasingly favor the use of superconducting quadrupoles for transport of particles at the higher energies. Transport systems using solenoids or beam guides do not appear to be generally competitive, but may have special applications to low momentum, large divergence beams, if the latter cannot conveniently be matched into a quadrupole system. (auth)

42105 IMPROVEMENT OF SURFACE CONDUCTIVITY OF COPPER AND ALUMINUM AT HIGH-FREQUENCIES, BY LOWERING OF TEMPERATURE. Biquard, F.; Septier, A. (Faculte des Sciences, Orsay, France). Nucl Instrum. Methods, 44: 18-28(Sept. 1966). (In French).

Experimental results are given for copper and aluminum microwave resonant cavities in S band and L band. The experimental gain on surface conductivity between room temperature and liquid helium temperature is 5.6 for copper and 7.4 for aluminum at a frequency of 3160 MHz. At 1420 MHz 5.3 is found for copper and 7.8 for aluminum. (M.O.W.)

42106 INEXPENSIVE LIQUID NITROGEN LEVEL CONTROL FOR COLD TRAPS. Perdue, P. T. (Oak Ridge National Lab., Tenn.). Nucl. Instrum. Methods, 44: 169-70(Sept. 1966). (ORNL-P-2236).

A circuit diagram is given for maintaining the liquid nitrogen level in cold traps for long periods of time. (M.O.W.)

42107 A LIQUID ^{3}He TARGET FOR HIGH ENERGY NUCLEAR EXPERIMENTS. Modena, I.; Montelatici, V.; Scaramuzzi, F. (CNEN, Frascati, Italy). Nucl. Instrum. Methods, 44: 175-8(Sept. 1966).

A liquid ^{3}He target was constructed for experiments of ^{3}He photodisintegration using the γ beam of the Frascati 1.1-Bev electron synchrotron. The cryostat is a development of a standard hydrogen–deuterium target in use with the Frascati electron synchrotron. The cryostat is described. (M.O.W.)

42108 SUPERCONDUCTING MEMORIES. Caswell, H. L. (International Business Machines Corp., Yorktown Heights, N. Y.). Onde Elec., 46: 635-42(June 1966). (In French).

The results of investigations on cryotrons are summarized with special attention being given to one type of cryotron memory, i.e., the cryogenic associative memory, and to one type of random access memory: the cryogenic continuous film memory. (auth)

42109 SUPERIMPOSED NORMAL AND SUPERCONDUCTING FILMS. I. TUNNELING CHARACTERISTICS IN ZERO FIELD. Guyon, E.; Martinet, A.; Mauro, S.; Meunier, F. (CNRS, Orsay, France). Phys. Kondens. Mater., 5: 123-40(1966).

Tunneling characteristics dI/dV were taken on both sides of "dirty" In–Bi/Zn superimposed films, the temperature T being such that In–Bi was superconducting and Zn normal. Most of the attention was devoted to the region $T \sim T_c$ where the experimental curves can be compared with a reasonably accurate microscopic theory. Reasonable agreement was found for the voltage scale and, more important, for the amplitude of the effects in the superconducting phase. (auth)

42110 ELECTRONIC EXCITATIONS IN A CLEAN TYPE-II SUPERCONDUCTOR IN HIGH FIELDS: TUNNEL EFFECT AND NUCLEAR RELAXATION. Phys. Kondens. Mater., 5: 141-56(1966). (In French).

Some properties of fermion-type excitations in a clean type II superconductor near the upper critical field are discussed. This situation is "ergodic" in the sense introduced by de Gennes and Tinkham. This ergodic behavior (in the absence of collisions) is due to the variations of the phase of the order parameter along a one-electron trajectory in a vortex lattice. The energy spectrum shows no gap, but is more singular than for "dirty" superconductors. The singularity stems from the electrons with paths nearly parallel to the field H. In tunnel experiments it was found that the singularity in the density of states is made weaker by the existence of diffuse scattering at the junction surface. The experiment was carried out on lead for $H \sim H_{c3}$ and gives qualitative agreement with the theoretical predictions. Nuclear relaxation rates are shown to depend sensitively on the bulk density of states. Effects related to the existence of an anisotropic Fermi surface are discussed. The latter may be interesting since the low-energy excitations have their velocity parallel to H. (auth)

42111 NEW, ATTENUATED WAVE MODE IN He II FILMS. Pollack, Gerald L. (Michigan State Univ., East Lansing). Contract AT(11-1)-1574. Phys. Rev., 149: 72-6(Sept. 9, 1966).

It is shown that if normal-fluid motion with a viscous force is allowed in He II films, then a new wave mode is predicted by the equations of motion. The film is described here by four equations: conservation of mass, conservation of energy, the usual superfluid thermohydrodynamic equation, and the normal-fluid equation with a viscous force per unit volume. The viscosity term is $\omega\rho r v_{nx}$, in which v_{nx} is the velocity of the normal fluid, ρ is the bulk helium density, ω is the angular frequency of the wave, and r is a dimensionless viscosity parameter. Two nontrivial wave modes are allowed: One corresponds to third sound, with a comparatively small attenuation, and the other is the new mode. Both modes are simultaneously waves in local film height, local film temperature, and superfluid and normal-fluid velocity. The new mode is heavily overdamped with an attenuation that rises from about 400 cm^{-1} at $r = 10^{-2}$, to about 10^4 cm^{-1} at $r = 10^3$, for waves of 10^3 cps in a 250 Å film. The velocity of the mode decreases with temperature in an interesting way: The maximum velocity at 1.2°K is about 900 cm/sec, at 2.0°K about 160 cm/sec, and at 2.15°K about 60 cm/sec. It is shown that these attenuations and velocities are of the same kind as have recently been observed as anomalies in third sound. It is suggested that this new mode is generally excited along with third-sound waves and that normal fluid can move in He II films. (auth)

42112 COMPRESSIBILITY OF LIQUID ^{4}He AS A FUNCTION OF PRESSURE. Grilly, E. R. (Los Alamos Scientific Lab., N. Mex.). Contract W-7405-Eng-36. Phys. Rev., 149: 97-101(Sept. 9, 1966). (LA-DC-7729).

The compressibility, $\beta = -(1/V)(\partial V/\partial P)_T$, of liquid ^{4}He was measured from 1 atm to the melting pressure and between 1.6 and 2.5°K. ΔV and ΔP were determined from deflections of the cell walls. The normal decrease of β with increasing P was observed except in an area below the λ line. For an isotherm crossing the λ line, β showed a minimum at $P < P_\lambda$ and a peak at P_λ. The minimum also occurred between the lowest T_λ (1.76°K) and 1.70°K. The variation of β with P near P_λ, relative to β at 2.20°K, followed an equation of the form $\beta_T - \beta_{2.2} = a - b \log |P - P_\lambda|$, where a and b for $P < P_\lambda$ are greater than a and b for $P > P_\lambda$. Between the T limits of the λ line, $(\partial\beta/\partial T)_P$ was definitely negative for P just above P_λ, but it approached zero for $P \gg P_\lambda$. (auth)

42113 EFFECT OF ATTRACTIVE FORCES ON THE SOLID-SUPERFLUID TRANSITION IN ^{4}He AT ABSOLUTE ZERO. Fernandez, J. F.; Gersch, H. A. (Georgia Inst. of Tech., Atlanta). Phys. Rev., 149: 154-64(Sept. 9, 1966).

The effect of attractive interactions between helium atoms on the solid-superfluid transition in ^{4}He at absolute zero is considered. It is found that the density of the solid-superfluid transition does not depend on the strength of the attractive interactions, but only on the mass of the particles and the strength of the repulsive interactions. The density at which the system reaches zero pressure increases with increasing strength of attractive forces, so that sufficiently large attractive forces can inhibit the transition. Quantitative estimates and comparisons are made of the zero-pressure density and of the transition density, for different masses and for different strengths of attractive interactions. (auth)

42114 CRITICAL CURRENTS IN THE SUPERCONDUCTING SURFACE SHEATH. Barnes, L. J.; Fink, H. J. (Atomics International, Canoga Park, Calif.). Contract AT-(11-1)-GEN-8. Phys. Rev., 149: 186-91 (Sept. 9, 1966).

Results are presented of magnetization measurements on Pb–Tl cylinders in axial magnetic fields of such magnitude that superconductivity is confined to the superconducting surface sheath. Specimens whose Ginzburg-Landau κ values range from 0.6 to 1.4 were investigated. For these cylindrical specimens a nonzero magnetization exists beyond the upper critical field H_{c2} up to a field H_{c3} (1.7 to 1.75 H_{c2}) identifiable with the surface nucleation field (1.695 H_{c2}). Evidence is presented that indicates the observed magnetization results from partial shielding of the interior of the cylinders by critical currents induced in the multiply connected surface sheath. Our experimental results are in quantitative accord with recent theoretical calculations of Fink and Barnes concerning the influence of critical sheath currents on the effective bulk-magnetization characteristics of a cylinder. It is observed that diamagnetic ($M < 0$) and paramagnetic ($M > 0$) shielding occur in uniformly increasing and decreasing fields, respectively, which is consistent with the existence of a multiconnected superconducting region which can carry a total current. The surface localization of the superconductivity involved is demonstrated by the proximity effects of electroplated normal metals on the specimens. Cu plating reduces both the magnetization and H_{c3} (~1.4 H_{c2}). Owing, perhaps, to their magnetic properties, electroplated Ni and Cr have a much more drastic effect than electroplated Cu. To the limit of experimental sensitivity, all traces of superconductivity above H_{c2} are removed by Ni and Cr platings. (auth)

42115 LOW-TEMPERATURE THERMODYNAMIC PROPERTIES OF VANADIUM. I. SUPERCONDUCTING AND NORMAL STATES. Radebaugh, Ray; Keesom, P. H. (Purdue Univ., Lafayette, Ind.). Phys. Rev., 149: 209-16(Sept. 9, 1966).

The specific heat of vanadium (resistivity ratio = 140) was measured in the superconducting and normal states between 0.5 and 5.4°K. The normal-state specific heat is given by $C_n = 9.82T + 0.035T^3 + C_{nuc}$ mJ $mole^{-1}$ deg^{-1}, where the term C_{nuc} arises from the interaction of the nuclear magnetic moments with the applied magnetic field. The coefficient of the cubic term corresponds to a Debye temperature θ_0 at 0°K of (382 ± 10)°K, which is slightly less than the value 399.3°K obtained from elastic measurements. The superconducting specific heat contains a term linear in T which is 0.52% of the normal-state linear term. This indicates the presence of a very small energy gap at the Fermi surface in addition to the normal gap. At all but the lowest temperatures the specific heat is governed by the normal energy gap and is in fair agreement with the BCS prediction. The agreement becomes excellent if the normal energy gap is assumed to be anisotropic with a maximum value of $3.52kT_c$ and a maximum of $3.20kT_c$, which is consistent with ultrasonic measurements. The superconducting transition temperature for this sample is (5.379 ± 0.004)°K with a total transition width of only about 1 mdeg. The intrinsic transition temperature for vanadium is estimated to be (5.414 ± 0.010)°K. (auth)

42116 LOW-TEMPERATURE THERMODYNAMIC PROPERTIES OF VANADIUM. II. MIXED STATE. Radebaugh, Ray; Keesom, P. H. (Purdue Univ., Lafayette, Ind.). Phys. Rev., 149: 217-31(Sept. 9, 1966).

The specific heat of a single-crystal vanadium sample (resistivity ratio = 140) has been measured in 12 different magnetic fields between 0.5 and 5.4°K to study the mixed

state. The specific heat above approximately H_c is found to be independent of sample history, which leads to a complete thermodynamic description of the mixed state. The upper critical field $H_{c2}(t)$ is found from the specific heat at high fields and from heating and cooling curves at low fields and is used with $H_c(t)$ determined from specific-heat measurements in part I of this investigation to obtain the parameter $\kappa_1(t) = H_{c2}(t)/\sqrt{2}H_c(t)$. The Ginzburg-Landau parameter $\kappa \equiv \kappa_1(1)$ is found to be 0.979 ± 0.010 for this sample and, when extrapolated to infinite electron mean free path, yields the value $\kappa_0 = 0.848 \pm 0.015 > 1/\sqrt{2}$, which proves that vanadium, like niobium, is an intrinsic type-II superconductor. The behavior of $\kappa_1(t)/\kappa$ for vanadium is shown to be nearly identical to that for niobium and is higher at all temperatures than the theoretical prediction of Gor'kov. In particular $\kappa_1(0)/\kappa$ is 1.50 ± 0.02 compared with the theoretical value 1.25, which points out the need for a refinement of the theory concerning intrinsic type-II superconductors. Magnetization curves are thermodynamically deduced from the specific-heat data and are used to find $H_{c1}(t)$, given by $1150(1 - t^2)$ Oe. In addition the curves appear to represent the average behavior of actual magnetization measurements in increasing and decreasing fields. The parameter $\kappa_2(t)$ calculated from the slopes of the deduced magnetization curves is in excellent agreement near t = 1 with the prediction of Maki and Tsuzuki, and at low temperatures approaches the value $\kappa_2(0)/\kappa = 2.66$. A reliable estimate of the Fermi-surface area, given by S/Sf = 0.714, is obtained from the value of κ_0, which then leads to the values $\lambda_L(0) = 398$ Å, $\xi_0 = 450$ Å, and l = 2450 Å. (auth)

42117 SUPERCONDUCTING PROPERTIES OF HIGH-PURITY NIOBIUM. Finnemore, D. K.; Stromberg, T. F.; Swenson, C. A. (Ames Lab., Ames, Iowa). Phys. Rev., 149: 231-43(Sept. 9, 1966). (IS-1194).

Precision magnetization data are given for high-purity niobium metal samples (resistance ratio $R_{300}/R^N_{4.2} = 1600 \pm 400$) over the range from 1.1°K to $T_c = 9.25$ (±0.01)°K. The thermodynamic critical-field curve, which is parabolic to 1%, is that to be expected for an intermediate-coupling superconductor. The magnetization curves are qualitatively like those associated with a type-II superconductor with $\kappa \sim 1$, but the detailed shape does not follow any theory. In particular, the magnetization increases linearly with a slope of 23 G/Oe from 1.005 H_{c1} to 1.025 H_{c1}, where a sharp break occurs to a smaller slope. The magnetization data at H_{c1} and in the region of H_{c2} are consistent with published specific-heat data. The magnitudes of H_{c2} and H_c are consistent with measured values of the penetration depth λ. Preliminary data are reported for H_{c3} as obtained from both resistive and a-c susceptibility measurements. (auth)

42118 EFFECT OF LOW-TEMPERATURE STRUCTURAL TRANSFORMATION ON ^{51}V KNIGHT SHIFTS AND ELECTRIC FIELD GRADIENTS IN V_3Si. Gossard, A. C. (Bell Telephone Labs., Murray Hill, N. J.). Phys. Rev., 149: 246-51(Sept. 9, 1966).

The nuclear magnetic resonance of ^{51}V in V_3Si has been observed in the presence of the low-temperature V_3Si structural transformation. Both the nuclear-electric-quadrupolar interactions and the Knight shift of the field for resonance are affected by the transformation, with two distinguishable vanadium sites evolving. The nuclear resonance resolves values of $e^2qQ = 2.674$ MHz and 3.262 MHz and Knight shift 0.41% and 0.45% for field perpendicular to the vanadium symmetry axis for the two sites, respectively. The changes result from changes in the electronic structure, the observed field-gradient change being some sixty times greater than the relative change in the point-charge contribution to the field gradient. The measurements were made in polycrystalline material, and present a means of detecting structural transformations in polycrystalline metals. The effects of possible further distortions within the unit cell are considered. (auth)

42119 RULES FOR THE ENERGY GAP AND CRITICAL FIELD OF SUPERCONDUCTORS. Sheahen, Thomas P. (Massachusetts Inst. of Tech., Cambridge). Contract SD-90. Phys. Rev., 149: 368-70(Sept. 9, 1966).

Two simple empirical rules are given by which to characterize the energy gap and critical field of most superconductors: for the reduced energy gap δ, $[\Delta(T)/\Delta(0)]^2 \equiv \delta^2 = \cos(\pi t^2/2)$, where $t = T/T_c$; and for the reduced critical field h, $h + D_0 \sin\pi h = 1 - t^2$, where D_0 is the maximum deviation from a parabola. An improved method of extrapolating critical-field data to 0°K is described. (auth)

42120 EFFECTIVE INTERACTION STRENGTH IN SUPERCONDUCTORS. Sheahen, Thomas P. (Massachusetts Inst. of Tech., Cambridge). Contract SD-90. Phys. Rev., 149: 370-7(Sept. 9, 1966).

A semiempirical extension of the BCS model to intermediate- and strong-coupling superconductors is used to derive a set of simple rules by which the following thermodynamic quantities can be related to one another: the absolute-zero energy gap $2\Delta_0$; the critical field H_0; the critical temperature T_c; the jump ΔC in specific heat at T_c; and the slope at T_c of the critical-field curve, $(dh/dt)_1$. The procedure determines an "effective interaction strength" N_0V^* (larger than the value of N_0V obtained from T_c/Θ_D) for each superconductor. A "temperature-variation" of this N_0V^* is the major departure from the original BCS model. N_0V^* is obtained for 9 superconductors from their specific-heat jumps, and used to predict values of the ratios $(dh/dt)_1$, Δ_0/kT_c, and $\gamma T_c^2/V_m H_0^2$ which agree well with experiment. The resulting values for the "effective cutoff" Θ_c lie close to $\Theta_D/9$. (auth)

42121 SUPERCONDUCTIVITY AND ELECTRONIC SPECIFIC HEAT IN THE SCANDIUM–ZIRCONIUM SYSTEM. Jensen, M. Anthony (Univ. of California, San Diego, La Jolla); Maita, J. P. Phys. Rev., 149: 409-14 (Sept. 9, 1966).

An investigation of the superconducting transition temperature and the electronic specific heat for the alloy system scandium–zirconium is reported. The results show that the alloys with the largest electronic specific heats are not superconducting down to 0.03°K. When compared with the other early transition metals (those with less than half-filled d shells), the data for this system indicate a sharp decrease in the strength of the net attractive electron-electron interaction as one decreases the number of d electrons (i.e., moves from zirconium to scandium). This behavior, combined with the apparently large exchange enhancement of the spin susceptibility in pure Sc, is very similar to the recently reported behavior near the filled end of the transition metals (i.e., near Pd). It is suggested that the proximity of a d-band edge may be causing the anomalous behavior in the superconductivity and the spin susceptibility for both regions of the transition metals. (auth)

42122 SUPERFLUID DENSITY AND SCALING LAWS FOR LIQUID HELIUM NEAR T_λ. Tyson, J. A. (Univ. of Chicago. Univ. of Wisconsin, Madison); Douglass, D. H. Jr. Phys. Rev. Lett., 17: 472-8(Aug. 29, 1966).

The superfluid density near T_λ is found to vary as $(T_\lambda - T)^\zeta$, where $\zeta = 0.666 \pm 0.006$, and the Josephson relation between the specific heat and the superfluid density is tested experimentally. It is shown that, assuming the Widom-Kadanoff scaling laws, the superfluid coherence length varies as $(T_\lambda - T)^{-\zeta}$. (auth)

42123 POTENTIAL ENERGY INTEGRALS FOR NON-OVERLAPPING ATOMIC WAVE FUNCTIONS. Roberts, P. J. (Univ. of Glasgow). Proc. Phys. Soc. (London), 89: 265-72(1966).

An analysis is presented of the potential energy integrals arising from the Einstein model of the solid inert gases at absolute zero. In this model two spherically symmetric nonoverlapping charge distributions of arbitrary form interact via an arbitrary two-body central potential. (auth)

42124 SUPERCONDUCTING CONTACT BETWEEN LEAD BASED AND NIOBIUM BASED ALLOYS. Carroll, K. J.; Laquer, H. L. (Los Alamos Scientific Lab., N. Mex.). Contract W-7405-eng-36. Rev. Sci. Instrum., 37: 1270(Sept. 1966). (LA-DC-7881).

A superconducting contact which is capable of carrying a persistent current of 30 amps in a field of about 100 G, for joining wires of Nb–Zr and Pb–Sn in a closed superconducting loop is described. The construction of this contact is discussed. (J.F.P.)

42125 LOW-FREQUENCY TRANSITIONS AND CRITICAL CURRENTS IN THE SUPERCONDUCTING SURFACE SHEATH. Rollins, R. W.; Silcox, J. (Cornell Univ., Ithaca, N. Y.). Solid State Commun., 4: 323-7(July 1966).

Direct observations of the waveform corresponding to the penetration of small, low-frequency a-c magnetic flux into a type II superconductor in superconducting sheath state were made. The model suggested by these experiments is confirmed by further measurements of the complex permeability and consistent with previous experiments. (auth)

42126 DE HAAS-VAN ALPHEN OSCILLATIONS IN THE CRITICAL TEMPERATURE OF TYPE II SUPERCONDUCTORS. Gunther, Leon (Tufts Univ., Medford, Mass.); Gruenberg, Leonard W. Solid State Commun., 4: 329-31 (July 1966).

It was demonstrated that the critical temperature $T_c(H)$ of a type II superconductor exhibits dHvA oscillations with the usual period μ/ω_c, where μ is the Fermi energy and $\omega_c = eH/mc$ is the cyclotron frequency. The result includes electron spin and is valid even outside the Ginzburg-Landau region. The feasibility of observing the effect at low temperatures through the oscillations of the resistivity in the transition region is demonstrated. (auth)

42127 SHIELDING PROPERTIES OF THE SUPERCONDUCTING SURFACE SHEATH. Fischer, Gaston; Klein, Rudolf; McEnvoy, J. P. (RCA Labs. Ltd., Zurich). Solid State Commun., 4: 361-5(July 1966).

Properties of the surface sheath of type I ($\kappa > 0.42$) and type II superconducting plates ($1/\sqrt{2} < \kappa < 2$) in a parallel magnetic field are investigated. It is shown that the changing external magnetic field induces currents in the surface sheath that lead to hysteretic behavior in the real part of the surface impedance R as a function of the applied field. The shielding of the bulk is most pronounced near the thermodynamical critical field H_c. The shielding properties in decreasing field seem to break down at H_c, even in type-II material with κ below a critical value. In an increasing field the bulk type I superconductor remains ideally diamagnetic up to a field higher than H_c. (auth)

42128 SOUND DISPERSION IN SUPERCONDUCTORS. Balkarei, Yu. I. (Lebedev Inst. of Physics, Moscow). Soviet Phys.-Solid State (Engl. Trans.), 8: 640-2(Sept. 1966).

Translated from Fiz. Tverd. Tela, 8: 797-801(Mar. 1966).

It is shown that for sound propagation in a superconductor in a narrow spectral region, when the wavelength is close to the size of a Cooper pair, there is a deviation from a linear dispersion law. (auth)

42129 ELECTRONIC MECHANISM OF SUPERCONDUCTIVITY. Geilikman, B. T. (Inst. of Physico-Technical, Moscow). Usp. Fiz. Nauk, 88: 327-45(Feb. 1966). (In Russian).

The feasibility is considered of superconductors having higher critical temperatures than are presently attainable. It is shown that a pure electronic mechanism leading to high critical temperatures, can exist in principle in the case of ordinary three-dimensional metals. Special attention is paid to two models: (1) a pure transition-group metal with two overlapping unfilled bands (or an ordered alloy of a metal with another metal (compound) with comparable concentrations of the two components and identical structure of the electron spectrum), and (2) an ordered alloy of a metal with a nonmetal, with comparable component densities, in the case when the electrons of the upper unfilled band of the shell of the nonmetal atom are not collectivized. The theoretically feasible critical temperature for the first model is found to be of the order of 100 to 1000°K. The conditions for appearance of superconductivity in the second model are more stringent. The Green's function and the energy gaps for the electrons for the case of free s electrons and strongly bound d or f electrons are calculated. (ATD)

42130 CONTAINMENT OF A SUPERCONDUCTING SPHERE BY A SYSTEM OF CIRCULAR CURRENTS. Beloozerov, V. N. Zh. Tekh. Fiz., 36: 852-9(May 1966). (In Russian).

The forces on a superconducting sphere due to the magnetic field of a system of circular windings are discussed. The sphere is assumed to be small compared with the radii of the windings. The potential energy of the sphere in the magnetic field is then equal to the scaler product of the magnetic moment of the sphere and the magnetic field strength, and is thus proportional to the square of the field strength. It is shown that the superconducting sphere can be supported against gravity by a single horizontal circular winding provided it is neither too heavy nor too light (for a given value of the current in the winding). If the sphere is too light it rises into a region where it is laterally unstable and falls off to the side. An arbitrarily light sphere can be stably supported by a system of two or more parallel coaxial circular windings, but the "rigidity" (second derivative of the potential energy at the equilibrium position) of such a system cannot be the same in all directions. Equal rigidity in all directions can be achieved by employing three mutually perpendicular systems of two parallel circular windings each. The forces on a superconducting sphere of finite radius due to the magnetic fields of circular windings are discussed briefly. Account is taken of the changes in the currents in the windings due to the motion of the sphere. (ATD)

42131 RF RESIDUAL LOSSES IN SUPERCONDUCTORS. Haden, C. Roland; Victor, Joe M.; Hartwig, William H. (Univ. of Texas, Austin). 8p. (CONF-660421-2). ORAU. Gmelin, AED-CONF-66-065-8.

From 18th Annual Southwestern IEEE Conference and Show, Dallas.

A study of the r-f residual losses in superconductors was made through use of a high Q resonant cavity in the frequency range 20 to 350 MHz. Results showed that the residual loss in tin with indium impurities and for other materials examined was hysteretic in nature. A model is proposed and compared with experimental results. (W.D. M.)

42132 MAGNETIC FLUX PENETRATION IN HARD SUPERCONDUCTING PLATES. Fast, R. W.; del Castillo, G. 5p. (CONF-660411-32). ORAU. Gmelin, AED-CONF-66-060-72.

From American Physical Society Meeting, Washington, D. C.

In order to more fully understand the difficulties encountered in shielding of magnetic fields with superconducting surfaces, the flux penetration in several type II superconductors was investigated. The procedure consisted of measuring the magnetic field in the gap between two parallel superconducting plates oriented normal to a uniform external field. Plates studied included niobium stannide, Nb–Ti alloy, Nb–25% Zr alloy, and Cerrobend 158 (50% Bi, 26.7% Pb, 13.3% Sn, 10% Cd). (W.D.M.)

42133 NEW APPROACH TO THE DETERMINATION OF EQUILIBRIUM MAGNETIZATION OF SUPERCONDUCTORS. Yntema, G. B.; Otter, F. A. Jr.; Burnham, J. B. (United Aircraft Research Labs., East Hartford, Conn.). 11p. (CONF-660327-6). ORAU. Gmelin, AED-CONF-66-050-17.

From American Physical Society Meeting, Durham, N. C.

Measurement of the equilibrium magnetization of type-II superconducting alloys as functions of temperature and of magnetic field was desired. However, the vortices are subject to pinning, which inhibits their assuming equilibrium configuration. Two approaches are described for measuring the magnetization without requiring that the vortices move. Using these two approaches, measurements were taken on Ti–37.5% Pb and Nb–1% Zr samples. Results are presented graphically. (W.D.M.)

42134 STUDY OF MECHANICAL FORCES ON TYPE 1 SUPERCONDUCTORS IN A MAGNETIC FIELD. Smith, David Robert (Rice Univ., Houston, Tex.). 87p. (CONF-660303-48). ORAU. Gmelin, AED-CONF-66-060-108.

Thesis. From American Physical Society, Conference of Neutron Cross Section Technology, Washington, D. C.

An investigation of the mechanical forces on superconducting strips of indium about 10^{-1} cm in thickness and strips of vacuum deposited tin about 8×10^{-5} cm thick due to their passage through magnetic fields was made with a torsion pendulum. At 4.2°K the thin films showed no observable eddy current damping, while the indium strips showed damping which increased with the magnetic field intensity. At temperatures corresponding to critical fields of about 50 gauss both materials showed damping which increased with the magnetic field intensity. This damping is clearly not due to eddy currents in the normal regions in the case of the tin films, since no eddy current damping was observed at 4.2°K. It is believed to be associated with the motion of normal superconducting boundaries and to the motion of flux lines against a resistive pinning force. An analysis of the data, assuming the dissipative force to be made up of a constant force plus a proportional to the first power of the velocity with which the samples pass through the field regions, indicates that the constant force is about the same for the films and the strips for corresponding degrees of flux penetration. There was also evidence of a conservative force which tended to expel the samples from the field regions and produced a flux penetration barrier opposing the entrance of the samples into the field regions. (auth)

42135 POTENTIAL OF SUPERCONDUCTING MAGNETS IN DESIGN ENGINEERING. Montgomery, D. Bruce (Massachusetts Inst. of Tech., Cambridge). New York, American Society of Mechanical Engineers, 1966, Preprint No. 66-MD-22, 12p., $1.50. (CONF-660519-2). ORAU.

From Design Engineering Conference and Show, Chicago.

Superconducting magnets are considered for a wide variety of applications. They are reviewed from the standpoint of economics, size and weight reduction possibilities, and as auxiliary devices in systems already requiring a helium environment. The basic properties of superconductivity are reviewed and their application to devices other than coils are suggested. A brief technology of superconducting magnets is given together with a discussion of the important aspects of the cryogenic environment. (auth)

Neutron Physics

See also REACTOR TECHNOLOGY — Criticality Studies

42136 (AD-637457) LOW VOLTAGE D-T NEUTRON SOURCE. Marion, Jerry B. (Armed Forces Radiobiology Research Inst., Bethesda, Md.). Jan. 1966. Contract DA-49-146-XZ-230. 83p. (AFRRI-CR-66-3). CFSTI $3.00 cy, $0.75 mn.

An analysis of the problems involved in the design and selection of equipment for the production of intense beams of 14-Mev neutrons is presented. Since the aim is to achieve total neutron yields in excess of 10^{13} sec^{-1}, a figure which considerably surpasses that commonly encountered with currently operating accelerators, it is necessary to extrapolate present performance to a considerable degree. Low-voltage accelerators in operation at the present time rarely produce d-c beam currents in excess of 1 mamp; currents of 600 μamp are considered high. The production of neutron yields of 10^{13} sec^{-1} will require beam currents greater than 10 mamp. This is a significant increase and gives rise to problems of ion source design, source cooling, beam optics, target preparation, mechanical target design, etc. These problems are analyzed individually. Certain conclusions are reached, and recommendations are made. (auth)

42137 (AEEW-M-661) A SUGGESTION FOR IMPROVING THE ACCURACY OF ^{240}Pu RESONANCE ESCAPE PROBABILITY MEASUREMENTS USING IRIDIUM FOILS. Maunders, E. J. (Atomic Energy Establishment, Winfrith (England)). June 1966. 12p. Dep. BIS $0.50. HMSO 2s. 6d.

An extension of the iridium technique for the measurement of ^{240}Pu resonance capture described by Jakeman and Maunders is suggested: in the original method the resonances above 2 ev introduced considerable unwanted contributions to the total reaction rate, which limited the accuracy of the method. A modification of the technique which minimizes these contributions by using the sandwich method with carefully optimized foil thicknesses and a filter of Cd–Ag alloy to eliminate contributions from the 5.36-ev resonance is suggested. The results of measurements made using this technique could be analyzed without the aid of a digital computer. (auth)

42138 (IN-1019) SLOW NEUTRON SCATTERING KERNELS FOR H_2O AT 423 DEG K AND 550 DEG K. McMurry, H. L. (Idaho Nuclear Corp., Idaho Falls). Aug. 1966. Contract AT(10-1)-1230. 9p. Dep. mn. CFSTI $1.00 cy, $0.50 mn.

The McMurry-Russell (MR) model for water assumes that 10% of the molecules are free, and the rest are divided equally between aggregates in which the effective masses for H scattering are 75 and 150. Each aggregate exhibits characteristic frequencies in the range $0 < E \leq 0.125$ ev which are chosen to make the calculated scattering agree with Brugger's room temperature data. A simple modification is described in which the fraction of free molecules in the MR model is adjusted to give a least squares fit to Haywood's 423°K data and to Page's 550°K data. The fractions of free molecules are 0.25 and 0.28, respectively. Agreement with the 423° data is reasonably good. Agreement with the 550° data is only fair. In both cases the modified MR model is in better agreement than the Nelkin (N) model. (auth)

42139 (IN-1020) MODEL FOR CALCULATING THE SLOW NEUTRON SCATTERING BY LIQUID D_2O. McMurry, H. L. (Idaho Nuclear Corp., Idaho Falls). Aug. 1966. Contract AT(10-1)-1230. 25p. Dep. mn. CFSTI $2.00 cy, $0.50 mn.

The Nelkin (N) model for room temperature water considers each H_2O molecule to posses free translational motion and assumes the intermolecular interaction produces single torsional oscillation of 0.06 ev. The McMurry-Russell (MR) model is a modification which allows for aggregates of H_2O molecules which exhibit l-f modes below 0.025 ev associated with group translation, together with intermediate modes with energies up to 0.125 ev associated with group rotations. Both the N and MR models assume that each H_2O molecule retains its three internal modes of 0.2, 0.46 and 0.46 ev. These models were scaled to suit D_2O by reducing the energies of the modes with characteristic energies in the range $0.025 < E \leq 0.125$ ev by $1/\sqrt{2}$, and by introducing the known internal D_2O frequencies. In addition, the scaled MR model (called MD in this work) was altered by selecting the fraction of free D_2O molecules to give a least squares fit to the experimental data. 17% of free D_2O molecules gives the scaled MR model which optimize the fit to the 22°C scattering law data of Haywood. This agreement is quite good and is superior to that obtained with the scaled N model. Agreement with recent double differential scattering data obtained by Whittemore using 0.157, 0.206 and 0.300 ev neutrons at 22°C is quite good for both the scaled MR and scaled N models. However, Whittemore's data show structure which is not predicted by either model. The scaled MR model with 53% free D_2O molecules optimizes agreement with Haywood's 150°C data. The agreement is fair at $\beta \leq 0.5$ and is superior to the scaled N model. For $\beta > 0.5$ both models give rather poor agreement. (auth)

42140 (JINR-P-2764) RASSEYANIE KILOVOL'TNYKH NEITRONOV SVINTSOM I ELEKTRICHESKAYA POLYARIZUEMOST NEITRONA. (Kev Neutron Scattering by Lead and Electrical Polarizability of Neutron). Aleksandrov, Yu. A.; Samosvat, G. S.; Sereter, Zh.; Choy Gen Sor (Joint Inst. for Nuclear Research, Dubna (USSR). Lab. of Neutron Physics). 1966. 8p. Dep. mn.

The angular distributions of neutrons scattered by lead at energies up to 25 kev were measured at angles of 30 to 150°. An analysis of the results shows that the magnitude of the electric polarizability coefficient of the neutron (α_n) is within the limits -4.7×10^{-42} cm^3 < α_n < 6.1×10^{-42} cm^3. (D.C.W.)

42141 (NAA-SR-11980(Vol.6)) UNICORN: A PROGRAM TO CALCULATE POINT CROSS SECTIONS FROM RESONANCE PARAMETERS. Otter, J. M. (Atomics International, Canoga Park, Calif.). June 30, 1966. Contract AT-11-1-GEN-8. 51p. Dep. mn. CFSTI $3.00 cy, $0.50 mn.

Unbroadened cross sections for l = 0 neutrons are calculated at energy points from resonance parameters using the Breit-Wigner line shape. The interference between resonance and potential scattering for multiple resonances is properly treated. Provision is made for spin-dependent potential scattering and adjustment to 2200 m/s cross-section values. The energy grid is optimized to provide a best representation using a specified number of points for an isolated resonance. The optimization is based on a symmetric line shape and is designed for use with logarithmic interpolation in the cross section and linear interpolation in energy. Under these conditions the magnitude of the error in the integral of the cross section in each interval is a constant percentage of the total integral. A calculation of the resonance integral in up to 50 groups is provided. The UNICORN code will accommodate a maximum of 100 resonances, 100 energy points per resonance, and 3900 total energy points. The energies and cross sections may be obtained on cards and in graphical displays. The code is written in FORTRAN IV. Execution time on the IBM 7094 is about 10 millisec/resonance/point including punched cards and graphs. (auth)

42142 (NP-16234) DIFFERENTIAL NEUTRON ALBEDO FOR THIN SLABS. Doty, D. R. (Naval Civil Engineering Lab., Port Hueneme, Calif.). Aug. 1966. 78p. (R-465). CFSTI $3.00 cy, $0.75 mn.

Data giving the experimental angular distribution of differential albedo for thermal neutrons incident upon thick scatterers of lead, high-density concrete, and iron were collected. Differential albedo of thermal neutrons on aluminum, iron, and polyethylene as a function of the material's thickness for given incident and exit angles is shown. These data are compared with a theoretical formula. Experimental verification of the theoretical formula is quite good for the angular variables. Asymptotic limits of the formula for thick and thin scatterers are as would be expected physically. The exponential dependence of the formula upon thickness agrees roughly within experimental errors. Reasons for inaccuracies in the magnitude of differential albedo are discussed. An extension to general albedo measurements for thin scatterers at any energy is described. This method, employing elemental scatterers, is shown to yield reliable results in the thermal region when the thickness of the material is less than one mean free path. The method also does away with the need for a collimated detector in differential albedo measurements for thin scatterers. (auth)

42143 (WANL-TNR-133(Rev.)) VARI-QUIR: A TWO-DIMENSIONAL TIME-DEPENDENT MULTI-GROUP DIFFUSION CODE. Riese, J. W.; Collier, George; Rieck, C. E. (Westinghouse Electric Corp., Pittsburgh, Pa. Astronuclear Lab.). Dec. 1965. Contract SNP-1. 196p. Dep. mn. CFSTI $6.00 cy, $1.25 mn.

A variational approximation was developed to solve the time-dependent neutron diffusion equations. The method was incorporated into a computer program, VARI-QUIR, which allows up to 4 energy groups and 6 precursors. A description and listing of the program are presented. (D.C.W.)

42144 EFFECT OF NUCLEAR SPIN CORRELATIONS ON THE SCATTERING OF NEUTRONS BY MOLECULES. Sinha, S. K.; Venkataraman, G. (Atomic Energy Establishment, Trombay, India). Phys. Rev., 149: 1-13(Sept. 9, 1966).

The scattering of slow neutrons by spherical-top molecules is discussed taking into account the correlations in nuclear spin caused by the presence of identical nuclei in the molecule. Matrix elements for the scattering are evaluated between different symmetrized states using group-theoretical methods. It is shown that coherent scattering can cause only those transitions which leave the symmetry of the total molecular wave function unchanged, while incoherent scattering can cause transitions between states of different symmetry. Explicit expressions for the cross section for scattering from methane are derived. These are different from those obtained by Michael recently in a treatment of the same problem. Formulas for the cross section for symmetric-top molecules are also derived. Numerical calculations have been performed for the scattering of 0.025-ev neutrons through a 10° scattering angle for methane gas at 10 and 300°K. It is found, contrary to Michael's observations, that at 10°K nuclear-spin correlations produce considerable differences in the scattering compared with the case where their effects are ignored. At 300°K, however, their effects are negligible. These findings are in accord with the predictions made earlier by Zemach and Glauber. (auth)

42145 MECHANISED EVALUATION OF NEUTRON CROSS SECTIONS. Parker, K. (Atomic Weapons Research Establishment, Aldermaston, England). 5p. (CONF-660303-40). ORAU. Gmelin, AED-CONF-66-034-26.

From American Physical Society, Conference of Neutron Cross Section Technology, Washington, D. C.

Possible ways of increasing the output of neutron cross section evaluations are discussed. The most promising appears to be direct analysis of data from the SCISRS tape on a digital computer using sophisticated curve fitting techniques. This method is illustrated by reference to scattering angular distributions and fast neutron capture and fission cross sections. The development of such methods could solve the problem of revision of existing evaluations in the light of new experimental results. The implications of this approach for the presentation of experimental and theoretical neutron cross section data are discussed. (auth)

Nuclear Properties and Reactions

Refer also to abstracts 41037, 41038, 41075, 41348, 41556, 41665, 41796, 42095, and 42523.

42146 (AD-638014) GAMMA RAYS RESULTING FROM INTERACTIONS OF 14.7 Mev NEUTRONS WITH SODIUM, SULFUR, CHLORINE, POTASSIUM, AND LEAD. Thompson, W. E.; Engesser, F. C. (Naval Radiological Defense Lab., San Francisco, Calif.). July 14, 1966. 28p. (USNRDL-TR-1043). CFSTI $2.00 cy, $0.50 mn.

The prompt gamma rays resulting from the interaction of 14.7-Mev neutrons with the nuclei of the elements sodium, sulfur, chlorine, potassium and lead, were investigated. Cross sections for the production of many of these gamma rays were measured by observing them with a carefully shielded detector during neutron bombardment of a given elemental sample. It is found that the (n,n'γ) process generally predominates and that gamma rays resulting from the de-excitation of the lowest energy levels, with one or two notable exceptions, are usually most prominent. Gamma rays attributable to (n,pγ), (n,$\alpha\gamma$), and (n,dγ) processes are also observed. In chlorine and potassium, gamma rays attributable to the (n,dγ) process are unusually preponderant. Some of the most important gamma rays are found to have the following elemental production cross sections (in millibarns per steradian at 90 deg): 0.44-Mev gamma ray from Na, 39.5 ± 4.5; 2.24-Mev gamma ray from S, 15.3 ± 1.7; 2.15-Mev gamma ray from Cl, 17.1 ± 2.0; 2.17-Mev gamma ray from K, 19.3 ± 2.5; and 2.62-Mev gamma ray from Pb, 20.3 ± 2.7. (auth)

42147 (AE-240) POSSIBLE ODD PARITY STATE OF ^{128}Xe. Broman, L.; Malmskog, S. G. (Aktiebolaget

Atomenergi, Stockholm (Sweden)). July 1966. 10p. Dep. mn.

Gamma lines in the decay of ^{128}I were measured using a Ge(Li) detector. The following gamma energies were obtained: 442.5 ± 0.05, 526.5 ± 0.5, 742.4 ± 1.0, 969.0 ± 1.0, and 1136.5 ± 2.0 kev. The 1136.5-kev transition defines a level in ^{128}Xe at 1579 ± 2 kev. From the log ft = 7.8 ± 0.3 of the β^- feeding, this level is believed to have an odd parity. Upper limits of gamma intensities for transitions around 530 kev are used to set a limit for the population of expected 0^+ level originating from the two-phonon quadrupole vibration. (auth)

42148 (BNWL-87) EVALUATION OF THE ACCURACY OF DECAY SCHEME CONSTANTS AND CALIBRATION STANDARDS FOR ^{137}Cs. Matsumoto, W. Y. (Battelle-Northwest, Richland, Wash. Pacific Northwest Lab.). July 1965. Contract AT(45-1)-1830. 20p. Dep. mn. CFSTI $1.00 cy, $0.50 mn.

A detailed review of published literature and an experimental cross-check program were made to assign "best estimates" to the ^{137}Cs decay-scheme constants and to the ASTM ^{137}Cs standard. A weighted estimate, with all the interrelated parameters considered, gave the following assignment of values: half life = 30.76 yr; β branching ratio = 0.954 for 518-kev β; internal conversion coefficient = 0.110; ASTM ^{137}Cs standard = 1.05×10^5 γ/sec/ml and 1.71×10^{14} atoms/ml. (S.F.L.)

42149 (CNAEM-34) PARAMETERS FOR THE FIRST NEUTRON RESONANCE IN ^{113}Cd. Akyuez, R. O.; Cansoy, C.; Domanic, F. (Cekmece Nuclear Research Center, Atomic Energy Commission, Istanbul (Turkey)). Dec. 1965. 17p. Dep. mn.

The total neutron cross section of ^{113}Cd was measured in the energy range from 0.025 to 1 ev using a crystal spectrometer with the Be(10I1) and NaCl(200) crystal planes as monochromators. A method for second-order correction was applied, and the resonance at 0.181 ev was fitted to a Breit-Wigner single-level formula by the method of least squares. The resonance parameters obtained from the analysis are: $E_0 = 0.181 \pm 0.003$ ev, $\sigma_0 = 7847 \pm 187$ barns, $r = 0.1087 \pm 0.0033$ ev and $r_n = 0.0791 \pm 0.0032 \times 10^{-3}$ ev assuming that the statistical weighing factor is $g = 3/4$. (auth)

42150 (COO-498-56) DIRECTIONAL CORRELATION MEASUREMENTS IN THE DECAY OF ^{160}Tb EMPLOYING A Ge-Li DETECTOR. Jaklevic, J. M.; Funk, E. G.; Mihelich, J. W. (Notre Dame Univ., Ind.). July 15, 1966. Contract AT(11-1)-498. 9p. (CONF-660906-14). Dep. mn. CFSTI $1.00 cy, $0.50 mn.

From International Conference on Nuclear Physics, Gatlinburg, Tenn.

A coincidence system employing a Ge-Li detector (planar, 1 cm diameter, 2 mm depletion depth) and a 3 in. × 3 in. NaI detector was used to measure gamma-gamma directional correlations in the decay of ^{160}Tb for cascades involving transitions of energies 87-879, 87-962, 87-1178, 87-1272, 216-962, 298-879, and 298-966 kev. (S.F.L.)

42151 (IN-1014) TABULATION OF THE ^{233}Pa TOTAL NEUTRON CROSS SECTION DATA. Simpson, F. B.; Codding, J. W. Jr. (Idaho Nuclear Corp., Idaho Falls). July 1966. Contract AT(10-1)-1230. 106p. Dep. mn. CFSTI $4.00 cy, $0.75 mn.

The total neutron cross section for ^{233}Pa was measured from 0.01 to 10,000 ev with the Materials Testing Reactor fast chopper. These data were taken at the 20-meter flight path with a resolution of 0.08 to 2.0 μsec/meter. Difficulties arise in the analysis of these cross section data because of the growth of the ^{233}U daughter into the sample as a function of time. Because of the lack of resonance parameters for ^{233}U above 18 ev, it is difficult to extract the effect of the ^{233}U contaminant above this energy. The sample used in making these measurements was produced by irradiating 280 grams of ^{232}Th in the Engineering Test Reactor for one cycle (approximately four weeks). This produced approximately 700 mg of chemically separated ^{233}Pa in an oxide form. The sample measured approximately 25,000 R/hr at one foot. Curves and tables are presented for the total neutron cross section as a function of energy. (auth)

42152 (JEN-159-DF/I-49) ESQUEMA DE DESINTEGRACION DEL ^{235}U. (Decay Scheme of the ^{235}U). Gaeta, R. (Junta de Energia Nuclear, Madrid (Spain). Division de Fisica). 1965. 134p. Dep. mn.

A study of the ^{231}Th excited levels from the alpha decay of ^{235}U was carried out. The alpha spectrum was measured by means of a semiconductor counter spectrometer with an effective resolution of 18 kev. Nineteen previously unreported lines were identified. The gamma spectrum was measured with thin samples of ^{235}U, free from decay products, and in such geometrical conditions that most of the interference effects were eliminated. The gamma-gamma coincidence spectra gave better knowledge of the transition between the several levels. (auth)

42153 (JINR-E-2824) ON MECHANISM OF THE PROTON TRANSFER REACTIONS. Volkov, V. V.; Vil'chinski, Ya. (Joint Inst. for Nuclear Research, Dubna (USSR). Lab. of Nuclear Reactions). 1966. 18p. Dep. mn.

The proton transfer reaction (^{12}C, ^{13}N) on ^{12}C, ^{27}Al, ^{51}V, ^{93}Nb, $^{107,109}Ag$, and ^{181}Ta target nuclei was investigated. The angular distributions at different energies, well above the Coulomb barrier, were measured. Distinct differences between the neutron and proton transfer reactions were revealed. The proton transfer cross section rapidly reduces with the increasing atomic number of the target. Moreover, the excitation functions decrease faster with decreasing energy than in the case of neutron transfer. The analysis of the experimental data, based on the single nucleon transfer reaction models of Frahn and Venter, and Kalinkin and Grabowski shows these differences. The observed specific behavior of the proton transfer reactions may be due to the Coulomb polarization of the proton wave functions. (auth)

42154 (JINR-E-2857) THE STRUCTURE OF THE GROUND AND EXCITED STATES OF DEFORMED ODD-MASS NUCLEI IN THE ACTINIDE REGION. Malov, L. A.; Solov'ev, V. G. (Joint Inst. for Nuclear Research, Dubna (USSR). Lab. of Theoretical Physics). 1966. 14p. Dep. mn.

The interaction of quasi-particles with quadrupole and octupole phonons in deformed odd-mass nuclei in the actinide region is calculated in the framework of the method of approximate second quantization. This interaction leads to the formation of low-lying collective nonrotational states and complex-structure states. Beta-vibrational and octupole phonons are more important in the actinide region than in the rare-earth one. Good agreement with experimental data was obtained. (auth)

42155 (JINR-P-2762) ISSLEDOVANIE IZLUCHENIYA ^{152}Tb. (The Decay of ^{152}Tb). Vil'ski, K.; Gromov, K. Ya.; Iorgensen, M.; Kuznetsov, V. V.; Kuznetova, M. Ya.; Nil'sen, O. B.; Skilbrait, O.; Urbanets, Ya.; Finger, M. (Joint Inst. for Nuclear Research, Dubna (USSR). Lab. of Nuclear Problems). 1966. 26p. Dep. mn.

The decay scheme of ^{152}Tb was investigated by measuring e^--γ and β^+-γ coincidence spectra and conversion-electron spectra. Many previously unreported levels of ^{152}Gd were identified, and spin-parity assignments were made. Branching ratios were also determined. (D.C.W.)

42156 (JINR-P-2813) NEKOTORYE OSOBENNOSTI MEKHANIZMA REAKTSII MNOGONUKLONNYKH PEREDACH. (Some Aspects of the Multi-Nucleon Transfer Reaction Mechanism). Vil'chinski, Ya.; Volkov, V. V.; Detsovski, P. (Joint Inst. for Nuclear Research, Dubna (USSR). Lab. of Nuclear Reactions). 1966. 12p. Dep. mn.

The reaction $^{27}Al(^{14}N,^{18}F)^{23}Na$ was investigated at 65.0, 78.7, 91.4, and 107.3 Mev. The energy distributions of the ^{18}F reaction products were measured at different angles. In addition to the products of the transfer reaction

$^{27}Al(^{14}N,^{18}F)^{23}N$, ^{18}F nuclei of significantly lower energy were observed in the energy distributions. An interpretation of the results in terms of two different mechanisms of the $^{27}Al(^{14}N,^{18}F)^{23}Na$ reaction is proposed. (D.C.W.)

42157 (JINR–P–2814) ISSLEDOVANIE IZLUCHENIYA ^{184}Re. (The Decay of ^{184}Re). Ageev, V.; Vrzal, Ya.; Klimenko, A.; Liptak, Ya.; Maidanyuk, V.; Urbanets, Ya.; Feoktistov, A. (Joint Inst. for Nuclear Research, Dubna (USSR). Lab. of Neutron Physics). 1966. 12p. Dep. mn.

Gamma spectra and conversion-electron spectra from the decay of ^{184}Re were measured using a Ge(Li) spectrometer and a magnetic β spectrometer, respectively. Internal-conversion coefficients were determined together with transition multipolarities. (D.C.W.)

42158 (JINR–P–2817) SKHEMA RASPADA ^{160}Ho. (Decay Mode of ^{160}Ho). Bonch-Osmolovskaya, N. A.; Vrzal, Ya.; Grigor'ev, E. P.; Liptak, Ya.; Urbanets, Ya. (Joint Inst. for Nuclear Research, Dubna (USSR). Lab. of Nuclear Problems). 1966. 18p. Dep. mn.

The decay mode of ^{160}Ho was studied. The γ spectrum was investigated using a semiconductor spectrometer with a germanium detector. The γ intensities and multipolarities of gamma transitions were determined. New data were introduced into the decay mode of ^{160}Ho. (auth)

42159 (JINR–P–2841) SPONTANNO DELYASHCHIISYA IZOMER S PERIODOM POLURASPADA 10^{-7} SEK. (Spontaneously Fissionable Isomer With the Half-Life Equal to 10^{-7} s). Gangrskii, Yu. P.; Markov, B. N.; Polikanov, S. M.; Yungklaussen, Kh. (Joint Inst. for Nuclear Research, Dubna (USSR). Lab. of Nuclear Reactions). 1966. 8p. Dep. mn.

A spontaneously fissioning isomer with a half life of $0.8 \pm 0.3 \times 10^{-7}$ sec was produced in ^{12}C reactions with ^{238}U. On the basis of the excitation function, the isomeric state was attributed to ^{246}Cf. The cross section for the production of the isomer was determined to be $1.2 \pm 0.5 \times 10^{-32}$ cm^2. (D.C.W.)

42160 (KAPL–3099) ^{12}C FAST NEUTRON CROSS SECTIONS AND LEGENDRE MOMENTS BELOW 15.0 Mev. Slaggie, E. L.; Reynolds, J. T. (Knolls Atomic Power Lab., Schenectady, N. Y.). June 30, 1966. Contract W-31-109-eng-52. 30p. Dep. mn. CFSTI $2.00 cy, $0.50 mn.

An evaluated library of cross sections and elastic scattering Legendre moments is given for ^{12}C between 0.01 and 15 Mev. The cross sections below 4 Mev and the moments below 7 Mev were calculated using a fitting formula based on a combined resonance and potential well theory. Above 8.4 Mev, the moments were obtained from a nonspherical optical potential calculation. These calculations are described. 46 references. (auth)

42161 (LA–DC–7878) STUDIES OF (d,pf) AND (t,pf) REACTIONS ON PLUTONIUM ISOTOPES. Britt, H. C.; Newsome, R. W. Jr.; Stokes, R. H. (Los Alamos Scientific Lab., Univ. of California, N. Mex.). [1966]. Contract W-7405-eng-36. 8p. (CONF-660716–1). Dep. mn. CFSTI $1.00 cy, $0.50 mn.

From Symposium on Recent Progress in Nuclear Physics with Tandems, Heidelberg, Germany.

The transition states available at the saddle point of fissioning ^{239}Pu and ^{240}Pu nuclei are studied by measuring the angular correlation of fragments from the fissioning nuclei excited in direct reactions. The experiments involve measuring proton spectra at laboratory angles of 120° and 130° for (t,pf) and (d,pf) reactions, respectively, in coincidence with fission fragments emitted at angles of 90° or 180° relative to the kinematic recoil angles for the fissioning nucleus. Experimental anisotropies are plotted vs. excitation energy from below threshold to 10 Mev. For each reaction, the relative fission probability ($p_f = \sigma_f/\sigma_p$) was approximately determined by integrating the fission angular correlations over all angles, assuming no azimuthal asymmetry. (S.F.L.)

42162 (LA–DC–8075) TOTAL REACTION CROSS SECTIONS FOR 14.5 Mev PROTONS FROM 22 SEPARATED ISOTOPES OF Ti, Fe, Ni, Cu, Zn, Zr, and Sn. Igo, G. J.; Dicello, J. F.; Rousch, M. L. (Los Alamos Scientific Lab., Univ. of California, N. Mex.). [1965]. Contract W-7405-eng-36. 9p. (CONF-660906–9). Dep. mn. CFSTI $1.00 cy, $0.50 mn.

From International Conference on Nuclear Physics, Gatlinburg, Tenn.

Total reaction cross sections σ_R were measured with ±2% accuracy using an improved beam attenuation; a counter technique employing a solid-state detector (200-kev resolution) to separate elastic events; 0.05-in. beam size to reduce finite size corrections; no metal collimators to minimize slit scattering; and a beam energy spread of 30 kev. The σ_R values plotted vs N (constant Z) increase significantly with increasing N. (auth)

42163 (LA–DC–8082) DIRECT AND COMPOUND-NUCLEUS REACTIONS FOR $^{32}S(d,p)^{33}S$ AT LOW ENERGIES. Leachman, R. B. (Los Alamos Scientific Lab., Univ. of California, N. Mex.). [1966]. Contract W-7405-eng-36. 9p. (CONF-660906–8). Dep. mn. CFSTI $1.00 cy, $0.50 mn.

From International Conference on Nuclear Physics, Gatlinburg, Tenn.

The contributions of direct-reaction and compound-nucleus mechanisms in the reaction $^{32}S(d,p)^{33}S$ were investigated. Excitation functions for the reaction were measured between 2.5 and 4.6 Mev at eight angles between 10 and 170°. The direct-reaction and compound-nucleus cross sections were obtained from the excitation functions by determining the fraction of direct reaction from fluctuation analyses. The experimental results were compared with the results of calculations. (D.C.W.)

42164 (LA–DC–8083) DETERMINATION OF SMALL WIDTHS IN THE CONTINUUM. Gibbs, W. R.; Fessenden, P.; Leachman, R. B. (Los Alamos Scientific Lab., Univ. of California, N. Mex.). [1965]. Contract W-7405-eng-36. 9p. (CONF-660906–13). ORAU.

From International Conference on Nuclear Physics, Gatlinburg, Tenn.

The determination of widths from fluctuation measurements is discussed for the case in which the experimental resolution is much larger than the width to be determined. An application of the technique to the determination of widths for ^{108}Cd, ^{110}Cd, ^{104}Pd, ^{76}Se, ^{116}Sn, and ^{90}Zr using (p,α_0) reactions on ^{75}As, ^{115}In, ^{103}Rh, ^{107}Ag, ^{109}Ag, and ^{89}Y is summarized. (D.C.W.)

42165 (MIT–2098–251, pp 16–20) LINEAR ACCELERATOR GROUP. (Massachusetts Inst. of Tech., Cambridge. Lab. for Nuclear Science).

A progress report is presented on the research activities of the linear accelerator group at M.I.T. Topics discussed are ^{9}Be(γ,n) data, photoneutron systematics, polarimeter, and collaboration with the University of Saskatchewan. (B.G.D.)

42166 (MIT–2098–251, pp 37–49) O.N.R. GENERATOR GROUP. (Massachusetts Inst. of Tech., Cambridge. Lab. for Nuclear Science).

A progress report is presented on the research activities of the O.N.R. group at M.I.T. Topics discussed are studies of energy levels in the $f_{\frac{7}{2}}$ shell, the ^{138}Ba(d,p) reaction, the ^{37}Cl(d,p) reaction, optical-model analysis and DWBA calculations, optical parameters for ^{3}He, ^{14}N(d,p) reaction, analog-state studies in the strontium isotopes, stripping analysis of the ^{128}Te(d,p) reaction, ground-state transition in $^{107}Ag(d,p)^{108}$Ag, collaboration with other universities, reaction studies from nickel isotopes, reaction studies from chromium isotopes, (d,p) and (d,d′) reactions on titanium isotopes, and reactions on zinc isotopes. (B.G.D.)

42167 (MIT–2098–251, pp 50–6) RADIOACTIVITY GROUP. (Massachusetts Inst. of Tech., Cambridge. Lab. for Nuclear Science).

A progress report is presented on the research activities of the Radioactivity Group at M.I.T. Topics discussed are measurements of magnetic and quadrupole moments of short-lived nuclear states using angular correlations

and Mössbauer techniques, and nuclear spectroscopy using the new high resolution germanium counters. (B.G.D.)

42168 (MIT–2098–251, pp 57-73) CYCLOTRON GROUP. (Massachusetts Inst. of Tech., Cambridge. Lab. for Nuclear Science).

A progress report is presented on research activities of the cyclotron group at M.I.T. Topics discussed are cyclotron operation and equipment, $^{40}Ca(\alpha,2\alpha)$ reactions, elastic and inelastic scattering of alpha particles, (α,p) reactions, $^{40}Ca(\alpha,\alpha'\gamma)$, and data analysis. (B.G.D.)

42169 (UCRL–14744, pp 1-18) NUCLEAR AND ATOMIC PHYSICS. (Lawrence Radiation Lab., Univ. of California, Livermore).

A report is presented on the theoretical and experimental aspects of nuclear and atomic physics. Topics discussed are Lehmann-Symonzik-Zimmermann (LSZ) formalism in the Lee model (V-Θ Sector), equivalent field theories and elementary particle democracy, strong interactions in the Limit $Z_3 = 0$, Gell-Mann Okubo Rule as a consequence of eightfoldedness, symmetries in first approximation S-matrix theory, helium inter-molecular potential, analysis of ^{13}C, shape of fission barrier for ^{242}Am, x-ray production in the L shell of copper by 25 to 1700 kev protons, fission cross sections of ^{235}U, excitation of the ground-state band of ^{19}F by 13.9 Mev proton scattering, quasi-elastic (p,n) scattering from scandium and titanium isotopes, excited states in ^{8}Be, high resolution studies of fission x rays and gamma rays, neutron diffraction-sodium superoxide, shell model calculations, and fitting of various (p,n) cross sections via the LOKI 9A Code. (B.G.D.)

42170 (UCRL–70045) HIGH-RESOLUTION STUDIES OF FISSION X RAYS AND GAMMA RAYS. John, W.; White, D. H.; Saunders, B. G.; Jewell, R. W.; Groves, D. (Lawrence Radiation Lab., Univ. of California, Livermore). Aug. 12, 1966. Contract W-7405-eng-48. 10p. (CONF-660812–1). Dep. mn. CFSTI $1.00 cy, $0.50 mn.

From 3rd Circular International Symposium, Lysekil, Sweden.

The spectra of gamma rays and x radiation from fission products were investigated using a bent-crystal spectrometer in three different arrangements. The source consisted of an Al–^{235}U foil exposed to a neutron flux from a pool-type reactor. Line intensities were determined, and the time dependence of the radiation was studied. (D.C.W.)

42171 (LA-tr–66-41) ENERGY DEPENDENCE OF ANGULAR DISTRIBUTION OF FRAGMENTS IN THE FISSION OF ^{233}U, ^{235}U, AND ^{239}Pu INDUCED BY NEUTRONS. Nesterov, V. G.; Smirenkin, G. N.; Shlak, D. L. (Gosudarstvennyi Komitet po Ispol'zovaniyu Atomnoi Energii SSSR, Obninsk. Fiziko-Energeticheskii Institut). Translated by A. D. Cernicek (Los Alamos Scientific Lab., Univ. of California, N. Mex.), from report FEI–33. 27p. Dep. mn. CFSTI $2.00 cy, $0.50 mn. JCL $2.60 fs, $1.01 mf.

The results of an investigation of the fission-fragment angular distributions in the neutron fission of ^{239}Pu, ^{233}U, and ^{235}U are presented. Measurements were made for ^{239}Pu and ^{233}U in the range of neutron energies from 0.08 to 1.5 Mev, while for ^{235}U the energy range was extended up to 6 Mev. The fragments were recorded using an electronic circuit that permitted the simultaneous counting of pulses from six ionization counters. (D.C.W.)

42172 ^{187}Re LEVEL AT 686 kev. Vasileva, N. Ann. Univ. Sofia, Fac. Sci. Phys., 59: No. 5, 1-4(1964-65). (In Russian).

Angular gamma-gamma correlations of 72 to 134 kev and 552 to 134 kev cascades were studied in order to determine the spin of the excited 686-kev level in ^{187}Re nuclei. The measurements of the first cascade correlations gave a mixing ratio of $\delta_{134} = +(0.11 \pm 0.04)$. Using the δ_{134} value and the angular correlation of the 552 to 134 kev cascade it was found that the spin of the 686-kev level is $5/2$. (G.O.Y.)

42173 PERTURBATION OF THE CRITICAL POTENTIAL FOR THE ELASTIC SCATTERING OF CHARGED PARTICLES. Lebon, G. (Univ., Liege). Bull. Soc. Roy. Sci. Liege, 35: 202-15(1966). (In French).

The critical potential corresponding to the scattering of a charged particle is determined by a perturbation method from the critical potential corresponding to the scattering of a neutral particle. The general results are applied to the case where the finite range interaction corresponds to a square well potential. (auth)

42174 MULTIPLICITY FACTOR OF NEUTRON FORMATION IN THE (μ,n) REACTIONS. Bobodzhanov, I. B.; Dzhuraev, A. A.; Azizkulov, N. Kh. Dokl. Akad. Nauk Tadzh. SSR, 9: No. 3, 12-14(1966). (In Russian).

The average number of neutrons $\bar{n}$ emitted during the capture of a meson(μ^-) by a nucleus is studied. The dependence of this average neutron emission on the atomic weight of the nucleus is expressed by $\bar{n} = (0.3 \pm 0.02)A^{1/3}$. (J.F.P.)

42175 NMR STUDIES OF ^{7}Li IN POLYCRYSTALLINE LITHIUM NITRIDE. Bishop, S. G.; Ring, P. J.; Bray, P. J. (Brown Univ., Providence). J. Chem. Phys., 45: 1525-31(Sept. 1, 1966).

The ^{7}Li NMR spectrum for polycrystalline lithium nitride was examined as a function of both temperature and magnetic field. Two central $m = 1/2$ to $m = -1/2$ transitions and two pairs of $m = \pm 3/2$ to $m = \pm 1/2$ satellite transitions were observed; the results were consistent with the presence of the two nonequivalent lithium sites in the known crystal structure of Li_3N. The quadrupole coupling constants for the two lithium sites, as determined from the frequency separation of the satellite transitions, are 288 ± 4 and 584 ± 6 kc/sec at room temperature. These values are in good agreement with those determined from the field dependence of the second-order quadrupolar widths of the two $m = 1/2$ to $m = -1/2$ transitions. The central transitions were examined as a function of temperature at a resonant frequency of 16 Mc/sec, where the linewidth is determined primarily by dipolar effects. As the temperature was increased from 77°K, the linewidths remained relatively constant at low temperatures but narrowed abruptly between roughly −75°C and room temperature. The observed narrowing was attributed to the diffusion of lithium ions. (auth)

42176 THERMAL FISSION YIELD OF ^{137}Cs IN ^{233}U. Ondrejcin, R. S. (E. I. du Pont de Nemours and Co., Aiken, S. C.). Contract AT(07-2)-1. J. Inorg. Nucl. Chem., 28: 1763-7(Sept. 1966). (TID–22386).

The thermal neutron fission yield of ^{137}Cs in ^{233}U was found to be 6.13 ± 0.13 per cent. ^{235}U and ^{233}U samples were irradiated in the ORNL Graphite Reactor. The samples were analyzed radiochemically to determine the amount of ^{137}Cs formed per unit weight of uranium. In the case of ^{235}U samples, the number of fissions was also determined. The apparent number of fissions for both isotopes was calculated from flux monitor data. Curves for flux depression in the uranium samples were developed from reactor parameters and comparison of fission product gamma activity with thick and thin ^{235}U and ^{233}U foils irradiated in an SRL reactor. From these curves, flux depression corrections were determined for the ^{233}U samples so that the number of fissions could be calculated; the validity of the flux correction was demonstrated with the ^{235}U samples. (auth)

42177 THE CHARGE AND MASS DISTRIBUTIONS IN FISSION OF URANIUM INDUCED BY 170 Mev PROTONS. Pappas, A. C. (Univ., Oslo); Hageboe, E. J. Inorg. Nucl. Chem., 28: 1769-85(Sept. 1966).

New fission yields were determined radiochemically for products between A = 100 and A = 140 from the reaction U(170 Mev p,f). The charge distribution curve is firmly established in the mass range $127 \leq A \leq 134$ and is found to be Gaussian with a full width at half maximum of 2.8 charge units. Additional data indicate that the same curve is valid from about A = 100 to about A = 140, and it has been used together with other fractional chain yields to establish Z_p, the most probable charge as a function of mass number. A complete mass distribution curve was

drawn. It is neither symmetric around a most probable mass nor does it have a broad flat maximum. (auth)

42178 THE INDEPENDENT YIELDS OF ^{86}Rb, ^{132}Cs, ^{134}Cs, AND ^{136}Cs IN THE THERMAL NEUTRON FISSION OF ^{235}U. McHugh, James A. (Knolls Atomic Power Lab., Schenectady, N. Y.). Contract W-31-109-eng-52. J. Inorg. Nucl. Chem., 28: 1787-90(Sept. 1966).

The independent yields for the shielded nuclides of rubidium and cesium in the thermal neutron fission of ^{235}U have been measured using high sensitivity mass spectrometric methods. The following yields were determined: ^{86}Rb, 2.40×10^{-5} per cent; ^{132}Cs, $<1.5 \times 10^{-7}$ per cent; ^{134}Cs, 8.9×10^{-6} per cent; and ^{136}Cs, 5.94×10^{-3} per cent. (auth)

42179 HALF-LIFE OF ^{101}Ag AND FORMATION CROSS SECTION FROM Ag AND In. Panontin, John A.; Caretto, Albert A. Jr. (Carnegie Inst. of Tech., Pittsburgh). Contract AT(30-1)-2897. J. Inorg. Nucl. Chem., 28: 1795-1801(Sept. 1966). (NYO-2897-16).

The half life of ^{101}Ag was determined to be 11.2 ± 0.1 min and its formation cross section from naturally occurring Ag with 200 and 400 Mev protons to be 12.4 ± 0.7 and 7.14 ± 0.01 mbarns, respectively, and from In to be 2.24 ± 0.10 and 5.15 ± 0.18 mbarns, respectively, also with 200 and 400 Mev protons. (auth)

42180 RECOIL MEASUREMENTS OF SUBNANOSECOND NUCLEAR LIFETIMES. Novakov, T. (Boris Kidric Inst. of Nuclear Sciences, Belgrade). Nucl. Instrum. Methods, 43: 199-208(1966).

The use of high-resolution electron spectrometers for recoil measurements of short nuclear lifetimes is discussed. The applications of the stopping foil method and the new electrostatic method to the measurements of half lives of nuclear states excited in alpha decay and in nuclear reactions is reviewed. (auth)

42181 ODD PARITY LEVELS EXCITED IN THE ^{37}Cl (p,γ)^{38}Ar REACTION. Erne, F. C.; Veltman, W. A. M.; Wintermans, J. A. J. M. (Univ., Utrecht). Nucl. Phys., 88: 1-11(1966).

From angular correlation and polarization measurements performed at two resonances in the ^{37}Cl(p,γ)^{38}Ar reaction, the spins and parities of levels at 4.49, 4.60, 5.67, 11.30 and 11.31 Mev were determined to be $J^{\pi} = 4^-$, 5^-, 5^-, 5^- and 5^-, respectively. The two high-energy states are very probably the (split) analogue of the first excited state in ^{38}Cl. The decay mainly proceeds, where possible, through M1 radiation, in five- and six-step cascades. The $5^- \rightarrow 5^-$ transitions are much stronger then the $5^- \rightarrow 4^-$ transitions. An explanation is suggested in terms of the predominant configurations involved. The experimental excitation energies are compared with energy values obtained in a recent shell-model calculation. (auth)

42182 MEASUREMENTS OF (p,γ) RESONANCE STRENGTHS IN THE s-d SHELL. Englebertink, G. A. P.; Endt, P. M. (Univ., Utrecht). Nucl. Phys., 88: 12-20 (1966).

Resonance strengths of selected resonances in the E_p = 0.3 – 2.1 Mev region in the (p,γ) reactions on ^{23}Na, ^{24}Mg, ^{25}Mg, ^{26}Mg, ^{27}Al, ^{28}Si, ^{29}Si, ^{30}Si, ^{31}P, ^{32}S, ^{34}S, ^{35}Cl, ^{37}Cl, ^{39}K, ^{41}K, and ^{40}Ca are compared through relative yield measurements, using targets of many different chemical compounds, each containing at least two of the investigated isotopes. If in a (N,Z) diagram lines are drawn between isotopes connected in this way, one obtains several closed cycles, providing internal checks on the measured strength ratios. The final best values of the relative strengths are obtained by least-squares analysis. The E_p = 621 kev ^{30}Si(p,γ)^{31}P resonance of which the strength is known from a γ-ray resonant absorption experiment, was used to convert the relative into absolute strengths. (auth)

42183 ^{10}B, ^{11}B, AND ^{6}Li INDUCED REACTIONS OF ^{27}Al. Ladenbauer-Bellis, I. M.; Morse, R. I.; Preiss, I. L. (Yale Univ., New Haven). Nucl. Phys., 88: 21-32 (1966). (YALE-2726-H-84).

The excitation functions of residual nuclei resulting from ^{10}B-, ^{11}B-, and ^{6}Li-induced reactions of ^{27}Al were measured. The angular distributions and recoil ranges of ^{24}Na, ^{18}F, and ^{32}P were found to correspond to values expected for complete fusion compound nucleus reactions. Statistical model calculations were found to agree with experimentally determined excitation functions for those products having masses comparable to or greater than the target, while lighter products such as ^{18}F can not be explained on the basis of single-particle and/or alpha cascades. (auth)

42184 EXPERIMENTAL STUDY OF ELASTIC PROTON-DEUTERON SCATTERING AT 155-Mev. Kuroda, K.; Michalowicz, A.; Poulet, M. (Institut de Physique Nucleaire, Orsay, France). Nucl. Phys., 88: 33-44(1966). (In French).

The cross section and the polarization of proton-deuteron elastic scattering at 155 Mev were measured with good energy resolution, in order to separate the elastic events from the inelastic ones. The differential cross sections are in good agreement with those of Postma and Wilson at 146 Mev, providing a correction of –8% according to their indication. The polarizations, however, differ from those of Postma and Wilson by 10 to 15% at the maximum polarization angles. The results are also compared with the theoretical curves recently given by Benoist and Gomez-Gimeno and independently by Kottle and Kowalski. (auth)

42185 EXPERIMENTAL STUDY OF INELASTIC PROTON-DEUTERON SCATTERING AT 155 Mev. Kuroda, K.; Michalowicz, A.; Poulet, M. (Institut de Physique Nucleaire, Orsay, France). Nucl. Phys., 88: 45-55(1966). (In French).

Measurements of the inelastic proton-deuteron cross sections and polarization in a region of small momentum transfer were made with a high-resolution magnetic spectrometer. The amplitude Σ_s and the polarization P_s associated with the transition which leaves the target nucleons in a singlet S-state were then obtained following Cromer's treatment of inelastic p-d scattering. The results are generally in good agreement with the theoretical predictions confirming Cromer's theory which introduces final interaction between the target nucleons. These parameters were also compared with the different solutions of nucleon-nucleon interaction with isospin T = 0. The best fit was obtained with the Hamada-Johnston potential. (auth)

42186 COULOMB EXCITATION OF LOW-ENERGY STATES IN ^{127}I, ^{121}Sb, AND ^{183}W. Thomas, M. F.; Grace, M. A. (Univ. of Oxford). Nucl. Phys., 88: 56-67(1966).

Values of B(E2) for the 38-kev state of ^{121}Sb, the 59- and 203-kev states of ^{127}I, and the 46.5-kev state of ^{183}W were obtained using Coulomb excitation by alpha particles and lithium ions. (D.C.W.)

42187 THE DECAY OF ^{192}Au. Nyman, B.; Johansson, A.; Bergman, C.; Baeckstroem, G. (Inst. of Physics, Uppsala). Nucl. Phys., 88: 63-80(1966).

The ^{192}Pt internal conversion spectrum following the decay of ^{192}Au was studied in detail using a high-precision beta spectrometer. The average accuracy of the energy and the relative K-line intensity determinations for the more than 200 established transitions is about two parts in 10^4 and 10%, respectively. Some tentative gamma intensities are also given. From the end-point energy of the position spectrum, a Q-value of 3514 ± 20 kev for the ^{192}Au decay was obtained. A level scheme comprising 42 excited levels and 140 transitions mainly on the basis of numerical relationships was constructed. (auth)

42188 A STUDY OF THE REACTION ^{10}B(^{3}He,pααα). Waggoner, M. A. (Univ. of Maryland, College Park. Univ. of Iowa, Iowa City); Etter, J. E.; Holmgren, H. D.; Moazed, C. Nucl. Phys., 88: 81-127(1966)

The ^{10}B(^{3}He,pααα) reaction was studied at bombarding energies of 2.45 and 6.00 Mev. These studies indicate that the ^{10}B + ^{3}He system proceeds to the four-body final state pααα primarily by sequential decay processes. Evidence was obtained for the occurrence of the following energeti-

cally allowed processes: $^{10}B + {}^3He \rightarrow p + {}^{12}C$, $^{12}C \rightarrow \alpha_1 + {}^8Be$, $^8Be \rightarrow \alpha_2 + \alpha_3$; $^{10}B + {}^3He \rightarrow \alpha_1 + {}^9B$, $^9B \rightarrow p + {}^8Be$, $^8Be \rightarrow \alpha_2 + \alpha_3$; $^{10}B + {}^3He \rightarrow \alpha_1 + {}^9B$, $^9B \rightarrow \alpha_2 + {}^5Li$, $^5Li \rightarrow \alpha_3 + p$; and $^{10}B + {}^3He \rightarrow {}^5Li + {}^8Be$, $^5Li \rightarrow p + \alpha_1$, $^8Be \rightarrow \alpha_2 + \alpha_3$. Spectroscopic information for many of the levels of the various intermediate systems was obtained. The results are consistent with the following J^π-assignments to the designated levels: (the decimal number indicates the energy of excitation of the level in Mev) ^9B: 2.34, $5/2^-$; 2.8, $1/2$. ^{12}C: 16.57, natural parity; 16.11, 2^+; 15.11, 1^+; 14.02, $J \geq 2$, natural parity; 13.34, $J \geq 1$, unnatural parity; 12.71, 1^+; 11.83, 2^-; 10.84, 1^-; 9.64, 3^-; 7.66, 0^+. Many of the above assignments are based primarily on previous work. (auth)

42189 ISOTOPE AND ISOMER SHIFTS IN MERCURY. Barrett, R. C. (Univ. of California, Berkeley). Nucl. Phys., 88: 128-36(1966).

Calculations were made of the change in the mean square charge radius of the mercury isotopes which results when a neutron is added to a doubly even core. Both the ground and isomeric states of the odd-mass isotopes were considered. First-order perturbation theory was used to obtain the amplitudes of monopole excitations of the proton core. The calculations were carried out by first assuming a conventional neutron-proton force and then using various density-dependent interactions. The results show a very marked A-dependence and achieve partial success in explaining the experimental shifts in the optical spectra. (auth)

42190 EXCITED STATES IN ^{6}Be AND ^{10}C. Mangelson, N.; Ajzenberg-Selove, F.; Reed, M.; Lu, C. C. (Univ. of California, Berkeley). Nucl. Phys., 88: 137-44(1966). (UCRL-16849).

The $^6Li(^3He,t)^6Be$ and $^{10}B(^3He,t)^{10}C$ reactions were studied at $E(^3He) = 30$ and 40 Mev. In ^{6}Be, an excited state is observed at $E_x = 1.67 \pm 0.08$ Mev ($\Gamma = 1.13 \pm 0.08$ Mev). In ^{10}C, in addition to the sharp ground and first excited states, level structure centered at $E_x = 5.28$ and 6.58 Mev is observed. (auth)

42191 THE APPLICATION OF THE SU(3) SHELL MODEL TO ^{9}Be. Adler, C.; Corcoran, T.; Mast, C. (Univ. of Notre Dame, Ind.). Nucl. Phys., 88: 145-68 (1966).

The normal and nonnormal parity levels, as well as the static properties of the ground state of ^{9}Be are investigated using the Elliott SU(3) shell model. The model predicts that the nonnormal (i.e., positive) parity levels from a $K = 1/2$ rotational band. Three different normal-parity energy level schemes are proposed, and it is shown that they each, to a good approximation, are composed of a $K = 3/2$ band and a $K = 1/2$ band. Each of the three normal-parity schemes involve an approximate degeneracy. For all three energy level schemes, the calculated ground-state quadrupole moment is in excellent agreement with experiment and does not aid in distinguishing between them. On the other hand, the ground state magnetic moment does depend significantly on the particular scheme chosen and favors a scheme that has a degeneracy at 2.50 Mev involving two levels with spin and parity assignment $1/2^-$ and $5/2^-$, respectively. It is concluded that the SU(3) shell model is capable of describing the ^{9}Be nucleus, and it is suggested that the normal-parity energy level scheme with the $1/2^-$, $5/2^-$ degeneracy is involved in this description. Finally, the results of some photodisintegration calculations are reported, which tend to confirm the preceeding conclusion. (auth)

42192 THE METASTABLE $d_{\frac{1}{2}}$ HOLE STATE IN ^{47}Sc. Bardin, T. T.; Runge, K.; Wu, C. S. (Columbia Univ., New York). Nucl. Phys., 88: 169-76(1966).

With a Ge(Li) detector, the γ spectrum of ^{47}Sc (populated by β decay of ^{47}Ca) was studied. The results obtained were two weak γ rays (0.5324 ± 0.0007 and 0.7640 ± 0.0007 Mev) were observed in the singles spectrum; the intensities of the γ transitions were determined to be $(0.17 \pm 0.02)\%$ of the total transition rate from the 1.2945-Mev level; from the delayed coincidence spectrum, the 0.7640-Mev line was found to be the only transition deexciting the metastable state; from the time-to-pulse-height spectrum, the half life was more accurately measured to be 270 ± 12 nsec. In addition, the technique of applying the Ge(Li) detector to coincidence work in spectroscopic studies is described. (auth)

42193 EVIDENCE FOR THE PRESENCE OF ALPHA CLUSTERS IN THE BORON ISOTOPES. Geesaman, Lynn B.; Knowles, H. B.; Mead, J. B. (Lawrence Radiation Lab., Livermore, Calif.). Nucl. Phys., 88: 177-92 (1966).

Thin aluminum-backed targets of ^{10}B and ^{11}B were bombarded with alpha particles of about 25 Mev. The alpha-particle momentum spectra taken at a lab angle of 46.4° were transformed to barycentric energy spectra after subtraction of background from the aluminum. A suggestion of four-body break-up of ^{10}B is thus obtained, but no such simple conclusion can be drawn from the ^{11}B spectrum. The types of fragments emitted were examined and were found to consist of ^{6}Li, ^{4}He and ^{2}H from the ^{10}B target and principally of ^{7}Li and ^{4}He from the ^{11}B target. Some evidence for the interesting two-body reaction $^{11}B(\alpha,{}^7Li)^8Be$ appears. (auth)

42194 AN ANALYSIS OF SOME SYNTHETIC CROSS-SECTION FLUCTUATION DATA. Dallimore, P. J.; Hall, I. (Nuclear Physics Lab., Oxford). Nucl. Phys., 88: 193-207(1966).

Excitation functions were synthesized according to the prescription of the statistical model of cross-section fluctuations. Examination of these indicates an insensitivity to the type of energy-level distribution employed; that the energy level overlap Γ/D need not be very large to permit a sensible fluctuation analysis in practice; and that the effects of a finite energy range of data are satisfactorily given by estimates which are also presented here. (auth)

42195 NEUTRON-PROTON CORRELATION EFFECTS IN SPHERICAL EVEN NUCLEI. Chen, H. T.; Goswami, A. (Western Research Univ., Cleveland). Nucl. Phys., 88: 208-14(1966).

The role of neutron-proton pairing correlations in the description of collective quadrupole states of even spherical nuclei with $40 < A < 70$ is studied. It is concluded that neutron-proton pairing correlations are significant in this region and with their inclusion one may be able to extend the region of applicability of the simple pairing plus quadrupole force model to all even spherical nuclei with $A > 40$. (auth)

42196 NEUTRON FISSION-EVAPORATION COMPETITION IN NUCLEI EMITTED IN THE BOMBARDMENT OF Bi BY PROTONS AT 100 TO 150 Mev. Le Beyec, Y.; Lefort, M.; Peter, J. (Institut de Physique Nucleaires, Orsay, France). Nucl. Phys., 88: 215-24(1966). (In French).

The cross sections were measured of polonium isotopes with mass numbers 197 to 203 produced in the bombardment of a bismuth target by 100 to 150 Mev protons. Since a fission-evaporation completion occurs at each step of the de-excitation process, the fission width for the de-excitation of every polonium nucleus from mass 198 to mass 210 and its dependence on the excitation energy can be deduced. It was shown that the total fission cross section of 120 mb is due to fission events occurring mainly on light polonium isotopes excited to excitation energies lower than 50 Mev. The neutron spectra at 0 and 90° were calculated, assuming that neutrons are emitted from excited nuclei before fission or from excited fragments. (auth)

42197 ON THE DECAY SERIES $^{138}Nd \rightarrow {}^{138}Pr \rightarrow {}^{138}Ce$. Gromov, K.; Demeter, I.; Schelev, Sch.; (and others) (Vereinigtes Institut fuer Kernforschung, Dubna, USSR). Nucl. Phys., 88: 225-34(1966). (In German).

The half life of ^{138}Nd was determined ($T_{\frac{1}{2}} = 5.2 \pm 0.1$ h). The half life of the ground state of $^{138}Pr(1^+)$ ($T_{\frac{1}{2}} = 1.5 \pm 0.15$ min) and the mass difference of the nucleides ^{138}Pr (1^+) and ^{138}Ce ($Q = 4460 \pm 40$ kev) were found. The energy difference of the isomeric state of ^{138}Pr ($T_{\frac{1}{2}} = 2.1$ h) and the ground state ($E = 330 \pm 60$ kev) was determined. The

log ft values for beta decay to the lower levels of ^{138}Ce from the ^{138}Pr(I^+) decay were calculated. The nature of the levels in the ^{138}Ce nucleus is discussed. (auth)

42198 A RESONANT ABSORPTION MEASUREMENT IN THE REACTION ^{26}Mg(p,γ)^{27}Al. van der Leun, C.; Jaspers, N. C. Burhoven (Rijksuniversiteit, Utrecht). Nucl. Phys., 88: 235-40(1966).

A resonant absorption measurement at the 1966-kev proton resonance in the reaction ^{26}Mg(p,γ)^{27}Al leads to an absolute determination of the resonance strength, $(2J + 1)\Gamma_p\Gamma_\gamma/\Gamma$, of 5.6 ± 1.8 eV. Normalization of previously published strengths of 120 resonances in the reaction ^{26}Mg(p,γ)^{27}Al, reduces these strengths by a factor of 2.7. (auth)

42199 PARTICLE-HOLE DESCRIPTION OF ^{28}Si AND ^{32}S. Farris, S. A.; Eisenberg, J. M. (Univ. of Virginia, Charlottesville). Nucl. Phys., 88: 241-56(1966). (ORO-2915-55).

Energy levels and transition rates are calculated for ^{28}Si and ^{32}S in the framework of the particle-hole model. Transitions between excited states as well as transitions to and from the ground state are considered. Particular attention is given to the low-lying energy levels and to the $J^\pi = 1^-$ states in the giant resonance regions of the two nuclei. A finite-range force is employed in the residual interaction. A spherical basis set is used in constructing the secular matrix and is limited to $0\hbar\omega$ and $1\hbar\omega$ excitations. Reasonable agreement is obtained for the positions of energy levels and many of the transition rates. Corrections to previous work in the literature on ^{28}Si giant resonance calculations are also presented. (auth)

42200 REACTIONS LEADING TO ^{37}Ar AND ^{37}K ENERGY LEVELS. McNally, J. H. (California Inst. of Tech., Pasadena). Nucl. Phys., 88: 257-72(1966).

Thirty-four ^{37}Ar levels were found with the ^{39}K(d,α)^{37}Ar and ^{35}Cl(^{3}He,p)^{37}Ar reactions, and the spectra of these two reactions are compared in a search for the $T = 3/2$ analogue to the ^{37}Cl ground state. The nuclear temperature calculated from the ^{37}Ar level density is 1.4 Mev. The angular distribution of the ^{39}K(d,α)^{37}Ar reaction to the lowest six levels at 10 Mev indicates a dominant direct interaction mechanism. The $2I + 1$ rule of the statistical model is found to be inapplicable. The ground-state Q-value of the ^{40}Ca(p,α)^{37}K reaction was measured to be −5179 ± 9 kev. This value implies a ^{37}K mass excess of −24804 ± 10 kev. (auth)

42201 LEVEL STRUCTURE OF NUCLEI WITH N = 29 AND $22 \leq Z \leq 26$. Ohnuma, Hajime (Tokyo Univ.). Nucl. Phys., 88: 273-84(1966).

Energy levels of ^{51}Ti, ^{52}V, ^{53}Cr, ^{54}Mn, and ^{55}Fe are calculated by the shell model with configuration mixing. The simple form of the effective n−p interaction is assumed and is taken to fit the energy levels of ^{56}Co and ^{50}Sc. Spectroscopic factors are also calculated in ^{50}Ti(d,p)^{51}Ti, ^{51}V(d,p)^{52}V, ^{52}Cr(d,p)^{53}Cr, and ^{54}Fe(d,p)^{55}Fe reactions. Overall agreements with experiments are obtained. For the odd-mass nuclei ^{51}Ti, ^{53}Cr, and ^{55}Fe, the results are satisfactory to explain the experiments below about 2 Mev in excitation energy. For the odd nuclei ^{52}V and ^{54}Mn, agreements are less unambiguous, but the general trends are reproduced. (auth)

42202 THE 16-min ^{241}Np ISOMER AND A SEARCH FOR ITS 3.4-hr ISOMER. Qaim, S. M. (Univ. of Birmingham, Eng.). Nucl. Phys., 88: 285-8(1966).

Some information on the decay data of 16-min ^{241}Np was obtained. A search for the 3.4-hr isomeric state showed that this activity probably does not exist. (auth)

42203 LEVELS AND TRANSITIONS IN ^{133}Cs. Thun, J. E.; Toernkvist, S.; Nielsen, K. Bonde; Snellman, H.; Falk, F.; Mocoroa, A. (Univ., Uppsala). Nucl. Phys., 88: 289-306(1966).

The decay of ^{133}Ba to levels of ^{133}Cs was studied. The energies of transitions in ^{133}Cs were determined from internal-conversion spectra recorded using an iron-free double-focusing spectrometer. Level energies, conversion line intensities, and conversion coefficients were obtained. Directional correlation measurements were also performed, and the electron-capture decay energy to the 437-kev level was determined. Transition probabilities were calculated for most of the transitions and were compared with predictions made by Kisslinger and Sorensen; the agreement was fairly good. The internal-conversion process of the retarded 1-forbidden M1 transitions was also considered; no evidence of penetration effects was obtained. (D.C.W.)

42204 THE REACTION (p,d) AT 156 Mev ON FLUORINE AND NITROGEN AND CONFIGURATION MIXING IN THE NUCLEI ^{13}N, ^{14}N, ^{18}F, AND ^{19}F. Bachelier, D.; Bernas, M.; Brissaud, I.; Radvanyi, P.; Roy, M. (Institut de Physique Nucleaire, Orsay, France). Nucl. Phys., 88: 307-20(1966). (In French).

The (p,d) reaction at 156 Mev on nitrogen and fluorine was studied to test a configuration-mixing description of the target and residual nuclei, and the single interaction pick-up mechanism. At this energy, a simple method is used to extract the relative spectroscopic factors for a given l for the whole spectrum. The comparison was made using spectroscopic factors calculated for nitrogen and fluorine with wave functions of Ripka and Giraud, and with the 1p wave functions of Cohen and Kurath for nitrogen. For nitrogen there is a good agreement between the experimental and theoretical spectroscopic factors especially when comparing with those calculated by Kurath where agreement is within about 20%. Such an agreement was also obtained for other nuclei of the 1p shell. For fluorine, the theoretical description seems qualitatively correct up to about 5-Mev excitation in ^{18}F. Excitation of the observed higher states must be assigned to pick-up in the inner 1p shell or to the contribution of more complex configurations. (auth)

42205 PARTICLE-HOLE EXCITATIONS IN ^{208}Pb. Gillet, V. (Centre d'Etudes Nucleaires, Saclay, Gif-sur-Yvette, France); Green, A. M.; Sanderson, E. A. Nucl. Phys., 88: 321-43(1966).

A good description of the known collective and non-collective odd-parity levels of ^{208}Pb may be obtained in terms of particle-hole excitations, with an interaction deduced from the spectroscopy of lighter closed shell nuclei. The random phase approximation appears to be essential for a correct prediction of transition rates; it does not require the introduction of any effective charge provided enough particle-hole configurations are included. No collective even-parity states are obtained with the model, even when $2\hbar\omega$ particle-hole configurations are included. (auth)

42206 EXCITATION FUNCTION FOR THE REACTION ^{197}Au(d,p)^{198}Au. Nassiff, S. J. (Comision Nacional de Energia Atomica, Buenos Aires); Quel, E.; Testoni, J.; Sandoval, E. Nucl. Phys., 88: 344-8(1966).

The excitation function for the reaction ^{197}Au(d,p)^{198}Au was experimentally determined using the stacked-foil technique. The energy of the deuterons in the incident beam was 27.5 Mev. The results were compared with calculated values based on the model proposed by Peaslee for a direct reaction mechanism. (auth)

42207 MEASUREMENT OF (n,2n) REACTION CROSS SECTIONS AT 14.8 Mev. Prasad, R.; Sarkar, D. C. (Muslim Univ., Aligarh, India). Nucl. Phys., 88: 349-52 (1966).

The activation cross sections for (n,2n) reactions on ^{140}Ce, ^{35}Cl, ^{168}Er, ^{179}Hf, ^{180}Hf, ^{115}In, ^{208}Pb, ^{31}P, ^{159}Tb, ^{184}W, and ^{186}W at 14.8 Mev were measured. (D.C.W.)

42208 SATURATION IN FINITE NUCLEI. Bhaduri, R. K. (McMaster Univ., Hamilton, Can.); Tomusiak, E. L. Nucl. Phys., 88: 353-60(1966).

It is concluded from a model calculation on finite nuclei that any effective two-nucleon force to be used for a Hartree-Fock calculation in the Ca region, or for heavier nuclei, should be chosen to give the correct saturation density in nuclear matter. For light nuclei like ^{16}O, however, reasonable saturation densities can be obtained by using forces without any short-range correlation. (auth)

42209 ANGULAR FUNCTIONS FOR A THREE-NUCLEON SYSTEM. Davies, B. (Univ. of New South Wales, Kensington). Nucl. Phys., 88: 361-72(1966).

Angular functions are developed which are suitable for writing down trial functions for variational and other types of calculations for a three-body nucleus. They are expressed in terms of a simple set of functions for the problem, first given by Derrick, and later extended to arbitrary states by Kalotas and Delves. (auth)

42210 STRIPPING FEATURES OF $^{6}Li(d,n)^{7}Be^{*}$ (0.43 Mev) AT E_d FROM 0.2 TO 0.8 Mev. Schier, W. A. (Univ., Basel); Michel, G.; Benenson, R. E. Nucl. Phys., 88: 373-84(1966).

Angular distributions of neutrons from the $^{6}Li(d,n)^{7}Be^{*}$ (0.43 Mev) reaction were obtained over the angular range 0 to 160° at deuteron energies of 0.24, 0.34, 0.44, 0.54, 0.64, and 0.84 Mev with an associated gamma time-of-flight measurement. All display $l_p = 1$ stripping patterns and are fitted with PWBA theory using a constant $r_0 = 5.7$ fm. The shapes of the 0.24 and 0.34 Mev distributions are fully reproduced with the PWBA distributions. A dispersion-theory interpretation of the break angle between PWBA theory and all available experimental data up to $E_d = 3.0$ Mev is in good agreement with the break angle calculated for a constant energy denominator of 8.16 Mev. (auth)

42211 MEASUREMENTS OF THE ENERGY LEVEL STRUCTURE OF Cr ISOTOPES USING (d,p) AND (p,p') REACTIONS. Macgregor, A.; Brown, G. (Bradford Inst. of Tech., Eng.). Nucl. Phys., 88: 385-410(1966).

Data on the energy levels of ^{50}Cr, ^{51}Cr, ^{52}Cr, ^{53}Cr, ^{54}Cr, and ^{55}Cr were obtained from a study of (d,p) and (p,p') reactions with the naturally occurring isotopes of chromium. Comparison of the (p,p') and (d,p) reactions leading to states of ^{53}Cr and ^{54}Cr show large differences in the population of the states at all excitation energies. The data reported are used to obtain information on the variation of the single-particle level density near the closed neutron shell. (auth)

42212 STUDY OF THE REACTION $p + {}^{9}Be \rightarrow d + {}^{8}Be$. Laugier, J. P.; Lemeille, C.; Marquez, L.; Saunier, N. (Centre d'Etudes Nucleaires, Saclay, France). Nucl. Phys., 88: 411-16(1966). (In French).

The energy spectra of the deuterons and alpha particles from the reaction $p + {}^{9}Be$ were measured using the Saclay tandem accelerator and a particle discrimination system. The deuteron spectra can be quantitatively explained if it is assumed that the reaction goes through the first excited state of ^{8}Be. The alpha spectra show peaks corresponding to the ground state and to the first and second excited states of ^{6}Li. (auth)

42213 SMALL ANGLE COMPTON SCATTERING WITH 17 Mev γ-RAYS FROM THE $^{7}Li(p,\gamma)^{8}Be$ REACTION. Peyman, A. A.; Scholz, W.; Sepp, G. (Univ. Freiburg i. B.). Nucl. Phys., 88: 417-23(1966).

The differential Compton scattering cross section for 17-Mev photons was measured from 1.33 to 7°. Compton electrons produced in NaI(Tl) crystals and plastic scintillators as scattering material were registered in coincidence with the scattered photons. Within the error limits, the results are consistent with both the Klein-Nishina formula and the correct expression for the Compton scattering cross section which includes the contributions of higher order corrections. In the angular range investigated, an upper limit of 15% of the Klein-Nishina cross section can be set for possible contributions to the total differential cross section from radiative corrections and double Compton scattering. (auth)

42214 CHARGED PHOTOPARTICLES FROM ^{165}Ho. Scanlon, P. J. (Queen's Univ., Kingston, Ont.). Nucl. Phys., 88: 424-32(1966).

A solid-state detector telescope was used for measurements on heavy charged photoparticles produced by the irradiation of ^{165}Ho with bremsstrahlung from a 70-Mev synchrotron. Photoproton spectra in the energy range 6.5 to 14 Mev are shown for measurements at 90 and 135° to the x-ray beam direction. Two peaks were observed in the proton spectra, at 9.25 and 12.25 Mev. The higher energy peak is less prominent at the backward angle. The energy of the protons in the lower-energy 9.25-Mev peak, plus the binding energy for protons in ^{165}Ho, is shown to be very nearly equal to the gamma energy that corresponds to the higher-energy peak of the split giant dipole resonance. A similar correlation is shown to exist for results by other authors on tantalum and praseodymium. At 90° the measured deuteron proton ratio was 0.04 and the triton/deuteron ratio was 0.25. The d/p ratio is similar to other measurements but the t/d ratio is about four times larger. (auth)

42215 THE DISTORTED WAVE t-MATRIX APPROXIMATION FOR THE (p,2p) REACTION. Lim, K. L. (Univ. of California, Davis. Univ. of Oregon, Eugene); McCarthy, I. E. Nucl. Phys., 88: 433-56(1966).

A refined distorted-wave approximation (DWA) for the (p,2p) reaction is discussed. The matrix element of the (p,p) t-matrix in an antisymmetrized distorted-wave representation is evaluated using a local spin-dependent model for the t-matrix which reproduces the correct (p,p) scattering in the absence of the nuclear core. The distorted waves are computed with potentials which fit elastic scattering in the corresponding proton-core system at the appropriate energy. The approximation is believed to exhaust the possibilities of DWA for a quasi-three-body reaction in a situation which is shown to be very sensitive to three-body effects. The approximation fails in a consistent and regular way for different target nuclei at different energies. The theoretical angular correlation curve is reproduced at angles which are too small. A good fit is obtained by increasing the distorting potential, which is responsible for three-body effects. A thorough parameter study and investigation of the model is made, and it is concluded that in low-energy (p,2p) experiments a situation exists which is sensitive to the details of a three-body theory and for which a DWA is inadequate. (auth)

42216 THE REACTIONS $^{20}Ne(n,\alpha)^{17}O$ AND $^{16}O(n,\alpha)^{13}C$ AT 14 Mev NEUTRONS. McDicken, W. N.; Jack, W. (Glasgow Univ.). Nucl. Phys., 88: 457-64(1966).

A counter telescope consisting of two thin proportional counters and a semiconductor detector was used to measure the absolute differential cross sections for the transitions $^{20}Ne(n,\alpha)^{17}O$ to the ground and first excited state of ^{17}O and $^{16}O(n,\alpha)^{13}C$ to the ground state of ^{13}C. The neutron energy was 14.1 Mev with a spread of ±35 kev. Evidence is presented for the belief that these reactions proceed by direct reaction mechanisms, and the possible mechanisms present are briefly discussed. (auth)

42217 ANGULAR DISTRIBUTIONS OF α-PARTICLES FROM THE REACTION $^{11}B(^{3}He,\alpha)^{10}B$. Lonergan, J. A.; Donahue, D. J. (Univ. of Arizona, Tucson). Nucl. Phys., 88: 465-73(1966).

The angular distributions of α-particles from the reaction $^{11}B(^{3}He,\alpha)^{10}B$ leading to the four lowest states in ^{10}B were measured for ^{3}He energies of 1.0, 1.8, and 2.15 Mev. The distributions were compared with predictions made from the plane-wave, Butler pick-up theory which was extended to the case of $(^{3}He,\alpha)$ reactions. The comparison indicates the presence of the direct interaction mechanism for the excitation of the three lowest states in ^{10}B. The α-particles associated with the formation of the 2.15-Mev state in ^{10}B were symmetric about 90° in the center-of-mass system. The excitation functions for the formation of the five lowest states in ^{10}B by the $^{11}B(^{3}He,\alpha)^{10}B$ reaction were measured for ^{3}He energies from 1.0 to 2.15 Mev. (auth)

42218 COULOMB EXCITATION IN THE PLATINUM ISOTOPES. Grodzins, L.; Borchers, R. R.; Hagemann, G. B. (Univ. of Copenhagen). Nucl. Phys., 88: 474-80 (1966).

Coulomb excitation experiments using 36-Mev oxygen ions were carried out on thick platinum targets enriched in ^{190}Pt and ^{198}Pt. The gamma rays were detected in a ≈ 2 cm^3 Ge(Li) detector. The relative $B(E2)_{ex}$ ($0^+ \rightarrow 2^+$) values show a maximum at ^{192}Pt, where the enhancement is ≈69. The $B(E2)_{ex}$ values were also obtained for ^{195}Pt;

they are in essential agreement with previous Coulomb excitation results. (auth)

42219 GYROMAGNETIC RATIO OF THE 564 kev STATE IN ^{122}Te. Auerbach, K.; Harms, B.; Siepe, K.; Wittkemper, G.; Koerner, H. J. (Univ., Hamburg). Phys. Lett., 22: 299-300(Aug. 15, 1966).

The g factor of the 564 kev first vibrational state in ^{122}Te was determined by perturbed angular correlations as g = +0.44 ± 0.06. This value is compared with the predictions of nuclear model calculations. (auth)

42220 SPECIFIC FEATURES OF THE PHOTODISINTEGRATION OF NUCLEI IN THE 1f-2p SHELL. Ishkhanov, B. S.; Kapitonov, I. M.; Majling, L. Phys. Lett., 22: 301-3(Aug. 15, 1966).

Features of the photodisintegration of 1f-2p shell nuclei connected with the existence of valence nucleons are discussed. Calculations are carried out for ^{58}Ni. (auth)

42221 FORM FACTORS FOR DWBA CALCULATIONS OF NEUTRON PICK-UP REACTIONS LEADING TO ISOBARIC ANALOGUE STATES. Stock, R. (Max-Planck Institut fuer Kernphysik, Heidelberg); Tamura, T. Contract W-7405-eng-26. Phys. Lett., 22: 304-7(Aug. 15, 1966). (ORNL-P-2282).

It is shown that if use is made of the solution of the Lane coupled-equations as the form factor in DWBA, the derived neutron pickup spectroscopic factor becomes sufficiently small to be consistent with the sum rule. (auth)

42222 DENSITY OF STATES OF DEGENERATE FERMI SYSTEMS WITH PERIODIC LEVEL SCHEMES. Kahn, P. B.; Rosenzweig, N. (Argonne National Lab., Ill.). Phys. Lett., 22: 307-9(Aug. 15, 1966).

An accurate and transparent asymptotic formula was derived for the density of states of a degenerate Fermi system with an arbitrary periodic independent-particle energy level scheme. The work generalizes, unifies, and simplifies earlier treatments of related problems. (auth)

42223 INFLUENCE OF COMPOUND NUCLEUS CONTRIBUTIONS ON (d,p) REACTIONS. Goldfarb, L. J. B.; Wong, K. K. (Univ. of Manchester, Eng.). Phys. Lett., 22: 310-12(Aug. 15, 1966).

The angular correlation, $W(\theta_\gamma)$, for ^{52}Cr(d,pγ)^{53}Cr with $\theta_p = 0$ or 180° and a variety of deuteron energies is computed using the DWBA. Comparison is given to predictions based on compound nucleus contributions, as calculated using the Hauser-Feshbach formalism. (auth)

42224 EXCITED LEVELS IN ^{3}He. Kim, C. C.; Bunch, S. M.; Devins, D. W.; Forster, H. H. (Univ. of Southern California, Los Angeles). Phys. Lett., 22: 314-15(Aug. 15, 1966).

The inelastic proton spectrum from the ^{3}He + p reaction was investigated in a search for excited states in ^{3}He. Possible evidence for the existence of virtual levels is discussed. (auth)

42225 SEARCH OF PARITY MIXING IN ^{180}Hf BY A MEASUREMENT OF THE CIRCULAR POLARIZATION OF γ RAYS. Bock, P.; Jenschke, B.; Schopper, H. (Technische Hochschule, Karlsruhe, Ger. Kernforschungszentrums, Karlsruhe, Ger.). Phys. Lett., 22: 316-17 (Aug. 15, 1966).

The circular polarization of the 57-kev transition as well as of the 501-kev cross-over transition was measured. Within experimental errors, no polarization was observed. (auth)

42226 INFLUENCE OF A RANDOMLY ORIENTED COLLINEAR COMBINED INTERACTION ON ANGULAR CORRELATIONS. Raghavan, R. S. (Univ., Bonn). Phys. Lett., 22: 318-20(Aug. 15, 1966).

Perturbations due to a randomly oriented collinear combined interaction on angular correlations are studied and applications to the determination of quadrupole moments of rare earth excited states are discussed. (auth)

42227 ISOSPIN QUINTUPLETS IN A = 20 NUCLEI. Loncke, P.; Pradal, J. (Institut de Physique Nucleaire, Orsay, France). Phys. Lett., 22: 320-2(Aug. 15, 1966).

It is shown that the T = 2 levels of ^{20}Ne can be interpreted in the framework of a simple shell model calculations, though the low-lying levels are known to be deformed. (auth)

42228 ZERO-RANGE TREATMENT OF THE THREE-BODY PHOTODISINTEGRATION CROSS SECTION OF ^{3}H AND ^{3}He. Knight, J. M. (Univ. of South Carolina, Columbia. Naval Ordnance Lab., White Oak, Md.); O'Connell, J. S.; Prats, F. Phys. Lett., 22: 322-5(Aug. 15, 1966).

A zero-range approach is used to construct bound and continuum state wave functions. The total and differential electric dipole photodisintegration cross sections for three-body breakup of ^{3}He and ^{3}H are calculated using these wave functions. (auth)

42229 MULTIPLE EXCITATION AND THE SHELL MODEL DESCRIPTION OF THE ^{90}Zr(p,p') REACTION. Love, W. G.; Satchler, G. R.; Tamura, T. (Oak Ridge National Lab., Tenn.). Contract W-7405-eng-26. Phys. Lett., 22: 325-7(Aug. 15, 1966). (ORNL-P-2323).

It is shown that multiple excitation effects are small for the inelastic scattering of 10 to 20 Mev protons from ^{90}Zr when a microscopic description of the reaction with shell model wavefunctions is used. (auth)

42230 SEARCH FOR PARITY MIXING IN THE 501 kev γ TRANSITION OF ^{180m}Hf. Blumberg, H.; Speidel, K.-H.; Schlenz, H.; Rasera, R. L.; Bodenstedt, E. (Univ., Bonn). Phys. Lett., 22: 328-30(Aug. 15, 1966).

The circular polarization of the 501 kev γ transition in ^{180m}Hf was measured as P_c (501 kev) ≤2%. Combining this result with the measurement of the 501 kev−332 kev $\gamma\gamma$ angular correlation the parity forbidden E2 content of the 501 kev radiation is found to be less than 0.2%. (auth)

42231 BRANCHING RATIOS IN ^{14}C AND ^{14}N. Carlson, R. R. (Univ. of Iowa, Iowa City). Phys. Rev., 148: 991-8(Aug. 19, 1966).

The ^{9}Be(^{7}Li,d)^{14}C and ^{10}B(^{6}Li,d)^{14}N reactions were used as sources of gamma-emitting excited states of ^{14}C and ^{14}N. Three-parameter measurements of E, dE/dx, and E_γ in 1024 × 1024 × 256-channel detail were used to identify deuteron groups and the gamma rays associated with them. Radiation from six bound levels in ^{14}C and from eight bound levels in ^{14}N was analyzed to give branching ratios. Results are generally in agreement with previous measurements where they have been made. Two unbound levels in ^{14}N are found to gamma-decay in competition with proton decay. (auth)

42232 6.92- TO 6.05-Mev E2 TRANSITION IN ^{16}O. Lowe, J. (Univ. of Birmingham, Eng. Brookhaven National Lab., Upton, N. Y.); Poletti, A. R.; Wilkinson, D. H. Phys. Rev., 148: 1045-50(Aug. 19, 1966). (BNL-10029).

The branching ratio of the $J^\pi = 2^+$ 6.92-Mev level of ^{16}O via the $J^\pi = 0^+$ 6.05-Mev level was measured to be R = 2.3 ± 0.5 × 10^{-4}. This corresponds to an E2 transition strength of several single-particle units and supports the suggestion that these two states are the lowest members of a rotational band. (auth)

42233 PROPERTIES OF EXCITED STATES IN ^{14}C. Alburger, D. E. (Brookhaven National Lab., Upton, N. Y. Institut de Recherches Nucleaires, Strasbourg); Gallmann, A.; Nelson, J. B.; Sample, J. T.; Warburton, E. K. Phys. Rev., 148: 1050-63(Aug. 19, 1966). (BNL-10082).

The 6.59-, 6.72-, 6.89-, and 7.34-Mev levels of ^{14}C, formed in the ^{13}C(d,p)^{14}C reaction, were studied by means of proton-gamma and gamma-gamma coincidence techniques, magnetic-pair spectrometer measurements, and observations with a Ge(Li) gamma-ray detector. Transition branches from the 6.59-Mev level are 6.59 → 6.09 (99.0 ± 0.4)% and 6.59 → 0 (1.0 ± 0.4)%. Gamma branches determined for the 6.72-Mev level are 6.72 → 6.09 (7 ± 2)% and 6.72 → 0 (93 ± 2)%. For the 7.34-Mev level the gamma branches are 7.34 → 6.72 (35 ± 7)%, 7.34 → 6.09 (47 ± 4)%, and 7.34 → 0 (18 ± 4)%. Multipolarity measurements with the magnetic pair spectrometer have shown that the 6.72-Mev transition is almost certainly E3 and that the 7.34-Mev transition is not E1. Gamma rays observed with the Ge(Li)

detector from the 6.72 → 0 and 6.59 → 6.09 transitions are neither Doppler-broadened nor Doppler-shifted, whereas the gamma rays from the 7.34 → 0, 7.34 → 6.09, and 6.89 → 6.09 transitions exhibit Doppler effects. Accurate gamma energies were measured for some of the cascade transitions. By combining the various observations with previous work, it is concluded that the 6.72-Mev level is $J^{\pi} = 3^-$ and the 7.34-Mev level is $J^{\pi} = 2^-$. Theoretical calculations were made for the various transition rates in ^{14}C and are compared with the experimental results. An incidental experimental result is a value of 495.33 ± 0.10 kev for the energy of the first excited state of ^{17}F. (auth)

42234 LIFETIME DETERMINATIONS FOR NUCLEI A = 10, 11, AND 12 FROM GAMMA-RAY DOPPLER SHIFTS. Warburton, E. K. (Brookhaven National Lab., Upton, N. Y.); Olness, J. W.; Jones, K. W.; Chasman, C.; Ristinen, R. A.; Wilkinson, D. H. Phys. Rev., 148: 1072-82(Aug. 19, 1966). (BNL-9804).

The Doppler-shift-attenuation technique was used to investigate the lifetimes of excited states of ^{10}Be, ^{10}B, ^{11}B, ^{11}C, and ^{12}C. Gamma rays from nuclear levels populated by d, ^3He, and α bombardment of thick Be and Cu–Be targets were detected with a lithium-drifted germanium detector at both forward and backward directions relative to the incident beam direction. Lifetimes were then extracted by comparing the differences in the Doppler shift as measured with the two targets. Gamma peaks from ^9Be + d were observed for the ^{10}Be 5.96 → 3.37, ^{10}Be 3.37 → 0, ^{10}B 3.59 → 0.72 and ^{10}B 5.16 → 2.15 transitions; and mean lifetimes of $<0.8 \times 10^{-13}$ sec, $1.6 \pm 0.3 \times 10^{-13}$ sec, $1.20 \pm 0.43 \times 10^{-13}$ sec, and $<0.8 \times 10^{-13}$ sec were obtained for the initial states of these transitions. The Doppler shift of the ^{12}C 4.43 → 0 transition was investigated using the $^9Be(\alpha,n)^{12}C$ reaction. A mean lifetime of 5.7×10^{-14} sec was obtained for the ^{12}C 4.43-Mev level. Levels in ^{11}B and ^{11}C were formed by the $^9Be(^3He,p)^{11}B$ and $^9Be(^3He,n)^{11}C$ reactions, and upper limits were set for the mean lifetimes of five levels in these nuclei. The strengths of known transitions from the ^{10}B 2.15- and 3.59-Mev levels are discussed in terms of the independent-particle model. The agreement is found to be generally good for the 3.59-Mev level and to be poor for the 2.15-Mev level. Several experimental and theoretical points remain to be clarified. (auth)

42235 QUADRUPOLE ELASTIC SCATTERING OF ALPHA PARTICLES BY POLARIZED NUCLEI. Kim, Y. N.; Thomas H. C. (Texas Technological Coll., Lubbock). Phys. Rev., 148: 1083-7(Aug. 19, 1966).

The effect of the charge distribution of target nuclei on elastic scattering between nuclei at an incident energy well below the Coulomb barrier was investigated in terms of the deviation from Rutherford scattering. The result of the calculation for the case in which the target nuclei are oriented during the collision is reported. For the head-on collision of alpha particles with ^{238}U and ^{181}Ta at 24 and 16 Mev, it is found that the deviations from Rutherford scattering should be about 18 and 20%, respectively, if the polarization of the target is complete. Therefore, it is concluded that the deviation should be large enough for detection even for a reasonable degree of polarization of the target. (auth)

42236 AVERAGE FLUCTUATION POTENTIAL AS EFFECTIVE INTERACTION IN COMPOSITE-SYSTEM SCATTERING. Hahn, Yukap (Univ. of Connecticut, Storrs). Phys. Rev., 148: 1088-96(Aug. 19, 1966).

Symmetric forms of the effective interactions both for the elastic and rearrangement collisions of composite systems are derived, and the distorted-wave amplitudes are constructed. Explicit forms of the effective-interaction potentials contain in common a single Green's function factor as the distortion effect of the indirect channels which appear only as intermediate states. Approximation methods to evaluate this factor are discussed in terms of the closure, unitarity, and certain self-consistency requirements, while the direct channels are treated exactly. The closure approximation gives rise to the average fluctuation potentials which contain the complex average energies as adjustable parameters. Preliminary attempts to estimate these parameters theoretically are described for some special cases. The resulting approximate expressions for the amplitudes retain explicitly information on the two-body interactions and the asymptotic boundary conditions for the direct channels. (auth)

42237 (d,^{6}Li) REACTIONS IN LIGHT ELEMENTS AND DISTORTED-WAVE BORN APPROXIMATION CALCULATIONS. Denes, L. J.; Daehnick, W. W.; Driskc, R. M. (Univ. of Pittsburgh). Phys. Rev., 148: 1097-1107 (Aug. 19, 1966).

Differential cross sections for (d,^{6}Li) reactions were measured for ^{13}C, ^{17}O, ^{18}O, and ^{19}F targets in addition to those reported previously for ^{12}C, ^{16}O, and ^{19}F. ^6Li particles were identified by using time-of-flight analysis in conjunction with energy analysis. (d,^{6}Li) reactions for all six targets investigated at incident deuteron energies near 15 Mev, have large total cross sections (4.2 to 0.6 mb). The angular distributions are diffraction-like and show forward peaking and minor sensitivity to energy changes of a few hundred kev. A theoretical interpretation of the (d,^{6}Li) reactions is given in terms of a simple direct four-nucleon transfer mechanism. Most calculations are made in the zero-range distorted-wave Born approximation (DWBA). The reaction form factor is calculated in the alpha transfer limit; an α cluster (with predictable quantum numbers) is assumed to exist in the target at the instant of the reaction and to be transferred as a whole. The cluster wave function is generated in a Saxon well of a depth determined by the α separation energy. Best-fit optical-model parameters for 15-Mev deuterons were used to generate the incident deuteron waves. All ^6Li distorted waves were based on an optical-model fit to the $^{12}C(^7Li,^7Li)$ ^{12}C scattering at 7 Mev. No adjustable parameters were used. In spite of these restrictions and the simplicity of the model, good agreement between data and calculations is observed for ^{12}C, ^{13}C, ^{16}O, ^{17}O, and ^{18}O. Agreement for $^{19}F(d,^6Li)^{15}N$ could be obtained only by parameter adjustments. The normalization of the DWBA predictions also appears to be in general agreement with the absolute magnitude for these reactions, and tentative spectroscopic factors for the reactions are obtained. (auth)

42238 ELASTIC AND INELASTIC ELECTRON SCATTERING FROM ^{12}C AND ^{16}O. Crannell, Hall (Stanford Univ., Calif.). Phys. Rev., 148: 1107-18(Aug. 19, 1966).

Electron elastic and inelastic scattering from ^{12}C and ^{16}O was studied for various scattered electron angles, using primary beam energies from 600 to 800 Mev. These studies cover a range of the square of the momentum transferred to the nucleus of 2.79 to 11.45 F^{-2} for ^{12}C, and 2.79 to 8.52 F^{-2} for ^{16}O. A procedure for subtracting the effects of energy loss due to radiation of the electrons is developed. With the resolution obtained in this experiment, it is possible to resolve elastically scattered electrons from inelastically scattered electrons. In many instances it is also possible to resolve electrons which have excited discrete nuclear levels in ^{12}C and ^{16}O. Inelastic electron scattering due to excitation of nuclear levels is observed for the 4.43-Mev 2^+ and 9.6-Mev 3^- levels in ^{12}C, and for the 6.1-Mev levels in ^{16}O. Differential cross sections for excitation of these levels as well as for elastic scattering are determined. Absolute values of the cross sections are obtained by comparison with known absolute proton cross sections. Analysis of the data using the first Born approximation shows that the root-mean-square radii of ^{12}C and ^{16}O are 2.40 ± 0.02 F and 2.65 ± 0.04 F, respectively. (auth)

42239 OBSERVATIONS OF THE MOESSBAUER EFFECT IN ^{133}Cs. Boyle, A. J. F.; Perlow, G. J. (Argonne National Lab., Ill.). Phys. Rev., 149: 165-70(Sept. 9, 1966).

In an extension ot measurements on the Mössbauer effect of the 81 kev transition in ^{133}Cs the isomer shifts of a variety of cesium chemicals, including the halides and the metal were measured. The measurements were done in transmission at 4.2°K using a source whose nominal composition was $^{133}BaAl_4$. The isomer shifts of the halides are shown to correlate linearly with the chemical shifts of their NMR frequencies. A fractional effect of

$(1.86 \pm 0.26) \times 10^{-4}$ was observed for the cesium metal, and the isomer shift with respect to $BaAl_4$ was -0.158 ± 0.057 mm/sec. When the latter is combined with the halogen shifts (which lead to an isomer shift of ~0.3 mm/sec for Cs^+), it is found that the cesium decay product of ^{133}Ba in $BaAl_4$ has the electron configuration $6s^2$. The existence of this species is supported by a plausibility argument in terms of the band structure of aluminum. The observed linewidth of the resonance in metallic cesium is 0.75 ± 0.18 mm/sec. In view of the source contribution, this is consistent with the natural linewidth. A spin-density-wave (SDW) ground state for Cs would lead to a hyperfine structure that was not observed. We conclude that for a linear SDW such as postulated for potassium by Overhauser, the linewidth indicates that the amplitude must be less than ~1% or the relaxation time less than 6×10^{-10} sec. An area analysis of the absorption in the metal leads to a recoilless fraction $f_{Cs} = 5.5 \times 10^{-5}$ and to the characteristic temperature $\Theta_M = 49 \pm 1°K$. In comparison, the Debye temperature at 0°K is $\Theta_D(0) = 40.5°$. From the shape of the function $\Theta_D(T)$ and the result $\Theta_M > \Theta_D(0)$, it is concluded that the phonon spectrum cuts off substantially higher than the frequency corresponding to $\Theta_D(0)$. A numerical calculation is made for the case of sodium where the spectrum is known and exhibits the predicted features. For this case a cancellation of two effects gives $\Theta_M = \Theta_D(0)$ within the error. (auth)

42240 SCATTERING AMPLITUDE FOR MULTIPOLE MIXTURES IN THE MOESSBAUER EFFECT. Wong, M. K. F. (Woodstock Coll., Md.). Phys. Rev., 149: 378-9(Sept. 9, 1966).

The scattering amplitude for multipole mixtures in the Mössbauer effect is worked out, from which other quantities, such as the absorption cross section and the complex refractive index, can be derived. The formula can also be used to measure E2/M1 mixing ratios and check time reversal invariance by means of the Mössbauer effect. (auth)

42241 ANALYSIS OF $_\Lambda{}^9Be$ AND $_\Lambda{}^{13}C$. Herndon, R. C. (Univ. of California, Livermore); Tang, Y. C. Contract W/7405-eng-48. Phys. Rev., 149: 735-43(Sept. 23, 1966). (UCRL-14874-T).

The hypernuclei $_\Lambda Be^9$ and $_\Lambda C^{13}$ are analyzed with the core nuclei treated in the alpha-particle model. Using a 2-body α-α potential that fits the low-energy $^1S_0$ phase shifts and an effective 3-body interaction which is introduced to simulate the effect of nucleon exchanges where all three alpha clusters are involved, the binding energy and charge form factors of ^{12}C can be correctly accounted for. The α-Λ interaction is obtained by folding a purely attractive Λ-nucleon potential into the nucleon density distribution of the alpha particle, with the depth determined from the binding energy B_Λ of $_\Lambda He^5$. Two α-Λ potentials are considered. These correspond to purely attractive Λ-nucleon interactions with intrinsic ranges appropriate to 2-pion and K-meson exchanges, respectively. The calculation is done with a Monte Carlo method, with both the upper and lower bounds of the eigenvalue determined. The results show that to obtain agreement with the experimentally determined values of B_Λ for $_\Lambda Be^9$ and $_\Lambda C^{13}$, it is necessary to use a Λ-nucleon potential with an intrinsic range less than about 1 F. Together with the conclusion reached by Bodmer, from a comparison of the hypernuclear results with the low-energy Λ-p scattering data, that purely attractive Λ-nucleon interactions with intrinsic ranges $b \lesssim 1$ F can be ruled out, the analysis gives a strong indication that the Λ-nucleon interaction is not purely attractive, but has a repulsive core. Also, it is found that the values for B_Λ are very sensitive to the structure of the core nuclei, which indicates that Λ particles may be used as a probe to study the structure of complex nuclei. (auth)

42242 STUDIES OF THE SHORT-LIVED ACTIVITIES ^{15}C, ^{17}F, ^{19}O, ^{20}F, AND ^{28}Al. Alburger, D. E.; Jones, K. W. (Brookhaven National Lab., Upton, N. Y.). Contract AT(30-2)-Gen-16. Phys. Rev., 149: 743-51(Sept. 23, 1966). (BNL-10153).

The short-lived activities ^{15}C, ^{17}F, ^{19}O, ^{20}F, and ^{28}Al were studied by bombarding targets with a mechanically chopped Van de Graaff deuteron beam and measuring the delayed gamma radiations with a lithium-drifted germanium detector. In the decay of ^{15}C, weak gamma rays of 8315 ± 6 and 9048 ± 4 kev were observed which correspond to beta-ray branches to the 8312- and 9052-kev states of ^{15}N with log ft values of 4.8 ± 0.3 and 3.7 ± 0.3, respectively. In the known beta decay of ^{19}O to the 1554-kev level of ^{19}F, the energy of this state is found to be 1553.9 ± 1.3 kev; and the measured gamma branching intensities agree with previous results. A weak gamma ray of 3334 ± 8 kev was observed in the beta decay of ^{20}F, corresponding to a beta branch to the 4969-kev state of ^{20}Ne with log ft = 6.9 ± 0.2. The energy of the ^{20}Ne first excited state was measured as 1632.6 ± 0.8 kev. The gamma ray emitted in the decay of ^{28}Al has an energy of 1777.8 ± 0.6 kev. Upper limits are given for other possible beta branches to known states in the decays of the various activities studied. (auth)

42243 EXACT SOLUTION TO OPTICAL-MODEL EQUATIONS FOR QUASI-ELASTIC (p,n) REACTIONS. Schwarcz, Ervin H. (Univ. of California, Livermore). Contract W-7405-eng-48. Phys. Rev., 149: 752-4 (Sept. 23, 1966). (UCRL-14873(Rev.1)).

The coupled optical-model equations describing quasi-elastic (p,n) reactions are solved exactly, and the results are compared with distorted-wave Born approximation (DWBA) solutions. It is shown that for reasonable values of the isobaric potential the DWBA deviates only slightly from the exact solution. Fits to experimental data are presented for $^{48}Ti(p,n)^{48}V$, $^{51}V(p,n)^{51}Cr$, and $^{52}Cr(p,n)^{52}Mn$. (auth)

42244 HOLE SELF-ENERGY CORRECTIONS IN THE BRUECKNER THEORY. Nuttall, J. (Texas A and M Univ., College Station). Phys. Rev., 149: 755-61(Sept. 23, 1966).

To study corrections to hole propagators in Brueckner theory, an extension of the Hugenholtz convolution theorem is proved. An integral equation is derived for a class of Brueckner hole corrections; and approximate solutions are obtained, one of which gives the usual prescription that makes holes propagate on the energy shell. The derivation shows which class of diagrams are included in this prescription and indicates that a more accurate treatment might be needed. (auth)

42245 COLLECTIVE NUCLEAR "BREATHING MODE" MODEL WITH APPLICATION TO ^4He MONOPOLE STATE. Werntz, Carl; Ueberall, H. (Catholic Univ. of America, Washington, D. C.). Phys. Rev., 149: 762-7(Sept. 23, 1966).

A collective model of the nuclear breathing mode is presented which avoids the usual assumption of a constant nuclear ground-state density. The 20.4-Mev 0^+ state in ^4He is treated as an example of such a breathing-mode state. (auth)

42246 ACCURATE EXCITATION ENERGIES OF ^{11}B STATES BELOW 7 Mev. Browne, C. P.; O'Donnell, F. H. (Univ. of Notre Dame, Ind.). Contract Nonr-1623(05). Phys. Rev., 149: 767-71(Sept. 23, 1966).

A recent precision measurement of gamma energy made with a lithium-drifted germanium detector disagrees with an earlier value of an excitation energy obtained by measurement of charged-particle energies. To investigate this discrepancy and to confirm the level assignment of the gamma-ray transition, excitation energies of ^{11}B states were measured using both the $^{10}B(d,p)^{11}B$ and $^9Be(^3He,p)^{11}B$ reactions. Particle energies were measured with a broad-range spectrograph calibrated with a ^{210}Po alpha source (5304.5 kev). Excitation energies determined with the data from the two reactions agree within 2.9 kev in all cases. The mean values are (in kev) 2124.4 ± 0.7, 4444.4 ± 1.4, 5018.9 ± 1.7, 6742.9 ± 1.8, and 6792.8 ± 1.8. The uncertainties are combinations of an uncertainty in the shape of the calibration curve with the standard deviation of the mean or the assumed internal error, whichever is greater. These uncertainties may be considered as standard deviations. The energy difference between the last two levels

was found to be 49.8 ± 0.3 kev. The value 6792.8 agrees exactly with the gamma energy, whereas this and the other excitation energies disagree by as much as 22 kev with earlier values from charged-particle measurement. (auth)

42247 REALISTIC POTENTIALS AND SHELL MODEL. [PART] I. Shakin, Carl M.; Svenne, Juris P.; Waghmare, Yeshwant R. (Massachusetts Inst. of Tech., Cambridge). Contract AT(30-1)-2098. Phys. Rev., 149: 772-7(Sept. 23, 1966). (MIT-2098-241).

Using the recent theory developed by Shakin for nuclear-structure calculations, energy-level calculations are made for realistic potentials such as the Yale potential and the nonlocal Tabakin potential. As examples, ^{90}Zr and ^{50}Ti are considered. The results for the spectra of these nuclei are compared with those of other authors and the experimental data. The agreement with the ^{50}Ti spectrum is good. In the case of ^{90}Zr, the agreement is improved if a configuration dependence for the effective interaction arising from the possibility of having different size parameters for the $g_{9/2}$ and $p_{1/2}$ orbits. The Yale potential yields better agreement with the experimental data than does the Tabakin potential. It is shown that the matrix elements of the Coulomb force between two protons in these nuclei do not affect the relative splittings of the energy levels by an appreciable amount. These matrix elements have a tendency to vary systematically with the total angular momentum for a given configuration. (auth)

42248 Λ_{10} APPROXIMATION FOR SELF-BOUND MANY-FERMION SYSTEMS. Puff, R.; Reiner, A. S.; Wilets, L. (Univ. of Washington, Seattle). Phys. Rev., 149: 778-84(Sept. 23, 1966).

Several approximations are investigated for self-bound many-fermion systems, each of which employs the Green's-function formalism together with a suitable factorization to close the otherwise infinite hierarchy of coupled integral equations. The particular approximations, which attempt to include the important two-body correlations for short-range forces, differ in the choice of propagator Λ for two-particle intermediate states in the T matrix used to calculate the two-body correlation function. The advantages and shortcomings of the choice $\Lambda_{00} \sim G_1^0 G_1^0$ have been noted previously and are not treated here. It is shown that the choice $\Lambda_{10} \sim G_1^0 G_1$, which appears in a "natural" factorization, is formulated in a manner which preserves much of the simplicity of the Λ_{00} approximation. (Numerical calculations using the Λ_{10} approximation are presented by Foster in the following paper.) The ground-state energies for three Λ approximations (Λ_{00}, Λ_{10}, and $\Lambda_{11} \sim G_1 G_1$) are expanded through third order in the interaction strength to facilitate comparison with each other and with the Brueckner-Goldstone series. Numerical comparison of these third-order contributions for a square-well potential is presented. Λ_{10} is in dramatically closer agreement with the full perturbation theory (for $k_0^0 c \leq 1$) than are the other Λ approximations or Brueckner theory. (auth)

42249 NUMERICAL CALCULATION OF THE GROUND-STATE PROPERTIES OF NUCLEAR MATTER USING THE Λ_{10} APPROXIMATION. Foster, Theodore C. (Univ. of Washington, Seattle). Phys. Rev., 149: 784-90(Sept. 23, 1966)

The consequences of one particular method of terminating the infinite chain of coupled Green's-function equations is investigated numerically for the case of nuclear matter. Of special interest is a comparison of this Λ_{10} theory with the Λ_{00} theory investigated previously. These two approximate theories rely on solution of a T-matrix equation, and they differ in the selection of the propagator for intermediate states. Using separable, nonlocal potentials the T-matrix equations are solved, and the bulk properties of the system are obtained. Results are presented for the energy and number densities, the effective mass, the nuclear compressibility, and the two-particle correlation function. It is found that the two theories give similar results, with Λ_{10} predicting several Mev less binding than Λ_{00} does. (auth)

42250 NORMALIZATION OF AND FINITE-RANGE EFFECTS IN (^{3}He,d) AND (t,d) REACTIONS. Bassel, R. H. (Oak Ridge National Lab., Tenn.). Contract W-7405-eng-26. Phys. Rev., 149: 791-7(Sept. 23, 1966). (ORNL-P-2109).

The effects of including a realistic wave function for the ^{3}He ion on the predictions of the distorted-wave theory for stripping and pickup reactions are studied in some detail. On the assumption that the ^{3}He ion and triton are similar, the results are carried over to reactions involving the triton. Good agreement with experiment is found. (auth)

42251 AZIMUTHAL ANGULAR DISTRIBUTION OF $^{12}C(\gamma,p_0)$. Kellogg, E. M.; Stephens, W. E. (Univ. of Pennsylvania, Philadelphia). Phys. Rev., 149: 798-800 (Sept. 23, 1966).

The azimuthal angular distribution of the photoprotons produced in the reaction $^{12}C(\gamma,p_0)^{11}C$ by monochromatic polarized gamma rays from $^3T(p,\gamma)^4He$ was measured for gamma energies of 21.3 and 21.6 Mev. The ratio R of the number of photoprotons with directions between 0 and 45° (with respect to the gamma-ray polarization) to the number between 45 and 90° was determined. The average observed ratio for R, 2.8 ± 0.7, is larger than but not inconsistent with that calculated for pure electric-dipole photon absorption, 2.08 ± 0.1. (auth)

42252 ANGULAR-CORRELATION STUDIES OF THE REACTIONS $^{16}O(^3He,\alpha\gamma)^{15}O$, $^{12}C(^3He,p\gamma)^{14}N$, AND $^{12}C(d,p\gamma)^{13}C$. Gorodetzky, S.; Freeman, R. M.; Gallmann, A.; Haas, F. (Institut de Recherches Nucleaires, Strasbourg). Phys. Rev., 149: 801-19(Sept. 23, 1966).

Mixing ratios of some gamma transitions in ^{15}O, ^{14}N, and ^{13}C were studied by particle-gamma angular-correlation measurements for the reactions $^{16}O(^3He,\alpha\gamma)^{15}O$, $^{12}C(^3He,p\gamma)^{14}N$, and $^{12}C(d,p\gamma)^{13}C$. The outgoing particles were detected close to 180° in an annular counter. For the ^{3}He beam energies available it was possible to study all the bound states of ^{14}N, but only the 5.18–5.24-Mev doublet (unresolved) and the 6.16-Mev level of ^{15}O could be studied in detail. An attempt was also made to obtain the mixing ratio of the ground-state transition from the 3.85-Mev level of ^{13}C. Spin assignments were verified wherever possible and the spin of the 5.24-Mev level of ^{16}O was established to be $\frac{5}{2}$. Gamma branching ratios were determined for the levels of ^{14}N and were generally in agreement with previous work. Strong evidence was found for a weak transition between the 5.10 and 3.95-Mev states of ^{14}N, but the previously reported transition between the 7.03- and 3.95-Mev states was not observed. Correlations for the $^{12}C(^3He,p\gamma)^{14}N$ reaction were measured at four different energies, since they can vary with energy. It was found from the correlations that the ^{14}N levels were strongly populated in the m = 0 substate. This was attributed to a direct interaction, possibly heavy-particle stripping. (auth)

42253 (^{3}He,d) REACTION ON ^{42}Ca AND ^{44}Ca. Schwartz, J. J.; Alford, W. Parker (Univ. of Rochester, N. Y.). Contract AT(30-1)-875. Phys. Rev., 149: 820-6 (Sept. 23, 1966). (UR-875-137).

Energy levels in ^{43}Sc and ^{45}Sc were studied using the (^{3}He,d) reaction on ^{42}Ca and ^{44}Ca at 10 and 11 Mev. Twenty-nine levels in ^{43}Sc and seventy-four levels in ^{45}Sc were observed below an excitation energy of 6.3 Mev. Angular distributions of the reaction deuterons were measured out to a laboratory angle of 50°. The angular distributions of the more intense groups were compared with the predictions of a distorted-wave Born-approximation calculation, and angular momentum transfers of l = 0, l = 1, l = 2, and l = 3 were identified. Most of the available $1f_{7/2}$ and 2p single-particle transition strength was observed. (auth)

42254 DECAY SCHEME AND GAMMA-GAMMA ANGULAR CORRELATIONS IN ^{60}Ni FOLLOWING THE DECAY OF 23-MIN ^{60}Cu. Shafroth, S. M. (Bartol Research Foundation, Swarthmore, Pa.); Wood, G. T. Phys. Rev., 149: 827-35(Sept. 23, 1966).

A decay scheme is given for ^{60}Cu which agrees with the main features of previous schemes. However, evidence was found for previously unreported feedings to levels at 4.08, 3.73, 3.39, 3.27, and 3.19 Mev. Analysis of single-crystal γ-ray spectra and spectra in coincidence with

1.33-Mev radiation and with annihilation radiation revealed, in addition to previously established γ rays, previously unreported weaker γ rays whose energies are 0.47, 0.50, 0.64, 0.95, 1.03, (1.10), 1.86, 1.94, 2.06, 2.40, 2.74, 3.19, and 3.27 Mev. No 3.52-Mev γ ray was found. The half life for ^{60}Cu was measured to be 22.9 ± 0.1 min. Angular-correlation measurements for γ rays of 0.83, 0.95, 1.03, and 1.79 Mev in coincidence with 1.33-Mev radiation were made. Spin-2 assignments resulted for levels at 2.16 and 3.12 Mev. E2/M1 mixing ratios $\delta = -1.2 \pm 0.3$ and 0.21 ± 0.04 were found for $2_1^+ \rightarrow 2_1^+$ transitions of 0.83 and 1.79 Mev, respectively. A spin-0 assignment for the 2.29-Mev level was made. The present γ-γ angular-correlation results are compared with results of a previous γ-γ angular-correlation study and with results of a ^{60}Ni(p,p′γ) γ-ray angular-distribution study. In the case of the E2/M1 mixing ratio for the 0.83-Mev γ ray arising from the 2.16-Mev level, the present value for δ is close to the value obtained from the (p,p′γ) study and disagrees with the previous radioactivity work. The negative sign of δ for this $2_2^+ \rightarrow 2_1^+$ transition is discussed in the light of new theoretical estimates by Greiner. The relation of the present experiment to other recent work is discussed. (auth)

42255 OPTICAL-MODEL ANALYSIS OF 30-Mev PROTON SCATTERING. Greenlees, G. W.; Pyle, G. J. (Univ. of Minnesota, Minneapolis). Phys. Rev., 149: 836-43(Sept. 23, 1966).

Elastic cross sections together with polarization data and reaction cross sections for the interaction of 30-Mev protons with ^{40}Ca, ^{56}Fe, ^{58}Ni, ^{59}Co, ^{60}Ni, Cu, ^{120}Sn, and ^{208}Pb were analyzed using the optical model. It was possible to obtain good fits to all the experimental data with a single set of geometrical parameters involving one diffuseness value but different radius parameters for the real central, the imaginary central, and the spin-orbit potentials. The new features revealed by this analysis include a spin-orbit radius parameter less than the corresponding central values and an imaginary diffuseness larger (0.7 F) than that required at lower energies (≈ 0.5 F). (auth)

42256 ^{59}Co(p,α)^{56}Fe AND ^{56}Fe(p,p′) REACTIONS. Vonach, H. K.; Huizenga, J. R. (Argonne National Lab., Ill.). Phys. Rev., 149: 844-53(Sept. 23, 1966).

Evaporation spectra of α particles from the ^{59}Co(p,α)^{56}Fe reaction and protons from the ^{56}Fe(p,p′) reaction were investigated with silicon surface-barrier detectors for proton-bombarding energies of 9 to 13.5 Mev. The α spectra are in good agreement with previous results. However, the proton spectra differ somewhat from earlier measurements. The anisotropy of the α particles from the ^{59}Co(p,α) reaction was measured as a function of α energy for proton-bombarding energies of 9 to 13.5 Mev. The level density and the spin-cutoff factor σ were calculated from the experimental results as a function of excitation energy in the range 3 to 9 Mev. The level density varies irregularly with excitation energy at the lower excitation energies and increases smoothly in an exponential manner at higher excitation energies. The nuclear temperature is in the range of 1.10 to 1.45 Mev and appears to increase slightly with excitation energy. The spin-cutoff factor σ increases from 3.5 to 3.8 in the excitation-energy range of 4 to 8 Mev. (auth)

42257 ENERGY-LEVEL STRUCTURE OF ^{40}Ca AS OBSERVED WITH THE ^{39}K(^{3}He,d)^{40}Ca REACTION. Erskine, John R. (Argonne National Lab., Ill.). Phys. Rev., 149: 854-62(Sept. 23, 1966).

The ^{39}K(^{3}He,d)^{40}Ca reaction was studied at a bombarding energy of 12 Mev with a broad-range magnetic spectrograph. Angular-distribution data were obtained for 15 levels which were observed in ^{40}Ca between 3.5- and 8.6-Mev excitation. Spectroscopic factors were extracted with a distorted-wave Born approximation analysis of the data. The major components of the $(d_{3/2}^{-1}f_{7/2})_{T=0}$, $(d_{3/2}^{-1}p_{3/2})_{T=0}$, and $(d_{3/2}^{-1}f_{7/2})_{T=1}$ configurations in ^{40}Ca were identified. The remarkably close agreement of the spacings and spectroscopic factors of the T = 1 states with their analogs in ^{40}K is hard to reconcile with the large Coulomb-mixing effects in the hole-particle calculations of Gillet and Sanderson. (auth)

42258 STUDY OF THE ^{14}N(p,γ)^{15}O REACTION. Evans, Albert E. (Naval Ordnance Lab., Silver Spring, Md.); Brown, Bernard; Marion, Jerry B. Phys. Rev., 149: 863-79(Sept. 23, 1966).

The reaction ^{14}N(p,γ)^{15}O was studied using an anticoincidence-shielded scintillation spectrometer. Excitation functions were measured for proton energies of 0.85–1.96 Mev. Resonances were found at bombarding energies of 1.061 ± 0.002, 1.55, 1.739 ± 0.002, and 1.800 ± 0.004 Mev, corresponding to the well-known excited states of ^{15}O at 8.283 ± 0.003, 8.75, 8.915 ± 0.003, and 8.972 ± 0.005 Mev. Gamma spectra show that the 8.28-Mev level decays to the ground state (54%), the 5.24-Mev level (43%), and the 6.18-Mev level (2%). In addition, coincidence spectra revealed a 1% branch through the 6.86-Mev level, which level decays to the 5.24-Mev level. No evidence was found for decay of the 8.28-Mev level to a previously reported level at 7.17 Mev. The 8.75-Mev level decays ⅔ by way of the 5.19-Mev level and ⅓ by way of the 6.18-Mev level. The 8.915-Mev level decays to the ground state (21%), the 5.19-Mev level (23%), the 6.18-Mev level (30%), and the 6.86-Mev level (26%). The 8.97-Mev level decays 93% to the ground state and 6% to the 5.19-Mev state. Based upon measured transition strengths and the angular distribution of the ground-state gamma rays, the spin of the 8.915-Mev level is established as ⅜; the 8.972-Mev level is $\frac{3}{2}^-$ or $\frac{1}{2}^-$, and the 6.86-Mev level has a spin of either ½ or ⅜. Off-resonance spectra for E_p near 1.2 Mev indicate direct capture into the 6.79-Mev level, the ground state, and also the 7.55-Mev level. The excitation function of radiation to ground from the bound states of ^{15}O indicate that the broad level of ^{15}O at 9.53 Mev decays almost entirely directly to the ground state or to the ground state and to unbound levels. (auth)

42259 RECOIL RANGES OF PRODUCTS FROM REACTIONS OF COPPER WITH 11-43-Mev ^{4}He IONS. Saha, G. B.; Porile, N. T. (Purdue Univ., Lafayette, Ind.). Contract AT(11-1)-1505. Phys. Rev., 149: 880-3(Sept. 23, 1966). (COO–1505–9).

Average projected ranges were determined for the following reactions of copper with 11–43-Mev ^{4}He ions: ^{65}Cu(α,n), ^{65}Cu(α,2n), ^{65}Cu(α,3n), ^{65}Cu(α,αn), and ^{63}Cu(α,n). The results were compared with calculations based on the assumption of compound-nucleus formation. Good agreement was obtained at all energies for the (α,xn) reactions. On the other hand, the ranges of ^{64}Cu are considerably smaller than those predicted by the theory indicating that there is a significant contribution of a direct process to the (α,αn) reaction. (auth)

42260 DECAY SCHEMES OF 43-DAY ^{115m}Cd AND 2.3-DAY ^{115g}Cd. Graeffe, G.; Tang, C.-W.; Coryell, C. D.; Gordon, G. E. (Massachusetts Inst. of Tech., Cambridge). Contract AT(30-1)-905. Phys. Rev., 149: 884-93(Sept. 23, 1966). (MIT-905-59).

The energy levels of ^{115}In were investigated by studying the decay schemes of isomeric ^{115}Cd using Ge(Li) gamma detectors and coincidence techniques. Gamma energies and intensities were determined as were conversion coefficients. Level spin-parity assignments were considered; the observation of the 106-kev transition indicates assignments of $\frac{5}{2}^-$ and $\frac{7}{2}^+$ for the levels at 829 and 943 kev, respectively. (D.C.W.)

42261 FISSION-FRAGMENT ENERGY-CORRELATION MEASUREMENTS FOR THE THERMAL-NEUTRON FISSION OF ^{239}Pu AND ^{241}Pu. Neiler, J. N.; Walter, F. J.; Schmitt, H. W. (Oak Ridge National Lab., Tenn.). Contract W-7405-eng-26. Phys. Rev., 149: 894-905(Sept. 23, 1966). (ORNL-P-2152).

Fission-fragment mass and energy distributions and mass-versus-energy correlations were obtained for ^{239}Pu and ^{241}Pu thermal-neutron-induced fission. Silicon surface-barrier detectors were used in energy-correlation measurements; absolute fragment energies were obtained by means of a recently developed mass-dependent energy calibration. Average total fragment kinetic energies

before neutron emission are found to be 177.7 ± 1.8 Mev for ^{239}Pu and 179.6 ± 1.8 Mev for ^{241}Pu. Detailed experimental results are given and are compared with those of other experiments. Observed fine structure in the fragment mass distribution and in the average total fragment kinetic energy as a function of mass is correlated with the energetically preferred even-even nucleon configurations in the fragments. New determinations of the root-mean-square width of the total-kinetic-energy distribution as a function of fragment mass show structure which also appears to be correlated with the energetically preferred even-even fragment configurations. Fission neutron and gamma-ray data of other experiments are used with the new fragment kinetic energies presented here to examine the total energy balance for fission for the two cases studied. A comparison of the two mass distributions shows the heavy-fragment groups almost superimposed; the light-fragment groups are separated almost uniformly by 2 amu. (auth)

42262 COULOMB DISPLACEMENT ENERGIES FROM ISOBARIC ANALOGUE RESONANCES. Long, D. D.; Richard, P.; Moore, C. F.; Fox, J. D. (Florida State Univ., Tallahassee). Phys. Rev., 149: 906-12(Sept. 23, 1966).

An analysis of isobaric analog resonances is performed to yield the Coulomb displacement energies. The resonances are produced in proton reactions on heavy nuclei. A discussion of the corrections to the resonance data is included. The Coulomb displacement energies can be fitted using the formula: $\Delta E_c = B_1 + B_2 Z/A^{\frac{1}{3}}$, where B_1 is found to be -1.032 ± 0.056 Mev, and B_2 is 1.448 ± 0.006 Mev. There is no evidence for shell, deformation, or pairing effects within the accuracy of this analysis; however, the effects that one would expect to find due to deformations are of the order of the errors in the experiment. The parameters obtained are compared with other measurements of Coulomb displacement energies. (auth)

42263 SEARCH FOR DOUBLE BETA DECAY IN ^{150}Nd. East, Larry V. (Case Inst. of Tech., Cleveland). Phys. Rev., 149: 913-22(Sept. 23, 1966).

Lower limits were obtained for the half life of the double beta decay of ^{150}Nd using thin plastic scintillation detectors surrounded by a large liquid scintillation anticoincidence shield. The experiment was performed 585m underground in the relatively low-radioactive-background environment of a salt mine. The observed count rates are consistent with a lower limit of 3×10^{17} years for the half life of the decay $^{150}\text{Nd} \rightarrow {}^{150}\text{Sm} + 2e^- + 2\bar{\nu}_e$ and 5×10^{18} years for the decay $^{150}\text{Nd} \rightarrow {}^{150}\text{Sm} + 2e^-$. A lower limit of $\sim 10^{17}$ years was also obtained for the single beta decay $^{150}\text{Nd} \rightarrow {}^{150}\text{Pm} + e^- + \bar{\nu}_e$. (auth)

42264 M, N, AND O SUBSHELL CONVERSION COEFFICIENTS IN ^{228}Th AND ^{240}Pu. Ramayya, A. V.; Van Nooijen, B.; Amtey, S. R.; Hamilton, J. H. (Vanderbilt Univ., Nashville). Phys. Rev., 149: 922-4(Sept. 23, 1966).

The M, N, and O subshell conversion coefficients of the 57.9-kev, $2^+ \rightarrow 0^+$ transition in ^{228}Th and the M and N subshell conversion coefficients of the 42.88-kev, $2^+ \rightarrow 0^+$ transition in ^{240}Pu were measured with an iron-free double-focusing spectrometer. In the case of ^{228}Th, conversion coefficients obtained for the M_1, M_2, M_3, $M_4 + M_5$, N_2, N_3, O_2, and O_3 shells are 0.89 ± 0.22, 19.1 ± 1.5, 17.8 ± 1.3, 0.55 ± 0.34, 5.16 ± 0.46, 4.97 ± 0.45, 1.33 ± 0.22, and 1.23 ± 0.20, respectively. For the transition in ^{240}Pu, the conversion coefficients of the M_1, M_2, M_3, N_1, N_2, N_3, and $N_4 + N_5$ are 5.6 ± 2.1, 107.2 ± 7.5, 97.8 ± 7.0, 2.9 ± 0.8, 28.2 ± 2.9, 28.7 ± 2.9, and 2.3 ± 1.0, respectively. Results from the M subshells are 15 ± 8% to 85 ± 45% higher than Rose's theoretical values after correcting for screening according to the semiempirical method of Chu and Perlman. The M-shell conversion-coefficient ratios for these E2 transitions agree with Rose's unscreened values within our experimental errors. This agreement suggests that the corrections due to screening for the different members in a particular shell are approximately the same. (auth)

42265 COLLECTIVE NUCLEAR STRUCTURE IN THE EVEN-EVEN SAMARIUM ISOTOPES. Seaman, G. G. (Yale Univ., New Haven); Greenberg, J. S.; Bromley, D. A.; McGowan, F. K. Phys. Rev., 149: 925-58(Sept. 23, 1966).

The level structure and transition matrix elements between collective states in the even-even isotopes of samarium (A = 148–154) were investigated using Coulomb excitation induced by ^{16}O ions. Both total and differential cross sections were measured for the de-excitation gamma radiation and for gamma radiation in coincidence with the inelastically scattered oxygen ions. Internal-conversion data also supplemented some phases of these studies. The existing information on these nuclei was extended to include higher spin states and previously unmeasured transition moments for both even- and odd-parity states. The predictions of the available phenomenological collective models were compared with this information, and it was found that although the latter models can account for some of the general features of the observed excitation spectra and transition matrix elements, they are deficient in explaining the details. In ^{152}Sm, where specific attention was devoted to the levels associated with the beta and gamma vibrations, the results indicate that for nuclei near the edges of the deformed region the axially symmetric model, with a first-order perturbation treatment of the rotational-vibrational interaction, is not adequate to explain the structure of low-lying states and that this mechanism can account for only 9% of the observed coefficient of the second-order term in the expansion of the excitation energy in an angular-momentum power series. The more exact account of centrifugal stretching, developed by Davydov and Chaban, presently produces the best overall fit, but a number of discrepancies with the data still remain and are discussed. (auth)

42266 ALTERATION OF THE DECAY CONSTANT OF ^{125m}Te BY CHEMICAL MEANS. Malliaris, A. C.; Bainbridge, Kenneth T. (Harvard Univ., Cambridge, Mass.). Contract Nonr-1866(19). Phys. Rev., 149: 958-64(Sept. 23, 1966).

The total rate of a nuclear transition which proceeds partially by internal conversion may be expected to change when alterations are produced in the states of the electrons concerned. Such alterations may be produced, for instance, by chemical means. Differences in the decay constant of the highly converted isomeric transitions of ^{125m}Te were measured using Te, TeO_2, and Ag_2Te (synthetic hessite). The results are: $\lambda(\text{Te}) - \lambda(\text{Ag}_2\text{Te}) = (2.59 \pm 0.18) \times 10^{-4}\lambda(\text{Te})$; $\lambda(\text{TeO}_2) - \lambda(\text{Ag}_2\text{Te}) = (2.23 \pm 0.18) \times 10^{-4}\lambda(\text{Te})$; $\lambda(\text{Te}) - \lambda(\text{TeO}_2) = (0.36 \pm 0.17) \times 10^{-4}\lambda(\text{Te})$. The errors are standard deviations arising mainly from the statistical fluctuations of the number of ionizing events which contributed to a measurement by the double-ionization-chamber balance method. The ionization currents were produced by the K x rays following the internal conversion process in the sources. Corrections were made for the effect of an initial 0.05% contamination of ^{123m}Te. Sources of errors are considered in detail. (auth)

42267 STUDIES OF FRAGMENT ANGULAR DISTRIBUTIONS IN THE FISSION OF ^{209}Bi AND ^{238}U INDUCED BY ALPHA PARTICLES OF ENERGIES UP TO 115 Mev. Kapoor, S. S.; Baba, H.; Thompson, S. G. (Univ. of California, Berkeley). Contract W-7405-eng-48. Phys. Rev., 149: 965-79(Sept. 23, 1966). (UCRL-16706).

Using semiconductor detectors, the fragment angular distributions were measured in the cases of fission of ^{209}Bi and ^{238}U induced by alpha particles of various energies ranging from 23 to 115 Mev. The cms angular distributions were analyzed by a least-squares fitting code to obtain the value of K_0^2 corresponding to the saddle-point excitation energy E_x^s for each bombarding energy. The transmission coefficients T_l and the mean square of the orbital angular momentum $\langle l^2 \rangle$ of the fissioning nucleus required for deducing K_0^2 were determined from optical-model calculations. For both the cases of compound nuclei of ^{213}At and ^{242}Pu, it is found that the values of K_0^2 increase more rapidly with E_x^s than expected on the basis of the Fermi-gas model irrespective of the assumptions made about the multiple-chance fissions. The fission cross sections of ^{238}U for alpha-particle energies up to 110 Mev, also measured in this work, permitted a check of the accuracy of the optical-

model calculations. The presence of direct interactions and their effects on the deduced values of K_0^2 were also investigated in detail in the case of the target nucleus ^{238}U. Using the standard expression for Γ_n/Γ_f, the first-chance values of K_0^2 were obtained and were further corrected for the estimated direct-interaction effects, in the case of the target nucleus ^{238}U. Even after allowance is made for the direct-interaction effects, the energy dependence of K_0^2 appears to be significantly different from that expected on the basis of the simple Fermi-gas model. These results can be explained within the framework of the Fermi-gas model if it is assumed that $J_{eff}/a_f^{\frac{1}{2}}$ increases significantly with the bombarding energy. It appears likely that these results suggest a rapid increase in the effective moment of inertia J_{eff} with the angular momentum, as can be expected on the basis of the observed steep variation in the saddle shapes with Z^2/A. (auth)

42268 LEVEL STRUCTURE OF ^{199}Au FROM DECAY OF ^{199}Pt. Prasad, K. G.; Sharma, R. P.; Thosar, B. V. (Tata Inst. of Fundamental Research, Bombay). Phys. Rev., 149: 980-?(Sept. 23, 1966).

The energy levels of ^{199}Au were investigated from the decay of 30-min ^{199}Pt. The high-resolution gamma spectra obtained from a Ge(Li) detector revealed three new gamma transitions of 187, 469, and 497 kev. A previously unreported energy level at 324 kev was suggested from the coincidence measurements, carried out with NaI(Tl) and Ge(Li) detectors. The possibility of an $11/2^-$ isomeric state expected in this odd-mass region of Au isotopes, was indicated at 549 kev. A study of the internal-conversion-electron spectrum with a surface-barrier detector has clearly shown conversion lines corresponding to 187-, 247-, 318-, and 544-kev gamma transitions, and their K-shell conversion coefficients are obtained as 0.16 ± 0.04, 0.34 ± 0.05, 0.19 ± 0.02, and 0.047 ± 0.004, respectively. These measurements have indicated that the 187-kev transition is almost pure E2 in character, while the 247-, 318-, and 544-kev transitions are mixtures of M1 and E2 in which the E2 component is very much enhanced. The gamma-gamma directional correlation of the 475-318-kev cascade was found to be $W(\theta) = 1 + (0.082 \pm 0.01) P2(\cos\theta) + (0.042 \pm 0.03) P_4(\cos\theta)$. The half life of the first excited state at 77 kev was determined to be 1.46 ± 0.12 nsec. Spin and parity assignments to the 77-, 318-, 324-, 544-, 736-, and 794-kev levels are based on these investigations, and the possible nature of these levels is discussed. (auth)

42269 STATISTICAL MODEL OF INTERMEDIATE STRUCTURE. Griffin, J. J. (Univ. of Wisconsin, Madison. Los Alamos Scientific Lab., N. Mex.). Phys. Rev. Lett., 17: 478-81(Aug. 29, 1966).

A model is proposed for the formation and decay of the average compound-nuclear state in which a weak two-body residual interaction causes transitions among the eigenstates of an independent-particle Hamiltonian that lie in the region dE^* near the compound-nuclear excitation energy E^*. The independent-particle model states are classified according to the number of particles and holes excited from the even-even ground state. (D.C.W.)

42270 SINGLE-PARTICLE WAVE FUNCTIONS OF CALCIUM ISOTOPES. Swift, A.; Elton, L. R. B. (Battersea Coll. of Technology, London). Phys. Rev. Lett., 17: 484-7(Aug. 29, 1966).

Single-particle wave functions were generated in an energy-dependent Woods-Saxon well. The parameters were adjusted so that the binding energies were fitted to the separation energies obtained from (e,ep) and (p,2p) reactions, as well as from mass differences, and the charge density of the protons, as obtained from the wave functions after folding in the finite proton size, was fitted to data on electron elastic scattering. (D.C.W.)

42271 COLLECTIVE CORRELATIONS IN ^{12}C. Drechsel, D.; Seaborn, J. B.; Greiner, W. (Univ., Frankfurt am Main). Phys. Rev. Lett., 17: 488-90(Aug. 29, 1966).

The coupling of giant resonances and surface oscillations in light nuclei is formulated in the particle-hole framework. It is shown that such coupling results in the splitting of the single one-particle, one-hole, 1^- collective state of ^{12}C into several components, improving the agreement of theoretical predictions for the photoabsorption cross section with experimental results. (D.C.W.)

42272 SINGLE-PARTICLE CALCULATIONS IN NUCLEAR FISSION. Primack, J. R. (Princeton Univ., N. J. California Inst. of Tech., Pasadena). Phys. Rev. Lett., 17: 539-41(Sept. 5, 1966).

The nuclear energy was calculated as a function of deformation by adding up the single-particle levels of a deformed shell model. It was found that nuclides of the transuranic region have barriers against fission with heights roughly in agreement with experimental observations. The location and width of the barriers differ somewhat from those calculated using the usual liquid-drop model. The barriers are considerably thinner, and the barrier peaks occur for smaller deformations. A method is proposed for calculating the effective mass in the nuclear deformational Hamiltonian. The calculated effective mass is two orders of magnitude larger than that given by the liquid-drop model assuming irrotational flow. The spontaneous fission rates are of about the right magnitude. (D.C.W.)

42273 EVIDENCE OF TERNARY FISSION AT LOWER ENERGIES. Iyer, R. H.; Cobble, J. W. (Purdue Univ., Lafayette, Ind.). Phys. Rev. Lett., 17: 541-5(Sept. 5, 1966). (COO-347-21).

Excitation functions for the formation of 21.3-hr ^{28}Mg and 2.9-hr ^{38}S in the fission of natural uranium induced by 20- to 40-Mev ^3He and ^4He ions were measured. The absolute cross sections for formation and the yields were measured using U foils and Ag catcher foils that collected the recoiling fragments in both the forward and backward directions parallel to the beam. Evidence that both the ^{28}Mg and ^{38}S result from true ternary fission was obtained. (D.C.W.)

42274 DEFORMED STATE ADMIXTURES IN ^{18}O. Benson, H. G.; Irvine, J. M. (Univ. of Manchester, Eng.). Proc. Phys. Soc. (London), 89: 249-64(1966).

Following the suggestion by Brown, a model of the nucleus ^{18}O was considered in which, in addition to the usual shell-model picture of two neutrons coupled to an inert ^{16}O core, a collective deformed state represented by a two-proton excitation in a deformed axially symmetric shell-model potential was also included. For a given model interaction (the Kallio-Kolltveit interaction), four fitted parameters (the oscillator constant, the effective charge and the single-particle spectrum), and two variational parameters (the deformation parameters), the lowest eight known positive-parity states in ^{18}O were reproduced to a good approximation, together with the two principal E2 transition rates. The predicted eigenvectors are in good agreement with the stripping experiments of Moreh and Daniels. (auth)

42275 AN INVESTIGATION OF THE STRUCTURE OF THE NUCLEAR SURFACE. Genczwein, F.; Voeroes, T. (Univ. for Technical Sciences, Budapest). Proc. Phys. Soc. (London), 89: 385-92(1966).

In a group of alpha-decay transuranic elements the structure of the nuclear surface was investigated. First, in the case of a short-cut-off potential it is shown that, by using a single-particle alpha wave function describing a "smooth" surface and by calculating the absolute emission rate, the ratio between the experimental and calculated values is a factor of about four-figure magnitude. If it is assumed that alpha particles do exist in the nuclear surface and if the alpha correlations are taken into account the difference between the calculated data and the experimental decay rate decreases to a significant degree; therefore it is very likely that the pre-existence of the quasi-alpha particles causes the roughness of the nuclear structure. Next, in the case of the Coulomb plus the Igo potential, the ratio of the experimental to the calculated value of the absolute emission rates differs by a factor of about 10 without and with alpha correlations. The role of alpha

correlations is to bring the barrier nearer to the nucleus, thus smoothing the "rough" nuclear surface. The alpha barrier begins at 8.18 fm, which is in good agreement with the inflection point of the theoretical alpha probability functions at 8.25 fm found by Mang and Rasmussen. (auth)

42276 QUASI-FREE PROTON SCATTERING AT 160 Mev. Gottschalk, B. (Northeastern Univ., Boston); Shlaer, W. J.; Strauch, K.; Wang, K. H. pp 703-18 of Proceedings of the Williamsburg Conference on Intermediate Energy Physics. Vol. II. Williamsburg, Va., College of William and Mary, 1966.

A discussion of the (p,2p) reaction is given. Measurements designed to test how closely the reaction behaves like a knock-out reaction are described. The scatter plot at 160 Mev, the binding energy, cross sections of p- and s-state events versus scattering angle, and the distorted momentum distributions are shown for carbon. Also given are some preliminary results for oxygen-16. (J.F.P.)

42277 SHELL-MODEL CALCULATION OF THE QUASI ELASTIC SCATTERING OF PROTONS FROM COMPLEX NUCLEI. Wall, N. S. (Univ. of Maryland, College Park). pp 719-29 of Proceedings of the Williamsburg Conference on Intermediate Energy Physics. Vol. II. Williamsburg, Va., College of William and Mary, 1966.

For the analysis a plane-wave impulse approximation is used, but the momentum distribution for nucleons in the nucleus is derived from an extreme shell model point of view. It is assumed that the momentum distribution for the 1s state is not too different from that given by the local nonenergy dependent potential. For the evaluation of the lower momentum an estimate of 75 Mev is used for the binding energy. Absorption is not taken into account since distortion in the spectrum would arise. (J.F.P.)

42278 CHANGES IN RADII BETWEEN NEIGHBOURING NUCLIDES. Elton, L. R. B.; Swift, A. (Battersea Coll. of Technology, London). pp 731-41 of Proceedings of the Williamsburg Conference on Intermediate Energy Physics. Vol. II. Williamsburg, Va., College of William and Mary, 1966.

The bulk properties of nuclear matter and specific shell effects are investigated from the properties of neighboring nuclides particularly different isotopes of a given element. Experimental and theoretical data are reviewed. (J.F.P.)

42279 COHERENT NEUTRON PROTON-HOLE EXCITATIONS IN NUCLEI. Fallieros, S.; Hughes, T. A.; Goulard, B. pp 743-8 of Proceedings of the Williamsburg Conference on Intermediate Energy Physics. Vol. II. Williamsburg, Va., College of William and Mary, 1966.

The possibility of coherent neutron proton-hole excitations in zirconium-90 is examined. A representation of the ground state and two typical n-$\bar{p}$ configurations are shown. The interaction between the various configurations and the relevant nuclear force component responsible for this interaction are illustrated. It is noted that the existence of the coherent n-$\bar{p}$ excitation is expected, and the existence of the giant dipole resonance is well-known. Both states can be described by definite values of the isotopic spin quantum number but are no longer members of the same isospin multiplet. (J.F.P.)

42280 OPTICAL MODEL PARAMETERS FOR COMPOSITE PARTICLES. Abul-Magd, A. Y.; El-Nadi, M. (Atomic Energy Establishment, Cairo). Progr. Theoret. Phys. (Kyoto), 35: 798-808(May 1966).

Approximate relations are given between the strengths and the shapes of real, imaginary and spin-orbit terms of the optical potentials for nucleons, deuterons, tritons, and ^{3}He-ions. (auth)

42281 NUCLEAR MATTER AND NUCLEAR FORCES. Akaisi, Yosinori (Kyoto Univ.); Takada, Kenjiro; Takagi, Shuji. Progr. Theoret. Phys. (Kyoto), 35: 978-80(May 1966).

The results for calculations using the reference spectrum method with correction terms neglected are reported for four types of nuclear forces. Numerical calculations were carried out for S, P, and D waves using the Gammel-Thaler, the Hamada-Johnson, and the two kinds of potentials derived by Watari and Tamagaki. The parameters are listed, and the phase shifts in the $^1S_0$ state are shown for the four potentials. The calculated binding energies are also shown. (J.F.P.)

42282 A NEW NUCLIDE: ^{52}Ti. Facetti, J. (Puerto Rico Nuclear Center); Fliegenheimer, J.; Trabal, E. Radiochim. Acta, 5: 143-5(June 1966).

The nuclide ^{52}Ti was produced in a reactor by neutron irradiation of Li_2TiF_6. Lithium enriched in ^{6}Li was used to prepare the compound. The half life is 49 ± 3 min. The mass number was established by identification of ^{52}V as the daughter product. The half life was confirmed by periodic milking of ^{52}V. Chemical procedures used for the preparation of Li_2TiF_6, the purification of ^{52}Ti, and the milking of ^{52}V are described. (auth)

42283 DIFFRACTION OF PROTONS. van Zyl, G. J.; Verleger, H. (Univ., Pretoria). Tydskr. Natuurwetenskappe, 4: 188-92(Dec. 1964). (In Afrikaans).

An experiment to obtain Fraunhofer diffraction with protons was performed successfully. The main difficulty which existed, namely that the diffraction pattern could not be resolved, was overcome by using an ion microscope assembly. Although the de Broglie wavelength of the protons cannot be determined accurately owing to the difficulty of measuring certain parameters in the ion microscope, it is yet possible to identify diffraction patterns. (auth)

42284 THE DECAY OF THE ISOTOPE ^{180}Os. Belyaev, B. N.; Gudov, V. I.; Kalyamin, A. V.; Krizhanskii, L. M.; Lilova, O. M. Yadern. Fiz., 4: 225-7(Aug. 1966). (In Russian).

The γ radiation of osmium obtained in the reaction ^{169}Tm(^{15}N,xn)Os was studied using a scintillation spectrometer. Levels with energies of 105, 230, 320, 400, 510, 880, 1050, and 1300 kev and the decay half life $T_{1/2}$ = 21 ± 2 min were found. (auth)

42285 STUDY OF THE DECAY SCHEME OF ^{179}Hf PRODUCED IN (n,γ) REACTIONS. Kramer, N. D.; Prokofev, P. T. (Inst. of Physics, Academy of Sciences, Latvian SSR). Yadern. Fiz., 4: 228-30(Aug. 1966). (In Russian).

The spectrum of conversion electrons emitted in the ^{178}Hf(n,γ)^{179}Hf reaction, was investigated by means of a β spectrograph. A decay scheme for the lower levels of ^{178}Hf is proposed using the results of measurements on (d,p) and (n,γ) reactions. (auth)

42286 γ-RAY SPECTRUM IN THE CAPTURE OF THERMAL NEUTRONS BY TELLURIUM. Groshev, L. V.; Demidov, A. M.; Shadiev, N. Yadern. Fiz., 4: 238-45 (Aug. 1966). (In Russian).

The spectrum of γ rays from the capture of thermal neutrons by tellurium was measured using a magnetic Compton spectrometer with the resolution 0.3%. The γ lines of various tellurium isotopes are identified for the measured spectrum. The most detailed data were obtained for the isotope ^{124}Te. The binding energy of the neutron in this isotope was determined to be 9410 ± 5 kev (auth)

42287 A NEW ISOTOPE ^{216}Ac. Rotter, Kh.; Demin, A. G.; Pashchenko, L. P.; Brinkmann, Kh. F. Yadern. Fiz., 4: 246-51(Aug. 1966). (In Russian).

A short-lived isotope ^{216}Ac produced in the reaction ^{209}Bi(^{12}C,5n)^{216}Ac was observed when Bi was bombarded by carbon ions. The measured values of the half life and α-particle energy $T_{1/2}$ = 0.39 ± 0.03 Mev msec and E = 9.14 + 0.03 Mev, agree with the α-decay systematics of nuclei with N = 127. The α-particle energies of ^{213}Rn, ^{214}Fr, and ^{215}Ra were also measured. The obtained values agree well with the data. Under certain assumptions concerning the decay scheme of these nuclei, reduced α-decay widths of nuclei with N = 127 were calculated and their relative behavior was discussed. (auth)

42288 LIFETIME OF INTERMEDIATE STATES. Baz, A. I. Yadern. Fiz., 4: 252-60(Aug. 1966). (In Russian).

A method is given for calculating the mean lifetime of intermediate states produced in nuclear reactions. A number of specific cases is discussed, and it is shown that the lifetime of an intermediate state can be large not only for Breit-Wigner resonances, but also in a number of other cases (virtual states, threshold states, etc.). It follows that the expression "quasistationary states" can be applied not only to resonances. It is shown that the experimental width Γ of the maximum in the cross section is not always connected with the mean lifetime T of the intermediate state by the relation $\Gamma T \sim h$. (auth)

42289 SPIN VALUES OF LOWER MULTIPLET STATES IN SPHERICAL ODD-ODD NUCLEI. Peker, L. K.; Novikov, Yu. N. Yadern. Fiz., 4: 261-4(Aug. 1966). (In Russian).

The rules for estimating the spin values of lower multiplet states (especially ground states) of spherical odd-odd nuclei were given, based on the analysis of experimental data. These rules coincide with that of Brennan-Bernstein only for configurations with the number of protons (neutrons) $n \neq \frac{1}{2}(2j+1)$ and for the nuclei with $A < 150$. Disagreement with Sliv' prediction for $A > 192$ and $n = \frac{1}{2}(2j+1)$ points out that the pn interaction can not be described by the terms of the form $V_{pn} = V_0(r) + V_1(r)(\sigma_p\sigma_n)$ and that additional forces have to be included. (auth)

42290 THE MECHANISM OF TWO NUCLEON TRANSFER REACTIONS. Timashev, S. F. Yadern. Fiz., 4: 265-8(Aug. 1966). (In Russian).

Experiments clarifying the mechanism of two-nucleon-transfer reactions are indicated on the basis of angular distribution calculations for the reactions (t,p) and (^{3}He,n). (auth)

42291 THE DEUTERON DISINTEGRATION BY 14 Mev NEUTRONS. Chernukhin, Yu. I.; Shuvalov, R. S. Yadern. Fiz., 4: 272-8(Aug. 1966). (In Russian).

The neutron spectra from the reaction n + d = 2n + p are calculated in the pole approximation for scattering angles (θ_0) of 10, 13, 20, and 28° and an energy of 14 Mev. A reasonable agreement between the theory and experimental observations is noted. An angle θ_0^{lim} is shown to exist, above which the interactions of final-state particles are much suppressed. It follows that to estimate the contributions of quadratic and more complicated diagrams spectra should be investigated under angles larger than θ^{lim}. (auth)

42292 SPONTANEOUSLY FISSIONING NEUTRON-DEFICIENT NEPTUNIUM ISOTOPE WITH THE HALF-LIFE 60 SEC. Kuznetsov, V. I.; Skobelev, N. K.; Flerov, G. N. Yadern. Fiz., 4: 279-81(Aug. 1966). (In Russian).

A previously unreported spontaneously fissioning product with a decay half life of 60 ± 5 sec was observed when ^{209}Bi was irradiated by an intensive flux of ^{22}Ne ions. The excitation function of this product was investigated. It is shown that the anomalous spontaneous fission of one of the neptunium isotopes ^{227}Np or ^{228}Np was observed in the reaction ^{209}Bi + ^{22}Ne. (auth)

42293 RADIATIVE CAPTURE CROSS SECTIONS OF 30 TO 170 kev NEUTRONS. Kononov, V. N.; Stavisskii, Yu. Ya.; Kolesov, V. E.; Dovbenko, A. G.; Nesterenko, V. S.; Moroka. V. I. Yadern. Fiz., 4: 282-92(Aug. 1966). (In Russian).

A method of measuring radiative capture cross sections for 30–170 kev neutrons is described. Nanosecond time-of-flight methods are used to determine the neutron energies. Capture events are detected according to prompt γ rays from the capture in a liquid scintillator detector. The results of neutron-capture cross section measurements are given for a natural mixture of Ta, W, and Re isotopes and for the separated tungsten isotopes ^{182}W, ^{183}W, ^{184}W, and ^{186}W. The experimentally measured cross sections are compared with calculations according to the statistical theory, using the nuclear optical model to calculate the neutron penetrabilities. (auth)

42294 OPTICAL MODEL ANALYSIS OF THE ELASTIC SCATTERING OF 13.6 Mev DEUTERONS ON MEDIUM WEIGHT NUCLEI. Nemets, O. F.; Sokolov, L. S.; Chernov, I. P.; Tokarevskii, V. V. (Inst. of Physics, Academy of Sciences, Ukrainian SSR). Yadern. Fiz., 4: 293-307 (Aug. 1966). (In Russian).

The elastic-scattering differential cross sections for deuterons on ^{50}Cr, ^{52}Cr, ^{54}Cr, ^{59}Co, ^{63}Cu, ^{65}Cu, Fe, ^{58}Ni, ^{60}Ni, ^{62}Ni, ^{64}Ni, and Ti were analyzed using the optical model. Three types of potentials were investigated: the Woods-Saxon potential and those with volume or surface absorption (the Gauss-type form-factor). It is shown that the Woods-Saxon potential does not give a suitable description of elastic scattering in the region of medium nuclei, whereas the other two types of potentials give an equally good agreement with the experimental data, if only 5 parameters are varied, leaving r_0 constant. The nuclei Ti and ^{50}Cr are exceptions, and for them the model with five parameters is inadequate. The regions in which the parameters V, W, a and r_ω are continuously multivalid, overlap for the isotopes ^{59}Co, ^{63}Cu, ^{65}Cu, ^{58}Ni, ^{60}Ni, ^{62}Ni, and ^{64}Ni, so that it is possible to describe the corresponding angular distributions by a single set of parameters. It is found that isotopic effects in the elastic scattering of deuterons can basically be explained by changing the nuclear radius according to the formula $R = r_0 A^{1/3}$. A comparison of the differential cross sections for neighboring even and odd nuclei show that the nuclear structure has little influence on the elastic scattering of deuterons. (auth)

42295 THE REACTION ^{15}N(d,α)^{13}C WITH 0.8 TO 1.8 Mev DEUTERONS. Titov, Yu. I.; Klyucharev, A. P.; Vypirailenko, V. D. Yadern. Fiz., 4: 308-13(Aug. 1966). (In Russian).

The reaction ^{15}N(d,α)^{13}C on a gaseous target was investigated using semiconductor detectors. Two resonances at 1.06 and 1.25 Mev were found in the excitation function, measured at the angle 47° in the deuteron energy region 0.8 to 1.8 Mev. An analysis of the angular distributions shows that the reaction involves the production of a compound nucleus. The 1.06-Mev resonance corresponds to a single-particle level in ^{17}O with the energy 14.97 Mev and spin and parity $5/2^+$. The 1.25-Mev resonance is produced by deuterons with the momentum 2; this corresponds to a level with spin and parity $5/2^-$ or $7/2^-$. However, both the width of the resonance and the value of the cross section indicates that this is not a single-particle level. (auth)

42296 THE REACTION ^{12}C(α,α')^{12*}C(9.64 Mev) → 3 α. Bormot, O. V.; Dolinov, V. K.; Melikov, Yu. V.; Tulinov, A. F. (Moscow State Univ.). Yadern. Fiz., 4: 316-24 (Aug. 1966). (In Russian).

The state of the nucleus ^{12*}C(9.64 Mev) produced in the reaction ^{12}C(α,α')^{12*}C (9.64 Mev) is shown to decay predominantly through the ground state of ^{8}Be: ^{12*}C (9.64 Mev) → $\alpha_1 + {}^8\mathrm{Be}_{gr} \rightarrow \alpha_1 + 2\alpha_2$. The ($\alpha',\alpha_1$) angular correlation functions were measured in the reaction plane at E_α = 25 Mev and $\psi_{\alpha'} = 30$ and 50° and at E_α = 20 Mev and $\psi_{\alpha'} = 30°$ in the laboratory system. The spin value of the 9.64-Mev level was found to be $J^\pi = 3^-$. The angular distribution of inelastically scattering particles at E_α = 25-Mev and the excitation function at $\psi_{\alpha'} = 30°$ in the laboratory system were measured. (auth)

42297 MULTIPARAMETRICAL INVESTIGATIONS OF FRAGMENTS IN THE FISSION OF ^{235}U BY THERMAL AND 5, 6, AND 7 Mev NEUTRONS. Vorobeva, V. G.; Dyachenko, P. P.; Kuzminov, B. D.; Tarasko, M. Z. Yadern. Fiz., 4: 325-31(Aug. 1966). (In Russian).

The dependence of the total kinetic energy of fragments on their mass was measured for the fission of ^{235}U by thermal and 5-, 6-, and 7-Mev neutrons. The energy of the fission fragments was measured using silicon surface-barrier counters. The total kinetic energy of fragments in the symmetrical fission of ^{235}U by thermal neutrons and by those with the energies 5, 6, and 7 Mev proved to be the same

within the limits of experimental error and to be equal to 157 Mev. (auth)

42298 SEARCH FOR LIGHT NEUTRON NUCLEI AMONG URANIUM FISSION PRODUCTS. Burmistrov, V. R.; Kiselev, B. G.; Shilin, V. A.; Kochetkov, V. L. (Inst. of Nuclear Physics, Academy of Sciences, Kazakhskoi SSR). Yadern. Fiz., 4: 332-6(Aug. 1966). (In Russian).

Hypothetical neutron nuclei n_0^3 and n_0^4, which can be produced in the thermal-neutron fission of ^{235}U, were sought by the method of Al and Sc activation in reactions accompanied by the emission of a charged particle. The trineutron and tetraneutron bound states were not observed. The upper limit on the product of the flux of the corresponding neutron nuclei and the cross section for the production of ^{28}Mg from $^{27}Al \leq 8.10^{-22}$ sec^{-1} and the cross section for the production of ^{43}K and ^{47}Ca from Sc is $\leq 2.10^{-18}$ sec^{-1} and $\leq 3.10^{-18}$ sec^{-1}, respectively. (auth)

42299 ANGULAR DISTRIBUTIONS AND NUMBER OF CASCADE NUCLEONS EMITTED BY NUCLEI INTERACTING WITH 660 Mev PROTONS. Konshin, V. A.; Matusevich, E. S.; Regushevskii, V. I. Yadern. Fiz., 4: 337-41(Aug. 1966). (In Russian).

Cascade nucleons were detected using bismuth indicators. The angular distributions of nucleons were measured in the region of angles from 10 to 160°. The number of cascade nucleons with energy higher than 60 Mev, emitted by nuclei between C and U, varies smoothly from 2.4 ± 0.3 to 1.75 ± 0.3. The results are compared with calculations. (auth)

42300 ANGULAR DISTRIBUTION OF HIGH ENERGY NEUTRONS EMITTED IN THE ABSORPTION OF POLARIZED μ^--MESONS IN Ca. Evseev, V. S.; Roganov, V. S.; Chernogorova, V. A.; Chang, Zhun-Wa; Shimchak, M. Yadern. Fiz., 4: 342-56(Aug. 1966). (In Russian).

The asymmetry coefficient B in the angular distribution of neutrons from μ^- capture in Ca was measured in the energy region $E_n = 6.7 - 20.7$ Mev. For high thresholds ($E_n \geq 18$ Mev) the asymmetry, corresponding to 100% residual polarization of the mesons (μ^-), is near to −1. This contradicts calculations based on the universal weak interaction theory. (auth)

42301 NONLOCAL SHELL MODEL PARAMETERS FOR NUCLEAR BOUND STATES. Ulrici, W.; Suessmann, G. (Institut fuer Theoretische Physik, Frankfurt am Main). Z. Naturforsch., 21a: 845-6(June 1966).

An attempt was made to determine the parameters of a nonlocal shell model by fitting the proton binding energies, charge radii, and mass defects of ^{121}Sb, ^{123}Sb, ^{209}Bi, ^{40}Ca, ^{59}Co, ^{197}Au, ^{115}In, and ^{32}S. In comparison with optical-model values, the results obtained indicate a notably larger nonlocality of 1.30 to 1.50 f-m correlated with a potential depth of 110 to 140 Mev. (D.C.W.)

42302 THE g-FACTOR IN THE 2^+ ROTATION STATES IN ^{166}Er AND ^{168}Er. Muenck, E.; Quitmann, D.; Huefner, S. (Technische Hochschule, Darmstadt, Ger.). Z. Naturforsch., 21a: 847-8(June 1966). (In German).

The magnetic hyperfine splittings of the 80-kev gamma rays of ^{166}Er and ^{168}Er were measured in $ErCl_3 \cdot 6H_2O$ by the Mössbauer technique using $TmAl_2$ and $HoAl_2$ sources. The following results were obtained: $g_R^{168}/g_R^{166} = 1.042 \pm 0.008$ and $g_R^{168} = 0.331 \pm 0.010$. (D.C.W.)

42303 THEORY OF THE INFLUENCE OF THE ENVIRONMENT ON γ-γ ANGULAR CORRELATION AND ITS ROTATIONAL DEPENDENCE. Tang, Lun-Han. Ann Arbor, Mich., Univ. of Michigan, 1965. 129p.

Thesis.

A theory of the influence of the environment on γ-γ angular correlations is presented. The theory is formulated by using the resolvent method, and the attenuation coefficient of the perturbed angular correlation function, which contains the effects of the changes of the states of the environment on the angular correlation, is obtained. In the solid environment, the effects of the lattice vibrations on the magnetic dipole-dipole coupling and the electric quadrupole coupling are analyzed by using the normal mode expansion of the lattice displacements; and the perturbed angular correlation function is shown to be a function of the crystal temperature as experimentally observed. In order to determine the nuclear electric quadrupole moments in an excited state, which can not be done by the usual microwave methods, a rotational technique is suggested; and the theory is developed for the case of asymmetric crystalline fields. For the special case of an axially symmetric crystalline field, the theory predicts the phase shifts in the rotational pattern of anisotropy. (Dissertation Abstr.)

42304 PROCEEDINGS OF THE WILLIAMSBURG CONFERENCE ON INTERMEDIATE ENERGY PHYSICS, FEBRUARY 10–12, 1966. VOLUME I. Williamsburg, Va., College of William and Mary, 1966. 481p. (CONF-660209(Vol.1)).

The conference included 28 papers 8 of which appeared previously in NSA. For abstracts of these papers see CONF-660209 in the Report Number Index. Separate abstracts were prepared for 20 papers. (J.F.P.)

For abstracts of individual sections see: 41661, 41890, 41891, and 42305–42321.

42305 EFFECTS OF NUCLEAR STRUCTURE IN MUATOMIC SPECTRA. Anderson, H. L. (Univ. of Chicago); McKee, R. J.; Hargrove, C. K.; Hincks, E. P. pp 1-14 of Proceedings of the Williamsburg Conference on Intermediate Energy Physics. Vol. I. Williamsburg, Va., College of William and Mary, 1966.

The use of the meson (μ) for exploring the shape of the nuclear charge distribution is shown. The spectra from meson (μ) capture in nuclei in the region of the $2p \rightarrow 1s$ transitions are given. The value of isotope shift from lead-206 to -208 was found to be 8.4 kev. Spectra for bismuth and gold are also studied. (J.F.P.)

42306 X-RAYS FROM MUONIC ATOMS WITH SPHERICAL OR NEARLY SPHERICAL NUCLEI. Cote, R. E. (Argonne National Lab., Ill.); Prestwich, W. J.; Raboy, S.; (and others). pp 51-75 of Proceedings of the Williamsburg Conference on Intermediate Energy Physics. Vol. I. Williamsburg, Va., College of William and Mary, 1966.

The x-ray spectra obtained from meson (μ) capture by atoms are discussed. These spectra are shown, and the structure is considered in the light of the solution of the Dirac equation for a point meson (μ) in the field of a finite nuclear charge distribution for the unperturbed meson (μ) wave functions and energy levels. (J.F.P.)

42307 MEASUREMENTS OF THE M1 AND E2 MUONIC h. f. s. OF ^{209}Bi, AND OF THE MUONIC ISOTOPE SHIFTS FOR ^{206}Pb, ^{207}Pb, AND ^{208}Pb. Telegdi, V. L. (Univ. of Chicago). pp 77-86 of Proceedings of the Williamsburg Conference on Intermediate Energy Physics. Vol. I. Williamsburg, Va., College of William and Mary, 1966.

A single meson (μ) beam was used to bombard a variety of targets in order to determine the hyperfine structure in bismuth and the meson (μ) isotope shifts in lead-206, -207, and -208. The x-ray spectra from bismuth and lead are shown, and the meson (μ) isotope shifts and isotope shift ratios are given. (J.F.P.)

42308 MUONIC X-RAY SPECTRA AND CHARGE DISTRIBUTION IN DEFORMED NUCLEI. Acker, H. L. (Univ. of Virginia, Charlottesville). pp 91-7 of Proceedings of the Williamsburg Conference on Intermediate Energy Physics. Vol. I. Williamsburg, Va., College of William and Mary, 1966.

In order to determine what details of the charge distribution of deformed nuclei may be expected from meson (μ) hyperfine structure relevant parameters are deduced from the muonic quadrupole splitting. Predictions from the Fermi distribution and those from a multipole expansion having a Fermi distribution for the monopole part and a Gaussian for the quadrupole distribution are also used to predict these parameters. It is found that the muonic hfs is a sensitive tool for investigating the charge distribution of deformed nuclei. (J.F.P.)

42309 MUONIC X-RAY STUDIES OF SPHERICAL NUCLEI. Daum, C. (CERN, Geneva); Backenstoss, G.; Sens, J. C.; deWit, S. A.; Acker, H. L. pp 99-133 of Proceedings of the Williamsburg Conference on Intermediate Energy Physics. Vol. I. Williamsburg, Va., College of William and Mary, 1966.

Negative mesons (μ) at 124 Mev/c were used to bombard targets of spherical and deformed nuclei, and an analysis of resulting x-ray spectra is discussed. The data are presented in the form of c-t diagrams. (J.F.P.)

42310 DETAILED ANALYSIS OF MUONIC X-RAY SPECTRUM FROM STRONGLY DEFORMED e-e NUCLEI. Runge, K.; Bardin, T. T.; Barrett, R.; Devons, S.; Hitlin, D.; Macagno, E. R.; Nissim-Sabat, C.; Rainwater, J.; Wu, C. S. (Columbia Univ., New York). pp 135-43 of Proceedings of the Williamsburg Conference on Intermediate Energy Physics. Vol. I. Williamsburg, Va., College of William and Mary, 1966.

X-ray spectra from measurements on meson (μ) atoms of ^{182}W, ^{184}W, ^{186}W, ^{238}U, and ^{152}Sm are presented. These spectra are shown and compared with calculated spectra. The transition probabilities B(E2) values are taken as determined by lifetime measurements of nuclear states or by Coulomb excitation, and only the radial matrix elements are computed from the hfs experimental splitting. (J.F.P.)

42311 PI-MESIC X-RAYS. Crowe, K. M. (Univ. of California, Berkeley). pp 145-73 of Proceedings of the Williamsburg Conference on Intermediate Energy Physics. Vol. I. Williamsburg, Va., College of William and Mary, 1966.

The semiconductor technique is used for the study of x-rays from meson (π) atoms, and preliminary data on the energy shifts for the s, p, d, and f states are shown for various elements. The design of the spectrometer used is given. (J.F.P.)

42312 PION INTERACTIONS WITH NUCLEI. Ericson, T. E. O. (CERN, Geneva). pp 187-205 of Proceedings of the Williamsburg Conference on Intermediate Energy Physics. Vol. I. Williamsburg, Va., College of William and Mary, 1966.

A study is made of the low-energy elastic meson (π) interactions with nuclei. It is assumed that the bound nucleons scatter mesons (π) in the same way as free nucleons. The interaction is taken as short range although both s- and p-wave (πN) interactions are permitted. Also the correct effective field for exciting a scatterer corresponding to the effective field exciting a scatterer and the average field in the medium for the classical dipole scattering of an electromagnetic wave in a dense medium is used. It is concluded that low-energy mesons (π) qualitatively see the nucleus as a dielectric medium with parameters describing the wave motion. (J.F.P.)

42313 TWO-NUCLEON EMISSION FOLLOWING ABSORPTION OF STOPPED NEGATIVE PIONS. Nordberg, M. E. Jr.; Kinsey, K. F.; Burman, R. L. (Univ. of Rochester, N. Y.). pp 207-22 of Proceedings of the Williamsburg Conference on Intermediate Energy Physics. Vol. I. Williamsburg, Va., College of William and Mary, 1966.

A beam of negative pions was brought to rest in a variety of light element targets ranging from ^{6}Li to ^{27}Al. The angular distributions of neutron-proton and neutron-neutron pairs emitted in the subsequent pion capture process were measured. The protons were detected in a scintillation counter telescope and the neutrons were detected in a plastic scintillation counter with an anti-coincidence guard counter. The threshold requirements discriminated against low-energy evaporation nucleons. The angular distributions peak strongly at 180°. These distributions and the comparison of n-n to p-n rates are discussed and compared with other similar measurements and theoretical analysis. (auth)

42314 PION CAPTURE AND NUCLEAR STRUCTURE. Davis, H.; Muirhead, H.; Woulds, J. N. (Univ. of Liverpool). pp 223-40 of Proceedings of the Williamsburg Conference on Intermediate Energy Physics. Vol. I. Williamsburg, Va., College of William and Mary, 1966.

Data from experiments on meson (π) capture by lithium-6, -7, carbon, silicon, and copper are presented. The positions of the peaks, the full width at half maximum, and the yields are given. The position of the peaks suggests the mechanism of a simple capture of a meson (π^-) on one nuclear proton leading to a free neutron and a gamma ray. (J.F.P.)

42315 RADIATIVE PION ABSORPTION IN COMPLEX NUCLEI. Anderson, D. K.; Eisenberg, J. M. (Univ. of Virginia, Charlottesville). pp 253-8 of Proceedings of the Williamsburg Conference on Intermediate Energy Physics. Vol. I. Williamsburg, Va., College of William and Mary, 1966.

Calculations of the radiative absorption of a meson (π) in oxygen-16 leading to nitrogen-16 plus a high-energy photon are discussed. Results of a multipole expansion of the electromagnetic field are given for the dipole cases. Also the results of a partial transition calculation using the unperturbed particle-hole basis wave functions are presented. (J.F.P.)

42316 DOUBLE CHARGE EXCHANGE. Solomon, J. (Princeton Univ., N. J.). pp 269-76 of Proceedings of the Williamsburg Conference on Intermediate Energy Physics. Vol. I. Williamsburg, Va., College of William and Mary, 1966.

A search was conducted for a $\Delta T_z = -2$ isobaric analog state in vanadium-51 and zirconium-90 produced through the double charge exchange scattering of mesons (π^+). The number of events per 10 Mev/c bins versus the momentum of the detected meson (π^-) is plotted. The analog states are not observed. It is concluded that the excitation of $\Delta T_z = -2$ isobaric analog states of the two nuclei expected to have favorable cross sections for the process does not compete significantly with other double charge exchange channels. (J.F.P.)

42317 MUON CAPTURE AND NUCLEAR STRUCTURE. Walecka, J. D. (Stanford Univ., Calif.). pp 297-326 of Proceedings of the Williamsburg Conference on Intermediate Energy Physics. Vol. I. Williamsburg, Va., College of William and Mary, 1966.

Meson (μ) capture by nuclei is reviewed. Theoretical and experimental results are presented. The exact magnitude of the induced pseudoscalar coupling constant is not known, but it appears to have the sign and order of magnitude of the Goldberger-Treiman value. There is no evidence against scalar and tensor couplings, and there is evidence that the predominant capture process is through the supermultiplet of the giant resonance. Also there is evidence from electron scattering of the presence of the spin-isospin members of the multiplet. (J.F.P.)

42318 MUON CAPTURE RATS IN COMPLEX NUCLEI. Welsh, R. E. (Coll. of William and Mary, Williamsburg, Va.); Eckhause, M.; Siegel, R. T.; Filippas, T. A. pp 411-18 of Proceedings of the Williamsburg Conference on Intermediate Energy Physics. Vol. I. Williamsburg, Va., College of William and Mary, 1966.

The results of a series of experiments for measuring negative meson (μ) disappearance rates in complex nuclei are summarized. This disappearance rate is found to be the sum of meson (μ) capture and decay rates which are obtained and given. The results of statistical fits of the data to the Fermi gas and Primakoff formulas are listed. (J.F.P.)

42319 OPTICAL MODELS FOR PION-NUCLEUS SCATTERING. Sternheim, M. M. (Univ. of Massachusetts, Amherst); Auerbach, E. pp 439-46 of Proceedings of the Williamsburg Conference on Intermediate Energy Physics. Vol. I. Williamsburg, Va., College of William and Mary, 1966.

The problem of calculating the elastic scattering of mesons (π) by nuclei is reviewed, and some optical model cal-

culations which are still in progress are discussed. Preliminary results are presented. (J.F.P.)

42320 PHASE SHIFT ANALYSIS FOR ELASTIC π^+-^{4}He SCATTERING IN THE ENERGY INTERVAL 100-160 Mev/c. Block, M. M.; Kenyon, I.; Keren, J.; Koetke, D.; Malhotra, P. K.; Walker, R.; Winzeler, H. pp 447-54 of Proceedings of the Williamsburg Conference on Intermediate Energy Physics. Vol. I. Williamsburg, Va., College of William and Mary, 1966.

The phase shift analysis of π^+-^{4}He elastic scattering is described. The purpose of this experiment is to study nuclear Coulomb interference effects at high momentum transfer with the eventual objective of measuring the meson (π) form factor, and to study light hypernuclei. The differential cross sections are plotted. (J.F.P.)

42321 INELASTIC π^+-^{4}He REACTIONS IN THE MOMENTUM RANGE 100-160 Mev/c. Block, M. M.; Kenyon, I.; Keren, J.; Koetke, D.; Malhotra, P. K.; Mazur, P.; Walker, R.; Winzeler, H. pp 455-9 of Proceedings of the Williamsburg Conference on Intermediate Energy Physics. Vol. 1. Williamsburg, Va., College of William and Mary, 1966.

Inelastic meson (π^+) scattering by helium-4 at 100 to 160 Mev/c in a bubble chamber is discussed. The detection of events of interest is described, and some of these events are shown. Cross sections obtained from the preliminary data are given. (J.F.P.)

42322 STATIC MOESSBAUER SEARCH FOR PARITY NONCONSERVATION IN ^{57m}Fe. Emmons, D. A.; Pond, T. A. (New York State Univ., Stony Brook). 12p. (CONF-660411-19). ORAU. Gmelin, AED-CONF-66-060-68.

From American Physical Society Meeting, Washington, D. C.

An attempt to observe nonconservation of parity in the 14.4-kev transition of ^{57}Fe is summarized. The intensity of the polarized photon beam resulting from the preferential absorption of photons of one helicity was recorded as a function of rapidly switching magnetic-field direction. Mössbauer spectra were obtained from ^{57}Fe in natural Fe and in Fe_2O_3. (D.C.W.)

42323 REGULARITIES AND FORMULAS FOR THE NUCLEAR MASSES. Witmer, Enos E. (Univ. of Pennsylvania, Philadelphia). 12p. (CONF-660411-37). ORAU. Gmelin, AED-CONF-66-060-88.

From American Physical Society Meeting, Washington, D. C.

It was previously proposed that the electron rest mass is the natural and logical unit of mass for nuclei and elementary particles and that if M^- is the mass of a nucleus or elementary particle expressed in terms of this unit, then the M^- both in the ground and excited states are very nearly of the form $I/2^n$, where I is an integer and n is a relatively small integer. It is shown that the available data on nuclear masses and excitation energies appear to support the proposals. Some mass formulas and regularities obtained using this mass unit are discussed. (D.C.W.)

42324 FLUCTUATION ANALYSIS OF ^{27}Al(p,α_0)^{24}Mg AND ^{27}Al(p,p$_3$)^{27}Al* CROSS SECTIONS. Mehta, M. K.; Divatia, A. S. (Atomic Energy Establishment, Trombay, India). 5p. (CONF-660411-23). ORAU. Gmelin, AED-CONF-66-060-64.

From American Physical Society Meeting, Washington, D. C.

A fluctuation analysis of the cross sections for the reactions ^{27}Al(p,α_0)^{24}Mg and ^{27}Al(p,p$_3$)^{27}Al* is outlined. The excitation curves considered were obtained at θ = 90 to 150° and for energies from 4.00 to 5.50 Mev, corresponding to excitation energies between 15.0 and 16.5 Mev in the compound nucleus ^{28}Si. On the basis of the fluctuation interpretation, the average level width for the compound nucleus ^{28}Si at an excitation between 15.0 and 16.5 Mev ranges from 14 to 22 kev. Evidence for resonance effects due to separate but interfering levels in the compound nucleus ^{28}Si was also obtained from the excitation curves. (D.C.W.)

42325 PROMPT FISSION NEUTRONS. Milton, J. C. D. 17p. (CONF-660320-15). ORAU. Gmelin, AED-CONF-66-051-53.

From American Chemical Society, 151st Meeting, Pittsburgh.

Neutron emission in fission is discussed with emphasis on the emission of scission neutrons. Some experimental results on the fission of ^{239}Pu and ^{235}U are presented, and neutron emission from individual fragments is also briefly considered. (D.C.W.)

42326 ISOMERIC CROSS-SECTION RATIOS FROM FAST-NEUTRON CAPTURE. Grench, H. A. (Lockheed Research Lab., Palo Alto, Calif.). 7p. (CONF-660303-37). ORAU. Gmelin, AED-CONF-66-034-18.

From American Physical Society, Conference on Neutron Cross Section Technology, Washington, D. C.

The results of some calculations of the total cross sections for fast-neutron capture by ^{113}In, ^{115}In, and ^{89}Y and of the cross sections for capture to isomeric states of ^{114}In, ^{116}In, and ^{90}Y are presented and are compared with experimental results. The sensitivity of the results to the value of the spin-cutoff factor is discussed. The ratios of the effective nuclear moment of inertia to the rigid-body moment, as calculated from the spin-cutoff factors, are presented for ^{114}In, ^{116}In, and ^{90}Y. (D.C.W.)

42327 WIDE ANGLE ELECTRON PAIR PRODUCTION AT HIGH ENERGY. Eisenhandler, E.; Feigenbaum, J.; Mistry, N.; Mostek, P.; Rust, D.; Silverman, A.; Sinclair, C.; Talman, R. (Cornell Univ., Ithaca, N. Y.). 29p. (CONF-660411-34). ORAU. Gmelin, AED-CONF-66-060-76.

From American Physical Society Meeting, Washington, D. C.

An experiment was performed to verify the results of Pipin and others which showed that the prediction of quantum electrodynamics for wide angle pair production was violated. The bremsstrahlung beam at 2 Bev passed through the target and the outgoing electron and positron trajectories are recorded for identification. The general trend of the data is shown and interpretations are discussed. (J.F.P.)

42328 THE HARTREE-FOCK METHOD IN THEORY AND PRACTICE. Villars, F. 17p. (CONF-660545-2). ORAU. Gmelin, AED-CONF-66-140-2.

From Midwest Conference on Theoretical Physics, Bloomington, Ind.

A discussion is given of a few issues connected with the conceptual basis of the Hartree-Fock method as applied to finite nuclei. The structure of the Hartree-Fock solutions and their nonuniqueness, the recovery of eigenstates of P and J (linear and angular momentum), and the problem of singular potentials are treated. (L.B.S.)

42329 ^{6}Li(^{12}C,d)^{16}O REACTION AT E_{CM}= 7 Mev. Loebenstein, H. M.; Mingay, D. W.; Winkler, H. C.; Zaidins, C. S. (California Inst. of Tech., Pasadena). 13p. (CONF-660411-22). ORAU. Gmelin, AED-CONF-66-060-51.

From American Physical Society Meeting, Washington, D. C.

The α width of the fourth excited state of ^{16}O was investigated by studying the ^{6}Li(^{12}C,d)^{16}O reaction. Angular distributions were measured at 7 Mev, and a few excitation functions were measured between 6 and 8 Mev. It was concluded that the fourth excited state of ^{16}O has an α width of the order of 0.1. (D.C.W.)

42330 DECAY OF THE FIRST T = $\frac{3}{2}$ STATE IN ^{13}C. Miller, Richard G.; Kavanagh, R. W. (California Inst. of Tech., Pasadena). 15p. (CONF-660411-42). ORAU. Gmelin, AED-CONF-66-060-53.

From American Physical Society Meeting, Washington D. C.

The location and decay modes of the first T = $\frac{3}{2}$ state of ^{13}C formed in the alpha-particle bombardment of ^{9}Be were investigated. The ^{9}Be + α and ^{12}C + n decay modes of the state were observed as well as decay by direct gamma capture to ^{13}C. (D.C.W.)

42331 GAMMA DECAY OF i-SPIN ANALOG RESONANCES IN ^{93}Tc AND ^{89}Y. Shafroth, S. M. (Franklin Inst., Swarthmore, Pa.); Legge, G. J. F. 10p. (CONF-660306-14). ORAU. Gmelin, AED-CONF-66-048-11.

From American Physical Society, Conference on Isobaric Spin, Tallahassee.

The decay of i-spin analog resonances in ^{93}Tc and ^{89}Y was investigated. The ^{92}Mo (p,γ) reaction was studied in the region of the 5.3-Mev s-wave analog-state resonance. No resonance in the E1 radiation to the 0.39-Mev $p_{\frac{1}{2}}$ proton-hole level in ^{93}Tc was found; an explanation was proposed. Resonances in the ^{88}Sr (p,γ) and ^{88}Sr (p,p') reactions at 6.1 and 7.5 Mev were also studied. (D.C.W.)

42332 FAST NEUTRON CROSS SECTIONS FOR THE ^{23}Na(n,γ)^{24}Na, ^{55}Mn(n,γ)^{54}Mn, ^{115}In(n,γ)^{116m}In, AND ^{165}Ho(n,γ)^{166}Ho REACTIONS. Menlove, H. O. (Lockheed Research Lab., Palo Alto, Calif.); Coop, K. L.; Grench, H. A.; Sher, R. 11p. (CONF-660303-39). ORAU. Gmelin, AED-CONF-66-034-17.

From American Physical Society, Conference of Neutron Cross Section Technology, Washington, D. C.

Neutron capture cross sections of ^{23}Na, ^{55}Mn, ^{115}In, and ^{165}Ho were measured by activation techniques at 16 neutron energies between approximately 1.0 and 19.5 Mev. Neutrons were produced by means of the T(p,n)^{3}He, D(d,n)^{3}He, ^{9}Be(α,n)^{12}C, and T(d,n)^{4}He reactions. The measurements were made relative to the fission cross section of ^{235}U for fast neutrons. A thermal irradiation was made in order to obtain cross sections normalized to the thermal activation cross sections of the irradiated samples and the thermal fission cross section of ^{235}U. The experimental cross section data show evidence of a peak in the vicinity of 15 Mev. (auth)

42333 RESONANCE ABSORPTION INTEGRAL OF RHENIUM. Karam, R. A.; Parkinson, T. F. (Univ. of Florida, Gainesville). 14p. (CONF-660303-41). ORAU. Gmelin, AED-CONF-66-034-12.

From American Physical Society, Conference of Neutron Cross Section Technology, Washington, D. C.

The activation resonance integral of Re was measured to be 657 ± 28 b (excluding 1/v absorption) for a lower energy limit of 0.53 ev. This value is based on the resonance integral of gold (1558b) and also depends on the thermal activation cross sections of ^{185}Re and ^{187}Re. When the uncertainties in these cross sections are considered, the cumulative error in the value obtained is estimated to be ±125 b. (auth)

42334 (^{3}He,t) INVESTIGATIONS OF IRON, NICKEL, AND ZIRCONIUM. Yavin, A. I.; Hoffswell, R. A.; Jones, L. H.; Noweir, T. M. (Univ. of Illinois, Urbana). 15p. (CONF-660306-9). ORAU. Gmelin, AED-CONF-66-048-4.

From American Physical Society, Conference on Isobaric Spin, Tallahassee.

Spectra of tritons from the bombardment of ^{54}Fe, ^{56}Fe, ^{57}Fe, ^{58}Ni, ^{60}Ni, ^{61}Ni, ^{62}Ni, ^{64}Ni, ^{90}Zr, ^{91}Zr, ^{92}Zr, and ^{94}Zr with 18-Mev ^{3}He^{2+} ions were recorded at a laboratory scattering angle of 40°. A pronounced triton peak, corresponding to the excitation of the isobaric analogue of the ground state of the target nucleus, was observed in each spectrum. The observed energy of this triton group was approximately constant for each isotope of the elements investigated. Observed Coulomb displacement energies for Fe and Ni are in reasonable agreement with those measured by Anderson, Wong, and McClure. A few other resolvable triton peaks corresponding to excitated analogue states as well as to low lying-nonalogue states in the residual nuclei were also observed. (auth)

42335 GAMMA-RAY TRANSITIONS IN ^{44}Ca. Cranston; White; Birkett. 13p. (CONF-660411-31). ORAU. Gmelin, AED-CONF-66-060-73.

From American Physical Society Meeting, Washington, D. C.

The energy levels of ^{44}Ca were investigated by observing gamma emission from thermal-neutron capture in ^{43}Ca. A level scheme is proposed. (D.C.W.)

42336 STUDY OF THE ^{13}C(α,n)^{16}O REACTION. Divatia, A. S.; Sekharan, K. K.; Mehta, M. K. (Atomic Energy Establishment, Trombay, India). 5p. (CONF-660411-17). ORAU. Gmelin, AED-CONF-66-060-54.

From American Physical Society Meeting, Washington, D. C.

The integrated cross section of the reaction ^{13}C(α,n)^{16}O was measured over the alpha energy range from 1.95 to 5.5 Mev. 20 resonances indicating levels in ^{17}O were observed; partial widths for several levels were calculated using the Breit-Wigner single-level dispersion theory. Two previously unreported resonances were observed at alpha energies of 5.30 and 5.42 Mev, corresponding to ^{17}O levels at 10.39 and 10.49 Mev. The integrated cross section for the inverse reaction ^{16}O(n,α)^{13}C was obtained by applying the reciprocity theorem for the neutron energy range from 3.95 to 6.5 Mev. (D.C.W.)

42337 COLLOQUE DE PHYSIQUE NUCLEAIRE SUR LES NOYAUX LEGERS. EXPOSES ET COMMUNICATIONS PRESENTES A LYON LES 26, 27 ET 28 JANVIER 1966. (Nuclear Physics Conference on Light Nuclei, Lyon, France January 26-28, 1966). J. Phys. (Paris), Colloq., No. 1, 1-160(1966). (CONF-660116).

Separate abstracts were written for 64 of the 69 papers included. For the remaining papers see entries under CONF-660116 in the Report Number Index. (S.F.L.)

42338 STRUCTURE OF LIGHT NUCLEI. Yoccoz, J. (Centre de Recherches Nucleaires, Strasbourg). J. Phys. (Paris), Colloq., No. 1, 3-9(1966). (In French).

Some recent developments in the understanding of the structure of light nuclei are reviewed. The various ways of choosing the single-particle wave functions and energies, the residual interaction, and the coupling scheme are analyzed. (auth)

42339 RECENT DEVELOPMENTS IN THE THEORY OF NUCLEAR REACTIONS. Bloch, Cl. (CEN, Saclay, Gif-sur-Yvette, France). J. Phys. (Paris), Colloq., No. 1, 10-16(1966). (In French).

A brief review of the ideas of the black-box theory of nuclear reactions, and a short account of the recent treatment of nuclear reactions as an extension of the shell model are given by taking proper account of the states of the continuum. The first numerical applications of this method are described for the square well, a schematic model of a photonuclear reaction, and a realistic model of photonuclear absorption on ^{16}O. Finally, the problems of intermediate resonances and statistical aspects in nuclear reactions are mentioned briefly. (auth)

42340 STUDY OF LIGHT NUCLEI BY ELECTROMAGNETIC INTERACTIONS. Isabelle, D. B. (Faculte des Sciences, Orsay, France). J. Phys. (Paris), Colloq., No. 1, 17-27(1966). (In French).

A brief summary of the expressions describing the interactions of electrons and photons with nuclei and a review of recent work on elastic and inelastic electron scattering are given. Particular emphasis is given to the dipole giant resonance. Also discussed are problems relating to nuclear matter. (auth)

42341 POLARIZATION OF PROTONS OF 152 Mev BY INELASTIC SCATTERING ON ^{12}C AND ^{40}Ca. Willis, A.; Geoffrion, B.; Marty, N.; Morlet, M.; Rolland, C.; Tatischeff, B. (Laboratoire Joliot-Curie, Orsay, France). J. Phys. (Paris), Colloq., No. 1, 33-4(1966). (In French).

Differential cross sections and polarization of 152-Mev protons inelastically scattered by 3.73- and 4.48-Mev levels of ^{40}Ca have been measured. The results for the 3.73-Mev level are compared with plane- and distorted-wave calculations. (auth)

42342 ELECTROMAGNETIC TRANSITIONS IN ^{16}O NUCLEI. Gorodetzky, S.; Brochard, F.; Chevallier, P.; Drouin, R. S.; Disdier, D.; Scheibling, F. (Institut de Recherches Nucleaires, Strasbourg). J. Phys. (Paris), Colloq., No. 1, 34-6(1966). (In French).

The electromagnetic decay modes from the ^{16}O levels

excited by the $^{15}N + p$ reaction through several resonances between $E_p = 400$ kev and $E_p = 1500$ kev have been studied. In particular for levels T = 1, the deduced partial widths are in agreement with those calculated from the wave functions given by V. Gillet and N. Vinh-Mau. (auth)

42343 REACTIONS $(\gamma,n\gamma')$ AND $(\gamma,p\gamma')$ ON ^{12}C AND ^{16}O IN THE GIANT RESONANCE REGION. Maison, J. M.; Langevin, M.; Loiseaux, J. M. (Laboratoire Joliot-Curie de Physique Nucleaire, Orsay, France). J. Phys. (Paris), Colloq., No. 1, 36-7(1966). (In French).

The emission of nucleons from giant resonance states of ^{12}C and ^{16}O to excited states of residual nuclei was studied. In ^{16}O the cross section for emission of neutrons and protons to the $\frac{3}{2}^-$ state in ^{15}O (6.16 Mev) and ^{15}N (6.32 Mev) shows a maximum at 23.5 Mev. 30% of excited states have positive parity. For ^{12}C the state at 25.5 Mev decreases to excited states $\frac{1}{2}^-$, $\frac{3}{2}^-$, $\frac{5}{2}^-$, and $(\frac{7}{2}^-)$ in ^{11}B and ^{11}C. (auth)

42344 QUINTUPLE ISOSPIN OF MASS 16 NUCLEI. Leonardi, R.; Loncke, P.; Pradal, J. (Institut de Physique Nucleaire, Orsay, France). J. Phys. (Paris), Colloq., No. 1, 37-9(1966). (In French).

Two perturbation methods are proposed in order to describe the T = 2 levels of ^{16}O. The first is based on the knowledge of the T = 1 state wave functions. The second one is with unperturbed ground state (Tamm-Dancoff). The results are in agreement with experiment. (auth)

42345 HOLE AND PARTICLE LEVELS OF ^{15}O AND ^{17}O. Bohigas, O. (Institut de Physique Nucleaire, Orsay, France). J. Phys. (Paris), Colloq., No. 1, 39-40(1966). (In French).

A theoretical study is presented of the hole and particle levels of ^{15}O and ^{17}O. A description is given of ^{15}O (^{17}O) as a mixture of 1 hole (1 particle) and 2 holes-1 particle (2 particles-1 hole). A zero-range force with a Soper mixture is used. The parameters of the force are fixed by fitting two-hole levels of the nuclei ^{14}N, ^{14}C, and ^{14}O. (auth)

42346 LEVELS OF ^{15}O EXCITED BY THE REACTION $^{14}N(d,n\gamma)^{15}O$ AT 6.3 Mev. Avignon, P.; Rosier, L. H.; Deschamps, Y. (Laboratoire de Physique Nucleaire, Orsay, France). J. Phys. (Paris), Colloq., No. 1, 40-2 (1966). (In French).

A biparametric analysis is made of both neutron and γ-ray spectra for the reaction $^{14}N(d,n\gamma)^{15}O$. Neutron angular distributions and relative intensities of neutron groups and γ rays are used to discuss spin and parity of ^{15}O levels below 10 Mev and to compare them with the levels of the mirror nucleus ^{15}N. (auth)

42347 LEVELS OF $^{24,25,26}Mg$ EXCITED BY THE REACTIONS (α,α'), $(\alpha,^3He)$, AND (α,t). Bruge, G. (Centre d'Etudes Nucleaires, Saclay, France); Faivre, J. C.; Vallois, G.; Bussiere, A.; Roussel, P. J. Phys. (Paris), Colloq., No. 1, 44-5(1966). (In French).

Inelastic scattering of α particles was used to study core-particle coupling in ^{24}Mg, ^{25}Mg, and ^{26}Mg and to populate collective states. Excitation of particle states was achieved by the (α,t) and $(\alpha,^3He)$ reactions. Energy-level diagrams are given. (S.F.L.)

42348 DETERMINATION OF COEFFICIENTS OF SPIN AND ISOSPIN MIXTURES OF AN EFFECTIVE NUCLEON-NUCLEON FORCE. Bassichis, W. H.; Levinson, C. A.; Ripka, G. (Centre d'Etudes Nucleaires, Saclay, Gif-sur-Yvette, France). J. Phys. (Paris), Colloq., No. 1, 48(1966). (In French).

The effects of the various spin and isospin exchange terms of the nucleon-nucleon residual interaction is investigated with a model force, commonly used in conjunction with the supermultiplet theory. (auth)

42349 STUDY OF THE REACTIONS $d + {}^7Li = n + 2\alpha$ AND $^6Li + T = n + 2\alpha$. Berrada, M. (Faculte des Sciences, Bordeaux); Laugier, J. P.; Lemeille, C.; Marquez, L.; Saunier, N. J. Phys. (Paris), Colloq., No. 1, 49-51 (1966). (In French).

The energy spectra of α particles from the reactions $d + {}^7Li \rightarrow n + 2\alpha$ and $T + {}^6Li \rightarrow n + 2\alpha$ have been measured. It is observed that in the second reaction there is a peak corresponding to the break up of a nuclear molecule, whereas in the first reaction this peak is absent. (S.F.L.)

42350 DISCUSSION OF THE RESULTS OBTAINED IN PICKUP REACTION ON ^9B AND ^{10}B NUCLEI AT 156 Mev. Bachelier, D.; Bernas, M.; Brissaud, I.; Detraz, C.; Radvanyi, P. (Institut de Physique Nucleaire, Orsay, France). J. Phys. (Paris), Colloq., No. 1, 51-5(1966). (In French).

A large number of levels are excited in the reactions $^{10}B(p,d)^9B$ and $^{11}B(p,d)^{10}B$ at 156 Mev. A comparison of the T = 1 levels of ^{10}B with the analog levels of ^{10}C from the reaction $^{12}C(p,t)^{10}C$. Discussion of the results is given: (a) in a rotational and in an intermediate coupling model scheme, and (b) on the basis of calculations of the 1p-shell effective interactions by S. Cohen and D. Kurath; in this case, excepting one level, agreement between experimental and calculated spectroscopical factors is better than 25% up to 8 Mev excitation energy in ^{10}B and better than 30% in ^9B. (auth)

42351 THE $^7Li(p,d)^6Li$ REACTION AT 100 Mev PROTON ENERGY. Lee, J. K. P.; Mark, S. K.; Moore, R. B. (McGill Univ., Montreal). J. Phys. (Paris), Colloq., No. 1, 55-7(1966).

Angular distributions of deuteron groups from the $^7Li(p,d)^6Li$ reaction leading to the ground state and the 2.2, 3.6, and 5.4 Mev excited states of ^6Li are reported. Results are discussed in the intermediate coupling shell model and the rotational model. (auth)

42352 QUASIELASTIC COLLISIONS ON α GROUPS IN ^{12}C BY 60 TO 120 Mev PROTONS. Jacquot, C.; Braun, H.; Gerber, J.-P.; Cueer, P. (Centre de Recherches Nucleaires, Strasbourg). J. Phys. (Paris), Colloq. No. 1, 57-9(1966). (In French).

The cross section of the reaction $^{12}C(p,p')\ \alpha + {}^8Be^*$ has been established by means of nuclear emulsions and was found to be 7 ± 2.8 mb at 120 Mev and 45 ± 15 mb at 60 Mev. The study of the spectator ^8Be gives an angular relation in connection with the excitation state of the ^8Be. This fact permits one to give an order of magnitude of the life time of $^8Be^*$ in its different levels and to obtain results as to the structure of the excited ^{12}C in this reaction. (auth)

42353 STUDY OF THE DEEXCITATION OF FIRST EXCITED LEVELS OF ^6He. Linck, I.; Linck, J.; Seltz, R.; Magnac-Valette, D. (Centre de Recherches Nucleaires, Strasbourg). J. Phys. (Paris), Colloq., No. 1, 59-60(1966). (In French).

A study was made of the relative probability of γ-ray deexcitation vs breakup of the 1.8-Mev level of ^6He into $\alpha + 2n$ via the ground state of ^5He. Bidimensional analysis of the coincidence spectra given by two solid-state detectors was used. (S.F.L.)

42354 STUDY OF CHARGED PRODUCTS IN THE REACTION $^9Be + d$ AT VERY LOW ENERGY (100 TO 200 kev). Ambrosino, G.; Crettez, J. P.; Lachkar, J.; Perchereau, J. (Laboratoire Maurice de Broglie, Bretigny-sur-Orge, France). J. Phys. (Paris), Colloq., No. 1, 62-4(1966). (In French).

Charged particles from the reaction $^9Be + d$ were studied for deuteron energies of 100 to 200 kev. The proton, triton, and α-particle angular distributions were found to be strongly anisotropic and not symmetric with respect to the plane perpendicular to the incident beam. The experimental results are explained by the interference of two levels of opposite parity of the compound nucleus initially formed. (S.F.L.)

42355 ISOBARIC MULTIPLETS IN LIGHT NUCLEI. Detraz, Cl. (Laboratoire Joliot-Curie de Physique Nucleaire, Orsay, France). J. Phys. (Paris), Colloq., No. 1, 64-6(1966). (In French).

The adequacy of isospin to describe excited states of very light nuclei and the importance of the determination of isobaric multiplet masses are discussed. Recent results on nuclei of mass 3, 4, 5, and 7 are presented. (auth)

42356 THEORETICAL STUDY OF THE REACTION $\pi^- + {}^4He \rightarrow \pi^+ + 4n$. Becker, F.; Schmit, C. (Institut de Physique Nucleaire, Orsay, France). J. Phys., (Paris), Colloq. No. 1, 66-7(1966). (In French).

Using the double-charge exchange theory, developed by F. Becker and Z. Maric, a study was made of two different states of the four-neutron system, and results compared with those of the CERN experiment [Phys. Letters 11: 244 (1964) and 19: 335(1965)]. (auth)

42357 STATES $^2P_{\frac{3}{2}}$ AND $^2P_{\frac{1}{2}}$ OF ^5He. Bilwes, R.; Bourotte, B.; Magnac-Valette, D. (Centre de Recherches Nucleaires, Strasbourg). J. Phys., (Paris), Colloq. No. 1, 68-9(1966). (In French).

Q-values were determined for the $^7Li(d,\alpha)^5He$ reaction using a Buechner-type heavy-particle spectrograph, and width measurements of the ground-state $^2P_{\frac{3}{2}}$ level of ^5He were made using an α-α coincidence method with semiconductor detectors. Evidence of the $^2P_{\frac{1}{2}}$ state of ^5He was sought using bidimensional analysis of the $^6Li(t,n)2\alpha$ reaction. (S.F.L.)

42358 PRELIMINARY RESULTS ON ^4Li, ^5Li, AND ^6Li OBTAINED BY (p,d) AND (p,t) REACTIONS ON ^6Li AND ^7Li AT 156 Mev. Bachelier, D.; Bernas, M.; Brissaud, I.; Chavy, F.; Radvanyi, P. (Institut de Physique Nucleaire, Orsay, France). J. Phys. (Paris), Colloq., No. 1, 70-1 (1966). (In French).

The energy spectra of deuterons and tritons were measured for the reactions $^6Li(p,d)^5Li$, $^6Li(p,t)^4Li$, $^7Li(p,d)^6Li$, and $^7Li(p,t)^5Li$ with incident proton energies of 156 Mev. Preliminary results are discussed for energy levels of ^4Li, ^5Li, and ^6Li. (S.F.L.)

42359 (n,d) SCATTERING BETWEEN 1 AND 5 Mev. Blanc, Daniel; Cambou, Francis; Vedrenne, Gilbert (Faculte des Sciences, Toulouse). J. Phys. (Paris), Colloq., No. 1, 71-3(1966). (In French).

The distribution of neutrons elastically scattered from deuterons is obtained from the recoil deuteron spectrum, recoil deuterons being produced in a deuterated benzene scintillator. The results obtained with neutron energy between 1 and 5 Mev are in reasonably good agreement with elastic scattering of protons from deuterons at the corresponding energies. (auth)

42360 STUDY OF (p,2p) REACTION AT 155 Mev ON ^7Li, ^9Be, AND ^{23}Na WITH AN ON-LINE COMPUTER. Arditi, M.; Roynette, J. C.; Ruhla, Ch.; Jacmart, J. C.; Mazloum, F.; Riou, M. (Institut de Physique Nucleaire, Orsay, France). J. Phys. (Paris), Colloq., No. 1, 73-6 (1966). (In French).

Reactions (p,2p) at 155 Mev have been restudied with a new experimental set-up combining two magnetic spectrometers, two spark chambers, and an on-line computer. Preliminary spectra on ^7Li, ^9Be, and ^{23}Na were obtained with an over-all energy resolution of 1.6 Mev. (auth)

42361 p-d ANGULAR CORRELATION IN THE REACTION $^{12}C(p,pd)^{10}B$ AT 155 Mev. Lhuillier, M.; Benoist-Gueutal, P. (Institut de Physique Nucleaire, Orsay, France). J. Phys. (Paris), Colloq., No. 1, 78-9(1966). (In French).

The differential cross section has been calculated for the reaction $^{12}C(p,pd)^{10}B$ assuming a knock-out mechanism (Born approximation). Two models have been used for ^{12}C: an independent-particle model with j-j coupling and a deuteron cluster model. Results of both of these models are similar, and comparison with experiment is qualitatively satisfactory. (auth)

42362 REACTION $^9Be(n,nn)\alpha\alpha$ AT 15 Mev. Bouchez, R.; Darves-Blanc, R.; Giorni, A.; Gondrand, J. C.; Perrin, C.; Perrin, P.; Quivy, P. (Univ., Grenoble, France). J. Phys. (Paris), Colloq., No. 1, 79-82(1966). (In French).

The $^9Be(n,2n)2\alpha$ reaction was analyzed at 15 Mev by double time-of-flight spectrometry. The results show a sequential process of two-body reactions. The decay of the 4- to 10-Mev ^9Be levels was observed, and the shift of the ^8Be (2+) free resonance by a third particle is discussed. (auth)

42363 PRECISE MEASUREMENT OF THE STOPPING POWER OF C, Au, Al, Ca, AND CaF_2 FOR 0.4 TO 6 Mev PROTONS. Gorodetzky, S.; Chevallier, A.; Armbruster, R.; Bergdolt, A. M.; Bres, M.; Pape, A.; Sens, J. C. (Institut de Recherches Nucleaires, Strasbourg). J. Phys. (Paris), Colloq., No. 1, 82-4(1966). (In French).

Measurements of the stopping powers of C, Ca, Al, Au, and CaF_2 have been made in the energy range 0.4 to 6 Mev. The experiments consisted in measuring the energy losses of the scattered Van de Graaff proton beams when thin stopping foils were interposed. Data were recorded either on paper or magnetic tapes and later processed on a computer. The numerous stopping foils were prepared under vacuum by methods appropriate to each. After a series of measurements the foils were weighed. All manipulations on Ca and CaF_2 were done either under vacuum or in an argon atmosphere. ^3He activation analysis showed that carbon and oxygen impurities were at low levels. (auth)

42364 EXCITATION OF 5.7 Mev LEVEL OF ^7Li BY (n,n') SCATTERING AT 14 Mev. Regis, V.; Nguyen Van Sen; Fiore, A.; Pham Dinh-Lien; Bouchez, R. (Univ., Grenoble, France). J. Phys. (Paris), Colloq., No. 1, 84-5 (1966). (In French).

Measurements made by time-of-flight spectrometry on 14-Mev neutrons scattered by ^7Li shows the existence of the 5.7-Mev level and suggests a level at 6.3 Mev. Angular distributions of neutrons for elastic and inelastic scattering from the 4.63-Mev level of ^7Li were also measured. (S.F.L.)

42365 ELASTIC SCATTERING OF DEUTERONS ON ^6Li AT 4 TO 6.5 Mev. Bruno, G.; Decharge, J.; Perrin, A.; Surget, G. (CEA, Paris). J. Phys. (Paris), Colloq., No. 1, 85-6(1966). (In French).

The excitation function at 115° for elastic scattering of deuterons by ^6Li for a deuteron energy range from 4 to 6.5 Mev was determined using coincidence between the scattered deuteron and the ^6Li recoil nucleus. (auth)

42366 DISSOCIATION OF ^6Li BY INTERACTION ON COMPLEX NUCLEI. Fleury, A.; Lagarde, M.; Simonoff, G. N. (Faculte des Sciences, Bordeaux). J. Phys. (Paris), Colloq., No. 1, 86-8(1966). (In French).

Comparison of the excitation function for the reaction $^{232}Th(d,2n)^{232}Pa$ with the function for ^{232}Pa formed by the interaction of $^6Li + {}^{232}Th$ indicates a high probability that ^6Li decays into deuterons and alpha particles by a stripping process. This dissociation decreases with increase of the energy of ^6Li. (auth)

42367 REACTIONS INDUCED IN CARBON BY FAST NEUTRONS. Huck, A.; Walter, G.; Coche, A. (Centre de Recherches Nucleaires, Strasbourg). J. Phys. (Paris), Colloq., No. 1, 88-9(1966). (In French).

Separation between α particles and recoil protons with an organic scintillator, was accomplished in order to investigate the α particle spectra resulting from fast neutron interactions with carbon atoms in stilbene. The total cross section for $^{12}C(n,\alpha_0)^9Be$ is given at $E_n = 16$ Mev ($\sigma = 49 \pm 16$ mb) and $E_n = 17$ Mev ($\sigma = 54 \pm 18$ mb). (auth)

42368 SPINS OF SOME T = 1 STATES IN ^{26}Al. Horvat, P.; Kump, P.; Vakselj, M. (Nuclear Inst. J. Stefan, Ljubljana). J. Phys. (Paris), Colloq., No. 1, 90-1(1966).

The T = 1 states in ^{26}Al with the energies 3.16 and 4.19 Mev have been studied by measuring the angular distributions and correlations. Spin and parity assignments have been found to be $J^\pi = 2^+$ for the 3.16-Mev level and $J^\pi = 4^+$ for the 4.19-Mev level. The transitions from these two levels are almost pure M1. (auth)

42369 STUDY OF NUCLEAR REACTIONS WITH A MAGNETIC SPECTROGRAPH. Gorodetzky, S.; Gallmann, A.; Fintz, P. (Institut de Recherches Nucleaires, Strasbourg). J. Phys. (Paris), Colloq., No. 1, 91-2(1966). (In French).

Energy levels of ^{13}C, ^{15}N, and ^{16}N were studied by the reactions $^{13}C(^3He,p)^{15}N$, $^{14}C(^3He,\alpha)^{13}C$, $^{14}C(^3He,p)^{16}N$, and $^{14}N(d,p)^{15}N$ using a Buechner-type magnetic spectrograph. (S.F.L.)

42370 STUDY OF (n,α) REACTION OF ^{16}O AT 14.9 Mev. Leroux, B.; Sordo, K.; Dalmas, J.; Chastel, R. (Faculte des Sciences, Bordeaux). J. Phys. (Paris), Colloq., No. 1, 93-4(1966). (In French).

The angular distribution of α particles was measured between 30° and 150° for the reaction $^{16}O(n,\alpha)^{13}C$ with incident-neutron energy of 14.9 Mev. A gaseous oxygen target, 1.7 mg/cm², was used, associated with a nuclear emulsion protected from the incident neutrons by a brass bar. Good separation of the α-particle group corresponding to the ground state of the residual nucleus was obtained. (S.F.L.)

42371 ABSOLUTE CROSS SECTIONS FOR ELASTIC SCATTERING OF DEUTERONS ON α PARTICLES BETWEEN 3 AND 14 Mev. Mani, G. S.; Sadeghi, A.; Tarrats, A. (Centre d'Etudes Nucleaires, Saclay, France). J. Phys. (Paris), Colloq., No. 1, 94-5(1966). (In French).

The absolute cross-sections for α + d elastic scattering have been measured for 20 angles ($47.1° \leq \theta_{C.M.} \leq 164.5°$) for deuteron energies between 3 and 14 Mev. (auth)

42372 ELASTIC AND INELASTIC SCATTERING OF PROTONS BY ^{7}Li. Bardolle, G.; Cabe, J.; Chretien, J. F.; Laurat, M. (CEA, Paris). J. Phys. (Paris), Colloq., No. 1, 96-7(1966). (In French).

The study of excitation functions and angular distributions for elastic and inelastic scattering of protons by ^{7}Li from 0.9 to 2 Mev shows a resonance at 1.030 Mev, strong interference between nuclear and Rutherford scattering, and two anomalies which occur at 1.400 Mev and at the $^{7}Li(p,n)^{7}Be$ threshold. (auth)

42373 ELASTIC SCATTERING OF NEUTRONS BY TRITIUM AT 14 Mev. Blanc, D.; Cambou, F.; Niel, M.; Vedrenne, G. (CNRS, Toulouse). J. Phys. (Paris), Colloq., No. 1, 98-9(1966). (In French).

Elastic scattering of neutrons from tritium is studied with a thin scatterer close to a CsI scintillator. The experimental distribution of recoil tritons produced by neutron impact gives the (n,t) elastic scattering cross section between 45° and 180° in the center-of-mass system. (auth)

42374 STUDY OF THE REACTIONS $^{10}B(d,\alpha)2^{4}He$ AND $^{9}Be(^{3}He,\alpha)2^{4}He$. Didier, D.; Duchemin, B.; Mouilhayrat, G., Perrault, F.; Thouvenin, P. (CEA, Paris). J. Phys. (Paris), Colloq., No. 1, 100-1(1966). (In French).

The $^{10}B(d,\alpha)2^{4}He$ and $^{9}Be(^{3}He,\alpha)2^{4}He$ reactions have been studied with two detectors by the coincidence method. In this experiment, the reactions mainly proceed through the levels of ^{8}Be. The respective contributions of these levels for both reactions are compared. (auth)

42375 STUDY OF ANGULAR DISTRIBUTIONS OF THE REACTION $^{32}S(n,\alpha_0)^{29}Si$ AT 2.5 TO 3.2 Mev. Chambon, B.; Billerey, R.; Salin, R.; Depraz, J. (Institut de Physique Nucleaire, Lyon). J. Phys. (Paris), Colloq., No. 1, 102-3 (1966). (In French).

The study of differential cross sections for the $^{32}S(n,\alpha_0)$ reaction for neutron energies from 2.5 to 3.2 Mev was made by low-resistivity silicon detectors. (auth)

42376 STUDY OF THE ELASTIC SCATTERING OF ELECTRONS BY ^{27}Al. Stovall, T.; Vinciguerra, D.; Bernheim, M. (Ecole Normale Superieure, Orsay, France). J. Phys. (Paris), Colloq., No. 1, 103-4(1966). (In French).

Theoretical expressions for the elastic-scattering electric and magnetic form factors for d-shell nuclei are presented. These expressions are compared with experimental results for aluminum-27. (auth)

42377 ELECTRON SCATTERING AT 180 DEG ON ^{12}C. Proca, G.; Isabelle, D.; Goldemberg, J. (Ecole Normale Superieure, Orsay, France). J. Phys. (Paris), Colloq., No. 1, 105-6(1966). (In French).

The characteristics of the levels of carbon-12 with excitation energies between 14 and 21 Mev were studied. Measurements were made by inelastic scattering of electrons at 180° with incident energies between 100 and 200 Mev. (auth)

42378 ELECTRON EXCITATION OF FIRST LEVELS OF ^{11}B. Riskalla, R.; Vinciguerra, D. (Ecole Normale Superieure, Orsay, France). J. Phys. (Paris), Colloq., No. 1, 106-7(1966). (In French).

The energy spectrum of electrons scattered from a ^{11}B target has been measured for momentum transfer between 0.6 and 1.4 F^{-1}. Preliminary results are given for the form factors of the first two excited levels. (auth)

42379 THEORETICAL STUDY OF THE CONTINUOUS SPECTRA OF GAMMA RAYS EMITTED IN NUCLEAR REACTIONS, MEASUREMENT OF MEAN LIVES. Mennrath, P. (Laboratoire de Physique Nucleaire, Bordeaux); Hubert, Ph.; Leccia, F.; Thibaud, J. P.; Stab, L. J. Phys. (Paris), Colloq., No. 1, 108-9(1966). (In French).

The continuous spectrum of a γ ray emitted during a nuclear reaction varies with the mean life of the electromagnetic transition, due to the Doppler effect. Calculations are made to show how this effect can be used to determine mean lives from γ-ray measurements. (S.F.L.)

42380 TEST OF $\alpha\alpha'\gamma$ ANGULAR CORRELATION ON ^{12}C AT 23 Mev. Jodogne, J. C. (Univ., Louvain, Belg.). J. Phys. (Paris), Colloq., No. 1, 110-11(1966). (In French).

By means of the inelastic scattering of α particles on the 2^+ levels of ^{12}C, the m = 2 and m = −2 substates are differently populated. The population ratios and the relative phases have been measured at different scattering angles. Comparison with theoretical predictions has met with little success. (auth)

42381 STUDY OF ELECTROMAGNETIC TRANSITIONS BY MEASUREMENT OF THE POLARIZATION DISTRIBUTION AND γ-γ ANGULAR CORRELATION. Gorodetzky, S.; Beck, F.; Bertini, R.; Bozek, E.; Chevallier, J.; Knipper, A. (Centre de Recherches Nucleaires, Strasbourg). J. Phys.,(Paris), Colloq., No. 1, 112-14 (1966). (In French).

Electromagnetic transitions from aligned levels can be studied without a detailed knowledge of the alignment process (nuclear reaction). The two methods used are (a) comparison of the angular distribution and plane polarization of the γ rays; and (b) γ-γ angular correlations as suggested by Litherland and Ferguson [Can. J. Phys., 39: 788(1961)]. The apparatus is briefly described, together with results for transitions in ^{12}B(955 kev), ^{13}C(170 kev), and ^{53}Mn (380, 910 and 1290 kev). (auth)

42382 STUDY OF ^{46}Sc LEVELS BY MEANS OF NEUTRON CAPTURE GAMMAS. Van Assche, P.; Gruber, U.; Maier, B. P.; Koch, H. R.; Schult, O. W. B. (Univ., Munich). J. Phys. (Paris), Colloq., No. 1, 115-16(1966). (In French).

The thermal neutron capture γ-ray spectrum of the reaction $^{45}Sc(n,\gamma)^{46}Sc$ has been measured with a bent-crystal γ spectrometer. For most levels of ^{46}Sc spin and parity assignments are proposed and discussed on the basis of the present experimental results. (auth)

42383 PARTICLE-GAMMA ANGULAR CORRELATIONS WITH DETECTION AT 180 DEG. Gorodetzky, S.; Freeman, R. M.; Gallmann, A.; Haas, F. (Institut de Recherches Nucleaires, Strasbourg). J. Phys. (Paris), Colloq., No. 1, 116-17(1966). (In French).

Particle-gamma angular correlations have been studied for the reactions $^{16}O(^{3}He,\alpha\gamma)^{15}O$, $^{12}C(^{3}He,p\gamma)^{14}N$, and $^{12}C(d,p\gamma)^{13}C$ for which the outgoing particles were detected near 180°. Spins of levels and mixing-ratios for the decay γ rays have been determined. (auth)

42384 THE "MULTIPOLIMETER" APPLICATION TO A STUDY OF ELECTROMAGNETIC TRANSITIONS. Gorodetzky, S.; Gallmann, A.; Coffin, J. P.; Frick, G.; Jundt, F. (Institut de Recherches Nucleaires, Strasbourg). J. Phys. (Paris), Colloq., No. 1, 118-20(1966). (In French).

A Siegbahn-Slätis intermediate-image magnetic spectrometer has been altered with the purpose of determining the multipolarity of electromagnetic transitions. A study

of the 8.92-Mev → 0 transition in ^{11}B and the 6.49 Mev → 0 transition in ^{11}C has shown the M1 and E2 character of these transitions, respectively. (auth)

42385 THEORY OF RADIATIVE CAPTURE OF π MESONS IN NUCLEI. Delorme, J. (Faculte des Sciences, Lyon); Ericson, T. J. Phys. (Paris), Colloq., No. 1, 120-1(1966). (In French).

The general amplitude for pion photoproduction is used to derive an effective Hamiltonian for the process $\pi^- + N(A,Z) \rightarrow N^*(A,Z-1) + \gamma$. The branching ratio is calculated in the closed approximation with the help of the Fermi-gas model. (auth)

42386 CONTRIBUTION TO A STUDY OF STRUCTURE OF LIGHT NUCLEI BY A STUDY OF THE ABSORPTION MECHANISMS OF K^- MESONS. Kurtz, N.; Baumann, G.; Gerber, J. P.; Braun, H.; Cueer, P. (Centre de Recherches Nucleaires, Strasbourg). J. Phys. (Paris), Colloq., No. 1, 122-4(1966). (In French).

The absorption of K^- mesons at rest by the light nuclei in emulsions is studied in stars emitting a fragment of ^8Li or a hyperfragment. The percentage of absorption by one nucleon and 2 nucleons is given and also the proportion of Λ and Σ emission. (auth)

42387 STUDY OF THE REACTION (d,p) WITH TOTAL INTERACTION IN THE EXCURSION METHOD. Maguin, C.; Pigeon, J. (Institut de Physique Nucleaire, Lyon). J. Phys. (Paris), Colloq., No. 1, 124-5(1966). (In French).

A theoretical differential cross section for the ^{28}Si-(d,p)^{29}Si reaction is given which assumes the outgoing proton in a central shell-model potential of the residual nucleus. A PWBA calculation shows a strong forward asymmetry. (auth)

42388 ELASTIC SCATTERING OF PROTONS OF 150 AND 80 Mev ON LIGHT NUCLEI AND THE OPTICAL POTENTIAL. Rolland, C.; Geoffrion, B.; Marty, N.; Morlet, M.; Tatischeff, B.; Willis, A. (Laboratoire de Physique Nucleaire, Orsay, France). J. Phys. (Paris), Colloq., No. 1, 126-8(1966). (In French).

Differential cross sections and polarizations were studied for protons elastically scattered at 80 and 150 Mev by ^6Li, ^7Li, ^{12}C, and ^{40}Ca. Results are presented along with parameters deduced from an optical potential analysis by an automatic search program. (S.F.L.)

42389 REACTIONS $^{12}C(\alpha,\alpha)$ AT 51 Mev AND $^{14}N(d,\alpha)$-^{12}C AND $^{14}N(d,d)$ AT 28.5 Mev. Vidal, J. L.; Bouche, R.; Fayard, C.; Feuvrais, L.; Gaillard, M.; Gaillard, P.; Gouanere, M.; Gusakow, M.; Lamot, G. H.; Pizzi, J. R. (Institut de Physique Nucleaire, Lyon). J. Phys. (Paris), Colloq., No. 1, 128-30(1966). (In French).

The α-particle energy spectrum from the reaction $^{14}N(d,\alpha)^{12}C$ was measured in the range 10° to 90° for laboratory coordinates. An optical-model program was used for analysis of angular distributions of deuterons scattered on ^{14}N and α particles scattered on ^{12}C at 28.5 and 51 Mev, respectively. A DWBA analysis was made for one of the transitions. (S.F.L.)

42390 ABSOLUTE CROSS SECTIONS OF THE REACTIONS $^{12}C(p,p)^{12}C$, $^{12}C(p,p')^{12}C^*$, $^{12}C(p,p'')^{12}C^*$ AND LEVELS OF ^{15}N. Mani, G. S.; Sadeghi, A.; Tarrats, A. (Centre d'Etudes Nucleaires, Saclay, France). J. Phys. (Paris), Colloq., No. 1, 130-2(1966). (In French).

Elastic and inelastic absolute cross sections for the reactions $^{12}C(p,p)^{12}C$, $^{12}C(p,p')^{12}C^*$, and $^{12}C(p,p'')^{12}C^*$ have been measured between 4.6 and 11.2 Mev incident energy. The results have been analyzed by the R-matrix formalism and by coupled-channel methods. (auth)

42391 STUDY OF (n,α) REACTIONS BY THE DISTORTED-WAVE METHOD. Fayard, C.; Lamot, G. H.; Massot, J. N.; Lafoucriere, J. (Institut de Physique Nucleaire, Lyon). J. Phys. (Paris), Colloq., No. 1, 132-4(1966). (In French).

$^{28}Si(n,\alpha)^{25}Mg$ and $^{16}O(n,\alpha)^{13}C$ reactions were studied by an exchange mechanism of direct interaction using the distorted-wave Born approximation. (auth)

42392 SCATTERING OF ALPHA PARTICLES ON ^9Be, ^{32}S, AND ^{31}P. Gregoire, G.; Macq, P. C. (Univ., Louvain, Belg.). J. Phys. (Paris), Colloq., No. 1, 136-8(1966). (In French).

Medium-energy alpha-particle elastic scattering on ^9Be, ^{32}S, and ^{31}P have been analyzed by the DWBA method. An I.1 coupling term in $^9Be(\alpha,\alpha)$ is not totally ruled out but would require more extensive analyses. Two phonon levels are clearly seen in $^{32}S(\alpha,\alpha)$ at 23.8 Mev. Inelastic angular distributions on the $3/2^+$ (1.27 Mev) and $5/2^+$ (2.23 Mev) levels of ^{31}P confirm their collective nature as a ^{32}S excited core coupled to a 2s $1/2$ hole. (auth)

42393 ELASTIC SCATTERING OF 14 Mev NEUTRONS BY POTASSIUM. Roturier, J.; Irigaray, J. L.; Lagardere, M.; Sonnaert, S.; Petit, G. Y. (Faculte des Sciences, Bordeaux). J. Phys. (Paris), Colloq., No. 1, 139-40(1966). (In French).

Experimental results for the total cross section and differential elastic scattering cross section are given for 14-Mev neutrons on ^{39}K. A theoretical analysis is made using a nonlocal optical model. Good agreement was found for $\sigma_{el}(\theta)$, but not for σ_T. (auth)

42394 SEPARATION OF REACTION MECHANISMS AT LOW ENERGY. Bassani, G. (Centre d'Etudes Nucleaires, Saclay, France); Cassagnou, Y.; Levi, C.; Mermaz, M.; Papineau, L.; Pappalardo. J. Phys. (Paris), Colloq., No. 1, 141-2(1966). (In French).

Reaction mechanisms for $^{27}Al(d,p)^{28}Al$, $^{24}Mg(d,p)^{25}Mg$, and $^{24}Mg(d,\alpha)^{22}Na$ have been separated by investigation of excitation functions and identification of Ericson fluctuations. Two wide resonance states were observed in ^{26}Al near 15 Mev. (S.F.L.)

42395 PROBABILITY DISTRIBUTIONS OF EXTREMES OF CROSS SECTIONS. Ericson, M.; Couchoud, S. (Faculte des Sciences, Lyon). J. Phys. (Paris), Colloq., No. 1, 142-4(1966). (In French).

The probability distributions for minima and maxima of nuclear cross sections are calculated to be approximately χ^2 distributions with one degree of freedom for minima and three degrees of freedom for maxima. (auth)

42396 EFFECTS OF POLARIZATION ON ERICSON FLUCTUATIONS. Dumazet, G.; Lambert, M. (Institut d'Etudes Nucleaires, Alger, France). J. Phys. (Paris), Colloq., No. 1, 145-6(1966). (In French).

In the continuum, the tensorial components of polarization have to exhibit Ericson fluctuations. The variance of these fluctuations is larger than for the cross sections. The more polarized the beam and/or the target, the greater are the fluctuations. (auth)

42397 APPLICATION OF A GRAPHICAL METHOD FOR CALCULATION OF $\sigma(\theta)$ OF STRIPPING. Massot, J. N.; El-Baz, E.; Lafoucriere, J. (Institut de Physique Nucleaire, Lyon). J. Phys. (Paris), Colloq., No. 1, 146-8 (1966). (In French).

It is shown how the graphical method of summation of Clebsch-Gordan coefficients extended to spherical harmonics easily gives differential cross sections of stripping reactions. (auth)

42398 ANGULAR DISTRIBUTIONS OF (t,α_0) REACTIONS ON LITHIUM, BORON, CARBON, AND OXYGEN. Seltz, R.; Gerardin, C.; Wery, M.; Magnac-Valette, D. (Centre de Recherches Nucleaires, Strasbourg). J. Phys. (Paris), Colloq., No. 1, 148-9(1966). (In French).

Angular distributions of (t,α_0) reactions on ^7Li, ^{10}B, ^{12}C, and ^{16}O for $1.5 \leq E_t \leq 3.25$ Mev were measured with thin targets and semiconductor detectors. The curves show peaks especially in the forward and backward direction and are very similar to angular distributions of (^3He,α) reactions on the same nuclei. (auth)

42399 STUDY OF (d,p) REACTIONS ON LIGHT NUCLEI AT LOW ENERGY. Beaumevieille, H.; Longequeue, N.; Longequeue, J. P.; Nguyen Van Sen (Univ., Grenoble, France). J. Phys.(Paris), Colloq., No. 1, 150-1(1966). (In French).

The strong backward intensity of the angular distributions of the (d,p) reactions ($E_d \simeq 300$ kev) on ^{16}O, ^{11}B, and ^{6}Li suggests a direct interaction mechanism, the angular distributions (d,α) being $\pi/2$ symmetric. An interpretation of the results for ^{16}O and ^{11}B by Coulomb stripping gives a good fit outside the resonances of the (d,α) reaction. (auth)

42400 CONTRIBUTION TO A STUDY OF THE REACTION $^{12}C(d,p)^{13}C$. Bruno, G.; Decharge, J.; Perrin, A.; Surget, G. (CEA, Paris). J. Phys. (Paris), Colloq., No. 1, 151-4(1966). (In French).

Excitation functions are given for $^{12}C(d,d)^{12}C$, and $^{12}C(d,p)^{13}C^*$ reactions at 120° for a deuteron energy range from 4 to 7 Mev. These curves show two new peaks corresponding to 14.70 and 15.26 Mev levels in ^{14}N. (auth)

Plasma Physics and Thermonuclear Processes

See also Fluid Physics and Thermodynamics

Refer also to abstracts 41120, 41121, 41123, 41554, 41692, 41699, 41708, 41712, 41715, 41717, 41723, 41741, 41750, 41751, 41754, 41756, 41764, 41766, 41768, 41770, 41772, and 42545.

42401 (AD-637854) EFFECTS OF PARTIAL IONIZATION AND PRESSURE ON HYDROMAGNETIC IONIZING WAVES. Physical Sciences Research Papers No. 239. Kushwaha, Ram S.; Rubin, Allen G. (Air Force Cambridge Research Labs., L. G. Hanscom Field, Mass.). June 1966. 15p. (AFCRL-66-429). CFSTI $1.00 cy, $0.50 mn.

The transverse hydromagnetic ionizing wave is studied theoretically without the assumption of infinite conductivity behind the wave. Finite gas pressures are included, as well as a variable degree of ionization behind the wave. The electric field in front of the wave is employed as a parameter. Jump conditions across the wave are solved. It is shown that finite pressure and variation of the degree of ionization are important in some regions. (auth)

42402 (IAE-1149) NEUSTOICHIVOST PLAZMY NA ZAPERTYKH CHASTITSAKH V TOROIDALNOI GEOMETRII. (Instability of Plasma with Captured Particles in Toroidal Geometry). Kadomtsev, B. B.; Pogutse, O. P. (Institut Atomnoi Energii, Gosudarstvennyi Komitet po Ispol'zovaniyu Atomnoi Energii SSSR, Moscow). [1966]. 24p. Dep. mn.

It is shown that instability similar to the instability of channel plasma in traps with magnetic mirrors can be developed in a toroidal discharge with longitudinal magnetic field. Such instability developed in particles captured between mirrors was investigated. (tr-auth)

42403 (IAE-1151) RAVNOVECIE PLAZMY V ZAMKNUTYKH TOROIDALNYKH MAGNITNYKH KONFIGURATSIYAKH. (Plasma Equilibrium in Confined Toroidal Magnetic Configurations). Shafranov, V. D. (Institut Atomnoi Energii, Gosudarstvennyi Komitet po Ispol'zovaniyu Atomnoi Energii SSSR, Moscow). [1966]. 14p. Dep. mn.

Distortions of magnetic field configurations caused by currents in plasma were studied in order to establish plasma equilibrium in magnetic fields. The strongest effects of plasma pressure in closed systems are exhibited by the plasma pinch toroidal shift outward from the center of curvature. This effect may change the shape of magnetic surfaces and even the topology of magnetic configurations. The shift of magnetic surfaces and general topology of toroidal equilibrate configurations are discussed. (tr-auth)

42404 (IC-66/45) WKB APPROXIMATION IN THE COMPLEX PLANE AND APPLICATIONS TO PLASMA THEORY. Skorupski, A. (International Centre for Theoretical Physics, Trieste (Italy)). May 1966. 38p. Dep. mn.

The following problems concerned with the WKB technique applied to the equation $d^2\psi/dz^2 + q^2(z)\psi = 0$ in the complex plane are considered: the errors and the applicability conditions along any line L, the properties of the Stokes and the anti-Stokes lines, and the connection formulas for zeros and simple poles of $q^2(z)$. The results obtained generalize those of N. Fröman and P. O. Fröman. Two typical applications are considered: (i) ionospheric propagation of the EM waves through a region with a resonance and a cutoff. An expression for the transmission coefficient is derived and it is shown to be exact for a simple model discussed by Budden, and (ii) evaluation of the eigenfrequencies for the "quasi-modes" introduced in plasma stability theory. For any number of zeros and poles of $q^2(z)$ in the complex plane the "quantization condition" specifying the eigenfrequencies is derived and reduced to a form convenient for approximations. It is shown that the location of poles of $q^2(z)$ defines a sector in the complex plane where the eigensolution $\psi(z)$ is not localized. (auth)

42405 (IPP-1/46) ENTWICKLUNG UND ERPROBUNG EINER HOCHAUFLOESENDEN PIEZOELEKTRISCHEN DRUCKSONDE. (Development and Testing of a Piezoelectric Pressure Probe With High-Resolving Power). Katsaros, W. (Institut fuer Plasmaphysik, G.m.b.H., Garching (West Germany)). Mar. 1966. 64p. Dep. mn.

Pressure measurements in rapidly varying dense plasmas are of great interest for plasma diagnostics. Such measurements are meaningful only if the smallest time interval which can be resolved by the equipment is at least three times shorter than the duration of the process to be investigated. The major purpose of this work is a development of piezoelectric probes with the aim of improving the presently available time resolving power by a factor of ~3. This purpose was approximately achieved and it turned out that further improvement appears impossible because of fundamental technical and physical limitations. A test of the probes was combined with pressure investigations in an inverse pinch. The results of the pressure measurements and of concurrent density determinations made it possible to carry out a detailed investigation of shock wave processes in an inverse pinch. The piezoelectric probe which was developed satisfies the following requirements: time resolving power about 80 ns; spatial resolving power about 0.5 mm; sensitivity about 5 torr/mv; and accuracy about ±10%. Since the piezoelectric transducer is quite sensitive against electrical perturbations from the plasma the pressure impulse which is to be investigated is transmitted to the transducer through a pressure guide. This pressure guide consists of a cylindrical quartz rod with diameter $\phi \approx 0.3$ mm and length $l = 150$ to 250 mm. In order to achieve a high sensitivity, a ceramic (P T.2) with very high piezoelectric coefficient is used. In order to obtain an accuracy of ±10%, a new calibrating method was developed. A high-voltage pulse excites a piezoelectric shock generator and this generator then yields a pressure pulse the amplitude and shape of which may be varied. This pulse is used for calibrating the probe. (auth)

42406 (IPP-2/47) ON THE IONIZATION OF BARIUM ON HOT RHENIUM SURFACES. Grieger, G. (Institut fuer Plasmaphysik, G.m.b.H., Garching (West Germany)). Apr. 1966. 43p. Dep. mn.

Due to both the high ionization and the high evaporation energy of barium, together with the high work function of rhenium it is expected that also for rather high temperatures of the emitter, the coating of the emitter surface by Ba atoms cannot be neglected. This coating has considerable influence on the work function of the emitter and on the individual desorption energies. On the other hand, a clean Re surface provides only a relatively small flux of thermally emitted electrons, so that it may be difficult to establish an electron sheath in front of the emitter. The properties of the system Ba–Re are evaluated. It is found that the relative potential distribution within the undisturbed part of the plasma column is unaffected by a change of the emitter properties. (auth)

42407 (IPP–2/48) UNTERSUCHUNG DER CAESIUM-PLASMA-DIODE MIT EINER NEUEN ELEKTRONEN-STRAHLSONDEN-TECHNIK. (Investigation of a Cesium Plasma Diode Using an Electron Beam Probing Technique). Ott, W. (Institut fuer Plasmaphysik, G.m.b.H., Garching (West Germany)). June 1966. 40p. Dep. mn.

The plasma in the diode was investigated experimentally with a ribbon-shaped electron beam. The ribbon beam is projected through the diode at a 45° angle to its axis and allowed to strike a fluorescent screen. Variations in the axial electric field of the diode cause the ribbon beam to be distorted. The image of the distorted beam as seen on the fluorescent screen then constitutes a plot of the axial electric field along the axis of the diode. The field plots so obtained are compared with a theory in which the collisions of the charge carriers are neglected. By means of this comparison it is possible to evaluate the neutralization parameter, the plasma density, and an average drift energy of the charge carriers. The results show that the theory correctly describes the different modes of the potential distribution and especially the transitions between modes of operation as long as the diode is free of oscillations. The stability of the different static potential distributions was also investigated. It was found experimentally and theoretically that the system is unstable if the electron emission is less than the ion emission and the collector potential is positive. (auth)

42408 (IPP–2/49) INTERFEROMETER FUER DREI WELLENLAENGEN: 2,5 mm, 4 mm UND 8 mm. (Interferometer for Three Wavelengths: 2,5 mm, 4 mm, and 8 mm). Michaelis, M. (Institut fuer Plasmaphysik, G.m.b.H., Garching (West Germany)). June 1966. 56p. Dep. mn.

The interferometer was designed to measure simultaneously the phase shifts of three superimposed microwave beams transmitted across a common plasma path. An "optical" transmission with teflon lenses, oversize waveguide, parallel plate filters, and wire grid was developed for the 2.5-mm wavelength and for the three wavelengths in the measurement channel. Conventional waveguides were used elsewhere. A zebra stripe display was obtained by means of long reference arms and provided direct phase-shift readings for all three wavelengths with a maximum sensitivity of 10°. A graphical method for error evaluation is given. The interferometer permits plasma density measurements between 10^{12} and 10^{14} particles/cc. (auth)

42409 (IPP–6/50) SPEZIELLE MAGNETOHYDROSTATISCHE AXIALSYMMETRISCHE MERIDIONALE GLEICHGEWICHTE. (Special Magnetohydrostatic, Axisymmetric Meridional Equilibria). Nuehrenberg, J. (Institut fuer Plasmaphysik, G.m.b.H., Garching (West Germany)). May 1966. 35p. Dep. mn.

An investigation was made of magnetohydrostatic, axisymmetric, meridional equilibria which are periodic along the axis of symmetry and for which the pressure tends monotonically and continuously towards zero as a function of the distance from the axis of symmetry. Analytical solutions are set up in the vicinity of the axis of symmetry; for a certain class of boundary value problems an approximation method is developed which reduces calculation of the equilibrium to solving a system of ordinary differential equations. (auth)

42410 (IPP–6/51) THE ELECTRICAL CONDUCTIVITY OF A PARTIALLY IONIZED ARGON–POTASSIUM PLASMA IN A MAGNETIC FIELD. Feneberg, W. (Institut fuer Plasmaphysik, G.m.b.H., Garching (West Germany)). Apr. 1966. 9p. Dep. mn.

In the case of small deviations from thermal equilibrium the second Enskog approximation is used as a starting point for solving the Boltzmann equation of the electrons in a partially ionized plasma. The distribution function is expanded according to Laguerre polynomials up to the order of 3. In this order the electrical conductivity of a Lorentz gas, which is known exactly, is obtained to an accuracy of roughly 5%. The approximation tested in this way was then used to calculate the conductivity of an argon–potassium mixture at electron temperatures between 2000 and 3500°K. If only the collisions between electrons and argon atoms are considered, the electric conductivity in the absence of a magnetic field would, in view of the Ramsauer effect, be greater by a factor of 2.8 than that obtained with an infinitely strong magnetic field. When the interaction with the potassium atoms and the Coulomb interactions are taken into account as well, the conductivity in the magnetic field varies by about 20%. (auth)

42411 (IPPJ–49) ON THE METHOD OF NUMERICAL COMPUTATION OF DISPERSIVE NONLINEAR EQUATION. Outi, Akizi; Yajima, Nobuo (Institute of Plasma Physics, Univ. of Nagoya (Japan)). June 1966. 12p. Dep. mn.

In order to examine the different schemes to obtain numerical solutions of dispersive nonlinear equations, a model equation is considered which is derived from the Schrödinger equation and is solvable exactly. By comparing the numerical solutions with the corresponding exact solutions it is found that Kruskal-Zabusky's scheme applied to the Kortweg-de Vries equation approximates the exact solution. (auth)

42412 (MIT–3221-19) PULSED ELECTRON-CYCLOTRON RESONANCE DISCHARGE EXPERIMENT. Technical Report No. 442. Fessenden, Thomas J. (Massachusetts Inst. of Tech., Cambridge. Research Lab. of Electronics). June 1, 1965. Contract AT(30-1)-3221. 84p. Dep. mn. CFSTI $3.00 cy, $0.75 mn.

Thesis.

Ideas useful in understanding the processes occurring in the experiments are developed. Motions of particles in a magnetic mirror field are considered with adiabatic approximations used. The loss of particles from a mirror because of collisions with the neutral background gas is considered. An estimate of the gain of energy that an electron experiences when it is accelerated by microwave fields in a nonuniform static magnetic field is presented. The experimental apparatus and the results of various experiments are described. Explanations of the observed experimental results and of the electron production and loss processes are presented. The small-angle scattering of electrons by neutrals is considered. The methods used in calibrating the diamagnetic signal probes are described. A new microwave perturbation technique is discussed which was developed in this study. The formulas that were used in studying the x-ray bremsstrahlung spectra of the electrons are presented. The evaluation of an integral used to indicate the effects of a distribution of electrons in energy on the decay of plasma electron density in a mirror is considered. (M.H.R.)

42413 (NASA-TN-D-2959) MONTE CARLO METHOD FOR THE CALCULATION OF TRANSPORT PROPERTIES IN A LOW-DENSITY IONIZED GAS. Goldstein, Charles M. (National Aeronautics and Space Administration, Cleveland, Ohio. Lewis Research Center). Sept. 1965. 56p. CFSTI $3.00 cy, $0.50 mn.

An introduction to the general Monte Carlo method is presented, along with a discussion of its scope of application to plasma physics. This is followed with a heuristic sketch of the method. The problem of electron flow through a perfect Lorentzian gas in a parallel-plane diode is then formulated. The Monte Carlo solution is discussed in detail along with the relevant computational techniques employed. (Pertinent concepts from the theory of random variables are included in an appendix.) The effects of mean free path on current-voltage characteristics, density distribution, and potential distribution are presented for two cases—monoenergetic and thermionic emission. Results indicate that electron-neutral elastic collisions can have a significant effect on the current-voltage characteristics for electrode separations as small as one mean free path in the case of thermionic emission, and one-half mean free path in the case of monoenergetic emission. (auth)

42414 (NP–16266) EQUILIBRIUM AND STABILITY OF A TOROIDAL SCREW PINCH. Rijnhuizen Report 66-

32, Bobeldijk, C.; Rietjens, L. H. Th.; van der Laan, P. C. T.; de Bats, F. Th. (Stichting voor Fundamenteel Onderzoek der Materie, Jutphaas (Netherlands). Instituut voor Plasma-Fysica). June 1966. 16p. Dep. mn.

A toroidal plasma column, produced and confined by a rapidly rising helical magnetic field is being studied. This "screw pinch" is of interest because it is in equilibrium and is completely reproducible. The discharge vessel is a quartz torus with major and minor diameters of 72 and 12 cm. Plasma currents (axial j_z and azimuthal j_θ) are induced by two orthogonal primary coils, which are simultaneously connected to capacitor banks (E_z = 5 kJ and E_θ = 7.5 kJ). Both circuits have a ringing frequency of 70 kHz. During the first microsecond the plasma collapses; then the column drifts about 0.5 cm to the outer wall and remains in this position, slightly off the tube axis, until the end of the first half cycle. The plasma is kept in this equilibrium position by the compression of the B_θ field between the plasma column and the metal shell surrounding the torus. The necessary gaps in the shell are constructed with special care. During the 7 μsec of the first half period no instabilities have been observed. This stable behavior is found even if the pitch of the magnetic field is varied between wide limits; expressed in terms of the axial current, a variation between approximately 4 to 12 times the Kruskal limiting current does not impair the reproducibility. A large-amplitude oscillation, excited by the implosion, is observed. The frequency agrees with the frequency of the stable m = 0, k = 0 mode, predicted by the normal mode analysis. From measured Stark broadening a density of 2×10^{16} cm^{-3} was derived, which corresponds to a compression ratio (radius of the tube divided by plasma radius) of 3. In a 15 micron Hg helium discharge a temperature of 20 ev has been measured. (auth)

42415 (TID–22928) HIGH TEMPERATURE PLASMAS BY LASER HEATING. Final Report. Sucov, E. W.; Pack, J. L.; Phelps, A. V.; Engelhardt, A. G. (Westinghouse Research Labs., Pittsburgh, Pa.). Apr. 6, 1966. Contract AT(30-1)-3472. 67p. Dep. mn. CFSTI $3.00 cy, $0.75 mn.

Studies were made of the confinement in a magnetic mirror of a plasma produced by focussing a Q-switched laser beam on aluminum targets in the form of disks, foils, and spheres. High speed photographs show that one component of the plasma generated from flat targets is asymmetric and moves toward the laser with a velocity of about 10^7 cm/sec. The plasma generated from ball targets is roughly symmetrical with respect to the origin and expands much more slowly. In the presence of a mirror magnetic field of ratio 2:1, the expansion velocities are not appreciably reduced. However, the duration of the luminosity from a slower constituent of the plasma is increased by a factor of about 5, i.e., from 1 μsec to about 5 μsec, indicating that some confinement has occurred. In addition, microwave interferometer measurements show the confinement of a slow component of the disk plasma in the magnetic field with an electron density of about 5×10^{11} cm^{-3} at times as late as 50 μsec. Electrostatic probes provide an independent verification of the maximum expansion velocity which corresponds to an ion kinetic energy of about 1.4 kev. Time integrated spectra of the plasma show lines from excited states of doubly ionized aluminum. Microwave attenuation measurements lead tc an apparent electron temperature of the order of 0.02 ev at times later than 1 μsec. Analysis of microwave and other data show that radial density gradients probably exist in some plasmas. (auth)

42416 (TID–23277) AEC POLICY AND ACTION PAPER ON CONTROLLED THERMONUCLEAR RESEARCH. (Atomic Energy Commission, Washington, D. C.). June 1966. 251p. Dep. mn. CFSTI $6.00 cy, $1.25 mn.

A review is presented of the scientific background for the controlled thermonuclear research program, including the nature of the problem, the methods of attack, etc. A brief survey is presented of the present status of research in controlled fusion, both in this country and abroad. The AEC policies are described. (M.O.W.)

42417 (UCRL–7170) MAGNETIC PULSE IN A COLD COLLISION-FREE PLASMA. Gonzales, Douglas E. (Lawrence Radiation Lab., Univ. of California, Livermore). Feb. 7, 1966. Contract W-7405-eng-48. 136p. Dep. mn. CFSTI $4.00 cy, $1.00 mn.

Thesis.

The steady-state motion of a magnetic disturbance propagating transverse to a uniform magnetic field in a cold collision-free plasma was investigated. Electrostatic interactions were ruled out by assuming that the plasma constituents have equal mass. The disturbance consists of a pulse—or series of pulses—of extra magnetic flux parallel to the original flux. Each pulse has the net effect of displacing the entire plasma among the direction of propagation. If the speed of the solitary disturbance is between one and two times the Alfvén speed in the undisturbed plasma, the individual particle orbits associated with the perturbation do not cross over one another. However, for speeds greater than this, particle crossovers occur corresponding to a symmetrical looped particle trajectory when viewed in a frame of reference moving with the disturbance. The nonlinearity of the plasma-field equations governing the multiple-stream loop region necessitates a numerical solution there, the external tail segments being specified by familiar single-valued analytic results. These solutions are also shown to be unique. In the event that extra stress is applied at the plasma boundary, not one but a series of pulses of extra flux is forced into the plasma. Physically, the extra stress is required to establish the steady-state periodic structure, since the individual pulses repel one another. Although the variation of the periodic solutions with pulse speed and extra stress is rather complex, their periodic structure corresponds closely to a superposition of solitary pulse solutions with regular spacings along the direction of propagation. In fact, multiple overlapping of the elementary looped trajectories result for some solutions when the propagation speed is greater than twice the undisturbed Alfvén speed. Rarefaction pulses with a net magnetic flux less than that of the reference state have also been found to exist, but only for the case of a total flux reversal. These solutions represent waves traveling in a direction opposite to that of the compression pulses described above when viewed in a frame moving with the mean particle velocity, and are related to them by a simple change of variables. Reduced "Rankine-Hugoniot" type relations for the magnetic shock problem are calculated on the basis that the multiple overlap pulses may effectively represent a finite temperature plasma. The actual shock transition linking two overlap states is concluded to be time dependent, and a model for investigating its structure is described. Procedures for utilizing the equal mass results in an analysis of the pulses generated in an unequal mass plasma are also given. (auth)

42418 (UCRL–14744, pp 37-48) RADIATION AND PLASMA PHYSICS. (Lawrence Radiation Lab., Univ. of California, Livermore).

Brief summaries of research are presented for the following: electromagnetic mass of the electron, many-atom effects in laser radiation, momentum transfer produced by focused laser giant pulses, nanosecond Q-spoiled laser pulses, frequency-dependent radiation transport, numerical computation of stellar dynamics, and plasma transport theory. (M.O.W.)

42419 (AD–636608) METHOD OF DETERMINING ELECTRON DENSITY DISTRIBUTION IN A PLASMA. Dushin, L. A.; Kononenko, V. I.; Skibenko, A. I. Translation of Russian Patent 167,524. 3p. (FTD-TT–65-748). CFSTI $1.00 cy, $0.50 mn.

A method is given for determining the electron density in a plasma by measuring the amplitude of a signal that has passed through it. The difference in this method and others is that measurements are made of the magnitude of damping of the amplitudes of microwave signals of several different frequencies that are selected so that at the moment a signal of one frequency is cut off the amplitude of one of the remaining signals experiences damping. (M.O.W.)

42420 (JPRS-36823) THE RIDDLE OF BALL LIGHTNING. Leonov, Roal'd Aleksandrovich. Translated from pp 3-75 of Zagadka Sharovoy Molnii, Academy of Sciences USSR, Nauka Publishers, Moscow, 1965. 72p. (TT-66-33253). CFSTI $3.00 cy, $0.75 mn.

An attempt was made to generalize everything that is known to science on the unusual properties of ball lightning, on the basis of a wide circle of sources. The puzzling mysteries, keen experiments, and bold hypotheses and modern theories of ball lightning are discussed. (M.O.W.)

42421 (NP-tr-1396) THE VACUUM SYSTEM OF OGRA-II. Butuzov, S. S.; Pustovoit, Yu. M.; Maslennikov, E. A. Translated for Culham Lab., Abingdon, Eng., from report IAE-1113. 23p. (CTO-299). Dep. mn. CFSTI $1.00 cy, $0.50 mn. JCL $2.60 fs, $0.89 mf.

The vacuum system in Ogra-II is described. It consists of an ion gun, a neutralization chamber, a differential pumping system and the working chamber in which the plasma is trapped. Calculations and experimental results are given for the differential pumping system, showing a pressure drop from 10^{-5} torr in the neutralization chamber to 10^{-9} torr at the entry into working chamber over a length of 3 meters, with a beam path aperture of area ~200 cm^2. The conditions are discussed under which heating and cooling of the device takes place, and pressures of ~10^{-10} torr are obtained in the trap without beam. The composition of the residual gases during the various stages of evacuation is given. Reasons are considered for the rise of pressure to 10^{-9} torr during the accumulation of the plasma, and methods for the pulsed pressure measurements in the working chamber in the presence of the accumulating plasmas are described. (auth)

42422 GRAVITATIONAL INSTABILITY OF ANISOTROPIC PLASMA. Gliddon, J. E. C. (Queen Mary Coll., London). Astrophys. J., 145: 583-8(Aug. 1966).

It is known that Jeans's criterion for instability of a self-gravitating gas is valid also for a homogeneous, rotating, low-density plasma permeated by a magnetic field. The criterion is independent of the magnetic field. It is shown that, if the plasma has an anisotropic velocity distribution, the plasma may exhibit hose instability as well as gravitational instability and the criterion for the latter is now dependent upon the magnetic field. (auth)

42423 PITCH-ANGLE DEPENDENCE OF FIRST-ORDER FERMI ACCELERATION AT SHOCK FRONTS. Jokipii, J. R. (Univ. of Chicago). Astrophys. J., 145: 616-22(Aug. 1966).

A model of first-order Fermi acceleration at shock fronts is extended to consider the angular distribution of the accelerated particles. In the model, particles trapped between a hydromagnetic shock front and a moving magnetic mirror are accelerated by a Fermi process. Scattering of the particles in pitch angle during acceleration was assumed to offset the decrease in pitch angle due to reflection from the moving mirror. The limit is considered in which scattering is assumed weak, although it is still strong enough to offset the effect of the mirror. An approximate energy sepctrum is obtained, and it is found that acceleration may be very efficient when the scattering is small. In particular, a mirror ratio $B_M/B_0 \sim 2$ may suffice to produce the observed energetic electron spectra observed near the Earth's bow shock. (auth)

42424 PLASMA EQUILIBRIUM IN A CIRCULAR MAGNETIC AXIS STELLARATOR. Shafranov, V. D. At. Energ. (USSR), 21: 47-9(June 1966). (In Russian).

The shift of plasma pinch from the center of curvature and distortion of the magnetic surface takes place during plasma placement into a magnetic trap. The shift of plasma pinch was computed for the case in which the transverse magnetic surface cross sections are close to a circular. The solution was obtained by the method of perturbation in linear approximation according to the dimensionless parameter $\beta\mu^2 R/b$ when β is the relation of plasma pressure to the pressure of the magnetic field, μ is the angle of torsion of magnetic field power line divided by 2π; R is the radius of the torus and b is the transverse dimension of the system. For solving in a simplified analytical field the vacuum magnetic field and surfaces are presented as an expansion according to the degree of distance from the magnetic field. The method may be satisfactorily used for resolving the distribution of equilibrated magnitudes considering the curvature of the system and intraplasma pinch. (R.V.J.)

42425 POSITIVE COLUMN IN A MAGNETIC FIELD. Forrest, J. R.; Franklin, R. N. (Oxford Univ.). Brit. J. Appl. Phys., 17: 1061-7(Aug. 1966).

A theoretical model for the behavior of the positive column of a low-pressure arc discharge in a magnetic field is developed. The model is applicable to "free-fall" conditions, in which ions are assumed to fall freely from their point of generation under the influence of a radial electrostatic potential gradient. For the case of a cylindrical plasma column, predictions are made for the variation with magnetic field of radial electron number-density profile, radial potential profile, wall number density, electron temperature and radial light emission profile. The constriction of a plasma column in a magnetic field is considered, and predictions from the above model are compared with measured radial light emission profiles from a mercury discharge, and also with the experimental results of previous authors. (auth)

42426 EFFECT OF STATIC MAGNETIC FIELD ON RADIATION THROUGH A PLASMA SHEATH. Seshadri, S. R. (Sylvania Electronic Systems, Waltham, Mass.); Yip, G. L. Can. J. Phys., 44: 1941-64(Sept. 1966).

The radiation characteristics of a filament of finite length with a triangular current distribution are investigated for the case in which it is situated along the axis of an infinitely long, axially magnetized column of uniform plasma. In general, the current filament will excite guided waves along the plasma column as well as space waves. The radiation pattern in the far zone and the radiation resistance of the current filament contributed by the space waves are studied as a function of the radius of the plasma column, the operating frequency of the source, the strength of the applied static magnetic field, and the length of the current filament with the current at its center kept constant. In particular, for various frequencies below the plasma frequency and for a particular radius of the plasma column, the radiation pattern and the radiation resistance are presented as a function of the strength of the applied static magnetic field. These results indicate that a significant improvement in the transmission through a plasma sheath can be obtained by a suitable application of a static magnetic field. A brief discussion of the characteristics of the possible guided waves along the plasma column is also included. (auth)

42427 NONLINEAR PROCESS IN A FINITE PLASMA. Etievant, Claude; Fidone, Ignazio; Laval, Guy; Olivain, Jack; Pellat, Rene; Perulli, Mariano (EURATOM-Commissariat a l'Energie Atomique, Fontenay-aux-Roses, France). Compt. Rend., Ser. B, 263: 19-21(July 4, 1966). (In French).

The study of nonlinear processes in infinite media shows that the energy and the pulse of the wave generated $(\omega, \vec{k})$ are determined by corresponding magnitudes of interacting waves. It is shown that in the case of radially limited media this result is not conserved integrally. (tr-auth)

42428 RESEARCH ON SHEATH FORMATION. Miyajima, Shigeki (Univ. of Nagoya, Japan). Denki Gakkai Zasshi, 85: 1200-7(July 1965). (In Japanese).

A discussion is presented of the plasma-sheath transition as a function of the electric current delivered to the sheath using a one-dimensional collisionless model and a set of macroscopic equations. From this treatment, the sheaths may be divided into two groups, depending on whether $\gamma^2 = 1$ or $\gamma^2 \neq 1$. In the equation $\gamma^2 = \Sigma C_s^2 T_s / \Sigma T_s$, the subscript s is for e (electron) and i (ion), and in the equation $C_s^2 = m_s v_{so}^2 / kT_s$, m_s is the mass, T_s the temperature, and V_{so} the velocity at the plasma-sheath boundary. When $\gamma^2 = 1$, then $n_e > n_i$ (or $n_i > n_e$) anywhere in the sheath, where n_s is the density; when $\gamma^2 \neq 1$ it is partly an electron excess and partly an ion excess region. When the condi-

tions $\gamma^2 = 1$ and $E_0 = 0$, where E_0 is the strength of electric field at the boundary, are satisfied, then for $C_i^2 > 1$ the pure ion excess sheath is formed and for $C_e^2 > 1$ the pure electron excess sheath is established. For $C_i^2 = C_e^2 = 1$, no sheath is developed, that is, the electric potential of a collector drawing out the electric current from the plasma is identical with the plasma potential. The stable sheath is formed only when $\gamma^2 \geq 1$, including the well-known Bohm criterion leading to the sheath formation. Calculations are also presented of the Langmuir probe curve, imposing the conditions $\gamma^2 = 1$ and $E_0 = 0$. The theoretical curve deviates from the classical theory showing that the resistance is zero at the plasma potential. (auth)

42429 EXCITATION OF ION PLASMA OSCILLATION BY ELECTRON BEAMS. Matsuura, Kenya; Ogawa, Kiyoshi; Yoseli, Morihiro; Kato, Kiyoe (Electrotechnical Lab., Tokyo). Denki Shikensho Iho, 30: 531-42(June 1966).

The excitation of the ion plasma oscillation is theoretically treated in relation to the plasma-electron beam system which is assumed to be composed of three components: ions, the medium electrons, and the beam electrons. In this three-component system the instability is different from the two-stream instability by the effects of the damping due to the medium electrons. The dispersion relations for these plasmas are derived by the linearized theory, and the approximate analyses and the numerical analyses are shown. From those results the physical meanings are considered and the theoretical guides for the experiments are given. (auth)

42430 NONLINEAR MAGNETOHYDRODYNAMIC WAVES. Polovin, R. V. (Inst. of Physics and Tech., Kharkov). Differentsial'nye Uravneniya, 1: 499-522 (Apr. 1965). (In Ukrainian).

A survey is presented of research on nonlinear, one-dimensional magnetohydrodynamic waves. A wide class of hyperbolic systems of partial quasi-linear equations is investigated. The significance of curves and their connection with waves of small amplitude are described. The simple wave theory, the question of Riemann invariants are discussed, and it is shown that in the absence of discontinuities the constant flow region can be bounded only by a simple wave. The character of the change of the profile of a simple wave during motion is discussed and it is shown that in a number of cases this change results in the formation of discontinuities. It is also shown that boundary conditions on discontinuous surfaces are obtained from conservation laws in integral form. It is shown that the conservation laws are satisfied not only by true discontinuities but also by extraneous solutions, and to exclude them, the conservation laws need to be supplemented by conditions of evolution. It is indicated that for waves of small intensity the difference between a shock wave and a self-similar wave (correct to magnitudes of second order inclusive) consists only in the sign of the density jump; from this it follows particularly that a change in a Riemann invariant in a weak shock wave is of the third order of smallness. It is shown that the use of these correlations allows a general solution to the problem of the decay of a discontinuity under initial conditions for waves of small intensity. The reasons are explained for the appearance of discontinuities when dissipation factors tend to zero and investigates the structure of a shock wave. (TCO)

42431 EFFECT OF RADIATION DECELERATION ON THE MOTION OF A RELATIVISTIC PARTICLE IN A UNIFORM MAGNETIC FIELD. Gernet, G. E. (Bonch-Bruevich Electrical Engineering Inst. of Communications, Leningrad). Dokl. Akad. Nauk SSSR, 168: 63-4(May 1, 1966). (In Russian).

The trajectory of a charged particle changes during motion in a magnetic field due to loss of energy caused by magnetic bremsstrahlung (synchrotron radiation). The following equation is derived for the change in energy: $dw/dt = -\delta[(w/w_\infty)^2 - 1]$, where $\omega = eH/mc$, $\delta = \frac{2}{3}e^4H^2/m^3c^5$ and $w_\infty = 1/\sqrt{1 - u_z^2}$, is the limiting value of w as $t \to \infty$. The integral of this equation is $w = w_\infty \mathrm{cth}\,(\delta t/w_\infty + C_0)$. The constant C_0 is determined from the condition $w = w_0$ at $t = 0$. It is shown that the transverse components of velocity are attenuated and disappear at $t \to \infty$. The energy is reduced to one-half in time $\sim 1/w_0\delta\sin^2\theta$ where θ is the angle between the initial velocity vector and the direction of the field. (ATD)

42432 DETERMINATION OF TEMPERATURE AND ELECTRON CONCENTRATION IN A PLASMA ARC FROM THOMSON SCATTERING OF LASER RADIATION. Malyshev, G. M.; Ostrovskaya, G. V.; Razdobarin, G. T.; Sokolova, L. V. (Ioffe Inst. of Physics and Tech., Leningrad). Dokl. Akad. Nauk SSSR, 168: 554-5(May 21, 1966). (In Russian).

The temperature and electron concentration in a d-c plasma arc in a magnetic field were determined from the scattering of laser radiation. The duration of the 25-j ruby laser operating at $\lambda = 6943$ Å was 0.5 μsec. The 800-Oe magnetic field was parallel to the discharge axis. The laser radiation was observed at a 90° angle from the incident radiation. This radiation was collected by lens L_5 from a volume 7 mm long and 0.6 mm in diameter into a solid angle of $\frac{1}{32}$ sterad. The discharge tube had a 50-mm diameter. The plasma under investigation was at the center of the discharge tube, 140 mm from the cathode. The laser pulse was activated in the middle of the discharge, the duration of which was several dozen seconds. The pressure of the helium flow in the tube was 0.2 mm Hg. Rayleigh scattering was used to calibrate the system. The slit width of the monochromator was 10 Å. The electron temperature determined from the halfwidth of the curve was $T = 1.8$ ev. The electron concentration was determined to be 2.5×10^{13} cm^{-3}. Since the parameter α was calculated to be much smaller than 1, the scattering of laser radiation by electrons was attributed to Thomson scattering. (ATD)

42433 SUMMARY OF ELECTRON SPIN RESONANCE TECHNIQUE AS APPLIED TO RADIATION-PRODUCED RADICALS. Livingston, Ralph (Oak Ridge National Lab., Tenn.). pp 3-26 of Electron Spin Resonance and the Effects of Radiation on Biological Systems. Snipes, Wallace (ed.). Washington, D. C., National Academy of Sciences–National Research Council, 1966.

This paper presents a brief discussion of ESR spectrometers, methods of production of free radicals by irradiation with gamma rays and with uv radiation, and quantitative assay of ESR spectra. Analysis is given of the ESR spectra of gamma-irradiated H_2SO_4, $HClO_4$, methyl alcohol, ethyl alcohol, and uv-photolyzed H_2O_2. (W.E.B.)

42434 PLASMA AND MEGAGAUSS FIELDS. Linhart, J. G. (Laboratorio Gas Ionizzati, Frasacati, Italy). pp 387-96 of EUR-2750.e.

In order to obtain plasma for nuclear fusion the product of plasma density n and the effective life-time τ of this plasma must be at least 10^{14}. Owing to many plasma instabilities it is difficult to achieve long confinement times and therefore, it is of interest to increase the density as much as possible. A high density ($n > 10^{19}$ ions/cm^3) thermonuclear plasma can be confined only by magnetic fields of the order of several megagauss. Criteria for such "pulsed" fusion reactors are derived and a survey is presented of several experimental approaches. Megagauss fields can be also used in plasma accelerators. Possible modes of operation of such accelerators are described. The generation of high magnetic fields is intimately connected with plasma behavior, as flux compression may be achieved by plasma liners and in any case in the final stages of a flux compression even a metallic liner resembles a plasma medium. Some experiments on plasma liners are described. (auth)

42435 LATERAL EXTRACTION OF NEGATIVE IONS FROM A LAYERED LOW PRESSURE DISCHARGE IN OXYGEN. Drost, H.; Klotz, H.-D.; Timm, U.; Pupke, H. (Forschungsgemeinschaft, Deutsche Akademie der Wissenschaften, Berlin. Institut fuer Biophysik, Berlin). Exp. Tech. Phys., 14: 47-56(1966). (In German).

The relation, occurring in the anodic extraction of negative ions from a stratified oxygen plasma, between stratification and pattern of the ion intensity with a lateral ion

extraction along the total discharge was investigated. The construction and operation of the apparatus that permits an ion detection up to 10^{-14} amp are described. The ion current curves obtained can be related to an increased content of the negative ions in the bright strata parts. A narrow series of strata caused a column with broad strata of corresponding broad ion current maxima. Current periodicities were drawn off along a column not detectable visually as stratified. An expansion of the extraction range to the Faraday dark space leads to the detection of maximum ion intensities in a plasma-free space. The phenomena are discussed in connection with the role of primary electrons in the formation of negative ions. (tr-auth)

42436 ELECTROMAGNETIC WAVES IN HOLLOW CONDUCTORS WITH ISOTROPIC PLASMA. Fruehauf, Uwe (Technische Univ., Dresden). Hochfrequenztech. Elektroakust., 73: 26-31(Feb. 1964). (In German).

The influence of an isotropic plasma on an electromagnetic wave, especially in practical applications of gas discharge tubes, is discussed. The determination of the dielectric constant and the electron concentration of a plasma is outlined. The variations of phase constant of a H_{11} hollow conductor wave are studied with the positive column of a glow discharge with the charge stream at constant pressure. With the tubes studied, phase rotations of up to 50° were obtained, corresponding to a relative variation of the phase constant of about 5%. If the charge current is increased, thereby increasing the electron density, a more pronounced influence on the hollow conductor waves is achieved. The charge regions of high electron concentration near the cathode may be used to vary the wave propagation. For such experiments a hollow conductor is sealed off at both ends and a filament introduced as cathode. (BBB)

42437 ROADBLOCKS IN THE PATH OF CONTROLLED FUSION. Bishop, A. S. IEEE (Inst. Elec. Electron. Eng.), Spectrum, 3: No. 7, 106-11(July 1966).

Progress in the field of controlled fusion is being slowed by inadequate confinement of the hot plasma, primarily due to instabilities of one type or another. The types of fusion devices are discussed together with the kinds of instabilities which arise in each type. The problems involved in the systematic reduction of the various energy reservoirs available to drive these instabilities are reviewed. (M.H.R.)

42438 ELECTRIC DIPOLE RADIATION THROUGH A FINITE CONICAL PLASMA SHEATH. Pridmore-Brown, D. C. (Aerospace Corp., El Segundo, Calif.). IEEE (Inst. Elec. Electron. Eng.) Trans. Antennas Propagation, AP-14: 428-33(July 1966).

An analysis was made of the role of diffraction effects or antenna pattern distortion in the so-called blackout problem, the sharp reduction in the effective transmission of information by radio between a reentry vehicle and a ground station. This reduction is observed as the vehicle enters the earth's atmosphere and becomes enveloped in a sheath of partially ionized gas or plasma. The ionized boundary layer that forms around a reentry vehicle is represented by a conical sheath having a surface impedance which is determined by the integrated electron density in the boundary layer. This cone can support surface currents that are induced in it by a Hertzian dipole antenna situated on its axis. The radiation pattern of such a structure at wavelengths short compared to the slant height is calculated by a perturbation technique. The calculation holds when the surface conductivity of the sheath varies linearly with distance from the apex of the cone. Plots are presented showing the effects of sheath strength, slant height, and antenna frequency on the patterns. (BBB)

42439 RF PROPAGATION AND ABSORPTION MEASUREMENTS IN A MAGNETOPLASMA NEAR ELECTRON CYCLOTRON RESONANCE. Miller, David B. (General Electric Co., King of Prussia, Pa.). IEEE (Inst. Elec. Electron. Eng.) Trans. Antennas Propagation, AP-14: 513-14(July 1966).

Measurements were made in a microwave plasma accelerator. In this device a continuous flow of gas is injected into the plasma chamber through the six peripheral ports. Circularly polarized microwave power at 8.35 Gcps is carried by the cylindrical waveguide (TE_{11} mode), passes through a half-wave dielectric window, continuously ionizes the injected gas flow, and energizes the plasma electrons in transverse cyclotron orbits. This magnetized plasma then interacts with the diverging magnetic field, converting the energy in transverse electron motion to longitudinal velocity of the total plasma. Calorimetric measurements of the accelerated plasma stream power indicated that best power conversion efficiency occurred when the dc magnetic field at the dielectric window was considerably above cyclotron resonance. The r-f propagation measurements were made, therefore, in order to discover the location at which the r-f power is actually being absorbed. The results show that the power is absorbed near the resonance point rather than immediately adjacent to the dielectric window. At higher magnetic field strengths, where efficiency was noted to be highest, the plasma is therefore created and accelerated in the free space region beyond the accelerator, thereby minimizing power loss to surrounding walls. (BBB)

42440 NETWORK REPRESENTATION FOR SPHERICAL WAVES IN A COMPRESSIBLE PLASMA. Wait, James R. (Inst. for Telecommunication Sciences and Aeronomy, Boulder, Colo.). IEEE (Inst. Elec. Electron. Eng.) Trans. Antennas Propagation, AP-14: 517-19(July 1966).

When an antenna is placed in an unbounded isotropic warm plasma, both electromagnetic and electroacoustic waves are irradiated. A hydrodynamic description of the plasma is attempted. A specific configuration which yields to this approach is a symmetrical biconical antenna which is surrounded by a rigid dielectric coating of outer radius $\underline{b}$. If the plasma, external to the coating, is homogeneous and unbounded, it is possible to calculate the radiated fields in a straightforward manner if the tangential fields over the aperture surface at $\underline{r} = \underline{a}$ are known. The concrete example considered is that of a slotted-sphere antenna which is encased by a dielectric coating. This may be regarded as a limiting case of the biconical structure when the angle between the two conical surfaces becomes very small. Another limiting situation is when the individual cones become vanishingly thin, in which case a center-fed linear antenna is obtained. This situation is interpreted in terms of a spherical coordinate system $(\underline{r}, \theta, \phi)$, chosen with polar axis $\theta = 0$ coinciding with the axis of the conical structure. External to the surface $\underline{r} = \underline{b}$, the fields are expressed as a sum of modes of both electromagnetic and electroacoustic types. The driving point impedance of the biconical structure is calculated in a straightforward manner once the radial wave impedance $Z_{\underline{n}}$ for mode $\underline{n}$ at the surface $\underline{r} = \underline{b}$ is known. An equivalent circuit was developed for the terminating impedance $Z_{\underline{n}}$ which takes account of the presence of both electromagnetic and electroacoustic waves in the external warm plasma. (BBB)

42441 RESONANCES OF A CYLINDRICAL CAVITY IN A LOSSY COMPRESSIBLE PLASMA. Burman, R. (Victoria Univ. of Wellington, New Zealand). IEEE (Inst. Elec. Electron. Eng.) Trans. Microwave Theory Tech., MTT-14: 251-2(May 1966).

Low frequency resonances are examined when the effects of losses and compressibility are small. A cylindrical cavity which is a free space region immersed in an isotropic compressible lossy plasma is considered. It is shown that the time constant with which the fields decay depends only on the electron collision frequency; it is independent of the compressibility and the mode number. This time constant is the same as that found for a spherical cavity in an isotropic slightly lossy, slightly compressible plasma. The fields oscillate with a real frequency which is independent of the losses. (BBB)

42442 INFLUENCE OF A H-F INHOMOGENEOUS FIELD ON A GASEOUS-DISCHARGE PLASMA. Grigorov,

G.; Popov, G.; Drazheva, L. (Univ., Sofia). Int. J. Electron., 20: 363-74(Apr. 1966). (In French).

The distribution of the parameters of a gaseous discharge plasma was studied in an h-f field which is inhomogeneous in three different forms. The results can be explained by the mean force F, created by the h-f field, and acting on the charged particles in the plasma. One of the forms studied, the Langmuir probe modulated by an h-f signal, is of particular interest for the classification of plasmas. (auth)

42443 ELECTRICAL CIRCUIT ANALOGUE OF ONE-DIMENSIONAL PLASMAS. Paik, S. F. (Northwestern Univ., Evanston, Ill.). Int. J. Electron., 20: 375-85(Apr. 1966).

A simple electrical circuit model is proposed to describe the r-f behavior of one-dimensional plasmas. The equivalent circuit consists of 'parametrically' coupled resonant circuits representing normal modes of the system. The energy conservation principle for a multivelocity stream model of the plasma is presented to show that it may be put into the form of the so-called Manley-Rowe relations. The circuit model of the two-stream system is analyzed in detail to show that the correct dispersion relation can be obtained from the circuit. The usefulness of circuit models as experimental tools is discussed. (auth)

42444 NOTE ON PLASMA ION OSCILLATIONS. Jones, J. M.; Emeleus, K. G. (Queen's Univ., Belfast). Int. J. Electron., 20: 387-9(Apr. 1966).

Experiments were performed on standing ion acoustic waves in hot-cathode, low-pressure, low-voltage discharges. Typical discharge parameters were current 20 mamp, voltage 33.5 v, and cathode-probe separation 1.125 cm. The variation of ion frequency with probe position is described. (M.O.W.)

42445 PLASMA DIAGNOSTIC METHODS UTILIZING LASERS. Rostas, Francois (Compagnie Generale d'Electricite, Marcoussis, France). J. Phys. (Paris), 27: 367-84(May-June 1966). (In French).

In the study of plasma properties, lasers have allowed the extension to optical frequencies of certain diagnostic methods which were first introduced at radiofrequencies. These methods are separated in two sets: interferometric methods, on the one hand, based on the measurement of the index of refraction of the plasma, with or without magnetic field, and, on the other hand, the methods employing the diffusion of light by free electrons (Thomson diffusion). Basic principles of each set of methods are first exposed and the various published experiments are then reviewed. Bibliographical references extend to the end of 1965. (auth)

42446 DETERMINATION OF ELECTRON CONCENTRATION OF PLASMA IN A REFLEX KLYSTRON. Chirkov, V. P. Izmeritel. Tekh., No. 6, 41-2(1966). (In Russian).

The use of a positive-repeller reflex klystron for diagnosing gas-discharge plasma is discussed; the plasma is created inside the klystron, and its electron concentration is determined. Two methods of plasma generation are possible: (1) two needle electrodes are inserted into the space between the resonator grids, and a voltage is applied to the needles; the plasma is formed due to the presence of residual gases; and (2) a plasma is injected into the resonator cavity by means of a plasma gun at right angles to the klystron axis. Interacting with the electron beam, the plasma is continuously withdrawn from the resonator by means of a special probe held at a potential positive with respect to the cathode. The plasma electron concentration is calculated from this formula:

$$N = \alpha \cdot \sin\frac{\varphi_0}{2} \cdot \frac{(U_1U_{02} - U_2U_{01})}{U_{01}\left(U_2 \cos\frac{\varphi_0}{2} - U_{02}\right)},$$

where $\alpha = (m\omega^2/8\pi^2e^2)$. A total net error of ±1% is expected; however, considering discharge-electrode effect on the beam, probe field, ion background, etc., the error may reach ±5 to ±10%. (TSS)

42447 ON SOME PECULIARITIES OF THE RAY THEORY OF CYLINDRICAL AND SPHERICAL WAVE PROPAGATION IN A WEAK NONHOMOGENEOUS PLASMA. II. Orlov, Yu. I. (Moscow Inst. of Power Engineering). Izv. Vyssh. Ucheb. Zaved., Radiofiz., 9: 657-65(1966). (In Russian).

By the ray-optics methods the problem was considered of the incidence of a cylindrical (spherical) electromagnetic wave on a nonhomogeneous plasma cylinder (sphere). It is shown that the finite curvature of a wave front and boundaries lead to peculiarities in the behavior of rays, the caustical surface and field. The peculiar caustic points were investigated and determined for hyperbolic and parabolic changes of the electron density N. The evolution of caustic surface is estimated when changing the position of source and the magnitude of gradient N. The plane of the problem parameters was divided into characteristical regions. (auth)

42448 THE KINETIC THEORY OF EM-WAVE REFLECTION FROM MOVING PLASMA. Miroshnichenko, V. I. Izv. Vyssh. Ucheb. Zaved., Radiofiz., 9: 666-74 (1966). (In Russian).

An oblique incident reflection of an electromagnetic wave is considered from a half-space filled with plasma. The plasma is moving in a medium where a slow wave may propagate ($V_\phi < c$). Under the assumption of a pure mirror and pure diffusion reflection of electrons from the boundary, general expressions were obtained for fields penetrating into plasma. The expressions for impedances and reflection factors were derived. The approximate values of reflection and absorption factors were calculated for limit cases of weak and strong spatial dispersion. (auth)

42449 ELECTROMAGNETIC WAVE SELF-FOCUSING IN ISOTROPIC PLASMA. Litvak, A. G. (Gorkii State Univ., USSR). Izv. Vyssh. Ucheb. Zaved., Radiofiz., 9: 675-80(1966). (In Russian).

Propagation is studied of two-dimensional electromagnetic waves of TM-type in an isotropic nonlinear plasma The possibility of self-focusing of these waves was shown, followed by formation of a stationary self-maintaining waveguide channel. The structure of self-consistent fields was calculated. If in the absence of field the plasma permittivity ϵ is negative, self-focusing is possible only when the wave power is greater than a critical one (for $\epsilon > 0$ on the axis). In a self-consistent solution, the transition through the point $\epsilon = 0$ is realized through discontinuity. (auth)

42450 NONLINEAR PHENOMENA IN PLASMA WAVEGUIDES. Virko, V. F.; Levitskii, S. M. (Kiev State Univ.). Izv. Vyssh. Ucheb. Zaved., Radiofiz., 9: 691-6 (1966). (In Russian).

The parameter changes of plasma waveguide are investigated with respect to the power of uhf signal, caused by electron density increase in plasma due to an additional gas ionization by uhf field. It is shown that the phase velocity of plasma-waveguide waves increases with the growth of the signal power but their damping decreases. The nonlinearity of plasma waveguide possesses a marked inertness. (auth)

42451 IMPROVED SURFACE-WAVE DESCRIPTION FOR SCATTERING FROM OVERDENSE PLASMAS. Wyatt, Philip J. (Defense Research Corp., Santa Barbara, Calif.). J. Appl. Phys., 37: 3641(Aug. 1966).

The normalized radar cross section as a function of electron density for a collisionless homogeneous plasma sphere is plotted. A technique is presented for describing surface-wave scattering in plasmas. (M.O.W.)

42452 GENERALIZED FULL-WAVE THEORY FOR ENERGY-DEPENDENT COLLISION FREQUENCIES. Deeks, D. G. (Radio and Space Research Station, Ditton Park, Slough, Eng.). J. Atmos. Terrest. Phys., 28: 839-46(Sept. 1966).

Equations are derived to describe the propagation of a plane electromagnetic wave through a magneto-ionic medium in which the collision frequency of mono-energetic electrons is proportional to the electron energy. It is

shown that no essentially new features are introduced into the results of full-wave calculations by the use of the generalized theory and that a suitable choice of effective classical collision frequency gives numerical results in good agreement with the more complicated theory. For an ionosphere at temperature T and for frequencies less than 100 kc/s the effective collision frequency, ν_{eff}, is related in the following way to the collision frequency, ν_M, appropriate to mono-energetic electrons with energy kT. $\nu_{eff} \simeq \frac{3}{2}\nu_M$ when $\omega_H \ll \nu_M$ and $\nu_{eff} \simeq \frac{5}{2}\nu_M$ when $\omega_H \gg \nu_M$; at higher frequencies ω_H is replaced by ω, the angular wave frequency. (auth)

42453 CHAPMAN-FERRARO HOLLOWS FOR A SYSTEM OF LINE CURRENTS ENVELOPED BY A STRATIFIED CORPUSCULAR FLUX. Hewson-Browne, R. C.; Windle, D. W. (Univ. of Sheffield, Eng.). J. Atmos. Terrest. Phys., 28: 847-60(Sept. 1966).

A stratified plasma stream of infinite conductivity is incident on the magnetic field of a system of parallel line currents. The magnetic field is confined to a hollow within the stream and the plasma particles are assumed to be specularly reflected at the hollow surface, a boundary condition which also serves as the hypersonic shockwave approximation. The method of solution is illustrated by considering the case of a stream comprising a number of uniform layers. In particular the case of a single line current only partially enveloped by a uniform stream and the case of a two-layered stream past a line dipole are considered. (auth)

42454 MAGNETOHYDRODYNAMIC FLOWS OF NONEQUILIBRIUM PLASMAS. Sherman, Arthur (General Electric Space Sciences Lab., Valley Forge, Pa.). J. Fluid Mech., 25: 621-37(July 1966).

Studies were made on the interaction between nonequilibrium ionization phenomena in a plasma and the nonuniform flow of that plasma. The characteristics of nonequilibrium conditions are reviewed for the uniform flow situation in which electric and magnetic fields may exist. In order to permit study of the nonuniform flow situation a single-fluid theory is proposed in which the electrical conductivity is assumed to be a function of the absolute magnitude of the current density. The resulting highly simplified system of equations are then used to formulate the Hartmann-flow problem. For this case the formerly linear problem becomes nonlinear. Despite this, solutions to within a quadrature are obtained when the Hall effect is neglected. The more complex problem including the Hall effect is solved numerically. Solutions showing velocity and current profiles are given. For certain values of the parameters governing the problem it is shown that no solutions exist. (auth)

42455 CLOSED-LINE AVERAGE MINIMUM-B CONFIGURATION. Johnson, John L.; Mosher, David (Princeton Univ., N. J.). Contract AT(30-1)-1238. J. Nucl. Energy: Pt. C, 8: 489-92(Sept.-Oct. 1966). (MATT-435).

A scheme of expansion about a uniform axial magnetic field is used to obtain closed-line configurations in which $\oint dl/B$ has a local maximum. The critical β for infinite-conductivity hydromagnetic ballooning modes is about unity in these systems. (auth)

42456 MOTION OF A CHARGED PARTICLE IN A COAXIAL PLASMA ACCELERATOR. Kulinski, S. (Inst. of Nuclear Research, Warsaw). J. Nucl. Energy: Pt. C, 8: 493-506(Sept.-Oct. 1966).

The motion of a single charged particle inside a coaxial plasma accelerator with static electric and magnetic fields E and B is considered. It is shown that the radial motion is periodic in time. The axial velocity averaged over one period depends on the polarity of electrodes and is also a function of the ratio q/m, where q is the charge and m is the mass of a particle. The conditions are stated for which these theoretical considerations can be applied to experimental devices. A comparison with the experimental results is presented showing relatively good agreement between theory and experiment. In particular it was possible to explain the dependence of the speed of the current sheet on the polarity of the central electrode. (auth)

42457 THERMAL BREMSSTRAHLUNG FROM INHOMOGENEOUS PLASMA. Cano, R.; Fidone, I.; Mattioli, M. (EURATOM-CEA, Fontenay-aux-Roses, France). J. Nucl. Energy: Pt. C, 8: 507-14(Sept.-Oct. 1966).

The microwave emission from a stationary plasma column having $n = 10^{14}$ cm^{-3} and $T_e \approx 10^{4\circ}$K was measured and interpreted taking into account the spatial distribution of the plasma density. An interference spectrometer with an indium antimonide detector was used in the wavelength range between $\lambda = 5$ mm and $\lambda = 0.5$ mm. Two kinds of spectra are discussed, those representing a black-body region at ω_p and those with a smaller intensity. Satisfactory agreement is found between theory and experiment for spectra presenting a black-body region while a discrepancy occurs around ω_p for spectra never attaining the black-body value. (auth)

42458 EQUILIBRIUM CONFIGURATION OF RAREFIED PLASMA IN MAGNETIC MIRROR SYSTEMS. Lacina, J. (Inst. of Plasma Physics, Prague). J. Nucl. Energy: Pt. C, 8: 515-31(Sept.-Oct. 1966).

On the basis of the first integrals of motion for a collisionless rarefied (low β) plasma confined by a magnetic mirror field, the equilibrium particle distribution function is evolved (stationary solution of Vlasov's equation) paying due respect to the plasma space-charge electric field and an external axially symmetric electric field. The macroscopic quantities (densities of particles, charge, current, pressure tensor, and mean kinetic energy) and the plasma boundaries are then derived from the distribution function. The computation of the electric potential and the conditions for plasma neutrality are discussed in detail. It is shown that plasma confined within a finite space can possess a charge density identically equal to zero (and hence also a zero plasma electric field) within the entire space only under definite assumptions as regards the distribution function of particles in the space of the integrals of motion with relation $m_+\overline{W}_+ = m_-\overline{W}_-$ (where m are the particle masses) applying between the mean kinetic energies $\overline{W}_+$ (energy per particle) of positive ions and electrons $\overline{W}_-$; as a result of the large difference in the masses of positive ions and electrons, this is manifested by hot electrons and cold ions. (auth)

42459 LINEARLY POLARIZED WAVES IN PLASMAS IN THE REGION OF THE ELECTRON CYCLOTRON FREQUENCY. Bachynski, M. P.; Gibbs, B. W. (RCA Victor Research Labs., Montreal). Contract AF 19(628)-4071. J. Nucl. Energy: Pt. C, 8: 533-9(Sept.-Oct. 1966).

Linearly polarized incident electromagnetic waves were propagated along the direction of a static magnetic field through a helium afterglow plasma in the frequency region of the electron cyclotron frequency. The experimental measurements illustrate clearly the behavior of the two transverse wave modes that the plasma can support. At high-electron densities the right-hand circularly polarized component is completely attenuated and the variation of the transmitted signal is due entirely to the left-hand circularly polarized component. Alternatively at low electron densities the plasma is transparent to the left-hand mode and the variation in transmitted signal is due to the right-hand mode. Detailed comparisons of measurements of the phase and intensity of the components of the electric field transmitted through the plasma in the same orientation as the incident polarization and cross-polarized to the incident polarization showed good agreement with theory. (auth)

42460 USE OF METALLIC SURFACES TO CONVERT HYDROGEN ATOMS TO IONS IN THE 50–3000 ev ENERGY RANGE. Voorhies, H. G.; Ohkawa, T. (General Atomic Div., General Dynamics Corp., San Diego, Calif.). J. Nucl. Energy: Pt. C, 8: 555-9(Sept.-Oct. 1966). (GA-6420(Rev.)).

A method is described for using untreated metal surfaces to convert hydrogen atoms to hydrogen ions in the 50 to 3000 ev energy range. The atoms are converted without an appreciable change in their energy. The efficiency of conversion is an order of magnitude less than the efficiency of

conversion in a gas (stripping) cell operated near its pressure of maximum efficiency, but the method is attractive in that no differential pumping system is required. (auth)

42461 MAGNETIC FIELD TOPOLOGY AND THE PROBLEM OF PLASMA CONTAINMENT. Skornyakov, G. V. (Ioffe Inst. of Physics and Tech., Leningrad). J. Nucl. Energy: Pt. C, 8: 561-75(Sept.-Oct. 1966).

Among the various magnetic systems designed for the containment of a high-temperature plasma, the most promising are close systems in which the magnetic field intensity increases towards the periphery. However, in the great majority of cases, the equations for the field lines of closed systems are non-integrable and an analytical study of the shape of the magnetic field lines, and even more so an analytical study of the motion of the charged particles and of plasma behavior in such fields, does not appear to be a very promising method of investigation. In any case, when studying containment problems, the actual detailed disposition of the magnetic field lines, and the details of the motion of the plasma inside the system, are not especially interesting. It is more important to know whether or not the plasma will remain within the confines of the closed volume. To solve this problem one turns quite naturally to the topological approach. Taking the crudest approximation, the motion of the charged particles occurs along the field lines of the magnetic field so that the first task is to analyse the topological characteristics of the field lines. In a number of cases the principal characteristics of the magnetic field may be determined on the basis of some quite general considerations of a topological nature. The main concern is to establish the general topological requirements of a field suitable for a magnetic trap and to provide a prescription for creating closed systems in which the magnetic field intensity increases towards the periphery. (auth)

42462 OBSERVATION OF THE INVERSE COLD-PLASMA RESONANCE IN CYLINDRICAL GEOMETRY. Weaver, J. M.; Wort, D. J. H. (Culham Lab., Abingdon, Eng.). J. Nucl. Energy: Pt. C, 8: 579-81(Sept.-Oct. 1966).

A small cylindrical column of plasma exhibits a dipole resonance at a frequency $\omega = \omega_p/\sqrt{2}$, independent of the radius of the column provided that this radius is much smaller than the free-space wavelength corresponding to frequency ω. Similarly, a cylindrical hole in a plasma (the reciprocal system) has a resonance at the same frequency. The resonance of the reciprocal system whose size is not small compared to the free space wavelength was observed, and it is shown that this resonance can be used to measure plasma density in a region well beyond the cutoff density for the frequency used. Experiments are described which confirm the theory of the resonance, indicate that the concept of a negative plasma dielectric constant is valid up to $\epsilon = -100$, and demonstrate a novel diagnostic technique using very simple equipment. (W.D.M.)

42463 DIPOLE RESONANCE OF CYLINDRICAL PLASMA COLUMNS IN A MAGNETO-PLASMA. Kawabe, Takaya (Tokyo Univ.). Kakuyugo-Kenkyu, 16: 516-21 (May 1966). (In Japanese).

Dipole resonance of a cylindrical plasma column was considered in the case in which it was embedded in a plasma and an external magnetic field was applied parallel to the axis of this column. They are treated quasi-statically, and the wave number of the magnetic field k_z was assumed to be very small and equal to zero. It is shown that the resonant frequency in the absence of external magnetic field increased as the density of external plasma increased. These results were compared with an earlier experiment. (auth)

42464 PINCH PHENOMENA IN A COAXIAL PLASMA GUN. Nakano, Yoshiei; Hirano, Katsumi (Tokyo Inst. of Tech.). Kakuyugo-Kenkyu, 17: 29-36(May 1966). (In Japanese).

A measurement is described of current density distribution in a coaxial plasma gun. A dip appears in its total discharge current at a certain time in its first half cycle. On the other hand, magnetic probe observations show that a pinch of the discharge occurs in front of the center electrode, then the current is cut off. This time coincides with that of the appearance of the dip in the total current. (auth)

42465 INSTABILITY OF UNIFORM PLASMA TURBULENCE. Gaylitis, A. (Inst. of Physics, Academy of Sciences, Latvian SSR). Latvijas PSR Zinat. Akad. Vestis, Fiz. Teh. Zinat. Ser., No. 4, 13-17(July-Aug. 1965). (In Russian).

It is shown that at a certain stage in the development of turbulence, instability of spatially uniform plasma and energy density distributions of turbulent oscillations may occur. Sufficient conditions are established for instability without precisely determining the time of its development or the final state which a plasma reaches after complete turbulence development. It is found that, roughly speaking, instability occurs when the ratio of the energy of plasma waves to the energy of the thermal motion of the plasma reaches the magnitude $8[1 - (\omega_0^2/\omega^2)] = 24\nu_{T1}(k^2/\omega_0^2)$. It is advantageous energy-wise for separate turbulence regions with reduced plasma density to be formed. (CFSTI)

42466 CALIBRATION TESTING OF THE JET OF A PLASMA GENERATOR. Fiorini, Vittorio (Istituto di Costruzioni Aeronautiche Scuola d'Ingegneria Aerospaziale, Rome). Missili, No. 1, 1-12(Jan.-Feb. 1964). (In Italian).

The methods used and the experimental results obtained on a first series of calibration tests of a plasma generator are reported. The generator has a design electrical output of 50 kw and operates with a mixture of Na and K metallic vapor. The pattern of the yield of the generator was determined as a function of the range of the gas for various degrees of the electrodes and is measured indirectly from the total enthalpy of the plasma. The data on the specific thermal flux is correlated with the total enthalpy of the jet by means of the Fay and Riddell formula. There is agreement between experimental and theoretical results. (J.S.R.)

42467 SEQUENT CORRELATIONS IN STOCHASTIC POINT PROCESSES. [PART] II. Srinivasan, S. K. (Indian Inst. of Tech., Madras); Koteswara Rao, N. V.; Vasudevan, R. Nuovo Cimento (10), 44A: 818-21(Aug. 1, 1966).

It is shown how differential equations can be obtained for the characteristic functional by the invariant embedding technique using the correlations in electromagnetic cascades. As point processes, a family of characteristic functionals which will generate different types of product densities and sequent correlations is defined. The application to two-time correlations in plasma is discussed. (J.F.P.)

42468 ELECTRIC MICROFIELD DISTRIBUTIONS IN PLASMAS. Hooper, C. F. Jr. (Univ. of Florida, Gainesville). Phys. Rev., 149: 77-91(Sept. 9, 1966).

A new method for calculating the distribution of electric microfields (high-frequency components) in a plasma is developed. Distributions are calculated at both a neutral and a charged point. The plasma is taken to be a system of N charged particles moving in a uniform neutralizing background. It is shown that this development allows for the inclusion of all correlations to a high degree of accuracy. This theory is then compared with the Holtsmark and Baranger-Mozer theories. A detailed analysis of all approximations is included, together with a Monte Carlo study. Numerical results are shown both graphically and in tabulated form. (auth)

42469 INVESTIGATION OF ELECTRONIC RECOMBINATION IN HELIUM AND ARGON AFTERGLOW PLASMAS BY MEANS OF LASER INTERFEROMETRIC MEASUREMENTS. Gusinow, M. A.; Gerardo, J. B.; Verdeyen, J. T. (Univ. of Illinois, Urbana). Phys. Rev., 149: 91-6(Sept. 9, 1966).

Two helium-neon laser interferometers were used to obtain the electron and neutral-atom densities in an afterglow plasma. The interferometric technique utilized allows one to obtain both the spatial and temporal dependence of

the electron decay. The two gases studied were helium and argon at 2–8 Torr and 0.3–0.8 Torr, respectively. The electron density was in the range of $2 \times 10^{13} < N_e < 10^{15}$ cm^{-3} and the electron temperature in the range $1000 < T_e < 7000$°K. The electron temperature was measured by comparing the relative atomic line intensities and by inference from the recombination coefficient. The electronic recombination in helium, argon, and helium–argon mixtures was found to be consistent with the predictions of Bates, Kingston, and McWhirter for collisional-radiative recombination. The electron temperature inferred from the measured recombination coefficient indicates a pronounced electron temperature gradient across the tube which is believed to be due to electron heating effects in the afterglow. (auth)

42470 RADIATIVE EQUILIBRIUM OF A FREE-ELECTRON GAS IN A UNIFORM MAGNETIC FIELD. Arunasalam, V. (Princeton Univ., N. J.). Phys. Rev., 149: 102-13(Sept. 9, 1966). (MATT–442).

The subject of radiative equilibrium of a free-electron gas in a uniform magnetic field is studied on the basis of Landau's quantized particle motion of the electrons and the "Golden Rule" of time-dependent perturbation theory. The analysis presented here is somewhat analogous to the quantum theory of blackbody radiation. It is shown that the radiative equilibrium between electrons and their radiation field arises as a consequence of a balance between the two competing processes: photon emission (spontaneous plus induced or stimulated emission) and photon absorption. A coupled set of equations, one describing the time evolution of the photon distribution function and the other describing the time evolution of the electron distribution function, is thus derived. A simple closed-form solution of the equation for the time rate of change of the photon distribution function is presented for situations where absorption exceeds the stimulated emission. This solution yields equations for the steady-state photon number density and the radiative relaxation time. It is shown that the steady-state photon number density is the familiar distribution function corresponding to Bose-Einstein statistics for "complete thermodynamic equilibrium." The conditions for the existence of overstabilities near the cyclotron frequency and its harmonics are also discussed. The equation for the time rate of change of the electron distribution function reduces, in the classical limit, to a Fokker-Planck equation in which there appear the usual "diffusion" and "dynamical friction" terms. In the classical limit, it is shown that this coupled set of equations (one describing the time evolution of the electromagnetic energy density and the other describing the time evolution of the electron distribution function) is self-consistent, by proving that the average rate of loss of z momentum of the electrons as predicted by one equation is equal to the average rate of gain of z momentum of their radiation field as predicted by the other equation. The z axis is chosen to be along the uniform magnetic field. (auth)

42471 HIGH-FREQUENCY EFFECT DUE TO THE AXIAL DRIFT VELOCITY OF A PLASMA COLUMN. Messiaen, A. M. (Ecole Royale Militaire, Brussels); Vandenplas, P. E. Phys. Rev., 149: 131-40(Sept. 9, 1966).

The scattering of a plane electromagnetic wave with normal incidence (E field perpendicular to the axis) by a plasma column in the presence of a static magnetic induction B_0 has been studied earlier. A heretofore unexplained effect, however, is the existence of a scattered axial field E_Z even when $B_0 = 0$. A mechanism responsible for this coupling between the E_Z and the transverse E field, in the absence of B_0, is investigated here, namely the role of an axial drift velocity v_d. The effect observed is a resonance peak of E_Z occurring at the same density for which there exists a resonance of the scattered transverse E field which is well explained by a uniform cold-plasma model. The same model is therefore assumed here. In this approximation the plasma can be described by a surface charge density Σ due to the HF polarization which gives rise to a surface current density $K = \Sigma v_d$. The boundary conditions then lead to the existence of an E_Z which, for $B_0 = 0$, has a $\sin\theta$ dependence when the exciting field has a $\cos\theta$ dependence. When $B_0 \neq 0$, a more complicated theoretical spectrum is obtained. Both the position and the angular dependence of the resonances are in very good agreement with experimental data. The effect predicted by this model is, however, more than an order of magnitude below that observed in a mercury plasma column. This phenomenon can be described as the plasma radio-frequency analog of the static field induced by the Roentgen-Eichenwald current. (auth)

42472 HIGH-FREQUENCY CONDUCTIVITY OF A PLASMA IN QUASI-EQUILIBRIUM. III. STUDY OF A TWO-TEMPERATURE PLASMA. Klevans, E. H.; Wu, C.-S. (California Inst. of Tech., Pasadena). Contract NAS-7-100. Phys. Rev., 149: 141-54(Sept. 9, 1966).

A general expression for the high-frequency conductivity of a homogeneous, isotropic plasma is obtained. The derivation is based on the use of the Bogoliubov-Born-Green-Kirkwood-Yvon hierarchy and therefore includes all effects due to the high-frequency field and the collective interactions up to first order in the plasma parameter. As an application of the general result, a two-temperature plasma with the electron temperature exceeding the ion temperature is studied in detail. It is found that when the ratio of the electron temperature to the ion temperature exceeds 100, there is an enhancement in the resistivity resulting from the excitation of incoherent ion waves. (auth)

42473 STABILITY OF PLASMA CONFINED BY A COLD-GAS BLANKET. Braams, C. M. (EURATOM-FOM Institut voor Plasma-Fysica, Rijnhuizen, Netherlands). Phys. Rev. Lett., 17: 470-1(Aug. 29, 1966).

A steady-state plasma, confined by a cold-gas blanket in a toroidal magnetic field, is stable against magnetohydrodynamic instabilities. A ring whirl will help to define the equilibrium position, to stabilize against deviations from the steady-state, and to allow a poloidal field component. (auth)

42474 EFFECT OF HALL CURRENT ON RAYLEIGH-TAYLOR INSTABILITY OF A PLASMA. Nayyar, N. K.; Trehan, S. K. (Goddard Space Flight Center, Greenbelt, Md.). Phys. Rev. Lett., 17: 526-8(Sept. 5, 1966).

It has been recently pointed out (Hosking, Phys. Rev. Letters, 15: 344(1965)) that the inclusion of Hall current in Ohm's law produces a new aperiodic instability in a wave number band which was previously stable in the classical problem of Rayleigh-Taylor instability for a plasma. However, it is shown that this result is incorrect and is a consequence of the fact that Hosking has not solved the problem with due regard to the boundary conditions. It is shown that the inclusion of Hall-current and electron-inertia terms in the generalized Ohm's law, in fact, do not have any effect on the development of Rayleigh-Taylor instability in hydromagnetics. (W.D.M.)

42475 TEMPERATURE MEASUREMENTS OF A LASER SPARK FROM SOFT-X-RAY EMISSION. Alcock, A. J.; Pashinin, P. P.; Ramsden, S. A. (National Research Council, Ottawa). Phys. Rev. Lett., 17: 528-30(Sept. 5, 1966).

Previous studies of laser sparks have shown that most of the energy of the beam is absorbed in the spark creating a high-density plasma, and that during the laser pulse the ionized region expands at high velocity into the beam. To eliminate uncertainties in previous measurements of electron temperature from soft x-ray emission, temperature measurements were made of laser sparks from the relative intensity of the x-ray flux transmitted through beryllium foils of different thickness. The x-ray emission was detected by means of two plastic scintillators (NE 102) each of which was optically coupled to a photomultiplier (Philips 56 AVP). (W.D.M.)

42476 CONVERGING CYLINDRICALLY SYMMETRICAL SHOCK WAVE IN THE PRESENCE OF DISSIPATIVE EFFECTS. Dyachenko, V. F.; Imshennik, V. S. Prikl. Mat. Mekh., 29: 993-6(1965). (In Russian).

The shock wave structure of a fully ionized plasma was studied, including dissipative effects. A cylindrical geom-

etry is assumed, and the governing equations consist of the ion-momentum equation, the ion-energy equation, and the electron-energy equation. The nondimensional parameters for the flow are then stated and the equations are solved numerically for a deuterium plasma. The largest difference between this solution and a fully self-similar case was observed at the cylinder axis during shock wave reflection. (TCO)

42477 BOUNDARY LAYERS IN A COMPLETELY IONIZED TWO-TEMPERATURE PLASMA. Gogosov, V. V. Prikl. Mat. Mekh., 30: 424-40(May-June 1966). (In Russian).

The equations derived by S. I. Braginskii, under certain simplifying assumptions of the author, were used to obtain the equations for the boundary layer in a completely ionized, two-temperature plasma. The results indicated that two temperature layers must be considered: the electron and the ion layers, within which the temperature of electrons and ions, respectively, are changed. Equations were derived to describe these layers; they indicated that the thickness of the electron temperature boundary layer is much larger than that of the ion layer. In some special cases, the electron boundary layer was absent. In addition to these layers, within which the electron and ion temperature changes suddenly, the existence of a "shielding" layer near the wall was also established. In this layer, the temperature difference caused by an external source near the wall, the temperature is arrived at by the simultaneous action of viscosity, Joule heating and thermal conductivity. The thickness of this layer was found to be $\delta = \sqrt{\varkappa_i/\gamma}$, whereby $\varkappa_i$ is the thermal conductivity and γ is the coefficient of the temperature gradient in the energy equation. It was also found that when the viscosity and thermal conductivity may be neglected in the external flux, a narrow "shielding" layer may also exist; this appears to be a characteristic of the two-temperature plasma and does not exist in the one-temperature system. (TTT)

42478 REMARKS ON EQUATIONS RELATING TO WAVE PROPAGATION IN AN INHOMOGENEOUS COMPRESSIBLE PLASMA. Burman, R. (Victoria Univ., Wellington, N. Z.). Proc. IEEE (Inst. Elec. Electron. Eng.), 54: 1069-70(Aug. 1966).

Equations describing wave propagation in an inhomogeneous anisotropic compressible plasma were considered previously (Proc. IEEE 53: 2124(1965)). The equation of motion used contains a term proportional to the gradient of the equilibrium pressure, ρ_0. The origin of the term in $\nabla\rho_0$ is shown and explained by the presence of an electrostatic or gravitational field. (M.H.R.)

42479 ENERGY RELATION FOR ACOUSTIC MODES IN A PLASMA. Lonngren, K. E. (State Univ. of Iowa, Iowa City). Proc. IEEE (Inst. Elec. Electron. Eng.), 54: 1101-2(Aug. 1966).

An energy relation was derived studying only the acoustic mode. Using this, a Lagrangian formalism was developed to determine the cross-sectional field distribution in an arbitrarily shaped waveguide. (M.H.R.)

42480 RADIATION IN A MOVING ANISOTROPIC PLASMA. Chawla, B. R.; Unz, H. (Univ. of Kansas, Lawrence). Proc. IEEE (Inst. Elec. Electron. Eng.), 54: 1103-5(Aug. 1966).

An alternative formulation of the problem of radiation in a moving anisotropic plasma is presented, using the exhaustive microscopic viewpoint of Lorentz. (M.H.R.)

42481 ELECTROMAGNETIC CHARACTERISTICS OF A BOUNDED PLASMA SLAB. Shockley, T. D. Jr. (North American Aviation, Inc., Tulsa, Okla.); Bowie, J. L. Proc. IEEE (Inst. Elec. Electron. Eng.), 54: 1105-6(Aug. 1966).

Some theoretical data are presented illustrating that the maximum magnitude of the reflection coefficient Γ_R occurs when the wall width is approximately $\lambda/4$, where λ is the wavelength in the wall material of the bounded plasma. The maximum magnitude of the reflection coefficient Γ_T occurs when the wall width is approximately $\lambda/2$. These data were obtained by solving the equations defining the E-field transmission and reflection coefficients on a digital computer. (M.H.R.)

42482 1965 GUTHRIE LECTURE. A REVIEW OF NUCLEAR FUSION RESEARCH. Adams, J. B. (United Kingdom Atomic Energy Authority, Abingdon, Eng.). Proc. Phys. Soc. (London), 89: 189-216(1966).

This lecture reviews the progress made towards releasing energy from the fusion of the light nuclei. To achieve this it is necessary to create an extremely hot plasma containing the light nuclei and to hold this plasma together long enough to obtain a net surplus of energy. The only promising way of confining such a hot plasma for sufficient times and isolating it from material surroundings is by means of magnetic fields. Unfortunately plasmas have shown themselves capable of escaping through magnetic fields by a number of forms of instability. The principles of magnetic confinement of plasmas are discussed and the main types of magnetic traps described. These are the open-ended magnetic bottles (Thetatrons, cusp) in which there is a sharp boundary between plasma and surrounding magnetic field, the open-ended adiabatic magnetic traps (magnetic mirrors) in which the plasma is immersed in a magnetic field, and closed adiabatic traps in which the plasma is immersed in a magnetic field whose lines of force close inside the system (toroidal pinch, Stellarators, etc.). The most important instability has been the interchange driven by charge separation of the plasma components caused by rapid motions of the plasma, as in Thetatrons, or more generally, by unfavorable magnetic field curvature, as in magnetic-mirror traps and in toroidal closed traps. In open-ended systems this instability has been overcome by designing traps with favorable magnetic field curvature (magnetic wells). In closed systems, shear in the magnetic field provides conducting paths which cancel the electric fields set up by charge separation, but this stabilizing effect is offset if the path lengths are too long or the plasma too resistive. More recently, closed systems with average favorable curvature of magnetic field lines have given stability when the connecting lengths between regions of favorable and unfavorable curvature are short enough. Smaller scale instabilities, associated with a variety of electrostatic waves which can propagate in the plasma and interact with groups of particles, are now proving troublesome. These can cause the plasma to diffuse very rapidly through the magnetic fields. Although these instabilities are fairly well understood theoretically, they are not yet controllable experimentally and new experiments using magnetic traps, designed to avoid interchange instabilities are being used to examine them. (auth)

42483 TEMPERATURE MEASUREMENTS IN SHOCK TUBES: TRANSITION PROBABILITIES FOR ARGON LINES. Coates, P. B.; Gaydon, A. G. (Imperial Coll. of Science and Tech., London). Proc. Roy. Soc. (London), Ser. A, 293: 452-68(Aug. 23, 1966).

The transition probabilities of 13 argon (ArI) spectrum lines between 4159 and 7635 Å were determined from their emission intensities from shock-heated argon. The equilibrium temperature was calculated from the measured speed of the incident shock in a detonating-driver type shock tube. Corrections for self-absorption in the stronger red lines were made by using theoretical values for the Stark line width. Results are compared with others obtained from measurement on arc plasmas or from theoretical calculations, and the accuracy of these values is discussed. The transition probabilities given should enable temperatures in the range 6000 to 15000°K in argon to be determined from the ratio of line intensities. (auth)

42484 ISOTHERMAL PLASMA OVEN. Agnew, Lewis; Summers, C. (Los Alamos Scientific Lab., N. Mex.). Contract W-7405-eng-36. Rev. Sci. Instrum., 37: 1224-9(Sept. 1966). (LA-DC-7857).

A tantalum oven that produces quiescent isothermal cesium plasmas at precisely known temperatures and pressures is described. The apparatus consists of a closed,

cesium-vapor filled tube heated by radiation within a resistance heated vacuum furnace. Plasma temperatures up to 2300°K and cesium vapor pressures up to 10 torr are obtainable. Temperatures are measured by calibrated unsheathed W/W–26% Re thermocouples. Cesium vapor pressures are known through careful control of the cesium condensation conditions. Designed especially for spectroscopic studies, the oven features two sapphire windows mounted on a line-of-sight axis through the plasma. Details of construction and operation are described. Performance data showing temperature profiles to 1% over a 10 cm length are given. (auth)

42485 COIL SYSTEMS FOR MEASURING CONDUCTIVITY AND VELOCITY OF PLASMA STREAMS. Rossow, Vernon J.; Posch, Rudolph E. (Ames Research Center, Moffett Field, Calif.). Rev. Sci. Instrum., 37: 1232-42(Sept. 1966).

A theoretical and experimental study is made of a device that measures the conductivity and velocity of plasma streams. The instrument consists of a primary coil and several secondary coils. Alternating current through the primary coil produces an oscillating magnetic field in the shape of a dipole. Positions of the secondary coils relative to the primary are such that they respond to distortions of the applied magnetic field of the primary that are brought about by the presence and motion of an electrically conducting fluid. These signals on the secondaries vary linearly with the conductivity and with the product of conductivity times velocity. Various possible coil arrangements and the results of tests conducted with a simple three coil configuration in an electric arc jet are presented. Details of the probe tested, its calibration, and its theoretical basis are described. Results obtained with the three coil system are in good agreement with theory. (auth)

42486 INTERACTION BETWEEN A FAST CHARGED PARTICLE AND NON-EQUILIBRIUM PLASMA. Radzievskii, V. N. (Inst. of Physics, Kiev). Ukr. Fiz. Zh., 11: 704-10(1966). (In Ukrainian).

The interaction between a fast charged particle with fluctuations of the electromagnetic field in nonequilibrium magneto-active plasma is studied. A general expression is obtained for the intensity of fluctuation losses of the particle during its spiral motion in the plasma. (auth)

42487 EFFECT OF GASEOUS ADMIXTURES TO ARGON UPON IONIZATION WORK FOR ALPHA RADIATION. Pawlowski, Z. (Warsaw Polytechnic). Zeszyty Nauk. Politech. Warszaw., No. 118, 43-54(1965). (In Polish).

An investigation was made to obtain a mixture of argon with another gas, which has a minimal ionization work for radiation. Tests were carried out with a pulsing chamber. A noticeable reduction of ionization work was found in the argon with gaseous admixtures having a lower ionization potential than the exciting potential of metastable argon states. This phenomenon is considered a result of collisions of the second kind of admixed molecules with metastable argon atoms. A minimal ionization work of 21.1 ev was obtained in the mixture of argon and acetylene as result of a resonant increase of the cross section of collisions leading to ionization. It was experimentally ascertained that the minimum of ionization work is provided by a mixture containing 0.8% of acetylene. Analysis of experimental data has shown that the decrease of ionization work occurring in the mixture of argon with acetylene at low pressure is caused by the process of dual collision between the metastable argon atoms and acetylene particles. As the pressure in acetylene increases the ionization work also increases as result of triple collisions between the metastable argon atoms and two particles of acetylene. (ATD)

42488 KINETIC ANALYSIS OF PLASMA COUETTE FLOW IN AN ELECTRIC FIELD. Shidlovskii, V. P. Zh. Prikl. Mekh. Tekh. Fiz., No. 1, 21-31(Jan.-Feb. 1966). (In Russian).

Steady-state flow of a fully ionized plasma between parallel plates in the presence of an electric field was investigated. The distribution functions of ions and electrons are determined from the Boltzmann kinetic equations, supplemented by equations for the electric field. The solution is constructed by means of one of the variations of the method of moments, and it is assumed that the momentum transfer is achieved only by the ions, and the heat transfer by the electrons. The analysis is performed taking into account the close collisions between particles for an arbitrary degree of plasma rarefaction. An example is given for calculating the basic flow characteristics. Boundary value problems, related to the presence of hard surfaces in the flow, have a much smaller practical importance in plasma dynamics than in gas dynamics. This is explained by the fact that plasma may exist only at very high temperatures the action of which causes some degree of destruction of most materials. As a rule, plasma is confined within certain boundaries not by solid walls, but by intense magnetic fields. However, an investigation of problems with boundary surfaces still presents a certain interest for the case of plasma. An approximate solution to one of the simplest problems of this kind is given. (ATD)

42489 CYLINDRICAL WAVES PROPAGATING ACROSS A MAGNETIC FIELD IN A RAREFIED PLASMA. Berezin, Yu. A. Zh. Prikl. Mekh. Tekh. Fiz., No. 1, 107-10(Jan.-Feb. 1966). (In Russian).

The profile of waves of finite amplitude in a rarefied plasma is determinable by two conflicting processes: nonlinear twisting and "smearing" due to dispersion effects. For waves propagating across a magnetic field in a cold rarefied plasma the dispersion law is such that the phase velocity of small oscillations decreases with decreasing length of the wave. Such a dispersion law leads to the possibility of the existence of stationary "compression" waves of finite amplitude (isolated and periodic). Some authors have investigated nonstationary plane waves moving across a magnetic field induced by increasing magnetic pressure on the plasma-vacuum boundary. The present author applies numerical integration of the corresponding equation system to the investigation of cylindrical waves propagating in a cold rarefied plasma across a high-intensity magnetic field. The results are important for experiments on rapid compression of plasma columns by a magnetic field under conditions when the plasma may be considered sufficiently rarefied. (ATD)

42490 DEPENDENCE OF THE RELATIVE POPULATION OF DISPLACED LEVELS OF A COPPER ATOM ON THE CONCENTRATION OF ELECTRONS IN THE PLASMA OF AN ARC DISCHARGE. Kiselevskii, L. I.; Snopko, V. N. Zh. Prikl. Spektrosk., Akad. Nauk BSSR, 2: 207-11(Mar. 1965). (In Russian).

The dependence of the relative population of levels of a copper atom e^4D_j with various probabilities of autoionization on the concentration of electrons in plasma is studied. The possibility of measuring N_e according to relative intensity of transitions from the displaced levels is shown. (auth)

42491 THE ROLE OF HELIUM IN HELIUM–XENON PLASMA. Ostapchenko, E. P.; Pugnin, V. I. Zh. Prikl. Spektrosk., Akad. Nauk BSSR, 2: 227-31(Mar. 1965). (In Russian).

In a He–Xe mixture at average pressures, a decrease in the population of the $5p^56s$ levels and an increase in the population of the $5p^56p$ xenon levels are observed for an increase in helium pressure. (auth)

42492 SPECTROSCOPIC INVESTIGATIONS OF A HIGH-CURRENT DISCHARGE IN THE AIR AT LOW DENSITIES. Nikolaevskii, L. S.; Simonenko, A. F.; Grenishin, S. G. Zh. Prikl. Spektrosk., Akad. Nauk BSSR, 4: 485-90 (June 1966). (In Russian).

The spectroscopic method was used to investigate an air plasma at 35,000°K, activated at different initial temperatures (p_0 = 0.01-10 mm Hg), in a discharge tube specially constructed for the purpose. In addition to the temperature, determinations were made of the concentration of the charged particles, the presence of thermodynamic equilibrium was established, and the emissivity of the air was measured. A diagram of the tube is given. The integral spectra with time in the region of 3000 to 7000 Å were

taken with a spectrophotometer with a diffraction grid with a reverse linear dispersion of 5Å/mm, and a type ISP-28 quartz spectrograph. The concentration of n_e electrons was determined from the width of the H_β hydrogen line. The temperature of the plasma was determined from the ratio of the intensities of the OII lines. A table shows the experimental values of the concentration of the component of an air plasma as a function of the initial pressure. Further data are presented to establish that the plasma is in a state of thermodynamic equilibrium. (ATD)

42493 INTERRUPTION OF A CURRENT PULSE BY A PLASMA SWITCH. Nikolaevskii, L. S.; Simonenko, A. F. Zh. Prikl. Spektrosk., Akad. Nauk BSSR, 3: 467-8(Nov. 1965). (In Russian).

A known method is used for limiting vibrations of a powerful discharge by grounding a current with a plasma jet ejected from a capillary, acting as a plasma switch, and making it possible to form a square pulse. The method may be used for physical experiments with pulse arcs. (auth)

42494 CONVECTIVE EXCITATION OF IONIC OSCILLATIONS OF A PLASMA BY A NONUNIFORM ELECTRON BEAM. Mikhailovskii, A. B.; Pashitskii, E. A. Zh. Tekh. Fiz., 36: 763-76(May 1966). (In Russian).

The excitation of ionic oscillations in a cylinder of homogeneous plasma in a uniform axial magnetic field by an inhomogeneous electron beam moving along the axis is described. Transverse velocities of the beam electrons are neglected, and it is assumed that the derivative of the distribution function of the beam electrons with respect to the longitudinal velocity is negative, so that the usual beam instability does not occur. It is found that the beam can, nevertheless, give rise to ionic oscillations in the plasma by a convective mechanism, provided the beam density varies in the transverse direction. Detailed calculations are given for a beam whose density is a Gaussian function of the distance from the axis. The calculations are based on the kinetic equation, and it is assumed that the ratio of the maximum beam density to the plasma density is small. It is found that both slow beams (beam velocity lower than the thermal velocity of the plasma electrons) and fast beams can give rise to a variety of ionic oscillations with frequencies ranging from far below the ion Larmor frequency to the hybrid frequency. Conditions are found for the excitation of different types of ionic oscillations and expressions are derived for the logarithmic increments of the different oscillations. The ionic oscillations excited by a slow beam are localized in the region of the beam, whereas those excited by a fast beam may propagate throughout the plasma. (ATD)

42495 ON THE ROLE OF CONVECTIVE EFFECTS IN THE EXCITATION OF ELECTRONIC OSCILLATIONS IN A PLASMA BY A BOUNDED BEAM. Mikhailovskii, A. B.; Yungwirt, K. (Inst. of Plasma Physics, Prague). Zh. Tekh. Fiz., 36: 777-90(May 1966). (In Russian).

The excitation of electronic oscillations in a homogeneous plasma cylinder in a uniform axial magnetic field by an inhomogeneous electron beam moving on the axis is discussed. Particular attention is given to excitation of oscillations that do not have axial symmetry; in this case there is effective a mechanism that does not come into play in the axially symmetric case and that involves radial drift of the beam electrons in the azimuthal electric field of the oscillations and the external magnetic field. The calculations are based on the kinetic equation of Vlasov, and only those oscillations are discussed whose frequencies are high compared with the ionic Larmor and Langmuir frequencies. Conditions for stability of the plasma are found and expressions are derived for the logarithmic increments of different instabilities with different assumptions concerning the velocity distribution of the beam electrons. When the transverse velocities of the beam electrons are finite, the convective mechanism contributes to the instability not only in the case of Cherenkov interaction between the particles and waves, but also in the case of the anomalous and normal Doppler effects. In addition to beams with square, Maxwellian, and delta-function velocity distributions, a beam is discussed in which the electrons rotate about the axis of the plasma cylinder. In the case of a very narrow beam of this type the usual convective effects play no role, but there appear instabilities that are due to another mechanism which has not yet been adequately studied. (ATD)

42496 KINETIC THEORY OF ELECTROMAGNETIC WAVES IN A BOUNDED MAGNETIZED PLASMA. I. Kondratenko, A. N. Zh. Tekh. Fiz., 36: 791-9(May 1966). (In Russian).

The linearized kinetic equations for the deviations of the ion and electron distribution functions from the Maxwellian form are employed to discuss the propagation parallel to a uniform external magnetic field of high-frequency electromagnetic waves in an infinite plasma layer of finite thickness. The results obtained are also applicable to a plasma cylinder, provided the radius of the cylinder is much larger than the wavelength. It is assumed that plasma particles striking the sharp boundaries of the plasma layer are either all specularly reflected or all diffusely reflected. The fields and distribution functions are expanded in Fourier series in the spatial coordinate perpendicular to the plasma layer, and equations are derived for the expansion coefficients. These equations could be solved completely for the case of specular reflection of the plasma particles, but the general solution is not given because of the complexity of the resulting dispersion equation. The equations are simplified for the case of small spatial dispersion (thermal velocities of the plasma particles small compared with the phase velocity of the waves) and the corresponding approximate dispersion equation is derived. The roots of the dispersion equation are not discussed. (ATD)

42497 ON THE VAVILOV-CHERENKOV EFFECT FOR SURFACE WAVES. Barsukov, K. A.; Naryshkina, L. G. (Moscow State Pedagogical Inst.). Zh. Tekh. Fiz., 36: 800-5(May 1966). (In Russian).

Surface waves induced on the infinite plane interface between a dielectric and the vacuum by a charged particle moving with constant velocity parallel to the boundary are discussed. Surface waves can propagate on such a boundary only if the dielectric constant of the dielectric is negative. When this is the case surface waves are excited by the charged particle regardless of its velocity. The case is discussed in detail of the boundary between the vacuum and a plasma whose dielectric constant is $1 - f_0^2/f(f - iF)$, where f_0 is the plasma frequency, f is the wave frequency, and F is the effective collision frequency. Formulas are derived for the energy and spectrum of the induced surface waves. When the velocity of the charged particle is very low the frequencies of the induced waves are concentrated near the value $f_0/2^{1/2}$, where they are strongly absorbed and cannot be observed; the induced waves become observable only when the velocity of the charged particle is large compared with $2.4c(F/f_0)$, where c is the velocity of light. The conclusion that the charged particle loses energy by polarization radiation at certain discrete frequencies is shown to be incorrect, and the mathematical error that led to this incorrect conclusion is pointed out. (ATD)

42498 INTERACTION OF ELECTROMAGNETIC WAVES AT THE BOUNDARY OF A PLASMA. Alanakyan, Yu. R. (Lebedev Physics Inst., Moscow). Zh. Tekh. Fiz., 36: 806-12(May 1966). (In Russian).

Equations describing the nonlinear interaction between surface waves on a plasma-vacuum boundary were used to discuss the interaction of two surface waves with a plane wave propagating in the vacuum or in the plasma. The interaction of two surface waves of different frequencies is first considered. It is shown that under certain conditions the components of the field that vary at the combination frequencies (the sum and difference frequencies and the two second harmonic frequencies) represent forced surface waves. Under other conditions the combination frequency components propagate as plane waves either in the vacuum alone or in both the vacuum and the plasma. When a plane wave is incident from outside onto a plasma-

vacuum boundary carrying two surface waves, there arise periodic time variations of the amplitudes of the surface waves. Expressions are derived for the frequency and amplitude of these beats. (ATD)

42499 CONVERSION OF A TRANSVERSE ELECTROMAGNETIC WAVE TO IONIC SOUND OSCILLATIONS OF A PLASMA WITH THE FORMATION OF AN INTERMEDIATE ELECTRONIC LANGMUIR WAVE. Danilkin, I. S. (Lebedev Physics Inst., Moscow). Zh. Tekh. Fiz., 36: 813-17(May 1966). (In Russian).

The technique of nonlinear optics is employed to discuss the two-stage conversion of transverse electromagnetic waves into ionic sound via intermediate longitudinal electronic waves in an infinite isotropic plasma in which the electron temperature considerably exceeds the ion temperature. Previous work on the direct conversion of transverse and Langmuir waves to ionic sound and of transverse to Langmuir waves indicates that the two-stage process will predominate for a wide range of frequencies and amplitudes of the interacting waves. Nonlinear optics equations for the simultaneous interaction of all three types of waves are discussed. A number of integrals of these equations are found and the solution is discussed for the case when transverse waves together with a small background of ionic sound are initially present. It is found that the initial presence of ionic sound considerably hinders the two-stage conversion of transverse waves to ionic sound by transforming Langmuir waves of the resonant frequency into Langmuir waves of other frequencies. (ATD)

42500 CONVERSION OF WAVES IN A NONUNIFORM PLASMA. Piliya, A. D. (Ioffe Inst. of Physics and Tech., Leningrad). Zh. Tekh. Fiz., 36: 818-26(May 1966). (In Russian).

The propagation of electromagnetic waves in an isotropic nonuniform plasma and their reflection, absorption, and conversion at a plane surface where the dielectric constant vanishes are discussed. Ion motions are neglected and the plasma density is assumed to depend only on the single coordinate z of a Cartesian system, to vanish for large negative values of z, and to increase monotonically with increasing z. Collisions are first neglected and the dielectric constant at the wave frequency is assumed to vanish at the plane z = 0. The Debye radius is assumed to be small compared with the inhomogeneity length a = ndz/dm of the plasma. With these assumptions approximate equations are derived for the propagation of electromagnetic waves. These equations are solved (using different approximations in the regions near and far from the singular plane z = 0) for a transverse electromagnetic wave polarized with the electric vector in the plane of incidence (the magnetic vector parallel to the z = 0 plane) and the coefficient describing conversion of the transverse waves to longitudinal waves is calculated. Dissipation of energy by electron collisions is then taken into account and the results are briefly compared with those of I. G. Denisov, who neglected spatial dispersion. Spatial dispersion is shown to be significant near the singular plane even when the collision frequency is high. Incidence of a longitudinal wave onto the singular plane is also discussed briefly. (ATD)

42501 MOTION IN SPATIALLY PERIODIC MAGNETIC FIELDS. Kovtun, R. I. Zh. Tekh. Fiz., 36: 827-42(May 1966). (In Russian).

The motion of a charged particle is described in a constant magnetic field consisting of a strong uniform field on which is superimposed a weak axially symmetric spatially periodic field. Only those trajectories are discussed that intersect the symmetry axis and remain sufficiently close to it. Asymptotic equations for the trajectories are derived by methods that are described in the monograph of Yu. A. Mitropol'skiy, to which reference is made for some details of the calculations. When the ratio v/L (v is the longitudinal velocity of the particle and L is the period of the spatial variation of the magnetic field) is close to the Larmor frequency, there occurs a slow periodic exchange of kinetic energy of forward motion with that of Larmor rotation. The exact resonance in which the frequency of this exchange vanishes is unstable. The condition that the strong component of the constant magnetic field be uniform is relaxed and this field is assumed to be a slowly varying function H(z) of the axial coordinate z. When the function H(z) has an appropriate form (which is calculated) the transfer of kinetic energy between the longitudinal and transverse motions of the charged particle becomes unidirectional and continuous. It is suggested that fields with this configuration may find practical application. (ATD)

42502 METHOD FOR CALCULATING THE ELECTROSTATIC FIELD OF A SYSTEM OF APERTURES. Tsyrlin, L. E. Zh. Tekh. Fiz., 36: 843-51(May 1966). (In Russian).

A technique is described for calculating approximately the axially symmetric electrostatic field of a system of circular apertures in parallel plane electrodes. The potential at each aperture is expanded in a series of Legendre polynomials of odd degree with the argument $(1 - r^2/a^2)^{1/2}$, where r is the distance from the axis and a is the radius of the aperture. The corresponding potential in the interelectrode regions is calculated and from the boundary conditions a set of linear equations is obtained for the expansion coefficients. The calculations for the case of two identical apertures are discussed in detail and it is shown that the method converges to the correct result in the two limiting cases when the two electrodes are very close together or very far apart. The method is illustrated by calculations for a three aperture lens, and the results obtained by retaining different numbers of terms are tabulated. Advantages of generality and simplicity are claimed for the method. (ATD)

42503 OSCILLATIONS OF AN INHOMOGENEOUS PLASMA CYLINDER. Yakimenko, I. P. (Kharkov State Univ.). Zh. Tekh. Fiz., 36: 868-76(May 1966). (In Russian).

A technique is described for calculating the conditions for propagation of E modes in an isotropic plasma waveguide of circular cross section in which the Langmuir frequency is a function of the distance from the axis. Such a technique is very desirable because experimentally realized plasma columns are practically always inhomogeneous in the radial direction. The plasma cylinder is divided into an arbitrary but finite number of cylindrical shells within each of which the plasma is homogeneous. The fields within each shell are expressed linearly in terms of modified Bessel functions of the first and second kinds and zeroth and first orders, and recurrence relations from which the coefficients in these expressions can be calculated are derived from the boundary conditions on the axis, at infinity, and on the surfaces between the several shells. These recurrence relations are relatively simple and are suitable for solution with a computer. The dispersion equation can be found with the aid of the recurrence relations. In the case of an inhomogeneous plasma waveguide there are a number (or a whole spectrum) of "cutoff" (absorption) frequencies; the present technique enables these to be calculated. The following simple cases are discussed by way of examples: a uniform cylindrical plasma waveguide; a plasma waveguide in a glass container, and a plasma waveguide on which there is formed a Langmuir layer in which the dielectric constant is unity. In the last case there occurs anomalous dispersion, and this is discussed. The technique as developed is applicable only to a cold plasma; it would be desirable to modify the technique so as to make it possible to take account of the effects of the thermal motions of the plasma electrons. (ATD)

42504 INVESTIGATION OF THE PLASMA INJECTED INTO A MAGNETIC TRAP WITH THE AID OF A CONICAL THETA PINCH. Alinovskii, N. I.; Iskol'dskii, A. M.; Nesterikhin, Yu. E.; Ponomarenko, A. G. Zh. Tekh. Fiz., 36: 877-80(May 1966). (In Russian).

The production and diagnosis are described for the plasma that was injected into a magnetic trap in the experiments of A. M. Iskol'dskiy et al. The plasmas (ion density about 10^{13} cm^{-3}) were produced with the aid of a conical theta-pinch. Approximately 0.1 cm^3 of D_2 or He was admitted to the vacuum chamber and a 2 μF 20-40 kv capacitor was discharged through the ionizing winding some

300 to 400 microsec later. The heated plasma entered the 150 cm long 16 cm diameter region between the two magnetic mirrors (mirror ratio ~1.4, magnetic field strength ≤3 kOe) through one of the mirrors, the field strength in which was less than that in the other by a factor of 1.3. Diagnosis of the plasma was effected with the aid of 0.4, 0.8, and 3 cm microwaves, an x-ray detector, an electrostatic analyzer, and a special ion collector similar to that described by M. V. Babykin et al. (ZhETF, 46, 511, 1964). The last was mounted in the region of one of the magnetic mirrors and was so designed that only ions with Larmor radii exceeding a preset value could reach the collecting electrode. A small number of high energy charged particles (energies up to 5 kev) were observed; these are ascribed to formation of a plasmoid in the conical plasma gun during the first half-period of the discharge. Most of the charged particles in the magnetic mirror machine had energies of the order of 100 ev; the density of particles with energies between 20 and 200 ev decreased exponentially with a time constant of 80 to 90 microsec. It is concluded that by means of external injection (fast theta-pinch) a plasma with a density of 10^{13} cm^{-3} and an average charged particle energy of 100 ev can be obtained in a magnetic mirror machine in which the magnetic field strength is between 1 and 3 kOe, and that such plasma can be employed to investigate the physics of collisionless shock waves. (ATD)

42505 INVESTIGATION OF A CONICAL INDUCTION PLASMA SOURCE. Kossyi, I. A.; Shpigel', I. S.; Dorofeev, E. V. (Lebedev Inst. of Physics, Moscow). Zh. Tekh. Fiz., 36: 881-91 (May 1966). (In Russian).

A two-stage electrodeless conical plasma gun was investigated in an effort to achieve a more efficient induction plasma source and to learn something about the operating mechanism of conical plasma guns. The auxiliary cone was 7 cm long with base diameters of 2.4 and 4 cm; the main cone was 20 cm long with base diameters of 4.7 and 11.4 cm. The distribution of both the longitudinal and radial components of the magnetic field in the main cone was measured with a ≤2 mm diameter magnetic probe, and the distribution of neutral gas on the axis of the system was determined with an ionization manometer. The properties of the plasmas were determined with a double electrostatic probe. The plasma source operated most efficiently when discharge through the main cone was delayed until plasma from the auxiliary cone had reached it. Under these conditions a current sheet was formed in the main cone 0.28 microsec after initiation of the discharge (the period of the oscillating discharge was approximately 2 microsec), whereas in single-stage operation the current sheet was not formed until the third half-period. The charged particle density in the plasma at the mouth of the gun was 3×10^{14} cm^{-3} and the electron temperature was 13 ev; the conductivity of the plasma in the main cone was of the order of 10^{14} cgs units. The plasma left the gun as a jet with a velocity of the order of 10^6 cm/sec, preceded by a leader in which the velocity exceeded 10^7 cm/sec. The charged particle density in the plasma produced by optimum two-stage operation was an order of magnitude greater than that in the plasma produced by single-stage operation with the same discharge energy. It is concluded that preliminary ionization considerably improves the operation of conical induction plasma guns. The processes taking place during operation of the gun are discussed briefly. Magnetic flux was entrained by the currents induced in the plasma, and during the second half-period the magnetic field on the axis of the gun was directed oppositely to the external field. (ATD)

42506 HOLLOW POSITIVE COLUMN IN A LONGITUDINAL MAGNETIC FIELD. Belousova, L. E. Zh. Tekh. Fiz., 36: 892-902 (May 1966). (In Russian).

The screw instability of a diffusing positive column in the form of a hollow cylindrical shell in a longitudinal magnetic field is discussed. The calculations are based on the equations of continuity and equations of motion for the ions and electrons with ionization processes and diffusion taken into account. Quasi-neutrality is assumed. First, there are derived equilibrium conditions for a hollow positive column. It is found that at a fixed gas pressure and with a fixed outer radius of the column, the electron temperature is higher in a hollow positive column than in a full cylindrical column, and increases with increasing inner radius. From the equilibrium conditions there are derived the linearized equations for a screw-type perturbation, and the stability conditions are obtained from the corresponding dispersion equation and are presented graphically. It is found that the presence of a hollow core in the cylindrical positive column inhibits both stabilizing and destabilizing factors, but that the latter are the more inhibited and the stability region of the hollow column is more extensive than that of a full cylindrical positive column. The effect of the magnetic field on the motions of the ions is calculated. The stability conditions thus found for a hollow positive column are identical in form with those obtained by Johnson and Jerde for a full cylindrical column, but the coefficients C_{11} and D_{11} occurring in them are given for the hollow case by different expressions. The critical magnetic field is discussed briefly. It is estimated that for a 1 cm radius column in He at a pressure of 1 mm Hg the critical field strength is 1.6 kOe for a full cylindrical column and 3.9 kOe for a hollow column with an inner radius of 0.5 cm. (ATD)

42507 EFFICIENT EXTRACTION OF ELECTRONS FROM A MODIFIED PENNING DISCHARGE. Kreindel', Yu. E. (Inst. of Radioelectronics and Electronic Technology, Tomsk, USSR). Zh. Tekh. Fiz., 36: 903-6 (May 1966). (In Russian).

Conditions for the efficient extraction of electrons from a Penning discharge were investigated. Measurements were made at pressures from a 5×10^{-5} to 2×10^{-2} mm Hg; at pressures below 5×10^{-4} mm Hg the pressure was uniform throughout the apparatus, but at higher pressures the gas was admitted directly to the discharge region and the pressure in the remainder of the apparatus was kept low by rapid pumping. Particular features of the present experiments were the use of a cylindrical anode rather than a ring, and the use of extraction electrodes of ferromagnetic material in order to distort the magnetic field in the vicinity of the opening in the anode wall. The distortion of the magnetic field was found greatly to enhance both the extraction efficiency and the extracted current at fixed pressure and discharge potential. The extraction efficiency increased approximately linearly with increasing potential of the extraction electrode with respect to the anode; this behavior is different from that previously observed in the case of high voltage pulsed Penning discharges. It is concluded that an appropriate distortion of the magnetic field in the vicinity of the opening in the anode wall makes possible efficient electron extraction from a high or low pressure stationary Penning discharge. (ATD)

42508 SOLUTION OF LAPLACE'S EQUATION FOR A PENNING DISCHARGE GAP. Ivanova, T. I.; Pustovalov, G. E.; Reikhrudel', E. M. (Moscow State Univ.). Zh. Tekh. Fiz., 36: 907-12 (May 1966). (In Russian).

Because of its practical significance in connection with design and study of Penning discharges, the electrostatic field is calculated of a charged cylinder of radius a and length 2L located midway between and with its axis perpendicular to two infinite parallel plane grounded electrodes separated by a distance of 2D. The problem is first solved rigorously by separation of variables in cylindrical coordinates r, θ z (origin of coordinates at the center of the cylindrical electrode), and a set of linear equations is derived from which the coefficients in the resulting expansion in a series of modified Bessel functions can be calculated. Because of the complexity of the calculations, a second, approximate, calculation technique is developed. This technique is based on the assumption of a particular relatively simple form, suggested by results of electrolytic tank measurements, for the potential in the region r = a, L < z < D. The limiting cases L → 0 and L → D are discussed, and numerical calculations for the case L/D = ½ are presented and compared with results of electrolytic tank measurements. The approximate calculations are least accurate near the edge of the cylindrical electrode; in this region

the error is 10-20%, when 10 terms of the series are employed and the error cannot be reduced below 5-10% even by using many more terms. The errors decrease rapidly with decreasing r, and four terms of the series given an accuracy of 1% in the region $r < 4a/5$. The first term alone of the series gives an accuracy of 1% on the axis. (ATD)

42509 HIGH-PRESSURE ELECTRODELESS DISCHARGE AND ITS MAGNETIC PROPERTIES. Mitin, R. V.; Pryadkin, K. K. Zh. Tekh. Fiz., 36: 913-19 (May 1966). (In Russian).

The results are reported of h-f electrodeless discharges in Kr, Xe, He, Ar, Ne, N_2, and O_2, and investigations of the magnetic properties of the plasmas. The discharges were produced in a 3-cm-diameter closed quartz tube mounted vertically within a winding (or one or several turns) that was excited at 20 MHz by an oscillator operating at a power level of 600 w or lower. The discharge was initiated at low pressure, and the pressure was then gradually raised. It was not possible to achieve high-pressure discharges in He, N_2, or O_2. The plasma in the Ne discharge was toroidal in form up to the highest pressure at which the discharge could be maintained (2.5×10^5 N/m^2). The plasmas in the Ar, Kr, and Xe discharges became almost spherical at a pressure of the order of 10^5 N/m^2, and with further increase of the pressure they floated to the top of the chamber. A discharge could be maintained in Xe at pressures up to 2.0×10^6 N/m^2, in Ar at pressures up to about 1.3×10^6 N/m^2, and in Kr at pressures up to about 0.6×10^6 N/m^2. The power radiated by the plasmas was measured with a thermopile, using a water filter to eliminate the thermal radiation from the hot wall of the discharge tube. The radiated power increased with increasing pressure and increasing atomic weight of the gas. The Xe discharge plasma at 2×10^6 N/m^2 radiated at the rate of approximately 400 w; this radiated power represents practically the full power developed by the exciting oscillator. The behavior of the plasmas in inhomogeneous magnetic fields of 200 to 300 Oe with gradients of the order of 100 Oe/cm was investigated. The plasmas were unexpectedly found to move toward the region of higher magnetic field strength, the paramagnetic force on the plasmas being of the order of the buoyant force. Under certain conditions the plasma in the magnetic field assumed the form of a torus and began to rotate about its axis at several hundred rpm. Measurements of the high-frequency magnetic field strength in the vicinity of the plasmas indicated that the high-frequency current circulating in the plasma was about 30% of the current in the exciting winding. From the high-frequency magnetic field measurements and the loading effect of the plasma on the oscillating circuit it was concluded that the Ar plasma at 3×10^5 N/m^2 was about 0.1% ionized and had a resistivity of 1000 mho/m, an electron density of 3×10^{21} m^{-3}, and a temperature of the order of 10,000°K. Two explanations are offered for the observed paramagnetic behavior of the plasmas. The first explanation involves rectification in the presence of a magnetic field of a small fraction (about one percent) of the high-frequency current in the plasma to provide a small dc circulating current giving rise to an induced magnetic moment. The rectification is ascribed to the influence of radial oscillations of the plasma due to the interaction of the circulating high-frequency current with the magnetic field. The rectifying action depends on the variation of the average cross section of the circulating current with the diameter of the plasma, and the rectified current can be of either sign, giving rise to either paramagnetic or diamagnetic behavior. The second explanation ascribes the magnetic behavior of the plasmas to the effects of ambipolar diffusion arising from their nonuniformity. Although ambipolar diffusion ordinarily results in diamagnetic behavior, it can give rise to paramagnetic behavior under some circumstances. It is suggested that both effects may cooperate to produce the observed behavior. In concluding, the authors note that the behavior of electrodeless high-frequency discharge plasmas may have something to do with ball lightning. (ATD)

42510 ON THE INFLUENCE OF THE SPACE CHARGE OF THE PARTICLES ON THE FOCUSING AND DISPERSION PROPERTIES OF THE ELECTROSTATIC FIELDS OF CYLINDRICAL AND PLANE ENERGY ANALYZERS. Shapovalov, A. S. (Saratov State Univ., USSR). Zh. Tekh. Fiz., 36: 920-30 (May 1966). (In Russian).

The effect of the space charge of the analyzed beam on the focusing and dispersion of a beam of charged particles in the field of a cylindrical capacitor is calculated and the results are compared with those previously obtained by the author for the case of a plane capacitor. The effect of space charge on the trajectories is calculated with the assumption that the angles θ and α are small. Nonlinear differential equations are written for the limiting trajectories of the beam and approximate solutions are obtained by first averaging the terms describing the spacecharge effect over the unperturbed orbit. To test the accuracy of this approximation the equations were solved numerically with a computer for several values of the parameters; comparison of the numerical solutions with the approximate solutions indicated that the latter were in error by not more than 1%. It is found that the effect of space charge is to shift the position of best focus, decrease the relative dispersion, limit the maximum attainable dispersion, and decrease the resolving power. The influence of a small space charge is found to decrease the size of the image of a point source on the inner cylindrical electrode; further increase of the space charge (i.e., increase of the beam current), however, leads to an increase in the size of the image. (ATD)

42511 ON THE POSSIBILITY OF COMPENSATING THE SPACE CHARGE OF PULSED ELECTRON BEAMS. Bosamykin, V. S.; Pavlovskii, A. I. Zh. Tekh. Fiz., 36: 958-60 (May 1966). (In Russian).

The effect of residual gas pressure on the passage of a pulsed electron beam through a metallic tube was investigated. The electron gun was activated with a 300 kv pulse with a short rise time and an approximately exponential decay with a half time of 12 μsec. The beam was collimated with the system of several 5 mm diameter apertures. At the output of the collimator the current density was 5 A/cm^2 and the angular spread of the beam was 5°. The apparatus is described. (M.O.W.)

42512 FOCUSING OF AN ION BEAM IN THE FIELD OF A CHARGED CURRENT-CARRYING RING. Lebedev, S. V.; Morozov, A. I. Zh. Tekh. Fiz., 36: 960-2 (May 1966). (In Russian).

From a general argument based on previous theoretical work of A. I. Morozov on electric and magnetic fields in plasmas, it is concluded that any focusing system containing both electric and magnetic fields will focus a low density beam with uncompensated space charge differently than it will focus a high density beam with compensated space charge (plasma). This conclusion is illustrated by calculation of the focal length of a charged current-carrying ring under the two conditions. The calculations are performed in the thin lens approximation, i.e., it is assumed that the focal length is much larger than the radius of the ring. It is found that in the case of a low density beam with uncompensated space charge the paraxial focal length is always positive, whereas in the case of a high density beam the focal length can have either sign. The difference between the focal lengths in the two cases is due to redistribution of the electric field as a result of the space charge induced in the high density space charge compensated beam. The expression derived for the induced space charge density is independent of the density of the beam. This means that if the density of the space charge compensated beam exceeds a certain value, further increase of the density will not lead to further change in the focal length. (ATD)

42513 STUDIES OF LOW CURRENT ARCS WITH HIGH FREQUENCY METHODS FOR PLASMA DIAGNOSIS. Prinzler, H. Dresden, Technical Univ., 1965. 97p. $2.00 Gmelin, AED-Diss. 65-365.

Thesis.

The general theory of high frequency plasma conduction is used for the calculation of a N plasma. The interaction between the arc and a resonator is studied using equivalent circuits. Generation of noise in arcs is investigated. Noise

in W cathodes is mostly shot-noise. Cold cathode noise is explained by a multiplication process. (Gmelin Inst.)

42514 IMPROVEMENTS IN OR RELATING TO INDUCTION COUPLED PLASMA GENERATORS. Hedger, Harry John (to United Kingdom Atomic Energy Authority). British Patent 1,033,392. June 22, 1966. Filed June 20, 1962.

A method is described for the initiation of a plasma discharge in induction coupled plasma generators that operate by passing a stream of gas suitably confined in a tube through an induction coil which is arranged to be connected to the output of a r-f generator. To initiate the discharge, an electrically conductive body located upstream of the induction coil is momentarily connected to the end of the induction coil that is farthest removed from the conducting body. The connection may be made directly or by way of a portion of a second coil that is connected in series with the induction coil. (B.L.M.)

42515 QUASI-FLUID TREATMENT FOR INTENSE ELECTRON BEAM FLOW. Roberts, A. S. Jr. (Old Dominion Coll., Norfolk, Va.). 27p. (CONF-660547-1). ORAU. Gmelin, AED-CONF-66-122-2.

From Virginia Academy of Science, 44th Annual Meeting, Harrisonburg, Va.

An attempt is made to account for collective interactions of beam particles via moments of the Boltzmann transport equation and use of an anisotropic stress tensor; a modified paraxial treatment is ultimately made. The objective is to describe the macroscopic behavior of an intense nonaccelerated beam of electrons in high vacuum (10^{-6} torr). The analytic model is constructed, governing equations are presented, and important constraining conditions are discussed. Presentation of the beam envelope trajectory equation is made and trajectory solutions which include self-magnetostatic and thermal effects are obtained. (W.D.M.)

42516 COAXIAL ACCELERATOR. Eisner, M.; Henson, R. M. (Texas A and M Univ., College Station). 11p. (CONF-650220-6). ORAU.

From American Physical Society, Southwest Meeting, Norman, Okla.

Modifications of the coaxial accelerator configuration for obtaining optical access in the desired direction are described. Photographs of the discharge are presented and discussed. (M.H.R.)

Shielding

Refer also to abstracts 41197, 41534, 41566, 41619, 41647, and 42142.

42517 ATTENUATION OF HIGH-ENERGY NEUTRON FLUXES IN HETEROGENEOUS SHIELDING. Zaitsev, L. N.; Komochkov, M. M.; Malkov, V. V.; Sychev, B. S.; Cherevatenko, E. P. At. Energ. (USSR), 21: 56-7(June 1966). (In Russian).

The distribution of neutrons of various energy groups in layer shielding was studied using neutron fluxes produced by beryllium target bombardment with 660-Mev protons. The neutron flux was recorded by ^{115}In, ^{31}P, and ^{12}C threshold detectors as a roentgen film of individual γ dosimeters. The shielding was formed by iron–water and iron–heavy concrete systems. The curves of neutron attenuation are plotted. (R.V.J.)

42518 SUMMARY OF ATTENUATION COEFFICIENTS OF MATERIALS FOR GAMMA RAYS FROM ^{60}Co. Kanamori, Yoshihiko (Mitsui Shipbuilding Engineering Co. Ltd., Japan). Mitsui Zosen Giho, No. 53, 45-53(Jan. 1966). (In Japanese).

^{60}Co is one of the most important gamma-ray emitting radioisotopes and is often utilized in gamma-ray research and industrial application. Generally in handling gamma rays in research and industry, attenuation coefficients of materials for these gamma rays are the most necessary and fundamental data to know the penetration characteristics of the rays through matter. Attenuation coefficients of materials for gamma rays from ^{60}Co are summarized with the technique to gain them experimentally or by calculations. (auth)

42519 DETERMINATION OF THE LINEAR ATTENUATION COEFFICIENT IN CONCRETE OF GAMMA RADIATION EMITTED BY ^{60}Co. Ivanov, I.; Ilies, F. Teh. Nucl., 8: 260-6(May 1965). (In Rumanian).

The method and the equipment are described for the determination of the attenuation coefficient of gamma rays in concretes of various mixtures. The installation consists of a G-M detector, type G-14H, connected to a Tesla electron counter, a ^{60}Co source of 22.54 mc, and a lead collimator. The material under investigation was placed between the source and the detector while between the latter and the material a second head collimator was inserted for avoiding the detection of backscattered radiations. The whole apparatus was enclosed in a lead protective cover. The measurements effected on test pieces made of various concretes are presented in table form and the coefficient of linear attenuation of gamma radiation emitted by ^{60}Co was computed for each concrete mixture. A computation example is given for thickness of a concrete protection screen against a radiation source of 100 c. (auth)

42520 TRANSMISSION OF ISOTROPICALLY INCIDENT ELECTRONS THROUGH SPACECRAFT HULL MATERIALS. Stromquist, Walter K. (Aerospace Corp., San Bernardino, Calif.); Sleeper, H. P. Jr.; McDermed, O. L. New York, American Institute of Aeronautics and Astronautics, 1966, Preprint No. 66-511, 13p, $1.50. (CONF-660632-9). ORAU.

From American Inst. of Aeronautics and Astronuatics, 4th Aerospace Sciences Meeting, Los Angeles.

Number transmission coefficients for isotropically incident electrons were determined for conditions suitable for spacecraft shield design. These coefficients were derived from narrow-beam measurements over a range of angles of incidence, from a related study. Experimental data at oblique angles of incidence had not previously been available, and theoretical analysis only extended to one-half the electron range, insufficient to include the range from which most of the transmitted dose is received in a spacecraft. The measurements covered the energy range from 0.5 to 2.5 Mev, and included three materials, aluminum, magnesium–lithium alloy, and polyethylene. The transmission coefficients are tabulated for each observed angle of incidence and for isotropic incidence. The transmission coefficients for oblique incidence, and thus for isotropic incidence, were found to differ significantly from those of equivalent path length at normal incidence. The isotropic coefficients were found to be nearly linear with respect to thickness except very near the maximum range. (auth)

42521 MOTION OF A CHARGED PARTICLE IN A MAGNETIC FIELD DUE TO A FINITE SOLENOID WITH APPLICATION TO SOLAR RADIATION PROTECTION. Helgesen, John O.; Spagnolo, Frank A. (Grumman Aircraft Engineering, Corp., Bethpage, N. Y.). New York, American Inst. of Aeronautics and Astronautics, 1966, Preprint No. 66-512, 26p., $1.50. (CONF-660632-1). ORAU.

From American Inst. of Aeronautics and Astronautics, 4th Aerospace Sciences Meeting, Los Angeles, Calif.

Many of the magnetic radiation shielding studies published to date have been based on the validity of some form of dipole approximation for the magnetic field. In this study, Lagrange's equations are used as a starting point from which certain conditions are established that enable one to determine the regions around a particular solenoid configuration that are inaccessible to charged particles of a given energy. A numerical-graphical analysis was devised in which coil dimensions, particle energies, etc., are varied. Coil radii up to 3 meters, length to radius ratio between 0.5 and 4, and particle kinetic energy up to 1 Bev were considered. The results show that a finite solenoid of a given magnetic moment is not as effective for radiation shielding as was indicated by studies where a dipole approximation to the field was used. These

results, together with a brief assessment of magnet requirements, indicate that materials must be developed that will maintain their superconductivity at field strengths exceeding 200 kilogauss before an effective shielding configuration can be obtained. (auth)

Solid State Physics

See *also* CHEMISTRY — Inorganic and Physical Chemistry
METALS, CERAMICS, AND OTHER MATERIALS — Properties and Structure

Refer also to abstracts 41379, 41412, and 41458.

42522 (COO–1533-2) STUDY OF INTERACTIONS BETWEEN f-SHELL TRANSITION IONS IN NON-METALLIC CRYSTALS. Annual Technical Progress Report, October 1, 1965–June 15, 1966. Carlson, Edward H. (Michigan State Univ., East Lansing. Dept. of Physics). June 20, 1966. Contract AT(11-1)-1533. 12p. Dep. mn. CFSTI $1.00 cy, $0.50 mn.

Several rare earth chlorides were investigated by nuclear magnetic and quadrupole resonance techniques. In $GdCl_3$, three Zeeman components of the pure quadrupole resonance line were observed for ^{35}Cl and ^{37}Cl below Curie temperature. These data were analyzed, giving for the electric field gradient asymmetry parameter η = 0.425; results are tabulated for internal magnetic field vs temperature. A crystal of $PrCl_3$ was studied in a ^3He bath at temperatures down to about 0.5°K. At the lowest temperature reached, the pure quadrupole line at 4.567 Mc was observed to split into two lines. A single crystal of $NdCl_3$ was studied down to about 0.5°K. Near the lowest temperature reached, the signal grew weak and disappeared. No splitting was observed. A sample of fifty-fifty mixture of $NdCl_3$ and $PrCl_3$ was examined by NMR at 77°K. No ^{35}Cl resonance was found, particularly at the frequencies expected for resonance in pure $NdCl_3$ and $PrCl_3$. (J.H.M.)

42523 (IS–1500(Sect. P)) ANNUAL SUMMARY RESEARCH REPORT IN PHYSICS. (Ames Lab., Iowa State Univ. of Science and Tech.). 79p.

Brief summaries are presented of research carried out at the Ames Laboratory in the fields of high-energy, medium-energy, low-energy, and solid-state physics. (M.O.W.)

42524 (NRL–6408) THE EMISSION SPECTRA OF VARIOUS THERMOLUMINESCENT MATERIALS. Gorbics, S. G. (Naval Research Lab., Washington, D. C.). Mar. 15, 1966. Contract AT(49-7)-1864. 12p. Dep. mn. CFSTI $1.00 cy, $0.50 mn.

The thermoluminescence emission spectra of various materials were determined using a quartz-prism spectrograph. The materials studied include: CaF_2:Mn, $CaSO_4$:Mn, $Li_2B_4O_7$:Mn, LiF(TLD-100), CaF_2(MBLE), and a terbium-activated lithium–aluminosilicate thermoluminescent glass. The spectra were measured photographically and corrected by means of an NBS quartz-iodine tungsten-filament standard of spectral irradiance. Precautions were taken to prevent spectral distortions resulting from the variation in sensitivity of the film as a function of wavelength, and from reciprocity-law failure. The present spectra are in general agreement with earlier measurements for CaF_2:Mn, $CaSO_4$:Mn, LiF(TLD-100), and CaF_2(MBLE). The radioluminescence spectra of CaF_2:Mn and $CaSO_4$:Mn were determined and found to be similar in shape and peak position to the thermoluminescence spectrum but were narrower. The radioluminescence spectrum of LiF(TLD-100), however, was wider than the thermoluminescence spectrum. The radioluminescence spectra of CaF_2(MBLE) extended far into the ultraviolet region. (auth)

42525 (ORNL-P-2466) ELECTRON SPIN RESONANCE SPECTRA OF Dy^{3+} IN ThO_2 AND CeO_2. Abraham, M. M.; Finch, C. B.; Raubenheimer, L. J.; El Saffar, Z. M.; Weeks, R. A. (Oak Ridge National Lab., Tenn.). Aug. 1966. Contract W-7405-eng-26. 11p. (CONF-660924-1). Dep. mn. CFSTI $1.00 cy, $0.50 mn.

From International Conference on Magnetic Resonance and Relaxation, 14th Colloque AMPERE, Ljubljana, Yugoslavia.

Single crystals of ThO_2 and CeO_2 (fluorite structure) doped with 0.5 atomic weight percent impurities of isotopically enriched Dy^{3+} (94% even-even isotopes) were grown. Electron spin resonance (ESR) measurements at ≃10 Gcps and liquid helium temperatures reveal spectra with symmetry axes along the 4 crystal [111] axes. For ThO_2 $g_{||} = 1.625 \pm 0.002$, $g_{\perp} = 9.95 \pm 0.05$ and for CeO_2 $g_{||} = 1.632 \pm 0.002$, $g_{\perp} = 9.98 \pm 0.05$. An additional line is observed and attributed to a $|\frac{1}{2}> \rightarrow |-\frac{1}{2}>$ transition between the levels of a ground state Γ_8 quartet in a cubic crystal field. For ThO_2, $g_{[100]} = 4.566$, $g_{[111]} = 4.323$, $g_{[110]} = 4.386$, and for CeO_2, $g_{[100]} = 4.433$, $g_{[111]} = 4.401$, $g_{[110]} = 4.411$ with 0.1% error. These data are sufficient for a calculation of the ratio of the cubic crystal field 4th and 6th order parameters. At 20°K no spectra were observed, which made it possible to detect a low lying Γ_7 doublet as observed in the case of the isomorphous CaF_2. All line widths were larger than those for other rare-earth ions in these crystals and were 20 to 40 gauss. (auth)

42526 REMARKS ON THE USE OF VERY HIGH PULSED FIELDS IN SOLID STATE RESEARCH. Olsen, J. L. (Swiss Federal Inst. of Tech., Zurich). pp 483-9 of EUR–2750.e.

Previous solid state experiments carried out in pulsed magnetic fields are summarized. The possibility of extending some of these experiments to the explosively generated high field region is discussed. The very short pulse length is found to be a very serious handicap. (auth)

42527 LOW-TEMPERATURE γ IRRADIATION AND TEMPERING OF INDIUM ANTIMONIDE. Mashovets, T. V.; Khansevarov, R. Yu. (Ioffe Inst. of Physics and Tech., Leningrad). Fiz. Tverd. Tela, 8: 1690-7(June 1966). (In Russian).

The complex character of the dependence of formation of γ radiation defects in n type material on exposure dose cannot be explained without the assumption of the presence of several different tempering processes occurring during radiation. Donor and acceptor components exist in monopolar tempering. The relative contribution of each process depends on the charge state of the defect. Samples of the n and p type with different initial concentrations as a result of irradiation attain a limiting state characterized by very close values of hole concentrations. This can be explained by the establishment of an equilibrium between formation processes and annealing processes of the acceptor component of defects only by the introduction of a supplementary hypothesis of the dependence of annealing on the degree of filling of the acceptor levels situated near E_F. On destruction of these levels, tempering is accelerated. Results on isochronous tempering of n and p type samples between 77°K and 300°K agree with previously published work; thus fundamental processes which always occur on irradiation of elementary defects occur here. The energetics of levels in the forbidden zone at various stages of irradiation for n type were examined. For the extreme case two levels are related to the radiation defect; apparently $E_c = -0.083$ ev is the donor and $E_v = 0.048$ ev the acceptor. (BBB)

42528 ANISOTROPY OF MAGNETIC RESONANCE OF ^{19}F NUCLEI IN A MONOCRYSTAL OF LaF_3. Lundin, A. G.; Gabuda, S. P. (Inst. of Physics, Krasnoyarsk, USSR). Fiz. Tverd. Tela, 8: 1889-94(June 1966). (In Russian).

The NMR spectrum of ^{19}F in monocrystals of LaF_3 between room temperature and –100°C at 15 and 37 Mc was studied. The spectrum may be resolved into two overlapping resonances; the dependence of the position of the max on the angle of rotation about the 100 and 001 axes is illustrated. Two types of F are distinguished in the crystal lattices, those at the apices of a triangular bipyramid about La and those at the vertices of the base triangle. At –16°C,

for the latter (F_I), $\sigma_{||} = (1.6 \pm 0.1) \times 10^{-4}$; $\sigma_{\perp} = (4.85 \pm 0.1) \times 10^{-4}$; for F_{II}, the former case $\sigma_{||} = (7.35 \pm 0.1) \times 10^{-4}$; $\sigma_{\perp} = (5.6 \pm 0.1) \times 10^{-4}$. For F_I it is also found that $p_{xx} = p_{yy} = 1.94$, $p_{zz} = 1.66$, $z_{eff} = -0.54$; for F_{II} $p_{xx} = p_{yy} = 1.66$, $p_{zz} = 1.86$, $z_{eff} = -0.18$. The electronic structure of the crystal is discussed. The diffusion constants for the two nonequivalent groups of F atoms have the same value. (BBB)

42529 APPLICATION OF THE INDOR TECHNIQUE TO HIGH RESOLUTION PROTON MAGNETIC RESONANCE SPECTRA: A NEGATIVE RING SPIN-SPIN COUPLING. Kowalewski, V. J.; de Kowalewski, D. G.; Ferra, E. C. (Univ. of Buenos Aires). J. Mol. Spectros., 20: 203-16 (July 1966).

Tickling and INDOR experiments are performed with a frequency swept, field/frequency locked high resolution proton magnetic resonance spectrometer, on a simple AB case and on an ABCD case with quadrupolar broadening due to ^{14}N. It is shown that the INDOR technique has in the last case definite advantages which permit the determination, in magnitude and sign, of the coupling between protons 2 and 6 in 3-acetylpyridine, in spite of the quadrupolar broadening. The result obtained is $J_{26} = -0.21$ cps. (auth)

42530 OBSERVATION AND STUDY OF A NEW COLOR CENTER IN IRRADIATED LITHIUM FLUORIDE: F_3^+. Farge, Y.; Toulouse, G.; Lambert, M. (Faculte des Sciences, Orsay, France). J. Phys. (Paris), 27: 287-94(May-June 1966). (In French).

The 4,500 Å absorption band in lithium fluoride is known as the M band. This band is in fact due to the superposed effects of the M center and another completely independent center. This new center corresponds to a 5,400 Å emission band which is the mirror image of its absorption band with respect to its 4,874 Å zero phonon line. The interaction with the lattice is interpreted by using a simple model and suggests a highly localized electronic structure (mostly linear coupling). The symmetry of this color center and its conversion into an R center by F light irradiation suggest that it is the F_3^+ center which was first observed by Schneider and Rabin in KCl and KBr. (auth)

42531 EFFECT OF TEMPERATURE ON THE ELECTRONIC INSTABILITY AND CRYSTALLINE PHASE CHANGE OF V_3Si-TYPE COMPOUNDS AT LOW TEMPERATURE. Labbe, J.; Friedel, J. (Faculte des Sciences, Orsay, France). J. Phys. (Paris), 27: 303-8(May-June 1966). (In French).

At very low temperatures the cubic phase of the intermetallic compounds of the type V_3Si is unstable. A Jahn Teller type of effect for the d band electrons can explain this instability. When the temperature is raised the effect is reduced and above a certain temperature T_m it is compensated by the action of the conduction electrons, which can reasonably be supposed to stabilize the cubic phase. It is at this temperature T_m that the change of structure from tetragonal to cubic phase occurs. (auth)

42532 PHOTOCURRENT AND THERMAL RELEASE TIME STUDIES OF URANIUM DIOXIDE. Iida, Shoji (Mitsubishi Atomic Power Industries, Inc., Ohmiya, Japan). Jap. J. Appl. Phys., 5: 752-5(Sept. 1966).

The photocurrent and thermal release time of trapped carriers in sintered uranium dioxide were measured at room temperature. The peak positions of photocurrent spectra indicated that the characteristic energy level of uranium dioxide is about 2.0 ~ 2.3 ev. This level was not affected by the O/U ratio; however, energy levels having smaller values than about 1.0 ev were affected by the O/U ratio. The measurement of thermal release time of trapped carriers also indicated that the shallow energy levels were affected by the O/U ratio. Infrared absorption spectra between 2.8μ and 45μ showed no particular absorption band, using powdered-film specimens, because the illuminating light source was too weak. (auth)

42533 VOLTAGE INDUCED BY AN ELECTRON BEAM IN A BULK SEMICONDUCTOR CRYSTAL. Munakata, Chusuke (Hitachi Ltd., Tokyo). Jap. J. Appl. Phys., 5: 756-63(Sept. 1966).

It is known that a voltage is induced by an electron beam as well as a light beam in a semiconductor crystal bar in which the resistivity is inhomogeneous. The voltage induced by an electron beam is considered and equations for the induced voltage are theoretically derived on a one-dimensional model for three special cases: linear, periodic, and abrupt resistivity-change. For the case of periodic resistivity-change, good agreement with experiment is obtained: in n-type Ge bar the calculated and the observed values are 7.9 μV and 6 μV respectively under the conditions that the current, the energy of the electrons, the change of the resistivity, and the periodic length are 2.5 mμA, 20 kev, 1 Ωcm, and about 0.024 cm, respectively. (auth)

42534 PROCESSING OF V_3Ga WIRES AND THEIR SUPERCONDUCTING PROPERTIES. Tachikawa, Kyoji; Tanaka, Yoshiaki (National Research Inst. for Metals, Tokyo). Jap. J. Appl. Phys., 5: 834(Sept. 1966).

V_3Ga wires were made by a new stepwise diffusion process and good superconducting properties were obtained. Five intermetallic compounds, i.e., V_3Ga, V_2Ga, V_3Ga_2, VGa, and VGa_2 were found in the V–Ga system. The process consisted of reacting a vanadium wire with molten gallium at 700°C to form VaG_2. Upon heat treatment at 800°C the VGa_2 is converted to V_3Ga_2. In a second-stage heat treatment the diffusion layer of V_3Ga_2 is converted to V_3Ga at 700°C. The transition temperature of the wire is lowered from 15 to 14°K as the baking temperature is raised from 700 to 1100°C. The critical current density of the V_3Ga layer made by this process is about 4×10^5 A/cm² in transverse magnetic fields of 30 kG at 4.2°K. (W.D.M.)

42535 EFFECT OF OXYGEN ADDITIONS ON THE STRUCTURE AND SUPERCONDUCTING PROPERTIES OF Zr–Nb ALLOYS. Bychkov, Yu. F.; Goncharov, I. N.; Khukhareva, I. S. Met. Metalloved. Chistykh Metal., Sb. Nauchn. Rabot, No. 5, 44-50(1966). (In Russian).

An investigation was made of the effect of oxygen additions on the critical current density (j_c) in Zr–Nb alloys, and on the β-solid solution decomposition that changes the magnitude of j_c. Electron-beam melted zirconium alloys containing 33 wt % Nb and 0.02 to 0.04 wt % O_2 were preforged at 800 to 900°C and cold rolled into a strip 1 mm thick, which was annealed at 900 to 950°C in oxygen, homogenized in vacuum at 1300°C for 1.5 hr, cold rolled to a thickness of 0.5 mm with process annealing at 500, 570, or 700°C for 1 hr, and then cold rolled into 0.05-mm foil without process annealing. The oxygen content in the foil varied from 0 to 1.0%. The critical current density (j_c) was measured in a magnetic field with an intensity, H, of up to 27 Oe parallel to the direction of rolling. It was found that alloying with up to 0.04 wt % O_2 had practically no effect on the magnitude of j_c; the dependence of j_c on H was the same as for alloys without oxygen. With oxygen content increasing from 0.1 to 0.25 wt %, the magnitude of j_c in specimens rolled without process annealing more than doubled and reached 4×10^4 amp/cm² in a field of 27 Oe The effect of oxygen was even more pronounced in foil rolled with process annealing, in which case the j_c of specimens containing 0.25% oxygen and annealed at 700°C reached 1.5×10^5 amp/cm². Thus, the j_c of Zr-base alloys can be significantly increased by alloying oxygen especially when cold deformation is followed by process annealing. Additions of oxygen substantially increased the hardness of alloys, although the hardness remains lower than that of niobium and niobium-base alloys. It appears that alloys with 25 to 35% Nb permit larger oxygen additions than the Nb-base alloys because of a smaller effect of oxygen on their ductility. The hardness of an alloy containing 33% Nb and 0.25% oxygen remained practically unchanged with annealing at 700°C, but decreased by 20 units in an alloy containing 26% Nb and 0.04% oxygen. Oxygen additions also caused separation of the β-solid solution into two solid solutions with a different concentration of the α-phase. The higher j_c in oxygen-rich alloys can be explained by the presence of finely dispersed inclusions with poor superconducting properties in the superconducting matrix, in particular, α-Zr inclusions with $T_c = 0.6$°K, which stabilize magnetic flux lines. (ATD)

42536 SCATTERING AND ENERGY LOSS OF ELECTRONS IN SILICON NEAR THE RADIATION DAMAGE THRESHOLD. George, G. G.; Stevens, P. R. C. (Atomic Weapons Research Establishment, Aldermaston, Eng.). Nucl. Instrum. Methods, 43: 278-84(Aug. 1966).

Measurements were made of scattering and energy loss of electrons in the energy range 100–400 kev, by single crystal silicon foils of thickness between 3 and 190 μm. The angular dispersion is found to be slightly less than predicted by the multiple scattering theory of Goudsmit and Saunderson, the best agreement being at the highest energy. The results are discussed briefly from the point of view of the interpretation of radiation damage anisotropy and threshold experiments. (auth)

42537 BINARY CENTERS PRODUCED BY LIGHT IN URANYL SALTS. Tolstoi, N. A.; Abramov, A. P.; Abramova, I. N. Opt. Spectros. (USSR) (Engl. Transl.), 20: 415-16(Apr. 1966).

Translated from Opt. Spektros., 20: 742-4(Apr. 1966).

A preliminary description is given of an unusual effect, which was discovered in uranyl salts excited by uv light at low temperature. The essence of the new phenomenon is as follows: if certain uranyl salts are exposed to a sufficiently high dose of initial uv excitation at liquid nitrogen temperature, both the stationary luminescence intensity, I, and relaxation time τ, decrease; the intensity, E, of that light by means of which the subsequent measurements of I and τ are carried out, can be as small as is desired. The described phenomenon was observed in uranyl sulfate, uranyl nitrate, and cesium uranyl nitrate, the greatest effect being observed in the latter. (M.H.R.)

42538 ELECTRON SPIN RESONANCE OF IRRADIATED SILICATE GLASSES. Sasakura, Hiroshi (Osaka Prefectural); Takeuchi, Nozomu. Osaka Furitsu Kogyo-Shoreikan Hokoku, No. 37, 7-11(Dec. 1965). (In Japanese).

Electron spin resonance of irradiated silicate-glasses containing impurities was investigated at room temperature. The spectrum of irradiated glass containing no impurities was attributed to trapped holes at an oxygen ion in a SiO_4 tetrahedral configuration in the glass structure. It showed considerable dipole-dipole broadening, presumably due to Na ion. The spectra of irradiated glasses containing V and Mn were further broadened by impurities. The interaction was possibly of Fermi-type, or of dipole-dipole type. (auth)

42539 FLUORESCENCE LIFETIMES OF HYDRATED SALTS OF EUROPIUM AND TERBIUM. Heber, J.; Hellwege, K. H.; Mangelsdorf, D.; Zieg, W. Phys. Kondens. Mater., 5: 89-99(1966). (In German).

At 300°K the fluorescent lifetimes of the levels $^5D_0$ of Eu^{3+} and $^5D_4$ of Tb^{3+} were measured in $RE(C_2H_5SO_4)_3 \cdot 9H_2O$, $RE(BrO_3)_3 \cdot 9H_2O$, $RECl_3 \cdot 6H_2O$, $RE(NO_3)_3 \cdot 6H_2O$, and $(RE)_2(SO_4)_3 \cdot 8H_2O$. The fluorescent lifetimes of the hydrated crystals were determined by radiationless transitions. An empirical relation can be obtained for the probability w for the radiationless transitions of the form $w = \text{const} \cdot \alpha_{RE} \cdot \alpha_{Lattice}$. The factors α_{RE} and $\alpha_{Lattice}$ depend only on the rare-earth ion or the lattice respectively. A structure of the interaction Hamiltonian between the rare-earth ion and the lattice is proposed, which leads to the empirically found relation. The influence of electron and x irradiation on the lifetime of the level $^5D_4$ in $TbCl_3 \cdot 6H_2O$ was investigated at 77°K. A decrease of the lifetime and a nonexponential decay of the fluorescence were found. By heating the crystal to room temperature, thermoluminescence and annealing of the irradiation defects were observed. (auth)

42540 SPIN-LATTICE RELAXATION OF RARE-EARTH IONS IN LaF_3. Schulz, M. B.; Jeffries, C. D. (Univ. of California, Berkeley). Phys. Rev., 149: 270-88(Sept. 9, 1966).

The spin-bath relaxation rate T_b^{-1} has been measured in the temperature range $1.3 < T < 5°K$ for each of the trivalent Kramers ions: Ce^{3+}, Nd^{3+}, Sm^{3+}, Gd^{3+}, Dy^{3+}, Er^{3+}, and Yb^{3+}, magnetically diluted in LaF_3. In three cases, Nd^{3+}, Er^{3+}, and Yb^{3+}, the temperature range was extended to $0.2 < T < 5°K$. All measurements were made by observing the transient recovery of the microwave paramagnetic resonance at the frequency $\nu \approx 9.3$ Gs/sec. The temperature dependence of the Orbach process $T_{1d}^{-1} \propto \exp(-\Delta/T)$ is displayed for Nd, Sm, and Er; and the Raman process $T_{1R}^{-1} \propto T^9$ is displayed for Nd, Er, and Yb. These do not depend on crystal orientation nor on the concentration of paramagnetic ions. The values $\Delta(Nd) = 57°K$ and $\Delta(Er) = 72°K$ are found to agree reasonably with the energy of the first crystal-field state, previously determined optically; we find $\Delta(Sm) = 50°K$. The direct process, $T_{1d}^{-1} \propto T$, is observed only for the lowest concentrations of paramagnetic ions: 0.1% Nd and 0.05% Er. For other ions and at higher concentrations the direct process was usually obscured by cross relaxation, probably to excited states of exchange coupled pairs or larger clusters of magnetic ions as evidenced by a temperature dependence $T_b^{-1} \propto \operatorname{csch}(\Delta'/kT)$, where Δ' is of order of the exchange energy. No clear-cut example of a phonon bottleneck, $T_b^{-1} \propto T^2$, is found. From optical data for Nd and Er, wave functions and crystal-field parameters are obtained, from which simple theoretical estimates of the relaxation rates are found to be in moderate agreement with the data. (auth)

42541 EXTENSION OF THE DISPERSION-RELATION MEASUREMENTS OF BERYLLIUM. Schmunk, R. E. (Phillips Petroleum Co., Idaho Falls, Idaho). Phys. Rev., 149: 450-6(Sept. 16, 1966).

The phonon dispersion-relation data for beryllium were extended for waves propagating in the $[01\bar{1}0]$ and $[11\bar{2}0]$ directions by recent neutron scattering measurements. Measurements were confined to phonons which have their polarization vectors aligned parallel to the hexagonal plane. Branches for the $[01\bar{1}0]$ direction of wave propagation designated TO($\parallel$) and TA($\parallel$) have intercept frequencies at the zone boundary of 1.72 and 1.21, respectively, in units of 10^{13} sec^{-1}. Comparison is made between these data and lattice-dynamical models of Gupta and Dayal, Iyengar et al., and DeWames et al. The model of DeWames et al. gives the best agreement with the data but further improvements are desired. The Rosenstock sum Rule which was applied to the dispersion-relation data for the symmetry directions indicates the presence of considerable nonelectrostatic or trace-variable forces. These forces are presumed to arise from the ion-core repulsion and the kinetic energy of the conduction electrons in beryllium. (auth)

42542 RE-EVALUATION OF SOME THERMODYNAMIC PROPERTIES OF GADOLINIUM METAL. Jelinek, F. J.; Gerstein, B. C.; Griffel, M.; Skochdopole, R. E.; Spedding, F. H. (Iowa State Univ., Ames). Phys. Rev., 149: 489-90(Sept. 16, 1966). (IS–1336).

The heat capacity of Gd metal was previously measured over the temperature range 15 to 355°K by M. Griffel et al. In this note, the γ coefficient (16×10^{-4} cal/g atom deg^2 in the original work) used in calculating the electronic specific heat of Gd was replaced by the more recent value of 22×10^{-4}, cal/g atom $deg.^2$ This leads to a slightly higher calculated Debye temperature and a subsequent readjustment of the lattice-specific-heat term. In addition, an error was discovered in the evaluation of the thermodynamic functions, particularly the (S_T^0) term. A Simpson's-rule integration procedure was applied to the original heat-capacity data and the thermodynamic functions were re-evaluated. These changes lead to a magnetic-entropy calculation considerably closer to the complete spin-order entropy, RIn8, than was reported in the original work. (auth)

42543 ELECTRON-IRRADIATION DAMAGE-RATE MEASUREMENTS IN ALUMINUM. Neely, H. H.; Bauer, Walter (Atomics International, Canoga Park, Calif.). Phys. Rev., 149: 535-9(Sept. 16, 1966).

The resistivity increase upon electron irradiation near 8°K of aluminum was measured as a function of incident electron energy from 0.19 to 1.6 Mev. A value of the displacement threshold energy of 16 ev was determined by

extrapolation of the damage-rate curve to zero damage production. A reasonable fit between the experimental and theoretical values of the displacement cross section was achieved with an effective threshold energy of 19 ev, a value of the Frenkel resistivity of $(1.32 \times 10^{-4}$ ohm cm)/(fractional concentration), and a unit step-displacement function. The tailing off in the damage rate near threshold that was observed in Cu, Au, and Pt is apparently absent in Al. (auth)

42544 HIGH-TEMPERATURE MAGNETIC SUSCEPTIBILITY OF LANTHANUM AND CERIUM METALS. Burr, C. R.; Ehara, S. (Univ. of California, Los Angeles). Phys. Rev., 149: 551-5(Sept. 16, 1966).

The magnetic susceptibilities of cerium and lanthanum metals were measured from room temperature through the melting point. Cerium has a unique fusion behavior with a negative melting slope which has been attributed to a 4f-5d electronic promotion. It is demonstrated that this promotion in cerium does not occur and that the small change in the susceptibility at cerium's two high-temperature phase transformations can be attributed almost entirely to changes in the Pauli susceptibility. A quantitative estimate of this change is found by comparison with the lanthanum high-temperature susceptibility. (auth)

42545 FORMATION OF A MAGNETIC PINCH IN InSb AND THE POSSIBILITY OF POPULATION INVERSION IN THE PINCH. Schmidt, Helmut (Boeing Scientific Research Labs., Seattle, Wash.). Phys. Rev., 149: 564-73 (Sept. 16, 1966).

A sufficiently strong current supported by an electron-hole plasma in InSb pinches. As the electron-hole gas is compressed by the current's magnetic field, the plasma temperature increases. The strong electron-phonon coupling, however, keeps the plasma temperature below the characteristic temperature of the optical phonons as long as the lattice remains cold. This early period of the pinch is discussed, which includes the initial contraction and some 10^{-7} sec thereafter. The collapse of the pinch may be halted by an increase of the plasma pressure caused by the exclusion principle or by the occurrence of impact ionization in the pinch's radial Hall field. An estimate of the particle density in the pinch shows that the conditions for population inversion may be satisfied, hence laser action due to stimulated electron-hole recombination might occur. This effect should influence the development of the pinch decisively. (auth)

42546 FLUX METHODS FOR TRANSPORT PROBLEMS IN SOLIDS WITH NONCONSTANT ELECTRIC FIELDS. Pulver, E. F., McKelvey, J. P. (Pennsylvania State Univ., University Park). Phys. Rev., 149: 617-23(Sept. 16, 1966).

Methods for the solution of one-dimensional steady-state transport problems, based on flux conservation in diffusion-recombination systems involving charged particles, are extended to cases where nonconstant electric fields act upon the particles of the system. In situations where the electric field is small enough so that the drift velocity is much less than the mean thermal speed, solutions for a system of coupled flux-conservation equations for the diffusion-recombination system can be obtained by use of the WKB method of approximation. From these solutions, expressions which involve integrals containing the field can be derived for the reflection and transmission coefficients of a material layer of arbitrary thickness. For the case where recombination may be neglected, the solutions are exact. Iterative methods are presented for obtaining the reflection and transmission coefficients of a material layer of arbitrary thickness under conditions where the requirements for the validity of the WKB method are not fulfilled. These methods are especially suitable for computer calculations. Expressions for the low-field reflection and transmission coefficients are obtained for a semiconductor surface space-charge layer in the case where bulk recombination is negligible. In the high field "hot-carrier" region, the fraction of flux which is reversed within a differential scattering layer is deduced empirically from symmetry properties and behavior in limiting cases. These expressions, though lacking any rigorous mathematical justification, are obtained independently of the carrier velocity distribution. (auth)

42547 THERMAL CONDUCTIVITY OF ELECTRON-IRRADIATED InSb. Vook, Frederick L. (Sandia Lab., Albuquerque, N. Mex.). Phys. Rev., 149: 631-6(Sept. 16, 1966).

Measurements were made of the change in low-temperature thermal conductivity of high-purity single-crystal InSb irradiated with 2-Mev electrons below 25°K. The additive thermal resistivity increases as the $\frac{3}{4}$ power of the time-integrated flux, in agreement with the recent theory of Erdös for strong impurity scattering. For equivalent low-temperature electron irradiations, the increase in the additive thermal resistivity for InSb is considerably larger than for GaAs, Ge, or Si. Concentration-dependent annealing stages are observed near 65 and 90°K. For light irradiations (p-type) the 65°K stage is the dominant annealing stage, and the previously observed 90°K stage (stage II) is completely absent. Measurements of the temperature dependence of the thermal conductivity after irradiation below successively higher anneal temperatures indicate that the defects anneal as point defects rather than form the precipitates observed for GaAs. (auth)

42548 RADIATIVE RECOMBINATION IN ANNEALED ELECTRON-IRRADIATED GaAs. Arnold, George W. (Sandia Lab., Albuquerque, N. Mex.). Phys. Rev., 149: 679-80(Sept. 16, 1966).

Broad-band emission peaking near 1.39 ev appears in Zn-doped GaAs in addition to the narrow bound-exciton emission at 1.49 ev. Electron irradiations at energies between 0.6 and 2.0 Mev for time-integrated fluxes of 1.3×10^{18} e/cm^2 quench all luminescence. For bombardment energies below a critical value, which lies between 1.0 and 1.5 Mev, isochronal annealing near 190°C causes the reappearance of the broad-band emission, which now is found to possess structure. The structure consists of three no-phonon lines at 1.4433, 1.4415, and 1.4402 ev which are repeated at intervals of the transverse acoustic phonon energy. The emission intensity is greatest for temperatures near 220°C. Further annealing at higher temperatures diminishes the intensity of the fine structure and the associated broad-band emission; complete disappearance occurs above 260°C. The emission is not regained upon annealing when the bombardment energy exceeds the critical value. It is suggested that direct lattice displacement occurs at the critical bombarding energy. This would correspond to a threshold displacement energy of 50 to 60 ev. It is also suggested that previous measurements of threshold energy (10 to 20 ev) in GaAs and other experimental observations may be due to known large concentrations ($\approx 10^{19}$ cm^3) of defects in as-grown GaAs, in the form of Ga-As interstitial pairs. (auth)

42549 ELECTRON PARAMAGNETIC RESONANCE AND ELECTRICAL PROPERTIES OF THE DOMINANT PARAMAGNETIC DEFECT IN ELECTRON-IRRADIATED p-TYPE SILICON. Almeleh, Nissim; Goldstein, Bernard (RCA Laboratories, Princeton, N. J.). Phys. Rev., 149: 687-92(Sept. 16, 1966).

Lattice defects having strong paramagnetic resonances are introduced into p-type silicon that has been bombarded with electrons. Studies were made on paramagnetic properties and growth of the dominant defect so introduced (the K center) as functions of electron flux and bombardment energy under conditions of different resistivities, impurity dopants, and illumination. The defect has a spin of $\frac{1}{2}$ and has g values of 2.0000, 2.0066, and 2.0056 for the principal magnetic axes, which lie along the $\langle 221 \rangle$, $\langle 1\bar{1}0 \rangle$, and $\langle 11\bar{4} \rangle$, crystallographic directions, respectively. No hyperfine interactions are observed. The introduction rates for the K center are 0.006, 0.025, 0.073, and 0.11 cm^{-1} at bombardment energies of 0.7, 1.3, and 6.6 Mev, respectively. The K center is independent of the p-type dopant. It is not a primary defect, but requires oxygen. At high integrated electron fluxes, the EPR-measured K-center concentration decreases; however, illumination and annealing experiments established that the defects are still present but

have a different charge state because they have trapped an electron. The EPR measurements were paralleled by Hall-effect measurements. We have associated the K center with a previously reported 0.3-ev defect level on the grounds that both require oxygen, that both have about the same introduction rates and bombardment energy dependence, and that the value of the Fermi level at which the K-center EPR absorption decreases sharply is about 0.3 ev. (auth)

42550 PRESSURE DEPENDENCE OF THE TA[100] ZONE-BOUNDARY PHONON FREQUENCY IN RUBIDIUM IODIDE. Saunderson, D. H. (Atomic Energy Research Establishment, Harwell, Eng.). Phys. Rev. Lett., 17: 530-3(Sept. 5, 1966).

The frequency of the TA[100] zone-boundary phonon was measured in rubidium iodide under hydrostatic pressures of 0 to 3.72 kbar by neutron inelastic scattering. A linear fit to the percentage decrease in frequency gave a value of 13.5 ± 0.9% when extrapolated to the NaCl–CsCl polymorphic transition pressure. (auth)

42551 FIELD ION MICROSCOPE STUDY OF NEUTRON-IRRADIATED TUNGSTEN. Attardo, M. (Brookhaven National Lab., Upton, N. Y.); Galligan, J. M. Phys. Status Solidi, 16: 449-57(1966). (BNL–9909).

A field-ion-microscope study of the damage introduced into tungsten by fast neutrons consisted of examining the type of damage as reflected in the vacancy content of the material and the removal of the vacancy content after various annealing treatments. Evidence presented shows that vacancies are removed from tungsten in stage IV. The observations also indicate the presence of depleted zones in the irradiated tungsten. (auth)

42552 MAGNETIC AND STRUCTURAL CHARACTERISTICS OF SOME EQUIATOMIC RARE-EARTH GERMANIDES. Buschow, K. H. J.; Fast, J. F. (Philips Research Labs., Eindhoven, Netherlands). Phys. Status Solidi, 16: 467-73(1966).

Magnetic and structural data are given for eleven rare earth-germanium intermetallic compounds represented by the formula RGe. The FeB type of structure is observed for R = La and Ce, while the CrB type is found for R = Pr, Nd, Sm, Gd, Tb, Dy, Ho, Er, and Y. The compounds LaGe and YGe are Pauli paramagnets. The compounds PrGe and NdGe are found to become ferromagnetically ordered upon cooling, whereas the compounds CeGe, SmGe, GdGe, TbGe, DyGe, and ErGe order antiferromagnetically. A field-induced transition from the antiferromagnetic state to a ferrimagnetic state is observed for the compound HoGe at 4.2°K when studied in moderate fields; when a pulsed field up to 80,000 Oe is used a second transition point is observed. The susceptibility at high temperatures of most of the compounds follows the Curie-Weiss law with effective moments close to those of the trivalent free rare earth ions. In the case of SmGe, a contribution to the susceptibility from higher multiplets is observed. (auth)

42553 MECHANISM OF SPUTTERING. Lehmann, Chr.; Sigmund, P. (Kernforschungsanlage, Juelich, Ger.). Phys. Status Solidi, 16: 507-11(1966).

It is shown that spot patterns in single-crystal sputtering do not necessarily arise as a consequence of focused collision sequences. Spots can be obtained if it is assumed that only the surface of a solid has a regular structure. The spot width is determined by the energy distribution in the collision cascade and the potential barrier at the surface. The contribution of focusons to sputtering is negligible at low bombarding energies because of the small penetration depth of the ions. Recent experimental results indicate that the average path length of focusons contributing to sputtering is extremely small even at high bombarding energies, so that the proposed sputtering mechanism should be dominant over the whole energy range. This result appears to be consistent with collision cascade theory if forward scattering is taken into account. (auth)

42554 ELECTRON MICROSCOPY OF IRRADIATION-INDUCED DEFECT CLUSTERS IN MAGNESIUM FLUORIDE. Barber, D. J. (Univ. of Essex, Colchester, Eng.). Phys. Status Solidi, 16: 531-47(1966).

The passage of electrons through thin crystals of magnesium fluoride produces point defects. These defects are mobile at temperatures normally attained under the electron beam, and they can give rise both to dislocation loops and to precipitate platelets. The aggregation of these radiation-induced defects can be controlled by using a cooled specimen stage in the electron microscope. This allows the growth and characteristics of the defect clusters to be studied. Dislocation loops lie on {011} planes and they sometimes show stacking fault contrast; their Burgers vectors are $\frac{1}{2}\langle 01\bar{1}\rangle$ and $\langle 01\bar{1}\rangle$. Prolonged irradiation can produce precipitates on and within the loops. Higher beam intensities produce precipitates directly. The nature of the loops and precipitates is discussed in relation to the production of point defects by ionization mechanisms and irradiation-stimulated migration. (auth)

42555 ELECTRICAL AND MAGNETIC PROPERTIES OF COLORED AND UNCOLORED CALCIUM FLUORIDE CRYSTALS. Ratnam, V. V. (Indian Inst. of Tech., Kharagpur). Phys. Status Solidi, 16: 549-57(1966).

The electrical and magnetic properties of uncolored calcium fluoride crystals and of specimens of these crystals colored by x rays and electrolysis are reported. The d-c conductivity and dielectric loss measurements of uncolored and x-ray colored CaF_2 crystals show that in a freshly prepared crystal the number of free negative ion vacancies is very small and the anti-Frenkel defects initially present are in the associated form. These points explain why, for irradiation at room temperature, the α-band (the F-band of this system) is not observed in optical absorption. The nature of the traps is also discussed in the context of the observed changes in the d-c conductivity accompanying the thermal bleaching of the color centers in an x-irradiated crystal. The temperature variation of the magnetic susceptibility indicates that x irradiation produces both paramagnetic and diamagnetic color centers. From the results of measurements on electrolytically colored crystals, the oscillator strength of the F-band is estimated as about 10^{-2}; this also explains why the formation of the α-band is not detected for room temperature x irradiation. (auth)

42556 COLOR CENTERS AND X-RAY LUMINESCENCE OF CALCIUM FLUORIDE CRYSTALS. Ratnam, V. V. (Indian Inst. of Tech., Kharagpur). Phys. Status Solidi, 16: 559-67(1966).

A study is made of differences in the coloration spectrum of calcium fluoride crystals obtained by x irradiation at different temperatures and by electrolysis. The changes occurring in the x-ray luminescence spectrum because of different irradiation temperatures are also considered. It is shown that the α- and β-bands, usually only observed in additive and electrolytic coloration, can also be produced by x irradiation if the irradiation temperature is between 180 and 250°C. The formation of the α-band (the F-band of this system) is difficult to detect at lower irradiation temperatures because of the small number of free negative ion vacancies at these temperatures and the low oscillator strength associated with this band. The changes observed in the x-ray luminescence spectrum for different irradiation temperatures are explained and the associated electronic processes are discussed briefly. (auth)

42557 NONRADIATIVE DESTRUCTION OF F CENTERS IN X-IRRADIATED KCl DOPED WITH ANIONIC IMPURITIES. Mukherjee, M. Ludwig; Bose, H. N. (Indian Inst. of Tech., Kharagpur). Phys. Status Solidi, 16: 591-8(1966).

A study is made of the thermoluminescent behavior and room temperature stability of F centers produced by x rays in KCl doped with some anionic impurities. A low percentage of KNO_3, KOH, and K_2CO_3 enhances the formation of F centers but a high percentage inhibits this formation. F centers in lightly doped samples stored in the dark and at room temperature are found to decay with time in two stages by some nonradiative processes. The thermo-

luminescence intensities of these samples are poor. In the case of KNO_3 doping, infrared absorption at 7.1 and 7.7 μm due to $(NO_3)^-$ and $(NO_2)^-$ ions decreases after irradiation by x rays suggesting decomposition of these complexes. It is suggested that the diffusion of decomposition products with trapped holes is responsible for the decay of F centers with time at room temperature. The activation energies for the diffusion processes are of the order of 0.98 and 1.05 ev in all the samples. With 1 mol % of KNO_3 doping, the F centers are almost undetectable. It is estimated that in this case the average distance between one nitrate or nitrite ion and an F center is of the order of 12 atomic units. (auth)

42558 MAGNETIC STRUCTURE OF SOLID OXYGEN. Collins, M. F. (Atomic Energy Research Establishment, Harwell, Eng.). Proc. Phys. Soc. (London), 89: 415-18 (1966).

Neutron powder patterns of solid α- and β-oxygen were taken. Comparison with x-ray and electron-diffraction patterns showed that α-oxygen is antiferromagnetic while β-oxygen is not. For the β phase there is strong evidence from the present neutron-diffraction data and from susceptibility measurements that the magnetic moments are not randomly aligned but that they exhibit short-range antiferromagnetic order. The magnetic structure of the α phase is commensurate with the lattice since the two observed magnetic lines have d spacings of twice the value for the nuclear lines, but the absence of an established atomic structure precludes detailed discussion of the magnetic order. (auth)

42559 SPIN-WAVE STIFFNESS AND ELECTRONIC STRUCTURE OF IRON–ALUMINUM AND IRON–GALLIUM ALLOYS. Antonini, B.; Stringfellow, M. W. (Atomic Energy Research Establishment, Harwell, Eng.). Proc. Phys. Soc. (London), 89: 419-26(1966).

The spin-wave stiffness D of a series of ferromagnetic iron–aluminum and iron–gallium alloys was measured by the neutron small-angle scattering technique. The experimental results were compared with the predictions of both a localized moment model and a simple band model, and it is found that both models were in fair agreement with the experimental measurements. The results of the fit to the band model suggest that in the iron–aluminum alloys the aluminum does not donate electrons to the 3d band of the alloy, while in the iron–gallium alloys each gallium atom contributes about one electron, which enters predominantly the spin-up sub-band. (auth)

42560 MAGNETIC STRUCTURE OF URANIUM MONOPHOSPHIDE. Curry, N. A. (Atomic Energy Research Establishment, Harwell, Eng.). Proc. Phys. Soc. (London), 89: 427-9(1966).

The magnetic structure of uranium monophosphide was determined by neutron diffraction, and shown to be the same as that of the mononitride. At 4°K the magnetic moment on a uranium ion is about 1.9 Bohr magnetons. The intensity of the strongest magnetic reflection shows a fairly abrupt change at about 30°K. (auth)

42561 A SIMPLE MODEL FOR DE-EXCITATION CURVES OF Ag-DOPED NaCl. Ruiz Mejia, Carlos (Univ. Nacional de Mexico). Rev. Mex. Fis., 15: 201-13 (1966). (In Spanish).

NaCl single crystals Ag-doped were irradiated with x rays at 40 kv. The de-excitation curves were determined and qualitatively explained by means of a simple luminescence model. The model was based on the assumption that a metastable level is created in the forbidden band of the NaCl electronic structure due to the presence of the silver ions. (auth)

42562 MECHANISM OF FORMATION OF M AND R CENTERS. Farge, Y.; Lambert, M.; Smoluchowski, R. (CNRS, Orsay, France). Solid State Commun., 4: 333-6 (July 1966). (In French).

The mechanism of M center formation ($\alpha + F \rightarrow F_2^+$ and $F_2^+ + e \rightarrow M$) was studied in LiF. A similar mechanism is proposed for the formation of R centers. (tr-auth)

42563 STABILITY AND PRODUCTION OF R′ CENTERS IN LITHIUM FLUORIDE. Hughes, A. E. (Atomic Energy Research Establishment, Harwell, Eng.). Solid State Commun., 4: 337-9(July 1966).

The effect of magnesium impurities on the thermal stability of an irradiation-induced color center in LiF is described. Measurements of the splitting of a zero-phonon line at 8328 Å under uniaxial stress show that the center has trigonal symmetry. These results and evidence for the production of these defects by conversion from R centers support the identification as an R′ center. (auth)

42564 EFFECT OF X-RAY IRRADIATION ON SOME PROPERTIES OF LITHIUM FLUORIDE SINGLE CRYSTALS. Golubeva, L. A.; Pchelinskaya, S. N.; Smiryagina, S. A.; Shishelov, A. A. (Kalinin State Univ., Leningrad). Soviet Phys.-Solid State (Engl. Trans.), 8: 546-8(Sept. 1966).

Translated from Fiz. Tverd. Tela, 8: 680-3(Mar. 1966).

The relationship between changes in the unit-cell volume of LiF crystals and the appearance in the cells of processes changing the dielectric losses is investigated. The change in lattice size was achieved by x irradiation and was measured by the change in density. The experiments conducted showed that when the irradiation dose was increased, the crystal lattice constant increased and tan δ changed. (auth)

42565 RECOMBINATION RADIATION OF α-SiC DUE TO ELECTRON BOMBARDMENT. Basov, N. G.; Bogdankevich, O. V.; Devyatkov, A. G. (Lebedev Inst. of Physics, Moscow). Soviet Phys.-Solid State (Engl. Trans.), 8: 643-4(Sept. 1966).

Translated from Fiz. Tverd. Tela, 8: 802-4(Mar. 1966).

Some results are reported of an investigation at low temperatures of the recombination radiation of α SiC excited by a beam of fast electrons. (auth)

42566 ELECTRON-NUCLEAR DOUBLE RESONANCE OF F CENTERS IN KCl AT ROOM TEMPERATURE (FIRST AND SECOND COORDINATION SPHERES). Deigen, M. F.; Ruban, M. A.; Gromoboi, Yu. S. (Inst. of Semiconductors, Academy of Sciences, USSR). Soviet Phys.-Solid State (Engl. Trans.), 8: 662-5(Sept. 1966).

Translated from Fiz. Tverd. Tela, 8: 826-31(Mar. 1966).

The angular variation of the electron-nuclear resonance (ENDOR) frequencies of F centers in KCl was investigated at room temperature for ions of the first and second coordination spheres surrounding the vacancy. The quadrupole triplet resolution for the first and second coordination spheres was obtained for various orientations of the crystal with respect to the external steady magnetic field. The contact and dipole-dipole hyperfine interaction constants as well as the quadrupole interaction constant were determined. (auth)

42567 CONCERNING THE NATURE OF THE IMPERFECTIONS PRODUCED IN DISLOCATION-FREE Si BY FAST-NEUTRON IRRADIATION. Kushnir, S. Kh.; Nikolaeva, L. G. (Inst. of Physics, Kiev). Soviet Phys.-Solid State (Engl. Trans.), 8: 790-1(Sept. 1966).

Translated from Fiz. Tverd. Tela, 8: 982-4(Mar. 1966).

Pure homogeneous n-type Si having a dislocation density of 1 to 2 cm^{-2} was irradiated in a reactor at about 70°C. The intensity of the anomalous transmission of x rays through the sample was measured on a double crystal spectrometer. Results indicate that irradiation by 1.4×10^{18} fast neutrons/cm^2 partially removed defects previously present in the crystal. (A.G.W.)

42568 PARTICLE WAVES AND DEFORMATION IN CRYSTALLINE SOLIDS. Fitzgerald, Edwin R. New York, Interscience Publishers, 1966. 258p. $11.95.

Wave mechanical calculations are described for macroscopic mechanical quantities such as transition velocities, non-elastic resonance frequencies, coefficients of sliding friction, and characteristic stresses. The calculations are made directly from a knowledge of Planck's constant, atomic mass, lattice spacing, and measured sound velocity. A modified wave-mechanical view is described, and some

of its far-reaching consequences are surveyed. In particular, an explanation of particle diffraction by crystals, an interesting relation between lattice dissociation energy and a mean elastic sound velocity, and the concept of a particle-wave oscillator are described. (M.O.W.)

42569 EFFECTS OF ORIENTATION AND ANNEALING ON JC VS. H. IN COLD-WORKED Nb–25% Zr. Rothwell, W. S.; Lindquist, P.; Rowcliffe, D. J. (Lockheed Research Labs., Palo Alto, Calif.). 17p. (CONF-660411-25). ORAU. Gmelin, AED-CONF-66-060-55.

From American Physical Society Meeting, Washington.

Critical current measurements were made on commercial Nb–25% Zr in the as-rolled condition and for four different anneals of 3 hr each at 500, 700, 850, and 1000°C. Curves show critical current vs. magnetic field (0 to 50 kG) for all relative orientations of rolling direction, current, and applied field. In general the level of the critical current increases from the as-rolled sample to a maximum for the 700 or 850°C samples and then decreases with the 1000°C sample. Comparison with structure studies indicates that maximum currents are sustained in the annealed specimens where the current anisotropy is removed and the laminar structure is replaced by a homogeneous precipitate. (A.G.W.)

42570 MOESSBAUER STUDIES OF RARE EARTH INTERMETALLIC COMPOUNDS. Nowik, I. (Bell Telephone Labs., Inc., Murray Hill, N. J.). 27p. (CONF-660113–4). ORAU. Gmelin, AED-CONF-66-058-4.

From Moessbauer Symposium, New York.

Recent Mössbauer studies of rare earth intermetallic compounds are reviewed. The usefulness of the Mössbauer effect in studying the magnetic and chemical properties of the intermetallics is demonstrated by a few examples. The various contributions to the magnetic hyperfine field acting on rare earth nuclei are discussed. In dysprosium intermetallic compounds except those containing Fe and Co the free ion hyperfine field is observed. In RFe_2 (R = Gd, Tb, Dy, Er, Tm) compounds conduction electrons contribute about 800 kOe to the magnetic hyperfine field. In divalent europium intermetallic compounds the magnetic hyperfine field is mainly due to core and conduction electron polarization. A correlation might exist between the magnetic hyperfine field and the isomeric shift in divalent Eu compounds. The validity of the existing theory of isomeric shifts was confirmed by the Mössbauer studies of the europium isotopes ^{151}Eu and ^{153}Eu. (auth)

42571 MEASUREMENT OF MAGNETIC FIELD DISTRIBUTIONS. Trousdale, William L.; Song, Cheng Jyi; Longworth, Goeffrey (Wesleyan Univ., Middletown, Conn.). 12p. (CONF-660113–2). ORAU. Gmelin, AED-CONF-66-058-1.

From Moessbauer Symposium, New York.

In situations where there is a large spread in hyperfine fields, the Mössbauer method provides a unique tool in the determination of this spread. An example of such a case is the hyperfine field distribution at iron nuclei in the ferromagnetic Fe–Pd alloys in the vicinity of the transition temperature. In 13.2 Fe–86.8 Pd, the iron atoms are assumed to be randomly distributed in the f.c.c. Pd structure. The important fractures of the Mössbauer spectra for this alloy are illustrated. A simple cluster model based on a molecular field calculation which relates the measured Mössbauer spectra to a magnetization distribution is presented. (W.D.M.)

42572 MOESSBAUER EFFECT IN GOLD MICROCRYSTALS. Marshall, S. W.; Wilenzick, R. M. (Tulane Univ., New Orleans). 11p. (CONF-660107–54). ORAU. Gmelin, AED-CONF-66-003-115.

From American Physical Society Meeting, New York.

Small crystals have phonon spectra different from the bulk solid for two reasons: long-wavelength phonons can not be sustained in small crystals and a large fraction of the atoms reside on the surface. Within the Debye continuum framework, a suitable phonon distribution function containing surface modes must be cut off at both a low-frequency and a high-frequency limit. An expression was derived for the recoilless fraction of gamma absorptions based on such a distribution function. The magnitude of the Mössbauer effect is thus a function of crystal size. The 77-kev Mössbauer transition in ^{197}Au was studied in gold microcrystals of 60 and 200 Å in diameter grown in a hydrosol and bound in gelatin. Measurements were made from 4.2 to 63°K while the platinum source was maintained at 4.2°K. These measurements indicate that the surface of the crystals are loosely bound to the gelatin and they yield characteristic temperatures of 8 and 163°K, and 23 and 173°K, respectively. These values are to be compared to 0 and 173°K found for a gold foil. (auth)

42573 REVIEW OF EXPERIMENTAL MEASUREMENTS OF LATTICE MODES IN TRANSITION METALS. Woods, A. D. B. (Atomic Energy of Canada Ltd., Chalk River, Ont.). 29p. (CONF-650932–5). ORAU. Gmelin, AED-CONF-65-292-2.

From Symposium on the Inelastic Scattering of Neutrons by Condensed Systems, Upton, N. Y.

A study was made of normal modes of vibration of crystalline lattices in transition metals using inelastic neutron scattering. Information concerning electron-phonon interactions is presented. Measured phonon dispersion curves are included for the group V and VI transition metals, and in particular for niobium and molybdenum and for alloys of these with one another. The results indicate that: (1) the phonon dispersion curves for these metals are dependent upon the details of the electronic structure acting through a strong electron-phonon interaction, (2) disordered alloys of these metals have a characteristic electronic band structure and phonon structure analogous to those for pure metals, and (3) the rigid band model is a reasonable approximation for this system. (J.H.M.)

42574 IMPULSE APPROXIMATION APPLIED TO ASSISTED FOCUSING. Weijsenfeld, C. H. (Univ., Utrecht). 14p. (CONF-640710–1). ORAU.

From Symposium on Atomic Collision Cascades in Radiation Damage, Harwell, Eng.

When a lattice atom in an f.c.c. crystal receives an impulse in a near ⟨100⟩ direction, it has to travel through a square consisting of four nearest neighbor atoms before hitting the next atom in the ⟨100⟩ row. An elaborate impulse approximation is shown to give a good agreement with machine calculations, if one is aware of the fact that the neighboring atoms are free, i.e., not bound to their lattice site for this sort of glancing collisions, as was wrongly assumed in earlier work. (M.O.W.)

42575 USE OF PRECISE SCHOTTKY DATA IN THE DETERMINATION OF THE SURFACE CHARACTERISTICS OF RHENIUM EMITTERS. D'Haenene, I. J.; Coomes, E. A. (Univ. of Notre Dame, Ind.). 9p. (CONF-660328–5). ORAU. Gmelin, AED-CONF-66-049-10.

From 26th Annual Conference on Physical Electronics, Cambridge, Mass.

The nature of the surface barrier in Re was studied through the Schottky effect. The two expected departures from Schottky linearity were found: the first order sigmoidal break caused by patches; and the second order periodic deviations, which are due to multiple reflection of emitted electrons traversing the surface barrier. Precise Schottky data taken on polycrystalline filaments in a coaxial Langmuir diode gave the following results: Richardson work function $e\phi_R = 4.856 \pm 0.015$ ev, and emission content $A_R = 57.16 \pm 0.33$ A/(cm°K)^2. The experimental periodic deviations were essentially coincident with those found for W, Mo, and Ta. In addition, the predicted (1/T) dependence of the periodic deviation amplitude was well confirmed. The experimental periodic deviations were found to be consistent with the Sommerfeld model for a $W_s \approx 22$ ev. By depositing fractional monolayer amounts of Mo on a pure Re filament, the Richardson work function was systematically changed from 4.86 to a minimum of 4.1 ev. Although large changes were found in A_R, no significant changes appeared in the periodic deviations. (auth)

REACTOR TECHNOLOGY

General

Refer also to abstract 41109.

42576 (AHSB(S)–R-107) SAFETY OF PRESSURE VESSELS AGAINST FAST FRACTURE. Irvine, W. H.; Bevitt, E.; Quirk, A. (Authority Health and Safety Branch, United Kingdom Atomic Energy Authority, Risley (England)). 1966. 13p. Dep. BIS $0.60. HMSO 3s. 0d.

The historical background of the UKAEA's present research programme on cyclic crack growth and fast fracture in pressure vessels is given and the significance and application of the experimental results from this programme in relation to reactor safety discussed. An outline is given of the direction of future work. (auth)

42577 (ANL–7230) REACTOR DEVELOPMENT PROGRAM PROGRESS REPORT, JUNE 1966. (Argonne National Lab., Ill.). June 1966. Contract W-31-109-eng-38. 96p. Dep. mn. CFSTI $3.00 cy, $0.75 mn.

Items of significant technical progress which have occurred in the specific reactor projects and the general engineering research and development programs are reported. Operation of the EBR-II, fast reactor physics, fuel development and reprocessing, and Na technology are described for the liquid metal cooled reactor program. Work under the general reactor technology program includes studies of theoretical reactor physics, high temperature materials, fuels and materials, engineering, chemical separations, and the Plutonium Recycle Experiment. The Argonne Advanced Research Reactor and Liquid Metal Fast Breeder Reactor development is reported. Nuclear safety studies include reactor kinetics, TREAT operations, energy transfer problems in reactor safety, and Pu volatility experiments. (H.D.R.)

42578 (ANL–7245) REACTOR DEVELOPMENT PROGRAM PROGRESS REPORT, JULY 1966. (Argonne National Lab., Ill.). Aug. 26, 1966. Contract W-31-109-eng-38. 81p. Dep. mn. CFSTI $3.00 cy, $0.75 mn.

Separate abstracts were prepared for the four included sections. (H.D.R.)

For abstracts of individual sections see: 42579, 42580, 42619, and 42670.

42579 (ANL–7245, pp 29-47) GENERAL REACTOR TECHNOLOGY. (Argonne National Lab., Ill.).

A method for computing effective resonance cross sections for epithermal energies is under development for application to the ARC system. Fuels and cladding materials development includes Th–U–Pu alloys, heat content of U–15 wt % Pu-6.5 wt % Ti alloy, mechanical properties of UO_2, Gd_2O_3 evaporation, U–S–O system properties, Ta corrosion in Li at high temperatures, and irradiation testing of ceramic fuel materials. The status of cladding materials being irradiated in EBR-II is tabulated. A neutron image-intensification system was tested and measurements were made on the thermal properties of irradiated AARR fuel plates. High-temperature mechanical properties were measured for V-15 wt % Ti-7.5 wt % Cr alloy. Master-slave manipulator systems and high-temperature instrument development are described, and processes for the recovery of U and Pu from low-enrichment fuels are examined. (H.D.R.)

42580 (ANL–7245, pp 60-73) NUCLEAR SAFETY. (Argonne National Lab., Ill.).

Fast reactor oxide fuel pins irradiated in TREAT were analyzed for burnup and transient fuel-clad interface temperatures were calculated. A failure analysis was performed on the meltdown experiment of an EBR-II Mark-I fuel pin in a TREAT flowing sodium loop. Materials behavior, equation of state, and energy transfer studies included a series of temperature drop experiments in water using a small nickel sphere attached to a swinging arm. A computer program was written to evaluate the data obtained with the swinging-arm apparatus, and heat transfer coefficients and heat fluxes were calculated. TREAT operations and tellurium fluoride chemistry are summarized. (H.D.R.)

42581 (ORNL–3875, pp 125-50) REACTOR INSTRUMENTATION AND CONTROLS. (Oak Ridge National Lab., Tenn.).

A progress report is presented on reactor instrumentation and control. Topics included are component development, analysis, theoretical and experimental investigations, control and instrument systems engineering, training and methods, in-pile irradiation, and MSRE project instrumentation. (B.G.D.)

42582 (WAPD-TM–534) FLASH: A PROGRAM FOR DIGITAL SIMULATION OF THE LOSS OF COOLANT ACCIDENT. Margolis, S. G.; Redfield, J. A. (Bettis Atomic Power Lab., Pittsburgh, Pa.). May 1966. Contract AT-11-1-GEN-14. 106p. Dep. mn. CFSTI $4.00 cy, $0.75 mn.

FLASH is a digital program which calculates flows, inventories, pressures and temperatures in the primary system during a loss-of-coolant accident. Starting with calculations of the rate of coolant efflux through assumed leaks, it calculates inflow from the fill system, inventory of water above and below the core, pressure drop across the core, flow through the core and loops, neutron and gamma heating in the fuel, and heat transfer from the fuel to the coolant. It calculates the fuel temperatures in both the hot and average channels of the core. Thus it provides a direct measure of the effectiveness of the system design and operating procedures in preventing fuel melting. (auth)

42583 (WAPD-Trans–34) ARRANGEMENT FOR DETECTING THE STICKING OF AN ARMATURE TO A MAGNET. Lang, Walter Translated for Bettis Atomic Power Lab., West Mifflin, Pa., from German Patent S97782. 8p. Dep. mn. JCL $1.10 fs, $0.80 mf.

A magnetic-field-responsive switching element is arranged in the magnet so that it is traversed by the leakage flux when the armature is released. Means are provided to concentrate the leakage flux on the switching element, which operates a signal or control circuit. (H.D.R.)

42584 METEOROLOGICAL MANUAL FOR REACTOR SAFETY ANALYSES. REPORT FROM THE SPECIAL COMMITTEE ON REACTOR SAFETY STANDARDS. Nippon Genshiryoku Gakkaishi, 10: No. 11, 2-17(Nov. 1965). (In Japanese).

Meteorological points in reactor safety analyses are dealt with on the basis of experiences gained in the past for large reactors. It consists of the following: meteorology for supposed reactor accidents (primary considerations, site considerations, examples of meteorological evaluations, diffusion equations, and selection of diffusion parameters), meteorology for normal reactor operation (diffusion process, standards, meteorology and radiation doses, and countermeasures), and items of observation and investigation. The appendixes include a guide for reactor site evaluations, diffusion equations, results of investigation for Tokai-mura, MPC and submersion, circumferential monitoring areas and radiation control areas, radiation doses from radioactive clouds, and experiments at JRR-2. (NSA of Japan)

Auxiliaries and Components

Refer also to abstract 41360.

42585 (ORNL–3875, pp 151-8) INSTRUMENTATION FOR REACTOR DIVISION TEST LOOPS. (Oak Ridge National Lab., Tenn.).

A progress report is presented on instrumentation for reactor division test loops at ORNL. Topics discussed are liquid-metal jet-pump test loop; instrumentation for po-

tassium loops, SNAP-50 corrosion loop, SNAP-8 corrosion loop, niobium-1% zirconium loop, pressurized water loop; and instrumentation for the intermediate water system. (B.G.D.)

42586 PRESSURE-APPLIED PROCESS FOR POURING HEAVY CONCRETE TO CONSTRUCT REACTOR SHIELDS. Fukuda, Otoji; Kimura, Keizo (Kajime Inst. Construction Tech., Japan). Kashima Kensetsu Gijutsu Kenkyusho Nenpo, No. 13, 275-85(Jan. 1965). (In Japanese).

The described construction was carried out in 1963 using 120 m^3 of concrete aggregate and 92 m^3 of barytes. The concrete mixer and its associated mortar pumps were installed close to the site of construction 10 meters above ground to prevent possible danger. The distribution of barytes pieces was carefully controlled to give as high a specific gravity as possible. To keep the mortar fluid and uniform during the process, the feeding rate was maintained to a suitable value. (NSA of Japan)

42587 IMPROVEMENTS IN CONTROL RODS FOR NUCLEAR REACTORS. Raievski, Victor (to EURATOM). British Patent 1,031,992. June 8, 1966. Priority date May 11, 1962, Italy.

A design is provided in which the cross section of the rod can be varied to provide uniform modification of the reactor reactivity. The rod may be formed of two or more elements slidable telescopically and may be individually or collectively withdrawn. Alternatively, the rod may be formed of sheet material bent to open cylindrical form which is wound to form a spiral, as viewed along the axis of the rod, to reduce the transverse dimensions of the rod. (B.L.M.)

42588 IMPROVEMENTS IN NUCLEAR REACTORS. Campbell, John William Edmund (to Babcock and Wilcox Ltd.). British Patent 1,036,896. July 20, 1966. Filed Apr. 29, 1963.

In a nuclear reactor arranged to be moderated by a liquid of which either the hydrogen or deuterium serves to effect the moderation, the fuel elements are arranged in a square array defining cruciform gaps to house cruciform control rods and followers for the control rods. The control rod and follower are dimensioned to afford a gap between the control rod and fissile material at the boundary of the space in which the control rod and follower are movable larger than the gap between the follower and the fissile material at the boundary. The gap between the control rod and the fissile material at the boundary of the space is so chosen that with the control rod inserted peaking of the thermal neutron flux adjacent to the control rod is substantially the same as that which occurs when the follower is in a position adjacent to the fuel element. (B.L.M.)

42589 IMPROVEMENTS IN AND RELATING TO ARTICULATED SUPPORTS. Bradshaw, Arthur Jeffrey; Robinson, John Albert (to Nuclear Power Plant Co. Ltd. A.E.I.-John Thompson Nuclear Energy Co. Ltd.). British Patent 1,037,606. July 27, 1966. Filed Oct. 9, 1964.

An articulate support design is described that is particularly concerned with a support for reactor guide tubes, and in its preferred form the support uses graphite wedge shaped blocks but the invention is not limited to this material. The support is applicable between two members each having a substantially plane annular supporting face with the supporting face of one member being similar to and disposed opposite to the supporting face of the other member. The supporting faces of the two members are spaced apart to provide annular space between the faces in which a number of the wedge shaped graphite blocks are arranged substantially in a single layer. The layer of supporting blocks comprises two opposing sets of an equal number of blocks with the blocks of each set being interposed between and in wedging engagement with the blocks of the other set. One set of blocks provides supporting contact substantially uniformly over the supporting face of one member, and the other set of blocks over the supporting face of the other member. Various embodiments of the general design are described in detail. (B.L.M.)

42590 NUCLEAR REACTOR. Cooke, Brian Frederick; Sutherland, Donald Mason (to Nuclear Power Plant Co. Ltd. A.E.I.-John Thompson Nuclear Energy Co. Ltd.). British Patent 1,037,841. Aug. 3, 1966. Filed Jan. 16, 1964.

An arrangement is described for providing access to the core of a graphite moderated gas-cooled reactor by means of passages opening through the concrete pressure vessel wall. The part of the vessel wall in which the passages are located has part of its outer surface enclosed by a further wall structure located opposite the pressure vessel wall. The enclosing wall is comprised of a metallic grid structure supporting on the side remote from the reactor core a floor comprised of prestressed concrete slabs and slabs of radiation-absorbing material. The metallic grid structure provides support for auxiliary components for the reactor and the enclosure defined by the further wall may include a door to permit an operator to enter the enclosure. A charging machine for the reactor moves over the surface formed by the radiation-absorbing material slabs and is connected to any selected standpipe by removing a slab opposite the standpipe and inserting a guide tube between the charge machine and the standpipe. (B.L.M.)

42591 CONTROL RODS. Dee, John B. Jr. (to General Dynamics Corp.). U. S. Patent 3,255,092. June 7, 1966. Filed Mar. 24, 1961.

An elongated reactor control rod is composed of several interchangeable parts or regions of neutron absorbing material and is suitable for use in different reactors with various parameters. A number of neutron-absorbing portions of predetermined geometric shape are arranged in the desired manner transversely across the control rod. Each portion contains a burnable poison, and the concentrations of the poisons vary between the portions. The varying concentrations are so selected and arranged that the effective neutron-absorbing cross-sectional area of the rod decreases in a programmed manner as a result of the burnout inward from the exterior of the rod. The various regions are arranged in concentric shells of different diameters nested one within the other; the nests of shells are disposed in vertically stacked relation; and the entire unit is contained within a stainless steel can with stainless steel spacers between adjacent units. (B.L.M.)

42592 IMPROVEMENTS IN OR RELATING TO NUCLEAR REACTOR INSTALLATIONS. Villadsen, Peter Mogens (to Aktieselskabet Burmeister and Wain's Maskin- og Skibsbyggeri). British Patent 1,034,375. June 29, 1966. Priority date Sept. 20, 1962, Denmark.

An installation for taking care of the pressure of vapor released from the rupture of a pressurized liquid circuit associated with a nuclear reactor includes a shell defining an outer containment, a reactor with the pressurized liquid circuit located within the containment, and wholly or partially liquid-filled condenser elements within the containment arranged so that the vapor from the reactor is forced to flow around the elements before impinging upon the shell. The condenser elements are located in one or more ducts that connect the reactor chamber with a separate chamber for receiving the escaping vapor and entrained air. The inlet and outlet openings of the duct are closed with diaphragms which are dimensioned to be broken at a small pressure difference. The ducts are normally closed, contain an inert gas, and have a water-absorbent medium, such as silica gel, disposed within them. (B.L.M.)

42593 IMPROVEMENTS IN OR RELATING TO MANIPULATING DEVICES FOR USE IN NUCLEAR REACTORS. Dodd, John Alan; Timbs, Arthur Edwards; Montgomery, Albert George (to United Kingdom Atomic Energy Authority). British Patent 1,034,866. July 6, 1966. Filed Mar. 25, 1963.

A manipulating device suitable for use as a refueling device for a nuclear reactor comprises a structural support member made up of a pillar having a support and locating means at its lower end and an assembly engaging member with means for extending the assembly engaging laterally outwardly from and retracting it inwardly toward

the structural support member. The engaging member has a lifting fork adapted to engage the lower end region of an assembly and releasable securing means for securing the upper end of an assembly. The device is particularly useful in refueling reactors not having a fixed moderator, for example, high temperature gas-cooled reactors using fuel units of moderator and fuel, fast reactors, and liquid-cooled reactors without permanent structural members in the core. (B.L.M.)

42594 CORE STRUCTURES FOR NUCLEAR REACTORS. Oliver, John (to Nuclear Power Plant Co., Ltd. A.E.I.-John Thompson Nuclear Energy Co. Ltd.). British Patent 1,034,941. July 6, 1966. Filed Mar. 6, 1964.

A solid moderator core structure for a nuclear reactor comprises an assembly of blocks of the moderator material having channels for fuel elements in the blocks. Interstitial blocks are located in spaces defined between laterally adjacent fuel channel-containing blocks. Cooling channels for the flow of cooling fluid are defined between the walls of laterally adjacent fuel channels-containing blocks and the interstitial blocks. Several embodiments of the general core design are described in detail. (B.L.M.)

42595 IMPROVEMENTS IN OR RELATING TO LIQUID MODERATED NUCLEAR REACTORS. Gratton, Charles Peter; Russell, Albert Henry; Lloyd, Albert Ivor (to Societe Anglo-Belge Vulcain SA). British Patent 1,032,396. June 8, 1966. Filed Nov. 19, 1962.

A core design for a liquid moderator reactor, particularly a pressurized water reactor, includes a cellular core lattice having a series of slots in the core arranged sequentially across the core so as to define at least one fuel free slab shaped zone penetrating the core. Control absorbers comprising one or more open ended hollow members of neutron absorbing material can be moved in the slots and are adapted to enclose liquid moderator when entered into the core. (B.L.M.)

42596 PRESSURE VESSELS. Barrett, Norman Thomas (to United Kingdom Atomic Energy Authority). British Patent 1,033,055. June 15, 1966. Filed May 25, 1962.

A prestressed concrete pressure vessel for a nuclear reactor defines a chamber which is at least part spherical or part spheroidal, and that part of the vessel that bounds the part spherical or spheroidal region is braced by a structure of tensioned tendons that are disposed in a lattice-work arrangement derived of two or more geodetic systems of which the poles are co-planar. The vessel is made up of a number of stressed panels. (B.L.M.)

42597 IMPROVEMENTS IN OR RELATING TO NUCLEAR REACTORS. Hackney, Stanley (United Kingdom Atomic Energy Authority). British Patent 1,038,087. Aug. 3, 1966. Filed Dec. 20, 1961.

Simplified shut-down facilities are described for a water cooled reactor in which the heat producing core includes fuel elements with a circulatable fluid heat transfer medium that is present as an intermediary between the fuel elements and the reactor coolant medium in a circuit separate from the coolant medium. The shut-down facilities include a valve through which the coolant medium is expelled to a degree to render the reactor non-reactive and means to check the expulsion to leave a pool of coolant of a depth such that the heat transfer medium continues in heat transfer relation with the pool. (B.L.M.)

42598 CORE ACCESS ASSEMBLY FOR NUCLEAR REACTORS. Pearson, Robin (to Nuclear Power Plant Co., Ltd. AEI-John Thompson Nuclear Energy Co., Ltd.). British Patent 1,035,631. July 13, 1966. Filed Nov. 3, 1964.

A multi-channel core access assembly is provided for a nuclear reactor of the type in which a neutron absorbing material is housed in a pressure vessel and in which the fuel in containers is located in channels in the core. The access assembly comprises guide passages extending from a group of fuel channels and merging into a single passage adjacent to the vessel walls. A single guide passage passes through the vessel wall or is connected to a duct in the vessel wall. The fuel elements in each channel are linked together and have an attached connecting member which passes through the guide passage from the channel and passes together with connecting members from other channels of the group through or into the duct in the vessel wall. The portions of connecting members lying within the single guide passage have a cross section such that space is provided to permit the passage of fuel elements, control rods, or the like. Each member has a flexible portion that may be either a bellows or a hinge at intervals along its length. Alternatively, the guide passages may terminate at a distance from the vessel wall, and a removable chute may be provided to connect the guide passages and the duct in the vessel wall. (B.L.M.)

Criticality Studies

Refer also to abstracts 41188, 42653, and 42674.

42599 (UJV–1424) SROVNANI TEORETICKEHO VYPOSTU LAPLASIANU MRIZE TEZKOVODNIHO REAKTORU S MERENIM NA KRITICKEM SOUBORU. (Comparisons of Theoretical Laplacian of Heavy-Water Reactor Lattice With the Measurements of the Critical Assembly). Sulc, P. (Ustav Jaderneho Vyzkumu, Ceskoslovenska Akademie Ved, Rez). 1966. 32p. Dep. mn.

A comparison between the calculated and measured Laplacian of a heavy water gas-cooled lattice cell with natural U fuel is given. The method of the correlation of the program PARAMETRY II is discussed together with the deficiencies of the calculational method. An estimate of the influence of incorrect values of some physical constants and geometrical characteristics on the Laplacian is made. In the conclusion some recommendations concerning the improvement of the calculational method are added and attention is devoted to necessary extension of the experimental material. (auth)

42600 CORRELATION OF TWO-GROUP THEORY WITH NEUTRON FLUX MEASUREMENTS IN A POOL-TYPE REACTOR. Coppersmith, W. C.; Meem, J. L. (Univ. of Virginia, Charlottesville). J. Nucl. Energy: Pt. A and B, 20: 635-48(Aug. 1966).

A method for determining reactor system parameters that employs a compilation of two-group theory and detailed flux measurements is presented. Application of the semi-empirical procedure is illustrated for the University of Virginia pool-type reactor, loaded to approximate two-region cylindrical geometry. Measurements were made of the fast and thermal fission-producing fluxes, using highly enriched U foils, both bare and Cd covered. The equivalent bare axial and radial components of the buckling were determined from the measurements, giving the principal buckling, μ^2. The related slowing down area, L_1^2, was adjusted so as to make two-group theory fit the experiment. The best value for the slowing-down area in the 0.40 Al-to-water mixture was found to be 42.5 cm^2 equivalent to an age of 38 cm^2. The slowing-down area in the water reflector was found to be 25.5 cm^2, in fair agreement with fission-to-thermal age measurements reported in the literature. (auth)

42601 PSEUDO-EXPONENTIAL DECAY OF A NEUTRON PULSE IN SMALL BERYLLIUM SYSTEMS. Wood, J. (Univ. of Birmingham, Eng.). J. Nucl. Energy: Pt. A and B, 20: 649-57(Aug. 1966).

The decay of a neutron pulse in Be is studied by solving, numerically, the homogeneous Boltzmann equation and fitting the amplitudes to an instantaneous slowing down source. The kernel used is the multi-phonon expansion, with a Debye phonon frequency distribution. It is found that for $B^2 < 0.033$ cm^{-2}, the neutron evolution is soon dominated by a single, exponentially decaying mode; but for $B^2 > 0.033$ cm^{-2}, it is likely that only a continuous spectrum of eigenvalues exists. However, this continuum exhibits an almost exponential behavior and is interpreted as possessing an effective decay constant. This effective decay constant is compared with experimental values, for

B^2 up to 0.1 cm^{-2}, and is suggested as an explanation of those measured decay constants which exceed $[\nu\Sigma]_{min}$. (auth)

Design and Feasibility

Refer also to abstracts 42588, 42591, and 42614.

42602 METHOD OF INCREASING THE SURFACE AREA OF A BOILED LIQUID AND IMPROVED NUCLEAR REACTORS EMBODYING THE METHOD. Lindstrom, Olle (to Allmanna Svenska Elektriska Aktiebolaget). British Patent 1,036,006. July 13, 1966. Filed Feb. 28, 1963.

A method for increasing the surface area of a boiling liquid surface comprises placing in the liquid surface one or more hollow screens opening downwardly into the liquid. Each screen is provided with holes or openings having a cross-sectional area, which, in the main, decreases in the upward direction. Each screen is so arranged that it is substantially covered by the boiling liquid surface, and the interior of the screen is filled by the boiling liquid. A flow of liquid-vapor mixture occurs outwardly through the holes of the screen. This method is applicable to either homogeneous or heterogeneous reactors containing a boiling coolant such as heavy and/or light water. (B.L.M.)

42603 IMPROVEMENTS IN OR RELATING TO NUCLEAR REACTORS. Taylor, Anthony James; Hawkins, Ronald James (to Babcock and Wilcox Ltd.). British Patent 1,036,883. July 20, 1966. Filed Oct. 31, 1961.

A design for a gas-cooled reactor is provided that includes support means for the core, heat exchanger, and neutron shield and that permits free or substantially free thermal expansion and contraction of the supporting means within the pressure vessel. The support means includes members in the form of rockable columns passing downwardly and extending through apertures in the pressure vessel. Sealing means include resilient sections, such as annular bellows members encircling the columns, adapted to permit relative movements between the columns and the pressure vessel due to differential thermal expansion and to seal the gaps between the apertures in the pressure vessel and the support members. Circulator means are arranged to circulate coolant through the core and heat exchangers as well as through the support means. (B.L.M.)

42604 IMPROVEMENTS IN GAS-COOLED NUCLEAR REACTORS. Taylor, Anthony James; McCabe, Terence Ivor (to Babcock and Wilcox Ltd.). British Patent 1,036,884. July 20, 1966. Filed Oct. 31, 1961.

A gas-cooled reactor includes the following parts: a core enclosed within a neutron shield, a steel pressure vessel enclosing the neutron shield, a heat exchanger located between the pressure vessel and the neutron shield, coolant circulating means for circulating the coolant sequentially through the core and over the heat exchanger, and a biological shield enclosing the pressure vessel. The heat exchange means includes individually closable passages that extend beneath the neutron shield and include part of the heat exchanger. The passages are adapted to discharge into a space contained in the pressure vessel, and a circulator disposed beneath the neutron shield is arranged to circulate coolant from the space in the pressure vessel upward through the core. As an alternative arrangement, a baffle wall may be disposed between the neutron shield and the pressure vessel with the passages lying between the baffle wall and the neutron shield so that the circulator withdraws coolant from between the baffle wall and the pressure vessel and returns coolant to the core through a shaft lying in the baffle wall. (B.L.M.)

42605 IMPROVEMENTS IN OR RELATING TO NUCLEAR REACTORS. (to Osterreichische Studiengesellschaft fur Atomenergie G.m.b.H.). British Patent 1,036,935. July 20, 1966. Priority date Aug. 4, 1962, Austria.

A nuclear reactor of the type in which the fission zone is occupied by a mass of active particles is described that provides for the actual changing of the volume of the reaction zone to prevent the lifting of the particles of fissionable material by the cooling gas entering the bottom of the reaction zone. The movable parts of the fission zone walls either form a part of or extend through the fission zone. Preferably, either the top cover of the reaction vessel is movable and urged downwardly or the bottom wall of the reactor vessel is movable and urged upwardly to provide pressure loading on the particles. Provision is made for discharge of the fission particles from the fission zone. (B.L.M.)

Fuels

Refer also to abstracts 41112 and 42625.

42606 (BNWL–252) K-III: A THREE-REGION KINETICS CODE IN FORTRAN-IV. Little, W. W. Jr. (Battelle-Northwest, Richland, Wash. Pacific Northwest Lab.). June 1966. Contract AT(45-1)-1830. 40p. Dep. mn. CFSTI $2.00 cy, $0.50 mn.

A coupled neutronics-heat transfer kinetics code written in FORTRAN-IV is described. The power variation is computed using a lumped parameter model with up to six precursor groups. The spatial temperature distribution in three regions is computed in plane, cylindrical, or spherical geometry. Up to 30 spatial nodes can be employed. Both linear and Doppler reactivity feedback mechanisms are available. Although running time is highly problem dependent, a typical case requires about two minutes of UNIVAC-1107 time. Input information, a sample case, and a FORTRAN-IV source deck listing are given in the appendices. (auth)

42607 (BNWL–298) PLUTONIUM UTILIZATION PROGRAM, FY-1967 THROUGH -1970. Program Analysis and Plans. Dawson, F. G. (comp.) (Battelle-Northwest, Richland, Wash. Pacific Northwest Lab.). July 1966. Contract AT(45-1)-1830. 45p. Dep. mn. CFSTI $2.00 cy, $0.50 mn.

The Hanford Plutonium Utilization Program includes Pu fuels development, chemical reprocessing studies, physics of Pu-fueled reactor systems, technical and economic optimization studies of Pu fueled reactors and Pu fuel cycles, and other research and development required to support the primary purposes of the program. The major program accomplishments to date and the scope of future investigations are summarized. (H.D.R.)

42608 (GEAP–5124) ACCURATE NUCLEAR FUEL BURNUP ANALYSES. Quarterly Progress Report No. 17, December 1965–February 1966. Rider, B. F.; Ruiz, C. P.; Peterson, J. P. Jr.; Jaech, J. L.; Seymour, R. S. (General Electric Co., Pleasanton, Calif. Vallecitos Atomic Lab.). Contract AT(04-3)-189. 43p. Dep. mn. CFSTI $2.00 cy, $0.50 mn.

Improvements were made in the program for computation of U and Pu fuel burnup from U, Pu, and Nd mass spectrometric measurements. The revised computer program is given with instructions for preparing input data cards. A list of programmed constants is included. (auth)

42609 (WAPD-T–1886) ^{233}U THORIUM SEED-BLANKET EXPERIMENTAL PROGRAM. Korsmeyer, J. D.; Milani, S.; Raab, H. F. Jr. (Bettis Atomic Power Lab., Pittsburgh, Pa.). Apr. 1966. Contract AT-11-1-GEN-14. 16p. (CONF-660606–18). Dep. mn. CFSTI $1.00 cy, $0.50 mn.

From American Nuclear Society Meeting, Denver, Colo.

The lattice characteristics of seed fuel elements containing ^{233}U and ^{235}U were measured in a series of small seed-blanket critical assemblies. The measurements included critical axial bucklings, seed power shapes, the ratio of epithermal to thermal thorium captures in blanket regions, and the ratio of epithermal to thermal ^{233}U fissions through seed and blanket regions. The experimental results are compared with calculations performed with diffusion theory, Monte Carlo, and neutron transport techniques. (H.D.R.)

42610 (AI-Trans-206) RESEARCH AND DETERMINATION OF RATES OF LEAKAGES OF NUCLEAR FUEL ELEMENTS. Block, M. N.; de Greeff, J. O. Translated for Atomics International, Canoga Park, Calif., from EURATOM Communication 688. 28p. Dep. mn. JCL $2.60 fs, $1.04 mf.

Nondestructive testing of nuclear fuel elements during and after the canning procedure is described. A review is given of existing detectors followed by a discussion of the signal interpretation problem, when adsorption has to be taken into account. Formulas are given for the different cases of leak rates and the Radiflo leak test is described. (tr-auth)

42611 (WAPD-Trans-33) PROCESS FOR THE PRODUCTION OF AN ESSENTIALLY FLAT FUEL ELEMENT FOR NUCLEAR REACTORS. Stohr, Jacques Andre; Genthron, Maurice. Translation of German Patent 1,192,332. 13p. Dep. mn. JCL $1.60 fs, $0.80 mf.

A process is described in which oxide fuel pellets are arranged in pre-formed protrusions on a metal sheet and covered with a second metal sheet. The sheets are bonded to the fuel by hydrostatic pressure and spot welded in the mid space between the fuel pieces and on the edges. The fuel element produced is in the form of a flat plate that is buckled in the areas that contain no fuel. (H.D.R.)

42612 FUEL TEMPERATURE MEASUREMENTS IN MIXED OXIDE ELEMENTS. Fisher, L.; Pendleton, J.; Pounder, J. O.; Washington, A. B. (United Kingdom Atomic Energy Authority, Dounreay, Eng.). Nucl. Eng., 11: 600-2(Aug. 1966).

A mixed oxide, $(Pu,U)O_2$, canned in stainless steel was developed for advanced fast reactors. It is characterized by low thermal conductivity, resulting in center fuel temperatures in the range 1500 to 2000°C, and high fission gas release. A void space or plenum is provided to limit fission gas pressure to a level which will not cause more than 1% creep strain in the can. A knowledge of center fuel temperature is of use in predicting the physics of a reactor system. Continuous measurements of the center fuel temperature and its variations due to fission gas poisoning were made in the Dounreay Fast Reactor. (F.S.)

42613 FUEL ELEMENT. Koutz, Stanley L. (to General Dynamics Corp.). U. S. Patent 3,252,869. May 24, 1966. Filed Feb. 12, 1963.

A self-purging fuel element for a high temperature gas-cooled reactor comprises a coolant gas previous graphite body having a bore extending through it, a number of spaced chambers adapted to receive fuel in the walls of the body and extending throughout the length of the body, and a hollow plug connected to one end of the body. The plug cooperates with the bore to form a venturi such that the pressure of the coolant gas passing through the body is reduced adjacent to the plug. The plug has communicating passageways between the chambers and the venturi by means of which the pressure in the chambers is reduced relative to the exterior and interior of the body inducing coolant gas flow into the chamber through the pervious walls of the body. This reduced pressure in the fuel chambers effects the purging of the fission products from the chambers. (B.L.M.)

42614 FUEL ARRANGEMENT FOR A NUCLEAR REACTOR. Frisch, Erling (to Westinghouse Electric Corp.). U. S. Patent 3,255,091. June 7, 1966. Filed Dec. 1, 1961.

A fuel arrangement for a nuclear reactor includes an elongated frame means within which a number of elongated fuel elements are disposed in generally parallel array. At least one grid member secured to and extending laterally across the frame is provided with openings through which the fuel elements extend. Resilient means extend into the openings to prevent lateral movement of the fuel elements. A removable handling fixture and retaining plate subassembly is provided on each end of the frame member so as to provide access to the fuel elements. Each end plate is provided with coolant passages that align with the fuel elements. (B.L.M.)

42615 FUEL PIN SPACERS. Leirvik, Raymond M. (to Babcock and Wilcox Co.). U. S. Patent 3,255,090. June 7, 1966. Filed Aug. 23, 1962.

As a spacer for reactor fuel pins or rods, a short section of tube is arranged concentrically about each fuel component in a bundle or assembly. The walls of the tube are formed with compound indentions. A portion of the wall is indented toward but out of contact with the fuel component that it surrounds. A relatively small surface of the initially indented surface is indented further inwardly so as to contact the surface of the component. At least three of these indented surfaces at equally spaced positions about the spacer serve to provide a resilient holding means for the fuel component. The spacer corners are partially cut away or slotted to permit improved and independent deflection characteristics for the individual wall surface of the spacers. (B.L.M.)

Power and Power-Breeder Reactors

Refer also to abstracts 41706, 41740, 42603, and 42604.

42616 (66-CNA-301) THE ROLE AND REQUIREMENTS OF HEAVY WATER IN CANADA AND THE WORLD. (Canadian Nuclear Association, Toronto (Ontario)). [1966]. 39p. (CONF-660516-15). Dep. mn.

From Annual Conference on Organic and Heavy Water Reactors, Winnipeg, Canada.

A forecast is presented of heavy water demand and supply to 1985 for heavy water moderated power reactors both in Canada and the World. The development of this forecast includes such requisite considerations as: basis for competitive heavy water reactors; basic nuclear power forecast; development of heavy water moderated power reactor forecast; heavy water inventory for current and future heavy water moderated power reactors; and existing and planned water production. The resultant forecast shows that currently planned production of heavy water in Canada will exceed Canadian demand during the forecast period. However, a nominal surplus is shown for the World prior to 1971 only. Beyond this date to 1985, an average deficiency of about 3,400 short tons per year may occur. (auth)

42617 (66-CNA-303) PROGRESS REPORT ON THE PICKERING GENERATING STATION. Morison, W. G. (Canadian Nuclear Association, Toronto (Ontario)). May 1966. 23p. (CONF-660516-14). Dep. mn.

From Annual Conference on Organic and Heavy Water Reactors, Winnipeg, Canada.

The design and construction of the Pickering power station is presently at an early stage. The design and site progress are summarized. A detailed table of design data and aerial views of the site are included. (D.L.C.)

42618 (66-CNA-312) EVALUATION OF CANDU: PHW FUELS. Aikin, A. M.; Howieson, J.; Pawliw, J. (Canadian Nuclear Association, Toronto (Ontario)). [1966]. 7p. (CONF-660516-8). Dep. mn.

From Annual Conference in Organic and Heavy Water Reactors, Winnipeg, Canada.

A history is presented of early fuel development with the NRX and NRU reactors, and the status of fuels is reviewed for each of the CANDU-PHW reactors: NPD, Douglas Point, and Pickering. Economics and future trends are considered briefly. (D.L.C.)

42619 (ANL-7245, pp 1-28) CIVILIAN POWER REACTORS. (Argonne National Lab., Ill.).

Sample preparation and the effects of the mounting unit are discussed for the proposed experiment to measure capture-to-fission ratios of ^{239}Pu and ^{241}Pu during power operation of the EBWR. Liquid-metal fast breeder reactor fuel development, cladding, and reprocessing are studied. Physics measurements were made in ZPR-3, ZPR-6, and ZPR-9. The status of ZPPR construction is outlined. Liquid Na coolant chemistry studies were conducted on the

determination of C in Na, and Na purification methods. Operation, modification, and testing in the EBR-II are summarized. (H.D.R.)

42620 (BAW-1280-39) SODIUM-HEATED STEAM GENERATOR DEVELOPMENT. Quarterly Progress Report, April–June 1966. (Babcock and Wilcox Co., Barberton, Ohio. Boiler Div.). July 19, 1966. Contract AT (11-1)-1280. 25p. Dep. mn. CFSTI $1.00 cy, $0.50 mn.

The preliminary design of the Prototype Steam Generator was completed and the design report, BAW-1280-28, was distributed. The detail design and fabrication of the steam generator are discussed. Fabrication is 70% complete. The status of the carbon transfer and effect on material properties and preliminary control and instrumentation studies is outlined. (H.D.R.)

42621 (CONF-660516-16) THE HWOCR PROGRAM. Storrs, Charles L. (Canadian Nuclear Association, Toronto (Ontario)). [nd]. Contract AT(38-1)-430. 9p. (66-CNA-315). Dep. mn. CFSTI $1.00 cy, $0.50 mn.

From Annual Conference on Organic and Heavy Water Reactors, Winnipeg, Canada.

General design features are described for three power plants utilizing the Heavy Water, Organic Cooled Reactor concept. The reference plant is a 1000 Mw(e) plant utilizing design parameters developed from a proposed demonstration plant based on existing technology. The third design goal is a very large dual-purpose power-desalting plant. (H.D.R.)

42622 (COO-285) AN EVALUATION OF THE ATOMICS INTERNATIONAL 1000 MWe FAST BREEDER REACTOR. (Chicago Operations Office (AEC), Ill. Reactor Engineering Div.). July 1966. 58p. Dep. mn. CFSTI $3.00 cy, $0.75 mn.

A conceptual design of a 1000 Mw(e) Liquid Metal Fast Breeder Reactor is compared to four similar conceptual designs evaluated in COO-279 (NSA 19: 10532). The similarities and differences between the Atomics International (AI) design and the previous four designs are discussed and certain nuclear properties of the AI study are reviewed. The result of a recalculation of some of the nuclear properties considered in COO-279 are given. (H.D.R.)

42623 (EUR-2996.f) LE REFRIGERANT ORGANIQUE DANS LE CADRE DU PROGRAMME ORGEL DE L'EURATOM. (The Organic Coolant for Euratom's ORGEL Program). Leny, J. C. (European Atomic Energy Community, Ispra (Italy). Joint Nuclear Research Center). Apr. 28, 1966. 20p. (CONF-660553-1). Dep. mn.

From Panel on Use of Organic Liquids as Reactor Coolants and Moderators, Vienna, Austria.

The various stages of the main research areas covered under the ORGEL Program are briefly reviewed. The organic liquid coolant chosen for the project is 0M2, a mixture of terphenyl isomers. The properties and performance of the coolant are discussed with regard to its effects on reactor characteristics and materials. The make-up costs for an ORGEL-type reactor are examined. (H.D.R.)

42624 (GA-6975) THE HTGR COATED PARTICLE FUEL. Goeddel, W. V.; Bokros, J. C. (General Dynamics Corp., San Diego, Calif. General Atomic Div.). Mar. 15, 1966. Contract AT(04-3)-167. 28p. (CONF-661003-3). Dep. mn. CFSTI $2.00 cy, $0.50 mn.

For Presentation at AIME Nuclear Metallurgy Symposium on High Temperature Nuclear Fuels, Delevan, Wis.

Comprehensive studies of coated particle fuels for the HTGR (High-Temperature Gas-cooled Reactor) are described. These studies are directed toward identifying and quantitatively defining the structural and environmental parameters influencing the behavior of pyrolytic-carbon-coated carbide fuel particles under conditions of high temperature, high burnup, and fast flux irradiation. Systematic studies of the relationship between the structure of pyrolytic carbon and its behavior under irradiation show that the most irradiation-stable carbon coatings will be those that are free of any preferred orientation, have densities as near theoretical as possible, and have maximum crystallinity to minimize irradiation-induced crystallite strains. Extensive irradiation testing of pyrolytic-carbon-coated carbide fuel particles shows that their stability is dependent on both environmental conditions (temperature and burnup) and material parameters (coating structure and geometry). Two- and three-layer pyrolytic-carbon coatings that have a low-density innermost layer and high-density isotropic outer layers have shown good stability during 10% to over 20% burnup at temperatures to over 1400°C. (auth)

42625 (GEAP-4466) EXPERIMENTAL STUDIES OF PLUTONIUM AND FISSION PRODUCT REDISTRIBUTION IN FAST REACTOR FUELS. Lauritzen, T. A.; Novak, P. E.; Davies, J. H. (General Electric Co., San Jose, Calif. Advanced Products Operation). Mar. 1966. Contract AT(04-3)-189. 17p. Dep. mn. CFSTI $1.00 cy, $0.50 mn.

An attempt is made to clarify the behavior of mixed-oxide fuels with regard to Pu and fission product redistribution and to assess both their magnitude and consequences on the operation of fast reactor systems. The Pu and fission product redistribution in mixed-oxide fuel operated above the melting point reduces the Doppler shutdown reactivity by 4 percent or less. (auth)

42626 (GEAP-4951) HIGH POWER DENSITY DEVELOPMENT PROJECT. Quarterly Progress Reports Nos. 21 and 22, June–November 1965. Holland, L. K. (comp.) (General Electric Co., San Jose, Calif. Atomic Power Equipment Dept.). Dec. 1, 1965. Contract AT(04-3)-361. 21p. Dep. mn. CFSTI $1.00 cy, $0.50 mn.

Fuel and physics development progress is reported for the High Power Density (HPD) Development Project. Microstructural changes in irradiated type-304 stainless steel cladding samples and the electron microscopic examination of failed, type-304 stainless steel cladding are discussed. Twenty-two developmental fuel assemblies continued to accumulate exposure in the Big Rock Point Reactor. An increase in off-gas activity indicated fuel rod failures have occurred in the reactor. The 600 Mw(e) HPD conceptual core design was completed, including the fuel cycle evaluation. The on-line computer continued to operate reliably. (H.D.R.)

42627 (GEAP-5051) DESIGN AND FABRICATION OF ESADA-VESR MARK III SUPERHEAT FUEL CLUSTERS. Lees, E. A.; Hazel, V. E.; Zeller, J. J.; Spalaris, C. N. (General Electric Co., San Jose, Calif. Atomic Power Equipment Dept.). Jan. 13, 1966. Contract AT(04-3)-189. 71p. Dep. mn. CFSTI $3.00 cy, $0.75 mn.

The design and fabrication of the ESADA-VESR (EVESR) Mark III fuel are described including details of fuel mechanical design, design calculations, fabrication development, and clad swaging. (auth)

42628 (GEAP-5145) DEVELOPMENT OF PULSED NEUTRON APPLICATION TO POWER REACTOR START-UP PROCEDURES. Quarterly Progress Report No. 16, January 1, 1966–March 31, 1966. Garelis, E.; Meyer, P. (General Electric Co., San Jose, Calif. Atomic Power Equipment Dept.). Apr. 1966. Contract AT(04-3)-189. 19p. Dep. mn. CFSTI $1.00 cy, $0.50 mn.

The merits of using a pseudo random neutron source excitation to measure reactor impulse response functions was investigated. A theoretical and experimental study is conducted, and results of the initial measurements are shown and discussed. As part of the theoretical development, the approach to obtain an exact solution of the time-dependent kinetic problem of a multiregion pulsed assembly is described, using a one-group symmetrically reflected diffusion theory model. (auth)

42629 (GEAP-5160) SOUTHWEST EXPERIMENTAL FAST OXIDE REACTOR DEVELOPMENT PROGRAM. Quarterly Report No. 8, February–April 1966. Horst, K. M. (comp.) (General Electric Co., San Jose, Calif. Advanced Products Operation). May 1966. Contract AT(04-3)-540. 124p. Dep. mn. CFSTI $4.00 cy, $0.75 mn.

Progress in the preoperational research and development

program of the SEFOR project is summarized. Program tasks described include: experimental program planning, experiments performed in the ZpR-III, fuel development, special instrumentation, steady-state and transient characteristics of the core assembly, reactivity controls required for experimentation, fuel handling, core design, and fuel fabrication. (H.D.R.)

42630 (HPR-66) DYNAMICS OF THE HALDEN BOILING WATER REACTOR. Eurola, T. (Institutt for Atomenergi, Halden (Norway). OECD Halden Reaktor Prosjekt). Dec. 1965. 57p. Dep. mn.

The dynamic behavior of the HBWR system with the second fuel charge is described in the light of experimental results on the unperturbed system and the system responses to various perturbations. The main features of a theoretical model describing the dynamics of a natural circulation boiling heavy water reactor are explained. The model is applied to the HBWR second fuel charge and the calculated and measured values are compared. (H.D.R.)

42631 (KFK-260) EXPERIMENTS TO EVALUATE REACTIVITY COEFFICIENTS WITH REACTOR OPERATING AT STEADY STATE CONDITIONS (STATIC EXPERIMENTS). Caldarola, L.; Haefele, W.; Schikarski, W. (Kernforschungszentrum, Karlsruhe (West Germany)). Feb. 1966. 42p. Dep. mn.

Three reactivity coefficients are defined: the global power coefficient referred to the reactor power, the global coolant temperature coefficient referred to the average coolant temperature, and the secondary radial expansion temperature coefficient referred to the coolant temperature rise in the reactor. Each coefficient is measured by a separate experiment in which the reactivity effects due to the other two are made equal to zero. The error analysis is developed with numerical examples referred to the Southwest Experimental Fast Oxide Reactor (SEFOR). With the aim of minimizing the total error, attention is given to the choice of the best power interval for the measurement of the global power coefficient. The control philosophy of the reactor system during the experiments is also studied. (auth)

42632 (NAA-SR-12060) 1000-Mwe FBR PARAMETRIC STUDY OF SECONDARY SODIUM-STEAM SYSTEM. Holz, H. B.; Schneider, G. (Atomics International, Canoga Park, Calif.). Aug. 31, 1966. Contract AT(11-1)-Gen-8. 151p. Dep. mn. CFSTI $5.00 cy, $1.00 mn.

Cost trends of major plant equipment for the secondary Na steam turbine portions of a LMFBR plant generating approximately 1000 Mwe are described. Eleven different combinations of secondary Na-steam generation systems and turbine plants were studied and compared on a differential cost basis, using a 2400 psi/1000°F-1000°F system as a base case. Incremental energy costs at the intermediate heat exchanger secondary outlet and inlet nozzles of 10, 20, and 30 cents per million Btu were assumed for capitalization of differential heat rates. The energy costs include fuel cycle costs as well as the variable portion of the capital, operation, and maintenance costs for the remaining portion of the plant. (F.S.)

42633 (ORNL-TM-1452) TEMPERATURES IN THE CLADDING UNDER THE SPACERS OF THE BONUS SUPERHEATER ASSEMBLIES. Sanders, J. P. (Oak Ridge National Lab., Tenn.). Apr. 22, 1966. Contract W-7405-eng-26. 14p. Dep. mn. CFSTI $1.00 cy, $0.50 mn.

The temperature distribution under the spacers presently used in the BONUS superheater assemblies was calculated with the HEATING program. A two-dimensional model in cylindrical coordinates (R, θ) was used for a 60° symmetrical segment. The results indicate that if a braze width at the point of contact of at least 40 mils can be obtained, the maximum temperature in the cladding will be less than 1200°F. (auth)

42634 (ORNL-TM-1453) TEMPERATURE DISTRIBUTION UNDER DIMPLES PROPOSED AS SPACERS IN THE BONUS SUPERHEATER ASSEMBLIES. Sanders, J. P. (Oak Ridge National Lab., Tenn.). Apr. 22, 1966. Contract W-7405-eng-26. 14p. Dep. mn. CFSTI $1.00 cy, $0.50 mn.

It has been proposed that dimples in the coolant tube be used as an alternative to the present space ring to center the clad fuel rod in the coolant stream in the BONUS superheater assemblies. The temperature distribution under such a dimple was investigated using the HEATING code. Calculations were made in two dimensions using cylindrical geometry and a 78.5° segment. It was found that lateral conduction could not dissipate heat from beneath the dimple sufficiently well to maintain temperatures in the cladding less than 1250°F. The only method of maintaining sufficiently low temperatures in the cladding was to insure good thermal contact between the cladding and the dimple. Sufficient contact might be obtained by placing three dimples around the same perimeter and constructing them to obtain an interference fit at the three points of contact. The dimples might be slightly flattened to the curvature of the fuel rod at the point of contact, and both metal surfaces should be clean and free of oxide film. (auth)

42635 (RISO-124) STUDY OF A PROPOSED HEAT TRANSFER EXPERIMENT WITH A MULTIROD ELEMENT, DOR DESIGN STUDY. Andersen, Rolf; Moyer, Carl B. (Danish Atomic Energy Commission, Risoe. Research Establishment). Dec. 1964. 140p. Dep. mn.

Various considerations pertinent to the design of experiments to obtain heat transfer information about the DOR 19-rod bundle fuel element are described. A comparison of analyses and data available in the literature shows that the lumped parameter or finite difference type of analysis can yield fairly accurate predictions of canning temperatures. Applied to typical DOR cases, the analysis predicts peripheral canning temperature variations of approximately 5°C about the mean provided that the fuel rods are properly aligned. A study of experimental methods suitable for simulating DOR reactor conditions indicates that no heating method can be designed at this time with any real assurance that it will provide an adequate simulation. A laboratory development program could probably lead to such a heater, but the time and expense involved would seem to be considerable. It is recommended that a simulation experiment not be attempted, and that the final verification of the fuel element heat transfer should be made as an in-pile experiment. (auth)

42636 (SWRI-1228-4-22) EVALUATION OF THE SERVICEABILITY OF THE ELK RIVER REACTOR PRESSURE VESSEL. Quarterly Report, April 1, 1966-June 30, 1966. Lautzenheiser, C. E. (Southwest Research Inst., San Antonio, Tex.). Aug. 1, 1966. Contract AT(11-1)-1228. 21p. Dep. mn. CFSTI $1.00 cy, $0.50 mn.

The work includes the study of the fatigue properties of steels and weldments, the study of neutron irradiation effects on the ductility and fatigue properties of steels and welds, and the development of remote nondestructive testing methods for the Elk River Reactor Pressure Vessel. (D.L.C.)

42637 (SWRI-1228-7-33) INVESTIGATION OF THE FABRICATION AND INSTALLATION OF THE LACBWR REACTOR PRESSURE VESSEL. Watson, Paul D. (Southwest Research Inst., San Antonio, Tex.). Aug. 4, 1966. Contract AT(11-1)-1228. 15p. Dep. mn. CFSTI $1.00 cy, $0.50 mn.

Fabrication specifications for the LaCrosse Boiling Water Reactor Pressure Vessel were reviewed, and the fabrication and erection operations were monitored. Some fabrication problems and their resolution are discussed. It is concluded that the fabrication and erection of the vessel assembly was performed satisfactorily in accordance with the specifications. (D.L.C.)

42638 (TID-23299) 237 MW KRB NUCLEAR POWER PLANT. Quarterly Report. (Kernkraftwerk Rwe-Bayerwerk G,m,b,H., Gundremmingen (West Germany)). 1965. 63p. (KRB-1965/4). Dep. mn. CFSTI $3.00 cy, $0.75 mn.

Progress is reported on the construction of the KRB power plant for the period Oct. 1 through Dec. 31, 1965.

Work was completed on the main building and assembly projects and the containment shell and solid waste storage facility were finished. The circulating loops and the hydraulic control rod drives were completed. Preoperational tests were carried out on the turbine, main and secondary cooling water units, instrument and operating air supplies, auxiliary boilers, and the waste processing unit. (H.D.R.)

42639 (UNC-5154) PERFORMANCE EVALUATION OF HEAT EXCHANGERS FOR SODIUM-COOLED REACTORS. Quarterly Technical Progress Report, April 1–June 30, 1966. Dischinger, R. H. (United Nuclear Corp., Elmsford, N. Y.). July 20, 1966. Contract AT(11-1)-1452. 35p. Dep. mn. CFSTI $2.00 cy, $0.50 mn.

Work toward evaluation of the thermal-hydraulic and structural performance of heat exchangers for Na-cooled reactor plants is reported The evaluation will be based on the results of tests of model heat exchangers [approximately 30 Mw(t)] in the Sodium Components Test Installation (SCTI). An intermediate heat exchanger and a steam generator are the first units to be tested. Data taken during plant shakedown was used to check out computer routines for the heat exchanger and steam generation units. It was found that minor modifications to these procedures are necessary. A recommendation was made suggesting that the Na level be carried at the maximum limit to reduce gas entrainment in the steam generator. Evaluation of the possibility of tube vibration in the heat exchangers continued. Review of heat exchanger test specifications was started. (J.R.D.)

42640 (WAPD-PWR-2210(Vol.1)) NUCLEAR PROTECTION SYSTEM. Instruction Book. (General Dynamics/Electronics, Rochester, N. Y.). Oct. 1, 1963. Contract AT(11-1)-Gen-14. 259p. Dep. mn. CFSTI $6.00 cy, $1.25 mn.

For Westinghouse Electric Corp., Pittsburgh, Pa. Atomic Power Div.

The Nuclear Protection System monitors neutron flux and coolant flow and maintains a safe operating level for the Shippingport PWR. Output signals are digital and are used to shut down the reactor by control rod insertion. The equipment also monitors and reads out the boiler feedwater flow and temperature which indicates the thermal output power of the reactor plant. Operating and maintenance instructions are presented for the system components, and a parts list is included. (H.D.R.)

42641 (WAPD-PWR-2213) PWR-2 FUEL HANDLING CRANE AND REFUELING TOOL. Instruction Book. (Stearns-Roger Corp., Denver, Colo. Nuclear Equipment Div.). Oct. 1, 1964. Contract AT(11-1)-Gen-14. 220p. Dep. mn. CFSTI $6.00 cy, $1.26 mn.

For Westinghouse Electric Corp., Atomic Power Div., Pittsburgh, Pa.

The bridge and trolley crane structure is used for positioning the refueling tool over the reactor to remove or replace fuel assemblies, to convey spent fuel assemblies to the storage area, and for transporting fresh fuel assemblies to the reactor. The refueling tool is designed to permit its insertion into the reactor vessel through the central access port in the reactor head. Detailed descriptions are given of the refueling crane and handling tool and their related components. Installation, testing, operation, and maintenance are described and a parts list and drawings are included. (H.D.R.)

42642 (WAPD-PWR-2216) STATIC INVERTER ROD DRIVE POWER SUPPLY. Instruction Book. (Thompson Ramo Wooldridge Inc., Cleveland, Ohio). Nov. 8, 1963. Contract AT-11-1-GEN-14. 206p. Dep. mn. CFSTI $6.00 cy, $1.25 mn.

For Westinghouse Electric Corp., Pittsburgh, Pa. Atomic Power Div.

The Rod Drive Power Supply to supply electrical power to a series of PWR control rod drive motors is essentially a static frequency changer, capable of changing a 60 cps three phase alternating current to a low frequency, phase sequence reversible, three phase, alternating current, or to direct current. The equipment consists of six frequency changers or units. The two major units of the power supply, the Rod Equipment Panel-Static Inverter Section and the Rod Control Transformer Panel, are described in detail. Installation, testing, operation, and maintenance of the equipment is discussed and drawings and a parts list are included. (H.D.R.)

42643 (WAPD-PWR-2217) PWR CORE 2 ROD CONTROL AND ROD POSITION EQUIPMENT. Instruction Book. (Westinghouse Electric Corp., East Pittsburgh, Pa. Assembled Switchgear and Devices Div.). Sept. 1963, Contract AT(11-1)-Gen-14. 367p. Dep. mn. CFSTI $7.00 cy, $1.75 mn.

For Westinghouse Electric Corp., Atomic Power Div., Pittsburgh, Pa.

The design, installation, testing, operation, and maintenance of the four major components of the PWR Core 2 control rod position and control equipment are described. The Rod Position Patchboard Panel, Rod Position Capacitor Panel, Rod Control Panel, and Rod Equipment Panel Programming Section are covered in separate chapters and remote and miscellaneous equipment is described. Drawings and parts lists are included for all components. (H.D.R.)

42644 (WAPD-PWR-2219) CORE 2 MAIN COOLANT PUMP MODEL M/M 8006-A1 FOR PWR NUCLEAR POWER STATION, SHIPPINGPORT, PENNSYLVANIA. Instruction Book 5710-33A. (Westinghouse Electric Corp., Cheswick, Pa. Atomic Equipment Div.). [nd]. Contract AT(11-1)-Gen-14. 109p. Dep. mn. CFSTI $4.00 cy, $0.75 mn.

The PWR Core 2 Main Coolant Pump is a vertical, single-stage centrifugal pump designed to pump large volumes of high pressure-high temperature water through a stainless steel pipe loops. The design, installation, operation, and maintenance are described in detail and a parts list and drawings are included. (H.D.R.)

42645 (WAPD-PWR-2222) PWR-CORE 2 STEAM GENERATOR. Instruction Book. (Foster Wheeler Corp., Livingston, N. J.). Sept. 1964. Contract AT(11-1)-Gen-14. 123p. Dep. mn. CFSTI $4.00 cy, $1.00 mn.

For Bettis Atomic Power Lab., West Mifflin, Pa.

The steam generator is the natural circulation type, consisting of a straight tube, fixed tube sheet exchanger horizontally oriented, and a separate horizontal steam drum connected to the heat exchanger by risers and downcomers. The design, installation, operation, and maintenance of the steam generator and gage glass are described and a parts list and drawings are included. (H.D.R.)

42646 (WAPD-PWR-2223) PWR CORE 2 STEAM GENERATOR. Instruction Book. (Babcock and Wilcox Co., New York). May 1964. Contract AT-11-1-GEN-14. 120p. Dep. mn. CFSTI $4.00 cy, $0.75 mn.

For Bettis Atomic Power Lab., West Mifflin, Pa.

The PWR Core 2 steam generator is of the natural circulation two-fluid type and consists of a horizontal U-tube straight-shell heat exchanger on which a separate steam drum is mounted. The steam generator is supported on saddles which are bolted to foundations. Installation procedures are described and operating and maintenance instructions are given. A parts list and engineering drawings are included. (H.D.R.)

42647 (WAPD-PWR-2226) PWR-2 AXIAL FLUX MEASUREMENT SYSTEM EQUIPMENT SPECIFICATION 568319. Instruction Book. (Eanco, Inc., Hatboro, Pa.). Mar. 1966. Contract AT(11-1)-Gen-14. 193p. Dep. mn. CFSTI $5.00 cy, $1.00 mn.

For Bettis Atomic Power Lab., West Mifflin, Pa.

The axial flux measurement system is designed to obtain periodic measurements of the neutron flux levels at specified locations in one quadrant of the PWR core at various power levels. The measurements are made by introducing neutron detector wires into designated fuel assemblies, irradiating the wires, and removing them for counting and flux mapping. The system includes six flux wire drive mechanisms located in a shielded access cubicle plus the

equipment required to transport the flux wires from the cubicle to the reactor. The system description, installation, calibration, operation, and maintenance are described. A parts list and drawings are included. (H.D.R.)

42648 (WAPD-PWR-2229) PWR-2 OMEGA SEAL WELDING MACHINE. Instruction Book. (Bettis Atomic Power Lab., Pittsburgh, Pa.). Apr. 1964. Contract AT-11-1-GEN-14. 255p. Dep. mn. CFSTI $6.00 cy, $1.25 mn.

The semi-automatic machine designed for welding of omega-type pressure boundary seals in the PWR Core 2 reactor vessel closure head is described. Descriptions, theory of operation, maintenance, and parts identifications are provided for the machine components, omega seal mockups, and test stands. Procedures are given for setting up, adjusting, and operating the machine. (H.D.R.)

42649 (WAPD-PWR-2230) PWR-2 OMEGA SEAL WELD CUTTING MACHINES FOR REFUELING PORT, CONTROL ROD MECHANISM PORTS, ORIFICE ADJUSTMENT PORTS. Instruction Book. (Bettis Atomic Power Lab., Pittsburgh, Pa.). Sept. 1964. Contract AT-11-1-GEN-14. 158p. Dep. mn. CFSTI $5.00 cy, $1.00 mn.

Portable units for cutting omega seal welds on the PWR-2 reactor ports and preparing them for rewelding are described. The mechanism port cutting machine cuts the control rod drive mechanism motor tube-to-nozzle seal welds and the 6 and 9 in. seal welds of the center port. The center port cutting machine cuts the 26 in. seal weld of the center port. The orifice port cutting machine cuts the 5 in. orifice port seal welds. Instructions are given for the assembly, use, and maintenance of these machines and a parts list and drawings are included. (H.D.R.)

42650 (WAPD-PWR-2232) PWR-2 REACTOR VESSEL CLOSURE HEAD SEAL WELD CUTTING MACHINE. Instruction Book. (Bettis Atomic Power Lab., Pittsburgh, Pa.). Oct. 1965. Contract AT-11-1-GEN-14. 80p. Dep. mn. CFSTI $3.00 cy, $0.75 mn.

Operating and maintenance procedures are described for the PWR-2 Reactor Vessel Closure Head Seal Weld Cutting Machine. The machine is designed to sever and prepare for rewelding the omega type closure seal between the reactor vessel and the PWR-2 core support flange and a similar omega seal between the core support flange and the reactor vessel closure head. A parts list and list of drawings is included. (H.D.R.)

42651 (WASH-1065) LIQUID SODIUM METAL COOLED FAST BREEDER REACTOR (LMFBR) PROGRAM. FUELS AND MATERIALS SUMMARY REPORT. (Division of Reactor Development and Technology (AEC), Washington, D. C. Fuels and Materials Branch). Jan. 1966. 41p. Dep. mn. CFSTI $1.00 cy, $0.50 mn.

The status of fuels and materials technology in the LMFBR program is reviewed and evaluated. Two metal fuel alloys that show promise are (U-Pu)Zr and (U-Pu)Ti. The U-Pu oxides and carbides currently offer the best potential for fast reactor fuel. Both fuels and cladding development are hampered by the lack of fast flux irradiation facilities. Limitations of the existing fast reactors, EBR-II and Fermi, make the design and construction of an adequate fast facility imperative to the development of economical and reliable fuels and materials. (H.D.R.)

42652 (EURFNR-92F) THE USE OF AUSTENITIC STEEL AS CONSTRUCTION MATERIAL FOR THE PRESSURE VESSEL OF THE FAST REACTOR "RAPSODIE." Guegnaud, A.; Roques, C. (Societe des Forges et Ateliers du Creusot, Paris (France)). Translation of report CEA-TP-1593. 37p. (CONF-777-1; EUR-1642.f). Dep. mn. CFSTI $2.00 cy, $0.50 mn.

Work Performed under United States–Euratom Fast Reactor Exchange Program.

From Symposium on Materials for Cooling Reactors with Sodium, New York, Nov. 1963.

Various factors which determine the selection of the base metal and the weld metal for the Rapsodie pressure vessel and sodium pipes are examined. High temperature creep, loading, and ductility properties are examined for stainless steels containing addition elements in small quantities. Creep and fracture properties are described for welded joints subjected to long-term tests. (H.D.R.)

42653 DOUNREAY FAST REACTOR: KINETIC COMPUTER ANALOG. James, P. R.; Tait, D. (United Kingdom Atomic Energy Authority, Dounreay, Eng.). Nucl. Eng., 11: 611-13(Aug. 1966).

Values for the fast acting feedback and control rod worth were rapidly obtained with an analog computer, and with the expenditure of a modest amount of reactor time all the principal feedback characteristics of the DFR were established. Hence a model of the reactor has been programmed and used to investigate the reactor response to coolant flow failures, reactivity steps, and control rod runaway accidents. More recently the computer has been programmed to act as an on-line reactivity monitor, and in this mode of operation it is invaluable for control rod calibration and measurement of the reactivity worth of perturbation samples. (auth)

42654 THE GAS TURBINE IN NUCLEAR POWER PLANTS. Colombi, Carlo. Termotecnica (Milan), 20: Suppl. to No. 5, 3-33(1966). (In Italian).

In order to be technically and economically feasible, it is essential that the turbines used in closed-cycle gas-turbine nuclear power plants have the smallest dimensions possible. The gas used as the reactor coolant and the working medium for the turbine influences the size of the turbine. Characteristics of the following coolant gases: air, neon, helium, and nitrogen are tabulated. (F.S.)

42655 ENGINEERING FOR COMMUNITY ACCEPTANCE. THE ARCHITECT-ENGINEER'S ROLE. Baron, S. (Burns and Roe, Inc., New York). 13p. (CONF-660429-5). ORAU. Gmelin, AED-CONF-66-098-13.

From American Power Conference, 28th Annual Meeting, Chicago.

Modern fossil fuel power plants have availability factors for power generation of over 90%. These high availabilities have been achieved by preventative maintenance programs, duplication of pumps, and the use of high quality equipment. Nuclear plants under the present cost competition have little or no standby equipment, and limit preventative maintenance to equipment, used in radioactive systems such as the primary system of the PWR, and the recirculating and feedwater system of the BWR. Utility operators, with multiple loops of these systems, may prefer isolation of a loop for direct or preventative maintenance. However, the low cost motivation by the bidder is so great that isolation of systems are not being offered in the fixed price turn-key bids. Whether these plants can achieve availabilities as high as 90% remains to be demonstrated. Design philosophies will change as experience is gained and these design changes can best be carried out by the architect-engineer in his traditional utility relationship. By achieving higher availability through greater design reliability, the public will be served by being assured of an uninterrupted power supply at a low cost-resulting from a highly competitive market for all the components of the nuclear power plant. (auth)

42656 IMPROVEMENTS IN NUCLEAR REACTORS. (to Societe Anglo-Belge Vulcain). British Patent 1,032,221. June 8, 1966. Priority date Mar. 23, 1962, Belgium.

A method for maintaining within operational limits the pressure of a nuclear reactor which has a pressurizer and a circuit through which flows a fluid that is a liquid in at least a portion of the circuit provides for simplified working of the pressurizer and simplification of most of the members required for such working and for the pressurizer regulation. No regulating device or means for additional heating of the fluid are required. The reactor is so designed that the total pressure of the primary fluid in the pressurizer is maintained at a value which is constantly adapted to the temperature of the fluid at its outlet from the reactor core. (B.L.M.)

42657 IMPROVEMENTS IN STEAM-GENERATING PLANT. Peters, Martin Charles (to Babcock and Wilcox

Ltd.). British Patent 1,037,634. Aug. 3, 1966. Filed Aug. 3, 1962.

A steam-generating plant including a liquid-metal cooled nuclear reactor is provided that attempts to eliminate the consequences of a tube failure in the heat exchanger that result in pressure surges which necessitate the use even in the pressure vessel of relatively thick walls. The reactor is connected in a primary coolant circuit arranged to operate at superatmospheric pressure with alkali metal primary coolant flowing in series through the reactor and a first heat exchanger. A second coolant circuit is arranged to operate in heat transfer relationship through the first heat exchanger and a second heat exchanger that provides steam generating surfaces. The secondary coolant comprises a suspension of solid particles in a gaseous fluid, both of which are substantially inert to heat exchange fluid inadvertently leaking at the first or second heat exchanger into the secondary coolant circuit. This secondary circuit operates at a superatmospheric pressure that is less than that of the primary coolant and less than the steam pressure of the secondary heat exchanger. Since neither the solid suspended material nor the gaseous fluid are rendered highly radioactive under irradiation by gamma rays, the secondary heat exchanger is located outside the biological shield enclosing the reactor and the first heat exchanger. (B.L.M.)

Process Heat Reactors

42658 (NP–16250) POTENTIALITIES AND POSSIBILITIES OF DESALTING FOR NORTHERN NEW JERSEY AND NEW YORK CITY. A Report by the Northeast Desalting Team. (Office of Saline Water, Washington, D. C.). Feb. 11, 1966. 112p. Dep.

The potentialities and possibilities of desalting are considered as a source of water supply to the area of New York City and the four northern counties of New Jersey. Desalting is explored in terms of its cost and relationship to the growing need for water and electrical power, the existing surface water supply system, and proposed additions to the surface system. Various design configurations, including nuclear, fossil, and refuse-disposal fuel sources and dual-purpose power-water production, are considered. (H.D.R.)

42659 WATER-ONLY PLANT STUDIES. Clark, Richard L. (Bechtel Corp., San Francisco). 18p. (CONF-660311–5). ORAU. Gmelin, AED-CONF-66-037-9.

From Symposium on Water Production Using Nuclear Energy, Tucson, Ariz.

Recent water desalting plant design studies are analyzed and a comparison is made of the cost of water from dual-purpose and water-only plants. The factors affecting the decision to build a water-only or a dual-purpose plant are discussed. Two approaches to reducing the cost of desalted water from water-only plants are compared. One approach is based on high temperature multistage flash evaporation while the other approach incorporates the low temperature Deep Pool Reactor concept. It is concluded that the cost of water is higher from a water-only desalting plant but a particular combination of conditions is necessary to justify a dual-purpose installation. Future process development may diminish the cost difference between dual-purpose and water-only operation. (auth)

Production Reactors

42660 (BNWL-SA–270) DYNAMIC ANALYSIS OF THE HANFORD DUAL-PURPOSE REACTOR PLANT USING ANALOG SIMULATION METHODS. Swanson, C. D.; Coughren, K. D.; Thieme, G. G. (Battelle-Northwest, Richland, Wash. Pacific Northwest Lab.). July 1965. Contracts AT(45-1)-1830; AT(45-1)-1350; AT(45-1)-1357. 41p. Dep. mn. CFSTI $2.00 cy, $0.50 mn.

Applications of analog simulation techniques to determine the dynamic characteristics and design adequacy of a large dual-purpose nuclear reactor plant are described. Methods used to simplify the plant model to permit simulation with available computing facilities are discussed. Typical studies included evaluation of plant safety instrumentation and trip settings, controller stability and performance for both small and large plant disturbances and various plant operating procedures. Results of typical studies are shown. (auth)

42661 (DPSPU–66-30-2) AXIAL POWER MONITORING WITH AN ON-LINE COMPUTER. Hurley, T. J. Jr. (Du Pont de Nemours (E. I.) and Co., Aiken, S. C. Savannah River Plant). June 1966. Contract AT(07-2)-1. 9p. (CONF-660606–17). Dep. mn. CFSTI $1.00 cy, $0.50 mn.

From American Nuclear Society Meeting, Denver, Colo.

On-line computer programs for a production reactor were developed for rapid determination of axial power distribution and calculation of the safety factor for film-boiling burnout of fuel surfaces. These programs operate concurrently to provide continual axial power monitoring and alarm functions. In use for over a year, the system has demonstrated speed and accuracy in gathering data, solving complex equations, and displaying useful information. It has thus been possible to operate closer to operating limits with added assurance of an adequate margin of safety. (auth)

Propulsion and Space

See also ENGINEERING — Space Propulsion

42662 (CONF-651101–84) NERVA REACTOR DEVELOPMENT STATUS. Esselman, W. H.; Arnold, W. H. (Westinghouse Electric Corp., Pittsburgh Pa. Astronuclear Lab.). Nov. 1965. Contract SNP-1. 27p. Dep. mn. CFSTI $2.00 cy, $0.50 mn.

From 13th Conference on Remote Systems Technology, Washington, D. C.

The Project Rover Reactor Development Program progress is summarized from its beginning in 1955. The development, testing, and evaluation of the KIWI, NRX, and NERVA reactors are described. (H.D.R.)

42663 (EGG–1183-1054) TEST CELL A CONTROL SYSTEMS. Report No. L-660. Budge, Ezra (Edgerton, Germeshausen, and Grier, Inc., Las Vegas, Nev.). June 1, 1964. Contract AT(29-1)-1183. 219p. Dep. mn. CFSTI $6.00 cy, $1.25 mn.

An installation and operation manual is presented for the Project Rover Test Cell A controls system instrumentation. Descriptions and diagrams are included for major systems, subsystems, and shared or common equipment. (H.D.R.)

42664 (IDO–17165) STEP PROJECT. Quarterly Technical Report, July 1965–September 1965. Dietz, K. A. (ed.) (Phillips Petroleum Co., Idaho Falls, Idaho. Atomic Energy Div.). July 1966. Contract AT(10-1)-205. 83p. Dep. mn. CFSTI $3.00 cy, $0.75 mn.

A steady-state power test, coupled-drum impulse transient tests, and cascaded step transient tests were conducted in the SNAPTRAN-1 experimental test program. The steady-state power test was conducted to determine the effect of ambient temperature changes in the core on the base reactivity and to calibrate nuclear instrumentation. The isothermal temperature coefficient of –0.11 ¢/°F was associated with the ambient temperature condition of the reactor core. The coupled-drum impulse transient tests were conducted to investigate the reactivity feedback behavior under conditions approaching reactor self-destruction, and the cascaded step transient tests were conducted to determine the feedback coefficient for average core temperatures in excess of 1200°F. H_2 pressure in SNAPTRAN fuel was measured during the SNAPTRAN-1 transient tests to obtain an understanding of the dynamics of hydrogen release from the ZrH lattice. The information obtained from the measurements was used in predicting the fuel behavior at energies which cause fuel damage. The SNAPTRAN-2 reactor and control systems were modified to ensure that the maximum reactivity could be inserted during the destructive test. The impulse-drum drive system was modified so the drums would be

stopped at the maximum reactivity position rather than being permitted to rotate from the minimum reactivity position through the maximum reactivity position and back to the minimum reactivity position. A preliminary measurement program was proposed for the SNAPTRAN-2 destructive test. Primarily, this program would provide information concerning energy generation and reactor disassembly. The instrumentation proposed for use in the destructive test was performance evaluated under environmental conditions similar to those expected during the test. The actual test conditions expected were simulated by detonating small charges of high explosives in air. These tests provided specific information concerning transducers and their associated instrumentation and provided general information concerning measuring and recording techniques. The proposed measurements and the results of the simulated tests are reported in detail. A method is being developed for calculating the spatial distribution of pressure within the LOFT primary-coolant system as a function of time during the first hundred milliseconds after blowdown. The discussion presented gives the theoretical basis for calculating acoustic wave propagation and reflection phenomena in a one-dimensional, uniform-area system. Also given are numerical solutions obtained through the use of a digital computer program (BURST) for cases of decompression of a uniform-area tube closed at one end and having a rupture disc at the other and containing pressurized, subcooled water with zero initial fluid velocity. As part of the LOFT radiological studies, a chemical method was developed for the rapid separation of Te and I_2 from other fission products and from each other. This method was developed to facilitate the measurement of biologically significant fission products in LOFT containment samples. After preliminary oxidation and reduction of I_2, Te was reduced to the metal and separated by filtration. I was absorbed as iodide by AgCl. The maximum expected concentrations of various fission products were calculated for the CDE and LOFT atmospheres after 1.16 days of cooling. The surface contamination after 11.6 days of cooling was also determined. The results obtained for atmospheric concentrations and surface contamination are presented in tabular form for comparison. Standard surfaces were selected for plateout studies to provide a basis for correlating data from different laboratories and simulated irradiation tests were conducted in a steam-air atmosphere to provide data concerning the behavior of mixed fission products and to determine decontamination factors for specific isotopes. Coated and stainless steel surfaces were contaminated with molecular I in an autoclave to determine the influence of steam pressure on contamination. Results of the decontamination of various coatings are given for the simulated irradiation plateout tests in which decontamination was performed by immersion techniques. The decontamination factors obtained by this method were similar to those obtained by spray decontamination. The coatings contaminated in molecular I were subjected to pressures of 5, 15, and 40 psig for 24 hours with the result that absolute iodine contamination decreased with increased pressure and the contamination of the coatings relative to that of stainless steel increased with pressure. A design study was made to determine the feasibility of a reactivity accident test using a small boiling water reactor core to model a typical large boiling water power reactor core. A proposed core design is presented and evaluated. (auth)

42665 (WCAP–2870) TEST AND ANALYSIS OF A MANIFOLD AND RE-ENTRANT TUBE ASSEMBLY. FEASIBILITY OF A CHEMICAL POISON LOOP SYSTEM. Engel, F. C.; Bishop, A. A. (Westinghouse Electric Corp., Pittsburgh, Pa. Atomic Power Div.). July 1966. Contract NAS 3-5215. 80p. (NASA-CR–54994).

An analytical and experimental model study was performed of a manifold and re-entrant tube chemical poison distribution system which are part of a rocket reactor control loop. The system operates by changing the concentration of the poison (CdS) in a water solution circulating through a large number (198) of parallel tubes which project from a manifold into the core. In order to meet the specifications that (1) the flow rate through all the tubes be uniform, (2) the injected chemical poison arrive at the top of the core within 0.2 second, and (3) the chemical solution concentration variation throughout the core should be within ±5%, a special manifold and re-entrant tube assembly was designed and a full size flow model was constructed of plexiglas and a series of tests performed to prove the design. (auth)

42666 IMPROVEMENTS IN RADIO CONTROLLED NUCLEAR ENERGY PROPELLED MARINE TOWING CRAFT. Pedrick, Arthur Paul. British Patent 1,032,689. June 15, 1966. Filed Mar. 3, 1965.

Unmanned nuclear powered marine towing crafts are proposed for operation around the Antarctic land mass in three Great Circle courses between three stations. The crafts would be maintained on course by the combination of short wave radio signals transmitted from interchange stations and from navigational satellites in orbit around the earth. The craft design, the reactor for powering the craft, and the control system are described in detail. (B.L.M.)

Research and Test Reactors

Refer also to abstract 42600.

42667 (66-CNA-309) WR-1: DESIGN AND CONSTRUCTION. Gray, K. J.; Graham, R. J. (Canadian Nuclear Association, Toronto (Ontario)). [1966]. 14p. (CONF-660516–11). Dep. mn.

From Annual Conference on Organic and Heavy Water Reactors, Winnipeg, Canada.

After a brief history and description of the Whiteshell Reactor No. 1, its construction is discussed in some detail. Organization, planning, schedule, work execution, and cost control are covered. (D.L.C.)

42668 (AECL–2552) THE COMMISSIONING OF WR-1. Summach, A. J. (Atomic Energy of Canada Ltd., Pinawa (Manitoba). Whiteshell Nuclear Research Establishment. Canadian Nuclear Association, Toronto (Ontario)). [1966]. 12p. (66-CNA-310; CONF-660516–10). Dep. mn.

From Annual Conference on Organic and Heavy Water Reactors, Winnipeg, Canada.

Significant aspects of the commissioning program, major system modifications and noteworthy test results are discussed including brief reference to initial operating experience. (auth)

42669 (AECL–2553) FUEL, MATERIALS, AND COOLANTS FOR WR-1. Robertson, R. F. S. (Atomic Energy of Canada Ltd., Pinawa (Manitoba). Whiteshell Nuclear Research Establishment. Canadian Nuclear Association, Toronto (Ontario)). [1966]. 14p. (66-CNA-311; CONF-660516–9). Dep. mn.

From Annual Conference on Organic and Heavy Water Reactors, Winnipeg, Canada.

The behavior of the WR-1 system of UO_2 fuel sheathed in zirconium alloy and cooled by an organic fluid flowing in a zirconium alloy pressure tube is described. (H.D.R.)

42670 (ANL–7245, pp 48–59) ADVANCED SYSTEMS RESEARCH AND DEVELOPMENT. (Argonne National Lab., Ill.).

Development progress is reported for the Argonne Advanced Research Reactor. Separate sections describe physics experiments and analyses, fuel and core development, and component development. (H.D.R.)

42671 (AWRE-R–5/66) URANIUM-FUELLED VERA REACTOR EXPERIMENTS. McTaggart, M. H.; Goodfellow, H.; Paterson, W. J.; Weale, J. W. (Atomic Weapons Research Establishment, Aldermaston (England)). July 1966. 89p. Dep. mn. BIS $2.40. HMSO 12s. 0d.

These experiments form part of a series designed to obtain information against which the nuclear data for ^{235}U and ^{238}U can be checked over the energy range 10 to 500 kev. Seven fast reactor assemblies are described. All the cores contained ^{235}U and graphite, and some also contained

^{238}U and H_2. Detailed measurements were made on four of the assemblies but for the other three assemblies the critical masses only were measured. (auth)

42672 (BNL-10388) THE EFFECT OF XENON ON SAFETY OF THE HFBR. Lellouche, G.; Chernick, J. (Brookhaven National Lab., Upton, N. Y.). July 1966. Contract AT(30-2)-Gen-16. 10p. (CONF-660606-16). Dep. mn. CFSTI $1.00 cy, $0.50 mn.

From American Nuclear Society Meeting, Denver.

The equations for the line model of reactor dynamics are presented and used to indicate the effect of xenon on High Flux Beam Reactor transients. (H.D.R.)

42673 (BNL-10483) THE DESIGN, TEST, AND USE OF THE BROOKHAVEN NATIONAL LABORATORY (BNL) REACTOR BYPASS FILTER FACILITY. McClintock, R. O. (Brookhaven National Lab., Upton, N. Y.). [nd]. Contract AT(30-2)-Gen-16. 9p. (CONF-660904-5). Dep. mn. CFSTI $1.00 cy, $0.50 mn.

For Presentation at 9th Air Cleaning Conference, Boston.

The BNL Reactor Bypass Filter Facility provides improved air cleaning in the event of a fuel element failure at either the Brookhaven Graphite Research Reactor (BGRR) or the High Flux Beam Reactor and allows the use of air cooling to combat a graphite fire at the BGRR. The system is designed to accommodate 100,000 cfm with high filtering efficiency from 96 absolute filters backed b activated charcoal filters. The system design and testing are described. (H.D.R.)

42674 (BNWL-221) PHYSICS EXPERIMENT: HIGH POWER DENSITY CORE OF THE PRTR. Worden, J. R.; Purcell, W. L.; Schmid, L. C. (Battelle-Northwest, Richland, Wash. Pacific Northwest Lab.). Jan. 1966. Contract AT(45-1)-1830. 33p. Dep. mn. CFSTI $2.00 cy, $0.50 mn.

A high power density (HPD) core is described for the Plutonium Recycle Test Reactor. The core consists of 54 clusters of UO_2-2 wt % PuO_2 fuel elements. The experimental program with the HPD core is designed to determine both the excess reactivity and fuel composition of the core as functions of time. The core will be irradiated in increments of 2 months duration, at which time fuel rods will be selected for isotopic analysis. Critical experiments will also be performed to determine reactivity coefficients associated with core burnup. (H.D.R.)

42675 (BNWL-272) INVESTIGATION OF THE COMBINED FAILURE OF A PRESSURE TUBE AND DEFECTED FUEL ROD IN PRTR. Freshley, M. D.; Wheeler, R. G.; Batch, J. M.; Hesson, G. M. (Battelle-Northwest, Richland, Wash. Pacific Northwest Lab.). May 13, 1966. Contract AT(45-1)-1830. 151p. Dep. mn. CFSTI $5.00 cy, $1.00 mn.

An incident involving the rupture of an intentionally defeated HPD UO_2-PuO_2 fuel rod and a Zircaloy pressure tube occurred in the Fuel Element Rupture Test Facility of PRTR. Evaluations of the fuel, pressure tube, and thermal-hydraulic conditions were made. A possible rupture mechanism is proposed. (D.L.C.)

42676 (BNWL-281) NEUTRONICS CHARACTERISTICS OF POSSIBLE DRIVER FUELS FOR THE FAST TEST REACTOR (FTR). Little, W. W. Jr.; Hardie, R. W. (Battelle-Northwest, Richland, Wash. Pacific Northwest Lab.). May 1966. Contract AT(45-1)-1830. 29p. Dep. mn. CFSTI $2.00 cy, $0.50 mn.

The principal neutronics characteristics of 14 possible driver fuels for the Fast Test Reactor (FTR) are described. The fuels considered are PuO_2-SS cermets, $(Pu-U)O_2$ and (Pu-U)C ceramics, and Pu-U-Zr metals. For each fuel, core volumes of 600 and 800 liters are studied. The cermet fueled reactors are found to produce the highest flux for a given power density. Unmoderated 600 and 800 liter ceramic fueled reactors appear to have only a marginal Doppler coefficient. The Doppler coefficient can be significantly increased by adding BeO to the core. (auth)

42677 (BNWL-SA-636) PLUTONIUM RECYCLE TEST REACTOR DECONTAMINATION FOLLOWING A MgO-PuO_2 FUEL ELEMENT FAILURE. Perrigo, L. D.; Demmitt, T. F.; Hayden, K. D.; Weed, R. D.; Ayres, J. A. (Battelle-Northwest, Richland, Wash. Pacific Northwest Lab.). Mar. 31, 1966. Contract AT(45-1)-1830. 10p. (CONF-660520-3). Dep. mn. CFSTI $1.00 cy, $0.50 mn.

From International Symposium on the Decontamination of Nuclear Installations, Harwell, Eng.

The rupture of an experimental MgO-PuO_2 fuel element in the PRTR resulted in high radiation fields, necessitating chemical decontamination. In a $3\frac{1}{2}$ month period of time, the PRTR fuel elements were discharged and cleaned in an ultrasonic bath, the heavy water primary coolant was cleaned, drained and stored, a chemical addition system was installed and the reactor was decontaminated, inspected, tested, filled with D_2O and recharged with cleaned fuel elements. The chemical decontamination was successfully completed in ten days. Decontamination factors ranged from 2.2 to 15.0. This reduction in activity has permitted ready access and maintenance of equipment. The levels following decontamination were, in fact, significantly lower than those encountered prior to the rupture. The reactor has operated since the decontamination for over 34 months without any adverse effects from this cleaning operation. (auth)

42678 (EUR-3051.e) COMPARISON OF DIFFERENT METHODS FOR THE KINETICS OF AN ESSOR REACTOR TYPE. Forti, G.; Rinaldini, C.; Vincenti, E. (European Atomic Energy Community, Ispra (Italy). Joint Nuclear Research Center). July 1966. 14p. Dep. mn.

With the aim of investigating the kind of representation needed in the kinetics calculation of a reactor made up of three quite different regions, like the ESSOR reactor, three approaches were used: a point model method, a nodal method subdividing the reactor in three spatial regions, and a direct numerical solution of the time dependent diffusion equations. The results lead to the conclusions that, for a large category of transients, the point model is a good representation of the ESSOR reactor. (auth)

42679 (IAN-R-1) GUIA GENERAL PARA IRRADIACIONES EN EL REACTOR DE ENSENANZA E INVESTIGACION IAN-R1. (General Guide for Irradiations in the Research and Experimental Reactor IAN-R1). Sandoval, Edmundo; Barragan, Antonio; Casabianca, Manuel (Instituto de Asuntos Nucleares, Bogota (Colombia). Division Reactor). Apr. 1965. 37p. Dep. mn.

The experimental irradiation facilities of the IAN-R1 reactor and the physical characteristics of these facilities are described. Basic information on the calculation of activities and reactivity is presented. The procedures that should be followed in order to obtain authorization for the use of the irradiation facilities are indicated. The most common errors in irradiation experiments are tabulated. (J.S.R.)

42680 (INR-698/IX-A/RP) MEASUREMENT OF NEUTRON DENSITY DISTRIBUTIONS IN MULTILAYER UNIT CELLS. II. RESULTS FOR ANNA REACTOR CELL WITH WATER, 14.0 CM LATTICE PITCH. Adamski, L.; Jozefowicz, E. T.; Jozefowicz, K.; Szechter, A. (Institute of Nuclear Research, Warsaw (Poland)). Mar. 1966. 20p. Dep.

Neutron density distribution in the ANNA elementary cell, using water moderation and 14.0 cm lattice pitch, was measured using the spiral wire detector method. The results are given in the form of distributions of bare and subcadmium Cu activities. A discussion of experimental errors and difficulties of the method is included. (auth)

42681 (IS-1500(Sect. R)) ANNUAL SUMMARY REPORT IN REACTOR UTILIZATION. (Ames Lab., Iowa State Univ. of Science and Tech.). 38p.

Research progress is summarized on the operation of the Ames Laboratory Research Reactor (ALRR). Modifications, operation, and characteristics of the ALRR are described and studies in support of ALRR experiments are reported. (H.D.R.)

42682 (LA-3508) ESTIMATES OF THE POSSIBILITY OF HYDROGEN EMBRITTLEMENT OF TANTALUM IN THE FRCTF. Wohlberg, Cornel (Los Alamos Scientific Lab., Univ. of California, N. Mex.). Aug. 18, 1965. Contract W-7405-eng-36. 51p. Dep. mn. CFSTI $3.00 cy, $0.50 mn.

An evaluation was made of the possibility of destructive hydriding of Ta in the FRCTF. The assumption was made that even if the Na used in the reactor is well gettered in advance, undetermined amounts of H_2 will get into the system during installation of fuel elements and subsequent operations. The partial pressures of H_2 over Na were estimated on the basis of data from the literature. Equilibria between the H_2 in the Na and Ta were calculated. The H_2 picked up by Ta from Na cold trapped at 125°C will reach an equilibrium value of 40 ppM. Na that is not continuously cold trapped may hydride the Ta at 600°C to levels well above the known $TaH_{0.76}$ phase. The literature gives little information of use on the embrittling effect of H_2 in the range of 500-600°C. However, a level of 800-900 ppM H_2 ($TaH_{0.48}$) will embrittle Ta at room temperature. Since the amounts of possible H_2 contamination from various sources can not be estimated (H_2O, air, oils), continuous cold trapping, or another method of removal, is definitely indicated. In order to visualize the actual amounts of H_2 that may be tolerated in the system, estimates were made of the total weights of H_2 that would need to be absorbed by the Ta for various concentrations. A conservative estimate is that 0.180 kg H_2 in the reactor may raise the H_2 content of the fuel capsules to about 1000 ppM. In all of the computations made, some rather extreme extrapolations had to be made because of lack of data, particularly on the partial pressures of H_2 over unsaturated Na solutions. These extrapolations and collateral assumptions were stressed to indicate the type of information that is needed. (auth)

42683 (ORNL-TM-1559) AN INTERVAL TIMER DESIGNED FOR USE DURING IRRADIATIONS AT THE HEALTH PHYSICS RESEARCH REACTOR. Thorngate, J. H. (Oak Ridge National Lab., Tenn.). Aug. 1966. Contract W-7405-eng-26. 26p. Dep. mn. CFSTI $2.00 cy, $0.50 mn.

An inexpensive, reliable timer was designed and constructed that allows reactor runs to be timed from an arbitrary starting point for periods up to 27 hours. Timing precision to 2.7 hours is 1 second and is 10 seconds up to 27 hours. Accuracy depends upon the constancy of the 60-Hertz line frequency but is within one cycle of this frequency. Manual timing of arbitrary reactor runs is also possible with this device as the timer will always stop when a reactor shutdown occurs whether or not the timer is controlling the reactor. (auth)

42684 (UCRL-7695(Rev.1)) REVISED SAFETY ANALYSIS REPORT FOR THE SUPER KUKLA PROMPT BURST REACTOR. Gilbert, W. S.; Kloverstrom, F. A.; Rienecker, F. Jr. (Lawrence Radiation Lab., Univ. of California, Livermore). Feb. 4, 1964. Contract W-7405-eng-48. 44p. Dep. mn. CFSTI $2.00 cy, $0.50 mn.

The Super Kukla is an all-metal prompt burst reactor designed for the irradiation of test samples. Site and facility descriptions are given and the reactor control systems and operational procedures are described. The operating characteristics and hazards from a maximum credible accident are analyzed, and operational experience with the reactor is presented. (H.D.R.)

42685 NUCLEAR REACTOR FOR CARRYING OUT IRRADIATION TESTS. Hofman, Walther (to Reactor Centrum Nederland). British Patent 1,032,250. June 8, 1966. Filed Dec. 18, 1964.

A facility is described for irradiating with uniform radiation a large number of objects such as plants or crops placed on a platform. The reactor core is surrounded with a biological shield with an irradiation channel positioned under the reactor extending through the shield and having a vertical center line. The walls of the channel are outside a cone whose vertex lies within the reactor core and whose vertical angle is 25 to 45°. The radiation from the channel issues into an irradiation chamber that communicates by means of sealable entrances with two other chambers, one for pre-treatment and the other for after-treatment of objects to be irradiated. Suitable shielding is provided so that the objects can be irradiated selectively with either neutrons or gamma rays. (B.L.M.)

WASTE DISPOSAL AND PROCESSING

See also BIOLOGY AND MEDICINE — Ecology
CHEMISTRY — Radiochemistry
CHEMISTRY — Separation Processes and Procedures
HEALTH AND SAFETY

42686 FINAL ELIMINATION AND BURIAL OF RADIOACTIVE WASTES. Soenksen, Dieter. At. Strom, 12: 58-60(May-June 1966). (In German).

Individual reports made at a lecture series on the disposal of radioactive wastes in Germany are compiled. Reports are included on legal and nuclear principles to be followed in waste disposal, the cavern project, preparation of the caverns, mining behavior, long-term safety, and thermal measurements on the tunnel installation Asse II. (J.S.R.)

42687 STUDY, USING RADIOACTIVE TRACERS OF THE DISTRIBUTION OF WASTE WATER IN A DISPOSAL PROCESS. Guizerix, J. (SAR-CEA, Grenoble, France). Cah. CERBOM (Cent. Etud. Rech. Biol. Oceanogr. Med.), 17: 109-23(1965). (In French).

The use of tracer methods for the study of pollution problems at a radioisotope laboratory is discussed. The waste solutions studied contained substances in solution, bacteria, and suspended particulates. Results using a radioactive tracer, ^{82}Br, and a colored tracer, rhodamine B, are compared. Studies showed that rhodamine B was adsorbed on particulates in the waste solution while ^{82}Br was distributed evenly. Calculations showed that one C of ^{82}Br was equivalent to 1 kg of rhodamine B when used as a tracer. Applications of both methods for studies of dispersion phenomenon in soil in the vicinity of the Danish Isotope Center are reported. (C.H.)

42688 ACTIVE EFFLUENT TREATMENT PLANT. Sumitani, Shozo; Muramatsu, Takio (Ebara Mfg. Co., Ltd., Japan). FAPIG (Tokyo), No. 38, 187-90(Oct. 1965). (In Japanese).

The course taken in the design and construction of the active effluent treatment plant and part of the facilities of the Tokai power plant is described. To the original plan of the effluent treatment plant considerable modifications, taking into consideration the conditions peculiar to Japan, were made, and supplementary technological information was supplied by the United Kingdom, by experiments, and by other tests. Descriptions are presented of the cartridge cooling pond system, which includes the following parts: a cooling pond for spent fuel; CO_2 gas neutralization, condensation and sedimentation facilities; sand-filter beds; cation-exchangers; CO_2 removal columns; anion-exchangers; facilities for regenerating columns, etc.; and instrumentation. (NSA of Japan)

42689 THE PROCESSING OF RADIOACTIVE WASTES: THE RECOVERY OF FISSION PRODUCTS AS SOURCES OF RADIATION OR ENERGY. Dejonghe, P. Mededel. Landbouwhogeschool Opzoekingssta. Staat Gent, 30: 1193-1214(1965). (In French).

In almost all the nuclear industries radioactive wastes are produced. According to their nature and activity level, these wastes are either dilute in nature, stored, or subjected to a purification procedure permitting storage of a small volume of concentrate and the release of the purified water or gas. Dilution in nature can be considered only after a profound study of the medium with particular attention to the phenomena of decantation, local concentration, and absorption in the biological cycle. More than 99% of the total volume of radioactive waste produced can be purified by evaporation or by chemical treatment and ion exchange. The concentrates are stored permanently in concrete or by dispersion in a mass of liquid asphalt. The major part of the waste with a specific activity higher than 1 C/l comes from the wet processing of irradiated fuel elements. In the USA an annual production of highly radioactive waste containing ^{90}Sr and ^{137}Cs can be predicted: 3000 MC in 1970, 20,000 MC in 1980, and 530,000 MC in 2000. These wastes contain very significant quantities of ^{147}Pm and ^{237}Np. These wastes are present in such a concentration that a selective separation of some fission products can be considered. Techniques of chemical precipitation or extraction were developed. Techniques for the separation of the fission products Cs, Sr, and Pm by treatment on mineral ion exchangers were developed. The Cs separated can be used in γ sources, the strontium can be used in energy sources, Pm can be considered as an energy source in some space applications, and ^{237}Np can be transformed into ^{238}Pu by irradiation in a high flux reactor. ^{238}Pu is a source of α energy. The production of concentrated liquid wastes can be avoided by the use of retreatment techniques of fuels by volatilization. In this case the fission products are present in a dry form and are less dangerous but the recovery is more difficult. (tr-auth)

42690 ADDITION OF LITHIUM VALUES IN CONVERSION OF FISSION-PRODUCT WASTES TO A GLASS-LIKE SOLID FOR DISPOSAL. Clark, W. E.; Fitzgerald, C. L.; Davis, G. D. (to U. S. Atomic Energy Commission). U. S. Patent 3,265,627. Aug. 9, 1966.

Methods of disposing of radioactive wastes in the form of a solid mass are given. An improved glass-like composition was produced by adding lithium and sodium values in a lithium-to-sodium ratio of 0.75 : 1 to 1.5 : 1 to a glass-forming mixture containing radioactive wastes and then heating the resulting mixture to its melting point. The addition of lithium and sodium reduced the melting temperature of the solids and decreased the water-solubility of the vitreous mass produced. (AEC)

GENERAL AND MISCELLANEOUS

42691 (IS–1500) ANNUAL SUMMARY RESEARCH REPORT OF CHEMISTRY, ENGINEERING, METALLURGY, PHYSICS, AND REACTOR DIVISIONS, JULY 1, 1965–JUNE 30, 1966. (Ames Lab., Iowa State Univ. of Science and Tech.). July 1966. Contract W-7405-eng-82. 494p. Dep. mn. CFSTI $7.94 cy, $2.25 mn.

Research progress is reported on chemistry, engineering, mathematics and computers, metallurgy, physics, and reactors. Separate abstracts were prepared for each section. (M.C.G.)

For abstracts of individual sections see: 40796, 41064, 41406, 41412, 42523, and 42681.

42692 (TID–3736) BIBLIOGRAPHIES OF ATOMIC ENERGY LITERATURE. Issued or in Progress During the Period, June–July 1966. (Division of Technical Information Extension (AEC), Oak Ridge, Tenn.). 15p. Dep. DTI Extension Free.

Seventy-two bibliographies are presented on atomic energy literature, issued and in preparation. Author, subject, and report number indexes are included. (B.G.D.)

42693 (TID–4043(Rev.3)) INDEX TO CONFERENCES RELATING TO NUCLEAR SCIENCE. Clark, Willie E.; Patterson, Carol B.; Pflueger, Margaret L. (eds.) (Division of Technical Information Extension (AEC), Oak Ridge, Tenn.). July 1966. 323p. Dep. mn. CFSTI $7.00 cy, $1.50 mn.

The index is divided into five categories: permuted titles and cities, dates, numbered conferences, report numbers, and a title list. (B.G.D.)

42694 (TID–4577(Rev.2)) DESCRIPTIVE CATALOGING GUIDE. (Division of Technical Information Extension (AEC), Oak Ridge, Tenn.). July 1966. 81p. CFSTI $1.00 cy, $0.75 mn.

Rules for descriptive cataloging for the U.S.A.E.C. Division of Technical Information Extension are given. The preparation of cataloging form and draft tapes, reproduction copy and computer tapes, program tapes including cataloging elements, and examples for each type of item descriptively cataloged are considered. Also discussed are descriptive cataloging elements including composition rules. The code configurations for descriptive cataloging flexowriters are shown. (J.F.P.)

42695 (TRG-Report–1200) SOME STATISTICAL TECHNIQUES FOR REDUCING THE NUMBER OF MEASUREMENTS DURING INSPECTION. Fenna, D. (Reactor Group, United Kingdom Atomic Energy Authority, Springfields (England)). Feb. 15, 1966. 19p. Dep. BIS $0.50. HMSO 2s. 6d.

Assessment of the minimum number of measurements necessary to maintain a statistically defined quality is an important means of keeping down inspection costs. Some of the most widely used sampling schemes are described. As an example, a simple sampling scheme is evolved which enables a specification and a set of inspection results to be fed into a Mercury computer program giving as output the required sampling scheme. (auth)

CORPORATE AUTHOR INDEX

This index contains entries for this period for all report literature and, in addition, for certain published literature items for which it is felt that a corporate approach is especially desirable, e.g., symposia, conference proceedings, and meetings.

Each entry under a corporate author is a shortened version of the title of the publication, followed by the *NSA* volume and abstract number. Report numbers are given in parentheses.

The phrase "Progress report" is abbreviated as "Prog. rpt.," permitting a more rapid and complete alphabetical arrangement of the titles without changing the location of the progress report titles in relation to the other titles.

A

AEROJET-GENERAL NUCLEONICS, SAN RAMON, CALIF.
Prog. rpt. on alkali metals evaluation program, 1–3/66, 20: 41438 (AGN-8187)
Prog. rpt. on alkali metals evaluation, 4–6/66, 20: 41439 (AGN-8198)

AEROPROJECTS, INC., WEST CHESTER, PA.
Prog. rpt. on ultrasonic instrumentation for nuclear applications, 6–7/66, 20: 41225 (NYO-3622-4)

AEROSPACE TECHNOLOGY DIV., LIBRARY OF CONGRESS, WASHINGTON, D. C.
Effects of ionizing radiation on animals and plants, 20: 40602 (AD-624934)

AGRICULTURAL RESEARCH COUNCIL, WANTAGE (ENGLAND). RADIOBIOLOGICAL LAB.
Radioactivity in milk, 1965, 20: 41186 (ARCRL-15)

AIR FORCE CAMBRIDGE RESEARCH LABS., L. G. HANSCOM FIELD, MASS.
Effects of partial ionization and pressure on hydromagnetic ionizing waves, 20: 42401 (AD-637854)

AKTIEBOLAGET ATOMENERGI, STOCKHOLM (SWEDEN).
Possible odd parity state of ^{126}Xe, 20: 42147 (AE-240)

ALLISON DIV., GENERAL MOTORS CORP., INDIANAPOLIS, IND.
Prog. rpt. on bimetallic liquid metal systems, 2–5/66, 20: 41419 (GMAD-3643-5)

AMES LAB., IOWA STATE UNIV. OF SCIENCE AND TECH.
Prog. rpt. on chemistry, engineering, metallurgy, physics, and reactor research, annual, 7/65–6/66, 20: 42691 (IS-1500)
Reactor utilization, 20: 42681 (IS-1500(Sect. R))
Research in chemistry, 20: 40796 (IS-1500(Sect. C))
Research in engineering, 20: 41064 (IS-1500(Sect. E))
Research in mathematics and computer research, 20: 41406 (IS-1500 (Sect. M and C))
Research in metallurgy, 20: 41412 (IS-1500(Sect. M))
Research in physics, 20: 42523 (IS-1500(Sect. P))
Uranium metal by carbon reduction of uranium oxide in vacuum, 20: 41411 (IS-1379)

ARGONNE CANCER RESEARCH HOSPITAL, CHICAGO, ILL.
Determination of absorbed dose for electron beam therapy, 20: 40741 (ACRH-25, pp 15-23)
Prog. rpt., semiannual, 3/66, 20: 40740 (ACRH-25)
Thin foil calorimeter for electron beam dosimetry, 20: 40742 (ACRH-25, pp 24-9)

ARGONNE NATIONAL LAB., ILL.
Advanced systems research and development, 20: 42670 (ANL-7245, pp 48-59)
Averages of interferometric measurements of thorium lines, 20: 40798 (ANL-7209)
Civilian power reactors, 20: 42619 (ANL-7245, pp 1-28)
General reactor technology, 20: 42579 (ANL-7245, pp 29-47)
Laboratory animal science, review of literature, 1–3/66, 20: 40493 (ANL-7300)
Measurement of beam profiles with thermoluminescent dosimeters, 20: 41530 (ANL-7196)
Nuclear safety, 20: 42580 (ANL-7245, pp 60-73)
Prog. rpt. on reactor development, 6/66, 20: 42577 (ANL-7230)
Prog. rpt. on reactor development, 7/66, 20: 42578 (ANL-7245)

ARIZONA AGRICULTURAL EXPERIMENT STATION, TUCSON.
Prog. rpt. on uptake of Sr by crops, 1966, 20: 40524 (TID-23271)

ARMED FORCES RADIOBIOLOGY RESEARCH INST., BETHESDA, MD.
Erythrocyte stem cell kinetics in postradiation rat, 20: 40603 (AD-635086)
Low voltage D-T neutron source, 20: 42136 (AD-637457)

ARMY ENGINEER NUCLEAR CRATERING GROUP, LIVERMORE, CALIF.
Trace elements in common rock types, 20: 41068 (PNE-5006)

ATOMIC ENERGY COMMISSION, WASHINGTON, D. C.
AEC policy and action paper on controlled thermonuclear research, 20: 42416 (TID-23277)

ATOMIC ENERGY ESTABLISHMENT, WINFRITH (ENGLAND).
Improving accuracy of ^{240}Pu resonance escape probability measurements using Ir, 20: 42137 (AEEW-M-661)

ATOMIC ENERGY OF CANADA LTD., CHALK RIVER (ONTARIO).
Conical-face high pressure rotary shaft seals, 20: 41074 (AECL-2551)
Radiolysis of ortho- and meta-terphenyl. II., 20: 40946 (AECL-2589)

ATOMIC ENERGY OF CANADA LTD., CHALK RIVER (ONTARIO). CHALK RIVER NUCLEAR LABS.
Radioactive tracer to study rate of exchange of water vapor between air and natural surfaces, 20: 41150 (AECL-2576)
Tritium hazards, 20: 41185 (AECL-2594)

ATOMIC ENERGY OF CANADA LTD., PINAWA (MANITOBA). WHITESHELL NUCLEAR RESEARCH ESTABLISHMENT.
Commissioning of WR-1, 20: 42668 (AECL-2552)
Fuel, materials, and coolants for WR-1, 20: 42669 (AECL-2553)
Microdetermination of C and H polyphenyls, fouling films, and terphenyl mixtures, 20: 40797 (AECL-2524)

ATOMIC ENERGY RESEARCH ESTABLISHMENT, HARWELL (ENGLAND).
High temperature graphite rig for scattering law experiments, 20: 41075 (AERE-R-5217)
Irradiation experiments with plutonium dioxide suspensions, 20: 41009 (AERE-R-3268)
Two crystallographic computer programs for lattice parameter refinement and for calculating expected line positions, 20: 41437 (AERE-R-5210)

ATOMIC WEAPONS RESEARCH ESTABLISHMENT, ALDERMASTON (ENGLAND).
Uranium-fueled VERA reactor experiments, 20: 42671 (AWRE-R-5/66)

ATOMICS INTERNATIONAL, CANOGA PARK, CALIF.
Effects of molecular diffusion of heat on fluid velocity measurements, 20: 41101 (NAA-SR-Memo-10848)
Possible mechanism for the activation of UC, 20: 40870 (NAA-SR-Memo-7310)
UNICORN: a program to calculate point cross sections from resonance parameters, 20: 42141 (NAA-SR-11980(Vol.6))
1000-Mwe FBR parametric study of secondary sodium–steam system, 20: 42632 (NAA-SR-12060)

AUSTRALIAN ATOMIC ENERGY COMMISSION RESEARCH ESTABLISHMENT, LUCAS HEIGHTS.
Stability of Lucas Heights area against possible seismic events, 20: 41148 (AAEC-TM-316)

AUTHORITY HEALTH AND SAFETY BRANCH, UNITED KINGDOM ATOMIC ENERGY AUTHORITY, RISLEY (ENGLAND).
Safety of pressure vessels against fast fracture, 20: 42576 (AHSB(S)-R-107)

B

BABCOCK AND WILCOX CO., BARBERTON, OHIO. BOILER DIV.
Prog. rpt. on Na-heated steam generator, 4–6/66, 20: 42620 (BAW-1280-39)
BABCOCK AND WILCOX CO., NEW YORK.
PWR Core 2 steam generator, 20: 42646 (WAPD-PWR-2223)
BATTELLE MEMORIAL INST., COLUMBUS, OHIO.
Fabrication of Be. I., 20: 41427 (NASA-TM-X-53453(Vol.1))
BATTELLE MEMORIAL INST., GENEVA (SWITZERLAND).
Prog. rpt. on mechanical properties of metals subjected to mechanical stress at elevated temperatures and neutron irradiation, 1–3/66, 20: 41445 (EURAEC-1622)
Prog. rpt. on mechanical properties of metals subjected to mechanical stress at elevated temperatures and neutron irradiation, annual, 1965, 20: 41495 (EURAEC-1621)
BATTELLE-NORTHWEST, RICHLAND, WASH. PACIFIC NORTHWEST LAB.
Chlorine recovery and radioiodine behavior in salt cycle process, 20: 41029 (BNWL-279)
Dynamic analysis of Hanford dual-purpose reactor plant using analog simulation methods, 20: 42660 (BNWL-SA-270)
Evaluation of accuracy of decay scheme constants and calibration standards for ^{137}Cs, 20: 42148 (BNWL-87)
High power density core of the PRTR, 20: 42674 (BNWL-221)
Investigation of combined failure of pressure tube and defected fuel rod in PRTR, 20: 42675 (BNWL-272)
K-III: three region kinetics code in FORTRAN-IV, 20: 42606 (BNWL-252)
Melting points of hypostoichiometric uranium dioxide, 20: 41441 (BNWL-224)
Neutron and high energy particle dosimeter for medical dosimetry applications, 20: 41262 (BNWL-SA-619)
Neutronics characteristics of possible driver fuels for the Fast Test Reactor, 20: 42676 (BNWL-281)
Physiological data telemetry system, 20: 41220 (BNWL-214)
Plutonium Recycle Test Reactor decontamination following MgO–PuO_2 fuel element failures, 20: 42677 (BNWL-SA-636)
Plutonium utilization program, FY 1967–1970, 20: 42607 (BNWL-298)
Prog. rpt. on atmospheric sciences, annual, 1965, 20: 41188 (BNWL-235-1)
BELFER GRADUATE SCHOOL OF SCIENCE, YESHIVA UNIV., NEW YORK.
Prog. rpt. on stable isotope studies, annual, 7/65–8/66, 20: 40873 (NYO-3462-2)
BETTIS ATOMIC POWER LAB., PITTSBURGH, PA.
FLASH: program for digital simulation of loss of coolant accident, 20: 42582 (WAPD-TM-534)
PWR-2 omega seal welding machine, 20: 42648 (WAPD-PWR-2229)
PWR-2 omega seal weld cutting machines for refueling port, control rod mechanism ports, orifice adjustment ports, 20: 42649 (WAPD-PWR-2230)
PWR-2 reactor vessel closure head seal weld cutting machine, 20: 42650 (WAPD-PWR-2232)
Uranium-233 thorium seed-blanket experimental program, 20: 42609 (WAPD-T-1886)
BETTIS ATOMIC POWER LAB., WEST MIFFLIN, PA.
PWR-Core 2 steam generator, 20: 42645 (WAPD-PWR-2222)
PWR Core 2 steam generator, 20: 42646 (WAPD-PWR-2223)
PWR-2 axial flux measurement system equipment specification 568319, 20: 42647 (WAPD-PWR-2226)
BRANDEIS UNIV., WALTHAM, MASS.
Classical statistical mechanics of the hard-core potential, 20: 41509 (AD-638830)
BRAZIL UNIV., RIO DE JANEIRO. INSTITUTO DE BIOFISICA.
Prog. rpt. on radiochemical and radioecological studies on Brazilian areas of high natural radiation, annual, 5/65–6/66, 20: 40522 (NYO-3273-7)
BROOKHAVEN NATIONAL LAB., UPTON, N. Y.
Calculations of hard sphere packings in large cylinders, 20: 41063 (BNL-997)
Design, test, and use of reactor bypass filter facility, 20: 42673 (BNL-10483)
Effect of Xe on safety of HFBR, 20: 42672 (BNL-10388)
Effects of chronic gamma irradiation on lichen communities, 20: 40517 (BNL-9437)
Extracorporeal irradiation of blood and lymph, 20: 40744 (BNL-10403)
Growth of phase space in high intensity proton beams due to nonuniform radial charge distribution, 20: 41531 (BNL-10528)
Interpretation of microbeam experiments for manned space flight, 20: 41187 (BNL-9468)
Necturus maculosus as experimental animal to study cellular injuries of irradiated gut, 20: 40607 (BNL-10518)
Symmetry principles in physics, 20: 41923 (BNL-956)
Tritiated thymidine as cytocidal agent in human leukemia, 20: 40743 (BNL-9374)
600 MHz r-f system for 200 Bev accelerator, 20: 41532 (BNL-10559)
BROWN UNIV., PROVIDENCE, R. I. DIV. OF ENGINEERING.
Continuum theory of plasticity on the macroscale and the microscale, 20: 41454 (NYO-2394-22)
BUREAU OF COMMERCIAL FISHERIES, GLOUCESTER, MASS. TECHNOLOGICAL LAB.
Prog. rpt. on study of irradiated-pasteurized fishery products, final, 10/64–9/65, 20: 41384 (TID-22833)
BUREAU OF MINES, ALBANY, OREG. ALBANY METALLURGY RESEARCH CENTER.
Prog. rpt. on metallurgy, 4–6/66, 20: 41429 (USBM-RC-1249)
Prog. rpt. on selected properties of Th with low ThO_2 additions, 7/65–6/66, 20: 41462 (USBM-RC-1245)

C

CALIFORNIA UNIV., DAVIS.
Prog. rpt. on ^{90}Sr and ^{137}Cs food chain relationships to deer and sheep, 9/65–6/66, 20: 40541 (UCD-34P104-3)
CALIFORNIA UNIV., DAVIS. SCHOOL OF VETERINARY MEDICINE.
Prog. rpt. on radiobiology, annual, 6/65–6/66, 20: 40539 (UCD-472-113)
Radionuclide toxicity, 20: 40540 (UCD-472-113, pp 17-56)
X-irradiation effects, 20: 40638 (UCD-472-113, pp 1-16)
CALIFORNIA UNIV., SAN FRANCISCO. MEDICAL CENTER.
Repair of chromosomal damage, 20: 40609 (CONF-660418-1)
CANADIAN NUCLEAR ASSOCIATION, TORONTO (ONTARIO).
Commissioning of WR-1, 20: 42668 (AECL-2552)
Evaluation of CANDU: PHW fuels, 20: 42618 (66-CNA-312)
Fuel, materials, and coolants for WR-1, 20: 42669 (AECL-2553)
HWOCR program, 20: 42621 (CONF-660516-16)
Prog. rpt. on Pickering Generating Station, 5/66, 20: 42617 (66-CNA-303)
Role and requirements of heavy water in Canada and World, 20: 42616 (66-CNA-301)
WR-1: design and construction, 20: 42667 (66-CNA-309)
CASE INST. OF TECH., CLEVELAND, OHIO. DEPT. OF METALLURGY.
Prog. rpt. on transformation of Zr–Nb alloys, 7/66, 20: 41443 (COO-588-12)
CEKMECE NUCLEAR RESEARCH CENTER, ATOMIC ENERGY COMMISSION, ISTANBUL (TURKEY).
Neutron activation analysis of Roman copper coins from 250–500 A.D. II., 20: 40800 (CNAEM-35)
Parameters for the first neutron resonance in ^{113}Cd, 20: 42149 (CNAEM-34)
Producing mutants resistant to Peronospora tabacina by seed treatment with radiation, 20: 40613 (N-66-18147)
CENTRE NATIONAL DE RECHERCHES METALLURGIQUES, LIEGE (BELGIUM).
Prog. rpt. on plastic fatigue embrittlement of reactor vessel steels, 1–3/66, 20: 41446 (EURAEC-1642)
CHANTIERS DE L'ATLANTIQUE PENHOET-LOIRE, PARIS (FRANCE).
Prog. rpt. on application of submerged arc welding process to thick plates, 4–6/66, 20: 41450 (EURAEC-1684)
CHICAGO OPERATIONS OFFICE (AEC), ILL. REACTOR ENGINEERING DIV.
Evaluation of the Atomics International 1000 Mwe fast breeder reactor, 20: 42622 (COO-285)
CHILDREN'S CANCER RESEARCH FOUNDATION, BOSTON, MASS.
Prog. rpt. [on preservation of human platelets], 1966, 20: 40496 (NYO-1753-3)
COLORADO STATE UNIV., FORT COLLINS. COLL. OF VETERINARY MEDICINE.
Prog. rpt. on effects of ionizing radiation on functional and structural status of bull testicle, final, 2/65–7/66, 20: 40610 (COO-895-9)
COLUMBIA UNIV., NEW YORK.
Replication and genetic exchange in genome of Escherichia coli K-12, 20: 40538 (TID-23238)
COLUMBIA UNIV., NEW YORK. COLL. OF PHYSICIANS AND SURGEONS.
Lung carcinomas in irradiated parabiotic rats, 20: 40614 (NYO-901-39)
COLUMBIA UNIV., NEW YORK. RADIOLOGICAL RESEARCH LAB.
Biophysics, 20: 40618 (NYO-2740-3, pp 166-215)
Prog. rpt. on research project, annual, 1/66, 20: 40617 (NYO-2740-3)
Radiobiology, 20: 40619 (NYO-2740-3, pp 216-57)
Radiological physics, 20: 41268 (NYO-2740-3, pp 5-165)
COMITATO NAZIONALE PER L'ENERGIA NUCLEARE, ROME (ITALY).
Void fraction measurement in boiling channel, 20: 41103 (RT-ING-(65)7)
COMMISSARIAT A L'ENERGIE ATOMIQUE, CADARACHE (FRANCE). CENTRE D'ETUDES NUCLEAIRES.

Multisphere technique. I., 20: 41280 (NP-tr-1410)
COMMISSARIAT A L'ENERGIE ATOMIQUE, FONTENAY-AUX-ROSES (FRANCE). CENTRE D'ETUDES NUCLEAIRES.
Fallout in France after second Chinese nuclear explosion, 20: 41189 (CEA-R-3020)
Fixation of metallic acetates on an anion-exchange resin, 20: 41030 (CEA-R-2994)
Study of pigs subjected to lethal dose of integral γ irradiation, 20: 40608 (CEA-R-3001)
COMMISSARIAT A L'ENERGIE ATOMIQUE, SACLAY (FRANCE). CENTRE D'ETUDES NUCLEAIRES.
Installation for analytic chemistry under irradiation, 20: 40799 (CEA-R-2887)
Tables of range and stopping power of chemical elements for charged particles of energy 0.5 to 500 Mev, 20: 41619 (CEA-R-3042)

D

DANISH ATOMIC ENERGY COMMISSION, RISOE. RESEARCH ESTABLISHMENT.
Heat transfer experiment with multirod element, DOR design study, 20: 42635 (RISO-124)
DARESBURY NUCLEAR PHYSICS LAB. (ENGLAND).
NINA: 4 Bev electron synchrotron, 20: 41535 (DNPL-1)
Prog. rpt. on 4 Bev electron synchrotron, 10/65, 20: 41536 (DNPL-2)
DELHI UNIV. (INDIA). DEPT. OF PHYSICS AND ASTROPHYSICS.
Higher symmetries of hadrons, 20: 41928 (NP-16191)
DEPARTMENT OF AGRICULTURE, WASHINGTON, D. C.
Gamma irradiation of fruits to extend market life, 20: 41385 (TID-23136)
DEPARTMENT OF NATIONAL HEALTH AND WELFARE, OTTAWA (ONTARIO). RADIATION PROTECTION DIV.
Data from Radiation Protection Programs, Vol. 4, No. 5, 20: 41198 (NP-16192)
DEUTSCHES ELEKTRONEN-SYNCHROTRON, HAMBURG (WEST GERMANY).
Applications of the maximum likelihood method in high energy physics, 20: 41790 (DESY-66/17)
Current commutation relations in the framework of general quantum field theory, 20: 41924 (DESY-66/19)
Radiative corrections to bremsstrahlung and pair production at high energies, 20: 41789 (DESY-66/16)
Shielding high-energy electrons: the neutron and muon components, 20: 41534 (DESY-66/18)
Small angle electron proton elastic scattering cross sections for momentum transfers between 10 and 105 f^{-2}, 20: 41791 (DESY-66/20)
DIVISION OF ISOTOPES DEVELOPMENT (AEC), WASHINGTON, D. C.
Conference on radiation preservation of foods, Kansas City, Missouri, 5/65, 20: 41383 (CONF-650552)
DIVISION OF REACTOR DEVELOPMENT AND TECHNOLOGY (AEC), WASHINGTON, D. C. FUELS AND MATERIALS BRANCH.
Fuels and materials, LMFBR program, 20: 42651 (WASH-1065)
DIVISION OF TECHNICAL INFORMATION EXTENSION, (AEC), OAK RIDGE, TENN.
Bibliographies of atomic energy literature issued or in progress during the period, 6–7/66, 20: 42692 (TID-3736)
Descriptive Cataloging Guide, 20: 42694 (TID-4577(Rev.2))
Index to conferences relating to nuclear science, 20: 42693 (TID-4043 (Rev.3))
Supplemental insert sheets for engineering materials list, 20: 41065 (TID-4100(Suppl.34))
DU PONT DE NEMOURS (E. I.) & CO., AIKEN, S. C. SAVANNAH RIVER LAB.
Control system for x-ray diffractometer scanning, 20: 41222 (DP-900)
Curium process development. III-1., 20: 41032 (DP-1010)
Dissolution of ion exchange resins in alkaline permanganate, 20: 41031 (DP-717)
Fission counter for routine isotopic analysis of Pu, 20: 41264 (DP-552)
Quantitative electrodeposition of actinides from isopropyl alcohol, 20: 41010 (DP-1048)
DU PONT DE NEMOURS (E. I.) & CO., AIKEN, S. C. SAVANNAH RIVER PLANT.
Axial power monitoring with an on-line computer, 20: 42661 (DPSPU-66-30-2)

E

EANCO, INC., HATBORO, PA.
PWR-2 axial flux measurement system equipment specification 568319, 20: 42647 (WAPD-PWR-2226)
EDGERTON, GERMESHAUSEN AND GRIER, INC., BEDFORD, MASS.
Timing and firing, Project Dribble, 20: 41070 (VUF-3021)
EDGERTON, GERMESHAUSEN AND GRIER, INC., LAS VEGAS, NEV.
Photo-optical instrumentation at Nuclear Rocket Development Station, 20: 41223 (EGG-1183-1244)
Test cell A control systems, 20: 42663 (EGG-1183-1054)
EDGERTON, GERMESHAUSEN AND GRIER, INC., SANTA BARBARA, CALIF.
Design of shielded source for irradiation of animal populations, 20: 40518 (CEX-63.10)
Motion sensing and its application to Project Wisp, 20: 41224 (EGG-1183-2078)
Prog. rpt. on transient radiation effects, optical, 1/65, 20: 41488 (EGG-1183-2013)
Prog. rpt. on transient radiation effects, electrical, 1/65, 20: 41489 (EGG-1183-2014)
Prog. rpt. on transient radiation effects, electrical, 5/65, 20: 41490 (EGG-1183-2029)
Prog. rpt. on transient radiation effects, optical, 5/65, 20: 41491 (EGG-1183-2030)
Prog. rpt. on transient radiation effects, optical, 8/65, 20: 41492 (EGG-1183-2039)
Prog. rpt. on transient radiation effects in electronic materials, 10/65, 20: 41493 (EGG-1183-2052)
EUROPEAN ATOMIC ENERGY COMMUNITY.
Comparison of different methods for kinetics of ESSOR reactor type, 20: 42678 (EUR-3051.e)
Conference on megagauss magnetic field generation by explosives, Frascati, Italy, 9/65, 20: 41076 (EUR-2750.e)
Conference on practical aspects of activation analyses with charged particles, Grenoble, France, 6/65, 20: 40801 (EUR-2957.d,f,e)
Influence of certain factors on number of leukocytes in blood, 20: 40612 (EUR-2711.f)
Isothermal transport processes in molten salts binary systems, 20: 40866 (EUR-2954.e)
Organic coolant for Euratom's ORGEL program, 20: 42623 (EUR-2996.f)
EUROPEAN ATOMIC ENERGY COMMUNITY, ISPRA (ITALY). JOINT NUCLEAR RESEARCH CENTER.
Comparison of different methods for kinetics of ESSOR reactor type, 20: 42678 (EUR-3051.e)
Influence of certain factors on number of leukocytes in blood, 20: 40612 (EUR-2711.f)
Isothermal transport processes in molten salts binary systems, 20: 40866 (EUR-2954.e)
Organic coolant for Euratom's ORGEL program, 20: 42623 (EUR-2996.f)
EUROPEAN ORGANIZATION FOR NUCLEAR RESEARCH, GENEVA (SWITZERLAND).
Studies on capture efficiencies of synchro-cyclotrons, 20: 41533 (CERN-66-27)
Track centering system for IEPs using vibrating reed track detector, 20: 41263 (CERN-66-23)

F

FLORIDA STATE UNIV., TALLAHASSEE. DEPT. OF CHEMISTRY.
Effect of changes in ionic medium on stability constant of $Eu(NO_3)^{+2}$, 20: 40876 (ORO-1797-2)
FLORIDA UNIV., GAINESVILLE. DEPT. OF PATHOLOGY.
Prog. rpt. on toxicology of nickel carbonyl, 10/65–7/66, 20: 40536 (ORO-3461-1)
FLORIDA UNIV., GAINESVILLE. DEPT. OF SOILS.
Prog. rpt. on effects of gamma radiation on soil microorganisms, final, 1966, 20: 40637 (ORO-2754-7)
FOSTER WHEELER CORP., LIVINGSTON, N. J.
PWR-Core 2 steam generator, 20: 42645 (WAPD-PWR-2222)
FRANCIS DELAFIELD HOSPITAL, NEW YORK. DEPT. OF PATHOLOGY.
Lung carcinomas in irradiated parabiotic rats, 20: 40614 (NYO-901-39)

G

GENERAL DYNAMICS CORP., SAN DIEGO, CALIF. GENERAL ATOMIC DIV.
HTGR coated particle fuel, 20: 42624 (GA-6975)
Prog. rpt. on effect of substructure on irradiation stability of ASTM A302 grade B steel, 4/66, 20: 41451 (GA-7101)
GENERAL DYNAMICS/ELECTRONICS, ROCHESTER, N. Y.
PWR nuclear protection system, 20: 42640 (WAPD-PWR-2210(Vol.1))
GENERAL ELECTRIC CO., PHILADELPHIA, PA. MISSILE AND SPACE DIV.
Thermal integration of electric power and life support systems for manned space stations, 20: 41679 (NASA-CR-543)
GENERAL ELECTRIC CO., PLEASANTON, CALIF. VALLECITOS ATOMIC LAB.
Prog. rpt. on accurate nuclear fuel burnup analyses, 12/65–2/66, 20: 42608 (GEAP-5124)
GENERAL ELECTRIC CO., RICHLAND, WASH. HANFORD ATOMIC PRODUCTS OPERATION.

Thermal stability of nitrate form anion resins in vented system, 20: 40877 (RL-SEP-823)
Uranium trioxide product specification analyses, 20: 40802 (HW-65402(Rev.1))

GENERAL ELECTRIC CO., SAN JOSE, CALIF. ADVANCED PRODUCTS OPERATION.
Experimental studies of plutonium and fission product redistribution in fast reactor fuels, 20: 42625 (GEAP-4466)
Prog. rpt. on SEFOR, 2–4/66, 20: 42629 (GEAP-5160)

GENERAL ELECTRIC CO., SAN JOSE, CALIF. ATOMIC POWER EQUIPMENT DEPT.
Design and fabrication of ESADA-VESR Mark III superheat fuel clusters, 20: 42627 (GEAP-5051)
Prog. rpt. on High Power Density development, 6–11/65, 20: 42626 (GEAP-4951)
Prog. rpt. on pulsed neutron application to power reactor start-up procedures, 1–3/66, 20: 42628 (GEAP-5145)

GENERAL ELECTRIC CO., SAN JOSE, CALIF. VALLECITOS ATOMIC LAB.
Prog. rpt. on stainless steel failure, 1–3/66, 20: 41418 (GEAP-5150)

GOSUDARSTVENNYI KOMITET PO ISPOL'ZOVANIYU ATOMNOI ENERGII SSSR, OBNINSK. FIZIKO-ENERGETICHESKII INSTITUT.
Energy dependence of angular distribution of fragments in the fission of ^{233}U, ^{235}U, and ^{239}Pu induced by neutrons, 20: 42171 (LA-tr-66-41)

H

HAMBURG UNIV. (WEST GERMANY). II. INSTITUT FUER EXPERIMENTALPHYSIK.
Current commutation relations in the framework of general quantum field theory, 20: 41924 (DESY-66/19)
Small angle electron proton elastic scattering cross sections for momentum transfers between 10 and 105 f^{-2}, 20: 41791 (DESY-66/20)

HARVARD SCHOOL OF PUBLIC HEALTH, BOSTON, MASS.
Prog. rpt. on radioisotopes in bones and Po in cigarette smoke, final, 3/63–6/66, 20: 41191 (HUX-3170-1)

HEALTH AND SAFETY LAB., NEW YORK OPERATIONS OFFICE (AEC), N. Y.
Prog. rpt. on fallout, 3–6/66, 20: 41131 (HASL-172)

I

IDAHO NUCLEAR CORP., IDAHO FALLS.
Model for calculating the slow neutron scattering by liquid D_2O, 20: 42139 (IN-1020)
Slow neutron scattering kernels for H_2O at 423°K and 550°K, 20: 42138 (IN-1019)
Tabulation of the ^{233}Pa total neutron cross section data, 20: 42151 (IN-1014)

IDAHO OPERATIONS OFFICE (AEC), IDAHO FALLS. HEALTH AND SAFETY DIV.
Dose to various body organs from inhalation or ingestion of soluble radionuclides, 20: 41193 (IDO-12054)
Prog. rpt. on controlled environmental radioiodine tests, 8/66, 20: 41192 (IDO-12053)

IIT RESEARCH INST., CHICAGO, ILL.
Neutron capture gamma ray techniques for nondestructive analysis of reactor burnable poisons, 20: 41112 (IITRI-578P11-54)
Prog. rpt. on radiation synthesis involving halogen compounds, final, 5/60–10/65, 20: 40948 (COO-578-3-32)
Prog. rpt. on Zy braze alloy development, 4–6/66, 20: 41425 (IITRI-578-P29-2)
Shelter habitability in existing buildings under fire exposure, 20: 41184 (AD-637806)

ILLINOIS STATE UNIV., NORMAL. DEPT. OF BIOLOGICAL SCIENCES.
Prog. rpt. on comparative mutagenesis of Neurospora, 6/63–9/66, 20: 40510 (TID-23137)

INDUSTRIAL NUCLEONICS CORP., COLUMBUS, OHIO.
Prog. rpt. on helicopter close-order formation keeping system, 5–7/65, 20: 41221 (COO-1471-1)

INSTITUT ATOMNOI ENERGII, GOSUDARSTVENNYI KOMITET PO ISPOL'ZOVANIYU ATOMNOI ENERGII SSSR, MOSCOW.
Behavior of live organisms in radiation fields, 20: 40519 (NP-16259)
Instability of plasma with captured particles in toroidal geometry, 20: 42402 (IAE-1149)
Mobilities and forms of ^{90}Sr, stable Sr and Ca in turf-podzolic and black earth soil, 20: 40520 (NP-16261)
Plasma equilibrium in confined toroidal magnetic configurations, 20: 42403 (IAE-1151)

INSTITUT DE RECHERCHES DE LA SIDERURGIE, ST. GERMAINE-EN-LAYE (FRANCE).
Prog. rpt. on base metal for research on brittle fracture of weldments, 5/65–4/66, 20: 41447 (EURAEC-1669)

INSTITUT FUER PLASMAPHYSIK, G.M.B.H. GARCHING (WEST GERMANY).
Development and testing of a piezoelectric pressure probe with high-resolving power, 20: 42405 (IPP-1/46)
Device for operating a closed-loop MHD generator with current density measuring facilities, 20: 41678 (IPP-3/40)
Electrical conductivity of a partially ionized Ar–K plasma in a magnetic field, 20: 42410 (IPP-6/51)
Interferometer for three wavelengths: 2.5 mm, 4 mm, and 8 mm, 20: 42408 (IPP-2/49)
Investigation of a cesium plasma diode using an electron beam probing technique, 20: 42407 (IPP-2/48)
Ionization of barium on hot rhenium surfaces, 20: 42406 (IPP-2/47)
Monte Carlo simulation of the flow of a KNUDSEN gas with due allowance for the sojourn time, 20: 42035 (IPP-2/41)
Special magnetohydrostatic, axisymmetric meridional equilibria, 20: 42409 (IPP-6/50)

INSTITUTE OF NUCLEAR RESEARCH, WARSAW (POLAND).
Automatic control-system for samples transport, 20: 41077 (INR-696/I/PL)
Determination of statistical parameters of triple coincidence circuit, 20: 41265 (INR-704/III/PL)
Measurement of neutron density distributions in multilayer unit cells. II., 20: 42680 (INR-698/IX-A/RP)
Study of zero and two prong antiproton-proton interactions at 3–4 Bev/c primary momentum, 20: 41792 (INR-708/VI/PL)
Thorium recovering from Polish thorium ores, 20: 41033 (INR-678/IV/C)

INSTITUTE OF PLASMA PHYSICS, UNIV. OF NAGOYA (JAPAN).
Numerical computation of dispersive nonlinear equation, 20: 42411 (IPPJ-49)

INSTITUTE OF RADIATION PHYSICS, HELSINKI (FINLAND).
Radiostrontium in milk, grass and some other biological samples in Finland, 20: 41134 (SFL-A3)

INSTITUTO DE ASUNTOS NUCLEARES, BOGOTA (COLOMBIA). DIVISION REACTOR.
General guide for irradiations in the research and experimental reactor IAN-R1, 20: 42679 (IAN-R-1)

INSTITUTO DE ENERGIA ATOMICA, SAO PAULO (BRAZIL).
Preparation of carrier-free ^{131}I from irradiated elemental tellurium, 20: 41399 (IEA-110)

INSTITUTT FOR ATOMENERGI, HALDEN (NORWAY). OECD HALDEN REAKTOR PROSJEKT.
Dynamics of the Halden Boiling Water Reactor, 20: 42630 (HPR-66)

INSTITUTT FOR ATOMENERGI, KJELLER (NORWAY).
Refractometric determination of U(VI) in aqueous and in TBP solutions, 20: 40804 (KR-108)

INSTITUTUL DE FIZICA ATOMICA, ACADEMIA R. P. R., BUCHAREST (ROMANIA).
Stable isotopes applications. I., 20: 41380 (IFA-IS-36)

INSTYTUT ELEKTROTECHNIKI, WARSAW (POLAND). ZAKLAD RADIOLOGII PRZEMYSLOWEJ.
Prog. rpt. on standard method for testing packaging of radioactive materials for radiation leakage, final, 2/64–10/65, 20: 41197 (NP-16172)

INTERNATIONAL ATOMIC ENERGY AGENCY, VIENNA (AUSTRIA).
Naturally occurring radionuclides in human tissues, 20: 40531 (A/AC.82/G/L-1045(Rev.1))

INTERNATIONAL CENTRE FOR THEORETICAL PHYSICS, TRIESTE (ITALY).
WKB approximation in complex plane and applications to plasma theory, 20: 42404 (IC-66/45)

ISTITUTO SUPERIORE DI SANITA', ROME (ITALY). LABORATORI DI FISICA.
Protection against x rays from apparatus for medical use, 20: 40733 (ISS-66/16)

J

JOINT INST. FOR NUCLEAR RESEARCH, DUBNA (USSR). LAB OF HIGH ENERGY.
Reduction of the energy spectra of non-stable particles according to their decay, 20: 41927 (JINR-P-2797)

JOINT INST. FOR NUCLEAR RESEARCH, DUBNA (USSR). LAB. OF NEUTRON PHYSICS.
Decay of ^{184}Re, 20: 42157 (JINR-P-2814)
Kev neutron scattering by lead and electrical polarizability of neutron, 20: 42140 (JINR-P-2764)

JOINT INST. FOR NUCLEAR RESEARCH, DUBNA (USSR). LAB OF NUCLEAR PROBLEMS.
Decay mode of ^{160}Ho, 20: 42158 (JINR-P-2817)
Decay of ^{152}Tb, 20: 42155 (JINR-P-2762)
Recoil proton polarization in elastic $\pi^- - p$ scattering at 300 Mev and the phase shift analysis of pion-nucleon scattering, 20: 41794 (JINR-E-2860)

JOINT INST. FOR NUCLEAR RESEARCH, DUBNA (USSR). LAB OF NUCLEAR REACTIONS.
Mechanism of the proton transfer reactions, 20: 42153 (JINR-E-2824)
Some aspects of the multi-nucleon transfer reaction mechanism, 20: 42156 (JINR-P-2813)
Spontaneously fissionable isomer with the half-life equal to 10^{-7} s, 20: 42159 (JINR-P-2841)
JOINT INST. FOR NUCLEAR RESEARCH, DUBNA (USSR). LAB OF THEORETICAL PHYSICS.
Classification of systems generalized wave functions, realizing the representations of L(n,n) and P(n,n) groups, 20: 42071 (JINR-P-2785)
Dispersion sum rules for strong and electromagnetic interactions, 20: 41793 (JINR-E-2822)
Interpretation of parafield as an usual field with an inner degree of freedom, 20: 41925 (JINR-P-2756)
Matrix elements of Lorentz transformation for unitary concept, 20: 41926 (JINR-P-2777)
Structure of the ground and excited states of deformed odd-mass nuclei in the actinide region, 20: 42154 (JINR-E-2857)
JUNTA DE ENERGIA NUCLEAR, MADRID (SPAIN). DIVISION DE FISICA.
Decay scheme of ^{238}U, 20: 42152 (JEN-159-DF/I-49)
JUNTA DE ENERGIA NUCLEAR, MADRID (SPAIN). DIVISION DE QUIMICA.
Separation of iodine and xenon fission radionuclides, 20: 41034 (JEN-160-DQ/I-54)

K

KENTUCKY UNIV., LEXINGTON. DEPT. OF CHEMISTRY.
Determination of Br in terrestrial and extraterrestrial materials, 20: 40811 (ORO-2670-13)
KERNFORSCHUNGSANLAGE, JUELICH (WEST GERMANY). INSTITUT FUER RADIOCHEMIE.
Double fluorides of Th, U, Np, and Pu of type $Me^{II}Me^{IV}F_6$ with LaF_3 structure, 20: 40867 (KFK-385)
Separation and radiochemical determination of fission element activities, 20: 40803 (KFK-387)
KERNFORSCHUNGSZENTRUM, KARLSRUHE (WEST GERMANY). INSTITUT FUER ANGEWANDTE KERNPHYSIK.
Experiments to evaluate reactivity coefficients with reactor operating at steady state conditions (static experiments), 20: 42631 (KFK-260)
KERNKRAFTWERK RWE-BAYERWERK G.M.B.H., GUNDREMMINGEN (WEST GERMANY).
Prog. rpt. on 237 Mw KRB nuclear power plant, 10–12/65, 20: 42638 (TID-23299)
KIEL UNIV. (WEST GERMANY). INSTITUT FUER ANGEWANDTE PHYSIK.
Development of pattern for stimulation of nerve fiber after studies of x-ray effects on stimulus threshold, 20: 40606 (BMwF-FBK-66-02)
KNOLLS ATOMIC POWER LAB., SCHENECTADY, N. Y.
Carbon-12 fast neutron cross sections and Legendre moments below 15.0 Mev, 20: 42160 (KAPL-3099)
Instrumentation for detection of maximum permissible burden of ^{60}Co lung contamination, 20: 41190 (CONF-660621-4)

L

LABORATOIRE DE L'ACCELERATEUR LINEAIRE, UNIV. DE PARIS, ORSAY (FRANCE).
Secondary emission monitor, 20: 41266 (LAL-1028)
LABORATORI NAZIONALI DI FRASCATI, COMITATO NAZIONALE PER L'ENERGIA NUCLEARE (ITALY).
Computation of the effects of errors of a magnetic channel on the final beam parameters, 20: 41538 (LNF-66/29)
LABORATORIO GAS IONIZZATI, COMITATO NAZIONALE PER L'ENERGIA NUCLEARE, FRASCATI (ITALY).
Conference on megagauss magnetic field generation by explosives, Frascati, Italy, 9/65, 20: 41076 (EUR-2750.e)
LAWRENCE RADIATION LAB., UNIV. OF CALIFORNIA, BERKELEY.
Approximations in the theory of rearrangement collisions and applications to a tractable model of charge exchange scattering, 20: 41624 (UCRL-17034)
Developments in technique for monitoring high-energy accelerator radiation, 20: 41276 (UCRL-16769)
Effects of thyroid hormones on cultured mammalian cells, 20: 40511 (UCRL-16776)
Explosion tests in gloved box with ether-air mixtures, 20: 41203 (UCRL-16259)
K+p inelastic interactions at 2.7 Bev/c, 20: 41804 (UCRL-17003)
Measurement of the relative branching ratio $K^+ \to \mu^+ + \nu / K^+ \to \pi^+ + \pi^0$, 20: 41801 (UCRL-16003)
Production of $K\bar{K}$ pairs in π^-p interactions, 20: 41802 (UCRL-16832)
Prog. rpt. on physics, semiannual, 11/65–4/66, 20: 41803 (UCRL-16863)
Surface ionization of cesium and thermionic emission from planar single crystals of tungsten, 20: 41681 (UCRL-11857)
System for measuring concentrations of atmospheric ^{222}Rn, 20: 41277 (UCRL-16952)
LAWRENCE RADIATION LAB., UNIV. OF CALIFORNIA, LIVERMORE.
Bibliography on elastic and inelastic p-p scattering, 20: 41800 (UCRL-14716)
Cathodic etching to prepare radioactive samples for oxygen determination, 20: 40817 (UCRL-14959)
Finite temperature thermodynamics for the modified Hartree-Fock electron gas, 20: 41623 (UCRL-14904)
Fission γ rays using Ge(Li) detector in conjunction with bent-crystal spectrometer, 20: 41278 (UCRL-70000)
Gamma mapping of liver with the digital computer, 20: 40747 (UCRL-14866)
High-resolution studies of fission x rays and gamma rays, 20: 42170 (UCRL-70045)
Long John thermo-gasdynamic research facility, 20: 41104 (UCRL-14841)
Magnetic pulse in a cold collision-free plasma, 20: 42417 (UCRL-7170)
Mechanisms that affect adsorption of methyl iodide on charcoal under humid conditions, 20: 41202 (UCRL-14990)
Nuclear and atomic physics, 20: 42169 (UCRL-14744, pp 1-18)
Prog. rpt. on noble-metal, metal sheathed thermocouples, final, 9/65, 20: 41461 (UCRL-7361(Pt.3))
Prog. rpt. on physics, 10/65–1/66, 20: 41512 (UCRL-14744)
Radiation and plasma physics, 20: 42418 (UCRL-14744, pp 37-48)
Revised safety analysis report for the Super Kukla prompt burst reactor, 20: 42684 (UCRL-7695(Rev.1))
Thermodynamic properties of matter, 20: 41513 (UCRL-14744, pp 19-36)
Very high magnetic fields produced by capacitor-bank discharge, 20: 41080 (UCRL-14831)
LOCKHEED MISSILES AND SPACE CO., PALO ALTO, CALIF.
Fabrication of Be. I., 20: 41427 (NASA-TM-X-53453(Vol.1))
LOS ALAMOS SCIENTIFIC LAB., UNIV. OF CALIFORNIA, N. MEX.
Beta-gamma radioactivity in environmental air at Los Alamos, New Mexico, 1965, 20: 41194 (LA-3516)
(d,pf) and (t,pf) reactions on Pu isotopes, 20: 42161 (LA-DC-7878)
Determination of small widths in the continuum, 20: 42164 (LA-DC-8083)
Direct and compound-nucleus reactions for $^{32}S(d,p)^{33}S$ at low energies, 20: 42163 (LA-DC-8082)
Estimates of possibility of H embrittlement of Ta in FRCTF, 20: 42682 (LA-3508)
Kiwi Transient Nuclear Test dose rate survey, 20: 41195 (LA-3519)
Large-scale electrorefining of Pu from Ga alloys, 20: 41035 (LA-2758)
Prog. rpt. on medium-energy physics, 7/66, 20: 41537 (LA-3587)
Solubilities of selected elements in liquid Pu. VIII., 20: 40868 (LA-3523)
Studies on the formation of Pu_2O_3 in the sintering of PuO_2, 20: 41426 (LA-3493)
Total reaction cross sections for 14.5 Mev protons from 22 separated isotopes of Ti, Fe, Ni, Cu, Zn, Zr, and Sn, 20: 42162 (LA-DC-8075)
Tritium contamination, 20: 41196 (LA-DC-7996)

M

MALLINCKRODT CHEMICAL WORKS, WELDON SPRING, MO. URANIUM DIV.
Calibration of Westphal balance and plummet, 20: 40869 (MCW-1473)
Electrolytic recovery of scrap uranium metal, 20: 41036 (MCW-1494)
MARYLAND UNIV., COLLEGE PARK. DEPT. OF PHYSICS AND ASTRONOMY.
Prog. rpt. on properties of K mesons and hyperons and related topics in high energy physics, 10/65–9/66, 20: 41799 (ORO-2504-96)
MASSACHUSETTS INST. OF TECH., CAMBRIDGE.
π_0 photoproduction at 3.0, 4.0, and 5.0 Bev for baryon four momentum transfers between 0.5 and 4.0 (Bev/c)^2, 20: 41798 (MIT-2098-265)
Search for fractionally charged, weakly interacting particles, 20: 41797 (MIT-2098-264)
MASSACHUSETTS INST. OF TECH., CAMBRIDGE. LAB. FOR NUCLEAR SCIENCE.
Cosmic ray group, 20: 41667 (MIT-2098-251, pp 1-13)
Cyclotron group, 20: 42168 (MIT-2098-251, pp 57-73)
Experiments and target-gas storage at the CEA at the time of the July 5, 1965 accident and fire, 20: 41539 (MIT-2098-259)
High energy accelerator physics group, 20: 41795 (MIT-2098-251, pp 21-36)
Linear accelerator group, 20: 42165 (MIT-2098-251, pp 16-20)
O.N.R. generator group, 20: 42166 (MIT-2098-251, pp 37-49)
Prog. rpt. on physics, 11/64–12/65, 20: 41510 (MIT-2098-251)
Radioactivity group, 20: 42167 (MIT-2098-251, pp 50-6)
Theoretical group, 20: 41796 (MIT-2098-251, pp 74-103)
MASSACHUSETTS INST. OF TECH., CAMBRIDGE. RESEARCH LAB. OF ELECTRONICS.

Pulsed electron-cyclotron resonance discharge experiment, 20: 42412 (MIT-3221-19)

MASSACHUSETTS UNIV., AMHERST. POLYMER RESEARCH INST.
Prog. rpt. on crystal orientation in irradiated polyethylene, final, 5/62–4/66, 20: 40949 (NYO-3003-29)

MATERIALS RESEARCH LAB., INC., RICHTON PARK, ILL.
Prog. rpt. on fracture toughness of reactor pressure vessel steels, 6–7/66, 20: 41444 (COO-1477-5)

MAX-PLANCK-INSTITUT FUER PHYSIK UND ASTROPHYSIK, MUNICH (WEST GERMANY).
Photoelectric recording device of high sensitivity and accuracy for spectrographs, 20: 41267 (MPI-PAE-P1-30/66)

MICHIGAN STATE UNIV., EAST LANSING. DEPT. OF PHYSICS
Prog. rpt. on interactions between f-shell transition ions in non-metallic crystals, annual, 10/1/65–6/15/66, 20: 42522 (COO-1533-2)

MICHIGAN UNIV., ANN ARBOR. DEPT. OF METEOROLOGY AND OCEANOGRAPHY.
Prog. rpt. on rain scavenging studies, 3/65–5/66, 20: 41130 (COO-1407-10)

MILAN UNIV. (ITALY). ISTITUTO DI GENETICA.
Revision frequency of waxy pollen type in normal and hypoploid maize plants, 20: 40509 (TID-22965)

MINNESOTA UNIV., MINNEAPOLIS.
Prog. rpt. on genetic control of physiological processes in higher plants, 1965-66, 20: 40532 (COO-1097-17)

MOUND LAB., MIAMISBURG, OHIO.
Analytical and instrumentation, 20: 40805 (MLM-1325, pp 63-70)
Differential thermal analysis study of impurities in plutonium, 20: 41452 (MLM-1172)
Prog. rpt., 1–3/66, 20: 41037 (MLM-1325)
Radioelements, 20: 41038 (MLM-1325, pp 9-62)

MOUNT SINAI HOSPITAL, NEW YORK. DEPT. OF HEMATOLOGY.
Tritiated thymidine as cytocidal agent in human leukemia, 20: 40743 (BNL-9374)

MSA RESEARCH CORP., EVANS CITY, PA.
Prog. rpt. on effect of high temperature Na on steels, 4–6/66, 20: 41420 (MSAR-66-149)

MUNICH UNIV. (WEST GERMANY).
Chemistry of Pm, 20: 40872 (NP-16254)

N

NATIONAL ACADEMY OF SCIENCES–NATIONAL RESEARCH COUNCIL, WASHINGTON, D. C. COMMITTEE ON NUCLEAR SCIENCE.
Activation analysis with charged particles, 20: 40806 (NAS-NS-3110)

NATIONAL AERONAUTICS AND SPACE ADMINISTRATION, CLEVELAND, OHIO. LEWIS RESEARCH CENTER.
Monte Carlo method for calculation of transport properties in a low-density ionized gas, 20: 42413 (NASA-TN-D-2959)

NATIONAL INST. FOR RESEARCH IN NUCLEAR SCIENCE, CHILTON (ENGLAND). RUTHERFORD HIGH ENERGY LAB.
Neutron dosimetry methods and experience on the 7 Bev proton synchrotron, Nimrod, 20: 41543 (RPP-R-2)
Nimrod electrostatic inflector, 20: 41542 (RHEL/R-125)

NATIONAL LEAD CO. OF OHIO, CINCINNATI.
Effects of graphite electrodes on carrier distillation of impurities in U_3O_8, 20: 40807 (NLCO-976)

NATIONAL RADIATION LAB., CHRISTCHURCH (NEW ZEALAND).
Prog. rpt. on environmental radioactivity in New Zealand, 1–3/66, 20: 40521 (NP-16270)

NAVAL CIVIL ENGINEERING LAB., PORT HUENEME, CALIF.
Differential neutron albedo for thin slabs, 20: 42142 (NP-16234)

NAVAL RADIOLOGICAL DEFENSE LAB., SAN FRANCISCO, CALIF.
Gamma rays resulting from interactions of 14.7 Mev neutrons with Na, S, Cl, K, and Pb, 20: 42146 (AD-638014)
Radiation-protection and recovery from radiation injury in endotoxin-treated mice, 20: 40732 (AD-636209)
Recovery from radiation injury in swine, 20: 40605 (AD-635735)
Treadmill exercise performance by aging irradiated rat, 20: 40604 (AD-635251)

NAVAL RESEARCH LAB., WASHINGTON, D. C.
Emission spectra of various thermoluminescent materials, 20: 42524 (NRL-6408)

NEW ENGLAND DEACONESS HOSPITAL, BOSTON, MASS. CANCER RESEARCH INST.
Biological chemistry, 20: 40533 (NYO-901-54, pp 16-19)
Biophysics: activation analysis in forensic medicine, 20: 40810 (NYO-901-54, pp 20-3)
Biophysics and radiation protection, 20: 40734 (NYO-901-54, pp 24-5)
Biostatistics and administration, 20: 40615 (NYO-901-54, pp 26-8)
Experimental pathology, 20: 40745 (NYO-901-54, pp 29-47)
Lung carcinomas in irradiated parabiotic rats, 20: 40614 (NYO-901-39)
Prog. rpt. [on biological problems in cancer and radiation], 5/65–4/66, 20: 40495 (NYO-901-54)
Radiobiology, 20: 40616 (NYO-901-54, pp 48-50)

NEW YORK STATE PSYCHIATRIC INST., NEW YORK.
Prog. rpt. on human chromosome analysis, final, 11/65, 20: 40497 (NYO-3400-1)

NEW YORK UNIV., N. Y. SCHOOL OF ENGINEERING AND SCIENCE.
Distribution of ^{226}Ra, ^{228}Ra, ^{210}Pb, and ^{228}Th in bone and soft tissue of Ra dial painters, 20: 40621 (NYO-3086-5)

NIJVERHEIDSORGANISATIE (TNO), THE HAGUE (NETHERLANDS).
Prog. rpt. on embrittlement in steel with respect to irradiation, 1–3/66, 20: 41494 (EURAEC-1617)

NORSK HYDRO'S INST. FOR CANCER RESEARCH, OSLO.
Cesium-137 in milk in Norway 1962–1966, 20: 41132 (NYO-3364-20)

NORSK RADIUMHOSPITAL, OSLO.
Cesium-137 in milk in Norway 1962–1966, 20: 41132 (NYO-3364-20)
Induced radioactivity in collimator system of a 31 Mev Brown Boveri betatron, 20: 41540 (NYO-3364-7(Rev.))

NORTH CAROLINA STATE COLL., RALEIGH.
Prog. rpt. on radiation genetics and radiation resistance in peanuts, annual, 7/65–6/66, 20: 40636 (ORO-1747-12)

NORTHWESTERN UNIV., EVANSTON, ILL. TECHNOLOGICAL INST.
Prog. rpt. on high temperature oxidation of metals, final, 2/62–5/66, 20: 41458 (TID-23268)

NOTRE DAME UNIV., IND.
Directional correlation measurements in decay of ^{160}Tb employing a Ge–Li detector, 20: 42150 (COO-498-56)

NUCLEAR MATERIALS AND EQUIPMENT CORP., APOLLO, PA.
Prog. rpt. on growth of single crystals of Pu, 1–3/66, 20: 41453 (NUMEC-3428-21)

NUKLEARNI INSTITUT "JOZEF STEFAN," LJUBLJANA (YUGOSLAVIA).
Mass spectrometric study on the isotope effect in secondary electron emission from metal surfaces by positive ions, 20: 41620 (NIJS-R-471)

O

OAK RIDGE NATIONAL LAB., TENN.
AEC–NASA space biology, 20: 40508 (ORNL-3922, pp 196-9)
AEC–NIH chemical carcinogenesis, 20: 40632 (ORNL-3922, pp 175-91)
AEC–NIH zonal ultracentrifuge development, 20: 40507 (ORNL-3922, pp 191-6)
Biochemical regulation, 20: 40506 (ORNL-3922, pp 168-73)
Biophysical and biochemical cytology, 20: 40581 (ORNL-3922, pp 50-1)
Biophysics, 20: 40504 (ORNL-3922, pp 146-60)
Bone marrow system for studying recovery from radiation injury, 20: 40634 (ORNL-P-2312)
Cell growth and differentiation, 20: 40499 (ORNL-3922, pp 69-79)
Cell physiology, 20: 40500 (ORNL-3922, pp 109-12)
Characterization of radioactive particulate aerosols by fibrous filter analyzer, 20: 41234 (ORNL-P-2436)
Chemical protection and enzyme catalysis, 20: 40719 (ORNL-3922, pp 136)
Computer program to calculate high-temperature thermodynamic functions, 20: 40875 (ORNL-TM-1599)
Creep-rupture properties of tungsten and tungsten-base alloys, 20: 41456 (ORNL-3992)
Cytochemistry and cell reproduction, 20: 40582 (ORNL-3922, pp 65-8)
Cytology and genetics, 20: 40623 (ORNL-3922, pp 32-49)
Data collection and analysis, 20: 41232 (ORNL-3875, pp 75-90)
Data on a set of trinomial distributions, 20: 41407 (ORNL-4004)
Detectors of ionizing particles and radiation, 20: 41271 (ORNL-3875, pp 44-52)
Drosophila cytology and genetics, 20: 40625 (ORNL-3922, pp 59-64)
Electrometers and accessories, 20: 41270 (ORNL-3875, pp 13-14)
Electron spin resonance spectra of Dy^{3+} in ThO_2 and CeO_2, 20: 42525 (ORNL-P-2466)
Enzymology, 20: 40503 (ORNL-3922, pp 137-45)
Estimation of beta radiation dose to skin by field instrument measurements, 20: 41274 (ORNL-TM-1581)
Fabrication and maintenance of electronic instruments, 20: 41229 (ORNL-3875, pp 21-3)
Fungal genetics, 20: 40624 (ORNL-3922, pp 52-8)
Human cytogenetics, 20: 40628 (ORNL-3922, pp 89-93)
Influence of age on susceptibility to radiation-induced life-shortening in mice, 20: 40633 (ORNL-P-2287)
Instrumentation for automatic control, 20: 41230 (ORNL-3875, pp 24-34)
Instrumentation for biomedical research, 20: 41231 (ORNL-3875, pp 35-43)
Instrumentation for reactor division test loops, 20: 42585 (ORNL-3875, pp 151-8)
Interval timer designed for use during irradiations at Health Physics Research Reactor, 20: 42683 (ORNL-TM-1559)
Lists of available and desired materials and available crystal-growth

references, 20: 40874 (ORNL-RMIC-5)
Low energy electron studies in indium and magnesium, 20: 41621 (ORNL-TM-1565)
Mammalian genetics, 20: 40627 (ORNL-3922, pp 84-8)
Mammalian recovery, 20: 40718 (ORNL-3922, pp 99-105)
Microbiology, 20: 40505 (ORNL-3922, pp 167)
Miscellaneous electronics development, 20: 41228 (ORNL-3875, pp 15-20)
Nanosecond circuitry and techniques, 20: 41227 (ORNL-3875, pp 1-3)
Nucleic acid chemistry, 20: 40501 (ORNL-3922, pp 113-14)
Nucleic acid enzymology, 20: 40535 (ORNL-3922, pp 128-35)
Operating guide for radiochemical laboratories at various activity levels, 20: 41199 (ORNL-TM-626)
Pathology and physiology, 20: 40502 (ORNL-3922, pp 115-27)
Plant physiology and photosynthesis, 20: 40631 (ORNL-3922, pp 161-6)
Preparation of charge materials for ORNL electromagnetic isotope separators, 20: 41400 (ORNL-3301(Suppl.1))
Process instrumentation and control systems engineering, 20: 41078 (ORNL-3875, pp 91-100)
Process instrumentation development, 20: 41233 (ORNL-3875, pp 101-24)
Prog. rpt. on biology, semiannual, 8/65–1/66, 20: 40498 (ORNL-3922)
Prog. rpt. on chemical applications of nuclear explosions, 4–6/66, 20: 41067 (ORNL-TM-1582)
Prog. rpt. on instrumentation and controls, annual, 9/65, 20: 41226 (ORNL-3875)
Prog. rpt. on synergistic effect of zero-G and radiation on white blood cells, annual, 6/64–6/65, 20: 40635 (ORNL-TM-1550)
Prog. rpt. on transuranium program, 2/28/65, 20: 41039 (ORNL-3880)
Pulse counting and analysis, 20: 41269 (ORNL-3875, pp 4-12)
Radiation immunology, 20: 40626 (ORNL-3922, pp 80-3)
Radiation microbiology, 20: 40629 (ORNL-3922, pp 94-8)
Radiation monitoring, 20: 41272 (ORNL-3875, pp 53-74)
Reactor instrumentation and controls, 20: 42581 (ORNL-3875, pp 125-50)
Replication and genetic exchange in genome of Escherichia coli K-12, 20: 40538 (TID-23238)
Review of ORNL electromagnetic separations program, 1965, 20: 41401 (ORNL-4006)
Separation of Sr and Ba by cation exchange, 20: 41040 (ORNL-TM-1342)
Subcellular and viral physiology, 20: 40630 (ORNL-3922, pp 106-8)
Support for the high-voltage accelerator program, 20: 41541 (ORNL-3875, pp 159-63)
Temperature dependence of response of lithium-drifted germanium detectors to gamma rays, 20: 41273 (ORNL-TM-1295)
Temperature distribution under dimples proposed as spacers in the BONUS superheater assemblies, 20: 42634 (ORNL-TM-1453)
Temperatures in the cladding under the spacers of the BONUS superheater assemblies, 20: 42633 (ORNL-TM-1452)
Urethane spray foaming, 20: 41200 (ORNL-TM-1551)

OERLIKON ELEKTRODENFABRIK EISENBERG G.M.B.H. (WEST GERMANY).
Prog. rpt. on breaking strength of weldments on heavy-gage tensile steels, 9–12/65, 20: 41410 (EURAEC-1612)
Prog. rpt. on breaking strength of weldments on heavy-gage tensile steels, 1–3/66, 20: 41448 (EURAEC-1670)

OESTERREICHISCHE STUDIENGESELLSCHAFT FUER ATOMENERGIE G.M.B.H., SEIBERSDORF. INSTITUT FUER CHEMIE.
Molecular plating. V., 20: 41011 (SGAE-CH-34/1966)

OESTERREICHISCHE STUDIENGESELLSCHAFT FUER ATOMENERGIE G.M.B.H., SEIBERSDORF. PHYSIK-INSTITUT.
Apparatus for motion transfer in a vacuum system, 20: 41125 (SGAE-PH-41/1966)

OFFICE OF SALINE WATER, WASHINGTON, D. C.
Potentialities and possibilities of desalting for Northern New Jersey and New York City, 20: 42658 (NP-16250)

OREGON STATE UNIV., CORVALLIS. DEPT. OF OCEANOGRAPHY.
Prog. rpt. on ecological studies of radioactivity in Columbia River and adjacent Pacific Ocean, annual, 7/65–6/66, 20: 40523 (RLO-1750-8 (Vol.1))

P

PENNSYLVANIA STATE UNIV., UNIVERSITY PARK. DEPT. OF AGRONOMY.
Accumulation of Ca, Sr, Mg, P and Zn by genotypes of corn under different soil fertility levels, 20: 40735 (NYO-2744-37)

PENNSYLVANIA STATE UNIV., UNIVERSITY PARK. DEPT. OF BIOPHYSICS.
Effects of irradiated medium on cellular functions of E. coli, 20: 40580 (NYO-2804-8)
Study on DNA degradation in Escherichia coli produced by ionizing radiation, 20: 40620 (NYO-2804-9)

PHILLIPS PETROLEUM CO. IDAHO FALLS, IDAHO., ATOMIC ENERGY DIV.
Prog. rpt. on STEP project, 7–9/65, 20: 42664 (IDO-17165)

PHYSIKALISCHES STAATSINSTITUT, HAMBURG (WEST GERMANY).
Current commutation relations in the framework of general quantum field theory, 20: 41924 (DESY-66/19)

PITTSBURGH UNIV., PA. DEPT. OF BIOCHEMISTRY AND NUTRITION.
Prog. rpt. on nuclear metabolism of DNA and RNA and sites of radiation sensitivity, 10/65–7/66, 20: 40534 (NYO-3621-1)

PRATT AND WHITNEY AIRCRAFT, MIDDLETOWN, CONN. CONNECTICUT ADVANCED NUCLEAR ENGINEERING LAB.
Heat capacity and enthalpy of UN from 0 to 1200C, 20: 40865 (CNLM-4461)
Physical properties of materials, 20: 41442 (CNLM-2393)
Viscosity of liquid K to 900°C, 20: 41460 (TIM-793)

PRODUCTION GROUP, UNITED KINGDOM ATOMIC ENERGY AUTHORITY, SELLAFIELD (ENGLAND).
Dissolution and preliminary purification of irradiated U fuel specimens, 20: 41042 (PG-Report-722)
Preparation of purified U_3O_8 from irradiated U, 20: 41041 (PG-Report-698)

PUBLIC HEALTH SERVICE, WASHINGTON, D. C.
Radionuclide analysis of environmental samples, 20: 40809 (NP-16235)

PUERTO RICO NUCLEAR CENTER, MAYAGUEZ.
Prog. rpt. on matrix isolation studies of products of γ-radiolysis of heterocyclic molecules, annual, 1965-66, 20: 40950 (PRNC-88)

R

RADIATION RESEARCH ASSOCIATES, INC., FORT WORTH, TEX.
Performance of enclosure shields in real fallout field, 20: 41201 (RRA-T55 and Summary)

RADIO CORP. OF AMERICA, LANCASTER, PA. DIRECT ENERGY CONVERSION DEPT.
Prog. rpt. on adsorption Cs reservoir, 4–6/66, 20: 41680 (NYO-3642-2)

RAND CORP., SANTA MONICA, CALIF.
Development of a radio signal from a nuclear explosion in the atmosphere, 20: 42046 (RM-4988)

REACTOR GROUP, UNITED KINGDOM ATOMIC ENERGY AUTHORITY, SPRINGFIELDS (ENGLAND).
Some statistical techniques for reducing the number of measurements during inspection, 20: 42695 (TRG-Report-1200)

RENSSELAER POLYTECHNIC INST., TROY, N. Y.
Decontamination of products from chemonuclear reactions, 20: 40951 (RPI-321-6)

RESEARCH AND ADVANCED DEVELOPMENT DIV., AVCO CORP., WILMINGTON, MASS.
Prog. rpt. on human chromosome analysis, final, 11/65, 20: 40497 (NYO-3400-1)

RESEARCH TRIANGLE INST., DURHAM, N. C.
Radiological recovery requirements, structures, and operations research. I., 20: 41179 (AD-635821)
Radiological recovery requirements, structures, and operations research. II., 20: 41180 (AD-635822)
Radiological recovery requirements, structures, and operations research. IV., 20: 41182 (AD-635824)
Radiological recovery requirements, structures, and operations research. III., 20: 41181 (AD-635823)

ROCKEFELLER UNIV., NEW YORK.
Prog. rpt. on genetic studies, annual, 6/65–6/66, 20: 40622 (NYO-3096-8)

ROCKY FLATS DIV., DOW CHEMICAL CO., GOLDEN, COLO.
Analysis of radioactive metals by spark source mass spectrography, 20: 40816 (RFP-699)
Compact, low-cost alpha counter, 20: 41275 (RFP-777)
Determination of Fe and Ni in U by atomic absorption spectrophotometry, 20: 40815 (RFP-698)
Mimic tool setter, 20: 41079 (RFP-666)
Pyroelectric sodium fluoride carrier distillation method for analysis of impurities in Pu, 20: 40814 (RFP-664)

ROCKY FLATS PLANT, DOW CHEMICAL CO., DENVER, COLO.
Optical emission spectrographic method for determination of ^{240}Pu in Pu materials, 20: 40813 (RFP-271)

RUTGERS–THE STATE UNIV. OF NEW JERSEY, NEW BRUNSWICK. DEPT. OF MECHANICAL ENGINEERING.
Solid density distribution in gas-solid pipe flow, 20: 41102 (NYO-2930-6)

RUTHERFORD HIGH ENERGY LAB., SCIENCE RESEARCH COUNCIL, CHILTON (ENGLAND).
Tables of vapor pressure and molar volume for liquid H and deuterium, 20: 40871 (NIRL-R-95)

S

SANDIA CORP., ALBUQUERQUE, N. MEX.
Craters from short-row charges and their interaction with pre-existing craters, 20: 41069 (SC-RR-66-324)
Generalized magnetohydrodynamic entrance flow model. I., 20: 42036 (SC-RR-66-356)
Photoconductivity processes in organic materials, 20: 40952 (SC-DC-66-1823)
Prog. rpt. on particle fallout and dispersion in the atmosphere, 12/65–2/66, 20: 41133 (SC-CR-66-2030)
Range and total ionization of low-energy recoil ions from alpha disintegrations in pure and binary gases, 20: 41622 (SC-DC-66-1564)
SANDIA CORP., LIVERMORE, CALIF.
Pressing hollow shapes from high-strength beryllium, 20: 41428 (SCL-DC-66-57)
SLOAN-KETTERING INST. FOR CANCER RESEARCH, NEW YORK.
Prog. rpt. on biological and clinical dosimetry, annual, 7/65–6/66, 20: 40746 (NYO-3510-2)
SOCIETA NAZIONALE METANODOTTI, MILAN (ITALY). LABORATORI REUNITI STUDI E RICERCHE.
Prog. rpt. on nondestructive analysis of irradiated fuel elements for ^{235}U and Pu, final, 11/63, 20: 40808 (NP-16212)
SOCIETE DES FORGES ET ATELIERS DU CREUSOT, PARIS (FRANCE).
Use of austenitic steel as construction material for the pressure vessel of the fast reactor "Rapsodie," 20: 42652 (EURFNR-92F)
SOUTHERN RESEARCH INST., BIRMINGHAM, ALA.
Mechanical behavior of grades RVD and AGOT graphites, 20: 41459 (TID-23288)
SOUTHWEST RESEARCH INST., SAN ANTONIO, TEX.
Fabrication and installation of LACBWR reactor pressure vessel, 20: 42637 (SWRI-1228-7-33)
Prog. rpt. on serviceability of Elk River Reactor pressure vessel, 4–6/66, 20: 42636 (SWRI-1228-4-22)
STANFORD LINEAR ACCELERATOR CENTER, STANFORD UNIV., CALIF.
Design of beam position and charge monitoring circuits for the Stanford two-mile accelerator, 20: 41544 (SLAC-63)
STANFORD RESEARCH INST., MENLO PARK, CALIF.
Area-wide shelter systems, 20: 41183 (AD-635931)
Fallout simulant development: sorption reactions of Ce, Cs, Ru, Sr, and Zr–Nb, 20: 41178 (AD-635547)
STATENS RADIOLOGISK-FYSISKE LABORATORIUM, OSLO (NORWAY).
Cesium-137 in milk in Norway 1962–1966, 20: 41132 (NYO-3364-20)
STEARNS-ROGER CORP., DENVER, COLO. NUCLEAR EQUIPMENT DIV.
PWR-2 fuel handling crane and refueling tool, 20: 42641 (WAPD-PWR-2213)
STICHTING VOOR FUNDAMENTEEL ONDERZOEK DER MATERIE, JUTPHAAS (NETHERLANDS). INSTITUUT VOOR PLASMA-FYSICA.
Equilibrium and stability of a toroidal screw pinch, 20: 42414 (NP-16266)
SYRACUSE UNIV. RESEARCH INST., N. Y. DEPT. OF CHEMISTRY.
Prog. rpt. on phase equilibria and specific volumes of liquid metals and alloys, 8/65–7/66, 20: 41455 (NYO-2731-7)

T

TECHNISCHE HOCHSCHULE, KARLSRUHE (WEST GERMANY).
Determination of natural and artificial radioactivity in water, 20: 40819 (CEA-tr-A-1883)
TECHNISCHE HOCHSCHULE, KARLSRUHE (WEST GERMANY). INSTITUT FUER THEORETISCHE KERNPHYSIK.
Peripheral model with absorption for the production process $\bar{p} + p \rightarrow \bar{N}^* + N^*$, 20: 41788 (BMwF-FBK-66-12)
TECHNISCHE UNIVERSITAET, BERLIN (WEST GERMANY).
Radiation chemical reactions in mixtures of phosphorus trichloride with olefins, 20: 40947 (BMwF-FBK-66-14)
TELEDYNE INDUSTRIES, INC., ALEXANDRIA, VA. EARTH SCIENCES DIV.
Seismic measurements of BUFF, 20: 41149 (AD-632956)
TENNESSEE UNIV., KNOXVILLE.
Low energy electron studies in indium and magnesium, 20: 41621 (ORNL-TM-1565)
Temperature dependence of response of lithium-drifted germanium detectors to gamma rays, 20: 41273 (ORNL-TM-1295)
TENNESSEE UNIV., KNOXVILLE. DEPT. OF CHEMICAL AND METALLURGICAL ENGINEERING.
Prog. rpt. on application of adiabatic calorimetry to metal systems, 9/65–8/66, 20: 41457 (ORO-3291-3)
TEXAS NUCLEAR CORP., AUSTIN.
Elemental trace analysis by charged particle and neutron activation, 20: 40812 (ORO-2980-14)
THOMPSON RAMO WOOLDRIDGE INC., CLEVELAND, OHIO.
PWR static inverter rod drive power supply, 20: 42642 (WAPD-PWR-2216)
TORONTO UNIV. (ONTARIO). INST. FOR AEROSPACE STUDIES.
Magnetohydrodynamic flow in the shock tube boundary layer with transverse magnetic field, 20: 42037 (UTIAS-115)
TRAVELERS RESEARCH CENTER, INC., HARTFORD, CONN.
Prog. rpt. on particle fallout and dispersion in the atmosphere, 12/65–2/66, 20: 41133 (SC-CR-66-2030)
TRW SYSTEMS, REDONDO BEACH, CALIF.
Prog. rpt. on radioisotope propulsion technology program, 1–3/66, 20: 41396 (STL-517-0042)
TUSKEGEE INST., ALA.
Prog. rpt. on differential absorption of Sr by plants, final, 3/66, 20: 40537 (TID-23052)

U

UNION CARBIDE CORP., OAK RIDGE, TENN. Y-12 PLANT.
Characterization of Y-12 U process materials correlated with in vivo experience, 20: 41204 (Y-1544-A)
Mechanical behavior of grades RVD and AGOT graphites, 20: 41459 (TID-23288)
UNION CARBIDE CORP., TONAWANDA, N. Y. LINDE DIV.
Prog. rpt. on thermal insulation, 4–6/66, 20: 41440 (ALO-3632-4)
UNION CARBIDE CORP., TUXEDO, N. Y. MINING AND METALS DIV.
Activation analysis with charged particles, 20: 40806 (NAS-NS-3110)
UNITED NUCLEAR CORP., ELMSFORD, N. Y.
Prog. rpt. on performance evaluation of heat exchangers for Na-cooled reactors, 4–6/66, 20: 42639 (UNC-5154)
UNITED STATES–EURATOM FAST REACTOR EXCHANGE PROGRAM.
Use of austenitic steel as construction material for the pressure vessel of the fast reactor "Rapsodie," 20: 42652 (EURFNR-92F)
UNITED STATES–EURATOM JOINT RESEARCH AND DEVELOPMENT PROGRAM.
Prog. rpt. on application of submerged arc welding process to thick plates, 4–6/66, 20: 41450 (EURAEC-1684)
Prog. rpt. on base metal for research on brittle fracture of weldments, 5/65–4/66, 20: 41447 (EURAEC-1669)
Prog. rpt. on breaking strength of weldments on heavy gage tensile steels, 9–12/65, 20: 41410 (EURAEC-1612)
Prog. rpt. on breaking strength of weldments on heavy-gage tensile steels, 1–3/66, 20: 41448 (EURAEC-1670)
Prog. rpt. on effect of substructure on irradiation stability of ASTM A302 grade B steel, 4/66, 20: 41451 (GA-7101)
Prog. rpt. on mechanical properties of metals subjected to mechanical stress at elevated temperatures and neutron irradiation, 1–3/66, 20: 41445 (EURAEC-1622)
Prog. rpt. on mechanical properties of metals subjected to mechanical stress at elevated temperatures and neutron irradiation, annual, 1965, 20: 41495 (EURAEC-1621)
Prog. rpt. on plastic fatigue embrittlement of reactor vessel steels, 1–3/66, 20: 41446 (EURAEC-1642)
Prog. rpt. on relationship of nitrogen content of austenitic stainless steel to stress corrosion, 3–5/66, 20: 41449 (EURAEC-1676)
Prog. rpt. on stainless steel failure, 1–3/66, 20: 41418 (GEAP-5150)
Prog. rpt. on Zy braze alloy development, 4–6/66, 20: 41425 (IITRI-578-P29-2)
UNIVERSITA CATTOLICA DEL SACRO CUORE DI MILANO, PIACENZA (ITALY). ISTITUTO DI GENETICA VEGETALE.
Reversion frequency of waxy pollen type in normal and hypoploid maize plants, 20: 40509 (TID-22965)
URS CORP., BURLINGAME, CALIF.
Peripheral radiological countermeasures, 20: 41177 (AD-632211)
USTAV JADERNEHO VYZKUMU, CESKOSLOVENSKA AKADEMIE VED, REZ.
Comparison of theoretical Laplacian of heavy-water reactor lattice with the measurements of the critical assembly, 20: 42599 (UJV-1424)
Determination of tungsten in iron by activation analysis, 20: 40818 (UJV-1368)
UTAH STATE UNIV., LOGAN.
Prog. rpt. on gamma irradiation effects on toxic responses of fish, 6/65–5/66, 20: 40611 (COO-1421-2)
UTAH STATE UNIV., LOGAN. DEPT. OF WILDLIFE RESOURCES.
Prog. rpt. on black-tailed jackrabbits in Curlew Valley, Northern Utah, 7/65–7/66, 20: 40494 (COO-1329-3)

V

VIRGINIA POLYTECHNIC INST., BLACKSBURG. DEPT. OF METALS AND CERAMIC ENGINEERING.
Prog. rpt. on relationship of nitrogen content of austenitic stainless steel to stress corrosion, 3–5/66, 20: 41449 (EURAEC-1676)

W

WASHINGTON UNIV., SEATTLE. DEPT. OF PHYSICS.
Prog. rpt. on theoretical nuclear physics, annual, 9/65–9/66, 20: 41511 (RLO-1388-501)
WESTINGHOUSE ELECTRIC CORP., CHESWICK, PA. ATOMIC EQUIPMENT DIV.
PWR Core 2 main coolant pump model M/M 8006-A1, 20: 42644 (WAPD-PWR-2219)
WESTINGHOUSE ELECTRIC CORP., EAST PITTSBURGH, PA. ASSEMBLED SWITCHGEAR AND DEVICES DIV.
PWR Core 2 rod control and rod position equipment, 20: 42643 (WAPD-PWR-2217)
WESTINGHOUSE ELECTRIC CORP., PITTSBURGH, PA. ASTRO-NUCLEAR LAB.
NERVA reactor development status, 20: 42662 (CONF-651101-84)
VARI-QUIR diffusion code, 20: 42143 (WANL-TNR-133(Rev.))
WESTINGHOUSE ELECTRIC CORP., PITTSBURGH, PA. ATOMIC POWER DIV.
Feasibility of chemical poison loop system, 20: 42665 (WCAP-2870)
PWR Core 2 rod control and rod position equipment, 20: 42643 (WAPD-PWR-2217)
PWR nuclear protection system, 20: 42640 (WAPD-PWR-2210(Vol.1))
PWR static inverter rod drive power supply, 20: 42642 (WAPD-PWR-2216)
PWR-2 fuel handling crane and refueling tool, 20: 42641 (WAPD-PWR-2213)
WESTINGHOUSE RESEARCH LABS., PITTSBURGH, PA.
High-temperature plasmas by laser heating, 20: 42415 (TID-22928)
WUERZBERG UNIV. (WEST GERMANY). INSTITUT FUER PHYSIKALISCHE CHEMIE.
Electrolytic deposition of beryllium from metallorganic complex-salts, 20: 40864 (BMwF-FBK-66-10)

PERSONAL AUTHOR INDEX

Each entry after an author's name is a shortened version of the title of the report or article, followed by the *NSA* volume and abstract number. Report numbers are given in parentheses.

The phrase "Progress report" is abbreviated as "Prog. rpt.," permitting a more rapid and complete alphabetical arrangement of the titles without changing the location of the progress report titles in relation to the other titles.

Because of problems involving the mechanical preparation of this index, all accent marks are omitted. The following changes in spelling have been introduced to reduce some of the confusion which might result from omitting the accents:

ä	becomes	ae
ö		oe
ø		oe
ü		ue (except in transliterated Chinese names)

A

ABBATTISTA, N., Nomogram for designing tunnel diode monostable circuits, 20: 41242

ABBATTISTA, N., Suggestions for improvements of timing circuits with tunnel diodes, 20: 41246

ABDULLAEV, V. M., Changes in eyes of monkeys affected with radiation sickness, 20: 40646

ABRAHAM, M. M., Electron spin resonance spectra of Dy^{3+} in ThO_2 and CeO_2, 20: 42525 (ORNL-P-2466)

ABRAHAMSON, S., Evidence demonstrating germinal selection in early premeiotic germ cells of Drosophila males, 20: 40670

ABRAMOV, A. P., Binary centers produced by light in uranyl salts, 20: 42537

ABRAMOVA, I. N., Binary centers produced by light in uranyl salts, 20: 42537

ABRAMS, Richard, Prog. rpt. on nuclear metabolism of DNA and RNA and sites of radiation sensitivity, 10/65–7/66, 20: 40534 (NYO-3621-1)

ABUL-MAGD, A. Y., Optical model parameters for composite particles, 20: 42280

ACHENER, P. Y., Prog. rpt. on alkali metals evaluation program, 1–3/66, 20: 41438 (AGN-8187)

ACHENER, P. Y., Prog. rpt. on alkali metals evaluation, 4–6/66, 20: 41439 (AGN-8198)

ACHEY, Phillip Mueller, Study on DNA degradation in Escherichia coli produced by ionizing radiation, 20: 40620 (NYO-2804-9)

ACKER, H. L., Muonic x-ray spectra and charge distribution in deformed nuclei, 20: 42308

ACKER, H. L., Muonic x-ray studies of spherical nuclei, 20: 42309

ACKERMAN, Frank J., Mechanisms that affect adsorption of methyl iodide on charcoal under humid conditions, 20: 41202 (UCRL-14990)

ADAIR, R. K., Search for heavy magnetic monopoles, 20: 41676

ADAMS, Duane A., Biological significance of the supersonic transport radiation environment, 20: 40525

ADAMS, J. B., Review of nuclear fusion research, 20: 42482

ADAMS, R. E., Characterization of radioactive particulate aerosols by fibrous filter analyzer, 20: 41234 (ORNL-P-2436)

ADAMSKI, L., Measurement of neutron density distributions in multilayer unit cells. II., 20: 42680 (INR-698/IX-A/RP)

ADKINS, K. F., Effect of single doses of x radiation on mandibular growth, 20: 40652

ADLER, C., Application of the SU(3) shell model to ^{9}Be, 20: 42191

AEBY, Jack W., Beta-gamma radioactivity in environmental air at Los Alamos, New Mexico, 1965, 20: 41194 (LA-3516)

AGARWAL, B. K., Peripheral model for K⁻-p collisions, 20: 41819

AGEEV, N. V., Analysis of nonmetallic inclusions in Mo and its alloys, 20: 41467

AGEEV, V., Decay of ^{184}Re, 20: 42157 (JINR-P-2814)

AGGSON, Th. L., Secondary emission monitor, 20: 41266 (LAL-1028)

AGNEW, Lewis, Isothermal plasma oven, 20: 42484

AGRAWALA, V. K., Cutkosky-Leon normalization conditions, 20: 41951

AIKIN, A. M., Evaluation of CANDU: PHW fuels, 20: 42618 (66-CNA-312)

AINSWORTH, E. J., Radiation-protection and recovery from radiation injury in endotoxin-treated mice, 20: 40732 (AD-636209)

AINSWORTH, E. J., Recovery from radiation injury in swine, 20: 40605 (AD-635735)

AJZENBERG-SELOVE, F., Excited states in ^{6}Be and ^{10}C, 20: 42190

AKAISI, Yoshinori, Nuclear matter and nuclear forces, 20: 42281

AKHIEZER, A. I., Photoformation of mesons on nucleons and SU(6) symmetry, 20: 41812

AKSEL'DORF, A. L., Radioisotope renography in diagnosis of a silent kidney, 20: 40775

AKYUEZ, R. O., Parameters for the first neutron resonance in ^{113}Cd, 20: 42149 (CNAEM-34)

ALANAKYAN, Yu. R., Interaction of electromagnetic waves at the boundary of a plasma, 20: 42498

ALBERTONI, S., Numerical computation methods for implosion processes, 20: 41088

ALBURGER, D. E., Properties of excited states in ^{14}C, 20: 42233

ALBURGER, D. E., Short-lived activities ^{15}C, ^{17}F, ^{19}O, ^{20}F, and ^{28}Al, 20: 42242

ALCOCK, A. J., Temperature measurements of a laser spark from soft-x-ray emission, 20: 42475

ALCOCK, N. W., Structure of uranyl triperoxide ion, 20: 40881

ALEKSANDROV, B. P., Influence of solution structure on the mobility of isotopic ions Li^{6+} and Li^{7+}, 20: 40930

ALEKSANDROV, Yu. A., Kev neutron scattering by lead and electrical polarizability of neutron, 20: 42140 (JINR-P-2764)

ALEXANDER, Peter, Significance of electron spin resonance measurements on irradiated biological macromolecules, 20: 40598

ALFORD, W. Parker, (Helium-3,d) reaction on ^{42}Ca and ^{44}Ca, 20: 42253

ALI, S. M., Use of gamma radiation in jute breeding, 20: 40681

ALIEVA, Sh. A., Synthesis and studies of Ga Y sulfides ($YGaS_3$) and In Y sulfides ($YInS_3$), 20: 40879

ALINOVSKII, N. I., Investigation of plasma injected into trap with conical theta pinch, 20: 42504

ALLEGRETTI, Nikso, Influence of x-irradiation on experimental allergic encephalomyelitis in rats, 20: 40728

ALLEN, Philip, Improvements in electric control or monitoring equipment or apparatus, 20: 41258

ALMEIDA, June D., Use of x rays to produce transmission pictures of virus models, 20: 40653

ALMELEH, Nissim, Electron paramagnetic resonance and electrical properties of the dominant paramagnetic defect in electron-irradiated p-type silicon, 20: 42549

AMATO, I., Dependence on microstructure of the high temperature properties of U oxide. Mo and U oxide. W cermets, 20: 41478

AMATO, J., Recent experiments on muonium, 20: 41661

AMBROSINO, G., Study of charged products in the reaction $^{9}Be + d$ at very low energy (100 to 200 kev), 20: 42354

AMBROSINO, Georges, Bound state of the positron in certain finely divided oxides, 20: 41629

AMEMIYA, Y., Preparation and test of MHD duct wall and electrode materials, 20: 41718

AMPELOGOVA, N. I., Extraction method for complex formation of Po with Cl and perchlorate ions, 20: 41052

AMTEY, S. R., M, N, and O subshell conversion coefficients in ^{228}Th and ^{240}Pu, 20: 42264
ANBAR, M., Mechanism of radiolysis of carbon dioxide, 20: 40996
ANDERS, H., Track centering system for IEPs using vibrating reed track detector, 20: 41263 (CERN-66-23)
ANDERSEN, Rolf, Heat transfer experiment with multirod element, DOR design study, 20: 42635 (RISO-124)
ANDERSON, D. K., Radiative pion absorption in complex nuclei, 20: 42315
ANDERSON, H. L., Effects of nuclear structure in mu-atomic spectra, 20: 42305
ANDERSON, J., Distribution of ^{47}Ca in the rat, 20: 40557
ANDERSON, V. L., Changes in quantitative traits of tribolium under irradiation and selection, 20: 40671
ANDRIANOV, V. V., Transition processes in superconducting magnetic systems, 20: 41760
ANIKINA, M., Search for new decay modes of the K^0_2-mesons, 20: 41903
ANISOVICH, V. V., Theory of reactions with formation of three particles near threshold, 20: 41900
ANSEL'M, A. A., Theory of reactions with formation of three particles near 20: 41900
ANTIPOV-KARATAEV, I. N., Radioactivity of soils and methods of measurement, 20: 41139
ANTOINE, J.-P., Electromagnetic form factor of the pion, 20: 41833
ANTONINI, B., Spin-wave stiffness and electronic structure of Fe–Al and Fe–Ga alloys, 20: 42559
ANTONOVA, T. D., Observations of intensity fluctuations in radio emission from the quasi-stellar source 3C-48 caused by heterogeneities of the interplanetary plasma, 20: 41598
ARCHER, H. P., Determination of non-linear parameters and their standard deviations from least-squares residuals, 20: 41518
ARDITI, M., Study of (p,2p) reaction at 155 Mev on ^{7}Li, ^{9}Be, and ^{23}Na with an on-line computer, 20: 42360
AREHART, T. A., Operating guide for radiochemical laboratories at various activity levels, 20: 41199 (ORNL-TM-626)
ARKENBOUT, G. J., Separation of lithium isotopes by countercurrent-exchange-electrolysis, 20: 41402
ARMANTROUT, C. E., Prog. rpt. on selected properties of Th with low ThO_2 additions, 7/65–6/66, 20: 41462 (USBM-RC-1245)
ARMBRUSTER, R., Precise measurement of the stopping power of C, Au, Al, Ca, and CaF_2 for 0.4 to 6 Mev protons, 20: 42363
ARNASON, G., Prog. rpt. on particle fallout and dispersion in the atmosphere, 12/65–2/66, 20: 41133 (SC-CR-66-2030)
ARNOLD, George W., Radiative recombination in annealed electron-irradiated GaAs, 20: 42548
ARNOLD, W. H., NERVA reactor development status, 20: 42662 (CONF-651101-84)
ARNUSH, Donald, Site testing for EMP hardness, 20: 41117
ARNY, Thomas T., Simple method for studying fragmentation in astrophysical systems, 20: 41593
ARONSON, Raphael, Physiological implications of laser beams, 20: 40691
AR-RASHID, Haron, Absorption correction in high-energy photoproduction of pions, 20: 41844
ARTHUR, Jett C. Jr., Post-irradiation grafted vinyl cellulose copolymers, 20: 40995
ARUNASALAM, V., Radiative equilibrium of a free-electron gas in a uniform magnetic field, 20: 42470
ARUTYUNYAN, E. G., Crystal structure of $Cs_3[UO_2(NCS)_5]$, 20: 40932
ASAM, U., Metabolism of ^{65}Zn by rats under influence of Prednisolone or Dexamethasone, 20: 40563
ATKINS, H. L., Practical modification of rectilinear scanner, 20: 40755
ATKINSON, D., Dynamical calculation of extinct bound states, 20: 41975
ATTARDO, M., Field ion microscope study of neutron-irradiated tungsten, 20: 42551
AUBERT, M., Radioactivity of plankton and of organic refuse, 20: 41146
AUERBACH, E., Optical models for pion-nucleus scattering, 20: 42319
AUERBACH, K., Gyromagnetic ratio of the 564 kev state in ^{122}Te, 20: 42219
AUERBACH, L., K^0_2 three-body decays and the $|\Delta I| = ½$ rules, 20: 41855
AUGUST, L. S., Energy dependence of proton-proton bremsstrahlung, 20: 41882
AURAND, K., Hazards resulting from discharge of radioactive wastes into municipal sewer systems, 20: 41217
AURELA, A. M., Measurements of the change ratio of cosmic-ray muons, 20: 41677
AVIGNON, P., Levels of ^{15}O excited by the reaction ^{14}N(d,nγ)^{15}O at 6.3 Mev, 20: 42346
AXFORD, W. I., Wind shear theory of the formation of temperate zone sporadic E layers, 20: 42067
AYRES, David S., Comparison of the lifetimes of positive and negative pions, 20: 41891
AYRES, J. A., Plutonium Recycle Test Reactor decontamination following MgO–PuO_2 fuel element failures, 20: 42677 (BNWL-SA-636)
AZEEM, M., Preparation of some ^{18}F labeled fluorides, 20: 41020
AZIZKULOV, N. Kh., Multiplicity factor of neutron formation in the (μ,n) reactions, 20: 42174
AZOEUF, Pierre, Installation for analytic chemistry under irradiation, 20: 40799 (CEA-R-2887)

B

BABA, H., Fission of ^{209}Bi and ^{238}U induced by alpha particles of energies up to 115 Mev, 20: 42267
BABENKOV, M. I., Svartholm-Siegbahn beta spectrometer with adjustable angular separation between source and detector, 20: 41348
BABIEVSKAYA, I. Z., Infrared absorption spectra of La, Gd, and Y nitrates, 20: 40886
BABKO, A. K., Determination of lanthanum in cerium oxide using paper chromatography, 20: 40859
BACALAO, P., Accretion and exchange of ^{85}Sr in trabecular and cortical bones, 20: 40684
BACHELIER, D., Discussion of the results obtained in pickup reaction on ^{9}B and ^{10}B nuclei at 156 Mev, 20: 42350
BACHELIER, D., Preliminary results on ^{4}Li, ^{5}Li, and ^{6}Li obtained by (p,d) and (p,t) reactions on ^{6}Li and ^{7}Li at 156 Mev, 20: 42358
BACHELIER, D., Reaction (p,d) at 156 Mev on fluorine and nitrogen, 20: 42204
BACHYNSKI, M. P., Linearly polarized waves in plasmas in the region of the electron cyclotron frequency, 20: 42459
BACKENSTOSS, G., Muonic x-ray studies of spherical nuclei, 20: 42309
BAECHMANN, K., Separation of lanthanides by thin-layer high-voltage electrophoresis, 20: 41046
BAECKMANN, A. V., Separation and radiochemical determination of element activities, 20: 40803 (KFK-387)
BAECKSTROEM, G., Decay of ^{192}Au, 20: 42187
BAEHR, Werner, Method for extraction of ^{137}Cs salts from irradiated nuclear fuel, 20: 41057
BAESSLER, K. H., Biological effects of irradiated fats, 20: 41391
BAESSLER, K. H., Nutritional value of irradiated potatoes, 20: 40576
BAEZ, A. P., Strontium-90 content in milk in Mexico, 20: 40854
BAGDASAR'YAN, Kh. S., Radiolysis of isopropanol and benzophenone and naphthalene is isopropanol in liquid state, 20: 41006
BAGINSKI, W. A., Oxidation studies of complex silicides for protective coatings, 20: 41424
BAGRAMYAN, E. R., Reaction of hypophyseal-adrenal system of irradiated rats to repeated stress, 20: 40655
BAILEY, R. E., Effects of molecular diffusion of heat on fluid velocity measurements, 20: 41101 (NAA-SR-Memo-10848)
BAILY, Norman A., Direct reading intracavitary dosimeter for use in radium therapy, 20: 41377
BAINBRIDGE, Kenneth T., Alteration of the decay constant of ^{125m}Te by chemical means, 20: 42266
BAINTON, K. F., MHD power generation experiments using seeded inert gases, 20: 41736
BAIRD, G. A., Solar minimum measurements of fast neutrons at high altitude, 20: 42055
BAKER, Dale E., Accumulation of Ca, Sr, Mg, P, and Zn by genotypes of corn under different soil fertility levels, 20: 40735 (NYO-2744-37)
BAKER, Edward J., Device for detecting and measuring high energy particles of predetermined energy level, 20: 41364
BAKULIN, E. A., Influence of solution structure on the mobility of isotopic ions Li^{6+} and Li^{7+}, 20: 40930
BALANCHANDRAN, A. P., Current algebras and meson-nucleon scattering lengths, 20: 41846
BALE, W. F., Determination of total iodine in radioactive iodide preparations of high specific activity, 20: 40553
BALKAREI, Yu. I., Sound dispersion in superconductors, 20: 42128
BALL, James S., η-Nucleon interaction and η production in π-nucleon scattering, 20: 41866
BALL, Robert C., Bacterial transport of radiophosphorus in a stream ecosyste..., 20: 40529
BALOGH, Tibor, Applications of the least squares method. I., 20: 41408
BALTER, Stephen, Extension of memorial system for implant dosimetry, 20: 40788
BALZHISER, R. E., Attenuation techniques for determination of void fractions in two-phase potassium flow, 20: 41111
BANDO, Masako, Large-angle elastic proton-proton scattering at high energy, 20: 41896
BANERJI, S., Arrow of time in homogeneous cosmological models, 20: 41611
BANGERTER, Roger O., New Σ decay parameters and test of $\Delta I = ½$ rule, 20: 41879
BANKS, Philip O., Evaluation of the decay constant of ^{235}U from lead isotope ratios, 20: 41176
BANKS, W. C., Lethal effects of ^{60}Co on mature White Leghorn chickens,

20: 40693
BANTYSH, A. N., Thermodynamic regularities in isotopic exchange. I., 20: 40924
BARANOV, V. I., Mobilities and forms of ^{90}Sr and Ca in turf-podzolic and black earth soil, 20: 40520 (NP-16261)
BARANOV, V. I., Sensitivity thresholds of radiometric analysis, 20: 41334
BARBARO-GALTIERI, Angelo, New Σ decay parameters and test of $\Delta I = \frac{1}{2}$ rule, 20: 41879
BARBER, D. J., Electron microscopy of irradiation-induced defect clusters in magnesium fluoride, 20: 42554
BARDACH, Herbert, Radioactive krypton simplifies temperature mapping of turbine blades, 20: 41114
BARDEEN, James M., Catalog of methods for studying the normal modes of radial pulsation of general-relativistic stellar models, 20: 41588
BARDIN, T. T., Detailed analysis of muonic x-ray spectrum from strongly deformed e-e nuclei, 20: 42310
BARDIN, T. T., Metastable $d_{3/2}$ hole state in ^{47}Sc, 20: 42192
BARDOLLE, G., Elastic and inelastic scattering of protons by ^{7}Li, 20: 42372
BARDSLEY, J. N., Electron resonances of the H_3^- ion, 20: 41656
BARDSLEY, J. N., Vibrational excitation and dissociative attachment in the scattering of electrons by hydrogen molecules, 20: 41657
BARELKO, E. V., Radiation chemical oxidation of butanol in aqueous solution at increased temperature, 20: 40983
BAREYRE, P., Measurement of the $\pi^{\pm}$p total effective cross section at T_π = 300 to 700 Mev, 20: 41830
BARINOV, G. V., Biological consequences of radioactive contamination of water bodies, 20: 40527
BARKER, Bruce M., One-graviton exchange interaction of elementary particles, 20: 41970
BARLOW, John S., Solar-flare induced increases in sea-level cosmic-ray intensities, 20: 40639
BARNES, L. J., Critical currents in the superconducting surface sheath, 20: 42114
BARON, S., Engineering for community acceptance. Architect-engineer's role, 20: 42655
BARRACHINA, M., Separation of iodine and xenon fission radionuclides, 20: 41034 (JEN-160-DQ/I-54)
BARRAGAN, Antonio, General guide for irradiations in the research and experimental reactor IAN-R1, 20: 42679 (IAN-R-1)
BARRETT, Norman Thomas, Pressure vessels, 20: 42596
BARRETT, R., Detailed analysis of muonic x-ray spectrum from strongly deformed e-e nuclei, 20: 42310
BARRETT, R. C., Isotope and isomer shifts in mercury, 20: 42189
BARRICK, C. W., Pyroelectric sodium fluoride carrier distillation method for analysis of impurities in Pu, 20: 40814 (RFP-664)
BARRY, P. J., Use of radioactive tracer to study rate of exchange of water vapor between air and natural surfaces, 20: 41150 (AECL-2576)
BARSHAY, Saul, CP violation with $|\Delta T| > \frac{1}{2}$: a re-examination of Truong's model for $K_2^0 \to 2\pi$, 20: 41872
BARSUKOV, K. A., Vavilov-Cherenkov effect for surface waves, 20: 42497
BARTEL, W., Small angle electron proton elastic scattering cross sections for momentum transfers between 10 and 105 f^{-2}, 20: 41791 (DESY-66/20)
BARTIS, F. J., Toroidal beta ray spectrometer, 20: 41309
BARTLETT, Alan C., Changes in quantitative traits of tribolium under irradiation and selection, 20: 40671
BARTLETT, Neil, Crystal structure and magnetic properties of pentafluoroxenonyl hexafluoroplatinate(V), 20: 40882
BASKIN, Yehuda, Uranium monosulfide–U monophosphide solid solutions, 20: 40936
BASOV, N. G., Recombination radiation of alpha SiC due to electron bombardment, 20: 42565
BASSANI, G., Separation of reaction mechanisms at low energy, 20: 42394
BASSEL, R. H., Normalization of and finite-range effects in (^{3}He,d) and (t,d) reactions, 20: 42250
BASSETTI, M., Computation of the effects of errors of a magnetic channel on the final beam parameters, 20: 41538 (LNF-66/29)
BASSETTO, A., Field-theoretical sum rules and mass-difference calculations, 20: 41824
BASSETTO, A., Vector meson bootstrap from singular N/D equations, 20: 41837
BASSICHIS, W. H., Determination of coefficients of spin and isospin mixtures of an effective nucleon-nucleon force, 20: 42348
BATCH, J. M., Investigation of combined failure of pressure tube and defected fuel rod in PRTR, 20: 42675 (BNWL-272)
BATES, Howard F., Proposed polar auroral radar system, 20: 42060
BATES, J. Lambert, Melting points of hypostoichiometric uranium dioxide, 20: 41441 (BNWL-224)
BATHOW, G., Shielding high-energy electrons: the neutron and muon components, 20: 41534 (DESY-66/18)
BATURICHEVA, Z. B., Effect of plastic deformation on light storage in crystals of NaI(Tl), 20: 41344
BAUER, Walter, Electron-irradiation damage-rate measurements in aluminum, 20: 42543
BAUM, S. J., Erythrocyte stem cell kinetics in postradiation rat, 20: 40603 (AD-635086)
BAUMANN, G., Contribution to a study of structure of light nuclei by a study of the absorption mechanisms of K$^-$ mesons, 20: 42386
BAUMGAERTNER, F., Tri(cyclopentadienyl)americium(III), 20: 40878
BAUMGARTNER, W. V., Neutron and high energy particle dosimeter for medical dosimetry applications, 20: 41262 (BNWL-SA-619)
BAW, P. S., Solid density distribution in gas-solid pipe flow, 20: 41102 (NYO-2930-6)
BAZ, A. I., Lifetime of intermediate states, 20: 42288
BEAUCHAMP, E. E., Operating guide for radiochemical laboratories at various activity levels, 20: 41199 (ORNL-TM-626)
BEAUMARIAGE, M. L., Premature incorporation of tritiated thymidine after irradiation of fibroblast and myoblast of chicken embryos, 20: 40587
BEAUMEVIEILLE, H., Study of (d,p) reactions on light nuclei at low energy, 20: 42399
BEBB, H. Barry, Generalized discrete-continuum radial integrals with Coulomb functions, 20: 41633
BEBIE, H., Lorentz- and spin-invariant elastic scattering of two spin-½ particles, 20: 41983
BECCHI, C., Connection between BBP and VPP verticles in the quark model, 20: 41876
BECK, F., Study of electromagnetic transitions by measurement of the polarization distribution and γ-γ angular correlation, 20: 42381
BECK, Robert Lamar, Measurement of the relative branching ratio $K^+ \to \mu^+ + \nu/K^+ \to \pi^+ + \pi^0$, 20: 41801 (UCRL-16003)
BECKER, F., Theoretical study of the reaction $\pi^- + {}^4He \to \pi^+ + 4n$, 20: 42356
BECKERS, J., Information on the axial-vector coupling constant through different current algebras, 20: 41955
BEDER, Douglas S., Diffraction scattering and form factors, 20: 41979
BEDER, Douglas S., Vector dominance and meson photoproduction, 20: 41869
BEDFORD, L. A. W., High temperature graphite rig for scattering law experiments, 20: 41075
BEEDER, R. H., Application of nuclear excavation to railroad use, 20: 41071
BELEVSKII, V. N., Decomposition of radicals in frozen aqueous solutions of $NaClO_4$ and $HClO_4$, 20: 40960
BELINFANTE, J. G., Cutkosky-Leon normalization conditions, 20: 41951
BELL, A. E., Changes in quantitative traits of tribolium under irradiation and selection, 20: 40671
BELL, M. C., Influence of dietary calcium, zinc, and oil upon uptake of ^{65}Zn by porcine blood cells, 20: 40556
BELL, W. A., Review of ORNL electromagnetic separations program, 1965, 20: 41401 (ORNL-4006)
BELLETTINI, G., Precision detector for high-energy neutral pions, 20: 41320
BELOOZEROV, V. N., Containment of superconducting sphere by circular currents, 20: 42130
BELOSLYUDOVA, G. A., Determination of ^{131}I, 20: 40852
BELOUSOVA, L. E., Hollow positive column in a longitudinal magnetic field, 20: 42506
BELOV, K. P., Rare earth ferromagnetics and antiferromagnetics, 20: 41483
BELYAEV, B. N., Decay of the isotope ^{180}Os, 20: 42284
BELYANCHIKOVA, M. A., Rare earth ferromagnetics and antiferromagnetics, 20: 41483
BEMPORAD, C., Precision detector for high-energy neutral pions, 20: 41320
BENDER, M. A., Prog. rpt. on synergistic effect of zero-G and radiation on white blood cells, annual, 6/64–6/65, 20: 40635 (ORNL-TM-1550)
BENDT, P. J., Large-angle neutron-proton C_{NN} parameter at 23.1 Mev, 20: 41877
BENENSON, R. E., Stripping features of $^6Li(d,n)^7Be^*$ (0.43 Mev) at E_d from 0.2 to 0.8 Mev, 20: 42210
BEN-NAIM, A., Solubility and thermodynamics of solution of Ar in mixtures of H_2O and D_2O, 20: 40897
BENNETT, G. W., Growth to phase space in high intensity proton beams due to nonuniform radial charge distribution, 20: 41531 (BNL-10528)
BENOIST-GUEUTAL, P., p-d Angular correlation in the reaction $^{12}C(p,pd)^{10}B$ at 155 Mev, 20: 42361
BENOIT-CATTIN, P., Energy distribution of He^+ ions produced by source with high-frequency electric excitation, 20: 41239
BENSON, H. G., Deformed state admixtures in ^{18}O, 20: 42274
BENVENUTI, P., Precision detector for high-energy neutral pions, 20: 41320
BEREZIN, Yu. A., Cylindrical waves propagating across a magnetic field in a rarefied plasma, 20: 42489
BEREZOVSKII, B. S., Protective action of phosphororganic preparation of nibufin on irradiated albino mice, 20: 40724

BERG, Claire Marjorie, Replication and genetic exchange in genome of Escherichia coli K-12, 20: 40538 (TID-23238)
BERG, Joseph W. Jr., Amplitudes and energies of primary seismic waves near Hardhat, Haymaker, and Shoal Bursts, 20: 41169
BERG, Roger, Changes in relative biological effectiveness of 35 Mev electron beam as function of tissue depth, 20: 40767
BERGDOLT, A. M., Precise measurement of the stopping power of C, Au, Al, Ca, and CaF_2 for 0.4 to 6 Mev protons, 20: 42363
BERGE, J. Peter, New Σ decay parameters and test of $\Delta I = \frac{1}{2}$ rule, 20: 41879
BERGHEDEN, C., Studies on allogenic inhibition. II., 20: 40588
BERGMAN, C., Decay of ^{192}Au, 20: 42187
BERGONZI, L., Pinhole camera in study of secondary emission in bodies exposed to irradiation, 20: 41321
BERGSTROM, James W., Semiconductor amplifying radiation detector, 20: 41361
BERLIN, A., Isothermal transport processes in molten salts binary systems, 20: 40866 (EUR-2954.e)
BERLYANT, S. M., Radiation cross linking of cable polyethylene insulation on large scale, 20: 41496
BERNADZIKOWSKI, R., Effect of the dose output on the electret effect in paraffin wax, 20: 41516
BERNAS, M., Discussion of the results obtained in pickup reaction on ^{9}B and ^{10}B nuclei at 156 Mev, 20: 42350
BERNAS, M., Preliminary results on ^{4}Li, ^{5}Li, and ^{6}Li obtained by (p,d) and (p,t) reactions on ^{6}Li and ^{6}Li at 156 Mev, 20: 42358
BERNAS, M., Reaction (p,d) at 156 Mev on fluorine and nitrogen, 20: 42204
BERNHEIM, M., Study of the elastic scattering of electrons by ^{27}Al, 20: 42376
BERNSTEIN, H. J., Electron spin resonance spectra of $N_2H_4^+$ and PF_2, 20: 40956
BERRADA, M., Study of the reactions $d + {}^{7}Li = n + 2\alpha$ and $^{6}Li + T = n + 2\alpha$, 20: 42349
BERRY, Arnold, Improvements in or relating to structural materials, 20: 41435
BERRY, R. K., Influence of dietary calcium, zinc, and oil upon uptake of ^{65}Zn by porcine blood cells, 20: 40556
BERTINI, R., Study of electromagnetic transitions by measurement of the polarization distribution and γ-γ angular correlation, 20: 42381
BERTOCCHI, L., Shadow model for the high-energy pion-proton elastic backward peak, 20: 41839
BERZI, Vittorio, Calculation of cross section of reaction $K + N \rightarrow K^* + N$, 20: 41898
BERZINA, I. G., Thermal stability of U fission products in monocrystalline muscovite for chemical etching, 20: 40889
BESANCON, J. E., Ferroelectric transducers, 20: 41684
BESANCON, J. E., Magnetic field compression, 20: 41081
BESANCON, J. E., Theory of magnetic field compression diffusion, surface instabilities, 20: 41090
BESEL, V. S., Temperature luminescence decay of ZnS:Ag monocrystals at excitation of radiation, 20: 41342
BEVITT, E., Safety of pressure vessels against fast fracture, 20: 42576 (AHSB(S)-R-107)
BHADURI, R. K., Saturation in finite nuclei, 20: 42208
BHALERAO, P. J., Circuit for preventing accumulation of experimental data when nuclear reaction rate exceeds preset value, 20: 41244
BHAT, A. N., Bis-2-pyridyl glycol as a reagent for gravimetric determination of U, Al, and Be, 20: 40849
BHATT, Y. M., Minor-element and trace-element content of marine environment on west coast of India, 20: 40572
BHATT, Y. M., Uptake of radionuclides by marine invertebrates from the west coast of India, 20: 40528
BHATTATHIRI, P. M. A., Uptake of radionuclides by marine invertebrates from the west coast of India, 20: 40528
BIANCHI, A., Mutagenesis in maize, 20: 40708
BIANCHI, A., Reversion frequency of waxy pollen type in normal and hypoploid maize plants, 20: 40509 (TID-22965)
BIANCHI, W. C., Use of tritium to measure movement of groundwater toward irrigation wells in Fresno County, California, 20: 41160
BIBB, A. E., Aqueous corrosion of zirconium single crystals, 20: 41423
BIEDENHARN, L. C., Generalizations of isoparity, 20: 41923
BIENERT, W. B., Experimental program to evaluate the feasibility of jet compressors for closed-Brayton-cycle MHD systems, 20: 41753
BILANIUK, O. M., Reliability of fractional registry of nuclear spectra, 20: 41315
BILDSTEIN, H., Molecular plating. V., 20: 41011 (SGAE-CH-34/1966)
BILLEREY, R., Study of angular distributions of the reaction $^{32}S(n,\alpha_0)^{29}Si$ at 2.5 to 3.2 Mev, 20: 42375
BILWES, R., States $^{2}P_{3/2}$ and $^{2}P_{1/2}$ of ^{3}He, 20: 42357
BIQUARD, F., Improvement of surface conductivity of Cu and Al at high frequencies, by lowering of temperature, 20: 42105
BIRKETT, Gamma-ray transitions in ^{44}Ca, 20: 42335
BIRKHOFF, R. D., Low energy electron studies in indium and magnesium, 20: 41621 (ORNL-TM-1565)
BIRMAN, B. I., Preparation of single crystals of refractory compounds, 20: 41480
BIRON, R. D., Experiments and target-gas storage at the CEA at the time of the July 5, 1965 accident and fire, 20: 41539 (MIT-2098-259)
BISCHOFF, K., Ionospheric absorption during solar eclipse on February 15, 1961. I., 20: 42051
BISCHOFF, K., Ionospheric absorption of short waves during solar eclipse of February 15, 1961. II., 20: 42052
BISHOP, A. A., Feasibility of chemical poison loop system, 20: 42665 (WCAP-2870)
BISHOP, A. S., Roadblocks in the path of controlled fusion, 20: 42437
BISHOP, S. G., NMR studies of ^{7}Li in polycrystalline lithium nitride, 20: 42175
BISWAS, S., Matter traversed by low-energy cosmic-ray nuclei in space, 20: 41675
BIZARD, G., Measurement of the $\pi^{\pm}$p total effective cross section at T_π = 300 to 700 Mev, 20: 41830
BIZOLLON, Ch. A., Application of radioisotopic dilution with incomplete extraction to determination of oligoelements in biology, 20: 40844
BLACKBURN, R., Alpha-particle radiolysis of the cyclohexane-S system, 20: 40990
BLACKWELL, Robert T., New radioprotector in E. coli, 20: 40737
BLAIR, D. T. A., Use of α irradiation in ionization coefficient measurements, 20: 41627
BLAKE, C. A. Jr., Prog. rpt. on chemical applications of nuclear explosions, 4–6/66, 20: 41067 (ORNL-TM-1582)
BLAKE, K. R., Elemental trace analysis by charged particle and neutron activation, 20: 40812 (ORO-2980-14)
BLANC, D., Elastic scattering of neutrons by tritium at 14 Mev, 20: 42373
BLANC, D., Energy distribution of He^+ ions produced by source with high-frequency electric excitation, 20: 41239
BLANC, Daniel, (n,d) Scattering between 1 and 5 Mev, 20: 42359
BLANC-LAPIERRE, A., Recent progress in the technique of particle accelerators: storage and collision rings, 20: 41559
BLAYLOCK, B. G., Cytogenetic study of Chironomidae inhabiting an area contaminated by radioactive waste, 20: 40530
BLESER, E., Design and performance of on-line wire spark chamber spectrometer, 20: 41297
BLEULER, E., Mass spectra of recoil nucleon states from inelastic ρ^0 production by pions of 12 and 18 Bev/c, 20: 41828
BLEWETT, John P., Resource letter PA-1 on particle accelerators, 20: 41546
BLINC, R., Electron spin resonance of irradiated $NaH_3(SeO_3)_2$ and $NaD_3(SeO_3)_2$, 20: 40972
BLINC, R., Nuclear magnetic resonance and relaxation of hexafluoride molecules in solid, 20: 40892
BLISKOVSKII, V. Z., Radioactivity of phosphorites, 20: 41174
BLOCH, Cl., Recent developments in the theory of nuclear reactions, 20: 42339
BLOCK, M. M., Inelastic π^{+-}-^{4}He reactions in the momentum range 100–160 Mev/c, 20: 42321
BLOCK, M. M., Phase shift analysis for elastic π^{+-}-^{4}He scattering in the energy interval 100–160 Mev/c, 20: 42320
BLOCK, M. N., Research and determination of rates of leakages of nuclear fuel elements, 20: 42610 (AI-Trans-206)
BLOEDORN, Fernando G., Computer dosimetry system for radium implants, 20: 40765
BLOKHINTSEV, D. I., Conditions of macroscopic causality for the scattering matrix, 20: 41962
BLOOM, E. D., Photoproduction of η mesons from 950 to 1100 Mev, 20: 41889
BLOUIN, Florine A., Post-irradiation grafted vinyl cellulose copolymers, 20: 40995
BLOXHAM, M. J. W., Certain physical-region singularities in S-matrix theory, 20: 41954
BLUMBERG, H., Search for parity mixing in the 501 kev γ transition of ^{180m}Hf, 20: 42230
BOARDMAN, C. R., Distribution in fracture permeability of granitic rock mass following contained nuclear explosion, 20: 41164
BOBELDIJK, C., Equilibrium and stability of a toroidal screw pinch, 20: 42414 (NP-16266)
BOBODZHANOV, I. B., Multiplicity factor of neutron formation in the (μ,n) reactions, 20: 42174
BOBYKIN, B. V., Svartholm-Siegbahn beta spectrometer with adjustable angular separation between source and detector, 20: 41348
BOCK, P., Search of parity mixing in ^{180}Hf by a measurement of the circular polarization of γ rays, 20: 42225
BOCKEMUEHL, Robert R., Semiconductor amplifying radiation detector, 20: 41361
BODENSTEDT, E., Search for parity mixing in the 501 kev γ transition of

^{180m}Hf, 20: 42230
BODILY, David M., Radiation chemistry of polyethylene. VIII., 20: 40964
BODILY, David M., Ultraviolet spectroscopy of irradiated polyethylene, 20: 40963
BOEDECKER, P. A., Determination of Au, Ir, and Pt in meteorites and natural materials by thermal-neutron activation analysis, 20: 40835
BOEHM, H., Irradiation effects on the mechanical properties of vanadium-base alloys, 20: 41506
BOEHM, S., Ionospheric absorption during solar eclipse on February 15, 1961. I., 20: 42051
BOELRIJK, N. A. I. M., Isotopic evidence for upper-cambrian or lower-ordovician granite emplacement in Vigo area, Spain, 20: 41153
BOERBOOM, A. J. H., Separation of lithium isotopes by countercurrent-exchange-electrolysis, 20: 41402
BOEV, A. G., Self-similar solution of nonsteady-state equations of a plane, laminar, magnetohydrodynamic boundary layer, 20: 42044
BOGARDUS, C. R. Jr., Complications and late changes following radiation therapy for carcinoma of eyelid and canthi, 20: 40689
BOGARDUS, Carl R. Jr., High-impedance vacuum tube voltmeter for use in radioisotope laboratory, 20: 41248
BOGARDUS, Carl R. Jr., Tandem elution of ^{99m}Tc generators, 20: 40754
BOGATYREV, V. L., Dissolution of $UO_2C_2O_4$ by ion exchange resins, 20: 40917
BOGDANKEVICH, O. V., Recombination radiation of alpha SiC due to electron bombardment, 20: 42565
BOGG, Richard F., Radiological health problems associated with operation of neutron generators, 20: 41215
BOGOYAVLENSKII, K. N., Effect of the annealing temperature and medium on the properties of molybdenum, 20: 41482
BOHIGAS, O., Hole and particle levels of ^{15}O and ^{17}O, 20: 42345
BOHN, Carole W., Electrodeposition of Cu–Mo alloys, 20: 41487
BOKOV, O. G., Remarks on the SU(6)$_w$ symmetry, 20: 42016
BOKROS, J. C., HTGR coated particle fuel, 20: 42624 (GA-6975)
BOLDYREV, V. V., Radiation effects on rate of silver nitrite thermal disintegration, 20: 41000
BOLON, G. C., π^0 photoproduction at 3.0, 4.0, and 5.0 Bev for baryon four momentum transfers between 0.5 and 4.0 (Bev/c)^2, 20: 41798 (MIT-2098-265)
BOLOTOV, V. N., Factors influencing the developing of discharge along trajectory of particle in spark chamber, 20: 41304
BOLOTOVSKII, B. M., Diffraction radiation, 20: 41523
BOLSUN, A. I., Polarization effects in the photoproduction of W-meson pairs on a nucleus, 20: 41901
BONAZZOLA, S., Equilibrium of a large assembly of particles in general relativity, 20: 42091
BONCHEV, Tsv, Iron-free asymmetric two-lens β spectrometer, 20: 41282
BONCH-OSMOLOVSKAYA, N. A., Decay mode of ^{160}Ho, 20: 42158 (JINR-P-2817)
BONCZAK, Boxyli, Efficiency of a hodoscope for registration of charged particles, 20: 41338
BONCZAK, Boxyli, Measurement of efficiency of liquid scintillation counters of large areas, 20: 41339
BOND, V. P., Iodine-125-DU (5-iodo-2'-deoxyuridine) in autoradiographic studies of cell proliferation, 20: 40666
BONDAR, I. A., Growing of rare earth silicate single crystals of oxyortho- and diortho-type from solution melt, 20: 40919
BONNET, G., Fluctuations of integral logarithmic period meter in random region, 20: 41237
BOOTH, A. H., Safety of radioisotopes in industry, 20: 41208
BORCHERS, R. R., Coulomb excitation in the platinum isotopes, 20: 42218
BORDENAVE-MONTESQUIEU, A., Energy distribution of He$^+$ ions produced by source with high-frequency electric excitation, 20: 41239
BORMOT, O. V., Reaction $^{12}C(\alpha,\alpha')^{12*}C(9.64\ Mev) \rightarrow 3\ \alpha$, 20: 42296
BOSAMYKIN, V. S., Compensating space charge of pulsed electron beams, 20: 42511
BOSE, H. N., Nonradiative destruction of F-centers in x-irradiated KCl doped with anionic impurities, 20: 42557
BOSTROEM, L., Numerical analysis of the time spectrum of delayed coincidences. I., 20: 41301
BOSTROEM, L., Numerical analysis of the time spectrum of delayed coincidences. II., 20: 41302
BOSTWICK, William E., Prog. rpt. on noble-metal, metal sheathed thermocouples, final, 9/65, 20: 41461 (UCRL-7361(Pt.3))
BOTSTEIN, Charles, Changes in relative biological effectiveness of 35 Mev electron beam as function of tissue depth, 20: 40767
BOUCHE, R., Reactions $^{12}C(a,a)$ at 51 Mev and $^{14}N(d,\alpha)^{12}C$ and $^{14}N(d,d)$ at 28.5 Mev, 20: 42389
BOUCHEZ, R., Excitation of 5.7 Mev level of ^{7}Li by (n,n') scattering at 14 Mev, 20: 42364
BOUCHEZ, R., Reaction ^{9}Be(n,nn)$\alpha\alpha$ at 15 Mev, 20: 42362
BOUCHIAT, C., Derivation of sum rules from the equal-time commutation relations for the space components of current densities, 20: 41958
BOUJOT, Jean-Paul, Tables of range and stopping power of chemical elements for charged particles of energy 0.5 to 500 Mev, 20: 41619 (CEA-R-3042)
BOULGER, F. W., Fabrication of Be. I., 20: 41427 (NASA-TN-X-53453 (Vol.1))
BOURGEON, Pierre, Fallout in France after second Chinese nuclear explosion, 20: 41189 (CEA-R-3020)
BOUROTTE, B., States $^3P_{3/2}$ and $^3P_{1/2}$ of ^{5}He, 20: 42357
BOWEN, D., Kρ three-body decays and the $|\Delta I| = \frac{1}{2}$ rules, 20: 41855
BOWEN, L. H., Solvent extraction of ^{18}F as tetraphenylstibonium fluoride, 20: 41021
BOWEN, T., Display lamp for counter logic, 20: 41314
BOWERSOX, D. F., Solubilities of selected elements in liquid Pu. VIII., 20: 40868 (LA-3523)
BOWIE, J. L., Electromagnetic characteristics of a bounded plasma slab, 20: 42481
BOWMAN, Kimiko O., Data on a set of trinomial distributions, 20: 41407 (ORNL-4004)
BOYD, A. W., Radiolysis of ortho- and meta-terphenyl. II., 20: 40946 (AECL-2589)
BOYD, J. H., Pion-pion interactions in π^-p reactions at 2.1 Bev/c, 20: 41858
BOYLE, A. J. F., Observations of the Moessbauer effect in ^{133}Cs, 20: 42239
BOYTSOV, V. E., Uranium and arsenic in hydrothermal process, 20: 41175
BOZEK, E., Study of electromagnetic transitions by measurement of the polarization distribution and γ-γ angular correlation, 20: 42381
BRAAMS, C. M., Stability of plasma confined by a cold-gas blanket, 20: 42473
BRACCINI, P. L., Precision detector for high-energy neutral pions, 20: 41320
BRACKENBUSH, L. W., Neutron and high energy particle dosimeter for medical dosimetry applications, 20: 41262 (BNWL-SA-619)
BRADFORD, R. R., Accumulation of Ca, Sr, Mg, P, and Zn by genotypes of corn under different soil fertility levels, 20: 40735 (NYO-2744-37)
BRADSHAW, Arthur Jeffrey, Improvements in and relating to articulated supports, 20: 42589
BRAMLAGE, William J., Gamma irradiation of fruits to extend market life, 20: 41385 (TID-23136)
BRANDMAIER, H. E., Two-dimensional electro-fluid dynamic channel flow, 20: 41696
BRANDT, E. N. Jr., Complications and late changes following radiation therapy for carcinoma of eyelid and canthi, 20: 40689
BRANSON, D., Cross-discontinuity condition in S-matrix theory, 20: 41966
BRASH, J. L., Photo- and radiation-induced cistrans isomerization of several 2-olefins, 20: 40965
BRAUN, H., Contribution to a study of structure of light nuclei by a study of the absorption mechanisms of K$^-$ mesons, 20: 42386
BRAUN, H., Quasielastic collisions on α groups in ^{12}C by 60 to 120 Mev protons, 20: 42352
BRAUN, R., Detector of fast neutrons with a moderator, 20: 41335
BRAUN, Ryszard, Gamma-ray scintillation spectrometer with NaI(Tl) single crystal, 20: 41336
BRAY, P. J., NMR studies of ^{7}Li in polycrystalline lithium nitride, 20: 42175
BREDERLOW, G., Device for operating a closed-loop MHD generator with current density measuring facilities, 20: 41678 (IPP-3/40)
BREGER, A. Kh., Radiation cross linking of cable polyethylene insulation on large scale, 20: 41496
BREININ, Goodwin M., Ocular lesions produced by an optical maser, 20: 40692
BREKHOVSKIKH, S. M., Radiation optical stability of quartz glass, 20: 41502
BREMER, Karl-Heinz, Hydrogen exchange in γ lactones, 20: 41017
BRENE, N., Leptonic decays of hadrons, 20: 41987
BRENNER, Morton W., Fast neutron measurements by threshold detectors in presence of 32 Mev x rays, 20: 41333
BRES, M., Precise measurement of the stopping power of C, Au, Al, Ca, and CaF_2 for 0.4 to 6 Mev protons, 20: 42363
BRESLOFF, Paul, Fine structure of lutein cells of x-irradiated rat ovary, 20: 40672
BRETTON, R. H., Gamma-radiation-induced ionic polymerization of pure liquid styrene. II., 20: 40978
BREWEN, J. G., Kinetics of chromatid aberrations induced in hamster cells by tritium-labeled thymidine, 20: 40686
BREZINA, Frantisek, Chemistry of the rare earth metals. XI., 20: 40909
BRICMAN, C., Measurement of the $\pi^\pm$p total effective cross section at T_π = 300 to 700 Mev, 20: 41830
BRIDWELL, L., Nanosecond time resolution in fission fragment x-ray lifetime experiments, 20: 41325
BRIGAUDEAU-VAISSIERE, Michele, Fixation of metallic acetates on an anion-exchange resin, 20: 41030 (CEA-R-2994)
BRIN, A., Magnetic field compression, 20: 41081

BRINKMANN, Kh. F., New isotope ^{216}Ac, 20: 42287
BRISSAUD, I., Discussion of the results obtained in pickup reaction on ^{9}B and ^{10}B nuclei at 156 Mev, 20: 42350
BRISSAUD, I., Preliminary results on ^{4}Li, ^{5}Li, and ^{6}Li obtained by (p,d) and (p,t) reactions on ^{6}Li and ^{7}Li at 156 Mev, 20: 42358
BRISSAUD, I., Reaction (p,d) at 156 Mev on fluorine and nitrogen, 20: 42204
BRITT, H. C., (d,pf) and (t,pf) reactions on Pu isotopes, 20: 42161 (LA-DC-7878)
BRITTEN, M. J. A., Radiation cataract: new evidence on radiation dosage to lens, 20: 40771
BROCHARD, F., Electromagnetic transitions in ^{16}O nuclei, 20: 42342
BROCKMAN, Herman, Prog. rpt. on comparative mutagenesis of Neurospora, 20: 40510 (TID-23137)
BRODIE, Arnold F., Oxidative phosphorylation in fractionated bacterial systems. XXII., 20: 40571
BRODSKII, A. M., Mechanism of radiation-thermal liquid phase conversions n-alkanes, 20: 40986
BRODY, M. D., Phase space representations of charged particle beams, 20: 41567
BRODY, T. A., Matrix elements and normalization coefficients in SU_n, 20: 42010
BROGAN, T. R., Hall configuration MHD generator studies, 20: 41761
BROGAN, Thomas R., Self-excited MHD generators, 20: 41709
BROMAN, L., Possible odd parity state of ^{128}Xe, 20: 42147 (AE-240)
BROMLEY, D. A., Collective nuclear structure in the even-even samarium isotopes, 20: 42265
BRONNIKOV, V. K., Temperature luminescence decay of ZnS:Ag mono-crystals at excitation of radiation, 20: 41342
BROOKS, C. R., Prog. rpt. on application of adiabatic calorimetry to metal systems, 9/65–8/66, 20: 41457 (ORO-3291-3)
BROS, J., Theoretical basis of the symmetrization postulate, 20: 42093
BROWN, Barbara L., Effect of radiation and actinomycin D therapy on incompletely removed mouse tumors, 20: 40762
BROWN, Bernard, ^{14}N(p,γ)^{15}O reaction, 20: 42258
BROWN, D. W., Radiation-induced polymerization of hexafluoropropylene at high temperature and pressure, 20: 40976
BROWN, G., Energy level structure of Cr isotopes, 20: 42211
BROWN, H. M., Germanium isotope fractionation, 20: 40933
BROWN, J. D., Pulse amplitude shifts in gas proportional x-ray detectors, 20: 41331
BROWN, K. B., Prog. rpt. on chemical applications of nuclear explosions, 4–6/66, 20: 41067 (ORNL-TM-1582)
BROWN, M. D., Some heavy-ion stopping powers, 20: 41647
BROWN, P. S., Prog. rpt. on particle fallout and dispersion in the atmosphere, 12/65–2/66, 20: 41133 (SC-CR-66-2030)
BROWN, Roger C., Determination of Cu in potato tissue using neutron activation analysis, 20: 40825
BROWNE, C. P., Accurate excitation energies of ^{11}B states below 7 Mev, 20: 42246
BROWNE, N. E., Prog. rpt. on particle fallout and dispersion in the atmosphere, 12/65–2/66, 20: 41133 (SC-CR-66-2030)
BROWNING, W. E. Jr., Characterization of radioactive particulate aerosols by fibrous filter analyzer, 20: 41234 (ORNL-P-2436)
BRUCE, R. S., Radioactivity in milk, 1965, 20: 41186 (ARCRL-15)
BRUGE, G., Levels of ^{24}Mg, ^{25}Mg, and ^{26}Mg excited by the reactions (α,α′), (α,^{3}He), and (α,t), 20: 42347
BRUNO, G., Contribution to a study of the reaction ^{12}C(d,p)^{13}C, 20: 42400
BRUNO, G., Elastic scattering of deuterons on ^{6}Li at 4 to 6.5 Mev, 20: 42365
BRUNTON, Donald C., Radiation gauging system with compensation for high background radiation intensities, 20: 41365
BRYAN, G. W., Accumulation of radionuclides by aquatic organisms of economic importance in United Kingdom, 20: 40578
BRYANT, A. R., Effect of Joule heating on diffusion of megagauss fields into metals, 20: 41087
BRYCE, A. J., Biological cleanability of surfaces using radioisotope tracer techniques, 20: 41218
BUBEN, N. Ya., Yield of stabilized charges in radiolysis of organic systems, 20: 40962
BUCELLA, F., Unitary-antisymmetric q-number terms in commutators of spatial current components, 20: 41985
BUCKLAND, Ernest Clifford, Improvements in and relating to separable electric connectors, 20: 41259
BUDGE, Ezra, Test cell A control systems, 20: 42663 (EGG-1183-1054)
BUGAENKO, L. T., Decomposition of radicals in frozen aqueous solutions of $NaClO_4$ and $HClO_4$, 20: 40960
BUGBY, Robert D., Visualization of lung by methods of scintiphotography, 20: 40749
BULLEN, J. M., Enhanced activity in the ionosphere E region at Cape Hallett and Campbell Island, 20: 42059
BUNCH, D. F., Dose to various body organs from inhalation or ingestion of soluble radionuclides, 20: 41193 (IDO-12054)
BUNCH, D. F., Prog. rpt. on controlled environmental radioiodine tests, 8/66, 20: 41192 (IDO-12053)
BUNCH, S. M., Excited levels in ^{3}He, 20: 42224
BUONANNI, R. M., Computation of the effects of errors of a magnetic channel on the final beam parameters, 20: 41538 (LNF-66/29)
BURCH, W. D., Prog. rpt. on transuranium program, 2/28/65, 20: 41039 (ORNL-3880)
BURGE, E. J., Wedge-shaped scintillation detector for magnetic spectrometer, 20: 41289
BURGERJON, J. J., Variable energy beam extraction from the Manitoba cyclotron, 20: 41557
BURGESS, E., Accretion and exchange of ^{85}Sr in trabecular and cortical bones, 20: 40684
BURKHALTER, P. G., Pulse amplitude shifts in gas proportional x-ray detectors, 20: 41331
BURKHANOV, G. S., Growing and plastic deformation of the single crystals of refractory metals and alloys, 20: 41481
BURKHARDT, H., Influence of wall radiation on the non-equilibrium electrical conductivity and on the ionization reaction time of a He–Cs plasma, 20: 41754
BURKHOLDER, Wendell E., Mating competition of γ-irradiated and non-irradiated male Trogoderma glabrum herbst, 20: 40673
BURMAN, R., Resonances of a cylindrical cavity in a lossy compressible plasma, 20: 42441
BURMAN, R., Wave propagation in an inhomogeneous compressible plasma, 20: 42478
BURMAN, R. L., Two-nucleon emission following absorption of stopped negative pions, 20: 42313
BURMANN, Franz J., Radionuclide analysis of environmental samples, 20: 40809 (NP-16235)
BURMISTROV, V. R., Light neutron nuclei among U fission products, 20: 42298
BURNETT, T. J., Operating guide for radiochemical laboratories at various activity levels, 20: 41199 (ORNL-TM-626)
BURNHAM, J. B., New approach to the determination of equilibrium magnetization of superconductors, 20: 42133
BURNHAM, M. W., Some experiments related to explosive driven MHD converters, 20: 41686
BURR, C. R., High-temperature magnetic susceptibility of lanthanum and cerium metals, 20: 42544
BURSON, Z. G., Design of shielded source for irradiation of animal populations, 20: 40518 (CEX-63.10)
BUSCHKE, Franz, Radiation therapy of carcinoma of vocal cord without mucosal reaction, 20: 40759
BUSCHOW, K. H. J., Magnetic and structural characteristics of some equiatomic rare-earth germanides, 20: 42552
BUSH, W. R., Tritium hazards, 20: 41185 (AECL-2594)
BUSSIERE, A., Levels of ^{24}Mg, ^{25}Mg, and ^{26}Mg excited by the reactions (α,α′), (α,^{3}He), and (α,t), 20: 42347
BUSSIERE, Paul, Determination of fluorine in gels of silica–alumina containing lead fluoride by fast neutron radioactivation, 20: 40845
BUTUZOV, S. S., Vacuum system of Ogra-II, 20: 42421 (NP-tr-1396)
BYCHKOV, Yu. F., Effect of oxygen additions on the structure and superconducting properties of Zr–Nb alloys, 20: 42535

C

CABE, J., Elastic and inelastic scattering of protons by ^{7}Li, 20: 42372
CADE, Stanford, Iatrogenics, 20: 40659
CAHILL, L. J. Jr., Structure of the magnetopause current layer, 20: 42068
CAILLAUD, Alain, Superconducting cavities for microtrons, 20: 41549
CALCANES, P. J., Experimental investigation of MHD channel flows at high Hartmann and Reynolds numbers, 20: 41707
CALDAROLA, L., Experiments to evaluate reactivity coefficients with reactor operating at steady state conditions (static experiments), 20: 42631 (KFK-260)
CALDERBANK, M., Wedge-shaped scintillation detector for magnetic spectrometer, 20: 41289
CALDWELL, D. O., Mass spectra of recoil nucleon states from inelastic ρ_0 production by pions of 12 and 18 Bev/c, 20: 41828
CALDWELL, David O., Comparison of the lifetimes of positive and negative pions, 20: 41891
CALUCCI, G., Cross-section for annihilation of a pair in two photons with gauge-invariant modification of the electron propagator, 20: 41822
CAMBOU, F., Elastic scattering of neutrons by tritium at 14 Mev, 20: 42373
CAMBOU, Francis, (n,d) Scattering between 1 and 5 Mev, 20: 42359
CAMERINI, U., Measurement of the $K_S^0 - K_L^0$ mass difference by the time dependent of strangeness, 20: 41922
CAMPBELL, Charles J., Optical maser as a retinal coagulator, 20: 40791
CAMPBELL, John William Edmund, Improvements in nuclear reactors,

20: 42588
CAMPO, Robert D., Fixation of ^{75}Se and ^{35}S onto protein-polysaccharides of bovine costal cartilage, 20: 40544
CANIGGIA, Angelo, Radiocalcium studies and histological findings in case of primary hyperparathyroidism, 20: 40552
CANO, G. L., Range and total ionization of low-energy recoil ions from alpha disintegrations in pure and binary gases, 20: 41622 (SC-DC-66-1564)
CANO, R., Thermal bremsstrahlung from inhomogeneous plasma, 20: 42457
CANSOY, C., Parameters for the first neutron resonance in ^{113}Cd, 20: 42149 (CNAEM-34)
CAP, F., Spinor calculus in Riemannian manifolds, 20: 42079
CAPELLA, A., Shadow model for the high-energy pion-proton elastic backward peak, 20: 41839
CAPENER, E. L., Ionization phenomena associated with solid-propellant rockets, 20: 41120
CAPPS, Richard H., SU(6)$_w$ and composite models of hadrons, 20: 42034
CAPRASSE, H., Modified one-nucleon exchange model in π-N scattering, 20: 41815
CAPRASSE, H., Regge pole analysis of $\pi^+ p \to \pi^0 N^{*++}$, 20: 41842
CARETTO, Albert A. Jr., Half-life of ^{101}Ag and formation cross section from Ag and In, 20: 42179
CARITHERS, W. C., Search for heavy magnetic monopoles, 20: 41676
CARLSON, Edward H., Prog. rpt. on interactions between f-shell transition ions in non-metallic crystals, annual, 10/1/65–6/15/66, 20: 42522 (COO-1533-2)
CARLSON, R. F., Energy dependence of proton-proton bremsstrahlung, 20: 41882
CARLSON, R. R., Branching ratios in ^{14}C and ^{14}N, 20: 42231
CARLSON, W. D., Prog. rpt. on effects of ionizing radiation on functional and structural status of bull testicle, final, 2/65–7/66, 20: 40610 (COO-895-9)
CAROVILLANO, R. L., Dynamical stability and boundary perturbations of the solar wind, 20: 41586
CARPETIS, C., Some aspects on the use of cryogenically cooled primary-windings system for an a-c MHD generator, 20: 41727
CARROLL, K. J., Superconducting contact between lead based and niobium based alloys, 20: 42124
CARROLL, Nicholas V., Spectral shift phenomenon of chloroquine, 20: 40954
CARTER, H. K., Germanium(Li)–NaI(Tl) coincidence system with multichannel analysis, 20: 41295
CARVER, Joseph H., Prog. rpt. on study of irradiated-pasteurized fishery products, final, 10/64–9/65, 20: 41384 (TID-22833)
CARVER, Robert L., Radioactivity apparatus for indicating properties of materials, 20: 41115
CASABIANCA, Manuel, General guide for irradiations in the research and experimental reactor IAN-R1, 20: 42679 (IAN-R-1)
CASHION, J. K., Calculated ion-to-molecule-ion ratios for electron-bombardment studies of molecular H, 20: 40893
CASIDA, John E., Synthesis of rotenone-6a-^{14}C on a semimicro scale, 20: 41013
CASIDA, John E., Synthesis of methylene-^{14}C-dioxyphenyl compounds, 20: 41014
CASIDA, John E., Synthesis of d-trans-chrysanthemumic acid-1-^{14}C and its antipode on semimicro scale, 20: 41015
CASSAGNOU, Y., Separation of reaction mechanisms at low energy, 20: 42394
CASTILLE, Y. P., Radiation-induced copolymerization of formaldehyde and styrene, 20: 40973
CASWELL, H. L., Superconducting memories, 20: 42108
CAVES, T., Deuteron quadrupole coupling constant in CH_3D, 20: 40894
CAWLEY, Robert G., Connection between the electromagnetic form factor and the propagator normalizations, 20: 41980
CECIL, R. A., Perfect thermodynamic vapor, 20: 42045
CEFALU, R., Nature and stability of system uranyl-benzohydroxamic acid in acid medium, 20: 40903
CERCIGNANI, C., Numerical computation methods for implosion processes, 20: 41088
CESARI, Leone, Radiocalcium studies and histological findings in case of primary hyperparathyroidism, 20: 40552
CHADWICK, Donald R., Observations derived from film packs used in nation-wide x-ray exposure study, 20: 41213
CHAKRABARTI, A., Unified unitary representation of Poincare group for particles of zero and positive rest mass, 20: 41940
CHAMBON, B., Study of angular distributions of the reaction $^{32}S(n,\alpha_0)^{29}Si$ at 2.5 to 3.2 Mev, 20: 42375
CHAMPETIER, J. L., Magnetic field compression, 20: 41081
CHAMPETIER, J. L., Theory of magnetic field compression diffusion, surface instabilities, 20: 41090
CHANANA, Arjun D., Tritiated thymidine as cytocidal agent in human leukemia, 20: 40743 (BNL-9374)
CHANDLER, A., Sequelae of LD/50 x-ray exposure of pre-implantation mouse embryo, 20: 40649
CHANG, C. C., Magnetohydrodynamic boundary layer between parallel streams of different magnetic fields and temperatures, 20: 42039
CHANG, Cho-ray, Effects of desolvation of a Pb–Sb alloy on the critical characteristics of superconductors, 20: 42099 (AD-636625)
CHANG, Chu-Chun, Separation of rare-earch metals by reversed-phase paper chromatography, 20: 41045
CHANG, Zhun-Wu, Angular distribution of high energy neutrons emitted in the absorption of polarized μ^--mesons in Ca, 20: 42300
CHAO, C. C., Superconductivity of LaAg, 20: 42101
CHAPMAN, R. L., Magnetic field compression techniques for metallic particle acceleration, 20: 41084
CHARKES, N. David, Value of ^{85}Sr bone scanning in radiation therapy, 20: 40794
CHARLESBY, A., Alpha-particle radiolysis of the cyclohexane-S system, 20: 40990
CHASMAN, C., Lifetime determinations for nuclei A = 10, 11, and 12 from gamma-ray Doppler shifts, 20: 42234
CHASTEL, R., Study of (n,α) reaction on ^{16}O at 14.9 Mev, 20: 42370
CHAVY, F., Preliminary results on ^4Li, ^5Li, and ^6Li obtained by (p,d) and (p,t) reactions on ^6Li and ^7Li at 156 Mev, 20: 42358
CHAWLA, B. R., Radiation in a moving anisotropic plasma, 20: 42480
CHEKHOVSKOI, V. Ya., Niobium and Zr carbides at temperatures between 1200 and 3500°K, 20: 41729
CHEN, H. T., Neutron-proton correlation effects in spherical even nuclei, 20: 42195
CHEN, Tsung-Shan, Focusing of electron beam from low-noise gun with different magnet systems. II., 20: 41551
CHEN, Tsung-Shan, Focusing of electron beam from low-noise gun with different magnet systems. III., 20: 41552
CHENG, I-p'ing, Effect of Y on high temperature oxidation of Mo, 20: 41421
CHEREDNICHENKO, I. M., Design of radioactive isotope instruments, 20: 41235
CHEREVATENKO, E. P., Attenuation of high-energy neutron fluxes in heterogeneous shielding, 20: 42517
CHERMALYKH, G. N., Frye-Warnock equation and the Froissart N/D method, 20: 42012
CHERNICK, J., Effect of Xe on safety of HFBR, 20: 42672 (BNL-10388)
CHERNOGOROVA, V. A., Angular distribution of high energy neutrons emitted in the absorption of polarized μ^--mesons in Ca, 20: 42300
CHERNOV, I. P., Optical model analysis of the elastic scattering of 13.6 Mev deuterons on medium weight nuclei, 20: 42294
CHERNUKHIN, Yu. I., Deuteron disintegration by 14 Mev neutrons, 20: 42291
CHESSELET, R., Measurement of radioactivity in the sea, 20: 41145
CHESSELET, R., Radioactivity of plankton and of organic refuse, 20: 41146
CHEVALLIER, A., Precise measurement of the stopping power of C, Au, Al, Ca, and CaF_2 for 0.4 to 6 Mev protons, 20: 42363
CHEVALLIER, J., Study of electromagnetic transitions by measurement of the polarization distribution and γ-γ angular correlation, 20: 42381
CHEVALLIER, P., Electromagnetic transitions in ^{16}O nuclei, 20: 42342
CHIKHLADZE, B. Ya., Use of the hollow cathode for the determination of gases in solids by the isotopic equilibrium method, 20: 41526
CHILASHVILI, G. A., Analytical properties of the non-relativistic amplitude, 20: 42019
CHILTON, F., Multiple subsurface spalling by underground nuclear explosions, 20: 41126
CHIPMAN, Walter A., Uptake and accumulation of ^{51}Cr by clam, 20: 40575
CHIRKOV, V. P., Determination of electron concentration of plasma in a reflex klystron, 20: 42446
CHIU, H. H., Two-dimensional electro-fluid dynamic channel flow, 20: 41696
CHIZHIK, V. I., Determining splitting in nuclear-resonance spectra, 20: 41254
CHKHAIDZE, L., Search for new decay modes of the K^+_3-mesons, 20: 41903
CHOPPIN, G. R., Effect of changes in ionic medium on stability constant of $Eu(NO_3)^{+2}$, 20: 40876 (ORO-1797-2)
CHOWN, J. B., Ionization phenomena associated with solid-propellant rockets, 20: 41120
CHOY GEN SOR, Kev neutron scattering by lead and electrical polarizability of neutron, 20: 42140 (JINR-P-2764)
CHRETIEN, J. F., Elastic and inelastic scattering of protons by ^7Li, 20: 42372
CHRISTIANSEN, Joern J., ESR of free radicals trapped in inert matrices at low temperature: P, PH_2, and As, 20: 40967
CHRISTIANSEN, Joern J., ESR of free radicals trapped in inert matrices at low temperature: CH_3, SiH_3, GeH_3, and SnH_3, 20: 40968
CHRISTOPHERSON, H. L., Calibration of Westphal balance and plummet, 20: 40869 (MCW-1473)
CHU, Florence C. H., Does prophylactic radiotherapy given for cancer of breast predispose to metastasis?, 20: 40793

CHUANG, Hsiang-lin, Isothermal sections at 1200°C of equilibrium diagrams of Mo–Ti–Zr and Mo–Nb–Zr, 20: 41464
CHUANG, Hsiang-lin, Molybdenum–Gd phase diagrams, 20: 41465
CHUANG, Yu-chih, Isothermal sections at 1200°C of equilibrium diagrams of Mo–Ti–Zr and Mo–Nb–Zr, 20: 41464
CHUANG, Yu-chih, Molybdenum–Gd phase diagrams, 20: 41465
CHUDOV, L. A., Numerical methods in gas dynamics, 20: 40038 (NASA-TT-F-360)
CHUKHLANTSEV, V. G., Preparation of granulated zirconyl phosphate by freezing and its ion exchange properties, 20: 41055
CHUPRIKOV, G. E., Growing and plastic deformation of the single crystals of refractory metals and alloys, 20: 41481
CHUTE, Rosanne N., Lung carcinomas in irradiated parabiotic rats, 20: 40614 (NYO-901-39)
CIAMPI, M., Features of a plasma ion source with hot cathode gas discharge, 20: 41403
CINI, J., Two-capsule program for comparing A302B steel from two manufacturers under specific irradiation conditions, 20: 41504
CIMORELLI, L., Void fraction measurement in boiling channel, 20: 41103 (RT-ING-(65)7)
CLANCY, B. E., Calculations of hard sphere packings in large cylinders, 20: 41063 (BNL-997)
CLARK, Gary Edwin, Gamma-gamma directional correlation, 20: 41371
CLARK, Richard L., Water-only plant studies, 20: 42659
CLARK, W. E., Addition of lithium values in conversion of fission-product wastes to a glass-like solid for disposal, 20: 42690
CLARK, Willie E., Index to conferences relating to nuclear science, 20: 42693 (TID-4043(Rev.3))
CLAYTON, R. N., Origin of saline formation waters. I., 20: 41161
CLEARY, R. E., Viscosity of liquid K to 900°C, 20: 41460 (TIM-793)
CLEMENT, G., Electroproduction of very high-energy muons, 20: 41805 (SLAC-Trans-46)
CLEWELL, Don B., Prevention of x-ray-induced leukemia in mice. I., 20: 40658
CLINE, D., Measurement of the K_S^0–K_L^0 mass difference by the time dependence of strangeness, 20: 41922
CLINGMAN, D. L., Experimental investigations of closed-loop MPD power generation, 20: 41741
COATES, P. B., Temperature measurements in shock tubes: transition probabilities for argon lines, 20: 42483
COBB, Joseph K., Electron-induced cascade showers in Cu and Pb at 1 Bev, 20: 41671
COBB, Lewis A., System for determining fluid flow rate in boreholes, 20: 41170
COBBLE, J. W., Evidence of ternary fission at lower energies, 20: 42273
COCHE, A., Reactions induced in carbon by fast neutrons, 20: 42367
COCHRAN, William R., Optical spectra of tripositive ^{224}Cm in lanthanum trichloride, 20: 40891
CODDING, J. W. Jr., Tabulation of the ^{233}Pa total neutron cross section data, 20: 42151 (IN-1014)
COFFIN, Don O., Tritium contamination, 20: 41196 (LA-DC-7996)
COFFIN, J. P., "Multipolimeter" application to a study of electromagnetic transitions, 20: 42384
COGBURN, Robert R., Mating competition of γ-irradiated and nonirradiated male Trogoderma glabrum herbst, 20: 40673
COHEN, Jeffrey M., Electromagnetic fields and rotating masses, 20: 41609
COHEN, Leon, Modification of radiosensitivity by porphyrins. II., 20: 40657
COHEN, S. L., Baryon mass differences in a model of broken unitary symmetry, 20: 41976
COHN, Jack, Geometry and Newtonian physics, 20: 42094
COLBY, L. J. Jr., Possible mechanism for the activation of UC, 20: 40870 (NAA-SR-Memo-7310)
COLE, Donald R., Radioprotective and anti-tumor effect of mixed bacterial toxins and anthramycin, 20: 40736
COLEMAN, J. A., Lithium compensated silicon focal plane detectors for electron scattering spectrometers, 20: 41326
COLEMAN, Sidney, Seven types of U(6), 20: 42031
COLI, M., Nomogram for designing tunnel diode monostable circuits, 20: 41242
COLI, M., Suggestions for improvements of timing circuits with tunnel diodes, 20: 41246
COLLICA, Carl J., Advantage of three combined diagnostic procedures with ^{131}I for evaluation of thyroid disorders, 20: 40756
COLLIER, George, VARI-QUIR diffusion code, 20: 42143 (WANL-TNR-133(Rev.))
COLLINS, G. B., Design and performance of on-line wire spark chamber spectrometer, 20: 41297
COLLINS, M. F., Magnetic structure of solid oxygen, 20: 42558
COLMAN, J. M., Timing and firing, Project Dribble, 20: 41070 (VUF-3021)
COLOMBI, Carlo, Gas turbine in nuclear power plants, 20: 42654
COLOMBO, R. L., Dependence on microstructure of the high temperature properties of U oxide. Mo and U oxide. W cermets, 20: 41478
COMANESCU, V., Electrode calibration for nuclear diagraphy, 20: 41165
COMBE, Rene, Superconducting cavities for microtrons, 20: 41549
COMPSTON, W., Radiometric ages of precambrian rocks from northwest division of western Australia, 20: 41159
COMUNETTI, Angelo, Gamma compensation of ionization chamber for detection of neutron flux in nuclear reactors, 20: 41360
CONDIT, Richard I., Area-wide shelter systems, 20: 41183 (AD-635931)
CONKLIN, J. W., Influence of age on susceptibility to radiation-induced life-shortening in mice, 20: 40633 (ORNL-P-2287)
CONNOLLY, T. F., Lists of available and desired materials and available crystal-growth references, 20: 40874 (ORNL-RMIC-5)
CONNOR, H. W. J., Radiolysis of ortho- and meta-terphenyl. II., 20: 40946 (AECL-2589)
CONTOGOURIS, A. P., Analytic and asymptotic properties of soluble N/D models, 20: 41961
CONTRE, M., Pressure-temperature phase diagram of beryllium, 20: 41485
CONTRERAS, Ma. de los Angeles, Determination of total iodine in radioactive iodide preparations of high specific activity, 20: 40553
CONWAY, John G., Optical spectra of tripositive ^{224}Cm in lanthanum trichloride, 20: 40891
COOK, John S., Photoreactivating enzyme in sea urchin egg, 20: 40543
COOK, Kenneth J., Automatic electron dosimetry system for a microwave linear accelerator, 20: 41323
COOK, L. H. Jr., Control system for x-ray diffractometer scanning, 20: 41222 (DP-900)
COOKE, Brian Frederick, Nuclear reactor, 20: 42590
COOMES, E. A., Use of precise Schottky data in the determination of the surface characteristics of Rh emitters, 20: 42575
COOP, K. L., Fast neutron cross sections for the ^{23}Na(n,γ)^{24}Na, ^{55}Mn(n,γ)^{56}Mn, ^{115}In(n,γ)^{116m}In, and ^{165}Ho(n,γ)^{166}Ho reactions, 20: 42332
COOPER, Martin J., Classical statistical mechanics of the hard-core potential, 20: 41509 (AD-638830)
COOPER, W. R., Sequelae of LD/50 x-ray exposure of pre-implantation mouse embryo, 20: 40649
COPPAGE, F. N., Photoconductivity processes in organic materials, 20: 40952 (SC-DC-66-1823)
COPPERSMITH, W. C., Correlation of two-group theory with neutron flux measurements in a pool-type reactor, 20: 42600
COPPI, Bruno, Origin of electron precipitations in the auroral zones, 20: 42056
CORALLO, R. A., Long John thermogasdynamic research facility, 20: 41104 (UCRL-14841)
CORBETT, James W., Electron radiation damage in semiconductors and metals, 20: 41508
CORBIN, L. T., Operating guide for radiochemical laboratories at various activity levels, 20: 41199 (ORNL-TM-626)
CORCORAN, T., Application of the SU(3) shell model to ^{9}Be, 20: 42191
CORYELL, C. D., Decay schemes of 43-day ^{115m}Cd and 2.3-day ^{115g}Cd, 20: 42260
COSTA, A., Surgery compared with radioiodine therapy in treatment of hyperthyroidism, 20: 40785
COTE, R. E., X-rays from muonic atoms with spherical or nearly spherical nuclei, 20: 42306
COTTER, David J., Ecological effects of short term exposures of ionizing radiation, 20: 40526
COTTERELL, Kenneth, Improvements in or relating to radiographic examination techniques, 20: 41116
COTTIER, H., Studies on lymphopoiesis. IV., 20: 40663
COTTINO, F., Surgery compared with radioiodine therapy in treatment of hyperthyroidism, 20: 40785
COUCHOUD, S., Probability distributions of extremes of cross sections, 20: 42395
COUEY, H. Melvin, Gamma irradiation of fruits to extend market life, 20: 41385 (TID-23136)
COUGHREN, K. D., Dynamic analysis of Hanford dual-purpose reactor plant using analog simulation methods, 20: 42660 (BNWL-SA-270)
COUNSELL, J. F., Thermodynamic properties of U compounds. II., 20: 40921
COURT, L., Long-term incidence of myxedema appearing after radiotherapy for cancer of larynx, 20: 40780
COWAN, M. Jr., Energy conversion efficiency in flux compression, 20: 41086
COWELL, Mary A. C., Prediction of dose of radioactive phosphorus in treatment of polycythemia vera, 20: 40774
COX, G. F., Measurements of the differential cross-section and polarization proton-proton scattering at about 143 Mev, 20: 41915
CRANNELL, H. L., Determination of relative efficiencies for multidetector system, 20: 41310
CRANNELL, Hall, Elastic and inelastic electron scattering from ^{12}C and ^{16}O, 20: 42238
CRANSTON, Gamma-ray transitions in ^{44}Ca, 20: 42335
CRAWFORD, Bevalyn B., Sign of the K_1^0–K_2^0 mass difference, 20: 41878
CRAWFORD, C. K., Phase space representations of charged particle beams,

20: 41567
CRAWFORD, Frank S. Jr., Sign of the K_1^0–K_2^0 mass difference, 20: 41878
CRAWLEY, Ralph Hugh Alfred, Decontamination of radioactive solutions, 20: 41061
CRENSHAW, John W., Response of DBA/2J mouse strain to acute ionizing radiation, 20: 40687
CRETTEZ, J. P., Study of charged products in the reaction $^9Be + d$ at very low energy (100 to 200 kev), 20: 42354
CROMER, Alan H., Analysis of π^--mesonic atoms, 20: 41665
CRONKITE, E. P., Extracorporeal irradiation of blood and lymph, 20: 40744 (BNL-10403)
CRONKITE, E. P., Studies on lymphopoiesis. IV., 20: 40663
CRONKITE, Eugene P., Tritiated thymidine as cytocidal agent in human leukemia, 20: 40743 (BNL-9374)
CRONSTROEM, C., Leptonic decays of hadrons, 20: 41987
CRONSTROEM, C., One-boson exchange potentials in nucleon-nucleon scattering, 20: 41899
CROSLEY, Phillip, Prog. rpt. on fracture toughness of reactor pressure vessel steels, 6–7/66, 20: 41444 (COO-1477-5)
CROUSE, D. J., Prog. rpt. on chemical applications of nuclear explosions, 4–6/66, 20: 41067 (ORNL-TM-1582)
CROWE, K. M., Pi-mesic x-rays, 20: 42311
CUEER, P., Contribution to a study of structure of light nuclei by a study of the absorption mechanisms of K^- mesons, 20: 42386
CUEER, P., Quasielastic collisions on α groups in ^{12}C by 60 to 120 Mev protons, 20: 42352
CUMMINGS, D. B., Electrical pulses from helical and coaxial explosive generators, 20: 41095
CURRIE, Douglas G., q-equivalent particle Hamiltonians. I., 20: 41941
CURRY, N. A., Magnetic structure of uranium monophosphide, 20: 42560
CURTIS, Howard J., Interpretation of microbeam experiments for manned space flight, 20: 41187 (BNL-9468)
CYROT, Michel, Spin-lattice relaxation in dirty superconducting alloys in high fields, 20: 42102
CZEPELSKA-SULKOWSKA, Barbara, Two-impulse neutron detector with plastic scintillator, 20: 41337
CZIRR, J. B., n-n S-wave scattering length from the neutron spectra of the reaction $\pi^- + d \rightarrow 2n + \gamma$, 20: 41914
CZYZEWSKI, Oleg, Study of zero and two prong antiproton-proton interactions at 3-4 Bev/c primary momentum, 20: 41792 (INR-708/VI/PL)

D

DABBS, J. W. T., Response of Si fission detectors to channeled ^{127}I and ^{40}Ar ions, 20: 41324
DABOUL, J., Departures from $\bar{U}_{12}$ in a relativistic quark model, 20: 41965
DA COSTA, R. C. T., Solution of the electromagnetic equations for rotating systems, 20: 42087
DAEHNICK, W. W., Reactions (d,^{6}Li) in light elements and distorted-wave Born approximation calculations, 20: 42237
DAGNAC, R., Energy distribution of He^+ ions produced by source with high-frequency electric excitation, 20: 41239
DAHM, A. J., Effective mass of positive and negative ions in liquid helium, 20: 41664
DAINTON, F. S., Important early stages in radiolysis of solid and liquid systems, 20: 40987
DALGARNO, A., Free-free transitions of electrons in gases, 20: 41626
DALITZ, R. H., Constraints on the statistical tensor for low-spin particles produced in strong interaction processes, 20: 41950
DALLIMORE, P. J., Analysis of some synthetic cross-section fluctuation data, 20: 42194
DALMAS, J., Study of (n,α) reaction on ^{16}O at 14.9 Mev, 20: 42370
DALY, N. R., Electron collisions in nitrogen, 20: 41652
DALY, N. R., Electron ionization of He^+, 20: 41653
DAMMERS, J., Nutrition experiments in pigs fattened with heat-decontaminated, γ-irradiated and untreated feeds, 20: 41394
D'ANGIO, Giulio J., Effect of radiation and actinomycin D therapy on incompletely removed mouse tumors, 20: 40762
DANIEL, G., Evidence demonstrating germinal selection in early premeiotic germ cells of Drosophila males, 20: 40670
DANIELSSON, L., Adsorption of number of elements from sulfuric acid solutions by anion exchange, 20: 40822
DANILKIN, I. S., Conversion of transverse EM wave to ionic sound oscillations of plasma, 20: 42499
DANNECKER, A., Determination of natural and artificial radioactivity in water, 20: 40819 (CEA-tr-A-1883)
DARENSKAYA, N. G., Behavior of live organisms in radiation fields, 20: 40519 (NP-16259)
DARGAN, C. L., Calculated magnetic electron drift velocities in H_2, N_2, O_2, air and C_2H_6, 20: 41628
DARVES-BLANC, R., Reaction $^9Be(n,nn)\alpha\alpha$ at 15 Mev, 20: 42362
DAS, H. A., Nondestructive activation analysis of antique gold coins, 20: 40829
DA SILVA, Constancio Pegano, Preparation of carrier-free ^{131}I from irradiated elemental tellurium, 20: 41399 (IEA-110)
DAUM, C., Muonic x-ray studies of spherical nuclei, 20: 42309
DAVID, J., Ferroelectric transducers, 20: 41684
DAVIES, B., Angular functions for a three-nucleon system, 20: 42209
DAVIES, J. H., Experimental studies of plutonium and fission product redistribution in fast reactor fuels, 20: 42625 (GEAP-4466)
DAVIS, Carl W., New radioprotector in E. coli, 20: 40737
DAVIS, G. D., Addition of lithium values in conversion of fission-product wastes to a glass-like solid for disposal, 20: 42690
DAVIS, H., Pion capture and nuclear structure, 20: 42314
DAVIS, W. R., Development of the covariant formulation of the conservation laws of general relativity, 20: 42080
DAWSON, F. G., Plutonium utilization program, FY 1967–70, 20: 42607 (BNWL-298)
DAY, Walter C., Trace elements in common rock types, 20: 41068 (PNE-5006)
DEARNALEY, G., Semiconductor counters for nuclear radiations, 20: 41352
DE BATS, F. Th., Equilibrium and stability of a toroidal screw pinch, 20: 42414 (NP-16266)
DEBEVEC, L., Mass spectrometric study on the isotope effect in secondary electron emission from metal surfaces by positive ions, 20: 41620 (NIJS-R-471)
DECHARGE, J., Contribution to a study of the reaction $^{12}C(d,p)^{13}C$, 20: 42400
DECHARGE, J., Elastic scattering of deuterons on ^{6}Li at 4 to 6.5 Mev, 20: 42365
DEE, John B. Jr., Control rods, 20: 42591
DEEKS, D. G., Generalized full-wave theory for energy-dependent collision frequencies, 20: 42452
DE GREEF, J. O., Research and determination of rates of leakages of nuclear fuel elements, 20: 42610 (AI-Trans-206)
DEGTYAREV, Yu. N., Combined determination of ^{90}Sr and ^{137}Cs, 20: 40853
DEGTYAREV, Yu. N., Determination of ^{131}I, 20: 40852
DEIGEN, M. F., ENDOR of F centers in KCl at room temperature, 20: 42566
DEJONGHE, P., Recovery of fission products as sources of radiation or energy, 20: 42689
DE KOWALEWSKI, D. G., Application of the ENDOR technique to high resolution proton magnetic resonance spectra, 20: 42529
DELACHE, Philippe, Some problems of radiative transfer in an atmosphere having a stellar wind, 20: 41618
DELBOURGO, R., Departures from $\bar{U}_{12}$ in a relativistic quark model, 20: 41965
DEL CASTILLO, G., Magnetic flux penetration in hard superconducting plates, 20: 42132
DELCROIX, V., Fluctuations of integral logarithmic period meter in random region, 20: 41237
DELL, R. M., Thermodynamic properties of U compounds. II., 20: 40921
DELL'ANTONIO, G.-F., Theorem on canonical commutation and anticommutation relations, 20: 42076
DELORME, J., Theory of radiative capture of π mesons in nuclei, 20: 42385
DE MARIA, D., Pinhole camera in study of secondary emission in bodies exposed to irradiation, 20: 41321
DE MEESTER, P., Choice of materials in nuclear technology, 20: 41413
DEMENTEV, V. A., Determination of specific activities by measurements of high-energy β-radiation, 20: 40833
DEMETER, I., Decay series $^{138}Nd \rightarrow {}^{138}Pr \rightarrow {}^{138}Ce$, 20: 42197
DEMIDOV, A. M., Capture of thermal neutrons by Te, 20: 42286
DEMIN, A. G., New isotope ^{216}Ac, 20: 42287
DEMMITT, T. F., Plutonium Recycle Test Reactor decontamination following MgO–PuO_2 fuel element failures, 20: 42677 (BNWL-SA-636)
DENES, L. J., Reactions (d,^{6}Li) in light elements and distorted-wave Born approximation calculations, 20: 42237
DENISOV, S. P., Isospin amplitudes for S-state pion photoproduction on nucleons, 20: 41906
DENISOVA, E. A., Clinical and dosimetric data on personnel operating a 10 Bev synchrophasotron, 20: 41206 (JPRS-36341, pp 10-17)
DENZEL, D. L., Experimental determination of the internal resistance matrix of MHD generator, 20: 41748
DE PAEPE, J.-C., Cervical cancer. Study of series of patients treated by radiations, 20: 40772
DEPCZYK, D., Test of the theory of alkaline earth metabolism by behaviour of ^{133}Ba in rats, 20: 40565
DEPRAZ, J., Study of angular distributions of the reaction $^{32}S(n,\alpha_0)^{29}Si$ at 2.5 to 3.2 Mev, 20: 42375
DESAI, Bipin R., Exchange of even- and odd-parity baryon-meson resonances and backward elastic scattering, 20: 41880
DE SANDO, R. J., Structures of Po and its compounds. I., 20: 41469
DESCHAMPS, Y., Levels of ^{15}O excited by the reaction $^{14}N(d,n\gamma)^{15}O$ at 6.3 Mev, 20: 42346
DESCHREIDER, A. R., Effects of gamma radiation on constituents of

wheat flour, 20: 40599
DE SIMONE, Jean Claude, Carrousel magnetoaerodynamic generator, 20: 41697
DESTREE, Rene, Construction and testing of auxiliary-arc electrodes, 20: 41745
DETHLEFSEN, Rolf, Experimental investigation of fluctuations in a non-equilibrium MHD plasma, 20: 41692
DETRAZ, C., Discussion of the results obtained in pickup reaction on ^{9}B and ^{10}B nuclei at 156 Mev, 20: 42350
DETRAZ, Cl., Isobaric multiplets in light nuclei, 20: 42355
DETSOVSKI, P., Some aspects of the multi-nucleon transfer reaction mechanism, 20: 42156 (JINR-P-2813)
DETTMANN, K., Convergence behavior of the Born series for rearrangement collisions, 20: 41642
DEURLOO, P. A., Refractometric determination of U(VI) in aqeuous and in TBP solutions, 20: 40804 (KR-108)
DEVINS, D. W., Excited levels in ^{3}He, 20: 42224
DEVISHEV, M. I., Factors influencing the developing of discharge along trajectory of particle in spark chamber, 20: 41304
DEVONS, S., Detailed analysis of muonic x-ray spectrum from strongly deformed e-e nuclei, 20: 42310
DEVYATKOV, A. G., Recombination radiation of alpha SiC due to electron bombardment, 20: 42565
DE WIT, S. A., Muonic x-ray studies of spherical nuclei, 20: 42309
DE WITT, W. D., Prog. rpt. on thermal insulation, 4–6/66, 20: 41440 (ALO-3632-4)
DE WOLF, M. Y., Laser induced prebreakdown and breakdown phenomena observed in cloud chambers, 20: 41375
DEWS, Jon R., Isotopic composition of lithium in chondrules, 20: 42061
D'HAENENE, I. J., Use of precise Schottky data in the determination of the surface characteristics of Rh emitters, 20: 42575
DHARWADKAR, S. R., Kinetics of thermal decomposition of UO_3. I., 20: 40899
DI BARTOLOMEO, M., Void fraction measurement in boiling channel, 20: 41103 (RT-ING-(65)7)
DICELLO, J. F., Total reaction cross sections for 14.5 Mev protons from ?? separated isotopes of Ti, Fe, Ni, Cu, Zn, Zr, and Sn, 20: 42162 (LA-DC-8075)
DICKINSON, L. A., Ionization phenomena associated with solid-propellant rockets, 20: 41120
DIDIER, D., Study of the reactions $^{10}B(d,\alpha)^{2}4He$ and $^{9}Be(^{3}He,\alpha)^{2}4He$, 20: 42374
DIENST, W., Irradiation effects on the mechanical properties of vanadium-base alloys, 20: 41506
DIENSTBIER, Z., Effects of irradiation on level of reduced nicotinamide nucleotides in rat liver homogenates, 20: 40583
DIETZ, K. A., Prog. rpt. on STEP project, 7–9/65, 20: 42664 (IDO-17165)
DIETZ, Klaus, Role of meson current in the determination of neutron form factors from elastic electron-deuteron scattering, 20: 41883
DIETZOLD, W., Differential thermal analysis of oxalate hydrates of rare earth metals, 20: 40900
DI GIUGNO, G., Measurement of the branching ratio $\omega \to$ neutrals/$\omega \to \pi^{+} + \pi^{-} + \pi^{0}$, 20: 41850
DI GREGORIO, C., Simple flux compression devices with small explosive charge, 20: 41094
DI LAZZARO, Maria A., Measurement of the cross section of coherent and incoherent scattering of 662-kev γ rays on bound electrons, 20: 41625
DILLI, S., Charge-transfer theory for interpretation of radiation-induced grafting of monomers to cellulose, 20: 40979
DIMICK, Keene P., Concentric tube and parallel plate electron capture detectors, 20: 40863
DI NANNO, L. R., Hall configuration MHD generator studies, 20: 41761
DINGLE, A. Nelson, Prog. rpt. on rain scavenging studies, 3/65–5/66, 20: 41130 (COO-1407-10)
DISCHINGER, R. H., Prog. rpt. on performance evaluation of heat exchangers for Na-cooled reactors, 4–6/66, 20: 42639 (UNC-5154)
DISDIER, D., Electromagnetic transitions in ^{16}O nuclei, 20: 42342
DIVATIA, A. S., Fluctuation analysis of $^{27}Al(p,\alpha_0)^{2}4Mg$ and $^{27}Al(p,p_3)^{27}Al^{*}$ cross sections, 20: 42324
DIVATIA, A. S., Study of the $^{13}C(\alpha,n)^{16}O$ reaction, 20: 42336
DMITRIEV, V. D., Integral radiant emissivity of W from 1200 to 2800°K, 20: 41525
DOBBS, J. M., K_{ρ} three-body decays and the $|\Delta I| = \frac{1}{2}$ rules, 20: 41855
DOBROVOLSKII, O. V., Critical wavelength in the system of a collisionless gas and solid medium in a homogeneous magnetic field, 20: 42041
DOBZHANSKY, Theodosius, Prog. rpt. on genetic studies, annual, 6/65–6/66, 20: 40622 (NYO-3096-8)
DODD, John Alan, Improvements in or relating to manipulating devices for use in nuclear reactors, 20: 42593
DODGE, Marilyn J., Effects of space radiations on refractive properties of optical glasses, 20: 41505
DODGE, W. R., Lithium compensated silicon focal plane detectors for electron scattering spectrometers, 20: 41326
DOLE, Malcolm, Radiation chemistry of polyethylene. VIII., 20: 40964
DOLE, Malcolm, Ultraviolet spectroscopy of irradiated polyethylene, 20: 40963
DOLGOV, A. D., Effects of violation of CP-invariance in radiative decays of neutral K-mesons, 20: 41905
DOLINOV, V. K., Reaction $^{12}C(\alpha,\alpha')^{12}*C(9.64\ Mev) \to 3\ \alpha$, 20: 42296
DOMANIC, F., Parameters for the first neutron resonance in ^{113}Cd, 20: 42149 (CNAEM-34)
DOMANSKI, T. M., Test of the theory of alkaline earth metabolism by behaviour of ^{133}Ba in rats, 20: 40565
DOMANUS, Jozef, Prog. rpt. on standard method for testing packaging of radioactive materials for radiation leakage, final, 2/64–10/65, 20: 41197 (NP-16172)
DOMANUS, Jozef, Radiation protection in industrial radiography, 20: 41212
DOMEN, S. R., Lithium compensated silicon focal plane detectors for electron scattering spectrometers, 20: 41326
DOMOKOS, G., Dynamics of strongly bound systems, 20: 41978
DONAHUE, D. J., Angular distributions of α-particles from the reaction $^{11}B(^{3}He,\alpha)^{10}B$, 20: 42217
DONDES, S., Decontamination of products from chemonuclear reactions, 20: 40951 (RPI-321-6)
DONNAN, M. Yates, Quantitative electrodeposition of actinides from isopropyl alcohol, 20: 41010 (DP-1048)
DONOEL, C., Premature incorporation of tritiated thymidine after irradiation of fibroblast and myoblast of chicken embryos, 20: 40587
DOPLICHER, S., Theorem on canonical commutation and anticommutation relations, 20: 42076
DOROFEEV, E. V., Investigation of a conical induction plasma source, 20: 42505
DOSHI, G. R., Uptake of radionuclides by marine invertebrates from the west coast of India, 20: 40528
DOTSON, Allen C., Yang-Mills groups and fields, 20: 41929
DOTY, R. R., Differential neutron albedo for thin slabs, 20: 42142 (NP-16234)
DOUGLASS, D. H. Jr., Superfluid density and scaling laws for liquid He near T_{λ}, 20: 42122
DOURY, Andre, Fallout in France after second Chinese nuclear explosion, 20: 41189 (CEA-R-3020)
DOVBENKO, A. G., Radiative capture cross sections of 30 to 170 kev neutrons, 20: 42293
DOWKER, J. S., Coulomb scattering for arbitrary spin, 20: 41990
DOWNES, J. S., Localized vibrations of trapped molecules, 20: 41651
DOWNEY, C. L., Uranium trioxide product specification analyses, 20: 40802 (HW-65402(Rev.1))
DOYLE, Margot, Prog. rpt., semiannual, 3/66, 20: 40740 (ACRH-25)
DRAGANOVIC, B., Dynamics of mineralization of fetal skeleton of chickens by use of ^{32}P and ^{45}Ca, 20: 40558
DRAGHICESCU, M., Autodyne installation for experiments on dynamic polarization of nuclei, 20: 41249
DRAPE, M., Long-term incidence of myxedema appearing after radiotherapy for cancer of larynx, 20: 40780
DRAZHEVA, L., Influence of a h-f inhomogeneous field on a gaseous-discharge plasma, 20: 42442
DRECHSEL, D., Collective correlations in ^{12}C, 20: 42271
DRESDEN, M., Universality of Lorentz invariance in particle physics, 20: 42032
DRESIA, H., Analysis of gases by absorption of soft γ radiation, 20: 40828
DREYER, Brenda B., Radioprotective and anti-tumor effect of mixed bacterial toxins and anthramycin, 20: 40736
DRISKO, R. M., Reactions $(d,^{6}Li)$ in light elements and distorted-wave Born approximation calculations, 20: 42237
DROST, H., Lateral extraction of negative ions from a layered low-pressure discharge in oxygen, 20: 42435
DROUIN, R. S., Electromagnetic transitions in ^{16}O nuclei, 20: 42342
DROZDOV, V. E., Radiation cross linking of cable polyethylene insulation on large scale, 20: 41496
DRUCKER, D. C., Continuum theory of plasticity on the macroscale and the microscale, 20: 41454 (NYO-2394-22)
DUBASOV, Yu. V., Thomas-Fermi-Dirac equation taking into account correlations for divalent radium ions, 20: 40929
DUBOIS, A., Design and testing of insulating walls and electrodes for MHD converters, 20: 41726
DUBOIS, Pierre, Carrousel magnetoaerodynamic generator, 20: 41697
DUCHEMIN, B., Study of the reactions $^{10}B(d,\alpha)^{2}4He$ and $^{9}Be(^{3}He,\alpha)^{2}4He$, 20: 42374
DUCHON, J., Measurement of the $\pi^{\pm}p$ total effective cross section at T_{π} = 300 to 700 Mev, 20: 41830
DUDELZAK, B., Small angle electron proton elastic scattering cross sections for momentum transfers between 10 and 105 f^{-2}, 20: 41791 (DESY-66/20)
DUFF, C. E., Effects of graphite electrodes on carrier distillation of

impurities in U_3O_8, 20: 40807 (NLCO-976)
DUHAMEL, L., Sequelae of LD/50 x-ray exposure of pre-implantation mouse embryo, 20: 40649
DUIVENSTIJN, A. J., Practical gamma spectrometry, 20: 41353
DUKE, P. J., Differential cross sections for $\pi^{\pm}p$ elastic scattering in the momentum range 875-1579 Mev/c, 20: 41857
DUKES, E. Kenneth, Quantitative electrodeposition of actinides from isopropyl alcohol, 20: 41010 (DP-1048)
DUKOWICZ, J. K., Magnetohydrodynamic flow in the shock tube boundary layer with transverse magnetic field, 20: 42037 (UTIAS-115)
DUMAZET, G., Effect of polarization on Ericson fluctuations, 20: 42396
DUMITRESCU, Gr., Results of radioiodine treatment in diabetes mellitus associated with hyperthyroidism, 20: 40790
DUNBAR, D. N. F., Charge exchange and dissociation cross sections for H_1^+, H_2^+, and H_3^+ ions of 2- to 50-kev energy incident upon H and the inert gases, 20: 41646
DUNCAN, R. N., Prog. rpt. on stainless steel failure, 1–3/66, 20: 41418 (GEAP-5150)
DUNN, M. J., Synthesis of ^{14}C-labeled bipyridylium salts, 20: 40941
DUPRE, N., Long-term incidence of myxedema appearing after radiotherapy for cancer of larynx, 20: 40780
DURSO, John W., Two-pion-exchange effects in NN scattering and consistency with π N scattering, 20: 41873
DUSHIN, L. A., Method of determining electron density distribution in a plasma, 20: 42419 (AD-636608)
DWORKIN, H. J., Study of metabolism of ^{18}F in dogs and its suitability for bone scanning, 20: 40554
DYACHENKO, P. P., Fragments in the fission of ^{235}U by thermal and 5, 6, and 7 Mev neutrons, 20: 42297
DYACHENKO, V. F., Converging cylindrically symmetrical shock wave in the presence of dissipative effects, 20: 42476
DYKHNE, A. M., Effective conductivity of non-homogeneous plasma in a magnetic field, 20: 41768
DZHAFAROV, I. G., Relationship between structure and polarization of particles in $l + \bar{l} \rightleftarrows p + \bar{p}$ reactions, 20: 41813
DZHAGATSPANYAN, R. V., Particle trajectories in radiation and chemical processes in pseudo-liquefied layer, 20: 40884
DZHAUGASHTIN, K. E., Results of theoretical investigations of MHD flows, 20: 41773
DZHURAEV, A. A., Multiplicity factor of neutron formation in the (μ,n) reactions, 20: 42174

E

EANDI, Richard D., Comparison of the lifetimes of positive and negative pions, 20: 41891
EAST, Larry V., Search for double beta decay in ^{150}Nd, 20: 42263
EATON, G. H., Measurements of the differential cross-section and polarization in proton-proton scattering at about 143 Mev, 20: 41915
EBEL, G., Peripheral model with absorption for the production process $\bar{p} + p \rightarrow \bar{N}^* + N^*$, 20: 41788 (BMwF-FBK-66-12)
ECKEL, J. F., Prog. rpt. on relationship of nitrogen content of austenitic stainless steel to stress corrosion, 3–5/66, 20: 41449 (EURAEC-1676)
ECKERT, H. G., Random events, pile-up, and summation in a fast-slow coincidence, 20: 41291
ECKHAUSE, M., Modular 100-Mc digital timer, 20: 41240
ECKHAUSE, M., Muon capture rate in complex nuclei, 20: 42318
EDEL, W., Nutrition experiments in pigs fattened with heat-decontaminated, γ-irradiated and untreated feeds, 20: 41394
EDELMAN, Fredkic, Is the brain an immunologically privileged site? II., 20: 40643
EDL, F. W., Apparatus for motion transfer in a vacuum system, 20: 41125 (SGAE-PH-41/1966)
EDWARDS, V. R. W., Wedge-shaped scintillation detector for magnetic spectrometer, 20: 41289
EFIMOV, G. V., Analytical properties of euclidean amplitudes, 20: 42021
EGELSTAFF, P. A., Localized vibrations of trapped molecules, 20: 41651
EGLIT, A. Kh., Mechanism of radiation-thermal liquid phase conversions of n-alkanes, 20: 40986
EHARA, S., High-temperature magnetic susceptibility of lanthanum and cerium metals, 20: 42544
EHMANN, W. D., Determination of Au, Ir, and Pt in meteorites and natural materials by thermal-neutron activation analysis, 20: 40835
EHRIG, R. J., Solid-state polymerization of diacetone acrylamide, 20: 40980
EICHELBERGER, J. F., Prog. rpt., 1–3/66, 20: 41037 (MLM-1325)
EICHMEIER, Joseph, Continuous recording of small air ions in closed rooms, 20: 42050
EINSTEIN, Fred, Crystal structure and magnetic properties of pentafluoroxenonyl hexafluoroplatinate(V), 20: 40882
EISENBERG, J. M., Particle-hole description of ^{28}Si and ^{32}S, 20: 42199
EISENBERG, J. M., Radiative pion absorption in complex nuclei, 20: 42315
EISENHANDLER, E., Wide angle electron pair production at high energy, 20: 42327
EISINGER, J., Electron spin resonance of irradiated deoxyribonucleic acid, 20: 40594
EISLER, J. D., Multiple subsurface spalling by underground nuclear explosions, 20: 41126
EISNER, M., Coaxial accelerator, 20: 42516
EKSPONG, A. G., Rate of energy loss for positive and negative pions, 20: 41826
EL-BAZ, E., Application of a graphical method for calculation of $\sigma(\theta)$ of stripping, 20: 42397
ELK, K., Variational principle in describing a many-particle system, 20: 42074
ELLIS, G. R. A., Frequency splitting of solar radio bursts, 20: 41606
ELMORE, W. C., Reliability of fractional registry of nuclear spectra, 20: 41315
EL-NADI, M., Optical model parameters for composite particles, 20: 42280
EL SAFFAR, Z. M., Electron spin resonance spectra of Dy^{3+} in ThO_2 and CeO_2, 20: 42525 (ORNL-P-2466)
EL-SHISHINI, M. M., Temperature dependence of response of lithium-drifted germanium detectors to gamma rays, 20: 41273 (ORNL-TM-1295)
ELSNER, B., Mass spectra of recoil nucleon states from inelastic ρ^0 production by pions of 12 and 18 Bev/c, 20: 41828
ELTON, L. R. B., Changes in radii between neighbouring nuclides, 20: 42278
ELTON, L. R. B., Single-particle wave functions of calcium isotopes, 20: 42270
ELY, Robert P. Jr., $Y\dagger$ resonant amplitudes between 1660 and 1900 Mev, 20: 41886
EMELEUS, K. G., Plasma ion oscillations, 20: 42444
EMELYANOV, V. S., Investigation of alloys of the Zr–C system, 20: 41471
EMERGY, Donald A., Prog. rpt. on radiation genetics and radiation resistance in peanuts, annual, 7/65–6/66, 20: 40636 (ORO-1747-12)
EMMONS, D. A., Static Moessbauer search for parity nonconservation in ^{57m}Fe, 20: 42322
EMSLEY, J. W., High resolution nuclear magnetic resonance spectroscopy. I., 20: 41255
ENDT, P. M., Measurements of (p,γ) resonance strengths in the s-d shell, 20: 42182
ENGEL, F. C., Feasibility of chemical poison loop system, 20: 42665 (WCAP-2870)
ENGELBERTINK, G. A. P., Measurements of (p,γ) resonance strengths in the s-d shell, 20: 42182
ENGELBRECHT, C. A., Symmetry properties of the strong interactions, 20: 42011
ENGELHARDT, A. G., High temperature plasmas by laser heating, 20: 42415 (TID-22928)
ENGESSER, F. C., Gamma rays resulting from interactions of 14.7 Mev neutrons with Na, S, Cl, K, and Pb, 20: 42146 (AD-638014)
ENGLAND, L. D., Elemental trace analysis by charged particle and neutron activation, 20: 40812 (ORO-2980-14)
ENGLISH, J. B., Measurement of the K_S^0–K_L^0 mass difference by the time dependence of strangeness, 20: 41922
ENO, Charles F., Prog. rpt. on effects of gamma radiation on soil microorganisms, final, 1966, 20: 40637 (ORO-2754-7)
ERBAN, J., Simple pulse interval analyser for scintillation scanning, 20: 41318
ERICSON, M., Probability distributions of extremes of cross sections, 20: 42395
ERICSON, T., Theory of radiative capture of π mesons in nuclei, 20: 42385
ERICSON, T. E. O., Pion interactions with nuclei, 20: 42312
ERLANSON, E. P., Thermal integration of electric power and life support systems for manned space stations, 20: 41679 (NASA-CR-543)
ERNE, F. C., Odd parity levels excited in the $^{37}Cl(p,\gamma)^{38}Ar$ reaction, 20: 42181
EROSHKIN, V. I., Radiation effects on rate of silver nitrite thermal disintegration, 20: 41000
ERSKINE, John R., Energy-level structure of ^{40}Ca as observed with the $^{39}K(^3He,d)^{40}Ca$ reaction, 20: 42257
ERWIN, A. R., Pion-pion interactions in π^-p reactions at 2.1 Bev/c, 20: 41858
ERWIN, A. R., Question of a K^+K^+ resonance, 20: 41856
ESSELMAN, W. H., NERVA reactor development status, 20: 42662 (CONF-651101-84)
ETIEVANT, Claude, Nonlinear process in a finite plasma, 20: 42427
ETTER, D. E., Differential thermal analysis study of impurities in plutonium, 20: 41452 (MLM-1172)
ETTER, J. E., Study of the reaction $^{10}B(^3He,pnnn)$, 20: 42188
EUROLA, T., Dynamics of the Halden Boiling Water Reactor, 20: 42630 (HPR-66)
EUSTIS, Robert H., MHD generator performance prediction including two-dimensional effects and wall leakage, 20: 41739

EVANS, Albert E., $^{14}N(p,\gamma)^{15}O$ reaction, 20: 42258
EVANS, E. P., Interrelationships of myeloid and lymphoid cells in lethally irradiated mice, 20: 40727
EVDOKIMOVA, T. P., Effect of radiation on composition of deoxyribonucleic acid in plants, 20: 40548
EVDOKIMOVA, V. V., Relations governing P-T phase diagrams and transformations under high pressures, 20: 41521
EVSEEV, V. S., Angular distribution of high energy neutrons emitted in the absorption of polarized μ^--mesons in Ca, 20: 42300
EVSTYUKHIN, A. I., Investigation of alloys of the Zr–C system, 20: 41471

F

FACETTI, J., New nuclide: ^{52}Ti, 20: 42282
FADINA, E. V., Pyrogallol–amidol developer for nuclear photo emulsions, 20: 41340
FAGAN, Walter, Nonuniform cooling of heat-generating cylinder or sphere, 20: 41106
FAHMY, Myrtle J., Biological organization in relation to differential gene response to mutagens, 20: 40706
FAHMY, O. G., Biological organization in relation to differential gene response to mutagens, 20: 40706
FAIVRE, J. C., Levels of ^{24}Mg, ^{25}Mg, and ^{26}Mg excited by the reactions (α,α'), $(\alpha,^3He)$, and (α,t), 20: 42347
FAIZI, N. H., Kinetics of polymerization of unsaturated oligomers with γ-rays by electroconductivity method, 20: 40999
FALEK, Arthur, Prog. rpt. on human chromosome analysis, final, 11/65, 20: 40497 (NYO-3400-1)
FALK, F., Levels and transitions in ^{133}Cs, 20: 42203
FALLA, D. F., Production of mesons in the nuclei of galaxies, 20: 41603
FALLIEROS, S., Coherent neutron proton-hole excitations in nuclei, 20: 42279
FAN, Liang-tseng, Heat transfer to MHD flow in the thermal entrance region of a flat duct, 20: 41105
FARGE, Y., Mechanism of formation of M and R centers, 20: 42562
FARGE, Y., New color center in irradiated lithium fluoride F_2^+, 20: 42530
FARRIS, S. A., Particle-hole description of ^{28}Si and ^{32}S, 20: 42199
FARROW, Joseph H., Does prophylactic radiotherapy given for cancer of breast predispose to metastasis?, 20: 40793
FARVAR, M. A., Attenuation techniques for determination of void fractions in two-phase potassium flow, 20: 41111
FASCIA, J. R., Aqueous corrosion of zirconium single crystals, 20: 41423
FAST, J. F., Magnetic and structural characteristics of some equiatomic rare-earth germanides, 20: 42552
FAST, R. W., Magnetic flux penetration in hard superconducting plates, 20: 42132
FAYARD, C., Reactions $^{12}C(\alpha,\alpha)$ at 51 Mev and $^{14}N(d,\alpha)^{12}C$ and $^{14}N(d,d)$ at 28.5 Mev, 20: 42389
FAYARD, C., Study of (n,α) reactions by the distorted-wave method, 20: 42391
FEDDEMA, J., X-ray television using plumbicon, 20: 40781
FEENEY, J., High resolution nuclear magnetic resonance spectroscopy. I., 20: 41255
FEIGENBAUM, J., Wide angle electron pair production at high energy, 20: 42327
FEINBERG, R. J., Instrumentation for detection of maximum permissible burden of ^{60}Co lung contamination, 20: 41190 (CONF-660621-4)
FEINENDEGEN, L. E., Iodine-125-DU (5-iodo-2'-deoxyuridine) in autoradiographic studies of cell proliferation, 20: 40666
FEKETE, T., Results of radioiodine treatment in diabetes mellitus associated with hyperthyroidism, 20: 40790
FELDL, E., Broad-range magnetic spectrograph system for routine angular distribution determinations, 20: 41306
FELDMANN, H.-H., Measuring method for the internal beam of a sector focussed cyclotron without disturbing the beam, 20: 41570
FELIX, H., Long-term incidence of myxedema appearing after radiotherapy for cancer of larynx, 20: 40780
FELTEN, James E., Radio electrons and magnetic fields in the galactic halo, 20: 41594
FENDLER, Heinz-Gerhard, Neutron dosimeter, 20: 41362
FENEBERG, W., Electrical conductivity of a partially ionized Ar–K plasma in a magnetic field, 20: 42410 (IPP-6/51)
FENG, Paul Y., Prog. rpt. on radiation synthesis involving halogen compounds, final, 5/60–10/65, 20: 40948 (COO-578-3-32)
FENNA, D., Some statistical techniques for reducing the number of measurements during inspection, 20: 42695 (TRG-Report-1200)
FEOKTISTOV, A., Decay of ^{184}Re, 20: 42157 (JINR-P-2814)
FER, Francis, Representation of an electron by a charged and coherent fluid, 20: 42077
FEREMANS, W., Comparison of effects on human blood cell chromosomes irradiated by x-rays, γ rays and electrons, 20: 40665
FERGUSON, Donald J., Application of thyroid scanning to study of transplantation, 20: 40516
FERNANDEZ, J. F., Effect of attractive forces on the solid-superfluid transition in ^4He at absolute zero, 20: 42113
FERRA, E. C., Application of the ENDOR technique to high resolution proton magnetic resonance spectra, 20: 42529
FERRIS, L. M., Hydrolysis of U, Th, and Al carbides in D_2O, 20: 40905
FERRY, B. N., Prog. rpt. on relationship of nitrogen content of austenitic stainless steel to stress corrosion, 3–5/66, 20: 41449 (EURAEC-1676)
FESSENDEN, P., Determination of small widths in the continuum, 20: 42164 (LA-DC-8083)
FESSENDEN, Thomas J., Pulsed electron-cyclotron resonance discharge experiment, 20: 42412 (MIT-3221-19)
FETROW, C., Broad-range magnetic spectrograph system for routine angular distribution determinations, 20: 41306
FEUVRAIS, L., Reactions $^{12}C(\alpha,\alpha)$ at 51 Mev and $^{14}N(d,\alpha)^{12}C$ and $^{14}N(d,d)$ at 28.5 Mev, 20: 42389
FICHTEL, C. E., Elemental abundances of low-energy cosmic rays in July 1964, 20: 41672
FICHTEL, C. E., Source spectra and composition of cosmic rays, 20: 41673
FICKEN, Vernon J., Tandem elution of ^{99m}Tc generators, 20: 40754
FIDONE, I., Thermal bremsstrahlung from inhomogeneous plasma, 20: 42457
FIDONE, Ignazio, Nonlinear process in a finite plasma, 20: 42427
FIGGINS, P. E., Purification of Pa from natural sources, 20: 41043
FILIPPAS, T. A., Muon capture rate in complex nuclei, 20: 42318
FINCH, C. B., Electron spin resonance spectra of Dy^{3+} in ThO_2 and CeO_2, 20: 42525 (ORNL-P-2466)
FINGER, M., Decay of ^{152}Tb, 20: 42155 (JINR-P-2762)
FINK, H. J., Critical currents in the superconducting surface sheath, 20: 42114
FINKEL', E. E., Radiation cross linking of cable polyethylene insulation on large scale, 20: 41496
FINNEMORE, D. K., Superconducting properties of high-purity niobium, 20: 42117
FINTZ, P., Study of nuclear reactions with a magnetic spectrograph, 20: 42369
FIORE, A., Excitation of 5.7 Mev level of ^7Li by (n,n') scattering at 14 Mev, 20: 42364
FIORINI, Vittorio, Calibration testing of jet of plasma generator, 20: 42466
FIRK, F. W. K., Fast neutron spectroscopy using the Yale electron linac and a new nanosecond time-of-flight system, 20: 41556
FIRKOWSKI, Ryszard, Efficiency of a hodoscope for registration of charged particles, 20: 41338
FIRTH, M., A 73 watt, 3°K He refrigerator using gas bearing turbines, 20: 41378
FISCHBEIN, W., Measurement of the K_S^0–K_L^0 mass difference by the time dependence of strangeness, 20: 41922
FISCHER, E. O., Tri(cyclopentadienyl)americium(III), 20: 40878
FISCHER, Gaston, Shielding properties of the superconducting surface sheath, 20: 42127
FISCHER, J., Design and performance of on-line wire spark chamber spectrometer, 20: 41297
FISCHER, W., Behavior of definite nitrides in Ti and Zr by determination of N, 20: 40820 (IS-Trans-37)
FISH, V. J., Thymic and splenic irradiation in treatment of acute lymphatic leukemia, 20: 40720
FISHER, L., Fuel temperature measurements in mixed oxide elements, 20: 42612
FITZGERALD, C. L., Addition of lithium values in conversion of fission-product wastes to a glass-like solid for disposal, 20: 42690
FITZGERALD, Edwin R., Particle waves and deformation in crystalline solids, 20: 42568
FIX, Richard C., Thermoluminescent dosimetry method, 20: 41370
FLAKS, Bojan, Fine structure of lutein cells of x-irradiated rat ovary, 20: 40672
FLEGENHEIMER, J., New nuclide: ^{52}Ti, 20: 42282
FLEISHMAN, D. G., Biological consequences of radioactive contamination of water bodies, 20: 40527
FLEMING, W. S., Electrolytic recovery of scrap uranium metal, 20: 41036 (MCW-1494)
FLEROV, G. N., Spontaneously fissioning neutron-deficient neptunium isotope with the half-life 60 sec, 20: 42292
FLETCHER, E. W. L., Use of x rays to produce transmission pictures of virus models, 20: 40653
FLEURY, A., Dissociation of ^6Li by interaction on complex nuclei, 20: 42366
FLOOR, P., Isotopic evidence for upper-cambrian or lower-ordovician granite emplacement in Vigo area, Spain, 20: 41153
FLORA, David H., Health physics problems in oil and gas well logging, 20: 41216
FLYNN, P. W., Prog. rpt. on effect of substructure on irradiation stability of ASTM A302 grade B steel, 4/66, 20: 41451 (GA-7101)

FLYNN, Robert J., Laboratory animal science, review of literature, 1–3/66, 20: 40493 (ANL-7300)
FOA, L., Precision detector for high-energy neutral pions, 20: 41320
FOCHT, Elizabeth F., Radiation cataract analysis and its uses in experimental fractionation, 20: 40690
FOMIN, G. S., Fabrication of thin plates from refractory carbides, 20: 41430
FONNUM, F., Radiochemical method for estimation of choline acetyltransferase, 20: 40584
FONTAINE, Jack H., Health physics problems in oil and gas well logging, 20: 41216
FONTES, J. C., Isotopic fractionation in water of crystallization of calcium sulfate, 20: 40836
FORCHERI, S., Isothermal transport processes in molten salts binary systems, 20: 40866 (EUR-2954.e)
FORD, C. E., Interrelationships of myeloid and lymphoid cells in lethally irradiated mice, 20: 40727
FORREST, J. R., Positive column in a magnetic field, 20: 42425
FORSTER, H. H., Excited levels in ^{3}He, 20: 42224
FORSYTH, P. D., Peak-to-total ratios and efficiencies for NaI crystal, 20: 41307
FORTI, G., Comparison of different methods for kinetics of ESSOR reactor type, 20: 42678 (EUR-3051.e)
FOSS, J., Search for fractionally charged, weakly interacting particles, 20: 41797 (MIT-2098-264)
FOSTER, R. J., Factors affecting biological action of mutagens, 20: 40717
FOSTER, Theodore C., Ground-state properties of nuclear matter using the Λ_{10} approximation, 20: 42249
FOWLER, J. H., Improved method for radioautography of erythropoietic cells labeled with ^{55}Fe or ^{59}Fe, 20: 40675
FOX, J. D., Coulomb displacement energies from isobaric analogue resonances, 20: 42262
FOX, J. D., Precise measurement of the K^+/K^- and π^+/π^- lifetime ratios, 20: 41884
FRADIN, Jean, Installation for analytic chemistry under irradiation, 20: 40799 (CEA-R-2887)
FRANCHI, L. L., Ultrastructure of male germ cells in rats x irradiated at birth, 20: 40683
FRANCOIS, D., Pressure-temperature phase diagram of beryllium, 20: 41485
FRANGOPOL, Maria, Measurement of radioactivity of ^{14}C using counter without window, 20: 41281
FRANKEVICH, E. L., Radiation effects on ion and electron processes occurring in condensed-phase hydrocarbons, 20: 40998
FRANKEVICH, E. L., Radiation-induced electric and photoconductivity in frozen heptane, 20: 41005
FRANKLIN, R. N., Positive column in a magnetic field, 20: 42425
FRANZEN, L. F., Characterization of radioactive particulate aerosols by fibrous filter analyzer, 20: 41234 (ORNL-P-2436)
FRAZER, Jack W., Cathodic etching to prepare radioactive samples for oxygen determination, 20: 40817 (UCRL-14959)
FRECK, David Vernon, Improvements relating to solid-state radiation detectors, 20: 41367
FRECK, David Vernon, Improvements relating to radiation detector apparatus, 20: 41368
FREED, Barry R., Extension of memorial system for implant dosimetry, 20: 40788
FREEDMAN, Daniel Z., Regge poles in unequal-mass scattering processes, 20: 41989
FREEMAN, J. M., Accurate measurement of relative efficiency of Ge(Li) gamma-ray detectors, 20: 41288
FREEMAN, R. M., Particle-gamma angular correlations with detection at 180°, 20: 42383
FREEMAN, R. M., Reactions $^{16}O(^{3}He,\alpha\gamma)^{15}O$, $^{12}C(^{3}He,p\gamma)^{14}N$, and $^{12}C(d,p\gamma)^{13}C$, 20: 42252
FRENCH, R. L., Performance of enclosure shields in real fallout field, 20: 41201 (RRA-T55 and Summary)
FRESHLEY, M. D., Investigation of combined failure of pressure tube and defected fuel rod in PKTR, 20: 42675 (BNWL-272)
FREUND, P. G. O., Noncompact groups in classifying hadrons, 20: 41982
FREUNDLICH, J., Radon effect with a copper counting tube, 20: 41372
FREY, Harold E. Jr., Effects of irradiated medium on cellular functions of E. coli, 20: 40580 (NYO-2804-8)
FREYTAG, E., Shielding high-energy electrons: the neutron and muon components, 20: 41534 (DESY-66/18)
FRICK, G., "Multipolimeter" application to a study of electromagnetic transitions, 20: 42384
FRIEDEL, J., Electronic instability and phase change of V_3Si-type compounds at low temperature, 20: 42531
FRIEDELL, Hymer L., Radioisotope scanning with system for information storage and controlled retrieval, 20: 40748
FRIEDMAN, I., Origin of saline formation waters. I., 20: 41161
FRISCH, Erling, Fuel arrangement for a nuclear reactor, 20: 42614
FRITSCH, C. A., Radiative heat transfer through an absorbing boundary layer, 20: 41108
FROEHLICH, H., Determination of electron lifetime in BF_3 proportional counters, 20: 41357
FROESE, Charlotte, Hartree-Fock parameters for the atoms helium to radon, 20: 41631
FROESE-GERTZEN, Edith E., Factors affecting biological action of mutagens, 20: 40717
FRONSDAL, Christian, Beyond SU(6), 20: 42030
FRUEHAUF, Uwe, Electromagnetic waves in hollow conductors with isotropic plasma, 20: 42436
FRY, W. F., Measurement of the $K_S^0-K_L^0$ mass difference by the time dependence of strangeness, 20: 41922
FRYE, Glenn M. Jr., Cosmic-ray electron flux above 4.7 Bv, 20: 41674
FUCHS, Norman H., Consistency conditions on the strong interactions, 20: 41861
FUEGER, G. F., Scintillation scanning with an 8-inch diameter Na iodide (Tl) crystal, 20: 40779
FUJII, T., Design and performance of on-line wire spark chamber spectrometer, 20: 41297
FUJIIE, Y., Role of excited atoms on nonequilibrium of partially ionized plasma, 20: 41757
FUJIMOTO, Masatoshi, Recent advances in ion-exchange-resin spot tests: 1960 to 1964. I., 20: 40827
FUJINO, H., MHD power generation experiments with K-seeded Ar plasmas, 20: 41781
FUKUDA, Otoji, Pressure-applied process for pouring heavy concrete to construct reactor shields, 20: 42586
FUKUI, Kenichi, Influence of addition of ethylene on γ induced alternating copolymerization of ethylenimine and C monoxide, 20: 40975
FUKUI, T., Preparation and test of MHD duct wall and electrode materials, 20: 41718
FULLAM, H. T., Thermal stability of nitrate form anion resins in vented system, 20: 40877 (RL-SEP-823)
FULTYN, R. V., Kiwi Transient Nuclear Test dose rate survey, 20: 41195 (LA-3519)
FUNABASHI, Koichi, Charge recombination in gamma-irradiated alkane glasses, 20: 40970
FUNK, E. G., Directional correlation measurements in decay of ^{160}Tb employing a Ge–Li detector, 20: 42150 (COO-498-56)
FURMAN, A. O., Determination of specific activities by measurements of high-energy β-radiation, 20: 40833
FURMAN, A. O., Testing counters of nuclear radiations of T-25-BFL type by aid of automatic apparatus, 20: 41285
FURTH, H. P., Use of pulse transformer to generate multi-megampere currents for high-field research, 20: 41092
FURUICHI, Jiro, Dynamic mechanical properties of polyoxymethylene. I., 20: 41500
FUSHIMI, K., Conductivity of a gas with suspension, 20: 41713
FUSHIMI, K., MHD power generator; E.T.L. Mark II, 20: 41714
FYTIZAS, E., Gamma radiation-induced dominant lethality to sperm of olive fruit fly, 20: 40674

G

GABUDA, S. P., Anisotropy of magnetic resonance of ^{19}F in LaF_3, 20: 42528
GABUDA, S. P., Nuclear magnetic resonance and electron structure of U, Th, and Zr, 20: 40931
GADYMOV, A. M., Synthesis and studies of Ga Y sulfides ($YGaS_3$) and In Y sulfides ($YInS_3$), 20: 40879
GAERTNER, Rudolf, Protective circuit for nuclear physics measuring apparatus, 20: 41260
GAETA, R., Decay scheme of ^{235}U, 20: 42152 (JEN-159-DF/I-49)
GAGARINSKII, Yu. V., Nuclear magnetic resonance and electron structure of U, Th, and Zr, 20: 40931
GAGNAIRE, D., Improvement of signal-to-noise ratio, 20: 41305
GAHMAN, R. L., Attenuation techniques for determination of void fractions in two-phase potassium flow, 20: 41111
GAIDOS, J. A., Measurement of the $K_S^0-K_L^0$ mass difference by the time dependence of strangeness, 20: 41922
GAILLARD, M., Reactions $^{12}C(\alpha,\alpha)$ at 51 Mev and $^{14}N(d,\alpha)^{12}C$ and $^{14}N(d,d)$ at 28.5 Mev, 20: 42389
GAILLARD, P., Reactions $^{12}C(\alpha,\alpha)$ at 51 Mev and $^{14}N(d,\alpha)^{12}C$ and $^{14}N(d,d)$ at 28.5 Mev, 20: 42389
GALANTE, Maurice, Radiation therapy in control of persistent thyroid cancer, 20: 40758
GALE, L. H., Radiation-initiated codimerization of methallyl chloride with unsaturates, 20: 40971
GALLANT, Ester M., Accumulation of beta activity from fallout on leaves, 20: 40579
GALLANT, Hermons, Electrodeless conductivity measurements within the

reaction zone of a combustion chamber, 20: 41710
GALLIGAN, J. M., Field ion microscope study of neutron-irradiated tungsten, 20: 42551
GALLIOT, J., Future of in situ detection method of γ activity of seawater, 20: 41147
GALLIOT, Jean, Radiocarbon content of deep and surface waters of north north Indian Ocean, 20: 41127
GALLMANN, A., "Multipolimeter" application to a study of electromagnetic transitions, 20: 42384
GALLMANN, A., Particle-gamma angular correlations with detection at 180°, 20: 42383
GALLMANN, A., Reactions $^{16}O(^3He,\alpha\gamma)^{15}O$, $^{12}C(^3He,p\gamma)^{14}N$, and $^{12}C(d,p\gamma)^{13}C$, 20: 42252
GALLMANN, A., Study of nuclear reactions with a magnetic spectrograph, 20: 42369
GAMBAROTTA, J.-P., Radioactivity of plankton and of organic refuse, 20: 41146
GANGRSKII, Yu. P., Spontaneously fissionable isomer with the half-life equal to 10^{-7} s, 20: 42159 (JINR-P-2841)
GANN, A., Some aspects on the use of cryogenically cooled primary-windings system for an a-c MHD generator, 20: 41727
GANNUTZ, T. P., Effects of chronic gamma irradiation on lichen communities, 20: 40517 (BNL-9437)
GARATTINI, S., Effect of radioprotectors on damage induced by alkylating agents on tumoural and normal tissues, 20: 40664
GARCIA, Eugene N., Simplified preparation of ^{99m}Tc sulfide colloid for liver scanning, 20: 40753
GARDNER, J. B., A 73 watt, 3°K He refrigerator using gas bearing turbines, 20: 41378
GARELICK, D., π^0 photoproduction at 3.0, 4.0, and 5.0 Bev for baryon four momentum transfers between 0.5 and 4.0 $(Bev/c)^2$, 20: 41798 (MIT-2098-265)
GARELICK, D., Search for fractionally charged, weakly interacting particles, 20: 41797 (MIT-2098-264)
GARELIS, E., Prog. rpt. on pulsed neutron application to power reactor start-up procedures, 1–3/66, 20: 42628 (GEAP-5145)
GARIBOTTI, C. R., Combined spin and G_2 symmetry, 20: 41972
GARNETT, J. L., Charge-transfer theory for interpretation of radiation-induced grafting of monomers to cellulose, 20: 40979
GATTO, R., Saturation of the SU_6 algebra and a possible classification group for hadrons, 20: 41968
GATTO, R., Unitary-antisymmetric q-number terms in commutators of spatial current components, 20: 41985
GATZ, Donald F., Prog. rpt. on rain scavenging studies, 3/65–5/66, 20: 41130 (COO-1407-10)
GAUL, H., Selection in M_1 generation after mutagenic treatment of barley seeds, 20: 40711
GAVRILOV, F. F., Temperature luminescence decay of ZnS:Ag monocrystals at excitation of radiation, 20: 41342
GAYDON, A. G., Temperature measurements in shock tubes: transition probabilities for argon lines, 20: 42483
GAYLITIS, A., Instability of uniform plasma turbulence, 20: 42465
GEBERT, E., Unit cell of γ-UO_3, 20: 40907
GEERK, Jens, Mass spectrometer, 20: 41261
GEESAMAN, Lyan B., Evidence for the presence of alpha clusters in the boron isotopes, 20: 42193
GEGUZIN, Ya. E., Thermal stability of U fission products in monocrystalline muscovite for chemical etching, 20: 40889
GEILIKMAN, B. T., Electronic mechanism of superconductivity, 20: 42129
GELERINTER, Edward, Electron spin resonance identification of N_2^- defect in x-irradiated sodium azide, 20: 40966
GELEZUNAS, V. L., Biological cleanability of surfaces using radioisotope tracer techniques, 20: 41218
GENCZWEIN, F., Structure of the nuclear surface, 20: 42275
GENDREAU, G., Improvement of profile of linear shims designed for separation of heavy isotopes, 20: 41405
GENNARI, C., Index of ^{85}Sr uptake in leg fractures, 20: 40542
GENNARI, Carlo, Radiocalcium studies and histological findings in case of primary hyperparathyroidism, 20: 40552
GENTHRON, Maurice, Production of essentially flat fuel element for nuclear reactors, 20: 42611 (WAPD-Trans-33)
GENTRY, Robert V., Anti-matter content of the Tunguska meteor, 20: 41607
GENUNCHE, Ano, Measurement of radioactivity of ^{14}C using counter without window, 20: 41281
GEOFFRION, B., Elastic scattering of protons of 150 and 80 Mev on light nuclei and the optical potential, 20: 42388
GEOFFRION, B., Polarization of protons of 152 Mev by inelastic scattering on ^{12}C and ^{40}Ca, 20: 42341
GEORGE, Claude, Finite-dimensional representations of some non-semisimple Lie algebras, 20: 41942
GEORGE, G. G., Scattering and energy loss of electrons in silicon near the radiation damage threshold, 20: 42536
GEORGE, W., Prog. rpt. on transient radiation effects, optical, 8/65, 20: 41492 (EGG-1183-2039)
GEORGE, W. D., Prog. rpt. on transient radiation effects, optical, 5/65, 20: 41491 (EGG-1183-2030)
GERARDIN, C., Angular distributions of (t,α_0) reactions on Li, B, C, and O, 20: 42398
GERARDO, J. B., Investigation of electronic recombination in helium and argon afterglow plasmas by means of laser interferometric measurements, 20: 42469
GERBER, J. P., Contribution to a study of structure of light nuclei by a study of the absorption mechanisms of K⁻ mesons, 20: 42386
GERBER, J.-P., Quasielastic collisions on α groups in ^{12}C by 60 to 120 Mev protons, 20: 42352
GERDS, A. F., Fabrication of Be. I., 20: 41427 (NASA-TM-X-53453 (Vol.1))
GERMANYUK, V. N., Experimental investigation of plasma using model MHD generators, 20: 41708
GERNET, G. E., Effect of radiation deceleration on the motion of a relativistic particle in a uniform magnetic field, 20: 42431
GERSCH, H. A., Effect of attractive forces on the solid-superfluid transition in ^4He at absolute zero, 20: 42113
GERSTEIN, B. C., Reevaluation of some thermodynamic properties of gadolinium metal, 20: 42542
GETOFF, N., ESR investigation of radical reactions in γ-irradiated frozen aqueous solutions of formic acid and formate, 20: 40994
GETOFF, N., Molecular plating. V., 20: 41011 (SGAE-CH-34/1966)
GHERMAN, Gr., Results of radioiodine treatment in diabetes mellitus associated with hyperthyroidism, 20: 40790
GHORMLEY, John A., Means for converting high energy radiation to electrical energy, 20: 41691
GIACCHETTI, Athos, Averages of interferometric measurements of thorium lines, 20: 40798 (ANL-7209)
GIBBS, B. W., Linearly polarized waves in plasmas in the region of the electron cyclotron frequency, 20: 42459
GIBBS, W. R., Determination of small widths in the continuum, 20: 42164 (LA-DC-8083)
GICHNER, T., Induction of chlorophyll chimeras by x rays and EMS in Arabidopsis thaliana, 20: 40710
GICHNER, Tomas, Chimerical structure of M_1 plants and its bearing on determination of mutation frequencies in Arabidopsis, 20: 40513
GICHNER, Tomas, Symposium on induction of mutations, Prague, 9/63, 20: 40705
GILBERT, W. S., Revised safety analysis report for the Super Kukla prompt burst reactor, 20: 42684 (UCRL-7695(Rev.1))
GILETTI, Bruno J., Isotopic ages from southwestern Montana, 20: 41163
GILINSKY, Victor, Development of a radio signal from nuclear explosion in the atmosphere, 20: 42046 (RM-4988)
GILL, P. S., Study of asymmetry in the lateral distribution of shower particles near sea level, 20: 41668
GILLESPIE, R. J., Preparation of some ^{18}F labeled fluorides, 20: 41020
GILLET, V., Particle-hole excitations in ^{208}Pb, 20: 42205
GINGRICH, James E., Isotopic power systems for manned missions, 20: 41398
GINZBURG, V. L., Space relativity: space research and theory of relativity, 20: 42075
GIORGI, M., Measurement of the branching ratio $\omega \to$ neutrals/$\omega \to \pi^+ + \pi^- + \pi^0$, 20: 41850
GIORNI, A., Reaction $^9Be(n,nn)\alpha\alpha$ at 15 Mev, 20: 42362
GIOVANNINI, Alberto, Regge symmetries of Clebsch-Gordan coefficients as a property of symmetric functions, 20: 42025
GIRIER, J. P., Thermal and radiochemical stability of aromatic and heterocyclic hydrocarbons, 20: 40991
GLASSER, M. Lawrence, Thermodynamic properties Bloch electrons in a magnetic field, 20: 41635
GLAUBITT, D., Metabolism of ^{65}Zn by rats under influence of Prednisolone or Dexamethasone, 20: 40563
GLAZUNOV, V. V., Adsorption of Cs on fluoroplast-4, polyethylene, and glass from aqueous solutions of sodium tetraphenylborate, 20: 40915
GLEESON, Austin M., Weak axial-vector currents and the baryon field, 20: 41981
GLEIZER, Yu. Ya., Radioisotope renography in diagnosis of a silent kidney, 20: 40775
GLIDDON, J. E. C., Gravitational instability of anisotropic plasma, 20: 42422
GLIGORE, V., Results of radioiodine treatment in diabetes mellitus associated with hyperthyroidism, 20: 40790
GLIMM, James, Schroedinger equation for quantum fields with nonlinear non-local scattering, 20: 41934
GLINSKA, Helina, Ten-year survival of patients with lymphogranulomatosis, following radiation therapy, 20: 40784
GLOERSEN, P., Neutral mass density measurements in repetitively pulsed coaxial plasma accelerator, 20: 41121
GODFREY, T. G., Computer program to calculate high-temperature thermo-

dynamic functions, 20: 40875 (ORNL-TM-1599)
GODIN, Yu. G., Investigation of alloys of the Zr–C system, 20: 41471
GOEBEL, C., Representations of strong coupling groups, 20: 42026
GOEDDEL, W. V., HTGR coated particle fuel, 20: 42624 (GA-6975)
GOERISCH, H., Separation of lanthanides by thin-layer high-voltage electrophoresis, 20: 41046
GOERZ, David J. Jr., Electron linear accelerator phasing method, 20: 41582
GOGOSOV, V. V., Boundary layers in a completely ionized two-temperature plasma, 20: 42477
GOKHALE, B. G., Forbidden transition L_{II}/N_{II} in the spectrum of Pt, 20: 41660
GOLDBERG, A., Prediction of dose of radioactive phosphorus in treatment of polycythemia, 20: 40774
GOLDBERG, E. D., Average diameter of erythrocytes under effect of radiation in human, 20: 40678
GOLDBERG, I., Separation of the relativistic perihelion precession from the precession due to the gravitational quadrupole moment, 20: 41610
GOLDBLATT, L, Laser induced prebreakdown and breakdown phenomena observed in cloud chambers, 20: 41375
GOLDEMBERG, J., Electron scattering at 180° on ^{12}C, 20: 42377
GOLDENBERG, Victor E., Lung carcinomas in irradiated parabiotic rats, 20: 40614 (NYO-901-39)
GOLDFARB, L. J. B., Influence of compound nucleus contributions on (d,p) reactions, 20: 42223
GOLDMAN, Leon, Applications of laser beam in cancer biology, 20: 40776
GOLDSHTEIN, M. I., Protective action of phosphororganic preparation of nibufin on irradiated albino mice, 20: 40724
GOLDSTEIN, Bernard, Electron paramagnetic resonance and electrical properties of the dominant paramagnetic defect in electron-irradiated p-type silicon, 20: 42549
GOLDSTEIN, Charles M., Monte Carlo method for calculation of transport properties in a low-density ionized gas, 20: 42413 (NASA-TN-D-2959)
GOLTSEV, V. P., Aging kinetics of Mo-base alloys, 20: 41466
GOLUB, M. A., Photo- and radiation-induced cistrans isomerization of several 2-olefins, 20: 40965
GOLUBEV, V. B., Decomposition of radicals in frozen aqueous solutions of $NaClO_4$ and $HClO_4$, 20: 40960
GOLUBEV, V. S., Determination of concentration of cesium atoms in a flow of argon and cesium by the radiation absorption method, 20: 41771
GOLUBEV, V. S., Investigation fo an electrical discharge in a magnetic field in the presence of a flow of gas, 20: 41770
GOLUBEVA, L. A., Effect of x-ray irradiation on some properties of lithium fluoride single crystals, 20: 42564
GOMULKIEWICZ, J., Effect of the dose output in the electret effect in paraffin wax, 20: 41516
GONCHAROV, I. N., Effect of oxygen additions on the structure and superconducting properties of Zr–Nb alloys, 20: 42535
GONCHAROVA, V. S., Effectiveness of the oxygen enrichment of air in MHD generator assemblies, 20: 41744
GONDRAND, J. C., Reaction ^{9}Be (n,nn)$\alpha\alpha$ at 15 Mev, 20: 42362
GONG, J. K., Accretion and exchange of ^{85}Sr in trabecular and cortical bones, 20: 40684
GONSHERY, Marvin E., Effects of space radiations on refractive properties of optical glasses, 20: 41505
GONZALES, Douglas E., Magnetic pulse in a cold collision-free plasma, 20: 42417 (UCRL-7170)
GOODFELLOW, H., Uranium-fueled VERA reactor experiments, 20: 42671 (AWRE-R-5/66)
GOODWIN, Paul N., Spectral measurements of 200- to 300-kv x rays, 20: 41322
GOOSEY, Malcolm H., Fission counter for routine isotopic analysis of Pu, 20: 41264 (DP-552)
GORBICS, S. G., Emission spectra of various thermoluminescent materials, 20: 42524 (NRL-6408)
GORDON, G. E., Decay schemes of 43-day ^{115m}Cd and 2.3-day ^{115g}Cd, 20: 42260
GORDY, Walter, ESR of free radicals trapped in inert matrices at low temperature: P, PH_2, and As, 20: 40967
GORDY, Walter, ESR of free radicals trapped in inert matrices at low temperature: CH_3, SiH_3, GeH_3, and SnH_3, 20: 40968
GORENFLO, R., Monte Carlo simulation of the flow of a KNUDSEN gas with due allowance for the sojourn time, 20: 42036 (IPP-2/41)
GORESLINE, H. E., Need for microbiological controls in legislation on irradiated food, 20: 41389
GORODETZKY, S., Electromagnetic transitions in ^{16}O nuclei, 20: 42342
GORODETZKY, S., "Multipolimeter" application to a study of electromagnetic transitions, 20: 42384
GORODETZKY, S., Particle-gamma angular correlations with detection at 180°, 20: 42383
GORODETZKY, S., Precise measurement of the stopping power of C, Au, Al, Ca, and CaF_2 for 0.4 to 6 Mev protons, 20: 42363
GORODETZKY, S., Reactions $^{16}O(^{3}He,\alpha\gamma)^{15}O$, $^{12}C(^{3}He,p\gamma)^{14}N$, and $^{12}C(d,p\gamma)^{13}C$, 20: 42252
GORODETZKY, S., Study of nuclear reactions with a magnetic spectrograph, 20: 42369
GORODETZKY, S., Study of electromagnetic transitions by measurement of the polarization distribution and γ-γ angular correlation, 20: 42381
GOROKHOV, I. M., Mass discrimination during measuring of isotopic composition of Sr and Rb made in mass spectrometer, 20: 40821
GOROWITZ, B., Neutral mass density measurements in repetitively pulsed coaxial plasma accelerator, 20: 41121
GOSSARD, A. C., Effect of low-temperature structural transformation on ^{51}V Knight shifts and electric field gradients in V_3Si, 20: 42118
GOSWAMI, A., Neutron-proton correlation effects in spherical even nuclei, 20: 42195
GOTTSCHALK, Alexander, Radioisotope scintiphotography with ^{99m}Tc and gamma scintillation camera, 20: 40750
GOTTSCHALK, B., Quasi-free proton scattering at 160 Mev, 20: 42276
GOTTSCHALK, W., Genetic control of the germ cell formation, 20: 40512
GOUANERE, M., Reactions $^{12}C(\alpha,\alpha)$ at 51 Mev and $^{14}N(d,\alpha)^{12}C$ and $^{14}N(d,d)$ at 28.5 Mev, 20: 42389
GOULARD, B., Coherent neutron proton-hole excitations in nuclei, 20: 42279
GOULD, Gordon, Physiological implications of laser beams, 20: 40691
GOURSKY, V., Phase-setting circuit at frequency of 100 MHz by transistors in avalanche region, 20: 41241
GOVAN, Ian O., Gamma mapping of liver with the digital computer, 20: 40747 (UCRL-14866)
GOVORKOV, A. B., Interpretation of parafield as an usual field with an inner degree of freedom, 20: 41925 (JINR-P-2756)
GOVORKOV, B. B., Isospin amplitudes for S-state pion photoproduction on nucleons, 20: 41906
GRABER, H. D., Method for analysis of pulse-height spectra, 20: 41292
GRACE, M. A., Coulomb excitation of low-energy states in ^{127}I, ^{121}Sb, and ^{183}W, 20: 42186
GRAEFFE, G., Decay schemes of 43-day ^{115m}Cd and 2.3-day ^{115g}Cd, 20: 42260
GRAF, D. L., Origin of saline formation waters. I., 20: 41161
GRAHAM, R. H., Parity-conserving hyperon decay and the pole model, 20: 41868
GRAHAM, R. J., WR-1: design and construction, 20: 42667 (66-CNA-309)
GRANNIS, P. D., Polarization in pion-proton scattering, 20: 41890
GRANT, M. A., Microdetermination of C and H polyphenyls, fouling films, and terphenyl mixtures, 20: 40797 (AECL-2524)
GRATTON, Charles Peter, Improvements in or relating to liquid moderated nuclear reactors, 20: 42595
GRAY, J. A., Equilibrium study of chloride and nitrate systems of Pr and Ni with tributyl phosphate and acid, 20: 40904
GRAY, Joyce, Interrelationships of myeloid and lymphoid cells in lethally irradiated mice, 20: 40727
GRAY, K. J., WR-1: design and construction, 20: 42667 (66-CNA-309)
GRAY, L., New determination of the ϕ spin and G parity, 20: 41881
GRECZ, N., Aspects of radiation D-values for spores of Clostridium botulinum, 20: 40601
GREEN, A. M., Particle-hole excitations in ^{208}Pb, 20: 42205
GREEN, J. K., Prog. rpt. on atmospheric sciences, annual, 1965, 20: 41188 (BNWL-235-1)
GREEN, Miles F., Linear accelerator simulator, 20: 41548
GREEN, R. M., Valley-to-peak ratios for zero-thickness sources, 20: 41312
GREENBERG, Arthur S., Comparison of the lifetimes of positive and negative pions, 20: 41891
GREENBERG, Harry B., Incidence of radiation fibrosis after radiotherapy for breast cancer, 20: 40773
GREENBERG, J. S., Collective nuclear structure in the even-even samarium isotopes, 20: 42265
GREENBERG, Michael L., Tritiated thymidine as cytocidal agent in human leukemia, 20: 40743 (BNL-9374)
GREENLEES, G. W., Optical-model analysis of 30-Mev proton scattering, 20: 42255
GREENWOOD, R. C., Neutron capture gamma ray techniques for nondestructive analysis of reactor burnable poisons, 20: 41112 (IITRI-578P11-54)
GREGG, Earle C., Radioisotope scanning with system for information storage and controlled retrieval, 20: 40748
GREGOIRE, G., Scattering of alpha particles on ^{9}Be, ^{32}S, and ^{31}P, 20: 42392
GREINER, E., Construction of high pressure diffusion cloud chamber, 20: 41356
GREINER, W., Collective correlations in ^{12}C, 20: 42271
GRENCH, H. A., Fast neutron cross sections for the $^{23}Na(n,\gamma)^{24}Na$, $^{55}Mn(n,\gamma)^{56}Mn$, $^{115}In(n,\gamma)^{116m}In$, and $^{165}Ho(n,\gamma)^{166}Ho$ reactions, 20: 42332
GRENCH, H. A., Isomeric cross-section ratios from fast-neutron capture, 20: 42326

GRENISHIN, S. G., Spectroscopic investigations of a high-current discharge in the air at low densities, 20: 42492
GRENS, John Z., Mechanisms that affect adsorption of methyl iodide on charcoal under humid conditions, 20: 41202 (UCRL-14990)
GRIBOVA, I. A., Clinical and dosimetric data on personnel operating a 10 Bev synchrophasotron, 20: 41206 (JPRS-36341, pp 10-17)
GRIEGER, G., Ionization of barium on hot rhenium surfaces, 20: 42406 (IPP-2/47)
GRIEM, Melvin L., Modification of radiation response of tissue by colchicine, 20: 40763
GRIFFEL, M., Reevaluation of some thermodynamic properties of gadolinium metal, 20: 42542
GRIFFIN, J. J., Statistical model of intermediate structure, 20: 42269
GRIGOR'EV, E. P., Decay mode of ^{160}Ho, 20: 42158 (JINR-P-2817)
GRIGOROV, G., Influence of a h-f inhomogeneous field on a gaseous-plasma, 20: 42442
GRILLY, E. R., Compressibility of liquid ^{4}He as a function of pressure, 20: 42112
GRIMISON, Alec, Prog. rpt. on matrix isolation studies of products of γ-radiolysis of heterocyclic molecules, annual, 1965–66, 20: 40950 (PRNC-88)
GRISARU, M. T., Observations concerning production amplitudes and models for $J^P = 3/2^+$ baryons, 20: 41836
GROB, Franz, Power supply installations for future spacecraft, 20: 41514 (AI-Trans-209)
GRODZINS, L., Coulomb excitation in the platinum isotopes, 20: 42218
GROEGER, D., Synthesis of radioactively labeled compounds. XV., 20: 41024
GROMOBOI, Yu. S., ENDOR of F centers in KCl at room temperature, 20: 42566
GROMOV, K., Decay series ^{138}Nd → ^{138}Pr → ^{138}Ce, 20: 42197
GROMOV, K. Yu., Decay of ^{152}Tb, 20: 42155 (JINR-P-2762)
GROSH, R. J., Radiative heat transfer through an absorbing boundary layer, 20: 41108
GROSHEV, L. V., Capture of thermal neutrons by Te, 20: 42286
GROSSE, Aristid V., Electrical and thermal conductivities of metals over their entire liquid range. III., 20: 41414
GROSSE, Aristid V., Electrical and thermal conductivities of metals over their entire liquid range. I., 20: 41476
GROSSE, Aristid V., Electrical and thermal conductivities of metals over their entire liquid range. II., 20: 41477
GROVE, G. R., Prog. rpt., 1–3/66, 20: 41037 (MLM-1325)
GROVES, D., High-resolution studies of fission x rays and gamma rays, 20: 42170 (UCRL-70045)
GROVES, D. J., Fission γ rays using Ge(Li) detector in conjunction with bent-crystal spectrometer, 20: 41278 (UCRL-70000)
GRUBER, John B., Optical spectra of tripositive ^{244}Cm in lanthanum trichloride, 20: 40891
GRUBER, U., Study of ^{46}Sc levels by means of neutron capture gammas, 20: 42382
GRUENBERG, H., Histologic and karyometric changes in salivary glands in man following exposure to ionizing radiation, 20: 40644
GRUENBERG, Leonard W., De Haas-Van Alphen oscillations in the critical temperature of type II superconductors, 20: 42126
GUAITANI, A., Effect of radioprotectors on damage induced by alkylating agents on tumoural and normal tissues, 20: 40664
GUAN, Wein-yen, Effects of desolvation of a Pb–Sb alloy on the critical characteristics of superconductors, 20: 42099 (AD-636625)
GUDOV, V. I., Decay of the isotope ^{180}Os, 20: 42284
GUEGNAUD, A., Use of austenitic steel as construction material for the pressure vessel of the fast reactor "rapsodie", 20: 42652 (EURFNR-92F)
GUENET, Jean-Louis, Study of pigs subjected to lethal dose of integral γ irradiation, 20: 40608 (CEA-R-3001)
GUENTHNER, K., Measurement of the asymmetry of bremsstrahlung from transversally polarized electrons, 20: 41662
GUERIN, Maurice, Studies in rats carrying lymphoblastic lymphosarcoma exposed to effect of electromagnetic waves associated with magnetic fields, 20: 40661
GUERRI, L., Numerical computation methods for implosion processes, 20: 41088
GUETLBAUER, F., ESR investigation of radical reactions in γ-irradiated frozen aqueous solutions of formic acid and formate, 20: 40994
GUIDERI, Renzo, Radiocalcium studies and histological findings in case of primary hyperparathyroidism, 20: 40552
GUIDINI, J., Contribution to a study of inelastic interactions between two ion beams, 20: 41666
GUILLON, Andre, Installation for analytic chemistry under irradiation, 20: 40799 (CEA-R-2887)
GUILLON, H., Phase-setting circuit at frequency of 100 MHz by transistors in avalanche region, 20: 41241
GUIZERIX, J., Distribution of waste water in a disposal process, 20: 42687
GUNDZIK, M. G., Current algebras and meson-nucleon scattering lengths, 20: 41846
GUNTHER, Leon, De Haas-Van Alphen oscillations in the critical temperature of type II superconductors, 20: 42126
GUPTA, R. D., Bis-2-pyridyl glycol as a reagent for gravimetric determination of U, Al, and Be, 20: 40849
GUPTA, S. K., Circuit for preventing accumulation of experimental data when nuclear reaction rate exceeds preset value, 20: 41244
GUPTA, S. L., Spectrophotometric and conductometric studies of complexes between UO_2^{++} and 2-hydroxy-3-naphthoic acid in aqueous medium, 20: 40898
GUPTA, Sharda Das, Radiation-induced grafting of mixed monomers on cotton fabric, 20: 40953
GUPTA, Suraj N., One-graviton exchange interaction of elementary particles, 20: 41970
GUPTA, Y. M., Peripheral model for K⁻-p collisions, 20: 41819
GUPTON, E. D., Estimation of beta radiation dose to skin by field instrument measurements, 20: 41274 (ORNL-TM-1581)
GURALNIK, G. S., Construction of nontrivial symmetry-breaking solutions in field theory, 20: 41969
GUREVICH, L. E., Instability of nonuniform current and field distribution, 20: 42040
GUREVICH, N. Yu., Effect of plastic deformation on light storage in crystals of NaI(Tl), 20: 41344
GURG, R. P., Development of thermoluminescent dosimeters at Trombay, 20: 41373
GURVICH, L. V., Composition and thermodynamic properties of the combustion products of natural fuels with ionizing additives, 20: 41785
GUSAKOW, M., Reactions $^{12}C(\alpha,\alpha)$ at 51 Mev and $^{14}N(d,\alpha)^{12}C$ and $^{14}N(d,d)$ at 28.5 Mev, 20: 42389
GUSELNIKOV, V. S., Separation of XeO_3 and HIO_3 in zirconium phosphate, 20: 41054
GUSEV, Yu. K., Chromatographic separation of xenon and iodine oxygen compounds, 20: 40851
GUSEV, Yu. K., Separation of XeO_3 and HIO_3 in zirconium phosphate, 20: 41054
GUSINOW, M. A., Investigation of electronic recombination in helium and argon afterglow plasmas by means of laser interferometric measurements, 20: 42469
GUS'KOVA, A. K., Clinical and dosimetric data on personnel operating a 10 Bev synchrophasotron, 20: 41206 (JPRS-36341, pp 10-17)
GUTHRIE, C. E., Operating guide for radiochemical laboratories at various activity levels, 20: 41199 (ORNL-TM-626)
GUTSCHOW, K., Changes in total leukocyte counts after exposure to whole-body doses of radiation, 20: 40697
GUYON, E., Superimposed normal and superconducting films. I., 20: 42109
GWINN, H. R., Preparation of charge materials for ORNL electromagnetic isotope separators, 20: 41400 (ORNL-3301(Suppl.1))
GYOERGYI, S., Iron-59 incorporation into rat erythrocytes after dose of L-methionine sulphoximine and after 600 r x-ray irradiation, 20: 40561

H

HAAS, F., Particle-gamma angular correlations with detection at 180°, 20: 42383
HAAS, F., Reactions $^{16}O(^3He,\alpha\gamma)^{15}O$, $^{12}C(^3He,p\gamma)^{14}N$, and $^{12}C(d,p\gamma)^{13}C$, 20: 42252
HACKNEY, Stanley, Improvements in or relating to nuclear reactors, 20: 42597
HADDOCK, R. P., n-n S-wave scattering length from the neutron spectra of the reaction $\pi^- + d \rightarrow 2n + \gamma$, 20: 41914
HADEISHI, Tetsuo, Spin exchange between the singly ionized Xe^+ ground state and the metastable state of neutral Xe, 20: 41650
HADEN, C. Roland, Radio-frequency residual losses in superconductors, 20: 42131
HAEFELE, W., Experiments to evaluate reactivity coefficients with reactor operating at steady state conditions (static experiments), 20: 42631 (KFK-260)
HAERM, R., Red giants of population II. IV., 20: 41587
HAGE, K. D., Prog. rpt. on particle fallout and dispersion in the atmosphere, 12/65–2/66, 20: 41133 (SC-CR-66-2030)
HAGEMANN, G. B., Coulomb excitation in the platinum isotopes, 20: 42218
HAGEMANN, R., Allele-induced instability in tomato, 20: 40713
HAGEN, C. R., Baryon mass differences in a model of broken unitary symmetry, 20: 41976
HAGEN, C. R., Construction of nontrivial symmetry-breaking solutions in field theory, 20: 41969
HAGEN, C. R., Higher-order poles in the S-matrix, 20: 41943
HAHN, H., Quasi-stellar radio sources, 20: 41608
HAHN, Yukap, Average fluctuation potential as effective interaction in composite-system scattering, 20: 42236
HAIMSON, Jacob, Collinear termination for high energy particle linear accelerators, 20: 41583

HAJDUKOVIC, S., Influence of DNA on reparation of germinal epithelium and spermatozoa of x-irradiated rats, 20: 40723
HAJDUKOVIC, Srdjan, Effect of postirradiation bleeding on proliferation of bone marrow cells in mice, 20: 40722
HAKEWESSELL, David B., Measurement of atmospheric density using gamma backscatter techniques, 20: 41257
HALAMA, H. J., 600 MHz r-f system for 200 Bev accelerator, 20: 41532 (BNL-10559)
HALL, I., Analysis of some synthetic cross-section fluctuation data, 20: 42194
HALL, L. L., Creep of ThO_2 and ThO_2–CaO solid solutions, 20: 41474
HALNAN, Keith E., Radiation cataract: new evidence on radiation dosage to lens, 20: 40771
HALPERN, M. B., Dynamical calculation of extinct bound states, 20: 41975
HAMADA, Ketsuhiro, Studies on bone marrow transplantation for hematopoietic disturbance, 20: 40726
HAMELIN, J., Improvement of profile of linear shims designed for separation of heavy isotopes, 20: 41405
HAMILTON, J. H., Germanium(Li)–NaI(Tl) coincidence system with multichannel analysis, 20: 41295
HAMILTON, J. H., M, N, and O subshell conversion coefficients in ^{228}Th and ^{240}Pu, 20: 42264
HAMMITT, A. G., Perfect thermodynamic vapor, 20: 42045
HAMNER, R. L., Method of rounding actinide oxide gel particles, 20: 40937
HANNOYER, H., Particle decay described by Lee model with Coulomb interaction, 20: 41909
HANSEN, C. J., Neutrino energy losses from vibrating neutron stars, 20: 41605
HANSEN, M. F., Effects of x-ray dosages on development of Heterakia gallinarum, 20: 40667
HANTMAN, R. L., Measurement of the K_S^0–K_L^0 mass difference by the time dependence of strangeness, 20: 41922
HARACZ, Richard D., One-graviton exchange interaction of elementary particles, 20: 41970
HARDER, B. R., Irradiation experiments with plutonium dioxide suspensions, 20: 41009 (AERE-R-3268)
HARDIE, R. W., Neutronics characteristics of possible driver fuels for the Fast Test Reactor, 20: 42676 (BNWL-281)
HARDY, Edward P. Jr., Prog. rpt. on fallout, 3–6/66, 20: 41131 (HASL-172)
HARGROVE, C. K., Effects of nuclear structure in mu-atomic spectra, 20: 42305
HARMS, B., Gyromagnetic ratio of the 564 kev state in ^{122}Te, 20: 42219
HARMSEN, D.-M., Production of hyperfragments by 1.5-Bev/c K⁻ mesons and studies of their decay properties, 20: 41911
HARPER, Paul V. Jr., Application of thyroid scanning to study of transplantation, 20: 40516
HARRELL, Wilhelmina, Pathogenesis of radiation-induced thymic lymphoma in mice, 20: 40677
HARRINGTON, L. C., Heat capacity and enthalpy of UN from 0 to 1200C, 20: 40865 (CNLM-4461)
HARRIS, Frank E., Studies of hydrogen-bonded systems. IV., 20: 40589
HARRIS, G., Prospects for the utilization of chemical ionization phenomena in MHD, 20: 41730
HARRIS, John W., Response of isolated leukocyte lysosomes to gamma irradiation, 20: 40685
HARTECK, P., Decontamination of products from chemonuclear reactions, 20: 40951 (RPI-321-6)
HARTH, W., Theory of secondary emission and of electron induced conductivity in insulators, 20: 41507
HARTING, D., Mass spectra of recoil nucleon states from inelastic ρ^0 production by pions of 12 and 18 Bev/c, 20: 41828
HARTMANN, C. Harold, Concentric tube and parallel plate electron capture detectors, 20: 40863
HARTWIG, William H., Radio-frequency residual losses in superconductors, 20: 42131
HASKELL, E. E. Jr., Use of tritium to measure movement of groundwater toward irrigation wells in Fresno County, California, 20: 41160
HASKELL, G. P., Superconducting focusing systems in high-energy physics, 20: 42104
HATADA, Motoyoshi, Intermediates of alpha-methylstyrene polymerization studied by pulse radiolysis, 20: 40985
HATTORI, Hiroyuki, Electron injection into betatron, 20: 41560
HATTORI, Hiroyuki, Shimadzu 26-Mev medical betatron, 20: 41564
HAUCK, H., Irradiation effects on the mechanical properties of vanadium-base alloys, 20: 41506
HAUPT, W., Random events, pile-up, and summation in a fast-slow coincidence, 20: 41291
HAVAS, Peter, Are zero rest mass particles necessarily stable?, 20: 41806
HAVLICEK, M., Physical representations of an infinite-dimensional Lie algebra, 20: 41937
HAWKING, S. W., Perturbations of an expanding universe, 20: 41590
HAWKINS, Ronald James, Improvements in or relating to nuclear reactors, 20: 42603
HAYASHI, I., Vacuum encapsulated lithium-drift detector telescope, 20: 41376
HAYASHI, Koichiro, ESR study on the radiation-induced polymerization of nitroethylene, 20: 40981
HAYASHI, Koichiro, Radiation-induced solid-state polymerization in binary systems. II., 20: 40977
HAYASHI, Takemi, 3°-plet model of elementary particles, 20: 41998
HAYDEN, K. D., Plutonium Recycle Test Reactor decontamination following MgO–PuO_2 fuel element failures, 20: 42677 (BNWL-SA-636)
HAZEL, V. E., Design and fabrication of ESADA-VESR Mark III superheat fuel clusters, 20: 42627 (GEAP-5051)
HEATON, H. T., Peak-to-total ratios and efficiencies for NaI crystal, 20: 41307
HEBEDA, E. H., Isotopic evidence for upper-cambrian or lower-ordovician granite emplacement in Vigo area, Spain, 20: 41153
HEBER, J., Fluorescence lifetimes of hydrated salts of europium and terbium, 20: 42539
HEDGER, Harry John, Improvements in or relating to induction coupled plasma generators, 20: 42514
HEGER, H., Studies of Panoramix radiographic technique and of radiation dose during Panoramix and mouth film exposure, 20: 40795
HEHEMANN, R. F., Prog. rpt. on transformation of Zr–Nb alloys, 7/66, 20: 41443 (COO-588-12)
HEIDEMANN, B., Protective action of cysteine on gonad development of in utero irradiated rats, 20: 40729
HEIL, H., Apparatus for alternate electron and ion treatment of surfaces with a micron size spot, 20: 41528
HEISER, William J., Crescent pattern of increased radioactivity in brain scanning, 20: 40789
HELDT, E., Mass spectrometric study on the isotope effect in secondary electron emission from metal surfaces by positive ions, 20: 41620 (NIJS-R-471)
HELGESEN, John O., Motion of a charged particle in a magnetic field due to a finite solenoid with application to solar radiation protection, 20: 42521
HELLER, S., Design and performance of on-line wire spark chamber spectrometer, 20: 41297
HELLSTROEM, K. E., Studies on allogenic inhibition. II., 20: 40588
HELLWEGE, K. H., Fluorescence lifetimes of hydrated salts of europium and terbium, 20: 42539
HELMKAMP, R. W., Determination of total iodine in radioactive iodide in radioactive iodide preparations of high specific activity, 20: 40553
HENDEE, William R., Thermoluminescent dosimetry of beta depth dose, 20: 40766
HENRIKSEN, Thormod, Electron spin resonance signals in irradiated proteins, 20: 40595
HENRY, G. Reading, Radiative corrections to high-energy inelastic electron scattering, 20: 42095
HENSE, U., Contribution of ionospheric F region to cosmic noise absorption, 20: 42048
HENSLEY II, J. C., Lethal effects of ^{60}Co on mature White Leghorn chickens, 20: 40693
HENSON, R. M., Coaxial accelerator, 20: 42516
HEPP, Klaus, Proof of the Bogoliubov-Parasiuk theorem on renormalization, 20: 41935
HERLACH, F., Conference on megagauss magnetic field generation by explosives, Frascati, Italy, 9/65, 20: 41076 (EUR-2750.e)
HERLACH, F., Faraday rotation in megagauss fields, 20: 41515
HERLACH, F., Magnetic field and current amplification with non-cylindrical explosive systems, 20: 41091
HERLACH, F., Results and limitations of cylindrical flux compression experiments, 20: 41085
HERLACH, F., Simple flux compression devices with small explosive charge, 20: 41094
HERMANN, R., Analytic continuation of group representations, 20: 41933
HERNDON, R. C., Analysis of $_{\Lambda}{}^{9}$Be and $_{\Lambda}{}^{13}$C, 20: 42241
HERP, Anthony, Depolymerization of hyaluronic acid by autoxidants and radiations, 20: 40591
HERPERS, U., Gamma-spectrometric determination of special reaction products of cosmic radiation in meteorites, 20: 41614
HERRMANN, M., Studies of multiple emission in electron emission processes, 20: 41529
HERTER, Frederic P., Rapid detection of tumor hormone dependency by radioisotopes, 20: 40566
HERZENBERG, A., Vibrational excitation and dissociative attachment in the scattering of electrons by hydrogen molecules, 20: 41657
HERZENBERT, A., Electron resonances of the H_2^- ion, 20: 41656
HESS, Richard Irwin, Production of $K\bar{K}$ pairs in π^-p interactions, 20: 41802 (UCRL-16832)
HESSON, G. M., Investigation of combined failure of pressure tube and defected fuel rod in PRTR, 20: 42675 (BNWL-272)

HEUSCH, C. A., Photoproduction of η mesons from 950 to 1100 Mev, 20: 41889
HEWSON-BROWNE, R. C., Chapman-Ferrano hollows for system of line currents enveloped by stratified corpuscular flux, 20: 42453
HEYLEN, A. E. D., Calculated magnetic electron drift velocities in H_2, N_2, O_2, air and C_2H_6, 20: 41628
HIEN, N. C., Design and performance of on-line wire spark chamber spectrometer, 20: 41297
HIGINBOTHAM, W., Design and performance of on-line wire spark chamber spectrometer, 20: 41297
HIKICHI, Kunio, Dynamic mechanical properties of polyoxymethylene. I., 20: 41500
HILBERT, Jerold W., Direct reading intracavitary dosimeter for use in radium therapy, 20: 41377
HILGERTOVA, J., Effects of irradiation on level of reduced nicotinamide nucleotides in rat liver homogenates, 20: 40583
HILL, John H., Cathodic etching to prepare radioactive samples for oxygen determination, 20: 40817 (UCRL-14959)
HILL, N. A., Observations on the strength and Young's modulus of BeO as a function of density and grain size, 20: 41473
HIMOE, E., Evidence demonstrating germinal selection in early premeiotic germ cells of Drosophila males, 20: 40670
HINCKS, E. P., Effects of nuclear structure in mu-atomic spectra, 20: 42305
HIRAMOTO, T., MHD power generation experiments with K-seeded Ar plasmas, 20: 41781
HIRANO, Katsumi, Pinch phenomena in a coaxial plasma gun, 20: 42464
HIRAYAMA, Minoru, X-η mixing and B_8 mass splittings, 20: 42005
HISKES, J. R., Formation of excited hydrogen atoms by charge exchange in ground state atoms, 20: 41634
HITLIN, D., Detailed analysis of muonic x-ray spectrum from strongly deformed e-e nuclei, 20: 42310
HODES, M. E., Prevention of x-ray-induced leukemia in mice. I., 20: 40658
HOEKSTRA, H., Unit cell of γ-UO_3, 20: 40907
HOFFSWELL, R. A., (^{3}He,t) investigations of Fe, Ni, and Zr, 20: 42334
HOFMAN, Walther, Nuclear reactor for carrying out irradiation tests, 20: 42685
HOGG, W. R., Photoproduction of charged pions from helium and hydrogen, 20: 41817
HOHMAN, Wayne, Intracellular distribution of calcium in mucosa of avian shell gland, 20: 40551
HOITINK, N. C., Physiological data telemetry system, 20: 41220 (BNWL-214)
HOLAN, T., Results of radioiodine treatment in diabetes mellitus associated with hyperthyroidism, 20: 40790
HOLLADAY, W. G., Application of π-N scattering results to Λ-K^0 production, 20: 41917
HOLLAND, L. K., Prog. rpt. on High Power Density development, 6–11/65, 20: 42626 (GEAP-4951)
HOLLO, L., Correlations between EM pulsations and the F2 layer, 20: 42054
HOLLOX, G. E., Effect of stoicheiometry on the yield stress of TiC and TiO_2, 20: 41475
HOLMGREN, H. D., Study of the reaction ^{10}B(^{3}He,p$\alpha\alpha\alpha$), 20: 42188
HOLZ, H. B., 1000-Mwe FBR parametric study of secondary sodium–steam system, 20: 42632 (NAA-SR-12060)
HOMMA, S., π^0 photoproduction at 3.0, 4.0, and 5.0 Bev for baryon four momentum transfers between 0.5 and 4.0 (Bev/c)^2, 20: 41798 (MIT-2098-265)
HOMMA, S., Search for fractionally charged, weakly interacting particles, 20: 41797 (MIT-2098-264)
HONCARIV, R., Effects of irradiation on frequency of chromosome aberrations in root tip of barley, 20: 40716
HONCARIVOVA, K., Effects of irradiation on frequency of chromosome aberrations in root tip of barley, 20: 40716
HONMA, T., Conductivity of a gas with suspension, 20: 41713
HOOPER, C. F. Jr., Electric microfield distributions in plasmas, 20: 42468
HOOPER, Frank F., Bacterial transport of radiophosphorus in a stream ecosystem, 20: 40529
HORST, K. M., Prog. rpt. on SEFOR, 2–4/66, 20: 42629 (GEAP-5160)
HORVAT, P., Spins of some T = 1 states in ^{26}Al, 20: 42368
HOSODA, T., Preparation and test of MHD duct wall and electrode materials, 20: 41718
HOUSTON, S. K., Lower bound to the reciprocal of the scattering length. II., 20: 41658
HOWIESON, J., Evaluation of CANDU: PHW fuels, 20: 42618 (66-CNA-312)
HOWLAND, J. W., Leukocyte response following simultaneous ionizing and microwave irradiation, 20: 40650
HRABOVCOVA, Alojzia, Betatron and the problem of protection in its use, 20: 41561
HUBBARD, J. Donald, Prevention of x-ray-induced leukemia in mice. I., 20: 40658
HUBERT, Ph., Theoretical study of the continuous spectra of gamma rays emitted in nuclear reactions, measurement of mean lives, 20: 42379
HUCK, A., Reactions induced in carbon by fast neutrons, 20: 42367
HUDSON, C., Motion sensing and its application to Project Wisp, 20: 41224 (EGG-1183-2078)
HUDSON, Michael John Bodenham, Decontamination of radioactive solutions, 20: 41061
HUEFNER, S., g-Factor in 2$^+$ rotation states in ^{166}Er and ^{168}Er, 20: 42302
HUERLIMANN, Theodor, Gamma compensation of ionization chamber for detection of neutron flux in nuclear reactors, 20: 41360
HUET, J. J., Stabilization of uranium monocarbide and production of the single-phase carbide, 20: 41431
HUFF, Dale D., Numerical model for hydrologic transport of radioactive aerosols from precipitation to water supplies, 20: 41141
HUGHES, A. E., Stability and production of R' centers in Li fluoride, 20: 42563
HUGHES, T. A., Coherent neutron proton-hole excitations in nuclei, 20: 42279
HUGHES, V. W., Recent experiments on muonium, 20: 41661
HUGHES, W. L., Iodine-125-DU (5-iodo-2'-deoxyuridine) in autoradiographic studies of cell proliferation, 20: 40666
HUIZENGA, J. R., Cobalt-59(p,α)^{56}Fe and ^{56}Fe(p,p') reactions, 20: 42256
HUME, R., Prediction of dose of radioactive phosphorus in treatment of polycythemia vera, 20: 40774
HUNDSTAD, Richard L., Electrode protection for magnetohydrodynamic generators, 20: 41689
HUNTER, J. H. Jr., Role of thermal instabilities in star formation, 20: 41601
HURLEY, T. J. Jr., Axial power monitoring with an on-line computer, 20: 42661 (DPSPU-66-30-2)
HUSAK, V., Simple pulse interval analyzer for scintillation scanning, 20: 41318
HUSSAIN, F., $p\bar{p}$ Annihilations at rest with representation mixing in SU_{6w}, 20: 41847
HUSSAIN, F., Semi-phenomenological analysis of nonleptonic hyperon decays in U_{12}, 20: 41831
HWANG, Ching-lai, Heat transfer to MHD flow in the thermal entrance region of a flat duct, 20: 41105
HYMAN, H. H., Raman spectrum and hydrolysis studies on hydrogen fluoride solutions of xenon oxide tetrafluoride, 20: 40906

I

IACOBELLI, R., Thermal diffusivity and conductivity measurements on metals and oxides at high temperatures, 20: 41479
IANCULOVICI, B., Autodyne installation for experiments on dynamic polarization of nuclei, 20: 41249
ICHIDA, Taizo, Influence of addition of ethylene on y induced alternating copolymerization of ethylenimine and C monoxide, 20: 40975
ICHIKAWA, R., Naturally occurring radionuclides in human tissues, 20: 40531 (A/AC.82/G/L-1045(Rev.1))
IGLOVA, L. V., Effectiveness of the oxygen enrichment of air in MHD generator assemblies, 20: 41744
IGNAT'EV, B. G., Fabrication of thin plates from refractory carbides, 20: 41430
IGNATOV, D. V., Analysis of nonmetallic inclusions in Mo and its alloys, 20: 41467
IGO, G. J., Total reaction cross sections for 14.5 Mev protons from 22 separated isotopes of Ti, Fe, Ni, Cu, Zn, Zr, and Sn, 20: 42162 (LA-DC-8075)
IGUMNOV, S. A., Application of delayed neutrons for coreless determination of U content in boreholes, 20: 41157
IIDA, S., Preparation and test of MHD duct wall and electrode materials, 20: 41718
IIDA, Shoji, Photocurrent and thermal release time studies of uranium dioxide, 20: 42532
IIO, Masahiro, Measurement of coronary circulation time with catheter-type micro G-M counter, 20: 40514
IJAZ, M. A., Neutral pion production in p-p interactions at 2.8 Bev/c, 20: 41920
ILIES, F., Determination of the linear attenuation coefficient in concrete of gamma radiation emitted by ^{60}Co, 20: 42519
ILINA, V. A., Displacements of atoms in alpha phase of neutron-bombarded carbon steel, 20: 41497
ILINSKAYA, T. A., Absorption spectra of uranium oxides. I., 20: 40916
IMADA, Yukuo, Studies on bone marrow transplantation for hematopoietic disturbance, 20: 40726
IMANI, K., Shock tube studies of magnetically induced non-equilibrium ionization in potassium seeded argon plasma, 20: 41715
IMSHENNIK, V. S., Converging cylindrically symmetrical shock wave in the presence of dissipative effects, 20: 42476

INGELS, S. E., Ductility of cross-rolled beryllium sheet: barrier or challenge, 20: 41433
INGRAM, M., General principles in microbiology of irradiated foods, 20: 41388
INO, Shiro, Fractional condensation of chloride vapor from chlorinated uranium ore, 20: 41048
INZELT-GERBER, E., Combined slit-collimator for measuring distribution of isotopes with γ activity, 20: 41012
IOFFE, V. A., Growing of rare earth aluminate single crystals with perovskite structure, 20: 40920
IOFFE, V. I., Instability of nonuniform current and field distribution, 20: 42040
IORGENSEN, M., Decay of ^{152}Tb, 20: 42155 (JINR-P-2762)
IRIGARAY, J. L., Elastic scattering of 14 Mev neutrons by K, 20: 42393
IRVINE, J. M., Deformed state admixtures in ^{18}O, 20: 42274
IRVINE, W. H., Safety of pressure vessels against fast fracture, 20: 42576 (AHSB(S)-R-107)
ISABELLE, D., Electron scattering at 180° on ^{12}C, 20: 42377
ISABELLE, D. B., Study of light nuclei by electromagnetic interactions, 20: 42340
ISAILA, M., Diverse schemes for flat topping the PPA, 20: 41569
ISHKHANOV, B. S., Specific features of the photodisintegration of nuclei in the 1f-2p shell, 20: 42220
ISKOL'DSKII, A. M., Investigation of plasma injected into trap with conical theta pinch, 20: 42504
ITO, Iwao, Measurement of coronary circulation time with catheter-type micro G-M counter, 20: 40514
ITO, Masayuki, Separation of ^{32}P from a ^{32}P–^{35}S mixture, 20: 41049
ITO, T., Experimental study of physical properties of combustion gas, 20: 41758
IVANCHENKO, I. M., Recoil proton polarization in elastic π^--p scattering at 300 Mev and the phase shift analysis of pion-nucleon scattering, 20: 41794 (JINR-E-2860)
IVANOV, A. B., Processes of interaction between high-temperature materials and gas flows in the duct of an MHD generator, 20: 41738
IVANOV, I., Determination of the linear attenuation coefficient in concrete of gamma radiation emitted by ^{60}Co, 20: 42519
IVANOV, V. N., Biological consequences of radioactive contamination of water bodies, 20: 40527
IVANOVA, T. I., Solution of Laplace's equation for a Penning discharge gap, 20: 42508
IVLEV, A. A., Thermodynamic regularities in isotopic exchange. I., 20: 40924
IWAMORI, Shigeru, Studies on bone marrow transplantation for hematopoietic disturbance, 20: 40726
IWASAKI, Yoichi, Masses of hadrons and pair states of quarks, 20: 42001
IWASHITA, Fumio, Accelerator, 20: 41572
IWASHITA, Fumio, Betatron and similar accelerators, 20: 41573
IWASHITA, Fumio, Device for accelerating an electron beam, 20: 41574
IWASHITA, Fumio, Method for deflecting accelerated charged particle, 20: 41575
IWASHITA, Fumio, Particle accelerating tube, 20: 41577
IWASHITA, Fumio, Particle accelerator, 20: 41578
IWASHITA, Fumio, Particle accelerator, 20: 41580
IYENGAR, K. V. K., Circuit for preventing accumulation of experimental data when nuclear reaction rate exceeds preset value, 20: 41244
IYER, R. H., Evidence of ternary fission at lower energies, 20: 42273
IZVEKOV, V. N., Preparation of single crystals of refractory compounds, 20: 41480

J

JACK, W., Reactions ^{20}Ne(n,α)^{17}O and ^{16}O(n,α)^{13}C at 14 Mev, 20: 42216
JACKSON, William D., Brayton cycle magnetohydrodynamic power generation, 20: 41706
JACMART, J. C., Study of (p,2p) reaction at 155 Mev on ^{7}Li, ^{9}Be, and ^{23}Na with an on-line computer, 20: 42360
JACOBS, Robert, Radiological health problems associated with operation of neutron generators, 20: 41215
JACOBS, Sydney, Incidence of radiation fibrosis after radiotherapy for breast cancer, 20: 40773
JACOBSON, Leon O., Prog. rpt., semiannual, 3/66, 20: 40740 (ACRH-25)
JACOBUS, David P., Response of DBA/2J mouse strain to acute ionizing radiation, 20: 40687
JACQUOT, C., Quasielastic collisions on α groups in ^{12}C by 60 to 120 Mev protons, 20: 42352
JAECH, J. L., Prog. rpt. on accurate nuclear fuel burnup analyses, 12/65–2/66, 20: 42608 (GEAP-5124)
JAGIELAK, J., Spectrum of scattered gamma radiation of ^{137}Cs in paraffin phantom, 20: 40792
JAHN, P., Construction of β spectrometer with a focusing angle $(\pi/2) \cdot \sqrt{13}$, 20: 41355
JAIN, B. D., Bis-2-pyridyl glycol as a reagent for gravimetric determination of U, Al, and Be, 20: 40849
JAIN, D. C., Effect of vibrational-rotational motion on the electric and magnetic properties of diatomic molecules, 20: 41659
JAKES, D., Magnesium, Sr, and Ba polyuranates, 20: 40901
JAKLEVIC, J. M., Directional correlation measurements in decay of ^{160}Tb employing a Ge–Li detector, 20: 42150 (COO-498-56)
JAMES, Clifford, Improvements in or relating to gauging instruments, 20: 41436
JAMES, P. R., Dounreay Fast Reactor: kinetic computer analog, 20: 42653
JAMESON, R. L., Magnetic-flux compression in explosion geometry, 20: 41093
JANETT, A., Studies on lymphopoiesis. IV., 20: 40663
JANOSSY, L., Lorentz principle and general theory of relativity. I., 20: 42072
JANOSSY, L., Lorentz principle and general theory of relativity. II., 20: 42073
JANSEN, C. R., Studies on lymphopoiesis. IV., 20: 40663
JARECKI, Tadeusz, Efficiency of a hodoscope for registration of charged particles, 20: 41338
JARVIS, O. N., Measurements of the differential cross-section and polarization in proton-proton scattering at about 143 Mev, 20: 41915
JASKOLA, M., Redrift treatment of Li-drifted Si detectors, 20: 41311
JASPERS, N. C. Burhoven, Resonant absorption measurement in the reaction ^{26}Mg(p,γ)^{27}Al, 20: 42198
JATCZAK, Jerzy, Efficiency of a hodoscope for registration of charged particles, 20: 41338
JATCZAK, Jerzy, Measurement of efficiency of liquid scintillation counters of large area, 20: 41339
JATCZAK, Jerzy, Measurement of the dose rate of unknown γ-radioactive substances, 20: 41025
JEFFRIES, C. D., Spin-lattice relaxation of rare-earth ions in LaF_3, 20: 42540
JELINEK, F. J., Reevaluation of some thermodynamic properties of gadolinium metal, 20: 42542
JENCKEL, Ludolf, Mass spectrometer, 20: 41261
JENKIN, J. G., Accurate measurement of relative efficiency of Ge(Li) gamma-ray detectors, 20: 41288
JENKINS, Robert K., Irradiation of some polysiloxanes in various gases, 20: 40974
JENKINS, Theodore M., Electron-induced cascade showers in Cu and Pb at 1 Bev, 20: 41671
JENSCHKE, B., Search of parity mixing in ^{180}Hf by a measurement of the circular polarization of γ rays, 20: 42225
JENSEN, M. Anthony, Superconductivity and electronic specific heat in the Sc–Zr system, 20: 42121
JENSEN, M. L., Bacteriogenic sulfur isotopic ratios in geology, 20: 41151
JEWELL, R. W., High-resolution studies of fission x rays and gamma rays, 20: 42170 (UCRL-70045)
JODOGNE, J. C., Test of α-γ angular correlation on ^{12}C at 23 Mev, 20: 42380
JOHANNES, R. E., Flux of ^{32}P and ^{65}Zn through a salt-marsh ecosystem, 20: 40573
JOHANSSON, A., Decay of ^{192}Au, 20: 42187
JOHN, W., Fission γ rays using Ge(Li) detector in conjunction with bent-crystal spectrometer, 20: 41278 (UCRL-70000)
JOHN, W., High-resolution studies of fission x rays and gamma rays, 20: 42170 (UCRL-70045)
JOHNE, S., Synthesis of radioactively labeled compounds. XV., 20: 41024
JOHNSON, A. J., Analysis of radioactive metals by spark source mass spectrography, 20: 40816 (RFP-699)
JOHNSON, A. J., Determination of Fe and Ni in U by atomic absorption spectrophotometry, 20: 40815 (RFP-698)
JOHNSON, D. M., Pressing hollow shapes from high-strength beryllium, 20: 41428 (SCL-DC-66-57)
JOHNSON, G. T., Mechanism of Ce uptake by Saccharomyces cerevisiae, 20: 40560
JOHNSON, John L., Closed-line average minimum-B configuration, 20: 42455
JOHNSON, T., Radiological recovery requirements, structures, and operations research. I., 20: 41179 (AD-635821)
JOHNSON, T., Radiological recovery requirements, structures, and operations research. II., 20: 41180 (AD-635822)
JOHNSTON, William H., Radioactive method of detection of hidden explosives, 20: 41066
JOKIPII, J. R., Pitch-angle dependence of first-order Fermi acceleration at shock fronts, 20: 42423
JONEK, Jan, Enzymes in cerebral tissue in various phases of acute irradiation syndrome, 20: 40590
JONEK, Teresa, Enzymes in cerebral tissue in various phases of acute irradiation syndrome, 20: 40590
JONES, D. C., Treadmill exercise performance by ageing irradiated rat, 20: 40604 (AD-635251)

JONES, D. P., Differential cross sections for $\pi^{\pm}$p elastic scattering in the momentum range 875-1579 Mev/c, 20: 41857
JONES, F. C., Transverse-momentum distribution of secondary particles from high-energy collisions, 20: 41845
JONES, Gary E., System for measuring concentrations of atmospheric ^{222}Rn, 20: 41277 (UCRL-16952)
JONES, J. J., Display lamp for counter logic, 20: 41314
JONES, J. M., Plasma ion oscillations, 20: 42444
JONES, J. R., Tritium labeling of compounds, 20: 41022
JONES, K. W., Lifetime determinations for nuclei A = 10, 11, and 12 from gamma-ray Doppler shifts, 20: 42234
JONES, K. W., Short-lived activities ^{15}C, ^{17}F, ^{19}O, ^{20}F, and ^{28}Al, 20: 42242
JONES, L. H., (^{3}He,t) investigations of Fe, Ni, and Zr, 20: 42334
JONES, L. V., Prog. rpt., 1-3/66, 20: 41037 (MLM-1325)
JONES, L. W., Mass spectra of recoil nucleon states from inelastic ρ^0 production by pions of 12 and 18 Bev/c, 20: 41828
JONES, M. S. Jr., Explosive driven linear MHD generators, 20: 41685
JONES, M. S. Jr., Pulsed electrical power generation from magnetically loaded explosives, 20: 41687
JONKE, A. A., Removal of actinide halides from alumina, 20: 41062
JONKE, Albert A., Removal of stainless-steel claddings from nuclear fuel elements, 20: 41000
JOON, K., Refractometric determination of U(VI) in aqueous and in TBP solutions, 20: 40804 (KR-108)
JORDAN, R. F., Generators of the de Sitter group for the hydrogen atom, 20: 41644
JOZEFOWICZ, E. T., Measurement of neutron density distributions in multilayer unit cells. II., 20: 42680 (INR-698/IX-A/RP)
JOZEFOWICZ, K., Measurement of neutron density distributions in multilayer unit cells. II., 20: 42680 (INR-698/IX-A/RP)
JUNDT, F., "Multipolimeter" application to a study of electromagnetic transitions, 20: 42384

K

KACAKI, J., Influence of DNA on reparation of germinal epithelium and spermatozoa of x-irradiated rats, 20: 40723
KADLECOVA, D., Combined treatment of tumors of oto-rhino-laryngeal region by methotrexate and irradiation, 20: 40782
KADOMTSEV, B. B., Instability of plasma with captured particles in toroidal geometry, 20: 42402 (IAE-1149)
KAETSU, Isao, Radiation-induced solid-state polymerization in binary systems. II., 20: 40977
KAGIYA, Tsutomu, Influence of addition of ethylene on γ induced alternating copolymerization of ethylenimine and C monoxide, 20: 40975
KAHN, B., Two-dimensional electro-fluid dynamic channel flow, 20: 41696
KAHN, P. B., Density of states of degenerate Fermi systems with periodic level schemes, 20: 42222
KAINDL, K., Microbiological studies on influence of heat and irradiation on survival of yeast, 20: 41387
KAJIKAWA, R., Pressurized discharge chamber, 20: 41294
KALININ, A. P., Morphological changes in thyroid gland following radioiodine administration, 20: 40657
KALISZ, J., Determination of statistical parameters of triple coincidence circuit, 20: 41265 (INR-704/III/PL)
KALLINNIKOV, A. E., Effect of gamma radiation on the mechanical characteristics of polyethylene terephthalate film, 20: 41501
KALMUS, George E., Y_1^1 resonant amplitudes between 1660 and 1900 Mev, 20: 41886
KALOGEROPOULOS, T., New determination of the ϕ spin and G parity, 20: 41881
KALYAMIN, A. V., Decay of the isotope ^{180}Os, 20: 42284
KAMAL, A. A., Ionization of relativistic electrons, 20: 41814
KAMAL, A. N., S-wave pion-pion scattering, 20: 41832
KAMIYAMA, Hideo, ESR study on the radiation-induced polymerization of nitroethylene, 20: 40981
KAMPELMACHER, E. H., Nutrition experiments in pigs fattened with heat-decontaminated, γ-irradiated and untreated feeds, 20: 41394
KANADA, Hiroyuki, Evidence for existence of a repulsive core in the Λ-N interaction, 20: 41894
KANAMORI, Yoshihiko, Attenuation coefficients of materials for γ rays from ^{60}Co, 20: 42518
KANAZAWA, A., Static baryon-meson bootstraps and SU_6 symmetry, 20: 41848
KANAZAWA, Akira, Dynamical approach to the leptonic decays of baryons, 20: 41999
KANDA, Frank A., Prog. rpt. on phase equilibria and specific volumes of liquid metals and alloys, 8/65-7/66, 20: 41455 (NYO-2731-7)
KANE, G. L., Observations concerning production amplitudes and models for $J^P = 3/2^+$ baryons, 20: 41836
KANELLAKOPULOS, B., Tri(cyclopentadienyl)americium(III), 20: 40878
KANKI, Takeshi, Fredholm theory of scattering, 20: 41993
KANTOR, M. M., Analysis of nonmetallic inclusions in Mo and its alloys, 20: 41467
KANTOROVICH, A., Systematics of hadrons under noncompact groups, 20: 41967
KAO, Lien-mei, Molybdenum-Gd phase diagrams, 20: 41465
KAPELNER, S. M., Viscosity of liquid K to 900°C, 20: 41460 (TIM-793)
KAPITONOV, I. M., Specific features of the photodisintegration of nuclei in the 1f-2p shell, 20: 42220
KAPITSA, S. P., Natural system of units in classical electrodynamics and electronics, 20: 41522
KAPOOR, S. S., Fission of ^{209}Bi and ^{238}U induced by alpha particles of energies up to 115 Mev, 20: 42267
KAPUSTIN, Yu. L., Accessory thoroughaninite in tuva nepheline syenites, 20: 41173
KAPUY, Ede, Electron correlation in atoms and molecules, 20: 41630
KARAEV, Z. Sh., Synthesis and studies of Ga Y sulfides ($YGaS_3$) and In Y sulfides ($YInS_3$), 20: 40879
KARAM, R. A., Resonance absorption integral of rhenium, 20: 42333
KARANOVIC, Dobrila, Effect of postirradiation bleeding on proliferation of bone marrow cells in mice, 20: 40722
KARANOVIC, Jovo, Effect of postirradiation bleeding on proliferation of bone marrow cells in mice, 20: 40722
KARDASHEV, A. V., Biological consequences of radioactive contamination of water bodies, 20: 40527
KARKHANAVALA, M. D., Kinetics of thermal decomposition of UO_3. I., 20: 40899
KARP, I. N., Experiments with an MHD generator model, 20: 41755
KARPLUS, M., Deuteron quadrupole coupling constant in CH_3D, 20: 40894
KARPOV, V. L., Radiation cross linking of cable polyethylene insulation on large scale, 20: 41496
KARRAS, T., Neutral mass density measurements in repetitively pulsed coaxial plasma accelerator, 20: 41121
KARTUZHIANSKII, A. L., Mechanism for increasing low-temperature sensitivity of nuclear photographic emulsions, 20: 41341
KAS'YANOV, V. A., Laminar EHD flow in plane exit cone, 20: 41110
KATAYAMA, Meiseki, Intermediates of alpha-methylstyrene polymerization studied by pulse radiolysis, 20: 40985
KATAYAMA, Yasuhisa, S_3 invariance and broken U_3 symmetry, 20: 42008
KATO, Kiyoe, Excitation of ion plasma oscillation by electron beams, 20: 42429
KATSAROS, W., Development and testing of a piezoelectric pressure probe with high-resolving power, 20: 42405 (IPP-1/46)
KATSURAI, M., MHD rotating machine: new type of a-c MHD power generator and turbine, 20: 41749
KATZ, A., Is the Heisenberg picture better than the Schroedinger picture?, 20: 42090
KAUFMANN, Klaus, Production of surface-barrier detectors for nuclear radiation, 20: 41363
KAVANAGH, R. W., Decay of the first T = 3/2 state in ^{13}C, 20: 42330
KAWABE, Takaya, Dipole resonance of cylindrical plasma columns in a magneto-plasma, 20: 42463
KAWADA, H., Shock tube studies of magnetically induced non-equilibrium ionization in potassium seeded argon plasma, 20: 41715
KAWAGUCHI, M., Absorption correction in high-energy photoproduction of pions, 20: 41844
KAWAGUCHI, Masaaki, Fredholm theory of scattering, 20: 41993
KAWATA, S., Detection of divergent α-rays and neutrons with multiple-wire spark counters, 20: 41317
KAYKOVA, T. M., Uranium and arsenic in hydrothermal process, 20: 41175
KAYLOR, John D., Prog. rpt. on study of irradiated-pasteurized fishery products, final, 10/64-9/65, 20: 41384 (TID-22833)
KAYUKAWA, Naoyuki, Performance of spatially constant B/ρ-type MHD generator with energy dissipation, 20: 41722
KAZEM, I., Preparation of ^{99m}Tc labeled human serum albumin, 20: 40944
KEECH, G. L., Determination of non-linear parameters and their standard deviations from least-squares residuals, 20: 41518
KEENAN, Thomas K., Lattice constants of 1:1 lithium tetravalent actinide pentafluorides, 20: 40888
KEESOM, P. H., Low-temperature thermodynamic properties of V. I., 20: 42115
KEESOM, P. H., Low-temperature thermodynamic properties of V. II., 20: 42116
KEISERUKHSKAYA, L. G., Synthesis and studies of Ga Y sulfides ($YGaS_3$) and In Y sulfides ($YInS_3$), 20: 40879
KELLER, L. P., Simple Marx high voltage pulse generator for wide gap spark chambers, 20: 41330
KELLEY, Arnold J., Atom-atom ionization mechanisms in Ar-Xe mixtures, 20: 41632
KELLOGG, E. M., Azimuthal angular distribution of $^{12}C(\gamma,p_0)$, 20: 42251
KELLY, Arnold J., Atom-atom ionization cross sections of the noble gases: Ar, Kr, and Xe, 20: 40896
KELLY, D. A., Effect of changes in ionic medium on stability constant

of $Eu(NO_3)^{+2}$, 20: 40876 (ORO-1797-2)
KEMMUNA, A., Radiation reactions of locally x-irradiated rat spleen isolated by operation, 20: 40702
KEMP, M. A. R., Differential cross sections for $\pi^{\pm}p$ elastic scattering in the momentum range 875-1579 Mev/c, 20: 41857
KEMP, William N., Radiotherapy, chemotherapy, and surgery in curative treatment in inoperable cervical cancer, 20: 40778
KENDALL, K., Radiation-protection and recovery from radiation injury in endotoxin-treated mice, 20: 40732 (AD-636209)
KENNEDY, I. R., Release of N from amino acids with ninhydrin for ^{15}N analysis, 20: 40824
KENNEDY, W. R., Beta-gamma radioactivity in environmental air at Los Alamos, New Mexico, 1965, 20: 41194 (LA-3516)
KENNELLEY, J. A., Electrolytic recovery of scrap uranium metal, 20: 41036 (MCW-1494)
KENNEY, Robert W., Comparison of the lifetimes of positive and negative pions, 20: 41891
KENYON, I., Inelastic π^{+-4}He reactions in the momentum range 100–160 Mev/c, 20: 42321
KENYON, I., Phase shift analysis for elastic π^{+-4}He scattering in the energy interval 100–160 Mev/c, 20: 42320
KEPLER, R. G., Photoconductivity processes in organic materials, 20: 40952 (SC-DC-66-1823)
KEPNER, Richard E., Prog. rpt. on ^{90}Sr and ^{137}Cs food chain relationships to deer and sheep, 9/65–6/66, 20: 40541 (UCD-34P104-3)
KEREN, J., Inelastic π^{+-4}He reactions in the momentum range 100–160 Mev/c, 20: 42321
KEREN, J., Phase shift analysis for elastic π^{+-4}He scattering in the energy interval 100–160 Mev/c, 20: 42320
KERIMOV, B. K., Relationship between structure and polarization of particles in $1+\bar{1} \rightleftarrows p+\bar{p}$ reactions, 20: 41813
KERN, H. E., Vacuum encapsulated lithium-drift detector telescope, 20: 41376
KERNAN, Anne, Y† resonant amplitudes between 1660 and 1900 Mev, 20: 41886
KERREBROCK, Jack L., Experimental investigation of fluctuations in a nonequilibrium MHD plasma, 20: 41692
KESSLER, P., Electroproduction of very high-energy muons, 20: 41805 (SLAC-Trans-46)
KEYSER, L. F., Infrared spectra of HCl and DCl in solid rare gases. II., 20: 40895
KHALFIN, L. A., Pauli principle and unstable elementary particles, 20: 42022
KHANSEVAROV, R. Yu., Low-temperature γ irradiation and tempering of InSb, 20: 42527
KHANSON, K. P., Effect of whole-body x-ray irradiation on activity of ATP-ase in rat liver mitochondria, 20: 40695
KHARE, S. P., Excitation of hydrogen molecules by electron impact, 20: 41645
KHARITONOV, Yu. Yu., Infrared absorption spectra of La, Gd, and Y nitrates, 20: 40886
KHEIFETS, L. I., Particle trajectories in radiation and chemical processes in pseudo-liquefied layer, 20: 40884
KHODAKOV, Yu. S., Dehydrogenating characteristics of Al oxide–Cr oxide catalysts, 20: 40943
KHOKHLOV, V. A., Viscosity of molten lanthanum trichloride and its mixtures with lanthanum dichloride, 20: 40925
KHOLOPOV, G. K., Integral radiant emissivity of W from 1200 to 2800°K, 20: 41525
KHOPKAR, S. M., Separation of silver from mixtures by cation-exchange chromatography, 20: 40847
KHORUSHAILOV, V. G., Effect of the annealing temperature and medium on the properties of molybdenum, 20: 41482
KHRUSHCHEV, V. G., Behavior of live organisms in radiation fields, 20: 40519 (NP-16259)
KHUKHAREVA, I. S., Effect of oxygen additions on the structure and superconducting properties of Zr–Nb alloys, 20: 42535
KIBA, T., Separation of technetium from rhenium by liquid-liquid extraction with potassium xanthate, 20: 40856
KIM, C. C., Excited levels in ^{3}He, 20: 42224
KIM, Y. N., Quadrupole elastic scattering of alpha particles by polarized nuclei, 20: 42235
KIMELDORF, D. J., Treadmill exercise performance by ageing irradiated rat, 20: 40604 (AD-635251)
KIMMEL, Hermann, Closing device for large-surface formed methane flow counter, 20: 41359
KIMURA, Keizo, Pressure-applied process for pouring heavy concrete to construct reactor shields, 20: 42586
KINCAID, Caleb B., Observations derived from film packs used in nationwide x-ray exposure study, 20: 41213
KING, G. A. M., Survey of F1 region in summer at solar minimum, 20: 42058
KING, J. H., Dynamical stability and boundary perturbations of the solar wind, 20: 41586
KINGSBURY, Charles A., NMR studies of H–deuterium exchange in carbonium ion systems, 20: 40945
KINOSHITA, Kiyoshi, Hidden channels and elementarity, 20: 42002
KINOSHITA, Toichiro, Forward scattering amplitude at high energy, 20: 42028
KINSEY, K. F., Two-nucleon emission following absorption of stopped negative pions, 20: 42313
KIRBY, H. W., Hydrolytic separations of protactinium, 20: 41044
KIRBY, H. W., Purification of Pa from natural sources, 20: 41043
KIRIN, I. S., Separation of XeO_3 and HIO_3 in zirconium phosphate, 20: 41054
KIRKO, I., Magnetohydrodynamics of condensed media, 20: 42042
KIRSCH, Michael A., Fixation of ^{75}Se and ^{35}S onto protein-polysaccharides of bovine costal cartilage, 20: 40544
KISDI, David, Field-theoretical method in the many-body problem. I., 20: 41931
KISELEV, B. G., Light neutron nuclei among U fission products, 20: 42298
KISELEVSKII, L. I., Dependence of the relative population of displaced levels of a copper atom on the concentration of electrons in the plasma of an arc discharge, 20: 42490
KISH, F., Radiolysis of isopropanol and benzophenone and naphthalene in isopropanol in liquid state, 20: 41006
KITA, Hideji, Non-trivial example of a relativistic quantum theory of particles without divergence difficulties, 20: 42000
KLAS, J., Errors of method of direct and inverse isotope dilution analysis by inexactness of radioactivity measurements, 20: 40831
KLECHKOVSKII, V. M., Effect of radiation on composition of deoxyribonucleic acid in plants, 20: 40548
KLEESE, R. A., Prog. rpt. on genetic control of physiological processes in higher plants, 1965–66, 20: 40532 (COO-1097-17)
KLEIN, E., Energy conversion with liquid metal working fluids in MHD Staustrahlrohr, 20: 41734
KLEIN, Georges, Carrousel magnetoaerodynamic generator, 20: 41697
KLEIN, Rudolf, Shielding properties of the superconducting surface sheath, 20: 42127
KLEMPNER, K. S., Design of radioactive isotope instruments, 20: 41235
KLEPPE, Lowell M., System for measuring concentrations of atmospheric ^{222}Rn, 20: 41277 (UCRL-16952)
KLEVANS, E. H., High-frequency conductivity of a plasma in quasi-equilibrium. III., 20: 42472
KLIMA, J., Magnesium, Sr, and Ba polyuranates, 20: 40901
KLIMANOVA, L. F., Factors influencing the developing of discharge along trajectory of particle in spark chamber, 20: 41304
KLIMENKO, A., Decay of ^{184}Re, 20: 42157 (JINR-P-2814)
KLOTZ, H.-D., Lateral extraction of negative ions from a layered low-pressure discharge in oxygen, 20: 42435
KLOVERSTROM, F. A., Revised safety analysis report for the Super Kukla prompt burst reactor, 20: 42684 (UCRL-7695(Rev.1))
KLUGOW, J., Detection and properties of π^0 mesons in multiple processes, 20: 41910
KLYUCHAREV, A. P., Reaction $^{18}N(d,\alpha)^{13}C$ with 0.8 to 1.8 Mev deuterons, 20: 42295
KNACKE, G., Activity of UCl_3 in the eutectic melt LiCl–KCl, 20: 40922
KNACKE, O., Anodic polarization of UC in the melt LiCl–KCl, 20: 40923
KNEZEVIC, Zvonko, Determination of ^{85}Sr, ^{106}Ru, ^{137}Cs, and ^{144}Ce by γ-spectroscopy, 20: 40837
KNIEPER, P. J., Heat transfer to MHD flow in the thermal entrance region of a flat duct, 20: 41105
KNIGHT, J. M., Zero-range treatment of the three-body photodisintegration cross section of ^3H and ^3He, 20: 42228
KNIPPER, A., Study of electromagnetic transitions by measurement of the polarization distribution and γ-γ angular correlation, 20: 42381
KNOEPFEL, H., Conference on megagauss magnetic field generation by explosives, Frascati, Italy, 9/65, 20: 41076 (EUR-2750.e)
KNOEPFEL, H., Faraday rotation in megagauss fields, 20: 41515
KNOEPFEL, H., Results and limitations of cylindrical flux compression experiments, 20: 41085
KNOEPFEL, H., Simple flux compression devices with small explosive charge, 20: 41094
KNOEPPEL, H., Magnetic field and current amplification with non-cylindrical explosive systems, 20: 41091
KNOPF, N. R., Two-capsule program for comparing A302B steel from two manufacturers under specific irradiation conditions, 20: 41504
KNOWLES, H. B., Evidence for the presence of alpha clusters in the boron isotopes, 20: 42193
KNYAZEV, D. A., Thermodynamic regularities in isotopic exchange. I., 20: 40924
KOBAYAKAWA, H., Pressurized discharge chamber, 20: 41294
KOBAYASHI, T., Gallium arsenide surface barrier diode as charged particle spectrometer, 20: 41313
KOBAZEV, E. I., Testing counters of nuclear radiations of T-25-BFL type by aid of automatic apparatus, 20: 41285
KOCH, H. R., Study of ^{46}Sc levels by means of neutron capture gammas,

20: 42382
KOCH, R. L., Experimental investigations of closed-loop MPD power generation, 20: 41741
KOCHEGURA, N. M., Antifriction and strength characteristics of materials subjected to neutron irradiation, 20: 41498
KOCHETKOV, V. L., Light neutron nuclei among U fission products, 20: 42298
KODA, Yoshio, Separation of ^{32}P from a ^{32}P–^{35}S mixture, 20: 41049
KOENIG, Daniel Rene, Surface ionization of cesium and thermionic emission from planar single crystals of tungsten, 20: 41681 (UCRL-11857)
KOERNER, H. J., Gyromagnetic ratio of the 564 kev state in ^{122}Te, 20: 42219
KOESTER, Charles J., Optical maser as a retinal coagulator, 20: 40791
KOETKE, D., Inelastic π^+-^{4}He reactions in the momentum range 100–160 Mev/c, 20: 42321
KOETKE, D., Phase shift analysis for elastic π^+-^{4}He scattering in the energy interval 100–160 Mev/c, 20: 42320
KOIDE, Tadashi, Measurement of coronary circulation time with catheter-type micro G-M counter, 20: 40514
KOLEROV, G. I., Conditions of macroscopic causality for the scattering matrix, 20: 41962
KOLESOV, V. E., Radiative capture cross sections of 30 to 170 kev neutrons, 20: 42293
KOLOUSEK, J., Iron-59 incorporation into rat erythrocytes after dose of L-methionine sulphoximine and after 600 r x-ray irradiation, 20: 40561
KOMAI, Kenichiro, Device for producing a pulsed charge-particle beam, 20: 41576
KOMAR, A. P., Instrument for determining intensity of gamma radiation, 20: 41284
KOMAROV, P. N., Influence of dose rate of γ radiation on kinetics of radiation-chemical oxidation of butanol, 20: 40984
KOMAROV, P. N., Oxidation of p-xylene induced by γ radiation, 20: 41002
KOMAROV, P. N., Radiation chemical oxidation of butanol in aqueous solution at increased temperature, 20: 40983
KOMOCHKOV, M. M., Attenuation of high-energy neutron fluxes in heterogeneous shielding, 20: 42517
KOMOV, A. G., Investigation by EPR method of the uv and γ-radiation induced free radicals in H_2O_2 in NH_3 solutions, 20: 41001
KONDRATENKO, A. N., Kinetic theory of EM waves in bounded magnetized plasma. I., 20: 42496
KONECNY, M., Combined treatment of tumors of oto-rhino-laryngeal region by methotrexate and irradiation, 20: 40782
KONONENKO, V. I., Method of determining electron density distribution in a plasma, 20: 42419 (AD-636608)
KONONOV, V. N., Radiative capture cross sections of 30 to 170 kev neutrons, 20: 42293
KONSHIN, V. A., Cascade nucleons emitted by nuclei interacting with 660 Mev protons, 20: 42299
KONZAK, C. F., Factors affecting biological action of mutagens, 20: 40717
KOPETSKII, Ch. V., Growing and plastic deformation of the single crystals of refractory metals and alloys, 20: 41481
KOPYLOV, G. I., Reduction of the energy spectra of non-stable particles according to their decay, 20: 41927 (JINR-P-2797)
KOPYLOW, B. A., Imitation of post-radiation damage to DNA under influence of extracts from irradiated potato bulbs, 20: 40562
KORBEL, Z., Real part of amplitude of elastic scattering of protons on deuterons at 8 Bev, 20: 41811
KOREN, Kristian, Cesium-137 in milk in Norway 1962–1966, 20: 41132 (NYO-3364-20)
KORNELSEN, E. V., Thermal desorption of inert gases from tungsten monocrystals, 20: 41463
KOROBOV, I. V., Thermodynamic properties of inorganic substances (handbook), 20: 41417
KOROGODIN, V. I., Problems of post-radiative cell restoration, 20: 40731
KOROLEV, A. M., Gradient invariance of the Lagrangian of a particle with nonlocal potential, 20: 41520
KOROLEVA, L. N., Growing of rare earth silicate single crystals of oxyortho- and diortho-type from solution melt, 20: 40919
KOROSTYLEVA, L. A., Hyperfine and isotope structure in the plutonium spectrum and its classification, 20: 41639
KORSMEYER, J. D., Uranium-233 thorium seed-blanket experimental program, 20: 42609 (WAPD-T-1886)
KORYAGINA, G. M., Effectiveness of the oxygen enrichment of air in MHD generator assemblies, 20: 41744
KOSMIDER, Stanislaw, Enzymes in cerebral tissue in various phases of acute irradiation syndrome, 20: 40590
KOSSYI, I. A., Investigation of a conical induction plasma source, 20: 42505
KOSTENKO, N. S., Effect of anion admixtures on luminescence and scintillation properties of monocrystals NaI(Tl), 20: 41347
KOTESWARA RAO, N. V., Sequent correlations in stochastic point processes. II., 20: 42467
KOTLYAREVSKII, D., Search for new decay modes of the K_2^0-mesons, 20: 41903
KOTONSKI, Z., Spectrum of scattered gamma radiation of ^{137}Cs in paraffin phantom, 20: 40792
KOTTMEIER, H.-L., High-voltage therapy of uterine carcinoma, 20: 40769
KOUTRAS, D. A., Minimum dose of potassium iodide which inhibits thyroidal radioiodine uptake, 20: 40564
KOUTZ, Stanley L., Fuel element, 20: 42613
KOVAL'CHUK, M. A., Radiolysis of mixed Co(III) nitroammoniates and Co(III) hexanitrites, 20: 41003
KOVALEV, A. V., Fabrication of thin plates from refractory carbides, 20: 41430
KOVBASUK, V. I., Plasma flow in the duct of a series-flow MHD generator, 20: 41698
KOVTUN, R. I., Motion in spatially periodic magnetic fields, 20: 42501
KOWALEWSKI, V. J., Application of the ENDOR technique to high resolution proton magnetic resonance spectra, 20: 42529
KOZLOVA, M. D., Preparation of carrier free ^{111}Ag, 20: 41023
KOZY, A., Analysis of radioactive metals by spark source mass spectrography, 20: 40816 (RFP-699)
KOZYREV, B. M., Influence of solvent on paramagnetic relaxation constant in liquid solutions of gadolinium nitrate, 20: 40928
KRAHE, J., Activity of UCl_3 in the eutectic melt LiCl–KCl, 20: 40922
KRAHE, J., Anodic polarization of UC in the melt LiCl–KCl, 20: 40923
KRAITZER, Ian C., Extraction of thoria and ceria from rare earth ores, 20: 41059
KRAMER, H., Method of producing hydrazine, 20: 41008
KRAMER, N. D., Decay scheme of ^{179}Hf produced in (n,γ) reactions, 20: 42285
KRASNOSHCHEKOV, M. M., Antifriction and strength characteristics of materials subjected to neutron irradiation, 20: 41498
KRAUSE, D. M., Use of ^{99m}Tc in studying thyroid physiology in mouse, 20: 40547
KRAYBILL, Henry L., Study of six-pronged interactions in π^+p collisions at 7 Bev/c, 20: 41919
KREBS, K. H., Mass spectrometric study on the isotope effect in secondary electron emission from metal surfaces by positive ions, 20: 41620 (NIJS-R-471)
KREHBIEL, H., Small angle electron proton elastic scattering cross sections for momentum transfers between 10 and 105 f^{-2}, 20: 41791 (DESY-66/20)
KREINDEL', Yu. E., Extraction of electrons from modified Penning discharge, 20: 42507
KRETSCHMER, R.-G., Ionospheric absorption during solar eclipse on February 15, 1961. I., 20: 42051
KRIEGER, Herman L., Radionuclide analysis of environmental samples, 20: 40809 (NP-16235)
KRIER, C. A., Oxidation studies of complex silicides for protective coatings, 20: 41424
KRISHNAMURTHY, T. M., Uptake of radionuclides by marine invertebrates from the west coast of India, 20: 40528
KRISTOFOVICH, B. G., Experiments with an MHD generator model, 20: 41755
KRITSKAYA, V. K., Displacements of atoms in alpha phase of neutron-bombarded carbon steel, 20: 41497
KRIVOKHATSKAYA, I. V., Radioactive isotopes in chemical research, 20: 41027
KRIVSKII, I. Yu., Principle of microcausality and "lack of remote action" in elementary particle theory, 20: 42014
KRIZHANSKII, L. M., Decay of the isotope ^{180}Os, 20: 42284
KROLIKOWSKI, W., Partial conservation of tensor current and electromagnetic form factors, 20: 41952
KRONGAUZ, V. A., Radiation yield of triplet molecules in radiolysis of benzene, 20: 40961
KRUEGER, W. F., Lethal effects of ^{60}Co on mature White Leghorn chickens, 20: 40693
KRUGER, C. H., Examination of the validity of the SAHA equation in a gas discharge, 20: 41751
KRUGER, Charles H., MHD generator performance prediction including two-dimensional effects and wall leakage, 20: 41739
KRUGER, Paul, Numerical model for hydrologic transport of radioactive aerosols from precipitation to water supplies, 20: 41141
KRUGLOV, S. P., Instrument for determining intensity of gamma radiation, 20: 41284
KUBO, Reijiro, Vertex function and renormalization constant Z_1, 20: 41893
KUCHOWICZ, B., Trajectories of massless particles in superdense stars, 20: 41596
KUHN, A., Recombination losses and influence on energy resolving power of p-i-n detectors, 20: 41283
KUHN, L., Development and use of semiconductor detectors, 20: 41287
KUJAWSKA, Janina, Comparison of measured and calculated doses in

radiation treatment of neoplasmas of head and neck, 20: 41210
KUKULA, F., Determination of tungsten in iron by activation analysis, 20: 40818 (UJV-1368)
KULESHOV, V. P., Investigation of a disintegrating Ar–Cs plasma by the microwave method, 20: 41699
KULINSKI, S., Motion of a charged particle in a coaxial plasma accelerator, 20: 42456
KULLANDER, S., Studies on capture efficiencies of synchro-cyclotrons, 20: 41533 (CERN-66-27)
KUMMER, Martin, Most general Clebsch-Gordan coefficients of the universal covering group of the inhomogeneous Lorentz group, 20: 41944
KUMP, P., Spins of some T = 1 states in ^{26}Al, 20: 42368
KUNARATNAM, N., Hypopituitary dwarfism following radiotherapy for nasopharyngeal carcinoma, 20: 40660
KUNTZE, M., Current generator for precision β spectrometer and measurements of conversion lines, 20: 41354
KURILENKO, A. I., Kinetics of polymerization of unsaturated oligomers with γ-rays by electroconductivity method, 20: 40999
KURODA, K., Experimental study of elastic proton-deuteron scattering at 155-Mev, 20: 42184
KURODA, K., Experimental study of inelastic proton-deuteron scattering at 155 Mev, 20: 42185
KURTZ, N., Contribution to a study of structure of light nuclei by a study of the absorption mechanisms of K$^-$ mesons, 20: 42386
KURZ, Richard J., Comparison of the lifetimes of positive and negative pions, 20: 41891
KUSHNIR, S. Kh., Imperfections produced in dislocation-free Si by fast-neutron irradiation, 20: 42567
KUSHWAHA, Ram S., Effects of partial ionization and pressure on hydromagnetic ionizing waves, 20: 42401 (AD-637854)
KUWATSUKA, Shozo, Synthesis of methylene-^{14}C-dioxyphenyl compounds, 20: 41014
KUZHETSOV, N. P., Separation of XeO_3 and HIO_3 in zirconium phosphate, 20: 41054
KUZIN, A. M., Imitation of post-radiation damage to DNA under influence of extracts from irradiated potato bulbs, 20: 40562
KUZIN, V. I., Absorption spectra of uranium oxides. I., 20: 40916
KUZ'MENKO, G. I., Laboratory and demonstration heavy-particle accelerators, 20: 41545 (AD-631586)
KUZMIN, V. N., Device for measuring median planes of magnetic fields in accelerators, 20: 41553
KUZMINOV, B. D., Fragments in the fission of ^{235}U by thermal and 5, 6, and 7 Mev neutrons, 20: 42297
KUZNETOVA, M. Ye., Decay of ^{152}Tb, 20: 42155 (JINR-P-2762)
KUZNETSOV, N. P., Chromatographic separation of xenon and iodine oxygen compounds, 20: 40851
KUZNETSOV, V. I., Spontaneously fissioning neutron-deficient neptunium isotope with the half-life 60 sec, 20: 42292
KUZNETSOV, V. V., Decay of ^{152}Tb, 20: 42155 (JINR-P-2762)
KUZNETSOVA, A. P., Displacements of atoms in alpha phase of neutron-bombarded carbon steel, 20: 41497
KYKER, G. C., Mechanism of Ce uptake by Saccharomyces cerevisiae, 20: 40560

L

LABBE, J., Electronic instability and phase change of V_3Si-type compounds at low temperatures, 20: 42531
LACHKAR, J., Study of charged products in the reaction ^{9}Be + d at very low energy (100 to 200 kev), 20: 42354
LACINA, J., Equilibrium configuration of rarefied plasma in magnetic mirror systems, 20: 42458
LADENBAUER-BELLIS, I. M., Boron-10, ^{11}B, and ^{6}Li induced reactions of ^{27}Al, 20: 42183
LADYGIN, B. Ya., Composition of products of radiative methanol oxidation, 20: 41004
LA FLEUR, P., Study of metabolism of ^{18}F in dogs and its suitability for bone scanning, 20: 40554
LAFOUCRIERE, J., Application of a graphical method for calculation of $\sigma(\theta)$ of stripping, 20: 42397
LAFOUCRIERE, J., Study of (n,α) reactions by the distorted-wave method, 20: 42391
LAGARDE, M., Dissociation of ^{6}Li by interaction on complex nuclei, 20: 42366
LAGARDERE, M., Elastic scattering of 14 Mev neutrons by K, 20: 42393
LAGERQUIST, R., Motion sensing and its application to Project Wisp, 20: 41224 (EGG-1183-2078)
LAGERQUIST, R. E., Design of shielded source for irradiation of animal populations, 20: 40518 (CEX-63.10)
LALOU, C., Measurement of radioactivity in the sea, 20: 41145
LALOU, C., Radioactivity of plankton and of organic refuse, 20: 41146
LAM, S. H., Stellar winds and the distribution of electrostatic potentials about stars, 20: 41617
LAMBERT, G., Radioactivity of the sea due to natural products and fallout, 20: 41144
LAMBERT, M., Effect of polarization on Ericson fluctuations, 20: 42396
LAMBERT, M., Mechanism of formation of M and R centers, 20: 42562
LAMBERT, M., New color center in irradiated lithium fluoride F$_1$, 20: 42530
LAMOT, G. H., Reactions ^{12}C(α,α) at 51 Mev and ^{14}N(d,α)^{12}C and ^{14}N(d,d) at 28.5 Mev, 20: 42389
LAMOT, G. H., Study of (n,α) reactions by the distorted-wave method, 20: 42391
LANDA, L. M., Radiation optical stability of quartz glass, 20: 41502
LANDE, K., K^0_2 three-body decays and the $|\Delta I| = \frac{1}{2}$ rules, 20: 41855
LANE, N. F., Free-free transitions of electrons in gases, 20: 41626
LANE, William B., Fallout simulant development: sorption reactions of Ce, Cs, Ru, Sr, and Zr–Nb, 20: 41178 (AD-635547)
LANG, H., Energy conversion with liquid metal working fluids in MHD Staustrahlrohr, 20: 41734
LANG, K., Biological effects of irradiated fats, 20: 41391
LANG, K., Nutritional value of irradiated potatoes, 20: 40576
LANG, Walter, Arrangement for detecting the sticking of an armature to a magnet, 20: 42583 (WAPD-Trans-34)
LANGE, D., Random events, pile-up, and summation in a fast-slow coincidence, 20: 41291
LANGE, R. C., Structures of Po and its compounds. I., 20: 41469
LANGEVIN, B., Isothermal transport processes in molten salts binary systems, 20: 40866 (EUR-2954.e)
LANGEVIN, M., Reaction (y,ny′) and (y,py′) on ^{12}C and ^{16}O in the giant resonance region, 20: 42343
LANGMANN, H. J., Reverse current of high-resistivity silicon surface-barrier counters, 20: 41300
LANGPAPE, Reinhart, Power supply installations for future spacecraft, 20: 41514 (AI-Trans-209)
LANSIART, A., Imagery of x and γ rays by gas-filled image intensifier, 20: 41299
LANZL, L. H., Determination of absorbed dose for electron beam therapy, 20: 40741 (ACRH-25, pp 15-23)
LAPIDUS, L. I., Recoil proton polarization in elastic π^--p scattering at 300 Mev and the phase shift analysis of pion-nucleon scattering, 20: 41794 (JINR-E-2860)
LAQUER, H. L., Superconducting contact between lead based and niobium based alloys, 20: 42124
LARSEN, R. S., Design of beam position and charge monitoring circuits for the Stanford two-mile accelerator, 20: 41544 (SLAC-63)
LARSON, R. A., Mimic tool setter, 20: 41079 (RFP-666)
LASH, Edward D., Antioxidant and prooxidant activity in ascites tumors, 20: 40642
LASSILA, K. E., Double poles and nonexponential decays in atomic physics, 20: 41649
LAUBEREAU, P., Tri(cyclopentadienyl)americium(III), 20: 40878
LAUE, H. J., Irradiation effects on the mechanical properties of vanadium-base alloys, 20: 41506
LAUGHLIN, John S., Extension of memorial system for implant dosimetry, 20: 40788
LAUGHLIN, John S., Prog. rpt. on biological and clinical dosimetry, annual, 7/65–6/66, 20: 40746 (NYO-3510-2)
LAUGIER, J. P., Reaction p + ^{9}Be → d + ^{8}Be, 20: 42212
LAUGIER, J. P., Study of the reactions d + ^{7}Li = n + 2α and ^{6}Li + T = n + 2α, 20: 42349
LAURAT, M., Elastic and inelastic scattering of protons by ^{7}Li, 20: 42372
LAURIKAINEN, K. V., One-boson exchange potentials in nucleon-nucleon scattering, 20: 41899
LAURITZEN, T. A., Experimental studies of plutonium and fission product redistribution in fast reactor fuels, 20: 42625 (GEAP-4466)
LAUTZENHEISER, C. E., Prog. rpt. on serviceability of Elk River Reactor pressure vessel, 4–6/66, 20: 42636 (SWRI-1228-4-22)
LAVAL, Guy, Nonlinear process in a finite plasma, 20: 42427
LAVAL, Guy, Origin of electron precipitations in the auroral zones, 20: 42056
LAVROVSKII, K. P., Mechanism of radiation-thermal liquid phase conversions of n-alkanes, 20: 40986
LAWDEN, M. D., Survey of F1 region in summer at solar minimum, 20: 42058
LAWLEY, A., Innovations in electron-beam zone refining of molybdenum, 20: 41434
LAWRENCE, J. H., Thymic and splenic irradiation in treatment of acute lymphatic leukemia, 20: 40720
LAWSON, E. M., Photoproduction of positive pions from helium and hydrogen, 20: 41816
LEACHMAN, R. B., Determination of small widths in the continuum, 20: 42164 (LA-DC-8083)
LEACHMAN, R. B., Direct and compound-nucleus reactions for ^{32}S(d,p)^{33}S at low energies, 20: 42163 (LA-DC-8082)

LEARY, J. A., Large-scale electrorefining of Pu from Ga alloys, 20: 41035 (LA-2758)
LEARY, J. A., Solubilities of selected elements in liquid Pu. VIII., 20: 40868 (LA-3523)
LEBEDEV, S. V., Focusing of an ion beam in the field of a charged current-carrying ring, 20: 42512
LEBEDEV, V. N., Clinical and dosimetric data on personnel operating a 10 Bev synchrophasotron, 20: 41206 (JPRS-36341, pp 10-17)
LEBEDEVA, G. A., Lesions of gastrointestinal tract in chronic radiation sickness caused by multiple x irradiation, 20: 40645
LE BEYEC, Y., Proton reactions with Bi at 100 to 150 Mev, 20: 42196
LEBLOND, C. P., Conference on radioautography in investigating protein synthesis, Montreal, 11/65, 20: 40567
LEBON, G., Perturbation of the critical potential for the elastic scattering of charged particles, 20: 42173
LECCIA, F., Theoretical study of the continuous spectra of gamma rays emitted in nuclear reactions, measurement of mean lives, 20: 42379
LECLANCHE, Y., Theory of magnetic field compression diffusion, surface instabilities, 20: 41090
LECOCQ, A., Determination of fluoride in fluorinated uranium compounds, 20: 40840
LEE, J. K. P., Reaction of $^{7}Li(p,d)^{6}Li$ at 100 Mev proton energy, 20: 42351
LEE, P. K., Kiwi Transient Nuclear Test dose rate survey, 20: 41195 (LA-3519)
LEES, E. A., Design and fabrication of ESADA-VESR Mark III superheat fuel clusters, 20: 42627 (GEAP-5051)
LEFORT, M., Proton reactions with Bi at 100 to 150 Mev, 20: 42196
LEGGE, G. J. F., Gamma decay of i-spin analog resonances in ^{93}Tc and ^{89}Y, 20: 42331
LEGGO, P. J., Radiometric ages of precambrian rocks from northwest division of western Australia, 20: 41159
LEHMANN, Chr., Mechanism of sputtering, 20: 42553
LEHMANN, H., Analytic properties of scattering amplitudes in two variables in general quantum field theory, 20: 41936
LEHNER, G., Maximum magnetic fields obtainable by flux compression, 20: 41082
LEIBFRIED, G., Convergence behavior of the Born series for rearrangement collisions, 20: 41642
LEIPZIGER, Stuart, Nonuniform cooling of heat-generating cylinder or sphere, 20: 41106
LEIRVIK, Raymond M., Fuel pin spacers, 20: 42615
LEITNAKER, J. M., Computer program to calculate high-temperature thermodynamic functions, 20: 40875 (ORNL-TM-1599)
LELLOUCHE, G., Effect of Xe on safety of HFBR, 20: 42672 (BNL-10388)
LELOUP, J., Imagery of x and γ rays by gas-filled image intensifier, 20: 41299
LEMEILLE, C., Reaction $p + {}^{9}Be \rightarrow d + {}^{9}Be$, 20: 42212
LEMEILLE, C., Study of the reactions $d + {}^{7}Li = n + 2\alpha$ and $^{6}Li + T = n + 2\alpha$, 20: 42349
LENARTOWICZ, J., Automatic control-system for samples transport, 20: 41077 (INR-696/I/PL)
LENGYEL, L., Internal resistance and potential drop in MHD generators, 20: 41700
LENIN, S. S., Determination of isotopic composition of U by absorption of α-radiation, 20: 40857
LENY, J. C., Organic coolant for Euratom's ORGEL program, 20: 42623 (EUR-2996.f)
LEON, M., Simple $\pi\pi\rho$ bootstrap model, 20: 41867
LEONARDI, R., Quintuple isospin of mass 16 nuclei, 20: 42344
LEONG, G. F., Recovery from radiation injury in swine, 20: 40605 (AD-635735)
LEONOV, Roal'd Aleksandrovich, Riddle of ball lightning, 20: 42420 (JPRS-36823)
LEONTIC, B. A., Low temperature spark chamber, 20: 41329
LEPETIT, H., Precision and calibration in determination of O by neutrons at 14 Mev, 20: 40846
LEQUEUX, J., Origin of cosmic particles, 20: 41669
LEROUX, B., Study of (n,α) reaction on ^{16}O at 14.9 Mev, 20: 42370
LESSARD, R. J., Study of metabolism of ^{18}F in dogs and its suitability for bone scanning, 20: 40554
LEUPOLD, Rodger L., Radiological health problems associated with operation of neutron generators, 20: 41215
LEVENTHAL, J. S., Use of tritium to measure movement of groundwater toward irrigation wells in Fresno County, California, 20: 41160
LEVI, C., Separation of reaction mechanisms at low energy, 20: 42394
LEVIN, E. M., Liquid immiscibility in the rare earth oxide–boric oxide systems, 20: 40910
LEVIN, F. S., Coupled-equations method for the scattering of identical particles. II., 20: 41870
LEVIN, Iddo, Improvements in or relating to electrolytic dissolution of spent U fuel elements, 20: 41056
LEVIN, V. I., Preparation of carrier free ^{111}Ag, 20: 41023
LEVINSON, C. A., Determination of coefficients of spin and isospin mixtures of an effective nucleon-nucleon force, 20: 42348
LEVITIN, R. Z., Rare earth ferromagnetics and antiferromagnetics, 20: 41483
LEVITSKII, S. M., Nonlinear phenomena in plasma waveguides, 20: 42450
LEVITT, S. H., Complications and late changes following radiation therapy for carcinoma of eyelid and canthi, 20: 40689
LEVITT, Seymour H., High-impedance vacuum tube voltmeter for use in radioisotope laboratory, 20: 41248
LEVITT, Seymour H., Tandem elution of ^{99m}Tc generators, 20: 40754
LEVITZ, N. M., Removal of actinide halides from alumina, 20: 41062
LEVITZ, Norman M., Removal of stainless-steel claddings from nuclear fuel elements, 20: 41060
LEVY, Arnoldo, Is the brain an immunologically privileged site? II., 20: 40643
LEVY-NAHAS, Monique, Finite-dimensional representations of some non-semisimple Lie algebras, 20: 41942
LEWIS, R., π^0 photoproduction at 3.0, 4.0, and 5.0 Bev for baryon four momentum transfers between 0.5 and 4.0 $(Bev/c)^2$, 20: 41798 (MIT-2098-265)
LEYMONIE, C., Prog. rpt. on application of submerged arc welding process to thick plates, 4–6/66, 20: 41450 (EURAEC-1684)
LHUILLIER, M., p-d Angular correlation in the reaction $^{12}C(p,pd)^{10}B$ at 155 Mev, 20: 42361
LI, Chao-wu, Molybdenum–Gd phase diagrams, 20: 41465
LI, Hsun, Effect of Y on high temperature oxidation of Mo, 20: 41421
LIBOFF, Richard L., Dynamics of certain spherical charge distributions, 20: 41517
LIBS, G., Resolution of charge preamplifier, 20: 41298
LIEB, Elliott, Quantum-mechanical extension of the Lebowitz-Penrose theorem on the Van Der Waals theory, 20: 42081
LIEBECQ-HUTTER, S., Premature incorporation of tritiated thymidine after irradiation of fibroblast and myoblast of chicken embryos, 20: 40587
LIEBERMAN, Kenneth W., Determination of Br in terrestrial and extra-terrestrial materials, 20: 40811 (ORO-2670-13)
LIELPETER, Yu. Yu., Applicability of the electrodynamic approximation in the theory of liquid–metal, induction MHD converters, 20: 41701
LIEVENS, F., Determination of fluoride in fluorinated uranium compounds, 20: 40840
LILOVA, O. M., Decay of the isotope ^{180}Os, 20: 42284
LIM, K. L., Distorted wave t-matrix approximation for the (p,2p) reaction, 20: 42215
LINCK, I., Study of the deexcitation of first excited levels of ^{6}He, 20: 42353
LINCK, J., Study of the deexcitation of first excited levels of ^{6}He, 20: 42353
LINDGREN, Nilo, Earthquake or explosion?, 20: 41155
LINDQUIST, P., Effects of orientation and annealing on Jc vs. H in cold-worked Nb-25% Zr, 20: 42569
LINDSAY, Stuart, Radiation therapy in control of persistent thyroid cancer, 20: 40758
LINDSTROM, Olle, Method of increasing the surface area of a boiled liquid and improved nuclear reactors embodying the method, 20: 42602
LINHART, J. G., Plasma and megagauss fields, 20: 42434
LINIECKI, J., Test of the theory of alkaline earth metabolism by behaviour of ^{133}Ba in rats, 20: 40565
LIPINSKI, Andrzej, Gamma-ray scintillation spectrometer with NaI(Tl) single crystal, 20: 41336
LIPINSKI, Andrzej, Measurement of efficiency of liquid scintillation counters of large area, 20: 41339
LIPINSKI, Andrzej, Measurement of the dose rate of unknown γ-radioactive substances, 20: 41025
LIPINSKI, Andrzej, Two-impulse neutron detector with plastic scintillator, 20: 41337
LIPINSKII, A., Detector of fast neutrons with a moderator, 20: 41335
LIPPERT, W., Contribution of ionospheric F region to cosmic noise absorption, 20: 42048
LIPPERT, W., Ionospheric absorption of short waves during solar eclipse February 15, 1961. III., 20: 42053
LIPTAK, Yu., Decay of ^{184}Re, 20: 42157 (JINR-P-2814)
LIPTAK, Yu., Decay mode of ^{160}Ho, 20: 42158 (JINR-P-2817)
LIPTON, James M., Locomotor behavior and neuromorphologic anomalies in prenatally and postnatally irradiated rats, 20: 40688
LITTLE, R., Photoproduction of positive pions from helium and hydrogen, 20: 41816
LITTLE, W. W. Jr., K-III: three region kinetics code in FORTRAN-IV, 20: 42606 (BNWL-252)
LITTLE, W. W. Jr., Neutronics characteristics of possible driver fuels for the Fast Test Reactor, 20: 42676 (BNWL-281)
LITVAK, A. G., Electromagnetic wave self-focusing in isotropic plasma, 20: 42449
LIU, Chung-Heng, Spin exchange between the singly ionized Xe^+ ground state and the metastable state of neutral Xe, 20: 41650

LIU, Y. S., Covariant density matrices for arbitrary spins, 20: 41960
LIVADAS, D., Minimum dose of potassium iodide which inhibits thyroidal radioiodine uptake, 20: 40564
LIVEY, D. T., Observations on the strength and Young's modulus of BeO as a function of density and grain size, 20: 41473
LIVINGSTON, Ralph, ESR technique as applied to radiation-produced radicals, 20: 42433
LLOYD, Albert Ivor, Improvements in or relating to liquid moderated nuclear reactors, 20: 42595
LLOYD, James Elgie, Improvements in or relating to preparation of uranium tetrafluoride, 20: 40935
LOBAR, W., Search for fractionally charged, weakly interacting particles, 20: 41797 (MIT-2098-264)
LOBKOWICZ, F., Precise measurement of the K^+/K^- and π^+/π^- lifetime ratios, 20: 41884
LOCKWOOD, Harold E., Photo-optical instrumentation at Nuclear Rocket Development Station, 20: 41223 (EGG-1183-1244)
LOEB, Julien, Coupling between h-f cavities and position of protons in synchrotron, 20: 41547
LOEBENSTEIN, H. M., Lithium-6(^{12}C,d)^{16}O reaction at E_{CM} = 7 Mev, 20: 42329
LOEFFLER, A. L. Jr., Experimental investigation of MHD channel flows at high Hartmann and Reynolds numbers, 20: 41707
LOEFFLER, Helmut, Measurement of gas velocities by radistion-modulation technique, 20: 41381
LOETZSCH, W., Application of neutron-capture γ spectroscopy for analytical purposes, 20: 41166
LOGAN, R. K., Analysis of the reaction $\pi^- + p \rightarrow \eta + n$ near threshold, 20: 41871
LOGUNOV, A. A., Asymptotic relations between the scattering amplitudes in local field theory, 20: 42015
LOISEAUX, J. M., Reaction $(\gamma,n\gamma')$ and $(\gamma,p\gamma')$ on ^{12}C and ^{16}O in the giant resonance region, 20: 42343
LOKEN, Merle K., Colloidal albumin ^{131}I as an agent for scanning liver and spleen, 20: 40777
LOKEN, Merle K., Visualization of lung by methods of scintiphotography, 20: 40749
LOMSADZE, Yu. M., Principle of microcausality and "lack of remote action" in elementary particle theory, 20: 42014
LONCKE, P., Isospin quintuplets in A = 20 nuclei, 20: 42227
LONCKE, P., Quintuple isospin of mass 16 nuclei, 20: 42344
LONERGAN, J. A., Angular distributions of α-particles from the reaction ^{11}B(^{3}He,α)^{10}B, 20: 42217
LONG, D. D., Coulomb displacement energies from isobaric analogue resonances, 20: 42262
LONGEQUEUE, J. P., Study of (d,p) reactions on light nuclei at low energy, 20: 42399
LONGEQUEUE, N., Study of (d,p) reactions on light nuclei at low energy, 20: 42399
LONGHURST, William M., Prog. rpt. on ^{90}Sr and ^{137}Cs food chain relationships to deer and sheep, 9/65–6/66, 20: 40541 (UCD-34P104-3)
LONGWORTH, Geoffrey, Measurement of magnetic field distributions, 20: 42571
LONGWORTH, J. W., Electron spin resonance of irradiated deoxyribonucleic acid, 20: 40594
LONNGREN, K. E., Energy relation for acoustic modes in a plasma, 20: 42479
LOPATIN, I. V., Instrument for determining intensity of gamma radiation, 20: 41284
LO SURDO, C., Current distribution in a Faraday-type segmented-electrode generator, 20: 41759
LOT, Fernand, Heavy ion accelerator of the Orsay nuclear physics laboratory, 20: 41563
LOTH, J. L., Velocity and density probe for steady nonequilibrium, supersonic flow, 20: 41702
LOUIS, Jean F., Studies on an alkali shock tube and on an MHD generator wind tunnel, 20: 41703
LOVE, L. O., Preparation of charge materials for ORNL electromagnetic isotope separators, 20: 41400 (ORNL-3301(Suppl.1))
LOVE, L. O., Review of ORNL electromagnetic separations program, 1965, 20: 41401 (ORNL-4006)
LOVE, W. G., Multiple excitation and the shell model description of the ^{90}Zr(p,p') reaction, 20: 42229
LOWE, J., 6.92- to 6.05-Mev E2 transition in ^{16}O, 20: 42232
LOWRY, R. E., Radiation-induced polymerization of hexafluoropropylene at high temperature and pressure, 20: 40976
LOZANO, L., Prospects for the utilization of chemical ionization phenomena in MHD, 20: 41730
LU, C. C., Excited states in ^{6}Be and ^{10}C, 20: 42190
LUCAS, A. C., Design of shielded source for irradiation of animal populations, 20: 40518 (CEX-63.10)
LUCAS, John C. Jr., Does prophylactic radiotherapy given for cancer of breast predispose to metastasis?, 20: 40793
LUCAS, Mary B., New radioprotector in E. coli, 20: 40737
LUCASSON, A., Experimental results obtained in low temperature electron irradiation of Pd, Mo, Zn, and α–U, 20: 41499
LUCASSON, P., Experimental results obtained in low temperature electron irradiation of Pd, Mo, Zn, and α–U, 20: 41499
LUCKEY, D., π^0 photoproduction at 3.0, 4.0, and 5.0 Bev for baryon four momentum transfers between 0.5 and 4.0 (Bev/c)^2, 20: 41798 (MIT-2098-265)
LUCKS, Herbert, Measurement of beam profiles with thermoluminescent dosimeters, 20: 41530 (ANL-7196)
LUKASIK, S. J., Magnetic-flux compression in explosion geometry, 20: 41093
LUNDIN, A. G., Anisotropy of magnetic resonance of ^{19}F in LaF_3, 20: 42528
LUNDIN, A. G., Nuclear magnetic resonance and electron structure of U, Th, and Zr, 20: 40931
LUNDQUIST, J. R., Chlorine recovery and radioiodine behavior in salt cycle process, 20: 41029 (BNWL-279)
LUO, H. L., Superconductivity of LaAg, 20: 42101
LUPPI, R., Faraday rotation in megagauss fields, 20: 41515
LUPPI, R., Magnetic field and current amplification with non-cylindrical explosive systems, 20: 41091
LVOV, V. V., Isotopic spectral analysis of He with use of isotopic filler, 20: 40861
L'VOVSKAYA, E. N., Clinical and dosimetric data on personnel operating a 10 Bev synchrophasotron, 20: 41206 (JPRS-36341, pp 10-17)
LYUBIMOV, G. A., Averaging magnetohydrodynamic flows and the applicability of the hydraulic approximation for calculating magnetohydrodynamic flow in ducts, 20: 41704
LYUBOSHITS, V. L., Spontaneous polarization of neutrons in magnetic and electric fields, 20: 41902

M

MAAS, Jean, Study of pigs subjected to lethal dose of integral γ irradiation, 20: 40608 (CEA-R-3001)
MACAGNO, E. R., Detailed analysis of muonic x-ray spectrum from strongly deformed e-e nuclei, 20: 42310
MACDONALD, Burns, Comparison of the lifetimes of positive and negative pions, 20: 41891
MAC GREGOR, A., Energy level structure of Cr isotopes, 20: 42211
MACHIROUX, R., Radiochromatography in gas phase, 20: 41019
MACIULAITIS, A., Experimental investigation of MHD channel flows at high Hartmann and Reynolds numbers, 20: 41707
MACKE, W., Variational principle in describing a many-particle system, 20: 42074
MAC KEOWN, P. K., Measurements of the charge ratio of cosmic-ray muons, 20: 41677
MACQ, P. C., Scattering of alpha particles on ^{9}Be, ^{32}S, and ^{31}P, 20: 42392
MADDOCK, Charlotte L., Effect of radiation and actinomycin D therapy on incompletely removed mouse tumors, 20: 40762
MADSHUS, Kjell, Cesium-137 in milk in Norway 1962–1966, 20: 41132 (NYO-3364-20)
MAGEE, John L., Charge recombination in gamma-irradiated alkane glasses, 20: 40970
MAGGIO, F., Nature and stability of system uranyl-benzohydroxamic acid in acid medium, 20: 40903
MAGLIONE, Anthony A., Advantage of three combined diagnostic procedures with ^{131}I for evaluation of thyroid disorders, 20: 40756
MAGNAC-VALETTE, D., Angular distributions of (t,α_0) reactions on Li, B, C, and O, 20: 42398
MAGNAC-VALETTE, D., States $^2P_{3/2}$ and $^2P_{1/2}$ of ^{5}He, 20: 42357
MAGNAC-VALETTE, D., Study of the deexcitation of first excited levels of ^{6}He, 20: 42353
MAGNERON, P., Improvement of signal-to-noise ratio, 20: 41305
MAGUIN, C., Study of the reaction (d,p) with total interaction in the excursion method, 20: 42387
MAHANTA, P., Baryon resonance decays in broken $U_3 \times U_3$, 20: 41843
MAHER, C. T., Detection of Ag in rainwater, 20: 40838
MAIANI, L., Saturation of the SU_6 algebra and a possible classification group for hadrons, 20: 41968
MAIDANYUK, V., Decay of ^{184}Re, 20: 42157 (JINR-P-2814)
MAIER, B. P., Study of ^{46}Sc levels by means of neutron capture gammas, 20: 42382
MAIER-BORST, W., Preparation of ^{99m}Tc labeled human serum albumin, 20: 40944
MAISON, J. M., Reaction $(\gamma,n\gamma')$ and $(\gamma,p\gamma')$ on ^{12}C and ^{16}O in the giant resonance region, 20: 42343
MAITA, J. P., Superconductivity and electronic specific heat in the Sc–Zr system, 20: 42121
MAITRA, S. C., Stationary dust-filled cosmological solution with $\Lambda = 0$ and without closed timelike lines, 20: 41599

MAJEROTTO, W., Spinor calculus in Riemannian manifolds, 20: 42079
MAJLING, L., Specific features of the photodisintegration of nuclei in the 1f-2p shell, 20: 42220
MAJUMDAR, Chanchal K., Effective mass of the positron in sodium, 20: 41853
MAKAROV, A. A., Structure of vector and axial currents in broken Ū(12) symmetry, 20: 41939
MAKAROVA, T. P., Electromigration method for studying complex formation of trivalent Pu in ethylenediaminetetraacetic acid solutions, 20: 40912
MAKAROVA, T. P., Electromigration method for studying complex Am(III) oxalates, 20: 40913
MAKSUMOV, M. N., Critical wavelength in the system of a collisionless gas and solid medium in a homogeneous magnetic field, 20: 42041
MALANIFY, J. J., Large-angle neutron-proton C_{NN} parameter at 23.1 Mev, 20: 41877
MALECKI, H., Detector of fast neutrons with a moderator, 20: 41335
MALECKI, Henryk, Gamma-ray scintillation spectrometer with NaI(Tl) single crystal, 20: 41336
MALHOTRA, P. K., Inelastic π^{+}-^{4}He reactions in the momentum range 100–160 Mev/c, 20: 42321
MALHOTRA, P. K., Phase shift analysis for elastic π^{+}-^{4}He scattering in the energy interval 100–160 Mev/c, 20: 42320
MALIKOV, M. M., Investigation of an electrical discharge in a magnetic field in the presence of a flow of gas, 20: 41770
MALININ, A. B., Preparation of carrier free ^{111}Ag, 20: 41023
MALITSON, Irving H., Effects of space radiations on refractive properties of optical glasses, 20: 41505
MALKES, L. Ya., Plastic scintillator with light yield proportional to the energy of outer electrons, 20: 41346
MALKINSON, Frederick D., Modification of radiation response of tissue by colchicine, 20: 40763
MAL'KOV, V. V., Attenuation of high-energy neutron fluxes in heterogeneous shielding, 20: 42517
MALLIARIS, A. C., Alteration of the decay constant of ^{125m}Te by chemical means, 20: 42266
MALLORY, Kenneth B., Electron linear accelerator phasing method, 20: 41582
MALMSKOG, S. G., Possible odd parity state of ^{128}Xe, 20: 42147 (AE-240)
MALOV, L. A., Structure of the ground and excited states of deformed odd-mass nuclei in the actinide region, 20: 42154 (JINR-E-2857)
MALYSHEV, G. M., Temperature and electron concentration in plasma arc from Thomson scattering, 20: 42432
MANAKA, Kazuo, Porcelain tubes, 20: 41579
MANDEL, L., Photon statistics and classical fields, 20: 41971
MANDL, Anita M., Population of germ cells in immature male rats following irradiation at birth, 20: 40682
MANDL, Anita M., Ultrastructure of male germ cells in rats x irradiated at birth, 20: 40683
MANDL, F., Electron resonances of the H_2^- ion, 20: 41656
MANDL, F., Vibrational excitation and dissociative attachment in the scattering of electrons by hydrogen molecules, 20: 41657
MANGELSDORF, D., Fluorescence lifetimes of hydrated salts of europium and terbium, 20: 42539
MANGELSON, N., Excited states in ^{6}Be and ^{10}C, 20: 42190
MANGIARACINA, A., Index of ^{85}Sr uptake in leg fractures, 20: 40542
MANI, G. S., Absolute cross sections for elastic scattering of deuterons on α particles between 3 and 14 Mev, 20: 42371
MANI, G. S., Absolute cross sections of the reactions ^{12}C(p,p)^{12}C, ^{12}C(p,p′)^{12}C*, ^{12}C(p,p″)^{12}C*, and levels of ^{15}N, 20: 42390
MANN, A. K., K_2^0 three-body decays and the $|\Delta I| = \frac{1}{2}$ rules, 20: 41855
MANN, B., Photoproduction of charged pions from helium and hydrogen, 20: 41817
MANTEL, Joseph, Automatic electron dosimetry system for a microwave linear accelerator, 20: 41323
MANUS, C., Contribution to a study of inelastic interactions between two ion beams, 20: 41666
MANUSHEV, B., Iron-free asymmetric two-lens β spectrometer, 20: 41282
MANZ, A., Angular distribution of mesons from nucleon collisions at 20 Bev/c, 20: 41829
MARANS, N. S., Solid-state polymerization of diacetone acrylamide, 20: 40980
MARCH, R. H., Measurement of the K_S^0–K_L^0 mass difference by the time dependence of strangeness, 20: 41922
MARCOWITZ, Stewart M., Measurement of beam profiles with thermoluminescent dosimeters, 20: 41530 (ANL-7196)
MARECEK, J., Determination of lanthanides in U by activation analysis, 20: 40832
MAREI, A. N., Movement of ^{90}Sr from fresh water bodies into the human organism, 20: 41142
MARGOLIS, S. G., FLASH, program for digital simulation of loss of coolant accident, 20: 42582 (WAPD-TM-534)
MARIC, Stjepan, Determination of ^{85}Sr, ^{106}Ru, ^{137}Cs, and ^{144}Ce by γ-spectroscopy, 20: 40837
MARINOV, M. S., Relativistic scattering of electrons on nuclei with arbitrary spins, 20: 41907
MARION, J. B., Peak-to-total ratios and efficiencies for NaI crystal, 20: 41307
MARION, Jerry B., Low voltage D-T neutron source, 20: 42136 (AD-637457)
MARION, Jerry B., ^{14}N(p,γ)^{15}O reaction, 20: 42258
MARK, S. K., Charged particle identification system using fast multiplier, 20: 41243
MARK, S. K., Reaction of ^{7}Li(p,d)^{6}Li at 100 Mev proton energy, 20: 42351
MARKER, D., P-p bremsstrahlung calculations, 20: 41921
MARKOV, B. N., Spontaneously fissionable isomer with the half-life equal to 10^{-7} s, 20: 42159 (JINR-P-2841)
MARKOVSKII, E. A., Antifriction and strength characteristics of materials subjected to neutron irradiation, 20: 41498
MARPLES, J. A. C., Two crystallographic computer programs for lattice parameter refinement and for calculating expected line positions, 20: 41437 (AERE-R-5210)
MARQUERINCK, J. E., X-ray television using plumbicon, 20: 40781
MARQUEZ, L., Reaction p + ^{9}Be → d + ^{8}Be, 20: 42212
MARQUEZ, L., Study of the reactions d + ^{7}Li = n + 2α and ^{6}Li + T = n + 2α, 20: 42349
MARSEL, J., Mass spectrometric study on the isotope effect in secondary electron emission from metal surfaces by positive ions, 20: 41620 (NIJS-R-471)
MARSHALL, S. J., Some experiments related to explosive driven MHD converters, 20: 41686
MARSHALL, S. W., Moessbauer effect in Au microcrystals, 20: 42572
MARSHALL, Wilton R., System for determining fluid flow rate in boreholes, 20: 41170
MARTIN, A., Extension of the axiomatic analyticity domain of scattering amplitudes by unitarity. II., 20: 41841
MARTIN, J. F., Thermodynamic properties of U compounds. II., 20: 40921
MARTIN, R. J., Synthesis of ^{14}C-labeled bipyridylium salts, 20: 40941
MARTIN, Shell E., Current and proposed Manned Spacecraft Center radiation safety program, 20: 41219
MARTINET, A., Superimposed normal and superconducting films. I., 20: 42109
MARTY, N., Elastic scattering of protons of 150 to 80 Mev on light nuclei and the optical potential, 20: 42388
MARTY, N., Polarization of protons of 152 Mev by inelastic scattering on ^{12}C and ^{40}Ca, 20: 42341
MARUYAMA, Masuo, Porcelain tubes, 20: 41579
MASAIKE, A., Pressurized discharge chamber, 20: 41294
MASEK, Tommy D., Plasma characteristics of electron bombardment ion engine, 20: 41123
MASHIREV, V. P., Thermodynamic properties of inorganic substances (handbook), 20: 41417
MASHOVETS, T. V., Low-temperature γ irradiation and tempering of InSb, 20: 42527
MASLENNIKOV, E. A., Vacuum system of Ogra-II, 20: 42421 (NP-tr-1396)
MASLENNIKOV, N. M., Experimental investigation of plasma using model MHD generators, 20: 41708
MASON, H. C., Acute effects of x-radiation upon mouse electrocardiogram, 20: 40648
MASSA, D., Radiation inactivation of foot and mouth disease virus, 20: 41392
MASSET, M., Effect of irrigation on absorption and localization of Cs and Sr in Oryza sativa L., 20: 40574
MASSOT, J. N., Application of a graphical method for calculation of $\sigma(\theta)$ of stripping, 20: 42397
MASSOT, J. N., Study of (n,α) reactions by the distorted-wave method, 20: 42391
MAST, C., Application of the SU(3) shell model to ^{9}Be, 20: 42191
MASTALKA, A., Determination of lanthanides in U by activation analysis, 20: 40832
MATHUR, V. S., CP violation and the neutral kaon complex, 20: 41849
MATOBA, T., Preparation and test of MHD duct wall and electrode materials, 20: 41718
MATOSIC, Miloje, Influence of x-irradiation on experimental allergic encephalomyelitis in rats, 20: 40728
MATSUBARA, S., Experimental study of physical properties of combustion gas, 20: 41758
MATSUDA, Satoshi, Sum rules for form factors of pseudoscalar hadron densities, 20: 41995
MATSUMOTO, W. Y., Evaluation of accuracy of decay scheme constants and calibration standards for ^{137}Cs, 20: 42148 (BNWL-87)
MATSUMURA, Go, Depolymerization of hyaluronic acid by autoxidants and radiations, 20: 40591
MATSUMURA, Hideaki, Studies on bone marrow transplantation for hematopoietic disturbance, 20: 40726

MATSUNAGA, S., MHD power generation experiments with K-seeded Ar plasmas, 20: 41781
MATSUOKA, Yoshito, Generalized and multiple eruptions during ^{60}Co radiotherapy of female genital cancer, 20: 40679
MATSUSHIMA, Satoshi, Apparent correlation between the lunar eclipse brightness and the solar wind, 20: 41604
MATSUSHITA, S., Study of blanketing sporadic E, 20: 42070
MATSUURA, Kenya, Excitation of ion plasma oscillation by electron beams, 20: 42429
MATSUZAKI, Isao, Hydrogen exchange between hydrogen, ethylene, or ethane during catalyzed hydrogenation of ethylene, 20: 40942
MATTHES, F., Differential thermal analysis of oxalate hydrates of rare earth metals, 20: 40900
MATTHIAS, E., Numerical analysis of the time spectrum of delayed coincidences. I., 20: 41301
MATTIOLI, M., Thermal bremsstrahlung from inhomogeneous plasma, 20: 42457
MATTSON, R., Improving routine measurements of artificial beta activity in air, 20: 41137
MATTSSON, Arne C. J., Self-excited MHD generators, 20: 41709
MATUMOTO, Ken-iti, Structure of baryons, 20: 42003
MATUMOTO, Ken-iti, Sub-hadronic and hadronic dynamics, 20: 42004
MATUSEVICH, E. S., Cascade nucleons emitted by nuclei interacting with 660 Mev protons, 20: 42299
MATVEEV, V. A., Dispersion sum rules for strong and electromagnetic interactions, 20: 41793 (JINR-E-2822)
MATVIENKO, V. I., Mechanism for increasing low-temperature sensitivity of nuclear photographic emulsions, 20: 41341
MATYUSHENKO, N. I., Morphology and texture of molybdenum and tungsten carbonyl deposits, 20: 41468
MAUNDERS, E. J., Improving accuracy of ^{240}Pu resonance escape probability measurements using Ir, 20: 42137 (AEEW-M-661)
MAURO, S., Superimposed normal and superconducting films. I., 20: 42109
MAXON, M. Stephen, Lehmann-Symanik-Zimmermann formalism in the Lee model (V-θ sector), 20: 41986
MAYBERRY, B. D., Prog. rpt. on differential absorption of Sr by plants, final, 3/66, 20: 40537 (TID-23052)
MAYEDA, T. K., Origin of saline formation waters. I., 20: 41161
MAZLOUM, F., Study of (p,2p) reaction at 155 Mev on ^{7}Li, ^{9}Be, and ^{23}Na with an on-line computer, 20: 42360
MAZUR, N. I., Experiments with an MHD generator model, 20: 41755
MAZUR, N. I., Investigation of phenomena at the cathode of an open-cycle MHD generator, 20: 41756
MAZUR, P., Inelastic $\pi^{+,-}$4He reactions in the momentum range 100–160 Mev/c, 20: 42321
MC AFEE, J. G., Scintillation scanning with an 8-inch diameter Na iodide (Tl) crystal, 20: 40779
MC CABE, Terence Ivor, Improvements in gas-cooled nuclear reactors, 20: 42604
MC CALL, J. R., Phase-space integrals and invariant-mass distributions with Monte Carlo techniques, 20: 41953
MC CALL, Richard C., Electron-induced cascade showers in Cu and Pb at 1 Bev, 20: 41671
MC CARTHY, I. E., Distorted wave t-matrix approximation for the (p,2p) reaction, 20: 42215
MC CASLIN, Joseph B., Developments in technique for monitoring high-energy accelerator radiation, 20: 41276 (UCRL-16769)
MC CAULEY, James E., Prog. rpt. on ecological studies of radioactivity in Columbia River and adjacent Pacific Ocean, annual, 7/65–6/66, 20: 40523 (RLO-1750-8(Vol.I))
MC CLENAHAN, Donald L., Gamma radiation effects on magnet wire, 20: 41503
MC CLINTOCK, R. O., Design, test, and use of reactor bypass filter facility, 20: 42673 (BNL-10483)
MC COLM, Douglas, Design of atomic and molecular beam resonance apparatus employing two-pole state selectors, 20: 41250
MC COY, H. E., Creep-rupture properties of tungsten and tungsten-base alloys, 20: 41456 (ORNL-3992)
MC CULLOCH, E. A., Improved method for radioautography of erythropoietic cells labeled with ^{55}Fe or ^{59}Fe, 20: 40675
MC CULLOCH, P. M., Frequency splitting of solar radio bursts, 20: 41606
MC DERMED, O. L., Transmission of isotropically incident electrons through spacecraft hull materials, 20: 42520
MC DICKEN, W. N., Reactions ^{20}Ne(n,α)^{17}O and ^{16}O(n,α)^{13}C at 14 Mev, 20: 42216
MC DOWELL, M. R. C., Electron-impact-induced $n \rightarrow n^1$ transitions in H atoms, 20: 41655
MC DOWELL, M. R. C., Impact parameter treatment of the excitation of atoms by charged particles, 20: 41654
MC ELROY, J. M., Small angle electron proton elastic scattering cross sections for momentum transfers between 10 and 105 f^{-2}, 20: 41791 (DESY-66/20)
MC ENVOY, J. P., Shielding properties of the superconducting surface sheath, 20: 42127
MC EWAN, A. C., Scattered radiation from a cuboid phantom, 20: 41211
MC GOWAN, F. K., Collective nuclear structure in the even-even samarium isotopes, 20: 42265
MC GUIRE, R., Prog. rpt. on transient radiation effects, optical, 8/65, 20: 41492 (EGG-1183-2039)
MC GUIRE, R. L., Prog. rpt. on transient radiation effects in electronic materials, 10/65, 20: 41493 (EGG-1183-2052)
MC HENRY, J. Roger, Two-probe nuclear device for determining the density of sediments, 20: 41156
MC HORSE, T. S., Use of ^{99m}Tc in studying thyroid physiology in mouse, 20: 40547
MC HUGH, James A., Independent yields of ^{86}Rb, ^{132}Cs, ^{134}Cs, and ^{136}Cs in the thermal neutron fission of ^{235}U, 20: 42178
MC KEE, H. B., Electrostatic probes for diagnostics in a collision-dominated weakly ionized plasma, 20: 41705
MC KEE, R. J., Effects of nuclear structure in mu-atomic spectra, 20: 42305
MC KELVEY, J. P., Flux methods for transport problems in solids with nonconstant electric fields, 20: 42546
MC KINNON, C. N. Jr., Explosive driven linear MHD generators, 20: 41685
MC KINNON, C. N. Jr., Pulsed electrical power generation from magnetically loaded explosives, 20: 41687
MC MULLEN, James M., Radiation gauging system with compensation for high background radiation intensities, 20: 41365
MC MURRY, H. L., Model for calculating the slow neutron scattering by liquid D_2O, 20: 42139 (IN-1020)
MC MURRY, H. L., Slow neutron scattering kernels for H_2O at 423°K and 550°K, 20: 42138 (IN-1019)
MC NALLY, J. H., Reactions leading to ^{37}Ar and ^{37}K energy levels, 20: 42200
MC NARY, Charles A., Brayton cycle magnetohydrodynamic power generation, 20: 41706
MC NAUGHTON, G. S., Radiation chemistry of liquid hydrogen sulfide, 20: 40997
MC NEIL, K. G., Valley-to-peak ratios for zero-thickness sources, 20: 41312
MC NEILL, Daniel, Radiation cataract analysis and its uses in experimental fractionation, 20: 40690
MC TAGGART, M. H., Uranium-fueled VERA reactor experiments, 20: 42671 (AWRE-R-5/66)
MEAD, J. B., Evidence for the presence of alpha clusters in the boron isotopes, 20: 42193
MECHL, Z., Combined treatment of tumors of oto-rhino-laryngeal region by methotrexate and irradiation, 20: 40782
MEDIN, S. A., Plasma flow in the duct of a series-flow MHD generator, 20: 41698
MEEM, J. L., Correlation of two-group theory with neutron flux measurements in a pool-type reactor, 20: 42600
MEENTS, W. F., Origin of saline formation waters. I., 20: 41161
MEGRUE, G. H., Rare-gas chronology of calcium-rich achondrites, 20: 41162
MEHTA, M. K., Fluctuation analysis of ^{27}Al(p,α_0)^{24}Mg and ^{27}Al(p,p$_3$)^{27}Al* cross sections, 20: 42324
MEHTA, M. K., Study of the ^{13}C(α,n)^{16}O reaction, 20: 42336
MEHTA, M. M., Effect of complexing agents on the disproportionation of U(V), 20: 40911
MEISNER, Gerald W., Sign of the K_1^0–K_2^0 mass difference, 20: 41878
MELIKOV, Yu. V., Reaction ^{12}C(α,α')^{12}*C(9.64 Mev) → 3 α, 20: 42296
MELISSINOS, A. C., Precise measurement of the K^+/K^- and π^+/π^- lifetime ratios, 20: 41884
MELTZER, David W., Catalog of methods for studying the normal modes of radial pulsation of general-relativistic stellar models, 20: 41588
MELTZER, David W., Normal modes of radial pulsation of stars at the end point of thermonuclear evolution, 20: 41589
MENES, J., Design and performance of on-line wire spark chamber spectrometer, 20: 41297
MENLOVE, H. O., Fast neutron cross sections for the ^{23}Na(n,γ)^{24}Na, ^{55}Mn(n,γ)^{56}Mn, ^{115}In(n,γ)^{116m}In, and ^{165}Ho(n,γ)^{166}Ho reactions, 20: 42332
MENNRATH, P., Theoretical study of the continuous spectra of gamma rays emitted in nuclear reactions, measurement of mean lives, 20: 42379
MEREDITH, W. J., Radiation cataract: new evidence on radiation dosage to lens, 20: 40771
MERMAZ, M., Separation of reaction mechanisms at low energy, 20: 42394
MERRIAM, George R. Jr., Radiation cataract analysis and its uses in experimental fractionation, 20: 40690
MESSIAEN, A. M., High-frequency effect due to the axial drift velocity of a plasma column, 20: 42471
MESSIAH, A. M. L., Theoretical basis of the symmetrization postulate, 20: 42093
MESTEL, L., Magnetic field of contracting gas cloud. I., 20: 41602

METZ, D. J., Gamma-radiation-induced ionic polymerization of pure liquid styrene. II., 20: 40978
MEUNIER, F., Superimposed normal and superconducting films. I., 20: 42109
MEYER, Helen Unger, Evidence demonstrating germinal selection in early premeiotic germ cells of Drosophila males, 20: 40670
MEYER, O., Reverse current of high-resistivity silicon surface-barrier counters, 20: 41300
MEYER, P., Prog. rpt. on pulsed neutron application to power reactor start-up procedures, 1–3/66, 20: 42628 (GEAP-5145)
MEYER, Ph., Derivation of sum rules from the equal-time commutation relations for the space components of current densities, 20: 41958
MEYER-BERKHOUT, U., Small angle electron proton elastic scattering cross sections for momentum transfers between 10 and 105 f^{-2}, 20: 41791 (DESY-66/20)
MIA, M. M., Use of gamma radiation in jute breeding, 20: 40681
MICHAELIS, A., Chelate formation as sensitizing factor in production of chromatid aberrations by radiomimetic agents, 20: 40715
MICHAELIS, M., Interferometer for three wavelengths: 2.5 mm, 4 mm, and 8 mm, 20: 42408 (IPP-2/49)
MICHAELSON, S. M., Leukocyte response following simultaneous ionizing and microwave irradiation, 20: 40650
MICHAELSON, Sol, X-ray induced hypothyroidism in dog, 20: 40698
MICHALOWICZ, A., Experimental study of elastic proton-deuteron scattering at 155-Mev, 20: 42184
MICHALOWICZ, A., Experimental study of inelastic proton-deuteron scattering at 155 Mev, 20: 42185
MICHEL, G., Stripping features of $^{6}Li(d,n)^{7}Be^{*}$ (0.43 Mev) at E_d from 0.2 to 0.8 Mev, 20: 42210
MICHON, G., Biological concentration factors in marine media, 20: 40546
MICKLEM, H. S., Interrelationships of myeloid and lymphoid cells in lethally irradiated mice, 20: 40727
MIDDELKOOP, W. C., Mass spectra of recoil nucleon states from inelastic ρ^0 production by pions of 12 and 18 Bev/c, 20: 41828
MIELNIKOWA, S. K., Imitation of post-radiation damage to DNA under influence of extracts from irradiated potato bulbs, 20: 40562
MIHELICH, J. W., Directional correlation measurements in decay of ^{160}Tb employing a Ge–Li detector, 20: 42150 (COO-498-56)
MIKHAILOVSKII, A. B., Convective excitation of ionic oscillations of a plasma by a nonuniform electron beam, 20: 42494
MIKHAILOVSKII, A. B., Convective effects in excitation of electronic oscillations in plasma, 20: 42495
MIKI, Kyosuke, Dynamic mechanical properties of polyoxymethylene. I., 20: 41500
MILANI, S., Uranium-233 thorium seed-blanket experimental program, 20: 42609 (WAPD-T-1886)
MILBERG, M. E., Continuous averaging technique for avoiding drift effects in x-ray scattering measurements, 20: 41327
MILDE, Helmut, Electrodeless conductivity measurements within the reaction zone of a combustion chamber, 20: 41710
MILEWSKI, J., Striated flow in the induction synchronous magnetogasdynamic generator, 20: 41711
MILLER, David B., R-f propagation and absorption measurements in magnetoplasma near electron cyclotron resonance, 20: 42439
MILLER, O. A., Radiolysis of ortho- and meta-terphenyl. II., 20: 40946 (AECL-2589)
MILLER, Richard G., Decay of the first $T = \frac{3}{2}$ state in ^{13}C, 20: 42330
MILLER, T. G., Diamond as a neutron scintillation counter, 20: 41290
MILTON, J. C. D., Prompt fission neutrons, 20: 42325
MINACHEV, Kh. M., Dehydrogenating characteristics of Al oxide–Cr oxide catalysts, 20: 40943
MINARIK, E. V., Isospin amplitudes for S-state pion photoproduction on nucleons, 20: 41906
MINCZEWSKI, J., Separation and enrichment of trace components in analytical chemistry, 20: 40850
MINGAY, D. W., Lithium-6(^{12}C,d)^{16}O reaction at E_{cm} = 7 Mev, 20: 42329
MIROSHNICHENKO, V. I., Kinetic theory of EM-wave reflection from moving plasma, 20: 42448
MISHCHENKO, V. T., Mixed sulfosalicylate complexes of rare earth elements, 20: 40926
MISSONI, G., Protection against x rays from apparatus for medical use, 20: 40733 (ISS-66/16)
MISSONI, Guido, Measurement of the cross section of coherent and incoherent scattering of 662-kev γ rays on bound electrons, 20: 41625
MISTRY, N., Wide angle electron pair production at high energy, 20: 42327
MISUTOVA, O., Effects of irradiation on frequency of chromosome aberrations in root tip of barley, 20: 40716
MITCHELL, F. A., Radiation-protection and recovery from radiation injury in endotoxin-treated mice, 20: 40732 (AD-636209)
MITCHNER, M., Electrostatic probes for diagnostics in a collision-dominated weakly ionized plasma, 20: 41705
MITCHNER, M., Examination of the validity of the SAHA equation in a gas discharge, 20: 41751
MITIN, R. V., High-pressure electrodeless discharge and its magnetic properties, 20: 42509
MITRIKOV, M., Iron-free asymmetric two-lens β spectrometer, 20: 41282
MITTRA, R., Interaction of electron beams with a modulated reactance surface, 20: 41519
MIYAJIMA, Shigeki, Research on sheath formation, 20: 42428
MIZOCK, Bernard J., Application of thyroid scanning to study of transplantation, 20: 40516
MKHITARYAN, A. M., Laminar EHD flow in plane exit cone, 20: 41110
MOAK, C. D., Response of Si fission detectors to channeled ^{127}I and ^{40}Ar ions, 20: 41324
MOAK, C. D., Some heavy-ion stopping powers, 20: 41647
MOAZED, C., Study of the reaction $^{10}B(^{3}He,p\alpha\alpha)$, 20: 42188
MOBLEY, R., Recent experiments on muonium, 20: 41661
MOCOROA, A., Levels and transitions in ^{133}Cs, 20: 42203
MODENA, I., Liquid ^{3}He target for high-energy nuclear experiments, 20: 42107
MOEBIUS, R., Differential thermal analysis of oxalate hydrates of rare earth metals, 20: 40900
MOHINDRA, V. K., Canadian fallout data for April 1965, 20: 41209
MOHINDRA, V. K., Reactor environment monitoring for April 1965, 20: 41136
MOHINDRA, V. K., Valley-to-peak ratios for zero-thickness sources, 20: 41312
MOISEIWITSCH, B. L., Lower bound to the reciprocal of the scattering length. II., 20: 41658
MOKHIR, E. P., Effect of anion admixtures on luminescence and scintillation properties of monocrystals NaI(Tl), 20: 41347
MOLCHANOVA, I. V., Behavior of microquantities of yttrium and cerium in soil, 20: 40914
MOLLIHAN, William V., Crescent pattern of increased radioactivity in brain scanning, 20: 40789
MOLMUD, Paul, Site testing for EMP hardness, 20: 41117
MOLNAR, S., Combined slit-collimator for measuring distribution of isotopes with γ activity, 20: 41012
MONASTYRSKAYA, A. R., Effectiveness of the oxygen enrichment of air in MHD generator assemblies, 20: 41744
MONSTER, J., Sulfur isotope abundances in evaporites and in ancient oceans, 20: 41135
MONTELATICI, V., Liquid ^{3}He target for high-energy nuclear experiments, 20: 42107
MONTGOMERY, Albert George, Improvements in or relating to manipulating devices for use in nuclear reactors, 20: 42593
MONTGOMERY, D. Bruce, High-strength conductors for supermagnets, 20: 41097
MONTGOMERY, D. Bruce, Potential of superconducting magnets in design engineering, 20: 42135
MONTH, Melvin, Role of meson current in the determination of neutron form factors from elastic electron-deuteron scattering, 20: 41883
MOODY, F. J., Maximum two-phase vessel blowdown from pipes, 20: 41107
MOON, Jack L., Scintillation alpha counter, 20: 41366
MOON, N. F., Study of metabolism of ^{18}F in dogs and its suitability for bone scanning, 20: 40554
MOORE, C. F., Broad-range magnetic spectrograph system for routine angular distribution determinations, 20: 41306
MOORE, C. F., Coulomb displacement energies from isobaric analogue resonances, 20: 42262
MOORE, M. F. C., Track centering system for IEPs using vibrating reed track detector, 20: 41263 (CERN-66-23)
MOORE, R. B., Charged particle identification system using fast multiplier, 20: 41243
MOORE, R. B., Reaction of $^{7}Li(p,d)^{6}Li$ at 100 Mev proton energy, 20: 42351
MOOS, W. S., Acute effects of x-radiation upon mouse electrocardiogram, 20: 40648
MORAVCSIK, Michael J., Non-dynamical structure of particle reactions, 20: 41992
MORAVEC, J., Magnesium, Sr, and Ba polyuranates, 20: 40901
MOREHOUSE, Roger L., ESR of free radicals trapped in inert matrices at low temperature: P, PH_2, and As, 20: 40967
MOREHOUSE, Roger L., ESR of free radicals trapped in inert matrices at low temperature: CH_3, SiH_3, GeH_3, and SnH_3, 20: 40968
MORET, R., Application of radioisotopic dilution with incomplete extraction to determination of oligoelements in biology, 20: 40844
MORETTI, S., Thermal diffusivity and conductivity measurements on metals and oxides at high temperatures, 20: 41479
MORGAN, A. N., Large-scale electrorefining of Pu from Ga alloys, 20: 41035 (LA-2758)
MORGAN, C. S., Creep of ThO_2 and ThO_2–CaO solid solutions, 20: 41474
MORGAN, I. L., Elemental trace analysis by charged particle and neutron activation, 20: 40812 (ORO-2980-14)
MORGULIS, N. D., Some properties of a plasma in helium and argon with added cesium and potassium vapors, 20: 41712

MORI, F., Conductivity of a gas with suspension, 20: 41713
MORI, F., MHD power generator; E.T.L. Mark II, 20: 41714
MORI, F., Shock tube studies of magnetically induced non-equilibrium ionization in potassium seeded argon plasma, 20: 41715
MORIKAWA, T., Experimental study of physical properties of combustion gas, 20: 41758
MORISON, W. G., Prog. rpt. on Pickering Generating Station, 5/66, 20: 42617 (66-CNA-303)
MORITA, Tohru, Derivation of the generalized Boltzmann equation in quantum statistical mechanics, 20: 42082
MORLET, M., Elastic scattering of protons of 150 and 80 Mev on light nuclei and the optical potential, 20: 42388
MORLET, M., Polarization of protons of 152 Mev by inelastic scattering on ^{12}C and ^{40}Ca, 20: 42341
MORLEY, M. J., Electrical pulses from helical and coaxial explosive generators, 20: 41095
MOROKA, V. I., Radiative capture cross sections of 30 to 170 kev neutrons, 20: 42293
MOROZOV, A. I., Focusing of an ion beam in the field of a charged current-carrying ring, 20: 42512
MORPURGO, G., Connection between BBP and VPP verticles in the quark model, 20: 41876
MORRIS, C., Diverse schemes for flat topping the PPA, 20: 41569
MORRIS, C. J., Cathodic etching to prepare radioactive samples for oxygen determination, 20: 40817 (UCRL-14959)
MORRIS, Nelle J., Post-irradiation grafted vinyl cellulose copolymers, 20: 40995
MORRIS, R. N., Analysis of radioactive metals by spark source mass spectrography, 20: 40816 (RFP-699)
MORRISON, R. J., Small angle electron proton elastic scattering cross sections for momentum transfers between 10 and 105 f^{-2}, 20: 41791 (DESY-66/20)
MORROW, Richard J., Anion-exchange separation techniques with methanol–water solutions of hydrochloric and nitric acids, 20: 40855
MORSE, R. I., Boron-10, ^{11}B, and ^{6}Li induced reactions of ^{27}Al, 20: 42183
MORTON, J. R., Electron spin resonance spectra of ^{15}N-centered radicals at low temperatures. II., 20: 40955
MORTON, J. R., Electron spin resonance spectra of $N_2H_4^+$ and PF_2, 20: 40956
MORTON, J. R., Electron spin resonance spectrum of ClO_4 trapped in irradiated $KClO_4$, 20: 40969
MORUCCI, J. P., Imagery of x and γ rays by gas-filled image intensifier, 20: 41299
MOSEVICH, A. N., Chromatographic separation of xenon and iodine oxygen compounds, 20: 40851
MOSEVICH, A. N., Separation of XeO_3 and HIO_3 in zirconium phosphate, 20: 41054
MOSHER, David, Closed-line average minimum-B configuration, 20: 42455
MOSHINSKY, M., Matrix elements and normalization coefficients in SU_n, 20: 42010
MOSICHEV, V. I., Isotopic spectral analysis of He with use of isotopic filler, 20: 40861
MOSS, M. K., Development of the covariant formulation of the conservation laws of general relativity, 20: 42080
MOSSEL, D. A. A., Radiation in decontamination of frozen proteinaceous staple foods, 20: 41390
MOSTEK, P., Wide angle electron pair production at high energy, 20: 42327
MOSZYNSKI, Jerzy R., End losses in MHD channels of variable cross section and their reduction, 20: 41716
MOTOCU, M., Results of radioiodine treatment in diabetes mellitus associated with hyperthyroidism, 20: 40790
MOUILHAYRAT, G., Study of the reactions $^{10}B(d,\alpha)^{2a}He$ and $^{9}Be(^{3}He,\alpha)^{2a}He$, 20: 42374
MOYER, Carl B., Heat transfer experiment with multirod element, DOR design study, 20: 42635 (RISO-124)
MOZECK, P., Selective activation in neutron activation analysis, 20: 40862
MOZLEY, J. M., Scintillation scanning with an 8-inch diameter Na iodide (Tl) crystal, 20: 40779
MUDGE, L. K., Chlorine recovery and radioiodine behavior in salt cycle process, 20: 41029 (BNWL-279)
MUEHLHAUSE, C. O., Material radiation environment, 20: 41527
MUELLER, A. J., Chimerical structure of M_1 plants and its bearing on determination of mutation frequencies in Arabidopsis, 20: 40513
MUELLER, Adolph, Radiation-produced electron spin resonance signals in nucleic acids, 20: 40593
MUELLER, F., Activity of UCl_3 in the eutectic melt LiCl–KCl, 20: 40922
MUELLER, F., Anodic polarization of UC in the melt LiCl–KCl, 20: 40923
MUENCK, E., g-Factor in 2^+ rotation states in ^{166}Er and ^{168}Er, 20: 42302
MUENKEL, J., Plasma diagnostics by microwave interferometry in MHD channels with the aid of an open waveguide, 20: 41717
MUIRHEAD, H., Pion capture and nuclear structure, 20: 42314
MUKHERJEE, M. Ludwig, Nonradiative destruction of F-centers in x-irradiated KCl doped with anionic impurities, 20: 42557
MUKOSEI, V. I., Particle trajectories in radiation and chemical processes in pseudo-liquefied layer, 20: 40884
MULLINS, L. J., Large-scale electrorefining of Pu from Ga alloys, 20: 41035 (LA-2758)
MUMME, I. A., Stability of Lucas Heights area against possible seismic events, 20: 41148 (AAEC-TM-316)
MUNAKATA, Chusuke, Voltage induced by an electron beam in a bulk semiconductor crystal, 20: 42533
MURAI, Y., Experimental study of physical properties of combustion gas, 20: 41758
MURAMATSU, Tokio, Active effluent treatment plant, 20: 42688
MURAYAMA, H., Highly active single particles in radioactive fallout, 20: 41138
MURPHY, P. G., Differential cross sections for $\pi^{\pm}p$ elastic scattering in the momentum range 875-1579 Mev/c, 20: 41857
MURRAY, Joseph J., New Σ decay parameters and test of $\Delta I = \frac{1}{2}$ rule, 20: 41879
MURRAY, Kenneth M., Radiation shielding at the NRL Linac facility, 20: 41566
MUSTAFINA, R. Kh., Effect of anion admixtures on luminescence and scintillation properties of monocrystals NaI(Tl), 20: 41347
MUSTO, R., Generators of O(4,1) for the quantum-mechanical hydrogen atom, 20: 41643
MYKLEBUST, R. L., Pulse amplitude shifts in gas proportional x-ray detectors, 20: 41331
MYTTENAERE, C., Effect of irrigation on absorption and localization of Cs and Sr in Oryza sativa L., 20: 40574

N

NACHTWEY, D. S., Recovery from radiation injury in swine, 20: 40605 (AD-635735)
NAGAHIRO, A., Preparation and test of MHD duct wall and electrode materials, 20: 41718
NAGASHIMA, Y., Precise measurement of the K^+/K^- and π^+/π^- lifetime ratios, 20: 41884
NAGATA, Nobuo, Studies on bone marrow transplantation for hematopoietic disturbance, 20: 40726
NAGORNAYA, L. L., Plastic scintillator with light yield proportional to the energy of outer electrons, 20: 41346
NAIDU, J. R., Minor-element and trace-element content of marine environment on west coast of India, 20: 40572
NAIDU, J. R., Uptake of radionuclides by marine invertebrates from the west coast of India, 20: 40528
NAIMAN, C. S., Laser induced prebreakdown and breakdown phenomena observed in cloud chambers, 20: 41375
NAITO, Seiichi, Broken symmetry and stability of particle-like states, 20: 41994
NAKAGAWA, Masami, 3*-plet model of elementary particles, 20: 41998
NAKAI, M. Y., Low energy electron studies in indium and magnesium, 20: 41621 (ORNL-TM-1565)
NAKAJIMA, Tsuyoshi, Hydrogen exchange between hydrogen, ethylene, or ethane during catalyzed hydrogenation of ethylene, 20: 40942
NAKAMAE, Tsunenori, Studies on bone marrow transplantation for hematopoietic disturbance, 20: 40726
NAKANISHI, Atsuo, Measurement of coronary circulation time with catheter-type micro G-M counter, 20: 40514
NAKANO, Yoshiei, Pinch phenomena in a coaxial plasma gun, 20: 42464
NAMBI, K. S. V., Development of thermoluminescent dosimeters at Trombay, 20: 41373
NANCE, R. L., Studies on the formation of Pu_2O_3 in the sintering of PuO_2, 20: 41426 (LA-3493)
NANEVICZ, J. E., Ionization phenomena associated with solid-propellant rockets, 20: 41120
NANGU, Makoto, Gaseous centrifuge and separation of argon isotopes, 20: 41404
NARIAI, Hidekazu, Applicability of a dust-like model to a collapsing or anti-collapsing star at high temperature, 20: 41612
NARIARI, Hidekazu, Behavior of the central region of a collapsing star with spherical symmetry and pressure gradient, 20: 41613
NARISAWA, Shizuo, Influence of addition of ethylene on γ induced alternating copolymerization of ethylenimine and C monoxide, 20: 40975
NARVAEZ, Richard, Curium process development. III-1., 20: 41032 (DP-1010)
NARYSHKINA, L. G., Vavilov-Cherenkov effect for surface waves, 20: 42497
NASSIFF, S. J., Excitation function for the reaction $^{197}Au(d,p)^{198}Au$, 20: 42206
NATARAJAN, T. K., Scintillation scanning with an 8-inch diameter Na iodide (Tl) crystal, 20: 40779

NATH, P., Perturbations of inelastic unitarity on dynamical calculations, 20: 41957
NATH, R., P-wave π-K$\bar{K}$ cross-section in the T = 1 state, 20: 41823
NAYYAR, N. K., Effect of Hall current on Rayleigh-Taylor instability of a plasma, 20: 42474
NEAL, Richard B., Electron linear accelerator phasing method, 20: 41582
NEELY, H. H., Electron-irradiation damage-rate measurements in aluminum, 20: 42543
NEFEDOV, V. D., Radioactive isotopes in chemical research, 20: 41027
NEILER, J. N., Fission-fragment energy-correlation measurements for the thermal-neutron fission of ^{239}Pu and ^{241}Pu, 20: 42261
NELSON, Walter R., Electron-induced cascade showers in Cu and Pb at 1 Bev, 20: 41671
NEMETS, O. F., Optical model analysis of the elastic scattering of 13.6 Mev deuterons on medium weight nuclei, 20: 42294
NEOKLADNOVA, L. N., Radiolysis of mixed Co(III) nitroammoniates and Co(III) hexanitrites, 20: 41003
NESTERENKO, V. S., Radiative capture cross sections of 30 to 170 kev neutrons, 20: 42293
NESTERIKHIN, Yu. E., Investigation of plasma injected into trap with conical theta pinch, 20: 42504
NESTEROV, V. G., Energy dependence of angular distribution of fragments in the fission of ^{233}U, ^{235}U, and ^{239}Pu induced by neutrons, 20: 42171 (LA-tr-66-41)
NEUBAUER, E. P., Uranium metal by carbon reduction of uranium oxide in vacuum, 20: 41411 (IS-1379)
NEUHOLD, John M., Prog. rpt. on gamma irradiation effects on toxic responses of fish, 6/65–5/66, 20: 40611 (COO-1421-2)
NEURATH, Peter W., Prog. rpt. on human chromosome analysis, final, 11/65, 20: 40497 (NYO-3400-1)
NEUREUTHER, A. R., Interaction of electron beams with a modulated reactance surface, 20: 41519
NEWMAN, Riley David, K$^+$p inelastic interactions at 2.7 Bev/c, 20: 41804 (UCRL-17003)
NEWSOME, R. W. Jr., (d,pf) and (t,pf) reactions on Pu isotopes, 20: 42161 (LA-DC-7878)
NEZHEVENKO, L. B., Fabrication of thin plates from refractory carbides, 20: 41430
NGUYEN-DUC, T., Systematics of hadrons under noncompact groups, 20: 41967
NGUYEN-NGOC, H., Small angle electron proton elastic scattering cross sections for momentum transfers between 10 and 105 f^{-2}, 20: 41791 (DESY-66/20)
NGUYEN VAN HIEU, Asymptotic relations between the scattering amplitudes in local field theory, 20: 42015
NGUYEN VAN HIEU, Matrix elements of Lorentz transformation for unitary concept, 20: 41926 (JINR-P-2777)
NGUYEN VAN HIEU, Structure of vector and axial currents in broken $\bar{U}$(12) symmetry, 20: 41939
NGUYEN VAN SEN, Excitation of 5.7 Mev level of ^{7}Li by (n,n′) scattering at 14 Mev, 20: 42364
NGUYEN VAN SEN, Study of (d,p) reactions on light nuclei at low energy, 20: 42399
NICHOLS, Lester D., Criteria for use of Rankine-MHD systems in space, 20: 41719
NICKSON, James J., Does prophylactic radiotherapy given for cancer of breast predispose to metastasis?, 20: 40793
NICODEMI, F., Current algebras and meson-nucleon scattering lengths, 20: 41846
NICODEMI, G., New determination of the ϕ spin and G parity, 20: 41881
NICOL, Ann T., Optical spectra of tripositive ^{244}Cm in lanthanum trichloride, 20: 40891
NIEBAUER, G., Injuries of the skin caused by light, 20: 40696
NIEL, M., Elastic scattering of neutrons by tritium at 14 Mev, 20: 42373
NIELSEN, K. Boade, Levels ar^{-1} transitions in ^{133}Cs, 20: 42203
NIEPEL, J., Separation of ^{90}Sr, ^{89}Sr, and ^{140}Ba from ashes of beef bones, milk, and fish, 20: 40858
NIETO, Michael Martin, Dynamical study of the Quark-Meson system, 20: 42029
NIGAM, A. N., Forbidden transition L_{II}/N_{II} in the spectrum of Pt, 20: 41660
NIKITIN, S. A., Rare earth ferromagnetics and antiferromagnetics, 20: 41483
NIKL, I., Effect of x-ray quality and ovarian location on genetic exposure in gynecological examinations, 20: 40770
NIKOLAEV, D. A., Concentration of water samples for determination of tritium, 20: 40826
NIKOLAEVA, L. G., Imperfections produced in dislocation-free Si by fast-neutron irradiation, 20: 42567
NIKOLAEVSKII, L. S., Interruption of a current pulse by a plasma switch, 20: 42493
NIKOLAEVSKII, L. S., Spectroscopic investigations of a high-current discharge in the air at low densities, 20: 42492
NIKOLSKII, V. G., Yield of stabilized charges in radiolysis of organic systems, 20: 40962
NIKULINA, I. G., Kinetics of polymerization of unsaturated oligomers with γ-rays by electroconductivity method, 20: 40999
NIKULINA, R. A., Plastic scintillator with light yield proportional to the energy of outer electrons, 20: 41346
NILAN, R. A., Factors affecting biological action of mutagens, 20: 40717
NILEWSKI, J., Modulated conductivity induction synchronous magnetogasdynamic generator, 20: 41683
NIL'SEN, O. B., Decay of ^{152}Tb, 20: 42155 (JINR-P-2762)
NISHIZAWA, Yoshihiko, Synthesis of rotenone-6a-^{14}C on a semimicro scale, 20: 41013
NISHIZAWA, Yoshihiko, Synthesis of d-trans-chrysanthemunic acid-1-^{14}C and its antipode on semimicro scale, 20: 41015
NISSIM-SABAT, C., Detailed analysis of muonic x-ray spectrum from strongly deformed e-e nuclei, 20: 42310
NIZZA, Pierre, Study of pigs subjected to lethal dose of integral γ irradiation, 20: 40608 (CEA-R-3001)
NODINE, John H., Digital computers in nuclear radiation counting, 20: 41319
NOLD, Max M., Biological significance of the supersonic transport radiation environment, 20: 40525
NORDBERG, M. E. Jr., Two-nucleon emission following absorption of stopped negative pions, 20: 42313
NORDEMANN, D., Measurement of radioactivity in the sea, 20: 41145
NORDMEYER, P., Metabolism of ^{65}Zn by rats under influence of Prednisolone or Dexamethasone, 20: 40563
NORMAN, Amos, Direct reading intracavitary dosimeter for use in radium therapy, 20: 41377
NORTHROP, D. C., Semiconductor counters for nuclear radiations, 20: 41352
NOVAK, P. E., Experimental studies of plutonium and fission product redistribution in fast reactor fuels, 20: 42625 (GEAP-4466)
NOVAKOV, T., Recoil measurements of subnanosecond nuclear lifetimes, 20: 42180
NOVIKOV, V., Search for new decay modes of the K_2^0-mesons, 20: 41903
NOVIKOV, Yu. N., Spin values of lower multiplet states in spherical odd-odd nuclei, 20: 42289
NOVIKOVA, N. R., Pyrogallol–amidol developer for nuclear photo emulsions, 20: 41340
NOWACKI, Pawel Jan, Analysis of a magnetohydrodynamic amplidyne, 20: 41720
NOWEIR, T. M., (^{3}He,t) investigations of Fe, Ni, and Zr, 20: 42334
NOWIK, I., Moessbauer studies of rare earth intermetallic compounds, 20: 42570
NUEHRENBERG, J., Special magnetohydrostatic, axisymmetric meridional equilibria, 20: 42409 (IPP-6/50)
NULMAN, Rebeca M., Strontium-90 content in milk in Mexico, 20: 40854
NUSSINOV, S., Theorem on the Clebsch-Gordan series in SU(n), 20: 41945
NUTTALL, J., Hole self-energy corrections in the Brueckner theory, 20: 42244
NUYTS, J., Generalizations of isoparity, 20: 41923
NYBOE, K., Redrift treatment of Li-drifted Si detectors, 20: 41311
NYGREN, D. R., n-n S-wave scattering length from the neutron spectra of the reaction $\pi^- + d \rightarrow 2n + \gamma$, 20: 41914
NYMAN, B., Decay of ^{192}Au, 20: 42187

O

OAKS, Dudley M., Concentric tube and parallel plate electron capture detectors, 20: 40863
O'BRIEN, J. F., Isotopic power sources, 20: 41397
OBUKHOVSKII, Yu. A., Preparation of single crystals of refractory compounds, 20: 41480
O'CONNELL, J. S., Zero-range treatment of the three-body photodisintegration cross section of ^{3}H and ^{3}He, 20: 42228
ODINOKOVA, V. A., Morphological changes in thyroid gland following radioiodine administration, 20: 40647
O'DONNELL, F. H., Accurate excitation energies of ^{11}B states below 7 Mev, 20: 42246
O'DONOVAN, Patrick J., M(12) potential model for nucleon-nucleon scattering, 20: 41973
ODUM, E. P., Flux of ^{32}P and ^{65}Zn through a salt-marsh ecosystem, 20: 40573
OGANEZOV, K. A., Use of the hollow cathode for the determination of gases in solids by the isotopic equilibrium method, 20: 41526
OGAWA, Kiyoshi, Excitation of ion plasma oscillation by electron beams, 20: 42429
OGIEVETSKII, V. I., Einstein's equations as describing a massless tensor field with spin 2, 20: 42078
OGIEVETSKII, V. I., Theory of a natural massive tensor field with spin 2, 20: 41938

O'HARE, S. A., Prog. rpt. on selected properties of Th with low ThO_2 additions, 7/65–6/66, 20: 41462 (USBM-RC-1245)
OHASHI, Y., Pressurized discharge chamber, 20: 41294
OHKAWA, T., Use of metallic surfaces to convert H atoms to ions in the 50–3000 ev energy range, 20: 42460
OHLENDORF, W., Nonequilibrium MHD generator using a nonseeded inert gas as working fluid, 20: 41721
OHNUMA, Hajime, Level structure of nuclei with N = 29 and $22 \leq Z \leq 26$, 20: 42201
OHSHIRO, Koji, Studies on bone marrow transplantation for hematopoietic disturbance, 20: 40726
OHTSUKI, Soji, Experiments on the propagation of normal region in a superconducting magnet, 20: 42100
OKABAYASHI, Tokoo, Broken symmetry and stability of particle-like states, 20: 41994
OKADA, A., Pressurized discharge chamber, 20: 41294
OKAMURA, Seizo, Radiation-induced solid-state polymerization in binary systems. II., 20: 40977
OKAWA, N., Separation of technetium from rhenium by liquid-liquid extraction with potassium xanthate, 20: 40856
OKONOV, E., Search for new decay modes of the K_2^0-mesons, 20: 41903
OKSMAN, J., Movements of radio aurora, 20: 42057
OKUBO, S., Inconsistency of canonical commutation relations among current densities, 20: 41964
OKUBO, S., Ultraviolet sensitivity of Bacillus subtilis bacteriophage SP02 and its infectious DNA, 20: 40676
OKUBO, S., Unitary-antisymmetric q-number terms in commutators of spatial current components, 20: 41985
OLIVAIN, Jack, Nonlinear process in a finite plasma, 20: 42427
OLIVEIRA, Colbar G., Interaction of the gravitational and spinor fields, 20: 42088
OLIVER, John, Core structures for nuclear reactors, 20: 42594
OLIVIERI, G., Kinetics of chromatid aberrations induced in hamster cells by tritium-labeled thymidine, 20: 40686
OLNESS, J. W., Lifetime determinations for nuclei A = 10, 11, and 12 from gamma-ray Doppler shifts, 20: 42234
OLSEN, B., Numerical analysis of the time spectrum of delayed coincidences. I., 20: 41301
OLSEN, B., Numerical analysis of the time spectrum of delayed coincidences. II., 20: 41302
OLSEN, J. L., Remarks on the use of very high pulsed fields in solid state research, 20: 42526
OMER, Guy C. Jr., Closed model universes with a cosmological constant, 20: 41591
ONCESCU, M., Electrode calibration for nuclear diagraphy, 20: 41165
ONDREJ, M., Influence of interaction between EDTA and x rays on mutation and crossover in Drosophila, 20: 40707
ONDREJCIN, R. S., Thermal fission yield of ^{137}Cs in ^{233}U, 20: 42176
O'NEILL, J. S., Observations on the strength and Young's modulus of BeO as a function of density and grain size, 20: 41473
ONODERA, Norihiko, Complications of extraperitoneal surgical radiation, 20: 40783
ORLENKO, P. A., Radiation cross linking of cable polyethylene insulation on large scale, 20: 41496
ORLIK, Leszek, Measurement of the dose rate of unknown γ-radioactive substances, 20: 41025
ORLOV, Yu. I., Peculiarities of ray theory of cylindrical and spherical wave propagation in plasma. II., 20: 42447
ORMANDZHIEV, Sl., Iron-free asymmetric two-lens β spectrometer, 20: 41282
ORTANDERL, Franz, Preparation of radioactively labeled pyridoxal-5′-phosphate, 20: 41016
OSAKI, S., Separation of technetium from rhenium by liquid-liquid extraction with potassium xanthate, 20: 40856
OSBORN, G. K., Treadmill exercise performance by ageing irradiated rat, 20: 40604 (AD-635251)
OSBORNE, L. S., π^0 photoproduction at 3.0, 4.0, and 5.0 Bev for baryon four momentum transfers between 0.5 and 4.0 $(Bev/c)^2$, 20: 41798 (MIT-2098-265)
OSBORNE, L. S., Search for fractionally charged, weakly interacting particles, 20: 41797 (MIT-2098-264)
OSTAPCHENKO, E. P., Role of He in He–Xe plasma, 20: 42491
OSTIC, Ronald G., Concentration and isotopic composition of lead in Toluca iron meteorite, 20: 42062
OSTLIND, D. A., Effects of x-ray dosages on development of Heterakis gallinarum, 20: 40667
OSTROVSKAYA, G. V., Temperature and electron concentration in plasma arc from Thomson scattering, 20: 42432
OTOKOZAWA, Jun, Compton scattering of vector photon by scalar nucleon, 20: 41897
OTSUKI, Shoichiro, Evidence for existence of a repulsive core in the A-N interaction, 20: 41894
OTT, W., Investigation of a cesium plasma diode using an electron beam probing technique, 20: 42407 (IPP-2/48)
OTTER, F. A. Jr., New approach to the determination of equilibrium magnetization of superconductors, 20: 42133
OTTER, J. M., UNICORN: a program to calculate point cross sections from resonance parameters, 20: 42141 (NAA-SR-11980(Vol.6))
OUDIN, J., Nuclear television, 20: 41099
OUTI, Akizi, Numerical computation of dispersive nonlinear equation, 20: 42411 (IPPJ-49)
OYAMA, Yoshitoshi, Gaseous centrifuge and separation of argon isotopes, 20: 41404
OZAWA, Yasutomo, Performance of spatially constant B/ρ-type MHD generator with energy dissipation, 20: 41722

P

PAAKKOLA, O., Radiostrontium in milk, grass, and some other biological samples in Finland, 20: 41134 (SFL-A3)
PACCANONI, F., Field-theoretical sum rules and mass-difference calculations, 20: 41824
PACCANONI, F., Vector meson bootstrap from singular N/D equations, 20: 41837
PACCO, M. G., Monte Carlo simulation of the flow of a KNUDSEN gas with due allowance for the sojourn time, 20: 42035 (IPP-2/41)
PACHNER, J., Radiation of a collapsing and anticollapsing body, 20: 41597
PACINI, F., Equilibrium of a large assembly of particles in general relativity, 20: 42091
PACK, J. L., High temperature plasmas by laser heating, 20: 42415 (TID-22928)
PADMAVATHI, S. V., Ionization of relativistic electrons, 20: 41814
PAI, S. I., Quasi-one-dimensional analysis of magnetogasdynamics, 20: 41723
PAIK, S. F., Electrical circuit analogue of one-dimensional plasmas, 20: 42443
PAKVASA, S., Parity-conserving hyperon decay and the pole model, 20: 41868
PALMA, V., Effect of radioprotectors on damage induced by alkylating agents on tumoural and normal tissues, 20: 40664
PALMER, W., Dynamics of strongly bound systems, 20: 41978
PANDE, D. N., Effect of deuteration on fluorescence lifetimes of uranyl salts, 20: 40887
PANONTIN, John A., Half-life of ^{101}Ag and formation cross section from Ag and In, 20: 42179
PANT, D. D., Effect of deuteration on fluorescence lifetimes of uranyl salts, 20: 40887
PANT, H. C., Effect of deuteration on fluorescence lifetimes of uranyl salts, 20: 40887
PAO, H. P., Magnetohydrodynamic boundary layer between parallel streams of different magnetic fields and temperatures, 20: 42039
PAPAGEORGIOU, Th., Considerations of radiation quantities and units in sense of theory of energy transfer, 20: 40787
PAPAGEORGIOU, M., Gamma radiation-induced dominant lethality to sperm of olive fruit fly, 20: 40674
PAPE, A., Precise measurement of the stopping power of C, Au, Al, Ca, and CaF_2 for 0.6 to 6 Mev protons, 20: 42363
PAPINEAU, L., Separation of reaction mechanisms at low energy, 20: 42394
PAPPALARDO, Separation of reaction mechanisms at low energy, 20: 42394
PAPPAS, A. C., Charge and mass distributions in fission of U induced by 170 Mev protons, 20: 42177
PAPPAS, W. S., Micron region pressure standard for uranium hexafluoride, 20: 41252
PARCHEVSKII, V. P., Biological consequences of radioactive contamination of water bodies, 20: 40527
PARDI, A. J., Effects of graphite electrodes on carrier distillation of impurities in U_3O_8, 20: 40807 (NLCO-976)
PARIS, Gy., Approximations to immersion type electrostatic lenses, 20: 41245
PARISEAU, Paul R., Compositions and process for removal of radioactive contaminants, 20: 41214
PARKER, C. V., Elemental trace analysis by charged particle and neutron activation, 20: 40812 (ORO-2980-14)
PARKER, K., Mechanised evaluation of neutron cross sections, 20: 42145
PARKER, S. I., Compact low-inductance spark chamber pulser, 20: 41293
PARKINSON, T. F., Resonance absorption integral of rhenium, 20: 42333
PARKS, J. G., Phase-space integrals and invariant-mass distributions with Monte Carlo techniques, 20: 41953
PARKS, W. F., Alternate commutation relations, 20: 41946
PARR, E. D., Prog. rpt. on alkali metals evaluation program, 1–3/66, 20: 41438 (AGN-8187)
PARSONS, M. J., Optimization of generator parameters and of overall thermal efficiencies for an MHD reactor system, 20: 41740

PASCUAL, L., Application of fluid switching to MHD energy conversion, 20: 41724
PASHCHENKO, L. P., New isotope ^{216}Ac, 20: 42287
PASHININ, P. P., Temperature measurements of a laser spark from soft-x-ray emission, 20: 42475
PASHITSKII, E. A., Convective excitation of ionic oscillations of a nonuniform electron beam, 20: 42494
PASTOREK, Richard, Chemistry of the rare earth metals. XL, 20: 40909
PASZTOR, L. C., Determination of rare earth inclusions in steel, 20: 41415
PATE, H., Design and performance of on-line wire spark chamber spectrometer, 20: 41297
PATEL, B., Uptake of radionuclides by marine invertebrates from the west coast of India, 20: 40528
PATERSON, W. J., Uranium-fueled VERA reactor experiments, 20: 42671 (AWRE-R-5/66)
PATIN, S. A., Absorption of artificial radionuclides by marine detritus, 20: 41140
PATTERSON, Carol B., Index to conferences relating to nuclear science, 20: 42693 (TID-4043(Rev.3))
PATTERSON, H. Wade, Developments in technique for monitoring high-energy accelerator radiation, 20: 41276 (UCRL-16769)
PATTON, Dennis D., Simplified preparation of ^{99m}Tc sulfide colloid for liver scanning, 20: 40753
PAUL, Roger A., Trace elements in common rock types, 20: 41068 (PNE-5006)
PAULIN, Robert, Bound state of the positron in certain finely divided oxides, 20: 41629
PAULUS, J., Interaction of tritium ions in selected energy ranges with gaseous butane, 20: 40938
PAVLIN, C., Application of fluid switching to MHD energy conversion, 20: 41724
PAVLOTSKAYA, F. I., Mobilities and forms of ^{90}Sr and Ca in turf-podzolic and black earth soil, 20: 40520 (NP-16261)
PAVLOVSKII, A. I., Compensating space charge of pulsed electron beams, 20: 42511
PAVLYUCHENKO, M. M., Effect of radioactive decay in solids on their relaxability, 20: 41018
PAWLIW, J., Evaluation of CANDU: PHW fuels, 20: 42618 (66-CNA-312)
PAWLOWSKI, Z., Effect of gaseous admixtures to argon upon ionization work for alpha radiation, 20: 42487
PCHELINSKAYA, S. N., Effect of x-ray irradiation on some properties of lithium fluoride single crystals, 20: 42564
PEARCE, D. W., Prog. rpt. on atmospheric sciences, annual, 1965, 20: 41188 (BNWL-235-1)
PEARSON, Robin, Core access assembly for nuclear reactors, 20: 42598
PEASLEE, D. C., (γ,ρ^0) as two-pion exchange, 20: 41821
PEDRICK, Arthur Paul, Improvements in radio controlled nuclear energy propelled marine towing craft, 20: 42666
PEKER, L. K., Spin values of lower multiplet states in spherical odd-odd nuclei, 20: 42289
PELETSKII, V. E., Investigation of high-melting metals in the temperature range 1300 to 3000°K, 20: 41762
PELLAT, Rene, Nonlinear process in a finite plasma, 20: 42427
PELLAT, Rene, Origin of electron precipitations in the auroral zones, 20: 42056
PENDLETON, J., Fuel temperature measurements in mixed oxide elements, 20: 42612
PENNA, Franco, E., Prog. rpt. on radiochemical and radioecological studies on Brazilian areas of high natural radiation, annual, 5/65–6/66, 20: 40522 (NYO-3273-7)
PEPPER, C. E., Effects of graphite electrodes on carrier distillation of impurities in U_3O_8, 20: 40807 (NLCO-976)
PERCHEREAU, J., Study of charged products in the reaction ^{9}Be + d at very low energy (100 to 200 kev), 20: 42354
PERDUE, P. T., Inexpensive liquid nitrogen level control for cold traps, 20: 42106
PERES, Asher, Saturation of quark forces in zero-triality states, 20: 41974
PERFILOV, N. A., Pyrogallol–amidol developer for nuclear photo emulsions, 20: 41340
PERICART, J., Design and testing of insulating walls and electrodes for MHD converters, 20: 41726
PERICART, M. J., Behavior of electrodes with electrically-conducting ceramic frontal faces on the Renardieres 8 Mw-test rig, 20: 41725
PERKINS, A. J., Prog. rpt. on transformation of Zr–Nb alloys, 7/66, 20: 41443 (COO-588-12)
PERLOW, G. J., Observations of the Moessbauer effect in ^{133}Cs, 20: 42239
PERLSTEIN, P., Mechanism of radiolysis of carbon dioxide, 20: 40996
PERRAULT, F., Study of the reactions ^{10}B(d,α)$^{2\,4}$He and ^{9}Be(^{3}He,α)$^{2\,4}$He, 20: 42374
PERRIGO, L. D., Plutonium Recycle Test Reactor decontamination following MgO–PuO_2 fuel element failures, 20: 42677 (BNWL-SA-636)
PERRIN, A., Contribution to a study of the reaction ^{12}C(d,p)^{13}C, 20: 42400
PERRIN, A., Elastic scattering of deuterons at ^{6}Li at 4 to 6.5 Mev, 20: 42365
PERRIN, C., Reaction ^{9}Be(n,nn)$\alpha\alpha$ at 15 Mev, 20: 42362
PERRIN, P., Reaction ^{9}Be(n,nn)$\alpha\alpha$ at 15 Mev, 20: 42362
PERRY, D. R., Neutron dosimetry methods and experience on the 7 Bev proton synchrotron, Nimrod, 20: 41543 (RPP-R-2)
PERSHAN, P. S., Electron spin resonance of irradiated deoxyribonucleic acid, 20: 40594
PERULLI, Mariano, Nonlinear process in a finite plasma, 20: 42427
PERUZZI, I., Measurement of the branching ratio $\omega \to$ neutrals/$\omega \to \pi^+ + \pi^- + \pi^0$, 20: 41850
PESCHKA, W., Some aspects on the use of cryogenically cooled primary-windings system for an a-c MHD generator, 20: 41727
PESKIN, R. L., Solid density distribution in gas-solid pipe flow, 20: 41102 (NYO-2930-6)
PETER, J., Proton reactions with Bi at 100 to 150 Mev, 20: 42196
PETERS, C. R., Continuous averaging technique for avoiding drift effects in x-ray scattering measurements, 20: 41327
PETERS, Martin Charles, Improvements in steam-generating plant, 20: 42657
PETERSON, J. P. Jr., Prog. rpt. on accurate nuclear fuel burnup analyses, 12/65–2/66, 20: 42608 (GEAP-5124)
PETIT, G. Y., Elastic scattering of 14 Mev neutrons by K, 20: 42393
PETRAS, M., Schroedinger theory of the static π-N interaction, 20: 41818
PETRICK, Michael, MHD generators operating with two-phase liquid metal flows, 20: 41728
PETROV, V. A., Niobium and Zr carbides at temperatures between 1200 and 3500°K, 20: 41729
PETROV, Yu. K., Device for measuring median planes of magnetic fields in accelerators, 20: 41553
PETROVIC, B., Contaminability of eggs by radionuclides in conditions of external radiocontamination, 20: 40559
PETROW, Henry G., Distribution of ^{226}Ra, ^{228}Ra, ^{210}Pb, and ^{228}Th in bone and soft tissue of Ra dial painters, 20: 40621 (NYO-3086-5)
PEYMAN, A. A., Small angle Compton scattering with 17 Mev γ-rays from the ^{7}Li(p,γ)^{8}Be reaction, 20: 42213
PFLEIDERER, Gerhard, Preparation of radioactively labeled pyridoxal-5′-phosphate, 20: 41016
PFLUEGER, Margaret L., Index to conferences relating to nuclear science, 20: 42693 (TID-4043(Rev.3))
PHAM DINH LIEN, Excitation of 5.7 Mev level of ^{7}Li by (n,n′) scattering at 14 Mev, 20: 42364
PHELPS, A. V., High temperature plasmas by laser heating, 20: 42415 (TID-22928)
PHILLIPS, G. W., Peak-to-total ratios and efficiencies for NaI crystal, 20: 41307
PHILLIPS, T. L., Radiation-protection and recovery from radiation injury in endotoxin-treated mice, 20: 40732 (AD-636209)
PHILLIPS, Will D., Explosion tests in gloved box with ether–air mixtures, 20: 41203 (UCRL-16259)
PICARD, Jean, Tables of range and stopping power of chemical elements for charged particles of energy 0.5 to 500 Mev, 20: 41619 (CEA-R-3042)
PICK, M., Relations between certain forms of ionospheric absorption and solar and geophysical phenomena, 20: 42047
PIERCE, G. E., Urethane spray foaming, 20: 41200 (ORNL-TM-1551)
PIGEON, J., Study of the reaction (d,p) with total interaction in the excursion method, 20: 42387
PIGMAN, Ward, Depolymerization of hyaluronic acid by autoxidants and radiations, 20: 40591
PIJCK, J., Determination of colloidal gold by thermal neutron radioactivation, 20: 40842
PILIYA, A. D., Conversion of waves in a nonuniform plasma, 20: 42500
PINAJIAN, J. J., Modified hypodermic syringe for liquid deposition of beta spectrometer samples, 20: 41296
PIPER, Arthur M., Atomic tools in developing water, 20: 41073
PIPER, R. D., Electrolytic recovery of scrap uranium metal, 20: 41036 (MCW-1494)
PIRKMAJER, E., Nuclear magnetic resonance and relaxation of hexafluoride molecules in solid, 20: 40892
PISARENKO, V. G., Dispersion sum rules for strong and electromagnetic interactions, 20: 41793 (JINR-E-2822)
PITTILLO, Robert F., New radioprotector in E. coli, 20: 40737
PITTS, J. H., Long John thermogasdynamic research facility, 20: 41104 (UCRL-14841)
PIZZI, J. R., Reactions ^{12}C(α,α) at 51 Mev and ^{14}N(d,α)^{12}C and ^{14}N(d,d) at 28.5 Mev, 20: 42389
PLANCHET, R. P., Timing and firing, Project Dribble, 20: 41070 (VUF-3021)
PLANTAMURA, V. L., Nomogram for designing tunnel diode monostable circuits, 20: 41242
PLANTAMURA, V. L., Suggestions for improvements of timing circuits

with tunnel diodes, 20: 41246
PLANTEVIN, J. P., Magnetic field compression, 20: 41081
PLANTEVIN, J. P., Theory of magnetic field compression diffusion, surface instabilities, 20: 41090
PLUEMER, F., Automatic beam current control on the electron accelerator, 20: 41550
PLUTA, K. M., Electron-impact-induced $n \rightarrow n'$ transitions in H atoms, 20: 41655
POBERAJ, S., Electron spin resonance of irradiated $NaH_3(SeO_3)_2$ and $NaD_3(SeO_3)_2$, 20: 40972
POGUTSE, O. P., Instability of plasma with captured particles in toroidal geometry, 20: 42402 (IAE-1149)
POLAK, L. S., Heterogeneous processes in radiation catalysis, 20: 40989
POLAR, Emine, Producing mutants resistant to Peronospora tabacina by seed treatment with radiation, 20: 40613 (N-66-18147)
POLETTI, A. R., 6.92- to 6.05-Mev E2 transition in ^{16}O, 20: 42232
POLIKANOV, S. M., Spontaneously fissionable isomer with the half-life equal to 10^{-7} s, 20: 42159 (JINR-P-2841)
POLIKARPOV, G. G., Biological consequences of radioactive contamination of water bodies, 20: 40527
POLIN, F., Dependence on microstructure of the high temperature properties of U oxide. Mo and U oxide. W cermets, 20: 41478
POL'KINA, R. I., Radiosensitizing action of naturally occurring pyrimidines, 20: 40668
POLLACK, Gerald L., New, attenuated wave mode in He II films, 20: 42111
POLOVIN, R. V., Nonlinear magnetohydrodynamic waves, 20: 42430
POLTORATSKII, N. I., Fabrication of thin plates from refractory carbides, 20: 41430
POLUBARINOV, I. V., Einstein's equations as describing a massless tensor field with spin 2, 20: 42078
POLUBARINOV, I. V., Theory of a natural massive tensor field with spin 2, 20: 41938
POLUEKTOV, N. S., Mixed sulfosalicylate complexes of rare earth elements, 20: 40926
POLUSHKIN, I. N., Some properties of a plasma in helium and argon with added cesium and potassium vapors, 20: 41712
POLYAKOV, A. M., Some consequences of the algebra of weak and electromagnetic currents, 20: 41949(T)
POMANOVA, E. S., Biological consequences of radioactive contamination of water bodies, 20: 40527
POMEROY, L. R., Flux of ^{32}P and ^{65}Zn through a salt-marsh ecosystem, 20: 40573
POMPE, W., Variational principle in describing a many-particle system, 20: 42074
POMRANING, G. C., Variational description of dissipative processes, 20: 41409
PONCELET, J., Prospects for the utilization of chemical ionization phenomena in MHD, 20: 41730
POND, T. A., Static Moessbauer search for parity nonconservation in ^{57m}Fe, 20: 42322
PONIZOVSKAYA, A. I., Clinical and dosimetric data on personnel operating a 10 Bev synchrophasotron, 20: 41206 (JPRS-36341, pp 10-17)
PONOMARENKO, A. G., Investigation of plasma injected into trap with conical theta pinch, 20: 42504
PONOMAREV, L. A., Effects of violation of CP-invariance in radiative decays of neutral K-mesons, 20: 41905
POPOV, G., Influence of a h-f inhomogeneous field on a gaseous-discharge plasma, 20: 42442
POPOV, N. I., Absorption of artificial radionuclides by marine detritus, 20: 41140
POPOV, V. A., Ionization and conductivity of hydrocarbon fuel combustion products, 20: 41731
POPP, R. A., Influence of age on susceptibility to radiation-induced life-shortening in mice, 20: 40633 (ORNL-P-2287)
PORAI-KOSHITS, M. A., Crystal structure of $Cs_3[UO_2(NCS)_5]$, 20: 40932
PORILE, N. T., Recoil ranges of products from reactions of Cu with 11-43-Mev ^4He ions, 20: 42259
PORTER, N. S., Physiological data telemetry system, 20: 41220 (BNWL-214)
POSCH, Rudolph E., Coil systems for measuring conductivity and velocity of plasma streams, 20: 42485
POSPELOV, A. A., Preparation of granulated zirconyl phosphate by freezing and its ion exchange properties, 20: 41055
POSPISIL, J., Effects of irradiation on level of reduced nicotinamide nucleotides in rat liver homogenates, 20: 40583
POTTER, R. C., Gamma-radiation-induced ionic polymerization of pure liquid styrene. II., 20: 40978
POULET, M., Experimental study of elastic proton-deuteron scattering at 155-Mev, 20: 42184
POULET, M., Experimental study of inelastic proton-deuteron scattering at 155 Mev, 20: 42185
POUNDER, J. O., Fuel temperature measurements in mixed oxide elements, 20: 42612
POWELL, J., Application in nuclear MHD cycles of non-equilibrium ionization from metastable molecular states excited by fission fragments, 20: 41732
POWELL, R. E., Electron collisions in nitrogen, 20: 41652
POWELL, R. E., Electron ionization of He^*, 20: 41653
POWERS, E. L., Contributions of electron paramagnetic resonance to understanding of radiation biology, 20: 40597
PRADAL, J., Isospin quintuplets in A = 20 nuclei, 20: 42227
PRADAL, J., Quintuple isospin of mass 16 nuclei, 20: 42344
PRASAD, K. G., Level structure of ^{199}Au from decay of ^{199}Pt, 20: 42268
PRASAD, Kedar N., Necturus maculosus as experimental animal to study cellular injuries of irradiated gut, 20: 40607 (BNL-10518)
PRASAD, R., Measurement of (n,2n) reaction cross sections at 14.8 Mev, 20: 42207
PRASIL, Z., Theory of radiation chemistry. I., 20: 40958
PRASIL, Z., Theory of radiation chemistry. II., 20: 40959
PRATS, F., Zero-range treatment of the three-body photodisintegration cross section of ^3H and ^3He, 20: 42228
PRATT, R. H., Generators of the de Sitter group for the hydrogen atom, 20: 41644
PRAVDINA, G. M., Behavior of live organisms in radiation fields, 20: 40519 (NP-16259)
PRAVDINA, G. M., Behavior of fish in zone of radiation sources, 20: 40656
PRAY, H. L., Low energy electron studies in indium and magnesium, 20: 41621 (ORNL-TM-1565)
PREISS, I. L., Boron-10, ^{11}B, and ^6Li induced reactions of ^{27}Al, 20: 42183
PREKEL, H. L., Innovations in electron-beam zone refining of molybdenum, 20: 41434
PREM, Lawrence L., Analytical and experimental results of the fluid metal MHD power conversion program, 20: 41733
PREMOLI, A., Void fraction measurement in boiling channel, 20: 41103 (RT-ING-(65)7)
PRENTICE, J. D., Differential cross sections for $\pi^\pm p$ elastic scattering in the momentum range 875-1579 Mev/c, 20: 41857
PREPARATA, G., Saturation of the SU_6 algebra and a possible classification group for hadrons, 20: 41968
PRESCOTT, C. Y., Photoproduction of η mesons from 950 to 1100 Mev, 20: 41889
PRESTON, A., Accumulation of radionuclides by aquatic organisms of economic importance in United Kingdom, 20: 40578
PRESTWICH, W. J., X-rays from muonic atoms with spherical or nearly spherical nuclei, 20: 42306
PRESTWICH, W. V., Determination of non-linear parameters and their standard deviations from least-squares residuals, 20: 41518
PRICE, J. H., Performance of enclosure shields in real fallout field, 20: 41201 (RRA-T55 and Summary)
PRIDMORE-BROWN, D. C., Electric dipole radiation through a finite conical plasma sheath, 20: 42438
PRIEM, H. N. A., Isotopic evidence for upper-cambrian or lower-ordovician granite emplacement in Vigo area, Spain, 20: 41153
PRIMACK, J. R., Single-particle calculations in nuclear fission, 20: 42272
PRINZ, W., Influence of Ca and Sr in the diet on the elimination of ^{85}Sr and ^{89}Sr by goats, 20: 40568
PRINZLER, H., Studies of low current arcs with high frequency methods for plasma diagnosis, 20: 42513
PRITCHARD, W. C., Studies on the formation of Pu_2O_3 in the sintering of PuO_2, 20: 41426 (LA-3493)
PROCA, G., Electron scattering at 180° on ^{12}C, 20: 42377
PRODAN, E. A., Effect of radioactive decay in solids on their relaxability, 20: 41018
PROKOFEV, P. T., Decay scheme of ^{179}Hf produced in (n,γ) reactions, 20: 42285
PROKSCH, E., Molecular plating. V., 20: 41011 (SGAE-CH-34/1966)
PROSKURNIN, M. A., Radiation chemical oxidation of butanol in aqueous solution at increased temperature, 20: 40983
PRUGOVECKI, Eduard, Axiomatic approach to the formalism of quantum mechanics. I., 20: 42083
PRUGOVECKI, Eduard, Axiomatic approach to the formalism of quantum mechanics. II., 20: 42084
PRUZANSKY, J., Method of producing hydrazine, 20: 41008
PRYADKIN, K. K., High-pressure electrodeless discharge and its magnetic properties, 20: 42509
PRZYTULA, M., Detector of fast neutrons with a moderator, 20: 41335
PRZYTULA, Marian, Gamma-ray scintillation spectrometer with NaI(Tl) single crystal, 20: 41336
PRZYTULA, Marian, Two-impulse neutron detector with plastic scintillator, 20: 41337
PSHEZHETSKII, S. YA., Heterogeneous processes in radiation catalysis, 20: 40989
PUFF, R., Λ_{10} approximation for self-bound many-fermion systems, 20: 42248

PUGNIN, V. I., Role of He in He–Xe plasma, 20: 42491
PUJIC, Zdravko, Determination of ^{85}Sr, ^{106}Ru, ^{137}Cs, and ^{144}Ce by γ-spectroscopy, 20: 40837
PULVER, E. F., Flux methods for transport problems in solids with non-constant electric fields, 20: 42546
PUPKE, H., Lateral extraction of negative ions from a layered low-pressure discharge in oxygen, 20: 42435
PURCELL, W. L., High power density core of the PRTR, 20: 42674 (BNWL-221)
PUSTOVALOV, G. E., Solution of Laplace's equation for a Penning discharge gap, 20: 42508
PUSTOVOIT, Yu. M., Vacuum system of Ogra-II, 20: 42421 (NP-tr-1396)
PYCHLAU, Herbert, Device for measurement of neutron radiation, 20: 41358
PYLE, G. J., Optical-model analysis of 30-Mev proton scattering, 20: 42255

Q

QAIM, S. M., 16-min ^{241}Np isomer and a search for its 3.4-hr isomer, 20: 42202
QUANG, Ho-kim, Three-nucleon potential, 20: 41838
QUARTERMAN, L. A., Raman spectrum and hydrolysis studies on hydrogen fluoride solutions of xenon oxide tetrafluoride, 20: 40906
QUEL, E., Excitation function for the reaction $^{197}Au(d,p)^{198}Au$, 20: 42206
QUINLAN, W. J., X-ray induced hypothyroidism in dog, 20: 40698
QUINN III, James L., Crescent pattern of increased radioactivity in brain scanning, 20: 40789
QUIRK, A., Safety of pressure vessels against fast fracture, 20: 42576 (AHSB(S)-R-107)
QUITMANN, D., g-Factor in 2^+ rotation states in ^{166}Er and ^{168}Er, 20: 42302
QUIVY, P., Reactions $^{9}Be(n,nn)\alpha\alpha$ at 15 Mev, 20: 42362
QUONG, James, Approximations in the theory of rearrangement collisions and applications to a tractable model of charge exchange scattering, 20: 41624 (UCRL-17034)

R

RAAB, W., Spinor calculus in Riemannian manifolds, 20: 42079
RABB, H. F. Jr., Uranium-233 thorium seed-blanket experimental program, 20: 42609 (WAPD-T-1886)
RABOY, S., X-rays from muonic atoms with spherical or nearly spherical nuclei, 20: 42306
RADEBAUGH, Ray, Low-temperature thermodynamic properties of V. I., 20: 42115
RADEBAUGH, Ray, Low-temperature thermodynamic properties of V. II., 20: 42116
RADEBOLD, R., Energy conversion with liquid metal working fluids in MHD Staustrahlrohr, 20: 41734
RADVANYI, P., Discussion of the results obtained in pickup reaction on ^{9}B and ^{10}B nuclei at 156 Mev, 20: 42350
RADVANYI, P., Preliminary results on ^{4}Li, ^{5}Li, and ^{6}Li obtained by (p,d) and (p,t) reactions on ^{6}Li and ^{7}Li at 156 Mev, 20: 42358
RADVANYI, P., Reaction (p,d) at 156 Mev on fluorine and nitrogen, 20: 42204
RADZIEVSKII, V. N., Interaction between a fast charged particle and non-equilibrium plasma, 20: 42486
RAGAZZONI, Gian D., Extension of memorial system for implant dosimetry, 20: 40788
RAGHAVAN, R. S., Influence of a randomly oriented collinear combined interaction on angular correlations, 20: 42226
RAHN, R. O., Electron spin resonance of irradiated deoxyribonucleic acid, 20: 40594
RAIEVSKI, Victor, Improvements in control rods for nuclear reactors, 20: 42587
RAINEY, V., Localized vibrations of trapped molecules, 20: 41651
RAINWATER, J., Detailed analysis of muonic x-ray spectrum from strongly deformed e-e nuclei, 20: 42310
RAKHIMOV, A. T., Magnetic hydrodynamics of flow in MHD ducts, 20: 41735
RALPH, J. C., MHD power generation experiments using seeded inert gases, 20: 41736
RAMADURAI, S., Matter traversed by low-energy cosmic-ray nuclei in space, 20: 41675
RAMAN, K., Evaluation of meson-baryon coupling constants from current divergences, 20: 41860
RAMANIAH, V. M., Preparation of carrier-free ^{131}I from irradiated elemental tellurium, 20: 41399 (IEA-110)
RAMASWAMI, D., Removal of actinide halides from alumina, 20: 41062
RAMASWAMI, Devabhaktuni, Removal of stainless-steel claddings from nuclear fuel elements, 20: 41060
RAMAYYA, A. V., Germanium(Li)–NaI(Tl) coincidence system with multichannel analysis, 20: 41295
RAMAYYA, A. V., M, N, and O subshell conversion coefficients in ^{228}Th and ^{240}Pu, 20: 42264
RAMKRISHNA, C. K., Oxidative phosphorylation in fractionated bacterial systems. XXII., 20: 40571
RAMSDEN, S. A., Temperature measurements of a laser spark from soft-x-ray emission, 20: 42475
RANGNEKAR, Asha V., Separation of silver from mixtures by cation-exchange chromatography, 20: 40847
RAO, A. Bhaskara, Study of asymmetry in the lateral distribution of shower particles near sea level, 20: 41668
RASERA, R. L., Search for parity mixing in the 501 kev γ transition of ^{180m}Hf, 20: 42230
RASHAD, A. R. M., Technique for measuring the scalar and tensor plasma conductivity using an induction type MHD device, 20: 41737
RASHAD, A. R. M., Theory and analysis of cylindrical induction-type MHD a-c power generators, 20: 41694
RASMUSSON, D. C., Prog. rpt. on genetic control of physiological processes in higher plants, 1965–66, 20: 40532 (COO-1097-17)
RASOR, N. S., Influence of negative ions on cesiated emitters, 20: 41695
RATNAM, V. V., Color centers and x-ray luminescence of calcium fluoride crystals, 20: 42556
RATNAM, V. V., Electrical and magnetic properties of colored and uncolored calcium fluoride crystals, 20: 42555
RAU, G., Duoplasmatron as negative ion source, 20: 41571
RAUBENHEIMER, L. J., Electron spin resonance spectra of Dy^{3+} in ThO_2 and CeO_2, 20: 42525 (ORNL-P-2466)
RAVERA, O., Effects of x-irradiation on various stages of life cycle of Physa acuta, 20: 40700
RAVIV, Szmuel, Improvements in or relating to electrolytic dissolution of spent U fuel elements, 20: 41056
RAYBECK, R. M., Determination of rare earth inclusions in steel, 20: 41415
RAZDOBARIN, G. T., Temperature and electron concentration in plasma arc from Thomson scattering, 20: 42432
READ, J. F., Alpha-particle radiolysis of the cyclohexane-S system, 20: 40990
REAGAN, Daryl, Scanning electron beam profile monitor, 20: 41562
REAMES, D. V., Elemental abundances of low-energy cosmic rays in July 1964, 20: 41672
REAMES, D. V., Source spectra and composition of cosmic rays, 20: 41673
RECAMI, Erasmo, Calculation of cross section of reaction $K + N \to K^* + N$, 20: 41898
REDFIELD, J. A., FLASH: program for digital simulation of loss of coolant accident, 20: 42582 (WAPD-TM-534)
REED, Jack W., Amplitude variability of explosion waves at long ranges, 20: 41158
REED, M., Excited states in ^{9}Be and ^{10}C, 20: 42190
REEVES, H., Some problems of nuclear astrophysics, 20: 41600
REGAN, R. E., Oxidation studies of complex silicides for protective coatings, 20: 41424
REGIS, V., Excitation of 5.7 Mev level at ^{7}Li by (n,n') scattering at 14 Mev, 20: 42364
REGUSHEVSKII, V. I., Cascade nucleons emitted by nuclei interacting with 660 Mev protons, 20: 42299
REIKHRUDEL', E. M., Solution of Laplace's equation for a Penning discharge gap, 20: 42508
REIN, Robert, Studies of hydrogen-bonded systems. IV., 20: 40589
REINER, A. S., A_{10} approximation for self-bound many-fermion systems, 20: 42248
REITAN, Arne, Radiative absorption of stopped pions by deuterons, 20: 41809
REJALI, Abbas M., Radioisotope scanning with system for information storage and controlled retrieval, 20: 40748
REKALO, M. P., Nonleptonic baryon decays in the static model with SU(6) symmetry, 20: 42023
REKALO, M. P., Photoformation of mesons on nucleons and SU(6) symmetry, 20: 41812
REKALO, M. P., Radiative decays of vector mesons in the SU(6) symmetry, 20: 41908
REKALO, M. P., Relations between interaction constants of vector mesons with baryons, 20: 42013
REKOV, A. I., Processes of interaction between high-temperature materials and gas flows in the duct of an MHD generator, 20: 41738
RENERO, I., Matrix elements and normalization coefficients in SU_n, 20: 42010
RENNINGER, G. H., Cutkosky-Leon normalization conditions, 20: 41951
RESECK, Karl G., MHD generator performance prediction including two-dimensional effects and wall leakage, 20: 41739
RESNIKOFF, M., Are the positive-parity mesons in the 405 multiplet?, 20: 41874

REY, C. A., Compact low-inductance spark chamber pulser, 20: 41293
REYERS-DEGLI INNOCENTI, I., Effect of radioprotectors on damage induced by alkylating agents on tumoural and normal tissues, 20: 40664
REYNOLDS, J. T., Carbon-12 fast neutron cross sections and Legendre moments below 15.0 Mev, 20: 42160 (KAPL-3099)
RICE, G., Optimization of generator parameters and of overall thermal efficiencies for an MHD reactor system, 20: 41740
RICH, Marvin A., Pathogenesis of radiation-induced thymic lymphoma in mice, 20: 40677
RICHARD, P., Coulomb displacement energies from isobaric analogue resonances, 20: 42262
RICHARDSON, J. Reginald, Energy dependence of proton-proton bremsstrahlung, 20: 41882
RICHTER, Alden P., Forecasting strong southwest winds at NRTS, 20: 41129
RICHTER, Karl, Measurement of gas velocities by radiation-modulation technique, 20: 41381
RIDER, B. F., Prog. rpt. on accurate nuclear fuel burnup analyses, 12/65–2/66, 20: 42608 (GEAP-5124)
RIECK, C. E., VARI-QUIR diffusion code, 20: 42143 (WANL-TNR-133 (Rev.))
RIEGER, R., Chelate formation as sensitizing factor in production of chromatid aberrations by radiomimetic agents, 20: 40715
RIEGER, R., Experimental induction of chromosomal aberrations in plants, 20: 40714
RIENECKER, F. Jr., Revised safety analysis report for the Super Kukla prompt burst reactor, 20: 42684 (UCRL-7695(Rev.1))
RIESE, J. W., VARI-QUIR diffusion code, 20: 42143 (WANL-TNR-133 (Rev.))
RIESENHUBER, Heinz, Separation of radioactive ions from their solutions, 20: 41058
RIETJENS, L. H. Th., Equilibrium and stability of a toroidal screw pinch, 20: 42414 (NP-16266)
RIGNEY, D. V., Viscosity of liquid K to 900°C, 20: 41460 (TIM-793)
RINALDINI, C., Comparison of different methods for kinetics of ESSOR reactor type, 20: 42678 (EUR-3051.e)
RING, P. J., NMR studies of ^{7}Li in polycrystalline lithium nitride, 20: 42175
RIOU, M., Study of (p,2p) reaction at 155 Mev on ^{7}Li, ^{9}Be, and ^{23}Na with an on-line computer, 20: 42360
RIPKA, G., Determination of coefficients of spin and isospin mixtures of an effective nucleon-nucleon force, 20: 42348
RIPLING, E. J., Prog. rpt. on fracture toughness of reactor pressure vessel steels, 6–7/66, 20: 41444 (COO-1477-5)
RIPPS, Harris, Ocular lesions produced by an optical maser, 20: 40692
RISKALLA, R., Electron excitation of first levels of ^{11}B, 20: 42378
RISTINEN, R. A., Lifetime determinations for nuclei A = 10, 11, and 12 from gamma-ray Doppler shifts, 20: 42234
RITCHIE, R. H., Low energy electron studies in indium and magnesium, 20: 41621 (ORNL-TM-1565)
RITTLER, M. Catherine, Optical maser as a retinal coagulator, 20: 40791
RIVERA, Joseph, Prog. rpt. on fallout, 3–6/66, 20: 41131 (HASL-172)
RIVIERE, Marcel-Rene, Studies in rats carrying lymphoblastic lymphosarcoma exposed to effect of electromagnetic waves associated with magnetic fields, 20: 40661
ROBERTS, A. S. Jr., Quasi-fluid treatment for intense electron beam flow, 20: 42515
ROBERTS, J. E., Dirac bra and ket formalism, 20: 42085
ROBERTS, N. L., Synthesis of ^{14}C-labelled bipyridylium salts, 20: 40941
ROBERTS, P. J., Potential energy integrals for nonoverlapping atomic wave functions, 20: 42123
ROBERTS, T. A., General principles in microbiology of irradiated foods, 20: 41388
ROBERTS, T. R., Large-angle neutron-proton C_{NN} parameter at 23.1 Mev, 20: 41877
ROBERTSON, R. F. S., Fuel, materials, and coolants for WR-1, 20: 42669 (AECL-2553)
ROBINSON, G. W., Infrared spectra of HCl and DCl in solid rare gases. II., 20: 40895
ROBINSON, J. Eugene, Computer dosimetry system for radium implants, 20: 40765
ROBINSON, John Albert, Couplings for tubular members, 20: 41100
ROBINSON, John Albert, Improvements in and relating to articulated supports, 20: 42589
ROBINSON, M. G., Irradiation of deoxyribonucleohistone solutions. I., 20: 40585
ROBINSON, M. G., Irradiation of deoxyribonucleohistone solutions. II., 20: 40586
ROCHESTER, L. S., Photoproduction of η mesons from 950 to 1100 Mev, 20: 41889
RODGERS, J. W., Vacuum encapsulated lithium-drift detector telescope, 20: 41376
ROEBBELEN, G., Effects of two endogenous factors on artificial mutagenesis in Arabidopsis thaliana, 20: 40709
ROFFMAN, B., Flux of ^{32}P and ^{65}Zn through a salt-marsh ecosystem, 20: 40573
ROGANOV, V. S., Angular distribution of high energy neutrons emitted in the absorption of polarized μ^--mesons in Ca, 20: 42300
ROGINSKII, V. A., Investigation by EPR method of the uv and γ-radiation induced free radicals in H_2O_2 in NH_3 solutions, 20: 41001
ROGOZKIN, B. D., Thermodynamic properties of inorganic substances (handbook), 20: 41417
ROLLAND, C., Elastic scattering of protons of 150 and 80 Mev on light nuclei and the optical potential, 20: 42388
ROLLAND, C., Polarization of protons of 152 Mev by inelastic scattering on ^{12}C and ^{40}Ca, 20: 42341
ROLLINS, R. W., Low-frequency transitions and critical currents in the superconducting surface sheath, 20: 42125
ROMAN, P., Effective $\Delta I = \frac{1}{2}$ rule in the three-pion decays of kaons, 20: 41840
ROMAN, P., Novel approach to nonleptonic weak hyperon decays, 20: 41834
ROMAN, P., Problems of physical interpretation connected with noncompact groups in particle physics, 20: 42033
ROMAN, P., Two-pion decays of kaons in a novel approach to nonleptonic weak processes, 20: 41835
ROMANO, V., Nature and stability of system uranyl-benzohydroxamic acid in acid medium, 20: 40903
ROMANOV, A. I., Processes of interaction between high-temperature materials and gas flows in the duct of an MHD generator, 20: 41738
ROMANOVSKY, V., Study of bottom layers in the deep parts of the Mediterranean Sea, 20: 41128
ROME, Martin, High temperature ruggedized multiplier phototubes, 20: 41374
RONSIVALLI, Louis J., Prog. rpt. on study of irradiated-pasteurized fishery products, final, 10/64–9/65, 20: 41384 (TID-22833)
ROOD, R. T., Solvent extraction of ^{18}F as tetraphenylstibonium fluoride, 20: 41021
ROOS, M., Leptonic decays of hadrons, 20: 41987
ROPER, L. David, Pion-nucleon phase shift analyses, 20: 41913
ROQUES, C., Use of austenitic steel as construction material for the pressure vessel of the fast reactor "rapsodie", 20: 42652 (EURFNR-92F)
ROSE, B., Experimental aspects of nucleon-nucleon scattering and polarization below 1 Bev, 20: 41918
ROSE, B., Measurements of the differential cross-section and polarization in proton-proton scattering at about 143 Mev, 20: 41915
ROSE, Joseph A., Computer dosimetry system for radium implants, 20: 40765
ROSEBROCK, T. L., Experimental investigations of closed-loop MPD power generation, 20: 41741
ROSEN, S. P., Parity-conserving hyperon decay and the pole model, 20: 41868
ROSENTHALL, Leonard, Radionuclide venography using ^{99m}Tc pertechnetate and gamma-ray scintillation camera, 20: 40752
ROSENZWEIG, N., Density of states of degenerate Fermi systems with periodic level schemes, 20: 42222
ROSICKY, Jaroslav, Chemistry of the rare earth metals. XI., 20: 40909
ROSIER, L. H., Levels of ^{15}O excited by the reaction $^{14}N(d,n\gamma)^{15}O$ at 6.3 Mev, 20: 42346
ROSLER, U., Zirconium and its alloys as materials for water-cooled nuclear reactors, 20: 41422
ROSLYAKOV, G. S., Numerical methods in gas dynamics, 20: 42038 (NASA-TT-F-360)
ROSNER, M., Efficiency of closed-loop MHD generators utilizing thermal non-equilibrium ionization, 20: 41742
ROSNER, M., Oil-fired MHD power plant, 20: 41743
ROSNY, G., Resolution of charge preamplifier, 20: 41298
ROSS, Marc, Photon dissociation model for vector-meson photoproduction, 20: 41863
ROSS, Marc, Regeneration effects in ω-ϕ production, 20: 41888
ROSSIEVSKII, G. I., Effectiveness of the oxygen enrichment of air in MHD generator assemblies, 20: 41744
ROSSIEVSKII, G. I., Effect of the capacity of electric power stations with MHD generators on their thermal efficiency, 20: 41769
ROSSOMAKHO, Yu. V., Effect of the annealing temperature and medium on the properties of molybdenum, 20: 41482
ROSSOW, Vernon J., Coil systems for measuring conductivity and velocity of plasma streams, 20: 42485
ROSTAS, Francois, Construction and testing of auxiliary-arc electrodes, 20: 41745
ROSTAS, Francois, Plasma diagnostic methods utilizing lasers, 20: 42445
ROTELLI, P., $p\bar{p}$ Annihilations at rest with representation mixing in SU_{6w}, 20: 41847
ROTELLI, P., Semi-phenomenological analysis of nonleptonic hyperon

decays in U_{12}, 20: 41831
ROTHBERG, J., Recent experiments of muonium, 20: 41661
ROTHWELL, W. S., Effects of orientation and annealing on Jc vs. H in cold-worked Nb-25% Zr, 20: 42569
ROTTER, Kh., New isotope ^{210}Ac, 20: 42287
ROTURIER, J., Elastic scattering of 14 Mev neutrons by K, 20: 42393
ROUSCH, M. L., Total reaction cross sections for 14.5 Mev protons from 22 separated isotopes of Ti, Fe, Ni, Cu, Zn, Zr, and Sn, 20: 42162 (LA-DC-8075)
ROUSE, Carl A., Accurate and stable numerical solutions to the Schroedinger equation, 20: 42097
ROUSSEL, P., Levels of ^{24}Mg, ^{25}Mg, and ^{26}Mg excited by the reactions (α,α') $(\alpha,^3He)$, and (α,t), 20: 42347
ROUSSELOT, Louis M., Radioprotective and anti-tumor effect of mixed bacterial toxins and anthramycin, 20: 40736
ROUX, G., Imagery of x and γ rays by gas-filled image intensifier, 20: 41299
ROWCLIFFE, D. J., Effects of orientation and annealing on Jc vs. H in cold-worked Nb-25% Zr, 20: 42569
ROY, M., Reaction (p,d) at 156 Mev on fluorine and nitrogen, 20: 42204
ROYNETTE, J. C., Study of (p,2p) reaction at 155 Mev on ^{7}Li, ^{9}Be, and ^{23}Na with an on-line computer, 20: 42360
ROZEN, A. A., Morphology and texture of molybdenum and tungsten carbonyl deposits, 20: 41468
ROZENFELD, M. L., Determination of absorbed dose for electron beam therapy, 20: 40741 (ACRH-25, pp 15-23)
RTISHCHEVA, N. P., Composition and thermodynamic properties of the combustion products of natural fuels with ionizing additives, 20: 41785
RUBAN, M. A., ENDOR of F centers in KCl at room temperature, 20: 42566
RUBENFELD, Sidney, Advantage of three combined diagnostic procedures with ^{131}I for evaluation of thyroid disorders, 20: 40756
RUBIN, Allen G., Effects of partial ionization and pressure on hydromagnetic ionizing waves, 20: 42401 (AD-637854)
RUEGG, H., Generalizations of isoparity, 20: 41923
RUELLE, D., Theorem on canonical commutation and anticommutation relations, 20: 42076
RUGH, R., Sequelae of LD/50 x-ray exposure of pre-implantation mouse embryo, 20: 40649
RUHLA, Ch., Study of (p,2p) reaction at 155 Mev on ^{7}Li, ^{9}Be, and ^{23}Na with an on-line computer, 20: 42360
RUIZ, C. P., Prog. rpt. on accurate nuclear fuel burnup analyses, 12/65–2/66, 20: 42608 (GEAP-5124)
RUIZ MEJIA, Carlos, Simple model for de-excitation curves of Ag-doped NaCl, 20: 42561
RUNGE, K., Detailed analysis of muonic x-ray spectrum from strongly deformed e-e nuclei, 20: 42310
RUNGE, K., Metastable $d_{3/2}$ hole state in ^{47}Sc, 20: 42192
RUNNELS, Sandra, Lethal effects of ^{60}Co on mature White Leghorn chickens, 20: 40693
RUSAKOV, A. A., Investigation of alloys of the Zr–C system, 20: 41471
RUSH, J. E., Application of π-N scattering results to Λ-K° production, 20: 41917
RUSSELL, Albert Henry, Improvements in or relating to liquid moderated nuclear reactors, 20: 42595
RUST, D., Wide angle electron pair production at high energy, 20: 42327
RUST, R. H., Prog. rpt. on genetic control of physiological processes in higher plants, 1965–66, 20: 40532 (COO-1097-17)
RUTLAND, D., Motion sensing and its application to Project Wisp, 20: 41224 (EGG-1183-2078)
RUUSKANEN, Vesa, Double poles and nonexponential decays in atomic physics, 20: 41649
RYABTSEV, N. G., Thermodynamic properties of inorganic substances (handbook), 20: 41417
RYAN, J. T., Radiological recovery requirements, structures, and operations research. I., 20: 41179 (AD-635821)
RYAN, J. T., Radiological recovery requirements, structures, and operations research. II., 20: 41180 (AD-635822)
RYAN, J. T., Radiological recovery requirements, structures, and operations research. IV., 20: 41182 (AD-635824)
RYL'KOV, V. V., Determining splitting in nuclear-resonance spectra, 20: 41254

S

SADEGHI, A., Absolute cross sections for elastic scattering of deuterons on α particles between 3 and 14 Mev, 20: 42371
SADEGHI, A., Absolute cross sections of the reactions ^{12}C(p,p)^{12}C, ^{12}C(p,p′)^{12}C*, ^{12}C(p,p″)^{12}C*, and levels of ^{15}N, 20: 42390
SAGALOVICH, V. V., Morphology and texture of molybdenum and tungsten carbonyl deposits, 20: 41468
SAGANE, Norio, Radiation-induced solid-state polymerization in binary systems. II., 20: 40977
SAHA, G. B., Recoil ranges of products from reactions of Cu with 11-43-Mev ^{4}He ions, 20: 42259
SAHNI, R. C., Effect of vibrational-rotational motion on the electric and magnetic properties of diatomic molecules, 20: 41659
SAITO, M., Static baryon-meson bootstraps and SU_6 symmetry, 20: 41848
SAITO, Y., Experimental studies of oil-fired MHD power generation, 20: 41780
SAKAI, Kenji, Evidence for existence of a repulsive core in the Λ-N interaction, 20: 41894
SAKATA, Harumi, Gaseous centrifuge and separation of argon isotopes, 20: 41404
SAKHAROV, A. D., Quark structure and masses of strongly interacting particles, 20: 42017
SAKITA, B., Higher symmetries of hadrons, 20: 41928 (NP-16191)
SAKUMA, T., Static baryon-meson bootstraps and SU_6 symmetry, 20: 41848
SAKUMA, Tetsuro, Dynamical approach to the leptonic decays of baryons, 20: 41999
SAKURAI, J. J., Relation between the pion-nucleon and the ρ-meson coupling constants from pion scattering lengths, 20: 41885
SALATSKAYA, M. I., Clinical and dosimetric data on personnel operating a 10 Bev synchrophasotron, 20: 41206 (JPRS-36341, pp 10-17)
SALETAN, Eugene J., q-equivalent particle Hamiltonians. I., 20: 41941
SALIN, R., Study of angular distributions of the reaction ^{32}S(n,α_0)^{29}Si at 2.5 to 3.2 Mev, 20: 42375
SALTER, R. M. Jr., n-n S-wave scattering length from the neutron spectra of the reaction $\pi^- + d \rightarrow 2n + \gamma$, 20: 41914
SALVAT, M., Device for operating a closed-loop MHD generator with current density measuring facilities, 20: 41678 (IPP-3/40)
SALVAT, M., Internal resistance and potential drop in MHD generators, 20: 41700
SALZER, Manfred, Double fluorides of Th, U, Np, and Pu of type $Me^{II}\,Me^{IV}F_6$ with LaF_3 structure, 20: 40867 (KFK-385)
SAMOKHVALOVA, L. I., Radiation yield of triplet molecules in radiolysis of benzene, 20: 40961
SAMOSVAT, G. S., Kev neutron scattering by lead and electrical polarizability of neutron, 20: 42140 (JINR-P-2764)
SAMPLE, J. T., Properties of excited states in ^{14}C, 20: 42233
SAMS, W. Mitchell Jr., Spectral shift phenomenon of chloroquine, 20: 40954
SAMSON, Stan, To encapsulate effectively scintillation crystals for x-ray diffraction work, 20: 41328
SAMUELS, E. R., Canadian fallout data for April 1965, 20: 41209
SAMUELS, E. R., Reactor environment monitoring for April 1965, 20: 41136
SANDBORG, Alan O., Particle detector of the semi-conductor type, 20: 41369
SANDERS, J. P., Temperatures in the cladding under the spacers of the BONUS superheater assemblies, 20: 42633 (ORNL-TM-1452)
SANDERS, J. P., Temperature distribution under dimples proposed as spacers in the BONUS superheater assemblies, 20: 42634 (ORNL-TM-1453)
SANDERSON, E. A., Particle-hole excitations in ^{208}Pb, 20: 42205
SANDOVAL, E., Excitation function for the reaction ^{197}Au(d,p)^{198}Au, 20: 42206
SANDOVAL, Edmundo, General guide for irradiations in the research and experimental reactor IAN-R1, 20: 42679 (IAN-R-1)
SANDRI, G., Stellar winds and the distribution of electrostatic potentials about stars, 20: 41617
SANDRU, P., Electrode calibration for nuclear diagraphy, 20: 41165
SANKAVICH, Melvin F., Generation of thermionic electricity from the thermal energy from nuclear combustion, 20: 41682 (LA-tr-66-32)
SANO, H., Moessbauer recoilless fraction in tin compounds, 20: 41637
SANTILLI, R. M., Connection between the complex Lorentz group with a real metric and the $U_{3,1}$ group, 20: 41852
SAPERSTEIN, Z. P., Prog. rpt. on Zy braze alloy development, 4–6/66, 20: 41425 (IITRI-578-P29-2)
SARAEVA, V. V., Composition of products of radiative methanol oxidation, 20: 41004
SARAIYA, S. C., Effect of complexing agents on the disproportionation of U(V), 20: 40911
SARGIN, Necla, Uranium and cobalt complexes of heterocyclically substituted formazans, 20: 40880
SARIC, W. S., Generalized magnetohydrodynamic entrance flow model. I., 20: 42036 (SC-RR-66-356)
SARKAR, D. C., Measurement of (n,2n) reaction cross sections at 14.8 Mev, 20: 42207
SARVER, J. F., Diffuse reflectance characteristics of monoclinic ZrO_2 as a function of purity, 20: 41486
SASAKI, Y., MHD power generation experiments with K-seeded Ar plasmas, 20: 41781
SASAKURA, Hiroshi, Electron spin resonance of irradiated silicate glasses, 20: 42538
SATCHLER, G. R., Multiple excitation and the shell model description of the ^{90}Zr(p,p′) reaction, 20: 42229
SAUER, F. M., Multiple subsurface spalling by underground nuclear

explosions, 20: 41126
SAIKEL, H., Molecular plating. V., 20: 41011 (SGAE-CH-34/1966)
SAUNDERS, B. G., Fission γ rays using Ge(Li) detector in conjunction with bent-crystal spectrometer, 20: 41278 (UCRL-70000)
SAUNDERS, B. G., High-resolution studies of fission x rays and gamma rays, 20: 42170 (UCRL-70045)
SAUNDERSON, D. H., Pressure dependence of the TA[100] zone-boundary phonon frequency in rubidium iodide, 20: 42550
SAUNIER, N., Reaction $p + {}^{9}Be \rightarrow d + {}^{8}Be$, 20: 42212
SAUNIER, N., Study of the reactions $d + {}^{7}Li = n + 2\alpha$ and ${}^{6}Li + T = n + 2\alpha$, 20: 42349
SAUROV, M. M., Movement of ${}^{90}Sr$ from fresh water bodies into the human organism, 20: 41142
SAUTIN, A., Variation of isotopic concentration in separated rare earths, 20: 40843
SAVITSKII, E. M., Growing and plastic deformation of the single crystals of refractory metals and alloys, 20: 41481
SAVKOVIC, N., Influence of DNA on reparation of germinal epithelium and spermatozoa of x-irradiated rats, 20: 40723
SCANLON, P. J., Charged photoparticles from ${}^{165}Ho$, 20: 42214
SCARAMUZZI, F., Liquid ${}^{3}He$ target for high-energy nuclear experiments, 20: 42107
SCARF, Frederick L., Wave-particle interactions in the solar wind, 20: 41615
SCHARA, M., Electron spin resonance of irradiated $NaH_3(SeO_3)_2$ and $NaD_3(SeO_3)_2$, 20: 40972
SCHATZMAN, E., Remarks on stellar evolutions. III., 20: 41584 (UCRL-Trans-10040)
SCHATZMAN, E., Remarks on stellar evolution. V., 20: 41585 (UCRL-Trans-10041)
SCHAUER, Carlotta V., Bibliography on elastic and inelastic p-p scattering, 20: 41800 (UCRL-14716)
SCHEIBLING, F., Electromagnetic transitions in ${}^{16}O$ nuclei, 20: 42342
SCHEINBERG, Labe C., Is the brain an immunologically privileged site? II., 20: 40643
SCHELEV, Sch., Decay series ${}^{138}Nd \rightarrow {}^{138}Pr \rightarrow {}^{138}Ce$, 20: 42197
SCHENCK, G. O., ESR investigation of radical reactions in γ-irradiated frozen aqueous solutions of formic acid and formate, 20: 40994
SCHENK, J., Method of optimalizing the electromagnet of a direct-current MHD generator, 20: 41746
SCHERBATSKOY, Serge A., Apparatus for nuclear well logging while drilling, 20: 41171
SCHERER, Volker, Chemistry of Pm, 20: 40872 (NP-16254)
SCHERZER, B. M. U., Monte Carlo simulation of the flow of a KNUDSEN gas with due allowance for the sojourn time, 20: 42035 (IPP-2/41)
SCHIAVON, P., Measurement of the branching ratio $\omega \rightarrow$ neutrals/$\omega \rightarrow \pi^+ + \pi^- + \pi^0$, 20: 41850
SCHIER, W. A., Stripping features of ${}^{8}Li(d,n){}^{7}Be^*$ (0.43 Mev) at E_d from 0.2 to 0.8 Mev, 20: 42210
SCHIFFER, Lewis M., Tritiated thymidine as cytocidal agent in human leukemia, 20: 40743 (BNL-9374)
SCHIKARSKI, W., Experiments to evaluate reactivity coefficients with reactor operating at steady state conditions (static experiments), 20: 42631 (KFK-260)
SCHINDLER, W. J., Use of ${}^{99m}Tc$ in studying thyroid physiology in mouse, 20: 40547
SCHLENDER, B., Tscherbyscheff approximation in partial functions, 20: 42043
SCHLENZ, H., Search for parity mixing in the 501 kev γ transition of ${}^{180m}Hf$, 20: 42230
SCHMERLING, E. R., Advances in ionospheric physics in the rocket and satellite era, 20: 42065
SCHMID, A., Changes in total leukocyte counts after exposure to whole-body doses of radiation, 20: 40697
SCHMID, A., Deposition and distribution of strontium in hen eggs, 20: 40569
SCHMID, L. C., High power density core of the PRTR, 20: 42674 (BNWL-221)
SCHMID, Paul, Gamma compensation of ionization chamber for detection of neutron flux in nuclear reactors, 20: 41360
SCHMIDT, C. F., Radiation resistance of spores of Clostridium botulinum type E, 20: 40699
SCHMIDT, D. L., Neutral pion production in p-p interactions at 2.8 Bev/c, 20: 41920
SCHMIDT, Helmut, Formation of a magnetic pinch in InSb and the possibility of population inversion in the pinch, 20: 42545
SCHMIDT, Herbert, Ocular lesions produced by an optical maser, 20: 40692
SCHMIDT, W., Small angle electron proton elastic scattering cross sections for momentum transfers between 10 and 105 f^{-2}, 20: 41791 (DESY-66/20)
SCHMIT, C., Theoretical study of the reaction $\pi^- + {}^{4}He \rightarrow \pi^+ + 4n$, 20: 42356
SCHMITT, H. W., Fission-fragment energy-correlation measurements for the thermal-neutron fission of ${}^{239}Pu$ and ${}^{241}Pu$, 20: 42261
SCHMITZ, F. K., Diffusion of actinide elements in UO_2, 20: 41484
SCHMUNK, R. E., Extension of the dispersion-relation measurements of beryllium, 20: 42541
SCHNADT, H., Prog. rpt. on breaking strength of weldments on heavy gage tensile steels, 9–12/65, 20: 41410 (EURAEC-1612)
SCHNEIDER, G., 1000-Mwe FBR parametric study of secondary sodium–steam system, 20: 42632 (NAA-SR-12060)
SCHNEIDER, R. T., Experimental investigation of closed-loop MPD power generation, 20: 41747
SCHNEIDER, W., Numerical analysis of the time spectrum of delayed coincidences. I., 20: 41301
SCHOEDEL, Juergen-Peter, Electron content of ionosphere from Faraday effect, 20: 42049
SCHOENEICH, J., Chromosomal aberrations in cancerostatic effectivity of chemotherapeutic agents, 20: 40550
SCHOLZ, F., Use of induced mutants to hybridization breeding in barley, 20: 40712
SCHOLZ, W., Small angle Compton scattering with 17 Mev γ-rays from the ${}^{7}Li(p,\gamma){}^{8}Be$ reaction, 20: 42213
SCHOPPER, H., Search of parity mixing in ${}^{180}Hf$ by a measurement of the circular polarization of γ rays, 20: 42225
SCHRAER, Harald, Intracellular distribution of calcium in mucosa of avian shell gland, 20: 40551
SCHREIBER, G. A., Pyroelectric sodium fluoride carrier distillation method for analysis of impurities in Pu, 20: 40814 (RFP-664)
SCHROEDER, H., Separation and radiochemical determination of fission element activities, 20: 40803 (KFK-387)
SCHROER, B., Current commutation relations in the framework of general quantum field theory, 20: 41924 (DESY-66/19)
SCHUBERT, G., Results of supervoltage therapy in gynecology, 20: 40768
SCHULT, O. W. B., Study of ${}^{46}Sc$ levels by means of neutron capture gammas, 20: 42382
SCHULTZ-GRUNOW, F., Experimental determination of the internal resistance matrix of MHD generator, 20: 41748
SCHULZ, D. F., Investigation of trace elements in sea-water by neutron-activation analysis, 20: 40834
SCHULZ, Hans Dietrich, Radiative corrections to bremsstrahlung and pair production at high energies, 20: 41789 (DESY-66/16)
SCHULZ, M. B., Spin-lattice relaxation of rare-earth ions in LaF_3, 20: 42540
SCHULZ, T., Energy conversion with liquid metal working fluids in MHD Staustrahlrohr, 20: 41734
SCHUTT, Paul F., Generation of thermionic electricity from the thermal energy from nuclear combustion, 20: 41682 (LA-tr-66-32)
SCHWARCZ, Erwin H., Exact solution to optical-model equations for quasi-elastic (p,n) reactions, 20: 42243
SCHWARTZ, J., Laser induced prebreakdown and breakdown phenomena observed in cloud chambers, 20: 41375
SCHWARTZ, J. J., (Helium-3,d) reaction on ${}^{42}Ca$ and ${}^{44}Ca$, 20: 42253
SCHWARTZ, Judah L., Finite temperature thermodynamics for the modified Hartree-Fock electron gas, 20: 41623 (UCRL-14904)
SCHWARTZ, Melvin, Radiation cataract analysis and its uses in experimental fractionation, 20: 40690
SCHWARTZ, Samuel, Modification of radiosensitivity by porphyrins. II., 20: 40657
SCHWARZ, George, Changes in relative biological effectiveness of 36 Mev electron beam as function of tissue depth, 20: 40767
SCHWARZSCHILD, M., Red giants of population II. IV., 20: 41587
SCIULLI, F. J., K_{β} three-body decays and the $|\Delta I| = \frac{1}{2}$ rules, 20: 41855
SCOTT, B. W., Apparatus for alternate electron and ion treatment of surfaces with a micron size spot, 20: 41528
SEABORN, J. B., Collective correlations in ${}^{12}C$, 20: 42271
SEAMAN, G. G., Collective nuclear structure in the even-even samarium isotopes, 20: 42265
SEAMAN, W., Radiometric method for determining neomycin on cotton, 20: 40823
SEARS, M. Bradley, Hydrolysis of U, Th, and Al carbides in D_2O, 20: 40965
SEATON, M. J., Variational principle for the scattering phase matrix, 20: 41991
SEGNER, W. P., Radiation resistance of spores of Clostridium botulinum type E., 20: 40699
SEGUINOT, J., Measurement of the $\pi^{\pm}$p total effective cross section at T_{π} = 300 to 700 Mev, 20: 41830
SEKHARAN, K. K., Study of the ${}^{13}C(\alpha,n){}^{16}O$ reaction, 20: 42336
SEKI, Ryoichi, Analysis of π^--mesonic atoms, 20: 41665
SEKIGUCHI, T., MHD rotating machine: new type of a-c MHD power generator and turbine, 20: 41749
SELIG, H. H., Raman spectrum and hydrolysis studies on hydrogen fluoride solutions of xenon oxide tetrafluoride, 20: 40906
SELLORS, Thomas Holmes, Management of cancer of lung, 20: 40786
SELLSCHOP, J. P. F., Problems in enrichment of tritium by thermal diffusion technique, 20: 41168
SELLSCHOP, J. P. F., Tritium measurements of subterranean waters in

some South African sites, 20: 41167
SELTZ, R., Angular distributions of (t,α_0) reactions on Li, B, C, and O, 20: 42398
SELTZ, R., Study of the deexcitation of first excited levels of ^{6}He, 20: 42353
SELZER, Adolph, Revised mechanics, 20: 42098
SEMAGIN, V. N., Conditioned reflexes in rats subjected to prenatal ionizing irradiation, 20: 40654
SEMENOV, L. F., Comparison of radiation sickness characteristics in various species of mammals, 20: 40694
SEN, P., Origin of SU_3 symmetry in elementary particles, 20: 41930
SENS, J. C., Muonic x-ray studies of spherical nuclei, 20: 42309
SENS, J. C., Precise measurement of the stopping power of C, Au, Al, Ca, and CaF_2 for 0.4 to 6 Mev protons, 20: 42363
SEPP, G., Small angle Compton scattering with 17 Mev γ-rays from the ^{7}Li(p,γ)^{8}Be reaction, 20: 42213
SEPTIER, A., Improvement of surface conductivity of Cu and Al at high frequencies, by lowering of temperature, 20: 42105
SERETER, Zh., Kev neutron scattering by lead and electrical polarizability of neutron, 20: 42140 (JINR-P-2764)
SERYAKOV, K. I., Analysis of shock wave propagation in Cs vapor, with allowance for radiation, 20: 41750
SESHADRI, S. R., Effect of static magnetic field on radiation through a sheath, 20: 42426
SETLOW, Jane K., Photoreactivating enzyme in sea urchin egg, 20: 40543
SETO, K., Static baryon-meson bootstraps and SU_6 symmetry, 20: 41848
SETO, Kenji, Weak interactions of leptons with U(12) symmetry, 20: 42009
SEVCHENKO, A. N., Photoconductivity of p-type silicon irradiated by fast electrons, 20: 41379
SEVERNYI, A. B., Magnetic fields of the sun and stars, 20: 41616
SEYHAN, Muvaffak, Uranium and cobalt complexes of heterocyclically substituted formazans, 20: 40880
SEYMOUR, R. S., Prog. rpt. on accurate nuclear fuel burnup analyses, 12/65–2/66, 20: 42608 (GEAP-5124)
SHADIEV, N., Capture of thermal neutrons by Te, 20: 42286
SHAFRANOV, V. D., Plasma equilibrium in confined toroidal magnetic configurations, 20: 42403 (IAE-1151)
SHAFRANOV, V. D., Plasma equilibrium in a circular magnetic axis stellarator, 20: 42424
SHAFROTH, S. M., Decay scheme and gamma-gamma angular correlations in ^{60}Ni following the decay of 23-min ^{60}Cu, 20: 42254
SHAFROTH, S. M., Gamma decay of i-spin analog resonances in ^{93}Tc and ^{89}Y, 20: 42331
SHAGISULTANOVA, G. A., Radiolysis of mixed Co(III) nitroammoniates and Co(III) hexanitrites, 20: 41003
SHAIKH, A. Q., Use of gamma radiation in jute breeding, 20: 40681
SHAKHTARIN, V. N., Investigation of d-c electromagnets with iron cores in MHD generator applications, 20: 41688
SHAKIN, Carl M., Realistic potentials and shell model. I., 20: 42247
SHALEK, Peter D., Uranium monosulfide–U monophosphide solid solutions, 20: 40936
SHALYGIN, V. A., Concentration of water samples for determination of tritium, 20: 40826
SHAPOVALOV, A. S., Influence of space charge on focusing and dispersion properties of electrostatic fields, 20: 42510
SHARMA, R. P., Level structure of ^{199}Au from decay of ^{199}Pt, 20: 42268
SHARON, B., Wide range thermostat for Moessbauer spectroscopy, 20: 41253
SHAROV, B. V., Displacements of atoms in alpha phase of neutron-bombarded carbon steel, 20: 41497
SHARP, R. T., Polynominal bases and isoscalar factors for SU(3), 20: 41947
SHARYGIN, L. M., Preparation of granulated zirconyl phosphate by freezing and its ion exchange properties, 20: 41055
SHAW, G., Use of multipoles in the fixed-t dispersion relations for photo-pion production, 20: 41851
SHAW, J. F., Examination of the validity of the SAHA equation in a gas discharge, 20: 41751
SHAW, J. L., Two crystallographic computer programs for lattice parameter refinement and for calculating expected line positions, 20: 41437 (AERE-R-5210)
SHCHEGEL'SKII, V. A., Recoil proton polarization in elastic π^--p scattering at 300 Mev and the phase shift analysis of pion-nucleon scattering, 20: 41794 (JINR-E-2860)
SHCHEGOLEV, G. M., Special thermodynamic features of high-temperature open cycles, 20: 41752
SHEA, Andrew W., Colloidal albumin ^{131}I as an agent for scanning liver and spleen, 20: 40777
SHEA, J. F., Liquid-liquid extraction of nonferrous metals, 20: 41047
SHEA, M. A., World-wide survey of vertical cosmic-ray cutoff rigidities determined by the trajectory-tracing method, 20: 42066
SHEAHEN, Thomas P., Effective interaction strength in superconductors, 20: 42120
SHEAHEN, Thomas P., Rules for the energy gap and critical field of superconductors, 20: 42119
SHEARER, James W., Very high magnetic fields produced by capacitor-bank discharge, 20: 41080 (UCRL-14831)
SHEFTEL, M. B., Classification of systems generalized wave functions, realizing the representations of L(m,n) and P(m,n) groups, 20: 42071 (JINR-P-2785)
SHEINDLIN, A. E., Niobium and Zr carbides at temperatures between 1200 and 3500°K, 20: 41729
SHEKHANOVA, I. A., Biological consequences of radioactive contamination of water bodies, 20: 40527
SHELINE, Glenn E., Radiation therapy in control of persistent thyroid cancer, 20: 40758
SHEPHERD, G. A., Determination of Fe and Ni in U by atomic absorption spectrophotometry, 20: 40815 (RFP-698)
SHER, R., Fast neutron cross sections for the ^{23}Na(n,γ)^{24}Na, ^{55}Mn(n,γ)^{56}Mn, ^{115}In(n,γ)^{116m}In, and ^{165}Ho(n,γ)^{166}Ho reactions, 20: 42332
SHERIDAN, C. W., Preparation of charge materials for ORNL electromagnetic isotope separators, 20: 41400 (ORNL-3301(Suppl.1))
SHERMAN, Arthur, Magnetohydrodynamic flows of nonequilibrium plasmas, 20: 42454
SHERMAN, Warren V., Radiation chemistry of solutions of chloromethanes in cyclohexane, 20: 40957
SHEVICK, Philip, Radioactivity apparatus for indicating properties of materials, 20: 41115
SHIDLOVSKII, V. P., Kinetic analysis of plasma Couette flow in an electric field, 20: 42488
SHIGEMITSU, Takao, Studies on bone marrow transplantation for hematopoietic disturbance, 20: 40726
SHIH, C., Experimental program to evaluate the feasibility of jet compressors for closed-Brayton-cycle MHD systems, 20: 41753
SHILIN, V. A., Light neutron nuclei among U fission products, 20: 42298
SHIMAMOTO, Susumu, Distribution of normal region after S-N transition in a superconducting magnet, 20: 42103
SHIMAMOTO, Susumu, Experiments on the propagation of normal region in a superconducting magnet, 20: 42100
SHIMCHAK, M., Angular distribution of high energy neutrons emitted in the absorption of polarized μ^--mesons in Ca, 20: 42300
SHIMOKAWA, K., Two-capsule program for comparing A302B steel from two manufacturers under specific irradiation conditions, 20: 41504
SHIMP, N. F., Origin of saline formation waters. I., 20: 41161
SHIOTA, M., Preparation and test of MHD duct wall and electrode materials, 20: 41718
SHIPP, John I., Regenerative collector target for long-term testing of electrical propulsion systems, 20: 41122
SHIRAKATA, H., MHD power generation experiments with K-seeded Ar plasmas, 20: 41781
SHISHELOV, A. A., Effect of x-ray irradiation on some properties of lithium fluoride single crystals, 20: 42564
SHLAER, W. J., Quasi-free proton scattering at 160 Mev, 20: 42276
SHLAK, D. L., Energy dependence of angular distribution of fragments in the fission of ^{233}U, ^{235}U, and ^{239}Pu induced by neutrons, 20: 42171 (LA-tr-66-41)
SHLANTSAR, F., Structural changes in uranium due to thermal cycles, 20: 41470
SHOCKLEY, T. D. Jr., Electromagnetic characteristics of a bounded plasma slab, 20: 42481
SHPIGEL', I. S., Investigation of a conical induction plasma source, 20: 42505
SHPILRAIN, E. E., Thermodynamics of a two-component liquid-metal power MHD assembly with injector, 20: 41778
SHTEFAN, V. V., Investigation of phenomena at the cathode of an open-cycle MHD generator, 20: 41756
SHUBINA, L. V., Plastic scintillator with light yield proportional to the energy of outer electrons, 20: 41346
SHUBINA, R. V., Raman analog of electronic and nuclear induction and echo, 20: 41640
SHUKLA, Shyama Kant, Paper chromatographic study of solution chemistry of Tc in hydrobromic acid, 20: 40918
SHULMAN, R. G., Electron spin resonance of irradiated deoxyribonucleic acid, 20: 40594
SHUMILOVSKII, N. N., Design of radioactive isotope instruments, 20: 41235
SHUMYATSKII, B. Ya., Effect of the capacity of electric power stations with MHD generators on their thermal efficiency, 20: 41769
SHUVALOV, R. S., Deuteron disintegration by 14 Mev neutrons, 20: 42291
SHVANGIRADZE, R. R., Use of the hollow cathode for the determination of gases in solids by the isotopic equilibrium method, 20: 41526
SICARD, F., Improvement of signal-to-noise ratio, 20: 41305
SIEGEL, Edward, Effects of thyroid hormones on cultured mammalian cells, 20: 40511 (UCRL-16776)

SIEGEL, Irwin M., Ocular lesions produced by an optical maser, 20: 40692
SIEGEL, R. T., Modular 100-Mc digital timer, 20: 41240
SIEGEL, R. T., Muon capture rate in complex nuclei, 20: 42318
SIEGEL, S., Unit cell of γ-UO_3, 20: 40907
SIEGERT, W., Effect of x irradiation on homozygote parent varieties and their crossed populations of barley, 20: 40701
SIEGFRIED, W., Prog. rpt. on mechanical properties of metals subjected to mechanical stress at elevated temperatures and neutron irradiation, 1/3/66, 20: 41445 (EURAEC-1622)
SIEGFRIED, W., Prog. rpt. on mechanical properties of metals subjected to mechanical stress at elevated temperatures and neutron irradiation, annual, 1965, 20: 41495 (EURAEC-1621)
SIEGLER, Richard, Pathogenesis of radiation-induced thymic lymphoma in mice, 20: 40677
SIEPE, K., Gyromagnetic ratio of the 564 kev state in ^{122}Te, 20: 42219
SIGMUND, P., Mechanism of sputtering, 20: 42553
SIGNELL, P., P-p bremsstrahlung calculations, 20: 41921
SIKSNA, Reinhards, Continuous recording of small air ions in closed rooms, 20: 42050
SILBAR, R. R., Are the positive-parity mesons in the 405 multiplet?, 20: 41874
SILBERBERG, Rein, Cosmic-ray modulations in the solar system and in interstellar space, 20: 41670
SILCOX, J., Low-frequency transitions and critical currents in the superconducting surface sheath, 20: 42125
SILER, William, Extension of memorial system for implant dosimetry, 20: 40788
SILIN, I. N., Recoil proton polarization in elastic π^--p scattering at 300 Mev and the phase shift analysis of pion-nucleon scattering, 20: 41794 (JINR-E-2860)
SILOBRCIC, V., Immunological tolerance in parental strain mice induced by F_1 hybrid spleen cells, 20: 40651
SILSBEE, Robert H., Electron spin resonance identification of N_2^- defect in x-irradiated sodium azide, 20: 40966
SILVER, Leon T., Evaluation of the decay constant of ^{235}U from lead isotope ratios, 20: 41176
SILVERMAN, A., Wide angle electron pair production at high energy, 20: 42327
SILVERMAN, M. D., Characterization of radioactive particulate aerosols by fibrous filter analyzer, 20: 41234 (ORNL-P-2436)
SILVESTRINI, V., Measurement of the branching ratio $\omega \to$ neutrals/$\omega \to \pi^+ + \pi^- + \pi^0$, 20: 41850
SIMINOVITCH, Louis, Improved method for radioautography of erythropoietic cells labeled with ^{55}Fe or ^{59}Fe, 20: 40675
SIMKOVA, M., Determination of tungsten in iron by activation analysis, 20: 40818 (UJV-1368)
SIMMONS, J. E., Large-angle neutron-proton C_{NN} parameter at 23.1 Mev, 20: 41877
SIMONENKO, A. F., Interruption of a current pulse by a plasma switch, 20: 42493
SIMONENKO, A. F., Spectroscopic investigations of a high-current discharge in the air at low densities, 20: 42492
SIMONOFF, G. N., Dissociation of ^6Li by interaction on complex nuclei, 20: 42366
SIMPSON, F. B., Tabulation of the ^{233}Pa total neutron cross section data, 20: 42151 (IN-1014)
SINA, H., Delayed reactions of urinary system and intestine after irradiation of uterine carcinoma, 20: 40703
SINCLAIR, C., Wide angle electron pair production at high energy, 20: 42327
SINDA, T., Contribution to a study of inelastic interactions between two ion beams, 20: 41666
SINGH, Gurdial, PMR spectra of some neopentyl derivatives of Hg, 20: 40908
SINGH, Virendra, Static bootstrap theory and application to pion-hyperon scattering, 20: 41862
SINGWI, K. S., Sum rules for a generalized frequency distribution function, 20: 42092
SINHA, M. K., Thermal desorption of inert gases from tungsten mono-crystals, 20: 41463
SINHA, S. K., Effect of nuclear spin correlations on the scattering of neutrons by molecules, 20: 42144
SINITSYN, N. M., Influence of acid ligands on complexing of uranyl with tri-n-butyl phosphine oxide, 20: 40885
SINITSYN, N. M., Investigation of the sorption of ruthenium by natural sorbents, 20: 40890
SINITSYNA, S. M., Influence of acid ligands on complexing of uranyl with tri-n-butyl phosphine oxide, 20: 40885
SINOTOVA, E. N., Radioactive isotopes in chemical research, 20: 41027
SKAGGS, L. S., Determination of absorbed dose for electron beam therapy, 20: 40741 (ACRH-25, pp 15-23)
SKAGGS, L. S., Thin foil calorimeter for electron beam dosimetry, 20: 40742 (ACRH-25, pp 24-9)
SKIBENKO, A. I., Method of determining electron density distribution in a plasma, 20: 42419 (AD-636608)
SKILBRAIT, O., Decay of ^{152}Tb, 20: 42155 (JINR-P-2762)
SKLAROFF, David M., Value of ^{88}Sr bone scanning in radiation therapy, 20: 40794
SKOBELEV, N. K., Spontaneously fissioning neutron-deficient neptunium isotope with the half-life 60 sec, 20: 42292
SKOCHDOPOLE, R. E., Reevaluation of some thermodynamic properties of gadolinium metal, 20: 42542
SKOLYSZEWSKI, Jan, Comparison of measured and calculated doses in radiation treatment of neoplasmas of head and neck, 20: 41210
SKORNYAKOV, G. V., Magnetic field topology and the problem of plasma containment, 20: 42461
SKORUPSKI, A., WKB approximation in complex plane and applications to plasma theory, 20: 42404 (IC-66/45)
SKROVE, J., Distribution in fracture permeability of granitic rock mass following contained nuclear explosion, 20: 41164
SKULSKII, I. A., Adsorption of Cs on fluoroplast-4, polyethylene, and glass from aqueous solutions of sodium tetraphenylborate, 20: 40915
SLADE, P., Synthesis of ^{14}C-labeled bipyridylium salts, 20: 40941
SLAGGIE, E. L., Carbon-12 fast neutron cross sections and Legendre moments below 15.0 Mev, 20: 42160 (KAPL-3099)
SLANCAR, F., Structural changes in uranium due to thermal cycles, 20: 41470
SLATTERY, Paul F., Study of six-pronged interactions in π^+p collisions at 7 Bev/c, 20: 41919
SLAUS, Ivo, Energy dependence of proton-proton bremsstrahlung, 20: 41882
SLAVIN, Joseph W., Prog. rpt. on study of irradiated-pasteurized fishery products, final, 10/64–9/65, 20: 41384 (TID-22833)
SLAVNOV, A. A., Lagrangian and hamiltonian for vector electrodynamics in Heisenberg representation, 20: 42020
SLEEPER, H. P. Jr., Transmission of isotropically incident electrons through spacecraft hull materials, 20: 42520
SLIVNIK, J., Nuclear magnetic resonance and relaxation of hexafluoride molecules in solid, 20: 40892
SLUNECKO, J., Determination of tungsten in iron by activation analysis, 20: 40818 (UJV-1368)
SLYSHKINA, S. A., Effect of radioactive decay in solids on their relaxability, 20: 41018
SMALLMAN, R. E., Effect of stoicheiometry on the yield stress of TiC and TiO_2, 20: 41475
SMART, Wesley M., Y_1^1 resonant amplitudes between 1660 and 1900 Mev, 20: 41886
SMELOV, V. S., Uranium extraction by trioctylamine–diisopentyl phosphoric acid mixture, 20: 41053
SMIRENKIN, G. N., Energy dependence of angular distribution of fragments in the fission of ^{233}U, ^{235}U, and ^{239}Pu induced by neutrons, 20: 42171 (LA-tr-66-41)
SMIRNOV, A. I., Radioactivity of phosphorites, 20: 41174
SMIRNOV, M. V., Viscosity of molten lanthanum trichloride and its mixtures with lanthanum dichloride, 20: 40925
SMIRYAGINA, S. A., Effect of x-ray irradiation on some properties of lithium fluoride single crystals, 20: 42564
SMIT, W. M., Separation of lithium isotopes by countercurrent-exchange-electrolysis, 20: 41402
SMITH, Alan R., Developments in technique for monitoring high-energy accelerator radiation, 20: 41276 (UCRL-16769)
SMITH, D. R., Electron spin resonance spectra of ^{15}N-centered radicals at low temperatures. II., 20: 40955
SMITH, David Robert, Study of mechanical forces of type 1 superconductors in a magnetic field, 20: 42134
SMITH, George W., Nuclear quadrupole resonance by nuclear induction, 20: 41648
SMITH, Janice L., Effect of ionizing radiation on animals and plants, 20: 40602 (AD-624934)
SMITH, L. H., Bone marrow system for studying recovery from radiation injury, 20: 40634 (ORNL-P-2312)
SMITH, L. H., Prog. rpt. on genetic control of physiological processes in higher plants, 1965–66, 20: 40532 (COO-1097-17)
SMITH, Lawrence H., Cosmic-ray electron flux above 4.7 Bv, 20: 41674
SMITH, P. F., Superconducting focusing systems in high-energy physics, 20: 42104
SMITH, R., Sequelae of LD/50 x-ray exposure of pre-implantation mouse embryo, 20: 40649
SMITH, S., Extension of the periodic table, 20: 41636
SMITH, T. F., Superconductivity of LaAg, 20: 42101
SMITH, W. A. Jr., Prog. rpt. on transient radiation effects, optical, 1/65, 20: 41488 (EGG-1183-2013)
SMITH, W. A. Jr., Prog. rpt. on transient radiation effects, electrical, 1/65, 20: 41489 (EGG-1183-2014)
SMITH, W. A. Jr., Prog. rpt. on transient radiation effects, electrical, 5/65, 20: 41490 (EGG-1183-2029)
SMITH, W. A. Jr., Prog. rpt. on transient radiation effects, optical, 5/65,

20: 41491 (EGG-1183-2030)
SMITH, W. H. Jr., Method of rounding actinide oxide gel particles, 20: 40937
SMITHSON, G. R. Jr., Liquid-liquid extraction of nonferrous metals, 20: 41047
SMOLUCHOWSKI, R., Mechanism of formation of M and R centers, 20: 42562
SMRZ, Pavel, Diffraction model for boson production at several Bev, 20: 41918
SMUTZ, M., Equilibrium study of chloride and nitrate systems of Pr and Nd with tributyl phosphate and acid, 20: 40904
SNELLMAN, H., Levels and transitions in ^{133}Cs, 20: 42203
SNIPES, Wallace, Conference on electron spin resonance and effects of radiation on biological systems, Gatlinburg, 5/65, 20: 40592
SNOPKO, V. N., Dependence of the relative population of displaced levels of a copper atom on the concentration of electrons in the plasma of an arc discharge, 20: 42490
SNOW, G. A., Prog. rpt. on properties of K mesons and hyperons and related topics in high energy physics, 10/65–9/66, 20: 41799 (ORO-2504-96)
SNYDER, Mark D., Dissolution of ion exchange resins in alkaline permanganate, 20: 41031 (DP-717)
SODEE, D. Bruce, Thyroid physiology utilizing intravenous sodium pertechnetate, 20: 40555
SOENKSEN, Dieter, Final elimination and burial of radioactive wastes, 20: 42686
SOFONEA, Liviu, Relativistic quantum concept of gravitation, 20: 42096
SOKOLOV, A. A., Relationship between structure and polarization of particles in $1 + \bar{1} \rightleftarrows p + \bar{p}$ reactions, 20: 41813
SOKOLOV, L. S., Optical model analysis of the elastic scattering of 13.6 Mev deuterons on medium weight nuclei, 20: 42294
SOKOLOVA, L. V., Temperature and electron concentration in plasma arc from Thomson scattering, 20: 42432
SOKOLOVA, S. I., Dissolution of $UO_2C_2O_4$ by ion exchange resins, 20: 40917
SOKOLOVSKAYA, T. I., Plastic scintillator with light yield proportional to the energy of outer electrons, 20: 41346
SOLIANI, G., Commutation rules between axial charges and axial divergences, 20: 41956
SOLMITZ, Frank T., New Σ decay parameters and test of $\Delta I = \frac{1}{2}$ rule, 20: 41879
SOLOMON, J., Double charge exchange, 20: 42316
SOLON, Leonard R., Ocular lesions produced by an optical maser, 20: 40692
SOLON, Leonard R., Physiological implications of laser beams, 20: 40691
SOLOV'EV, V. G., Structure of the ground and excited states of deformed odd-mass nuclei in the actinide region, 20: 42154 (JINR-E-2857)
SOMMER, G., Theorem on high-energy scattering amplitudes, 20: 41963
SOMOGYI, C., Sequelae of LD/50 x-ray exposure of pre-implantation mouse embryo, 20: 40649
SOMON, J. P., Magnetic fields obtained by flux compression, 20: 41083
SOMON, J. P., Magnetic fields obtained by flux compression, 20: 41089
SONG, Cheng X Jyi, Measurement of magnetic field distributions, 20: 42571
SONI, R. N., Spectrophotometric and conductometric studies of complexes between UO_2^{2+} and 2-hydroxy-3-naphthoic acid in aqueous medium, 20: 40898
SONKA, J., Effects of irradiation on level of reduced nicotinamide nucleotides in rat liver homogenates, 20: 40583
SONNAERT, S., Elastic scattering of 14 Mev neutrons by K, 20: 42393
SONNERUP, B., Structure of the magnetopause current layer, 20: 42068
SOOVIK, T. A., Mechanism of radioluminescence of alkali metal halide crystal phosphors, 20: 41343
SOOYIK, T., Mechanism of radioluminescence in crystal phosphors of alkali metal halides, 20: 41007
SORDO, K., Study of (n,α) reaction on ^{16}O at 14.9 Mev, 20: 42370
SOWDEN, R. G., Irradiation experiments with plutonium dioxide suspensions, 20: 41009 (AERE-R-3268)
SPAGNOLO, Frank A., Motion of a charged particle in a magnetic field due to a finite solenoid with application to solar radiation protection, 20: 42521
SPALARIS, C. N., Design and fabrication of ESADA-VESR Mark III superheat fuel clusters, 20: 42627 (GEAP-5051)
SPALEK, Jan, Neutron capture gamma ray techniques for nondestructive analysis of reactor burnable poisons, 20: 41112 (IITRI-578P11-54)
SPECTOR, Mozart I., Observations derived from film packs used in nation-wide x-ray exposure study, 20: 41213
SPEDDING, F. H., Reevaluation of some thermodynamic properties of gadolinium metal, 20: 42542
SPEIDEL, K.-H., Search for parity mixing in the 501 kev γ transition of ^{180m}Hf, 20: 42230
SPIELBERG, N., Elimination of intensity dependent shifts in proportional counter pulse height distributions, 20: 41332
SPINDEL, William, Prog. rpt. on stable isotope studies, annual, 7/65–8/66, 20: 40873 (NYO-3462-2)
SPIVAK, V., Improvement of signal-to-noise ratio, 20: 41305
SREEKUMARAN, C., Minor-element and trace-element content of marine environment on west coast of India, 20: 40572
SREENIVASAN, N., Matter traversed by low-energy cosmic-ray nuclei in space, 20: 41675
SRINIVASAN, S. K., Sequent correlations in stochastic point processes. II., 20: 42467
SRIVASTAVA, K. D., Nimrod electrostatic inflector, 20: 41542 (RHEL/R-125)
SRIVASTAVA, Y. N., Perturbations of inelastic unitary on dynamical calculations, 20: 41957
STAAB, Edward V., Colloidal albumin ^{131}I as an agent for scanning liver and spleen, 20: 40777
STAB, L., Theoretical study of the continuous spectra of gamma rays emitted in nuclear reactions, measurement of mean lives, 20: 42379
STAEHLE, M., Influence of wall radiation on the non-equilibrium electrical conductivity and on the ionization reaction time of a He–Cs plasma, 20: 41754
STAGG, M. S., Impact testing of radioactive samples, 20: 41113
STAHL, Kurt, Power supply installations for future spacecraft, 20: 41514 (AI-Trans-209)
STAMM, H. H., Separation and radiochemical determination of fission element activities, 20: 40803 (KFK-387)
STANDEN, H., Synthesis of ^{14}C-labeled bipyridylium salts, 20: 40941
STANFORD, G., Sequelae of LD/50 x-ray exposure of pre-implantation mouse embryo, 20: 40649
STANIC, B. V., Motion of a charged particle in an axially symmetric nonstationary magnetic field, 20: 41558
STANNETT, V., Radiation-induced copolymerization of formaldehyde and styrene, 20: 40973
STANSBURY, E. E., Prog. rpt. on application of adiabatic calorimetry to metal systems, 9/65–8/66, 20: 41457 (ORO-3291-3)
STARIK, I. E., Extraction method for complex formation of Po with Cl and perchlorate ions, 20: 41052
STARK, R., Measurement of the $K_S^0 - K_L^0$ mass difference by the time dependence of strangeness, 20: 41922
STARK, Virgil, Devices for protection against radioactive fallout, 20: 41118
STATHAM, Eric, Improvements in or relating to gauging instruments, 20: 41436
STAUFFER, A. D., Impact parameter treatment of the excitation of atoms by charged particles, 20: 41654
STAVISSKII, Yu. Ya., Radiative capture cross sections of 30 to 170 kev neutrons, 20: 42293
STEARNS, Brenton F., Comparison of the lifetimes of positive and negative pions, 20: 41891
STECKEL, L. M., Characterization of Y-12 U process materials correlated with in vivo experience, 20: 41204 (Y-1544-A)
STEEN, Heather, Determination of Cu in potato tissue using neutron activation analysis, 20: 40825
STEFANSKI, R., Search for heavy magnetic monopoles, 20: 41676
STEHLIK, G., Microbiological studies on influence of heat and irradiation on survival of yeast, 20: 41387
STEIN, G., Action of ^{60}Co γ rays and trenimon on nucleus and nucleolus of cancer cells, 20: 40704
STEIN, R., Multiple emission of fragments with charge ≥3 after disintegration of heavy nuclei in ionographic emulsions, 20: 41827
STEIN, Richard S., Prog. rpt. on crystal orientation in irradiated polyethylene, final, 5/62–4/66, 20: 40949 (NYO-3003-29)
STEINBERG, M., Method of producing hydrazine, 20: 41008
STEINBERG, M., Progress in chemonuclear and radiation chemical process development, 20: 40988
STEINMANN, O., Symmetry postulate and cluster property, 20: 42089
STEINRUECKEN, D., Behavior of definite nitrides in Ti and Zr by determination of N, 20: 40820 (IS-Trans-37)
STEPANOV, A. V., Electromigration method for studying complex formation of trivalent Pu in ethylenediaminetetraacetic acid solutions, 20: 40912
STEPANOV, A. V., Electromigration method for studying complex Am(III) oxalates, 20: 40913
STEPANOV, V. P., Viscosity of molten lanthanum trichloride and its mixtures with lanthanum dichloride, 20: 40925
STEPHENS, C. L., Photo- and radiation-induced cistrans isomerization of several 2-olefins, 20: 40965
STEPHENS, Lloyd D., Developments in technique for monitoring high-energy accelerator radiation, 20: 41276 (UCRL-16769)
STEPHENS, W. E., Azimuthal angular distribution of ^{12}C(γ,p_0), 20: 42251
STEPINSKI, Marian, Measurement of efficiency of liquid scintillation counters of large area, 20: 41339
STEPISNIK, J., Electron spin resonance of irradiated $NaH_3(SeO_3)_2$ and $NaD_3(SeO_3)_2$, 20: 40972
STERLIGOV, O. D., Dehydrogenating characteristics of Al oxide–Cr oxide catalysts, 20: 40943
STERN, G., Two-capsule program for comparing A302B steel from two manufacturers under specific irradiation conditions, 20: 41504

STERNHEIM, M. M., Optical models for pion-nucleus scattering, 20: 42319
STEVENS, P. R. C., Scattering and energy loss of electrons in silicon near the radiation damage threshold, 20: 42536
STEVENSON, M. Lynn, New Σ decay parameters and test of $\Delta I = \frac{1}{2}$ rule, 20: 41879
STEWART, D. F., Crystal structure and magnetic properties of penta-fluoroxenonyl hexafluoroplatinate(V), 20: 40882
STEWART, D. Jr., Radiometric method for determining neomycin on cotton, 20: 40823
STEWART, R. B., Microdetermination of C and H polyphenyls, fouling films, and terphenyl mixtures, 20: 40797 (AECL-2524)
STICHEL, P., Current commutation relations in the framework of general quantum field theory, 20: 41924 (DESY-66/19)
STOCK, Arthur, Preparation of radioactively labeled pyridoxal-5′-phosphate, 20: 41016
STOCK, R., Form factors for DWBA calculations of neutron pick-up reactions leading to isobaric analogue states, 20: 42221
STODOLSKY, Leo, Photon dissociation model for vector-meson photo-production, 20: 41863
STODOLSKY, Leo, Regeneration effects in ω-φ production, 20: 41888
STOECKLER, H. A., Moessbauer recoilless fraction in tin compounds, 20: 41637
STOHR, Jacques Andre, Production of essentially flat fuel element for nuclear reactors, 20: 42611 (WAPD-Trans-33)
STOKES, R. H., (d,pf) and (t,pf) reactions on Pu isotopes, 20: 42161 (LA-DC-7878)
STOLYAROVA, E. L., Applied spectrometry of ionizing radiation, 20: 41279 (AEC-tr-6698)
STORRS, Charles L., HWOCR program, 20: 42621 (CONF-660516-16)
STOVALL, T., Study of the elastic scattering of electrons by ^{27}Al, 20: 42376
STRACK, William C., Solar-electric propulsion system performance for 0.1-AU solar probe mission, 20: 41124
STRAIN, R. V., Uranium metal by carbon reduction of uranium oxide in vacuum, 20: 41411 (IS-1379)
STRAKHOVA, A. V., Uranium extraction by trioctylamine–diisopentyl phosphoric acid mixture, 20: 41053
STRASHININ, E. P., Experiments with an MHD generator model, 20: 41755
STRASHININ, E. P., Investigation of phenomena at the cathode of an open-cycle MHD generator, 20: 41756
STRAUCH, K., Quasi-free proton scattering at 160 Mev, 20: 42276
STREMNITZER, H., Regge pole analysis of $\pi^+ p \to \pi^0 N^{*++}$, 20: 41842
STRIGANOV, A. R., Hyperfine and isotope structure in the plutonium spectrum and its classification, 20: 41639
STRINGFELLOW, M. W., Spin-wave stiffness and electronic structure of Fe–Al and Fe–Ga alloys, 20: 42559
STROEMME, Aksel, Cesium-137 in milk in Norway 1962–1966, 22: 41132 (NYO-3364-20)
STROEMME, Aksel, Induced radioactivity in collimator system of a 31 Mev Brown Boveri betatron, 20: 41540 (NYO-3364-7(Rev.))
STROHMEIER, W., Electrolytic deposition of beryllium from metallorganic complex-salts, 20: 40864 (BMwF-FBK-66-10)
STROMBERG, T. F., Superconducting properties of high-purity niobium, 20: 42117
STROMQUIST, Walter K., Transmission of isotropically incident electrons through spacecraft hull materials, 20: 42520
STRONG, Robert Edmund, Improvements in or relating to structural materials, 20: 41435
STRUMINSKII, B. V., Dispersion sum rules for strong and electromagnetic interactions, 20: 41793 (JINR-E-2822)
STRYCKMANS, Pierre A., Tritiated thymidine as cytocidal agent in human leukemia, 20: 40743 (BNL-9374)
STUART, Richard N., Finite temperature thermodynamics for the modified Hartree-Fock electron gas, 20: 41623 (UCRL-14904)
SUBBA RAO, B. N., Simple formula for the transmission and absorption of monoenergetic electrons, 20: 41638
SUCHKOV, I. I., Investigation of alloys of the Zr–C system, 20: 41471
SUCOV, E. W., High temperature plasmas by laser heating, 20: 42415 (TID-22928)
SUELZLE, L. R., Determination of relative efficiencies for multidetector system, 20: 41310
SUESSMANN, G., Nonlocal shell model parameters for nuclear bound states, 20: 42301
SUITA, T., Role of excited atoms on nonequilibrium of partially ionized plasma, 20: 41757
SUKHANOV, A. D., Lagrangian and hamiltonian for vector electrodynamics in Heisenberg representation, 20: 42020
SUKHANOV, A. D., Non-linear Heisenberg operators in quantum field theory, 20: 42018
SULC, P., Comparison of theoretical Laplacian of heavy-water reactor lattice with the measurements of the critical assembly, 20: 42599 (UJV-1424)
SULLIVAN, J. D., W-meson production in $\pi^- + p \to W^- + p$ interactions, 20: 41859
SUMIDA, A., Experimental study of physical properties of combustion gas, 20: 41758
SUMITANI, Shozo, Active effluent treatment plant, 20: 42688
SUMMACH, A. J., Commissioning of WR-1, 20: 42668 (AECL-2552)
SUMMERS, C., Isothermal plasma oven, 20: 42484
SUMNER, Cyril R., System for determining fluid flow rate in boreholes, 20: 41170
SUNDARAM, A. K., Effect of complexing agents on the disproportionation of U(V), 20: 40911
SUNDERMAN, F. William Jr., Prog. rpt. on toxicology of nickel carbonyl, 10/65–7/66, 20: 40536 (ORO-3461-1)
SUNTA, C. M., Development of thermoluminescent dosimeters at Trombay, 20: 41373
SUPKO, Peter R., Biological significance of the supersonic transport radiation environment, 20: 40525
SURGET, G., Contribution to a study of the reaction $^{12}C(d,p)^{13}C$, 20: 42400
SURGET, G., Elastic scattering of deuterons on ^{6}Li at 4 to 6.5 Mev, 20: 42365
SUROEGIN, L. M., Radiation cross linking of cable polyethylene insulation on large scale, 20: 41496
SUTCLIFFE, L. H., High resolution nuclear magnetic resonance spectroscopy. I., 20: 41255
SUTHERLAND, Donald Mason, Nuclear reactor, 20: 42590
SVENNE, Juris P., Realistic potentials and shell model. I., 20: 42247
SWANSON, C. D., Dynamic analysis of Hanford dual-purpose reactor plant using analog simulation methods, 20: 42660 (BNWL-SA-270)
SWANSON, W. P., Applications of the maximum likelihood method in high energy physics, 20: 41790 (DESY-66/17)
SWENSON, C. A., Superconducting properties of high-purity niobium, 20: 42117
SWIFT, A., Changes in radii between neighbouring nuclides, 20: 42278
SWIFT, A., Single-particle wave functions of calcium isotopes, 20: 42270
SYASKIN, Yu. M., Thermodynamics of a two-component liquid-metal power MHD assembly with injector, 20: 41778
SYCHEV, B. S., Attenuation of high-energy neutron fluxes in heterogeneous shielding, 20: 42517
SYCHEV, V. V., Transition processes in superconducting magnetic systems, 20: 41760
SYMONS, C. R., Mass spectra of recoil nucleon states from inelastic ρ^0 production by pions of 12 and 18 Bev/c, 20: 41828
SYNAKH, V. S., Cross section for double bremsstrahlung in ee-collisions in the small angles approximation, 20: 41904
SYROVOI, V. A., Theory of regular electrostatic charged particle beams, 20: 41524
SYSOEV, L. A., Preparation of single crystals of refractory compounds, 20: 41480
SZECHTER, A., Measurement of neutron density distributions in multilayer unit cells. II., 20: 42680 (INR-698/IX-A/RP)
SZEWALSKI, R., Modulated conductivity induction synchronous magnetogasdynamic generator, 20: 41683
SZYMANSKA, Danuta, Thorium recovering from Polish thorium ores, 20: 41033 (INR-678/IV/C)
SZYMCZYK, Wislawa, Comparison of measured and calculated doses in radiation treatment of neoplasmas of head and neck, 20: 41210

T

TACHIKAWA, Kyoji, Processing of V_3Ga wires and their superconducting properties, 20: 42534
TAHA, M. O., Reduced-amplitude equations for two- and three-particle systems. II., 20: 41959
TAIT, D., Dounreay Fast Reactor: kinetic computer analog, 20: 42653
TAKADA, Kenjiro, Nuclear matter and nuclear forces, 20: 42281
TAKADA, Yoshio, Large-angle elastic proton-proton scattering at high energy, 20: 41896
TAKAGI, Shoji, Nuclear matter and nuclear forces, 20: 42281
TAKAHASHI, S., Preparation and test of MHD duct wall and electrode materials, 20: 41718
TAKAKURA, Koichi, Bevatron (35-Mev), 20: 41555
TAKAMATSU, Toshiaki, Radiation-induced graft copolymerization of styrene to polyvinyl chloride. I., 20: 40992
TAKAMATSU, Toshiaki, Radiation-induced graft copolymerization of styrene to polyvinyl chloride. II.,
TAKASHIMA, Yoichi, Gaseous centrifuge and separation of argon isotopes, 20: 41404
TAKAYANAGI, S., Gallium arsenide surface barrier diode as charged particle spectrometer, 20: 41313
TAKEUCHI, Nozomu, Electron spin resonance of irradiated silicate glasses, 20: 42538
TAKHTAMYSHEV, G., Search for new decay modes of the K_2^0-mesons, 20: 41903

TALANTOV, V. V., Morphological changes in thyroid gland following radioiodine administration, 20: 40647

TALINI, N., Features of a plasma ion source with hot cathode gas discharge, 20: 41403

TALMAN, R., Wide angle electron pair production at high energy, 20: 42327

TAMAOKI, T., Experimental studies of oil-fired MHD power generation, 20: 41780

TAMURA, T., Form factors for DWBA calculations of neutron pick-up reactions leading to isobaric analogue states, 20: 42221

TAMURA, T., Multiple excitation and the shell model description of the $^{90}Zr(p,p')$ reaction, 20: 42229

TAN, B. C., Hypopituitary dwarfism following radiotherapy for nasopharyngeal carcinoma, 20: 40660

TANAKA, K., Permutation symmetry in strong interactions, 20: 41984

TANAKA, Osamu, Betatron (35-Mev), 20: 41555

TANAKA, Sho, Composition of hadrons and mass splittings, 20: 42007

TANAKA, Yoshiaki, Processing of V_3Ga wires and their superconducting properties, 20: 42534

TANG, C.-W., Decay schemes of 43-day ^{115m}Cd and 2.3-day ^{115g}Cd, 20: 42260

T'ANG, Ch'ung-hung, Isothermal sections at 1200°C of equilibrium diagrams of Mo–Ti–Zr and Mo–Nb–Zr, 20: 41464

TANG, Lun-Hua, Theory of the influence of the environment on γ-γ angular correlation and its rotational dependence, 20: 42303

TANG, Y. C., Analysis of $_{\Lambda}{}^{9}Be$ and $_{\Lambda}{}^{13}C$, 20: 42241

TANGUY, H., Influence of certain factors on number of leukocytes in blood, 20: 40612 (EUR-2711.f)

TANI, S., Infinity of potential strength, 20: 42027

TANIMOTO, Junichi, Studies on bone marrow transplantation for hematopoietic disturbance, 20: 40726

TAO WONG TEK, Matrix elements of Lorentz transformation for unitary concept, 20: 41926 (JINR-P-2777)

TAPPER, R. J., Tables of vapor pressure and molar volume for liquid H and deuterium, 20: 40871 (NIRL-R-95)

TARASKO, M. Z., Fragments in the fission of ^{235}U by thermal and 5, 6, and 7 Mev neutrons, 20: 42297

TARASOV, V. I., Thermodynamic properties of inorganic substances (handbook), 20: 41417

TARONI, A., Numerical computation methods for implosion processes, 20: 41088

TARRATS, A., Absolute cross sections for elastic scattering of deuterons on α particles between 3 and 14 Mev, 20: 42371

TARRATS, A., Absolute cross sections of the reactions $^{12}C(p,p)^{12}C$, $^{12}C(p,p')^{12}C^*$, $^{12}C(p,p'')^{12}C^*$, and levels of ^{15}N, 20: 42390

TATARINSKII, V. S., Concentration of water samples for determination of tritium, 20: 40826

TATI, Takeo, Picture of strong interactions, 20: 42006

TATISCHEFF, B., Elastic scattering of protons of 150 and 80 Mev on light nuclei and the optical potential, 20: 42388

TATISCHEFF, B., Polarization of protons of 152 Mev by inelastic scattering on ^{12}C and ^{40}Ca, 20: 42341

TAUBENHEIM, J., Contribution of ionospheric F region to cosmic noise absorption, 20: 42048

TAUBENHEIM, J., Ionospheric absorption during solar eclipse on February 15, 1961. I., 20: 42051

TAUBENHEIM, J., Ionospheric absorption of short waves during solar eclipse of February 15, 1961. II., 20: 42052

TAUTZ, M., Analytical consideration of fetal gonad burden in isotope placentography, 20: 40680

TAYLOR, Anthony James, Improvements in or relating to nuclear reactors, 20: 42603

TAYLOR, Anthony James, Improvements in gas-cooled nuclear reactors, 20: 42604

TAYLOR, D. M., Metabolism of ^{47}Sc produced by the decay of ^{47}Ca in vivo, 20: 40545

TAYLOR, Herbert Arthur, Improvements in or relating to preparation of uranium tetrafluoride, 20: 40935

TEFFT, M., Radioisotopic scanning as an aid in planning radiation therapy, 20: 40757

TEFFT, Melvin, Effect of radiation and actinomycin D therapy on incompletely removed mouse tumors, 20: 40762

TELEGDI, V. L., Measurements of the M1 and E2 muonic h.f.s. of ^{209}Bi and of the muonic isotope shifts for ^{206}Pb, ^{207}Pb, and ^{208}Pb, 20: 42307

TEMPLETON, W. L., Accumulation of radionuclides by aquatic organisms of economic importance in United Kingdom, 20: 40578

TENDLER, Moses D., Radioprotective and anti-tumor effect of mixed bacterial toxins and anthramycin, 20: 40736

TENO, J., Hall configuration MHD generator studies, 20: 41761

TERADA, K., Separation of technetium from rhenium by liquid-liquid extraction with potassium xanthate, 20: 40856

TESCH, K., Shielding high-energy electrons: the neutron and muon components, 20: 41534 (DESY-66/18)

TESTONI, J., Excitation function for the reaction $^{197}Au(d,p)^{198}Au$, 20: 42206

TETENYI, Pal, Activities of the Isotope Institute of the National Atomic Energy Committee, 20: 41386 (JPRS-36895)

TETZLAFF, K. H., Analysis of gases by absorption of soft γ radiation, 20: 40828

TEWKSBURY, S., Precise measurement of the K^+/K^- and π^+/π^- lifetime ratios, 20: 41884

TEWKSBURY, T. L., Liquid-liquid extraction of nonferrous metals, 20: 41047

THEILACKER, Walter, Hydrogen exchange in γ lactones, 20: 41017

THIBAUD, J. P., Theoretical study of the continuous spectra of gamma rays emitted in nuclear reactions, measurement of mean lives, 20: 42379

THIEME, G. G., Dynamic analysis of Hanford dual-purpose reactor plant using analog simulation methods, 20: 42660 (BNWL-SA-270)

THIRLAWAY, Henry I. S., Seismology and fundamental geology, 20: 41152

THODE, H. G., Sulfur isotope abundances in evaporites and in ancient oceans, 20: 41135

THOMAS, D. L., Photoproduction of charged pions from helium and hydrogen, 20: 41817

THOMAS, H. C., Quadrupole elastic scattering of alpha particles by polarized nuclei, 20: 42235

THOMAS, M. F., Coulomb excitation of low-energy states in ^{127}I, ^{121}Sb, and ^{183}W, 20: 42186

THOMAS, W. I., Accumulation of Ca, Sr, Mg, P, and Zn by genotypes of corn under different soil fertility levels, 20: 40735 (NYO-2744-37)

THOMMERET, J., Future of in situ detection method of γ activity of seawater, 20: 41147

THOMMERET, Jean, Radiocarbon content of deep and surface waters of north Indian Ocean, 20: 41127

THOMMERET, Yolande, Radiocarbon content of deep and surface waters of north Indian Ocean, 20: 41127

THOMPSON, J. S., Nucleic acid metabolism in thymus and related organs of mice after estradiol and irradiation, 20: 40577

THOMPSON, P., Recent experiments on muonium, 20: 41661

THOMPSON, S. G., Fission of ^{209}Bi and ^{238}U induced by alpha particles of energies up to 115 Mev, 20: 42267

THOMPSON, W. E., Gamma rays resulting from interactions of 14.7 Mev neutrons with Na, S, Cl, K, and Pb, 20: 42146 (AD-638014)

THOMPSON, Willie Ellison, Improvements in electric control or monitoring equipment or apparatus, 20: 41258

THOMSON, R. A. E., Leukocyte response following simultaneous ionizing and microwave irradiation, 20: 40650

THORNE, Kip S., Catalog of methods for studying the normal modes of radial pulsation of general-relativistic stellar models, 20: 41588

THORNE, Kip S., Normal modes of radial pulsation of stars at the end point of thermonuclear evolution, 20: 41589

THORNGATE, J. H., Interval timer designed for use during irradiations at Health Physics Research Reactor, 20: 42683 (ORNL-TM-1559)

THOSAR, B. V., Level structure of ^{199}Au from decay of ^{199}Pt, 20: 42268

THOUVENIN, P., Study of the reactions $^{10}B(d,\alpha)^{24}He$ and $^{9}Be(^{3}He,\alpha)^{24}He$, 20: 42374

THRESHER, J. J., Differential cross sections for $\pi^{\pm}p$ elastic scattering in the momentum range 875-1579 Mev/c, 20: 41857

THUKRAL, S. P., Continuous monitor for radioactive fallout in air, 20: 41303

THUN, H., Stability of lanthanide complexes with mandelate and atrolactate, 20: 40902

THUN, J. E., Levels and transitions in ^{133}Cs, 20: 42203

THUNELL, S., Determination of ^{59}Fe in hemin of peripheral red blood cells and of red cells in bone-marrow cultures, 20: 40830

TILBURY, R. S., Activation analysis with charged particles, 20: 40806 (NAS-NS-3110)

TILL, J. E., Improved method for radioautography of erythropoietic cells labeled with ^{55}Fe or ^{59}Fe, 20: 40675

TILTON, Elvin W., Mating competition of γ-irradiated and nonirradiated male Trogoderma glabrum herbst, 20: 40673

TIMASHEV, S. F., Mechanism of two nucleon transfer reactions, 20: 42290

TIMBS, Arthur Edwards, Improvements in or relating to manipulating devices for use in nuclear reactors, 20: 42593

TIMM, U., Lateral extraction of negative ions from a layered low-pressure discharge in oxygen, 20: 42435

TIMMERMANS, W., Hot drawing of thin walled Zircaloy-2, 20: 41432

TIMROT, D. L., Investigation of high-melting metals in the temperature range 1300 to 3000°K, 20: 41762

TIPTON, D. L., Experimental investigations of closed-loop MPD power generation, 20: 41741

TITLYANOVA, A. A., Behavior of microquantities of yttrium and cerium in soil, 20: 40914

TITOV, V. B., Mechanism of radiation-thermal liquid phase conversions of n-alkanes, 20: 40986

TITOV, Yu. I., Reaction $^{15}N(d,\alpha)^{13}C$ with 0.8 to 1.8 Mev deuterons, 20: 42295

TKACHEV, L. G., Structure of vector and axial currents in broken $\bar{U}(12)$ symmetry, 20: 41939
TKACHEV, V. D., Photoconductivity of p-type silicon irradiated by fast electrons, 20: 41379
TOCHIN, V. A., Yield of stabilized charges in radiolysis of organic systems, 20: 40962
TODD, Paul, Reversible and irreversible effects of radiations upon reproductive capacity of human cells, 20: 40725
TODORIKI, Itaru, Experiments on the propagation of normal region in a superconducting magnet, 20: 42100
TODOROV, I. T., Asymptotic relations between the scattering amplitudes in local field theory, 20: 42015
TODOROV, P., Iron-free asymmetric two-lens β spectrometer, 20: 41282
TOERNKVIST, S., Levels and transitions in ^{133}Cs, 20: 42203
TOKAREVSKII, V. V., Optical model analysis of the elastic scattering of 13.6 Mev deuterons on medium weight nuclei, 20: 42294
TOKARSKAJA, B. I., Imitation of post-radiation damage to DNA under influence of extracts from irradiated potato bulbs, 20: 40562
TOKUDA, N., Static baryon-meson bootstraps and SU_6 symmetry, 20: 41848
TOLBERT, Bert M., Radiation chemistry of proteins in dry state, 20: 40596
TOLMACH, I. M., Spatial effects in an MHD duct with segmented electrodes, 20: 41763
TOLMACHEV, Yu. M., Absorption spectra of uranium oxides. I., 20: 40916
TOLSTOI, N. A., Binary centers produced by light in uranyl salts, 20: 42537
TOMASSINI, C., Reversion frequency of waxy pollen type in normal and hypoploid maize plants, 20: 40509 (TID-22965)
TOMITA, Kenji, Applicability of a dust-like model to a collapsing or anti-collapsing star at high temperature, 20: 41612
TOMIZAWA, Satoshi, Fractional condensation of chloride vapor from chlorinated uranium ore, 20: 41048
TOMLINSON, R. W. S., Distribution of ^{47}Ca in the rat, 20: 40557
TOMPKINS, K. W., Performance of enclosure shields in real fallout field, 20: 41201 (RRA-T55 and Summary)
TOMUSIAK, E. L., Saturation in finite nuclei, 20: 42208
TONOOKA, Yasuhiko, Gaseous centrifuge and separation of argon isotopes, 20: 41404
TOPA, A., Electrode calibration for nuclear diagraphy, 20: 41165
TORIYAMA, Hideaki, Shimadzu 26-Mev medical betatron, 20: 41564
TOROPOV, N. A., Growing of rare earth silicate single crystals of oxyortho- and diortho-type from solution melt, 20: 40919
TOROPOVA, M. A., Radioactive isotopes in chemical research, 20: 41027
TOSI, M. P., Sum rules for a generalized frequency distribution function, 20: 42092
TOULOUSE, G., New color center in irradiated lithium fluoride F_3^+, 20: 42530
TOURTELLOTTE, Charles D., Fixation of ^{75}Se and ^{35}S onto protein-polysaccharides of bovine costal cartilage, 20: 40544
TOURYAN, K. J., Generalized magnetohydrodynamic entrance flow model. I., 20: 42036 (SC-RR-66-356)
TOUSSET, J., Precision and calibration in determination of O by neutrons at 14 Mev, 20: 40846
TOUSSET, J., Variation of isotopic concentration in separated rare earths, 20: 40843
TOYODA, Akira, 3*-plet model of elementary particles, 20: 41998
TRABAL, E., New nuclide: ^{52}Ti, 20: 42282
TRAHIN, M., Improvement of profile of linear shims designed for separation of heavy isotopes, 20: 41405
TRAVING, G., Tschebyscheff approximation in partial functions, 20: 42043
TREHAN, S. K., Effect of Hall current on Rayleigh-Taylor instability of a plasma, 20: 42474
TREMBLY, Lynn D., Amplitudes and energies of primary seismic waves near Hardhat, Haymaker, and Shoal Bursts, 20: 41169
TRENDALL, A. F., Radiometric ages of precambrian rocks from northwest division of western Australia, 20: 41159
TREVES, D., Wide range thermostat for Moessbauer spectroscopy, 20: 41253
TRICE, Siebert W., Bomb and fallout shelters, 20: 41119
TRIES, B., Some aspects on the use of cryogenically cooled primary-windings system for an a-c MHD generator, 20: 41727
TRIGER, S. A., Theory of the stability of sound in a nonhomogeneous plasma, 20: 41764
TRIPATHY, Kishore Chandra, Baryon-antibaryon scattering and the collinear U(3) X U(3) symmetry, 20: 41977
TRIPP, Robert D., New Σ decay parameters and test of $\Delta I = \frac{1}{2}$ rule, 20: 41879
TRIVEDI, U., Low-energy π-N phase shifts, 20: 41864
TROISE, G., Measurement of the branching ratio $\omega \to$ neutrals/$\omega \to \pi^+ + \pi^- + \pi^0$, 20: 41850
TROLINGER, James D., Regenerative collector target for long-term testing of electrical propulsion systems, 20: 41122
TROTTER, James, Crystal structure and magnetic properties of pentafluoroxenonyl hexafluoroplatinate(V), 20: 40882
TROUSDALE, William L., Measurement of magnetic field distributions, 20: 42571
TROZERA, T. A., Prog. rpt. on effect of substructure on irradiation stability of ASTM A302 grade B steel, 4/66, 20: 41451 (GA-7101)
TRUITT, J., Characterization of radioactive particulate aerosols by fibrous filter analyzer, 20: 41234 (ORNL-P-2436)
TSAI, Y. S., Thick-target bremsstrahlung and secondary-particle production by electrons, 20: 41875
TSAO, She-wen, Effects of desolvation of a Pb–Sb alloy on the critical characteristics of superconductors, 20: 42099 (AD-636625)
TSIRLIN, Yu. A., Effect of plastic deformation on light storage in crystals of NaI(Tl), 20: 41344
TSIRLIN, Yu. A., Plastic scintillator with light yield proportional to the energy of outer electrons, 20: 41346
TSITSIPIS, J. A., Gamma radiation-induced dominant lethality to sperm of olive fruit fly, 20: 40674
TSU, T. C., Magnetohydrodynamic power generation, 20: 41693
TSU, T. C., Optimization studies of MHD-steam plants, 20: 41765
TSUJI, Kozo, ESR study on the radiation-induced polymerization of nitroethylene, 20: 40981
TSYRLIN, L. E., Calculating electrostatic field of system of apertures, 20: 42502
TULINOV, A. F., Reaction $^{12}C(\alpha,\alpha')^{12*}C(9.64\ Mev) \to 3\ \alpha$, 20: 42296
TULINOVA, N. I., Influence of injection pulse duration on capture of electrons in a betatron, 20: 41565
TUREKIAN, K. K., Investigation of trace elements in sea-water by neutron-activation analysis, 20: 40834
TURKOT, F., Design and performance of on-line wire spark chamber spectrometer, 20: 41297
TURNER, C. M., Growth of phase space in high intensity proton beams due to nonuniform radial charge distribution, 20: 41531 (BNL-10528)
TUROS, A., Automatic control-system for samples transport, 20: 41077 (INR-696/I/PL)
TUROS, A., Diode function generator for identification of charged particles, 20: 41308
TYAPKIN, A. A., Recoil proton polarization in elastic π^--p scattering at 300 Mev and the phase shift analysis of pion-nucleon scattering, 20: 41794 (JINR-E-2860)
TYREE, W. H., Compact, low-cost alpha counter, 20: 41275
TYSON, J. A., Superfluid density and scaling laws for liquid He near T_λ, 20: 42122
TYURYUKANOVA, E. B., Mobilities and forms of ^{90}Sr and Ca in turf-podzolic and black earth soil, 20: 40520 (NP-16261)
TZANAKAKIS, M. E., Gamma radiation-induced dominant lethality to sperm of olive fruit fly, 20: 40674

U

UCHIYAMA-CAMPBELL, F., Analysis of the reaction $\pi^- + p \to \eta + n$ near threshold, 20: 41871
UDGAONKAR, Bhalchandra M., Static bootstrap theory and application to pion-hyperon scattering, 20: 41862
UEBERALL, H., Collective nuclear "breathing mode" model with application to ^{4}He monopole state, 20: 42245
UEDA, Hideo, Measurement of coronary circulation time with catheter-type micro G-M counter, 20: 40514
UEDA, Kozuo, Grafting of vinyl chloride onto polyethylene by pre-irradiation method, 20: 40982
UGLUM, J., π^0 photoproduction at 3.0, 4.0, and 5.0 Bev for baryon four momentum transfers between 0.5 and 4.0 (Bev/c)^2, 20: 41798 (MIT-2098-265)
UGLUM, J., Search for fractionally charged, weakly interacting particles, 20: 41797 (MIT-2098-264)
UHLIR, M., Structure of vector and axial currents in broken $\bar{U}(12)$ symmetry, 20: 41939
UHLMANN-HAMBURG, G., Results of supervoltage therapy in gynecology, 20: 40768
UKRAINTSEV, E. V., Mechanism of Th and U extraction by mono- and diisopentyl esters of methylphosphonic acid, 20: 41050
UKRAINTSEV, E. V., Zirconium extraction by di- and monoisopentyl esters of methylphosphonic acid, 20: 41051
ULINICH, F. R., Magnetic hydrodynamics of flow in MHD ducts, 20: 41735
ULRICI, W., Nonlocal shell model parameters for nuclear bound states, 20: 42301
ULYANOV, K. N., Relaxation processes in non-equilibrium plasma, 20: 41766
UMEMURA, Isao, 3*-plet model of elementary particles, 20: 41998
UMREIKO, D. S., Absorption properties and stability of uranyl compounds at increased temperatures, 20: 40927
UNNI, C. K., Uptake of radionuclides by marine invertebrates from the west coast of India, 20: 40528
UNRUH, C. M., Neutron and high energy particle dosimeter for medical dosimetry applications, 20: 41262 (BNWL-SA-619)

UNTEREGGER, P., Spinor calculus in Riemannian manifolds, 20: 42079
UNZ, H., Radiation in a moving anisotropic plasma, 20: 42480
UPPULURI, V. R. Rao, Data on a set of trinomial distributions, 20: 41407 (ORNL-4004)
UPTON, A. C., Influence of age on susceptibility to radiation-induced life-shortening in mice, 20: 40633 (ORNL-P-2287)
URBANETS, Ya., Decay of ^{152}Tb, 20: 42155 (JINR-P-2762)
URBANETS, Ya., Decay of ^{184}Re, 20: 42157 (JINR-P-2814)
URBANETS, Ya., Decay mode of ^{160}Ho, 20: 42158 (JINR-P-2817)
URUSOV, I. D., MHD duct design, 20: 41767
USHIO, Kazuhiro, Distribution of normal region after S-N transition in a superconducting magnet, 20: 42103
USHIO, Kazuhiro, Experiments on the propagation of normal region in a superconducting magnet, 20: 42100
UTO, H., K^0_2 three-body decays and the $|\Delta I| = \frac{1}{2}$ rules, 20: 41855

V

VACQUIE, S., Energy distribution of He^+ ions produced by source with high-frequency electric excitation, 20: 41239
VAEHAETALO, Soini, Determination of pulmonary tissue factor in ^{60}Co teletherapy, 20: 40760
VAETH, Jerome M., Radiation therapy of carcinoma of vocal cord without mucosal reaction, 20: 40759
VAIMAN, Marcel, Study of pigs subjected to lethal dose of integral γ irradiation, 20: 40608 (CEA-R-3001)
VAKSELJ, M., Spins of some T = 1 states in ^{26}Al, 20: 42368
VALCKX, F. P. G., Vibrational dissociation and dissociation in cascade of H_2^+ ions by collisions with molecules of a gas, 20: 41663
VALLADAS, G., Measurement of the $\pi^\pm$p total effective cross section at T_π = 300 to 700 Mev, 20: 41830
VALLEBONA, A., Carcinogenic and leukemic activity of ionizing radiations, 20: 41207
VALLEBONA, A., Influence of ionizing radiations on human heredity, 20: 40662
VALLOIS, G., Levels of ^{24}Mg, ^{25}Mg, and ^{26}Mg excited by the reactions (α,α′), (α,^{3}He), and (α,t), 20: 42347
VAN ASSCHE, P., Study of ^{46}Sc levels by means of neutron capture gammas, 20: 42382
VAN DE GRAAFF, Robert Jemison, Apparatus for the acceleration of charged particles, 20: 41581
VAN DEN BRENK, H. A. S., Increased radiosensitivity of skin and normal tissues in high pressure O, 20: 40721
VAN DEN BRENK, H. A. S., Relation of dose-fractionation of x-rays and its spacing in time to skin damage, 20: 40764
VANDENPLAS, P. E., High-frequency effect due to the axial velocity of a plasma column, 20: 42471
VAN DER BEKEN, H., Fluctuations of integral logarithmic period meter in random region, 20: 41237
VAN DER LAAN, P. C. T., Equilibrium and stability of a toroidal screw pinch, 20: 42414 (NP-16266)
VANDERLEEN, W., Stability of lanthanide complexes with mandelate and atrolactate, 20: 40902
VAN DER LEUN, C., Resonant absorption measurement in the reaction ^{26}Mg(p,γ)^{27}Al, 20: 42198
VAN ELST, H. C., Prog. rpt. on embrittlement in steel with respect to irradiation, 1–3/66, 20: 41494 (EURAEC-1617)
VANGEEL, J., Stabilization of uranium monocarbide and production of the single phase carbide, 20: 41431
VAN HORN, William H., Peripheral radiological countermeasures, 20: 41177 (AD-632211)
VAN MONTFOORT, J. E., Faraday rotation in megagauss fields, 20: 41515
VAN NOOIJEN, B., Germanium(Li)–NaI(Tl) coincidence system with multichannel analysis, 20: 41295
VAN NOOIJEN, B., M, N, and O subshell conversion coefficients in ^{228}Th ^{240}Pu, 20: 42264
VAN OERS, W. T. H., Energy dependence of proton-proton bremsstrahlung, 20: 41882
VANOLI, F., Measurement of the branching ratio $\omega \to$ neutrals/$\omega \to \pi^+ + \pi^- + \pi^0$, 20: 41850
VAN SANT, J. H., Long John thermogasdynamic research facility, 20: 41104 (UCRL-14841)
VAN SCHOTHORST, M., Nutrition experiments in pigs fattened with heat-decontaminated, γ-irradiated and untreated feeds, 20: 41394
VANSELOW, K., Development of pattern for stimulation of nerve fiber after studies of x-ray effects on stimulus threshold, 20: 40606 (BMwF-FBK-66-02)
VANYO, James P., Closed model universes with a cosmological constant, 20: 41591
VAN ZYL, C. P., Measurements of the differential cross-section and polarization in proton-proton scattering at about 143 Mev, 20: 41915
VAN ZYL, G. J., Diffraction of protons, 20: 42283
VARDENGA, G., Search for new decay modes of the K^0_2-mesons, 22: 41903
VAS, K., Radiation resistance of enzymes in foods irradiated against microbial damage, 20: 40600
VASARU, Gheorghe, Stable isotopes applications. I., 20: 41380 (IFA-IS-36)
VASHAKIDZE, I. Sh., Analytical properties of the non-relativistic amplitude in a soluble three-particle model, 20: 42019
VASILEVA, N., Rhenium-187 level at 686 kev, 20: 42172
VASILEVA, N. N., Duration of scintillation of monocrystals of CaI(Te) as function of concentration of activator, 20: 41345
VASILEVSKII, I. M., Recoil proton polarization in elastic π^--p scattering at 300 Mev and the phase shift analysis of pion-nucleon scattering, 20: 41794 (JINR-E-2860)
VASKA, L., Hydrido-deuterio-complexes of iridium, 20: 40883
VASUCEVAN, R., Sequent correlations in stochastic point processes. II., 20: 42467
VDOVENKO, M. E., Determination of lanthanum in cerium oxide using paper chromatography, 20: 40859
VDOVENKO, M. E., Photometric determination of La by Xylenol Orange in presence of Complexone III, 20: 40860
VDOVENKO, V. M., Thomas-Fermi-Dirac equation taking into account corrections for divalent radium ions, 20: 40929
VEDEL, J., Ferroelectric transducers, 20: 41684
VEDENOV, A. A., Effective conductivity of non-homogeneous plasma in a magnetic field, 20: 41768
VEDRENNE, G., Elastic scattering of neutrons by tritium at 14 Mev, 20: 42373
VEDRENNE, Gilbert, (n,d) Scattering between 1 and 5 Mev, 20: 42359
VEJE, L., Leptonic decays of hadrons, 20: 41987
VEJVODA, E., Optical emission spectrographic method for determination of ^{240}Pu in Pu materials, 20: 40813 (RFP-271)
VELASQUEZ, Joseph, Radiation cataract analysis and its uses in experimental fractionation, 20: 40690
VELEMINSKY, J., Induction of chlorophyll chimeras by x rays and EMS in Arabidopsis thaliana, 20: 40710
VELEMINSKY, Jiri, Chimerical structure of M_1 plants and its bearing on determination of mutation frequencies in Arabidopsis, 20: 40513
VELEMINSKY, Jiri, Symposium on induction of mutations, Prague, 9/63, 20: 40705
VELTEN, Richard J., Radionuclide analysis of environmental samples, 20: 40809 (NP-16235)
VELTMAN, M., Divergence conditions and sum rules, 20: 41988
VELTMAN, W. A. M., Odd parity levels excited in the ^{37}Cl(p,γ)^{38}Ar reaction, 20: 42181
VENEZIANO, G., Unitary-antisymmetric q-number terms in commutators of spatial current components, 20: 41985
VENKATANADHACHARI, G., Cytological abnormalities in irradiated M rice, 20: 40641
VENKATANADHACHARI, G., Polygenic variability in irradiated cultivated rice N.P. 130, 20: 40640
VENKATARAMAN, G., Effect of nuclear spin correlations on the scattering of neutrons by molecules, 20: 42144
VENVERLOO, L. A. J., Practical gamma spectrometry, 20: 41353
VERBA, J. W., Energy dependence of proton-proton bremsstrahlung, 20: 41882
VERBEEK, F., Stability of lanthanide complexes with mandelate and atrolactate, 20: 40902
VERDEYEN, J. T., Investigation of electronic recombination in helium and argon afterglow plasmas by means of laser interferometric measurements, 20: 42469
VERHAGEN, B. Th., Problems in enrichment of tritium by thermal diffusion technique, 20: 41168
VERHAGEN, B. Th., Tritium measurements of subterranean waters in some South African sites, 20: 41167
VERLEGER, H., Diffraction of protons, 20: 42283
VEROE, J., Correlations between EM pulsations and the F2 layer, 20: 42054
VERSCHURE, R. H., Isotopic evidence for upper-cambrian or lower-ordovician granite emplacement in Vigo area, Spain, 20: 41153
VERVEER, P., Vibrational dissociation and dissociation in cascade of H_2^+ ions by collisions with molecules of a gas, 20: 41663
VERYATIN, U. D., Thermodynamic properties of inorganic substances (handbook), 20: 41417
VICTOR, Joe M., Radio-frequency residual losses in superconductors, 20: 42131
VIDAL, Alberto, Interaction of the gravitational and spinor fields, 20: 42088
VIDAL, C.-R., Photoelectric recording device of high sensitivity and accuracy for spectrographs, 20: 41267 (MPI-PAE-P1-30/66)
VIDAL, J. L., Reactions ^{12}C(α,α) at 51 Mev and ^{14}N(d,α)^{12}C and ^{14}N(d,d) at 28.5 Mev, 20: 42389
VIEGAS, J. R., Examination of the validity of the SAHA equation in a gas discharge, 20: 41751

VIL'CHINSKI, Ya., Mechanism of the proton transfer reactions, 20: 42153 (JINR-E-2824)
VIL'CHINSKI, Ya., Some aspects of the multi-nucleon transfer reaction mechanism, 20: 42156 (JINR-P-2813)
VILLADSEN, Peter Mogens, Improvements in or relating to nuclear reactor installations, 20: 42592
VILLAR, M. A., Separation of iodine and xenon fission radionuclides, 20: 41034 (JEN-160-DQ/I-54)
VILLARS, F., Hartee-Fock method in theory and practice, 20: 42328
VILLET, G., Measurement of the $\pi^{\pm}$p total effective cross section at T_{π} = 300 to 700 Mev, 20: 41830
VIL'SKII, K., Decay of ^{152}Tb, 20: 42155 (JINR-P-2762)
VINCENTI, E., Comparison of different methods for kinetics of ESSOR reactor type, 20: 42678 (EUR-3051.e)
VINCIGUERRA, D., Electron excitation of first levels of ^{11}B, 20: 42378
VINCIGUERRA, D., Study of the elastic scattering of electrons by ^{27}Al, 20: 42376
VINOGRADOV, A. P., Composition of meteorites, 20: 42064
VINOKUROV, E. K., Effectiveness of the oxygen enrichment of air in MHD generator assemblies, 20: 41744
VINOKUROV, E. K., Effect of the capacity of electric power stations with MHD generators on their thermal efficiency, 20: 41769
VIRKO, V, F., Nonlinear phenomena in plasma waveguides, 20: 42450
VISHNEVSKAYA, G. P., Influence of solvent on paramagnetic relaxation constant in liquid solutions of gadolinium nitrate, 20: 40928
VISHNYAKOV, V. V., Recoil proton polarization in elastic π^--p scattering at 300 Mev and the phase shift analysis of pion-nucleon scattering, 20: 41794 (JINR-E-2860)
VISWANATHAN, R., Uptake of radionuclides by marine invertebrates from the west coast of India, 20: 40528
VITALE, Branko, Influence of x-irradiation on experimental allergic encephalomyelitis in rats, 20: 40728
VITKEVICH, V. V., Observations of intensity fluctuations in radio emission from the quasi-stellar source 3C-48 caused by heterogeneities of the interplanetary plasma, 20: 41598
VITSHAS, A. F., Determination of concentration of cesium atoms in a flow of argon and cesium by the radiation absorption method, 20: 41771
VITSHAS, A. F., Investigation of an electrical discharge in a magnetic field in the presence of a flow of gas, 20: 41770
VLASOV, V. I., Observations of intensity fluctuations in radio emission from the quasi-stellar source 3C-48 caused by heterogeneities of the interplanetary plasma, 20: 41598
VOBECKY, M., Determination of lanthanides in U by activation analysis, 20: 40832
VODROS, Daniel, Characteristics of self-extinguishing Geiger-Mueller counting tubes, 20: 41286
VOELKER, W., Analysis of gases by absorption of soft γ radiation, 20: 40828
VOEROES, T., Structure of the nuclear surface, 20: 42275
VOGEL, Marcel J., Uranium and lanthanide activated alkaline earth molybdate and tungstate phosphors, 20: 40934
VOGG, Hubert, Method for extraction of ^{137}Cs salts from irradiated nuclear fuel, 20: 41057
VOHRA, K. G., Continuous monitor for radioactive fallout in air, 20: 41303
VOLKER, A. R., Determination of density of rock by the γ-absorption method, 20: 41154
VOLKOV, V. V., Mechanism of the proton transfer reactions, 20: 42153 (JINR-E-2824)
VOLKOV, V. V., Some aspects of the multi-nucleon transfer reaction mechanism, 20: 42156 (JINR-P-2813)
VOLKOV, Yu. M., Electrical conductivity and electron energy balance in non-equilibrium plasma, 20: 41772
VONACH, H. K., Cobalt-59(p,α)^{56}Fe and ^{58}Fe(p,p') reactions, 20: 42256
VON BAEYER, Hans, Polynominal bases and isoscalar factors for SU(3), 20: 41947
VON BAEYER, Hans C., Diffraction model for boson production at several Bev, 20: 41918
VON BRIESEN, H. Jr., Precise measurement of the K^+/K^- and π^+/π^- lifetime ratios, 20: 41884
VOOK, Frederick L., Thermal conductivity of electron-irradiated InSb, 20: 42547
VOORHIES, H. G., Use of metallic surfaces to convert H atoms to ions in the 50–3000 ev energy range, 20: 42460
VOROB'EVA, I. V., Thermal stability of U fission products in monocrystalline muscovite for chemical etching, 20: 40889
VOROBEVA, V. G., Fragments in the fission of ^{235}U by thermal and 5, 6, and 7 Mev neutrons, 20: 42297
VORTMAN, L. J., Craters from short-row charges and their interaction with pre-existing craters, 20: 41069 (SC-RR-66-324)
VOSKRESENSKII, G. V., Diffraction radiation, 20: 41523
VOSKRESENSKII, V. Yu., Investigation of high-melting metals in the temperature range 1300 to 3000°K, 20: 41762
VOTRUBA, J., Physical representations of an infinite-dimensional Lie algebra, 20: 41937
VOUTILAINEN, Antero, Determination of pulmonary tissue factor in ^{60}Co teletherapy, 20: 40760
VRZAL, Ya., Decay of ^{154}Re, 20: 42157 (JINR-P-2814)
VRZAL, Ya., Decay mode of ^{160}Ho, 20: 42158 (JINR-P-2817)
VUKSANOVIC, Mario M., Pregnancy following ovarian irradiation, 20: 40761
VULIS, L. A., Observations of mercury flowing along a trough in a transverse magnetic field, 20: 41774
VULIS, L. A., Results of theoretical investigations of MHD flows, 20: 41773
VYPIRAILENKO, V. D., Reaction ^{15}N(d,α)^{13}C with 0.8 to 1.8 Mev deuterons, 20: 42295

W

WAGGONER, M. A., Study of the reaction ^{10}B(^{3}He,*paaa*), 20: 42188
WAGHMARE, Yeshwant R., Realistic potentials and shell model. I., 20: 42247
WAGNER, Frederic H., Prog. rpt. on black-tailed jackrabbits in Curlew Valley, Northern Utah, 7/65–7/66, 20: 40494 (COO-1329-3)
WAGNER, H. N. Jr., Scintillation scanning with an 8-inch diameter Na iodide (Tl) crystal, 20: 40779
WAGNER, H. P., Studies on lymphopoiesis. IV., 20: 40663
WAGNER, J. Bruce Jr., Prog. rpt. on high temperature oxidation of metals, final, 2/62–5/66, 20: 41458 (TID-23268)
WAGNER, K. H., Energy conversion with liquid metal working fluids in MHD Staustrahlrohr, 20: 41734
WAGNER, V., Isothermal transport processes in molten salts binary systems, 20: 40866 (EUR-2954.e)
WAIT, James R., Network representation for spherical waves in a compressible plasma, 20: 42440
WAKEFIELD, James, Improvements relating to solid-state radiation detectors, 20: 41367
WALECKA, J. D., Muon capture and nuclear structure, 20: 42317
WALKER, P., Synthesis of ^{14}C-labeled bipyridylium salts, 20: 40941
WALKER, R., Inelastic $\pi^{+,-}$-^{4}He reactions in the momentum range 100–160 Mev/c, 20: 42321
WALKER, R., Phase shift analysis for elastic $\pi^{+,-}$-^{4}He scattering in the energy interval 100–160 Mev/c, 20: 42320
WALKER, S. M., Radiological recovery requirements, structures, and operations research. I., 20: 41179 (AD-635821)
WALKER, S. M., Radiological recovery requirements, structures, and operations research. III., 20: 41181 (AD-635823)
WALKER, Terry, System for determining fluid flow rate in boreholes, 20: 41170
WALKER, W. D., Pion-pion interactions in π^-p reactions at 2.1 Bev/c, 20: 41858
WALKER, W. D., Question of a K^+K^+ resonance, 20: 41856
WALKER, W. W., Response of Si fission detectors to channeled ^{127}I and ^{40}Ar ions, 20: 41324
WALL, L. A., Radiation-induced polymerization of hexafluoropropylene at high temperature and pressure, 20: 40976
WALL, N. S., Shell-model calculation of the quasi elastic scattering of protons from complex nuclei, 20: 42277
WALLIS, G., Interpretation of plasma resonances on topside ionograms, 20: 42063
WALSCHON, E. G., Simple Marx high voltage pulse generator for wide gap spark chambers, 20: 41330
WALSH, Charles J., Particle detector of the semi-conductor type, 20: 41369
WALSH, G., Prog. rpt. on transient radiation effects, optical, 8/65, 20: 41492 (EGG-1183-2039)
WALSH, G., Prog. rpt. on transient radiation effects in electronic materials, 10/65, 20: 41493 (EGG-1183-2052)
WALSH, G. E., Prog. rpt. on transient radiation effects, optical, 1/65, 20: 41488 (EGG-1183-2013)
WALSH, G. E., Prog. rpt. on transient radiation effects, electrical, 1/65, 20: 41489 (EGG-1183-2014)
WALSH, G. E., Prog. rpt. on transient radiation effects, optical, 5/65, 20: 41491 (EGG-1183-2030)
WALTER, F. J., Fission-fragment energy-correlation measurements for the thermal-neutron fission of ^{239}Pu and ^{241}Pu, 20: 42261
WALTER, G., Reactions induced in carbon by fast neutrons, 20: 42367
WALZ, Richard N., Nuclear static eliminators design and development, 20: 41395
WAMANACHARYA, G. S., Separation of Sr and Ba by cation exchange, 20: 41040 (ORNL-TM-1342)
WAN, J. K. S., Electron spin resonance spectra of $N_2H_4^+$ and PF_2, 20: 40956
WANG, Jiunming, Regge poles in unequal-mass scattering processes, 20: 41989
WANG, K. H., Quasi-free proton scattering at 160 Mev, 20: 42276
WANG, Yen, Thyroid scanning using gamma camera, 20: 40751

WANIEK, R. W., Use of pulse transformer to generate multi-megampere currents for high-field research, 20: 41092
WARBURTON, E. K., Lifetime determinations for nuclei A = 10, 11, and 12 from gamma-ray Doppler shifts, 20: 42234
WARBURTON, E. K., Properties of excited states in ^{14}C, 20: 42233
WARBURTON, J. A., Detection of Ag in rainwater, 20: 40838
WARBURTON, J. A., Detection of Ag in rainwater, 20: 40839
WARD, D. E., A 73 watt, 3°K He refrigerator using gas bearing turbines, 20: 41378
WARD, E. H., Effect of changes in ionic medium on stability constant of $Eu(NO_3)^{+2}$, 20: 40876 (ORO-1797-2)
WARREN, Shields, Lung carcinomas in irradiated parabiotic rats, 20: 40614 (NYO-901-39)
WARTY, M. D., Phase-shift analysis of K^+-proton elastic scattering at 910 Mev/c, 20: 41825
WASHINGTON, A. B., Fuel temperature measurements in mixed oxide elements, 20: 42612
WATANABE, Keiji, S-matrix method for calculation of radiative correction for $\pi^+ \to \pi^0 e^+ \nu$, 20: 41865
WATEL, G., Contribution to a study of inelastic interactions between two ion beams, 20: 41666
WATERMAN, Thomas E., Shelter habitability in existing buildings under fire exposure, 20: 41184 (AD-637806)
WATSON, D. D., Method for analysis of pulse-height spectra, 20: 41292
WATSON, Paul D., Fabrication and installation of LACBWR reactor pressure vessel, 20: 42637 (SWRI-1228-7-33)
WATSON, R. D., Conical-face high pressure rotary shaft seals, 20: 41074 (AECL-2551)
WAY, S., Optimization studies of MHD-steam plants, 20: 41765
WAY, Stewart, Electrode protection for magnetohydrodynamic generators, 20: 41689
WAY, Stewart, Part-load operation of MHD power plants, 20: 41775
WEALE, J. W., Uranium-fueled VERA reactor experiments, 20: 42671 (AWRE-R-5/66)
WEAVER, J. M., Observation of the inverse cold-plasma resonance in cylindrical geometry, 20: 42462
WEAVER, Merle L., Determination of Cu in potato tissue using neutron activation analysis, 20: 40825
WEBBER, Milo M., Simplified preparation of ^{99m}Tc sulfide colloid for liver scanning, 20: 40753
WEBER, G., Small angle electron proton elastic scattering cross sections for momentum transfers between 10 and 105 f^{-2}, 20: 41791 (DESY-66/20)
WEED, R. D., Plutonium Recycle Test Reactor decontamination following MgO–PuO_2 fuel element failures, 20: 42677 (BNWL-SA-636)
WEEKS, R. A., Electron spin resonance spectra of Dy^{3+} in ThO_2 and CeO_2, 20: 42525 (ORNL-P-2466)
WEENING, W. E., Synthesis and several properties of deuterated organic compounds, 20: 40940
WEH, H., Energy conversion with liquid metal working fluids in MHD Staustrahlrohr, 20: 41734
WEIJSENFELD, C. H., Impulse approximation applied to assisted focusing, 20: 42574
WEINBERG, A., Question of a K^+K^+ resonance, 20: 41856
WEISS, J. J., Irradiation of deoxyribonucleohistone solutions. I., 20: 40585
WEISS, J. J., Irradiation of deoxyribonucleohistone solutions. II., 20: 40586
WELIN, Eric, Mineralogy of Sweden. IV., 20: 41172
WELLY, J. D., End losses in MHD generators, 20: 41776
WELSH, R. E., Modular 100-Mc digital timer, 20: 41240
WELSH, R. E., Muon capture rate in complex nuclei, 20: 42318
WENGERT, Paul A. Jr., Fixation of ^{75}Se and ^{35}S onto protein-polysaccharides of bovine costal cartilage, 20: 40544
WENTZEL, Donat G., Interstellar clouds and Petschek's mechanism for dissipating magnetic fields, 20: 41595
WERLE, J., Relativistic theory of reactions, 20: 42024
WERNER, Richard W., Gamma mapping of liver with the digital computer, 20: 40747 (UCRL-14866)
WERNTZ, Carl, Collective nuclear "breathing mode" model with application to ^4He monopole state, 20: 42245
WERTENBACH, H., Separation and radiochemical determination of fission element activities, 20: 40803 (KFK-387)
WERY, M., Angular ditributions of (t,α_0) reactions on Li, B, C, and O, 20: 42398
WEST, C. M., Characterization of Y-12 U process materials correlated with in vivo experience, 20: 41204 (Y-1544-A)
WEST, E., Pion-pion interactions in π^-p reactions at 2.1 Bev/c, 20: 41858
WEYMANN, Ray, Energy spectrum of radiation in the expanding universe, 20: 41592
WHEATLEY, G. H., Vacuum encapsulated lithium-drift detector telescope, 20: 41376
WHEELER, C. M., Irradiation of deoxyribonucleohistone solutions. I., 20: 40585
WHEELER, C. M., Irradiation of deoxyribonucleohistone solutions. II., 20: 40586
WHEELER, R. G., Investigation of combined failure of pressure tube and deflected fuel rod in PRTR, 20: 42675 (BNWL-272)
WHEELER, Robert V., Measurement of beam profiles with thermoluminescent dosimeters, 20: 41530 (ANL-7196)
WHITAKER, R. O., Experimental investigations of closed-loop MPD power generation, 20: 41741
WHITE, Gamma-ray transitions in ^{44}Ca, 20: 42335
WHITE, D. H., Fission γ rays using Ge(Li) detector in conjunction with bent-crystal spectrometer, 20: 41278 (UCRL-70000)
WHITE, D. H., High-resolution studies of fission x rays and gamma rays, 20: 42170 (UCRL-70045)
WHITE, D. H., K_2^0 three-body decays and the $|\Delta I| = \frac{1}{2}$ rules, 20: 41855
WHITE, J. W., Localized vibrations of trapped molecules, 20: 41651
WHITE, L., Fuel element heat transfer near dimple braces, 20: 41109
WHITE, Richard L., Rapid detection of tumor hormone dependency by radioisotopes, 20: 40566
WHITFIELD, J. F., Effects of radiation and inhibitors of oxidative phosphorylation on nuclear structure of rat thymocytes, 20: 40549
WHITING, P. W., Black eye colors of Mormoniella, 20: 40669
WHITIS, Van, Thick-target bremsstrahlung and secondary-particle production by electrons, 20: 41875
WHITMAN, Alan M., Characteristics of plasma probes in an MHD working fluid, 20: 41782
WHITTAKER, J. K., Lithium compensated silicon focal plane detectors for electron scattering spectrometers, 20: 41326
WHITTENBERGER, James L., Prog. rpt. on radioisotopes in bones and Po in cigarette smoke, final, 3/63–6/66, 20: 41191 (HUX-3170-1)
WIECH, G., Ultrahigh vacuum grating spectrograph with glacing incidence for studies of soft x rays, 20: 41350
WIEDERMANN, M., Simple pulse interval analyzer for scintillating scanning, 20: 41318
WILDIN, M. W., Radiative heat transfer through an absorbing boundary layer, 20: 41108
WILENZICK, R. M., Moessbauer effect in Au microcrystals, 20: 42572
WILETS, L., Λ_{10} approximation for self-bound many-fermion systems, 20: 42248
WILHELM, H. A., Uranium metal by carbon reduction of uranium oxide in vacuum, 20: 41411 (IS-1379)
WILHELM, H. E., Experimental investigation of closed-loop MPD power generation, 20: 41747
WILIN, Colin, Charge independence in high-energy scattering from deuterons, 20: 41887
WILKIE, D., Fuel element heat transfer near dimple braces, 20: 41109
WILKINSON, D. H., Lifetime determinations for nuclei A = 10, 11, and 12 from gamma-ray Doppler shifts, 20: 42234
WILKINSON, D. H., 6.92- to 6.05-Mev E2 transition in ^{16}O, 20: 42232
WILLI, Alfred V., Calculations of kinetic isotope effects for iodide exchange and for solvolysis of methyl iodide, 20: 40939
WILLIAMS, D. N., Theoretical basis of the symmetrization postulate, 20: 42093
WILLIAMS, I. R., Monte Carlo calculation of source-to-detector geometry, 20: 41316
WILLIAMS, J. F., Charge exchange and dissociation cross sections for H_1^+, H_2^+, and H_3^+ ions of 2- to 50-kev energy incident upon H and the inert gases, 20: 41646
WILLIAMS, J. F., Extraction of positive ions from electrodeless discharge, 20: 41251
WILLIAMS, R. F., Fabrication of Be. I., 20: 41427 (NASA-TM-X-53453 (Vol.I))
WILLIAMSON, Claude Francis, Tables of range and stopping power of chemical elements for charged particles of energy 0.5 to 500 Mev, 20: 41619 (CEA-R-3042)
WILLIS, A., Elastic scattering of protons of 150 and 80 Mev on light nuclei and the optical potential, 20: 42388
WILLIS, A., Polarization of protons of 152 Mev by inelastic scattering on ^{12}C and ^{40}Ca, 20: 42341
WILSON, B. G., Solar minimum measurements of fast neutrons at high altitude, 20: 42055
WILSON, R. R., The 10-Bev electron synchrotron at Cornell, 20: 41568
WINCHELL, H. S., Thymic and splenic irradiation in treatment of acute lymphatic leukemia, 20: 40720
WINDLE, D. W., Chapman-Ferraro hollows for system of line currents enveloped by stratified corpuscular flux, 20: 42453
WINKLER, H. C., Lithium-6(^{12}C,d)^{16}O reaction at E_{cm} = 7 Mev, 20: 42329
WINTERBERG, F., Magnetic acceleration of a superconducting solenoid to hypervelocities, 20: 41554
WINTERMANS, J. A. J. M., Odd parity levels excited in the $^{37}Cl(p,\gamma)^{38}Ar$ reaction, 20: 42181
WINTERNITZ, P., Structure of vector and axial currents in broken U(12) symmetry, 20: 41939
WINZELER, H., Inelastic π^+-^4He reactions in the momentum range 100–160 Mev/c, 20: 42321

WINZELER, H., Phase shift analysis for elastic π^{+}-^{4}He scattering in the energy interval 100–160 Mev/c, 20: 42320
WISNIEFF, Stanley F., Radioactive krypton simplifies temperature mapping of turbine blades, 20: 41114
WITMER, Enos E., Regularities and formulas for the nuclear masses, 20: 42323
WITTEL, H., Wall losses by radiation in oil-fired MHD generator, 20: 41777
WITTENBERG, L. J., Differential thermal analysis study of impurities in plutonium, 20: 41452 (MLM-1172)
WITTKEMPER, G., Gyromagnetic ratio of the 564 kev state in ^{122}Te, 20: 42219
WOELFLE, R., Gamma-spectrometric determination of special reaction products of cosmic radiation in meteorites, 20: 41614
WOHLBERG, Cornel, Estimates of possibility of H embrittlement of Ta in FRCTF, 20: 42682 (LA-3508)
WOLF, E., Photon statistics and classical fields, 20: 41971
WOLFENDALE, A. W., Measurements of the charge ratio of cosmic-ray muons, 20: 41677
WOLFF, Sheldon, Repair of chromosomal damage, 20: 40609 (CONF-660148-1)
WOLGAST, R., ESR investigation of radical reactions in γ-irradiated frozen aqueous solutions of formic acid and formate, 20: 40994
WOLK, I., Solution of the electromagnetic equations for rotating systems, 20: 42087
WOLSKI, Maciej, Radiation protection in industrial radiography, 20: 41212
WOLSKI, W., Transistorized nuclear magnetometer, 20: 41247
WOLTER, R., Hazards resulting from discharge of radioactive wastes into municipal sewer systems, 20: 41217
WONG, K. K., Influence of compound nucleus contributions on (d,p) reactions, 20: 42223
WONG, M. K. F., Scattering amplitude for multipole mixtures in the Moessbauer effect, 20: 42240
WOOD, Donald E., Activation analysis in the metals industry, 20: 40848
WOOD, G. T., Decay scheme and gamma-gamma angular correlations in ^{60}Ni following the decay of 23-min ^{60}Cu, 20: 42254
WOOD, J., Pseudo-exponential decay of a neutron pulse in small beryllium systems, 20: 42601
WOODARD, John D., Mechanical behavior of grades RVD and AGOT graphites, 20: 41459 (TID-23288)
WOODS, A. D. B., Review of experimental measurements of lattice modes in transition metals, 20: 42573
WOODS, R. W., Thermal integration of electric power and life support systems for manned space stations, 20: 41679 (NASA-CR-543)
WOODWELL, G. M., Effects of chronic gamma irradiation on lichen communities, 20: 40517 (BNL-9437)
WORDEN, J. R., High power density core of the PRTR, 20: 42674 (BNWL-221)
WORT, D. J. H., Observation of the inverse cold-plasma resonance in cylindrical geometry, 20: 42462
WOULDS, J. N., Pion capture and nuclear structure, 20: 42314
WRIGHT, P. L., Influence of dietary calcium, zinc, and oil upon uptake of ^{65}Zn by porcine blood cells, 20: 40556
WU, C. S., Detailed analysis of muonic x-ray spectrum from strongly deformed e-e nuclei, 20: 42310
WU, C.-S., High-frequency conductivity of a plasma in quasi-equilibrium. III., 20: 42472
WU, C. S., Metastable $d_{5/2}$ hole state in ^{47}Sc, 20: 42192
WU, Tsung-fan, Search for new decay modes of the K_2^0-mesons, 20: 41903
WUNDER, K., Radiation chemical reactions in mixtures of phosphorus trichloride with olefines, 20: 40947 (BMwF-FBK-66-14)
WYATT, Philip J., Improved surface-wave description for scattering from overdense plasmas, 20: 42451
WYMAN, M. E., Nanosecond time resolution in fission fragment x-ray lifetime experiments, 20: 41325

Y

YABUKI, Haruichi, Remark on the condition, $Z_3 = 0$, 20: 41997
YAFFE, P. E., Prog. rpt. on transformation of Zr–Nb alloys, 7/66, 20: 41443 (COO-588-12)
YAGLENKO, V. T., Observations of mercury flowing along a trough in a transverse magnetic field, 20: 41774
YAJIMA, Nobuo, Numerical computation of dispersive nonlinear equation, 20: 42411 (IPPJ-49)
YAKH'YAEV, R. Sh., Relationship between structure and polarization of particles in $1 + \bar{1} \rightleftarrows p + \bar{p}$ reactions, 20: 41813
YAKIMENKO, I. P., Oscillations of an inhomogeneous plasma cylinder, 20: 42503
YAKIMOVICH, K. A., Thermodynamics of a two-component liquid-metal power MHD assembly with injector, 20: 41778
YAKOVLEV, B. S., Radiation-induced electric and photoconductivity in frozen heptane, 20: 41005
YAKOVLEVA, L. A., Comparison of radiation sickness characteristics in various species of mammals, 20: 40694
YAKUBENKO, A. E., Calculation of the boundary layer at the electrode of a plane MHD generator, 20: 41779
YAKUTOVICH, M. V., Fabrication of thin plates from refractory carbides, 20: 41430
YAMADA, Masao, Self-consistent method for anomalous magnetic moments of baryons, 20: 41996
YAMAGATA, Noboru, Analytical methods for stable and radioactive cesium, 20: 40841
YAMAGUCHI, Kenji, Gaseous centrifuge and separation of argon isotopes, 20: 41404
YAMAGUCHI, Yoshio, Intermediate boson production by nucleon-pair annihilation, 20: 41892
YAMAMOTO, M., Experimental studies of oil-fired MHD power generation, 20: 41780
YAMAMOTO, M., MHD power generator; E.T.L. Mark II, 20: 41714
YAMAMOTO, M., Shock tube studies of magnetically induced non-equilibrium ionization in potassium seeded argon plasma, 20: 41715
YAMAMOTO, Yoshitaka, Large angle proton-proton scattering and real part of the scattering amplitude, 20: 41895
YAMAOKA, Hitoshi, ESR study on the radiation-induced polymerization of nitroethylene, 20: 40981
YAMDAGNI, N. K., Rate of energy loss for positive and negative pions, 20: 41826
YANG, C. N., Symmetry principles in physics, 20: 41923 (BNL-956)
YANG, Hsiu-Hsio, Separation of rare-earth metals by reversed-phase paper chromatography, 20: 41045
YANO, S., MHD power generation experiments with K-seeded Ar plasmas, 20: 41781
YASUNO, Masaru, Evidence for existence of a repulsive core in the Λ-N interaction, 20: 41894
YAVIN, A. I., (^{3}He,t) investigations of Fe, Ni, and Zr, 20: 42334
YEH, Hsuan, Characteristics of plasma probes in an MHD working fluid, 20: 41782
YEN, James T., Magnetohydrodynamic power generation as affected by viscosity and non-equilibrium ionization, 20: 41783
YEN, James T., Penetration of solar wind particles into earth's magnetosphere, 20: 42069
YEROUCHALMI, D., Testing of materials and structures intended for MHD conversion in a 200-kw experimental duct, 20: 41784
YEROUCHALMI, M. D., Behavior of electrodes with electrically-conducting ceramic frontal faces on the Renardieres 8 Mw-test rig, 20: 41725
YIN, Yao-te, Effect of Y on high temperature oxidation of Mo, 20: 41421
YIP, G. L., Effect of static magnetic field on radiation through a plasma sheath, 20: 42426
YNDURAIN, F. J., S-matrix formalism, charge renormalization, and definition of the Hamiltonian in a simple field-theoretical model, 20: 41948
YNTEMA, G. B., New approach to the determination of equilibrium magnetization of superconductors, 20: 42133
YOCCOZ, J., Structure of light nuclei, 20: 42338
YOCK, P. C. M., Distorted-wave one-pion-exchange model for inelastic proton-proton scattering, 20: 41820
YOKOKAWA, Yukimoto, Dynamic mechanical properties of polyoxymethylene. I., 20: 41500
YOKOTA, Hisao, Influence of addition of ethylene on γ induced alternating copolymerization of ethylenimine and C monoxide, 20: 40975
YOKOYAMA, K., MHD rotating machine: new type of a-c MHD power generator and turbine, 20: 41749
YONNET, J., Measurement of the $\pi^{\pm}$p total effective cross section at T_{π} = 300 to 700 Mev, 20: 41830
YOSELI, Morihiro, Excitation of ion plasma oscillation by electron beams, 20: 42429
YOSHIDA, Hiroshida, ESR study on the radiation-induced polymerization of nitroethylene, 20: 40981
YOUDALE, T., Effects of radiation and inhibitors of oxidative phosphorylation on nuclear structure of rat thymocytes, 20: 40549
YOUNG, F. C., Peak-to-total ratios and efficiencies for NaI crystal, 20: 41307
YOUNG, Jensen, Explosion tests in gloved box with ether–air mixtures, 20: 41203 (UCRL-16259)
YOUNG, K. K., K_2^0 three-body decays and the $|\Delta I| = \frac{1}{2}$ rules, 20: 41855
YOUNG, W. E., Optimization studies of MHD-steam plants, 20: 41765
YOUNG, William E., Electrode protection for magnetohydrodynamic generators, 20: 41689
YU, Pao-lo, Prevention of x-ray-induced leukemia in mice. I., 20: 40658
YUHAS, John M., Response of DBA/2J mouse strain to acute ionizing radiation, 20: 40687
YUN, S. K., Effective $\Delta I = \frac{1}{2}$ rule in the three-pion decays of kaons, 20: 41840
YUN, S. K., Novel approach to nonleptonic weak hyperon decays, 20: 41834
YUN, S. K., Two-pion decays of kaons in a novel approach to nonleptonic weak processes, 20: 41835

YUNGKLAUSSEN, Kh., Spontaneously fissionable isomer with the half-life equal to 10^{-7} s, 20: 42159 (JINR-P-2841)
YUNGMAN, V. S., Composition and thermodynamic properties of the combustion products of natural fuels with ionizing additives, 20: 41785
YUNGVIRT, K., Convective effects in excitation of electronic oscillations in plasma, 20: 42495

Z

ZABOROWSKI, H., Multisphere technique. I., 20: 41280 (NP-tr-1410)
ZACHAROV, B., Mass spectra of recoil nucleon states from inelastic ρ^0 production by pions of 12 and 18 Bev/c, 20: 41828
ZAIDINS, C. S., Lithium-6(^{12}C,d)^{16}O reaction at E_{cm} = 7 Mev, 20: 42329
ZAITSEV, L. N., Attenuation of high-energy neutron fluxes in heterogeneous shielding, 20: 42517
ZAKHAROV, V. I., Pyrogallol–amidol developer for nuclear photo emulsions, 20: 41340
ZAMAN, Arif Uz, Covariant density matrices for arbitrary spins, 20: 41960
ZANE, R., Moessbauer effect velocity drive linearized by shape correction, 20: 41238
ZARET, Milton M., Ocular lesions produced by an optical maser, 20: 40692
ZASTAVENKO, L. G., Theory of classical particles with dipole moments, 20: 41807
ZASTAVENKO, L. G., Theory of Dirac's classical electron, 20: 41808
ZATSEPINA, L. N., Mobilities and forms of ^{90}Sr, stable Sr and Ca in turf-podzolic and black earth soil, 20: 40520 (NP-16261)
ZAUDERER, Bert, Electrical loss mechanisms in linear MHD generators operating at large Hall parameters, 20: 41787
ZAUDERER, Bert, Experimental study of the relaxation process and the magnitude of nonthermal ionization in an MHD generator, 20: 41786
ZELDOVICH, Ya. B., Quark structure and masses of strongly interacting particles, 20: 42017
ZELLER, J. J., Design and fabrication of ESADA-VESR Mark III superheat fuel clusters, 20: 42627 (GEAP-5051)
ZELLER, M., n-n S-wave scattering length from the neutron spectra of the reaction $\pi^- + d \rightarrow 2n + \gamma$, 20: 41914
ZEL'VENSKII, Ya. D., Concentration of water samples for determination of tritium, 20: 40826
ZENDLE, R., Instrumentation for detection of maximum permissible burden of ^{60}Co lung contamination, 20: 41190 (CONF-660621-4)
ZENKEVICH, V. B., Transition processes in superconducting magnetic systems, 20: 41760
ZEPKO, G. W., Magnetic-flux compression in explosion geometry, 20: 41093
ZHIBRITSKII, V. K., Determination of concentration of cesium atoms in a flow of argon and cesium by the radiation absorption method, 20: 41771
ZHIKHAREVA, T. V., Resonance phenomena in the elastic scattering of electrons by He atoms. II., 20: 41641
ZHURAVLEVA, M., Search for new decay modes of the K_2^0-mesons, 20: 41903
ZIEG, W., Fluorescence lifetimes of hydrated salts of europium and terbium, 20: 42539
ZIEMINSKI, A., Diode function generator for identification of charged particles, 20: 41308
ZIMERING, S., Prog. rpt. on mechanical properties of metals subjected to mechanical stress at elevated temperatures and neutron irradiation, 1/3/66, 20: 41445 (EURAEC-1622)
ZIMERING, S., Prog. rpt. on mechanical properties of metals subjected to mechanical stress at elevated temperatures and neutron irradiation, annual, 1965, 20: 41495 (EURAEC-1621)
ZIMIN, E. P., Experimental investigation of the ionization and conductivity of hydrocarbon fuel combustion products in the presence of solid particles with a small electron work function, 20: 41731
ZIMMER, F., Detection of slow electrons produced in vacuum by flow counter with pressure stage, 20: 41351
ZIMMER, Glenn W., Radiation shielding at the NRL Linac facility, 20: 41566
ZIMMER, K. G., Some unusual topics in radiation biology, 20: 40515
ZIMMER, W. H., Uranium trioxide product specification analyses, 20: 40802 (HW-65402(Rev.1))
ZIPF, K., Changes in total leukocyte counts after exposure to whole-body doses of radiation, 20: 40697
ZIPF, K., Deposition and distribution of strontium in hen eggs, 20: 40569
ZIPOY, David M., Topology of some spheroidal metrics, 20: 42086
ZIPPRICH, F., Decontamination of products from chemonuclear reactions, 20: 40951 (RPI-321-6)
ZLATAREVA, A., Iron-free asymmetric two-lens β spectrometer, 20: 41282
ZOBEL, W., Temperature dependence of response of lithium-drifted germanium detectors to gamma rays, 20: 41273 (ORNL-TM-1295)
ZONDERHUIS, J., Nondestructive activation analysis of antique gold coins, 20: 40829
ZONN, Z. N., Growing of rare earth aluminate single crystals with perovskite structure, 20: 40920
ZOPPETTI, G., Surgery compared with radioiodine therapy in treatment of hyperthyroidism, 20: 40785
ZORIN, V. A., Radiation cross linking of cable polyethylene insulation on large scale, 20: 41496
ZUBER, Kurt, Neutron activation analysis of Roman copper coins from 250–500 A. D. II., 20: 40800 (CNAEM-35)
ZUCKER, M., Application in nuclear MHD cycles of non-equilibrium ionization from metastable molecular states excited by fission fragments, 20: 41732
ZUPANCIC, I., Nuclear magnetic resonance and relaxation of hexafluoride molecules in solid, 20: 40892
ZYULIKOVA, A. G., Effect of radiation on composition of deoxyribonucleic acid in plants, 20: 40548

SUBJECT INDEX

Main entries in this index are generally specific materials, things, and processes. These are followed by modifiers that describe the properties of, and processes applied to, the main entries.

The number preceding the colon is the *NSA* volume number, and the number following is the abstract number. The designation (R) following the abstract number indicates that the abstract is of a progress report; (P) indicates a patent; and (T) indicates a translation. Abstracts for reports other than progress reports carry no letter designation. References to report numbers, where appropriate, are included after the abstract number of the citation. Published literature (journal article or book) is identifiable by the absence of a report number.

The user should bear in mind that the ideas presented in the original literature, rather than key words, have been indexed. The indexers have tried to select what seemed the most probable and logical place to look for typical information. Since it is not possible to anticipate where a user would look for information, numerous cross references are included in cumulative indexes to assist him in his search.

Experience in using an index of this type will be the best guide in obtaining the desired information, and a consideration of synonymous or closely related terms will prove valuable.

Information must be so indexed as to be of the greatest use to the greatest number of users. This requires that a topic be indexed to headings that most specifically describe it and not ordinarily to the headings that describe its ultimate use, nor to the general class headings that include the specific headings. For example, information on the treatment of thyroid disease with I-131 would be indexed under Thyroid Gland and under Iodine Isotopes I-131, but not necessarily under Radiotherapy. A study of the effects of x radiation on hair would be indexed under both X Radiation and Hair. However, the information would not be indexed under the experimental animal, e.g., Rats, unless the report discusses the effects on rat hair as compared with the effect on the hair of other animals.

The broad, general class headings are used only for general information or for comprehensive reports or articles.

Subject Heading Styles

Generally, the direct form of subject entry is used rather than inverted headings, e.g., Amino Acids rather than Acids, Amino; Helium Isotopes He-4 rather than Helium—isotopes He-4 or Helium—He-4 isotopes. Note, however, that in some cases parenthetic modifying terms or inverted headings of the form Neutrons, Fast are used in preference to a direct entry that would result in the scattering of information. Organic compounds are usually entered in the index in the inverted form so that substituted compounds can be listed near the parent compound; e.g., Benzene, Bromo- rather than Bromobenzene. In general, the style of nomenclature used is that of Chemical Abstracts, except that some items listed in that publication as subheadings are elevated to form part of the main heading; e.g., Butyric Acid, Methyl Ester rather than Butyric Acid—methyl ester.

Alphabetization

Main headings are alphabetized word-by-word. A parenthetic qualifier following a main heading is disregarded in alphabetizing unless there are two or more headings identical except for the parenthetic qualifier, in which case the qualifier determines the order. Headings involving Greek letters are arranged as if the names of the letters were spelled out.

Examples:

M-Capture
  see Electron Capture
Magnesium
Magnesium Alloys
Manganese Fluorides
Manganese(II) Fluorides
Mesons
Mesons (π)
Mesons (ρ)
3-Pentanol, 2,4-Dimethyl-
2-Pentanol, 2-Methyl-
2-Pentanol, 4-Methyl-

Nomenclature of Inorganic Compounds

Inorganic compounds are indexed in the direct form, listing cations in the order of increasing valence in the case of polycationic salts of varying valence and in alphabetic order for polycationic salts in which all cations have the same valence; e.g., Sodium Aluminum Silicates and Potassium Sodium Sulfates.

Multicomponent Alloys and Other Systems

Multicomponent alloys, except well-known trade names, are indexed under a main heading in the form "element alloy" for each element in the alloy. The modifier begins with element symbols for each component arranged alphabetically as if the English name for the element were spelled out.

Example: Copper-Gold Alloy is indexed
  Copper Alloys
    Cu-Au...
  Gold Alloys
    Cu-Au...

Well-known alloys such as Zircaloy-2 are indexed directly to the trade name; cross references referring from each component of the alloy to the entry for the trade name appear in cumulative indexes.

Multicomponent systems of non-metallic elements are indexed in a manner similar to alloys except the main heading used contains the word "Systems" in place of "Alloys."

Example: Silicon–Tungsten Systems are indexed
  Silicon Systems
    Si-W...
  Tungsten Systems
    Si-W...

Multicompound systems and mixtures of compounds are indexed under the main heading for each component com-

pound; the modifiers begin with an alphabetical listing of compound formulas.

Example: Lead Titanate–Lead Zirconate is indexed
Lead Titanates
$PbTiO_3$-$PbZrO_3$...
Lead Zirconates
$PbTiO_3$-$PbZrO_3$...

A mixed system of compounds and elements is indexed using a combined form of the above conventions, e.g., a dispersion of copper and alumina would be indexed

Aluminum Oxides
Al_2O_3-Cu...
Copper Systems
Al_2O_3-Cu..

Physical States and Configurations of Materials

Specification of the physical state, if other than normal, or geometric configuration of the material is included in the modifying phrase, i.e., liquid metals would be indexed to the metal with "liquid" in the modifier, and carbon crucibles would be indexed to Carbon with "crucibles" appropriately placed in the modifier and also to Crucibles if appropriate.

Modifying Phrases

The modifiers appearing under a main heading are written specifically to describe the relation of the item being indexed to that main heading. The modifier, therefore, will generally contain more useful information about that relation than will a title or a phrase written to be used under every main heading assigned to the item. Effort is exerted to begin the modifier with the word judged to be of greatest use to the greatest number of users; this, however, does not obviate the need to consider all modifiers under the main heading(s) of interest.

Modifiers are usually intended to form a meaningful phrase when combined with the main heading. Some are intended to be read following the main heading, e.g., the entry Hydrogen—sorption by charcoal is read "hydrogen sorption by charcoal"; however, as a result of placing the important word first, many modifiers must be arranged for smooth reading, e.g., Formaldehyde—yields in radiolysis of ethyl ether, effects of deuterium on is read "effects of deuterium on formaldehyde yields in radiolysis of ethyl ether" and Uranium—crystal structure of, effect of cooling rate on allotropic transformations in is read "effect of cooling rate on allotropic transformations in crystal structure of uranium." Prepositions are sometimes omitted if no ambiguity results.

Special characters are added to modifiers in the field of physics; if the modifier does not establish the experimental or theoretical character of a reference, a symbol (E), (T), or (E/T) is placed immediately after the modifying phrase and before the journal reference number. The value of this identification has been established by the American Institute of Physics.

A

ABDOMEN
pre-surgical radiotherapy of peritoneal lymphocysts, 20: 40783
radiation effects on, following therapy, 20: 40659
ABSTRACTS
descriptive cataloging guide for, 20: 42694 (TID-4577(Rev.2))
ACCELERATOR TUBES
design, 20: 41577(P)
design of porcelain, 20: 41579(P)
ACCELERATORS
beam deflection system for, 20: 41575(P)
beam injection system for, development of, 20: 41537(R) (LA-3587)
beam spill properties of, test display lamp for, 20: 41314
charged-particle motion in optical systems for, phase space representations of, 20: 41567
control and instrumentation for, development of, 20: 41537(R) (LA-3587)
design, 20: 41578(P)
design of electron, 20: 41572(P)
design of electron, with irradiation window, 20: 41574(P)
design of traveling-wave, for hypervelocity solenoids, 20: 41554
design with forced cooling, 20: 41580(P)
development, 20: 41546
drift tubes for, development of Alvarez, 20: 41537(R) (LA-3587)
fabrication and operation of deuterium and proton dischargers- for demonstration and laboratory use, 20: 41545(T) (AD-631586)
magnetic fields in, design of Permalloy transducers for measuring median surfaces of, 20: 41553
power amplifiers for, development of, 20: 41537(R) (LA-3587)
power supplies for, development of, 20: 41537(R) (LA-3587)
radiation monitoring of, instrumentation and techniques for, 20: 41276 (UCRL-16769)
storage and collision rings for, design and performance of, 20: 41559
wave guides for, development of, 20: 41537(R) (LA-3587)
ACCELEROMETERS
development for motion sensing, 20: 41224 (EGG-1183-2078)
ACCIDENTS
location of criticality in processing plants or storage areas, equipment for, 20: 41349
ACETATES
carbon-14-labeled, use in estimation of choline acetyltransferase, 20: 40584
effects on uranyl complexes with tributylphosphine oxide, 20: 40885
ACETIC ACID, ALLYL ESTERS
radioinduced codimerization of methyallyl chloride with, 20: 40971
ACETIC ACID, [(CARBOXYMETHYLIMINO) BIS(ETHYLENENITRILO)] TETRA-
analytical use in cation exchange separation of barium and strontium, 20: 41040 (ORNL-TM-1342)
effects on removal of plutonium-239 from mice, 20: 40745(R) (NYO-901-54, pp 29-47)
ACETIC ACID, (ETHYLENEDIAMINE) TETRA-
effects on Drosophila, genetic, 20: 40707
effects on frequency of chromosome aberrations induced by radiomimetic agents in *Vicia faba*, 20: 40715
uptake of chromium-51-labeled, by clams, 20: 40575
use in determination of lanthanum, 20: 40860
use in rinsing fallout particles from leaves, 20: 40579
ACETIC ACID, (ETHYLENEDIAMINE) TETRA- COMPLEXES
with plutonium, electromigration studies on, 20: 40912
ACETIC ACID, (*N*-HYDROXYETHYLETHYLENEDIAMINE) TRI-
analytical use in cation exchange separation of barium and strontium, 20: 41040 (ORNL-TM-1342)
ACETIC ACID, IODO-
radiosensitizing effects of, electron spin resonance studies, 20: 40598
ACETIC ACID, VINYL ESTER
radioinduced codimerization of methyallyl chloride with, 20: 40971
radioinduced graft polymerization to cotton cellulose, properties of products formed by gamma, 20: 40995
ACETONE
effects on paramagnetic relaxation constant of gadolinium nitrate, 20: 40928
radiolysis of, EPR studies of yields of stabilized charges in low-temperature, 20: 40962
use in rinsing fallout particles from leaves, 20: 40579
yields in gamma radiolysis of liquid 2-propanol, effects of benzophenone and naphthalene additions on, 20: 41006
ACETONITRILE
vibrations of trapped, in β-quinol clathrates, localized, 20: 41651
ACETOPHENONE
radiolysis of, EPR studies of yields of stabilized charges in low-temperature, 20: 40962
ACETYLENE
acetylene–Ar, ionization potential of, alpha excitation, 20: 42487
production by chemonuclear synthesis, 20: 40988
ACOUSTIC WAVES
production in plasma, from electromagnetic waves, (T), 20: 42499
propagation in compressible plasma, network representation of, 20: 42440
ACRIDINES
effects on mutation induction in Neurospora, in absence of light, 20: 40510(R) (TID-23137)
ACRYLAMIDE
radioinduced solid-state polymerization of, with other organic compounds, 20: 40977
ACRYLAMIDE, *N*-(1,1-DIMETHYL-3-OXOBUTYL)-
radioinduced polymerization of, electron, 20: 40980
ACRYLAMIDE POLYMERS
electrophoretic analysis of, using urea, 20: 40534(R) (NYO-3621-1)
ACRYLIC ACID
radioinduced solid-state polymerization of, with other organic compounds, 20: 40977
acrylic acid–styrene, radioinduced graft polymerization cotton fabric, properties of products formed in gamma, 20: 40953
ACRYLONITRILES
radioinduced graft polymerization to cotton cellulose, properties of products formed by gamma, 20: 40995
acrylonitrile–methyl methacrylate, radioinduced graft polymerization to cotton fabric, properties of products formed in gamma, 20: 40953
ACTINIDE HALIDES
separation of, from alumina by volatility process using fluorine and nitrogen gases, 20: 41062(P)
ACTINIDE OXIDES
preparation of spherical gel particles of, 20: 40937(P)
ACTINIDES
deposition of, from isopropyl alcohol solutions, electrolytic, 20: 41010 (DP-1048)
diffusion in uranium dioxide, mechanism of, 20: 41484
nuclear energy levels of deformed odd-A, collective, (T), 20: 42154 (JINR-E-2857)
separation from rare earths by ion exchange using mixed solvent systems, 20: 40855
ACTINIUM
separation of protactinium from, by hydrolysis in hydrochloric acid, 20: 41044
ACTINIUM ISOTOPES Ac-216
alpha decay of, from bismuth-209 (C-12,5n) reactions, (E), 20: 42287
ACTINIUM ISOTOPES Ac-227
separation from francium-223 by ion exchange, 20: 41038(R) (MLM-1325, pp 9-62)
ACTINIUM ISOTOPES Ac-228
gamma spectra, 20: 41038(R) (MLM-1325, pp 9-62)
ACTINOMYCIN
radiosensitivity effects on chromosomes in *Vicia faba* root cells, x, 20: 40581(R) (ORNL-3922, pp 50-1)
therapeutic effects on mouse tumors, in combination with radiotherapy, 20: 40762
ACTIVATION ANALYSIS
applications in forensic medicine, 20: 40810(R) (NYO-901-54, pp 20-3)
equipment and procedures for, in metals industry, 20: 40848
method for chloride in water, neutron, 20: 41418(R) (GEAP-5150)
methods for deuteron, of metal surfaces, 20: 40812 (ORO-2980-14)
methods for, using charged particles, 20: 40801 (EUR-2957.d.f.e)
neutron filters for selective activation in, 20: 40862
research progress on neutron, 20: 40796(R) (IS-1500(Sect.C))
use of charged particles in, review on, 20: 40806 (NAS-NS-3110)
ACTIVATION DETECTORS
design of metal-foil, 20: 41358(P)
use for accelerator radiation monitoring, 20: 41276 (UCRL-16769)
ADDITION COMPOUNDS
vibrations of trapped molecules in β-quinol clathrates, localized, 20: 41651
ADENINE
ratio to thymine in potato tuber DNA, effects of radiotoxins on, 20: 40562
ADENOSINE, 2-FLUORO-
radiation-sensitizing effect on *Escherichia coli*, diminishing effect of SPATA, 20: 40737
ADENYL PYROPHOSPHATASE
radiation effects on activity of rat liver mitochondria, x, 20: 40695
ADRENAL GLANDS
radiation effects on ascorbic acid content in rat, effects of excision of left gland on, 20: 40655
ADSORPTION
methyl iodide, breakthrough curves, 20: 41202 (UCRL-14990)
AEROSOLS

filtration of radioactive, development of fibrous filter analyzer for, 20: 41234 (ORNL-P-2436)
monthly average of total radioactivity in West Germany, 20: 40570
AGE
carbon-14 measurements of sea water, 20: 41127
effect of, comparison of fission product absorption by young and mature leaves, 20: 40579
effect on exercise performance of x irradiated rats, 20: 40604 (AD-635251)
effects of, on lead-210 and radium-226 content in blood of radium dial painters, 20: 40621 (NYO-3086-5)
effects on charging of transfer DNA with leucine and phenylalanine in rat liver, 20: 40506(R) (ORNL-3922, pp 168-73)
effects on chromosomes in man, 20: 40745(R) (NYO-901-54, pp 29-47)
effects on secondary antibody-forming potential in mice, 20: 40626(R) (ORNL-3922, pp 80-3)
radiosensitivity effects on mouse life spans, x, 20: 40633 (ORNL-P-2287)
radiosensitivity effects on rat spermatogenesis, x, 20: 40682
radiosensitivity effects on germ cell ultrastructure in male rats, x, 20: 40683
radiosensitivity effects on gastropods, x, 20: 40700
AGE ESTIMATION
rubidium-87/strontium-86 method of, for Precambrian rocks of Western Australia, 20: 41159
strontium-87/-86 method for, 20: 41153
strontium-87/-86 method of, for Precambrian rocks of Western Australia, 20: 41159
AGING
effects of microbial flora on mouse, 20: 40502(R) (ORNL-3922, pp 115-27)
effects of supersonic transport environment, 20: 40525
AGRICULTURE
use of induced mutations in barley hybridization breeding, 20: 40712
AIR
cleaning of, BNL Reactor Bypass Filter Facility design for, 20: 42673 (BNL-10483)
electric discharges in, plasma properties from, 20: 42492
electron drift velocities in, magnetic field effect on, (T), 20: 41628
maximum permissible concentration of tritium, 20: 41185 (AECL-2594)
properties as working medium in closed-cycle turbine, 20: 42654
radioactivity content of, from fallout in West Germany, 20: 40570
radioactivity measurements in New Zealand, 20: 40521(R) (NP-16270)
supply for KRB reactor, testing of, 20: 42638(R) (TID-23299)
AIRCRAFT
fitting with zinc sulfide detection system for atmospheric diffusion studies, 20: 41188(R) (BNWL-235-1)
signaling system for helicopters, isotopic gamma-ray, 20: 41221(R) (COO-1471-1)
ALANINE
radioprotective effect on damage induced by alkylating agents, 20: 40664
ALANINE, PHENYL-
effects on Drosophila, genetic, 20: 40706
uptake by transfer RNA of, in adult and fetal rat liver, 20: 40506(R) (ORNL-3922, pp 168-73)
ALBUMINS
preparation of technetium-99-labeled serum, 20: 40944
radioinduced decomposition of wheat flour, gamma, 20: 40599
tracer use of radioisotope-labeled, for placentography, gonadal dose to fetuses from, 20: 40680
use in scintiphotography of lung, 20: 40750
use of iodine-131-labeled, as scanning agent for liver and spleen, 20: 40777
use of serum, as radiation protection factor, 20: 40658
ALCOHOLS
carbon-11 recoil reactions in, 20: 40796(R) (IS-1500(Sect.C))
effects on paramagnetic relaxation constant of gadolinium nitrate, 20: 40928
ALGAE
phosphorus-32 adsorption on, in salt-marsh ecosystems, 20: 40573
phosphorus-32 adsorption on, in salt-marsh ecosystems, 20: 40573
strontium and calcium absorption by, 20: 40524(R) (TID-23271)
ALIZARIN RED S COMPLEXES
use in intravital staining of bone, 20: 40652
ALKALI METAL HALIDES
radioinduced luminescence of crystal phosphors of, effects of thallium on, 20: 41007
scintillation properties of thallium-activated, 20: 41007
ALKALI METAL SULFATES
alkali metal bisulfate–sulfamic acid, properties as decontaminating solution for aluminum or zirconium, 20: 41214(P)
ALKALI METALS
content in meteorites, 20: 42064
properties of, research program on, 20: 41439(R) (AGN-8198)
ALKALINE EARTH METALS
content in meteorites, 20: 42064
metabolism in rats, testing of Marshall's theory for, 20: 40565
ALKALINE EARTH MOLYBDATES
preparation of lanthanide- and uranium-activated phosphors of, 20: 40934
ALKALINE EARTH TUNGSTATES
preparation of lanthanide- and uranium-activated phosphors of, 20: 40934(P)
ALKALOIDS
effects of vinblastine, on megakaryocytes and platelets in rats, 20: 40502(R) (ORNL-3922, pp 115-27)
ALKANES
radiolysis of glasses of, charge recombination in gamma, 20: 40970
yields of deuterated, in hydrolysis of aluminum, thorium, and uranium carbides in heavy water, 20: 40905
ALKENES
saturation of, method for determining, 20: 40796(R) (IS-1500(Sect.C))
yields of deuterated, in hydrolysis of aluminum, thorium, and uranium carbides in heavy water, 20: 40905
ALKYNES
yields of deuterated, in hydrolysis of aluminum, thorium, and uranium carbides in heavy water, 20: 40905
ALLOYS
book: *Data Book on Physical Properties of Materials*, 20: 41442 (CNLM-2393)
book: *Electron Radiation Damage in Semiconductors and Metals*, 20: 41508
ALPHA DECAY
systematics for nuclei with N = 127, (T), 20: 42287
ALPHA PARTICLES
analysis of tissues for, 20: 41191(R) (HUX-3170-1)
attenuation by nuclei at 0.1 to 500 Mev, tables for, 20: 41619 (CEA-R-3042)
calculation of dose from, to radium dial painters, 20: 40621 (NYO-3086-5)
content in water near Canadian reactors, 20: 41136
detection and measurement of, scintillation counter for, 20: 41366(P)
detection and measurement of, design of low-cost portable counter for, 20: 41275 (RFP-777)
detection of divergent, performance of multiple-wire spark counters for, 20: 41317
detection of, design and performance of lithium-drift telescope silicon detectors for, 20: 41376
detection of, development of survey meters for, 20: 41272(R) (ORNL-3875, pp 53-74)
detection using triethylamine-sensitized nuclear emulsions, 20: 41341
deuteron elastic scattering at 3 to 14 Mev, absolute cross sections for, (E), 20: 42371
dosimetry with solid state track detectors, medical uses, 20: 41262 (BNWL-SA-619)
effects on cyclohexane, effects of sulfur on yields in, 20: 40990
effects on human kidney cells, factors affecting RBE, 20: 40725
interactions with gases, properties of recoil ions from, 20: 41622 (SC-DC-66-1564)
reactions ($\alpha,\alpha'\gamma$) with calcium-40 at 30 Mev, gamma spectra from, (E), 20: 42168(R) (MIT-2098-251, pp 57-73)
reactions (α,f) with bismuth-209 and uranium-238 at 23 to 115 Mev, fragment angular distributions in, (E), 20: 42267
reactions (α,f) with uranium-238 at 20 to 40 Mev, ternary fission in, (E), 20: 42273
reactions (α,γ) with beryllium-9, carbon-13 energy-level transitions from, (E), 20: 42330
reactions (α,n) with carbon-13 at 1.95 to 5.5 Mev, oxygen-17 energy levels from, (E), 20: 42336
reactions (α,n) with beryllium-9, carbon-12 energy level lifetimes from, 20: 42234
reactions with copper-63 and copper-65 at 11 to 43 Mev, recoil ranges in, (E), 20: 42259
scattering by antimony-121, iodine-127, and tungsten-183, energy-level transitions from inelastic, (E), 20: 42186
scattering by beryllium-9, phosphorus-31, and sulfur-32, DWBA analysis of elastic, (T), 20: 42392
scattering by calcium isotopes and titanium-50, energy levels from elastic and inelastic, (E), 20: 42168(R) (MIT-2098-251, pp 57-73)
scattering by carbon-12 at 23 Mev, angular correlations in inelastic, (E), 20: 42380
scattering by carbon-12 at 51 Mev, elastic, (E/T), 20: 42389
scattering by carbon-12 at 20 and 25 Mev, inelastic, (E), 20: 42296
scattering by polarized nuclei at 16 and 24 Mev, quadrupole effect in elastic, (T), 20: 42235
use in activation analysis, review on, 20: 40806 (NAS-NS-3110)
ALPHA SOURCES
preparation of thin, by electrodeposition of actinides from isopropyl

alcohol, 20: 41010 (DP-1048)
use in ionization coefficient measurements in gases, 20: 41627
ALUMINUM
decontamination of, method and solution for, 20: 41214(P)
determination by atomic absorption spectroscopy using induction-coupled plasmas, 20: 40796(R) (IS-1500(Sect.C))
determination in americium and plutonium by spark-source mass spectrography, 20: 40816 (RFP-699)
determination in bauxite, activation, 20: 40812 (ORO-2980-14)
determination in plutonium by carrier distillation methods, spectrographic, 20: 40814 (RFP-664)
determination in uranium trioxide by emission spectrography, 20: 40802 (HW-65402(Rev.1))
determination in uranium(IV-VI) oxides, effects of graphite electrode grade on carrier-distillation spectroscopic, 20: 40807 (NLCO-976)
determination of, in nickel base alloy by deuteron activation methods, 20: 40812 (ORO-2980-14)
determination using bis-2-pyridyl glycol, effects of pH on gravimetric, 20: 40849
effects on electrodeposition of actinides from isopropyl alcohol solutions, 20: 41010 (DP-1048)
effects on oxidation resistance of refractory metal disilicides, 20: 41424
effects on phase transformations in gallium–plutonium alloy and plutonium, differential thermal analysis of, 20: 41452 (MLM-1172)
effects on sorption of cerium and yttrium by soil, 20: 40914
electric conductivity of liquid, 20: 41476
electric conductivity enhancement at low temperatures, surface, 20: 42105
electron penetration of, for spacecraft shielding, (E), 20: 42520
helium and hydrogen ion attenuation at 0.1 to 500 Mev, tables for, 20: 41619 (CEA-R-3042)
ion ranges at 10 to 100 Mev, bromine and iodine, 20: 41647
laser beam reactions with, magnetic mirror containment of plasma from, 20: 42415 (TID-22928)
neutron differential reflection by slabs of, thermal, (E/T), 20: 42142 (NP-16234)
performance as neutron threshold detector in presence of x rays, 20: 41333
preparation of single crystals of, 20: 41064(R) (IS-1500(Sect.E))
properties for use as thermal shielding at high temperatures in vacuum, 20: 41440(R) (ALO-3632-4)
proton energy losses in, (E), 20: 42363
radiation damage in, 0.19- to 1.6-Mev electron, 20: 42543
reactions with niobium pentoxide at high temperatures, for production of niobium metal, 20: 41412(R) (IS-1500(Sect. M))
reactions with pollucite at 950 to 1050°C, for cesium separation, 20: 41412(R) (IS-1500(Sect. M))
reactions with vanadium pentoxide at high temperatures, for production of vanadium metal, 20: 41412(R) (IS-1500(Sect. M))
separation of silver from, by cation exchange chromatography, 20: 40847
thermal conductivity of liquid, estimation of, 20: 41477
use in shielding against gamma radiation, 20: 40518 (CEX-63.10)
x-ray emission spectra of, L and K, (E), 20: 41350
ALUMINUM ALLOYS
interactions with gas flow in MHD generators, 20: 41738
Al–Cu, fatigue softening of, factors affecting, 20: 41412(R) (IS-1500 (Sect. M))
Al–Fe, elastic properties of iron-base single-crystal, 20: 41412(R) (IS-1500(Sect. M))
Al–Fe, spin-wave stiffness, neutron-diffraction analysis of, (E), 20: 42559
Al–Fe, tensile properties of intermetallic compound, 20: 41412(R) (IS-1500(Sect. M))
Al–Li, crystal structure of intermetallic compounds, 20: 41412(R) (IS-1500(Sect. M))
Al–Y, crystal structure of intermetallic-compound polymorphs of, 20: 41412(R) (IS-1500(Sect. M))
ALUMINUM CARBIDES
hydrolysis of, in heavy water, products and rate of, 20: 40905
ALUMINUM ISOTOPES Al-26
content in iron meteorites, (E), 20: 41614
energy levels at 3.16 and 4.19 Mev, spins and parities of, (E), 20: 42368
ALUMINUM ISOTOPES Al-27
boron-10 reactions at 0 to 110 Mev, excitation functions for, (E), 20: 42183
boron-11 reactions at 0 to 110 Mev, excitation functions for, (E), 20: 42183
carbon-12 reactions (C-12,N-13) with, angular distributions from, (E), 20: 42153 (JINR-E-2824)
deuteron reactions (d,p) with, mechanism of, (T), 20: 42394
electron elastic scattering, (T), 20: 42376
energy level widths, (E), 20: 42198
lithium-6 reactions at 0 to 110 Mev, excitation functions for, (E), 20: 42183
nitrogen-14 reactions (N-14,F-18) at 65.0 to 107.3 Mev, (E), 20: 42156 (JINR-P-2813)
proton inelastic scattering at 4.00 to 5.50 Mev, cross sections for, (E/T), 20: 42324
proton reactions (p,α) at 4.00 to 5.50 Mev, cross sections for, (E/T), 20: 42324
proton reactions (p,γ) at 0.3 to 2.1 Mev, resonance strengths for, (E), 20: 42182
ALUMINUM ISOTOPES Al-28
beta decay, (E), 20: 42242
ALUMINUM OXIDES
ion exchange properties for xenon oxide in iodate and periodate solutions, 20: 40851
preparation and properties of α-corundum single crystals, 20: 41480
properties for high-temperature insulation of thermocouples, 20: 41461(R) (UCRL-7361(Pt.3))
resistivity of crushable, at high temperature, 20: 42579(R) (ANL-7245, pp 29-47)
separation of, from actinide halides by volatility process using fluorine and nitrogen gases, 20: 41062(P)
yields from potash alum solution, gravimetric estimation of, 20: 40849
Al_2O_3–Cr_2O_3, properties for use in dehydrogenation of butane, 20: 40943
Al_2O_3–Cr_2O_3–K_2O, properties for use in dehydrogenation of butane, 20: 40943
Al_2O_3–Cr_2O_3–Nd_2O_3, properties for use in dehydrogenation of butane, 20: 40943
Al_2O_3–Cr_2O_3–Pr_2O_3, properties for use in dehydrogenation of butane, 20: 40943
Al_2O_3–SiO_2, analysis of lead fluoride-containing gels of, for fluoride by fast-neutron radioactivation, 20: 40845
ALUMINUM SYSTEMS
Al–Si, microstructure model of, 20: 41454 (NYO-2394-22)
Al–UO_2, extrusion of, for tube production, 20: 41412(R) (IS-1500 (Sect. M))
AMERICIUM
analysis by spark-source mass spectrography, 20: 40816 (RFP-699)
separation from einsteinium and californium by ion exchange using hydrochloric acid–methanol solvent system, 20: 40855
separation from irradiated targets by Clanex and Tramex processes, 20: 41039(R) (ORNL-3880)
AMERICIUM COMPLEXES
with oxalic acid, electromigration studies on, 20: 40913
AMERICIUM ISOTOPES
separation by electromagnetic methods, 20: 41401(R) (ORNL-4006)
AMERICIUM ISOTOPES Am-241
use as reference source in air density measurements, 20: 41257
AMERICIUM ISOTOPES Am-242
fission barrier of, shape of, (E), 20: 42169(R) (UCRL-14744, pp 1-18)
AMERICIUM ISOTOPES Am-243
preparation of, in Transuranium Processing Plant, 20: 41039(R) (ORNL-3880)
AMERICIUM, TRICYCLOPENTADIENYL-
preparation and properties of, 20: 40878
AMES RESEARCH REACTOR
development and operation, July 1965–June 1966, 20: 42681(R) (IS-1500(Sect. R))
AMETHOPTERIN
effects on oto-rhino-laryngeal tumors, 20: 40782
AMIDOL
amidol-pyrogallol, use as developer for nuclear photoemulsions, 20: 41340
AMINES
analysis of virgin and degraded, in curium purification process, 20: 41032 (DP-1010)
AMINO ACIDS
analysis for nitrogen-15 in legume root, use of ninhydrin in colorimetric, 20: 40824
analysis for, in γ irradiated deoxyribonucleohistone solutions, 20: 40586
radiation effects on dry, electron spin resonance studies of, 20: 40596
radioinduced free radicals in, endothermic decay of x, 20: 40504(R) (ORNL-3922, pp 146-60)
radioinduced free radicals in, electron spin resonance studies, 20: 40595
radiolysis of, in deoxyribonucleohistone and histone solutions, gamma, 20: 40585
AMINOPTERIN
radiation-sensitizing effect on *Escherichia coli*, diminishing effect of SPATA, 20: 40737
AMMINES
radiolysis of tetraamminedinitritocobalt nitrate and triamminecobalt trinitrate, mechanism of gamma and uv, 20: 41003
AMMONIA

production by chemonuclear synthesis, 20: 40988
radiolysis of, formation of hydrazine from, 20: 41008(P)
vibrations of trapped, in molecular sieves, 20: 41651
NH_3–H_2O_2, radioinduced free radicals in frozen solutions of, ESR spectral studies on gamma and uv, 20: 41001

AMMONIUM ACID SULFATES
ammonium bisulfate–sulfamic acid, properties as decontaminating solution for aluminum or zirconium, 20: 41214(P)

AMMONIUM FLUOPHOSPHATES
radiation effects on, ESR spectra of radicals from, 20: 40956

AMMONIUM THIOCYANATES
NH_4SCN–HNO_3–TBP, use in chromatographic separation of rare earths, thorium, and uranium, 20: 41045

AMMONIUM YTTRIUM NITRATES
binding energies in, infrared spectral studies of, 20: 40886

AMPHIBIANS
radiation effects on necturus intestine, 20: 40607 (BNL-10508)

AMPLIFIERS
circuit for protection of input stage of linear, design of, 20: 41260(P)
description of variable-gain pulse, using photoconductive control element, 20: 41269(R) (ORNL-3875, pp 4-12)
design and performance of hybrid pre-, for spectrometers, 20: 41298
design of wide-band low-noise charge-sensitive pre-, 20: 41269(R) (ORNL-3875, pp 4-12)
development of h-f low-noise transistorized wide-bandwidth, 20: 41227(R) (ORNL-3875, pp 1-3)
operation and testing of nuclear pulse, elimination of undershoot in, 20: 41269(R) (ORNL-3875, pp 4-12)
pulse shaping in nuclear pulse, minimum-noise, 20: 41269(R) (ORNL-3875, pp 4-12)
simulation of pulse, transfer-function, 20: 41228(R) (ORNL-3875, pp 15-20)

ANIMAL CELLS
aminoacyl-sRNA in neoplastic and normal human, preparation of, 20: 40632(R) (ORNL-3922, pp 175-91)
antioxidant and prooxidant components in mouse ascites tumor, 20: 40642
book: *Problems of Post-Radiative Cell Restoration*, 20: 40731
calcium distribution in avian shell gland, 20: 40551
chromosome aberrations induced by ^{3}H-thymidine, 20: 40686
cytokinetics of human spleen, using diffusion chamber techniques, 20: 40632(R) (ORNL-3922, pp 175-91)
DNA synthesis in Ehrlich ascites carcinoma, relation to histone fractions, 20: 40534(R) (NYO-3621-1)
effects of dose-fractionation of x rays on population dynamics, 20: 40764
effects of vinblastine on rat megakaryocyte, 20: 40502(R) (ORNL-3922, pp 115-27)
growth in semisolid agar of mouse, infected with Rauscher leukemia virus, 20: 40502(R) (ORNL-3922, pp 115-27)
growth in tissue culture, effects of thyroid hormones on, 20: 40511 (UCRL-16776)
histones from Ehrlich ascites carcinoma, quantitative analysis, 20: 40534(R) (NYO-3621-1)
lymphopoiesis of thoracic duct cells, 20: 40663
macromolecular synthesis in nuclei of mammalian, 20: 40534(R) (NYO-3621-1)
protein biosynthesis in, autoradiography of, 20: 40567
radiation effects on mouse marrow, factors affecting recovery from x, 20: 40634 (ORNL-P-2312)
radiation effects on cultured hamster and HeLa, lethal, effects of calchicine on low-dose x, 20: 40618(R) (NYO-2740-3, pp 166-215)
radiation effects on cultured, biological, uv and x, 20: 40623(R) (ORNL-3922, pp 32-49)
radiation effects on fine structure of lutein, from rat ovary, x, 20: 40672
radiation effects in rats on male germ, following exposure at birth, x, 20: 40683
radiation effects on reproductive capacity of human kidney, factors affecting particulate, 20: 40725
radiation effects on nuclear structure, gamma, 20: 40549
radiation effects on DNA synthesis in chick fibroblast and myoblast, x, 20: 40587
radiation effects on liver or lymphoma cells incubated with phytohemagglutinin, x, 20: 40588
radioinduced chromosome aberrations in Chinese hamster, β, 20: 40628(R) (ORNL-3922, pp 89-93)
radioinduced chromosome aberrations in, repair mechanisms for, 20: 40609 (CONF-660418-1)
subcellular components of rat liver, separation by B-XV zonal centrifuge rotor, 20: 40507 (ORNL-3922, pp 191-6)
use of 5-^{125}I-2′-deoxyuridine as thymidine analogue for autoradiography, 20: 40666

ANIMAL REPRODUCTION
radiation effects on female mouse, genetic control of x, 20: 40627(R) (ORNL-3922, pp 84-8)
radiation effects on number of offspring and sterility of Tribolium, x, 20: 40671
radiation effects on gastropod, effects of age at exposure on x, 20: 40700
radiation effects on fish, from radioisotope decay, 20: 40527

ANIMALS
bibliography on laboratory management, 20: 40493 (ANL-7300)
book: *Problems of Post-Radiative Cell Restoration*, 20: 40731
design of shielded source for irradiation of, 20: 40518 (CEX-63.10)
effects of jackrabbit, on population density, 20: 40494(R) (COO-1329-4)
radiation effects on behavior, gamma, 20: 40519 (NP-16259)
radiation effects on, effects of age, species, and strain on, 20: 40602 (AD-624934)
radiation effects on protein metabolism in, 20: 40602 (AD-624934)
radioinduced injuries to, ecological effects on recovery from, review of, 20: 40526
radioisotope accumulation by ocean-dwelling, 20: 41145

ANION EXCHANGE MATERIALS
sorptive properties for metals in sulfuric acid solutions, 20: 40822
thermal stability of nitrate-form resins in vented system, 20: 40877 (RL-SEP-823)

ANNEALING
effects of medium and temperature of, on molybdenum properties, 20: 41482
effects on radiation damage in graphite, 20: 42551

ANOXIA
protective effects on mice exposed to sublethal radiation, 20: 40732 (AD-636209)
radiosensitivity effects on human kidney cells, particulate, 20: 40725

ANTENNAS
signal propagation from reentering space vehicle, diffraction effects on, 20: 42438
signal propagation in compressible plasma, network representation of, 20: 42440

ANTHRACENE
radiation effects on, effects of partial absorption on beta, 20: 40504(R) (ORNL-3922, pp 146-60)
radiation effects on photoconductivity processes in, x, 20: 40952 (SC-DC-66-1823)

ANTHRANILIC ACID, METHYL ESTER
preparation of nitrogen-15-labeled, method for, 20: 41024

ANTIBARYONS
interactions with baryons, collinear U(3) ⊗ U(3) symmetry for, 20: 41977

ANTIBIOTICS
use of anthramycin for radiation protection, 20: 40736

ANTIBODIES
effects of auto-, on tumor transplants following x-radiation cure of previously transplanted tumors, 20: 40643
effects of auto-, in etiology of CNS diseases, 20: 40643
effects of content of, on counts of erythrocyte polymers, 20: 40626(R) (ORNL-3922, pp 80-3)
effects of incubation with hemagglutinin, irradiated cancer and normal cells, 20: 40588
formation of secondary, in mice of varying ages, 20: 40626(R) (ORNL-3922, pp 80-3)
production in mice, morphologic changes in spleen lymphatic tissue during, 20: 40632(R) (ORNL-3922, pp 175-91)
radiation effects on mouse production of, x, 20: 40626(R) (ORNL-3922, pp 80-3)
radiation effects on lymphoma or liver cells incubated with phytohemagglutinin, x, 20: 40588
response of, diffusion chamber technique for determining cytokinetics of, 20: 40632(R) (ORNL-3922, pp 175-91)
synthesis of, studies on, 20: 40503(R) (ORNL-3922, pp 137-45)

ANTIFERROMAGNETIC MATERIALS
book: *Rare Earth Ferromagnetics and Antiferromagnetics*, 20: 41483

ANTIGENS
clearance of rat and sheep erythrocyte, in mouse blood, selenium-75 tracer study of, 20: 40503(R) (ORNL-3922, pp 137-45)
isolation of spleen particles containing, by gonal centrifugation, 20: 40623(R) (ORNL-3922, pp 32-49)
lymph cell contact with foreign H-2, effects on irradiated mouse lymphoma cells of, 20: 40588
possible production of, in tissues during radiotherapy, 20: 40679
separation of, from blood platelets that affect vascular permeability, 20: 40496(R) (NYO-1753-3)

ANTIMONY
determination in copper coins by neutron activation methods, 20: 40800 (CNAEM-35)
determination in plutonium by carrier distillation methods, spectrographic, 20: 40814 (RFP-664)
determination in seawater, activation, 20: 40834
determination of, spectrophotometric, 20: 40796(R) (IS-1500(Sect.C))
separation from products of fission-fragment-induced radiolysis, 20: 40951

(RPI-321-6)
separation of silver from, by cation exchange chromatography, 20: 40847
ANTIMONY ALLOYS
Sb–Cd, phase studies, 20: 41455(R) (NYO-2731-7)
Sb–In, magnetic pinch in crystals of, population inversion in, 20: 42545
Sb–In, radioinduced defects in n-type, during tempering, 20: 42527
Sb–In, thermal conductivity of 2-Mev-electron-irradiated, 20: 42547
Sb–Na, solubility in sodium halide melts, 20: 40796(R) (IS-1500(Sect.C))
Sb–Pb, superconducting critical currents for, desolvation effects on, 20: 42099(T) (AD-636625)
ANTIMONY ISOTOPES Sb-121
energy-level transitions from Coulomb excitation by alpha particles at 1.30 and 1.50 Mev, (E), 20: 42186
ANTIMONY ISOTOPES Sb-124
determination in water, 20: 40819(T) (CEA-tr-A-1883)
ANTIMONY ISOTOPES Sb-125
beta activity measurements in France, 20: 41189 (CEA-R-3020)
content in fallout from Chinese nuclear test, May 1965, 20: 41130(R) (COO-1407-10)
ANTIMONY ISOTOPES Sb-126
yields of isomeric, in proton fission of uranium at 170 Mev, 20: 42177
ANTIMONY ISOTOPES Sb-127
yields in proton fission of uranium at 170 Mev, 20: 42177
ANTIMONY ISOTOPES Sb-128
yields in proton fission of uranium at 170 Mev, 20: 42177
ANTIMONY ISOTOPES Sb-129
yields in proton fission of uranium at 170 Mev, 20: 42177
ANTIMONY ISOTOPES Sb-130
yields in proton fission of uranium at 170 Mev, 20: 42177
ANTINUCLEONS
interactions with nucleons, intermediate boson production in annihilation, (T), 20: 41892
ANTIPROTONS
annihilation on protons in Tunguska meteor, properties of, 20: 41607
interactions with protons at 2.7 Bev/c, final states from, 20: 42523(R) (IS-1500(Sect.P))
interactions with protons, differential cross section for $\bar{N}^*N^*$ production in, (T), 20: 41788 (BMwF-FBK-66-12)
interactions with protons at 3 to 4 Bev/c, two- and zero-prong, (E), 20: 41792 (INR-708/VI/PL)
interactions with protons, polarization and structure relations for annihilation, (T), 20: 41813
interactions with protons, representation mixing in broken SU_{6w} for annihilation, 20: 41847
ARGON
acetylene–Ar, ionization potential of, alpha excitation, 20: 42487
alpha-particle interactions with, properties of recoil ions from, 20: 41622 (SC-DC-66-1564)
cesium concentration in flowing, method for determining, (E), 20: 41771
content in meteoric feldspar and pyropene, 20: 41162
design of potassium-seeded MHD generator, 20: 41678 (IPP-3/40)
electric conductivity in Brayton cycle MHD power generation, (T), 20: 41706
electric conductivity in plasma of, in magnetic field, (E), 20: 41770
electric conductivity of cesium-seeded plasma of, (E), 20: 41772
electric conductivity of potassium-seeded plasma of, (T), 20: 42410 (IPP-6/51)
electric discharges in, high-pressure electrodeless, (E), 20: 42509
electron energy balance in cesium-seeded plasma of, (E), 20: 41772
electronic recombination in afterglow plasma of, laser interferometric measurements of, (E), 20: 42469
hydrogen ion reactions at 50 to 150 kev, proton production in, (E), 20: 41663
ionization kinetics in cesium-seeded plasma of, (E), 20: 41703
ionization levels at 1400°K of potassium-seeded, (E), 20: 41736
ionization of potassium-seeded, magnetically induced non-equilibrium, (E), 20: 41715
ionization of, cross sections for shock-produced, 20: 40896
ionization relaxation process for, in MHD generator, 20: 41786
ionization using alpha excitation, acetylene addition effects on, 20: 42487
oscillations in potassium–seeded plasma of, (E), 20: 41692
plasma of, effective recombination coefficient of cesium-seeded, (E), 20: 41699
plasma of, electric potential distribution in potassium-seeded, (E), 20: 41708
potential energy integrals at 0°K of solid, (T), 20: 42123
properties as working fluid in Brayton power cycle, 20: 41398
properties of alkali-seeded plasma of, 20: 41712
scattering on nickel at 12 to 25 kev, secondary electrons from, 20: 41620 (NIJS-R-471)
solubility and thermodynamic properties of, in mixtures of deuterium oxide and water, 20: 40897
temperature measurement in shock-heated, transition probabilities for spectra used in, 20: 42483
use in MHD generators of nonseeded, (T), 20: 41721
use of potassium-seeded, in JAERI MHD generators, (E), 20: 41781
Ar–Xe, ionization of, at 5000 to 9000°K, shock-induced atom-atom, 20: 41632
ARGON ISOTOPES
separation of, design of gas centrifuges for, 20: 41404
ARGON ISOTOPES Ar-37
energy levels, (E), 20: 42200
ARGON ISOTOPES Ar-38
energy-level quantum numbers and transitions, (E), 20: 42181
ARGON ISOTOPES Ar-40
detection of, response of silicon fission chamber for, 20: 41324
ARGON SYSTEMS
Ar–ethylene, alpha particle interactions with, recoil ion properties from, 20: 41622 (SC-DC-66-1564)
ARGONNE ADVANCED RESEARCH REACTOR
development, 20: 42577(R) (ANL-7230)
development and testing, 20: 42670(R) (ANL-7245, pp 48-59)
fuel plates for, thermal conductivity of irradiated, 20: 42579(R) (ANL-7245, pp 29-47)
ARGONNE SYNCHROTRON
beam profile of, use of thermoluminescent dosimeters for determining, 20: 41530 (ANL-7196)
ARSENIC
determination in americium and plutonium by spark-source mass spectrography, 20: 40816 (RFP-699)
determination in plutonium by carrier distillation methods, spectrographic, 20: 40814 (RFP-664)
effects on uranium sulfide structure in hydrothermal deposits, 20: 41175
separation of silver from, by cation exchange chromatography, 20: 40847
ARSENIC FLUORIDES
preparation of fluorine-18-labeled, 20: 41020
ARSENIC SYSTEMS
As–S–Se, sintering mechanism of, 20: 41064(R) (IS-1500(Sect.E))
ARSINE
radiation effects on, in krypton at 4.2°K, ESR of free radicals from gamma, 20: 40967
ASCORBIC ACID
radiation effects on content of, in monkey eye tissues, γ, 20: 40646
radiation effects on content in rat adrenals of, 20: 40655
ASTROPHYSICS
electromagnetic fields and rotating masses, 20: 41609
gravitational collapse models for quasars, (T), 20: 41608
nuclear reaction cross section requirements for, 20: 41600
research programs on, 20: 41511(R) (RLO-1388-501)
ATLANTIC OCEAN
measurements of radioactivity in, 20: 41147
strontium-90 content in waters of, 1965 and 1966, 20: 41131(R) (HASL-172)
ATMOSPHERE
analysis for cesium-137 and strontium-90 in surface, method for, 20: 40853
density of, equipment for measurement of, 20: 41257
detection and measurement of fission products, in France after Chinese nuclear explosion, 20: 41189 (CEA-R-3020)
fallout dispersion and transport in, mathematical model for, 20: 41133(R) (SC-CR-66-2030)
fallout transport from, to water supplies, 20: 41141
fission product monitoring, 1965 and 1966, 20: 41131(R) (HASL-172)
neutron flux in, solar minimum measurements of fast, 20: 42055
particle scavenging of, by rain water, 20: 41130(R) (COO-1407-10)
radiation dose from inhaled or ingested radioactive methyl iodide in, 20: 41192(R) (IDO-12053)
radioactivity in Canadian, α and β, April 1965, 20: 41209
radioactivity in, near Canadian reactors, 20: 41136
radioactivity of, in Canada, April, 1966, 20: 41198 (NP-16192)
radon-222 content in, charcoal adsorption technique for determining, 20: 41277 (UCRL-16952)
ATMOSPHERE EXPOSURE CHAMBERS
parameters of, for carcinogenesis in mice, 20: 40632(R) (ORNL-3922, pp 175-91)
ATOMIC BEAMS
production of, optimum design of equipment for, 20: 41250
ATOMIC CLOUDS
rain scavenging of fallout from, 20: 41130(R) (COO-1407-10)
ATOMIC ENERGY COMMISSION
thermonuclear research policies of, 20: 42416 (TID-23277)
ATOMIC ENERGY, LEGAL ASPECTS
microbiological controls in, of food irradiation, 20: 41389

ATOMIC EXPLOSIONS
dynamics of certain spherical charge distributions, 20: 41517
effect on subsurface spalling of earth, 20: 41126
electromagnetic pulses from, effect on buried command posts and missile launch complexes, 20: 41117
fallout in France after second Chinese, 20: 41189 (CEA-R-3020)
fallout particles from, characteristics of highly active, 20: 41138
fission product formation by, 20: 41144
radio waves produced by gamma flux from atmospheric, (T), 20: 42046 (RM-4988)
seismic waves from Haymaker, Hardhat, and Shoal, 20: 41169
shelter systems for protection against, 20: 41183 (AD-635931)
timing and firing of, 20: 41070 (VUF-3021)
use in copper ore mining, 20: 41067(R) (ORNL-TM-1582)
use in excavation for railroad relocation, 20: 41071
use of underground in water development and management, 20: 41073
uses of, in United States, 20: 41072
ATOMIC PHYSICS
generalized discrete-continuum radial integrals with Coulomb functions, 20: 41633
research programs on, 20: 41511(R) (RLO-1388-501)
ATOMIC WEAPONS
civilian defense measures for, Project Harbor evaluation of, 20: 40738
effects on nuclear warfare and human sociological behavior, 20: 40738
motion of, sensing device for, 20: 41224 (EGG-1183-2078)
ATOMS
charge exchange scattering, model for, 20: 41624 (UCRL-17034)
collisions, convergence behavior of Born series for rearrangement, (T), 20: 41642
electron structure of, prediction of, 20: 41636
energy levels of, electron correlations for, 20: 41630
energy levels of, resonance fluorescence from, (T), 20: 41649
structure of, calculation of Hartree-Fock parameters for, 20: 41631
AUDITORY ORGANS
treatment of tumors of, by radiation and methotrexate, 20: 40782
AURORAL STORMS
electron precipitation in, origin of, (T), 20: 42056
intensity over Cape Hallett and Campbell Island, 20: 42059
location of, radar system for, 20: 42060
AUSTRALIA
rock in western, age of Precambrian, 20: 41159
silver content in rainwater from silver iodide-seeded clouds in, 20: 40838
AUTORADIOGRAPHY
bone marrow cell proliferation studies using tritiated thymidine, 20: 40722
book: *The Use of Radioautography in Investigating Protein Synthesis*, 20: 40567
determination of fluorine-18 distribution in dog bone using, 20: 40554
of amphibian intestine labeled with tritiated thymidine, 20: 40607 (BNL-10518)
of erythropoietic cells labeled with iron-55 and iron-59, 20: 40675
radioisotope-labeled albumins for placental, gonadal dose to fetuses from, 20: 40680
use for dosimetry of beta particles from injected tritiated thymidine in bone marrow nuclei, 20: 40743 (BNL-9374)
use for leak detection in shielded shipping containers, 20: 41197(R) (NP-16172)
use in studies of vaginal epithelia in mice, 20: 40502(R) (ORNL-3922, pp 115-27)
use of 5-^{125}I-2'-deoxyuridine as thymidine analogue for bone marrow cells, 20: 40666
AUXINS
effects on development of wheat parenchyma growing without mitosis, 20: 40631(R) (ORNL-3922, pp 161-6)

B

BACTERIA
adsorption of zinc-65 on, in salt-marsh ecosystems, 20: 40573
Bacillus subtilis, infection with DNA from SP02 bacteriophage, 20: 40676
effects of near-ultraviolet radiation on succinic oxidase metabolism in *Mycobacterium phlei*, 20: 40571
malic-lactic transhydrogenase in, preparation from *Micrococcus lactilyticus*, 20: 40505(R) (ORNL-3922, pp 167)
phosphorus-32 adsorption on, in salt-marsh ecosystems, 20: 40573
radiation effects on differentiating spores of *Bacillus megaterium*, repair of uv, 20: 40504(R) (ORNL-3922, pp 146-60)
radiation effects on *Hemophilus influenzae*, uv, 20: 40623(R) (ORNL-3922, pp 32-49)
radioprotective effects of products of, 20: 40736
radiosensitivity of soil, gamma, 20: 40637(R) (ORO-2754-7)
role in cutaneous eruptions during radiotherapy of female genital cancer, 20: 40679
thymineless, studies on, 20: 40632(R) (ORNL-3922, pp 175-91)
tracer use of phosphorus-32-labeled, for testing cleanability of biologically contaminated surfaces, 20: 41218
tryptophan metabolism in Pseudomonas, enzyme reactions for, 20: 40533(R) (NYO-901-54(p.16-19)
use in rat brain homogenate for induction of experimental allergic encephalomyelitis, 20: 40728
BACTERIOPHAGES
attachment of fl, to male strains of *E. coli*, 20: 40504(R) (ORNL-3922, pp 146-60)
buoyant density and survival of, effects of dilution treatments and osmotic shock on, 20: 40500(R) (ORNL-3922, pp 109-12)
characteristics of P1kc, 20: 40504(R) (ORNL-3922, pp 146-60)
effects of colicine on cells infected with, 20: 40535(R) (ORNL-3922, pp 128-35)
electron spin resonance spectrometry of nucleic acid of, 20: 40593
isolation of messenger, 20: 40535(R) (ORNL-3922, pp 128-35)
radiation effects on bromouracil-substituted DNA of T3, uv, 20: 40504(R) (ORNL-3922, pp 146-60)
radiation effects on T3, role of *E. coli* in repair of uv, 20: 40504(R) (ORNL-3922, pp 146-60)
radiation effects on chromosomes of, repair mechanisms for, 20: 40609 (CONF-660418-1)
radiation effects on developing *Escherichia coli* complexes with, uv, 20: 40618(R) (NYO-2740-3, pp 166-215)
radiation effects on, genetic, uv, 20: 40623(R) (ORNL-3922, pp 32-49)
radiation effects on, SH compound protection, gamma, 20: 40515
SP02 of *Bacillus subtilis*, uv sensitivity compared with that of its infectious DNA, 20: 40676
thymine dimer transfer in T4v$^-$, 20: 40504(R) (ORNL-3922, pp 146-60)
BALANCES
calibration Westphal, for density measurements, 20: 40869 (MCW-1473)
BARITE CONCRETES
pouring for construction of shields for Kyoto University research reactor, 20: 42586
BARIUM
determination in fission product solutions, method for, 20: 40803 (KFK-387)
determination in plutonium by carrier distillation methods, spectrographic, 20: 40814 (RFP-664)
determination in seawater, activation, 20: 40834
diffusion of hydrogen in, 20: 41412(R) (IS-1500(Sect. M))
distribution of, in neutron-irradiated plutonium dioxide suspensions, 20: 41009 (AERE-R-3268)
ionization on hot rhenium surfaces, (T), 20: 42406 (IPP-2/47)
proton reactions with neutral ground state of, formation of excited hydrogen atoms in, (T), 20: 41634
scattering on beryllium–copper alloy at 5 kev, secondary electrons from, 20: 41620 (NIJS-R-471)
separation from ashes of beef bones, milk, and fish, 20: 40858
separation from strontium by ion exchange on granulated zirconyl phosphate, 20: 41055
separation from strontium by cation exchange using DTPA and HEDTA as eluants, 20: 41040 (ORNL-TM-1342)
separation of silver from, by cation exchange chromatography, 20: 40847
BARIUM BROMIDES
vapor pressure enthalpies and equations for, 20: 41412(R) (IS-1500 (Sect. M))
BARIUM FLUORIDES
solubility in double fluorides of neptunium, plutonium, thorium, and uranium, 20: 40867 (KFK-385)
BaF_2–LiF–UF_4, uses as electrolyte in electrolytic recovery of scrap uranium metal, 20: 41036 (MCW-1494)
BARIUM IODIDES
vapor pressure enthalpies and equations for, 20: 41412(R) (IS-1500 (Sect. M))
BARIUM ISOTOPES Ba-133
decay, (E), 20: 42203
metabolism in rats as indicator of alkaline earth metabolism, 20: 40565
BARIUM ISOTOPES Ba-140
beta activity measurements in France, 20: 41189 (CEA-R-3020)
BARIUM NEPTUNIUM FLUORIDES
preparation, properties, and structure of, 20: 40867 (KFK-385)
BARIUM THORIUM FLUORIDES
preparation, properties, and structure of, 20: 40867 (KFK-385)
BARIUM TITANATES
performance in ferroelectric transducers, 20: 41684
BARIUM URANATES
preparation, properties, and spectra of, 20: 40901
BARIUM URANIUM FLUORIDES
preparation, properties, and structure of, 20: 40867 (KFK-385)

BARLEY
effects of alkylating sulfonates on, biological, 20: 40717
genetic control of strontium-89 and calcium-45 accumulation, 20: 40532(R) (COO-1097-17)
radiation effects on, effects of zygosity on x, 20: 40701
radiation effects on, genetic, γ, 20: 40716
radiation effects on, genetic, x, 20: 40717
radioinduced mutations of, selection in first generation plants from exposed seeds, x, 20: 40711
use of chemically induced mutations in hybridization breeding of, 20: 40712
use of radioinduced mutations in hybridization breeding of, 20: 40712
BARYONS
classification in irreducible representations of noncompact groups, 20: 41967
classification in D_5 group, 20: 41972
classification in noncompact groups, 20: 41982
composite models for, in $SU(6)_W$, 20: 42034
decay of Lee model for electromagnetic field effects on, (T), 20: 41909
decay of, broken U(12) for leptonic, 20: 41939
decay of, dynamic self-consistency requirement for leptonic, (T), 20: 41999
decays of, static model with SU(6) symmetry for nonleptonic, 20: 42023
decays of, two-angle Cabibbo theory of leptonic, 20: 41987
interactions of, weak axial-vector currents for, 20: 41981
interactions of, weak magnetism in U(12) symmetry for weak, 20: 42009
interactions with mesons, SU(3) invariant coupling constants for, 20: 41976
interactions with antibaryons, collinear U(3) ⊗ U(3) symmetry for, 20: 41977
interactions with mesons, permutation symmetry in, 20: 41984
interactions with vector mesons, unitary symmetry for moderately strong, 20: 42013
interactions with mesons, $SU(6)_W$ symmetry scheme for, 20: 42016
interactions with baryons, SU(3) symmetry for, (T), 20: 41799(R) (ORO-2504-96)
interactions with mesons, bootstrap model and SU_6 symmetry for, 20: 41848
interactions with mesons in broken SU(3) symmetry, strong coupling constants for, 20: 41860
interactions with mesons, exchange of even- and odd-parity resonances in, 20: 41880
magnetic moments of, strong interaction SU(2) and SU(3) for anomalous, 20: 41996
mass differences of, model of broken unitary symmetry for, 20: 41976
masses and quark structure of, 20: 42017
production amplitudes for $J^P = ½^+$, effect of inelastic processes on, 20: 41836
production in neutrino interactions, broken U(12) for, 20: 41939
structure of, Rutherford-type model for, 20: 42003
symmetry for, beyond SU(6), 20: 42030
symmetry for, 3* plet model for, 20: 41998
symmetry group for classification of, saturation of SU(6), 20: 41968
BARYONS, RESONANCE
classification in irreducible representations of noncompact groups, 20: 41967
classification in irreducible representations of noncompact groups, 20: 41967
decays of, sum rule for, 20: 41843
model for $N\frac{1}{3}N\pi$ vertex, quark, 20: 41876
production and properties of Y_1^*, in meson (K^-)-neutron interactions at 0.8 to 1.1 Bev/c, (E), 20: 41886
production in neutrino interactions, broken U(12) for, 20: 41939
production of N* (1236) in meson (K^+) interactions at 2.7 Bev/c, (E), 20: 41804 (UCRL-17003)
production of N* pairs, in antiproton-proton interactions, (T), 20: 41788 (BMwF-FBK-66-12)
production of N^{*+} (1238) and N^{*+} (1430), in distorted-wave OPE model for proton-proton inelastic interactions, 20: 41820
production of N* (1688) and N* (1928) in meson (π)-proton interactions at 875 to 1579 Mev/c, (E), 20: 41857
production of N* (1920), in mesons (π^-) interactions with protons at 2.1 Bev/c, (E), 20: 41858
production of N* (1236) and N* (1518), in proton-proton interactions at 2.8 Bev/c, (E), 20: 41920
production of N*(1688), in proton-antiproton interactions at 3 to 4 Bev/c, (E), 20: 41792 (INR-708/VI/PL)
production of Y* (1385) in meson (K^-)-proton interactions, peripheral model for charge-state interference in, 20: 41819
properties of, maximum likelihood method for determining, 20: 41790 (DESY-66/17)
stability in broken symmetry, 20: 41994
BAUXITE
analysis for aluminum and silicon, activation, 20: 40812 (ORO-2980-14)
BEANS
base composition of nucleic acid fractions in root cells of Vicia, 20: 40631(R) (ORNL-3922, pp 161-6)
BEHAVIOR
effects of nuclear warfare on human sociological, 20: 40738
radiation effects on locomotor, in rats, x, 20: 40688
radiation effects on gastropod reproductive, effects of age at exposure on x, 20: 40700
radiation effects on animals, gamma, 20: 40519 (NP-16259)
radiation effects on rat conditioned reflex, following fetal exposure, 20: 40654
radiation effects on carp food selection, gamma, 20: 40656
BENZENE
radiolysis of, EPR studies of yields of stabilized charges in low-temperature, 20: 40962
radiolysis of, stilbene isomerization by triplet molecules from gamma, 20: 40961
benzene–bromotrifluoromethane, radiolysis of, mechanism and yields of products in gamma, 20: 40948(R) (COO-578-3-32)
BENZENE, ETHYL-
radiolysis of, EPR studies of yields of stabilized charges in low-temperature, 20: 40962
BENZENE, FLUORO-
yields in gamma radiolysis of benzene–bromotrifluoromethane, mechanism of, 20: 40948(R) (COO-578-3-32)
BENZOHYDROXAMIC ACID
complexes with uranyl ions, stability of, 20: 40903
BENZOPHENONE
effects on yields in gamma radiolysis of liquid and vitreous 2-propanol, 20: 41006
3,4-BENZOPYRENE
radiosensitivity effects on bacterial DNA, uv, 20: 40632(R) (ORNL-3922, pp 175-91)
p-BENZOQUINONE, TRIS(1-AZIRIDINYL)-
effects of, combined with γ radiation on HeLa cells, 20: 40704
BERYLLIUM
analysis for carbon, nitrogen, and oxygen by deuteron activation methods, 20: 40812 (ORO-2980-14)
analysis for impurities in, methods for, 20: 41416
analysis of, for oxygen, equipment used in activation methods for, 20: 40848
crystal structure and properties of, 20: 41416
deposition from complexes on copper or silver, electrolytic, 20: 40864 (BMwF-FBK-66-10)
determination in plutonium by carrier distillation methods, spectrographic, 20: 40814 (RFP-664)
determination using bis-2-pyridyl glycol, effects of pH on gravimetric, 20: 40849
electric conductivity of, as function of temperature, 20: 41485
fabrication of, technology survey on, 20: 41427 (NASA-TM-X-53453 (Vol.1))
forming of cross-rolled sheets of, techniques for, 20: 41433
helium and hydrogen ion attenuation at 0.1 to 500 Mev, tables for, 20: 41619 (CEA-R-3042)
ion ranges at 10 to 100 Mev, bromine and iodine, 20: 41647
phase diagram of, pressure-temperature, 20: 41485
phonon dispersion-relation measurements for, by neutron scattering, 20: 42541
preparation, 20: 41416
pressing hollow shapes of, method development, 20: 41428 (SCL-DC-66-57)
proton reactions with neutral ground state of, formation of excited hydrogen atoms in, (T), 20: 41634
purification by distillation and zone refining of, methods for, 20: 41416
x-ray emission spectra of, L and K, (E), 20: 41350
BERYLLIUM ALLOYS
interactions with gas flow in MHD generators, 20: 41738
Be–Cu, ion scattering at 5 kev, secondary electrons from, 20: 41620 (NIJS-R-471)
Be–Cu, properties as magnet material, 20: 41097
BERYLLIUM ISOTOPES Be-6
energy levels, (E), 20: 42190
energy levels of, from helium-3–helium-4 reactions (He-3,n) at 26 Mev, (E), 20: 42169(R) (UCRL-14744, pp 1-18)
energy levels of, from proton reactions (p,n) with lithium-6 at 11.6 and 12.6 Mev, (E), 20: 42169(R) (UCRL-14744, pp 1-18)
BERYLLIUM ISOTOPES Be-7
beta activity measurements in France, 20: 41189 (CEA-R-3020)
production in neutron reactions with nuclei, (E), 20: 41276 (UCRL-16769)
BERYLLIUM ISOTOPES Be-8
energy levels, (E), 20: 42352

BERYLLIUM ISOTOPES Be-9
alpha elastic scattering by, DWBA analysis of, (T), 20: 42392
alpha reactions (α,γ) with, carbon-13 energy-level transitions from, (E), 20: 42330
alpha reactions (α,n) with, carbon-12 energy-level lifetimes from, (E), 20: 42234
description using SU(3) shell model, (T), 20: 42191
deuteron reactions at 100 to 200 kev, angular distributions of protons, tritons, and alpha particles from, (E), 20: 42354
helium-3 reactions (He-3,p) with, boron-11 energy levels from, (E), 20: 42246
helium-3 reactions (He-3,α)2α with, coincidence studies of, (E), 20: 42374
helium-3 reactions (He-3,n) and (He-3,p) with, boron-11 and carbon-11 energy-level lifetimes from, (E), 20: 42234
lithium-7 reactions (Li-7,d) with, carbon-14 energy-level transitions from, (E), 20: 42231
neutron reactions (n,2n)2α at 15 Mev, mechanism of, (E), 20: 42362
proton reactions (p,2p) at 155 Mev, proton energy spectra from, (E), 20: 42360
proton reactions (p,α) and (p,d) at 7 to 9 Mev, (E), 20: 42212

BERYLLIUM ISOTOPES Be-10
energy-level lifetimes from gamma Doppler shifts, (E), 20: 42234

BERYLLIUM OXIDES
strength and Young's modulus of, effects of density and grain size on, 20: 41473
yields from beryllium sulfate solution, gravimetric estimation of, 20: 40849

BERYLLIUM SYSTEMS
neutron decay constants in, 20: 42601

BETA PARTICLES
content in water near Canadian reactors, 20: 41136
daily average of total activity in air in West Germany, 20: 40570
detection and measurement of, using Geiger-Mueller counters and anticoincidence techniques, 20: 40833
dosimetry in and on skin using field-type instruments, 20: 41274 (ORNL-TM-1581)
dosimetry in bone marrow nuclei of, from injected tritiated thymidine, autoradiographic method, 20: 40743 (BNL-9374)
dosimetry of, for polycythemia therapy, 20: 40774
effects combined with zero-gravity on induction of chromosome aberrations in leukocytes, 20: 40635(R) (ORNL-TM-1550)
effects on anthracene and sodium iodides, effects of partial absorption on, 20: 40504(R) (ORNL-3922, pp 146-60)
effects on chromosomes in Chinese hamster cells, aberrant, 20: 40628(R) (ORNL-3922, pp 89-93)
effects on electret effect in paraffin wax, (E), 20: 41516
effects on fish spawning, 20: 40527
effects on hybrid development in frogs, 20: 40535(R) (ORNL-3922, pp 128-35)
effects on rice seed, chlorophyll mutations from, 20: 40641
effects on thymidine metabolism in thyroid cell nuclei in mice, 20: 40616(R) (NYO-901-54, pp 48-50)
hyaluronic acid depolymerization by, 20: 40591
measurement of fallout activity in New Zealand, 20: 40521(R) (NP-16270)
radioinduced mutations in rice, 20: 40640
uptake by leaves from fallout, 20: 40579

BETA SPECTROMETERS
current generator for precision, development of, 20: 41354
description of two-lens, with correction coils, 20: 41282
design and performance of flat magnetic, with 324.5° focusing angle, 20: 41355
design and performance of b = 1 toroidal, for short-period beta emitter study, 20: 41309
design of double focusing magnetic, with lithium compensated silicon focal plane detectors, 20: 41326
detector system for use with Stanford, calibration technique for multi-, 20: 41310
performance of double focusing, with adjustable angular separation, 20: 41348
sample deposition for, hypodermic syringe design modification for liquid, 20: 41296
use for recoil measurements of subnanosecond nuclear lifetimes, 20: 42180

BETATRONS
beam injection pulse duration effects on electron capture in, 20: 41565
bremsstrahlung collimator system of 3 Mev Brown Boveri, induced radioactivity of, 20: 41540 (NYO-3364-7(Rev.))
design, 20: 41573(P)
design and performance of 35-Mev, for industrial and medical use, 20: 41555
effects on human erythrocyte diameter and volume from occupational exposure to, 20: 40678
electron injection in, maximum x-ray output from, 20: 41560
performance of 24-Mev, for medical use, 20: 41564
radiation monitoring system for, 20: 41561
use in cancer therapy in gynecology, 20: 40768

BEVATRON
development and operation, 20: 41803(R) (UCRL-16863)

BIBENZYL
yields in gamma radiolysis of sulfur hexafluoride–toluene, 20: 40948(R) (COO-578-3-32)

BIBLIOGRAPHIES
of atomic energy literature, 20: 42692 (TID-3736)
on accelerators, 20: 41546
on analytical methods for cesium-137, 20: 40841
on beryllium fabrication, 20: 41427 (NASA-TM-X-53453(Vol.1))
on calorimetry of metals, 20: 41457(R) (ORO-3291-3)
on chemistry of promethium, 20: 40872 (NP-16254)
on determination of bromine in terrestrial and extraterrestrial materials by neutron activation, 20: 40811 (ORO-2670-13)
on elastic and inelastic proton-proton scattering, 20: 41800 (UCRL-14716)
on laboratory animal science, 20: 40493 (ANL-7300)
on physical properties of materials, 20: 41442 (CNLM-2393)
on preparation, properties, and uses of deuteriated organic compounds, 20: 40940
on stable isotopes in chemistry, geology, and physics, 20: 41380(T) (IFA-IS-36)
on thermal insulation, 20: 41440(R) (ALO-3632-4)

BINDING ENERGY
calculation of nuclear D-, P-, and S-wave, 20: 42281

BIOCHEMISTRY
effects of hepatomas on trout, 20: 40632(R) (ORNL-3922, pp 175-91)
radiation effects on fish embryo and prelarvae, 20: 40527
radiation effects on wheat flour, gamma, 20: 40599

BIOLOGICAL MATERIALS
analysis of, for trace elements by radioisotopic dilution, 20: 40844
molecular structure in, determined by neutron-diffraction analysis, 20: 40632(R) (ORNL-3922, pp 175-91)
radiation effects on, parameters of x, 20: 40504(R) (ORNL-3922, pp 146-60)
radioisotope accumulation by organic debris in oceans, 20: 41146

BIOLOGICAL MODELS
use in mutation studies on peanuts, 20: 40636(R) (ORO-1747-12)

BIOLOGICAL STRESS
effects of dilution treatment and osmotic shock, on buoyant density and survival in bacteriophages, 20: 40500(R) (ORNL-3922, pp 109-12)

BIOLOGICAL SYSTEMS
bound water in, calorimetric determination of, 20: 40500(R) (ORNL-3922, pp 109-12)
effects of nuclear warfare on, 20: 40738

BIOMETRY
analysis of variance of progenies of irradiated peanuts, 20: 40636(R) (ORO-1747-12)

BIOSYNTHESIS
book: *The Use of Radioautography in Investigating Protein Synthesis*, 20: 40567
radiation effects on chick DNA, x, 20: 40587

BIPHENYL
properties as working fluid in Rankine power cycle, 20: 41398
yields in gamma radiolysis of sulfur hexafluoride–toluene, 20: 40948(R) (COO-578-3-32)

BIPYRIDINES
effects on frequency of chromosome aberrations induced by radiomimetic agents in *Vicia faba*, 20: 40715
labeling with carbon-14, 20: 40941

BISMUTH
analysis for tellurium, spectrophotometric, 20: 40805(R) (MLM-1325, pp 63-70)
determination in plutonium by carrier distillation methods, spectrographic, 20: 40814 (RFP-664)
determination of, using isoöctylthioglycolate, 20: 40796(R) (IS-1500 (Sect.C))
meson (μ^-) capture by, nuclear charge distribution determination from, (E), 20: 42305
meson (μ^-) capture by, x-ray spectra from, (E), 20: 42306
photon reactions (γ,n) with, energy spectra from, (E), 20: 42165(R) (MIT-2098-251, pp 16-20)
preparation of single crystals of, 20: 41064(R) (IS-1500(Sect.E))
separation from tin by reversed-phase chromatography, 20: 40796(R) (IS-1500(Sect.C))
separation of silver from, by cation exchange chromatography, 20: 40847
use in fission chambers, 20: 41276 (UCRL-16769)

BISMUTH ALLOYS
Bi–Cd–Pb–Sn, magnetic flux penetration in superconducting, (E), 20: 42132
Bi–In, tunneling in superconducting films of, superimposed on normal zinc films, (E), 20: 42109
Bi–Na, solubility in sodium halide melts, 20: 40796(R) (IS-1500(Sect.C))
Bi–Pb, extraction of cadmium from, 20: 41064(R) (IS-1500(Sect.E))
Bi–Pb, wetting reactions with stainless steel, 20: 41064(R) (IS-1500 (Sect.E))
Bi–Sn, distribution of tin in, 20: 41064(R) (IS-1500(Sect.E))
Bi–Sn, solidification of, effects of electric fields on, 20: 41412(R) (IS-1500(Sect. M))
BISMUTH ISOTOPES Bi-209
alpha fission at 23 to 115 Mev, fragment angular distributions in, (E), 20: 42267
carbon-12 reactions (C-12,5n) with, actinium-216 production in, (E), 20: 42287
meson (μ^-) capture by, E2 and M1 hyperfine structure determination from, (E), 20: 42307
neon-22 reactions with, production of spontaneously fissioning neptunium isotope in, (E), 20: 42292
proton fission at 100 to 150 Mev, (E), 20: 42196
proton reactions (p,xn) at 75 to 160 Mev, production of polonium isotopes in, (E), 20: 42196
BISMUTH SYSTEMS
Bi–Te, phase studies, 20: 41455(R) (NYO-2731-7)
BISMUTH TELLURIDES
crystal structure of, 20: 41455(R) (NYO-2731-7)
BITOLYLS
yields in gamma radiolysis of sulfur hexafluoride–toluene, 20: 40948(R) (COO-578-3-32)
BLAST EFFECTS
shelter systems for protection against, 20: 41183 (AD-635931)
BLOOD
analysis for iron-59 in hemin in red cells in, method for, 20: 40830
analysis of, for ceruloplasmin, copper, and zinc by radioisotopic dilution, 20: 40844
antigenicity of rat and sheep erythrocytes in mouse, selenium-75 tracer study of, 20: 40503(R) (ORNL-3922, pp 137-45)
determination of fluorine-18 activity after oral and intravenous administration in dogs, 20: 40554
effects of simultaneous x radiation and microwaves on leukocytes and hematocrit, 20: 40650
effects of x ray and L-methionine on iron-59 metabolism, 20: 40561
glucose levels in, following iodine-131 therapy for diabetes-hyperthyroidism, 20: 40790
irradiation of, extracorporeal, effects on lymphocyte content, 20: 40744 (BNL-10403)
leukocyte number in human, factors affecting, 20: 40612 (EUR-2711.f)
radiation effects on proteolytic activity of, 20: 40602 (AD-624934)
radioinduced inactivation of foot and mouth disease virus in, of swine carcases, γ, 20: 41392
separation of granulocytes from red cells by sedimentation, 20: 40496(R) (NYO-1753-3)
therapy of thrombocytopenia using frozen blood platelets, 20: 40496(R) (NYO-1753-3)
urea nitrogen content in, of deer and sheep, 20: 40541(R) (UCD-34P104-3)
BLOOD CELLS
analysis for iron-59 in hemin in, method for, 20: 40830
radioinduced chromosome aberrations in human, 20: 40665
uptake of zinc-65 and other radioisotopes, effects of dietary calcium, zinc, and corn oil on, 20: 40556
use of iron-55 and iron-59 for autoradiography of, 20: 40675
BLOOD CIRCULATION
measurement of dog coronary, using phosphorus-32 tracer and new catheter-type micro G-M counter, 20: 40514
radiation effects on content of leukocytes in rat, mechanisms involved, 20: 40697
BLOOD FORMATION
effects of lymphoid and myeloid transplants on, in lethally x-irradiated mice, 20: 40727
BLOOD PICTURE
radiation effects on swine, x, 20: 40605 (AD-635735)
radiation effects on swine, γ, 20: 40608 (CEA-R-3001)
radiation effects on human, low-dose, 20: 40612 (EUR-2711.f)
radiation effects on, in mice irradiated *in utero*, 20: 40649
BLOOD PLASMA
iron-59 and water-content in rats, 20: 40561
strontium-85 activity in dogs, 20: 40684
BLOOD PLATELETS
antigenic properties of, affecting vascular permeability, 20: 40496(R) (NYO-1753-3)
effects of vinblastine on rat, 20: 40502(R) (ORNL-3922, pp 115-27)
life span of infused frozen, in thrombocytopenic patients, 20: 40496(R) (NYO-1753-3)
preservation by freezing, effects of cryoprotective drugs on, 20: 40496(R) (NYO-1753-3)
BLOOD SERUM
technetium-99-labeled albumins from, preparation of, 20: 40944
tracer use of radioisotope-labeled albumins in, for placentography, gonadal dose to fetuses from, 20: 40680
BLOOD VESSELS
radium-226 and lead-210 content in radium dial painters, 20: 40621 (NYO-3086-5)
use of radioisotope angiography in kidney function studies, 20: 40775(T)
visualization using gamma-ray scintillation camera, 20: 40752
BLOOD VOLUME
use of erythrocyte, in determination of dosimetry of phosphorus-32 therapy for polycythemia, 20: 40774
BODY WATER
content and turnover in deer and sheep, tracer study, using T_2O, 20: 40541(R) (UCD-34P104-3)
BOILERS
cost analysis of, for sodium-steam system, 20: 42632 (NAA-SR-12060)
description and operation of PWR Core 2, instruction manual, 20: 42645 (WAPD-PWR-2222)
design and operation of PWR Core 2, instruction manual, 20: 42646 (WAPD-PWR-2223)
development and testing for sodium-cooled reactors, 20: 42639(R) (UNC-5154)
development of sodium-heated, 20: 42620(R) (BAW-1280-39)
testing of, for KRB reactor, 20: 42638(R) (TID-23299)
BOILING
area of, method for increasing, 20: 42602(P)
detection in liquid metals, ultrasonic flowmeter for, 20: 41225(R) (NYO-3622-4)
void fractions in, impedance method of measuring, 20: 41103 (RT-ING-(65)7)
BOILING REACTORS
design of, with increased boiling surface, 20: 42602(P)
fuel element cladding for, corrosion testing of, 20: 41418(R) (GEAP-5150)
reactivity accident tests of, core design for, 20: 42664(R) (IDO-17165)
BONDS
disulfide, radiation effects in proteins, 20: 40596
BONE MARROW
analysis for iron-59 in hemin in red blood cells in, method for, 20: 40830
cell proliferation in, after bleeding of x-irradiated mice, 20: 40722
effects of injected tritiated thymidine on, in leukemia patients, cytocidal, 20: 40743 (BNL-9374)
radiation effects on cells of mouse, factors affecting recovery from x, 20: 40634 (ORNL-P-2312)
radiation effects on erythrocyte stem cell kinetics in rat, 20: 40603 (AD-635086)
radiation effects on swine, γ, 20: 40608 (CEA-R-3001)
radioinduced inactivation of foot and mouth disease virus in, of swine carcasses, γ, 20: 41392
radioprotective effects in mice, x, 20: 40718(R) (ORNL-3922, pp 99-105)
radioprotective effects in mice of, combined with AET or glutathione treatment, 20: 40719(R) (ORNL-3922, pp 136)
radioprotective effects of transplants of mouse, mechanism for x, 20: 40727
radiosensitivity effects in mice, effects of estradiol on x, 20: 40577
recolonization in x-irradiated mice of, following lymphoid or myeloid transplants, 20: 40727
therapy for hematopoietic anomalies induced by cancer chemo- or radiotherapy, 20: 40726
use of 5-^{125}I-2′-deoxyuridine as thymidine analogue for autoradiography, 20: 40666
BONE TUMORS
pathology of plutonium-239-induced, in mice, 20: 40745(R) (NYO-901-54, pp 29-47)
BONES
analysis for naturally-occurring radioisotopes, in sarcoma patients, 20: 41191(R) (HUX-3170-1)
analysis for radium-226, strontium-89, and strontium-90, 20: 40809 (NP-16235)
calcium-47 uptake by rat, 20: 40557
determination of biological half-life for radium in, from radium dial painters, 20: 40621(R) (NYO-3086-5)
distribution of radium-226, radium-228, lead-210, and thorium-228 in radium dial painters, 20: 40621 (NYO-3086-5)
histology of, before and after removal of parathyroid adenoma, 20: 40552
lead-210 content in human, 20: 40531 (A/AC.82/G/L-1045(Rev.1))
plutonium-239 effects on mouse, pathological, 20: 40745(R) (NYO-901-

54, pp 29-47)
polonium-210 content in human, 20: 40531 (A/AC.82/G/L-1045(Rev.1))
radiation effects on mandibular growth of rat, x, 20: 40652
radiation injury of subcutaneous, following therapy, 20: 40659
radiocalcium studies and histological findings in osteitis fibrosa cystica generalisata of von Recklinghausen, 20: 40552
radium-226 content in human, 20: 40531 (A/AC.82/G/L-1045(Rev.1))
radium-228 content in human, 20: 40531 (A/AC.82/G/L-1045(Rev.1))
scandium-47 and calcium-47 metabolism in rats, 20: 40545
scanning in dogs using fluorine-18, 20: 40554
separation of barium-140, strontium-89, and strontium-90 from ashes of beef, 20: 40858
strontium-85 accretion and exchange in dog trabecular and cortical, 20: 40684
strontium-85 uptake by fractured human, 20: 40542
strontium-90 content in, of yearling deer, 20: 40541(R) (UCD-34P104-3)
strontium-90 content of, sampled in 1965, 20: 41131(R) (HASL-172)
thorium-228 content in human, 20: 40531 (A/AC.82/G/L-1045(Rev.1))
use of strontium-85 scanning for location of metastases of, for radiotherapy, 20: 40794
x-ray spectral distributions in, 20: 41322

BORON
analysis of, for oxygen by neutron activation methods, 20: 40846
content in common rock types, 20: 41068 (PNE-5006)
determination in americium and plutonium by spark-source mass spectrography, 20: 40816 (RFP-699)
determination in plutonium by carrier distillation methods, spectrographic, 20: 40814 (RFP-664)
determination in uranium(IV-VI) oxides, effects of graphite electrode grade on carrier-distillation spectroscopic, 20: 40807 (NLCO-976)
determination in uranium dioxide fuel pellets, 20: 41112 (IITRI-578P11-54)
determination of, in nickel base alloy by deuteron activation methods, 20: 40812 (ORO-2980-14)
effects on oxidation resistance of refractory metal disilicides, 20: 41424
helium and hydrogen ion attenuation at 0.1 to 500 Mev, tables for, 20: 41619 (CEA-R-3042)
proton reactions with neutral ground state of, formation of excited hydrogen atoms in, (T), 20: 41634

BORON FLUORIDES
preparation of fluorine-18-labeled, 20: 41020
use in proportional counters, for neutron dosimetry in accelerator environment, 20: 41543 (RPP-R-2)

BORON ISOTOPES
alpha-particle structures in, (E), 20: 42193

BORON ISOTOPES B-9
energy levels, (E), 20: 42188
energy levels, (E/T), 20: 42350

BORON ISOTOPES B-10
alpha-cluster formation in alpha reactions and scattering near 25 Mev, (E), 20: 42193
deuteron reactions (d,p) with, boron-11 energy levels from, (E), 20: 42246
deuteron reactions (d,α)2α with, coincidence studies of, (E), 20: 42374
energy level excitation in helium-3 reactions (He-3,α) with boron-11 at 1.0 to 2.15 Mev, (E), 20: 42217
energy levels, (E/T), 20: 42350
energy-level lifetimes from gamma Doppler shifts, (E), 20: 42234
fabrication on compact absorbers of, for neutron spectrometers, 20: 41272(R) (ORNL-3875, pp 53-74)
helium-3 reactions (He-3,p3α) at 2.45 and 6.00 Mev, 20: 42188
helium-3 reactions (He-3,t) at 30 and 40 Mev, carbon-10 energy levels from, (E), 20: 42190
lithium-6 reactions (Li-6,d) with, nitrogen-14, energy-level transitions from, (E), 20: 42231
proton reactions (p,d) at 156 Mev, boron-9 energy levels from, (E/T),
reactions with aluminum-27 at 0 to 110 Mev, excitation functions for, (E), 20: 42183
triton reactions (t,α_0) at 1.5 to 3.25 Mev, angular distributions for, (E), 20: 42398

BORON ISOTOPES B-11
alpha-cluster formation in alpha reactions and scattering near 25 Mev, (E), 20: 42193
deuteron reactions (d,p) at 300 kev, angular distributions for, (E/T), 20: 42399
electron scattering by, energy level excitation in, (E), 20: 42378
energy level transitions of, multipolarity in 8.92 Mev → 0, (E), 20: 42384
energy levels, (E), 20: 42246
energy levels, (E), 20: 42378
energy levels from carbon-12 (y,py') reaction, (E), 20: 42343
energy-level lifetimes from gamma Doppler shifts, (E), 20: 42234
helium-3 reactions (He-3,α) at 1.0 to 2.15 Mev, alpha angular distributions from, (E/T), 20: 42217
proton reactions (p,d) at 156 Mev, boron-10 energy levels from, (E/T), 20: 42350
reactions with aluminum-27 at 0 to 110 Mev, excitation functions for, (E), 20: 42183

BORON ISOTOPES B-12
energy level at 955 kev, gamma decay of, (E), 20: 42381

BORON NITRIDES
properties for high-temperature insulation of thermocouples, 20: 41461(R) (UCRL-7361(Pt.3))

BORON OXIDES
B_2O_3–Dy_2O_3, liquid immiscibility in, 20: 40910
B_2O_3–Er_2O_3, liquid immiscibility in, 20: 40910
B_2O_3–Eu_2O_3, liquid immiscibility in, 20: 40910
B_2O_3–Gd_2O_3, liquid immiscibility in, 20: 40910
B_2O_3–Ho_2O_3, liquid immiscibility in, 20: 40910
B_2O_3–La_2O_3, liquid immiscibility in, 20: 40910
B_2O_3–Lu_2O_3, liquid immiscibility in, 20: 40910
B_2O_3–Nd_2O_3, liquid immiscibility in, 20: 40910
B_2O_3–Sc_2O_3, liquid immiscibility in, 20: 40910
B_2O_3–Sm_2O_3, liquid immiscibility in, 20: 40910
B_2O_3–Tm_2O_3, liquid immiscibility in, 20: 40910
B_2O_3–Yb_2O_3, liquid immiscibility in, 20: 40910
B_2O_3–Y_2O_3, liquid immiscibility in, 20: 40910

BOSONS
decay of intermediate, rate for, (T), 20: 41892
field theory for, paraquantization in, 20: 41925 (JINR-P-2756)
field theory for, Lie algebra and Schroedinger equation for quantum, 20: 41934
field theory for, commutation relations for, 20: 41946
interactions with fermions, Lehmann-Symonzik-Zimmermann formalism in Lee model for, (T), 20: 42169(R) (UCRL-14744, pp 1-18)
photoproduction of pair of circularly polarized intermediate vector, on lead 208, (E), 20: 41901
production of intermediate, from antinucleon-nucleon annihilation, (T), 20: 41892
production of W, in meson (π^-) interactions with protons at 2 to 5 Bev, cross sections for, (T), 20: 41859

BOUNDARY LAYER
heat transfer through absorbing, radiative, 20: 41108
magnetohydrodynamic, effect of magnetic fields and temperatures on, 20: 42039
magnetohydrodynamic plane, equations for, 20: 42044

BRAIN
crescent pattern of increased radioactivity in scanning, 20: 40789
enzyme assays of cerebral tissues during acute radiation syndrome, 20: 40590
immune response to transplanted tumors in mouse, following x radiation cure of previously transplanted tumors, 20: 40643
radiation effects on, deuteron, 20: 41187 (BNL-9468)
radioinduced abnormalities in rats, x, 20: 40688
radioinduced microencephaly in male mouse, effects of age at exposure on x, 20: 40633 (ORNL-P-2287)
radiotherapy of tumors of, laser, 20: 40776
reparative effects of DNA from, on sperm of x-irradiated rat, 20: 40723
use of improved scintillation scanner for radiodiagnosis, 20: 40779
use of pertechnetate in studying extracellular space, 20: 40750

BRAZIL
radiochemical and radioecological studies in areas of high natural radiation, 20: 40522(R) (NYO-3273-7)

BRAZING ALLOYS
development of zirconium-base, for fuel assemblies, 20: 41425(R) (IITRI-578-P29-2)

BREASTS
radiotherapy of cancer, 20: 40773
radiotherapy of cancer of, effects on metastases of x, 20: 40793

BREMSSTRAHLUNG
emission in electron-electron interactions, cross sections for double-, 20: 41904
production at high energies, cross sections for, 20: 41789 (DESY-66/16)
production by electron interactions with thick targets, 20: 41875
production from polarized electron reactions with nuclei at 300 kev, asymmetry function for, (E), 20: 41662
production from proton reactions with hydrogen and deuterium, 20: 41916
production in proton-proton interactions at 33.5 and 46 Mev, energy dependence of cross sections for, (E), 20: 41882
production in proton-proton interactions at 50 Mev, (T), 20: 41921
reactions with helium and hydrogen, meson (π^+) production from, (E), 20: 41816
reactions with helium and hydrogen below 330 Mev, mesons (π^-) and (π^+), relative yields from, (E), 20: 41817
reactions with nuclei at 2 Bev, quantum electrodynamic violation in wide angle pair production from, (E), 20: 42327

BROMIDE IONS
bromine-82 exchange between, and tetrabromoplatinate ions, 20: 40796(R)

(IS-1500(Sect.C))
BROMINE
determination in extraterrestrial and terrestrial materials, activation, 20: 40811 (ORO-2670-13)
effects on yields in gamma radiolysis of carbon tetrachloride, 20: 40948(R) (COO-578-3-32)
helium and hydrogen ion attenuation at 0.1 to 500 Mev, tables for, 20: 41619 (CEA-R-3042)
BROMINE IONS
ranges in materials at 10 to 100 Mev, 20: 41647
BROMINE ISOTOPES Br-82
exchange between bromide and tetrabromoplatinate ions, 20: 40796(R) (IS-1500(Sect.C))
use as tracer for waste solution dispersion in soil, 20: 42687
BRONZE
radiation effects on antifriction and strength properties of lead, neutron, 20: 41498
BROOKHAVEN BEAM RESEARCH REACTOR
accidents in, facility design for air cleaning following, 20: 42673 (BNL-10483)
safety of, effect of xenon on, 20: 42672 (BNL-10388)
BROOKHAVEN REACTOR
accidents in, facility design for air cleaning following, 20: 42673 (BNL-10483)
BUBBLE CHAMBERS
data analysis of, track centering system for flying spot digitizers for, 20: 41263 (CERN-66-23)
development and operation at LRL, 20: 41803(R) (UCRL-16863)
refrigerator for, design and performance of 3°K helium, 20: 41378
BUILDING MATERIALS
fabrication using cement and depleted uranium, 20: 41435(P)
BUTADIENE
yields from catalytic dehydrogenation of butane, 20: 40943
BUTANE
dehydrogenation of, effects of neodymium and praseodymium oxides on catalytic properties of aluminum–chromium system for, 20: 40943
tritium ion reactions at 3 to 6000 ev with, (E), 20: 40938
yields of deuterated, in hydrolysis of aluminum, thorium, and uranium carbides in heavy water, 20: 40905
BUTANE, 2,3-EPOXY-
effects on maize, genetic, 20: 40708
1-BUTANOL
radioinduced oxidation of aqueous solutions of, effects of dose rate and temperature on gamma, 20: 40983
radioinduced oxidation of aqueous solutions of, effects of dose rate on kinetics of gamma, 20: 40984
2-BUTANONE
radiolysis of, EPR studies of yields of stabilized charges in low-temperature, 20: 40962
BUTENES
yields from catalytic dehydrogenation of butane, 20: 40943
yields of deuterated, in hydrolysis of aluminum, thorium, and uranium carbides in heavy water, 20: 40905
BUTYL PHOSPHATES
analysis for uranium, refractometric, 20: 40804 (KR-108)
solvent properties for polonium in chloride and perchlorate solutions, 20: 41052
$HCl–NdCl_3–PrCl_3–TBP–H_2O$, separation factors for neodymium and praseodymium in, 20: 40904
$Nd(NO_3)_3–HNO_3–Pr(NO_3)_3–TBP–H_2O$, separation factors for neodymium and praseodymium in, 20: 40904
$NH_4SCN–HNO_3–TBP$, use in chromatographic separation of rare earths, thorium, and uranium, 20: 41045
BUTYRIC ACID, 4-AMINO-2-HYDROXY-
preparation of nitrogen-15-labeled, method for, 20: 41024

C

CADARACHE REACTORS (RAPSODIE)
pressure vessel for, austenitic steel testing for, 20: 42652(T) (EURFNR-92F)
CADMIUM
determination in plutonium by carrier distillation methods, spectrographic, 20: 40814 (RFP-664)
determination in uranium dioxide fuel pellets, 20: 41112 (IITRI-578P11-54)
determination of, developments in resin spot tests for, 20: 40827
electric conductivity of liquid, 20: 41476
helium and hydrogen ion attenuation at 0.1 to 500 Mev, tables for, 20: 41619 (CEA-R-3042)
separation from tin by reversed-phase chromatography, 20: 40796(R) (IS-1500(Sect.C))
CADMIUM ALLOYS
Bi–Cd–Pb–Sn, magnetic flux penetration in superconducting, (E), 20: 42132
Sb–Cd, phase studies, 20: 41455(R) (NYO-2731-7)
CADMIUM CARBONATES
carbon-14 decay in labeled, effects of, on reactivity, 20: 41018
CADMIUM IONS
spectra of, electronic absorption, 20: 40796(R) (IS-1500(Sect.C))
CADMIUM ISOTOPES Cd-113
neutron total cross section from 0.025 to 1 ev, resonance parameters from, (E), 20: 42149 (CNAEM-34)
CADMIUM ISOTOPES Cd-115
decay of isomeric, (E), 20: 42260
uptake by swine blood cells in vitro, effects of dietary calcium, zinc, and corn oil on, 20: 40556
CADMIUM SULFIDES
preparation and properties of single crystals of, effects of crystallization temperature on, 20: 41480
radiation effects on n-type, gamma and thermal neutron, 20: 41271(R) (ORNL-3875, pp 44-52)
CADMIUM TELLURIDES
radiation effects on n-type, gamma and thermal neutron, 20: 41271(R) (ORNL-3875, pp 44-52)
CADMIUM THORIUM FLUORIDES
preparation, properties, and structure of, 20: 40867 (KFK-385)
CALCIUM
absorption by algae and fungi, 20: 40524(R) (TID-23271)
content and distribution in chicken eggs, effects of dietary strontium and calcium on, 20: 40569
content in sea water from Indian Ocean, uptake of marine organisms, 20: 40572
content in total diet and milk in Finland, 20: 41134 (SFL-A3)
determination by atomic absorption spectroscopy using induction-coupled plasmas, 20: 40796(R) (IS-1500(Sect.C))
determination in americium and plutonium by spark-source mass spectrography, 20: 40816 (RFP-699)
determination in environmental samples, 20: 40809 (NP-16235)
determination in plutonium by carrier distillation methods, spectrographic, 20: 40814 (RFP-664)
determination in uranium trioxide by emission spectrography, 20: 40802 (HW-65402(Rev.1))
effects on strontium-85 and strontium-89 excretion by goats, 20: 40568
heat of fusion and transformation temperature of, 20: 41412(R) (IS-1500(Sect. M))
helium and hydrogen ion attenuation at 0.1 to 500 Mev, tables for, 20: 41619 (CEA-R-3042)
intracellular distribution in avian shell gland, 20: 40551
meson (μ^-) capture using polarized meson (μ^-), neutron angular distribution from, (E), 20: 42300
migration in turf-podzolic and black earth soil, 20: 40520 (NP-16261)
preparation of pure, by distillation, 20: 41455(R) (NYO-2731-7)
proton energy losses in, (E), 20: 42363
proton reactions with neutral ground state of, formation of excited hydrogen atoms in, (T), 20: 41634
purification of, by sublimation, 20: 41412(R) (IS-1500(Sect. M))
radiation effects on content in soils, effects of soil type on gamma, 20: 40637(R) (ORO-2754-7)
ratio of strontium-90 to, in milk in Great Britain, 20: 41186 (ARCRL-15)
uptake by corn plants, effects of soil fertility on, 20: 40735 (NYO-2744-37)
uptake by rice, effects of irrigation on, 20: 40574
CALCIUM ALLOYS
Ca–Mg, heat capacity of intermetallic compound, at 4 to 287°K, 20: 41412(R) (IS-1500(Sect. M))
Ca–Mg, heat of fusion of intermetallic compound, 20: 41412(R) (IS-1500(Sect. M))
Ca–Yb, crystal structure and electric conductivity of, 20: 41412(R) (IS-1500(Sect. M))
Ca–Zn, heat of fusion of intermetallic compound, 20: 41412(R) (IS-1500(Sect. M))
Ca–Zn, thermodynamic properties of, 20: 41412(R) (IS-1500(Sect. M))
CALCIUM BROMIDES
vapor pressure enthalpies and equations for, 20: 41412(R) (IS-1500 (Sect. M))
CALCIUM CHLORIDES
heat of fusion, 20: 41412(R) (IS-1500(Sect. M))
CALCIUM FLUORIDES
magnetic behavior of electrolytically colored crystals of, (E), 20: 42555
proton energy losses in, (E), 20: 42363
radiation effects on electric and magnetic properties of crystals of, x, (E), 20: 42555
radiation effects on color and x-ray luminescence of, as function of temperature, x, 20: 42556
radioluminescence spectra of manganese-activated, 20: 42524 (NRL-

6408)
sintering mechanisms of, 20: 41064(R) (IS-1500(Sect.E))
solubility in double fluorides of neptunium, plutonium, thorium, and uranium, 20: 40867 (KFK-385)
spectra of electrolytically colored crystals of, 20: 42556
thermoluminescence emission spectra of manganese-activated, 20: 42524 (NRL-6408)
thermoluminescence emission spectra of, 20: 42524 (NRL-6408)
use in thermoluminescent dosimeters, 20: 41373

CALCIUM IODIDES
vapor pressure enthalpies and equations for, 20: 41412(R) (IS-1500 (Sect. M))

CALCIUM ISOTOPES
nuclear wave functions for, single-particle, (T), 20: 42270

CALCIUM ISOTOPES Ca-40
alpha elastic and inelastic scattering by, energy levels from, (E), 20: 42168(R) (MIT-2098-251, pp 57-73)
alpha reactions ($\alpha,\alpha'\gamma$) at 30 Mev, gamma spectra from, (E), 20: 42168(R) (MIT-2098-251, pp 57-73)
energy levels, (E), 20: 42257
proton elastic scattering at 30 Mev, optical-model analysis of, (T), 20: 42255
proton elastic scattering at 80 and 150 Mev, differential cross sections and polarizations for, (E/T), 20: 42388
proton inelastic scattering at 152 Mev, differential cross sections and polarization of, (E), 20: 42341
proton quasi-elastic scattering below 160 Mev, shell-model calculations, 20: 42277
proton reactions (p,γ) at 0.3 to 2.1 Mev, resonance strengths for, (E), 20: 42182
proton reactions (p,α) at 11 Mev, Q-values for, (E), 20: 42200
proton reactions at 30 Mev, optical model analysis of total cross sections for, (T), 20: 42255

CALCIUM ISOTOPES Ca-42
alpha elastic and inelastic scattering by, energy levels from, (E), 20: 42168(R) (MIT-2098-251, pp 57-73)
helium-3 reactions (He-3,d) at 10 and 11 Mev, scandium-43 energy levels from, (E), 20: 42253

CALCIUM ISOTOPES Ca-43
neutron capture by, calcium-44 energy-level transitions from thermal, (E), 20: 42335

CALCIUM ISOTOPES Ca-44
alpha elastic and inelastic scattering by, energy levels from, (E), 20: 42168(R) (MIT-2098-251, pp 57-73)
energy-level transitions from thermal-neutron capture by calcium-43, (E), 20: 42335
helium-3 reactions (He-3,d) at 10 and 11 Mev, scandium-45 energy levels from, (E), 20: 42253
proton reactions (p,d) with, energy spectra from, (E), 20: 42168(R) (MIT-2098-251, pp 57-73)

CALCIUM ISOTOPES Ca-45
dynamics and intestinal absorption studies on hyperparathyroidism, 20: 40552
genetic control of accumulation in barley and wheat, 20: 40532(R) (COO-1097-17)
intracellular distribution in avian shell gland, 20: 40551
use in bone mineralization dynamics studies, 20: 40558

CALCIUM ISOTOPES Ca-47
beta decay, (E), 20: 42192
dynamics and intestinal absorption studies on hyperparathyroidism, 20: 40552
metabolism in rat bones, 20: 40545
production in thermal-neutron fission of uranium-235, (E), 20: 42298
rate of exchange of, in rat tissues, power function for, 20: 40557
uptake by bones, muscle and skin of rats of various ages, 20: 40557

CALCIUM ISOTOPES Ca-48
alpha elastic and inelastic scattering by, energy levels from, (E), 20: 42168(R) (MIT-2098-251, pp 57-73)

CALCIUM ISOTOPES Ca-50
alpha elastic and inelastic scattering by, energy levels from, (E), 20: 42168(R) (MIT-2098-251, pp 57-73)

CALCIUM NEPTUNIUM FLUORIDES
preparation, properties, and structure of, 20: 40867 (KFK-385)

CALCIUM NITRATES
use as buffer in determination of lanthanum using Complexone III and Xylenol Orange, 20: 40860

CALCIUM OXIDES
CaO–ThO_2, creep of polycrystalline at 1465°C, effects of stress on, 20: 41474

CALCIUM PLUTONIUM(IV) FLUORIDES
preparation, properties, and structure of, 20: 40867 (KFK-385)

CALCIUM SULFATES
isotopic fractionation of oxygen-18 in water of crystallization of, 20: 40836
radioluminescence spectra of manganese-activated, 20: 42524 (NRL-6408)
thermoluminescence emission spectra of manganese-activated, 20: 42524 (NRL-6408)

CALCIUM SYSTEMS
Ca–O, phase studies, 20: 41412(R) (IS-1500(Sect. M))

CALCIUM THORIUM FLUORIDES
preparation, properties, and structure of, 20: 40867 (KFK-385)

CALCIUM TUNGSTATES
preparation and properties of single crystals of, effects of crystallization temperature on, 20: 41480

CALCIUM URANIUM FLUORIDES
preparation, properties, and structure of, 20: 40867 (KFK-385)

CALIFORNIUM
separation from americium and curium, by ion exchange using hydrochloric acid–methanol solvent system, 20: 40855

CALIFORNIUM ISOTOPES Cf-246
production of isomeric, in uranium-238 (C-12,4n) reactions, (E), 20: 42159 (JINR-P-2841)

CALORIMETERS
design and performance of adiabatic, for metal systems, 20: 41457(R) (ORO-3291-3)
design for electron beam dosimetry, 20: 40742(R) (ACRH-25, pp 24-9)
design of adiabatic, for use at 4.2 to 350°K, 20: 40796(R) (IS-1500 (Sect.C))
use of total intensity, for absolute dose measurements for field emission electron generator, 20: 40746(R) (NYO-3510-2)

CALORIMETRY
use in determining bound water in biological systems, 20: 40500(R) (ORNL-3922, pp 109-12)

CAMBRIDGE SYNCHROTRON
explosion and fire in, factors affecting, 20: 41539 (MIT-2098-259)

CAMERAS
design of high-speed, for study of nuclear rocket engines, 20: 41223 (EGG-1183-1244)
design of television, for use in nuclear atmosphere, 20: 41099

CANADA
environs monitoring near reactors in, April 1965, 20: 41136
fallout monitoring, April, 1966, 20: 41198 (NP-16192)
fallout monitoring in, April 1965, 20: 41209
heavy water production in, 20: 42616 (66-CNA-301)

CANADIAN REACTORS
environs monitoring, April, 1966, 20: 41198 (NP-16192)

CANDU REACTOR
environs monitoring, April 1965, 20: 41136
fuel development for, status, 20: 42618 (66-CNA-312)

CAPTURE-TO-FISSION RATIOS
measurement of, time-of-flight system with on-line computer for, 20: 41232(R) (ORNL-3875, pp 75-90)

CARBAMIC ACID, DIETHYLDITHIO-, SODIUM SALTS
use for therapy of nickel carbonyl poisoning and thallium sulfate poisoning in man, 20: 40536(R) (ORO-3461-1)

CARBAMIC ACID, ETHYL ESTER
effects as spray foam for sealing air leaks, 20: 41200 (ORNL-TM-1551)

CARBIDES
melting points of, equipment and methods for, 20: 41412(R) (IS-1500 (Sect. M))

CARBON
addition of trace-amounts to chromium–nickel steel, method for, 20: 41418(R) (GEAP-5150)
bremsstrahlung reactions with, quantum electrodynamic violation in wide angle pair production from, (E), 20: 42327
carburization reactions with iron and steel under vacuum, 20: 41412(R) (IS-1500(Sect. M))
chemical reactions with uranium oxides at high temperatures, kinetics of, 20: 41411 (IS-1379)
content in arc-melted rhenium–tungsten ingots, 20: 41429(R) (USBM-RC-1249)
corrosive effects of liquid sodium-dissolved, on stainless steel at high temperatures, 20: 41420(R) (MSAR-66-149)
determination in hydrogenated polyphenyls, fouling films, and terphenyl mixtures, 20: 40797 (AECL-2524)
determination in liquid sodium from recirculating test loops, 20: 41420(R) (MSAR-66-149)
determination in sodium, method for, 20: 42619(R) (ANL-7245, pp 1-28)
determination of, in nickel base alloy by deuteron activation methods, 20: 40812 (ORO-2980-14)
determination of, on beryllium surfaces by deuteron activation methods, 20: 40812 (ORO-2980-14)
distribution in stainless steel, effects of liquid metal loop conditions on, 20: 41419(R) (GMAD-3643-5)
effects of traces of, on corrosion of chromium–nickel steel, 20: 41418(R)

(GEAP-5150)
effects on phase transformations in gallium–plutonium alloy and plutonium, differential thermal analysis of, 20: 41452 (MLM-1172)
effects on silica-base thermal insulators at high temperatures, 20: 41440(R) (ALO-3632-4)
effects on thorium tensile properties at 100 to 1000 ppm, 20: 41412(R) (IS-1500(Sect. M))
flux in primary cosmic radiation, (E), 20: 41672
helium and hydrogen ion attenuation at 0.1 to 500 Mev, tables for, 20: 41619 (CEA-R-3042)
ion ranges at 10 to 100 Mev, bromine and iodine, 20: 41647
meson (π^-) capture below 140 Mev, gamma spectra from, (E), 20: 42314
proton energy losses in, (E), 20: 42363
proton reactions (p,2p) at 160 and 460 Mev, quasi-free, (E), 20: 42276
proton reactions with neutral ground state of, formation of excited hydrogen atoms in, (T), 20: 41634
proton scattering by, maximum likelihood method for analysis of polarization from, 20: 41790 (DESY-66/17)
reactions at high temperatures with urania, for metal production, 20: 41412(R) (IS-1500(Sect. M))
reactions with vanadium pentoxide at high temperatures, for production of vanadium metal, 20: 41412(R) (IS-1500(Sect. M))
separation from gallium–plutonium alloys by zone refining, method evaluation for, 20: 41453(R) (NUMEC-3428-21)
separation from thorium by electrotransport, 20: 41412(R) (IS-1500 (Sect. M))
uptake by niobium–zirconium alloys in liquid metals, 20: 41419(R) (GMAD-3643-5)

CARBON DIOXIDES
determination in sea water, 20: 40523(R) (RLO-1750-8(Vol.1))
effects on leaky and nonleaky mutants in Neurospora, 20: 40624(R) (ORNL-3922, pp 52-8)
radiolysis of frozen aqueous solutions of, ESR spectral studies on radical reactions in, 20: 40994
radiolysis of, mechanism of gamma and x, 20: 40996
reactions with copper and copper–gold alloys at 1000°C, 20: 41458(R) (TID-23268)
reactions with uranium carbide, effects of hydrogen on, 20: 40870 (NAA-SR-Memo-7310)
CO_2–CO, reactions with iron–titanium alloys at 900 to 1100°C, 20: 41458(R) (TID-23268)

CARBON IONS
effects on human kidney cells, factors affecting RBE, 20: 40725

CARBON ISOTOPES C-10
energy levels, (E), 20: 42190

CARBON ISOTOPES C-11
energy level transitions of, multipolarity in 6.49 Mev → 0, (E), 20: 42384
energy levels from carbon-12 ($\gamma,n\gamma'$) reaction, (E), 20: 42343
energy-level lifetimes from gamma Doppler shifts, (E), 20: 42234
reactions of recoil, in irradiated alcohols and hydrocarbons, 20: 40796(R) (IS-1500(Sect.C))

CARBON ISOTOPES C-12
alpha elastic scattering at 51 Mev, (E/T), 20: 42389
alpha inelastic scattering at 20 and 25 Mev, (E), 20: 42296
alpha inelastic scattering at 23 Mev, angular correlations in, (E), 20: 42380
carbon-12 reactions (C-12,N-13) with, angular distributions from, (E), 20: 42153 (JINR-E-2824)
coupling of giant resonance and surface oscillations in, (T), 20: 42271
deuteron reactions (d,pγ) with, carbon-13 energy-level spins and transitions from, (E), 20: 42252
deuteron reactions (d,pγ) with, proton-gamma angular correlations in, (E), 20: 42383
deuteron reactions (d,p) at 4 to 7 Mev, excitation functions for, (E), 20: 42400
deuteron scattering at 4 to 7 Mev, (E), 20: 42400
electron elastic and inelastic scattering at 600 to 800 Mev, cross sections for, (E/T), 20: 42238
electron elastic scattering at 100 to 200 Mev, 20: 42377
energy levels, (E), 20: 42352
energy levels, (E), 20: 42188
energy levels between 14 and 21 Mev, (E), 20: 42377
energy-level lifetimes from gamma Doppler shifts, (E), 20: 42234
gamma reactions ($\gamma,n\gamma'$) with, carbon-11 energy levels from, (E), 20: 42343
gamma reactions (γ,p) at 21.3 and 21.6 Mev, azimuthal proton angular distribution from, (E), 20: 42251
gamma reactions ($\gamma,p\gamma'$) with, boron-11 energy levels from, (E), 20: 42343
helium-3 reactions (He-3,pγ) with, nitrogen-14 energy-level spins and transitions from, (E), 20: 42252
helium-3 reactions (He-3,pγ), proton-gamma angular correlations in, (E), 20: 42383
neutron cross sections from 0.01 to 15 Mev, 20: 42160 (KAPL-3099)
neutron elastic scattering at 1 to 10 Mev, angular distributions from, (E), 20: 41556
neutron reactions with, beryllium-7 production in, (E), 20: 41276 (UCRL-16769)
neutron reactions (n,α_0) at 16 and 17 Mev, total cross sections for, 20: 42367
proton elastic and inelastic scattering at 4.6 to 11.2 Mev, absolute cross sections for elastic, (E/T), 20: 42390
proton elastic scattering at 80 and 150 Mev, differential cross sections and polarizations for, (E/T), 20: 42388
proton reactions ($p,p'\alpha$) at 60 and 120 Mev, cross sections for, (E), 20: 42352
proton reactions (p,pd) at 155 Mev, differential cross sections for, (T), 20: 42361
reactions (C-12,d) with lithium-6 at 6 to 8 Mev, oxygen-16 energy levels from, (E), 20: 42329
reactions (C-12,N-13) with aluminum-27, carbon-12, niobium-93, silver-107, silver-108, tantalum-181, and vanadium-51, (E), 20: 42153 (JINR-E-2824)
reactions (C-12,4n) with uranium-238, production of isomeric californium-246 in, (E), 20: 42159 (JINR-P-2841)
reactions (C-12,5n) with bismuth-209, actinium-216 production in, (E), 20: 42287
triton reactions (t,α_0) at 1.5 to 3.25 Mev, angular distributions for, (E), 20: 42398

CARBON ISOTOPES C-13
alpha reactions (α,n) at 1.95 to 5.5 Mev, oxygen-17 energy levels from, (E), 20: 42336
deuteron reactions (d,Li-6) at 15 Mev, differential cross sections for, (E/T), 20: 42237
effects in solvolysis and iodine-131 exchange reactions of methyl iodide, kinetic, 20: 40939
energy level at 170 kev, gamma decay of, (E), 20: 42381
energy levels, (E), 20: 42369
energy levels from oxygen-16(n,α) reaction, (E), 20: 42370
energy-level spins and transitions, (E), 20: 42252
energy-level transitions from beryllium-9 (α,γ) reactions, 20: 42330
helium-3 reactions (He-3,p) with, nitrogen-15 energy levels from, (E), 20: 42369

CARBON ISOTOPES C-14
content in deep waters of Pacific Ocean, 20: 41127
content of deep and surface waters of Indian Ocean, 20: 41127
decay in cadmium carbonate, effects on reactivity of, 20: 41018
determination in atmosphere, equipment design for, 20: 40734(R) (NYO-901-54, pp 24-5)
effects of thymidine labeled with, on mitosis in hamster cells, 20: 40686
energy levels from carbon-13 (d,p) reactions, (E), 20: 42233
energy-level transitions in, branching ratios for, (E), 20: 42231
helium-3 reactions (He-3,α) with, carbon-13 energy levels from, (E), 20: 42369
helium-3 reactions (He-3,p) with, nitrogen-16 energy levels from, (E), 20: 42369
incorporation in bipyridylium salts, 20: 40941
incorporation in chrysanthemumic acid, method for, 20: 41015
incorporation in methylenedioxyphenyl compounds, methods for, 20: 41014
incorporation in rotenone on semimicro scale, 20: 41013
radioactivity measurement using windowless counters, 20: 41281
use as tracer for estimation of choline acetyltransferase, 20: 40584
use as tracer in determining microsome production in antibody-forming cells, 20: 40626(R) (ORNL-3922, pp80-3)

CARBON ISOTOPES C-15
beta decay, (E), 20: 42242

CARBON MONOXIDES
monitoring of content in fallout shelters during fires, 20: 41184 (AD-637806)
production by chemonuclear synthesis, 20: 40988
production in gamma and x radiolysis of carbon dioxide, mechanism of, 20: 40996
radioinduced polymerization with ethylenimine, effects of ethylene on, 20: 40975
radiolysis of, decontamination of products from fission-fragment, 20: 40951 (RPI-321-6)
CO_2–CO, reactions with iron–titanium alloys at 900 to 1100°C, 20: 41458(R) (TID-23268)

CARBON STEEL
radiation effects on crystal lattice of, neutron, 20: 41497

CARBON SYSTEMS
C–Fe, precipitates in, crystal structure and growth of, 20: 41412(R) (IS-1500(Sect. M))
C–Hf–W, creep-rupture properties of Sylvania A, 20: 41456 (ORNL-3992)
C–N–O–U, preparation and high-temperature properties of stoichiometric, 20: 41429(R) (USBM-RC-1249)

C–O–U, preparation and properties of oxycarbide phases of, 20: 41429(R) (USBM-RC-1249)
C–U–UO_2, phase studies, 20: 41412(R) (IS-1500(Sect. M))
C–Y, phase studies, 20: 41412(R) (IS-1500(Sect. M))
C–Zr, preparation and properties of alloys of, 20: 41471

CARBON TETRACHLORIDE
radiolysis of, mechanism and yields of products in gamma, 20: 40948(R) (COO-578-3-32)
reactions with thorium oxalate for production of thorium tetrachloride, 20: 41412(R) (IS-1500(Sect. M))
solvent properties for fluorine-18 in irradiated lithium carbonate, 20: 41021
solvent properties for technetium and rhenium, 20: 40856
yields in gamma radiolysis of bromo- and chlorotrifluoromethane, mechanism of, 20: 40948(R) (COO-578-3-32)
carbon tetrachloride–cyclohexane, radiolysis of, mechanism of transfer mechanism in, 20: 40957

CARBONIUM COMPOUNDS
deuterium-hydrogen exchange in cations derived from, NMR studies on, 20: 40945

CARBONYLS
determination in radiation processed sea foods, chemical, 20: 41384(R) (TID-22833)
effects on wholesomeness of radiation processed sea foods, 20: 41384(R) (TID-22833)
ionization and bond dissociations of, critical potentials for, 20: 40796(R) (IS-1500(Sect.C))

CARCINOGENESIS
effects of polonium-210 attached to tobacco smoke particles on bronchial epithelium, 20: 41191(R) (HUX-3170-1)
radioinduced in man, 20: 40659
radioinduced in mice, effects of age at exposure on x, 20: 40633 (ORNL-P-2287)
studies of chemical, development of tissue culture lines for, 20: 40632(R) (ORNL-3922, pp 175-91)

CARCINOMAS
chromosome aberrations induced by nitrogen mustard and triethylenemelamine, with and without added nicotinic amide, in, 20: 40550
effects of radioprotective drugs on damage induced by alkylating agents, 20: 40664
effects of radiotherapy of uterine, on the intestine and urinary system, 20: 40703
high-voltage therapy of uterine, at radium clinic in Stockholm, 20: 40769
induced in mice in inhalation chambers, 20: 40632(R) (ORNL-3922, pp 175-91)
phosphorus-32 uptake by, as indication of hormonal response of, 20: 40566
pulmonary fibrosis after radiotherapy of breast, 20: 40773
radiation effectiveness for lung, review of, 20: 40786
radiation effects on HeLa cells combined with trenimon, gamma, 20: 40704
radioinduced, in parabiotic rats by total-body x irradiated, 20: 40614 (NYO-901-39)
radioinduction of, in occupationally exposed persons, 20: 41207
radiotherapy of adeno-, laser, 20: 40776
radiotherapy of canthi and eyelid, injuries from gamma and x, 20: 40689
radiotherapy of cervical, radium and x, 20: 40772
radiotherapy of female genital, cutaneous eruptions following, 20: 40679
radiotherapy of laryngeal, myxedema development following x, 20: 40780
radiotherapy of nasopharyngeal, effects on pituitary function of x, 20: 40660
radiotherapy of thyroid, 20: 40758
radiotherapy of vocal cord, 20: 40759
radiotherapy of, in gynecology using supervoltage x rays, 20: 40768
response of gastrointestinal, to combined colchicine and radiation therapy, 20: 40763
treatment of oto-rhino-laryngeal by radiation and methotrexate, 20: 40782
use of intracavitary cobalt-60 therapy in uterine, 20: 40761

CARDIOGRAPHY
radiation effects on mouse, x, 20: 40648

CAROTENOIDS
decomposition of, in wheat flour, gamma, 20: 40599

CARTILAGE
selenium-75 and sulfur-35 fixation to protein-polysaccharides of, 20: 40544

CASCADE SHOWERS
production of electron-photon, in copper and lead at 1 Bev, 20: 41671

CATALYSIS
radioinduced, review of, 20: 40989

CATALYSTS
radioactive, effeciency and uses of, 20: 40989

CATARACTS
analysis of radiation-induced, 20: 40690
radiation-induced, in mice, 20: 40649
radioinduced in mice and rabbits, RBE of neutrons and x, 20: 40618(R) (NYO-2740-3, pp 166-215)
radioinduced in mice, by intrauterine exposure to x, 20: 40619(R) (NYO-2740-3, pp 216-57)

CATION EXCHANGE MATERIALS
radiation effects on soil, gamma, 20: 40637(R) (ORO-2754-7)

CATTLE
cesium-137 content in milk from Norweigian, March 1962 to 1966, 20: 41132 (NYO-3364-20)
radiation effects on function and structure of bull testicle, x, 20: 40610(R) (COO-895-9)
radiation effects on function and structure of bull testicle, x, 20: 40610(R) (COO-895-9)
selenium-75 and sulfur-35 metabolism in cartilage of, 20: 40544

CAVES
development and standardization in UK, 20: 41098

CAVITY RESONATORS
superconducting, for microtrons, 20: 41549

CELLULOSE
radioinduced grafting of styrene on, theory of, 20: 40979
radioinduced graft polymerization of cotton, to acrylonitrile, methyl methacrylate, and vinyl acetate, properties of products formed by gamma, 20: 40995
use in thin-layer high-voltage electrophoresis of rare earths, 20: 41046

CEMENTS
cements–depleted uranium, fabrication of structural members using, 20: 41435(P)

CENTRIFUGAL PUMPS
description and operation of, for PWR Core 2 coolant, 20: 42644 (WAPD-PWR-2219)
speed detectors for, design of, 20: 41233(R) (ORNL-3875, pp 101-24)

CENTRIFUGATION
gradient separation methods for, 20: 40507(R) (ORNL-3922, pp 191-6)
of lymph extracorporeal, for depletion of lymphocytes, 20: 40744 (BNL-10403)

CERAMIC MATERIALS
book: *Data Book on Physical Properties of Materials*, 20: 41442 (CNLN-2393)
properties of complex, conference on, 20: 41472

CERIUM
atomic structure of, calculation of Hartree-Fock parameters for, 20: 41631
determination in fission product solutions, method for, 20: 40803 (KFK-387)
determination in steel, procedure for, 20: 41415
distribution of, in neutron-irradiated plutonium dioxide suspensions, 20: 41009 (AERE-R-3268)
heat of fusion and transformation temperature of, 20: 41412(R) (IS-1500(Sect. M))
liquid, solubility of tantalum and tungsten in, at high temperatures, 20: 41412(R) (IS-1500(Sect. M))
magnetic susceptibility of, high temperature, (E), 20: 42544
meson (μ^-) capture by, x-ray spectra from, (E), 20: 42306
properties of allotropes of, at low temperatures, 20: 41412(R) (IS-1500 (Sect. M))
separation from products of fission-fragment-induced radiolysis, 20: 40951 (RPI-321-6)
separation of silver from, by cation exchange chromatography, 20: 40847
separation of, from other lanthanides by thin-layer high-voltage electrophoresis, 20: 41046
sorption by soil, effects of acidity and concentration on, 20: 40914

CERIUM ALLOYS
Ce–Mg, thermodynamics of formation of intermetallic compounds, 20: 41412(R) (IS-1500(Sect. M))
Ce–Zn, heat of fusion of intermetallic compound, 20: 41412(R) (IS-1500(Sect. M))

CERIUM CHLORIDES
preparation by cerium oxide reactions with carbonyl chloride, 20: 41412(R) (IS-1500(Sect. M))

CERIUM COMPLEXES
with mandelic acid, stability of, 20: 40902

CERIUM FLUORIDES
CeF_3–SrF_2, solubility studies on, 20: 40867 (KFK-385)

CERIUM IONS
spin-lattice relaxation of, in lanthanum fluorides, 20: 42540

CERIUM ISOTOPES
separation by electromagnetic methods, 20: 41401(R) (ORNL-4006)

CERIUM ISOTOPES Ce-138
energy levels, (E), 20: 42197

CERIUM ISOTOPES Ce-140
neutron reactions (n,2n) at 14.8 Mev, activation cross section for, (E),

20: 42207
CERIUM ISOTOPES Ce-141
beta activity measurements in France, 20: 41189 (CEA-R-3020)
content in fallout and plankton of Mediterranean Sea, 2963, 20: 41146
determination in water, 20: 40819(T) (CEA-tr-A-1883)
CERIUM ISOTOPES Ce-144
beta activity measurements in France, 20: 41189 (CEA-R-3020)
contamination of eggs by, penetration and internal distribution, 20: 40559
content in detritus from Indian Ocean, 20: 41140
content in fallout and plankton of Mediterranean Sea, 1963, 20: 41146
content in fallout from Chinese nuclear test, May 1965, 20: 41130(R) (COO-1407-10)
properties of, in isotopic power sources, 20: 41397
sorption reactions of, on minerals, 20: 41178 (AD-635547)
uptake by marine mollusks, 20: 40528
uptake by Saccharomyces cervisiae, mechanism of, 20: 40560
use in gamma backscattering density measurements, 20: 41257
CERIUM NITRATES
binding energies in, infrared spectral studies of, 20: 40886
CERIUM OXALATES
thermal decomposition of hydrates of, differential thermal analysis of products of, 20: 40900
CERIUM OXIDES
analysis for lanthanum by paper chromatography and photometry, 20: 40859
dysprosium ion ESR spectra of, 20: 42525 (ORNL-P-2466)
separation from rare earth ores, 20: 41059(P)
CERMETS
book: *Data Book on Physical Properties of Materials*, 20: 41442 (CNLM-2393)
electric and mechanical properties of thoria–thorium, 20: 41462(R) (USBM-RC-1245)
electric conductivity of molybdenum–urania and tungsten–urania, effects of microstructure on, 20: 41478
preparation and properties of thorium-thoria, 20: 41429(R) (USBM-RC-1249)
CESIUM
concentration in flowing argon at 400 to 800°C, (E), 20: 41771
determination in fission product solutions, method for, 20: 40803 (KFK-387)
determination in seawater, activation, 20: 40834
electric conductivity of liquid, 20: 41476
electric potential distribution in plasma diode of, (E/T), 20: 42407 (IPP-2/48)
emission from cesium-adsorbed tungsten cathodes, work functions for, 20: 41681 (UCRL-11857)
helium and hydrogen ion attenuation at 0.1 to 500 Mev, tables for, 20: 41619 (CEA-R-3042)
production of plasma of, design and performance of isothermal tantalum oven for, 20: 42484
properties for heat pipe uses, preparations for measurement of, 20: 41438(R) (AGN-8187)
separation from pollucite by reactions with aluminum at 950 to 1050°C, 20: 41412(R) (IS-1500(Sect. M))
separation from products of fission-fragment-induced radiolysis, 20: 40951 (RPI-321-6)
separation from strontium by ion exchange on granulated zirconyl phosphate, 20: 41055
separation from waste solutions, 20: 42689
shock wave propagation in plasma of, (E), 20: 41750
sorption from aqueous sodium tetraphenylborate solutions by glass, polyethylene, and Teflon, 20: 40915
thermal conductivity of liquid, estimation of, 20: 41477
thermionic emission from, influence of negative ions on, (T), 20: 41695
thermodynamic properties of, measurement for space power systems, 20: 41438(R) (AGN-8187)
thermodynamic properties of, research on liquid and vaporous, 20: 41439(R) (AGN-8198)
uptake by rice, effects of irrigation on, 20: 40574
use in jet compressor closed-cycle Brayton MHD systems, 20: 41753
viscosity of liquid, at 55 to 1063°C, 20: 41438(R) (AGN-8187)
CESIUM ALUMINUM SILICATES
separation of cesium from, process for, 20: 41412(R) (IS-1500(Sect. M))
CESIUM COPPER CHLORIDES
magnetic susceptibility at 1.3 to 150°K, 20: 40796(R) (IS-1500(Sect.C))
CESIUM FLUORIDES
Cs–CsF, thermionic emission from, influence of negative ions on, (T), 20: 41695
CESIUM IODIDES
radiation effects on thallium-activated, x, (T), 20: 41344
scintillation of tellurium-activated, duration of, (T), 20: 41345
CESIUM IONS
emission from cesium-adsorbed tungsten cathodes, work functions for, 20: 41681 (UCRL-11857)
CESIUM ISOTOPES Cs-131
use in myocardial scanning, 20: 40748
CESIUM ISOTOPES Cs-132
yields in thermal neutron fission of uranium-235, 20: 42178
CESIUM ISOTOPES Cs-133
energy-level quantum numbers and transitions, (E), 20: 42203
Mossbauer effect in, 20: 42239
CESIUM ISOTOPES Cs-134
yields in thermal neutron fission of uranium-235, 20: 42178
CESIUM ISOTOPES Cs-136
yields in thermal neutron fission of uranium-235, 20: 42178
CESIUM ISOTOPES Cs-137
activity measurements in milk in Great Britain, 20: 41186 (ARCRL-15)
contamination of eggs by, penetration and internal distribution, 20: 40559
content in Canadian milk, 1966, 20: 41198 (NP-16192)
content in Canadian milk, April 1965, 20: 41209
content in detritus from Indian Ocean, 20: 41140
content in fallout from Chinese nuclear test, May 1965, 20: 41130(R) (COO-1407-10)
content in fallout in India, 20: 40572
content in human bones and tissues, 20: 40570
content in Norweigian milk, March 1962 to 1966, 20: 41132 (NYO-3364-20)
content in waters near Canadian reactors, April 1965, 20: 41136
decay scheme constants of, assignment of "best estimates" to, (E), 20: 42148 (BNWL-87)
determination in environmental samples, 20: 40809 (NP-16235)
determination in food, soil, and surface atmosphere, 20: 40853
determination in radioisotope mixtures using simultaneous equations, gamma spectrometric, 20: 40837
determination in water, 20: 40819(T) (CEA-tr-A-1883)
determination of trace amounts of, review on methods for, 20: 40841
measurement in milk samples in New Zealand, 20: 40521(R) (NP-16270)
properties of, in isotopic power sources, 20: 41397
separation from irradiated reactor fuel, method for, 20: 41057(P)
sorption reactions of, on minerals, 20: 41178 (AD-635547)
uptake by browsing deer and sheep, food-chain factors affecting, 20: 40541(R) (UCD-34P104-3)
uptake by marine crabs and mollusks, 20: 40528
uptake by rice, effects of irrigation on, 20: 40574
uptake by swine blood cells in vitro, effects of dietary calcium, zinc, and corn oil on, 20: 40556
use as gamma source in well logging, 20: 41165
use in gamma source to measure density and concentration of silts, 20: 41156
yields in thermal neutron fission of uranium-233 and -235, 20: 42176
CESIUM ISOTOPES Cs-144
determination in radioisotope mixtures using simultaneous equations, gamma spectrometric, 20: 40837
CESIUM NITRATES
$CsNO_3$–$AgNO_3$, diffusion and transport processes in molten, on ceramic oxides, 20: 40866 (EUR-2954.e)
$CsNO_3$–$NaNO_3$, diffusion and transport processes in molten, on ceramic oxides, 20: 40866 (EUR-2954.e)
CESIUM SYSTEMS
Cs–CsF, thermionic emission from, influence of negative ions on, (T), 20: 41695
CESIUM URANYL NITRATES
radioinduced binary centers in, uv, 20: 42537(T)
CESIUM URANYL THIOCYANATES
crystal structure of $Cs_3[UO_2(NCS)_5]$, 20: 40932
CHARCOAL
methyl iodide adsorption on, under humid conditions, 20: 41202 (UCRL-14990)
use in determining radon-222 content in atmosphere, 20: 41277 (UCRL-16952)
CHARGED PARTICLE BEAMS
deflection in accelerators, method of, 20: 41575(P)
effects on human kidney cells, factors affecting RBE, 20: 40725
focusing and transport of, feasibility of high-field superconducting systems for, 20: 42104
focusing in electrostatic fields, space charge effects on, 20: 42510
kinetics of electrostatic, 20: 41524
production of pulsed, device for, 20: 41576(P)
properties in magnetic channels, effects of channel errors on, 20: 41538 (LNF-66/29)
CHARGED PARTICLES
angular distributions of Fermi-accelerated, at shock fronts, 20: 42423
detection and identification of, design and performance of fast transistor multiplication circuit for, 20: 41243
detection and identification of, design and performance of diode function generator for, 20: 41308
detection and measurement of, semiconductor detector for, 20: 41369(P)

diffraction by optical inhomogeneities, (T), 20: 41523
dosimetry with solid state track detectors, medical uses, 20: 41262 (BNWL-SA-619)
interactions in magneto-active nonequilibrium plasma, particle loss intensity from, (T), 20: 42486
interactions with electromagnetic fields, gradient invariance of lagrangian for, 20: 41520
motion in axially symmetric nonstationary magnetic field, (T), 20: 41558
motion in coaxial plasma accelerators, (T), 20: 42456
motion in electrostatic lenses, phase space representations of, 20: 41567
motion in magnetic fields, radiation deceleration effects on, (T), 20: 42431
motion in spatially periodic magnetic fields, 20: 42501
motion in superconducting solenoid field, 20: 42521
motion in vacuum-bounded plasma, Cherenkov surface waves from, 20: 42497
photoproduction on holmium-165 at 70 Mev, (E), 20: 42214
scattering by nuclei, critical potential perturbation for, (T), 20: 42173
scattering cross section of arbitrary spin, Coulomb, (T), 20: 41990
use in activation analysis, review on, 20: 40806 (NAS-NS-3110)
use in activation analysis, 20: 40801 (EUR-2957.d.f.e)

CHEMICAL ANALYSIS
methods for cesium-137 in trace amounts, review on, 20: 40841

CHEMICAL PROPHYLAXIS
book: *Problems of Post-Radiative Cell Restoration*, 20: 40731

CHEMICALS AND REAGENTS
radioinduced synthesis of, economics of, 20: 40988

CHEMISTRY
book: *Radioactive Isotopes in Chemical Research*, 20: 41027
stable isotopes in, 20: 41380(T) (IFA-IS-36)

CHEMOTHERAPY
effectiveness for inoperable cervical cancer, in combination with radiotherapy and surgery, 20: 40778
effects of cancer, on hematopoietic system, effects of bone marrow transplants on, 20: 40726
testing of cancerostatic drugs in, mouse chromosome idiogram studies, 20: 40550

CHICKENS
bone mineralization dynamics in fetal, 20: 40558
calcium distribution in shell gland, 20: 40551
effects of dietary strontium and calcium on content and distribution of strontium in eggs of, 20: 40569
radiation injuries to White Leghorn, determination of $LD_{50/30}$, γ, 20: 40693

CHIMERAS
chlorophyll, induction in *Arabidopsis thaliana* by x radiation and ethyl methanesulfonate treatment of seeds, 20: 40710
induced in parental mice by spleen cell transplants from hybrid offspring, 20: 40651
marking of rat-mouse, with lactate dehydrogenases, 20: 40503(R) (ORNL-3922, pp 137-45)

CHLORAMPHENICOL
effects on *E. coli* mitosis, 20: 40630(R) (ORNL-3922, pp 106-8)

CHLORELLA
radiosensitivity of soil, gamma, 20: 40637(R) (ORO-2754-7)

CHLORIDE IONS
effects on reactions of chromium(II) with vanadium(III), 20: 40796(R) (IS-1500(Sect.C))

CHLORIDES
determination in water, neutron activation, 20: 41418(R) (GEAP-5150)
separation of polonium from, by solvent extraction using TBP in benzene, 20: 41052

CHLORINATION
of uranium ores in Japan, fractional condensation of chloride vapor from, 20: 41048
particle motion effects on radiochemical, 20: 40884

CHLORINE
content in common rock types, 20: 41068 (PNE-5006)
determination in americium and plutonium by spark-source mass spectrography, 20: 40816 (RFP-699)
effects on yields in gamma radiolysis of carbon tetrachloride, 20: 40948(R) (COO-578-3-32)
helium and hydrogen ion attenuation at 0.1 to 500 Mev, tables for, 20: 41619 (CEA-R-3042)
neutron reactions at 14.7 Mev, gamma emission in, (E), 20: 42146 (AD-638014)
separation by liquefaction at −100°C, effect of iodine volatility on, 20: 41029 (BNWL-279)

CHLORINE ISOTOPES Cl-35
helium-3 reactions (He-3,p) at 11.5 Mev, argon-37 energy levels from, (E), 20: 42200
neutron reactions (n,2n) at 14.8 Mev, activation cross section for, (E), 20: 42207
proton reactions (p,γ) at 0.3 to 2.1 Mev, resonance strengths for, (E), 20: 42182

CHLORINE ISOTOPES Cl-37
proton reactions (p,γ) at 1.088 and 1.092 Mev, argon-38 energy levels from, (E), 20: 42181
proton reactions (p,γ) at 0.3 to 2.1 Mev, resonance strengths for, (E), 20: 42182

CHLORINE OXIDES
decomposition of, from gamma radiolysis of frozen solutions of perchloric acid and sodium perchlorate, ESR studies of, 20: 40960

CHLOROFORM
chloroform–cyclohexane, radiolysis of, mechanism of transfer mechanism in, 20: 40957

CHLOROPHYLLS
radiation effects on content in leaves of jute, gamma, 20: 40681
radiation effects in producing mutations involving rice, beta, thermal neutron, and x, 20: 40641
radioinduced chimeras of, in plants, 20: 40710

CHOLESTEROL
radiation effects on levels of dog, x, 20: 40698

CHOLINE, ACETYL-
carbon-14-labeled, formation from labeled acetate, 20: 40584

CHONDROITIN SULFATES
sulfur-35 labeled, in bovine cartilage, 20: 40544

CHROMATOGRAPHY
detectors in gas, thermal conductivity response of catalytic combustion, 20: 41230(R) (ORNL-3875, pp 24-34)
equipment for gas phase radio-, design and performance of, 20: 41019
equipment for gas, concentric tube and parallel plate electron capture detectors, 20: 40863

CHROMIUM
crystal lattice vibrations in, inelastic neutron scattering measurements of, 20: 42573
determination in americium and plutonium by spark-source mass spectrography, 20: 40816 (RFP-699)
determination in plutonium by carrier distillation methods, spectrographic, 20: 40814 (RFP-664)
determination in seawater, activation, 20: 40834
determination in uranium trioxide by emission spectrography, 20: 40802 (HW-65402(Rev.1))
determination in uranium(IV-VI) oxides, effects of graphite electrode grade on carrier-distillation spectroscopic, 20: 40807 (NLCO-976)
ductility of, effects of nitrogen on, 20: 41412(R) (IS-1500(Sect. M))
effects on oxidation resistance of refractory metal disilicides, 20: 41424
effects on phase transformations in gallium–plutonium alloy and plutonium, differential thermal analysis of, 20: 41452 (MLM-1172)
scattering on beryllium–copper alloy at 5 kev, secondary electrons from, 20: 41620 (NIJS-R-471)

CHROMIUM ALLOYS
ductility of, effects of composition, crystal structure, and heat treatments on, 20: 41412(R) (IS-1500(Sect. M))
Cr–Hf, phase diagrams, 20: 41412(R) (IS-1500(Sect. M))
Cr–Ni, corrosion by aqueous iron chloride, effects of carbon, manganese, and silicon traces on, 20: 41418(R) (GEAP-5150)
Cr–Ti–V, mechanical properties at high temperatures, 20: 42579(R) (ANL-7245, pp 29-47)
Cr–U, corrosive effects of liquid, on tantalum and yttrium, 20: 41064(R) (IS-1500(Sect.E))
Cr–U, melting point of, effects of impurities on eutectic, 20: 41064(R) (IS-1500(Sect.E))

CHROMIUM CARBIDES
production in type 316 stainless steel by high-temperature liquid potassium, 20: 41419(R) (GMAD-3643-5)

CHROMIUM CHLORIDES
uptake of chromium-51-labeled, by clams, 20: 40575

CHROMIUM IONS
reactions with cobalt cyanide complexes, 20: 40796(R) (IS-1500(Sect.C))
reactions with vanadium ions, effects of chloride ions on, 20: 40796(R) (IS-1500(Sect.C))

CHROMIUM ISOTOPES Cr-50
deuteron elastic scattering at 13.6 Mev, optical model analysis of, (T), 20: 42294
deuteron reactions (d,p) at 10 Mev, (E), 20: 42211
energy level structure, (E), 20: 42211
proton inelastic scattering at 11 and 12 Mev, (E), 20: 42211
proton reactions (p,p') with, energy levels from, (E), 20: 42166(R) (MIT-2098-251, pp 37-49)

CHROMIUM ISOTOPES Cr-51
energy level structure, (E), 20: 42211
radiation dose to human, from isotope placentography, 20: 40680
uptake by clams, effects of valency on, 20: 40575

CHROMIUM ISOTOPES Cr-52

deuteron elastic scattering at 13.6 Mev, optical model analysis of, (T), 20: 42294
deuteron reactions (d,p) with, chromium-53 energy levels from, (T), 20: 42201
deuteron reactions (d,p) at 10 Mev, (E), 20: 42211
deuteron reactions (d,pγ) at 6.6 to 11 Mev, angular correlations for, (T), 20: 42223
energy level structure, (E), 29: 42211
helium-3 reactions (He-3,α) at 18 Mev, DWBA calculations for, 20: 42221
proton inelastic scattering at 11 and 12 Mev, (E), 20: 42211
proton reactions (p,p') with, energy levels from, (E), 20: 42166(R) (MIT-2098-251, pp 37-49)

CHROMIUM ISOTOPES Cr-53
deuteron reactions (d,p) at 10 Mev, (E), 20: 42211
energy level structure, (E), 20: 42211
energy-level structure of, calculations using shell model with configuration mixing, (T), 20: 42201
proton inelastic scattering at 11 and 12 Mev, (E), 20: 42211
proton reactions (p,p') with, energy levels from, (E), 20: 42166(R) (MIT-2098-251, pp 37-49)

CHROMIUM ISOTOPES Cr-54
deuteron reactions (d,p) at 10 Mev, (E), 20: 42211
energy level structure, (E), 20: 42211
proton inelastic scattering at 11 and 12 Mev, (E), 20: 42211
proton reactions (p,p') with, energy levels from, (E), 20: 42166(R) (MIT-2098-251, pp 37-49)

CHROMIUM ISOTOPES Cr-55
energy level structure, (E), 20: 42211

CHROMIUM OXIDES
Al_2O_3–Cr_2O_3, properties for use in dehydrogenation of butane, 20: 40943
Al_2O_3–Cr_2O_3–K_2O, properties for use in dehydrogenation of butane, 20: 40943
Al_2O_3–Cr_2O_3–Nd_2O_3, properties for use in dehydrogenation of butane, 20: 40943
Al_2O_3–Cr_2O_3–Pr_2O_3, properties for use in dehydrogenation of butane, 20: 40943

CHROMIUM STEEL
Cr–Mo–Ni, properties of Super-Elso, effects of heat treatments on, 20: 41447(R) (EURAEC-1669)
Cr–Mo–V, rupture mechanisms of, determination by time-to-rupture tests, 20: 41445(R) (EURAEC-1622)
Cr–Ni, corrosion by aqueous dichromate-nitric acid, 20: 41418(R) (GEAP-5150)
Cr–Ni, preparation of, containing controlled-impurity carbon, manganese, and silicon, 20: 41418(R) (GEAP-5150)

CHROMOSOMES
aberrations in people with high radium and thorium body-burdens, 20: 40522(R) (NYO-3273-7)
analysis of human, semi-automatic system for, 20: 40497(R) (NYO-3400-1)
configuration of *E. coli* polysome, 20: 40503(R) (ORNL-3922, pp 137-45)
genetic control of, in mutant peas, 20: 40512
induction of aberrations in plant, by chemicals, 20: 40714
induction of aberrations in plant, by radiomimetic agents, effects of chelating compounds on, 20: 40715
induction of aberrations in mouse carcinoma and sarcoma cell, by nitrogen mustard and triethyleneamine, with and without added nicotinic amide, 20: 40550
length measurements of, electromechanical aids for, 20: 41231(R) (ORNL-3875, pp 35-43)
pattern of Drosophila, 20: 40706
ploidy of maize, effects on reversion frequency of, 20: 40509 (TID-22965)
radiation effects on mouse sex, x, 20: 40627(R) (ORNL-3922, pp 84-8)
radiation effects on ratio of induced x to autosome lethals in Drosophila, gamma, 20: 40670
radiation effects on rice, beta, thermal neutron, and x, 20: 40641
radiation effects on mouse, 20: 40649
radioinduced aberrations in Chinese hamster cell, β, 20: 40628(R) (ORNL-3922, pp 89-93)
radioinduced aberrations in Chinese hamster cell, β, 20: 40628(R) (ORNL-3922, pp 89-93)
radioinduced aberrations in leukocyte, synergistic effects of zero-gravity on, 20: 40635(R) (ORNL-TM-1550)
radioinduced aberrations in *Vicia faba*, protective effects of actinomycin D against x, 20: 40581(R) (ORNL-3922, pp 50-1)
radioinduced aberrations of, repair mechanisms for, 20: 40609 (CONF-660418-1)
radioinduced aberrations in Drosophila oocyte, frequency of crossover-suppressing x, 20: 40625(R) (ORNL-3922, pp 59-64)
radioinduced aberrations of human, 20: 40745(R) (NYO-901-54, pp 29-47)
radioinduced aberrations in human blood cell, 20: 40665
radioinduced aberrations, gamma, 20: 40681
radioinduced aberrations in hamster cells, from ^{3}H-thymidine, 20: 40686
radioinduced aberrations in plant, 20: 40714
radioinduced aberrations in barley root tip, effects of dose rate of γ, 20: 40716
radioinduced aberrations in Chironomus, from waste disposal, 20: 40530
radioinduced loss and nondisjunction in Drosophila X, effects of zygosity on x, 20: 40625(R) (ORNL-3922, pp 59-64)
radioinduced sister chromatid exchanges in hamster and human, x, 20: 40628(R) (ORNL-3922, pp 89-93)
radioinduced transfer of *E. coli* Hfr, uv, 20: 40629(R) (ORNL-3922, pp 94-8)
replication in bacteria, 20: 40538 (TID-23238)
sensitivity of Drosophila, to EDTA, 20: 40707
tandem duplication in Drosophila, effects on recombination, 20: 40625(R) (ORNL-3922, pp 59-64)
translocations in Drosophila, use as crossover suppressors, 20: 40625(R) (ORNL-3922, pp 59-64)
use as markers in mouse lymphoid and myeloid transplants, 20: 40727
use of idiograms of, to evaluate cancerostatic therapeutic agents, 20: 40550

CIRCUITS
design and performance of fast transistor multiplication, for charged particle identification, 20: 41243
design for analyzing plasma oscillations, 20: 42443
design for data cutoff at preset value, for nuclear reactions, 20: 41244
design of monostable tunnel diode, nomogram for, 20: 41242
design of, for protection of linear amplifier input stage, 20: 41260(P)

CIVILIAN DEFENSE
measures for nuclear warfare, Project Harbor evaluation of, 20: 40738
radiological countermeasures for postattack protection, requirements for, 20: 41177 (AD-632211)
radiological countermeasures for postattack protection, 20: 41179 (AD-635821)
radiological countermeasures for postattack protection, requirements for, 20: 41180 (AD-635822)
radiological countermeasures for postattack protection, requirements for, 20: 41181 (AD-635823)
radiological countermeasures for postattack protection, requirements for, 20: 41182 (AD-635824)
use of community resources for shelter systems in San Jose, California, 20: 41183 (AD-635931)

CLANEX PROCESS
development, 20: 41039(R) (ORNL-3880)

CLAYS
sorptive properties for radioruthenium in different solutions, 20: 40890

CLEANING
methods for metallic thermal insulation foils, 20: 41440(R) (ALO-3632-4)
of biologically contaminated surfaces, tracer techniques for ultrasonic, 20: 41218
use of cathodic etching method for, of radioactive surfaces for oxygen determination, 20: 40817 (UCRL-14959)

CLOSTRIDIUM
radiation effects on food-borne, review, 20: 41388
radioinduced spore inactivation in, factors affecting dose required for, 20: 40601
radiosensitivity of type E spores of, γ, 20: 40699
ribosome function in, studies of, 20: 40503(R) (ORNL-3922, pp 137-45)

CLOTHING
analysis for neomycin in cotton, radiometric method for, 20: 40823
contamination monitor for shoes, design of, 20: 41272(R) (ORNL-3875, pp 53-74)

CLOUD CHAMBERS
design and performance of diffusion, for below 65 atm., 20: 41356
radioinduced prebreakdown and breakdown in, laser, 20: 41375

COATINGS
oxidation resistance of silicide, effects of additives on, 20: 41424

COBALT
determination in americium and plutonium by spark-source mass spectrography, 20: 40816 (RFP-699)
determination in copper coins by neutron activation methods, 20: 40800 (CNAEM-35)
determination in plutonium by carrier distillation methods, spectrographic, 20: 40814 (RFP-664)
determination in seawater, activation, 20: 40834
uptake by marine mollusks, 20: 40528

COBALT ALLOYS
Co–Hf, crystal structure of intermetallic compounds, 20: 41412(R) (IS-1500(Sect. M))
Co–Hf, phase studies, 20: 41412(R) (IS-1500(Sect. M))
Co–Ni–Sc, crystal structure of Laves phases in, 20: 41412(R) (IS-1500 (Sect. M))
Co–Pr, crystal structure of Laves phases in, 20: 41412(R) (IS-1500 (Sect. M))
Co–Tm, crystal structure of Laves phases in, 20: 41412(R) (IS-1500 (Sect. M))

Co–Zr, crystal structure of intermetallic compounds, 20: 41412(R) (IS-1500(Sect. M))
Co–Zr, elastic properties of Laves-phase intermetallic compound, 20: 41412(R) (IS-1500(Sect. M))

COBALT COMPLEXES
radioinduced formation of cobalt-58 in, 20: 40796(R) (IS-1500(Sect.C))
tetrabutylammonium-tris-acetylacetonato, crystal structure, 20: 40796(R) (IS-1500(Sect.C)
with heterocyclicly substituted formazan, 20: 40880

COBALT COMPOUNDS
radiolysis of tetraamminedinitritocobalt nitrate, triamminecobalt trinitrate, and sodium nitritocobaltate, mechanism of gamma and uv, 20: 41003

COBALT CYANIDE COMPLEXES
reactions with chromium ions, 20: 40796(R) (IS-1500(Sect.C))

COBALT ISOTOPES
radioactive, effects on human erythrocyte diameter and volume from occupational exposure to, 20: 40678

COBALT ISOTOPES Co-58
reactions of recoil, in irradiated cobalt complexes, 20: 40796(R) (IS-1500(Sect.C))

COBALT ISOTOPES Co-59
deuteron elastic scattering at 13.6 Mev, optical model analysis of, (T), 20: 42294
proton elastic scattering at 30 Mev, optical-model analysis of, (T), 20: 42255
proton reactions (p,α) at 9 to 13.5 Mev, iron-56 energy levels from, (E), 20: 42256
proton reactions at 30 Mev, optical-model analysis of total cross sections for, (T), 20: 42255

COBALT ISOTOPES Co-60
decay scheme, (E), 20: 42254
detection of insoluble, deposited in lungs, 20: 41190 (CONF-660621-4)
determination in water, 20: 40819(T) (CEA-tr-A-1883)
distribution in mollusks of Columbia River estuary, 20: 40523(R) (RLO-1750-8(Vol.1))
gamma attenuation measurements for, in concretes, 20: 42519
permissible limits for lung burden of, 20: 41190 (CONF-660621-4)
uptake by swine blood cells in vitro, effects of dietary calcium, zinc, and corn oil on, 20: 40556
use as gamma source in well logging, 20: 41165

COBALT OXIDES
crystal structure of lithium-doped, 20: 41458(R) (TID-23268)
properties lithium-doped single-crystal, at 900 to 1200°C, 20: 41458(R) (TID-23268)

COCKCROFT-WALTON ACCELERATORS
radiological hazards of, used as neutron generators, 20: 41215

COILS
design and performance of system of, for plasma jet electric conductivity and velocity measurements, 20: 42485

COINCIDENCE CIRCUITS
design for identifying and analyzing charged particles, 20: 41269(R) (ORNL-3875, pp 4-12)
performance of triple, mathematical methods for determining statistical parameters for, 20: 41265 (INR-704/III/PL)

COINCIDENCE COUNTERS
design and performance of germanium–sodium iodide, with multichannel analysis, 20: 41295
design of alpha-gamma, for studies on thorium-227 decay, 20: 41038(R) (MLM-1325, pp 9-62)
efficiency of, for charged particle detection, 20: 41338
performance of fast-slow, pile-up, random events, and summation in, 20: 41291
pulse analyzer for delayed coincidences, computer analysis for time spectra from, 20: 41301
time spectra of delayed coincidences in multichannel, decay constant evaluation for excited nuclear levels from, 20: 41302
use in determination of void fraction in potassium flow, 20: 41111

COLCHICINE
effects on radiosensitivity of cultured hamster and HeLa cells of normal and carbon-14 labeled, 20: 40618(R) (NYO-2740-3, pp 166-215)
use in modification of radiation response of tissues, 20: 40763

COLICINS
effects on phage-infected cells, 20: 40535(R) (ORNL-3922, pp 128-35)

COLLIMATORS
design and fabrication of neutron, for ALRR, 20: 42681(R) (IS-1500 (Sect. R))
design and performance of combined slit-, for measuring linear gamma-activity distribution, 20: 41012
design of, for scintillation scanners, 20: 40779
design of, for use with rectilinear scanner, 20: 40755

COLLOIDS
preparation of Tc_2S_7, for use in liver scanning, 20: 40753
use of iodine-131-labeled albumin, as scanning agent for liver and spleen, 20: 40777

COLORIMETRY
developments in, using ion exchange resins, 20: 40827

COLUMBIA RIVER
ecology of estuary of, tracer study, 20: 40523(R) (RLO-1750-8(Vol.1))

COMBUSTION
ionization in hydrocarbon, (E), 20: 41731
ionization measurements in reaction zone of, (E), 20: 41710

COMPRESSORS
operation of jet, for closed-Brayton-cycle MHD systems, 20: 41753

COMPTON EFFECT
small-angle scattering of 17-Mev gamma radiation, 20: 42213

COMPUTER PROGRAMS
BURNUP, for nuclear fuel burnup analysis, 20: 42608(R) (GEAP-5124)
BURST, for fluid transient analysis in rupture of pressurized-water systems, 20: 42664(R) (IDO-17165)
COHEN, for crystal lattice parameters, 20: 41437 (AERE-R-5210)
description of general digital frequency-response, 20: 42581(R) (ORNL-3875, pp 125-50)
development for analysis of ionization chamber dosimetry data, 20: 41268(R) (NYO-2740-3, pp 5-165)
DIAN, for simulation of analog operation, 20: 41064(R) (IS-1500(Sect.E))
dosimetry of radon seed implants, 20: 40788
FLASH, for loss-of-coolant accident analysis, 20: 42582 (WAPD-TM-534)
for cost analysis of chemical processing plants, 20: 41064(R) (IS-1500 (Sect.E))
for determining lattice parameters using least-squares analysis, FORTRAN-II for IBM-1620, 20: 40805(R) (MLM-1325, pp 63-70)
for fallout dispersion calculations for 10 to 90 km altitude source, in FORTRAN 4 for CDC-3600, 20: 41133(R) (SC-CR-66-2030)
for heat transfer analysis of small spheres to liquid coolants, 20: 42580(R) (ANL-7245, pp 60-73)
for pulse height spectra analysis from gamma scintillation detectors, for IBM 7094, 20: 41292
for source-to-detector geometry, in FORTRAN, 20: 41316
for thermocouple calibration, 20: 41232(R) (ORNL-3875, pp 75-90)
for trinomial distribution calculations, 20: 41407 (ORNL-4004)
for yttrium crystallography, 20: 41412(R) (IS-1500(Sect. M))
FORTRAN, for analysis of radiological decontamination data, 20: 41180 (AD-635822)
GENSTRUK, for crystal lattice line positions, 20: 41437 (AERE-R-5210)
HEATING, for fuel cladding temperature analysis, 20: 42633 (ORNL-TM-1452)
HEATING, for temperature distribution under BONUS fuel rod spacers, 20: 42634 (ORNL-TM-1453)
K-III, for fuel element temperature distribution analysis, 20: 42606 (BNWL-252)
MATE, for flow analysis of reactor chemical poison distribution system, 20: 42665 (WCAP-2870)
MIDAS, for calculations of stream functions for long-range trajectory construction on constant-entropy surfaces, from radiosonde data, 20: 41188(R) (BNWL-235-1)
MIDAS, for evaluation of evaporative losses of falling rain drops, 20: 41188(R) (BNWL-235-1)
PARAMETRY II, for Laplacian calculation in reactor lattice, 20: 42599 (UJV-1424)
PLOTHEAT, for thermodynamic functions for compounds, FORTRAN 63 CDC 1604A, 20: 40875 (ORNL-TM-1599)
SIMPLE SAMPLE, for statistical sampling, 20: 42695 (TRG-Report-1200)
UNICORN, for calculation of point cross sections from resonance parameters, FORTRAN IV for IBM 7094, 20: 42141 (NAA-SR-11980 (Vol.6))
VARI-QUIR, for solution of time-dependent two-dimensional multigroup neutron diffusion equations, 20: 42143 (WANL-TNR-133(Rev.))

COMPUTERS
gamma mapping of liver, 20: 40747 (UCRL-14866)
performance of digital, in nuclear radiation counting, 20: 41319
performance of, for reactor axial power monitoring, 20: 42661 (DPSPU-66-30-2)
process simulation on, digital, by analog methods, 20: 41064(R) (IS-1500 (Sect.E))
programming and use at LRL, 20: 41803(R) (UCRL-16863)
research programs on, 20: 41406(R) (IS-1500(Sect. M and C))
use for analysis of radiological decontamination data, 20: 41180 (AD-635822)
use in analysis of sphere packing in cylindrical vessels, 20: 41063 (BNL-997)
use in analyzing human chromosomes, 20: 40497(R) (NYO-3400-1)
use in calculations of radiation fields produced by radium needle implants, 20: 40765
use in evaluation of neutron cross sections, 20: 42145

use of analog, for Hanford N-Reactor dynamic analysis, 20: 42660 (BNWL-SA-270)
use of analog, to investigate DFR characteristics, 20: 42653
use of, for conducting civil defense decontamination analysis, 20: 41179 (AD-635821)

CONCRETES
gamma attenuation in, measurements for cobalt-60, 20: 42519
neutron differential reflection by slabs of, thermal, (E/T), 20: 42142 (NP-16234)
prestressed, for reactor pressure vessels, 20: 42596(P)
shielding measurements in heavy, electrons, mesons (μ), and neutrons, 20: 41534 (DESY-66/18)
use as insulation in MHD generators of high temperature, (T), 20: 41738
concretes–Fe, neutron attenuation in, 20: 42517

CONFERENCES
see also introduction to Report Number Index
Electron Spin Resonance and the Effects of Radiation on Biological Systems, Gatlinburg, Tenn., May 10–12, 1965, 20: 40592
index for nuclear-science oriented, 20: 42693 (TID-4043(Rev.3))

CONNECTORS (ELECTRIC)
design of separable, for reactor fuel elements, 20: 41259(P)

CONSTANTS AND CONVERSION FACTORS
for radiation dose estimations for body organs from inhaled or ingested soluble radionuclides, 20: 41193 (IDO-12054)

CONSTITUTION DIAGRAMS
pressure-temperature, and prediction of crystal structure alterations, (T), 20: 41521
thermodynamic data estimation from, methods for, 20: 41412(R) (IS-1500 (Sect. M))

CONTAMINATION
of eggs by radioisotopes in surrounding air and dust, 20: 40559
strontium-90 and cesium-137, in milk in Great Britain, 20: 41186 (ARCRL-15)

CONVEYERS
design for irradiation facility, 20: 41077 (INR-696/1/PL)

COPPER
analysis of coins of, for antimony, cobalt, gold, indium, silver, and tin by neutron activation methods, 20: 40800 (CNAEM-35)
coating with beryllium, electrolytic, 20: 40864 (BMwF-FBK-66-10)
content in sea water from Indian Ocean, uptake by marine organisms, 20: 40572
determination in americium and plutonium by spark-source mass spectrography, 20: 40816 (RFP-699)
determination in plutonium by carrier distillation methods, spectrographic, 20: 40814 (RFP-664)
determination in uranium(IV-VI) oxides, effects of graphite electrode grade on carrier-distillation spectroscopic, 20: 40807 (NLCO-976)
determination of, using isooctylthioglycolate, 20: 40796(R) (IS-1500 (Sect.C))
determination of, in potato tissue using neutron activation and electrodeposition, 20: 40825
determination of, developments in resin spot tests for, 20: 40827
determination of, in blood by radioisotopic dilution, 20: 40844
effects on phase transformations in gallium–plutonium alloy and plutonium, differential thermal analysis of, 20: 41452 (MLM-1172)
effects on plasma electron densities in arc discharges, 20: 42490
electric conductivity of liquid, 20: 41476
electric conductivity enhancement at low temperatures, surface, 20: 42105
fatigue softening of, factors affecting, 20: 41412(R) (IS-1500(Sect. M))
helium and hydrogen ion attenuation at 0.1 to 500 Mev, tables for, 20: 41619 (CEA-R-3042)
magnetic field diffusion in, Joule heating effects on, 20: 41087
meson (π^-) capture below 140 Mev, gamma spectra from, (E), 20: 42314
oxidation by carbon dioxide at 1000°C, 20: 41458(R) (TID-23268)
properties as magnet material, 20: 41097
properties for use as thermal shielding at high temperatures in vacuum, 20: 41440(R) (ALO-3632-4)
proton elastic scattering at 30 Mev, optical-model analysis of, (T), 20: 42255
proton inelastic scattering at 25 to 1700 kev, x-ray production in L shell from, (E), 20: 42169(R) (UCRL-14744, pp 1-18)
proton reactions at 30 Mev, optical-moded analysis of total cross sections for, (T), 20: 42255
radiation effects on antifriction and strength properties of, neutron, 20: 41498
radioinduced cascade showers at 1 Bev in, 20: 41671
separation from leach solutions by solvent extraction, 20: 41067(R) (ORNL-TM-1582)
separation from tin by reversed-phase chromatography, 20: 40796(R) (IS-1500(Sect.C))
separation of silver from, by cation exchange chromatography, 20: 40847
specific heats of, methods of measuring, 20: 41457(R) (ORO-3291-3)
thermal conductivity of liquid, estimation of, 20: 41477

COPPER ALLOYS
Al–Cu, fatigue softening of, factors affecting, 20: 41412(R) (IS-1500 (Sect. M))
Be–Cu, ion scattering at 5 kev, secondary electrons from, 20: 41620 (NIJS-R-471)
Be–Cu, properties as magnet material, 20: 41097
Cu–Au, crystal structure of intermetallic compound, effects of gold diffusion on, 20: 41412(R) (IS-1500(Sect. M))
Cu–Au, oxidation by carbon dioxide at 1000°C, 20: 41458(R) (TID-23268)
Cu–Au, specific heat of intermetallic compound, 20: 41457(R) (ORO-3291-3)
Cu–Mo, electrodeposition, optimal conditions for, 20: 41487
Cu–Y, phase studies, 20: 41412(R) (IS-1500(Sect. M))
Cu–Zr, properties as magnet material, 20: 41097

COPPER COMPLEXES
with dimethylglyoxime, infrared spectra of, 20: 40796(R) (IS-1500 (Sect.C))

COPPER ISOTOPES
proton reactions at 14.5 Mev, total cross sections for, (E), 20: 42162 (LA-DC-8075)

COPPER ISOTOPES Cu-63
alpha reactions at 11 to 43 Mev, recoil ranges in, (E), 20: 42259
deuteron elastic scattering at 13.6 Mev, optical model analysis of, (T), 20: 42294

COPPER ISOTOPES Cu-64
determination in antique gold coins by activation and gamma spectrometry, 20: 40829
uptake by swine blood cells in vitro, effects of dietary calcium, zinc, and corn oil on, 20: 40556

COPPER ISOTOPES Cu-65
alpha reactions at 11 to 43 Mev, recoil ranges in, (E), 20: 42259
deuteron elastic scattering at 13.6 Mev, optical model analysis of, (T), 20: 42294

COPPER MINERALS
mining of, use of atomic explosions in, 20: 41067(R) (ORNL-TM-1582)

CORROSION
instrumentation for SNAP-8 and -50, 20: 42585(R) (ORNL-3875, pp 151-8)

CORROSION LOOPS
design and operation of liquid potassium, 20: 41419(R) (GMAD-3643-5)
testing stainless steel walls of liquid-metal, for nitrogen diffusion, 20: 41419(R) (GMAD-3643-5)

CORTICOSTERONES
effects on enzyme reactions in developing rats, 20: 40533(R) (NYO-901-54, pp 16-19)

COSMIC ALPHA PARTICLES
intensity modulations in solar system and interstellar space, (T), 20: 41670

COSMIC ELECTRONS
distribution in showers near sea level, asymmetry in lateral, (E), 20: 41668
flux of primary, above 4.7 Bv, 20: 41674
interactions in copper and lead at 1 Bev, cascade showers from, 20: 41671

COSMIC MESONS
intensity variations of, (E), 20: 41667(R) (MIT-2098-251, pp 1-13)

COSMIC MESONS (μ)
charge ratio of, (E), 20: 41677
distribution in showers near sea level, asymmetry in lateral, (E), 20: 41668

COSMIC NEUTRINOS
emission from vibrating neutron stars, energy losses in, 20: 41605
motion in superdense stars, (T), 20: 41596

COSMIC NUCLEONS
interactions with cosmic nucleons and photons, production of magnetic monopoles by, (E/T), 20: 41676

COSMIC PARTICLES
composition and flux of $Z \geq 3$ nuclei in primary, (E), 20: 41672
origin of, (T), 20: 41669
propagation of nuclei in primary, in space, 20: 41675
use of deuteron microbeam to simulate effects of, 20: 41187 (BNL-9468)

COSMIC PHOTONS
interactions with cosmic nucleons, production of magnetic monopoles by, (E/T), 20: 41676

COSMIC PROTONS
intensity modulations in solar system and interstellar space, (T), 20: 41670

COSMIC RADIATION
composition and flux of $Z \geq 3$ nuclei in primary, (E), 20: 41672
composition and source spectra of $Z \geq 3$ nuclei in galactic, 20: 41673
composition of primary, performance of CsI(Tl) detectors for determining,

20: 41667(R) (MIT-2098-251, pp 1-13)
cutoff rigidities determined by trajectory-tracing method, vertical, (E), 20: 42066
effects on etiology of multiple sclerosis, 20: 40639
interactions in atmosphere, production of magnetic monopoles by, (E/T), 20: 41676
propagation of nuclei in primary, in space, 20: 41675
research programs on gamma and x, (E), 20: 41667(R) (MIT-2098-251, pp 1-13)
COSMIC SHOWERS
measurements of air, in Bolivian joint experiment, (E), 20: 41667(R) (MIT-2098-251, pp 1-13)
particle distribution near sea level in, asymmetry in lateral electron and meson (μ), (E), 20: 41668
COSMOLOGY
dynamics of certain spherical charge distributions, 20: 41517
electromagnetic fields and rotating masses, 20: 41609
equilibrium of large assembly of particles in general relativity, 20: 42091
expansion of universe, energy spectra of radiation in, 20: 41592
homogeneous models in relativistic, arrow of time in, 20: 41611
method for studying fragmentation in astrophysical systems, 20: 41593
models of universe, closed, 20: 41591
relativity theory for, general, 20: 42075
solution of Einstein's field equations for dust-filled universe, 20: 41599
CRATERS
formation of, effect of single- or row-charge on, 20: 41069 (SC-RR-66-324)
production by nuclear explosions, 20: 41071
CREEP
radioinduced in metals, extrapolation method for neutron, 20: 41495(R) (EURAEC-1621)
CRITICAL ASSEMBLIES
physics measurements in ZPR-3, -6, and -9, 20: 42619(R) (ANL-7245, pp 1-28)
physics measurements in VERA, of fast reactor assembly properties, 20: 42671 (AWRE-R-5/66)
safety analysis of Super Kukla, 20: 42684 (UCRL-7695(Rev.1))
ZPR-III, criticality studies of SEFOR core in, 20: 42629(R) (GEAP-5160)
CROSS SECTIONS
measurement of stripping, by graphical methods, 20: 42397
probability distributions for extremes of, (T), 20: 42395
statistical analysis of fluctuations in, for nuclear reactions, (T), 20: 42194
CRUCIBLES
fabrication of yttria, method for, 20: 41412(R) (IS-1500(Sect. M))
performance of graphite, in containment of tantalum at 5000°K, 20: 41414
performance of yttria, for carbothermic reduction of uranium oxides, 20: 41411 (IS-1379)
CRUSTACEA
radioisotope accumulation by ocean-dwelling, 20: 40546
RNA synthesis in brine shrimp, role of DNA in, 20: 40535(R) (ORNL-3922, pp 128-35)
uptake of radioisotopes by marine, 20: 40528
uptake of radioisotopes by, factors affecting, 20: 40578
CRYOGENICS
magnet cooling for MHD generators, (T), 20: 41727
CRYOSTATS
design of liquid helium-3, 20: 42107
design of liquid nitrogen, 20: 42106
CRYSTAL STRUCTURE
book: *Electron Radiation Damage in Semiconductors and Metals*, 20: 41508
book: *Particle Waves and Deformation in Crystalline Solids*, 20: 42568
computer programs for lattices and line positions of, 20: 41437 (AERE-R-5210)
continuum theory of plasticity in, 20: 41454 (NYO-2394-22)
effects of, on electric conductivity of urania-base cermets, 20: 41478
effects on properties of type 302B steel, 20: 41451(R) (GA-7101)
research progress on, 20: 40796(R) (IS-1500(Sect.C))
CRYSTALLOGRAPHY
computer program for determining lattice parameters using least-squares analysis, 20: 40805(R) (MLM-1325, pp 63-70)
CRYSTALS
dislocation of, conference on, 20: 41472
impulse focusing in, 20: 42574
optical properties of potassium chloride, effects of pulsed electrons on, 20: 41492(R) (EGG-1183-2039)
phase determination for protein, using anomalous scattering data and isomorphous replacement, 20: 40632(R) (ORNL-3922, pp 175-91)
radioinduced center production in potassium chloride, electron, 20: 41493(R) (EGG-1183-2052)
strength of nonmetallic, conference on, 20: 41472
CULTURE MEDIA
effects of gamma-irradiated, on *E. coli* physiology, 20: 40580 (NYO-2804-8)
effects of, on radiosensitivity of *Clostridium botulinum* spores, 20: 40601
CUMENE
radiolysis of, EPR studies of yields of stabilized charges in low-temperature, 20: 40962
CURIUM
separation from einsteinium and californium by ion exchange using hydrochloric acid–methanol solvent system, 20: 40855
separation from irradiated fuels by solvent extraction using amines, analysis of solvent in, 20: 41023 (DP-1010)
separation from irradiated targets by Clanex and Tramex processes, 20: 41039(R) (ORNL-3880)
CURIUM ISOTOPES Cm-242
preparation of, in Transuranium Processing Plant, 20: 41039(R) (ORNL-3880)
properties of, in isotopic power sources, 20: 41397
CURIUM ISOTOPES Cm-244
preparation of, in Transuranium Processing Plant, 20: 41039(R) (ORNL-3880)
properties of, in isotopic power sources, 20: 41397
spectra of trivalent, in lanthanum trichloride, absorption and emission, 20: 40891
CYCLOHEXANE
radiation effects on, effects of sulfur on alpha and gamma, 20: 40990
radiolysis of, EPR studies of yields of stabilized charges in low-temperature, 20: 40962
radiolysis of, isomerization of stilbene by free radicals from gamma, 20: 40961
carbon tetrachloride–cyclohexane, radiolysis of, mechanism of transfer mechanism in, 20: 40957
chloroform–cyclohexane, radiolysis of, mechanism of transfer mechanism in, 20: 40957
chloromethane–cyclohexane, radiolysis of, mechanism of transfer mechanism in, 20: 40957
dichloromethane–cyclohexane, radiolysis of, mechanism of transfer mechanism in, 20: 40957
CYCLOHEXENE
cyclohexene–PCl_3, radiolysis of, effects of temperature on yields of products in gamma, 20: 40947 (BMwF-FBK-66-14)
CYCLOPROPANECARBOXYLIC ACID, 2,2-DIMETHYL-3-(2-METHYL-PROPENYL)-
preparation of carbon-14-labeled, 20: 41015
CYCLOTRONS
beam of Karlsruhe, apparatus for measuring phase of internal, 20: 41570
cavity resonators for, superconducting, 20: 41549
collision ring for Orsay, design, testing, and performance of, 20: 41559
design and performance of Manitoba, with variable beam extraction, 20: 41557
design of heavy ion Orsay, 20: 41563
development and operation of LRL 88 in., 20: 41803(R) (UCRL-16863)
CYLINDERS
cooling of heat-generating solid, temperature distributions in, 20: 41106
packing spheres in, computer analysis of, 20: 41063 (BNL-997)
CYSTEINE
radioprotective effect on damage induced by alkylating agents, 20: 40664
radioprotective effects on rats, x, 20: 40729
CYSTINE, (*p*-SULFAMOYLPHENYL)ARSYLENE-
use as radioprotective agent for *E. coli*, 20: 40737
CYTIDINE
synthesis in Amblystoma iris epithelium, effects of lens removal on, 20: 40499(R) (ORNL-3922, pp 69-79)
CYTIDINE, 2'-DEOXY-
content in *Vicia faba*, root cells, effects of thymidine on, 20: 40581(R) (ORNL-3922, pp 50-1)
CYTOCHROME C
synthesis in Ustilago, 20: 40503(R) (ORNL-3922, pp 137-45)
CYTOCHROMES
role in bacterial metabolism, 20: 40571
CYTOLOGY
calcium-45 content in microsomes and mitochondria of shell gland mucosa, 20: 40551
radiation damage to leukocytes, role of lysosomes, 20: 40685
radiation effects on fine structure of rat ovarian cells, x, 20: 40672
radiation effects on rat primordial germ cell, following exposure at birth, x, 20: 40682
radiation effects on fish embryo and prelarvae, 20: 40527
radiation effects on salivary gland, following cobalt-60 therapy, 20: 40644
use for testing cancerostatic therapeutic agents in cancer cells, 20: 40550

use of mitotic index for generation time studies on lymph cells, 20: 40663
CYTOSINE
cytosine-guanine, radioinduced tunneling and tautomeric equilibria in, 20: 40589

D

DATA RECORDING SYSTEMS
design for heat transfer facility, 20: 41104 (UCRL-14841)
for gamma mapping of liver, 20: 40747 (UCRL-14866)
readout for device to measure density of silts, 20: 41156
use in radiography, 20: 41116(P)
DATA TABULATIONS
book: *Data Book on Physical Properties of Materials*, 20: 41442 (CNLM-2393)
book: *Thermodynamic Properties of Inorganic Substances (Handbook)*, 20: 41417
for charged particle attenuation in nuclei at 0.1 to 500 Mev, 20: 41619 (CEA-R-3042)
neutron cross sections for carbon-12 from 0.01 to 15 Mev, 20: 42160 (KAPL-3099)
DECANE
radiolysis of, EPR studies of yields of stabilized charges in low-temperature, 20: 40962
DECANE, DICYCLOHEXYL-
radiolysis of, EPR studies of yields of stabilized charges in low-temperature, 20: 40962
DECONTAMINATING SOLUTIONS
design for aluminum or zirconium, 20: 41214(P)
DECONTAMINATION
methods for surfaces in LOFT containment, 20: 42664(R) (IDO-17165)
of PRTR after failure of magnesia–plutonia fuel element, 20: 42677 (BNWL-SA-636)
of urban areas during postattack period, requirements, 20: 41179 (AD-635821)
of urban areas during postattack period, 20: 41180 (AD-635822)
of urban areas during postattack period, requirements for, 20: 41181 (AD-635823)
of urban areas during postattack period, requirements for, 20: 41182 (AD-635824)
process for metal, 20: 41214(P)
DEER
body water content and turnover in, tracer study, using T_2O, 20: 40541(R) (UCD-34P104-3)
cesium-137 content in browsing, effects of food-chain on, 20: 40541(R) (UCD-34P104-3)
physiology of digestion in, 20: 40541(R) (UCD-34P104-3)
strontium-90 content in browsing, effects of food-chain on, 20: 40541(R) (UCD-34P104-3)
strontium-90 content in bones of yearling, 20: 40541(R) (UCD-34P104-3)
urea nitrogen content in blood of, 20: 40541(R) (UCD-34P104-3)
DEHYDROGENASES
electrophoretic mobility of Drosophila alcohol, chemically-induced mutation for altering, 20: 40625(R) (ORNL-3922, pp 59-64)
isolation and properties of Drosophila alcohol, 20: 40503(R) (ORNL-3922, pp 137-45)
use of lactate, as a marker in rat-mouse chimeras, 20: 40503(R) (ORNL-3922, pp 137-45)
DENSITOMETERS
design of radiometric, for atmosphere, 20: 41257
development for liquid metals, 20: 41455(R) (NYO-2731-7)
DENSITY
measurement of, calibration of Westphal balance and plummet for, 20: 40869 (MCW-1473)
measurement of, equipment for, 20: 41156
DETERGENTS
use in rinsing fallout particles from leaves, 20: 40579
DETONATION WAVES
amplitudes of atmospheric, from underground nuclear, 20: 41158
DIMETHYLAMINE, *N*-NITROSO-
effects on Neurospora, mutagenic, 20: 40632(R) (ORNL-3922, pp 175-91)
DEUTERIOORGANIC COMPOUNDS
preparation, properties, and uses of, review on, 20: 40940
DEUTERIUM
content in oil well brines, 20: 41161
detection in solar atmosphere, design and performance of device for, 20: 41667(R) (MIT-2098-251, pp 1-13)
effects in solvolysis and iodine-131 exchange reactions of methyl iodide, kinetic, 20: 40939
effects on ESR spectra of irradiated sodium acid selenites, 20: 40972
effects on fluorescence lifetime of potassium uranyl sulfates and uranyl sulfates, (E), 20: 40887
exchange with hydrogen in carbonium ion systems, NMR studies on, 20: 40945
exchange with hydrogen during nickel-catalyzed hydrogenation of ethylene, 20: 40942
ionization of, by electron bombardment, 20: 40893
magnetic susceptibility and rotational magnetic moment of molecular, (T), 20: 41659
proton reactions with, bremsstrahlung production from, (E), 20: 41916
shock wave propagation in plasma of, dissipative effects on, (T), 20: 42476
vapor pressures and molar volumes of liquid, tanles of, 20: 40871 (NIRL-R-95)
yields in hydrolysis of aluminum, thorium, and uranium carbides in heavy water, 20: 40905
DEUTERIUM HYDRIDES
magnetic susceptibility and rotational magnetic moment of, (T), 20: 41659
DEUTERONS
attenuation by nuclei at 0.1 to 500 Mev, tables for, 20: 41619 (CEA-R-3042)
effects on brain, eye, and hair follicles, 20: 41187 (BNL-9468)
interactions with mesons (π^-), nonradiative and radiative absorption ratios for atomic s-orbitals for, (T), 20: 41809
interactions with protons at 8 Bev, real part of amplitude of elastic, (E), 20: 41811
interactions with neutrons at 14 Mev, neutron spectra from disintegration, (T), 20: 42291
interactions with protons at 155 Mev, elastic, (E), 20: 42184
interactions with protons at 155 Mev, inelastic, (E), 20: 42185
interactions with electrons, neutron electromagnetic form factors from, (T), 20: 41883
interactions with mesons (π) at high energies, charge independence in, (T), 20: 41887
interactions with electrons, polarization effects in, (T), 20: 41907
interactions with mesons (π^-), neutron-neutron S-wave scattering length from, (E), 20: 41914
interactions with protons below 1 Bev, review of polarization in, (E), 20: 41916
neutron elastic scattering at 1 to 5 Mev, angular distributions for, (E), 20: 42359
nuclear quadrupole coupling constant of, in CH_3D, 20: 40894
reactions (d,α) with nitrogen-15 at 0.8 to 1.8 Mev, oxygen-17 energy levels from, (E), 20: 42295
reactions (d,α) with lithium-7, Q-values for, (E), 20: 42357
reactions (d,α)2α with boron-10, coincidence studies of, (E), 20: 42374
reactions (d,α) with nitrogen-14, alpha energy spectra from, (E), 20: 42389
reactions (d,α) with magnesium-24, mechanism of, (T), 20: 42394
reactions (d,α) with potassium-39 at 10 and 11 Mev, argon-37 energy levels from, (E), 20: 42200
reactions (d,Li-6) with light nuclei at 15 Mev, differential cross sections for, (E/T), 20: 42237
reactions (d,n) with tritium, design of neutron source using low-voltage accelerators, 20: 42136 (AD-637457)
reactions (d,n) with lithium-6 at 0.2 to 0.8 Mev, (E/T), 20: 42210
reactions (d,n)2α with lithium-7, of alpha particle energy spectra from, (E), 20: 42349
reactions (d,pf) with plutonium-239, angular correlations in, (E), 20: 42161 (LA-DC-7878)
reactions (d,pγ) with carbon-12, carbon-13 energy-level spins and transitions from, (E), 20: 42252
reactions (d,pγ) with carbon-12, proton-gamma angular correlations in, (E), 20: 42383
reactions (d,pγ) with chromium-52 at 6.6 to 11 Mev, angular correlations for, (T), 20: 42223
reactions (d,p) with sulfur-32 at 2.5 to 4.6 Mev, (E/T), 20: 42163 (LA-DC-8082)
reactions (d,p) with boron-10, boron-11 energy levels from, (E), 20: 42246
reactions (d,p) with nitrogen-14, energy levels from, (E), 20: 42369
reactions (d,p) with silicon-28, differential cross sections for, (T), 20: 42387
reactions (d,p) with aluminum-27 and magnesium-24, mechanism of, (T), 20: 42394
reactions (d,p) with boron-11, lithium-6, and oxygen-16 at 300 kev, angular distributions for, (E/T), 20: 42399
reactions (d,p) with carbon-12 at 4 to 7 Mev, excitation functions for, (E), 20: 42400
reactions (d,p) with chromium-52, iron-54, titanium-50, and vanadium-51, 20: 42201
reactions (d,p) with gold-197 at 10.2 to 26.9 Mev, excitation function for, (E), 20: 42206
reactions (d,p) with chromium isotopes at 10 Mev, (E), 20: 42211
reactions (d,p) with carbon-13, carbon-14 energy levels from, (E), 20: 42233

reactions with beryllium-9 at 100 to 200 kev, angular distributions of protons, tritons, and alpha particles from, (E), 20: 42354
reactions with nuclei, approximate relations for strengths and shapes of optical potentials for, 20: 42280
scattering by alpha particles at 3 to 14 Mev, absolute cross sections for elastic, (E), 20: 42371
scattering by lithium-6 at 4 to 6 Mev, excitation function at 115° for elastic, (E), 20: 42365
scattering by nitrogen-14 at 28.5 Mev, elastic, (E/T), 20: 42389
scattering by nuclei with Z = 22 to 29 at 13.6 Mev, optical-model analysis of elastic, (T), 20: 42294
use in activation analysis, review on, 20: 40806 (NAS-NS-3110)

DEXAMETHASONE
effects on zinc-65 metabolism in rats, 20: 40563

DIABETES
use of iodine-131 in therapy of, when associated with hyperthyroidism, 20: 40790

DIAMONDS
performance as scintillator for gamma and neutron detection, 20: 41290

DIET
digestibility and palatibility of browse, of deer and sheep, factors affecting, 20: 40541(R) (UCD-34P104-3)
effects of calcium, zinc, and corn oil in swine, on *in vitro* uptake of various radioisotopes by blood cells, 20: 40556
effects of calcium and strontium in, on elimination of strontium-85 and strontium-89 in goats, 20: 40568
effects of calcium and strontium in chicken, on egg content of strontium, 20: 40569
effects of irradiated oils in, on rats, 20: 41391
effects of irradiated potatoes in, on rats, 20: 40576
strontium-90 contamination in human, factors affecting, 20: 41142
strontium-90 to calcium ratio in Finnish, 20: 41134 (SFL-A3)

DIETHYLAMINE, *N*-NITROSO-
effects on Neurospora, mutagenic, 20: 40632(R) (ORNL-3922, pp 175-91)

DIFFERENTIAL EQUATIONS
solution of time-dependent, variational formalism for, 20: 41409

DILATOMETERS
calibration, 20: 41449(R) (EURAEC-1676)

DIOXANE
effects on paramagnetic relaxation constant of gadolinium nitrate, 20: 40928
radiolysis of, EPR studies of yields of stabilized charges in low-temperature, 20: 40962

DIRECT ENERGY CONVERSION DEVICES
design using radiation and salt solutions, 20: 41691(P)

DISEASES
radiodiagnosis of brain, using pertechnetate-99m scanning, 20: 40789
radioinduced inactivation of virus for foot and mouth, in tissues of infected animals, gamma, 20: 41392
radiotherapy of Hodgkin's, survival following, 20: 40784
skin, role of solar radiation in etiology of, review of, 20: 40696
survey of infectious, in irradiated mammals, 20: 40694

DISTILLATION
use in trace analysis, 20: 40850

DISTILLATION APPARATUS
design for calcium purification, 20: 41455(R) (NYO-2731-7)

DOGS
coronary circulation time in, measurement using phosphorus-32 and a new catheter-type micro G-M counter, 20: 40514
fluorine-18 metabolism studies, 20: 40554
hematologic response to simultaneous ionizing and microwave irradiation, 20: 40650
radiation effects on beagle, pathological x, 20: 40638(R) (UCD-472-113, pp 1-16)
radiation sickness in, gamma and x, 20: 40694
radioinduced hypothyroidism in, effects on metabolism of x, 20: 40698
radioinduced lesions in gastrointestinal tract of, multiple x, 20: 40645
radium-226 toxic effects in beagles, 20: 40540(R) (UCD-472-113, pp 17-56)
strontium content of tissues, effects of age on, 20: 40540(R) (UCD-472-113, pp 17-56)
strontium-85 accretion and exchange in bones of, 20: 40684
strontium-90 toxic effects in beagles, 20: 40540(R) (UCD-472-113, pp 17-56)
thyroid transplant effectiveness in, use of pertechnetate-99 to measure, 20: 40516
zinc content of tissues, effects of age on, 20: 40540(R) (UCD-472-113, pp 17-56)

DOSIMETERS
design of neutron, 20: 41362(P)
design of thermoluminescent, for charged and uncharged particles, 20: 41370(P)
design of thermoluminescent, for measurement of beta depth dose, 20: 40766
design, fabrication, and performance of calcium fluoride and lithium fluoride thermoluminescent, 20: 41373
development of small silver activated metaphosphate glass rod, for γ rays, 20: 40734(R) (NYO-901-54, pp 24-5)
energy dependence of lithium fluoride, for high energy radiation, 20: 40746(R) (NYO-3510-2)
medical uses of, for neutrons and high energy particles, 20: 41262 (BNWL-SA-619)
performance of neutron, for accelerator environment, 20: 41543 (RPP-R-2)
solid state track devices for neutrons and high energy particles, 20: 41262 (BNWL-SA-619)
testing of CD-V-742, 20: 41272(R) (ORNL-3875, pp 53-74)
use of thermoluminescent, for determining beam profiles of ANL proton synchrotron, 20: 41530 (ANL-7196)

DOUNREAY FAST REACTOR
reactivity of, analog computer analysis of, 20: 42653

DROPS
mass transfer rates from, 20: 41064(R) (IS-1500(Sect.E))

DROSOPHILA
alcohol dehydrogenases of, isolation and properties, 20: 40503(R) (ORNL-3922, pp 137-45)
chromosome translocations in, use as crossover suppressors, 20: 40625(R) (ORNL-3922, pp 59-64)
crossing-over frequency in, meiotic origin of temperature-induced, 20: 40625(R) (ORNL-3922, pp 59-64)
effects of phenylalanine and trimethylenemelamine on, genetic, 20: 40706
EMS-induced mutation in, for altering electrophoretic mobility of alcohol dehydrogenases, 20: 40625(R) (ORNL-3922, pp 59-64)
enzyme activity during development of, 20: 40623(R) (ORNL-3922, pp 32-49)
genetic studies on natural populations of, 20: 40622(R) (NYO-3096-8)
mutations induced by EDTA in, 20: 40707
radiation effects on genetics of populations of, x, 20: 40622(R) (NYO-3096-8)
radiation effects on germinal selection in premeiotic germ cells, gamma, 20: 40670
radiation effects on, genetic, x, 20: 40706
radioinduced chromosome aberrations in oocytes of, frequency of crossover-suppressing x, 20: 40625(R) (ORNL-3922, pp 59-64)
radioinduced loss and nondisjunction of X chromosomes in, effects of zygosity on x, 20: 40625(R) (ORNL-3922, pp 59-64)
radioinduced mutations in, effects of EDTA on x, 20: 40707
recombination in genes of, effects of tandem duplication on, 20: 40625(R) (ORNL-3922, pp 59-64)
sex-linked lethal mutations in, single-hit effects on, 20: 40515
tritium uptake by female, from mating with labeled males, 20: 40625(R) (ORNL-3922, pp 59-64)

DRUGS
effects of cryoprotective, on preservation of frozen blood platelets, 20: 40496(R) (NYO-1753-3)
effects on hyperthyroidism of mercazol, bone marrow transplants for hematopoietic injuries from, 20: 40726
use of radioprotective, in combination with alkylating agents for tumor chemotherapy, 20: 40664

DUCTILITY
of pressure-vessel steels, effects of fatigue on, 20: 41446(R) (EURAEC-1624)

DUSTS
fallout particles in airborne, characteristics of, 20: 41138

DYES
use of rhodamine B in studying bottom layers of Mediterranean Sea, 20: 41128

DYSPROSIUM
determination by x-ray-fluorescence methods, 20: 40796(R) (IS-1500 (Sect.C))
determination in uranium dioxide fuel pellets, 20: 41112 (IITRI-578P11-54)
determination of, in uranium by neutron activation methods, 20: 40832
liquid, solubility of tantalum in, at high temperatures, 20: 41412(R) (IS-1500(Sect. M))
liquid, solubility of tungsten in, at high temperatures, 20: 41412(R) (IS-1500(Sect. M))
purification by sublimation, 20: 41412(R) (IS-1500(Sect. M))
thermodynamic properties of, at 0°C to melting point, 20: 41412(R) (IS-1500(Sect. M))

DYSPROSIUM ALLOYS
Dy–Mg, thermodynamics of formation of intermetallic compounds, 20: 41412(R) (IS-1500(Sect. M))

DYSPROSIUM CHLORIDES
preparation by lanthanum oxide reactions with carbonyl chloride, 20: 41412(R) (IS-1500(Sect. M))

DYSPROSIUM IONS
electron spin resonance spectra in cerium oxides and thorium oxides, 20: 42525 (ORNL-P-2466)
spin-lattice relaxation of, in lanthanum fluorides, 20: 42540
DYSPROSIUM ISOTOPES Dy-160
energy-level transitions from beta decay of terbium-160, (E), 20: 42150 (COO-498-56)
energy-level transitions from decay of holmium-160, (E), 20: 42158 (JINR-P-2817)
DYSPROSIUM OXALATES
thermal decomposition of hydrates of, differential thermal analysis of products of, 20: 40900
DYSPROSIUM OXIDES
B_2O_3–Dy_2O_3 liquid immiscibility in, 20: 40910

E

EARTH
structure of, use of nuclear explosions for determining internal, 20: 41152
ECOLOGY
absorption of zinc-65 and phosphorus-32 in salt marsh ecosystem, 20: 40573
biological significance of supersonic transport radiation environment, 20: 40525
Brazilian areas of high natural radiation, 20: 40522(R) (NYO-3273-7)
effects of radioactive contamination in bodies of water on biological organisms, 20: 40527
effects of, on recovery of ecosystems from radioinduced damage, review of, 20: 40526
of Columbia River estuary and adjacent Pacific Ocean, 20: 40523(R) (RLO-1750-8(Vol.1))
phosphorus-32 transport studies in, 20: 40529
radiation effects on forest lichens, gamma, 20: 40517 (BNL-9437)
radioactive contamination in New Zealand, 20: 40521(R) (NP-16270)
studies in jackrabbit, 20: 40494(R) (COO-1329-4)
survey of environmental radioactivity in West Germany, 20: 40570
EGGS
phosvitin isolation and purification from vertebrate, 20: 40499(R) (ORNL-3922, pp 69-79)
radiation effects on Arbacia, effects of AET on x, 20: 40619(R) (NYO-2740-3, pp 216-57)
radiation effects on gastropod, effects of age at exposure on x, 20: 40700
radioisotope contamination of, from environment, 20: 40559
strontium distribution in chicken, effects of dietary strontium and calcium on, 20: 40569
uracil-containing compounds in frog, properties of, 20: 40535(R) (ORNL-3922, pp 128-35)
EINSTEINIUM
separation from americium and curium, by ion exchange using hydrochloric acid–methanol solvent system, 20: 40855
ELECTRETS
radioinduced, in paraffin wax, beta, (E), 20: 41516
ELECTRIC ARCS
properties of low-current, for plasma diagnostics, 20: 42513
ELECTRIC CONDENSERS
performance for high magnetic field production, 20: 41080 (UCRL-14831)
ELECTRIC CONDUCTIVITY
calculation of liquid metal, methods for, 20: 41476
of urania-base cermets, effects of microstructure on, 20: 41478
radiation effects on isochronal recovery of, in molybdenum, palladium, zinc, and α-uranium, electron, 20: 41499
ELECTRIC CONTROL SYSTEMS
monitoring means for, 20: 41258(P)
ELECTRIC DISCHARGE
anodic extraction from low-pressure, in oxygen, (E), 20: 42435
electric conductivity of, in argon and cesium-seeded argon, (E), 20: 41770
electron density in plasma of, copper energy level effects on, 20: 42490
electron extraction in modified Penning, 20: 42507
in air, plasma properties from, 20: 42492
initiation in induction coupled plasma generators, 20: 42514(P)
ion extraction from electrodeless, positive, 20: 41251
kinetics of positive column of, with magnetic field, (T), 20: 42425
Penning, Laplace equation for, 20: 42508
vibrations of, plasma switch for, (E), 20: 42493
properties of high-pressure electrodeless, in gases, 20: 42509
ELECTRIC FIELDS
effects on solidification of metals, 20: 41412(R) (IS-1500(Sect. M))
plasma flow in, Couette, 20: 42488
ELECTRIC INSULATORS
radiation effects on polymeric, 20: 41489(R) (EGG-1183-2014)
radiation effects on film insulation for magnet wires, gamma, 20: 41503
radiation effects on electric conductivity of, electron, (T), 20: 41507
radioinduced cross-linking of cable polyethylene, 20: 41496
ELECTRIC PROBES
current-voltage characteristics for Langmuir-type, (E), 20: 41705
design for measuring combustion chamber ionization, 20: 41120
theory of, in nonequilibrium high-pressure plasma, 20: 41782
ELECTRICITY
production by direct conversion of nuclear energy, 20: 41691(P)
ELECTRODES
calibration for nuclear diography, 20: 41165
construction and testing of auxiliary-arc, for MHD generators, (E), 20: 41745
design and testing of regenerative collector, 20: 41122
design for MHD converters, 20: 41726
effect of temperature and beam energy on collector, 20: 41122
sputtering of, control of, 20: 41122
testing of ceramic, for Renardieres 8-Mw MHD test rig, 20: 41725
ELECTRODYNAMICS
units in classical, electron system of, (T), 20: 41522
ELECTROHYDRODYNAMICS
fluid flow in plane exit cone-with barodiffusion and space charge, 20: 41110
ELECTROLYTIC CELLS
development of, for fluoride determination in presence of uranium, 20: 40840
use of aqueous alkaline and acid, for dissolution of aluminum-clad uranium fuel elements, 20: 41056(P)
ELECTROLYTIC POLISHING
methods for alloys and metals using perchloric acid, 20: 41412(R) (IS-1500(Sect. M))
ELECTROMAGNETIC FIELDS
charged-particle interactions with, gradient invariance of lagrangian for, 20: 41520
effect of nuclear-explosion, on buried command posts and missile launch complexes, 20: 41117
effects of rotating mass shells on, (T), 20: 41609
effects on baryon decay in charged baryon and meson, Lee model for, 20: 41909
effects on lymphoblastic lymphosarcomas in rats, 20: 40661
ELECTROMAGNETIC LENSES
feasibility of high-field superconducting, 20: 42104
ELECTROMAGNETIC PUMPS
design for sodium, 20: 41064(R) (IS-1500(Sect.E))
ELECTROMAGNETIC SEPARATION
development of, review of 1965, 20: 41401(R) (ORNL-4006)
ion sources for isotope, design and performance of plasma, 20: 41403
shim design for heavy-isotope, 20: 41405
ELECTROMAGNETIC WAVES
absorption in ionosphere during solar eclipse, measurement of, 20: 42051
absorption in ionosphere during solar eclipse, measurement of, 20: 42052
conversion to sound waves in plasma, (T), 20: 42499
effects of high-frequency, on gaseous-discharge plasma, 20: 42442
interactions in dense plasma, surface, (T), 20: 42451
interactions in vacuum-bounded plasma, surface, 20: 42498
interactions with plasma, cylindrical and spherical, (T), 20: 42447
interactions with moving plasma, reflection of, (T), 20: 42448
propagation in bounded magnetoplasma, kinetic theory of, 20: 42496
propagation in compressible plasma, network representation of, 20: 42461
propagation in helium afterglow plasma of linearly polarized, (E), 20: 42459
propagation in ionosphere, electron density determination from, 20: 42001
propagation in ionosphere, WKB approximation for, (T), 20: 42404 (IC-66/45)
propagation in ionosphere, collision frequencies for, (T), 20: 42452
propagation in isotropic cylindrical plasma, properties of, 20: 42436
propagation in isotropic plasma, self-focusing from, (T), 20: 42449
propagation in nonuniform plasma, conversion of, 20: 42500
propagation in plasma, diffraction effects on, 20: 42438
propagation in plasma, nonlinear waveguide phenomena for, 20: 42450
ELECTROMETERS
construction of differential, with MOS-FET transistors, 20: 41270(R) (ORNL-3875, pp 13-14)
ELECTRON BEAMS
dosimetry of absorbed dose of therapeutic, 20: 40741(R) (ACRH-25, pp 15-23)
dosimetry systems for, 20: 41323
dosimetry, design of calorimeter for, 20: 40742(R) (ACRH-25, pp 24-9)
effects of pulsed, on optical transmission by potassium chloride crystals, 20: 41492(R) (EGG-1183-2039)
effects on lifetime of $^5D_4$ level in terbium chlorides, (E), 20: 42539
effects on magnesium fluoride crystals, electron microscopy of, 20: 42558
effects on recombination radiation of silicon carbide crystals, (E),

20: 42565(T)
effects on refractive properties of optical glasses and silica, 20: 41505
flow of unaccelerated, quasi-fluid treatment of, 20: 42515
focusing in magnet systems, outer electron trajectories in, 20: 41551
focusing in magnet systems, outer electron trajectories in, 20: 41552
interactions with plasma, excitation of ion oscillations in, 20: 42494
interactions with plasma, convective effects of electron oscillations in, 20: 42495
interactions with modulated reactance surface, 20: 41519
interactions with gases in metallic tubes, pressure effects on, 20: 42511
interactions with n-type germanium, voltage induction by, (E/T), 20: 42533
ion plasma oscillation excitation by, (T), 20: 42429
relative biological effectiveness of, as function of tissue depth, 20: 40767
use for heating, design of high voltage power supply for, 20: 41228(R) (ORNL-3875, pp 15-20)
use in zone refining of molybdenum, equipment and methods for, 20: 41434
uses in production of thorium from magnesium–thorium sponge, 20: 41412(R) (IS-1500(Sect. M))
uses of pulsed, in studies of radiation effects on electronic materials, 20: 41493(R) (EGG-1183-2052)

ELECTRON MICROSCOPY
of irradiation-induced defects in magnesium fluorides, 20: 42554
sample etching for, electronic controller for, 20: 41230(R) (ORNL-3875, pp 24-34)
uses in phase studies of niobium–zirconium alloys, 20: 41443(R) (COO-588-12)

ELECTRON PAIRS
annihilation into two photons, cross sections for, (T), 20: 41822
photoproduction from electron interactions with thick targets, secondary, 20: 41875
production from bremsstrahlung reactions with nuclei at 2 Bev, quantum electrodynamic violation in wide angle, (E), 20: 42327
production from meson (π^-) reactions in emulsions at 17 Bev/c, (E), 20: 41814

ELECTRON SOURCES
design for use in mass spectrometers, 20: 40796(R) (IS-1500(Sect.C))
design of, for alternate electron or ion beam production for surface treatment, 20: 41528

ELECTRON TUBES
plasma electron concentration in reflex klystron, (T), 20: 42446

ELECTRONIC EQUIPMENT
book: *Nuclear Instrumentation*, 20: 41256
design of circuit for breakdown protection of proportional counters, 20: 41268(R) (NYO-2740-3, pp 5-165)
fabrication and maintenance of, 20: 41229(R) (ORNL-3875, pp 21-3)

ELECTRONICS
units in classical, electron system of, (T), 20: 41522

ELECTRONS
absorption and transmission of monoenergetic, theory for, 20: 41638
attenuation measurements in thin films of indium and magnesium, 20: 41621 (ORNL-TM-1565)
book: *Electron Radiation Damage in Semiconductors and Metals*, 20: 41508
density in plasma from seeded aluminized propellants, 20: 41120
detection and measurement of low energy, description of proportional counter for, 20: 41351
detection of, design and performance of lithium-drift telescope silicon detectors for, 20: 41376
drift velocities in gases, magnetic field effect on, (T), 20: 41628
effects of high energy, on human blood cell chromosomes, comparison with x ray and gamma ray effects, 20: 40665
effects on aluminum at 0.19 to 1.6 Mev near 8°K, 20: 42543
effects on color centers in lithium fluoride crystals, 20: 42530
effects on emission spectra of zinc-doped gallium arsenide at 0.6 to 2 Mev, 20: 42548
effects on graft polymerization of styrene to polyvinyl chloride in liquid and vapor phases, 20: 40992
effects on insulator electric conductivities, (T), 20: 41507
effects on molybdenum, palladium, alpha-uranium, and zinc at 11 to 7°K, 20: 41499
effects on p-type silicon, photoconductivity spectrum from damage from, 20: 41379
effects on p-type silicon, paramagnetic defects from, 20: 42549
effects on polymerization of diacetone acrylamide, 20: 40980
effects on proteins, electron spin resonance studies of, 20: 40595
effects on terphenyl, 20: 40946 (AECL-2589)
effects on thermal conductivity of antimony–indium alloy at 2 Mev, 20: 42547
electron spin resonance of excited states of, in irradiated deoxyribonucleic acid, 20: 40594
emission from tungsten cathodes in cesium diodes, work functions for, 20: 41681 (UCRL-11857)
emission in modified Penning discharges, 20: 42507
emission processes of, Poisson curves for multiple, 20: 41529
energy loss and scattering by single crystal silicon foils at 100 to 400 kev, near radiation damage threshold, (E), 20: 42536
gamma scattering by gold, uranium, and zinc atoms at 662 kev, (E), 20: 41625
gases of, sum rules for generalized frequency distribution function for, 20: 42092
injection into betatrons, maximum x-ray output from, 20: 41560
interactions of free gas of, in uniform magnetic field, 20: 42470
interactions with protons at 3.7 to 5.9 Bev, cross sections for momentum transfer of 10 and 105 F^{-2} in, (E), 20: 41791 (DESY-66/20)
interactions with positrons, polarization and structure relations for annihilation, (T), 20: 41813
interactions with photons at 17.6 Mev, cross section for Compton, (E), 20: 42213
interactions with thick targets, bremsstrahlung and secondary-particle production by, 20: 41875
interactions with deuterons, neutron electromagnetic form factors from, (T), 20: 41883
interactions with electrons, cross section for double-bremsstrahlung emission in, 20: 41904
interactions with deuterons, polarization effects in, (T), 20: 41907
lifetime and losses in boron trifluoride proportional counters, factors for, 20: 41357
magnetic susceptibility in uniform magnetic field, 20: 41635
measurement of absorbed dose from high energy, 20: 40746(R) (NYO-3510-2)
penetration into magnetosphere, solar wind, (T), 20: 42069
precipitation in auroral zone, origin of, (T), 20: 42056
production and losses in F1 region at summer solar minimum, 20: 42058
reactions of, in radiolysis of hydrocarbons, 20: 40998
reactions with atoms, excitation cross sections, (T), 20: 41654
reactions with atomic hydrogen, cross sections, (T), 20: 41655
reactions with helium ions, ionization, (E), 20: 41653
reactions with hydrogen ions, resonances, (T), 20: 41656
reactions with lead and lithium at 6 to 25 Bev, mesons (μ) production in, (E), 20: 41805(T) (SLAC-Trans-46)
reactions with light nuclei, review of, 20: 42340
reactions with nitrogen molecules, ionization cross section, (E), 20: 41652
reactions with nuclei at 300 kev, asymmetry function for external bremsstrahlung from, (E), 20: 41662
reactions with potassium chloride, F center production by, 20: 41493(R) (EGG-1183-2052)
recombination of, in gamma-irradiated alkane glasses, 20: 40970
relative biological efficiency of high energy, comparison with x radiation and gamma radiation, 20: 40665
scattering by aluminum-27, elastic, (T), 20: 42376
scattering by boron-11, energy level excitation in, (E), 20: 42378
scattering by carbon-12 at 100 to 200 Mev, elastic, (E), 20: 42377
scattering by carbon-12 and oxygen-16 at 600 to 800 Mev, cross sections for, (E/T), 20: 42238
scattering by d-shell nuclei, form factors for elastic, (T), 20: 42376
scattering by helium, resonance phenomena in elastic, 20: 41641(T)
scattering by helium and hydrogen, lower bound to reciprocal of length of, (T), 20: 41658
scattering by hydrogen molecules, excitation in, 20: 41645
scattering by hydrogen molecules, vibrational excitation and dissociative attachment in, (T), 20: 41657
scattering by light nuclei, review of, 20: 42340
scattering by nuclei at high energies, radiative corrections to inelastic, 20: 42095
scattering in gases, free-free transition calculations for, 20: 41626
shielding measurements in heavy concrete, 20: 41534 (DESY-66/18)
theory of Dirac's classical, analysis using simplified Price energy-momentum tensor, 20: 41808
theory of, represented as charged and coherent fluid, (T), 20: 42077
transmission of isotropically incident, through spacecraft hull materials, (E), 20: 42520
transport in a low-density ionized gas, Monte Carlo method for calculating, 20: 42413 (NASA-TN-D-2959)

ELECTROPHORESIS
technique for analytical, on polyacrylamide gels using urea, 20: 40534(R) (NYO-3621-1)
use of discontinuous, flat-bed, as a preparatory system, 20: 40502(R) (ORNL-3922, pp 115-27)

ELECTROSTATIC FIELDS
calculation for system of apertures, method for, 20: 42502
determination for Penning discharge gaps, (T), 20: 42508

ELECTROSTATIC LENSES
charged-particle focusing in, space charge effects on, 20: 42510

charged-particle motion in, phase space representations for, 20: 41567
electric potential distribution for immersion-type, paraxial-ray equation for, 20: 41245
ELECTROSTATICS
kinetics of charged particle beams, 20: 41524
ELEMENTARY PARTICLES
binding energies for, dispersion theory for large, 20: 41978
book: *Relativistic Theory of Reactions*, 20: 42024
classification in D_5 group, 20: 41972
classification of strongly interacting, in noncompact groups, 20: 41982
classification of, physical representations of irreducible Lie algebra for, 20: 41937
commutation rules for, between axial charges and divergences, 20: 41956
compositeness conditions for, renormalization constants for Z_3 factors for, 20: 41997
conference, 20: 41912
current algebra for, sign of strangeness-conserving axial-vector coupling constant from, 20: 41955
decay of, energy spectra from, (T), 20: 41927 (JINR-P-2797)
decay of, maximum likelihood method for determining branching ratios in two-step, 20: 41790 (DESY-66/17)
density matrices for arbitrary-spin, covariant, 20: 41960
diffraction scattering and form factors of strongly interacting, 20: 41979
form factors for pseudoscalar hadron densities, sum rules for, 20: 41995
form factors for, relation between propagator normalizations and electromagnetic, 20: 41980
interactions at high energies, Regge poles in unequal-mass, (T), 20: 41989
interactions at high energies, review of forward amplitudes for strong, 20: 42028
interactions at high energies, transverse-momentum distribution of secondary particles from, (T), 20: 41845
interactions of arbitrary spin, cross sections for Coulomb, 20: 41990
interactions of spin-½, Lorentz- and spin-invariant elastic, 20: 41983
interactions of spinless, elementarity and hidden channels in S-wave two-channel two-body, (T), 20: 42002
interactions of SU(3) × SU(3) algebra for electromagnetic and weak, 20: 41949(T)
interactions of, asymptotic relations between amplitudes for, 20: 42015
interactions of, charge renormalization, hamiltonian, and S-matrix in model for, 20: 41948
interactions of, constraints on statistical tensor for low-spin particles produced in strong, 20: 41950
interactions of, Froissart N/D method and Frye-Warnock equation for, 20: 42012
interactions of, Lee model for production and elastic-scattering amplitudes for, 20: 41986
interactions of, microcausality and lack of remote action in theory for amplitudes of, 20: 42014
interactions of, nondynamical structure of, (T), 20: 41992
interactions of, nontrivial relativistic quantum theory for, 20: 42000
interactions of, one-graviton-exchange, 20: 41970
interactions of, permutation symmetry in strong, 20: 41984
interactions of, properties of strong, (T), 20: 42006
interactions of, properties of soluble N/D models for, 20: 41961
interactions of, perturbation of inelastic unitarity on calculations for strong, 20: 41957
interactions of, representations of strong coupling groups for, 20: 42026
interactions of, research programs on strong, 20: 41796(R) (MIT-2098-251, pp 74-103)
interactions of, sum rules for coupling of, 20: 41988
interactions of, theory of three particle production in, 20: 41900
interactions of, urbaryon-pair effect suppression in, (T), 20: 42004
interactions with degenerate pseudoscalar meson octet at 0.49 Bev, quark-meson bootstrap from, 20: 42029
kinetics of one-dimensional, q-equivalent hamiltonians and lagrangians for, 20: 41941
mass distributions and phase-space integrals for many-body systems of, invariant, 20: 41953
masses and quark structure of strongly interacting, 20: 42017
masses of hadrons, quark pair states for, 20: 42001
model of, zero-triality states in quark, 20: 41974
models of, inconsistency of cononical commutation relations among current densities in, 20: 41964
photoproduction of fractionally-charged, weakly interacting, 20: 41797 (MIT-2098-264)
properties of unstable, symmetrization principle for, 20: 42022
research on, survey on experimental, 20: 41803(R) (UCRL-16863)
research programs on, 20: 41511(R) (RLO-1388-501)
research with bubble chambers, survey of, 20: 41803(R) (UCRL-16863)
resonances of, maximum likelihood method for determining abundances, masses, and widths of, 20: 41790 (DESY-66/17)
space-time regions for high energy and momentum, special relativity theory for, 20: 42075
spin density matrix elements of, maximum livelihood method for determining, 20: 41790 (DESY-66/17)
structure of strongly interacting, partial conservation of tensor current for electromagnetic, 20: 41952
sum rules for, derivation from equal-time commutation relations for space components of current densities, 20: 41958
symmetries for hadron, lectures on higher, 20: 41928 (NP-16191)
symmetry for positive and zero rest-mass, unified unitary representation of Poincare group in, 20: 41940
symmetry for strongly interacting, isospin and octet model for, 20: 42011
symmetry for, axial and vector current structure in broken U(12), 20: 41939
symmetry for, beyond SU(6), 20: 42030
symmetry for, Clebsch-Gordan coefficients for Regge, 20: 42025
symmetry for, finite-dimensional representations of nonsemisimple Lie algebras for, 20: 41942
symmetry for, mass splitting and X-η mixing in SU(3), 20: 42005
symmetry for, matrix elements and normalization coefficients in SU(n), 20: 42010
symmetry for, most general Clebsch-Gordan coefficients for, 20: 41944
symmetry for, noncompact groups in, 20: 42033
symmetry for, origin of SU(3), 20: 41930
symmetry for, particle-like state stability in broken, 20: 41994
symmetry for, polynomial bases and isoscalar factors for SU(3), 20: 41947
symmetry for, relativistic U(6), 20: 42031
symmetry for, relation between U(3.1) groups and complex Lorentz group with real metric in, 20: 41852
symmetry for, representations of Lie and Poincaré groups for, 20: 42071 (JINR-P-2785)
symmetry for, S(3) invariance in broken U(3), 20: 42008
symmetry for, $SU(6)_W$, 20: 42034
symmetry for, theorem on Clebsch-Gordan series in SU(n), 20: 41945
symmetry group for strongly interacting, saturation of SU(6), 20: 41968
symmetry group representations for, analytic continuation of, 20: 41933
symmetry groups for, generalization of isoparity for internal, 20: 41932
symmetry principles for, 20: 41923 (BNL-956)
symmetry structure of, Lorentz transformations for, 20: 42032
symmetry theory for, research programs on SU(6) and U(12), 20: 41796(R) (MIT-2098-251, pp 74-103)
theory for, Cutkosky-Leon normalization conditions for Bethe-Salpeter amplitudes in bootstrap, 20: 41951
theory of classical, generalization of dipole moments in, 20: 41807
theory of, research programs on, 20: 41796(R) (MIT-2098-251, pp 74-103)
ELEMENTS
atomic structure of, calculation of Hartree-Fock parameters for, 20: 41631
composition of $Z \geq 3$, in primary cosmic radiation, 20: 41672
determination of trace, in biological materials by radioisotopic dilution, 20: 40844
electron structure of, prediction of, 20: 41636
thermodynamic functions for, computer program for calculating, 20: 40875 (ORNL-TM-1599)
ELK RIVER POWER REACTOR
pressure vessel serviceability evaluation, 20: 42636(R) (SWRI-1228-4-22)
EMBRYOLOGY
radiation effects on *Heterakis gallinarum*, x, 20: 40667
EMBRYOS
locomotor behavior and neuromorphologic anomalies in rats irradiated prenatally, 20: 40688
radiation effects on mouse, lethal, RBE of neutrons and x, 20: 40618(R) (NYO-2740-3, pp 166-215)
radiation effects on mouse, cataractogenetic, x, 20: 40619(R) (NYO-2740-3, pp 216-57)
radiation effects on gastropod, effects of age at exposure on x, 20: 40700
radiation effects on fish, 20: 40527
radiation effects on post-mitotic uptake of tritiated thymidine by fibroblast and myoblast cultures from chick, x, 20: 40587
radiation effects on mouse, 20: 40649
ENCEPHALOMYELITIS
radiation effects on development of allergic, in rats following injection of rat brain homogenates and *Mycobacterium tuberculosis*, x, 20: 40728
ENDOXAN
radioprotective effect on damage induced by alkylating agents, 20: 40664
use in uterine cancer therapy in combination with radiotherapy and surgery, 20: 40778
ENERGY
transfer by elastic nuclear collisions, 20: 40515
ENGINEERING
engineering materials list, 20: 41065 (TID-4100(Suppl. 34))

ENZYMES
activation and properties of tryptophan pyrrolase and tyrosine transaminase, 20: 40523(R) (NYO-901-54, pp 16-19)
activity of D Nase and DNA polymerase in Drosophila, effects of developmental stage on, 20: 40623(R) (ORNL-3922, pp 32-49)
activity of DNA polymerase, in puromycin-treated synchronized mammalian cells, 20: 40504(R) (ORNL-3922, pp 146-60)
assay of tryptophan synthetase, using carbon-14 tracer techniques in yeasts, 20: 40582(R) (ORNL-3922, pp 65-8)
book: *The Use of Radioautography in Investigating Protein Synthesis*, 20: 40567
effects of hydrocortisone on activity of tyrosine transaminase and tryptophan pyrrolase in developing rats, 20: 40533(R) (NYO-901-54, pp 16-19)
effects of near ultraviolet on flavoprotein, cytochrome-b and succinic oxidase in bacteria, 20: 40571
effects of viruses on host cell aminoacyl-sRNA, 20: 40632(R) (ORNL-3922, pp 175-91)
electron spin resonance signals from irradiated, 20: 40595
histochemical assays of, in cerebral tissues during acute radiation syndrome, 20: 40590
inactivation of rat liver α-ketoglutarate transaminase, mechanism of *in vitro*, 20: 40506(R) (ORNL-3922, pp 168-73)
induction of rat liver α-ketoglutarate transaminase, pyridoxine, 20: 40506(R) (ORNL-3922, pp 168-73)
induction of tyrosine transaminase, in rat liver by insulin, 20: 40506(R) (ORNL-3922, pp 168-73)
inhibition of valyl-tRNA synthetase, by oligonucleotides, 20: 40503(R) (ORNL-3922, pp 137-45)
isolation of ribosome-tRNA synthetase, from *E. coli* by molecular seiving, 20: 40503(R) (ORNL-3922, pp 137-45)
levels associated with DNA synthesis at entry into S phase, factors affecting, 20: 40534(R) (NYO-3621-1)
levels in Reuber hepatomas, hormonal control *in vitro*, 20: 40506(R) (ORNL-3922, pp 168-73)
preparation of aminoacyl-sRNA, from neoplastic and normal human cells, 20: 40632(R) (ORNL-3922, pp 175-91)
preparation of malic-lactic transhydrogenase, from *Micrococcus lactilyticus*, 20: 40505(R) (ORNL-3922, pp 167)
properties of exonuclease, 20: 40534(R) (NYO-3621-1)
properties of malic-lactic transhydrogenase, effects on reaction between pyridine nucleotides and substrate, 20: 40505(R) (ORNL-3922, pp 167)
purification of DNA polymerase, methods for, 20: 40504(R) (ORNL-3922, pp 146-60)
radiation effects on β-glucuronidase and aryl sulfatase from lysosomes, 20: 40685
radiochemical method for estimation of choline acetyltransferase, 20: 40584
radioinduced inactivation of dry, 20: 40596
radioinduced inactivation of, electron spin resonance studies, 20: 40598
radioinduced structural changes in, effects on activity, 20: 40596
radiosensitivity of food, effects of purity on, 20: 40600
reactions in neoplastic cells, 20: 40533(R) (NYO-901-54(p.16-19))
reactions of phenylalanine-RNA synthetase, with RNA, 20: 40503(R) (ORNL-3922, pp 137-45)
role in photoreactivation of ultraviolet damage in sea urchin eggs, 20: 40543
transfer RNA and multiple aminoacyl-RNA synthetase, partition studies on, 20: 40535(R) (ORNL-3922, pp 128-35)

EPIDEMIOLOGY
aspects of irradiating proteinaceous food, 20: 41390

EQUIPMENT AND PROCEDURES
description of, for thermal conductivity in metals and oxides, 20: 41479
development for radioinduced optical effects in materials, 20: 41488(R) (EGG-1183-2013)
for analysis of human chromosomes, 20: 40497(R) (NYO-3400-1)
for performance testing of thermal insulation, 20: 41440(R) (ALO-3632-4)
for studies on bottom layers of Mediterranean Sea, 20: 41128

ERBIUM
helium and hydrogen ion attenuation at 0.1 to 500 Mev, tables for, 20: 41619 (CEA-R-3042)
liquid, solubility of tantalum in, at high temperatures, 20: 41412(R) (IS-1500(Sect. M))
liquid, solubility of tungsten in, at high temperatures, 20: 41412(R) (IS-1500(Sect. M))
nuclear hyperfine interactions in, Moessbauer studies of, 20: 42523(R) (IS-1500(Sect.P))
photon reactions (γ,n) with, energy spectra from, (E), 20: 42165(R) (MIT-2098-251, pp 16-20)
purification by sublimation, 20: 41412(R) (IS-1500(Sect. M))
thermodynamic properties of, at 0°C to melting point, 20: 41412(R) (IS-1500(Sect. M))

ERBIUM ALLOYS
Er–Mg, thermodynamics of formation of intermetallic compounds, 20: 41412(R) (IS-1500(Sect. M))

ERBIUM COMPLEXES
with α-methylmandelic acid, stability of, 20: 40902
with sulfosalicyclic acid, spectra of, effects of other rare earths on absorption, 20: 40926

ERBIUM IONS
spin-lattice relaxation of, in lanthanum fluorides, 20: 42540

ERBIUM ISOTOPES Er^{-166}
energy levels of, g-factors for 2⁺ rotational, (E), 20: 42302

ERBIUM ISOTOPES Er^{-168}
energy levels of, g-iactors for 2⁺ rotational, (E), 20: 42302
neutron reactions (n,2n) at 14.8 Mev, activation cross section for, (E), 20: 42207

ERBIUM OXALATES
thermal decomposition of hydrates of, differential thermal analysis of products of, 20: 40900

ERBIUM OXIDES
sintering mechanisms of, 20: 41064(R) (IS-1500(Sect.E))
B_2O_3–Er_2O_3, liquid immiscibility in, 20: 40910

ERYTHROCYTES
clearance of rat and sheep, in mouse blood, selenium-75 tracer study of, 20: 40503(R) (ORNL-3922, pp 137-45)
cytokinetics of rat, using diffusion chamber techniques, 20: 40632(R) (ORNL-3922, pp 175-91)
effects of x ray and L-methionine on iron-59 metabolism, 20: 40561
production of polymers of, effects of antibody titer on, 20: 40626(R) (ORNL-3922, pp 80-3)
radiation effects on counts of mouse, fast neutron, 20: 40502(R) (ORNL-3922, pp 115-27)
radiation effects on diameter and volume of human, resulting from occupational exposure, 20: 40678
radiation effects on volume of, in polycythemic patients, use in dosimetry determination, 20: 40774

ERYTHROPOIESIS
autoradiography of cells, using iron-55 and iron-59, 20: 40675
radiation effects on rat, tracer study of x, 20: 40603 (AD-635086)

ERYTHROPOIETIN
purification and separation, 20: 40502(R) (ORNL-3922, pp 115-27)

ESCHERICHIA COLI
bacteriophage attachment to male strains of, 20: 40504(R) (ORNL-3922, pp 146-60)
conjugation in F⁻ and Hfr strains of, 20: 40629(R) (ORNL-3922, pp 94-8)
conjugation of K12, DNA transfer during, 20: 40504(R) (ORNL-3922, pp 146-60)
donor pili in Hfr, role of, 20: 40629(R) (ORNL-3922, pp 94-8)
genes in K-12 strains, characterization of, 20: 40629(R) (ORNL-3922, pp 94-8)
growth in gamma-irradiated culture media of, physiological effects, 20: 40580 (NYO-2804-8)
mitosis in, effects of chloramphenicol on, 20: 40630(R) (ORNL-3922, pp 106-8)
mutants of, use for studies in germfree mice, 20: 40629(R) (ORNL-3922, pp 94-8)
phenylalanine transfer RNA from, methylation of, 20: 40503(R) (ORNL-3922, pp 137-45)
phenylalanine transfer RNA in, physical characteristics of, 20: 40503(R) (ORNL-3922, pp 137-45)
phosphorus-32 transport in stream ecosystems by, 20: 40529
polysome configuration in, 20: 40503(R) (ORNL-3922, pp 137-45)
radiation effects on mitosis in, factors affecting x, 20: 40630(R) (ORNL-3922, pp 106-8)
radiation effects on DNA in, effects of benzopyrene on uv, 20: 40632(R) (ORNL-3922, pp 175-91)
radiation effects on developing phage complexes with, uv, 20: 40618(R) (NYO-2740-3, pp 166-215)
radiation effects on DNA metabolism in, tracer study, γ, 20: 40620 (NYO-2804-9)
radioinduced chromosome transfer by, mechanism for uv, 20: 40629(R) (ORNL-3922, pp 94-8)
radioinduced mutants of, genetics and physiology of uv, 20: 40629(R) (ORNL-3922, pp 94-8)
radioprotective effect of SPATA, 20: 40737
radiosensitivity effects of protein synthesis in, x, 20: 40629(R) (ORNL-3922, pp 94-8)
replication and genetic exchange in genome, 20: 40538 (TID-23238)
RNA from, analysis of, 20: 40501(R) (ORNL-3922, pp 113-14)
RNA structure in, effects of deoxyribonucleotide transferase on, 20: 40535(R) (ORNL-3922, pp 128-35)
role in repair of uv-induced damage in phage T3, 20: 40504(R) (ORNL-3922, pp 146-60)

ESOPHAGUS
treatment of tumors of, by radiation and methotrexate, 20: 40782

ESTRADIOL
effects on immune system and lymphatic tissues in adult and newborn mice, 20: 40577
effects on mouse thymus, 20: 40577
radiosensitivity effects on immune system and lymphatic tissue in mice of, effects of bone marrow transplants on x, 20: 40577
ETHANE
electron drift velocities in, magnetic field effect on, (T), 20: 41628
yields of deuterated, in hydrolysis of aluminum, thorium, and uranium carbides in heavy water, 20: 40905
ETHANE, HEXAFLUORO-
yields in gamma radiolysis of carbon tetrachloride, 20: 40948(R) (COO-578-3-32)
ETHANE, IODO-
exchange reactions of radioiodine between methyl iodide and, radiochromatography equipment for studies on, 20: 41019
ETHANETHIOL, 2-AMINO-
radioprotective effect on damage induced by alkylating agents, 20: 40664
radioprotective effects of, electron spin resonance studies, 20: 40598
radiosensitivity effects on human kidney cells, particulate, 20: 40725
ETHANOL
effects on vertebrate phosvitin, 20: 40499(R) (ORNL-3922, pp 69-79)
electron spin resonance spectra of, 20: 42433
radiolysis of, EPR studies of yields of stabilized charges in low-temperature, 20: 40962
ETHERS
explosion tests in gloved box, 20: 41203 (UCRL-16259)
ETHYL ETHER
effects on radioinduced polymerization of styrene with formaldehyde, 20: 40973
ETHYL SULFATES
chemical and physical properties and mutagenic action of di-, on barley seeds, 20: 40717
ETHYLENE
alpha-particle interactions with, properties of recoil ions from, 20: 41622 (SC-DC-66-1564)
effects on gamma-induced polymerization of carbon monoxide with ethylenimine, 20: 40975
hydrogenation of, deuterium–hydrogen exchange during nickel-catalyzed, 20: 40942
production by chemonuclear synthesis, 20: 40988
radioinduced polymerization of, 20: 40988
reactions with muonium, review of, 20: 41661
yields of deuterated, in hydrolysis of aluminum, thorium, and uranium carbides in heavy water, 20: 40905
Ar–ethylene, alpha particle interactions with, recoil ion properties from, 20: 41622 (SC-DC-66-1564)
ethylene–N_2, alpha-particle interactions with, properties of recoil ions from, 20: 41622 (SC-DC-66-1564)
ETHYLENE, CHLORO-
radioinduced graft polymerization to polyethylenes, pre-irradiation method for, 20: 40982
ETHYLENE, CHLORO- POLYMERS
radioinduced graft polymerization to styrene in liquid and vapor phases, rate of electron and gamma, 20: 40992
radioinduced polymerization with styrene, rate of gamma, 20: 40993
ETHYLENE GLYCOL
production by chemonuclear synthesis, 20: 40988
ETHYLENE, NITRO-
radioinduced polymerization of, ESR study of gamma, 20: 40981
ETHYLENE POLYMERS
effects on coating on potassium bromide windows for infrared analysis of heavy metal systems, 20: 40805(R) (MLM-1325, pp 63-70)
electron penetration of, for spacecraft shielding, (E), 20: 42520
neutron differential reflection by slabs of, thermal, (E/T), 20: 42142 (NP-16234)
radiation effects on ultraviolet absorption spectra of, gamma, 20: 40963
radiation effects on crystal orientation in, x, 20: 40949(R) (NYO-3003-29)
radiochlorination of, effects of suspended particle trajectory on, 20: 40884
radioinduced cross-linking of, cable insulation, 20: 41496
radioinduced graft polymerization to vinyl chloride, pre-irradiation method for, 20: 40982
radiolysis of, EPR studies of yields of stabilized charges in low-temperature, 20: 40962
radiolysis of, ultraviolet absorption spectroscopy of free radicals from, gamma, 20: 40964
sorptive properties for cesium from aqueous sodium tetraphenylborate solutions, 20: 40915
ETHYLENE, TETRAFLUORO- POLYMERS
sorptive properties for cesium from aqueous sodium tetraphenylborate solutions, 20: 40915
ETHYLENIMINE
radioinduced polymerization with carbon monoxide, effects of ethylene on, 20: 40975
EUROPIUM
content in common rock types, 20: 41068 (PNE-5006)
determination by x-ray-fluorescence methods, 20: 40796(R) (IS-1500 (Sect.C))
determination in uranium dioxide fuel pellets, 20: 41112 (IITRI-578P11-54)
determination of, in uranium by neutron activation methods, 20: 40832
liquid, solubility of tantalum and tungsten in, at high temperatures, 20: 41412(R) (IS-1500(Sect. M))
separation of, from other lanthanides by thin-layer high-voltage electrophoresis, 20: 41046
EUROPIUM ALLOYS
Eu–Pb, phase diagrams, 20: 41412(R) (IS-1500(Sect. M))
EUROPIUM BROMATES
fluorescent lifetime of $^5D_0$ level of trivalent europium ions in, (E/T), 20: 42539
EUROPIUM CHLORIDES
fluorescent lifetime of $^5D_0$ level of trivalent europium ions in, (E/T), 20: 42539
EUROPIUM COMPLEXES
with α-methylmandelic acid, stability of, 20: 40902
with sulfosalicyclic acid, composition of, fluorometric study of, 20: 40926
EUROPIUM ETHYL SULFATES
fluorescent lifetime of $^5D_0$ level of trivalent europium ions in, (E/T), 20: 42539
EUROPIUM IONS
fluorescence, 20: 40796(R) (IS-1500(Sect.C))
fluorescent lifetime of $^5D_0$ level of trivalent, in hydrated salts, (E/T), 20: 42539
EUROPIUM ISOTOPES Eu-152
energy level transitions in, conversion electron spectra from, (E), 20: 41348
EUROPIUM ISOTOPES Eu-154
energy level transitions in, conversion electron spectra from, (E), 20: 41348
EUROPIUM NITRATES
fluorescent lifetime of $^5D_0$ level of trivalent europium ions in, (E/T), 20: 42539
stability constant of $(EuNO_3)^{2+}$, in various ionic media, 20: 40876 (ORO-1797-2)
EUROPIUM OXALATES
thermal decomposition of hydrates of, differential thermal analysis of products of, 20: 40900
EUROPIUM OXIDES
determination in uranium dioxide fuel pellets, 20: 41112 (IITRI-578P11-54)
B_2O_3–Eu_2O_3, liquid immiscibility in, 20: 40910
EUROPIUM SULFATES
fluorescent lifetime of $^5D_0$ level of trivalent europium ions in, (E/T), 20: 42539
EUROPIUM THORIUM FLUORIDES
preparation, properties, and structure of, 20: 40867 (KFK-385)
EVAPORATION
equations for surface-to-air concentration gradients, 20: 41150 (AECL-2576)
EXERCISE
radiation effects combined with aging on performance of treadmill, by rats, 20: 40604 (AD-635251)
EXPERIMENTAL BOILING WATER REACTOR
reactivity of plutonium-fueled, 20: 42577(R) (ANL-7230)
EXPERIMENTAL BREEDER REACTOR-II
development and operation of, June 1966, 20: 42577(R) (ANL-7230)
development and operation, July 1966, 20: 42619(R) (ANL-7245, pp 1-20)
fuel meltdown studies in TREAT, 20: 42580(R) (ANL-7245, pp 60-73)
fuel pin burnup testing, 20: 42580(R) (ANL-7245, pp 60-73)
EXPERIMENTAL GAS COOLED REACTOR
operator training simulator for, 20: 42581(R) (ORNL-3875, pp 125-50)
EXPLOSIONS
craters formation by short-row charges in, 20: 41069 (SC-RR-66-324)
ether–nitrogen and ether–air in gloved box, 20: 41203 (UCRL-16259)
wave amplitudes from, variability of, 20: 41158
EXPLOSIVES
cratering by cast TNT, 20: 41069 (SC-RR-66-324)
detection of hidden, using gamma rays from tracers, 20: 41066(P)
EXTENSOMETERS
design for metal samples, 20: 41451(R) (GA-7101)
performance in liquid sodium at high temperatures, 20: 41420(R) (MSAR-66-149)
EYES
cataract induction resulting from radon gold seed implants, 20: 40771

corneal opacities in x-irradiated mice, 20: 40649
gamma crystallins in lens regenerates of Salamander, 20: 40499(R) (ORNL-3922, pp 69-79)
lens explants of frog, effects of alcohol on lens-inducing ability of, 20: 40499(R) (ORNL-3922, pp 69-79)
nuclei acids in Amblystoma, effects of lens removal on synthesis of, 20: 40499(R) (ORNL-3922, pp 69-79)
physiological effects of laser beams on retina of, 20: 40691
radiation effects on rabbit, laser, 20: 40692
radiation effects on, deuteron, 20: 41187 (BNL-9468)
radiation effects on cell morphology and histochemistry of monkey, γ, 20: 40646
radiation effects on, instrument designed for retinal coagulation, 20: 40791
radiation injury on human, following therapy of canthus and eyelid carcinomas, 20: 40689
radio-induced cataracts, dosimetry studies, 20: 40690
use of bovine, for studies on effects of alpha-emitting isotopes, 20: 41191(R) (HUX-3170-1)

F

FALLOUT
absorption and retention of, by vegetal mechanisms, 20: 41141
analysis of Chinese 1965 nuclear test, 20: 41130(R) (COO-1407-10)
atmospheric transfer processes in France after Chinese nuclear explosion, 20: 41189 (CEA-R-3020)
beta activity from, in leaves during growing season in Delaware, Ohio, 20: 40579
content in Marine environment on west coast of India, 20: 40572
content in Norweigian milk, March 1962 to 1966, 20: 41132 (NYO-3364-20)
deposition in rain water, effects of storm cell characteristics on, 20: 41130(R) (COO-1407-10)
determination in water, 20: 40819(T) (CEA-tr-A-1883)
development of agronomic practices to reduce uptake of radioisotopes from, 20: 40735 (NYO-2744-37)
dispersion and transport in atmosphere, methematical model for, 20: 41133(R) (SC-CR-66-2030)
distribution in ocean waters, 1945 to 1963, 20: 41144
gamma radiation dose measurements for, 20: 41180 (AD-635822)
monitoring in air, design and performance of instrument for continuous beta, 20: 41303
monitoring in Canada, April, 1966, 20: 41198 (NP-16192)
monitoring in Canada, April 1965, 20: 41209
monitoring in Finland, 1960 through 1965, 20: 41134 (SFL-A3)
monitoring in Mediterranean Sea, 1963, 20: 41145
monitoring in Mediterranean Sea, 1963, 20: 41146
monitoring in stratosphere, 1965, 20: 41131(R) (HASL-172)
monitoring of global, 1965 and 1966, 20: 41131(R) (HASL-172)
particles in, properties of highly active, 20: 41138
preparation of synthetic, 20: 41178 (AD-635547)
protection against, for city populations, 20: 41183 (AD-635931)
radiation dose estimations for postattack, 20: 41177 (AD-632211)
radioactivity measurements in air, water, soil, and milk in New Zealand, 20: 40521(R) (NP-16270)
shelters against, portable on fixed, 20: 41118(P)
shelters against, design of precast concrete, 20: 41119(P)
sorption of synthetic, on minerals, 20: 41178 (AD-635547)
survey of radioactivity and radiation burden from, in West Germany, 20: 40570
transport from atmosphere to water supplies, 20: 41141
uptake by aquatic organisms in United Kingdom, 20: 40578
use of multilayer iron and water enclosure shields in real field, 20: 41201 (RRA-T55 and Summary)
FAST CERAMIC REACTOR
fuel development for, 20: 42625 (GEAP-4466)
FAST REACTORS
design of 1000 Mw(e) sodium-cooled, evaluation of, 20: 42622 (COO-285)
development of LMFBR, 20: 42577(R) (ANL-7230)
fuel development for, 20: 42577(R) (ANL-7230)
fuel development for, 20: 42619(R) (ANL-7245, pp 1-28)
fuel reprocessing, development for, 20: 42577(R) (ANL-7230)
fuels and materials development for LMFBR, 20: 42651 (WASH-1065)
heat transfer system for, cost analysis of secondary sodium-steam, 20: 42632 (NAA-SR-12060)
reactivity coefficients of, steady state evaluation of, 20: 42631 (KFK-260)
reactivity measurements on uranium-fueled assemblies, 20: 42671 (AWRE-R-5/66)
FAST TEST REACTOR
fuels for, neutron physics of driver, 20: 42676 (BNWL-281)
FATIGUE
effects on ductility of pressure-vessel steels, 20: 41446(R) (EURAEC-1624)
FATTY ACIDS
capillary ripple propagation in, damping of, 20: 40796(R) (IS-1500 (Sect.C))
FECES
Salmonella populations in, of swine fed heat-treated or γ-irradiated meals, 20: 41394
FEED MATERIALS
preparation for electromagnetic isotope separators, 20: 41400 (ORNL-3301(Suppl.1))
FEEDBACK SYSTEMS
design and performance of, for Mossbauer effect measurements for pulse analyzers, 20: 41238
FELDSPARS
ages of meteoric, estimation of, 20: 41162
FERMIONS
decay of Lee model for electromagnetic field effects on, (T), 20: 41909
energy levels of degenerate systems of, density of, 20: 42222
field theory for, paraquantization in, 20: 41925 (JINR-P-2756)
interactions of identical, coupled-equations method for, 20: 41870
interactions with bosons, Lehmann-Symonzik-Zimmermann formalism in Lee model for, (T), 20: 42169(R) (UCRL-14744, pp 1-18)
theory of many-body systems of, hole self-energy corrections in Brueckner, (T), 20: 42244
theory of self-bound many-body systems of, 20: 42248
FERROMAGNETIC MATERIALS
book: *Rare Earth Ferromagnetics and Antiferromagnetics*, 20: 41483
FETUSES
chicken, bone mineralization dynamics studies, 20: 40558
radiation dose to human, from isotope placentography, 20: 40680
radiation effects on mouse, x, 20: 40619(R) (NYO-2740-3, pp 216-57)
radiation effects on nervous system in rat, 20: 40654
RNA synthesis in rat, 20: 40506(R) (ORNL-3922, pp 168-73)
FIELD EMISSION MICROSCOPY
use in study of neutron-irradiated tungsten, 20: 42551
FIELD FORTIFICATIONS
testing for electromagnetic pulse hardness, 20: 41117
FIELD THEORY
boson fields in quantum, Lie algebra and Schroedinger equation for, 20: 41934
commutation relations among current densities in, inconsistency of canonical, 20: 41964
commutation relations for Bose, 20: 41946
commutators of spatial current components in, unitary-antisymmetric Schwinger terms in, 20: 41985
current commutation relations in general quantum, 20: 41924 (DESY-66/19)
Einstein field equations for dust-filled universe, solution of, 20: 41599
Einstein's vacuum field equations, solution using spheroidal coordinates, 20: 42086
Feynman diagrams in euclidean formulation of quantum, 20: 42021
field equations in, symmetry-breaking solutions to, 20: 41969
field interactions in, neutral mass spin-2 tensor, 20: 41938
formalism for many-body systems, 20: 41931
Heisenberg operators in quantum, nonlinear, 20: 42018
paraquantization in, interpretation of boson-fermion, 20: 41925 (JINR-P-2756)
propagator normalizations in, relation between electromagnetic form factor and, 20: 41980
renormalization in quantum, Bogoliubov-Parasiuk theorem on, 20: 41935
research at LRL, 20: 41803(R) (UCRL-16863)
research programs on, 20: 41511(R) (RLO-1388-501)
FILTERS
design of light, for optical systems used in radiation effects measurements, 20: 41491(R) (EGG-1183-2030)
development for radioactive particulate aerosols, 20: 41234 (ORNL-P-2436)
fallout collection during ascent and descent of balloon-borne, 20: 41131(R) (HASL-172)
testing of ALRR ventilation system, 20: 42681(R) (IS-1500(Sect. R))
FINLAND
fallout monitoring, 1960 through 1965, 20: 41134 (SFL-A3)
FIRES
monitoring of heat smoke and toxic gases from, in fallout shelters, 20: 41184 (AD-637806)
FISH
biochemical characteristics of hepatomatous trout, 20: 40632(R) (ORNL-3922, pp 175-91)
ecology of, in Columbia River estuary and Northeast Pacific, tracer study, 20: 40523(R) (RLO-1750-8(Vol.1))
manganese-54 and zinc-65 content in Northeast Pacific Ocean, 20: 40523(R) (RLO-1750-8(Vol.1))
phosphorus-32 uptake by, from *E. coli* in stream ecosystems, 20: 40529

radiation effects on rainbow trout, γ, 20: 40611(R) (COO-1421-2)
radiation effects on spawning in, from radioisotope decay, 20: 40527
radiation effects on food selection behavior in carp, gamma, 20: 40656
radioactivity content of, from fallout in West Germany, 20: 40570
radioactivity in Columbia River estuary and Northeast Pacific Ocean, 20: 40523(R) (RLO-1750-8(Vol.I))
radioisotope accumulation by ocean-dwelling, 20: 40546
separation of barium-140, strontium-89, and strontium-90 from ashes of, 20: 40858
soluble amino-acid-incorporating system in liver of trout, 20: 40632(R) (ORNL-3922, pp 175-91)
strontium-90 content in Baltic herring, 1965, 20: 41134 (SFL-A3)
uptake of radioisotopes by, factors affecting, 20: 40578

FISSION
neutron emission in, research on, 20: 42325
theory using single-particle model, 20: 42272

FISSION CHAMBERS
design for determining plutonium-240 content in plutonium, 20: 41264 (DP-552)
development of bismuth, 20: 41276 (UCRL-16769)
response of silicon, to channeled argon-40 and iodine-127 ions, 20: 41324

FISSION FRAGMENTS
angular distribution in neutron fission of plutonium-239, uranium-233, and uranium-235, (E), 20: 42171(T) (LA-tr-66-41)
angular distributions in alpha fission of bismuth-209 and uranium-238 at 23 to 115 Mev, (E), 20: 42267
dosimetric use of tracks of, in plastics, 20: 41262 (BNWL-SA-619)
energy and mass distributions from thermal-neutron fission of plutonium-239 and plutonium-241, (E), 20: 42261
energy in neutron fission of uranium-235, mass dependence of total, (E), 20: 42297
excitation of metastable molecular states in MHD cycles, ionization from, (T), 20: 41732
use in chemonuclear reactions, contamination from, 20: 40951 (RPI-321-6)

FISSION PRODUCTS
accumulation in oceans, 1945 to 1963, 20: 41144
age determinations of, in fallout from Chinese nuclear test, May 1965, 20: 41130(R) (COO-1407-10)
age of, beta spectroscopy for estimating, 20: 41137
analysis for elements in solutions of, methods for, 20: 40803 (KFK-387)
atmospheric transfer processes in France after Chinese nuclear explosion, 20: 41189 (CEA-R-3020)
beta activity from, in leaves during growing season, 20: 40579
buildup in samarium–uranium dioxide sandwiches, 20: 41112 (IITRI-578P11-54)
contamination of eggs, 20: 40559
content in detritus from Indian Ocean, 20: 41140
delayed neutron emission, 20: 42681(R) (IS-1500(Sect. R))
determination in uranium trioxide by beta and gamma counting, 20: 40802 (HW-65402(Rev.1))
determination in water, 20: 40819(T) (CEA-tr-A-1883)
diffusion in sea water of fallout, 20: 41144
diffusion from glass fibers in radiation sources for chemonuclear reactions, 20: 40951 (RPI-321-6)
distribution in mixed-oxide fast reactor fuels, 20: 42625 (GEAP-4466)
distribution of, in neutron-irradiated plutonium dioxide suspensions, 20: 41009 (AERE-R-3268)
effects on ALRR reactivity, 20: 42681(R) (IS-1500(Sect. R))
gamma spectra and x-ray spectra of uranium-235, (E), 20: 42170 (UCRL-70045)
generator design and fabrication for ALRR, 20: 42681(R) (IS-1500 (Sect. R))
metabolism by marine organisms of, 20: 40546
monitoring in atmosphere, 1965 and 1966, 20: 41131(R) (HASL-172)
release in LOFT, sampling and analysis of, 20: 42664(R) (IDO-17165)
removal from LOFT containment surfaces, 20: 42664(R) (IDO-17165)
separation from irradiated uranium fuel, method for, 20: 41042 (PG-Report-722)
separation of iodine and xenon isotopes from uranium, methods for, 20: 41034 (JEN-160-DQ/I-54)
separation of, from waste solutions for use as radiation sources, 20: 42689
thermal stability of, from uranium, in monocrystalline muscovite during chemical etching, 20: 40889
yields in proton fission of uranium at 170 Mev, 20: 42177

FLAVINES
effects on thymine dimer formation and monomerization, 20: 40504(R) (ORNL-3922, pp 146-60)

FLOWMETERS
calibration of magnetic, for sodium, 20: 41064(R) (IS-1500(Sect.E))
design and operation of ultrasonic, molten metals and fused salts, 20: 41225(R) (NYO-3622-4)
design using tracers for use in boreholes, 20: 41170(P)

FLUID FLOW
analysis of MHD, in entrance section of plane channels, 20: 42036 (SC-RR-66-356)
determination of vapor in two-phase, 20: 41111
diffusion coefficients in, measurement of self-, 20: 41064(R) (IS-1500 (Sect.E))
magnetohydrodynamic, hydraulic approximation for, in ducts, 20: 41704
magnetohydrodynamic, equations for striated-layer, (T), 20: 41711
magnetohydrodynamic, application of switching in, (T), 20: 41724
magnetohydrodynamic, theory of boundary-layer and impact-wave, 20: 41735
magnetohydrodynamic, theory of plane, 20: 41773
measurement in boreholes, equipment for, 20: 41170(P)
model for two-phase, in constant-area adiabatic pipes, 20: 41107
research on, 20: 42038(T) (NASA-TT-F-360)
two-dimensional MHD, analysis of, 20: 41696
velocity and density probe for supersonic, 20: 41702
void fraction in two-phase, impedance measurement of, 20: 41103 (RT-ING-(65)7)

FLUID FLOW (LAMINAR)
in MHD fluid, heat transfer to, 20: 41105
magnetohydrodynamic, boundary layer analysis of parallel stream, 20: 42039
magnetohydrodynamic, plane boundary layer for, (T), 20: 42044

FLUID FLOW (TURBULENT)
magnetohydrodynamic, of mercury in channel, (E), 20: 41707
measurement in circular pipes, 20: 41102 (NYO-2930-6)
velocity in liquid metal stream, noise analysis of, 20: 41101 (NAA-SR-Memo-10848)

FLUORIDES
determination of, in presence of uranium, electrolytic, 20: 40840
effects on disproportionation of uranium(V), 20: 40911

FLUORINE
determination in americium and plutonium by spark-source mass spectrography, 20: 40816 (RFP-699)
determination of, in silica–alumina gels containing lead fluoride, by fast-neutron radioactivation, 20: 40845
helium and hydrogen ion attenuation at 0.1 to 500 Mev, tables for, 20: 41619 (CEA-R-3042)

FLUORINE ISOTOPES
nucleon configuration mixing, (E), 20: 42204

FLUORINE ISOTOPES F-17
beta decay, (E), 20: 42242

FLUORINE ISOTOPES F-18
energy levels, (E), 20: 42204
incorporation in arsenic, boron, phosphorus, selenium, and sulfur fluorides, 20: 41020
metabolism in dogs, 20: 40554
preparation of carrier-free, using neutron-irradiated lithium carbonate, 20: 41021
separation from irradiated lithium carbonate by solvent extraction using carbon tetrachloride, 20: 41021
use in bone scanning, 20: 40554

FLUORINE ISOTOPES F-19
deuteron reactions (d,Li-6) at 15 Mev, differential cross sections for, (E/T), 20: 42237
nuclear magnetic resonance in monocrystal of lanthanum fluoride, anisotropy of, 20: 42528
nuclear magnetic resonance spectra of, in solid molybdenum, osmium, platinum, plutonium, tungsten, and uranium hexafluorides, 20: 40892
proton elastic and inelastic scattering at 13.9 Mev, excitation of ground state band from, (E), 20: 42169(R) (UCRL-14744, pp 1-18)
proton reactions (p,d) at 156 Mev, fluorine-18 energy levels from, (E), 20: 42204
spectra of, in thorium, uranium, and zirconium tetrafluorides, NMR, 20: 40931

FLUORINE ISOTOPES F-20
beta decay, (E), 20: 42242

FLUORINE SYSTEMS
F–N, use in removal of actinide halides from alumina, 20: 41062(P)

FLUOXYMESTERONE
use in uterine cancer therapy in combination with radiotherapy and surgery, 20: 40778

FOOD
analysis for cesium-137 and strontium-90, method for, 20: 40853
hazards from contamination of, evolution, 20: 41217
radiation effects on carp selection of, gamma, 20: 40656
radiation preservation of, review of developments in, 20: 41383 (CONF-650552)
radioactivity content of, from fallout in West Germany, 20: 40570
radiopreservation of proteinaceous, review, 20: 41390
radiopreservation of, microbiological controls in legislation on,

20: 41389
radiosensitivity of enzymes in, 20: 40600
radiosterilization of swine, effects on Salmonella contamination, 20: 41394
radiosterilization of, review of microbiological aspects of, 20: 41388
FOOD IRRADIATION FACILITIES
operational feasibility of Marine Products Development Irradiator for processing commercial shipments, 20: 41384(R) (TID-22833)
FORESTS
radiation effects on lichens in, gamma, 20: 40517 (BNL-9437)
FORMALDEHYDE
production by chemonuclear synthesis, 20: 40988
production in radioinduced oxidation of methanol, 20: 41004
radioinduced polymerization of, with styrene in bulk and solution, gamma, 20: 40973
FORMAMIDE
spectra of quadrupole coupling in, NMR, 20: 40805(R) (MLM-1325, pp 63-70)
FORMAZAN
complexes of heterocyclicly substituted, with cobalt and uranium, 20: 40880
FORMIC ACID
production by chemonuclear synthesis, 20: 40988
radiolysis of frozen aqueous solutions of, ESR spectral studies on radical reactions in, 20: 40994
FRACTURE TESTS
methods for A302B stainless steel, 20: 41444(R) (COO-1477-5)
FRANCE
fallout after Chinese nuclear explosion, 20: 41189 (CEA-R-3020)
FRANCIUM ISOTOPES Fr-214
alpha decay, (E), 20: 42287
FRANCIUM ISOTOPES Fr-223
gamma spectra, 20: 41038(R) (MLM-1325, pp 9-62)
half life, 20: 41038(R) (MLM-1325, pp 9-62)
separation from members of actinium-227 decay chain by ion exchange, 20: 41038(R) (MLM-1325, pp 9-62)
FREE RADICALS
effects in radiation biology, electron spin resonance studies, 20: 40597
electron spin resonance spectra of trapped, in gamma-irradiated arsine and phosphine, 20: 40967
electron spin resonance spectra of trapped, in gamma-irradiated germanium hydride, methane, silicon hydride, and tin hydride, 20: 40968
electron spin resonance of, in irradiated sodium acid selenites, 20: 40972
electron spin resonance spectroscopy of radiation-induced, 20: 42433
radiation effects on, in *Clostridium botulinum* spores, 20: 40601
radioinduced in amino acids, endothermic decay of x, 20: 40504(R) (ORNL-3922, pp 146-60)
radioinduced in frozen ammonia and hydrogen peroxide solutions, ESR spectral studies on gamma and uv, 20: 41001
radioinduction in deoxyribonucleic acid, electron spin resonance studies, 20: 40594
radioinduction in proteins, electron spin resonance studies, 20: 40595
reactions of, electron spin resonance studies, 20: 40598
transformation properties of, in irradiated sodium acid selenites, 20: 40972
yields of from gamma radiolysis of polyethylene, uv spectral studies of, 20: 40964
FROGS
isolation and properties of a uracil-containing compound in eggs of, 20: 40535(R) (ORNL-3922, pp 128-35)
optic cupts in Xenopus, effects of alcohol on lens-inducing ability of, 20: 40499(R) (ORNL-3922, pp 69-79)
radiation effects on hybrid development in, 20: 40535(R) (ORNL-3922, pp 128-35)
FRUCTOSE
radiation effects on metabolism in bull testicle, x, 20: 40610(R) (COO-895-9)
FRUITS
radiation processing of, effects on storage life, 20: 41385 (TID-23136)
FUEL CELLS
evaluation for sun mission, 20: 41124
FUNGI
cytochrome C synthesis in Ustilago, 20: 40503(R) (ORNL-3922, pp 137-45)
radioinduced mutations in tobacco for resistance to *Peronospora tabacina*, gamma, neutron, and x, 20: 40613 (N-66-18147)
radiosensitivity of soil, gamma, 20: 40637(R) (ORO-2754-7)
strontium absorption, 20: 40524(R) (TID-23271)
FURAN, TETRAHYDRO-
radiolysis of, EPR studies of yields of stabilized charges in low-temperature, 20: 40962
FURAN, TETRAHYDRO-2-METHYL-
effects on gamma-induced polymerization of nitroethylene, 20: 40981
radiolysis of, EPR studies of yields of stabilized charges in low-temperature, 20: 40962
FURNACES
development of induction-melting, for reactive metals, 20: 41429(R) (USBM-RC-1249)
performance of, for carbide-casting, 20: 41429(R) (USBM-RC-1249)
FUSED SALTS
boiling in, ultrasonic flowmeter for detection of, 20: 41225(R) (NYO-3622-4)

G

GADOLINIUM
content in common rock types, 20: 41068 (PNE-5006)
determination by x-ray-fluorescence methods, 20: 40796(R) (IS-1500 (Sect.C))
determination in uranium dioxide fuel pellets, 20: 41112 (IITRI-578P11-54)
determination of, in mixture of rare earths, errors in neutron activation methods of, 20: 40843
determination of, in uranium by neutron activation methods, 20: 40832
helium and hydrogen ion attenuation at 0.1 to 500 Mev, tables for, 20: 41619 (CEA-R-3042)
liquid, solubility of tantalum in, at high temperatures, 20: 41412(R) (IS-1500(Sect. M))
liquid, solubility of tungsten in, at high temperatures, 20: 41412(R) (IS-1500(Sect. M))
specific heat at 400 to 1500°K, values of electronic, 20: 41412(R) (IS-1500(Sect. M))
thermodynamic properties of, at 0°C to melting point, 20: 41412(R) (IS-1500(Sect. M))
thermodynamic properties of, re-evaluation of, 20: 42542
GADOLINIUM ALLOYS
Gd–Mg, thermodynamics of formation of intermetallic compounds, 20: 41412(R) (IS-1500(Sect. M))
Gd–Mo, phase studies of, 20: 41465
Gd–Pb, phase studies, 20: 41412(R) (IS-1500(Sect. M))
GADOLINIUM CHLORIDES
magnetic properties from NMR and NQR studies, 20: 42522(R) (COO-1533-2)
GADOLINIUM COMPLEXES
with α-methylmandelic acid, stability of, 20: 40902
GADOLINIUM IONS
spin-lattice relaxation of, in lanthanum fluorides, 20: 42540
GADOLINIUM ISOTOPES Gd-152
energy levels from beta decay of terbium-152, (E), 20: 42155 (JINR-P-2762)
GADOLINIUM NITRATES
binding energies in, infrared spectral studies of hydrated, 20: 40886
paramagnetic relaxation of liquid solutions of, effects of solvent on, 20: 40928
GADOLINIUM OXALATES
thermal decomposition of hydrates of, differential thermal analysis of products of, 20: 40900
GADOLINIUM OXIDES
evaporation-rate measurements, 20: 42579(R) (ANL-7245, pp 29-47)
B_2O_3–Gd_2O_3, liquid immiscibility in, 20: 40910
GAGES
design for ovality measurement, 20: 41436(P)
design of radiometric, for use in high background, 20: 41365(P)
production and use of radiometric, in Hungary, 20: 41386(T) (JPRS-36895)
GALAXIES
cosmic particle origin in, (T), 20: 41669
electron emission from halo of, magnetic field determination from radio, 20: 41594
formation of, 20: 41585(T) (UCRL-Trans-10041)
meson (π) production in centers of, model for, 20: 41603
perturbations in expanding, 20: 41590
GALLIUM
determination in americium and plutonium by spark-source mass spectrography, 20: 40816 (RFP-699)
determination in plutonium by carrier distillation methods, spectrographic, 20: 40814 (RFP-664)
GALLIUM ALLOYS
Ga–Fe, spin-wave stiffness, neutron-diffraction analysis of, (E), 20: 42559
Ga–Pu, effects of impurities on phase transformations in, differential thermal analysis of, 20: 41452 (MLM-1172)
Ga-Pu, separation of plutonium from, electrorefining processes for, 20: 41035 (LA-2758)

Ga–Pu, zone refining of carbon-contaminated rods, method evaluation, 20: 41453(R) (NUMEC-3428-21)
Ga–V, preparation of V_3Ga, 20: 42534
Ga–V, superconductivity of V_3Ga in 30 kG fields, 20: 42534

GALLIUM ARSENIDES
performance of scintillation detectors of, as charged-particle spectrometer, 20: 41313
radiation effects on emission spectra in zinc-doped, 0.6- to 2-Mev electron, 20: 42548

GALLIUM YTTRIUM SULFIDES
preparation and properties of, 20: 40879

GAMETES
formation in radioinduced mutants of peas, genetic control of, 20: 40512
radiation effects on germinal selection in Drosophila, gamma, 20: 40670

GAMMA CAMERAS
detection of tumors of liver, brain and other organs, 20: 40747 (UCRL-14866)
performance for detection of secondary emission from tissue exposed to high-energy γ radiation, 20: 41321
use of scintillation, for radiodiagnosis, 20: 40750
use of scintillation, for radiodiagnosis, 20: 40751
use of scintillation, for blood vessel visualization, 20: 40752

GAMMA DECAY
polarization and gamma-gamma angular correlations for energy-level transitions, (E), 20: 42381

GAMMA RADIATION
absorption by gases, analysis by, 20: 40828
absorption in rock, determination of density by, (E), 20: 41154
angular correlations of, effects of environment on γ-γ, (T), 20: 42303
attenuation by lead, 20: 41197(R) (NP-16172)
attenuation in concretes, measurements for cobalt-60, 20: 42519
attenuation in shielding materials, coefficients for, 20: 42518
coincidence measurements of, semiconductor-scintillation system for, 20: 41295
cutaneous reaction to, in cobalt-60 radiotherapy of female genital cancer, 20: 40679
detection and analysis of cosmic, research programs on, (E), 20: 41667(R) (MIT-2098-251, pp 1-13)
detection and measurement of fallout, 20: 41180 (AD-635822)
detection and measurement in sea water, development of immersible scintillation probe for, 20: 41147
detection and measurement of, from deposited cobalt-60 in lungs, 20: 41190 (CONF-660621-4)
detection of 500- to 1500-kev, efficiency of germanium detectors for, 20: 41288
detection of, computer analysis for scintillation detector pulse height spectra for, 20: 41292
detection of, design and performance of diamond scintillation detector for, 20: 41290
detection of, design and performance of gas-filled image intensifier spark chamber for, 20: 41289
detection of, directional correlation coefficients for, 20: 41371
detection using lithium-drifted germanium detectors, temperature dependence of response of, 20: 41273 (ORNL-TM-1295)
dose distribution at soil surface, 20: 40518 (CEX-63.10)
dose distributions for uterine carcinoma, 20: 40769
dose effects of, on free radical yield in nucleic acid irradiation, 20: 40593
dose effects on animal behavior, 20: 40519 (NP-16259)
dose measurement determination for pulmonary tissue, 20: 40760
dose rate survey following KIWI-TNT destruct excursion, 20: 41195 (LA-3519)
dose response to lethal, in mice, 20: 40687
dosimetry for therapy, 20: 40787
dosimetry in intracavitary therapy, design and use of system for, 20: 41377
dosimetry in mouse phantoms, 20: 41268(R) (NYO-2740-3, pp 5-165)
dosimetry of, performance of small wall-less tissue equivalent proportional detector for, 20: 41268(R) (NYO-2740-3, pp 5-165)
dosimetry using silver activated metaphosphate glass rods, 20: 40734(R) (NYO-901-54, pp 24-5)
effects of polymerization of nitroethylene, 20: 40981
effects of, combined with heat treatments on yeasts, 20: 41387
effects of, combined with trenimon on HeLa cells, 20: 40704
effects of, combined with mitomycin on cancer, bone marrow transplants for hematopoietic injuries from, 20: 40726
effects on acute lymphatic, use in leukemia, radiotherapy, 20: 40720
effects on alkane glasses, charge recombination in, 20: 40970
effects on amino acids in deoxyribonucleohistone and histone solutions, 20: 40585
effects on ammonium hexafluorophosphate, ESR studies of, 20: 40956
effects on aromatic and simple fluorocarbons, mechanism and yields of products in, 20: 40948(R) (COO-578-3-32)
effects on arsine and phosphines, ESR of free radicals from, 20: 40967
effects on barley, genetic, effects of chronic dose rate on, 20: 40716
effects on binding of histone to DNA in deoxynucleohistone, 20: 40586
effects on carbon dioxide, mechanism of, 20: 40996
effects on chickens, determination of lethal dose of, 20: 40693
effects on chloromethanes in cyclohexane, transfer mechanism in, 20: 40957
effects on codimerization of methallyl chloride with unsaturated compounds, 20: 40971
effects on constituents of wheat flour, 20: 40599
effects on culture media, effects of *E. coli* of, 20: 40580 (NYO-2804-8)
effects on cyclohexene–phosphorus trichloride, effects of temperature on yields of products in, 20: 40947 (BMwF-FBK-66-14)
effects on cyclohexane, effects of sulfur on yields in, 20: 40990
effects on cytology and function of human salivary glands following radiotherapy with cobalt-60, 20: 40644
effects on deoxyribonucleic acid, electron spin resonance studies of, 20: 40594
effects on DNA metabolism in *Escherichia coli*, tracer study, 20: 40620 (NYO-2804-9)
effects on electron spin resonance in lettuce seeds, effects of hydration on, 20: 40631(R) (ORNL-3922, pp 161-6)
effects on eye tissues in monkeys, 20: 40646
effects on eyes following therapy of canthus and eyelid carcinomas, effects of dose on, 20: 40689
effects on film-insulated magnet wire, 20: 41503
effects on fish, biological, 20: 40611(R) (COO-1421-2)
effects on food selection by carp, 20: 40656
effects on foot and mouth disease virus in tissues of infected animals, 20: 41392
effects on free radical induction in frozen ammonia and hydrogen peroxide solutions, ESR spectral studies on, 20: 41001
effects on frozen aqueous solutions of carbon dioxide, carbonates, formate, and formic acid, ESR spectral studies on, 20: 40994
effects on germanium hydride, methane, silicon hydride, and tin hydride, ESR studies of, 20: 40968
effects on germinal selection in Drosophila germ cells, 20: 40670
effects on graft polymerization of cotton fabric to methyl methacrylate and styrene mixtures with monomers, 20: 40953
effects on graft polymerization of vinyl chloride to polyethylenes, 20: 40982
effects on graft polymerization of styrene to polyvinyl chloride in liquid and vapor phases, 20: 40992
effects on graft polymerization of styrene to poly(vinyl chloride), 20: 40993
effects on graft polymerization of cotton cellulose to acrylonitrile, methyl methacrylate, and vinyl acetate, properties of products formed by, 20: 40995
effects on heterocyclic molecules, 20: 40950(R) (PRNC-88)
effects on human blood cell chromosomes, comparison with x ray and high energy electron effects, 20: 40665
effects on indium antimonide during tempering, 20: 42527
effects on ionic polymerization of styrene, kinetic study of, 20: 40978
effects on levels of reduced pyridine nucleotides in rat liver homogenates, 20: 40583
effects on lichen communities, 20: 40517 (BNL-9437)
effects on liquid hydrogen sulfide, effects of 2,2-diphenyl-1-picrylhydrazyl and iodine on yields in, 20: 40997
effects on liquid and vitreous 2-propanol, effects of benzophenone and naphthalene additions on, 20: 41006
effects on lysosomes from rabbit leukocytes, 20: 40685
effects on mammals, 20: 40694
effects on mechanical properties of polyoxymethylene at −30 to 150°C, 20: 41500
effects on mechanical properties of polyethylene terephthalate film, 20: 41501
effects on n-type cadmium sulfides and cadmium tellurides, 20: 41271(R) (ORNL-3875, pp 44-52)
effects on nuclear structure of rat thymocytes, 20: 40549
effects on optical stability of quartz, 20: 41502
effects on oxidation of aqueous solutions of butanol, effects of dose rate and temperature on, 20: 40983
effects on oxidation of aqueous solutions of butanol, effects of dose rate on kinetics of, 20: 40984
effects on oxidation of *p*-xylene, effects of temperature on kinetics of, 20: 41002
effects on plants, genetic, 20: 40714
effects on polyethylene, uv adsorption spectroscopy of, 20: 40964
effects on polymerization of styrene with formaldehyde, 20: 40973
effects on polymerization of carbon monoxide with ethylenimine, effects of ethylene on, 20: 40975
effects on polymerization of hexafluoropropylene at high pressure and 100 to 230°C, 20: 40976

effects on polymerization of resins, electroconductivity measurements on kinetics of, 20: 40999
effects on potassium perchlorate, ESR studies of, 20: 40969
effects on potassium sulfamate, ESR studies at 77°K of, 20: 40955
effects on radiolysis of frozen solutions of perchloric acid and sodium perchlorate, decomposition of radicals from, 20: 40960
effects on refractive properties of optical glasses and silica, 20: 41505
effects on Salmonella populations in swine meal, 20: 41394
effects on silicone polymers, in various gaseous atmospheres, 20: 40974
effects on sodium hydrogen selenite and sodium deuterium selenite, EPR studies of, 20: 40972
effects on soil and soil organisms, 20: 40637(R) (ORO-2754-7)
effects on spores of *Clostridium botulinum* type E, 20: 40699
effects on storage life and wholesomeness of sea foods, 20: 41384(R) (TID-22833)
effects on storage life of fruits, 20: 41385 (TID-23136)
effects on swine, pathological, 20: 40608 (CEA-R-3001)
effects on terphenyl, 20: 40946 (AECL-2589)
effects on tetraamminedinitritocobalt nitrate, tramminecobalt trinitrate, and sodium nitritocobaltate, mechanism of, 20: 41003
effects on the mating competitiveness of male *Trogoderma glabrum*, 20: 40673
effects on the reproduction of the olive fruit fly, 20: 40674
effects on thymidine metabolism in thyroid cell nuclei in mice, 20: 40616(R) (NYO-901-54, pp 48-50)
effects on tobacco resistance to blue mold disease, mutagenic, 20: 40613 (N-66-18147)
effects on triplet molecule and free radical formation in benzene and cyclohexane, stilbene isomerization studies of, 20: 40961
effects on ultraviolet absorption spectra of polyethylene, 20: 40963
energy transfer by, theory of, 20: 40787
enzyme inactivation by, electron spin resonance studies of, 20: 40596
flux from atmospheric nuclear explosion, radio waves produced by, (T), 20: 42046 (RM-4988)
genetic effects on peanuts, 20: 40636(R) (ORO-1747-12)
genetic effects on jute seeds, 20: 40681
health physics problems of, in well logging, 20: 41216
interactions with electrons at 17.6 Mev, cross section for Compton, (E), 20: 42213
measurement of linear distribution of, design and performance of slit-collimator for, 20: 41012
measurement of, intensity in ALRR, 20: 42681(R) (IS-1500(Sect. R))
penetration into shields in real fallout field, 20: 41201 (RRA-T55 and Summary)
personnel monitoring by test films in industrial radiography in Poland, 20: 41212
production in proton-proton interactions at 33.5 and 46 Mev, angular distribution of, (E), 20: 41882
radiological health problems of, from neutron generators, 20: 41215
radiotherapy of cervix carcinoma in pregnant women using, 20: 40761
reactions (γ,p) with carbon-12 at 21.3 and 21.6 Mev, azimuthal proton angular distribution from, (E), 20: 42251
reactions with holmium-165 at 70 Mev, charged-particle production in, (E), 20: 42214
reactions with tissues, detection of secondary emissions from, using γ cameras, 20: 41321
relative biological efficiency of, comparison with x radiation and high energy electrons, 20: 40665
RNase inactivation, single-hit effects, 20: 40515
scattering by electrons of gold, uranium, and zinc atoms at 662 kev, (E), 20: 41625
scattering in paraffin phantom, spectra of cesium-137, 20: 40792
spectra from uranium-235 fission products, (E), 20: 42170 (UCRL-70045)
therapeutic effects of, on uterine carcinoma, when combined with radium therapy, 20: 40769
use in cancer therapy in gynecology, 20: 40768
use in detection of hidden explosives, 20: 41066(P)
use in pre-surgery treatment of peritoneal tumors, 20: 40783
use in well logging during drilling, 20: 41171(P)
use of thermal-neutron-capture, to measure burnable poisons in reactor fuels, 20: 41112 (IITRI-578P11-54)

GAMMA SOURCES
use in helicopter signaling system, 20: 41221(R) (COO-1471-1)
use in measuring sediment density and concentration, 20: 41156
use in radiography, 20: 41116(P)
use in void fraction determination in two-phase flow, 20: 41111

GAMMA SPECTRA
from nuclear reactions, use in mean-life measurements, (T), 20: 42379

GAMMA SPECTROMETERS
analysis of detritus from Indian Ocean, 20: 41140
design and performance of, with sodium iodide crystal, 20: 41336
design of, for bore-hole exploration in iron ores, 20: 41166
development of lithium-drifted germanium bent-crystal, for studying fission gammas, 20: 41278 (UCRL-70000)
use for determining cesium-137 in milk, 20: 41132 (NYO-3364-20)
use in oil well prospecting, 20: 41165
use to determine activity of technetium-99m and iodine-125, 20: 40547

GAMMA SPECTROSCOPY
book: *Practical Gamma Spectrometry*, 20: 41353(T)

GAS CENTRIFUGES
design and performance of, for isotope separation, 20: 41404

GAS COOLED REACTORS
coolants for, evaluation of, 20: 42654
core access arrangement for, 20: 42590(P)
core assembly design for graphite-moderated, 20: 42598(P)
design, 20: 42603(P)
design, 20: 42604(P)
fuel element design for, self-purging, 20: 42613(P)
fuel element heat transfer near dimple braces in, 20: 41109
use in single-loop MHD Brayton cycle power plants, (T), 20: 41706

GAS FLOW
analysis of, using radiation modulation techniques, 20: 41381
magnetohydrodynamic, boundary layer in shock tube, 20: 42037 (UTIAS-115)
magnetohydrodynamic, analysis of quasi-one-dimensional, (T), 20: 41723
magnetohydrodynamic, boundary layers in crossed fields in, (T), 20: 41779
research on, 20: 42038(T) (NASA-TT-F-360)
simulation of Knudsen, Monte Carlo, 20: 42035 (IPP-2/41)

GAS FLOW (LAMINAR)
magnetohydrodynamic, theory of plane, 20: 41773

GASES
analysis of, by absorption of soft gammas, 20: 40828
detection in boiling channels, impedance method for, 20: 41103 (RT-ING-(65)7)
determination in solids, spectral isotopic, (T), 20: 41526
dynamics of system of self-gravitating particles in collisionless, in magnetic fields, (T), 20: 42041
electric discharges in, electron extraction in Penning, 20: 42507
electron beam interactions with, pressure effects on, 20: 42511
electron drift velocities in, magnetic effect on, (T), 20: 41628
electron free-free transitions in, method for calculating, 20: 41626
electron transport in low-density ionized, Monte Carlo method for calculating, 20: 42413 (NASA-TN-D-2959)
ionization coefficient measurements in, alpha-particle irradiation in, 20: 41627
radiolysis of, quasi-equilibrium theory for determining yields in, 20: 40958
reactions with solids, potential energy curves for, 20: 40796(R) (IS-1500(Sect.C))
thermodynamic properties of electron, in magnetic fields, 20: 41635
thermodynamics of modified Hartree-Fock electron, 20: 41623 (UCRL-14904)
transfer properties of, analysis of heat and momentum, 20: 41104 (UCRL-14841)
gas–solid, flow in pipes, 20: 41102 (NYO-2930-6)

GASTROINTESTINAL TRACT
anatomy study of, comparison of different ruminants, 20: 40541(R) (UCD-34P104-3)
radioinduced lesions of, in dog, x, 20: 40645

GEIGER-MUELLER TUBES
performance of self-extinguishing, 20: 41286
use in gamma survey meter, 20: 41349

GENES
characterization of *E. coli* K-12, 20: 40629(R) (ORNL-3922, pp 94-8)
effects of mutant, on germ cell formation in peas, 20: 40512
marker frequency in *Escherichia coli*, 20: 40538 (TID-23238)
radioinduced mutations in eye color changes in Mormoniella, 20: 40669
radiosensitivity of Drosophila, x, 20: 40706
recombination in Drosophila, effects of tandem duplication on, 20: 40625(R) (ORNL-3922, pp 59-64)
reversion frequency of maize, effects of ploidy on, 20: 40509 (TID-22965)
sensitivity to chemical mutagens of specific loci of Drosophila, 20: 40706

GENETICS
chromosome marking in, use for reversion frequency studies, 20: 40509 (TID-22965)
chromosome replication and exchange in bacteria, 20: 40538 (TID-23238)
effects of genotype on mineral metabolism in corn plants, 20: 40735 (NYO-2744-37)
effects of supersonic transport environment, 20: 40525
effects of x-radiosensitivity on barley, 20: 40701
gene response to x radiation and chemical mutagens, 20: 40706
radiation effects on peanuts, gamma, 20: 40636(R) (ORO-1747-12)
radiation effects and sources and their effect on human, review of,

20: 40662
radiation effects on quantitative traits of Tribolium, x, 20: 40671
radiation effects on jute in Pakistan, 20: 40681
radioinduced eye color mutations in Mormoniella, x, 20: 40669
uptake of strontium in barley and wheat, 20: 40532(R) (COO-1097-17)
GEOLOGY
bacteriogenic sulfur isotopic ratios in, 20: 41151
rock formations at Lucas Heights, 20: 41148 (AAEC-TM-316)
stable isotopes in, 20: 41380(T) (IFA-IS-36)
GEOMAGNETIC FIELDS
multiple sclerosis incidence in relation to, 20: 40639
plasma interactions with, analysis of solar wind, (T), 20: 42453
GEOMAGNETIC STORMS
properties of, solar flare effects on, 20: 42047
GERMANIUM
efficiency of detectors of, for gammas at 500 to 1500 kev, 20: 41288
electron beam interactions in n-type, voltage induction by 20-kev, (E/T), 20: 42533
helium and hydrogen ion attenuation at 0.1 to 500 Mev, tables for, 20: 41619 (CEA-R-3042)
liquid, electrotransport of solutes in, 20: 41412(R) (IS-1500(Sect. M))
lithium incorporation in, method for, 20: 41367(P)
performance of detectors of lithium-drifted, for gamma rays, 20: 41273 (ORNL-TM-1295)
production and encapsulation of detectors of lithium-drifted, 20: 41271(R) (ORNL-3875, pp 44-52)
use in gamma coincidence counters , 20: 41295
GERMANIUM ALLOYS
Ge–rare earth, crystal structure and magnetic properties of intermetallic, 20: 42552
GERMANIUM HYDRIDES
radiation effects on, in krypton at 4.2°K, ESR of free radicals from gamma, 20: 40968
GERMANIUM ISOTOPES
fractionation of, processes in, 20: 40933
separation by electromagnetic methods, 20: 41401(R) (ORNL-4006)
GERMANIUM ISOTOPES Ge-70
exchange with germanium-76 in germanium compounds, effects of temperature and binding energy on, 20: 40933
GERMANIUM ISOTOPES Ge-76
exchange with germanium-70 in germanium compounds, effects of temperature and binding energy on, 20: 40933
GLANDS
calcium distribution in mucosa of shell, 20: 40551
GLASS
Faraday rotation in crown, in megagauss fields, 20: 41515
properties of, for neutron environments, 20: 41099
radiation effects on refractive properties of optical, electron and gamma, 20: 41505
radiation effects on silicate, electron spin resonance studies of, 20: 42538
sorptive properties for cesium from aqueous sodium tetraphenylborate solutions, 20: 40915
GLASS TEXTILES
properties and testing of, for thermal insulation spacer materials, 20: 41440(R) (ALO-3632-4)
GLOBULIN
determination of ceruloplasmin in blood, by radioisotopic dilution, 20: 40844
metabolism in rats of, effects of irradiated oils in diet on, 20: 41391
use of serum, as radiation protection factor, 20: 40658
GLOVE BOXES
explosion testing of ether–nitrogen and ether–air in, 20: 41203 (UCRL-16259)
GLUCOSE
levels in blood and urine following iodine-131 therapy for diabetes-hyperthyroidism, 20: 40790
GLUTAMIC ACID
radiation effects on dry, electron spin resonance studies of, 20: 40596
GLUTATHIONE
radioprotective effects on survival in mice, x, 20: 40719(R) (ORNL-3922, pp 136)
radioprotective effects in mice of, combined with bone marrow transplants, x, 20: 40719(R) (ORNL-3922, pp 136)
GLUTEN
radiation effects on wheat flour, gamma, 20: 40599
GLYCINE
radioprotective effect on damage induced by alkylating agents, 20: 40664
GLYCOGEN
radiation effects on content of, in monkey eye tissues, γ, 20: 40646
GLYOXIME, DIMETHYL- COMPLEXES
with copper and nickel, infrared spectra of, 20: 40796(R) (IS-1500 (Sect.C))
GOATS
strontium-85 and strontium-89 excretion by, effects of dietary calcium and strontium on, 20: 40568
GOLD
analysis for copper-64 and gold-198 and silver-110 in antique coins of, by activation and gamma spectrometry, 20: 40829
content in meteorites, 20: 42064
determination in copper coins by neutron activation methods, 20: 40800 (CNAEM-35)
determination in meteorites and natural materials by thermal neutron activation, 20: 40835
determination in plutonium by carrier distillation methods, spectrographic, 20: 40814 (RFP-664)
determination in pharmaceuticals, activation, 20: 40842
determination in seawater, activation, 20: 40834
determination of, using isooctylthioglycolate, 20: 40796(R) (IS-1500 (Sect.C))
determination of, developments in resin spot tests for, 20: 40827
diffusion effects of, on crystal structure of copper–gold alloys, 20: 41412(R) (IS-1500(Sect. M))
electric conductivity of liquid, 20: 41476
gamma scattering by electrons of, at 662 kev, (E), 20: 41625
gold-197 Mössbauer effect in small crystals of, (E), 20: 42572
helium and hydrogen ion attenuation at 0.1 to 500 Mev, tables for, 20: 41619 (CEA-R-3042)
ion ranges at 10 to 100 Mev, bromine and iodine, 20: 41647
meson (μ^-) capture by, nuclear charge distribution determination from, (E), 20: 42305
proton energy losses in, (E), 20: 42363
thermal conductivity of liquid, estimation of, 20: 41477
use in seed implants for radiotherapy, 20: 40771
GOLD ALLOYS
Au–Na, solubility in sodium halide melts, 20: 40796(R) (IS-1500(Sect.C))
Au–Pr, phase studies, 20: 41412(R) (IS-1500(Sect. M))
Cu–Au, crystal structure of intermetallic compound, effects of gold diffusion on, 20: 41412(R) (IS-1500(Sect. M))
Cu–Au, oxidation by carbon dioxide at 1000°C, 20: 41458(R) (TID-23268)
Cu–Au, specific heat of intermetallic compound, 20: 41457(R) (ORO-3291-3)
GOLD ISOTOPES Au-192
beta decay, (E), 20: 42187
GOLD ISOTOPES Au-197
deuteron reactions (d,p) at 10.2 to 26.9 Mev, excitation function for, (E), 20: 42206
meson (μ^-) capture by, x-ray spectra from, (E), 20: 42306
Mössbauer effect in small crystals of gold, (E), 20: 42572
GOLD ISOTOPES Au-198
determination in antique gold coins by activation and gamma spectrometry, 20: 40829
use as gamma source in well logging, 20: 41165
use in liver scanning, 20: 40748
use of colloidal, for liver and spleen scanning, 20: 40777
GOLD ISOTOPES Au-199
energy levels, (E), 20: 42268
GONADS
effect of ovarian location on radiation exposure in gynecological examinations, 20: 40770
radiation dose to fetal, from isotope placentography, 20: 40680
radiation dose to, during radiotherapy for ovarian carcinoma, effects on pregnancy, 20: 40761
radiation dose to, during jaw radiography, 20: 40795
radiation effects on function and structure of bull testicle, single whole-body or fractionated x, 20: 40610(R) (COO-895-9)
radiation effects on lutein cells of rat ovary, x, 20: 40672
radiation effects on olive fruit fly, γ, 20: 40674
radiation effects on germ cell populations in rat testes, following exposure at birth, x, 20: 40683
radioprotective effects of cysteine on rat, x, 20: 40729
reparative effects of DNA from, on sperm of x-irradiated rat, 20: 40723
GONIOMETERS
design and fabrication of, for ALRR neutron diffractometer, 20: 42681(R) (IS-1500(Sect. R))
GRAIN GROWTH
kinetics of ledge motion in, at dislocation interfaces, 20: 41412(R) (IS-1500(Sect. M))
GRAIN STRUCTURE
effects on corrosion of chromium–nickel steel, 20: 41418(R) (GEAP-5150)
GRANITES
age of, in northwest Spain, strontium-87/-86 determination of, 20: 41153
effects of nuclear explosion on fracture permeability of, 20: 41164
radioactivity induced in, by underground nuclear explosions, (T),

20: 41068 (PNE-5006)
GRAPHITE
effects of grades of electrodes of, on carrier-distillation spectroscopy, 20: 40807 (NLCO-976)
mechanical behavior of RVD and AGOT under stress, 20: 41459 (TID-23288)
neutron scattering by, equipment for study of, 20: 41075 (AERE-R-5217)
performance in containment of tantalum at 5000°K, 20: 41414
GRAPHITE MODERATED REACTORS
core access arrangement for, 20: 42590(P)
core assembly design for gas-cooled, 20: 42598(P)
fuel element heat transfer near dimple braces in, 20: 41109
GRASS
beta activity from fallout, 20: 40579
methyl iodide deposition on, effects of meteorological conditions, tracer study, 20: 41192(R) (IDO-12053)
strontium-90 content in Finnish, 1963 and 1964, 20: 41134 (SFL-A3)
GRAVITATION
collapse of quasars, models for, 20: 41608
effects of Zero-6 on induction of chromosome aberrations in leukocytes, synergistic effects of radiation on, 20: 40635(R) (ORNL-TM-1550)
Einstein's vacuum field equations, solution using spheroidal coordinates, 20: 42086
equilibrium of relativistic configuration of particles, 20: 42091
field interactions in, Einstein equations for spin-2 massless tensor, 20: 42078
field interactions with spinor fields, 20: 42088
geodetic lines in field of, equations for, 20: 42073
graviton exchange in elementary particles interactions, 20: 41970
motion sensing gage for, 20: 41224 (EGG-1183-2078)
plasma instabilities in field of, magneto-, 20: 42422
quadrupole moment effect on sunspots and solar flares, 20: 41610
quantum theory of, relativistic, 20: 42096
relativity theory for, general, 20: 42075
theory of, research on, 20: 41803(R) (UCRL-16863)
GREAT BRITAIN
radioactivity in milk, 20: 41186 (ARCRL-15)
radioisotope uptake by aquatic organisms in, 20: 40578
GROUND WATERS
flow rates of, use of tritium in determining, 20: 41160
use of tritium in measurement of subterranean, 20: 41167
GROWTH
bone mineralization studies in fetal chickens, 20: 40558
effects of gamma-irradiated soils on plant, 20: 40637(R) (ORO-2754-7)
radiation effects on mandibular, of rats, x, 20: 40652
GROWTH FAILURE
radioinduction of pituitary hypodwarfism following radiotherapy of nasopharyngeal carcinoma, 20: 40660
GUANINE
cytosine-guanine, radioinduced tunneling and tautomeric equilibria in, 20: 40589
GUINEA PIGS
behavior response to gamma radiation, 20: 40519 (NP-16259)
enzyme assays of cerebral tissues during acute radiation syndrome, 20: 40590
radiation sickness in, gamma and x, 20: 40694
GUNDREMMINGEN POWER REACTOR
development, Oct.–Dec. 1965, 20: 42638(R) (TID-23299)

H

HAFNIUM
determination in seawater, activation, 20: 40834
determination in uranium dioxide fuel pellets, 20: 41112 (IITRI-578P11-54)
HAFNIUM ALLOYS
Co–Hf, crystal structure of intermetallic compounds, 20: 41412(R) (IS-1500(Sect. M))
Co–Hf, phase studies, 20: 41412(R) (IS-1500(Sect. M))
Cr–Hf, phase diagrams, 20: 41412(R) (IS-1500(Sect. M))
Hf–Mo, aging kinetics of, at 1300 to 1500°K, 20: 41466
Hf–Ni, crystal structure of intermetallic compounds, 20: 41412(R) (IS-1500(Sect. M))
HAFNIUM CARBIDES
hardness of cast, at 20 to 1500°C, 20: 41429(R) (USBM-RC-1249)
oxidation of cast, by air at 450 to 800°C, 20: 41429(R) (USBM-RC-1249)
HAFNIUM IODIDES
thermophysical properties at 1300 to 3000°K, (E), 20: 41762
HAFNIUM ISOTOPES Hf-178
neutron reactions (n,γ) with, hafnium-179 decay scheme from, (E), 20: 42285
HAFNIUM ISOTOPES Hf-179
decay scheme from hafnium-178 (n,γ) reactions, 20: 42285
neutron reactions (n,2n) at 14.8 Mev, activation cross section for, (E), 20: 42207
HAFNIUM ISOTOPES Hf-180
energy level transitions in, parity mixing in, (E), 20: 42225
energy level transitions in, parity mixing in 501-kev, (E), 20: 42230
neutron reactions (n,2n) at 14.8 Mev, activation cross section for, (E), 20: 42207
HAFNIUM SULFIDES
vaporization, 20: 40796(R) (IS-1500(Sect.C))
HAFNIUM SYSTEMS
C–Hf–W, creep-rupture properties of Sylvania A, 20: 41456 (ORNL-3992)
HAIR
radiation effects on, deuteron, 20: 41187 (BNL-9468)
HALDEN BOILING REACTOR
kinetics of, perturbation effects on, 20: 42630 (HPR-66)
HALIDES
chemistry of heavy metal, 20: 40796(R) (IS-1500(Sect.C))
content in meteorites, 20: 42064
HALL EFFECT
analysis of, in incompressible flow with variable conductivity, 20: 42036 (SC-RR-66-356)
HAMBURG ELECTRON SYNCHROTRON
shielding measurements, 20: 41534 (DESY-66/18)
HAMSTERS
radioinduced chromosome aberrations, from ^{3}H-thymidine, 20: 40686
HANDBOOKS AND MANUALS
book: *Data Book on Physical Properties of Materials*, 20: 41442 (CNLM-2393)
on radionuclide analysis of environmental samples, 20: 40809 (NP-16235)
on thermodynamic properties of inorganic substances, 20: 41417
HANDS
radiation effects on, in handling collimator system of 3 Mev Brown Boveri betatron, 20: 41540 (NYO-3364-7(Rev.))
HANFORD AREA (WASH.)
design of radio-telemetered meterological and radiation data network, 20: 41188(R) (BNWL-235-1)
spectral distribution of atmospheric turbulence, 1964 and 1965, 20: 41188(R) (BNWL-235-1)
HANFORD PRODUCTION REACTORS
simulation of N, dynamic analysis using analog, 20: 42660 (BNWL-SA-270)
HARDENING
theory of dispersion and precipitation, in metal-base materials, 20: 41454 (NYO-2394-22)
HARWELL SYNCHROTRON
beam inflection system for, development of electrostatic, 20: 41542 (RHEL/R-125)
HASTELLOY X
properties for high-temperature vacuum enclosure construction, 20: 41440(R) (ALO-3632-4)
HAYNES 25 ALLOY
properties for high-temperature vacuum enclosure construction, 20: 41440(R) (ALO-3632-4)
HEAD
radiotherapy of tumors of, dosimetry for x, 20: 41210
HEALTH PHYSICS
physiological data for reactor personnel, telemetering system for, 20: 41220 (BNWL-214)
problems of, in well logging, 20: 41216
problems with Cockcroft-Walton neutron generators, 20: 41215
HEART
blood circulation time in dog, measurement using phosphorus-32 and a new catheter-type micro G-M counter, 20: 40514
radiation injuries to mouse, x, 20: 40648
HEAT
measurement of radiant fluxes at window openings during burning of fallout shelters, 20: 41184 (AD-637806)
HEAT EXCHANGERS
development and testing for sodium-cooled reactors, 20: 42639(R) (UNC-5154)
HEAT-RESISTING ALLOYS
rupture mechanisms of types S590 and S816, determination by time-to-rupture tests, 20: 41445(R) (EURAEC-1622)
HEAT TRANSFER
analysis in DOR, simulation methods for, 20: 42635 (RISO-124)
coefficient of, for heat-generating solid cylinders and spheres, 20: 41106
from nickel spheres to water, 20: 42580(R) (ANL-7245, pp 60-73)
in MHD fluid in thermal entrance region, 20: 41105
of AGR fuel rods near dimple braces, 20: 41109
radiative, through absorbing boundary layer, 20: 41108
void fractions in boiling-channel, impedance method of measuring, 20: 41103 (RT-ING-(65)7)
HEAT TRANSFER SYSTEMS

cost analysis of, 20: 42632 (NAA-SR-12060)
design for MGD flow analysis, 20: 41104 (UCRL-14841)

HEATERS
development for testing thermal insulation, 20: 41440(R) (ALO-3632-4)

HEAVY WATER ORGANIC-COOLED REACTOR
design, 20: 42621 (CONF-660516-16)

HEAVY WATER REACTORS
control rod design for, to reduce flux peaking, 20: 42588(P)
design of boiling, with increased boiling surface, 20: 42602(P)
heat transfer in DOR, simulation methods for, 20: 42635 (RISO-124)
heavy water for, forcast of demand and supply to 1985, 20: 42616 (66-CNA-301)
kinetics of ESSOR, methods for analysis of, 20: 42678 (EUR-3051.e)

HELIUM
analysis for helium-3 and -4, photoelectric, 20: 40861
bremsstrahlung reactions with, mesons (π^+) production from, (E), 20: 41816
bremsstrahlung reactions below 330 Mev, meson (π^-) and (π^+) yields from, (E), 20: 41817
effective mass of positive and negative ions in liquid, (E), 20: 41664
electric conductivity in Brayton cycle MHD power generation, (T), 20: 41706
electric conductivity of cesium-seeded plasma of, (E), 20: 41772
electric conductivity of cesium-seeded plasma of, wall-radiation effects on, (T), 20: 41754
electric discharges in, high-pressure electrodeless, (E), 20: 42509
electromagnetic wave propagation in plasma of, linearly polarized, 20: 42459
electron elastic scattering by, resonance phenomena in, 20: 41641(T)
electron energy balance in cesium-seeded plasma of, (E), 20: 41772
electron excitation cross sections, (T), 20: 41654
electron free-free transitions in, method for calculating, 20: 41626
electron scattering lengths for, lower bound to reciprocal of, (T), 20: 41658
electronic recombination in afterglow plasma of, laser interferometric measurements of, (E), 20: 42469
helium and hydrogen ion attenuation at 0.1 to 500 Mev, tables for, 20: 41619 (CEA-R-3042)
ionization reaction time of cesium-seeded plasma of, wall-radiation effects on, (T), 20: 41754
positron scattering lengths for, lower bound to reciprocal of, (T), 20: 41658
potential energy integrals at 0°K of solid, (T), 20: 42123
properties as working fluid in Brayton power cycle, 20: 41398
properties as working medium in closed-cycle turbine, 20: 42654
properties of alkali-seeded plasma of, 20: 41712
proton reactions with neutral ground state of, formation of excited hydrogen atoms in, (T), 20: 41634
sound wave mode in films of liquid II, attenuated, (T), 20: 42111
use in jet compressor closed-cycle Brayton MHD systems, 20: 41753
use in low temperature spark chamber, 20: 41329

HELIUM IONS
attenuation by nuclei at 0.1 to 500 Mev, tables for, 20: 41619 (CEA-R-3042)
concentration in atmosphere, 20: 42065
destruction of doubly ionized, in confined electron beam, (E), 20: 41653
effects on human kidney cells, factors affecting RBE, 20: 40725
electron ionization of, (E), 20: 41653
production of, energy spectra from h-f ion source for, 20: 41239

HELIUM ISOTOPES He-3
attenuation by nuclei at 0.1 to 500 Mev, tables for, 20: 41619 (CEA-R-3042)
content in meteoric feldspar and pyropene, 20: 41162
determination in helium, photoelectric, 20: 40861
photon reactions (γ,2p) with, wave functions for, 20: 42228
preparation of liquid, for nuclear targets, 20: 42107
proton inelastic scattering at 30.2 Mev, energy levels from, (E), 20: 42224
reactions (He-3,$\alpha\gamma$) with oxygen-16, oxygen-15 energy-level spins and transitions from, (E), 20: 42252
reactions (He-3,α) with carbon-14, energy levels from, (E), 20: 42369
reactions (He-3,α)2α with beryllium-9, coincidence studies of, (E), 20: 42374
reactions (He-3,$\alpha\gamma$) with oxygen-16, alpha-gamma angular correlations in, (E), 20: 42383
reactions (He-3,α) with boron-11 at 1.0 to 2.15 Mev, alpha angular distributions from, (E/T), 20: 42217
reactions (He-3,α) with chromium-52 at 18 Mev, DWBA calculations for, 20: 42221
reactions (He-3,d) with nuclei, calculations using distorted-wave theory, 20: 42250
reactions (He-3,d) with calcium-42 and calcium-44 at 10 and 11 Mev, (E), 20: 42253
reactions (He-3, d) with potassium-39 at 12 Mev, calcium-40 energy levels from, (E), 20: 42257
reactions (He-3,f) with uranium-238 at 20 to 40 Mev, ternary fission in, (E), 20: 42273
reactions (He-3,n) with helium-4 at 26 Mev, beryllium-6 energy levels from, (E), 20: 42169(R) (UCRL-14744, pp 1-18)
reactions (He-3,n) with nuclei, angular distributions from, (T), 20: 42290
reactions (He-3,n) and (He-3,p) with beryllium-9, boron-11 and carbon-11 energy-level lifetimes from, (E), 20: 42234
reactions (He-3,pγ) with carbon-12, nitrogen-14 energy-level spins and transitions from, (E), 20: 42252
reactions (He-3,pγ) with carbon-12, proton-gamma angular correlations in, (E), 20: 42383
reactions (He-3,p3α) with boron-10 at 2.45 and 6.00 Mev, (E), 20: 42188
reactions (He-3,p) with beryllium-9, boron-11 energy levels from, (E), 20: 42246
reactions (He-3,p) with carbon-13 and carbon-14, energy levels from, (E), 20: 42369
reactions (He-3,p) with chlorine-35 at 11.5 Mev, argon-37 energy levels from, (E), 20: 42200
reactions (He-3,t) with iron isotopes, nickel isotopes, and zirconium isotopes at 18 Mev, (E), 20: 42334
reactions (He-3,t) with boron-10 and lithium-6 at 30 and 40 Mev, (E), 20: 42190
reactions with nuclei, approximate relations for strengths and shapes of optical potentials for, 20: 42280
use in activation analysis, review on, 20: 40806 (NAS-NS-3110)

HELIUM ISOTOPES He-4
compressibility of liquid, as function of pressure, 20: 42112
density of superfluid, near transition temperature, 20: 42122
description using collective model with breathing-mode state, (T), 20: 42245
determination in helium, photoelectric, 20: 40861
helium-3 reactions (He-3,n) at 26 Mev, beryllium-6 energy levels from, (E), 20: 42169(R) (UCRL-14744, pp 1-18)
meson (π^-) reactions (π^-,π^+4n) with, (T), 20: 42356
meson (π^+) elastic scattering at 100 to 160 Mev/c, phase shift analysis for, (E), 20: 42320
meson (π^+) inelastic scattering at 100 to 160 Mev/c, (E), 20: 42321
superfluid transition at absolute zero in, effect of attractive forces on solid-, (T), 20: 42113

HELIUM ISOTOPES He-5
energy levels $^2P_{3/2}$ and $^2P_{1/2}$ for, (E/T), 20: 42357

HELIUM ISOTOPES He-6
energy level at 1.8 Mev, de-excitation of, (E), 20: 42353

HELIUM SYSTEMS
He–Xe, energy levels of ionized, pressure effects on, 20: 42491

HEMATOPOIESIS
radiation effects on leukocyte, gamma and x, 20: 40694
role in recovery from radiation injury in endotoxin-treated mice, 20: 40732 (AD-636209)

HEMATOPOIETIC SYSTEM
effects of cancer chemo- or radiotherapy on, effects of bone marrow transplants on, 20: 40726

HEMINS
analysis for iron-59 in, of bone marrow and peripheral red blood cells, method for, 20: 40830

HEMORRHAGE
effects on bone marrow cell proliferation in x-irradiated mice, 20: 40722

HEPTANE
radiation effects on electric and photoconductivity in frozen, mechanism of, 20: 41005

2-HEPTENE
radioinduced and photoinduced isomerizatio of, effects of benzene on, 20: 40965

HETEROCYCLIC COMPOUNDS
radiolysis of, matrix isolation studies of products from gamma, 20: 40950(R) (PRNC-88)

HETEROGENEOUS REACTORS
design of boiling, with increased boiling surface, 20: 42602(P)

HEXAMETHYLENETETRAMINE
nuclear quadrupole resonance absorption in, (E/T), 20: 41648

HEXANE
radiolysis of, EPR studies of yields of stabilized charges in low-temperature, 20: 40962

2-HEXENE
radioinduced and photoinduced isomerization of, effects of benzene on, 20: 40965

HIGH TEMPERATURE SEPARATION PROCESSES
electron-beam floating zone unit for, 20: 41434

HIPPURIC ACID, *o*-IODO-, SODIUM SALTS
use as contrast material in renography, 20: 40775(T)

HISTOCHEMISTRY

enzyme determination in cerebral tissues during acute radiation syndrome, 20: 40590
HISTONES
fractionation of, methods for, 20: 40534(R) (NYO-3621-1)
HOISTS
design for PWR Core 2 fuel handling, 20: 42641 (WAPD-PWR-2213)
HOLMIUM
liquid, solubility of tantalum in, at high temperatures, 20: 41412(R) (IS-1500(Sect. M))
liquid, solubility of tungsten in, at high temperatures, 20: 41412(R) (IS-1500(Sect. M))
magnetic susceptibility of, frequency dependence of, 20: 40796(R) (IS-1500(Sect.C))
photon reactions (γ,n) with, energy spectra from, (E), 20: 42165(R) (MIT-2098-251, pp 16-20)
thermodynamic properties of, at 0°C to melting point, 20: 41412(R) (IS-1500(Sect. M))
HOLMIUM ALLOYS
Ho–Mg, thermodynamics of formation of intermetallic compounds, 20: 41412(R) (IS-1500(Sect. M))
HOLMIUM COMPLEXES
with α-methylmandelic acid, stability of, 20: 40902
HOLMIUM ISOTOPES Ho-160
decay of, dysprosium-160 energy-level transitions from, (E), 20: 42158 (JINR-P-2817)
HOLMIUM ISOTOPES Ho-165
gamma reactions at 70 Mev, charged-particle production in, (E), 20: 42214
meson (μ^-) capture by, x-ray spectra from, (E), 20: 42306
neutron radiative capture cross section from 1.0 to 19.5 Mev, (E), 20: 42332
HOLMIUM NITRATES
specific gravity of aqueous solutions of, 20: 40796(R) (IS-1500(Sect.C))
HOLMIUM OXALATES
thermal decomposition of hydrates of, differential thermal analysis of products of, 20: 40900
HOLMIUM OXIDES
analysis for rare earth impurities by neutron activation, 20: 40796(R) (IS-1500(Sect.C))
B_2O_3–Ho_2O_3, liquid immiscibility in, 20: 40910
HORMONES
effects of androgens on tumor growth, prediction by tumor uptake of phosphorus-32, 20: 40566
effects on enzyme levels in Reuber hepatomas, 20: 40506(R) (ORNL-3922, pp 168-73)
radiation effects on production of ovarian, x, 20: 40672
HUMIDITY
radiosensitivity effects of, on radioinduced electron spin resonance signals in lettuce seeds, γ, 20: 40631(R) (ORNL-3922, pp 161-6)
radiosensitivity effects on tobacco mutations, 20: 40613 (N-66-18147)
HYALURONIC ACID
depolymerization by x radiation, beta radiation and autoxidants, 20: 40591
HYDRAZINE
production by chemonuclear synthesis, 20: 40988
production of, by radiolysis of ammonia, 20: 41008(P)
HYDRAZYL, DIPHENYLPICRYL-
effects on yields in gamma radiolysis of liquid hydrogen sulfide, 20: 40997
HYDROAROMATIC COMPOUNDS
crystal structure of, determination of nonbonded potential parameters from, 20: 40796(R) (IS-1500(Sect.C))
HYDROBROMIC ACID
reactions with pertechnetate ions, paper chromatographic studies on, 20: 40918
HYDROCARBONS
carbon-11 recoil reactions in, 20: 40796(R) (IS-1500(Sect.C))
effects on parallel plate electron capture detector response, 20: 40863
radiolysis of, ion and electron processes in condensed-phase, 20: 40998
HYDROCHLORIC ACID
corrosive effects of aqueous, on stainless steel at 650°F, 20: 41418(R) (GEAP-5150)
effects on palladium–titanium alloy and Zircaloy-2, 20: 41039(R) (ORNL-3880)
solvent properties for stainless steel cladding on fuel elements, 20: 41060(P)
spectra of normal and deuterated polymers of, in solid rare gases, infrared, 20: 40895
HCl–$NdCl_3$–$PrCl_3$–TBP–H_2O, separation factors for neodymium and praseodymium in, 20: 40904
HYDROFLUORIC ACID
hydrolysis of xenon tetrafluoride oxide in, Raman spectra of products of, 20: 40906
reactions with uranium(IV) oxide to prepare uranium(IV) fluoride, fluidized-bed process for, 20: 40935(P)
HYDROGEN
bremsstrahlung reactions with, mesons (π^+) production from, (E), 20: 41816
bremsstrahlung reactions below 330 Mev, meson (π^+) yields from, (E), 20: 41817
determination in hydrogenated polyphenyls, fouling films, and terphenyl mixtures, 20: 40797 (AECL-2524)
determination in liquid sodium from recirculating test loops, 20: 41420(R) (MSAR-66-149)
diffusion in barium, 20: 41412(R) (IS-1500(Sect. M))
diffusion in thorium hydrides, 20: 42523(R) (IS-1500(Sect.P))
effects of absorbed, on ductility of type 304 stainless steel, 20: 41418(R) (GEAP-5150)
effects on chemical reactivity of uranium carbide in water vapor, 20: 40870 (NAA-SR-Memo-7310)
effects on tantalum in FRCTF, evaluation of possible, 20: 42682 (LA-3508)
effects on vanadium embrittlement, mechanisms of, 20: 41412(R) (IS-1500(Sect. M))
electron drift velocities in, magnetic field effect on, (T), 20: 41628
electron excitation cross sections, (T), 20: 41654
electron free-free transitions in, method for calculating, 20: 41626
electron impact excitation of molecular, 20: 41645
electron scattering by molecular, vibrational excitation and dissociative attachment in, (T), 20: 41657
electron scattering lengths for, lower bound to reciprocal of, (T), 20: 41658
electron-impact-induced $n \rightarrow n'$ transitions in atomic, (T), 20: 41655
exchange reactions with tritium between lactones and water, effects of triethylamine catalyst on, 20: 41017
exchange with deuterium in carbonium ion systems NMR studies on, 20: 40945
exchange with deuterium during nickel-catalyzed hydrogenation of ethylene, 20: 40942
generators of O(4,1) group for quantum-mechanical atom of, (T), 20: 41643
generators of O(4,1) group for atom of, 20: 41644
helium and hydrogen ion attenuation at 0.1 to 500 Mev, tables for, 20: 41619 (CEA-R-3042)
hydrogen ion reactions at 2 to 50 kev, charge exchange and dissociation cross sections for, 20: 41646
hydrogen ion reactions at 50 to 150 kev, proton production in, (E), 20: 41663
hyperon (Σ^-) absorption time in, (E), 20: 41799(R) (ORO-2504-96)
ionization of, by electron bombardment, 20: 40893
isotopic ratio in oil well brines, 20: 41161
magnetic susceptibility and rotational magnetic moment of molecular, (T), 20: 41659
partial functions for, Tschebyscheff approximation for, 20: 42043
positron scattering lengths for, lower bound to reciprocal of, (T), 20: 41658
production by chemonuclear synthesis, 20: 40988
production of excited atoms of, by charge exchange in ground-state atoms, (T), 20: 41634
proton reactions with, bremsstrahlung production from, (E), 20: 41916
radiation effects on catalytic chemisorption of, 20: 40989
reactions of, from gamma radiolysis of frozen solutions of perchloric acid and sodium perchlorate, ESR studies of, 20: 40960
reactions with vanadium impurities for purification, 20: 41412(R) (IS-1500(Sect. M))
scattering on metallic surfaces of atomic, ion production from, (E), 20: 42460
vapor pressures and molar volumes of liquid, tables of, 20: 40871 (NIRL-R-95)
yields in gamma radiolysis of liquid hydrogen sulfide, effects of 2,2-diphenyl-1-picrylhydrazyl and iodine on, 20: 40997
yields in gamma radiolysis of liquid 2-propanol, effects of benzophenone and naphthalene additions on, 20: 41006
HYDROGEN ION CONCENTRATION
influence of, on variability in wheat and barley growth in different soils, 20: 40532(R) (COO-1097-17)
HYDROGEN IONS
attenuation by nuclei at 0.1 to 500 Mev, tables for, 20: 41619 (CEA-R-3042)
charge exchange and dissociation cross sections for 2- to 50-kev, incident upon hydrogen and inert gases, 20: 41646
dissociation in collisions with gas molecules at 50 to 150 kev, (E), 20: 41663
electron resonances of molecular, (T), 20: 41656
interactions with nitrogen ions at 20 to 250 kev, cross sections for inelastic, (E), 20: 41666

production on metallic surfaces at 50 to 3000 ev, (E), 20: 42460
HYDROGEN PEROXIDES
electron spin resonance spectra of, 20: 42433
production by chemonuclear synthesis, 20: 40988
NH_3–H_2O_2, radioinduced free radicals in frozen solutions of, ESR spectral studies on gamma and uv, 20: 41001
HYDROGEN SULFIDES
radiolysis of liquid, effects of 2,2-diphenyl-1-picrylhydrazyl and iodine on yields in gamma, 20: 40997
HYDROGEN SYSTEMS
H–La, phase studies, 20: 41412(R) (IS-1500(Sect. M))
H–V, phase studies, 20: 41412(R) (IS-1500(Sect. M))
HYDROGEN TRITIDES
thermal diffusion of, for tritium enrichment, 20: 41168
HYDROMAGNETIC WAVES
charged particle scattering on, angular distributions from, 20: 42423
properties of nonlinear, (T), 20: 42430
HYDROXYL RADICAL
decomposition of, from gamma radiolysis of frozen solutions of perchloric acid and sodium perchlorate, ESR studies of, 20: 40960
effects on radiolysis of amino acids in deoxyribonucleohistone solutions, 20: 40585
HYPERFRAGMENTS
decay properties, (E), 20: 41911
description of ${}_{\Lambda}Be^{9}$ and ${}_{\Lambda}C^{13}$, (T), 20: 42241
production in meson (K^-) interactions in nuclear emulsions at 1.5 Bev/c, 20: 41911
HYPERONS
decay of, pole model for parity-conserving, 20: 41868
decay of, sum rule for S-wave amplitude of nonleptonic weak, 20: 41998
decays of, amplitudes for nonleptonic, 20: 41834
decays of, semiphenomenological analysis in U(12) of nonleptonic, 20: 41831
interactions with mesons (π), static bootstrap theory and Lie group for, 20: 41862
HYPERONS (Λ)
interactions with nucleons, repulsive core in S state in, (T), 20: 41894
production in meson (π^-)-proton interactions at 900 Mev, (T), 20: 41917
HYPERONS (Λ^0)
production in meson (K^-)-proton interactions at 0.9 to 1.0 Mev/c, (E), 20: 41799(R) (ORO-2504-96)
HYPERONS (Ω)
decay of, broken U(12) for leptonic, 20: 41939
HYPERONS (Ω^-)
production amplitudes for, effect of inelastic processes on, 20: 41836
HYPERONS (Σ)
decay parameters as test of $\Delta I = \frac{1}{2}$ rule, (E), 20: 41879
HYPERONS (Σ^-)
absorption time in liquid hydrogen, (E), 20: 41799(R) (ORO-2504-96)
decay of, branching ratio for $\Lambda e^{\pm}\nu$, (E), 20: 41799(R) (ORO-2504-96)
interactions with protons at 150 Mev/c, cross sections for, (E), 20: 41799(R) (ORO-2504-96)
production in meson (K^-)-proton interactions at 0.9 to 1.0 Mev/c, (E), 20: 41799(R) (ORO-2504-96)
HYPERONS (Σ^0)
decay of, test of time reversal invariance in $\Lambda e^- e^+$, (E), 20: 41799(R) (ORO-2504-96)
HYPERONS (Σ^+)
decay of, branching ratio for $\Lambda e^{\pm}\nu$, (E), 20: 41799(R) (ORO-2504-96)
interactions with protons at 161.5 Mev/c, cross sections for, (E), 20: 41799(R) (ORO-2504-96)
production in meson (K^-)-proton interactions at 0.9 to 1.0 Mev/c, (E), 20: 41799(R) (ORO-2504-96)
HYPERTHYROIDISM
association with diabetes, use of iodine-131 therapy in, 20: 40790
chemotherapy for, bone marrow transplants for agranulocytosis induced by, 20: 40726
radiotherapy with iodine-131 and surgical treatment of, comparison of, 20: 40785
HYPOTHYROIDISM
myxedema following x radiotherapy of laryngeal cancer, 20: 40780

I

IGNEOUS ROCKS
age of southwest Montana, determination of, 20: 41163
analysis for bromine, activation, 20: 40811 (ORO-2670-13)
radioactivity induced in, by underground nuclear explosions, (T), 20: 41068 (PNE-5006)
uranium minerals in, in Sweden, 20: 41172
IMAGE BRIGHTNESS INTENSIFIERS
use of, in television monitoring of x-ray fluoroscopy, 20: 40781
IMMUNE REACTIONS
radiation effects on rat tumor graft, electromagnetic, 20: 40661
response of mice to tumor transplants after previous implantation and x-radiation cure, 20: 40643
tolerance induced by hybrid spleen cells in parental strain mice, 20: 40651
IMPACT SHOCK
use in materials testing, remotely operated equipment for, 20: 41113
IN-PILE LOOPS
instrumentation for potassium, 20: 42585(R) (ORNL-3875, pp 151-8)
instrumentation for liquid-potassium jet-pump test, 20: 42585(R) (ORNL-3875, pp 151-8)
instrumentation for pressurized water, 20: 42585(R) (ORNL-3875, pp 151-8)
INCONEL
properties of 600 and 625, for high-temperature vacuum enclosure construction, 20: 41440(R) (ALO-3632-4)
INDENE, 1-(4-DIMETHYLAMINOBENZYLIDINE)-
metabolism in rats, 20: 40632(R) (ORNL-3922, pp 175-91)
INDEXES
of conferences relating to nuclear science, 20: 42693 (TID-4043 (Rev.3))
INDIA
marine organisms off west coast of, trace element uptake by, 20: 40572
uptake of radioisotopes by marine invertebrates, 20: 40528
INDIAN OCEAN
carbon-14 content of deep and surface waters of, 20: 41127
measurements of radioactivity in, 20: 41147
radioisotope distribution in, 20: 41140
trace element content in sea water from, uptake by marine organisms, 20: 40572
INDIUM
determination in copper coins by neutron activation methods, 20: 40800 (CNAEM-35)
determination in plutonium by carrier distillation methods, spectrographic, 20: 40814 (RFP-664)
electron beam attenuation in thin films of, 20: 41621 (ORNL-TM-1565)
mechanical forces on superconducting, magnetic field effects on, (E), 20: 42134
meson (μ^-) capture by, x-ray spectra from, (E), 20: 42306
photon reactions (γ,n) with, energy spectra from, (E), 20: 42165(R) (MIT-2098-251, pp 16-20)
proton reactions at 200 and 400 Mev, formation cross section and half life of silver-101 yields in, 20: 42179
vaporization rates from molten, 20: 41064(R) (IS-1500(Sect.E))
INDIUM ALLOYS
Bi–In, tunneling in superconducting films of, superimposed on normal zinc films, (E), 20: 42109
In–Pb, vaporization rates from molten, 20: 41064(R) (IS-1500(Sect.E))
In–Zn, diffusion coefficients of liquid, 20: 41064(R) (IS-1500(Sect.E))
Sb–In, magnetic pinch in crystals of, population inversion in, 20: 42545
Sb–In, radioinduced defects in n-type, during tempering, 20: 42527
Sb–In, thermal conductivity of 2-Mev-electron-irradiated, 20: 42547
INDIUM ARSENIDES
thermal expansion at low temperatures, 20: 42523(R) (IS-1500(Sect.P))
INDIUM ISOTOPES In-113
neutron capture by, cross sections for production of isomeric indium-114 in fast, (E), 20: 42326
INDIUM ISOTOPES In-115
energy levels from decay of isomeric cadmium-115, (E), 20: 42260
neutron capture by, cross sections for production of isomeric indium-116 in fast, 20: 42326
neutron radiative capture cross section from 1.0 to 19.5 Mev, (E), 20: 42332
neutron reactions (n,2n) at 14.8 Mev, activation cross section for, (E), 20: 42207
INDIUM YTTRIUM SULFIDES
preparation and properties of, 20: 40879
5-INDOLOL, 3-(2-AMINOETHYL)-
radioprotective effect on damage induced by alkylating agents, 20: 40664
INDUSTRIAL HYGIENE
lung exposure from uranium process materials, 20: 41204 (Y-1544-A)
standard for handling radioisotopes, safety record from, 20: 41208
INFORMATION RETRIEVAL SYSTEMS
television replay system for medical data, 20: 40748
INFRARED RADIATION
effects on human skin, review of, 20: 40696
INFRARED SPECTROMETERS
recording systems for, design of photoelectric, 20: 41267 (MPI-PAE-P1-30/66)
INSECTICIDES
effects with carbon-14-labeled-synergists on toxicity to houseflies, 20: 41014
preparation of carbon-14-labeled agents to be used as synergists with,

20: 41014
INSECTS
effects of insecticides with carbon-14-labeled synergists on houseflies, toxic, 20: 41014
phosphorus-32 uptake by, from *E. coli* in stream ecosystems, 20: 40529
radiation effects on Tribolium pupal weight and reproductive fitness, x, 20: 40671
radiation effects on the mating competitiveness of male *Trogoderma glabrum*, γ, 20: 40673
radiation effects on the reproductive systems of the olive fruit fly, γ, 20: 40674
radioinduced chromosome aberrations in Chironomus, from waste disposal, 20: 40530
INSTRUMENTATION
design for Charpy impact testing of metals, 20: 41451(R) (GA-7101)
development for dosage control in tumor therapy, 20: 41323
development of timing and firing, for Dribble Program, 20: 41070 (VUF-3021)
electromagnetic interference in circuits of, 20: 41228(R) (ORNL-3875, pp 15-20)
fabrication and maintenance of, 20: 41229(R) (ORNL-3875, pp 21-3)
for SEFOR, development of, 20: 42629(R) (GEAP-5160)
manufacturing of isotopic and nucleonic, developments in Poland, 20: 41236
monitoring means for, 20: 41258(P)
INSTRUMENTS
book: *Nuclear Instrumentation*, 20: 41256
design and use of optical density analyzer, 20: 40502(R) (ORNL-3922, pp 115-27)
performance of radiometric, 20: 41235
radioisotope scanner with system for information storage and retrieval, 20: 40748
INSULIN
induction of tyrosine transaminase by, in rat liver, 20: 40506(R) (ORNL-3922, pp 168-73)
INTERFEROMETERS
design for phase shift measurements of three superimposed microwave beams, 20: 42408 (IPP-2/49)
INTERMETALLIC COMPOUNDS
crystal structure of magnesium–strontium, 20: 41455(R) (NYO-2731-7)
electric conductivity of molybdenum–nickel, effects of temperature on, 20: 41457(R) (ORO-3291-3)
preparation of high-purity crystals of, 20: 40874 (ORNL-RMIC-5)
INTESTINE
calcium-45 and calcium-47 absorption in a case of parathyroid adenoma, 20: 40552
injury to, following radiotherapy of uterine carcinoma, 20: 40703
radiation effects on epithelial cells of rats and amphibians, 20: 40607 (BNL-10518)
INVERTEBRATES
distribution of zinc-65 in Columbia River estuary, 20: 40523(R) (RLO-1750-8(Vol.1))
ecology of marine, in Columbia River estuary and Northeast Pacific, tracer study, 20: 40523(R) (RLO-1750-8(Vol.1))
radioactivity in Columbia River estuary and Northeast Pacific Ocean, 20: 40523(R) (RLO-1750-8(Vol.1))
IODATES
separation of xenon oxides from, by ion exchange chromatography, 20: 40851
IODIC ACID
separation from xenon oxide using zirconium phosphate, 20: 41054
IODIDE IONS
iodine-131 exchange between, and methyl iodide, 20: 40939
IODINE
determination of total, in radioactive iodide preparations, 20: 40553
distribution of, in neutron-irradiated plutonium dioxide suspensions, 20: 41009 (AERE-R-3268)
effects on yields in gamma radiolysis of liquid hydrogen sulfide, 20: 40997
helium and hydrogen ion attenuation at 0.1 to 500 Mev, tables for, 20: 41619 (CEA-R-3042)
meson (μ^-) capture by, x-ray spectra from, (E), 20: 42306
photon reactions (γ,n) with, energy spectra from, (E), 20: 42165(R) (MIT-2098-251, pp 16-20)
radiation effects on levels of dog protein-bound, x, 20: 40698
release of fission product, by reactor fuel elements, 20: 41202 (UCRL-14990)
separation from products of fission-fragment-induced radiolysis, 20: 40951 (RPI-321-6)
IODINE CHLORIDES
decomposition of ICl_3 to ICl in gas streams, 20: 41029 (BNWL-279)
IODINE IONS
ranges in materials at 10 to 100 Mev, 20: 41647
IODINE ISOTOPES
effects on metabolism of radioactive, following therapy, 20: 40659
exchange between ethyl iodide and methyl iodide, radiochromatography equipment for studies on, 20: 41019
radioactive, effects on human erythrocyte diameter and volume from occupational exposure to, 20: 40678
IODINE ISOTOPES I-125
use as tracer in thyroid metabolism studies, 20: 40547
use in labeling 2′-deoxyuridine for autoradiography, 20: 40666
IODINE ISOTOPES I-126
reactions of recoil, in irradiated potassium iodate, 20: 40796(R) (IS-1500(Sect.C))
IODINE ISOTOPES I-127
detection of, response of silicon fission chamber for, 20: 41324
energy-level transitions from Coulomb excitation by alpha particles at 3.3 Mev, (E), 20: 42186
IODINE ISOTOPES I-128
decay of, xenon-128 energy-level quantum numbers and transitions from, (E), 20: 42147 (AE-240)
IODINE ISOTOPES I-131
beta activity measurements in France, 20: 41189 (CEA-R-3020)
contamination of eggs by, penetration and internal distribution, 20: 40559
content in human thyroid gland, 20: 40570
controlled environmental deposition of, CERT program, 20: 41192(R) (IDO-12053)
conversion ratio of protein-bound, in thyroid patients, 20: 40756
determination in environmental samples, 20: 40809 (NP-16235)
determination in milk and vegetable rinses, method for, 20: 40852
determination in water, 20: 40819(T) (CEA-tr-A-1883)
determination of total iodine in preparations labeled with, 20: 40553
effects on thymidine metabolism in cell nuclei of mouse thyroid, 20: 40616(R) (NYO-901-54, pp 48-50)
exchange between methyl iodide and iodide ions, 20: 40939
morphological change induction in thyroid by, 20: 40647
production of carrier-free, by neutron irradiation of tellurium, 20: 41399 (IEA-110)
radiation dose to children from ingested, in milk, effects of season on, 20: 41192(R) (IDO-12053)
radiation effects on uptake of, by dog thyroid, x, 20: 40698
radioactivity of milk from incorporated, analytical model for, 20: 41192(R) (IDO-12053)
radioactivity of thyroid gland from incorporated, analytical model for, 20: 41192(R) (IDO-12053)
scavenging by rain and snow of stack gas, 20: 41188(R) (BNWL-235-1)
separation from gas streams, effect of volatility on, 20: 41029 (BNWL-279)
separation from uranium fission products by distillation, method for, 20: 41034 (JEN-160-DQ/I-54)
separation of carrier-free, from irradiated tellurium oxide, 20: 41026(P)
uptake by human thyroid, effects of potassium iodide on, 20: 40564
uptake by swine blood cells in vitro, effects of dietary calcium, zinc, and corn oil on, 20: 40556
use as gamma source in well logging, 20: 41165
use as tracer in renographic diagnosis of kidney function, 20: 40775(T)
use in labeling colloidal albumin for scanning agent, 20: 40777
use in lung scanning, 20: 40748
use in scintiphotography studies of lungs, 20: 40749
use in thyroid physiology studies, 20: 40555
use in thyroid scanning, 20: 40751
use in treatment of hyperthyroidism, performance compared to surgery, 20: 40785
use of albumin labeled with, for placentography, gonadal dose to fetus from, 20: 40680
IODINE ISOTOPES I-132
radiation dose to human, from isotope placentography, 20: 40680
separation from uranium fission products by distillation, method for, 20: 41034 (JEN-160-DQ/I-54)
IODINE ISOTOPES I-133
separation from uranium fission products by distillation, method for, 20: 41034 (JEN-160-DQ/I-54)
IODINE ISOTOPES I-134
separation from uranium fission products by distillation, method for, 20: 41034 (JEN-160-DQ/I-54)
IODINE ISOTOPES I-135
separation from uranium fission products by distillation, method for, 20: 41034 (JEN-160-DQ/I-54)
ION BEAMS
focusing by charged current-carrying ring, 20: 42512
separation of isotopic, shim magnet design for, 20: 41405
ION EXCHANGE
strontium, strontium-90 and calcium in soils, 20: 40520 (NP-16261)
use in trace analysis, 20: 40850
ION EXCHANGE MATERIALS

dissolution of radioactive, by alkaline potassium permanganate, 20: 41031 (DP-717)
sorptive properties for xenon oxide in iodate and periodate solutions, 20: 40851
use in analytical spot tests, 20: 40827
ION EXCHANGE PROCESSES
design for decontamination of cooling-pond waters, 20: 41061(P)
ION PUMPS
rare earth cathodes in diode, 20: 40796(R) (IS-1500(Sect.C))
ION SOURCES
design and performance of plasma, for isotope separation, 20: 41403
design of, for alternate electron or ion beam production for surface treatment, 20: 41528
development of electrodeless discharge, 20: 41251
development of lithium duoplasmatron, 20: 41571
ion energy distribution from h-f, helium, 20: 41239
IONIZATION
use for neutron dosimetry in accelerator environment, 20: 41543 (RPP-R-2)
use of chemical, in MHD conversion, (T), 20: 41730
IONIZATION CHAMBERS
current fluctuations in, produced by gamma and neutron sources, 20: 41271(R) (ORNL-3875, pp 44-52)
design and performance of gamma-compensated, for neutron detection in reactors, 20: 41360(P)
design for neutron dosimetry, 20: 41268(R) (NYO-2740-3, pp 5-165)
fabrication and testing of, 20: 41271(R) (ORNL-3875, pp 44-52)
performance for leak detection in containers for radioactive materials, 20: 41197(R)
performance for proton beam dosimetry, 20: 41268(R) (NYO-2740-3, pp 5-165)
stability testing of, 20: 41268(R) (NYO-2740-3, pp 5-165)
use for dosimetry of electron beams, 20: 40741(R) (ACRH-25, pp 15-23)
IONOSPHERE
cosmic noise absorption in F region of, 20: 42048
disturbances in E-region, activities from, 20: 42059
electromagnetic wave absorption during solar eclipse, measurement of, 20: 42051
electromagnetic wave absorption during solar eclipse, measurement of, 20: 42052
electromagnetic wave propagation in, WKB approximation for, (T), 20: 42404 (IC-66/45)
electromagnetic wave propagation in, collision frequencies for, (T), 20: 42452
electron density determination in, using Faraday effect, 20: 42049
electron density in, detection by radio-wave absorption during solar eclipse, 20: 42053
electron density in F2 region of, correlation of electromagnetic pulsations with, 20: 42054
electron distribution above peak of F region, 20: 42065
electron production and losses in F1 region, at summer solar minimum, 20: 42058
electron temperature in, measurements summary of, 20: 42065
exploration of, summary of advances in, 20: 42065
ionization from cosmic rays, summary of observations of, 20: 42065
plasma resonance in, measurements summary of, 20: 42065
plasma resonances on topside ionograms, interpretation of, (E/T), 20: 42063
radiation absorption in, solar flare effects on, 20: 42047
radio aurora backscattering, 20: 42057
radio-wave absorption during solar eclipse, (E), 20: 42053
sporadic E layer in, blanketing, 20: 42070
sporadic E layers of, wind shear theory of formation of temperate zone, 20: 42067
whistlers in, observed by rockets and satellites, 20: 42065
IONS
charge exchange scattering, model for, 20: 41624 (UCRL-17034)
density in ion-engine plasma, 20: 41123
effective mass of positive and negative, in liquid helium, (E), 20: 41664
monitoring of air, in closed rooms, 20: 42050
radioinduction in sulfur-containing proteins, 20: 40598
reactions of, in radiolysis of hydrocarbons, 20: 40998
sputtering of single crystals by, mechanism of, 20: 42553
IRIDIUM
determination in meteorites and natural materials by thermal neutron activation, 20: 40835
IRIDIUM ALLOYS
Ir–Rh, air oxidation testing of, 20: 41396(R) (STL-517-0042)
IRIDIUM COMPLEXES
deuterio-hydride, preparation and structure of, 20: 40883
IRIDIUM FLUORIDES
preparation and evaluation for electromagnetic separation of iridium isotopes, 20: 41400 (ORNL-3301(Suppl.1))
IRIDIUM ISOTOPES
separation of, preparation of iridium fluorides for electromagnetic, 20: 41400 (ORNL-3301(Suppl.1))
IRIDIUM ISOTOPES Ir-192
conversion electron spectra of, (E), 20: 41354
determination in water, 20: 40819(T) (CEA-tr-A-1883)
IRON
analysis for tungsten, activation, 20: 40818 (UJV-1368)
analysis of, for silicon, equipment used in activation methods for, 20: 40848
carburization of, effects of impurities on vacuum, 20: 41412(R) (IS-1500 (Sect. M))
content in sea water from Indian Ocean, uptake by marine organisms, 20: 40572
determination in americium and plutonium by spark-source mass spectrography, 20: 40816 (RFP-699)
determination in plutonium by carrier distillation methods, spectrographic, 20: 40814 (RFP-664)
determination in seawater, activation, 20: 40834
determination in uranium trioxide by emission spectrography, 20: 40802 (HW-65402(Rev.1))
determination in uranium(IV-VI) oxides, effects of graphite electrode grade on carrier-distillation spectroscopic, 20: 40807 (NLCO-976)
determination in uranium by atomic absorption spectrophotometry, 20: 40815 (RFP-698)
determination of, developments in resin spot tests for, 20: 40827
deuteron elastic scattering at 13.6 Mev, optical model analysis of, (T), 20: 42294
effects on electrodeposition of actinides from isopropyl alcohol solutions, 20: 41010 (DP-1048)
effects on phase transformations in gallium–plutonium alloy and plutonium, differential thermal analysis of, 20: 41452 (MLM-1172)
effects on reflectance of zirconium oxides, 20: 41486
effects on sorption of cerium and yttrium by soil, 20: 40914
helium and hydrogen ion attenuation at 0.1 to 500 Mev, tables for, 20: 41619 (CEA-R-3042)
influence of, content of soils on wheat and barley growth variations, 20: 40532(R) (COO-1097-17)
magnetic fields in low-temperature, De Haas-Van Alphen effect from, 20: 42523(R) (IS-1500(Sect.P))
neutron differential reflection by slabs of, thermal, (E/T), 20: 42142 (NP-16234)
performance as neutron threshold detector in presence of x rays, 20: 41333
radiation effects on antifriction and strength properties of cast, neutron, 20: 41498
separation of protactinium from, by selective dissolution, 20: 41044
separation of silver from, by cation exchange chromatography, 20: 40847
use in multilayer enclosure shields in real fallout field, 20: 41201 (RRA-T55 and Summary)
Al–Fe, tensile properties of intermetallic compound, 20: 41412(R) (IS-1500(Sect. M))
IRON ALLOYS
Al–Fe, elastic properties of iron-base single-crystal, 20: 41412(R) (IS-1500(Sect. M))
Al–Fe, spin-wave stiffness, neutron-diffraction analysis of, (E), 20: 42559
Fe–Ni–Sc, crystal structure of Laves phases in, 20: 41412(R) (IS-1500 (Sect. M))
Fe–Pd, hyperfine field distribution at iron nuclei, Mössbauer measurement of, (E), 20: 42571
Fe–Ti, oxidation by carbon dioxide–monoxide mixtures at 900 to 1100°C, mechanisms of, 20: 41458(R) (TID-23268)
Ga–Fe, spin-wave stiffness, neutron-diffraction analysis of, (E), 20: 42559
IRON CARBONYLS
molecular structure, 20: 40796(R) (IS-1500(Sect.C))
IRON CHLORIDES
corrosive effects on steels, effects of impurities on, 20: 41418(R) (GEAP-5150)
corrosive effects on irradiated stainless steels, 20: 41418(R) (GEAP-5150)
IRON COMPLEXES
use in scintiphotography of kidney, 20: 40750
IRON(III) HYDROXIDES
use in separation of phosphorus-32 from sulfur-35, 20: 41049
IRON ISOTOPES
helium-3 reactions (He-3,t) at 18 Mev, (E), 20: 42334
proton reactions at 14.5 Mev, total cross sections for, (E), 20: 42162 (LA-DC-8075)
IRON ISOTOPES Fe-54
deuteron reactions (d,p) with, iron-55 energy levels from, (T), 20: 42201

helium-3 reactions (He-3,t) at 18 Mev, (E), 20: 42334
IRON ISOTOPES Fe-55
autoradiography of erythropoietic cells labeled with, 20: 40675
energy-level structure of, calculations using shell model with configuration mixing, (T), 20: 42201
IRON ISOTOPES Fe-56
energy levels, (E), 20: 42256
helium-3 reactions (He-3,t) at 18 Mev, (E), 20: 42334
proton elastic scattering at 30 Mev, optical-model analysis of, (T), 20: 42255
proton reactions at 30 Mev, optical-model analysis of total cross sections for, (T), 20: 42255
IRON ISOTOPES Fe-57
energy-level transitions in, parity nonconservation in 14.4-kev, (E), 20: 42322
helium-3 reactions (He-3,t) at 18 Mev, (E), 20: 42334
IRON ISOTOPES Fe-59
autoradiography of erythropoietic cells labeled with, 20: 40675
determination in hemin in bone marrow and peripheral red blood cells, method for, 20: 40830
effects of x ray and L-methionine sulphoximine on metabolism of, in rat blood, 20: 40561
radiation effects on intestinal uptake in rats, x, 20: 40607 (BNL-10518)
uptake by mouse spleen, use in assessing radiosensitivity of marrow cells, 20: 40634 (ORNL-P-2312)
uptake by swine blood cells *in vitro*, effects of dietary calcium, zinc, and corn oil on, 20: 40556
use for measurement of x irradiated rat erythropoiesis, 20: 40603 (AD-635086)
IRON ORES
bore-hole exploration of, design of gamma spectrometer for, 20: 41166
IRON OXIDES
phase studies, 20: 41458(R) (TID-23268)
thermodynamic properties of wüstite, at 950 to 1250°C, 20: 41458(R) (TID-23268)
IRON(III) OXIDES
sintering mechanisms of, 20: 41064(R) (IS-1500(Sect.E))
IRON SILICIDES
deformation of single-crystal, mechanism of, 20: 41412(R) (IS-1500 (Sect. M))
deformation of, interactions of superlattices in, 20: 41412(R) (IS-1500 (Sect. M))
IRON SULFIDES
corrosive effects of aqueous, on stainless steel at 650°F, 20: 41418(R) (GEAP-5150)
IRON SYSTEMS
C–Fe, precipitates in, crystal structure and growth of, 20: 41412(R) (IS-1500(Sect. M))
concretes–Fe, neutron attenuation in, 20: 42517
Fe–H_2O, neutron attenuation in, 20: 42517
Fe–Si, elastic properties of iron-base single-crystal, 20: 41412(R) (IS-1500(Sect. M))
IRRADIATION FACILITIES
conveyor belt design for, 20: 41077 (INR-696/I/PL)
description of IAN-R1 reactor, 20: 42679 (IAN-R-1)
design of swimming pool reactor, for large-scale irradiations, 20: 42685(P)
development of ALRR fast neutron, 20: 42681(R) (IS-1500(Sect. R))
dosimetry of fast neutron, for chronic exposure of mice, 20: 40504(R) (ORNL-3922, pp 146-60)
window design for electron accelerator, 20: 41574(P)
IRRADIATION TECHNIQUES
for blood and lymph, extracorporeal, 20: 40744 (BNL-10403)
ISOQUINOLINE
radiolysis of, yields in, 20: 40991
thermal decomposition, 20: 40991
ISOQUINOLINE, 3-METHYL-
radiolysis of, yields in, 20: 40991
thermal decomposition, 20: 40991
ISOTOPE EFFECTS
of deuterium and carbon-13 on methyl iodide solvolysis, calculation of force constants for kinetic, 20: 40939
of deuterium on ESR spectra of irradiated sodium acid selenites, 20: 40972
ISOTOPE SEPARATION METHODS
book: *Radioactive Isotopes in Chemical Research*, 20: 41027
design of ALRR electromagnetic separator, 20: 42681(R) (IS-1500 (Sect. R))
thermodynamic regularities in, by exchange, 20: 40924
ISOTOPES
use in implant therapy, dosimetry studies, 20: 40746(R) (NYO-3510-2)
ISOTOPIC EQUILIBRATION
use in analysis, errors in direct or inverse, 20: 40831
use in spectral determination of gases in solids, 20: 41526
ISOTOPIC EXCHANGE
between bromide and tetrabromoplatinate ions, 20: 40796(R) (IS-1500 (Sect.C))
between germanium compounds, effects of temperature and binding energy on, 20: 40933
thermodynamic regularities in reactions of, 20: 40924

J

JAPAN
fallout monitoring, 1962 and 1964, 20: 41138
JAWS
radiography of, dose to gonads during, 20: 40795
JUTE
radiation effects on seeds, mutation studies, gamma, 20: 40681

K

KAOLINITES
adsorption of zinc-65 on, in salt-marsh ecosystems, 20: 40573
phosphorus-32 adsorption on, in salt-marsh ecocystems, 20: 40573
KIDNEYS
radiation effects on cells from human, effects of fractionated doses on particulate, 20: 40725
radiation injury of subcutaneous, following therapy, 20: 40659
radioisotope renography using Hippuran, 20: 40775(T)
reparative effects of DNA from, on sperm of x-irradiated rat, 20: 40723
scanning of, using radioisotopes, 20: 40757
use of pertechnetate in renal scanning, 20: 40750
zinc-65 content in rat, effects of dexamethasone and prednisolone on, 20: 40563
KRYPTON
electric discharges in, high-pressure electrodeless, (E), 20: 42509
ionization of, cross sections for shock-produced, 20: 40896
potential energy integrals at 0°K of solid, (T), 20: 42123
properties as working fluid in Brayton power cycle, 20: 41398
scattering on beryllium–copper alloys and nickel at 5 to 25 kev, secondary electrons from, 20: 41620 (NIJS-R-471)
KRYPTON ISOTOPES Kr-85
use in temperature mapping of turbine blades, 20: 41114

L

LA CROSSE BOILING WATER REACTOR
pressure vessel fabrication and installation, quality control of, 20: 42637 (SWRI-1228-7-33)
LABORATORIES
development and standardization in UK, 20: 41098
safety guide for radiochemical, 20: 41199 (ORNL-TM-626)
LABORATORY EQUIPMENT
design and use of silicone cage, for polycythemia induction in mice, 20: 40718(R) (ORNL-3922, pp 99-105)
design of, to study graphite scattering of neutrons, 20: 41075 (AERE-R-5217)
development of, for Transuranium Processing Plant, 20: 41039(R) (ORNL-3880)
fabrication and operation of deuterium and proton accelerators-dischargers, 20: 41545(T) (AD-631586)
LACTATES
effects on disproportionation of uranium(V), 20: 40911
LACTIC ACID, 2-METHYL-
use in thin-layer high-voltage electrophoresis of rare earths, 20: 41046
LACTONES
hydrogen-tritium exchange reactions between water and, effects of triethylamine catalyst on, 20: 41017
preparation of tritium-labeled, effects of triethylamine catalyst on, 20: 41017
LAMPREYS
phosphorus-32 uptake by, from *E. coli* in stream ecosystems, 20: 40529
LANTHANUM
atomic structure of, calculation of Hartree-Fock parameters for, 20: 41631
determination in cerium oxide by paper chromatography and photometry, 20: 40859
determination in steel, procedure for, 20: 41415
determination of, in aqueous solutions, using Complexone III and Xylenol Orange, 20: 40860
determination of, in uranium by neutron activation methods, 20: 40832
liquid, solubility of tantalum and tungsten in, at high temperatures, 20: 41412(R) (IS-1500(Sect. M))
magnetic susceptibility of, high temperature, (E), 20: 42544
photon reactions (γ,n) with, energy spectra from, (E), 20: 42165(R) (MIT-2098-251, pp 16-20)

preparation of high-purity, by calcium reduction of fluorides of, 20: 41412(R) (IS-1500(Sect. M))
solubility in lutetium at 500°C, 20: 41412(R) (IS-1500(Sect. M))
superconductivity of, effects of crystal imperfections on, 20: 41412(R) (IS-1500(Sect. M))
La–$LaCl_3$, viscosity of, effects of temperature on, 20: 40925

LANTHANUM ALLOYS
Ag–La, superconductivity of, effects of pressure on, 20: 42101
La–Mg, thermodynamics of formation in intermetallic compounds, 20: 41412(R) (IS-1500(Sect. M))

LANTHANUM ALUMINATES
preparation of monocrystals of, with perovskite structure, 20: 40920

LANTHANUM BORIDES
electric conductivity of nitrogen-powdered, (T), 20: 41713
interactions with gas flow in MHD generators, 20: 41738

LANTHANUM CHLORIDES
preparation by lanthanum oxide reactions with carbonyl chloride, 20: 41412(R) (IS-1500(Sect. M))
spectra of trivalent curium-244 in, absorption and emission, 20: 40891
viscosity of, effects of temperature on, 20: 40925
La–$LaCl_3$, viscosity of, effects of temperature on, 20: 40925

LANTHANUM COMPLEXES
with mandelic acid, stability of, 20: 40902
with sulfosalicyclic acid, effect of, on absorption spectra of erbium and neodymium complexes, 20: 40926

LANTHANUM FLUORIDES
fluorine-19 NMR in monocrystal of, anisotropy of, 20: 42528
spin-lattice relaxation of rare earth ions in, at 1.3 to 5°K, 20: 42540

LANTHANUM IODIDES
electric and magnetic properties of $LaI_{2.42}$, 20: 40796(R) (IS-1500 (Sect.C))

LANTHANUM ISOTOPES La-140
beta activity measurements in France, 20: 41189 (CEA-R-3020)

LANTHANUM NITRATES
binding energies in, infrared spectral studies of hydrated, 20: 40886

LANTHANUM OXALATES
thermal decomposition of hydrates of, differential thermal analysis of products of, 20: 40900

LANTHANUM OXIDES
B_2O_3–La_2O_3, liquid immiscibility in, 20: 40910

LANTHANUM SILICATES
preparation of $La_2O(SiO_4)$ monocrystals, 20: 40919

LANTHANUM SYSTEMS
H–La, phase studies, 20: 41412(R) (IS-1500(Sect. M))

LARVAE
method for producing Mormoniella diapause, 20: 40582(R) (ORNL-3922, pp 65-8)

LARYNX
radiotherapy of carcinoma of, 20: 40759
radiotherapy of cancer of, myxedema development following x, 20: 40780
treatment of tumors of, by radiation and methotrexate, 20: 40782

LEAD
content in Toluca iron meteorite, 20: 42062
determination in americium and plutonium by spark-source mass spectrography, 20: 40816 (RFP-699)
determination in plutonium by carrier distillation methods, spectrographic, 20: 40814 (RFP-664)
electron reactions at 6 to 25 Bev, mesons (μ) production in, (E), 20: 41805(T) (SLAC-Trans-46)
gamma attenuation in, 20: 41197(R) (NP-16172)
heat of fusion, 20: 41412(R) (IS-1500(Sect. M))
helium and hydrogen ion attenuation at 0.1 to 500 Mev, tables for, 20: 41619 (CEA-R-3042)
meson (μ^-) capture by, nuclear charge distribution determination from, (E), 20: 42305
neutron differential reflection by slabs of, thermal, (E/T), 20: 42142 (NP-16234)
neutron reactions at 14.7 Mev, gamma emission in, (E), 20: 42146 (AD-638014)
neutron scattering at low energy, neutron polarization in, (E), 20: 42140 (JINR-P-2764)
preparation of single crystals of, 20: 41064(R) (IS-1500(Sect.E))
radioinduced cascade showers at 1 Bev in, 20: 41671
separation from tin by reversed-phase chromatography, 20: 40796(R) (IS-1500(Sect.C))
use in shielding against gamma radiation, 20: 40518 (CEX-63.10)
use of liquid, as cathode in electrolysis of LiCl–KCl–UCl_3 melt, 20: 40923
vaporization rates from molten, 20: 41064(R) (IS-1500(Sect.E))

LEAD ALLOYS
Bi–Cd–Pb–Sn, magnetic flux penetration in superconducting, (E), 20: 42132
Bi–Pb, extraction of cadmium from, 20: 41064(R) (IS-1500(Sect.E))
Bi–Pb, wetting reactions with stainless steel, 20: 41064(R) (IS-1500 (Sect.E))
Eu–Pb, phase diagrams, 20: 41412(R) (IS-1500(Sect. M))
Gd–Pb, phase studies, 20: 41412(R) (IS-1500(Sect. M))
In–Pb, vaporization rates from molten, 20: 41064(R) (IS-1500(Sect.E))
Pb–Na, solubility in sodium halide melts, 20: 40796(R) (IS-1500(Sect.C))
Pb–Tl, magnetic susceptibilities of, 20: 41412(R) (IS-1500(Sect. M))
Pb–Tl, magnetization of superconducting, (E), 20: 42133
Pb–Tl, superconductivity in, effects of plating on, 20: 42114
Pb–Y, phase diagrams, 20: 41412(R) (IS-1500(Sect. M))
Pb–Yb, phase diagrams, 20: 41412(R) (IS-1500(Sect. M))
Pd–Tl, elastic properties of fcc, 20: 41412(R) (IS-1500(Sect. M))
Sb–Pb, superconducting critical currents for, desolvation effects on, 20: 42099(T) (AD-636625)

LEAD CERIUM FLUORIDES
preparation, properties, and structure of, 20: 40867 (KFK-385)

LEAD FLUORIDES
solubility in double fluorides of neptunium, plutonium, thorium, and uranium, 20: 40867 (KFK-385)

LEAD ISOTOPES
content in Toluca iron meteorite, 20: 42062

LEAD ISOTOPES Pb-206
content in uranothorite and zircon, 20: 41176
meson (μ^-) capture by, isotope shift determination from, (E), 20: 42305
meson (μ^-) capture by, E2 and M1 hyperfine structure determination from, (E), 20: 42307

LEAD ISOTOPES Pb-207
content in uranothorite and zircon, 20: 41176
meson (μ^-) capture by, E2 and M1 hyperfine structure determination from, (E), 20: 42307
photon reactions (γ,n) with, energy spectra from, (E), 20: 42165(R) (MIT-2098-251, pp 16-20)

LEAD ISOTOPES Pb-208
energy-level positions and transitions in particle-hole model, (T), 20: 42205
meson (μ^-) capture by, isotope shift determination from, (E), 20: 42305
meson (μ^-) capture by, E2 and M1 hyperfine structure determination from, (E), 20: 42307
neutron reactions (n,2n) at 14.8 Mev, activation cross section for, 20: 42207
photon reactions (γ,n) with, energy spectra from, (E), 20: 42165(R) (MIT-2098-251, pp 16-20)
photon reactions at 50 Bev, circularly polarized intermediate vector boson pair production from, (E), 20: 41901
proton elastic scattering at 30 Mev, optical-model analysis of, (T), 20: 42255
proton reactions at 30 Mev, optical-model analysis of total cross sections for, (T), 20: 42255

LEAD ISOTOPES Pb-210
bone content in sarcoma patients, 20: 41191(R) (HUX-3170-1)
content in human bones and teeth, 20: 40531 (A/AC.82/G/L-1045 (Rev.1))
distribution in bone and soft tissue of radium dial painters, 20: 40621 (NYO-3086-5)

LEAD ISOTOPES Pb-211
gamma spectra, 20: 41038(R) (MLM-1325, pp 9-62)

LEAD ISOTOPES Pb-212
gamma spectra, 20: 41038(R) (MLM-1325, pp 9-62)

LEAD NEPTUNIUM FLUORIDES
preparation, properties, and structure of, 20: 40867 (KFK-385)

LEAD THORIUM FLUORIDES
preparation, properties, and structure of, 20: 40867 (KFK-385)

LEAD URANIUM FLUORIDES
preparation, properties, and structure of, 20: 40867 (KFK-385)

LEAD ZIRCONATES
performance in ferroelectric transducers, 20: 41684

LEAK DETECTORS
standards for use in testing radioactive material containers, 20: 41199(R) (NP-16172)

LEAKS
effects of urethan spray foam for sealing air, 20: 41200 (ORNL-TM-1551)

LEAVES
radiation effects on jute, gamma, 20: 40681
uptake of beta activity from fallout during growing season in Delaware, Ohio, 20: 40579

LEPTONS
interactions of, U(12) symmetry for weak, 20: 42009

LEUCINE
uptake by transfer RNA of, in adult and fetal rat liver, 20: 40506(R) (ORNL-3922, pp 168-73)

LEUKEMIA
immunity in rats to transplantable, 20: 40502(R) (ORNL-3922, pp 115-27)
prevention of x-ray-induced, in mice, 20: 40658

radiation effects on incidence in cancer patients, 20: 40745(R) (NYO-901-54, pp 29-47)
radioinduction of, in occupationally exposed persons, 20: 41207
radiotherapy of human, using tritiated thymidine, 20: 40743 (BNL-9374)
radiotherapy using extracorporeal irradiation of blood, 20: 40744 (BNL-10403)
treatment by radiation of thymus and spleen, 20: 40720

LEUKOCYTES
effects of endotoxin on numbers in irradiated mice, 20: 40732 (AD-636209)
effects of radioprotective drugs on damage induced by alkylating agents, 20: 40664
life span of frozen human, in leukopenic rats, 20: 40496(R) (NYO-1753-3)
number in blood of man, factors affecting, 20: 40612 (EUR-2711.f)
radiation effects on counts of mouse, fast neutron, 20: 40502(R) (ORNL-3922, pp 115-27)
radiation effects on human, uv, 20: 40581(R) (ORNL-3922, pp 50-1)
radiation effects on formation of, in thymus, 20: 40677
radiation effects on lysosomes from rabbit polymorphonuclear, gamma, 20: 40685
radiation effects on numbers of, in rats, mechanisms for, x, 20: 40697
radioinduced chromosome aberrations in, synergistic effects of zero-gravity, 20: 40635(R) (ORNL-TM-1550)
radioinduced sister chromatid exchanges in human, x, 20: 40628(R) (ORNL-3922, pp 89-93)
response to simultaneous ionizing and microwave irradiation, 20: 40650
separation of granulocytes from red cells by sedimentation, 20: 40496(R) (NYO-1753-3)

LEUKOPENIA
bone marrow transplants for, induced by mercazol therapy for hyperthyroidism, 20: 40726

LEVEL INDICATORS
design of molten metal and salt, 20: 41233(R) (ORNL-3875, pp 101-24)
design of resistance-type liquid metal, 20: 41233(R) (ORNL-3875, pp 101-24)
use in motion sensing systems, 20: 41224 (EGG-1183-2078)

LICHENS
radiation effects on forest communities of, gamma, 20: 40517 (BNL-9437)

LIFE SPANS
effects of irradiated-oils in rat diet on, 20: 41391
effects of jackrabbit, on population density, 20: 40494(R) (COO-1329-4)
radiation effects on mouse, effects of age at exposure on x, 20: 40633 (ORNL-P-2287)
radiation effects on mammalian, gamma and x, 20: 40694
radiation effects on gastropod, effects of age at exposure on x, 20: 40700
radiation effects on mouse, protective effects of nibufin against x, 20: 40724
radioprotective effects of cysteine on rat, x, 20: 40729

LIGHT
effects on human skin, review of, 20: 40696
production of, using radioisotopes, 20: 41393
propagation in space, Lorentz principle for, 20: 42072
propagation in space, Lorentz principle for, 20: 42073
radiation effects on rat response to, following fetal exposure, 20: 40654
reflectance by aluminum, copper and nickel foils, effects of cleaning on, 20: 41440(R) (ALO-3632-4)
response of 56 AVP photomultiplier tubes to Neher-source, 20: 41491(R) (EGG-1183-2030)

LIGHT SOURCES
design and performance of, using radioisotopes, 20: 41393

LIGHTNING
properties of ball, survey on, 20: 42420(T) (JPRS-36823)

LIGNITES
water content of, gamma-absorption determination of, 20: 41154

LIMBS
pains and paresis-like symptoms resulting from pre-surgery radiation of peritoneal lymphocysts, 20: 40783
strontium-85 uptake by fractures of, 20: 40542

LINEAR ACCELERATORS
beam current of electron, design and performance of control device for, 20: 41550
beam monitor for electron, properties of secondary emission, 20: 41266 (LAL-1028)
beam phasing for electron, method for, 20: 41582(P)
design modification and performance of Yale electron, 20: 41556
development and operation of LRL electron, 20: 41803(R) (UCRL-16863)
dosimetry system for electron, 20: 41323
shielding for NRL, effectiveness of gamma rays, neutrons and x-ray, (T), 20: 41566
use in food radiopreservation, 20: 41383 (CONF-650552)
use of simulated, for training radiographers, 20: 41548
waveguide structure with collinear termination for, design of, 20: 41583(P)

LIPIDS
radiopreservation of, effects on rats, 20: 41391

LIQUID METAL COOLED REACTORS
boiler and heat exchanger development and testing for, 20: 42639(R) (UNC-5154)
cooling system technology, 20: 42577(R) (ANL-7230)
design of 1000 Mw(e) sodium-cooled fast, evaluation of, 20: 42622 (COO-285)
development of LMFBR, 20: 42577(R) (ANL-7230)
fuel development for, 20: 42619(R) (ANL-7245, pp 1-28)
fuels and materials development for LMFBR, 20: 42651 (WASH-1065)
heat transfer system for, cost analysis of secondary sodium-steam, 20: 42632 (NAA-SR-12060)
steam generating plant for, design of, 20: 42657(P)
steam generator development for sodium, 20: 42620(R) (BAW-1280-39)

LIQUIDS
particle motion in layers of pseudo, in chemical and radiative processes, 20: 40884
radiolysis of, review of mechanisms in, 20: 40987
surface area of boiling, method for increasing, 20: 42602(P)

LITHIUM
corrosive effects on tantalum at 1200°C, 20: 42579(R) (ANL-7245, pp 29-47)
effects on conversion of radioactive wastes to glass-like solids for disposal, 20: 42690(P)
effects on crystals of cobaltous oxide and nickel oxide, 20: 41458(R) (TID-23268)
electric conductivity of liquid, 20: 41476
electron reactions at 6 to 25 Bev, mesons (μ) production in, (E), 20: 41805(T) (SLAC-Trans-46)
helium and hydrogen ion attenuation at 0.1 to 500 Mev, tables for, 20: 41619 (CEA-R-3042)
incorporation in germanium, 20: 41367(P)
properties for heat pipe uses, preparations for measurement of, 20: 41438(R) (AGN-8187)
separation from meteorites, 20: 42061
thermal conductivity of liquid, estimation of, 20: 41477
thermodynamic properties of, research on liquid and vaporous, 20: 41439(R) (AGN-8198)
use in MHD-cycle systems in space, (T), 20: 41719

LITHIUM ALLOYS
Al–Li, crystal structure of intermetallic compounds, 20: 41412(R) (IS-1500(Sect. M))
Li–Mg, electron penetration of spacecraft shielding of, (E), 20: 42520
Li–Na, density and miscibility of liquid, 20: 41455(R) (NYO-2731-7)

LITHIUM ALUMINUM SILICATES
thermoluminescence emission spectra of terbium-activated, 20: 42524 (NRL-6408)

LITHIUM AMERICIUM FLUORIDES
preparation and crystal structure of, 20: 40888

LITHIUM BORATES
thermoluminescence emission spectra of manganese-activated, 20: 42524 (NRL-6408)

LITHIUM CARBONATES
separation of fluorine-18 from irradiated, by solvent extraction using carbon tetrachloride, 20: 41021

LITHIUM CHLORIDES
LiCl–KCl, activity of uranium(III) chloride in eutectic melts of, 20: 40922
LiCl–KCl–UCl_3, polarization of uranium carbide electrode in melts of, anodic, 20: 40923
LiCl–KCl, thermodynamic properties of, calculation from phase diagrams, 20: 41412(R) (IS-1500(Sect. M))

LITHIUM CURIUM FLUORIDES
preparation and crystal structure of, 20: 40888

LITHIUM FLUORIDES
radiation effects on electric properties and unit cell volume of crystals of, x, (E), 20: 42564(T)
radioinduced color center (F_2^+) in, electron, 20: 42530
radioinduced color centers in, mechanism of formation of, 20: 42562
radioinduced color centers in, production and stability of, (E), 20: 42563
radioluminescence spectra of, 20: 42524 (NRL-6408)
thermoluminescence emission spectra of, 20: 42524 (NRL-6408)
use in dosimeters for high energy radiation, 20: 40746(R) (NYO-3510-2)
use in thermoluminescent dosimeters, 20: 41373
BaF_2–LiF–UF_4, uses as electrolyte in electrolytic recovery of scrap uranium metal, 20: 41036 (MCW-1494)

LITHIUM IODIDES
radiation effects on thallium-activated, x, (T), 20: 41344

LITHIUM IONS
production of negative, in duoplasmatrons, 20: 41571

LITHIUM ISOTOPES
content in Bruderheim and Bjurbole meteorites, 20: 42061

separation of, by countercurrent-exchange-electrolysis, 20: 41402
LITHIUM ISOTOPES Li-4
energy levels, (E), 20: 42358
LITHIUM ISOTOPES Li-5
energy levels, (E), 20: 42358
LITHIUM ISOTOPES Li-6
carbon-12 reactions (C-12,d) at 6 to 8 Mev, oxygen-16 energy levels from, (E), 20: 42329
deuteron elastic scattering at 4 to 6 Mev, excitation function at 115° for, (E), 20: 42365
deuteron reactions (d,p) at 300 kev, angular distributions for, (E/T), 20: 42399
deuteron reactions (d,n) at 0.2 to 0.8 Mev, (E/T), 20: 42210
dissociation by interaction with complex nuclei, 20: 42366
energy levels, (E/T), 20: 42351
energy levels, (E), 20: 42358
helium-3 reactions (He-3,t) at 30 and 40 Mev, beryllium-6 energy levels from, (E), 20: 42190
meson (π^-) capture below 300 Mev, gamma and neutron spectra from, (E), 20: 42314
mobility of ionic, effects of structure of lithium nitrate solution on, 20: 40930
photon reactions (γ,np) with, coincidence measurements of, 20: 42165(R) (MIT-2098-251, pp 16-20)
proton elastic scattering at 80 and 150 Mev, differential cross sections and polarizations for, (E/T), 20: 42388
proton reactions (p,n) at 11.6 and 12.6 Mev, beryllium-6 energy levels from, (E), 20: 42169(R) (UCRL-14744, pp 1-18)
proton reactions (p,d) at 156 Mev, lithium-5 energy levels from, (E), 20: 42358
proton reactions (p,t) at 156 Mev, lithium-4 energy levels from, (E), 20: 42358
reactions (Li-6,d) with boron-10, nitrogen-14 energy-level transitions from, (E), 20: 42231
reactions with aluminum-27 at 0 to 110 Mev, excitation functions for, (E), 20: 42183
scattering by tungsten-183, energy-level transitions from inelastic, (E), 20: 42186
triton reactions (t,n)2α with alpha particle energy spectra from, (E), 20: 42349
LITHIUM ISOTOPES Li-7
deuteron reactions (d,n)2α with, alpha particle energy spectra from, (E), 20: 42349
deuteron reactions (d,α) with, Q-values for, (E), 20: 42357
energy level at 5.7 Mev, excitation by neutron scattering at 14 Mev, (E), 20: 42364
lithium-7 (Li-7,d) with beryllium-9, carbon-14 energy-level transitions from, (E), 20: 42231
meson (π^-) capture below 300 Mev, gamma and neutron spectra from, (E), 20: 42314
mobility of ionic, effects of structure of lithium nitrate solution on, 20: 40930
neutron inelastic scattering at 14 Mev, excitation of 5.7-Mev level by, (E), 20: 42364
nuclear magnetic resonance spectra of, in polycrystalline lithium nitride, 20: 42175
proton elastic and inelastic scattering at 0.9 to 2 Mev, excitation functions and angular distributions for, (E), 20: 42372
proton elastic scattering at 80 and 150 Mev, differential cross sections and polarizations for, (E/T), 20: 42388
proton reactions (p,d) at 100 Mev, lithium-6 energy levels from, (E/T), 20: 42351
proton reactions (p,d) at 156 Mev, lithium-6 energy levels from, (E), 20: 42358
proton reactions (p,t) at 156 Mev, lithium-5 energy levels from, (E), 20: 42358
proton reactions (p,2p) at 155 Mev, proton energy spectra from, (E), 20: 42360
scattering by tungsten-183, energy-level transitions from inelastic, (E), 20: 42186
triton reactions (t,α_0) at 1.5 to 3.25 Mev, angular distributions for, (E), 20: 42398
LITHIUM NEPTUNIUM FLUORIDES
preparation and crystal structure of, 20: 40888
LITHIUM NITRATES
effects of structure of solution of, on mobility of ionic lithium-6 and -7, 20: 40930
LITHIUM NITRIDES
nuclear magnetic resonance spectra of lithium-7 in polycrystalline, 20: 42175
LITHIUM PLUTONIUM FLUORIDES
preparation and crystal structure of, 20: 40888
LIVER
α-ketoglutarate transaminase in rat, induced by pyridoxine, 20: 40506(R) (ORNL-3922, pp 168-73)
cells from rat, use of B-XV zonal centrifuge rotor for separating subcellular components from, 20: 40507(R) (ORNL-3922, pp 191-6)
function in rats of, effects of irradiated oils in diet on, 20: 41391
gamma mapping with digital computer, 20: 40747 (UCRL-14866)
lysosome studies on mouse, after treatment with mixed bacterial toxins and anthramycin, 20: 40736
protein synthesis in cancerous and normal trout, 20: 40632(R) (ORNL-3922, pp 175-91)
radiation effects on levels of reduced pyridine nucleotides in homogenates from rat, γ, 20: 40583
radiation effects on cells of, incubated with phytohemagglutinin, x, 20: 40588
reparative effects of DNA from, on sperm of x-irradiated rat, 20: 40723
RNA synthesis in fetal rat, 20: 40506(R) (ORNL-3922, pp 168-73)
scanning of, using radioisotopes, 20: 40757
scanning, using technetium-99m sulfide colloid, 20: 40753
soluble amino-acid-incorporating system in trout, 20: 40632(R) (ORNL-3922, pp 175-91)
transfer RNA in adult and fetal rat, uptake of leucine and phenylalanine by, 20: 40506(R) (ORNL-3922, pp 168-73)
tyrosine transaminase induction in rat, by insulin, 20: 40506(R) (ORNL-3922, pp 168-73)
use of improved scintillation scanner for radiodiagnosis, 20: 40779
use of iodine-131-labeled colloidal albumin as scanning agent, 20: 40777
LOOPS
flow in liquid metal, measurement of, 20: 41064(R) (IS-1500(Sect.E))
LOS ALAMOS MOLTEN PLUTONIUM REACTOR EXPERIMENTS
hydrogen embrittlement of tantalum in FRCTF, evaluation of possible, 20: 42682 (LA-3508)
LOS ALAMOS SCIENTIFIC LAB., N. MEX.
accelerator building and site planning at, 20: 41537(R) (LA-3587)
environs monitoring, 1965, 20: 41194(R) (LA-3516)
LOW INTENSITY TEST REACTOR
control and safety systems for, modifications to, 20: 42581(R) (ORNL-3875, pp 125-50)
experimental facilities for, pneumatic tube, 20: 42581(R) (ORNL-3875, pp 125-50)
LUMINESCENT DETECTORS
development of silver activated metaphosphate glass rod, for γ rays, 20: 40734(R) (NYO-901-54, pp 24-5)
LUNGS
absorption of tritium oxide through, 20: 41185 (AECL-2594)
carcinogenic effects of polonium-210, 20: 41191(R) (HUX-3170-1)
fibrosis following use of radiotherapy for breast cancer, 20: 40773
phantom of, preparation of masonite, 20: 41190 (CONF-660621-4)
polonium-210 content in, effects of cigarette smoking on, 20: 40531 (A/AC.82/G/L-1045(Rev.1))
radiation injury of subcutaneous, following therapy, 20: 40659
radiotherapy effectiveness for cancer of, review of, 20: 40786
radiotherapy of, effects of tissue factor on dose, 20: 40760
uranium octoxide deposition in, effects of chemical composition and particle size on, 20: 41204 (Y-1544-A)
use of improved scintillation scanner for radiodiagnosis, 20: 40779
visualization by scintiphotography, 20: 40749
LUTETIUM
determination in fission product solutions, method for, 20: 40803 (KFK-387)
determination in holmium oxides by neutron activation, 20: 40796(R) (IS-1500(Sect.C))
liquid, solubility of tantalum in, at high temperatures, 20: 41412(R) (IS-1500(Sect. M))
liquid, solubility of tungsten in, at high temperatures, 20: 41412(R) (IS-1500(Sect. M))
purification by sublimation, 20: 41412(R) (IS-1500(Sect. M))
solubility in lanthanum at 500°C, 20: 41412(R) (IS-1500(Sect. M))
thermodynamic properties of, at 0°C to melting point, 20: 41412(R) (IS-1500(Sect. M))
LUTETIUM ALLOYS
Lu–Mg, thermodynamics of formation of intermetallic compounds, 20: 41412(R) (IS-1500(Sect. M))
LUTETIUM CHLORIDES
chemical properties of aqueous solutions of, 20: 40796(R) (IS-1500 (Sect.C))
density of aqueous solutions of, 20: 40796(R) (IS-1500(Sect.C))
LUTETIUM OXALATES
thermal decomposition of hydrates of, differential thermal analysis of products of, 20: 40900
LUTETIUM OXIDES
B_2O_3–Lu_2O_3, liquid immiscibility in, 20: 40910
LYMPH
centrifugation of, extracorporeal, effects on lymphocyte content in blood

and lymph system, 20: 40744 (BNL-10403)
irradiation of, extracorporeal, effects on lymphocyte content, 20: 40744 (BNL-10403)
LYMPH CELLS
effects of antibody production on morphology of spleen, 20: 40632(R) (ORNL-3922, pp 175-91)
generation time studies using tritiated thymidine, 20: 40663
radiation effects on content in blood and lymph, extracorporeal exposure, 20: 40744 (BNL-10403)
radioprotective effects of transplants of mouse, mechanism for x, 20: 40727
LYMPH SYSTEM
cytokinetic studies on calf thoracic duct lymphoid cells using tritiated thymidine, 20: 40663
DNA and RNA synthesis in mouse, effects of estradiol on, 20: 40577
effects of extracorporeal irradiation of lymph on lymphocyte population of, 20: 40744 (BNL-10403)
radiation effects on tumors of rat, electromagnetic, 20: 40661
radiation effects on DNA and RNA synthesis in marrow-protected mice, effects of estradiol on x, 20: 40577
radiation effects on lymphomas in, incubated with phytohemagglutinin, x, 20: 40588
radiation effects on cells of, incubated with phytohemagglutinin, x, 20: 40588
radioinduced inactivation of foot and mouth disease virus in, of swine carcasses, γ, 20: 41392
radioinduced metastases in human, following therapy for breast cancer, 20: 40793
radiotherapy of lymphogranulomatosis, survival following, 20: 40784
LYSINE
separation of component rich in, from Ehrlick ascites carcinoma cells, 20: 40534(R) (NYO-3621-1)
LYSOSOMES
effects on mouse, following therapy with mixed bacterial toxins and anthramycin, 20: 40736
radiation effects on suspensions of, γ, 20: 40685
LYSOZYME
electron spin resonance signals from irradiated, 20: 40595
radioinduced inactivation of dry, 20: 40596

M

MACHINE TOOLS
mimic setter for single point tool bits on two-axis numerical control turning, 20: 41079 (RFP-666)
MACHINING
gaging device for oval-bore, 20: 41436(P)
MAGNESIUM
determination by atomic absorption spectroscopy using induction-coupled plasmas, 20: 40796(R) (IS-1500(Sect.C))
determination in americium and plutonium by spark-source mass spectrography, 20: 40816 (RFP-699)
determination in plutonium by carrier distillation methods, spectrographic, 20: 40814 (RFP-664)
determination of, in nickel base alloy by deuteron activation methods, 20: 40812 (ORO-2980-14)
effects on phase transformations in gallium–plutonium alloy and plutonium, differential thermal analysis of, 20: 41452 (MLM-1172)
effects on radioinduced color centers in lithium fluorides, (E), 20: 42563
electron beam attenuation in thin films of, 20: 41621 (ORNL-TM-1565)
heat of fusion, 20: 41412(R) (IS-1500(Sect. M))
influence of, content of soils on wheat and barley growth variations, 20: 40532(R) (COO-1097-17)
proton reactions with neutral ground state of, formation of excited hydrogen atoms in, (T), 20: 41634
radiation effects on soil content of, effects of soil type on gamma, 20: 40637(R) (ORO-2754-7)
uptake by corn plants, effects of soil fertility on, 20: 40735 (NYO-2744-37)
MAGNESIUM ALLOYS
interactions with gas flow in MHD generators, 20: 41738
Ca–Mg, heat capacity of intermetallic compound, at 4 to 287°K, 20: 41412(R) (IS-1500(Sect. M))
Ca–Mg, heat of fusion of intermetallic compound, 20: 41412(R) (IS-1500(Sect. M))
Ce–Mg, thermodynamics of formation of intermetallic compounds, 20: 41412(R) (IS-1500(Sect. M))
Dy–Mg, thermodynamics of formation of intermetallic compounds, 20: 41412(R) (IS-1500(Sect. M))
Er–Mg, thermodynamics of formation of intermetallic compounds, 20: 41412(R) (IS-1500(Sect. M))
Gd–Mg, thermodynamics of formation of intermetallic compounds, 20: 41412(R) (IS-1500(Sect. M))
Ho–Mg, thermodynamics of formation of intermetallic compounds, 20: 41412(R) (IS-1500(Sect. M))
La–Mg, thermodynamics of formation of intermetallic compounds, 20: 41412(R) (IS-1500(Sect. M))
Li–Mg, electron penetration of spacecraft shielding of, (E), 20: 42520
Lu–Mg, thermodynamics of formation of intermetallic compounds, 20: 41412(R) (IS-1500(Sect. M))
Mg–Nd, thermodynamics of formation of intermetallic compounds, 20: 41412(R) (IS-1500(Sect. M))
Mg–Pr, thermodynamics of formation of intermetallic compounds, 20: 41412(R) (IS-1500(Sect. M))
Mg–Sc, phase diagrams, 20: 41412(R) (IS-1500(Sect. M))
Mg–Sm, thermodynamics of formation of intermetallic compounds, 20: 41412(R) (IS-1500(Sect. M))
Mg–Sn, Moessbauer measurements in, 20: 41637
Mg–Sr, crystal structures of intermetallic compounds of, 20: 41455(R) (NYO-2731-7)
Mg–Tb, thermodynamics of formation of intermetallic compounds, 20: 41412(R) (IS-1500(Sect. M))
Mg–Th, thorium production from sponge, using electron-beam melting, 20: 41412(R) (IS-1500(Sect. M))
Mg–Tm, thermodynamics of formation of intermetallic compounds, 20: 41412(R) (IS-1500(Sect. M))
Mg–Zn, heat of fusion of intermetallic compound, 20: 41412(R) (IS-1500(Sect. M))
MAGNESIUM FLUORIDES
radioinduced defect clusters in, electron microscopy of, 20: 42554
MAGNESIUM ISOTOPES Mg-24
deuteron reactions (d,p) with, mechanism of, (T), 20: 42394
deuteron reactions (d,α) with, mechanism of, (T), 20: 42394
energy levels of, excited by alpha particles, 20: 42347
proton reactions (p,γ) at 0.3 to 2.1 Mev, resonance strengths for, (E), 20: 42182
MAGNESIUM ISOTOPES Mg-25
energy levels of, excited by alpha particles, 20: 42347
proton reactions (p,γ) at 0.3 to 2.1 Mev, resonance strengths for, (E), 20: 42182
MAGNESIUM ISOTOPES Mg-26
energy levels of, excited by alpha particles, 20: 42347
proton reactions (p,γ) at 0.3 to 2.1 Mev, resonance strengths for, (E), 20: 42182
proton reactions (p,γ) at 1.966 Mev, resonance strength for, (E), 20: 42198
MAGNESIUM ISOTOPES Mg-28
production in thermal-neutron fission of uranium-235, (E), 20: 42298
MAGNESIUM OXIDES
properties for high-temperature insulation of thermocouples, 20: 41461(R) (UCRL-7361(Pt.3))
sintering mechanisms of, 20: 41064(R) (IS-1500(Sect.E))
use in MHD duct walls, preparation and testing for, (E), 20: 41718
MAGNESIUM URANATES
preparation, properties, and spectra of, 20: 40901
MAGNETIC FIELDS
acceleration of superconducting solenoids in traveling, 20: 41554
charged particle motion in, radiation deceleration effects on, (T), 20: 42431
charged particle motion in axially symmetric nonstationary, (T), 20: 41558
charged-particle beam parameters in channels of, effects of channel errors on, 20: 41538 (LNF-66/29)
charged-particle motion in spatially periodic, 20: 42501
compression by explosives, energy conversion efficiency in, 20: 41086
compression devices for, noncylindrical explosive, 20: 41091
compression devices for, using explosives, 20: 41094
compression devices for, design of explosive, 20: 41095
compression in cylindrical liners, limitations of, 20: 41083
compression in explosion geometry, 20: 41093
compression of cylindrical, limitations of, 20: 41085
compression of cylindrical, diffusion limitations of, 20: 41089
compression of, devices for, 20: 41096
compression of, diffusion limitations of, 20: 41082
compression of, diffusion and surface instabilities in, (T), 20: 41090
compression of, properties of, 20: 41081
compression properties of, calculation of implosive, 20: 41088
compression techniques for metallic particle acceleration, development of, 20: 41084
design for isotopic beam separation, 20: 41405
diffusion in metals, Joule heating effects on, 20: 41087
dynamics of system of self-gravitating particles in collisionless gases in, 20: 42041
effects of megagauss, on Faraday rotation in glass and quartz, 20: 41515
effects on radio-wave transmission through plasma sheath, (T),

20: 42426
effects on shielding properties of superconducting surface sheaths, (E), 20: 42127
effects on type-I superconductors in, mechanical forces, (E), 20: 42134
effects on type-II superconductors in superconducting sheath state, (E/T), 20: 42125
effects on wave propagation in rarefied plasma, (T), 20: 42489
electric conductivity of nonhomogeneous plasma in, (T), 20: 41768
electric discharge in argon flow in, (E), 20: 41770
electron beam focusing in, outer electron trajectories in, 20: 41551
electron beam focusing in, outer electron trajectories in, 20: 41552
electron magnetic susceptibility in uniform, 20: 41635
expansion about uniform axial, for closed-line average minimum-B configuration, 20: 42455
flow of mercury in transverse, hydraulics of, (E), 20: 41774
ion beam focusing in current-carrying ring, 20: 42512
observations of stellar and solar, (E/T), 20: 41616
penetration in Type-II superconducting plates, (E), 20: 42132
plasma containment in megagauss, 20: 42434
plasma interactions with line current, analysis of, (T), 20: 42453
plasma stability in toroidal, with longitudinal fields, 20: 42402 (IAE-1149)
plasma stability in toroidal, 20: 42403 (IAE-1151)
production of large, pulse transformers for, 20: 41092
production of large, using capacitor-bank discharges, 20: 41080 (UCRL-14831)
properties of contracting gas cloud, 20: 41602
properties of interstellar, Petschek's mechanism for dissipating, 20: 41595
superconductor suspension in, force calculations for spherical, 20: 42130
topological characteristics for plasma containment, 20: 42461
use in motion sensing systems, 20: 41224 (EGG-1183-2078)
use of large pulsed, in solid state research, 20: 42526

MAGNETIC MIRROR MACHINES
plasma injection using theta-pinch device, properties of, 20: 42504

MAGNETIC MIRRORS
plasma configuration in, rarefied, (T), 20: 42458
plasma containment in, laser-produced, 20: 42415 (TID-22928)
plasma stability in, relation to toroidal confined, 20: 42402 (IAE-1149)

MAGNETIC MONOPOLES
production in cosmic radiation, (E/T), 20: 41676

MAGNETIC RESONANCE
conference on use of, to determine biological effects of radiation, 20: 40592
deoxyribonucleic acid studies using, after irradiation, 20: 40594
enzyme inactivation studies using, 20: 40596
free radical studies by, in radiation biology, 20: 40597
measurement of ENDOR of F centers in potassium chloride, 20: 42566)T)
nucleic acid studies using, qualitative and quantitative results, 20: 40593
protein studies using, after irradiation, 20: 40595
radioinduced in lettuce seeds, effects of hydration on, 20: 40631(R) (ORNL-3922, pp 161-6)
spectra of electron, of irradiated silicate glasses, 20: 42538
techniques for radiation-produced radicals, 20: 42433
use in radioprotective compound studies, 20: 40598
use in radiosensitizing compound studies, 20: 40598

MAGNETIC SUSCEPTIBILITY
measurement of metal, methods for, 20: 41455(R) (NYO-2731-7)

MAGNETO-OPTICAL ROTATION
properties in crown glass and quartz, in megagauss fields, 20: 41515

MAGNETOHYDRODYNAMIC CELLS
construction of closed-cycle potassium-seeded argon, 20: 41678 (IPP-3/40)
design, 20: 41696
design and testing of NaK and potassium, 20: 41733
design of a-c rotating machine, 20: 41749
design of E.T.L. Mark II, 20: 41714
design of pebble-bed inert-gas, 20: 41736
design of segmented-electrode amplidyne, 20: 41720
design of self-excited Faraday-type, 20: 41709
design of two-phase liquid metal, 20: 41734
design of U- and T-duct, (T), 20: 41767
design of walls and electrodes for, 20: 41726
design optimization of power plants using, (T), 20: 41765
design to eliminate pressure gradient changes with lead changes, 20: 41690(P)
efficiency and stability of large inert-gas, (T), 20: 41703
efficiency of closed-loop, with thermal nonequilibrium ionization, (T), 20: 41742
efficiency of liquid-metal injector, (T), 20: 41778
efficiency of Rankine-cycle, using "perfect thermodynamic vapor", 20: 42045
electric and hydraulic properties of oil-fired, (E), 20: 41780
electric characteristics, (T), 20: 41748
electric characteristics of JAERI, (E), 20: 41781
electric conductivity of nitrogen with suspended powder in, (T), 20: 41713
electric conductivity in plasmas of, scalar and tensor, (E), 20: 41737
electric conductivity of helium–cesium plasma in, wall-radiation effects on, (T), 20: 41754
electric conductivity of combustion gas in, (E), 20: 41758
electric current distribution in Faraday-type, (T), 20: 41700
electric current distribution in Faraday-type segmented-electrode, (T), 20: 41759
electric current density distribution in segmented-electrode, (T), 20: 41763
electric loss mechanisms in linear, operating at large Hall parameters, 20: 41787
electric potential and current at cathode of, (E), 20: 41756
electric properties of plasma in, (E), 20: 41708
electrical characteristics of combustion, under open-flame conditions, 20: 41755
electrode construction and testing for, auxiliary-arc, (E), 20: 41745
electrode development for Renardieres 8-Mw, 20: 41725
electrode protection method for, 20: 41689(P)
end losses in, (T), 20: 41776
end losses in liquid-metal variable cross section, reduction of, (T), 20: 41716
flow in ducts of, boundary-layer and impact-wave theory of, 20: 41735
flow in induction, striated, (T), 20: 41711
flow in, analysis of two-dimensional channel, 20: 41696
flow in, hydraulic approximation for, (T), 20: 41704
flow turbulence of mercury in, (E), 20: 41707
fluid flow in duct of series-flow, (T), 20: 41698
fluid switching in, (T), 20: 41724
fuel combustion with ionizing additives for, composition and thermodynamic properties of products in, (T), 20: 41785
gas flow in, boundary layer calculations for, (T), 20: 41779
ionization effects on low-temperature operation of closed-loop, nonequilibrium, (E), 20: 41747
ionization from metastable molecular states excited by fission fragments in, (T), 20: 41732
ionization in combustion chamber of, (E), 20: 41710
ionization in reaction zone of, chemical, (T), 20: 41730
ionization in, effects of excited atoms on nonequilibrium, (E), 20: 41757
ionization in, magnetically induced nonequilibrium, (E), 20: 41715
ionization in, magnetically induced, (E), 20: 41786
ionization relaxation processes in, (E), 20: 41786
magnet design for, cryogenically cooled, 20: 41727
magnet parameters for, optimalizing, (T), 20: 41746
magnets for, design of, 20: 41688
materials and structures for 200-kw, testing of, 20: 41784
materials for walls and electrodes, preparation and testing of, (E), 20: 41718
materials interaction with gas flow in, (E), 20: 41738
operation at part load in power plants, (T), 20: 41775
operation of nonequilibrium, with nonseeded argon, (T), 20: 41721
operation with jet compressors of closed-cycle, (E/T), 20: 41753
operation with two-phase liquid metal flows, 20: 41728
performance in power plants, (E), 20: 41769
performance of closed-loop, (E), 20: 41741
performance of cylindrical induction-type, (T), 20: 41694
performance of Hall-type, (E), 20: 41761
performance of induction synchronous, with modulated conductivity, 20: 41683
performance of spatially constant B/ρ-type, with energy losses, (T), 20: 41722
performance of Stanford, effects of wall leakage on, (E/T), 20: 41739
performance using oxygen enrichment, (T), 20: 41744
plasma diagnostics in, microwave interferometry for, (E), 20: 41717
plasma fluctuations effects on performance of, 20: 41692
plasma properties in explosive-driven, 20: 41686
plasma properties and flow in circular, (T), 20: 41697
power generation by, viscosity and nonequilibrium ionization effects on, 20: 41783
properties of explosive-driven, (E), 20: 41685
properties of magnetically-loaded, explosive-driven, 20: 41687
relaxation processes in nonequilibrium plasma of, (T), 20: 41766
theory of liquid-metal induction, 20: 41701
thermal loss to walls in oil-fired, by radiation, (E), 20: 41777
thermodynamics of high-temperature open-cycle, (T), 20: 41752
use in power plants, (T), 20: 41693
use in Rankine-cycle space power systems, (T), 20: 41719
use in reactor power plants, optimization of parameters for, (T), 20: 41740
use in single-loop MHD Brayton cycle power plants, (T), 20: 41706

use in steam power plants, (T), 20: 41743
MAGNETOHYDRODYNAMICS
boundary-layer flow in, effect of magnetic fields and temperatures on free laminar, 20: 42039
electric current density in quasi-one-dimensional, (T), 20: 41723
equilibrium in, axisymmetric meridional, (T), 20: 42409 (IPP-6/50)
flow in shock tubes, boundary layer, 20: 42037 (UTIAS-115)
flow of mercury, hydraulics of, (E), 20: 41774
flow of nonequilibrium plasma, (T), 20: 42454
fluid flow in, analysis of conducting incompressible, 20: 42036 (SC-RR-66-356)
fluid flow in, boundary layer for plane laminar, 20: 42044
fluid flow in, theory of plane laminar, 20: 41773
heat transfer to MHD fluid, 20: 41105
ionization of hydrocarbon combustion products, (T), 20: 41731
of system of collisionless gas with self-gravitating particles in magnetic fields, 20: 42041
plasma probe theory for, 20: 41782
power generation principles, (T), 20: 41693
research by Soviet and Latvian scientists, 20: 42042
stability of sound in nonhomogeneous plasma, (T), 20: 41764
stability of, nonuniform current and field distribution effects on, 20: 42040
thermodynamic vapor, properties of "perfect", (T), 20: 42045
MAGNETOMETERS
design and performance of transistorized autodyne, 20: 41247
design for superconducting materials, 20: 41228(R) (ORNL-3875, pp 15-20)
MAGNETOSPHERE
boundary of, magnetic-field component perpendicular to, 20: 42068
boundary of, magnetic structure on attitude of, 20: 42068
solar wind particle penetration into, (T), 20: 42069
MAGNETS
armature release in, detection device for, 20: 42583(T) (WAPD-Trans-34)
design for d-c MHD generators, (T), 20: 41746
design for MHD cells, 20: 41688
materials for 50-225 KG, 20: 41097
properties of superconducting, (T), 20: 42135
radiation effects on film-insulated wires for, gamma, 20: 41503
superconducting, transition processes in, (E), 20: 41760
MAIZE
effects of epoxybutane and methanesulfonate on, genetic, 20: 40708
metabolism of minerals in, genetic control of, 20: 40735 (NYO-2744-37)
radiation effects on genetic, neutrons, 20: 40618(R) (NYO-2740-3, pp 166-215)
radiation effects on, genetic, x, 20: 40708
reversion frequency in, effects of ploidy on, 20: 40509 (TID-22965)
uptake of calcium, magnesium, phosphorus, strontium, and zinc by hybrids of, effects of soil fertility on, 20: 40735 (NYO-2744-37)
MALEIC ANHYDRIDE
radioinduced codimerization of methyallyl chloride with, 20: 40971
MAN
carcinoma radioinduction in, 20: 41207
chromosome preparation from, semi-automatic system for, analysis, 20: 40497(R) (NYO-3400-1)
distribution of radium-226, radium-228, lead-210 and thorium-228 in radium painters, 20: 40621 (NYO-3086-5)
effects of nuclear warfare on sociological behavior in, 20: 40738
iodine-131 uptake by thyroid in, effects of potassium iodide on, 20: 40564
leukemia radioinduction in, 20: 41207
leukocyte number in blood of, factors affecting, 20: 40612 (EUR-2711.f)
myxedema in, following x radiotherapy of laryngeal cancer, 20: 40780
radiation and skin diseases, solar, review of, 20: 40696
radiation burden from fallout, in West Germany, 20: 40570
radiation dose from inhaled or ingested iodine-131-methyl iodide in, 20: 41192(R) (IDO-12053)
radiation dose from ingested iodine-131 in milk by children, effects of season on, 20: 41192(R) (IDO-12053)
radiation dose from inhaled iodine-131 in, 20: 41192(R) (IDO-12053)
radiation effects on spermatogonia in, x, 20: 40627(R) (ORNL-3922, pp 84-8)
radiation effects on leukocytes from, uv, 20: 40581(R) (ORNL-3922, pp 50-1)
radiation effects on, following therapy, 20: 40659
radiation effects on pituitary function in, following nasopharyngeal carcinoma therapy, x, 20: 40660
radiation effects on genetics of, review, 20: 40662
radiation effects on, from supersonic transport environment, 20: 40525
radiation injury on eyes of, following therapy of canthus and eyelid carcinomas, 20: 40689
radiation protection of patients during diagnostic and therapeutic radiography, 20: 40733 (ISS-66/16)
radioinduced carcinogenesis in, 20: 40659
radioinduced cytologic changes in salivary glands of, following cobalt-60 radiotherapy, 20: 40644
radioinduced sister chromatid exchanges in leukocytes of, x, 20: 40628(R) (ORNL-3922, pp 89-93)
radioisotope body-burden estimations in Brazil, 20: 40522(R) (NYO-3273-7)
radiotherapy of leukemia in, using tritiated thymidine injections, 20: 40743 (BNL-9374)
strontium-90 uptake by, factors affecting, 20: 41142
therapy of thrombocytopenia using infusions of frozen blood platelets, 20: 40496(R) (NYO-1753-3)
uranium oxide deposition in lungs of, effects of chemical composition and particle size on, 20: 41204 (Y-1544-A)
MANDELIC ACID
complexes with rare earths, stability of, 20: 40902
MANDELIC ACID, α-METHYL-
complexes with rare earths, stability of, 20: 40902
MANGANESE
addition of trace-amounts to chromium–nickel steel, method for, 20: 41418(R) (GEAP-5150)
content in sea water from Indian Ocean, uptake by marine organisms, 20: 40572
determination in americium and plutonium by spark-source mass spectrography, 20: 40816 (RFP-699)
determination in plutonium by carrier distillation methods, spectrographic, 20; 40814 (RFP-664)
effects of traces of, on corrosion of chromium–nickel steel, 20: 41418(R) (GEAP-5150)
effects on phase transformations in gallium–plutonium alloy and plutonium, differential thermal analysis of, 20: 41452 (MLM-1172)
influence of, content of soils on wheat and barley growth variations, 20: 40532(R) (COO-1097-17)
uptake by rice, effects of irrigation on, 20: 40574
MANGANESE ALLOYS
Mn–Ni–Sc, crystal structure of Laves phases in, 20: 41412(R) (IS-1500 (Sect. M))
Mn–U, corrosive effects of liquid, on tantalum and yttrium, 20: 41064(R) (IS-1500(Sect.E))
Mn–U, melting point of, effects of impurities on eutectic, 20: 41064(R) (IS-1500(Sect.E))
MANGANESE IONS
effects on electron spin resonance spectra of irradiated silicate glasses, 20: 42538
MANGANESE ISOTOPES Mn-53
content in iron meteorites, (E), 20: 41614
energy levels of, gamma decay of, (E), 20: 42381
MANGANESE ISOTOPES Mn-54
beta activity measurements in France, 20: 41189 (CEA-R-3020)
content in fish in Northeast Pacific Ocean, 20: 40523(R) (RLO-1750-8 (Vol.1))
distribution in mollusks of Columbia River estuary, 20:40523(R) (RLO-1750-8(Vol.1))
energy-level structure of, calculations using shell model with configuration mixing, (T), 20: 42201
uptake by marine mollusks, 20: 40528
uptake by swine blood cells in vitro, effects of dietary calcium, zinc, and corn oil on, 20: 40556
MANGANESE ISOTOPES Mn-55
neutron radiative capture cross section from 1.0 to 19.5 Mev, (E), 20: 42332
MANGANESE STEEL
Mn–Mo, properties of type 302B, effects of fabrication and heating on, 20: 41451(R) (GA-7101)
Mn–Mo–V, properties of Ammo, variations in samples of, 20: 41447(R) (EURAEC-1669)
MARITIME REACTORS
design for radio-controlled towing craft, 20: 42666(P)
MASERS (OPTICAL)
beam effects on prebreakdown and breakdown in cloud chambers, 20: 41375
beam reactions with aluminum targets, magnetic mirror containment of plasma from, 20: 42415 (TID-22928)
design of instrument for retinal coagulation using, 20: 40791
effects on rabbit eyes, 20: 40692
effects on rabbit eyes, 20: 40791
electron temperatures of, soft x-ray emission determination of, (E), 20: 42475
physical properties of significance as a hazard to personnel, 20: 40691
use for plasma electron density determination, 20: 42432
use in cancer research and radiotherapy, review, 20: 40776
use in motion detection, 20: 41224 (EGG-1183-2078)

use in plasma diagnostics, 20: 42445
MASS SPECTROGRAPHY
spark source methods of, efficiency of, 20: 40796(R) (IS-1500(Sect.C))
MASS SPECTROMETERS
description of, 20: 41261(P)
design of, for simultaneous collection of positive and negative ions, 20: 40796(R) (IS-1500(Sect.C))
design of, phase space representations for charged-particle motion for, 20: 41567
electron gun design for, 20: 40796(R) (IS-1500(Sect.C))
MASS TRANSFER
of AGR fuel rods on dimple brace configurations, 20: 41109
MATERIALS TESTING
equipment and methods for comparison of neutron effects on steels, 20: 41504
equipment for impact-shock, 20: 41113
ether–nitrogen and ether–air explosions in gloved box, 20: 41203 (UCRL-16259)
facility design for collector targets, 20: 41122
method for pressure vessel steel, 20: 41444(R) (COO-1477-5)
nondestructive methods of, for reactor fuels, 20: 41112 (IITRI-578P11-54)
nondestructive method for surface, neutron device for, 20: 41115(P)
nondestructive remote methods development for Elk River Reactor pressure vessel, 20: 42636(R) (SWRI-1228-4-22)
nondestructive, methods for leak-testing reactor fuel elements, 20: 42610(T) (AI-Trans-206)
steel samples for research on brittle fracture of weldments, 20: 41447(R) (EURAEC-1669)
MATERIALS TESTING REACTOR
experimental facilities for, fuel irradiation, 20: 42581(R) (ORNL-3875, pp 125-50)
MATHEMATICS
equation for determination of rupture-time curves of metals, 20: 41495(R) (EURAEC-1621)
equations for prediction of particle deposition on ground from elevated source, 20: 41188(R) (BNWL-235-1)
generalized discrete-continuum radial integrals with Coulomb functions, 20: 41633
methods of least squares, application of, 20: 41408
research programs on, 20: 41406(R) (IS-1500(Sect. M and C))
solution of time-dependent differential equations, variational formalism for, 20: 41409
trinomial expansions in, computer program for calculating, 20: 41407 (ORNL-4004)
MATING
radiation effects on the competitiveness of male *Trogoderma glabrum* during, γ, 20: 40673
MATTER
binding energy of nuclear, D-, P-, and S-wave, 20: 42281
properties of nuclear, ground-state, (T), 20: 42249
theory of nuclear, two-body correlations in, 20: 42248
thermodynamic properties of, (T), 20: 41513(R) (UCRL-14744, pp 19-36)
MEATS
radiosterilization of, feasibility of, 20: 41390
MECHANICS
many-body problem in statistical, variational principles for, 20: 42074
MEDICAL PERSONNEL
radiation effects on health and fertility of dentists and radiologists, 20: 40615(R) (NYO-901-54, pp 26-8)
radiation effects on diameter and volume of erythrocytes of, from occupational exposure, 20: 40678
radiation protection during radiography, 20: 40733 (ISS-66/16)
MEDICINE
forensic, applications of activation analysis in, 20: 40810(K) (NYO-901-54, pp 20-3)
solid state track dosimeters for, use with neutrons and high-energy particles, 20: 41262 (BNWL-SA-619)
x-ray dosimetry in, film pack survey of, 20: 41213
MEDITERRANEAN SEA
bottom layers in, studies on, 20: 41128
fallout monitoring of, 1963, 20: 41145
fallout monitoring, 1963, 20: 41146
measurements of radioactivity in, 20: 41147
MEIOSIS
effects of suppressible mutations and super-suppressors on Saccharomyces, 20: 40582(R) (ORNL-3922, pp 65-8)
genetic control of, in mutant peas, 20: 40512
radiation effects on rice chromosomes during, beta, thermal neutron, and x, 20: 40641
role in temperature-induced crossing-over frequency in Drosophila, 20: 40625(R) (ORNL-3922, pp 59-64)
MELAMINE, TRIETHYLENE-
effects on Drosophila, genetic, 20: 40706
effects on Paramecium, mutagenic, 20: 40632(R) (ORNL-3922, pp 175-91)
MEMBRANES
radiation effects on properties of nerve, x, 20: 40606 (BMwF-FBK-66-02)
MEMORY DEVICES
properties of cryogenic associative and continuous film, (T), 20: 42108
MERCURY
determination in seawater, activation, 20: 40834
determination of, using isoöctylthioglycolate, 20: 40796(R) (IS-1500 (Sect.C))
determination of, developments in resin spot tests for, 20: 40827
electric conductivity of liquid, 20: 41476
emission properties of targets of, 20: 41122
flow in magnetic fields, hydraulics of, (E), 20: 41774
flow in MHD ducts, turbulence at high Hartmann and Reynolds numbers, (E), 20: 41707
ionization in MHD duct, excited atom effects on nonequilibrium, (E), 20: 41757
photon reactions (γ,n) with, energy spectra from, (E), 20: 42165(R) (MIT-2098-251, pp 16-20)
properties as working fluid in Rankine power cycle, 20: 41398
scattering on beryllium–copper alloys and nickel at 5 to 25 kev, secondary electrons from, 20: 41620 (NIJS-R-471)
separation from tin by reversed-phase chromatography, 20: 40796(R) (IS-1500(Sect.C))
solubility in organic compounds, tracer studies of, 20: 40796(R) (IS-1500(Sect.C))
spallation of, use in accelerator radiation monitoring, 20: 41276 (UCRL-16769)
thermal conductivity of liquid, estimation of, 20: 41477
MERCURY HALIDES
neopentyl derivatives of, mercury-199 proton coupling in, PMR spectral studies on, 20: 40908
MERCURY ISOTOPES
nuclear charge distribution in, isomeric and isotopic effects on, (T), 20: 42189
radioactive, effects on human erythrocyte diameter and volume from occupational exposure to, 20: 40678
separation by electromagnetic methods, 20: 41401(R) (ORNL-4006)
spectra of, isomer and isotope shifts in optical, (T), 20: 42189
MERCURY ISOTOPES Hg-197
use in brain scanning, 20: 40748
use in labeling mercurihydroxypropane for scanning agent, 20: 40777
MERCURY ISOTOPES Hg-199
proton coupling in neopentyl derivatives of mercury, PMR spectral studies on, 20: 40908
MERCURY ISOTOPES Hg-203
use as gamma source in well logging, 20: 41165
MESIC ATOMS
absorption ratios for s-orbitals in deuterium π^-, nonradiative and radiative, 20: 41809
energy level shifts and line widths of π, (E), 20: 41803(R) (UCRL-16863)
theory for light π^-, 20: 41665
x-ray spectra from μ^-, (E), 20: 42306
x-ray spectra from μ^-, isotope shifts from, (E), 20: 42307
x-ray spectra from μ, (E), 20: 42309
x-ray spectra from μ, (E/T), 20: 42310
x-ray spectra from π, in even-even nuclei, (E), 20: 42311
x-ray spectra from μ, nuclear charge distribution determination from, (E), 20: 42305
MESONS
classification in irreducible representations of noncompact groups, 20: 41967
classification in noncompact groups, 20: 41982
composite models for, in $SU(6)_W$, 20: 42034
composition and mass splitting of octets of pseudoscalar and vector, 20: 42007
decays of vector SU(6) symmetry for radiative, 20: 41908
decays of, two-angle Cabibbo theory of leptonic, 20: 41987
electrodynamic fields and groups for vector, Yang-Mills, 20: 41929
form factors of pseudoscalar, sum rules for, 20: 41995
interactions of degenerate pseudoscalar octet of, with triplet elementary particles, (T), 20: 42029
interactions of pseudoscalar, P-wave amplitude for, 20: 41837
interactions with baryons, SU(3) invariant coupling constants for, 20: 41976
interactions with baryons, permutation symmetry in, 20: 41984
interactions with baryons, unitary symmetry for moderately strong, 20: 42013
interactions with baryons, $SU(6)_W$ symmetry scheme for, 20: 42016
interactions with baryons, bootstrap model and SU_6 symmetry for, 20: 41848
interactions with baryons in broken SU(3) symmetry, strong coupling constants for, 20: 41860

interactions with baryons, exchange of even- and odd-parity resonances in, 20: 41880
interactions with equal-mass scalar mesons, renormalization constant Z_1 and vertex function for, 20: 41893
mass formula for positive-parity, 405 multiplet, 20: 41874
masses and quark structure of, 20: 42017
model for, U_{12} invariance in relativistic quark, 20: 41965
model of, binding energy for relativistic degenerate quark, 20: 41978
photoproduction of vector, photon dissociation model for, 20: 41863
photoproduction of, vector dominance approximation for, 20: 41869
photoproduction on nucleons, SU(6) symmetry for, (T), 20: 41812
production in proton interactions with nucleons in emulsions at 20 Bev/c, (E/T), 20: 41829
symmetry for, beyond SU(6), 20: 42030
symmetry group for classification of, saturation of SU(6), 20: 41968
theory of, commutation relations in pseudoscalar-pseudovector, 20: 41964

MESONS, RESONANCE
classification in D_5 group, 20: 41972
mass formula for positive-parity, 405 multiplet, 20: 41874
model for $\rho\pi\pi$ vertex, quark, 20: 41876
production cross sections of A_2, D, E, and ϕ, in meson (π^-)-proton interactions at 2.0 to 4.0 Bev/c, (E), 20: 41802 (UCRL-16832)
production in meson (π^+)-proton interactions via two-meson (π) exchange, (T), 20: 41918
production of K* (891) in meson (K^+)-proton interactions at 2.7 Bev/c, (E), 20: 41804 (UCRL-17003)
properties of, maximum likelihood method for determining, 20: 41790 (DESY-66/17)
stability in broken symmetry, 20: 41994

MESONS (η)
decay of, search for C violation in 3π, (E/T), 20: 41854
exchange in nucleon-nucleon interactions, 20: 41899
interactions with nucleons from meson (π)-nucleon interaction, (T), 20: 41866
mixing in SU(3), 20: 42005
photoproduction on protons at 0.95 to 1.1 Bev, differential cross sections for, (E), 20: 41889
production from meson (π^-)-nucleon interactions, cross section lower limit determination from, (E), 20: 41910
production in meson (π^-)-proton interactions at 558 to 900 Mev, cross sections for, (E/T), 20: 41871

MESONS (f^0)
spin of, from meson (π^-) proton interactions at 10 Bev/c, (E), 20: 41795(R) (MIT-2098-251, pp 21-36)

MESONS (K)
decay of, 3π, (T), 20: 41900
decays of, amplitudes for 2π, 20: 41835
decays of, effective $\Delta I = \frac{1}{2}$ rule in 3π, 20: 41840
interactions with nucleons, scattering lengths for, (T), 20: 41846
interactions with nucleons, cross sections for, (T), 20: 41898
pair production in meson (π^-)-proton interactions at 2.0 to 4.0 Bev/c, (E), 20: 41802 (UCRL-16832)
production of pairs of, in π-π P-wave interactions, 20: 41823

MESONS (K^-)
capture at rest by light nuclei in emulsions, (E), 20: 42386
interactions in nuclear emulsions at 1.5 Bev/c, production and decay properties of hyperfragments from, (E), 20: 41911
interactions with protons at 4.2 Bev/c, strangeness-1 and -2 events in, (E), 20: 41799(R) (ORO-2504-96)
interactions with protons at 0.9 to 1.0 Mev/c, Λ^0, $\Sigma^\pm$, and $\bar{K}^0$ production in, (E), 20: 41799(R) (ORO-2504-96)
interactions with protons, peripheral model for Y* charge-state interference in, 20: 41819
interactions with neutrons at 0.8 to 1.1 Bev/c, Y$_1^*$ resonant amplitudes from, (E), 20: 41886
lifetime relative to mesons (K^+), (E), 20: 41884

MESONS (K^0)
decay modes of K_2^0, 20: 41903
decay of, CP violation in 2π, 20: 41849
decay of, test of $\Delta I = \frac{1}{2}$ rule for leptonic, (E), 20: 41799(R) (ORO-2504-96)
decay rate of long-lived, absolute three-body, (E), 20: 41855
decays of, branching ratios for 2π, 20: 41872
decays of, CP violation in radiative, 20: 41905
interactions of K_1^0 with protons, total cross sections for, (E), 20: 41799(R) (ORO-2504-96)
lifetime of short-lived, (E), 20: 41855
mass difference (K_S^0–K_L^0), (E), 20: 41922
mass difference of K_1^0 and K_2^0, measurement of sign of, (E), 20: 41878
mass differences (K_S^0–K_1^0), 20: 41872
production in meson (π^-)-proton interactions at 900 Mev, (T), 20: 41917

MESONS ($\bar{K}^0$)
production in meson (K^-)-proton interactions at 0.9 to 1.0 Mev/c, (E), 20: 41799(R) (ORO-2504-96)

MESONS (K^+)
decay of, branching ratio of $\pi 2$ and $\mu 2$ modes of, 20: 41801 (UCRL-16003)
interactions with protons at 2.7 Bev/c, K* (891), N* (1236), and ω production from, (E), 20: 41804 (UCRL-17003)
interactions with protons at 910 Mev/c, phase-shift analysis of, 20: 41825
interactions with protons at 3.5 Bev/c, existence of K^+K^- resonance in, (E), 20: 41856
lifetime relative to mesons (K^-), (E), 20: 41884
photoproduction on protons at 2.6 to 2.7 Bev, differential cross sections for, (E), 20: 41795(R) (MIT-2098-251, pp 21-36)

MESONS ($K_{\mu 3}^+$)
decay of, branching ratio relative to mesons ($K_{\pi 2}^+$), 20: 41801 (UCRL-16003)

MESONS (K_{e3}^+)
decay of, meson (μ^+) polarization from, (E), 20: 41799(R) (ORO-2504-96)

MESONS ($K_{\pi 3}^+$)
decay of, branching ratio relative to mesons ($K_{\pi 2}^+$) for, 20: 41801 (UCRL-16003)

MESONS (μ)
capture by nuclei, conference on, 20: 42304
magnetic moment of, experiment for measuring anomalous, 20: 41810
production in electron reactions with lead and lithium at 6 to 25 Bev, (E), 20: 41805(T) (SLAC-Trans-46)
shielding measurements in heavy concrete, 20: 41534 (DESY-66/18)

MESONS (μ^-)
capture by atoms, x-ray spectra from, (E), 20: 42306
capture by bismuth-209, E2 and M1 hyperfine structure determination from, (E), 20: 42307
capture by complex nuclei, (E), 20: 42318
capture by deformed nuclei, nuclear charge distribution determination from hfs spectra from, (E), 20: 42308
capture by deformed and spherical nuclei, x-ray spectra from, (E), 20: 42309
capture by lead isotopes, isotope shifts from, (E), 20: 42307
capture by nuclei, nuclear charge distribution determination from, (E), 20: 42305
capture by nuclei, review of, 20: 42317
capture by nuclei, mass dependence of average neutron emission from, (E/T), 20: 42174
capture by oxygen-16, coherent antiproton-neutron excitations from, (T), 20: 42279
capture of polarized, by calcium, neutron angular distribution from, (E), 20: 42300

MESONS (ω)
decay of, branching ratio for, (E), 20: 41850
decay of, meson (ϕ) production in, (T), 20: 41888
exchange in nucleon-nucleon interactions, 20: 41899
mixing in SU(3), 20: 42005
photoproduction of, photon dissociation model for, 20: 41863
production in meson (K^+)-proton interactions at 2.7 Bev/c, (E), 20: 41804 (UCRL-17003)

MESONS (ϕ)
mixing in SU(3), 20: 42005
photoproduction of, photon dissociation model for, 20: 41863
production in meson (π^-)-proton interactions at 2.0 to 4.0 Bev/c, (E), 20: 41802 (UCRL-16832)
regeneration of, from mesons (ω), (T), 20: 41888
spin and G parity of, (E), 20: 41881

MESONS (π)
capture by nuclei, conference on, 20: 42304
capture by oxygen-16, radiative, (T), 20: 42315
exchange in meson (π^+)-proton interactions, two-body, (T), 20: 41918
exchange in photon-nucleon interactions, two-body, (T), 20: 41821
form factor of, electromagnetic, (T), 20: 41833
interactions of, $\pi\pi p$ bootstrap model for, 20: 41867
interactions with nucleons at 300 Mev, phase shift analysis of, (E), 20: 41794 (JINR-E-2860)
interactions with nucleons, modified one-nucleon exchange model for, 20: 41815
interactions with bound nucleus at low energies, (T), 20: 42312
interactions with nucleons, Schroedinger theory for static, 20: 41818
interactions with mesons (π), P-wave meson (K) pair production cross section in T = 1 state, 20: 41823
interactions with mesons (π) at low energies, S-wave phase shifts for, 20: 41832
interactions with mesons (π), meson (ρ) exchange in, 20: 41837
interactions with mesons (π), analyticity domain of amplitude for, 20: 41841
interactions with nucleons, scattering lengths for, (T), 20: 41846
interactions with mesons (π) from meson (π^-)-proton interactions at

2.1 Bev/c, (E), 20: 41858
interactions with mesons (π), consistency conditions on strong, 20: 41861
interactions with nucleons, consistency conditions on strong, 20: 41861
interactions with hyperons, static bootstrap theory and Lie group for, 20: 41862
interactions with nucleons at low energies, modified effective-range approximation for, 20: 41864
interactions with nucleons, meson (η) production and interaction from, (T), 20: 41866
interactions with nucleons, consistency of nucleon-nucleon interaction with, (T), 20: 41873
interactions with mesons (π), quark model for $\rho\pi\pi$ vertex in, 20: 41876
interactions with nucleons, quark model for $N\frac{3}{3}N\pi$ vertex in, 20: 41876
interactions with nucleons, meson (π)-nucleon and meson (ρ) coupling constants from scattering lengths in, (T), 20: 41885
interactions with deuterons at high energies, charge independence in, (T), 20: 41887
interactions with nucleons, theory of three particle production in, 20: 41900
interactions with nucleons, review of phase shift analyses for, 20: 41913
photoproduction of, fixed-t dispersion relations for, 20: 41851
photoproduction on nucleons, amplitudes for, (T), 20: 41996
production in galaxies, model for, 20: 41603
reactions with nuclei at low energies, (T), 20: 42312
scattering by nuclei, optical models for elastic, (T), 20: 42319
scattering of cloud, in proton-proton interactions at high energies, 20: 41896

MESONS (π^-)
capture by nuclei below 300 Mev, gamma and neutron spectra from, (E), 20: 42314
capture by nuclei, radiative, (T), 20: 42385
interactions with protons at 6 to 18 Bev/c, cross sections for elastic charge-exchange, (E), 20: 41795(R) (MIT-2098-251, pp 21-36)
interactions with protons at 10 Bev/c, $2\pi^0$ mass spectra from, (E), 20: 41795(R) (MIT-2098-251, pp 21-36)
interactions with protons at 10 Bev/c, spin of mesons (f^0) from, (E), 20: 41795(R) (MIT-2098-251, pp 21-36)
interactions with protons at 2.0 to 4.0 Bev/c, cross sections for A_2, D, E, and ϕ mesons production in, (E), 20: 41802 (UCRL-16832)
interactions with protons at 2.0 to 4.0 Bev/c, $K\bar{K}$ production in, (E), 20: 41802 (UCRL-16832)
interactions with protons at 300 Mev, recoil polarization from, (E), 20: 41794 (JINR-Ł-2860)
interactions with deuterons, nonradiative and radiative absorption ratios for atomic s-orbitals for, (T), 20: 41809
interactions with nucleons at 12 and 18 Bev/c, recoil nucleon states from inelastic meson (ρ^0) production in, (E), 20: 41828
interactions with protons at 300 to 700 Mev, total cross sections for, (E), 20: 41830
interactions with protons at 875 to 1579 Mev/c, cross sections for elastic, (E), 20: 41857
interactions with protons at 2.1 Bev/c, π-π interactions and N* (1920) production in, (E), 20: 41858
interactions with protons at 2 to 5 Bev, cross section for W boson production in, (T), 20: 41859
interactions with protons at 558 to 900 Mev, cross sections for, (E/T), 20: 41871
interactions with protons at 323 to 900 Mev/c, polarization in, (E), 20: 41890
interactions with nucleons, cross section lower limit for, (E), 20: 41910
interactions with deuterons, neutron-neutron S-wave scattering length from, (E), 20: 41914
interactions with protons at 900 Mev, hyperon (Λ) and meson (K^0) production from, (T), 20: 41917
lifetime, (E), 20: 41891
lifetime relative to mesons (π^+), (E), 20: 41884
production from bremsstrahlung reactions with helium below 330 Mev, (E), 20: 41817
range in nuclear emulsions at 78 and 90 Mev/c, 20: 41826
reactions (π^-,2n) and (π^-,np) with light nuclei, neutron-neutron and neutron-proton pair angular distributions from, (E), 20: 42313
reactions (π^-,π^+ 4n) with helium-4, (T), 20: 42356
reactions in light nuclei, phenomenological analysis of, 20: 41665
reactions in nuclear emulsions at 17 Bev/c, electron pair production from, (E), 20: 41814

MESONS (π^0)
detection and measurement using photon detector, 20: 41320
mass spectra of π^0-π^0, from meson (π^-)-proton interactions at 10 Bev/c, (F), 20: 41795(R) (MIT-2098-251, pp 21-36)
photoproduction on protons, (E), 20: 41798 (MIT-2098-265)
photoproduction on nucleons, isospin amplitudes for S-state, 20: 41906
production from particle interactions at 8 Bev/c, kinematic properties from multiple, (E), 20: 41910
production in proton-proton interactions at 2.8 Bev/c, (E), 20: 41920

MESONS (π^+)
decay of, S-matrix method for radiative correction for, 20: 41865
interactions with protons at 300 to 700 Mev, total cross sections for, (E), 20: 41830
interactions with protons at 8 Bev/c, shadow model for elastic backward peak in, (T), 20: 41839
interactions with protons at 4 and 8 Bev/c, Regge-pole analysis of, 20: 41842
interactions with protons at 875 to 1579 Mev/c, cross sections for elastic, (E), 20: 41857
interactions with protons at 900 to 1580 Mev/c, polarization in, (E), 20: 41890
interactions with protons via two-meson (π) exchange, (T), 20: 41918
interactions with protons at 7 Bev/c, effective mass spectra from, (E), 20: 41919
lifetime, (E), 20: 41891
lifetime relative to mesons (π^-), (E), 20: 41884
photoproduction on protons at 2.6 to 2.7 Bev, differential cross sections for, (E), 20: 41795(R) (MIT-2098-251, pp 21-36)
photoproduction on protons at high energies, absorption correction in, 20: 41844
production from bremsstrahlung reactions with hydrogen and helium below 330 Mev, (E), 20: 41817
range in nuclear emulsions at 78 and 90 Mev/c, 20: 41826
reactions with vanadium-51 and zirconium-90 at 220 to 320 Mev/c, double charge exchange in, (E), 20: 42316
scattering by helium-4 at 100 to 160 Mev/c, phase shift analysis for elastic, (E), 20: 42320
scattering by helium-4 at 1000 to 160 Mev/c, inelastic, (E), 20: 42321
yields from bremsstrahlung reactions with helium and hydrogen, absolute, 20: 41816

MESONS (ρ)
exchange in meson (π)-nucleon interactions, coupling constant for, 20: 41885
exchange in nucleon-nucleon interactions, 20: 41899
exchange in photon-nucleon interactions, (T), 20: 41821
mass and width of, from meson (π) interactions, 20: 41837
mass and width of, *mmp* bootstrap model for, 20: 41867
photoproduction of, photon dissociation model for, 20: 41863

MESONS (ρ^-)
mass relative to meson (ρ^0), field-theoretical sum rules for calculating, 20: 41824

MESONS (ρ^0)
mass relative to mesons ($\rho^\pm$), field-theoretical sum rules for calculating, 20: 41824
production in meson (π^-) interactions with nucleons at 12 and 18 Bev/c, recoil nucleon states from inelastic, (E), 20: 41828
production in photon-proton interactions via two-meson (π) exchange, (T), 20: 41918

MESONS (ρ^+)
mass relative to meson (ρ^0), field-theoretical sum rules for calculating 20: 41824

MESONS (X)
mixing in SU(3), 20: 42005

METABOLIC DISEASES
radioinduced hypothyroidism in dogs, x, 20: 40698

METABOLISM
basal, effects of iodine-131 therapy for diabetes-hyperthyroidism, 20: 40790
bone mineralization studies in fetal chickens, 20: 40558
calcium and strontium, in algae, 20: 40524(R) (TID-23271)
chromium-51, in clams, 20: 40575
double label experiments on thyroid with technetium-99m and iodine-125, 20: 40547
effects of heat-treated and γ-irradiated meals on swine, 20: 41394
of fluorine-18, in dogs, 20: 40554
of scandium-47 and calcium-47 in rat bones, 20: 40545
of 1-(4-dimethylaminobenzylidene) indene in rats, 20: 40632(R) (ORNL-3922, pp 175-91)
radiation effects on, in soil organisms, gamma, 20: 40637(R) (ORO-2754-7)
radiation effects on human, from iodine therapy, 20: 40659
radiation effects on protein, in animals, 20: 40602 (AD-624934)
rat protein, effects of irradiated potatoes in diet on, 20: 40576
succinic oxidase, in *Mycobacterium phlei*, 20: 40571
theory of alkaline earth, use of barium-133 retention in rats for testing Marshall's, 20: 40565
use of iodine-131 and technetium-99m in study of thyroid, 20: 40555

METALLIC FOILS
properties of, effects of temperature and time on low-pressure, 20: 41440(R) (ALO-3632-4)

METALLURGY
book: *International Conference on Beryllium Metallurgy*, Grenoble, May 17–20, 1965, 20: 41416
METALS
acceleration of milligram mass, magnetic field compression techniques for, 20: 41084
analysis for nitrogen and oxygen by carrier-gas fusion extraction, 20: 40796(R) (IS-1500(Sect.C))
book: *Data Book on Physical Properties of Materials*, 20: 41442 (CNLM-2393)
book: *Electron Radiation Damage in Semiconductors and Metals*, 20: 41508
content in meteorites, 20: 42064
corrosion test for liquid, · 20: 41064(R) (IS-1500(Sect.E))
deformation and rupture mechanisms of, determination by activation energies, 20: 41445(R) (EURAEC-1622)
design of level indicators for molten, 20: 41233(R) (ORNL-3875, pp 101-24)
diffusion coefficients of liquid, · 20: 41064(R) (IS-1500(Sect.E))
distillation of liquid, flash, · 20: 41064(R) (IS-1500(Sect.E))
electric conductivities of liquid, effects of Z on, 20: 41476
flow of, void fraction detection in, 20: 41111
flowmeter for liquid, ultrasonic, · 20: 41225(R) (NYO-3622-4)
magnetic field diffusion in, Joule heating effects on, 20: 41087
magnetoresistance measurements using high pulsed fields, 20: 42526
preparation of radioactive, for oxygen determination, cathodic etching method for, · 20: 40817 (UCRL-14959)
purification by electrotransport, survey on, 20: 41412(R) (IS-1500 (Sect. M))
radiation effects on creep of, extrapolation method for neutron, 20: 41495(R) (EURAEC-1621)
scattering of hydrogen on surfaces of, ion production from, 20: 42460
separation from uranium by fixation of acetate on anion-exchange resins, 20: 41030 (CEA-R-2994)
separation of nonferrous, by liquid-liquid extraction, review on, 20: 41047
solidification of, effects of electric fields on, 20: 41412(R) (IS-1500 (Sect. M))
sorption from sulfuric acid solutions by anion exchange materials, 20: 40822
spectra of heavy, effects of polyethylene coating on potassium bromide windows for infrared, · 20: 40805(R) (MLM-1325, pp 63-70)
use in MHD conversion systems of two-phase liquid, 20: 41734
vapor, thermodynamic properties of "perfect", (T), 20: 42045
METASTASES
detection of bone, by strontium-85 scanning, 20: 40794
effects of radiotherapy, surgery, and other treatments on growth of tumor, 20: 40745(R) (NYO-901-54, pp 29-47)
radiation effects on, following therapy for breast cancer, 20: 40793
METEORITES
ages of Estherville, Haraija, Juvinos, Shergotty, and Stannern, 20: 41162
aluminum-26 and manganese-53 content and radiation ages of iron, (E), 20: 41614
analysis for bromine, activation, 20: 40811 (ORO-2670-13)
analysis for gold, iridium, and platinum by thermal neutron activation, 20: 40835
analysis for lead, and uranium, activation, 20: 42062
composition and classification of, 20: 42064
lithium isotopic composition of Bruderheim and Bjurbole, 20: 42061
METEOROLOGY
effects of wind and precipitation on fallout dispersion, · 20: 41133(R) (SC-CR-66-2030)
effects on deposition of methyl iodide on grass, · 20: 41192(R) (IDO-12053
isentropic stream functions and trajectories, computer analysis of radiosonde data on, · 20: 41188(R) (BNWL-235-1)
manual of, for reactor safety analysis, 20: 42584
performance of radio-telemetering system for data accumulation on, 20: 41188(R) (BNWL-235-1)
rain scavenging of atmosphere particulate matter, · 20: 41130(R) (COO-1407-10)
wind predictions for National Reactor Testing Station, 20: 41129
METEORS
explosion of Tunguska, anti-matter, 20: 41607
METHACRYLIC ACID, METHYL ESTER
effects on isomerization of stilbene in gamma radiolysis of benzene and cyclohexane, 20: 40961
radioinduced graft polymerization to cotton cellulose, properties of products formed by gamma, 20: 40995
acrylonitrile–methyl methacrylate, radioinduced graft polymerization to cotton fabric, properties of products formed in gamma, 20: 40953
methyl methacrylate–styrene, radioinduced graft polymerization to cotton fabric, properties of products formed in gamma, 20: 40953
METHANE
deuteron nuclear quadrupole coupling constant in deuterated, 20: 40894
electric properties of combustion products of, (E), 20: 41731
neutron scattering by, effect of nuclear spin correlations on, 20: 42144
radiation effects on, in krypton at 4.2°K, ESR of free radicals from gamma, 20: 40968
vibrations of trapped, in β-quinol clathrates, localized, 20: 41651
yields in gamma radiolysis of liquid 2-propanol, effects of benzophenone and naphthalene additions on, 20: 41006
yields of deuterated, in hydrolysis of aluminum, thorium, and uranium carbides in heavy water, 20: 40905
methane–H_2O, tritium exchange in, · 20: 41067(R) (ORNL-TM-1582)
METHANE, BROMO-
effects on soils, sterilization, 20: 40637(R) (ORO-2754-7)
METHANE, BROMOTRIFLUORO-
radiolysis of, effects of temperature on yields of products in gamma, 20: 40948(R) (COO-578-3-32)
radiolysis of, mechanism and yields of products in gamma, · 20: 40948(R) (COO-578-3-32)
yields in gamma radiolysis of carbon tetrachloride in presence of bromine, 20: 40948(R) (COO-578-3-32)
benzene–bromotrifluoromethane, radiolysis of, mechanism and yields of products in gamma, 20: 40948(R) (COO-578-3-32)
METHANE, CHLORO-
chloromethane–cyclohexane, radiolysis of, mechanism of transfer mechanism in, 20: 40957
METHANE, CHLOROTRIFLUORO-
radiolysis of, mechanism and yields of products in gamma, · 20: 40948(R) (COO-578-3-32)
yields in gamma radiolysis of carbon tetrachloride in presence of chlorine, 20: 40948(R) (COO-578-3-32)
METHANE, DIBROMODIFLUORO-
yields in gamma radiolysis of bromotrifluoromethane, mechanism of, 20: 40948(R) (COO-578-3-32)
METHANE, DICHLORO-
effects on radioinduced polymerization of styrene with formaldehyde, 20: 40973
dichloromethane–cyclohexane, radiolysis of, mechanism of transfer mechanism in, 20: 40957
METHANE, DICHLORODIFLUORO-
yields in gamma radiolysis of chlorotrifluoromethane, mechanism of, 20: 40948(R) (COO-578-3-32)
METHANE, DIPHENYL-
radiolysis of, EPR studies of yields of stabilized charges in low-temperature, 20: 40962
METHANE, IODO-
adsorption on charcoal under humid conditions, · 20: 41202 (UCRL-14990)
deposition on grass of atmospheric, tracer study, · 20: 41192(R) (IDO-12053)
exchange reactions of radioiodine between ethyl iodide and, radiochromatography equipment for studies on, 20: 41019
iodine-131 exchange between, and iodide ions, 20: 40939
metabolism in man of inhaled or ingested, tracer study, · 20: 41192(R) (IDO-12053)
solvolysis of, effects of carbon-13 and deuterium on, 20: 40939
METHANESULFONIC ACID, ETHYL ESTER
chemical and physical properties and mutagenic action on barley seeds, 20: 40717
effects on, 20: 40513
effects on *Arabidopsis thaliana*, genetic, 20: 40710
effects on barley, genetic, 20: 40712
effects on Drosophila genes, mutagenic, 20: 40625(R) (ORNL-3922, pp 59-64)
effects on maize, genetic, 20: 40708
effects on Neurospora, mutagenic, 20: 40632(R) (ORNL-3922, pp 175-91)
METHANOL
electron spin resonance spectra of, 20: 42433
radioinduced oxidation of, yields in, 20: 41004
radiolysis of, quasi-equilibrium theory calculations of yields from gas-phase, 20: 40959
vibrations of trapped, in β-quinol clathrates, localized, 20: 41651
METHIONINESULFOXIMINE
effects on iron-59 metabolism in rats, 20: 40561
METROLOGY
carbon-14 content of Indian Ocean, 20: 41127
MEXICO
strontium-90 content of milk in, 1963 to 1965, 20: 40854
MICE
aging in ICR, effects of microbial flora on, 20: 40502(R) (ORNL-3922, pp 115-27)
antibody production in, morphologic changes in spleen lymphatic tissue during, 20: 40632(R) (ORNL-3922, pp 175-91)
antibody-forming potential in, effects of age on secondary, 20: 40626(R)

(ORNL-3922, pp 80-3)
autoradiography of erythropoietic cells, 20: 40675
behavior response to gamma radiation, 20: 40519 (NP-16259)
chemotherapy of Ehrlich carcinoma and sarcoma 180 by radioprotective drugs and alkylating agents, 20: 40664
chronic irradiation of, dosimetry of fast neutron source for, 20: 40504(R) (ORNL-3922, pp 146-60)
effect of hematoporphyrin on radiosensitivity of rhabdomyosarcoma, 20: 40657
effects of combined radiation and actinomycin D therapy on tumors, 20: 40762
effects of dose-time factors on radiotherapy of skin damage, 20: 40764
effects of estradiol on immune system and lymphatic tissue in adult and newborn, 20: 40577
fission neutron dosimetry in phantom, 20: 41268(R) (NYO-2740-3, pp 5-165)
gamma dosimetry in phantom, 20: 41268(R) (NYO-2740-3, pp 5-165)
hybrid spleen cells of, induced immunological tolerance in parental strain, 20: 40651
immune response to transplanted tumors in, following x-radiation cure of previously-transplanted tumors, 20: 40643
immunity to myxofibrosarcomas after serial passage in, 20: 40502(R) (ORNL-3922, pp 115-27)
immunity to transplanted leukemia viruses in, 20: 40502(R) (ORNL-3922, pp 115-27)
mutations induced by DNA in, methods for testing, 20: 40627(R) (ORNL-3922, pp 84-8)
plutonium-239 effects on bones of, carcinogenic, 20: 40745(R) (NYO-901-54, pp 29-47)
polycythemia induction in, by confinement in silicone rubber cages, 20: 40718(R) (ORNL-3922, pp 99-105)
radiation effects on sex chromosomes in, x, 20: 40627(R) (ORNL-3922, pp 84-8)
radiation effects on life spans in, effects of age at exposure on x, 20: 40633 (ORNL-P-2287)
radiation effects on bone marrow cells in, factors affecting recovery from x, 20: 40634 (ORNL-P-2312)
radiation effects on, protective effects of bone marrow against x, 20: 40718(R) (ORNL-3922, pp 99-105)
radiation effects on, protective effects of transplants of parental tissue against x, 20: 40718(R) (ORNL-3922, pp 99-105)
radiation effects on survival of, protective effects of AET or glutathione combined with bone marrow transplants against x, 20: 40719(R) (ORNL-3922, pp 136)
radiation effects on blood cell counts in fast neutron, 20: 40502(R) (ORNL-3922, pp 115-27)
radiation effects on embryos of, lethal, RBE of neutrons and x, 20: 40618(R) (NYO-2740-3, pp 166-215)
radiation effects on embryos of, cataractogenetic, x, 20: 40619(R) (NYO-2740-3, pp 216-57)
radiation effects on development of, exposed *in utero* to x, 20: 40619(R) (NYO-2740-3, pp 216-57)
radiation effects on antibody production in, x, 20: 40626(R) (ORNL-3922, pp 80-3)
radiation effects on DBA/2J strain, gamma, 20: 40687
radiation effects on, protective effects of nibufin on x, 20: 40724
radiation effects on, mechanism for protective effects of lymphoid and myeloid cell transplants against x, 20: 40727
radiation effects on embryos, 20: 40649
radiation effects on hybrid, grafted with skin from parents, 20: 40651
radiation effects on immune system and lymphatic tissue in estradiol-injected, effects of marrow transplants on x, 20: 40577
radiation effects on lymphoma cells incubated with phytohemaglutinin in, x, 20: 40588
radiation effects on oxidative activity of tissues, x and ultraviolet, 20: 40642
radiation injuries to hearts of, x, 20: 40648
radiation protection and recovery in endotoxin-treated, 20: 40732 (AD-636209)
radiation sickness in, gamma and x, 20: 40694
radioinduced mutations in spermatogonia of, effects of dose on frequency of x, 20: 40627(R) (ORNL-3922, pp 84-8)
radioinduced sterilization in female, genetic control of x, 20: 40627(R) (ORNL-3922, pp 84-8)
radioprotective effects of mixed bacterial toxins and anthramycin, liver and spleen studies, 20: 40736
radiosensitivity of tumors of, effects of uracil on x, 20: 40668
survival curves of, following total body irradiation, 20: 40767
thymic lymphoma induced by radiation, pathogenesis studies, 20: 40677
thyroid metabolism studies, 20: 40547
use of carcinoma and sarcoma cells of, for testing cancerostatic therapeutic agents, 20: 40550
use of iodine-131-labeled colloidal albumin as scanning agent, 20: 40777
vaginal epithelia in, autoradiographic studies of, 20: 40502(R) (ORNL-3922, pp 115-27)
x-irradiated, bone marrow cell proliferation after bleeding of, 20: 40722
x-ray-induced leukemia, protection against, 20: 40658

MICHIGAN, LAKE
strontium-90 content in waters and land areas surrounding, 20: 41131(R) (HASL-172)

MICROORGANISMS
control in irradiated foods of, legislation on, 20: 41389
effects on aging in ICR mice, 20: 40502(R) (ORNL-3922, pp 115-27)
radiation effects on food-borne, review, 20: 41388
radiation effects on, in proteinaceous food, 20: 41390

MICROSOMES
calcium-45 content in shell gland mucosa cells, 20: 40551
function of ribosomes in Clostridium, 20: 40503(R) (ORNL-3922, pp 137-45)
production in antibody-forming cells, tracer study using carbon-14 of, 20: 40626(R) (ORNL-3922, pp 80-3)
role in protein synthesis, 20: 40503(R) (ORNL-3922, pp 137-45)

MICROWAVE EQUIPMENT
design for plasma diagnostics, 20: 41120
design of waveguide with collinear termination for linear accelerators, 20: 41583(P)
use in remote surveillance, 20: 41224 (EGG-1183-2078)
use of open waveguide in plasma diagnostics, (E), 20: 41717

MICROWAVES
absorption in magnetoplasma, near electron cyclotron resonance, 20: 42439
attenuation by rocket exhaust plasma, 20: 41120
diagnostic use for plasma, open waveguide method for, (E), 20: 41717
effects of combined, and x radiation on hematologic response of dogs, 20: 40650
emission from stationary inhomogeneous plasma, (E/T), 20: 42457
phase shifts of three superimposed beams, interferometer for measuring, 20: 42408 (IPP-2/49)
propagation in magnetoplasma, near electron cyclotron resonance, 20: 42439
use for plasma electron density determination, 20: 42419(T) (AD-636608)

MILK
analysis for iodine-131, strontium-89, and strontium-90, 20: 40809 (NP-16235)
analysis for iodine-131, method for, 20: 40852
analysis for strontium-90, 20: 40854
cesium-137 and strontium-90 content of Canadian, 20: 41198 (NP-16192)
cesium-137 content in Canadian, April 1965, 20: 41209
cesium-137 content in Norweigian, March 1962 to 1966, 20: 41132 (NYO-3364-20)
measurements of strontium-90 and cesium-137 activity in Great Britain, 20: 41186 (ARCRL-15)
radioactivity content of, from fallout in West Germany, 20: 40570
radioactivity measurements in New Zealand, 20: 40521(R) (NP-16270)
radioactivity of, analytical model for iodine-131, 20: 41192(R) (IDO-12053)
separation of barium-140, strontium-89, and strontium-90 from ashes of, 20: 40858
strontium-85 and strontium-89 excretion in goat, effects of dietary calcium and strontium on, 20: 40568
strontium-89 and strontium-90 content in, in Finland, 1960 through 1965, 20: 41134 (SFL-A3)
strontium-90 content in Canadian, April 1965, 20: 41209
strontium-90 content of global samples, 1965 and 1966, 20: 41131(R) (HASL-172)
strontium-90 content of, in Mexico, 1963 to 1965, 20: 40854

MINERAL DEPOSITS
genesis of, using sulfur isotopic ratios in studying, 20: 41151

MINERALS
analysis for gold, iridium, and platinum by thermal neutron activation, 20: 40835

MITOCHONDRIA
calcium-45 content in shell gland mucosa cells, 20: 40551
radiation effects on number in lutein cells of rat ovary, x, 20: 40672
radiation effects on adensosine triphosphatase activity in rat liver, x, 20: 40695

MITOMYCINS
effects of mitomycin C combined with gamma radiation on cancer, bone marrow transplants for hematopoietic injuries from, 20: 40726
radioprotective effect on damage induced by alkylating agents, 20: 40664

MITOSIS
effects of chloramphenicol on *E. coli*, 20: 40630(R) (ORNL-3922, pp 106-8)
frequency in hamster cells after pulse-labeling with thymidine, 20: 40686
radiation effects on *E. coli*, factors affecting, 20: 40630(R) (ORNL-3922,

pp 106-8)
radiation effects on human leukocyte, uv, 20: 40581(R) (ORNL-3922, pp 50-1)
radiation effects in human blood cells, 20: 40665
radiation effects on rat spermatogonial, following exposure at birth, x, 20: 40682
radiation effects in rats on male germ cell, following exposure at birth, x, 20: 40683
radiation effects on DNA synthesis during, in chick fibroblasts and myoblasts, x, 20: 40587
MOLECULAR BEAMS
production of, optimum design of equipment for, 20: 41250
MOLECULAR STRUCTURE
determination of, for biological molecules using neutron-diffraction analysis, 20: 40632(R) (ORNL-3922, pp 175-91)
MOLECULES
electron interaction energies in diatomic, 20: 40796(R) (IS-1500(Sect.C))
electron scattering by diatomic, theory of resonances in, 20: 41657
energy levels of, electron correlations for, 20: 41630
neutron scattering by, effect of nuclear spin correlations on, 20: 42144
nuclear magnetic resonance spectra of, performance of INDOR technique for, 20: 42529
orbitals in, contour diagrams for localized, 20: 40796(R) (IS-1500 (Sect.C))
research programs on physics of, 20: 41511(R) (RLO-1388-501)
MOLLUSKS
chromium-51 uptake by clam, chemical and physical factors affecting, 20: 40575
cobalt-60, manganese-54, and zinc-65 content in Columbia River estuary, 20: 40523(R) (RLO-1750-8(Vol.1))
radiation effects on *Physa acuta*, following exposure at various stages of life cycle, x, 20: 40700
radioisotope accumulation by ocean-dwelling, 20: 40546
uptake of radioisotopes by marine, 20: 40528
uptake of radioisotopes by, factors affecting, 20: 40578
uptake of trace elements by Indian Ocean, use as biological indicator, 20: 40572
MOLTEN SALT REACTOR EXPERIMENT
computer programming for, 20: 41232(R) (ORNL-3875, pp 75-90)
data collection and analysis for, 20: 41232(R) (ORNL-3875, pp 75-90)
instrumentation development for, 20: 42581(R) (ORNL-3875, pp 125-50)
metallurgical test rig for, on-line digital control of, 20: 42581(R) (ORNL-3875, pp 125-50)
operator training simulator for, 20: 42581(R) (ORNL-3875, pp 125-50)
stability analysis and dynamic testing programs for, 20: 42581(R) (ORNL-3875, pp 125-50)
MOLYBDENUM
crystal lattice vibrations in, inelastic neutron scattering measurements of, 20: 42573
deposition from carbonyl decomposition, temperature effects on, 20: 41468
determination in fission product solutions, method for, 20: 40803 (KFK-387)
determination in plutonium by carrier distillation methods, spectrographic, 20: 40814 (RFP-664)
determination in uranium trioxide by emission spectrography, 20: 40802 (HW-65402(Rev.1))
determination of, developments in resin spot tests for, 20: 40827
distribution of, in neutron-irradiated plutonium dioxide suspensions, 20: 41009 (AERE-R-3268)
helium and hydrogen ion attenuation at 0.1 to 500 Mev, tables for, 20: 41619 (CEA-R-3042)
lattice defects in single-crystal, effects of annealing on, 20: 41434
microstructure of, effects of melting method on inclusions in, 20: 41467
oxidation at high temperatures, 20: 41421
performance as adsorption cesium reservoirs, 20: 41680(R) (NYO-3642-2)
preparation and properties of single crystals of, 20: 41481
preparation of single crystals of, using electron-beam zone refining, 20: 41434
properties of, effects of annealing medium and temperature on, 20: 41482
radiation effects on, at 11 to 7°K, electron, 20: 41499
separation from niobium, tantalum, and tungsten by solvent extraction using methyl isobutyl ketone, 20: 40796(R) (IS-1500(Sect.C))
separation from tin by reversed-phase chromatography, 20: 40796(R) (IS-1500(Sect.C))
solubility in plutonium at 700 to 1000°C, 20: 40868 (LA-3523)
thermophysical properties at 1300 to 3000°K, (E), 20: 41762
x-ray emission spectra of, L and K, (E), 20: 41350
MOLYBDENUM ALLOYS
microstructure of, effects of melting method on inclusions in, 20: 41467
Cu–Mo, electrodeposition, optimal conditions for, 20: 41487
Gd–Mo, phase studies of, 20: 41465
Hf–Mo, aging kinetics of, at 1300 to 1500°K, 20: 41466
Mo–Nb, crystal lattice vibrations in, inelastic neutron scattering measurements of, 20: 42573
Mo–Nb, preparation and properties of single crystals of, 20: 41481
Mo–Nb–Zr, phase studies of, isothermal sections at 1200°C in, 20: 41464
Mo–Ni, electric conductivity of, effects of crystal structure on, 20: 41457(R) (ORO-3291-3)
Mo–Ni, specific heats of, methods of measuring, 20: 41457 (ORO-3291-3)
Mo–Re–W, recovery of scrap, methods for, 20: 41429(R) (USBM-RC-1249)
Mo–Ti, aging kinetics of, at 1300 to 1500°K, 20: 41466
Mo–Ti, preparation and properties of single crystals of, 20: 41481
Mo–Ti–Zr, phase studies of, isothermal sections at 1200°C in, 20: 41464
Mo–W, preparation and properties of single crystals of, 20: 41481
Mo–Y, oxidation at high temperatures, effects of yttrium content on, 20: 41421
Mo–Zr, aging kinetics of, at 1300 to 1500°K, 20: 41466
MOLYBDENUM BROMIDES
solubility and molecular weight of, in liquid bromine, 20: 40796(R) (IS-1500(Sect.C))
MOLYBDENUM CARBIDES
formation as inclusions in molybdenum and molybdenum alloys, 20: 41467
MOLYBDENUM CARBONYLS
azulene-, crystal structure, 20: 40796(R) (IS-1500(Sect.C))
thermal decomposition of, properties of deposits from, 20: 41468
MOLYBDENUM FLUORIDES
fluorine-19 NMR and spin-lattice relaxation in, 20: 40892
MOLYBDENUM ISOTOPES Mo-92
proton reactions (p,γ) with, gamma decay of analog resonances in, (E) 20: 42331
MOLYBDENUM ISOTOPES Mo-93
energy-level density and transitions, (E), 20: 42331
MOLYBDENUM SILICIDES
oxidation at reduced pressures, effects of additives on, 20: 41424
MOLYBDENUM STEEL
Cr–Mo–Ni, properties of Super-Elso, effects of heat treatments on, 20: 41447(R) (EURAEC-1669)
Cr–Mo–V, rupture mechanisms of, determination by time-to-rupture tests, 20: 41445(R) (EURAEC-1622)
Mn–Mo, properties of type 302B, effects of fabrication and heating on, 20: 41451(R) (GA-7101)
Mn–Mo–V, properties of Ammo, variations in samples of, 20: 41447(R) (EURAEC-1669)
MOLYBDENUM SYSTEMS
Mo–UO_2, electric conductivity of cermet, effects of microstructure on, 20: 41478
MONAZITES
radioecological studies in Brazil, 20: 40522(R) (NYO-3273-7)
MONKEYS
behavior response to gamma radiation, 20: 40519 (NP-16259)
radiation effects on development of, exposed *in utero* to x, 20: 40619(R) (NYO-2740-3, pp 216-57)
radiation effects on, localized vs. whole-body γ and x, 20: 40694
radiation effects on eye tissues of, γ, 20: 40646
MONTANA
geological dating in southwest, potassium–argon and rubidium–strontium, 20: 41163
MONTE CARLO METHOD
use for calculating source-to-detector geometry, 20: 41316
use for electron transport properties in a low-density ionized gas, 20: 42413 (NASA-TN-D-2959)
use in determination of radiation penetration into enclosure shields in fallout field, 20: 41201 (RRA-T55 and Summary)
MONTMORILLONITES
adsorption of zinc-65 on, in salt-marsh ecosystems, 20: 40573
phosphorus-32 adsorption on, in salt-marsh ecosystems, 20: 40573
MOON
brightness of, correlation to solar wind, 20: 41604
MORPHOLOGY
radiation effects on fine structure of ovarian cells, x, 20: 40672
radiation effects on fish embryo and prelarvae, 20: 40527
thyroid, changes induced by iodine-131, 20: 40647
MÖSSBAUER EFFECT
in rare earth intermetallic compounds, review, 20: 42570
measurement in cesium-133, 20: 42239
measurement in tin compounds, 20: 41637
scattering amplitude for multipole mixtures in, 20: 42240
spectroscopy of, design and performance of wide range vacuum thermostat for, 20: 41253

use in measurement of hyperfine field distribution, (T), 20: 42571
use in sensing motion, 20: 41224 (EGG-1183-2078)
velocity drive linearization by shape correction, 20: 41238
MOUTH
radiography of, Panoramix method for, 20: 40795
MUCOSA
calcium distribution in avian shell gland, 20: 40551
MULTIPLE SCLEROSIS
immune reaction as a possible mechanism in etiology of, 20: 40643
radiation effects as possible etiology of, cosmic, 20: 40639
MUONIUM
hyperfine structure of, review of, 20: 41661
reactions with atoms and molecules, review of, 20: 41661
MUSCLES
calcium-47 uptake by rat, 20: 40557
MUSCOVITES
etching of monocrystalline, thermal stability of uranium fission products in chemical, 20: 40889
MUTAGENS
effects of alkylating sulfonates on barley, biological, 20: 40717
effects of chemicals, in Neurospora, 20: 40510(R) (TID-23137)
effects of chemical, on autogenic development of mutations in *Arabidopsis thaluna*, 20: 40709
effects of sixteen chemical, on chromosome aberration induction in plants, 20: 40714
MUTATIONS
characterization of Neurospora leaky and nonleaky, effects of carbon dioxide on, 20: 40624(R) (ORNL-3922, pp 52-8)
classification in Saccharomyces, 20: 40582(R) (ORNL-3922, pp 65-8)
detection in first generation plants of *Arabidopsis thalia* grown from mutagen-treated seed, 20: 40513
induced by alkylating sulfonates in barley, 20: 40717
induced by chemicals in Neurospora, 20: 40510(R) (TID-23137)
induced by chemicals, in Drosophila, 20: 40706
induced by chemicals in plants, effects of exogenous factors on, 20: 40709
induced by EDTA in Drosophila, 20: 40707
induced by ethyl methanesulfonate in plants, 20: 40710
induced by ethyl methanesulfonate in barley, use for hybridization breeding, 20: 40712
induced by triethylene melamine during mitosis in Paramecium, 20: 40632(R) (ORNL-3922, pp 175-91)
induced in mice by DNA, methods for testing, 20: 40627(R) (ORNL-3922, pp 84-8)
induced in Neurospora by methanesulfonate, 20: 40632(R) (ORNL-3922, pp 175-91)
induced in Neurospora by diethyl- and dimethylnitrosamine, 20: 40632(R) (ORNL-3922, pp 175-91)
induction by chemicals in maize, reaction mechanisms of, 20: 40708
radiation effects on, in man, 20: 40662
radiation effects in causing chlorophyll, in rice, mechanisms for, 20: 40641
radioinduced in barley, effects of dose fractionation on x, 20: 40701
radioinduced in barley, selection in first generation plants, x, 20: 40711
radioinduced in barley, use for hybridization breeding, 20: 40712
radioinduced in barley, x, 20: 40717
radioinduced in Drosophila, x, 20: 40622(R) (NYO-3096-8)
radioinduced in Drosophila, x, 20: 40706
radioinduced in Drosophila, effects of EDTA on x, 20: 40707
radioinduced in *E. coli*, genetics and physiology of uv, 20: 40629(R) (ORNL-3922, pp 94-8)
radioinduced in food-borne microorganisms, 20: 41388
radioinduced in jute, gamma, 20: 40681
radioinduced in maize, reaction mechanisms of x, 20: 40708
radioinduced in mouse spermatogonia, effects of dose on frequency of x, 20: 40627(R) (ORNL-3922, pp 84-8)
radioinduced in Neurospora, complementation between nonallelic, x, 20: 40624(R) (ORNL-3922, pp 52-8)
radioinduced in Neurospora, photoreactivation of uv, 20: 40624(R) (ORNL-3922, pp 52-8)
radioinduced in plants, effects of exogenous factors on, 20: 40709
radioinduced in plants, x, 20: 40710
radioinduced in tomatoes, somatic conversion in x, 20: 40713
radioinduced, effects on eye color in Mormoniella, x, 20: 40669
radioinduced, effects of tunneling and tautomeric equilibria in guanine-cytosine base pair on, 20: 40589
radioinduced, in peanuts, 20: 40636(R) (ORO-1747-12)
rice, induced by beta particles, thermal neutrons, or x rays, 20: 40640
sex-linked lethal, in *Drosophila*, 20: 40515
use of *E. coli*, for studies in germfree mice, 20: 40629(R) (ORNL-3922, pp 94-8)

N

NAPHTHALENE
effects on yields in gamma radiolysis of liquid and vitreous 2-propanol, 20: 41006
radiolysis of, yields in, 20: 40991
thermal decomposition, 20: 40991
NAPHTHALENE, 1-METHYL-
radiolysis of, yields in, 20: 40991
thermal decomposition, 20: 40991
NAPHTHALENE, 2-METHYL-
radiolysis of, yields in, 20: 40991
thermal decomposition, 20: 40991
3-NAPHTHOIC ACID, 2-HYDROXY-
complexes with uranyl ions, preparation and properties of, 20: 40898
NATIONAL REACTOR TESTING STATION
wind prediction for, strong southwest, 20: 41129
NATURAL WATERS
analysis for tritium, thermal diffusion method for, 20: 41168
NAVAL VESSELS
design of radio-controlled nuclear, 20: 42666(P)
NECK
radiotherapy of tumors of, dosimetry for x, 20: 41210
NEMATODES
radiation effects on development of *Heterakis gallinarum* embryos, x, 20: 40667
NEODYMIUM
atomic structure of, calculation of Hartree-Fock parameters for, 20: 41631
determination in steel, procedure for, 20: 41415
helium and hydrogen ion attenuation at 0.1 to 500 Mev, tables for, 20: 41619 (CEA-R-3042)
liquid, solubility of tantalum and tungsten in, at high temperatures, 20: 41412(R) (IS-1500(Sect. M))
separation factor for, in chloride and nitrate systems containing TBP, 20: 40904
NEODYMIUM ALLOYS
Mg–Nd, thermodynamics of formation of intermetallic compounds, 20: 41412(R) (IS-1500(Sect. M))
NEODYMIUM ALUMINATES
preparation of monocrystals of, with perovskite structure, 20: 40920
NEODYMIUM CHLORIDES
magnetic properties from NMR and NQR studies, 20: 42522(R) (COO-1533-2)
$HCl–NdCl_3–PrCl_3–TBP–H_2O$, separation factors for neodymium and praseodymium in, 20: 40904
NEODYMIUM COMPLEXES
with mandelic acid and α-methylmandelic acid, stability of, 20: 40902
with sulfosalicyclic acid, spectra of, effects of other rare earths on absorption, 20: 40926
NEODYMIUM IONS
spin-lattice relaxation of, in lanthanum fluorides, 20: 42540
NEODYMIUM ISOTOPES Nd-138
beta decay, (E), 20: 42197
NEODYMIUM ISOTOPES Nd-150
beta decay of, double, (E), 20: 42263
NEODYMIUM NITRATES
$Nd(NO_3)_3–HNO_3–Pr(NO_3)_3–TBP–H_2O$, separation factors for neodymium and praseodymium in, 20: 40904
NEODYMIUM OXALATES
thermal decomposition of hydrates of, differential thermal analysis of products of, 20: 40900
NEODYMIUM OXIDES
effects on catalytic properties of aluminum oxide–chromium oxide systems, 20: 40943
$Al_2O_3–Cr_2O_3–Nd_2O_3$, properties for use in dehydrogenation of butane, 20: 40943
$B_2O_3–Nd_2O_3$, liquid immiscibility in, 20: 40910
NEOMYCIN
determination in cotton clothing, radiometric method for, 20: 40823
NEON
electric conductivity in Brayton cycle MHD power generation, (T), 20: 41706
electric discharges in, high-pressure electrodeless, (E), 20: 42509
electron free-free transitions in, method for calculating, 20: 41626
helium and hydrogen ion attenuation at 0.1 to 500 Mev, tables for, 20: 41619 (CEA-R-3042)
potential energy integrals at 0°K of solid, (T), 20: 42123
properties as working fluid in Brayton power cycle, 20: 41398
properties as working medium in closed-cycle turbine, 20: 42654
proton reactions with neutral ground state of, formation of excited hydrogen atoms in, (T), 20: 41634
scattering on beryllium–copper alloys and nickel at 5 to 25 kev,

secondary electrons from, 20: 41620 (NIJS-R-471)
use in low temperature spark chamber, 20: 41329
NEON ISOTOPES Ne-20
energy levels of, T = 2, 20: 42227
neutron reactions (n,α) at 14.1 Mev, angular distributions for, (E), 20: 42216
NEON ISOTOPES Ne-21
content in meteoric feldspar and pyropene, 20: 41162
NEON ISOTOPES Ne-22
reactions with bismuth-209, production of spontaneously fissioning neptunium isotope in, (E), 20: 42292
NEPTUNIUM
separation from waste solutions, 20: 42689
NEPTUNIUM ISOTOPES
production of spontaneously fissioning, in neon-22 reactions with bismuth-209, 20: 42292
NEPTUNIUM ISOTOPES Np-241
decay of isomeric, (E), 20: 42202
NERVES
radiation effects on leg, gamma, 20: 40783
radiation effects on membrane properties and action potential of, x, 20: 40606 (BMwF-FBK-66-02)
NERVOUS SYSTEM
radiation effects on central, following therapy, 20: 40659
radiation effects on fetal rat, 20: 40654
NEUROSPORA
effects of diethyl- and dimethylnitrosamine on, mutagenic, 20: 40632(R) (ORNL-3922, pp 175-91)
effects of methanesulfonate on, mutagenic, 20: 40632(R) (ORNL-3922, pp 175-91)
mutagenic effects of acridines on, in absence of light, 20: 40510(R) (TID-23137)
mutants in, effects of carbon dioxide on leaky and nonleaky, 20: 40624(R) (ORNL-3922, pp 52-8)
radioinduced inactivation of, mechanism for photoreactivation of uv, 20: 40629(R) (ORNL-3922, pp 94-8)
radioinduced mutations in, photoreactivation of uv, 20: 40624(R) (ORNL-3922, pp 52-8)
radioinduced nonallelic mutations in, x, 20: 40624(R) (ORNL-3922, pp 52-8)
RNA in, characterization of, 20: 40535(R) (ORNL-3922, pp 128-35)
simulated space flight tests for biocompatibility, 20: 40508(R) (ORNL-3922, pp 196-9)
NEUTRINOS
decay and relativistic properties, (T), 20: 41806
emission from high-temperature stars, surface intensity and stellar energy loss from, (T), 20: 41612
NEUTRON CAPTURE CROSS SECTIONS
measurement at 30 to 170 kev, method of, 20: 42293
NEUTRON CROSS SECTIONS
calculation of point, from resonance parameters, computer program for, 20: 42141 (NAA-SR-11980(Vol.6))
data evaluation using computers, 20: 42145
library for carbon-12 from 0.01 to 15 Mev, 20: 42160 (KAPL-3099)
NEUTRON-DIFFRACTION ANALYSIS
use for determining structures of biological molecules, 20: 40632(R) (ORNL-3922, pp 175-91)
NEUTRON DIFFRACTOMETERS
development, 20: 40796(R) (IS-1500(Sect.C))
shielding design and fabrication for, 20: 42681(R) (IS-1500(Sect. R))
NEUTRON MONOCHROMATORS
use for determining molecular structure in biological materials, 20: 40632(R) (ORNL-3922, pp 175-91)
NEUTRON PHOTOGRAPHY
image-intensification system testing, 20: 42579(R) (ANL-7245, pp 29-47)
NEUTRON RESONANCE CROSS SECTIONS
calculation of, development of methods for epithermal energies, 20: 42579(R) (ANL-7245, pp 29-47)
NEUTRON SOURCES
design using deuteron reactions (d,n) with tritium, with low-voltage accelerators, 20: 42136 (AD-637457)
development of pulsed, for power reactor startup, 20: 42628(R) (GEAP-5145)
dosimetry of fast neutron, for chronic exposure of mice, 20: 40504(R) (ORNL-3922, pp 146-60)
health physics problems of, in well logging, 20: 41216
health problems of, 20: 41215
use in nondestructive testing of materials, 20: 41115(P)
NEUTRON SPECTROMETERS
boron-10 absorbers for, fabrication of compact, 20: 41272(R) (ORNL-3875, pp 53-74)
design for slow neutrons, 20: 42681(R) (IS-1500(Sect. R))
design of remotely-operated low-energy, 20: 41272(R) (ORNL-3875, pp 53-74)
NEUTRON SPECTROSCOPY
development using stars in nuclear emulsions, 20: 41276 (UCRL-16769)
multisphere technique for, 20: 41280(T) (NP-tr-1410)
NEUTRONS
absorption resonance integral for rhenium, (E), 20: 42333
absorption resonance escape probability in plutonium-240, measurement using iridium foils, 20: 42137 (AEEW-M-661)
attenuation in concrete-iron and iron-water systems, 20: 42517
capture by rhenium isotopes, tantalum isotopes, and tungsten isotopes at 30 to 170 kev, cross sections for, (E), 20: 42293
capture-to-fission ratio measurements, design of time-of-flight system with on-line computer for, 20: 41232(R) (ORNL-3875, pp 75-90)
decay constants in beryllium systems, 20: 42601
density distributions in multilayer unit cells, 20: 42680 (INR-698/IX-A/RP)
detection in reactors, design and performance of gamma-compensated ionization chamber for, 20: 41360(P)
detection of divergent, performance of multiple-wire spark counters for, 20: 41317
detection of, design and performance of diamond scintillation detector for, 20: 41290
detection of, design and performance of two-impulse scintillation detector for, 20: 41337
detection of, design of metal-foil activation detector for, 20: 41358(P)
detection of, design of spherical boron trifluoride proportional counter for, 20: 41271(R) (ORNL-3875, pp 44-52)
diffusion equations for, computer program for solution of time-dependent two-dimensional multigroup, 20: 42143 (WANL-TNR-133(Rev.))
dosimetry in accelerator environment, methods for, 20: 41543 (RPP-R-2)
dosimetry of first- and multiple-collision, multisphere technique for, 20: 41280(T) (NP-tr-1410)
dosimetry of, design of ionization chamber for, 20: 41268(R) (NYO-2740-3, pp 5-165)
dosimetry of, performance of proportional detectors for, 20: 41268(R) (NYO-2740-3, pp 5-165)
dosimetry with solid state track detectors, medical uses, 20: 41262 (BNWL-SA-619)
effects on antifriction and strength properties of structural materials, 20: 41498
effects on aqueous suspensions of plutonium dioxide, 20: 41009 (AERE-R-3268)
effects on chromosomes, repair mechanisms for, 20: 40609 (CONF-660418-1)
effects on creep of metals at high temperature, extrapolation method for, 20: 41495(R) (EURAEC-1621)
effects on crystal lattice of carbon steel, 20: 41497
effects on embryos of mice, RBE of x radiation, 20: 40618(R) (NYO-2740-3, pp 166-215)
effects on eyes, cataractogenetic, RBE of x radiation, 20: 40618(R) (NYO-2740-3, pp 166-215)
effects on maize, genetic, 20: 40618(R) (NYO-2740-3, pp 166-215)
effects on mechanical properties of vanadium-base alloys, 20: 41506
effects on pressure vessel steels, 20: 41494(R) (EURAEC-1617)
effects on steels, method for comparison of, 20: 41504
effects on steels, equipment for measuring, 20: 41113
effects on tobacco resistance to blue mold disease, mutagenic, 20: 40613 (N-66-18147)
flux distributions in swimming-pool reactors, correlation with two-group diffusion theory, 20: 42600
flux measurements of, multisphere technique for, 20: 41280(T) (NP-tr-1410)
flux measurements in PWR Core 2, system description for, 20: 42647 (WAPD-PWR-2226)
flux monitoring system development, 20: 42579(R) (ANL-7245, pp 29-47)
form factors from deuteron-electron interactions, electromagnetic, (T), 20: 41883
interactions with deuterons at 14 Mev, neutron spectra from disintegration, (T), 20: 42291
interactions with protons at 23.1 Mev, spin correlation parameter for, (E), 20: 41877
interactions with mesons (K^-) at 0.8 to 1.1 Bev/c, Y_1^1 resonant amplitudes from, (E), 20: 41886
interactions with protons below 1 Bev, review of polarization in, (E), 20: 41916
mass relative to protons, field-theoretical sum rules for calculating, 20: 41824
photoproduction on nuclei, energy spectra from, (E), 20: 42165(R) (MIT-2098-251, pp 16-20)
polarization in electric and magnetic fields, 20: 41902
reactions (n,α_0) with carbon-12 at 16 and 17 Mev, total cross sections for, 20: 42367

reactions (n,α) with oxygen-16 at 14.9 Mev, alpha angular distribution from, (E), 20: 42370
reactions (n,α_0) with sulfur-32 from 2.5 to 3.2 Mev, differential cross sections for, (E), 20: 42375
reactions (n,α) with oxygen-16 and silicon-28, DWBA analysis of, (T), 20: 42392
reactions (n,α) with neon-20 and oxygen-16 at 14.1 Mev, angular distributions for, (E), 20: 42216
reactions (n,f) with plutonium-239, uranium-233, and uranium-235, energy dependence of fission-fragment angular distribution in, (E), 20: 42171(T) (LA-tr-66-41)
reactions (n,γ) with hafnium-178, hafnium-179 decay scheme from, (E), 20: 42285
reactions (n,γ) with palladium-108 and silver-109, preparation of carrier-free silver-111 by, 20: 41023
reactions (n,2n) with nuclei at 14.8 Mev, activation cross sections for, (E), 20: 42207
reactions (n,2n)2α with beryllium-9 at 15 Mev, mechanism of, (E), 20: 42362
reactions in nuclear emulsions at 20 to 300 Mev, gray prong per star analysis of, (E), 20: 41276 (UCRL-16769)
reactions with chlorine, lead, potassium, sodium, and sulfur at 14.7 Mev, gamma emission in, (E), 20: 42146 (AD-638014)
reactions with protactinium-233 at 0.01 ev to 10 kev, total cross sections for, (E), 20: 42151 (IN-1014)
reactions with tellurium, production of iodine-131 in, 20: 41399 (IEA-110)
scattering by beryllium, measurement of dispersion relation by, 20: 42541
scattering by carbon-12 at 1 to 10 Mev, differential elastic, (E), 20: 41556
scattering by deuterons at 1 to 5 Mev, angular distributions for elastic, (E), 20: 42359
scattering by graphite, equipment for, 20: 41075 (AERE-R-5217)
scattering by lead at low energy, neutron polarization in, (E), 20: 42140 (JINR-P-2764)
scattering by lithium-7 at 14 Mev, excitation of 5.7 Mev level by inelastic, (E), 20: 42364
scattering by molecules, effect of nuclear spin correlations on, 20: 42144
scattering by potassium-39 at 14 Mev, cross sections for elastic, (E/T), 20: 42393
scattering by tritium at 14 Mev, differential cross sections for elastic, (E), 20: 42373
scattering cross sections for, optical model analysis of, 20: 41796(R) (MIT-2098-251, pp 74-103)
shielding measurements in heavy concrete, 20: 41534 (DESY-66/18)
spectra in ALRR, nuclear emulsion analysis, 20: 42681(R) (IS-1500 (Sect. R))

NEUTRONS, DELAYED
emission by fission products, 20: 42681(R) (IS-1500(Sect. R))
use in uranium determination in boreholes, 20: 41157

NEUTRONS, EPITHERMAL
dosimetry of, detector for, 20: 41362(P)

NEUTRONS, FAST
capture by indium-113, indium-115, and yttrium-89, cross sections for isomer production in, (E), 20: 42326
capture cross sections for holmium-165, indium-115, manganese-55, and sodium-23 from 1.0 to 19.5 Mev, radiative, (E), 20: 42332
detection and measurement of, design of silver-activated zinc sulfide sandwiched scintillation detectors for, 20: 41335
dosimetry of, detector for, 20: 41362(P)
effects on blood cells in mice, 20: 40502(R) (ORNL-3922, pp 115-27)
effects on defects in silicon crystals, (E), 20: 42567(T)
effects on mechanical properties of cladding materials, 20: 42579(R) (ANL-7245, pp 29-47)
effects on terphenyl, 20: 40946 (AECL-2589)
effects on tungsten, annealing of, 20: 42551
flux in atmosphere, solar minimum measurements of, 20: 42055
reactions (n,f) with uranium-235 at 5, 6, and 7 Mev, mass dependence of total fission-fragment energy in, (E), 20: 42297
sources for chronic exposure of mice, dosimetry, 20: 40504(R) (ORNL-3922, pp 146-60)

NEUTRONS, FISSION
dosimetry in mouse phantoms, 20: 41268(R) (NYO-2740-3, pp 5-165)

NEUTRONS, PROMPT
emission of, research on, 20: 42325
lifetime in ALRR, 20: 42681(R) (IS-1500(Sect. R))

NEUTRONS, THERMAL
capture by calcium-43, calcium-44 energy-level transitions from, (E), 20: 42335
capture by tellurium isotopes, gamma spectra from, (E), 20: 42286
detection of, development of survey meters for, 20: 41272(R) (ORNL-3875, pp 53-74)
dosimetry of, detector for, 20: 41362(P)
effects on n-type cadmium sulfides and cadmium tellurides, 20: 41271(R) (ORNL-3875, pp 44-52)
effects on rice seed, chlorophyll mutations from, 20: 40641
gamma rays from capture of, nondestructive technique to defect burnable poisons in fuel materials, 20: 41112 (IITRI-578P11-54)
radioinduced mutations in rice, 20: 40640
reactions (n,f) with plutonium-239 and plutonium-241, fission-fragment energy and mass distributions in, (E), 20: 42261
reactions (n,f) with uranium-235, mass dependence of fission-fragment energy, (E), 20: 42297
reactions (n,f) with uranium-235, search for three- and four-body neutron bound states in, (E), 20: 42298
reactions (n,f) with uranium-235, cesium-132, -134, and -136 and rubidium-86 yields in, 20: 42178
reactions (n,f) with uranium-233 and -235, cesium-137 yields in, 20: 42176
reactions (n,γ) with scandium-45, gamma spectra from, (E), 20: 42382
reflection by slabs of aluminum, concrete, iron, lead, and polyethylene, differential, 20: 42142 (NP-16234)
scattering by water-d_2, model for calculating, (T), 20: 42139 (IN-1020)
scattering kernels for water at 423 and 550°K, (T), 20: 42138 (IN-1019)

NEW JERSEY
water supply for New York City area of, desalting evaluation for, 20: 42658 (NP-16250)

NEW YORK
water supply for New York City area of, desalting evaluation for, 20: 42658 (NP-16250)

NEW ZEALAND
environmental radioactivity measurements, 20: 40521(R) (NP-16270)

NICKEL
determination in americium and plutonium by spark-source mass spectrography, 20: 40816 (RFP-699)
determination in plutonium by carrier distillation methods, spectrographic, 20: 40814 (RFP-664)
determination in uranium trioxide by emission spectrography, 20: 40802 (HW-65402(Rev.1))
determination in uranium(IV-VI) oxides, effects of graphite electrode grade on carrier-distillation spectroscopic, 20: 40807 (NLCO-976)
determination in uranium by atomic absorption spectrophotometry, 20: 40815 (RFP-698)
effects as catalyst on hydrogenation of ethylene, deuterium–hydrogen exchange in, 20: 40942
effects on phase transformations in gallium–plutonium alloy and plutonium, differential thermal analysis of, 20: 41452 (MLM-1172)
heat transfer to water by spheres of, 20: 42580(R) (ANL-7245, pp 60-73)
helium and hydrogen ion attenuation at 0.1 to 500 Mev, tables for, 20: 41619 (CEA-R-3042)
ion ranges at 10 to 100 Mev, bromine and iodine, 20: 41647
ion scattering at 12 to 25 kev, secondary electrons from, 20: 41620 (NIJS-R-471)
magnetic fields in low-temperature, De Haas-Van Alphen effect from, 20: 42523(R) (IS-1500(Sect.P))
properties for use as thermal shielding at high temperatures in vacuum, 20: 41440(R) (ALO-3632-4)

NICKEL ALLOYS
analysis of, for trace impurities by deuteron activation methods, 20: 40812 (ORO-2980-14)
Co–Ni–Sc, crystal structure of Laves phases in, 20: 41412(R) (IS-1500 (Sect. M))
Fe–Ni–Sc, crystal structure of Laves phases in, 20: 41412(R) (IS-1500 (Sect. M))
Hf–Ni, crystal structure of intermetallic compounds, 20: 41412(R) (IS-1500(Sect. M))
Mn–Ni–Sc, crystal structure of Laves phases in, 20: 41412(R) (IS-1500 (Sect. M))
Mo–Ni, electric conductivity of, effects of crystal structure on, 20: 41457(R) (ORO-3291-3)
Mo–Ni, specific heats of, methods of measuring, 20: 41457(R) (ORO-3291-3)
Ni–Ti, crystal structure of equi-atomic, model of, 20: 41412(R) (IS-1500(Sect. M))
Ni–Zr, crystal structure of intermetallic compounds, 20: 41412(R) (IS-1500(Sect. M))

NICKEL CARBONYLS
metabolism in rats, tracer study, 20: 40536(R) (ORO-3461-1)
poisoning in man, use of dithiocarb for therapy of, 20: 40536(R) (ORO-3461-1)
toxicity in rats, 20: 40536(R) (ORO-3461-1)

NICKEL CHLORIDES
metabolism in rats, tracer study, 20: 40536(R) (ORO-3461-1)

NICKEL COMPLEXES
with dimethylglyoxime, infrared spectra of, 20: 40796(R) (IS-1500 (Sect.C))

NICKEL ISOTOPES
helium-3 reactions (He-3,t) at 18 Mev, (E), 20: 42334
proton reactions at 14.5 Mev, total cross sections for, (E), 20: 42162 (LA-DC-8075)

NICKEL ISOTOPES Ni-58
deuteron elastic scattering at 13.6 Mev, optical model analysis of, (T), 20: 42294
helium-3 reactions (He-3,t) at 18 Mev, (E), 20: 42334
photon reactions (γ,n) and (γ,p) with, properties of, (T), 20: 42220
proton elastic scattering at 30 Mev, optical-model analysis of, (T), 20: 42255
proton reactions at 30 Mev, optical-model analysis of total cross sections for, (T), 20: 42255

NICKEL ISOTOPES Ni-60
deuteron elastic scattering at 13.6 Mev, optical model analysis of, (T), 20: 42294
energy-level transitions, (E), 20: 42254
helium-3 reactions (He-3,t) at 18 Mev, (E), 20: 42334
proton elastic scattering at 30 Mev, optical-model analysis of, (T), 20: 42255
proton reactions at 30 Mev, optical-model analysis of total cross sections for, (T), 20: 42255

NICKEL ISOTOPES Ni-61
helium-3 reactions (He-3,t) at 18 Mev, (E), 20: 42334

NICKEL ISOTOPES Ni-62
deuteron elastic scattering at 13.6 Mev, optical model analysis of, (T), 20: 42294
helium-3 reactions (He-3,t) at 18 Mev, (E), 20: 42334

NICKEL ISOTOPES Ni-64
deuteron elastic scattering at 13.6 Mev, optical model analysis of, (T), 20: 42294
helium-3 reactions (He-3,t) at 18 Mev, (E), 20: 42334

NICKEL OXIDES
crystal structure of lithium-doped, 20: 41458(R) (TID-23268)

NICKEL STEEL
Cr–Mo–Ni, properties of Super-Elso, effects of heat treatments on, 20: 41447(R) (EURAEC-1669)
Cr–Ni, corrosion by aqueous dichromate-nitric acid, 20: 41418(R) (GEAP-5150)
Cr–Ni, corrosion by aqueous iron chloride, effects of carbon, manganese, and silicon traces on, 20: 41418(R) (GEAP-5150)
Cr–Ni, preparation of, containing controlled-impurity carbon, manganese, and silicon, 20: 41418(R) (GEAP-5150)

NICOTINAMIDES
effects on chromosome aberration induction in carcinoma and sarcoma cells by nitrogen mustard and triethylamine, 20: 40550

NIOBIUM
crystal lattice vibrations in, inelastic neutron scattering measurements of, 20: 42573
determination by atomic absorption spectroscopy using induction-coupled plasmas, 20: 40796(R) (IS-1500(Sect.C))
oxidation of, effects of specimen shape and stress on, 20: 41412(R) (IS-1500(Sect. M))
preparation and properties of single crystals of, 20: 41481
preparation by reduction of pentoxide of, using aluminum, 20: 41412(R) (IS-1500(Sect. M))
separation from molybdenum, tantalum, and tungsten by solvent extraction using methyl isobutyl ketone, 20: 40796(R) (IS-1500(Sect.C))
separation of protactinium from, by selective precipitation from oxalic-hydrochloric acid mixtures, 20: 41043
separation of protactinium from, by hydrolysis in oxalic and hydrochloric acid, 20: 41044
superconducting properties of high-purity, (E), 20: 42117
thermophysical properties at 1300 to 3000°K, (E), 20: 41762
x-ray emission spectra of, L and K, (E), 20: 41350

NIOBIUM ALLOYS
Mo–Nb, crystal lattice vibrations in, inelastic neutron scattering measurements of, 20: 42573
Mo–Nb, preparation and properties of single crystals of, 20: 41481
Mo–Nb–Zr, phase studies of, isothermal sections at 1200°C in, 20: 41464
Nb–Sn, magnetic flux penetration in superconducting, (E), 20: 42132
Nb–Ti, magnetic flux penetration in supe conducting, (E), 20: 42132
Nb–Ti–V, radiation effects on mechanical properties up to 750°C, neutron, 20: 41506
Nb–U, production of niobium-base, method for, 20: 41412(R) (IS-1500 (Sect. M))
Nb–W, preparation and properties of single crystals of, 20: 41481
Nb–Zr, corrosion by liquid potassium at high temperatures, 20: 41419(R) (GMAD-3643-5)
Nb–Zr, corrosion of zirconium-base, by steam at high temperatures, 20: 41422
Nb–Zr, critical currents in, effects of annealing and orientation on, (E), 20: 42569
Nb–Zr, ductility of zirconium-base, effects of high temperatures on, 20: 41422
Nb–Zr, magnetic flux penetration in superconducting, (E), 20: 42132
Nb–Zr, magnetization of superconducting, (E), 20: 42133
Nb–Zr, mechanical properties of, effects of oxygen on, 20: 41412(R) (IS-1500(Sect. M))
Nb–Zr, phase studies of, 20: 41443(R) (COO-588-12)
Nb–Zr, propagation of normal region in superconducting solenoid of, 20: 42100
Nb–Zr, structure and superconducting properties of, effects of oxygen on, 20: 42535
Nb–Zr, uptake of carbon, nitrogen, and oxygen by, in liquid metal loops, 20: 41419(R) (GMAD-3643-5)

NIOBIUM CARBIDES
electric resistance at 1200 to 3500°K, 20: 41729
hardness of cast, at 20 to 1500°C, 20: 41429(R) (USBM-RC-1249)
interactions with gas flow in MHD generators, 20: 41738
oxidation of cast, by air at 450 to 800°C, 20: 41429(R) (USBM-RC-1249)
preparation and properties of cast, 20: 41429(R) (USBM-RC-1249)
radiation capacity at 1200 to 3500°K, 20: 41729

NIOBIUM CHLORIDES
separation from tantalum chloride, methods for, 20: 41064(R) (IS-1500 (Sect.E))

NIOBIUM COMPLEXES
acetonitrile, crystal structure of, 20: 40796(R) (IS-1500(Sect.C))

NIOBIUM ISOTOPES Nb-93
carbon-12 reactions (C-12,N-13) with, angular distributions from, (E), 20: 42153 (JINR-E-2824)

NIOBIUM ISOTOPES Nb-95
beta activity measurements in France, 20: 41189 (CEA-R-3020)
content in fallout and plankton of Mediterranean Sea, 1963, 20: 41146
content in fallout from Chinese nuclear test, May 1965, 20: 41130(R) (COO-1407-10)
determination in sea water, gamma spectrometric, 20: 41145
sorption reactions of, on minerals, 20: 41178 (AD-635547)

NIOBIUM OXYCHLORIDES
chlorination kinetics of, 20: 41064(R) (IS-1500(Sect.E))

NIOBIUM SILICIDES
oxidation at reduced pressures, effects of additives on, 20: 41424

NIOBIUM SULFIDES
vaporization of, thermodynamics of, 20: 40796(R) (IS-1500(Sect.C))

NITRATES
thermal stability of anion resins in form of, in vented system, 20: 40877 (RL-SEP-823)

NITRIC ACID
corrosive effects of aqueous dichromate solutions of, on chromium–nickel steel, 20: 41418(R) (GEAP-5150)
isotopic substitution in, partition function ratios at 20 to 2000°K for nitrogen-15 and oxygen-18, 20: 40873(R) (NYO-3462-2)
separation from water by extraction in pulse columns, 20: 41064(R) (IS-1500(Sect.E))
separation of zirconium from, by solvent extraction using di- and monoisopentyl esters of methylphosphonic acid, 20: 41051
HNO_3–NO, nitrogen-15 fractionation in, effects of temperature on, 20: 40873(R) (NYO-3462-2)
HNO_3–$UO_2(NO_3)_2$–H_2O, refractive index measurements on, 20: 40804 (KR-108)
$Nd(NO_3)_3$–HNO_3–$Pr(NO_3)_3$–TBP–H_2O, separation factors for neodymium and praseodymium in, 20: 40904
NH_4SCN–HNO_3–TBP, use in chromatographic separation of rare earths, thorium, and uranium, 20: 41045

NITROGEN
alpha-particle interactions with, properties of recoil ions from, 20: 41622 (SC-DC-66-1564)
content in arc-melted rhenium–tungsten ingots, 20: 41429(R) (USBM-RC-1249)
determination in liquid sodium from recirculating test loops, 20: 41420(R) (MSAR-66-149)
determination in metals by carrier-gas fusion extraction, 20: 40796(R) (IS-1500(Sect.C))
determination in titanium and zirconium nitrides, comparison of hot extraction and Kjeldahl methods for, 20: 40820(T) (IS-Trans-37)
determination of, on beryllium surfaces by deuteron activation methods, 20: 40812 (ORO-2980-14)
diffusion in stainless steel, effects of temperature on, 20: 41419(R) (GMAD-3643-5)
effects on brittle-ductile transitions in chromium, 20: 41412(R) (IS-1500(Sect. M))
effects on microstructure of type 304 stainless steel wire, dilatometric, 20: 41449(R) (EURAEC-1676)
electric conductivity of LaB_6 powder suspended in, (T), 20: 41713
electric discharges in, high-pressure electrodeless, (E), 20: 42509

electron drift velocities in, magnetic field effect on, (T), 20: 41628
electron free-free transitions in, method for calculating, 20: 41626
electron ionization cross sections of molecular, (E), 20: 41652
explosion tests in gloved box, 20: 41203 (UCRL-16259)
flux in primary cosmic radiation, (E), 20: 41672
helium and hydrogen ion attenuation at 0.1 to 500 Mev, tables for, 20: 41619 (CEA-R-3042)
hydrogen ion reactions at 2 to 50 kev, charge exchange and dissociation cross sections for, 20: 41646
incorporation in 4-amino-2-hydroxybutyric acid and methyl ester of anthranilic acid, 20: 41024
properties as working medium in closed-cycle turbine, 20: 42654
radiation effects on content in soils, effects of soil type on gamma, 20: 40637(R) (ORO-2754-7)
reactions with uranium carbide, effects of hydrogen on, 20: 40870 (NAA-SR-Memo-7310)
release from amino acids using ninhydrin, nitrogen-15 determination by, 20: 40824
separation from oxygen by gas chromatography, 20: 40805(R) (MLM-1325, pp 63-70)
separation from thorium by electrotransport, 20: 41412(R) (IS-1500 (Sect. M))
uptake by niobium–zirconium alloys in liquid metals, 20: 41419(R) (GMAD-3643-5)
urea, content in blood of deer and sheep, 20: 40541(R) (UCD-34P104-3)

NITROGEN IONS
interactions with hydrogen ions at 20 to 250 kev, cross sections for inelastic, (E), 20: 41666
radioinduced formation of N_3^- in sodium azides, ESR studies of x, 20: 40966

NITROGEN ISOTOPES
nucleon configuration mixing, (E), 20: 42204

NITROGEN ISOTOPES N-13
energy levels, (E), 20: 42204

NITROGEN ISOTOPES N-14
deuteron elastic scattering at 28.5 Mev, (E/T), 20: 42389
deuteron reactions (d,nγ) with oxygen-15 energy levels from, (E), 20: 42346
deuteron reactions (d,p) with, nitrogen-15 energy levels from, (E), 20: 42369
deuteron reactions (d,α) with, alpha energy spectra from, (E), 20: 42389
energy levels, (E), 20: 42400
energy-level spins and transitions, (E), 20: 42252
energy-level transitions in, branching ratios for, (E), 20: 42231
neutron reactions with, beryllium-7 production in, (E), 20: 41276 (UCRL-16769)
proton reactions (p,γ) at 0.85 to 1.96 Mev, oxygen-15 energy levels from, (E), 20: 42258
proton reactions (p,d) at 156 Mev, nitrogen-13 energy levels from, (E), 20: 42204
reactions (N-14,F-18) with aluminum-27 at 65.0 to 107.3 Mev, (E), 20: 42156 (JINR-P-2813)

NITROGEN ISOTOPES N-15
determination in amino acids in legume root nodules, use of ninhydrin in colorimetric, 20: 40824
deuteron reactions (d,α) at 0.8 to 1.8 Mev, oxygen-17 energy levels from, (E), 20: 42295
electron spin resonance of, in gamma-irradiated potassium sulfamate, 20: 40955
energy levels, (E), 20: 42369
energy levels from oxygen-16 (γ,pγ′) reaction, (E), 20: 42343
fractionation in nitric acid–nitric oxide system, effects of temperature on, 20: 40873(R) (NYO-3462-2)
proton reactions (p,γ) with, oxygen-16 energy levels from, (E), 20: 42342
reactions (N-15,xn) with thulium-169, beta decay of osmium-180 from, (E), 20: 42284
substitution in nitrogen compounds, partition function ratios at 20 to 2000°K for, 20: 40873(R) (NYO-3462-2)

NITROGEN ISOTOPES N-16
energy levels, (E), 20: 42369

NITROGEN MUSTARDS
effects on chromosome aberration induction in carcinoma and sarcoma cells, effects of nicotinamide on, 20: 40550

NITROGEN OXIDES
determination of, in presence of hydrogen, methane, and nitrogen by gas chromatography, 20: 40805(R) (MLM-1325, pp 63-70)
effects in radiation biology, electron spin resonance studies, 20: 40597
isotopic substitution in, partition function ratios at 20 to 2000°K for nitrogen-15 and oxygen-18, 20: 40873(R) (NYO-3462-2)
production by chemonuclear synthesis, 20: 40988
reactions with muonium, review of, 20: 41661
HNO_3–NO, nitrogen-15 fractionation in, effects of temperature on, 20: 40873(R) (NYO-3462-2)

NITROGEN SYSTEMS
C–N–O–U, preparation and high-temperature properties of stoichiometric, 20: 41429(R) (USBM-RC-1249)
ethylene–N_2, alpha-particle interactions with, properties of recoil ions from, 20: 41622 (SC-DC-66-1564)
F–N, use in removal of actinide halides from alumina, 20: 41062(P)
N–O, radiolysis of, decontamination of products from fission-fragment, 20: 40951(RPI-321-6)
N–Y, phase studies, 20: 41412(R) (IS-1500(Sect. M))

NITROSYL BROMIDES
isotopic substitution in, partition function ratios at 20 to 2000°K for nitrogen-15 and oxygen-18, 20: 40873(R) (NYO-3462-2)

NITROSYL CHLORIDES
isotopic substitution in, partition function ratios at 20 to 2000°K for nitrogen-15 and oxygen-18, 20: 40873(R) (NYO-3462-2)

NITROSYL FLUORIDES
isotopic substitution in, partition function ratios at 20 to 2000°K for nitrogen-15 and oxygen-18, 20: 40873(R) (NYO-3462-2)

NITROUS ACID
isotopic substitution in, partition function ratios at 20 to 2000°K for nitrogen-15 and oxygen-18, 20: 40873(R) (NYO-3462-2)

NITROXY FLUORIDES
isotopic substitution in, partition function ratios at 20 to 2000°K for nitrogen-15 and oxygen-18, 20: 40873(R) (NYO-3462-2)

NITRYL CHLORIDES
isotopic substitution in, partition function ratios at 20 to 2000°K for nitrogen-15 and oxygen-18, 20: 40873(R) (NYO-3462-2)

NITRYL FLUORIDES (NO,F)
isotopic substitution in, partition function ratios at 20 to 2000°K for nitrogen-15 and oxygen-18, 20: 40873(R) (NYO-3462-2)

NORWAY
cesium-137 content in milk from, March 1962 to 1966, 20: 41132 (NYO-3364-20)

NOSE
treatment of tumors of, by radiation and methotrexate, 20: 40782

NOZZLES
development for Poodle propulsion system, 20: 41396(R) (STL-517-0042)
inspection of pressure-vessel, ultrasonic devices for, 20: 42636(R) (SWRI-1228-4-22)

NPD REACTOR
environs monitoring, April 1965, 20: 41136
fuel development for, status, 20: 42618 (66-CNA-312)

NPD-2 REACTOR
environs monitoring, April 1965, 20: 41136

NRX REACTOR
environs monitoring, April 1965, 20: 41136

NUCLEAR ELECTRIC MOMENTS
measurement of quadrupole, for excited states, method for, (T), 20: 42303

NUCLEAR EMULSIONS
meson (π^-) reactions at 17 Bev/c, electron pair production from, (E), 20: 41814
meson ($\pi^\pm$) range in, at 78 and 90 Mev/c, 20: 41826
particle track developer for, properties of amidol-pyrogallol, 20: 41340
proton interactions at 25 Bev in, multiple fragment emission in, 20: 41827
scanning of nuclear spectra registered in, reliability of fractional, 20: 41315
sensitivity of triethylamine-sensitized, for uranium-233 alpha radiation, 20: 41341
use for monitoring accelerator radiation, 20: 41276 (UCRL-16769)
use for neutron dosimetry in accelerator environment, 20: 41543 (RPP-R-2)
use in ALRR neutron spectra analysis, 20: 42681(R) (IS-1500(Sect. R))
use in space research, (E), 20: 41803(R) (UCRL-16863)

NUCLEAR ENGINEERING
materials for use in, survey of, 20: 41413

NUCLEAR MAGNETIC RESONANCE
book: *High Resolution Nuclear Magnetic Resonance Spectroscopy, Vol. I*, 20: 41255
measurement of, performance of INDOR technique for, 20: 42529

NUCLEAR MODELS
formulation of statistical compound-nucleus, (T), 20: 42269
hole self-energy corrections in Brueckner theory, 20: 42244

NUCLEAR MODELS (COLLECTIVE)
formulation with breathing-mode state, (T), 20: 42245

NUCLEAR MODELS (OPTICAL)
development for meson (π) elastic scattering, (T), 20: 42319
exact solution of equations of, for analysis (p,n) reactions, 20: 42243
potentials for composite particles, approximate relations for strengths and shapes of, 20: 42280
use in analysis of neutron scattering cross section data, 20: 41796(R) (MIT-2098-251, pp 74-103)

NUCLEAR MODELS (SHELL)

nuclear bound states in nonlocal, · 20: 42301
potentials for calculation of nuclear properties, (T), · 20: 42247
wave functions for calculation of nuclear properties, (T), · 20: 42247
wave functions for calculation of nuclear properties, (T), · 20: 42247
wave functions

NUCLEON SHOWERS
production by proton reactions with nuclei from Z = 6 to 92 at 660 Mev, (E), 20: 42299
NUCLEONS
form factors of, electromagnetic, 20: 41952
interactions of, dispersion sum rules for electromagnetic and strong, (T), 20: 41793 (JINR-E-2822)
interactions of, two-pion-exchange potential for three-body, 20: 41838
interactions of, weak axial-vector currents for, 20: 41981
interactions with nucleons in M(12) symmetry, SU(3) symmetry breaking effects in, 20: 41973
interactions with mesons (π) at 300 Mev, phase shift analysis of, (E), 20: 41794 (JINR-E-2860)
interactions with photons, SU(6) symmetry for meson production in, (T), 20: 41812
interactions with mesons (π) in nuclei at low energies, (T), 20: 42312
interactions with mesons (π), modified one-nucleon exchange model for, 20: 41815
interactions with mesons (π), Schroedinger theory for static, 20: 41418
interactions with photons, two-meson (π) exchange in, (T), 20: 41821
interactions with mesons (π^-) at 12 and 18 Bev/c, recoil states from inelastic meson (ρ^0) production in, (E), 20: 41828
interactions with protons at 20 Bev/c, multiple meson production, (E/T), 20: 41829
interactions with mesons (K) and (π), scattering lengths for, (T), 20: 41846
interactions with mesons (π), consistency condition on strong, 20: 41861
interactions with mesons (π) at low energies, modified effective-range approximation for, 20: 41864
interactions with mesons (π), meson (η) production and interaction from, (T), 20: 41866
interactions with mesons (η) from meson (π)-nucleon interactions, (T), 20: 41866
interactions with photons, vector dominance approximation for meson production in, 20: 41869
interactions with nucleons, two-pion-exchange effects in, (T), 20: 41873
interactions with mesons (π), consistency of nucleon-nucleon interactions with, (T), 20: 41873
interactions with mesons (π), quark model for $N\frac{1}{2}_3N\pi$ vertex in, 20: 41876
interactions with mesons (π), meson (π)-nucleon and meson (ρ) coupling constants from scattering lengths in, (T), 20: 41885
interactions with antinucleons, intermediate boson production in annihilation, (T), 20: 41892
interactions with hyperons (Λ), repulsive core in S state in, (T), 20: 41894
interactions with massless vector photons, large t limit for sixth-order diagrams for Compton, 20: 41897
interactions with mesons (K), cross sections for, (T), 20: 41898
interactions with nucleons, one-boson exchange potentials for, (T), 20: 41899
interactions with mesons (π) and photons, theory of three particle production in, 20: 41900
interactions with photons, isospin amplitudes for S-state meson (π^0) production in, 20: 41906
interactions with mesons (π^-), cross section lower limit for, (E), 20: 41910
interactions with mesons (π), phase shift analyses for, 20: 41913
photon reactions with, meson (π) production amplitudes for, (T), 20: 41996
reactions with nuclei, approximate relations for strengths and shapes of optical potentials for, 20: 42280
theory of many-body systems of, hole self-energy corrections in Brueckner, (T), 20: 42244
wave functions for three-body systems of, (T), 20: 42209
NUCLEOPROTEINS
radiation effects on, electron spin resonance studies, 20: 40598
NUCLEOSIDES
electron spin resonance spectrometry of irradiated, 20: 40593
NUCLEOTIDES
effects of radiophosphorus on composition of, in plants, 20: 40548
inhibition of valyl-tRNA synthetase by oligo-, 20: 40503(R) (ORNL-3922, pp 137-45)
radiation effects on levels of reduced pyridine, in rat liver homogenates, γ, 20: 40583
NUCLEOTIDES, DESOXY-
electron spin resonance spectrometry of irradiated, 20: 40593

O

OAK RIDGE NATIONAL LAB., TENN.
containment research installation at, construction of, 20: 41078(R) (ORNL-3875, pp 91-100)
data collection and analysis at, 20: 41232(R) (ORNL-3875, pp 75-90)
radiation warning and communication system at, expansion and modernization of, 20: 41272(R) (ORNL-3875, pp 53-74)
radio communication system at, description of, 20: 41272(R) (ORNL-3875, pp 53-74)
OCEANOGRAPHY
carbon-14 studies during International Indian Ocean Expedition, 20: 41127
tracer studies of Columbia River estuary and Northeast Pacific, 20: 40523(R) (RLO-1750-8(Vol.1))
OCTANE, 2,7-DIMETHYL-
radiolysis of, EPR studies of yields of stabilized charges in low-temperature, 20: 40962
2-OCTENE
radioinduced and photoinduced isomerization of, effects of benzene on, 20: 40965
OIL DEPOSITS
origin of brines in, 20: 41161
properties for, equipment development for radiometric, 20: 41165
OILS
radiopreservation of, effects on rats, 20: 41391
OLIGOMYCIN
effects on nuclear structure of rat thymocytes, 20: 40549
OPTICAL SYSTEMS
design for measurement of radioinduced effects in materials, 20: 41488(R) (EGG-1183-2013)
design for measurement of radioinduced effects in materials, 20: 41491(R) (EGG-1183-2030)
design of, for measuring radioinduced effects in materials, 20: 41493(R) (EGG-1183-2052)
development for measurement of radioinduced effects in materials, 20: 41492(R) (EGG-1183-2039)
radiation effects on transparency, recovery from, 20: 41099
ORES
analysis for silver, equipment used in activation methods for, 20: 40848
ORGANIC CHEMISTRY
book: *Radioactive Isotopes in Chemical Research*, 20: 41027
ORGANIC COOLED REACTORS
heat transfer in DOR, simulation methods for, 20: 42635 (RISO-124)
kinetics of ESSOR, methods for analysis of, 20: 42678 (EUR-3051.e)
ORGANIC MODERATED REACTORS
control rod design for, to reduce flux peaking, 20: 42588(P)
ORGANISMS
radioisotope uptake by hydrobiont, 20: 40527
ORGANS
radiation dose from inhaled or ingested soluble radionuclides, dose conversion factors for estimation of, 20: 41193 (IDO-12054)
radioisotope scanning in, design and performance of gas-filled intensifier spark chamber for, 20: 41298
use of pertechnetate in scintiscanning of, 20: 40750
ORGEL REACTOR
coolant properties for, 20: 42623 (EUR-2996.f)
ORNL FAST BURST REACTOR
operation of, internal timer design for, 20: 42683 (ORNL-TM-1559)
ORNL HIGH FLUX ISOTOPE REACTOR
design of fuel cladding-failure detectors, 20: 41272(R) (ORNL-3875, pp 53-74)
servomechanisms of, testing of power-regulating, 20: 42581(R) (ORNL-3875, pp 125-50)
testing of, hydrodynamic and vibrational, 20: 42581(R) (ORNL-3875, pp 125-50)
ORNL RESEARCH REACTOR
boiling detector for, development of, 20: 42581(R) (ORNL-3875, pp 125-50)
experimental facilities for, pneumatic tube, 20: 42581(R) (ORNL-3875, pp 125-50)
experimental facilities for, capsule test, 20: 42581(R) (ORNL-3875, pp 125-50)
radiation warning and communication system at, performance of, 20: 41272(R) (ORNL-3875, pp 53-74)
OSMIUM FLUORIDES
fluorine-19 NMR and spin-lattice relaxation in, 20: 40892
OSMIUM ISOTOPES Os-180
beta decay of, rhenium-180 energy levels from, (E), 20: 42284
OSMIUM ISOTOPES Os-186
gamma emission from first 2+ state of, Mössbauer scattering of, (E), 20: 42167(R) (MIT-2098-251, pp 50-6)
OXALATE COMPLEXES
with americium, electromigration studies on, 20: 40913
OXALATES
effects on uranyl complexes with tributylphosphine oxide, 20: 40885

OXALIC ACID
effects on disproportionation of uranium(V), 20: 40911
OXIDATION
radiation effects on, in mouse tumor cells, 20: 40642
OXIDIZING AGENTS
effects of aut-, on depolymerization of hyaluronic acid, 20: 40591
OXYGEN
content in arc-melted rhenium–tungsten ingots, 20: 41429(R) (USBM-RC-1249)
corrosive effects of liquid sodium-dissolved, on stainless steel at high temperatures, 20: 41420(R) (MSAR-66-149)
depletion in fire zones of fallout shelters, 20: 41184 (AD-637806)
determination by activation analysis, 20: 40796(R) (IS-1500(Sect.C))
determination in liquid sodium from recirculating test loops, 20: 41420(R) (MSAR-66-149)
determination in metals by carrier-gas fusion extraction, 20: 40796(R) (IS-1500(Sect.C))
determination of, in radioactive metals, cathodic etching method for surface cleaning for, 20: 40817 (UCRL-14959)
determination of, on beryllium surfaces by deuteron activation methods, 20: 40812 (ORO-2980-14)
determination of, in boron by neutron activation analysis, 20: 40846
determination of, in beryllium, equipment used in activation methods for, 20: 40848
determination of, in steel, equipment used in activation methods for, 20: 40848
effects in radiation biology, electron spin resonance studies, 20: 40597
effects of, on radiosensitivity of tobacco mutations, 20: 40613 (N-66-18147)
effects on mechanical properties of niobium–zirconium alloys, 20: 41412(R) (IS-1500(Sect. M))
effects on structure and superconducting properties of niobium–zirconium alloys, 20: 42535
electric discharges in, high-pressure electrodeless, (E), 20: 42509
electron drift velocities in, magnetic field effect on, (T), 20: 41628
electron excitation cross sections, (T), 20: 41654
electron free-free transitions in, method for calculating, 20: 41626
flux in primary cosmic radiation, (E), 20: 41672
gradients in Mediterranean Sea, 20: 41128
helium and hydrogen ion attenuation at 0.1 to 500 Mev, tables for, 20: 41619 (CEA-R-3042)
ionization in low-pressure discharge, anion extraction during, (E), 20: 42435
isotopic composition of, in oil well brines, 20: 41161
magnetic structure of solid, neutron-diffraction study, (E), 20: 42558
production in gamma and x radiolysis of carbon dioxide, mechanism of, 20: 40996
proton reactions (p,2p) at 160 and 460 Mev, quasi-free, (E), 20: 42276
proton reactions with neutral ground state of, formation of excited hydrogen atoms in, (T), 20: 41634
radiation effects on metabolism in bull testicle, x, 20: 40610(R) (COO-895-9)
radiation effects on uptake of, by mouse heart, x, 20: 40648
radiosensitizing effects of, electron spin resonance studies, 20: 40598
reactions with muonium, review of, 20: 41661
reactions with uranium carbide, effects of hydrogen on, 20: 40870 (NAA-SR-Memo-7310)
separation from nitrogen by gas chromatography, 20: 40805(R) (MLM-1325, pp 63-70)
separation from thorium by electrotransport, 20: 41412(R) (IS-1500 (Sect. M))
uptake by niobium–zirconium alloys in liquid metals, 20: 41419(R) (GMAD-3643-5)
use of high pressure, to increase radiosensitivity of tissues, 20: 40721
OXYGEN IONS
diffusion in yttrium oxide, 20: 41064(R) (IS-1500(Sect.E))
OXYGEN ISOTOPES O-15
energy levels from oxygen-16 (γ,nγ') reaction, (E), 20: 42343
energy levels from nitrogen-14 (d,nγ) reaction, (E), 20: 42346
energy levels of, hole and particle, (T), 20: 42345
energy-level spins and transitions, (E), 20: 42252
energy-level spins and transitions, (E), 20: 42258
OXYGEN ISOTOPES O-16
deuteron reactions (d,p) at 300 kev, angular distributions for, (E/T), 20: 42399
electron elastic and inelastic scattering at 600 to 800 Mev, cross sections for, (E/T), 20: 42238
energy levels from lithium-6 (C-12,d) reactions, width of 7.12-Mev, (E), 20: 42329
energy levels of, electromagnetic decay modes of, (E), 20: 42342
energy levels of, perturbation theory for isospin T = 2, 20: 42344
energy-level transitions in, branching ratio for E2, (E), 20: 42232
gamma reactions (γ,nγ') with, oxygen-15 energy levels from, (E), 20: 42343
gamma reactions (γ,pγ') with, nitrogen-15 energy levels from, (E), 20: 42343
gamma reactions with, theory of, 20: 42339
helium-3 reactions (He-3,$\alpha\gamma$) with, oxygen-15 energy-level spins and transitions from, (E), 20: 42252
helium-3 reactions (He-3,$\alpha\gamma$) with, alpha-gamma angular correlations in, (E), 20: 42383
meson (μ^-) capture by, coherent antiproton-neutron excitations from, (T), 20: 42279
meson (π^-) capture by radiative, (T), 20: 42315
neutron reactions with, beryllium-7 production in, (E), 20: 41276 (UCRL-16769)
neutron reactions (n,α) at 14.9 Mev, alpha angular distribution from, (E), 20: 42370
neutron reactions (n,α) with, DWBA analysis of, (T), 20: 42391
neutron reactions (n,α) at 14.1 Mev, angular distributions for, (E), 20: 42216
photon reactions (γ,n) with, polarization effects in neutron yield from giant dipole resonance region from, (E), 20: 41556
scattering by platinum isotopes at 36 Mev, inelastic, (E), 20: 42218
triton reactions (t,α_0) at 1.5 to 3.25 Mev, angular distributions for, (E), 20: 42398
OXYGEN ISOTOPES O-17
deuteron reactions (d,Li-6) at 15 Mev, differential cross sections for, (E/T), 20: 42237
energy levels for nitrogen-15 (d,α) reactions at 0.8 to 1.8 Mev, (E), 20: 42295
energy levels from carbon-13 (α,n) reactions at 1.95 to 5.5 Mev, (E), 20: 42336
energy levels of, hole and particle, (T), 20: 42345
OXYGEN ISOTOPES O-18
content in oil well brines, 20: 41161
description using shell model with admixture of deformed states, (T), 20: 42274
deuteron reactions (d,Li-6) at 15 Mev, differential cross sections for, (E/T), 20: 42237
fractionation in water of crystallization of calcium sulfate, 20: 40836
substitution in nitrogen compounds, partition function ratios at 20 to 2000°K, 20: 40873(R) (NYO-3462-2)
OXYGEN ISOTOPES O-19
beta decay, (E), 20: 42242
OXYGEN SYSTEMS
Ca–O, phase studies, 20: 41412(R) (IS-1500(Sect. M))
C–N–O–U, preparation and high-temperature properties of stoichiometric, 20: 41429(R) (USBM-RC-1249)
C–O–U, preparation and properties of oxycarbide phases of, 20: 41429(R) (USBM-RC-1249)
N–O, radiolysis of, decontamination of products from fission-fragment, 20: 40951 (RPI-321-6)
O–S–U, phase studies, 20: 42579(R) (ANL-7245, pp 29-47)
OZONE
production by chemonuclear synthesis, 20: 40988

P

PACIFIC OCEAN
ecology of Northeast, tracer study, 20: 40523(R) (RLO-1750-8(Vol.1))
PACKAGING
evaluation of plastic film materials for radiation processed sea foods, 20: 41384(R) (TID-22833)
PAIR PRODUCTION
cross sections for, at high energies, 20: 41789 (DESY-66/16)
PALLADIUM
determination in plutonium by carrier distillation methods, spectrographic, 20: 40814 (RFP-664)
radiation effects on, at 11 to 7°K, electron, 20: 41499
PALLADIUM ALLOYS
Fe–Pd, hyperfine field distribution at iron nuclei, Mössbauer measurement of, (E), 20: 42571
Pd–Sn, Moessbauer measurements in, 20: 41637
Pd–Ti, corrosion by hydrochloric acid, 20: 41039(R) (ORNL-3880)
PALLADIUM ISOTOPES Pd-108
neutron reactions (n,γ), use of, in preparation of carrier-free silver-111, 20: 41023
PANCREAS
zinc-65 content in rat, effects of dexamethasone and prednisolone on, 20: 40563
PARABIOSIS
radioinduced lung carcinoma in rats, 20: 40614 (NYO-901-39)
PARAFFIN
gamma scattering in phantom of, spectra of cesium-137, 20: 40792
radioinduced electret effect in, beta, 20: 41516

PARAMECIUM
mutations induced in, by triethylene melamine, 20: 40632(R) (ORNL-3922, pp 175-91)
radiation effects, genetic, x, 20: 40623(R) (ORNL-3922, pp 32-49)
PARASITES
radiation effects on development of *Hetemkis gallinarum* embryos, x, 20: 40667
PARATHYROID EXTRACTS
effects on nuclear structure of rat thymocytes, 20: 40549
PARATHYROID GLANDS
radiocalcium studies and histological findings in case of hyperparathyroidism, 20: 40552
PARTICLE STATISTICS
many-body problem in statistical mechanics, variational principles for, 20: 42074
many-body problem in, hard-core potential, 20: 41509 (AD-638830)
PARTICLE TRACKS
dosimetric use of, in plastics, 20: 41262 (BNWL-SA-619)
PARTICLES
biological effects of heavy ionizing components of galactic and solar flare, 20: 40525
deposition on ground of, from elevated source, mathematical prediction of, 20: 41188(R) (BNWL-235-1)
distribution in two-phase flow, 20: 41102 (NYO-2930-6)
dynamics of systems of self-gravitating, in collisionless gases in magnetic fields, (T), 20: 42041
equilibrium of large assembly of, in general relativity, 20: 42091
motion along geodesics in 4-space, Newtonian equations of, 20: 42094
motion of suspended, effects of, on chemical and radiative processes in pseudo-liquified layer, 20: 40884
scavenging of atmospheric, by rain water, 20: 41130(R) (COO-1407-10)
PATHOLOGY
cutaneous eruptions in cobalt-60 therapy of female genital cancer, 20: 40679
of radiation-induced thymic lymphoma in mice, 20: 40677
thyroid, lesions induced by iodine-131, 20: 40647
PEACH BOTTOM POWER REACTOR
fuels for, performance under irradiation of, 20: 42624 (GA-6975)
PEAS
radioinduced mutants of, genetic control of germ cell formation in, 20: 40512
PEAT
sorptive properties for radioruthenium in different solutions, 20: 40890
PEBBLE BED REACTORS
design of, with variable core volume, 20: 42605(P)
2-PENTANONE, 4-METHYL-
solvent properties for molybdenum, niobium, tantalum, and tungsten, 20: 40796(R) (IS-1500(Sect.C))
1-PENTENE
radioinduced codimerization of methyallyl chloride with, 20: 40971
2-PENTENE
radioinduced and photoinduced isomerization of, effects of benzene on, 20: 40965
PERCHLORATE IONS
effects on uranyl complexes with tributylphosphine oxide, 20: 40885
electron spin resonance spectra of trapped, in gamma-irradiated potassium perchlorate, 20: 40969
PERCHLORATES
separation of polonium from, by solvent extraction using TBP in benzene, 20: 41052
PERCHLORIC ACID
electron spin resonance spectra of, 20: 42433
radiolysis of frozen solutions of, ESR studies of decomposition of radicals from gamma, 20: 40960
PERIODATES
separation of xenon oxides from, by ion exchange chromatography, 20: 40851
PERIODIC SYSTEMS
phase diagrams of the elements, pressure-temperature, (T), 20: 41521
PEROXIDES
induced in *E. coli* by growth on gamma-irradiated culture media, 20: 40580 (NYO-2804-8)
production in radioinduced oxidation of methanol, 20: 41004
PERSONNEL
exposure monitoring of, in industrial radiography in Poland, 20: 41212
radiation effects on accelerator operations, 20: 41206(T) (JPRS-36341, pp 10-17)
radiation effects on diameter and volume of erythrocytes of, from occupational exposure, 20: 40678
radiation hazards to sewage worker, from radioactive waste disposal in sewage systems, 20: 41217
radiation properties of lasers as a potential hazard to, 20: 40691
radiation protection of, using lasers for therapy, 20: 40776
tritium hazards to laboratory, 20: 41185 (AECL-2594)
PERTECHNETATE IONS
reactions with concentrated hydrobromic acid, paper chromatographic studies on, 20: 40918
PERTECHNETATES
preparation of technetium-99m sulfide colloid from, 20: 40753
use in mice thyroid metabolism studies, 20: 40547
use in scintiphotography of thyroid and brain, 20: 40750
use in scintiphotography of blood vessels, 20: 40752
use in thyroid physiology studies, 20: 40555
use of pertechnetate-99 to measure survival of thyroid transplants, 20: 40516
PESTICIDES
analysis of, electron capture parallel plate detector response for, 20: 40863
PHANTOMS
gamma reactions in, detection of secondary emission from, 20: 41321
preparation of masonite lung, 20: 41190 (CONF-660621-4)
radiation scattering from a cuboid shaped tissue-equivalent, factors affecting angular variation of, 20: 41211
use in dosimetric measurements for pelvic radiographs and fluoroscopic examinations, 20: 40770
use of head and neck, for x-ray dosimetry, 20: 41210
use of mouse, for fission neutron and γ dosimetry, 20: 41268(R) (NYO-2740-3, pp 5-165)
PHARMACEUTICALS
analysis for colloidal gold, activation, 20: 40842
PHARYNX
effects of carcinomas of naso-, effects on pituitary function of x, 20: 40660
PHASE STUDIES
solute equilibrium between two phases, interface curvature effects on, 20: 41412(R) (IS-1500(Sect. M))
PHENOL
viscosities of aqueous, 20: 41455(R) (NYO-2731-7)
PHENOL, DINITRO-
effects on nuclear structure of rat thymocytes, 20: 40549
PHONONS
distribution function in small crystals, (E/T), 20: 42572
PHOSGENE
reactions with lanthanide oxides and thoria, for production of chlorides, 20: 41412(R) (IS-1500(Sect. M))
reactions with yttria for production of yttrium chloride, 20: 41412(R) (IS-1500(Sect. M))
PHOSPHATE ROCKS
uranium content of, distribution of, 20: 41174
PHOSPHINE OXIDE, TRIBUTYL-
complexes with uranyl salts, preparation and properties of, effects of acid ligands, on, 20: 40885
PHOSPHINE OXIDES
preparation and properties of, for use as solvent, 20: 40796(R) (IS-1500 (Sect.C))
PHOSPHINES
radiation effects on, in krypton at 4.2°K, ESR of free radicals from gamma, 20: 40967
PHOSPHINIC ACID, DIBUTYL-, *p*-NITROPHENYL ESTER
radioprotective effects of, in x irradiated mice, 20: 40724
PHOSPHONIC ACID, METHYL, DIISOAMYL ESTER
solvent properties for thorium and uranium, 20: 41050
solvent properties for zirconium, 20: 41051
PHOSPHONIC ACID, METHYL-, MONOISOAMYL ESTER
solvent properties for thorium and uranium, 20: 41050
solvent properties for zirconium, 20: 41051
PHOSPHORIC ACID, BIS(2-ETHYLHEXYL) ESTER
solvent properties for rare earths, 20: 41064(R) (IS-1500(Sect.E))
PHOSPHORIC ACID, DIISOAMYL ESTER
diisoamyl phosphate–trioctylamine, solvent properties for uranium, mechanism of, 20: 41053
PHOSPHORS
development of radioactivated luminous, for space applications, 20: 41219
light yield of polystyrene, containing 1% PBE, 20: 41346
preparation for use in x-ray diffraction studies, sealing process for, 20: 41328
preparation of lanthanide- and uranium-activated alkaline earth molybdate and tungstate, 20: 40934(P)
radioinduced luminescence of thallium-activated alkali metal halides, 20: 41007
scintillation efficiency of thallium-activated alkali halide crystals, 20: 41343
use of sodium iodide, for neutron dosimetry in accelerator environment, 20: 41543 (RPP-R-2)
PHOSPHORUS

content in sea water from Indian Ocean, uptake by marine organisms, 20: 40572
determination in americium and plutonium by spark-source mass spectrography, · 20: 40816 (RFP-699)
determination in plutonium by carrier distillation methods, spectrographic, 20: 40814 (RFP-664)
determination in uranium trioxide by emission spectrography, 20: 40802 (HW-65402(Rev.1))
performance as neutron threshold detector in presence of x rays, 20: 41333
radiation effects on content in soils, effects of soil type on gamma, 20: 40637(R) (ORO-2754-7)
separation of, from sulfur by co-precipitation with ferric hydroxide, 20: 41049
uptake by corn plants, effects of soil fertility on, 20: 40735 (NYO-2744-37)
uptake differences in varieties of barley, 20: 40532(R) (COO-1097-17)
PHOSPHORUS CHLORIDES
cyclohexene–PCl_3, radiolysis of, effects of temperature on yields of products in gamma, 20: 40947 (BMwF-FBK-66-14)
PHOSPHORUS FLUORIDES
preparation of fluorine-18-labeled, 20: 41020
PHOSPHORUS ISOTOPES
effects on DNA composition in plants, 20: 40548
radioactive, effects on human erythrocyte diameter and volume from occupational exposure to, 20: 40678
PHOSPHORUS ISOTOPES P-31
alpha elastic scattering by, DWBA analysis of, (T), 20: 42392
neutron reactions (n,2n) at 14.8 Mev, activation cross section for, (E), 20: 42207
proton reactions (p,γ) at 0.3 to 2.1 Mev, resonance strengths for, (E), 20: 42182
PHOSPHORUS ISOTOPES P-32
determination in water, 20: 40819(T) (CEA-tr-A-1883)
distribution in stream ecosystems by *E. coli*, 20: 40529
dosimetry of, for polycythemia therapy, 20: 40774
effects on anthracene and sodium iodides, effects of partial absorption on, 20: 40504(R) (ORNL-3922, pp 146-60)
hyaluronic acid depolymerization by, 20: 40591
incorporation in pyridoxal-5'-phosphate, method for, 20: 41016
metabolism in salt-marsh ecosystems, 20: 40573
preparation of carrier-free, 20: 41049
tracer use of bacteria-incorporated, for testing cleanability of biologically contaminated surfaces, 20: 41218
use in bone mineralization dynamics studies, 20: 40558
use in detection of hormonal response of tumors, 20: 40566
use in measurement of coronary circulation time in dogs, catheter-type micro G-M counter for detection of, 20: 40514
PHOSPHOTYL FLUORIDES
preparation of fluorine-18-labeled, 20: 41020
PHOTOCHEMISTRY
role of enzymes in photoreactivation of ultraviolet damage in sea urchin eggs, 20: 40543
PHOTOELECTRIC CELLS
recording system for uv and infrared spectral line intensities, design of, 20: 41267 (MPI-PAE-P1-30/60)
PHOTOGRAPHIC FILM
analysis for particle tracks, centering system for flying spot digitizers for, 20: 41263 (CERN-66-23)
radiation effects on, · 20: 41223 (EGG-1183-1244)
use for neutron dosimetry in accelerator environment, 20: 41543 (RPP-R-2)
use for surveying medical x-ray sources, 20: 41213
PHOTOGRAPHIC FILM DETECTORS
performance for beta dosimetry of skin, 20: 41274 (ORNL-TM-1581)
use in industrial radiography in Poland, 20: 41212
PHOTOGRAPHY
control system for microfiche printer, automatic, · 20: 41230(R) (ORNL-3875, pp 24-34)
method of, in radiation environments, · 20: 41223 (EGG-1183-1244)
use in studying bottom layers of Mediterranean Sea, 20: 41128
PHOTOMULTIPLIER TUBES
design and performance of highly ruggedized, for high-temperature scintillation counting, 20: 41374
gating of large-area photocathode, 20: 41269(R) (ORNL-3875, pp 4-12)
response of 56 AVP to Neher light sources, 20: 41491(R) (EGG-1183-2030)
testing of 20-pin sockets for, 20: 41228(R) (ORNL-3875, pp 15-20)
PHOTONS
decay and relativistic properties, (T), 20: 41806
emission in electron-electron interactions, cross sections for double-, 20: 41904
interactions with nucleons, meson (π) production amplitudes for, (T), 20: 41996
interactions with protons at 2.6 to 2.7 Bev, differential cross sections for meson (K^+) and mesons (π^+) production in, (E), 20: 41795(R) (MIT-2098-251, pp 21-36)
interactions with protons, mesons (π^0) production cross sections for, (E), 20: 41798 (MIT-2098-265)
interactions with nucleons, SU(6) symmetry for meson production in, (T), 20: 41812
interactions with bound and free protons, meson (π^+) yields from, (E), 20: 41816
interactions with bound and free protons below 330 Mev, meson (π) yields from, (E), 20: 41817
interactions with electrons at 17.6 Mev, cross section for Compton, (E), 20: 42213
interactions with nucleons, two-meson (π) exchange in, (T), 20: 41821
interactions with protons at high energies, absorption correction for meson (π^+) production in, 20: 41844
interactions with nucleons, vector dominance approximation for meson production in, 20: 41869
interactions with protons at 0.95 to 1.1 Bev, differential cross section for meson (η) production in, (E), 20: 41889
interactions with scalar nucleons, large t limit for sixth-order diagrams for Compton, 20: 41897
interactions with nucleons, theory of three particle production in, 20: 41900
interactions with nucleons, isospin amplitudes for S-state meson (π^0) production in, 20: 41906
interactions with protons, meson (ρ^0) production via two-meson (π) exchange in, (T), 20: 41918
motion in superdense stars, (T), 20: 41596
reactions (y,n) with nuclei, energy spectra from, (E), 20: 42165(R) (MIT-2098-251, pp 16-20)
reactions (y,np) with lithium-6, coincidence measurements of, 20: 42165(R) (MIT-2098-251, pp 16-20)
reactions (y,n) and (y,p) with nickel-58, properties of, (T), 20: 42220
reactions (y,n) with oxygen-16, polarization effects in neutron yield from giant dipole resonance region from, (E), 20: 41556
reactions (y,2n) with tritium, wave functions for, 20: 42228
reactions (y,2p) with helium-3, wave functions for, 20: 42228
reactions with lead-208 at 50 Bev, circularly polarized intermediate vector boson pair production from, (E), 20: 41901
reactions with light nuclei, review of, · 20: 42340
reactions with silicon-28 at 16 to 60 Mev, cross sections for, (E), 20: 42523(R) (IS-1500(Sect.P))
theory for, semiclassical field, 20: 41971
PHYSICAL CHEMISTRY
book: *Radioactive Isotopes in Chemical Research*, 20: 41027
PHYSICS
conference on intermediate-energy, · 20: 42304
conference on intermediate-energy, 20: 41912
stable isotopes in, 20: 41380(T) (IFA-IS-36)
symmetry principles in, 20: 41923 (BNL-956)
PHYSIOLOGY
effects of laser beams on, importance in biomedical uses, 20: 40691
effects of, combined with radiation on food enzymes, 20: 40600
radiation effects on human, following therapy, 20: 40659
radiation effects on fish embryo and prelarvae, 20: 40527
use of iodine-131 and technetium-99m in study of thyroid, 20: 40555
PICKERING POWER REACTOR
design and site development, summary, 20: 42617(R) (66-CNA-303)
fuel development for, status, 20: 42618 (66-CNA-312)
PIEZOELECTRIC CRYSTALS
development and testing of plasma pressure probe, 20: 42405 (IPP-1/46)
PIGMENTS
radiation effects on wheat flour carotenoid, gamma, 20: 40599
PINCH DEVICES
stability of toroidal screw, 20: 42414 (NP-16266)
PINCH EFFECT
electron-hole plasma, in antimony–indium crystals, 20: 42545
properties in coaxial plasma jets, 20: 42464
PIPES
flow in, two-phase, · 20: 41102 (NYO-2930-6)
flow rates and blowdown transients in, two-phase, 20: 41107
PITUITARY GLAND
radiation effects on function of human, following nasopharyngeal carcinoma therapy, 20: 40660
radiation effects on rat, effects of repeated exposure on, 20: 40655
PLACENTA
autoradiography of human, gonadal dose in fetuses from, 20: 40680
polonium-210 content in human, 20: 40531 (A/AC.82/G/L-1045(Rev.1))
PLANETS
angular momentum exchange between sun and, 20: 41610

PLANKTON
ecology of, in Columbia River estuary and Northeast Pacific, tracer study, 20: 40523(R) (RLO-1750-8(Vol.1))
radioactivity in Columbia River estuary and Northeast Pacific Ocean, 20: 40523(R) (RLO-1750-8(Vol.1))
radioisotope accumulation by ocean-dwelling, 20: 41146
radioisotope accumulation by ocean-dwelling, 20: 40546
PLANT CELLS
book: *Problems of Post-Radiative Cell Restoration*, 20: 40731
radioinduced chromosome aberrations in, repair mechanisms for, 20: 40609 (CONF-660418-1)
PLANT RESPIRATION
role of γ-irradiated culture media on *E. coli*, 20: 40580 (NYO-2804-8)
PLANTS
analysis for cesium-137, strontium-89, and strontium-90, 20: 40809 (NP-16235)
analysis for iodine-131 in vegetable rinses, method for, 20: 40852
book: *Problems of Post-Radiative Cell Restoration*, 20: 40731
chlorophyll chimera induction in *Arabidopsis thaliana*, by x radiation and ethyl methanesulfonate treatment of seeds, 20: 40710
effects of phenyl ethylurethane on *Arabidopsis thaliana*, effects of exogenous factors on mutagenic, 20: 40709
effects of radiophosphorus on DNA composition, 20: 40548
induction of chromosome aberrations by chemicals in *Vicia faba*, 20: 40714
induction of chromosome aberrations in *Vicia faba* by radiomimetic agents in, effects of chelating compounds on, 20: 40715
light emission from, use of Kerr-cell shutter for measuring delayed-, 20: 41231(R) (ORNL-3875, pp 35-43)
light emission from, use of digital memory oscilloscope to measurement of delayed-, 20: 41231(R) (ORNL-3875, pp 35-43)
mutation detection in first generation *Arabidopsis thalia*, grown from mutagen-treated seed, 20: 40513
pyrimidine synthesis in root cells of *Vicia faba*, effects of thymidine on, 20: 40581(R) (ORNL-3922, pp 50-1)
radiation effects on genetics of peanut, gamma, 20: 40636(R) (ORO-1747-12)
radiation effects on jute, mutation studies, gamma, 20: 40681
radioactivity content of, from fallout in West Germany, 20: 40570
radioinduced chromosome aberrations in *Vicia faba*, γ and x, 20: 40714
radioinduced electron spin resonance signals in seeds of lettuce, effects of hydration on γ, 20: 40631(R) (ORNL-3922, pp 161-6)
radioinduced injuries to, ecological effects on recovery from, review of, 20: 40526
radioinduced mutations of *Arabidopsis thaliana*, effects of exogenous factors on x, 20: 40709
radioisotope accumulation by ocean-dwelling, 20: 41145
strontium uptake, 20: 40524(R) (TID-23271)
strontium uptake by edible parts of, effects of calcium content of soil and plant species on, 20: 40537(R) (TID-23052)
uptake of beta activity from fallout during growing season in Delaware, Ohio, 20: 40579
uptake of radioisotopes by, factors affecting, 20: 40578
PLASMA
acceleration, charged-particle motion in coaxial, (T), 20: 42456
acoustic wave propagation in compressible, network representation of, 20: 42440
acoustic wave propagation in, energy relation for, 20: 42479
boundary layer in ionized two-temperature, (T), 20: 42477
charged-particle interactions with magneto-active nonequilibrium, particle loss intensity from fast, (T), 20: 42486
charged-particle motion in vacuum-bounded, Cherenkov surface waves from, 20: 42497
compression, wave propagation during, (T), 20: 42489
containment in closed systems, magnetic field topology for, (T), 20: 42461
containment in cold-gas blanket, stability of, 20: 42473
containment in magnetic field, theory of, 20: 42425
containment in thermonuclear devices, using megagauss fields, 20: 42434
containment of laser-produced, in magnetic mirrors, 20: 42415 (TID-22928)
containment of, review of problems in, 20: 42437
diagnostic probe for supersonic flow in, 20: 41702
diagnostics by microwave interferometry, open waveguide method for, (E), 20: 41717
diagnostics in coaxial jets, photographic determination for, 20: 42516
diagnostics in collision-dominated weakly ionized, electrostatic probe for, (E), 20: 41705
diagnostics of cold, inverse resonance in cylindrical geometry, 20: 42462
diagnostics of electric arc, using laser beams, 20: 42432
diagnostics of magnetic mirror machine injected, 20: 42504
diagnostics of, low-current arcs for, 20: 42513
diagnostics using laser beams, review on, 20: 42445
diagnostics, interferometer for three wavelengths, 20: 42408 (IPP-2/49)
diagnostics, piezoelectric pressure probe for, 20: 42405 (IPP-1/46)
dynamics of certain spherical charge distributions, 20: 41517
electric conductivity in MHD, scalar and tensor, (E), 20: 41737
electric conductivity of helium–cesium, effect of wall radiation on, (T), 20: 41754
electric conductivity of nonhomogeneous, in magnetic field, (T), 20: 41768
electric conductivity in argon and helium nonequilibrium, (E), 20: 41772
electric conductivity of potassium-seeded argon, (T), 20: 42410 (IPP-6/51)
electric conductivity of two-temperature, high-frequency, in quasi-equilibrium, (T), 20: 42472
electric discharges in, method of initiation of, 20: 42514(P)
electric microfield distribution in, (T), 20: 42468
electric potential distribution in column of, thermionic emitter effects on, 20: 42406 (IPP-2/47)
electric potential distribution in cesium diode, (E/T), 20: 42407 (IPP-2/48)
electric properties of, in MHD generators, (E), 20: 41708
electric properties of potassium-seeded argon, shock tube studies of, (E), 20: 41715
electromagnetic properties of bounded slab of, 20: 42481
electromagnetic wave propagation in isotropic cylindrical, properties of, 20: 42436
electromagnetic wave propagation in, diffraction effects on, 20: 42438
electromagnetic wave propagation in compressible, network representation of, 20: 42440
electromagnetic wave interactions with nonhomogeneous, cylindrical and spherical, (T), 20: 42447
electromagnetic wave interaction with moving, reflection of, (T), 20: 42448
electromagnetic wave propagation in isotropic, self-focusing from, (T), 20: 42449
electromagnetic wave propagation in, nonlinear waveguide phenomena for, 20: 42450
electromagnetic wave interactions in dense, surface, (T), 20: 42451
electromagnetic wave propagation in helium afterglow, linearly polarized, (E), 20: 42459
electromagnetic wave scattering by, column of high-frequency effect due to axial drift velocity in, (T), 20: 42471
electromagnetic wave propagation in bounded magneto-, kinetic theory of, 20: 42496
electromagnetic wave interactions in vacuum-bounded, surface, 20: 42498
electromagnetic wave conversion to ionic sound oscillations in, (T), 20: 42499
electromagnetic wave propagation in nonuniform, conversion of, 20: 42500
electromagnetic-wave effects on gaseous-discharge, h-f inhomogeneous, 20: 42442
electron beam flow, quasi-fluid treatment of unaccelerated, 20: 42515
electron beam interactions with, excitation of ion oscillations in, 20: 42494
electron beam interactions with, convective effects of electron oscillations in, 20: 42495
electron concentration in reflex klystron, (T), 20: 42446
electron density and conductivity of argon–cesium, in shock tube, 20: 41703
electron density determination in, using microwaves, 20: 42419(T) (AD-636608)
electron density in arc discharge, copper energy level effects on, 20: 42490
electron energy balance in nonequilibrium argon and helium, (E), 20: 41772
electron kinetics of Couette-flow, in an electric field, (T), 20: 42488
electronic recombination in helium and argon afterglow, laser interferometric measurements of, (E), 20: 42469
electrostatic probe theory for high-pressure nonequilibrium, 20: 41782
energy levels of helium–xenon, pressure effects on, 20: 42491
equation for, in ion engines, 20: 41123
flow in duct of series-flow MHD generator, 20: 41698
flow of fully ionized, between parallel plates, (T), 20: 42488
hydromagnetic configurations, closed-line average minimum-B, (E), 20: 42455
hydromagnetic wave propagation, ionization and gas pressure effects on, (T), 20: 42401 (AD-637854)
interactions with line current magnetic fields, analysis of, (T), 20: 42453
ion extraction from low-pressure oxygen, negative, (E), 20: 42435
ion oscillations in electric discharge, properties of, (E), 20: 42444
ionization in, validity of SAHA equation in nonequilibrium, (T), 20: 41751
ionization near cathodes of MHD generator, (T), 20: 41756
ionization reaction time of helium–cesium, effect of wall radiation on, (T),

20: 41754
kinetics in magnetic field, variation of cylindrical column of, (T), 20: 42425
kinetics of, dispersive nonlinear equation for, 20: 42411 (IPPJ-49)
kinetics of, sequent correlations for stochastic point processes in, (T), 20: 42467
magnetic field interactions with free-electron, radiative equilibrium in, 20: 42470
magnetic pulse in cold collision-free, 20: 42417 (UCRL-7170)
magnetohydrodynamics flow of nonequilibrium, (T), 20: 42454
microwave absorption and propagation in magneto-, near electron cyclotron resonance, 20: 42439
microwave attenuation by rocket exhaust, 20: 41120
microwave diagnostics of disintegrating argon–cesium, (E), 20: 41699
microwave emission from stationary inhomogeneous, (E/T), 20: 42457
oscillation excitation by electron beams, (T), 20: 42429
oscillations in inhomogeneous cylindrical, (T), 20: 42503
oscillations in nonequilibrium argon–potassium, (E), 20: 41692
oscillations in one-dimensional, circuit analog for analyzing, 20: 42443
oscillations in, convective effects of electron beam excitation of, 20: 42495
oscillations in, electron beam excitation of ion, 20: 42494
particle transport in, (T), 20: 42418(R) (UCRL-14744, pp 37-48)
production of cesium, design and performances of isothermal tantalum oven for, 20: 42484
production of, conical induction apparatus for, 20: 42505
properties in explosive-driven MHD cells, 20: 41686
properties of alkali-seeded helium and argon, (E), 20: 41712
properties of rarefied, in magnetic mirror systems, (T), 20: 42458
properties of, in closed-loop MHD generator, (E), 20: 41741
properties of, produced by microwave energy at electron-cyclotron frequency, 20: 42412 (MIT-3221-19)
radiation in moving anisotropic, 20: 42480
radio-wave transmission through, magnetic field effects on, (T), 20: 42426
relaxation processes in nonequilibrium, (T), 20: 41766
research policies of AEC, 20: 42416 (TID-23277)
research programs on interplanetary, (E), 20: 41667(R) (MIT-2098-251, pp 1-13)
resonances in cylindrical magneto-, dipole, 20: 42463
resonances in lossy compressible, in cylindrical cavity, 20: 42441
sheath formation as a function of delivered electric current in, 20: 42428
shock wave propagation in cesium, (E), 20: 41750
shock wave propagation in, dissipative effects on, (T), 20: 42476
sound stability in nonhomogeneous, (T), 20: 41764
spectra of high-temperature air, properties of, 20: 42492
stability in magnetic mirrors, relation to toroidal confined, 20: 42402 (IAE-1149)
stability in toroidal stellarators, 20: 42424
stability of anisotropic magneto-, gravitational, 20: 42422
stability of argon and argon–cesium, (E), 20: 41770
stability of hollow positive column, in longitudinal magnetic fields, 20: 42506
stability of toroidal confined, with longitudinal fields, 20: 42402 (IAE-1149)
stability of toroidal confined, 20: 42403 (IAE-1151)
stability of toroidal screw pinch, 20: 42414 (NP-16266)
stability of, Hall-current effects on Rayleigh-Taylor, (T), 20: 42474
stability of, review of problems in, 20: 42437
stability of, review, (T), 20: 42482
stability theory for, WKB approximation for, (T), 20: 42404 (IC-66/45)
stabilization of uniform turbulent, 20: 42465
wave propagation in finite, nonlinear processes in, (T), 20: 42427
wave propagation in inhomogeneous incompressible, equations relating to, 20: 42478
wave propagation in rarefied, magnetic field effects on, (T), 20: 42489

PLASMA JETS
calibration testing of electric discharge, 20: 42466
density measurements in repetitively pulsed coaxial, 20: 41121
diagnostics of coaxial, design modifications for photographic, 20: 42516
electric conductivity and velocity of, design and performance of coil system for measuring, 20: 42485
pinch properties in coaxial, 20: 42464
properties of conical induction, 20: 42505

PLASTICITY
continuum theory of, for structural materials, 20: 41454 (NYO-2394-22)

PLASTICS
development of device using silicon diode and plastic scintillators for measurement of absorbed electron dose, 20: 40746(R) (NYO-3510-2)
diffusion of tritium through, 20: 41196 (LA-DC-7996)
use as scintillator for two-impulse neutron detector, 20: 41337
use for detection of particulate radiations, 20: 41262 (BNWL-SA-619)
use in nanosecond x-ray scintillation detectors, 20: 41325

PLATES
fabrication of zirconium carbide, methods for, 20: 41430
fluid flow between parallel, 20: 41105
welding of thick steel, specimen testing for, 20: 41450(R) (EURAEC-1684)

PLATINATES
pentafluoroxenonyl hexafluoro-, crystal structure and magnetic properties of, 20: 40882

PLATING
design of equipment for radioactive material, 20: 41268(R) (NYO-2740-3, pp 5-165)

PLATINUM
analysis for impurities by neutron activation, 20: 40796(R) (IS-1500 (Sect.C))
determination in meteorites and natural materials by thermal neutron activation, 20: 40835
energy levels of, magnetic moments of 2^+, (E), 20: 42167(R) (MIT-2098-251, pp 50-6)
x radiation spectra, forbidden transitions in, 20: 41660

PLATINUM ALLOY COUPLES
Pt/Pt–Rh, insulation for, testing at high temperatures, 20: 41461(R) (UCRL-7361(Pt.3))

PLATINUM COMPLEXES
with bromine, bromine-82 exchange between, and bromide ions, 20: 40796(R) (IS-1500(Sect.C))

PLATINUM COUPLES
Pt/Pt–Rh, insulation for, testing at high temperatures, 20: 41461(R) (UCRL-7631(Pt.3))

PLATINUM FLUORIDES
fluorine-19 NMR and spin-lattice relaxation in, 20: 40892

PLATINUM ISOTOPES Pt-190
energy level transitions from oxygen-16 inelastic scattering at 36 Mev, (E), 20: 42218

PLATINUM ISOTOPES Pt-192
energy level transitions from oxygen-16 inelastic scattering at 36 Mev, (E), 20: 42218
energy levels from gold-192 decay, (E), 20: 42187

PLATINUM ISOTOPES Pt-194
energy level transitions from oxygen-16 inelastic scattering at 36 Mev, (E), 20: 42218

PLATINUM ISOTOPES Pt-195
energy level transitions from oxygen-16 inelastic scattering at 36 Mev, (E), 20: 42218

PLATINUM ISOTOPES Pt-196
energy level transitions from oxygen-16 inelastic scattering at 36 Mev, (E), 20: 42218

PLATINUM ISOTOPES Pt-198
energy level transitions from oxygen-16 inelastic scattering at 36 Mev, (E), 20: 42218

PLATINUM ISOTOPES Pt-199
energy levels, (E), 20: 42268

PLATINUM XENON FLUORIDES
crystal structure and magnetic properties of pentafluoroxenonyl hexafluoroplatinate, 20: 40882

PLOWSHARE PROJECT
cratering studies for excavation of sea-level canal, 20: 41069 (SC-RR-66-324)
effect single- or row-charges on craters, 20: 41069 (SC-RR-66-324)
excavation for railroad relocation, 20: 41071
review, 20: 41072
use of underground nuclear explosions in water supply management, 20: 41073

PLUTONIUM
analysis by spark-source mass spectrography, 20: 40816 (RFP-699)
analysis for impurities by optical emission spectroscopy, 20: 40805(R) (MLM-1325, pp 63-70)
analysis for impurities, carrier distillation method for spectrographic, 20: 40814 (RFP-664)
burnup analysis of, computer program for, 20: 42608(R) (GEAP-5124)
determination in uranium trioxide by alpha spectroscopy, 20: 40802 (HW-65402(Rev.1))
determination of, in irradiated fuel elements by alpha spectroscopy, nondestructive, 20: 40808(R) (NP-16212)
diffusion in uranium dioxide, methods for measuring, 20: 41484
distribution in mixed-oxide fast reactor fuels, 20: 42625 (GEAP-4466)
effects of impurities on phase transformations in, differential thermal analysis of, 20: 41452 (MLM-1172)
electrorefining of, in presence of gallium, 20: 41035 (LA-2758)
growth of delta single crystals of, method for, 20: 41453(R) (NUMEC-3428-21)
plutonium-240 content in, design of fission counter for determining, 20: 41264 (DP-552)
recovery from low enrichment fuel, processes for, 20: 42579(R)

(ANL-7245, pp 29-47)
separation from irradiated uranium fuel, method for, 20: 41042 (PG-Report-722)
solvent properties for molybdenum at 700 to 1000°C, 20: 40868 (LA-3523)
spectra of, hyperfine and isotope structure in, 20: 41639(T)
use for reactor fuel, Hanford Utilization Program for, 20: 42607 (BNWL-298)
volatility safety experiments, 20: 42577(R) (ANL-7230)

PLUTONIUM ALLOYS
Ga–Pu, effects of impurities on phase transformations in, differential thermal analysis of, 20: 41452 (MLM-1172)
Ga–Pu, separation of plutonium from, electrorefining processes for, 20: 41035 (LA-2758)
Ga–Pu, zone refining of carbon-contaminated rods, method evaluation, 20: 41453(R) (NUMEC-3428-21)
Pu–Th–U, thermal conductivity measurements, 20: 42579(R) (ANL-7245, pp 29-47)
Pu–Ti–U, development for LMFBR fuel, 20: 42651 (WASH-1065)
Pu–Ti–U, heat content measurement to 1150°C, 20: 42579(R) (ANL-7245, pp 29-47)
Pu–U–Zr, development for LMFBR fuel, 20: 42651 (WASH-1065)
Pu–U–Zr, performance as FTR fuel, 20: 42676 (BNWL-281)

PLUTONIUM CARBIDES
PuC–UC, development for LMFBR fuel, 20: 42651 (WASH-1065)
PuC–UC, performance as FTR fuel, 20: 42676 (BNWL-281)

PLUTONIUM COMPLEXES
with EDTA, electromigration studies on, 20: 40912

PLUTONIUM COMPOUNDS
analysis for plutonium-240 by emission spectrography, 20: 40813 (RFP-271)

PLUTONIUM(VI) FLUORIDES
fluorine-19 NMR and spin-lattice relaxation in, 20: 40892

PLUTONIUM ISOTOPES
separation by electromagnetic methods, 20: 41401(R) (ORNL-4006)

PLUTONIUM ISOTOPES Pu-238
content in stratosphere of, from SNAP-9A burnup, 20: 41131(R) (HASL-172)
properties of, in isotopic power sources, 20: 41397
reactions in dilute nitric acid, equilibrium, 20: 41038(R) (MLM-1325, pp 9-62)
separation from uranium-234, methods for, 20: 41038(R) (MLM-1325, pp 9-62)
valence studies on, 20: 41038(R) (MLM-1325, pp 9-62)

PLUTONIUM ISOTOPES Pu-239
deuteron reactions (d,pf) with, angular correlations in, (E), 20: 42161 (LA-DC-7878)
effects on mice, effects of DTPA treatment on carcinogenic, 20: 40745(R) (NYO-901-54, pp 29-47)
neutron fission at 0.08 to 1.5 Mev, energy dependence of fission-fragment angular distribution in, (E), 20: 42171(T) (LA-tr-66-41)
neutron fission of, fission-fragment energy and mass distributions in thermal, (E), 20: 42261
neutron fission of, neutron emission in, 20: 42325
preparation of foil samples, 20: 42619(R) (ANL-7245, pp 1-28)
triton reactions (t,pf) with, angular correlations in, (E), 20: 42161 (LA-DC-7878)

PLUTONIUM ISOTOPES Pu-240
content in plutonium, design of fission counter for determining, 20: 41264 (DP-552)
determination in plutonium compounds by emission spectrography, 20: 40813 (RFP-271)
internal-conversion coefficients for 42.88-kev transition in, (E), 20: 42264
neutron absorption resonance escape probability in, measurement using iridium foils, 20: 42137 (AEEW-M-661)
triton reactions (t,pf) with, angular correlations in, 20: 42161 (LA-DC-7878)

PLUTONIUM ISOTOPES Pu-241
neutron fission of, fission-fragment energy and mass distributions in thermal, (E), 20: 42261
preparation of foil samples, 20: 42619(R) (ANL-7245, pp 1-28)

PLUTONIUM(IV) OXIDES
analysis for plutonium-240 by emission spectrography, 20: 40813 (RFP-271)
production of, for use in HFIR, 20: 41039(R) (OENL-3880)
radiation effects on aqueous suspensions of, neutron, 20: 41009 (AERE-R-3268)
sintering of, formation of Pu_2O_3 in, 20: 41426 (LA-3493)
PuO_2–stainless steel, performance as FTR fuel, 20: 42676 (BNWL-281)
PuO_2–UO_2, development for LMFBR fuel, 20: 42651 (WASH-1065)
PuO_2–UO_2, fission product and plutonium migration in, 20: 42625 (GEAP-4466)

PLUTONYL NITRATES
complexes with pyridine, spectral studies on, 20: 41038(R) (MLM-1325, pp 9-62)
crystal structure, 20: 41038(R) (MLM-1325, pp 9-62)

PNEUMATIC SYSTEMS
modifications to ALRR rabbit delivery, 20: 42681(R) (IS-1500(Sect. R))

POLAND
exposure monitoring of personnel in industrial radiography, 20: 41212

POLLEN
reversion frequency in maize, effects of ploidy on, 20: 40509 (TID-22965)

POLONIUM
crystal structure of alpha and beta, x-ray diffraction studies on, 20: 41469
separation from chloride and perchlorate solutions by solvent extraction using TBP in benzene, 20: 41052

POLONIUM ISOTOPES
production in proton reactions (p,xn) with bismuth-209 at 75 to 160 Mev, 20: 42196

POLONIUM ISOTOPES Po-208
decay of, weak alpha and electron-capture, 20: 41038(R) (MLM-1325, pp 9-62)

POLONIUM ISOTOPES Po-209
decay of, weak alpha and electron-capture, 20: 41038(R) (MLM-1325, pp 9-62)

POLONIUM ISOTOPES Po-210
carcinogenic effects on bronchial epithelium, 20: 41191(R) (HUX-3170-1)
content in human bones and teeth, 20: 40531 (A/AC.82/G/L-1045 (Rev.1))
content in human soft tissues and placenta, 20: 40531 (A/AC.82/G/L-1045(Rev.1))
half life, 20: 41038(R) (MLM-1325, pp 9-62)
properties of, in isotopic power sources, 20: 41397
use in radioactive static eliminators, 20: 41395

POLYCRYSTALS
creep and plastic flow of, conference on, 20: 41472

POLYCYTHEMIA
induction in mice by confinement in silicone rubber cages, 20: 40718(R) (ORNL-3922, pp 99-105)
radiotherapy of, method for dosimetry of phosphorus-32, 20: 40774

POLYMERIZATION
radioinduced in thymine, effects of temperature on uv, 20: 40504(R) (ORNL-3922, pp 146-60)

POLYMERS
effects on Drosophila, genetic, 20: 40706
excision of pyrimidine, method for *in vitro*, 20: 40504(R) (ORNL-3922, pp 146-60)
radiation effects on electric conductivity of, 20: 41489(R) (EGG-1183-2014)
transfer of thymine, in phages, 20: 40504(R) (ORNL-3922, pp 146-60)

POLYOXYMETHYLENES
radiation effects on mechanical properties at −30 to 150°C, gamma, 20: 41500

POLYPHENYLS
analysis of hydrogenated, for carbon and hydrogen, 20: 40797 (AECL-2524)

POLYSACCHARIDES
selenium-75 and sulfur-35 fixation to protein-, in cartilage, 20: 40544

POODLE PROPULSION SYSTEMS
development, Jan.–Mar. 1966, 20: 41396(R) (STL-517-0042)
fuel capsules for, creep analysis of, 20: 41396(R) (STL-517-0042)
reentry testing of, 20: 41396(R) (STL-517-0042)

POPULATIONS
dynamics of jackrabbit, 20: 40494(R) (COO-1329-3)
mutation studies on irradiated peanuts, 20: 40636(R) (ORO-1747-12)
radiation burden from fallout, in West Germany, 20: 40570
radiation effects on lichen, in oak-pine forest, gamma, 20: 40517 (BNL-9437)
radiation effects on chromosomes in Chironomus, from waste disposal, 20: 40530
radiation hazards to municipal, from waste disposal in sewage systems, 20: 41217
radiation protection during postattack period, requirements for, 20: 41177 (AD-532211)
shielded source for irradiation of animal, 20: 40518 (CEX-63.10)

PORCELAIN
use in accelerator tubes, 20: 41579(P)

PORPHYRINS
effect on radiosensitivity of mouse tumors, 20: 40657

POSITRONS
interactions with electrons, polarization and structure relations for annihilation, (T), 20: 41813
lifetime and origin in powered oxides, (E), 20: 41629
mass in sodium, band effective, 20: 41853
scattering by helium and hydrogen, lower bound to reciprocal of length of, (T), 20: 41658

systems, 20: 40943
Al_2O_3–Cr_2O_3–K_2O, properties for use in dehydrogenation of butane, 20: 40943

POTASSIUM PERCHLORATES
radiation effects on, ESR of perchlorate radicals trapped in gamma, 20: 40969

POTASSIUM PERMANGANATES
use in dissolution of radioactive ion exchange resins, 20: 41031 (DP-717)

POTASSIUM SULFAMATE
radiolysis of single-crystal nitrogen-15-enriched, ESR study at 77°K of gamma, 20: 40955

POTASSIUM URANYL SULFATES
fluorescence lifetime of, effects of deuteration on, 20: 40887

POTATOES
analysis of tissues of, for copper using neutron activation and electrodeposition, 20: 40825
determination of nutritional value of irradiated, on rats, 20: 40576
DNA synthesis in tubers of, effects of radiotoxins on, 20: 40562

POWDER METALLURGY
method for pressing beryllium into high-strength shapes, 20: 41428 (SCL-DC-66-57)

POWER BREEDER REACTORS
design of 1000 Mw(e) sodium-cooled fast, evaluation of, 20: 42622 (COO-285)
development of LMFBR, 20: 42577(R) (ANL-7230)
fuel development for thorium–uranium-233 seed-blanket, 20: 42609 (WAPD-T-1886)
fuel development for, 20: 42619(R) (ANL-7245, pp 1-28)
fuels and materials development for LMFBR, 20: 42651 (WASH-1065)
heat transfer system for, cost analysis of secondary sodium-steam, 20: 42632 (NAA-SR-12060)

POWER CYCLES
design of Brayton and Rankine, for manned space stations, 20: 41679 (NASA-CR-543)
working fluids for Rankine and Brayton, evaluation of, 20: 41398

POWER PLANTS
design of MHD, using seeded inert gases, 20: 41736
design optimization of MHD, (T), 20: 41765
efficiency of closed-loop MHD, 20: 41742
efficiency of liquid-metal MHD, (T), 20: 41778
efficiency of MHD, with oxygen enrichment, (T), 20: 41752
efficiency of oil-fired MHD, (T), 20: 41743
efficiency of reactor–MHD, thermal, (T), 20: 41740
fission fragment ionization in MHD cycles, (T), 20: 41732
operation at part load of MHD, (T), 20: 41775
operation of Brayton cycle MHD, (T), 20: 41706
performance of MHD, (E), 20: 41769
principles of MHD, (T), 20: 41693
space, criteria for Rankine-MHD, 20: 41719
spacecraft, review, 20: 41514(T) (AI-Trans-209)

POWER REACTORS
core access arrangement for, 20: 42590(P)
design of gas-cooled, 20: 42603(P)
design of gas-cooled, 20: 42604(P)
design of pebble-bed, with variable core volume, 20: 42605(P)
development of High Power Density, June–Nov. 1965, 20: 42626(R) (GEAP-4951)
economics of dual-purpose, 20: 42658 (NP-16250)
economics of dual-purpose, 20: 42659
fuel development for CANDU-PHW, status, 20: 42618 (66-CNA-312)
kinetics of ESSOR, methods for analysis of, 20: 42678 (EUR-3051.e)
neutron density fluctuations in, compressible fluid model for determining, 20: 42581(R) (ORNL-3875, pp 125-50)
pressure control in pressurized-water, method for, 20: 42656(P)
reactivity coefficients of, steady state evaluation of, 20: 42631 (KFK-260)
startup of, impulse response measurements, 20: 42628(R) (GEAP-5145)
use in MHD power plants, (T), 20: 41693
use in power plants combining MHD generators, (T), 20: 41740

POWER SUPPLIES
design and operation of, for reactor control rod drive motors in PWR, 20: 42642 (WAPD-PWR-2216)
design for ALRR neutron chopper, 20: 42681(R) (IS-1500(Sect. R))
design of high-voltage, for electron beam heating, 20: 41228(R) (ORNL-3875, pp 15-20)
development of isotopic, using Brayton and Rankine cycles, 20: 41398
evaluation of isotope, 20: 41397

PRASEODYMIUM
atomic structure of, calculation of Hartree-Fock parameters for, 20: 41631
liquid, solubility of tantalum and tungsten in, at high temperatures,

20: 41412(R) (IS-1500(Sect. M))
photon reactions (γ,n) with, energy spectra from, (E), 20: 42165(R) (MIT-2098-251, pp 16-20)
separation factor for, in chloride and nitrate systems containing TBP, 20: 40904
PRASEODYMIUM ALLOYS
Au–Pr, phase studies, 20: 41412(R) (IS-1500(Sect. M))
Co–Pr, crystal structure of Laves phases in, 20: 41412(R) (IS-1500 (Sect. M))
Mg–Pr, thermodynamics of formation of intermetallic compounds, 20: 41412(R) (IS-1500(Sect. M))
PRASEODYMIUM ALUMINATES
preparation of monocrystals of, with perovskite structure, 20: 40920
PRASEODYMIUM CHLORIDES
magnetic properties from NMR and NQR studies, 20: 42522(R) (COO-1533-2)
$HCl–NdCl_3–PrCl_3–TBP–H_2O$, separation factors for neodymium and praseodymium in, 20: 40904
PRASEODYMIUM COMPLEXES
with mandelic acid and α-methylmandelic acid, stability of, 20: 40902
PRASEODYMIUM ISOTOPES Pr-138
beta decay, (E), 20: 42197
PRASEODYMIUM ISOTOPES Pr-141
meson (μ^-) capture by, x-ray spectra from, (E), 20: 42306
PRASEODYMIUM ISOTOPES Pr-144
content in fallout from Chinese nuclear test, May 1965, 20: 41130(R) (COO-1407-10)
PRASEODYMIUM NITRATES
specific gravity of aqueous solutions of, 20: 40796(R) (IS-1500(Sect.C))
$Nd(NO_3)_3–HNO_3–Pr(NO_3)_3–TBP–H_2O$, separation factors for neodymium and praseodymium in, 20: 40904
PRASEODYMIUM OXALATES
thermal decomposition of hydrates of, differential thermal analysis of products of, 20: 40900
PRASEODYMIUM OXIDES
effects on catalytic properties of aluminum oxide–chromium oxide systems, 20: 40943
$Al_2O_3–Cr_2O_3–Pr_2O_3$, properties for use in dehydrogenation of butane, 20: 40943
PRECIPITATION, ATMOSPHERIC
fallout content in Canadian, April 1965, 20: 41209
fallout transport to water supplies by, 20: 41141
radioactivity of, in Canada, April, 1966, 20: 41198 (NP-16192)
strontium-90 content in global, 1965 and 1966, 20: 41131(R) (HASL-172)
PRECIPITATION, CHEMICAL
use in trace analysis, 20: 40850
PREDNISOLONE
effects on zinc-65 metabolism in rats, 20: 40563
PREGNANCY
effects of ovarian irradiation on, 20: 40761
PRESSURE
control of, in reactors, method for, 20: 42656(P)
effect on leak rate of conical-face seals, 20: 41074 (AECL-2551)
effects on polymorphic transformations of the elements, (T), 20: 41521
pulsations at high loading ratios, 20: 41102 (NYO-2930-6)
PRESSURE GAGES
calibration of uranium hexafluoride, design and performance of micron region standard for, 20: 41252
PRESSURE VESSELS
containment shells, design for pressurized water reactors, 20: 42592(P)
crack growth mechanisms in steel, 20: 42576 (AHSB(S)-R-107)
design of prestressed concrete, 20: 42596(P)
development and testing of AARR, 20: 42670(R) (ANL-7245, pp 48-59)
fabrication and installation of La Crosse BWR, quality control of, 20: 42637 (SWRI-1228-7-33)
fracture of steel, testing for fast, 20: 42576 (AHSB(S)-R-107)
materials for Rapsodie, testing of austenitic steel, 20: 42652(T) (EURFNR-92F)
materials for reactor, fatigue embrittlement of steel, 20: 41446(R) (EURAEC-1624)
materials for, testing type 302B steel for, 20: 41451(R) (GA-7101)
port weld cutting machines for PWR Core 2, instruction manual, 20: 42649 (WAPD-PWR-2230)
radioinduced embrittlement of steel, neutron, 20: 41494(R) (EURAEC-1617)
seal weld cutting machine for PWR Core 2, instruction manual, 20: 42650 (WAPD-PWR-2232)
seal welding machine for PWR Core 2, instruction manual, 20: 42648 (WAPD-PWR-2229)
serviceability evaluation of Elk River Reactor, 20: 42636(R) (SWRI-1228-4-22)
PRESSURIZED WATER REACTORS
core design for, 20: 42595(P)
fuel assemblies for, zirconium alloy brazes for, 20: 41425(R) (IITRI-578-P29-2)
pressure control in, method for, 20: 42656(P)
PRINCETON SYNCHROTRON
magnet current of, schemes for flat topping for maximizing stability in, 20: 41569
PROCESS HEAT REACTORS
economics for desalination, 20: 42658 (NP-16250)
economics for desalination, 20: 42659
PROMETHIUM
chemistry, 20: 40872 (NP-16254)
separation from waste solutions, 20: 42689
separation of, from other lanthanides by thin-layer high-voltage electrophoresis, 20: 41046
PROMETHIUM COMPOUNDS
preparation and properties of, 20: 40872 (NP-16254)
PROMETHIUM ISOTOPES Pm-147
properties of, in isotopic power sources, 20: 41397
PROPANE
yields of deuterated, in hydrolysis of aluminum, thorium, and uranium carbides in heavy water, 20: 40905
2-PROPANOL
radiolysis of liquid and vitreous, effects of benzophenone and naphthalene additions on gamma, 20: 41006
radiolysis of, EPR studies of yields of stabilized charges in low-temperature, 20: 40962
PROPELLANTS
injection of plasma-jet, port modifications for, 20: 41121
PROPENE, 3-CHLORO-2-METHYL-
radioinduced codimerization of, with unsaturated compounds, 20: 40971
PROPENE, HEXAFLUORO-
radioinduced polymerization of, at high pressure and 100 to 230°C, 20: 40976
PROPENE POLYMERS
radiation effects on crystal orientation in, x, 20: 40949(R) (NYO-3003-29)
PROPORTIONAL DETECTORS
circuit design for breakdown protection of, 20: 41268(R) (NYO-2740-3, pp 5-165)
description of, for low energy electrons, 20: 41351
design and fabrication of spherical boron trifluoride, for neutron detection, 20: 41271(R) (ORNL-3875, pp 44-52)
design of low-cost portable alpha, 20: 41275 (RFP-777)
design of methane-flow, closing device for, 20: 41359(P)
electron lifetime and loss factors in boron trifluoride, 20: 41357
performance for neutron dosimetry, 20: 41268(R) (NYO-2740-3, pp 5-165)
performance of cylindrical and spherical, for dosimetry, 20: 41268(R) (NYO-2740-3, pp 5-165)
performance of small wall-less tissue equivalent, for γ microdosimetry, 20: 41268(R) (NYO-2740-3, pp 5-165)
pulse height distributions from, elimination of intensity dependent shifts in, 20: 41332
pulse height in x-ray gas, shifts in, 20: 41331
radon-222 effects on count rate of copper, 20: 41372
use of BF_3, for neutron dosimetry in accelerator environment, 20: 41543 (RPP-R-2)
use of, surrounded by G-M anticoincidence ring, for subterranean water measurements, 20: 41167
PROPULSION
chemical, performance in solar probe mission, 20: 41124
electrical, testing systems for, 20: 41122
ion engine for, analytical model for plasma in, 20: 41123
plasma jet, engine design for, 20: 41121
solar-electric, performance in solar probe mission, 20: 41124
PROTACTINIUM
separation from actinium, radium, and thorium by various methods, 20: 41044
separation of, from niobium, by selective precipitation from oxalic-hydrochloric acid mixtures, 20: 41043
PROTACTINIUM ISOTOPES Pa-233
neutron total cross sections at 0.01 ev to 10 kev, (E), 20: 42151 (IN-1014)
PROTEINS
amino acid destruction in deoxyribonucleohistone solutions following gamma radiation, 20: 40585
biosynthesis in yeasts, effects of super-suppressible mutants on, 20: 40582(R) (ORNL-3922, pp 65-8)
book: *The Use of Radioautography in Investigating Protein Synthesis*, 20: 40567
determination of iodine content in iodine-131 labeled, 20: 40553
effect of irradiated potato, in diet of rats, 20: 40576
electron spin resonance signals from irradiated, 20: 40595
isolation and purification of phosvitin, from vertebrate eggs, 20: 40499(R) (ORNL-3922, pp 69-79)

phase determination for crystals of, using anomalous scattering data and isomorphous replacement, 20: 40632(R) (ORNL-3922, pp 175-91)
radiation effects on binding of histone to DNA in deoxyribonucleohistone, gamma, 20: 40586
radiation effects on metabolism in animals, 20: 40602 (AD-624934)
radiation effects, in lysosome suspensions, gamma, 20: 40685
radioinduced decomposition of wheat flour, gamma, 20: 40599
radioinduced inactivation of dry, 20: 40596
radioinduced inactivation of, electron spin resonance studies, 20: 40598
radioinduced structural changes in, effects on activity, 20: 40596
radiosensitivity effects in *E. coli* of synthesis of, x, 20: 40629(R) (ORNL-3922, pp 94-8)
role in bacterial metabolism, 20: 40571
role of microsomes in synthesis of, 20: 40503(R) (ORNL-3922, pp 137-45)
selenium-75 fixation to, in protein-polysaccharides of cartilage, 20: 40544
structures of, use of uranium for determining, 20: 40632(R) (ORNL-3922, pp 175-91)
sulfur-containing, ion radioinduction in, 20: 40598
synthesis in cancerous and normal trout liver, 20: 40632(R) (ORNL-3922, pp 175-91)

PROTON BEAMS

emittance area growth of, with nonuniform radial charge distribution, 20: 41531 (BNL-10528)
energy of, design of range wheel for determining, 20: 41228(R) (ORNL-3875, pp 15-20)

PROTON TOTAL CROSS SECTIONS

measurement for nuclei with Z = 22 to 50 at 14.5 Mev, 20: 42162 (LA-DC-8075)

PROTONS

annihilation on antiprotons in Tunguska meteor, properties of, 20: 41607
attenuation by nuclei at 0.1 to 500 Mev, tables for, 20: 41619 (CEA-R-3042)
detection of, design and performance of lithium-drift telescope silicon detectors for, 20: 41376
diffraction patterns for, using ion microscopy, 20: 42283
dosimetry of, performance of ionization chamber and accesory equipment for, 20: 41268(R) (NYO-2740-3, pp 5-165)
dosimetry with solid state track detectors, medical uses, 20: 41262 (BNWL-SA-619)
effects on optical stability of quartz, 20: 41502
energy losses in aluminum, calcium, calcium fluoride, carbon, and gold at 0.4 to 6 Mev, (E), 20: 42363
interactions in nuclear emulsions at 25 Bev, multiple fragment emission in, 20: 41827
interactions of bound and free, with photons, meson (π^+) production from, (E), 20: 41816
interactions of bound and free, with photons below 330 Mev, meson (π) yields from, (E), 20: 41817
interactions with antiprotons at 2.7 Bev/c, final states from, 20: 42523(R) (IS-1500(Sect.P))
interactions with photons at 2.6 to 2.7 Bev, differential cross sections for mesons (K^+) and mesons (π^+) production in, (E), 20: 41795(R) (MIT-2098-251, pp 21-36)
interactions with mesons (π^-) at 6 to 18 Bev/c, cross sections for elastic charge-exchange, (E), 20: 41795(R) (MIT-2098-251, pp 21-36)
interactions with mesons (π^-) at 10 Bev/c, $2\pi^0$ mass spectra from, (E), 20: 41795(R) (MIT-2098-251, pp 21-36)
interactions with mesons (π^-) at 10 Bev/c, spin of mesons (f^0) from, (E), 20: 41795(R) (MIT-2098-251, pp 21-36)
interactions with photons, mesons (π^0) production cross sections for, (E), 20: 41798 (MIT-2098-265)
interactions with mesons (K^-) at 4.2 Bev/c, strangeness-1 and -2 events in, (E), 20: 41799(R) (ORO-2504-96)
interactions with mesons (K^-) at 0.9 to 1.0 Mev/c, Λ^0, $\Sigma^\pm$, and K^0 production in, (E), 20: 41799(R) (ORO-2504-96)
interactions with hyperons ($\Sigma^\pm$) at 150 to 161.5 Mev/c, cross sections for, (E), 20: 41799(R) (ORO-2504-96)
interactions with mesons $K^\pm_2$, total cross sections for, (E), 20: 41799(R) (ORO-2504-96)
interactions with protons, bibliography on, 20: 41800 (UCRL-14716)
interactions with mesons (π^-) at 2.0 to 4.0 Bev/c, cross sections for A_2, D, E, and ϕ mesons production in, (E), 20: 41802 (UCRL-16832)
interactions with mesons (π^-) at 2.0 to 4.0 Bev/c, $K\bar{K}$ production in, (E), 20: 41802 (UCRL-16832)
interactions with mesons (K^+) at 2.7 Bev/c, K* (891), N* (1236), and ω production from, (E), 20: 41804 (UCRL-17003)
interactions with antiprotons, differential cross section for $\bar{N}^*N^*$ production in, (T), 20: 41788 (BMwF-FBK-66-12)
interactions with antiprotons at 3 to 4 Bev/c, two- and zero-prong, (E), 20: 41792 (INR-708/VI/PL)
interactions with deuterons at 8 Bev, real part of amplitude of elastic, (E), 20: 41811
interactions with antiprotons, polarization and structure relations for annihilation, (T), 20: 41813
interactions with deuterons at 155 Mev, elastic, (E), 20: 42184
interactions with deuterons at 155 Mev, inelastic, (E), 20: 42185
interactions with electrons at 3.7 to 5.9 Bev, cross sections for momentum transfer of 10 and 105 F^{-2} in, (E), 20: 41791 (DESY-66/20)
interactions with mesons (π^-) at 300 Mev, recoil polarization from, (E), 20: 41794 (JINR-E-2860)
interactions with mesons (K^-), peripheral model for Y* charge-state interference in, 20: 41819
interactions with protons, nucleon isobar production in distorted-wave OPE model for inelastic, 20: 41820
interactions with mesons (K^+) at 910 Mev/c, phase-shift analysis of, 20: 41825
interactions with nucleons in emulsions at 20 Bev/c, multiple meson production in, (E/T), 20: 41829
interactions with mesons ($\pi^\pm$) at 300 to 700 Mev, total cross sections for, (E), 20: 41830
interactions with mesons (π^+) at 8 Bev/c, shadow model for elastic backward peak in, 20: 41839
interactions with mesons (π^+) at 4 and 8 Bev/c, Regge-pole analysis of, 20: 41842
interactions with photons at high energies, absorption correction for meson (π^+) production in, 20: 41844
interactions with antiprotons, representation mixing in SU_{6_w} for annihilation, 20: 41847
interactions with mesons (K^+) at 3.5 Bev/c, existence of K^+K^- resonance in, (E), 20: 41856
interactions with mesons ($\pi^\pm$) at 875 to 1579 Mev/c, cross sections for elastic, (E), 20: 41857
interactions with mesons (π^-) at 2.1 Bev/c, π-π interactions and N* (1920) production in, (E), 20: 41858
interactions with mesons (π^-) at 2 to 5 Bev, cross section for W boson production in, (T), 20: 41859
interactions with mesons (π^-) at 558 to 900 Mev, cross sections for, (E/T), 20: 41871
interactions with neutrons at 23.1 Mev, spin correlation parameter for, (E), 20: 41877
interactions with protons at 33.5 and 46 Mev, angular distribution of gamma rays from, (E), 20: 41882
interactions with photons at 0.95 to 1.1 Bev, differential cross sections for meson (η) production in, (E), 20: 41889
interactions with mesons (π^-) and (π^+) at 323 to 1150 Mev/c, polarization in, (E), 20: 41890
interactions with protons at high energies, real part of amplitude for, (T), 20: 41895
interactions with protons at high energies, properties of large-angle, (T), 20: 41896
interactions with protons at 143 Mev, differential cross section and polarization from, (E), 20: 41915
interactions with deuterons, protons, and neutrons below 1 Bev, review of polarization in, (E), 20: 41916
interactions with mesons (π^-) at 900 Mev, hyperon (Λ) and meson (K^0) production from, (T), 20: 41917
interactions with photons, meson (ρ^0) production via two-meson (π) exchange in, (T), 20: 41918
interactions with mesons (π^+) via two-meson (π) exchange, (T), 20: 41918
interactions with mesons (π^+) at 7 Bev/c, effective mass spectra from, (E), 20: 41919
interactions with protons at 2.8 Bev/c, meson (π^0) production in, (E), 20: 41920
interactions with protons at 50 Mev, bremsstrahlung production in, (T), 20: 41921
interactions with protons at 33.5 and 46 Mev, energy dependence of bremsstrahlung cross sections for, (E), 20: 41882
mass relative to neutrons, field-theoretical sum rules for calculating, 20: 41824
penetration into magnetosphere, solar wind, (T), 20: 42069
production in hydrogen ion collisions with gas molecules, 20: 41663
reactions (d,p) with calcium-44, energy spectra from, (E), 20: 42168(R) (MIT-2098-251, pp 57-73)
reactions (p,α) with aluminum-27 at 4.00 to 5.50 Mev, cross sections for, (E/T), 20: 42324
reactions (p,α) with calcium-40 at 11 Mev, Q-values for, (E), 20: 42200
reactions (p,α) and (p,d) with beryllium-9 at 7 to 9 Mev, (E), 20: 42212
reactions (p,α) with cobalt-59 at 9 to 13.5 Mev, iron-56 energy levels from, (E), 20: 42256
reactions (p,d) and (p,d) with lithium-6 and lithium-7, energy levels from, (E), 20: 42358
reactions (p,d) with boron-10 and boron-11 at 156 Mev, (E/T), 20: 42350
reactions (p,d) with lithium-7 at 100 Mev, lithium-6 energy levels from,

(E/T), 20: 42351
reactions (p,d) with fluorine-19 and nitrogen-14 at 156 Mev, (E), 20: 42204
reactions (p,d) with nuclei, form factors for DWBA calculations of, 20: 42221
reactions (p,f) with uranium at 170 Mev, yields in, 20: 42177
reactions (p,f) with bismuth-209 at 100 to 150 Mev, (E), 20: 42196
reactions (p,γ) with molybdenum-92 and strontium-88, analog resonances in, (E), 20: 42331
reactions (p,γ) with nitrogen-15, oxygen-16 energy levels from, (E), 20: 42342
reactions (p,γ) with chlorine-37 at 1.088 and 1.092 Mev, argon-38 energy levels from, (E), 20: 42181
reactions (p,γ) with nuclei with Z = 10-20 at 0.3 to 2.1 Mev, resonance strengths for, (E), 20: 42182
reactions (p,γ) with magnesium-26 at 1.966 Mev, resonance strength for, (E), 20: 42198
reactions (p,n) with scandium and titanium isotopes at 15.25 Mev, angular distributions for quasielastic, (E), 20: 42169(R) (UCRL-14744, pp 1-18)
reactions (p,n) with lithium-6 at 11.6 and 12.6 Mev, beryllium-6 energy levels from, (E), 20: 42169(R) (UCRL-14744, pp 1-18)
reactions (p,n) with nuclei, exact solution of optical-model equations for, (T), 20: 42243
reactions (p,p') with chromium isotopes, energy levels from, (E), 20: 42166(R) (MIT-2098-251, pp 37-49)
reactions (p,p'α) at 60 and 120 Mev, cross sections for, (E), 20: 42352
reactions (p,pd) with carbon-12 at 155 Mev, differential cross sections for, (T), 20: 42361
reactions (p,xn) with bismuth-209 at 75 to 160 Mev, production of polonium isotopes, (E), 20: 42196
reactions (p,2p) with carbon and oxygen at 160 and 460 Mev, quasi-free, (E), 20: 42276
reactions (p,2p) with beryllium-9, lithium-7, and sodium-23 at 155 Mev, (E), 20: 42360
reactions (p,2p) with nuclei, calculations using distorted-wave t-matrix approximation, (T), 20: 42215
reactions with deuterium and hydrogen, bremsstrahlung production from, (E), 20: 41916
reactions with heavy nuclei, Coulomb displacement energies from isobaric analog resonances in, (E), 20: 42262
reactions with indium and silver at 200 and 400 Mev, cross section and half life of silver-101 yields in, 20: 42179
reactions with neutral ground-state atoms, formation of excited hydrogen atoms from, (T), 20: 41634
reactions with nuclei from Z = 22 to 50 at 14.5 Mev, total cross sections for, (E), 20: 42162 (LA-DC-8075)
reactions with nuclei with A = 40 to 208 at 30 Mev, optical-model analysis of total cross sections for, 20: 42255
reactions with nuclei from Z = 6 to 92 at 660 Mev, cascade nucleon emission in, (E), 20: 42299
scattering by aluminum-27 at 4.00 to 5.50 Mev, cross sections for inelastic, (E/T), 20: 42324
scattering by calcium-40 below 160 Mev, shell-model calculations for quasi-elastic, 20: 42277
scattering by calcium-40 at 152 Mev, differential cross sections and polarization for inelastic, (E), 20: 42341
scattering by carbon, maximum likelihood method for analysis of polarization from, 20: 41790 (DESY-66/17)
scattering by carbon-12 at 4.6 to 11.2 Mev, absolute cross sections for elastic and inelastic, (E/T), 20: 42390
scattering by chromium isotopes at 11 and 12 Mev, inelastic, (E), 20: 42211
scattering by copper at 25 to 1700 kev, x-ray production in L shell from inelastic, (E), 20: 42169(R) (UCRL-14744, pp 1-18)
scattering by fluorine-19 at 13.9 Mev, excitation of ground state band from, (E), 20: 42169(R) (UCRL-14744, pp 1-18)
scattering by helium-3 at 30.2 Mev, energy levels from inelastic, (E), 20: 42224
scattering by iron-56 at 9 to 13.5 Mev, inelastic, (E), 20: 42256
scattering by light nuclei at 80 and 150 Mev, differential cross sections and polarizations for, (E/T), 20: 42388
scattering by lithium-7 at 0.9 to 2 Mev, excitation functions and angular distributions for elastic and inelastic, (E), 20: 42372
scattering by nuclei with A = 40 to 208 at 30 Mev, optical-model analysis of elastic, (T), 20: 42255
scattering by zirconium-90 at 10 to 20 Mev, multiple excitation and shell model description of inelastic, 20: 42229
use in activation analysis, review on, 20: 40806 (NAS-NS-3110)

PROTOZOA
cytology and metabolism of *Rhynchosciara angelae*, 20: 40623(R) (ORNL-3922, pp 32-49)
phosphate metabolism in *Tetrahymena pyriformis*, 20: 40623(R) (ORNL-3922, pp 32-49)
radiation effects on cell division of the ciliate *Spathidium spathula*, x, 20: 40623(R) (ORNL-3922, pp 32-49)

PSEUDOUREA, 2-(2-AMINOETHYL)-2-THIO-
effects on x irradiated Arbacia eggs, 20: 40619(R) (NYO-2740-3, pp 216-57)
radioprotective effects on survival in mice, x, 20: 40719(R) (ORNL-3922, pp 136)
radioprotective effects in mice of, combined with bone marrow transplants, x, 20: 40719(R) (ORNL-3922, pp 136)
radioprotective effect on damage induced by alkylating agents, 20: 40664

PUERTO RICO POWER REACTOR
fuel elements for, cladding temperatures in superheater, 20: 42633 (ORNL-TM-1452)
superheater assembly fuel rod spacers, temperature distribution under, 20: 42634 (ORNL-TM-1453)

PULMONARY ABSORPTION
effects of chemical composition and particle size of uranium oxides on, 20: 41204 (Y-1544-A)

PULSE ANALYZERS
description of, for neutron kinetic energy measurement, 20: 42681(R) (IS-1500(Sect. R))
design for scintiscanning, 20: 41318
Mossbauer effect linearized velocity drive for, design and performance of feedback system for measuring, 20: 41238
signal-to-noise ratio for Intertechnique SA 40, for use with Varian A-60 spectrometer, 20: 41305
time spectra for delayed coincidences in multichannel, computer analysis for, 20: 41301
timing circuits for, design and performance of phase-setting, 20: 41241

PULSE GENERATORS (ELECTRONICS)
design and performance of Marx high-voltage, for wide-gap spark chambers, 20: 41330
design of explosive, for magnetic field compression, 20: 41095
design of variable-rate kv, 20: 41227(R) (ORNL-3875, pp 1-3)

PULSE TRANSFORMERS
performance for large magnetic field production, 20: 41092

PUPAE
radiation effects on weight of Tribolium, x, 20: 40671

PURINES
analysis in *E. coli* RNA, 20: 40501(R) (ORNL-3922, pp 113-14)
analysis of nucleic acid, in root cells of Vicia, 20: 40631(R) (ORNL-3922, pp 161-6)

PYRIDINE, 3-ACETYL-
nuclear magnetic resonance spectra of, using INDOR technique, 20: 42529

PYRIDINE COMPLEXES
with plutonyl nitrate, spectral studies on, 20: 41038(R) (MLM-1325, pp 9-62)

PYRIDINES
reaction with substrate of enzyme-bound, effects of malic-lactic transhydrogenase on, 20: 40505(R) (ORNL-3922, pp 167)

PYRIDOXINE
induction of α-ketoglutarate transaminase in rat liver by, 20: 40506(R) (ORNL-3922, pp 168-73)
phosphate, preparation of phosphorus-32- and tritium-labeled, 20: 41016

PYRIMIDINES
analysis in *E. coli* RNA, 20: 40501(R) (ORNL-3922, pp 113-14)
analysis of nucleic acid, in root cells of Vicia, 20: 40631(R) (ORNL-3922, pp 161-6)
dimer excision from, method for *in vitro*, 20: 40504(R) (ORNL-3922, pp 146-60)
role in cleavage delay in Arbacia, 20: 40543
synthesis in *Vicia faba*, effects of thymidine on, 20: 40581(R) (ORNL-3922, pp 50-1)

PYRITES
uranium content in, effect of weathering on, 20: 41174

PYROGALLOL
amidol-pyrogallol, use as developer for nuclear photoemulsions, 20: 41340

PYROXENES
ages of meteoric, estimation of, 20: 41162

Q

QUALITY CONTROL
methods for, statistical, 20: 42695 (TRG-Report-1200)

QUANTOMETERS
design for measuring intensity of gamma radiation, 20: 41284

QUANTUM ELECTRODYNAMICS
operators in, Heisenberg representation for lagrangian and hamiltonian, 20: 42020
propagator normalizations in, relation between electromagnetic form factor and, 20: 41980

theory of, research programs on, 20: 41796(R) (MIT-2098-251, pp 74-103)
Yang-Mills gauge groups in, 20: 41929
QUANTUM MECHANICS
book: *Particle Waves and Deformation in Crystalline Solids*, 20: 42568
canonical commutation and anticommutation relations in, 20: 42076
derivation of generalized Boltzmann equation in statistical, 20: 42082
extension of Lebowitz-Penrose theorem on van der Waals theory, 20: 42081
formalism in, Dirac bra and ket, 20: 42085
formalism of, axiomatic approach to, 20: 42083
formalism of, axiomatic approach to, 20: 42084
generators of O(4,1) group for hydrogen atom, (T), 20: 41643
generators of O(4,1) group for the hydrogen atom, 20: 41644
many-body problem in, variational principles for, 20: 42074
particle system in, symmetrization postulate for cluster property of, 20: 42089
spin systems in, comparison of Heisenberg and Schroedinger theory for, 20: 42090
statistical, research programs on, 20: 41511(R) (RLO-1388-501)
statistics of particle in condensed system in, sum rules for generalized frequency distribution function for, 20: 42092
symmetrization postulate for identical particles in, 20: 42093
symmetry principles in, 20: 41923 (BNL-956)
wave equations in, stable numerical solutions for Schroedinger, 20: 42097
wave functions for three-nucleon systems, (T), 20: 42209
wave functions in, classification of systems of generalized, 20: 42071 (JINR-P-2785)
QUARTZ
Faraday rotation in megagauss fields, 20: 41515
radiation effects on optical stability of, gamma and proton, 20: 41502
QUARTZ FIBERS
properties and testing of, for thermal insulation spacer materials, 20: 41440(R) (ALO-3632-4)
QUINOLINE, 7-CHLORO-4-[[4-(DIETHYLAMINO)-1-METHYLBUTYL] AMINO]-
diphosphate, radiation effects on, spectral studies on uv, 20: 40954
QUINOLINES
radiolysis of, yields in, 20: 40991
thermal decomposition, 20: 40991

R

RABBITS
effects of Shope papilloma virus on, mechanism for tumorigenic, 20: 40632(R) (ORNL-3922, pp 175-91)
population dynamics in, 20: 40494(R) (COO-1329-3)
radiation dose for $LD_{50/30}$ in, x, 20: 40494(R) (COO-1329-3)
radiation effects on leukocyte lysosomes, gamma, 20: 40685
radiation effects on eyes of, laser, 20: 40692
radiation effects on eyes of, laser source instrument for obtaining, 20: 40791
radiation sickness in, gamma and x, 20: 40694
RADAR
effects of combined, and x radiation on hematologic response of dogs, 20: 40650
RADIATION
book: *Electron Radiation Damage in Semiconductors and Metals*, 20: 41508
color center production in lithium fluoride by, mechanism of, 20: 42562
dose curves for induction of chromosome aberrations by tritium-labeled thymidine, 20: 40686
dose estimations for fallout, 20: 41177 (AD-632211)
dose to various body organs from inhalation or ingestion of soluble radionuclides, dose conversion factors based on ICRP for estimation of, 20: 41193 (IDO-12054)
dosimetry in food irradiation, principles of, 20: 41388
dosimetry of charged and uncharged, 20: 41370(P)
effect on silicate glasses, electron spin resonance studies of, 20: 42538
effects of ionizing, on human genetics, review of, 20: 40662
effects of short-term ionizing, on ecosystems, review of, 20: 40526
effects of, combined with heat, physiological methods, or refrigeration on food enzymes, 20: 40600
effects on adrenal-hypophyseal system in rats, effects of repeated exposure on, 20: 40655
effects on animals, biological, 20: 40602 (AD-624934)
effects on aqueous salt solution, generation of electricity by, 20: 41691(P)
effects on chromosomes in man, 20: 40745(R) (NYO-901-54, pp 29-47)
effects on cladding materials, 20: 42579(R) (ANL-7245, pp 29-47)
effects on *Clostridium botulinum* spores, factors affecting dose required for inactivation, 20: 40601
effects on conditioned reflexes in fetally-exposed rats, 20: 40654
effects on electric and photoconductivity in frozen heptane, mechanism of, 20: 41005
effects on health and fertility of dentists and radiologists, statistical analysis of, 20: 40615(R) (NYO-901-54, pp 26-8)
effects on isomerization of 2-hexene, 2-heptene, 2-octene, and 2-pentene, 20: 40965
effects on isoquinolines, naphthalenes, and quinoline, products in, 20: 40991
effects on leukocyte number in blood of man, low-dose, 20: 40612 (EUR-2711.f)
effects on liquid tetratriacontane as function of temperature, mechanism of, 20: 40986(T)
effects on luminescence decay of zinc sulfide monocrystals, 20: 41342
effects on materials, survey of, 20: 41413
effects on materials, equipment for optical measurement of, 20: 41488(R) (EGG-1183-2013)
effects on oxidation of methanol, 20: 41004
effects on photographic film, 20: 41223 (EGG-1183-1244)
effects on polymeric electric insulators, 20: 41489(R) (EGG-1183-2014)
effects on polymerization of acrylic monomers in binary systems, 20: 40977
effects on tissues following radiotherapy, 20: 40659
energy transfer by, theory of, 20: 40787
enzyme inactivation by, electron spin resonance studies of, 20: 40596
injuries to intestine and urinary system following uterine carcinoma therapy, 20: 40703
linear energy transfer studies, relation to relative biological effectiveness of electron beams, 20: 40767
radioecological studies in Brazilian areas of high natural, 20: 40522(R) (NYO-3273-7)
reactions with reactor materials, review, 20: 41527
spectra of recombination, from electron-excited silicon carbide crystals, (E), 20: 42565(T)
use in studying genetic control of germ cell formation in peas, 20: 40512
use of computers to calculate and store data describing fields produced by radium needle implants, 20: 40765
RADIATION CHEMISTRY
enzyme inactivation studies, 20: 40596
radiolysis of solid and liquid systems, survey of, 20: 40987
yields of gas-phase radiolysis, use of quasi-equilibrium theory to determine, 20: 40958
RADIATION DETECTION INSTRUMENTS
book: *Nuclear Instrumentation*, 20: 41256
calibration of multidetector, technique for, 20: 41310
calibration of, for space application, 20: 41219
data accumulation systems for, circuit for preset value cutoff for, 20: 41244
design and performance of photon, for high-energy mesons (π^0), 20: 41320
design for detecting high-energy particles in radiation environment, 20: 41364(P)
design for use in high background, 20: 41365(P)
manufacturing of isotopic and nucleonic, developments in Poland, 20: 41236
performance of windowless, for carbon-14 measurements, 20: 41281
testing counting characteristics of, automatic system for, 20: 41285
RADIATION DETECTION INSTRUMENTS (ION CURRENT TYPE)
development of alpha and thermal neutron survey meters, 20: 41272(R) (ORNL-3875, pp 53-74)
RADIATION DETECTION INSTRUMENTS (PULSE TYPE)
circuit for protection of linear amplifier input stage, 20: 41260(P)
design and performance of diode function generator, for charged particle identification, 20: 41308
design of alpha scintillation, 20: 41366(P)
design of catheter-type micro Geiger-Mueller counter for use in coronary blood circulation rates using phosphorus-32, 20: 40514
design using solid state detector, 20: 41368(P)
efficiency of large-area liquid scintillator, 20: 41339
gain stabilizing system for, 20: 41112 (IITRI-578P11-54)
use for accelerator radiation monitoring, 20: 41276 (UCRL-16769)
use for uranium determination in boreholes, 20: 41157
use of modified rectilinear scintillation, for radiodiagnosis, 20: 40755
RADIATION DETECTORS
development of scanner, with system for medical information storage and retrieval, 20: 40748
gamma-gamma directional correlation coefficients for, 20: 41371
geometry of, program for source-to-detector, 20: 41316
RADIATION INJURIES
book: *Problems of Post-Radiative Cell Restoration*, 20: 40731
carcinoma induction in occupationally exposed persons, 20: 41207
ecological effects on recovery from, review of, 20: 40526
effects of galactic radiation on cells at altitudes of 70,000 ft, 20: 40525
free radical effects on, electron spin resonance studies, 20: 40597
in man following radiotherapy, 20: 40659

laser beam induced, in eyes of rabbits, 20: 40692
leukemia induction in occupationally exposed persons, 20: 41207
myxedema resulting from x radiotherapy of laryngeal cancer, 20: 40780
pathology of, in monkeys exposed *in utero* to x, 20: 40619(R) (NYO-2740-3, pp 216-57)
pathology of, neurohumoral mechanisms of remote, 20: 40602 (AD-624934)
production in thyroid by radiotherapy, 20: 40647
protective effects of endotoxin in mice, 20: 40732 (AD-636209)
pulmonary fibrosis after radiotherapy of breast cancer, 20: 40773
recovery of rat hematopoietic system from x, 20: 40603 (AD-635086)
recovery of swine from, 20: 40605 (AD-635735)
repair mechanisms for radioinduced chromosome aberrations, 20: 40609 (CONF-660418-1)
salivary gland cytologic changes following cobalt-60 radiotherapy, 20: 40644
skin diseases caused by light, human, review of, 20: 40696

RADIATION MONITORING
Canadian reactor, April 1965, 20: 41136
equipment design for nuclear excursion, 20: 41349
fallout in New Zealand and Pacific areas, 20: 40521(R) (NP-16270)
instrument for continuous beta activity, design and performance, 20: 41303
personnel in industrial radiography in Poland, 20: 41212
program at ORNL, 20: 41272(R) (ORNL-3875, pp 53-74)
survey of accelerator personnel, 20: 41206(T) (JPRS-36341, pp 10-17)

RADIATION PROTECTION
area-wide shelter systems in San Jose, California, 20: 41183 (AD-635931)
book: *Problems of Post-Radiative Cell Restoration*, 20: 40731
endotoxin and hypoxia effects on mice exposed to sublethal radiation, 20: 40732 (AD-636209)
methods for, during radiotherapy by technique modification, 20: 40659
methods for, using laser therapy, 20: 40776
of *Escherichia coli*, using 3,3′-[(*p*-Sulfamoylphenyl)arsylenedithio]dialanine, 20: 40737
of mice, against x-ray induced leukemia, 20: 40658
personnel monitoring in industrial radiography in Poland, 20: 41212
procedures during diagnostic and therapeutic radiography, 20: 40733 (ISS-66/16)
procedures for persons using neutron generators, 20: 41215
procedures in well logging, 20: 41216
special equipment development and research at NASA Manned Spacecraft Center, 20: 41219
standards for clinics and hospitals, 20: 40739
use of mixed bacterial toxins and anthramycin, 20: 40736
use of television in monitoring fluoroscopic x rays as means of, 20: 40781

RADIATION SICKNESS
effects of nibufin on mouse, x, 20: 40724
effects on enzyme content of cerebral tissues, 20: 40590
induced in dog by multiple x irradiation, 20: 40645
manifestations in mammals, 20: 40694
radiation effects on eye tissues of monkeys suffering, γ, 20: 40646

RADIATION SOURCES
design of laser instrument for retinal coagulation in radiotherapy, 20: 40791
design of shielded, for animal populations, 20: 40518 (CEX-63.10)
preparation for isotopic power generators, 20: 41397
production and use in Hungary, 20: 41386(T) (JPRS-36895)
production from recovered fission products, 20: 42689
use of polonium–beryllium, in uranium determination in boreholes, 20: 41157

RADIATION TARGET CANS
design for comparison of neutron effects on steels, 20: 41504
design of liquid helium-3, 20: 42107

RADIATION TARGETS
preparation of plutonium dioxide, for HFIR, 20: 41039(R) (ORNL-3880)

RADIO ASTRONOMY
frequency splitting in solar bursts, 20: 41606

RADIO WAVES
absorption in ionosphere during solar eclipse, (E), 20: 42053
backscattering of radio aurora, 20: 42057
emission from atmospheric nuclear explosion, gamma flux produced, (T), 20: 42046 (RM-4988)
emission from sun, frequency splitting in, 20: 41606
transmission through plasma sheath, magnetic field effects on, (T), 20: 42426

RADIOACTIVE CONTAMINATION
determination in LOFT atmosphere after blowdown, 20: 42664(R) (IDO-17165)
evaluation of, for postattack protection, 20: 41177 (AD-632211)
monitoring of environmental, in New Zealand, 20: 40521(R) (NP-16270)

RADIOACTIVE MATERIALS
analysis of, development of remote-control equipment for, 20: 40799 (CEA-R-2887)
plating, design of equipment for, 20: 41268(R) (NYO-2740-3, pp 5-165)
separation from cooling-pond water by ion exchange, 20: 41061(P)
PuO_2–UO_2, performance as FTR fuel, 20: 42676 (BNWL-281)
PuO_2–UO_2, thermal properties, 20: 42612

PLUTONIUM RECYCLE TEST REACTOR
decontamination of, after failure of magnesia–plutonia fuel element, 20: 42677 (BNWL-SA-636)
failure of pressure tube and defected fuel rod in FERTF of, combined, 20: 42675 (BNWL-272)
reactivity of high power density core for, 20: 42674 (BNWL-221)

PLUTONYL IONS
stability in dilute nitric acid, 20: 41038(R) (MLM-1325, pp 9-62)
shipping containers for, leak detection in, 20: 41197(R) (NP-16172)

RADIOACTIVE STATIC ELIMINATORS
design and development of, using polonium-210, 20: 41395

RADIOACTIVE WATERS
decontamination of, from cooling ponds, ion-exchange method for, 20: 41061(P)

RADIOACTIVITY
book: *Radioactivity of Soils and Methods of Measurement*, 20: 41139
effects of fallout fission products on ocean, 20: 41144
measurements of strontium-90 and cesium-137 in milk in the United Kingdom, 20: 41186 (ARCRL-15)
monitoring atmospheric beta, method for, 20: 41137
monitoring in atmosphere, performance of radio-telemetering system for, 20: 41188(R) (BNWL-235-1)
survey of fallout, in West Germany, 20: 40570

RADIOAPPLICATORS
computer programs for radium implant dosimetry, 20: 40788
use of computers to calculate radiation fields produced by radium needle implants, 20: 40765
use of radon gold seed implants for therapy of eye tumors, 20: 40771

RADIOBIOLOGY
conference on electron spin resonance use in, to determine biological effects of radiation, 20: 40592
energy transfer by elastic nuclear collisions, 20: 40515
free radical effects in, electron spin resonance studies, 20: 40597
radioprotection using SH compounds, 20: 40515
single-hit effects, 20: 40515

RADIOCHEMISTRY
analysis of detritus from Indian Ocean, 20: 41140
analytical procedures in, 20: 40799 (CEA-R-2887)
conference on, at Lyon, May 13, 1965, 20: 41028
estimation of choline acetyl transferase using carbon-14-labeled acetate, 20: 40584
safety guide for laboratories, 20: 41199 (ORNL-TM-626)

RADIODERMATITIS
production by gamma radiation in therapy of female genital cancer, 20: 40679

RADIODIAGNOSIS
background suppression during scintiscan, design and use of pulse analyzer for, 20: 41318
blood vessel visualization by scintiphotography, 20: 40752
bone scanning for fluorine-18 uptake, 20: 40554
gamma mapping of the liver with the digital computer, 20: 40747 (UCRL-14866)
liver scanning, using technetium-99m sulfide colloid, 20: 40753
lung visualization by scintiphotography, 20: 40749
radioisotope renography of kidneys, 20: 40775(T)
scintillation scanning with eight-inch sodium iodide crystal, 20: 40779
scintiphotography of liver and spleen, 20: 40777
thyroid scanning with technetium-99m and iodine-131, 20: 40555
use of gamma camera for, thyroid gland, 20: 40751
use of iodine-131 for evaluation of thyroid disorders, 20: 40756
use of modified rectilinear scanner for, 20: 40755
use of pertechnetate in, 20: 40750
use of pertechnetate-99m in brain scanning, 20: 40789
use of phantoms in dosimetric measurements for pelvic radiographs, 20: 40770

RADIOFREQUENCY SPECTROMETERS
design and performance of, for NMR splitting, 20: 41254
design of superheterodyne, for observing ENDOR of F centers, 20: 42566(T)
pulse analyzer Intertechnique SA 40 for Varian A-60, signal-to-noise ratio for, 20: 41305

RADIOGRAPHY
dosimetry of medical, survey using film packs, 20: 41213
effect of x-ray quality and ovarian location on genetic exposure in gynecological examinations, 20: 40770
effects on human erythrocyte diameter and volume from occupational exposure to, 20: 40678
equipment and techniques for, 20: 41116(P)

fluoroscopic x-ray, television equipment for monitoring, 20: 40781
method for mouth, 20: 40795
personnel monitoring in industrial, in Poland, 20: 41212
radiation hazards of diagnostic and therapeutic, 20: 40733 (ISS-66/16)
use in production of transmission pictures of virus models, 20: 40653

RADIOISOTOPES
availability and specifications of, 20: 41382
behavior in soils, 20: 41139
book: *Radioactive Isotopes in Chemical Research*, 20: 41027
catalog and price list, 20: 41382
contamination of eggs by fission products, 20: 40559
content of naturally occurring, in sarcoma patients, 20: 41191(R) (HUX-3170-1)
deposition of, use of molecular plating for quantitative, 20: 41011 (SGAE-CH-34/1966)
detection in human organs, design and performance of gas-filled image intensifier spark chamber for, 20: 41299
determination in environmental samples, laboratory manual for, 20: 40809 (NP-16235)
determination of small quantities of, 20: 41139
effects on human erythrocyte diameter and volume from occupational exposure to, 20: 40678
health physics problems of, in well logging, 20: 41216
identification of, using gamma dose rate measurements, 20: 41025
industrial use of, safety record for, 20: 41208
maximum permissible concentration of, in seawater in Bombay region, India, 20: 40528
preparation and use in Hungary, 20: 41386(T) (JPRS-36895)
preparation of films of, by molecular plating, 20: 41011 (SGAE-CH-34/1966)
radiation dose to body organs from inhalation or ingestion of soluble, dose conversion factors for estimation of, 20: 41193 (IDO-12054)
separation of ionic, from solutions, method for, 20: 41058(P)
toxicity of 150, as compared to plutonium-239, 20: 41199 (ORNL-TM-626)
uptake by aquatic organisms in United Kingdom, 20: 40578
uptake by hydrobionts, 20: 40527
uptake by marine crabs and mollusks from west coast of India, 20: 40528
uptake by plants, 20: 41139
use for visible light production, 20: 41393
use in food radiopreservation, 20: 41383 (CONF-650552)
use in instruments, 20: 41235
use in scanning as aid in radiotherapy, 20: 40757
uses in industry and medicine, performance of digital computers for data interpretation in, 20: 41319

RADIOLOGICAL DEFENSE
decontamination of urban areas during postattack period, requirements, 20: 41179 (AD-635821)
decontamination of urban areas during postattack period, requirements for, 20: 41180 (AD-635822)
decontamination of urban areas during postattack period, requirements for, 20: 41181 (AD-635823)
decontamination of urban areas during postattack period, requirements for, 20: 41182 (AD-635824)
during postattack period, requirements for, 20: 41177 (AD-632211)

RADIOLOGICAL TELEMETERING SYSTEMS
performance of radio-, for area monitoring, 20: 41188(R) (BNWL-235-1)

RADIOMETRIC ANALYSIS
measurements in, sensitivity thresholds of, 20: 41334

RADIOMIMETIC SUBSTANCES
effects of vinblastine, on megakaryocytes and platelets in rats, 20: 40502(R) (ORNL-3922, pp 115-27)
effects on *Vicia faba*, effects of chelating agents on genetic, 20: 40715

RADIOPROTECTIVE COMPOUNDS
effects of nibufin, on lethally x-irradiated mice, 20: 40724
effects of SH compounds on phage inactivation by gamma radiation, 20: 40515
effects on damage induced by alkylating agents, 20: 40664
mechanisms of, electron spin resonance studies, 20: 40598

RADIOSENSITIVITY
chicken, difference between sexes, 20: 40693
effects of chemicals on, electron spin resonance studies, 20: 40598
effects of varying, on recovery processes of ecosystems, review of, 20: 40526
factors affecting spore, in *Clostridium botulinum*, 20: 40601
modification of, by porphyrins in mice, 20: 40657
of *Corchorus* species (jute), gamma, 20: 40681
resistance of peanuts to gamma radiation, 20: 40636(R) (ORO-1747-12)
skin and tissues, use of hyperbaric oxygen to increase, 20: 40721
uv, comparison of *Bacillus subtilis* bacteriophage SP02 and its infectious DNA, 20: 40676

RADIOSENSITIZERS
effects of sparsomycin on *E. coli* grown in SPATA, 20: 40737
effects of uracil on mouse tumors, x, 20: 40668

RADIOSTERILIZATION
dose required for, of animal carcasses infected with foot and mouth disease, 20: 41392
effects of oil, on rats, 20: 41391
effects on enzymes in food, effects of dose on, 20: 40600
effects on storage life and wholesomeness of sea foods, 20: 41384(R) (TID-22833)
mating competitiveness after, in male *Trogoderma glabrum*, 20: 40673
microbiological aspects of food, review, 20: 41388
microbiological problems in, of foods, 20: 41383 (CONF-650552)
of fruits, effects on storage life, γ, 20: 41385 (TID-23136)
of haddock homogenates innoculated with type E *Clostridium botulinium* spores, 20: 40699
review of proteinaceous food, 20: 41390
status of food, in the United States, 20: 41383 (CONF-650552)

RADIOTHERAPY
bone scanning with strontium-85 prior to, 20: 40794
combined use of colchicine and x rays in, 20: 40763
complications of pre-surgical radiation of peritoneal lymphocysts, 20: 40783
cutaneous eruptions in, of female genital cancer, 20: 40679
dosimetry for phosphorus-32, using erythrocyte volume, 20: 40774
dosimetry of absorbed dose for electron beam, 20: 40741(R) (ACRH-25, pp 15-23)
dosimetry of electron beams for, 20: 40742(R) (ACRH-25, pp 24-9)
dosimetry of intracavitary radium, design and use of system for, 20: 41377
dosimetry system for electron, 20: 41323
effectiveness for inoperable cervical cancer, in combination with drugs and surgery, 20: 40778
effects of cancer, on hematopoietic system, effects of bone marrow transplants on, 20: 40726
effects of combined actinomycin D therapy and, on mouse tumors, 20: 40762
effects of dose-time factors on skin, 20: 40764
effects of nasopharyngeal carcinoma, on pituitary function, 20: 40660
effects of pulmonary tissue factor on dose, 20: 40760
effects on intestine and urinary system following, of uterine carcinoma, 20: 40703
effects on leukemia incidence in cancer patients, 20: 40745(R) (NYO-901-54, pp 29-47)
effects on survival in patients with hodgkin's disease, 20: 40784
effects on thymus and spleen, in leukemia patients, 20: 40720
effects on tissues, review, 20: 40659
equipment for, design of 35-Mev betatron, 20: 41555
equipment for, linear accelerator simulator, 20: 41548
equipment for, performance of 24-Mev betatron, 20: 41564
iodine-131 versus surgery for hyperthyroidism, relative merits of, 20: 40785
laryngeal cancer, myxedema development following, 20: 40780
memorial system for implant dosimetry, 20: 40788
of cancer, enhancing effect of hyperbaric oxygen, 20: 40721
of cervical carcinoma, radium and x, 20: 40772
of thyroid carcinoma, 20: 40758
of vocal cord carcinoma, 20: 40760
radiation fibrosis after use of, for breast cancer, 20: 40773
radiation field measurements around isotope implants, 20: 40746(R) (NYO-3510-2)
radioinduced injuries to the salivary glands following cobalt-60, 20: 40644
supervoltage, in cancer therapy in gynecology, 20: 40768
thyroid lesion induction by, 20: 40647
use for lung cancer, review of, 20: 40786
use of combined cobalt and radium, for uterine carcinoma, 20: 40769
use of computer dosimetry system for radium implants, 20: 40765
use of iodine-131 in diabetes associated with hyperthyroidism, 20: 40790
use of laser beams in, physiological effects of, 20: 40691
use of laser instrument for retinal coagulation, 20: 40791
use of radioisotope scanning as aid in, 20: 40757
use of radon gold seed implants for eyelid tumors, 20: 40771
use of ultraviolet and radium for oto-rhino-laryngeal tumors, 20: 40782

RADIOTOXICITY
effects of tissue extracts on DNA synthesis in potato tubers, 20: 40562
safety guide for isotopes, based on inhalation hazards, 20: 41199 (ORNL-TM-626)

RADIUM
body burden in people of Brazil, 20: 40522(R) (NYO-3273-7)
dosimetry in intracavitary therapy, design and use of system for, 20: 41377
effects on eyes following therapy of canthus and eyelid carcinomas, effects of dose on, 20: 40689

effects on human erythrocyte diameter and volume from occupational exposure to, 20: 40678
health physics problems of, in well logging, 20: 41216
separation of protactinium from, by hydrolysis in hydrochloric acid, 20: 41044
therapeutic effects on uterine carcinoma, when combined with cobalt therapy, 20: 40769
therapeutic effects on cervical carcinoma, 20: 40772
use in cancer therapy in gynecology in conjunction with x rays, 20: 40768
use in seed implants, dosimetry studies, 20: 40788
use of ultraviolet and radium for oto-rhino-laryngeal tumors, 20: 40782

RADIUM IONS
electron polarizability and magnetic susceptibility of, Thomas-Fermi-Dirac equation for, 20: 40929

RADIUM ISOTOPES Ra-215
alpha decay, (E), 20: 42287

RADIUM ISOTOPES Ra-223
energy levels of, lifetime of 286.1-kev, (E), 20: 42167(R) (MIT-2098-251, pp 50-6)
gamma spectra, 20: 41038(R) (MLM-1325, pp 9-62)
gamma spectra of, energy levels in, 20: 41038(R) (MLM-1325, pp 9-62)
separation from francium-223 by ion exchange, 20: 41038(R) (MLM-1325, pp 9-62)

RADIUM ISOTOPES Ra-226
bone content in sarcoma patients, 20: 41191(R) (HUX-3170-1)
content in human bone and teeth, 20: 40531 (A/AC.82/G/L-1045(Rev.1))
content in human soft tissues, 20: 40531 (A/AC.82/G/L-1045(Rev.1))
determination in environmental samples, 20: 40809 (NP-16235)
distribution in bone and soft tissue of radium dial painters, 20: 40621 (NYO-3086-5)
toxicity in dogs, 20: 40540(R) (UCD-472-113, pp 17-56)

RADIUM ISOTOPES Ra-228
content in human bones, 20: 40531 (A/AC.82/G/L-1045(Rev.1))
distribution in bone and soft tissue of radium dial painters, 20: 40621 (NYO-3086-5)

RADON
determination in environmental samples, 20: 40809 (NP-16235)
use in seed implants for radiotherapy, 20: 40771
use in seed implants, dosimetry studies, 20: 40788

RADON ISOTOPES Rn-213
alpha decay, (E), 20: 42287

RADON ISOTOPES Rn-222
content in atmosphere, charcoal adsorption technique for determining, 20: 41277 (UCRL-16952)
effects on copper proportional detector count rate, 20: 41372

RAIN WATER
analysis for cesium-137, strontium-89, and strontium-90, 20: 40809 (NP-16235)
analysis for silver, ion-exchange separation in, 20: 40839
analysis of, for silver from silver iodide-seeded clouds in Australia, 20: 40838
evaporative losses of falling drops, computer analysis of, 20: 41188(R) (BNWL-235-1)
radioactivity from, strontium-90, 20: 41139
scavenging of atmospheric particular matter by, 20: 41130(R) (COO-1407-10)

RAMAN EFFECT
pulse techniques in, analog of electronic and nuclear spin induction and echo, 20: 41640(T)

RARE EARTH ALLOYS
Ge–rare earth, crystal structure and magnetic properties of intermetallic, 20: 42552

RARE EARTH CARBIDES
determination in steel, procedure for, 20: 41415

RARE EARTH COMPLEXES
stability constants for, 20: 40796(R) (IS-1500(Sect.C))
with sulfosalicyclic acid, composition of, spectrophotometric and fluorometric studies of, 20: 40926

RARE EARTH COMPOUNDS
Mössbauer studies of intermetallic, review, 20: 42570

RARE EARTH ISOTOPES
energy levels of, quadrupole moments of excited, 20: 42226

RARE EARTH MINERALS
processing for ceria and thoria recovery, 20: 41059(P)

RARE EARTH NITRATES
binding energies in, infrared spectral studies of, 20: 40886

RARE EARTH OXALATES
thermal decomposition of hydrates of, differential thermal analysis of products of, 20: 40900

RARE EARTH OXIDES
determination in steel, procedure for, 20: 41415

RARE EARTH SULFIDES
determination in steel, procedure for, 20: 41415

RARE EARTHS
analysis for gadolinium, errors in neutron activation methods of, 20: 40843
analysis for tantalum and tungsten, spectrophotometric, 20: 40796(R) (IS-1500(Sect.C))
analysis for trace impurities, spectrophotometric, 20: 40796(R) (IS-1500(Sect.C))
book: *Rare Earth Ferromagnetics and Antiferromagnetics*, 20: 41483
determination by mass spectrography, 20: 40796(R) (IS-1500(Sect.C))
determination by x-ray-fluorescence methods, 20: 40796(R) (IS-1500 (Sect.C))
determination in americium and plutonium by spark-source mass spectrography, 20: 40816 (RFP-699)
determination of, in uranium by neutron activation analysis, 20: 40832
effects on fish spawning, 20: 40527
properties as cathode material for ion pumps, 20: 40796(R) (IS-1500 (Sect.C))
purification of, methods for, 20: 41412(R) (IS-1500(Sect. M))
separation by ion-exchange elution processes, 20: 40796(R) (IS-1500 (Sect.C))
separation by reversed-phase column partition chromatography, 20: 40796(R) (IS-1500(Sect.C))
separation by solvent extraction using bis(2-ethylhexyl)phosphate, 20: 41064(R) (IS-1500(Sect.E))
separation by thin-layer high-voltage electrophoresis, 20: 41046
separation from actinides by ion exchange using mixed solvent systems, 20: 40855
separation from thorium and uranium by chromatography using ammonium thiocyanate–nitric acid–TBP, 20: 41045
specific heat of, model of electronic, 20: 41412(R) (IS-1500(Sect. M))

RARE GASES
desorption from tungsten monocrystals following ion bombardment, 20: 41463
effects on human kidney cells, factors affecting RBE, 20: 40725
hydrogen ion reactions at 2 to 50 kev, charge exchange and dissociation cross sections for, 20: 41646
ionization in alkali-seeded plasma of, nonequilibrium, (T), 20: 41751
spectra of polymers of normal and deuterated hydrochloric acid in, infrared, 20: 40895

RATE METERS
use of gamma, for radioisotope identification, 20: 41025

RATS
α-ketoglutarate transaminase in liver of, mechanism for *in vitro* inactivation of, 20: 40506(R) (ORNL-3922, pp 168-73)
α-ketoglutarate transaminase in liver of, induced by pyridoxine, 20: 40506(R) (ORNL-3922, pp 168-73)
autoradiography of bone marrow cells, 20: 40666
behavior response to gamma radiation, 20: 40519 (NP-16259)
calcium-47 distribution in bones, muscle and skin of, 20: 40557
comparison of effects of radiation and inhibitors of oxidative phosphorylation on thymocytes, 20: 40549
effects of dose-time factors on radiotherapy of skin damage, 20: 40764
effects of irradiated oils in diet on, 20: 41391
effects of irradiated potatoes in diet on, 20: 40576
effects of x ray and L-methionine sulphoximine on iron-59 metabolism in erythrocytes, 20: 40561
enzyme reactions in, effects of hydrocortisone on, 20: 40533(R) (NYO-901-54, pp 16-19)
fate of leukemia transplants in, immunological basis for, 20: 40502(R) (ORNL-3922, pp 115-27)
life span of frozen human leukocytes, in leukopenic, 20: 40496(R) (NYO-1753-3)
locomotor behavior and neuromorphologic anomalies after pre- and postnatal radiation, 20: 40688
metabolism barium-133 in, used for testing theory of alkaline earth metabolism, 20: 40565
metabolism of nickel chloride and nickel carbonyl in, tracer studies, 20: 40536(R) (ORO-3461-1)
metabolism of 1-(4-dimethylaminobenzylidene) indene in, 20: 40632(R) (ORNL-3922, pp 175-91)
nickel carbonyl toxic effects in, 20: 40536(R) (ORO-3461-1)
phosphorus-32 uptake by tumors in, as prediction of response to hormone treatment, 20: 40566
radiation effects combined with aging on exercise performance of,
radiation effects on adrenal-hypophyseal system in, effects of repeated exposure on, 20: 40655
radiation effects on conditioned reflexes in fetally-exposed, 20: 40654
radiation effects on intestinal mucosa, x, 20: 40607 (BNL-10518)
radiation effects on fine structure of ovarian cells, x, 20: 40672
radiation effects on spermatogenesis in, following exposure at birth, x, 20: 40682
radiation effects on ultrastructure of male germ cells in, following exposure at birth, x, 20: 40683

radiation effects on adenosine triphosphatase activity in liver mitochondria of, x, 20: 40695
radiation effects on leukocyte counts in, whole-body x, 20: 40697
radiation effects on spleen of, effects of fractionated doses on regeneration of x, 20: 40702
radiation effects on experimental allergic encephalomyelitis in, x, 20: 40728
radiation effects on, protective effects of cysteine against x, 20: 40729
radiation effects on lymphoblastic lymphosarcomas in, electromagnetic, 20: 40661
radiation effects on levels of reduced pyridine nucleotides in liver homogenates from, γ, 20: 40583
radiation effects on erythropoiesis in, x, 20: 40603 (AD-635086) 20: 40604 (AD-635251)
radiation effects on mandibular growth, x, 20: 40652
radiation sickness in, gamma and x, 20: 40694
radio-induced cataracts, dosimetry studies, 20: 40690
radioinduced lung carcinoma in parabiotic, total-body, x, 20: 40614 (NYO-901-39)
radiosensitivity of skin in air and hyperbaric oxygen, 20: 40721
reparative effects of DNA on, after total body x-irradiation, 20: 40723
RNA synthesis in fetal, 20: 40506(R) (ORNL-3922, pp 168-73)
scandium-47 and calcium-47 metabolism in bones, 20: 40545
subcellular components of liver cells from, separation by B-XV zonal centrifuge rotor, 20: 40507(R) (ORNL-3922, pp 191-6)
transfer RNA in liver of adult and fetal, uptake of leucine and phenylalanine by, 20: 40506(R) (ORNL-3922, pp 168-73)
tyrosine transaminase induction in liver of, by insulin, 20: 40506(R) (ORNL-3922, pp 168-73)
zinc-65 metabolism in, effects of dexamethasone and prednisolone on, 20: 40563

REACTOR CONTROL RODS
design for liquid moderated reactors to prevent flux peaking, 20: 42588(P)
design of multiregion burnable-poison, 20: 42591(P)
design of variable cross section, for uniform reactivity control, 20: 42587(P)
drive control equipment for PWR Core 2, 20: 42643 (WAPD-PWR-2217)
drive mechanism power supply for PWR, description and operation of, 20: 42642 (WAPD-PWR-2216)
magnet replacement in ALRR, 20: 42681(R) (IS-1500(Sect. R))
position control equipment for PWR Core 2, 20: 42643 (WAPD-PWR-2217)
release of magnetically suspended, detection device for, 20: 42583(T) (WAPD-Trans-34)

REACTOR CONTROL SYSTEMS
description of, for Shippingport PWR, 20: 42640 (WAPD-PWR-2210(Vol.1))
design model study of chemical poison distribution system for rocket reactor, 20: 42665 (WCAP-2870)
design of shutdown, using coolant expulsion, 20: 42597(P)
for SEFOR, development of, 20: 42629(R) (GEAP-5160)

REACTOR COOLANTS
analysis of sodium for carbon, 20: 42619(R) (ANL-7245, pp 1-28)
properties of OM2, for ORGEL reactor, 20: 42623 (EUR-2996.f)
purification of sodium, 20: 42619(R) (ANL-7245, pp 1-28)

REACTOR COOLING SYSTEMS
coolant pump for PWR Core 2, instruction manual, 20: 42644 (WAPD-PWR-2219)
development and testing of AARR, 20: 42670(R) (ANL-7245, pp 48-59)
development for KRB reactor, 20: 42638(R) (TID-23299)
development for KRB reactor, 20: 42638(R) (TID-23299)
failures of pressurized-water, computer program for analysis of, 20: 42664(R) (IDO-17165)
testing of, for KRB reactor, 20: 42638(R) (TID-23299)

REACTOR EXPERIMENTAL FACILITIES
beam-tube development for AARR, 20: 42670(R) (ANL-7245, pp 48-59)

REACTOR FUEL ELEMENTS
adsorption of fission product iodine from, on charcoal, 20: 41202 (UCRL-14990)
analysis of irradiated, for uranium-235 and plutonium, nondestructive, 20: 40808(R) (NP-16212)
boiling burnout of, computer system for monitoring, 20: 42661 (DPSPU-66-30-2)
cladding dissolution from, using atomized hydrochloric acid, 20: 41060(P)
cladding for, fast neutron radiation damage, 20: 42579(R) (ANL-7245, pp 29-47)
cladding of, corrosion testing of stainless steel for, 20: 41418(R) (GEAP-5150)
cladding temperature in BONUS, computer analysis of, 20: 42633 (ORNL-TM-1452)
design of EVESR Mark III, 20: 42627 (GEAP-5051)
design of self-purging, for gas-cooled reactors, 20: 42613(P)
development for CANDU-PHW reactors, status, 20: 42618 (66-CNA-312)
development for High Power Density Project, 20: 42626(R) (GEAP-4951)
development for thorium–uranium-233 seed-blanket reactor, 20: 42609 (WAPD-T-1886)
fabrication for pressurized-water reactors, brazing alloys for, 20: 41425(R) (IITRI-578-P29-2)
fabrication of EVESR Mark III, 20: 42627 (GEAP-5051)
handling device for PWR Core 2, description and operation, 20: 42641 (WAPD-PWR-2213)
heat transfer coefficient of solid cylindrical and spherical, 20: 41106
heat transfer of DOR 19-rod bundles, simulation of, 20: 42635 (RISO-124)
processing of spent aluminum-clad uranium, electrolytic dissolution method for, 20: 41056(P)
properties of high-temperature, experiment simulator for determining, 20: 41233(R) (ORNL-3875, pp 101-24)
radiography of, method and equipment for, 20: 41116(P)
storage at Lucas Heights, site evaluation for, 20: 41148 (AAEC-TM-316)
support design for, 20: 42614(P)
temperature distribution in two-region, computer program for, 20: 42606 (BNWL-252)
testing of leak rates of, nondestructive methods for, 20: 42610(T) (AI-Trans-206)
thermocouples for, design of electric connectors for, 20: 41259(P)

REACTOR FUEL ELEMENTS (CERAMIC)
development for FTR, neutronic aspects of, 20: 42676 (BNWL-281)
production of aluminum–urania, by extrusion, 20: 41412(R) (IS-1500 (Sect. M))
radiation testing of, 20: 42579(R) (ANL-7245, pp 29-47)
temperature measurements on mixed-oxide, 20: 42612

REACTOR FUEL PINS
burnup of, TREAT tests on, 20: 42580(R) (ANL-7245, pp 60-73)
meltdown in flowing sodium, TREAT tests on, 20: 42580(R) (ANL-7245, pp 60-73)
spacer design for, 20: 42615(P)

REACTOR FUEL PLATES
development and testing of AARR, 20: 42670(R) (ANL-7245, pp 48-59)
fabrication of, process for, 20: 42611(T) (WAPD-Trans-33)
thermal conductivity of AARR irradiated, 20: 42579(R) (ANL-7245, pp 29-47)

REACTOR FUEL RODS
bores in, equipment for measurement of ovality of, 20: 41436(P)
failure of defected plutonia–urania, in combination with pressure tube in PRTR, 20: 42675 (BNWL-272)
handling facilities at SEFOR, development of, 20: 42629(R) (GEAP-5160)
heat transfer in AGR, near dimple braces, 20: 41109
mass transfer in AGR, on dimple brace configurations, 20: 41109
spacers in BONUS assemblies, temperature distribution under, 20: 42634 (ORNL-TM-1453)

REACTOR FUELS
analysis for burnable poisons, radiometric, 20: 41112 (IITRI-578P11-54)
burnup analysis of, computer program for, 20: 42608(R) (GEAP-5124)
burnup in ALRR, reactivity changes from, 20: 42681(R) (IS-1500(Sect. R))
cycle costs for High Power Density, 20: 42626(R) (GEAP-4951)
development for fast reactors, 20: 42577(R) (ANL-7230)
development for fast reactors, 20: 42579(R) (ANL-7245, pp 29-47)
development for FTR, neutronic aspects of, 20: 42676 (BNWL-281)
development for LMFBR, 20: 42619(R) (ANL-7245, pp 1-28)
development for LMFBR, 20: 42651 (WASH-1065)
development for SEFOR, 20: 42629(R) (GEAP-5160)
development of plutonium, Hanford program for, 20: 42607 (BNWL-298)
fission product distribution in mixed-oxide fast, 20: 42625 (GEAP-4466)
performance of carbon-coated carbide particles for HTGR, 20: 42624 (GA-6975)
plutonium distribution in mixed-oxide fast, 20: 42625 (GEAP-4466)
preparation of irradiated uranium, for mass spectrometry, 20: 41042 (PG-Report-722)
processing for plutonium and uranium recovery, methods for, 20: 42579(R) (ANL-7245, pp 29-47)
reprocessing, development for fast reactors, 20: 42577(R) (ANL-7230)
separation of cesium-137 from irradiated, method for, 20: 41057(P)
temperature effects on SNAPTRAN, hydrogen release measurements, 20: 42664(R) (IDO-17165)

REACTOR MATERIALS
radiation reactions with, in reactor environment, review, 20: 41527

REACTOR MATRICES
criticality studies of, computer program for, 20: 42599 (UJV-1424)
design, 20: 42594(P)
design, 20: 42614(P)
design of liquid-moderated, 20: 42595(P)

REACTOR MODERATORS

design of solid-block, 20: 42594(P)
effect of, in ALRR beam tubes, 20: 42681(R) (IS-1500(Sect. R))
neutron decay constants in beryllium, 20: 42601
REACTOR SAFETY
analysis for fast power reactors, reactivity coefficients measurement, 20: 42631 (KFK-260)
analysis for Super Kukla prompt burst reactor, 20: 42684 (UCRL-7695 (Rev.1))
analysis of, meteorological manual for, 20: 42584
containment shell for pressurized water reactors, 20: 42592(R)
loss-of-coolant accident analysis, computer program for, 20: 42582 (WAPD-TM-534)
pressure vessel fast fracture testing, 20: 42576 (AHSB(S)-R-107)
research programs on, 20: 42577(R) (ANL-7230)
systems for, design of BNL air cleaning, 20: 42673 (BNL-10483)
xenon effects on HFBR, 20: 42672 (BNL-10388)
REACTOR SAFETY EXPERIMENTS
blowdown in LOFT, acoustic phenomena during, 20: 42664(R) (IDO-17165)
destructive test SNAPTRAN-2, measurement program for, 20: 42664(R) (IDO-17165)
fission product release in LOFT, sampling and analysis of, 20: 42664(R) (IDO-17165)
fuel meltdown studies in TREAT, 20: 42580(R) (ANL-7245, pp 60-73)
operation of TREAT, June 1966, 20: 42577(R) (ANL-7230)
operation of TREAT, 20: 42580(R) (ANL-7245, pp 60-73)
reactivity feedback during transients, SNAPTRAN-1 tests of, 20: 42664(R) (IDO-17165)
REACTOR SHIELDING
design and construction of heavy-concrete, at Kyoto University, 20: 42586
REACTOR SIMULATORS
use of analog, for Hanford N-Reactor dynamic analysis, 20: 42660 (BNWL-SA-270)
REACTOR TUBES
design of moderator-containing, 20: 42589(P)
failure of pressure, in combination with defected fuel rod in PRTR, 20: 42675 (BNWL-272)
REACTORS
components, radiation environment, and radiation processes in, review, 20: 41527
control training simulator for, 20: 42581(R) (ORNL-3875, pp 125-50)
coolant loss accidents in, computer program for analysis of, 20: 42582 (WAPD-TM-534)
core design for solid-moderated, 20: 42594(P)
development, 20: 42578(R) (ANL-7245)
experimental radiation from, in West Germany, 20: 40570
fuels and materials development, 20: 42577(R) (ANL-7230)
loading device for, design of, 20: 42593(P)
neutron detection in, design and performance of gamma-compensated ionization chamber for, 20: 41360(P)
pressure vessel for, prestressed concrete, 20: 42596(P)
reactivity of, cross-power spectral density analyzer for measuring, 20: 42581(R) (ORNL-3875, pp 125-50)
reactivity period meters for, performance of integral logarithmic, 20: 41237
RECOIL IONS
use in activation analysis, review on, 20: 40806 (NAS-NS-3110)
REFLECTION
properties of aluminum, copper, and nickel foils for light, effects of cleaning on, 20: 41440(R) (ALO-3632-4)
REFRACTORY MATERIALS
book: *Thermodynamic Properties of Inorganic Substances (Handbook)*, 20: 41417
REFRIGERATION
design and performance of 3°K helium refrigerator for bubble chambers, 20: 41378
REGENERATION
effects of *in vitro* growth on salamander lens, 20: 40499(R) (ORNL-3922, pp 69-79)
radiation effects on rat spleen, effects of fractionated doses on x, 20: 40702
RELATIVITY THEORY
conservation laws of general, development of covariant formulation of, 20: 42080
electromagnetic equations for rotating systems in, 20: 42087
equilibrium of large assembly of particles in, 20: 42091
formalism for revised, 20: 42098
gravitational field in general, 20: 42075
Lorentz principle in general, 20: 42072
Lorentz principle in general, 20: 42073
Lorentz transformation in, matrix elements of, 20: 41926 (JINR-P-2777)
particle motion along geodesics in 4-space in, Newtonian equations of, 20: 42094
research programs on general, 20: 41511(R) (RLO-1388-501)
spinor calculus in Riemannian manifolds of general, 20: 42079
REMOTE-CONTROL EQUIPMENT
design and development of master-slave components, 20: 42579(R) (ANL-7245, pp 29-47)
design for impact-testing, 20: 41113
design for vacuum systems, 20: 41125 (SGAE-PH-41/1966)
design of radio-controlled, nuclear powered, towing vessels, 20: 42666(P)
development and operation of, for use in analysis of radioactive materials, 20: 40799 (CEA-R-2887)
development and standardization at UKAEA, 20: 41098
fuel handling facilities at SEFOR, development of, 20: 42629(R) (GEAP-5160)
manipulator for reactor fueling, 20: 42593(P)
RENÉ-41
properties for high-temperature vacuum enclosure construction, 20: 41440(R) (ALO-3632-4)
RESEARCH REACTORS
description of IAN-R1 irradiation facilities, 20: 42679 (IAN-R-1)
environs monitoring at McMaster University, April 1965, 20: 41136
neutron density distribution in ANNA, 20: 42680 (INR-698/IX-A/RP)
RESINS
effects on dissolution of uranyl oxalate, 20: 40917
radioinduced polymerization of, electroconductivity measurements on kinetics of gamma, 20: 40999
thermal stability of nitrate-form anion, in vented system, 20: 40877 (RL-SEP-823)
use in analytical spot tests, 20: 40827
RETICULO-ENDOTHELIAL SYSTEM
uptake of iodine-131-labeled colloidal albumin by cells of, 20: 40777
use of pertechnetate colloid for studying, 20: 40750
RHENIUM
determination by atomic absorption spectroscopy using induction-coupled plasmas, 20: 40796(R) (IS-1500(Sect.C))
ionization of barium on hot surface of, (T), 20: 42406 (IPP-2/47)
neutron absorption resonance integral, (E), 20: 42333
preparation and properties of single crystals of, 20: 41481
separation of, from technetium, by extraction using potassium xanthate and carbon tetrachloride, 20: 40856
surface characteristics of emitters of, 20: 42575
RHENIUM ALLOYS
Mo–Re–W, recovery of scrap, methods for, 20: 41429(R) (USBM-RC-1249)
Re–W, analysis for total composition of powdered, results of, 20: 41429(R) (USBM-RC-1249)
Re–W, content of carbon, nitrogen, and oxygen in arc-melted ingots of, 20: 41429(R) (USBM-RC-1249)
Re–W, creep rates of, 20: 41396(R) (STL-517-0042)
Re–W, extrusion and properties of tubular, 20: 41429(R) (USBM-RC-1249)
Re–W, mechanical properties of arc-melted and powder-metallurgy processed, 20: 41429(R) (USBM-RC-1249)
RHENIUM ISOTOPES
neutron capture cross section at 30 to 170 kev, (E), 20: 42293
RHENIUM ISOTOPES Re^{180}
energy levels from beta decay of osmium-180, (E), 20: 42284
RHENIUM ISOTOPES Re-184
decay of, conversion-electron and γ spectra from, (E), 20: 42157 (JINR-P-2814)
RHENIUM ISOTOPES Re-187
energy levels of, spin of 686-kev, 20: 42172
RHENIUM OXIDES
chemistry of, 20: 41412(R) (IS-1500(Sect. M))
RHENIUM SULFIDES
chemistry of, 20: 41412(R) (IS-1500(Sect. M))
RHODAMINE B
use as tracer for waste solution dispersion in soil, 20: 42687
use in studying bottom layers of Mediterranean Sea, 20: 41128
RHODIUM
helium and hydrogen ion attenuation at 0.1 to 500 Mev, tables for, 20: 41619 (CEA-R-3042)
RHODIUM ALLOY COUPLES
Pt/Pt–Rh, insulation for, testing at high temperatures, 20: 41461(R) (UCRL-7631(Pt.3))
RHODIUM ALLOYS
Ir–Rh, air oxidation testing of, 20: 41396(R) (STL-517-0042)
RHODIUM ISOTOPES Rh-105
yields in proton fission of uranium at 170 Mev, 20: 42177
RHODIUM ISOTOPES Rh-106
beta activity measurements in France, 20: 41189 (CEA-R-3020)
determination in water, 20: 40819(T) (CEA-tr-A-1883)
RIBONUCLEASE
radiation effects in air and in nitrogen, gamma, 20: 40515
radioinduced inactivation of dry, 20: 40596

RIBONUCLEASE, DEOXY-
radioinduced inactivation of dry, 20: 40596
RIBONUCLEIC ACID
analysis of *E. coli*, using microtechniques, 20: 40501(R) (ORNL-3922, pp 113-14)
charging of transfer, with leucine and phenylalanine in adult and fetal rat liver, 20: 40506(R) (ORNL-3922, pp 168-73)
coding properties, fractionation, and interspecies reactions of Neurospora, 20: 40535(R) (ORNL-3922, pp 128-35)
electron spin resonance spectrometry of irradiated, 20: 40593
metabolism in Ehrlich ascites carcinoma cells, 20: 40534(R) (NYO-3621-1)
methylation of *E. coli* phenylalanine transfer, 20: 40503(R) (ORNL-3922, pp 137-45)
physical characteristics of *E. coli* phenylalanine transfer, 20: 40503(R) (ORNL-3922, pp 137-45)
radiation effects on synthesis in marrow-protected mice, effects of estradiol on x, 20: 40577
reactions with phenylalanine-RNA synthetase, 20: 40503(R) (ORNL-3922, pp 137-45)
structure of T2 infected *E. coli*, effects of oligodeoxyribonucleotide transferase on, 20: 40535(R) (ORNL-3922, pp 128-35)
synthesis in fetal rat liver, 20: 40506(R) (ORNL-3922, pp 168-73)
synthesis of brine shrimp, role of DNA in, 20: 40535(R) (ORNL-3922, pp 128-35)
RIBONUCLEIC ACID, DESOXY-
effects of radiophosphorus on nucleotide composition of, 20: 40548
effects of, from various organs on reparation of sperm of x-irradiated rat, 20: 40723
electron spin resonance spectrometry of irradiated, 20: 40593
electron spin resonance spectroscopy of irradiated, 20: 40594
measurements of renewal of, using labeled thymidine, 20: 40666
mutagenic effects in mice, methods for testing, 20: 40627(R) (ORNL-3922, pp 84-8)
mutagenic specificity of, in Drosophila, 20: 40706
photoreactivation of, in uv irradiated Hemophilus influenza by yeast enzyme, 20: 40543
radiation effects on *E. coli*, effects of benzopyrene on uv, 20: 40632(R) (ORNL-3922, pp 175-91)
radiation effects on bromouracil-substituted, of phage T3, uv, 20: 40504(R) (ORNL-3922, pp 146-60)
radiation effects on metabolism in *Escherichia coli*, γ, 20: 40620 (NYO-2804-9)
radiation effects on synthesis in marrow-protected mice, effects of estradiol on x, 20: 40577
radiation effects on binding to histone in deoxyribonucleohistone solution, gamma, 20: 40586
radiation effects on synthesis of, by chick fibroblasts and megoblasts, x, 20: 40587
radiation effects on, in *Clostridium botulinum* spores, 20: 40601
radiation protection by histone OH scavenged radicals, 20: 40585
radioinduced degradation in *Escherichia coli*, γ, 20: 40620 (NYO-2804-9)
role of brine shrimp, in synthesizing, 20: 40535(R) (ORNL-3922, pp 128-35)
synthesis at entry into S phase, factors affecting enzyme levels associated with, 20: 40534(R) (NYO-3621-1)
synthesis in Ehrlich ascites carcinoma cells, relation to histone fractions, 20: 40534(R) (NYO-3621-1)
synthesis in potato tubers, effects of radiotoxins on, 20: 40562
transfer in bacterial conjugation, 20: 40504(R) (ORNL-3922, pp 146-60)
uv sensitivity of infectious, from *Bacillus subtilis* bacteriophage SP02 bacteriophage SP02 compared with that of the total phage, 20: 40676
RICE
effects of irrigation of, on uptake of cesium-137 and strontium-90, 20: 40574
mutations induced by beta particles, thermal neutrons, and x rays, 20: 40640
radiation effects on seeds of, mutations arising from β, thermal neutron, or x, 20: 40641
ROCKET MOTORS
materials for high-power, properties of, 20: 41414
ROCKET REACTORS
control by chemical poison, model design study of manifold and reentrant tube assembly for, 20: 42665 (WCAP-2870)
development of NRX, review of, 20: 42662 (CONF-651101-84)
testing of, control systems manual for NRDS Test Cell A, 20: 42663 (EGG-1183-1054)
testing of, design of photo-optical equipment for, 20: 41223 (EGG-1183-1244)
ROCKET REACTORS (KIWI)
development of, review of, 20: 42662 (CONF-651101-84)
radiation dose rate survey for KIWI-TNT destruct test, 20: 41195 (LA-3519)
ROCKETS
ionization phenomena in solid-propellant, 20: 41120
ROCKS
age of Western Australian Precambrian, 20: 41159
age Precambrian, of southwest Montana, 20: 41163
analysis for bromine, activation, 20: 40811 (ORO-2670-13)
density of, gamma-absorption method for determining, 20: 41154
effects of nuclear explosion on fracture permeability, granitic, 20: 41164
element contents of, trace, 20: 41068 (PNE-5006)
radioactivity induced in, by underground nuclear explosions, (T), 20: 41068 (PNE-5006)
spalling by underground nuclear explosions, 20: 41126
sulfur-34 distribution in sedimentary, variations in, 20: 41135
RODS
bores in, equipment for measurement of ovality of, 20: 41436(P)
ROOTS
analysis for nitrogen-15 in amino acids in legume, use of ninhydrin in colorimetric, 20: 40824
cesium-137 content in rice, effects of irrigation on, 20: 40574
radiation effects on cells in *Vicia faba*, protective effects of actinomycin D against x, 20: 40581(R) (ORNL-3922, pp 50-1)
ROSE BENGAL
use of iodine-131 labeled for liver and spleen scanning, 20: 40777
ROTARY SEALS
design of conical-face, high-pressure, rotary-shaft, 20: 41074 (AECL-2551)
ROTENONE
preparation of carbon-14-labeled, on semimicro scale, 20: 41013
ROTIFIERS
radiosensitivity of soil, gamma, 20: 40637(R) (ORO-2754-7)
ROTORS
use of B-IX zonal, for isolating respiratory syncytial viruses, 20: 40507(R) (ORNL-3922, pp 191-6)
use of B-XV zonal centrifuge, for separating components of rat liver cells, 20: 40507(R) (ORNL-3922, pp 191-6)
RUBIDIUM
content in Spanish rock, 20: 41153
determination in seawater, activation, 20: 40834
electric conductivity of liquid, 20: 41476
isotopic composition in, mass discrimination in spectrometric measurements on, 20: 40821
properties as working fluid in Rankine power cycle, 20: 41398
properties for heat pipe uses, preparations for measurement of, 20: 41438(R) (AGN-8187)
thermal conductivity of liquid, estimation of, 20: 41477
thermodynamic properties of, measurement for space power systems, 20: 41438(R) (AGN-8187)
thermodynamic properties of, research on liquid and vaporous, 20: 41439(R) (AGN-8198)
RUBIDIUM CARBONATES
preparation and evaluation for electromagnetic separation of rubidium isotopes, 20: 41400 (ORNL-3301(Suppl.1))
RUBIDIUM COMPOUNDS
magnetic susceptibility of RbO_2^- at 1.3 to 300°K in, 20: 40796(R) (IS-1500(Sect.C))
RUBIDIUM IODIDES
crystal structure, neutron inelastic scattering determination of, (E), 20: 42550
RUBIDIUM ISOTOPES
composition in rubidium, mass discrimination in spectrometric measurements on, 20: 40821
separation of, preparation of rubidium carbonates for electromagnetic, 20: 41400 (ORNL-3301(Suppl.1))
RUBIDIUM ISOTOPES Rb-86
content in Australian Precambrian rock, 20: 41159
yields in thermal neutron fission of uranium-235, 20: 42178
RUBIES
preparation and properties of single crystals of, effects of crystallization temperature on, 20: 41480
RUTHENIUM
separation from copper leach solutions by ion exchange, 20: 41067(R) (ORNL-TM-1582)
separation from products of fission-fragment-induced radiolysis, 20: 40951 (RPI-321-6)
RUTHENIUM CHLORIDE COMPLEXES
sorption of solutions of radioactive, by natural sorbents, 20: 40890
RUTHENIUM FLUORIDES
preparation and evaluation for electromagnetic separation of ruthenium isotopes, 20: 41400 (ORNL-3301(Suppl.1))
RUTHENIUM ISOTOPES
separation of, preparation of ruthenium fluorides for, 20: 41400 (ORNL-3301(Suppl.1))
sorption of solutions of radioactive, by natural sorbents, 20: 40890

RUTHENIUM ISOTOPES Ru-103
content in fallout and plankton of Mediterranean Sea, 1963, 20: 41146
determination in sea water, gamma spectrometric, 20: 41145
sorption reactions of, on minerals, 20: 41178 (AD-635547)
RUTHENIUM ISOTOPES Ru-104
content in detritus from Indian Ocean, 20: 41140
RUTHENIUM ISOTOPES Ru-106
beta activity measurements in France, 20: 41189 (CEA-R-3020)
content in fallout and plankton of Mediterranean Sea, 1963, 20: 41146
content in fallout in India, 20: 40572
determination in radioisotope mixtures using simultaneous equations, gamma spectrometric, 20: 40837
determination in sea water, gamma spectrometric, 20: 41145
determination in water, 20: 40819(T) (CEA-tr-A-1883)
RUTHENIUM NITRATE COMPLEXES
sorption of solutions of radioactive, by natural sorbents, 20: 40890
RUTHENIUM NITROSYL NITRATES
sorption of solutions of radioactive, by natural sorbents, 20: 40890
RUTILES
preparation and properties of single crystals of, effects of crystallization temperature on, 20: 41480

S

SAFETY
accidents in well logging, 20: 41216
use of urethan spray foam for containment, 20: 41200 (ORNL-TM-1551)
SAFETY HAZARDS
control of industrial, from use of radioisotopes, 20: 41208
cosmic ray particles for space flight, 20: 41187 (BNL-9468)
experiments for evaluation of radiological, 20: 41178 (AD-635547)
from radioactive waste disposal in municipal sewage systems, 20: 41217
laboratory guides for radiotoxicity of isotopes, 20: 41199 (ORNL-TM-626)
protective measures against tritium oxide, 20: 41185 (AECL-2594)
tests, evaluations and special equipment development at NASA Manned Spacecraft Center, 20: 41219
SALAMANDERS
gamma crystallins in, lens nuclei of, during Wolfian lens regeneration, 20: 40499(R) (ORNL-3922, pp 69-79)
lens regeneration in, effects of *in vitro* growth on, 20: 40499(R) (ORNL-3922, pp 69-79)
nucleic acid synthesis in iris epithelium of, effects of lens removal on, 20: 40499(R) (ORNL-3922, pp 69-79)
SALICYLIC ACID, SULFO-
complexes with rare earths, composition of, fluorometric and spectrophotometric studies of, 20: 40926
SALIVARY GLANDS
radioinduced cytologic and functional changes in human, following cobalt-60 radiotherapy, 20: 40644
SALMONELLA
radiation effects on populations of, in swine meal, γ, 20: 41394
radiopreservation of food contaminated with, review, 20: 41390
SALTS
design of level indicators for molten, 20: 41233(R) (ORNL-3875, pp 101-24)
determination in sea water, 20: 40523(R) (RLO-1750-8(Vol.1))
SAMARIUM
content in common rock types, 20: 41068 (PNE-5006)
determination in uranium dioxide fuel pellets, 20: 41112 (IITRI-578P11-54)
determination of, in uranium by neutron activation methods, 20: 40832
liquid, solubility of tungsten in, at high temperatures, 20: 41412(R) (IS-1500(Sect. M))
photon reactions (γ,n) with, energy spectra from, (E), 20: 42165(R) (MIT-2098-251, pp 16-20)
scattering on beryllium–copper alloy at 5 kev, secondary electrons from, 20: 41620 (NIJS-R-471)
SAMARIUM ALLOYS
Mg–Sm, thermodynamics of formation of intermetallic compounds, 20: 41412(R) (IS-1500(Sect. M))
Sm–Zn, crystallographic and thermodynamic data on intermetallic compound, 20: 41412(R) (IS-1500(Sect. M))
SAMARIUM ALUMINATES
preparation of monocrystals of, with perovskite structure, 20: 40920
SAMARIUM BROMIDES
density of aqueous solutions of, 20: 40796(R) (IS-1500(Sect.C))
SAMARIUM COMPLEXES
with mandelic acid and α-methylmandelic acid, stability of, 20: 40902
SAMARIUM IONS
spin-lattice relaxation of, in lanthanum fluorides, 20: 42540
SAMARIUM ISOTOPES
energy levels of even-even, collective, (E), 20: 42265
SAMARIUM ISOTOPES Sm-148
energy levels of, collective, (E), 20: 42265
SAMARIUM ISOTOPES Sm-150
energy levels of, collective, (E), 20: 42265
SAMARIUM ISOTOPES Sm-152
energy levels of, collective, (E), 20: 42265
x-ray spectra from μ^- mesic atoms of, (E/T), 20: 42310
SAMARIUM ISOTOPES Sm-154
energy levels of, collective, (E), 20: 42265
SAMARIUM NITRATES
binding energies in, infrared spectral studies of, 20: 40886
specific gravity of aqueous solutions of, 20: 40796(R) (IS-1500(Sect.C))
SAMARIUM OXIDES
determination in uranium dioxide fuel pellets, 20: 41112 (IITRI-578P11-54)
B_2O_3–Sm_2O_3, liquid immiscibility in, 20: 40910
SAMARIUM SILICATES
preparation of $Sm_2O(SiO_4)$ monocrystals, 20: 40919
SAMPLING
equipment and techniques of sea water and estuary silts, 20: 40523(R) (RLO-1750-8(Vol.I))
fallout in air, water, soil, and milk in New Zealand, 20: 40521(R) (NP-16270)
of sea foods for bacteriological studies, 20: 41384(R) (TID-22833)
statistical techniques for, 20: 42695 (TRG-Report-1200)
SANDS
sorptive properties for radioruthenium in different solutions, 20: 40890
SARCOMAS
chromosome aberrations induced by nitrogen mustard and triethylene-amine, with and without added nicotinic amide, in, 20: 40550
effects of combined radiation and actinomycin D therapy on mouse, 20: 40762
effects of porphyrins on radiosensitivity of rhabdomyo-, 20: 40657
leukemogenic properties of myxofibro-, after serial passage in mice, 20: 40502(R) (ORNL-3922, pp 115-27)
radiation effects on rat lymphoblastic lympho-, electromagnetic, 20: 40661
radioisotope content of bones of patients with, 20: 41191(R) (HUX-3170-1)
SAVANNAH RIVER PRODUCTION REACTORS
operation of, computer system for axial power monitoring, 20: 42661 (DPSPU-66-30-2)
SCALERS
design of d-c to 100 Mc, 20: 41269(R) (ORNL-3875, pp 4-12)
SCANDIUM
determination in plutonium by carrier distillation methods, spectrographic, 20: 40814 (RFP-664)
determination in seawater, activation, 20: 40834
liquid, solubility of tantalum in, at high temperatures, 20: 41412(R) (IS-1500(Sect. M))
thermodynamic properties of, at 0°C to melting point, 20: 41412(R) (IS-1500(Sect. M))
SCANDIUM ALLOYS
Co–Ni–Sc, crystal structure of Laves phases in, 20: 41412(R) (IS-1500 (Sect. M))
Fe–Ni–Sc, crystal structure of Laves phases in, 20: 41412(R) (IS-1500 (Sect. M))
Mg–Sc, phase diagrams, 20: 41412(R) (IS-1500(Sect. M))
Mn–Ni–Sc, crystal structure of Laves phases in, 20: 41412(R) (IS-1500 (Sect. M))
Sc–Zr, superconducting transition temperature and electronic specific heat of, 20: 42121
SCANDIUM ISOTOPES Sc-43
energy levels, (E), 20: 42253
SCANDIUM ISOTOPES Sc-45
energy levels, (E), 20: 42253
neutron reactions (n,γ) at thermal energies, gamma spectra from, (E), 20: 42382
proton reactions (p,n) at 15.25 Mev, angular distributions for quasi-elastic, (E), 20: 42169(R) (UCRL-14744, pp 1-18)
SCANDIUM ISOTOPES Sc-46
energy levels, (E), 20: 42382
SCANDIUM ISOTOPES Sc-47
energy levels of, lifetime of metastable hole state in, (E), 20: 42192
metabolism in rat bones, 20: 40545
SCANDIUM OXIDES
B_2O_3–Sc_2O_3, liquid immiscibility in, 20: 40910
SCANDIUM SILICATES
preparation of $Sc_2O(SiO_4)$ monocrystals, 20: 40919
SCATTERING
amplitude for three-particle inelastic, analytical properties of, 20: 42019
amplitudes at high energies, review of forward, (T), 20: 42028
amplitudes for two- and three-particle, reduced, 20: 41959
amplitudes for, general quantum field theory for analytic properties of, 20: 41936
amplitudes in, Lee model for production and elastic, 20: 41986

amplitudes of, properties of N/D, 20: 41961
amplitudes of, theorem on high-energy, 20: 41963
convergence behavior of Born series for rearrangement, (T), 20: 41642
diffraction of charged particles by optical inhomogeneities, 20: 41523
electron elastic-scattering form factors for d-shell nuclei, (T), 20: 42376
frequency distribution function of, sum rules for generalized, 20: 42092
interaction potentials for composite systems, (T), 20: 42236
ion–atom charge exchange, model for, 20: 41624 (UCRL-17034)
phase matrix, variational principle for, (T), 20: 41991
potential for singular, infinity of strength of, (T), 20: 42027
S-matrix for, higher-order poles in, 20: 41943
S-matrix for, most general Clebsch-Gordan coefficients for, 20: 41944
S-matrix for, relativistic Lee model for, 20: 41948
S-matrix in, crossing principle in, 20: 41803(R) (UCRL-16863)
S-matrix theory for, symmetries in first-approximation, 20: 42169(R) (UCRL-14744, pp 1-18)
S-matrix theory for, physical-region singularities in, 20: 41954
S-matrix theory in, unitarity in, 20: 42020
S-matrix theory of, macroscopic causality conditions in, 20: 41962
S-matrix theory of, cross-discontinuity condition in, 20: 41966
theory for nonrelativistic, Fredholm, 20: 41993
theory of, N/D method for extinct bound states in, 20: 41975

SCINTILLATION DETECTORS
design and performance of diamond, for gamma rays and neutrons, 20: 41290
design and performance of two-impulse neutron, with plastic scintillator, 20: 41337
design and performance of thin plastic and sodium iodide nanosecond, for x-ray lifetime determinations, 20: 41325
design of silver-activated zinc sulfide sandwiched, for fast neutrons, 20: 41335
development of immersible gamma probe for direct measurement of activity in sea water, 20: 41147
development of, for measurement of absorbed dose from high energy electrons, 20: 40746(R) (NYO-3510-2)
efficiency and peak-to-peak ratio for sodium iodide crystal, absolute, 20: 41307
efficiency of large-area liquid, 20: 41339
logic of, circuit for test display lamp for, 20: 41314
performance at high temperatures, using highly ruggedized photomultiplier tubes, 20: 41374
performance for beta dosimetry of skin, 20: 41274 (ORNL-TM-1581)
performance for determination measurement of cobalt-60 deposited in lungs, 20: 41190 (CONF-660621-4)
performance for leak detection in containers for radioactive materials, 20: 41197(R) (NP-16172)
performance for zero-thickness sources, valley-to-peak ratios for, 20: 41312
performance of gallium arsenide, as charged-particle spectrometer, 20: 41313
performance of thallium-activated cesium iodide, for determining composition of primary cosmic rays, 20: 41667(R) (MIT-2098-251, pp 1-13)
performance of wedge-shaped, for magnetic spectrometer, 20: 41289
pulse height spectra from, computer analysis for gamma, 20: 41292
response of alpha, in gamma and neutron backgrounds, 20: 41271(R) (ORNL-3875, pp 44-52)
use in counting tritiated thymidine transferred to females by labeled Drosophila males, 20: 40625(R) (ORNL-3922, pp 59-64)
use in determining activity of technetium-99m and iodine-125, 20: 40547
use in helicopter signaling system, 20: 41221(R) (COO-1471-1)
use in measuring sediment density and concentration, 20: 41156
use in medical diagnosis, design of pulse analyzer for suppressing background during, 20: 41318
use in radiodiagnosis, comparison of 8 inch with 3 inch crystal, 20: 40779
use in radiography, 20: 41116(P)
use in renography for kidney function studies, 20: 40775(T)
use in void fraction detection in potassium flow, 20: 41111

SEA URCHINS
photoreactivating enzyme in eggs, 20: 40543
radiation effects on eggs of, effects of AET on x, 20: 40619(R) (NYO-2740-3, pp 216-57)

SEA WATER
analysis for bromine in sediments in, activation, 20: 40811 (ORO-2670-13)
analysis for carbon dioxide and salts, 20: 40523(R) (RLO-1750-8(Vol.1))
analysis for trace elements, activation, 20: 40834
carbon-14 content of deep and surface, of north Indian Ocean, 20: 41127
chemical properties of, effects of depth and temperature on, 20: 40523(R) (RLO-1750-8(Vol.1))
chromium-51 in, uptake by clams of, 20: 40575
desalination of, evaluation for New Jersey–New York City area, 20: 42658 (NP-16250)
desalination using reactors, economics of, 20: 42659
gamma activity in, direct measurement using immersible scintillation probe, 20: 41147
gamma spectrometric analysis for fallout fission products, 20: 41145
oxygen gradients in Mediterranean, 20: 41128
radioactivity of Northeast Pacific Ocean, effects of Hanford waste solutions on, 20: 40523(R) (RLO-1750-8(Vol.1))
radioactivity of, effects of fallout fission products on, 1945 to 1963, 20: 41144
radioactivity of, effects of fallout fission product accumulation by plankton on, 20: 41146
radioisotope distribution between suspended materials and Indian Ocean, 20: 41140
sulfur-34 distribution in ancient, variations in, 20: 41135
trace elements in Indian Ocean by marine organisms, 20: 40572
uptake of fallout fission products by marine organisms from, 20: 40546

SEAFOOD
radiation processing of, effects on storage life and wholesomeness, 20: 41384(R) (TID-22833)
radiation processing of fish fillets and clam and lobster meats, 20: 41384(R) (TID-22833)
radiosensitivity of *Clostridium botulinum* type E spores on homogenates of haddock, γ, 20: 40699
sampling for bacteriological studies, 20: 41384(R) (TID-22833)

SEALS AND GLANDS
design for tubular members, 20: 41100(P)

SEDIMENTATION
phosphorus-32 adsorption on, in salt-marsh ecosystems, 20: 40573
phosphorus-32 adsorption on, in salt-marsh ecosystems, 20: 40573
sulfur-34 distribution in, variations in, 20: 41135

SEED
nuclei in wheat, microspectrophotometric study of properties of, 20: 40631(R) (ORNL-3922, pp 161-6)
radiation effects on chromosomes of *Vicia faba*, repair mechanisms for, 20: 40609 (CONF-660418-1)
radiation effects on jute, gamma, 20: 40681
radiation effects on rice, chlorophyll mutations from β, thermal neutron, or x, 20: 40641
radioinduced electron spin resonance signals in lettuce, effects of hydration on γ, 20: 40631(R) (ORNL-3922, pp 161-6)
radioinduced mutations in barley, x, 20: 40711
radioinduced mutations in rice, beta, thermal neutron, or x, 20: 40640
radiosensitivity of sprouting barley, γ, 20: 40716
radiosensitivity of tobacco, factors affecting, 20: 40613 (N-66-18147)

SEIGNETTOELECTRIC MATERIALS
performance of barium titanates and lead zirconates, in ferroelectric transducers, 20: 41684

SEISMIC WAVES
amplitude of BUFF-event, 20: 41149 (AD-632956)
displacement amplitude and energy variations with distance by, 20: 41169

SEISMOLOGY
data on BUFF event, analysis of, 20: 41149 (AD-632956)
stability of Lucas Heights area, review, 20: 41148 (AAEC-TM-316)
use in detecting nuclear underground explosions and geological studies, 20: 41152

SEISMOMETERS
arrays of, for investigating earthquake mechanism, 20: 41152
development and performance of large-aperture arrays, 20: 41155

SELENIUM
content in meteorites, 20: 42064
determination in seawater, activation, 20: 40834

SELENIUM FLUORIDES
preparation of fluorine-18-labeled, 20: 41020

SELENIUM ISOTOPES Se-75
fixation to protein-polysaccharides of bovine cartilage, 20: 40544
tracer use in mouse immunological studies, 20: 40503(R) (ORNL-3922, pp 137-45)
uptake by swine blood cells in vitro, effects of dietary calcium, zinc, and corn oil on, 20: 40556
use in gamma backscattering density measurements, 20: 41257
use in pancreas scanning, 20: 40748

SELENIUM SYSTEMS
As–S–Se, sintering mechanism of, 20: 41064(R) (IS-1500(Sect.E))

SEMEN
radiation effects on bull, biochemical, x, 20: 40610(R) (COO-895-9)

SEMICONDUCTOR DETECTORS
book: *Semiconductor Counters for Nuclear Radiations*, 20: 41352
current in high-resistivity n-silicon, reverse, 20: 41300
design and performance, 20: 41369(P)
design and use for intracavitary dosimetry in radium therapy, 20: 41377
design of amplifying, 20: 41361(P)
design, fabrication, and performance of vacuum encapsulated lithium-drift

telescope, 20: 41376
development and use, review of, 20: 41287
development of, for measurement of absorbed electron dose, 20: 40746(R) (NYO-3510-2)
efficiency of germanium, for gammas at 500 to 1500 kev, 20: 41288
energy resolving power of p-i-n, recombination less effects on, 20: 41283
fabrication and performance of lithium compensated silicon focal plane, for beta spectrometers, 20: 41326
fabrication of lithium-drifted germanium, 20: 41367(P)
fabrication of p-type silicon, 20: 41363(P)
lifetime and homogeneity of p-i-n, methods for measuring, 20: 41283
production and encapsulation of lithium-drifted germanium, 20: 41271(R) (ORNL-3875, pp 44-52)
response of lithium-drifted germanium, to gamma rays, temperature dependence of, 20: 41273 (ORNL-TM-1295)

SEMICONDUCTORS
book: *Electron Radiation Damage in Semiconductors and Metals*, 20: 41508
carrier transport in, with nonconstant electric fields, (T), 20: 42546
doping of oxide, mechanisms of, 20: 41458(R) (TID-23268)
electron beam interactions in, voltage induction by, (E/T), 20: 42533
performance of redrift-treated lithium-drifted silicon, 20: 41311

SEPARATION PROCESSES
use in trace analysis, 20: 40850

SEWAGE SYSTEMS
radioactive waste discharge in municipal, hazards from, 20: 41217

SEX
radiosensitivity differences in chickens depending on, γ, 20: 40693

SHEEP
body water content and turnover in, tracer study, using T_2O, 20: 40541(R) (UCD-34P104-3)
cesium-137 content in browsing, effects of food-chain on, 20: 40541(R) (UCD-34P104-3)
physiology of digestion in, 20: 40541(R) (UCD-34P104-3)
strontium-90 content in browsing, effects of food-chain on, 20: 40541(R) (UCD-34P104-3)
urea nitrogen content in blood of, 20: 40541(R) (UCD-34P104-3)

SHELTERS
design of portable on fixed, 20: 41118(P)
design of precast fallout, 20: 41119(P)
evaluation of, for postattack protection, 20: 41177 (AD-632211)
habitability of fallout, under fire exposure, 20: 41184 (AD-637806)
plans for area-wide, in city community, 20: 41183 (AD-635931)

SHIELDED CONTAINERS
design for shipping tritium, 20: 41196 (LA-DC-7996)
leak detection in, autoradiographic and radiometric methods for, 20: 41197(R) (NP-16172)

SHIELDING
analysis of performance of, in real fallout field, 20: 41201 (RRA-T55 and Summary)
design for handling ALRR components, 20: 42681(R) (IS-1500(Sect. R))
design of collapsible on fixed, for personnel, 20: 41118(P)
design of radiation source, for irradiating natural animal populations, 20: 40518 (CEX-63.10)
development of, for space applications, 20: 41219
electron transmission through spacecraft, isotropically incident, (E), 20: 42520
fabrication using cement and depleted uranium, 20: 41435(P)
magnetic, charged particle motion around superconducting solenoid, 20: 42521
requirements of, for neutron generators, 20: 41215

SHIELDING MATERIALS
gamma attenuation coefficients for, cobalt-60, 20: 42518

SHIPPING
containers for radioactive materials, leak detection in, 20: 41197(R) (NP-16172)
shielded container design for tritium, 20: 41196 (LA-DC-7996)

SHIPPINGPORT PRESSURIZED WATER REACTOR
control of, nuclear protection system description, 20: 42640 (WAPD-PWR-2210(Vol.1))
control rod position and control equipment, instruction manual for Core 2, 20: 42643 (WAPD-PWR-2217)
control rod power supply for, instruction manual, 20: 42642 (WAPD-PWR-2216)
coolant pumps for Core 2, instruction manual, 20: 42644 (WAPD-PWR-2219)
fuel handling tool for Core 2, instruction manual, 20: 42641 (WAPD-PWR-2213)
neutron flux measurements in Core 2, system description for, 20: 42647 (WAPD-PWR-2226)
steam generator for Core 2, description and operation of, 20: 42645 (WAPD-PWR-2222)
steam generator for Core 2, description and operation of, 20: 42646 (WAPD-PWR-2223)
weld cutting machines for Core 2 vessel ports, instruction manual, 20: 42649 (WAPD-PWR-2230)
weld cutting machine for Core 2 vessel seal, instruction manual, 20: 42650 (WAPD-PWR-2232)
welding machine for Core 2 omega seal, instruction manual, 20: 42648 (WAPD-PWR-2229)

SHOCK TUBES
design of argon–cesium, for MHD generators, 20: 41703
energy losses due to radiation in, (E), 20: 41750
magnetohydrodynamic flow in, boundary layer, 20: 42037 (UTIAS-115)
plasma ionization in, potassium-seeded argon, (E), 20: 41715
temperature measurement in, transition probabilities for argon lines for, 20: 42483

SHOCK WAVES
effect on spall gaps in subsurface layers of earth, 20: 41126
pressure probe for plasma diagnostics, piezoelectric, 20: 42405 (IPP-1/46)
propagation in plasma, dissipative effects on, (T), 20: 42476
propagation in solids, profiles for, (T), 20: 41513(R) (UCRL-14744, pp 19-36)

SILANE
radiation effects on, in krypton at 4.2°K, ESR of free radicals from gamma, 20: 40968

SILICON
addition of trace-amounts to chromium–nickel steel, method for, 20: 41418(R) (GEAP-5150)
current in high-resistivity semiconductors of n-type, reverse, 20: 41300
determination in americium and plutonium by spark-source mass spectrography, 20: 40816 (RFP-699)
determination in bauxite, activation, 20: 40812 (ORO-2980-14)
determination in plutonium by carrier distillation methods, spectrographic, 20: 40814 (RFP-664)
determination in uranium trioxide by emission spectrography, 20: 40802 (HW-65402(Rev.1))
determination in uranium(IV-VI) oxides, effects of graphite electrode grade on carrier-distillation spectroscopic, 20: 40807 (NLCO-976)
determination of, in iron, equipment used in activation methods for, 20: 40848
development of device containing plastic scintillator and diodes of, for measurement of absorbed dose from high energy electrons, 20: 40746(R) (NYO-3510-2)
effects of additions of, to sintering properties of beryllium powders, 20: 41428 (SCL-DC-66-57)
effects of traces of, on corrosion of cheomium–nickel steel, 20: 41418(R) (GEAP-5150)
effects on phase transformations in gallium–plutonium alloy and plutonium, differential thermal analysis of, 20: 41452 (MLM-1172)
electric properties of paramagnetic defect in electron-irradiated p-type, 20: 42549
electron energy loss and scattering at 100 to 400 kev in single crystal foils of, near radiation damage threshold, (E), 20: 42536
electron paramagnetic resonance of electron-irradiated p-type, 20: 42549
fabrication of detectors of p-type, 20: 41363(P)
helium and hydrogen ion attenuation at 0.1 to 500 Mev, tables for, 20: 41619 (CEA-R-3042)
meson (π^-) capture below 140 Mev, gamma spectra from, (E), 20: 42314
performance as neutron threshold detector in presence of x rays, 20: 41333
performance of redrift-treated lithium-drifted detectors of, 20: 41311
radiation effects on defects in crystals of, fast neutron, (E), 20: 42567(T)
radioinduced damage in p-type, photoconductivity spectrum from electron, 20: 41379
response of fission chambers of, to channeled argon-40 and iodine-127 ions, 20: 41324
use in lithium compensated focal plane detectors, for beta spectrometers, 20: 41326
use in vacuum encapsulated lithium-drift telescope detectors, 20: 41376
x-ray emission spectra of, L and K, (E), 20: 41350

SILICON CARBIDES
interactions with gas flow in MHD generators, 20: 41738
radiation spectra of electron-excited crystals of, (E), 20: 42565(T)

SILICON ISOTOPES
separation of, preparation of silicon sulfides for electromagnetic, 20: 41400 (ORNL-3301(Suppl.1))

SILICON ISOTOPES Si-28
deuteron reactions (d,p) with, differential cross section for, (T), 20: 42387
energy-level positions and transitions in, calculations using particle-hole model, (T), 20: 42199
neutron reactions (n,α) with, DWBA analysis of, (T), 20: 42391
photon reactions at 16 to 60 Mev, cross sections for, (E), 20: 42523(R)

(IS-1500(Sect.P))
proton reactions (p,γ) at 0.3 to 2.1 Mev, resonance strengths for, (E), 20: 42182
SILICON ISOTOPES Si-29
proton reactions (p,γ) at 0.3 to 2.1 Mev, resonance strengths for, (E), 20: 42182
SILICON ISOTOPES Si-30
proton reactions (p,γ) at 0.3 to 2.1 Mev, resonance strengths for, (E), 20: 42182
SILICON OXIDES
radiation effects on refractive properties of high-purity fused, electron and gamma, 20: 41505
Al_2O_3–SiO_2, analysis of lead fluoride-containing gels of, for fluoride by fast-neutron radioactivation, 20: 40845
SILICON SULFIDES
preparation and evaluation for electromagnetic separation of silicon isotopes, 20: 41400 (ORNL-3301(Suppl.1))
SILICON SYSTEMS
Al–Si, microstructure model of, 20: 41454 (NYO-2394-22)
Fe–Si, elastic properties of iron-base single-crystal, 20: 41412(R) (IS-1500(Sect. M))
SILICONE POLYMERS
radiation effects on, in various gaseous atmospheres, gamma, 20: 40974
SILICOORGANIC COMPOUNDS
radiolysis of, EPR studies of yields of stabilized charges in low-temperature, 20: 40962
SILTS
analysis for bromine in deep-sea, activation, 20: 40811 (ORO-2670-13)
content of manganese-54 and zinc-65 in Columbia River, 20: 40523(R) (RLO-1750-8(Vol.1))
density and concentration of, equipment for measuring, 20: 41156
radioisotope accumulation by organic ocean, 20: 41146
sorptive properties for radioruthenium in different solutions, 20: 40890
SILVER
coating with beryllium, electrolytic, 20: 40864 (BMwF-FBK-66-10)
content in meteorites, 20: 42064
determination in copper coins by neutron activation methods, 20: 40800 (CNAEM-35)
determination in plutonium by carrier distillation methods, spectrographic, 20: 40814 (RFP-664)
determination in seawater, activation, 20: 40834
determination of, using isooctylthioglycolate, 20: 40796(R) (IS-1500 (Sect.C))
determination of, in rainwater from silver iodide-seeded clouds in Australia, 20: 40838
determination of, in rainwater, ion-exchange separation in, 20: 40839
determination of, in ores, equipment used in activation methods for, 20: 40848
electric conductivity of liquid, 20: 41476
helium and hydrogen ion attenuation at 0.1 to 500 Mev, tables for, 20: 41619 (CEA-R-3042)
ion ranges at 10 to 100 Mev, bromine and iodine, 20: 41647
proton reactions at 200 and 400 Mev, formation cross section and half life of silver-101 yields in, 20: 42179
separation from mixtures by cation exchange chromatography, 20: 40847
thermal conductivity of liquid, estimation of, 20: 41477
SILVER ALLOYS
Ag–La, superconductivity of, effects of pressure on, 20: 42101
SILVER CHLORIDES
thermochemical properties of, 20: 40922
SILVER ISOTOPES Ag-101
half life and formation cross section of, from proton reactions on indium and silver at 200 and 400 Mev, 20: 42179
SILVER ISOTOPES Ag-107
carbon-12 reactions (C-12,N-13) with, angular distributions from, (E), 20: 42153 (JINR-E-2824)
SILVER ISOTOPES Ag-109
carbon-12 reactions (C-12,N-13) with, angular distributions from, (E), 20: 42153 (JINR-E-2824)
SILVER ISOTOPES Ag-110
determination in antique gold coins by activation and gamma spectrometry, 20: 40829
SILVER ISOTOPES Ag-111
preparation of carrier-free, from neutron-irradiated palladium, 20: 41023
SILVER ISOTOPES Ag-112
yields in proton fission of uranium at 170 Mev, 20: 42177
SILVER NITRATES
$CsNO_3$–$AgNO_3$, diffusion and transport processes in molten, on ceramic oxides, 20: 40866 (EUR-2954.e)
SILVER NITRITES
radiation effects on rate of thermal decomposition of, x, 20: 41000
SINGLE CRYSTALS
defects in lithium-doped cobaltous oxide, at 900 to 1200°C, analysis of, 20: 41458(R) (TID-23268)
elastic properties of iron-base, in aluminum–iron alloys, 20: 41412(R) (IS-1500(Sect. M))
elastic properties of iron-base, in iron–silicon systems, 20: 41412(R) (IS-1500(Sect. M))
growth rate of, effect of vertical temperature gradient on controlled, 20: 41064(R) (IS-1500(Sect.E))
preparation, 20: 41412(R) (IS-1500(Sect. M))
preparation of, 20: 41064(R) (IS-1500(Sect.E))
preparation of high-purity inorganic, 20: 40874 (ORNL-RMIC-5)
production of delta-plutonium, methods for, 20: 41453(R) (NUMEC-3428-21)
sputtering by ions, mechanism of, 20: 42553
SINTERING
kinetics of, effects of temperature on, 20: 41064(R) (IS-1500(Sect.E))
SKELETON
mineralization dynamics of, in fetal chickens, 20: 40558
radiation effects on, in mice irradiated *in utero*, 20: 40649
scandium-47 and calcium-47 metabolism in rats, 20: 40545
SKIN
absorption of tritium oxide through, 20: 41185 (AECL-2594)
beta dosimetry of, using fueld-type instruments, 20: 41274 (ORNL-TM-1581)
calcium-47 uptake by rat, 20: 40557
cutaneous reactions of, to radiotherapy of female genital cancer, 20: 40679
effects of dose-time factors on radiotherapy of rat, 20: 40764
immune response to transplanted tumors in mouse, following x-radiation cure of previously transplanted tumors, 20: 40643
radiation doses to, in gynecological examination, 20: 40770
radiation effects on human, solar, review of, 20: 40696
radiosensitivity of, in air and in hyperbaric oxygen, 20: 40721
response of mycosis fungoides to combined colchicine and radiation therapy of, 20: 40763
SKIN GRAFTING
effects of extracorporeal irradiation of blood or lymph on graft take, 20: 40744 (BNL-10403)
tolerance to, in hybrid x irradiated mice given skin from parents, 20: 40651
SKIN LESIONS
radiotherapy of, laser, 20: 40776
SMOKES
iodide scavenging by rain and snow from Hanford stock gases, measurement of, 20: 41188(R) (BNWL-235-1)
polonium-210 content in tobacco, effects on lung content of cigarette smokers, 20: 40531 (A/AC.82/G/L-1045(Rev.1))
SNAILS
phosphorus-32 uptake by, from *E. coli* in stream ecosystems, 20: 40529
radiation experiments on, single-hit curves, 20: 40515
SNOW
evaporation of, surface-to-air concentration gradients in analysis of, 20: 41150 (AECL-2576)
SODIUM
analysis for carbon, method for, 20: 42619(R) (ANL-7245, pp 1-28)
determination in americium and plutonium by spark-source mass spectrography, 20: 40816 (RFP-699)
determination in uranium trioxide by emission spectrography, 20: 40802 (HW-65402(Rev.1))
effects on conversion of radioactive wastes to glass-like solids for disposal, 20: 42690(P)
electric conductivity of liquid, 20: 41476
flowmeters for, calibration of magnetic, 20: 41064(R) (IS-1500(Sect.E))
helium and hydrogen ion attenuation at 0.1 to 500 Mev, tables for, 20: 41619 (CEA-R-3042)
hydrogen content in, effects on embrittlement of tantalum, 20: 42682 (LA-3508)
liquid corrosive effects on stainless steel at high temperatures, 20: 41420(R) (MSAR-66-149)
liquid, analysis for contaminants, emission spectrographic, 20: 41420(R) (MSAR-66-149)
liquid, analysis of test-loop recirculated, for carbon, hydrogen, nitrogen, and oxygen, 20: 41420(R) (MSAR-66-149)
neutron reactions at 14.7 Mev, gamma emission in, (F), 20: 42146 (AD-638014)
positron mass in, band effective, 20: 41853
properties as working fluid in Rankine power cycle, 20: 41398
properties for heat pipe uses, preparations for measurement of, 20: 41438(R) (AGN-8187)
pump for, induction, 20: 41064(R) (IS-1500(Sect.E))
purification of, development of methods for, 20: 42619(R) (ANL-7245, pp 1-28)
sampling of cold-trapped, method for, 20: 41420(R) (MSAR-66-149)
technology for fast reactors, 20: 42577(R) (ANL-7230)

thermal conductivity of liquid, estimation of, 20: 41477
thermodynamic properties of, research on liquid and vaporous, 20: 41439(R) (AGN-8198)

SODIUM ACID CARBONATES
radiolysis of frozen aqueous solutions of, ESR spectral studies on radical reactions in, 20: 40994

SODIUM ALLOYS
Au–Na, solubility in sodium halide melts, 20: 40796(R) (IS-1500(Sect.C))
Bi–Na, solubility in sodium halide melts, 20: 40796(R) (IS-1500(Sect.C))
K–Na, phase studies, 20: 41455(R) (NYO-2731-7)
K–Na, use in MHD generators with two-phase flow, 20: 41728
K–Na, use in MHD conversion systems, 20: 41733
Li–Na, density and miscibility of liquid, 20: 41455(R) (NYO-2731-7)
Na–Sn, solubility in sodium halide melts, 20: 40796(R) (IS-1500(Sect.C))
Na–Tl, crystal structure of intermetallic compounds, 20: 41412(R) (IS-1500(Sect. M))
Na–Tl, solubility in sodium halide melts, 20: 40796(R) (IS-1500(Sect.C))
Pb–Na, solubility in sodium halide melts, 20: 40796(R) (IS-1500(Sect.C))
Sb–Na, solubility in sodium halide melts, 20: 40796(R) (IS-1500(Sect.C))

SODIUM AZIDES
radioinduced formation of N_3^- defects in, studies of x, 20: 40966

SODIUM CARBONATES
radiolysis of frozen aqueous solutions of, ESR spectral studies on radical reactions in, 20: 40994

SODIUM CHLORIDES
corrosive effects of aqueous, on stainless steel at 650°F, 20: 41418(R) (GEAP-5150)
effects on DNA-histone linkages in irradiated deoxyribonucleohistone solutions, 20: 40586
radiation effects on silver-doped, model for de-excitation curves of x, 20: 42561

SODIUM CHROMATES
uptake of chromium-51-labeled, by clams, 20: 40575

SODIUM FLUORIDES
use in fluorine-18 metabolism studies, 20: 40554

SODIUM FORMATES
radiolysis of frozen aqueous solutions of, ESR spectral studies on radical reactions in, 20: 40994

SODIUM HALIDES
solvent properties for intermetallic sodium compounds, 20: 40796(R) (IS-1500(Sect.C))

SODIUM IODIDES
effects on NMR spectra of formamide, 20: 40805(R) (MLM-1325, pp 63-70)
efficiency and peak-to-peak ratio for scintillation detectors of, absolute, 20: 41307
performance of detectors of, voltage-to-peak ratios for zero-thickness sources, 20: 41312
preparation for use in x-ray diffraction studies, sealing process for, 20: 41328
radiation effects on thallium-activated, x, (T), 20: 41344
radiation effects on, effects of partial absorption on beta, 20: 40504(R) (ORNL-3922, pp 146-60)
scintillation properties of monocrystals of, impurity effects on, 20: 41347
use in gamma coincidence counters, 20: 41295
use in nanosecond x-ray scintillation detectors, 20: 41325

SODIUM IONS
effects on electron spin resonance spectra of irradiated silicate glasses, 20: 42538

SODIUM ISOTOPES Na-22
use as gamma source in well logging, 20: 41165

SODIUM ISOTOPES Na-23
neutron radiative capture cross section from 1.0 to 19.5 Mev, (E), 20: 42332
proton reactions (p,2p) at 155 Mev, proton energy spectra from, (E), 20: 42360
proton reactions (p,γ) at 0.3 to 2.1 Mev, resonance strengths for, (E), 20: 42182

SODIUM NITRATES
$CsNO_3$–$NaNO_3$, diffusion and transport processes in molten, on ceramic oxides, 20: 40866 (EUR-2954.e)
$NaNO_3$–$TlNO_3$, diffusion and transport processes in molten, on ceramic oxides, 20: 40866 (EUR-2954.e)

SODIUM OXIDES
magnetic susceptibility of NaO_2, at 63°K to room temperature, (E), 20: 42169(R) (UCRL-14744, pp 1-18)

SODIUM PERCHLORATES
radiolysis of frozen solutions of, ESR studies of decomposition of radicals from gamma, 20: 40960

SODIUM SALTS
effects on growth of *Clostridium botulinum* Type E in sea foods, 20: 41384(R) (TID-22833)

SODIUM SELENITES
radiation effects on single-crystal $NaH_3(SeO_3)_2$, effects of deuterium on EPR spectra from gamma, 20: 40972

SODIUM TETRAPHENYLBORATES
sorption of cesium from aqueous solutions of, by glass, polyethylene, and Teflon, 20: 40915

SODIUM TUNGSTATES
enthalpy of, at 50 to 260°C, 20: 41412(R) (IS-1500(Sect. M))

SOILS
analysis for cesium-137 and strontium-90, method for, 20: 40853
analysis for moisture using neutron scattering, 20: 41115(P)
book: *Radioactivity of Soils and Methods of Measurement*, 20: 41139
effects of fertility levels of, on uptake of calcium, magnesium, phosphorus, strontium, and zinc by corn plants, 20: 40735 (NYO-2744-37)
effects of irrigating, on cesium-137 and strontium-90 uptake by rice, 20: 40574
effects of, on radiosensitivity of tobacco mutations, 20: 40613 (N-66-18147)
ion content variability studies, 20: 40532(R) (COO-1097-17)
mobilities of stable strontium, strontium-90 and calcium, 20: 40520 (NP-16261)
radiation effects on, gamma, 20: 40637(R) (ORO-2754-7)
radioactivity content of, from fallout in West Germany, 20: 40570
radioactivity measurements in New Zealand, 20: 40521(R) (NP-16270)
sorptive properties for radioruthenium in different solutions, 20: 40890
sorptive properties for cerium and yttrium, effects of acidity and concentration on, 20: 40914
stable strontium, strontium-90 and calcium mobilities in turf-podzolic and black earth, 20: 40520 (NP-16261)
strontium uptake by edible plants from, effects of calcium content on, 20: 40537(R) (TID-23052)
translocation of strontium and calcium, 20: 40524(R) (TID-23271)
waste solution dispersion in, tracer study, 20: 42687

SOLAR BATTERIES
evaluation for sun mission, 20: 41124

SOLAR FLARES
effects on etiology of multiple sclerosis, 20: 40639
effects on solar and geophysical phenomena, 20: 42047
hazards at supersonic transport altitudes, 20: 40525
production of, angular momentum exchange between planet and sun as mechanism for, 20: 41610

SOLAR RADIATION
charged-particle penetration into magnetosphere, (T), 20: 42069
dynamics of solar wind, (T), 20: 41617
effects on human skin, review of, 20: 40696
model for solar wind, boundary perturbations and stability of, 20: 41586
modulation of cosmic protons and helium nuclei by, (T), 20: 41670
particle-wave interactions in solar wind, fluid models for, 20: 41615
plasma flow in solar wind, correlation to lunar eclipse brightness, 20: 41604

SOLENOIDS
acceleration of superconducting, to hypervelocities, (T), 20: 41554
charged particle motion in field of superconducting, 20: 42521
performance for magnetic flux compression, 20: 41091
propagation of normal region in niobium–zirconium superconducting, 20: 42100
superconducting, distribution of normal region after quenching of, (E), 20: 42103

SOLID PROPELLANTS
exhaust plasma from, microwave attenuation in, 20: 41120

SOLID SOLUTIONS
lattice models of, for correction of Vegard's law, 20: 41412(R) (IS-1500 (Sect. M))

SOLID STATE REACTIONS
phase formation in type 316 stainless steel at high temperatures, chi, 20: 41419(R) (GMAD-3643-5)

SOLIDS
analysis for gases, spectral isotopic, (T), 20: 41526
radiation effects on catalytic properties of, 20: 40989
radiolysis of, review of mechanisms in, 20: 40987
reactions with gases, potential energy curves for, 20: 40796(R) (IS-1500(Sect.C))
shock propagation in, profiles for, (T), 20: 41513(R) (UCRL-14744, pp 19-36)
gas–solid, flow in pipes, 20: 41102 (NYO-2930-6)

SOLUTIONS
separation of radioactive ions from, method for, 20: 41058(P)

SOLVENT EXTRACTION PROCESSES
developments in, for nonferrous metals, review on, 20: 41047

SONIC INSPECTION
device development for pressure vessel nozzles, 20: 42636(R) (SWRI-1228-4-22)

SOUND
propagation in superconductors, (T), 20: 42128(T)

radiation effects on rat response to, following fetal exposure, 20: 40654
SOUTHWEST EXPERIMENTAL FAST OXIDE REACTOR
design and development, 20: 42629(R) (GEAP-5160)
reactivity coefficients of, steady state evaluation of, 20: 42631 (KFK-260)
SOVIET UNION
strontium-90 content in drinking water and food in, 20: 41142
SOYBEANS
strontium-89 and calcium-45 accumulation, 20: 40532(R) (COO-1097-17)
SPACE
light propagation in, Lorentz principle for, 20: 42072
light propagation in, Lorentz principle for, 20: 42073
magnetic fields in interstellar, Petschek's mechanism for dissipating, 20: 41595
plasma instability in interstellar, gravitational and magnetic effects on, 20: 42422
plasma perturbations in interstellar, fragmentations from, 20: 41593
SPACE FLIGHT
effects of cosmic ray particles on body tissues, 20: 41187 (BNL-9468)
effects of radiation and zero-gravity on leukocyte chromosome aberration induction, 20: 40635(R) (ORNL-TM-1550)
effects of simulated, on biocompatibility of Neurospora, 20: 40508 (ORNL-3922, pp 196-9)
exposure to space radiation during, 20: 41219
interaction experiment for Gemini-3, 20: 40508(R) (ORNL-3922, pp 196-9)
power plants for, review of types of, 20: 41514(T) (AI-Trans-209)
use of simulated, for testing Habrobracon, 20: 40508(R) (ORNL-3922, pp 196-9)
SPACE MEDICINE
biological significance of supersonic transport radiation environment, 20: 40525
SPACE VEHICLES
electron shielding for, (E), 20: 42520
power plants for, review of types of, 20: 41514(T) (AI-Trans-209)
power sources for, use of isotopic, 20: 41397
power supplies for, evaluation of Brayton and Rankine cycles for, 20: 41398
power supplies for manned space stations, Brayton and Rankine, 20: 41679 (NASA-CR-543)
propulsion of, materials testing facility for electrical, 20: 41122
reentry plasma sheath of, signal diffraction effects in, 20: 42438
SPAIN
granites in northwestern, ages of, 20: 41153
SPALLATION
of mercury, use in accelerator radiation monitoring, 20: 41276 (UCRL-16769)
SPARK CHAMBERS
data analysis of, track centering system for flying spot digitizers for, 20: 41263 (CERN-66-23)
design and performance of gas-filled image intensifier, for gamma and x rays from radioisotopes in human organs, 20: 41299
design and performance of low temperature, using helium and neon gas, 20: 41329
design and performance of pressurized discharge, at 33 kg/cm² and room temperature, 20: 41294
design and performance on on-line wire spectrometer, for 5- to 30-Bev/c particles, 20: 41297
operation of wide-gap, design and performance of Marx high-voltage pulse generator for, 20: 41330
particle trajectories in, factors influencing discharge development along, 20: 41304
performance of multiple-wire, for divergent alpha particles and neutrons, 20: 41317
voltage pulser for, design and performance of compact low-inductance, 20: 41293
SPECTROMETERS
design and performance of on-line wire spark chamber, for 5- to 30-Bev/c particles, 20: 41297
design of broad-range system for magnetic, using nuclear emulsions, 20: 41306
detectors in multi-unit arrays for, gaps between, 20: 41315
evaluation for clinical use, 20: 40734(R) (NYO-901-54, pp 24-5)
performance of gallium arsenide detector, for charged particles, 20: 41313
performance of, with hybrid preamplifier, 20: 41298
recording system for uv, design of photoelectric, 20: 41267 (MPI-PAE-P1-30/66)
scintillation detectors for magnetic, performance of, 20: 41289
stabilization system for, development of digital pulse-height analyzer, 20: 41269(R) (ORNL-3875, pp 4-12)
SPECTROSCOPY
book: *High Resolution Nuclear Magnetic Resonance Spectroscopy, Vol. I*, 20: 41255
research progress in, 20: 40796(R) (IS-1500(Sect.C))
use of lasers for cancer, advantages of, 20: 40776
SPERM
radiation effects on morphology and viability of bull, x, 20: 40610(R) (COO-895-9)
radioinduced dominant lethality in, of olive fruit fly, 20: 40674
reparative effects of DNA from various organs on, after x-irradiation, 20: 40723
SPERMATOGENESIS
radiation effects on human, x, 20: 40627(R) (ORNL-3922, pp 84-8)
radiation effects on bull, x, 20: 40610(R) (COO-895-9)
radiation effects on rat, following exposure at birth, x, 20: 40682
radiation effects on germ cell ultrastructure during rat, following exposure at birth, x, 20: 40683
radioinduced mutations in mice during, frequency of x, 20: 40627(R) (ORNL-3922, pp 84-8)
SPHERES
cooling of heat-generating solid, temperature distributions in, 20: 41106
packing in cylindrical vessels, computer analysis of, 20: 41063 (BNL-997)
SPLEEN
DNA and RNA synthesis in mouse, effects of estradiol on, 20: 40577
effects of radioprotective drugs on damage induced by alkylating agents, 20: 40664
iron-59 uptake by mouse, use in assessing radiosensitivity of marrow cells, 20: 40634 (ORNL-P-2312)
lymph cells in mouse, effects of antibody production on morphology of, 20: 40632(R) (ORNL-3922, pp 175-91)
lysosome studies on mouse, after treatment with mixed bacterial toxins and anthramycin, 20: 40736
mouse hybrid, transplanted cells inducing tolerance in parental mouse strain, 20: 40651
radiation effects on DNA and RNA synthesis in marrow-protected mice, effects of estradiol on x, 20: 40577
radiation effects on cells of, incubated with phytochemagglutinin, x, 20: 40588
radiation injury on rat, effects of fractionated doses on regeneration of x, 20: 40702
radiotherapy of, in leukemia, 20: 40720
recolonization in x-irradiated mice of, following lymphoid or myeloid transplants, 20: 40727
reparative effects of DNA from, on sperm of x-irradiated rat, 20: 40723
use of extract as radiation protection factor, 20: 40658
use of iodine-131-labeled colloidal albumin as scanning agent, 20: 40777
SPORES
radiation effects on differentiating bacterial, repair of uv, 20: 40504(R) (ORNL-3922, pp 146-60)
radioinduced inactivation of *Clostridium botulinum*, factors affecting dose required for, 20: 40601
radiosensitivity of *Clostridium botulinum* type E, γ, 20: 40699
SPRAYS
effects of urethan foam, on air leaks in buildings, 20: 41200 (ORNL-TM-1551)
SPUTTERING
control of, in regenerative collector target, 20: 41122
mechanism of single-crystal, 20: 42553
STABLE ISOTOPES
use in chemistry, geology, and physics, 20: 41380(T) (IFA-IS-36)
STACK DISPOSAL
iodide scavenging by rain and snow from Hanford stack gases, measurements, 20: 41188(R) (BNWL-235-1)
STAINLESS STEEL
carbon content of, effects of liquid metal loop conditions on, 20: 41419(R) (GMAD-3643-5)
chemical reactions with liquid potassium at high temperatures, carbides and phases from, 20: 41419(R) (GMAD-3643-5)
corrosion by aqueous iron chloride, effects of carbon, manganese, and silicon traces on, 20: 41418(R) (GEAP-5150)
corrosion by water, effects of dissolved impurities on, 20: 41418(R) (GEAP-5150)
corrosion of type 316, by liquid potassium at high temperatures, 20: 41419(R) (GMAD-3643-5)
crystal structure of type 304, dilatometric effects of nitrogen on, 20: 41449(R) (EURAEC-1676)
fracture strength measurement at room temperature, method for, 20: 41444(R) (COO-1477-5)
hydrogenation of type 304, effects on ductility, 20: 41418(R) (GEAP-5150)
mechanical properties of type 316, corrosive effects on air and liquid potassium at high temperatures on, 20: 41419(R) (GMAD-3643-5)
mechanical properties of, corrosive effects of contaminated high-temperature liquid sodium on, 20: 41420(R) (MSAR-66-149)
mechanical properties of type 304, at 1200°F in air and helium,

20: 41420(R) (MSAR-66-149)
properties of austenitic, for Rapsodie pressure vessel, 20: 42652(T) (EURFNR-92F)
radiation effects on fuel cladding of type 304, 20: 42626(R) (GEAP-4951)
radiation effects on corrosion by iron chloride, 20: 41418(R) (GEAP-5150)
removal from fuel elements using atomized hydrochloric acid, 20: 41060(P)
rupture mechanisms of type 304, determination by time-to-rupture tests, 20: 41445(R) (EURAEC-1622)
thermal conductivity of, measurement at high temperatures, 20: 41479
wetting by lead–bismuth eutectics, 20: 41064(R) (IS-1500(Sect.E))
PuO_2–stainless steel, performance as FTR fuel, 20: 42676 (BNWL-281)

STANDARDS
design and performance of, for uranium hexafluoride pressure gages in micron region, 20: 41252

STANFORD LINEAR ACCELERATOR
beam position and charge monitoring circuits for, design and performance of, 20: 41544 (SLAC-63)
beam profile monitor for, design and performance of, 20: 41562

STARCHES
radiation effects on wheat flour, gamma, 20: 40599

STARS
collapse of high-temperature, model with neutrino surface intensity and energy loss for gravitational, 20: 41612
electrostatic potential distribution around, from stellar winds, (T), 20: 41617
evolution of population II red giants, 20: 41587
evolution of, axial rotations in, 20: 41584(T) (UCRL-Trans-10040)
formation of, 20: 41585(T) (UCRL-Trans-10041)
formation of, thermal instability role in, 20: 41601
magnetic field of collapsing, 20: 41602
magnetic fields of, (E/T), 20: 41616
neutrino energy losses from vibrating neutron, 20: 41605
neutrino motion in superdense, (T), 20: 41596
properties of central region of collapsing, with spherical symmetry and pressure gradient, 20: 41613
properties of quasars, (T), 20: 41608
pulsations from, normal modes of radial, 20: 41588
pulsations from, normal modes of radial, 20: 41589
radiations from collapsing and anticollapsing, 20: 41597
radio emission from 3C-48 quasar, intensity fluctuations of, 20: 41598

STATISTICS
dynamics of certain spherical charge distributions, 20: 41517
quantum mechanical derivation of generalized Boltzmann equation, 20: 42082
quantum-mechanical extension of Lebowitz-Penrose theorem on van der Waals theory, 20: 42081

STEAM
effects on soils, sterilization, 20: 40637(R) (ORO-2754-7)
steam–water, effect of pipe and entrance properties on flow rates of, 20: 41107

STEAM POWER PLANTS
design using liquid-metal cooled reactor, 20: 42657(P)

STEEL
analysis for rare earth inclusions, procedure for, 20: 41415
analysis of, for oxygen, equipment used in activation methods for, 20: 40848
carburization of, effects of impurities on vacuum, 20: 41412(R) (IS-1500 (Sect. M))
crystal structure and stress relief of thick-plate, 20: 41450(R) (EURAEC-1684)
ductility of pressure-vessel effects of fatigue on, 20: 41446(R) (EURAEC-1624)
properties as magnet material, 20: 41097
properties testing for use in Elk River Reactor pressure vessel, 20: 42636(R) (SWRI-1228-4-22)
radiation effects on antifriction and strength properties of No. 45, neutron, 20: 41498
radiation effects on embrittlement of pressure-vessel, neutron, 20: 41494(R) (EURAEC-1617)
radiation effects on, method for comparison of neutron, 20: 41504
radioinduced embrittlement of, remotely controlled equipment for evaluating, 20: 41113
strength of pearlitic and spheroidized, analysis of, 20: 41454 (NYO-2394-22)
welds of heavy-gage, research programs on strength of, 20: 41410(R) (EURAEC-1612)
welds of high-tensile, preparation for research on strength of, 20: 41448(R) (EURAEC-1670)

STELLARATORS
plasma equilibrium in toroidal magnetic axis, 20: 42424

STERILITY
radioinduced in jute, gamma, 20: 40681

STILBENE
isomerization of, by triplet molecules and free radicals from gamma radiolysis of benzene and cyclohexane, 20: 40961
radiolysis of, in cyclohexane and benzene, 20: 40961

STRATOSPHERE
fission-product monitoring by balloon filters, 1965, 20: 41131(R) (HASL-172)
strontium-90 content in, 1963 to 1966, 20: 41131(R) (HASL-172)

STRESS CORROSION
effects of nitrogen on type 304 stainless steel, 20: 41449(R) (EURAEC-1676)

STRONTIUM
content and distribution in chicken eggs, effects of dietary strontium and calcium on, 20: 40569
content in sea water from Indian Ocean, uptake by marine organisms, 20: 40572
content in Spanish rock, 20: 41153
content in tissues of young and aged dogs, 20: 40540(R) (UCD-472-113, pp 17-56)
determination in environmental samples, 20: 40809 (NP-16235)
determination in fission product solutions, method for, 20: 40803 (KFK-387)
determination in seawater, activation, 20: 40834
effects on strontium-85 and strontium-89 excretion by goats, 20: 40568
isotopic composition in, mass discrimination in spectrometric measurements on, 20: 40821
migration in turf-podzolic and black earth soil, 20: 40520 (NP-16261)
proton reactions with neutral ground state of, formation of excited hydrogen atoms in, (T), 20: 41634
scattering on beryllium–copper alloy at 5 kev, secondary electrons from, 20: 41620 (NIJS-R-471)
separation from ashes of beef bones, milk, and fish, 20: 40858
separation from barium and cesium by ion exchange on granulated zirconyl phosphate, 20: 41055
separation from barium by cation exchange using DTPA and HEDTA as eluants, 20: 41040 (ORNL-TM-1342)
separation from products of fission-fragment-induced radiolysis, 20: 40951 (RPI-321-6)
separation from waste solutions, 20: 42689
separation of silver from, by cation exchange chromatography, 20: 40847
uptake by corn plants, effects of soil fertility on, 20: 40735 (NYO-2744-37)
uptake by crops and factors affecting translocation in soil, 20: 40524(R) (TID-23271)
uptake by edible plants, effects of calcium content of soil and plant species, tracer study, 20: 40537(R) (TID-23052)
uptake by rice, effects of irrigation on, 20: 40574

STRONTIUM ALLOYS
Mg–Sr, crystal structures of intermetallic compounds of, 20: 41455(R) (NYO-2731-7)

STRONTIUM BROMIDES
vapor pressure enthalpies and equations for, 20: 41412(R) (IS-1500 (Sect. M))

STRONTIUM CERIUM FLUORIDES
preparation, properties, and structure of, 20: 40867 (KFK-385)

STRONTIUM FLUORIDES
solubility in double fluorides of neptunium, plutonium, thorium, and uranium, 20: 40867 (KFK-385)
CeF_3–SrF_2, solubility studies on, 20: 40867 (KFK-385)

STRONTIUM IODIDES
vapor pressure enthalpies and equations for, 20: 41412(R) (IS-1500 (Sect. M))

STRONTIUM ISOTOPES
composition in strontium, mass discrimination in spectrometric measurements on, 20: 40821

STRONTIUM ISOTOPES Sr-80
determination in environmental samples, 20: 40809 (NP-16235)

STRONTIUM ISOTOPES Sr-85
determination in radioisotope mixtures using simultaneous equations, gamma spectrometric, 20: 40837
excretion by goats, effects of dietary calcium and strontium on, 20: 40568
sorption reactions of, on minerals, 20: 41178 (AD-635547)
uptake and exchange in bones of dogs, 20: 40684
uptake by fractured human bones, 20: 40542
use in bone scanning, 20: 40748
use in bone scanning, value to radiotherapy, 20: 40794

STRONTIUM ISOTOPES Sr-86
content in Australian Precambrian rock, 20: 41159
content in Spanish granites, age estimation from, 20: 41153

STRONTIUM ISOTOPES Sr-87
content in Australian Precambrian rock, 20: 41159
content in Spanish granites, age estimation from, 20: 41153
STRONTIUM ISOTOPES Sr-88
proton reactions (p,γ) with, gamma decay of analog resonances in, (E), 20: 42331
STRONTIUM ISOTOPES Sr-89
content in Finnish milk, 1960 through 1965, 20: 41134 (SFL-A3)
content in waters near Canadian reactors, April 1965, 20: 41136
determination in environmental samples, 20: 40809 (NP-16235)
energy-level density and transitions, (E), 20: 42331
excretion by goats, effects of dietary calcium and strontium on, 20: 40568
genetic control of accumulation in barley and wheat, 20: 40532(R) (COO-1097-17)
movement in calcareous soils, 20: 40524(R) (TID-23271)
STRONTIUM ISOTOPES Sr-90
activity measurements in milk in Great Britain, 20: 41186 (ARCRL-15)
concentration and distribution in soils, 20: 41139
contamination of eggs by, penetration and internal distribution, 20: 40559
content in Baltic herring, 1965, 20: 41134 (SFL-A3)
content in bones of yearling deer, 20: 40541(R) (UCD-34P104-3)
content in bones sampled in 1965, 20: 41131(R) (HASL-172)
content in Canadian milk and wheat, 1966, 20: 41198 (NP-16192)
content in Canadian milk, April 1965, 20: 41209
content in detritus from Indian Ocean, 20: 41140
content in fallout in India, 20: 40572
content in Finnish milk, 1960 through 1965, 20: 41134 (SFL-A3)
content in human bones and tissues, 20: 40570
content in Lake Michigan waters and surrounding land areas, 20: 41131(R) (HASL-172)
content in milk in Mexico, 1963 to 1965, 20: 40854
content in milk, 1965 and 1966, 20: 41131(R) (HASL-172)
content in stratosphere, 1963 to 1966, and predictions to 1968, 20: 41131(R) (HASL-172)
content in waters near Canadian reactors, April 1965, 20: 41136
deposition in precipitation, global, 1965 and 1966, 20: 41131(R) (HASL-172)
deposition of, use of molecular plating for quantitative, 20: 41011 (SGAE-CH-34/1966)
determination in food, soil, and surface atmosphere, 20: 40853
determination in milk, 20: 40854
determination in water, 20: 40819(T) (CEA-tr-A-1883)
effects on fish spawning, 20: 40527
measurement in milk samples in New Zealand, 20: 40521(R) (NP-16270)
measurement in rain samples in New Zealand, 20: 40521(R) (NP-16270)
migration in turf-podzolic and black earth soil, 20: 40520 (NP-16261)
properties of, in isotopic power sources, 20: 41397
toxicity in dogs, 20: 40540(R) (UCD-472-113, pp 17-56)
translocation from maternal skeleton to progeny during gestation and lactation, 20: 40540(R) (UCD-472-113, pp 17-56)
transport from atmosphere to water supplies, 20: 41141
uptake by browsing deer and sheep, food-chain factors affecting, 20: 40541(R) (UCD-34P104-3)
uptake by man of, through drinking water and food chain, 20: 41142
uptake by rice, effects of irrigation on, 20: 40574
use in beta applicators, 20: 40766
STRONTIUM NEPTUNIUM FLUORIDES
preparation, properties, and structure of, 20: 40867 (KFK-385)
STRONTIUM PLUTONIUM FLUORIDES
preparation, properties, and structure of, 20: 40867 (KFK-385)
STRONTIUM THORIUM FLUORIDES
preparation, properties, and structure of, 20: 40867 (KFK-385)
STRONTIUM TITANATES
preparation and properties of single crystals of, effects of crystallization temperature on, 20: 41480
STRONTIUM URANATES
preparation, properties, and spectra of, 20: 40901
STRONTIUM URANIUM FLUORIDES
preparation, properties, and structure of, 20: 40867 (KFK-385)
STRUCTURES
air leaks in, effects of urethan spray foam on, 20: 41200 (ORNL-TM-1551)
design for protection of cameras and film, 20: 41223 (EGG-1183-1244)
radiological decontamination of, postattack requirements for, 20: 41179 (AD-635821)
radiological decontamination of, postattack, requirements for, 20: 41180 (AD-635822)
radiological decontamination of, postattack requirements for, 20: 41181 (AD-635823)
radiological decontamination of, postattack requirements for, 20: 41182 (AD-635824)
STYRENE
effects on isomerization of stilbene in gamma radiolysis of benzene and cyclohexane, 20: 40961
radioinduced grafting of, on cellulose theory of, 20: 40979
radioinduced graft polymerization with poly(vinyl chloride), rate of gamma, 20: 40993
radioinduced graft polymerization to polyvinyl chloride in liquid and vapor phases, rate of electron and gamma, 20: 40992
radioinduced ionic polymerization of, kinetic study of gamma, 20: 40978
radioinduced polymerization of, with formaldehyde in bulk and solution, gamma, 20: 40973
radiolysis of, EPR studies of yields of stabilized charges in low-temperature, 20: 40962
acrylic acid–styrene, radioinduced graft polymerization to cotton fabric, properties of products formed in gamma, 20: 40953
methyl methacrylate–styrene, radioinduced graft polymerization to cotton fabric, properties of products formed in gamma, 20: 40953
STYRENE, α-METHYL-
radiolysis of, identification of intermediates in polymerization from pulse, 20: 40985
STYRENE POLYMERS
radiation effects on photoconductivity processes in, x, 20: 40952 (SC-DC-66-1823)
radiolysis of, EPR studies of yields of stabilized charges in low-temperature, 20: 40962
scintillation light yield from, 20: 41346
SUCCINIC OXIDASE
effects of near-ultraviolet radiation on activity of, in bacteria, 20: 40571
SULFAMIC ACID
alkali metal bisulfate–sulfamic acid, properties as decontaminating solution for aluminum or zirconium, 20: 41214(P)
ammonium bisulfate–sulfamic acid, properties as decontaminating solution for aluminum or zirconium, 20: 41214(P)
sulfamic acid–sulfuric acid, properties as decontaminating solution for aluminum or zirconium, 20: 41214(P)
SULFATE IONS
effects on uranyl complexes with tributylphosphine oxide, 20: 40885
SULFATES
effects on disproportionation of uranium(V), 20: 40911
SULFIDES
determination in radiation processes sea foods, chemical, 20: 41384(R) (TID-22833)
effects on wholesomeness of radiation processed sea foods, 20: 41384(R) (TID-22833)
SULFUR
content in meteorites, 20: 42064
determination in americium and plutonium by spark-source mass spectrography, 20: 40816 (RFP-699)
determination in uranium trioxide, turbidimetric, 20: 40802 (HW-65402 (Rev.1))
effects on alpha and gamma radiolysis of cyclohexane, 20: 40990
neutron reactions at 14.7 Mev, gamma emission in, (E), 20: 42146 (AD-638014)
separation of phosphorus from, by co-precipitation with ferric hydroxide, 20: 41049
yields in gamma radiolysis of liquid hydrogen sulfide, effects of 2,2-diphenyl-1-picrylhydrazyl and iodine on, 20: 40997
SULFUR CHLORIDES
preparation and evaluation for electromagnetic separation of sulfur isotopes, 20: 41400 (ORNL-3301(Suppl.1))
SULFUR DIOXIDES
determination in waste gases, by absorption of soft gammas, 20: 40828
SULFUR FLUORIDES
preparation of fluorine-18-labeled, 20: 41020
SF_6–toluene, radiolysis of, mechanism and yields of products in gamma, 20: 40948(R) (COO-578-3-32)
SULFUR ISOTOPES
radioactive, effects on human erythrocyte diameter and volume from occupational exposure to, 20: 40678
separation by electromagnetic methods, 20: 41401(R) (ORNL-4006)
separation of, preparation of disulfur dichloride for electromagnetic, 20: 41400 (ORNL-3301(Suppl.1))
use of stable, in determining origin of sulfides, 20: 41151
SULFUR ISOTOPES S-32
alpha elastic scattering by, DWBA analysis of, (T), 20: 42392
deuteron reactions (d,p) at 2.5 to 4.6 Mev, (E/T), 20: 42163 (LA-DC-8082)
energy-level positions and transitions in, calculations using particle-hole model, (T), 20: 42199
neutron reactions (n,α_0) at 2.5 to 3.2 Mev, 20: 42375
proton reactions (p,γ) at 0.3 to 2.1 Mev, resonance strengths for, (E), 20: 42182
use in studying genesis of mineral deposits, 20: 41151
SULFUR ISOTOPES S-34
distribution in ancient oceans and evaporites, variations in, 20: 41135

proton reactions (p,γ) at 0.3 to 2.1 Mev, resonance strengths for, (E), 20: 42182
use in studying genesis of mineral deposits, 20: 41151
SULFUR ISOTOPES S-35
effects on rice seed, chlorophyll mutations from, 20: 40641
fixation to protein-polysaccharides of bovine cartilage, 20: 40544
radioinduced mutations in rice, 20: 40640
SULFUR SYSTEMS
As–S–Se, sintering mechanism of, 20: 41064(R) (IS-1500(Sect.E))
O–S–U, phase studies, 20: 42579(R) (ANL-7245, pp 29-47)
SULFURIC ACID
effects as leaching agent on recovery of thorium from thorium ores, 20: 41033 (INR-678/IV/C)
electron spin resonance spectra of, 20: 42433
sorption of metals from solutions of, by anion exchange materials, 20: 40822
sulfamic acid–sulfuric acid, properties as decontaminating solution for aluminum or zirconium, 20: 41214(P)
SULFURYL FLUORIDE
preparation of fluorine-18-labeled, 20: 41020
SUN
angular momentum exchange between planets and, 20: 41610
magnetic fields of, (E/T), 20: 41616
radiative transfer between chromosphere and corona, stellar wind effects on, 20: 41618
radio waves from, frequency splitting of, 20: 41606
sunspot phenomenon of, gravitational quadrupole moment effect on, 20: 41610
SUPERCONDUCTIVITY
critical temperatures in, models for high, 20: 42129
of lanthanum, effects of crystal imperfections on, 20: 41412(R) (IS-1500(Sect. M))
transition, propagation of normal region in niobium–zirconium solenoid during, 20: 42100
SUPERCONDUCTORS
acceleration to hypervelocities of Type-II, magnetic, 20: 41554
contact between niobium–zirconium and lead–tin, design and fabrication of, 20: 42124
critical currents of antimony-lead, desolvation effects on, 20: 42099(T) (AD-636625)
critical currents in surface sheaths of, effects of copper, chromium, and nickel plating on, 20: 42114
critical currents in niobium–zirconium, effects of annealing and orientation on, (E), 20: 42569
critical field and energy gap of, rules for, 20: 42119
critical temperature of type-II, de Haas-van Alphen oscillations in, (T), 20: 42126
excitations in type-II, properties of fermion-type, 20: 42110
magnetic field suspension of spherical, force calculations for, 20: 42130
magnetic fields of, design of magnetometer for, 20: 41228(R) (ORNL-3875, pp 15-20)
magnetic flux penetration in Type-II, (E), 20: 42132
magnetization of Type-II, equilibrium, (E), 20: 42133
mechanical forces on type-I, in magnetic fields, (E), 20: 42134
properties of high-purity niobium, (E), 20: 42117
properties of niobium–zirconium alloy, effects of oxygen on, 20: 42535
residual losses in, r-f, (E), 20: 42131
sound dispersion in, (T), 20: 42128(T)
spin-lattice relaxation time of dirty type-II, in high fields, (T), 20: 42102
structural transformation in V_3Si, vanadium-51 Knight shifts and field gradients during, 20: 42118
surface sheaths of type-II, responses to applied field, (E/T), 20: 42125
surface sheaths of, shielding properties of, (E), 20: 42127
temperature effects on electronic stability and crystal structure of V_3Si-type, 20: 42531
thermal capacity and transition temperature in the scandium–zirconium system of, 20: 42121
thermal capacity of mixed state in vanadium, at 0.5 and 5.4°K, 20: 42116
thermal capacity of normal and superconducting vanadium, at 0.5 to 5.4°K, 20: 42115
thermodynamic properties of, use of effective interaction strength to predict, 20: 42120
transitions in solenoid, distribution of normal region after, (E), 20: 42103
tunneling in superimposed normal and conducting films, (E), 20: 42109
use in cryotron memory devices, (T), 20: 42108
use in high-field electromagnetic lenses, 20: 42104
use in magnets, design engineering from, (T), 20: 42135
uses for magnets, transition of solenoid windings to normal state in, (E), 20: 41760
SUPERFLUIDITY
density of helium-4 near transition temperature, 20: 42122
SUPERHEATERS (NUCLEAR)
spacers in BONUS assemblies, temperature distribution under, 20: 42634 (ORNL-TM-1453)
SURFACE WATERS
phosphorus-32 distribution in stream, by *E. coli*, 20: 40529
radioactive contamination of, effects on hydrobionts, 20: 40527
radioactivity from fallout in, 1965 and 1966, 20: 41131(R) (HASL-172)
radioactivity in, near Canadian reactors, α and β, 20: 41136
uptake of strontium-90 by man through drinking water and food chain, 20: 41142
SURFACES
biological cleanability of, tracer technique for, 20: 41218
electron and ion beam treatment of, sources for, 20: 41528
SURGERY
effectiveness for cervical cancer in combination with drugs and radiotherapy, 20: 40778
use in treatment of hyperthyroidism, performance compared with iodine-131, 20: 40785
SUSPENSIONS
radioisotope distribution between Indian Ocean sea water and, 20: 41140
SWEDEN
cobalt and radium therapy of uterine carcinomas, 20: 40769
SWIMMING POOL REACTORS
design for large-scale irradiation tests, 20: 42685(P)
neutron flux distributions in, correlation with two-group diffusion theory, 20: 42600
SWINE
effect of calcium, zinc, and corn oil in diet on the in vitro uptake of various radioisotopes by blood cells of, 20: 40556
radiation effects on, pathological γ, 20: 40608 (CEA-R-3001)
radioinduced inactivation of foot and mouth disease virus in tissues of, γ, 20: 41392
radiosensitivity of, effects of conditioning exposure on x, 20: 40605 (AD-635735)
Salmonella infections in, fed heat-treated or γ-irradiated meals, 20: 41394
SYENITES
uranites in nepheline, 20: 41173
SYNCHROCYCLOTRONS
beam capture efficiencies of, 20: 41533 (CERN-66-27)
radiation dosimetry around high-energy, 20: 41206(T) (JPRS-36341, pp 10-17)
SYNCHROTRONS
coupling of h-f cavities to proton positions in, nonlinear technique for, 20: 41547
design of 10-Bev electron, at Cornell, 20: 41568
development of NINA 4-Bev electron, 20: 41535 (DNPL-1)
development of NINA 4-Bev electron, 20: 41536(R) (DNPL-2)
neutron dosimetry methods for Nimrod, 20: 41543 (RPP-R-2)
radio frequency system for, design of 600-Mc, 20: 41532 (BNL-10559)
SYNERGISTIC ACTION
of gamma rays and triethylene benzoquinone on HeLa cell nuclei, 20: 40704
of heat treatments and γ radiation on yeasts, 20: 41387
SYSTEMS FOR NUCLEAR AUXILIARY POWER
radioisotopes for, evaluation of, 20: 41397
reactivity transient tests in SNAPTRAN-1, step, 20: 42664(R) (IDO-17165)
testing of SNAPTRAN-2, destructive, 20: 42664(R) (IDO-17165)
SYSTEMS FOR NUCLEAR AUXILIARY POWER (SNAP-9)
reentry burnup of 9A, effects on plutonium-238 content in stratosphere, 20: 41131(R) (HASL-172)
SYSTEMS FOR NUCLEAR AUXILIARY POWER (SNAP-10)
fuel for 10A, hydrogen pressure measurements in, 20: 42664(R) (IDO-17165)

T

TANTALUM
corrosion by chromium–uranium and manganese–uranium eutectics, 20: 41064(R) (IS-1500(Sect.E))
corrosion by lithium at 1200°C, 20: 42579(R) (ANL-7245, pp 29-47)
crystal lattice vibrations in, inelastic neutron scattering measurements of, 20: 42573
determination in americium and plutonium by spark-source mass spectrography, 20: 40816 (RFP-699)
determination in rare earths, spectrophotometric, 20: 40796(R) (IS-1500 (Sect.C))
determination in seawater, activation, 20: 40834
helium and hydrogen ion attenuation at 0.1 to 500 Mev, tables for, 20: 41619 (CEA-R-3042)

hydrogen embrittlement in FRCTF, evaluation of possible, 20: 42682 (LA-3508)
photon reactions (γ,n) with, energy spectra from, (E), 20: 42165(R) (MIT-2098-251, pp 16-20)
preparation and properties of single crystals of, 20: 41481
properties for use as thermal shielding at high temperatures in vacuum, 20: 41440(R) (ALO-3632-4)
separation from molybdenum, niobium, and tungsten by solvent extraction using methyl isobutyl ketone, 20: 40796(R) (IS-1500(Sect.C))
solubility in liquid lanthanides at high temperatures, 20: 41412(R) (IS-1500(Sect. M))
thermophysical properties at 1300 to 3000°K, (E), 20: 41762
use in isothermal ovens for plasma production, 20: 42484

TANTALUM CARBIDES
containment at 5000°K, rotating graphite crucible for, 20: 41414
hardness of cast, at 20 to 1500°C, 20: 41429(R) (USBM-RC-1249)
oxidation of cast, by air at 450 to 800°C, 20: 41429(R) (USBM-RC-1249)

TANTALUM CHLORIDES
phase studies, 20: 40796(R) (IS-1500(Sect.C))
separation from niobium chloride, methods for, 20: 41064(R) (IS-1500 (Sect.E))

TANTALUM COMPLEXES
acetonitrile, crystal structure of, 20: 40796(R) (IS-1500(Sect.C))

TANTALUM ISOTOPES
neutron capture cross section at 30 to 170 kev, (E), 20: 42293

TANTALUM ISOTOPES Ta-181
alpha elastic scattering at 16 and 24 Mev, quadrupole effect in, (T), 20: 42235
carbon-12 reactions (C-12,N-13) with, angular distributions from, (E), 20: 42153 (JINR-E-2824)
meson (μ^-) capture by, x-ray spectra from, (E), 20: 42306

TANTALUM SILICIDES
oxidation at reduced pressures, effects of additives on, 20: 41424

TARTARIC ACID COMPLEXES
with yttrium, spectra and thermal decomposition of, 20: 40909

TECHNETIUM
separation from products of fission-fragment-induced radiolysis, 20: 40951 (RPI-321-6)
separation of, from rhenium, by extraction using potassium xanthate and carbon tetrachloride, 20: 40856

TECHNETIUM ISOTOPES Tc-93
energy-level density and transitions, (E), 20: 42331

TECHNETIUM ISOTOPES Tc-99
determination in water, 20: 40819(T) (CEA-tr-A-1883)
preparation of albumin-incorporated, 20: 40944
radiation dose to human, from isotope placentography, 20: 40680
tandem elution of, from generators, 20: 40754
use as tracer in thyroid metabolism studies, 20: 40547
use in brain scanning, 20: 40748
use in brain scanning, 20: 40789
use in development of rectilinear scanner, 20: 40755
use in liver scanning, 20: 40753
use in radiodiagnosis with scintiphotography, 20: 40750
use in radiodiagnosis with scintiphotography, 20: 40752
use in scintiphotography studies of lungs, 20: 40749
use in thyroid physiology studies, 20: 40555
use of pertechnetate-99 to measure survival of thyroid transplants, 20: 40516

TECHNICAL REPORTS
descriptive cataloging guide for, 20: 42694 (TID-4577(Rev.2))

TEETH
lead-210 content in human, 20: 40531 (A/AC.82/G/L-1045(Rev.1))
polonium-210 content in human, 20: 40531 (A/AC.82/G/L-1045(Rev.1))
radium-226 content in human, 20: 40531 (A/AC.82/G/L-1045(Rev.1))

TEKTITES
analysis for bromine, activation, 20: 40811 (ORO-2670-13)

TELEMETERING SYSTEMS
design and performance of physiological data, 20: 41220 (BNWL-214)
design of radiometric, for atmosphere, 20: 41257
performance of radio-, for meteorological data accumulation, 20: 41188(R) (BNWL-235-1)

TELEVISION EQUIPMENT
design for use in reactors, 20: 41099
design of, for monitoring x-ray fluoroscopy, 20: 40781
use in retrieval of medical data, 20: 40748

TELLURIUM
content in meteorites, 20: 42064
determination in bismuth, spectrophotometric, 20: 40805(R) (MLM-1325, pp 63-70)
determination in fission product solutions, method for, 20: 40803 (KFK-387)
distribution of, in neutron-irradiated plutonium dioxide suspensions, 20: 41009 (AERE-R-3268)
neutron reactions with, production of iodine-131 in, 20: 41399 (IEA-110)

TELLURIUM FLUORIDES
reactions of volatile, on solid sorbents, 20: 42580(R) (ANL-7245, pp 60-73)

TELLURIUM ISOTOPES
neutron capture by, gamma spectra from thermal, (E), 20: 42286

TELLURIUM ISOTOPES Te-122
energy levels of, gyromagnetic ratio of 564-kev vibrational, (E), 20: 42219

TELLURIUM ISOTOPES Te-125
half life of isomeric, dependence on chemical state, (E), 20: 42266
yields of isomeric, in proton fission of uranium at 170 Mev, 20: 42177

TELLURIUM ISOTOPES Te-127
yields of isomeric, in proton fission of uranium at 170 Mev, 20: 42177

TELLURIUM ISOTOPES Te-128
yields in proton fission of uranium at 170 Mev, 20: 42177

TELLURIUM ISOTOPES Te-129
yields of isomeric, in proton fission of uranium at 170 Mev, 20: 42177

TELLURIUM ISOTOPES Te-130
yields in proton fission of uranium at 170 Mev, 20: 42177

TELLURIUM ISOTOPES Te-131
yields of isomeric, in proton fission of uranium at 170 Mev, 20: 42177

TELLURIUM ISOTOPES Te-132
yields in proton fission of uranium at 170 Mev, 20: 42177

TELLURIUM ISOTOPES Te-133
yields of isomeric, in proton fission of uranium at 170 Mev, 20: 42177

TELLURIUM OXIDES
separation of carrier-free iodine-131 from irradiated, 20: 41026(P)

TELLURIUM SYSTEMS
Bi–Te, phase studies, 20: 41455(R) (NYO-2731-7)
Te–Tl, phase studies, 20: 41455(R) (NYO-2731-7)

TEMPERATURE
effect on thyroid/serum ratios of pertechnetates in mouse, 20: 40547
effects in radiation biology, electron spin resonance studies, 20: 40597
effects of, combined with γ radiation on yeasts, 20: 41387
effects of, combined with radiation on food enzymes, 20: 40600
effects of, on radiosensitivity of *Clostridium botulinum* spores, 20: 40601
effects of, on radiosensitivity of tobacco mutations, 20: 40613 (N-66-18147)
effects on crossing-over frequency in Drosophila, meiotic origin of, 20: 40625(R) (ORNL-3922, pp 59-64)
effects on polymorphic transformations of the elements, (T), 20: 41521
effects on radioinduced coloration and x-ray luminescence of calcium fluorides, 20: 42556
effects on uv-induced dimerization of thymine, 20: 40504(R) (ORNL-3922, pp 146-60)
measurement system for, development of differential optical, 20: 41233(R) (ORNL-3875, pp 101-24)
profiles of, in thermal entrance region, 20: 41105
radiosensitivity effects on mouse marrow cells, x, 20: 40634 (ORNL-P-2312)
radiosensitivity effects of, on spores of *Clostridium botulinum* type E, γ, 20: 40699

TERBIUM
determination by x-ray-fluorescence methods, 20: 40796(R) (IS-1500 (Sect.C))
determination in holmium oxides by neutron activation, 20: 40796(R) (IS-1500(Sect.C))
liquid, solubility of tantalum in, at high temperatures, 20: 41412(R) (IS-1500(Sect. M))
liquid, solubility of tungsten in, at high temperatures, 20: 41412(R) (IS-1500(Sect. M))
thermodynamic properties of, at 0°C to melting point, 20: 41412(R) (IS-1500(Sect. M))

TERBIUM ALLOYS
Mg–Tb, thermodynamics of formation of intermetallic compounds, 20: 41412(R) (IS-1500(Sect. M))

TERBIUM BROMATES
fluorescent lifetime of $^5D_4$ level of trivalent terbium ions in, (E/T), 20: 42539

TERBIUM CHLORIDES
fluorescent lifetime of $^5D_4$ level of trivalent terbium ions in, (E/T), 20: 42539
radiation effects on lifetime of $^5D_4$ level in, electron and x, (E), 20: 42539

TERBIUM COMPLEXES
with sulfosalicyclic acid, composition of, fluorometric study of, 20: 40926

TERBIUM ETHYL SULFATES
fluorescent lifetime of $^5D_4$ level of trivalent terbium ions in, (E/T), 20: 42539

TERBIUM IONS

fluorescent lifetime of $^5D_4$ level of trivalent, in hydrated salts, (E/T), 20: 42539

TERBIUM ISOTOPES Tb-152
beta decay of, gadolinium-152 energy levels from, (E), 20: 42155 (JINR-P-2762)

TERBIUM ISOTOPES Tb-159
meson (μ^-) capture by, x-ray spectra from, (E), 20: 42306
neutron reactions (n,2n) at 14.8 Mev, activation cross section for, (E), 20: 42207

TERBIUM ISOTOPES Tb-160
beta decay of, γ-γ directional correlations in, (E), 20: 42150 (COO-498-56)

TERBIUM NITRATES
fluorescent lifetime of $^5D_4$ level of trivalent terbium ions in, (E/T), 20: 42539

TERBIUM OXALATES
thermal decomposition of hydrates of, differential thermal analysis of products of, 20: 40900

TERBIUM SULFATES
fluorescent lifetime of $^5D_4$ level of trivalent terbium ions in, (E/T), 20: 42539

TEREPHTHALIC ACID, ETHYLENE POLYMER ESTERS
radiation effects on mechanical properties of, gamma, 20: 41501

TERPHENYL
analysis of mixtures of isomers of, for carbon and hydrogen, 20: 40797 (AECL-2524)
effects on yields in radiolysis of tetratriacontane as function of temperature, 20: 40986(T)
properties as coolant for ORGEL reactor, 20: 42623 (EUR-2996.f)
properties of Santowax ON as WR-1 coolant, 20: 42669 (AECL-2553)
radiolysis of, effects of LET and dose rate in, 20: 40946 (AECL-2589)

TESTOSTERONE
effects of dihydro-, on tumor growth, prediction by tumor uptake of phosphorus-32, 20: 40566
propionate of, use in cancer therapy in combination and radiotherapy and surgery, 20: 40778

TETRATRIACONTANE
radiolysis of liquid, mechanism and temperature effects in, 20: 40986(T)

TEXTILES
radioinduced graft polymerization to methyl methacrylate and styrene mixtures with monomers, gamma, 20: 40953

THALLIUM
determination of, developments in resin spot tests for, 20: 40827
effects on luminescence of alkali halides, 20: 41007
photon reactions (γ,n) with, energy spectra from, (E), 20: 42165(R) (MIT-2098-251, pp 16-20)

THALLIUM ALLOYS
Na–Tl, crystal structure of intermetallic compounds, 20: 41412(R) (IS-1500(Sect. M))
Na–Tl, solubility in sodium halide melts, 20: 40796(R) (IS-1500(Sect.C))
Pb–Tl, magnetic susceptibilities of, 20: 41412(R) (IS-1500(Sect. M))
Pb–Tl, magnetization of superconducting, (E), 20: 42133
Pb–Tl, superconductivity in, effects of plating on, 20: 42114
Pd–Tl, elastic properties of fcc, 20: 41412(R) (IS-1500(Sect. M))

THALLIUM ISOTOPES Tl-204
determination in water, 20: 40819(T) (CEA-tr-A-1883)

THALLIUM ISOTOPES Tl-207
energy levels of, lifetime 351-kev, (E), 20: 42167(R) (MIT-2098-251, pp 50-6)

THALLIUM NITRATES
$NaNO_3$–$TlNO_3$, diffusion and transport processes in molten, on ceramic oxides, 20: 40866 (EUR-2954.e)

THALLIUM SULFATES
poisoning in man, use of dithiocarb for therapy of, 20: 40536(R) (ORO-3461-1)

THALLIUM SYSTEMS
Te–Tl, phase studies, 20: 41455(R) (NYO-2731-7)

THERAPY
bleeding effects on bone marrow cell proliferation in x-irradiated rats, 20: 40722
DNA effects on sperm of x-irradiated rat, 20: 40723

THERMAL CONDUCTIVITY
calculation of liquid metal, methods for, 20: 41477
mathematical analysis of, 20: 41101 (NAA-SR-Memo-10848)
measurement of, equipment for metals and oxides at high temperatures, 20: 41479

THERMAL CYCLING
effects on microstructure of uranium, 20: 41470

THERMAL DIFFUSION
equipment for tritium enrichment by, 20: 41168

THERMAL INSULATION
development for thermocouples, resistivity of alumina, 20: 42579(R) (ANL-7245, pp 29-47)
development for use at 400 to 1800°F in vacuum, 20: 41440(R) (ALO-3632-4)
performance of silica-base, effects of carbon on high-temperature, 20: 41440(R) (ALO-3632-4)
radioinduced cross-linking of polyethylene, 20: 41496
spacer materials for, properties and testing silica-based, 20: 41440(R) (ALO-3632-4)
testing of thermocouple, at high temperatures, 20: 41461(R) (UCRL-7631(Pt.3))

THERMAL RADIATION
shielding by injections into boundary layers, 20: 41108

THERMIONIC CELLS
cesium reservoir for, development of adsorption, 20: 41680(R) (NYO-3642-2)
design of nuclear-fueled, 20: 41682(T) (LA-tr-66-32)
electric potential distribution in cesium, electron beam probe for, (E/T), 20: 42407 (IPP-2/48)
electron emission from tungsten electrodes in cesium, work functions for, 20: 41681 (UCRL-11857)
ionization of barium on hot rhenium surfaces, 20: 42406 (IPP-2/47)

THERMOCOUPLES
connection to fuel elements, connector for, 20: 41259(P)
development at ORNL, 20: 41233(R) (ORNL-3875, pp 101-24)
fabrication damage of, evaluation of as-purchased, 20: 41461(R) (UCRL-7631(Pt.3))
insulation for use with, testing of, 20: 41461(R) (UCRL-7361(Pt.3))
scanning system for, development of, 20: 41078(R) (ORNL-3875, pp 91-100)
use for measuring velocity of fluids, limits to, 20: 41101 (NAA-SR-Memo-10848)

THERMODYNAMICS
book: *Thermodynamic Properties of Inorganic Substances (Handbook)*, 20: 41417
calculations for compounds, computer program for, 20: 40875 (ORNL-TM-1599)

THERMOLUMINESCENT DETECTORS
design of, for charged and uncharged particle dosimetry, 20: 41370(P)
design, fabrication, and performance of calcium fluoride and lithium fluoride dosimeter, 20: 41373
use for neutron dosimetry in accelerator environment, 20: 41543 (RPP-R-2)
use in measurement of yttrium-90 beta depth dose, 20: 40766

THERMOMETRY
development in high-temperature, at ORNL, 20: 41233(R) (ORNL-3875, pp 101-24)

THERMONUCLEAR EXPLOSIONS
fission product formation by, 20: 41144

THERMONUCLEAR REACTIONS
plasma containment for, review of, (T), 20: 42482
research policies of AEC, 20: 42416 (TID-23277)

THERMONUCLEAR REACTORS
plasma containment for, using megagauss fields, 20: 42434
plasma containment and stability in, review of problems of, 20: 42437
plasma containment in, review of, (T), 20: 42482
research policies of AEC, 20: 42416 (TID-23277)
vacuum system of Ogra-II, design of, 20: 42421(T) (NP-tr-1396)

THERMOSTATS
design and performance of wide range vacuum, for Mossbauer spectroscopy, 20: 41253

THIOCYANATE IONS
effects on uranyl complexes with tributylphosphine oxide, 20: 40885

THIOCYANATES
effects on disproportionation of uranium(V), 20: 40911

THORIUM
body burden in people of Brazil, 20: 40522(R) (NYO-3273-7)
content in meteorites, 20: 42064
criticality studies on seed-blanket reactor fuel containing, 20: 42609 (WAPD-T-1886)
preparation by electron-beam melting of magnesium–thorium sponge, 20: 41412(R) (IS-1500(Sect. M))
purification by electrotransport, 20: 41412(R) (IS-1500(Sect. M))
recovery from thorium ores by leaching with sulfuric acid, 20: 41033 (INR-678/IV/C)
separation from rare earths and uranium by chromatography using ammonium thiocyanate–nitric acid–TBP, 20: 41045
separation from uranium by solvent extraction using di- and monoisopentyl esters of methylphosphonic acid, 20: 41050
separation of protactinium from, by hydrolysis in nitric acid, 20: 41044
separation of silver from, by cation exchange chromatography, 20: 40847
separation of, from lanthanides by coprecipitation with zirconium iodate, 20: 40832
spectra of, interferometric measurements of lines in, 20: 40798 (ANL-

7209)
tensile properties of, effects of carbon traces on, 20: 41412(R) (IS-1500 (Sect. M))
THORIUM ALLOYS
Mg–Th, thorium production from sponge, using electron-beam melting, 20: 41412(R) (IS-1500(Sect. M))
Pu–Th–U, thermal conductivity measurements, 20: 42579(R) (ANL-7245, pp 29-47)
THORIUM CARBIDES
hydrolysis of, in heavy water, products and rate of, 20: 40905
THORIUM(IV) CHLORIDES
heat of fusion and transformation temperature of, 20: 41412(R) (IS-1500(Sect. M))
preparation by chlorination of thorium oxalates using carbon tetrachloride, 20: 41412(R) (IS-1500(Sect. M))
preparation by lanthanum oxide reactions with carbonyl chloride, 20: 41412(R) (IS-1500(Sect. M))
$ThCl_4$–Th, phase studies, 20: 41412(R) (IS-1500(Sect. M))
THORIUM(IV) FLUORIDES
spectra of fluorine-19 in, NMR, 20: 40931
THORIUM HYDRIDES
hydrogen diffusion in, 20: 42523(R) (IS-1500(Sect.P))
THORIUM ISOTOPES
separation by electromagnetic methods, 20: 41401(R) (ORNL-4006)
THORIUM ISOTOPES Th-227
decay of, alpha-gamma coincidence spectra of, 20: 41038(R) (MLM-1325, pp 9-62)
gamma spectra, 20: 41038(R) (MLM-1325, pp 9-62)
separation from francium-223 by ion exchange, 20: 41038(R) (MLM-1325, pp 9-62)
THORIUM ISOTOPES Th-228
bone content in sarcoma patients, 20: 41191(R) (HUX-3170-1)
content in human bones, 20: 40531 (A/AC.82/G/L-1045(Rev.1))
distribution in bone and soft tissue of radium dial painters, 20: 40621 (NYO-3086-5)
internal-conversion coefficients for 57.9-kev transition in, (E), 20: 42264
separation from uranium-232/233 by residue adsorption, 20: 41038(R) (MLM-1325, pp 9-62)
THORIUM ISOTOPES Th-229
separation from uranium-232/233 by residue adsorption, 20: 41038(R) (MLM-1325, pp 9-62)
separation from uranium-233 by cation exchange, 20: 41038(R) (MLM-1325, pp 9-62)
THORIUM ISOTOPES Th-231
energy levels from alpha decay of uranium-235, (E), 20: 42152 (JEN-159-DF/I-49)
THORIUM ISOTOPES Th-234
separation from uranium-238 by anion exchange, 20: 41038(R) (MLM-1325, pp 9-62)
THORIUM ORES
thorium recovery from, by leaching with sulfuric acid, 20: 41033 (INR-678/IV/C)
THORIUM OXALATES
reactions with carbon tetrachloride for production of thorium tetrachloride, 20: 41412(R) (IS-1500(Sect. M))
THORIUM OXIDES
content in uranites, 20: 41173
THORIUM(IV) OXIDES
creep of polycrystalline at 1465°C, effects of stress on, 20: 41474
dysprosium ion ESR spectra of, 20: 42525 (ORNL-P-2466)
separation from rare earth ores, 20: 41059(P)
$CaO–ThO_2$, creep of polycrystalline at 1465°C, effects of stress on, 20: 41474
ThO_2–W, creep-rupture properties, 20: 41456 (ORNL-3992)
Th–ThO_2, electric and tensile properties of sintered-compact extrusions of, using submicron thoria, 20: 41429(R) (USBM-RC-1249)
Th–ThO_2, electric and mechanical properties of thoria-dispersion-strengthened, 20: 41462(R) (USBM-RC-1245)
Th–ThO_2, properties of compacted dispersions of, using micron-size thoria, 20: 41429(R) (USBM-RC-1249)
THORIUM SYSTEMS
$ThCl_4$–Th, phase studies, 20: 41412(R) (IS-1500(Sect. M))
Th–ThO_2, electric and tensile properties of sintered-compact extrusions of, using submicron thoria, 20: 41429(R) (USBM-RC-1249)
Th–ThO_2, electric and mechanical properties of thoria-dispersion-strengthened, 20: 41462(R) (USBM-RC-1245)
Th–ThO_2, properties of compacted dispersions of, using micron-size thoria, 20: 41429(R) (USBM-RC-1249)
THRESHOLD DETECTORS
performance of neutron, in presence of x rays, 20: 41333
performance of neutron, in accelerator environment, 20: 41543 (RPP-R-2)
use for monitoring accelerator radiation, 20: 41276 (UCRL-16769)
THULIUM
determination in holmium oxides by neutron activation, 20: 40796(R) (IS-1500(Sect.C))
determination of, in uranium by neutron activation methods, 20: 40832
liquid, solubility of tantalum in, at high temperatures, 20: 41412(R) (IS-1500(Sect. M))
liquid, solubility of tungsten in, at high temperatures, 20: 41412(R) (IS-1500(Sect. M))
thermodynamic properties of, at 0°C to melting point, 20: 41412(R) (IS-1500(Sect. M))
THULIUM ALLOYS
Co–Tm, crystal structure of Laves phases in, 20: 41412(R) (IS-1500 (Sect. M))
Mg–Tm, thermodynamics of formation of intermetallic compounds, 20: 41412(R) (IS-1500(Sect. M))
THULIUM CHLORIDES
chemical properties of aqueous solutions of, 20: 40796(R) (IS-1500 (Sect.C))
density of aqueous solutions of, 20: 40796(R) (IS-1500(Sect.C))
THULIUM ISOTOPES Tm-169
nitrogen-15 reactions (N-15,xn) with, beta decay of osmium-180 from, (E), 20: 42284
THULIUM OXALATES
thermal decomposition of hydrates of, differential thermal analysis of products of, 20: 40900
THULIUM OXIDES
$B_2O_3–Tm_2O_3$, liquid immiscibility in, 20: 40910
THYMIDINE
effects of tritiated, on Chinese hamster cells, aberrant, 20: 40628(R) (ORNL-3922, pp 89-93)
effects of tritiated, on hybrid development in frogs, 20: 40535(R) (ORNL-3922, pp 128-35)
effects of tritium-labeled on hamster chromosomes, 20: 40686
effects on pyrimidine synthesis in *Vicia faba*, 20: 40581(R) (ORNL-3922, pp 50-1)
radiation effects on metabolism in mouse thyroid cell nuclei, 20: 40616(R) (NYO-901-54, pp 48-50)
radiation effects on uptake of tritium-labeled, by chick fibroblasts and myoblasts during mitosis, 20: 40588
synthesis in Amblystoma iris epithelium, effects of lens removal on, 20: 40499(R) (ORNL-3922, pp 69-79)
tritium-labeled, use in bone marrow cell proliferation studies, 20: 40722
use of high-specific-activity tritium-labeled, for leukemia therapy, 20: 40743 (BNL-9374)
use of tritiated in labeling intestinal mucosa, 20: 40607 (BNL-10518)
use of tritiated, for generation time studies on lymph cells, 20: 40663
use of 5-^{125}I-2′-deoxyuridine as analogue for autoradiography, 20: 40666
THYMINE
dimerization and monomerization of, in presence of proflavine, 20: 40504(R) (ORNL-3922, pp 146-60)
effects of deprivation of, on *Escherichia coli*, biological, 20: 40618(R) (NYO-2740-3, pp 166-215)
free radicals of, electron spin resonance studies, 20: 40594
metabolism in *Escherichia coli*, tracer study, 20: 40620 (NYO-2804-9)
phage transfer of dimers of, from parent to progeny, 20: 40504(R) (ORNL-3922, pp 146-60)
radioinduced dimerization of, effects of temperature on uv, 20: 40504(R) (ORNL-3922, pp 146-60)
ratio to adenine in potato tuber DNA, effects of radiotoxins on, 20: 40562
THYMUS GLAND
effects on estradiol action in irradiated and newborn mice, 20: 40577
histones from, quantitative analysis, 20: 40534(R) (NYO-3621-1)
radiation-induced lymphoma in mice, 20: 40677
radiotherapy of, in leukemia, 20: 40720
recolonization in x-irradiated mice of, following lymphoid or myeloid transplants, 20: 40727
reparative effects of DNA from, on sperm of x-irradiated rat, 20: 40723
THYROID GLAND
effects of physiological state of, on survival of transplants of, use of scanning to measure, 20: 40516
gland radiodiagnosis using iodine-131 for diseases of, 20: 40756
iodine-131 content in humans in West Germany, 20: 40570
iodine-131 uptake by human, effects of potassium iodide on, 20: 40564
metabolism studies using technetium-99m and iodine-125, 20: 40547
morphological changes in, induced by iodine-131, 20: 40647
radiation effects on thymidine metabolism in cell nuclei of mouse, 20: 40616(R) (NYO-901-54, pp 48-50)
radiation effects on iodine-131 uptake by dog, x, 20: 40698
radioactivity of, analytical model for iodine-131, 20: 41192(R) (IDO-12053)
radiotherapy of carcinoma of, 20: 40758
radium-226 and lead-210 content in radium dial painters, 20: 40621 (NYO-3086-5)

scanning of, using iodide crystal Magnascanner and Anger's gamma camera, 20: 40751
use of pertechnetate in studying trapping mechanism of, 20: 40750
use of salivary iodine-131/plasma protein-bound iodine-131 as index of activity, 20: 40756
use of sodium pertechnetate for diagnosis of diseases of, 20: 40555

THYROID HORMONES
effects of exogenous, on iodine-131 uptake and serum protein-bound iodine levels in x-irradiated dogs, 20: 40698
reaction mechanisms of, on mammalian cells, 20: 40511 (UCRL-16776)

THYRONINE, TRIIODO-
effects on cultured mammalian cells, physiological, 20: 40511 (UCRL-16776)

THYROXINE
effects on cultured mammalian cells, physiological, 20: 40511 (UCRL-16776)

TIMING CIRCUITS
design and linearity of modular 100 Mc digital, 20: 41240
design and performance of phase-setting, for pulse analyzers and time-of-flight measurements, 20: 41241
design for HPRR operation, 20: 42683 (ORNL-TM-1559)
performance of zero crosser, minimum slowing time for, 20: 41246

TIN
determination in copper coins by neutron activation methods, 20: 40800 (CNAEM-35)
determination in plutonium by carrier distillation methods, spectrographic, 20: 40814 (RFP-664)
electric conductivity of liquid, 20: 41476
heat of fusion, 20: 41412(R) (IS-1500(Sect. M))
helium and hydrogen ion attenuation at 0.1 to 500 Mev, tables for, 20: 41619 (CEA-R-3042)
magnetoresistance of, 20: 42523(R) (IS-1500(Sect.P))
mechanical forces on superconducting, magnetic field effects on, (E), 20: 42134
photon reactions (γ,n) with, energy spectra from, (E), 20: 42165(R) (MIT-2098-251, pp 16-20)
preparation of single crystals of, 20: 41064(R) (IS-1500(Sect.E))
separation from other metals by reversed-phase chromatography, 20: 40796(R) (IS-1500(Sect.C))
superconducting r-f residual losses in, (E), 20: 42131
use of liquid, as cathode in electrolysis of LiCl–KCl–UCl_3 melt, 20: 40923

TIN ALLOYS
Bi–Cd–Pb–Sn, magnetic flux penetration in superconducting, (E), 20: 42132
Bi–Sn, distribution of tin in, 20: 41064(R) (IS-1500(Sect.E))
Bi–Sn, solidification of, effects of electric fields on, 20: 41412(R) (IS-1500(Sect. M))
Mg–Sn, Moessbauer measurements in, 20: 41637
Na–Sn, solubility in sodium halide melts, 20: 40796(R) (IS-1500(Sect.C))
Nb–Sn, magnetic flux penetration in superconducting, (E), 20: 42132
Pd–Sn, Moessbauer measurements in, 20: 41637

TIN HYDRIDES
radiation effects on, in krypton at 4.2°K, ESR of free radicals from gamma, 20: 40968

TIN ISOTOPES
proton reactions at 14.5 Mev, total cross sections for, (E), 20: 42162 (LA-DC-8075)
separation by electromagnetic methods, 20: 41401(R) (ORNL-4006)
separation of, preparation of tin sulfides for electromagnetic, 20: 41400 (ORNL-3301(Suppl.1))

TIN ISOTOPES Sn-120
proton elastic scattering at 30 Mev, optical-model analysis of, (T), 20: 42255
proton reactions at 30 Mev, optical-model analysis of total cross sections for, (T), 20: 42255

TIN ISOTOPES Sn-127
yields in proton fission of uranium at 170 Mev, 20: 42177

TIN ISOTOPES Sn-128
yields in proton fission of uranium at 170 Mev, 20: 42177

TIN ISOTOPES Sn-129
yields in proton fission of uranium at 170 Mev, 20: 42177

TIN ISOTOPES Sn-130
yields in proton fission of uranium at 170 Mev, 20: 42177

TIN SULFIDES
preparation and evaluation for electromagnetic separation of tin isotopes, 20: 41400 (ORNL-3301(Suppl.1))

TISSUE CULTURES
cell growth in, effects of thyroid hormones on, 20: 40511 (UCRL-16776)
development for chemical carcinogenesis studies, 20: 40632(R) (ORNL-3922, pp 175-91)
DNA polymerase activity in synchronized mammalian, treated with puromycin, 20: 40504(R) (ORNL-3922, pp 146-60)
growth in semisolid agar of mouse, infected with Rauscher leukemia virus, 20: 40502(R) (ORNL-3922, pp 115-27)
radiation effects on hamster and HeLa cells in, lethal, effects of calchicine on low-dose x, 20: 40618(R) (NYO-2740-3, pp 166-215)
radiation effects on animal cells in, biological, uv and x, 20: 40623(R) (ORNL-3922, pp 32-49)
radiation effects combined with trenimon on HeLa cell, γ, 20: 40704
radiation effects on reproductive capacity of human kidney, factors affecting particulate, 20: 40725
radiation effects on DNA synthesis in chick fibroblast and myoblast, x, 20: 40587
radioinduced chromosome aberrations in Chinese hamster cell, β, 20: 40628(R) (ORNL-3922, pp 89-93)
radioprotective effects of transplants of mouse lymphoid or myeloid, mechanism for x, 20: 40727

TISSUE HOMOGENATES
radiation effects on levels of reduced pyridine nucleotides in rat liver, x, 20: 40583
radiosensitivity effects on mouse marrow cells, x, 20: 40634 (ORNL-P-2312)

TISSUE TRANSPLANTS
mouse hybrid spleen cells as, in parental strain, induced immunological tolerance from, 20: 40651
radiation effects on rat immunity to tumor, electromagnetic, 20: 40661
radiation effects on hybrid mice grafted with skin of parent mice, 20: 40651
thyroid, use of technetium-99 to measure effectiveness of, 20: 40516
tolerance of hybrid mice to skin, from parents, 20: 40651
tumor immune response of mice after previous transplants and x-radiation cure, 20: 40643

TISSUES
analysis for alpha-emitting radioisotopes, 20: 41191(R) (HUX-3170-1)
cesium-137 and strontium-90 content in rice panicle, effects of irrigation on, 20: 40574
chromium-51 content in clam soft, 20: 40575
development of wheat parenchyma, effects of auxins on, 20: 40631(R) (ORNL-3922, pp 161-6)
distribution of radium-226, radium-228, lead-210, and thorium-228 in radium dial painters, 20: 40621 (NYO-3086-5)
effects of radioprotective drugs on damage induced by alkylating agents, 20: 40664
electron beam irradiation in mice, 20: 40767
extracts from irradiated potato, effects on DNA synthesis, 20: 40562
gamma reactions in, detection of secondary emission from, 20: 41321
histological examination of irradiated bull testicle, 20: 40610(R) (COO-895-9)
polonium-210 content in human soft, 20: 40531 (A/AC.82/G/L-1045 (Rev.1))
radiation injury of subcutaneous, following therapy, 20: 40659
radioprotective effects of parental, in mice, x, 20: 40718(R) (ORNL-3922, pp 99-105)
radium-226 content in human soft, 20: 40531 (A/AC.82/G/L-1045(Rev.1))
use of hyperbaric oxygen to increase radiosensitivity of, 20: 40721
use of well counting to determine fluorine-18 activity, 20: 40554
x-ray spectral distributions in, 20: 41322

TITANIUM
determination in plutonium by carrier distillation methods, spectrographic, 20: 40814 (RFP-664)
determination of, developments in resin spot tests for, 20: 40827
deuteron elastic scattering at 13.6 Mev, optical model analysis of, (T), 20: 42294
effects on oxidation resistance of refractory metal disilicides, 20: 41424
effects on reflectance of zirconium oxides, 20: 41486

TITANIUM ALLOYS
Cr–Ti–V, mechanical properties at high temperatures, 20: 42579(R) (ANL-7245, pp 29-47)
Fe–Ti, oxidation by carbon dioxide–monoxide mixtures at 900 to 1100°C, mechanisms of, 20: 41458(R) (TID-23268)
Mo–Ti, aging kinetics of, at 1300 to 1500°K, 20: 41466
Mo–Ti, preparation and properties of single crystals of, 20: 41481
Mo–Ti–Zr, phase studies of, isothermal sections at 1200°C in, 20: 41464
Nb–Ti, magnetic flux penetration in superconducting, (E), 20: 42132
Nb–Ti–V, radiation effects on mechanical properties up to 750°C, neutron, 20: 41506
Ni–Ti, crystal structure of equi-atomic, model of, 20: 41412(R) (IS-1500(Sect. M))
Pd–Ti, corrosion by hydrochloric acid, 20: 41039(R) (ORNL-3880)
Pu–Ti–U, development for LMFBR fuel, 20: 42651 (WASH-1065)
Pu–Ti–U, heat content measurement to 1150°C, 20: 42579(R) (ANL-7245, pp 29-47)
Ti–V, radiation effects on mechanical properties up to 750°C, neutron, 20: 41506

Ti–Zr, electric conductivity of, effects of temperature on, 20: 41457(R) (ORO-3291-3)
Ti–Zr, phase diagram for, 20: 41457(R) (ORO-3291-3)
TITANIUM BORIDES
interactions with gas flow in MHD generators, 20: 41738
TITANIUM CARBIDES
interactions with gas flow in MHD generators, 20: 41738
preparation and properties of cast, 20: 41429(R) (USBM-RC-1249)
yield stress of, effects of nonstoichiometric defects on, 20: 41475
TITANIUM ISOTOPES
proton reactions at 14.5 Mev, total cross sections for, (E), 20: 42162 (LA-DC-8075)
separation by electromagnetic methods, 20: 41401(R) (ORNL-4006)
TITANIUM ISOTOPES Ti-46
proton reactions (p,n) at 15.25 Mev, angular distributions for quasi-elastic, (E), 20: 42169(R) (UCRL-14744, pp 1-18)
TITANIUM ISOTOPES Ti-47
proton reactions (p,n) at 15.25 Mev, angular distributions for quasi-elastic, (E), 20: 42169(R) (UCRL-14744, pp 1-18)
TITANIUM ISOTOPES Ti-48
proton reactions (p,n) at 15.25 Mev, angular distributions for quasi-elastic, (E), 20: 42169(R) (UCRL-14744, pp 1-18)
TITANIUM ISOTOPES Ti-49
proton reactions (p,n) at 15.25 Mev, angular distributions for quasi-elastic, (E), 20: 42169(R) (UCRL-14744, pp 1-18)
TITANIUM ISOTOPES Ti-50
deuteron reactions (d,p) with, titanium-51 energy levels from, (T), 20: 42201
proton reactions (p,n) at 15.25 Mev, angular distributions for quasi-elastic, (E), 20: 42169(R) (UCRL-14744, pp 1-18)
triton reactions (t,p) with, titanium-52 production by, (E), 20: 42282
TITANIUM ISOTOPES Ti-51
energy-level structure of, calculations using shell model with configuration mixing, (T), 20: 42201
TITANIUM ISOTOPES Ti-52
production by titanium-50 (t,p) reactions, (E), 20: 42282
TITANIUM NITRIDES
analysis for nitrogen, comparison of hot extraction and Kjeldahl methods for, 20: 40820(T) (IS-Trans-37)
TITANIUM OXIDES
yield stress of, effects of nonstoichiometric defects on, 20: 41475
TITANIUM SULFIDES
crystal structure, 20: 40796(R) (IS-1500(Sect.C))
vaporization of, thermodynamics of, 20: 40796(R) (IS-1500(Sect.C))
TOBACCO
carcinogenic effects of polonium-210 atoms attached to, 20: 41191(R) (HUX-3170-1)
polonium-210 content in smoke from, effects on lung content of cigarette smokers, 20: 40531 (A/AC.82/G/L-1045(Rev.1))
radioinduced mutants for resistance to blue mold disease in, gamma, neutron, and x, 20: 40613 (N-66-18147)
TOKAI-MURA POWER REACTOR
waste processing facility for, 20: 42688
TOLUENE
radiolysis of, EPR studies of yields of stabilized charges in low-temperature, 20: 40962
SF_6–Toluene, radiolysis of, gaseous, mechanism and yields of products in gamma, 20: 40948(R) (COO-578-3-32)
TOLUENE, α,α,α-TRIFLUORO-
yields in gamma radiolysis of benzene–bromotrifluoromethane, mechanism of, 20: 40948(R) (COO-578-3-32)
TOMATOES
radioinduced mutations of, somatic conversion in x, 20: 40713
TOXINS
production of *Clostridium botulinum* Type E, in radiation processed sea foods, effects of sodium salt dip on, 20: 41384(R) (TID-22833)
radioprotective and anti-tumor effects of mixed bacterial, 20: 40736
use of endo-, as radioprotective agent, 20: 40732 (AD-636209)
TRACER TECHNIQUES
book: *Radioactive Isotopes in Chemical Research*, 20: 41027
design of, for detecting hidden explosives, 20: 41066(P)
research on, in Hungary, 20: 41386(T) (JPRS-36895)
review of stable-isotope, 20: 41380(T) (IFA-IS-36)
use for gas flow analysis, 20: 41381
use of tritium in, assessment of, 20: 41022
TRACER TECHNIQUES (BIOLOGY)
bone marrow cell proliferation studies using tritiated thymidine, 20: 40722
bone mineralization dynamics studies in fetal chickens, 20: 40558
use of pertechnetate-99 to measure survival of thyroid transplants, 20: 40516
TRACER TECHNIQUES (ENGINEERING)
development of, using krypton-85, 20: 41114
TRACER TECHNIQUES (GEOLOGY)
health physics problems in well logging, 20: 41216
TRACER TECHNIQUES (HYDROLOGY)
use for study of waste solution dispersion in soil, 20: 42687
TRACER TECHNIQUES (MEDICINE)
detection of hormonal response of tumors by use of phosphorus-32, 20: 40566
iodine determination in radioactive iodide samples, 20: 40553
TRACER TECHNIQUES (METEOROLOGY)
turbulence and molecular transport of snow, 20: 41150 (AECL-2576)
use of zinc sulfide tracer and aircraft detection system for, 20: 41188(R) (BNWL-235-1)
TRACER TECHNIQUES (OCEANOGRAPHY)
use of fallout fission products as tracers for, 20: 40546
TRADESCANTIA
radiation effects on chromosomes of, repair mechanisms, 20: 40609 (CONF-660418-1)
TRAMEX PROCESS
development, 20: 41039(R) (ORNL-3880)
TRANSDUCERS
design of Permalloy, for measuring median surfaces of magnetic fields in accelerators, 20: 41553
properties of terroelectric, 20: 41684
TRANSISTORS
properties of h-f, amplification and noise, 20: 41227(R) (ORNL-3875, pp 1-3)
properties of MOS-FET, 20: 41270(R) (ORNL-3875, pp 13-14)
TRANSITION METALS
crystal lattice vibrations in, inelastic neutron scattering measurements of, 20: 42573
TRANSURANIC ELEMENTS
nuclear surface structure of alpha-emitting, (T), 20: 42275
processing plant instrumentation and valves, 20: 41078(R) (ORNL-3875, pp 91-100)
production of, development of facility for, 20: 41039(R) (ORNL-3880)
TREES
beta activity from fallout on leaves of silver maple, horsechestnut, boxelder, and pine, 20: 40579
TRIETHYLAMINE
effects as catalyst on hydrogen-tritium exchange reactions between lactones and water, 20: 41017
effects on chromosome aberration induction in carcinoma and sarcoma cells, effects of nicotinamide on, 20: 40550
TRIOCTYLAMINE
diisoamyl phosphate–trioctylamine, solvent properties for uranium, mechanism of, 20: 41053
TRITIUM
concentration by thermal diffusion, 20: 41168
concentration in water, method for, 20: 40826
content in atmosphere and ground waters of San Joaquin Valley, 20: 41160
determination in environmental samples, 20: 40809 (NP-16235)
determination in water, method for, 20: 40826
deuteron reactions (d,n) with, design of neutron sources using low-voltage accelerators, 20: 42136 (AD-637457)
diffusion through plastic, 20: 41196 (LA-DC-7996)
effects of thymidine labeled with, on chromosomes, 20: 40686
effects on hybrid development in frogs, 20: 40535(R) (ORNL-3922, pp 128-35)
exchange between water and methane, 20: 41067(R) (ORNL-TM-1582)
exchange reactions with hydrogen between lactones and water, effects of triethylamine catalyst on, 20: 41017
incorporation in compounds, assessment of, 20: 41022
incorporation in pyridoxal-5′-phosphate, method for, 20: 41016
ionization of, by electron bombardment, 20: 40893
neutron elastic scattering at 14 Mev, differential cross sections for, (E), 20: 42373
photon reactions (γ,2n) with, wave functions for, 20: 42228
radiation effects on uptake of thymidine-incorporated, by chick fibroblasts and myoblasts during mitosis, x, 20: 40587
radiation hazards to laboratory personnel, 20: 41185 (AECL-2594)
subterranean water supply measurement, 20: 41167
thymidine-labeling with, use in bone marrow cell proliferation studies, 20: 40722
use in neutron generators, health problems of, 20: 41215
use of in determining body water content and turnover in deer and sheep, 20: 40541(R) (UCD-34P104-3)
use of thymidine labeled with high-specific-activity, for therapy of human leukemia, 20: 40743 (BNL-9374)
use of thymidine labeled with, for cytokinetic studies, 20: 40663
use to measure groundwater velocity, 20: 41160
TRITIUM IONS
reactions with butane at 3 to 6000 ev, (E), 20: 40938
TRITONS

attenuation by nuclei at 0.1 to 500 Mev, tables for, 20: 41619 (CEA-R-3042)
reactions (t,α_0) with boron-10, carbon-12, lithium-7, and oxygen-16 at 1.5 to 3.25 Mev, angular distributions for, (E), 20: 42398
reactions (t,d) with nuclei, calculations using distorted-wave theory, 20: 42250
reactions (t,n)2α with lithium-6, energy spectra of α particles from, (E), 20: 42349
reactions (t,pf) with plutonium-239 and -240, angular correlations in, (E), 20: 42161 (LA-DC-7878)
reactions (t,p) with titanium-50, titanium-52 production by, (E), 20: 42282
reactions (t,p) with nuclei, angular distributions from, (T), 20: 42290
reactions with nuclei, approximate relations for strengths and shapes of optical potentials for, 20: 42280
use in activation analysis, review on, 20: 40806 (NAS-NS-3110)

TRYPSIN
electron spin resonance signals from irradiated, 20: 40595
radioinduced inactivation of dry, 20: 40596
radioinduced inactivation of, electron spin resonance studies, 20: 40598
sensitivity of *Arbacia* extract to, 20: 40543

TRYPTOPHAN
determination in tissues, 20: 40533(R) (NYO-901-54, pp 16-19)
metabolism of, enzyme reactions for, 20: 40533(R) (NYO-901-54, pp 16-19)

TUBES
corrosion of stainless steel, by high-temperature liquid sodium, 20: 41419(R) (GMAD-3643-5)
coupling for, design of, 20: 41100(P)
fabrication of Zircaloy-2 and zirconium, by hot drawing, 20: 41432
production of aluminum–uranium, by extrusion, 20: 41412(R) (IS-1500 (Sect. M))

TUMORS
antioxidant and prooxidant activity in ascites, 20: 40642
brain, immune response of mice to transplantation after cure of prior transplants, 20: 40643
detection with scintillation camera, 20: 40747 (UCRL-14866)
effects of hepatoma, on biochemical characteristics of trout, 20: 40632(R) (ORNL-3922, pp 175-91)
effects of malignant, on protein synthesis in trout liver, 20: 40632(R) (ORNL-3922, pp 175-91)
effects of radioprotective drugs on damage induced by alkylating agents, 20: 40664
enzyme levels in Reuber hepatoma, hormonal control *in vitro*, 20: 40506(R) (ORNL-3922, pp 168-73)
enzyme reactions in, 20: 40533(R) (NYO-901-54(p.16-19))
induced in rabbits by Shope papilloma virus, mechanism for, 20: 40632(R) (ORNL-3922, pp 175-91)
location of metastases from, using strontium-85 scanning, 20: 40794
modification of radiosensitivity of, by colchicine, 20: 40763
pathology of bladder, breast, and uterine, in man, and effects of radiotherapy, surgery, and other treatments on metastastic growth, 20: 40745(R) (NYO-901-54, pp 29-47)
phosphorus-32 uptake by, as indication of hormonal response of, 20: 40566
prognosis of bladder, breast, and uterine, tests for, 20: 40745(R) (NYO-901-54, pp 29-47)
radiation effects on peritoneal lymphocysts, pre-surgery, 20: 40783
radiation effects on lymphoma, incubated with phytohemagglutinin, 20: 40588
radiation effects on mouse liver or lymphoid, incubated with phytohemagglutinin, x, 20: 40588
radiation-induced lymphoma in mice, 20: 40677
radiocalcium kinetic studies before and after removal of parathyroid, 20: 40552
radiosensitivity of mouse, effects of uracil on x, 20: 40668
radiotherapy of brain, laser, 20: 40776
radiotherapy of breast, effects on metastases of x, 20: 40793
radiotherapy of head and neck, dosimetry for x, 20: 41210
radiotherapy of head and neck, dosimetry for, 20: 41210
radiotherapy of lung, using γ radiation, 20: 40760
radiotherapy of lymphogranulomatosis, survival following, 20: 40784
radiotherapy of melanoma, laser, 20: 40776
therapy of uterine, effectiveness of combination of drugs, radiotherapy, and surgery, 20: 40778

TUNGSTEN
cesium atom and ion emission from cesium-adsorbed cathodes of, work functions for, 20: 41681 (UCRL-11857)
creep-rupture properties of powder-metallurgy and thermochemically deposited, 20: 41456 (ORNL-3992)
crystal lattice vibrations in, inelastic neutron scattering measurements of, 20: 42573
deposition from carbonyl decomposition, temperature effects on, 20: 41468
desorption of inert gases from, following ion bombardment, 20: 41463
determination in americium and plutonium by spark-source mass spectrography, 20: 40816 (RFP-699)
determination in iron, activation, 20: 40818 (UJV-1368)
determination in rare earths, spectrophotometric, 20: 40796(R) (IS-1500 (Sect.C))
electron emission from single crystals of, work functions for, 20: 41681 (UCRL-11857)
emissivity at 1200 to 2600°K, integral radiant, (T), 20: 41525
performance as adsorption cesium reservoirs, 20: 41680(R) (NYO-3642-2)
photon reactions (y,n) with, energy spectra from, (E), 20: 42165(R) (MIT-2098-251, pp 16-20)
preparation and properties of single crystals of, 20: 41481
radiation damage in, effects of annealing on fast neutron, 20: 42551
scattering on beryllium–copper alloy at 5 kev, secondary electrons from, 20: 41620 (NIJS-R-471)
separation from molybdenum, niobium, and tantalum by solvent extraction using methyl isobutyl ketone, 20: 40796(R) (IS-1500(Sect.C))
solubility in liquid lanthanides at high temperatures, 20: 41412(R) (IS-1500(Sect. M))

TUNGSTEN ALLOYS
Mo–Re–W, recovery of scrap, methods for, 20: 41429(R) (USBM-RC-1249)
Mo–W, preparation and properties of single crystals of, 20: 41481
Nb–W, preparation and properties of single crystals of, 20: 41481
Re–W, analysis for total composition of powdered, results of, 20: 41429(R) (USBM-RC-1249)
Re–W, content of carbon, nitrogen, and oxygen in arc-melted ingots of, 20: 41429(R) (USBM-RC-1249)
Re–W, creep rates of, 20: 41396(R) (STL-517-0042)
Re–W, extrusion and properties of tubular, 20: 41429(R) (USBM-RC-1249)
Re–W, mechanical properties of arc-melted and powder-metallurgy processed, 20: 41429(R) (USBM-RC-1249)

TUNGSTEN CARBIDES
plasticity of, effects of microstructure on, 20: 41454 (NYO-2394-22)

TUNGSTEN CARBONYLS
thermal decomposition of, properties of deposits from, 20: 41468

TUNGSTEN CHLORIDES
preparation, 20: 40796(R) (IS-1500(Sect.C))

TUNGSTEN FLUORIDES
fluorine-19 NMR and spin-lattice relaxation in, 20: 40892

TUNGSTEN ISOTOPES
neutron capture cross section at 30 to 170 kev, (E), 20: 42293

TUNGSTEN ISOTOPES W-182
neutron capture cross section at 30 to 170 kev, (E), 20: 42293
x-ray spectra from μ^- mesic atoms of, (E/T), 20: 42310

TUNGSTEN ISOTOPES W-183
energy-level transitions from Coulomb excitation by alpha particles and lithium ions, (E), 20: 42186
neutron capture cross section at 30 to 170 kev, (E), 20: 42293

TUNGSTEN ISOTOPES W-184
neutron capture cross section at 30 to 170 kev, (E), 20: 42293
neutron reactions (n,2n) at 14.8 Mev, activation cross section for, 20: 42207
x-ray spectra from μ^- mesic atoms of, (E/T), 20: 42310

TUNGSTEN ISOTOPES W-186
neutron capture cross section at 30 to 170 kev, (E), 20: 42293
neutron reactions (n,2n) at 14.8 Mev, activation cross section for, 20: 42207
x-ray spectra from μ^- mesic atoms of, (E/T), 20: 42310

TUNGSTEN SILICIDES
oxidation at reduced pressures, effects of additives on, 20: 41424

TUNGSTEN SYSTEMS
C–Hf–W, creep-rupture properties of Sylvania A, 20: 41456 (ORNL-3992)
ThO_2–W, creep-rupture properties, 20: 41456 (ORNL-3992)
W–UO_2, electric conductivity of cermet, effects of microstructure on, 20: 41478

TURBINE BLADES
temperature mapping of, using krypton-85, 20: 41114

TURBINES
closed-cycle gas, evaluation for nuclear power plants, 20: 42654
closed-cycle gas, working media for, 20: 42654
cost analysis of, for sodium-steam system, 20: 42632 (NAA-SR-12060)
design of MHD, 20: 41749
testing of, for KRB reactor, 20: 42638(R) (TID-23299)

U

ULTRASONICS
use for cleaning biologically contaminated surfaces, tracer techniques for testing efficiency of, 20: 41218
use in boiling detection in liquid metals, 20: 41225(R) (NYO-3622-4)

ULTRAVIOLET RADIATION
effect on oxidative phosphorylation in bacteria, 20: 40571
effects on ascites tumor antioxidant activity, 20: 40642
effects on bromouracil-substituted DNA of phage T3, 20: 40504(R) (ORNL-3922, pp 146-60)
effects on chloroquine phosphate, spectral studies on uv, 20: 40954
effects on chromosome transfer in *E. coli* Hfr, mechanisms for, 20: 40629(R) (ORNL-3922, pp 94-8)
effects on chromosomes, repair mechanisms for, 20: 40609 (CONF-660418-1)
effects on deoxyribonucleic acid, electron spin resonance studies of, 20: 40594
effects on developing *Escherichia coli*-phage complexes, 20: 40618(R) (NYO-2740-3, pp 166-215)
effects on differentiating bacterial spores, repair of, 20: 40504(R) (ORNL-3922, pp 146-60)
effects on *E. coli*, genetics and physiology of mutagenic, 20: 40629(R) (ORNL-3922, pp 94-8)
effects on *E. coli* DNA, effects of benzopyrene on, 20: 40632(R) (ORNL-3922, pp 175-91)
effects on *Escherichia coli*, effects of nutrients on biological, 20: 40618(R) (NYO-2740-3, pp 166-215)
effects on free radical induction in frozen ammonia and hydrogen peroxide solutions, ESR spectral studies on, 20: 41001
effects on hamster cells intissue culture, biological, 20: 40623(R) (ORNL-3922, pp 32-49)
effects on *Hemophilus influenzae*, 20: 40623(R) (ORNL-3922, pp 32-49)
effects on human leukocytes, 20: 40581(R) (ORNL-3922, pp 50-1)
effects on human skin, review of, 20: 40696
effects on lipid peroxidation in mouse liver, 20: 40642
effects on Neurospora, mechanism for photoreactivation of, 20: 40629(R) (ORNL-3922, pp 94-8)
effects on Neurospora, photoreactivation of mutagenic, 20: 40624(R) (ORNL-3922, pp 52-8)
effects on oto-rhino-laryngeal tumors, 20: 40782
effects on phage T3, role of *E. coli* B/r in repair of, 20: 40504(R) (ORNL-3922, pp 146-60)
effects on tetraamminediaitritocobalt nitrate, triamminecobalt trinitrate, and sodium nitritocobaltate, mechanism of, 20: 41003
effects on thymine, effects of temperature on dimerization, 20: 40504(R) (ORNL-3922, pp 146-60)
effects on uranyl salts, binary centers from, 20: 42537(T)
photoreactivation of damage induced by, in sea urchin eggs, 20: 40543
sensitivity to, comparison of *Bacillus subtilis* bacteriophage SP02 and its infectious DNA, 20: 40676

UNDERGROUND EXPLOSIONS
air-blast wave amplitudes from, 20: 41158
detection and identification of, seismometers for, 20: 41155
detection of, seismological equipment for, 20: 41152
effects on fracture permeability of granitic rock mass, 20: 41164
radioactivity induced by, effect of trace element on, 20: 41068 (PNE-5006)
seismic measurements on BUFF event, 20: 41149 (AD-632956)
seismic waves from Haymaker, Hardhat, and Shoal, 20: 41169
spalling by, multiple subsurface, 20: 41126
timing and firing instrumentation for, 20: 41070 (VUF-3021)
use in water supply management, 20: 41073

URACIL
compounds in frog eggs of, properties of, 20: 40535(R) (ORNL-3922, pp 128-35)
radiosensitizing effects on mouse tumors, x, 20: 40668

URACIL, 5-FLUORO-
radioprotective effect on damage induced by alkylating agents, 20: 40664

URANINITES
composition of, in nepheline syenites of Tuva, 20: 41173
detection in nepheline syenites in Tuva, 20: 41173

URANIUM
analysis for iron and nickel by atomic absorption spectrophotometry, 20: 40815 (RFP-698)
analysis for trace materials, comparison of methods for, 20: 40850
analysis of, for lanthanides by neutron activation methods, 20: 40832
burnup analysis of, computer program for, 20: 42608(R) (GEAP-5124)
content in meteorites, 20: 42064
content in meteoric feldspar and pyropene, 20: 41162
content in phosphorites, weathering effect on, 20: 41174
content in sea water from Indian Ocean, uptake by marine organisms, 20: 40572
content in Toluca iron meteorite, 20: 42062
determination in aqueous and TBP solutions, refractometric, 20: 40804 (KR-108)
determination in uranium trioxide, gravimetric, 20: 40802 (HW-65402 (Rev.1))
determination of, developments in resin spot tests for, 20: 40827
determination using bis-2-pyridyl glycol, effects of pH on gravimetric, 20: 40849
dissolution and purification of irradiated fuel of, for mass spectrometry, 20: 41042 (PG-Report-722)
distribution in phosphorites, 20: 41174
gamma scattering by electrons of, at 662 kev, (E), 20: 41625
helium and hydrogen ion attenuation at 0.1 to 500 Mev, tables for, 20: 41619 (CEA-R-3042)
isotopic composition of natural, 20: 41176
microstructure of, effects of thermal cycling on, 20: 41470
production by oxide reduction using carbon, kinetics of, 20: 41411 (IS-1379)
proton fission in, product yields at 170 Mev, 20: 42177
purification of irradiated, 20: 41041 (PG-Report-698)
radiation effects on alpha-, at 11 to 7°K, electron, 20: 41499
recovery from low enrichment fuel, processes for, 20: 42579(R) (ANL-7245, pp 29-47)
separation by solvent extraction using diisoamyl phosphate–trioctylamine, mechanism of, 20: 41053
separation from fission products and plutonium, method for, 20: 41042 (PG-Report-722)
separation from irradiated fuels, 20: 41041 (PG-Report-698)
separation from metal scraps, electrolytic process for, 20: 41036 (MCW-1494)
separation from ores by chlorination and fractional condensation of vapor, 20: 41048
separation from other metals by fixation of acetate on anion-exchange resins, 20: 41030 (CEA-R-2994)
separation from rare earths and thorium by chromatography using ammonium thiocyanate–nitric acid–TBP, 20: 41045
separation from thorium by solvent extraction using di- and monoisopentyl esters of methylphosphonic acid, 20: 41050
separation of silver from, by cation exchange chromatography, 20: 40847
thermal stability of fission products of, in monocrystalline muscovite during chemical etching, 20: 40889
use of, for determining protein structures, 20: 40632(R) (ORNL-3922, pp 175-91)
cements–depleted uranium, fabrication of structural members using, 20: 41435(P)

URANIUM ALLOYS
Cr–U, corrosive effects of liquid, on tantalum and yttrium, 20: 41064(R) (IS-1500(Sect.E))
Cr–U, melting point of, effects of impurities on eutectic, 20: 41064(R) (IS-1500(Sect.E))
Mn–U, corrosive effects of liquid, on tantalum and yttrium, 20: 41064(R) (IS-1500(Sect.E))
Mn–U, melting point of, effects of impurities on eutectic, 20: 41064(R) (IS-1500(Sect.E))
Nb–U, production of niobium-base, method for, 20: 41412(R) (IS-1500 (Sect. M))
Pu–Th–U, thermal conductivity measurements, 20: 42579(R) (ANL-7245, pp 29-47)
Pu–Ti–U, development for LMFBR fuel, 20: 42651 (WASH-1065)
Pu–Ti–U, heat content measurement to 1150°C, 20: 42579(R) (ANL-7245, pp 29-47)
Pu–U–Zr, development for LMFBR fuel, 20: 42651 (WASH-1065)
Pu–U–Zr, performance as FTR fuel, 20: 42676 (BNWL-281)

URANIUM BORIDES
development of, for burnable poison fuels, 20: 42670(R) (ANL-7245, pp 48-59)

URANIUM CARBIDES
hydrolysis of, in heavy water, products and rate of, 20: 40905
polarization of electrode of, in eutectic melt of LiCl–KCl–UCl_3, anodic, 20: 40923
precipitation of, during carbon reduction of uranium oxides, 20: 41411 (IS-1379)
reactions with carbon dioxide, nitrogen, oxygen, and water vapor, effects of hydrogen on, 20: 40870 (NAA-SR-Memo-7310)
stabilization of mono-, by arc melting in argon–nitrogen, 20: 41431
PuC–UC, development for LMFBR fuel, 20: 42651 (WASH-1065)
PuC–UC, performance as FTR fuel, 20: 42676 (BNWL-281)

URANIUM CARBONITRIDES
preparation of single-phase, 20: 41431

URANIUM(III) CHLORIDES
activity of, in eutectic melt of LiCl–KCl, EMF measurements of, 20: 40922
thermochemical properties of, 20: 40922
LiCl–KCl–UCl_3, polarization of uranium carbide electrode in melts of, anodic, 20: 40923

URANIUM COMPLEXES
with benzohydroxamic acid, stability of ionic, 20: 40903
with heterocyclicly substituted formazan, 20: 40880

with tri-*n*-butylphosphine oxide, preparation and properties of, effects of acid ligands on, 20: 40885
with 2-hydroxy-3-naphthoic acid, preparation and properties of, 20: 40898

URANIUM COMPOUNDS
analysis for fluoride in presence of, electrolytic, 20: 40840

URANIUM DEPOSITS
geologic structure of hydrothermal, 20: 41175

URANIUM(IV) FLUORIDES
preparation by reaction of hydrofluoric acid with uranium dioxide, fluidized-bed process for, 20: 40935(P)
spectra of fluorine-19 in, NMR, 20: 40931
BaF_2–LiF–UF_4, uses as electrolyte in electrolytic recovery of scrap uranium metal, 20: 41036 (MCW-1494)

URANIUM(VI) FLUORIDES
fluorine-19 NMR and spin-lattice relaxation in, 20: 40892
pressure standard for, micron-region, 20: 41252

URANIUM IONS
magnetic moment in uranium monophosphide, (E), 20: 42560

URANIUM ISOTOPES
determination of composition of, by measuring alpha radiation absorption, 20: 40857
electromagnetic separation of, shim design for, 20: 41405
separation by electromagnetic methods, 20: 41401(R) (ORNL-4006)

URANIUM ISOTOPES U-228
preparation of, for oxygen determination, cathodic etching method for, 20: 40817 (UCRL-14959)

URANIUM ISOTOPES U-232
separation from thorium-228/229 by residue adsorption, 20: 41038(R) (MLM-1325, pp 9-62)

URANIUM ISOTOPES U-233
criticality studies on seed-blanket reactor fuel containing, 20: 42609 (WAPD-T-1886)
gamma spectra, 20: 41038(R) (MLM-1325, pp 9-62)
neutron fission at 0.08 to 1.5 Mev, energy dependence of fission-fragment angular distribution in, (E), 20: 42171(T) (LA-tr-66-41)
neutron fission of, cesium-137 yields in thermal, 20: 42176
separation from thorium-228/229 by residue adsorption, 20: 41038(R) (MLM-1325, pp 9-62)
separation from thorium-229 by cation exchange, 20: 41038(R) (MLM-1325, pp 9-62)
storage facility for liquid, instrumentation for, 20: 41078(R) (ORNL-3875, pp 91-100)

URANIUM ISOTOPES U-234
determination of ratio with uranium-238 in samples by measuring alpha radiation absorption, 20: 40857
separation from aged plutonium-238, methods for, 20: 41038(R) (MLM-1325, pp 9-62)

URANIUM ISOTOPES U-235
alpha decay of, thorium-231 energy levels from, (E), 20: 42152 (JEN-159-DF/I-49)
decay constant and abundance ratio, 20: 41176
decay constant of, lead-207/-206 ratio determination of, 20: 41176
determination in uranium trioxide by mass spectrometry, 20: 40802 (HW-65402(Rev.1))
determination of, in irradiated fuel elements by alpha spectroscopy, nondestructive, 20: 40808(R) (NP-16212)
neutron fission at 0.08 to 1.5 Mev, energy dependence of fission-fragment angular distribution in, 20: 42171(T) (LA-tr-66-41)
neutron fission at 5, 6, and 7 Mev, mass dependence of total fission-fragment energy in, (E), 20: 42297
neutron fission of, cesium-137 yields in thermal, 20: 42176
neutron fission of, cesium-132, -134, and -136 and rubidium-86 yields in thermal, 20: 42178
neutron fission of, gamma spectra and x-ray spectra of fission products from, (E), 20: 42170 (UCRL-70045)
neutron fission of, mass dependence of total fission-fragment energy in thermal, (E), 20: 42297
neutron fission of, measurement of delayed neutrons from, 20: 41157
neutron fission of, neutron emission in, 20: 42325
neutron fission of, search for three- and four-body neutron bound states in, (E), 20: 42298

URANIUM ISOTOPES U-238
alpha elastic scattering at 16 and 24 Mev, quadrupole effect in, (T), 20: 42235
alpha fission at 23 to 115 Mev, fragment angular distributions in, (E), 20: 42267
alpha fission at 20 to 40 Mev, ternary, (E), 20: 42273
carbon-12 reactions (C-12,4n) with, production of isomeric californium-246 in, 20: 42159 (JINR-P-2841)
decay constant and abundance ratio, 20: 41176
determination of ratio with uranium-234 in samples by measuring alpha radiation absorption, 20: 40857
helium-3 reactions (He-3,f) at 20 to 40 Mev, ternary fission in, (E), 20: 42273
separation from thorium-234 by anion exchange, 20: 41038(R) (MLM-1325, pp 9-62)
x-ray spectra from μ^- mesic atoms of, (E/T), 20: 42310

URANIUM MINERALS
occurrence of secondary, in Sweden, 20: 41172

URANIUM NITRIDES
enthalpy and thermal capacity of, at 0 to 1200°C, 20: 40865 (CNLM-4461)
thermodynamic properties of, at 11 to 320°K, 20: 40921

URANIUM ORES
chlorination of Japanese, fractional condensation of chloride vapor from, 20: 41048
presence of quartz-pitchblende-arsenic, in hydrothermal deposits of, 20: 41175

URANIUM OXIDES
chemical composition and particle size of 22, effects on lung deposition, 20: 41204 (Y-1544-A)
reduction by carbon, kinetics of, 20: 41411 (IS-1379)

URANIUM(IV) OXIDES
analysis for burnable poisons, radiometric, 20: 41112 (IITRI-578P11-54)
diffusion of actinides in, mechanism of, 20: 41484
diffusion of plutonium in, methods for measuring, 20: 41484
energy levels of sintered, photocurrent spectra of, (E), 20: 42532
mechanical properties at high temperatures, 20: 42579(R) (ANL-7245, pp 29-47)
melting points of hypostoichiometric, 20: 41441 (BNWL-224)
properties of, for WR-1 fuel, 20: 42669 (AECL-2553)
reactions with hydrofluoric acid to prepare uranium(IV) fluoride, fluidized-bed process for, 20: 40935(P)
reduction to metal by carbothermic reactions, 20: 41412(R) (IS-1500 (Sect. M))
thermal conductivity of, measurement at high temperatures, 20: 41479
trapped carriers in, thermal release time of, (E), 20: 42532
vaporization mechanisms, 20: 41064(R) (IS-1500(Sect.E))
Al–UO_2, extrusion of, for tube production, 20: 41412(R) (IS-1500 (Sect. M))
C–U–UO_2, phase studies, 20: 41412(R) (IS-1500(Sect. M))
Mo–UO_2, electric conductivity of cermet, effects of microstructure on, 20: 41478
PuO_2–UO_2, development for LMFBR fuel, 20: 42651 (WASH-1065)
PuO_2–UO_2, fission product and plutonium migration in, 20: 42625 (GEAP-4466)
PuO_2–UO_2, performance as FTR fuel, 20: 42676 (BNWL-281)
PuO_2–UO_2, thermal properties, 20: 42612
W–UO_2, electric conductivity of cermet, effects of microstructure on, 20: 41478

URANIUM(IV-VI) OXIDES
analysis for impurities, effects of graphite electrode grade on carrier-distillation spectroscopic, 20: 40807 (NLCO-976)
deposition in lungs of particulates of, 20: 41204 (Y-1544-A)
preparation, 20: 41041 (PG-Report-698)
properties of, 20: 41204 (Y-1544-A)
yields from uranyl nitrate solutions, gravimetric estimation of, 20: 40849

URANIUM(V) OXIDES
disproportionation of, effects of lactate, thiocyanate, sulfate, oxalic acid, and fluoride on, 20: 40911
spectra of, infrared absorption, 20: 40916

URANIUM(VI) OXIDES
particle size determination on powders of, 20: 40802 (HW-65402(Rev.1))
preparation and structure of single crystals of gamma-, 20: 40907
production of, specification analyses for, 20: 40802 (HW-65402(Rev.1))
thermal decomposition of alpha-, kinetics of, 20: 40899

URANIUM PEROXIDES
crystal structure of tetravalent ionic UO_3, 20: 40881

URANIUM PHOSPHIDES
magnetic structure of, neutron-diffraction study of, (E), 20: 42560
UP–US, preparation and phase studies of, 20: 40936(P)

URANIUM SULFIDES
composition of, effect of arsenic on, 20: 41175
UP–US, preparation and phase studies of, 20: 40936(P)

URANIUM SYSTEMS
C–N–O–U, preparation and high-temperature properties of stoichiometric, 20: 41429(R) (USBM-RC-1249)
C–O–U, preparation and properties of oxycarbide phases of, 20: 41429(R) (USBM-RC-1249)
C–U–UO_2, phase studies, 20: 41412(R) (IS-1500(Sect. M))
O–S–U, phase studies, 20: 42579(R) (ANL-7245, pp 29-47)

URANOTHORITES
lead-207/-206 ratio in, 20: 41176

URANYL CARBONATES
deposition in Stripa iron ore mines in Sweden, 20: 41172

URANYL NITRATES
hydrolysis of hexahydrate of, 20: 41038(R) (MLM-1325, pp 9-62)
properties and spectra of, in aqueous cyclohexanone solutions, effects of temperature on, 20: 40927
radioinduced binary centers in, uv, 20: 42537(T)
HNO_3–$UO_2(NO_3)_2$–H_2O, refractive index measurements on, 20: 40804 (KR-108)
URANYL OXALATES
dissolution by ion exchange resins, 20: 40917
URANYL SULFATES
fluorescence lifetime of, effects of deuteration on, 20: 40887
properties and spectra of, in aqueous sulfuric acid solutions, effects of temperature on, 20: 40927
radioinduced binary centers in, uv, 20: 42537(T)
UREA
use in analytical electrophoresis of polyacrylamide gels, 20: 40534 (NYO-3621-1)
UREA, THIO-
radioprotective effect on damage induced by alkylating agents, 20: 40664
URETHANS
phenyl ethyl, effects on plants, genetic, effects of exogenous factors on, 20: 40709
URIDINE, 5-BROMO-2'-DEOXY-
radiosensitivity effects on human kidney cells, particulate, 20: 40725
URIDINE, 5-IODO-2'-DEOXY-
radiosensitivity effects on human kidney cells, particulate, 20: 40725
URIDINES, 2'-DEOXY-
use of iodine-125-labeled as thymidine analogue for autoradiography, 20: 40666
URINARY TRACT
injury to, following radiotherapy of uterine carcinoma, 20: 40703
URINE
determination of fluorine-18 activity after oral and intravenous administration in dogs, 20: 40554
glucose levels in, following iodine-131 therapy for diabetes-hyperthyroidism, 20: 40790
iron-59 and water-content in rats, 20: 40561
UTERUS
radiotherapy of cancer of, system for dosimetry of intracavitary radium, 20: 41377
radiotherapy of cancer of, cutaneous eruptions following, 20: 40679
radiotherapy of carcinomas of, urinary system injuries following, 20: 40703
radiotherapy of cancer of, using x rays and gamma rays, 20: 40768
radiotherapy of carcinoma, 20: 40769
radiotherapy of carcinoma of, radium and x, 20: 40772
therapy of cancer of, using combination of drugs, radiotherapy, and surgery, 20: 40778

V

VACUUM SYSTEMS
design for Ogra-II, 20: 42421(T) (NP-tr-1396)
materials for high-temperature, development and testing of, 20: 41440(R) (ALO-3632-4)
motion transfer in, device for, 20: 41125 (SGAE-PH-41/1966)
VAGINA
epithelial studies in mouse, autoradiographic method for, 20: 40502(R) (ORNL-3922, pp 115-27)
radioinduced cornification of cells in rat, x, 20: 40673
radiotherapy of cancer of, system for dosimetry of intracavitary radium, 20: 41377
radiotherapy of cancer of, cutaneous eruptions following, 20: 40679
radiotherapy of cancer of, using betatron, 20: 40768
VALENCY
effects on chromium-51 uptake by clams, 20: 40575
VALLECITOS SUPERHEAT REACTOR
fuel clusters for, design and fabrication of Mark III, 20: 42627 (GEAP-5051)
VAN DE GRAAFF ACCELERATORS
description of tandem, 20: 41581(P)
development of 5-Mv, 20: 41541(R) (ORNL-3875, pp 159-63)
VANADIUM
crystal lattice vibrations in, inelastic neutron scattering measurements of, 20: 42573
determination in plutonium by carrier distillation methods, spectrographic, 20: 40814 (RFP-664)
effects on oxidation resistance of refractory metal disilicides, 20: 41424
embrittlement by hydrogen, mechanisms of, 20: 41412(R) (IS-1500 (Sect. M))
helium and hydrogen ion attenuation at 0.1 to 500 Mev, tables for, 20: 41619 (CEA-R-3042)
preparation and properties of single crystals of, 20: 41481
preparation by reduction of pentoxide of, using aluminum and carbon, 20: 41412(R) (IS-1500(Sect. M))
purification by hydrogen reactions, 20: 41412(R) (IS-1500(Sect. M))
thermal capacity of normal and superconducting, at 0.5 to 5.4°K, 20: 42115
thermal capacity of mixed state in, at 0.5 and 5.4°K, 20: 42116
VANADIUM ALLOYS
Cr–Ti–V, mechanical properties at high temperatures, 20: 42579(R) (ANL-7245, pp 29-47)
Ga–V, preparation of V_3Ga, 20: 42534
Ga–V, superconductivity of V_3Ga in 30 kG fields, 20: 42534
Nb–Ti–V, radiation effects on mechanical properties up to 750°C, neutron, 20: 41506
Ti–V, radiation effects on mechanical properties up to 750°C, neutron, 20: 41506
VANADIUM IODIDES
vapor pressure and equilibrium reactions, 20: 40796 (IS-1500(Sect.C))
VANADIUM IONS
effects on electron spin resonance spectra of irradiated silicate glasses, 20: 42538
reactions with chromium ions, effects of chloride ions on, 20: 40796(R) (IS-1500(Sect.C))
VANADIUM ISOTOPES V-51
carbon-12 reactions (C-12,N-13) with, angular distributions from, (E), 20: 42153 (JINR-E-2824)
deuteron reactions (d,p) with, vanadium-52 energy levels from, (T), 20: 42201
meson (π^+) reactions at 220 to 320 Mev/c, double charge exchange in, (E), 20: 42316
VANADIUM ISOTOPES V-52
energy-level structure of, calculations using shell model with configuration mixing, (T), 20: 42201
VANADIUM OXIDES
reduction to metal by reactions with aluminum and carbon, 20: 41412(R) (IS-1500(Sect. M))
VANADIUM SILICIDES
crystal structure of, phase temperature effects on, 20: 42531
electronic instability, temperature effects on, 20: 42531
structural transformation in V_3Si, vanadium-51 Knight shifts and field gradients during, 20: 42118
VANADIUM STEEL
Cr–Mo–V, rupture mechanisms of, determination by time-to-rupture tests, 20: 41445(R) (EURAEC-1622)
Mn–Mo–V, properties of Ammo, variations in samples of, 20: 41447(R) (EURAEC-1669)
VANADIUM SYSTEMS
H–V, phase studies, 20: 41412(R) (IS-1500(Sect. M))
VELA PROJECT
instrumentation for Salmon Event, 20: 41070 (VUF-3021)
seismic measurements on underground explosions in, 20: 41149 (AD-632956)
VENTILATION
filter system modification and testing in ALRR, 20: 42681(R) (IS-1500(Sect. R))
VESPIDAE
diapause larvae in Mormoniella, method for producing, 20: 40582(R) (ORNL-3922, pp 65-8)
radioinduced eye color mutations in Mormoniella, x, 20: 40669
simulated flight tests for Habrobracon, 20: 40508(R) (ORNL-3922, pp 196-9)
VESSELS
packing spheres in cylindrical, computer analysis of, 20: 41063 (BNL-997)
storage of tritium, in plastic bags, hazards of, 20: 41196 (LA-DC-7996)
VINYL ALCOHOL POLYMERS
radiolysis of, EPR studies of yields of stabilized charges in low-temperature, 20: 40962
VIRUSES
effects of Rauscher leukemia, on growth of mouse cells in semisolid agar, 20: 40502(R) (ORNL-3922, pp 115-27)
effects on aminoacyl-sRNA synthetase systems in host cells, 20: 40632(R) (ORNL-3922, pp 175-91)
effects on rabbits on Shope papilloma, mechanisms for tumorigenic, 20: 40632(R) (ORNL-3922, pp 175-91)
immunity in mice to transplanted leukemia, 20: 40502(R) (ORNL-3922, pp 115-27)
interaction with host, physiology of, 20: 40632(R) (ORNL-3922, pp 175-91)
isolation of respiratory syncytial, by B-IX zonal rotors, 20: 40507(R) (ORNL-3922, pp 191-6)
radiation effects on food-borne, review, 20: 41388
radiography of models of, 20: 40653
radioinduced inactivation of foot and mouth disease, in tissues of

infected animals, gamma, 20: 41392
use of sheep spleen extract as protection against Rauscher, 20: 40658
VISCOMETERS
design and operation of, for liquid metals, 20: 41455(R) (NYO-2731-7)
design of, for use with liquid metals, 20: 41460 (TIM-793)
VISCOSITY
effect on leak rate of conical-face seals, 20: 41074 (AECL-2551)
VITAMIN K
role in bacterial metabolism, 20: 40571
VOLTMETERS
design of high-impedance vacuum tube, 20: 41248

W

WASTE DISPOSAL
effects of radioactive, on hydrobionts, 20: 40527
effects of radioactive, on Chironomus chromosome aberrations, 20: 40530
hazards from radioactive, in municipal sewage systems, 20: 41217
principles of, legal and nuclear, in Germany, 20: 42686
safety in tunnel or cavern, 20: 42686
WASTE PROCESSING
equipment and method for, at Tokai Power Station in Japan, 20: 42688
fixation method of, effects of adding lithium and sodium to glass-forming mixture in, 20: 42690(P)
methods of, recovery of fission products as energy and radiation sources in, 20: 42689
radiation monitoring system for, effluent, 20: 41272(R) (ORNL-3875, pp 53-74)
testing of KRB reactor facility for, 20: 42638(R) (TID-23299)
WASTE SOLUTIONS
flow in soils, tracer studies of, 20: 42687
WATER
analysis for radioisotopes, 20: 40819(T) (CEA-tr-A-1883)
analysis for radium-226, 20: 40809 (NP-16235)
analysis for tritium, method for, 20: 40826
analysis of reactor-coolant, for chlorides by neutron activation, 20: 41418(R) (GEAP-5150)
content in blood plasma and urine of rats, 20: 40561
corrosive effects on zirconium single crystals at 680°F, 20: 41423
determination in lignites by gamma absorption, 20: 41154
determination in soils by neutron scattering, 20: 41115(P)
effects in radiation biology, electron spin resonance studies, 20: 40597
hazards from contamination of drinking, evaluation, 20: 41217
heat transfer to, from high temperature fuel particles, 20: 42580(R) (ANL-7245, pp 60-73)
hydrogen-tritium exchange reactions between lactones and, effects of triethylamine catalyst on, 20: 41017
neutron scattering kernels at 423 and 550°K, thermal, (T), 20: 42138 (IN-1019)
origin of brines in oil wells, 20: 41161
oxygen-18/-16 ratio in saline, in oil wells, 20: 41161
properties as working fluid in Rankine power cycle, 20: 41398
radioactivity content of, from fallout in West Germany, 20: 40570
radioactivity in, methods for measuring, 20: 40819(T) (CEA-tr-A-1883)
radioactivity measurements in New Zealand, 20: 40521(R) (NP-16270)
strontium-90 contamination in drinking, factors affecting uptake by man, 20: 41142
use in multilayer enclosure shields in real fallout field, 20: 41201 (RRA-T55 and Summary)
vibrations of trapped, in molecular sieves, 20: 41651
x-ray spectral distributions in, 20: 41322
$Fe-H_2O$, neutron attenuation in, 20: 42517
$HCl-NdCl_3PrCl_3-TBP-H_2O$, separation factors for neodymium and praseodymium in, 20: 40904
$HNO_3-UO_2(NO_3)_2-H_2O$, refractive index measurements on, 20: 40804 (KR-108)
H_2O-D_2O, solvent properties for argon, 20: 40897
methane–H_2O, tritium exchange in, 20: 41067(R) (ORNL-TM-1582)
$Nd(NO_3)_3-HNO_3-Pr(NO_3)_3-TBP-H_2O$, separation factors for neodymium and praseodymium in, 20: 40904
steam–water, effect of pipe and entrance properties on flow rates of, 20: 41107
WATER-d_2
demand and supply for heavy water reactors, forcast to 1985, 20: 42516 (66-CNA-301)
effects on products in hydrolysis of aluminum, thorium, and uranium carbides, 20: 40905
hazards of tritium from, to skin of laboratory personnel, 20: 41185 (AECL-2594)
neutron scattering by, model for calculating thermal, (T), 20: 42139 (IN-1020)
H_2O-D_2O, solvent properties for argon, 20: 40897
WATER COOLED REACTORS
design of boiling, with increased boiling surface, 20: 42602(P)
materials for, properties of niobium–zirconium alloys as, 20: 41422
shutdown system for, 20: 42597(P)
WATER MODERATED REACTORS
control rod design for, to reduce flux peaking, 20: 42588(P)
core design for, 20: 42595(P)
WATER SUPPLIES
development and management of, use of atomic explosion in, 20: 41073
radioactivity from fallout in, 1965 and 1966, 20: 41131(R) (HASL-172)
strontium-90 hydrologic transport to, from atmosphere, 20: 41141
use of tritium in measuring subterranean, in South Africa, 20: 41167
WATER VAPOR
effect on external surface adsorption capacity of charcoal for methyl iodide, 20: 41202 (UCRL-14990)
reactions with uranium carbide, effects of hydrogen on, 20: 40870 (NAA-SR-Memo-7310)
WELDING
instrumentation and control systems for automatic, 20: 41230(R) (ORNL-3875, pp 24-34)
of thick steel plates, specimen testing for, 20: 41450(R) (EURAEC-1684)
WELDS
cutting machine for, for PWR Core 2, instruction manual, 20: 42649 (WAPD-PWR-2230)
cutting machine for, for PWR Core 2, instruction manual, 20: 42650 (WAPD-PWR-2232)
mechanical properties of high-tensile steels, preparations for research on, 20: 41448(R) (EURAEC-1670)
mechanical properties of heavy-gage steel, preparations for research on, 20: 41410(R) (EURAEC-1612)
properties testing for use in Elk River Reactor pressure vessel, 20: 42636(R) (SWRI-1228-4-22)
WELL LOGGING
equipment for flow measurements in boreholes, 20: 41170(P)
equipment for gamma-gamma, during drilling, 20: 41171(P)
equipment for gamma, electrode calibration for, 20: 41165
health physics problems in, 20: 41216
method of, using delayed neutrons, 20: 41157
WELLS
isotopic composition of brines in oil, 20: 41161
WHEAT
calcium content in Canadian, 20: 41198 (NP-16192)
development of parenchyma in, effects of auxins on, 20: 40631(R) (ORNL-3922, pp 161-6)
genetic control of strontium-89 and calcium-45 accumulation, 20: 40532(R) (COO-1097-17)
properties of nuclei in seeds of, microspectrophotometric study of, 20: 40631(R) (ORNL-3922, pp 161-6)
radiation effects on constituents of flour of, gamma, 20: 40599
strontium-90 content in Canadian, 1966, 20: 41198 (NP-16192)
WHITE OAK CREEK
radioactive waste disposal in White Oak Lake and, effects on Chironomus cytogenetics, 20: 40530
WHITESHELL REACTOR NO. 1
commissioning program, 20: 42668 (AECL-2552)
construction of, 20: 42667 (66-CNA-309)
coolant behavior in, 20: 42669 (AECL-2553)
fuel behavior in, 20: 42669 (AECL-2553)
materials behavior in, 20: 42669 (AECL-2553)
WIND
predictions of, at National Reactor Testing Station, 20: 41129
WINDOWS
design of irradiation, for electron accelerators, 20: 41574(P)
WIRES
crystal structure of nitrided type 304 stainless steel, dilatometric studies of, 20: 41449(R) (EURAEC-1676)
radiation effects on film-insulated magnet, gamma, 20: 41503
WORMS
radiation effects on African giant and red wiggler, gamma, 20: 40637(R) (ORO-2754-7)

X

X RADIATION
bleeding effects on bone marrow cell proliferation in mice following, 20: 40722
detection and analysis of cosmic, research programs on, (E), 20: 41667(R) (MIT-2098-251, pp 1-13)
detection of, design and performance of gas-filled image intensifier spark chamber for, 20: 41299
detection of, pulse height shifts in gas proportional detectors for, 20: 41331
dose distributions for uterine carcinoma, 20: 40769
dose effects on cataract induction, 20: 40771

dose effects on chromosome aberrations in human blood cells, 20: 40665
dose for $LD_{50/30}$ in jackrabbits, 20: 40494(R) (COO-1329-3)
dose fractionation effects on cataracts of rats, 20: 40690
dosimetry during mouth radiography, 20: 40795
dosimetry for therapy of head and neck neoplasms, 20: 41210
dosimetry of medical, survey using film packs, 20: 41213
effects combined with aging on rat exercise performance, 20: 40604 (AD-635251)
effects of combined, and microwaves on hematologic response of dogs, 20: 40650
effects of multiple radiation sickness on induction of lesions in dog gastrointestinal tract, 20: 40645
effects of porphyrin on sensitivity of mouse sarcoma to, 20: 40657
effects of pre- and postnatal on locomotor behavior and neuromorphologic anomalies in rats, 20: 40688
effects of various doses on rat leukocyte counts, whole-body, 20: 40697
effects on adensonine triphosphatase activity in rat liver mitochondria, 20: 40695
effects on amino acids, endothermic decay of free radicals induced by, 20: 40504(R) (ORNL-3922, pp 146-60)
effects on antibody production in mice, 20: 40626(R) (ORNL-3922, pp 80-3)
effects on antigenticity of mouse liver on lymphoid cells incubated with phytohemagglutinin, 20: 40588
effects on *Arabidopsis thaliana*, genetic, 20: 40710
effects on Arbacia eggs, effects of AET on, 20: 40619(R) (NYO-2740-3, pp 216-57)
effects on ascites tumor antioxidant activity, 20: 40642
effects on barley, effects of zygosity on, 20: 40701
effects on barley, genetic, 20: 40711
effects on barley, genetic, 20: 40712
effects on barley, genetic, 20: 40717
effects on biological materials, parameters of, 20: 40504(R) (ORNL-3922, pp 146-60)
effects on carbon dioxide, mechanism of, 20: 40996
effects on carrier mobility and trap density in anthracene and polystyrene, 20: 40952 (SC-DC-66-1823)
effects on cell division of the ciliate *Spathidium spathula*, 20: 40623(R) (ORNL-3922, pp 32-49)
effects on chromosomes in Chinese hamster cells and human leukocytes, 20: 40628(R) (ORNL-3922, pp 89-93)
effects on chromosomes, repair mechanisms for, 20: 40609 (CONF-660418-1)
effects on chromosomes in Drosophila oocytes, frequency of crossover-suppressing aberrant, 20: 40625(R) (ORNL-3922, pp 59-64)
effects on color and x-ray luminescence of calcium fluorides as function of temperature, 20: 42556
effects on crystal orientation in ethylene and propene polymers, 20: 40949(R) (NYO-3003-29)
effects on cultured hamster and HeLa cells, lethal, effects of calchicine on, 20: 40618(R) (NYO-2740-3, pp 166-215)
effects on development of mice exposed *in utero*, 20: 40619(R) (NYO-2740-3, pp 216-57)
effects on development of monkeys exposed *in utero*, 20: 40619(R) (NYO-2740-3, pp 216-57)
effects on development of *Heterakis gallinarum* embryos, 20: 40667
effects on development of experimental allergic encephalomyelitis in rats, 20: 40728
effects on DNA synthesis in chick fibroblasts and myoblasts, 20: 40587
effects on dogs, pathological, 20: 40638(R) (UCD-472-113, pp 1-16)
effects on Drosophila populations, genetic, 20: 40622(R) (NYO-3096-8)
effects on Drosophila, genetic, 20: 40706
effects on Drosophila, genetic, 20: 40707
effects on *E. coli*, effects of protein synthesis on, 20: 40629(R) (ORNL-3922, pp 94-8)
effects on electric and magnetic properties of calcium fluoride crystals, (E), 20: 42555
effects on electric properties and unit cell volume of lithium fluoride crystals, 20: 42564(T)
effects on embryos of mice, RBE of neutrons, 20: 40618(R) (NYO-2740-3, pp 166-215)
effects on *Escherichia coli*, effects of nutrients on biological, 20: 40618(R) (NYO-2740-3, pp 166-215)
effects on eyes following therapy of canthus and eyelid carcinomas, 20: 40689
effects on eyes, cataractogenetic, RBE of neutrons, 20: 40618(R) (NYO-2740-3, pp 166-215)
effects on F-center formetion in doped potassium chlorides, 20: 42557
effects on function and structure of bull testicle, single whole-body or fractionated dose, 20: 40610(R) (COO-895-9)
effects on growth of mouse tumors, sensitizing effects of uracil on, 20: 40668
effects on human cells in culture, biological, 20: 40623(R) (ORNL-3922, pp 32-49)
effects on human erythrocyte diameter and volume from occupational exposure to, 20: 40678
effects on human kidney cells, factors affecting RBE, 20: 40725
effects on human spermatogonia, 20: 40627(R) (ORNL-3922, pp 84-8)
effects on hybrid mice grafted with skin from parents, 20: 40651
effects on immune system and lymphatic tissues in estradiol-injected mice, effects of marrow transplants on, 20: 40577
effects on intestinal cells of rats and amphibians, 20: 40607 (BNL-10518)
effects on iron-59 metabolism in rat blood, 20: 40561
effects on life spans in mice, effects of age at exposure on, 20: 40633 (ORNL-P-2287)
effects on lifetime of $^5D_4$ level in terbium chlorides, (E), 20: 42539
effects on lutein cells of rat ovary, 20: 40672
effects on maize, genetic, 20: 40708
effects on mammals, 20: 40694
effects on metastases following therapy for breast cancer, 20: 40793
effects on mice, mechanism for protective effects of lymphoid and myeloid cell transplants against, 20: 40727
effects on mice, protective effects of bone marrow against, 20: 40718(R) (ORNL-3922, pp 99-105)
effects on mice, protective effects of transplants of parental tissue against, 20: 40718(R) (ORNL-3922, pp 99-105)
effects on mice, protective effects of nibufin against, 20: 40724
effects on mitosis in *E. coli*, factors affecting, 20: 40630(R) (ORNL-3922, pp 106-8)
effects on mortality gastropods exposed at various stages of life cycle, 20: 40700
effects on mouse embryos, cataractogenetic, 20: 40619(R) (NYO-2740-3, pp 216-57)
effects on mouse embryos, 20: 40649
effects on mouse heart and resultant electrocardiograms, 20: 40648
effects on mouse marrow cells, factors affecting recovery from, 20: 40634 (ORNL-P-2312)
effects on mouse spermatogonia, effects of dose on frequency of mutagenic, 20: 40627(R) (ORNL-3922, pp 84-8)
effects on mouse sex chromosomes, aberrant, 20: 40627(R) (ORNL-3922, pp 84-8)
effects on nerves, physiological, 20: 40606 (BMwF-FBK-66-02)
effects on nonallelic mutations in Neurospora, 20: 40624(R) (ORNL-3922, pp 52-8)
effects on Paramecium, genetic, 20: 40623(R) (ORNL-3922, pp 32-49)
effects on performance of neutron threshold detectors, 20: 41333
effects on pituitary function following nasopharyngeal carcinoma therapy, 20: 40660
effects on plants, genetic, effects of exogenous factors on, 20: 40709
effects on plants, genetic, 20: 40714
effects on pupal weight and reproductive fitness of Tribolium, 20: 40671
effects on rat spleen, effects of fractionated doses on regeneration of, 20: 40702
effects on rate of thermal decomposition of silver nitrite, 20: 41000
effects on rats, hematological, 20: 40603 (AD-635086)
effects on rats, protective effects of cysteine against, 20: 40729
effects on rice seed, chlorophyll mutations from, 20: 40641
effects on silver-doped sodium chlorides at 40 kv, de-excitation curves from, 20: 42561
effects on sodium azide, ESR studies of, 20: 40966
effects on spermatogenesis in rats following exposure at birth, 20: 40682
effects on survival in mice, protective effects of AET or glutathione combined with bone marrow treatments against, 20: 40719(R) (ORNL-3922, pp 136)
effects on swine, effects of conditioning exposure on pathological, 20: 40605 (AD-635735)
effects on tobacco resistance to blue mold disease, mutagenic, 20: 40613 (N-66-18147)
effects on tomato seeds, genetic, 20: 40713
effects on transplanted tumors in mice, immune response to subsequently transplanted tumors, 20: 40643
effects on ultrastructure of male germ cells in rats following exposure at birth, 20: 40683
effects on *Vicia faba* chromsomes, protective effects of actinomycin D against aberrant, 20: 40581(R) (ORNL-3922, pp 50-1)
effects on X chromosomes in heterozygous and homozyzous Drosophila females, 20: 40625(R) (ORNL-3922, pp 59-64)
emission from fission fragments, design and performance of nanosecond scintillation detectors for determining half life from, 20: 41325
emission from laser spark of soft, determination of electron temperatures by, (E), 20: 42475
fluoroscopic, television equipment for monitoring, 20: 40781
hyaluronic acid depolymerization by, 20: 40591
induction of hypothyroidism in dogs and resulting effects on metabolism, 20: 40698

induction of lung carcinoma in rats by total-body, 20: 40614 (NYO-901-39)
personnel monitoring by test films in industrial radiography in Poland, 20: 41212
prevention of leukemia induced by, using sheep spleen extract, 20: 40658
production from electron oscillations in betatrons, maximum, 20: 41560
production in proton inelastic scattering by copper at 25 to 1700 kev, L shell, (E), 20: 42169(R) (UCRL-14744, pp 1-18)
radioinduced mutations in rice, 20: 40640
radioinduction of eye color mutations in Mormoniella, 20: 40669
relation of dose-fractionation and spacing in time to skin damage, 20: 40764
relative biological efficiency of, comparison with gamma radiation and high energy electrons, 20: 40665
reparative effects of DNA on rat sperm following total body, 20: 40723
scattering from a cuboid shaped tissue-equivalent phantom, factors affecting angular variation of, 20: 41211
single dose effects on mandibular growth, 20: 40652
single-hit effects by, on Drosophila, water snails, and RNase, 20: 40515
spectra from uranium-235 fission products, (E), 20: 42170 (UCRL-70045)
spectra in therapy beam, in 200 to 300 kvp range, 20: 41322
standardized technique of radiotherapy for breast cancer, 20: 40773
supervoltage, in cancer therapy in gynecology, 20: 40768
therapeutic effects on cervical carcinoma, 20: 40772
transmission through silicon, fast-neutron effects on, (E), 20: 42567(T)
use in production of transmission pictures of virus models, 20: 40653

X-RAY-DIFFRACTION ANALYSIS
of phases in type 316 stainless steel subjected to high temperatures, 20: 41419(R) (GMAD-3643-5)

X-RAY DIFFRACTOMETERS
design modification of, with continuous averaging technique for avoiding drift effects in scattering measurements, 20: 41327
goniometer scanning of, design of program controller for, 20: 41222 (DP-900)

X-RAY FLUORESCENCE ANALYSIS
dosimetry of medical, survey using film packs, 20: 41213

X-RAY SOURCES
use in radiography, 20: 41116(P)
use of beta-excited, in helicopter signaling system, 20: 41221(R) (COO-1471-1)

X-RAY SPECTROMETERS
design and performance of semiconductor detector, for π-mesic atom spectra, 20: 42311
design of ultrahigh vacuum grating, with grazing incidence, 20: 41350

XANTHATES
solvent properties for technetium and rhenium, 20: 40856

XENON
buildup in ALRR, reactivity change from, 20: 42681(R) (IS-1500(Sect. R))
effects on safety of HFBR, 20: 42672 (BNL-10388)
electric discharges in, high-pressure electrodeless, (E), 20: 42509
ionization of, cross sections for shock-produced, 20: 40896
ionization processes in MHD generator, (E), 20: 41786
potential energy integrals at 0°K of solid, (T), 20: 42123
properties as working fluid in Brayton power cycle, 20: 41398
scattering on beryllium–copper alloys and nickel at 5 to 25 kev, secondary electrons from, 20: 41620 (NIJS-R-471)
separation from products of fission-fragment-induced radiolysis, 20: 40951 (RPI-321-6)
spin-exchange collisions between singly-ionized ground state and metastable state of neutral, (E), 20: 41650
Ar–Xe, ionization of, at 5000 to 9000°K, shock-induced atom-atom, 20: 41632

XENON COMPOUNDS
with platinum fluorides, structure and magnetic properties of, 20: 40882

XENON FLUORIDE OXIDES
hydrolysis of, in hydrofluoric acid solutions, Raman spectra of products of, 20: 40906

XENON FLUORIDES
fluorine-19 NMR and spin-lattice relaxation in, 20: 40892

XENON ISOTOPES Xe-128
energy-level quantum numbers and transitions from decay of iodine-128, (E), 20: 42147

XENON ISOTOPES Xe-131
formation of metastable, by beta decay of iodine-131 in compounds, 20: 40851

XENON ISOTOPES Xe-133
separation from uranium fission products, method for, 20: 41034 (JEN-160-DQ/I-54)
use in scintiphotography studies of lungs, 20: 40749

XENON ISOTOPES Xe-135
separation from uranium fission products, method for, 20: 41034 (JEN-160-DQ/I-54)

XENON OXIDES
separation from iodic acid using zirconium phosphate, 20: 41054
separation from iodate and periodate solutions by ion exchange chromatography, 20: 40851

XENON SYSTEMS
He–Xe, energy levels of ionized, pressure effects on, 20: 42491

XYLENE
properties as working fluid in Rankine power cycle, 20: 41398
radiation effects on oxidation of, effects of temperature on kinetics of, 20: 41002

XYLENOL ORANGE
use in the determination of lanthanum, 20: 40860

Y

YEASTS
cerium-144 uptake by *Saccharomyces cerevisiae*, mechanism of, 20: 40560
effects of heat treatments combined with γ radiation on *Saccharomyces cerevisiae*, 20: 41387
mutations in Saccharomyces, super-suppressors as addition-deletion, 20: 40582(R) (ORNL-3922, pp 65-8)
tryptophan synthetase assay in, using carbon-14 tracer techniques, 20: 40582(R) (ORNL-3922, pp 65-8)

YTTERBIUM
determination in holmium oxides by neutron activation, 20: 40796(R) (IS-1500(Sect.C))
liquid, solubility of tantalum and tungsten in, at high temperatures, 20: 41412(R) (IS-1500(Sect. M))

YTTERBIUM ALLOYS
Ca–Yb, crystal structure and electric conductivity of, 20: 41412(R) (IS-1500(Sect. M))
Pb–Yb, phase diagrams, 20: 41412(R) (IS-1500(Sect. M))

YTTERBIUM CHLORIDES
chemical properties of aqueous solutions of, 20: 40796(R) (IS-1500 (Sect.C))

YTTERBIUM COMPLEXES
with α-methylmandelic acid, stability of, 20: 40902

YTTERBIUM IONS
spin-lattice relaxation of, in lanthanum fluorides, 20: 42540

YTTERBIUM ISOTOPES Yb-170
energy level transitions in, conversion coefficients for, (E), 20: 42523(R) (IS-1500(Sect.P))

YTTERBIUM OXALATES
thermal decomposition of hydrates of, differential thermal analysis of products of, 20: 40900

YTTERBIUM OXIDES
Yb_2O_3–Yb_2O_3, liquid immiscibility in, 20: 40910

YTTERBIUM SILICATES
preparation of $Yb_2O(SiO_4)$ and $Yb_2Si_2O_7$ monocrystals, 20: 40919

YTTRIUM
corrosion by chromium–uranium and manganese–uranium eutectics, 20: 41064(R) (IS-1500(Sect.E))
deformation of polycrystalline, effects of second phases on, 20: 41412(R) (IS-1500(Sect. M))
extrusion of, methods for, 20: 41412(R) (IS-1500(Sect. M))
helium and hydrogen ion attenuation at 0.1 to 500 Mev, tables for, 20: 41619 (CEA-R-3042)
liquid, solubility of tantalum and tungsten in, at high temperatures, 20: 41412(R) (IS-1500(Sect. M))
preparation of high-purity, methods for, 20: 41412(R) (IS-1500(Sect. M))
purification by electrotransport, 20: 41412(R) (IS-1500(Sect. M))
separation from products of fission-fragment-induced radiolysis, 20: 40951 (RPI-321-6)
sorption by soil, effects of acidity and concentration on, 20: 40914

YTTRIUM ALLOYS
Al–Y, crystal structure of intermetallic-compound polymorphs of, 20: 41412(R) (IS-1500(Sect. M))
Cu–Y, phase studies, 20: 41412(R) (IS-1500(Sect. M))
Mo–Y, oxidation at high temperatures, effects of yttrium content on, 20: 41421
Pb–Y, phase diagrams, 20: 41412(R) (IS-1500(Sect. M))

YTTRIUM CHLORIDES
preparation by reactions of carbonyl chloride with yttria, 20: 41412(R) (IS-1500(Sect. M))
reduction for preparation of metal, methods for, 20: 41412(R) (IS-1500 (Sect. M))

YTTRIUM COMPLEXES
with sulfosalicyclic acid, effect of, on absorption spectra of erbium and neodymium complexes, 20: 40926
with tartaric acid, spectra and thermal decomposition of, 20: 40909

YTTRIUM ISOTOPES Y-89
energy-level density and transitions, (E), 20: 42331
neutron capture by, cross sections for production of isomeric yttrium-90

in fast, (E), 20: 42326
YTTRIUM ISOTOPES Y-90
deposition of, use of molecular plating for quantitative, 20: 41011 (SGAE-CH-34/1966)
determination in water, 20: 40819(T) (CEA-tr-A-1883)
use in beta applicators, 20: 40766
YTTRIUM NITRATES
binding energies in, infrared spectral studies of ammoniated, 20: 40886
YTTRIUM OXALATES
thermal decomposition of hydrates of, differential thermal analysis of products of, 20: 40900
YTTRIUM OXIDES
elastic properties of, 20: 41064(R) (IS-1500(Sect.E))
fabrication of crucibles of, method for, 20: 41412(R) (IS-1500(Sect. M))
preparation by calcination of yttrium oxalate in air, 20: 41064(R) (IS-1500(Sect.E))
preparation of single crystal, 20: 41064(R) (IS-1500(Sect.E))
properties for carbon reduction crucibles, 20: 41411 (IS-1379)
properties for high-temperature insulation of thermocouples, 20: 41461(R) (UCRL-7361(Pt.3))
reactions with carbonyl chloride for production of yttrium chloride, 20: 41412(R) (IS-1500(Sect. M))
sintering mechanisms of, 20: 41064(R) (IS-1500(Sect.E))
B_2O_3–Y_2O_3, liquid immiscibility in, 20: 40910
YTTRIUM SILICATES
preparation of $Y_2O(SiO_4)$ monocrystals, 20: 40919
YTTRIUM SYSTEMS
C–Y, phase studies, 20: 41412(R) (IS-1500(Sect. M))
N–Y, phase studies, 20: 41412(R) (IS-1500(Sect. M))

Z

ZINC
content in tissues of young and aged dogs, 20: 40540(R) (UCD-472-113, pp 17-56)
determination in americium and plutonium by spark-source mass spectrography, 20: 40816 (RFP-699)
determination in plutonium by carrier distillation methods, spectrographic, 20: 40814 (RFP-664)
determination in seawater, activation, 20: 40834
determination of, in blood by radioisotopic dilution, 20: 40844
electric conductivity of liquid, 20: 41476
films of, tunneling in superconducting bismuth–indium films superimposed on, (E), 20: 42109
gamma scattering by electrons of, at 662 kev, (E), 20: 41625
heat of fusion, 20: 41412(R) (IS-1500(Sect. M))
influence of, content of soils on wheat and barley growth variations, 20: 40532(R) (COO-1097-17)
preparation of single crystals of, 20: 41064(R) (IS-1500(Sect.E))
radiation effects on, at 11 to 7°K, electron, 20: 41499
separation from tin by reversed-phase chromatography, 20: 40796(R) (IS-1500(Sect.C))
separation of silver from, by cation exchange chromatography, 20: 40847
uptake by corn plants, effects of soil fertility on, 20: 40735 (NYO-2744-37)
ZINC ALLOYS
Ca–Zn, heat of fusion of intermetallic compound, 20: 41412(R) (IS-1500(Sect. M))
Ca–Zn, thermodynamic properties of, 20: 41412(R) (IS-1500(Sect. M))
Ce–Zn, heat of fusion of intermetallic compound, 20: 41412(R) (IS-1500(Sect. M))
In–Zn, diffusion coefficients of liquid, 20: 41064(R) (IS-1500(Sect.E))
Mg–Zn, heat of fusion of intermetallic compound, 20: 41412(R) (IS-1500(Sect. M))
Sm–Zn, crystallographic and thermodynamic data on intermetallic compound, 20: 41412(R) (IS-1500(Sect. M))
ZINC ISOTOPES
proton reactions at 14.5 Mev, total cross sections for, (E), 20: 42162 (LA-DC-8075)
ZINC ISOTOPES Zn-65
content in fish in Northeast Pacific Ocean, 20: 40523(R) (RLO-1750-8 (Vol.1))
content in invertebrates in Columbia River estuary, 20: 40523(R) (RLO-1750-8(Vol.1))
content in sediments in Columbia River estuary, 20: 40523(R) (RLO-1750-8(Vol.1))
distribution in mollusks of Columbia River estuary, 20: 40523(R) (RLO-1750-8(Vol.1))
metabolism in rats of, effects of dexamethasone and prednisolone on, 20: 40563
metabolism in salt marsh ecosystems, 20: 40573
uptake by marine mollusks, 20: 40528
uptake by swine blood cells in vitro, effects of dietary calcium, zinc, and corn oil on, 20: 40556
use as gamma source in well logging, 20: 41165
ZINC SULFIDES
radiation effects on scintillation properties of silver-activated, 20: 41342
ZIRCALOY-2
corrosion by hydrochloric acid at 35 to 105°C, 20: 41039(R) (ORNL-3880)
corrosion by steam at high temperatures, 20: 41422
ductility of, effects of high temperatures on, 20: 41422
fabrication of tubes of, by hot drawing, 20: 41432
ZIRCONIUM
corrosion of single crystals of, by water at 680°F, 20: 41423
decontamination of, method and solution for, 20: 41214(P)
determination in fission product solutions, method for, 20: 40803 (KFK-387)
determination in seawater, activation, 20: 40834
distribution of, in neutron-irradiated plutonium dioxide suspensions, 20: 41009 (AERE-R-3268)
fabrication of tubes of, by hot drawing, 20: 41432
helium and hydrogen ion attenuation at 0.1 to 500 Mev, tables for, 20: 41619 (CEA-R-3042)
separation from nitric acid solutions by solvent extraction using di- and monoisopentyl esters of methylphosphonic acid, 20: 41051
separation of silver from, by cation exchange chromatography, 20: 40847
ZIRCONIUM ALLOYS
development and evaluation of binary, for fuel assembly brazing, 20: 41425(R) (IITRI-578-P29-2)
Co–Zr, crystal structure of intermetallic compounds, 20: 41412(R) (IS-1500(Sect. M))
Co–Zr, elastic properties of Laves-phase intermetallic compound, 20: 41412(R) (IS-1500(Sect. M))
Cu–Zr, properties as magnet material, 20: 41097
Mo–Nb–Zr, phase studies of, isothermal sections at 1200°C in, 20: 41464
Mo–Ti–Zr, phase studies of, isothermal sections at 1200°C in, 20: 41464
Mo–Zr, aging kinetics of, at 1300 to 1500°K, 20: 41466
Nb–Zr, corrosion by liquid potassium at high temperatures, 20: 41419(R) (GMAD-3643-5)
Nb–Zr, corrosion of zirconium-base, by steam at high temperatures, 20: 41422
Nb–Zr, critical current in, effects of annealing and orientation on, (E), 20: 42569
Nb–Zr, ductility of zirconium-base, effects of high temperatures on, 20: 41422
Nb–Zr, magnetic flux penetration in superconducting, (E), 20: 42132
Nb–Zr, magnetization of superconducting, (E), 20: 42133
Nb–Zr, mechanical properties of, effects of oxygen on, 20: 41412(R) (IS-1500(Sect. M))
Nb–Zr, phase studies of, 20: 41443(R) (COO-588-12)
Nb–Zr, propagation of normal region in superconducting solenoid of, 20: 42100
Nb–Zr, structure and superconducting properties of, effects of oxygen on, 20: 42535
Nb–Zr, uptake of carbon, nitrogen, and oxygen by, in liquid metal loops, 20: 41419(R) (GMAD-3643-5)
Ni–Zr, crystal structure of intermetallic compounds, 20: 41412(R) (IS-1500(Sect. M))
Pu–U–Zr, development for LMFBR fuel, 20: 42651 (WASH-1065)
Pu–U–Zr, performance as FTR fuel, 20: 42676 (BNWL-281)
Sc–Zr, superconducting transition temperature and electronic specific heat of, 20: 42121
Ti–Zr, electric conductivity of, effects of temperature on, 20: 41457(R) (ORO-3291-3)
Ti–Zr, phase diagram for, 20: 41457(R) (ORO-3291-3)
ZIRCONIUM BORIDES
interactions with gas flow in MHD generators, 20: 41738
use in MHD duct electrodes, preparation and testing for, (E), 20: 41718
ZIRCONIUM CARBIDES
electric resistance at 1200 to 3500°K, 20: 41729
fabrication into thin plates, methods for, 20: 41430
interactions with gas flow in MHD generators, 20: 41738
oxidation of cast, by air at 450 to 800°C, 20: 41429(R) (USBM-RC-1249)
preparation and properties of cast, 20: 41429(R) (USBM-RC-1249)
radiation capacity at 1200 to 3500°K, 20: 41729
ZIRCONIUM FLUORIDES
spectra of fluorine-19 in, NMR, 20: 40931
ZIRCONIUM HYDROXIDES
ion exchange properties for xenon oxide in iodate and periodate solutions, 20: 40851
ZIRCONIUM IODATES

use in separation of thorium-234 from lanthanides, 20: 40832
ZIRCONIUM ISOTOPES
helium-3 reactions (He-3,t) at 18 Mev, (E), 20: 42334
proton reactions at 14.5 Mev, total cross sections for, (E), 20: 42162 (LA-DC-8075)
ZIRCONIUM ISOTOPES Zr-90
energy level excitations in, coherent antiproton-neutron, (T), 20: 42279
helium-3 reactions (He-3,t) at 18 Mev, (E), 20: 42334
meson (π^+) reactions at 220 to 320 Mev/c, double charge exchange in, (E), 20: 42316
proton inelastic scattering at 10 to 20 Mev, multiple excitation and shell model description of, 20: 42229
ZIRCONIUM ISOTOPES Zr-91
helium-3 reactions (He-3,t) at 18 Mev, (E), 20: 42334
ZIRCONIUM ISOTOPES Zr-92
helium-3 reactions (He-3,t) at 18 Mev, (E), 20: 42334
ZIRCONIUM ISOTOPES Zr-94
helium-3 reactions (He-3,t) at 18 Mev, (E), 20: 42334
ZIRCONIUM ISOTOPES Zr-95
beta activity measurements in France, 20: 41189 (CEA-R-3020)
content in fallout and plankton of Mediterranean Sea, 1963, 20: 41146
content in fallout from Chinese nuclear test, May 1965, 20: 41130(R) (COO-1407-10)
determination in sea water, gamma spectrometric, 20: 41145
sorption reactions of, on minerals, 20: 41178 (AD-635547)
uptake by marine mollusks, 20: 40528
ZIRCONIUM NITRIDES
analysis for nitrogen, comparison of hot extraction and Kjeldahl methods for, 20: 40820(T) (IS-Trans-37)
ZIRCONIUM OXIDES
formation and properties of, on zirconium single crystals in water, 20: 41423
interactions with gas flow in MHD generators, 20: 41738
preparation of high-purity, 20: 41486
reflectance of monoclinic, as function of purity, 20: 41486
use in MHD duct walls, preparation and testing for, (E), 20: 41718
ZIRCONIUM PHOSPHATES
ion exchange properties for xenon oxide in iodate and periodate solutions, 20: 40851
properties for separation of iodic acid and xenon oxide, 20: 41054
ZIRCONIUM SYSTEMS
C–Zr, preparation and properties of alloys of, 20: 41471
ZIRCONS
lead-207/-206 ratio in, 20: 41176
ZIRCONYL PHOSPHATES
ion exchange properties of granulated, 20: 41055
preparation of granulated, by freezing, 20: 41055

REPORT NUMBER INDEX

Reports, conference papers and proceedings, numbered translations, and patents abstracted during the period are included in this index. Each item is listed by report number; this is followed by the abstract number and a brief notation regarding public availability. The index entries show which reports are on file in the depository libraries, which reports have been published in open-literature journals (journal citation given), and which reports can be purchased (source and price). Whenever a report is identified by more than one number, cross references from secondary to primary report numbers are cited.

The report number codes apply to AEC reports unless designated otherwise. Non-AEC reports are identified by parenthetical notes after the report codes; e.g., (non-AEC), (British), (Canadian), (French). The note (Misc.) identifies those codes used for both USAEC and non-AEC reports. Patents are listed under the heading "PATENTS"; the country of origin is included in parentheses.

A comprehensive listing of both AEC and non-AEC report codes is contained in TID-85(5th Rev.), *Report Number Series Used by the Division of Technical Information in Cataloging Reports.* This information is also included in the Cumulative Report Number Index (issued annually).

Public Availability of USAEC Reports

All USAEC reports abstracted in *NSA* are available to the public through one or more of the following sources:

(1) Depository libraries in the United States, in other countries, and in international agencies. A list of these depositories appears on the inside covers of each issue of *NSA*.

(2) Scientific and technical journals or other publications.

(3) Microcard Editions, Inc., in Microcard and micronegative form. Orders and inquiries should be sent to: Accounting and Shipping Department, West Salem, Wisconsin 54669.

(4) Clearinghouse for Federal Scientific and Technical Information, U. S. Department of Commerce, Springfield, Virginia 22151.

(5) Superintendent of Documents, U. S. Government Printing Office, Washington, D. C. 20402.

Public Availability of Non-AEC Reports

U. S. Reports. Many reports of U. S. Government agencies are available to the public from the Clearinghouse for Federal Scientific and Technical Information (CFSTI). This availability is given when known. Such reports should be ordered by AD number or NASA-N number. If availability is not shown, inquiries may be directed to CFSTI. In the case of NP numbers, inquiries should be by title and author.

Non-U. S. Reports. Many reports of atomic energy establishments of other countries are deposited in the libraries listed on the inside covers of each issue of *NSA*.

Additionally, the following have made their reports available as indicated.

AUSTRALIA

Australian Atomic Energy Commission Research Establishment. Available upon request from the Library, Australian Atomic Research Establishment, Private Mail Bag, Sutherland, New South Wales, Australia.

BELGIUM

Centre d'Étude de l'Énergie Nucléaire. Available upon request to individuals and organizations, from the Centre d'Étude de l'Énergie Nucléaire (CEN), 31, Rue Belliard, Bruxelles, Belgium.

CANADA

Atomic Energy of Canada Limited. For sale by the Technical Information Officer, Atomic Energy of Canada Limited, Chalk River, Ontario, Canada. Copies are also deposited in libraries in the United Kingdom.

National Research Council of Canada. Available from the National Research Council of Canada, Ottawa 2, Ontario, Canada.

DENMARK

Atomic Energy Commission Research Establishment, Risø. Available on exchange from the Library, Danish Atomic Energy Commission, Risø, Roskilde, Denmark. Also for sale by Jul. Gjellerup, Booksellers, 87 Sölvgade, København K., Denmark.

Danatom. Available on loan from Research Establishment, Risø, Roskilde, Denmark. Copies are available from Danatom, Aurehøjvej 2, Hellerup, Denmark.

EURATOM

Reports from the Commission of the European Atomic Energy Community are available from: Presses academiques europeennes, 98, chaussee de Charleroi, Brussels 6, Belgium; and Office central de vente des publications des Communautes eurodeennes 2, place de Metz, Luxemburg.

FRANCE

Commissariat à l'Énergie Atomique. Inquiries for reports numbered 1-2199 should be addressed to Commissariat à l'Énergie Atomique, Service Central de Documentation, Centre d'Études Nucléaires de Saclay, Boite Postale No. 2, Gif-sur-Yvette (S. et O.), France. Reports numbered 2200 and above are available from La Documentation Francaise, 16 Rue Lord-Byron, Paris VIII, France.

Service Central de Protection contre les Rayonnements Ionisants. Copies are available from Ministère de la Santé Publique, Service Central de Protection contre les Rayonnements Ionisants, B. P. n° 35—LE VESINET (S. et O.), France.

GERMANY

Deutsches Elektronen-Synchrotron DESY. Copies are available from Deutsches Elektronen-Synchrotron Desy, Dokumentation, 2000 Hamburg-Gr. Flottbek 1, Notkestieg 1, Germany.

Gesellschaft für Kernforschung mbH (KFK). Copies are available from Gesellschaft für Kernforschung mbH, 75 Karlsruhe, Postfach 947, Germany. Copies are also deposited in many national nuclear centers in the world.

Kernforschungsanlage. Copies may be ordered from Zentralbibliothek der Kernforschungsanlage Jülich, Jülich, Bundesrepublik Deutschland.

Hahn-Meitner-Institute für Kernforschung. Available without charge from Hahn-Meitner-Institute für Kernforschung Berlin, Bibliothek, Glienicker Strasse 100, 1 Berlin

39, Germany. Copies are deposited in many national nuclear centers in the world.

Johann-Wolfgang-Goethe Universität, Frankfurt Am Main, Institut für Kernphysik, (IKF). Copies are available from Gmelin Institut, 40-42 Varrentrappstrasse, Frankfurt (Main), West Germany.

ISRAEL

Israel Atomic Energy Commission. Available without charge from Ministry of Defence/Atomic Energy Commission, Soreq Research Establishment, Yavne, Israel. Copies are deposited in libraries in Israel and in other countries.

ITALY

Centro Informazioni Studi Esperienze (CISE). For sale at CISE Press Office, Casella Postale 3986, Milano, Italy. Copies are deposited in libraries in Italy.

Comitato Nazionale per l'Energia Nucleare. Copies are available from Comitato Nazionale per l'Energia Nucleare, Divisione Affari Internazionali e Studi Economici, Ufficio Pubblicazioni, Via Belisario, 15, Roma, Italy.

JAPAN

Japan Atomic Energy Research Institute (JAERI). Available from the Staff Supply Cooperative of Japan Atomic Energy Research Institute (JAERI), 1-1 Tamura-Cho, Shiba, Minato-Ku, Tokyo, Japan. Copies are deposited in depositories in Tokyo, Nagoya, and Osaka.

Nagoya University. Copies are available from Research Information Center, Institute of Plasma Physics, Nagoya University, Nagoya, Japan.

University of Tokyo. Available free of charge from Institute for Nuclear Study, University of Tokyo, Tanashi-Machi, Kitatama-gun, Tokyo, Japan.

NETHERLANDS

Reactor Centrum Nederland. For sale by Reactor Centrum Nederland, 112 Scheveningseweg, 's-Gravenhage, The Netherlands. Copies are deposited in university libraries in Holland and in many national nuclear centers in the world.

NEW ZEALAND

Institute of Nuclear Sciences. Copies are available from Librarian, Institute of Nuclear Sciences, D.S.I.R., Private Bag, Lower Hutt, New Zealand. Copies are deposited in other countries.

NORWAY

Forsvarets Forskningsinstitutt. Copies available from Norwegian Defence Research Establishment, Library, P. O. Box 25, Kjeller, Norway.

Institutt for Atomenergi. "KR" reports are available on an exchange basis from the Library, Institutt for Atomenergi, Box 40, Kjeller, Norway. Other series are not generally available to the public.

Norwegian Reactor School. Copies are available from The Library, Institutt for Atomenergi, P. O. Box 40, Kjeller, Norway.

PAKISTAN

Atomic Energy Center. Copies are available from Atomic Energy Center, P. O. Box 658, Lahore, (West Pakistan).

POLAND

Reports of the Polish nuclear institutes are published by the Nuclear Energy Information Center of the Government Commissioner for Use of Nuclear Energy. Copies are available from Ośrodek Informacji o Energii Jądrowej, Warszawa, PKiN, Poland.

SPAIN

Junta de Energia Nuclear. "JEN" reports are available without charge from Servicio de Documentation, Junta de Energia Nuclear, Ciudad Universitaria, Madrid (3), Spain.

SWEDEN

Aktiebolaget Atomenergi. "AE" reports are for sale from Aktiebolaget Atomenergi, Library Section, Box 43041, Stockholm 43, Sweden. Bibliographies and literature surveys of the VDDIT- series may be obtained from Aktiebolaget Atomenergi, Information Office, Scientific and Technical Information, Box 43041, Stockholm 43, Sweden. Other series are not generally available to the public. Organizations in the atomic energy field may obtain copies from Aktiebolaget Atomenergi. Microcopy of AE reports is available from the International Documentation Centre, Tumba, Sweden.

SWITZERLAND

CERN European Organization for Nuclear Research. Available without charge from CERN European Organization for Nuclear Research, Geneva 23, Switzerland. Copies are deposited in libraries in 13 countries.

Eidgenössisches Institut für Reaktorforschung. "EIR" reports are available from Eidgenössiches Institut für Reaktorforschung, c/o Bibliothek, Würenlingen/Ag, Switzerland.

TURKEY

Turkish Atomic Energy Commission. Copies are available free of charge from T.A.E.C., Çekmece Nuclear Research Center, P. O. Box 1, Airport, İstanbul, Turkey.

UNITED KINGDOM

United Kingdom Atomic Energy Authority. Some reports are for sale in the United States by the British Information Service (BIS), 845 Third Avenue, New York, N. Y. 10022. United Kingdom reports generally may be purchased from Her Majesty's Stationery Office, London. Copies not for sale by Her Majesty's Stationery Office may be purchased in microcopy form from Micro Methods Limited, East Ardsley, Wakefield, Yorks, England. Report copies are deposited in a large number of libraries in England, depositories of the USAEC in the United States and abroad, and in most national nuclear centers throughout the world.

Conferences

Published conference proceedings as well as individual unpublished papers from conferences are included in this index. A CONF number is assigned to the conference if published proceedings are received and also if only a single paper is received. The base number used is year-month-sequence. Thus, the number CONF-650101 would indicate that the conference was held in 1965, in January, and that this was the first January 1965 conference so received. This number would be assigned to complete published proceedings, or if individual papers are received, the base number would be extended to include a paper number, i.e., CONF-650101-1. As additional papers are received, they will be assigned consecutive numbers in the series, CONF-650101-1, 2, 3, 4, etc. This numbering system ensures that all papers received from a conference will be associated with that conference in this index.

If published proceedings are received after the receipt of individual papers, the complete proceedings will be abstracted and the abstract number will appear in this index with the base CONF number.

Abbreviations Used in Availability Column

AECL	For sale by Atomic Energy of Canada Ltd., Chalk River, Ontario, Canada.
BIS	For sale by British Information Service, 845 Third Avenue, New York, N. Y. 10022
CFSTI	For sale by the Clearinghouse for Federal Scientific and Technical Information, U.S. Department of Commerce, Spring-

field, Virginia 22151. The symbol "cy" indicates that the format of the item sold may be either a printed document or a photographic reproduction (two-thirds of original size) depending upon the availability of printed stock. The indicated price is for either format. The symbol "mn" is used to indicate that copy is also available in the form of micronegatives (microfiche).

Dep. — AEC reports: Full-size copy is on deposit in the depository libraries both inside and outside the United States. These reports are also for sale by Microcard Editions, Inc., Accounting and Shipping Department, West Salem, Wisconsin 54669.

Non-AEC reports: Full-size copy on deposit in the depository libraries in the United States only.

Dep.(mc) — Same as for Dep., except copy is in Microcard form.

Dep.(mn) — Same as for Dep., except copy is in micronegative (microfiche) form.

DSIR — For sale by the National Lending Library for Science and Technology (D.S.I.R.), Boston Spa, Yorkshire, England.

DTI Extension — Available from the U. S. Atomic Energy Commission, Division of Technical Information Extension, P. O. Box 62, Oak Ridge, Tennessee 37830.

EM — Blueprints and microcopy of AEC engineering drawings are available from Clearinghouse for Federal Scientific and Technical Information, U. S. Department of Commerce, Springfield, Virginia 22151. Current prices of the CAPE- packages may be obtained from this address. TID-4100, available from the Division of Technical Information Extension, P. O. Box 62, Oak Ridge, Tennessee 37831, contains information on all the CAPE- packages for sale.

Gmelin — Available at a nominal charge and under the AED- number shown from Atomic Energy Documentation Center, Gmelin Institute, 40-42 Varrentrappstrasse Frankfurt (Main), West Germany.

GPO — For sale by the Superintendent of Documents, Government Printing Office, Washington, D. C. 20402.

HMSO — Her Majesty's Stationery Office, London.

IAEA — Available from the International Atomic Energy Agency, Vienna, Austria, and from its sales agencies in various countries throughout the world. A list of these agencies is found in each STI/DOC and STI/PUB publication.

JCL — For sale by the Special Libraries Association Translation Center, John Crerar Library, 35 West 33rd Street, Chicago, Illinois 60616.

LC — For sale by the Library of Congress, Photoduplication Service, Washington, D. C. 20540.

NAS — National Academy of Sciences, National Research Council, Washington, D. C. 20418.

NRC — For sale by the National Research Council of Canada, Ottawa, Ontario, Canada.

ORAU — Available on interlibrary loan from the Library, Oak Ridge Associated Universities, Post Office Box 117, Oak Ridge, Tennessee 37830.

ORINS — See ORAU.

UKAEA, London — Available from United Kingdom Atomic Energy Authority, 11 Charles II Street, London, S. W. 1.

UN — United Nations Bookshop, United Nations Headquarters, New York, New York.

USGS — Available free of charge from the U. S. Geological Survey, Washington, D. C. 20242.

ZLDI — Zentralstelle Für Luftfahrtdokumentation Und-Information, Maria-Theresia-Strasse 21, Munich 27, Germany.

[The symbols "ph," "mf," and "fs" are used to designate that copy is available only in photostat, microfilm, or facsimile form. The symbol "mn" is used to designate that copy is available in micronegative (microfiche) form. The symbol "cy" is used to designate full size or photographically enlarged copy (two-thirds of original size).]

Report No.	Abstract No.	Availability
NUMERICAL	**(Misc.)**	
66-CNA-301	20-42616	Dep. mn
66-CNA-303	20-42617	Dep. mn
66-CNA-309	20-42667	Dep. mn
66-CNA-310	20-42668	See AECL-2552
66-CNA-311	20-42669	See AECL-2553
66-CNA-312	20-42618	Dep. mn
66-CNA-315	20-42621	See CONF-660516-16
A-AC–	**(Misc.)**	
82/G/L-1045 (Rev.1)	20-40531	
AAEC-TM–	**(Australian)**	
316	20-41148	Dep. mn
ACRH–		
25	20-40740	Dep. mn. CFSTI $4.00 cy, $1.00 mn
AD–	**(Misc.)**	
624934	20-40602	CFSTI $1.00 cy, $0.50 mn
631586	20-41545	CFSTI $1.00 cy, $0.50 mn
632211	20-41177	CFSTI $5.00 cy, $1.00 mn
632956	20-41149	CFSTI $2.00 cy, $0.50 mn
635086	20-40603	CFSTI $2.00 cy, $0.50 mn
635251	20-40604	CFSTI $1.00 cy, $0.50 mn
635547	20-41178	CFSTI $2.00 cy, $0.50 mn
635735	20-40605	CFSTI $1.00 cy, $0.50 mn
635821	20-41179	CFSTI $3.00 cy, $0.75 mn
635822	20-41180	CFSTI $6.00 cy, $1.25 mn
635823	20-41181	CFSTI $6.00 cy, $1.25 mn
635824	20-41182	CFSTI $6.00 cy, $1.50 mn
635931	20-41183	CFSTI $6.00 cy
636209	20-40732	CFSTI $2.00 cy, $0.50 mn
636608	20-42419	CFSTI $1.00 cy, $0.50 mn
636625	20-42099	CFSTI $1.00 cy, $0.50 mn
637457	20-42136	CFSTI $3.00 cy, $0.75 mn
637806	20-41184	CFSTI $4.00 cy, $1.00 mn
637854	20-42401	CFSTI $1.00 cy, $0.50 mn
638014	20-42146	CFSTI $2.00 cy, $0.50 mn
638830	20-41509	CFSTI $3.00 cy, $0.75 mn
AE–	**(Non-AEC)**	
240	20-42147	Dep. mn
AEC-tr–	**(For complete listing see TID-4025)**	
6698	20-41279	Dep. mn. CFSTI $8.25 cy, $2.25 mn
AECL–	**(Canadian)**	
2465	20-40955	Can. J. Chem., 44: 1951-5(1966)
2524	20-40797	Dep. mn. AECL $0.50
2551	20-41074	Dep. mn. AECL $1.00
2552	20-42668	Dep. mn
2553	20-42669	Dep. mn
2576	20-41150	Dep. mn. AECL $0.50
2589	20-40946	Dep. mn. AECL $0.50
2594	20-41185	Dep. mn. AECL $0.50
AEEW-M–	**(British)**	
661	20-42137	Dep. BIS $0.50. HMSO 2s. 6d.
AERE-R–	**(British)**	
3268	20-41009	Dep. mn
4901	20-41736	See CONF-660704-131
5142	20-41288	Nucl. Instrum. Methods, 43: 269-77(1966)
5210	20-41437	Dep. BIS $1.60. HMSO 8s.
5217	20-41075	Dep. BIS $0.60. HMSO 3s.
AFCRL–	**(Non-AEC)**	
66-429	20-42401	See AD-637854
AFRRI-CR–	**(Non-AEC)**	
66-3	20-42136	See AD-637457
AFRRI-SR–	**(Non-AEC)**	
66-4	20-40603	See AD-635086
AGN–	**(Misc.)**	
8187	20-41438	Dep. mn. CFSTI $2.00 cy, $0.50 mn
8198	20-41439	Dep. mn. CFSTI $1.00 cy, $0.50 mn

Report No.	Abstract No.	Availability
AHSB(S)–	**(British)**	
R-107	20-42576	Dep. BIS $0.60. HMSO 3s. 0d.
Al-Trans–		
206	20-42610	Dep. mn. JCL $2.60 fs, $1.04 mf
209	20-41514	Dep. mn. JCL $1.60 fs, $0.80 mf
ALO–		
3632-4	20-41440	Dep. mn. CFSTI $3.00 cy, $0.75 mn
ANL–		
7196	20-41530	Dep. mn. CFSTI $1.00 cy, $0.50 mn
7209	20-40798	Dep. mn. CFSTI $2.00 cy, $0.50 mn
7230	20-42577	Dep. mn. CFSTI $3.00 cy, $0.75 mn
7245	20-42578	Dep. mn. CFSTI $3.00 cy, $0.75 mn
7300	20-40493	Dep. mn. CFSTI $3.00 cy, $0.50 mn
ARCRL–	**(British)**	
15	20-41186	Dep. mn. BIS $0.50. HMSO 2s. 6d.
ATD–	**(Non-AEC)**	
65-110	20-40602	See AD-624934
AWRE-R–	**(British)**	
5/66	20-42671	Dep. mn. BIS $2.40. HMSO 12s. 0d.
BAW–	**(Misc.)**	
1280-39	20-42620	Dep. mn. CFSTI $1.00 cy, $0.50 mn
BLG–	**(Belgian)**	
347	20-41432	Metallurgie (Mons, Belg.), 2: 43-8(1964)
348	20-41431	Metallurgie (Mons, Belg.), 2: 31-42(1964)
351	20-41413	Ing. Bl. (Antwerp), No. 10, 1-8(1965)
BMwF-FBK–	**(German)**	
66-02	20-40606	Dep. mn
66-10	20-40864	Dep. mn. DM 1,60
66-12	20-41788	Dep. mn. DM 3,00
66-14	20-40947	Dep. mn
BNL–		
956	20-41923	Dep. mn. CFSTI $1.00 cy, $0.50 mn
997	20-41063	Dep. mn. CFSTI $2.00 cy, $0.50 mn
9374	20-40743	Dep. mn. CFSTI $1.00 cy, $0.50 mn
9437	20-40517	Dep. mn. CFSTI $1.00 cy, $0.50 mn
9468	20-41187	Dep. mn. CFSTI $1.00 cy, $0.50 mn
9690	20-40939	Can. J. Chem., 44: 1889-97(1966)
9804	20-42234	Phys. Rev., 148: 1072-82(1966)
9897	20-41297	Nucl. Instrum. Methods, 44: 1-17(1966)
9909	20-42551	Phys. Status Solidi, 16: 449-57(1966)
9956	20-40755	Amer. J. Roentgenol., Radium Therapy Nucl. Med., 97: 888-95(1966)
9963	20-41162	J. Geophys. Res., 71: 4021-7(1966)
9974	20-40666	Exp. Cell Res., 43: 107-19(1966)
10021	20-41546	Amer. J. Phys., 34: 742-52(1966)
10029	20-42232	Phys. Rev., 148: 1045-50(1966)
10082	20-42233	Phys. Rev., 148: 1050-63(1966)
10146	20-41863	Phys. Rev., 149: 1172-81(1966)
10153	20-42242	Phys. Rev., 149: 743-51(1966)
10386	20-41888	Phys. Rev. Lett., 17: 563-8(1966)
10388	20-42672	Dep. mn. CFSTI $1.00 cy, $0.50 mn
10403	20-40744	ORAU
10483	20-42673	Dep. mn. CFSTI $1.00 cy, $0.50 mn
10518	20-40607	Dep. mn. CFSTI $1.00 cy, $0.50 mn
10528	20-41531	Dep. mn. CFSTI $1.00 cy, $0.50 mn
10559	20-41532	Dep. mn. CFSTI $1.00 cy, $0.50 mn
BNWL–		
87	20-42148	Dep. mn. CFSTI $1.00 cy, $0.50 mn
214	20-41220	Dep. mn. CFSTI $1.00 cy, $0.50 mn
221	20-42674	Dep. mn. CFSTI $2.00 cy, $0.50 mn
224	20-41441	Dep. mn. CFSTI
235-1	20-41188	Dep. mn. CFSTI $2.00 cy, $0.50 mn
252	20-42606	Dep. mn. CFSTI $2.00 cy, $0.50 mn
272	20-42675	Dep. mn. CFSTI $5.00 cy, $1.00 mn
279	20-41029	Dep. mn. CFSTI $1.00 cy, $0.50 mn
281	20-42676	Dep. mn. CFSTI $2.00 cy, $0.50 mn
298	20-42607	Dep. mn. CFSTI $2.00 cy, $0.50 mn
BNWL-SA–		
270	20-42660	Dep. mn. CFSTI $2.00 cy, $0.50 mn
619	20-41262	Dep. mn. CFSTI $1.00 cy, $0.50 mn
636	20-42677	Dep. mn. CFSTI $1.00 cy, $0.50 mn

Report No.	Abstract No.	Availability
CAPE–		
1472	20-41349	EM
CEA-R–	(French)	
2887	20-40799	Dep. mn
2994	20-41030	Dep. mn
3001	20-40608	Dep. mn
3020	20-41189	Dep. mn
3042	20-41619	Dep. mn
CEA-tr–	(French)	
A-1883	20-40819	Dep. mn. JCL $6.60 fs, $2.09 mf
CERN–	(European Organization for Nuclear Research)	
66-23	20-41263	Dep. mn
66-27	20-41533	Dep. mn
CEX–		
63.10	20-40518	Dep. mn. CFSTI $1.00 cy, $0.50 mn
CNAEM–	(Turkish)	
18	20-40613	See N-66-18147
34	20-42149	Dep. mn
35	20-40800	Dep. mn
CNLM–	(Misc.)	
2393	20-41442	Dep. mn. CFSTI $3.00 cy, $0.75 mn
4461	20-40865	Dep. mn. CFSTI $1.00 cy, $0.50 mn
CONF-578–	(Conference on the Physics of Electromagnetic Separation Methods, Orsay, France, July 1962)	
17	20-41405	ORAU
CONF-777–	(Symposium on Materials for Cooling Reactors with Sodium, New York, Nov. 1963)	
1	20-42652	See EURFNR-92F
CONF-630916–	20-40705	(Symposium on Induction of Mutations and the Mutation Process, Prague, Sept. 26–28, 1963) Prague, Publishing House of the Czechoslovak Academy of Sciences, 1965
CONF-640710–	(Symposium on Atomic Collision Cascades in Radiation Damage, Harwell, England, July 13–16, 1964)	
1	20-42574	ORAU
CONF-640931–	20-41143	(International Symposium on Pollution of Marine Media, Nice, Sept. 15–17, 1964) Cah. CERBOM (Cent. Etud. Rech. Biol. Oceanogr. Med.), 17: 1-153(1965)
CONF-650220–	(American Physical Society, Southwest Meeting, Norman, Okla., Feb. 25–27, 1965)	
6	20-42516	ORAU
CONF-650311–	(Conference on Analytical Chemistry and Applied Spectroscopy, Pittsburgh, Mar. 5, 1965)	
6	20-41415	ORAU
CONF-650412–	(IEEE Convention, Las Vegas, Nev., Apr. 13, 1965)	
2	20-41398	ORAU
CONF-650448–	(Semismological Society of Americ , Annual Meeting, St. Louis, Apr. 12–14, 1965)	
1	20-41169	ORAU. Gmelin, AED-CONF-65-227-1
CONF-650508–	20-41416	(International Conference on Beryllium Metallurgy, Grenoble, France, May 20, 1965) Paris, Presses Universitaires de France, 1966
CONF-650540–	(American Industrial Hygiene Assn. Meeting, Houston, Tex., May 4–7, 1965)	
7	20-41219	ORAU
CONF-650552–	20-41383	(Institute of Food Technologists, 25th Annual Meeting, Kansas City, Mo., May 16–20, 1965) Dep. mn. CFSTI $1.25 cy, $0.75 mn
CONF-650561–	20-40592	(Symposium on Electron Spin Resonance in Biology, Gatlinburg, Tenn., May 1965) $4.00
CONF-650573–	20-41028	(Meeting of National Analytical Radiochemistry Group, Lyon, May 13, 1965) Villeurbanne, France, Institut de Physique Nucleaire de Lyon, 1965
CONF-650652–	20-29438	(6th International Conference on Radiocarbon and Tritium Dating, Pullman, Wash., June 7–11, 1965) Dep. mn. CFSTI $8.00 cy, $3.25 mn
19	20-41372	ORAU. Gmelin, AED-CONF-65-158-28
20	20-41167	ORAU. Gmelin, AED-CONF-66-176-2
21	20-41168	ORAU. Gmelin, AED-CONF-66-176-1
CONF-650667–	20-40801	(1st Meeting on the Practical Aspects of Activation Analysis with Charged Particles, Grenoble, France, June 23, 1965) See EUR-2957.d,f,e
CONF-650833–	20-17288	(4th International Conference on the Physics of Electronic and Atomic Collisions, Quebec, Canada, Aug. 3–7, 1965) New York, Science Bookcrafters, Inc.
1	20-41663	ORAU. Gmelin, AED-CONF-65-315-46
2	20-41666	ORAU. Gmelin, AED-CONF-65-315-18
CONF-650836–	(7th International Conference on Phenomena in Ionized Gases, Beograd, Yugoslavia, Aug. 22–27, 1965)	
3	20-41620	See NIJS-R-471
CONF-650924–	(Workshop Conference on Space Radiation Biology, Berkeley, Calif., Sept. 7–10, 1965)	
1	20-41187	See BNL-9468
CONF-650932–	20-34803	(Symposium on the Inelastic Scattering of Neutrons by Condensed Systems, Upton, N. Y., Sept. 1965) See BNL-940
5	20-42573	ORAU. Gmelin, AED-CONF-65-292-2
CONF-650937–	20-41076	(Conference on Megagauss Magnetic Field Generation by Explosives and Related Experiments, Frascati, Italy, Sept. 21–23, 1965) See EUR-2750.e
CONF-650962–	(6th Electrical Insulation Conference, New York, Sept. 13–16, 1965)	
3	20-41503	ORAU. Gmelin, AED-CONF-65-240-2
CONF-650965–	(1st International Conference on Medical Physics, Harrogate, England, Sept. 1965)	
2	20-40742	See ACRH-25, pp 24-9
CONF-650969–	(International Meeting on Physical and Clinical Dosimetry of Fast Electrons, Rome (City), Sept. 28, 1965)	
1	20-40741	See ACRH-25, pp 15-23
CONF-650973–	(National Water Well Assn., Houston, Tex., Sept. 21, 1965)	
1	20-41073	ORAU
CONF-650974–	(15th Brazilian Congress, Rio de Janeiro, Sept. 19–25, 1965)	
1	20-41399	See IEA-110
CONF-650975–	(16th Meeting of the International Committee of Thermodynamics and Electrochemical Kinetics, Budapest, Hungary, Sept. 5–19, 1966)	
1	20-40866	See EUR-2954.e
CONF-651015–	(American Physical Society Meeting, Chicago, Oct. 7, 1965)	
26	20-41664	ORAU. Gmelin, AED-CONF-65-312-61
CONF-651101–	20-3647 20-9102	(American Nuclear Society, Winter Meeting, Washington, D. C., Nov. 15–18, 1965)
84	20-42662	Dep. mn. CFSTI $2.00 cy, $0.50 mn
85	20-41566	ORAU. Gmelin, AED-CONF-65-332-139
CONF-651108–	(Symposium on Isotope Techniques, Urbana, Ill., Nov. 10–12, 1965)	
6	20-41141	ORAU. Gmelin, AED-CONF-65-347-11

Report No.	Abstract No.	Availability
7	20-41150	See AECL-2576
CONF-651213–	**(American Physical Society, Winter Meeting in the West, Los Angeles, Dec. 20–22, 1965)**	
5	20-42030	ORAU. Gmelin, AED-CONF-65-400-3
CONF-660104–	**(Symposium on Magnet Flat Topping for Rapid Cycling Particle Accelerators, Princeton, N. J., Jan. 31–Feb. 1, 1966)**	
2	20-41568	ORAU. Gmelin, AED-CONF-66-174-1
3	20-41569	ORAU. Gmelin, AED-CONF-66-174-2
CONF-660107–	**(American Physical Society Meeting, New York, Jan. 26–29, 1966)**	
54	20-42572	ORAU. Gmelin, AED-CONF-66-003-115
55	20-41919	ORAU. Gmelin, AED-CONF-66-003-122
CONF-660113–	**(Mossbauer Symposium, New York, Jan. 25, 1966)**	
2	20-42571	ORAU. Gmelin, AED-CONF-66-058-1
4	20-42570	ORAU. Gmelin, AED-CONF-66-058-4
CONF-660116–	**20-42337**	**(Nuclear Physics Conference on Light Nuclei, Lyon, France, Jan. 26–28, 1966) J. Phys. (Paris), Colloq., No. 1, 1-160(1966)**
CONF-660201–	**(Conference on Analytical Chemistry and Applied Spectroscopy, Pittsburgh, Feb. 1966)**	
3	20-40863	ORAU. Gmelin, AED-CONF-66-117-2
CONF-660205–	**(Metallurgical Society of the American Institute of Mining, Metallurgical, and Petroleum Engineers, New York, Feb. 1966)**	
6	20-41485	ORAU. Gmelin, AED-CONF-66-021-8
CONF-660207–	**(Radioisotope Applications in Aerospace Symposium, Dayton, Ohio, Feb. 15–17, 1966)**	
23	20-41393	ORAU. Gmelin, AED-CONF-66-011-34
24	20-41374	ORAU. Gmelin, AED-CONF-66-011-33
25	20-41257	ORAU. Gmelin, AED-CONF-66-011-38
CONF-660209–	**(Conference on Intermediate Energy Physics, Williamsburg, Va., Feb. 9–11, 1966)**	
Vol.1	20-42304	
Vol.2	20-41912	
14	20-41921	ORAU. Gmelin, AED-CONF-66-023-14
CONF-660212–	**(Radiation Research Society, 14th Annual Meeting, Coronado, Calif., Feb. 13–16, 1966)**	
11	20-40698	ORAU. Gmelin, AED-CONF-66-016-11
CONF-660217–	**(Symposium on Interdisciplinary Aspects of Radiative Energy Transfer, Philadelphia, Feb. 24–26, 1966)**	
3	20-41618	ORAU. Gmelin, AED-CONF-66-013-7
CONF-660303–	**(American Physical Society, Conference of Neutron Cross Section Technology, Washington, D. C., Mar. 22–24, 1966)**	
37	20-42326	ORAU. Gmelin, AED-CONF-66-034-18
39	20-42332	ORAU. Gmelin, AED-CONF-66-034-17
40	20-42145	ORAU. Gmelin, AED-CONF-66-034-26
41	20-42333	ORAU. Gmelin, AED-CONF-66-034-12
48	20-42134	ORAU. Gmelin, AED-CONF-66-060-108
CONF-660304–	**20-33646**	**(Institute of Electrical and Electronics Engineers, Scintillation and Semiconductor Counter Symposium, Washington, D. C., Mar. 2–4, 1966) Trans. Nucl. Sci., NS-13: No. 3, 1-601(1966)**
22	20-41376	ORAU. Gmelin, AED-CONF-66-020-44
CONF-660306–	**(American Physical Society, Conference on Isobaric Spin, Tallahassee, Mar. 17–19, 1966)**	
9	20-42334	ORAU. Gmelin, AED-CONF-66-048-4
14	20-42331	ORAU. Gmelin, AED-CONF-66-048-11
CONF-660311–	**(Symposium on Water Production Using Nuclear Energy, Tucson, Ariz., Mar. 30–Apr. 1, 1966)**	
5	20-42659	ORAU. Gmelin, AED-CONF-66-037-9
CONF-660320–	**(American Chemical Society, 151st Meeting, Pittsburgh, Mar. 22–31, 1966)**	
15	20-42325	ORAU. Gmelin, AED-CONF-66-051-53
CONF-660324–	**(26th Annual Conference on Physical Electronics, Cambridge, Mass., Mar. 21–23, 1966)**	
5	20-41695	ORAU. Gmelin, AED-CONF-66-036-5
CONF-660326–	**(7th Symposium on Engineering Aspects of Magnetohydrodynamics, Princeton, N. J., Mar. 30–Apr. 1, 1966)**	
1	20-41696	ORAU. Gmelin, AED-CONF-66-047-4
2	20-41692	ORAU. Gmelin, AED-CONF-66-047-1
3	20-42045	ORAU. Gmelin, AED-CONF-66-047-3
CONF-660327–	**(American Physical Society Meeting, Durham, N. C., Mar. 28–31, 1966)**	
6	20-42133	ORAU. Gmelin, AED-CONF-66-050-17
CONF-660328–	**(26th Annual Conference on Physical Electronics, Cambridge, Mass., Mar. 21–23, 1966)**	
5	20-42575	ORAU. Gmelin, AED-CONF-66-049-10
CONF-660330–	**(Conference on Modern Methods of Weather Forecasting and Analysis, Chicago, Ill., Mar. 23–25, 1966)**	
1	20-41129	ORAU. Gmelin, AED-CONF-66-072-1
CONF-660401–	**(American Meteorological Society, American Geophysical Union, Annual Joint Meeting, Washington, D. C., Apr. 19, 1966)**	
8	20-42070	ORAU. Gmelin, AED-CONF-66-061-15
11	20-42068	ORAU. Gmelin, AED-CONF-66-061-18
CONF-660411–	**(American Physical Society Meeting, Washington, D. C., Apr. 25–28, 1966)**	
17	20-42336	ORAU. Gmelin, AED-CONF-66-060-54
19	20-42322	ORAU. Gmelin, AED-CONF-66-060-68
22	20-42329	ORAU. Gmelin, AED-CONF-66-060-51
23	20-42324	ORAU. Gmelin, AED-CONF-66-060-64
25	20-42569	ORAU. Gmelin, AED-CONF-66-060-55
26	20-42097	ORAU. Gmelin, AED-CONF-66-060-67
27	20-41917	ORAU. Gmelin, AED-CONF-66-060-62
28	20-42066	ORAU. Gmelin, AED-CONF-66-060-61
30	20-41918	ORAU. Gmelin, AED-CONF-66-060-57
31	20-42335	ORAU. Gmelin, AED-CONF-66-060-73
32	20-42132	ORAU. Gmelin, AED-CONF-66-060-72
34	20-42327	ORAU. Gmelin, AED-CONF-66-060-76
36	20-41617	ORAU. Gmelin, AED-CONF-66-060-75
37	20-42323	ORAU. Gmelin, AED-CONF-66-060-88
38	20-42034	ORAU. Gmelin, AED-CONF-66-060-89
39	20-42027	ORAU. Gmelin, AED-CONF-66-060-90
40	20-42025	ORAU. Gmelin, AED-CONF-66-060-109
41	20-41665	ORAU. Gmelin, AED-CONF-66-060-112
42	20-42330	ORAU. Gmelin, AED-CONF-66-060-53
44	20-41922	ORAU. Gmelin, AED-CONF-66-060-106
45	20-42028	ORAU. Gmelin, AED-CONF-66-060-104
47	20-42029	ORAU. Gmelin, AED-CONF-66-060-102
CONF-660414–	**(2nd International Conference on Electron and Ion Beam Science and Technology, New York, Apr. 17–20, 1966)**	
2	20-41528	ORAU. Gmelin, AED-CONF-66-119-3
4	20-41434	ORAU. Gmelin, AED-CONF-66-119-4
6	20-41567	ORAU. Gmelin, AED-CONF-66-119-5
7	20-41123	ORAU. Gmelin, AED-CONF-66-119-8
CONF-660418–	**(IAEA Meeting on the Genetical Aspects of Radiosensitivity: Mechanisms of Repair, Vienna, Apr. 18–22, 1966)**	
1	20-40609	Dep. mn. CFSTI $1.00 cy, $0.50 mn
CONF-660419–	**(IEEE Region 6 Annual Conference, Tucson, Ariz., Apr. 26–28, 1966)**	
2	20-41694	ORAU. Gmelin, AED-CONF-66-057-2
3	20-41397	ORAU. Gmelin, AED-CONF-66-057-3
CONF-660421–	**(18th Annual Southwestern IEEE Conference and Show, Dallas, Apr. 20–22, 1966)**	
2	20-42131	ORAU. Gmelin, AED-CONF-66-065-8
CONF-660428–	**(Federation of American Societies for Experimental Biology, 50th Meeting, Atlantic City, N. J., Apr. 11–16, 1966)**	
1	20-40577	ORAU. Gmelin, AED-CONF-66-075-2

Report No.	Abstract No.	Availability
CONF-660429–		**(American Power Conference, 28th Annual Meeting, Chicago, Ill., Apr. 26–28, 1966)**
5	20-42655	ORAU. Gmelin, AED-CONF-66-098-13
CONF-660430–		**(Ohio Academy of Science, 75th Annual Meeting, Columbus, Ohio, Apr. 21–23, 1966)**
3	20-40579	ORAU. Gmelin, AED-CONF-66-105-2
5	20-41487	ORAU. Gmelin, AED-CONF-66-105-3
CONF-660431–		**(Symposium on Hot Atom Chemistry, Lafayette, Ind., Apr. 1–2, 1966)**
4	20-40938	ORAU. Gmelin, AED-CONF-66-120-4
CONF-660432–		**(Aerospace Medical Assn., 37th Annual Scientific Meeting, Las Vegas, Nev., Apr. 18–21, 1966)**
1	20-41218	ORAU. Gmelin, AED-CONF-66-077-1
CONF-660433–		**(American Radium Society, 48th Annual Meeting, Phoenix, Ariz., Apr. 13–16, 1966)**
1	20-41377	ORAU. Gmelin, AED-CONF-66-064-2
2	20-40793	ORAU. Gmelin, AED-CONF-66-064-3
3	20-40794	ORAU. Gmelin, AED-CONF-66-064-4
CONF-660437–		**(Society of Automotive Engineers, National Aeronautic Meeting, New York, Apr. 25–28, 1966)**
1	20-41433	ORAU
CONF-660438–		**(International Quantum Electronics Conference, Phoenix, Ariz., Apr. 12–15, 1966)**
2	20-41375	ORAU. Gmelin, AED-CONF-66-078-5
CONF-660439–		**(Conference on Ground-Based Aeronomic Studies of the Lower Ionosphere, Ottawa, Ontario, Canada, Apr. 11–15, 1966)**
2	20-42067	ORAU. Gmelin, AED-CONF-66-063-2
CONF-660440–		**(American Physical Society, New England Section, Spring Meeting, Providence, R. I., Apr. 8–9, 1966)**
1	20-42098	ORAU. Gmelin, AED-CONF-66-106-3
CONF-660505–	**20-27419**	**(American Ceramic Society Meeting, Washington, D. C., May 7–12, 1966) Hinsdale, Ill., American Nuclear Society, 1966**
5	20-41527	ORAU. Gmelin, AED-CONF-66-103-4
6	20-41486	ORAU. Gmelin, AED-CONF-66-103-6
11	20-41424	ORAU. Gmelin, AED-CONF-66-103-14
CONF-660506–		**(American Inst. of Chemical Engineers, Nuclear Engineering Div. Symposium, Columbus, Ohio, May 15, 1966)**
5	20-41111	ORAU. Gmelin, AED-CONF-66-133-6
CONF-660507–		**(Symposium for the Disposal of Radioactive Wastes into Sea, Oceans, and Surface Waters, Vienna, May 17, 1966)**
9	20-40573	ORAU
17	20-41128	ORAU
18	20-41140	ORAU
20	20-40574	ORAU
21	20-40529	ORAU
22	20-41142	ORAU
23	20-40575	ORAU
24	20-40528	ORAU
25	20-40572	ORAU
26	20-40578	ORAU
27	20-41217	ORAU
30	20-40700	ORAU
31	20-40530	ORAU
32	20-40527	ORAU
CONF-660516–		**(Annual Conference on Organic and Heavy Water Reactors, Winnipeg, Canada, May 30–June 1, 1966)**
8	20-42618	See 66-CNA-312
9	20-42669	See AECL-2553
10	20-42668	See AECL-2552
11	20-42667	See 66-CNA-309
14	20-42617	See 66-CNA-303
15	20-42616	See 66-CNA-301
16	20-42621	Dep. mn. CFSTI $1.00 cy, $0.50 mn
CONF-660519–		**(Design Engineering Conference and Show, Chicago, May 9–12, 1966)**
2	20-42135	ORAU
CONF-660520–		**(International Symposium on the Decontamination of Nuclear Installations, Harwell, England, May 4–6, 1966)**
3	20-42677	See BNWL-SA-636
CONF-660539–		**(American Society for Microbiology, 66th Annual Meeting, Los Angeles, Calif., May 1–5, 1966)**
3	20-40571	ORAU. Gmelin, AED-CONF-66-114-3
CONF-660540–		**(Conference on Non-Compact Groups in Particle Physics, Milwaukee, Wis., May 4–6, 1966)**
1	20-42033	ORAU. Gmelin, AED-CONF-66-113-1
3	20-42026	ORAU. Gmelin, AED-CONF-66-113-2
6	20-42032	ORAU. Gmelin, AED-CONF-66-113-3
CONF-660542–		**(Society of Photographic Scientists and Engineers Meeting, San Francisco, Calif., May 9–13, 1966)**
1	20-41505	ORAU
CONF-660545–		**(Midwest Conference on Theoretical Physics, Bloomington, Ind., May 20–21, 1966)**
1	20-42031	ORAU. Gmelin, AED-CONF-66-140-1
2	20-42328	ORAU. Gmelin, AED-CONF-66-140-2
CONF-660547–		**(Virginia Academy of Science, 44th Annual Meeting, Harrisonburg, Virginia, May 4–7, 1966)**
1	20-42515	ORAU. Gmelin, AED-CONF-66-122-2
4	20-41920	ORAU. Gmelin, AED-CONF-66-121-1
CONF-660548–		**(Freiburg Medical Society Meeting, Freiburg, Germany, May 1966)**
1	20-40744	See BNL-10403
CONF-660549–		**(6th Annual Packaging Industry Technical Conference, Hartford, Conn., May 10–12, 1966)**
1	20-41395	ORAU. Gmelin, AED-CONF-66-141-1
CONF-660550–		**(Kansas Academy of Science, 98th Annual Meeting, Topeka, Kan., May 5–7, 1966)**
1	20-41371	ORAU. Gmelin, AED-CONF-66-139-1
CONF-660553–		**(Panel on Use of Organic Liquids as Reactor Coolants and Moderators, Vienna, Austria, May 9–13, 1966)**
1	20-42623	See EUR-2996.f
CONF-660605–		**(Cryogenic Engineering Conference, Boulder, Colo., June 13–15, 1966)**
9	20-41539	See MIT-2098-259
CONF-660606–	**20-34872**	**(American Nuclear Society Meeting, Denver, June 19–23, 1966) Trans. Amer. Nucl. Soc., 9: 1-322(1966)**
16	20-42672	See BNL-10388
17	20-42661	See DPSPU-66-30-2
18	20-42609	See WAPD-T-1886
CONF-660609–		**(International Symposium on Food Irradiation Meeting, Karlsruhe, Germany, June 6–10, 1966)**
5	20-40601	ORAU
14	20-41387	ORAU
16	20-40576	ORAU
17	20-41391	ORAU
18	20-41394	ORAU
19	20-40699	ORAU
20	20-41389	ORAU
21	20-41390	ORAU
22	20-41392	ORAU
24	20-40600	ORAU
25	20-41388	ORAU
27	20-40599	ORAU
CONF-660621–		**(Health Physics Society, 11th Annual Meeting, Houston, Tex., June 27–30, 1966)**
4	20-41190	Dep. mn. CFSTI $1.00 cy, $0.50 mn
6	20-41196	See LA-DC-7996
10	20-41216	ORAU. Gmelin, AED-CONF-66-193-2
13	20-41215	ORAU. Gmelin, AED-CONF-66-193-5
15	20-41373	ORAU. Gmelin, AED-CONF-66-193-8
CONF-660627–		**(American Society for Testing and Materials, 69th Annual Meeting, Atlantic City, N. J., June 27–July 1, 1966)**
3	20-41454	See NYO-2394-22

Report No.	Abstract No.	Availability
4	20-41506	ORAU. Gmelin, AED-CONF-66-198-2
5	20-41504	ORAU. Gmelin, AED-CONF-66-198-3
CONF-660628–	**(International Inst. of Refrigeration Commission I Meeting, Boulder, Colo., June 16–18, 1966)**	
4	20-41378	ORAU. Gmelin, AED-CONF-66-173-9
CONF-660630–	**(Vacuum Metallurgy Conference, New York, June 27–29, 1966)**	
1	20-41411	See IS-1379
CONF-660632–	**(American Inst. of Aeronautics and Astronautics, 4th Aerospace Sciences Meeting, Los Angeles, Calif., June 27–29, 1966)**	
1	20-42521	ORAU
5	20-41124	ORAU
6	20-41122	ORAU
8	20-42069	ORAU
9	20-42520	ORAU
CONF-660634–	**(Conference on the Recovery of Irradiated Cells by Herceg Novi, Yugoslavia, June 23–24, 1966)**	
1	20-40634	See ORNL-P-2312
CONF-660635–	**(International Colloquium on Radiations and Aging, Semmering, Austria, June 23–24, 1966)**	
2	20-40633	See ORNL-P-2287
CONF-660704–	**(Magnetohydrodynamic Electrical Power Generation, 2nd International Symposium, Salzburg, July 4–8, 1966)**	
92	20-41697	ORAU
93	20-41698	ORAU
94	20-41699	ORAU
95	20-41700	ORAU
96	20-41701	ORAU
97	20-41702	ORAU
98	20-41703	ORAU
99	20-41704	ORAU
100	20-41705	ORAU
101	20-41706	ORAU
102	20-41707	ORAU
103	20-41708	ORAU
104	20-41709	ORAU
105	20-41710	ORAU
106	20-41711	ORAU
107	20-41712	ORAU
108	20-41713	ORAU
109	20-41714	ORAU
110	20-41715	ORAU
111	20-41716	ORAU
112	20-41717	ORAU
113	20-41718	ORAU
114	20-41719	ORAU
115	20-41720	ORAU
116	20-41721	ORAU
117	20-41722	ORAU
118	20-41723	ORAU
119	20-41724	ORAU
120	20-41725	ORAU
121	20-41726	ORAU
122	20-41727	ORAU
123	20-41728	ORAU
124	20-41729	ORAU
125	20-41730	ORAU
126	20-41731	ORAU
127	20-41732	ORAU
128	20-41733	ORAU
129	20-41734	ORAU
130	20-41735	ORAU
131	20-41736	ORAU
132	20-41737	ORAU
133	20-41738	ORAU
134	20-41739	ORAU
135	20-41740	ORAU
136	20-41741	ORAU
137	20-41742	ORAU
138	20-41743	ORAU
139	20-41744	ORAU
140	20-41745	ORAU
141	20-41746	ORAU
142	20-41747	ORAU
143	20-41748	ORAU
144	20-41749	ORAU
145	20-41750	ORAU
146	20-41751	ORAU
147	20-41752	ORAU
148	20-41753	ORAU
149	20-41754	ORAU
150	20-41755	ORAU
151	20-41756	ORAU
152	20-41757	ORAU
153	20-41758	ORAU
154	20-41759	ORAU
155	20-41760	ORAU
156	20-41761	ORAU
157	20-41762	ORAU
158	20-41763	ORAU
159	20-41764	ORAU
160	20-41765	ORAU
161	20-41766	ORAU
162	20-41767	ORAU
163	20-41768	ORAU
164	20-41769	ORAU
165	20-41770	ORAU
166	20-41771	ORAU
167	20-41772	ORAU
168	20-41773	ORAU
169	20-41774	ORAU
170	20-41775	ORAU
171	20-41776	ORAU
173	20-41777	ORAU
174	20-41778	ORAU
175	20-41779	ORAU
176	20-41780	ORAU
177	20-41781	ORAU
178	20-41782	ORAU
179	20-41783	ORAU
180	20-41784	ORAU
181	20-41785	ORAU
182	20-41786	ORAU
183	20-41787	ORAU
CONF-660705–	**(IEEE Annual Conference, Palo Alto, Calif., July 18–22, 1966)**	
3	20-40952	See SC-DC-66-1823
CONF-660708–	**(Institute of Electrical and Electronics Engineers, Summer Meeting, New Orleans, La., July 1966)**	
3	20-41693	ORAU
CONF-660716–	**(Symposium on Recent Progress in Nuclear Physics with Tandems, Heidelberg, Germany, July 18–21, 1966)**	
1	20-42161	See LA-DC-7878
CONF-660804–	**(Society of Photo-Optical Instrumentation Engineers, 11th Annual Symposium, St. Louis, Mo., Aug. 22–26, 1966)**	
1	20-41223	See EGG-1183-1244
CONF-660805–	**(International Conference on Solvent Extraction, Goteborg, Sweden, Aug. 27–Sept. 1, 1966)**	
2	20-40876	See ORO-1797-2
CONF-660807–	**(Symposium on Neutron Monitoring for Radiological Protection, Vienna, Austria, Aug. 29, 1966)**	
2	20-41543	See RPP-R-2
CONF-660808–	**(13th International Conference on High Energy Physics, Berkeley, Calif., Aug. 31–Sept. 7, 1966)**	
9	20-41798	See MIT-2098-265
10	20-41797	See MIT-2098-264
CONF-660810–	**(8th Annual Rocky Mountain Spectroscopy Conference, Denver, Colo., Aug. 8, 1966)**	
1	20-40816	See RFP-699
2	20-40814	See RFP-664
3	20-40815	See RFP-698
CONF-660811–	**(American Physical Society Meeting, Mexico City, Mexico, Aug. 29–31, 1966)**	
1	20-41622	See SC-DC-66-1564
CONF-660812–	**(3rd Circular International Symposium, Lysekil, Sweden, Aug. 21–27, 1966)**	

Report No.	Abstract No.	Availability
1	20-42170	See UCRL-70045
CONF-660904–	**(9th Air Cleaning Conference, Boston, Mass., Sept. 13–16, 1966)**	
5	20-42673	See BNL-10483
6	20-41202	See UCRL-14990
10	20-41234	See ORNL-P-2436
CONF-660906–	**(International Conference on Nuclear Physics, Gatlinburg, Tenn., Sept. 12–17, 1966)**	
8	20-42163	See LA-DC-8082
9	20-42162	See LA-DC-8075
13	20-42164	See LA-DC-8083
14	20-42150	See COO-498-56
24	20-41278	See UCRL-70000
CONF-660912–	**(FAO/IAEA Symposium on the Use of Isotopes in Plant Nutrition and Physiology Studies, Vienna, Austria, Sept. 5–9, 1966)**	
1	20-40735	See NYO-2744-37
CONF-660917–	**(Gastrointestinal Radiation Injury Symposium, Richland, Washington, Sept. 25–28, 1966)**	
1	20-40607	See BNL-10518
CONF-660920–	**(1st International Congress of the International Radiation Protection Assn., Rome, Italy, Sept. 5–10, 1966)**	
5	20-41276	See UCRL-16769
CONF-660921–	**(International Colloquium on Intense Magnetic Fields, Their Production and Their Application, Grenoble, France, Sept. 12–14, 1966)**	
1	20-41080	See UCRL-14831
CONF-660924–	**(International Conference on Magnetic Resonance and Relaxation, 14th Colloque AMPERE, Ljubljana, Yugoslavia, Sept. 6–11, 1966)**	
1	20-42525	See ORNL-P-2466
CONF-661003–	**(AIME Nuclear Metallurgy Symposium on High Temperature Nuclear Fuels, Delevan, Wis., Oct. 3–5, 1966)**	
3	20-42624	See GA-6975
CONF-661005–	**(Symposium on Solid-State and Chemical Radiation Dosimetry, Vienna, Austria, Oct. 3, 1966)**	
1	20-41262	See BNWL-SA-619
COO–		
264-316	20-41982	Phys. Rev., 149: 1257-9(1966)
264-321	20-41973	Phys. Rev., 149: 1128-31(1966)
285	20-42622	Dep. mn. CFSTI $3.00 cy, $0.75 mn
347-21	20-42273	Phys. Rev. Lett., 17: 541-5(1966)
498-56	20-42150	Dep. mn. CFSTI $1.00 cy, $0.50 mn
578-3-32	20-40948	Dep. mn. CFSTI $3.00 cy, $0.75 mn
588-12	20-41443	Dep. mn. CFSTI $2.00 cy, $0.50 mn
818-79	20-41674	Phys. Rev., 149: 1013-17(1966)
878-12	20-40642	Arch. Biochem. Biophys., 115: 332-6(1966)
881-59	20-41858	Phys. Rev., 149: 1089-1113(1966)
881-68	20-41922	See CONF-660411-44
895-9	20-40610	Dep. mn. CFSTI $2.00 cy, $0.50 mn
1088-18	20-40963	J. Chem. Phys., 45: 1428-32(1966)
1088-19	20-40964	J. Chem. Phys., 45: 1433-9(1966)
1097-17	20-40532	Dep. mn. CFSTI $2.00 cy, $0.50 mn
1329-3	20-40494	Dep. mn. CFSTI $2.00 cy, $0.50 mn
1391-5	20-40658	Cancer Res., 26: 1780-6(1966)
1407-10	20-41130	Dep. mn. CFSTI $2.00 cy, $0.50 mn
1421-2	20-40611	Dep. mn. CFSTI $2.00 cy, $0.50 mn
1471-1	20-41221	Dep. mn. CFSTI $2.00 cy, $0.50 mn
1477-5	20-41444	Dep. mn. CFSTI $1.00 cy, $0.50 mn
1505-9	20-42259	Phys. Rev., 149: 880-3(1966)
1533-2	20-42522	Dep. mn. CFSTI $1.00 cy, $0.50 mn
1545-4	20-41984	Phys. Rev., 149: 1264-8(1966)
CTO–	**(Non-AEC)**	
299	20-42421	For translation see NP-tr-1396
DESY–	**(German)**	
66/16	20-41789	Dep. mn
66/17	20-41790	Dep. mn
66/18	20-41534	Dep. mn
66/19	20-41924	Dep. mn
66/20	20-41791	Dep. mn

Report No.	Abstract No.	Availability
DNPL–	**(British)**	
1	20-41535	Dep. mn
2	20-41536	Dep. mn
DP–		
552	20-41264	Dep. mn. CFSTI $1.00 cy, $0.50 mn
717	20-41031	Dep. mn. CFSTI $1.00 cy, $0.50 mn
900	20-41222	Dep. mn. CFSTI $1.00 cy, $0.50 mn
1010	20-41032	Dep. mn. CFSTI $2.00 cy, $0.50 mn
1048	20-41010	Dep. mn. CFSTI $1.00 cy, $0.50 mn
DPSPU–		
66-30-2	20-42661	Dep. mn. CFSTI $1.00 cy, $0.50 mn
DUBNA REPORTS	**(Russian)**	
See JINR (Russian)		
EDR–	**(Misc.)**	
4719	20-41419	See GMAD-3643-5
EFINS–	**(Misc.)**	
66-32	20-41982	See COO-264-316
66-40	20-41973	See COO-264-321
EGG–		
1183-1054	20-42663	Dep. mn. CFSTI $6.00 cy, $1.25 mn
1183-1244	20-41223	ORAU
1183-2013	20-41488	Dep. mn. CFSTI $1.00 cy, $0.50 mn
1183-2014	20-41489	Dep. mn. CFSTI $1.00 cy, $0.50 mn
1183-2029	20-41490	Dep. mn. CFSTI $1.00 cy, $0.50 mn
1183-2030	20-41491	Dep. mn. CFSTI $1.00 cy, $0.50 mn
1183-2039	20-41492	Dep. mn. CFSTI $1.00 cy, $0.50 mn
1183-2052	20-41493	Dep. mn. CFSTI $1.00 cy, $0.50 mn
1183-2078	20-41224	Dep. mn. CFSTI $3.00 cy, $0.75 mn
1183-2054	20-40518	See CEX-63.10
EUR–	**(European Atomic Energy Community)**	
1642.f	20-42652	See EURFNR-92F
2711.f	20-40612	Dep. mn
2750.e	20-41076	Belgian American Bank and Trust Co., New York, $12.00
2825	20-41410	See EURAEC-1612
2830	20-41494	See EURAEC-1617
2834	20-41495	See EURAEC-1621
2835	20-41445	See EURAEC-1622
2837	20-41446	See EURAEC-1624
2862	20-41448	See EURAEC-1670
2871	20-41450	See EURAEC-1684
2954.e	20-40866	Dep. mn
2957.d,f,e	20-40801	Dep. mn
2996.f	20-42623	Dep. mn
3051.e	20-42678	Dep. mn
EURAEC–		
1612	20-41410	Dep. mn. CFSTI $1.00 cy, $0.50 mn
1617	20-41494	Dep. mn. CFSTI $1.00 cy, $0.50 mn
1621	20-41495	Dep. mn. CFSTI $1.00 cy, $0.50 mn
1622	20-41445	Dep. mn. CFSTI $1.00 cy, $0.50 mn
1624	20-41446	Dep. mn. CFSTI $2.00 cy, $0.50 mn
1633	20-41418	See GEAP-5150
1634	20-41451	See GA-7101
1669	20-41447	Dep. mn. CFSTI $2.00 cy, $0.50 mn
1670	20-41448	Dep. mn. CFSTI $1.00 cy, $0.50 mn
1676	20-41449	Dep. mn. CFSTI $2.00 cy, $0.50 mn
1679	20-41425	See IITRI-578-P29-2
1684	20-41450	Dep. mn. CFSTI $1.00 cy, $0.50 mn
EURFNR–	**(Misc.)**	
92F	20-42652	Dep. mn. CFSTI $2.00 cy, $0.50 mn
FTD-HT–	**(Non-AEC)**	
66-191	20-41545	For translation see AD-631586
FTD-TT–	**(Non-AEC)**	
65-748	20-42419	For translation see AD-636608
65-887	20-42099	For translation see AD-636625
GA–	**(Misc.)**	
6420(Rev.)	20-42460	J. Nucl. Energy: Pt. C, 8: 555-9(1966)
6975	20-42624	Dep. mn. CFSTI $2.00 cy, $0.50 mn
7101	20-41451	Dep. mn. CFSTI $1.00 cy, $0.50 mn

Report No.	Abstract No.	Availability
GEAP–	**(Misc.)**	
4466	20-42625	Dep. mn. CFSTI $1.00 cy, $0.50 mn
4951	20-42626	Dep. mn. CFSTI $1.00 cy, $0.50 mn
5051	20-42627	Dep. mn. CFSTI $3.00 cy, $0.75 mn
5124	20-42608	Dep. mn. CFSTI $2.00 cy, $0.50 mn
5145	20-42628	Dep. mn. CFSTI $1.00 cy, $0.50 mn
5150	20-41418	Dep. mn. CFSTI $2.00 cy, $0.50 mn
5160	20-42629	Dep. mn. CFSTI $4.00 cy, $0.75 mn
GMAD–		
3643-5	20-41419	Dep. mn
HASL–		
172	20-41131	Dep. mn. CFSTI $8.00 cy, $2.25 mn
HPR–	**(Norwegian)**	
66	20-42630	Dep. mn
HUX–		
3170-1	20-41191	Dep. mn. CFSTI $3.00 cy, $0.75 mn
HW–		
65402(Rev.1)	20-40802	Dep. mn. CFSTI $1.00 cy, $0.50 mn
IAE–	**(Non-AEC)**	
1149	20-42402	Dep. mn
1151	20-42403	Dep. mn
IAN-R–	**(Colombia)**	
1	20-42679	Dep. mn
IBJ–	**(Polish)**	
See INR		
IC–	**(Misc.)**	
66/45	20-42404	Dep. mn
IDO–		
12053	20-41192	Dep. mn. CFSTI $2.00 cy, $0.50 mn
12054	20-41193	Dep. mn. CFSTI $2.00 cy, $0.50 mn
17165	20-42664	Dep. mn. CFSTI $3.00 cy, $0.75 mn
IEA–	**(Brazilian)**	
110	20-41399	Dep. mn
IFA-IS–	**(Rumanian)**	
36	20-41380	Dep. mn. JCL $4.60 fs, $1.61 mf
IITRI–	**(Misc.)**	
578P11-54	20-41112	Dep. mn. CFSTI $2.00 cy, $0.50 mn
578P29-2	20-41425	Dep. mn. CFSTI $1.00 cy, $0.50 mn
1193-54	20-41112	See IITRI-578P11-54
B6064-2	20-41425	See IITRI-578-P29-2
IN–		
1014	20-42151	Dep. mn. CFSTI $4.00 cy, $0.75 mn
1019	20-42138	Dep. mn. CFSTI $1.00 cy, $0.50 mn
1020	20-42139	Dep. mn. CFSTI $2.00 cy, $0.50 mn
INR–	**(Non-AEC)**	
678/IV/C	20-41265	Dep.
696/I/PL	20-41077	Dep.
698/IX-A/RP	20-42680	Dep.
704/III/PL	20-41265	Dep.
708/VI/PL	20-41792	Dep.
IPP–	**(Non-AEC)**	
1/46	20-42405	Dep. mn
2/41	20-42035	Dep. mn
2/47	20-42406	Dep. mn
2/48	20-42407	Dep. mn
2/49	20-42408	Dep. mn
3/40	20-41678	Dep. mn
6/46	20-42035	See IPP-2/41
6/50	20-42409	Dep. mn
6/51	20-42410	Dep. mn
IPPJ–	**(Japanese)**	
49	20-42411	Dep. mn
IPST-Cat.–	**(Russian)**	
1456	20-42038	For translation see NASA-TT-F-360
IS–		
1194	20-42117	Phys. Rev., 149: 231-43(1966)
1235	20-40904	J. Inorg. Nucl. Chem., 28: 2015-24(1966)
1336	20-42542	Phys. Rev., 149: 489-90(1966)
1379	20-41411	Dep. mn. CFSTI $2.00 cy, $0.50 mn
1500	20-42691	Dep. mn. CFSTI $7.94 cy, $2.25 mn
IS-Trans–		
37	20-40820	Dep. mn. JCL $2.60 fs, $0.83 mf
ISS–	**(Italian)**	
66/16	20-40733	Dep. mn
JEN–	**(Spanish)**	
159-DF/I-49	20-42152	Dep. mn
160-DQ/I-54	20-41034	Dep. mn
JINR–	**(Russian)**	
E-2822	20-41793	Dep. mn
E-2824	20-42153	Dep. mn
E-2857	20-42154	Dep. mn
E-2860	20-41794	Dep. mn
P-2756	20-41925	Dep. mn
P-2762	20-42155	Dep. mn
P-2764	20-42140	Dep. mn
P-2777	20-41926	Dep. mn
P-2785	20-42071	Dep. mn
P-2797	20-41927	Dep. mn
P-2813	20-42156	Dep. mn
P-2814	20-42157	Dep. mn
P-2817	20-42158	Dep. mn
P-2841	20-42159	Dep. mn
JPRS–	**(Non-AEC)**	
36341	20-41205	CFSTI $4.00 cy, $0.75 mn
36823	20-42420	CFSTI $3.00 cy, $0.75 mn
36895	20-41386	CFSTI $1.00 cy, $0.50 mn
K-L–		
6096	20-41252	Rev. Sci. Instrum., 37: 1217-19(1966)
KAPL–		
3099	20-42160	Dep. mn. CFSTI $2.00 cy, $0.50 mn
KAPL-P–		
2280	20-41423	Trans. Met. Soc. AIME, 230: 415-19(1964)
KFK–	**(German)**	
260	20-42631	Dep. mn
385	20-40867	Dep. mn
387	20-40803	Dep. mn
KR–	**(Norwegian)**	
108	20-40804	Dep. mn
KRB–	**(German)**	
1965/4	20-42638	See TID-23299
LA–		
2758	20-41035	Dep. mn. CFSTI $2.00 cy, $0.50 mn
3493	20-41426	Dep. mn. CFSTI $2.00 cy, $0.50 mn
3508	20-42682	Dep. mn. CFSTI $3.00 cy, $0.50 mn
3516	20-41194	Dep. mn. CFSTI $2.00 cy, $0.50 mn
3519	20-41195	Dep. mn. CFSTI $3.00 cy, $0.50 mn
3523	20-40868	Dep. mn. CFSTI $1.00 cy, $0.50 mn
3587	20-41537	Dep. mn. CFSTI $3.00 cy, $0.75 mn
LA-DC–		
7537	20-41877	Phys. Rev. Lett., 17: 481-4(1966)
7729	20-42112	Phys. Rev., 149: 97-101(1966)
7857	20-42484	Rev. Sci. Instrum., 37: 1224-9(1966)
7878	20-42161	Dep. mn. CFSTI $1.00 cy, $0.50 mn
7881	20-42124	Rev. Sci. Instrum., 37: 1270(1966)
7886	20-40888	Inorg. Nucl. Chem. Lett., 2: 153-6(1966)
7996	20-41196	Dep. mn. CFSTI $1.00 cy, $0.50 mn
8075	20-42162	Dep. mn. CFSTI $1.00 cy, $0.50 mn
8082	20-42163	Dep. mn. CFSTI $1.00 cy, $0.50 mn
8083	20-42164	ORAU
LA-tr–		
66-32	20-41682	Dep. mn. JCL $1.60 fs, $0.80 mf

Report No.	Abstract No.	Availability
66-41	20-42171	Dep. mn. CFSTI $2.00 cy, $0.50 mn. JCL $2.60 fs, $1.01 mf
LAL–	**(French)**	
1028	20-41266	
LNF–	**(Italian)**	
66/29	20-41538	Dep. mn
MATT–		
435	20-42455	J. Nucl. Energy: Pt. C, 8: 489-92(1966)
442	20-42470	Phys. Rev., 149: 102-13(1966)
MCW–		
1473	20-40869	Dep. mn. CFSTI $1.00 cy, $0.50 mn
1494	20-41036	Dep. mn. CFSTI $1.00 cy, $0.50 mn
MIT–	**(Misc.)**	
905-59	20-42260	Phys. Rev., 149: 884-93(1966)
2098-241	20-42247	Phys. Rev., 149: 772-7(1966)
2098-246	20-41820	Nuovo Cimento (10), 44A: 777-83(1966)
2098-251	20-41510	Dep. mn. CFSTI $4.00 cy, $0.75 mn
2098-259	20-41539	Dep. mn. CFSTI $1.00 cy, $0.50 mn
2098-265	20-41798	Dep. mn. CFSTI $1.00 cy, $0.50 mn
2098-264	20-41797	Dep. mn. CFSTI $1.00 cy, $0.50 mn
3221-19	20-42412	Dep. mn. CFSTI $3.00 cy, $0.75 mn
MLM–		
1172	20-41452	Dep. mn. CFSTI $1.00 cy, $0.50 mn
1313J	20-41469	J. Inorg. Nucl. Chem., 28: 1837-46(1966)
1325	20-41037	Dep. mn. CFSTI $3.00 cy, $0.75 mn
MPI-PAE–	**(German)**	
P1-30/66	20-41267	Dep. mn
MSAR–	**(Misc.)**	
66-149	20-41420	Dep. mn. CFSTI $3.00 cy, $0.75 mn
N–	**(Misc.)**	
66-14667	20-40602	See AD-624934
66-18147	20-40613	CFSTI $1.00 cy, $0.50 mn
NAA-SR–		
11980(Vol.6)	20-42141	Dep. mn. CFSTI $3.00 cy, $0.50 mn
12060	20-42632	Dep. mn. CFSTI $5.00 cy, $1.00 mn
NAA-SR-Memo–		
7310	20-40870	Dep. mn. CFSTI $1.00 cy, $0.50 mn
10848	20-41101	Dep. mn. CFSTI $2.00 cy, $0.50 mn
NAS-NS–	**(Misc.)**	
3110	20-40806	Dep. mn. CFSTI $1.00 cy, $0.50 mn
NASA-CR–	**(Misc.)**	
543	20-41679	CFSTI $4.25 cy, $1.50 mn
54994	20-42665	See WCAP-2870
NASA-TM–	**(Misc.)**	
X-53453(Vol.1)	20-41427	
NASA-TN–	**(Misc.)**	
D-2959	20-42413	CFSTI $3.00 cy, $0.50 mn
NASA-TT–	**(Non-AEC)**	
F-360	20-42038	CFSTI $5.00 cy, $1.00 mn
NIJS-R–	**(Yugoslavian)**	
471	20-41620	Dep. mn
NIRL-R–	**(British)**	
95	20-40871	Dep. mn. BIS $0.60. HMSO 3s.
NLCO–		
976	20-40807	Dep. mn. CFSTI $1.00 cy, $0.50 mn
NP–	**(AEC File No. for Non-AEC Reports)**	
16172	20-41197	Dep. mn
16191	20-41928	Dep. mn
16192	20-41198	Dep. mn
16212	20-40808	Dep. mn
16234	20-42142	CFSTI $3.00 cy, $0.75 mn
16235	20-40809	
16250	20-42658	Dep.
16254	20-40872	Dep. mn
16259	20-40519	Dep. mn
16261	20-40520	Dep. mn
16266	20-42414	Dep. mn
16270	20-40521	Dep. mn
NP-tr–	**(AEC File No. for Non-AEC Translations)**	
1396	20-42421	Dep. mn. CFSTI $1.00 cy, $0.50 mn. JCL $2.60 fs, $0.89 mf
1410	20-41280	Dep. mn. JCL $5.60 fs, $1.76 mf
NRC–	**(Canadian)**	
9057	20-40956	Can. J. Chem., 44: 1957-9(1966)
NRDL-TRC–	**(Non-AEC)**	
16	20-41184	See AD-637806
NRL–	**(Misc.)**	
6408	20-42524	Dep. mn. CFSTI $1.00 cy, $0.50 mn
NRL-F–	**(Non-AEC)**	
20	20-40521	See NP-16270
NUMEC–		
3428-21	20-41453	Dep. mn. CFSTI $1.00 cy, $0.50 mn
NYO–		
901-39	20-40614	Dep. mn. CFSTI $1.00 cy, $0.50 mn
901-54	20-40495	Dep. mn. CFSTI $3.00 cy, $0.75 mn
1753-3	20-40496	Dep. mn. CFSTI $3.00 cy, $0.75 mn
2150-12	20-40966	J. Chem. Phys., 45: 1703-9(1966)
2394-22	20-41454	Dep. mn. CFSTI $3.00 cy, $0.75 mn
2731-7	20-41455	Dep. mn. CFSTI $3.00 cy, $0.75 mn
2740-3	20-40617	Dep. mn. CFSTI $6.00 cy, $1.25 mn
2744-37	20-40735	Dep. mn. CFSTI $1.00 cy, $0.50 mn
2804-8	20-40580	Dep. mn. CFSTI $3.00 cy, $0.75 mn
2804-9	20-40620	Dep. mn. CFSTI $3.00 cy, $0.75 mn
2897-16	20-42179	J. Inorg. Nucl. Chem., 28: 1795-1801(1966)
2930-6	20-41102	Dep. mn. CFSTI $2.00 cy, $0.50 mn
3003-29	20-40949	Dep. mn. CFSTI $1.00 cy, $0.50 mn
3086-5	20-40621	Dep. mn. CFSTI $5.00 cy, $1.00 mn
3096-8	20-40622	Dep. mn. CFSTI $1.00 cy, $0.50 mn
3273-7	20-40522	Dep. mn. CFSTI $4.00 cy, $0.75 mn
3364-7(Rev.)	20-41540	Dep. mn. CFSTI $1.00 cy, $0.50 mn
3364-20	20-41132	Dep. mn. CFSTI $2.00 cy, $0.50 mn
3399-49	20-41983	Phys. Rev., 149: 1260-3(1966)
3399-50	20-41643	Phys. Rev., 148: 1274-5(1966)
3399-52	20-41860	Phys. Rev., 149: 1122-5(1966)
3399-63	20-41846	Nuovo Cimento (10), 44A: 1257-61(1966)
3400-1	20-40497	Dep. mn. CFSTI $2.00 cy, $0.50 mn
3462-2	20-40873	Dep. mn. CFSTI $3.00 cy, $0.75 mn
3510-2	20-40746	Dep. mn. CFSTI $2.00 cy, $0.50 mn
3621-1	20-40534	Dep. mn. CFSTI $1.00 cy, $0.50 mn
3622-4	20-41225	Dep. mn. CFSTI $1.00 cy, $0.50 mn
3642-2	20-41680	Dep. mn. CFSTI $2.00 cy, $0.50 mn
ORNL–		
3301(Suppl.1)	20-41400	Dep. mn. CFSTI $1.00 cy, $0.50 mn
3875	20-41226	Dep. mn. CFSTI $5.00 cy, $1.00 mn
3880	20-41039	Dep. mn. CFSTI $3.00 cy, $0.75 mn
3922	20-40498	Dep. mn. CFSTI $6.00 cy, $1.25 mn
3992	20-41456	Dep. mn. CFSTI $3.00 cy, $0.50 mn
4004	20-41407	Dep. mn. CFSTI $3.00 cy, $0.75 mn
4006	20-41401	Dep. mn. CFSTI $2.00 cy, $0.50 mn
ORNL-P–	**(Misc.)**	
82	20-40669	Genetics, 54: 639-55(1966)
1563	20-40686	Radiat. Res., 28: 779-92(1966)
1794	20-40905	J. Inorg. Nucl. Chem., 28: 2055-9(1966)
2109	20-42250	Phys. Rev., 149: 791-7(1966)
2121	20-41647	Phys. Rev., 149: 244-5(1966)
2122	20-41296	Nucl. Instrum. Methods, 43: 385(1966)
2152	20-42261	Phys. Rev., 149: 894-905(1966)
2198	20-41324	Rev. Sci. Instrum., 37: 1131-4(1966)
2236	20-42106	Nucl. Instrum. Methods, 44: 169-70(1966)
2246	20-40543	Biochem. Biophys. Res. Commun., 24: 285-9(1966)
2282	20-42221	Phys. Lett., 22: 304-7(1966)
2287	20-40633	Dep. mn. CFSTI $1.00 cy, $0.50 mn
2306	20-41316	Nucl. Instrum. Methods, 44: 160-2(1966)
2312	20-40634	Dep. mn. CFSTI $1.00 cy, $0.50 mn

Report No.	Abstract No.	Availability
2323	20-42229	Phys. Lett., 22: 325-7(1966)
2436	20-41234	Dep. mn. CFSTI $1.00 cy, $0.50 mn
2466	20-42525	Dep. mn. CFSTI $1.00 cy, $0.50 mn
ORNL-RMIC–	**(Oak Ridge National Lab.)**	
5	20-40874	Dep. mn. CFSTI $3.00 cy, $0.50 mn
ORNL-TM–		
626	20-41199	Dep. mn. CFSTI $1.00 cy, $0.50 mn
1295	20-41273	Dep. mn. CFSTI $3.00 cy, $0.75 mn
1342	20-41040	Dep. mn. CFSTI $1.00 cy, $0.50 mn
1452	20-42633	Dep. mn. CFSTI $1.00 cy, $0.50 mn
1453	20-42634	Dep. mn. CFSTI $1.00 cy, $0.50 mn
1550	20-40635	Dep. mn. CFSTI $2.00 cy, $0.50 mn
1551	20-41200	Dep. mn. CFSTI $1.00 cy, $0.50 mn
1559	20-42683	Dep. mn. CFSTI $2.00 cy, $0.50 mn
1565	20-41621	Dep. mn. CFSTI $3.00 cy, $0.75 mn
1581	20-41274	Dep. mn. CFSTI $1.00 cy, $0.50 mn
1582	20-41067	Dep. mn. CFSTI $1.00 cy, $0.50 mn
1599	20-40875	Dep. mn. CFSTI $2.00 cy, $0.50 mn
ORO–		
1747-12	20-40636	Dep. mn. CFSTI $1.00 cy, $0.50 mn
1797-2	20-40876	Dep. mn. CFSTI $1.00 cy, $0.50 mn
2504-96	20-41799	Dep. mn. CFSTI $1.00 cy, $0.50 mn
2670-13	20-40811	Dep. mn. CFSTI $5.00 cy, $1.00 mn
2754-7	20-40637	Dep. mn. CFSTI $2.00 cy, $0.50 mn
2915-55	20-42199	Nucl. Phys., 88: 241-56(1966)
2980-14	20-40812	Dep. mn. CFSTI $2.00 cy, $0.50 mn
3291-3	20-41457	Dep. mn. CFSTI $2.00 cy, $0.50 mn
3461-1	20-40536	Dep. mn. CFSTI $1.00 cy, $0.50 mn
PAN–	**(Polish)**	**(This series of reports was terminated in 1965. Subsequent reports are identified by the code INR)**
PATENTS	**(British)**	**(4s. 6d. each, U. K. Patent Office)**
1,031,992	20-42587	
1,032,121	20-41436	
1,032,221	20-42656	
1,032,250	20-42685	
1,032,396	20-42595	
1,032,585	20-41100	
1,032,689	20-42666	
1,033,055	20-42596	
1,033,392	20-42514	
1,034,375	20-42592	
1,034,817	20-41061	
1,034,866	20-42593	
1,034,941	20-42594	
1,035,522	20-41690	
1,035,631	20-42598	
1,036,006	20-42602	
1,036,646	20-41435	
1,036,720	20-41258	
1,036,883	20-42603	
1,036,884	20-42604	
1,036,896	20-42588	
1,036,935	20-42605	
1,037,291	20-40935	
1,037,524	20-41056	
1,037,606	20-42589	
1,037,634	20-42657	
1,037,783	20-41259	
1,037,841	20-42590	
1,038,041	20-41367	
1,038,042	20-41368	
1,038,087	20-42597	
1,038,711	20-41116	
PATENTS	**(German)**	
1,215,263	20-41358	
1,216,444	20-41359	
1,216,996	20-41260	
1,216,997	20-41362	
1,217,351	20-41057	
1,218,073	20-41363	
1,218,626	20-41360	
1,218,964	20-41058	
1,219,140	20-41581	
1,219,254	20-41261	

Report No.	Abstract No.	Availability
PATENTS	**(Japanese)**	
1965-20834	20-41576	
1965-20835	20-41575	
1965-20836	20-41574	
1965-20837	20-41573	
1965-20838	20-41572	
1965-20959	20-41577	
1965-20960	20-41578	
1965-22291	20-41579	
1965-26720	20-41580	
PATENTS	**(Spanish)**	
311,107	20-41026	
PATENTS	**(U. S.)**	**($0.50 each, U. S. Patent Office)**
3,251,159	20-41119	
3,252,754	20-41059	
3,252,869	20-42613	
3,255,046	20-41691	
3,255,090	20-42615	
3,255,091	20-42614	
3,255,092	20-42591	
3,255,119	20-41214	
3,255,346	20-41365	
3,255,347	20-41170	
3,255,350	20-41370	
3,255,351	20-41369	
3,255,352	20-41066	
3,255,353	20-41171	
3,256,434	20-41115	
3,256,436	20-41366	
3,256,440	20-41118	
3,259,767	20-41689	
3,264,070	20-41062	
3,264,223	20-40936	
3,264,379	20-40937	
3,264,515	20-41583	
3,264,568	20-41582	
3,265,602	20-41008	
3,265,627	20-42690	
3,265,628	20-40934	
3,265,895	20-41364	
3,265,899	20-41361	
3,268,303	20-41060	
PG-Report–	**(British)**	
698	20-41041	Dep. BIS $0.30. HMSO 1s. 9d.
722	20-41042	Dep. BIS $0.30. HMSO 1s. 3d.
PNE–		
5006	20-41068	Dep. mn. CFSTI $1.50 cy, $0.50 mn
PRNC–		
88	20-40950	Dep. mn. CFSTI $1.00 cy, $0.50 mn
R–	**(Misc.)**	
59-6	20-40809	See NP-16235
465	20-42142	See NP-16234
RFP–		
271	20-40813	Dep. mn. CFSTI $1.00 cy, $0.50 mn
664	20-40814	Dep. mn. CFSTI $2.00 cy, $0.50 mn
666	20-41079	Dep. mn. CFSTI $1.00 cy, $0.50 mn
698	20-40815	Dep. mn. CFSTI $1.00 cy, $0.50 mn
699	20-40816	Dep. mn. CFSTI $2.00 cy, $0.50 mn
777	20-41275	Dep. mn. CFSTI $1.00 cy, $0.50 mn
RHEL/R–	**(British)**	
125	20-41542	Dep. mn. BIS $0.50. HMSO 2s. 6d.
RISO–	**(Danish)**	
124	20-42635	Dep. mn
RL-SEP–		
823	20-40877	Dep. mn. CFSTI $2.00 cy, $0.50 mn
RLO–		
1388-501	20-41511	Dep. mn. CFSTI $2.00 cy, $0.50 mn
1750-8(Vol.1)	20-40523	Dep. mn. CFSTI $6.00 cy, $1.50 mn
RM–	**(Misc.)**	
4988	20-42046	

Report No.	Abstract No.	Availability
RPI–	(Misc.)	
321-6	20-40951	Dep. mn. CFSTI $4.00 cy, $1.00 mn
RPP-R–	(British)	
2	20-41543	Dep. mn
RRA–	(Misc.)	
T55 and Summary	20-41201	
RT-ING–	(Italian)	
(65)7	20-41103	Dep. mn
SC-CR–		
66-2030	20-41133	Dep. mn. CFSTI $3.00 cy, $0.75 mn
SC-DC–		
66-1564	20-41622	Dep. mn. CFSTI $1.00 cy, $0.50 mn
66-1823	20-40952	Dep. mn. CFSTI $1.00 cy, $0.50 mn
SC-R–		
66-886	20-41158	J. Acoust. Soc. Amer., 39: 980-1(1966)
SC-RR–		
66-324	20-41069	Dep. mn. CFSTI $2.00 cy, $0.75 mn
66-356	20-42036	Dep. mn. CFSTI $3.00 cy, $0.50 mn
SCL-DC–		
66-57	20-41428	Dep. mn. CFSTI $1.00 cy, $0.50 mn
SFL–	(Finnish)	
A3	20-41134	Dep. mn
SGAE-CH–	(Austrian)	
34/1966	20-41011	Dep.
SGAE-PH–	(Austrian)	
41/1966	20-41125	Dep. mn
SLAC–		
63	20-41544	Dep. mn. CFSTI $3.00 cy, $0.75 mn
SLAC-PUB–		
144	20-41859	Phys. Rev., 149: 1114-21(1966)
163	20-41671	Phys. Rev., 149: 201-8(1966)
184	20-41875	Phys. Rev., 149: 1248-57(1966)
186	20-41562	Rev. Sci. Instrum., 37: 1190-1(1966)
SLAC-Trans–		
46	20-41805	Dep. mn
STL–	(Misc.)	
517-0042	20-41396	Dep. mn. CFSTI $5.00 cy, $1.00 mn
SWRI–		
1228-4-22	20-42636	Dep. mn. CFSTI $1.00 cy, $0.50 mn
1228-7-33	20-42637	Dep. mn. CFSTI $1.00 cy, $0.50 mn
TID–		
3736	20-42692	Dep. DTI Extension Free
4043(Rev.3)	20-42693	Dep. mn. CFSTI $7.00 cy, $1.50 mn
4100(Suppl.34)	20-41065	Dep. DTI Extension Free
4577(Rev.2)	20-42694	CFSTI $1.00 cy, $0.75 mn
21223	20-40560	Mycologia, 58: 91-9(1966)
22386	20-42176	J. Inorg. Nucl. Chem., 28: 1763-7(1966)
22833	20-41384	Dep. mn. CFSTI $5.00 cy, $1.00 mn
22834	20-41873	Phys. Rev., 149: 1234-42(1966)
22859	20-41921	See CONF-660209-14
22928	20-42415	Dep. mn. CFSTI $3.00 cy, $0.75 mn
22965	20-40509	ORAU
23052	20-40537	Dep. mn. CFSTI $1.00 cy, $0.50 mn
23136	20-41385	Dep. mn. GPO $0.15
23137	20-40510	Dep. mn. CFSTI $1.00 cy, $0.50 mn
23238	20-40538	Dep. mn. CFSTI $3.00 cy, $0.75 mn
23268	20-41458	Dep. mn. CFSTI $3.00 cy, $0.75 mn
23271	20-40524	Dep. mn. CFSTI $2.00 cy, $0.50 mn
23277	20-42416	Dep. mn. CFSTI $6.00 cy, $1.25 mn
23288	20-41459	Dep. mn. CFSTI $5.00 cy, $1.00 mn
23299	20-42638	Dep. mn. CFSTI $3.00 cy, $0.75 mn
TIM–	(Misc.)	
793	20-41460	Dep. mn. CFSTI $1.00 cy, $0.50 mn
TRG-Report–	(British)	
1200	20-42695	Dep. BIS $0.50. HMSO 2s. 6d.
TT–	(Canadian)	
65-50138	20-42038	For translation see NASA-TT-F-360
66-32773	20-41205	See JPRS-36341
66-33253	20-42420	See JPRS-36823
66-33325	20-41386	See JPRS-36895
UCD–		
34P104-3	20-40541	Dep. mn. CFSTI $3.00 cy, $0.50 mn
472-113	20-40539	Dep. mn. CFSTI $3.00 cy, $0.75 mn
UCRL–		
7170	20-42417	Dep. mn. CFSTI $4.00 cy, $1.00 mn
7361(Pt.3)	20-41461	Dep. mn. CFSTI $1.00 cy, $0.50 mn
7695(Rev.1)	20-42684	Dep. mn. CFSTI $2.00 cy, $0.50 mn
11670(Rev.)	20-41250	Rev. Sci. Instrum., 37: 1115-23(1966)
11857	20-41681	Dep. mn. CFSTI $7.00 cy, $1.50 mn
13195(Rev.1)	20-41126	J. Geophys. Res., 71: 3923-7(1966)
13206	20-41224	See EGG-1183-2078
14292(Rev.2)	20-41164	J. Petrol. Technol., 619-23(1966)
14312	20-40855	Talanta, 13: 1265-74(1966)
14667	20-41953	Nuovo Cimento (10), 44A: 768-76(1966)
14678	20-41634	J. Nucl. Energy: Pt. C, 8: 577-8(1966)
14716	20-41800	Dep. mn. CFSTI $1.00 cy, $0.50 mn
14744	20-41512	Dep. mn. CFSTI $3.00 cy, $0.50 mn
14831	20-41080	Dep. mn. CFSTI $1.00 cy, $0.50 mn
14841	20-41104	Dep. mn. CFSTI $2.00 cy, $0.50 mn
14866	20-40747	Dep. mn. CFSTI $2.00 cy, $0.50 mn
14873(Rev.1)	20-42243	Phys. Rev., 149: 752-4(1966)
14874-T	20-42241	Phys. Rev., 149: 735-43(1966)
14904	20-41623	CFSTI $3.00 cy
14959	20-40817	Dep. mn. CFSTI $1.00 cy, $0.50 mn
14990	20-41202	Dep. mn. CFSTI $1.00 cy, $0.50 mn
16003	20-41801	Dep. mn. CFSTI $3.00 cy, $0.75 mn
16259	20-41203	Dep. mn. CFSTI $1.00 cy, $0.50 mn
16401	20-41238	Nucl. Instrum. Methods, 43: 333-7(1966)
16654	20-41293	Nucl. Instrum. Methods, 43: 361-4(1966)
16693	20-41854	Phys. Rev., 149: 1044-51(1966)
16702	20-41966	Nuovo Cimento (10), 44A: 1081-90(1966)
16706	20-42267	Phys. Rev., 149: 965-79(1966)
16728	20-41979	Phys. Rev., 149: 1208-12(1966)
16769	20-41276	Dep. mn. CFSTI $1.00 cy, $0.50 mn
16776	20-40511	Dep. mn. CFSTI $5.00 cy, $1.00 mn
16781	20-41869	Phys. Rev., 149: 1203-7(1966)
16832	20-41802	Dep. mn. CFSTI $3.00 cy, $0.75 mn
16849	20-42190	Nucl. Phys., 88: 137-44(1966)
16863	20-41803	Dep. mn. CFSTI $3.00 cy, $0.75 mn
16938	20-41878	Phys. Rev. Lett., 17: 492-5(1966)
16939	20-41879	Phys. Rev. Lett., 17: 495-8(1966)
16952	20-41277	Dep. mn. CFSTI $2.00 cy, $0.50 mn
16961	20-41886	Phys. Rev. Lett., 17: 556-61(1966)
17003	20-41804	Dep. mn. CFSTI $3.00 cy, $0.75 mn
17034	20-41624	Dep. mn. CFSTI $3.00 cy, $0.75 mn
70000	20-41278	Dep. mn. CFSTI $1.00 cy, $0.50 mn
70045	20-42170	Dep. mn. CFSTI $1.00 cy, $0.50 mn
UCRL-Trans–		
10040	20-41584	Dep. mn. JCL $1.60 fs, $0.80 mf
10041	20-41585	Dep. mn. JCL $2.60 fs, $1.01 mf
UJV–	(Czechoslovakian)	
1368	20-40818	Dep. mn
1424	20-42599	Dep. mn
UNC–	(Misc.)	
5154	20-42639	Dep. mn. CFSTI $2.00 cy, $0.50 mn
UR–		
875-107	20-41943	J. Math. Phys. (N. Y.), 7: 989-90(1966)
875-125	20-41969	Phys. Rev., 149: 1017-26(1966)
875-129	20-41849	Nuovo Cimento (10), 44A: 1268-71(1966)
875-137	20-42253	Phys. Rev., 149: 820-6(1966)
875-138	20-41976	Phys. Rev., 149: 1138-44(1966)
875-152	20-41884	Phys. Rev. Lett., 17: 548-52(1966)
URS–	(Non-AEC)	
646-4	20-41177	See AD-632211
USBM-RC–		
1245	20-41462	Dep. mn. CFSTI $1.00 cy, $0.50 mn

Report No.	Abstract No.	Availability
1249	20-41429	Dep. mn. CFSTI $3.00 cy, $0.50 mn
USNRDL-TR–	**(Misc.)**	
1017	20-40604	See AD-635251
1023	20-40732	See AD-636209
1025	20-40605	See AD-635735
1043	20-42146	See AD-638014
USNRDL-TRC–	**(Non-AEC)**	
5	20-41177	See AD-632211
16(Vol.1)	20-41179	See AD-635821
16(Vol.2)	20-41180	See AD-635822
16(Vol.3)	20-41181	See AD-635823
16(Vol.4)	20-41182	See AD-635824
UTIAS–	**(Canadian)**	
115	20-42037	
VUF–		
3021	20-41070	Dep. mn
WANL-TNR–	**(Misc.)**	
133(Rev.)	20-42143	Dep. mn. CFSTI $6.00 cy, $1.25 mn
WAPD-PWR–		
2210(Vol.1)	20-42640	Dep. mn. CFSTI $6.00 cy, $1.25 mn
2213	20-42641	Dep. mn. CFSTI $6.00 cy, $1.26 mn
2216	20-42642	Dep. mn. CFSTI $6.00 cy, $1.25 mn
2217	20-42643	Dep. mn. CFSTI $7.00 cy, $1.75 mn
2219	20-42644	Dep. mn. CFSTI $4.00 cy, $0.75 mn
2222	20-42645	Dep. mn. CFSTI $4.00 cy, $1.00 mn
2223	20-42646	Dep. mn. CFSTI $4.00 cy, $0.75 mn
2226	20-42647	Dep. mn. CFSTI $5.00 cy, $1.00 mn
2229	20-42648	Dep. mn. CFSTI $6.00 cy, $1.25 mn
2230	20-42649	Dep. mn. CFSTI $5.00 cy, $1.00 mn
2232	20-42650	Dep. mn. CFSTI $3.00 cy, $0.75 mn
WAPD-T–		
1886	20-42609	Dep. mn. CFSTI $1.00 cy, $0.50 mn
WAPD-TM–	**(Misc.)**	
534	20-42582	Dep. mn. CFSTI $4.00 cy, $0.75 mn
WAPD-Trans–		
33	20-42611	Dep. mn. JCL $1.60 fs, $0.80 mf
34	20-42583	Dep. mn. JCL $1.10 fs, $0.80 mf
WASH–		
1065	20-42651	Dep. mn. CFSTI $1.00 cy, $0.50 mn
WCAP–	**(Misc.)**	
2870	20-42665	
Y–		
1544-A	20-41204	Dep. mn. CFSTI $3.00 cy, $0.50 mn
YALE–		
2726-H-84	20-42183	Nucl. Phys., 88: 21-32(1966)

DEPOSITORIES OF USAEC REPORTS

In Countries Other than the U.S.

ARGENTINA
Buenos Aires, Comisión Nacional de Energía Atómica
AUSTRALIA
Canberra, Australian National Library
Sutherland, New South Wales, Australian Atomic Energy Commission
AUSTRIA
Vienna, Zentral Bibliothek der Physikalischen Institute der Universität
BELGIUM
Mol-Donk, Centre d'Etude de l'Energie Nucleaire
BOLIVIA
La Paz, Comisión Nacional de Energia Nuclear
BRAZIL
Rio de Janeiro, Instituto Brasileiro de Bibliografia e Documentacao
São Paulo, Instituto de Energia Atomica, Cidade Universitaria São Paulo
BURMA
Rangoon, Union of Burma Applied Research Institute, Atomic Energy Center Library
CANADA
Hamilton, McMaster University
Ottawa, National Research Council Library
Vancouver, University of British Columbia
CHILE
Santiago, Departamento de Fisica, Universidad de Chile
CHINA
Hsinchu, Taiwan, Free China, National Tsing Hua University
COLOMBIA
Bogota, Instituto De Asuntos Nucleares
COSTA RICA
San Pedro, University of Costa Rica Library
DENMARK
Risö, Danish Atomic Energy Commission
ECUADOR
Quito, Escuela Politécnica Nacional
EL SALVADOR
San Salvador, Universidad de El Salvador, Biblioteca de Energia Nuclear
FINLAND
Helsinki, Teknillisen Korkeakoulun Kirjasto
FRANCE
Gif-sur-Yvette, Centre d'Etudes Nucléaires de Saclay
Paris, Académie des Sciences
GERMANY
Berlin, Hahn-Meitner-Institut für Kernforschung Berlin
Frankfurt/Main, Gmelin-Institut
Munich, Technische Hochschule, Bibliothek
GHANA
Accra, University College of Ghana
GREECE
Athens, Nuclear Research Center "Democritus"
GUATEMALA
Guatemala, Comisión Nacional de Energía Nuclear
INDIA
Bombay, Department of Atomic Energy
IRAN
Tehran, Tehran University Nuclear Centre
IRAQ
Baghdad, Iraqi Atomic Energy Commission
IRELAND
Dublin, University College
ISRAEL
Rehovoth, Israel Atomic Energy Commission
ITALY
Rome, Centro di Studi Nucleari della Casaccia
Rome, Comitato Nazionale per l'Energia Nucleare
JAPAN
Tokyo, National Diet Library
KOREA
Seoul, Office of Atomic Energy
LEBANON
Beirut, Lebanese National Council for Scientific Research
LUXEMBOURG
Luxembourg, Ministry of Transport and Electricity
MALAYSIA
Kuala Lumpur, University of Malaysia
MEXICO
Mexico, D.F., Comisión Nacional de Energía Nuclear
NETHERLANDS
The Hague, Reactor Centrum Nederland
NEW ZEALAND
Lower Hutt, Institute of Nuclear Sciences
NIGERIA
Ibadan, University of Ibadan
NORWAY
Lillestrøm, Institutt för Atomenergi
PAKISTAN
Lahore, West Pakistan, Atomic Energy Centre
PERU
Lima, Junta de Control de Energia Atomica
PHILIPPINE REPUBLIC
Manila, Philippine Atomic Energy Commission
POLAND
Warsaw, Biura Pelnomocnika Rzadu do Spraw Wykorzystania Energii Jadrowej
PORTUGAL
Sacavem, Junta de Energía Nuclear
REPUBLIC OF SOUTH AFRICA
Pretoria, Atomic Energy Board Library
REPUBLIC OF THE CONGO
Leopoldville, Université Lovanium
SPAIN
Madrid, Junta de Energía Nuclear, Biblioteca Documentación y Publicaciones, Ciudad Universitaria
SWEDEN
Nyköping, Aktiebolaget Atomenergi
SWITZERLAND
Zürich, Eidgenössische Technische Hochschule, Bibliothek
THAILAND
Bangkok, Office of the Thai Atomic Energy Commission, Department of Science
TURKEY
Ankara, Turkish Atomic Energy Commission, Atomic Energy Library
UNITED ARAB REPUBLIC
Cairo, Atomic Energy Commission
UNITED KINGDOM
Birmingham, Central Library
Boston Spa, National Lending Library for Science and Technology
Kingston upon Hull, Central Library
Liverpool, Central Library
London, Central Library, Acton
London, National Reference Library
London, Science Museum Library, South Kensington
Manchester, Central Library
Newcastle upon Tyne, Central Library
Nottingham, Central Library
Sheffield, Central Library
URUGUAY
Montevideo, Comision Nacional de Energia Atomica
VENEZUELA
Caracas, Instituto Venezolano de Investigaciones Científicas
VIET-NAM
Saigon, Atomic Energy Office
YUGOSLAVIA
Belgrade, Federal Commission for Nuclear Energy

In International Agencies

AUSTRIA
Vienna, International Atomic Energy Agency
BELGIUM
Brussels, La Bibliotheque EURATOM
FRANCE
Paris, European Nuclear Energy Agency, O.E.C.D.
ITALY
Ispra, EURATOM Research Center
SWITZERLAND
Geneva, United Nations Library

UNITED STATES
GOVERNMENT PRINTING OFFICE
DIVISION OF PUBLIC DOCUMENTS
WASHINGTON, D.C. 20402

OFFICIAL BUSINESS

POSTAGE AND FEES PAID
U.S. GOVERNMENT PRINTING OFFICE

TECHNICAL PROGRESS REVIEWS

The Division of Technical Information, U. S. Atomic Energy Commission, also publishes the Technical Progress Reviews, a series of four quarterly journals on nuclear technology. These journals, compiled by specialists and recognized authorities, summarize, evaluate, and reference the progress of development in four important fields.

Isotopes and Radiation Technology P. S. Baker, A. F. Rupp, and associates, Oak Ridge National Laboratory. Reviews AEC-sponsored projects and related significant worldwide developments in radioisotopes and radiation technology.

Nuclear Safety Wm. B. Cottrell, W. H. Jordan, J. P. Blakely, and associates, Nuclear Safety Information Center, Oak Ridge National Laboratory. Covers topics relevant to the analysis and control of hazards associated with nuclear reactors and with operations involving fissionable materials and the products of nuclear fission.

Power Reactor Technology Argonne National Laboratory. Reviews research, development, design practices, and operating experiences associated with power reactors, including aerospace applications.

Reactor Materials E. M. Simons and associates, Battelle Memorial Institute. Covers the properties, behavior, and fabrication processes of materials used in nuclear reactors and associated equipment.

Availability

SUBSCRIPTION RATE: The Technical Progress Reviews may be purchased from the Superintendent of Documents, U. S. Government Printing Office, Washington, D. C. 20402. *Nuclear Safety* at $3.00 per year for each subscription or $1.00 per issue; each of the other journals at $2.50 per year or $0.70 per issue.

POSTAGE: Postpaid within the United States, Canada, Mexico, and all Central and South American countries except Argentina, Brazil, Guyana, French Guiana, Surinam, and British Honduras. For these Central and South American countries and all other countries, add $0.75 for each annual subscription or $0.20 for a single issue.

REMITTANCE: Payment should be by check, money order, or document coupons and MUST accompany order. Remittances from foreign countries should be made by international money order or draft on an American bank payable to the Superintendent of Documents or by UNESCO book coupons.